Introduction to NUCLEAR REACTOR PHYSICS

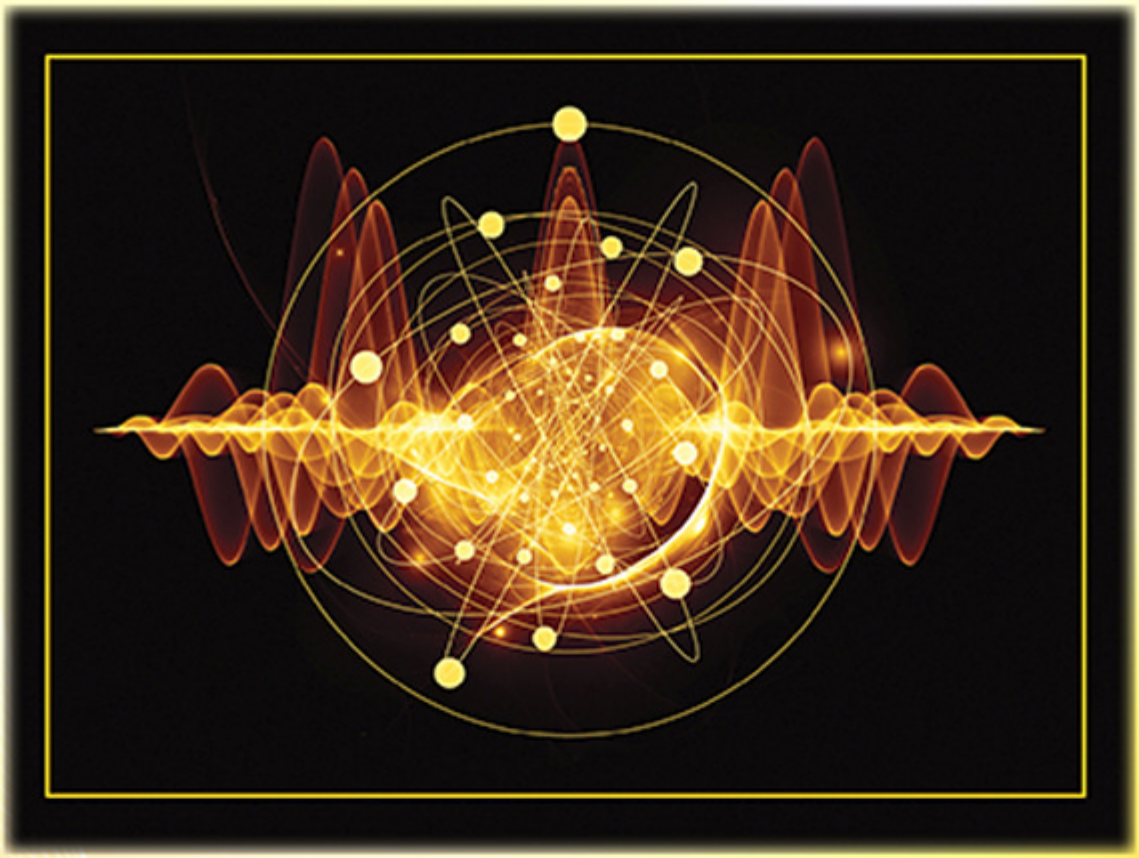

Robert E. Masterson

CRC Press
Taylor & Francis Group

Introduction to Nuclear Reactor Physics

Introduction to Nuclear Reactor Physics

Robert E. Masterson, ScD

CRC Press
Taylor & Francis Group
Boca Raton London New York

CRC Press is an imprint of the
Taylor & Francis Group, an **informa** business

CRC Press
Taylor & Francis Group
6000 Broken Sound Parkway NW, Suite 300
Boca Raton, FL 33487-2742

© 2018 by Taylor & Francis Group, LLC
CRC Press is an imprint of Taylor & Francis Group, an Informa business

No claim to original U.S. Government works

Printed on acid-free paper

International Standard Book Number-13: 978-1-4987-5148-3 (Hardback)

This book contains information obtained from authentic and highly regarded sources. Reasonable efforts have been made to publish reliable data and information, but the author and publisher cannot assume responsibility for the validity of all materials or the consequences of their use. The authors and publishers have attempted to trace the copyright holders of all material reproduced in this publication and apologize to copyright holders if permission to publish in this form has not been obtained. If any copyright material has not been acknowledged please write and let us know so we may rectify in any future reprint.

Except as permitted under U.S. Copyright Law, no part of this book may be reprinted, reproduced, transmitted, or utilized in any form by any electronic, mechanical, or other means, now known or hereafter invented, including photocopying, microfilming, and recording, or in any information storage or retrieval system, without written permission from the publishers.

For permission to photocopy or use material electronically from this work, please access www.copyright.com (http://www.copyright.com/) or contact the Copyright Clearance Center, Inc. (CCC), 222 Rosewood Drive, Danvers, MA 01923, 978-750-8400. CCC is a not-for-profit organization that provides licenses and registration for a variety of users. For organizations that have been granted a photocopy license by the CCC, a separate system of payment has been arranged.

Trademark Notice: Product or corporate names may be trademarks or registered trademarks, and are used only for identification and explanation without intent to infringe.

Library of Congress Cataloging-in-Publication Data

Names: Masterson, Robert, 1950- author.
Title: Introduction to nuclear reactor physics / Robert Masterson.
Description: Boca Raton : Taylor & Francis, a CRC title, part of the Taylor & Francis imprint, a member of the Taylor & Francis Group, the academic division of T&F Informa, plc, [2017]
Identifiers: LCCN 2016052983 | ISBN 9781498751483 (hardback : acid-free paper)
Subjects: LCSH: Nuclear reactors. | Nuclear physics. | Nuclear power plants.
Classification: LCC QC786.5 .M375 2017 | DDC 621.48/31--dc23
LC record available at https://lccn.loc.gov/2016052983

Visit the Taylor & Francis Web site at
http://www.taylorandfrancis.com

and the CRC Press Web site at
http://www.crcpress.com

This book is dedicated to the great men and women who created the nuclear power industry and helped to make it what it is today.

This book is further dedicated to my old friend and colleague John Cowley, who claims that he will read every line of it even though he may not understand all of it.

Finally, this book is dedicated to my late wife Carol, who encouraged me to undertake this effort, but never lived to see it fully completed.

Table of Contents

Preface xxi
Credits and Acknowledgments xxv
Author xxvii

CHAPTER 1

Nuclear Power in the World Today 1

1.1 Popular Types of Reactors and Their Design Characteristics 1
1.2 Number of Power Reactors in the World Today 1
1.3 Power Reactor Architectures 2
1.4 Power Reactors and Their Design Parameters 6
1.5 Schematic of a Nuclear Power Plant 7
1.6 Coolants Used in Nuclear Power Plants 8
1.7 Types of Nuclear Reactor Fuel 12
1.8 Properties of Nuclear Fuel 12
1.9 Reactor Pressure Vessels and Their Properties 13
1.10 Thermal Energy Production from Nuclear Fuel Rods 16
1.11 Fuel Rod Cladding 17
1.12 Nuclear Fuel Assemblies 19
1.13 PWR, BWR, and LMFBR Fuel Assemblies 20
1.14 Number of Fuel Rods in a Reactor Fuel Assembly 21
1.15 Fuel Rods in Square Fuel Assemblies 22
1.16 Fuel Rods in Hexagonal Fuel Assemblies 23
1.17 Other Fuel Assemblies: CANDU Fuel Assemblies 23
1.18 Characteristics of Reactor Fuel Assemblies 24
1.19 Design Parameters for Reactor Fuel Assemblies 26
1.20 Characteristics of Reactor Cores 26
1.21 Core Composition 28
1.22 Lattice Geometries 30
1.23 Unit Cells 31
1.24 The Infinite Lattice Approximation 32
1.25 Accounting for the Fuel-to-Cladding Gap 33
1.26 Fuel Assembly Loading Schemes 34
1.27 Reactor Refueling Cycles 37
1.28 An Overview of Nuclear Fuel Management 38
1.29 Core Loading Patterns 40
1.30 Ways to Measure the Amount of Nuclear Fuel That Has Been Burned 41
1.31 Alternative Ways for Measuring the Burnup of the Fuel 43
1.32 Other Important Nuclear Reactor Properties (Power Density and Thermal Efficiency) 44
1.33 Power Density 44
1.34 Thermal Efficiency 45
1.35 Control Rods and Their Function 47
1.36 Comparing PWR Control Rods and BWR Control Rods 48
1.37 Use of the Scram Button and the Word SCRAM 51
1.38 Maintaining the Criticality of the Core over Time 51
1.39 Electrical Generating Systems in a Nuclear Power Plant 51
1.40 Steam Generators in Nuclear Power Plants 51
1.41 Steam Turbines 53
1.42 Steam Generator and Steam Turbine Pairing 53
1.43 Electrical Generators 53
1.44 Common Measurements of Electrical Energy Production 55
1.45 Reviewing What We Have Just Learned 58
References 58
Books and Textbooks 58
Web References 58
Questions for the Student 59
Exercises for the Student 63

CHAPTER 2

Neutrons and Other Important Particles of Reactor Physics 67

2.1 Reactor Physics and the Study of the Neutron 67
2.1.1 Nuclear Particles and Particle Types 67
2.2 Visualizing the Atomic Nucleus 70
2.3 Basic Laws of the Nuclear World: The Conservation of Mass/Energy, Momentum, and Charge 71
2.4 Units for Measuring Nuclear Mass 71
2.5 Protons and Neutrons: The Building Blocks of the Atomic Nucleus 73
2.6 Gluon and the Nuclear Force Field 75
2.7 Yukawa Potential and the Coulomb Potential 76
2.8 Visualizing the Nuclear Binding Force 76
2.9 Nucleus and Its Surface 79
2.10 Density of the Atomic Nucleus 79
2.11 How the Number of Neutrons Affects the Stability of a Nucleus 80
2.12 Other Factors That Affect Nuclear Stability 80

2.13 Differences between Chemical and Nuclear Bonds 82
2.13.1 Difference #1: The Strength of the Nuclear and Chemical Bonds 82
2.13.2 Difference #2: The Existence of Discrete Energy Levels 82
2.13.3 Difference #3: The Range of the Chemical and Nuclear Forces 84
2.14 How Nuclear Energy Is Measured 85
2.15 Estimating the Energy of the Neutron, the Proton, and the Electron 86
2.16 Conservation of Linear Momentum in Particle Reactions 89
2.17 Momentum Conservation in Reactions Involving Photons 91
2.18 Conservation of the Baryon Number in Nuclear Reactions 92
2.19 Some Final Observations 92
2.20 Effects of Relativity on Particle Behavior 93
2.21 Effect of Motion on Particle Behavior and Radioactive Decay 95
2.22 Relationship between the Mass and the Energy of Matter Particles 96
2.23 Behavior of Nuclear Particles at Very High Speeds 97
2.24 Converting Particle Energies to Particle Velocities 99
2.25 Relationship between the Energy of a Neutron and Its Velocity 100
2.26 Speed of Photon Propagation in a Material Medium 101
2.27 Controlling the Behavior of Nuclear Particles without an Electrical Charge 102
2.28 Connecting the Microscopic World to the Macroscopic One 103
2.29 Calculating Nuclear Energy from $E = mc^2$ 103
2.30 Understanding Nuclear Energy Production 105
2.31 Converting the Kinetic Energy of Nuclear Particles into Thermal Energy and Heat 105
References 107
Books and Textbooks 107
Web References 107
Additional References 107
Questions for the Student 108
Exercises for the Student 111

CHAPTER 3
Nuclear Particles, Processes, and Reactions 115

3.1 Nuclear Particle Behavior 115
3.2 Determining the Behavior of Particles with an Electric Charge 115
3.3 The Behavior of Neutrons 117
3.4 Prompt and Delayed Neutrons 118
3.4.1 The Prompt Neutron Energy Spectrum 118
3.4.2 Understanding the Terms in the Watt Equation 119
3.5 The Delayed Neutron Fraction 120
3.6 Types of Neutron Interactions 120
3.7 Modeling the Emission of a Neutron from an Atomic Nucleus 122
3.8 Coordinate System Independence during Particle Collisions 123
3.9 Momentum Conservation for a Multiparticle System 125
3.10 What Happens When a Neutron Hits an Atomic Nucleus 127
3.11 Including Photons and Neutrinos in Common Particle Collisions 129
3.12 The Physics of Head-On Collisions 130
3.13 Particle Backscattering 132
3.14 Finding the Energy Loss in a Head-On Elastic Collision 133
3.15 The Energy Loss in a Glancing Collision 135
3.16 Neutron Energy Loss as a Function of Scattering Angle 138
3.17 Scattering Angles in the Laboratory and Center of Mass Systems 138
3.18 A More Detailed Look at the Interaction of Neutrons with Matter 141
3.19 Reviewing Elastic Neutron Scattering 141
3.20 Reviewing Inelastic Neutron Scattering 142
3.21 Neutron Beam Generators 143
3.22 Generating Cold Neutron Beams 143
3.23 Understanding the Difference between Neutron Capture and Neutron Absorption 144
3.24 Neutrons and Their Role in the Nuclear Fission Process 145
3.25 Examining the Nuclear Fission of Uranium-235 in More Detail 147
3.25.1 Outcome 1 147
3.25.2 Outcome 2 147
3.26 Fission Products and Fission Product Poisons 148
3.27 The Energetics of Nuclear Fission 148
3.28 Standard Notation Used to Describe Different Nuclear Reactions 149
3.29 Some Final Observations regarding Elastic Scattering Reactions 150
3.30 Neutron Moderators and Neutron Kinetic Energy Loss 152
3.31 Using a Neutron Balance Equation to Model the Behavior of Large Numbers of Neutrons 152
3.32 Scattering Angles and Scattering Probabilities 152

3.33 Scattering Angles in Inelastic Collisions 155
3.34 Neutron Scattering in Heavy Materials 155
3.35 Defining the Differential Scattering Probability 156
3.36 The Scattering of Alpha Particles 158
3.37 The Rutherford Scattering Formula 158
References 160
Books and Textbooks 160
Web References 160
Additional References 160
Questions for the Student 161
Exercises for the Student 163

CHAPTER 4
Nuclear Cross Sections, Reaction Probabilities, and Reaction Rates 167

4.1 Nuclear Cross Sections and Their Uses 167
4.2 Types of Nuclear Cross Sections 167
4.3 Reaction Resonances and Nuclear Cross Sections 171
4.4 Reaction Resonances and Compound Nucleus Formation 172
4.5 Nuclear Cross Sections and Reaction Rates 174
4.6 Finding Energy-Dependent Reaction Rates 176
4.7 Fast and Thermal Neutron Cross Sections 177
4.8 Cross Sections with More than Two Energy Groups 179
4.9 Multigroup Approximation 180
4.10 Fission Cross Sections for Neutrons Having Any Kinetic Energy 181
4.11 Absorption Cross Sections for Neutrons Having Any Energy 182
4.12 Radiative Capture 183
4.13 Scattering Cross Sections for Neutrons with Any Kinetic Energy 184
4.14 Nuclear Properties of Hydrogen and Deuterium 186
4.15 Methods for Estimating the Total Cross Section 187
4.16 Converting Microscopic Cross Sections to Macroscopic Ones 189
4.17 A Brief Chemical Primer 189
4.18 A Practical Example of a Cross Section Calculation 190
4.19 Finding the Cross Sections for a Pure Material 191
4.20 Relationship between the Physical Density and the Atomic Density 192
4.21 Finding Macroscopic Cross Sections for a Complex Nuclear Material 193
4.22 Public Cross Section Libraries 194
4.23 Measuring Avogadro's Number 196
4.24 Uranium Dioxide and Its Properties 198
4.25 Important Cross Section Naming Conventions 200
References 200
Books and Textbooks 200
Web References 201
Additional References 201
Questions for the Student 202
Exercises for the Student 204

CHAPTER 5
Cross Section Libraries and Sources of Practical Nuclear Data 207

5.1 Sources of Nuclear Cross Section Data 207
5.2 A Very Important Table with Three Distinct Parts 207
5.3 Online Plotting Tools (A Tool for Plotting Nuclear Cross Sections—*ENDFPLOT*) 215
5.4 Cross Sections and ENDF/B Nomenclature 215
5.5 Comparison of Cross Sections for Common Nuclear Materials 217
5.6 Finding the Number of Atoms or Molecules in a Given Sample of Material 219
5.7 Other Applications 221
5.8 Thermal Cross Sections for 1/v and Non-1/v Absorbers 221
5.9 Thermal Energy Group Cross Sections 223
5.10 Cross Sections and the Behavior of the Neutron Flux near a Reaction Resonance 225
5.11 Creating Neutron Cross Section Libraries from Raw Data 226
5.12 Finding the Neutron Energy Spectrum to Build a Group Cross Section Library 232
5.13 Collapsing the Group Cross Sections When Needed 233
5.14 Conserving the Reaction Rates When Collapsing to a Single Energy Group 235
5.15 Group Flux and Average Flux within a Group 239
5.16 Using Large Numbers of Energy Groups 241
5.17 Realistic Reactor Design Practices 243
5.18 A Simple Design Exercise 244
5.19 Cross Section Naming Conventions 246
References 247
Books and Textbooks 247
Web References 248
Additional References 248
Questions for the Student 249
Exercises for the Student 250

CHAPTER 6

Nuclear Fuels, Nuclear Structure, the Mass Defect, and Radioactive Decay 255

6.1 Elements, Isotopes, and Nuclear Fuels 255
6.2 The Periodic Table 255
6.3 Elements and Isotopes in the Periodic Table 257
6.4 Man-Made Elements 259
6.5 Fractional Atomic Weights and Their Meaning 262
6.6 Effect of Binding Energy on Isotopic Rest Mass 264
6.7 Fundamental Origins of Fission and Fusion 265
6.8 The Mass Defect and Its Origin 265
6.9 Nuclear Binding Energy Curve 268
6.10 Energy Released due to Missing Nuclear Mass 270
6.11 Physical Basis for the Shape of the Nuclear Binding Energy Curve 271
6.12 Liquid Drop Model of the Atomic Nucleus 273
6.12.1 The Volume Energy Term 275
6.12.2 The Surface Energy Term 275
6.12.3 The Electrical Energy Term 275
6.12.4 The Asymmetry Energy Term 276
6.12.5 The Pairing Energy Term 276
6.13 Interpreting the Results 276
6.14 Shell Model of the Nucleus 278
6.15 How Nuclear Fission Is Related to Nuclear Structure 279
6.16 Nuclear Fuels and Their Properties 280
6.17 Difference between Controlled and Uncontrolled Nuclear Reactions 282
6.18 The Process of Uranium Enrichment 283
6.19 Man-Made Elements and Nuclear Fuels 285
6.20 The Element Neptunium 285
6.21 The Element Plutonium 286
6.22 Production of Plutonium-239 286
6.23 Plutonium-239 Decay 288
6.24 Other Isotopes of Plutonium 289
6.25 Radioactivity and Radioactive Decay 289
6.26 Force Imbalances and the Origin of Radioactivity 289
6.27 Statistical Probability Distributions Associated with Radioactive Decay 292
6.28 Laws of Radioactive Decay 294
6.29 Exponential Functions and Their Relationship to Radioactive Decay 295
6.30 Equations Governing a Sample of Several Radioactive Elements 296
6.31 Measuring the Radioactive Decay Rate 298
6.32 Extensions to Radioactive Materials That Can Both Multiply and Decay 300
6.33 Time-Dependent Activity of a Radioactive Material 300
6.34 Half-Life of a Radioactive Material 301
6.35 Half-Lives, Average Lives, Decay Constants, and Doubling Times 302
6.36 Understanding the Equations of Secular Equilibrium 304
6.37 A Stable Daughter and a Radioactive Parent 306
6.38 Isotopic Stability and the Periodic Table 306
6.39 Radiation Released by Radioactive Materials 308
6.40 Gamma Rays in Nuclear Power Plants 309
6.41 How Nuclear Decay Heat Is Produced 309
References 310
Books and Textbooks 310
Web References 310
Additional References 310
Questions for the Student 311
Exercises for the Student 314

CHAPTER 7

Nuclear Fission and Nuclear Energy Production 319

7.1 Converting Mass into Energy 319
7.2 Fission and Fusion: A Review of Fundamental Concepts 319
7.3 Uranium and Its Characteristics 321
7.4 Energy Output: Fission versus Fusion 323
7.5 Splitting of the Uranium Atom: The Process of Induced Fission 323
7.6 Understanding the Fission of Uranium-235 324
7.7 Capture and Fission Channels for U-235 324
7.7.1 Channel 1: Capture 325
7.7.2 Channel 2: Fission 326
7.8 Fission Neutron Energy Spectrum 327
7.9 Fast, Epithermal, and Thermal Energy Ranges for Nuclear Fission 329
7.10 Mass Distribution of the Fission Fragments 330
7.11 Amount of Energy Released from the Fission of Different Nuclear Materials 330
7.12 Neutrons Released per Fission 332
7.13 Neutrons Released per Neutron Absorbed 333
7.14 The Value of Eta for Different Fuel Mixtures 335
7.15 Nuclear Energy Release versus Chemical Energy Release 337
7.15.1 An Interesting Comparison 338
7.16 Energy Release per Fission 338
7.17 The Origin of Nuclear Energy 338
7.18 The Threshold Energy for Fission 340
7.18.1 The Critical Energy of Fission 341

7.19 Some Examples of the Amount of Energy Produced 342
7.20 Differences in Fission Product and Uranium and Plutonium Masses 343
7.21 Types of Nuclear Chain Reactions 344
7.22 The Speed of a Nuclear Chain Reaction 348
7.23 Neutron Velocities at Different Neutron Energies 350
7.24 The Total Energy Released by a Fission Reaction 351
7.25 Electrical versus Thermal Energy Production 352
7.26 Finding the Uranium Consumption Rate over Time 352
7.27 Prompt Neutrons and Their Origin 353
7.28 Delayed Neutrons and Their Origin 353
7.29 Buildup of Xenon and Samarium 357
7.30 Cumulative Effect of the Buildup of Fission Product Poisons 358
References 359
Books and Textbooks 359
Web References 360
Additional References 360
Questions for the Student 361
Exercises for the Student 363

CHAPTER 8

Neutron Slowing Down Theory, Neutron Moderators, and Reactor Coolants 367

8.1 Introduction 367
8.2 Neutron Moderators and Their Function 367
8.3 Reactor Coolant Comparisons 368
8.4 Common Reactor Coolants and Their Properties 369
8.4.1 Category I: Thermal Water Reactor Coolants 369
8.4.2 Category II: Gas Reactor Coolants 370
8.4.3 Category III: Fast Reactor or Liquid Metal Coolants 370
8.5 Fast Reactors versus Thermal Reactors 371
8.6 Advantages to Moderating a Neutron 374
8.7 The Relationship between the Temperature, the Energy, and the Velocity of a Moderated Neutron 376
8.8 The Origin of the Term Thermal Neutron 378
8.9 The Apparent Temperature of a Fission Neutron 379
8.10 Neutron Slowing Down Theory 380
8.11 The Energy Staircase 380
8.12 The Lethargy and Its Application to Neutron Slowing Down Theory 382
8.13 Collisions between Neutrons and More Complex Materials 384
8.14 The Moderating Ratio 385
8.15 The Maxwell–Boltzmann Probability Distribution 387
8.16 The Origin of the Maxwell–Boltzmann Probability Distribution 388
8.17 Maxwell's Derivation of the Maxwell–Boltzmann Probability Distribution 388
8.18 Boltzmann's Constant and Its Relationship to the Maxwell–Boltzmann Probability Distribution 390
8.19 Heavy Water and Some of Its Uses 392
8.20 The Process of Heavy Water Production 393
References 394
Books and Textbooks 394
Web References 395
Additional References 395
Questions for the Student 396
Exercises for the Student 397

CHAPTER 9

The Neutron Multiplication Factor, the Reactivity, and the Four-Factor Formula 399

9.1 Uses for the Macroscopic Fission and Absorption Cross Sections 399
9.2 Meaning of the Effective Multiplication Factor 401
9.3 Relationship between the Effective Multiplication Factor and the Neutron Life Cycle 402
9.4 Finding the Effective Multiplication Factor and the Infinite Multiplication Factor with More than One Energy Group 404
9.5 Defining the Reactivity 405
9.6 Units for the Reactivity 407
9.7 Effect of Delayed Neutrons on the Value of the Reactivity 407
9.8 Using the Four-Factor and Six-Factor Formulas to Determine When a Reactor Becomes Critical 408
9.9 Unit Cells 408
9.10 Representing the Fuel to Cladding Gap 410
9.11 The Infinite Lattice Approximation 411
9.12 Four-Factor Formula for an Infinite Reactor Lattice 412
9.13 The First Factor: The Eta of the Fuel 415
9.14 The Second Factor: The Fast Fission Factor 416
9.15 The Third Factor: The Thermal Utilization 417
9.16 The Fourth Factor: The Resonance Escape Probability 419
9.17 Effects of Resonance Self-Shielding on the Resonance Escape Probability 422

9.18 Classical Form of the Four-Factor Formula 423
9.19 Representative Values of the Four Factors for a Reactor Lattice 423
9.20 Understanding the Neutron Life Cycle in a CANDU Reactor Unit Cell 423
9.21 Understanding the Neutron Life Cycle in a Westinghouse PWR Unit Cell 425
9.22 Understanding the Behavior of the Neutron Population in a Typical Reactor Unit Cell 426
9.23 How the Factors in the Four-Factor Formula Are Affected by Burnup 427
9.24 Understanding the Limitations of the Four-Factor Formula 427
9.25 Definitions of the Instantaneous Reactivity and the Net Reactivity 429
9.26 How Fuel Burnup Affects the Net Reactivity 430
9.27 Cross Sections Used to Calculate the Infinite Multiplication Factor and the Reactivity in Thermal Water Reactors 433
References 434
Books and Textbooks 434
Web References 434
Additional References 434
Questions for the Student 435
Exercises for the Student 436

CHAPTER 10

Neutron Leakage, Reactor Criticality, and the Six-Factor Formula 439

10.1 Understanding the Purpose of the Six-Factor Formula 439
10.2 Finding the Value of $K_{effective}$ from K_∞ in a Finite Reactor Lattice 439
10.3 Calculating the Fast and Thermal Nonleakage Probabilities 441
10.4 Physical Significance of the Six Factors 443
10.5 Criticality and Core Composition 444
10.6 Moderator to Fuel Ratio and the Four-Factor Formula 446
10.7 Optimal Moderator to Fuel Ratios and the Effect of the Pitch on the Value of K 448
10.8 Comparing Hexagonal Fuel Assemblies to Square Ones 450
10.9 Using the Six-Factor Formula to Predict When a System Becomes Critical 451
10.10 Some Limitations of the Four-Factor Formula and the Six-Factor Formula 452
10.11 Applying the Six-Factor Formula to the Great Natural Nuclear Reactors of Oklo 453
10.12 Estimating the Critical Size of the Oklo Reactors 455
10.13 Other Applications of the Six-Factor Formula 456
10.14 Reactor Characteristics and Some Typical Values of the Neutron Flux 456
10.15 Understanding the Relationship between the Flux and Power 456
10.16 Representative Values of the Flux and the Enrichment 457
10.17 Thermal to Fast Neutron Flux Ratios in Thermal Water Reactors 458
10.18 Comparing the Shape of the Fast and Thermal Buckling 459
10.19 Comparing Core Power Densities 460
References 462
Books and Textbooks 462
Web References 463
Additional References 463
Questions for the Student 464
Exercises for the Student 466

CHAPTER 11

An Introduction to Neutron Diffusion Theory and Fick's Law of Diffusion 469

11.1 Neutrons and Their Flow through Matter 469
11.2 Definition of the Neutron Density 470
11.3 Definition of the Neutron Flux 471
11.4 Definition of the Neutron Current 473
11.5 Fick's Law of Diffusion 474
11.6 Neutron Diffusion Coefficient and Its Meaning 478
11.7 Some Limitations of Fick's Law 483
11.8 Introduction to the Neutron Diffusion Equation 484
11.9 Writing an Equation to Conserve Neutrons 485
11.10 Adding Sources and Sinks to the Neutron Conservation Equation 487
11.11 Derivation of the Time-Dependent Neutron Diffusion Equation 488
11.12 Steady-State Neutron Diffusion Equation 489
11.13 Steady-State Neutron Diffusion Equation with an External Neutron Source 490
11.14 Standard Form of the Steady-State Neutron Diffusion Equation 491
11.15 Boundary Conditions for the Neutron Diffusion Equation 493
11.16 Boundary Conditions for More than One Energy Group 494
11.17 Defining the Neutron Diffusion Length 495
11.18 Neutron Diffusion Distance 496

11.19 Neutron Mean Free Path and Its Relationship to Diffusion Theory 499
11.20 Monte Carlo Method: An Alternative to Neutron Diffusion Theory 500
11.21 Diffusion Theory versus Transport Theory 502
11.22 Use of Neutron Diffusion Theory with Control Rods 503
11.23 Assumptions about Neutron Diffusion Theory near a Cylindrical Control Rod 504
11.24 Other Uses for the Extrapolation Distance 505
11.25 Using Diffusion Theory near a BWR Control Rod 506
11.26 How the Diffusion Distance Is Derived 507
11.27 Finding the Diffusion Distance from a Point Source 508
11.28 Neutron Scattering and the Size of the Neutron Diffusion Coefficient 510
References 512
Books and Textbooks 512
Web References 513
Additional References 513
Questions for the Student 514
Exercises for the Student 516

CHAPTER 12

Multigroup Neutron Diffusion Theory 519

12.1 Multigroup Neutron Diffusion Theory and Its Applications 519
12.2 Introduction to Multigroup Theory 519
12.3 Energy-Dependent Diffusion Equation 519
12.4 Introducing the Two-Group Approximation 520
12.5 Multigroup Cross Sections 522
12.6 Deriving the Multigroup Approximation 523
12.7 Defining Scattering Cross Sections between Energy Groups 524
12.8 Multigroup Diffusion Coefficients 525
12.8.1 Alternative Definitions for the Diffusion Coefficient 526
12.9 Neutron Diffusion Equation with Two Energy Groups 526
12.10 Cramer's Rule 530
12.11 Solving the Inhomogeneous Neutron Diffusion Equation with Two Energy Groups 532
12.12 Solving the Two-Group Diffusion Equations in a Finite Reactor Core 532
12.13 Deriving the Six-Factor Formula from the Neutron Diffusion Equation 533
12.14 Modified One-Group Neutron Diffusion Theory 534
12.15 Working with the N-Speed Neutron Diffusion Equation 535
12.16 Matrix Form of the Multigroup Diffusion Equations 536
12.17 Fast and Thermal Flux Shapes Predicted by Two-Group Theory 537
12.18 Popular Multigroup Neutron Diffusion Theory Programs 539
12.19 Reactor Licensing Applications 539
12.20 Performing a Reactor Licensing Analysis with TRACE 540
12.21 Parameters to Use with the Multigroup Equations 542
References 543
Books and Textbooks 543
Web References 543
Additional References 544
Questions for the Student 545
Exercises for the Student 546

CHAPTER 13

Solutions to the Steady-State Neutron Diffusion Equation 549

13.1 Solutions to the Steady-State Neutron Diffusion Equation for Slab Reactor 549
13.2 Correlating the Power Level to the Neutron Flux 552
13.3 A Physical Interpretation for the Geometric Buckling 553
13.4 Design Parameters for Different Reactors 555
13.5 Boundary Conditions for the Neutron Flux 555
13.6 Solutions to the Neutron Diffusion Equation in Common Reactor Geometries 556
13.7 Understanding the Neutron Flux in a Three-Dimensional Rectangular Reactor 556
13.8 Understanding the Flux Shape in a Three-Dimensional Spherical Reactor 559
13.9 Understanding the Flux Shape in a Three-Dimensional Cylindrical Reactor 560
13.10 Understanding the Flux Shape in an Infinite Cylindrical Reactor 563
13.11 Finding the Peak-to-Average Power Ratio in a Bare Core 564
13.12 Flux and Power Shaping 565
13.13 Benefits of Reflected Reactors 566
13.14 Flux Shapes for Fast and Thermal Neutrons in a Reflected Thermal Reactor 566
13.15 Defining the Reflector Savings and the Albedo 567
13.16 Deriving the Reflector Savings from the Diffusion Equation 571
13.17 Predicting the Size of a Critical Reactor 574

13.18 Differences between the Geometric Buckling with One and Two Energy Groups 576
13.19 Optimum Sizes and Shapes for Reactor Cores 578
13.20 Calculating the Critical Mass for Bare Reactors Having Different Sizes and Shapes 580
13.21 Estimating the Effect of a Reflector on the Critical Mass 581
13.22 Saving Fuel with a Neutron Reflector 581
13.23 Dependence of the Buckling and Diffusion Coefficient on Temperature 582
13.24 Temperature Dependence of the Neutron Mean Free Path 587
13.25 Solutions to the Neutron Diffusion Equation with More than One Homogeneous Region 587
13.26 How to Model a Fuel Assembly next to a Reflector 592
13.27 Other Topics 594
References 594
Books and Textbooks 594
Web References 595
Additional References 595
Questions for the Student 596
Exercises for the Student 599

CHAPTER 14

Solving the Neutron Diffusion Equation with a Radioactive Source Term 601

14.1 Solutions to the Diffusion Equation with No Fissionable Materials 601
14.2 Types of Neutron Sources 602
14.3 General Solutions to the Neutron Diffusion Equation 603
14.4 Solutions to the Diffusion Equation with a Neutron Source on the Boundaries 604
14.5 Simple Planar Neutron Source 605
14.6 Point Sources of Neutrons 607
14.7 Radiation Field from a Point Source in a Vacuum 608
14.8 Understanding the Principle of Superposition 610
14.9 Some Additional Observations regarding the Principle of Superposition 610
14.10 Finding the Neutron Flux from Multiple Point Sources 613
14.11 Applying the Principle of Superposition to Neutrons in a Vacuum 614
14.12 Applying the Principle of Superposition to Light Waves 614
14.13 Simulating Line Sources of Neutrons 617
14.14 Solutions to the Neutron Diffusion Equation in a Diffusive Medium with a Distributed Source 618
14.15 Solving the Neutron Diffusion Equation with a Distributed Source 619
14.16 Two Diffusive Regions with a Distributed Neutron Source in the Interior One 621
14.17 Vacuum Boundary Conditions for the Diffusion Equation 623
14.18 Defining an Energy-Dependent Extrapolation Distance 625
14.19 A Planar Neutron Source with the Extrapolated Boundary Condition 626
14.20 Solutions to the Neutron Diffusion Equation with More than One Material Region 629
14.21 Introduction to the Iterative Power Method 630
14.22 Convergence Criteria and Numerical Errors 632
14.23 Solutions to the Neutron Diffusion Equation near a Burnable Poison 633
14.24 Time-Dependent Effects 636
14.25 Comparing the Neutron Diffusion Equation to Laplace's Equation, Poisson's Equation, and Helmholtz's Equation 637
14.26 Time-Dependent Neutron Diffusion Theory 639
References 640
Books and Textbooks 640
Web References 640
Additional References 641
Questions for the Student 642
Exercises for the Student 644

CHAPTER 15

Time-Dependent Reactors and Their Behavior 647

15.1 Time-Dependent Reactor Behavior 647
15.2 Time-Dependent Neutron Production 648
15.3 Delayed Neutrons and Their Importance 649
15.4 Isotopes That Produce Delayed Neutrons 653
15.5 Visualizing How Delayed Neutrons Are Produced 655
15.6 Time-Dependent Diffusion Equation without Delayed Neutrons 656
15.7 Finding Simple Solutions to the Time-Dependent Diffusion Equation Using the Separation of Variables Method 656
15.8 Defining the Reactor Period 659
15.9 Understanding the Life Cycle of a Prompt Neutron 661

15.10 Time-Dependent Diffusion Equation with Delayed Neutrons 662
15.11 Finding the Time-Dependent Neutron Flux and Fission Product Concentrations 664
15.12 The Reactor Period and the Reactor Power 667
References 668
Books and Textbooks 668
Web References 668
Additional References 669
Questions for the Student 670
Exercises for the Student 671

CHAPTER 16

The Point Kinetics Approximation and the Inhour Equation 673

16.1 Deriving the Inhour Equation 673
16.2 Graphical Solutions to the Inhour Equation 677
16.3 Exact Solutions to the Inhour Equation 679
16.4 Reactor Period with Delayed Neutrons 679
16.5 Understanding Time-Dependent Reactor Behavior 681
16.5.1 Normal or Planned Shutdown 681
16.5.2 Emergency Shutdown 682
16.5.3 Prompt Critical Behavior 682
16.6 Conventional Units for Measuring the Reactivity-Dollars and Cents 683
16.7 Deriving the Prompt Jump and the Prompt Drop Approximations 685
16.8 Normal Reactor Behavior and Normal Reactivity Swings 689
16.8.1 Large Positive Reactivity Changes (Increases) 690
16.8.2 Large Negative Reactivity Changes (Decreases) 691
16.8.3 Supercritical Transients 693
16.8.4 Prompt Supercritical Transient 693
16.9 Solutions to the Inhour Equation with Six Delayed Neutron Groups 694
16.10 Time-Dependent Behavior of Fast Reactors 696
16.11 Finding the Asymptotic Reactor Period 696
16.12 Flux and Power Changes Starting from an Arbitrary State 698
16.13 Understanding the Origin of the Term "Inhour" 699
16.14 History of the Inhour Equation and the Unit of the Inhour 700
16.15 Using the Reactor Period to Measure the Worth of a Control Rod 702
16.16 Measuring the Point Kinetics Parameters 702
16.17 Other Applications of the Point Kinetics Equations 703
16.18 Examining the Validity of the Point Kinetics Approximation 703
16.19 Estimating the Instantaneous Reactor Power Level as a Function of Time 704
16.20 Ways to Measure the Point Kinetics Parameters 708
16.21 The Rod Drop Method 708
16.22 The Rod Oscillator Method 709
16.23 The Pulsed Neutron Source Method 710
16.24 Reactor Noise Analysis 711
References 712
Books and Textbooks 712
Web References 713
Additional References 713
Questions for the Student 714
Exercises for the Student 716

CHAPTER 17

Burnup, Depletion, and Temperature Feedback 719

17.1 Tracking the Burnup of Nuclear Fuel 719
17.2 Factors That Affect the Life of the Fuel 721
17.3 Buildup of Plutonium in the Core 721
17.4 Plutonium Production Rate in a Typical Thermal Water Reactor 723
17.5 Estimating the Amount of Energy Produced from Plutonium in a Thermal Water Reactor Core 723
17.6 Changes to the Isotopic Composition of the Core 724
17.6.1 Burnable Poisons and Other Neutron Poisons 724
17.6.2 Soluble Neutron Poisons and Their Function 724
17.7 Fuel Management and Plant Operation 726
17.8 Power Profiles in Low-Leakage Cores 728
17.9 How Temperature Affects the Reactivity of the Core 731
17.10 Moderator Temperature Coefficient 732
17.11 Effect of Boric Acid on the Moderator Temperature Coefficient 733
17.12 Temperature Feedback with Nucleate or Bulk Boiling 733
17.13 Understanding the Void Coefficient of the Reactivity 734
17.14 The Void Coefficient and Load Following 735
17.15 Understanding the Fuel Temperature Coefficient 737
17.16 Doppler Broadening and Its Effect on the Resonance Escape Probability 737

17.17 Other Factors That Affect the Fuel Temperature Coefficient 740
17.18 Time Dependence of the Core Temperature Coefficients 741
17.19 Regulatory Requirements Governing Sudden Reactivity Changes 742
17.20 Compliance with the Compendium of Federal Regulations and 10 CFR50 743
17.21 Curve-Fitting Methods for Nuclear Data 744
17.22 The Least Squares Method 744
17.23 Power Coefficient of the Reactivity 747
17.24 Finding the Temperature Defect and the Power Defect 749
17.25 Isothermal Temperature Coefficient 749
17.26 Calculating the Power Coefficient during Start-Up 749
17.27 Calculating the Temperature and Power Defects 750
17.28 Control Systems and Thermal Feedback 751
17.29 Temperature Feedback and the TRIGA Reactor 752
17.30 Understanding How a TRIGA Reactor Works 752
17.31 Power Pulses in a TRIGA Reactor 756
17.32 Reviewing the Effects of Thermal and Temperature Feedback 757
17.33 Some Additional Observations regarding Temperature Feedback 757
References 759
Books and Textbooks 759
Web References 759
Additional References 760
Questions for the Student 761
Exercises for the Student 762

CHAPTER 18

Long-Term Changes to the Reactivity of the Core 765

18.1 Tracking the Long-Term Reactivity 765
18.2 Core Reactivity as a Function of Burnup 767
18.3 Reactivity Changes in One-, Two-, and Three-Batch Cores 768
18.4 Single-Batch Cores versus Multi-Batch Cores 769
18.5 Reactivity Behavior of an N-Batch Core 771
18.6 Optimizing the Fuel-Loading Pattern within a Given Cycle 774
18.7 Optimizing a Reactor Core 775
18.8 Fuel Assembly–Loading Patterns 776
18.9 Core Power Profile as a Function of Burnup 778
18.9.1 Maintaining the Fuel Pin Temperatures within Established Limits 778
18.10 Axial Zoning Schemes 778
18.11 Burnable Poisons within an Individual Fuel Assembly 779
18.12 Burnable Poisons Inside of Reactor Fuel Assemblies 781
18.13 Effect of Burnable Poisons on the Flux Shape 782
18.14 Mathematical Description of the Depletion Process 782
18.15 Fission Product Buildup 784
18.16 Understanding the Buildup of Xenon-135 and Samarium-149 789
18.17 Equilibrium Concentrations of Xenon-135 and Samarium-149 789
18.18 Behavior of Xenon-135 and Samarium-149 after Shutdown 791
18.19 Xenon Buildup and "Reactor Dead Time" 792
18.20 The Concentration of Samarium-149 after Shutdown 792
18.21 Comparing Fission Product Poisoning in Fast and Thermal Reactors 793
18.22 Yields of Other Important Fission Products 793
18.23 Cumulative Effect of the Fission Product Poisons 794
18.24 Reactivity Change Caused by the Buildup of Fission Products 795
18.25 Cross Section for a Hypothetical Fission Product 797
References 799
Books and Textbooks 799
Web References 800
Additional References 800
Questions for the Student 801
Exercises for the Student 802

CHAPTER 19

Fuel Assembly Homogenization and Reaction Rate Conservation 805

19.1 A Closer look at the Neutron Diffusion Equation 805
19.2 Spatial Homogenization of a Reactor Fuel Assembly 807
19.3 Popular Neutron Diffusion Theory Codes and Their Applications 809
19.4 Homogenizing a Spatially Heterogeneous Region of Space 809
19.5 Examples of How the Homogenization Process Works 812
19.6 Fuel Assembly Homogenization and Reactor Super Cells 814

19.7 Some Interesting Relationships between the Size, Shape, and Composition of a Reactor Core 815
19.8 Thermal Disadvantage Factors and Fuel Assembly Homogenization 819
References 819
Books and Textbooks 819
Web References 820
Additional References 820
Questions for the Student 821
Exercises for the Student 824

CHAPTER 20
Control Rods, Burnable Poisons, and Chemical Shim 827

20.1 Control Rods and Their Function 827
20.2 Control Rods and Their Origin 828
20.3 Control Rod Designs 830
20.4 Control Rod Materials 834
20.5 Burnable and Nonburnable Poisons 835
20.6 Soluble Neutron Poisons and Chemical Shim 836
20.7 Burnable Poisons within a Fuel Assembly 838
20.8 Burnable Poisons within a Reactor as a Whole 839
20.9 Effect of Burnable Poisons on the Neutron Flux Shape 840
20.10 Burnable Poison Locations in a Reactor Core 841
20.11 Using Soluble Boron (or Solbor) as a Reactor Control System 841
20.12 Reactivity Changes Induced by Control Rods 842
20.13 Reactivity Changes Induced by Chemical Shim 843
20.14 Correlating the Reactivity Change to the Chemical Shim Concentration 844
20.15 Converting from PPM to Grams per Liter 846
20.16 Boric Acid Injection Systems 847
20.17 Comparing PWR and BWR Control Rods 847
20.18 Control Rod Banks and Control Rod Guide Tubes 848
20.19 Origin of the Word SCRAM 850
20.20 Maintaining the Criticality of the Core over Time 851
20.21 Defining the Worth of a Control Rod 853
20.22 Estimating the Effect of a Control Rod on the Reactivity 854
20.23 How the Control Rod Worth Changes When the Flux Shape Changes 856
20.24 Reactivity Corrections to Account for Partially Inserted Control Rods 858
20.25 Effect of the Fuel Type on the Control Rod Worth 862
20.26 Semantic Differences in the Definition of the Control Rod Worth 863
20.27 Effect of Control Rods on the Axial Power Profile 863
20.28 Fast Reactor Control Rods 864
20.29 Control Rod Materials and Their Cross Sections 867
20.30 Control Rod Design Parameters 868
20.31 Reactor Control Systems and Their Limitations 868
20.32 Alternative Forms of Reactivity Control 868
References 870
Books and Textbooks 870
Web References 871
Additional References 871
Questions for the Student 872
Exercises for the Student 874

CHAPTER 21
Fission Products, Xenon Transients, and Reactor Accidents 877

21.1 Importance of Fission Product Poisons 877
21.2 Reactivity Changes due to Fission Product Poisons Like Xenon 878
21.3 Xenon Behavior during Start-Up, Equilibrium, and Shutdown 878
21.4 Scenario I: Xenon following Start-Up 879
21.5 Scenario II: Equilibrium Xenon 880
21.5.1 Case 1: A Low Thermal Flux 881
21.5.2 Case 2: A Moderate Thermal Flux 881
21.5.3 Case 3: A High Thermal Flux 881
21.6 Scenario III: Shutdown Xenon 882
21.7 Reactor Dead Time and Its Implications 885
21.8 Nonintuitive Xenon Behavior 886
21.9 Power Control and Demand Management to Avoid Xenon Imbalances in the Core 887
21.10 Reactivity Changes due to Samarium Buildup and Decay 888
21.10.1 Case 1: The Samarium Concentration following Reactor Start-Up 889
21.10.2 Case 2: Equilibrium Samarium 890
21.10.3 Case 3: Samarium after Shutdown 891
21.11 Nuclear Properties of Xenon-135 and Samarium-149 893
21.12 How the Reactor Accident at Chernobyl Occurred 894
21.13 Design Features of the Chernobyl Reactor 895
21.14 Buildup of Xenon in the Chernobyl Core 896
21.15 The Chernobyl Accident and Its Aftermath 897

21.16 Comparing Chernobyl to Other Reactor Accidents 898
21.17 Accident Severity and the INES Scale 899
21.18 Lessons Learned from the Chernobyl Disaster 900
21.19 Computer Programs Used to Model Reactor Transients and Reactor Accidents: TRAC, TRACE, RETRAN, and RELAP 902
21.20 Typical Applications for TRACE 903
21.21 Using Realistic Cross Sections for Xenon and Samarium 906
References 906
Books and Textbooks 906
Web References 906
Additional References 907
Questions for the Student 908
Exercises for the Student 910

CHAPTER 22

An Introduction to Neutron Transport Theory 911

22.1 An Introduction to Neutron Transport Theory 911
22.2 Diffusion Theory versus Transport Theory 912
22.3 Diffusion Theory Concepts in Transport Theory Terminology 913
22.4 Deriving the Neutron Transport Equation 917
22.5 Finding the Scattering Rate for an Arbitrary Neutron 919
22.6 Boundary Conditions for the Neutron Transport Equation 920
22.7 Reducing the Transport Equation to a More Conventional Form 920
22.8 Showing When Solutions to the Transport Equation Reduce to Solutions to the Diffusion Equation 922
22.9 Simplifications to Neutron Transport Theory 922
22.9.1 Category I: The Steady-State Transport Equation 923
22.9.2 Category II: The One-Group or One-Speed Transport Equation 923
22.9.3 Category III: The Transport Equation for a Homogeneous Material 923
22.9.4 Category IV: The Transport Equation for a Homogeneous Material with Isotropic Scattering 923
22.9.5 Category V: The Transport Equation with Isotropic Source Terms 924
22.10 Difficulties with Obtaining a Solution to the Neutron Transport Equation 924
22.11 Deriving the Diffusion Theory Approximation 926
22.12 Introducing the P_N and S_N Approximations 929
22.13 P_N Approximation 929
22.14 S_N Approximation 933
22.15 Applying the S_N Method to a Spherical Source 935
22.16 Unit Vector and Dimensional Gradient in More than One Dimension 937
22.17 Numerical Methods for Solving the Time-Dependent Transport Equation 939
22.18 Using the Transport Equation with Pure Scatters and Absorbers 941
22.19 Ray Effects and Their Origin 943
22.20 Multigroup Neutron Transport Equation 944
22.21 How Boundary Conditions Are Handled in Neutron Transport Theory and Neutron Diffusion Theory 946
22.22 Common Types of Neutron Boundary Conditions 946
22.23 Initial Conditions for Time-Dependent Problems 946
22.24 Boundary Conditions at a Material Interface 947
22.25 Vacuum Boundary Conditions 948
22.26 Diffusion Coefficients and the P_1 Approximation 950
22.27 Commercial Computer Programs Used to Solve the Neutron Transport Equation 952
22.28 Other Approaches for Solving the Neutron Transport Equation 952
22.29 Visualizing the Angular Neutron Flux 953
References 954
Books and Textbooks 954
Web References 954
Additional References 954
Questions for the Student 955
Exercises for the Student 956

CHAPTER 23

The Monte Carlo Method and Its Applications to Nuclear Science and Engineering 959

23.1 An Introduction to the Monte Carlo Method 959
23.2 Random Number Generators and Statistical Probability Distributions 962
23.3 Steps in a Monte Carlo Calculation 966
23.3.1 Step 1: Establish an Initial Direction of Motion and an Initial Particle Energy E 966

23.3.2 Step 2: Find the Distance to the First Collision 967
23.3.3 Step 3: Determine the Type of Collision 968
23.3.4 Step 4: Determine the Direction That the Particle Exits the Collision 968
23.3.5 Step 5: Store the Case History for the Particle until It Is Destroyed or Leaves the System 970
23.3.6 Step 6: Repeat the Same Process for the Next Particle 970
23.4 Pros and Cons of Monte Carlo Calculations 971
23.5 Statistical Analysis Phase 971
23.6 The Monte Carlo Method and Moore's Law of Computing 971
23.7 Determining the Error in a Monte Carlo Calculation 973
23.8 Error Reduction Schemes 974
23.9 Computer Programs That Implement the Monte Carlo Method 978
23.10 Monte Carlo Calculation of the Fast Fission Factor 981
23.11 Dealing with a Cylindrical Geometry in a Monte Carlo Simulation 985
23.12 Monte Carlo Calculation of the Resonance Escape Probability 986
23.13 Extensions of the Monte Carlo Method to Control Rods 989
23.14 Skewed Probability Distributions 990
23.15 Finding the Scattering Angles in a Monte Carlo Calculation 991
23.16 Generating Asymmetric Scattering Angles 994
23.17 Using Random Walks to Simulate Particle Diffusion 997
23.18 Generating Truly Random Numbers 999
References 1002
Books and Textbooks 1002
Web References 1002
Additional References 1002
Questions for the Student 1003
Exercises for the Student 1003

APPENDIX A
Important Nuclear and Physical Constants 1005

A.1 Physical Constants and Their Values 1005
A.2 Units of Energy and Power 1006
A.3 Relationship between Number of Fissions per Second and Thermal Energy Production 1006
A.4 Time and Decay Conversion Factors and Constants 1006
A.5 Units of the Reactivity 1006

APPENDIX B
Unit Systems and Conversion Factors 1007

B.1 Common Unit Systems 1007
B.2 Prefixes, Primary Units, and Derived Units 1007
B.3 Temperature Conversion Formulas 1009

APPENDIX C
Nuclear Cross Sections and Reaction Rates 1011

C.1 Nuclear Cross Sections 1011
C.2 Repositories for Nuclear Cross-Section Data 1011
C.3 Tools for Plotting Nuclear Cross-Section Data 1011
C.4 Converting from Microscopic Cross Sections to Macroscopic Ones 1015
C.5 Some Comments on Cross-Section Naming Conventions 1018
C.6 Finding the Neutron Production Rate 1019
C.7 Nuclear Reaction Rates for the Fast and Thermal Energy Groups 1019
C.8 Power Production from Cross-Section Libraries 1021
C.9 Using Non-1/v Correction Factors to Find Thermal Group Cross Sections 1021
C.10 Temperature-Dependent Reaction Rates 1022

APPENDIX D
Physical Properties of Important Nuclear Materials 1023

D.1 Physical Properties of Important Nuclear Materials and Their Uses 1023

APPENDIX E
Atomic Mass Tables, Half-Lives, and Natural Abundances 1027

E.1 Atomic Mass Tables, Half-Lives, and Natural Abundances 1027
E.2 Finding the Amount of Energy Released from Table E.1 1027
E.3 Important Fission Products 1033

APPENDIX F
Delayed Neutron Emitters and Their Nuclear Properties 1035

F.1 Delayed Neutron Emitting Materials 1035
F.2 Features of Delayed Neutrons 1035
F.3 The Role of Bromine-87 1038

APPENDIX G

Attenuation Coefficients for Radiation Shields 1039

G.1 Types of Attenuation Coefficients and Their Uses 1039
G.2 Attenuation of a Photon Beam 1041
G.3 Distinguishing between X-Rays and Gamma Rays 1041

APPENDIX H

Diffusion Coefficients, Transport Cross Sections, and Mean Free Paths 1043

H.1 Neutron Diffusion Coefficient 1043
H.2 Fick's Law of Diffusion 1043
H.3 Neutron Diffusion Coefficients for Pure Scatters 1046
H.4 Finding the Cosine of the Neutron Scattering Angle 1046
H.5 Reasons for Using the Transport Cross Section Instead of the Total Cross Section 1046
H.6 Understanding the Mean Free Path 1047
H.7 The Diffusion Coefficient and the Mean Free Path 1047
H.8 Typical Values of the Diffusion Coefficient, the Mean Free Path, and the Transport Cross Section for Nuclear Materials 1048
H.9 The Transport Correction Factor 1048

APPENDIX I

Diffusion Parameters for Common Nuclear Materials 1049

I.1 Reactor Diffusion Parameters 1049

APPENDIX J

Common Integrals Used in Nuclear Science and Engineering 1051

J.1 Common Integrals 1051
J.2 Definite versus Indefinite Integrals 1051
J.3 Useful References 1051
Web References 1052

APPENDIX K

Bessel Functions That Appear in the Study of Nuclear Science and Engineering 1053

K.1 Bessel Functions and Their Origin 1053
K.2 Types of Bessel Functions 1053
K.3 Bessel Functions of the First and Second Kind 1053
K.4 Modified Bessel Functions of the First and Second Kind 1054
K.5 Using Bessel Functions to Find the Flux Shape in a Bare Cylindrical Reactor 1057
Web References 1059

Index 1061

PREFACE

P.1 Overview of This Book

Nuclear engineering is in the midst of a long overdue renaissance, but few reactor physics books have been written to support this renaissance on a worldwide scale. Instructors are often asked to choose between books that are either too advanced or too elementary to meet the needs of a specific curriculum. Thus, many instructors have chosen to develop their own course notes or to ask students to buy several reactor physics books in order to cover the material that is required to fulfill the needs of a specific curriculum. In addition, many reactor physics books intended for undergraduates do not discuss the multigroup neutron diffusion equation or multigroup neutron diffusion theory and its applications. Instead, simple analytical solutions are presented to the diffusion equation for idealized reactor geometries with a single energy group. These solutions do not account for the presence of the reflector, and at an undergraduate level, they do not discuss the neutron transport equation or the Monte Carlo method. In addition, their computational underpinnings are almost never discussed.

To provide the attention these important areas deserve, this book endeavors to cover many subjects of interest to the reactor physicist as well as anyone interested in pursuing a career in nuclear science and engineering. The subject matter is inclusive enough to meet the needs of junior and senior undergraduates, but it is also broad enough and advanced enough to meet the needs of first-year graduate students. Thus this book is intended to be a comprehensive, accessible, and easy-to-use reference that will be an excellent addition to any nuclear engineering curriculum. It may also be used as an introductory or intermediate level textbook that the student can read prior to taking more advanced courses in the field. To achieve these goals, this book makes extensive use of color images, links to the Internet, computer graphics, and other innovative techniques to illustrate the concepts that are important to a modern nuclear engineer. The subject matter is broad enough and deep enough to support a nuclear engineering degree program at the B.S. or M.S. level.

P.2 Topics Covered: Reactor Physics, Reactor Dynamics, and Nuclear Particle Transport

P.2.1 Basic Reactor Physics

Holistically speaking, this book is designed to be used for a one-semester or two-semester course in the physics of nuclear power. To achieve this objective, considerable attention is paid to the behavior of the neutron and its interaction with matter. The nature of elastic, inelastic, head-on, and glancing collisions is explored. X-rays, gamma rays, and other nuclear particles of interest to the field of reactor physics are also discussed. Various reactor types, reactor fuel cycles, radioisotopes, radioactive materials, and various aspects of reactor design and operation are explored. Chapter 7 is devoted to the nuclear chain reaction as well as other important concepts required to understand how fission reactors work. In addition to these topics, other important topics such as neutron diffusion theory, the neutron diffusion equation, Fick's Law of Diffusion, and both steady state and time-dependent reactor behavior are explored. Both steady state and time-dependent solutions to the neutron diffusion equation are presented. The Inhour equation, the Point Kinetics Approximation, and Xenon transients are explored. These subjects are enhanced by a discussion of reactor accidents, the INES Scale of accident severity, the neutron transport equation, and the Monte Carlo method. Single-group, two-group, and multigroup neutron diffusion theories are also discussed.

In addition to these important topics, neutron slowing down theory is discussed. This theory includes how fission neutrons are converted into thermal and epithermal neutrons and how neutron moderators are used to perform this function. Slowing down theory is applied to many different moderators and reactor coolants. The average energy loss per collision is determined for elastic scattering events. The dependence of neutron energy loss on the scattering angle is also discussed. Useful parameters such as the lethargy and moderating ratio are defined and applied to practical problems. The "energy staircase" that illustrates how neutrons lose energy as they move through a reactor lattice is illustrated pictorially in Chapter 8. Next, this book describes the differences between neutron transport theory and neutron diffusion theory. The neutron transport equation and the neutron diffusion equation are derived from first principles. The angular neutron flux is compared to the isotropic neutron flux, and for isotropic particle flows, the current is expressed as the gradient of the particle flux. This discussion is preceded by a derivation of the Four-Factor formula, the Six-Factor formula, and Fick's Law of Diffusion. Each factor in the four- and six-factor formulas is derived and discussed. Representative values are provided for these factors. Control rods, burnable poisons, chemical shim, burnup and depletion, and long-term changes to the isotopic composition of the core are discussed.

P.2.2 Reactor Dynamics and Nuclear Particle Transport

Next, the text attempts to provide a broad and relatively practical overview of reactor dynamics and nuclear particle transport. Time-dependent reactor behavior is initially discussed at an elementary level, which includes a presentation of the Prompt Jump and the

Prompt Drop approximations. Then it is extended to more advanced topics including the Point Kinetics approximation, the two-root Inhour equation, and the seven-root Inhour equation. (Other introductory textbooks only discuss the two-root Inhour equation.) The origins of the Inhour, the Infinite multiplication factor, and the Effective multiplication factor are discussed. The fast and thermal nonleakage probabilities are derived from first principles. The reactivity is defined using both absolute and relative units. Several equations are presented for the control rod worth, and its value is expressed as a function of the delayed neutron fraction. The relationship between the reactivity and the reactor period is explored. Temperature feedback and other forms of thermal feedback such as the nuclear Doppler effect, the fuel temperature coefficient, the moderator temperature coefficient, and the void coefficient of the reactivity are examined for different reactor types. The time frames associated with these feedback mechanisms are discussed as well. Regulatory issues are explored, and important reactor design parameters, such as the Moderator Fuel Ratio (or MFR), are added to the discussion. The coverage of reactor physics is extensive, and in many cases it exceeds the level of coverage presented in far more expensive reactor physics books.

P.3 Sources of Nuclear Data

This text also provides an extensive discussion of nuclear cross-section libraries and valuable sources of nuclear data. The cross sections used are based on the ENDF and JENDL databases, although other sources of nuclear data are referenced as well. The text then attempts to create an operational multigroup cross-section library from raw experimental nuclear data. It discusses ultrafine libraries, course libraries, and how the process of cross-section collapsing is implemented. It illustrates how cross-section data can be plotted using ENDFPLOT and other online plotting tools. As a bonus, it describes the process of fuel assembly and fuel rod homogenization. It starts with a discussion of bare reactors and then extends this discussion to include reactors with both radial and axial reflectors. The concept of the reflector savings is discussed. Particular attention is paid to the temperature dependence of nuclear cross sections, diffusion coefficients, and leakage rates. Once the neutrons become thermal neutrons, the Maxwell–Boltzmann probability distribution is discussed. (Here it is also derived, while in most other textbooks, it is simply discussed.)

P.4 Other Important Topics

On a nuts-and-bolts level, real nuclear engineering is discussed. Many topics are presented that build on the foundation created in our companion book (see Section P.7). These topics include a discussion of reactor core design, fuel rod design, and fuel assembly design. Containment buildings, power plant thermal cycles, and nuclear steam supply systems are discussed at both an operational level and at a design level. The containment buildings that failed at Fukushima and Chernobyl are discussed as well. The role of suppression pools and passive heat removal systems are explored. Modern reactor designs, such as the Westinghouse AP-1000, the AREVA EPR, and the GE Advanced Boiling Water Reactor (ABWR) and Simplified Boiling Water Reactor (SBWR), are also discussed. In our companion book, the Zirconium–water reaction and the buildup of hydrogen gas during a severe reactor accident or LOCA is explored. The energetics of the Zirconium–water reaction is discussed. Other topics of interest include radioactivity, radioactive decay, decay heat generation, and the Wigner–Way equation. The decay heat generated by both the fission products and the Actinides is explored. Radioactive decay chains, the Bateman equations, and secular equilibrium are discussed. The nuclear fuel cycle is presented for both fast and thermal reactors. The attributes and drawbacks of various nuclear fuels are discussed.

In addition to PWRs, BWRs, gas reactors, and LMFBRs, the neutronic characteristics of mobile power reactors (MPRs) and military reactors are explored. Their refueling cycles are also compared to those of commercial power reactors. Because of its novel design and unusual stability, the design of the TRIGA reactor is discussed in some detail (see Chapter 17). The advantages of heavy water are compared and contrasted to those of light water. Various reactor safety analysis and reactor licensing codes such as RELAP, TRAC, and TRACE are discussed within the framework of modern reactor physics. Monte Carlo, Transport Theory, and Neutron Diffusion Theory codes are discussed as well.

P.5 Neutron Transport Theory and the Monte Carlo Method

On a somewhat more advanced level, several chapters (including Chapters 22 and 23) are dedicated to a discussion of neutron transport theory and the Monte Carlo method. The neutron transport equation is derived from first principles. The angular neutron flux is then discretized using the discrete ordinates method and the S_N method. The P_N method for solving the neutron transport equation is presented in addition to the P_1 approximation. The Monte Carlo method is then introduced to the reader in Chapter 23. Since Monte Carlo methods require the use of random numbers, both hardware and software random number generators are discussed. Algorithms for generating random numbers are provided for reactor physicists. Practical applications of PDFs, CDFs, and inverse CDFs are presented in Chapter 23. The characteristic features of statistical probability distributions are explored. The primary differences between neutron transport theory and neutron diffusion theory are discussed. The angular neutron current and the angular neutron flux are defined and

compared to the conventional neutron current and the conventional neutron flux. The transport cross section and the transport mean free path are directly derived from the P1 approximation. Finally, variance reduction methods and other error reduction schemes are introduced for reducing the statistical uncertainties in a Monte Carlo calculation. As far as the author and the publisher are aware, this is the only introductory reactor physics book that attempts to discuss these subjects at a working level. The relationship between the Monte Carlo method and neutron game theory is explored.

P.6 Topics of Historical Interest to Nuclear Scientists and Engineers

This book, as well as its companion book *Nuclear Engineering Fundamentals: A Practical Perspective*, provides a unique historical perspective on the nuclear power industry that is not available in other textbooks. This perspective may be of interest to anyone seeking to know how the nuclear industry was founded, and which people were responsible for creating it. Its origins dating back to the early days of the Manhattan Project are explored in the companion book. The use of the first PWR in the Nuclear Navy is discussed. The history of the U.S. Nuclear Navy is discussed from the viewpoint of a reactor physicist.

The text also presents a historical narrative of how the nuclear power industry originated in the United States and then became prevalent throughout the rest of the world. For example, in its companion book, the relationship between George Westinghouse and Nicola Tesla, which led to the founding of the Westinghouse Nuclear Energy Corporation, is explored. The Borax experiments that led to the creation of the first BWR are discussed. Finally, the origins of the modern LMFBR, dating back to the Clementine reactor at Los Alamos, are discussed. This includes a discussion of the design of modern containment buildings, including the GE Mark I, Mark II, and Mark III containments, and the containment buildings used for the Westinghouse AP-1000. The contributions of the many great men to the field of nuclear engineering are explored within the context of its companion book. These historical figures include Hyman Rickover, James Maxwell, Ludwig Boltzmann, Albert Einstein, Enrico Fermi, Robert Oppenheimer, Edward Teller, Glenn Seaborg, Freeman Dyson, Nikola Tesla, Richard Feynman, George Westinghouse, and John von Neumann (one of the inventors of the modern computer, computer game theory, and the Monte Carlo method). Several other figures of historical importance in the field, such as Gordon Moore (the cofounder of Intel and one of the inventors of the modern microprocessor), are also discussed.

P.7 Relationship of This Book to Its Companion Book

As alluded to previously, this text book is intended to be the second book of a two-book set. Its companion volume, *Nuclear Engineering Fundamentals: A Practical Perspective* (which is also available from CRC Press), provides the introductory material that students should be exposed to before taking a reactor physics class. It begins by discussing common types of reactors (including PWRs, BWRs, gas reactors, Military Reactors, and LMFBRs) as well as their various design and operational parameters. It discusses the interaction of radiation with matter, radiation detection and protection, and radiation shielding. Radioactivity is discussed in Chapter 6 and the nuclear chain reaction is discussed in Chapter 7. In addition to these important topics, a great deal of attention is paid to the nuclear fuel cycle, the uranium enrichment process, various uranium enrichment technologies, and the interaction of radiation with matter. The advantages (and drawbacks) of different types of nuclear waste disposal and fast and thermal breeder reactors are discussed. The Thorium fuel cycle is also presented and compared to conventional uranium and plutonium fuel cycles. The economic trade-offs associated with each of these fuel cycles are discussed. The extraction of uranium from sea water is explored. This book also describes the neutron life cycle, nuclear cross sections and reaction rates, single group and multigroup cross sections, compound nucleus formation, the Liquid Drop Model and the Shell models of nuclear structure, and the mass defect of the nucleus. It is the first mainstream nuclear engineering textbook the publisher is aware of that presents a modern view of the theory of radioactive decay (including the nature of the weak force and the application of Feynman diagrams). As a bonus, it also presents the first publicly available derivation of Einstein's famous equation $E = mc^2$ in an introductory nuclear engineering textbook.

Consequently, we believe the reader will find this two-book set to be an excellent introductory set of books for teaching modern nuclear engineering to many different types of nuclear scientists and engineers. Combined together, these two books contain literally thousands of homework problems, worked examples, and illustrations to explain the principles of reactor physics. As opposed to many other textbooks, a great deal of work has gone into ensuring that the writing style is warm and inviting rather than classical and dry. While this may seem to be a bit unorthodox at first, we believe that it will ultimately broaden the appeal of the book and make it easier for the general population to embrace the concept of nuclear power as a whole.

P.8 Potential for Course and Curriculum Customization

This textbook takes a slightly different approach than classical reactor physics books because it is designed to be *as modular as possible*. This inherent modularity allows the instructor to mix, match, and interchange the chapters in a variety of different ways to match the needs of a specific curriculum. In other words, *it allows the subject of reactor physics to be taught on many different levels and*

to many different audiences. The initial chapters (Chapters 1 through 12) can be used for an introductory reactor physics class (at a level similar to that employed by Lamarsh), and the later chapters are appropriate for a more advanced class (at a level similar to that used by Duderstadt or Stacy). Hence, this book can be used to create *two separate reactor physics courses* (an introductory course and an advanced course) that can be used for a two-semester curriculum. This inherent modularity allows the instructor to find the most appropriate type of presentation for a specific curriculum. This extensive modularity may also be of some benefit to those who would like to vary their core curriculum from time to time. The overall text is broad enough and deep enough to accommodate most of these needs. Several customized courses can also be developed from the material provided.

P.9 Modularity, Cost Effectiveness, and Flexibility

In conclusion, we hope that you will find this book to be a thoroughly modern alternative to classical reactor physics books that are much more expensive or much harder to read. It provides a thorough introduction to the subject of reactor physics that is wide-ranging in its intended scope and cuts a broad swath across many areas of interest to the nuclear scientist and engineer. This book and its companion book are the first mainstream nuclear engineering textbooks to be printed in full color. Taken together, *they contain more than 3000 worked homework problems, examples, questions, and sample problems* for the interested student or reader. This is between *five and ten times* the number of homework problems that are provided in other comparable textbooks. A solution key for these problems is also available to accredited faculty members and instructors. Because of their inherent flexibility and modularity, these books can provide a modern and cost-effective way to teach nuclear engineering courses to undergraduates and first-year graduate students. In some cases, a three-semester or four-semester course can be fashioned from the subject matter provided. Every effort has been made to make the information presented in this book as accurate as possible. In the event an error is found, please report it to *orders@taylorandfrancis.com* and it will be corrected in the next edition.

Finally, we sincerely hope that you will enjoy the warm and inviting writing style and the beautiful color images. We hope that it will inspire you to embrace the renaissance in the nuclear power industry that is occurring in the world today. We hope that you will enjoy reading this book and that you will find it to be an interesting and rewarding experience.

Robert E. Masterson, ScD (MIT)

Credits and Acknowledgments

The author wishes to thank the many faculty, students, and industry professionals who contributed their thoughts and comments to the completion of this book. In particular, he would like to thank:

- Kord Smith and Lulu Li from the Nuclear Engineering Department of MIT
- Igor Bolotnov and Maria Avramova from the North Carolina State University
- Jim Turso from Pennsylvania State University
- Harry Goodman from Louisiana State University
- Shripad Revankar from Purdue University
- Yaron Danon from Rensselaer Polytechnic Institute
- Mahmoud Massoud from the University of Maryland, College Park
- Dr. Tom Boulette, previously from Boston Edison and the US NRC
- Eddy Cardentey from the Westinghouse Nuclear Corporation
- Mark Pierson and Dewey Spangler from Virginia Polytechnic University
- William L. Dunn from Kansas State University
- Mike Driscoll, previously from the Nuclear Engineering Department at MIT
- The students and staff of Virginia Tech
- And lastly for his inspiration and support, Ken Ball, now dean of engineering at George Mason University

Finally, I would like to express my gratitude to the editors at CRC Press and in particular to Jonathan Plant, whose vision and perseverance has made a book of this scope, color, depth, and breadth possible.

Author

Robert E. Masterson earned an MS and a PhD (ScD) in nuclear science and engineering at the Massachusetts Institute of Technology and a BS in physics at the University of Notre Dame. He has published extensively in the Transactions of the ANS (the American Nuclear Society) and has been a member of the society for many years.

Dr. Masterson has also served over the years as affiliate professor of nuclear science and engineering at the Virginia Polytechnic Institute and has an extensive background in the fields of reactor safety, reactor design and analysis, reactor thermal hydraulics, numerical analysis, reactor physics, reactor dynamics, nuclear medicine, and nuclear particle transport. The author has more than 20 years of experience in the field of nuclear science and engineering and worked for Westinghouse Nuclear Energy Systems at the Hanford site. He is president of a major technology consulting firm and is also the author of *Nuclear Engineering Fundamentals: A Practical Perspective*, which can also be obtained from CRC Press.

In addition to his work in nuclear science and engineering, he has founded and cofounded several companies and has held many noteworthy management, advisory, and strategic positions. His global e-mail address is drbobmasters@gmail.com, where he welcomes feedback and suggestions regarding his books.

1

Nuclear Power in the World Today

1.1 Popular Types of Reactors and Their Design Characteristics

Five basic types of nuclear power plants can be commonly found in the world today. These reactors use different combinations of coolants and different types of fuel (usually isotopes of uranium and plutonium) to generate the power the world needs. The ability of a reactor to produce electric power over long periods of time is dependent upon the type of coolant, the composition of the core, and the enrichment of the fuel. All reactors must be able to produce more neutrons than they consume for the fission chain reaction to be sustainable. We will have more to say about this in future chapters of the book. *Control rods* are then used to absorb these excess neutrons and keep the chain reaction under control. On a high level, it is possible to characterize the commercial nuclear reactors in the world today into *five broad categories*:

1. *Pressurized water reactors (PWRs)*
2. *Boiling water reactors (BWRs)*
3. *Heavy water reactors (HWRs)*
4. *Gas-cooled reactors (GCRs)*
5. *Liquid metal fast breeder reactors (LMFBRs)*

PWRs and BWRs use light water (i.e., ordinary water) to cool the core, while HWRs, like the *CANada Deuterium Uranium* (or *CANDU*) reactor, use heavy water as the moderator and the coolant.

Heavy water absorbs fewer neutrons than light water does, and because of this, reactors that are cooled with heavy water do not need enriched uranium to be able to operate successfully. However, they can also use enriched uranium if the need arises. All commercial nuclear power plants have a certain number of design features in common, including the need for fuel rods, control rods, and some type of liquid or gaseous coolant to cool the core. With the exception of GCRs (such as the AGR and the HTGR), which can sometimes use the *Brayton thermal cycle* to produce power, all other reactors use the *Rankine thermal cycle* to generate steam that is sent to the power turbines. PWRs, HWRs, and LMFBRs have two coolant loops (a primary and a secondary loop), while BWRs and GCRs have only one. As we discussed in our companion book,* many LMFBRs have a third coolant loop (sometimes called an *intermediate loop*) to isolate the coolant in the core from the steam generators. This prevents the liquid sodium in the core from interacting with the water in the *Nuclear Steam Supply System* (or *NSSS*) and introducing radioactivity into the steam that drives the power turbines. This reduces the chance that any radioactive materials will be released into the environment.

1.2 Number of Power Reactors in the World Today

The number of power reactors in the world has increased steadily since the 1950s. Figure 1.1 shows how the number of power reactors has changed between the time that they were first introduced and the present day. Today there are approximately 436 nuclear power plants in operation in 31 countries (see Figure 1.2), and in some countries, they are responsible for generating a large fraction of the total electrical demand. These nuclear power plants are usually implemented using a *base-loading model*, since the cost of the fuel is a very small part of the cost of power production. The current generation of commercial nuclear power plants has a total electrical output of about 374 GW, and there are an additional 65 power plants under construction in China, India, and Russia with a projected capacity of about 65 GW (see Table 1.1). The number of new reactors under construction is shown in Figure 1.3.

By far the most common type of commercial nuclear reactor in the world today is the PWR, which is manufactured and designed by *Westinghouse*, *AREVA*, and a number of other vendors. Table 1.2 shows the breakdown of the current-installed base by reactor type. Notice that PWRs represent about 2/3 of the world's nuclear generating capacity. BWRs, which are manufactured and designed by the *General Electric Company* (GE), are the next most common type of reactor in the world. They account for about

* See *Nuclear Engineering Fundamentals: A Practical Perspective*, by R.E. Masterson, CRC Press (2017).

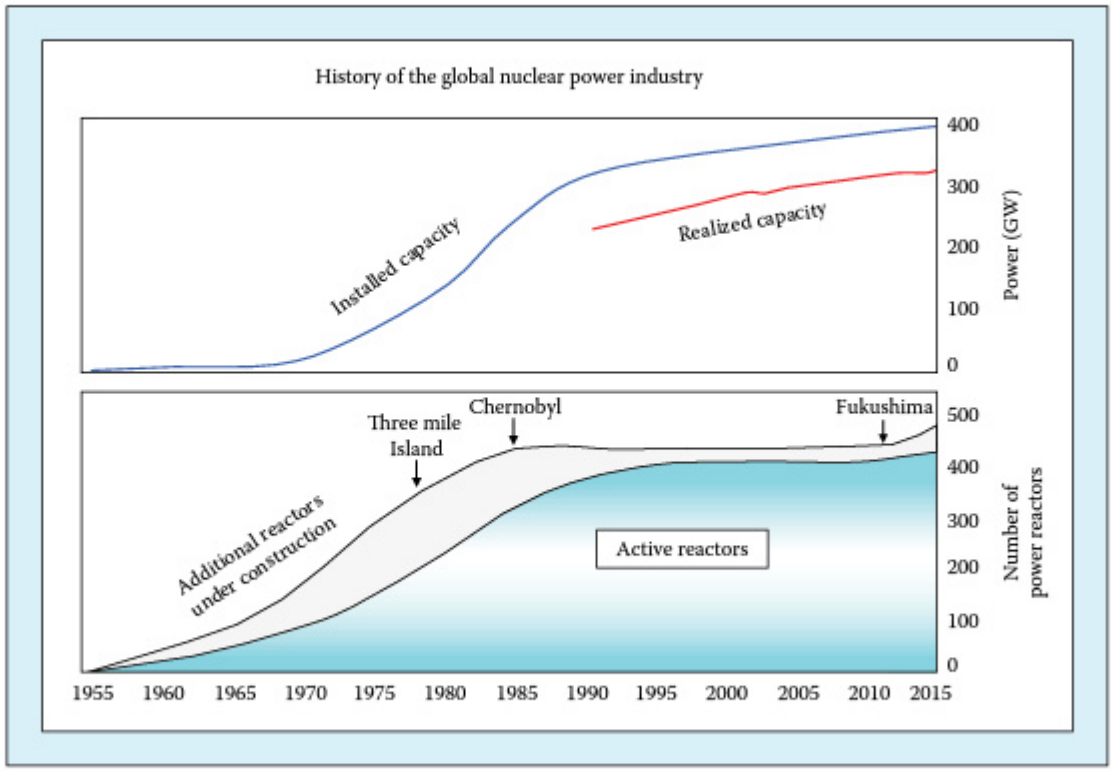

FIGURE 1.1 The number of nuclear power plants operating in the world as a function of time. (Based on data provided by The World Nuclear Association.)

1/4 of the current installed base. (Other reactors such as fast and gas reactors are then responsible for the remainder.) The percentage of electrical power generated in each country by nuclear power plants is shown in Figure 1.4. Notice that nuclear power generates about 20% of the total electrical power in the United States, while it generates almost 80% of the electrical power in France. Countries that do not have a great deal of coal and oil tend to rely more heavily on nuclear power than countries where these resources are readily available. Because of this, Saudi Arabia and most Arabic countries do not generate any of their electrical power from nuclear power plants, while countries like France and Switzerland rely on them quite heavily. However, Saudi Arabia and the UAE have expressed an interest in building large numbers of nuclear power plants in the future. Thus nuclear power has become an almost universally accepted way for generating at least part of the world's electricity. More information about the role of nuclear power plants in the world today can be found at the following Website:

http://www.euronuclear.org/info/encyclopedia/n/nuclear-power-plant-world-wide.htm.

which is maintained by the European Nuclear Association. Now we would like to turn our attention to the *high level design* or *architecture* of a nuclear power plant.

1.3 Power Reactor Architectures

Fundamentally speaking, the basic architecture of all nuclear power plants is similar. The basic architecture of the five major types of power plants is shown in Figure 1.5. In most cases, the core can be thought of as a "*black box*" that generates the heat that is supplied to the *Nuclear Steam Supply System (NSSS)*. The neutronic characteristics of the core are very specific, and they affect how easy (or hard) a reactor is to control. Generally speaking, water reactors are easier to control than LMFBRs because they have a "softer" neutron energy spectrum and more delayed neutrons (see Chapter 15). The behavior of GCRs is somewhat different.

Nearly all reactor types (except LMFBRs) rely on the coolant that flows past the fuel rods to slow down the neutrons that are needed to sustain the nuclear chain reaction. In these reactors, the coolant is also known as "the *moderator*" (because it moderates or reduces the speed of the fission neutrons, and therefore makes it easier for them to be absorbed). The moderator is the first way that a nuclear chain reaction can be controlled. If the moderator were to be removed from the core of a thermal water reactor, the fission process would suddenly shut down, and the power generation rate would be substantially reduced. (The only power that would be produced would then be the power produced by the decay heat.)

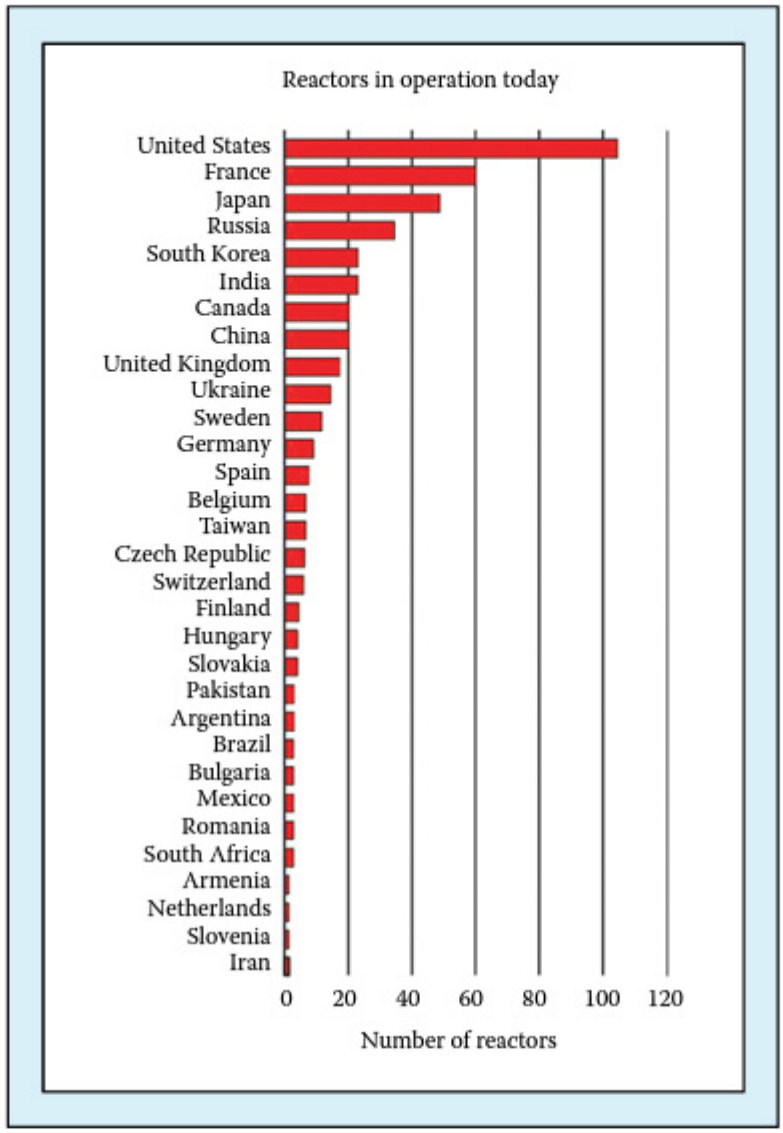

FIGURE 1.2 The number of nuclear reactors in operation, worldwide—by country. (Courtesy of the IAEA. Date: January 2013.)

However, the same is not necessarily true for LMFBRs because the loss of liquid sodium (a weak neutron moderator) can sometimes lead to very large reactivity insertions. (This is discussed in more detail in Chapters 15 and 16.)

Hence, the type of coolant used, its flow rate, its temperature, and its density all have an effect on how the core behaves. The enrichment of the fuel and the size of the fuel rods determine how hot the fuel rods can become and how easily the heat can be removed from the core. The flow rate, the temperature, and the pressure of the coolant then determine the *thermodynamic efficiency* of the power plant. In PWRs, HWRs, AGRs, and LMFBRs, the coolant leaving the core transfers its heat to an intermediate device known as a *steam generator*. The steam generator then transfers this heat to the secondary loop where it causes the water in the secondary loop to boil and to turn into steam. The steam then turns the power turbines to generate the electricity that is produced. The primary loops and the secondary loops in these plants are completely separate from one another. This ensures that any radioactivity that is produced in the primary loop does not enter the secondary loop.

The *NSSS* uses a *Rankine cycle* to recondense the steam after it leaves the power turbines. Waste heat is rejected from the plant by passing it through a device called a *condenser*. The waste heat then makes its way to a cooling pond, a lake, a river, or a cooling tower. This is essentially how a *power plant thermal cycle* works. (Power plant thermal cycles are discussed in more detail in our companion book.*) The coolant is then returned to the core to be reheated again. Both the primary and the secondary loops have different flow rates, and the flow rates must be balanced so that the secondary loop removes exactly the same amount of heat as the primary loop produces. The core deposits its heat in the primary loop, and the process continues until the plant has to be refueled. BWRs use a similar process except that the secondary loop is removed from the plant entirely.

* See *Nuclear Engineering Fundamentals: A Practical Perspective*, by R.E. Masterson, CRC Press (2017).

TABLE 1.1
Number of Nuclear Power Plants in the World Today (Either in Operation or Under Construction)

	Reactors in Operation (Jan 2013)		Reactors under Construction (Jan 2013)		Reactors Planned (Jan 2013)		Reactors Proposed (Jan 2013)		Uranium Required (2012)
Country	#	MWE	#	MWE	#	MWE	#	MWE	Metric Tons
Argentina	2	935	1	745	1	33	2	1,400	124
Armenia	1	376	0	0	1	1,060			64
Bangladesh	0	0	0	0	2	2,000	0	0	0
Belarus	0	0	0	0	2	2,400	2	2,400	0
Belgium	7	5,943	0	0	0	0	0	0	995
Brazil	2	1,901	1	1,405	0	0	4	4,000	321
Bulgaria	2	1,906	0	0	1	950	0	0	313
Canada	19	13,531	0	0	2	1,500	3	3,800	1,694
Chile	0	0	0	0	0	0	4	4,400	0
China	16	12,918	29	29,990	51	59,800	120	123,000	6,550
Czech Republic	6	3,764	0	0	2	2,400	1	1,200	583
Egypt	0	0	0	0	1	1,000	1	1,000	0
Finland	4	2,741	1	1,700	0	0	2	3,000	471
France	58	63,130	1	1,720	1	1,720	1	1,100	9,254
Germany	9	12,003	0	0	0	0	0	0	1,934
Hungary	4	1,880	0	0	0	0	2	2,200	331
India	20	4,385	7	5,300	18	15,100	39	45,000	937
Indonesia	0	0	0	0	2	2,000	4	4,000	0
Iran	1	915	0	0	2	2,000	1	300	170
Israel	0	0	0	0	0	0	1	1,200	0
Italy	0	0	0	0	0	0	10	17,000	0
Japan	50	44,396	3	3,036	10	13,772	3	4,000	4,636
Jordan	0	0	0	0	1	1,000			0
Kazakhstan	0	0	0	0	2	600	2	600	0
Korea DPR (North)	0	0	0	0	0	0	1	950	0
Korea RO (South)	23	20,787	4	5,205	5	7,000	0	0	3,967
Lithuania	0	0	0	0	1	1,350	0	0	0
Malaysia	0	0	0	0	0	0	2	2,000	0
Mexico	2	1,600	0	0	0	0	2	2,000	279
Netherlands	1	485	0	0	0	0	1	1,000	102
Pakistan	3	725	2	680	0	0	2	2,000	117
Poland	0	0	0	0	6	6,000	0	0	0
Romania	2	1,310	0	0	2	1,310	1	655	177
Russia	33	24,164	10	9,160	17	24,180	20	20,000	5,488
Saudi Arabia	0	0	0	0	0	0	16	17,000	0
Slovakia	4	1,816	2	880	0	0	1	1,200	307
Slovenia	1	696	0	0	0	0	1	1,000	137
South Africa	2	1,800	0	0	0	0	6	9,600	304
Spain	7	7,002	0	0	0	0	0	0	1,355
Sweden	10	9,399	0	0	0	0	0	0	1,394
Switzerland	5	3,252	0	0	0	0	3	4,000	527
Thailand	0	0	0	0	0	0	5	5,000	0
Turkey	0	0	0	0	4	4,800	4	5,600	0
Ukraine	15	13,168	0	0	2	1,900	11	12,000	2,348
UAE	0	0	1	1,400	3	4,200	10	14,400	0
United Kingdom	16	10,038	0	0	4	6,680	9	12,000	2,096
United States	104	102,215	1	1,218	13	15,660	13	21,600	19,724
Vietnam	0	0	0	0	4	4,000	6	6,700	0
World	436	374,108	65	65,139	167	184,415	317	359,655	67,990
	No.	MWe	No.	MWe	No.	MWe	No.	MWe	tons U
	Reactors operable		Reactors under construction		On order or planned		Proposed		Uranium required

Source: IAEA. Date: January 2013.

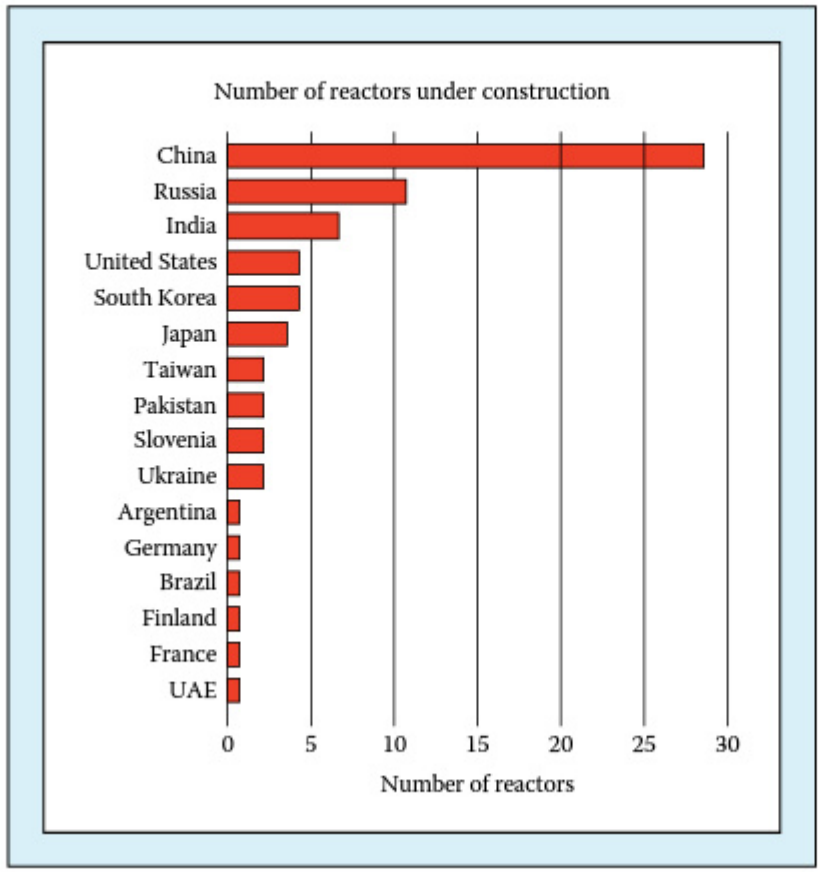

FIGURE 1.3 The number of nuclear reactors under construction, worldwide—by country. (Courtesy of the IAEA. Date: January 2013.)

TABLE 1.2
Number of Commercial Power Reactors in the World Today as a Function of Their Design Type (PWR, BWR, AGR, LMFBR, etc.) as of January 2010

Reactor Type	Main Countries	Number	GWe	Fuel	Coolant	Moderator	Percent of World Total
Pressurized water reactor (PWR)	United States, France, Japan, Russia, China	271	270.4	Enriched UO_2	Water	Water	
Boiling water reactor (BWR)	United States, Japan, Sweden	84	81.2	Enriched UO_2	Water	Water	
Pressurized heavy water reactor "CANDU" (PHWR)	Canada	48	27.1	Natural UO_2	Heavy water	Heavy water	
Gas-Cooled reactor (AGR and Magnox)	United Kingdom	17	9.6	Natural U (metal), enriched UO_2	CO_2	Graphite	
Light water graphite reactor (RBMK and EGP)	Russia	11 + 4	10.4	Enriched UO_2	Water	Graphite	
Fast neutron reactor (LMFBR)	Russia	1	0.6	PuO_2 and UO_2	Liquid sodium	None	
Total number in operation		436	399.3				100

Source: World Nuclear Association.

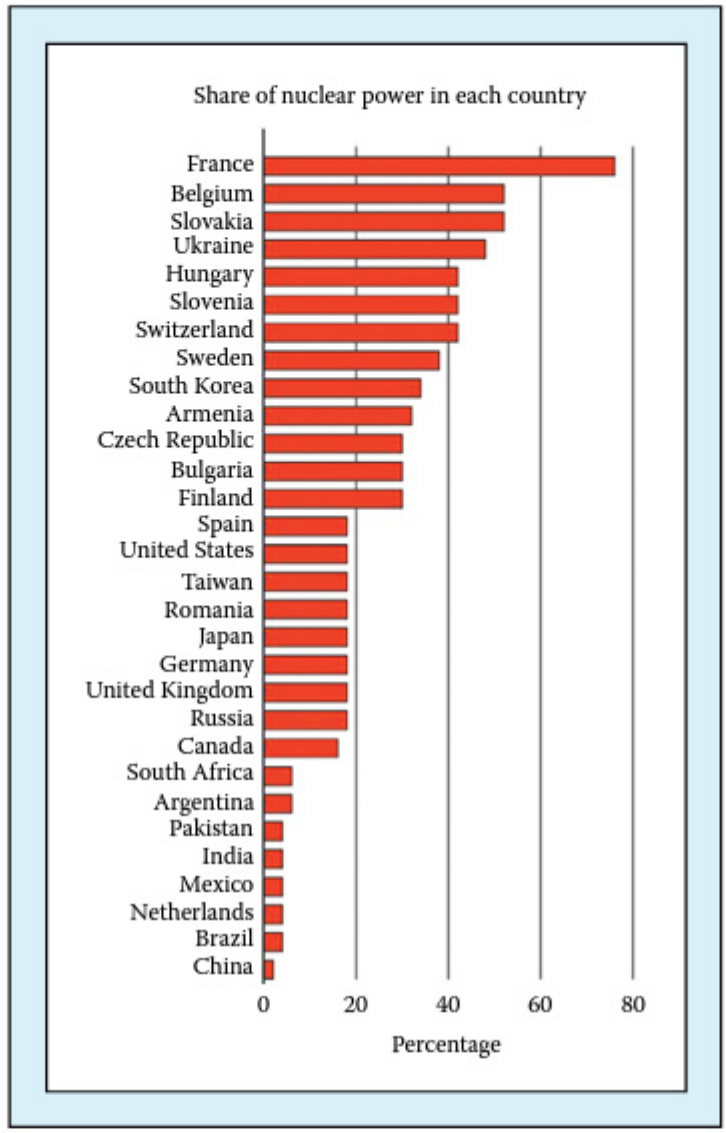

FIGURE 1.4 The share of power in each country generated by nuclear power plants. (Courtesy of the IAEA. Date: January 2013.)

In BWRs, the steam generated in the core is sent directly to the steam turbines, and so *BWRs do not require steam generators*. (However, they still use a *steam dryer* at the top of the pressure vessel to remove moisture from the steam.) Eliminating the secondary loop reduces the cost of building the plant because it is no longer necessary to have two separate loops. This also eliminates the need to build two or three steam generators, which can be very large and expensive. BWRs also use the Rankine thermal cycle to extract energy from the core. AGRs use a gaseous coolant, and so they can theoretically use another power plant thermal cycle called the *Brayton thermal cycle. The major difference between these two cycles is that the working coolant in a Rankine cycle boils (i.e., it undergoes a change of phase), while in a Brayton cycle, it is a gas that does not*. However, most AGRs use the Rankine cycle just like thermal water reactors do. The efficiency of these thermal cycles is plant specific, and it can range from about 28% for a PHWR to about 42% for a LMFBR. Most commercial PWRs and BWRs today have thermal efficiencies between 32% and 35%. These efficiencies are discussed in more detail in our companion book.*

1.4 Power Reactors and Their Design Parameters

Each reactor type uses a slightly different type of fuel, and the number of fuel assemblies can vary depending on the design of the core and its power rating. These parameters have also changed over time as new designs have been introduced to replace older ones. In this section, we would like to compare and contrast the fuel assemblies that are used in each reactor type. The design of a fuel assembly affects the behavior of the core from a neutronic, thermal-hydraulic, and safety

* See for example *Nuclear Engineering Fundamentals: A Practical Perspective*, by R.E. Masterson, CRC Press (2017).

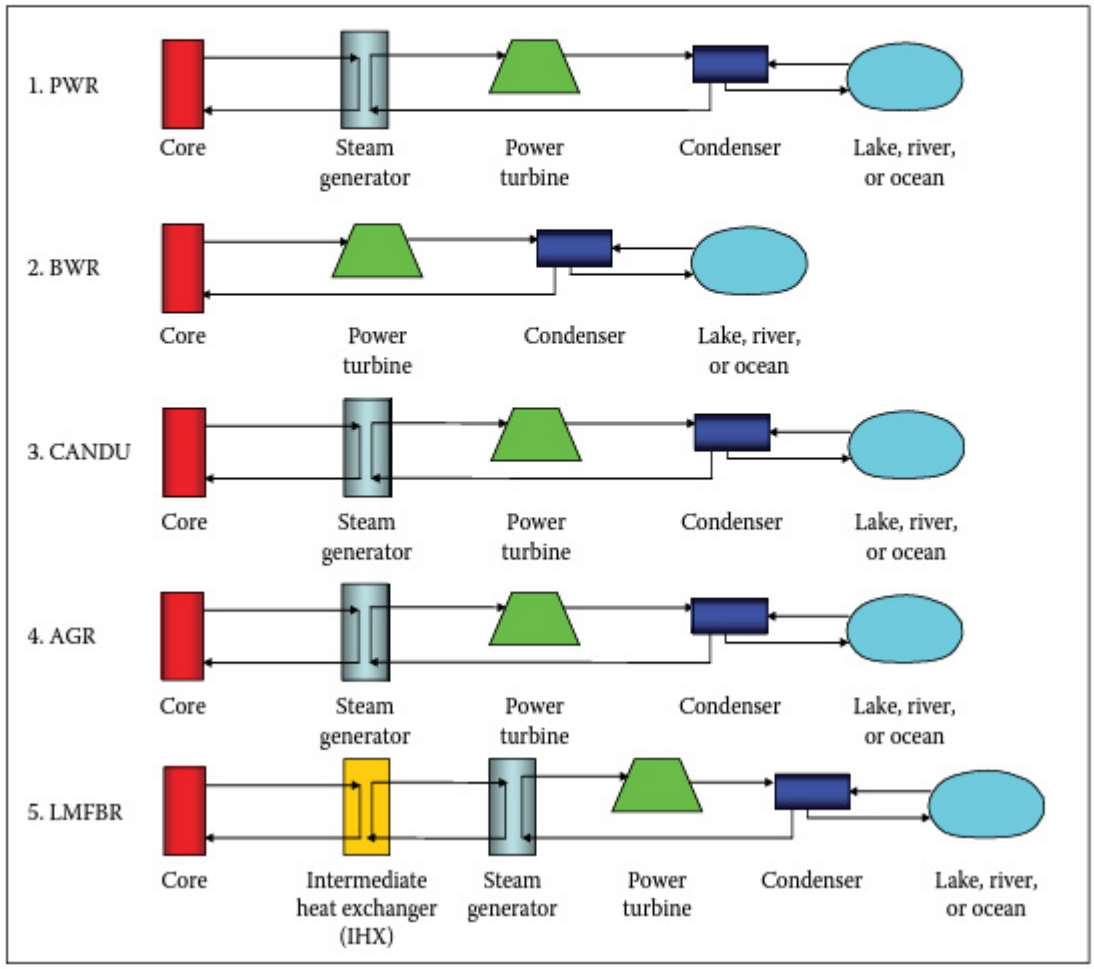

FIGURE 1.5 The basic architectures of different reactor types: PWR, pressurized water reactor; BWR, boiling water reactor; CANDU, Canadian heavy water reactor; LMFBR, liquid metal fast breeder reactor; and AGR, or advanced gas reactor. Notice that all designs have a great many features in common.

perspective. Reactor vendors have never created a "standard fuel assembly," and so each vendor tends to use its own designs for the fuel and the cladding. However, these designs tend to have a great deal in common, and here we would like to describe the similarities and differences between them. Their basic design features are summarized in Table 1.3. These numbers represent *industry averages*, and significant differences can exist from one reactor type to the next.

1.5 Schematic of a Nuclear Power Plant

Several pictures of a nuclear power plant are shown in Figure 1.6(a) and Figure 1.6(b). These diagrams are representative of the size and complexity of most commercial nuclear power plants. The *reactor core* is where the nuclear energy is generated. Notice that the core is just one of a large number of other components in the plant. Some of the remaining components include the piping system, the steam generators, the power turbines, the spent fuel pool, the containment building, and the condenser. Aside from the reactor and the containment building, most nuclear reactors are remarkably similar to the design of coal-fired power plants. Of course the power source is different, but after the coolant is heated, it must pass through almost the same identical components that a coal-fired power plant would use. A very crude diagram of these components is shown in Figure 1.5. In future sections, we will attempt to discuss each of these components, and explain their functions in more detail. Thus it is usually appropriate to introduce several quantities that can be used to describe the performance of a nuclear power plant. Each quantity is described in Table 1.4. Here, the formal definition of these quantities is given as well as the units in which they are measured. In Table 1.4, we have decided to use the *International System of Units* or the *metric system* wherever possible. It is interesting to observe that many of these quantities are, in fact, *dimensionless*. Consequently, they can be used to characterize the relative performance of all types of reactors on an apples-to-apples basis.

The design of a nuclear power plant is a monumental task that involves implementing literally hundreds or even thousands of specific design tradeoffs. While there is no single design that optimizes all of these tradeoffs, most nuclear power plants

TABLE 1.3
Design Parameters of a Modern Nuclear Power Plant (by Reactor Size or Type)

Feature	PWR	BWR	CANDU PWR (HWR)	AGR	LMFBR
Coolant (primary loop)	Light water	Light water	Heavy water	Carbon dioxide	Liquid sodium
Pressure (primary loop) (MPa/PSI)	15.50 (2250)	7.15 (1040)	10 (1450)	4.25 (615)	~0.1 (20)
Temperature (primary loop)[a] (°C)	330	293	310	640	540
Coolant (secondary loop)	Light water	N/A	Light water	Light water	Light water
Pressure (secondary loop) (MPa/PSI)	6.9 (1000)	N/A	4.7 (680)	17.0 (2450)	17.5 (2500)
Temperature (secondary loop)[a] (°C)	285	N/A	260	545	490
Type of fuel	Enriched uranium	Enriched uranium	Natural uranium	Enriched uranium	Uranium and plutonium
Average enrichment (%)	4–5	3–4	0.71	~3	~15–20 Pu
Fuel assembly shape	Square	Square	Concentric circles of rods	Concentric circles of rods	Hexagonal
Cladding	Zircaloy-4	Zircaloy-2	Zircaloy-4	Stainless steel	Stainless steel
Moderator	H_2O	H_2O	D_2O	Graphite	None
Classification	Thermal converter	Thermal converter	Thermal converter	Thermal converter	Fast breeder
Thermal efficiency (%)	34	32	29	42	40
Steam generators	Yes	No	Yes	Yes	Yes
Steam generator type	U tube	N/A	U tube	Helical coil	Helical coil
Core power density (kW/L)	105	52	12	2.7	~400
Average burnup (MWD/ton)	50,000	50,000	7,500	20,000	110,000

Source: Todreas, N. and Kazimi, M.S., *Nuclear Systems*, Vol. 1, CRC Press, Boca Raton, FL, 2008.
[a] The temperatures shown are the maximum average loop temperatures.

are designed to achieve a reasonable compromise between cost, safety, size, longevity, efficiency, and thermal-hydraulic performance. In recent years, there has also been a trend toward reducing the number of components (i.e., pipes, valves) that an individual reactor can use. This can be achieved through better systems design and optimization. Finally, there has been a trend toward more modular designs in an attempt to save money and to improve system reliability. *Modular designs* also have the advantage that a specific class of nuclear power plants can be scaled to a much larger size by simply using larger numbers of the same identical components (for example, the steam generators in a PWR). In this way, every nuclear power plant can use at least some of the same components that smaller versions of the same design use. Light water is used primarily because of its availability and low cost, and also because its thermodynamic properties are well known and well understood. The only problem with light water is that it cannot be used in fast reactors because it contains a high concentration of hydrogen. Light water can also be overly corrosive to the reactor piping system at times.

Modern nuclear power plants also use at least some *passive safety systems*, and the purpose of these systems is to limit the amount of operator intervention that is required in the event of a reactor accident. One of the other design goals of these systems is to limit the number of "surprises" that can occur in the unlikely event of a reactor accident. These safety systems can react much faster to unusual events than human beings, and by design, they are intended to limit the scope of a reactor accident as soon as it begins. We will discuss several of these safety systems as we proceed further into the chapter.

1.6 Coolants Used in Nuclear Power Plants

Many factors go into selecting a reactor coolant, and some of the most important factors include *cost, availability, neutronic performance, and thermal-hydraulic performance*. As Table 1.5 shows, nuclear reactors utilize a variety of coolants, but not all coolants are suitable for all reactor types. Reactor coolants can be further subdivided into three broad categories, which are shown below:

1. *Fluids (such as water)*
2. *Liquid metals*
3. *Gases*

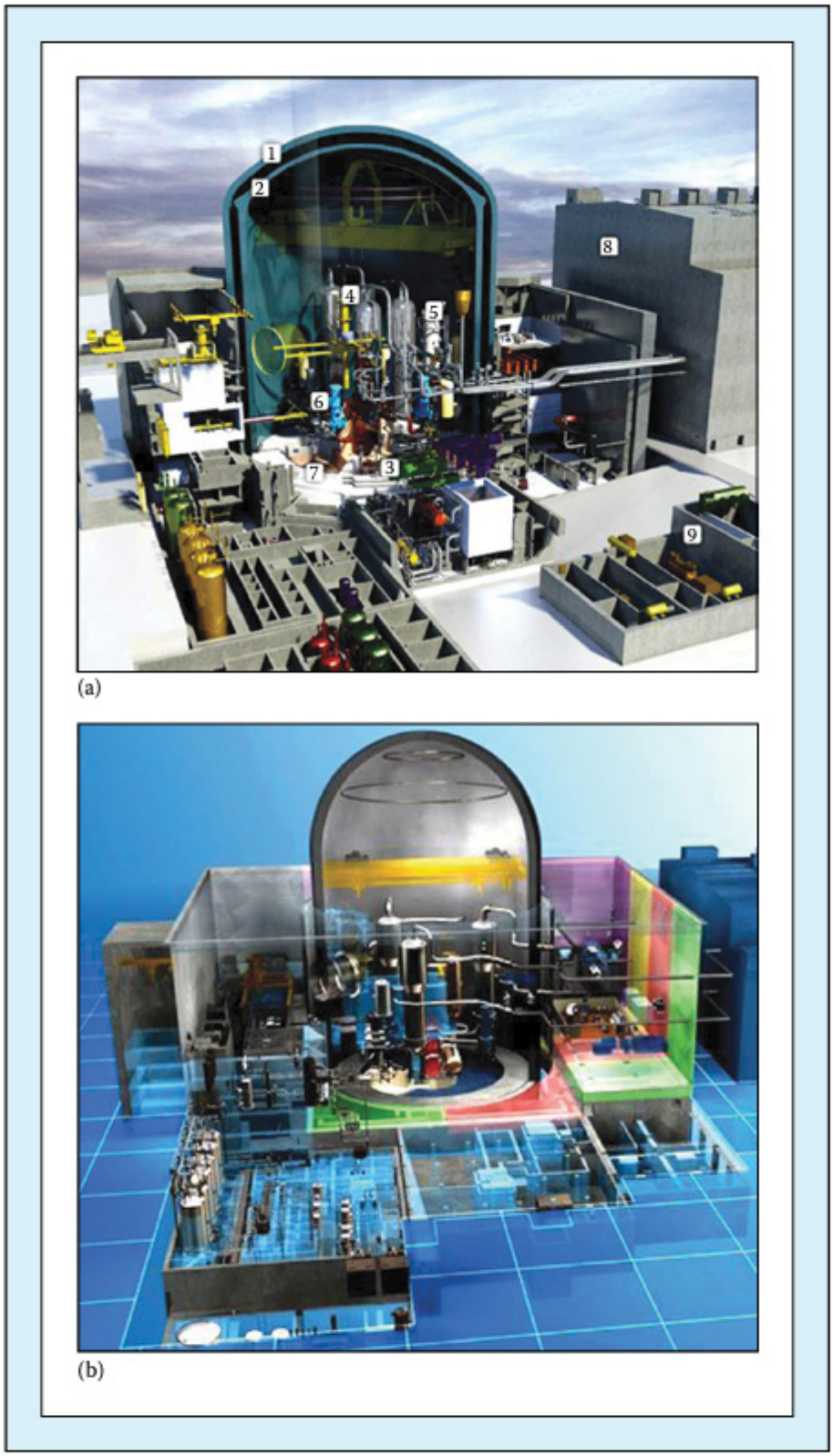

FIGURE 1.6 (a) A schematic of a modern nuclear power plant. The numbers 1 through 9 in the figure refer to 1, the containment building; 2, the steel liner; 3, the reactor core; 4, the steam generators; 5, the pressurizer; 6, the reactor coolant pumps; 7, the fuel storage area; 8, the building housing the steam turbines and the electrical generators; and 9, the auxiliary storage building. (b) Another schematic view of a modern nuclear power plant. (a: Courtesy of AREVA; b: Courtesy of Westinghouse.)

TABLE 1.4
Useful Terms Used to Describe a Nuclear Power Plant

Useful Terms and Their Definitions
Coolant: A fluid that circulates through the core and removes heat generated by the nuclear chain reaction. A coolant is also needed for the nuclear steam supply system (see the text below) to generate electric power.
Moderator: A material, usually with a low atomic mass, that is placed in the core to slow down or moderate fission neutrons so that more of them can be absorbed by the fuel. Typical moderating materials include light water, heavy water, carbon (graphite), and the metal beryllium.
Coolant Channel: A flow channel, usually inside of a fuel assembly, where the coolant flows through over the hot fuel rods and removes heat from the core. In some reactors (like BWRs), the coolant is allowed to boil, while in other reactors (like PWRs and GCRs), it is generally not.
Structure: Supporting materials inside of a reactor core such as the support plates, the grid spacers, the orifice plates, and the metallic tubes that surround the fuel (also known as the cladding). The structure may also include the reactor pressure vessel and other structural components inside of the core.
Core: The area inside of the pressure vessel where the nuclear chain reaction occurs. Normally the core is made up of hundreds of individual fuel assemblies arranged in square or triangular arrays, although this does not always have to be the case. The core also contains the control rods and some instrumentation tubes.
Blanket: An area surrounding the core, usually in a fast breeder reactor, where additional breeding of nuclear fuel occurs. Most fast reactors are surrounded by a radial blanket as well as an axial one. Typical materials used in the blanket include U-238, depleted uranium, and Thorium-232.
Pressure Vessel: A large and heavy cylindrical container, usually 6–9 in. thick, which houses the core. The coolant in the pressure vessel usually flows through the core under very high pressure, and this is one of the reasons why the pressure vessel is named. Not all pressure vessels are cylindrical in shape. In fact, some can also be spherical.
Shielding: A combination of materials, usually consisting of metal and concrete, that are used to shield reactor personnel and the general public from the radiation produced in the core and in the rest of the power plant. The containment building is another type of radiation shield, and also one of the most important ones.
Nuclear Steam Supply System: The piping system, the steam generators, the steam turbines, the pumps, the condenser, and the other components of the cooling system that cool the reactor core and supply steam to the power turbines. The nuclear steam supply system is also called the NSSS.
Steam Turbines: Large, bulky rotating devices inside of a nuclear power plant that are used to take the high pressure steam generated by the reactor core, and delivered by the NSSS, to turn a number of shafts at very high speed, which are connected to electrical generators. The electrical generators then generate the electricity that the power plant produces.
Electrical Generators: Large rotating devices that are connected to the steam turbines or the power turbines to produce the electricity that is generated by the plant.
Pressurizer: A device connected to the nuclear steam supply system of a PWR to maintain the pressure level in the primary coolant loop and to prevent the coolant from boiling. Note: This device is used in PWRs only and is not used in BWRs, LMFBRs, or AGRs.
Steam Generators: Large, complex devices used in PWRs to transfer energy from the primary coolant loop to the secondary coolant loop and produce steam in the process. Steam generators usually contain thousands of individual tubes through which the hot coolant flows to transfer energy to the colder coolant and produce large quantities of steam.

TABLE 1.5
Characteristics of Some Common Reactor Coolants

Coolant	Particle Economy	Heat Transfer Ability	Availability	Cost
Water (light)	Good	Good	Excellent	Low
Water (heavy)	Excellent	Good	Fair	High
Liquid metals	Good	Excellent	Excellent	Moderate
Gases	Good	Fair	Excellent	Low

By far the most common reactor coolant is ordinary water (or H_2O). Sometimes ordinary water is also called *light water*. PWRs and BWRs use light water to cool the core, and the only difference is that BWRs allow the coolant to boil, while PWRs do not—except near the top of the core (see Figure 1.7). CANDU reactors use heavy water as the coolant in their primary loop and light water as the coolant in their secondary loop. *Heavy water* serves as both the moderator and the coolant. Heavy water differs from ordinary water because it has an additional neutron attached to the hydrogen nuclei in the water molecule. Sometimes a hydrogen nucleus with this extra neutron is called *deuterium*. Thus *CANDU reactors are sometimes called HWRs*, or *Heavy Water Reactors. In some books, they are also called Pressurized Heavy Water Reactors, or PHWRs*.

Water works very well as the coolant in thermal reactors because it also serves as the moderator. However, it does not work well in fast reactors because it contains two hydrogen atoms in the water molecule, and these atoms cause the neutrons in a fast reactor to slow down too quickly. Consequently, *fast reactors must use liquid metal coolants (such as liquid sodium, potassium, lead, and sometimes mercury) instead of water to remove the heat from the core*. These liquid metals have excellent heat conduction and retention capabilities, and they can more easily remove the large amounts of heat that fast reactors produce. (Lead is also used as a coolant in military reactors and in naval propulsion systems.)

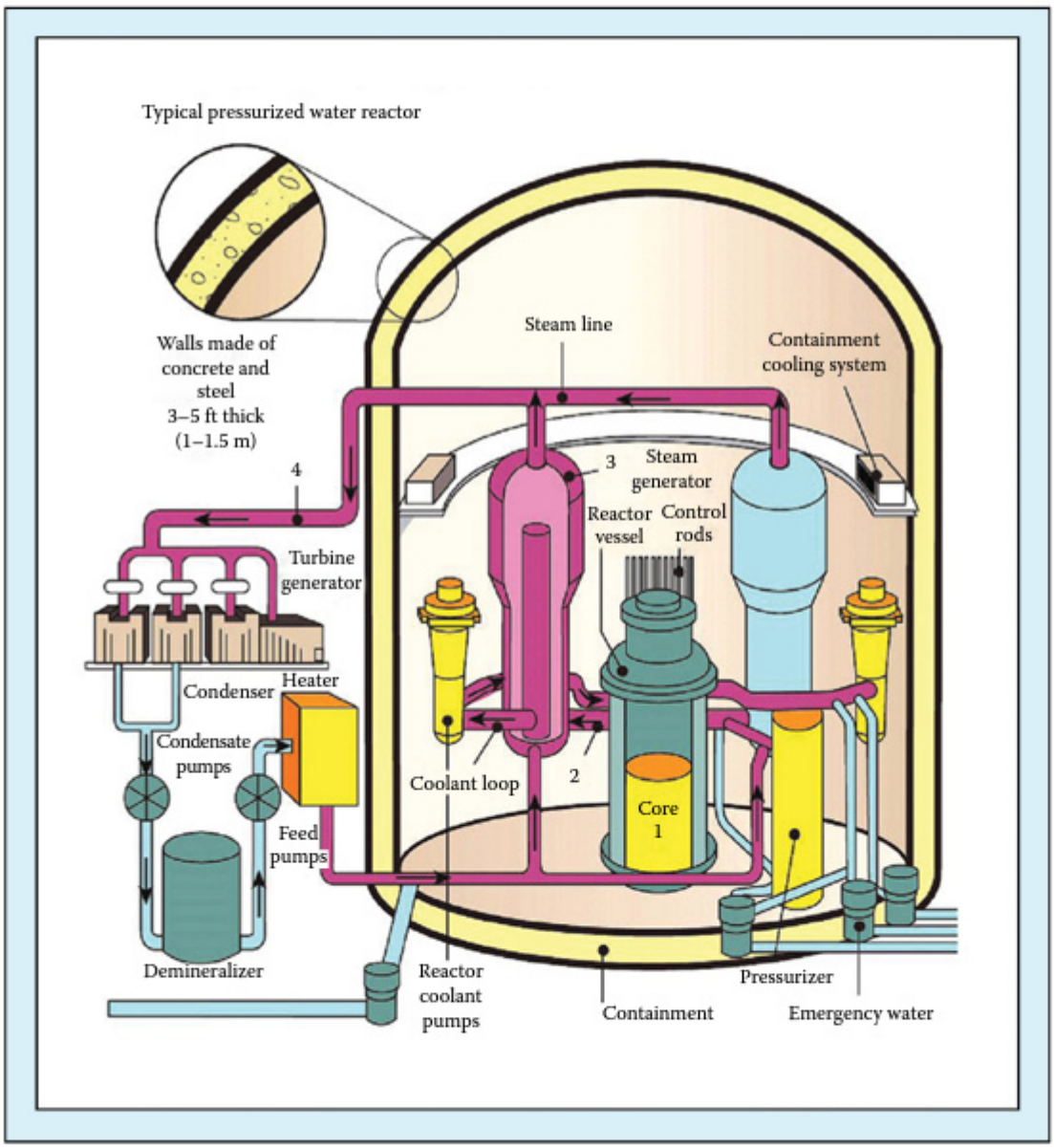

FIGURE 1.7 A typical PWR. Here 1, core; 2, primary loop; 3, steam generators; and 4, secondary loop. (Courtesy of the U.S. NRC.)

Particle economy is also a major factor when deciding the best type of coolant to use. CANDU reactors use natural uranium fuel, and they cannot use moderators such as light water that have high absorption cross sections because there are simply not enough neutrons to go around. However, *the neutron absorption cross sections for heavy water are about 500 times lower than they are for light water*, and so heavy water is an ideal moderating material to use in these reactors in spite of its limited availability and cost. The values of the cross sections for these materials are presented in Appendix C.

1.7 Types of Nuclear Reactor Fuel

A nuclear fuel is a material that causes nuclear energy to be produced. Only a couple of elements in the Periodic Table (see Chapter 6) can be used as commercial nuclear fuels, and some variations of the same element (called isotopes) turn out to be better nuclear fuels than others. To create useful heat and power, a nuclear fuel has to be "burned."

Nuclear fuel is consumed when a uranium or plutonium atom splits apart by absorbing a low energy neutron. Only certain isotopes of uranium and plutonium, called *fissile isotopes*, have this unusual property. Examples of these isotopes include U-233, U-235, Pu-239, and Pu-241. Other varieties of uranium and plutonium, including U-238, Pu-240, and Pu-242, can also absorb a low energy neutron, but they will not *split apart or fission* when they do so. Instead, they are converted into other materials, which may undergo radioactive decay. Incidentally, this is how most of the lead in the world today was created today. Lead is an excellent shielding material that is commonly used in the construction of *radiation shields*. Radiation shields are discussed in great detail in our companion book.* Isotopes of uranium and plutonium with even numbers of protons and neutrons are called *fertile materials*.

The number immediately following the prefixes for U and Pu refers to an element's atomic number, that is, the total number of protons and neutrons in its nucleus. Hence in this case, U-235 is a fissile material, while U-238 is a fertile one. The properties of these fertile and fissile materials are presented in Table 1.6. *Notice that an element is defined by the total number of protons in the nucleus, while different isotopes of the element are defined by the total number of neutrons in the nucleus*. This distinction is discussed in considerable detail in many nuclear engineering textbooks.

1.8 Properties of Nuclear Fuel

Uranium is almost a perfect nuclear fuel because it is relatively abundant in nature, and in fact, it is more plentiful on Earth than either silver or gold (see Table 1.7). However, this is not true in the universe as a whole, where silver and gold far exceed the amounts of naturally occurring uranium. Plutonium does not exist naturally in significant quantities, but it can be created by exposing Uranium-238 to a source of neutrons. Sometimes this process is called *breeding*. The uranium in the earth's crust consists of Uranium-238 (about 99.3% by weight) and about 0.71% by weight of Uranium-235. (Small amounts of Uranium-234 are also present.) This type of uranium is commonly referred to as *natural uranium*. Both uranium and plutonium are heavy metals that have nearly the same appearance as silver (see Figure 1.8). Unfortunately, for reasons that were explained earlier in the chapter, natural uranium is not a particularly good nuclear fuel (except in CANDU reactors) because the coolant or moderator absorbs too many neutrons to allow the reactor to stay critical. *Because of this, there are not enough neutrons left in the core to sustain a nuclear chain reaction*. To compensate for this neutron deficiency, the concentration of U-235 in light water reactors is artificially raised to between 2.5% and 5% using a process called *uranium enrichment*. The enriched fuel is then called *enriched uranium*. The process for enriching uranium is not particularly complicated, but it does take a fair amount of technological infrastructure. The interested reader should consult our companion book.* to learn more about how this process works. The *uranium enrichment process* can also be used to make the material that is used in nuclear weapons.

TABLE 1.6
Nuclear Fuels and Their Properties

Isotope	Classification	Number of Protons	Number of Neutrons	Discover
Th-232	Fertile	90	142	Berzelius
U-233	Fissile	92	141	Klaproth
U-235	Fissile	92	143	Klaproth
U-238	Fertile[a]	92	146	Klaproth
Pu-239	Fissile	94	145	Seaborg
Pu-241	Fissile	94	147	Seaborg

[a] However, even fertile isotopes like U-238 can produce power under certain conditions.

* See *Nuclear Engineering Fundamentals: A Practical Perspective*, by R.E. Masterson, CRC Press (2017).

TABLE 1.7
Natural Abundance of Various Nuclear Fuels in the Earth's Crust

Isotope	Classification	Natural Abundance	Half-Life (Years)	Created from
U-233	Fissile	Does not exist in nature	159,200	Th-232
U-235	Fissile	0.71%	703,800,000	N/A
U-238	Fertile	99.4%	4.468 billion	N/A
Pu-239	Fissile	Does not exist in nature	24,100	U-238
Pu-241	Fissile	Does not exist in nature	14	Pu-239

Note: See Chapter 6 for more information on this subject.

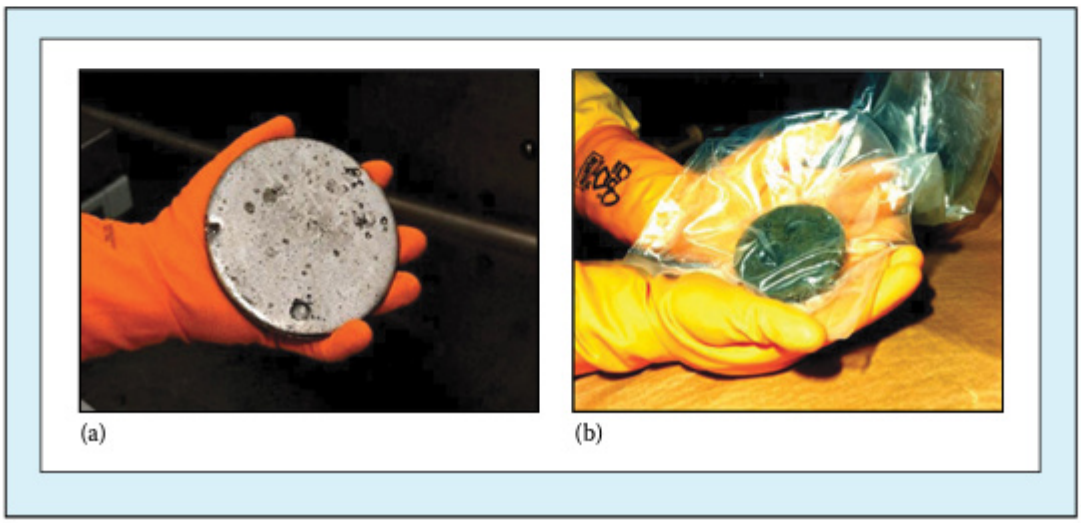

FIGURE 1.8 Two common nuclear fuels—uranium (a) and plutonium (b) in their metallic form. (Courtesy of the U.S. NRC.)

The original process for enriching natural uranium was called the *gaseous diffusion process*. This process was first implemented during the Second World War. Unfortunately, this process turned out to be very expensive and consumed large amounts of electric power. The gaseous diffusion process uses *Uranium Hexafluoride* gas (or UF_6) to separate the lighter U-235 molecules from the heavier and more abundant U-238 ones by passing the gas through porous membranes called *gaseous diffusion stages.* The lighter U-235F_6 molecules pass through the membranes more easily than the U-238F_6 molecules do. Recently, the gaseous diffusion process has been replaced by the *centrifugal separation process* and the *laser enrichment process*, which are both more energy efficient. The centrifugal enrichment process is the dominant uranium enrichment process in the world today. It is so popular because it uses only about 2% as much electricity as the gaseous diffusion process does, and it also has a much smaller physical footprint. The laser enrichment process, which uses industrial lasers to separate U-235 from U-238, uses even less electricity, but it has only recently been deployed on a commercial scale. These three processes are compared to each other in Figure 1.9. The enriched uranium is then mixed with two oxygen atoms to form a ceramic compound called *uranium dioxide* or *UO_2. Uranium dioxide is the most common nuclear fuel in the world today.* Its nuclear and physical properties are well known and well understood, and they are discussed in many nuclear engineering text books.* *Uranium dioxide* also has a very high melting point (about 2850°C or 5160°F) and it is dimensionally and thermally stable. It is generally considered to be a very good nuclear fuel.

1.9 Reactor Pressure Vessels and Their Properties

For a variety of reasons, the core of a nuclear reactor is surrounded by a large physical structure called the pressure vessel. A *pressure vessel* is a large stainless steel or concrete container that holds the fuel assemblies, the control rods, and the coolant in place. The pressure vessel serves as a radiation shield to keep the radiation that is produced in the core from leaking into the rest of the plant. It also serves to pressurize the reactor coolant in PWRs and BWRs, and this pressurization process tends to increase the thermal efficiency of the plant. Reactor pressure vessels can be built in a variety of different sizes and shapes, but the ones used in PWRs and BWRs are primarily cylindrical in shape.

* See *Nuclear Engineering Fundamentals: A Practical Perspective*, by R.E. Masterson, CRC Press (2017).

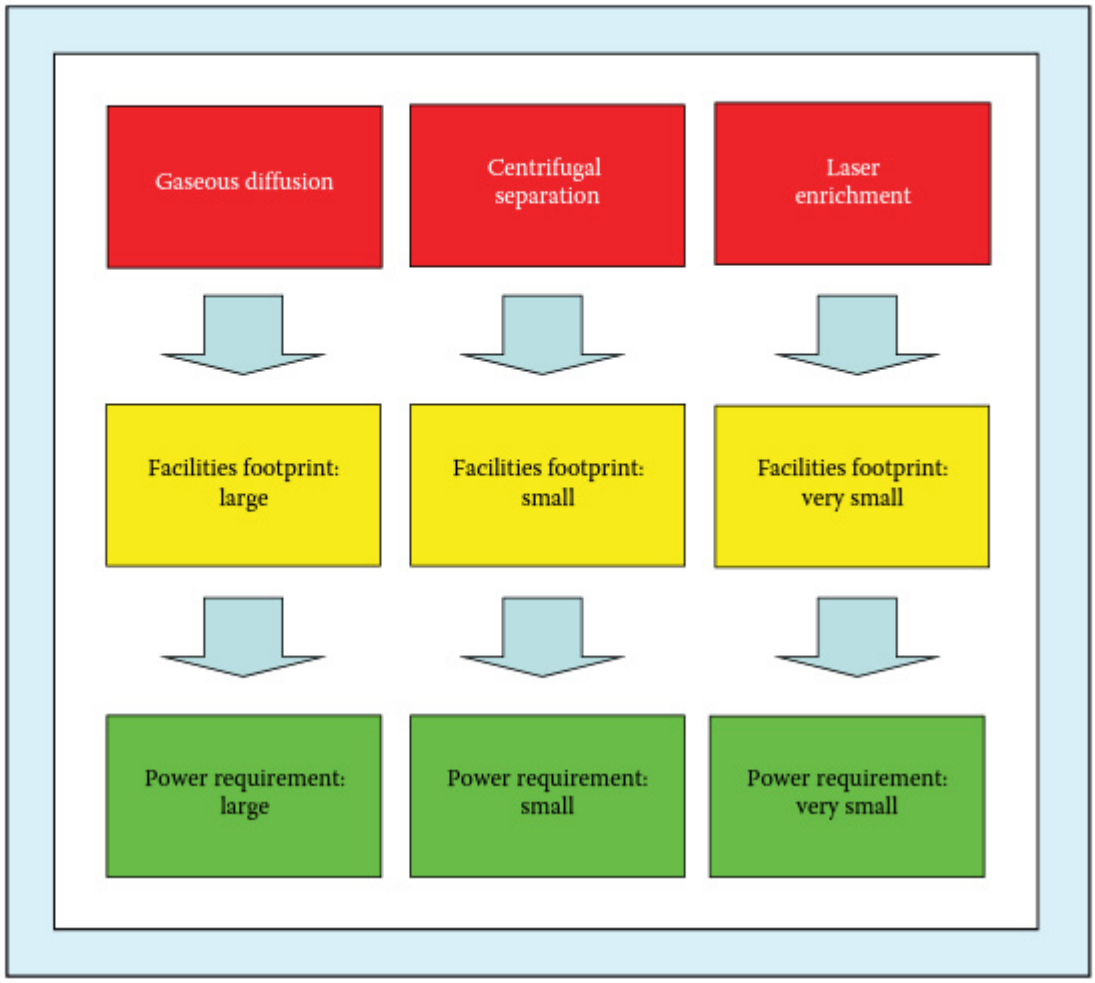

FIGURE 1.9 The three processes of uranium enrichment compared.

Pressure vessels are sized to the thermal output of the core, and some pressure vessels can be as much as 20 m high and 20 m wide. However, on average, most reactor pressure vessels are much smaller than this. The size of the pressure vessels that are used in commercial nuclear power plants are shown in Figure 1.10 and in Table 1.8. *Generally speaking, PWRs have much smaller pressure vessels than BWRs do* (~13 m high and ~5 m wide vs. ~21 m high and ~6 m wide for a reactor having the same power output). In other words, they have about half of the overall volume in spite of the fact that the average power density is twice as high (~105 vs. ~52 kW/L). They are also about 50% thicker to account for the increased system pressure (~2250 PSI vs. ~1050 PSI) (Figure 1.10).

The materials used in reactor pressure vessels vary slightly depending upon the design of the core as a whole. PWRs and BWRs use low carbon steel with a stainless steel liner to increase the life of the pressure vessel and to keep it from becoming brittle as it is exposed to high levels of radiation for prolonged periods of time (typically 40 or 50 years). AGRs, on the other hand, use pressure vessels made out of prestressed concrete with a steel liner because they are so large.

Finally, fast reactors cooled with liquid metals use relatively thin stainless steel pressure vessels because the operating pressure is so low (about 15 PSI). The thickness of these pressure vessels is dictated primarily by the type of coolant and the power density of the core. No two reactor pressure vessels are exactly the same, although their construction has become more standardized in recent years because of a trend toward more modular designs. The thickness of several pressure vessels is shown in Table 1.9. In general, for the same material, the thickness increases as the pressure difference between the inside and the outside of the pressure vessel is increased. Interestingly enough, *the relationship between the system pressure and the pressure vessel thickness is not a linear one*. The AMSE and the ANS first established standards for the construction of reactor pressure vessels in the 1970s. Since then, these standards have undergone several major

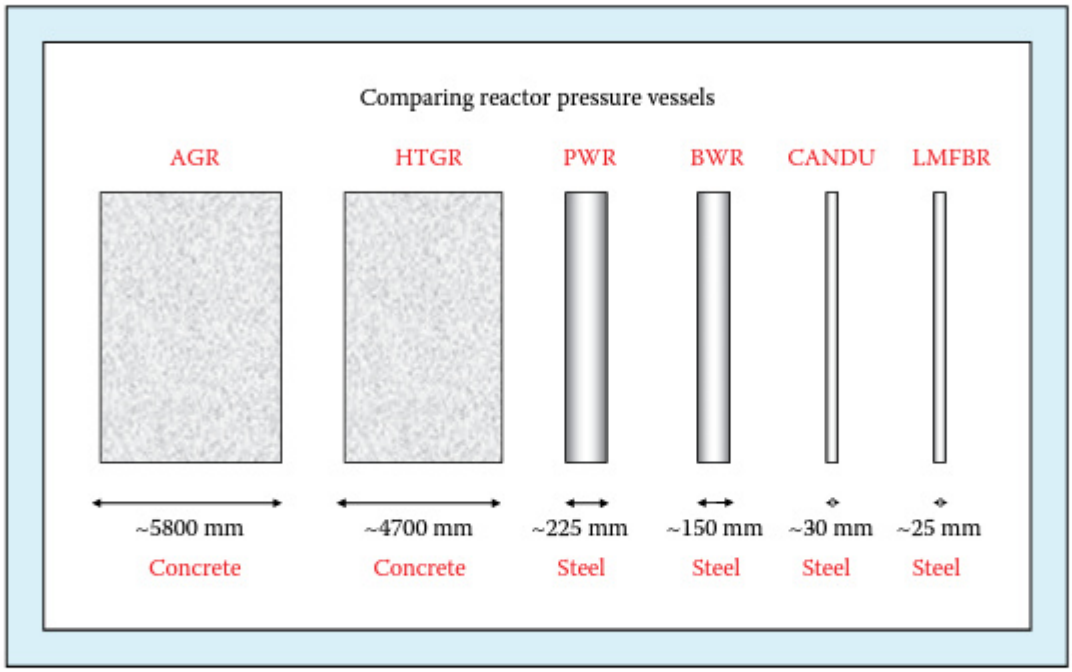

FIGURE 1.10 The thickness of different reactor pressure vessels. (From Todreas, N. and Kazimi, M.S., *Nuclear Systems*, Vol. 1, CRC Press, Boca Raton, FL, 2008.)

TABLE 1.8
Reactor Pressure Vessel Sizes

Reactor Type	Pressure Vessel Height (m)[a]	Pressure Vessel Width or Diameter (m)[a]	Wall Thickness (mm)	Composition	Other Features
PWR	13.4	4.83	224	SS clad carbon steel	N/A
BWR	21.6	6.05	152	SS clad carbon steel	N/A
CANDU	4.0	7.6	28.6	Stainless steel	Pressure tubes
HTGR	14.4	11.3	4720	Reinforced concrete	Steel liners
AGR	21.9	20.3	5800	Reinforced concrete	Steel lined
LMFBR[b]	19.5	21.0	25	Stainless steel	Pool type

Source: Todreas, N. and Kazimi, M.S., *Nuclear Systems*, Vol. 1, CRC Press, Boca Raton, FL, 2008.
Note: For CANDU reactors and LMFBRs, the pressure vessel is sometimes called the "reactor vessel."
[a] Inside dimensions.
[b] Pool-type LMFBR.

TABLE 1.9
Thickness and Design Pressure of Some Common Reactor Pressure Vessels

Reactor Type	Operating Pressure (MPa)	Operating Pressure (PSI)	Wall Thickness (mm)	Wall Thickness (in.)
PWR	15.5	2250	225	8.86
BWR	7.15	1050	150	5.90
CANDU	10.0	1450	30	1.20
HTGR	5.0	725	25	1.00
AGR	4.3	625	4700	158.05
LMFBR	~0.1	15.0	5800	228.35

FIGURE 1.11 A view of the internal structure of a BWR pressure vessel. (a) Full view; (b) detailed view. (Courtesy of TEPCO—see *http://cryptome.org/eyeball/daiichi-npp15/daiichi-photos15.htm*.)

revisions. Today these standards can be found in *Section III of the ASME Boiler and Pressure Vessel code*. The interested reader can order copies of these standards directly from the ANS or the ASME. All reactor pressure vessels are manufactured according to these standards today (see Figure 1.11).

1.10 Thermal Energy Production from Nuclear Fuel Rods

Nuclear power is produced by *nuclear fuel rods*, which are located in the core. These rods, in turn, are grouped together to form what are known as nuclear *fuel assemblies*. Fuel assemblies can have anywhere from 50 to 400 fuel rods. The design of these assemblies is discussed in Section 1.12. Nuclear fuel rods contain uranium or plutonium atoms combined together with two oxygen atoms to form ceramic compounds called *uranium dioxide* and *plutonium dioxide* (UO_2 and PuO_2). Between 95% and 97% of the uranium in most commercial power reactors is Uranium-238 and the remaining 3%–5% is Uranium-235. Uranium and plutonium dioxide have very high melting points, and in general, they are dimensionally, thermally, and structurally stable. A schematic view of a nuclear fuel rod is shown in Figure 1.12. The uranium dioxide and the plutonium dioxide in these rods is then compressed together to form what is called a nuclear *fuel pellet*.

A typical rod consists of several hundred fuel pellets stacked together into vertical or horizontal arrays. Normally the fuel pellets are cylindrical in shape, but this does not always have to be the case. The enrichment of the fuel is specified by the owner or operator of the nuclear power plant or by the reactor vendor who built the plant. The average enrichment of the fuel in a fresh core is between 3.5% and 5.0% for light water reactors (BWRs or PWRs), although these numbers have tended to increase over time as uranium has become more expensive and fuel has been allowed to remain in the core longer.

The size of a fuel pellet is dictated by the rate at which heat must be removed from the rod. The fuel pellets are then inserted into the rods, which are stacked to the correct height, welded shut, filled with a pressurized gas, and sealed. Not all of fuel rods or fuel pellets have the same size, and their actual dimensions can vary considerably from one reactor type to the next. In fact, they can even vary from one PWR or BWR to the next. Fuel pellets used in PWRs and BWRs have an average diameter of about 0.9 cm. PWR fuel pellets are slightly smaller than BWR fuel pellets because of the respective differences in the power densities between the two designs. The sizes of these pellets are compared in Table 1.10. In general, the higher the power density of the core is, the smaller the fuel pellet must be to safely remove the heat. The parameters shown in Table 1.10 can be considered to be "typical" in the sense that they represent *industry average* values over many different designs.

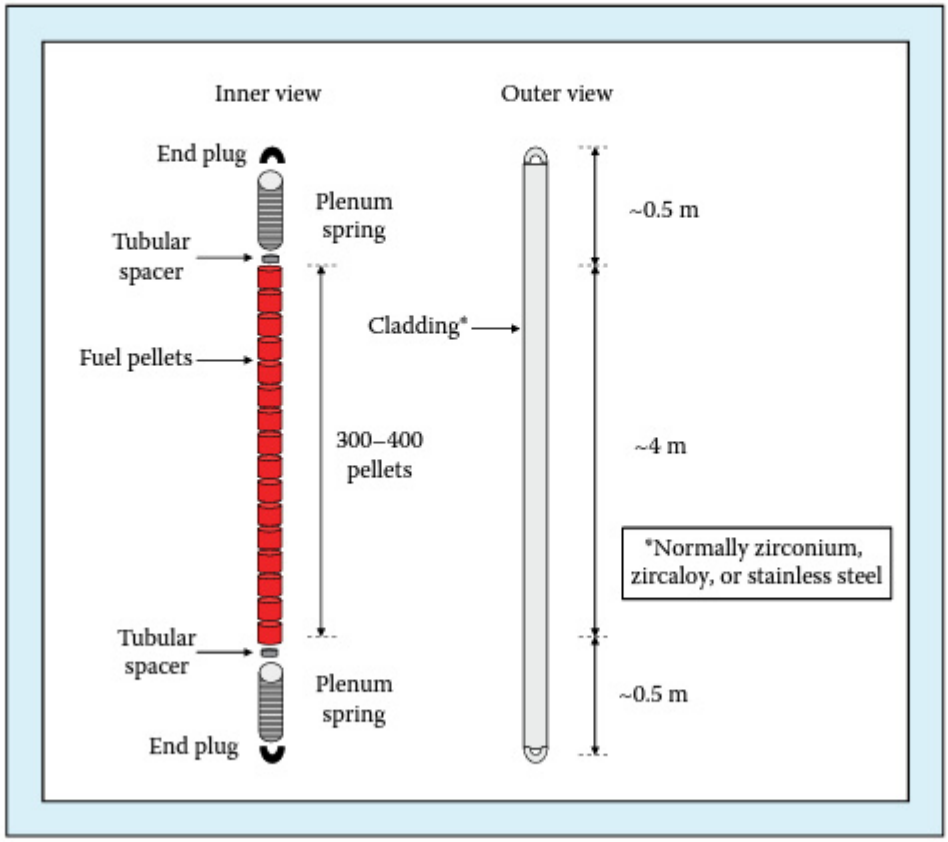

FIGURE 1.12 A picture of a nuclear fuel rod from a PWR and its internal structure.

TABLE 1.10
Properties of Nuclear Fuel Pellets Used in Different Types of Reactors

Reactor Type	BWR	PWR	CANDU	AGR	LMFBR
Fuel pellet diameter (typical) (cm)	1.0–1.1	0.7–0.9	1.2–1.4	1.4–1.5	0.6–0.8
Fuel pellet height (typical) (cm)	1.0–1.1	1.2–1.3	1.4–1.6	1.4–1.5	0.6–0.8
Fuel pellet volume (typical) (cm^3)	~1	~0.8	~2	~2.5	~0.25
Fuel pellet composition	UO_2	UO_2	UO_2	UO_2	PuO_2/UO_2
Enrichment (typical)[a] (%)	1.8–2.6	2.6–4.5	0.711	2.2–2.6	15–18 Pu
Number of fuel pellets per fuel rod (typical)[b]	~380	~360	~30	~20	~360

Source: Todreas, N. and Kazimi, M.S., *Nuclear Systems*, Vol. 1, CRC Press, Boca Raton, FL, 2008.

[a] Representative range (for a fresh core).

[b] Assumes a 12 ft long or 4 m long fuel rod, and a 50 cm long CANDU fuel bundle.

1.11 Fuel Rod Cladding

The fuel pellets used in commercial nuclear power plants are surrounded by a thin metal casing called *the cladding*. The cladding separates the fuel from the coolant, and in the case of a light water reactor, the coolant also serves as the moderator. Most materials used for the cladding have relatively low neutron absorption cross sections (less than 1 barn) so as not to seriously affect the overall neutron economy of the core. (The actual values of these cross sections are presented in Appendix C). A cross-sectional view of a typical fuel rod is shown in Figure 1.13. Fuel rods such as this come in two primary configurations: those that are cylindrical in shape, and those that are cylindrical and annular in shape. Both types of fuel rods have advantages and drawbacks. Most light water reactors use solid cylindrical fuel rods because of their simplicity and relatively low cost. A solid cylindrical fuel rod is probably one of the best-understood parts of any nuclear power plant. However, when high temperatures and high power densities are required, annular fuel pellets are better at removing the heat than solid fuel pellets are. This is also true in certain types of reactor transients that are important to ensuring the overall safety of the core.

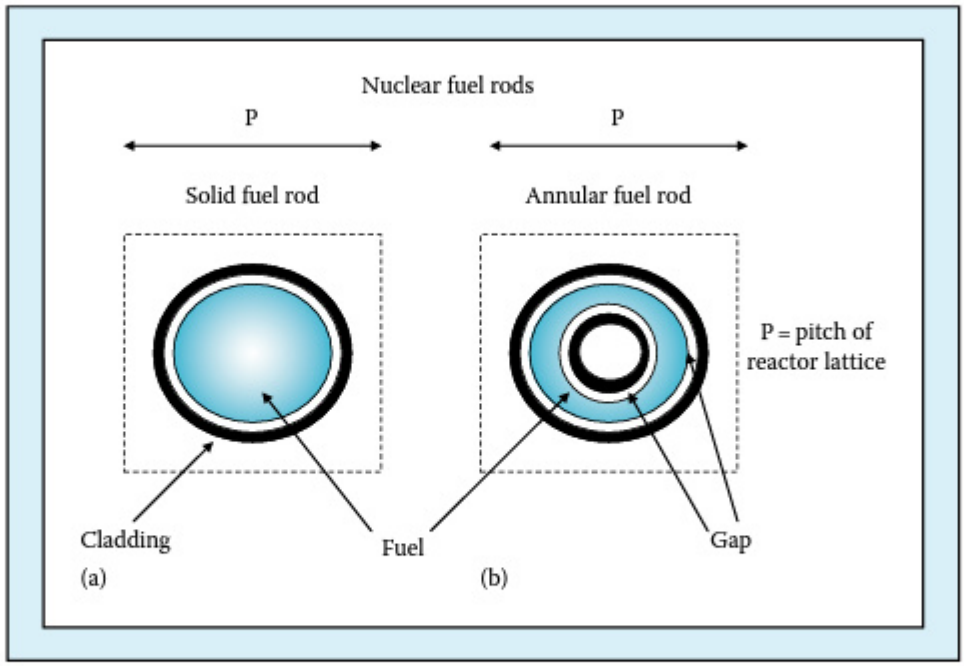

FIGURE 1.13 A cross-sectional view of two different types of nuclear fuel rods—(a) a solid fuel rod and (b) an annular fuel rod. Here P is the "pitch" of the reactor lattice, which is defined as the centerline-to-centerline spacing between adjacent fuel rods.

Many materials can be used for the cladding. Historically, the cladding in nuclear power plants was made from *zirconium* (Zr) or *stainless steel* (SS). Reactors designed in the 1950s and the 1960s used cladding that was made primarily from *Zirconium* or one of its alloys. The average cladding thickness at that time was about 1 mm. Unfortunately, the Zirconium used in the cladding absorbed too many neutrons because it contained the element hafnium, which is a strong thermal neutron absorber. These cladding materials absorbed more neutrons than was ideal from a design perspective, and so more advanced alloys like *Zircaloy-2* and *Zircaloy-4* were developed. These alloys had much lower neutron absorption rates, and so less fuel was needed to keep the core critical. In the 1970s and 1980s, it then became possible to shrink the thickness of the cladding to improve neutron economy as well. *The latest generation of fuel assemblies now have cladding with an average thickness of about two-thirds of a millimeter (0.60 mm), and the gap between the cladding and the fuel now has an average thickness of about 1/10th of a millimeter (0.10 mm)*. Consequently, the distance between the surface of the fuel and the surface of the cladding is now about 0.70 mm (0.60 + 0.10 mm) in most modern light water reactors. BWRs manufactured by General Electric tend to have the highest average cladding thickness (0.66 mm–0.88 mm), while CANDU reactors and AGRs tend to have the lowest (about 0.40 mm). PWRs and LMBFRs with an average thickness of about 0.57 mm tend to fall somewhere between these two extremes. The thickness of the cladding used in each reactor type is shown in Table 1.11.

Not surprisingly, the thickness of the other major cladding material (stainless steel) has remained about the same—even though it absorbs more thermal neutrons and has a lower melting point. In the design and manufacture of nuclear fuel rods, the goal is to create as many fuel rods as possible that are exactly the same as each other to that they can be put together into larger groups of rods called *fuel assemblies*. Sometimes a group of these rods is also called a *rod bundle*. We will now discuss how fuel assemblies are designed. Like any other component of the plant, reactor vendors will supply nuclear fuel and nuclear fuel rods to utilities in any form that is desired.

TABLE 1.11
Cladding Materials Used in Different Reactor Designs

Reactor Type	BWR	PWR	CANDU	AGR	LMFBR
Cladding geometry	Cylindrical	Cylindrical	Cylindrical	Cylindrical	Annular
Cladding material	Zircaloy-2	Zircaloy-4	Zircaloy-4	Stainless steel	Stainless steel
Cladding thickness (avg.) (mm)	~0.75	0.57	0.42	0.37	0.56
Gap thickness (avg.) (mm)	~0.1	~0.1	~0.1	~0.1	~0.1
Fuel rod pitch (avg.) (mm)	13–16	12.6	14–15	~25	~10

TABLE 1.12
Composition of Various Alloys of Zircaloy, Which Is a Common Cladding Material Used for Nuclear Fuel Rods (The Percentages of Each Element Are Shown Below)

Material	Zircaloy-2	Zircaloy-4	Stainless Steel (316)
Zirconium	98.00	98.00	~0.0
Tin	1.2–1.7	1.2–1.7	~0.0
Iron	0.07–0.20	0.18–0.24	70.0–80.0
Chromium	0.05–0.15	0.07–0.13	16.0–18.0
Nickel	0.03–0.08	0.002–0.007	10.0–14.0
All other	<0.01	<0.01	4.0–5.0
Melting point (°C)	1850	1850	1400

Cladding materials used today have a very high thermal conductivity, and generally speaking, they have good resistance to the X-rays and gamma rays produced by the fuel. *Zircaloy* is much better than stainless steel in this regard. It has a very low thermal absorption cross section, and because of this, it allows more thermal neutrons to be absorbed by the fuel. There are two versions of the alloy Zircaloy in widespread use today: *Zircaloy-2, which is used primarily in BWRs, and Zircaloy-4, which is used primarily in PWRs*. The properties of these two alloys are compared in Table 1.12. Notice that Zircaloy-4 has a slightly more Iron and Chromium than Zircaloy-2. *It also has much less Nickel*. The amount of tin and Zirconium in both alloys is about the same. An excellent article discussing the physical properties of these two materials can be found at the following URL:

http://web.ornl.gov/info/reports/1962/3445605716311.pdf.

The melting points of Zircaloy-2 and Zircaloy-4 are nearly identical. The *gap* between the fuel pellets and the inner surface of the cladding is then filled with *pressurized helium* to improve the flow of heat across the rod. Sometimes this gap is referred to as the *fuel-cladding gap*. The pressure of the helium inside of the rod is normally set equal to the ambient pressure of the reactor environment in which the rod will be placed. In the case of a BWR, this turns out to be about 1050 PSIA, and in the case of a PWR, this turns out to be about 2250 PSIA. Although the size of the gap can vary somewhat from one design to the next, most reactors have a fuel-cladding gap of about 0.10 mm. (The industry average gap in modern PWRs and BWRs today tends to be about 0.09 mm.) *Normally, the gap is about one-quarter to one-third the thickness of the cladding*. The smaller the gap, the easier it is to remove heat from the fuel when the reactor is operating. However, if the gap is too small, the chance of the cladding being breached may be increased because of the mechanical interaction between the cladding and the fuel. Over time, the design of most fuel rods has been changed to minimize these competing effects as the burnup of the fuel has been increased.

1.12 Nuclear Fuel Assemblies

Once the nuclear fuel rods have been built, they are assembled into clusters of rods called *nuclear fuel assemblies*. Within each fuel assembly, the rods are separated from each other using sets of ingeniously designed grids or spacers. The reactor coolant (usually water) is then designed to flow between the fuel rods to remove the heat from the rods. The most common types of fuel assemblies, such as those used in PWRs and in BWRs, are simple rectangular arrays of rods. About 70% of the commercial nuclear reactors in the United States are PWRs, and most of the remaining commercial power reactors are BWRs. Today, these reactors generate enough electricity to supply about 20% of the United States' total electrical needs. Holistically speaking, neither type of reactor has an overwhelming advantage over the other, although PWRs have been in operation longer and they have certain perceived advantages when it comes to the power density and the reactivity control (see Chapter 20). These advantages are due to the fact that the average power output of PWR fuel is about twice that of a BWR (per liter) and because the control rods in a PWR will automatically fall into the core in the event of a reactor emergency under the influence of gravity alone—whereas in BWRs, they have to be inserted mechanically into the core from below. On the other hand, PWRs have an extra coolant loop and an extra steam generator per loop, and these additional parts may add some cost and complexity that BWRs are able to avoid. The safety records for both reactors have been excellent, and within the United States, not a single civilian has been killed in a nuclear-power-related accident in the last 50 years. During this same period of time, approximately 2 million people have been killed or injured on the nation's highways, and several million have died from drug overdoses. Thus commercial nuclear power plants, at least on a statistical basis, are extremely safe machines.

1.13 PWR, BWR, and LMFBR Fuel Assemblies

PWR fuel assemblies contain large numbers of cylindrical fuel rods bundled together into square arrays having 15, 17, or 19 rods per side. A typical PWR fuel assembly having $17 \times 17 = 289$ fuel rods and control rods is shown in Figure 1.14. The fuel rods are usually about 12 ft long (~4 m), although their overall length can vary considerably depending upon the design of the core. The control rods are made of boron or cadmium. The fuel pellets are loaded into the fuel rods by first welding one end of the rods completely shut. A spring is then inserted into the rod to hold the fuel pellets in position, and then the fuel pellets are placed on top of it. The fuel rods are designed so that an additional space, or *fission gas plenum*, about 2 ft in length, is provided near the top and the bottom of the rods to allow the gaseous fission products to accumulate. A picture of a fuel rod used in a PWR is shown in Figure 1.12. The fuel pin springs hold the fuel pellets together and reduce the axial stress on the rod. Notice that there is one spring and one plenum or spacer at each end of the rod (top and bottom) for the fission gases to accumulate. The rod is then evacuated and filled with a conductive gas like Helium. Helium helps to improve the heat transfer coefficient across the fuel-cladding gap. In PWRs, the fuel rods contain enough fuel pellets to create an active core height between 3 and 4 m. In PWRs, they are then pressurized to about 2200 PSI (1.55×10^7 Pa), and in BWRs, they are pressurized to about 1000 PSI (about 6.9×10^6 Pa). The fuel rods are designed to withstand these pressures easily. The rod ends are then welded shut, and the fuel rods are placed in a vacuum chamber to test for leaks. If a rod successfully passes this "leak test," then it is etched in a nitric–hydrofluoric acid bath and cleaned with high pressure steam. This produces an outer surface film that is corrosion resistant and has a very clean finish. The fuel rods are then ready to be assembled into fuel assemblies.

Interspersed between the fuel rods are *control rods*, which are made from *cadmium or boron* to absorb excess neutrons. A considerable amount of time and effort goes into the design of a nuclear fuel assembly, and a typical fuel assembly can weigh several metric tons. *There are about as many different fuel assembly designs as there are types of commercial airplanes*. The major difference between these designs is in the spacing between the fuel rods and the location of the control rods. The centerline-to-centerline spacing is called the *rod pitch* P. There are also differences due to the overall geometry of a fuel assembly (hexagonal, square, or circular), and whether or not the fuel assemblies are surrounded by a thin tube of metal called a "*can*," a "*sheath*," or a *shroud*. Figure 1.14 shows a cross-sectional view of a modern PWR fuel assembly. There are many variations on this particular design, including the number of fuel rods and the location and number of control rods. Normally, PWRs have fuel rods arranged in rectangular arrays, with 15×15 or 17×17 rods per side. A good example of this is illustrated in Figure 1.15.

In LMFBRs, the fuel assemblies are *hexagonal* rather than rectangular in shape. See Figure 1.16. We will not discuss these fuel assemblies in detail here except to say that it is theoretically possible to get a higher power output out of a hexagonal-shaped assembly than a rectangular one because of the way that the rods are packed together. This makes fuel assemblies with hexagonal arrays a desirable thing to have in high power applications. BWR fuel assemblies are similar to PWR fuel assemblies except that they are smaller, and they have "cans" around them to separate them from one another from a thermal-hydraulic and neutronic perspective. The number of fuel pins per assembly is also less (usually 60 to 80), and the surrounding cans are usually made of stainless steel.

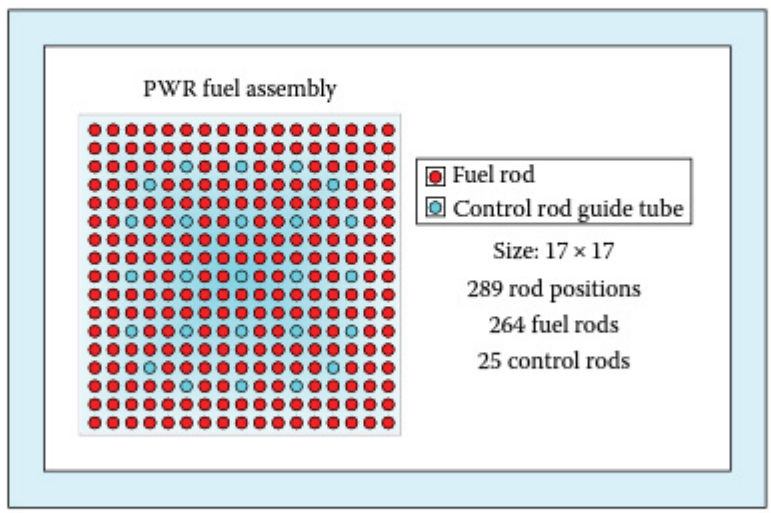

FIGURE 1.14 A cross-sectional view of a modern PWR fuel assembly. Today PWR fuel assemblies can have either 17 or 19 rods per side.

FIGURE 1.15 A picture of a PWR fuel assembly ready to be loaded into a reactor core. (Courtesy of the U.S. NRC.)

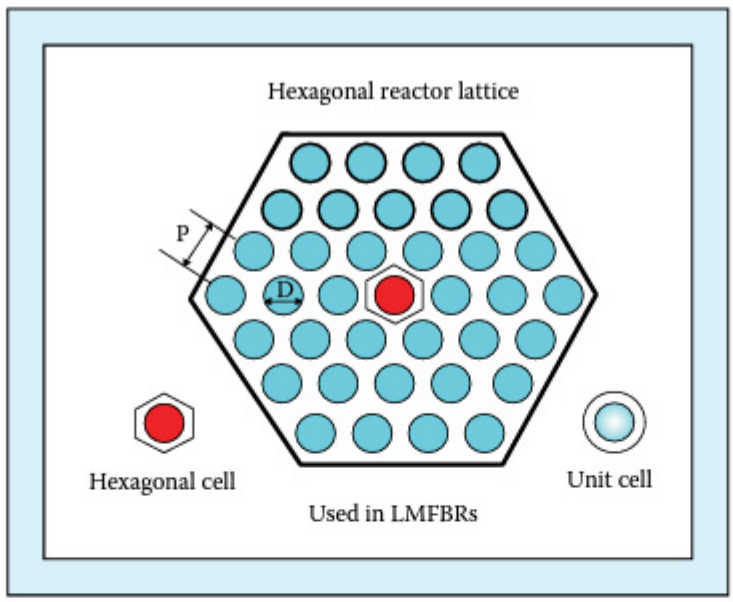

FIGURE 1.16 A cross-sectional view of a modern LMFBR fuel assembly.

1.14 Number of Fuel Rods in a Reactor Fuel Assembly

One other major difference between reactor fuel assemblies is the number of fuel rods and control rods they contain. Modern PWRs have upwards of 200 rods per fuel assembly, while BWRs can have as few as 60. LMFBRs tend to mimic PWRs in this respect, while CANDU reactors and AGRs have only about 40 rods per assembly. The average number of rods in each design is presented in Table 1.13. Note that the number of rods within an assembly can vary greatly from one reactor type to the next. Again, it is important to remember that these numbers represent *industry averages* and that some additional variation may occur within each generation of a specific reactor type. A BWR fuel assembly with an outer "can" is shown in Figure 1.17. In general, it is much smaller than its PWR counterpart. Sometimes the outer can is also called a *sheath* or a *shroud*.

TABLE 1.13
Typical Fuel Assembly Design Parameters by Reactor Classification

Reactor Type	Manufacturer	Fuel Assembly Characteristics	Fuel Rods per Assembly	Fuel Assembly Geometry	Fuel Assembly Orientation
BWR	General Electric	8–9 rods per side	64–81[a]	Square	Vertical
PWR	Westinghouse	13–17 rods per side	169–289[a]	Square	Vertical
CANDU	Atomic Energy of Canada	5–7 concentric rings	28–45[a]	Cylindrical	Horizontal
AGR	National Nuclear	Concentric rings	190[a]	Cylindrical	Vertical
LMFRB	Westinghouse	7–9 rods per side	169–271[a]	Hexagonal	Vertical

[a] Typical range—exact numbers can vary from those shown.

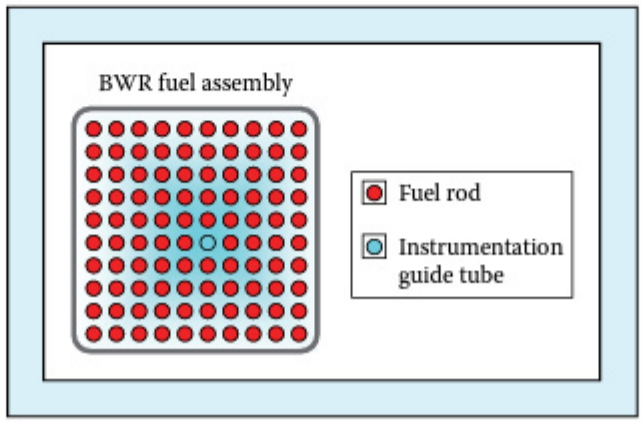

FIGURE 1.17 A modern BWR fuel assembly with its surrounding "Can" and no control blade.

1.15 Fuel Rods in Square Fuel Assemblies

The number of fuel rods in a square fuel assembly can be found by simply multiplying the number of fuel rods along each side of the assembly and then subtracting the number of these slots that are intended for control rods and instrumentation guide tubes. Table 1.14 shows the types of fuel rods that can be found in an assembly as a function of the number of rods the assembly contains. In a square reactor lattice, the number of "corner" rods always stays the same, while the number of interior rods and side rods increases as the size of the fuel assembly is increased.

TABLE 1.14
Number of Fuel Rods That Are Theoretically Possible in a Square Fuel Assembly

Rows of Rods	Interior Rods	Side Rods	Corner Rods	Total Rods
1	1	0	0	1
2	0	0	4	4
3	1	4	4	9
4	4	8	4	16
5	9	12	4	25
6	16	16	4	36
7	25	20	4	49
8	36	24	4	64
9	49	28	4	81
N	**$(N-2)^2$ for N > 1**	**4 (N − 2) for N > 1**	**4 for N > 1**	**N^2**

TABLE 1.15
Number of Fuel Rods That Are Theoretically Possible in a Hexagonal Fuel Assembly as a Function of the "Ring Count"

Rings of Rods	Interior Rods	Side Rods	Corner Rods	Total Rods
1	7	0	0	7
2	7	6	6	19
3	19	12	6	37
4	37	18	6	61
5	61	24	6	91
6	91	30	6	127
7	127	36	6	169
8	169	42	6	217
9	217	48	6	271
n	**Σ_n 6n + 1 for n > 1**	**6 (N_{rings} − 1) for n > 1**	**6 for n > 1**	**N = Σ_n 6n + 1**

1.16 Fuel Rods in Hexagonal Fuel Assemblies

As one can imagine, the number of fuel rods in a hexagonal fuel assembly follows a similar set of combinatorial rules. To find the total number of fuel rods that a hexagonal fuel assembly contains, we simply find the total number of "*rings*" n that are used in the assembly. For each ring number, we multiply by 6, and then add 1 to the total. The expression to calculate the total number of rods is then $N_{RODS} = \Sigma_n 6n+1$, where n is the ring number and N is the total number of rods. The exact numbers of rods are shown in Table 1.15 as the ring number increases. Thus, the total number of "corner" rods is always 6, and the number of side rods is six times the number of rings minus six, or 6 (N_{rings} − 1). Table 1.15 shows the total number of fuel rods that are theoretically possible in a fuel assembly of this type as a function of the number of rings. The formulas for each type of rod (edge, corner, or interior) are also shown. Thus the total number of fuel rods of all types is given by

Fuel Rods in a Hexagonal Fuel Assembly Having N Rings

$$N_{RODS} = \sum_{n=1}^{N} 6n+1 \tag{1.1}$$

where N is the number of rings. For reasons that we will subsequently discuss, *a hexagonal fuel assembly has about 16% more fuel rods for the same volume of space than a square fuel assembly does*. This percentage assumes that the size of the fuel rods is identical. The total number of rods for 8 and 9 rings is 217 and 271, respectively. By comparison, square fuel assemblies 17 rods wide and 19 rods wide will have 289 and 361 rods, respectively. As before, these numbers include the spaces that are reserved for control rods and instrumentation guide tubes.

1.17 Other Fuel Assemblies: CANDU Fuel Assemblies

The word CANDU is an acronym for a *CANada Deuterium Uranium* reactor. *It is a Canadian-designed PHWR that can be fueled with natural uranium, enriched uranium, or a mixture of these fuels (and even plutonium in some cases)*. The fuel is imbedded in a ceramic oxide matrix, and the fuel pellets are loaded into the core *horizontally* rather than vertically. CANDU reactors were originally developed from a German design that was proposed by Nazi Germany during the Second World War, but it was not fully implemented until after the war was won. *In CANDU reactors, the fuel assemblies are positioned horizontally in the core*, and the fuel assemblies are then referred to as *fuel bundles*. The fuel bundles are not permanently sealed in the way that PWR fuel rods are. Instead they consist of arrays of horizontal *pressure tubes* which can be opened from the side. Because of this, CANDU reactors can be refueled by opening the side of a pressure tube and inserting fresh fuel into it with a refueling machine. *This allows the core to be refueled while the reactor is still operating*. In the trade, this process is called *online refueling*. The fuel bundles are submerged in a large cylindrical tank called a *Calandria*, which is then filled with heavy water or D_2O. A picture of a Calandria, as well as a fuel bundle containing the pressure tubes, is shown in Figure 1.18. The D_2O in this case is very close to atmospheric pressure, and the D_2O within the Calandria is used to moderate the neutrons. A more detailed discussion of neutron moderation is provided in Chapter 8. A picture of the Calandria as well as one of the fuel bundles inside of it is shown in Figure 1.18.

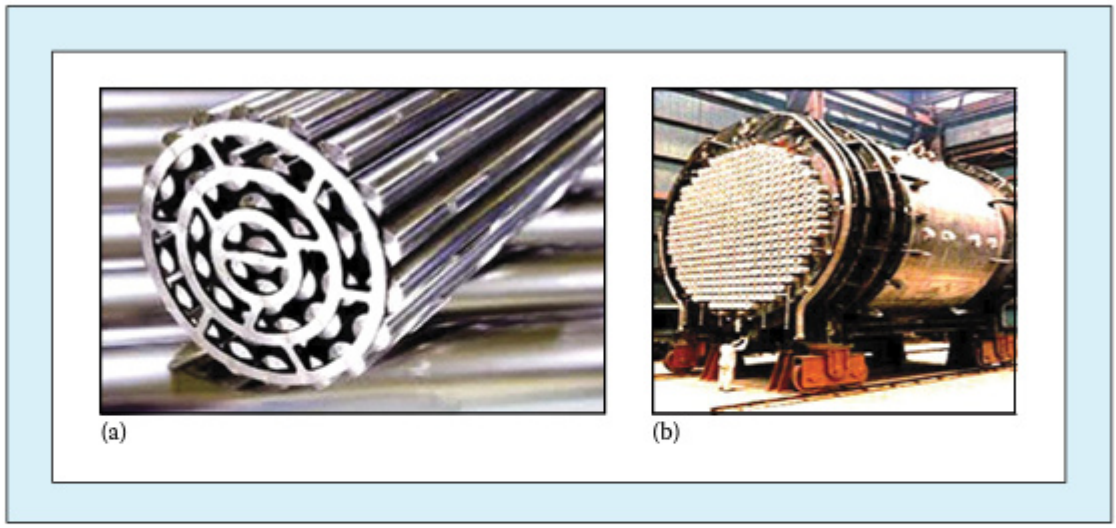

FIGURE 1.18 (a) One of the fuel bundles from a CANDU PHWR and (b) the Calandria in which they are placed. The pressure tubes operate at about two-thirds the pressure of a conventional PWR or about 10 MPa.

The fuel rods in a CANDU reactor are about 50 cm long, and they are assembled into *fuel bundles* that are approximately 10 cm in diameter. A fuel bundle can consist of 28, 37, or 43 fuel elements arranged in several concentric rings around a central axis (see Figure 1.18(a)). Their short length means that they do not require the massive support structures that fuel rods in ordinary BWRs or PWRs do. CANDU reactor fuel does not attain a very high burnup, and it cannot remain in the core for very long before it has to be replaced. This means that the fuel rods in a CANDU reactor do not need a very large fuel-to-cladding gap, and they do not have to be pressurized with an inert gas like the fuel rods in conventional LWRs do. CANDU reactors have a great deal of appeal in developing countries because one does not have to have a uranium enrichment plant to provide the fuel for them. The overall size of a CANDU reactor can be reduced substantially by using slightly enriched uranium rather than natural uranium fuel. An average enrichment of about 1.2% appears to achieve the best balance between the extra cost of enriching the uranium and the money that can be saved by using a smaller pressure vessel. The CANDU reactor is a remarkable achievement because it can run on natural uranium alone. The uranium is again mixed with oxygen to produce a uranium dioxide or UO_2 fuel pellet. UO_2 is a complex ceramic material with a very high melting point (~2865°C). In fact, its melting point is similar to the melting point of the heat shield used on the U.S. *space shuttle*. The fuel pellets in a CANDU reactor rarely melt because the core power density is so low. The volumetric power density is compared to that of other reactor types in our companion book.*

1.18 Characteristics of Reactor Fuel Assemblies

Reactor fuel assemblies come in many different sizes and shapes, and there is no such thing as a "standard" reactor fuel assembly. However, they do have many design features in common. In this section, we would like to focus primarily on these features and how fuel assemblies can be used to construct a reactor core. A large PWR core can have between 175 and 225 fuel assemblies, and a large BWR core can have between 700 and 800 of them. *Light water reactor fuel assemblies are designed to have an average burnup of about 50,000 Mega Watt Days (MWD) per metric ton. This means that the fuel rods may have to stay in the core for 3 or 4 years*. During this time, they continue to generate heat and power, and the heat generated is proportional to the number of fuel assemblies and the average power density of the core.

Large LMFBRs, on the other hand, can have about 600 fuel assemblies (that are normally hexagonal in shape), but in a fast reactor, some of these fuel assemblies are used for the core and other fuel assemblies, which surround them, are used to create *the blanket* region, where new nuclear fuel is bred. The core contains a high concentration of plutonium and the blanket contains either U-238, depleted uranium, or thorium. *The power density in the core of a LMFBR can be extremely high. In fact, it can be 5–10 times higher than the power density of an average light water reactor core*. The relationship between the core and the blanket is shown in Figure 1.19. Sometimes LMFBRs are designed to employ an axial blanket as well as a radial one. Hence the upper and lower 10%–20% of each fuel assembly contains fertile material (U-238 or Thorium-232) that is used to create new reactor fuel. *Fast reactor fuel assemblies are designed to have an average burnup of over 100,000 MWD per metric ton. This is at least twice the burnup of an average light water reactor fuel assembly*. The rods in the radial blanket may also be larger than the fuel rods in the core (again refer to Figure 1.19).

* See *Nuclear Engineering Fundamentals: A Practical Perspective*, by R.E. Masterson, CRC Press (2017).

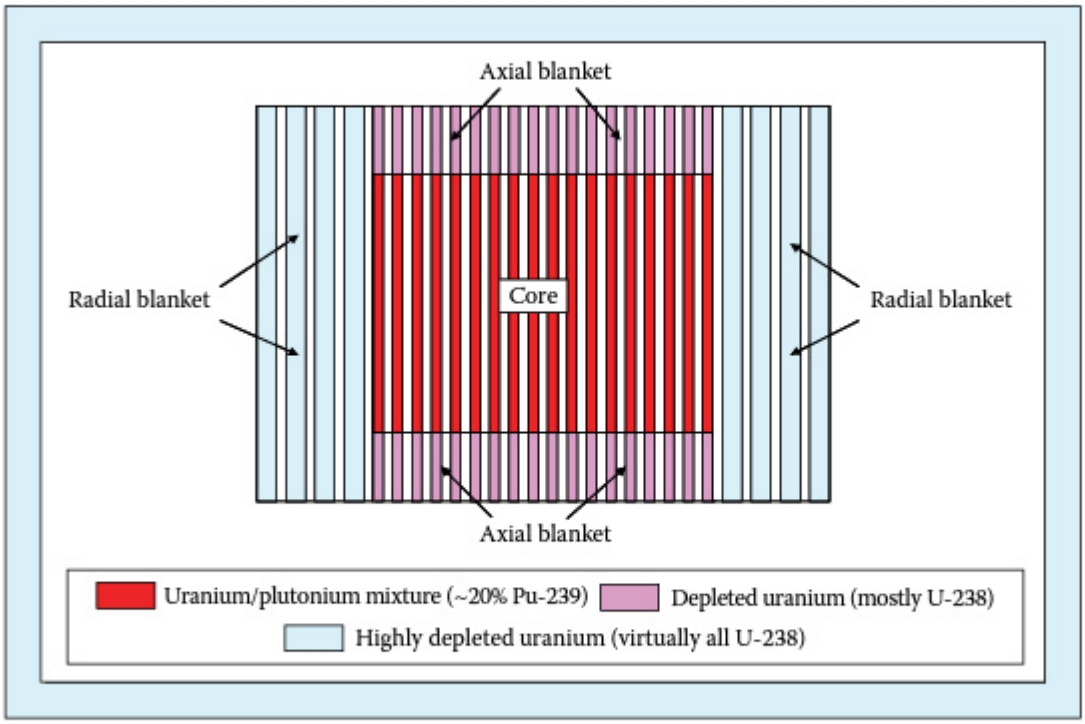

FIGURE 1.19 The core and blanket regions of a plutonium-fueled fast breeder reactor. (Additional reference: *http://www.ati.ac.at/fileadmin/files/research_areas/ssnm/nmkt/11_LMFBR.pdf*.)

It is not uncommon for the uranium atoms in an entire PWR core to weigh between 100 and 150 metric tons, and this is also true of the fuel assemblies in a BWR core. PWR, BWR, and LMFBR fuel assemblies are about 4 m long, and the active fuel height is about 3.5 m. CANDU and gas reactor fuel assemblies are not as long as PWR or BWR fuel assemblies, and between 8 and 12 of them are normally stacked vertically or horizontally to create the core. A CANDU reactor core is about 6 m long, and gas reactor cores tend to be 8–10 m high. LMFBR cores are about the same size as PWR cores. The characteristics of these cores are compared in Table 1.16. The *pitch of the fuel rods* in reactor fuel assemblies (the centerline-to-centerline spacing between the fuel rods) can also vary from one type of reactor to the next. The pitch also depends on the shape of a fuel assembly, and this concept is illustrated pictorially in Figure 1.20. The pitch of the rods in a modern PWR is about 12.6 mm, while the pitch of the fuel rods in a modern BWR is about 14.37 mm. The pitch of the fuel rods in a fast reactor fuel assembly (which is hexagonal in shape) is about 9.8 mm. CANDU reactor fuel assemblies, which are sometimes referred to as *fuel bundles*, have a typical pitch of about 14.6 mm. Finally, gas reactors can have a fuel rod pitch of between 23 mm and 37 mm. Not surprisingly, these fuel assemblies also have the lowest average power density (2.5 kW/L to 8.5 kW/L).

TABLE 1.16
Design Parameters for Some Common Reactor Cores

Reactor Type	Fuel Assembly Geometry	Type of Fuel	Rod Pitch (mm)	Coolant	Moderator	Fuel Rod Length (m)
PWR	Square	Enriched UO_2	12.60	H_2O	H_2O	3.88
BWR	Square	Enriched UO_2	14.37	H_2O	H_2O	4.09
CANDU	Concentric circles	Natural UO_2	14.60	D_2O[a]	D_2O	0.49
HTGR	Hexagonal block	Enriched UO_2	23.00	He	Graphite	0.79
AGR	Concentric circles	Enriched UO_2	37.00	CO_2	Graphite	1.04
LMFBR	Hexagonal	PuO_2	9.80	Liquid Na	Not used	2.70

Note: The numbers shown are approximate and can vary depending on the exact design.

[a] Primary loop only; secondary loop uses H_2O.

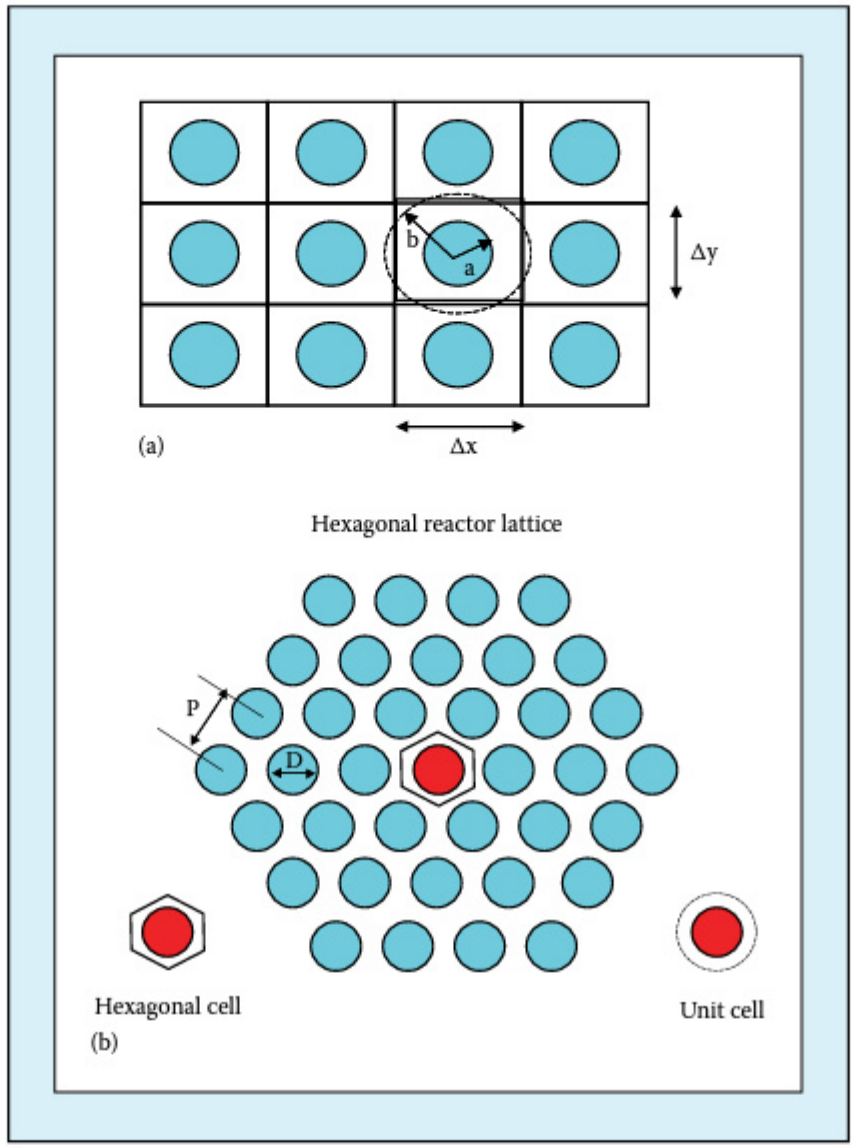

FIGURE 1.20 (a) An equivalent cylindrical unit cell in a standard reactor lattice. (b) A hexagonal reactor lattice and its equivalent cylindrical unit cell(s). These figures also show the relationship of the pitch to the size of a typical unit cell.

1.19 Design Parameters for Reactor Fuel Assemblies

Examples of the design parameters used for modern reactor fuel assemblies are shown in Table 1.17, as well as the dimensions of the fuel rods used in the current generation of western PWRs and BWRs. Notice that there can be a considerable variation in the values of these parameters. In particular, there can be even more differences than the differences presented here.

1.20 Characteristics of Reactor Cores

Reactor cores are constructed from arrays of fuel rods grouped together into larger structures known as *nuclear fuel assemblies*. Within each fuel assembly, the rods are deployed in a manner similar to that shown in Figure 1.21. A nuclear fuel assembly can have between 50 and 300 fuel rods, and the number of rods can vary greatly depending upon how a reactor is designed. The exact arrangement of these rods depends upon whether the fuel assembly is square, circular, or hexagonal in shape. A picture of some fuel assemblies from a Westinghouse PWR is shown in Figure 1.22. For reasons that are discussed in our companion book, PWR, BWR, and LMFBR fuel assemblies can have slightly different sizes and shapes. When it comes to light water reactors, BWRs have the largest cores, and PWRs have the smallest. Gas reactor cores are much larger because their average power density is so low (<10 kW/L). The parameters of these cores are

TABLE 1.17
Some Modern Fuel Assembly Design Parameters

Name	BWR	PWR	CANDU PHWR	HTGR	AGR	LMFBR
			Different reactor types and their design parameters			
Manufacturer	General Electric	Westinghouse	Atomic Energy of Canada	General Atomic	National Nuclear	Novatome
Coolant	Water	Water	Water (heavy)	He	CO_2	Sodium
Moderator	Water	Water	Deuterium	Graphite	Graphite	None
Neutron Energies	Thermal	Thermal	Thermal	Thermal	Thermal	Fast
Purpose	Converter	Converter	Converter	Converter	Converter	Breeder
			Type of fuel			
Composition	UO_2	UO_2	UC/ThO_2	UO_2	UO_2	PuO_2/UO_2
Geometry	Cylindrical pellet	Cylindrical pellet	Cylindrical pellet	Coated microspheres	Cylindrical pellet	Cylindrical or annular pellet
Average fissile content (%)	~3.5	~4.0	0.711	90–95	~2.5	15–18
Fissile material	U-235	U-235	U-235	U-235	U-235	Pu-239
Fertile material	U-238	U-238	U-238	Th-232	U-235	U-238
			Fuel pins			
Geometry	Pellet stack in cylindrical tube	Pellet stack in cylindrical tube	Pellet stack in cylindrical tube	Microspheres in cylindrical tube	Pellet stack in cylindrical tube	Pellet stack in cylindrical tube
Diameter (mm)	12.27	9.50	13.10	15.70	14.89	8.65 (core) 15.80 (blanket)
Cladding	Zircaloy-2	Zircaloy-4	Zircaloy-4	Graphite	Stainless steel	Stainless steel
Cladding thickness (mm)	0.813	0.57	0.42	N/A	0.38	0.65
			Fuel assemblies			
Geometry	8 × 8 square lattice	17 × 17 square lattice	Concentric circles	Hexagonal graphite blocks	Concentric circles	Hexagonal lattice
Rod pitch (mm)	16.2	12.6	14.6	N/A	25.7	9.70 (core) 17.0 (blanket)
Number of fuel rod locations	64	289	37	76	37	271 (core) 91 (blanket)
Number of fuel rods	62	264	37	76	36	271 (core) 91 (blanket)
Outer dimension (mm)	139	214	102	360	190 (inner)	173

Source: Todreas, N. and Kazimi, M.S., *Nuclear Systems*, Vol. 1, CRC Press, Boca Raton, FL, 2008.
Note: The actual numbers can vary from those shown.

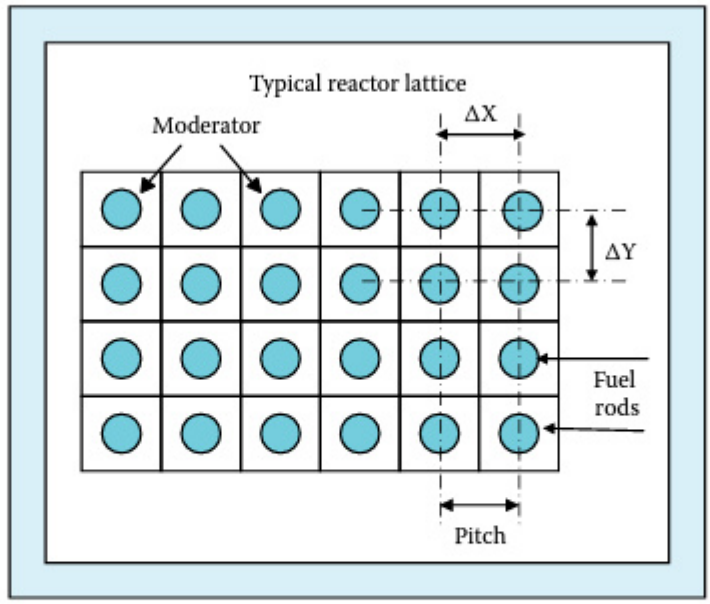

FIGURE 1.21 A simple reactor lattice with the fuel rods arranged in a square array. Large numbers of these rods are then grouped together to form fuel assemblies, and large numbers of fuel assemblies are then grouped together to form reactor cores. Hence, reactor cores consist of large repetitive arrays of fuel rods such as the ones shown above.

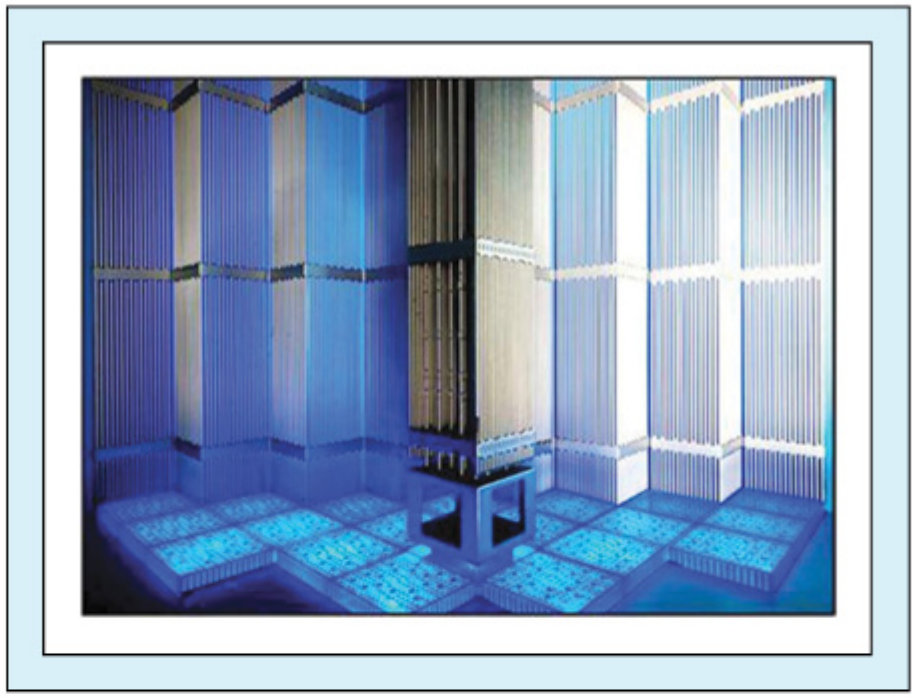

FIGURE 1.22 Examples of PWR fuel assemblies and the fuel rods from which they are made.

compared in Table 1.16. Reactor cores are constructed from large arrays of fuel rods and fuel assemblies. These cores and their composition are discussed in future sections.

1.21 Core Composition

Reactor behavior is determined by the material composition of the core. In light water reactors, the fuel occupies about 25% of the active core volume. This number is design dependent, and it also depends on the pitch of the lattice (see Figure 1.21). In PWRs and BWRs, the fuel pins are constructed from a compound called *uranium dioxide* (or UO_2) in which two oxygen atoms are bound to each uranium atom. This creates a ceramic compound (see Chapter 10 of our

companion book) that is generally black or dark gray in color. Uranium dioxide has a very high melting point, and it is the world's most popular nuclear fuel. The pie chart shown in Figure 1.23 illustrates the composition of a typical light water reactor core in which uranium dioxide is used as the fuel. In this figure, the word "fuel" refers to the uranium dioxide contained in the fuel rods. The word "structure" refers to the cladding surrounding the fuel rods, as well as the control rods and all of other structural materials (grid spacers), inlet and outlet plenums, etc., that are needed to hold them in place. The remainder of the core then consists of moderator or reactor coolant.

In PWRs and BWRs, water is used to cool the core. In BWRs the water boils, and in PWRs it generally does not. The cooling water (H_2O) is sometimes called *light water*. Other reactors, such as CANDU reactors, use *heavy water* or D_2O rather than light water to moderate the neutrons produced in the core. (The specific reasons for this are discussed in Chapter 8.) Heavy water is also called *deuterium dioxide* and it is chemically similar to light water, but its nuclear properties are different. It absorbs fewer neutrons than light water does, and therefore allows reactors cooled by it to use natural uranium fuel. In thermal water reactors, there are a number of reasons why the materials in the core tend to have these specific ratios. First, these ratios are needed to achieve the highest possible reaction rates and allow the most uranium-235 to be burned over a long period of time. Second, enough coolant must be available to remove the heat from the core, and also to "slow down" the fission neutrons to thermal energies so that additional fission neutrons can be produced. Finally, about one-quarter of the total volume of the core must be reserved for the structural materials required to hold the core together (see Figure 1.23). A certain amount of additional structure is also needed so that a reactor can operate for long periods of time without having the fuel rods and the control rods bend or bow.

The ratio of the amount of the moderator to the amount of the fuel is known as the *moderator-to-fuel ratio*. Most light water reactors—for both safety and performance reasons—operate with *moderator-to-fuel ratios*, or MFRs, somewhere between 2:1 and 4:1 to 1. In most LWRs, the moderator is also used as the coolant. The value of the moderator-to-fuel ratio is determined primarily by the *pitch* of the reactor lattice P, which is the centerline-to-centerline spacing between adjacent fuel rods (see Figures 1.16 and 1.21). A low moderator-to-fuel ratio requires a very tightly packed reactor lattice with the fuel rods very close together, while a higher moderator-to-fuel ratio allows the fuel rods to be spaced further apart. The power density, or the power output per liter of fuel assembly volume, is also inversely proportional to the moderator-to-fuel ratio. For moderator-to-fuel ratios close to 2, the amount of structural material in the core (including the cladding) is

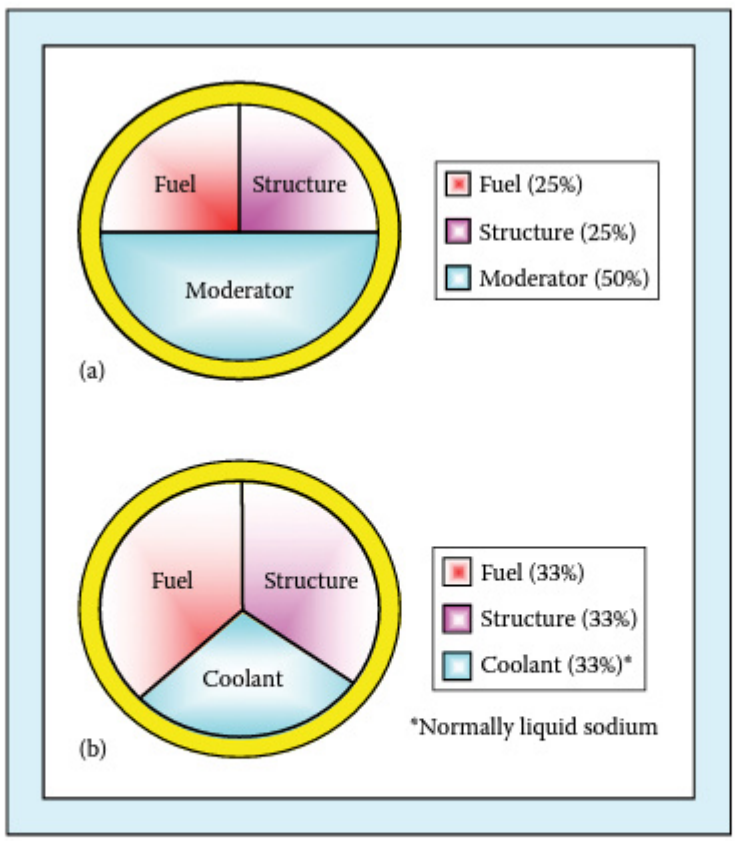

FIGURE 1.23 (a) The core composition in a typical light water reactor with a fuel rod pitch of about 1.5. (b) The core composition in a typical LMFBR with a fuel rod pitch of about 1.5.

approximately equal to the volume of the fuel. This fuel-to-structure ratio (1:1) is commonly used by most reactor designers today. Figure 1.21 illustrates how this is related to a reactor fuel assembly as a whole. Assuming that the fuel rods are cylindrical in shape and that the lattice has a square pitch, it can be shown that the pitch P of the lattice is related to the diameter D of the fuel rods by

Relationship between Rod Pitch, Rod Diameter, and Moderator-to-Fuel Ratio

$$P^2 = \frac{\pi D^2}{4} \times (MFR + 1) \tag{1.2}$$

which the reader is encouraged to derive. Equivalently, Equation 1.2 can be written as

$$P^2 = \pi R^2 \times (MFR + 1) \tag{1.3}$$

where MFR is the moderator-to-fuel ratio, expressed as the ratio of the volume of the moderator V_M to the volume of the fuel V_F or

$$MFR = \frac{V_M}{V_F} \tag{1.4}$$

The moderator-to-fuel ratio is a dimensionless number. Hence, any two of the three variables in Equation 1.2 (MFR, P or D) can be used to determine the other. For example, if the moderator-to-fuel ratio is 3, then Equation 1.2 says that the pitch of the lattice must be $P = \sqrt{\pi} \cdot D$. Conversely, if two adjacent fuel rods are allowed to just touch each other so that P = D, then this would correspond to a moderator to fuel ratio of $MFR = (P^2 - \pi R^2)/\pi R^2 = (4 - \pi)/\pi = 0.273$. This is the smallest possible value for the moderator-to-fuel ratio when the reactor lattice is square. *The design of most light water reactor fuel assemblies requires a moderator-to-fuel ratio between 2 and 4.* (The exact reasons for this ratio are discussed in Chapter 10.) However, many of them are safety related.

Student Exercise 1.1

For the reactor lattice shown in Figure 1.21, show that $P^2 = \pi R^2 \times (MFR + 1)$ where P is the pitch of the lattice, and R is the diameter of a fuel rod. Hint: Start with the basic equation $MFR = V_M/V_F$ to begin your derivation.

1.22 Lattice Geometries

A square reactor lattice is by far the most common reactor lattice in use today. Commercial PWRs and BWRs use this lattice, as well as many research reactors. However, it is not the only one that can be used. Other reactors (such as LMFBRs) require higher power densities within their fuel assemblies, and this in turn can be achieved by arranging the fuel rods in the assemblies in the hexagonal configuration shown in Figure 1.20(b). The hexagons within the figure can be further subdivided into *equilateral triangles* (see Figure 1.24) that define the centerline-to-centerline rod spacing, or the pitch P

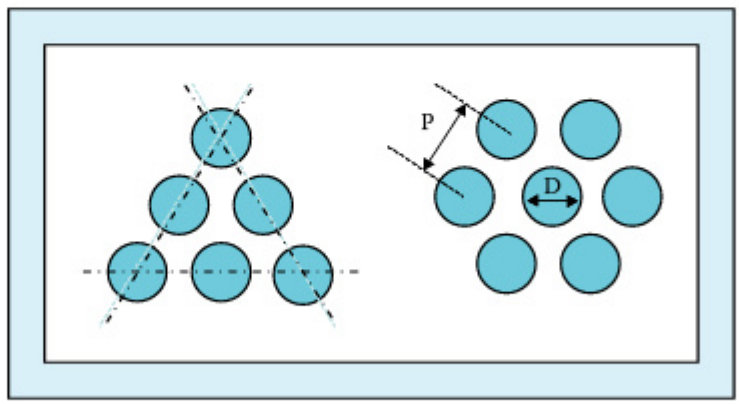

FIGURE 1.24 A hexagonal lattice of fuel rods that is used in an LMFBR.

of the lattice. Relative to a square lattice with the same fuel rods and the same enrichment, a hexagonal lattice has a power density that is about *16% higher* for the same amount of space. This in turn means that it is possible to get more power out of a core of comparable size.

Military and space-bound reactors tend to prefer this arrangement for their fuel pins because the reactor vessel can be made smaller and space is usually at a premium. However, each type of array offers its own unique advantages, and when more moderator is required to increase the thermal neutron population, it is usually easier to simply increase the enrichment of the fuel than it is to move to a hexagonal arrangement of pins with a reduced pitch. The remainder of the core consists of a combination of moderator (or coolant) and structure. *In most light water reactors, the coolant takes up 45%–50% of the total core volume, with another 20%–30% consumed by the structural materials, the control rods, and the metal cladding in which the fuel rods are encased*. Of course, these numbers can vary slightly from one design to the next, and can therefore be thought of as "industry averages." The reactor vendor or fuel assembly supplier should be consulted to determine what the exact ratio is for a particular design. This ratio may also change somewhat when the control rods are withdrawn from the core and replaced by the coolant. Exercise 1.2 asks the reader to compute these ratios for a square reactor lattice of infinite length in the x and y directions. Sometimes a lattice of this type is called an *infinite lattice*, and performing design calculations with an infinite lattice is called the *infinite lattice approximation*. We will have more to say about the infinite lattice approximation in Chapter 9. The infinite lattice approximation was used to design some of the world's first reactors.

1.23 Unit Cells

Sometimes it is convenient to replace a fuel rod and the coolant that surrounds the rod by what is known as a *unit cell*. A unit cell is the fundamental building block of a reactor lattice. A unit cell allows the design parameters of different fuel assemblies to be compared on an "apples-to-apples" basis. A unit cell is basically a simple way to compare the material ratios that a fuel assembly contains on a geometry-independent basis. A square and a hexagonal lattice and their equivalent unit cells are shown in Figure 1.20. Notice that these unit cells can be either square or cylindrical in shape. To calculate the outer radius of a cylindrical unit cell, one simply calculates the area of the square unit cell in the reactor lattice, and then equates the two areas to find the radius of the equivalent cell as if it were cylindrical. This approach is sometimes called the *equivalent annulus approximation*, and this approximation is also used in reactor thermal-hydraulic design (see Reference 2). The equivalent radius of the unit cell can then be found by solving the following equation for the value of R_{cell}

$$\pi R_{cell}^2 = \Delta x^2 \tag{1.5}$$

in which case it is easy to see that

$$R_{cell} = \frac{\Delta x}{\sqrt{\pi}} \tag{1.6}$$

or $R_{cell} = P/\sqrt{\pi}$, since the pitch P of the lattice is equal to Δx in this case. The radius of the fuel R_{fuel} and the radius of the cladding R_{clad} within an individual fuel rod are then the same as before. The total volume of the fuel, the cladding, and the moderator (or coolant) in the unit cell can then be found from

$$V_{fuel} = \pi R_{fuel}^2 \Delta z \tag{1.7}$$

$$V_{clad} = \pi R_{clad}^2 \Delta z - \pi R_{fuel}^2 \Delta z \tag{1.8}$$

and

$$V_{mod} = \pi R_{cell}^2 \Delta z - \pi R_{clad}^2 \Delta z \tag{1.9}$$

where Δz is the length in the axial direction. Notice that the length cancels from these equations when the volume ratios are found.

Student Exercise 1.2

In modern-day PWRs, the spacing between the centers of the adjacent fuel rods is about 2 cm, and a typical fuel rod is about 1.2 cm in diameter. Assuming that the gap between the cladding and the fuel is about 0.3 mm, and that the cladding is about 1 mm thick, what is the percentage of fuel, moderator, and structural material (i.e., the cladding) in this configuration?

1.24 The Infinite Lattice Approximation

In elementary reactor design, each fuel assembly is assembled from an infinite array of identical unit cells, which are normally placed side by side. These unit cells are then used to construct what is called the *reactor lattice*. In nuclear science and engineering, this assumption is sometimes called *the infinite lattice approximation*. When the unit cells within an assembly are all identical, it becomes easier to calculate the power profile because the neutron flux does not change appreciably from one cell to the next (except near the edges of the assembly). Hence, the average reaction rates within the assembly are nearly the same as those for the individual cells. The neutron flux shape in this case resembles that shown in Figure 1.25. Notice that the shape of the fast flux is different than the shape of the thermal flux.

For example, modern PWR fuel assemblies are usually configured with 17 rods per side (see Figure 1.14) although this number can vary between 13 and 19. This represents a total of $17 \times 17 = 289$ possible locations for the fuel rods and the control rods. In Figure 1.14, 25 of these locations—or about 8% of the total—are reserved for instrumentation and control rods. This means that even if a fuel assembly happens to be very large, the moderator-to-fuel ratio can vary by about ±10% depending upon whether the control rods are fully inserted or fully withdrawn. However, not all of the fuel assemblies in a commercial PWR core contain the same number of control rods. (In some Westinghouse PWRs, only one-quarter of the fuel assemblies do.) These fuel assemblies are then subdivided into *control assemblies* and *shutdown assemblies*. Control assemblies are used to shape the power profile and change the reactor power level slowly, while, shutdown assemblies are used to shut the core down. These assemblies are discussed in more detail in Chapter 20.

In principle, there is no difference between a unit cell in a hexagonal lattice and a unit cell in a square lattice when the infinite lattice approximation is used. In a hexagonal lattice, a representative unit cell (such as the one shown in Figure 1.20) then becomes a *hexagon*. Irrespective of the cell shape, there are certain combinations of materials that are more effective than others in obtaining a critical system. We will quantify these exact combinations when we explore the *four-factor formula* in Chapter 9. *The four-factor formula can then be thought of as a mathematical representation of the infinite lattice approximation because it assumes that a reactor consists of an infinite number of identical unit cells in which the effects of neutron leakage can be ignored.* This then makes it easier to perform a reactor criticality calculation.

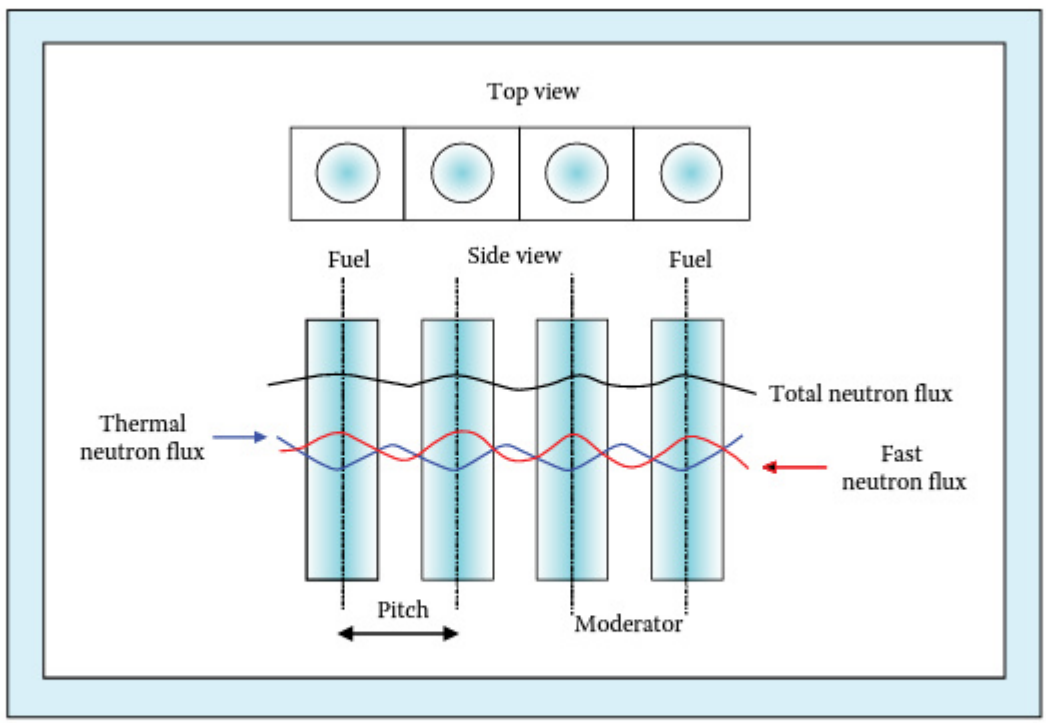

FIGURE 1.25 The neutron population in an infinite lattice of identical fuel rods. These unit cells are then used to construct what is known as the *infinite lattice approximation*. In this figure, the fast flux peaks in the fuel and the thermal flux peaks in the moderator. In thermal water reactors, there are about two fast neutrons for every thermal neutron.

1.25 Accounting for the Fuel-to-Cladding Gap

In practice, real reactor unit cells must take into account the small gap between the fuel and the cladding. Sometimes this gap is called the *fuel-to-cladding gap*. In light water reactors, this gap typically has a thickness between 0.08 and 0.12 mm. (Its exact size is discussed in Chapter 11 of our companion book.) This gap allows the fuel pellets to expand and contract slightly as the temperature of the core is changed. *The purpose of this gap is similar in principle to the expansion joints between the sections of the road surface on a bridge*. It allows the fuel to expand and contract without allowing it to buckle or crack. This gap is typically filled with a *conductive gas* such as *helium* to improve the heat flow between the surface of the fuel pin and the cladding. The thermal performance of a reactor fuel rod depends on the design of this gap.

Another important feature of a cylindrical unit cell is that it simplifies the process of calculating the moderator-to-fuel ratio and the fuel-to-cladding ratio because the values of π and Δz cancel when calculating the actual volumes. It then follows that

$$\frac{V_{mod}}{V_{fuel}} = \frac{\pi R_{cell}^2 \Delta z - \pi R_{clad}^2 \Delta z}{\pi R_{fuel}^2 \Delta z} = \frac{R_{cell}^2 - R_{clad}^2}{R_{fuel}^2} \tag{1.10}$$

$$\frac{V_{clad}}{V_{fuel}} = \frac{\pi R_{clad}^2 \Delta z - \pi R_{fuel}^2 \Delta z}{\pi R_{fuel}^2 \Delta z} = \left(\frac{R_{clad}}{R_{fuel}}\right)^2 - 1 \tag{1.11}$$

and

$$\frac{V_{cell}}{V_{fuel}} = \frac{\pi R_{cell}^2 \Delta z}{\pi R_{fuel}^2 \Delta z} = \frac{R_{cell}^2}{R_{fuel}^2} \tag{1.12}$$

While we have only chosen to illustrate this process for a rectangular lattice, the same approach can be extended to a hexagonal or triangular one. When this is done, the ratio V_{clad}/V_{fuel} remains the same, but the values of V_{mod}/V_{fuel} and V_{cell}/V_{fuel} are approximately 1/1.16 = 0.86 or about 14% lower. This means that the average volume of the fuel in a hexagonal fuel assembly is about 16% *higher* than it is in rectangular fuel assembly having the same *fuel rod pitch* P, and centerline-to-centerline spacing.

In LMFBRs, this tends to reduce the amount of the coolant required by about 20% because the additional coolant is no longer needed to create thermal neutrons. Moreover, in most fast reactors, the fuel assemblies are surrounded by metal "cans" or "sheaths" to keep the coolant from expanding into other fuel assemblies that may have a lower power rating. This causes the overall composition of a fast reactor core to be different than the composition of a thermal reactor core. A typical breakdown of the material composition (fuel, structure, and coolant) for a thermal reactor core and a fast reactor core is summarized in Figure 1.23. In the fast reactor, between 35% and 40% of the core is fuel, about 1/3 of the core is structural material, and the remainder of the core is the coolant. Notice that the coolant is not referred to as the moderator in this case because moderation of the fission neutrons is no longer required. Sometimes, the fuel rods contain plutonium dioxide (or PuO_2) instead of just uranium dioxide (or UO_2). Reactor fuel that contains both uranium dioxide and plutonium dioxide is called *mixed oxide* or *MOX fuel*. MOX fuel is commonly used in LMFBRs and other types of breeder reactors. In fact, it can be used in thermal water reactors to breed plutonium as well.

Student Exercise 1.3

Suppose that the fuel assemblies in the same PWR contain control rods, burnable poisons, and additional structural materials that are equal in volume to approximately five times the volume of the cladding above. What is the total percentage of fuel, moderator, and structural materials (including the cladding, the control rods, the burnable poisons, and the other structural materials) in this design?

Student Exercise 1.4

Part 1: Suppose that you wish to build a reactor fuel assembly out of nuclear fuel pellets having a diameter of 1 cm with a fuel-to-cladding gap of 0.5 mm and surrounded by a tube of zirconium cladding having a thickness of approximately 1 mm.

If the fuel rods made from these parts are deployed in a rectangular array with a pitch P (centerline-to-centerline spacing) of 2 cm, calculate the moderator-to-fuel ratio, the cladding-to-fuel ratio, and the unit cell-to-fuel ratio for this configuration.

Part 2: Moreover, on a per volume basis, calculate the percentage of the fuel assembly that consists of the fuel, the moderator, and the cladding. You may ignore the presence of the control rods and other structural materials in the assembly when doing your calculations.

Part 3: Repeat your calculations for a similar fuel assembly in which the pitch P has been reduced to 1.75 but all other parameters remain the same. By what percentage has the volume of the fuel increased in this case?

1.26 Fuel Assembly Loading Schemes

Once the composition of each fuel assembly has been specified, the fuel assemblies are then placed in periodic arrays to form what is known as the *reactor core*. Normally reactor cores are designed to be cylindrical in shape (see Figure 1.26), although this does not always have to be the case. The motivation behind placing the fuel assemblies in the core then becomes getting as much power as possible out of the fuel before the fuel assemblies have to be replaced. This is equivalent to requiring that the burnup of the fuel should be as high as possible, and that the average temperature of the fuel should be as uniform as possible for as long as possible. The *burnup* of the fuel is usually measured in *Megawatt days per metric ton*, or MWD/T, and the *volumetric power density* of the fuel is usually measured in *kW/L*. (These quantities are discussed in more detail later in the chapter.) However, in LWRs today, the typical burnup of the fuel is between 40,000 and 75,000 MWD/T. (The exact burnup limit is determined by the details of the reactor and how frequently the core is to be refueled.) At the beginning of life (BOL), fresh PWR and BWR fuel assemblies are capable of producing average power densities between 110 kW/L and 55 kW/L. Because of the way they are designed and operated, a PWR will always have a slightly higher power density than a BWR. However, these power densities may decline to as little as 25 kW/L to 12 kW/L when the fuel is fully burned. The spent fuel assemblies then need to be replaced, and one must be able to decide which spent fuel assemblies can be reused for another fuel cycle, and which ones cannot. The most depleted fuel assemblies are then sent to the fuel holding tank. There are many competing factors that affect how to load and burn the fuel in an optimal manner. The actual process of doing this is known as the *fuel assembly loading pattern*.

In the early days of the nuclear industry, knowing how these factors interacted with each other was more of an art than a science. However, in recent years, a number of elaborate computer programs have been written that can make this process easier to rationalize once the underlying physics and economics is clearly understood. Because of this, many different types of fuel management strategies are possible. As we will see in future chapters, the greatest possible amount of energy can be released from the fuel by minimizing what is known as the *peak-to-average power ratio* across the core over time. This can best be done by distributing the fuel assemblies radially in such a way that the enrichments of all of the fuel assemblies are not the same. In fact, it can be shown that the greatest average burnup

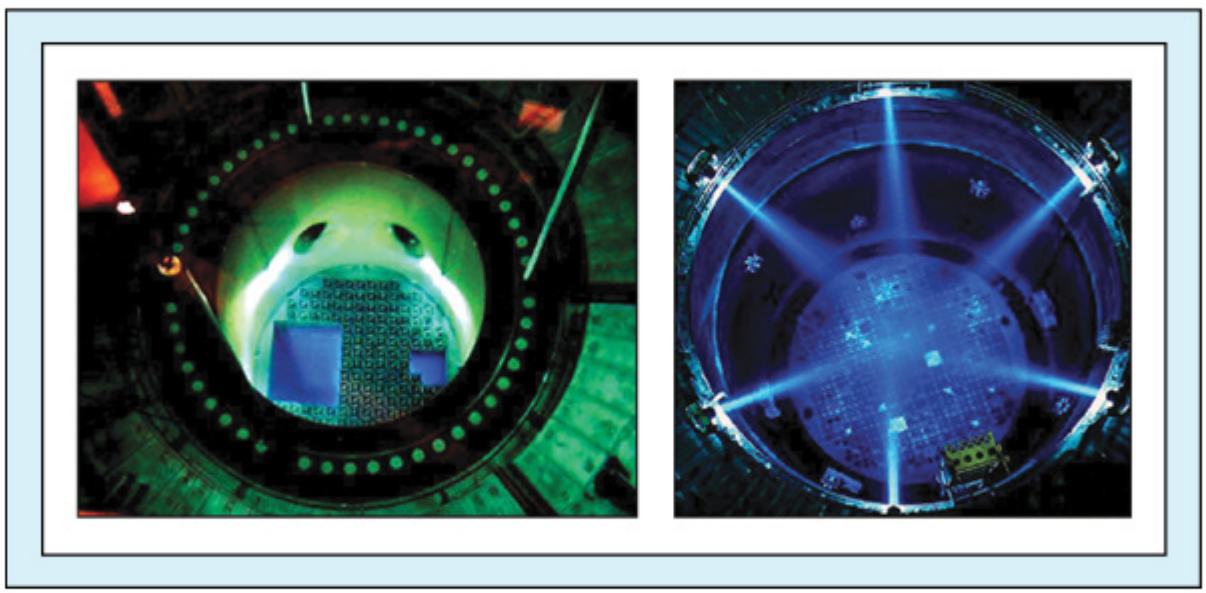

FIGURE 1.26 Two pictures of a reactor core and pressure vessel as seen from above. In both cases, the pressure vessel is cylindrical in shape and the core, which consists of many fuel assemblies, is roughly cylindrical in shape. This configuration helps to reduce the neutron leakage rate and improve the performance of the fuel.

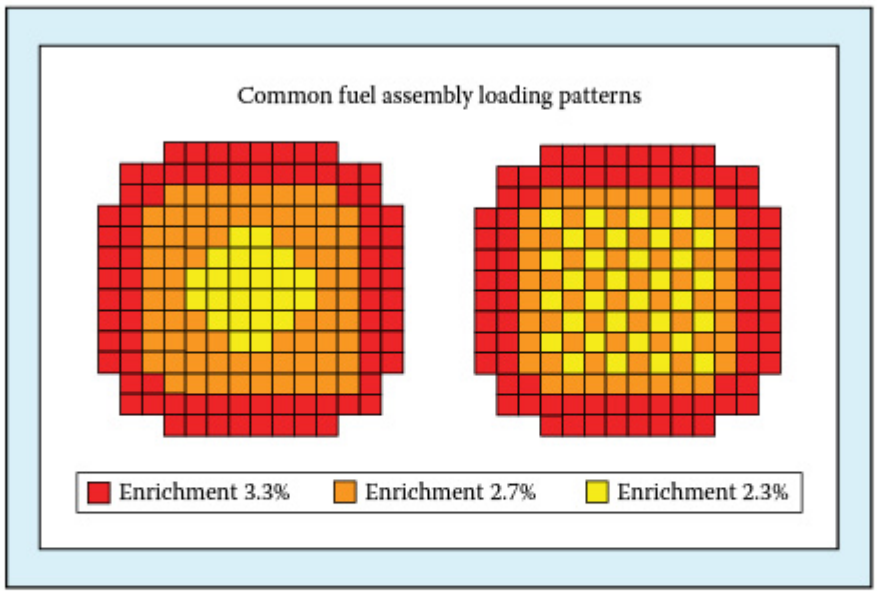

FIGURE 1.27 Some simple fuel assembly loading pattern.

can be achieved by making the power distribution inside of the core as uniform as possible. In a cylindrical core such as the one shown in Figure 1.26, it can be shown that a uniform radial and axial enrichment will result in a peak-to-average power ratio of about 3.6:1. In Chapter 13, we will give an exact explanation of how this ratio can be obtained.

In other words, this requires the fuel rods at the center of the core to be operated at approximately 3.6 times the average temperature of the fuel rods in the reactor as a whole. This also means that the fuel rods along the periphery of the core must be operated at about one-fifth of the temperature of the fuel rods at the center. In general, *the best way to flatten the core power distribution is to place the fuel assemblies with a lower average enrichment near the center of the core, and those with a higher average enrichment around the periphery*. This is why the fuel assemblies are usually loaded into the core in the manner shown in Figure 1.27. It should be intuitively obvious that flattening the power profile in the radial direction solves only half of the problem. To achieve the best possible results, the power distribution must also be made as flat as possible in the axial direction. It is also possible to employ a technique known as *axial zoning* to make the axial power profile as uniform as possible. In this technique, the fuel pellets within each fuel assembly are stacked in such a way that the average enrichment to also allowed to vary in the axial direction.

The potential of axial zoning can be enhanced by introducing materials directly into the fuel that are known as *burnable poisons*. As the name implies, these poisons also burn as the fuel is burned, but they do so in a way that allows as much power as possible to be extracted from an individual fuel assembly before it has to be replaced. This requires a choice to be made between a number of competing factors such as the length of the refueling cycle, the average enrichment of the core, and the manner in which the fuel assemblies are deployed. A different burnable poison strategy may also be needed if a low-leakage refueling scheme is used instead of an out-in or checkerboard one. See Chapter 20 for more details regarding the pros and cons associated with each of these particular schemes. Just as in the case of a *radial zoning* scheme, the fuel pellets with a lower average enrichment are placed near the center of the rods, and the fuel pellets with the highest average enrichment are placed near the ends. In a typical 12 ft (4 m) fuel rod, this allows the 700 to 800 fuel pellets within the rod to be stacked in a number of different axial configurations. Several axial zoning schemes are illustrated in Figure 1.28. With the correct combinations of radial and axial zoning, it is possible to achieve a much more acceptable peak-to-average power ratio.

In practice, with a well-designed fuel management strategy, it is possible to achieve a peak-to-average power ratio close to 1.3 over the life of the fuel. This requires a very sophisticated operating plan, and in particular, great care must be taken to ensure that the control rods are inserted and withdrawn in such a way that they do not introduce any unnecessary peaks or dips in the global power distribution. Over much shorter periods of time, their individual movements may cause additional spikes in the peak-to-average power ratio, but these will be averaged out over time if the fuel management strategy and the operating plan supporting it are well designed. Over longer periods of time, the axial power profiles get flatter as the fuel is burned. In principle, reactors can be designed with almost any conceivable *refueling cycle*. For example, military reactors—such as those used on nuclear aircraft carriers and submarines—are designed to be refueled once every 40 or 50 years. This requires a very high enrichment of U-235 (usually between 90% and 95%), and a very high power density in the core. On a per kilowatt basis, military reactors tend to be much smaller than their commercial

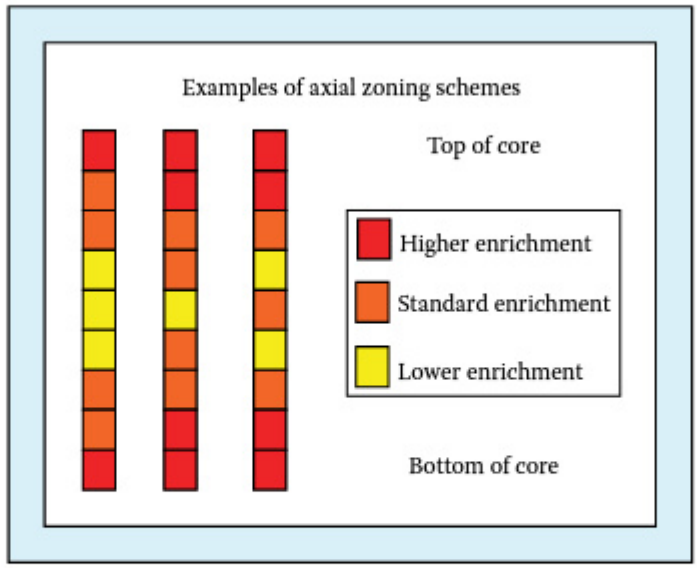

FIGURE 1.28 An example of some axial zoning schemes that are used to flatten the core power shape.

and industrial counterparts, and they also have a much higher power output per liter of fuel. Nuclear aircraft carriers and nuclear submarines are the two most common types of ships that use these very high-powered reactors.

A picture of the *nuclear aircraft carrier USS George Washington* is shown in Figure 1.29. The reactor in this carrier has a 50-year refueling cycle. In contrast to military reactors, most commercial power reactors in the United States use an 18-month, a 2-year, or a 3-year refueling cycle. Depending on the design of the core, and the type of the nuclear fuel that is used, 1/4 to 1/3 of the fuel assemblies are replaced at a time. There has been considerable economic pressure on utilities recently to keep their nuclear power plants running as long as possible. As a result of this, the time interval between refuelings has been gradually increased, while the amount of time required per refueling has remained about the same (usually about 30 days). This has put considerable pressure on power plant refueling and operating personnel to replace the fuel during normal refueling cycles as quickly as possible. The *climate* in a country (or a particular group of countries) can also have a big effect on when a reactor needs to be refueled. In most parts of the world, it is common to shut down a reactor for refueling during periods when the demand for electricity is low. In northern Europe, including the United Kingdom, Germany, France, and Sweden, the demand for electricity peaks during the winter months (because the electricity is needed to heat many homes), so a reactor is usually refueled during the summer.

FIGURE 1.29 The U.S. nuclear-powered aircraft carrier the USS *George Washington* on the left, and a U.S. nuclear-powered submarine on the right. In carriers and submarines such as this, the reactors are designed to be refueled once every 40 or 50 years.

1.27 Reactor Refueling Cycles

In the United States, the demand for power peaks in both the winter and the summer months (due to heating and air-conditioning), and so 12- or 18-month refueling cycles with the refueling occurring in the spring or the fall are far more common. As we will see later, the length of a refueling cycle is driven by the need to get as much energy out of the fuel as possible. Before a reactor can be refueled, it is necessary to gradually reduce the power level of the core for a period of 5–10 days so that the amount of decay heat from the fuel rods can be reduced. This means that full power may not be restored, on average, for a period of up to about 30 + 10 = 40 days after the refueling process begins. During this time, a utility may have to purchase the replacement power from an alternative source. To keep the number of "up days" as high as possible, fuel suppliers have gradually raised the average enrichment of the fuel. This has made it possible to extend the amount of time between one refueling cycle and the next.

Because of these trends, the average enrichment of a fuel assembly is much higher today than it was 20 years ago. This trend is likely to continue for the foreseeable future because it is the easiest way to increase the power output from the core, or lengthen the time between refueling cycles for a given power rating. Some reactors, such as the CANDU reactor and the AGR, have been able to avoid this problem entirely because of the unique way in which their fuel assemblies are designed. In these reactors, the fuel within an assembly can be accessed directly without removing the fuel assembly from the core. Thus, the old fuel can be replaced with new fuel while the reactors are still online. This form of refueling is known as *continuous refueling* or *online refueling*. The refueling is done using an automated refueling machine such as the one shown in Figure 1.30. The CANDU reactors are currently the most common alternative to conventional PWRs and BWRs when this type of refueling method is required. Traditional reactors such as PWRs and BWRs have to be shut down to remove the depleted fuel. There can also be a significant lead time between when a reactor needs to be refueled and when the fresh fuel needs to be ordered. The actual lead time varies depending upon the fuel supplier that is used, but in general, orders for new fuel assemblies are placed by utilities between 12 and 18 months in advance of the time when the reactor is scheduled to be shut down for refueling. This assumes that one-quarter to one-third of the fuel assemblies are to be replaced at a time. In general, this is needed to get the most energy out of the fuel as possible. Mixing fresh fuel with the burned fuel allows the burned fuel to be burned more completely than if a reactor is run based on just the burned fuel alone. Except for the time interval of about 1 month between the time when a reactor is shut down for refueling, and the time when it can be restarted, it is expected to be up and running and generating useful power all the time. The economics of the nuclear power industry are critically dependent on this basic assumption.

In a nuclear power plant, the cost of generating electricity depends weakly on the cost of the fuel. In most reactors, this happens to be a small fraction of the total cost of generating electricity (the largest fraction is the capital investment in the plant itself), but since the fuel is a relatively expensive item, there is an economic incentive to get as much energy out of it as possible. The burnup of nuclear fuel (see Section 1.30) is normally measured in the units of Megawatt days per metric ton (MWD/ton). Because the cost of uranium has continued to rise over the years (see Chapter 10 of our companion book),

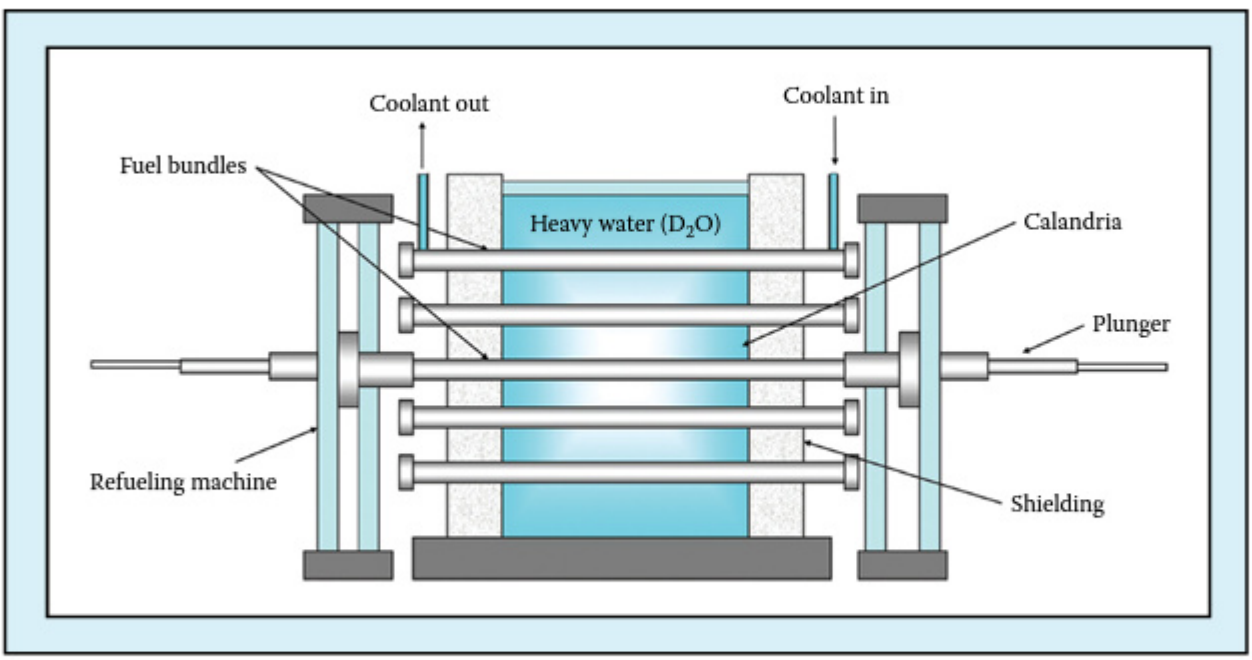

FIGURE 1.30 A cross-sectional view of a refueling machine used to refuel a CANDU reactor while it is operating. (Picture provided by the author.)

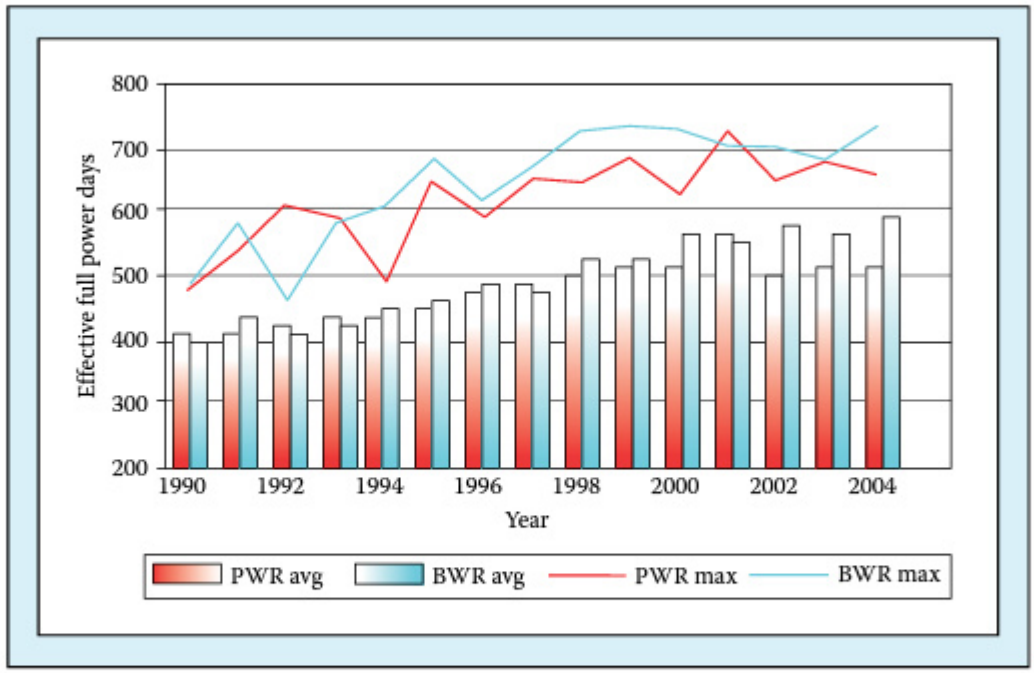

FIGURE 1.31 The average length of the refueling cycle for reactors operated in the United States since 1990. (From IAEA.)

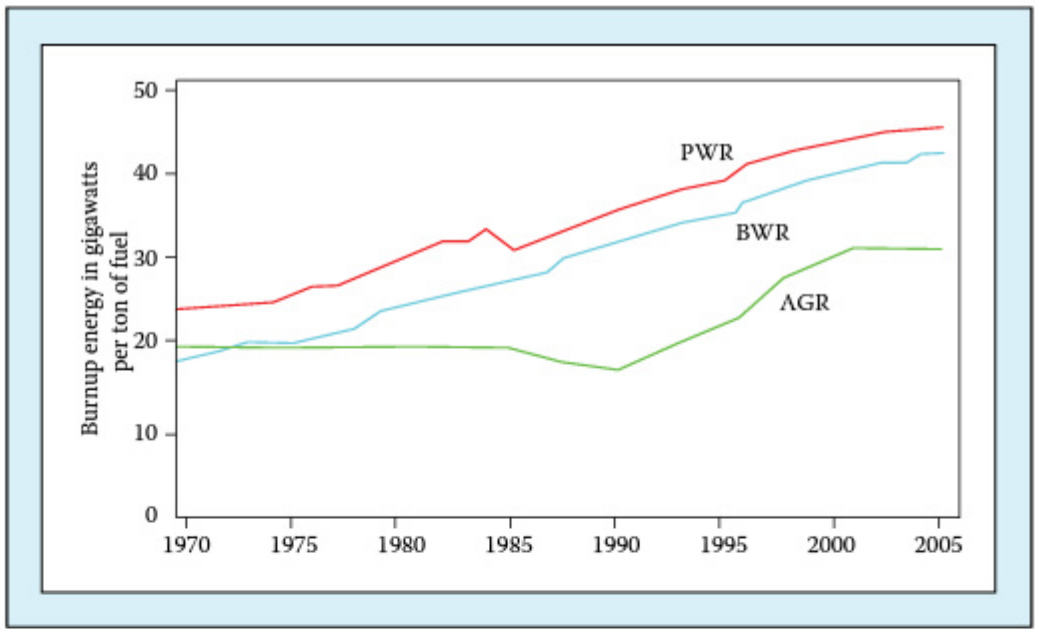

FIGURE 1.32 An illustration of how the average burnup of fuel in nuclear reactors has changed as a function of time since the 1970s. (Data provided by the IAEA.)

the average burnup of the fuel has doubled in light water reactors since the mid-1970s. This has been done by increasing the average enrichment of the fuel rods from 2.5% to about 4.5% today, with a current maximum being about 4.95% for a light water reactor in the western world. In some countries, the cost of generating nuclear power has been reduced even further by increasing their nominal power by about 5% for PWRs and as much as 20% for BWRs. Hence, as the burnup of the fuel has increased, the time between refuelings has increased as well. The overall trends are shown in Figures 1.31 and 1.32.

1.28 An Overview of Nuclear Fuel Management

Once the refueling intervals and the core power level have been specified, the average enrichment of a fuel assembly can be found with the help of a computer program. However, it is then up to the reactor operator to determine how the fuel

assemblies need to be arranged to optimize the amount of power that can be produced between the times that the reactor is shut down for maintenance and refueling. The exact arrangement of the assemblies is dictated by the *fuel management strategy* that the operator of a particular reactor chooses to use. Many computer programs have been written to optimize these competing factors, and many patents have been filed to protect the loading patterns (or LPs) that are used. *Nuclear fuel management is the process of loading and reloading the fuel in such a way that the energy output of the fuel can be optimized while keeping the core critical at all times*. Normally, this requires the power profile in the core to be as flat as possible, and the product of the neutron flux ϕ and the enrichment e determines what the local power level P will be.

As we have seen, *the greatest possible amount of energy can be extracted from the fuel by making the radial and axial power profiles as uniform as possible*. However, when the need arises to shut down the plant and replace some of the fuel, only 1/4 to 1/3 of the fuel assemblies are normally replaced at the same time. The rest are allowed to stay in the core, where they can either remain intact or where they can be moved to another location. Knowing exactly what fuel assemblies to replace and what fuel assemblies to move depends upon how much of their uranium has been burned. This can be estimated if the total amount of energy produced per fuel assembly is known. However, knowing where to put them after this has been established requires a fair amount of analysis, planning, and skill. In some refueling strategies, the most depleted fuel assemblies are removed from the center of the core and placed in a holding tank to be cooled down. The remaining fuel assemblies, which are generally located along the periphery of the core, are then moved inward to replace them. The partially burned fuel assemblies along the periphery are then replaced by fresh ones, and the process continues whenever the reactor needs to be shut down and refueled.

In nuclear fuel management, this practice is sometimes called "*out-in refueling*." In still other common refueling schemes, the fuel assemblies along the periphery are kept intact, while the fuel assemblies close to the center of the core are constantly reshuffled in what amounts to a large checkerboard. The fuel assemblies along the periphery are only replaced every third or fourth cycle, while some of the fuel assemblies in the center may be replaced whenever the reactor is shut down. This practice is known as "*checkerboard refueling,*" and it is normally considered to be an improvement over in-out refueling. An example of the out-in refueling process is illustrated in Figure 1.33. In general, there is no "perfect" refueling scheme that can be used to optimize the burnup of the fuel under all conditions. However, calculating

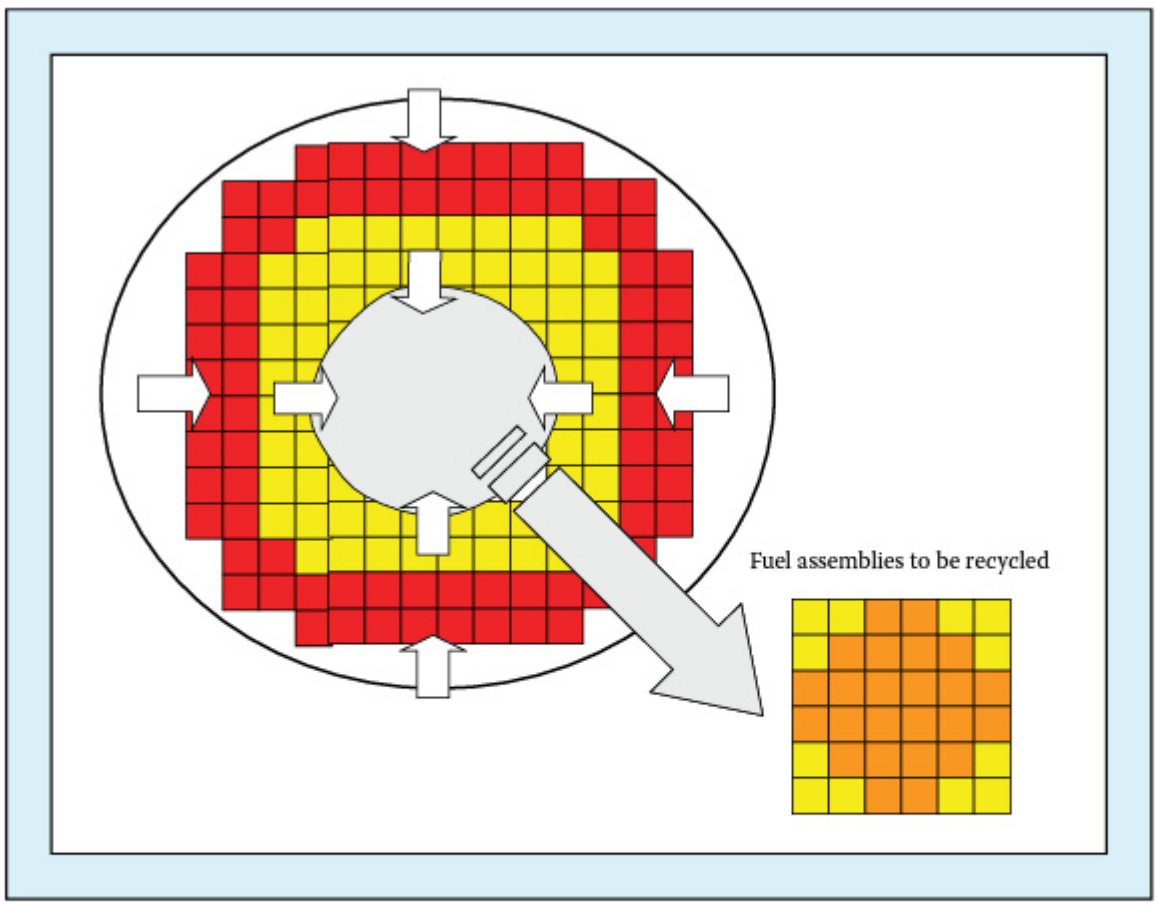

FIGURE 1.33 An example of an "out-in" refueling scheme. Notice that the inner assemblies in this scheme are sent to a holding tank to be cooled and recycled.

the burnup of the fuel with a computer program may allow one to develop some strategies that are more optimal than others over a long period of time. Each reactor vendor usually offers a slightly different strategy to optimize the burnup of its particular type of fuel. Various consulting services may also be provided to arrive at an optimal refueling plan. The fuel assemblies to be removed are then sent to a holding tank to be cooled and recycled. Normally, the "cooling off process" can take several weeks to several months. The spent fuel assemblies may then be moved to a local storage facility for further cooling and reprocessing.

1.29 Core Loading Patterns

When a reactor needs to be shut down for refueling, the design of the *core loading pattern*, or the *"LP,"* determines how efficiently the plant can be operated until the next scheduled refueling. The first goal of a nuclear utility is to control the local power peaks resulting from the physical arrangement of the fuel assemblies within the core itself. Fresh fuel assemblies tend to amplify the local power shape, while fuel with a large accumulated burnup will tend to depress it (see Figure 1.34). Hence, if too many fresh fuel assemblies are located too close together, it is possible to create a local power peak (or hot spot) that will limit how "hot" the reactor can be operated before the fuel begins to melt. In Chapter 20 we will see that this leads to a number of heuristic "rules" that can be applied to prevent this from occurring.

In general, it is *standard operating procedure* (or *SOP*) in light water reactors to keep some fuel assemblies in the core for another burnup cycle, in addition to removing old fuel assemblies and inserting new ones. It is also standard practice to "shuffle" the remaining fuel assemblies around to keep the power profile in the core (radially and axially) as uniform as possible for another cycle. A modern PWR has about 200 fuel assemblies, so if quarter-core symmetry (either reflective or rotational) is maintained, as is standard practice, then there are about 1100 different LPs that can be used assuming that only one-third to one-quarter of the assemblies are replaced at a time. *Finding the optimal pattern out of over 1000 patterns can be a daunting task. In some ways, it can be equivalent to finding a needle in a haystack* (see Chapter 4). Although it is becoming increasingly possible to solve an optimization problem of this magnitude, most utilities still prefer to rely on human designers and engineers to come up with an optimal core design. If the utility wishes to operate

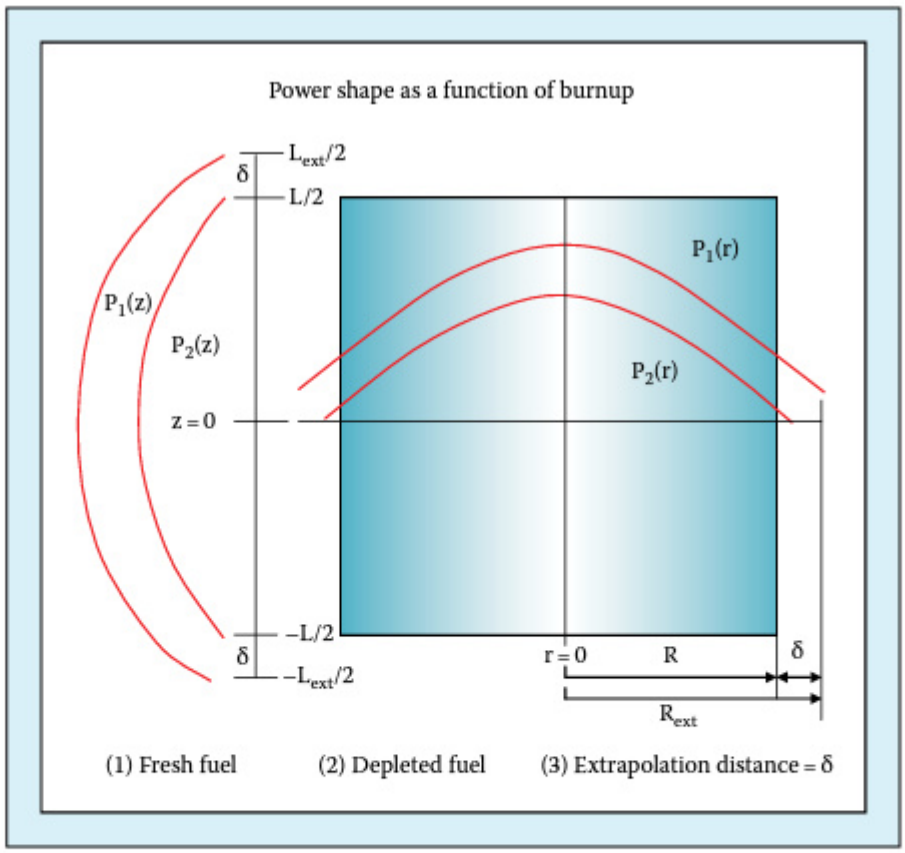

FIGURE 1.34 At the beginning of life, a bare cylindrical core has a cosinusoidal power shape when all of the fuel assemblies have exactly the same enrichment. Notice that the radial and axial power profiles become flatter as the fuel is burned. This causes any large radial and axial power peaks such as the ones shown earlier to become smaller over time.

a plant for 40 or 50 years, then limiting the amount of local power peaking may come into direct conflict with limiting the amount of neutron leakage from the core to reduce the radiation damage to the reactor pressure vessel. Hence the structural integrity of the pressure vessel may determine the design of the fuel assemblies that can be used in the outer one or two rows of the core. Again, this is a topic that requires additional discussion. In some cases, reactor vendors have begun using specially modified fuel assemblies to reduce the neutron leakage rate in the radial direction in proximity to the water reflector and the pressure vessel wall.

Student Exercise 1.5

Using the knowledge that you have just acquired, show that the volume of the fuel in triangular or hexagonal lattice is approximately 16% greater than the volume of the fuel in a square lattice that has the same rod pitch P and the same rod diameter D. Hint: You may use Figures 1.20 and 1.24 to assist you with your derivation.

1.30 Ways to Measure the Amount of Nuclear Fuel That Has Been Burned

The amount of energy that a fuel assembly can produce determines how long it can stay in the core before it has to be replaced. This energy is directly proportional to the number of fuel atoms (U-235, U-233, or Pu-239 atoms) that are put into the fuel assembly when it is built, and then the number of those atoms that are burned while the reactor continues to operate. It is easy to see that the total rate at which these atoms are destroyed is directly proportional to the product of the number of fuel atoms in the core when the reactor is turned on (at $t = 0$) $N_o = N(0)$ multiplied by the operating power P, and then adjusted for the enrichment of the fuel e. If the power level is reasonably constant for a period of time, the number of fuel atoms ΔN that will be burned in a time interval Δt is

$$\Delta N = -NP \times f\Delta t \tag{1.13}$$

where

f is a function of the type of fuel
P is the power level
Δt is the time interval that a reactor operates at that power

The minus sign in this expression is used to indicate that the number of fuel atoms will always *decrease* as the fuel is burned. In differential form, Equation 1.13 may also be written as

$$dN = -NP \times f dt \tag{1.14}$$

or

$$\frac{dN}{N} = -P \times f\,dt. \tag{1.15}$$

Integrating each side, the solution is then

$$N(t)^{U\text{-}235} = N(0)^{U\text{-}235} e^{-Pft} = N_o{}^{U\text{-}235} e^{-Pft} \tag{1.16}$$

where N_o is the number of uranium-235 atoms in the fuel at $t = 0$.

Hence, for a U-235-fueled light water reactor operating at a constant power level P, we have just shown that the number of uranium-235 atoms in a fuel assembly will fall *exponentially* with time. This is illustrated in Figure 1.35 for a number of different power levels corresponding to progressively higher values of the reactor power. In other words, the more fuel that is added to the core for a given power level P, the longer it will last before it has to be replaced. Notice that the total number of U-235 atoms, which determines the initial value of N, is determined by the enrichment of the fuel e. If the value of e is small, then very little power will be produced because there are not many Uranium-235 atoms to split apart. Conversely, if the enrichment is high, there will be plenty of U-235 atoms to split apart, and the fuel assembly will be able to generate useful power for a long period of time. Again, the initial enrichment of the fuel determines the value of $N(0)^{U\text{-}235}$ or $N_o{}^{U\text{-}235}$ in this case.

Notice that the number of U-235 atoms is nearly a linear function of the enrichment except when e becomes very large ($e > 10\%$). However, for reasonable values of e (between 2.5% and 5%), a linear relationship between the enrichment and

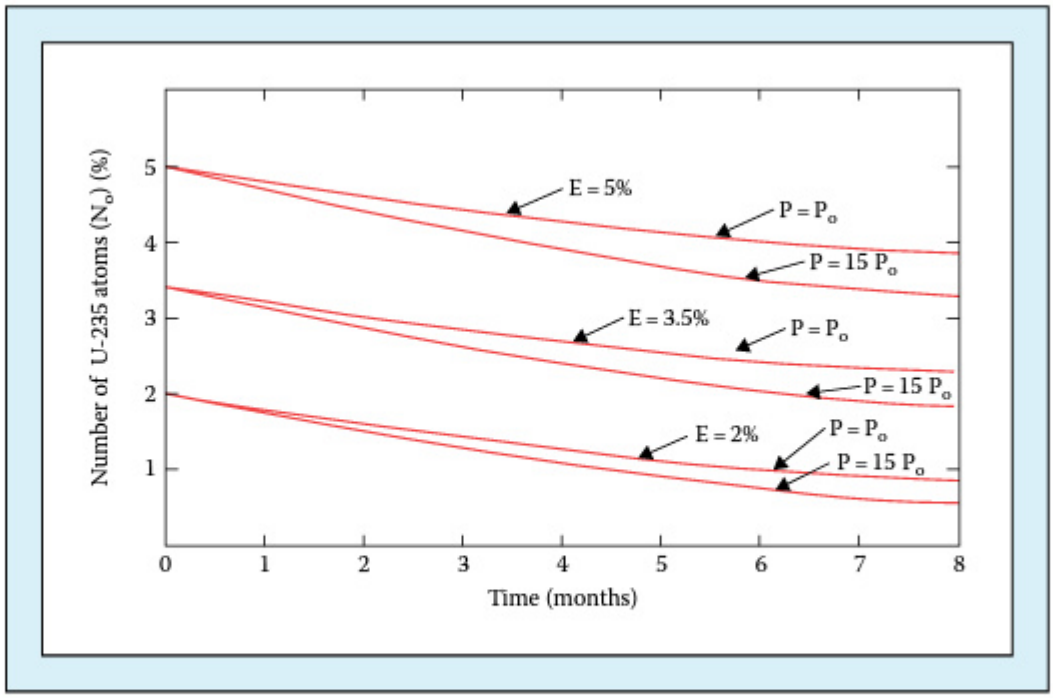

FIGURE 1.35 The number of uranium-235 atoms as a function of the enrichment e and the power level P.

the number of U-235 atoms can almost always be assumed. A fuel assembly will normally be kept in the core until it is no longer capable of producing more neutrons than it absorbs. When this happens, its effective multiplication factor (see Chapter 7) falls below 1.0, and the fuel assembly must be replaced by a fresh fuel assembly for the reactor to continue to operate. A fuel assembly that reaches the end of its useful life and needs to be replaced is said to be *depleted or spent*. For light water reactors, this normally occurs when the number of U-235 atoms (by weight) falls below about 1.5%. At this point, the fission products and other neutron poisons in the fuel assembly simply absorb more neutrons than the remaining fuel is able to produce. There are currently two widely accepted ways to measure the burnup of the U-235 atoms as they are consumed:

- First, we can measure the amount of energy released over a long period of time divided by the mass of the fuel that releases it.
- Second, we can measure the actual percentage of the uranium or plutonium atoms in the fuel and that are burned during this period of time.

Hence, it is possible in principle to measure the "*burnup*" as both the fraction of the fuel atoms that have been split apart and as the actual energy released by a known amount of the fuel in gigawatt days/metric ton or a similar unit. In the first case, the fraction of the atoms that are split apart is usually measured in *fissions per initial heavy metal atom (FIMAs)*. When the total burnup is expressed as a percentage of the atoms available to be burned, then calculating the amount of burnup becomes very simple: because if 3% of the initial heavy metal atoms have undergone fission, then the burnup will be exactly 3%. This way of measuring the burnup is very simple, and it is also quite appealing to those who are analytically inclined because it can be used to calculate exactly how many atoms of unburned fuel are still available.

Unfortunately, this number is difficult to measure while a reactor is operating, and because of this, most utilities and nuclear fuel suppliers prefer to use the alternative definition (of energy released per unit mass) instead. Consequently, we will also adhere to this convention and define *the burnup of the fuel as the total amount of energy released by the fuel over a period of time divided by the mass of the fuel that is actually being burned*. This mass must include all U-233, U-235, U-238, and Pu-239 atoms in the fuel (if applicable). We can write this in the form of an equation as follows:

Definition of the Burnup (BU)

$$\text{BU} = \frac{\text{Energy output} \times \text{Days of continuous operation}}{\text{Mass of the fuel}} \tag{1.17}$$

and we will always use the symbol BU to refer to the burnup of the fuel in this case. In most countries, the energy output is expressed in units of Mega-Watts of thermal power (MWT), and not in the units of Mega-Watts of electrical power (MWE), which of course is about three times less. (1000 MWE is approximately equal to 3300 MWT because of the plant thermal cycle.) For example, if a reactor contains 100 metric tons of uranium and operates at a power level of 3300 MWT for 365 days, the total burnup of the fuel will be

$$\text{Burnup}\left(\text{in MWD/ton}\right) = \frac{3{,}300\ \text{MWT} \times 365\ \text{days}}{100\ \text{metric tons}} \approx 12{,}000\ \text{MWD/ton} \tag{1.18}$$

where the abbreviation MWD/ton refers to *Mega Watt Days per metric ton of uranium*. If only 1/3 of the fuel in the reactor is replaced at a time, and the reactor operates for about 1 year (365 days) between refuelings, then this fuel will be in the reactor for an average of 3 years. In this case, the total burnup of the fuel at the end of this 3-year period will be

$$\text{BU} = \frac{3{,}300 \times 365 \times 3\ \text{years}}{100} \approx 36{,}000\ \text{MWD/ton} \tag{1.19}$$

Before Y2K, this was about the average burnup of the fuel that could be obtained from a commercial light water reactor before it had to be refueled. Since that time, there has been a strong incentive to increase the burnup of the fuel to reduce the cost of the electricity that a plant produces. This has led to an average increase in the enrichment of fuel for thermal water reactors (except the CANDU reactor) from about 3.3% to about 4.5%, and this in turn has allowed about ¼ of the fuel to be replaced at a time instead of just 1/3. Accordingly, it is not unusual today for the average burnup of the fuel in a modern PWR or BWR after 4 years to be

$$\text{BU} = \frac{3{,}300 \times 365 \times 4\ \text{years}}{100} \approx 48{,}000\ \text{MWD/ton} \tag{1.20}$$

or about 50,000 MWD/ton. Of course, even higher average burnups are possible depending on how the fuel assemblies are distributed spatially, the fuel management scheme that is used, and what the average enrichment of the fuel is that is allowed by the NRC. These factors are all interrelated to one another, and all that can really be said is that the longer the fuel remains in the core, the higher the burnup of the fuel will be.

Eventually, a point is reached when the fuel becomes so depleted that it is no longer possible to maintain the core in a critical state—even when all of the control rods are withdrawn. This is usually the key parameter that determines when the fuel needs to be replaced. The best way to predict when this occurs is to monitor the value of the reactivity of the core as a whole. When it gets close to 0 (with the control rods withdrawn), then the reactor must be shut down for refueling. We will discuss the reactivity in more detail in future chapters (specifically in Chapters 9, 10, 15, and 16), and then we will be in a position to show you how it is used. So many maintenance operations are scheduled during refueling outages that the length of the outage (typically about 1 month) is effectively independent of the number of fuel assemblies to be moved to other locations in the core or replaced. Hence almost all utilities that own a nuclear power plant purchase their replacement power to coincide with this 30-day period when the reactor needs to be refueled.

1.31 Alternative Ways for Measuring the Burnup of the Fuel

There are many alternative ways in which the burnup of the fuel can be measured. In some countries, the burnup is measured in MWD/kg of uranium, and in most European countries, it is measured in GWD (GigaWatt Days) per metric ton. Most utilities use one of these two basic units to measure and warrant their fuel, in addition to the more conventional unit of a MWD/ton. The conversion factors between these various unit systems are summarized below:

Converting between MWD/ton and MWD/kg

$$1\ \text{GWD/ton} = 1000\ \text{MWD/ton}$$
$$1\ \text{MWD/kg} = 1\ \text{GWD/ton} \tag{1.21}$$

As one might expect, many measurements of fuel performance are directly correlated to the burnup. Some properties of the structural materials (such as the cladding and the pressure vessel) are also correlated to the value of the *fluence*

(which is the fast flux integrated over time), which in turn is related to the dislocation density or the "*DPA*." Converting between the percentage of the fuel that has been burned and the energy that has been released requires a knowledge of E_f, the energy released per fission. As we will see in Chapter 7, a typical value for E_f is about 200 MeV/fission. This refers to the amount of *recoverable energy* released per fission. (Another 5% of this energy is essentially unrecoverable.) At least at thermal energies, this value varies only slightly from Uranium-233 to Uranium-235 to Plutonium-239. With this in mind, the maximum atomic burnup rate of a fuel rod that has an enrichment of about 10%, which includes the fissioning of the fissile materials in the fuel (such as U-233, U-235, or Pu-239), is equivalent to about 250,000 MWD per metric ton.

In other words, burning just 10% of the heavy metal uranium and plutonium atoms is approximately equal to a burnup of just under *250,000 MWD/MT*. We can apply this metric to infer that burning up 1% of the total heavy metal atoms in the fuel corresponds to a burnup of about 25,000 MWD/ton, and burning up 2% of the total heavy metal atoms in the fuel corresponds to a burnup of about 50,000 MWD/ton. Conversely, a burnup of 75,000 MWD/ton would correspond to approximately 3% of the fertile and fissionable materials in the core being burned away. This makes equating the energy released to the number of fuel atoms burned a relatively easy thing to do.

1.32 Other Important Nuclear Reactor Properties (Power Density and Thermal Efficiency)

Two other extremely important properties of a nuclear power plant are the *power density of the core* and the *thermal efficiency of the plant*. Both of these parameters are a function of the design of the core and the *Nuclear Steam Supply System*. The nuclear steam supply system is used to convert the heat generated in the core into high pressure and high temperature steam. The steam is then used to turn the blades of a steam turbine, which is connected to an electrical generator to produce electric power. In the following sections, we would like to discuss these two parameters and show how they are related to each other. In future chapters, we will then explore the relationship between them in more detail.

1.33 Power Density

The power density of a reactor core is defined as the power P produced in the core divided by the volume of the core V_{CORE}. *The volume in this case refers to the active core volume*. The heat Q that is produced is often equated to the thermal power output $P_{THERMAL}$. Hence an alternative definition of the core power density is

PD = Power Density

$$PD = \frac{Q}{V_{CORE}} = \frac{P_{THERMAL}}{V_{CORE}} \tag{1.22}$$

Reducing the volume of the core and keeping the power output constant increases the power density, while increasing the volume of the core and keeping the power output constant decreases it. In general, *reactor designers try to keep the core power density as high as possible because this reduces the size of the core and it also helps to reduce the cost of constructing the plant. Normally the power density is limited by the rate that heat can be removed from the fuel rods*. Cores that have high power densities tend to have thin fuel rods (because it is easier to remove heat from a thin fuel rod than it is from a thicker one). Consequently, a PWR will have thinner fuel rods than a BWR, and a BWR will have thinner fuel rods than a GCR.

If the type of coolant and the system pressure are fixed, the diameter of a fuel rod normally falls as the power density increases. If the power density gets too high (say beyond 120 kW/L), a conventional coolant (such as liquid water) may have to be replaced by a liquid metal to remove the heat. Hence the power density, the system pressure, and the type of coolant are intimately related to one another. This means that all three variables must be taken into account when designing a core to meet a particular need. The power densities of some common reactor cores are shown in Figure 1.36. The power densities quoted here represent *industry averages* over many different designs. Notice that the power densities can range from about 3 kW/L in a GCR to about 300 kW/L in an LMFBR. *In some Russian fast breeder reactors, power densities as high as 500 kW/L have been reported*. By any standard, this is a very high core power density.

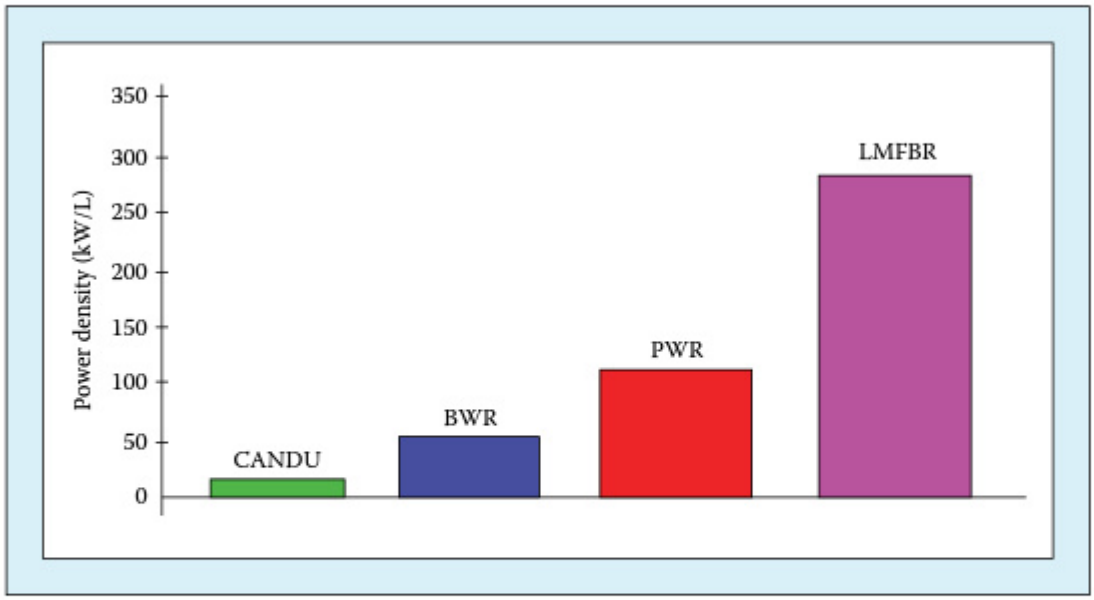

FIGURE 1.36 A comparison of the power densities of modern PWR, BWR, and LMFBR cores. The differences in the power densities are attributable primarily to differences in the enrichment of the fuel. Note that LMFBRs use a hexagonal lattice, while PWRs and BWRs use a square one.

1.34 Thermal Efficiency

Once heat is generated in the core, it is the responsibility of the nuclear steam supply system to remove this heat from the core and turn it into useful electricity. In most reactors, this is done by converting the heat into steam that is then fed to what is known as a *steam turbine* or a *power turbine*. An electric generator is then attached to the shaft of the steam turbine, and turning the arms of this generator causes electric power to be produced. On a very high level, this process is illustrated in Figure 1.37.

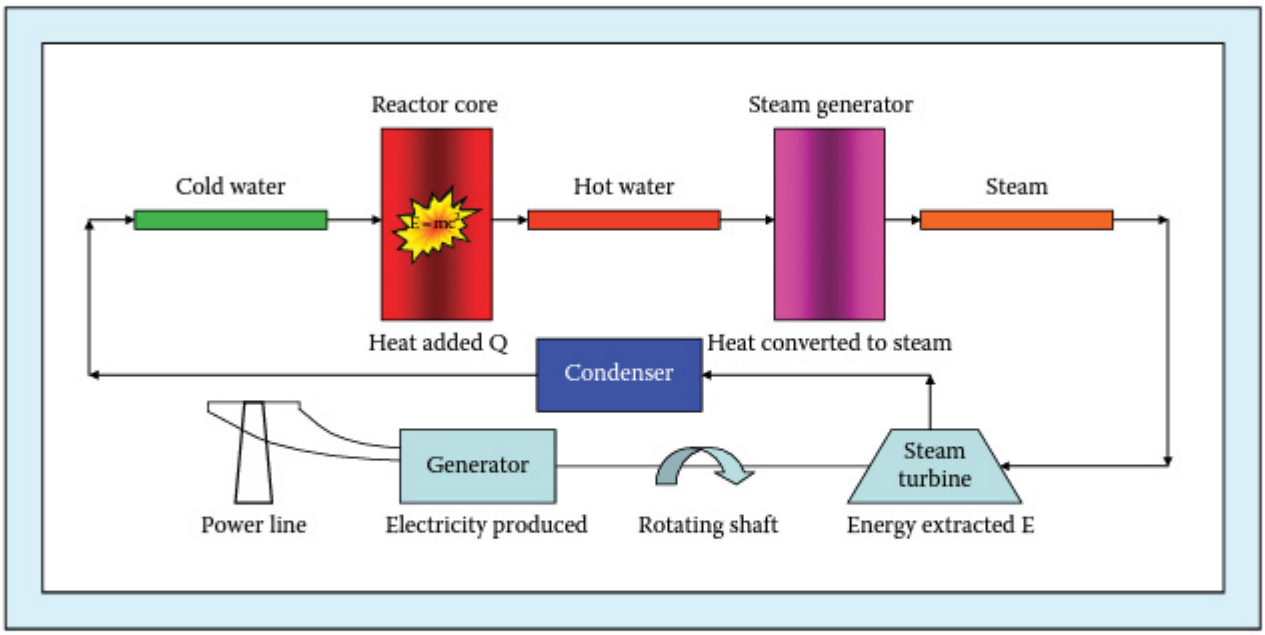

FIGURE 1.37 How the energy conversion process from heat to electricity works in a typical PWR.

TABLE 1.18
Thermal Efficiencies of Common Commercial Power Reactors in the World Today

Type of Reactor	Manufacturer	Average Thermal Efficiency (%)
CANDU	Atomic Energy of Canada, Ltd.	29–30
BWR	General Electric	32–34
PWR	Westinghouse	33–34
LMFBR	Novatome	43
AGR	National Nuclear	43
HTGR	General Atomic	48

Source: Todreas, N. and Kazimi, M.S., *Nuclear Systems*, Vol. 1, CRC Press, Boca Raton, FL, 2008.

Notes: The numbers shown are approximate. The actual thermal efficiencies may vary from those shown.

The *thermal efficiency* of a power plant η is defined as the ratio of the electric power produced by the plant to the amount of thermal energy produced in the core. If the amount of heat produced in the core is Q, and the electrical power produced is P, then the definition of the thermal efficiency is

$$\eta = \mathbf{TE} = \mathbf{Thermal\ Efficiency}$$

$$\eta = \frac{P(\mathrm{MWE})}{Q(\mathrm{MWT})} \tag{1.23}$$

This definition is used in most reactor thermal-hydraulic books. Notice that the electrical power output P is measured in MWE (electric) and the thermal power output is measured in MWT (thermal). The reader should not confuse these two terms because they refer to entirely different things. *The thermal efficiency is a dimensionless number*. The actual thermal efficiency is defined by the type of plant thermal cycle that is used. Most nuclear power plants use a *Rankine thermal cycle* to convert the heat generated in the core into useful power. However, GCRs can theoretically use a *Brayton thermal cycle* to achieve the same effect. The characteristics and attributes of both of these cycles are discussed in our companion book.*

However, the larger temperature difference ΔT there is between the temperature of the coolant in the core and the heat sink to which this thermal energy is released, the greater the thermal efficiency of the power plant will be. This is the same regardless of whether we are dealing with a nuclear power plant or a coal-fired power plant. Hence, many of the components of the NSSS that are used in fossil-fired power plants are also used in nuclear ones. Notice that gas reactors and LMFBRs tend to have the highest thermal efficiencies (in the range of 40%–48%). Conventional PWRs and BWRs tend to have a thermal efficiency of about 33%, although this number can vary somewhat from one power plant to the next. Sometimes additional "tricks" such as reheat and regeneration can be used to extract more efficiency from a reactor thermal cycle. The thermal efficiencies of these different types of reactors are shown in Table 1.18.

The number of coolant loops in the NSSS also has some effect on the thermal efficiency. Generally speaking, PWRs have two loops (a primary loop and a secondary loop), and the coolant in the primary loop is a liquid, while the coolant in the secondary loop is a vapor. BWRs have only one loop (a primary loop) because the coolant is intentionally allowed to boil. Finally, LMFBRs can have as many as three separate loops to separate the heat-generating loop in the core from the steam-generating loop, which is connected to the power turbines. Each of these reactors also has variations on these basic designs. For example, within a particular coolant loop (primary, secondary, or tertiary), additional sub-loops (called *coolant legs*) may exist to carry the energy transferred by the coolant. In a large PWR, the coolant flow through the primary loop may then be handled by three or four of these additional sub-loops. Each of these sub-loops may then have a separate reactor coolant pump (or RCP) and steam generator (or SG) attached to them. Hence a 1000 MWE PWR may have as many as four separate steam generators and RCPs. BWRs have multiple sub-loops within the primary loop as well. The sub-loop that receives the hot coolant from the core is called the *hot leg*, and the sub-loop that feeds the cold coolant back to the core is called the *cold leg*. Because all of the components of a nuclear power plant must be redundant, commercial power reactors have at least two hot and cold legs. The most severe reactor accident is normally assumed to occur when there is massive failure of one of the coolant pipes in the hot leg. When modeling the consequences of such a reactor accident, a double-ended *guillotine pipe break* of the main coolant pipe in the hot leg is normally assumed to be the most catastrophic type of break that can occur.*

* See *Nuclear Engineering Fundamentals: A Practical Perspective*, by R.E. Masterson, CRC Press (2017).

1.35 Control Rods and Their Function

In nuclear power plants, the control rods have a number of important functions to perform. First, they can be used to either raise or lower the power level of the core by changing the value of the *reactivity* ρ, which is defined in Chapter 9:

Definition of the Reactivity

$$\rho = \frac{K_{effective} - 1}{K_{effective}} \tag{1.24}$$

Here $K_{effective}$ is the ratio of the neutron production rate to the neutron destruction rate, which is also called the *effective multiplication factor* of the core. Changing the reactivity changes the reactor period, and this needs to be taken into account when a control rod is moved. Secondly, when put in the context of an overall operating plan, they can help to shape the flux and eliminate hot spots and flux peaks and to promote a more complete burnup of the fuel. Third, they can help to keep a reactor critical by compensating for changes in the reactivity due to the introduction of burnable poisons and soluble poisons and the burnup of the fuel. Fourth, control rods are the first line of defense when it comes to shutting down a reactor quickly and reliably in the event that an unforeseen safety problem (such as a loss of coolant accident) occurs.

Withdrawing a control rod from the core will tend to increase the core power since fewer thermal neutrons will be absorbed by the materials inside of the rod. Conversely, moving a control rod further into the core will have exactly the opposite effect because more free neutrons will be absorbed. Control rods are usually designed so that each incremental movement in the position of a control rod will correspond to a known reactivity change (+ or −). For example, if a control rod has a total of 20 possible vertical positions (see Figure 1.38), each position will change the reactivity by 1/20th of this amount. The actual amount that the reactivity is changed depends on how a reactor is designed. However, in most reactor designs, an incremental change in the position of a *control rod bank* will change the *reactivity* by *one cent* to *one-half of one cent*. A fully withdrawn rod will have no net contribution to the reactivity. However, each time a control rod bank is inserted into the core by 1/20th of its length, the reactivity will be reduced by ½ cent or 1 cent. Thus a fully inserted control rod bank will be able to reduce the total reactivity by a total of 10–20 cents, while a control rod bank that is inserted halfway into the core will be able to change the reactivity by only half of this amount. Finally, they can be used as an emergency control system to quickly and reliably shut the reactor down in the event of an unforeseen problem or a safety issue. The reactivity will be formally defined in Chapter 9. Until that time, the definition given earlier should be used.

According to the U.S. NRC, the formal definition of a control rod is

The U.S. NCR's Definition of a Control Rod

A rod, plate, or tube containing a material such as hafnium, boron, etc., used to control the power level of a nuclear reactor. By absorbing neutrons, a control rod prevents the neutrons from causing further fissions.

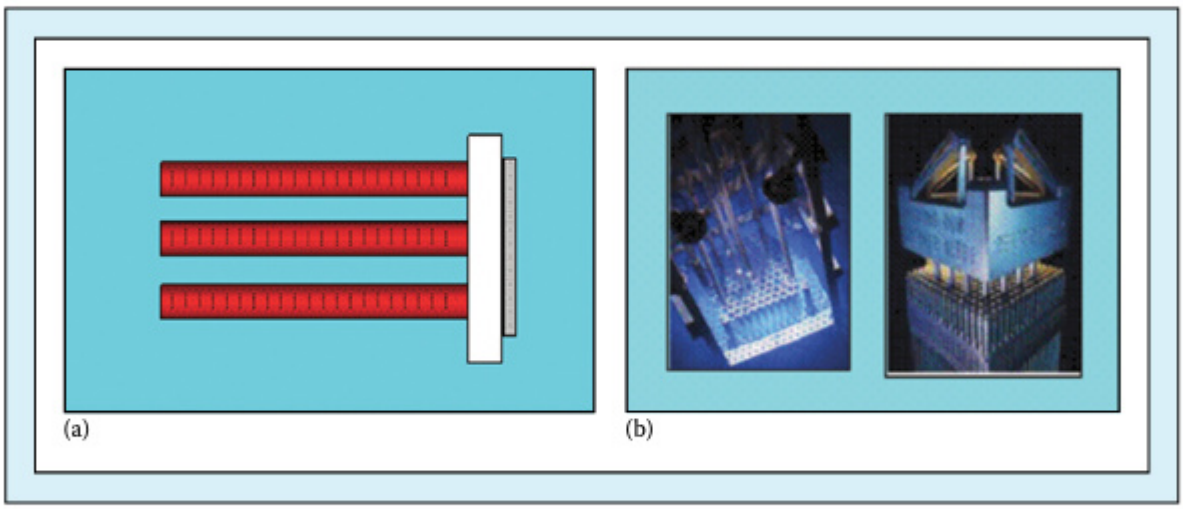

FIGURE 1.38 (a) A group of control rods (shown sideways) and a control rod drive assembly with graduations on the rod. Each graduation is ~0.1 cent of reactivity. (b) A fuel assembly with the control rods partially inserted into the core. (Pictures provided by the author and Westinghouse Nuclear Energy Systems.)

Today control rods are also designed to use silver, indium, cadmium, and boron carbide (B_4C). Hence, control rods are a very important component of any reactor core. Without them, it would be virtually impossible to control the power level when quick changes to the neutron population are required in response to sudden temperature or reactivity changes in the core. Control rods can also come in many different sizes and shapes, and they are generally optimized to the needs of a particular design. *BWRs have cruciform-shaped control rods*, while most other types of reactors (such as *PWRs and LMFBRs*) *have cylindrical-shaped ones*. Some *research reactors* also use *plate-type* or *rectangular* control rods, but these control rods are generally not as common as those used in other designs.

1.36 Comparing PWR Control Rods and BWR Control Rods

For a number of reasons, BWRs and PWRs have taken a slightly different evolutionary path when it has come to the design of their control rods. During normal operation, the moderator in a BWR is intended to boil throughout much of the core, while the water in a PWR is only designed to undergo *nucleate boiling* near the top of the core. Because of this, the coolant exiting a BWR must employ a *steam dryer* to remove the excess moisture from the steam at the top of the pressure vessel head, and because of space limitations, the presence of the steam dryer makes it impractical to mechanically insert the control rods into the core from above. Consequently, *BWRs have tended to adopt a design where the control rods are inserted into the core from below, while the control rods in a PWR are inserted into the core from above*. In addition, because the control rods are inserted into the core from opposite directions, the shapes of the control rods are very different in these two designs. For example, *PWRs use finger-shaped control rods* that are similar in shape to the fuel rods themselves, while BWRs use *cruciform-shaped control rods* that are much larger and more rigid than their PWR counterparts. Both designs are illustrated in Figure 1.39. The direction of insertion is also shown in Figure 1.40, and in both cases, the fuel rods are shown in dark gray or light blue, and the control rods are shown in red. Because the control rods in a BWR are so much larger than the control rods in a PWR, they have a much greater control rod worth (or negative reactivity per rod). In BWRs, a single cruciform-shaped control rod is normally surrounded by *four fuel assemblies*. The enrichments of the rods in the fuel assemblies are then varied to flatten the radial power profile. A picture of the central control rod and four of the surrounding assemblies is shown in Figure 1.41. In some designs, more fuel rods are used in each assembly.

In a PWR, each cluster of control rods is inserted into the core from above using a *mechanical drive system*. The drive system is attached to the pressure vessel head using a large number of electromagnets. In the event the reactor needs to be shut down quickly, the power to the electromagnets is cut by pushing a *scram button* on the control panel (see Figure 1.42), and the rods fall into the core under the force of gravity alone. This is an example of what is called an *emergency reactor shutdown, or "scram."* The design of the control rod linkages and the electromagnets that allow the control rods to fall into the core goes back to the early days of the U.S. nuclear submarine program, and the designs that

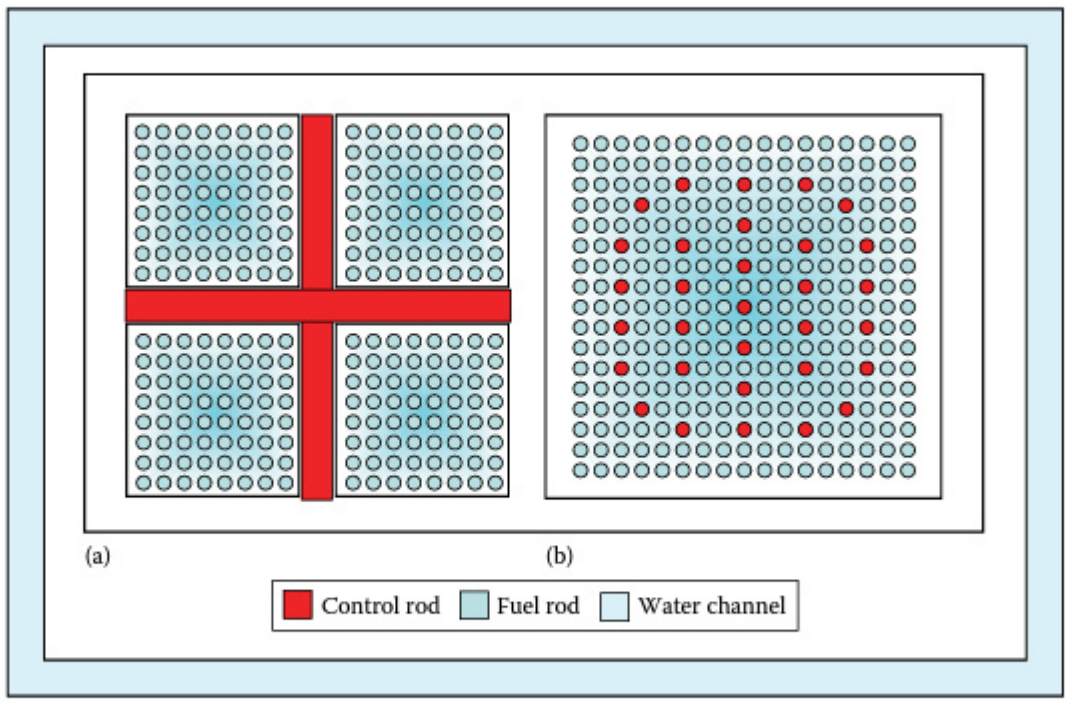

FIGURE 1.39 The fuel assemblies and control rods in a BWR (a) and in a PWR (b) directly compared.

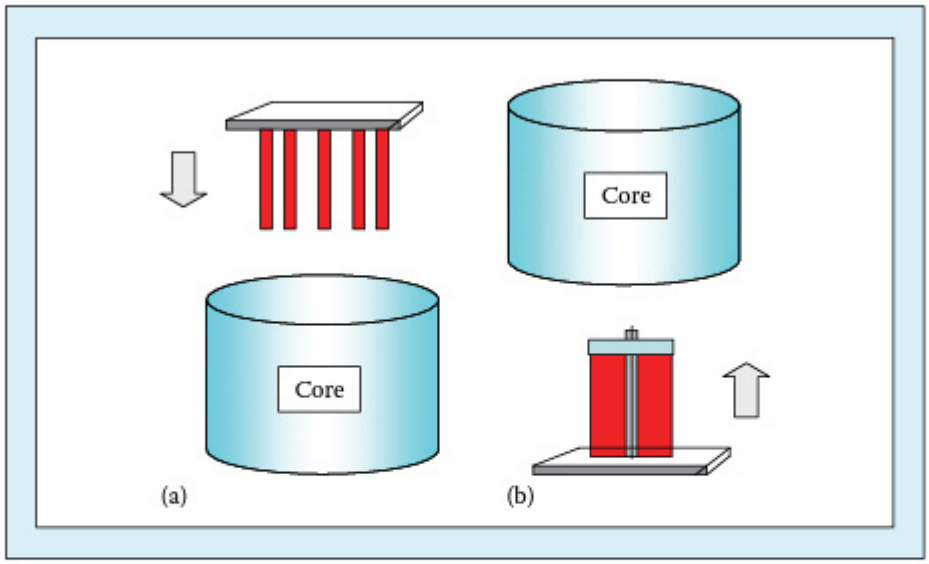

FIGURE 1.40 Control rods are inserted into the core in opposite directions in a PWR (a) and a BWR (b). This has been part of their standard design for about 50 years.

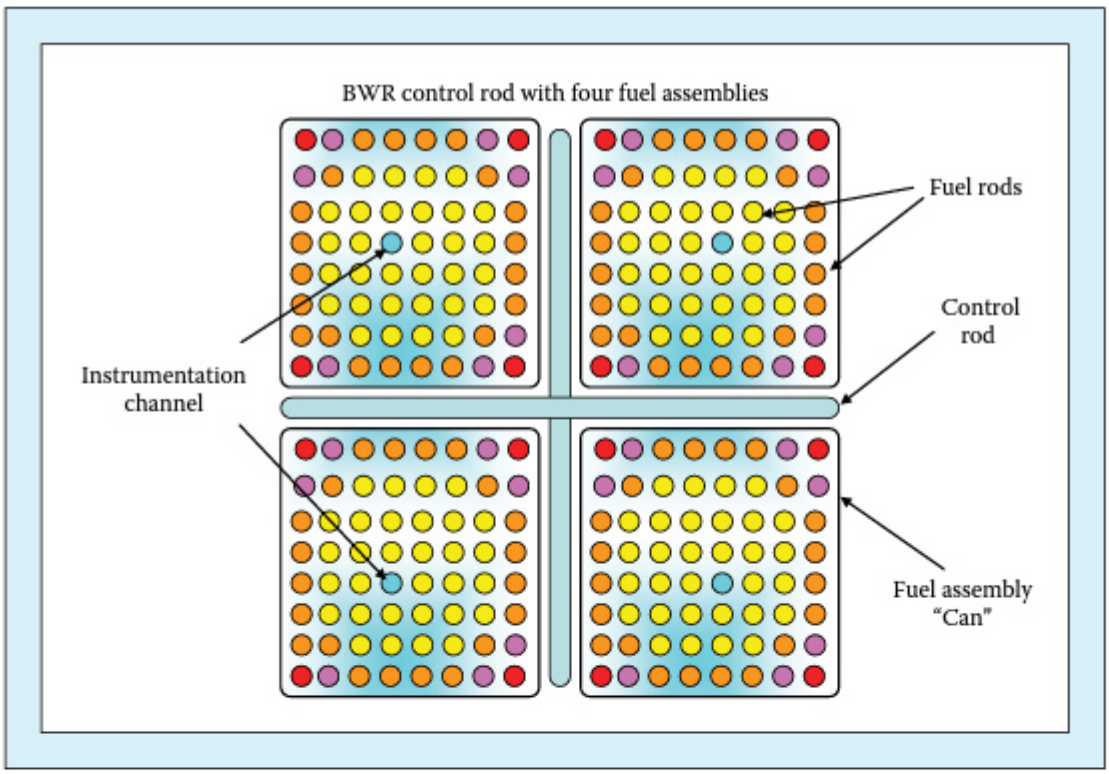

FIGURE 1.41 A picture of a BWR control rod surrounded by four fuel assemblies. The enrichments of the rods in each assembly are then varied to flatten the radial power profile and to optimize the performance of the fuel. In each fuel assembly, the different colored rods are used to represent different enrichments. The blue "hole" in the center of the assemblies is typically an instrumentation channel.

are used today are not much different than the designs that were used 50 years ago. The control rod scram system in a PWR is an example of a *passive safety system* because once the *scram button* is pushed, the rods fall into the core without the need for human intervention. (The scram button cuts off the electricity to the upper part of the pressure vessel and this "pulls the plug" on the electromagnets.)

On the other hand, BWRs use a high-pressure hydraulic system to insert the control rods into the core from below. As we mentioned previously, these rods are generally larger and heavier than their PWR counterparts, *and in most cases,*

FIGURE 1.42 A picture of the scram button on a reactor control panel. (Picture provided by wikimedia.org—see file: NS Savannah SCRAM MD1.jpg.)

their reactivity is larger as well. The hydraulic pressure exerted on the rods from below provides the necessary lifting force required to insert them into the core. Internally, a cruciform-shaped control rod consists of

- A solid neutron-absorbing material in metallic form, or
- A hollow chamber into which many hollow tubes filled with B_4C powder can be placed

The design of these rods has evolved considerably over the years, and the materials that are used in most control rods today (e.g., hafnium and iridium) are considerably different from those which were used several decades ago. *In a reactor physics calculation, it is usually possible to model the rods in a BWR as sheets of black neutron-absorbing material and to calculate their worth by treating them as a planar sheet of absorbing material located in an otherwise homogeneous region of the core*. It can be shown that a typical control rod will have a negative rod worth of about -0.2β, or $W = -0.0013/0.0065 \approx -20$ cents per rod. A 1000 MW (3000 MWT) BWR will have about 150 of these rods. This puts the total control rod worth for a large BWR at about −$25.00 on a system-wide basis. By comparison, a comparable PWR will have about 40% as many control rods (~60 clusters vs. 150), and their aggregate negative reactivity will be about −$11.00. The average rod worth is still about -0.2β, or $W = -0.0013/0.0065 \approx -20$ cents per cluster. Each cluster has about 20 finger-shaped control rods, so an individual finger-shaped control rod in a PWR will have a negative reactivity of −20 cents/20 or about −1 cent per rod. The total rod worth is only about 40% as much in a PWR as it is in a BWR because of the presence of the chemical shim. Furthermore, only about ¼ of the fuel assemblies in a typical PWR are actually be equipped with control rods.

Student Exercise 1.6

In an advanced reactor physics class, it can be shown that a modern PWR might not have enough negative reactivity to prevent the core from going critical with a fresh batch of fuel based on the reactivity (i.e., the neutron-absorbing characteristics) of the control rods alone.

This design decision was probably the result of a carefully thought out cost savings initiative, and much internal analysis probably occurred before the final design decision was made. Since control rods and their drive mechanisms are very expensive, putting more control rods into a PWR to allow it to be subcritical under any conditions could increase the total cost of a reactor by several percent.

If you were a reactor operator or a utility shareholder, do you agree with this basic design decision?

1.37 Use of the Scram Button and the Word SCRAM

When reactors were first installed on nuclear submarines, the word *scram* was invented by engineers to indicate that a condition existed where a reactor had to be shut down or "scrammed" immediately. The word "scram" then became an abbreviation for what was called a "*safety control rod axe man.*" However, today its meaning has changed, and now it is intended to indicate the *SCRAM* or emergency shutdown of any type of commercial or military reactor, which is usually initiated by the reactor operator by pushing the *scram button* on the control panel (see the pictures in Figure 1.41). In commercial power reactors, this emergency shutdown process is also called a "*reactor trip*," but the exact usage of this term is not universal, and sometimes it varies from country to country. In most PWRs and BWRs, a reactor SCRAM is now part of the emergency shutdown procedure that all reactors are required to undergo during a routine safety test. However, when they are ready to be refueled, a more gradual rod insertion process is required.

1.38 Maintaining the Criticality of the Core over Time

During normal reactor operation, the amount of fuel in the core decreases monotonically with time if the power level P remains constant. If the reactor is designed to operate for a long period of time without being refueled, then additional fuel in excess of what is required to achieve criticality must be added to the core before it is started up. The *positive reactivity* generated by this excess fuel must then be balanced with *negative reactivity* introduced by other sources. These sources can include moveable control rods and burnable poisons, and in the case of PWRs, this neutron-absorbing capacity is augmented further by introducing a strong neutron-absorbing material, or poison into the coolant in the form of *boric acid*, or *chemical shim*. A cold, clean core always has more fuel than it needs to become critical. *In a commercial power reactor, it is not uncommon for the reactor to contain more than 30% more fuel than it needs to achieve a critical state. Without neutron absorbing materials to compensate for this excess reactivity, a typical (unpoisoned) $K_{effective}$ for a PWR is about 1.40 at start-up, and the corresponding $K_{effective}$ for a BWR at start-up is about 1.33. This corresponds to an excess reactivity at start-up of about \$45.00 for a PWR and about \$38.00 for a BWR - assuming they are fueled with U-235.* By design, the positive reactivity produced by this excess fuel is always balanced by the negative reactivity from the reactor's control rods, or in the case of a PWR, from both the control rods and the boric acid that is dissolved in the coolant. The control rods are inserted into the core just far enough to keep the reactor in a subcritical state until a decision is made to start it up. In PWRs, this excess reactivity is also held in check by the boron dissolved in the coolant. Once a reactor is started up, the control rods are gradually withdrawn to compensate for the reduction in the reactivity due to the buildup of xenon, and the increase in the operating temperature of the fuel. This process of withdrawing the control rods continues for several hours until it has reached its desired operating state. In PWRs, the boron concentration in the coolant is also reduced for the same reason. Once the reactor has reached its intended power level, the amount of fuel in the core starts to monotonically decrease with time as a result of the elevated neutron flux. *So although a reactor may initially start its life with much more fuel than it needs to stay critical, this excess fuel is what allows it to operate for long periods of time after initial criticality has been achieved.* We will have more to say about this process in Chapters 17 and 18, where the effects of burnup and depletion are discussed.

1.39 Electrical Generating Systems in a Nuclear Power Plant

Basically, a nuclear power plant can be thought of as a large thermonuclear furnace that generates heat by splitting apart atoms of uranium or plutonium instead of burning fossil fuels like coal and natural gas. The heat generated in this process is eventually converted into steam, and the steam drives a *steam turbine* and an *electrical generator* to produce the electricity that is generated by the plant. In this section, we would like to illustrate exactly how this process occurs, and how the thermal energy generated by the plant in MWT (Mega Watts Thermal) can be converted to electricity in MWE (Mega Watts Electric). Some reactors use coolants other than water (such as carbon dioxide or liquid metals) to cool the core, but with the exception of GCRs, which can sometimes use a Brayton cycle, all other commercial nuclear reactors use a Rankine thermal cycle to turn the electrical generators and to produce useful power from the heat that is generated in the core. The *Rankine thermal cycle* assumes that the working fluid (which in most nuclear power plants is water) can undergo a change of phase, while the *Brayton thermal cycle*, which GCRs are capable of using, assumes that it cannot.

1.40 Steam Generators in Nuclear Power Plants

With the exception of BWRs, all modern nuclear power plants use a device called a steam generator to convert the hot water produced in the core into steam to turn the power turbines. Steam generators are large and relatively complex devices that take hot water produced by the core and cooler water from another cooling loop (usually called the secondary loop) and convert it into steam. The primary loops which transfer the heat from the core to the steam generators are shown in Figure 1.43. Most steam generators have no moving parts. However, designing one to work properly can be extremely

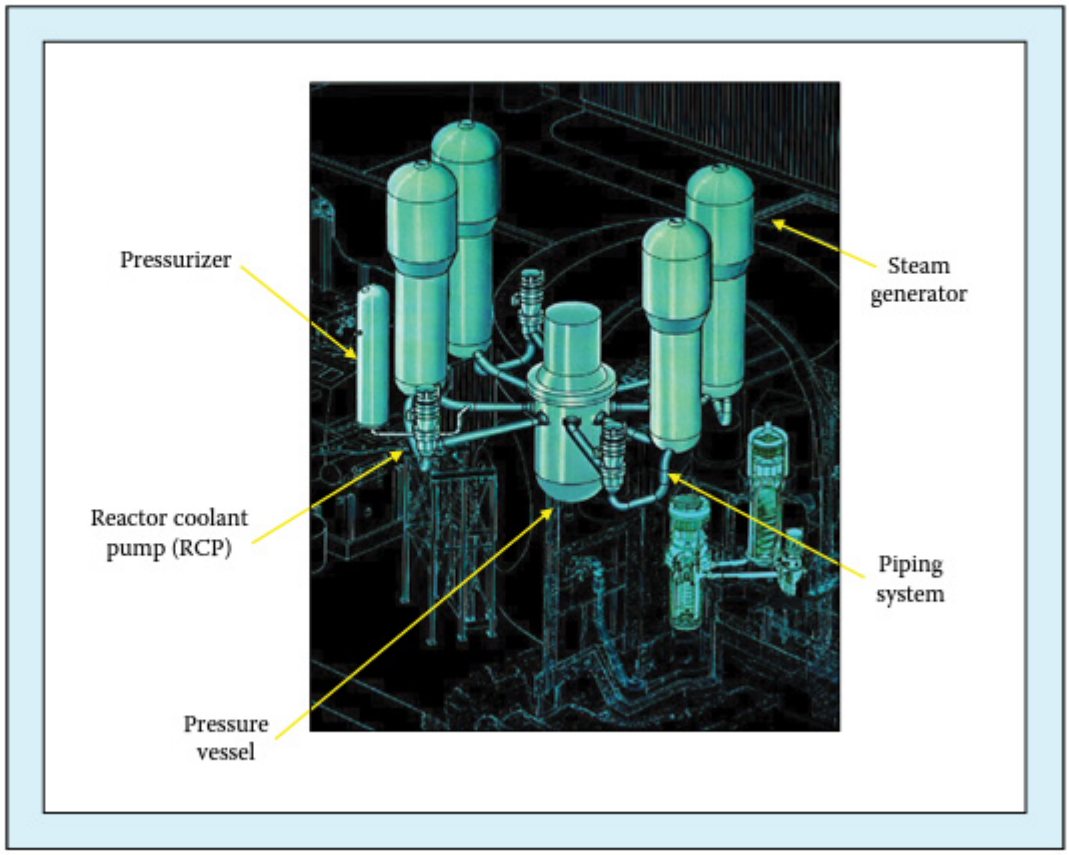

FIGURE 1.43 The RCPs, the steam generators, the pressurizer, the reactor vessel, and the primary coolant loops in a large PWR. (Courtesy of Westinghouse—see *http://me1065.wikidot.com/nuclear-pressurized-water-reactor-pwr*.)

difficult because it involves a very detailed knowledge of heat transfer, fluid flow, water chemistry, and material technology. Steam generators today tend to come in two basic designs. The first design is called a *once-through steam generator (OTSG)*, and the other is called a *UTUBE steam generator*. OTSGs can be 60–80 ft high (20–25 m), and UTUBE steam generators are about 1/3 of that height. In a typical PWR, hot water from the core enters a steam generator with a pressure of between 2200 and 2250 PSI, and at a temperature of about 325°C (620°F). In this state, it is said to be a *saturated liquid*. In other words, it contains as much thermal energy as it can without boiling. The cooler water from the secondary loop enters the steam generator at a pressure of about 900 PSI and at a temperature of about 220°C (430°F). The steam on the secondary side emerges from the steam generator at a temperature of about 275°C (540°F). In this state, it is said to be *completely saturated*, and it also has an *exit quality* equal to one. There are no water droplets remaining in the steam at this point, and if the steam is heated even further, it then becomes *superheated*.* The physical state of the coolant entering and leaving the steam generators is summarized in Table 1.19. In many designs, the thermal efficiency can be increased even further by providing an additional 5 to 10 degrees Centigrade of superheat.

Power turbines prefer this kind of steam because it is extremely hot and dry. Hence, they can run for a long time without the impellers being damaged or eroding. The tubes inside of the steam generators are typically made of noncorrosive

TABLE 1.19
Temperatures and the Pressures of the Coolant Entering and Leaving the Primary and the Secondary Sides of the Steam Generators in a Typical PWR

Side of the NSSS	Pressure (MPa, Absolute)	Inlet Temperature (°C)	Outlet Temperature (°C)
Primary side (tube side)	15.5	325 (saturated water)	275 (liquid water)
Secondary side (shell side)	6.2	220 (liquid water)	275 (saturated steam)

Note: These numbers can vary somewhat depending on the design.

* Thus superheated steam can have more energy than saturated steam does.

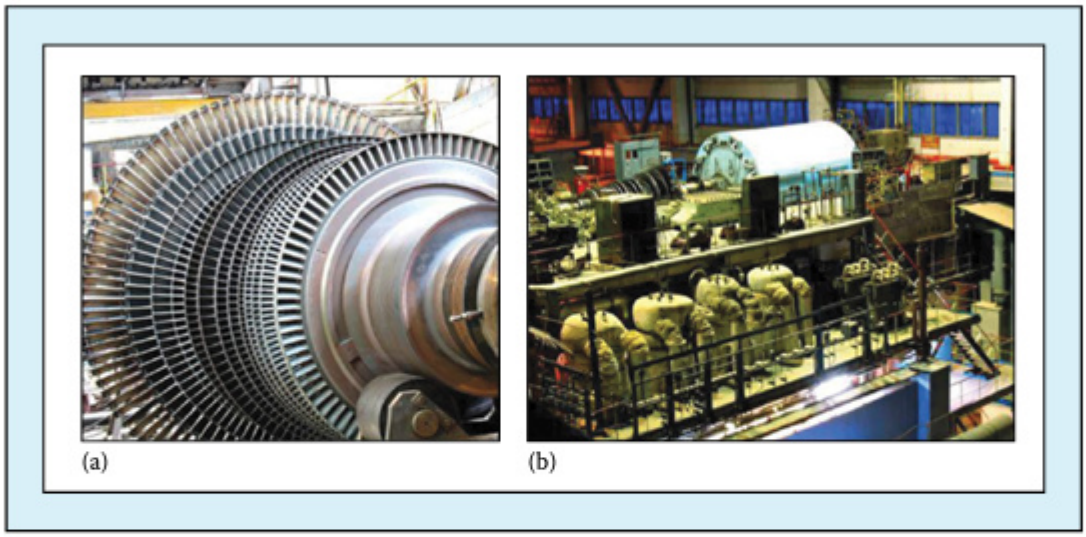

FIGURE 1.44 A large steam turbine in a nuclear power plant (a) and another steam turbine being repaired (b).

metals or exotic alloys of stainless steel. These high-performance alloys and superalloys have been used in steam generators for many years, and they are specifically designed not to rust or corrode. Some commonly used alloys that meet these requirements include type 316 stainless steel, Alloy 400, Alloy 600MA (that is mill annealed), Alloy 600TT (that is thermally treated), Alloy 690TT, and Alloy 800Mod. References to other alloys can also be found in the literature. Steam generators in a "typical" PWR in the United States have the operating conditions shown in Table 1.19.

1.41 Steam Turbines

Once the steam is produced by a steam generator, it is passed through the secondary loop into a device known as a *steam turbine*. In a nuclear power plant, steam turbines are also called *power turbines*. In today's power plants, steam turbines are normally located *outside* the containment building. When the steam enters the power turbine, it causes the blades of the turbine to turn, and this kinetic energy is eventually transferred to a rotating shaft. (The actual rate of rotation depends on how fast the turbine is designed to spin.) We will have more to say about this presently. Figure 1.44 shows the inside of a modern steam turbine. The modern turbine was invented by an Englishman by the name *Charles Parsons*.

1.42 Steam Generator and Steam Turbine Pairing

In PWRs, the steam generators and steam turbines tend to come in matched pairs. There are a number of design reasons for this that are generally related to the specifics of the plant thermal cycle. However, almost all PWRs have this basic design in common. *The major difference between two PWRs with different power levels is that they can have different numbers of steam generators or power turbines attached to the core. Generally speaking, another steam generator and/or turbine set is added to the plant for each additional 500, 750, or 1000 MW of thermal power that is required.* This way both the steam generators and steam turbines can be designed as "matched pairs" to optimize the amount of electrical power that is produced. This also helps reactor vendors to design plants that are cheaper and more modular. If a higher power output is required, one simply adds a larger core and another steam generator/steam turbine pair set to the secondary loop. This design concept forms the basis for what are called *advanced modular reactors* (or AMRs) today. *Hence, a modern nuclear power plant that generates 1000 MW of electrical power (or about 3000 MWT of thermal power) will typically have three or four large steam generators inside of the containment building*. (The steam turbines are normally located outside of the containment building in the *auxiliary building*.) However, each of these steam generator/steam turbine pairs is essentially an identical clone of each other, and so if we can understand how one of them works, then we can understand how all of them work. We would now like to discuss the electrical generators that are attached to the shafts of the steam turbines.

1.43 Electrical Generators

An electrical generator is a device that takes the mechanical energy from a rotating shaft and converts it into electric power. In nuclear power plants, this is achieved by attaching the electrical generator to a steam turbine. The modern-day electrical generator was first proposed by an Englishman by the name *Michael Faraday* in 1861. An electrical generator can be found

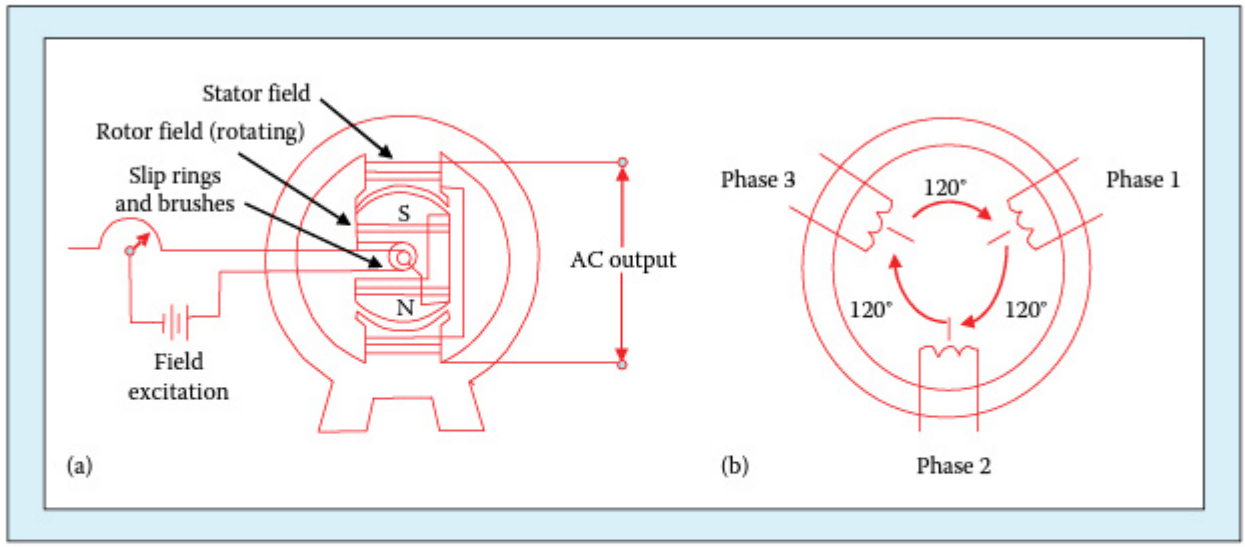

FIGURE 1.45 A single-phase generator (a) can produce single-phase AC power, while a three-phase generator (b) can produce three-phase AC power. The current is then summed in the three-phase generator to generate a three-phase AC current (refer to the phase diagram in Figure 1.46).

at the heart of every nuclear power plant in the world today. An *electrical generator* is simply a large rotating device that converts mechanical power from a rotating shaft into electrical power. It does so by creating some relative motion between a stationary magnetic field (called a *stator*) and a rotating conductor (called a *rotor*). In an electrical generator, the shaft usually rotates and the magnetic coils that are used to generate the electricity are usually fixed. However, this does not always have to be the case. *The fixed coils are called the stator and the moving shaft is called the rotor* (see Figure 1.45).

The faster the rotor turns, the more power the generator produces. It should come as no surprise that most of the AC power in the modern industrial world is produced in this way. Nuclear power plants typically use electrical generators having three or four pole rotors. These rotors are used because the temperatures and pressures in the NSSS are more suitable to three and four pole generators than those having just one or two. *The electrical output from the poles is combined together to produce an alternating current*. Figure 1.46 shows the actual process that is used to generate the electrical current that reaches your home. *The number of poles is determined by the rate that the shaft turns the generator. The shaft of an electrical generator in a nuclear power plant rotates at about 1800 revolutions per minute.* Hence the output of the three poles is combined together to produce the alternating current that is generated. In comparison, a hydroelectric generator rotates at a speed of about 100 RPM. In these generators, 72 poles are used to obtain the same effect. Of course, this number varies slightly depending upon how the power-producing device is designed. More information about the design of electrical generators can be found at the following website:

http://www.asope.org/pdfs/AC_Electrical_Generators_ASOPE.pdf

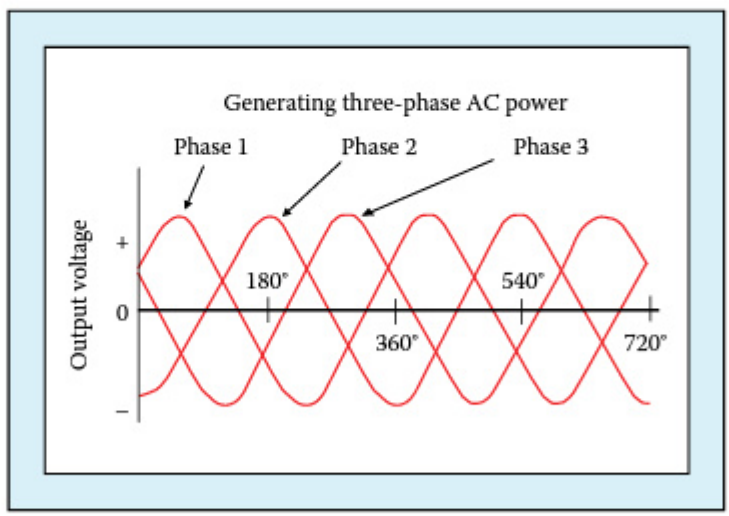

FIGURE 1.46 How the voltages are summed together to a form the three-phase current that enters your home.

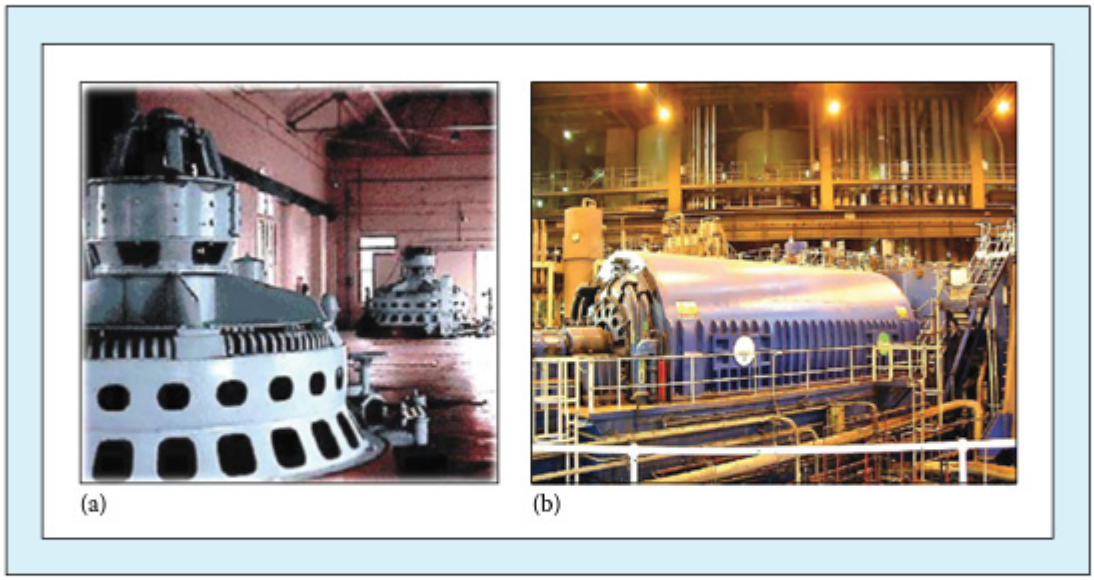

FIGURE 1.47 A large electrical generator used in a dam (a), and a similar generator used in a nuclear power plant (b). Note the immense scale and size that these electrical generators can have.

AC power having three phases is called *three-phase power*. It is generally preferable to other forms of AC power because it uses less electrical conducting material to transmit the same electric power than equivalent single-phase or two-phase systems with an identical voltage. For this reason and others, the concept of alternating current was first patented by Nikola Tesla in 1887 and 1888, and it subsequently came into widespread use at the beginning of the nineteenth century. In a three-pole generator, the poles are arranged in such a way that the individual currents from each pole vary sinusoidally at the same frequency but with a different phase. The peaks and troughs of their respective waveforms are intentionally offset by 1/3 of a cycle to provide three complementary alternating currents with a phase separation of 120°. The electrical power that is produced in this way is called three-phase power. Three-phase power is the most common form of electrical power in the world today, and most of the electrical power in the world is generated in this way. In the United States and a few other countries, three-phase power is generally not allowed to enter a person's home. Even in the areas where it does, it is typically split out at the main *distribution box*, and most residential appliances are powered by electric current that has only one phase. However, a three-phase current is still used in most of North America to power electric stoves, electric clothes dryers, and some types of dishwashers. So if your electricity is generated by a nuclear power plant, then this is the form that it will eventually arrive to your home. Figure 1.47 shows a large electrical generator that is used in a hydroelectric dam (on the left) and another generator that is used in a nuclear power plant (on the right). A typical generator can be between 5 and 10 m long, and it can weigh *several thousand tons*. The exact size and shape depends on the rating of the generator, and how many generators are needed to generate the total electrical output that is required.

Consequently, nuclear power plants having between 8 and 16 large generators are fairly common. Each generator is then tasked with the job of generating between 20 and 100 MW of electrical power. For a variety of reasons, electric generators above 100 MWE are not in wide-spread use today. If you have ever been to one of the world's large dams, such as the *Hoover Dam* in North America, or the *Three Gorges Dam* in China, you can begin to appreciate the size of these monumental machines. So in summary, a nuclear reactor creates the heat to generate the power, the steam generators convert this heat into high pressure steam, and the power turbines use this steam to turn the rotating shafts of large devices called electrical generators. The movement of the rotors past the stators inside of the generators then generates an electric current that is then sent to the power grid. Different types of power plants have different designs for these devices, but the basic principle behind them is essentially the same. The ratio of the electrical energy produced by the generators to the thermal energy produced by the core is then known as the *thermal efficiency* of the plant.

1.44 Common Measurements of Electrical Energy Production

The electrical generators in a nuclear power plant produce electricity in exactly the same way as the generators in a coal-fired power plant. The only significant difference is that the electrical generators in a coal-fired plant turn at a slightly higher speed because the steam reaching the steam turbines from the boilers is hotter (i.e., it has a higher energy content

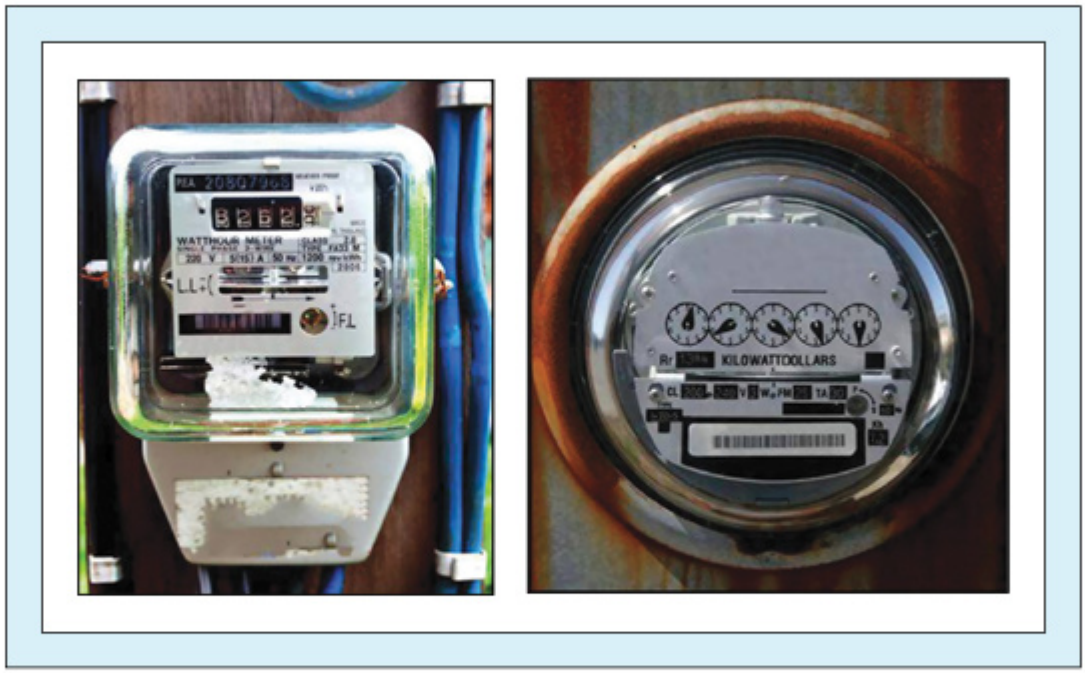

FIGURE 1.48 Two pictures of electric meters showing the usage of electricity in kilowatt hours.

or specific enthalpy h). The alternating current produced by the electrical generators is then sent to the electrical power grid, where it ultimately makes its way to your home. In Chapter 7, we will learn that every joule of electrical energy produced per second is equivalent to one watt of electrical power. In other words,

Converting Joules to Watts

$$1 \text{ J/s} = 1 \text{ W} \tag{1.25}$$

Electric utilities normally measure the amount of electricity that reaches your home in a slightly different unit of energy consumption called the *kilowatt hour. A kilowatt hour is the amount of energy consumed by multiplying the number of watts of electric power used per hour times the number of hours*. In other words, it is equivalent to 1000 J of electricity being used per second times the number of seconds in an hour (3600 seconds). For this reason, *1 kW Hour is equivalent to 1000 watt-hours or 3.6 MJ of electricity*. Electric meters such as those used in Figure 1.48 measure the amount of electricity that is consumed in this way.

Because the thermal efficiency of most commercial nuclear power plants is about 33%, the reactor core in one of these plants must generate approximately three times as many joules of thermal energy to produce 1 kWh. In other words, *1 kWh requires a nuclear power plant to produce approximately 3 × 3.6 = 10.8 MJ of thermal power*. The electric utility then bills you for this power based on the number of kilowatt hours you receive. In Canada, China, India, and the United States, a kilowatt hour of electricity costs about 12 cents (the actual numbers vary between 6 and 15 cents). Hence, every time the core of a nuclear reactor produces 10.8 MJ of thermal power, an electric utility charges you 12 cents (in USD) for this electrical power. It is helpful to keep these numbers in mind as we proceed further into this book. Fortunately, nuclear power plants can produce electricity much more cheaply than other types of power plants can, and this is one of the reasons why there are so many nuclear reactors in operation in the world today.

Example Problem 1.1

A kilowatt hour of electricity requires a nuclear power plant or a coal-fired power plant to produce 1000 J of electrical energy for 1 hour (3600 seconds), or 3,600,000 J. Suppose that a nuclear power plant produces 1000 MW of electricity for 1 day. How many kilowatt hours of electricity does it produce in this period of time?

Solution Since 1 kWh = 3,600,000 J, a 1000 MWE nuclear power plant will produce 1,000,000,000 J/s × 3,600 s/h × 24 h/day = 8.64×10^{13} J of energy = 8,640,000,000,000 J/3,600,000 J/kWh = 24,000,000 kWh in a single 24-hour day. [Ans.]

FIGURE 1.49 The Empire State Building in New York City is a famous tourist attraction. The annual electric bill for the Empire State Building is about 100 million dollars—a truly astronomical amount of money, even by today's standards, which the tenants of the building gladly pay!

Example Problem 1.2

Suppose that the cost of retail electric power in the New York City metropolitan area is 15 cents per kWh. Estimate the electric bill for the Empire State Building (see Figure 1.49) if it uses 1 million 100 W electric light bulbs for 1 day.

Solution In 1 hour, 1 million electric light bulbs using 100 W of electricity will use 100,000 kWh of electricity. In a 24-hour day, these same electric light bulbs will use 2,400,000 kWh of electricity. If the cost of 1 kWh of electricity is 15 cents, the electric bill for the Empire State Building will be 15 cents/kWh × 2,400,000 kWh = $360,000 USD for 1 day! In reality, the Empire State Building purchases electric power from Con Edison (the local electric utility) at a wholesale cost of about 10 cents per kWh, so the electricity still costs about $250,000 USD per calendar day. [Ans]

Example Problem 1.3

Suppose that a cylindrical reactor core 3 m high and 3 m wide has a thermal power output of 2200 MW. What type of reactor do you expect this to be? What do you expect the thermal efficiency to be, and how much electricity do you expect this reactor to produce?

Solution Since the reactor core is cylindrical in shape, its total volume is $V = \pi R^2 H = 3.14 \times 150^2 \times 300 = 21{,}205{,}125$ $cm^3 = 21{,}205$ L. Since its total power output is 2,200 MW (2,200,000 kW), its average power density is P/V = 103.75 kW/L. Hence, the reactor is most likely to be a PWR. Modern PWRs have a thermal efficiency between 33% and 34%. Therefore, we expect this reactor to generate between 725 and 750 MW of electric power. [Ans.]

1.45 Reviewing What We Have Just Learned

Finally, we would like to take a moment to review what we have just learned, because in future chapters, we will attempt to discuss the neutronic characteristics of many of these reactors in more detail. Basically, there are five types of commercial power reactors in widespread use in the world today. They are:

1. Pressurized water reactors
2. Boiling water reactors
3. Heavy water reactors (which are another variation of the pressurized water reactor)
4. Gas-cooled reactors
5. Liquid metal fast breeder reactors

Counting the reactors currently under construction, there will be approximately 500 commercial nuclear power plants in operation by the year 2020. PWRs are the most common type of reactor in use today (accounting for about two-thirds of the world's nuclear generating capacity), and BWRs are the second most common commercial reactor type. On average, these reactors supply about 20% of the world's electric power. In some countries like France, this number is considerably higher (about 80%). In the foreseeable future, it is likely that the number of commercial nuclear power plants in the world will continue to increase, and within 50 to 60 years, there will probably be 1000 commercial nuclear power plants in operation around the world.

In general, nuclear power plants have had an extraordinary safety record, and only three major reactor accidents have occurred since the nuclear power industry was founded in the 1950s (TMI, Chernobyl, and Fukushima). However, Fukushima was caused by a natural disaster beyond the stated design limits of the plant, and so it could have been avoided if the large earthquake off the coast of Japan did not occur. So in spite of these unfortunate incidents, nuclear power will continue to play a major role in meeting the world's energy needs as oil, coal, natural gas, and other natural resources continue to decline. Consequently, the number of nuclear power plants in the world will continue to increase for the foreseeable future. In future chapters of this book, we will attempt to show you how these plants behave and operate on a daily basis. We will then attempt to explore their neutronic performance and the methods through which this performance is achieved.

Example Problem 1.4

Suppose that the average cost of retail electric power in Washington, DC, is 10 cents per kWh. Using this number, estimate what it would cost to run a single 100 W electric light bulb in a Washington, DC, home for 1 day.

Solution In 1 day, a 100 W light bulb would use 2.4 kWh of electricity. At a cost of 10 cents per kWh, the light bulb would cost 24 cents to run in your home for a day. [Ans.]

References

Books and Textbooks

1. Lamarsh, J.R. and Baratta, A.J. *Introduction to Nuclear Engineering*, Prentice Hall, Upper Saddle River, NJ (2001).
2. Todreas, N. and Kazimi, M.S. *Nuclear Systems*, Vol. 1, CRC Press, Boca Raton, FL (2008).
3. Duderstadt, J. and Hamilton, L. *Nuclear Reactor Analysis*, John Wiley & Sons, New York (1976).
4. El-Wakil, M.M. *Nuclear Heat Transport*, American Nuclear Society, La Grange Park, IL (1981).
5. Waltar, A.E. and Reynolds, A.B. *Fast Breeder Reactors*, Pergamon Press, London, England (1981).
6. Lamarsh, J.R. *Introduction to Nuclear Reactor Theory*, second printing, Addison-Wesley Publishing Company, Inc., New York (1972).
7. Glasstone, S. and Sesonske, A. *Nuclear Reactor Engineering*, 3rd edn., Van Nostrand Reinhold Company, New York (1981).
8. Shultis, K. and Faw, R. *Fundamentals of Nuclear Science and Engineering*, 2nd edn., CRC Press, Boca Raton, FL (2008).
9. Masterson, R.E. *Nuclear Engineering Fundamentals: A Practical Perspective*, CRC Press, Boca Raton, FL (2017).

Web References

1. *http://inventors.about.com*.
2. *http://www.westinghousenuclear.com/*.
3. *http://en.wikipedia.org/wiki/Nikola_Tesla*.
4. *http://en.wikipedia.org/wiki/Steam_turbine*.
5. *http://en.wikipedia.org/wiki/Thomas_Edison*.
6. *http://en.wikipedia.org/wiki/Electric_generator*.
7. *http://www.asope.org/pdfs/AC_Electrical_Generators_ASOPE.pdf*.
8. *http://www.britannica.com/EBchecked/topic/641020/George-Westinghouse*.
9. *http://www.ge-energy.com/products_and_services/products/steam_turbines/*.
10. *http://www.westinghousenuclear.com/Our_Company/history/george_westinghouse.shtm*.

Questions for the Student

The following questions cover the material presented in this chapter. They are designed to test how well the student has acquired a working knowledge of the subject matter.

1. Name at least four types of nuclear particles that are produced in a reactor core.
2. How many times higher is the coolant pressure in a PWR than it is in a BWR?
3. Which reactor has a thicker pressure vessel—a PWR or a BWR?
4. Conceptually speaking, what is the difference between a fission product and a fission fragment?
5. What material is used in the construction of a gas reactor pressure vessel?
6. In what document can the standards for the construction of nuclear reactor pressure vessels be found?
7. What is the most common type of nuclear reactor in use in the world today?
8. What country has the most commercial nuclear power plants in operation today?
9. What is the second most common type of nuclear reactor in use in the world today?
10. Approximately how many commercial nuclear power plants are in operation in the world today?
11. How many coolant loops does a CANDU reactor have?
12. Who invented the modern steam turbine which is found in nuclear power plants today?
13. What coolant is used in the primary loop of a CANDU reactor, and what coolant is used in the secondary loop?
14. What component is the shaft of a steam turbine connected to in a nuclear power plant?
15. What is the frequency of the alternating current produced by the electrical generators in a modern nuclear power plant, and how many phases does this current have?
16. What are the two basic types of steam generators that are used in nuclear power plants today?
17. Name at least one type of reactor that does not require a steam generator.
18. Which reactor has a thicker pressure vessel—a BWR or an LMFBR?
19. What are the inlet and outlet temperatures from the steam generators in the primary loop of a PWR?
20. At what temperature does the steam leaving the secondary loop of these steam generators become completely saturated?
21. In a water steam mixture, what is the definition of the quality x?
22. What term is used to describe the sub-loops within the primary loop of a PWR?
23. Some steam generators are also designed to produce superheated steam. What does the term "superheated steam" refer to, and why is superheated steam preferable to saturated steam?
24. Why are liquid metal coolants used in fast reactors? Can you name at least three of these coolants?
25. Who did George Westinghouse originally buy the patents from that led to the rise of the Westinghouse Electric Corporation, which is now the largest supplier of nuclear power plants in the world today?
26. What are the inlet and outlet temperatures from the steam generators in the secondary loop of a PWR?
27. What is the steam-generating system in a nuclear power plant called?
28. What industrial country has the largest percentage of its electrical power generated by nuclear power plants today?
29. Who was the first person to show that alternating current has lower electrical transmission line losses than direct current?
30. What country has the most commercial nuclear reactors under construction today?
31. What is the fundamental difference between a coal-fired power plant and a nuclear power plant? Do you think coal-powered power plants produce higher energy steam or lower energy steam than nuclear power plants do?
32. What famous thermal cycle do most of the nuclear reactors in the world use today?
33. Which reactor of the following four reactor types has the highest core power density, and which reactor has the lowest: PWRs, BWRs, CANDU reactors, and LMFBRs?
34. What type of fuel does a commercial PWR use?
35. What reactor uses heavy water and natural uranium fuel?
36. What reactor has three separate coolant loops, and why does it have this many loops?
37. In the nuclear power business, what does the term NSSS refer to?
38. Who is the primary manufacturer of BWRs in the world?
39. What is the thermal efficiency of a typical PWR?
40. Approximately what percentage of the electric power in the United States is generated by nuclear power?
41. What is the shape of the control rods in a PWR, and what is the shape of the control rods in a BWR?
42. Which reactor has a higher thermal efficiency—a PWR, a BWR, or an LMFBR?
43. In the nuclear power business, what is the word SCRAM an abbreviation for?
44. Suppose that 1 g of uranium is completely converted into energy in a nuclear power plant. Assuming that the plant thermal cycle is 33% efficient, now how many kilowatt hours of electricity does this produce?

45. At the average cost of electricity in the world today, approximately how many dollars of electricity does this 1 g of burned uranium produce?
46. Assume that 1 kg of uranium ore costs $100, and that it contains 0.711% U-235. Assuming that all of the U-235 is ultimately recoverable, how many kilograms of natural uranium does it take to produce 1 g of U-235?
47. Using the information presented in Questions 44, 45, and 46, estimate the fuel cost per kilowatt hour for a typical nuclear power plant in the world today (excluding enrichment and fabrication costs).
48. What percentage of the commercial nuclear reactors in the world today are PWRs?
49. Where is the fuel "bred" in a fast breeder reactor? Name two of the most common breeding materials in a breeder reactor and the isotopes of uranium or plutonium that they breed.
50. What industrial country has the highest percentage of its electrical power generated by nuclear power plants?
51. What is the average thermal efficiency of a CANDU reactor?
52. Write a mathematical expression for the definition of the power density for a nuclear reactor core.
53. What are the four primary functions of a reactor control rod?
54. Approximately how many commercial nuclear power plants are there in operation in the world today?
55. Which has a higher average burnup—a fast reactor fuel assembly or a thermal reactor fuel assembly?
56. Nuclear power plants are a major competitor to coal-fired power plants in the world today. Is the energy content of the cooling water in the core of a nuclear reactor higher or lower than that in the boilers of a modern coal-fired power plant?
57. What is the typical outlet temperature of the water from a commercial PWR core, and what is the typical outlet temperature from the steam from one of its steam generators?
58. If you were put in charge of building a nuclear power plant today, what type of nuclear power plant would you build and why?
59. What is the minimum diameter and the maximum diameter of the fuel pellets that are used in most commercial nuclear power plants?
60. What is the single most important factor, except for the material composition, that determines the size of a nuclear fuel pellet?
61. Name three common materials that can be used for the cladding in a PWR or a BWR.
62. How thick is the cladding in a typical PWR fuel assembly?
63. What is the primary ceramic material that nuclear fuel pellets are made from today?
64. What is the concentration of U-235 in a fresh PWR fuel pellet?
65. How thick is the fuel-to-cladding gap in a commercial thermal water reactor fuel rod?
66. What is the name of the gas that is normally added to reactor fuel rods to increase their thermal conductivity and to improve the heat transfer coefficient across the fuel/cladding gap?
67. What does the "pitch" of a reactor lattice refer to?
68. How many fuel rods are there in modern fuel PWR assemblies?
69. How many fuel rods can be found in a modern BWR fuel assembly?
70. What fraction of the fuel assemblies in a PWR core normally contain control rods?
71. If you shut down a nuclear reactor to be refueled, and the fuel rods are still giving off a lot of radioactive decay heat, what is the one thing you do NOT want to do while the reactor is cooling down?
72. How many fuel assemblies can be found in the core of a large commercial BWR?
73. Name two common geometries that are used for reactor fuel assemblies.
74. What is the purpose of the steel shroud or "can" that surrounds a BWR or LMFBR fuel assembly?
75. How many fuel assemblies can be found in a large PWR core?
76. What fuel assembly geometry has the highest theoretical power density?
77. What is the purpose of introducing burnable poisons into a reactor fuel assembly?
78. Name three common burnable poisons.
79. What does the term uranium enrichment refer to?
80. What are the control rods in most reactors made from?
81. From which direction are the control rods normally inserted into the core of a PWR?
82. From which direction are the fuel rods normally inserted into the core of a BWR?
83. Using the numbers presented earlier in the chapter, how much thermal power would a typical PWR fuel assembly generate?
84. For the same volumetric power output, which type of fuel assembly has a smaller pitch—a square fuel assembly or a hexagonal one?
85. What is the shape of an American BWR control rod?
86. Using the numbers presented earlier in the chapter, how much thermal power does a typical BWR fuel assembly generate?

87. Which type of reactor has the highest volumetric heat generation rate?
88. What is the electrical power output of a commercial PWR with about 200 fuel assemblies?
89. How thick is the cladding that covers the fuel rods in a BWR?
90. What percentage of the overall length of a PWR fuel rod contains fissionable material (i.e., UO_2 or PuO_2)?
91. How long is a typical PWR fuel assembly in an American PWR?
92. What alloy of zirconium is used for the fuel rods in a BWR?
93. What percentage of the overall length of a PWR fuel rod does NOT contain fissionable material, and what is this additional region called?
94. What alloy of zirconium is used for the cladding in a PWR? What is the composition of this alloy?
95. Approximately what percentage of the fuel rods in a commercial PWR fail under normal operating conditions?
96. What is the shape of a standard PWR fuel rod?
97. In what units is the burnup of the fuel usually measured?
98. What is another term for the heavy water that is used as the moderator in a CANDU reactor?
99. Fill in the following sentence with the appropriate word or phrase: As a design rule for a LWR, the fuel-to-cladding gap should be approximately _____ of the thickness of the cladding. (Hint: you may want to refer to our companion book.)
100. What percentage of the core of a PWR consists of fuel or fuel rods by volume?
101. Does an LMFBR fuel assembly have a higher average burnup or a lower average burnup than a water reactor fuel assembly? Explain the reason why there is a difference.
102. Now consider three separate types of commercial power reactors—a PWR, a BWR, and a CANDU reactor. Which one of these reactors has the lowest average power density and which one has the highest? What factors do you think determine the power density for each design?
103. There are two different types of commercial PWRs—the Westinghouse and Areva PWR and the CANDU PHWR. What are the moderating materials that are used to produce thermal neutrons in each of these designs?
104. What is the average concentration of U-235 in a CANDU reactor fuel rod?
105. Approximately how many fuel rods are there in a large 1000 MWE PWR?
106. What type of material is normally used to surround the fuel rods in an LMFBR fuel assembly?
107. How is the power level in a BWR increased or decreased without having to move any of the control rods?
108. If the power to the reactor control system in a PWR is suddenly interrupted, a PWR can still be shutdown safely. Exactly how does a PWR effect a safe shutdown in this case?
109. Name three common materials that can be used for reactor control rods and two common materials that can be used for burnable poisons.
110. What is the U.S. NRC's definition of a reactor control rod?
111. When discussing the Canadian PHWR, what does the term CANDU stand for?
112. What is the advantage of adding a burnable poison to a reactor fuel assembly?
113. In addition to uranium-235, what other fissile materials can be used in reactor fuel rods?
114. What isotope of Boron absorbs the most neutrons in a reactor control rod?
115. How long can military reactors (in nuclear warships and submarines) be operated before they need to be refueled?
116. Where are the spent fuel assemblies that are removed from a reactor core initially stored?
117. If a 17 × 17 PWR fuel assembly contains control rods, approximately how many control rods does the fuel assembly contain?
118. What is the standard outage period for a commercial water reactor when it is time for the reactor to be refueled?
119. Name at least one type of western reactor that can be refueled while the reactor is still operating.
120. Approximately what percentage of the core of a thermal water reactor is composed of the structure and the coolant?
121. In what direction are the fuel assemblies positioned in a CANDU reactor?
122. Complete the following sentence with the appropriate word or phrase: In a high temperature gas reactor, the fuel consists primarily of small _____.
123. What is the ratio of the thickness of the cladding in a General Electric BWR to the thickness of the cladding in a Westinghouse PWR?
124. Why is the fuel-to-cladding gap about the same in a PWR as it is in a BWR?
125. Complete the following sentence with the appropriate word or phrase: The reactor accident at Fukushima, Japan, was an example of a loss of _____ event.
126. Name two places where a spent fuel pool can be found in a nuclear power plant.
127. During the 1970s, the average enrichment of the fuel in a PWR core was between 2.5% and 3.0%. What is the average enrichment of the fuel assemblies in a PWR today, and what is the maximum enrichment a fuel assembly can have?
128. What material does the Calandria in a CANDU reactor hold?

129. What two materials do the coolant pumps in a CANDU reactor pump?
130. If you wanted to build a military power reactor, what enrichment would you use for the fuel rods and why?
131. In what units is the power density of the fuel in a nuclear power plant usually measured?
132. In addition to their high melting point, the heat tiles that are used in the U.S. Space Shuttle and the uranium dioxide fuel pellets that are used in reactor fuel rods have one additional feature in common. Can you describe what this additional feature is?
133. Why are the sides of most fuel pellets usually chamfered or beveled before they are put into a fuel rod?
134. When uranium dioxide fuel is allowed to burn in a reactor core for a period of time, its structure changes and a central void may develop in some of the fuel pins. What is this change in density called, and as a result of it, is the fuel less dense or more dense than it was before?
135. What is the only reactor in the world that can run on natural uranium fuel?
136. What is the melting point of uranium dioxide (or UO_2) which is the most common type of material used for reactor fuel rods today?
137. What is the metal structure that surrounds the core of a PWR called?
138. Earlier in the chapter, we mentioned that uranium dioxide fuel pellets can undergo some structural changes when they are burned. What is the name of the hole in the middle of a uranium dioxide fuel pellet when this occurs?
139. What is the maximum recommended temperature that the uranium dioxide fuel in a PWR should be operated at during normal operating conditions?
140. What concept does an annular fuel rod use to achieve a higher volumetric power level than a solid fuel rod?
141. Suppose that reactor A is operated at a power level of PA and reactor B is operated at a reactor power level of PB. If PA is twice PB, and the two reactor cores are identical, how much more decay heat is released from the core of reactor A after time t than from reactor B?
142. What does the term AGR refer to?
143. Name a computer program that can be used to predict the burnup of PWR fuel assemblies over a long period of time.
144. What is the fuel rod pitch in a typical LMFBR?
145. In addition to its high melting point and its relatively low production cost, what is another advantage of using uranium dioxide in reactor fuel rods?
146. What is the "pressure vessel" that surrounds the core in a CANDU reactor called?
147. Name two common thermal cycles that most nuclear reactors use today.
148. When a nuclear utility decides to do its own nuclear fuel management, what person in the utility is generally responsible for ensuring that the maximum amount of energy can be extracted from each fuel assembly before it is removed from the core?
149. Why is it generally not a good idea to operate the uranium dioxide fuel pins in thermal water reactor above an average temperature of about 1200°C?
150. What is the "active" height of the fuel in a modern PWR core?
151. What process(es) for enriching natural uranium rely on the use of molecules of Uranium Hexafluoride gas?
152. In a Westinghouse PWR, what is the height of the fission gas plenum immediately above and below the fuel pins?
153. At what temperatures do Zircaloy-2 and Zircaloy-4 begin to melt?
154. What is the most common type of cladding used in BWRs today?
155. What two types of reactors have fuel pins that are approximately the same height and width?
156. If you were designing a light water reactor today that used stainless steel cladding, what is the highest temperature you would be able to operate the cladding at before it would begin to melt?
157. Name three popular ways of enriching natural uranium fuel.
158. In a typical nuclear fuel rod, what is the "width" of the fuel-to-cladding gap?
159. What is the typical thickness of the cladding in a commercial BWR today?
160. What is the name of the region immediately above and below the fuel pins in a light water reactor fuel rod? What is its function?
161. Name two reasons why Zirconium is used instead of Stainless steel in light water reactor fuel rods.
162. What is the melting point of the Zirconium metal from which reactor alloys such as Zircaloy-2 and Zircaloy-4 are made?
163. What is the percentage of Zirconium metal in Zircaloy-2 and Zircaloy-4?
164. Why is the cladding slightly thinner in a PWR than it is in a BWR?
165. What is the average volumetric power density in a modern PWR core?
166. What is the average thermal output of a typical PWR fuel assembly and what is the average thermal output of a typical BWR fuel assembly?

167. Fill in the following sentence with the appropriate word or phrase: _____ is used as a cladding material in PWRs and _____ is used as a cladding material in BWRs.
168. From a materials perspective, what is the primary difference between Zircaloy-2 and Zircaloy-4?
169. Who invented the modern steam turbine?
170. Kilowatt hour is equivalent to approximately how many megajoules of electric power?
171. If 1 kWh of electrical power costs approximately 12 cents, how much does it cost to operate a 1 kW air conditioner continuously for 1 week?
172. Relative to other forms of electric power generation, do you think that nuclear power is more expensive or less expensive than some of the alternatives?
173. What is the purpose of a fast breeder reactor?
174. Can a thermal water reactor also serve as a breeder reactor?
175. What is the purpose of a steam generator in a nuclear power plant?
176. What types of reactors do not have steam generators?
177. Do nuclear power plants generate alternating current or direct current?
178. Why is uranium dioxide used as a nuclear fuel?
179. When the fuel in a nuclear fuel rod consists of a combination of uranium dioxide and plutonium dioxide, what is it called?
180. Name three isotopes of uranium and two isotopes of plutonium that can be used as practical nuclear fuels.

Exercises for the Student

Exercise 1.1

A reactor core 3 m high and 5 m wide is cylindrical in shape. If its thermal power output is 3000 MW, what do you expect its electrical output to be? What type of reactor is this most likely to be, and what is the average core power density?

Exercise 1.2

Suppose that a research reactor core 1 m on a side has a thermal power output 100 MW. If the reactor core contains 16 fuel assemblies in the shape of a cube, what do you expect the average power output and the average power density of an individual fuel assembly to be?

Exercise 1.3

A plutonium-fueled fast breeder reactor has an electrical power output of 500 MW. If the core is cooled with liquid sodium, what does the total volume of the core have to be, and what is its thermal power output?

Exercise 1.4

A thermal water reactor is cooled with light water where the coolant enters the core with an average energy content or enthalpy of 1.3 megajoules (MJ) per kilogram and exits the core with an average energy content or enthalpy of 1.5 MJ per kilogram. If the reactor is a PWR with an electrical power output of 1000 MWE, what must the average flow rate through the core be to remove the heat generated by the nuclear chain reaction?

Exercise 1.5

A well-designed thermal water reactor can produce retail electrical power at a cost to the consumer of between 8 and 12 cents per kWh. Using the average of these values, calculate the amount of revenue that a 1000 MWE nuclear power plant can produce by operating at full power for a single calendar day. How much revenue is lost when it must be shut down for refueling every 18 months? Assume that the average down time in this case is 30 calendar days.

Exercise 1.6

A CANDU reactor with a thermal efficiency of 29% is being compared to a Westinghouse PWR with a thermal efficiency of 34%. If the fuel cost for the CANDU reactor is 10% less than the cost of the fuel for the Westinghouse PWR (because the fuel for the CANDU reactor does not have to be enriched), which power plant will generate electricity more cheaply if the capital cost for the two power plants is exactly the same? Assume that the capacity factor for both power plants is the same as well.

Exercise 1.7

Reactor A operates at a capacity factor of 87% and reactor B operates at a capacity factor of 92%. If reactors A and B have exactly the same fuel cycle cost, and the thermal efficiency of reactor A is 32% while the thermal efficiency of reactor B is 34%, which reactor generates nuclear power more cheaply? If the cost of the electric power being produced by reactor A is 10 cents per kWh, what is the cost of the electric power being produced by reactor B?

Exercise 1.8

Earlier in the chapter, we learned that the core exit temperature of an LMFBR is considerably higher than it is for a PWR. Using representative values for these two numbers, and assuming that the heat in both cases is rejected from the condenser at an average temperature of 150°C, how do the maximum theoretical thermal efficiencies of these two reactors compare?

Exercise 1.9

Suppose that the wall thickness of a reactor pressure vessel increases as the square root of the maximum system pressure. Using this fact alone, estimate the ratio of the thickness of the pressure vessel in a PWR to the thickness of a pressure vessel in a BWR. Assume that the reactor pressure vessels are made out of the same material in each case.

Exercise 1.10

A wise man comes to you and claims that it is possible to design a new type of reactor that converts half of all the heat that is produced in the core into electric power. Is this a realistic claim to make in light of what you have learned so far in this chapter? If so, what type of reactor would this be most likely to be? What type of reactor thermal cycle would it use?

Exercise 1.11

Suppose that you are asked to reduce the power density in a reactor core by a factor of two. If the flow rate remains the same, and ordinary water is used to cool the core, approximately how much can the system pressure be reduced in the primary coolant loop before the water begins to boil? Assume that the initial pressure in the primary loop is 2000 PSI.

Exercise 1.12

Suppose that two reactors have fuel rods that are exactly 1 cm in diameter. Reactor A has a square lattice with a pitch of 12 cm and Reactor B has a square lattice with a pitch of 15 cm. If the enrichment of the fuel rods is exactly the same, what is the ratio of the power density of the core in Reactor A to the power density of the core in Reactor B?

Exercise 1.13

A small commercial PWR contains 49 fuel assemblies arranged in a 7×7 square. How much uranium is used in this reactor, and what do you expect its thermal output and its electrical output to be?

Exercise 1.14

A BWR core is made up of 200 fuel assemblies. What do you expect its thermal power output and its electrical power output to be? If it is refueled every 2 years, and one-quarter of the core is replaced at that time, how much new uranium will be required for the core reload?

Exercise 1.15

Using the data presented earlier in the chapter, calculate the weight of the fuel pellets in a BWR, PWR, CANDU, AGR, and LMFBR fuel rod. You may assume that the density of uranium dioxide in these fuel pellets is 10 gm/cm^3.

Exercise 1.16

Suppose that a PWR fuel assembly contains 200 fuel rods. Using the data presented earlier in the chapter, calculate how much pure uranium is required to create a PWR fuel assembly if the uranium dioxide (UO_2) used in the fuel rods is approximately 88% uranium by weight.

Exercise 1.17

Earlier in the chapter, we discussed several types of commercial power reactors and the average enrichment of the fuel assemblies in their cores. They included the CANDU PHWR, the BWR, the LMFBR, and the PWR. Please rank each of these reactors—based on their typical operating parameters, from those having the highest average enrichment to those having the lowest average enrichment. Why is the CANDU reactor the only reactor that can run on natural uranium?

Exercise 1.18

In practice, the volume of the fuel in an hexagonal fuel assembly is approximately 16% greater than the volume of the fuel in a square fuel assembly that has the same diameter fuel rods D and the same rod pitch P. Prove this assertion by comparing the volumes of the fuel and the moderator in a square and hexagonal reactor lattice. You may ignore the presence of the cladding and the fuel-to-cladding gap for the purpose of this comparison.

2

Neutrons and Other Important Particles of Reactor Physics

2.1 Reactor Physics and the Study of the Neutron

Reactor physics is the study of the neutron and its behavior. Reactor physics can be used to study how neutrons and gamma rays scatter off of atomic nuclei and how they lose kinetic energy in the process. The behavior of a large number of neutrons can be described by what is known as the *neutron diffusion equation*, and when the angular flow of neutrons becomes anisotropic, by what is known as the *neutron transport equation*. A subfield of reactor physics that deals with the energy loss of neutrons (and therefore their transition from high energies to low energies) is called *neutron slowing down theory*. Slowing down theory is introduced to the reader in Chapter 8 of this book, and it is also discussed in our companion book, where neutron moderators and reactor coolants are presented to the reader for the first time.*

As an alternative to neutron diffusion theory and neutron transport theory, the behavior of individual neutrons can be described by a statistically based approach called the *Monte Carlo method*, which was originally developed from the study of *game theory*. The Monte Carlo method attempts to simulate the lives of millions of individual neutrons with a computer program, and from the results of these simulations or *case histories*, the aggregate behavior of the particle population can be inferred. If the results of these simulations are averaged over millions of individual particles, then the predictions of the Monte Carlo method converge to those of diffusion theory and transport theory. Finally, each of these methods is appropriate to use under certain conditions, and in some cases, all three methods can be used interchangeably. The merits and drawbacks of each method are compared and contrasted in Figure 2.1. Note that except for very simple geometric shapes such as spheres, rectangles, and cylinders, each of these methods requires a computer program to obtain meaningful results. Finally, transport theory and the Monte Carlo method can be used to perform *radiation shielding* and *radiation streaming* calculations as well as simpler calculations involving particle transport in spatially homogeneous materials. In geometries where the material composition becomes spatially dependent or where strong particle sources and sinks appear, the flow of neutrons and photons can become highly directional or *anisotropic* and diffusion theory can no longer be used with confidence. When this occurs, transport theory and the Monte Carlo method must be used to describe the particle flow. However, they are harder to implement and require a higher level of programming expertise than neutron diffusion theory does. Consequently, most practical problems involving real reactors are solved numerically rather than analytically. Numerical methods for doing this are discussed in great detail in Volume II of this book, where reactor dynamics and nuclear particle transport are also explored.†

2.1.1 Nuclear Particles and Particle Types

In the nuclear world, neutrons can be thought of as electrically neutral particles whose behavior can be described by the laws of classical mechanics. In other words, their behavior is determined by the laws of energy and momentum conservation. Neutrons have a diameter of about 1×10^{-14} cm, which is about a million-billion times smaller than a chicken egg. In other words, they are very small and heavy nuclear particles. From a practical perspective, the interactions of neutrons with other nuclear particles have many similarities to the collisions of objects such as *billiard balls* on a pool table (see Chapter 3). These collisions can be either *elastic* or *inelastic* in nature. *Neutron slowing down theory is usually based on the premise that these collisions are elastic collisions in which energy is conserved. Hence, slowing down theory rarely concerns itself with inelastic collisions such as those that involve the process of compound nucleus formation*. More information on compound nucleus formation can be found in Chapters 4 and 7 of this book and also in other chapters of our companion book.*

* See *Nuclear Engineering Fundamentals: A Practical Perspective* by R.E. Masterson, CRC Press (2017).

† See *Contemporary Nuclear Reactor Physics with an Introduction to Reactor Dynamics, Computational Methods, and Nuclear Particle Transport* by R.E. Masterson, CRC Press (2020).

Diffusion theory	Transport theory	Monte Carlo method
Normally applied to just neutrons	Can be used for either neutrons or photons	Can be applied to almost any nuclear particle
Relatively simple to use for homogeneous materials	Can be complicated to use even for homogeneous materials	Straightforward to use but requires a lot of computer time
Requires the neutron flux to be isotropic	Should be used when the neutron flux becomes angularly anisotropic	Can be used to model both isotropic and anisotropic particle flows
Can be derived from neutron transport theory	Can be used for radiation streaming calculations	Can be used for any geometric shape and is commonly used to design radiation shields

FIGURE 2.1 A comparison of neutron diffusion theory, neutron transport theory, and the Monte Carlo method.

Neutrons are part of a larger family of atomic particles called *Baryons* also include protons and more fundamental nuclear particles called *quarks*. *Hadrons* are also a subset of this particle family, and the term "Hadron" is sometimes used to refer to both protons and neutrons. The relationship between these elementary particles is depicted in Figure 2.2. The neutron population in a reactor core can stay the same, or it can change as a function of time. Time-independent neutron populations are described by what is known as the *steady-state neutron diffusion equation*, and time-dependent neutron populations are described by what is known as the *time-dependent neutron diffusion equation*. Both of these equations can be used to predict the neutron population in operational nuclear reactors. However, the approach they use to do so is slightly different.

Neutrons and protons are the building blocks of the material world. Thus they are referred to as *matter particles* because they are used to create the matter from which our industrial civilization is built. Each neutron and proton is held together by *force particles* that are constructed from more elementary particles called *quarks*. (Quarks are discussed extensively in our companion book.) Hydrogen, which is the lightest element, contains one proton surrounded by one electron. Uranium, which

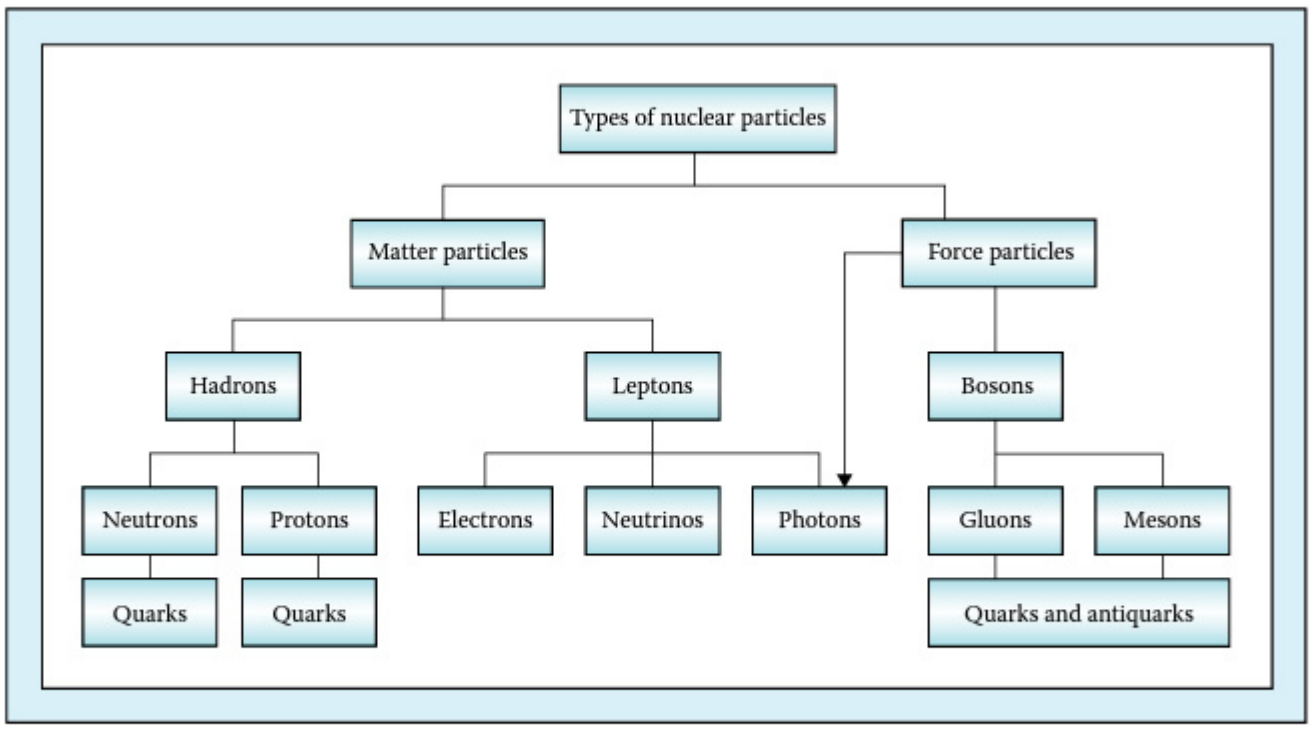

FIGURE 2.2 The primary nuclear particles from which atoms and other nuclear particles are formed.

is the heaviest naturally occurring element, contains 92 protons and between 141 and 146 neutrons. The protons and neutrons in the nucleus are then held together by force particles called *gluons*, which in turn consist of quark and antiquark pairs. Under normal conditions, neutrons and protons are bound together to form a small and extremely dense structure called the *atomic nucleus*. The atomic nucleus can contain different numbers of neutrons and protons, and this is what makes one element fundamentally different from another. An atom that contains different numbers of protons is called an *element*, and an atom that contains the same number of protons but different numbers of neutrons is called an *isotope* of that element. There are 92 naturally occurring elements and about 20 man-made ones. These elements are then used to construct the *Periodic Table*, which is discussed in Chapter 9 of our companion book.* About 3000 individual isotopes can be constructed from these natural and man-made elements. For reasons that we will subsequently discuss, heavier elements tend to be less stable and more radioactive than lighter ones. This radioactivity can be attributed to the *weak force* of nuclear structure. Hence, the weak force tends to destabilize the atomic nucleus, while the strong nuclear force (which is carried by the gluons) tends to hold it together.

The atomic nucleus is then surrounded by swarms of *electrons* that revolve around it in many different paths. Like the planets in our solar system and the comets and meteors within it, some of the electrons have elliptical orbits, while others may have circular ones. Still others have orbits resembling the shape of ellipsoids and barbells. In general, the more kinetic energy an electron has, the more eccentric its orbit will be. In an electrically neutral atom, the number of protons and electrons is always the same. The electrons swarm around the nucleus at about 10% of the speed of light in a structure that has become known as the *electron cloud*. The paths these electrons follow are *probability distributions* that are sometimes referred to as *orbitals*. Hence, an orbital is a graphical representation of the probability that an electron will be in a certain place in space at a particular time. The sum of all its possible locations then defines the shape of the orbital, and its most probable location is defined by where the orbital has the highest overall probability density. Pictures of atomic orbitals can be found in many physics and chemistry books. When a nuclear orientation is required, the reader is referred to our companion book* to see what some of these orbitals look like.

Protons and neutrons inside the nucleus also follow a preferred set of paths or orbitals, although the forces that hold them together are considerably more complicated than those that control the electrons. *The nucleus of an atom is held together by force particles called gluons*. A gluon has a diameter of about 1×10^{-16} cm. A typical atomic nucleus has a diameter of about 10^{-12} cm, and the surrounding electron cloud has a diameter of between 0.25×10^{-8} and 1.6×10^{-8} cm. Hence, there are about eight orders of magnitude difference between the size of the electron cloud and the size of a gluon. Hydrogen, which is the lightest element, has the smallest electron cloud, while heavier elements like cesium (Cs) and uranium (U) have the largest. The size of the electron cloud is determined primarily by the orbital paths the electrons follow within the cloud. Heavy atoms have six or seven different types of orbitals, while lighter atoms (such as hydrogen) have only one. Several pictures of the atom and the nucleus are shown in Figure 2.3. The simplest orbitals are essentially *spherical* in shape.

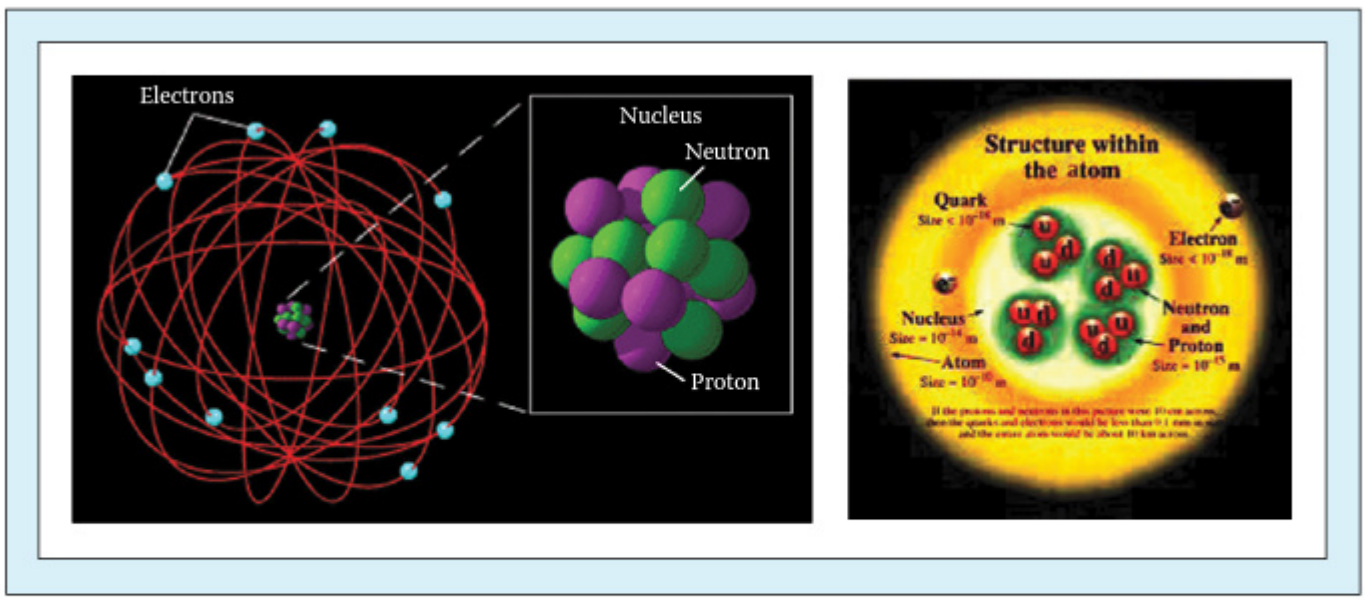

FIGURE 2.3 A picture of the nucleus of a simple atom. (Courtesy of Google Images.)

* See *Nuclear Engineering Fundamentals: A Practical Perspective*, by R.E. Masterson, CRC Press (2017).

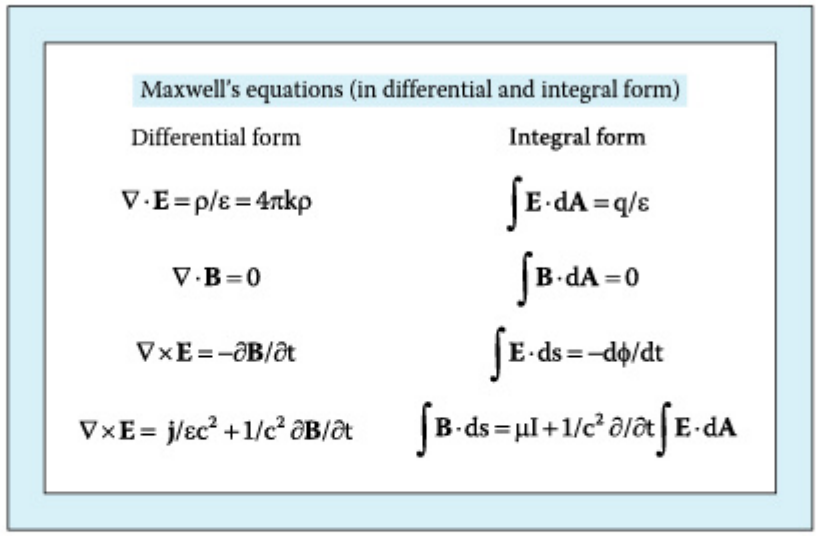
Maxwell's equations (in differential and integral form)
Differential form
Integral form
$\nabla \cdot \mathbf{E} = \rho/\varepsilon = 4\pi k\rho$
$\int \mathbf{E} \cdot d\mathbf{A} = q/\varepsilon$
$\nabla \cdot \mathbf{B} = 0$
$\int \mathbf{B} \cdot d\mathbf{A} = 0$
$\nabla \times \mathbf{E} = -\partial \mathbf{B}/\partial t$
$\int \mathbf{E} \cdot ds = -d\phi/dt$
$\nabla \times \mathbf{E} = j/\varepsilon c^2 + 1/c^2\, \partial \mathbf{B}/\partial t$
$\int \mathbf{B} \cdot ds = \mu I + 1/c^2\, \partial/\partial t \int \mathbf{E} \cdot d\mathbf{A}$

FIGURE 2.4 Maxwell's equations of electricity and magnetism, written in both differential and integral forms.

2.2 Visualizing the Atomic Nucleus

At the heart of an atom is a small and a very dense structure called the *atomic nucleus*. The nucleus has a diameter of about 1×10^{-12} cm, and almost 99.999% of the mass of an atom (in the form of protons and neutrons) is contained within it. Protons and neutrons are relatively heavy matter particles that have a unique set of physical properties including mass, charge, and spin. They are the *building blocks* from which the material universe is made. Sometimes this matter is also called *Baryonic matter*. All elements in the universe have an atomic nucleus that contains at least one proton and one or more neutrons. (The sole exception to this rule is the element hydrogen, which, in its basic form, has no neutrons at all.) Hydrogen is the lightest element in the Periodic Table (see Chapter 6), and the heaviest naturally occurring element is uranium. Natural uranium can have up to 146 neutrons in its nucleus (to create U-238), but when isotopic stability is taken into account, it cannot have any more.

In order to understand how a nuclear power plant works, it is necessary to understand the types of particles that allow a nuclear chain reaction to occur. It is also important to understand the types of radiation that are produced by these particles, as well as the ways in which this radiation can interact with matter. There are many different types of nuclear particles, and each of them interacts with matter in an entirely different way. Moreover, no two types of nuclear particles behave in exactly the same way, and particles with an electrical charge (like the electron and the proton) behave differently than those that do not (such as the neutron, the photon, and the neutrino). Particles with an electric charge interact with other charged particles over very long distances (by nuclear standards), and their behavior as a whole is described by *Maxwell's equations* of electricity and magnetism, which are shown in Figure 2.4. Normally, these equations, their implications, and their solutions are discussed in a college physics class. Maxwell's equations can be written in either integral or differential form.

Particles that do not possess an electric charge interact over much shorter distances (with the exception of a photon or a light wave) and in aggregate; their behavior is governed by Newton's Laws of Motion. Finally, when one reaches the size of the atom or the nucleus, *quantum mechanical effects* begin to come into play. The combination of these effects (plus charge, mass and momentum, and quantum mechanics) then determines the way in which a particular nuclear particle behaves. In this chapter, we would like to discuss the types of particles that are important to the behavior of a nuclear power plant as a whole. This will lead us to a detailed discussion of the neutron and its properties. *When it comes to building or operating a nuclear power plant, the neutron is by far the most important nuclear particle to understand.* Other less important particles that must be considered to understand the process of radioactive decay and the overall energy generation rate in the core are *the proton, the electron, the photon, and the neutrino*. However, these particles obey some additional physical laws that determine what types of nuclear reactions are possible and what types of reactions are not.

Example Problem 2.1

Suppose that a Uranium-238 atom has 92 protons in its nucleus. How many electrons must it have in its electron cloud to be electrically neutral?

Solution For an atom to be electrically neutral, and not an ion, it must have the same number of electrons as the number of protons. In the case of Uranium, this means that it must have 92 electrons orbiting the atomic nucleus. [Ans].

2.3 Basic Laws of the Nuclear World: The Conservation of Mass/Energy, Momentum, and Charge

In addition to Newton's Laws of Motion, the Laws of Electromagnetism, and Einstein's formulation of Special and General Relativity, there are three other conservation laws that all particles in a nuclear reactor must obey:

1. *The Conservation of Mass and Energy*
2. *The Conservation of Momentum*
3. *The Conservation of Charge*

Some knowledge of these conservation laws, plus an understanding of basic quantum mechanics and wave motion, is sufficient to understand how a nuclear reactor works. The meaning of these conservation laws should be clear to anyone who has taken an elementary class in college chemistry or physics. *These laws simply state that whatever the mass, energy, momentum, and charge of an object (or a system of objects) is at the beginning of a reaction, the mass, energy, momentum, and charge must be the same at the end of the reaction, no matter how many material objects or particles are involved*. These laws place some constraints on the types of particles that can come out of a nuclear reaction if we know the mass, energy, momentum, and charge of the particles that go into the reaction. So in short, these are the "rules" that reactor physicists use to decide what types of nuclear reactions are possible and what types of nuclear reactions are not. The *spin* of a nuclear particle also determines what types of particle interactions are possible. In general, the spin is also a conserved nuclear property.

2.4 Units for Measuring Nuclear Mass

In the early days of the nuclear power business, there was no commonly accepted unit to measure the mass of the nuclear particles that were known to exist at the time (which included the electron, the neutron, and the proton). The *Atomic Mass Unit*, or *AMU*, was designed to solve this problem. By convention, *one AMU is defined as exactly 1/12th of the rest mass of one electrically neutral atom of the isotope Carbon-12.*

The Definition of the AMU

1 AMU is defined as exactly 1/12th of the rest mass of one electrically neutral atom of the isotope Carbon-12.

Since Carbon-12 has exactly six protons and six neutrons, one AMU is exactly equal to the average atomic weight of one proton and one neutron, plus the small extra mass of half an electron. This also means that the proton has an atomic mass slightly less than the neutron. In the SI unit system, the atomic mass unit is sometimes given the symbol "u." In these units of measurement, the difference between the rest mass of a neutron and a proton shows up in the third decimal place, for example, *Proton = 1.0073 AMU* and *Neutron = 1.0087 AMU*, respectively. Table 2.1 lists the rest masses of all three particles in more modern units, or electron volts (eV)/c^2. An electron volt is the kinetic energy required to move an electron through a potential difference of one volt. One MeV is then equal to one million electron volts, or 1×10^6 eV. *Appendix A* lists the values of all of the physical constants that we will use for this purpose.

Compared to the proton or the neutron, *the electron is a much lighter particle (about 2000 times lighter)* that circles the atomic nucleus in complex electronic orbits called *orbitals or shells*. It is responsible for the chemical bonds that bond atoms together, and it is found in nature in great abundance. *It is responsible for the chemical reactions that we experience in everyday life*. Electrons have a negative charge of −1 and they can also be released by the decay of a neutron (which has no charge) into an electron and a proton. The proton, of course, has a positive change of +1. Electrons, like protons and neutrons, are matter particles because they have real mass (about 5.486×10^{-4} AMU), even when they are at rest. The rest masses, the charges, and the spins of the electron, the neutron, and the proton are shown in Table 2.1. In more conventional units, the relationship between 1 AMU and a gram is

TABLE 2.1
Atomic Properties of the Proton, the Neutron, and the Electron

Particle	Type	Mass (kg)	Mass (AMU)	Mass (MeV/c^2)	Spin	Charge
Proton	Baryon	1.672623×10^{-27}	1.0073	938.28	½	+1
Neutron	Baryon	1.674929×10^{-27}	1.0087	939.57	½	0
Electron	Lepton	9.109390×10^{-31}	0.0005	0.511	½	−1

Source: Courtesy of Wikipedia—see *https://en.wikipedia.org/wiki/Neutron*, *https://en.wikipedia.org/wiki/Electron*, and *https://en.wikipedia.org/wiki/Proton*.

The Value of the AMU

$$1 \text{ AMU} = 1.6605402 \times 10^{-24} \text{ g} = 931.494 \text{ MeV/c}^2 \quad (2.1)$$

Notice that we could also have obtained the same result using Einstein's equation $E = m_o c^2$ to convert the energy of a particle into its rest mass:

Einstein's Famous Equation

$$E = m_o c^2 \quad (2.2)$$

Sometimes reactor physicists use Einstein's equation to express the rest mass of the neutron, the proton, and the electron in units of MeV/c², since this is the most natural way to measure the rest masses when Einstein's equation (Equation 2.2) is used. In this "natural" unit system, *1 AMU = 931.494 MeV/c²* or $1.6605389 \times 10^{-24}$ g, and the rest masses of the proton, the neutron, and the electron are given by

Proton, Neutron, and Electron Rest Masses in AMU, MeV/c², and grams

$$\text{Proton:} \quad 1.00728 \text{ AMU} = 938.28 \text{ MeV/c}^2 = 1.6726485 \times 10^{-24} \text{ g} \quad (2.3)$$

$$\text{Neutron:} \quad 1.00866 \text{ AMU} = 939.57 \text{ MeV/c}^2 = 1.6749544 \times 10^{-24} \text{ g} \quad (2.4)$$

$$\text{Electron:} \quad 0.000549 \text{ AMU} = 0.5110034 \text{ MeV/c}^2 = 9.109534 \times 10^{-28} \text{ g} \quad (2.5)$$

In later chapters, we will find that Equations 2.3, 2.4, and 2.5 can be extremely useful when it comes to calculating the amount of energy E that the fission of a uranium or plutonium nucleus can release. The utility of this concept is illustrated in some of the exercises at the end of the chapter. Because the masses of most nuclear particles are so small, masses in the nuclear world are rarely expressed in kilograms. Instead, grams or AMUs are the preferred way in which they are measured and used. The quarks that determine the masses of the proton and the neutron in Equations 2.3 and 2.4 are shown in Figure 2.5. Notice that the neutron consists of two *down quarks* and an up quark and the proton consists of two *up quarks* and

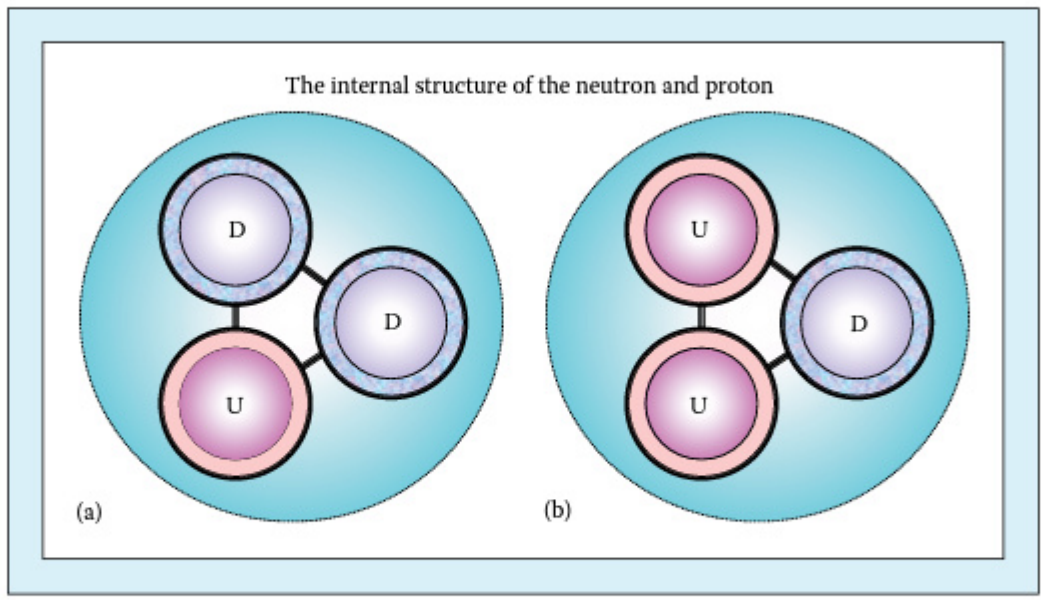

FIGURE 2.5 A graphic model of the internal structure of the neutron (a) and the proton (b). Although they appear to be immutable particles at the atomic level, in reality they consist of more fundamental particles called quarks. The symbol U refers to an "up" quark and the symbol D refers to a "down" quark. The neutron consists of two down quarks and an up quark, and the proton consists of two up quarks and a down quark (b).

a down quark. Since the down quarks are slightly heavier than the up quarks, the neutron is slightly heavier than the proton. In fact, the mass difference between the neutron and the proton is approximately equal to twice the mass of the electron.

Example Problem 2.2

What is the ratio of the mass of the electron to that of the proton?

Solution From Table 2.1, the mass of the electron is 0.0005 AMU and the mass of the proton is 1.0073 AMU. Their ratio is 1/1839. [Ans.]

2.5 Protons and Neutrons: The Building Blocks of the Atomic Nucleus

Another element that is frequently encountered in the study of nuclear science and engineering is the element *Plutonium*. Plutonium is heavier than Uranium, and it does not exist naturally because it tends to decay too quickly to be present in measureable quantities in nature. However, Plutonium is produced in nuclear reactors in significant amounts, and in some reactors, about 1/3rd of the power is generated from it. The amount of an element that appears in nature is called its *natural abundance*. The most common isotopes (or varieties) of Plutonium are Pu-238, Pu-239, Pu-240, and Pu-241. Pu-238 is used as a power source in *interplanetary space probes*. *The number of protons inside a nucleus defines an element, and the number of neutrons inside the same nucleus defines an isotope of that element*. Because of this, Uranium has 92 protons in the nucleus, and Plutonium has 94. The number of protons and neutrons then determines the isotope of a particular element (i.e., U-238, Pu-239, or Pu-241). Isotopes are discussed in more detail in Chapter 6.

Protons and neutrons are small nuclear particles that are about 10,000 times smaller than the nucleus itself—or approximately 10^{-14} cm in diameter. Hence we are talking about very, very small particles of matter with a very high density here. The primary difference between a neutron and a proton (except for a small difference in their rest masses) is that *a neutron is electrically "neutral"* (i.e., it has a charge of 0), whereas a proton is not electrically neutral, and it has a positive charge of +1. Neutrons are also slightly more massive than protons, and so they can be thought of as having an atomic weight approximately equal to the weight of a proton and an electron combined (plus a small amount of binding energy that keeps the two of them together). Neutrons have the interesting property that they can only exist outside the nucleus for about *15 minutes* before they decay into a proton, an electron, and occasionally some photons. On a nuclear time frame, where most events happen in a billionth of a second, this turns out to be a very long period of time. Their counterparts—the protons—are far more stable, and they are believed to have a half-life of at least 50 billion years. As a matter of fact, no one has ever seen a proton decay (although it has been hypothesized to occur for some time). They can exist outside of the nucleus, and they can exist in this state essentially forever without decaying into something else. In some models of nuclear field theory, they simply live forever—although exactly how long "forever" is still a subject of some debate. And even when they are outside the nucleus, their half-lives are much greater than the current *age of the universe* (which is about 14.4 billion years).

Because protons have a positive electrical charge, they respond to electric and magnetic forces in much the same way that electrons do. (However, in this case, the directions of their reactions are reversed.) Hence, we can easily manipulate them, focus them into beams, and send them wherever we want. Their electrical charge allows us to create "*atom smashers*" and the *nuclear accelerators* that are used to probe the internal structure of the nucleus. (This is why protons and electrons can be used to treat certain types of cancers by focusing them into narrow and highly directed beams.) As a matter of fact, some parts of the nuclear engineering field today have branched out into the area of *nuclear medicine* as the healthcare business has continued to expand, and the population has continued to age. *Neutrons* are responsible for most of the reactions that occur in a fission reactor and are therefore the basis of the nuclear power industry as a whole. They have no electrical charge, and because of this, we cannot direct them, change their direction, or focus them into a specific area of space with electric and magnetic fields. (In fact, the word "neutron" was invented to describe the fact that the neutron is an *electrically neutral* particle.) Because of this lack of electric charge, they obey a *diffusion equation* similar to the diffusion equation that describes the motion of the particles of a diffuse gas. However, they are amenable to some level of control because they can be absorbed by, or reemitted by, the nuclei of other atoms through which they must pass.

Some relatively common elements like Boron and Cadmium, which we will study in more detail in future chapters, also have the ability to absorb free neutrons in the event that we generate too many of them. Hence, these elements can be used to create the *control rods* in a nuclear reactor core—which are used to control the power output of the reactor and the scope of the nuclear chain reaction. Even if the neutrons are moving very quickly (at a speed of several thousand meters per second), an element like *Boron* or *Cadmium* can "reach out" and capture one of these neutrons if they get too close to the nucleus. Other isotopes of the elements such as *Xenon* and *Samarium* are even more adept at capturing free neutrons that happen to come in contact with them. We will discuss exactly how they do this in Chapter 4. Neutrons are members of a family of very heavy nuclear particles called *Hadrons*. The probability that they will be absorbed by an

atomic nucleus depends in part on the speed at which they are moving. *Fast neutrons*, which can move at speeds between 10,000 and 20,000 km/s, have a very low probability of being absorbed because they are simply not around the nucleus long enough for the nucleus to reach out and "grab" them. *Slow neutrons*, on the other hand, are much easier to absorb because they move much more slowly (between speeds of 2 and 3 km/s). Because they move so slowly, they are much easier, figuratively, for a nucleus to reach out and "grab them." Hence, they are much easier to absorb.

We can use this property of the neutron to control the number of neutrons that are available at any one time to participate in a nuclear chain reaction. Hence, the speed at which a neutron travels (or its kinetic energy) is one of the principal properties that can be used to control the size and speed of a nuclear chain reaction. This behavior allows us to design a nuclear power plant in which a chain reaction can be controlled. We will have more to say about this process in Chapter 7. In nuclear physics, the probability that a nuclear particle interacts with another nuclear particle is called its "*nuclear cross section*." For historical reasons, the probability of absorption or emission is measured in the units of "*barns*." Hence, nuclear cross sections are also measured in "barns." Figure 2.6 shows some nuclear interaction cross sections as a function of the kinetic energy (and therefore the speed) of a neutron for both fast and slow neutrons in the vicinity of the nucleus of a boron atom. *In general, slow-moving neutrons are approximately 100 times more likely to be absorbed than very fast-moving neutrons. Nuclear reaction probabilities* were historically measured in the units of barns because people believed that getting two protons or neutrons to interact together was like trying to hit "the broad side of a barn." This terminology became popular in the 1940s, and it has continued to exist until the current day. From a reactor designer's point of view, the control of neutrons, including their creation, reabsorption, and reemission from the nuclei of a few very specific elements, is one of the most important parameters in building an operational nuclear reactor.

Before we discuss how neutrons can be manipulated (by changing their speed), we would first like to mention that *protons and neutrons are not fundamental particles—at least as far as the universe itself is concerned*. By this we mean

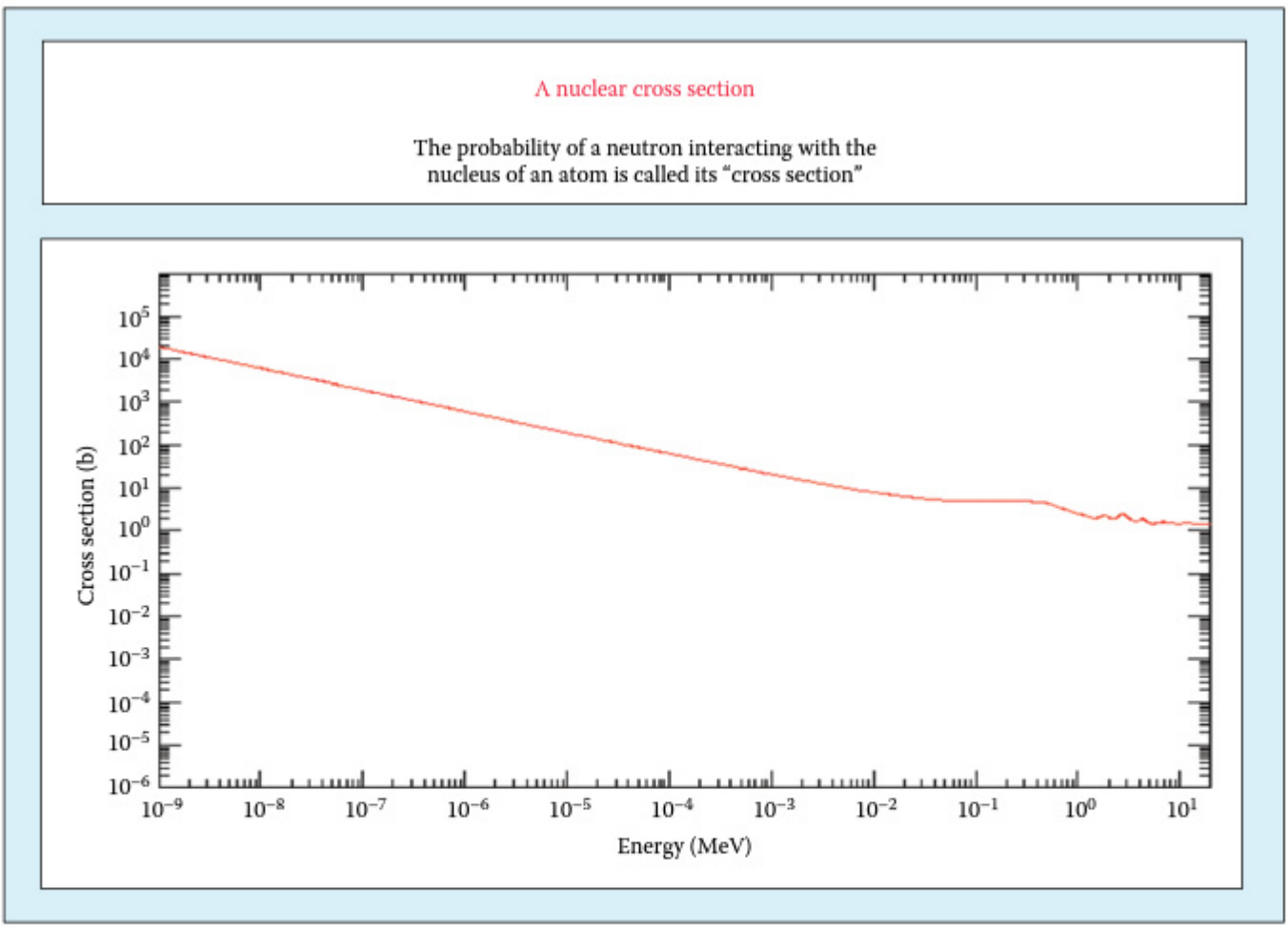

FIGURE 2.6 The probability of a fast- and slow-moving neutron being scattered or absorbed by a Boron-10 atom (in barns) as a function of the neutron's speed (or kinetic energy E). Notice that the slower the neutron moves past the boron atom, the higher the probability is that it will be scattered or absorbed. The reaction probabilities here are measured in barns. (Picture generated by ENDFPLOT.)

that they are made out of still more fundamental particles called *quarks*. The quarks, and the particles that hold them together called *gluons* (for the nuclear "glue"), are the true fundamental particles from which the universe is built, and these are the particles that determine how a nuclear power plant behaves. Unfortunately, quarks are not discussed in most nuclear science and engineering books, and so one is left to conclude that the neutrons are all that matter. However, this is not necessarily true if one looks into things at a much deeper level. This is particularly true when one explores the process of *radioactive decay*. The process of *radioactivity* is discussed in more detail in Chapter 6.

2.6 Gluon and the Nuclear Force Field

For a long time, nuclear scientists and engineers wondered why the nucleus of the atom did not fly apart or disintegrate when there was more than one electrically charged proton inside of it. After all, each proton was known to possess a positive charge of +1, so when two or more identical protons were put together, they should repel each other, and the nucleus of each element (beyond hydrogen—which has only one proton) should theoretically become unstable and subsequently disintegrate. However, when all the elements in the universe were analyzed individually and arranged in the periodic table (which we will discuss in Chapter 6), this did not turn out to be the case. Indeed, some scientists concluded that some other type of force had to be present to hold the nucleus of every atom together in spite of the attempts of *electromagnetic force* (remember that it follows the inverse square law $F = k*q_1*q_2/(r_1 - r_2)^2$—which is quite strong at these distances)—to rip it apart. Then in the early 1930s, a Japanese physicist by the name of *Hideki Yukawa* (who later won the Nobel Prize in Physics for his theory of the nuclear force) proposed that there must be a stronger nuclear force, of an extremely short range (with an effective range of about 10^{-15} cm), that overwhelmed the repulsive forces between the protons and provided the "glue" to hold the nucleus together (Figure 2.7). This force eventually became known as the *strong nuclear force*. The nuclear force F on a proton or a neutron could be found by taking the derivative of a potential function, U, which Yukawa proposed to have the following form:

$$U_Y(r) = \frac{-g^2 e^{-ymr}}{r} \tag{2.6}$$

where

y was an empirical constant, called the *Yukawa constant*, which was determined experimentally
r was the distance from the center of the nucleus

Here g is a *scaling constant*, m is the mass of the affected particle, and r is the radial distance to the particle. This potential eventually became known as the *Yukawa potential*. When Murray Gell-Mann, George Zweig, and others from Cal Tech first proposed the existence of quarks in the 1960s, they independently came to the conclusion that another set of quarks (consisting of a quark and an antiquark pair) must come together inside the nucleus to create a special kind of particle

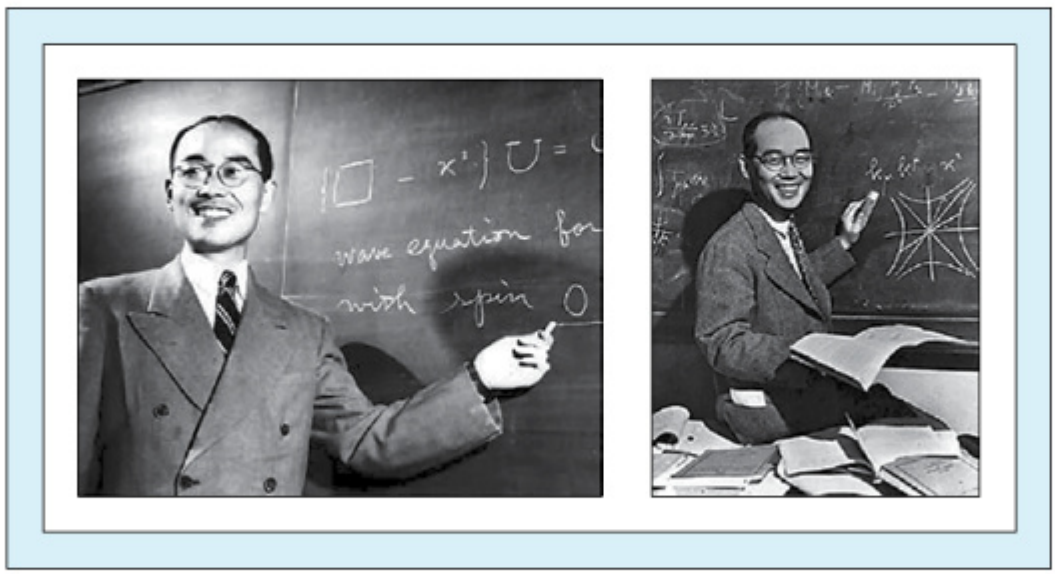

FIGURE 2.7 Two pictures of Hideki Yukawa who invented the Yukawa potential to describe the range of the nuclear force field. (Pictures provided by Wikipedia.)

called the *gluon*. The purpose of the gluon was to hold the protons and neutrons together, even when they were confined to the limited space inside of the nucleus itself (about 10^{-36} cm^3). *The gluon was subsequently found to also hold the nucleus of the atom together, in addition to providing the internal "glue" of the neutrons and protons themselves. In more recent times, the gluon has become recognized as the particle in nature that holds together the nucleus of each atom—and therefore the structure of all the heavy matter in the universe*. A Helium nucleus bound together by gluons is shown in Figure 2.9, where the black lines represent the bonds created by the gluons. Gluons can only exist within the nucleus itself—and they cannot exist in nature as independent or freestanding particles.

The gluons are then said to be the carriers of the strong nuclear force field. They are extremely massive particles that exist in the nucleus for only very short periods of time. Although the nuclear force that holds the nucleus together has a very short range (on the order of 10^{-15} cm), it is over *100 times stronger* than the electrical forces that seek to repel the protons from each other at these distances. It is responsible for the stability of all atomic nuclei upon which the nuclear power industry is based.

2.7 Yukawa Potential and the Coulomb Potential

Because the nuclear force defined by the Yukawa potential holds the nucleus together, it is important to understand how the Yukawa potential compares to the Coulomb potential when it comes to its effect on protons and neutrons. The Coulomb potential is defined by

$$U_C(r) = \frac{-g^2 e^{-mr}}{r} \tag{2.7}$$

Of course, the Coulomb potential has absolutely no effect on uncharged particles (like neutrons), so we must compare the strength of the Coulomb potential to the strength of the Yukawa potential only when we are dealing with protons. In this case, the mass of the particle carrying the electromagnetic field (the photon) is zero (m = 0), and $e^{-mr} = e^0 = 1$. Consequently, the equation $U_C(r) = -g^C e^{-mr}/r$ reduces to

$$U_C(r) = \frac{-g^2}{r} \tag{2.8}$$

which is the more common form of the Coulomb potential that can be found in many textbooks. This equation can be further simplified to read

$$U_C(r) = \frac{-k}{r} \tag{2.9}$$

where Coulomb's constant, k, is simply $\sqrt{g^2}$. Now suppose that we plot the long range strength of the Yukawa potential and the Coulomb potential in Figure 2.8. It is obvious that the Coulomb potential acts over a much larger distance than the Yukawa potential does. In fact, the range of the Coulomb potential is essentially infinite, while the Yukawa potential falls to zero as soon as we move outside the nucleus. The strength of the nuclear force on the protons is then given by

$$F_{NUCLEAR} = \frac{dU_Y(r)}{dr} \tag{2.10}$$

and the strength of the electrical forces on the protons is given by

$$F_{ELECTRICAL} = \frac{dU_C(r)}{dr} \tag{2.11}$$

We will leave it to the student as an exercise to compare the strength of these two forces at a typical distance between two protons (of approximately 10^{-13} cm) orbiting inside the nucleus. However, for appropriate values of the scaling constant g and the mass of the gluon m, it is easy to show that the nuclear force is many times stronger than the electrical force. This is therefore the fundamental process that holds the nucleus of an atom together (see Figure 2.9).

2.8 Visualizing the Nuclear Binding Force

The other interesting property of the gluons is that they can only consist of *quark and antiquark pairs. In other words, the gluons consist of pure energy formed by the reactive combination of a quark and an antiquark* (a particle of matter and a particle of antimatter). However, instead of completely annihilating each other, which particles of matter and antimatter

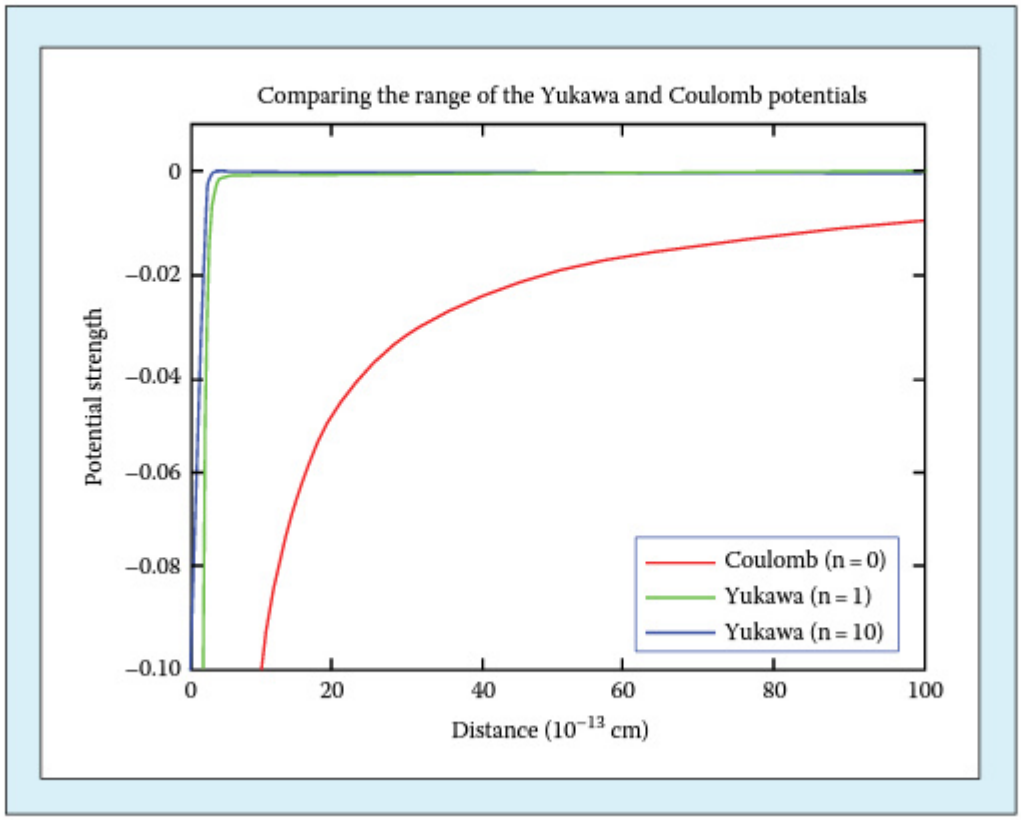

FIGURE 2.8 Comparing the Yukawa and the Coulomb potential as a function of distance.

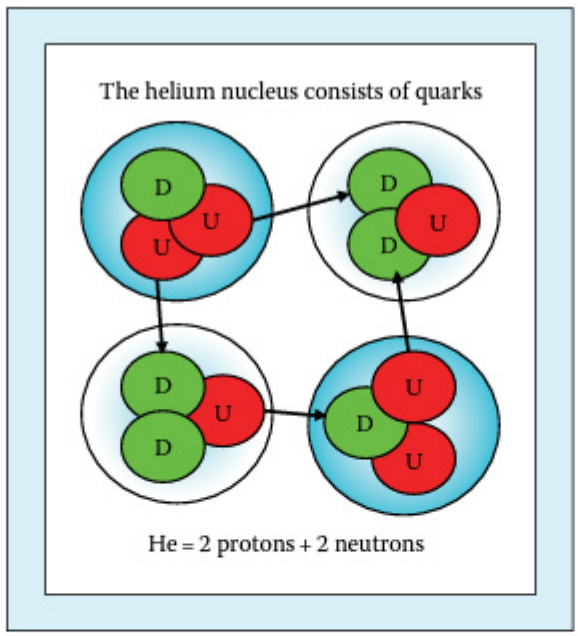

FIGURE 2.9 A helium nucleus held together by gluons that are represented by the black lines.

always do, they stay together just long enough to bind the protons and the neutrons together into a stable orbital configuration. *You can think of them as the two ends of a bar magnet or the two ends of a very strong spring, where the matter particles—the up quark and the down quark—are the particles at the ends of the spring.* The "bond" between them has several unusual characteristics that we do not observe in the chemical bonds that hold ordinary atoms together:

- ⊙ First, it is many times stronger than the binding energy of a comparable chemical bond (in general, *millions of times stronger*).

- Second, the bond goes in and out of existence as the gluons appear and disappear in accordance with the Heisenberg Uncertainty Principle (see Section 1.14 of our companion book*).
- Third, and most importantly, the bond actually gets *stronger* the further away the quarks are from each other.

This astonishing result has very wide-reaching implications. In other words, *the strength of the nuclear force field actually increases the further away the quarks are from each other! No other force that we know of in nature, including electromagnetism and gravity, behaves in this way*. However, at the end of the day, it is this fundamental mechanism that is ultimately responsible for the strength of the nuclear force field. This was also the property of the nuclear binding force that was first hypothesized by Hideki Yukawa in 1930. In order to help us appreciate what we have just said, consider the "picture" of the proton shown in Figure 2.10. To the best of our knowledge, this is the most accurate picture of the proton that we can draw. It also shows how the nuclear binding force, carried by the gluons, holds the proton together. There are three gluons (consisting of three quark–antiquark pairs), represented by the small red, green, and blue spheres in Figure 2.10. They bind together the larger up and down quarks (also represented by the larger red, green, and blue spheres). All of these gluons, as well as the up quarks and down quarks, have well-defined masses, charges, and spins. If you add up the contributions from all of the parts, you will come up with the mass, the charge, and the spin of the proton! In order for all of the parts to sum up to the correct answer, the electrical charge of the gluon must be 0.

This is obvious if you think about it, because a gluon consists of a quark–antiquark pair, and we know from our previous discussion of antimatter that antimatter particles have the same charge as particles of normal matter but that their charge has the opposite sign. Another consequence of the existence of the gluons is that the binding energy of the nucleus, or the amount of energy contained in a nuclear bond, can vary slightly from one element to the next. Figure 2.13 shows the average binding energy of a nucleon (a nuclear matter particle such as a proton or a neutron) as a function of the total number of nucleons (the total number of protons and neutrons) in the nucleus. For most elements, the *nuclear binding energy* is about 8 MeV per nucleon, but it can vary from a high of about 8.8 MeV for iron to much lower values for hydrogen and helium. For uranium, it is about 7.6 MeV. Elements of an intermediate atomic weight (say, 60) are more tightly bound than much heavier or lighter elements are. This is one of the reasons why we cannot generate any energy by splitting apart the nucleus of an Iron atom (having the symbol Fe), while we can generate a lot of additional energy by splitting apart a uranium atom, or by fusing together two hydrogen atoms to form a helium atom. *The bonds are simply weaker when elements are very heavy or very*

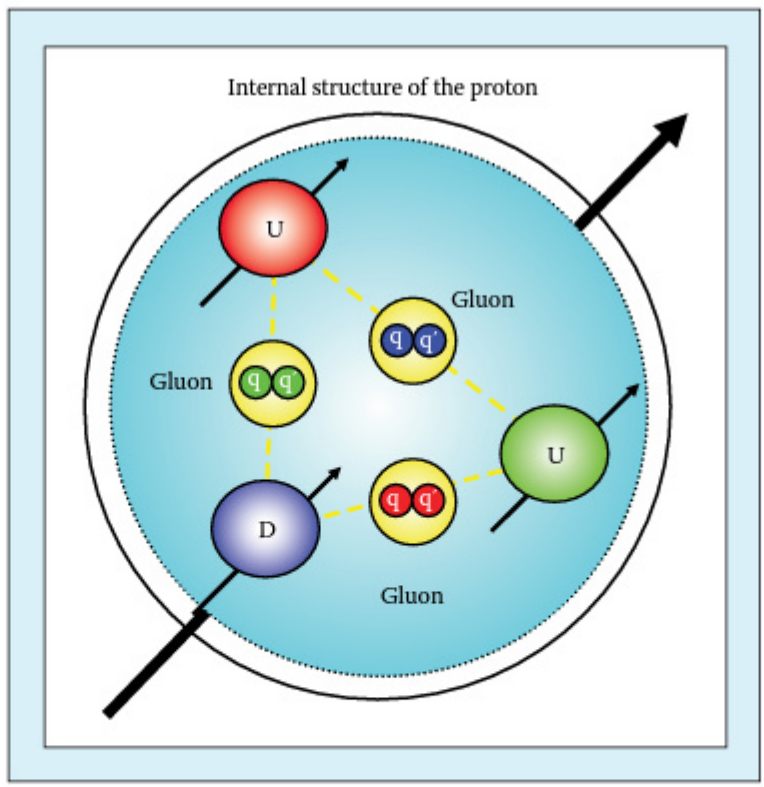

FIGURE 2.10 A picture illustrating the internal structure of the proton.

* See *Nuclear Engineering Fundamentals: A Practical Perspective*, by R.E. Masterson, CRC Press (2017).

light, and we can take advantage of this fact in both fission reactors and fusion reactors to generate useful electrical power. However, as of the writing of this book, a practical fusion reactor has not yet been built. Sometimes Figure 2.13 is called the *nuclear binding energy curve*, and we will explore it in more detail in Chapter 6.

Example Problem 2.3

Suppose that we do a hypothetical thought experiment where an atom is 100 m across. What would the approximate size of the nucleus be in this case?

Solution The nucleus of a typical atom is approximately 1×10^{-4} the size of the electron cloud. So if an atom were 100 m across, the nucleus would be $0.0001 \times 100\ \text{m} \cong 0.01$ m, or about 1 cm in diameter. [Ans.]

2.9 Nucleus and Its Surface

Strictly speaking, an atomic nucleus does not have a well-defined surface. Instead, its outer surface undulates slightly because of the motions of the protons and neutrons inside of it. In some ways, it can be thought of as *a drop of incompressible fluid with an outer surface that undulates slightly as it moves*. Classically, the diameter of the nucleus is given by the equation

Equation for the Diameter of the Nucleus

$$D = 2.5\ A^{1/3} \times 10^{-13}\ \text{cm} \tag{2.12}$$

where A is the *Baryon number* (the number of protons and neutrons) in the nucleus. The protons and neutrons may occasionally move across this boundary (e.g., during the process of electron capture), but on average, this is as far as the nuclear force field, which is carried by the gluons, can reach. Because the protons in the nucleus tend to repel each other due to their electric charge, they normally orbit closer to the edge of the nucleus than the neutrons do, and this fact is reflected in many modern models of nuclear structure (see Chapter 6).

Example Problem 2.4

Suppose that the nucleus of an atom consists of 30 protons and 34 neutrons. What should the approximate diameter of the nucleus be?

Solution According to Equation 2.12, the diameter of the nucleus is $D = 2.5A^{1/3} \times 10^{-13}$ cm. Since the nucleus contains 30 protons and 34 neutrons, the atomic number is $A = Z + N = 64$. The diameter of the nucleus is therefore $D = 2.5 \times (64)^{1/3} \times 10^{-13}\ \text{cm} = 2.5 \times 4 \times 10^{-13}\ \text{cm} = 1 \times 10^{-12}$ cm. This particular combination happens to be an isotope of the element Zinc (Zn). [Ans].

2.10 Density of the Atomic Nucleus

The nucleus is a very dense structure. In fact, it is millions of times denser than any other structure we know of in nature. The total mass of the nucleus $m_{NUCLEUS}$ can be written as the sum of the masses of the nucleons it contains. So to a first approximation, neglecting the binding forces, the mass of the nucleus is given by

$$m_{NUCLEUS} = A \times m_{NUCLEON} \tag{2.13}$$

where A is the atomic number (the number of nucleons or the total number of protons Z and neutrons N):

$$A = Z + N \tag{2.14}$$

and $m_{NUCLEON}$ is the average mass of a nucleon (about 1 AMU or $1.6605402 \times 10^{-24}\ \text{g} = 1.6605402 \times 10^{-27}$ kg). The density $\rho_{NUCLEUS}$ of the nucleus (in kg/m^3) can be found from

$$\rho_{NUCLEUS} = \frac{m_{NUCLEUS}}{V_{NUCLEUS}} \tag{2.15}$$

where V is the volume in cubic meters. If the nucleons are roughly spherical in shape, then we can write

$$V_{NUCLEUS} = \frac{4}{3}\pi r^3 \cdot A \tag{2.16}$$

which leads us to conclude that

$$\rho_{NUCLEUS} = \frac{m_{NUCLEUS}}{V_{NUCLEUS}} = \frac{A \times m_{NUCLEON}}{A \times 4/3\pi r^3} \tag{2.17}$$

where r is the radius of an average nucleon. Solving for $\rho_{NUCLEUS}$ then gives

Equation for the Density of the Nucleus

$$\rho_{NUCLEUS} = \frac{3\, m_{NUCLEON}}{\pi r^3} \tag{2.18}$$

This equation implies that the *density of the average nucleus is approximately* 1.8×10^{17} *kg/m*^{3} *or* 1.8×10^{11} *kg/cm*^{3}. *Hence, the nucleus is a very dense structure indeed!* This explains why many particles simply bounce off of it instead of being absorbed.

Example Problem 2.5

Suppose that we were able to fill a container one meter square with the material used in an atomic nucleus. If the material has the same density as an average atomic nucleus, how many times more massive would this container be than the Statue of Liberty, which weighs 450,000 pounds (about 225 tons)?

Solution The Statue of Liberty weighs 450,000 pounds, or 204,116 kg. One cubic meter of pure nuclear material weighs 1.8×10^{17} kg. So the nuclear material in this container would weigh $1.8 \times 10^{17}/2.04 \times 10^5 = 8.82 \times 10^{11}$ times more than the Statue of Liberty. [Ans.]

2.11 How the Number of Neutrons Affects the Stability of a Nucleus

Long before anyone knew about the existence of quarks and gluons, scientists knew that atoms with larger numbers of protons seemed to need a much larger number of neutrons for their nuclei to remain stable. When they plotted the number of neutrons against the number of protons for all of the naturally occurring elements in the Periodic Table, they found an interesting relationship that we would like to present to you now. They found that the number of neutrons in the nucleus increased at a greater rate than the number of protons and that the constant of proportionality between the two of them seemed to increase as elements became heavier. In other words, the relationship between the number of protons and the number of neutrons was not at all a linear one. They ultimately concluded that the extra neutrons were needed to keep the protons from getting too close together and therefore destabilizing the nucleus as the result of the electrical forces between them.

Today, we realize that this is a direct consequence of the interplay between the electromagnetic forces (which are carried by photons) and the nuclear forces (which are carried by the gluons). The relationship between the number of protons and the number of neutrons as a function of the atomic number can be seen in Figure 2.11. If we are dealing with very heavy elements like Uranium and Plutonium, there are, on average, about 1.5 neutrons for every proton to maintain the stability of the nucleus as a whole. This seems to be a magic number that is neither too big nor too small—but just about right to hold the nucleus together. For lighter and intermediate elements, like aluminum and carbon, this ratio is much closer to 1.0. For example, Oxygen-16 has eight protons and eight neutrons. Yet it is remarkably stable and has a half-life of about 20 billion years. When the nucleus of a heavy element undergoes a fission event, some of the by-products of the nuclear chain reaction (e.g., the fission products) are "neutron rich" relative to the ideal ratios shown in Figure 2.11.

When this happens, the fission by-products (like Cesium, Rubidium, and Barium) generally emit an additional neutron to bring their neutron-to-proton ratio back into balance. These neutrons have a special place in the field of reactor physics, and they are called "*delayed neutrons*." The important thing to remember before we move on is that the isotopes we observe in nature are needed to keep the nuclei of atoms together as the atoms get heavier. Without them, the electrical forces generated by the protons would tear the nuclei apart, and the world would be a much different place than it is today.

2.12 Other Factors That Affect Nuclear Stability

There are still other factors that affect the stability of an average atomic nucleus. Because of the gluons, most atomic nuclei are structurally stable for very long periods of time—thousands, hundreds of thousands, or even millions of years. *This is particularly true of nuclei that have EVEN numbers of protons and neutrons*. Somehow, being put together this

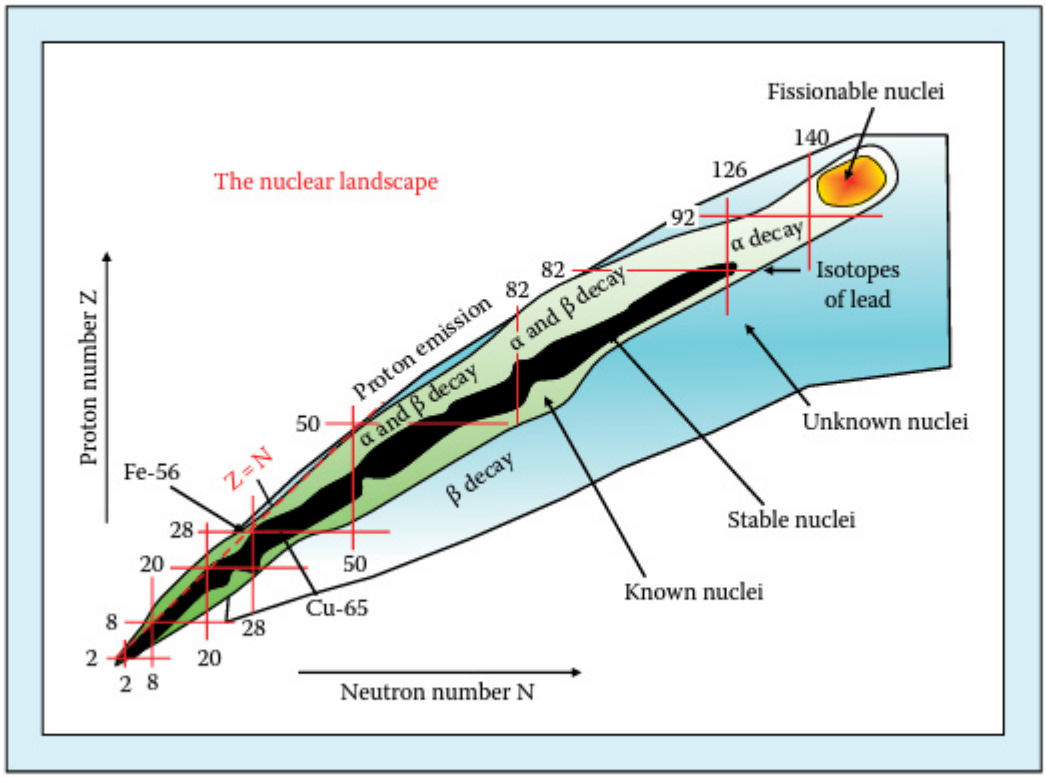

FIGURE 2.11 The nuclear landscape—how the stability of the isotopes is affected by the number of protons and neutrons in the nucleus.

way makes them more stable than if the numbers of protons and neutrons are ODD. However, there are a number of exceptions to this rule, for example, the stability of Uranium-236 compared to the stability of Uranium-235. (In this case, U-236 has a half-life of 23.4 million years, while U-235 has a half-life of about 700 million years.) The half-lives of all the common isotopes of uranium are shown in Table 2.2. A picture of the uranium atom, including the number of protons (Z) and the number of neutrons (N) in the Uranium-238 nucleus, is shown in Figure 2.12.

However, nature has also produced certain elements (and their isotopes) that are naturally unstable, and given enough time, they will disintegrate into simpler atoms or elements, radiating light (photons), electrons, protons, neutrons, and energetic ions (nuclear fragments without their associated electrons) in the process. Plutonium-239 is an example of one of these isotopes. The kinetic energy these decay products carry can cause the materials that they are created from

TABLE 2.2
Half-Lives of Most Common Isotopes of the Element Uranium

Isotope of the Element Uranium	Radioactive Half-Life	Exists in Nature
U-230	20.8 days	No
U-231	4.2 days	No
U-232	~70 years	No
U-233	159,000 years	No
U-234	247,000 years	Yes
U-235	704,000,000 years	Yes
U-236	23,400,000 years	Trace amounts only
U-237	6.75 days	No
U-238	4,460,000,000 years	Yes
U-239	23.5 minutes	No
U-240	14.1 hours	No

Source: ChemicalElements.com.

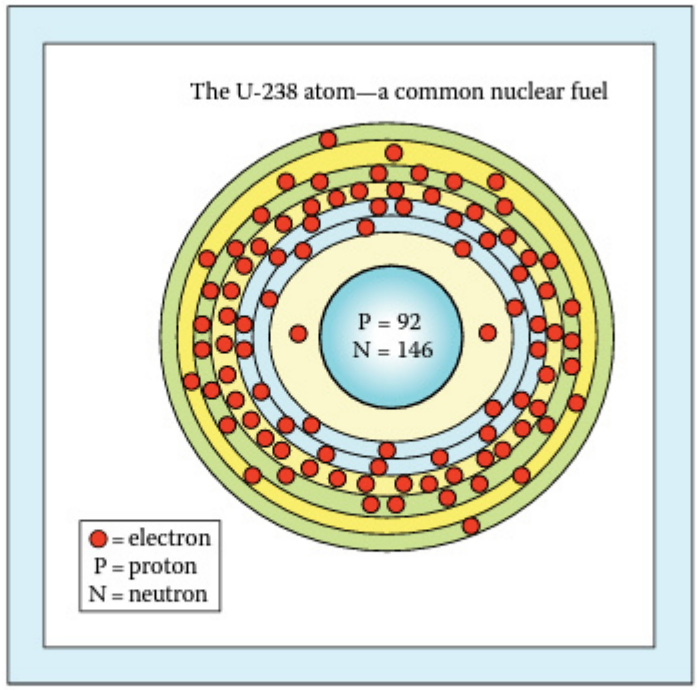

FIGURE 2.12 A picture of the Uranium-238 atom, which has 92 protons and 146 neutrons.

to radiate, glow, and give off significant amounts of heat. Elements can also be *induced* to become unstable and decay artificially through the absorption of an extra neutron or neutrons—giving off large amounts of energy in the process. If the kinetic energy of these radioactive by-products can create enough heat to heat water (or another coolant) and drive the blades in a turbine and an electric generator, then electric power can be generated as the result of a large number of these reactions.

2.13 Differences between Chemical and Nuclear Bonds

2.13.1 Difference #1: The Strength of the Nuclear and Chemical Bonds

As you have probably surmised by now, the electrons that whirl around the nucleus of an atom are held together in their orbits by *electrical forces* carried by energetic photons. The electrons move around the nucleus in preferred orbits, patterns of motion, or *shells*. *These electrical forces are the result of the exchange of photons between the electrons, or between the protons in the nucleus, and the electrons in their shells*. As you probably learned in high school chemistry, it only takes a few electron volts (or eV) to dislodge an electron from the outer shell of an atom. This means that the binding force of an electron, which is responsible for the chemical reactions that we experience in everyday life, is a very weak force indeed. On the other hand, the "binding energy" of a nucleon, which holds particles like protons and neutrons together in the nucleus, is on the order of a million times greater, for example, 8 MeV versus a few eV. See Figure 2.13.

Electrons are the particles in nature that enable chemical reactions to occur. Nucleons are the particles in nature that allow nuclear reactions to occur. Because of the difference in the strength of these forces, the energy that is released in a nuclear reaction is generally many times greater than the energy that is released in a chemical one. There are two final differences between the electrical forces and the nuclear ones that we would like to mention here.

2.13.2 Difference #2: The Existence of Discrete Energy Levels

The electrons that orbit around the nucleus of an atom do so only in discrete energy levels defined by the Schrödinger Wave Equation. This property of the atom means that any electron captured by an atom can only orbit the atom at certain specific energies that can be studied and measured. *When an electron moves from one energy level to the next, it must give up or absorb exactly the amount of energy needed for it to fit into the next energy level. It cannot absorb any more or any less. This excess energy is always given off in the form of a photon. This was Einstein's fundamental finding in his study of the photoelectric effect*. See Figure 2.15 for a picture of the absorption lines for elemental hydrogen.

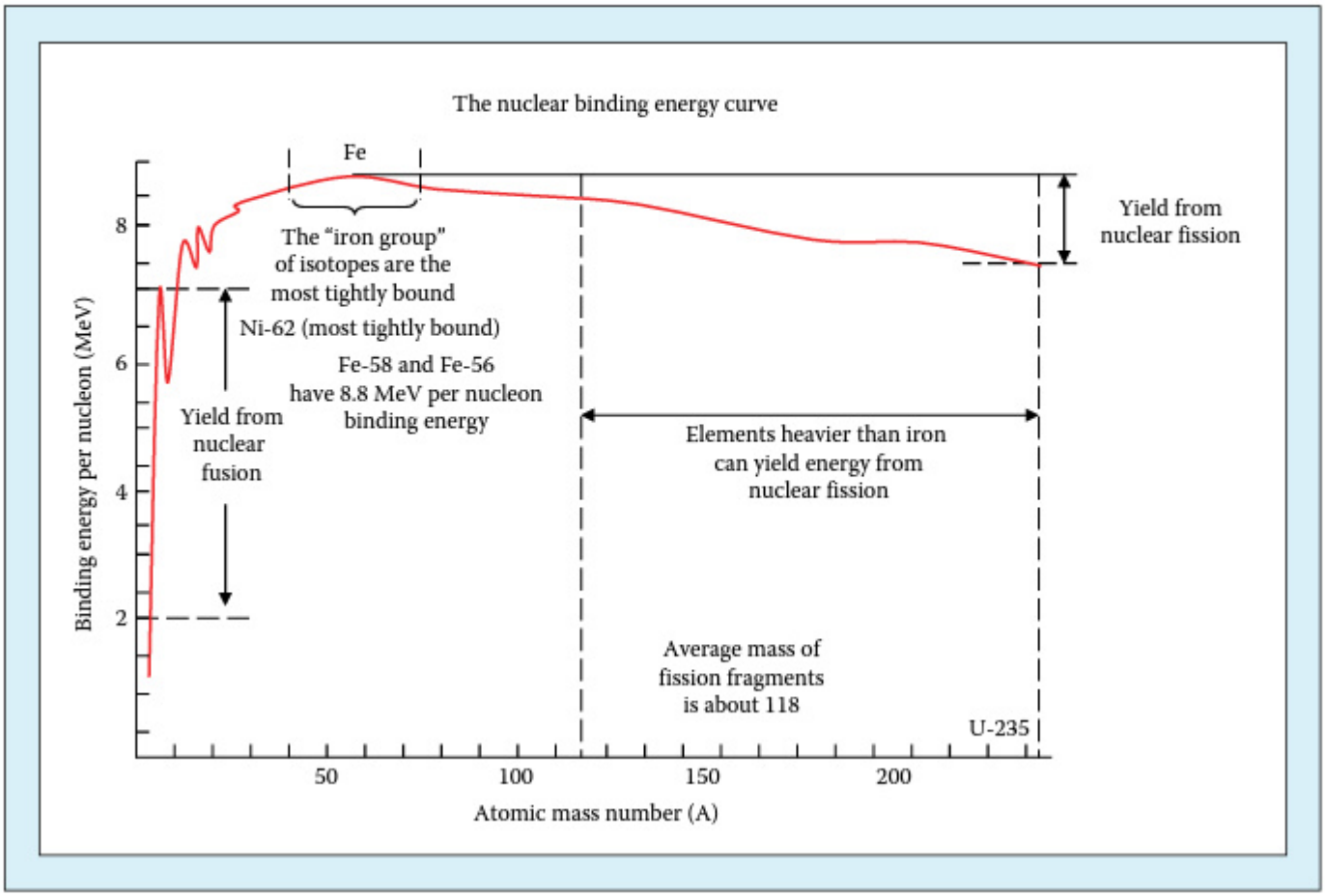

FIGURE 2.13 How the nuclear binding energy varies with the number of protons and neutrons in the atomic nucleus. Sometimes this figure is referred to as the "Nuclear Bonding Energy Curve."

In other words, the energy of the electrons is "quantized" into discrete levels that are *INTEGRAL MULTIPLES of Planck's constant*, h. Photons, which are the carriers of the electromagnetic force, also carry their energy E away in multiples of Planck's constant as well (Figure 2.14):

$$E = fh \tag{2.19}$$

where
f is the frequency of vibration
h is Planck's constant

The discrete structure of these energy levels has been known for many years, and it is responsible for the energy spectrum of the individual elements, including the dark bands, or the absorption lines that are observed in the spectrum of light coming from distant stars through telescopes. (This is one way that the chemical composition of a star can be determined at a great distance.) Because of this quantization of the electron energy levels, each element has its own unique electromagnetic signature when it interacts with a light wave. The absorption lines for the sun are compared to the bright star Vega in Figure 2.15. Sometimes these lines are also known as the *Fraunhofer lines*. Notice how well you can see the *Balmer absorption lines* for hydrogen in the spectrum of the star Vega. This indicates that Vega is a very young star with a lot of hydrogen in its core, while the sun is a middle-aged star with less hydrogen to burn. This is how we know what elements the stars are made out of and what the overall abundance of the individual elements in the universe is! Away from the effects of the nucleus, free electrons are free to have any energy that they desire. In other words, their energy spectrum is continuous there. However, in the vicinity of the nucleus, their energy levels must be *quantized*, and this fact can never be ignored in determining their position and behavior.

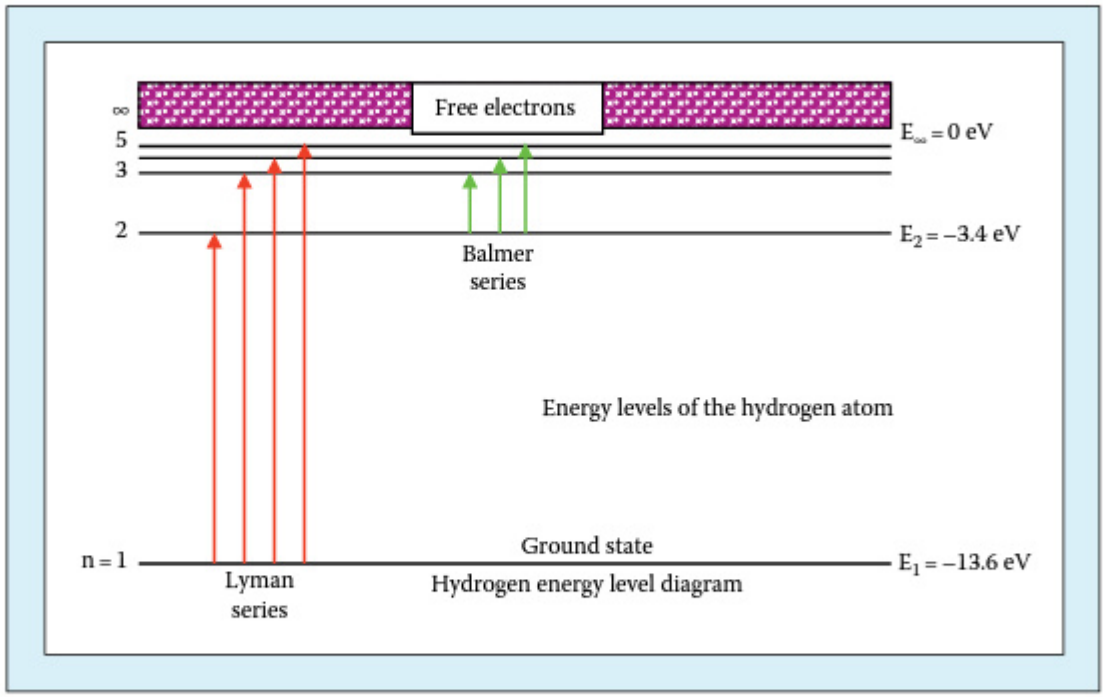

FIGURE 2.14 The energy levels of the electrons in a hydrogen atom.

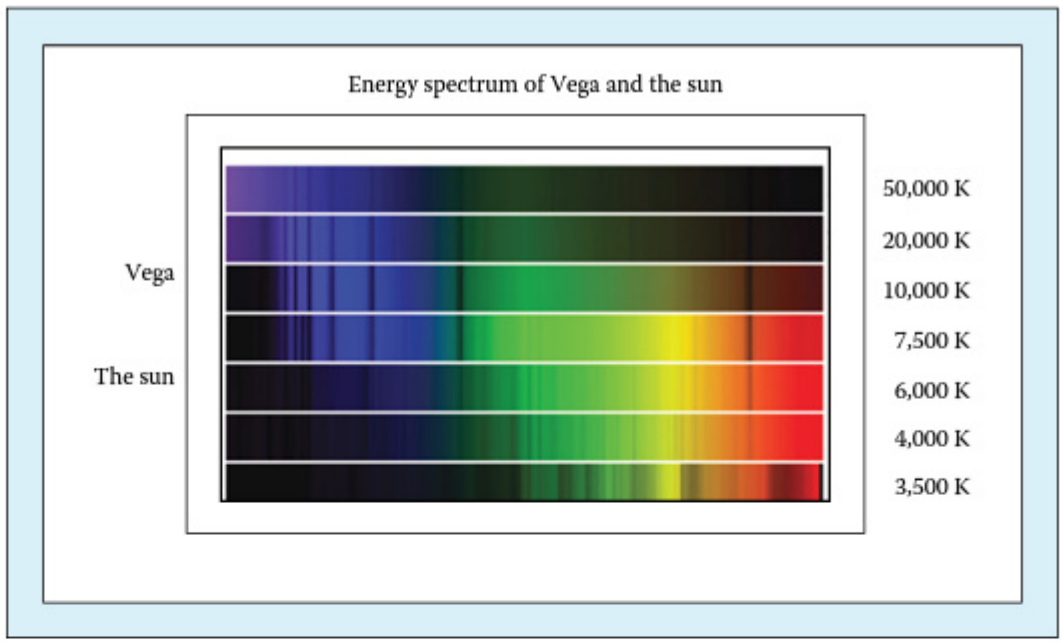

FIGURE 2.15 The absorption lines in the energy spectrum of the sun compared to those of the bright star Vega. (Adapted from a spectral image provided by NASA.)

2.13.3 Difference #3: The Range of the Chemical and Nuclear Forces

The third difference between the electrical forces and the nuclear ones is that electrical forces have an extremely long range, which, for all intents and purposes, is an infinite one. We know this from *Coulomb's Law* that we first studied in high school chemistry or physics. Here the electrical force F between two charges is proportional to only the product of the two charges q_1 and q_2 and inversely proportional to the square of the distance r between them:

$$F = \frac{kq_1 * q_2}{r^2} \tag{2.20}$$

where k is *Coulomb's constant. No matter how great the distance r between the two charges is, there is some force acting on the charges*. This electrical force is transferred between the charges by particles of light called photons (which are simply another variety of a force particle). Nuclear forces, on the other hand, can only exist within the confines of the nucleus itself. They cannot go out and "grab" something in one of the electron shells. Only the electrical force between the protons and the electrons can do that. They therefore, by design, have only a very short range (on the order of 10^{-12} cm). They are, in fact, "muscle-bound" in this respect. So in conclusion, there are three major differences between the nuclear forces, which are responsible for nuclear power, and the electrical ones, which are responsible for all of the world's chemistry:

1. The nuclear forces are *much* stronger than the electrical ones. (The binding energies per particle are on the order of one million times greater—so the bonds are much harder to break.)
2. The energy levels of the electrons around the nucleus are quantized, whereas the energy levels of the protons and the neutrons in the nucleus are *not* quantized to the same extent.
3. The nuclear forces have a *much shorter* range than the electrical forces. For example, they have a range of about 10^{-12} cm versus an essentially infinite one when photons (the carriers of the electromagnetic force) are involved. All of these factors influence the way in which a reactor behaves in one way or another. It is always important to keep them in mind when we get into a discussion of the reactions of the individual particles, or in chain reactions, where many particles are involved.

2.14 How Nuclear Energy Is Measured

Mostly for historical reasons, the release of nuclear energy is almost always measured today in the units of *electron volts. An electron volt is defined as the amount of energy acquired by an electron falling through a potential difference of one volt* (see Figure 2.16). According to this definition, an electron volt is approximately equal to 1.6×10^{-19} J. So 1 MeV—or 1 million electron volts—is approximately equal to 1×10^{6} eV $\times$ 1.6×10^{-19} J/eV = 1.6×10^{-13} J.

The Size of an Electron Volt

$$1\,\text{eV} = 1.6 \times 10^{-19}\ \text{J} \tag{2.21}$$

Perhaps the easiest way to visualize what an electron volt implies is to imagine an electron that starts at the negative plate of a parallel plate capacitor and moves to the positive plate after a period of time. The positive plate is at a voltage that is one volt higher than the negative plate, and so the energy that is acquired by the electron as it moves between the two plates is what an electron volt means. Numerically, it is easy to show that one joule is equal to 6.2×10^{18} eV, and so it follows from this simple relationship that *it takes 6.2×10^{20} eV/s to light a 100 W light bulb*. When a uranium nucleus splits apart, approximately 200 MeV of recoverable energy is released per fission. This means that *a single nuclear fission event will create $2 \times 10^{8} \times 1.6 \times 10^{-19} = 3.2 \times 10^{-11}$ J of heat. In other words, approximately 3.125×10^{10} fissions, or 30 billion fissions per second, are required to generate 1 W of thermal power!* Hence we may write

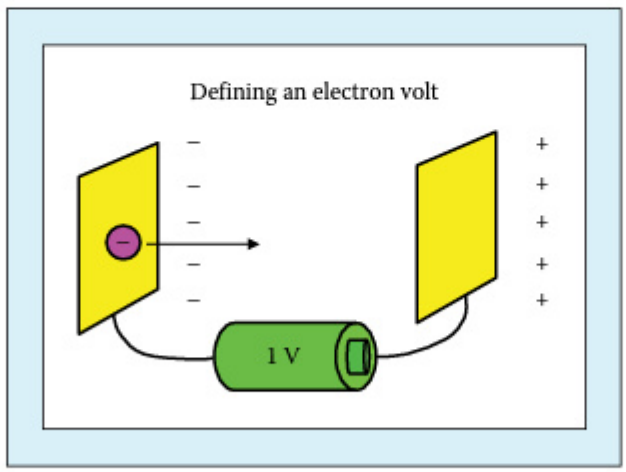

FIGURE 2.16 A simple way to visualize the definition of an electron volt.

Converting Fissions to Watts

30 billion fissions per second ≅ 1 W of thermal power (2.22)

If you think about it, this is an astonishing number. For example, it implies that if a nuclear power plant is 33% efficient (which means that 3000 MW of thermal power is required to produce 1000 MW of electrical power), then approximately $3 \times 10^9 \times 3.125 \times 10^{10} \cong 100$ billion-billion fissions per second are required for a 1000 MW nuclear power plant to generate 1000 MW of electrical power. *This requires the coordination of literally trillions of atoms and trillions of neutrons per second to achieve this rate of energy production.* This point is often lost upon the casual reader whenever the science of nuclear power is discussed.

2.15 Estimating the Energy of the Neutron, the Proton, and the Electron

As you have undoubtedly surmised by now, most of the energy of a matter particle comes from the mass of the particle itself. *When we measure this natural mass in a laboratory, we find that neutrons have more "mass" than protons do and protons have more mass than electrons do.* We refer to the natural mass that a particle possesses when it is at rest as the particle's "*rest mass*," and it is usually measured in Atomic Mass Units, or AMUs. According to Einstein, the rest mass, m_o, and the *rest energy* of a particle are two different manifestations of the same thing. The rest energy of any material object with a rest mass of m_o is given by

Mass and Energy Equivalence

$$E = m_o c^2 \quad (\text{for all energies } E) \tag{2.23}$$

where

E is the energy
c is the speed of light

Conversely, if we know the energy E of a particle, the total mass m of the particle at any speed is given by

Deducing Mass from Energy

$$m = \frac{E}{c^2} \tag{2.24}$$

In addition to this rest energy, particles can possess additional energy due to the fact that they are moving relative to the person who is observing them. This additional energy of the motion of a particle is called the *kinetic energy* of a particle. Except at very high speeds (close to the speed of light), the kinetic energy of a particle is given by the simple classical expression

Kinetic Energy

$$K = \frac{1}{2} m_o v^2 \quad \text{for "normal" velocities } (v < 1/10c) \tag{2.25}$$

where

K is the kinetic energy
m_o is the "rest mass" of a particle
v is the velocity (or speed) at which the particle moves

At higher speeds, the more accurate and more fundamentally correct equation for the kinetic energy is

Kinetic Energy

$$K = \frac{1}{2} m_o v^2 + \frac{3}{8} m_o v^4/c^2 + \frac{5}{16} m_o v^6/c^4 \quad \text{for "high" velocities } (v \geq 1/10c) \tag{2.26}$$

where
v is the velocity of the particle
c is the speed of light

The reason why this equation exists is that the mass of any matter particle is a function of the velocity that it travels relative to the person who is observing it. In other words, the mass of any material object is a function of its velocity v:

$$M = m(v) \tag{2.27}$$

and according to Einstein, the exact expression for this relationship is

$$m(v) = \frac{m_o}{\sqrt{1 - v^2/c^2}} \tag{2.28}$$

The total mass of a matter particle is therefore a unique number only when the particle is at rest. In this case, the expression for the relativistic mass reduces to

$$m = \frac{m_o}{\sqrt{1}} = m_o \tag{2.29}$$

which is the value for the rest mass of a nuclear particle when $v = 0$. *At any speed v greater than 0, the mass of a matter particle is greater than when it is at rest.* Only when its total speed is zero does it have a unique value—and this value is the minimum value that it can attain. This expression for the kinetic energy K of a matter particle can be found by taking Einstein's equation for the total energy of the particle $E = mc^2$ and subtracting the corresponding expression for the rest energy m_oc^2 of the particle. The difference between these two is the kinetic energy K that the matter particle possesses; hence, we may write

Kinetic Energy of a Matter Particle

$$K = mc^2 - m_oc^2 \tag{2.30}$$

If we expand the first term $m = m_o/\sqrt{1 - v^2/c^2}$ for the velocity-dependent mass m in a Taylor series, the first few terms in the Taylor series are

$$\frac{m_o}{\sqrt{1 - v^2/c^2}} = m_o\left(1 + \frac{1}{2}v^2/c^2 + \frac{3}{8}v^4/v^4 + \frac{5}{16}v^6/c^6 + \cdots + \text{higher-order terms}\right) \tag{2.31}$$

which leads us to the conclusion that

$$K = mc^2 - m_oc^2 = m_oc^2\left(1 + \frac{1}{2}v^2/c^2 + \frac{3}{8}\,v^4/c^4 + \frac{5}{16}v^6/c^6 + \cdots\right) - m_oc^2 \tag{2.32}$$

or

$$K = \frac{1}{2}m_ov^2 + \frac{3}{8}m_ov^4/c^2 + \frac{5}{16}\,m_ov^6/c^4 \tag{2.33}$$

This expression for the kinetic energy K is simply an alternative form of Einstein's equation with the higher-order terms removed. Notice that when $v < 0.1c$, or about 10% of the speed of light, the difference between the classical expression for the kinetic energy

$$K = \frac{1}{2}m_ov^2 \tag{2.34}$$

and the corresponding relativistic expression is minimal (less than 1%). Now let us take a look at the magnitude of each of these terms to understand what this equation really means. In one form of radioactive decay, alpha particles are typically emitted from a heavy nucleus at about 5% of the speed of light, or $V = 0.05c$. Here the error between the "classical" and the relativistic equations is very small, since the size of the terms in the equation for the kinetic energy is

$$K = \tfrac{1}{2}m_oc^2\left(0.0025 + \tfrac{3}{4} \times 0.00000625 + 5/8 \times 0.000000016\right) \tag{2.35}$$

At this speed (<0.1c), the higher-order terms in the equation for the kinetic energy make almost no contributions to the total kinetic energy of the particle and can therefore be ignored. However, in another form of radioactivity, called beta decay, electrons may be emitted from the nucleus with a velocity of about 60% of the speed of light, or V = 0.6c. Here, the error between the "classical" result and the relativistic result can be very large.

For example, let's look at the size of this error when v = 0.6c (60% of the speed of light). In this case, $m = \frac{m_0}{\sqrt{1-v^2/c^2}} = \frac{m_0}{\sqrt{1-(0.6c)^2/c^2}} = \frac{m_0}{\sqrt{0.64}} = 1.25\, m_0$. So, the error in the value of the momentum or the energy of a particle due to the difference in the value of the mass is about 25% in this case (i.e., $\Delta m = 1.25\, m_o - m_o = 0.25\, m_o$). *This means that we cannot use just the rest mass of a particle to calculate its energy or its momentum when the velocity becomes a significant fraction of the speed of light (say v > 0.1c). We must then use the velocity-dependent mass instead. We can express this observation with the following important guideline:*

An Important Guideline

Whenever the speed of a matter particle (such as a proton, a neutron, or an electron) is less than about 10% of the speed of light (v < 0.1c), the mass of the matter particle can be approximated by its rest mass m_o.

At these speeds, the relativistic mass m differs from the rest mass by less than 1%, and so the error in the calculation of the kinetic energy $K = \frac{1}{2}mv^2$ or the momentum p = mv is also less than 1%.

Figure 2.17 shows how the mass of a matter particle changes as its speed increases. *This increase in mass is due to an effect called the Higgs mechanism*, which is discussed in our companion book.* Generally speaking, the relativistic equation for the mass, that is, $m(v) = m_o/\sqrt{1-v^2/c^2}$, of a matter particle *must* be used to find the correct energy or momentum of a matter particle whenever v > 0.1c. This applies to protons, neutrons, and electrons. Otherwise, the results of our calculations will not be correct! However, for v < 0.1c, the normal rest mass m_o can be used (which will result in a very small error—typically <1%). Neutrons and protons that are released from the nucleus of an atom can carry this kinetic energy with them as they escape and heat up the surrounding structural material and coolant. Electrons can also carry away kinetic energy from a nuclear reaction (since they are also particles with a rest mass). High-energy electrons

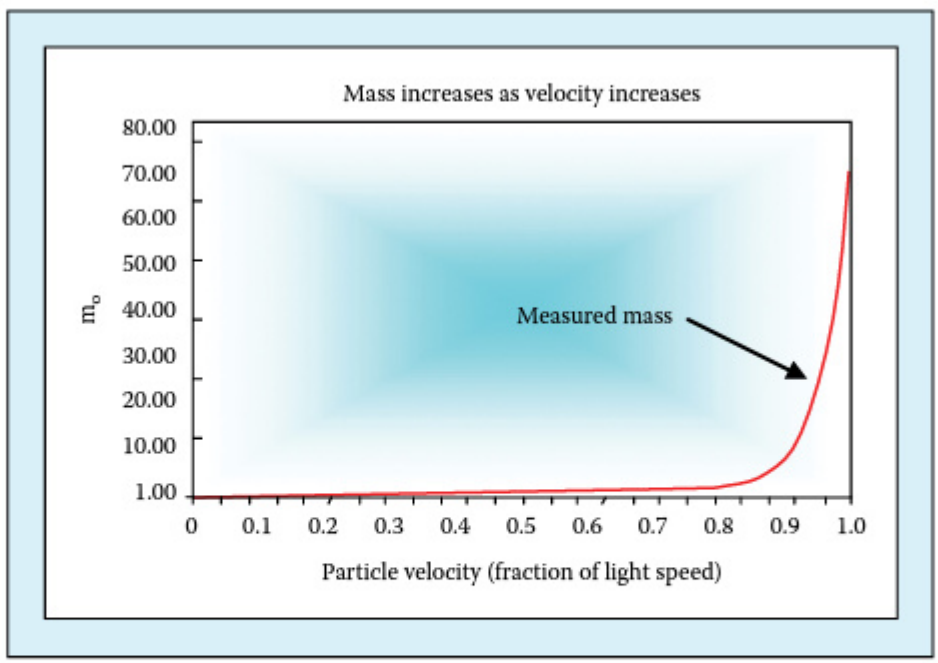

FIGURE 2.17 The mass of a matter particle as a function of its velocity. Note that as the velocity approaches the speed of light c, the mass becomes effectively infinite.

* See *Nuclear Engineering Fundamentals: A Practical Perspective*, by R.E. Masterson, CRC Press (2017).

TABLE 2.3
Spins and Symbols for Some Common Nuclear Particles

Nuclear Particle	Antiparticle	Symbol	Spin	Type
Proton	Antiproton	P or P^-	½	Matter
Neutron	Antineutron	N or P^-	½	Matter
Electron	Positron	e^- or e^+	½	Matter
Photon	None	γ	1	Force
Quark	Antiquark	Q or Q^-	½	Can be both
Meson	Antimeson	K or K^- and π or π^-	0 or 1	Force
Neutrino	Antineutrino	ν or ν^-	½	N/A

are sometimes called "*Beta Rays*." The total energy E_T of any matter particle with rest mass m is then the sum of the rest energy E_r and the kinetic energy E_k of the particle, or $E_T = E_r + E_k = m_o c^2 + \frac{1}{2} m_o v^2 + \frac{3}{8} m_o v^4/c^2 +$ higher-order terms. We will come back to this equation on many occasions throughout this book now that we know how to calculate the total energy of a neutron, a proton, or an electron (see Table 2.3).

Since the photon is not a matter particle, it has no rest mass, and the equations given earlier do not apply to it. Instead, we must use the equation

$$E_\gamma = hf \tag{2.36}$$

to calculate its kinetic energy, where h is a fundamental constant of nature called Planck's constant. Planck's constant appears in many important equations of quantum mechanics, and it also appears in the *Heisenberg uncertainly principle*, which relates the uncertainty in a particle's position to the uncertainty in a particle's momentum. The particles in the atomic nucleus obey the Heisenberg uncertainty principle as well. These equations make it possible to calculate the energy released by any nuclear reaction if we know the number of particles and the types of particles that are involved. Since energy is always conserved in nuclear reactions, we now have a useful tool that we can use to predict the exact contributions of the fission fragments to the total energy that is released.

Example Problem 2.6

Using the knowledge you have just acquired, calculate the error in the kinetic energy of a matter particle when the classical expression $K = \frac{1}{2} mv^2$ is used to calculate its kinetic energy instead of the more accurate relativistic expression $K = mc^2 - m_o c^2$ for the general case where the matter particle is traveling at 10% of the speed of light (v = 0.1c).

Solution We can find the error in this case by taking the difference between the rest mass m_o of the particle and the "relativistic mass" $m = m_0/\sqrt{1 - v^2/c^2}$ when m = 0.1c. In this case, the difference is $m = m_0/\sqrt{1 - v^2/c^2} = m_0/\sqrt{1 - (0.1\ c)^2/c^2} = m_0/\sqrt{0.99} = 1.01\ m_0$ or $\Delta m = 1.01\ m_0 - m_0 = 0.01 m_0$. So the error in the momentum or the energy due to the difference in the mass is usually about 1% in this case. [Ans.]

2.16 Conservation of Linear Momentum in Particle Reactions

As opposed to the angular momentum or spin, the linear momentum P of a matter particle such as a neutron can be found by simply applying Newton's laws of motion and multiplying its mass M times its velocity V. In other words, *the linear momentum of a matter particle* is given by

$$\mathbf{P} = m\mathbf{v} \tag{2.37}$$

where m is the mass of the particle at a linear velocity **v**. At normal speeds (less than about 10% of the speed of light), it can be shown that the mass of a nuclear particle is not affected very much by a particle's velocity. Therefore, at low speeds, the assumption that the mass m is a constant, which is equivalent to the rest mass m_o, is usually a good one. However, at higher speeds, Einstein showed that the mass of a matter particle actually increases relative to the mass that

it has when it is at rest. This is a real effect that is observed every day when the speed of a particle gets beyond a certain point. The exact dependence of a particle's mass on its velocity is given by

$$m(v) = \frac{m_o}{\sqrt{1-(v/c)^2}} \tag{2.38}$$

where

m_o is the mass measured for the particle when it is at rest
c is the speed of light

This means that at particle speeds greater than about 0.10c, it is appropriate to use the following expression to calculate the momentum P of a matter particle:

$$\mathbf{P} = \frac{m_o \mathbf{v}}{\sqrt{1-(v/c)^2}} \tag{2.39}$$

If we expand the denominator of Equation 2.39 in a Taylor series and keep only the first few terms, we find that the momentum at higher velocities can also be calculated from

Linear Momentum

$$P = m_0 v + 1/2 m_0 v^3/c^2 + 3/8 m_0 v^5/c^4 \quad \text{for "high" velocities } (v \geq 1/10c) \tag{2.40}$$

where

m_0 is the rest mass
the first term $\mathbf{P} = m_0\mathbf{v}$ is again the standard classical result

In Figure 2.17, you can see how large the mass of a matter particle and therefore the momentum P = mv can get as we approach the speed of light. It is rare for a neutron or a proton produced in a nuclear reaction to have a velocity much greater than 0.20c. However, it is quite common for electrons (such as those produced in beta decay) to have an average velocity of about 0.60c. It is also true in certain cases that electrons can be ejected from fuel rods at speeds greater than 0.75c. In this case, the electrons may be responsible for a unique form of light blue radiation called *Cherenkov radiation* (see Chapter 6 of our companion book, which can also be seen in *spent fuel pools*). In the nuclear world, we can express the conservation of linear momentum by writing

Conservation of Linear Momentum

$$\text{Momentum in} = \text{Momentum out}$$

$$\sum \mathbf{P}_{in}(i) = \sum \mathbf{P}_{out}(j) \quad \text{over } i = 1\ldots I \text{ and } j = 1\ldots J \tag{2.41}$$

Here again, the sums must be taken over all of the particles going into a reaction and over all of the particles coming out of a reaction. *If one of the particles is missing, Equation 2.41 will not balance, and momentum will not be conserved.* It goes without saying that the linear momentum, whether it is calculated for a particular particle from Equation 2.39 or Equation 2.40, is a *vector* quantity. In other words, the momentum can always be written as

$$\mathbf{P} = \mathbf{i} \cdot P_x + \mathbf{j} \cdot P_y + \mathbf{k} \cdot P_z \tag{2.42}$$

where **i**, **j**, and **k** are the unit vectors in the x, y, and z directions, respectively. This means that the components of the momentum in the x direction must always balance before and after the reaction, as well as the components in the y and z directions (Figure 2.18). We can express this fact by writing

$$\sum \mathbf{P}_{x\,in}(i) = \sum \mathbf{P}_{x\,out}(j) \quad \text{for } i = 1\ldots I \text{ and } j = 1\ldots J \quad \text{and} \tag{2.43}$$

$$\sum \mathbf{P}_{y\,in}(i) = \sum \mathbf{P}_{y\,out}(j) \quad \text{for } i = 1\ldots I \text{ and } j = 1\ldots J \quad \text{and} \tag{2.44}$$

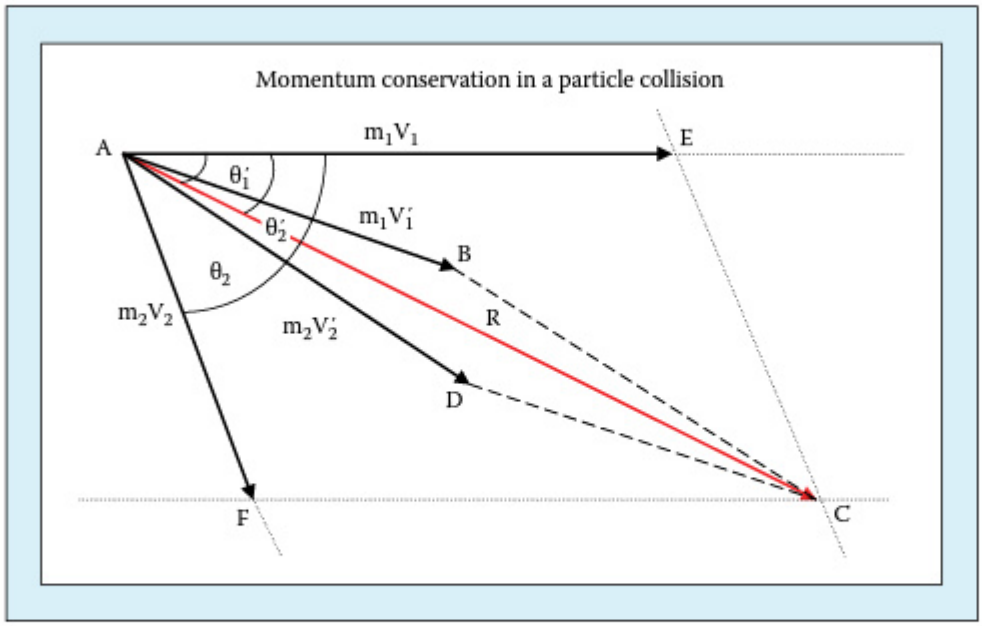

FIGURE 2.18 A diagram depicting the conservation of momentum when two arbitrary objects collide. The initial velocities of the two objects are V_1 and V_2, and the final velocities are V_1' and V_2'. Note that the length of the resulting momentum vector R is always conserved in each case; that is to say, it has the same length before and after the collision.

$$\sum \mathbf{P}_{z\,in}(i) = \sum \mathbf{P}_{z\,out}(j) \quad \text{for } i = 1\ldots I \text{ and } j = 1\ldots J \tag{2.45}$$

If the momentum is not parallel to one of the coordinate axes, the x, y, and z components can be found by simply projecting the magnitude of the momentum P onto each axis using the simple geometric relationships

$$\mathbf{P}_x = P\cos\theta \tag{2.46}$$

$$\mathbf{P}_y = P\sin\theta \tag{2.47}$$

$$\mathbf{P}_z = P\cos\varphi \tag{2.48}$$

where θ and φ are the angles of the momentum vector with respect to the x- and z-axes.

2.17 Momentum Conservation in Reactions Involving Photons

The momentum of a photon cannot be calculated like the momentum of an ordinary matter particle because the photon has no rest mass. For photons, an alternative procedure must be used to calculate P. The momentum of a photon P is related to its energy E by the following equation:

$$\mathbf{P} = \frac{E}{c} \tag{2.49}$$

which is discussed in many elementary physics books. Here the constant c is again the speed of light. This means that if we know either the energy of the photon E or its wavelength λ, we can calculate its momentum from one of the following equations:

Conservation of Linear Momentum for a Photon

$$\mathbf{P} = \frac{E}{c} \quad \text{or} \quad \mathbf{P} = f\left(\frac{h}{c}\right) = \frac{h}{\lambda} \tag{2.50}$$

where

f is the frequency
h is Planck's constant
λ has the dimensions of length

Once we have obtained the momentum of the photon **P**, it can be substituted into one of the previous equations to ensure that linear momentum is conserved. With Equations 2.42 through 2.48, we can, in principle, predict the velocity splits of the particles coming out of a reaction if we know their rest masses. Conversely, we can use these two equations to predict their angular distribution as well. There are many more complex examples of this in real life, but no matter what the degree of complexity is, the conservation of momentum always applies. This applies to both the linear momentum of Newtonian mechanics, which gives the correct scattering angles and velocities, and to the angular momentum of the particles, which is determined by their spin.

2.18 Conservation of the Baryon Number in Nuclear Reactions

There is actually a fourth conservation law that many nuclear particles obey. This law is called the *Conservation of the Baryon Number* A, where the reader may recall from our previous discussion that the number of *Baryons* (A or B) is equal to the number of protons plus the number of neutrons; for example,

$$\text{A or B} = Z + N \tag{2.51}$$

where
Z is the number of protons
N is the number of neutrons

It then follows that

Conservation of the Number of Nucleons or the Baryon Number

$$A_{IN} = A_{OUT}$$

where

$$A_{IN} = N_{IN} + Z_{IN}$$

$$A_{OUT} = N_{OUT} + Z_{OUT} \tag{2.52}$$

The reason why this expression is valid is that all Baryons (protons and neutrons) consist of more fundamental particles called quarks. Since the quarks themselves are fundamental particles that at normal energies cannot be created or destroyed, the next layer of matter particles from which they are built (the protons and neutrons) must follow this same basic methodology as well. *The conservation of the Baryon number is therefore equivalent to saying that the number of nucleons that go into a nuclear reaction must be equal to the number of nucleons that come out of the reaction*. This is especially true when a nucleus splits into a number of smaller parts (in a fission reaction) or when a nucleus is combined into a fewer number of parts (in a fusion reaction). In either case, the total number of nucleons (protons plus neutrons) must always be conserved. Again, this places certain constraints on which reactions are possible and which ones are not. *If a reaction does not comply with this rule, it is simply not allowed*. The following problem illustrates a practical example of this principle.

Example Problem 2.7

Problem: Suppose that a Uranium-235 nucleus absorbs a neutron and then decides to split apart. If it splits into one fission product that has 110 nucleons, how many protons and neutrons will there be in the second fission product if three additional neutrons are released in the process?

Solution Because the total number of protons and neutrons in this reaction must be conserved, 235 + 1 = 236 Baryons go into the reaction, and therefore 236 Baryons must come out of the reaction. Since one of the fission products has 110 nucleons (or baryons), the other one must have 236 – 110 – 3 = 123 protons and neutrons. [Ans.]

2.19 Some Final Observations

Notice that the Conservation of the Baryon Number does not say anything about the number of protons and neutrons that each nuclear reaction must produce. This is because many different combinations of these two numbers are possible. *The Law of Baryon conservation only requires that the sum of the number of protons and neutrons going into a reaction must be equal to the sum of the number of protons and neutrons coming out of a reaction. It does NOT say anything about*

what the neutron-to-proton ratio (N/Z) going into the reaction or coming out of the reaction must be. This ratio is never a constant, but instead it is determined by a statistical probability distribution that varies from one type of nuclear reaction to the next. As we will see in Chapter 7, the N-to-Z ratio is both element and isotopic dependent.

2.20 Effects of Relativity on Particle Behavior

When nuclear particles (excluding the photon) move at very high speeds, their behavior is governed by the laws of *Special Relativity*. Essentially, their mass increases with their speed (but not linearly), and when their speed exceeds about 10% of the speed of light (0.10c), then we can no longer use their classical rest masses m_o to calculate their energy E and momentum P correctly. Instead, we must use a more general expression for their relativistic mass m(v), which is a function of their apparent velocity v. The specific expression to use in this case is

$$M(v) = \frac{m_o}{\sqrt{1-(v/c)^2}} \tag{2.53}$$

Another interesting consequence of the Theory of Relativity is that *time slows down as the speed of a particle increases*, and this has an effect on the rate that certain nuclear reactions can occur. The relationship between the speed of time t′ of a particle in motion and the speed of time t when the same particle is at rest is given by

$$t' = \gamma t \tag{2.54}$$

where γ is called the *time dilation factor*. The appropriate expression to use for γ is

$$\gamma = \sqrt{1-(v/c)^2} \tag{2.55}$$

γ is also called the *Lorentz "shrinkage factor,"* in honor of *H.A. Lorentz*, who first discovered it. A picture of Lorentz is shown in Figure 2.19, and the equations of Lorentz transformation are shown in Figure 2.20. The Lorentz transformation

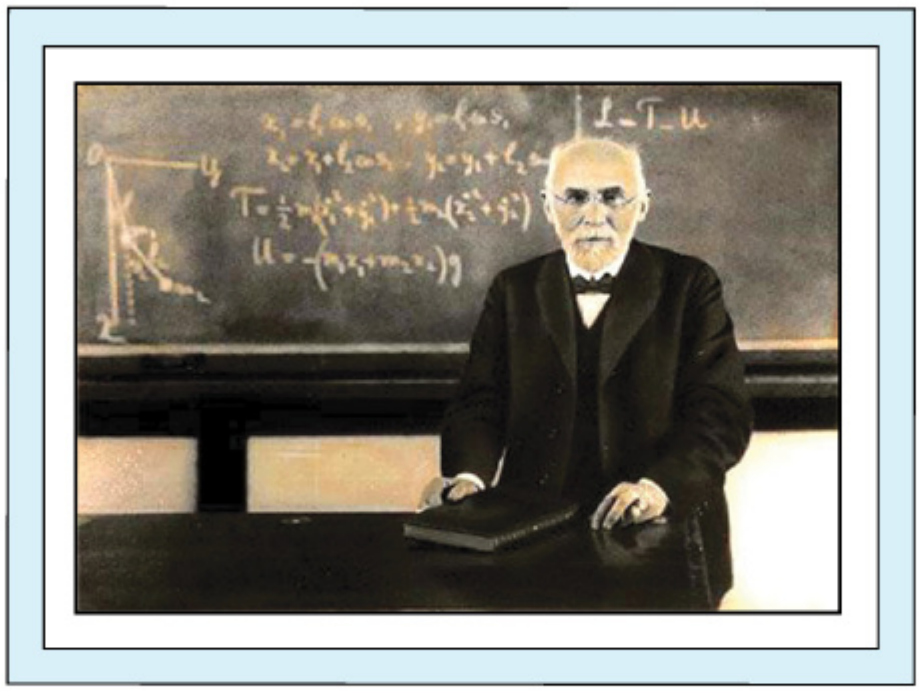

FIGURE 2.19 A picture of the Dutch scientist H.A. Lorentz, who invented the Lorentz transformation of space and time. (Picture provided by Wikipedia.)

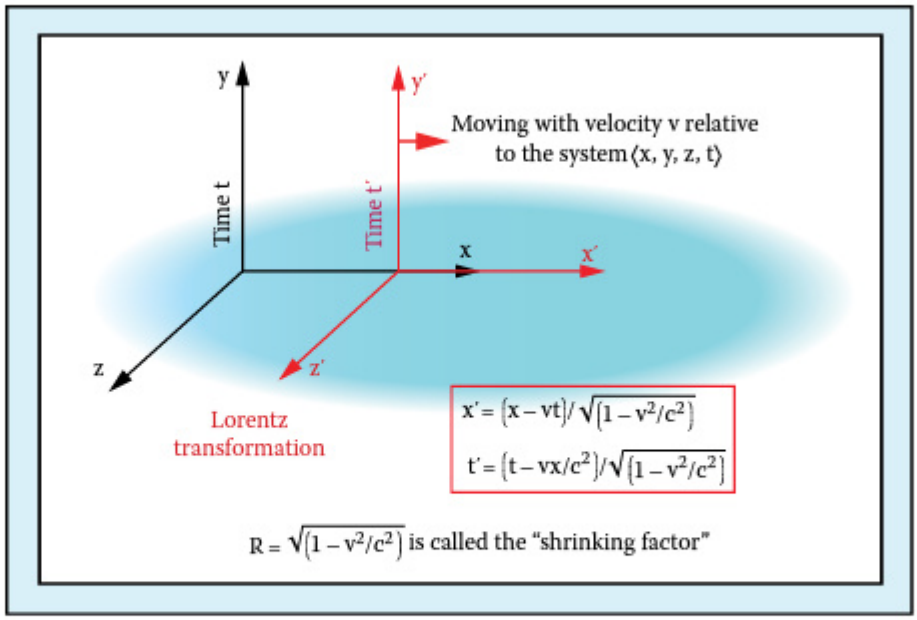

FIGURE 2.20 The equations of the Lorentz transformation, which relate the dilation of space and time.

can also be applied to electric and magnetic fields, but we will not discuss these effects here. However, they are discussed in some of the references at the end of the chapter. From Equations 2.54 and 2.55, it is easy to deduce that as $v \rightarrow c$, the term $\sqrt{1-(v/c)^2}$ gets very small and that the time in the reference frame that is moving gets very small as well (see Figure 2.21). *In other words, time slows down the faster you move.* This effect is hardly noticeable at the normal velocities that you would drive your car at (about 1 part in a billion), but when v gets greater than about one-half the speed of light, things start to slow down dramatically. For every hour of time that passes for a person at rest (see Figure 2.22), only several minutes will pass for a person who is in motion. The amount of time that passes for a person in motion is compared to the time that passes for a person who is at rest in Figure 2.22. *At 86% of the speed of light, a moving clock will slow down to about half of its normal speed.* This effect is not linear with velocity because of the square root in the expression for γ (the time dilation factor). Today, *global positioning systems*, including the GPS in your car, take

FIGURE 2.21 A picture of the International Space Station where time moves more slowly than it does on earth. (Picture courtesy of NASA.)

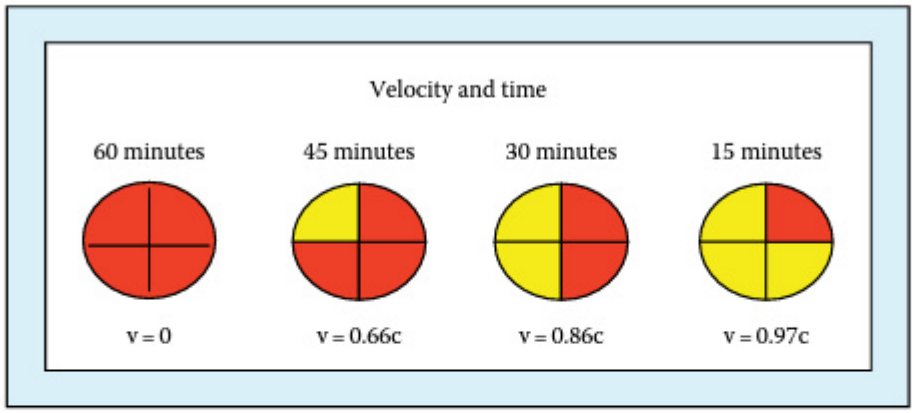

FIGURE 2.22 The slowing down of a physical clock as the velocity of a particle approaches the speed of light c.

advantage of this fact to precisely determine your location at any point on the Earth's surface. This strange phenomenon also affects the way that nuclear particles decay.

Student Exercise 2.1

An astronaut is orbiting the earth at a speed of 17,500 miles/h. If he orbits the earth for an entire year at this speed, how much slower is his clock than an identical clock on the surface of the Earth?

2.21 Effect of Motion on Particle Behavior and Radioactive Decay

Special relativity predicts that nuclear particles alter their behavior as their speed increases relative to a person who is observing them. There are several famous examples of this behavior that are of practical importance to the nuclear industry as a whole. First, a free neutron emitted from a uranium nucleus has an average lifetime of about 15 minutes. It will then decay into a neutron and a proton. If a nuclear reactor were aboard a spaceship, the average lifetime of the neutron would increase relative to the lifetime of a neutron in a reactor here on earth. We can actually measure this effect when a *cesium atomic clock* is brought on board the *International Space Station* (see Figure 2.21).

The cesium atoms in the clock vibrate slightly slower than the cesium atoms in the six atomic clocks on earth that are used to keep the world time. On earth, these clocks are accurate to about 16 digits (i.e., 1×10^{-16} seconds). On the space station, the cesium clock immediately shows a different value for the time in the last 3 and 4 digits. There is no difference between the cesium clocks that are in motion and at rest except that the cesium atoms in the clock on the space station are vibrating slower.

Another famous example of the effects of relativity can be seen in the collisions of particles in a nuclear particle accelerator. In a very large accelerator like the *TEVATRON* or the *Large Hadron Collider (LHC)* at *CERN*, alternating electric and magnetic fields in the rings of the collider can easily accelerate a proton or another relatively massive particle to 99.999% of the speed of light. When a proton that is moving at these speeds hits another object and decays, the reaction actually occurs in slow motion—at least relative to the same process when it occurs at much lower speeds. This is because the energies and the velocities of the particles are so high. Finally, the effect of *time dilation* can be observed in what are known as *cosmic ray showers*. Here very high-energy particles and composite nuclei hit the earth's upper atmosphere at speeds that approach 20%–30% of the speed of light. At these speeds, they decay much more slowly than their counterparts on the surface of the earth. In other words, *the process of radioactive decay is affected by how fast a decaying object is moving as well*. For an atom that can undergo radioactive decay, the half-life of the atom is increased from $T_{1/2}$ to $T'_{1/2} = T_{1/2}/\gamma$, where $\gamma = \sqrt{1-(v/c)^2}$ is again the time dilation factor. The mesons that carry the weak force in the atomic nucleus apparently slow down according to this rule as well. The following exercise illustrates how nuclear particles behave when their speed is increased relative to the person who is observing them. In classical physics, this person is also referred to as the *observer*.

Student Exercise 2.2

Consider a neutron that is ejected from a uranium nucleus in a nuclear reactor when the nucleus undergoes the process of nuclear fission. If the neutron has a kinetic energy E of 2 MeV, what is its velocity when it is ejected from the nucleus? Assume that the velocity of the neutron can be found from its kinetic energy E using the following equation: $V = \sqrt{2E/m}$.

Show that this yields a speed of 1.2×10^7 m/s. If the free neutron has an average lifetime of 13.7 minutes outside the nucleus when it is sitting at rest, what is its average lifetime if it is traveling with an energy of 2 MeV? Assume that it does not hit anything in the process to slow it down.

2.22 Relationship between the Mass and the Energy of Matter Particles

Particles like the proton, the neutron, and the electron are part of a family of nuclear particles called the *matter particles*. As the name implies, they always appear to have a measurable mass—even when they are at rest and not in motion. According to Einstein, the mass of a matter particle that is at rest is *less* than the mass of a matter particle that is moving with a velocity v. For matter particles, this relationship is expressed by the equation

$$m = \frac{m_o}{\sqrt{1-(v/c)^2}} \tag{2.56}$$

where

v is the velocity of motion
c is the speed of light
m_o is the mass that we measure for these particles when they are at rest

Sometimes this mass is called the *rest mass*. Now if we take the square root $\sqrt{1-(v/c)^2}$ in the denominator of Equation 2.56 and expand it in a *Taylor Series*, we find that

$$\sqrt{1-\left(\frac{v}{c}\right)^2} = \left(1-\left(\frac{v}{c}\right)^2\right)^{-1/2} = \left(1+\frac{1}{2}\left(\frac{v}{c}\right)^2+\frac{3}{8}\left(\frac{v}{c}\right)^4+\frac{5}{16}+\left(\frac{v}{c}\right)^6+\cdots\right) \tag{2.57}$$

So if we know the rest mass m_o of a matter particle and its velocity v, then its mass at any arbitrary speed is given by

$$m = \frac{m_o}{\sqrt{1-(v/c)^2}} \tag{2.58}$$

or

$$m(v) = m_o\left(1+\frac{1}{2}\left(\frac{v}{c}\right)^2+\frac{3}{8}\left(\frac{v}{c}\right)^4+\frac{5}{16}\left(\frac{v}{c}\right)^6+\cdots\right) \tag{2.59}$$

Now let us come back to the most famous of all of Einstein's equations, $E = mc^2$. If we substitute our new found expression for the mass m into it, we find that

$$E = m_o c^2 + \frac{1}{2}m_o v^2 + \cdots \tag{2.60}$$

At very low velocities ($v \ll c$), we can neglect all but the first two terms, in which case we obtain

$$E \approx m_o c^2 + \frac{1}{2}m_o v^2 \tag{2.61}$$

The first term in Equation 2.61, $m_o c^2$, is the *rest energy of a particle*, and the second term is its classical kinetic energy $\frac{1}{2}m_o v^2$. In virtually every textbook that discusses nuclear reactor physics, particle energies for the neutron, the proton, and the electron are quoted and measured in this way. For example, the kinetic energy of an average fission neutron is about 2 MeV, although some neutrons are emitted at lower energies, and some are emitted at energies as high as 10 or 15 MeV. Hence, at all but the very highest speeds ($v > 0.10c$), the classical equation for the kinetic energy of a matter particle can be used with little or no error

$$KE = \frac{1}{2}m_o v^2 \tag{2.62}$$

However, in the rare event that the speed of a matter particle exceeds about 10% of the speed of light, then it is better to use the more exact and relativistically correct result

$$KE = \frac{1}{2}m_o v^2 + \frac{3}{8}m_o v^4/c^2 + \frac{5}{16}m_o v^6/c^4 \tag{2.63}$$

when calculating the kinetic energy. In other words, both of these expressions are applicable to particles that have a finite rest mass m_o.

Student Exercise 2.3

Suppose that the radioactive half-life of a Barium isotope that is used in a nuclear medical instrument is 2.5×10^{12} seconds. If the instrument is sent from Boston to Hong Kong in a plane flying at an average speed of 1,000 miles an hour, and the cities are 12,000 miles apart, how much more of the isotope will remain when it arrives on the ground in Hong Kong than would be the case it it were simply manufactured in Hong Kong instead?

2.23 Behavior of Nuclear Particles at Very High Speeds

In classical physics, a matter particle is defined as one that has a measurable rest mass m; in other words, a particle is a matter particle when its mass $m > 0$ and, at the same time, $v = 0$. The electron, the proton, the neutron, and the quark (as well as their antiparticles) are all examples of particles that follow this rule. Their rest masses and their equivalent rest energies, calculated by using the equality $E = m_o c^2$, are shown in Table 2.4. The fact that these particles have a finite rest

TABLE 2.4
Mass of a Nuclear Particle as Its Speed Increases

Fraction of Light Speed (v/c)	Relative Mass of Moving Particle
0.00000	1.00
0.05000	1.00
0.10000	1.01
0.15000	1.01
0.20000	1.02
0.25000	1.03
0.30000	1.05
0.35000	1.07
0.40000	1.09
0.45000	1.12
0.50000	1.15
0.55000	1.20
0.60000	1.25
0.65000	1.32
0.70000	1.40
0.75000	1.51
0.80000	1.67
0.85000	1.90
0.90000	2.29
0.95000	2.20
0.97500	2.50
0.99000	7.09
0.99600	11.19
0.99950	31.63
0.99990	70.71

The initial mass or rest mass is normalized to 1.0.

mass has profound consequences when it comes to how they behave at much higher speeds. *At normal speeds (usually less than about 10% of the speed of light), it can be shown that the mass of a nuclear particle is not affected much by the particle's velocity*. Therefore, at low speeds, the assumption that the mass m is a constant is usually a good one. However, at higher speeds, Einstein showed that the mass of a matter particle actually increases relative to the mass that it has when it is at rest. This is a real physical effect that is observed every day when the speed of a particle gets beyond a certain point. The exact dependence of a particle's mass on its velocity is given by

$$m(v) = \frac{m_o}{\sqrt{1-(v/c)^2}} \tag{2.64}$$

where

m_o is the mass measured for the particle when it is at rest
c is the speed of light

If we expand the denominator of Equation 2.64 in a Taylor series and keep only the first few terms, we find that the mass of a matter particle at higher velocities can also be calculated from

Mass as a Function of Particle Velocity

$$m(v) = m_o + \frac{1}{2}m_o v^2/c^2 + \frac{3}{8}m_o v^4/c^4$$
$$\Rightarrow m(v) = m_o\left(1 + \frac{1}{2}v^2/c^2 + \frac{3}{8}v^4/c^4\right) \tag{2.65}$$
for "high" velocities $(v \geq 1/10c)$

where

the first term m_o is the standard rest mass of course
v is the velocity usually measured in meters per second

The classical assumption of m being constant is good to about 1 part in 200 (or 0.5%) if v = 1/10th c. However, at particle speeds greater than about 0.10c, it is better to include the higher-order terms in the mass calculation, or to use Equation 2.56 directly. This increase in the mass of a particle as its speed increases makes the particle heavier and heavier the closer we get to the speed of light. The mass of the matter particle having a rest mass of m_o is shown in Table 2.4 and in Figure 2.23 for various values of v as we approach the speed of light c. It is easy to see that at 99% of the speed of light, the mass of a matter particle will increase by a factor of about 7, and at 99.99% of the speed of light, the mass of a matter particle will increase by a factor of about 70. This makes it very difficult to accelerate nuclear particles beyond a certain point because all that happens is that their energy and momentum increase indefinitely with very little additional increase in the velocity. As we have seen, the momentum P increases as

$$P = \frac{m_o v}{\sqrt{1-(v/c)^2}} \tag{2.66}$$

and the energy E increases as

$$E = \frac{m_o c^2}{\sqrt{1-(v/c)^2}} \tag{2.67}$$

which in the case of the momentum is even greater than the increase in the rest mass alone. Using the previous Taylor series expansions, the energy and the momentum both vary with velocity as

Energy at High Velocities

$$E = m_o c^2 + \frac{1}{2}m_o v^2 + \frac{3}{8}mv^4/c^2 \tag{2.68}$$
for "high" velocities $(v \geq 1/10c)$

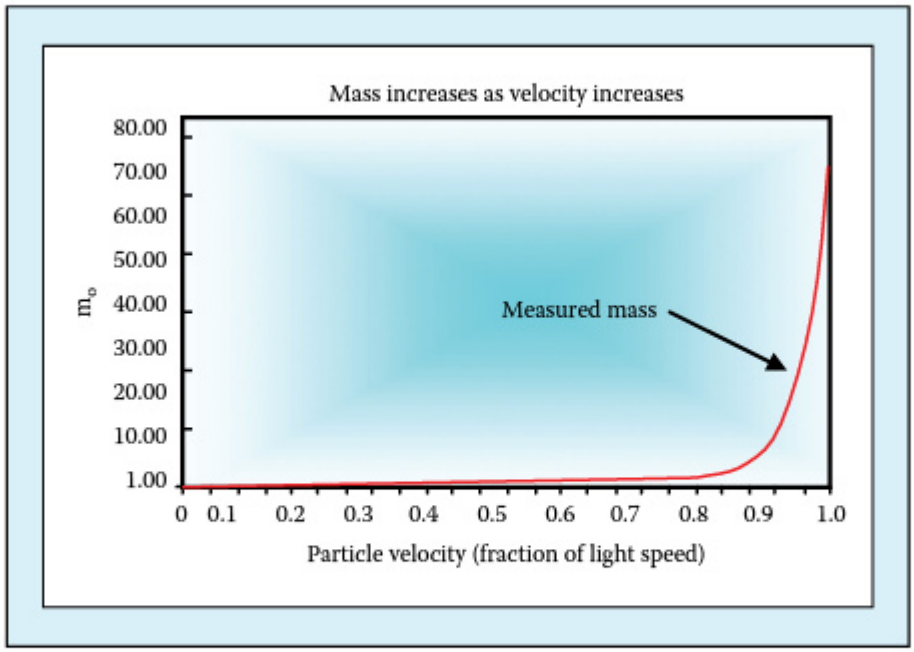

FIGURE 2.23 The mass of a nuclear particle as its speed increases.

and

Momentum at High Velocities

$$P = m_o v + 1/2 m v^3/c^2 + 3/8 m_o v^5/c^4 \quad \text{for "high" velocities } (v \geq 1/10c) \tag{2.69}$$

where the first terms in each case $P = m_o v$ and $E = m_o c^2$ and $K = \frac{1}{2} m_o v^2$ are the standard classical results. *When evaluating the outcome of a particular reaction, it is always important to consider the effect that this mass increase can have.* Otherwise, it may be difficult to determine if the kinetic energy and momentum have been conserved. For example, in certain types of inelastic scattering reactions that we will discuss in Chapter 3, the nucleus simply absorbs the excess energy and momentum, until a gamma ray is released at a much later time. The nucleus vibrates in an excited state, but its kinetic motion alone is not sufficient for energy and momentum to be conserved.

2.24 Converting Particle Energies to Particle Velocities

At low velocities relative to the speed of light ($v < 0.1c$), it is entirely legitimate to calculate the velocity of a matter particle (but not the photon) from the classical expression

$$V = \sqrt{\frac{2E}{m}} \tag{2.70}$$

if we know the kinetic energy E, since $E = \frac{1}{2} m V^2$. To do the conversion, we can use the rest masses shown in Table 2.2. To convert from electron volts to joules, the following expressions can be used:

Definition of the Electron Volt and Its Value in Joules

$$\begin{aligned} 1\ \text{eV} &= (\text{charge of one electron}) \cdot (1\ \text{V}) \\ &= (1.60 \times 10^{-19}\ \text{C}) \cdot (1.00\ \text{V}) \\ &= 1.60 \times 10^{-19}\ \text{J} \end{aligned} \tag{2.71}$$

With this definition, we can see that *1 million electron* volts = *1 MeV* = $(1.00 \times 10^6)(1.60 \times 10^{-19}\ \text{J}) = 1.60 \times 10^{-13}$ J. To convert from joules and kilograms to meters and centimeters, the following expression can be used:

$$1\left(\text{J/kg}\right)^{1/2} = 1\ \text{m/s} \tag{2.72}$$

This all works perfectly well as long as the particle velocities are small relative to the speed of light, but what happens if the energies become much higher? We know from Equation 2.68 that

$$E = \frac{1}{2}m_o v^2 + \frac{3}{8}m_o v^4/c^2 \tag{2.73}$$

While this is still an approximation at very, very high speeds, it can be used with little error for neutron and proton energies up to about 100 MeV. Since this equation is quadratic in v, we can solve for v if we know m and E. If we make the following substitution $s = v^2$ in Equation 2.73, we obtain

$$E = \frac{1}{2}m_o s + \frac{3}{8}c^2 m_o s^2 \tag{2.74}$$

$$\Rightarrow 3s^2 + 4c^2 s - 8Ec^2/m_o = 0 \tag{2.75}$$

This equation can be solved for s using the quadratic formula* $s = [-b \pm \sqrt{b^2 - 4ac}\,]/2a$. After plugging in the appropriate values for a, b, and c, we obtain

$$s = -2c^2/3 \pm 4c\sqrt{c^2 + 6E/m_o} \tag{2.76}$$

Solving for s and throwing out the negative root, we find that

$$s = 4c\sqrt{c^2 + 6E/m_o} - 2c^2/3 \tag{2.77}$$

so the particle velocity at much higher speeds can be found from the expression

$$v = \sqrt{s} = \sqrt{4c\sqrt{c^2 + 6E/m_o} - 2c^2/3} \tag{2.78}$$

where m_o is the rest mass. With this equation, we can calculate v given E and m up to much higher energies (say, $v \leq c/2$) with little error. Of course, this equation does not apply to the photon because the photon always travels at the speed of light.

2.25 Relationship between the Energy of a Neutron and Its Velocity

We can estimate how fast a neutron is traveling through a reactor core if we know the value of its kinetic energy E. The classical expression for the kinetic energy $E = \frac{1}{2}mv^2$ is relatively accurate for kinetic energies up to about 100 MeV, because even at 100 MeV, the kinetic energy of a neutron is only about one-tenth of its rest mass energy (939.55 MeV). If the velocity of the neutron is measured in meters per second and its kinetic energy is measured in MeV, then its energy E is related to its velocity v by

The Energy–Velocity Equation (for a Neutron or Proton)

$$E = 5.227 \times 10^{-15}\, v^2\ (\text{MeV}) \tag{2.79}$$

* The quadratic formula states that the equation $ax^2 + bx + c = 0$ has the solution $x = \{-b \pm \sqrt{b^2 - 4ac}\,\}/2a$. Additional information on the quadratic formula is available at *http://www.mathsisfun.com/algebra/quadratic-equation-derivation.html*. The quadratic formula is usually introduced to students in a high school algebra class.

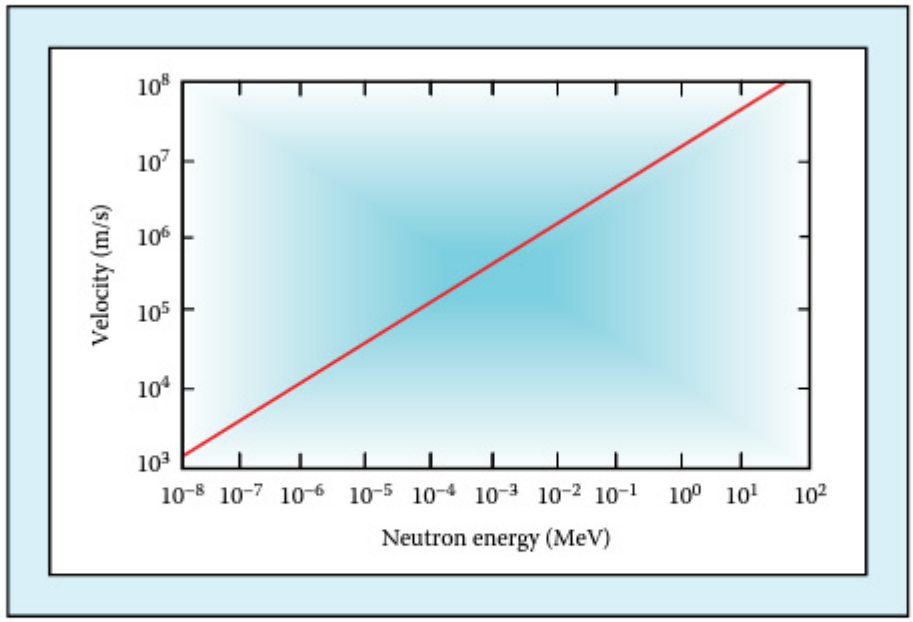

FIGURE 2.24 A graph showing the relationship between a neutron's speed v and its kinetic energy E.

and its velocity v is related to its energy E by

The Velocity–Energy Equation (for a Neutron or Proton)

$$v = 1.383 \times 10^7 \, E^{1/2} \, (\text{m/s}) \tag{2.80}$$

Figure 2.24 shows a graph of these equations for kinetic energies and velocities of interest to the average nuclear scientist and engineer. In other words, a 1 MeV neutron has a speed of about 6×10^6 m/s, and a 0.025 MeV neutron has a speed of about 2187 m/s. Thus, a slow-moving or "thermal" neutron would be able to cross the width of a reactor pressure vessel (about 4 m) in just 0.0018 seconds. Photons normally travel much faster than this, and even when their speed is reduced because they must bounce off of atoms as they move, their rate of transport across an object the size of a reactor pressure vessel is essentially instantaneous. Their speed of propagation in different materials is discussed in the next section, and for transparent materials, the reduction in their apparent speed is related to a parameter known as the *index of refraction*.

2.26 Speed of Photon Propagation in a Material Medium

The speed of light in empty space is 299,792,458 m/s, or about 186,282 miles/s, and according to the theory of relativity, *the speed of light is the maximum speed at which all energy, matter, and information in the universe can travel*. It is the speed at which all massless particles (such as the photon) and their associated fields can travel in a vacuum. It is also the speed that gravitational waves are predicted to travel. The value of the speed of light is the same regardless of the motion of the source or the inertial reference frame in which it is measured. In other words, *the speed of light does not depend upon how fast an observer is moving*. As we have just seen, the speed of light c interrelates space and time and also appears in Einstein's famous equation $E = mc^2$ of mass–energy equivalence.

The speed at which light travels through transparent materials, such as air or water, is always *less* than the speed it travels through a vacuum. This is because the photons in a light wave have to bounce off of atoms in their path as they move. The ratio between c and the speed v at which light travels in a material is called the index of refraction of the material. The formal definition of the refractive index is $n = c/v$, where n is always greater than 1.0. The refractive index of some common materials is shown in Table 2.5. In most cases, the index of refraction is also a function of the photon's wavelength. When it comes to visible light, the refractive index of glass is about 1.5, which means that light in glass travels at approximately 67% of the speed it travels in empty space, or about 200,000 km/s. The refractive index for visible light in air is 1.000293, so the speed of light in air is 299,705 km/s (just 88 km/s slower than c). The speed of light comes into

TABLE 2.5
Values for the Refractive Index of Some Common Materials

Material	Refractive Index	Speed of Propagation (m/s)
Empty space (the vacuum)	1.00000	299,792,458
Air at STP	1.00029	299,705,000
Ice	1.31	229,000,000
Water at 20°C	1.33	225,563,910
Typical crown glass	1.52	197,368,420
Crown glasses	1.52–1.62	~189,873,420
Diamond	2.417	124,120,810

play in nuclear engineering because the rate at which particles decay is a function of their speed. As the speed increases, the decay rate slows down, and this can affect how far a neutron can travel before it decays.

Example Problem 2.8

If the kinetic energy of the neutron is 2 MeV when it is first emitted from an atomic nucleus, what is its velocity, and what fraction of the velocity of the speed of light is this?

Solution According to Figure 2.24, a 2 MeV neutron has an initial velocity of about 1.2×10^7 m/s. Since the velocity of light is about 3×10^8 m/s, the neutron is emitted from the nucleus at about 4% of the speed of light. [Ans.]

2.27 Controlling the Behavior of Nuclear Particles without an Electrical Charge

In the early 1900s, scientists began to realize that many nuclear particles (notably neutrons, photons, and neutrinos) were not affected by the presence of electric or magnetic fields. In particular, they found that the paths of light waves and neutrons could *NOT BE BENT* by an electric or magnetic field. In general, the motion of an electrically neutral particle (except a light wave) must be described by an equation called a *diffusion equation*, which the neutrons in a reactor must also obey. Gravity can affect the motion of these particles, but it is so weak relative to the other forces of nature that there are very few problems in which gravity has any real effect until we have to deal with objects the size of mountains.

Because the paths of neutrons cannot be affected by electric or magnetic fields, Maxwell's equations of electricity and magnetism (see Section 2.1) *DO NOT APPLY* to them. Their motion must be modeled using either a neutron transport equation or a simplified form of the transport equation called a diffusion equation. The form of the transport equation that is used in the nuclear industry to predict the motion of neutrons and photons is called the *Boltzmann transport equation.* A simplified form of this equation is shown in Figure 2.25. Under certain conditions that we will subsequently

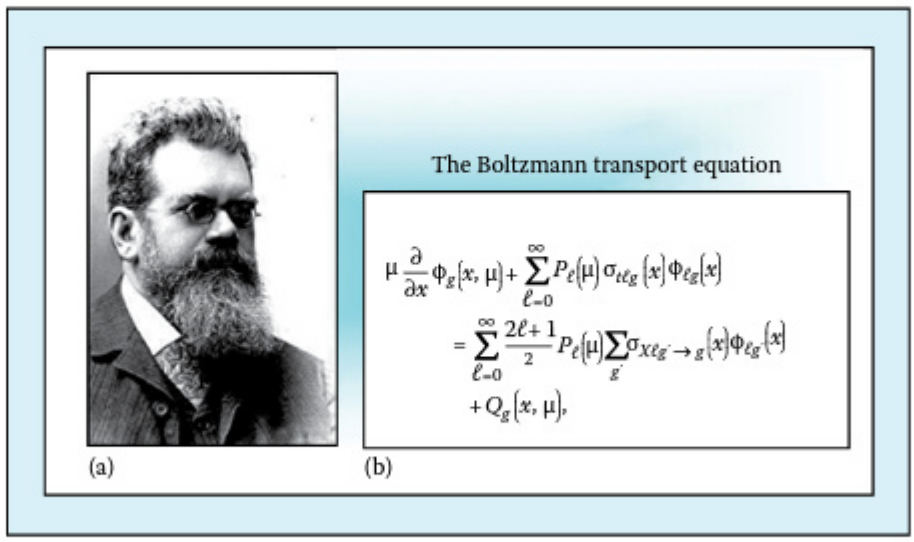
The Boltzmann transport equation
$$\mu \frac{\partial}{\partial x}\Phi_g(x,\mu)+\sum_{\ell=0}^{\infty}P_\ell(\mu)\sigma_{t\ell g}(x)\Phi_{\ell g}(x) = \sum_{\ell=0}^{\infty}\frac{2\ell+1}{2}P_\ell(\mu)\sum_{g'}\sigma_{x\ell g'\to g}(x)\Phi_{\ell g'}(x) + Q_g(x,\mu),$$
(a)
(b)

FIGURE 2.25 A picture of Ludwig Boltzmann (a) and the multigroup neutron transport equation (b) that bears his name. (Boltzmann's picture provided by Wikipedia.)

discuss in Chapter 22, the Boltzmann transport equation can be reduced to a simpler equation called the *neutron diffusion equation*. Together these two equations can be used to solve virtually any particle transport problem in nuclear science and engineering. Solving these two equations requires some knowledge of differential and integral equations that we will attempt to provide as we proceed further into this book. In most cases, they must be solved *numerically* because reactor geometries are simply too complex for analytical solutions to be readily available. The neutron diffusion equation is derived in Chapter 11, and its solutions are presented in Chapters 12 through 16. The neutron transport equation is normally discussed in more advanced textbooks, although we will also discuss it in Chapter 22.*

2.28 Connecting the Microscopic World to the Macroscopic One

Some of the material we have discussed so far may be hard to relate to the process of nuclear power production—particularly if one happens to be a nuts and bolts engineer. However, now that we have been able to describe how the nuclear world works, we would like to discuss how the equations we have just presented can be used to describe the nuclear reactions that occur inside a nuclear power plant. This will eventually lead to a discussion of nuclear processes and nuclear cross sections. We will then use what we have learned to predict the rate that neutrons (and other nuclear particles) can be created and destroyed. *In general, trillions of nuclear particles are created and destroyed in a nuclear reactor every second. The total energy E that is produced in the core is then equal to the mass deficit Δm for the total number of particle interactions multiplied by the square of the speed of light c.* This energy can be found from Einstein's equation

$$E = \Delta mc^2 \tag{2.81}$$

of mass–energy equivalence. In a reactor, it shows up in the form of heat Q that we can measure and use to produce useful power. We will discuss the process that allows this to occur as we proceed further into the book. *However, not all of this energy is deposited as heat, and about 5% of it turns out to be unrecoverable.*

Recoverable and Unrecoverable Nuclear Energy

$$Q \cong 0.95\,\Delta mc^2\,(\text{recoverable}) \tag{2.82}$$

$$Q \cong 0.05\,\Delta mc^2\,(\text{unrecoverable}) \tag{2.83}$$

The recoverable component of this energy (which we can measure as heat) is then equal to about 0.95 Δmc^2. *The remainder of this energy is carried off by small ghostlike particles called neutrinos and cannot be recovered by any physical process we know of today.* On a nuclear level, the amount of recoverable energy per fission turns out to be about 200 MeV. The amount of unrecoverable energy is then about 10 MeV. Here the term MeV is equal to one million electron volts, and one million electron volts is equal to $1.60217653 \times 10^{-13}$ J. The definition of the electron volt (eV) was presented in a previous section.

2.29 Calculating Nuclear Energy from E = mc²

The nuclear power industry in the world today is a direct consequence of Einstein's equation $E = mc^2$, which was first proposed by Albert Einstein in 1905. *Einstein's equation suggests that there is a fundamental relationship between mass and energy*, and it also implies that a small amount of mass m is equivalent to a very large amount of energy E. The constant of proportionality between these two interrelated properties is then the square of the speed of light (which happens to be a very large number!). Since the value of c^2 is 8.99×10^{16} m^2/s^2, Einstein's equation implies that 1 kg of a material (such as uranium) is equivalent to about 8.99×10^{16} J of thermal energy. This is as much energy as a 24.5 megaton bomb can release! Eventually, Einstein's equation led to the development of the first nuclear power plants and the first atomic bomb.

In other words, modern nuclear engineers have Einstein's equations to thank for the existence of the nuclear power industry in the world today! Since his original derivation was presented in 1905, several alternative derivations have been proposed. In any event, Einstein's equation is still considered to be the most tangible by-product of the *theory of*

* For example, see *Nuclear Reactor Analysis*, by Duderstadt and Hamilton (described in Reference 4).

special relativity. It appears everywhere today—on billboards, on the Internet, in YouTube videos, and even on the back of smartphones. In other words,

$E = mc^2$ is the defining equation of the nuclear age

Later the value of m was subsequently interpreted as the *velocity-dependent mass* of a particle m(v) that is of course different from its rest mass m_o. This interpretation led physicists to conclude that the kinetic energy of a nuclear particle is given by

$$KE = mc^2 - m_oc^2 \tag{2.84}$$

which is again a commonly used result. The *total energy* E of a nuclear particle is then the sum of its potential energy PE and its kinetic energy KE:

$$\text{Total energy } E = PE + KE \tag{2.85}$$

This further implies that since the kinetic energy is given by $KE = mc^2 - m_oc^2$, the potential energy PE must be equal to

$$PE = m_oc^2 \tag{2.86}$$

The sum of the two is then the total energy $E = mc^2$ (Figure 2.26). *According to this definition, the photon (which has no rest mass) has no potential energy.* The value of m used in this equation is simply

$$m = \frac{m_o}{\sqrt{1-(v/c)^2}} \tag{2.87}$$

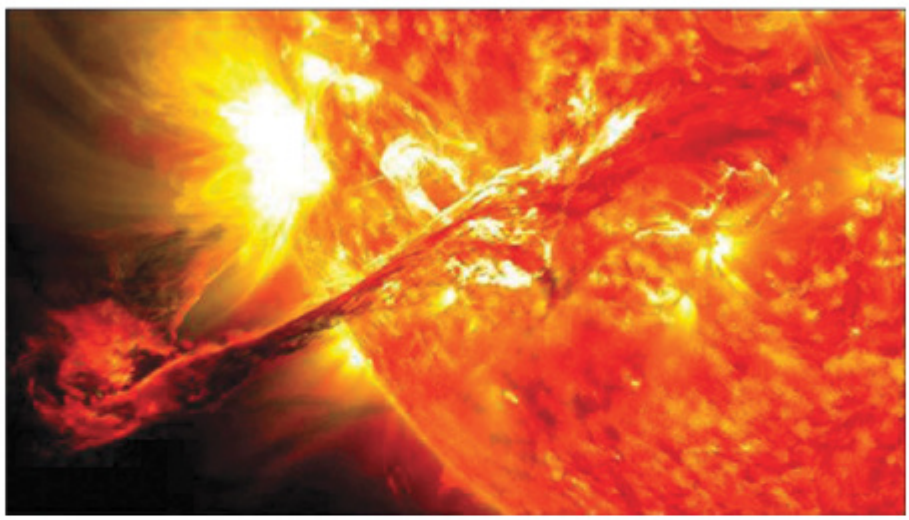

A solar flare caused by the process of nuclear fusion

FIGURE 2.26 Einstein's famous equation $E = mc^2$ implies that the mass m and the energy E of an object are interchangeable. It explains how nuclear energy is produced in the interior of stars and how atomic bombs can be produced by the process of nuclear fission. In both cases, a small amount of mass is converted into a large amount of energy. The constant of proportionality between the amount of mass that is lost and the amount of energy that is produced is c^2, which is the square of the speed of light. The speed of light (about 300,000,000 m/s or 186,000 miles/s) is a very large number. In the picture given earlier, mass is converted into energy in the sun's interior by thermonuclear fusion. The corona that surrounds the sun is a glowing plasma of gas with an average temperature of several million degrees. The large plume of gas on the left is a solar flare. Occasionally, the Earth is also hit by solar flares. (Picture provided by NASA.)

In future chapters, we will explore some additional implications of this important equation. For now, it is important to keep in mind that the *mass of a matter particle is the least when it is at rest*. As soon as it starts to move, its mass increases because some of the energy required to set it in motion becomes part of the particle itself and can no longer be separated from it. The following example shows when this can become important.

Example Problem 2.9

A particle with a rest mass of m_o is moving through a nuclear reactor at 60% of the speed of light. Using the equations given earlier, derive an expression for the kinetic energy that this particle must have.

Solution According to the equations of special relativity, the kinetic energy of a particle with a finite rest mass is given by $KE = mc^2 - m_oc^2$, where the value of m is given by $m = m_o/\sqrt{1-(v/c)^2}$. At 60% of the speed of light ($v = 0.6c$), the value of m is $m = m_o/\sqrt{1-(v/c)^2} = m_o/\sqrt{1-0.36} = m_o/\sqrt{0.64} = m_o/0.8 = 1.25m_o$. Therefore, the kinetic energy of the particle is equal to $KE = 1.25\ m_oc^2 - m_oc^2 = 0.25\ m_oc^2$. [Ans.]

2.30 Understanding Nuclear Energy Production

Finally, Einstein's equation can be used to predict the amount of energy released by the fission process in a reactor core. Thermal energy is produced in a nuclear power plant by the process of *nuclear fission*, and it is eventually distributed through the core by alpha, beta, and gamma rays and by other by-products of the fission process. Most of this heat is deposited in the fuel, but a few percent of it is deposited in the coolant and the cladding. Gamma rays also deposit some of their energy in the pressure vessel wall. Most of the energy produced by the fission process is carried away by radioactive *fission products* that are also produced when an atomic nucleus splits apart. Fission products are given the symbol FP, while alpha, beta, and gamma rays are given the symbols α, β, *and* γ, respectively. *Alpha particles* refer to *ionized helium nuclei, beta rays* refer to high-energy electrons and positrons, and *gamma rays* refer to high-energy photons. In addition to these numerous nuclear particles and fission products, several neutrons are released when an atomic nucleus splits apart. The kinetic energy of these neutrons and other nuclear particles is eventually transformed into *heat*, which increases the temperature of the core. Coolant is then pumped through the core to remove this heat, and the heated coolant is eventually sent to the nuclear steam supply system to generate electric power.

2.31 Converting the Kinetic Energy of Nuclear Particles into Thermal Energy and Heat

Once an atomic nucleus splits apart, the fission products and fission neutrons that are released from it move away from the disintegrated nucleus at very high speeds, which are normally much faster than any man-made vehicle can go, but in a nuclear power plant the mass of the by-products is always *less* than the mass of the original nucleus. The *mass deficit* Δm between the mass of the original nucleus and the mass of all of the by-products is directly proportional to the kinetic energy of the by-products. The kinetic energy of the by-products (the fission products and the fission neutrons) is then

$$KE = \Delta mc^2 \tag{2.88}$$

where c is the speed of light (~300,000,000 m/s). Because the speed of light is such a large number, Equation 2.88 implies that a very small reduction in the total mass Δm of the reactants can result in a large amount of energy being produced. The kinetic energy KE of the nuclear particles that are produced in the fission process can then be represented by

$$KE = \sum_{n=1}^{N}\left(\frac{1}{2}m_nv_n^2\right) \tag{2.89}$$

where

N is the number of particles that are produced

v_n is their velocity

This kinetic energy is also equal to the energy ΔE that is released when a small amount of mass Δm is converted into pure energy. Thus, the kinetic energy of all of these particles is equivalent to

$$KE = \sum_{n=1}^{N}\left(\frac{1}{2}m_n v_n^2\right) = \Delta mc^2 \tag{2.90}$$

and this is the energy that eventually shows up in the form of *heat* Q. Moreover, the *First Law of Thermodynamics* (which is discussed in many thermodynamics books) states that this kinetic energy must show up in the form of heat and that the heat produced must always be conserved. We can express this fact by requiring that

$$Q = KE = \sum_{n=1}^{N}\left(\frac{1}{2}m_n v_n^2\right) = \Delta mc^2 \tag{2.91}$$

When gamma rays are produced, an additional term must be added to the summation above to account for the presence of these gamma rays. This can be done by expanding the summation to read

$$Q = KE = \sum_{n=1}^{N}\left(\frac{1}{2}m_n v_n^2\right) + \sum_{m=1}^{M} hf_m = \Delta mc^2 \tag{2.92}$$

where

M is the number of gamma rays
h is Planck's constant
f is their frequency of vibration (in cycles per second)

The value of *Planck's constant* is approximately 6.6×10^{-34} kg · m²/s or $6.6260695 \times 10^{-34}$ J seconds = $4.1356675 \times 10^{-15}$ eV seconds. *Thus, a 1 MeV gamma ray has a vibrational frequency of* $f = 1 \times 10^6$ *eV/*$4.1356675 \times 10^{-15}$ *eV seconds* $\cong 2.42 \times 10^{20}$ *Hz*. In other words, the kinetic energy of a gamma ray is directly proportional to its frequency of vibration. Finally, there are many different ways in which an atomic nucleus can split apart if it absorbs a passing neutron, and each way results in a slightly different amount of nuclear energy being produced. Each fission event also produces different types of fission products with different atomic masses and different numbers of fission neutrons. For U-235 and Pu-239, some of the by-products of the fission process are

Examples of the Nuclear Fission Process for Uranium-235 and Plutonium-239

$$\begin{aligned}
&{}^{1}_{0}n + {}^{235}_{92}U \rightarrow {}^{236}_{92}U \rightarrow {}^{140}_{55}Cs + {}^{93}_{37}Rb + 3\,{}^{1}_{0}n + Q' \\
&{}^{1}_{0}n + {}^{235}_{92}U \rightarrow {}^{236}_{92}U \rightarrow {}^{139}_{56}Ba + {}^{94}_{36}Kr + 3\,{}^{1}_{0}n + Q'' \\
&{}^{1}_{0}n + {}^{235}_{92}U \rightarrow {}^{236}_{92}U \rightarrow {}^{142}_{54}Xe + {}^{92}_{38}Sr + 2\,{}^{1}_{0}n + Q''' \\
&{}^{1}_{0}n + {}^{235}_{92}U \rightarrow {}^{236}_{92}U \rightarrow {}^{141}_{56}Ba + {}^{92}_{36}Kr + 3\,{}^{1}_{0}n + Q'''' \\
&{}^{1}_{0}n + {}^{235}_{92}U \rightarrow {}^{236}_{92}U \rightarrow {}^{142}_{56}Ba + {}^{92}_{36}Kr + 2\,{}^{1}_{0}n + Q''''' \\
&{}^{1}_{0}n + {}^{235}_{92}U \rightarrow {}^{236}_{92}U \rightarrow {}^{144}_{56}Ba + {}^{90}_{36}Kr + 2\,{}^{1}_{0}n + Q'''''' \\
&{}^{1}_{0}n + {}^{235}_{92}U \rightarrow {}^{236}_{92}U \rightarrow {}^{134}_{54}Xe + {}^{100}_{38}Sr + 2\,{}^{1}_{0}n + Q''''''' \\
&{}^{1}_{0}n + {}^{239}_{94}Pu \rightarrow {}^{240}_{94}Pu \rightarrow {}^{148}Ce_{58} + {}^{89}Kr_{36} + 3\,{}^{1}_{0}n + Q''''''''
\end{aligned} \tag{2.93}$$

where the kinetic energy released, Q, has a value between 190 and 220 MeV, and additional kinetic energy is released when the fission products decay. In Equation 2.93, the superscripts ′, ″, ‴, ⁗, etc., are intended to indicate that the same amount of kinetic energy is *NOT* released all of the time. In fact, it depends on the fission products that are produced as well as the number of neutrons that leave the reaction. The *average amounts* of energy released for different nuclear

fuels vary from about 210 MeV to about 215 MeV. (The exact amounts are presented in Chapter 7.) In Equation 2.93, it is assumed that this kinetic energy is eventually converted into thermal energy or heat. Of course, the *unrecoverable* kinetic energy is carried away by light, ghostlike particles called the *neutrinos*. The neutrinos pass right through the earth and distribute this kinetic energy somewhere between the stars. Why so many neutrinos are created in these reactions is one of the great unsolved problems of modern physics, and the solution to this problem may shed some light on the fate of the universe itself.

Example Problem 2.10

In a nuclear reaction, the masses of the particles leaving the reaction weigh 0.22 AMU less than the masses of the particles entering the reaction. Based on this fact alone, how much energy will ten reactions of this type produce per second?

Solution Earlier in the chapter, we found that 1 AMU has an energy content of 1 AMU = 931.494 MeV/c^2. Since 0.22 AMUs of mass are converted into energy in each reaction, Einstein's equation tells us that the energy released in a single reaction is $E = \Delta mc^2 = 0.22 \times 931.494\ \text{MeV}/c^2 \times c^2 = 204.95$ MeV. Therefore, ten reactions will produce a total of 2049.5 MeV/s. Eventually this energy will show up in the form of *heat*. [Ans.]

References

Books and Textbooks

1. Kaplan, I. *Nuclear Physics*, Addison-Wesley, Reading, MA (1965).
2. Eisberg, R. *Fundamentals of Modern Physics*, John Wiley & Sons, New York (1961).
3. Resnick, R. and Halliday, D. *Fundamentals of Physics*, John Wiley & Sons, New York (1967).
4. Duderstadt, J. and Hamilton, L. *Nuclear Reactor Analysis*, John Wiley & Sons, New York (1976).
5. Lamarsh, J.R. and Baratta, A.J. *Introduction to Nuclear Engineering*, Prentice Hall, Upper Saddle River, NJ (2001).
6. Feynman, R.P., Leighton, R. and Sands, M. *The Feynman Lectures on Physics*, Narosa Publishing House, New Delhi, India (2011).
7. Shultis, K. and Faw, R. *Fundamentals of Nuclear Science and Engineering*, 2nd edn., CRC Press, Boca Raton, FL (2008).
8. Masterson, R.E. *Nuclear Engineering Fundamentals: A Practical Perspective*, CRC Press, Boca Raton, FL (2017).

Web References

1. *http://www.1728.org/freqwave.htm.*
2. *http://en.wikipedia.org/wiki/Neutrino.*
3. *http://www.crystalinks.com/phila.html.*
4. *http://en.wikipedia.org/wiki/Antimatter.*
5. *http://home.web.cern.ch/topics/antimatter.*
6. *http://plato.stanford.edu/entries/equivME/.*
7. *http://en.wikipedia.org/wiki/Maxwell's_equations.*
8. *https://www.youtube.com/watch?v=202fU9qIVK4.*
9. *https://www.youtube.com/watch?v=ChjyCR8V2Bg.*
10. *http://en.wikipedia.org/wiki/Lorentz_transformation.*
11. *http://en.wikipedia.org/wiki/Philadelphia_Experiment.*
12. *http://hyperphysics.phy-astr.gsu.edu/hbase/electric/maxeq.html.*
13. *http://hyperphysics.phy-astr.gsu.edu/hbase/nuclear/nucuni.html.*
14. *http://hyperphysics.phy-astr.gsu.edu/hbase/particles/neutrino.html.*
15. *http://en.wikipedia.org/wiki/Mass%E2%80%93energy_equivalence.*
16. *http://www.mathsisfun.com/algebra/quadratic-equation-derivation.html.*
17. *http://www.natureworldnews.com/articles/5968/20140210/mass-neutrinos-accurately-calculated-first-time-physicists-report.htm.*

Additional References

- Important physical constants used by nuclear scientists and engineers can be found in *Appendix A*.
- Unit systems and their conversion factors can be found in *Appendix B*.
- Nuclear cross sections for many important nuclear materials can be found in *Appendix C*.
- Physical properties of important nuclear materials can be found in *Appendix D*.
- Atomic masses, half-lives, and natural abundances can be found in *Appendix E*.

Questions for the Student

The following questions cover the material presented in this chapter and, in some cases, previous chapters as well. They are designed to test how well the student has acquired a working knowledge of the subject matter.

1. Name three fundamental conservation laws that all nuclear particles must obey.
2. Name an additional conservation law that the protons and the neutrons inside the nucleus of an atom must obey.
3. What is the Law of the Conservation of Energy?
4. What is the Law of the Conservation of Momentum?
5. What is the Law of the Conservation of Charge?
6. What is a Feynman Diagram, and what does it represent?
7. What is a simple equation for the momentum of a particle of mass m?
8. What is the equation for the energy of a photon?
9. If a photon is ejected from an atomic nucleus with twice the energy of another photon, how do the frequencies of the two photons compare?
10. Neutrinos are created in a nuclear reactor all of the time. What percentage of the energy do they carry away, and where does this energy go?
11. What is Planck's constant, and who discovered it?
12. What is a positron, and what is its corresponding matter particle?
13. If there were such a thing as an antiproton, and we shot one through a magnetic field at right angles to the field, what would we observe, relative to doing the same thing with a normal proton?
14. What is the classical expression for the kinetic energy of a proton?
15. What is the energy equivalent of one atomic mass unit, or AMU?
16. What symbol is sometimes used for the atomic mass instead of the AMU?
17. If a proton were traveling close to the speed of light, how would this equation change?
18. In a classical sense, is the momentum of a particle a scalar or a vector quantity?
19. What is the "rest mass" of a matter particle?
20. What is an electron volt? What is a KeV and an MeV?
21. What is the relationship between a photon's frequency and its wavelength?
22. Fill in the following sentence with the appropriate word or phrase: A photon with a wavelength of 10 cm is sometimes called a _____ wave.
23. How long does a neutron live inside the nucleus of an atom?
24. What is a photon with a frequency of 10^{+15} cycles/s called?
25. What is a photon with a frequency of 10^{+18} cycles/s called?
26. What is a photon with a frequency of 10^{+22} cycles/s called?
27. What is a photon with a frequency of 10^{+10} cycles/s called?
28. Which one of these would you use to cook something in a microwave oven?
29. If a neutron outside the nucleus of an atom (also called a free neutron) were to decay into some other particles, what would these particles most likely to be?
30. What conservation laws would you use to predict the by-products of the decay process?
31. Does a radio wave have a higher energy or lower energy than a microwave?
32. In a reaction involving the fission of an atomic nucleus, what is the symbol "Q" normally used to refer to?
33. At what frequency (in cycles per second) is a typical gamma ray emitted from a reactor core?
34. What is an AMU, and why was it originally invented?
35. What is a neutrino, and how thick would a lead plate have to be to have a 50% chance of stopping one?
36. If all of the momentum of a matter particle of mass m_o and velocity v was transferred to a photon, what would the energy E of the photon be?
37. What would be its wavelength?
38. What is the electrical charge of a Quark?
39. What is the atomic weight of a proton in AMUs and in MeV/c^2?
40. What is the atomic weight of a neutron in AMUs and in MeV/c^2?
41. What is the atomic weight of an electron in AMUs and in MeV/c^2?
42. Does a photon have any rest mass?
43. There are two forms of radioactive beta decay—B^- decay and B^+ decay. What particle is emitted in B+ decay?
44. By convention, how is the AMU defined?
45. At what speed does a matter particle have its least possible mass?
46. What is the difference in the atomic weight between a neutron and a proton?

47. By what fundamental process can a neutron be converted into a proton and an electron?
48. Does a neutrino have any rest mass?
49. What charge does a photon have?
50. What charge does a proton have?
51. Fill in the following sentence with the appropriate word or phrase: A photon with a wavelength the same size as a large building is sometimes called a _____ wave.
52. What types of particles require Maxwell's four equations of electricity and magnetism to predict their behavior?
53. What charge does a neutron have?
54. Approximately how many times heavier is a neutron than an electron?
55. What equation can be used to relate the energy of a photon to its momentum?
56. What charge does an electron have?
57. What is the name of the antimatter particle that is the mirror image of the normal electron?
58. What is an alpha particle, and what is its mass in AMUs?
59. When an alpha particle acquires two additional electrons, what does it then become?
60. Fill in the following sentence with the appropriate word or phrase: All neutrons and protons are held together by _____ particles that in turn are constructed from more elementary particles called _____.
61. Write an expression for the kinetic energy of a matter particle in terms of its relativistic mass and its rest mass.
62. What charge (or charges) can an alpha particle have?
63. What is a "first-order" particle interaction?
64. What particle is the carrier of the electrical force between the electrons surrounding the nucleus and the protons inside the nucleus?
65. What is the speed of a photon in empty space?
66. There are two forms of radioactive beta decay—B^- decay and B^+ decay. What particle is emitted in B^- decay?
67. What is the most commonly observed particle in a nuclear reactor core?
68. Fill in the following sentence with the appropriate word or phrase: Neutron diffusion theory can be used to find the neutron flux in a reactor fuel assembly when the neutron flux is angularly _____.
69. Fill in the following sentence with the appropriate word or phrase: _____ is a subfield of reactor physics that deals with the slowing down of neutrons through a series of _____ and _____ collisions.
70. What particle is the antiparticle of the electron, and what charge does it have?
71. Using Maxwell's relationship between the energy and the momentum of a photon, show that the momentum of a photon is related to its frequency of vibration by p = hf//c.
72. If a helium nucleus is converted into a helium ion with a charge of $^+1$, how many electrons must be emitted in this process to allow for the conservation of charge?
73. Fill in the following sentence with the appropriate word or phrase: The _____ method is a statistical method that can be used to emulate the behavior of neutrons and other subatomic particles.
74. Fill in the following sentence with the appropriate word or phrase: _____ is a deterministic method that can be used to find the shape of the neutron flux in the vicinity of a nuclear control rod.
75. What is the most important nuclear particle in the study of nuclear reactor physics?
76. Fill in the following sentence with the appropriate word or phrase: Neutron transport theory is based on an equation called the _____.
77. Approximately what percent of the energy released in a nuclear reaction involving neutrinos is normally unrecoverable?
78. What is antimatter, and how does it differ from ordinary matter?
79. Fill in the following sentence with the appropriate word or phrase: Between _____ and _____ MeV of kinetic energy is released from the thermal fission of U-235.
80. What nuclear particle is its own antiparticle?
81. How is a positron different from an ordinary electron?
82. What reactions in a nuclear reactor core lead to the creation of positrons?
83. Fill in the following sentence with the appropriate word or phrase: According to electromagnetic theory, a _____ ray has the same wavelength as the diameter of the nucleus of an atom.
84. What reactions in a nuclear reactor core require the creation of a neutrino?
85. What does the Second Law of Thermodynamics tell us about the direction of heat flow in a nuclear reactor?
86. What is the equation that relates the energy of a matter particle to its rest mass and then to its velocity-dependent mass?
87. If a matter particle having a rest mass of m_o is traveling at approximately 86% of the speed of light, what would we measure for the mass m of this matter particle at that particular speed?

88. What equation is generally referred to as the defining equation of the nuclear age?
89. Name the by-products of the fission reaction that carry away most of the kinetic energy that is produced.
90. How many joules of energy are approximately equal to one electron volt?
91. As it pertains to the nucleus of an atom, what is the Baryon number, and how is it conserved?
92. In all nuclear reactions, does it necessarily follow that the number of neutrons going into a reaction must always be equal to the number of neutrons coming out of a reaction?
93. Why does the mass of a nuclear particle (with the exception of the photon) increase as its velocity increases?
94. What is the difference between a matter particle and a force particle?
95. When an atomic nucleus splits apart, what is the minimum number of fission neutrons that can be released?
96. What fundamental nuclear property is conserved by the First Law of Thermodynamics?
97. What is the name of the nuclear force that is responsible for radioactive decay?
98. Write down an equation for the density of the atomic nucleus.
99. What is the average velocity of a fission neutron when it is first released from an atomic nucleus?
100. Approximately how long after a uranium atom absorbs a free neutron is it likely to split apart?
101. Below what fraction of the speed of light is it generally acceptable to use the expression for the rest mass of a particle without making an error in the calculation of its mass or its momentum?
102. What deterministic equation can be used to find the shape of the neutron flux in a spatially homogeneous medium?
103. At what kinetic energy does an electron become a relativistic particle?
104. What purpose does the neutrino serve in the process of radioactive beta decay?
105. If an electron and a positron happen to collide with each other in a reactor core, what happens during the collision?
106. When an atomic nucleus splits apart, what is the maximum number of fission neutrons that can be released?
107. What two famous equations are needed to predict the transport of particles in nuclear systems?
108. What type of equation do the smoke particles in a room filled with dry air obey?
109. Fill in the following sentence with the appropriate word or phrase: According to electromagnetic theory, a _____ ray has the same wavelength as the diameter of an atom's electron cloud.
110. At what energy must an electron be treated as a relativistic particle in a reactor core?
111. If one calculates the velocity of a 10 MeV neutron using classical mechanics, how much error does this introduce into the calculation?
112. Name three ways in which nuclear bonds are different from chemical ones.
113. It is a well-known fact that the half-life of a nuclear particle increases as it moves faster. Suppose that the half-life of a nuclear particle is 1 second when it is measured at rest in a laboratory coordinate system. If it then starts to move at approximately 97% of the speed of light, what is its corresponding half-life in this case?
114. In general, what type of atomic nucleus is more likely to be more stable—one with an even number of nucleons or one with an odd number of nucleons?
115. In the field of nuclear science and engineering, what is the definition of a nucleon?
116. At what velocity does an electron become a relativistic particle?
117. Earlier in the chapter, we showed that neutrons cannot be affected by the presence of electric or magnetic fields. Because of this, what two equations are required to predict the behavior of neutrons in a nuclear reactor core?
118. In a Monte Carlo simulation, what is the lifetime of individual nuclear particle called?
119. A Plutonium-239 nucleus absorbs a thermal neutron and decides to split itself apart. Write down at least one equation describing what happens next.
120. What is the average kinetic of a fission neutron?
121. As an alternative to the Monte Carlo method, what deterministic equation can be used to find the angularly dependent neutron flux in the presence of a strong neutron absorber?
122. What two elements in the Periodic Table have the highest binding energy per nucleon and are therefore the hardest to break apart?
123. Approximately how long after an atomic nucleus splits apart is the first fission neutron released?
124. What is the most probable kinetic energy of an average fission neutron?
125. In the standard symbol for Uranum-238, what does the number 238 refer to?
126. Who is H.A. Lorentz and what was his primary contribution to the field of nuclear science and engineering?
127. When kinetic energy is released by the fission process, what form of energy does this kinetic energy ultimately become in a reactor core?
128. Name the process that is most directly responsible for the production of nuclear energy in our Sun.

129. A Uranium-235 nucleus absorbs a thermal neutron. Write down three equations describing the possible outcome of this reaction. Is the amount of kinetic energy released the same in each case?
130. Name two methods—a deterministic method and a statistical one—that can be used to perform radiation shielding calculations.
131. Fill in the following sentence with the appropriate word or phrase: Protons and neutrons are held together by particles called _____ which in turn consist of quark and antiquark pairs.
132. Suppose that someone decides to use neutron diffusion theory to predict the shape of the neutron flux in the vicinity of a fuel rod. Is this an appropriate thing to do?
133. How many naturally occurring elements are there and approximate how many man-made ones are there in addition to these?
134. Approximately how many isotopes can be constructed from all the known elements in the Periodic Table?
135. Suppose that a nuclear particle that weighs exactly 1 AMU is converted into pure energy. How much kinetic energy will be released in the process and what nuclear particles will appear to carry away this energy?
136. What contribution did Hideki Yukawa make to the field of nuclear science and engineering?
137. Suppose that a nuclear engineer decides to use neutron diffusion theory to predict the shape of the neutron flux in the vicinity of a control rod. Is this an appropriate thing to do?
138. What is the fundamental difference between an element and an isotope?
139. Name four isotopes of uranium and plutonium that are commonly used as nuclear fuels.
140. What is the most popular nuclear fuel in the world today?
141. Approximately how many times stronger are the nuclear bonds used to hold the nucleus together than the chemical bonds used to hold atoms together?
142. What is the heaviest nuclear fuel?
143. Who is Ludwig Boltzmann and what famous equation did he invent? What is this equation used for by reactor physicists today?
144. Excluding the elements hydrogen and helium, what is the average nuclear binding energy per nucleon of a typical element in the Periodic Table?
145. Nuclear fission releases kinetic energy by splitting the nucleus of an atom apart. What is the name of the process that releases energy by combining the nuclei of two lighter elements together?
146. What is the name of the thermal energy produced by the process of nuclear fission?
147. Fill in the following sentence with the appropriate word or phrase: Nuclear particles decay more _____ when they are moving at very high speeds.
148. What commonly observed nuclear particles are used to construct an atomic nucleus?
149. When referring to the number of nucleons in an atomic nucleus, what do the symbols A, Z, and N represent?
150. What elements in the Periodic Table have the smallest number of nucleons and what elements have the largest?

Exercises for the Student

Exercise 2.1

If the neutron eventually slows down to a kinetic energy of 0.025 eV, through repeated collisions with other atoms, it eventually comes into thermal equilibrium with its environment. In this case, what is the average velocity of a free neutron when it finally reaches thermal equilibrium?

Exercise 2.2

A very high-speed proton having a kinetic energy of 10 MeV can be created in a particle accelerator. What is the velocity of the proton inside the accelerator?

Exercise 2.3

Part 1: What is the minimum frequency that a Gamma Ray emitted from the nucleus of a radioactive atom must have to create an electron–positron pair in a nuclear reaction such as "pair production?"
Part 2: What is the wavelength of the gamma ray in this case?
Part 3: If the electron is emitted from the reaction at an angle of 30° in a standard Cartesian coordinate system, what angle is the positron emitted at, and what are the x and y components of the momentum of the positron in this case?
Part 4: Show that spin and charge are conserved in this reaction.

Exercise 2.4

Suppose that the gamma ray is emitted from the nucleus of a Carbon-12 atom with a frequency of 5×10^{20} Hz.

Part 1: What is its wavelength and what is its energy?
Part 2: What is the value of its linear momentum as well?
Part 3: What is the ratio of the frequency of this gamma ray to the frequency of a photon produced by a GE "soft white" light bulb in your home?

Exercise 2.5

A carbon-12 nucleus has a number of internal energy levels that correspond to different orbital configurations of the protons and neutrons inside it. These energy levels are shown in Chapter 6. Suppose that a Carbon-12 nucleus in an excited state emits a gamma ray from the highest energy level shown and then transitions itself to its most stable state, which corresponds to the lowest energy shown.

Part 1: What is the energy of the gamma ray that is emitted in this process?
Part 2: Suppose that the gamma ray then collides with the nucleus of a hydrogen atom and is subsequently absorbed. What velocity does the hydrogen nucleus recoil away from this reaction? You may assume in this case that the collision with the hydrogen atom is an elastic one.
Part 3: Suppose that the hydrogen nucleus subsequently decides to emit another gamma ray with 10% of the energy of the original gamma ray. What is the frequency and the wavelength of the emitted gamma ray in this case?

Exercise 2.6

Derive an expression for the momentum of a photon that is based on its frequency of vibration f.

Exercise 2.7

Suppose that an electron and a positron happen to collide with each other in a nuclear reactor core and that the velocity of each particle is relatively small compared to the speed of light. What is the energy and the frequency of the photon that is created in the process?

Exercise 2.8

In simple terms, explain why the photon has no rest mass.

Exercise 2.9

A small nuclear reactor produces 500,000 MeV of thermal energy each second. How many neutrons per second does it have to convert entirely into energy to do this?

Exercise 2.10

A fission neutron is emitted from a plutonium-239 nucleus with an initial kinetic energy of 10 MeV. What is its speed in meters per second immediately after it is born?

Exercise 2.11

Suppose that 500 billion uranium atoms are split apart every second in a fuel rod in a low-power research reactor. If 200 MeV of kinetic energy is released in each fission reaction, how many watts of power does the fuel rod produce every second?

Exercise 2.12

Suppose that a particle is traveling through empty space at 30,000 m/s. What is the percentage difference between the rest mass of the particle and its relativistic mass?

Exercise 2.13

The International Space Station orbits the earth at a speed of about 11,000 m/s. A Cesium clock to be installed on the space station has a frequency of 9,192,631,770 cycles/s on the earth. What will the frequency of the same clock be aboard the International Space Station?

Exercise 2.14

What is the ratio of the speed of light in empty space to the speed of light in air? If the refractive index of a diamond is 2.417, what is the speed of light in a diamond?

Exercise 2.15

A gamma ray produced in a nuclear reactor has a frequency of 1×10^{20} cycles/s. What is its wavelength and what is its energy?

Exercise 2.16

We mentioned earlier in the chapter that some photons can have the same wavelength as the diameter of an atom and other photons can have the same wavelength as the diameter of the nucleus. What energy does a photon have to have a wavelength the size of an atom, and what energy does it have to have a wavelength the size of the nucleus?

Exercise 2.17

A photon produced in a nuclear reactor core has an energy of 1 MeV. What is its momentum?

Exercise 2.18

An electron and a positron that are initially moving very slowly collide with one another and release a gamma ray in the process (Figure 2.27). The gamma ray is ejected at an angle of 60° with respect to the positive x-axis. (See the following diagram.) What is the energy of the gamma ray, what is its frequency of vibration, and what is its momentum in the positive x direction?

Exercise 2.19

Consider the Yukawa potential for a nuclear particle with rest mass m. Show that in the case of the photon (which carries the electromagnetic field and has a rest mass of zero), the Yukawa potential reduces to the potential function that is used to derive Coulomb's Law.

Exercise 2.20

Derive Coulomb's Law from the potential function discussed earlier.

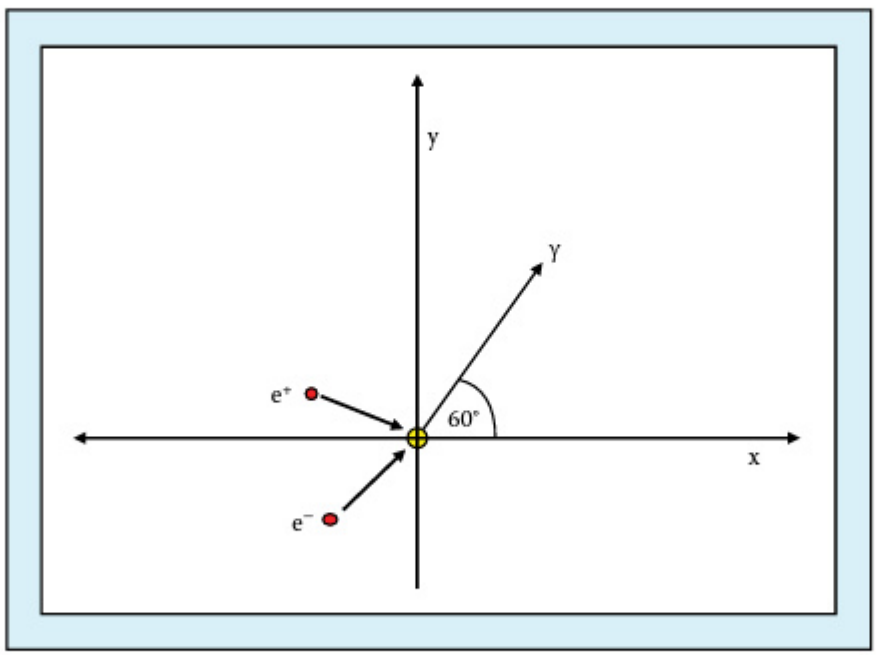

FIGURE 2.27 An electron and a positron colliding to produce a gamma ray.

Exercise 2.21

A common formula for the diameter of the nucleus is $D = C \times A^{1/3}$, where A is the atomic mass number of the nucleus (the number of protons plus the number of neutrons) and C is an empirically determined constant on the order of 1.5×10^{-13} cm. Use this formula to estimate the diameters of the Uranium-235 nucleus, where A = 235, and the Carbon-14 nucleus, where A = 14. What is the ratio of the diameter of the Uranium-235 nucleus to the Carbon-14 nucleus in this case?

Exercise 2.22

Derive an expression for the volume V of an atomic nucleus from the formula presented earlier. Is the volume proportional to the number of nucleons in this case?

Exercise 2.23

Suppose that a new element called "Unobtainium" is discovered to have 120 protons and 200 neutrons. What is the neutron-to-proton ratio of this element, and what percent larger is the volume of this nucleus than the volume of the U-238 nucleus?

Exercise 2.24

The wavelength of a particle λ is related to its momentum p by the formula $\lambda = h/p$, where h is the value of Planck's constant. At nonrelativistic energies (less than about 10% of the speed of light), the momentum p is related to the kinetic energy E of a particle by the following formula: $p = \sqrt{2m_o E}$, where m_o is the rest mass. In the case of a neutron, show that this expression reduces to $\lambda = 2.86 \times 10^{-9}/\sqrt{E}$, where λ is the wavelength of the neutron in centimeters and E is the kinetic energy of the neutron in eV. Using this formula, calculate the wavelength of a 4 MeV neutron.

Exercise 2.25

For a 1 MeV neutron traveling through a reactor, use the formula given earlier to calculate the average wavelength of the neutron.

Exercise 2.26

When a fission neutron produced in a reactor core slows down to the lowest possible energy it can obtain, it is called a thermal neutron. When it reaches this energy, its most probable energy is 0.025 eV. Under these conditions, how does its wavelength compare to the diameter of an ordinary atom?

Exercise 2.27

Fission neutrons are produced with an average energy of 2 MeV. How fast does a 2 MeV fission neutron travel through a reactor core?

Exercise 2.28

Suppose that a small amount of nuclear material is assembled into the shape of a diamond on a diamond ring, which has an average volume of about 1×10^{-3} cm^3. How much does this small volume of nuclear material weigh, and how does the weight of this nuclear "diamond" compare to the weight of the Empire State Building?

3

Nuclear Particles, Processes, and Reactions

3.1 Nuclear Particle Behavior

In this chapter, we would like to continue our study of nuclear particles, and in particular, we would like to discuss how nuclear particles interact with each other and with the materials in a nuclear power plant. *Reactor physics* is the study of the behavior of these particles, and in particular, it is the study of the behavior of the neutron. Consequently, we would like to study how these particles interact with each other from a number of different perspectives. Reactors produce several different types of nuclear particles (see Figure 3.1), and in addition to affecting the structural materials in the core, they can also affect human beings who are exposed to them. The particles produced in the fuel rods of a nuclear reactor include

- Neutrons
- Protons
- Electrons
- Neutrinos
- Alpha particles
- Beta particles
- Gamma rays

Gamma rays are high-energy photons that can possess energies up to about 20 MeV. These nuclear particles can be further subdivided into two basic categories:

1. Those that carry an electric charge (protons, electrons, alpha particles, and beta rays)
2. Those that do not carry an electric charge (neutrons, photons, neutrinos, and γ-rays)

Each of these particles interacts with the matter differently, and the characteristics of this reaction are a function of the speed the particles are moving. Very energetic and high-speed particles cannot be easily stopped by most materials. If the particle does not have an electric charge, then it is even harder to stop. The behavior of an electrically neutral particle such as a neutron can be modeled to a high degree of accuracy by assuming that the neutron and the object it collides with (i.e., an atomic nucleus) are simply atomic billiard balls having different masses, m_1 and m_2, and different velocities, v_1 and v_2. In other words, these types of reactions can be modeled by assuming that the neutron and the nucleus participate in what is known as an *elastic collision*. Elastic collisions can be further subdivided into *head-on collisions* and *glancing collisions*. Elastic collisions are the most common collisions in a nuclear power plant, but they are not the only ones. Other collisions where an incoming particle is temporarily absorbed and then reemitted are called *inelastic collisions*.

3.2 Determining the Behavior of Particles with an Electric Charge

The outcome of an elastic collision can be determined from the laws of classical mechanics. If a nucleus does not absorb a neutron, it normally scatters it. However, charged particles behave in an entirely different way than neutrons and other electrically neutral particles do. The electrical forces acting on charged particles operate over much longer distance scales. These electrical forces are described by *Coulomb's law* (see Equation 3.1), which states that the electrical force F_E between two charged particles is inversely proportional to the square of the distance between them and directly proportional to the product of their electric charges q_1 and q_2. Hence, in addition

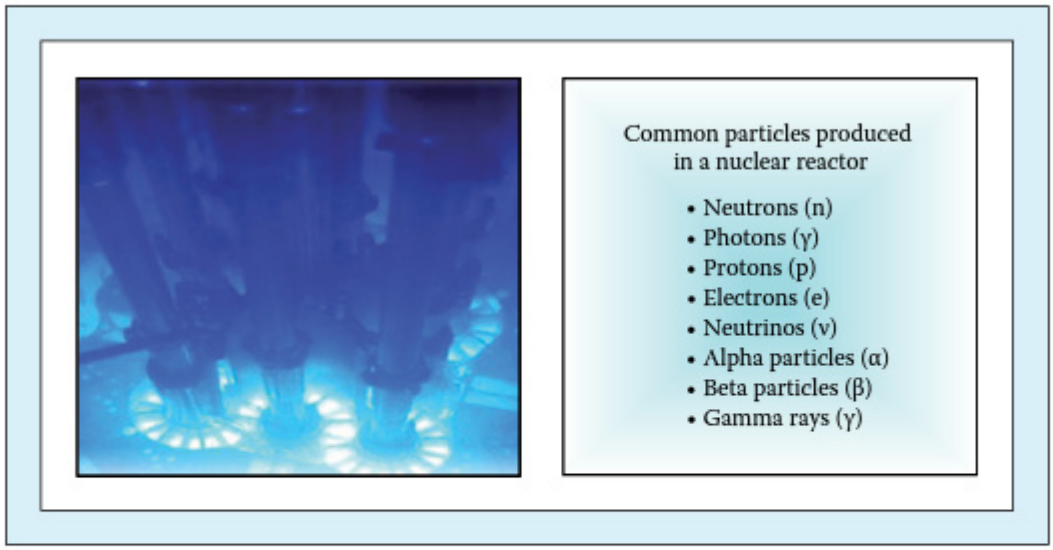

FIGURE 3.1 Some of the more common particles produced in a nuclear reactor. The most common particle is the neutron, but it cannot be seen directly by the human eye. However, another form of radiation called Cherenkov radiation can be seen directly by the human eye. This radiation is produced when high-speed electrons interact with the surrounding water and release a bluish white light. This light is also emitted from spent fuel pools. (The picture on the left was provided by the US NRC.)

to just scattering off of each other, protons, electrons, and alpha particles can also experience a long-distance electrical force whose magnitude is given by

Force between Two Charged Particles

$$F_E = m\frac{dr}{dt} = \frac{kq_1 \cdot q_2}{r^2} \tag{3.1}$$

Applies to protons and electrons but **not** to photons or neutrons

On a quantum level, this force is due to the process of *photon exchange*. Photon exchange can be visualized graphically using what are known as *Feynman diagrams*. A Feynman diagram depicting the collision of two electrons is shown in Figure 3.2.

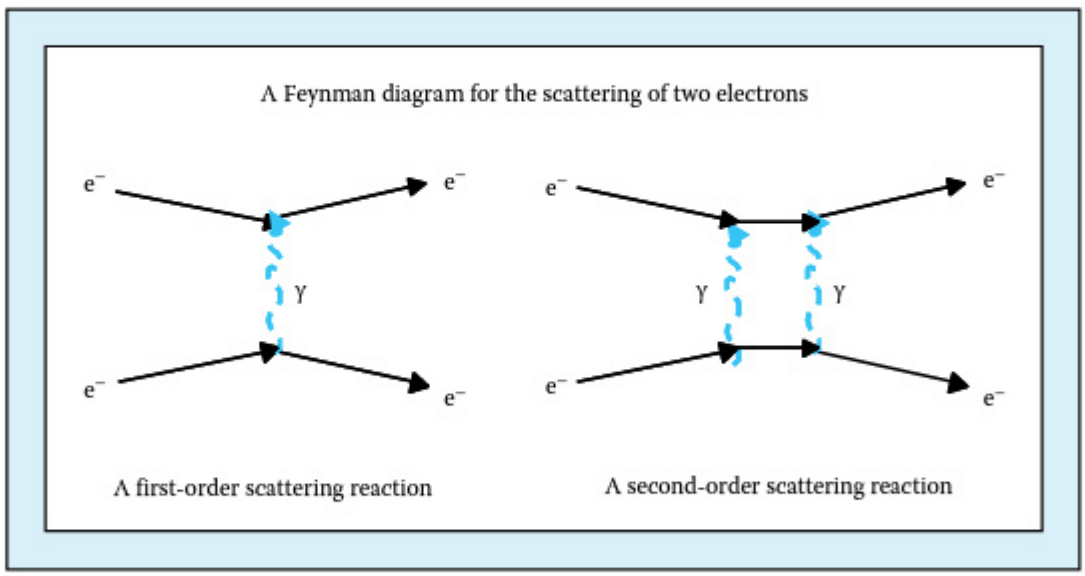

FIGURE 3.2 A Feynman diagram depicting a collision between two electrons where one or more virtual photons (represented by the symbol γ) are exchanged to transfer the electrical force. The Feynman diagram for the scattering of two protons is the same.

Other Feynman diagrams were discussed in Chapter 2. The force constant k used in Coulomb's law is called *Coulomb's constant*, and it has a value of $k = 8.98 \times 10^9$ N m²/Coulomb². The *Coulomb* is the electric charge of a single electron or proton, and it has the value of $q = \pm 1.6 \times 10^{-19}$ Coulombs in the SI unit system. If either q_1 or q_2 is zero, the electrical force vanishes entirely, and this means that we can predict the outcome of a collision from a simple energy and momentum balance. In particular, if the collision is an elastic one, both the energy and the momentum must be conserved, and the energy and the momentum of the particles coming out of the collision must be equal to the energy and momentum of the particles going into the collision. Then, we can write

The Conservation of Energy

$$E_{OUT} = E_{IN} \tag{3.2}$$

where

E_{IN} is the energy of the particles coming into a reaction
E_{OUT} is the energy of the particles coming out of the reaction

In order for momentum to be conserved, we can also write

The Conservation of Momentum

$$\mathbf{P}_{OUT} = \mathbf{P}_{IN} \tag{3.3}$$

where

$\mathbf{P}_{IN}$ is the momentum of the particles coming into a reaction
$\mathbf{P}_{OUT}$ is the momentum of the particles coming out of the reaction

Equations 3.2 and 3.3 only imply that the total energy and momentum of the particles are conserved. These equations *do NOT imply* that the energies and the momenta of the individual particles remain the same. Of course, the linear momentum **P** in Equation 3.3 is a *vector* quantity, and the kinetic energy E in Equation 3.2 is a *scalar* quantity. Thus, the momentum of each particle has both a magnitude and a direction, while the energy has only a magnitude in each case.

An important feature of these equations is that if we know the energy and the momentum of a specific set of particles going into a collision, then we can predict the energy and the momentum of the same particles coming out of the collision. If one of these particles happens to be a neutron, then we can also predict the amount of energy the neutron loses as the result of the collision. Later on, we will see that this energy loss can be described by an elegant mathematical framework that has become known as *neutron slowing down theory*. Slowing down theory is discussed in many reactor physics books, and it is also discussed in Chapter 8 of this book.

3.3 The Behavior of Neutrons

Now let us turn our attention to how neutrons and other electrically neutral particles behave. The behavior of neutrons is of great practical importance to the nuclear power industry as a whole. In particular, the way in which a neutron loses kinetic energy as it moves is essential to understanding how a nuclear power plant behaves. In reactor physics, the process by which a neutron loses kinetic energy through a sequence of elastic scattering collisions is called *neutron slowing down theory* (see Section 3.2). Slowing down theory normally does not concern itself with inelastic scattering collisions, which can take place between neutrons and very heavy atoms (such as Uranium and Plutonium nuclei, which can have many possible excited states). A neutron that exists outside of the atomic nucleus is called a *free neutron*, while a neutron that exists inside of the nucleus is called a *bound neutron.* Free neutrons have *a half-life of about 15 minutes*, while the half-life of a bound neutron is effectively infinite. Here the *half-life* is defined as the amount of time required for exactly half the neutrons in a sample of nuclear material to decay. A common reaction involving the decay of a neutron is

The Process of Neutron Decay

$$n \rightarrow p^{+} + e^{-} \tag{3.4}$$

where the neutron decays into a proton and an electron. In this particular reaction, the spin, the charge, the energy, and the momentum of the incoming and outgoing particles are conserved (see Chapter 2). Basically, the decay of a neutron involves converting a down quark inside of the neutron into an up quark, and this causes the neutron to become a proton. An energetic electron is also released in the process. When this process occurs inside of an

atomic nucleus, it is called radioactive *beta decay*. Beta decay is responsible for most of the *decay heat* that is generated in nuclear fuel rods (see Chapter 6).

3.4 Prompt and Delayed Neutrons

Neutrons can be produced in reactor cores in two distinct ways:

1. First, they can be produced when an atomic nucleus splits apart or "fissions." (These neutrons are usually released within 1 billionth of a second after the nucleus first disintegrates.) The resulting neutrons are called *prompt fission neutrons* because they appear *promptly* or essentially *instantaneously* after the nucleus splits apart.
2. Second, smaller numbers of less energetic neutrons are produced much later from the by-products, or *fission products*, of the fission process. These additional neutrons are called *delayed neutrons*, and delayed neutrons normally appear between one-tenth of a second and 100 seconds after the fission products are produced. (The exact timing is a function of the type of fission product, and not all fission products are radioactive enough to produce delayed neutrons.) The average kinetic energy of a delayed neutron is about one-third of that of a prompt neutron (see Chapter 7). Otherwise, the properties of delayed neurons and prompt neutrons are identical.

3.4.1 The Prompt Neutron Energy Spectrum

Now let us compare the kinetic energies of prompt neutrons to those of delayed neutrons. In general, prompt *fission neutrons are created with a distribution of kinetic energies between about 1 keV and 10 MeV*. The exact energies with which they are produced are governed by a statistical probability distribution called the *"Watt curve,"* and fission neutrons are more likely to be produced with certain energies than others. The Watt curve for prompt fission neutrons created from the thermal fission of Uranium-235 is shown in Figure 3.3. Historically, this curve was named after an American physicist named B.E. Watt, who first measured it in 1952. According to this curve, prompt fission *neutrons have a most probable kinetic energy of about 0.75 MeV, and this energy corresponds to the peak of the curve* shown in Figure 3.3. In other words, the most probable energy is the energy with which they are most likely to be produced. The energies of the prompt neutrons described by this curve can also be fit to a statistical probability distribution of the form

Prompt Neutron Energy Distribution

$$P_P(E) = 0.453\ e^{-1.036E} \sinh\left\{\sqrt{(2.29E)}\right\} \tag{3.5}$$

Equation 3.5 is *normalized* so that the area under the curve represented by the Watt distribution is equal to 1.0. The *average kinetic energy* <E> of a prompt neutron is then given by the area under the curve $A = \int P_P(E)\, dE$, divided by the energy

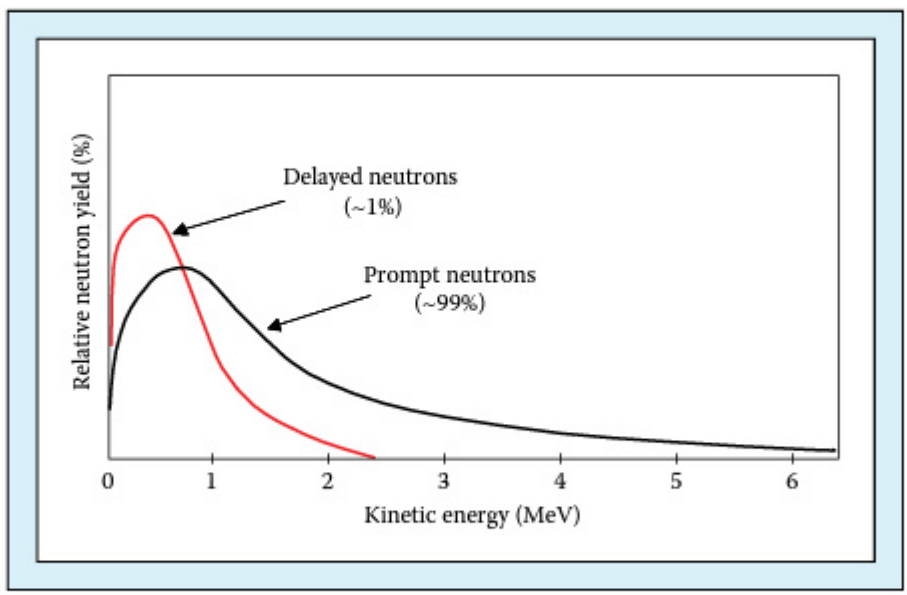

FIGURE 3.3 The neutron energy spectrum of "prompt" neutrons and "delayed" neutrons produced from the thermal fission of Uranium-235. The prompt neutron energy spectrum is often called the "Watt curve."

range in which the neutrons are produced: $\Delta E = E_{high} - E_{low} \cong 10$ MeV. *Hence, the average energy of a prompt neutron produced from the thermal fission of U-235 is*

Average Energy of a Prompt Fission Neutron

$$<E> = \frac{A}{\Delta E} = \frac{\int_E P_P(E)dE}{\int_E dE} = \int_E P_P(E)\frac{dE}{\Delta E} \cong 2 \text{ MeV} \tag{3.6}$$

Thus it can be seen that the average kinetic energy of a prompt fission neutron is about 2 MeV and the most probable kinetic energy of a prompt fission neutron is about 0.75 MeV. Occasionally prompt neutrons are produced with kinetic energies greater than 10 MeV, but these events are relatively rare, statistically speaking. Hence, 10 MeV is usually taken to be the "top" of the prompt neutron energy range, although some books extend this range to about 15 MeV. In general, only about one-tenth of one percent (<0.1%) of prompt neutrons are produced with kinetic energies above 10 MeV.

3.4.2 Understanding the Terms in the Watt Equation

The subscript P in Equations 3.5 and 3.6 refers to the fact that the Watt curve applies to "prompt" neutrons, and the function sinh(x) that appears in the Watt equation is called the *hyperbolic sine*. Values of the hyperbolic sine and similar trigonometric functions can be found in most elementary calculus books, and their values are also tabulated on the Internet. Its complementary function—called the *hyperbolic cosine*—is defined in the same way as the hyperbolic sine, except that the minus sign in the numerator is replaced by a plus sign. Hence the definitions of the hyperbolic sine and cosine are

Hyperbolic Sine and Cosine

$$\sinh(x) = \frac{\left(e^x - e^{-x}\right)}{2}$$
$$\cosh(x) = \frac{\left(e^x + e^{-x}\right)}{2} \tag{3.7}$$

Later we will find that the hyperbolic sine and cosine appear in many other equations in nuclear science and engineering. Notice that the prompt neutron energy spectrum illustrated in Figure 3.3 is shown in MeV. Later on, we will learn that prompt neutrons are produced about 10^{-12} seconds after an atomic nucleus splits apart. In other words, their creation is essentially an *instantaneous* process. Both prompt neutrons and delayed neutrons are also discussed in our companion book.* Except for their lower kinetic energies, delayed neutrons are identical in every respect to prompt neutrons. The percentage of delayed neutrons produced is also a function of the type of nuclear fuel that is used (see Chapter 7). Delayed neutrons play an important role in time-dependent reactor behavior because they make a reactor easier to control (see Section 3.5). Delayed neutrons have a most probable kinetic energy of about 0.3 MeV and an average kinetic energy of about 0.6 MeV. Delayed neutrons also "thermalize" more quickly than prompt fission neutrons do. (The exact thermalization times are discussed in Chapter 10, and there the thermalization times are related to another important parameter of reactor physics called the *neutron age*. Ironically, the neutron age is measured in the units of area rather than time.) Finally, it can be shown that the neutron age is proportional to the time it takes a fast neutron to become a thermal neutron. Hence its value can be determined experimentally because it also is equal to one sixth of the square of the distance a neutron travels (as the crow flies) between the location it is emitted as a fast neutron and the location it is absorbed as a thermal neutron. For fission neutrons travelling through light water, a typical value of the neutron age is about 25 square centimeters. For the same

* See *Nuclear Engineering Fundamentals: A Practical Perspective*, by R.E. Masterson, CRC Press (2017).

TABLE 3.1
Average Characteristics of Prompt and Delayed Neutrons

	Time of Appearance (s)[a]	Average Kinetic Energy (MeV)	Most Probable Kinetic Energy (MeV)
Prompt neutrons	$\sim 10^{-12}$	2.00	0.74
Delayed neutrons	0.1–100	0.60	0.30
	U-233	**U-235**	**Pu-239**
Prompt-to-delayed neutron ratio	385	154	500

Source: Duderstadt, J. and Hamilton, L. *Nuclear Reactor Analysis*, John Wiley & Sons, New York, 1976.
[a] After initial fission.

neutrons travelling through heavy water, the value of the neutron age increases to about 130 square centimeters.* We will have more to say about the uses of the neutron age in Chapters 10, 11, and 12.

3.5 The Delayed Neutron Fraction

In the fields of reactor kinetics and reactor control, which are important to the behavior of time-dependent reactors, the ratio of the number of delayed neutrons produced to the total number of neutrons produced (both prompt and delayed) is another meaningful nuclear parameter. This parameter is sometimes called the *delayed neutron fraction* β, *and it is defined as*

Definition of the Delayed Neutron Fraction

$$\beta = \frac{\text{Number of delayed neutrons}}{\left(\text{Number of prompt neutrons} + \text{Number of delayed neutrons}\right)} \tag{3.8}$$

Normally less than 1% of neutrons produced in a reactor are delayed neutrons. Hence, delayed neutrons usually constitute less than 1% of the total neutron population, except during very fast and severe transients, where their percentage can temporarily rise above 1%. The delayed neutron fraction is also a function of the type of nuclear fuel that is used. In particular, a reactor fueled with Pu-239 has fewer delayed neutrons than a reactor fueled with U-235. The actual ratios are presented in Table 3.1 and expanded upon in Chapter 7.

Delayed neutrons play an important role in the time-dependent reactor behavior because they are produced slowly enough to make it possible for the reactor control system to respond to changes in the neutron population before too many neutrons or too few neutrons are produced. In other words, delayed neutrons are what allow the nuclear chain reaction to be controlled. *Without delayed neutrons, commercial power reactors would be almost impossible to control*. The study of delayed neutrons is part of the field of *reactor kinetics*, which is introduced to the reader in Chapters 15 and 16 of this book. The delayed neutron fraction also appears in another famous equation of reactor physics and reactor kinetics called the *Inhour equation*. Among other things, the Inhour equation can be used to predict how the core-wide neutron population increases or decreases with time.

3.6 Types of Neutron Interactions

Because free neutrons are electrically neutral particles, the only way they can interact with ordinary matter is to collide with it. Most of the time, this matter happens to be an atomic nucleus. (However, a neutron can also hit another neutron or nuclear particle on some occasions.) When a neutron hits an atomic nucleus, it can be either scattered off of the nucleus or it can be absorbed by it. It can also destabilize the nucleus and cause it to split apart or "fission." Thus nuclear power can be produced in this way. The kinetic energy a neutron imparts to an atomic nucleus can be substantial in some cases.

If a nucleus absorbs a neutron and subsequently emits a γ-ray after absorbing the neutron to return to a more stable state, the process of neutron absorption and γ-ray emission is called *radiative capture*. For a Uranium-235 nucleus, radiative capture occurs about 15% of the time. The other 85% of the time, the nucleus simply "fissions" after absorbing the neutron. In future sections, we will see that the dynamics of this process can become quite complicated. The probability of a particular reaction occurring is then described by what is known as a *reaction cross section*. Separate cross sections

* See *An Introduction to Nuclear Engineering*, by Lamarsh, J.R. and Baratta, A.J., Prentice Hall Publishing, Upper Saddle River, NJ (2001).

exist for scattering than they do for capture, fission, or absorption. Cross sections for scattering can also be subdivided into those for elastic scattering and those for inelastic scattering. Inelastic scattering reactions almost always involve the creation of a *compound nucleus*, whose properties are discussed in Chapter 4. Thus a neutron traveling through a reactor core can interact with an atomic nucleus in four different ways:

1. It can "elastically scatter" off of the nucleus (where the kinetic energy of both particles is conserved and no additional particles are produced).
2. It can "inelastically scatter" off of the nucleus (where other nuclear particles are produced or the nucleus is put into an excited state by subsequently absorbing and reemitting the neutron). When this occurs, the kinetic energy of the particles participating in the collision may *not* be conserved (since the nucleus may be temporarily put into a highly excited state).
3. It can lead to a "radiative capture event" (where γ-rays may be produced after absorbing the incoming neutron). The neutron normally remains inside of the nucleus and a new isotope of the same element is formed. (However, the nucleus may then transform the neutron inside of the nucleus into an electron and a proton, and an entirely new element may be formed. See Equation 3.4.)
4. It can cause the atomic nucleus to split apart or "fission" (where the atomic nucleus splits apart after absorbing the incoming neutron). After splitting apart, it may release two or three additional neutrons. As discussed previously, these additional neutrons are also called *prompt fission neutrons*.

Now let us make some comments about how the process of elastic scattering works. Elastic scattering is the most common way in which neutrons lose energy if they are not absorbed. *When an incoming neutron hits an atomic nucleus, the process is similar to two billiard balls colliding with each other on a billiards table* (see Figure 3.4). However, the neutron and the atomic nucleus are much smaller, and they are normally traveling at much higher speeds. All atoms (with the exception of hydrogen) are heavier than the incoming neutron itself, so if one were to extrapolate this mass difference back to the game of billiards, we would find that there would be a mass difference of approximately 240 between the lightest balls on the table, which would represent the neutrons, and the heaviest balls on the table, which would represent the uranium and plutonium nuclei. *Depending on the energy of the incoming neutron and the types of atoms that it collides with, a free neutron can take between 20 and 1000 collisions to "slow down" as it moves. Eventually, these collisions reduce its average kinetic energy from 2 MeV to about 0.025 eV.*

Finally, when a neutron reaches this energy, its average kinetic energy can neither increase nor decrease, and it is said to be in *thermal equilibrium* with its environment. In a thermal water reactor, such as a PWR or BWR, this energy loss can take about 10^{-4} seconds to occur. Neutrons that acquire a kinetic energy less than 1 eV are called *thermal neutrons*. In practice, about 1/3 of the neutrons in a thermal water reactor are thermal neutrons. The remaining 2/3 of the neutrons have kinetic energies above 0.025 eV and are therefore called either *epithermal* or *fast* neutrons. The energy ranges for epithermal and fast neutrons are discussed in Chapters 4 and 5.

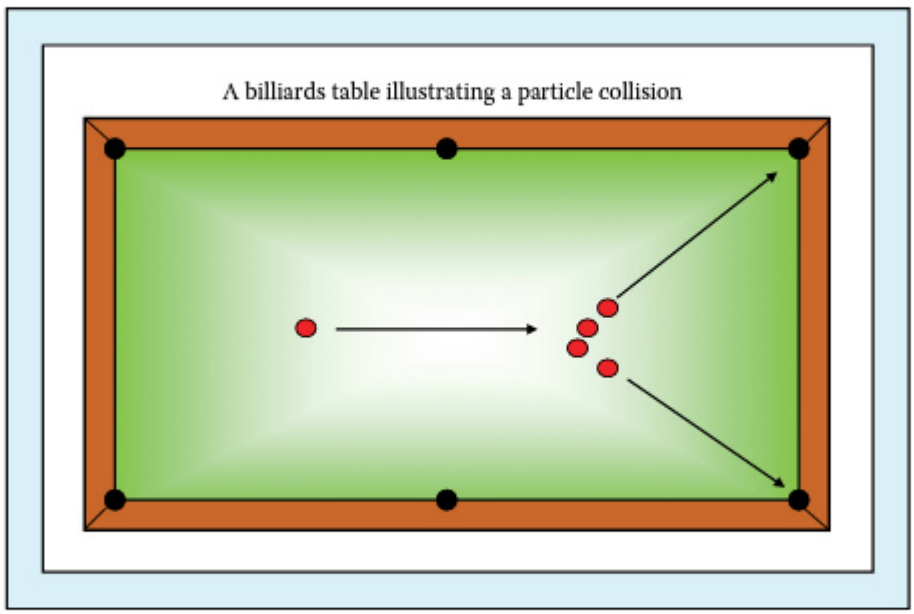

FIGURE 3.4 An illustration of the game of billiards, where two billiard balls collide in a set of elastic collisions. This process is similar to the process that occurs in a reactor when a neutron collides with an atomic nucleus that is in its path.

3.7 Modeling the Emission of a Neutron from an Atomic Nucleus

Suppose that an atomic nucleus, such as the one shown in Figure 3.5, becomes energetically unstable and decides to emit a neutron in the positive x direction after absorbing it at a previous time. This process can occur if the nucleus does not have the correct neutron-to-proton ratio (N/Z). Then, the conservation of momentum requires that the linear momentum of the nucleus and the neutron in the x direction before and after the reaction must be conserved:

Momentum Conservation during Spontaneous Neutron Emission

Momentum Before = Momentum After

$$MV = M'V' + m'v' \tag{3.9}$$

where

M is the mass of the nucleus before the collision
M′ is the mass of the nucleus after the collision
V is the velocity of the nucleus before the collision
V′ is the velocity of the nucleus after the collision
m′ and v′ are the mass and velocity of the emitted neutron(s), respectively

Because linear momentum is a vector quantity, the nucleus will move away from the reaction in exactly the *opposite direction* of the neutron because this is the only way that the linear momentum of the system can be conserved. As long as only two particles are involved in this process, then it is easy to see that this must always be the case. However, when more than two particles are involved, then it is necessary to assume that the neutron and the nucleus will *not* move in exactly the opposite direction.

In most cases, the target nucleus can be assumed to be stationary (or nearly stationary) before a neutron or another atomic particle is emitted. In this case, it is possible to set V = 0 in Equation 3.9. Then, Equation 3.9 implies that $V' = -v'(m'/M)$ in a spontaneous emission process. The speed that the nucleus exits the reaction is directly proportional to the mass ratio m/M of the neutron to the nucleus. Now, let us assume that the mass of the nucleus is measured in AMUs so that the mass of the nucleus after the particle is emitted is given by the symbol A. Then, we may write

$$V' = -v'\left(\frac{m'}{A}\right) \tag{3.10}$$

Using Equation 3.10, we can then predict what happens when the nucleus ejects a proton, a neutron, or even an electron. For a proton or a neutron, the value of m′ in AMUs is approximately equal to 1 (see Chapter 2). Therefore, the ratio of the velocity to the nucleus V′ to the velocity of the ejected neutron v′ is

$$V' = -\left(\frac{1}{A}\right)v' \tag{3.11}$$

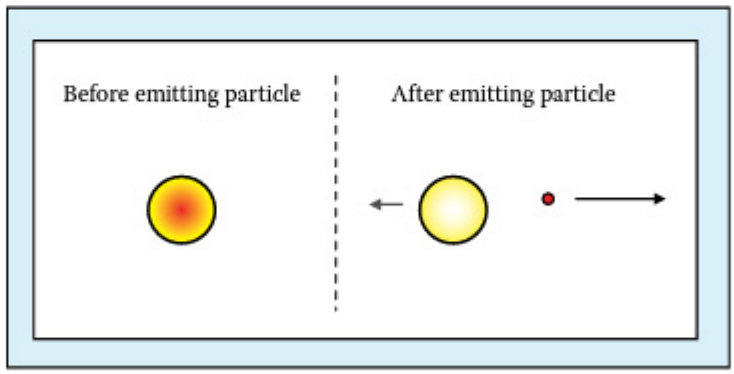

FIGURE 3.5 An example of spontaneous particle emission where the nucleus spontaneously emits another particle. This particle can be a γ-ray, a proton, a neutron, or an electron.

which depends entirely on the mass of the nucleus and the neutron. The nucleus is simply too heavy for the neutron to have much effect on it. Now let us see if we can understand what Equation 3.10 implies. If the atom has a reasonably heavy nucleus, say with 50 protons and 50 neutrons so that A = 100, then its recoil velocity will be

$$V' = -0.01v' \tag{3.12}$$

In other words, the atom (including the nucleus and the whole electron cloud surrounding it) will only move away at 1% of the velocity of the ejected particle if the particle happens to be a neutron. Now let us try the same exercise with an electron, which is about 2000 times lighter. Then, $m' \sim 0.0005$ and $V' = -0.000005v'$. *In other words, when the electron is ejected, the nucleus hardly moves at all.*

Example Problem 3.1

In Chapter 2, we learned that approximately 30 billion nuclear fissions are required every second to produce one watt of *thermal* power. Using this information, estimate how many fissions are required per second to produce 3000 MW of thermal energy from a thermal water reactor.

Solution We know that 3000 MW of thermal power requires 3,000,000,000 as many neutrons as it does to produce 1 watt of thermal power. Therefore, the number of neutrons required to produce 1000 MW of electricity per second (or 3000 MW of thermal power) is $3{,}000{,}000{,}000 \times 30{,}000{,}000{,}000 = 9 \times 10^{19}$ fission neutrons per second. *This is 90 billion billion nuclear fissions every second.* [Ans.]

3.8 Coordinate System Independence during Particle Collisions

When analyzing the outcome of an emission event, one can normally assume that the particle and the nucleus will move in opposite directions. In other words, if a neutron is emitted in the x direction, there is no y component or z component of the motion to consider. However, most nuclear reactions do not occur along a single coordinate direction, and so it is necessary to understand how momentum and energy can be conserved in this case. Now consider the problem shown in Figure 3.6 where a particle having mass m′ is *not* emitted parallel to the x-axis.

In this case, the y component of the momentum must be taken into account to ensure that the total linear momentum is conserved. Suppose that we refer to the x component of the momentum before and after the emission as P_X and P'_X and the y component of the momentum before and after the emission as P_Y and P'_Y. Then, the conservation of the momentum along the x direction requires that $P'_X = P_X$, and the conservation of the momentum along the y direction requires

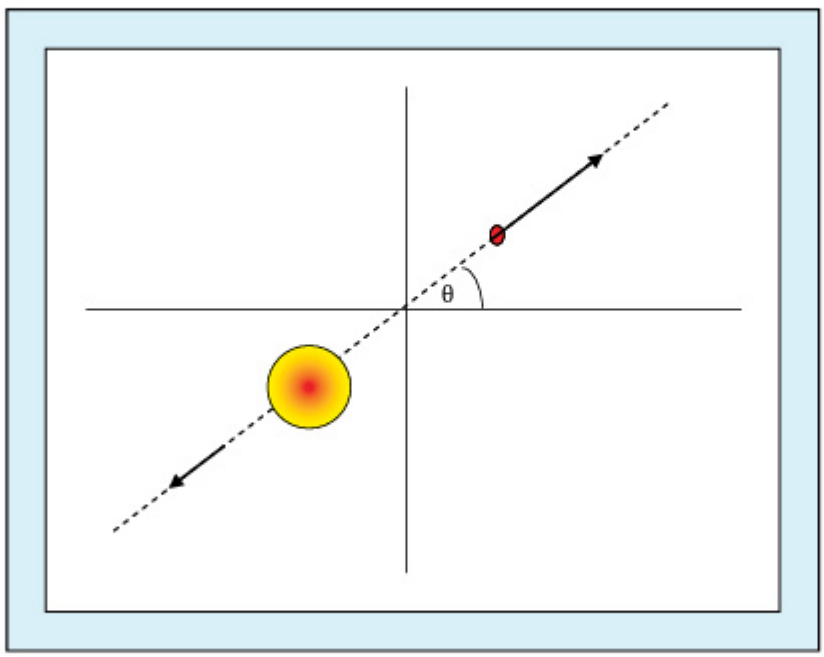

FIGURE 3.6 An example of spontaneous particle emission at an angle with respect to the x- and y-axes.

that $P'_Y = P_Y$. *In other words, we must independently conserve the x component and y component of the linear momentum for the total momentum to be conserved*. Using the expressions for each of these terms, we see that

$$MV_x = M'V'_x + m'v'_x \quad \text{(for the x direction)} \tag{3.13}$$

$$MV_y = M'V'_y + m'v'_y \quad \text{(for the y direction)} \tag{3.14}$$

If we assume that the nucleus that emits the particle is stationary or is nearly so, then we can set $V_x = V_y \approx 0$, and using Figure 3.6, it is easy to see that we can write

$$V'_x = -v'_x\left(\frac{m'}{M}\right) \quad \text{(for the x direction)} \tag{3.15}$$

$$V'_y = -v'_y\left(\frac{m'}{M}\right) \quad \text{(for the y direction)} \tag{3.16}$$

Now suppose that the particle is emitted with a velocity v′ at an arbitrary angle θ with respect to the x-axis. Then, using simple geometrical principles, the components of its velocity along the x- and y-axes are

$$v'_x = v'\cos\theta \tag{3.17}$$

$$v'_y = v'\sin\theta \tag{3.18}$$

On substituting these values into Equations 3.15 and 3.16, we obtain

Finding the Velocity of the Nucleus

$$V'_x = -v'\cos\theta\left(\frac{m'}{M}\right)$$
$$V'_y = -v'\sin\theta\left(\frac{m'}{M}\right) \tag{3.19}$$

where v′ is the speed of the emitted particle.

These expressions can be used to find the final velocity of the nucleus along the x- and y-axes as long as we know the masses, the ejection angle of the particle, and the velocity of the ejected particle. Then, how do we calculate the final velocity of the nucleus V′? We can find the final velocity V′ by simply applying the *Pythagorean theorem* and realizing that $(V')^2 = (V'_x)^2 + (V'_y)^2$. It therefore follows that

$$V' = \sqrt{(V'_x)^2 + (V'_y)^2} \tag{3.20}$$

If we substitute $V'_x = -v'\cos\theta(m'/M)$ and $V'_y = -v'\sin\theta(m'/M)$ into Equation 3.20 and perform the required math, we obtain

$$V' = \sqrt{\left[v'\left(\frac{m'}{M}\right)\right]^2\left(\sin^2\theta + \cos^2\theta\right)} \tag{3.21}$$

or

$$V' = v'\left(\frac{m'}{M}\right) \tag{3.22}$$

where we have used the fact that $\sin^2\theta + \cos^2\theta = 1$.

In other words, no matter how the x- and y-axes are aligned, the result is exactly the same. If we know the velocity of the ejected particle and the masses of the various parts, then we know how the nucleus and the electron cloud that surrounds it will behave. Although we have not demonstrated it here, the same argument can be extended to three spatial dimensions (where we need to consider the x, y, and z directions) rather than just two (x and y). This is because the linear momentum **P** is a vector, and no matter what coordinate system or number of dimensions that are used, the magnitude of the total velocity V and therefore the total momentum **P = MV** must always be the same.

The only thing that changes is the percentage of the vectors P'_X, P_X, P'_Y, P_Y, and P'_Z, P_Z, which are projected along each coordinate direction. It is also possible in some situations that the total mass M′ of the nucleus after a matter particle is ejected from it will be significantly less than the initial mass M. In this case, we must consider *both* the velocity of the ejected particle *and* the change in the mass of the parent nucleus to calculate the final velocities correctly. We will explore this concept in more detail in the discussion that follows.

3.9 Momentum Conservation for a Multiparticle System

Now suppose that we would like to generalize our previous discussion to include a much larger system of particles similar to what we might encounter in a reactor core. In this case, the environment we are dealing with would consist of N particles (which would consist primarily of neutrons), and each particle n might have a different mass m_n or a different velocity $\mathbf{v}_n$. Then, the sum of the products of all of the masses and all of the velocities will always add up to the same vector P, which we will call the *total momentum of the system* P—even though the number of particles and their velocities might change over time (see Figure 3.7). We can express this fact by writing

$$\mathbf{P} = \sum_i m_i \mathbf{v}_i = m_1\mathbf{v}_1 + m_2\mathbf{v}_2 + m_3\mathbf{v}_3 + \cdots + m_n\mathbf{v}_n \tag{3.23}$$

or in a simpler form

$$P = \sum_i \mathbf{P}_i = \mathbf{P}_1 + \mathbf{P}_2 + \mathbf{P}_3 + \cdots + \mathbf{P}_n \tag{3.24}$$

where both the summations are over all particles from i = 1 to i = N. Then, if **P** is the total momentum prior to the beginning of the interactions between these particles and **P′** is the total momentum at the end of these interactions, then the conservation of linear momentum requires that

$$\mathbf{P}' = \sum \mathbf{P}'_i = \mathbf{P}'_1 + \mathbf{P}'_2 + \mathbf{P}'_3 + \cdots + \mathbf{P}'_n = \mathbf{P}_1 + \mathbf{P}_2 + \mathbf{P}_3 + \cdots + \mathbf{P}_n \tag{3.25}$$

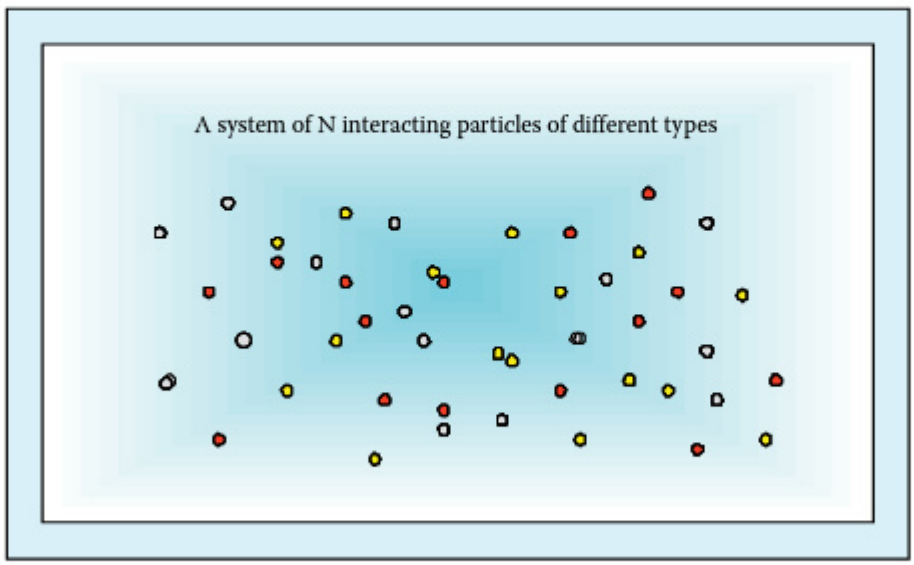

FIGURE 3.7 An N particle system having many different masses and velocities.

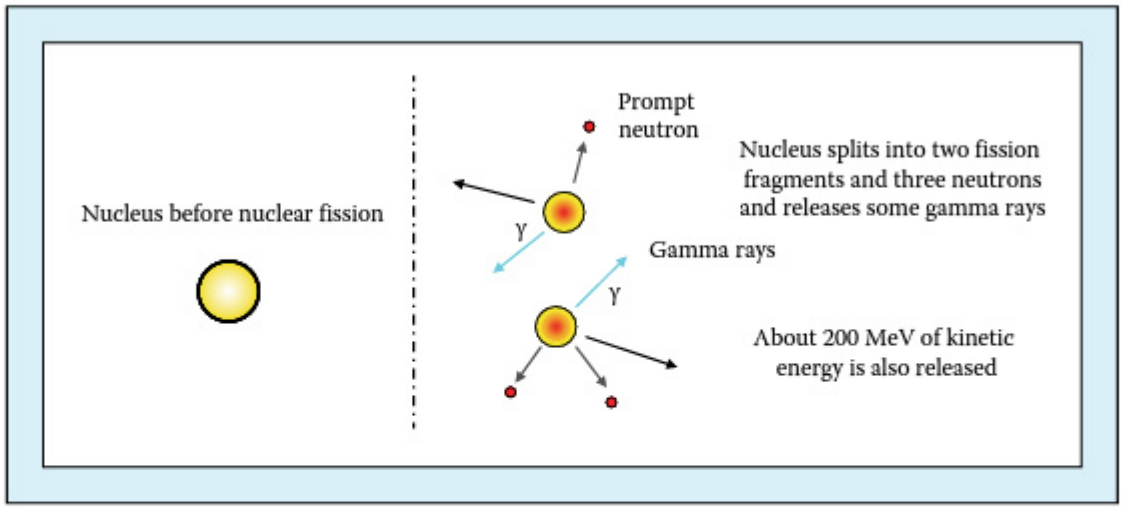
Nucleus before nuclear fission
Prompt neutron
Nucleus splits into two fission fragments and three neutrons and releases some gamma rays
γ
Gamma rays
γ
About 200 MeV of kinetic energy is also released

FIGURE 3.8 A uranium nucleus before and after it splits apart.

and $\mathbf{P}' = \mathbf{P}$ always. Notice that we are only referring to the total momentum of the particle population here. It immediately follows from our previous discussion that the total momentum in the x direction and the y direction must also be conserved because the momentum is a vector quantity. Hence,

$$\mathbf{P}'_x = \mathbf{P}_x \quad (\text{for the x direction}) \tag{3.26}$$

$$\mathbf{P}'_y = \mathbf{P}_y \quad (\text{for the y direction}) \tag{3.27}$$

Armed with these very simple principles, it is possible to predict how neutrons behave statistically when they collide with target nuclei in the core. These nuclei can be present in the fuel, the moderator, or the coolant.

To illustrate a practical application of this principle, suppose that the uranium nucleus in Figure 3.8 decides to split apart. The nucleus has already absorbed a neutron, but because the speed of the neutron is so low and the mass of the nucleus is so high, we can assume from our previous discussion that the velocity V′ of the nucleus at the start of the fission process is approximately equal to 0. The total momentum at the beginning of the reaction is therefore P ~ 0. We can represent this by drawing the point P1 in Figure 3.8. If the result of this reaction (which is quite typical) is that the nucleus splits into eight parts—say two fission fragments, three neutrons, two γ-rays, and a neutrino (not shown)—then each of these parts will have its own unique momentum and its own unique direction. However, the final momentum of the sum of the eight parts, which we can represent graphically by the sum of all the arrows in Figure 3.9, must be exactly equal to the momentum of the original nucleus before the process started or $\mathbf{P} = \sum_i \mathbf{P}_i = 0$.

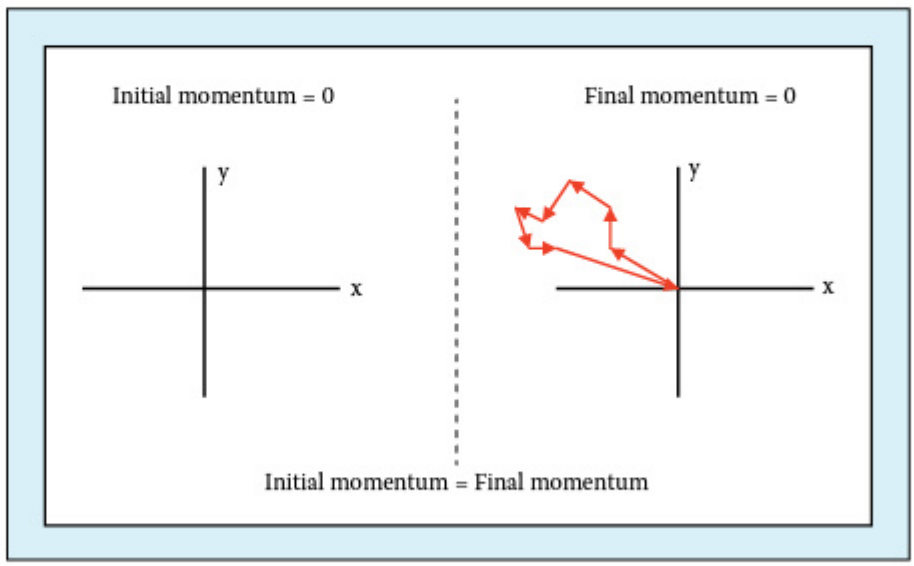

FIGURE 3.9 The sum of the momentum vectors of particles that come out of the same reaction where the target nucleus is initially at rest.

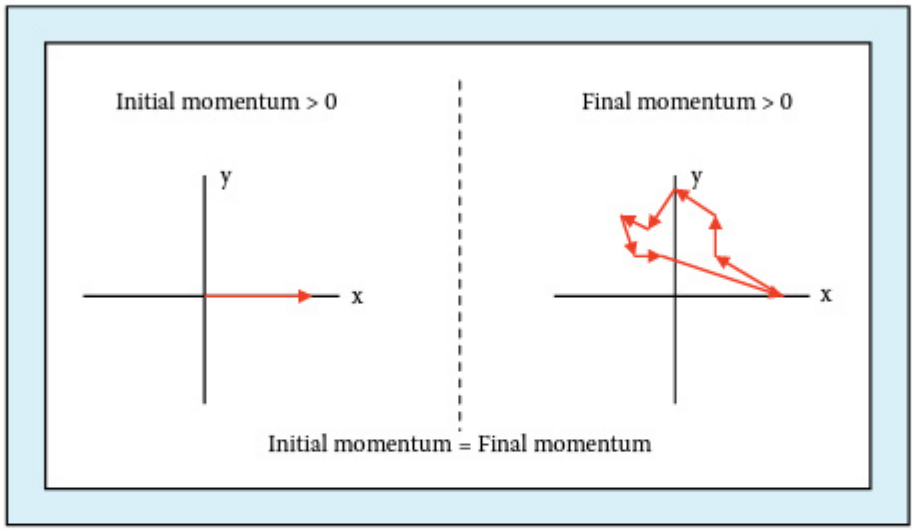

FIGURE 3.10 The sum of the momentum vectors of particles that come out of the same reaction where the target nucleus is moving to the right with a velocity V.

In other words, *the total momentum does not change between the beginning of the reaction and the end of the reaction no matter how the particles decide to distribute themselves*. Now, let us consider the second reaction shown on the left-hand side of Figure 3.10 where the target nucleus has a velocity V and a momentum **P** = **MV** before it splits into several different parts. What does the sum of the eight momentum vectors look like in this case? The result is shown on the right-hand side of Figure 3.10. *Notice that the initial motion of the target nucleus simply displaces the other eight momentum vectors. At the end of the process, the eight momentum vectors still add up to the initial momentum vector P = MV!*

The number 8 is not a magic number that we have made up to convince you that this result is correct. If the reaction had only released two neutrons instead of three and only one γ-ray (instead of two), then the results would have been exactly the same. In the next section, we will learn that this is true even when some of the particles coming out of the reaction, like the photons, do not have any rest mass at all. Even then, the sum of the arrows will always go back to the original momentum vector (which is defined by its direction and its length), and the total momentum before the reaction P must equal the total momentum P′ after the reaction. The particles may have completely different energies, but the total momentum will remain the same. This can be very handy when trying to understand the angular distribution of the individual particles (θ_1, θ_2, θ_3, θ_4, θ_5, θ_6, θ_7, and θ_8) that fly out of a nucleus after it has undergone a fission event. The linear momentum of the system is always conserved. In the example we used, the number of particles we picked was just a formality. A different number of particles could have also been used.

Student Exercise 3.1

Show that if a neutron is moving at a velocity V at an angle θ with respect to the x- and y-axes and an angle ϕ with respect to the z-axis, then the sum of the squares of the momentum along each coordinate direction will always be conserved.

3.10 What Happens When a Neutron Hits an Atomic Nucleus

In a previous section, we assumed that the linear momentum **P** of all of the particles was zero. In other words, we assumed that the system of particles could be described by requiring that $\mathbf{P_X} = 0$, $\mathbf{P_Y} = 0$, and $\mathbf{P_Z} = 0$. In many solids and liquids and even in most gases at low temperatures, this turns out to be a reasonably good assumption to make. However, as we pointed out in Section 3.4, some neutrons can be created with very high energies (E > 1 MeV), and therefore they can possess some very high velocities as well. In a nuclear reactor, these neutrons eventually interact with other atomic nuclei that happen to be in their way. When this occurs, a neutron will scatter off of a nucleus, and both the neutron and the target nucleus can move away from each other along a different path. In this case, the incoming neutron has so much energy that it is no longer possible to assume that $\langle \mathbf{P} \rangle = 0$. Whenever this occurs, the incoming neutron velocity v cannot be ignored when predicting the outcome of the collision. In this case, we must go back to our original equations and require that

$$\mathbf{P}' = \mathbf{P} \neq 0 \tag{3.28}$$

We can also write this explicitly for a two-particle system (an incoming neutron of velocity v and a relatively stationary nucleus having an initial velocity V) as

$$M'V' + m'v' = MV + mv \tag{3.29}$$

where

M is the mass of the nucleus before the collision
M′ is the mass of the nucleus after the collision
V is the velocity of the nucleus before the collision
V′ is the velocity of the nucleus after the collision
m and v are the mass and the velocity of the neutron before the collision
m′ and v′ are the mass and the velocity of the neutron after the collision

Depending on whether or not the neutron is absorbed by the nucleus, or just scatters off of it, the value of M′ can be greater than M(M′ > M) or the same as M(M′ = M). Most interactions of high-speed neutrons with matter can be understood in this way. It is easy to see that the same approach can also be extended to handle neutrons that are moving at *relativistic speeds* (i.e., v > 0.1c). In this case, it is no longer possible to assume that the mass m of the neutron is the same as the neutron rest mass m_o, and we must write

$$m = \frac{m_o}{\sqrt{\left[1-(v/c)^2\right]}} \tag{3.30}$$

which implies that

$$M'V' + \frac{m_o v'}{\sqrt{\left[1-(v'/c)^2\right]}} = MV + \frac{m_o v}{\sqrt{\left[1-(v/c)^2\right]}} \tag{3.31}$$

when M ≫ m and M′ ≫ m′. Hence, when dealing with very-high-speed neutrons, we must use this expression and the corresponding expression for the conservation of energy

Energy Conservation in a Particle Collision

Energy Out = Energy In

$$E' = E \tag{3.32}$$

to calculate the final velocities properly. We can illustrate how the kinetic energy E of an incoming neutron (in MeV) is related to its actual velocity as it travels through matter with the following example. Most heavy nuclei do not routinely travel at such high speeds, and so for M > 12 AMU (which is true for the element carbon), the mass of the nucleus before and after the collision can generally be assumed to be equal to the rest mass as follows:

$$M' \approx M \approx M_o \tag{3.33}$$

Interactions with uranium and plutonium atoms can be modeled in a similar way.

Example Problem 3.2

Using the classical expression for the neutron kinetic energy E (see Chapter 2), calculate the velocity v of a 2 MeV neutron before it collides with the nucleus of a nearly stationary atom. What percentage of the speed of light is the neutron traveling at in this case?

Solution In Chapter 2, we learned that the classical expression for the kinetic energy $E = 1/2\ mv^2$ turns out to be relatively accurate for neutron energies up to about 100 MeV, because even at 100 MeV, the kinetic energy of a neutron is only about one-tenth of its rest mass energy (939.55 MeV). If the velocity is measured in meters per second, and the kinetic energy E is measured in MeV, the velocity is related to the energy by $v = 1.383 \times 10^7 \sqrt{E}$. Since E = 2 MeV, $v = 1.955 \times 10^7$ m/s. Since the speed of light is 3×10^8 m/s, the 2 MeV neutron is only traveling at $0.1955 \times 10^8/3 \times 10^8 =$ 6.5% of the speed of light. [Ans.]

3.11 Including Photons and Neutrinos in Common Particle Collisions

In the previous problem, we did not include the effects of relativity in our calculations because we assumed that most of the particles that were emitted had velocities that were low relative to the speed of light ($v \ll c$). We also did not include the effects of photons in our analysis. However, photons are produced in very large numbers in a reactor core (in the form of energetic γ-rays), and some nuclear particles, like the electrons that are emitted in beta decay, have an average velocity that is large relative to the speed of light (say between 0.5c and 0.7c). In this case, it is no longer appropriate to assume that the laws of classical mechanics apply, and we must use the relativistic equations for the energy and the momentum that were derived in Chapter 2.

This implies that we must replace m_o, the rest mass that we measure in the laboratory (LAB), with $m = m_o\sqrt{[(1(v/c)^2]}$. This simple fix works well for every nuclear particle except the photon. However, because *the photon has no rest mass* at all ($m_o = 0$), we cannot use the same expressions that we applied previously because $m_o = 0$. In the case of the photon, it can be shown (see Chapter 2) that the photon's energy E_γ is related to its momentum p_γ by the equation

Energy and Momentum of a Photon

$$E_\gamma = p_\gamma c \tag{3.34}$$

where

$E_\gamma = hf$
h is Planck's constant
f is the frequency of vibration (in cycles per second)
c is the speed of light

In the case of the neutrino, it has such a low rest mass that it can be ignored in most calculations. However, its momentum cannot be ignored, and so we can assume with very little error that its momentum and its energy are related in a similar way as follows:

$$E_v = p_v v \tag{3.35}$$

where v is the velocity of the neutrino. Hence, some of the particles produced in the core need to be treated differently than the neutron or the proton, and in this case, the expressions in Table 3.2 must be used. Now, let us ask the following two questions that we have been unable to answer so far:

1. How do we find the final velocity of the original nucleus when it loses some of its original mass (e.g., when its mass is reduced from M to M′) after a neutron, proton, or alpha particle is ejected from it?
2. How do we find the final velocity of the nucleus if only a photon (which has no rest mass) is emitted from it instead of a neutron?

Let us start by considering the answer to question 1 first. If we substitute the value of E′ into our earlier example, then the equation for the conservation of linear momentum becomes

$$MV = M'V' + m'v' \tag{3.36}$$

or

TABLE 3.2
Summary of the Appropriate Equations to Use When Calculating Energy and Momentum in a Nuclear Reaction

Particle Name	Symbol	Particle Type	Equation for Kinetic Energy ($v \ll c$)	Equation for Linear Momentum
Proton	P	Matter particle	$1/2\ m_o V^2$	mV
Neutron	N	Matter particle	$1/2\ m_o V^2$	mV
Electron	e^-	Matter particle	$1/2\ m_o V^2$	mV
Photon	γ	Force particle	hf	hf/c

$$MV = M'V' + \sqrt{(2m'E')} \tag{3.37}$$

and finally, when we solve for V′, we obtain

$$V' = \left(\frac{M}{M'}\right)V - \left(\frac{1}{M'}\right)\sqrt{(2m'E')} \tag{3.38}$$

if we are dealing with an ejected particle of rest mass m′ and energy E′. Now let us provide the answer to question 2. In this case, the photon has no rest mass, but it definitely has energy and momentum, so the appropriate equation to use is

$$V' = \left(\frac{M}{M'}\right)V - \left(\frac{1}{M'c}\right)E'_{\gamma} \tag{3.39}$$

and in the case of the neutrino, the same argument (which has a slight error) leads to conclude that

$$V' = \left(\frac{M}{M'}\right)V - \left(\frac{1}{M'c}\right)E'_{v} \tag{3.40}$$

It is important to realize that these arguments can be applied to any number of particles as long as we know what their final energies are. Now let us show how these equations can be applied to a neutron that participates in a head-on elastic collision.

3.12 The Physics of Head-On Collisions

Occasionally, a neutron will hit an atomic nucleus "head-on." When this occurs, the neutron either will be absorbed by the nucleus or will bounce off one of the particles inside of it and scatter back in exactly the opposite direction from which it came. In physics books, this type of collision is called a *head-on collision*. What happens in this case depends on the atomic weight A of the target nucleus as well as the mass ratio of the neutron to the nucleus. We would like to illustrate this principle for you with a few simple examples. From our previous discussion, we saw from the conservation of momentum (and also the conservation of energy) that the final velocities of the neutron and the atomic nucleus, V'_N and V'_A, are related to their initial velocities V_N and V_A by the following equations:

$$V'_N = V_N\frac{(M_N - M_A)}{(M_N + M_A)} + V_A\frac{(2M_A)}{(M_N + M_A)} \tag{3.41}$$

$$V'_A = V_A\frac{(M_A - M_N)}{(M_N + M_A)} + V_N\frac{(2M_N)}{(M_N + M_A)} \tag{3.42}$$

where

M_N is the mass of the neutron
M_A is the mass of the atom

If the atom is stationary, or nearly so, then we can set $V_A = 0$. In this case, the final velocities of the neutron and the atom can be found from the initial velocity of the incoming neutron from the equations

$$V'_N = V_N\frac{(M_N - M_A)}{(M_N + M_A)} \tag{3.43}$$

$$V'_A = V_N\frac{(2M_N)}{(M_N + M_A)} \tag{3.44}$$

To arrive at these equations, we used the fact that the kinetic energy and the momentum of the nucleus and the neutron were conserved. Now, let us see exactly what these equations imply. To do so, consider two entirely different scenarios involving the collision of a neutron with an atomic nucleus. In the first case, assume that the neutron hits a hydrogen nucleus, which has an atomic mass of 1 ($M_A = 1$) in a head-on collision. In the second case, assume that the neutron hits a Uranium-235 nucleus, which has an atomic mass of 235 ($M_A = 235$) in a head-on collision. Since the neutron has an atomic mass of 1 ($M_N = 1$), the final velocities for both particles will be represented by Equation 3.45.

Now, let us reflect on what each of these scenarios implies. *In the first scenario, when the neutron has a head-on collision with the nucleus of a hydrogen atom, the final velocity of the neutron—due to the conservation of momentum—is zero*. In other words, the neutron has been able to transfer virtually all of its kinetic energy and momentum to the hydrogen nucleus, and at the end of the collision, it has virtually none left. If you think about it, this is exactly what happens when two billiard balls collide on a pool table. Except for the small amount of energy that is lost in the "click," the energy and momentum of the billiard balls must be conserved, and when the incoming ball stops, the other ball continues with the same momentum or speed (as long as the collision is elastic and frictionless)

The Velocity of an Atomic Nucleus When It Is Hit by a Neutron

For Hydrogen:

$$V'_N = 0 \quad V'_A = V_N$$

For Uranium-235: (3.45)

$$V'_N = -\left(\frac{117}{118}\right)V_N \quad V'_A = \left(\frac{1}{118}\right)V_N$$

This means that a hydrogen atom can take a high-speed neutron, which is emitted from a Uranium-235 nucleus with an average velocity of about 14,000,000 m/s, and slow it down to thermal speeds (which are about 2200 m/s) in just a single head-on elastic collision. Hence, hydrogen has become a very popular neutron moderator in commercial water reactors, where it is combined with oxygen to form the reactor coolant.

Now, let us turn our attention to what happens when the same fission neutron collides with a uranium nucleus, which may also be present in the fuel. Obviously, the uranium nucleus is much heavier than the hydrogen nucleus, and because of this, we would expect the rate of momentum transfer to be different. When the neutron is not absorbed, it ricochets back in the opposite direction at over 99% of the speed that it collided with the uranium nucleus. *In other words, it acts like a tennis ball that has just bounced off of a brick wall*. The remaining 1% of the forward speed of the neutron is transferred to the uranium nucleus, which receives a slight kick forward as a result of the collision. The results of both collisions are illustrated in Figure 3.11.

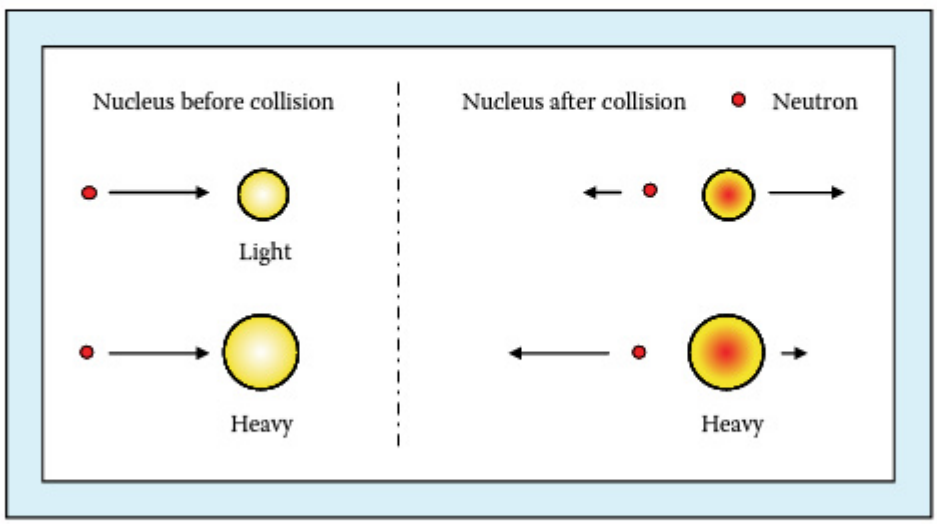

FIGURE 3.11 The results of two head-on elastic collisions with different atoms. The top one is a light one, and the bottom one is a heavy one. Note that the linear momentum is conserved in both cases.

Now let us turn our attention to another phenomenon that sometimes occurs when the speed of the incoming neutron is lower. If the neutron approaches a U-235 nucleus at exactly the right speed (which happens to be about 2200 m/s), then the neutron can be absorbed by the U-235 nucleus, and it sticks to the nucleus rather than bouncing away from it. *This is similar to what happens when a small snowball hits a much larger one at just the right speed, and the two snowballs stick together rather than flying apart*. In this case, the initial momentum must be equal to the final momentum

$$M_N V_N + M_A V_A = (M_N + M_A) V'_A \tag{3.46}$$

and due to the conservation of momentum, the final velocity of the combined structure must be

$$V'_A = \frac{(M_N V_N + M_A V_A)}{(M_N + M_A)} \tag{3.47}$$

Finally, if the nucleus is initially at rest so that $V_A = 0$, we have

$$V'_A = \frac{V_N M_N}{(M_N + M_A)} \tag{3.48}$$

3.13 Particle Backscattering

One of the remarkable things about the equations we have just discussed is that they allow us to infer the masses of particles in an elastic collision by just observing their final velocities. In the early days of the nuclear industry (see Chapter 2), scientists did not always know the masses of the radioactive materials they were using, and so they conducted *scattering experiments* to determine what their masses might be. If we take a look at Equation 3.43 more closely, we see that the velocity of a particle bouncing off of a stationary nucleus in a head-on collision is just

$$V'_N = V_N \frac{(M_N - M_A)}{(M_N + M_A)} \tag{3.49}$$

where

M_N is the mass of the neutron
M_A is the mass of the target nucleus

However, the value of M_N in this equation can be the mass of any nuclear particle that is shot at the nucleus. If this particle happens to be an alpha particle (with $M_N = 4$), then Equation 3.43 can be rewritten as

$$V'_\alpha = V_\alpha \frac{(4 - M_A)}{(4 + M_A)} \tag{3.50}$$

or

$$V'_\alpha = V_\alpha \frac{(4 - A)}{(4 + A)} \tag{3.51}$$

Here, the subscript α refers to the fact that the incoming particle is an alpha particle (rather than a neutron) and A now refers to the mass of the target nucleus. If we shoot some alpha particles at an atomic nucleus where we do not know the value of A, then we can *infer* the value of A by observing how the alpha particles react.

If the atomic nucleus is *heavier* than the incoming alpha particles, then $A > 4$, and the numerator will be a *negative number*. This means that some of the alpha particles will *backscatter* (if they happen to hit the atomic nucleus directly), *and we can conclude from this simple observation that the atomic nucleus must be heavier than the incoming alpha particles*. Conversely, consider what happens if the alpha particles *do not* backscatter from the target nucleus. In this case, the alpha particles must be *heavier* than the atomic nucleus, and the value of the numerator must be positive. Finally, suppose that we shoot alpha particles at the target nucleus, and the velocities of the alpha particles do not change at all.

In this third scenario, we must conclude that the alpha particles have transferred all of their kinetic energy to the atomic nucleus and that the atomic nucleus is in fact a helium nucleus. Furthermore, we can infer the mass of the atomic nucleus, A, by simply taking the ratio of the initial alpha particle velocity to the final alpha particle velocity. The mass of the atomic nucleus is therefore

$$A = \frac{4\left(V_\alpha - V'_\alpha\right)}{\left(V_\alpha + V'_\alpha\right)} \tag{3.52}$$

Hence, by simply observing how the alpha particles behave, we can infer what the mass of the atomic nucleus must be. Moreover, we can generalize these equations to *any nuclear reaction* in which the masses of the incoming particles are known. This is one way in which an elastic scattering experiment can be used to determine what the underlying structure of a nuclear material must be.

Example Problem 3.3

Suppose that we fire a beam of alpha particles at an atomic nucleus and we find that some of the alpha particles are scattered at an angle of greater than 90°. What can be concluded from this simple observation?

Solution If some of the alpha particles are scattered back at an angle of greater than 90°, we must conclude that the velocity of the alpha particles is negative, and from Equation 3.51, we must conclude that $A > 4$. In other words, the atomic nucleus must have a mass greater than that of the incoming alpha particles. [Ans.]

We would now like to turn our attention to how the energies of the incoming particles behave.

3.14 Finding the Energy Loss in a Head-On Elastic Collision

We can also use the principle of energy conservation to calculate how much energy a neutron with an atomic mass of $M_N \approx 1$ AMU loses in a single elastic collision with a target nucleus having a mass of M_A AMU. If we keep the same notation that we used previously, the conservation of energy in an elastic collision requires that

$$\left(\frac{1}{2}\right)M_N V_N^2 + \left(\frac{1}{2}\right)M_A V_A^2 = \left(\frac{1}{2}\right)M_N V_N'^2 + \left(\frac{1}{2}\right)M_A V_A'^2 \tag{3.53}$$

Now, suppose that the nucleus of the atom that the neutron is colliding with is essentially at rest relative to the speed of the neutron. In this case, $V_A \sim 0$, and we have

$$\left(\frac{1}{2}\right)M_N V_N^2 - \left(\frac{1}{2}\right)M_N V_N'^2 = \left(\frac{1}{2}\right)M_A V_A'^2 \tag{3.54}$$

or

$$\Delta E = \left(\frac{1}{2}\right)M_A V_A'^2 \tag{3.55}$$

Finally, we know from Equation 3.48 that

$$V'_A = \frac{V_N M_N}{\left(M_N + M_A\right)} \tag{3.56}$$

so

$$\Delta E = \left(\frac{1}{2}\right)M_A V_A'^2 \quad \text{or} \quad \Delta E = \left(\frac{1}{2}\right)M_N V_N^2 \cdot \left(\frac{M_A}{\left(M_N + M_A\right)}\right)^2 \tag{3.57}$$

In other words, Equation 3.57 states that the total change in the energy of the neutron ΔE as the result of a collision with an atom of mass M_A is equal to the initial kinetic energy of the neutron $(1/2)\, M_N V_N^2$ times a constant of proportionality, which we will call α. According to the expression we have just presented, the value of α is

$$\alpha = \frac{(M_A - M_N)^2}{(M_A + M_N)^2} \tag{3.58}$$

This constant of proportionality is sometimes called the *energy decrement per collision*. Since $M_N = 1$ for a neutron, Equation 3.58 reduces to

$$\alpha = \frac{(M_A - 1)^2}{(M_A + 1)^2} \tag{3.59}$$

In some textbooks, this notation is further simplified by replacing the atomic mass of the target nucleus M_A by the symbol A, where A is the atomic mass in AMU, and by recognizing that the atomic mass of the neutron M_N is approximately equal to 1 AMU. In this case, the energy decrement per collision becomes

Neutron Energy Decrement per Collision

$$\alpha = \frac{(A - 1)^2}{(A + 1)^2} \tag{3.60}$$

where A is the atomic mass in AMU of the atom that the neutron is colliding with. *Equation 3.60 appears frequently in the study of nuclear science and engineering, and it is also discussed on many occasions in our companion book.* It allows us to calculate how much energy a neutron loses in a single head-on elastic collision* with a target nucleus. If the neutron collides with the same type of atom over and over again, it will lose exactly this fraction of its energy each time. In other words, its energy E declines at a rate that is proportional to αE, or

Relationship of the Initial Energy E to the Final Energy E′ after One Head-On Elastic Collision

$$E' = \alpha E \tag{3.61}$$

where

E is the initial energy before the collision
E′ is the final energy after the collision

In general, this means that $\Delta E = E - E' = E(1 - \alpha)$, so the smaller the value of α, the greater the total energy loss will be. In the case of *repetitive elastic collisions*, it also follows from Equation 3.61 that

$$E'' = \alpha E' = \alpha\alpha E \tag{3.62}$$

and

$$E''' = \alpha\alpha\alpha E, \quad \text{and so on.} \tag{3.63}$$

We can generalize this result to the case of n successive collisions by writing

Relationship of the Initial Energy E to the Final Energy E′ after n Head-On Elastic Collisions

$$E'_n = \alpha^n E \tag{3.64}$$

* See *Nuclear Engineering Fundamentals: A Practical Perspective*, by R.E. Masterson, CRC Press (2017).

where
E'_n is the energy of the neutron after the nth collision
E is the initial energy before any of the collisions occurred

This is a very important result that is of great importance to the field of nuclear science and engineering.

3.15 The Energy Loss in a Glancing Collision

The equations above are based on the assumption that both the neutron and the nucleus will emerge from a collision and move along exactly the opposite directions as they did before the collision. We would now like to generalize our discussion to include the case where the neutron does NOT hit the nucleus directly. In other words, we would like to generalize our discussion to include collisions called *glancing collisions*. In these types of collisions, the nucleus and the neutron move away from each other in different directions that correspond to scattering angles θ_1 and θ_2, which add up to the total scattering angle θ, which is observed in the laboratory coordinate system. In other words, in the derivation that follows, we will assume that $\theta = \theta_1 + \theta_2$.

When two particles participate in such a collision, this type of collision is referred to as a *glancing collision*. We would like to start our derivation for the energy loss by referring to Figure 3.12. As long as the energy and linear momentum are conserved, it is possible to represent the momentum before and after the collision by the vector diagram shown in Figure 3.12. Applying the *law of cosines* to the momentum vectors p'_n and p'_a after the collision and knowing that they must be equal to the total momentum p_n before the collision, it is easy to see that the initial and final momenta are related by

Initial and Final Momentum in a Glancing Collision

$$(p_n)^2 = (p'_n)^2 + (p_a)^2 - 2p'_n\, p'_a \cos\theta \tag{3.65}$$

where
p_n is the initial momentum of the neutron
p'_n is the final momentum of the neutron
p'_a is the final momentum of the atom

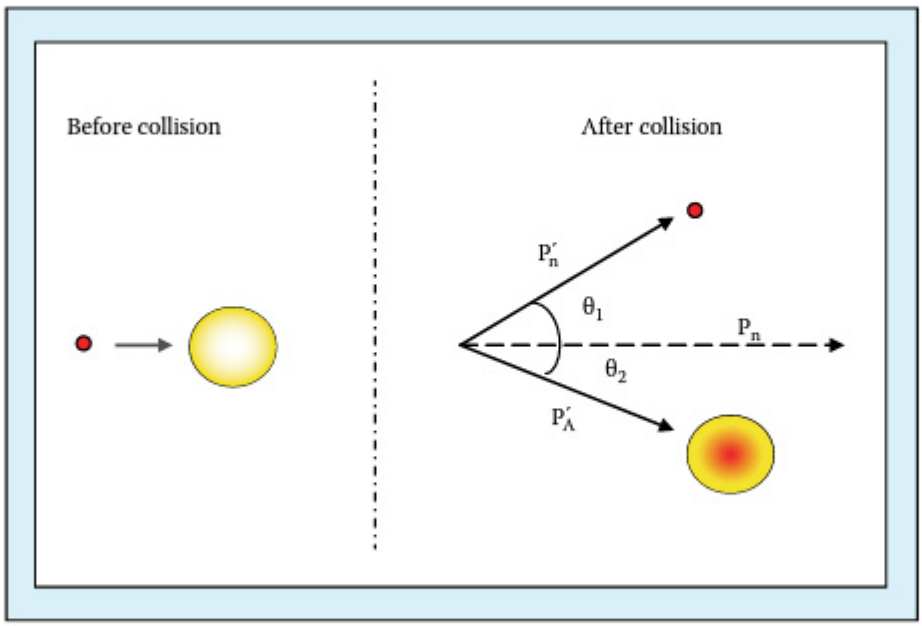

FIGURE 3.12 A neutron and an atomic nucleus undergoing elastic scattering.

From our discussion earlier in the chapter, we also know that

$$p^2 = 2EM_n \quad \text{and} \quad p_n'^2 = 2E'M_n \quad \text{and} \quad p_a'^2 = 2E_a'M_a \tag{3.66}$$

where
E is the energy of the incoming neutron
E′ is its final energy
M_n is its mass

This allows us to write Equation 3.65 as

$$2EM_n = 2E'M_n + 2E_a'M_a - 2\sqrt{(2E'M_n)}\sqrt{(2E_a'M_a)}\cos\theta \tag{3.67}$$

or

$$M_nE = M_nE' + M_aE_a' - 2\sqrt{(M_nM_aE'E_a')}\cos\theta \tag{3.68}$$

Recognizing that the mass of the neutron M_n is approximately 1 AMU and that the mass of the atom is A AMUs, we can then write

$$E = E' + AE_a' - 2\sqrt{(AE_a'E')}\cos\theta \tag{3.69}$$

and finally realizing that $E = E' + E_a'$ or $E_a' = E - E'$, we can eliminate E_a' from this equation to obtain

$$(1+A)E' - 2\sqrt{(E'E)}\cos\theta + (1-A)E = 0 \tag{3.70}$$

Equation 3.70 can be solved for the final neutron energy E′ if we know the initial neutron energy E. After some work and a lot of rearrangement, we obtain

Initial and Final Energy in a Glancing Collision

$$E' = \alpha' E$$
$$\text{where } \alpha' = \{(1+\alpha)/2 + (1-\alpha)/2 \cdot \cos\theta\} \tag{3.71}$$

and $\alpha = (A-1)^2/(A+1)^2$. *Equation 3.71 therefore establishes a direct relationship between the initial and final energies of the neutron and its scattering angle for any type of elastic collision*. It should be apparent that if the neutron hits a hydrogen atom and backscatters along the direction from which it initially came, then Equation 3.71 reduces to

$$E' = \alpha E \tag{3.72}$$

because $\theta_1 = 180°$. In other words, this is exactly the same result we obtained previously for a head-on collision with $\alpha = (A-1)^2/(A+1)^2$. Thus, *the energy loss in an elastic scattering collision is proportional to the cosine of the scattering angle*. To elaborate on this further, consider the case of a hydrogen atom where A = 1. In this case, the value of α′ is

$$\alpha' = 0.5(1+\cos\theta) \tag{3.73}$$

TABLE 3.3
Average Energy Loss per Collision for a Neutron Elastically Scattering Off of a Hydrogen Atom for Different Values of the Neutron Scattering Angle θ

Scattering Angle θ (°)	Value of α′	Value of ΔE	Percentage Energy Loss (per Collision)
0	1.00	0	0
30	0.93	0.07	7
45	0.85	0.15	15
60	0.75	0.25	25
75	0.63	0.37	37
90	0.50	0.50	50
135	0.15	0.85	85
180	0.00	1.00	100

Now, let us consider what happens to the final energy of the neutron E′ for various values of α′ and θ. In this case, the fractional energy loss is ΔE = E − E′. In a single elastic collision, the energy loss is given by

$$\Delta E = (1 - \alpha') = 0.5(1 - \cos\theta) \tag{3.74}$$

When θ = 0, the neutron's trajectory is not changed, and ΔE = 0. Conversely, when θ = 180°, the neutron hits the hydrogen nucleus head-on and comes to a complete stop. In this case, ΔE = 1 (100%), and all of its kinetic energy is lost. Table 3.3 shows the values of the fractional energy loss ΔE for various values of the neutron scattering angle θ. *Thus, the neutron energy loss always increases as the scattering angle is increased*. The general trend is shown for a number of important elements in Figure 3.13. In each case, the energy loss per collision reaches its maximum value when θ = 180° and the particle *backscatters*. Conversely, when the scattering angle is 0, the neutron misses the target nucleus completely, and its kinetic energy remains unchanged. Notice that all we needed to arrive at these results were a simple energy and momentum balance.

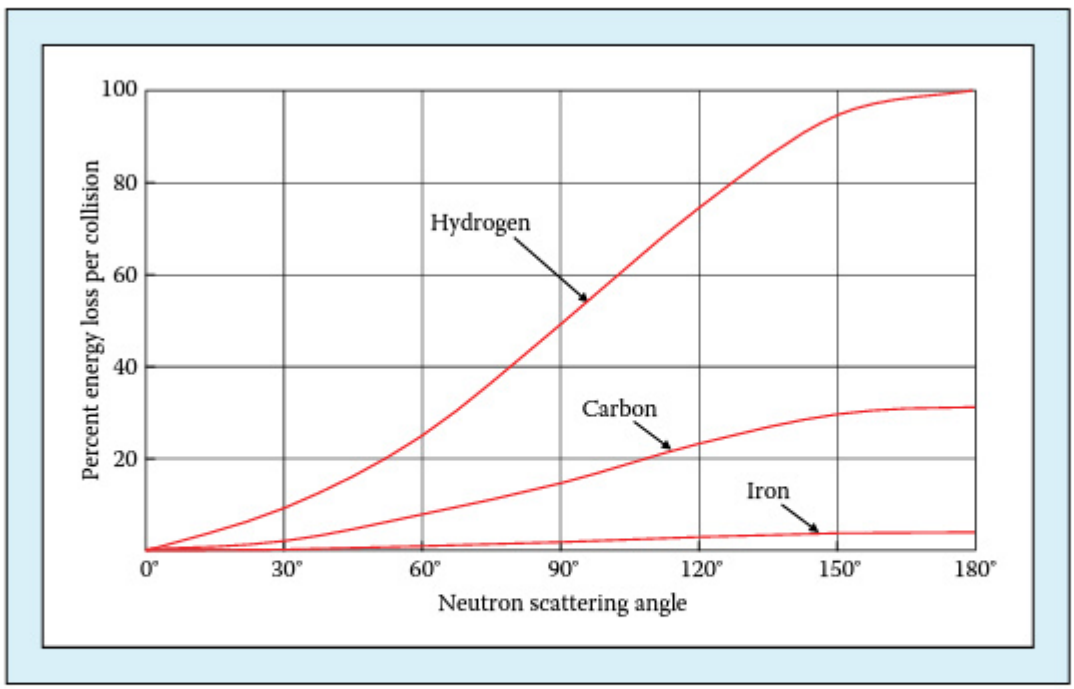

FIGURE 3.13 The percentage energy loss per collision for neutrons scattered off of hydrogen, carbon, and iron atoms for different values of the neutron scattering angle θ.

3.16 Neutron Energy Loss as a Function of Scattering Angle

Now that we have a direct relationship between the scattering angle θ and the neutron energy loss ΔE for an elastic collision, we would like to explore how much energy can be lost when a random combination of direct and indirect collisions occurs. *In a head-on collision, we know that the maximum energy loss in a collision is $\Delta E = E(1-\alpha)$ when $\theta = 180°$, and we know in a glancing collision that $\theta = 0$, so the minimum energy loss in this case is 0* (since we know from Equation 3.67 that E′ = E). So heuristically, we can to a first approximation assume that the *average* energy loss of a neutron under either of these conditions can be found by taking the average of the maximum and minimum energy loss; that is,

$$\Delta E = \frac{E(1-\alpha)}{2} \tag{3.75}$$

which is exactly the average value of the two previous results. Interestingly enough, the same result can be obtained from another approach based on the use of a *scattering kernel*, which is presented in Chapter 22* and in Reference 10. By applying this kernel, it can be shown that *the average cosine of the neutron scattering angle* $\langle\cos\theta\rangle$ is related to the atomic mass A of the atom that scatters the neutron by the following relationship:

The Scattering Angle of a Neutron and the Mass of the Target Nucleus

$$\langle\cos\theta\rangle = \frac{2}{3A} \tag{3.76}$$

Notice that this equation can also be written as $\langle\theta\rangle = \cos^{-1}(2/3A)$, which means that for large values of A, $\langle\cos\theta\rangle \to 0$, and $\langle\theta\rangle = \cos^{-1}(0) \to 90°$. In other words, *Equation 3.76 shows that when a neutron is scattered by a heavy nucleus with a large value of A, the average scattering angle approaches 90°*. This means that the scattering becomes isotropic and that any scattering angle from 0° to 180° is equally probable. On the other hand, if a neutron is scattered off of a hydrogen atom where $\langle\cos\theta\rangle = 2/3$, the average scattering angle becomes

$$\langle\theta\rangle = \cos^{-1}\left(\frac{2}{3}\right) = 48° \tag{3.77}$$

This type of scattering is sometimes referred to as *forward scattering* since the average scattering angle $\langle\theta\rangle$ is always less than 90°.

Example Problem 3.4

A neutron scatters off of a Carbon-12 nucleus, which is frequently used as a moderating material in thermal graphite reactors. If the scattering reaction is an elastic one, what is the average scattering angle of the neutron? What percentage of the initial kinetic energy of the neutron is lost in a single elastic collision of this type?

Solution The average scattering of the neutron is given by $\langle\theta\rangle = \cos^{-1}(2/3A)$. Since A = 12, $\langle q\rangle = \cos^{-1}(2/36) = 86.5°$. According to Equation 3.67, $\alpha' = \{(1+\alpha)/2 + (1-\alpha)/2 \cdot \cos\theta\} = 0.86 + 0.14\cos\theta$. The fractional energy loss is therefore $\Delta E = 0.14(1-\cos\theta) = 0.14(1-\cos\theta) = 0.14 \times (1-0.06) = 0.13 = 13\%$. [Ans.]

3.17 Scattering Angles in the Laboratory and Center of Mass Systems

One of the interesting features of elastic scattering is that the scattering angle in the center of mass (COM) reference frame (where it is normally easier to perform a calculation) is *different* than the scattering angle in the laboratory reference frame (where we generally measure and interpret the results of these experiments). *In fact, even when the scattering process is completely isotropic in the COM reference frame, it is NOT isotropic in the LAB reference frame where we do most of our work. This means that the neutron diffusion coefficient D and the neutron mean free path λ, which we will study extensively in Chapter 11, are NOT the same in each reference frame.*

* See *Nuclear Engineering Fundamentals: A Practical Perspective*, by R.E. Masterson, CRC Press (2017).

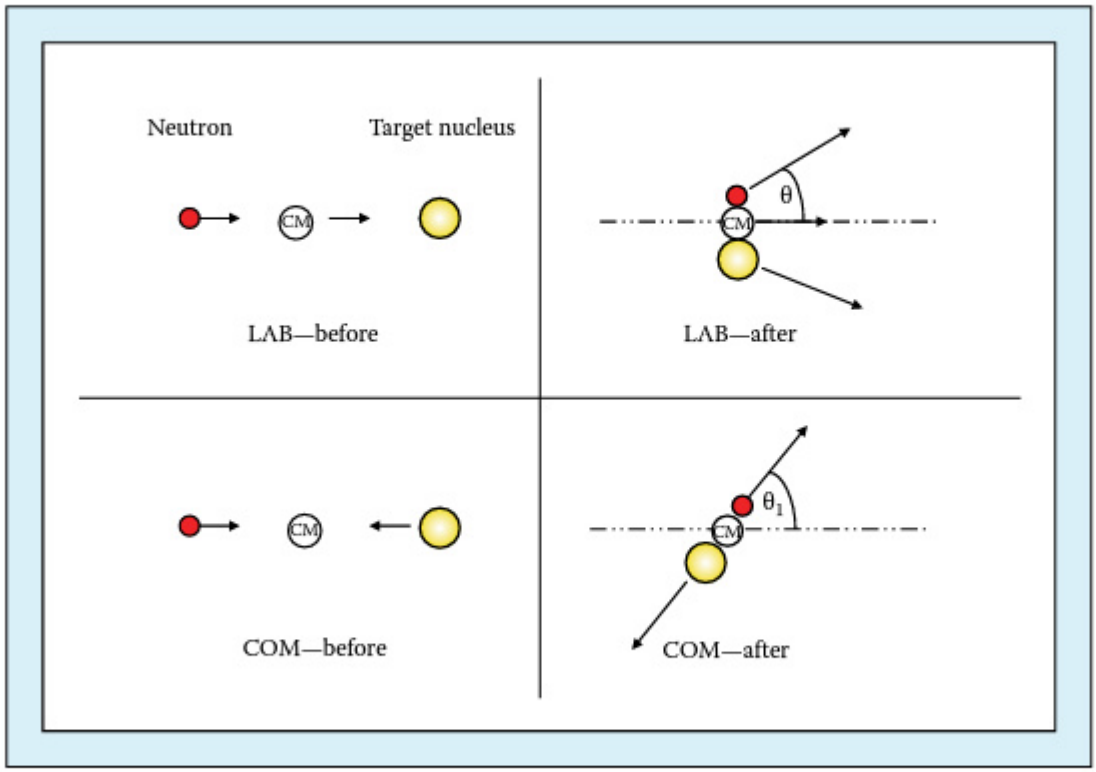

FIGURE 3.14 Comparing a collision in the laboratory and center of mass coordinate systems.

To understand why this occurs, consider the diagram shown in Figure 3.14, which shows a neutron colliding with an atomic nucleus. In the COM reference frame, the COM never moves, and this makes it easier to perform an energy and momentum balance. Because $v_{CM} = 0$, the total momentum P_{CM} in the COM system must be zero as well. If we try to relate the energy in one coordinate system to the energy in the other, we find that

$$E' = \left[\frac{(1+\alpha)}{2} + \cos\theta_1 \cdot \frac{(1-\alpha)}{2}\right]E = \alpha' E \tag{3.78}$$

where

E is the initial neutron energy
E′ is the final neutron energy
θ_1 is the scattering angle in the COM system

Here, again $\alpha' = \{(1+\alpha)/2 + (1-\alpha)/2 \cdot \cos\theta\}$ and $\alpha = [(A-1)/(A+1)]^2$. Now let us consider what Equation 3.78 implies. First, it implies that the energy transfer from the neutron to the nucleus is a function of the scattering angle in the COM system. For example, when $\theta_1 = 0$, the neutron loses no energy and $E' = E$. Moreover, it implies that the maximum energy loss occurs when $\theta_1 = 180°$, in which case $E' = [(1+\alpha)/2 + \cos\theta_1 \cdot (1-\alpha)/2]E = \alpha E$. Hence, the maximum amount of energy loss in an elastic collision with a stationary atomic nucleus is $\Delta E = E' - E = (1-\alpha)E$. This is consistent with the equations we presented earlier.

The second major implication of our analysis is that the energy loss in the COM system depends on only scattering angle and the atomic mass A of the target nucleus and nothing else. As A gets larger, the energy loss per collision gets smaller, and when A is 238 (which it is for a nucleus like Uranium-238), the largest possible energy loss ΔE is 1.7%. Moreover, it is easy to see that when the scattering is completely isotropic in the COM system, the average neutron energy after a single elastic collision is

$$E' = \left[\frac{(1+\alpha)}{2}\right]E \tag{3.79}$$

since $\theta_1 = 90°$ and $\cos 90° = 0$. What is even more interesting is that when we try to calculate the relationship between the probability of a neutron scattering into a differential solid angle $d\theta_1$ and the differential energy loss dE associated with

this scattering angle, we find that *when the scattering process is isotropic in the COM system*, the scattering probability distribution as a function of the initial neutron energy E becomes

Probability of the Neutron Kinetic Energy E Becoming E′

$$P(E \to E')dE' = \frac{1}{((1-\alpha)E)} \cdot dE' \tag{3.80}$$

in the LAB coordinate system. Equation 3.80 is sometimes called the *neutron scattering kernel* for elastic neutron scattering. Finally, the relationship between the scattering angle θ_l in the COM system and the scattering angle θ in the LAB coordinate system is

Relationship between the Neutron Scattering Angles in the LAB and COM Coordinate Systems

$$\cos\theta = \frac{(1 + A\cos\theta_l)}{\sqrt{(A^2 + 2A\cos\theta_l + 1)}} \tag{3.81}$$

Thus, if the elastic scattering process is completely isotropic in the COM system so that $\theta_l = 90°$ and $\cos 90° = 0$, then $\cos\theta = \sqrt{1/(A^2+1)}$, and *the scattering angle θ in the LAB coordinate system is* $\theta = \cos^{-1}\left(\sqrt{1/(A^2+1)}\right)$, *which is NOT isotropic for any finite value of A*.

The Scattering Angle in the LAB Coordinate System When There Is Isotropic Elastic Scattering in the COM System

$$\cos\theta = \frac{1}{\sqrt{(A^2+1)}} \tag{3.82}$$

In particular, *the neutron in the LAB system attempts to forward scatter, and the amount of forward scattering is greater for lighter elements than it is for heavier ones*. For example, if the neutron hits a hydrogen atom with A = 1, then $\theta = \cos^{-1}(1/\sqrt{2}) = 45°$, and if it hits a U-238 nucleus where A = 238, then $\theta \approx \cos^{-1}(1/238) = 89.76°$. Now suppose that we take Equation 3.81 and integrate it over all possible scattering angles between 0° and 180°. When we do so, we find that

$$\langle\cos\theta\rangle = \int_0^{\pi} \frac{(1 + A\cos\theta_l)}{\sqrt{(A^2 + 2A\cos\theta_l + 1)}} d\theta_l = \frac{2}{(3A)} \tag{3.83}$$

or

$$\langle\cos\theta\rangle = \frac{0.67}{A} \tag{3.84}$$

In other words, when the elastic scattering process is completely isotropic in the COM system, the average cosine of the scattering angle in the LAB system is given by Equation 3.84, and moreover, the average scattering angle is always a positive number.

This example shows that there will always be some forward scattering in the laboratory coordinate system (where we live and work every day) and that the amount of forward scattering for neutrons is greater for light elements than it is for heavy ones. We made use of this fact in our companion book* when we attempted to explain the difference between neutron diffusion theory and neutron transport theory. In particular, *forward scattering is one of the justifications for creating the neutron transport cross section*, which we will formally discuss in Chapter 22. The transport cross section is derived using what is known as the *P1 approximation*. The P1 approximation is the basis for many transport theory calculations, and it is also used in the design or radiation shields.*

* See *Nuclear Engineering Fundamentals: A Practical Perspective*, by R.E. Masterson, CRC Press (2017).

Example Problem 3.5

Suppose that a neutron scattering collision is completely isotropic when observed in the COM coordinate system. If a neutron scatters off of a Carbon-12 nucleus in this system, what scattering angle would we observe in the LAB coordinate system if the scattering angle in the COM system is 90°? What would be the average cosine of the scattering angle?

Solution The scattering angles in the COM and the LAB coordinate systems are related by the equation $\cos\theta = (1 + A\cos\theta_1)/\sqrt{\left(A^2 + 2A\cos\theta_1 + 1\right)}$. Since $\theta_1 = 90°$ in the COM system, $\cos\theta = 1/\sqrt{A^2 + 1}$ in the LAB coordinate system. For a Carbon-12 nucleus, the value of A is 12, so $\cos\theta = 1/\sqrt{12^2 + 1} = 0.083$ and $\theta = 85.24°$. The average cosine of the scattering angle will be $\langle\cos\theta\rangle = 0.67/A = 0.0558$. [Ans.]

3.18 A More Detailed Look at the Interaction of Neutrons with Matter

Before moving on to other topics, now let us take a moment to review the types of reactions that can occur in a nuclear power plant. In the core, *there are four fundamental ways that neutrons can "interact" with an atomic nucleus when their wave functions overlap*. These modes of interaction include the following:

1. *Elastic scattering* collisions where the kinetic energy of the colliding particles is always conserved.
2. *Inelastic scattering* collisions where some of the kinetic energy of the colliding particles is transferred to a third particle (such as a photon) or where one of the colliding particles is forced into an energetic state.
3. *Absorption and capture* reactions where the neutron is absorbed by the atomic nucleus. In an absorption reaction, the incoming particle is absorbed and not reemitted. In a capture reaction, the incoming particle is absorbed and then a nuclear photon is emitted.
4. *Nuclear fission* reactions where the neutron is absorbed by the nucleus before it splits apart. This latter reaction is responsible for the thermal energy that a nuclear thermal energy plant produces.

The relative probability of a neutron interacting with a nucleus is a function of the size of the nucleus and the relative velocity difference between the nucleus and the approaching neutron. However, it is possible to model these events using Newtonian mechanics (see Chapter 2) as long as we do not look too closely at the details of the individual reactions. In other words, we can predict how the particles leave the reaction if we look at only the inputs and outputs from a distance.

3.19 Reviewing Elastic Neutron Scattering

In addition to head-on collisions and glancing collisions, collisions can also be classified according to the function they serve. *By far, the most common way for a neutron to interact with an atomic nucleus is to scatter off of it elastically*. This requires the *wave functions* of the nucleus and the neutron to "overlap" quantum mechanically in some way. An example of this process is shown in Figure 3.15. The incoming neutron transfers some of its energy to the nucleus,

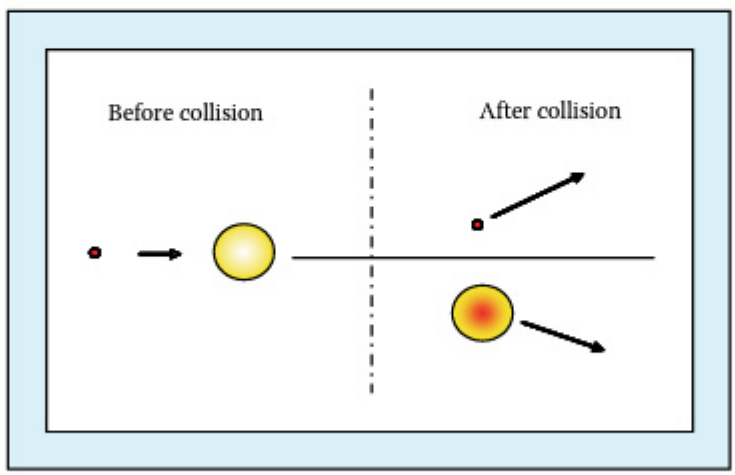

FIGURE 3.15 An example of an elastic scattering event.

and since energy and momentum are conserved, the energy loss of the neutron can be calculated from the following formula (see Section 3.15):

$$\Delta E = E - E' = \left(1 - \alpha'\right)E \tag{3.85}$$

where course $\alpha' = \{(1+\alpha)/2 + (1-\alpha)/2 \cdot \cos\theta_l\}$, $\alpha = (A-1)^2/(A+1)^2$, and A is the mass of the target nucleus in AMU. The larger the scattering angle θ_l, the larger the energy loss becomes. The energy loss is greatest when $\theta_l = 180°$, in which case $\Delta E = (1-\alpha)E$.

3.20 Reviewing Inelastic Neutron Scattering

An inelastic scattering collision is similar to an elastic one, except that the incoming neutron transfers some of its kinetic energy to an intermediate particle that is emitted after the collision. In an inelastic collision, the target nucleus absorbs the neutron and enters into what is called an *excited state*. The resulting kinetic energies of the neutron and the target nucleus will now be somewhat less than the kinetic energy of the incoming neutron alone. The energy difference between the initial and final particles is sometimes called the *excitation energy* of the nucleus. Depending on how the nucleus and the neutron interact, it can be shown that there is a chance that the neutron may be temporarily absorbed by the nucleus before being emitted again. *From a distance, this can give the appearance that the neutron has bounced off of the nucleus, while in fact, it has actually been absorbed by the nucleus and subsequently reemitted. This type of reaction is shown in Figure 3.16 and is called an inelastic scattering reaction*. Electrons and other nuclear particles can also participate in inelastic scattering collisions.

If the target nucleus is stationary or nearly so before the collision, then the neutron must have a kinetic energy *greater* than the excitation energy of the nucleus, or this type of reaction will not occur. *Therefore, this type of inelastic scattering only occurs at energies above 1 MeV, when the incoming neutron has enough kinetic energy to send the nucleus of a heavy element into an excited state. The excited nucleus eventually returns to a stable state by emitting a photon. Heavy elements usually have lower energy thresholds for inelastic scattering reactions than lighter elements do. In general, the probability of a neutron scattering inelastically is smaller than the probability of it scattering elastically*.

The resulting nucleus that is formed in an inelastic scattering reaction is sometimes called a *"compound nucleus."* Essentially the neutron and the target nucleus merge together to form a "compound" structure for a brief period of time (about one millionth of a second). These specific reactions may also cause *"resonances"* or resonance peaks to develop in the absorption and scattering probabilities where the probability of the nucleus absorbing the incoming neutron is higher than it is at others. These resonances appear as sharp peaks in the absorption and scattering probabilities when the reaction probability is plotted as a function of the incoming neutron energy E. We will have more to say about this process in Chapter 4. Hence, although inelastic scattering appears to be superficially as simple as elastic scattering, it is not. In nuclear science and engineering, inelastic neutron scattering is almost always due to compound nucleus formation.

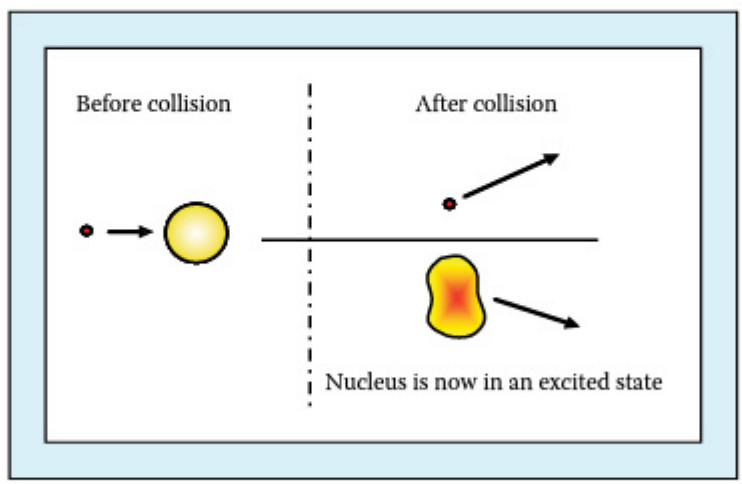

FIGURE 3.16 An inelastic scattering event where the nucleus is left in an excited state.

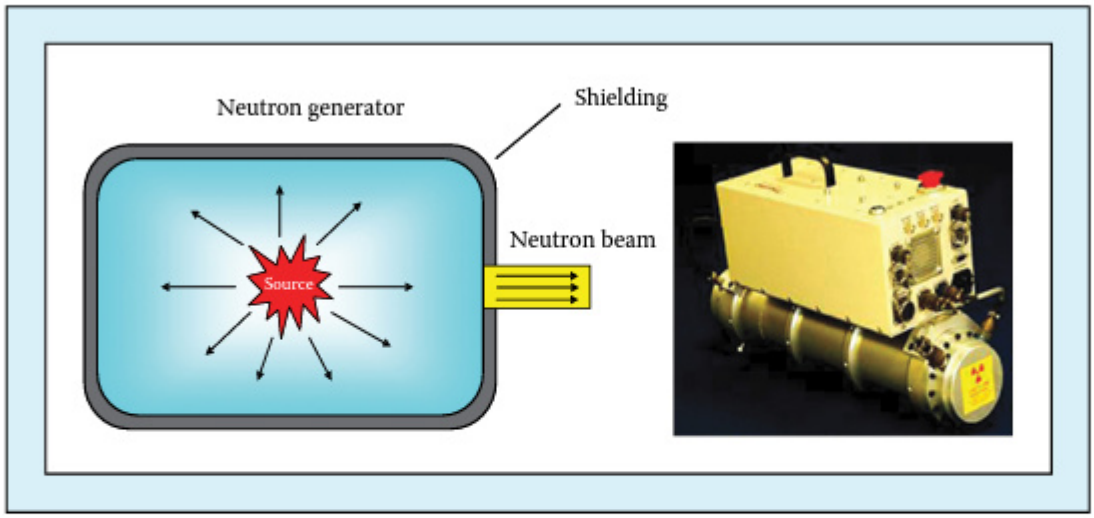

FIGURE 3.17 The Thermo Scientific™ MP 320 neutron generator is a lightweight, portable neutron generator that generates about 100,000,000 neutrons per second. The model shown in the picture weighs 12 kg (or about 25 lb). The beam steering mechanism in these devices is usually just a simple pipe with shielding around it on all sides. (The picture on the right was provided by Thermo Scientific and can be found on Google Images.)

3.21 Neutron Beam Generators

Neutron scattering experiments can be used to understand the atomic structure of many solids and liquids. Neutron scattering experiments are used to determine the exact positions, motions, and magnetic moments of atoms by investigating how neutrons collide with them and then measuring the change in the kinetic energy and the momentum of particles going into and out of the reactions. Experimental data obtained from these scattering experiments can then be used to infer the internal structure of the atom or molecule that is being investigated.

In Chapter 2, we mentioned that *neutrons are subatomic particles that cannot be focused into narrow beams or "steered" using electric and magnetic fields because they do not possess an electric charge*. However, they are produced in nuclear reactors and nuclear accelerators in very large numbers, and they can still be focused to a certain extent by providing a narrow channel or "tube" between the source of the neutrons and the target which is to receive them (see Figure 3.17). If enough shielding is placed around the tube, many of the neutrons hitting the shield will be absorbed or deflected in another direction, and the only neutrons that remain become a narrow beam of unattenuated neutrons. Machines that generate neutron beams are called *neutron beam generators*. A picture of a commercial neutron beam generator is shown in Figure 3.17. Most neutron beam generators are small devices that weigh no more than 100 lb (about 40 kg). When a nuclear reactor is used to generate one of these beams, the neutron beams normally originate from a number of preferred channels or "ports" that emanate from the reactor vessel itself. (The exact configuration of these ports depends on how the reactor is designed.) *Normally, research reactors are designed with these ports, while power reactors are not*.

3.22 Generating Cold Neutron Beams

In some scattering experiments, it is necessary to create a neutron beam that is as *monoenergetic* as possible (e.g., for the purpose of cross-section measurements). In practice, it is not always possible to create a completely monoenergetic neutron beam because not all of the neutrons are emitted with exactly the same energy and some of them tend to scatter from the sides of the tube at least a few times before they hit their intended target. However, it is possible to come reasonably close to a true monoenergetic beam by creating what is known as an *ultracold beam*. The design of a device that produces such a beam is shown in Figure 3.18.

In ultracold beams, neutron energies are forced to converge to kinetic energies close to zero. At these energies, the energy range of the beam narrows, and the only neutrons that remain are essentially those at thermal energies where $E \leq 0.025$ eV. Hence, the average energies converge close to 0, which is why the beam appears to be "cooled." Unfortunately, neutrons in these beams do not move very quickly compared to fast neutrons (about 2000 m/s), and so their penetrating power is rather limited. As mentioned previously, cold neutron beams are used to perform thermal cross-section measurements.

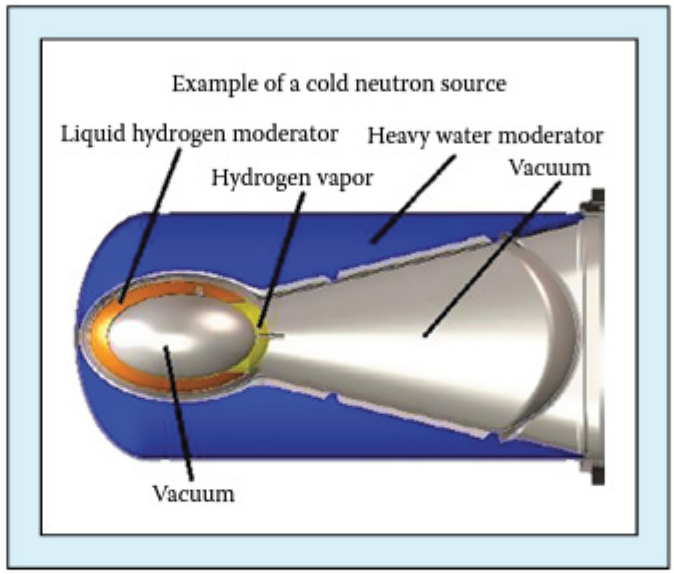

FIGURE 3.18 An example of a cold neutron source that is capable of producing neutrons at about the same temperature as liquid hydrogen.

3.23 Understanding the Difference between Neutron Capture and Neutron Absorption

If a neutron is not scattered when it hits an atomic nucleus, then it will be either captured or absorbed. In this case, the incoming neutron is captured by a target nucleus of mass A, and a new isotope is formed with an atomic mass of A + 1. Thus, $A + n \rightarrow A + 1$.

In reactions of this type, one element is not changed into another element because the number of protons remains the same. *However, the addition of the extra neutron can cause the nucleus to become heavier, and a new isotope is subsequently formed. Sometimes, the absorption of the neutron also forces the new isotope into an excited state. The new isotope then returns to a more stable state by emitting a photon. The neutron is lost in the process and is not reemitted again* (see Figure 3.19).

In principle, there is a subtle difference between what it means to be captured and what it means to be absorbed. Sometimes, a capture reaction is called a "*radiative capture reaction*" because the neutron is first captured by the nucleus, and then some radiation is subsequently emitted in the form of a photon. In a pure absorption reaction, this radiation is not emitted, and the nucleus simply absorbs the neutron before becoming another isotope. Since the nucleus does not split apart, the absorption process is different than the fission process. Hence, the difference between an absorption reaction and a capture reaction can be summarized in the following way:

$$\text{In an absorption reaction}: \quad n + A = (A+1)$$
$$\text{In a capture reaction}: \quad n + A = (A+1) + \text{gamma rays}$$

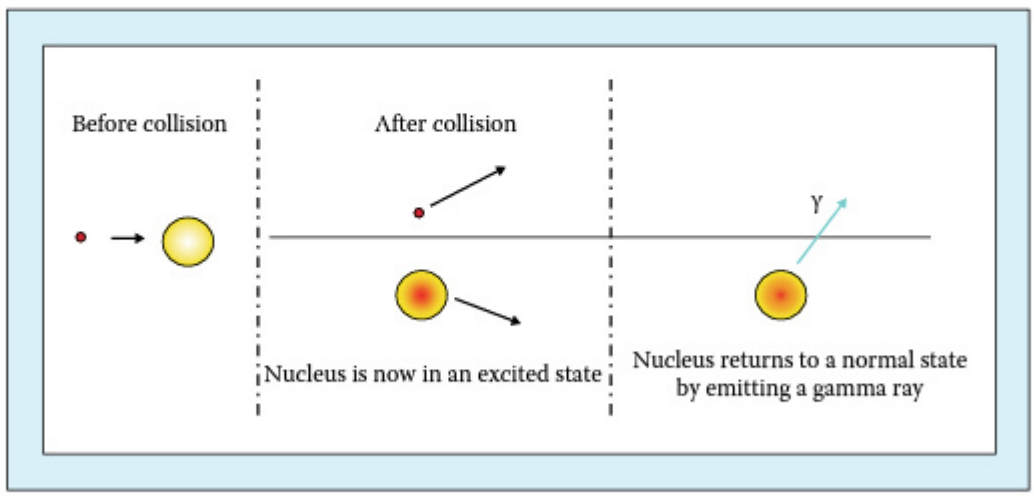

FIGURE 3.19 An example of neutron absorption that leads to radiative capture and γ-ray emission.

A typical photon released from a radiative capture process has a kinetic energy of about 1 MeV. Hence, photons of this type are normally considered to be gamma rays (see Chapter 2). In fuels like U-235 and Pu-239, *radiative capture occurs about 20% of the time a low-energy neutron is absorbed. The rest of the time, the nucleus splits apart according to the fission process that is described in the next section*. The probability of either event occurring also increases as the speed of the incoming neutron is decreased. At "low speeds," corresponding to less than about 10% of the speed of light, the kinetic energy E and the velocity v of the neutron are related by the simple classical equation

$$E = \frac{1}{2} m_o v^2 \tag{3.86}$$

where m_o is the *rest mass* of the neutron. At high speeds that are greater than about 10% of the speed of light, the kinetic energy E and the velocity v of the neutron are related by another equation:

$$E = \frac{1}{2} \frac{m_o v^2}{\sqrt{\left(1 - v^2/c^2\right)}} \tag{3.87}$$

in which the actual mass increases according to the following equation:

$$m(v) = \frac{m_o}{\sqrt{\left(1 - v^2/c^2\right)}} \tag{3.88}$$

As we discovered in Chapter 2, this is a real effect that cannot be ignored when calculating the relationship between v and E when the neutron energies become high.

3.24 Neutrons and Their Role in the Nuclear Fission Process

When an incoming neutron is captured by a Uranium-233, Uranium-235, or Plutonium-239 nucleus, the neutron may cause the nucleus to split apart or "fission" into two smaller parts of approximately the same mass (see Chapter 7). These parts are first *called "fission fragments" and after they acquire some additional orbital electrons, they become known as "fission products."* In addition to these fission products, some additional neutrons, neutrinos, γ-rays, and about 210 MeV of kinetic energy are also released in the process (see Figure 3.20).

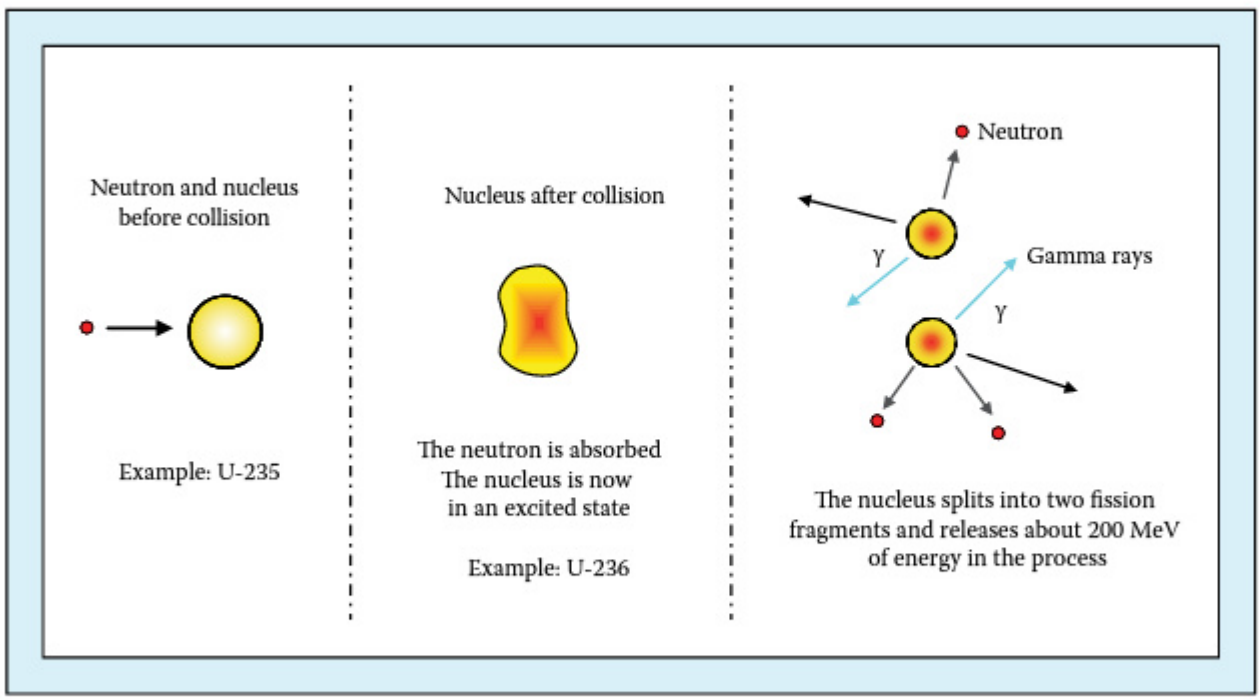
Neutron and nucleus before collision
Example: U-235
Nucleus after collision
The neutron is absorbed
The nucleus is now in an excited state
Example: U-236
Neutron
γ
Gamma rays
γ
The nucleus splits into two fission fragments and releases about 200 MeV of energy in the process

FIGURE 3.20 An example of the process of nuclear fission.

The fission products carry away approximately 170 MeV of the kinetic energy that is produced, but they do not carry away all of it. (The fission product mass distribution is discussed in Chapters 7 and 18.) The fission products leaving the reaction are normally smaller nuclei that have been forced into an excited state by the fission process. They deexcite over time through the subsequent emission of beta rays (energetic electrons), γ-rays, and *"delayed" neutrons*. We will have more to say about the properties of these neutrons in Chapter 7. The energy released from a typical fission process is shown in Table 3.4. Normally, the distribution of this kinetic energy is slightly different for U-233 or Pu-239 than it is for U-235. An additional 20 MeV of kinetic energy is released when the fission products decay. This energy is distributed among delayed neutrons, beta particles, and the delayed γ-rays that accompany the fission product decay process. Most of this energy is released within 100 seconds after the initial fission reaction, but some of it may be released even later.

Figure 3.21 shows the exact timing of the events that occur. *Depending on how it is viewed, the fission process can be considered to consist of between four and six distinct steps*. Some textbooks treat these steps differently than others. When the fission process begins (step 1), a neutron (shown in green) strikes the nucleus of a uranium or plutonium atom (shown in yellow), causing the nucleus to become unstable and deform. If the amount of deformation becomes large enough (late step 2), the nucleus splits into two smaller parts called fission fragments (step 3) and releases between two and three fission neutrons in the process. These neutrons are released so quickly, and they have so much kinetic energy that they are called "prompt" neutrons. About 10^{-12} seconds later, the two fission fragments come to rest by colliding with other atoms in their immediate vicinity and, in doing so, emit a number of energetic photons or γ-rays (which are shown in blue). At this point, the fission fragments become what are known as *fission products*.

TABLE 3.4
Kinetic Energies of Particles in a Typical Fission Reaction

Particles Produced	Particle Kinetic Energies (MeV)	Type of Energy
Fission products (3)	170	Recoverable immediately
Fission product decay	20	Recoverable after 100 seconds
Fission neutrons (2–4)	5	Recoverable immediately
γ-rays	5	Recoverable immediately
Neutrinos	10	Not recoverable

Note: An average nuclear fission produces about 210 MeV of kinetic energy, but only about 200 MeV of this is recoverable. The rest is carried away by strange particles called neutrinos and ends up being distributed somewhere between the stars.

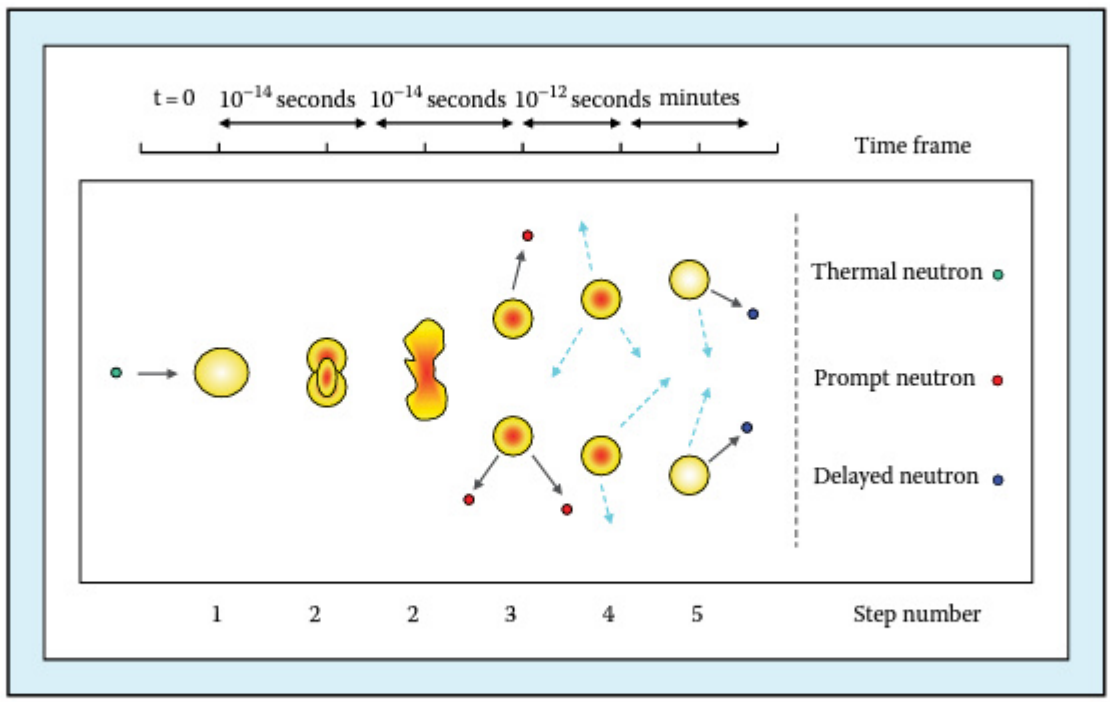

FIGURE 3.21 The five steps of nuclear fission and their respective timescales.

The fission products attract additional electrons to their electron clouds, and in doing so, they sometimes emit additional photons. In step 5, the fission products emit additional neutrons called "delayed" neutrons (which are less energetic than prompt neutrons), more γ-rays, and additional electrons. Each fission product then decays with its own characteristic half-life, and over time, these radioactive fission products become stable. Each fission product has its own unique decay chain, and *there is at least one decay chain for each fission product that is produced.*

3.25 Examining the Nuclear Fission of Uranium-235 in More Detail

There are several things that can happen when a Uranium-235 nucleus absorbs a thermal neutron. Similar processes also occur when a neutron is absorbed by a Uranium-233 or Plutonium-239 nucleus. In this section, we would like to describe two of the more common of them and their relative probabilities of occurrence. When the nucleus first absorbs the neutron, it transforms itself into a U-236 nucleus. The U-236 nucleus starts to shake violently and acts as if it wants to split apart. Within about 10^{-12} seconds, it starts down one of the two primary paths called *reaction channels*. We would now like to discuss what happens after it decides to make this choice.

3.25.1 Outcome 1

About 14% of the time, the U-236 nucleus continues to oscillate until it emits a high-energy photon (or γ-ray). Then, it settles down into a lower energy state and becomes a "stable" U-236 atom. The "half-life" of U-236 is about 24 million years. The γ-ray carries away about 1 MeV of kinetic energy from the excited nucleus. The resulting process is called *radiative capture* because the capture of a neutron causes the nucleus to radiate a γ-ray. In other words, after the nucleus captures the neutron, it does not necessarily mean that the nucleus will split apart or "fission."

3.25.2 Outcome 2

However, about 86% of the time, the U-236 nucleus becomes unstable and splits into a number of smaller and more energetic parts. Each of these parts is called a *fission fragment*. In every reaction, two fission fragments are produced. (However, some additional neutrons or gamma rays may be emitted as well.) This process creates most of the thermal energy that is produced in a reactor core.

Some of the By-Products of the Process of Nuclear Fission

$$^{1}_{0}\mathrm{n} + {}^{235}_{92}\mathrm{U} \rightarrow {}^{236}_{92}\mathrm{U} \rightarrow {}^{140}_{55}\mathrm{Cs} + {}^{93}_{37}\mathrm{Rb} + 3\,{}^{1}_{0}\mathrm{n} + \mathrm{Q}'$$

$$^{1}_{0}\mathrm{n} + {}^{235}_{92}\mathrm{U} \rightarrow {}^{236}_{92}\mathrm{U} \rightarrow {}^{139}_{56}\mathrm{Ba} + {}^{94}_{36}\mathrm{Kr} + 3\,{}^{1}_{0}\mathrm{n} + \mathrm{Q}''$$

$$^{1}_{0}\mathrm{n} + {}^{235}_{92}\mathrm{U} \rightarrow {}^{236}_{92}\mathrm{U} \rightarrow {}^{142}_{54}\mathrm{Xe} + {}^{92}_{38}\mathrm{Sr} + 2\,{}^{1}_{0}\mathrm{n} + \mathrm{Q}'''$$

$$^{1}_{0}\mathrm{n} + {}^{235}_{92}\mathrm{U} \rightarrow {}^{236}_{92}\mathrm{U} \rightarrow {}^{141}_{56}\mathrm{Ba} + {}^{92}_{36}\mathrm{Kr} + 3\,{}^{1}_{0}\mathrm{n} + \mathrm{Q}''''$$

$$^{1}_{0}\mathrm{n} + {}^{235}_{92}\mathrm{U} \rightarrow {}^{236}_{92}\mathrm{U} \rightarrow {}^{142}_{56}\mathrm{Ba} + {}^{92}_{36}\mathrm{Kr} + 2\,{}^{1}_{0}\mathrm{n} + \mathrm{Q}'''''$$

$$^{1}_{0}\mathrm{n} + {}^{235}_{92}\mathrm{U} \rightarrow {}^{236}_{92}\mathrm{U} \rightarrow {}^{144}_{56}\mathrm{Ba} + {}^{90}_{36}\mathrm{Kr} + 2\,{}^{1}_{0}\mathrm{n} + \mathrm{Q}''''''$$

$$^{1}_{0}\mathrm{n} + {}^{235}_{92}\mathrm{U} \rightarrow {}^{236}_{92}\mathrm{U} \rightarrow {}^{134}_{54}\mathrm{Xe} + {}^{100}_{38}\mathrm{Sr} + 2\,{}^{1}_{0}\mathrm{n} + \mathrm{Q}'''''''$$

(Most of these by-products are radioactive)

There are about 20 ways that a U-236 nucleus can split apart in a reactor core. (Figure 3.21 simply depicts one of them.) The most common by-products of this process are Strontium-94 and Xenon-150, with two neutrons, and Barium-141 and Krypton-92, with three neutrons. Frequently, a U-236 nucleus will also split into Barium-137 and Krypton-97. It may also split into Barium-141 and Krypton-92. It can split into Strontium-94 and Xenon-140, and finally, it can split into Cesium-140 and Rubidium-93. The equations governing these reactions are shown in the blue box above. Many other combinations of fission products are also possible.

In these reactions, the symbol Q stands for the quantity of kinetic energy E that is released. Notice that the value of Q depends on the fission products that are released. This energy can be further subdivided into

1. The kinetic energy of the fission fragments
2. The kinetic energy of the fission neutrons
3. The kinetic energy of the γ-rays

Now, let us examine each of these by-products separately.

TABLE 3.5
Time Frames for the Maximum Buildup of Xenon-135 and Samarium-149 in a Thermal Water Reactor after Start-Up and Shutdown

	Times When the Maximum Concentrations of Xenon-135 and Samarium-149 Are Reached	
	Time after Start-Up (Hours)	Time after Shutdown (Hours)
Xenon-135	40	12
Samarium-149	300	300

3.26 Fission Products and Fission Product Poisons

After the fission process is complete, the ejected fission products decay into other fission products, and some of these fission products can absorb almost as many neutrons as the control rods can. Between 50 and 100 different fission products are produced in this process, but only a few of them can affect the way in which a reactor behaves. A fission product that is capable of absorbing large numbers of neutrons is called a *neutron poison*. By far the most important neutron poison is *Xenon-135. It is about 5000 times more likely to absorb a low-energy neutron than a U-235 nucleus is*, and because of this, its buildup must be very carefully monitored and controlled over the lifetime of the core.

Another relatively important fission product that absorbs fewer neutrons is Samarium-149. *Samarium-149 has only about 20% the poisoning effect that Xenon-135 has, but its buildup must also be carefully monitored and controlled. The rate at which these two fission products build up and decay is governed by what is known as a radioactive decay chain.* (These decay chains are discussed in Chapter 6.) Because each fission product is part of a different decay chain that begins with the fission of U-235, the rate of buildup and the rate of burn down are also different for each chain (and for other fission products in different chains).

Normally, Xenon-135 reaches its maximum concentration in a thermal water reactor about 40 hours after the reactor is started up. When the same reactor is shut down, the Xenon-135 concentration will become even higher because there are no fission neutrons left to burn off the excess Xenon-135 that is already in place. However, Samarium-149 is part of a different decay chain, and so its buildup and burn down are completely different (see Chapter 7). Samarium-149 reaches its maximum concentration about 300 hours (about 12 days) after a reactor is started up. After shutdown, the samarium concentration continues to increase until it stabilizes after about 13 days. This is about 25 times longer than it takes xenon to reach its postshutdown peak (300 hours vs. 12 hours). Like xenon, the final concentration of samarium also depends on the reactor power level prior to shutdown. If the power level is higher, then more xenon and samarium will be produced. The time frames associated with the maximum buildup of Xenon-135 and Samarium-149 are shown in Table 3.5. These neutron poisons are very important in thermal water reactors (such as PWRs and BWRs) but not in fast reactors such as LMFBRs. In fast reactors, the neutron energies are too high for xenon and samarium to be effective neutron poisons.

3.27 The Energetics of Nuclear Fission

The ability of an atomic nucleus to participate in a fission reaction is determined by a parameter called the *average binding energy per nucleon* (see Chapter 7). Atoms like iron and nickel have a high binding energy per nucleon, while nuclear fuels like uranium and plutonium have a low binding energy per nucleon. When atoms have a low binding energy per nucleon, they can split apart without adding any additional energy to their nuclei under certain conditions. The kinetic energy that must be added to a nucleus to cause it to split apart is called the *critical energy of fission*. The critical energy of fission is given the symbol E_{CRIT}, and it is shown for several heavy elements in Table 3.6.

The critical energy of fission is determined by the internal structure of the nucleus. It is also determined by the orbital configurations the protons and neutrons tend to assume. If a uranium or plutonium atom absorbs a passing neutron, a compound nucleus will be formed with a total energy equal to its initial energy plus the kinetic energy of the neutron. *If the kinetic energy of the neutron is greater than the critical energy of fission, then the compound nucleus will split apart even if it happens to absorb a neutron with essentially no additional energy.* For example, if a U-235 nucleus absorbs a thermal neutron with a kinetic energy around 0.025 eV, it will immediately transform itself into a U-236 nucleus, which is one of the compound nuclei listed in Table 3.4. The U-236 nucleus has 1.1 MeV more energy than it needs—even if the neutron it absorbs has almost no kinetic energy at all. Hence, the U-236 nucleus immediately splits apart and releases

TABLE 3.6
Critical Energies Required for the Nucleus of a Heavy Atom to Deform Enough to Split Apart

Fissioning Nucleus	Compound Nucleus	Critical Energy, E_{CRIT} (in MeV)	Binding Energy of the Least Tightly Bound Neutron**
Th-232	No	5.9	**
Th-233	Yes	6.5	5.1
U-233	No	5.5	**
U-234	Yes	4.6	6.6
U-235	No	5.75	**
U-236	Yes	5.3	6.4
U-238	No	5.85	**
U-239	Yes	5.5	4.9
Pu-239	No	5.5	**
Pu-240	Yes	4.0	6.4

Source: Lamarsh, J.R. *Introduction to Nuclear Reactor Theory*, second printing, Addison-Wesley Publishing Company, Inc., Reading, MA, 1972.
Note: The critical energies of fission and the binding energies are given in MeV.

two fission products in the process. The propensity of a nuclear fuel to undergo fast or thermal fission is determined by the critical binding energies in Table 3.4. *The formation of a compound nucleus is generally a prerequisite for the fission process to occur*. For example, heavy elements such as plutonium and uranium have an average binding energy of about 7.6 MeV per nucleon, while lighter elements like barium and krypton (which are also common fission products) have an average binding energy of about 8.5 MeV per nucleon. So, if a U-235 nucleus were to fission into a Barium-141 atom and a Krypton-92 atom, it would release about $235 \times (8.5 - 7.6\ \text{MeV}) \cong 210$ MeV of kinetic energy in the process. However, only 200 MeV of this energy is recoverable because the neutrinos carry the rest of it away (about 10 MeV per fission). (Neutrinos were introduced to the reader in Chapter 2.)

3.28 Standard Notation Used to Describe Different Nuclear Reactions

Depending on the type of reactions that occur, neutrons can interact with nuclear fuel rods in about a dozen different ways. To describe these reactions, a *standard naming convention* is sometimes used. Figure 3.22 shows the most common naming conventions that are applied to reactions involving neutrons. To illustrate the use of this nomenclature, suppose that neutron n impinges on a target nucleus T and forms a resultant nucleus R, which leads to the release of an outgoing particle of type o. This interaction is represented by the symbol T (n,o), R, where R is the new nucleus. The letters separated by the commas in the parentheses represent the incoming and outgoing particles.

To describe a reaction without regard to a specific set of particles, only the terms between the parentheses are normally used. Hence, the references to T and R are sometimes deleted when referring to reactions of this type. If a nucleus absorbs a neutron and emits a proton, this reaction is represented by (n, p), and if a nucleus absorbs a neutron and emits a γ-ray, then this reaction is represented by (n, γ). Similarly, if a nucleus absorbs a neutron and emits two neutrons with different energies, this reaction is represented by the symbol (n, 2n). Many other types of reactions can also be represented in this way. Normally, nuclear reaction probabilities are tabulated in what is known as a *cross-section library*. (Chapter 5 describes how these cross-section libraries are built.)

Example Problem 3.6

Assume that a Uranium-239 nucleus absorbs a passing low-speed neutron. How much kinetic energy must the incoming neutron have to cause the nucleus to split apart? Approximately how fast must the neutron be traveling?

Solution According to Table 3.6, the neutron must have a kinetic energy of $5.5 - 4.9 = 0.6$ MeV. In a reactor, the velocity v of a neutron (in meters per second) is related to its kinetic energy E (in MeV) by the equation $v = 1.383 \times 10^7\ E^{1/2}$, which was first introduced to the reader in Chapter 2. Hence, if the neutron has a kinetic energy of 0.6 MeV, it must have a velocity greater than 1.07×10^7 m/s to cause a Uranium-239 nucleus to split apart. Another nucleus, such as the Uranium-234 nucleus, will have an entirely different set of properties than the Uranium-239 nucleus does. [Ans].

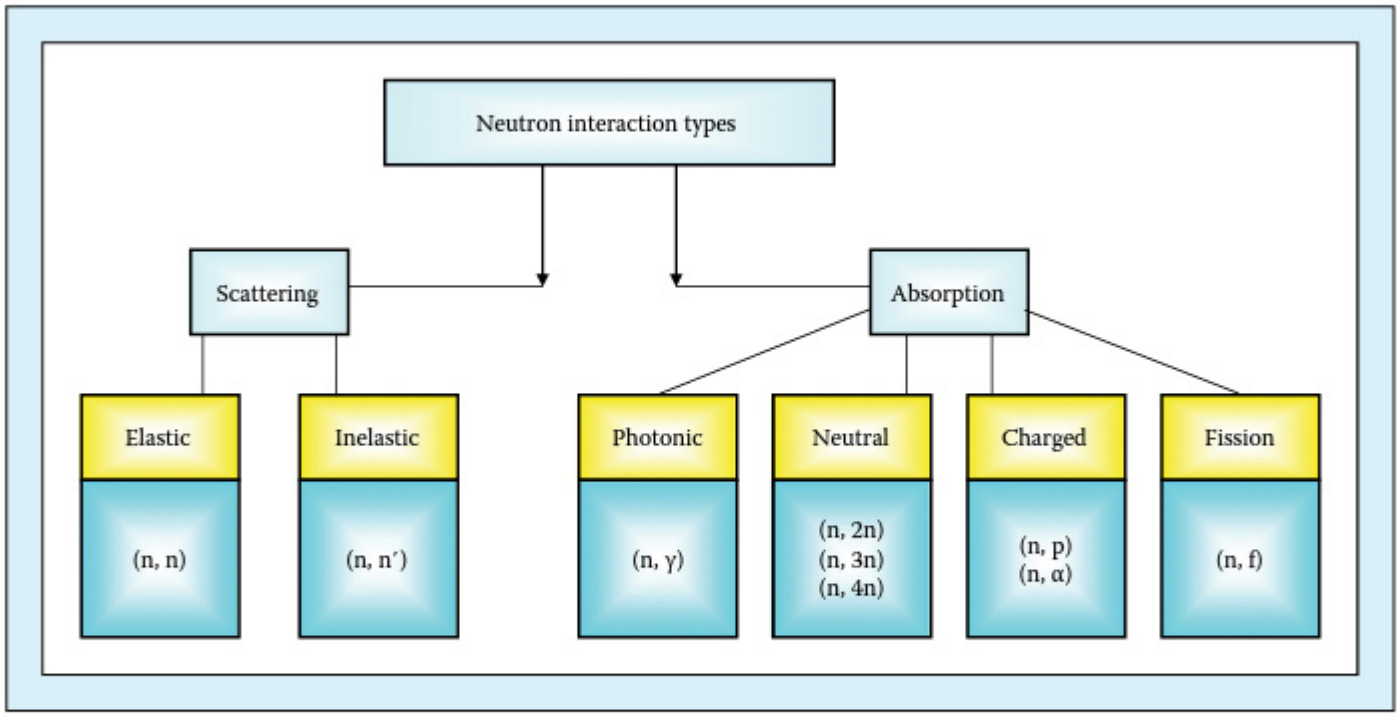

FIGURE 3.22 A summary of common neutron reactions that can occur in a nuclear reactor. The letters separated by the commas indicate the incoming and outgoing particles.

3.29 Some Final Observations regarding Elastic Scattering Reactions

As we mentioned earlier, scattering reactions can be subdivided into two basic categories called elastic scattering reactions and inelastic scattering reactions. In elastic scattering reactions, the total kinetic energy of the neutron and the target nucleus are conserved. Hence, the total kinetic energy of the particles going into the reaction is equal to the total kinetic energy of the particles coming out of the reaction. This allows us to write

A Requirement for Elastic Scattering

$$E_{OUT} = E_{IN}\left(\text{Nucleus and neutron}\right) \tag{3.89}$$

However, the kinetic energy between the two particles can be distributed in many different ways, and the final energies are therefore a function of the neutron scattering angles θ. The greater the scattering angle, the more energy the neutron loses and the more energy the target nucleus gains. In elastic scattering reactions, no additional nuclear particles (such as photons) are produced. Thus, a second requirement for an elastic scattering reaction to occur is

An Additional Requirement for Elastic Scattering

$$\text{PARTICLES}_{OUT} = \text{PARTICLES}_{IN} \tag{3.90}$$

The momentum of the incoming and outgoing particles is also conserved in these reactions. When a neutron collides with a stationary nucleus, the kinetic energy transferred to the target nucleus is also a function of the target nucleus's weight. If the neutron has an initial energy E and encounters an atomic nucleus with an atomic weight of A, then the average kinetic energy E′ of the neutron after the collision will be $(1 - \alpha)E/2$, where $\alpha = (A - 1)^2/(A + 1)^2$ for a head-on collision. After some additional manipulation, it can be shown that the preceding expression relating the initial and final neutron energies can also be written as

The Equation for Average Energy of a Neutron after an Elastic Collision

$$E' = \frac{2AE}{(A+1)^2} \tag{3.91}$$

TABLE 3.7
Average Number of Collisions Required to Convert a Fission Neutron to a Thermal Neutron in an Elastic Scattering Reaction

Element	Atomic Weight A	Number of Collisions
Hydrogen	1	27
Deuterium	2	31
Helium	4	48
Beryllium	9	92
Carbon	12	119
Uranium	238	2175

Source: Los Alamos report by P. Rinard.

where E is again the neutron's initial kinetic energy. Hence the easiest way to reduce the kinetic energy of a high-speed neutron is to use a target nucleus with a very small value of A. In fact, the most efficient way to reduce its speed (i.e., to *moderate* it) is to have it collide with a hydrogen nucleus, in which case A = 1. Then the final energy E′ will have a value of E/2, and so the *average* energy loss in an elastic collision will be exactly 50%. Equation 3.91 also implies that a fission neutron that is born with a kinetic energy of 2 MeV can have its kinetic energy reduced to 1 MeV in a single elastic collision with a hydrogen nucleus, and after two elastic collisions, its average kinetic energy will fall to 0.5 MeV. *Thus, the energy loss falls off as approximately*

$$E'_n = \left(\frac{1}{2}\right)^n E_o \tag{3.92}$$

where
n is the number of elastic collisions
E_o is the initial neutron energy

In Chapter 8, we will discover that the kinetic energy of the fission neutrons will eventually be reduced to the point that it cannot fall any further. In this case, the fission neutrons are said to be in thermal equilibrium with their environment, and both their average and most probable kinetic energies obey what is known *as a Maxwell–Boltzmann probability distribution*. In this state, their most probable kinetic energy will be only 0.025 eV, which is about *80 million times less* than the kinetic energy with which they were initially born. It is relatively easy to show that this energy is reached after about 27 elastic collisions with a hydrogen atom.

If another moderator is used instead and the target nucleus is different, then the average number of elastic collisions required to thermalize a fission neutron depends on the atomic weight of the nucleus (i.e., the value of A). Table 3.7 shows the average number of elastic collisions required to "thermalize" a fission neutron in this case. By inspecting this table, one can see that the number of elastic collisions required to thermalize a fission neutron increases as the atomic weight of the target nucleus is increased. For example, for a Carbon-12 atom, 119 collisions would be required for the neutron to reach thermal energies, and in the case of Uranium-238, the number of collisions would be about 2175. For this reason, hydrogen is a very popular material when it comes to slowing down neutrons, and the most common reactor coolant is light water (or H_2O), which has two hydrogen atoms attached to each oxygen atom (see Chapter 8). *Water is also a very effective reactor coolant because it is able to remove larger amounts of heat from the core than other materials can*. Normally, not all of the collisions that occur in a reactor are elastic ones, and if a neutron happens to collide with a heavier nucleus (such as the nucleus of a uranium or plutonium atom), an inelastic collision can also occur. The process of inelastic scattering is discussed again in Section 3.33.

Example Problem 3.7

Show that equation $E' = 1/2(1 - \alpha)E$, which frequently arises in the study of elastic collisions, is equivalent to the equation $E' = 2AE/(A + 1)^2$, which we presented earlier in this section.

Solution In the equation $E' = 1/2(1 - \alpha)E$, the value of α is given by $\alpha = (A - 1)^2/(A + 1)^2$. The value of $(1 - \alpha)$ is therefore $[(A + 1)^2 - (A - 1)^2/(A + 1)^2 = [A^2 + 2A + 1 - A^2 + 2A - 1]/(A + 1)^2 = 4A/(A + 1)^2$. The value of E′ is therefore $E' = 2AE/(A + 1)^2$, which is equivalent to Equation 3.91. [Ans.]

3.30 Neutron Moderators and Neutron Kinetic Energy Loss

Most reactors (with the exception of fast reactors) require a material called a *neutron moderator* to slow down the fission neutrons. At lower energies, these neutrons can be absorbed more easily by the uranium and plutonium atoms, and this allows additional fission neutrons to be produced to sustain the chain reaction. However, neutron moderators can also absorb some of the incoming neutrons that are scattering off of them, and when neutron moderation becomes necessary, the material selected for the moderator should have a low absorption rate as well as a high scattering one. Hence, elemental hydrogen (which is found in the cooling water used in thermal water reactors) is an attractive moderating material because it requires fewer collisions than other materials to achieve a specific neutron energy loss (see Table 3.7). However, it also has a larger absorption cross section than another popular moderator (deuterium or heavy hydrogen) for thermal neutrons. Because of this, deuterium absorbs fewer neutrons than ordinary hydrogen does, and this is one of the reasons why heavy water or D_2O (which reactors such as the Canadian CANDU reactor use) is sometimes preferred to light water or H_2O when the enrichment of the nuclear fuel is low. Hence the ability of a material to scatter neutrons elastically must be compared to the ability of the same material to absorb these neutrons when selecting the optimum moderator for a specific fuel.* The physics of neutron moderation is discussed in Chapter 8 where the nuances of *neutron slowing down theory* are also discussed.

3.31 Using a Neutron Balance Equation to Model the Behavior of Large Numbers of Neutrons

Earlier in the chapter, we showed that elastic neutron scattering could be described with the laws of classical mechanics, which were invented by Isaac Newton long before the first nuclear reactors were built. When neutron velocities are greater than about 10% of the speed of light, we can apply a relativistic correction factor

The Relativistic Correction Factor for the Rest Mass

$$m(v) = \frac{m_o}{\sqrt{\left(1 - v^2/c^2\right)}} \tag{3.93}$$

to the neutron rest mass m_o, which appears in Newton's energy and momentum equations. The final energies and velocities of the scattered neutrons can then be determined in this way.

However, when this process must be repeated over millions or even billions of individual collisions, the details of an individual collision become less important, and the behavior of the neutron population (while it can still be described by the laws of classical mechanics) can be modeled more conveniently by using what is known as a *neutron diffusion equation*. The neutron diffusion equation is introduced to the reader in Chapter 11, and some of its solutions are presented in Chapters 12 and 13. Hence large neutron populations are rarely modeled by following the motions of individual neutrons, except when performing simulations of particle populations using what is known as a *Monte Carlo method* (which is also discussed in Chapter 23). Once the neutron population becomes so large that it becomes impractical to follow the path of each neutron, then a "neutron balance equation" must be constructed to describe the aggregate behavior of the neutron population. (In reactor physics, this neutron balance equation then becomes the time-dependent neutron diffusion equation or the time-dependent neutron transport equation.) Constructing this equation requires us to define additional parameters such as the neutron flux Φ and the neutron diffusion coefficient D. Finally, it requires us to define what are called neutron cross sections for scattering, fission, and absorption. These cross sections will be presented to the reader in Chapters 4 and 5. Hence a cross section can be thought of as a convenient way to model the collective behavior of large numbers of neutrons when it becomes impractical to model the behavior of each of them individually. The neutron diffusion equation is then used to describe the behavior of these neutrons in an *Eulerian reference frame*. Almost all nuclear science and engineering is performed in this reference frame. Now let us make some final observations about neutron scattering angles and neutron scattering probabilities.

3.32 Scattering Angles and Scattering Probabilities

In practice, not all neutrons scatter off an atomic nucleus in exactly the same way. Free neutrons and other nuclear particles follow *scattering probability distributions* when interacting with a nucleus on a nuclear scale. Over large numbers of these collisions, the angular distribution of the scattered neutrons $P(\theta)$ can be plotted as a function of the kinetic energy

* The thermal absorption cross section of light water is about 0.644 barns, and the thermal absorption cross section of heavy water is about 0.00133 barns (see Appendix C). Hence, light water is approximately 0.644/0.00133 = 485 times more likely than heavy water to absorb a thermal neutron.

E of the incoming neutron and the atomic mass A of the target nucleus. In this section, we would like to briefly discuss how these *scattering probability distribution functions* can be defined. We would then like to demonstrate how they can be used to define another important variable, which is called the neutron *scattering cross section*. The neutron scattering cross section can then be used to define the diffusion coefficient in the neutron diffusion equation, which was discussed in Section 3.31. Neutron scattering cross sections are among the most important variables in all of nuclear science and engineering, and so we would like to take some time to describe how they can be deduced from the outcome of a neutron scattering experiment. We would then like to extend this experiment to include the scattering of alpha particles as well.

To begin our discussion, consider an elastic scattering reaction, whose probability of occurrence is represented by the microscopic scattering cross section σ_s. This scattering cross section consists of both an elastic part and an inelastic part, which we will call σ_{el} and σ_{in}. The angular probability distribution of the scattered neutrons P (θ) has an energy dependence, which is determined by the structure of the target nucleus, and the average scattering angle <θ> can be deduced from a simple energy and momentum balance. The neutron simply scatters off of the atomic nucleus in a direct (i.e., head-on) or indirect (i.e., glancing) scattering reaction, and the energy loss per collision ΔE is proportional to the scattering angle θ. The angular distribution of the scattered neutrons obeys a statistical probability distribution function similar to the one shown in Figure 3.23. The average scattering angle of an individual neutron <θ> is then given by the average of all the individual scattering angles $\theta_1, \theta_2, \theta_3, \ldots, \theta_N$ defined by the angular probability distribution P(θ):

$$\langle\theta\rangle = \frac{\int_0^{2\pi} P(\theta)\,d\theta}{\int_0^{2\pi} d\theta} = \left(\frac{1}{2\pi}\right)\int_0^{2\pi} P(\theta)\,d\theta \tag{3.94}$$

Normally, the shape of P(θ) is determined by performing an experiment. However, it can also be derived from first principles if we are willing to make some simplifying assumptions. For elastic scattering, the average cosine of the scattering angle u = cos <θ> is related to the atomic weight A of the target nucleus by the following equation:

$$u = \frac{2}{3A} \tag{3.95}$$

which implies that <θ> = cosine^{-1} (2/3A) = arc cosine (2/3A).

In other words, when an incoming neutron elastically scatters off of a heavy nucleus (where the value of A is large), the average scattering angle approaches 90°, and when an incoming neutron scatters off of a very light nucleus such as hydrogen (where A is 1), the average scattering angle is <θ> ≈ cosine^{-1} (.667) ≈ 48° (see Figure 3.24). When the same

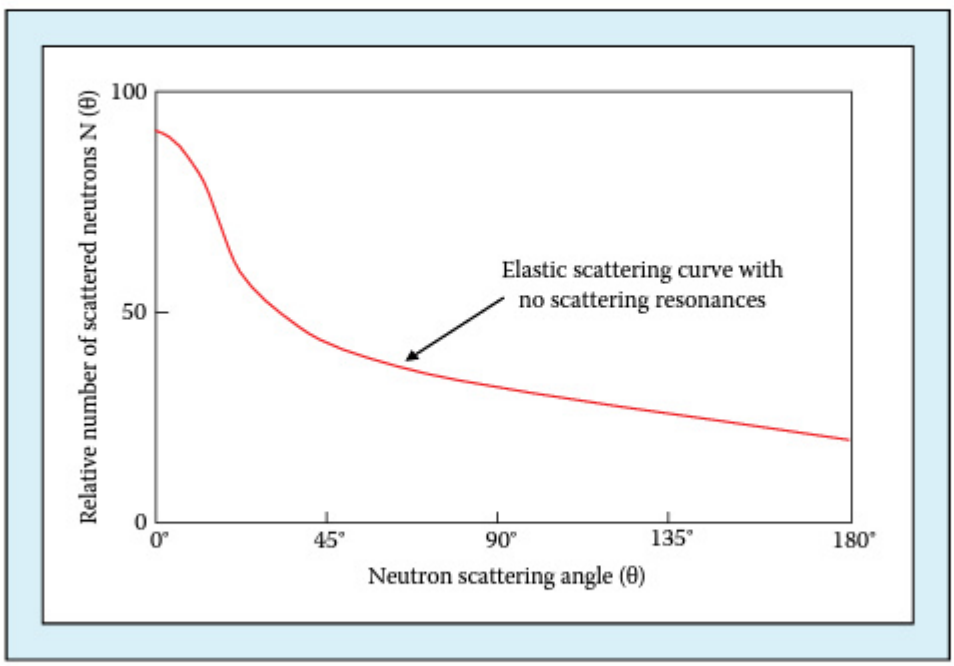

FIGURE 3.23 The angular distribution of the scattered neutrons as a function of the neutron scattering angle.

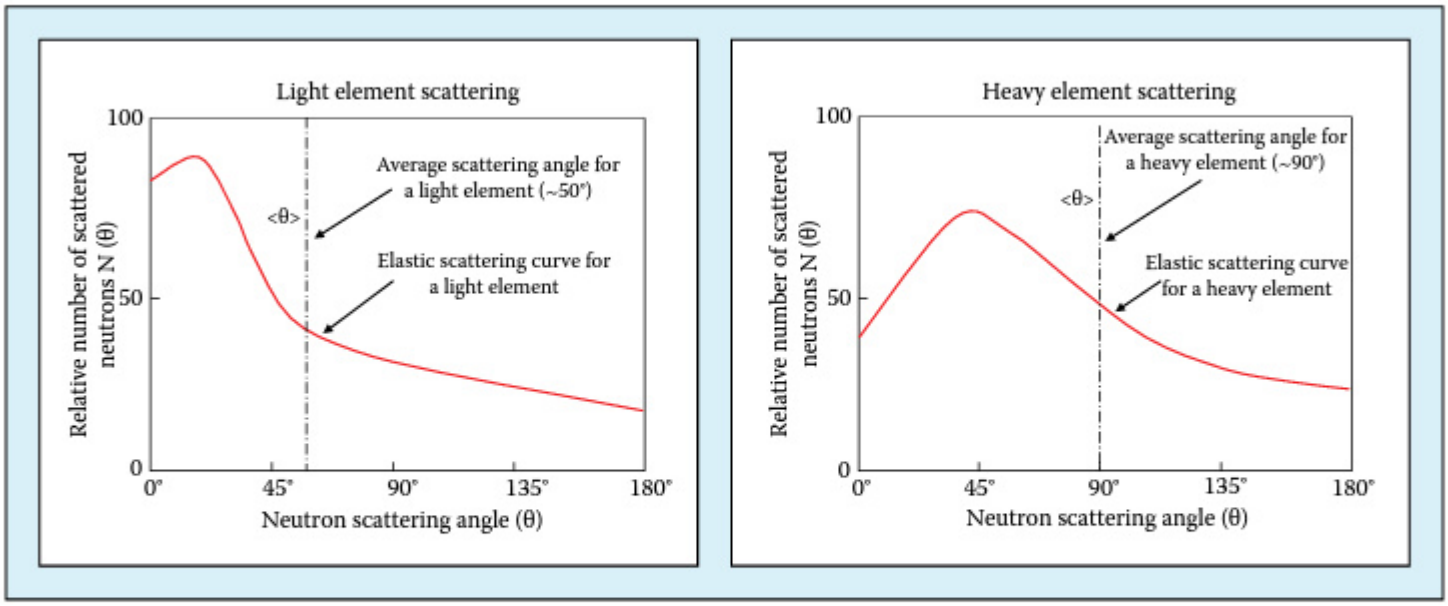

FIGURE 3.24 A comparison of the neutron scattering angles for light and heavy elements.

process is applied to 3D problems, a beam of incoming neutrons can scatter off of an atomic nucleus of mass A in many different angular directions, but an "average" neutron will be scattered into the *differential solid angle dΩ* defined by the value of θ and another angular variable ϕ that is used to represent the azimuthal direction. Exactly where the neutron is scattered azimuthally into the cone bounded by this solid angle cannot be determined in advance as long as the target nucleus is assumed to be spherical in shape. *All that can be said is that it will be scattered somewhere into the cone whose average scattering angle is defined by* <θ> (see Figure 3.25).

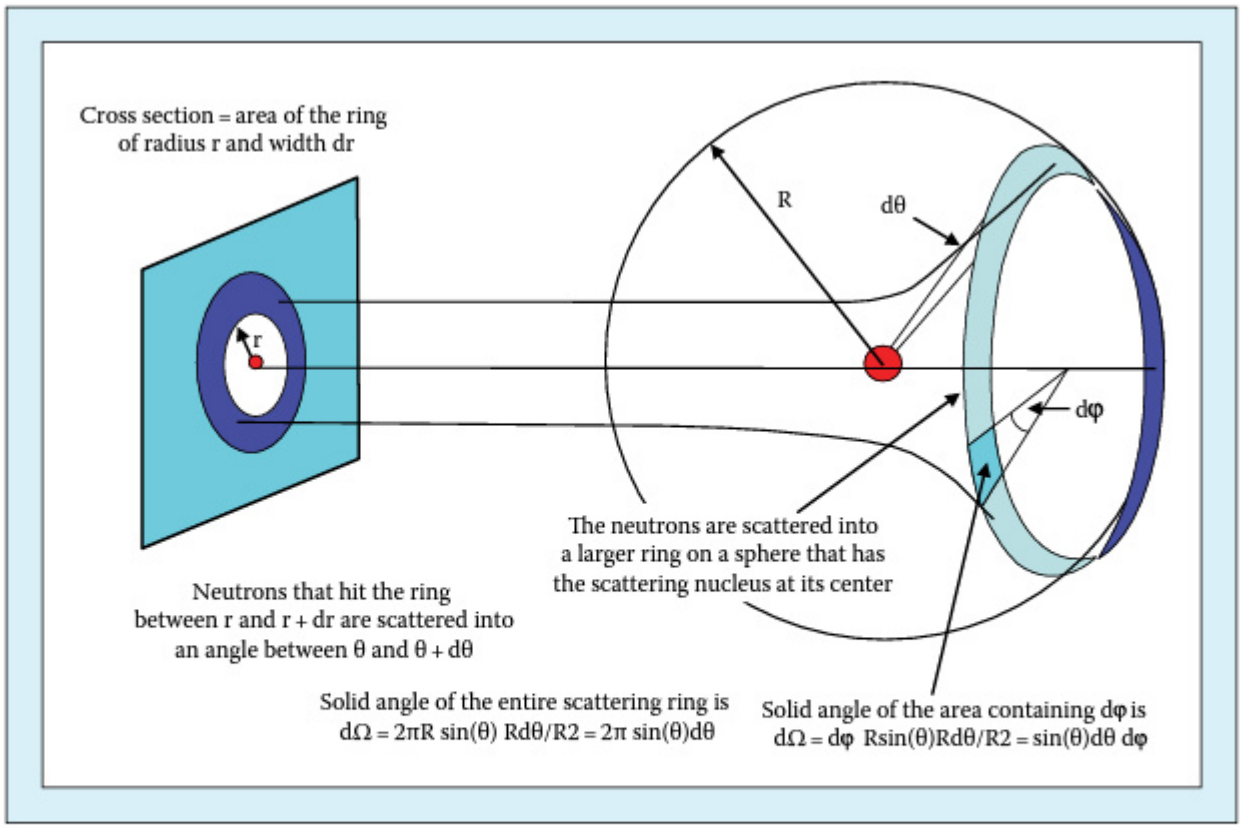
Cross section = area of the ring of radius r and width dr
r
R
dθ
dφ
The neutrons are scattered into a larger ring on a sphere that has the scattering nucleus at its center
Neutrons that hit the ring between r and r + dr are scattered into an angle between θ and θ + dθ
Solid angle of the entire scattering ring is dΩ = 2πR sin(θ) Rdθ/R2 = 2π sin(θ)dθ
Solid angle of the area containing dφ is dΩ = dφ Rsin(θ)Rdθ/R2 = sin(θ)dθ dφ

FIGURE 3.25 The scattering cone of some neutrons in a neutron scattering experiment. (Adapted from a picture published at HyperPhysics.com.)

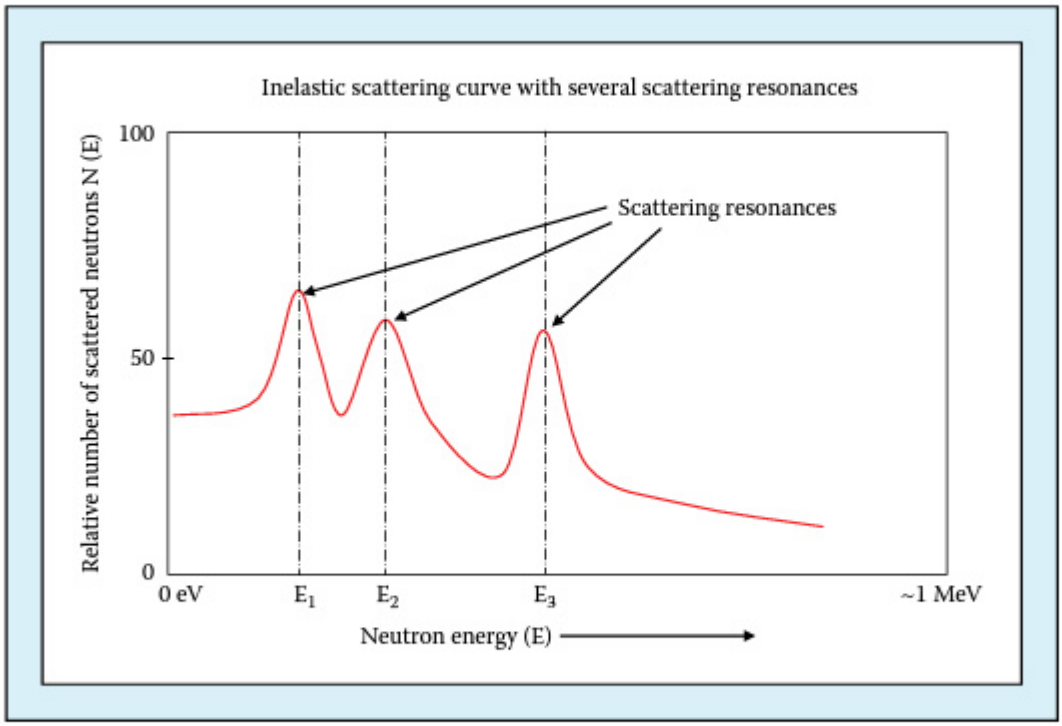

FIGURE 3.26 The energy-dependent scattering of a neutron beam due to scattering resonances at E_1, E_2, and E_3. (The scattering angle near each scattering resonance is completely isotropic.)

3.33 Scattering Angles in Inelastic Collisions

In inelastic collisions, the target nucleus absorbs a neutron and subsequently reemits it in a random direction that has nothing to do with the original direction from which it came. From a distance, this gives the impression that the neutron has scattered off of the target nucleus, when in fact it has been absorbed and reemitted again. However, the probability of the nucleus absorbing the neutron and subsequently reemitting it is energy dependent. In fact, it is much more likely to occur at certain energies called *resonance energies* than it is at others (Figure 3.26).

This means that the angular distribution of the emitted neutrons P(θ, E) changes as the kinetic energy of the incoming neutron is changed. In particular, very large and heavy nuclei exhibit specific energies called *resonance energies* where these *scattering resonances* or enhanced reaction probabilities occur. Physically, each of these scattering resonances corresponds to an excited state in which a compound nucleus is produced for a short period of time. Thus, when a neutron inelastically scatters off of a heavy nucleus at one of these energies, the angular distribution of the scattered neutrons will exhibit additional peaks at the energies where these scattering resonances occur (see Figure 3.26).

Then, the angular probability distribution function $P_{in}(\theta, A, E)$ becomes energy dependent, and the percentage of neutrons scattered in a given direction depends on the energy difference E between the target nucleus T and the incoming neutron n. However, these scattering resonances are normally not found in lighter elements because their nuclear structure is simpler and they possess fewer excited states. Finally, it is important to keep in mind that the *neutrons emitted from an inelastic scattering event will be emitted isotropically* (with the same probability in each angular direction), and therefore after the neutron is absorbed, the target nucleus does not remember where the incoming neutron came from. *Thus, the scattering process is isotropic at the energies where these scattering resonances occur*. (See Figure 3.26.) However, it is *NOT* isotropic when the scattering becomes elastic.

3.34 Neutron Scattering in Heavy Materials

In heavy elements such as thorium, uranium, and plutonium, the total scattering probability consists of an inelastic part $P_{in}(A, E)$, which is angularly isotropic, and an elastic part $P_{el}(\theta, E, A)$, which has an angular dependence and an energy dependence. Thus, the total angular distribution P(θ, E, A) of the scattered neutrons is the sum of the elastic part $P_{el}(\theta, E, A)$ and the inelastic part $P_{in}(A, E)$:

$$P_{TOTAL}(\theta, E, A) = P_{ELASTIC}(\theta, E, A) + P_{INELASTIC}(A, E) \tag{3.96}$$

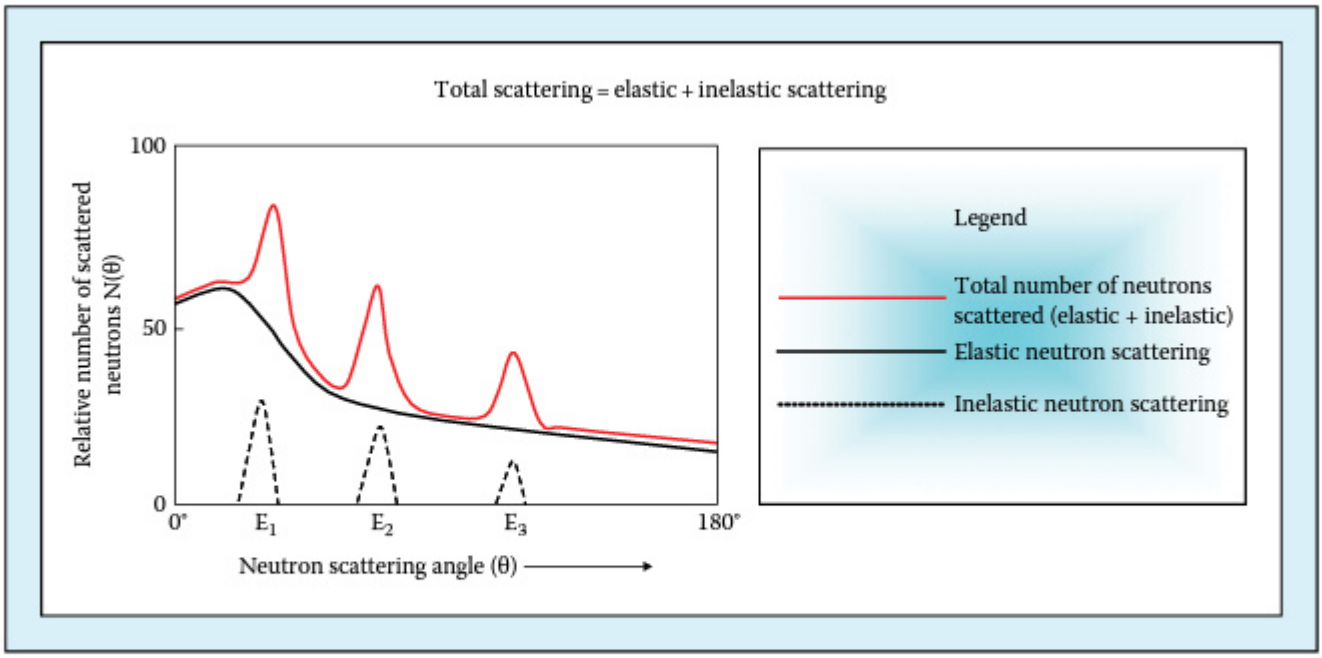

FIGURE 3.27 The total number of neutrons scattered at a particular energy E is the sum of the neutrons scattered both elastically and inelastically.

The scattering probabilities for many heavy elements can be thought of in this way (see Figure 3.27). Normally, the angular dependence is of little practical importance when dealing with the total scattering probability P_{TOTAL}, but when neutron diffusion theory no longer applies, the angular dependence of the scattered neutrons becomes important because it determines the shape of the *angular neutron flux* $\phi(r, \theta, \varphi, E)$ that appears in the neutron transport equation. Again, the neutron transport equation is discussed in Chapter 22.

3.35 Defining the Differential Scattering Probability

The derivative of the angular neutron scattering function $P(\theta)$ is called the *differential scattering probability*, $dP/d\theta$. However, because incoming neutrons can be scattered anywhere into the cone centered about this scattering angle, they can scatter into any *azimuthal scattering angle* φ as well. This means that the value of θ is usually replaced by the value of the *solid angle directional vector* $\Omega = \mathbf{i} \cdot \sin\theta\cos\theta + \mathbf{j} \cdot \sin\theta\sin\theta + \mathbf{k} \cdot \cos\theta$ when the differential scattering probability is found. Thus, the differential scattering probability is written as

$$\text{Differential scattering probability} = \frac{dP}{d\Omega} \tag{3.97}$$

where now $d\Omega$ is understood to be the *differential solid angle* into which the neutrons are scattered. Integrating this normalized differential scattering probability over all of the possible scattering angles from $\theta = 0°–360°$ (or $0–2\pi$) and $\phi = 0–2\pi$ gives

$$P = \int_0^{4\pi} \frac{dP}{d\Omega}\, d\Omega = 1.0 \tag{3.98}$$

which means that the total probability of the neutrons scattering into all solid angles is 1.0 (100%). In two dimensions, this angular integral becomes

$$\int_{\text{All}\Omega} d\Omega = \int_0^{2\pi} d\theta = 2\pi \tag{3.99}$$

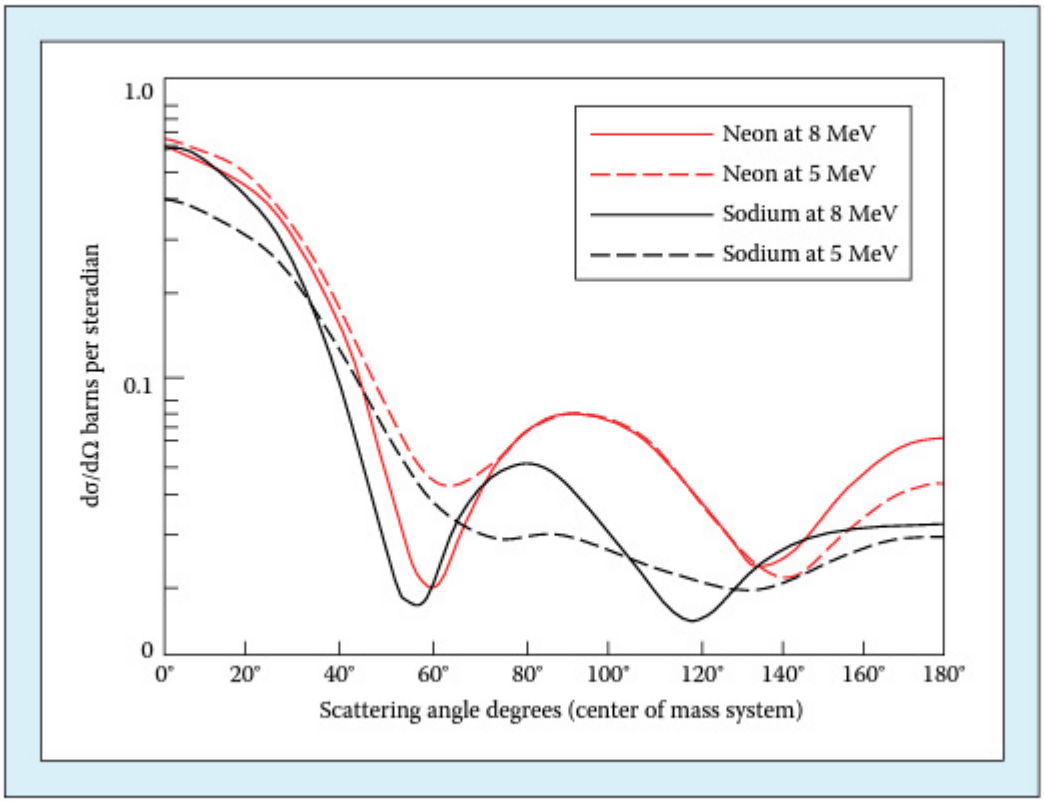

FIGURE 3.28 The neutron scattering probabilities for sodium and neon expressed in terms of their differential scattering cross sections $d\sigma/d\Omega$. Notice that as the neutron energy is increased, more nuclear structure becomes apparent.

which is just the area of a circle ($2\pi r$) with $r = 1$. In our companion book, we will learn that the differential scattering probability can be related to another important variable called the *differential scattering cross section*. In this case, $dP/d\Omega$ is simply rewritten as $d\sigma/d\Omega$, where now σ is the *microscopic scattering cross section* for the material in question. When angular scattering probabilities are expressed in this way, the value of $d\sigma/d\Omega$ is called the *differential scattering cross section*. The total scattering cross section σ_s is then found by integrating the differential scattering cross section over all possible solid angles

$$\sigma_s = \int_0^{2\pi} \frac{d\sigma}{d\Omega} d\Omega \tag{3.100}$$

The value of $d\sigma/d\Omega$ (see Figure 3.28) *is expressed in barns per steradian, and the value of σ_s is expressed in barns*. In the next chapter, we will discover that the *barn* is a unit of nuclear cross-sectional area equal to 1×10^{-24} cm^2 and that there are $4\pi = 12.56$ steradians in all of the solid angles in a complete sphere. Hence, when the elastic and inelastic scattering cross sections are tabulated in nuclear cross-section libraries, their values are integrated over all solid angles, and they are normally quoted in barns alone. In conclusion, *the process of neutron scattering can consist of both elastic and inelastic parts*, and inelastic scattering becomes more prevalent as the mass of the target nucleus is increased. The total probability of a neutron scattering is energy dependent, and both elastic (or potential scattering) and inelastic scattering (which creates a compound nucleus) must be taken into account when attempting to find the total scattering probability.

Example Problem 3.8

In neutron scattering experiments, neutrons can be thought of as hard objects consisting of three quarks that are roughly spherical in shape. Suppose that a high-speed neutron of radius r scatters off of an oxygen nucleus of radius R and that the differential scattering cross section for this reaction is $d\sigma/d\Omega = (r + R)^2/4$. What is the total scattering cross section σ_s for the neutron?

Solution The total scattering cross section σ is simply the differential scattering cross section dσ/dΩ integrated over all solid angles between 0 and 2π, or $\sigma_s = \int_0^{2\pi} d\sigma/d\Omega \; d\Omega$. Performing the required integration yields $\sigma_s = \pi(r + R)^2$. So, in this case, the total cross section is just the area of the circle where the neutron and the oxygen nucleus overlap, and the radius of this circle is $R' = r + R$. [Ans.]

3.36 The Scattering of Alpha Particles

Before proceeding to Chapter 4, we would like to take a moment to discuss the scattering of alpha particles, which are ionized helium atoms with the electrons removed. In 1909, *Hans Geiger* and *Ernest Marsden* (see Chapter 6 of our companion book*) first discovered that alpha particles emitted from certain radioactive materials sometimes "backscattered" from heavy elements at angles greater than 90°, which was physically impossible unless the atomic nucleus was more massive than the alpha particles themselves. In 1913, this led *Ernest Rutherford* (who was later renamed *Lord Rutherford* by the Queen of England) to conclude that the positive charge in an atom is concentrated in a small structure that we call the nucleus today and that the size of the nucleus had to be less than about 10^{-12} cm. Because alpha particles have an electrical charge of +2, they do not scatter in the same way that neutrons do.

Example Problem 3.9

In most atoms, the radius of a neutron is about 10,000 times smaller than the radius of the nucleus. Using this fact and the results presented in the previous problem(s), derive an expression for the total scattering cross section of a neutron elastically scattering off of an atomic nucleus of radius R.

Solution In the previous problem, we learned that the total elastic scattering cross section for the neutron was $\sigma_s = \pi(r + R)^2$. In the case when $r \ll R$, the expression for the scattering cross section reduces to $\sigma_s = \pi R^2$, where R is the radius of the atomic nucleus. This scattering cross section is sometimes called the scattering cross section for *potential scattering*, and it is used extensively in other nuclear engineering textbooks (see, e.g., Reference 8) to calculate the scattering rate. [Ans.]

3.37 The Rutherford Scattering Formula

Rutherford worked out a formula for the scattering of these alpha particles using some of the same techniques that were presented earlier in this chapter. Rutherford's formula eventually became known as the *Rutherford scattering formula*, and its specific form for elastic particle scattering was

The Rutherford Scattering Formula

$$N(\theta) = \frac{NnLZ^2k^2e^4}{\left(4r^2E^2\sin^4(\theta/2)\right)} \tag{3.101}$$

where

N is the number of incident alpha particles
n is the number of atoms per unit volume in the target material
L is the thickness of the target (in cm)
e is the electron's charge
k is Coulomb's constant
r is the target to detector distance (in cm)
E is the kinetic energy of the alpha particle
θ is the scattering angle (in degrees)
Z is the charge of the alpha particle

The Rutherford scattering formula is discussed in many undergraduate textbooks, and so we will not derive it here. However, its derivation may be found at the following website:

http://en.wikipedia.org/wiki/Rutherfword_scattering

* See *Nuclear Engineering Fundamentals: A Practical Perspective*, by R.E. Masterson, CRC Press (2017).

which is part of the Wikipedia domain. When Rutherford first derived his formula, he assumed that the scattering of alpha particles from an atomic nucleus could be modeled by a Coulomb force term and treated as a particle orbit. However, when one looks into the process of Coulomb scattering more closely, one finds that the scattering process can be treated statistically in terms of cross sections, which are discussed in Chapter 4. For a detector at a specific angle θ with respect to an incident neutron beam, the number of neutrons per unit area $N(\theta)$ striking the detector is given by Rutherford's formula (Equation 3.101). Rutherford's formula was a fundamental breakthrough in the field of atomic physics at the time because it matched the data that Geiger and Marsden had acquired several years earlier (see Figure 3.29). It also confirmed that elastic scattering occurred with nuclear particles all of the time. In other words, it showed that elastic scattering could occur with both charged particles (alpha particles) and uncharged particles (neutrons).

Eventually, people discovered that Rutherford's formula could also be applied to protons as alpha particles. Thus, scattering experiments helped early scientists to understand the structure of the atomic nucleus. This allowed scientists to design reactors based on neutron scattering probabilities and the average amount of energy that a neutron could lose in an elastic scattering collision. To convert Rutherford's formula into a differential scattering probability,

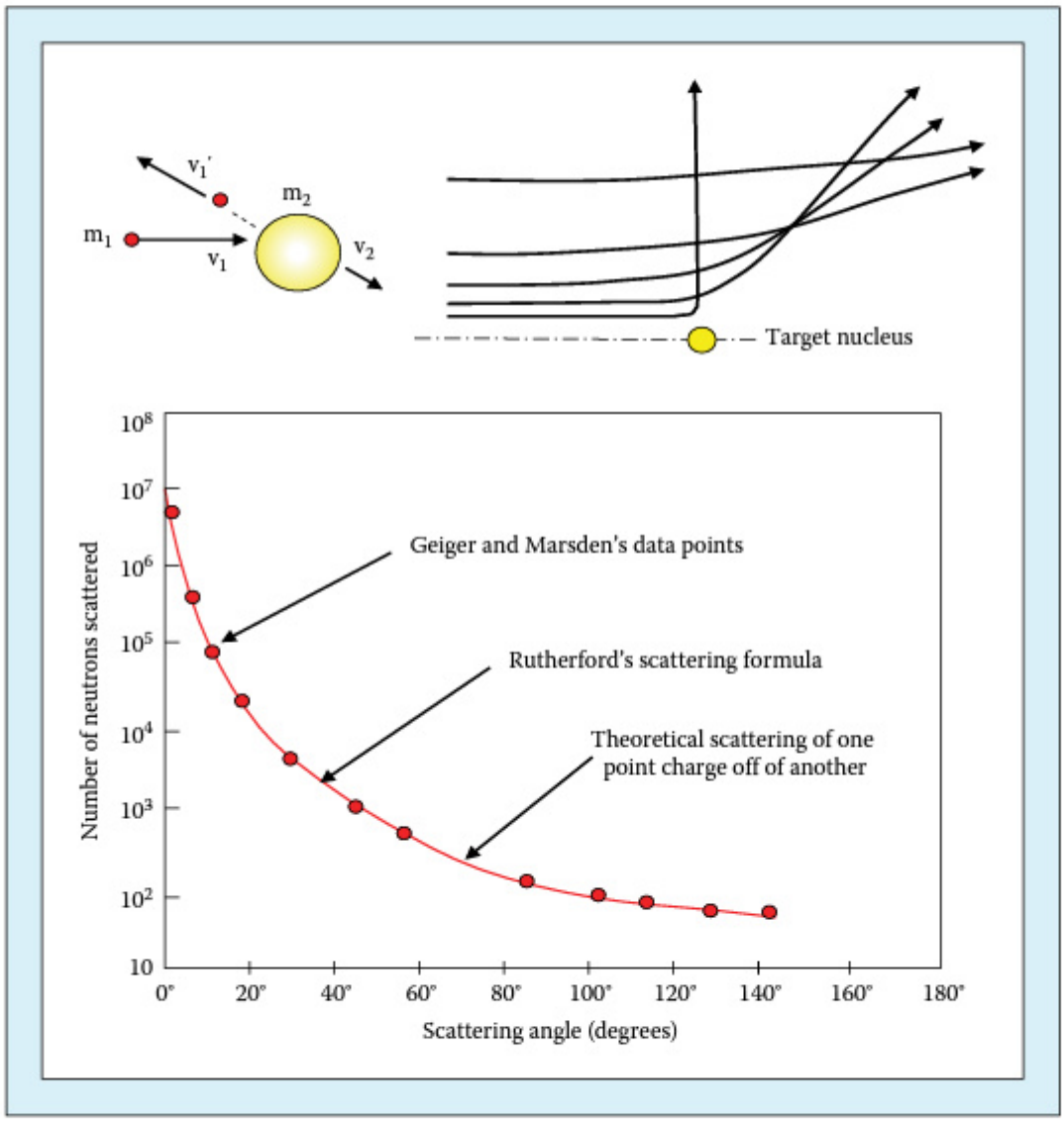

FIGURE 3.29 In 1909, Geiger and Marsden showed that the number of scattered alpha particles was consistent with a small, concentrated positive structure that we now call the nucleus. At angles above 140°, the nucleus appeared to be a point positive charge, so these data did not measure the size of the nucleus itself. When the scattering departed from the shape predicted by Coulomb's law, it could be inferred that another force was coming into play. In scattering reactions between alpha particles and heavy atoms, the scattering angle never becomes greater than about 140°. This implies that the nucleus is much heavier than the alpha particle that is scattering off of it. (Data provided by HyperPhysics; see hyperphysics.com.)

one simply divides both sides of Equation 3.101 by N. Then, the normalized angular distribution of the scattered particles becomes

$$P(q) = \frac{nLZ^2k^2e^4}{\left(4r^2E^2\sin^4(\theta/2)\right)} \tag{3.102}$$

and the differential scattering cross section is dP/dθ. Now let us proceed to Chapter 4, where the total scattering cross section is defined.

Example Problem 3.10

A common expression for the radius of an atomic nucleus is $R = 1.25\,A^{1/3} \times 10^{-13}$ cm, where A is the atomic mass number (i.e., the number of protons and neutrons the nucleus contains). Use this equation to derive the potential scattering cross section for a neutron from the nucleus of a carbon-12 atom.

Solution In the previous problem, we learned that the total elastic scattering cross section can be found from $\sigma_s = \pi R^2$, where R is the radius of the atomic nucleus. Since $R = 1.25\,A^{1/3} \times 10^{-13}$ cm, another expression for the elastic scattering cross section is

$$\sigma_s = \pi R^2 = 4.9\ A^{2/3} \times 10^{-26}\ \text{cm}^2.$$

In the case of Carbon-12, A = 12, so $\sigma_s = \pi R^2 = 4.9\,A^{2/3} \times 10^{-26}$ cm^2 $= 0.259 \times 10^{-24}$ cm^2 = 0.259 barns, where 1 barn = 1×10^{-24} cm^2. The use of the *barn* as a unit of neutron scattering is discussed in more detail in the next chapter. [Ans.]

References

Books and Textbooks

1. Shultis, K. and Faw, R. *Fundamentals of Nuclear Science and Engineering*, 2nd edn., CRC Press, Boca Raton, FL (2008).
2. Feynman, R.P., Leighton, R. and Sands, M. *The Feynman Lectures on Physics*, Narosa Publishing House, New Delhi, India (2011).
3. Glasstone, S. and Eedlund, M.C. *The Elements of Nuclear Reactor Theory, D*, Van Nostrand Company, Inc., New York (1952).
4. Watt, B.E. Energy spectrum of neutron from thermal fission of 235U, *Physical Review*, **87**, number 6 (1952).
5. Lamarsh, J.R. *Introduction to Nuclear Reactor Theory*, second printing, Addison-Wesley Publishing Company, Inc., Reading, MA (1972).
6. Glasstone, S. and Sesonske, A. *Nuclear Reactor Engineering*, 3rd edn., Van Nostrand Reinhold Company, New York (1981).
7. Kaplan, I. *Nuclear Physics*, Addison-Wesley, Reading, MA (1965).
8. Lamarsh, J.R. and Baratta, A.J. *Introduction to Nuclear Engineering*, Prentice Hall, Upper Saddle River, NJ (2001).
9. Stacey, W.M. *Nuclear Reactor Physics,* 2nd edn., John Wiley & Sons, New York (2007).
10. Duderstadt, J. and Hamilton, L. *Nuclear Reactor Analysis*, John Wiley & Sons, New York (1976).
11. Lewis, E. *Fundamentals of Nuclear Reactor Physics*, Academic Press, Boston, MA (2008).
12. Resnick, R. and Halliday, D. *Fundamentals of Physics*, John Wiley & Sons, New York (1967).
13. Eisberg, R. *Fundamentals of Modern Physics*, John Wiley & Sons, New York (1961).
14. Masterson, R.E. *Nuclear Engineering Fundamentals: A Practical Perspective*, 1st edn., CRC Press, Boca Raton, FL (2017).

Web References

1. *http://en.wikipedia.org/wiki/Coulomb's_law.*
2. *http://en.wikipedia.org/wiki/Virtual_particle.*
3. *http://en.wikipedia.org/wiki/Coulomb's_constant.*
4. *http://en.wikipedia.org/wiki/Rutherford_scattering.*
5. *http://en.wikipedia.org/wiki/Scattering_cross-section.*
6. *http://hyperphysics.phy-astr.gsu.edu/hbase/electric/elefor.html.*

Additional References

- Important physical constants used by nuclear scientists and engineers can be found in *Appendix A*.
- Unit systems and their conversion factors can be found in *Appendix B*.
- Nuclear cross sections for many important nuclear materials can be found in *Appendix C*.
- Physical properties of important nuclear materials can be found in *Appendix D*.
- Atomic masses, half-lives, and natural abundances can be found in *Appendix E*.

Questions for the Student

The following questions cover the material presented in this chapter, and in some cases, previous chapters as well. They are designed to test how well the student has acquired a working knowledge of the subject matter.

1. At least six different types of nuclear particles are produced in a reactor core. What are the names of each of these particles?
2. Suppose that two billiard balls collide with each other on a pool table. The que ball hits another billiard ball, and the que ball comes to a complete stop. Why does it do so?
3. Fill in the following sentence with the appropriate word or phrase: γ-rays and neutrinos are members of a larger family of nuclear particles called _____.
4. What are the conventional Greek symbols for a γ-ray and a neutrino?
5. In the elastic scattering collision of a fission neutron with an atomic nucleus, is more energy lost in a head-on collision or in a glancing collision?
6. Write the equation that can be used to find the electrical force between two protons separated by a distance r in an atomic nucleus.
7. Write an equation that determines the final energy E′ of a neutron in an elastic scattering collision when the initial kinetic energy E is known.
8. Write an expression for the energy decrement per collision α for a neutron scattering off of the nucleus of a carbon atom. In the case of Carbon-12, what does the value of the energy decrement per collision become?
9. In a fuel assembly consisting of several different nuclear materials having different atomic weights, is the value of the energy decrement per collision the same for each material?
10. What is the most probable energy that a prompt neutron can be emitted from the thermal fission of a Uranium-235 nucleus?
11. What is the average energy that a prompt neutron is emitted from the thermal fission of a U-235 nucleus?
12. What is the fundamental difference between an elastic scattering collision and an inelastic one?
13. What temporary nuclear structure is formed in an inelastic scattering reaction?
14. Earlier in the chapter, we mentioned that neutron scattering cross sections are normally measured in the units of barns. If a neutron scattering cross section has a value of 5 barns, what is its area in square centimeters?
15. What nuclear particle has a higher kinetic energy—an x-ray or a γ-ray?
16. What is the rest mass of a photon?
17. Write an equation for the decay of a free neutron into two other nuclear particles. Is charge conserved in this reaction?
18. What is the process of neutron decay within an atomic nucleus called?
19. What is the average lifetime of a free neutron after it leaves an atomic nucleus?
20. Name the four fundamental ways that a neutron can interact with an atomic nucleus when their wave functions overlap.
21. What is the fundamental difference between a radiative capture process and the more common reaction that involves the simple absorption of a low-energy neutron?
22. In an inelastic scattering reaction with a neutron, how long does a compound nucleus normally exist?
23. Under what conditions can we assume that the collision of a neutron with an atomic nucleus will be an elastic one?
24. Suppose that a neutron with a kinetic energy E happens to collide with an alpha particle that is initially at rest. What will be the final kinetic energy E′ of the neutron after a single "head-on" elastic scattering collision?
25. What will be the final kinetic energy E′ of the neutron if the scattering angle happens to be 45°?
26. What are the four basic types of neutron interactions that were discussed in this chapter?
27. What is the easiest way to get a uranium nucleus to absorb a neutron that is produced in a nuclear reactor?
28. What is the average scattering angle of a neutron that hits a nucleus with an atomic weight of 10?
29. What material would be more effective to use as a neutron moderator—uranium, carbon, or hydrogen?
30. Suppose that a neutron hits a stationary uranium-238 nucleus. What is the maximum amount of energy that can be lost in a single elastic collision?
31. Suppose that the incoming velocity v of a neutron that collides with a Uranium-235 atom is 100,000 m/s. If the collision is a head-on elastic one, what is the velocity of the neutron when it leaves the collision?
32. Write an equation for the conservation of momentum during the process of spontaneous particle emission.
33. A neutron scattering experiment with an unknown material reveals that the average scattering angle of an incoming neutron is 88°. What is the atomic weight of the material that the neutrons are scattering off of?
34. What is the definition of the critical energy of fission?
35. Light water and heavy water are both excellent moderating materials. What is one advantage that light water has over heavy water?

36. Fill in the following sentence with the appropriate word or phrase: The energy loss in an elastic scattering collision is proportional to the _____ of the scattering angle.
37. What type of nucleus is normally created during an inelastic scattering collision?
38. When the nucleus in the previous problem returns to unexcited state, what particle in addition to a neutron is it likely to emit in the process?
39. Draw a Feynman diagram for the scattering of two protons.
40. Draw a Feynman diagram for the elastic scattering of two neutrons.
41. Approximately how many head-on collisions does it take for a fission neutron colliding with a Carbon-12 nucleus to slow down to thermal speeds?
42. What is a common application for a neutron scattering experiment?
43. A neutron hits an atomic nucleus in a head-on collision and ricochets back in the opposite direction with nearly the same speed as its initial speed. What can you conclude from this reaction about the weight of the target nucleus?
44. In the derivation of the equations for elastic neutron scattering, what does the symbol $\theta 1$ refer to?
45. Suppose that a particular nuclear reaction in a cross-section library is represented by the symbols (n, 2γ + n). What does this specific nomenclature tell you about the reaction?
46. What is the probability that the absorption of a thermal neutron by a U-235 nucleus will NOT result in the nucleus splitting apart?
47. What is the critical energy of fission of a Pu-239 nucleus?
48. What is the value of Coulomb's constant k, which defines the strength of the electrical force between two charged particles in Coulomb's law?
49. Suppose that two nuclear particles collide with one another, and it is later discovered that the kinetic energy of the two particles is not conserved. What type of scattering reaction is this called?
50. What is the equation relating the rest mass of a neutron m_o to its actual mass when it is traveling at more than 10% of the speed of light?
51. Write an explicit expression for the hyperbolic sine—sinh (E) that appears in the following expression for the energy distribution of the prompt fission neutrons $P_p(E) = 0.453e^{-1.036E} \sinh\left\{\sqrt{(2.29\,E)}\right\}$.
52. Write an expression for the hyperbolic cosine of x.
53. Why do most elastic scattering curves show more neutrons scattering from an atomic nucleus at a small scattering angle than at a large one?
54. Write a simple expression for the average scattering angle θ of a neutron scattering off of an atomic nucleus of weight A.
55. When a Uranium-235 nucleus absorbs a thermal neutron and does not split apart, what does it ultimately become?
56. Name at least six fission products that can be produced when a U-235 nucleus splits apart.
57. What is the value of Coulomb's constant in the MKS unit system?
58. Suppose that a fast-moving neutron is absorbed by a target nucleus and, within 10^{-10} seconds, is reemitted by the same nucleus. If the reaction is a scattering reaction, what type of reaction is this reaction called?
59. How many collisions with a uranium atom does it take for a fission neutron to slow down from 2 MeV to 0.025 eV?
60. When an inelastic scattering reaction occurs, what do you expect to see in a plot of the number of neutrons scattered as a function of their initial energy?
61. Why is the emission probability in an inelastic scattering reaction the same in all angular directions?
62. What is the charge of a neutron that can be found in a nuclear reactor in Coulombs?
63. What is the electric charge of an electron in Coulombs in the MKS unit system?
64. A fission neutron scatters off of an atomic nucleus with a scattering angle of 30°. If a second neutron with exactly the same energy scatters off of the same nucleus but the scattering angle is 60°, which neutron (the first or the second) loses more kinetic energy in the collision?
65. A neutron scatters off of a Carbon-12 nucleus in a graphite block in a thermal gas reactor. What is the expected scattering angle of the neutron if the collision with the nucleus is an elastic one?
66. On average, what type of material will have a larger average scattering angle for a fission neutron produced in a nuclear fuel rod—hydrogen or uranium?
67. What type of scattering reaction is normally associated with the formation of a scattering resonance?
68. Write an equation for the average fractional energy loss ΔE of a neutron in an elastic collision with an iron atom having an atomic weight of 66.
69. Write an equation for the average fractional energy loss ΔE of a neutron in an elastic collision with a Carbon-12 atom having an atomic weight of 12.
70. Sometimes, when a neutron hits an atomic nucleus, it is temporarily absorbed by the nucleus before it is reemitted. Approximately how long does it take for this reemission process to occur in an inelastic scattering reaction?

71. Suppose that an experiment reveals that the average scattering angle of a neutron is 75°. What is the atomic weight of the material with which the neutron is scattering?
72. Write down an equation for the average fractional energy loss ΔE of a neutron in an elastic collision with a U-238 atom having an atomic weight of 238.
73. Based on the nuclear processes you have studied in this chapter, do you think that hydrogen or carbon is a more effective neutron moderator?
74. Is the angular distribution of the neutrons emerging from an inelastic scattering reaction isotropic or anisotropic?
75. When particles including neutrons and alpha particles are scattered in three dimensions, the angular direction of the scattered particles is normally measured in steradians. How many steradians are there in a unit sphere of radius 1?
76. Light water and heavy water are both excellent moderating materials. What is one advantage that heavy water has over light water?
77. How many angles are required to uniquely define the scattering direction of a scattered neutron in three dimensions?
78. Sometimes, when a neutron hits an atomic nucleus, it is temporarily absorbed by the nucleus before it is reemitted. What can you say about the angular distribution of the neutrons emerging from this reaction?
79. How many types of generic neutron scattering are there, and what are their names?
80. In the derivation of the equations for elastic neutron scattering, what does the symbol θ_2 refer to?
81. In general, what type of neutron scattering has a stronger energy dependence—elastic or inelastic?
82. A target nucleus has an atomic mass of A. What is its atomic mass immediately after being hit by a neutron in an inelastic scattering collision?
83. A neutron hits an atomic nucleus in a head-on collision and comes to a complete stop. What can you conclude from this reaction about the weight of the target nucleus?
84. Do the equations governing the scattering angle of a neutron following an elastic scattering reaction have any explicit energy dependence?
85. A particle scattering cross section usually consists of an elastic and an inelastic part. What specific component of the scattering cross section does not have an explicit angular dependence?
86. If the scattering angle of a neutron is decreased in an elastic scattering reaction, does the energy loss of the neutron increase or decrease?
87. In a scattering experiment involving neutrons emitted from a nuclear fuel rod, what is the quantity $d\sigma/d\Omega$ called, and what units does it normally have?
88. In any 3D scattering problem, particles will scatter from a target nucleus in a direction defined by the angular unit vector Ω. Write an explicit expression for this unit vector in terms of the particle scattering angles θ and φ.

Exercises for the Student

Exercise 3.1

In the center of mass system, a neutron elastically scatters off of a hydrogen atom at an angle of 45°. What does the scattering angle appear to be to a person watching this collision in the laboratory coordinate system?

Exercise 3.2

When the elastic scattering process in the center of mass system is completely isotropic, show that the final energy of a neutron is given by the equation $E' = [(1 + \alpha)/2]E$, where $\alpha = [(A - 1)/(A + 1)]^2$. If a neutron scatters off of a carbon atom, what is the final neutron energy if the initial neutron energy is 1 MeV?

Exercise 3.3

Suppose that two fission products are released from the fission of a Uranium-235 atom with a total kinetic energy E of 170 MeV. If the first fission product is 20% heavier than the second, what is the ratio of the kinetic energy carried by the second fission product to the kinetic energy carried by the first?

Exercise 3.4

Suppose that the scattering angle for an elastic collision of a neutron with an atomic nucleus in a nuclear fuel rod is observed to be 45°. What was the atomic mass A of the nucleus that the neutron hits if the scattering angle was 90° in the COM system? From your knowledge of nuclear materials, what element did the neutron collide with in the fuel rod?

Exercise 3.5

A single neutron with a kinetic energy of 10 MeV collides with U-238 nucleus in the COM coordinate system. Show that the maximum possible energy loss in a single elastic collision is given by $\Delta E_{MAX} = E' - E = (1-\alpha)E$ and that the most probable energy loss is given by $\Delta E_{MP} = E' - E = (1-\alpha)/2 \cdot E$. For a collision with a U-238 nucleus, what is the maximum and most probable energy loss after a single elastic collision?

Exercise 3.6

Suppose that two nuclear particles collide with each other in a head-on elastic collision. The mass of the first nuclear particle is m_1 and the mass of the second nuclear particle is m_2. If m_2 is initially at rest, show that a necessary and sufficient condition for the first particle to backscatter from the second is $m_1 < m_2$ and that a necessary and sufficient condition for the first particle to continue moving in the same direction after the collision is $m_2 < m_1$.

Exercise 3.7

Suppose that two nuclear particles are traveling through a reactor pressure vessel and that they deposit their kinetic energy in a series of elastic collisions as they go. If the first particle travels at twice the speed of the second particle, and the rest mass of the first particle is twice the rest mass of the second, what is the ratio of their kinetic energies in this case?

Exercise 3.8

An atomic nucleus initially at rest in a reactor core collides with another nuclear particle whose initial velocity is 10,000 m/s. After just one collision, the nuclear particle comes to a complete stop, and the atomic nucleus heads off in the same direction with the same average velocity. What can we conclude about the mass of the atomic nucleus in this case? If the incoming particle is an alpha particle, what element did the alpha particle collide with?

Exercise 3.9

In the scenario described in Exercise 3.8, what type of collision must occur between the nuclear particles in a real reactor, and what particles do you think participated in this collision if the atomic nucleus was a hydrogen atom?

Exercise 3.10

Suppose that you conduct a neutron scattering experiment where a beam of neutrons is directed at a small spherical container containing hydrogen gas. What is the average scattering angle of the neutrons emerging from this experiment?

Exercise 3.11

Using the knowledge you have just acquired, estimate the average scattering angle of a neutron scattering off of a uranium atom in a nuclear fuel rod in an elastic collision.

Exercise 3.12

A neutron hits an atomic nucleus in a head-on collision and comes to a complete stop. It loses all of its kinetic energy in the process. If an identical neutron then scatters off of the same atomic nucleus at an angle of 60° in the COM system, what fraction of its kinetic energy does it lose in a single elastic collision?

Exercise 3.13

A neutron undergoes three successive elastic collisions with a carbon nucleus and then collides twice with a helium nucleus. If the initial kinetic energy of the neutron is 1 MeV, what is the final kinetic energy of the neutron if all five of these collisions are head-on collisions?

Exercise 3.14

A low-energy neutron scatters off of the nucleus of a water molecule surrounding a nuclear fuel rod, and its energy is reduced by 20%. Approximately how much is the velocity of the neutron reduced in this case?

Exercise 3.15

Suppose that an atomic nucleus of mass m_2 collides with a second nuclear particle of mass m_1. If the atomic nucleus is initially at rest, and the velocity of the second nuclear particle is reduced by 50%, what is the mass of the atomic nucleus? Assume that the mass of the second nuclear particle is 1 AMU.

Exercise 3.16

Regardless of the force between a neutron and a target nucleus in an elastic collision, show that the target nucleus must be more massive than an incoming neutron to get a neutron scattering angle greater than 90°.

4

Nuclear Cross Sections, Reaction Probabilities, and Reaction Rates

4.1 Nuclear Cross Sections and Their Uses

When scientists first began to explore the structure of the atom, they were surprised to learn that the atom consisted primarily of *empty space* and that within this empty space there was a very small and extremely dense structure called the atomic *nucleus*, which was later discovered to have a diameter of about 10^{-12} cm (see Chapter 2). When they attempted to shoot other particles into the atom to break it apart, they found that the particles normally went right through the atom without hitting anything at all! Their experiments were equivalent to shooting a bullet into a *haystack* that has a small metal object (which is represented by the nucleus) inside of it. (In a real haystack, the nucleus would be about the size of a flea.) Most of the time, the bullet hits nothing but straw and passes completely through the haystack. However, occasionally it hits the metal object inside of it and scatters or ricochets away. Refer to Figure 4.1 to visualize the dynamics of this process. In the early days of the nuclear industry, scientists invented a way to measure the probability that an incoming particle (such as a neutron) would actually "hit" the nucleus and cause a nuclear reaction to occur. For this purpose, they invented the concept of the nuclear cross section.

Essentially, a *nuclear cross section* is a convenient way of measuring the *probability* that an incoming particle will hit the nucleus (or another comparably sized object like an electron) and, as the result of that collision, cause a particular nuclear reaction or set of reactions to occur. There is a direct correlation between the size of a nuclear cross section and the cross-sectional area of the nucleus that the incident particle is trying to hit. A larger cross-sectional area means that there will be a higher probability for a reaction to occur, and a smaller cross-sectional area means that the probability will be lower. The standard unit for measuring nuclear cross sections is a unit called the *barn*, (σ), which has a value of 10^{-24} cm^2. Hence a barn is roughly equivalent to the cross-sectional area of an atomic nucleus (i.e., $A = \pi * D^2/4$, where the diameter of the nucleus D is about 10^{-12} cm). (Refer to Figure 4.2 to get an idea of exactly how small a cross-sectional area of 10^{-24} cm can be.) In comparison, 1 *Angstrom*, a common unit for measuring the wavelength of light in the fields of chemistry and optics, is about 10^{-8} cm, and the atomic nucleus itself is about 1 *femtometer* (1×10^{-12} cm) in diameter. Hence the electron cloud in Figure 4.2 is about 1 Angstrom in diameter, while the nucleus is about 10,000 times smaller than this. Historically, the term "barn" was invented because it was believed that the early scientists who were shooting particles at the nucleus were having a hard time *hitting the broad side of a barn*. Over the years, the term became imbedded in the culture of the nuclear industry, and now all nuclear reaction probabilities are measured in this way.

4.2 Types of Nuclear Cross Sections

Cross sections can be defined for any type of process that involves a collision between two nuclear or subatomic particles, including the scattering of photons, the scattering of electrons, and the absorption of a neutron by an atomic nucleus. To determine the value of a nuclear cross section, one simply points a beam of particles with a well-defined energy at an object and measures the attenuation of the beam as it passes through the object. The object is then referred to as the "target." By convention, most targets are constructed from materials 1 cm thick and the attenuation of the beam depends on the type of material that is used.

Particle detectors can then be placed around the target to count the number of particles that are scattered by the nuclei in the target material. By counting the number of particles that are scattered per second (and their angular distribution—see Chapter 3), one can then deduce the number of particles that are deflected or absorbed. The cross section for a particle being removed from the beam is called the *removal cross section* for that particle. The value of this cross section depends not only on the type of particle that is shot at the target but also what the target is made from and the energy of the particles in the beam. The *total reaction cross section* can then be thought of as a measure of the probability that a scattering or absorption reaction will occur. A nuclear cross section is usually represented in

FIGURE 4.1 Shooting a bullet into a haystack with a small metal object inside of it can sometimes be an exercise in futility.

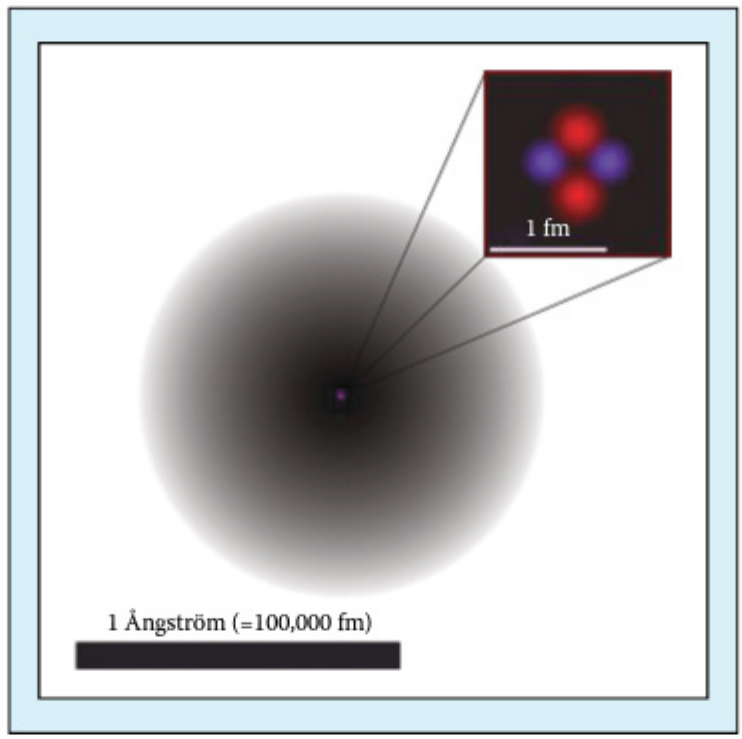

FIGURE 4.2 An illustration of what "hitting the broad side of a barn" means the blue and red dot at the center of the atom has the area of about one "barn." (Picture provided by Wikipedia.)

the literature by the Greek symbol σ (*rho*), although other symbols are sometimes used. The number of particles that are scattered and the number of particles that are absorbed can vary tremendously depending upon the target and

1. The energy of the incoming particle
2. The type of particle
3. The material from which the target is made

No single one of these three factors dominates the other two. However, all nuclear cross sections (including scattering, absorption, and fission) exhibit *some* dependence on the energy of the incoming particles. Figure 4.3 shows the neutron fission and absorption cross sections for some common nuclear materials including several nuclear fuels. What is striking about this figure is that the neutron energy, when measured from low (thermal) to high (fast) in the vertical direction, has

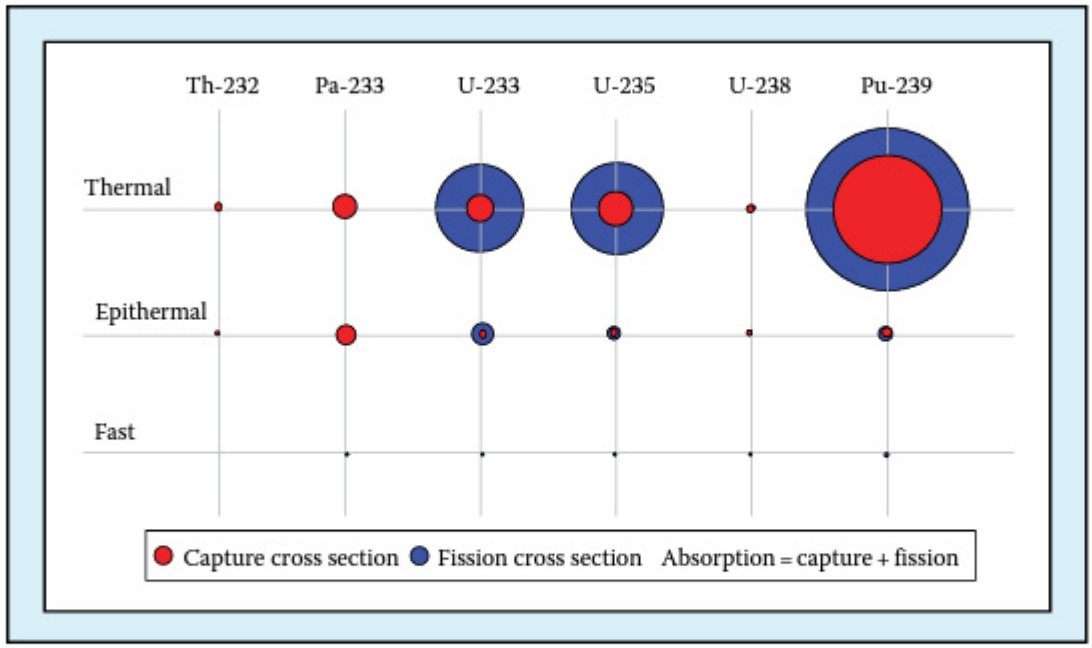

FIGURE 4.3 Reaction probabilities for some common nuclear materials at different neutron energies. Defined in this way, a thermal neutron has a kinetic energy of about 0.025 eV, an intermediate or "epithermal" neutron has a kinetic energy between about 1 eV and 100 keV, and a fast neutron has a kinetic energy of 1 MeV or higher.

a large influence on how large the apparent cross sections of many nuclear materials can be. For example, it can be seen that there is a difference of almost 10,000 between the size of the absorption cross section for Plutonium-239 at low energies (~270 barns) and the same cross section at higher energies (~0.027 barns). Since the size of the target nucleus is a function of the number of protons and neutrons (Z + N) it contains, small atoms will only present a small cross-sectional area to the incoming particles and larger atoms will present a larger one. So, there must also be some other processes at work that make the plutonium nucleus appear to an incoming neutron to be so large at some energies and to be so small at others. In fact, this strange behavior can be attributed to the wave-like nature of nuclear particles (or matter waves) that we rarely encounter in our everyday existence, but becomes quite real when we approach atomic and nuclear distance scales of less than 10^{-8} cm. If the reader has ever taken a class in *quantum mechanics*, then they are undoubtedly familiar with this effect (which is illustrated in Figure 4.4).

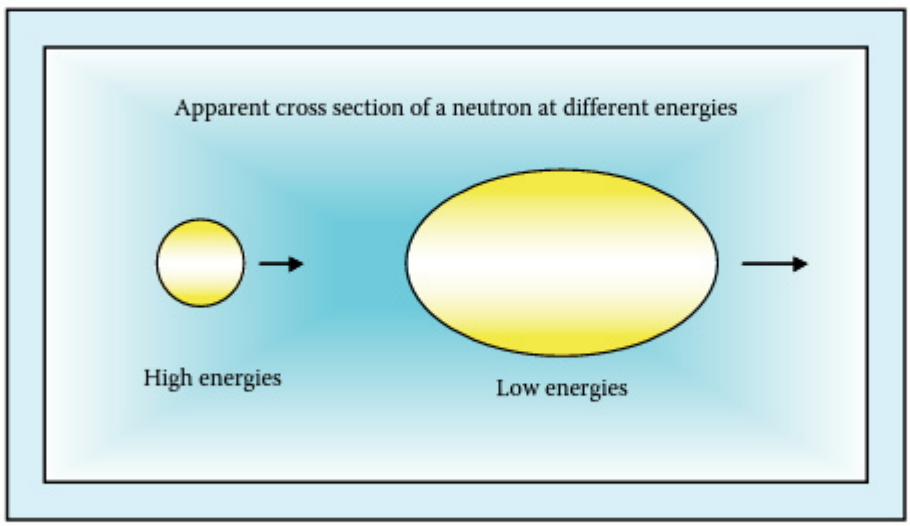

FIGURE 4.4 The apparent wavelength of a neutron and the area it can "touch" as a function of its energy. According to the predictions of the *theory of quantum mechanics*, the way in which we view a simple particle like a neutron or a photon can depend on the energy (and hence the wavelength) that we view it at. (Picture drawn by the author.)

A neutron, like any other elementary particle, does not have an absolute size or shape. How "large" or "small" it appears depends on its kinetic energy relative to the person who is observing it. So while it may appear to shrink as its kinetic energy is increased, it will also appear to grow larger as its kinetic energy is decreased. At high kinetic energies (say E > 1 MeV), neutrons and other subatomic particles such as photons behave more like point-sized chunks of matter than they do like waves, and due to the *Heisenberg uncertainty principle* (see Chapters 1 and 2 of our companion book*), their corresponding wavelengths are very small. This limits the extent to which they can spread out while they move, and so their cross sections at these energies are typically very small. On the other hand, as their kinetic energies become lower, their wavelengths increase and they begin to spread out spatially as they move. This increases the extent to which they can "reach out," bend around objects, and interact with the nucleus as they move. The further this influence extends, and the longer that the neutron is close to the nucleus (due to its lower speed), the larger an atomic cross section will be. Note that this applies to both scattering cross sections and absorption cross sections. So, particles like neutrons—because they do not have an electric charge—tend to always have larger cross sections when their kinetic energy is low than when their kinetic energy is high. We will encounter many examples of this behavior in future chapters of this book. There are four basic types of nuclear cross sections that we will encounter in our study of neutrons. They include

1. A cross section for *scattering*—represented by the symbol σ_s
2. A cross section for *absorption*—represented by the symbol σ_a
3. A cross section for *fission*—represented by the symbol σ_f
4. A cross section for *capture*—represented by the symbol σ_c

At low or thermal energies (E < 1 eV), the absorption cross sections are usually the largest of the four. (Their actual size is dependent on the specific isotopes that a neutron interacts with.) A *total nuclear cross section* σ_t can then be defined to represent the sum of the probabilities that a neutron will be scattered or absorbed:

$$\sigma_t = \sigma_s + \sigma_a = \sigma_s + \sigma_c + \sigma_f \tag{4.1}$$

A total absorption cross section σ_a can also be defined that represents the probability to either be captured without causing a nucleus to fission σ_c or to be captured and causing a nucleus to fission σ_f:

$$\sigma_a = \sigma_c + \sigma_f \tag{4.2}$$

For neutrons, the capture cross section σ_c defined in this way is sometimes called the *radiative capture* cross section because the capture of a thermal neutron by a heavy nucleus can sometimes cause a photon or an energetic gamma ray to be released. In this case, the symbol σ_c is sometimes replaced by the symbol σ_γ; for example,

$$\sigma_a = \sigma_\gamma + \sigma_f \tag{4.3}$$

Depending upon the specific process involved, the cross section for the capture of a photon can be further subdivided into

A cross section for the *photoelectric effect*, σ_{pe}
A cross section for *Compton scattering*, σ_{cs}
A cross section for *pair production*, σ_{pp}

In other words, the total scattering cross section for a photon can be written as $\sigma_\gamma = \sigma_{pe} + \sigma_{cs} + \sigma_{pp}$. Each process depends on the energy of the incoming photon, which can be a light wave, an *x-ray*, or a *gamma ray*. To a certain extent, the reaction rates are also a function of the internal structure of the *electron cloud*. Sometimes, the energy dependence of these nuclear cross sections is suppressed to keep the notation simple. Moreover, the kinetic energy of a fission neutron can sometimes extend up to 15 MeV, although most of the time 10 MeV is considered to be the upper limit of this energy range. Since neutrons do not carry an electric charge, the effects that *electrical forces* have on the values of their reaction cross sections can be neglected and only the effects due to *nuclear forces* need to be considered to predict their behavior from a quantitative perspective.

* See *Nuclear Engineering Fundamentals: A Practical Perspective*, by R.E. Masterson, CRC Press (2017).

Example Problem 4.1

An isotope of plutonium has a thermal fission cross section of 747.40 barns, a thermal capture cross section of 270.33 barns, and a thermal scattering cross section of 7.7 barns. What is the thermal absorption cross section of this isotope?

Solution By definition, the absorption cross section is the sum of the capture cross section and the fission cross section. Therefore, the thermal absorption cross section is $\sigma_a = \sigma_f + \sigma_c$ = 747.40 barns + 270.33 barns = 1017.73 barns. [Ans.]

4.3 Reaction Resonances and Nuclear Cross Sections

Every cross section is a function of the internal structure of the atom that it represents. Similarly, nuclear cross sections can be explained in terms of the internal structure of the nucleus (and sometimes the internal energy levels it has). While the internal structure of the nucleus is not as well known as that of the electron cloud (see Chapter 9), there is still a very high degree of correlation between how the nucleus behaves and the values of the nuclear cross sections that describe it. Fission, absorption, and even scattering cross sections have certain energies where the probability of a reaction occurring is much higher than it is at others. These energies result in peaks in the value of the reaction cross sections that are sometimes called *reaction resonances*. In many cases, these reaction resonances are separate and distinct from one another, but at neutron energies above 10 keV, they can overlap and can become difficult to distinguish from one another. Most of the time, these resonances are due to nuclei temporarily absorbing an incoming neutron before reemitting it again. When a nucleus absorbs a neutron, the kinetic energy of the neutron temporarily forces the nucleus into an *excited state*, where the excess kinetic energy needs to be released before the nucleus can return to a more stable state. A nucleus in which this occurs is sometimes called a *compound nucleus* (see Chapter 3).

Compound nucleus formation is the underlying process behind most of the nuclear reaction resonances that are observed in nature. Most resonances involving the scattering and absorption of neutrons are less than 100 eV across, and many of them—particularly at lower energies—have an average width of no more than 1–5 eV. Of course, their width is a function of the internal structure of the nucleus, and this in turn is a function of the number of protons and neutrons that it contains. An example of compound nucleus formation that gives rise to one of these reaction resonances is shown in Figure 4.5. There is a brief period of time (typically on the order of about 10^{-8} seconds) where the incoming neutron disappears entirely before it is reemitted by the target nucleus again. As we mentioned in Chapter 3, the angular distribution of the emitted neutron *is isotropic in the center of mass system*.

In other words, the emission angle of the emitted neutron does not depend on the angle from which the original neutron came. A simple diagram showing some of these scattering and absorption resonances is shown in Figure 4.6.

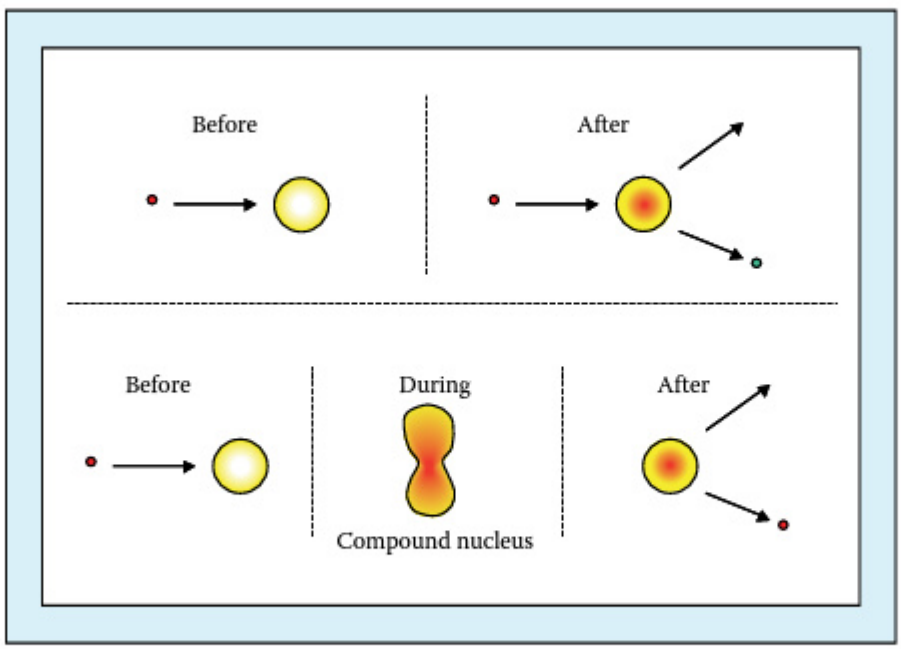

FIGURE 4.5 Process of simple elastic scattering compared to the process of inelastic scattering with compound nucleus formation. Top: the process of simple elastic scattering. Bottom: the process of inelastic scattering with compound nucleus formation.

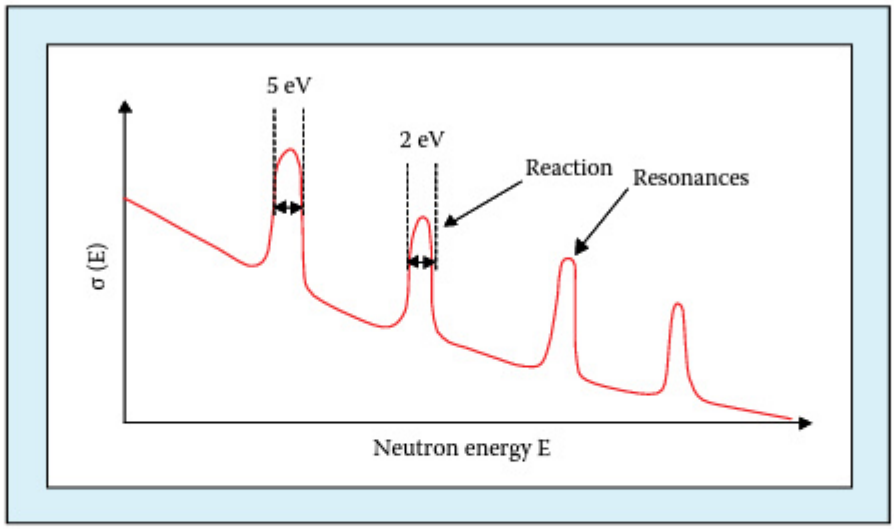

FIGURE 4.6 Reaction resonances of a typical nucleus as a function of the incoming neutron energy E. Note that most resonances are between 1 and 5 eV in width.

Notice that the reaction resonances tend to be very narrow (1–10 eV) and they are also symmetrical in shape. This behavior is typical of heavy elements where the nucleus can have many different energy levels and excited states.

Example Problem 4.2

For the same isotope that was discussed in Example Problem 4.1, what is the probability that when the isotope absorbs a thermal neutron the nucleus will split apart into two pieces, and what is the probability that it will not?

Solution What we are essentially asking for here is what is the probability that there will be a fission reaction, and what is the probability that absorbing the neutron will not cause the nucleus to fission. The probability of having a thermal neutron cause the nucleus to fission is $\sigma_f/\sigma_a = 747.4/1017.73 = 0.734 = 73.4\%$, and the probability of the thermal neutron just being captured is $\sigma_c/\sigma_a = 270.33/1017.73 = 0.266 = 26.6\%$. Note that the sum of these two probabilities must add up to 1.0 since $\sigma_f/\sigma_a + \sigma_c/\sigma_a = (\sigma_f + \sigma_c)/\sigma_a = \sigma_a/\sigma_a = 1.0 = 100\%$. [Ans.]

4.4 Reaction Resonances and Compound Nucleus Formation

The *probability* that a compound nucleus will be formed and that a reaction resonance will appear greatly increases if the *excitation energy* added to the nucleus by the incident neutron corresponds to one of the internal energy levels or *excited states* of the nucleus itself (again refer to Chapter 3). Scattering and absorption cross sections almost always exhibit resonance peaks at neutron kinetic energies that correspond to these excited states, which are sometimes called *quantum states*. Figure 4.7 illustrates where these peaks or *reaction resonances* can be found in the scattering and absorption cross sections of Sodium-23, a relatively stable isotope of sodium and a key ingredient of common table salt (NaCl). Each element and each isotope of a particular element will have its own unique resonance energy structure, but, in general, the heavier a nucleus is, the more internal energy states it will have, and the more closely these states will be spaced together. In lighter elements, there will be many fewer excited states, and the spacing between these states and the ground state will be greater. Because of this, the resonances in the cross sections of most light elements begin to occur at much higher energies than the comparable resonances in their heavier counterparts. Furthermore, the resonances of lighter elements tend to be more widely spaced, and most of the time, they have a smaller capture to scattering cross section ratio.

One of the interesting features of heavy elements is that their absorption and scattering resonances appear to suddenly stop at about 10 keV. Within the nucleus, however, this is far from true because there are so many internal resonances involved. However, above 10 keV they become so closely spaced together that they cannot be resolved experimentally without considerable time and expense. In other words, the smooth curves for the absorption and scattering cross sections tend to mask the unresolved resonances beneath them (which can number in the hundreds or even the thousands). The presence of these resonances must be resolved by statistical analysis until more precise experimental measurements can

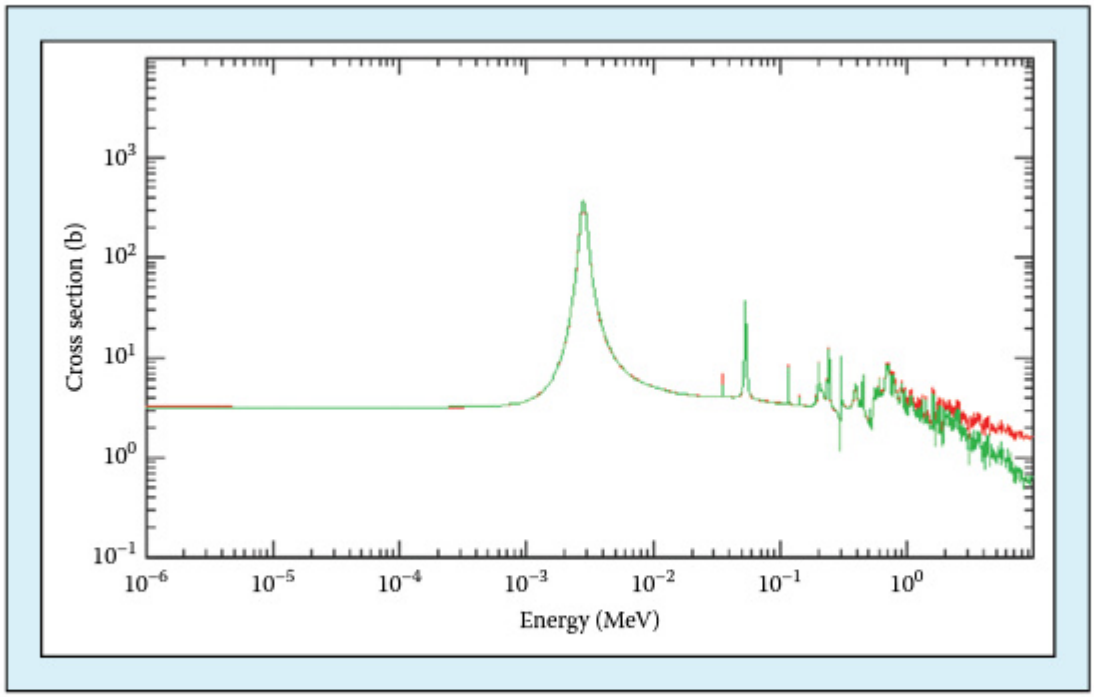

FIGURE 4.7 Total cross section (in red) and the scattering cross section (in green) for Sodium-23, a common isotope of the element sodium. The width of a resonance is represented by the symbol Γ.

be made. When the kinetic energy of an incoming neutron falls below about 1 keV, the individual absorption and scattering resonances become much easier to resolve. This relationship continues when accounting for the effects of neutron capture and moderation as well. For example, when the resonances are spaced widely apart, most of the absorption or scattering will take place within an interval ±Γ about the resonance energy peak. Sometimes the symbol Γ is called the *half-width of a reaction resonance*, and these half-widths occur frequently in the study of the nuclear Doppler effect, which is discussed in great detail in Chapter 17. This means that fission neutrons traveling through the *resonance energy region* (see Chapter 5) will have a finite probability of falling into one of these reaction resonances and being further scattered or absorbed.

The probability of escaping these resonances can be found by calculating a parameter called the resonance integral I. The *resonance integral* is a measure of the probability that a neutron will be absorbed (or scattered) by a resonance if it falls within an energy interval that corresponds to the resonance's bell-shaped curve. If the probability of being captured in resonance i is given by $PC_i = CI_i$, where C is an empirical constant, then the probability of *not* being captured in resonance i is given by $P_i = 1 - CI_i$, where P_i is called the *resonance escape probability* from the resonance. If N is the total number of absorption resonances that the neutron passes, then the probability of escaping all of them and not being captured at all is given by

$$P = P_1 \times P_2 \times P_3 \times P_4 \times \cdots \times P_N \tag{4.4}$$

In many nuclear textbooks, this number is also called the *total resonance escape probability P*, and alternatively it can be found from the equation

$$P = e^{-CI} \tag{4.5}$$

where C is the same empirical constant and the resonance integral I is now the sum of the contributions from all of the individual absorption resonances

$$I = \sum_i I_i \tag{4.6}$$

where i = 1, 2, 3, 4, …, N. This parameter is widely used in the calculation of nuclear reaction rates, and its properties are discussed in more detail in Chapter 9. There we will derive the *four-factor formula*, which is one of the most famous equations in all of nuclear science and engineering. The four-factor formula was used in the early days of the nuclear power industry to determine when a reactor lattice would become critical and when it would not. Unfortunately, the four factor formula did not account for the effects of neutron leakage on the effective multiplication factor, and so its use was restricted primarily to large reactor lattices with repetitive and identical unit cells.

Student Exercise 4.1

Considering the total cross section and the scattering cross section only of the hypothetical isotope discussed in the previous problems, what is the probability that a thermal neutron will be scattered by an isotope of this material if such a reaction were to occur?

Example Problem 4.3

Suppose that one atom of a hypothetical material scatters a thermal neutron and another atom of the same material scatters a fast neutron. If the thermal scattering cross section is 7.7 barns and the fast scattering cross section is 6.98 barns, how much more likely is it for the thermal neutron to be scattered than the fast one?

Solution Since each of the scattering cross sections is just a measure of the probability that a scattering event will occur, a thermal neutron is 7.7/6.98 = 1.1 times more likely to be scattered than a fast neutron is. [Ans.]

4.5 Nuclear Cross Sections and Reaction Rates

Suppose that we would like to measure the rate that nuclear reactions occur in the sample of material shown in Figure 4.8. Suppose that the sample is bombarded with a beam of neutrons from the left with a well-defined kinetic energy E. The nuclei of the atoms within the material are represented by the small black dots in the figure. Since the atoms inside of the target consist primarily of empty space, it is normally not realistic to assume that every neutron in the beam will hit one of these atoms. In fact, most of the neutrons will pass right through the target and they will not hit anything at all! (They will simply emerge on the other side.) However, a small fraction of them will actually "hit" an atomic nucleus inside of the material, and we can use this fact to calculate the number of neutrons per second that are captured, scattered, and absorbed. We would further like to assume that all of the neutrons in the beam have approximately the same kinetic

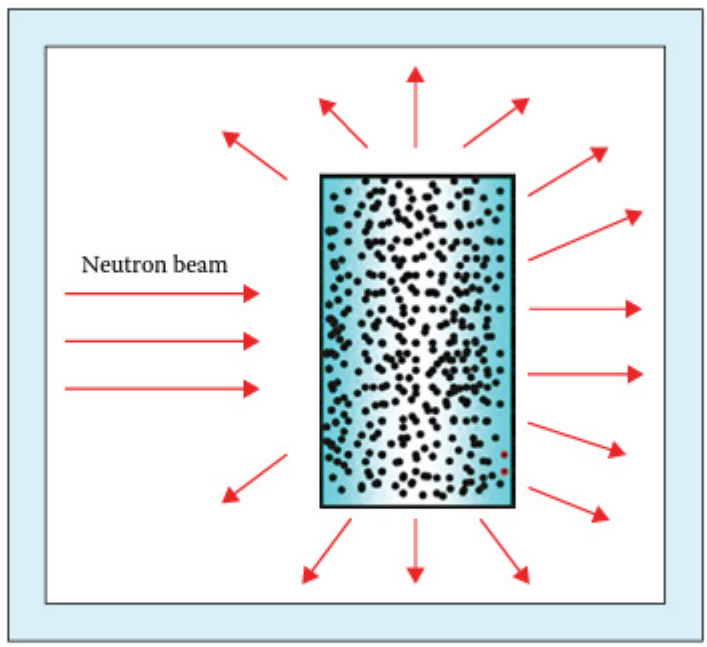

FIGURE 4.8 A slab of uniform target material being bombarded by a beam of incoming neutrons. Some of the neutrons hit the atoms in the target and are scattered or absorbed. However, the majority of the neutrons pass directly through the material and do not hit anything at all.

energy, so that at least to start, we can neglect the dependence of the cross sections on the kinetic energy of the incoming neutrons. In this case, the nuclear *reaction rate*, R, which is the number of reactions that occur per cubic centimeter per second, can be calculated from the following equation

The Nuclear Reaction Rate (in reactions per cubic centimeter per second)

$$R_x = \phi\Sigma_x$$

where

$$\Sigma_x = \sigma_{x1}N_1 + \sigma_{x2}N_2 + \sigma_{x3}N_3 + \sigma_{x4}N_4 + \cdots + \sigma_{xN}N_N \tag{4.7}$$

where

R_x is the number of reactions of type x, per cubic centimeter per second

Φ is the *particle flux*, or the number of incoming particles hitting an area of the target per second (usually in the units of particles/cm^2/s)

σ_x^j is the *microscopic cross section* for reaction type x, and isotope j in a predefined area (usually in *barns* or cm^2)

N_j is the number of the atoms in the material of isotope j—per cubic centimeter (or atoms/cm^3)

Σ_x is the *macroscopic cross section* for reaction type x, with dimensions of per unit length (usually 1/cm)

Equation 4.7 is sometimes called a *rate equation* because it allows us to calculate the rate at which a particular nuclear reaction x = (fission, absorption, capture, or scattering) will occur. Notice that the reaction rates, at least for nuclear reactions, are always *additive* in nature. In other words, for a known nuclear material, we can always write

$$\Sigma_{total} = \Sigma_{x1} + \Sigma_{x2} + \Sigma_{x3} + \Sigma_{x4} + \cdots + \Sigma_{xN} \tag{4.8}$$

and if we know the value of the particle flux Φ, we can also write

$$R_{total} = \Phi\Sigma_{total} = \Phi\left(\Sigma_{x1} + \Sigma_{x2} + \Sigma_{x3} + \Sigma_{x4} + \cdots + \Sigma_{xN}\right) = R_{x1} + R_{x2} + R_{x3} + R_{x4} + \cdots + R_{xN} \tag{4.9}$$

So no matter what the reaction rate for a single nuclear process, R_x, is, the sum of the cross sections will always equal the total cross section for that process, and the sum of the reaction rates will always equal the total reaction rate. It does not matter whether we are talking about neutrons, protons, electrons, or alpha particles. Their reaction rates can all be calculated from Equation 4.9—and only the values of ϕ and Σ will change. Equation 4.7 is also very important when it comes to understanding how neutrons react with matter because *it defines the macroscopic cross section Σ as the product of microscopic cross section for a single atom and the number of atoms N that are present in the material*.

The more atoms there are to hit in a material, the more times that we can multiply the reaction rate for a single atom by the number of atoms that are present. In other words, $R_x = \phi V\Sigma_x$ is the *total reaction rate* for the entire material, where V is the volume of the material. Thus the total reaction rate is based on *the volume* V of the material—and not just on its cross-sectional area A. This distinction becomes important when working with the neutron diffusion equation, which is derived and discussed in Chapters 11 through 14. There we will attempt to predict the behavior of large numbers of neutrons by assuming that the collisions between neutrons and the materials in a reactor core are similar to the collisions between the particles of a *diffuse gas*. Hence a diffusion equation is an obvious equation to use to describe the behavior of large numbers of neutrons under these conditions.

Example Problem 4.4

Suppose that there are 0.0334×10^{24} molecules of water in a volume of material 1 cm^2 and 1 cm thick. If the microscopic scattering cross section for a water molecule at 1 MeV is 10 barns, what is the macroscopic scattering cross section Σ_s for water for the neutrons at this energy?

Solution The macroscopic scattering cross section for water is defined as $\Sigma_s = \sigma_s N_{H_2O}$. If N_{H_2O} is the number of molecules of water in a volume of space equal to 1 cm^3, or $N_{H_2O} = 0.0334 \times 10^{24}$ molecules, then $\Sigma_s = 0.0334 \times 10^{24} \times 10 \times 10^{-24}$ cm^2 = 0.334 cm^{-1}. [Ans.]

One of the interesting features of Equation 4.7 is that the exponents in the terms on the right-hand side tend to cancel when we start to plug in realistic numbers. This is because typical microscopic cross sections are on the order of 10×10^{-24} cm^2 per atom, and there are about 10^{23} atoms in a cubic centimeter of most materials. When we multiply these two numbers together, we will usually end up with a number that is relatively close to unity! This makes it easy

to work with macroscopic cross sections because we can develop an intuitive feel for what their correct orders of magnitude should be. Practically speaking, the physical distinction between a *macroscopic cross section* and a microscopic one is that the macroscopic cross section is a *property* of a specific lump of material (like its color, its density, or its mass), while the *microscopic cross section* is an intrinsic property of the atoms from which the material is made (like the number of electrons revolving around the nucleus, or what the average diameter of the atomic nucleus is). In our previous examples, we assumed that the neutron flux ϕ did not have an energy dependence (since we were dealing with a monochromatic neutron beam). This is, of course, a gross simplification that we will shortly attempt to correct.

Example Problem 4.5

Now suppose that the same volume of water in Example Problem 4.4 is exposed to a neutron flux of 100 neutrons/cm^2/s. How many neutrons per second will be scattered by the water in this case, and how many neutrons will be scattered in 10 seconds?

Solution From our previous discussion (Equation 4.7), we know that the number of neutrons scattered per second will be given by $R_s = \phi V \Sigma_s$. So in 1 second, the number of neutrons scattered by the water will be $R_s = 100 \times 1 \times 0.334 =$ approximately 33 neutrons, and in 10 seconds, the total number of neutrons scattered will be 10 seconds × 33 neutrons per second = 333 neutrons. [Ans.].

4.6 Finding Energy-Dependent Reaction Rates

In practice, all reaction rates are energy dependent. The correct form of Equation 4.7 to account for this dependence is

$$R_x^j(E) = \phi(E)\Sigma_x^j(E) \tag{4.10}$$

for any neutron energy E and any isotope j. Here, the reaction type x can be a, c, f, s, or t. If we want to find the total reaction rate R_x for a beam with an arbitrary distribution of neutron energies (rather than a monoenergetic beam), then we must integrate the product of the neutron flux and the macroscopic cross section over every neutron energy in the beam. That is,

$$R_x = \int_E \phi(E)\Sigma_x(E)dE \tag{4.11}$$

or

$$R_x = N\int_E \phi(E)\sigma_x(E)dE \tag{4.12a}$$

where N is the total number of atoms per cubic centimeter, and again the limits of integration are from $E_1 = 0$ to $E_2 = 10$ MeV since neutron energies rarely exceed 10 MeV. Again, this results in a reaction rate that is measured in reactions per cubic centimeter per second. To find the total reaction rate, we must then multiply by the volume of the material through which the neutrons are passing. Hence, the total reaction rate becomes

$$R_{total} = R_x \times V \tag{4.12b}$$

where V is the volume of the material containing the target atoms. Example Problem 4.6 presents a practical example of how the reaction rates can be found with this equation.

Example Problem 4.6

A material has a one-group macroscopic scattering cross section Σ_s of 0.50 cm^{-1}. How many neutrons will be scattered passing through a sample of this material 1 cm thick and 2 cm on a side if the flux is one million neutrons per square centimeter per second?

Solution By definition, $R_s = \phi\Sigma_s$ is the rate that the neutrons will be scattered by one cubic centimeter of this material. Therefore, in a target with a volume of 4 cubic centimeters, the total scattering rate is $R_s = \phi\Sigma_s V = 1{,}000{,}000 \times 0.5 \times 4 =$ 2,000,000 neutrons per second. In this case, the neutrons hit only a small fraction of the atoms in the target material. [Ans.]

4.7 Fast and Thermal Neutron Cross Sections

In Section 4.2, we learned that the values of almost all nuclear cross sections are dependent on the kinetic energy of the incoming neutrons. Thermal neutrons with very low energies are much more likely to be absorbed than fast neutrons with higher energies, and almost all reactors are designed to take advantage of this fact. Specifically, this energy dependence can be accounted for by rewriting Σ_a and Σ_f as $\Sigma_a(E)$ and $\Sigma_f(E)$, where E is the kinetic energy of the incoming neutron(s). In most reactors, the reaction rates are found by further subdividing the fission and absorption cross sections into two separate parts: (1) the first part for calculating the reaction rates for fast neutrons and (2) the second part for calculating the reaction rates for thermal neutrons. By convention, a *fast neutron* is defined to have a kinetic energy of about 1 MeV and a *thermal neutron* is defined to have a kinetic energy of about 0.025 eV. (The actual dividing line between what is a "thermal" neutron cross section and what is a "fast" neutron cross section is somewhat arbitrary, but in practice a neutron energy of about 1 eV is usually considered to be a good compromise.) It goes without saying that the neutrons will always have a distribution of energies that we can measure if we wish to determine how many are moving at high speeds and how many are moving at low speeds. In principle, there is also no reason to arbitrarily subdivide the neutron energy spectrum into just two regions that we have chosen to call "fast" and "thermal." However, their physical behavior is so different at higher energies than it is at lower energies that it is natural to segment them and to think about their behavior in this way.

In Chapter 11, we will present a formal definition of the *neutron flux* to show how fast and thermal neutrons fit into this scheme. However, it should be clear by now that if we consider ~1 eV to be the dividing line between neutrons that are considered "thermal" and neutrons that are considered "fast," then we can define two *energy groups* to hold all of these neutrons, and that the total number of neutrons flowing through the surface of a material can be represented by subdividing the neutron flux $\phi(E)$ into these two energy groups as well. Thought of in this way, we can define the *thermal neutron flux* ϕ_T as

$$\phi_T = \int_E \phi(E)dE \tag{4.13}$$

where the limits of integration E_o and E_1 are from $E_o = 0$ and $E_1 = 1$ eV, and we can define the *fast neutron flux* ϕ_F as

$$\phi_F = \int_E \phi(E)dE \tag{4.14}$$

where the limits of integration are $E_1 = 1$ eV and $E_2 \sim 10$ MeV. For any type of reaction x, the reaction rates can then be conserved by defining

$$R_x = \phi\Sigma_x \tag{4.15}$$

if all of the neutrons are in a single energy group, and ϕ is the "one-group" flux, and

$$R_x = \phi_F\Sigma_{xF} + \phi_T\Sigma_{xT} \tag{4.16}$$

if all of the neutrons are in two energy groups, and where ϕ_F is the fast flux and ϕ_F is the thermal flux. It goes without saying that the one-group flux ϕ contains neutrons from both energy groups and that it must always be defined as $\phi = \phi_T + \phi_F$ to conserve the total number of neutrons and also to conserve the reaction rate; for example,

$$\phi\Sigma_x = \phi_F\Sigma_{xF} + \phi_T\Sigma_{xT} \tag{4.17}$$

where Σ_{xF} and Σ_{xT} are the fast and thermal cross sections for reaction type x, respectively. There are then four primary ways in which fast and thermal neutrons can interact with matter (scattering, capture, fission, and absorption), and we can represent any of these by simply setting x = s, c, f, or a. Finally, it follows that the absorption cross section must always be defined as

$$\Sigma_a = \Sigma_f + \Sigma_c \tag{4.18}$$

and that the total cross section must always be defined as

$$\Sigma_t = \Sigma_f + \Sigma_c + \Sigma_s = \Sigma_a + \Sigma_s \tag{4.19}$$

where we have suppressed the energy dependence for the moment to simplify the notation. Figure 4.9 shows the cross sections for U-235 and U-238 as a function of incoming neutron energy. The fission cross section for a thermal neutron

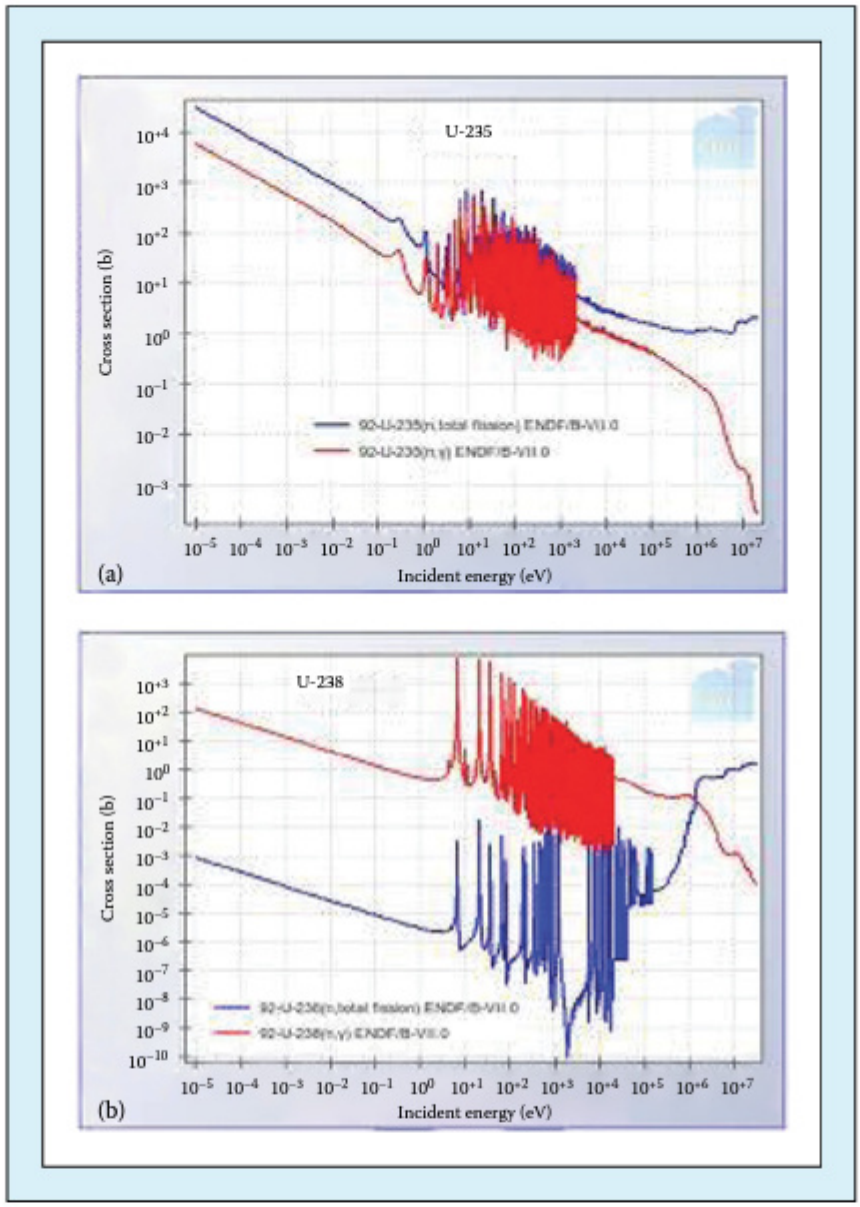

FIGURE 4.9 Neutron absorption and fission cross sections for Uranium-235 and Uranium-238.

hitting U-235 is about 600 barns, and the cross section for capture only σ_c is about 100 barns. Conversely, the fission cross section for a thermal neutron hitting U-238 (which becomes Plutonium-239 and then starts to decay rather quickly by geological standards) is about 10 barns. As we will see in Chapter 7, most nuclear materials that create fission neutrons create them with a distribution of energies between about 0.5 and 10 MeV. The *most probable energy* at which a neutron is created in this distribution is about 0.75 MeV, and the average energy at which a neutron is created is about 2 MeV. These numbers vary only slightly from one type of nuclear fuel to the next.

A typical thermal water reactor will have a distribution of neutrons that peaks at energies where the "fast "neutrons are initially produced (1–2 MeV), and then again where the thermal neutrons tend to accumulate (~0.025 eV), before they are ultimately absorbed. These two characteristic peaks are shown in the neutron energy spectrum in Figure 4.10. The "fast" neutrons fall into the bin on the right-hand side of the dividing line (which we previously established at about 1 eV), and the thermal neutrons fall into the bin to the left of it. This dividing "line" will of course vary depending upon the way in which the fast and thermal cross sections are defined. It should be immediately obvious from inspecting this figure that the number of fast neutrons is greater than the number of thermal neutrons when the total neutron energy spectrum is drawn in this way. This is a feature of the neutron energy spectrum that virtually all thermal reactors have in common. Because of this, our previous decision to divide the neutron energy spectrum into what we

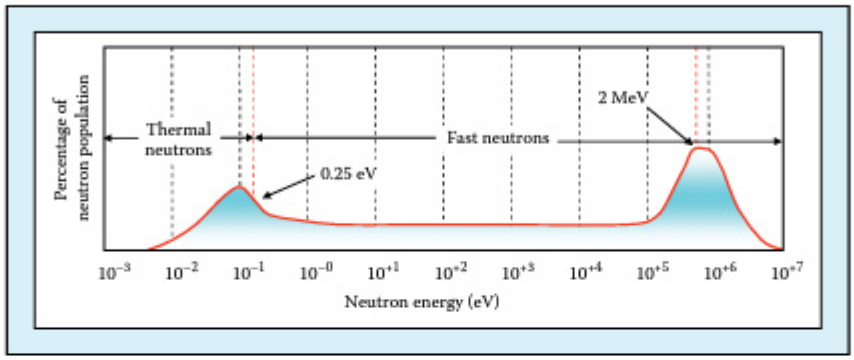

FIGURE 4.10 A typical thermal reactor neutron energy spectrum.

consider to be "fast neutrons" and what we consider to be "thermal neutrons" has a number of practical advantages that may only now become apparent.

For example, only when the neutron flux is subdivided in this way can the nuclear reaction rates, which are proportional to the product of the energy-dependent cross sections and the neutron flux, be calculated with enough accuracy to make a reactor function properly. We will subsequently learn that the spatial shape of the neutron flux can be different in the fuel than it is in the moderator and that this shape is also different as a function of the neutron kinetic energy E. This is one reason why it is so difficult to calculate the reaction rates properly in a fuel assembly where the fuel and the moderator are physically separated. Nevertheless, this turns out to be the optimum way to build a reactor when all the reaction rates are taken into account. In *general, the neutron energy spectrum in a thermal reactor will have about 65% of its neutrons in the "fast" energy range and about 35% of its neutrons in the "thermal" energy range*. Of course, these numbers can vary slightly from one thermal reactor design to the next, but, on average, these are the weights that must be assigned to the total neutron flux when both fast and thermal cross sections are available to calculate the reaction rates.

4.8 Cross Sections with More than Two Energy Groups

In practice, there is no reason to arbitrarily restrict our discussion to problems involving only fast and thermal neutrons. In principle, any number of cross sections, differentiated by different energy ranges, can be used. We could, for example, subdivide the neutron energy spectrum into three energy ranges instead of just two. Energy range 3 could be from 0 to 1 eV, energy range 2 could be from 1 eV to about 10 keV (where the resonances in the absorption and fission cross sections usually stop), and energy range 1 could be from 10 keV to 10 MeV. In this case, knowing the dependence of each cross section on the neutron energy, for example, $\Sigma(E)$, we could *define*

$$\Sigma = \Sigma_{E1} + \Sigma_{E2} + \Sigma_{E3} \tag{4.20}$$

where

$$\Sigma_{E3} = \frac{\int_E \Sigma(E)\phi(E)dE}{\int_E \phi(E)dE} \quad \text{where } E_0 = 0 \text{ and } E_1 = 1 \text{ eV} \tag{4.21}$$

$$\Sigma_{E2} = \frac{\int_E \Sigma(E)\phi(E)dE}{\int_E \phi(E)dE} \quad \text{where } E_1 = 1 \text{ eV and } E_2 = 10 \text{ keV} \tag{4.22}$$

$$\Sigma_{E1} = \frac{\int_E \Sigma(E)\phi(E)dE}{\int_E \phi(E)dE} \quad \text{where } E_2 = 10 \text{ keV and } E_3 = 10 \text{ MeV} \tag{4.23}$$

and in the case of the neutron flux ϕ

$$\phi = \phi_{E1} + \phi_{E2} + \phi_{E3} \tag{4.24}$$

where

$$\phi_{E3} = \int_{E} \phi(E)dE \quad \text{where } E_0 = 0 \text{ and } E_1 = 1 \text{ eV} \tag{4.25}$$

$$\phi_{E2} = \int_{E} \phi(E)dE \quad \text{where } E_1 = 1 \text{ eV and } E_2 = 10 \text{ keV} \tag{4.26}$$

$$\phi_{E1} = \int_{E} \phi(E)dE \quad \text{where } E_2 = 10 \text{ keV and } E_3 = 10 \text{ MeV} \tag{4.27}$$

Each energy interval so defined is then called an *energy "group."* Therefore, the group flux ϕ_g would be the total flux of neutrons in energy group g (where g = 1, 2, 3, …, G), and the reaction cross section Σ_g would be the total reaction cross section for the neutrons in energy group g (g = 1, 2, 3, …, G).

4.9 Multigroup Approximation

It is easy to extend the logic mentioned earlier to any number of energy groups that do not necessarily have to be the same width or have the same spacing. Refer to Figure 4.11 to see how partitioning the neutron energy spectrum works. *In nuclear science and engineering, neutrons with the highest energies are usually assigned to the lowest energy group (g = 1), and neutrons with the lowest energies are usually assigned to the highest energy group (g = G).* There is some logic behind this reasoning because it allows us to write scattering cross sections between the higher energy groups and the lower energy groups as $E_{1\to2}$ or $E_{2\to3}$ (and more generally as $\Sigma_{Sg'g}$). This also allows us to write $\Delta E_g = E_{g-1} - E_g$ (where g = 1, 2, 3, …, G). In general, the energy intervals ΔE_g do not have to all be the same size, and in practice, they are normally *not*. Similarly, this allows us to define the *group flux* ϕ_g as

The Definition of the Group Flux

$$\phi_g = \int_{E} \phi(E)dE$$

or

$$\phi_g = \int_{E} n(E) \cdot v(E)dE \tag{4.28}$$

where the energy integral is now from E_g to E_{g-1}, n(E) is the energy-dependent neutron density, and v(E) is the energy-dependent neutron velocity. *Notice that the group flux as it is defined in Equation 4.28 represents the total number of neutrons per cm²/s within an arbitrary energy group g, that is, having energies between E_{g-1} and E_g.*

In layman's terms, what we have just discussed is part of a branch of nuclear reactor theory called *multigroup theory*—because reactors are normally designed by breaking the neutron energy spectrum into multiple energy groups—and

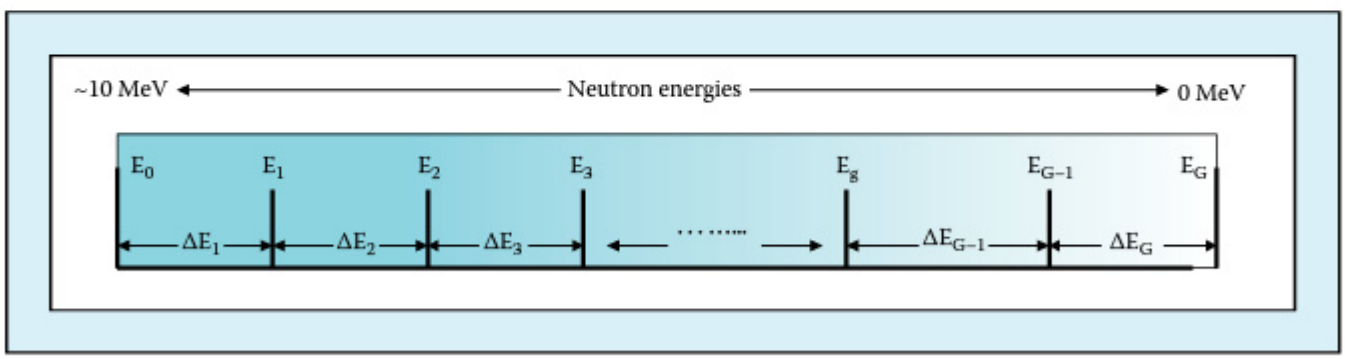

FIGURE 4.11 A multigroup neutron energy partitioning scheme.

calculating the reaction rates for each energy group. The sum of the reaction rates from all of the energy groups then becomes the total reaction rate. Today, cross section libraries with up to 50 energy groups are common, and some people have attempted to create cross section libraries with as many as 2000 energy groups. The objective of these libraries is to be able to predict the neutron energy spectrum with enough accuracy so that the reaction rates can be calculated with more accuracy as well. In reactor design today, computer programs are normally written to perform this work with great precision and speed. We will discuss how these programs work in the next chapter.

4.10 Fission Cross Sections for Neutrons Having Any Kinetic Energy

When it comes to fission cross sections, there is a considerable difference between the behavior of *fissile materials* (which have odd atomic numbers) and *fertile materials* (which have even ones). This difference is often overlooked in cursory discussions of the subject, but it is extremely relevant to how the nuclear fuels in a reactor perform. For *fissile materials*, like U-233, U-235, and Pu-239, the fission cross sections tend to have a 1/v shape in the thermal energy range (where v is the velocity of the neutron) and are usually quite large (500–1000 barns) for popular nuclear fuels. In Chapter 5, we will learn that these materials are called *1/v absorbers*.

Above the thermal energy range (E > 1 eV), large narrow *resonances* begin to develop in most cross sections, and these resonances can continue to persist for some time. Most of these resonances decrease in height and widen in the keV range (due to a number of competing factors) until they eventually disappear above about 10 keV when the fission cross sections fall below a couple of barns. In the high keV and MeV energy ranges, the fission cross sections show only a slight reduction in their value with increasing values of the neutron energy. At very high energies, their fission cross sections usually have values of only a couple of barns. *Fertile* isotopes, on the other hand (those with *even atomic numbers* like U-238, Pu-240, and Th-232), have fission cross sections that behave in an entirely different way. These fertile isotopes have very small fission cross sections in the thermal energy range, and these cross sections become almost negligible at much higher neutron energies. The fission cross sections for both fissile and fertile materials are shown in Figures 4.12 and 4.13. As a rule of thumb, fissile materials normally have fission cross sections that are 10–100 times larger than fertile materials do.

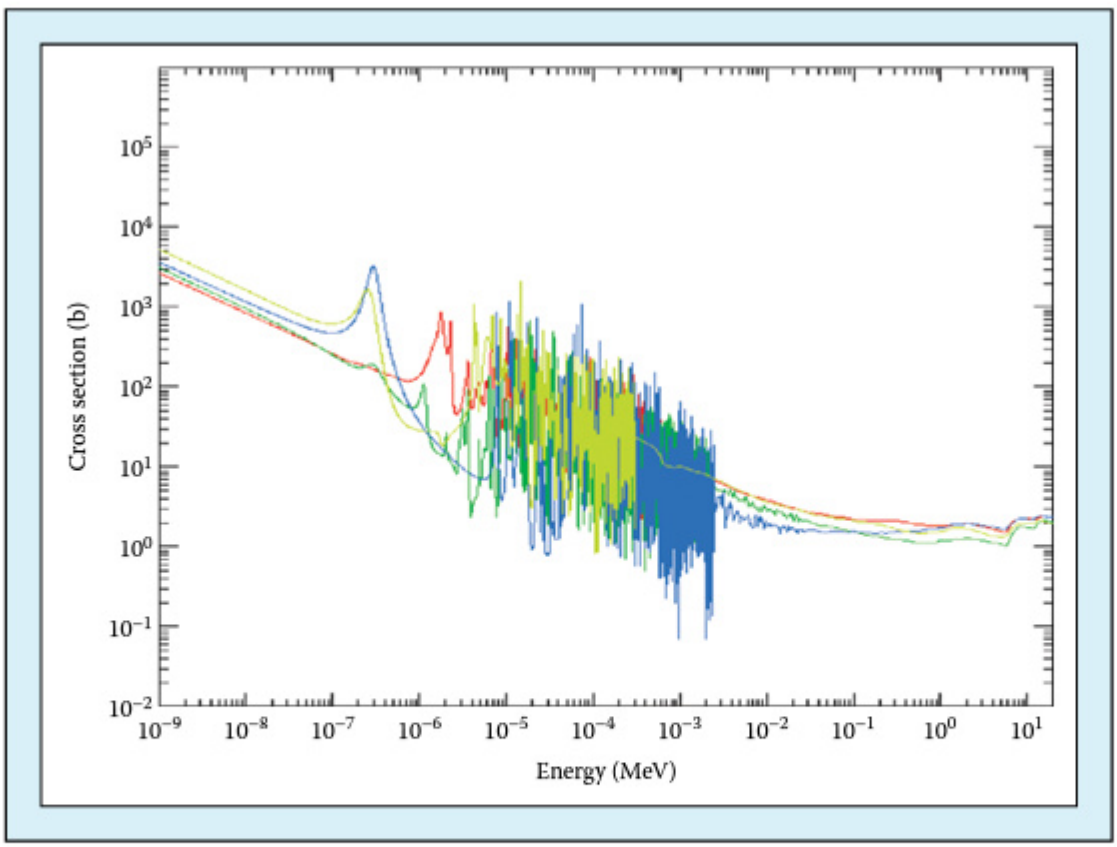

FIGURE 4.12 Fission cross sections for the fissile elements—Uranium-233 (red), Uranium-235 (green), Plutonium-239 (blue), and Plutonium-241 (light green).

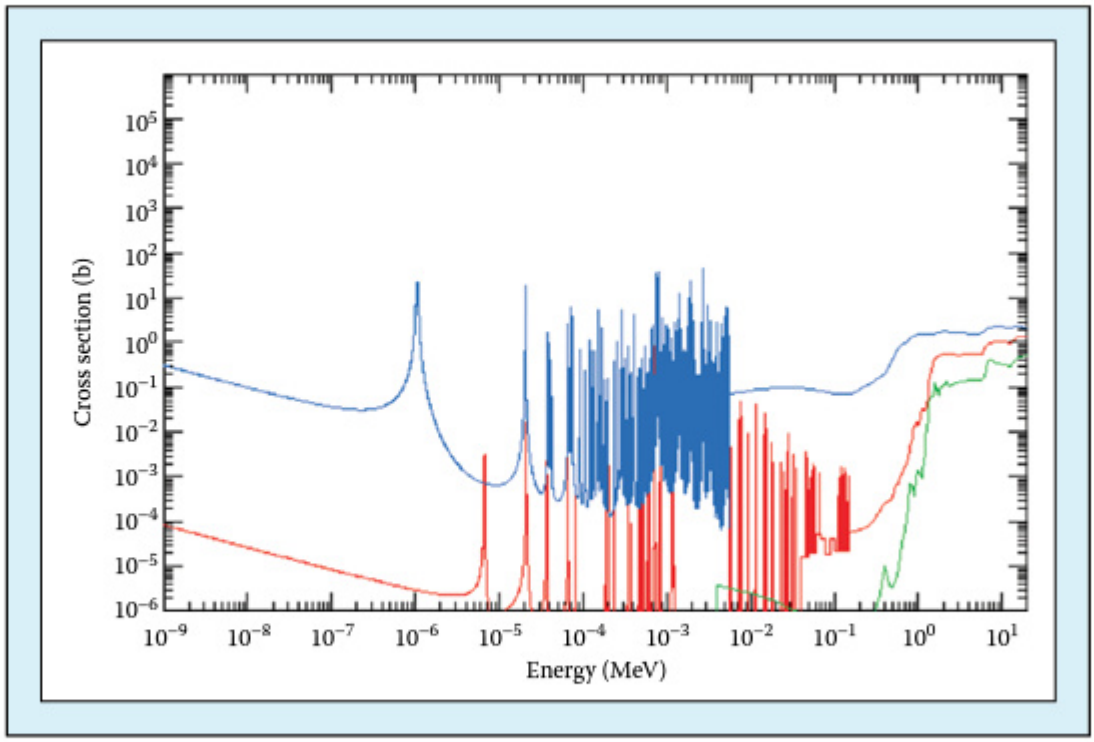

FIGURE 4.13 Fission cross sections for Uranium-238 (red), Plutonium-240 (blue), and Thorium-232 (green).

4.11 Absorption Cross Sections for Neutrons Having Any Energy

As we mentioned previously, the absorption cross sections for many elements tend to fall off as 1/v at low neutron energies (say E < 2 eV). In particular, many nuclear materials and heavy isotopes exhibit this behavior. Because the kinetic energy of a neutron is proportional to the *square* of its velocity, this is equivalent to saying that the absorption cross sections tend to fall off as $1/\sqrt{(E)}$, at low (E < 2 eV) neutron energies. That is, if σ_{at} is the value of the thermal absorption cross section for an isotope at 0.025 eV, then the thermal absorption cross section at any energy below 2 eV is given by

The Energy-Dependent Cross Section for a 1/v Absorber

$$\sigma_a(E) = \frac{\sqrt{(0.025)}}{\sqrt{(E)}\sigma_{at}} \tag{4.29}$$

This happens to be a very important equation if one happens to know the absorption cross sections at 0.025 eV. Light elements can exhibit this *1/v behavior* as well. For some light elements, this 1/v behavior can continue up to very high neutron energies because these elements do not have the absorption resonances that are typical of heavy materials like U-238. Hydrogen and deuterium are two common examples of materials that exhibit this particular behavior. However, for heavy and intermediate elements, the absorption cross sections start to oscillate wildly just above the thermal energy range. These oscillations, or *resonance peaks*, are associated with the existence of metastable energy levels in the nucleus of the atom. The reader may recall from our earlier discussion that these absorption or scattering resonances are caused by the creation of a *compound nucleus* in which the incoming neutron and the target nucleus coalesce into a single excited nucleus for a brief period of time. We will not get into the details of why these metastable energy levels exist, except to say that even the nucleus has some energy states and orbital configurations where it is more receptive to absorbing a neutron than others. Whenever the incoming neutron has exactly enough energy to correspond to one of these excited states, the probability of compound nucleus formation and therefore the probability of creating an absorption resonance are much higher. At higher energies, these resonances eventually begin to damp themselves out, and the curves for the absorption cross sections tend to become continuous again. Eventually, "normal" smooth cross section behavior is again restored.

4.12 Radiative Capture

In practice, it is very common for a nucleus to capture a neutron, and then after a brief period of time, to retain the neutron by emitting one or two photons in its place. Many nuclear processes involving the absorption of a free neutron will lead to the emission of gamma ray and an increase in the atomic weight of the target nucleus that is roughly equal to the mass of the neutron that has been absorbed. For example, a common isotope of iron, Fe-56, whose cross sections are shown in Figure 4.14, can create a compound nucleus by absorbing a neutron to create another isotope of iron called Fe-57. The new nucleus can then become stable again by emitting a high-energy photon, or *gamma ray*. This process, which is called *radiative capture*, is illustrated by the following example:

The Radiative Capture Process

$$\text{Fe-56} + \text{n} \rightarrow \text{Fe-57}^* \rightarrow \text{Fe-57} + \gamma \qquad (4.30)$$

radiative capture

Here, the asterisk* represents the excited Iron-57 nucleus and γ is the symbol for the gamma ray. The radiative capture cross section $\sigma\gamma$ for this type of reaction can be divided into roughly three distinct regions that are a function of the energy E of the incident neutron. These regions correspond roughly to the *thermal energy region* (region I), an *epithermal or resonance energy region* (region II), and an energy region above the resonance region that is called the *fast region*, or region III. In the first and lowest energy region, the radiative capture cross section $\sigma\gamma$ varies as 1/v, or $1/\sqrt{E}$, where v and E are the neutron velocity and the neutron energy, respectively. In some textbooks, this is known as the *1/v region*. Materials that possess this behavior are called 1/v absorbers, and those that do not exhibit this behavior are called non-1/v absorbers. If the radiative capture cross section is plotted on a *logarithmic scale*, as most cross sections are, then a 1/v absorber will have a cross section that is a straight line with a *slope of –1/2*. This can be seen in Figure 4.15 in which the 1/v region and the first absorption resonance are shown for U-233.

Most nuclei exhibit a 1/v behavior in this region. Two notable exceptions to this rule are Xenon-135, which is an important neutron absorber, and Samarium-149, which is also an important non-1/v absorber. As we will see in subsequent chapters, both these materials play an important role in determining the time-dependent behavior of a reactor. Beyond the 1/v region, there is a region that is sometimes dominated by compound nucleus formation. Here, many absorption resonances can develop. At the lower end of this second energy range, the absorption resonances are initially separate and distinct from one another. However, as the neutron energy increases, the resonances begin to crowd together and overlap to the extent that they can no longer be individually resolved. Then, the radiative capture cross section

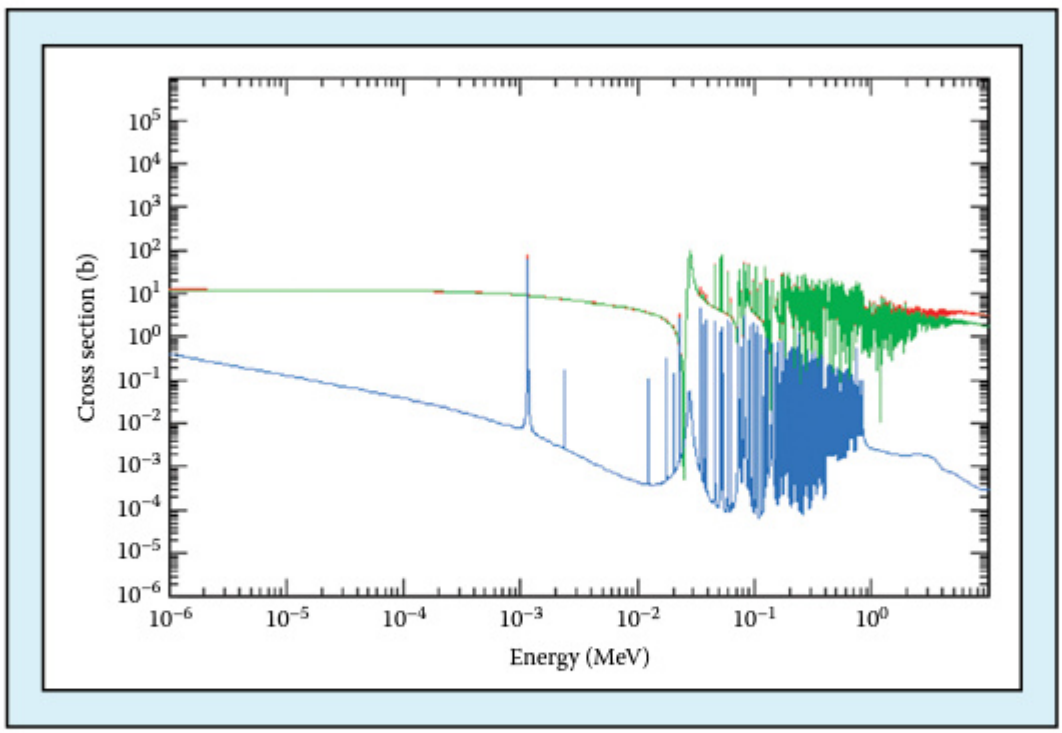

FIGURE 4.14 Neutron interaction cross sections for the element Iron-56. The scattering resonances above 1 keV are shown in green, and the resonances due to radiative capture are shown in blue. Notice how narrow most of the individual resonances are.

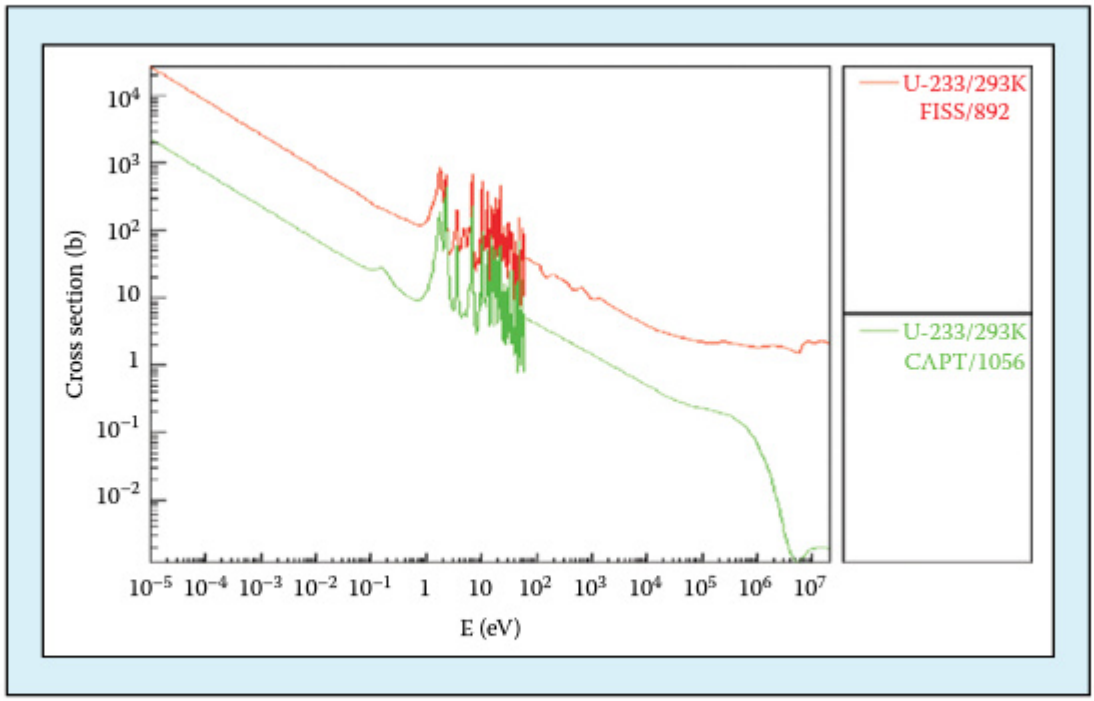

FIGURE 4.15 The capture and fission cross sections for Uranium-233 at room temperature (293°K) as drawn by ENDFPLOT.

becomes a smooth function of the neutron energy again. Hence capture cross sections tend to behave in a similar way to fission cross sections as the energy of the incident neutron is raised.

4.13 Scattering Cross Sections for Neutrons with Any Kinetic Energy

Compared to the fission and absorption cross sections we discussed in earlier sections, scattering cross sections (at least for the neutrons in a reactor core) are a relatively boring affair. However, they still deserve some attention because of their ability to take fast neutrons, and through a series of successive collisions, turn them into slow neutrons, or "thermal" ones. In multigroup theory, scattering cross sections between energy groups are usually written as $\Sigma_{gg'}$, where the higher energy group is g and the lower energy group is g′. In other words, Σ_{12} refers to the scattering cross section from energy group 1 to energy group 2, and Σ_{23} refers to the scattering cross section from energy group 2 to energy group 3. Whenever $g' \geq g$, a group scattering cross section will have a finite value. This is because "down scattering" (e.g., scattering from a higher energy group) to a lower energy group is always allowed. Similarly, scattering within the same group ($g' = g$) is allowed as well. The only time $\Sigma'_{gg} = 0$ is when $g' < g$. In general, only the cross sections for "up scattering" between groups are zero. This nomenclature remains consistent no matter how many energy groups are used to represent the neutron energy spectrum. An example of how multigroup scattering works is shown in Figure 4.16. The scattering cross sections for most elements interacting with low-energy neutrons are relatively small (between 10 and 100 barns), and they remain relatively constant as a function of the incident neutron energy E (see Figure 4.17). The scattering process is usually elastic, and it is very similar to a collection of billiard balls of different sizes and velocities bouncing around on a billiard table.

The one significant exception to this rule is the scattering cross section for hydrogen in a water molecule. This cross section can rise dramatically at low energies rather than remaining constant. Like the radiative capture cross section, the scattering of a neutron can be conceptually subdivided into three separate regions that depend on the energy E of the incident neutron. In the first and lowest energy region, the scattering cross sections are small and almost constant. The scattering in this region does not occur through compound nucleus formation, and the neutrons are scattered elastically by simply bouncing off of the surface of the nucleus rather than being absorbed by it. This form of scattering, in which the neutron simply bounces off of the surface of the nucleus—as in a collision between two billiard balls—is known as *potential scattering*, and it can also occur when the nucleus is bombarded by an incoming proton as well. The cross section for the *elastic scattering* in this region is given by

The Cross Section for Potential Scattering

$$\sigma_s = \pi D^2/4 \quad \text{(for potential scattering)} \tag{4.31}$$

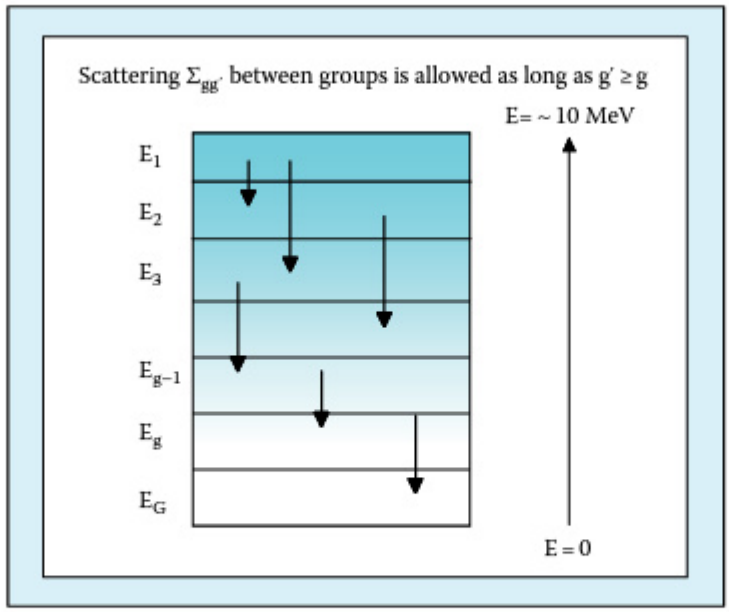

FIGURE 4.16 An example of multigroup scattering.

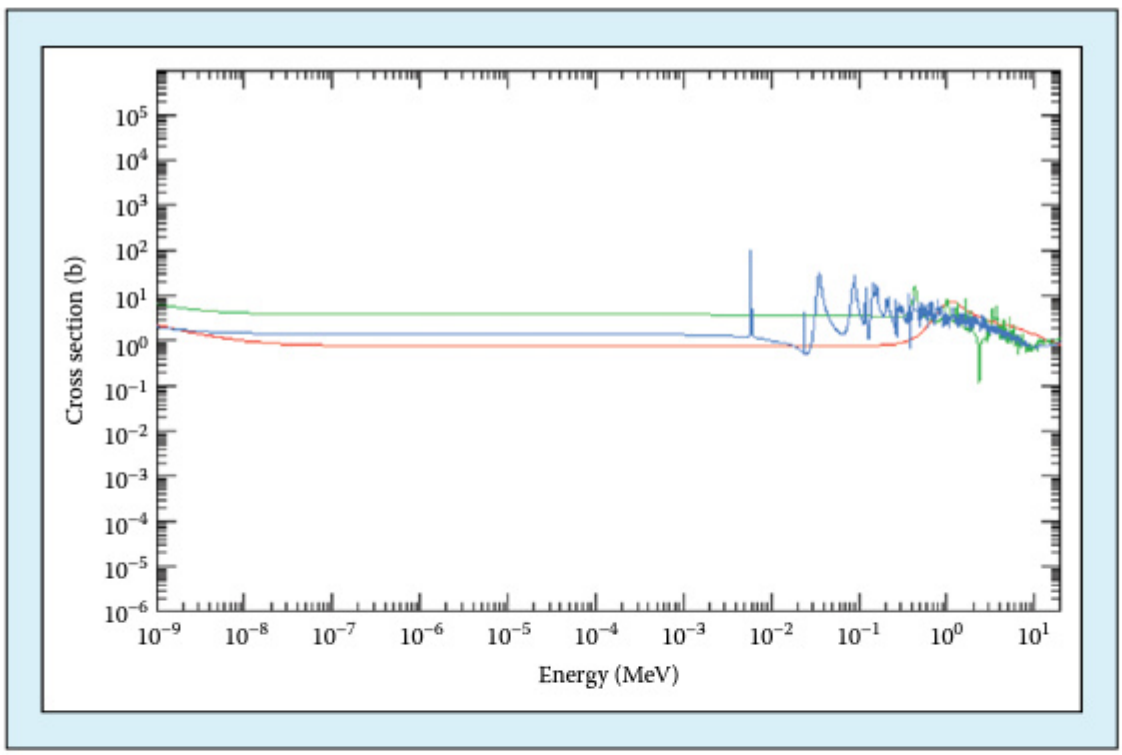

FIGURE 4.17 Scattering cross sections for some light elements such as helium (red), oxygen (green), and aluminum (blue).

where D is the radius of the target nucleus. Notice that it is theoretically possible to estimate the diameter of the target nucleus from this equation if the elastic scattering cross section σ_s is known. Just above the potential scattering region, scattering resonances begin to develop due to compound nucleus formation. Scattering in this region can be either *elastic or inelastic*. When an *inelastic scattering* event occurs, the nucleus decides to keep some of the energy of the incoming neutron, which it may later emit in the form of an energetic photon γ, and so *linear momentum* is no longer conserved. Just as in the case of the absorption resonances, the scattering resonances are initially several electron volts wide, but as the neutron energy increases, they begin to overlap and a point is eventually reached where it is no longer possible to

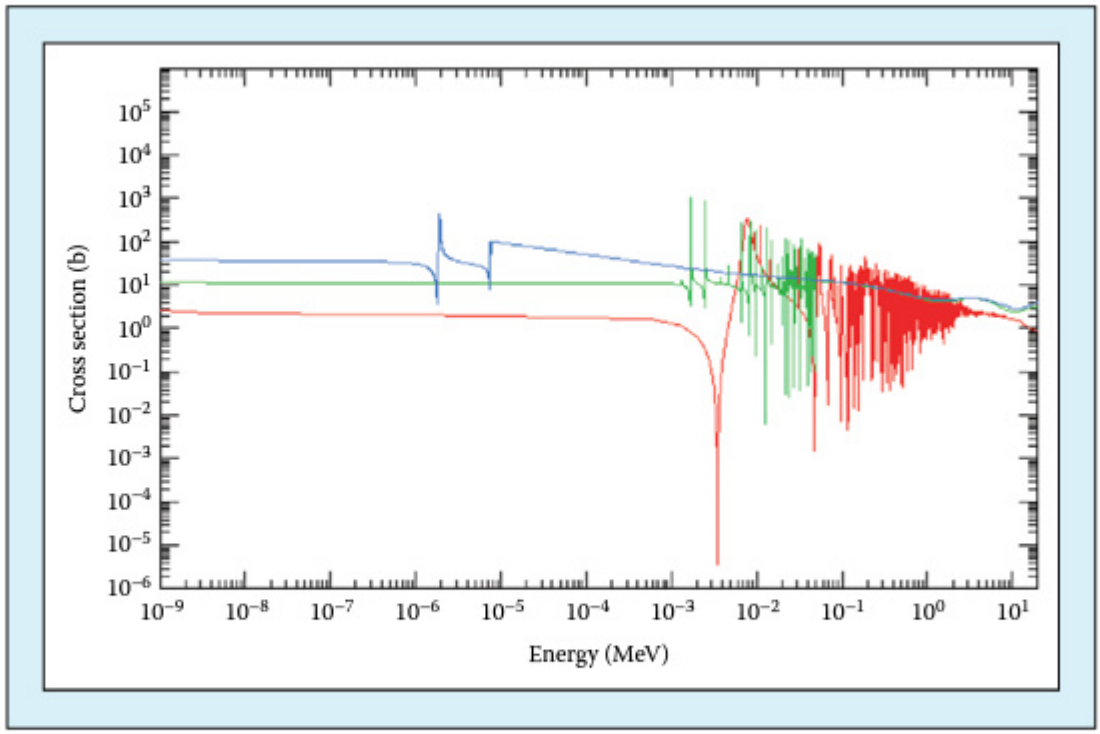

FIGURE 4.18 Scattering cross sections for some heavy elements such as Iron-54 (red), Lead-204 (green), and Thorium-228 (blue). (This picture was created with ENDFPLOT, which we will discuss in Chapter 5.)

distinguish one scattering resonance from the next. Finally, at very high energies, these resonances disappear completely, and the scattering cross sections again become very smooth and predictable.

When dealing with elements of a light and intermediate atomic weight (helium, oxygen, aluminum, etc.), scattering cross sections can remain relatively constant up to neutron energies of a couple of keV. There small resonances can develop, but they gradually become lower and broader as the energy level is increased. In heavy elements (see Figure 4.18), there are simply more ways for a neutron to be scattered. As a result, the scattering cross sections for many heavy elements have scattering resonances that can develop over a wider energy range. In some heavy elements, these resonances can start at incident neutron energies just above one electron volt. The scattering resonances in Thorium-228 are one such example of this behavior. Hence it should be clear that the energy of a neutron has a profound effect on its reaction rate. In order to successfully design, build, and operate a nuclear reactor, neutron cross sections have to be known with a high degree of accuracy. Today, accurate values of almost every known neutron cross section have been compiled into a few large electronic libraries that are available to the nuclear and scientific community. We will briefly touch on the largest and most famous of these libraries in the next chapter.

Example Problem 4.7

A material has a one-group macroscopic scattering cross section Σ_s of 0.10 cm^{-1} and a one-group macroscopic absorption cross section Σ_a of 0.40 cm^{-1}. What is the probability that a neutron will be absorbed when passing through a sample of this material?

Solution By definition, $\Sigma_a/(\Sigma_a + \Sigma_s)$ is the probability that a neutron will be absorbed by this material. Since $\Sigma_s = 0.10$ and $\Sigma_a = 0.40$, there is a 0.4/0.5 = 80% chance that the neutron will be absorbed and there is a 20% chance that it will be scattered. [Ans.]

4.14 Nuclear Properties of Hydrogen and Deuterium

Some lighter isotopes (notably *hydrogen* and *deuterium*) are used in certain types of reactors in very large quantities. Because they are very simple, their nuclei tend to interact with neutrons in a simpler way than many of the other materials that we have discussed. The hydrogen nucleus consists of only a single proton and the deuterium nucleus consists

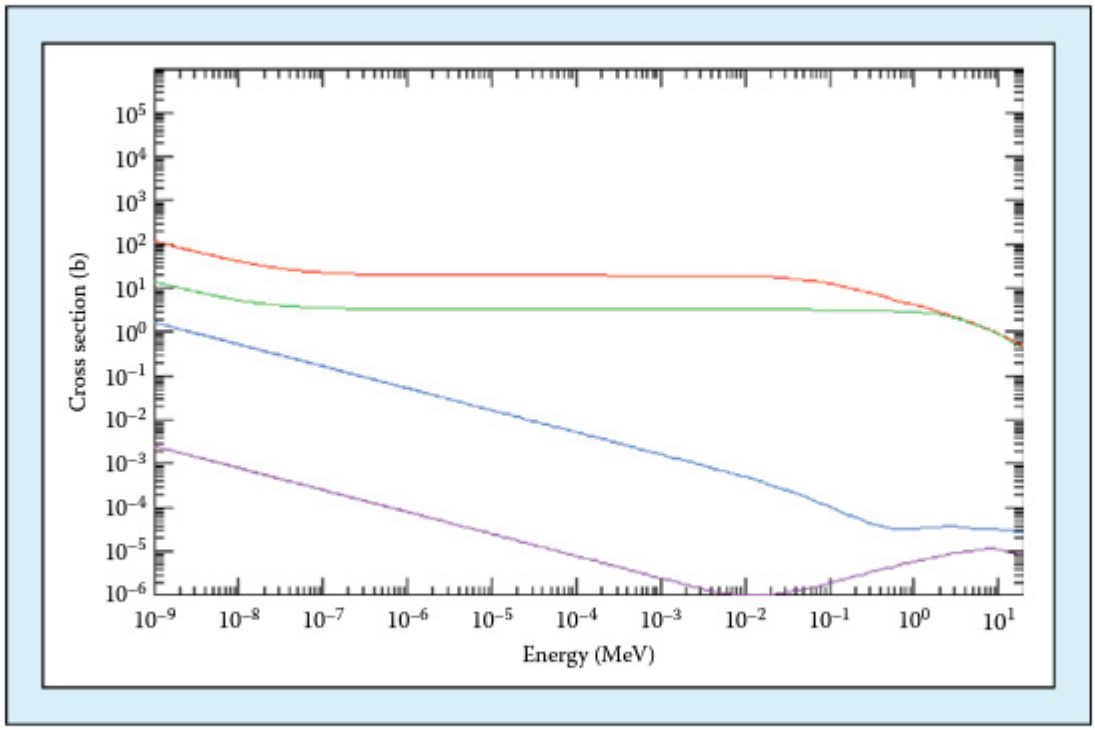

FIGURE 4.19 Elastic scattering cross sections of hydrogen and deuterium (shown in red and green) and their radiative capture cross sections (shown in blue and purple). Note the 1/v behavior of the capture process.

of just a proton and a neutron. *As a result of this simplicity, a neutron interacting with either a hydrogen or deuterium atom will not form a compound nucleus*. Consequently, hydrogen and deuterium do *not* have any scattering or absorption resonances in their nuclear cross sections.

Their scattering cross sections are essentially constant from thermal energies to about 10 keV (see Figure 4.19), and their radiative capture cross sections are pure 1/v at all energies. Compared to heavier materials, the nuclei of hydrogen and deuterium have no excited states, and so there can be no inelastic scattering at any neutron energy E. This can also be seen in any of the ENDF/B libraries, which we will formally present in Chapter 5.

Example Problem 4.8

Find the diameter of a deuterium nucleus from the elastic scattering data shown in Figure 4.19.

Solution From Figure 4.19, it can be seen that the elastic scattering cross section for deuterium (shown in green) is about 6 barns in the thermal energy range. Since there are no scattering resonances in this region, it can be assumed that there is no compound nucleus formation and that the only scattering that can occur is potential scattering. In this case, the diameter of the nucleus can be found from $D = \sqrt{(4\sigma_s/\pi)}$, so $D = \sqrt{4\times\left(6\times10^{-24}/\pi\right)} \approx 4.9\times10^{-12}$ cm. This result is representative of the diameter of a small and simple nucleus near the top of the periodic table (see Chapter 6 for more details). [Ans.]

4.15 Methods for Estimating the Total Cross Section

As we discussed earlier, the *total cross section* for a material is defined as the sum of the cross sections for all possible reactions a nuclear particle can participate in. In reactions involving the formation of a compound nucleus, the total cross section can consist of the sum of the cross sections of 40 or 50 different reaction types. However, many of these reaction types have a very low probability of occurrence, and in practice, it is possible to represent the total cross section as the sum of just the most important processes; namely,

The Definition of the Total Cross Section

$$\sigma_t = \sigma_s + \sigma_a = \sigma_{se} + \sigma_{si} + \sigma_\gamma + \sigma_r + \sigma_f \tag{4.32}$$

where σ_γ is the cross section for radiative capture, σ_r is the total cross section for resonance capture, and σ_{se} and σ_{si} are the cross sections for elastic and inelastic scattering. In most elements, the fission cross section σ_f is zero, and so the variation of σ_t with energy depends upon only how σ_s, σ_r, and σ_γ behave with E. At low energies (beneath the range of the absorption resonances), it is therefore easy to see that σ_t is given by

The Total Cross Section beneath the Absorption Resonances

$$\sigma_t(E) = \left(\frac{\pi}{4}\right)D^2 + \frac{C}{\sqrt{E}} \tag{4.33}$$

where

C is a constant that is isotope specific
D is the diameter of the atomic nucleus
E is the energy of the incident neutron

In this case, it is interesting to observe that the expression for $\sigma_t(E)$ consists of only two parts—the first part being due to the *elastic scattering* of the neutron due to potential scattering effects and the second part being due to the *radiative capture* of the incoming neutron in the 1/v region (which is proportional to the inverse square root of the neutron energy). If the first part is much larger than the second, then the total cross section is constant at low energies and is dominated primarily by *potential scattering*. Conversely, if the second part is much larger than the first, then the material is a 1/v absorber below the resonance energy range and the potential scattering process is less important. When the contributions from the absorption and scattering resonances are added back in, the term σ_r can dominate the behavior up to a couple of keV. Then, σ_t will become smooth again, and the total cross section will only change gradually as the total neutron energy is increased. In Chapter 2, we learned that the diameter D of an atomic nucleus can be estimated to some degree of accuracy from the equation

Diameter of the Atomic Nucleus

$$D = 2.5\,A^{1/3} \times 10^{-13}\ \text{cm} \tag{4.34}$$

where *A is the atomic mass number* or the total number of protons and neutrons (A = Z + N) that the nucleus contains. It therefore follows that Carbon-12 (with an atomic mass number of 12) has a nuclear diameter of about $D = 2.5 \times (12)^{1/3} = 4.75 \times 10^{-13}$ cm, while a heavy nucleus like U-238 has a diameter of about $D = 2.5 \times (238)^{1/3} = 1.5 \times 10^{-12}$ cm. The diameters of several common atomic nuclei are shown in Table 4.1. Isotopes of chromium, nickel, copper, and zinc, which have an atomic mass number of 64, have a nuclear diameter of exactly 1×10^{-12} cm. This corresponds to a cross-sectional area for the nucleus of $\pi/4 \times 10^{-24}$ cm^2, or just about 1 barn.

TABLE 4.1
Diameters (in cm) of Several Common Atomic Nuclei

Element	Symbol	Atomic Weight	$A^{1/3}$	D ($\times 10^{-12}$ cm)
Hydrogen	H	1	1	0.25
Carbon	C	12	2.3	0.55
Oxygen	O	16	2.5	0.62
Aluminum	Al	27	3.0	0.75
Iron	Fe	56	3.8	0.95
Copper	Cu	64	4.0	1.00
Zirconium	Zr	91	4.4	1.10
Silver	Ag	108	4.7	1.18
Gold	Au	197	4.7	1.42
Thorium	Th	232	6.0	1.50
Uranium	U	238	6.1	1.52

Source: Wikipedia—see *https://en.wikipedia.org/wiki/Atomic_radius*.

With this in mind, it is easy to see that the total microscopic cross section at low energies, just beneath the range of the absorption resonances, is given by

The Total Cross Section beneath the Absorption Resonances

$$\sigma_t(E) = 6.25\pi A^{2/3} + \frac{C}{\sqrt{E}} \tag{4.35}$$

where

C is a constant that is isotope specific
A is the atomic mass number
E is the energy of the incident neutron

Notice that the value of $A^{2/3}$ that appears here is similar in form to the surface area term that appears in the *semiempirical mass formula*, which we will discuss in Chapter 6. The semiempirical mass formula can used to determine the rest mass of a nucleus from the number of protons and neutrons it contains.

4.16 Converting Microscopic Cross Sections to Macroscopic Ones

Sometimes, the microscopic cross section for a nuclear material is available, and we would like to use it to calculate the macroscopic cross section. Because *the microscopic cross section represents the reaction probability for just a single atom*, we need to know how many atoms there are in a specific material since the macroscopic cross section enables us to determine the reaction rate when more than one atom or nucleus is involved. Many years ago, chemical engineers established a direct relationship between the weight of a material in grams, its molecular weight M (which depends upon its atomic structure), and the number of atoms or molecules it contains. This was based upon the use of a quantity that has become known today in the science of chemistry and physics as *the mole*. In the sections that follow, we would like to discuss the mole and how it is used today in many important branches of nuclear science and engineering to help convert microscopic cross sections into macroscopic ones.

4.17 A Brief Chemical Primer

The *mole* is a unit of *chemical measurement* that allows one to calculate the number of atoms (or molecules) of a material that are contained within a sample of a known physical weight and molecular composition. It is one of the basic units in the *International System of Measurement*, and for many years it has been referred to scientifically by the symbol of "mol." Hence, 5 moles of a material is written as 5 mol, whereas 1.5 moles of a material is written as 1.5 mol. The name mole was originally derived from the German unit of measurement called the *Mol*, which in turn was derived from the German word *Molekül* (or molecule). The modern usage of the term was first introduced to the field of chemistry by the German chemist *Wilhelm Ostwald* around 1894. His picture is shown in Figure 4.20. The mole is defined as the amount of a substance that contains as many elementary *entities* (which can be either atoms, molecules, ions, or electrons) as there are atoms in 12 g of the isotope Carbon-12. *In other words, when we apply this definition, we see that 1 mol of pure Carbon-12 weighs exactly 12 g*.

The experimentally determined value of the number of atoms or molecules in 1 mol of a material was originally believed to be $6.02214179 \times 10^{23}$ atoms or molecules/mol. Recent measurements now set this value at $6.02214078 \times 10^{23}$ atoms or molecules, which is recognized as the exact value of *Avogadro's number* A_o today. The current definition of the mole was approved for general use by the International Standards Organization (or the ISO) in 1964. Earlier definitions had been based on the atomic mass of hydrogen (about 1 g of Hydrogen-1 gas, excluding its heavy isotopes), the atomic weight of oxygen, and the relative atomic mass of Oxygen-16. It turned out that these four different definitions were equivalent to one another to within an absolute accuracy of about 1%. However, the version based upon the use of Carbon-12 is acknowledged as the most widely accepted version of the standard today. *Hence, Avogadro's number of $A_o = 6.02214078 \times 1023$ atoms, molecules, ions, or electrons per mole is now quoted in terms of this slightly more accurate value*.

According to this definition, a mole of a pure substance has a mass in grams exactly equal to that substance's molecular weight M or atomic mass A; for example, 1 mol of Calcium-40 has an approximate weight of 40 g because Ca-40 has a mass of 39.9625906 AMU on the C-12 scale. In other words, the numerical value of a substance's molecular or atomic weight in atomic mass units is the same as that of its molar mass—the mass of 1 mol of that substance—in grams. For example, 1 mol of NH_3 has 6.022×10^{23} *molecules* and weighs about 17 g, 1 mol of copper has 6.022×10^{23} *atoms* and weighs about 63.54 g, and 1 mol of uranium dioxide (UO_2) has 6.022×10^{23} *molecules* and weighs about

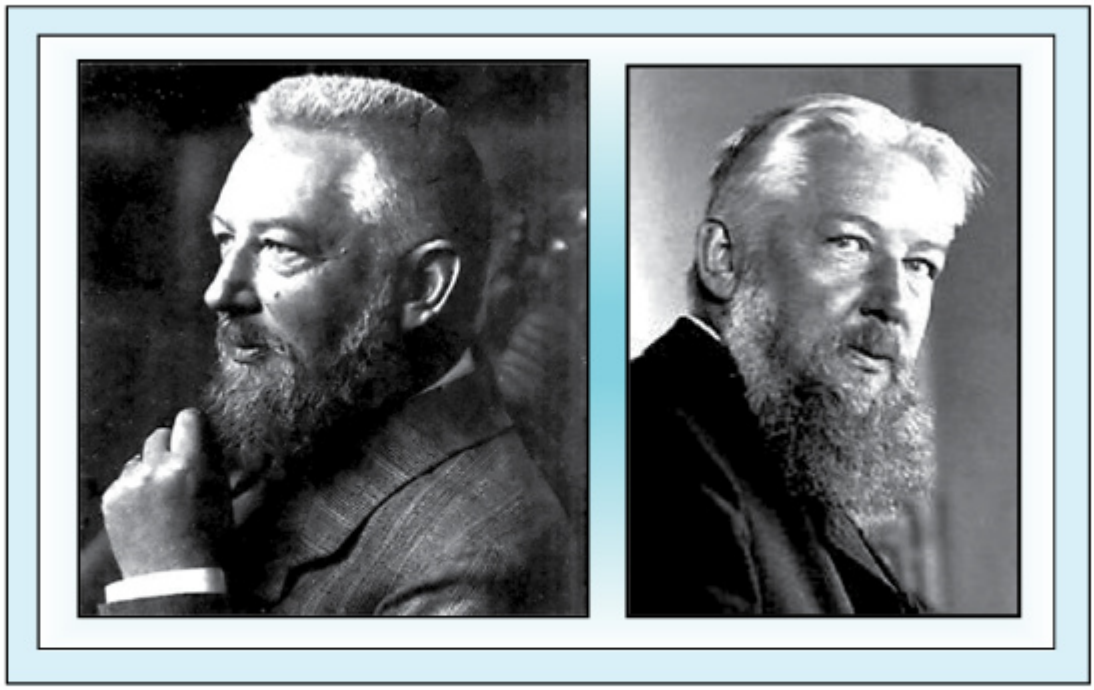

FIGURE 4.20 Friedrich Wilhelm Ostwald, the inventor of what is known today as the mole, was a German chemist. He received the Nobel Prize in Chemistry in 1909 for his work on catalysis, chemical equilibrium, and reaction velocities. He was also a professor at Harvard University for about a year. (Pictures provided by Google Images.)

$(238 + 2 \times 16) = 270$ g. Conversely, 12 g of pure carbon (C), 18 g of water (H_2O), and 44 g of carbon dioxide (CO_2), etc., all contain exactly the same number of particles—6.022×10^{23} particles, which corresponds to the constant represented by Avogadro's constant A_o. In other textbooks, Avogadro's number is also represented by the symbol A′. Nevertheless, the meaning of these two symbols is exactly the same.

4.18 A Practical Example of a Cross Section Calculation

The aforementioned relationship makes it relatively easy to find the number of atoms that there are in a gram of a material if we know its molecular weight M. We simply calculate the number of molecules that there are in a gram and then multiply by the number of atoms per molecule. For example, if 1 g of water (H_2O) has $A_o/M = 1/18 \times A_o$ molecules in it, then 1 g of water will have $1/18 \times A_o$ atoms of oxygen and $1/9 \times A_o$ atoms of hydrogen. Irrespective of the complexity of the underlying substance, the same basic equation always applies. This makes it easy to find the number of atoms that are needed to calculate the macroscopic cross section of nuclear materials and hence the nuclear reaction rate R. It is possible to express what we have just said as a simple equation that relates the number of atoms or molecules in 1 g of a material to the weight of the material itself. We simply calculate the number of atoms or molecules per gram, which is given by

The Number of Atoms or Molecules per Gram

$$N = \frac{A_o}{M} \tag{4.36}$$

and then multiply by the physical density ρ to get the number of atoms or molecules per cubic centimeter. Knowing the molecular structure, it is then a simple matter to determine the number of individual atoms that a specific volume of the material will contain. If we are dealing with a material that is made up of only *a single* isotope or element, then the total number of atoms N per cubic centimeter of that material is given by

The Number of Atoms per Cubic Centimeter

$$N = \frac{\rho A_o}{M} \tag{4.37}$$

where

ρ is the physical density of the material (in g/cm^3)

M is the *molecular weight* of a mole of the material (which is just the total number of protons and neutrons it contains)

A_o is Avogadro's number, which is equal to the number of atoms of the material in a mole, or $A_o = 6.022 \times 10^{23}$ atoms/mol

In other words, if we know what the density ρ of a material is, we can multiply its physical density by Avogadro's number and divide by the molecular weight M to find the number of atoms it has.

4.19 Finding the Cross Sections for a Pure Material

It is important to bear in mind that Equation 4.37 only works for *pure materials* that contain only a single isotope. For materials like this, the macroscopic cross section for scattering is given by $\Sigma_s = N\sigma_s$, and the macroscopic cross section for absorption is given by $\Sigma_a = N\sigma_a$. We can illustrate how both macroscopic cross sections can be found by considering some typical materials such as hydrogen and carbon. In the case of hydrogen, we know that M = 1, and $A_o = 6.022 \times 10^{23}$ atoms/mol, so the number of hydrogen atoms in a cubic centimeter of hydrogen gas is

$$N_H = \rho_H \cdot 6.022 \times 10^{23}$$

Similarly, for a material like pure carbon, which has a molecular weight of 12, we know that M = 12, and $A_o = 6.022 \times 10^{23}$ atoms/mol, so the number of carbon atoms in a cubic centimeter of Carbon-12 is

$$N_C = \rho_C \cdot 0.501 \times 10^{23}$$

If we know the microscopic absorption and scattering cross sections for Carbon-12, which are $\sigma_a = 0.669$ barns and $\sigma_s = 66.97$ barns, respectively, in the thermal energy range then the macroscopic absorption and scattering cross sections for Carbon-12 are

$$\Sigma_a = N_C\sigma_a = 0.501 \times 10^{23}/\text{cm}^3 \times 0.669 \times 10^{-24}\ \text{cm}^2 = 0.033\ \text{cm}^{-1} \quad (\text{for absorption})$$

$$\Sigma_s = N_C\sigma_s = 0.501 \times 10^{23}/\text{cm}^3 \times 66.97 \times 10^{-24}\ \text{cm}^2 = 0.33\ \text{cm}^{-1} \quad (\text{for scattering})$$

where 1 barn = 10^{-24} cm^2. Hence thermal neutrons interacting with carbon atoms are ten times more likely to be scattered than to be absorbed. It should be noted here that a carbon atom cannot fission, so $\sigma_f = 0$ and $\sigma_a = \sigma_c + \sigma_f = \sigma_c$. This same approach can be used to find the macroscopic cross section for *any* pure substance as long as we know its molecular weight M. It does not matter whether the substance is a liquid, a solid, or a gas. It should also be obvious that we can use the same principle in reverse to calculate the microscopic cross section if we know what the macroscopic cross section is since the microscopic cross section in barns can be found for any reaction type × by simply dividing by the macroscopic cross section for that reaction type. In other words,

Converting a Macroscopic Cross Section to a Microscopic Cross Section

$$\sigma_x = \frac{\Sigma_x}{N} \tag{4.38}$$

or, more explicitly,

$$\sigma_x = \frac{M\Sigma_x}{\rho A_o} \tag{4.39}$$

where ρ is the physical density and x is the reaction type (c, f, a, or s).

Equation 4.39 turns out to be a very powerful relationship that can be used to convert a microscopic cross section to a macroscopic one (or vice versa). It does not matter whether the material is a solid, a liquid, or a gas. The value of x

can refer to a fission reaction, in which case x = f, a scattering reaction, in which case x = s, or an absorption reaction, in which case x = a. Thus the total macroscopic cross section Σ_t can be expressed as the sum of the individual macroscopic cross sections, where t = f + s + a. This allows us to write

$$\Sigma_t = \Sigma_f + \Sigma_s + \Sigma_a \tag{4.40}$$

or more precisely

$$\Sigma_t = N\left(\sigma_f + \sigma_s + \sigma_a\right) \tag{4.41}$$

In some tabulations of nuclear cross section data, including a famous one provided by the *Brookhaven National Laboratory* (see Chapter 5), only the values of Σ_t and Σ_s or their microscopic counterparts are typically given. In this case, it can be *assumed* that $\Sigma_a = \Sigma_t - \Sigma_s$. This presentation works well, except when the isotopes of fissile materials like uranium and plutonium are involved in which case $\Sigma_f \neq 0$ and $\Sigma_a = \Sigma_f + \Sigma_c$.

4.20 Relationship between the Physical Density and the Atomic Density

In future sections of this book, we will be asked to convert the *physical density* of a material (in g/cm^3) into the number of atoms there are in 1 cm^3 of the material (the *atomic density*), and we will have to be able to convert the number of the atoms N in a cubic centimeter (or 1/cm^3) of the material into a physical density ρ. In the previous section, we introduced the equation

Converting the Physical Density to the Atomic Density

$$N = \frac{\rho A_o}{M} \tag{4.42}$$

to help us convert the physical density into the atomic density. Here, ρ is the density of the material (in g/cm^3), M is the molecular weight of a mole of the material (which is just the total number of protons and neutrons), and A_o is an empirical constant called Avogadro's number, which is equal to the number of atoms of the material in a mole, or $A_o = 6.022 \times 10^{23}$ atoms/mol. Equation 4.42 is more than just a simple way to convert microscopic cross sections into macroscopic ones. In fact, it is the fundamental link between the *physical density* of a material ρ (which we can measure because it has weight) and its *atomic density* N, which we cannot measure directly without a complex experiment. If we solve this equation for ρ, the fundamental relationship between the atomic density N and the physical density ρ is then

$$\rho = \frac{NM}{A_o} \tag{4.43}$$

where, as before, A_o is Avogadro's number and M is the molecular weight (which is just the number of protons and neutrons the material contains). In other words, if we know the atomic density of the material N (in atoms/cm^3), we can multiply the atomic density by the molecular weight M and divide by Avogadro's number A_o to find the physical density. Conversely, if we know the physical density ρ, we can multiply the physical density by Avogadro's number and divide it by the molecular weight M to find the number of atoms there are. Used in this way, Equation 4.43 is not only applicable to *any pure substance* but it is also applicable to composite materials like water (H_2O), which is used as a reactor coolant, and uranium dioxide (UO_2), from which most nuclear fuel pellets are made. We can illustrate how this process works with a couple of simple examples. Suppose that we know the atomic density N of three common materials that are used in a reactor core.

They are water (H_2O), graphite (C), which is a common neutron moderator, and natural uranium U fuel. Their atomic densities N_{H2O}, N_C, and N_U are shown in Table 4.2, as well as their molecular weights. Then how does one determine what a cubic centimeter of each of these materials weighs? We simply use the equations we have just presented to find them. When we do the math, we obtain the physical densities ρ_{H2O}, ρ_C, and ρ_U that are shown in Table 4.2. It is also worth noting that with the exception of some rare gases, the large exponents in Avogadro's number A_o and in the atomic density N almost always cancel each other out.

TABLE 4.2
Physical Densities and the Atomic Densities for Some Common Nuclear Materials

Name	Atomic Number (Z)	Chemical Symbol	Physical Density ρ (g/cm³)	Atomic Density N Atoms or Molecules per cm³ (×10²⁴)	Atomic or Molecular Weight[a] (Z + N)
Carbon	6	C	1.60	0.0802	12
Uranium	92	U	19.10	0.0483	238
Water (light)	—	H_2O	1.00	0.0334	18

[a] In practice, many elements have more than one isotope, and therefore the actual atomic or molecular weight will differ slightly from the whole numbers presented here. However, for many calculations, the amount of error introduced by using these whole numbers is negligible.

Example Problem 4.9

Suppose that the physical density ρ of uranium dioxide is 10 g/cm³. What is the atomic density N for this material?

Solution We know from Equation 4.42 that $N = \rho A_o/M$. Uranium dioxide has 1 uranium atom with an atomic weight of 238 and 2 oxygen atoms with an atomic weight of 16 each. Therefore, the total molecular weight of UO_2 is 238 + 2(16) = 270. Therefore, the atomic density for uranium dioxide is $N_{UO2} = 10 \times 6.022 \times 10^{23}/270 = 2.23 \times 10^{22}$ atoms/cm³. [Ans.]

4.21 Finding Macroscopic Cross Sections for a Complex Nuclear Material

In our previous discussion, we did not explain how we were able to determine the total number of atoms, ρ^j, of a particular element or isotope j in a material. Since this is an important thing to be able to do properly, we would now like to demonstrate how we can find the macroscopic scattering, absorption, and fission cross sections based on only the knowledge of a material's physical properties. The number of atoms in any material made up of more than one isotope (where j = 1 to N) can be quite laborious to calculate. However, if we know the *molecular weight* of the material and how many atoms there are per molecule (e.g., what the molecular composition is), then there is a useful relationship that we can use to obtain the answer. This relationship was first developed by chemists in the early 1800s to understand the atomic composition of liquids and gases. It is equally applicable to all of the materials that we use in nuclear reactors today. This relationship says that the number of atoms of any element j in a complex material or compound can be found from the equation

The Number of Atoms in a Complex Material

$$N^j = \frac{\rho A_o C^j}{M} \tag{4.44}$$

where

ρ is the physical density of the material (in g/cm³)
A_o is Avogadro's number = 6.022×10^{23} atoms/mol
M is the molecular weight (of a mole) of the material
C^j is the number of atoms of element or isotope j in one molecule of the material (or the atomic "count")
N is the number of atoms of element j per cubic centimeter (which is also known as the atomic material density)

Equation 4.44 relates the physical density of the material, ρ, the molecular weight of the material, M, and the molecular composition of the material, C, to the atomic density N_i of each element or isotope inside of it. We can illustrate how Equation 4.44 works with the following example.

Example 4.1

Suppose that we would like to apply Equation 4.44 to find the number of atoms of uranium and oxygen in a UO_2 (uranium dioxide) fuel pellet. These fuel pellets are used in many different types of reactors because of their chemical and physical stability. Suppose that we wish to find the number of atoms of uranium and oxygen in a pellet of enriched uranium. Most pellets like this contain uranium that is enriched to a concentration of about 4% U-235 and 96% U-238. Let us further

assume that every uranium atom is bonded to two oxygen atoms to produce a molecule of uranium dioxide (UO_2). We know that UO_2 has a molecular weight of 270 and a density of 10 g/cm^3. In other words, we know the following values for UO_2: $\rho = 10$ g/cm^3, $M = 270$, $A_o = 6.022 \times 10^{23}$ atoms/mol, and $C_{U\text{-}235} = 0.04$, $C_{U\text{-}238} = 0.96$, and $C_{O\text{-}16} = 2.0$. If we substitute these values into Equation 4.44, we obtain

- $N_{u235} = 0.223 \times 10^{23} \times 0.04 = 0.0089 \times 10^{23} = 8.9 \times 10^{20}$ atoms/cm^3
- $N_{u238} = 0.223 \times 10^{23} \times 0.96 = 0.2140 \times 10^{23} = 2.14 \times 10^{22}$ atoms/cm^3
- $N_{O16} = 0.223 \times 10^{23} \times 2.0 = 0.4460 \times 10^{23} = 4.46 \times 10^{22}$ atoms/cm^3

Thus these are the *number of atoms* that a neutron would "see" if it went through 1 cm^3 of UO_2. If the neutron was traveling at thermal energies (say where E ~ .025 eV), it would see a total microscopic cross section σ_t for U-238 of 4.6 barns, a σ_t for U-235 of 703 barns, and a σ_t for O-16 of 3.87 barns. (We will show you where these values came from in Chapter 5.) Therefore, continuing with the math, we would find that the total macroscopic cross sections for the U-235, U-238, and O-16 in a typical light water reactor fuel rod would be

- $\Sigma_{U235} = \sigma_{tU235} N_{u235} = 8.9 \times 10^{20}$ atoms/cm$^3 \times 703 \times 10^{-24}$ cm^2/atom $= 0.625$/cm
- $\Sigma_{U238} = \sigma_{tU238} N_{u238} = 2.14 \times 10^{22}$ atoms/cm$^3 \times .6 \times 10^{-24}$ cm^2/atom $= 0.248$/cm
- $\Sigma_{O16} = \sigma_{tO16} N_{O16} = 4.46 \times 10^{22}$ atoms/cm$^3 \times 3.87 \times 10^{-24}$ cm^2/atom $= 0.172$/cm

and their corresponding mean free paths would be

- $\lambda_{U235} = 1/\Sigma_{U235} = 1.6$ cm
- $\lambda_{U238} = 1/\Sigma_{U238} = 4.0$ cm
- $\lambda_{O16} = 1/\Sigma_{O16} = 4.8$ cm

This would mean that a "typical" neutron at thermal energies would have to travel an average distance of 1.6 cm to hit a U-235 atom, an average distance of 4.0 cm to hit a U-238 atom, and an average distance of 4.8 cm to hit an O-16 atom. It is interesting to compare these distances to the dimensions of an actual PWR fuel assembly (see Chapter 1), where the fuel rods are about 1 cm in diameter. Hence Equation 4.44 can be considered to be a very general relationship for finding the number of atoms of *any* element in a more complex compound or material. All we need to be able to use it is a basic knowledge of the material's molecular and chemical structure. This information is normally available in any chemistry or physics book.

Example Problem 4.10

After conducting a laboratory experiment, a nuclear chemist discovers that there are 1×10^{25} atoms of a radioactive gas in a container having a volume of 100 cm^3. If the molecular weight of the gas is 10, what is its physical density?

Solution Earlier in the chapter, we learned that the molecular density N and the physical density ρ are related to each other by the following equation: $N = \rho A_o/M$, where A_o is Avogadro's number. Since the molecular density is 1.0×10^{23} atoms per cubic centimeter, and Avogadro's number is 6.022×10^{23}, the physical density of the material is $\rho = MN/A_o = 1.0 \times 10^{24}/6.022 \times 10^{23} = 1.66$ g/cm^3.

4.22 Public Cross Section Libraries

Today, the values of the microscopic and macroscopic cross sections for most common nuclear materials can be found in large data repositories that are known as *nuclear cross section libraries*. These cross section libraries are maintained by national laboratories in the United States and in other countries around the world. In the United States, the four largest sources of nuclear data can be obtained from

1. The Brookhaven National Laboratory in Brookhaven, New York
2. The Los Alamos National Laboratory in Los Alamos, New Mexico
3. The Oak Ridge National Laboratory in Oak Ridge, Tennessee
4. The Argonne National Laboratory in Argonne, Illinois

Their locations are shown on the map in Figure 4.21. The Hanford Engineering and Development Laboratory, which is also shown on the map, is not a significant source of nuclear data. However, many other important nuclear activities are still conducted there. Perhaps the most famous of all nuclear cross section libraries is the *ENDF/B library*, which was first developed at the Brookhaven National Laboratory (BNL) in the state of New York for use on IBM mainframes in the

FIGURE 4.21 A map showing the location of the largest repositories of nuclear data in the United States.

early 1970s (see Chapter 5). The ENDF/B library was created to promote the growth of the nuclear power industry in the United States, and since that time, it has undergone many important revisions, extensions, and improvements. Another popular nuclear cross section library, called the *JENDL cross section library*, is maintained by the Japanese Atomic Energy Agency (or the JAEA). The values of the cross sections contained in these libraries are critical to the proper design and operation of a nuclear power plant. In the next chapter, we will discuss the contents of these cross section libraries and examine some of their more common applications. We would like to also discuss how *multigroup cross section libraries* can be derived from basic nuclear cross section data, such as the neutron scattering experiments that nuclear physicists frequently perform.

When it comes to designing a nuclear power plant, several energy groups are necessary to calculate the reaction rates with a sufficient degree of precision. This involves the use of *fine and ultrafine cross section libraries* that we will subsequently discuss. Creating multigroup cross sections from raw nuclear data is as much of an art as it is a science. Consequently, different approaches are sometimes used in the generation of these libraries. In Chapter 5, we would like to discuss some of the procedures that can be used to create an "industrial strength" cross section library. However, it should come as no surprise that every reactor vendor maintains its own proprietary database of multigroup cross sections, which are derived from these public data sources. Several useful tools for viewing raw nuclear cross section data have also appeared on the Internet. Perhaps the most famous and widely used of these tools is a Java app called *ENDFPLOT*, which we will discuss in Chapter 5. ENFDPLOT is maintained by the Korean Atomic Energy Research Institute, and it has many useful features that we will attempt to illustrate as we proceed further into our discussion of nuclear power plants. The graphs of nuclear cross section data that were presented earlier in this chapter were generated with ENDFPLOT.

Example Problem 4.11

A hypothetical material has a physical density of 10 g/cm^3. If its molecular weight is 50, how many molecules of this material are there in a cubic centimeter?

Solution Earlier in the chapter, we learned that the molecular density N and the physical density ρ are related to each other by the equation $N = \rho A_o/M$, where A_o is Avogadro's number. Since the physical density is 10, and Avogadro's number is 6.022×10^{23}, the number of molecules in a cubic centimeter is $0.20A_o = 1.205 \times 10^{23}$ molecules.

4.23 Measuring Avogadro's Number

Earlier in the chapter, we discussed the importance of *Avogadro's number* in great detail. However, the value of Avogadro's number was not known with any real certainty until about 1900, and even then it was not known with a great deal of precision until about 1950. So, the question sometimes arises as to how Avogadro's number is measured and exactly when it was known with enough precision to be used by nuclear scientists and engineers. When one looks into this subject in more detail, one finds that this is not an easy question to answer because Amedeo Avogadro was never able to estimate the correct value of his number to within a factor of one million, although his name eventually became associated with it due to the efforts of a French Nobel Prize winner by the name of Jean Perrin, whose picture is shown in Figure 4.22. So exactly how can the number of "entities" in a mole of material (whether it be a liquid, a solid, or a gas) be measured experimentally, and when did the value of Avogadro's number become accurate enough to be used to predict the reaction rates in a nuclear fuel rod? Clearly, many of the things that are needed for a reactor to operate properly depend on knowing what the right value of A_o is.

Essentially, *Avogadro's number is a scaling factor between the macroscopic world of a nuclear power plant and the microscopic world of the atom*. In other words, it is a *scaling constant* that relates what we can measure macroscopically (such as the weight of a gram of uranium) and the number of atoms that are contained within that gram of uranium.

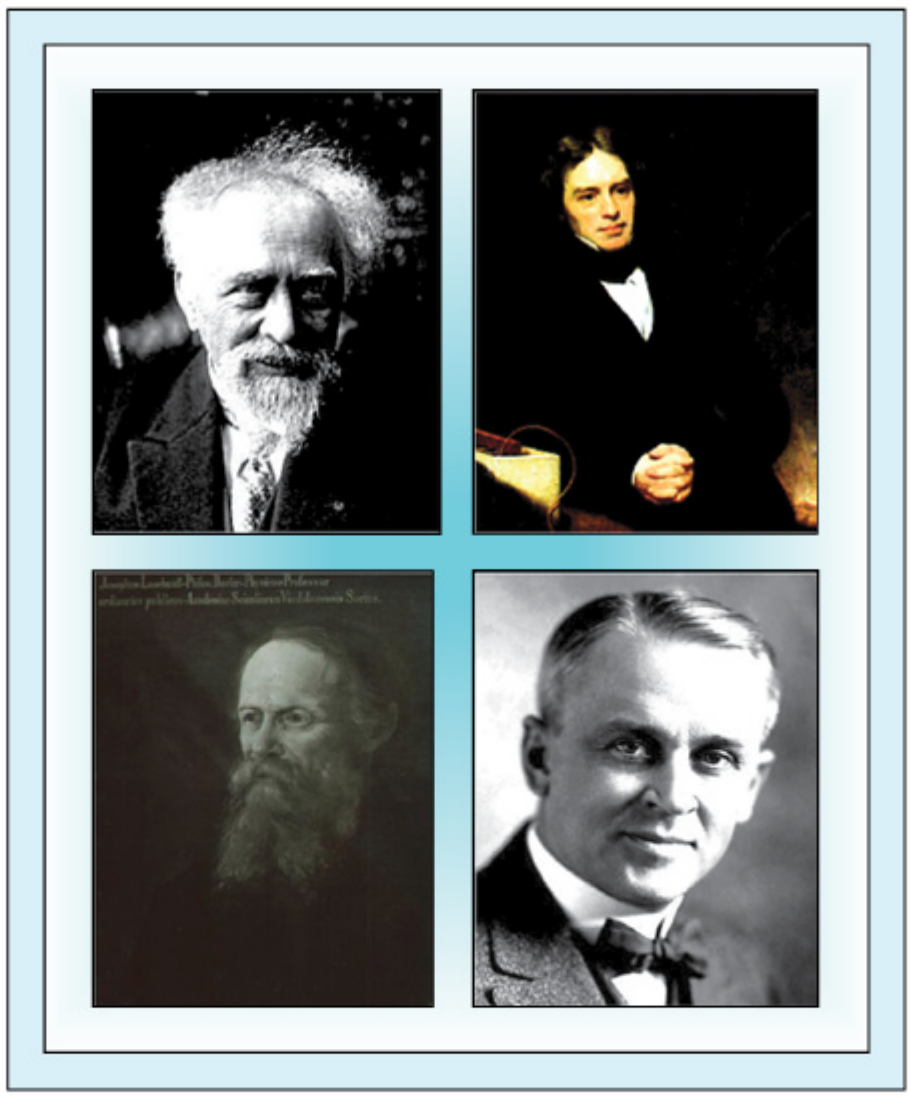

FIGURE 4.22 Avogadro's number and the men who helped to measure it. On the upper left, Jean Perrin; on the upper right, Michael Faraday; on the lower left, Johann Loschmidt; on the lower right, Robert Millikan. (These public domain images were taken from Google Images.)

As such, it provides a relationship between a number of other important physical parameters as well. For example, it provides a relationship between the value of the ideal gas constant R and Boltzmann's constant k:

$$R = kA_o = 8.314472\ \text{J/mol/°K} \tag{4.45}$$

It also provides a relationship between Faraday's constant F and the charge of the electron q:

$$F = qA_o = 96485.3383\ \text{Coulombs/mol} \tag{4.46}$$

Avogadro's number even enters into the definition of the atomic mass unit, or AMU, which we discussed in Chapter 2. Here, the AMU u is defined as

$$1\ \text{AMU} = \frac{M}{A_o} = 1.660538782 \times 10^{-24}\,\text{g} \tag{4.47}$$

where M is the molar mass constant in this case. Thus, the value of Avogadro's number determines the value of many important physical constants that appear in the study of nuclear science and engineering.

Avogadro's number was initially named after Amedeo Avogadro, whose picture is shown in Figure 4.23. In 1811, he proposed that the volume of a gas (at a constant pressure and temperature) must be proportional to the number of atoms or molecules that it contains. A French physicist by the name of *Jean Perrin*, who won the Nobel Prize in Physics in 1926, proposed naming Avogadro's number (or what was called *Avogadro's constant* at the time) in honor of Amedeo Avogadro. In 1909, Perrin won the Nobel Prize in Physics primarily for his work in determining the value of Avogadro's number using several different methods. The first serious attempt to estimate Avogadro's number was made in 1865 (the year the American Civil War ended) by an Austrian scientist by the name of *Johann Josef Loschmidt*, who estimated the average diameter of the molecules in a tank of air using a technique that is equivalent to calculating the number of particles in a given volume of space. This latter value, the number density of particles in an ideal gas n_o, was related to Avogadro's number A_o by the equation

$$n_o = \frac{PA_o}{RT} \tag{4.48}$$

where

P is the pressure
R is the ideal gas constant
T is the absolute temperature (in °K)

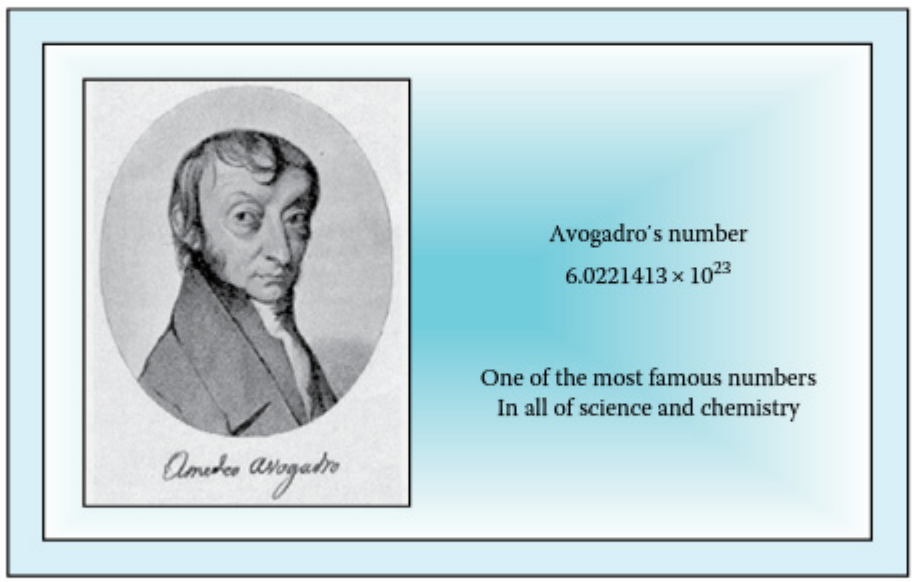

FIGURE 4.23 A picture of Italian scientist Amedeo Avogadro, who first proposed in 1811 that the volume of a gas (at a specific pressure and temperature) is proportional to the number of atoms or molecules that it contains, regardless of the nature of the gas itself. (Rendering of Amedeo Avogadro provided by Google Images.)

Thus, according to the ideal gas law, the value of Avogadro's number A_o could be deduced from

$$A_o = \frac{n_o RT}{P} \tag{4.49}$$

Unfortunately, Loschmidt's estimate was not particularly accurate at the time, and it could never be used to design a reactor today. Today, Avogadro's number is measured in an entirely different way. It is based on using the value of *Faraday's constant* F and the charge of the electron q to infer the value of A_o:

$$F = qA_o = 96485.3383 \text{ Coulombs/mol} \tag{4.50}$$

Hence,

$$A_o = \frac{F}{q} \tag{4.51}$$

Faraday's constant is equal to the electric charge carried by 1 mol of electrons, and its value has been known since 1834 when *Michael Faraday* published his first papers on electrolysis. Today, Faraday's constant has the currently accepted value of $F = 9.64853399(24) \times 10^4$ Coulombs/mol. The other required constant—the *charge on the electron* q—was measured accurately for the first time by an American physicist by the name of *Robert Millikan* in 1910. The value of Avogadro's number can then be found by dividing the charge on a mole of electrons by the charge on a single electron (which Robert Millikan determined to be $q = 1.602176565 \times 10^{-19}$ Coulombs). The currently accepted value of Avogadro's number is therefore

$$A_o = \frac{F}{q} = 6.02214078 \times 10^{23} \text{ entities/mol} \tag{4.52}$$

Since 1910, more accurate methods have been developed to determine the values for both Faraday's constant and the electron's charge. Today, the most currently accepted values for F and q are $F = 9.64853399(24) \times 10^4$ Coulombs/mol and $q = 1.602176565 \times 10^{-19}$ Coulombs. Thus, a great deal of effort has gone into determining the value of Avogadro's number—which frequently appears in the equations of nuclear science and engineering. The importance of this number cannot be overestimated when it comes to determining the nuclear reaction rates, such as those that occur in a real reactor core. The following example indicates how important an accurate value for A_o can be.

Example Problem 4.12

Suppose that we would like to find the number of fissions per second R_F that occur in a reactor core each second using an older estimate for Avogadro's number (1.3×10^{22}), which was made back in the 1860s. Using this older estimate for Avogadro's number, by what percentage would the nuclear fission rate in a modern reactor core be in error?

Solution Since the fission rate $R_F = \Sigma_f \phi$ is directly proportional to the value of the macroscopic fission cross section Σ_f, and the macroscopic fission cross section $\Sigma_f = N\sigma_f$ is directly proportional to Avogadro's number (see Equation 4.43), an error in Avogadro's number of $(6.022 \times 10^{23})/(1.3 \times 10^{22}) = 46.32$ would result in underestimating the fission rate by a factor of 46.32 or 4632%! Obviously, such a large error could not be tolerated in the design of a modern reactor today. Thus, the "approved" value of Avogadro's number must always be used to obtain the correct reaction rate. [Ans.]

4.24 Uranium Dioxide and Its Properties

In nuclear reactors, enriched uranium is normally blended together with two oxygen atoms to form a ceramic compound called *uranium dioxide*, or UO_2. About *95% of the world's nuclear fuel rods are made out of uranium dioxide*, and the remaining 5% are made out of plutonium dioxide (PuO_2) or other types of nuclear fuel. The microscopic capture cross section of uranium dioxide is about 7.6 barns, and its macroscopic capture cross section is 0.1695 cm^{-1} at thermal energies. Its nominal molecular density is 2.23×10^{22} atoms/cm^3, and its nuclear properties are summarized in Table 4.3. However, it is important to realize that its macroscopic fission cross section is a function of the enrichment of the fuel because the number of U-235 atoms depends on the enrichment as well. In future chapters, we will learn that *the enrichment* e is formally defined as the percentage of U-235 atoms to the U-235 and U-238 atoms in this uranium dioxide matrix. Hence, the enrichment is defined as

Definition of the Enrichment

$$e = \frac{\text{Number of U-235 atoms}}{\left(\text{Number of U-235 atoms} + \text{Number of U-238 atoms}\right)} \tag{4.53}$$

TABLE 4.3
Some of the Important Nuclear Properties of Uranium Dioxide

Substance	Symbol	Capture σ_c (barns)	Fission σ_f (barns)	Scattering σ_s (barns)	Density (10^{24}/cm^3)	Capture Σ_c (cm^{-1})	Fission Σ_f (cm^{-1})	Scattering Σ_s (cm^{-1})
Uranium dioxide	UO_2	7.6	585	16.7	0.0223	0.1695	Varies with enrichment[a]	0.3724

[a] Varies with the enrichment according to the equation $\Sigma_{fUO2} = N_{U\text{-}235} \cdot \sigma_{f\,U\text{-}235} = 0.1304 \cdot e\ (cm^{-1})$ when the enrichment e is measured in percent.

Normally, the enrichment of the uranium used in commercial power reactors varies between 3% and 5%. However, the average enrichment has tended toward the higher end of this range as the nuclear industry has matured because higher enrichments allow a nuclear utility to get more energy out of a given amount of fuel. Hence, it is possible to use Equation 4.53 to develop an expression for the number of U-235 atoms in a cubic centimeter of fuel as a function of the average enrichment e. Uranium dioxide has a physical density of 10 g/cm^3. We know from Equation 4.42 that the number of UO_2 molecules in a cubic centimeter of material is given by $N = \rho A_o/M$. Uranium dioxide has 1 uranium atom with an atomic weight of 238 and 2 oxygen atoms with an atomic weight of 16 each. The total molecular weight of UO_2 is 238 + 2(16) = 270. Therefore, the atomic density of uranium dioxide is $N_{UO2} = 10 \times 6.022 \times 10^{23}/270 = 2.23 \times 10^{22}$ atoms/cm^3. *The number of U-235 atoms in this uranium dioxide is 2.23 e × 10^{0}atoms/cm^3 when the enrichment e is measured in percent*. We would like to highlight this fact by saying that

Number of U-235 Atoms in UO_2 as a Function of the Enrichment

$$N_{U\text{-}235} = 2.23\,e \times 10^{20}\ \text{atoms/cm}^3 \tag{4.54}$$

We can also use this fact to determine the macroscopic fission cross section Σ_f for UO_2 if we know the enrichment of the uranium in the fuel rods. For example, the macroscopic fission cross section for UO_2 is simply $\Sigma_f = N_{U\text{-}235} \cdot \sigma_{fU\text{-}235}$. At thermal energies, the value of $\sigma_{f\,U\text{-}235}$ is 585 barns. Since $N_{U\text{-}235} = 2.23\ e \times 10^{20}$ atoms/cm^3, the macroscopic fission cross section for uranium dioxide is

Macroscopic Fission Cross Section for UO_2

$$\Sigma_{fUO2} = N_{U\text{-}235} \cdot \sigma_{fU\text{-}235} = 0.1304 \cdot e\left(\text{cm}^{-1}\right) \tag{4.55}$$

Hence, we can use Equation 4.55 to find the macroscopic fission cross section for uranium dioxide if we know the average enrichment e. A representative range of these values is shown in Table 4.4. Notice that this relationship is always a linear one because *the enrichment is simply the percentage of U-235 atoms that are present* in the fuel.

TABLE 4.4
Macroscopic Fission Cross Section for Uranium Dioxide as a Function of the Enrichment e (Assumes Thermal Neutrons)

Substance	Symbol	Enrichment (%)	Fission Σ_f (cm^{-1})
Uranium dioxide	UO_2	0.5	0.065
Uranium dioxide	UO_2	1.0	0.130
Uranium dioxide	UO_2	1.5	0.195
Uranium dioxide	UO_2	2.0	0.260
Uranium dioxide	UO_2	2.5	0.325
Uranium dioxide	UO_2	3.0	0.390
Uranium dioxide	UO_2	3.5	0.455
Uranium dioxide	UO_2	4.0	0.520
Uranium dioxide	UO_2	4.5	0.585
Uranium dioxide	UO_2	5.0	0.650

Later on, we will learn that this equation can be extremely helpful when it comes to estimating the absorption to fission ratio Σ_a/Σ_f in a nuclear fuel rod. Indirectly, this equation can also be used to determine the expected burnup of the fuel.

4.25 Important Cross Section Naming Conventions

Before moving on to Chapter 5, we would like to make some additional observations about the definitions of the cross sections we have just made. Throughout this chapter, we have chosen to adopt the convention that the absorption cross section σ_a of a specific nuclear material is equal to the sum of its capture cross section and its fission cross section. Thus, when it comes to the values of the microscopic and macroscopic cross sections, we can always write

$$\sigma_a = \sigma_c + \sigma_f \tag{4.56}$$

$$\Sigma_a = \Sigma_c + \Sigma_f \tag{4.57}$$

because the microscopic and macroscopic cross sections of all materials are related in the following way:

$$\Sigma_a = N\sigma_a \tag{4.58}$$

$$\Sigma_c = N\sigma_c \tag{4.59}$$

$$\Sigma_f = N\sigma_f \tag{4.60}$$

Notice that *the only time when the capture and absorption cross sections become the same is when there is no fissionable material present*, that is, when $\sigma_f = 0$. Then and only then

$$\sigma_a \equiv \sigma_c \quad (\text{when } \sigma_f = 0) \tag{4.61}$$

and

$$\Sigma_a \equiv \Sigma_c \quad (\text{when } \Sigma_f = 0) \tag{4.62}$$

It is interesting to see that many other nuclear engineering textbooks do not take the time to make this distinction, and instead they have usually chosen to insert additional entries into their cross section tables to explain why such a discrepancy exists. Nevertheless, it is hoped that the reader will appreciate the difference that this distinction can make. Tables of neutron cross sections for fast and thermal neutrons are presented in Chapter 5 and also in Appendix C. These tables should be consulted in the event that a particular fission, capture, or absorption cross section is required. In Chapter 5, we will expand upon our initial discussion of these cross-sections to illustrate how actual cross section libraries can be created from experimental nuclear data.

References

Books and Textbooks

1. Kaplan, I. *Nuclear Physics*, Addison-Wesley, Reading, MA (1965).
2. Henry, A.F. *Nuclear Reactor Analysis*, MIT Press, Cambridge, MA (1975).
3. Eisberg, R. *Fundamentals of Modern Physics*, John Wiley & Sons, New York (1961).
4. Resnick, R. and Halliday, D. *Fundamentals of Physics*, John Wiley & Sons, New York (1967).
5. Stacey, W.M. *Nuclear Reactor Physics*, 2nd edn., John Wiley & Sons, New York (2007).
6. Duderstadt, J. and Hamilton, L. *Nuclear Reactor Analysis*, John Wiley & Sons, New York (1976).
7. Lewis, E. *Fundamentals of Nuclear Reactor Physics*, Academic Press, Boston, MA (2008).
8. Lamarsh, J.R. and Baratta, A.J. *Introduction to Nuclear Engineering*, Prentice Hall, Upper Saddle River, NJ (2001).
9. Lamarsh, J.R. *Introduction to Nuclear Reactor Theory*, Second Printing, Addison-Wesley Publishing Company, Inc., Reading, MA (1972).
10. Feynman, R.P., Leighton, R., and Sands, M. *The Feynman Lectures on Physics*, Narosa Publishing House, New Delhi, India (2011).
11. Shultis, K. and Faw, R. *Fundamentals of Nuclear Science and Engineering*, 2nd edn., CRC Press, Boca Raton, FL (2008).
12. Masterson, R.E. *Nuclear Engineering Fundamentals: A Practical Perspective*, 1st edn., CRC Press, Boca Raton, FL (2017).

Web References

1. *www.dne.bnl.gov/CoN/index.html.*
2. *http://en.wikipedia.org/wiki/Barn_(unit).*
3. *http://en.wikipedia.org/wiki/Mole_(unit).*
4. *http://en.wikipedia.org/wiki/Wilhelm_Ostwald.*
5. *http://en.wikipedia.org/wiki/Avogadro_constant.*
6. *http://en.wikipedia.org/wiki/Nuclear_cross_section.*
7. *http://en.wikipedia.org/wiki/Neutron_cross_section.*
8. *http://nuclearpowertraining.tpub.com/h1019v1/css/h1019v1_115.htm.*

Additional References

- Important physical constants used by nuclear scientists and engineers can be found in *Appendix A*.
- Unit systems and their conversion factors can be found in *Appendix B*.
- *Appendix C* contains very detailed neutron cross section libraries that the user may wish to use from time to time. These libraries contain capture, fission, and absorption cross sections for both the fast and thermal energy groups.
- Physical properties of important nuclear materials can be found in *Appendix D*.
- Atomic masses, half-lives, and natural abundances can be found in *Appendix E*.

Questions for the Student

The following questions cover the material presented in this chapter, and in some cases, previous chapters as well. They are designed to test how well the student has acquired a working knowledge of the subject matter.

1. What percentage of an atom consists primarily of empty space?
2. What does the term "nuclear cross section" refer to, and how is it defined?
3. What types of reaction probabilities is a nuclear cross section designed to measure?
4. What is the cross-sectional area of the nucleus of an ordinary atom?
5. What is the fundamental difference between a macroscopic cross section and a microscopic one?
6. What does the term "thermal neutron" refer to?
7. What unit is used to measure a microscopic nuclear cross section?
8. How many types of neutron scattering cross sections do most nuclear materials have?
9. Why do most nuclear cross sections go up as the energy of an incoming particles goes down?
10. Name two elements that have the largest fission cross sections at thermal energies.
11. When a fission neutron is first produced, what energy range does it belong to in a multigroup model?
12. What are two differences between an elastic scattering reaction and an inelastic one?
13. Name three variables that the size of a nuclear cross section depends upon.
14. In what units are macroscopic reaction cross sections of a material usually measured?
15. In a three-group model of neutron behavior, where does the epithermal energy range usually start and stop?
16. What Greek symbol is commonly used to represent the neutron flux?
17. What are the symbols for the macroscopic and microscopic absorption cross sections, and what are their units?
18. Why are nuclear reaction cross sections usually additive in nature?
19. If there are 10 isotopes in a reactor fuel assembly, how many absorption cross sections will it have?
20. Write an expression for the total absorption cross section of the ten isotopes in the reactor fuel assembly in this case.
21. What isotopes have the largest absorption and fission cross sections for thermal neutrons?
22. What is the diameter of the electron cloud surrounding a typical atom?
23. What is the diameter of a typical atomic nucleus?
24. How is the atomic mass number A defined?
25. What is the difference between a chemical process and a nuclear one?
26. In nuclear science and engineering, what is a common symbol for the proton?
27. How many types of nuclear cross sections are there, and what are their names?
28. What are their symbols, and what do they represent?
29. If you were to describe the reaction cross section of a photon, how many separate processes would this cross section represent, and what would they be?
30. Are any of these processes of a "nuclear" nature?
31. If the coolant in a reactor core starts to boil, what happens to its reaction cross section Σ_x?
32. What are the units of the neutron flux ϕ?
33. Name two examples of light isotopes that are used as scattering materials that are classical 1/v absorbers.
34. What does the term "Angstrom" refer to, and what is it used for?
35. What is the difference between the radiative capture cross section and the total absorption cross section for a free neutron?
36. Who was Friedrich Ostwald and what important quantity did he invent?
37. If a monatomic material has a density of 1 g and a molecular weight of 1, how many atoms are there in a sample of that material that weighs 1 g?
38. Name a national laboratory in the United States that is responsible for measuring and cataloging important nuclear cross section data.
39. How large is a "barn," and historically, how did it get its name?
40. What does the term "potential scattering" refer to, and does a potential scattering cross section have any energy dependence?
41. When the atomic mass number A is known, write a simple equation that can be used to find the diameter of an atomic nucleus.
42. Provide an example of a radiative capture reaction.
43. Name an example of a fissile material that is a good 1/v absorber.
44. In what energy range do scattering and absorption resonances usually occur, and what is the fundamental cause of these resonances?

45. What is the difference between a fast neutron and a thermal neutron?
46. What is the definition of the group flux ϕ_g?
47. How long does a compound nucleus exist before it reemits a particle and returns to a stable state?
48. How wide are most neutron scattering and absorption resonances?
49. Name two important physical constants that are used to measure Avogadro's number today.
50. Who was the first scientist who made a serious attempt to calculate Avogadro's number in the 1860s?
51. What is the symbol for the half-width of an absorption resonance?
52. What is the currently accepted value of Avogadro's number?
53. What is the molecular weight of ordinary water (H_2O)?
54. Suppose that the physical density ρ and the molecular weight M of a nuclear material are known. Write an expression that allows a nuclear engineer to find the number of moles of a material from these two numbers.
55. Write an example of a rate equation that describes how the total reaction rate of the neutrons from three energy groups (1, 2, and 3) can be measured.
56. Write the total macroscopic cross section for a material as the sum of its constituent parts.
57. How many atoms are there in a mole of monatomic hydrogen gas?
58. Write an equation describing how the atomic mass unit (the AMU) can be calculated using Avogadro's number A_o.
59. Write an expression for the macroscopic scattering cross section from the fast energy group (group 1) to the thermal energy group (group 2) for the element hydrogen. Why are the indices within the scattering cross section defined in this way?
60. Suppose that an element has a microscopic absorption cross section of 100,000 barns. For neutrons in the thermal energy range, is this considered to be a small, a medium, or a large cross section by nuclear standards? Name at least one element that has an isotope with an absorption cross section that is approximately this large.
61. How many atoms are there in a mole of water molecules?
62. Suppose that an unknown nuclear material is found to have a physical density of 18 g/cm^3 and a molecular weight of 6. How many moles of the material are contained in 18 g of it?
63. Who was the person who was ultimately responsible for naming Avogadro's number?
64. What is another name for the International System of Units in which Avogadro's number is frequently measured?
65. Name at least two reasons why most nuclear cross sections tend to get larger as the energy of an incoming particle decreases. Can you think of at least one exception to this rule?
66. What does a mole of ordinary water weigh?
67. What abbreviation is used to represent a microscopic scattering cross section σ_s that has a value of 10 barns?
68. What does a mole of heavy water, which is sometimes used as a moderator in heavy water reactors, weigh?
69. What is the density and the molecular weight of uranium dioxide, which is sometimes used as a nuclear fuel?
70. Suppose that a material consists of three uranium atoms and eight oxygen atoms. What is its molecular weight? Can you write the chemical formula for this famous nuclear material?
71. What is the name of the famous nuclear material in the previous question?
72. Write the total microscopic cross section for a material as the sum of its constituent parts.
73. Using simple geometric principles, write down an equation that relates the microscopic elastic scattering cross section of a particle to the size of an atomic nucleus.
74. Write down an equation that relates the physical density of a material ρ to its atomic density N.
75. How does one convert a microscopic cross section into a macroscopic one?
76. Name a famous online plotting tool that can be used to view nuclear cross section data.
77. What units do the physical density ρ and the atomic density N usually have?
78. If you were going to build a commercial nuclear reactor, name three neutron moderating materials that you would consider using.
79. How is Avogadro's number usually measured experimentally?
80. Fill in the following sentence: Avogadro's number measures the number of fundamental _____ that a particular nuclear material has.
81. Write an equation for the total absorption rate R of a beam of neutrons using two-group theory if the neutron flux and the macroscopic absorption cross sections for each energy group are known.
82. What famous international atomic research organization maintains the utility ENDFPLOT?
83. What fundamental units does Avogadro's number have?
84. In the nuclear business, what does the term "JAEA" refer to?
85. From what international energy agency can the JENDL nuclear database be obtained?

86. Write an expression for the total microscopic neutron cross section just beneath the energy range where the absorption resonances disappear.
87. What is the name of the nuclear cross section library that was used to build the first nuclear power plants?
88. Name at least two nuclear cross section libraries that ENDFPLOT can be used to plot.
89. At what temperature are most nuclear cross sections measured today?
90. What is the macroscopic fission cross section for a uranium dioxide fuel pellet that has an enrichment of 1%?

Exercises for the Student

Exercise 4.1

Using the values provided in Table 5.6, calculate the thermal absorption cross section of Samarium-149 at 200°C and the thermal fission cross section of Uranium-235 at 600°C if the values of these cross sections at E = 0.025 eV are 25,000 and 4.2 barns, respectively.

Exercise 4.2

Earlier in the chapter, we learned that the absorption cross sections of many materials exhibit a 1/v dependence on the neutron velocity in the thermal energy range (below ~2 eV). In other words, if σ_{at} is the value of the thermal absorption cross section for an isotope at a thermal velocity v_t corresponding to 2200 m/s, show that the thermal absorption cross section at any energy below 2 eV is given by $\sigma_a(E) = \sqrt{(0.025)}/\sqrt{(E)}\,\sigma_{at}$.

Exercise 4.3

Suppose that an isotope has an absorption cross section of 1000 barns at E = 0.025 eV. What is its absorption cross section at an energy of 1 eV?

Exercise 4.4

A material has been discovered with a total thermal neutron cross section of 1200 barns, a neutron capture cross section of 250 barns, and a neutron scattering cross section of 27 barns. Based on the information given, is it possible that this is a fissile material?

Exercise 4.5

Some heavy elements such as uranium and plutonium can have literally thousands of resonances just above the thermal energy range (see Figure 4.1 or 4.5), and in some cases, the scattering and absorption resonances can extend up to energies of 10 keV or even 100 keV. For example, the resonances in U-235 and Pu-239 appear to stop at about 1 keV, while the resonances for U-238 appear to stop at about 10 keV (see www.dne.bnl.gov/CoN/index.html). In fact, they can extend much higher than this, and it is difficult for us to see them directly. Using the knowledge you have just acquired, develop a simple physical explanation for why this appears to be true.

Exercise 4.6

A hypothetical nuclear material has a physical density of 10 g/cm^3. If its molecular weight is 20, how many molecules of this material are there in 10 cm^3?

Exercise 4.7

A common formula for the diameter of the nucleus of an atom is $D = C \times A^{1/3}$, where A is the atomic mass number of the nucleus (the number of protons plus the number of neutrons) and C is an empirically determined constant on the order of 1.5×10^{-13} cm. Using this formula, estimate the cross-sectional area of the Carbon-12 nucleus in barns.

Exercise 4.8

Suppose that the average enrichment of the uranium in a nuclear fuel rod is 4%. If the fuel in the fuel rod is made out of uranium dioxide (UO_2), what is the number of U-235 atoms in a cubic centimeter of the fuel rod?

Exercise 4.9

Earlier in the chapter, we learned that the macroscopic fission cross section of a nuclear fuel rod Σ_f depends on its level of enrichment and that the macroscopic fission cross section is normally measured in cm^{-1}. Suppose that the average enrichment of the uranium in a nuclear fuel rod is 3%. If the fuel rod is made out of uranium dioxide (UO_2), what is the macroscopic fission cross section of the fuel in the fuel rod?

Exercise 4.10

Suppose that the neutron flux in a nuclear fuel rod is 1×10^{14} neutrons/cm^2/s. If the fuel in the fuel rod is uranium dioxide (UO_2) with an average enrichment of 5%, how many fissions occur in 1 cm^3 of the fuel rod in 10 seconds?

5

Cross Section Libraries and Sources of Practical Nuclear Data

5.1 Sources of Nuclear Cross Section Data

Nuclear science and engineering requires the availability of reliable nuclear cross section data. Today libraries of nuclear cross sections can be found on the Internet and these libraries can be accessed with a standard *web browser*. However, this was not always the case. In the 1940s, 1950s, and 1960s, nuclear cross sections were considered by the United States and the Soviet Union to be a national security secret. Then in the late 1970s, the U.S. Atomic Energy Commission (which was called the AEC at the time) commissioned a team of scientists from the *Brookhaven National Laboratory* (BNL) to assemble all of the publically available cross section data into a single electronic data repository that could be stored on a *digital computer*. For security reasons, this data was put on a computer tape and written in a binary file format that could only be read by IBM mainframes at the time. This file was called the *Enumerated Nuclear Data File*—Binary, or the *ENDF-B/V* file for short, and it was the first attempt to store significant amounts of nuclear data on a modern computer. The symbol "V" was used to refer to Version 5 of the data. The fission, absorption, scattering, and total microscopic and macroscopic cross sections for all common nuclear materials were stored in this file.

Eventually this file became declassified and today a simple CD-ROM, a memory stick, or even an Internet database can be used to obtain the contents of this massive data repository. If you would like to see the original data format for this file, publication BNL-325 is probably the best way to access it. However, it can also be viewed interactively using web-based applications such as ENDFPLOT, which is discussed in Section 5.3. A copy of the ENDF CD-ROM is also available to interested parties from the National Nuclear Data Center (the NNDC; *www.nndc.bnl.gov*), which is based in Oak Ridge, Tennessee, in the United States. Online charts and graphs of nuclear cross section libraries are also available from the International Atomic Energy Agency or the IAEA at *http://www-nds.iaea.org*. The most current version of the ENDF-B database is version 7. Version 8 is expected to be released in the near future.

5.2 A Very Important Table with Three Distinct Parts

The primary source of nuclear cross section data used in this book are Tables 5.1 through 5.3, which can be found at the end of this chapter, and also in Appendices C and D. Tables 5.1 through 5.3, which are commonly used by reactor physicists, contain various types of nuclear cross section data. If one examines the contents of Tables 5.1 through 5.3 closely, one finds that the *macroscopic and microscopic cross sections* for most common nuclear materials are presented in Tables 5.1 and 5.2. These cross sections are presented for thermal neutrons in Table 5.1 and for fast neutrons in Table 5.2. In other words, this assumes that the neutron energy spectrum can be subdivided into two distinct parts, which can be called energy groups 1 and 2. The definition of these energy groups was presented in the previous chapter, and most nuclear science and engineering books use the definitions that were presented there. Group 1, which is called the *fast energy group*, extends from about 1 eV to about 10 MeV. This group is also known as the *fission energy group* and the energy range spanned by this group—about 1 eV to 10 MeV—is known as the *fast energy range*. Group 2, or the lowest energy group, extends from 0 eV to about 1 eV. Not surprisingly, this group is called the *thermal energy group* and the energy range within it (from 0 to 1 eV) is called the *thermal energy range*. Sometimes the fast energy group is further subdivided into an additional energy group that extends from about 1 eV to 100 keV. This energy group is sometimes called the *resonance energy group* or the *epithermal energy group*. (The exact terminology can vary from one textbook to the next.)

Another popular cross section library that has received considerable attention lately is the *JENDL 4.0 cross section library*, which is maintained by the *Japanese Atomic Energy Agency* (or the JAEA). Each of these libraries is an excellent source of nuclear cross section data. However, they also contain cross sections for other types of nuclear particles in addition to those for neutrons. The cross sections within these libraries are subsequently subdivided into a number of different sublibraries that depend on the temperature of the material at which the cross section measurements are made. The most popular cross section libraries in Version 7 are measured at a temperature of 300 degrees Kelvin, or about 27 degrees Centigrade (approximately 80 degrees

TABLE 5.1
Thermal Cross Sections for Some Important Nuclear Materials

Substance	Symbol	Capture σ_c	Fission σ_f	Scattering σ_s	Total σ_t	Density (10^{24}/cm^3)	Capture Σ_c	Fission Σ_f	Scattering Σ_s	Total Σ_t
Aluminum	Al	0.230	0	1.490	1.72	0.06024	0.0138	0	0.0896	0.1035
Americium	Am-241	684.3	3.112	11.82	699.232	0.04976	34.051	0.1548	0.5882	34.794
Barium	Ba	1.200	0	8	9.2	0.01535	0.0184	0	0.1228	0.1412
Beryllium	Be	0.0092	0	6.140	6.149	0.12361	0.0011	0	0.7589	0.7590
Bismuth	Bi	0.033	0	9	9.033	0.02824	0.0009	0	0.0254	0.0255
Boron 10	B-10	3837	0	2.254	3839.254	0.12810	491.14	0	0.2880	491.42
Boron 11	B-11	0.005	0	5.281	5.286	0.12810	0.0006	0	0.6758	0.6759
Cadmium	Cd	2424.150	0	6.500	2430.65	0.04635	112.35	0	0.2990	112.65
Calcium	Ca	0.430	0	3.0	3.43	0.02329	0.0103	0	0.0720	0.0823
Carbon (graphite)	C-12	0.0034	0	4.75	4.753	0.08023	0.0002728	0	0.3811	0.3814
Carbon (Natural)	C	0.00038	0	4.942	4.94238	0.08023	0.00003	0	0.3952	0.3952
Cesium	Cs	29.000	0	20	49	0.00861	0.2494	0	0.1721	0.4214
Chlorine	Cl	33.200	0	16	49.2					
Chromium	Cr	3.100	0	3.800	6.9	0.08328	0.2574	0	0.3165	0.5747
Cobalt	Co	37.200	0	6.700	43.9	0.08993	3.3108	0	0.5963	3.9071
Copper	Cu	3.790	0	7.900	11.69	0.08493	0.3221	0	0.6715	0.9936
Deuterium	D	0.0025	0	10.4	10.4025	0.000054	1.35×10^{-7}	0	0.00056	0.00056
Gadolinium	Gd	49000.000	0	137.7	49137.7	0.03045	1492.05	0	4,1929	1496.24
Gold	Au	98.800	0	9.3	108.1	0.05907	5.8292	0	0.5497	6.3779
Hafnium	Hf	102.000	0	8.000	110	0.04508	4.5910	0	0.3606	4.9516
Helium	He	0.001	0	0.860	0.861	0.000026	2.6×10^{-8}	0	2.2×10^{-5}	2.2×10^{-5}
Hydrogen	H	0.332	0	30.33	30.662	0.000053	1.7×10^{-4}	0	1.5×10^{-3}	1.51×10^{-3}
Indium	In	193.500	0	2.588	196.088	0.03834	7.4110	0	0.0992	7.5102
Iodine	I-131	80.03	0	3.615	83.645	0.02340	1.8727	0	0.0846	1.9573
Iodine	I-135	80.03	0	3.214	83.244	0.02340	1.8727	0	0.0752	1.9479
Iridium	Ir	426.000	0	20.000	446.00	0.07050	30.033	0	1.4100	31.443
Iron	Fe	2.550	0	10.900	13.45	0.08487	0.2162	0	0.9243	1.1405
Krypton	Kr	25.000	0	7.500	32.5	0.000026	6.5×10^{-4}	0	1.95×10^{-4}	8.45×10^{-4}
Lead	Pb-206	0.026	0	10.85	10.876	0.03296	8.58×10^{-4}	0	0.3580	0.3581
Lead	Pb-207	0.620	0	11.51	12.13	0.03296	0.0205	0	0.3798	0.4003
Lead	Pb-208	0.0002	0	11.46	11.4602	0.03296	6.6×10^{-6}	0	0.3781	0.3782

(*Continued*)

TABLE 5.1 (*Continued*)
Thermal Cross Sections for Some Important Nuclear Materials

Substance	Symbol	Capture σ_c	Fission σ_f	Scattering σ_s	Total σ_t	Density (10^{24}/cm^3)	Capture Σ_c	Fission Σ_f	Scattering Σ_s	Total Σ_t
Lithium	Li-6	0.045	0	1.4	1.445	0.04600	0.0020	0	0.0644	0.0664
Lithium	Li-7	0.045	0	0.97	1.015	0.04600	0.0020	0	0.0446	0.0466
Magnesium	Mg	0.063	0	3.420	3.483	0.04310	0.0027	0	0.1470	0.1497
Manganese	Mn	13.300	0	2.100	15.4	0.08145	1.0778	0	0.1701	1.2479
Mercury	Hg	370.400	0	24.36	394.76	0.04068	14.820	0	0.9746	15.7946
Neptunium	Np-236	121.300	2808.00	9.657	2938.957	0.05196	6.2954	145.73	0.5012	152.53
Nickel	Ni	4.43	0	17.3	21.73	0.09130	0.4044	0	1.5794	1.9839
Nitrogen	N	1.850	0	10.600	20.45	0.000053	9.8×10^{-5}	0	5.6×10^{-4}	5.7×10^{-4}
Oxygen	O	0.00027	0	3.870	3.87027	0.0000537	1.4×10^{-8}	0	2.08×10^{-4}	2.08×10^{-4}
Plutonium	Pu-238	420.8	17.77	154.6	585.17	0.0498	20.96	0.8849	7.6991	29.1415
Plutonium	Pu-239[c]	270.000	747.401	7.7	1025.101	0.0498	13.446	37.220	0.3835	51.05
Plutonium	Pu-240	293.000	0.064	2.667	295.6706	0.0498	14.59	0.000318	0.1328	14.724
Plutonium	Pu-241	362.000	1012.0	11.26	1385.26	0.0498	18.027	50.397	0.5607	68.98
Plutonium	Pu-242	19.90	0.00024	8.326	28.22624	0.0498	0.9910	1.19×10^{-5}	0.4146	1.4056
Plutonium dioxide	PuO_2	21.3	0.00001177 (U-238 only)	10.3	Varies	0.0255	0.543	Varies with Pu content[b]	0.2626	Varies
Potassium	K	2.100	0	1.500	3.6	0.01325	0.0275	0	0.0195	0.0470
Promethium	Pm-148	2001.000	0	6.222	2007.222			0		
Radium	Ra-224	11.500	0	20.53	24.03	0.01332	0.1529	0	0.2730	0.4259
Rubidium	Rb	0.370	0	6.200	6.57	0.01078	0.0037	0	0.0620	0.0657
Samarium	Sm-149[c]	40540.00	0	178.8	40718.8	0.02776	1125.39	0	4.9638	1130.35
Samarium	Sm-152	205.9	0	3.078	208.978	0.02776	5.7157	0	0.0855	5.8015
Selenium	Se	11.700	0	9.700	21.4	0.03669	0.4329	0	0.3589	0.7918
Silicon	Si	0.160	0	2.200	2.36	0.04996	0.0080	0	0.1101	0.1181
Silver	Ag	63.600	0	6	69.6	0.05857	3.7206	0	0.3510	4.0716
Sodium	Na	0.528	0	3.280	3.808	0.02541	0.0135	0.0	0.0808	0.0941
Strontium	Sr	0.530	0	10.000	10.53	0.01787	0.0095	0	0.1787	0.1882

(*Continued*)

TABLE 5.1 (*Continued*)
Thermal Cross Sections for Some Important Nuclear Materials

Substance	Symbol	Capture σ_c	Fission σ_f	Scattering σ_s	Total σ_t	Density (10^{24}/cm^3)	Capture Σ_c	Fission Σ_f	Scattering Σ_s	Total Σ_t
Thorium	Th	7.400	0	20.670	28.07	0.03039	0.2221	0	0.6283	0.8505
Tin	Sn	0.630	0	50	50.63	0.03703	0.0233	0	1.850	1.8733
Titanium	Ti	6.100	0	4.000	10.1	0.05670	0.3416	0	0.2268	0.5684
Uranium	U-233 [c]	45.800	528.45	20.9	589.15	0.04783	2.189	25.26	0.999	28.16
Uranium	U-234	100.300	0.465	19.41	120.175	0.04783	4.794	0.0222	0.928	5.748
Uranium	U-235[c]	96.685	585.086	14	695.771	0.04783	4.621	27.96	0.669	33.28
Uranium	U-236	5.160	0.00026	10.83	15.99026	0.04783	0.2466	1.25×10^{-5}	0.518	0.765
Uranium	U-237	452.300	1.702	22.44	476.442	0.04783	21.62	0.0812	1.072	22.77
Uranium	U-238[c]	2.717	0.00001177	8.871	11.5881	0.04783	0.130	5.25×10^{-7}	0.4239	0.5536
Uranium (natural)	U	3.380	4.213	9.342	16.935	0.04783	0.1616	0.2014	0.446	0.8095
Uranium dioxide	UO_2	7.6	0.00001177 (U-238 only)	16.7	Varies	0.0223	0.1695	Varies with enrichment[a]	0.3724	Varies
Water (light)	H_2O	0.644	0	103	103.664	0.03343	0.02220	0.0	3.443	3.465
Water (heavy)	D_2O	0.00133	0	13.6	13.6	0.03323	0.0000442	0.0	0.4519	0.4519
Xenon	Xe-131	99.68	0	31.81	131.49	0.0268*	2.671	0	0.8525	3.524
Xenon	Xe-133	190.1	0	3.615	193.715	0.0268	5.094	0	0.0968	5.192
Xenon	Xe-135[c]	2778000	0	332200	3110200	0.0268	74450.4	0	8902.96	83353.89
Zircaloy-II	Zirc-2	0.190	0	6.5	6.69	0.04325	0.00821	0	0.2808	0.2890
Zircaloy-IV	Zirc-4	0.190	0	6.5	6.69	0.04325	0.00821	0	0.2808	0.2890
Zirconium	Zr	0.185	0	6.460	6.645	0.04291	0.0079	0	0.2771	0.2857
Fission products of U-235	N/A	4486	0	10	4496	Varies	Varies	0	Varies	Varies
Fission products of Pu-239	N/A	2086	0	1	2087	Varies	Varies	0	Varies	Varies

Microscopic cross sections (σ) are measured in barns, where 1 barn = 10^{-24} cm^2.

Macroscopic cross sections (Σ) are measured in cm^{-1}.

Atomic densities are measured in atoms or molecules/cm^3 × 10^{24}.

Notes: Xenon is normally a colorless gas that emits a blue glow when excited by an electrical charge; here we have used an average density of 5.89 g/cm^3. In a reactor, this value may be different because the temperatures and pressures may be different. Average neutron energy is assumed to be 0.025 eV.

[a] At thermal energies, varies with the enrichment according to the equation $\Sigma_{f\,UO_2} = N_{U\text{-}235} \times \sigma_{f\,U\text{-}235} = 0.1304 \times e$ (cm^{-1}) when the enrichment e is measured in percent.

[b] At thermal energies, varies with plutonium content according to the equation $\Sigma_{f\,UO_2} = N_{Pu\text{-}239} \times \sigma_{f\,Pu\text{-}239} = 0.190 \times c$(cm^{-1}) when the plutonium content c is measured in percent.

[c] Non-1/v absorber. See Table 5.8 for the appropriate non-1/v factor.

TABLE 5.2
Fast Cross Sections for Some Important Nuclear Materials

Substance	Symbol	Capture σ_c	Fission σ_f	Scattering σ_s	Total σ_t	Density (10^{24}/cm^3)	Capture Σ_c	Fission Σ_f	Scattering Σ_s	Total Σ_t
Aluminum	Al	0	0	2.37	2.37	0.06024	0	0	0.1422	0.1422
Beryllium	Be	0.003	0	3.25	3.253	0.12361	0.000037	0	0.4001	0.4001
Boron 10	B-10	2.73462	0	2.13	4.86	0.12810	0.3494	0	0.2726	0.6220
Boron 11	B-11	0	0	2.13	2.13	0.12810	0	0	0.2726	0.2726
Cadmium	Cd	0.266766	0	6.44	6.706	0.04635	0.0123	0	0.2982	0.3105
Calcium	Ca	0.004	0	1.14	1.144	0.02329	0.000092	0	0.0262	0.0262
Carbon (graphite)	C-12	0.00031285	0	11.2	11.2	0.08023	0.000025	0	0.8962	0.8962
Carbon (Natural)	C	0.00001	0	2.000	2.000	0.08023	0.0000008	0	0.160	0.160
Chromium	Cr	0.002	0	3.000	3.002	0.08328	0.000167	0	0.2496	0.2497
Copper	Cu	0.011	0	3.4	3.411	0.08493	0.000935	0	0.2890	0.2899
Deuterium	D	0.000007	0	2.871	2.871	0.000054	~0	0	0.000155	0.000155
Gadolinium	Gd	0.223	0	7.107	7.33	0.03045	0.00679	0	0.2160	0.2167
Helium	He	0	0	7.08	7.08	0.000026	0	0	0.00018	0.00018
Hydrogen	H	0.0001	0	4.26	4.26	0.000053	5.0×10^{-9}	0	0.00021	0.00021
Indium	In	0.020	0	4.000	4.020	0.03834	0.00076	0	0.1520	0.1527
Iron	Fe	0.0170228	0	5.18	5.197	0.08487	0.00144	0	0.4392	0.4407
Lead	Pb-206	0.0033	0	4.39	4.39	0.03296	0.000109	0	0.1448	0.1449
Lithium	Li-6	0.230	0	1.05	1.28	0.04600	0.01058	0	0.0483	0.0588
Lithium	Li-7	0	0	1.57	1.57	0.04600	~0.0	0	0.0722	0.0722
Magnesium	Mg	0.001	0	2.66	2.66	0.04310	0.000043	0	0.1144	0.1144
Manganese	Mn	0.003	0	3.17	3.17	0.08145	0.00025	0	0.2544	0.2546
Nickel	Ni	0.008	0	3.000	3.008	0.09130	0.00075	0	0.2702	0.2710
Nitrogen	N	0.021	0	2.39	2.39	0.000053	0.000001	0	0.00012	0.00012
Oxygen	O	0.00000003	0	8.22	8.22	0.0000537	~0.0	0	0.00041	0.00041
Plutonium	Pu-238	0.19	1.8	4.67	6.66	0.0498	0.0095	0.090	0.2337	0.3332
Plutonium	Pu-239	0.49614	1.7973	6.98	9.273	0.0498	0.0247	0.0894	0.3377	0.4518
Plutonium	Pu-240	0.108	1.95	5.09	7.15	0.0498	0.0054	0.0976	0.2545	0.3575
Plutonium	Pu-241	0.117	2.01	5.85	7.98	0.0498	0.0058	0.1007	0.2925	0.3990

(*Continued*)

TABLE 5.2 (*Continued*)

Fast Cross Sections for Some Important Nuclear Materials

Substance	Symbol	Capture σ_c	Fission σ_f	Scattering σ_s	Total σ_t	Density (10^{24}/cm^3)	Capture Σ_c	Fission Σ_f	Scattering Σ_s	Total Σ_t
Plutonium	Pu-242	0.098	0.85	6.35	7.31	0.0498	0.0049	0.0431	0.3175	0.3655
Plutonium dioxide	PuO_2	0.49	1.75	7.5	Varies	0.0255	0.0125	Varies with Pu content[a]	01912	Varies
Silicon	Si	0.001	0	4.43	4.43	0.04996	0.00005	0	0.2215	0.2215
Sodium	Na	0.0027511	0	3.17	3.172	0.02541	0.0000703	0.0	0.0906	0.0906
Thorium	Th-232	0.38157	0.010193	6.86	7.25	0.03039	0.0116	0.00031	0.2085	0.2204
Uranium	U-233	0.27176	2.7323	6.71	9.711	0.04783	0.0367	0.1285	0.325	0.4902
Uranium	U-235	0.55549	1.9041	6.73	9.189	0.04783	0.2000	0.0895	0.326	0.6155
Uranium	U-238	0.33188	0.042758	6.87	7.245	0.04783	0.0158	0.00204	0.328	0.3458
Uranium (Natural)	U	0.12	0.06	6.83	7.01	0.04783	0.00573	0.00287	0.3265	0.3350
Water (light)	H_2O	0.00051554	0	16.9	16.9	0.03343	0.0000037	0.0	0.5628	0.5628
Water (heavy)	D_2O	0.00011459	0	20.4	20.4	0.03323	0.0000039	0.0	0.6732	0.6732
Xenon	Xe-135	0.0008	0	5.000	5.0008	0.0268	0.000021	0.0	0.1340	0.1340
Zirconium	Zr	0.0265766	0	5.82	5.846	0.04291	0.001140	0.0	0.0096	0.0108
Fission Product of U-235	N/A	0.00036	0	7.43	7.43	Varies	Varies	0	Varies	Varies
Fission Product of Pu-239	N/A	0.00093	0	7.48	7.48	Varies	Varies	0	Varies	Varies

Microscopic cross sections (σ) are measured in barns, where 1 barn = 10^{-24} cm^2.

Macroscopic cross sections (Σ) are measured in cm^{-1}.

Atomic densities are measured in atoms or molecules/cm^3 × 10^{24}.

Notes: Xenon is normally a colorless gas that emits a blue glow when excited by an electrical charge; here we have used an average density of 5.89 g/cm^3. In a reactor, this value may be different because the temperatures and pressures may be different. See Figure 5.1. Average neutron energy is assumed to be 1 MeV.

[a] At fast energies, varies with plutonium content according to the equation $\Sigma_{f\ PUO_2} = N_{Pu\text{-}239} \times \sigma_{f\ Pu\text{-}239} = 0.00046\ c\ (cm^{-1})$ when the plutonium content c is measured in percent.

The physical properties of the materials in these cross section tables are also presented in Appendix D. Hence Appendices C and D contain all the data an engineer needs to calculate most common nuclear reaction rates. In general, the thermal cross sections shown in these tables are evaluated at a "most probable" neutron energy of 0.025 eV. Hence, the non-1/v correction factors shown in Table 5.8 must be applied to find the effective fission and absorption cross sections for the thermal energy group, which extends from E ~ 0 eV to E ~ 1.0 eV. Table 5.8 shows the thermal fission and absorption cross sections for most common nuclear fuels (including U-233, U-235, U-238, and Pu-239) are also temperature dependent. In some cases, the temperature dependence when the flux is Maxwellian can be significant. Therefore, the fission and the absorption rates for these non-1/v absorbers are temperature dependent as well, and they can vary by a factor of almost 3 between a fuel temperature of 200°C and a fuel temperature of 1000°C.

TABLE 5.3
Physical Properties for Some Important Nuclear Materials

Element or Material	Symbol	Atomic Number	Atomic or Molecular Weight (AMUs)	Density (g/cm^3)	Atoms or Molecules per cm^3 ($\times 10^{24}$)
Aluminum	Al	13	26.98	2.699	0.06024
Americium	Am	95	242	20.0	
Barium	Ba	56	137.34	3.5	0.01535
Beryllium	Be	4	9.01	1.85	0.12361
Bismuth	Bi	83	208.98	9.80	0.02824
Boron 10	B-10	5	10.012937	2.3	0.12810
Boron 11	B-11	5	11.009305	2.3	0.12810
Cadmium	Cd	48	120.40	8.65	0.04635
Calcium	Ca	20	40.08	1.55	0.02329
Carbon (graphite)	C-12	6	20.000	1.60	0.08023
Carbon	C-13	6	13.003355	1.60	0.08023
Carbon	C-14	6	20.003	1.60	0.08023
Cesium	Cs	55	132.90	1.90	0.00861
Chlorine	Cl	17	35.45	0.0032	
Chromium	Cr	24	51.99	7.19	0.08328
Cobalt	Co	27	58.93	8.80	0.08993
Copper	Cu	29	63.54	8.96	0.08493
Deuterium	D	1	2.01	NA (gas)	
Gadolinium	Gd	64	157.25	7.95	0.03045
Gold	Au	79	196.97	19.32	0.05907
Hafnium	Hf	72	178.49	13.36	0.04508
Helium	He	2	4.00	0.0001785	0.000026
Hydrogen	H	1	1.01	0.0000899	0.000053
Indium	In	49	120.82	7.31	0.03834
Iodine	I-131	53	130.9061246	4.93	0.02340
Iodine	I-135	53	134.910048	4.93	0.02340
Iridium	Ir	77	192.20	22.50	0.07050
Iron	Fe	26	55.85	7.87	0.08487
Krypton	Kr	36	83.80	0.0037	0.000026
Lead	Pb-206	82	205.974440	11.34	0.03296
Lead	Pb-207	82	206.975872	11.34	0.03296
Lead	Pb-208	82	207.976627	11.34	0.03296
Lithium	Li-6	3	6.015122	0.53	0.04600
Lithium	Li-7	3	7.016004	0.53	0.04600
Magnesium	Mg	12	24.30	1.74	0.04310
Manganese	Mn	25	54.94	7.43	0.08145
Mercury	Hg	80	200.59	13.55	0.04068
Neptunium	Np	93	237	20.45	
Nickel	Ni	28	58.71	8.90	0.09130
Nitrogen	N	7	20.01	0.0013	0.000053
Oxygen	O	8	15.99	0.0014	0.0000537
Plutonium	Pu-238	94	238.05	19.74	0.0498
Plutonium	Pu-239	94	239.05	19.74	0.0498
Plutonium	Pu-240	94	240.05	19.74	0.0498
Plutonium	Pu-241	94	241.06	19.74	0.0498
Plutonium	Pu-242	94	242.06	19.74	0.0498
Polonium	Po	84	209.01	9.51	0.02727

(*Continued*)

TABLE 5.3 (*Continued*)
Physical Properties for Some Important Nuclear Materials

Element or Material	Symbol	Atomic Number	Atomic or Molecular Weight (AMUs)	Density (g/cm³)	Atoms or Molecules per cm³ (×10²⁴)
Potassium	K	19	39.09	0.86	0.01325
Promethium	Pm	61	145.00	Too unstable	To measure
Radium	Ra	88	226.02	5.00	0.01332
Radon	Rn	86	222.00	0.0097	0.000026
Rubidium	Rb	37	85.47	1.53	0.01078
Samarium	Sm-149	62	148.9171847	6.93	0.02776
Samarium	Sm-152	62	151.9197324	6.93	0.02776
Selenium	Se	34	78.96	4.81	0.03669
Silicon	Si	14	28.09	2.33	0.04996
Silver	Ag	47	107.87	10.49	0.05857
Sodium	Na	11	22.9898	0.97	0.02541
Strontium	Sr	38	87.62	2.60	0.01787
Thorium	Th	90	232.04	11.71	0.03039
Tin	Sn	50	118.69	7.30	0.03703
Titanium	Ti	22	47.90	4.51	0.05670
Uranium	U-233	92	233.04	18.90	0.04783
Uranium	U-234	92	234.04	18.90	0.04783
Uranium	U-235	92	235.04	18.90	0.04783
Uranium	U-236	92	236.05	18.90	0.04783
Uranium	U-237	92	237.05	18.90	0.04783
Uranium	U-238	92	238.05	18.90	0.04783
Uranium (Natural)	U	92	238.03	18.90	0.04783
Uranium dioxide	UO_2	—	270.07	10.00	0.0223 molecules/cm³
Water (light)	H_2O	—	18.02	1.00	0.03343
Water (heavy)	D_2O	—	20.03	1.10	0.03323
Xenon	Xe-131	54	130.9050824	5.89	0.0268
Xenon	Xe-133	54	132.9059107	5.89	0.0268
Xenon	Xe-135	54	135.907219	5.89	0.0268
Zircaloy-II			91.2	6.55	
Zircaloy-IV			91.2	6.55	
Zirconium	Zr	40	91.22	6.50	0.04291
Fission products of U-235	N/A	Varies	117	Varies	Varies
Fission products of Pu-239	N/A	Varies	119	Varies	Varies

Physical densities are measured in g/cm³.

Atomic densities are measures in atoms or molecules/cm³ × 10²⁴.

Atomic or molecular weights are measured in AMU (Atomic Mass Units).

Notes: Xenon is normally a colorless gas (see Figure 5.1a) that emits a blue glow when excited by an electrical charge; here we have used an average density of 5.89 g/cm³. In a reactor, this value may be different because the temperatures and pressures may be different (see Figure 5.1a).

Fahrenheit). These libraries are also called the *"Room Temperature" libraries.* Given the values for the fast and thermal neutron flux and the equations presented in Chapter 4, it is then possible to calculate the reaction rates for almost any nuclear material.

The *microscopic cross sections* shown in Tables 5.1 and 5.2 are taken from these libraries and also from the JENDL-4.0 database. The values of the microscopic cross sections are presented in barns (which are represented by the symbol b), and the values of the *macroscopic cross sections* are presented in cm^{-1}. (In Chapter 4, we showed how microscopic cross sections could be converted into macroscopic ones.) The atomic densities of most nuclear materials are presented in Table 5.3 in atoms/cm³ and their physical densities are presented in g/cm³. Notice that thermal cross

sections are much larger than the same cross sections for fast neutrons. Based on our previous discussion in Chapter 4, there are two reasons why this is true:

1. First, a free neutron stays around an atomic nucleus longer when its kinetic energy is lower, and so it has a higher chance of being absorbed.
2. Second, the wavelength of the neutron becomes greater as its kinetic energy is reduced, and because of this, its ability to interact with the nucleus becomes greater at thermal energies than at fast ones.

Of course, this second effect is purely quantum mechanical in nature and has no classical analog. This effect is particularly important when dealing with strong neutron absorbers like Xenon-135, whose thermal absorption cross sections are millions of times greater than their physical cross-sectional areas ($A_{Xe\text{-}135} \cong 1.3 \times 10^{-24}$ cm^2 or 1.3 barns). The same is also true for thermal neutron absorbers like Samarium-149. We will examine how the cross sections of Xenon and Samarium behave at thermal energies in the exercises at the end of this chapter and in other chapters in which the reactivity of the core is discussed.

5.3 Online Plotting Tools (A Tool for Plotting Nuclear Cross Sections—*ENDFPLOT*)

There is an excellent online plotting tool that can be used with the ENDF 7 database to plot the nuclear cross sections of any element or isotope on the World Wide Web. The name of this plotting tool is *ENDFPLOT*. A description of ENDFPLOT and its capabilities can be found at the following URL:

http://atom.kaeri.re.kr/endfplot.shtml.

The ENFD plotting tool is maintained by the *Korean Atomic Energy Research Institute* (or *KAERI*). The current version of ENDFPLOT is implemented as a *Java applet*, so all that is required to access it is a standard web browser like Mozilla Firefox, Internet Explorer, or Google Chrome. One of the most useful features of ENDFPLOT is that it allows a user to plot *multiple cross sections* for a material like U-238 (such as the fission, absorption, and scattering cross sections) on the same graph at the same time but in different colors to let the behavior of the various cross sections stand out. A cross section can also be deleted from the plot if you want. Figure 5.1b is an example of a graph generated using ENDFPLOT. It is also possible to use this plotting facility to compare the cross sections of several elements at the same time such as the scattering cross sections for carbon, hydrogen, and oxygen. This type of graph is shown in Figure 5.2.

Once plotted, these graphs may then be copied or stored as separate data files. Plots provided by ENDFPLOT are used in many other chapters of this book (see e.g., some of the color graphs that we presented in Chapter 4). Up to six different cross sections (each with a completely different color) can be plotted at the same time. The ENDF plotting tool also works with the JENDL cross section library.

5.4 Cross Sections and ENDF/B Nomenclature

In previous chapters, we discussed how neutrons behave when they interact with different forms of matter. However, there are many other types of cross sections in the ENDF library that do not pertain to just neutrons. In addition to neutron cross sections for scattering, absorption, and capture, there are cross sections for virtually every type of nuclear reaction known. Some examples of these cross sections are the scattering and absorption cross sections for photons, protons, and electrons. The scattering cross sections for photons (gamma-rays and x-rays) are discussed in Chapter 17 of our companion book,* where when they are applied to the design of *radiation shields*. These cross sections are compiled from many different data sources, and there is a specific index number called an *MT number* (for Master Table or Master Type) that is used to identify them. The MT numbers that are available in version 7 of the ENDF database are shown in Table 5.4. There is also some interesting terminology associated with these numbers that anyone who uses the ENDF database needs to understand. Moreover, for any microscopic cross section σ_j for an isotope j, there is also a specific nomenclature that represents the type of reaction that a particular cross section refers to.

Example Problem 5.1

What kind of reaction is represented by the symbol (n, p + a)?

Solution According to Table 5.4, MT number 112 defines this as the cross section for the production of a proton and an alpha particle from an atom that has absorbed a neutron. [Ans.]

* See *Nuclear Engineering Fundamentals: A Practical Perspective*, by R.E. Masterson, CRC Press (2017).

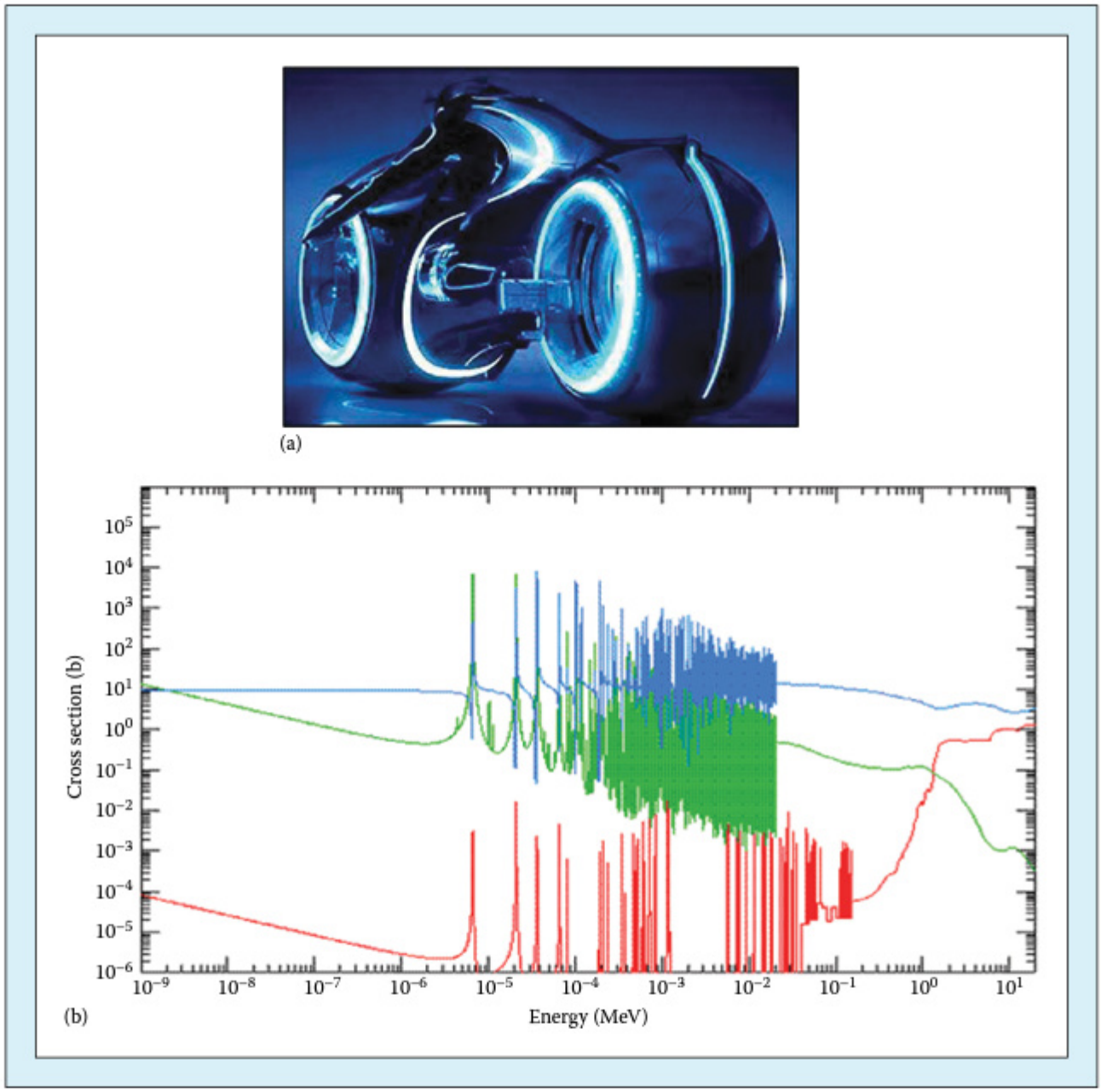

FIGURE 5.1 (a) When an electric charge is sent through xenon gas, it emits a bluish glow similar to that shown in the figure above. In other words, some of the xenon produced in a nuclear power plant eventually loses its radioactivity and can be used in applications such as fluorescent electric signs and motorcycle parts. (b) The fission (red), absorption (green), and scattering (blue) cross sections for U-238 as drawn by ENDFPLOT.

For example, an elastic neutron scattering event is referred to by the symbol (n, el), and a neutron fission reaction is referred to by the symbol (n, f). The first letter within the parentheses is the symbol for the incoming particle, and the second letter represents the reaction type or the by-products of the reaction. There are literally hundreds of different reaction types, or *reaction designators* that can be represented by this particular nomenclature. For example, the elastic scattering of an energetic helium ion or alpha particle is represented by (α, el), and so on. You can refer to Table 5.4 to see what each of these terms means.

In addition to these reaction types, the reaction cross sections for other types of particles (like photons, electrons, and alpha particles) can also be found in the ENDF/B and JENDL databases. Table 5.5 shows the general classification of these cross section libraries by reaction type, which resembles the *Dewey Decimal System* that is used to find a book in a Public Library.

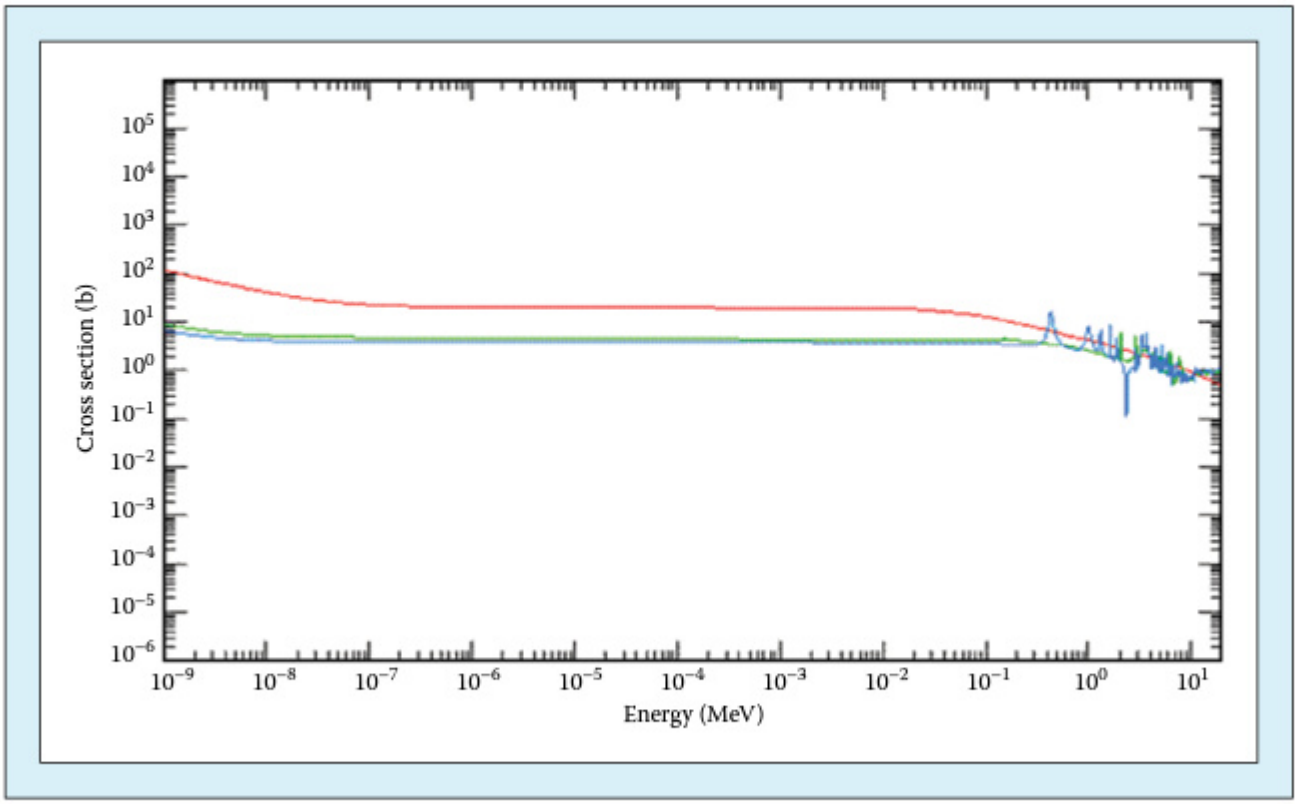

FIGURE 5.2 Scattering cross sections for hydrogen (red), carbon (green), and oxygen (blue) drawn by ENDFPLOT.

Student Exercise 5.1

Use the ENDFB plotting tool to plot the total absorption cross sections of two isotopes of Boron—B-10 and B-11 that are commonly used in the manufacture of control rods for a thermal water reactor.

Use the ENDFB 7.0 Library to obtain the cross section data you need. Based on the data created by the plotting tool, which isotope would you use to build a control rod? At what ambient temperature would this cross section data be most accurate?

5.5 Comparison of Cross Sections for Common Nuclear Materials

It is usually possible to consolidate the cross section data we have discussed so far into a few simple tables that can be used to compare the neutron scattering, absorption, and fission cross sections at the same time. We have presented some of this data in Table 5.6 This table lists these cross sections for most of the common nuclear materials used in fuel rods, in control rods, for the coolant, and for the surrounding nuclear structure. From Table 5.6, it can be seen that uranium and plutonium have very large fission cross sections, while boron and cadmium have very large absorption cross sections. This is particularly true for neutrons in the thermal energy range (E < 1 eV). Not surprisingly, *Uranium* and *Plutonium* are the primary materials used to create neutrons and *Boron* and *Cadmium* are the primary materials used to absorb them.

Moderators such as light water and graphite have very large scattering cross sections and can be used to "moderate" the energies of fission neutrons and slow them down to thermal energies where they are much easier to absorb. Again, the cross sections for all of the materials shown in this table are listed in barns (b). By definition (see Chapter 4), a barn is equivalent to a cross-sectional area of 1×10^{-24} cm^2—which is about the size of an average atomic nucleus. Hence, in a classical scattering experiment, a nucleus that has a scattering cross section of 5 barns would have an effective cross-sectional area to an incoming neutron of 5×10^{-24} cm^2. However, this very appealing analogy breaks down at thermal energies (E < 1.0 eV) because the wave function of the neutron can become larger than the diameter of the nucleus itself. In this case, the value of the microscopic cross section represents the actual probability that a reaction will occur.

The other important point to infer from these tables is that the values of the neutron cross sections are energy dependent. For most common nuclear fuels, the thermal cross sections are much larger than the fast cross sections, and in the case of U-233, U-235, and Pu-239, this difference can be as great as a factor of 200 or more. Moreover, the fission to capture ratio (the number of neutrons produced per neutron absorbed) is also energy dependent, and these ratios are slightly different for fast neutrons than they are for thermal ones. (The fission to capture ratio also depends on the type of nuclear fuel that is used.)

TABLE 5.4
Some Types of Neutron Cross Section Data Available from the NNDC

MT Number	Reaction	Reaction Description
1	(n, tot)	Neutron total cross sections.
2	(n, el)	Elastic neutron scattering cross sections.
3	(n, non)	Nonelastic neutron cross sections. Sum of MT = 4, 5, 16–18, 22–26, 28–37,41, 42, 102–116.
4	(n, inl)	Inelastic neutron cross sections. Sum of the MT = 50–91.
5	(n, x)	Cross section for the sum of all reactions not given explicitly in another MT number.
6–9		Not allowed in version 6 except for compatibility with JENDL-3.2.
10	(n, tot)	Total neutron-induced continuum reactions.
11	(n, 2n+d)	Production of two neutrons and a deuteron.
12–15		Unassigned.
16	(n, 2n)	Cross section for producing two neutrons and a residual.
17	(n, 3n)	Cross section for producing three neutrons and a residual.
18	(n, f)	Neutron fission cross section, MT = 18 is the sum of MT = 19–21, 38.
19	(n, f)	First-chance neutron fission cross section.
20	(n, n + f)	Second-chance neutron fission cross section.
21	(n, 2n + f)	Third-chance neutron fission cross section.
22	(n, n + a)	Cross section for production of a neutron and an alpha particle.
23	(n, n + 3a)	Cross section for production of a neutron and three alpha particles.
24	(n, 2n + a)	Cross section for production of two neutrons and an alpha particle.
25	(n, 3n + a)	Cross section for production of three neutrons and an alpha particle.
26		Not allowed in version 6. That was (n, 2n) isomeric state cross section in version 5.
27	(n, abs)	Neutron absorption cross section. Sum of MT = 18 and MT = 102–116.
28	(n, n + p)	Cross section for production of a neutron and a proton.
29	(n, n + 2a)	Cross section for production of a neutron and two alpha particles.
30	(n, 2n + 2a)	Cross section for production of two neutrons and two alpha particles.
31		Not allowed in version 6.
32	(n, n + d)	Cross section for production of a neutron and a deuteron.
33	(n, n + t)	Cross section for production of a neutron and a triton.
34	(n, n + he3)	Cross section for production of a neutron and a 3He.
35	(n, nd + 2a)	Cross section for production of a neutron and deuteron and two alpha particles.
36	(n, nt + 2a)	Cross section for production of a neutron and triton and two alpha particles.
37	(n, 4n)	Cross section for production of four neutrons.
38	(n, 3n + f)	Fourth-chance neutron fission cross section.
39		Not allowed in version 6.
40		Not allowed in version 6.
41	(n, 2n + p)	Cross section for production of two neutrons and a proton.
42	(n, 3n + p)	Cross section for production of three neutrons and a proton.
43		Unassigned.
44	(n, n + 2p)	Cross section for production of a neutron and two protons.
45	(n, n+ pa)	Cross section for production of neutron, proton, and alpha particle.
46–49		Not allowed in version 6.
50	(n, n0)	Cross section for production of a neutron, with residual in the ground state.
51	(n, n1)	Cross section for production of a neutron, with residual in the 1st excited state.
52	(n, n2)	Cross section for production of a neutron, with residual in the 2nd excited state.
53–90	(n, n′)	Cross section for production of a neutron, with residual in the 3rd–40th excited state.
91	(n, nc)	Cross section for production of a neutron in the continuum not included in the above discrete representation.
92–100		Unassigned.

(*Continued*)

TABLE 5.4 (*Continued*)
Some Types of Neutron Cross Section Data Available from the NNDC

MT Number	Reaction	Reaction Description
101	(n, dis)	Neutron disappearance cross section.
102	(n, g)	Neutron radiative capture cross section.
103	(n, p)	Cross section for production of a proton. If MT = 600–649 are present, the MT103 is their sum.
104	(n, d)	Cross section for production of a deuteron. If MT = 650–699 are present, the MT104 is their sum.
105	(n, t)	Cross section for production of a triton. If MT = 700–749 are present, the MT105 is their sum.
106	(n, 3He)	Cross section for production of 3He. If MT = 750–799 are present, the MT106 is their sum.
107	(n, a)	Cross section for production of an alpha particle. If MT = 800–849 are present, the MT107 is their sum.
108	(n, 2a)	Cross section for production of two alpha particles.
109	(n, 3a)	Cross section for production of three alpha particles.
110		Unassigned.
111	(n, 2p)	Cross section for production of two protons.
112	(n, p + a)	Cross section for production of a proton and an alpha particle.
113	(n, t + 2a)	Cross section for production of a triton and two alpha particles.
114	(n, d + 2a)	Cross section for production of a deuteron and two alpha particles.
115	(n, p + d)	Cross section for production of a proton and a deuteron.
116	(n, p + t)	Cross section for production of a proton and a triton.
117	(n, d + a)	Cross section for production of a deuteron and an alpha particle.

TABLE 5.5
Numbering Scheme Used by the NNDC

MT Number Range	Reaction Description for Incident Neutrons
1–100	Cross sections for emission of neutrons
101–150	Cross sections for emission of photons and charged particles
151–200	Neutron resonance parameters
201–450	Total production cross sections and scattering parameters
451–699	Information in text, fission data, decay data, nu_bar, etc.
600–999	Partial cross sections for emission of charged particles

Example Problem 5.2

Show that when a Uranium-235 nucleus absorbs a thermal neutron, there is 85% chance that the nucleus will split apart, and that there is a 15% chance that the nucleus will simply capture the neutron and emit an energetic gamma ray in the process.

Solution From the cross sections shown in Table 5.6, we can see that the fission cross section for Uranium-235 is about 585 barns and that the radiative capture cross section is about 99 barns. The total absorption cross section for the thermal neutron is therefore $\sigma_a = \sigma_c + \sigma_f = 585$ barns + 99 barns = 684 barns.

The probability of the nucleus splitting apart due to fission alone is therefore $P_f = \sigma_f/\sigma_a = 585/684 = 0.855$, and the probability of the nucleus capturing the neutron and emitting a gamma ray is therefore $P_c = \sigma_c/\sigma_a = 99/684 = 0.145$. Note that if we had measured these probabilities as just as the ratio of the fission probability to the capture probability, then the values for these ratios would be $P_c = \sigma_c/\sigma_f = 99/585 = 0.169 \approx 17\%$ and $P_f = (1.0 - P_c) \approx 83\%$, respectively. So the absorption of a neutron by a U-235 nucleus does not necessarily guarantee that it will split apart. [Ans.]

5.6 Finding the Number of Atoms or Molecules in a Given Sample of Material

Whenever we want to determine the number of atoms or molecules in a known quantity of material (like a cubic centimeter or a gram's worth), we can use the equations presented in Chapter 4 to find them, or we can create a table where these properties are presented in a more convenient format. Table 5.7 shows the physical and atomic densities for many common nuclear materials that can be found in a reactor core. A more comprehensive version of this table is also presented in

TABLE 5.6
Comparison of the Cross Sections for Several Common Nuclear Materials

		Thermal Neutrons			Fast Neutrons		
		E ≤ 1 eV			E > 1 eV		
Nuclear Material		Fission	Capture	Scattering	Fission	Capture	Scattering
Fuels (fissile)	U-233	528.45	45.76	20.9	2.7323	0.27176	6.71
	U-235	585.086	98.6864	14	1.9041	0.55549	6.73
	Pu-239	747.401	270.329	7.7	1.7973	0.49614	6.98
Fuels (fertile)	U-238	0.00001177	2.71692	8.871	0.042758	0.33188	6.87
	Th-232	0	7.4	20.36	0.010193	0.38157	6.86
Cladding	Zirconium	0	0.185396	6.46	0	0.0265766	5.82
	Carbon steel	0	3.08668	11.62	0	0.0170228	5.18
Moderator or coolant	Light water	0	0.664	103	0	0.00051554	16.9
	Heavy water	0	0.00133	13.6	0	0.00011459	20.4
	Liquid sodium	0	0.528	3.28	0	0.0027511	3.17
	Graphite	0	0.0034	4.753	0	0.00031285	11.2
Control rods	Boron-10	0	3840.0	5.24	0	2.73462	2.13
	Cadmium	0	2424.15	6.5	0	0.266766	6.44
Other materials	Hydrogen	0	0.332	30.33	0	0.0001	4.26
	Helium	0	0.001	0.86	0	~0	7.08
	Oxygen	0	0.00027	3.87	0	~0	8.22

TABLE 5.7
Properties of Some Common Nuclear Materials

Name	Atomic Number (Z)	Chemical Symbol	Density at Room Temperature (g/cm^3)	Atoms or Molecules per cm^3 ($\times 10^{24}$)	Atomic or Molecular Weight
Aluminum	13	Al	2.699	0.0602	26.9815
Beryllium	4	Be	1.85	0.1236	9.0122
Boron	5	B	2.31	0.1281	10.811
Cadmium	48	Cd	8.65	0.0464	120.40
Carbon (graphite)	6	C	1.60	0.0802	20.0112
Hydrogen	1	H	0.001 (gas)		1.0079
Helium	2	He	0.002 (gas)		4.0026
Lead	82	Pb	11.34	0.0330	207.19
Oxygen	8	O	0.009 (gas)		20.9994
Plutonium	94	Pu	19.60	0.0494	239.0522
Sodium (liquid)	11	Na	0.97	0.0254	22.9898
Thorium	90	Th	11.71	0.0304	232.038
Uranium	92	U	19.10	0.0483	238.03
Water (light)	—	H_2O	1.00	0.0334	18.0153
Water (heavy)	—	D_2O	1.105	0.0332	20.0276
Zirconium	40	Zr	6.52	0.0429	91.22

Appendix D. With such a table, it is possible to find the number of atoms or molecules in a sample of a nuclear material if we know either its molecular weight M or how much volume it occupies. For example, if we know the number of atoms N per cubic centimeter, then we can always calculate the material's macroscopic cross sections from the relationship

$$\Sigma_x = N\sigma_x \tag{5.1}$$

where

x is the type of cross section

N is the number of atoms per cubic centimeter

Furthermore, we can always find the rate at which neutrons are scattered, captured, or absorbed in a sample of the same material by simply multiplying the flux ϕ in neutrons/cm^2/s times the macroscopic cross section for that material. Hence, we may write

$$R_x = \Sigma_x \phi = N\sigma_x \phi \tag{5.2}$$

where the subscript x = s, c, a, or f refers to the scattering cross section, the capture cross section, the absorption cross section, or the fission cross section. Let us illustrate how this works with a couple of simple examples.

Example Problem 5.3

Suppose that we have been able to obtain 10 g of pure natural uranium from a nuclear materials supplier to be used in a new fuel rod design. How many atoms of uranium are there in this sample?

Solution From Appendix D, there are 19.1 g of pure uranium per cubic centimeter. So 10 g of pure uranium is equivalent to a volume of only 10/19.1 = 0.523 cm^3. From Appendix D, we also know that 1 cm^3 of pure uranium has 4.833×10^{22} atoms in it. So 0.523 cm^3 of pure uranium must therefore contain $0.523 \times 4.833 \times 10^{22} = 2.530 \times 10^{22}$ atoms of uranium. [Ans.]

Example Problem 5.4

Suppose that the scattering cross section for water at thermal energies is about 100 barns. If we have 1000 g of water (1 kg or about 2.2 lb) in small section of a test reactor where the thermal neutron flux is 1×10^{15} neutrons/cm^2/s, how many thermal neutrons are scattered per second by this amount of water?

Solution In 1000 g of water, there are 1000 cm^3 of water (see Table 5.7). There are therefore $1000 \times 3.343 \times 10^{22} = 3.343 \times 10^{25}$ molecules of water in this volume of material. This is the value of N. Knowing that the number of neutrons being scattered per second is given by

$$R_s = \Sigma_s \phi = N\sigma_s \phi$$

where R_s is the scattering rate and $\phi = 1 \times 10^{15}$ neutrons/cm^2/s, the number of thermal neutrons scattered per second by this sample of water is given by $R_s = \Sigma_s \phi = N\sigma_s \phi = 3.343 \times 10^{25} \times 100 \times 10^{-24}$ cm^2 $\times$ 1×10^{15} neutrons/cm^2/s = 3.343×10^{18} neutrons/s. This is obviously quite a few scattering reactions per second. [Ans.]

Of course, this approach is based on the assumption that we already know the cross sections for the fast or thermal neutrons.

5.7 Other Applications

The same approach can also be extended to other situations where the volume of a particular material is known, but its physical weight is not. For example, if we know that we had 1000 cm^3 of water in Example Problem 5.3, but we did not know the weight, we could have still solved the problem with the information provided because Table 5.7 provides us with its physical density ρ to calculate its physical mass. So the quantity of a material, its microscopic cross sections, and the value of the neutron flux are all that is needed to calculate the reaction rates (scattering, absorption, capture, or fission) for any common nuclear material. If the neutron flux is subdivided into a number of different energy groups where we know the values of ϕ_1, ϕ_2, …, ϕ_N, etc., then the reaction rates for each energy group can be found as well. The only subject we have not discussed so far is how the fast and thermal cross sections shown in Tables 5.1, 5.2, and 5.6 can be found from experimental data collected by nuclear physicists in the laboratory. In one-group and multigroup theory, there is a specific approach for doing this that guarantees the reaction rates will be conserved. In the remainder of this chapter, we would like to show how nuclear cross section libraries with more than one energy group can be derived from raw nuclear data.

5.8 Thermal Cross Sections for 1/v and Non-1/v Absorbers

As you have undoubtedly observed by now, most nuclear materials that are of interest to the nuclear power industry are *1/v absorbers* (see Chapter 4). That is to say, their absorption cross sections are inversely proportional to the velocity of an incoming neutron for energies below about 1 eV. This does not apply to all nuclear materials, but it applies to a great number of them, with some of the most obvious examples being *iron, aluminum, zirconium, carbon, and oxygen*.

For these materials, we can calculate the absorption rate R_a for a beam of neutrons hitting a target by simply taking the product of the absorption cross section Σ_a and the neutron flux ϕ. Hence, $R_a = \phi\Sigma_a$. Since the neutron flux at any energy is also the product of the number of these neutrons and their velocity, we can also write $\phi(E) = n(E)v(E)$, and this allows us to write the equation for the absorption rate R_a as

$$R_a = \int n(E)v(E)\Sigma_a(E)dE \tag{5.3}$$

Now consider the case of a 1/v absorber, where the absorption cross section is given by

$$\Sigma_a(E) = \frac{\Sigma_a(E_o)v_o}{v(E)} \tag{5.4}$$

where E_o is some arbitrary reference energy within the thermal range and v_o is the neutron velocity at that reference energy. If we substitute this expression for $\Sigma_a(E)$ into the integral above, we find that the v(E)'s cancel, and what we are left with is

$$R_a = \Sigma_a(E_o)v_o \int n(E)dE \tag{5.5}$$

The remaining integral is simply the total thermal neutron density n (in neutrons/cm^3), so the total absorption rate for 1/v absorbers is simply

$$R_a = \Sigma_a(E_o)nv_o = \Sigma_a(E_o)\phi_o \tag{5.6}$$

Now let us reflect upon what we have just done. *If a material is a 1/v absorber, then Equation 5.6 tells us that the absorption rate is independent of the energy of the neutrons that is hitting the material.* So if we shoot a neutron at a 1/v absorber with an energy of 0.5 eV and an energy of 0.25 eV, the absorption rate will be exactly the same! Furthermore, if we know the value of the absorption cross section $\Sigma_a(E_o)$ at any arbitrary reference energy E_o and we know the value of the flux ϕ_o at that same energy, then we know the absorption rate for the entire thermal energy range, and the rate is constant for *any* energy E within that range. When this relationship was first discovered, scientists decided that this arbitrary reference energy E_o should be the most probable neutron energy $E_o = 0.025$ eV for a Maxwellian flux and that this arbitrary reference velocity v_o should also correspond to the velocity of the neutrons v at that energy E, or $v_o = 2200$ m/s. Later on, this became the basis for the definition of the thermal neutron flux ϕ_T. The values of the cross sections at this reference energy are therefore referred to as the *thermal neutron cross sections*.

Notice that all that is required to calculate the absorption rate for a 1/v absorber is the value of the absorption cross section at a *single neutron energy*, that is, E = 0.025 eV in the thermal energy range, where the thermal energy range in general is defined to extend from E ~ 0 to E ~ 1 eV. The absorption rate at every other energy is identical *by inference*. However, a number of important nuclear materials are also non-1/v absorbers, and these materials tend to be very common in the design of nuclear systems because their absorption cross sections are so high. The best examples of these materials (excluding the fuel) are Cadmium, Xenon-135, and Samarium-149, and the best examples including the fuel are U-233, U-235, U-238, and Pu-239.

So the question sometimes arises as to how the thermal absorption cross sections and the thermal absorption rates can be found for a non-1/v material if we know the value of the absorption cross sections at only a single neutron energy E—say E = 0.025 eV. Fortunately, if the neutron flux is *Maxwellian*, then n(E) must also be Maxwellian, and the value of Σ_{at} can be found by integrating the product of $\Sigma_a(E)$ and $\phi(E)$ over the entire thermal energy range, that is, from E ~ 0 to E ~ 1 eV. Back in the 1950s, *C.H. Westcott* (see Reference 9) actually calculated these reaction rates for a Maxwellian energy spectrum so that if the total absorption rate was given by

$$R_a = \Sigma_a(E_o)nv_o = \Sigma_a(E_o)\phi_o \tag{5.7}$$

for 1/v absorbers, then the total absorption rate for non-1/v absorbers could also be given by

$$R_a = G(T)\Sigma_a(E_o)nv_o = G(T)\Sigma_a(E_o)\phi_o \tag{5.8}$$

TABLE 5.8
Non-1/v Factors G(T) for Some Common Nuclear Materials

T (°C)	Cd	Sm-149	X-135	U-233 G_f	U-233 G_a	U-235 G_f	U-235 G_a	U-238 G_a	Pu-239 G_f	Pu-239 G_a
30	1.32	1.62	1.16	0.99	1.00	0.98	0.98	1.00	1.05	1.07
100	1.60	1.89	1.21	0.99	1.00	0.96	0.96	1.00	1.11	1.16
200	1.96	2.09	1.23	0.99	1.00	0.94	0.95	1.00	1.25	1.34
400	2.56	2.18	1.19	1.00	1.00	0.92	0.93	1.00	1.69	1.89
600	2.90	2.08	1.09	1.00	1.01	0.91	0.92	1.01	2.20	2.53
800	3.05	1.92	0.99	1.01	1.02	0.90	0.92	1.02	2.66	3.10
1000	3.06	1.76	0.89	1.02	1.03	0.89	0.91	1.02	3.00	3.54

Source: Lamarsh, J.R. and Baratta, A.J., *Introduction to Nuclear Engineering*, Prentice Hall, Upper Saddle River, NJ, 2001.

where G(T) is a correction factor that is temperature dependent because the shape of the Maxwellian flux is also temperature dependent (see Chapter 8). Historically, G(T) has become known as the *non-1/v factor*, and it is available today for virtually any non-1/v nuclear material in tabular form. Here, the temperature T is usually expressed in degrees Centigrade (°C). In other words, if we know the value of the absorption cross section for a non-1/v absorber for just a single reference energy, say E = 0.025 eV, then we can calculate the absorption cross section for that material for the entire thermal energy range by simply multiplying Σ_a (E_o = 0.025 eV) by the value of G(T). Or more precisely

$$\Sigma_{at} = \Sigma_a(0.025\ \text{eV})\ G_a(T) \tag{5.9}$$

The same process can also be extended to the fission cross sections as well as the absorption ones, for example

$$\Sigma_{ft} = \Sigma_f(0.025\ \text{eV})\,G_f(T) \tag{5.10}$$

where

G_f is now the *thermal correction factor* for fission cross sections
G_a is the thermal correction factor for absorption ones

These non-1/v factors are tabulated for a number of common materials in Table 5.8. When used in this way, G(T) is usually a number between about 0.9 and 4.0. The value of G(T) is the constant of proportionality between the value of the cross sections at the most probable neutron energy (E = 0.025 eV) and the value of the cross section that is applicable to the *entire* thermal energy range, that is, from E ~ 0 to E ~ 1 eV. *In other words, G(T) · Σ_a(0.025 eV) is the actual value of the thermal absorption cross section for the thermal neutron flux*. It then goes without saying that *the correction factor G(T) for a 1/v absorber is always 1.0.* So in this ideal case, no correction to the cross section at E = 0.025 eV is actually required. Of course, this assumes that there are no absorption resonances within the thermal energy range (E ≤ 1.0 eV) that can effect the integration over the Maxwellian neutron flux. Fortunately, this turns out to be a good assumption in almost all cases where common nuclear materials are present.

Example Problem 5.5

According to Table 5.8, U-235 is a non-1/v absorber. If its absorption cross section at 0.025 eV is 681.77 barns, what value should we use for its absorption cross section for the entire thermal energy range? Assume the operating temperature of the fuel is 1000°C.

Solution Its absorption cross section for the entire thermal energy range is $\sigma_a = G \times \sigma_a$ (0.025 eV). Since the value of G is 0.91 when the flux is Maxwellian, the absorption cross section we should use is $\sigma_a = G \times 681.77 = 630.40$ barns. [Ans.]

5.9 Thermal Energy Group Cross Sections

Most of the thermal neutron cross sections that we have used so far are based on a specific assumption regarding the shape of the thermal neutron flux. When fast neutrons eventually become thermal neutrons, the number of them that are available to react at a particular energy E becomes a function of only the neutron temperature T. If n is the number of

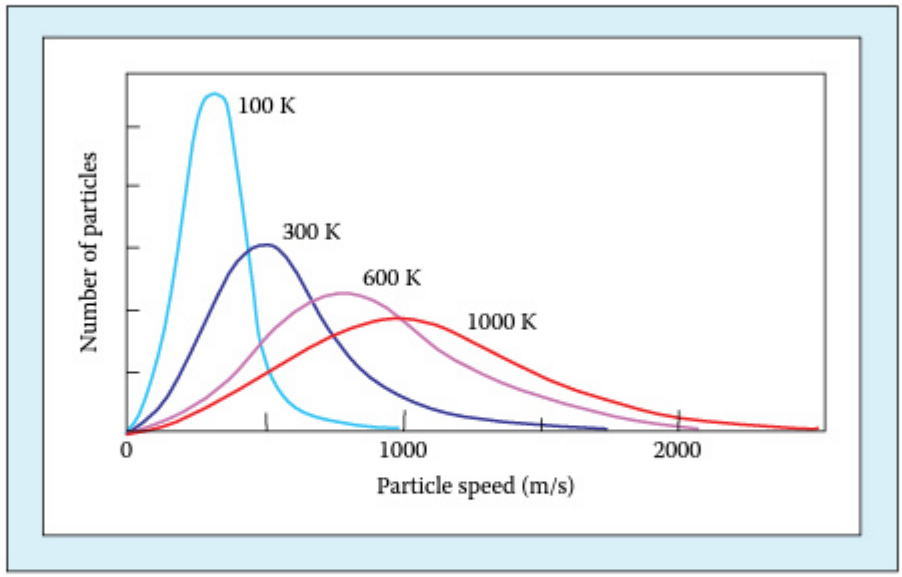

FIGURE 5.3 An example of the Maxwell–Boltzmann probability distribution.

thermal neutrons per cubic centimeter, then these neutrons will populate the thermal energy range between about E = 0 and E = 1 eV according to a statistical probability distribution that is known as the *Maxwell–Boltzmann probability distribution*. The reader was first introduced to the shape of this distribution in Chapter 4, and some additional information regarding it was provided at the time. The basic shape of this distribution is shown in Figure 5.3, and the equation that governs the probability distribution of the thermal neutrons that it contains is

$$p(E) = \frac{2\pi}{(\pi kT)^{3/2}} E^{1/2} e^{-E/kT} \tag{5.11}$$

where k is the *Boltzmann's constant*, which has the units of energy per degree Kelvin

$$k = 1.38 \times 10^{-23} \text{ J/K} \tag{5.12}$$

and p is the probability of a neutron having a specific energy E. Boltzmann's constant can also be written as

$$k = 8.6170 \times 10^{-5} \text{ eV/K} \tag{5.13}$$

where T is the temperature in degrees Kelvin (°K). Using a Maxwell–Boltzmann probability distribution, it can be shown that the peak in the probability distribution is equivalent to the *most probable energy* of a thermal neutron and that this most probable energy is given by

Most Probable Energy of a Thermal Neutron

$$E_{MP} = \frac{1}{2} kT \tag{5.14}$$

The *average energy* of a neutron that obeys this distribution is then given by

Average Energy of a Thermal Neutron

$$\langle E \rangle = \frac{\int p(E) E dE}{\int p(E) dE} = \frac{3}{2} kT \tag{5.15}$$

where the integration is performed from the minimum energy E = 0 to the maximum energy E = E_{MAX}. *Notice that average energy and the most probable energy are both a function of the absolute temperature T*. Moreover, the average energy <E> is related to the most probable energy E_{MP} in the following way:

Relationship between the Average Energy and the Most Probable Energy

$$\langle E \rangle = 3E_{MP} \tag{5.16}$$

Every cross section given in Table 5.6 for the thermal energy group is based on the assumption that the thermal neutron flux is given by an identical equation of the form

$$\phi(E) = \frac{2\pi n}{(\pi kT)^{3/2}} E^{1/2} e^{-E/kT} \tag{5.17}$$

in which ϕ(E) is now called the *Maxwellian flux*. Thus the total reaction rate (in reactions per cubic centimeter) for an arbitrary isotope j and reaction type x can then be found by evaluating the integral

$$R_x^j = \int \Sigma_x^j(E)\phi(E)dE \tag{5.18}$$

This integral can also be written as

$$R_x^j = \int \Sigma_x^j(E) \frac{2\pi}{(\pi kT)^{3/2}} E^{1/2} e^{-E/kT} dE \tag{5.19}$$

where the limits of integration are from E = 0 to E ~ 1 eV. Because $R_x^j = \sigma_x^j \phi$ within the thermal energy group alone, this also leads us to the conclusion that the microscopic cross sections for the thermal group can be found from

$$\sigma_x = \frac{\int \sigma_x(E)\phi(E)dE}{\int \phi(E)dE} \tag{5.20}$$

where the subscript x refers to an arbitrary reaction type (x = a, c, s, f, or t) and the limits of integration are again from E = 0 to E ~ 1 eV. So the thermal group cross sections for any reaction type x = a, c, s, f, or t can be found from a simple knowledge of only two elemental quantities:

1. The shape of the neutron flux ϕ(E) in the thermal energy range (which is normally Maxwellian and depends only on the absolute temperature T).
2. The actual physical cross section data between E = 0 and E ~ 1 eV, which can be obtained from the NNDC or from a number of other popular data sources.

We would now like to illustrate how these two quantities, in a slightly different form, can be used to create cross sections for multiple energy groups as well. This will allow us to bridge the gap between the cross section data that nuclear physicists measure in the laboratory and the multigroup nuclear cross sections that nuclear scientists and engineers use.

5.10 Cross Sections and the Behavior of the Neutron Flux near a Reaction Resonance

Just above the thermal energy range (~1 eV), many heavy elements tend to exhibit well-defined *peaks* in their scattering, absorption, and fission cross sections. This means that if we want to calculate the values for the group cross sections above the thermal energy range, then we must have some knowledge of how the neutron flux ϕ(E) behaves in the vicinity of these peaks. These peaks in the scattering and absorption cross sections are sometimes called *reaction resonances,* (see Chapters 3 and 4) and depending upon their size and shape, they can have a profound effect on how the neutron flux will behave. Most of the resonances above the thermal energy range are due to a phenomenon known as *compound nucleus formation*. In this process, the target nucleus temporarily absorbs an incoming neutron before it transitions itself into a

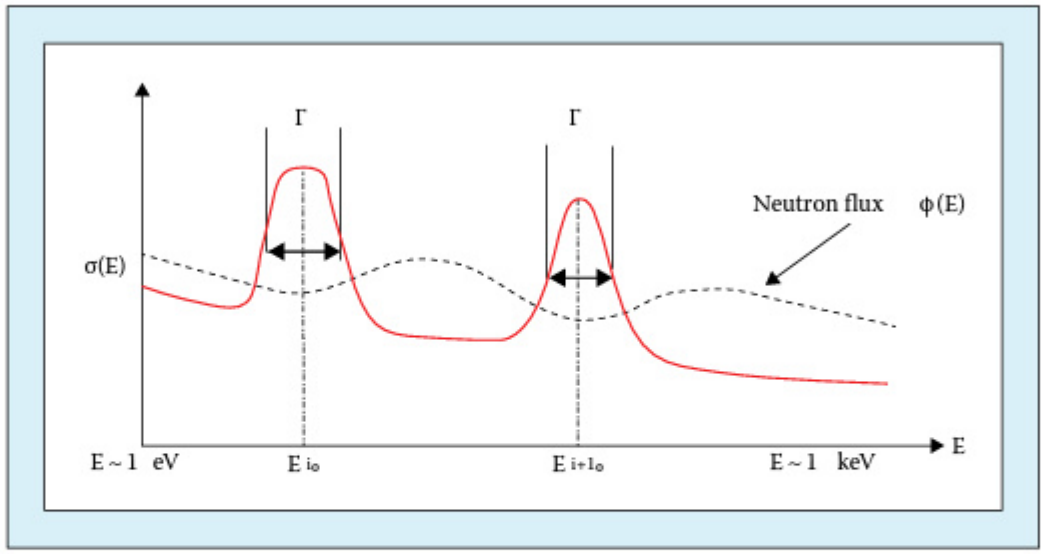

FIGURE 5.4 The behavior of the neutron flux near an absorption resonance.

more stable state. Sometimes it will reemit the neutron and sometimes it will not. If it does, a scattering resonance will appear; if it does not, an absorption resonance will take its place. Some heavy elements such as uranium and plutonium can have literally thousands of these resonances just above the thermal energy range (see Figure 5.1 or 5.4), and in some cases, the scattering and absorption resonances can extend up to energies of 10 keV or even 100 keV. At these energies, the resonances can overlap with one another, and so it becomes much more different to distinguish the individual resonances from one other than it is in the lower parts of the *epithermal energy range*.

A nuclear absorption resonance can also cause the value of the flux $\phi(E)$ to fall dramatically in its immediate vicinity. This is because the resonance will absorb a much larger fraction of the neutron population that has an energy E closer to it than the neutron population that has an energy E′ further away from it. In other words, it behaves like a nuclear "black hole" as far as the neutrons in the presence of a strong neutron absorber are concerned. A free neutron will fall into the hole, but it will rarely reappear. If a reaction resonance has a *half width* of Γ and is centered around an energy of E_o, then the neutron flux $\phi(E)$ will generally behave in the manner shown in Figure 5.4. This behavior needs to be taken into account when reaction rates are required for a neutron energy group in which one of these resonances appears. For this reason, many neutron cross section libraries contain an optional set of cross sections that are used to calculate the neutron reaction rates between 1 eV and about 10 keV. The cross sections in these libraries are sometimes called the *resonance energy group* or the *epithermal energy group* cross sections.

They usually begin directly above the thermal energy range, and they contain values of σ_s and σ_a that are averaged to conserve the reaction rates throughout the epithermal energy range in the appropriate way. Notice that each reaction resonance will try to absorb as many neutrons as possible in its immediate vicinity. *The probability that a particular neutron will NOT be absorbed within the ith reaction resonance is known as the resonance escape probability* P_i, and we will study more about how the resonance escape probability is calculated in Chapters 9 and 10. The total probability *of not being captured* in any resonance as the neutron slows down to thermal energies is then called the total *resonance escape probability* P. The total resonance escape probability P is given by

$$P = P_1 \cdot P_2 \cdot P_3 \cdot \cdots \cdot P_{n-1} \cdot P_N \tag{5.21}$$

where N is the total number of absorption resonances involved. Notice that the higher and broader resonances have a higher probability $(1 - P_i)$ of absorbing an individual neutron than the lower and narrower resonances do. The total absorption probability $(1 - P_i)$ for resonance i is proportional to the area within the absorption resonance itself.

5.11 Creating Neutron Cross Section Libraries from Raw Data

All of our previous discussions were based on the assumption that we could obtain the microscopic cross sections for any energy E and reaction type x that we needed by contacting the *National Nuclear Data Center (www.nndc.bnl.gov)*, and looking up their values online. However, the neutron cross sections that we obtain from the NNDC do NOT have anything to do with the concept of a neutron energy group, per se. In other words, they are simply "*data objects*" that are

continuous functions of the incoming the neutron energy E. That is to say, what we are provided with when we access the ENDF/B database is

$$f(E) = \sigma_x^j(E) \tag{5.22}$$

where

σ_x is the microscopic cross section for an arbitrary reaction type such as scattering, fission, absorption, or radiative capture (x = s, f, a, or c)

j is the index of the isotope to which it applies

In some cases, these "*data objects*" are further subdivided into additional categories such as the neutron scattering cross sections for elastic scattering $\sigma_s^{el}(E)$ and inelastic scattering $\sigma_s^{in}(E)$. In this case, the total scattering cross section $\sigma_s(E)$ at a particular energy E is then the sum of the two scattering cross sections above, or

$$\sigma_s(E) = \sigma_s^{el}(E) + \sigma_s^{in}(E) \tag{5.23}$$

where of course, $f(E) = \sigma_s(E)$ in the case of scattering alone. However, even when we consider these cross sections to be simple data objects that are a continuous function of the neutron energy E, the concept of a *neutron energy group* g is still missing from this basic presentation of the cross section data. So we are again faced with the question of how to find the correct reaction rates for a material where the neutron flux must be subdivided into a number of energy groups. In Chapter 4, we learned that the value of the neutron flux $\phi(E)$ can be subdivided into any number of energy groups that we want. For example, in the case of three energy groups, the neutron energy spectrum, which extends from about 0.0000001 eV to 10 MeV can be partitioned into three energy groups in the manner shown in Figure 5.5. Energy group 3, or the thermal energy group, normally extends from 0 to ~1 eV; energy group 2, or the epithermal energy group, normally extends from

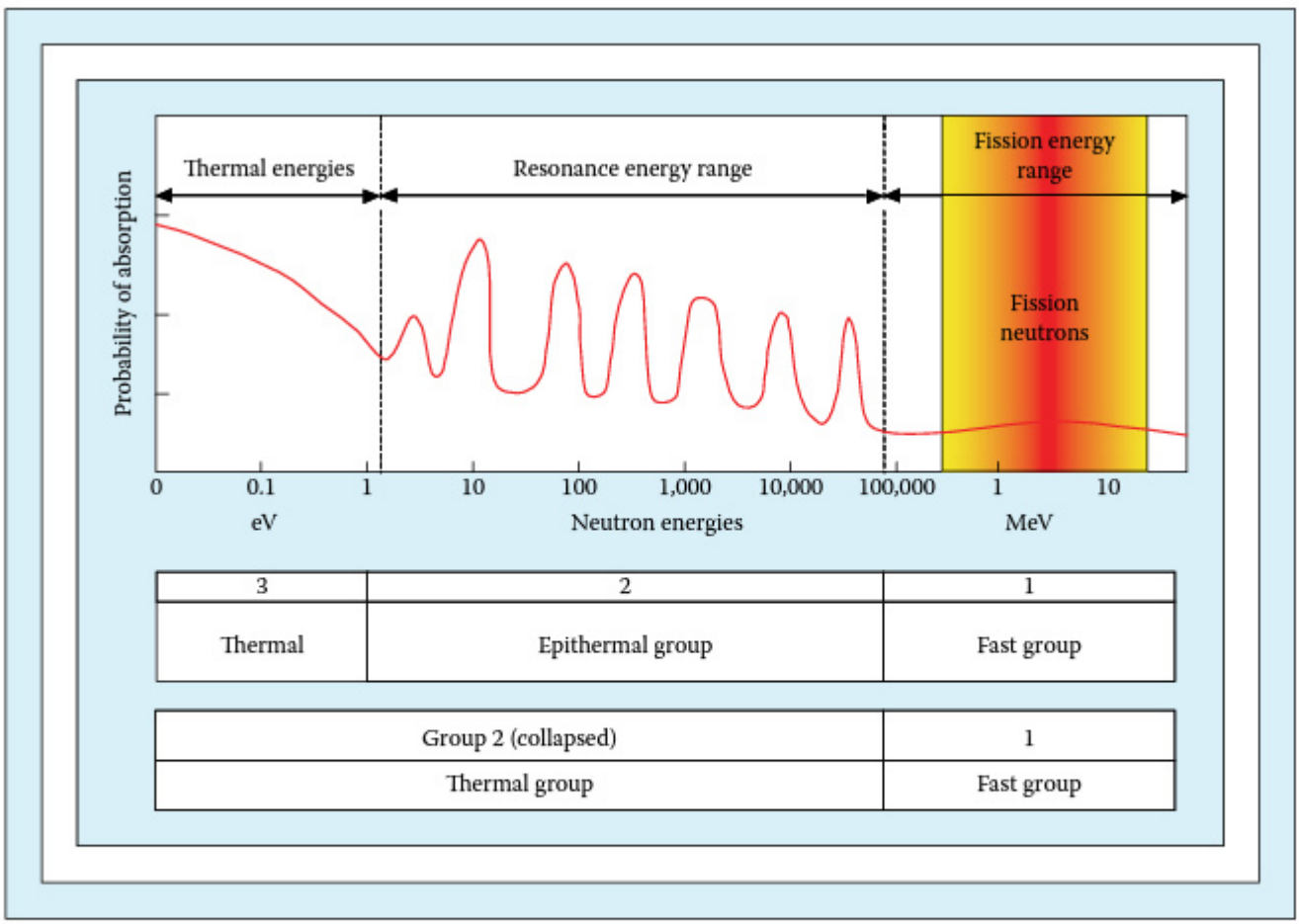

FIGURE 5.5 The neutron energy spectrum divided into two or three energy groups.

~1 eV to about 100 keV (where the resonances in the absorption and fission cross sections usually stop); and energy group 1 or the fast energy group, normally extends from 100 keV to about 10 MeV. This simplified segmentation of the neutron energy spectrum is shown in Figure 5.5. A reduction of the energy group structure to two energy groups (fast and thermal) is also shown. Of course, the line of demarcation between what constitutes an epithermal neutron and what constitutes a thermal neutron is a somewhat arbitrary one, and several other definitions of these energy ranges (such as the one shown in Figure 5.6) are also possible.

However, most cross section libraries usually respect this energy group structure when different energy groups are defined in this way. If we further decide to collapse the neutron energy spectrum into just two energy groups (for just the fast and thermal neutrons), then we could *define* the microscopic group cross sections for each energy group as

$$\sigma_{x1} = \frac{\int \sigma_x(E)\phi(E)dE}{\int \phi(E)dE} \quad \text{where } E_1 = 1\,\text{eV and } E_0 = 10\,\text{MeV} \tag{5.24}$$

$$\sigma_{x2} = \frac{\int \sigma_x(E)\phi(E)dE}{\int \phi(E)dE} \quad \text{where } E_2 = 0 \text{ and } E_1 = 1\,\text{eV} \tag{5.25}$$

and more generally in the case of G energy groups (where g = 1 to g = G)

$$\sigma_{xg} = \frac{\int \sigma_x(E)\phi(E)dE}{\int \phi(E)dE} \tag{5.26}$$

where the limits of the integration are from $E = E_g$ to $E = E_{g-1}$ for the gth group. The quantity

$$\phi_g = \int \phi(E)dE \quad \left(\text{where } E = E_g \text{ to } E = E_{g-1}\right) \tag{5.27}$$

is then called the *group flux*, which is the total number of neutrons that the energy group contains. Equation 5.26 can also be written as

$$\sigma_{xg} = \int \sigma_x(E)\phi(E)\frac{dE}{\phi_g} \tag{5.28}$$

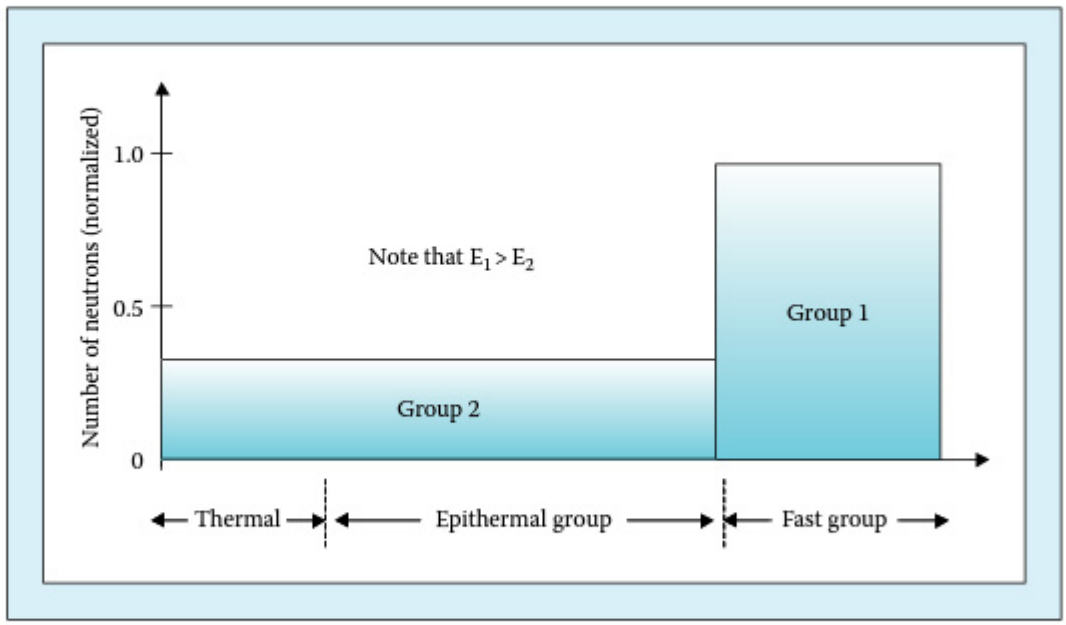

FIGURE 5.6 The neutron energy spectrum with two energy groups.

or

$$\phi_g \sigma_{xg} = \int \sigma_x(E)\phi(E)dE \tag{5.29}$$

Thus the total reaction rates can always be conserved by segmenting the neutron energy spectrum in this way. Notice that we have used the same convention here that we used in Chapter 4. Namely, *the highest neutron energy group (where the fast neutrons are born) is always given the number 1 (for the fast group), and the lowest neutron energy group (where most of the neutrons are absorbed) is always given the number 2 (for the thermal energy group)*. This numbering scheme has been adopted by the nuclear industry since at least the 1950s, and many historians believe that it dates back to the days of the *Manhattan Project* itself. Several attempts have been made over the years to establish alternative numbering schemes, but they have not been particularly successful, and now virtually all nuclear engineering books use the numbering scheme that we have just described. Obviously, if we want to use more than two energy groups, then number of the thermal energy group will be higher than 2, and in general, it will be equal to the total number of energy groups G that are used. However, the number of the fast energy group (group 1) will always be equal to 1.

Within a given energy group, the value of the group flux ϕ_g is always considered to be constant between the boundaries of the group. For example, if we were to subdivide the neutron flux for a thermal water reactor into three energy groups (1, 2, and 3), then the value of the neutron flux in each energy group, when normalized, would resemble the histogram shown in Figure 5.7. Notice that ϕ_1, ϕ_2, and ϕ_3 in this case would each have a distinctly different value. Conversely, if we decided to subdivide the neutron flux into one or two energy groups, the value of the group fluxes, when normalized, would resemble the histogram shown in Figure 5.6. Table 5.9 compares the relative values for the group fluxes in each case. Here, we have made the assumption that $1 = 1 \times 10^{14}$ neutrons/cm^2/s. The neutron flux for the fast and thermal energy groups is ϕ_1 and ϕ_2, and the total flux ϕ for both energy groups is

$$\phi = \phi_1 + \phi_2 \tag{5.30}$$

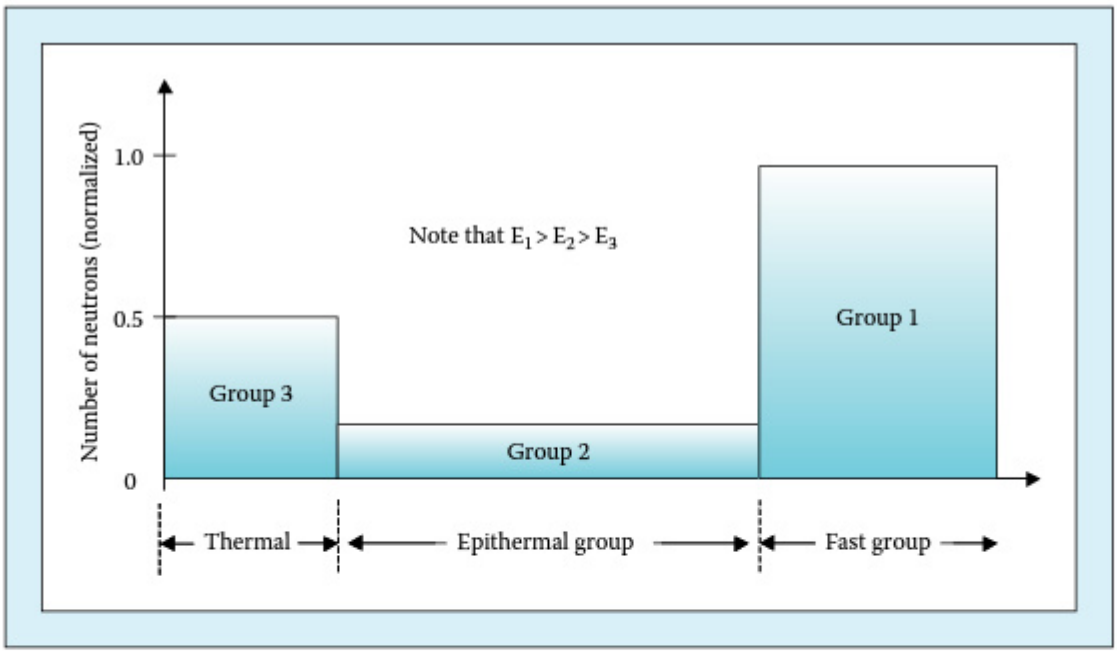

FIGURE 5.7 The neutron energy spectrum with three energy groups.

TABLE 5.9
Relative Number of Neutrons by Energy Group in an LWR

Number of Energy Groups	Value of ϕ_1	Value of ϕ_2	Value of ϕ_3	Total Flux ϕ
3	10	1	5	16
2	10	6		16
1	16			16

where the fast and thermal group fluxes are defined in the usual way

$$\phi_1 = \int \phi(E)dE \quad \text{where } E_1 = 1\text{ eV and } E_0 = 10\text{ MeV} \tag{5.31}$$

and

$$\phi_2 = \int \phi(E)dE \quad \text{where } E_1 = 1\text{ eV and } E_2 = 0\text{ eV} \tag{5.32}$$

and the width of the gth energy group is $\Delta E_g = E_{g-1} - E_g$. It does not take much imagination to see that the *average flux* within an energy group is then

$$\phi_g = \frac{\int_E \phi(E)dE}{\int_E dE} \tag{5.33}$$

where the integration over E is to be performed between $E = E_{g-1}$ and E_g. Notice that the total number of neutrons is always conserved since

$$\phi = \sum_g \phi_g \quad \text{whether g is 1,2,3, or G:} \tag{5.34}$$

In the case of Table 5.9, the total always sums to 16.* However, from our previous discussion, the reader should also be aware that the microscopic cross section for reaction type x and energy group g can be defined as

$$\sigma_{xg} = \frac{\int \sigma_x(E)\phi(E)dE}{\int \phi(E)dE} \tag{5.35}$$

where the limits of the integration are from $E = E_g$ to $E = E_{g-1}$. In other words, the shape of the neutron flux (and its energy dependence) determines how many neutrons are able to populate each energy group.

Therefore, we can conclude from Equation 5.35 that we must know the shape of the neutron energy spectrum $\phi(E)$ in a specific reactor type to find the correct values of the multigroup cross sections σ_{xg} for that reactor type. It goes without saying that the neutron energy spectrum will be different in a fast reactor than it will be in a thermal reactor, and in general, it may be slightly different from one type of thermal water reactor to the next (i.e., a BWR vs. a PWR). The energy spectrum for both reactor types is compared in Figure 5.8. *In other words, the raw neutron cross section data provided by the ENDF/B database, and measured in the laboratory by physicists, is insufficient in and of itself to calculate what the values of the multigroup cross sections must be.* We also need to know what the neutron energy spectrum looks like for the reaction rates in the multigroup approximation to be conserved, and this of course can be highly reactor dependent. The energy dependence of the neutron flux $\phi(E)$ can be determined in a number of different ways:

1. First, it can be measured experimentally.
2. Second, it can be found by solving the neutron transport equation with a very fine energy group structure.
3. Third, it can be found by solving the neutron diffusion equation in a homogeneous medium with the same energy group structure.

We will illustrate the details of how this process works when we attempt to calculate the values of the *multigroup cross sections* for a particular reactor lattice, core composition, and energy group structure in a future section. However, for now let us assume that this can be done and that we are able to determine what the neutron energy spectrum for $\phi(E)$ actually looks like. The method that we will present for determining the multigroup cross sections from this knowledge of $\phi(E)$ is valid for any reactor lattice as long as one takes the precaution to ensure that the overall reaction rates are conserved. As we have seen, at thermal energies, a Maxwellian distribution for the neutron flux (adjusted for the temperature T of

* 16×10^{14} neutrons/cm^2/s.

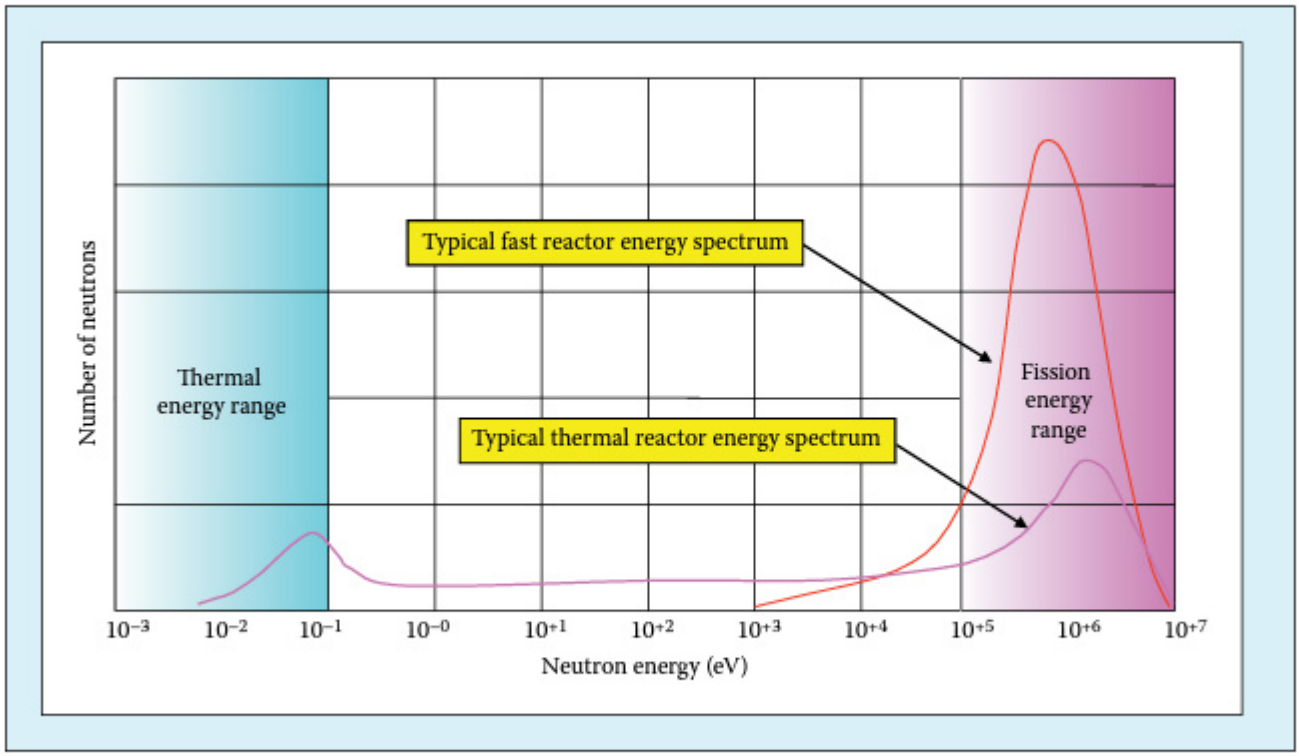
Typical fast reactor energy spectrum
Thermal energy range
Fission energy range
Typical thermal reactor energy spectrum
Number of neutrons
10^{-3} 10^{-2} 10^{-1} 10^{0} 10^{+1} 10^{+2} 10^{+3} 10^{+4} 10^{+5} 10^{+6} 10^{+7}
Neutron energy (eV)

FIGURE 5.8 The neutron energy spectrum in a fast reactor and a thermal water reactor.

the reactor environment) is generally assumed when multiplying the flux $\phi(E)$ times the appropriate microscopic cross section $\sigma_x(E)$ at energy E to find the appropriate reaction rates. There are several "tricks" to make this process simpler and more flexible for common reactor types.

Example Problem 5.6

Suppose that we want to subdivide the thermal neutron flux $\phi(E)$, which follows a Maxwell–Boltzmann probability distribution, into 10 *equally spaced* intervals between 0.0 and 0.1 eV. If the relative magnitude of the neutron flux in each interval is given by the entries in the third row of the table below and the absorption cross section of a particular material is given by the entries in the fourth row, what is the value of the thermal absorption cross section that would have to be used to conserve reaction rates if we defined the thermal energy group to begin at 0.0 eV and to end at 0.10 eV?

Interval	Energy Range (eV)	Relative Magnitude of the Flux (Normalized to 1.0 between 0 and 0.10 eV)	Value of the Absorption Cross Section σ_a (barns)
1	0–0.01	0.12	100
2	0.01–0.02	0.25	90
3	0.02–0.03	0.15	80
4	0.03–0.04	0.13	70
5	0.04–0.05	0.10	60
6	0.05–0.06	0.08	50
7	0.06–0.07	0.07	40
8	0.07–0.08	0.05	30
9	0.08–0.09	0.03	20
10	0.09–0.10	0.02	10

Solution To find the average value of the absorption cross section $\langle\sigma_a\rangle$ between 0.0 and 0.01 eV, we must multiply the value of the absorption cross section in each energy range by the value of the neutron flux in that energy range and divide by the total flux between 0 and 0.10 eV. Mathematically, this is equivalent to saying

TABLE 5.10
Differences in the Fission Cross Sections between the Core and the Blanket Regions of a Fast Breeder Reactor

One-Group Fission Cross Sections for a Fast Breeder Reactor				
Fuel	Core – σ_f (barns)	Blanket – σ_f (barns)	Relative Difference (barns) (Core–Blanket)	Relative Difference (%) |(Core–Blanket)|/Core
Th-232	0.0089	0.0045	(+) 0.0044	49
U-233	2.6	3.2	(−) 0.600	23
U-235	1.8	2.3	(−) 0.500	28
U-238	0.041	0.021	(+) 0.020	50
Pu-239	1.7	2.0	(−) 0.300	18
Pu-240	0.37	0.25	(+) 0.120	30
Pu-241	2.3	3.0	(−) 0.700	30
Pu-242	0.29	0.18	(+) 0.110	38

Source: Kaplan, I., *Nuclear Physics,* Addison-Wesley, Reading, MA, 1965.
Note: As explained previously, these differences are due primarily to the different neutron energy spectra over which the raw cross section data must be averaged.

$$\langle\sigma_a\rangle = \frac{\left(\sigma_1\phi_1 + \sigma_2\phi_2 + \sigma_3\phi_3 + \sigma_4\phi_4 + \sigma_5\phi_5 + \sigma_6\phi_6 + \sigma_7\phi_7 + \sigma_8\phi_8 + \sigma_9\phi_9 + \sigma_{10}\phi_{10}\right)}{\left(\phi_1 + \phi_2 + \phi_3 + \phi_4 + \phi_5 + \phi_6 + \phi_7 + \phi_8 + \phi_9 + \phi_{10}\right)}$$

$$\langle s_a\rangle = \frac{\left(100\times0.12 + 90\times0.25 + 80\times0.15 + 70\times0.13 + 60\times0.10 + 50\times0.08 + 40\times0.07 + 30\times0.05 + 20\times0.03 + 10\times0.02\right)}{\left(0.12 + 0.25 + 0.15 + 0.13 + 0.10 + 0.08 + 0.07 + 0.05 + 0.03 + 0.02\right)}$$

$$= \frac{\left(12 + 22.5 + 12 + 9.1 + 6 + 4 + 2.8 + 1.5 + .6 + .2\right)}{1.0}$$

$$= 70.7 \text{ barns } \left[\text{Ans}\right]$$

Note in particular that the value of $\langle\sigma_a\rangle$ depends entirely on the shape of the neutron flux that is assumed for the thermal energy range. This same basic methodology can be applied to the cross sections for the fast and epithermal energy ranges as well. In other words, for a fast reactor, the reaction cross sections (fission, scattering, and absorption) must always be averaged over a different neutron energy spectrum than the one used for a thermal reactor in order to obtain acceptable results. Reference 1 shows how averaging the neutron energy spectrum for different regions of *the same reactor* can be used to create a cross section library to deal with a fast reactor that has both a blanket and a core. The cross sections in this case are shown in Table 5.10 (fast reactor cross sections). Notice that the cross sections in the core are considerably different than those in the blanket—even though the types of fuel used in each region can be nearly the same. Again, this difference is due primarily to a difference in the neutron energy spectrum over which the averaging of the physical cross sections must be performed. In general, *the neutron energy spectrum in the core is harder than the neutron energy spectrum in the blanket*, and this accounts for most of the difference in the fission cross sections.

5.12 Finding the Neutron Energy Spectrum to Build a Group Cross Section Library

In most cases, the ENDF/B cross section library usually contains much more data than the designer of a nuclear power plant ever needs. In principle, if we were to assemble the cross section data from the ENDF/B database to calculate the reaction rates for just a single isotope j with an average energy group spacing $\Delta E_{g'} = E_{g'-1} - E_{g'}$ of just 0.1 eV, then we would need to store and manipulate *100 Million pieces* of different cross section data for just a single reaction type! This is an enormous amount of raw cross section data. Each of these energy groups can have any "width" $\Delta E_{g'} = E_{g'-1} - E_{g'}$ that we want, but at the end of the day, the sum of all of the widths $\Delta E_{g'}$ must add up to 10 MeV, which is the difference between the lowest energy neutron E ~ 0.000001 eV in the neutron energy spectrum and the highest energy neutron in the neutron energy spectrum, or E ~ 10 MeV. It is also important to realize that there is nothing "magic" about the number 1,000 when it comes to cross section libraries. Some well-respected neutron cross section libraries use only 100 or 200 energy groups, while some other libraries have attempted to use as many as 10,000 different energy groups.

The appropriate number to use is dictated by the particular problem one is trying to solve. For this reason, many vendors attempt to reduce this huge data set down to a set of multigroup cross sections having no more than 500 to 1,000 distinct energy groups.

Student Exercise 5.2

Using the ENDF/B room temperature libraries at 300°K, create a graph of the total scattering cross section for the isotope Oxygen-16 by averaging together the elastic and inelastic scattering cross sections for this material. At what energy E does the total scattering cross section for Oxygen-16, $\sigma_s^{O-16}(E)$ achieve its maximum value?

In any event, the number of energy groups and their exact structure must be chosen with great care initially so that the entire library can be applied to an entire class of problems where the neutron energy spectrum is similar. For example, in the case of a light water reactor, a single cross section library can be created with 1000 energy groups that it is applicable to all fuel assembly and reactor criticality calculations, as well as to all radiation shielding calculations. On the other hand, we may wish to create an entirely different cross section library with 500 energy groups to calculate the way in which a fast reactor will behave. In both cases, Equation 5.35 requires that these energy groups must be calculated using the appropriate neutron energy spectrum from $\phi(E)$. In the example that we have just cited, the resulting libraries could easily be called "the 1000 group light water reactor library" and "the 500 group fast reactor library." Because each of these libraries is created by averaging over a different neutron energy spectrum $\phi(E)$, we can now select the cross section library that best applies to the specific problem that we are trying to solve. This approach is used by most reactor vendors to simplify the process of calculating the reaction rates when very precise calculations are required. The cross section libraries produced in this way are sometimes called "superfine" or *hyperfine cross section libraries* because so many different energy groups are used.

5.13 Collapsing the Group Cross Sections When Needed

In practice, a nuclear engineer rarely requires 1000 energy groups for most routine criticality calculations. Because of this, most reactor designers use a process known as "*cross section collapsing*" to reduce the multigroup cross sections to a much smaller number of "working" energy groups. The resulting cross sections still conserve the total reaction rate for an arbitrary reaction type R_x. However, instead of having to deal with 1000 energy groups, most calculations only have to be performed with 2 or 3. To create a set of collapsed cross sections, the equation

$$\sigma_{xg} = \frac{\sum_{g'} \sigma_{xg'} \phi_{g'} \Delta E_{g'}}{\sum_{g'} \phi_{g'} \Delta E_{g'}} \tag{5.36}$$

still requires the values of the "hyperfine" neutron flux $\phi_{g'}$ in each energy group G′.

We can then collapse these hyperfine cross sections to a smaller number of energy groups G in the following way. First, consider a set of G′ finely spaced energy groups with energy group boundaries $E_{g'}$, with g′ = 1…G′ and another set of "broader" energy group cross sections with a coarser energy group structure consisting of G groups with energy group boundaries E_g, where g = 1…G, and in general G ≪ G′. A basic requirement for reducing the total number of energy groups from G′ (which can be as many as 1000) to G (which can be much smaller) is that the energy group boundaries of both the coarse and the fine energy groups must end in the same place. This can be at any neutron energy we want, but in general, the boundaries must match wherever a larger number of energy groups G′ is to be collapsed into a smaller number of energy groups G. A cross section in the coarse group structure is then obtained from

$$\sigma_{xg} = \frac{\sum_{g'} \sigma_{xg'} \phi_{g'} \Delta E_{g'}}{\sum_{g'} \phi_{g'} \Delta E_{g'}} \tag{5.37}$$

where $\Delta E_{g'} = E_{g-1'} - E_{g'}$ and the summation over g′ covers all the g′ energy groups whose energy boundaries lie within those of the gth group. This process must be repeated for energy groups g = 1, g = 2,…, g = G until the collapsed cross sections for all G coarser energy groups are found. The G group set may be the final set that we use to do our work, or it may not. This is entirely dependent on the problem we are trying to solve. The *coarse group constants* obtained in this way then constitute the *"collapsed" or "coarse" cross section set*. The general strategy for collapsing the energy groups

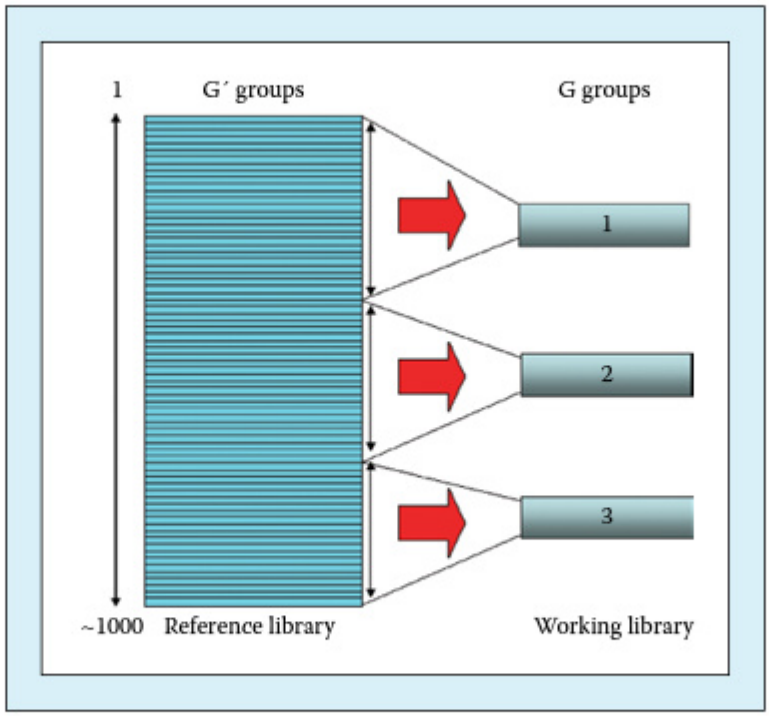

FIGURE 5.9 The procedure for converting fine group cross sections into course group cross sections in a multigroup method.

is shown in Figure 5.9 and in the flow chart in Figure 5.10. Note that the methodology presented here does not place any restrictions on how we can average the "fine" multigroup cross sections together in order to calculate the "coarse" multigroup cross sections. In this sense, the "fine" multigroup cross sections represent a "reference cross section library" that we can reuse over and over again if we know the values of ϕ_1, ϕ_2,…, ϕ_g,…, and ϕ_G and also the values of σ_{x1}, σ_{x2},…, σ_{xg},…, and σ_{xG}. We can simply store their values in a database and access them whenever we need to. This reduces the normal wear and tear that is usually associated with such an ambitious exercise.

The process of collapsing the fine group cross sections into the coarse group cross sections can be easily automated with a digital computer. Sometimes the set of G cross sections is the final set one chooses to use to calculate the reaction rates, and sometimes it is not. In some cases, a reactor designer may choose to create a set of *intermediate group cross sections* with say, 50–100 energy groups, and then to do a set of initial calculations with these. A nuclear engineer can then continue to collapse the energy groups down into as few energy groups as we want. Adding a third energy group for the epithermal or resonance energy range can also improve the accuracy of the cross section library in some cases. However, adding more energy groups than this is sometimes not worth the effort that it requires. In general, there is no exact answer to how many energy groups are required to create a successful design. In thermal water reactors, a single energy group is usually not enough to calculate the reaction rates with the accuracy that is required. For this reason, serious calculations of the neutron flux in thermal water reactors rely on the use of at least two energy groups—which we have previously referred to as the "fast" and "thermal" energy groups to obtain realistic results. The only way to know for sure what the "optimum" number of energy groups to use in a particular design is to compare the reaction rates for say two or three energy groups, with the reaction rates that are calculated using more energy groups. For example, we can compare the values of R_x calculated with 1000 energy groups to the value of R_x calculated with 3. If the difference in the results is small, then this is generally a good indication that we have reached the point of diminishing returns.

Student Exercise 5.3

Another excellent source of neutron cross section data is the JENDL 4.0 database, which is maintained by the Japanese Atomic Energy Agency. The JENDL database can be accessed from the Internet using a standard web browser, and the URL for this excellent resource is *http://wwwndc.jaea.go.jp/NuC/index.html*.

When you first start to use the JENDL database, you will notice that the total thermal cross section for natural uranium is 16.93 barns, while the Maxwellian averaged total thermal cross section for natural uranium is 18.04 barns. How do you explain the apparent difference between the values of these two cross sections, and which one would you use if you were put in charge of designing a thermal water reactor? Be prepared to justify your answers and your conclusions.

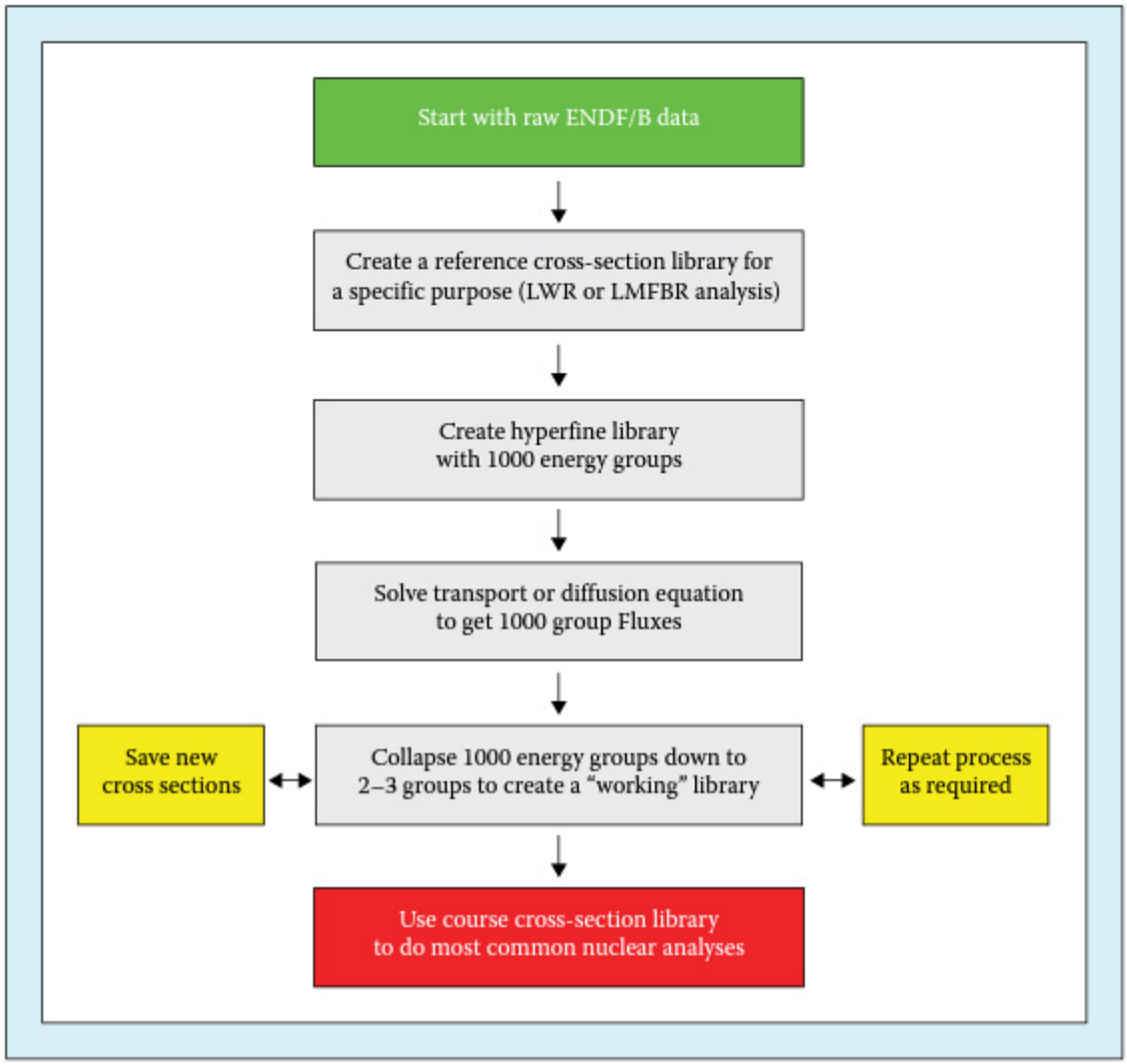
Start with raw ENDF/B data
Create a reference cross-section library for a specific purpose (LWR or LMFBR analysis)
Create hyperfine library with 1000 energy groups
Solve transport or diffusion equation to get 1000 group Fluxes
Save new cross sections
Collapse 1000 energy groups down to 2–3 groups to create a "working" library
Repeat process as required
Use course cross-section library to do most common nuclear analyses

FIGURE 5.10 A chart of how a "reference" cross-section library and a "working" cross section library are created.

5.14 Conserving the Reaction Rates When Collapsing to a Single Energy Group

Because finding the neutron flux shape can overwhelm even the most powerful computer when a large number of energy groups are involved, most reactor designers attempt to find the shape of the neutron flux $\phi(E)$ in a unit cell with only two or three energy groups, and to then collapse these energy groups into a single neutron energy group that represents the behavior of the unit cell as a whole. This is part of a larger process called *spatial homogenization* that is required to homogenize a unit cell or a fuel assembly that can be constructed from a number of these representative unit cells. There is a rigorous process for doing this that virtually all reactor designers use. We will have more to say about how this process works in Chapter 19. However, we would like to show you how it works for a single unit cell at this time. We will neglect the presence of the cladding to keep the calculations simple, and we will also assume that the width ΔE_g of each energy group is the same. In a future chapter, we will discuss how the same cross sections can be found when the energy groups have a different width and when the internal geometry is more complex.

Now consider for the moment the simple unit cell shown in Figure 5.11 that contains only fuel and moderator atoms. Suppose furthermore that we have the two-group fission and absorption cross sections Σ_{fg} and Σ_{ag} available for each material and that we have already found the values of the fast and thermal flux ϕ_1 and ϕ_2 by running a computer program that solves the neutron diffusion equation. We also know the volume of the fuel and the moderator in the unit cell. Let us again call these volumes V^{fuel} and V^{mod}. Then according to the two-group theory, the total absorption rates for the fuel and the moderator are

$$R_a^{fuel} = N^{fuel}\sigma_{a1}^{fuel}\phi_1^{fuel}V^{fuel} + N^{fuel}\sigma_{a2}^{fuel}\phi_2^{fuel}V^{fuel} \tag{5.38}$$

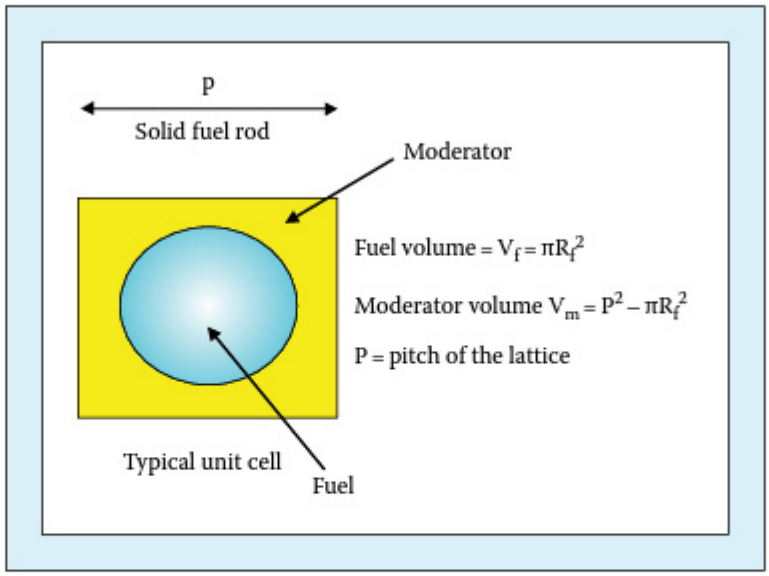

FIGURE 5.11 A typical unit cell used to calculate the reaction rates in a reactor lattice.

$$R_a^{mod} = N^{mod}\sigma_{a1}^{mod}\phi_1^{mod}V^{mod} + N^{mod}\sigma_{a2}^{mod}\phi_2^{mod}V^{mod} \tag{5.39}$$

where

The subscript 1 represents the fast energy group
The subscript 2 represents the thermal energy group

These equations may also be written as

$$R_a^{fuel} = \left(\Sigma_{a1}^{fuel}\phi_1^{fuel} + \Sigma_{a2}^{fuel}\phi_2^{fuel}\right)V^{fuel} \tag{5.40}$$

and

$$R_a^{mod} = \left(\Sigma_{a1}^{mod}\phi_1^{mod} + \Sigma_{a2}^{mod}\phi_2^{mod}\right)V^{mod} \tag{5.41}$$

where we have used the fact that

$$\Sigma_{a1}^{fuel} = N^{fuel}\sigma_{a1}^{fuel} \tag{5.42}$$

$$\Sigma_{a1}^{mod} = N^{mod}\sigma_{a1}^{mod} \tag{5.43}$$

and

$$\Sigma_{a2}^{fuel} = N^{fuel}\sigma_{a2}^{fuel} \tag{5.44}$$

$$\Sigma_{a2}^{mod} = N^{mod}\sigma_{a2}^{mod} \tag{5.45}$$

are the fast and thermal group absorption cross sections. Similarly, the expressions for the total fission rates in the fuel and the moderator are

$$R_f^{fuel} = \left(\Sigma_{f1}^{fuel}\phi_1^{fuel} + \Sigma_{f2}^{fuel}\phi_2^{fuel}\right)V^{fuel} \tag{5.46}$$

and

$$R_f^{mod} = \left(\Sigma_{f1}^{mod}\phi_1^{mod} + \Sigma_{f2}^{mod}\phi_2^{mod}\right)V^{mod} \tag{5.47}$$

where

$$\Sigma_{f1}^{fuel} = N^{fuel}\sigma_{f1}^{fuel} \tag{5.48}$$

$$\Sigma_{f1}^{mod} = N^{mod}\sigma_{f1}^{mod} \tag{5.49}$$

and

$$\Sigma_{f2}^{fuel} = N^{fuel}\sigma_{f2}^{fuel} \tag{5.50}$$

$$\Sigma_{f2}^{mod} = N^{mod}\sigma_{f2}^{mod} \tag{5.51}$$

are the analogous fast and thermal fission cross sections.

Notice that the fuel and the moderator do not necessarily have the same volumes, and in general, ϕ_1^{fuel} and ϕ_2^{fuel}, ϕ_1^{mod} and ϕ_2^{mod}, and V^{fuel} and V^{mod} can all have different values from one another. The expressions for R_a^{fuel} and R_a^{mod}, and R_f^{fuel} and R_f^{mod} therefore represent the true reaction rates in the entire unit cell. Now suppose that we would like to replace the two-group flux and the two-group cross sections in the unit cell with values for ϕ^{fuel} and ϕ^{mod}, Σ_a^{fuel} and Σ_a^{mod}, and Σ_f^{fuel} and Σ_f^{mod} that allow us to use only the equivalent one-group cross sections instead. How can this be done? The answer is that we can do this only if we can guarantee that the reaction rates predicted by one-group theory are the same as the reaction rates predicted by two-group theory. In other words, we must "collapse" the cross sections and the neutron flux from two energy groups to one energy group, and in doing so, we must insist that

$$R_a^{fuel} = R_{a1}^{fuel} + R_{a2}^{fuel} \tag{5.52}$$

$$R_a^{mod} = R_{a1}^{mod} + R_{a2}^{mod} \tag{5.53}$$

and

$$R_f^{fuel} = R_{f1}^{fuel} + R_{f2}^{fuel} \tag{5.54}$$

$$R_f^{mod} = R_{f1}^{mod} + R_{f2}^{mod} \tag{5.55}$$

and for the flux to be conserved, we must also insist that

$$\phi = \phi_1 + \phi_2 \tag{5.56}$$

Now let us write out one of these equations in more detail to show what is involved. For the case of the fuel, we must require that

$$\Sigma_a^{fuel}\phi^{fuel}V^{fuel} = \left(\Sigma_{a1}^{fuel}\phi_1^{fuel} + \Sigma_{a2}^{fuel}\phi_2^{fuel}\right)V^{fuel} \tag{5.57}$$

$$\Sigma_f^{fuel}\phi^{fuel}V^{fuel} = \left(\Sigma_{f1}^{fuel}\phi_1^{fuel} + \Sigma_{f2}^{fuel}\phi_2^{fuel}\right)V^{fuel} \tag{5.58}$$

and for the case of the moderator we must require that

$$\Sigma_a^{mod}\phi^{mod}V^{mod} = \left(\Sigma_{a1}^{fuel}\phi_1^{mod} + \Sigma_{a2}^{mod}\phi_2^{mod}\right)V^{mod} \tag{5.59}$$

since the fission cross sections Σ_f^{mod}, Σ_{f1}^{mod}, and Σ_{f2}^{mod} are usually 0 there. So in general, for a portion of the lattice having a total volume V we must insist that

$$\Sigma_x\phi V = \left(\Sigma_{x1}\phi_1 + \Sigma_{x2}\phi_2\right)V \tag{5.60}$$

or

$$\Sigma_x \phi = \left(\Sigma_{x1}\phi_1 + \Sigma_{x2}\phi_2\right) \tag{5.61}$$

where

$$\phi = \phi_1 + \phi_2 \tag{5.62}$$

Therefore, when we collapse the reaction rates from two energy groups to one energy group, the equations that must always be used to do so are

$$\Sigma_x = \frac{\left(\Sigma_{x1}\phi_1 + \Sigma_{x2}\phi_2\right)}{\left(\phi_1 + \phi_2\right)} \tag{5.63}$$

or

$$\sigma_x = \frac{\left(\sigma_{x1}\phi_1 + \sigma_{x2}\phi_2\right)}{\left(\phi_1 + \phi_2\right)} \tag{5.64}$$

This is the only way that the reaction rates can be conserved for an arbitrary reaction type x. These final two expressions are a special case of a much more general result in which we have temporarily assumed that the size of each energy group ΔE_g is the same. It is a simple matter to extend what we have just learned to more than two energy groups of an arbitrary width ΔE_g by requiring that

$$\Sigma_x = \sum_g \frac{\left(\Sigma_{xg}\phi_g \Delta E_g\right)}{\phi} \tag{5.65}$$

or

$$\sigma_x = \sum_g \frac{\left(\sigma_{xg}\phi_g \Delta E_g\right)}{\phi} \tag{5.66}$$

where the summation shown is over all energy groups from g = 1 to g = G, and the total flux is defined as

$$\phi = \sum_g \phi_g \quad (g = 1, 2, \ldots, G) \tag{5.67}$$

If there is more than one isotope in each region of the unit cell, then we must repeat this process for each isotope j. Obviously, any number of energy groups can be collapsed into one energy group in this way, and when simple ballpark calculations of the criticality are to be performed, it is more computationally efficient to use the one-group cross sections we have derived rather than the more complex multigroup cross sections provided by multigroup theory. There are many computer programs available today that automate this process entirely. Again, for a computer program to predict the reaction rates accurately, it must always generate values for the one-group flux and for the one-group cross sections that will allow this to occur. The example below gives a practical example of how this can be done. Obviously, the process of collapsing the multigroup cross sections uses exactly the opposite approach that we have used to expand them. Collapsing the cross sections makes the calculations of the group reaction rates simpler and more efficient, while expanding them allows us to be more accurate if we are willing to put up with the additional time and computational expense. For this reason, calculations with several energy groups are usually done within an individual fuel assembly or unit cell itself, while calculations with fewer energy groups are usually done between fuel assemblies or when groups of fuel assemblies are involved.

Example Problem 5.7

Suppose that the neutron flux $\phi(E)$ in a thermal water reactor has been subdivided into three energy groups between 0.0 and 1 eV. If the relative magnitude of the flux in each of these energy groups is shown in the table below, and the absorption cross section of the fuel is given by the entries in the fourth row of the table, what is the value of the thermal absorption cross section when all three of these groups are collapsed into a single energy group that spans the range from 0 to 1 eV?

Group	Energy Range (eV)	Relative Magnitude of the Group Flux (Normalized to 1.0 between 0 and 1 eV)	Value of the Absorption Cross Section Σ_a (cm^{-1})
3	0.0–0.2	0.5	10
2	0.2–0.5	0.3	5
1	0.5–1.0	0.2	1

Solution From the data given previously, the average value of the absorption cross section $<\Sigma_a>$ for the fuel between E = 0 eV and E = 1 eV can be found from the expression

$$<\sigma_a> = \frac{\sum_g \left(\Sigma_{ag}\phi_g \Delta E_g\right)}{\sum_g \phi_g \Delta E_g}$$

where the summation $\sum$ is to be performed over all energy groups from g =1 to 3. Now in the case of groups 1, 2, and 3, the values of ΔE_g are $\Delta E_1 = 0.5$, $\Delta E_2 = 0.3$, and $\Delta E_3 = 0.2$, the values of ϕ_1, ϕ_2, and ϕ_3 are $\phi_1 = 0.2$, $\phi_2 = 0.3$, and $\phi_3 = 0.5$, and the values of Σ_{a1}, Σ_{a2}, and Σ_{a3} are $\Sigma_{a1} = 1$, $\Sigma_{a2} = 5$, and $\Sigma_{a3} = 10$.

The average value of the absorption cross section $<\Sigma_a>$ between E = 0 eV and E = 1 eV is then

$$<\Sigma_a> = \frac{\left(\Sigma_{a1}\phi_1\Delta E_1 + \Sigma_{a2}\phi_2\Delta E_2 + \Sigma_{a3}\phi_3\Delta E_3\right)}{\left(\phi_1\Delta E_1 + \phi_2\Delta E_2 + \phi_3\Delta E_3\right)}$$

$$= \frac{\left(1\times 0.2\times 0.5 + 5\times 0.3\times 0.3 + 10\times 0.5\times 0.2\right)}{\left(0.2\times 0.5 + 0.3\times 0.3 + 0.5\times 0.2\right)}$$

or

$$<\Sigma_a> = \frac{\left(0.1 + 0.45 + 1\right)}{\left(0.1 + 0.09 + 0.1\right)} = \frac{1.55}{0.29} = 5.34 \text{ cm}^{-1} \left[\text{Ans.}\right]$$

There is no simple rule that covers all possible scenarios that can occur. However, if we homogenize the spatial structure of the core as well, then fewer energy groups are usually required, and if we want to know the details of what is going on within an individual fuel assembly or unit cell, then more energy groups are usually needed to obtain the appropriate level of accuracy. In a future chapter, we would like to turn our attention to how the neutrons that are created in energy group 1 (the fast energy group) move into other energy groups, and what this implies in terms of how a reactor should be designed. This will lead us into a general discussion of what is known as "*neutron slowing down theory*," which is an aid in determining what type of moderating materials should be used.

5.15 Group Flux and Average Flux within a Group

For anyone who is new to the field of nuclear science and engineering, it is sometimes easier to understand what the *group flux* ϕ_g represents if we visualize the neutron flux $\phi(E)$ as a continuous function of the neutron kinetic energy E. If we plot the value of ϕ as a function of E, then the variable ϕ can rise or fall any way we want as the neutron energy is changed. This is no different conceptually than the simple function f(x), which we have drawn at the top of Figure 5.12. Because we are dealing exclusively with neutrons in this case, all that we have done is to substitute ϕ for f and E for x. As long as we require $\phi(E)$ to be continuous, then everything that we learned in elementary calculus is immediately applicable to

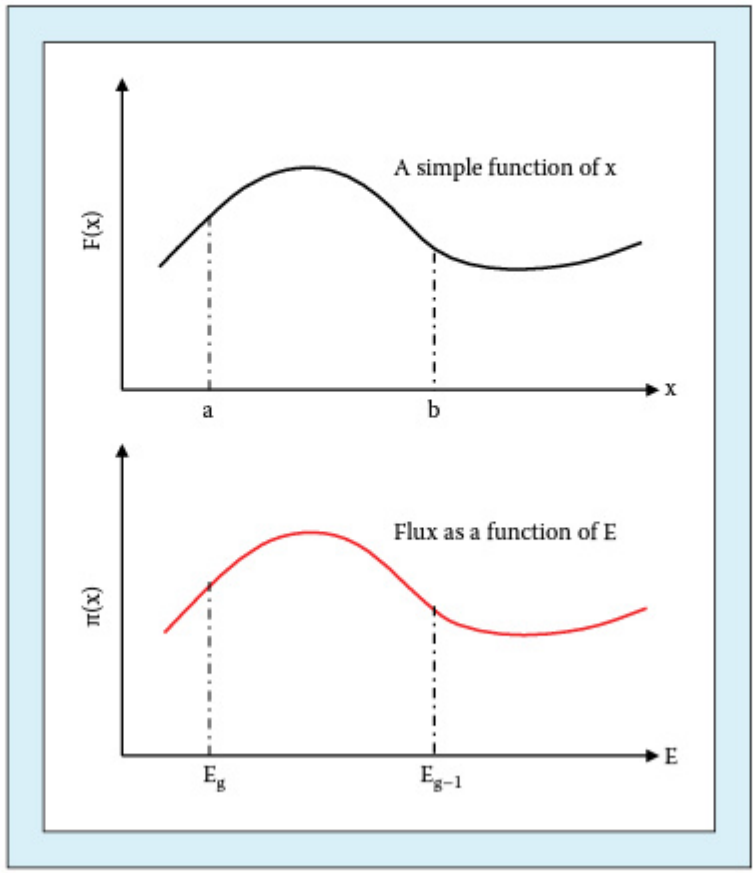

FIGURE 5.12 A simple function showing the energy dependence of the neutron flux and an arbitrary energy group that extends from $E = E_{g-1}$ to $E = E_g$ and has a width $\Delta E_g = E_{g-1} - E_g$.

the definitions we have created for the group flux. Integrating $\phi(E)$ between $E = E_g$ and $E = E_{g-1}$ is equivalent to finding the area under the curve between $E = E_g$ and $E = E_{g-1}$, where i is the number of "intervals" we choose to use to find the area under the curve, and $\Delta E_g = E_g - E_{g-1} = \sum_i \Delta E_i$. *Thus the group flux ϕ_g is simply the total number of neutrons under the curve between $E = E_g$ and $E = E_{g-1}$, and the average flux within group g $\langle\phi_g\rangle$ is the group flux ϕ_g divided by the width of the energy interval $\Delta E_g = E_g - E_{g-1}$ in which these neutrons are found.*

Consequently, we can write

Definition of the Group Flux

$$\phi_g = \int \phi(E)\,dE$$
$$= \text{Area under the curve}\left(\text{between } E_g \text{ and } E_{g-1}\right) \tag{5.68}$$

and

The Average Flux within a Group

$$\langle\phi_g\rangle = \int \phi(E)\,dE \Big/ \int dE = \int \phi(E)\,dE/\Delta E_g$$
$$= \phi_g/\Delta E_g$$
$$= \text{Area under the curve/width of the group}$$
$$\left(\text{between } E_g \text{ and } E_{g-1}\right) \tag{5.69}$$
$$\text{and}$$
$$\Delta E_g = E_g - E_{g-1} = \text{width of group}$$

Notice that the group flux is simply the total number of neutrons within an energy group, while the average group flux is the total number of neutrons per eV. To find the group flux from the average flux, we must multiply the average flux by the width of the energy group ΔE_g (in eV):

$$\phi_g = <\phi_g> \cdot \Delta E_g \tag{5.70}$$

Again we are just trying to find the total number of neutrons under the curve. Notice that this definition does not place any restrictions on what the size of the neutron energy groups can be. Only the limits of integration determine where one-group ends and the next group begins. All that the calculus requires is that there must be G energy groups in all, and that the energy-dependent flux from which they are derived must be continuous, so that in one-group theory, G = 1, and in multigroup theory, G > 1. Clearly, if we are dealing with just a single energy group, then the limits of integration for the neutron flux are $E_{LOW} = 0$ and $E_{HIGH} \sim 10$ MeV, and all of the neutrons between those limits belong to this single energy group.

5.16 Using Large Numbers of Energy Groups

Many people who are exposed to the field of nuclear science and engineering for the first time sometimes ask why so many energy groups are required for a reactor physics calculation. After all, we could simply take the one-group cross sections we presented in Chapter 4 and use the following prescription to calculate the value of the reaction rate R_x for any particular process

$$R_x = \Sigma_x \phi = N\sigma_x \phi \tag{5.71}$$

where x = a, c, f, s, or t, etc. *The reason why this is the case is that the additional energy groups are needed to get the correct values for the nuclear reaction rates—especially when we have to take the spatial heterogeneity of a reactor core into account*. There are certain phenomena such as the shape of the thermal flux in the vicinity of the reflector, the fuel rods and control rods that we can simply not estimate accurately unless we can distinguish between how the fast neutrons behave and how the thermal neutrons behave. We will learn more about what this spatial structure looks like when we study the shape of the neutron flux in Chapter 13, which also provides solutions to the neutron diffusion equation for these geometries.

Moreover, we need to understand this spatial structure in more detail to even find the reaction rates in a single unit cell under certain conditions. Simply stated, we cannot do this unless we can distinguish between how the fast and thermal neutrons behave. Finally, when we introduce the reader to the neutron diffusion equation in Chapter 11, we will find that this spatial dependence becomes even more important when the neutron mean free path becomes very short. Specifically, it becomes important when the neutron mean free path λ is less than about *three times* the size of the smallest spatial structures that we need to analyze. So while fast neutrons are energetic enough to avoid having to deal with most of this structural detail (because their mean free paths are so long), we cannot apply the same logic to thermal neutrons because their mean free paths are too short. In fact, because of the presence of the absorption resonances in the fuel (see Figure 5.4), an epithermal energy group is sometimes needed to account for the presence of these resonances upon the reaction rates as well. So the *Calculus of Newton*—which students normally study in their first calculus class—provides us with the tools we need to make this happen. The Calculus of Newton allows us to find the area under the curves in Figures 5.12 and 5.13—and this is the key quantity we need to get the correct values of the reaction rates within an arbitrary neutron energy group g. Only in this case, we are forced to break the area under each curve into several pieces, and to find the areas of each of these pieces individually.

This is the price that we have to pay to get the spatial detail we need. Similarly, the group cross sections

$$\sigma_{xg} = \frac{\int \sigma_x(E)\phi(E)dE}{\int \phi(E)dE} \quad g = 1,2,3,\ldots,G \tag{5.72}$$

require us to perform a similar set of integrations across each energy group. In this case, we must take the product of the neutron flux and the microscopic cross sections $R_x(E) = \phi(E)\sigma_x(E)$ at each energy E and integrate them to find the area under the curve between $E = E_g$ and $E = E_{g-1}$. Again, this is the same thing as taking two simple functions from the calculus of Newton, f(x) and g(x), multiplying them together, and integrating them to find the area under the curve as well. The similarities can again be seen in the inputs to the process in Figure 5.13 and the output of the process, which is shown in Figure 5.14. Only in this case, to find the "average" value of g(x) or $\sigma_x(E)$ within an energy group, we must divide the

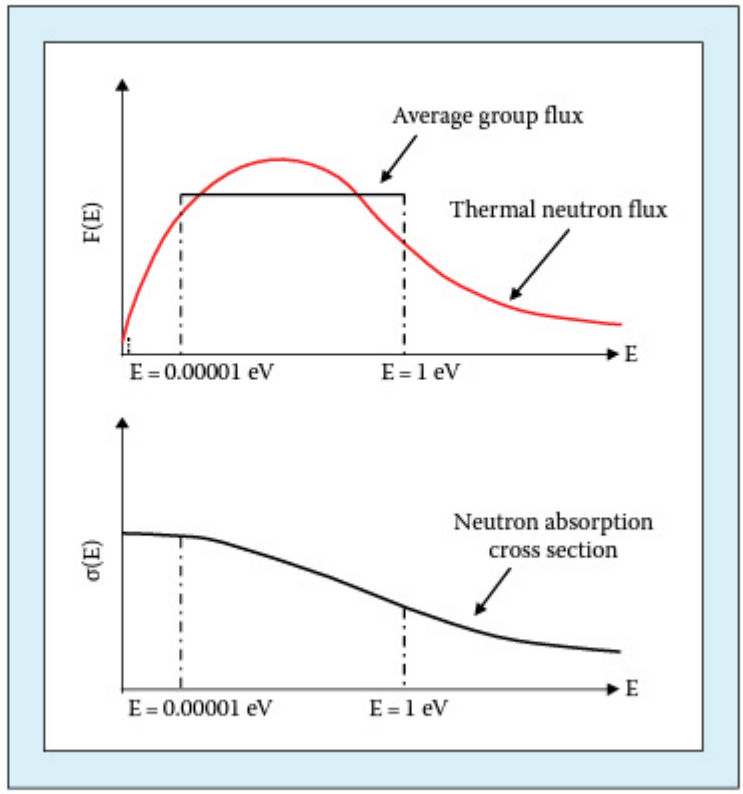

FIGURE 5.13 The behavior of the neutron flux and an absorption cross section in the thermal energy range.

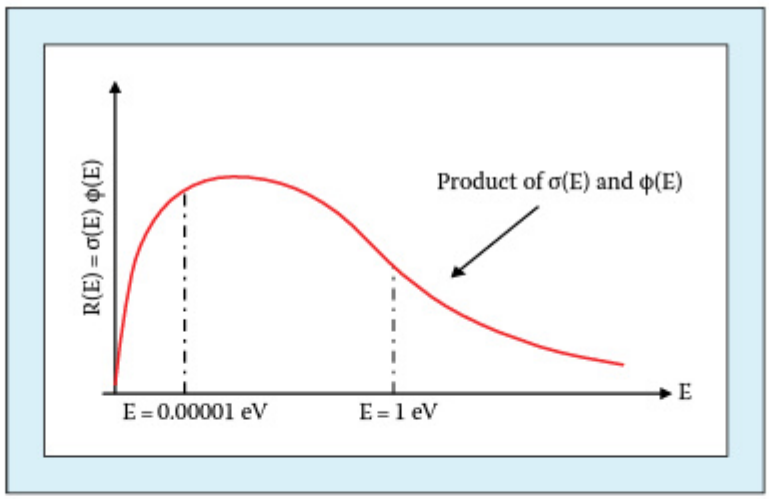

FIGURE 5.14 The reaction rate R(E) as a function of the neutron kinetic energy E.

result by the total value of f(x) (or $\phi(E)$ in this case) to get the numbers to work out. Using the "traditional" definition of the group flux $\phi_g = \int \phi(E)\, dE$, we see that this again leads us to conclude that

$$\sigma_{xg} = \frac{\int \sigma_x(E)\phi(E)dE}{\int \phi(E)dE} \tag{5.73}$$

or

$$\sigma_{xg} = \int \sigma_x(E)\phi(E)\frac{dE}{\phi_g} \tag{5.74}$$

where $\phi_g = \int \phi(E)\, dE$. Thus the energy integral $\int dE = \Delta E_g = E_g - E_{g-1} = \sum_i \Delta E_i$ provides the appropriate *weighting function* for all of the reaction rates to work out. Hence the objective of one-group theory is to find the area under these curves between $E_{LOW} = 0$ and $E_{HIGH} \sim 10$ MeV, and in multigroup theory, the objective is to find the area under these curves for many different energy groups (g = 1, 2, 3,…, G). Otherwise, we cannot predict the reaction rates correctly if all of this spatial detail and energy dependence is ignored. Stated another way, we certainly cannot find the "hot spots" in an individual fuel assembly unless we know where the thermal neutron flux peaks, and this requires a different value for ϕ_2 than we would calculate for ϕ or just ϕ_1.

Student Exercise 5.4

One of the interesting consequences of our discussion so far is *that the average flux $\langle\phi_g\rangle$ within an energy group is not the same as the group flux.* Using the equations presented earlier, demonstrate mathematically how these two terms are different and derive an expression to convert the flux within an energy group into the group flux.

Why is it important to have this distinction in the field of nuclear engineering, and what additional value does it provide? What does the *average flux* within an energy group represent?

Example Problem 5.8

Consider the following histogram, which represents the neutron energy spectrum in a thermal water reactor:

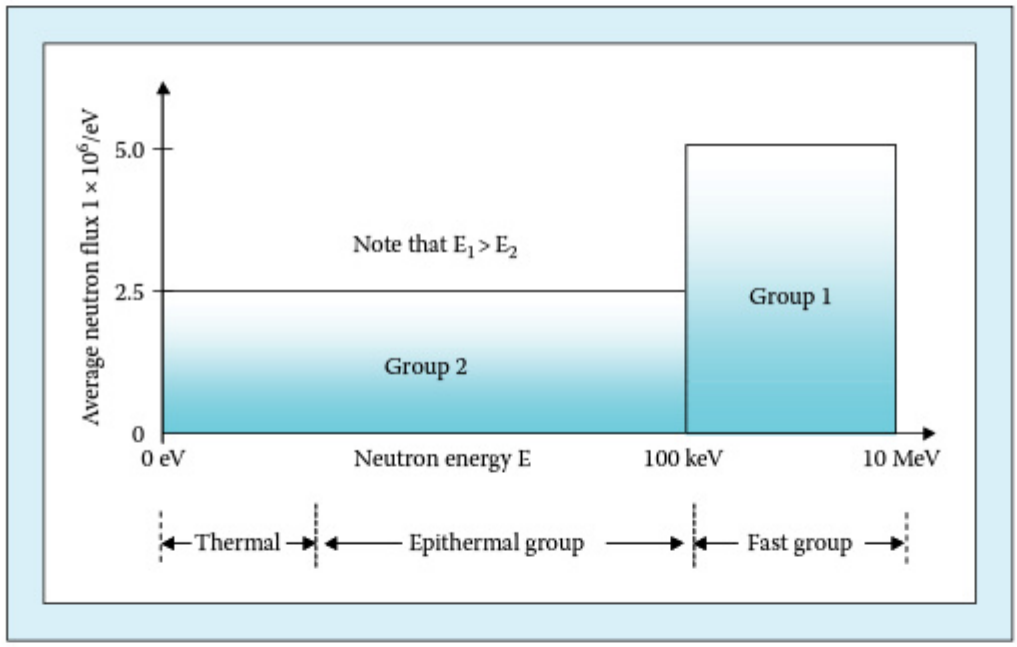

If the Y axis shows the *average neutron flux* $\langle\phi_g\rangle$, what is the group flux ϕ_1 for the fast energy group (Group 1) and what is the group flux ϕ_2 for the thermal and epithermal energy groups (Group 2)?

Solution The group flux ϕ_g is related to the average flux $\langle\phi_g\rangle$ by the equation $\phi_g = \langle\phi_g\rangle \cdot \Delta E_g$, where ΔE_g is the width of the energy group. The lowest energy group, which contains the thermal and epithermal neutrons, is 100 keV = 1×10^5 eV wide, and the fast energy group is 9.9 MeV = 9.9×10^6 eV wide. The fast group flux is therefore $\phi_1 = \langle\phi_1\rangle \cdot \Delta E_1 = 5 \times 10^6 \times 9.9 \times 10^6 = 4.95 \times 10^{13}$ neutrons/cm^2/s, and the thermal and epithermal group flux is therefore $\phi_2 = \langle\phi_2\rangle \cdot \Delta E_2 = 2.5 \times 10^6 \times 1 \times 10^5 = 2.5 \times 10^{11}$ neutrons/cm^2/s. Notice that the fast flux is much larger than the thermal flux in this case. [Ans.]

5.17 Realistic Reactor Design Practices

Assuming that we know the values for the group fluxes ϕ_g and the multigroup cross sections Σ_g^j (j being the index of the material in question and g being the index of the energy group), we can calculate how many neutrons are absorbed by the materials in a reactor core per second and how many additional neutrons are created by the process of nuclear fission per second. The ratio of these two numbers then allows us to determine whether the neutron population in the core as a whole will increase, decrease, or remain the same as a function of time. In a future chapter, we will introduce a number

TABLE 5.11
Thermal Cross Sections Required to Calculate the Effective Multiplication Factor in Neutron Diffusion Theory

Thermal Macroscopic Cross Sections for Some Important Nuclear Materials						
Name	Use	$\sum_c$ (cm^{-1})	$\sum_f$ (cm^{-1})	$\sum_a$ (cm^{-1})	$\sum_s$ (cm^{-1})	$\sum_t$ (cm^{-1})
Light water (H_2O)	Coolant/moderator	0.02220	0.0	0.02220	3.443	3.465
Heavy water (D_2O)	Coolant/moderator	0.0000442	0.0	0.0000442	0.4519	0.4519
Liquid sodium (Na)	Coolant	0.0135	0.0	0.0135	0.0808	0.0941
U-233	Fuel	2.189	25.26	27.449	0.999	28.16
U-235	Fuel	4.621	27.96	32.581	0.669	33.28
U-238	Fuel	0.130	5.25×10^{-7}	0.130	0.4239	0.5536
Pu-239	Fuel	13.446	37.220	50.666	0.3835	51.05

Sources: Duderstadt, J. and Hamilton, L., *Nuclear Reactor Analysis*, John Wiley & Sons, New York, 1976; Lamarsh, J.R. and Baratta, A.J., *Introduction to Nuclear Engineering*, Prentice Hall, Upper Saddle River, NJ, 2001.

TABLE 5.12
Fast Cross Sections Required to Calculate the Effective Multiplication Factor in Neutron Diffusion Theory

Fast Macroscopic Cross Sections for Some Important Nuclear Materials						
Name	Use	$\sum_c$ (cm^{-1})	$\sum_f$ (cm^{-1})	$\sum_a$ (cm^{-1})	$\sum_s$ (cm^{-1})	$\sum_t$ (cm^{-1})
Light water (H_2O)	Coolant/moderator	0.0000037	0.0	0.0000037	0.5628	0.5628
Heavy water (D_2O)	Coolant/moderator	0.0000039	0.0	0.0000039	0.6732	0.6732
Liquid sodium (Na)	Coolant	0.0000703	0.0	0.0000703	0.0906	0.0906
U-233	Fuel	0.0367	0.1285	0.1652	0.3250	0.4902
U-235	Fuel	0.2000	0.0895	0.2895	0.3260	0.6155
U-238	Fuel	0.0158	0.00204	0.0178	0.3280	0.3458
Pu-239	Fuel	0.0247	0.0894	0.1141	0.3377	0.4518

Sources: Duderstadt, J. and Hamilton, L., *Nuclear Reactor Analysis*, John Wiley & Sons, New York, 1976; Lamarsh, J.R. and Baratta, A.J., *Introduction to Nuclear Engineering*, Prentice Hall, Upper Saddle River, NJ, 2001.

of analytical expressions to predict how the neutron population behaves under these conditions. This will lead us to the definition of the *effective multiplication factor* K_{eff} and the *reactivity* ρ (both of which are simple dimensionless numbers under most circumstances). If we are able to find numerical values for K_{eff} or ρ, we can then determine exactly how the neutron population will behave.

When it comes to designing a reactor core, the most important quantities required to calculate the effective multiplication factor are the macroscopic fission and absorption cross sections for the fuel and the moderator. In the early stages of reactor design, the one-group values for these parameters are normally used, and when the process of detailed design begins, the one-group values are replaced by their multigroup equivalents. While there is no single process that can be used for all reactor designs, every process used by commercial reactor designers today relies on the values of $\sum_f$ and $\sum_a$. Consequently, we would like to summarize the values of these important parameters for some common nuclear materials. Table 5.11 shows the values of the macroscopic cross sections that are used for thermal diffusion theory calculations, and Table 5.12 shows the values of the same parameters that are used for fast neutron diffusion theory calculations. Since each macroscopic cross section has the units of inverse centimeters (cm^{-1}), we can estimate the total reaction rate within any region of the core by simply multiplying these cross sections by the values of the fast and thermal flux and then multiplying them again by the total volume V of the fuel and the moderator. (The exact approach was outlined in Section 5.12). *To begin a design, many designers simply use the cross sections for the thermal energy group for their one-group calculations.*

5.18 A Simple Design Exercise

To illustrate the difference between one-group and two-group theory, suppose that we would like to calculate the reaction rates with one energy group and then with more than one energy group. To begin with, consider a reactor that is fueled

with pure U-235. If the reactor is a thermal water reactor, about 1/3 of the neutrons will be thermal neutrons and 2/3 of the neutrons will be fast neutrons (see Figure 5.7). Suppose that the total neutron flux in a typical fuel assembly (fast plus thermal) is 1×10^{14} neutrons/cm^2/s. Approximately 2/3 of the neutrons will have an energy above 1 eV, and approximately 1/3 of the neutrons will have an energy below 1 eV. So if the total neutron flux is 1×10^{14} neutrons/cm^2/s, the thermal neutron flux will be 3.33×10^{13} neutrons/cm^2/s and the fast neutron flux will be 6.67×10^{13} neutrons/cm^2/s. When we ignore the fast neutrons entirely, the reaction rates are

$$R_f = \Sigma_{f2}\phi_2 = 0.9310 \times 10^{15} \text{ fissions/s/cm}^3 \tag{5.75}$$

$$R_a = \Sigma_{a2}\phi_2 = 1.085 \times 10^{15} \text{ absorptions/s/cm}^3 \tag{5.76}$$

since the thermal flux is $\phi_2 = 3.33 \times 10^{13}$ neutrons/cm^2/s. When we add the fast neutrons back into the mix, and use a true two-group model, we get

$$R_f = \Sigma_{f1}\phi_1 + \Sigma_{f2}\phi_2 = 0.9370 \times 10^{15} \text{ fissions/s/cm}^3 \tag{5.77}$$

$$R_a = \Sigma_{a1}\phi_1 + \Sigma_{a2}\phi_2 = 1.1042 \times 10^{15} \text{ absorptions/s/cm}^3 \tag{5.78}$$

In other words, the difference between the predictions of the one-group model (with thermal neutrons only) and the two-group model (with both fast and thermal neutrons) is about 0.6% for the fission rate and about 1.8% for the absorption rate. *This indicates that when we apply a two-group model to the center of a reactor core, the two-group model is about 1% more accurate than the one-group model* for this hypothetical problem. However, we had to use *both* the fast and thermal cross sections to arrive at this conclusion, and the fast flux was different than the thermal neutron flux in this case ($\phi_1 \neq \phi_2$). Moreover, our analysis also shows that the difference in the effective multiplication factors is at least as great because without the fast neutrons, the ratio of R_f to R_a is

$$R_f/R_a \left(\text{without fast neutrons}\right) = 0.858 \tag{5.79}$$

and the ratio with fast neutrons is

$$R_f/R_a \left(\text{with fast neutrons}\right) = 0.848 \tag{5.80}$$

which is a difference of 1.1%. In most cases, a two-group model is between 1% and 2% more accurate than a one-group model under similar conditions. However, in a fast reactor, between 10 or 20 energy groups are sometimes needed to achieve the same result. The exact difference depends on how the multigroup cross sections are defined, but in general, the accuracy will continue to improve until the number of energy groups reaches 10 to 20. Then any additional increase in the number of energy groups will have a negligible effect on the reaction rates. This is particularly true when it comes to estimating the effective multiplication factor because the values of the multigroup flux appear in both the numerator and the denominator. See Chapter 10 to see how the effective multiplication factor is defined.

Example Problem 5.9

Using Equations 5.75 through 5.78, estimate the percentage error in the fission and absorption rates when the fast neutrons are ignored in a thermal water reactor fuel rod.

Solution According to Equations 5.75 and 5.77, the difference in the fission rate is 0.9370×10^{15} fissions/s/cm^3 $- 0.9310 \times 10^{15}$ fissions/s/cm^3 $= 0.006 \times 10^{15}$ fissions/s/cm^3 $\approx 0.6\%$. When we use Equations 5.76 and 5.78, we find that the difference in the absorption rate is 1.1042×10^{15} absorptions/s/cm^3 $- 1.085 \times 10^{15}$ absorptions/s/cm^3 $= 0.0192 \times 10^{15}$ absorptions/s/cm^3 $\approx 1.7\%$. Hence, there is a greater error in the absorption rate than there is in the fission rate in this case. [Ans.]

TABLE 5.13
Macroscopic Fission Cross Section for Plutonium Dioxide (PuO_2) as a Function of the Plutonium Content c

Substance	Symbol	Plutonium Content (%)	Fission Cross Section Σ_f (cm^{-1})
Plutonium dioxide	PuO_2	2.5	0.475
Plutonium dioxide	PuO_2	5.0	0.950
Plutonium dioxide	PuO_2	7.5	1.425
Plutonium dioxide	PuO_2	10.0	1.900
Plutonium dioxide	PuO_2	12.5	2.375
Plutonium dioxide	PuO_2	15.0	2.850
Plutonium dioxide	PuO_2	17.5	3.325
Plutonium dioxide	PuO_2	20.0	3.800
Plutonium dioxide	PuO_2	22.5	4.275
Plutonium dioxide	PuO_2	25.0	4.750

Assumes only thermal neutrons cause the plutonium to fission.

Example Problem 5.10

Develop a table that shows the macroscopic fission cross section $\sum_f$ of plutonium dioxide (PuO_2) as a function of its plutonium content c using the fact that at thermal energies, the fission cross section varies with plutonium content according to the equation $\Sigma_{f\,PuO2} = N_{Pu\text{-}239} \cdot \sigma_{f\,Pu\text{-}239} = 0.190 \cdot c\ (cm^{-1})$ when the plutonium content c is measured in percent.

Solution The results are shown in Table 5.13. Clearly this is a very interesting result because it shows that the macroscopic fission for PuO_2 is about 46% higher than the same cross section for UO_2. In other words, in a thermal water reactor, we would only need about $1/1.46 \approx 68\%$ as much plutonium to generate the same amount of thermal energy. This is one of the reasons Pu-239 is so highly prized as a nuclear fuel. [Ans.]

Example Problem 5.11

Suppose that energy groups 142, 143, and 144 in an ultrafine cross-section library have scattering cross sections of 2.5, 2.8, and 3.1 barns, respectively. If the energy groups have the same width and they are exposed to a neutron flux where the number of neutrons in each energy group is 1.0×10^8 neutrons/cm^2/s, 0.9×10^8 neutrons/cm^2/s, and 0.8×10^8 neutrons/cm^2/s, respectively, what is the effective scattering cross section when all three of these groups are collapsed into a single energy group?

Solution The effective scattering cross section in this case can be found from the equation $\sigma_{sg} = \Sigma_{g'}\sigma_{sg'}\phi_{g'}\Delta E_{g'}/E_{g'}\phi_{g'}\Delta E_{g'}$, where $g' = 142$, 143, and 144. Since all three groups have the same width, the values of $\Delta E_{g'}$ cancel from the numerator and the denominator, and we are left with $\sigma_s = (2.5 \times 1.0 + 2.8 \times 0.9 + 3.1 \times 0.8)/(1.0 + 0.9 + 0.8) = 7.5/2.7 = 2.77$ barns as the "effective" scattering cross section for the collapsed group. [Ans.]

5.19 Cross Section Naming Conventions

Throughout this chapter and in Appendices B and C, we have used the fact that the absorption cross section is equal to the sum of its capture and fission cross sections. Thus, when it comes to either a microscopic or macroscopic cross section, we are able to write

$$\sigma_a = \sigma_c + \sigma_f \tag{5.81}$$

$$\sum\nolimits_a = \sum\nolimits_c + \sum\nolimits_f \tag{5.82}$$

because the microscopic and macroscopic cross sections of all materials are related in the following way:

$$\sum\nolimits_a = N\sigma_a \tag{5.83}$$

$$\sum_c = N\sigma_c \tag{5.84}$$

$$\sum_f = N\sigma_f \tag{5.85}$$

Notice that *the only time when the capture and absorption cross sections become identical is when there is no fissionable material present*, because in this case $\sigma_f = 0$. Then and only then can we say that

$$\sigma_a \equiv \sigma_c \left(\text{when } \sigma_f = 0\right) \tag{5.86}$$

$$\sum_a \equiv \sum_c \left(\text{when } \sum_f = 0\right) \tag{5.87}$$

It is interesting to observe that many other reference books (see e.g., Reference 6) do not make this distinction, and instead have chosen to insert additional entries into their cross section tables to explain why such a discrepancy exists. However, this book does not present fundamental nuclear cross section data in this way, and it is hoped that the reader will appreciate the difference that this important distinction can make. Tables of neutron cross section data for the fast and thermal energy groups are also presented in Appendix C. These tables should be used in the event that a particular fission, capture, or absorption cross section is required. These tables are slightly more general versions of Tables 5.1 through 5.3, 5.6, and 5.7 that can be found in this chapter. Extended versions of Tables 5.1 through 5.3 are also presented in the appendices.

Example Problem 5.12

According to Table 5.8, U-233, U-235, U-238, and Pu-249 are all non-1/v absorbers. If their absorption cross sections at 0.025 eV are 574.25 barns, 681.77, 2.717, and 1017.40 barns, what values should we use for their absorption cross sections for the entire thermal energy range? Assume the operating temperature of the fuel is 1000°C.

Solution Their absorption cross sections for the entire thermal energy range can be found from the equation $\sigma_a = G \times \sigma_a$ (0.025 eV), where G is the non-1/v factor shown in Table 5.8. Since the values of G for U-233, U-235, U-238, and Pu-239 are 1.02, 0.91, 1.02, and 3.54, respectively when the flux is Maxwellian and the operating temperature of the fuel is 1000°C, the absorption cross sections we should use are $\sigma_{a233} = 1.02 \times 574.25 = 585.74$ barns, $\sigma_{a235} = 0.91 \times 681.77 = 630.40$ barns, $\sigma_{a238} = 1.02 \times 2.717 = 2.771$ barns, and $\sigma_{a239} = 3.54 \times 1017.40 = 3601.60$ barns. Notice that each of these cross sections can be interpreted as the thermal group cross sections in this case because the thermal energy range is defined to exist between 0 and 1 eV. [Ans.]

References

Books and Textbooks

1. Kaplan, I. *Nuclear Physics*, Addison-Wesley, Reading, MA (1965).
2. Henry, A.F. *Nuclear Reactor Analysis*, MIT Press, Cambridge, MA (1975).
3. Stacey, W.M. *Nuclear Reactor Physics*, 2nd edn., John Wiley & Sons, New York (2007).
4. Duderstadt, J. and Hamilton, L. *Nuclear Reactor Analysis*, John Wiley & Sons, New York (1976).
5. Lewis, E. *Fundamentals of Nuclear Reactor Physics*, Academic Press Boston, MA (2008).
6. Lamarsh, J.R. and Baratta, A.J. *Introduction to Nuclear Engineering*, Prentice Hall, Upper Saddle River, NJ (2001).
7. Cochran, R.G. and Toulfanidis, N. *The Nuclear Fuel Cycle: Analysis and Management*, American Nuclear Society, La Grange Park, IL (1999).
8. Shultis, K. and Faw, R. *Fundamentals of Nuclear Science and Engineering*, 2nd edn., CRC Press, Boca Raton, FL (2008).
9. Westcott, C.H. The specification of neutron flux and nuclear cross-sections in reactor calculations, *Journal of Nuclear Energy*, **2**, 59 (1955).
10. Glasstone, S. and Eedlund, M.C. *The Elements of Nuclear Reactor Theory, D*, Van Nostrand Company, Inc., New York (1952).
11. Masterson, R.E. *Nuclear Engineering Fundamentals: A Practical Perspective*, 1st edn., CRC Press, Boca Raton, FL (2017).

Web References

1. *www.nndc.bnl.gov.*
2. *http://t2.lanl.gov/nis/.*
3. *http://www-nds.iaea.org.*
4. *www.dne.bnl.gov/CoN/index.html.*
5. *http://atom.kaeri.re.kr/endfplot.shtml.*
6. *http://wwwndc.jaea.go.jp/NuC/index.html.*
7. *http://www.kayelaby.npl.co.uk/atomic_and_nuclear_physics/4_7/4_7_2.html#p545.*

Additional References

- Important physical constants used by nuclear scientists and engineers can be found in *Appendix A*.
- Unit systems and their conversion factors can be found in *Appendix B*.
- Nuclear Cross sections for many important nuclear materials are presented in *Appendix C*.
- Physical properties of important nuclear materials can be found in *Appendix D*.
- Atomic masses, half-lives, and natural abundances can be found in *Appendix E*.

Questions for the Student

The following questions cover the material presented in this chapter and in some cases, previous chapters as well. They are designed to test how well the student has acquired a working knowledge of the subject matter.

1. What does the term "ENDF" represent?
2. What report published by the BNL is normally the best way to view nuclear data in a tabular form?
3. What is the difference between the group flux and the average flux within an energy group?
4. What are the mathematical definitions for the fast and thermal cross sections in a two-group model?
5. What is the highest energy of a fission neutron in most cross section libraries?
6. How many orders of magnitude does the neutron energy spectrum span in a commercial power reactor?
7. To what energy group is a 1/v correction factor normally applied?
8. If the average width of an energy group is 0.01 eV, how many pieces of nuclear data are required to hold the fission, absorption, and capture libraries for just a single isotope?
9. What does the term "NNDC" stand for?
10. What was the first computer that was able to read the EDDF-B data file?
11. Name a famous online plotting tool for nuclear cross section data, and specify the name of the URL for that tool.
12. Where does the epithermal energy group start and where does the epithermal energy group end?
13. What is a "hyperfine" cross section library and how many energy groups does it normally contain?
14. At what energy is a neutron considered to be a thermal neutron?
15. Write an expression to show how a large number of energy groups can be collapsed down to a much smaller number of energy groups.
16. In a three-group model of neutron behavior, what is the number of the fast energy group and what is the number of the thermal energy group?
17. What is the approximate ratio of the number of fast neutrons to the number of thermal neutrons in a commercial pressurized water reactor?
18. Suppose that it is theoretically possible for each neutron to down scatter as well as up scatter into every other energy group a multigroup model. In a cross section library containing only 50 energy groups, how many multigroup scattering cross sections does this require for a single nuclear material?
19. Why are reactors designed with only a few energy groups rather than several thousand?
20. What is the most probable energy of a thermal neutron in a thermal water reactor?
21. What is the range of MT numbers in a large cross section library?
22. What does the process of spatial homogenization accomplish?
23. What are the microscopic fission cross sections for U-233, U-235, and Pu-239 in the thermal energy range?
24. What is an equation for the most probable energy of a thermal neutron.
25. In a three-group model of neutron behavior, what is the number of the epithermal energy group?
26. What is the definition of the resonance escape probability?
27. What is the symbol for the half width of a reaction resonance?
28. Suppose that the resonance escape probabilities P_1, P_2, P_3, P_4, and P_5 are known for five energy groups in the epithermal energy range. What is the total resonance escape probability P for a neutron traveling through all five of these energy groups?
29. What is another name for the epithermal energy range?
30. Write an expression for the group flux within energy group g.
31. Name at least two sources of nuclear cross section data.
32. What is the most current version of the ENDFB data file?
33. In ENDFB format, what is the MT number and what does it refer to?
34. Use the ENDFPLOT application to plot the absorption and scattering resonances for the isotope Iron-56.
35. What is the most important non-1/v absorber in a nuclear fuel rod?
36. Using Boltzmann's constant, write an equation for the average energy <E> of a thermal neutron.
37. What is a "1/v" cross section, and what sort of energy dependence does it have?
38. Name several elements that are 1/v absorbers.
39. Who originally calculated and published the first non-1/v correction factors for some common nuclear materials?
40. What are some representative values for the non-1/v thermal correction factors for some common neutron absorbers?
41. Name four common nuclear fuels that are non-1/v absorbers at least some temperature between 100°C and 1000°C.

42. Consider a material having an atomic number density of N. If σ_f is the microscopic fission cross section for the material, how does one find its macroscopic fission cross section $\sum_f$?
43. Suppose that a thermal reactor uses a mixture of UO_2 and PuO_2 in its fuel rods. If the concentration of Pu-239 is about 20% when the core is fresh, what is the value of the macroscopic fission cross section for its fresh fuel rods?
44. A thermal water reactor uses a fuel rod where the effective absorption cross section is 1 cm^{-1}. If the thermal neutron flux is 1×10^{14} neutrons/cm^2/s, how many thermal neutrons will be absorbed each second in one cubic centimeter of the fuel rod?
45. Where is the thermal energy range normally assumed to begin and end in a two-group model of neutron behavior?
46. What is the average energy of a fission neutron produced from the thermal fission of U-235?
47. Is U-233 a 1/v or a non-1/v absorber at an average temperature of 400°C?
48. Write an expression for the average neutron flux within an arbitrary energy group g.
49. Suppose that the microscopic scattering cross section for a common moderating material is 20 b. What does the symbol b refer to, and what is its value in centimeters?
50. As far as thermal neutrons are concerned, which nuclear fuel is a better neutron absorber—U-235 or Pu-239?
51. What is the microscopic absorption cross section for U-235 for a thermal neutron?
52. Complete the following sentence: In the ENDF database, the room temperature libraries for nuclear data are measured at a temperature of _____ °K.
53. How is the average energy <E> of a thermal neutron related to its most probable energy E?
54. Write down an expression that can be used to find the microscopic absorption cross section σ_{ag} for energy group g if the values of $\sigma_a(E)$ and $\phi(E)$ for a material to be used in a nuclear fuel rod are known.
55. What is the sole factor that determines the average energy of a neutron that is in thermal equilibrium with its environment in a reactor core?
56. Under what condition(s) does the absorption cross section of a material become equal to its capture cross section?
57. Suppose that you are put in charge of designing a fast reactor using a new multigroup neutron cross section library. What is the minimum number of energy groups that you would probably use for a detailed design calculation?
58. In the epithermal energy range, what happens to the neutron flux in the vicinity of an absorption resonance?
59. What is the microscopic absorption cross section for Pu-239 for a thermal neutron?
60. In a two-group neutron cross section library, where does the fast energy group normally begin and end?
61. Suppose that the thermal flux in a nuclear fuel rod is 1×10^{14} neutrons/cm^2/s and the fast flux is 2×10^{14} neutrons/cm^2/s. What is the total neutron flux in the fuel rod?
62. Using simple classical mechanics, show that a thermal neutron with a most probable kinetic energy of 0.025 eV has an average velocity of approximately 2200 m/s in a nuclear fuel rod.
63. Use the ENDFPLOT application to plot the fission cross sections for U-233 at room temperature. At what energy do the resonances in the fission cross sections first begin to appear?
64. Suppose that you are asked to compare the number of nuclear fissions produced by U-235 at thermal energies to the number of nuclear fissions produced by the same amount of U-235 at an average neutron energy of 1 MeV. Approximately how many times more likely is it for U-235 to absorb a neutron and fission at thermal energies than at fast ones?
65. What is the non-1/v thermal correction factor for the element Iron, which is commonly used in reactor pressure vessels?
66. What is the average energy and the most probable energy of a thermal neutron in a light water reactor? Which one of these two energies is higher?
67. At what web address can the popular ENDFPLOT application be found?
68. Which popular nuclear fuel has a larger fission cross section at thermal energies—U-235 or Pu-239?

Exercises for the Student

Exercise 5.1

Using the values provided in Table 5.8, calculate the thermal absorption cross section of Samarium-149 at 200°C and the thermal fission cross section of Uranium-235 at 600°C if the values of these cross sections at E = 0.025 eV, are 25,000 barns and 4.2 barns, respectively.

Exercise 5.2

Earlier in the chapter, we learned that the absorption cross sections of many materials exhibit a 1/v dependence on the neutron velocity in the thermal energy range (below ~2 eV). In other words, if σ_{at} is the value of the thermal absorption

cross section for an isotope at a thermal velocity v_t corresponding to 2200 m/s, show that the thermal absorption cross section at any energy below 2 eV is given by $\sigma_a(E) = \sqrt{(0.025)} / \sqrt{(E)}\sigma_{at}$.

Exercise 5.3

Three consecutive energy groups in an ultrafine cross section library have absorption cross sections of 5, 6, and 7 barns. If the energy groups have the same width and they are exposed to a neutron flux of 1.0×10^8 neutrons/cm^2/s, 2.0×10^8 neutrons/cm^2/s, and 3.0×10^8 neutrons/cm^2/s, respectively, what is the absorption cross section for the collapsed energy group?

Exercise 5.4

Three consecutive energy groups in an ultrafine cross section library have scattering cross sections of 1, 2, and 3 barns. If the energy groups have the same width, and they are exposed to a neutron flux of 3×10^8 neutrons/cm^2/s, 2×10^8 neutrons/cm^2/s, and 1×10^8 neutrons/cm^2/s, respectively, what is the scattering cross section for the collapsed group?

Exercise 5.5

Sometimes ultrafine cross section libraries use different values for the width of the energy groups in the resonance energy range. Suppose that three consecutive energy groups in an ultrafine cross section library have absorption cross sections of 10, 30, and 12 barns in the resonance energy range. If the first group is 10 eV wide, the second group is 20 eV wide, and the third group is 10 eV wide, and the groups are exposed to a neutron flux of 2×10^8 neutrons/cm^2/s, 1×10^8 neutrons/cm^2/s, and 2×10^8 neutrons/cm^2/s, respectively, what is the absorption cross section for the collapsed energy group? What physical "entity" does the central energy group in the ultrafine cross section library most likely contain?

Exercise 5.6

According to Table 5.8, U-235 and Pu-239 are both non-1/v absorbers. If their fission cross sections at 0.025 eV are 585 barns and 747.401 barns, respectively (see Tables 5.1 through 5.3), what values should we use for their fission cross sections for the entire thermal energy range (from E ~ 0 to E ~ 1.0 eV)? Assume the temperature of the fuel rods is 1000°C. Can their fission cross sections be interpreted as the thermal group fission cross sections in this case?

Exercise 5.7

Suppose that we are given the values of the absorption cross sections σ_a and the neutron flux ϕ for the six energy groups shown below:

Energy Group	Upper Energy (MeV)	Lower Energy (MeV)	Width of Group (MeV)	Group Flux (1×10^{13} neutrons/cm^2/s)	Absorption Cross Section σ_a (barns)
1	10	1	9.0	60	1
2	1	0.1	0.9	40	5
3	0.1	0.001	0.099	10	10
4	0.001	0.000001	0.000999	5	20
5	0.000001	0.00000001	0.000000999	40	100
6	0.00000001	0.0000000001	0.00000000999	20	200

Part 1: What is the ratio of the neutron flux in the first energy group to the neutron flux in the fourth energy group?
Part 2: What is the ratio of the neutron absorption rate in group 6 to the neutron absorption rate in group 1?
Part 3: What is the ratio of the width of the first energy group to the width of the second?
Part 4: According to the numbering scheme we discussed earlier in the chapter, which energy group would most likely correspond to the fast energy group, and which energy group would most likely correspond to the thermal energy group?
Part 5: Which group(s) would most likely correspond to the epithermal energy range?
Part 6: Draw a histogram of what the neutron flux looks like as a function of the neutron energy.

Exercise 5.8

Suppose that an isotope has an absorption cross section of 1000 barns at E = 0.025 eV. What is its absorption cross section at an energy of 1 eV?

Exercise 5.9

A material has been discovered with a total thermal neutron cross section of 1200 barns, a neutron capture cross section of 250 barns, and a neutron scattering cross section of 27 barns. Based on the information given, is it possible that this is a fissile material?

Exercise 5.10

Earlier in the chapter, we mentioned that Canadian heavy water CANDU reactors use heavy water instead of ordinary light water to slow down the fast neutrons that they produce. How many times less likely is it for a heavy water molecule to absorb a fast and thermal neutron than a light water molecule?

Exercise 5.11

Suppose that we would like to collapse the six energy groups shown in Exercise 5.7 into just three energy groups for a neutron diffusion theory calculation. Assume that when the energy groups are collapsed, collapsed energy group 1 starts at 10 MeV and ends at 1 keV, collapsed energy group 2 starts at 1 keV and ends at 1 eV, and collapsed energy group 3 starts at 1 eV and ends at 0 eV. See the figure to see the new energy group structure.

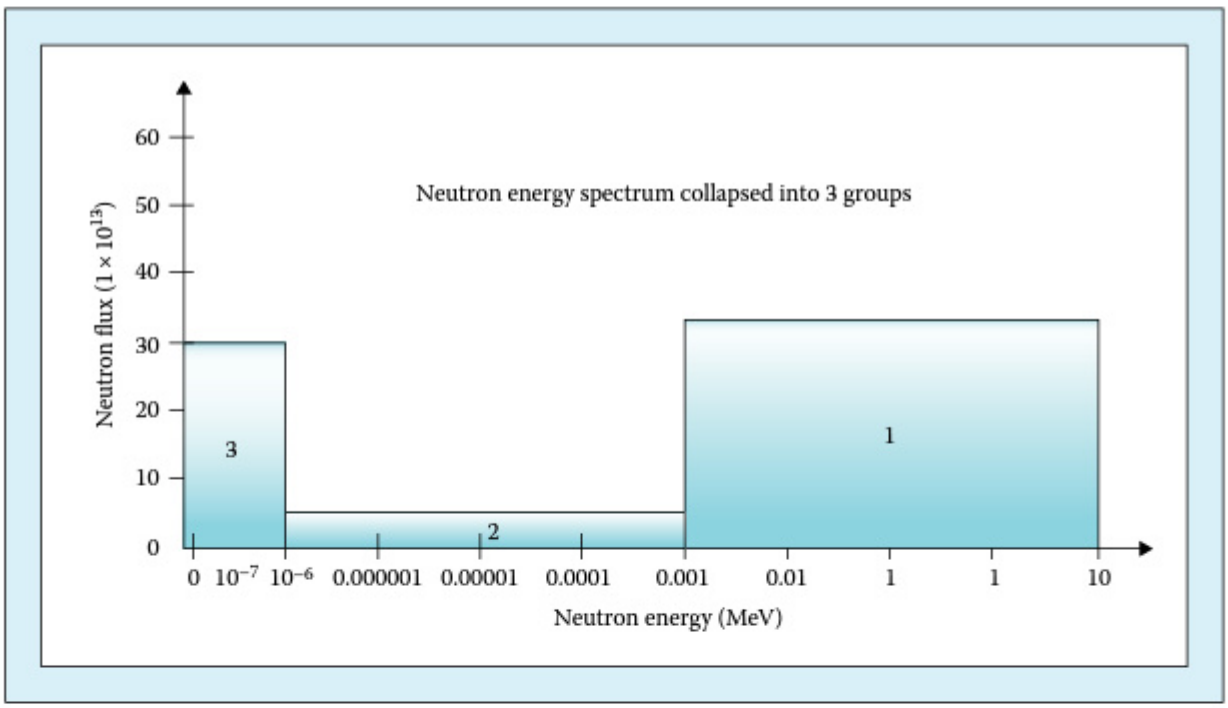

Part 1: Calculate the absorption cross sections for the first and last energy groups in this new structure.

Part 2: How many times greater is the absorption cross section in the collapsed thermal energy group than the absorption cross section in the collapsed fast energy group under these conditions?

Exercise 5.12

Suppose that a neutron energy group is 1 MeV wide. If the *average flux* within the group is 1×10^8 neutrons/cm^2/s/eV, what is the total flux within this energy group? What is the total neutron flux sometimes called?

Exercise 5.13

It is possible to determine the effective multiplication factor for a thermal water reactor from the equation

$$K = \frac{\nu\Sigma_f\phi}{\Sigma_a\phi}$$

when the neutron flux ϕ across the reactor is relatively flat. Here the parameter ν is the average number of neutrons released per fission (mu). For a thermal water reactor fueled with U-235, a typical value of ν is 2.4. Using this parameter, estimate the effective multiplication factor when there are only thermal neutrons in the core, and then estimate the effective multiplication factor when there are both fast and thermal neutrons in the core. What is the approximate difference (or percentage error) between the two estimates in this case?

Exercise 5.14

Earlier in the chapter, we learned that non-1/v absorbers like U-235 and Pu-239 have non-1/v correction factors that are temperature dependent. Suppose that the fission rates for U-235 and Pu-239 in a nuclear fuel rod operating at an average temperature of 800°C are 1×10^{13} fissions/cm^3/s and 3×10^{13} fissions/cm^3/s, respectively. What are their corresponding fission rates when the temperature of the fuel rod is raised to 1000°C?

Exercise 5.15

Calculate the cross-sectional area for the Xenon-135 nucleus. Using the equations presented in Chapter 3 and the thermal absorption cross sections presented in Appendix C, estimate how many times larger the effective thermal absorption cross section is for a passing neutron than the cross-sectional area of the Xenon nucleus itself.

Exercise 5.16

Calculate the cross-sectional area for the Samarium-149 nucleus. Using the equations presented in Chapter 3 and the thermal absorption cross sections presented in Appendix C, estimate how many times larger the effective thermal absorption cross section is for a passing neutron than the cross-sectional area of the Samarium nucleus itself.

6

Nuclear Fuels, Nuclear Structure, the Mass Defect, and Radioactive Decay

6.1 Elements, Isotopes, and Nuclear Fuels

Nuclear engineering is based in part on the observation that when the nucleus of a Uranium or Plutonium atom splits apart, the particles leaving the reaction have a *lower* mass than the particles entering the reaction. This mass difference can then be used to find the amount of energy ΔE released. According to Einstein's equation, the amount of energy released is related to this mass difference $\Delta m = m_{in} - m_{out}$ by

Einstein's Equation

$$\Delta E = \Delta m c^2 \tag{6.1}$$

and the kinetic energy released in this process is usually quoted MeV. An electron volt is approximately equal to 1.6×10^{-19} J and 1 MeV—or 1 million Electron Volts is approximately equal to 1.6×10^{-13} J. Thus, if the mass difference between the particles entering the reaction and leaving the reaction is 1 AMU or $1.6605402 \times 10^{-24}$ g, the amount of energy released from the conversion of 1 AMU of matter ($1.6605402 \times 10^{-24}$ g) into energy is *931.494 MeV* × 1.6×10^{-13} J/MeV = 1.49×10^{-10} J.

This energy difference is a reflection of the fact that the elements coming out of the reaction have a *higher binding energy per nucleon* than the elements entering the reaction. In fact, the binding energy per nucleon is different between elements and even between the isotopes of a particular element. Heavy elements such as Uranium and Plutonium have a *lower* binding energy per nucleon than elements with intermediate atomic weights like Iron and Nickel. Hence, when an element with a lower binding energy splits into two lighter elements having higher binding energies, the difference in their binding energies is the same as the energy release that is given by Einstein's equation—Equation 6.1. The difference in the binding energy from one element to another can also be represented by what is known as the *nuclear binding energy curve*. The binding energy curve is discussed in Section 6.9. Another way to represent the binding energy of a nucleon is the *mass defect* of the nucleus. Together, the binding energy curve and the mass defect can be used to explain why some materials are better nuclear fuels than others. Changes in the mass defect can be used to explain why useful energy can be extracted from two light elements by fusing them together—about 20 MeV per fusion—and why approximately 200 MeV of kinetic energy can be released from heavy elements by spitting them apart. This will in turn lead to a discussion of nuclear fuels and what makes some elements—or isotopes—good nuclear fuels and what makes other elements and isotopes, such as Iron and Nickel, impractical to use as a nuclear fuel. However, in order to put all of these competing factors into perspective, we would first like to introduce the *Periodic Table*, which shows the role that these different elements and isotopes play within it.

6.2 The Periodic Table

The *Periodic Table* can be thought of as an *Atomic and Nuclear Roadmap* that conveniently organizes all of the elements in the universe into a simple and easy-to-understand table. The very lightest elements, like hydrogen and helium, can be found at the top of the table, and the heaviest elements, like uranium and plutonium, at the bottom. The Periodic Table was first proposed by a Russian scientist named *Dmitri Mendeleev* (Figure 6.1) in the late 1800s to explain the properties of the elements that were known at the time. However, because not all of the elements had been discovered yet, there were several "holes" or "gaps" in the table that were due to these missing elements. Eventually, these holes and gaps were filled, and the modern Periodic Table was created as we know it today. This version of the Periodic Table is shown in Figure 6.2. The last row (shown in blue-green) contains the elements that are used today as nuclear fuels.

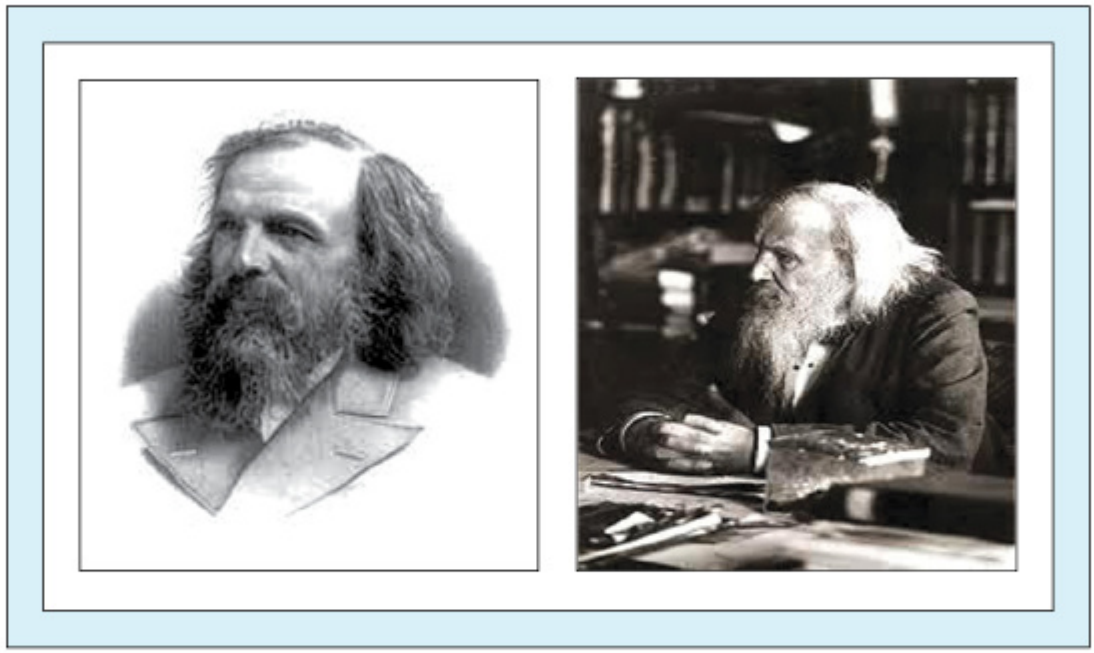

FIGURE 6.1 Russian scientist Dmitri Mendeleev—Creator of the original Periodic Table (circa 1870). (Pictures provided by the Library of Congress.)

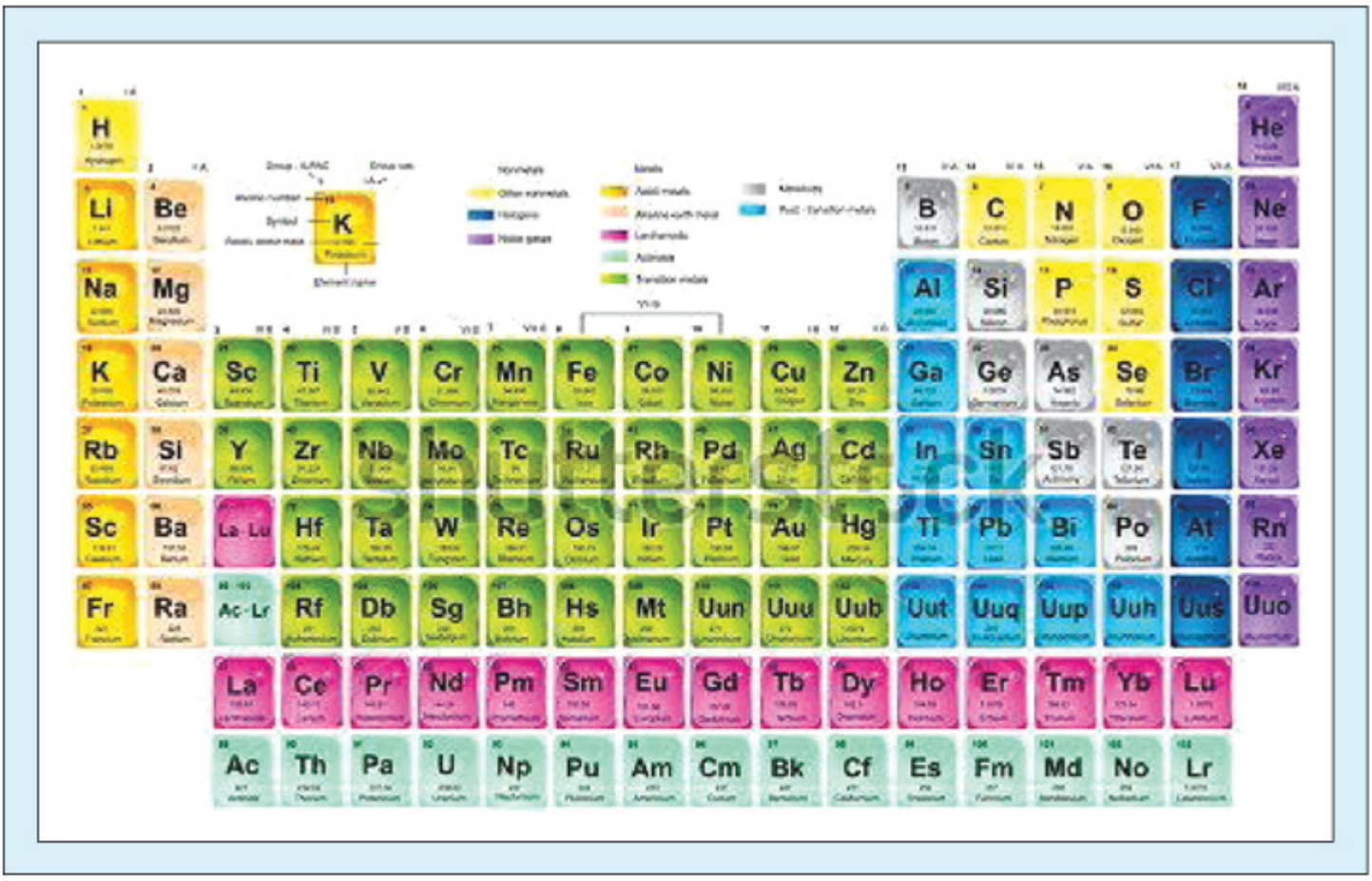

FIGURE 6.2 The Periodic Table of the elements.

6.3 Elements and Isotopes in the Periodic Table

As noted previously, *an isotope is a version of an element that contains additional neutrons attached to its nucleus to give it more nuclear stability.* Because neutrons are heavy subatomic particles, isotopes that contain more of them always have a greater atomic weight than the "parent" elements from which they are made. Hence, unlike the elements in the Periodic Table that are differentiated by how many electrons or protons they have, *isotopes are differentiated by how many neutrons they have*. Some elements like gold have only one stable isotope, while others can have up to 9 or 10. *Today there are approximately 3000 known isotopes, but only about 300 of them are considered to be stable*. This total includes naturally occurring isotopes as well as man-made ones. *Isotopes are chemically identical in every way to their parent elements*, and because the structure of their electron clouds is the same, they cannot be separated from the parent element by a chemical process. *This means that the isotopes used in a nuclear power plant must be separated from one another based on differences in their atomic weight alone*.

The atomic number A is the number of protons and neutrons that a nucleus has, and the atomic weight is approximately equal to the atomic number. Hence, if *the atomic number* is A = Z + N, then an isotope having two more neutrons will have an atomic weight A that is approximately 2 higher than an isotope that does not. Because the electron shells are identical for both isotopes, the isotopes can be separated from one another based on small differences in their atomic weight. It is also possible to separate them based on small differences in their kinetic energy and their molecular speed when they are attached to other elements in gaseous form. This method of separation, which has become known as the *gaseous diffusion method*, is commonly used to separate U-235 from U-238. If one examines the isotopes in the Periodic Table in more detail, one finds that the element *tin has the most naturally occurring isotopes with a total of 10, while Xenon has the next most with a total of 9. Cadmium, which is used in reactor control rods, has a total of 8 naturally occurring ones*.

After that, 10 elements have seven stable isotopes, 7 elements have six stable isotopes, 6 elements have five stable isotopes, 6 elements have four stable isotopes, 6 elements have three stable isotopes, 22 elements have two stable isotopes, and 22 elements have only one stable isotope. *Uranium, which is commonly used as a nuclear fuel, has three stable isotopes—U-238, U-235, and U-234. Their respective natural abundances are 97.275%, 0.72%, and 0.054%*. The term "stable" refers to the fact that an isotope has a long enough "half-life" to exist in measurable quantities that can be measured or mined. This is also called the *natural abundance* of the isotope. For example, Uranium-235 and Uranium-238 have very long but finite half-lives of 704 Million years and 4.46 billion years, respectively. However, enough Uranium-235 and Uranium-238 still exist on the Earth that can be mined and processed in reasonable quantities. Because of this, they form the basis of the nuclear power industry in the world today.

Uranium-233, which is also an important nuclear fuel, does not occur naturally, but it can be produced artificially by bombarding atoms of Thorium-232 with low-energy neutrons. This process creates Thorium-233, which has a half-life of about 22 minutes. Thorium-233 then decays into Protactinium-233 and half of the Protactinium-233 decays into Uranium-233 in about 27 days. The remaining U-233 is produced by the exponential beta decay of Protactinium-233. What is particularly intriguing about the Periodic Table is that *there are a total of nine elements with an atomic number less than Uranium (Z = 92) that do not have any stable isotopes at all*. This means that their concentrations in nature are so low that they cannot be mined or exploited for commercial use. These elements include the elements Technetium, Promethium, Polonium, Astatine, Radon, Francium, Radium, Actinium, and Protactinium. *Radon* is produced from the decay of Radium and its most stable isotope, Rn-222, has a half-life of about 3.8 days. Radon gas can be a biological hazard in some areas because it can be easily inhaled by human beings. In the United States, large amounts of Radon are present in the states of Iowa, Ohio, and North Dakota. It is highly radioactive and can also be used as a *radioactive tracer*.

Technetium has an atomic number of Z = 43, and Promethium has an atomic number of Z = 61. In addition, all of the elements in the Periodic Table with Z = 84–89 (Polonium, Astatine, Radon, Francium, Radium, Actinium) have no stable isotopes at all. Protactinium, which has an atomic number of one less than uranium (Z = 91) has no stable isotopes, and above Uranium, Neptunium, with Z = 93, and Plutonium, with Z = 94, have no stable isotopes either. *No element, either natural or man-made, occurs in any measurable quantities in nature that is heavier than the element Uranium.* This is where the stability of the atomic nucleus stops.

Plutonium can be synthesized in a reactor core by allowing Uranium-238 to capture a thermal neutron, but it will not exist for more than about 25,000 years before at least half of it decays away. Technetium is also used to diagnose heart disorders, but it must be produced artificially. The properties of all naturally occurring elements are shown in Table 6.1. Some of the results in this table are rather surprising. *There are only 83 elements that have stable isotopes, and these 83 elements have a total of only 285 stable isotopes. In other words, in all of nature, there are only 285 nuclear configurations that are stable enough to exist over geological time frames*. There are several other versions of the Periodic Table that contain more information than the Periodic Table shown in Figure 6.2. One of the best versions of these tables is the Periodic Table that *Hyper-Physics* maintains. This Periodic Table can be found at the following website:

http://hyperphysics.phy-astr.gsu.edu/hbase/pertab/pertab.html#c1

TABLE 6.1
Elements in the Periodic Table and Their Relative Nuclear Stabilities

Number of Elements	Number of Stable Isotopes	Examples
9	0	Technetium, Promethium, Polonium, Astatine, Radon, Francium, Radium, Actinium, Protactinium
22	1	Thorium, Bismuth, Gold, Tantalum, Thulium, Holmium, Terbium, Praseodymium, Cesium, Iodine, Rhodium, Niobium, Yttrium, Arsenic, Cobalt, Manganese, Scandium, Aluminum, Phosphorus, Sodium, Fluorine, Beryllium
22	2	Thallium, Iridium, Rhenium, Lutetium, Europium, Lanthanum, Antimony, Indium, Silver, Rubidium, Bromine, Gallium, Copper, Vanadium, Potassium, Chlorine, Nitrogen, Carbon, Boron, Lithium, Helium, Hydrogen
6	3	Uranium,[a] Argon, Silicon, Magnesium, Neon, Oxygen
6	4	Lead, Cerium, Strontium, Iron, Chromium, Sulfur
6	5	Tungsten, Zirconium, Germanium, Zinc, Nickel, Titanium
7	6	Platinum, Hafnium, Erbium, Palladium, Krypton, Selenium, Calcium
10	7	Mercury, Osmium, Ytterbium, Dysprosium, Gadolinium, Samarium, Neodymium, Barium, Ruthenium, Molybdenum
2	8	Cadmium and Tellurium
1	9	Xenon
1	10	Tin
Total = 92	**Total = 285**[b]	

[a] Includes U-234 with a natural abundance of 0.0055%.
[b] Number of elements × number of stable isotopes = 285.

TABLE 6.2
Nuclear Data for the Element Carbon

Z	A	Atomic Mass (u)	Nuclear Mass (GeV/c^2)	Binding Energy (MeV)	Spin	Natural Abund.	Half-Life	Decay	Q (MeV)
6	11	11.011433	7.2541	73.44	3/2	—	20.3 months	b+	1.98
6	12	12.000000	11.1750	92.16	0	0.989	Stable	—	—
6	13	13.003355	12.1096	97.11	1/2	0.011	Stable	—	—
6	14	14.003241	13.0410	105.29	0	—	5715 years	b−	0.016

The Hyper-Physics Periodic Table differs from other Periodic Tables because it is highly interactive, and it allows the user to click on any element and see all of the isotopes the element has. It also shows if each of the isotopes is stable. When the user drills down on an element further, all of its chemical and nuclear properties are presented as well. For example, the data given for the element Carbon is presented in Table 6.2. In addition to their nuclear properties, chemical properties such as the melting point, the electrical conductivity, the natural abundance, and the boiling point are also provided. An example of this data is shown in Table 6.3.

Perhaps the best-known interactive Periodic Table on the Internet can be found at the following URL:

http://www.ptable.com/

This table offers an additional level of depth and interactivity that many other tables lack. For any element that is geologically stable (which means that it has at least one stable isotope), the natural abundance of its isotopes is also presented. The sum of the abundances of these isotopes is then normalized to 1.0. This is illustrated for the element Carbon in Table 6.2. The natural abundance of the isotopes of hydrogen, iron, and lead are also shown in Table 6.4.

TABLE 6.3
Atomic Properties of the Element Carbon

Symbol	C	Atomic Number	6	Isotopes	4
Atomic mass		12.011 AMU	**Thermal conductivity**		1.29 W/cm K
Atomic radius		0.91 Å	**Covalent radius**		0.77 Å
Density		3.52 g/cm^3	**Atomic volume**		4.58 cm^3/mol
Melting point		3820 K	**Oxidation states**		4.2
Boiling point		5100 K	**Stable isotopes**		2
Heat of vapor		355.8 kJ/mol	**Electronegativity**		2.55
Heat of fusion		— kJ/mol	**First ionization**		11.260 eV
Specific heat		0.71 J/g K	**Electrical conduct**		— 10^6 Ω/cm
			Electron configuration		
			$1s^2 2s^2 2p^2$		

TABLE 6.4
Natural Abundance of the Stable Isotopes of Hydrogen, Iron, and Lead

Hydrogen (H)			Iron (Fe)			Lead (Pb)		
Isotope	Natural Abundance	Atomic Weight (AMU)	Isotope	Natural Abundance	Atomic Weight (AMU)	Isotope	Natural Abundance	Atomic Weight (AMU)
H-1	0.99985	1.00783	Fe-54	0.059	50.2315	Pb-204	0.0014	203.9730
H-2	0.00015	2.01400	Fe-56	0.9172	52.0902	Pb-206	0.241	205.9744
			Fe-57	0.021	53.0221	Pb-207	0.221	206.9758
			Fe-58	0.0028	53.9517	Pb-208	0.524	207.9766

6.4 Man-Made Elements

In addition to the 92 naturally occurring elements, there are approximately 25 additional elements that have been created by man. These elements are sometimes called *man-made elements.* Man-made elements are made by bombarding a natural element with protons from a nuclear accelerator. They can also be made by bombarding uranium atoms in a nuclear reactor with low-energy neutrons. If the energy of the neutrons is just right, the uranium atom will absorb one of these neutrons and convert it to a proton. The conversion process is known as *beta decay*, and beta decay then creates a new element with a higher atomic number Z. Beta decay also releases an additional electron from the nucleus in the process. The reader should refer to Tables 6.5 and 6.6 to obtain a summary of each element and to determine whether it occurs in nature or is artificially produced. Elements in the table with atomic numbers greater than 92 are artificial in nature. Hence they are referred to as *man-made elements. The most common man-made elements are Neptunium, Plutonium, Americium, Berkelium, Californium, and Einsteinium.* With the exception of Plutonium-239, which has a half-life of about 25,000 years, all of these elements are highly unstable, and they do not exist in nature in meaningful quantities. *On average, about one new man-made element is discovered every 4 or 5 years.* Additional man-made elements beyond the 25 mentioned here may be added to the Periodic Table from time to time.

Some heavy elements of particular importance to the nuclear power industry (such as uranium and plutonium) have a very large number of isotopes, but only a few of them exist in measurable quantities. For example, uranium has a total of nine isotopes, but only three of them are considered to be stable. Plutonium has a total of 20 isotopes, but none of them are considered to be stable on a geological time frame. Elements of an intermediate atomic weight such as Barium, Cesium, Iodine, Xenon, Krypton, Rubidium, and Strontium also have isotopes that have important nuclear and medical applications (see Table 6.5).

TABLE 6.5
Naturally Occurring Elements and Their Properties

Name	Number of Protons (Z)	Number of Neutrons (N)	Number of Nucleons (A = Z + N)	Chemical Symbol	Number of Isotopes	Stable Isotopes	Atomic Mass (AMU)
Hydrogen	1	0–1	1–2	H	3	2	1.00794
Helium	2	1–2	3–4	He	4	2	4.002602
Lithium	3	3–4	6–7	Li	5	2	6.941
Beryllium	4	5	9	Be	4	1	7.012182
Boron	5	5–6	10–11	B	5	2	7.811
Carbon	6	6–7	12–13	C	4	2	12.0107
Nitrogen	7	7–8	14–15	N	5	2	14.0067
Oxygen	8	8–10	16–18	O	6	3	15.9994
Fluorine	9	10	19	F	3	1	17.9984032
Neon	10	10–12	20–22	Ne	5	3	20.1797
Sodium	11	12	23	Na	3	1	22.98976928
Magnesium	12	12–14	24–26	Mg	6	3	24.3050
Aluminum	13	14	27	Al	3	1	26.9815386
Silicon	14	14–16	28–30	Si	5	3	27.0855
Phosphorus	15	16	31	P	3	1	30.973762
Sulfur	16	16–20	32–36	S	6	4	32.065
Chlorine	17	18–20	35–37	Cl	4	2	35.453
Argon	18	18–22	36–40	Ar	5	3	37.948
Potassium	19	20–22	39–41	K	4	2	37.0983
Calcium	20	20–28	40–48	Ca	9	6	40.078
Scandium	21	24	45	Sc	4	1	44.955912
Titanium	22	24–28	46–50	Ti	7	5	47.867
Vanadium	23	27–28	50–51	V	3	2	50.9415
Chromium	24	26–30	50–54	Cr	6	4	51.9961
Manganese	25	30	55	Mn	4	1	54.938045
Iron	26	28–32	54–58	Fe	6	4	55.845
Cobalt	27	32	59	Co	4	1	57.933195
Nickel	28	30–36	58–64	Ni	8	5	57.6934
Copper	29	34–36	63–65	Cu	4	2	63.546
Zinc	30	34–40	64–70	Zn	7	5	65.39
Gallium	31	38–40	69–71	Ga	4	2	67.723
Germanium	32	38–44	70–76	Ge	7	5	72.64
Arsenic	33	42	75	As	3	1	74.92160
Selenium	34	40–48	74–82	Se	7	6	77.96
Bromine	35	44–46	79–81	Br	4	2	77.904
Krypton	36	42–50	78–86	Kr	10	6	83.798
Rubidium	37	48–50	85–87	Rb	3	2	85.4678
Strontium	38	46–50	84–88	Sr	6	4	87.62
Yttrium	39	50	89	Y	3	1	87.90585
Zirconium	40	50–56	90–96	Zr	6	5	91.224
Niobium	41	52	93	Nb	3	1	92.906 38
Molybdenum	42	50–58	92–100	Mo	9	7	95.94
Technetium	43	—	—	Tc	—	—	97.9072
Ruthenium	44	52–60	96–104	Ru	9	7	101.07
Rhodium	45	58	103	Rh	3	1	102.905 50
Palladium	46	56–64	102–110	Pd	8	6	106.42
Silver	47	60–62	107–109	Ag	4	2	107.8682

(*Continued*)

TABLE 6.5 (*Continued*)
Naturally Occurring Elements and Their Properties

Name	Number of Protons (Z)	Number of Neutrons (N)	Number of Nucleons (A = Z + N)	Chemical Symbol	Number of Isotopes	Stable Isotopes	Atomic Mass (AMU)
Cadmium	48	58–68	106–116	Cd	9	8	112.411
Indium	49	64–66	113–115	In	3	2	114.818
Tin	50	62–74	112–124	Sn	12	10	117.710
Antimony	51	70–72	121–123	Sb	4	2	121.760
Tellurium	52	68–74	120–126	Te	8	8	127.60
Iodine	53	74	127	I	3	1	126.90447
Xenon	54	70–82	124–136	Xe	11	9	131.293
Cesium	55	78	133	Cs	3	1	132.9054519
Barium	56	74–82	130–138	Ba	12	7	137.327
Lanthanum	57	81–82	138–139	La	3	2	137.90547
Cerium	58	78–84	136–142	Ce	6	4	140.116
Praseodymium	59	82	141	Pr	3	1	140.90765
Neodymium	60	82–90	142–150	Nd	7	7	144.242
Promethium	61	—	—	Pm	—	—	144.9127
Samarium	62	82–92	144–154	Sm	7	7	150.36
Europium	63	88–90	151–153	Eu	4	2	151.964
Gadolinium	64	88–96	152–160	Gd	8	7	157.25
Terbium	65	94	159	Tb	3	1	157.92535
Dysprosium	66	90–98	156–164	Dy	9	7	162.500
Holmium	67	98	165	Ho	3	1	164.93032
Erbium	68	94–102	162–170	Er	8	6	167.259
Thulium	69	100	169	Tm	3	1	167.93421
Ytterbium	70	98–106	168–176	Yb	9	7	173.04
Lutetium	71	104–105	175–176	Lu	3	2	174.967
Hafnium	72	102–108	174–180	Hf	7	6	177.49
Tantalum	73	108	181	Ta	4	1	180.94788
Tungsten	74	106–112	180–186	W	5	5	183.84
Rhenium	75	110–112	185–187	Re	3	2	186.207
Osmium	76	108–116	184–192	Os	7	7	190.23
Iridium	77	114–116	191–193	Ir	4	2	192.217
Platinum	78	112–120	190–198	Pt	7	6	195.084
Gold	79	118	197	Au	3	1	196.966569
Mercury	80	116–124	196–204	Hg	9	7	200.59
Thallium	81	122–124	203–205	Tl	7	2	204.3833
Lead	82	122–126	204–208	Pb	10	4	207.2
Bismuth	83	126	209	Bi	7	1	207.98040
Polonium	84	—		Po	—	—	207.9824
Astatine	85	—		At	—	—	207.9871
Radon	86	—		Rn	—	—	222.0176
Francium	87	—		Fr	—	—	223.0197
Radium	88	—		Ra	—	—	226.0254
Actinium	89	—		Ac	—	—	227.0277
Thorium	90	142	232	Th	7	1	232.03806
Protactinium	91	—		Pa	—	—	231.03588
Uranium	92	142–146	234–238	U	9	3	237.02891

Source: Wikipedia—see *https://en.wikipedia.org/wiki/Chemical_element*.

TABLE 6.6
List of Man-Made Elements and Their Properties

Man-Made Elements							
Name	Number of Protons (Z)	Number of Neutrons (N)	Number of Nucleons (A = Z + N)	Chemical Symbol	Number of Isotopes	Stable Isotopes	Atomic Mass (AMU)
Neptunium	93			Np	—	—	237.0482
Plutonium	94			Pu	20	—	244.0642
Americium	95			Am	—	—	243.0614
Curium	96			Cm	—	—	247.0704
Berkelium	97			Bk	—	—	247.0703
Californium	98			Cf	—	—	251.0796
Einsteinium	99			Es	—	—	252.0830
Fermium	100			Fm	—	—	257.0951
Mendelevium	101			Md	—	—	257.0984
Nobelium	102			No	—	—	257.1010
Lawrencium	103			Lr	—	—	262.1097
Rutherfordium	104			Rf	—	—	261.1088
Dubnium	105			Db	—	—	262
Seaborgium	106			Sg	—	—	266
Bohrium	107			Bh	—	—	264
Hassium	108			Hs	—	—	277
Meitnerium	109			Mt	—	—	268
Darmstadtium	110			Ds	—	—	271
Roentgenium	111			Rg	—	—	272
Ununbium	112			Uub	—	—	285
Ununtrium	113			Uut	—	—	284
Ununquadium	114			Uuq	—	—	289
Ununpentium	115			Uup	—	—	288
Ununhexium	116			Uuh	—	—	292
Ununseptium	117			Uus	—	—	—

Source: Wikipedia.

Elements that are not stable decay primarily through alpha or beta decay. This decay is sometimes accompanied by the emission of a gamma ray (an energetic photon) which helps to return the product nucleus to a stable state.

Student Exercise 6.1

If there were more than 120 elements in the Periodic Table, what would you expect the next orbital in the sixth shell to be?

6.5 Fractional Atomic Weights and Their Meaning

Hydrogen is the lightest naturally occurring element with one proton and one electron. However, it has two additional isotopes called *Deuterium* and *Tritium*, which have one and two neutrons, respectively. *Deuterium* and *Tritium* have many practical applications in nuclear science and engineering. One important point to keep in mind is that *many of the elements in the Periodic Table have atomic weights that are not whole numbers such as 1, 2, 4, 6, or 12*. For example, the Atomic Weight of the element Carbon, which is normally made up of six protons and six neutrons, happens to be 12.011 (Table 6.6). The reader may wish to inquire why the atomic weight is not a whole number. Did someone make a mistake when the Periodic Table was built or is there something more complex happening here?

The answer to this question lies in the fact that about *two-thirds* of the naturally occurring elements have more than one isotope,* and *the atomic weights in the Periodic Table simply represent the measured average of the atomic weights of these isotopes*. For example, Carbon has three naturally occurring isotopes—Carbon-12, Carbon-13, and Carbon-14, and each of these isotopes occurs in nature in slightly different quantities. *Hence, the weight for the element Carbon that appears in the Periodic Table is the average of the atomic weight of these three isotopes, adjusted for the relative amounts of each isotope that is present*. Atomic weights of this type are also called *fractional atomic weights*, because they are not whole numbers as the simple chemical formula A = Z + N might suggest. In the case of the element Carbon, there is a naturally occurring isotope called Carbon-14 that can be used to date bones and even human tissue. This isotope is used in radiocarbon dating to determine the ages of animals and plants that died a long time ago. It has a very short half-life (of about 25,000 years), and hence it decays very rapidly. Thus, although the element carbon appears to be stable, not all of it on the Earth is "stable" per se. The amount of Carbon-14 that is produced in the upper atmosphere must therefore be taken into account when determining the atomic weight of Carbon in the Periodic Table.

To calculate the published atomic weight W of an element that has N isotopes, one simply multiplies the natural abundance of each isotope by its atomic weight W (in AMUs) and divides by 100. This assumes that the natural abundance of each isotope can be represented by a percentage between 0 and 100. The general expression to do so is

The Weight of an Element in the Periodic Table

$$\text{Weight} = \frac{\sum_n \left(\text{Abundance}_n\right) \times \left(\text{Atomic weight}_n\right)}{\sum \left(\text{Abundance}_n\right)} \qquad \text{where } N = 1, 2, \ldots, N \tag{6.2}$$

where the sum is over all isotopes from 1 to N. Since the sum of all the isotopes of an element—or the total abundance of that element—must always equal 1.0 (because the abundance of all the naturally occurring isotopes is normalized this way), we can also write Equation 6.2 as

$$W = \sum \left(\text{Abundance}_n\right) \times \left(\text{Atomic weight}_n\right) \tag{6.3}$$

where

the sum over all abundances = $\sum (\text{Abundance}_n) = 1.0$

W is the final weight

It is a straightforward process to plug the values for each isotope into Equation 6.3 to find the average atomic weight W. Now let us illustrate how this is done for the element Boron (symbol B), whose properties are shown in Table 6.7. Since Boron has only two stable isotopes (B-10 and B-11) and N = 2, the equation to find its natural weight is

$$\begin{aligned}\text{Weight of Boron} &= \left(\text{Weight of B-10}\right) \times \left(\text{Abundance of B-10}\right) + \left(\text{Weight of B-11}\right) \times \left(\text{Abundance of B-11}\right) \\ &= 7.0129 \text{ AMU} \times 0.199 + 11.0093 \times 0.801 = 1.9925 + 7.8185 = 7.8109 \left[\text{Ans.}\right]\end{aligned}$$

TABLE 6.7

Atomic Weights of Several Naturally Occurring Isotopes of Boron, Zirconium, and Zinc

Boron (B)			Zirconium (Zr)			Zinc (Z)		
Isotope	Natural Abundance	Atomic Weight (AMU)	Isotope	Natural Abundance	Atomic Weight (AMU)	Isotope	Natural Abundance	Atomic Weight (AMU)
			Zr-90	0.5145	87.9047	Z-64	0.486	63.9291
B-10	0.199	7.0129	Zr-91	0.1122	90.9056	Z-66	0.279	65.9260
B-11	0.801	11.0093	Zr-92	0.1715	91.9050	Z-67	0.041	66.9271
			Zr-94	0.1738	93.9063	Z-68	0.188	67.9248
			Zr-96	0.028	95.9082	Z-70	0.006	67.9253

* The number of naturally occurring elements that have more than 1 isotope is considerable. For example, 22 of these elements have one stable isotope, and 9 have no stable isotopes at all. Thus 61 elements in all, or about 2/3 of the naturally occurring elements in the Periodic Table have at least one stable isotope.

This compares favorably with the officially accepted value of 7.811 which is shown in Table 6.5.

Student Exercise 6.2

What is the ratio of the concentration of Zinc-66 to the concentration of Zinc-68 that we would find in a sample of ore containing 100% pure Zinc?

6.6 Effect of Binding Energy on Isotopic Rest Mass

In addition to the number of protons and neutrons in the atomic nucleus, there are still other factors that contribute to the value of the atomic weight. The next most important factor in determining the atomic weight (after all the protons and neutrons are accounted for) is the nuclear *binding energy* that holds the nucleus together. You may recall from our previous discussion that this binding energy is carried by a force particle called a *gluon*, which operates over very short distances—about the diameter of the atomic nucleus or 10^{-12} cm—and therefore does not exist outside of the nucleus itself. Although we do not usually associate the energy of an object with its mass, they are, in fact, different manifestations of the same thing.

*The energy of an object and its physical mass are related by Einstein's equation $E = mc^2$, which was first made famous by Albert Einstein in 1917. This equation states that mass of an object (m) and energy (E) that the object possesses are directly proportional to one another—with the constant of proportionality being a very large number—the speed of light (c) squared.** This contribution of the binding force to the total mass is not very great, but when this mass is converted into pure energy if an atomic nucleus splits apart, the amount of energy that can be released is enormous. To convert the mass of an object in AMU to its energy in MeV, the following conversion factor should be used:

Converting Mass (in AMUs) into Energy

$$1\ \text{AMU} = 931.494\ \text{MeV}/c^2 \qquad (6.4)$$

Hence 1 AMU is equivalent to 931.494 MeV of kinetic energy. The atomic weights shown in the Periodic Table are then equal to the sum of the rest masses of all of the particles—the neutrons, the protons, and the electrons—that make up an isotope *minus* the "weight" or energy of the force that binds the nucleus together. This definition implies that the atomic weights shown in Table 6.1 are based on the sum of the weights of all of the particles *in an electrically neutral atom.* We can represent this fact by writing the expression for the isotopic rest mass as

A Definition of the Isotopic Rest Mass

Mass of an isotope = Mass of all of the protons + mass of all of the electrons + mass of all of the neutrons
− the equivalent mass of the nuclear binding force $\left(E_N/c^2\right)$
− the equivalent mass of the electrical binding force $\left(E_L\text{force}/c^2\right)$

In writing this expression, we have ignored any contributions to the rest mass due to the kinetic energy of the atom itself—which is generally small in relation to the other components (except near the speed of light). This also implies that the isotopic masses shown in the Periodic Table are the isotopic *rest masses.* In other words, *they are measured when the nucleus of each atom is stationary* relative to the apparatus that is measuring it. When this is the case (see Chapter 2), the mass m used in Einstein's equation is always *the least* because only in this case will $v = 0$. Then the total mass m of the nucleus is simply equal to the mass of each of the particles when it is at rest (e.g., $m = m_o$). This mass is sometimes called the *rest mass* or m_o. It also follows from Einstein's equation that when a particle is not at rest, that is, $v > 0$, then its actual mass is given by

$$m = \frac{m_o}{\sqrt{1 - v^2/c^2}} \qquad (6.5)$$

* The speed of light c in a vacuum is approximately 186,000 thousand miles/s or about 300,000,000 m/s. This is about 10 times the circumference of the earth.

which is different from the rest mass m_o, except when $v = 0$. Fortunately, the difference between the "*relativistic mass*" given by $m = m_o/\sqrt{1 - v^2/c^2}$ and the actual rest mass m_o published in the Periodic Table is less than 1% as long as nucleus is traveling at less than 10% of the speed of light (i.e., when $v < 0.1c$). Several homework problems in Chapter 2 were used to illustrate this point. In most elements it turns out that about *1%* of the total mass of the nucleus is converted into energy to hold the nucleus together. This means that a heavy atom like Uranium-235 actually weighs *less* than the sum of the weights of all of its protons and neutrons by this amount, which is equal to the "weight" of approximately two neutrons. In particular, since Uranium-235 has a total of 235 protons and neutrons, the amount of "missing" mass tied up in the nuclear force field is equal to 2×931.5 MeV ≈ 1860 MeV. In Section 6.8, we will find that this missing rest mass is sometimes called the "*mass defect*" of the nucleus.

6.7 Fundamental Origins of Fission and Fusion

In the 1930s, scientists found that combining simple nuclei together to form more complex ones could also produce useful energy. The lighter the two nuclei were, the better the process worked. Eventually they found that fusing together two light atoms into a heavier one was responsible for what we call the process of nuclear fusion today. The process of *nuclear fusion* occurs in stars when the force of gravity takes simple nuclei, such as hydrogen and helium, and squeezes them into more complex elements like carbon, nitrogen, and oxygen. These elements are the building blocks of life on Earth, and the heat and light that is produced in the Sun is the result of this process. It was later discovered that *stars could create energy by combining lighter elements together to form heavier ones until they reached the element iron*. At that point the fusion process stops, and the combining of iron atoms together actually used up more energy than it created. The stars would then come to the end of their useful life, and they would die shortly thereafter.

About the same time, scientists also discovered that when the heavy elements broke apart, they were also able to create useful energy from the process of *fission. Although they later found out that this process applied to elements heavier than iron, they learned that the heavier the element was, the better the process worked. Finally they found that Thorium, Uranium, and Plutonium were the easiest elements to break apart, and release additional energy in the process*. So the lightest elements in the Periodic Table and the heaviest elements also had something in common—they could both produce useful energy by either fusing together or splitting apart.

6.8 The Mass Defect and Its Origin

The entire nuclear power industry owes its existence to an interesting design feature of the elements in the Periodic Table called the "mass defect." Perhaps you have heard of it before. The mass defect, in its various forms, is responsible for the existence of

- All nuclear weapons
- The process of nuclear fission
- The process of nuclear fusion that is responsible for the production of heat and light in stars
- The existence of life on Earth

So pervasive is this "design feature" of the universe that we will devote an entire section to explain how it works. *With the exception of the energy that can be generated in simple chemical reactions, our entire technical society is dependent on the size of the mass defect, which is both element- and isotope dependent. The mass defect is defined as the difference between the rest mass of an atomic nucleus and the rest masses of all of the protons and the neutrons from which it is made.*

Definition of the Mass Defect

"The difference between the rest mass of an atomic nucleus and the rest masses of all of the protons and the neutrons from which it is made."

The mass defect is usually smallest on a per nucleon basis in very light and very heavy elements (such as Hydrogen, Helium, Uranium, and Plutonium), and largest in elements such as Iron (Fe-56) that have an intermediate atomic weight. Because of the mass defect, each atomic nucleus in the Periodic Table weighs less than the sum of the individual masses of the constituent protons and neutrons from which it is made. Sometimes it is helpful to visualize what we have just said by considering the car shown in Figure 6.3 which is made up of many different parts. Each of these parts will have a specific mass M_{part} that should add up to the total mass of the car M_{car}. When looked upon in this way, the mass defect is

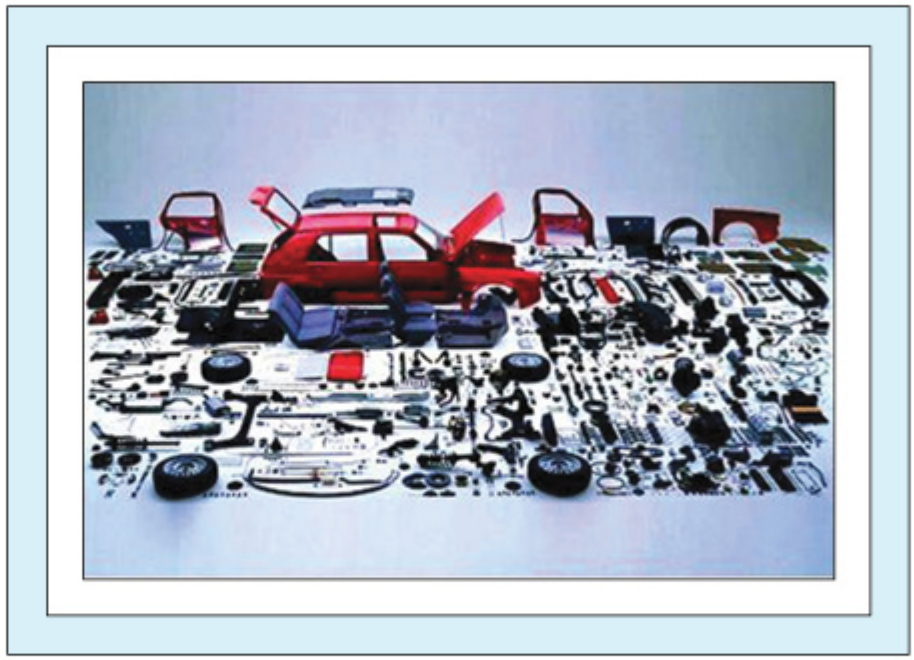

FIGURE 6.3 The mass defect is no different conceptually than building a car that weighs less than the sum of its parts. This "design feature" of the universe is responsible for converting the "weight" of some of the car parts into pure energy that holds the car together. On average, about 1% of the rest mass of an isotope is converted into the energy of the nuclear force field. This is one way to estimate the "strength" of the nuclear force field that holds the nucleus of the atom together. (Picture Courtesy of Google Images.)

equivalent to saying that when a car is assembled from many different car parts, *the assembled car weighs less than the sum of the parts from which it is made*! In other words, the mass defect implies that

$$M_{part\,1} + M_{part\,2} + M_{part\,3} + \cdots + M_{part\,N} < M_{car} \tag{6.6}$$

where

M_{car} is the total mass of the car

$M_{part\,(i)}$ is the mass of each individual part

In other words, every atom in the universe possesses this strange property that enables it to weigh less than the mass of the pieces from which it is made!

This "missing" nuclear mass is called the "*mass defect*," and it is based on Einstein's assertion that mass and energy are interchangeable ($E = mc^2$). *Thus the mass defect is a measure of the strength of the nuclear force field—and in particular, the total binding energy that holds the nucleus together. Generally speaking, the mass defect is on the order of about 1% of the total rest mass of the parts that make up the nucleus. It is usually manifested in the form of gluons that form quark–anti-quark pairs*. The implications of the mass defect can be most easily understood by considering the following example from an elementary chemistry class.

Suppose that we consider the Helium-4 nucleus shown in Figure 6.4, which consists of two protons and two neutrons. In this case, there are four parts—two protons and two neutrons—from which the nucleus, or in this case, our hypothetical "car," is made up of. The rest masses of the protons and the neutrons in AMUs are

Proton and Neutron Rest Masses

$$\text{Proton: } 1.00728 \text{ AMU} = 937.28 \text{ MeV/c}^2$$
$$\text{Neutron: } 1.00866 \text{ AMU} = 937.36 \text{ MeV/c}^2 \tag{6.7}$$

Ignoring the contributions of the two electrons for the moment, the measured mass of the nucleus in the laboratory is 4.00153 AMU, whereas the sum of the masses of the two protons and the two neutrons is

Protons: 2×1.00728 AMU = 2.01456 AMU
Neutrons: 2×1.00866 AMU = 2.01732 AMU

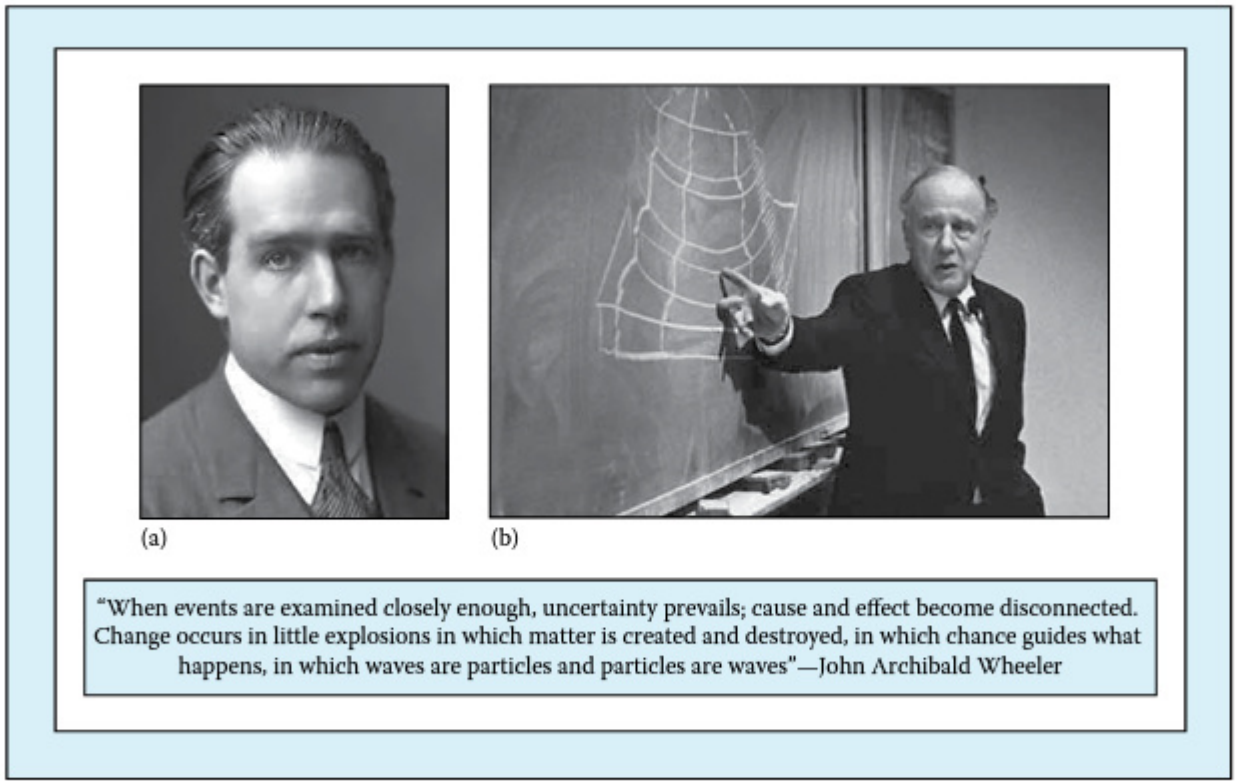
(a)
(b)
"When events are examined closely enough, uncertainty prevails; cause and effect become disconnected. Change occurs in little explosions in which matter is created and destroyed, in which chance guides what happens, in which waves are particles and particles are waves"—John Archibald Wheeler

FIGURE 6.4 Two of the three inventors of the liquid drop model of nuclear structure—Niels Bohr (a) and John Archibald Wheeler (b). John Archibald Wheeler was also the thesis advisor of Richard Feynman. (Pictures provided by Wikipedia.)

which is equal to 4.03188 AMU. In other words, the Helium-4 nucleus weighs less than the two protons and neutrons from which it is made, and the missing mass is called the "mass defect." In this case, the size of the mass defect is

$$\Delta m = 4.03188\ \text{AMU} - 4.00153\ \text{AMU} = 0.03035\ \text{AMU}$$

When we do this exercise with other atoms, the result is always the same. Every element and every isotope of every element has a mass deficit that we can measure in AMUs. It is often helpful to convert this missing rest mass Δm into the nuclear binding energy that it represents. The equation to do so is

$$\Delta E = \Delta m c^2 \tag{6.8}$$

From our previous discussion, you may recall that 1 AMU and the rest energy are related to each other through the following conversion factors:

Mass and Energy Conversions

$$1\ \text{AMU} = 1.66054 \times 10^{-27}\ \text{kg} = 931.494\ \text{MeV}/c^2 \tag{6.9}$$

where in the case of a Helium-4 atom, we have

$$\Delta E = \Delta m c^2 = 0.03035\ \text{AMU} \times 931.494\ \text{MeV}/c^2/\text{AMU} \times c^2 = 27.27\ \text{MeV}.$$

In other words, if we were able to fuse two neutrons and two protons together, we would be able to release an amount of energy equal to 27.27 MeV. The mass of the resulting isotope produced by doing this would be *less* than the mass of the "parts" that were used to make it. Using $\Delta E = \Delta m c^2$, it is easy to see that the "missing mass" created by making a Helium-4 atom out of two protons and neutrons would be equal to 0.03035 AMU, or about 1% of its rest mass. This is precisely what happens in the sun when lighter elements are fused together by gravity to form heavier ones.

Student Exercise 6.3

What is the highest number of neutrons and the lowest number of neutrons that we can find in a naturally occurring sample of Zinc?

6.9 Nuclear Binding Energy Curve

In Chapter 2, we also learned that *the nucleus* is an extremely small and dense structure that consists of protons and neutrons. Several illustrations of the atom and its nucleus are shown in Figure 6.5. On average, the higher the binding energy is per nucleon, the more stable an atomic nucleus will be. Hence a nucleus with a higher average binding energy is bound together more tightly than a nucleus with a lower one. If we take the mass defect Δm and divide it by the total number of protons Z and neutrons N in a specific isotope, then we can define the average nuclear binding energy BE that each proton or neutron possesses:

$$BE = \frac{\Delta m}{Z + N} \tag{6.10}$$

This equation can also be written as $\Delta E/c^2 \cdot (1/A)$, where $A = Z + N$ is the total number of *nucleons* (protons and neutrons) that the nucleus possesses. *Hence the nuclear binding energy is normally quoted in MeV per nucleon*. When we calculate the binding energy of all of the elements in the Periodic Table, starting with the lightest element hydrogen and ending with the heaviest naturally occurring element uranium, we get the curve shown in Figure 6.6. This curve is called the nuclear *binding energy curve*, and it is one of the most important curves in all of nuclear science and engineering. Notice that the binding energy is different from one element to the next, and in fact, is also isotope dependent. The binding energy per nucleon varies from about 2 MeV for helium to about 10 MeV for iron. *The average binding energy for an element in the Periodic Table is about 8 MeV per nucleon*. Hence a nucleus with 150 nucleons will have

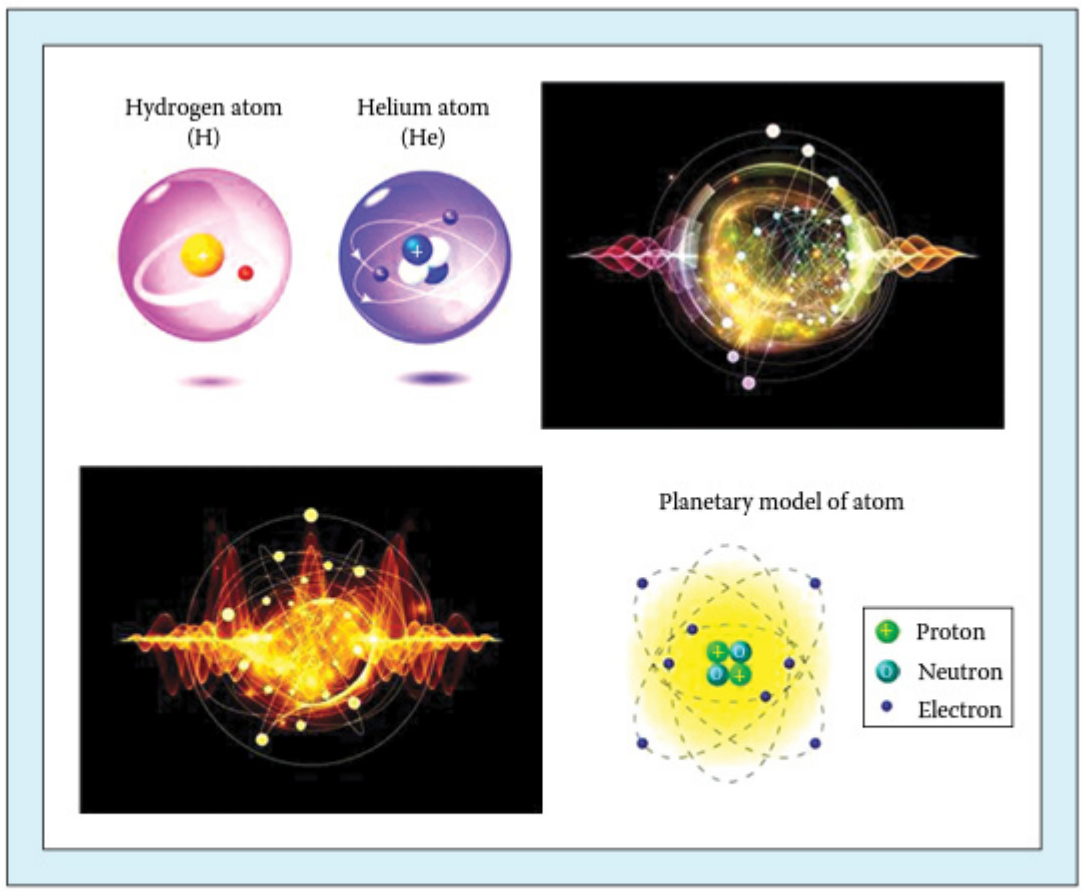

FIGURE 6.5 The classical, planetary, and wave function views of the atom.

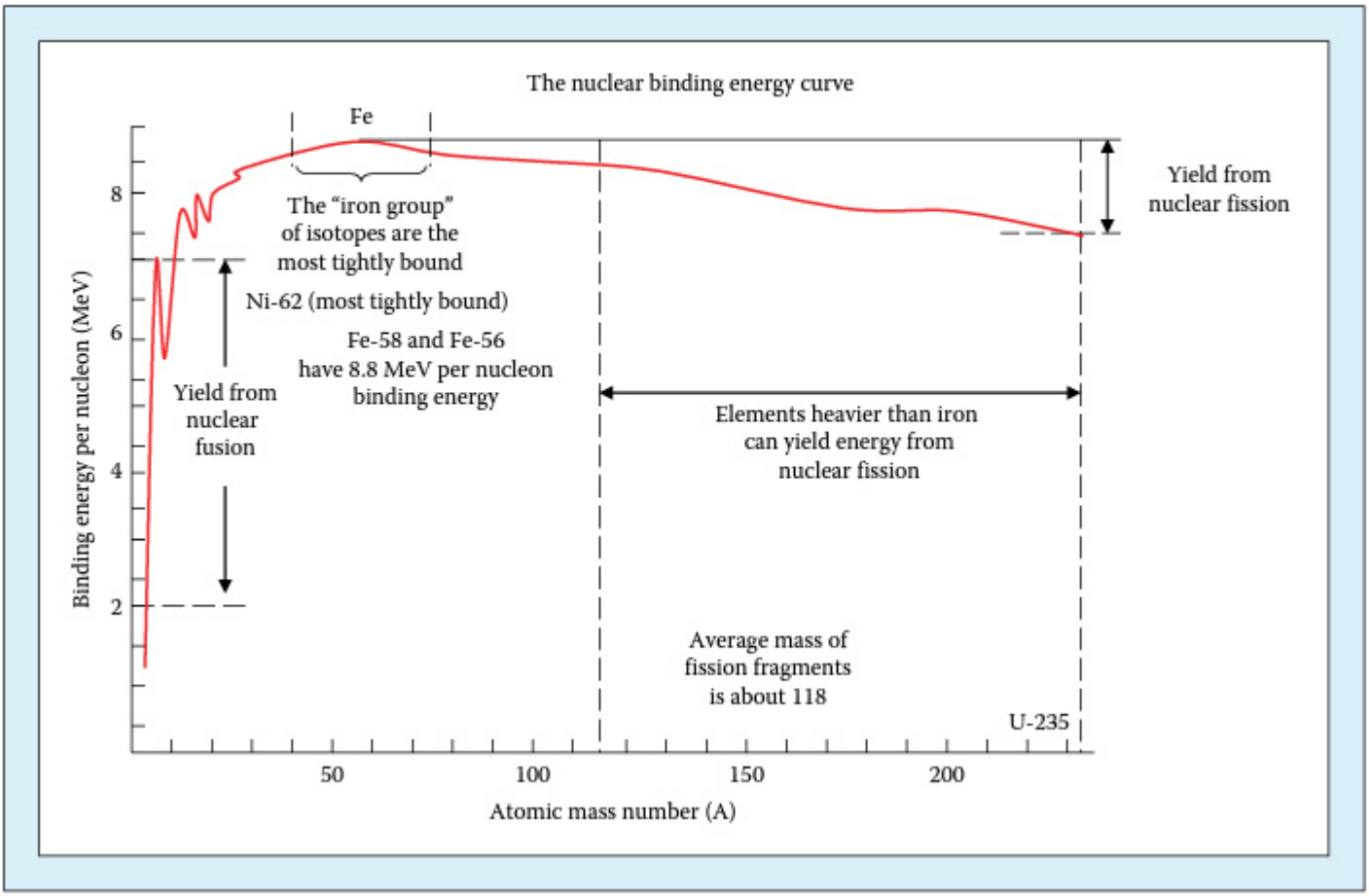

FIGURE 6.6 The shape of the nuclear binding energy curve.

a binding energy of about 150 × 8 MeV = 1200 MeV. Approximately 1% of the mass of the nucleus is converted into the bonds required to hold the nucleus together.

For a number of practical reasons, the binding energy curve has a great deal of influence on how nuclear reactors behave. First, it shows that both heavy and light nuclei can release useful energy by transforming themselves into nuclei that have an intermediate atomic weight. This is possible because the binding energy difference between an element of intermediate atomic weight and one of higher or lower atomic weight can be converted directly into useful kinetic energy in the form of heat and light. This energy can be expressed as ΔE and it can be found from the equation $\Delta E = \Delta mc^2$. *The implications of this are that very heavy elements and very light elements can both be useful power sources if we can find a way to split them apart or fuse them together*. Either process results in a net release of useful energy because only the elements in the middle of the binding energy curve (such as iron) have no useful energy to give. We can illustrate how this works again with a very simple example from elementary chemistry. Using the binding energy curve, we can estimate the energy released in the fission of uranium-235.

For a Uranium-235 nucleus to split apart, it must absorb a neutron and convert itself into Uranium-236. From this curve, we can see that heavy elements (like uranium-235) have a mean binding energy of about 7.5 MeV per nucleon. For elements of intermediate atomic weight, like Barium and Iodine (with an average mass about 140), the binding energy per nucleon is about 8.5 MeV. This difference in the total binding energy between a single large nucleus and two smaller fission fragments (which are assumed to be about equal in mass) is about 210 MeV. This turns out to be about the average amount of energy released when a uranium-235 nucleus splits apart. We can illustrate what we have said in more detail by considering the fission of a uranium-235 atom into a barium-141 atom and a krypton-92 atom. This is just one of about 20 different ways in which U-235 can split into smaller parts that are also known as fission fragments. See Chapter 7 for a discussion of this process and the fission products that are produced. Before the U-235 nucleus absorbs a neutron, and becomes U-236, it has a binding energy of 235 times ~ 7.6 MeV = 1790.4 MeV. For the fission products barium and krypton, however, the binding energies are 141 times ~ 7.4 MeV (barium) = 1184.4 MeV and 92 times ~ 7.5 MeV (krypton) = 782 MeV. The sum of these binding energies is 1966.4 MeV. The difference,

which is 1966.4 MeV − 1790.4 MeV = 176 MeV, is the energy released when the Uranium-235 nucleus splits apart. This compares favorably with the actual value of 177.001 MeV that we will show you in Section 6.10 using much more precise estimates of the nuclear masses to four decimal places. The value for mass defect, or the actual differences in the masses of the nuclear particles before and after the reaction, will give exactly the same result. The difference in the nuclear masses $\Delta m = \Sigma AMU_{in} - \Sigma AMU_{out}$ multiplied by the speed of light squared will always give the total energy that is released

$$\Delta E = \Delta mc^2 \tag{6.11}$$

It is simply a matter of taste whether the value of the mass defect or the actual nuclear masses should be used.

A final implication of what we have just said is that it would be impossible to generate any useful energy if the binding energies of all of the elements in the Periodic Table were exactly the same. In this case, the value of Δm would always be zero, and by inference, the value of ΔE would also be zero as well. *Hence, the fact that the stars burn, that life exists on earth, and that nuclear power is possible all owe their existence to the fact that the mass defect Δm varies from one element to the next.* The entire universe appears to be designed to take advantage of this simple fact.

Student Exercise 6.4

Using the data presented in Table 6.2, calculate the atomic weight of Carbon to four decimal places. How does this compare to the value that we previously quoted of 12.011 AMU?

6.10 Energy Released due to Missing Nuclear Mass

Sometimes it is confusing to discuss nuclear reactions in terms of the nuclear binding energy alone. An alternative way to understand why nuclear fission releases more energy than it consumes is to look at the masses of the particles going into the reaction, and the masses of the particles leaving the reaction. To do so, we simply need to apply the principles of mass and energy conservation that we discussed in Chapter 2. Since the nucleus is made up of many more of these particles, the same basic principle applies. There are simply more moving parts (in the form of protons and neutrons) to keep track of. In the case of Uranium-235, we know that adding a neutron (with a mass of 1.00866 AMU) will convert the U-235 nucleus into U-236. This causes the U-236 nucleus (which has a rest mass of 236.0456 AMU) to become unstable, and it will break into two fission products and two or three neutrons about 80% of the time. (The other 20% of the time, it will not break apart, but it will release the excess energy by emitting an energetic photon or gamma ray.) There are many common ways, or decay channels, that U-236 uses to split apart. We will illustrate two of them for you that involve different isotopes of Barium and Krypton. This process is by no means confined to the creation of Barium and Krypton alone. Many other by-products of the fission process, involving the generation of Cs-133, I-135, Sr-88, Xe-136, Sr-90, and Zr-93, will result in very similar results. The first reaction involves splitting U-235 into Barium-141 and Krypton-92, and releasing *three neutrons* in the process. The governing reaction is

$$^{1}_{0}n + ^{235}_{92}U \rightarrow ^{236}_{92}U \rightarrow ^{141}_{56}Ba + ^{92}_{36}Kr + 3^{1}_{0}n \tag{6.12}$$

When the exact masses of the final products are added together, the sum is found to be appreciably less than the sum of the exact masses of uranium-235 and the original neutron. This difference in mass appears as energy given by $E = mc^2$ (where c is the velocity of light). The second way is which Uranium-236 can fission to split into Barium-144 and Krypton-90 and release *two neutrons* in the process. The governing reaction in this case is

$$^{1}_{0}n + ^{235}_{92}U \rightarrow ^{236}_{92}U \rightarrow ^{144}_{56}Ba + ^{90}_{36}Kr + 2^{1}_{0}n \tag{6.13}$$

Now let us add up the masses of the by-products in each case. In the first case, where U-236 splits into Ba-141 and Kr-92 and three neutrons, the sum of the masses of the by-products is

Ba-141 nuclear mass = 140.8833 AMU
Kr-92 nuclear mass = 91.9021 AMU
Three neutron rest masses = 3.0256 AMU
Total nuclear mass = 235.811 AMU

And in the second case, where U-236 splits into Ba-144 and Kr-90 and two neutrons, the sum of the masses of the by-products is

Ba-144 nuclear mass = 143.9229 AMU
Kr-90 nuclear mass = 87.9195 AMU
Two neutron rest masses = 2.0173 AMU
Total nuclear mass = 235.860 AMU

In the first case, the mass difference is 236.0456 AMU − 235.811 AMU = 0.235 AMU or 217.902 MeV. In the second case, the mass difference is 236.0456 AMU − 235.860 = 0.186 AMU or 173.259 MeV. In this last example, the mass differences are about 20% less than we would encounter in other reactions involving the generation of Cs-133, I-135, Sr-88, Xe-136, Sr-90, and Zr-93.

Averaged over all possible combinations of the fission fragments and the by-products of the fission of U-235, the mass difference on average turns out to be about 0.225 AMU—or about 210 MeV (see Equation 6.6). Using Einstein's equation $\Delta E = \Delta mc^2$, we find that this is the energy released in the fission of a single heavy nucleus. If we were to repeat the results with Pu-239 instead of U-235, the results would be essentially the same. This is how the missing mass from the fission of a heavy nucleus is converted directly into useable kinetic energy, light, and heat. The fact that the mass of the particles coming out of a reaction is less than the mass of the particles coming into the reaction is what makes nuclear fusion and fission work. *Both fission and fusion are examples of exothermic reactions because they both release more energy than they consume*.

6.11 Physical Basis for the Shape of the Nuclear Binding Energy Curve

There are some interesting technical reasons why the nuclear binding energy curve has the shape it does. As one can see from Figure 6.7, the binding energy E_b decreases as the mass of an average element is increased or decreased. The binding energy is *NOT* the same for every element in the Periodic Table. *The binding energy only stays the same for elements that have an intermediate atomic weight*. By this we mean elements that have an atomic weight between about 40 and 120 AMU. We would like to share some of the reasons with you why this is the case. In the 1940s, *George Gamow*, *Niels Bohr*, and *John Archibald Wheeler* proposed a theory to successfully explain the shape of the binding energy curve. They used a simple mathematical model to explain why the binding energy of the nuclear force behaves the way it does.

Their work resulted in an equation that can be used to predict the binding energy of the nucleus as a function of the number of protons Z and neutrons N that it contains. It is instructive to examine the assumptions they used in deriving this equation because it is helpful to understand how the nucleus works. This equation can be used to explain why elements with an intermediate atomic weight, such as iron and nickel, have high binding energies per nucleon and are stable over geologic periods of time, while other elements have lower binding energies and are not. *It should be obvious that if the binding energy per nucleon was the same for all of the elements in the Periodic Table, then the nuclear power industry would not exist because splitting a heavy element into two lighter ones would not release any energy. This would mean that there would be absolutely no energy released when atoms were split apart or fused together*.

Example Problem 6.1

Calculate the binding energy of an alpha particle that is occasionally released from a U-235 or Pu-239 nucleus during the process of radioactive decay.

Solution An alpha particle consists of two protons with a mass of 1.00728 AMU and two neutrons with a mass of 1.00866 AMU. The configuration is shown in the attached figure. For an alpha particle, the mass of the parts is 4.03188 AMU, and the mass of the alpha particle itself is 4.00153 AMU. Accordingly, the mass difference is 0.0304 AMU or 28.3 MeV. [Ans.]

In other words, the earth would be a very dead place and the stars (which rely on the process of nuclear fusion) would not shine. The universe would be an extremely dull place indeed. Splitting elements apart (by nuclear fission) or combining them together (by nuclear fusion) would be a futile exercise because the binding energy would be the same for both the original elements and their by-products. We would now like to introduce to you the equation that Gamow, Bohr, and Wheeler developed to explain why the shape of the binding energy curve varies as from one element to the next and how it also varies between the individual isotopes that a particular element may have. Some features of this theory, which we

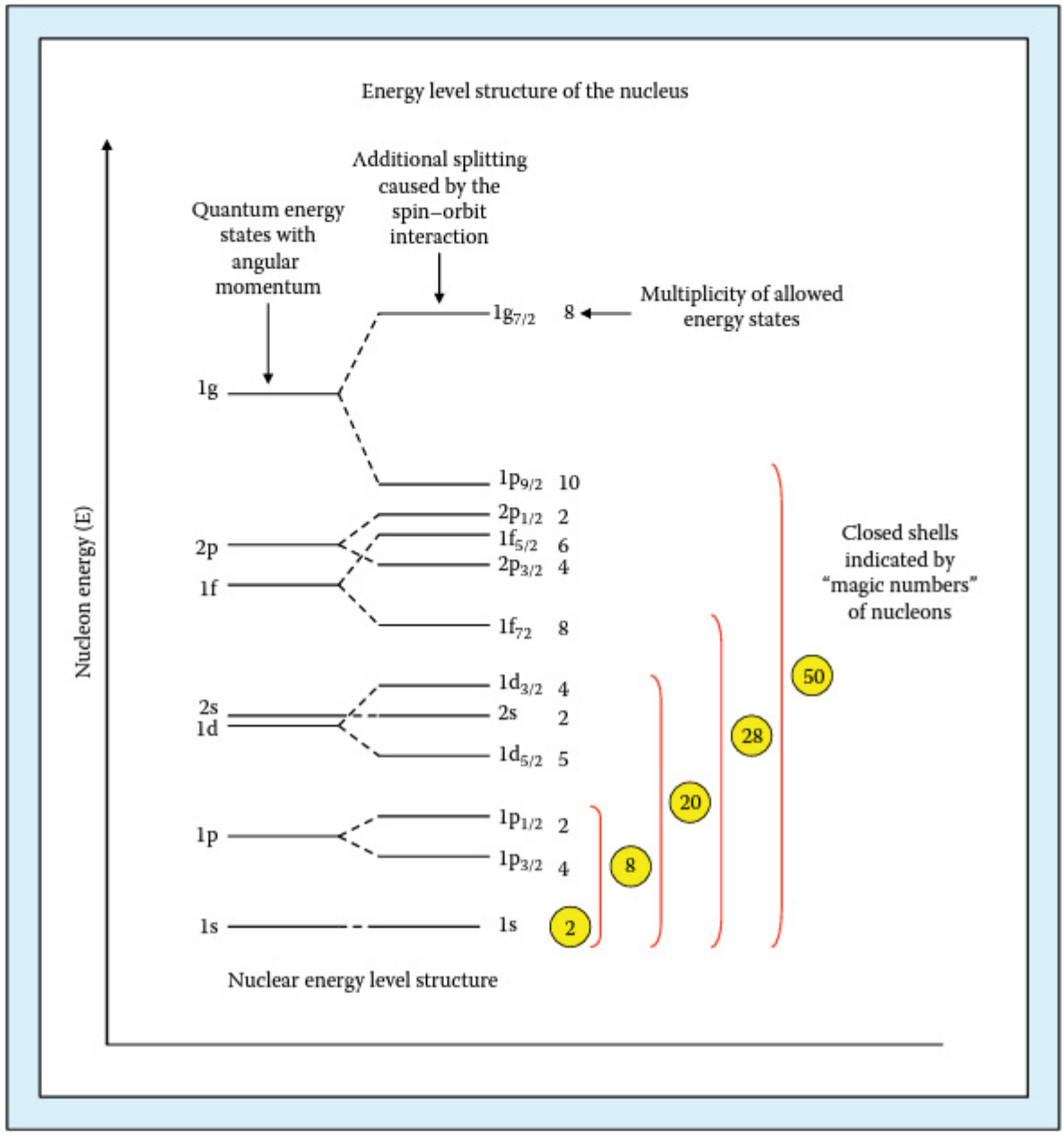

FIGURE 6.7 The orbital configurations and the energy levels of the atomic nucleus based on a potential energy well.

will refer to as the *Pairing Energy* and the *Asymmetry Energy*, can be deduced from the Laws of Quantum Mechanics, while other features of the theory cannot be. *The theory that they developed to explain the shape of the nuclear binding energy curve is based on the assumption that the nucleus can be modeled as a drop of incompressible fluid that has surface tension and can be deformed slightly to be either spherical or elliptical in shape*. Hence, both the theory and the equation derived from it are called the "*Liquid Drop Model*" of nuclear structure. The thinking behind the liquid drop model is illustrated in Figure 6.8. Because the nucleus is so dense relative to the electron cloud that surrounds it, modeling the nucleus in this way is not entirely without merit. There are also some physical arguments that can be used to justify proceeding in this way (see Figure 6.9).

Example Problem 6.2

Sometimes it's hard to appreciate how powerful the nuclear binding force can be. Suppose that we would like to compare the average binding energy of a proton or neutron in an alpha particle to the binding energy of the electron circling a hydrogen atom. Using the information provided in the previous exercise, and remembering that the ionization energy of

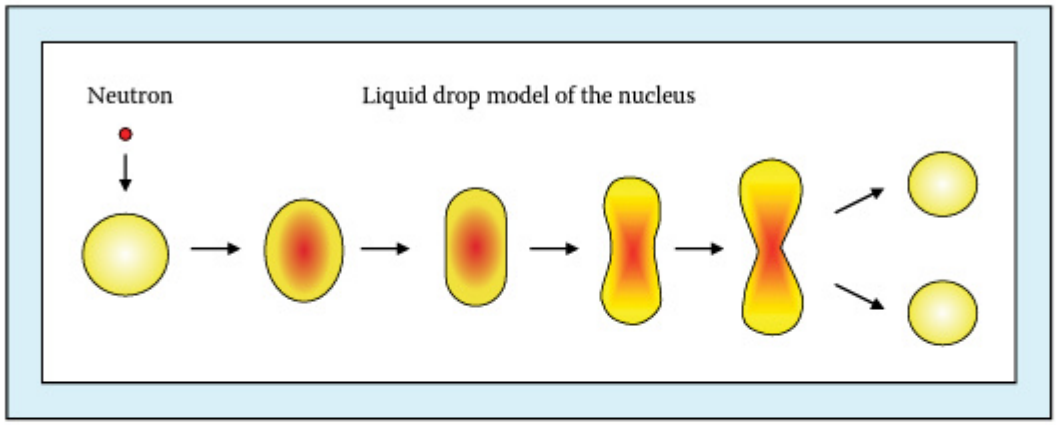

FIGURE 6.8 The liquid drop model is an attempt to model the behavior of the nucleus as a drop of incompressible fluid that can be deformed slightly if the energy is just right. Like a drop of liquid water, it can flex and if it absorbs enough energy, it can oscillate or even split into two parts. The liquid drop model takes the factors that are responsible for causing this behavior into account.

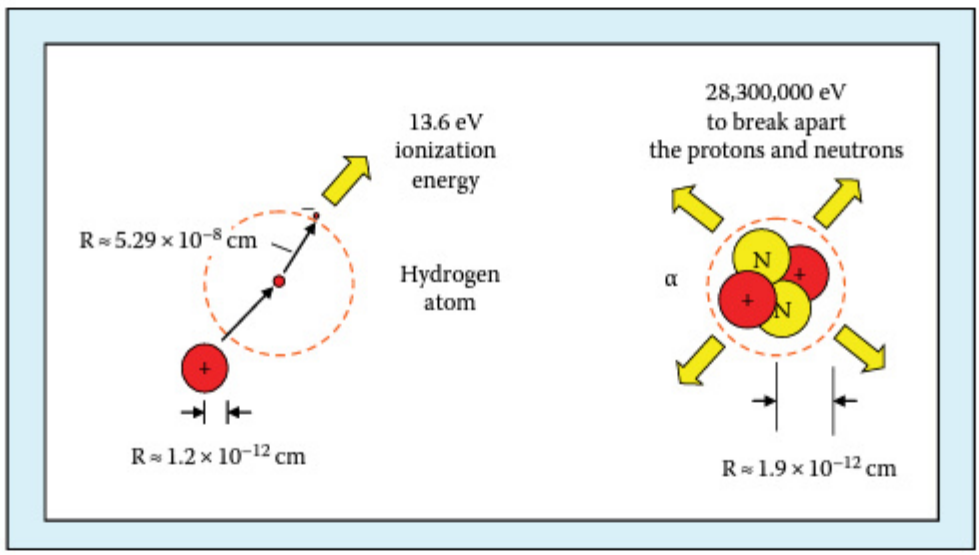

FIGURE 6.9 Comparing the binding energies on an atomic and nuclear scale.

an electron in a hydrogen atom is 13.6 eV, how many times greater is the nuclear binding energy than the energy required to keep the electron bound to the hydrogen atom?

Solution In Example Problem 6.1, we learned that the nuclear binding energy for an alpha particle is 28.3 MeV. This is an average of approximately 7.1 MeV per nucleon. In other words, it takes 7,100,000 eV to break apart an alpha particle, and release one of its protons or neutrons. This is a factor of approximately 7,100,000/13.6 = 522,000 times greater than the binding energy of an electron to the nucleus of the hydrogen atom. [Ans.]

Thus the nuclear binding force is about a million times stronger than the electrical binding force in this respect.

6.12 Liquid Drop Model of the Atomic Nucleus

Before quarks were proposed by Murray Gell-Mann and George Zweig, *George Gamow*, *Niels Bohr*, and *John Archibald Wheeler* developed the *Liquid Drop Model* to explain how the binding energy E_B of the nucleus varies as a function of the number of protons and neutrons it contains (Figure 6.9). In our discussion of this model, we will again let Z refer to the number of protons and N to the number of neutrons. Following our earlier conventions, we will use the atomic number A

to represent the total number protons and neutrons (e.g., A = N + Z) or the number of *nucleons* that the nucleus contains. According to our previous definitions, the mass of the nucleus M can be found from the following equation:

$$M = Z \cdot M_P + N \cdot M_N - E_B/c^2 \tag{6.14}$$

where

M_P is the rest mass of the proton
M_N is the rest mass of the neutron
E_B is the total *binding energy* of the nucleus

The theory that Gamow, Bohr, and Wheeler developed assumes that the nuclear binding energy can be written as the sum of *five* distinct terms:

The Binding Energy Curve Equation

$$E_B = C_V A - C_S A^{2/3} - C_E\, Z(Z-1)/A^{1/3} - C_A (A-2Z)^2/A + C_P(A,Z) \tag{6.15}$$

where each of these terms has a different physical meaning and significance. When defined in this way, a positive value of the binding energy E_B means that there is enough energy contained in the nuclear force field to keep the nucleus together. If the binding energy happens to become 0 or negative (due to the contributions from the second, third, and fourth terms), then the nucleus will simply fly apart because there is not enough available energy to hold it together. *The strength of the nuclear force field is represented primarily by the value of the first term. This term always has a very large positive value and is referred to in many textbooks as "The Volume Term."* The volume term assumes that the nuclear binding energy is directly proportional to the volume V of the nucleus being bound. To a first approximation, this turns out to be a very realistic assumption because this is where the nuclear bonds are found. The greater the total volume V, the more nuclear bonds there will be, and the greater the binding energy must also be. As we saw in Chapter 2, this finding is also consistent with our initial observation that the diameter of the nucleus D also varies with the number of nucleons (A = N + Z) that it contains. To a first approximation, this relationship can be written as

$$D = 2.5A^{1/3} \times 10^{-13}\ \text{cm} \tag{6.16}$$

which gives a total diameter for a Uranium-235 nucleus (A = 235) of about 1.5×10^{-12} cm. Since the volume V is proportional to the cube of the radius when the nucleus is roughly spherical in shape, that is, $V = 4/3\pi R^3$, it also follows that the total volume V is directly proportional to the total number of protons and neutrons A that the nucleus contains, or

$$V = C_V A \tag{6.17}$$

where C_V is a constant of proportionality.

The value of this constant is usually determined empirically. The second term in the Liquid Drop Model is called the *Surface Area or the Surface Tension Term*, and it is proportional to the surface area S of the nucleus itself. As we will see shortly, it is an attempt to modify the geometrical contributions to the nuclear binding energy from the calculation of the volume of the nucleus alone. Physically, this makes considerable sense if you can assume that the range of the nuclear force is limited by the range of the gluons themselves. For a number of historical reasons, the third term is usually referred to as the *Coulomb Term. It is also called the Electrical Energy Term.* Its magnitude is inversely proportional to the average distance between the protons in the nucleus, and it attempts to capture the repulsive energy of the electrical field by summing over all of the protons that contribute to the field.

If you have taken a previous E&M course, it is roughly equivalent to the electrical potential energy U of a spherical ball of charge. The fourth term is smaller than the first three terms and is sometimes called the Asymmetry Term. It attempts to capture the predictions of the Pauli exclusion principle, which states that a nucleus with the same numbers of neutrons and protons (N = Z) will have a lower total energy E than one that does not. Although this may be intuitively obvious, a proof of the derivation of this term is beyond the scope of our cursory discussion here. The fifth term represented by the expression C_P (A,Z) was the last term to be added historically to the Liquid Drop Model to attempt to calculate the binding energy of the nucleus as a whole. This term is referred to as the *Pairing Term*, and it is again the product of an empirical constant divided by the inverse square root of the volume. It is a relatively simple way to account for the spin energy, or the angular momentum, that certain proton and neutron combinations may have. Depending on the particular combinations involved, it may make either a positive, a negative, or a zero contribution to the total energy of the system.

In most instances, it is about the same size as the Asymmetry Term. It is a function of both the atomic number A and the number of protons Z. We would now like to discuss each of these terms in greater detail and see how they affect the binding energy of a specific isotope.

6.12.1 The Volume Energy Term

The first term is called the *volume energy term*, and it consists of two parts: the coefficient C_V and the total number of protons and neutrons in the nucleus A, where A = N + Z. Since the volume of the nucleus V is proportional to the number of protons and neutrons inside of it, and the number of nuclear bonds also depends on A, this is a logical way to measure the energy of the nuclear force field. Since the nuclear force that is carried by the gluons affects both protons and neutrons in essentially the same way, this term depends on the value of A and not just Z. This, of course, is to be expected. Since the nuclear binding force affects both protons and neutrons, and the total number of nuclear bonds is given by A (A − 1)/2, one would expect the volume energy to be proportional to $A^2 - A$. However, the nuclear force has a very limited range, and a given nucleon may only interact strongly with its nearest and next nearest neighbors. Therefore, the number of pairs of particles that actually interacts with is roughly proportional to A, which gives the volume term its simple form. We will not discuss how the coefficient C_V can be derived, but several quantum mechanical arguments place the theoretical value at 17–18 MeV. This turns out to be quite close to the value that is actually observed experimentally.

6.12.2 The Surface Energy Term

The second term that appears in the expression for the binding energy can be found by taking the product of Cs and $A^{2/3}$ is called the *surface energy*, or *surface tension term*. This term is also used to model the strength of the nuclear force, but it does so by making a correction to the value predicted by the volume term alone. The volume term is based on the assumption that the nuclear force has a long enough range to efficiently reach across the entire diameter of the nucleus and bind together equally all of the nucleons that are contained within that volume of space. While this is a good assumption for the protons and neutrons deep within the nucleus, the protons and the neutrons on the surface do not have as many nearest neighbors, and so a correction factor is needed to account for the fact that they are not bound as tightly as the ones in the interior. Without this correction, we would not be able to model the binding energy in heavy nuclei properly. If we assume that the volume of the nucleus V is proportional to A, then the radius R should be proportional to $A^{1/3}$. The surface area should then be proportional to R^2, or $A^{2/3}$. This explains why the surface term is proportional to $A^{2/3}$. It can also be shown using similar arguments that Cs should have a similar value to Cv. This places the value of Cs in the range of 17–18 MeV. This is not far from the experimentally measured results.

6.12.3 The Electrical Energy Term

The third term in Equation 6.18 is called the electrical energy term. It is sometimes referred to as the *Coulomb energy term*. Both of these names for this term have appeared in the literature from time to time. The Coulomb energy term is based on the assumption that the nucleus can be modeled as a spherical object having *uniform charge density*, where the charges that are contained inside of the sphere happen to be protons in this case. Classically, the potential energy E of such a distribution of charges can be shown to be given by

$$E = \frac{3}{5}\left(\frac{1}{4\pi\varepsilon}\right)\left(\frac{Q^2}{R}\right) \tag{6.18}$$

where
Q is the total charge
R is the radius of the sphere

In the case of the nucleus, we can approximate the values of both R and Q by noting that

$$R = r_o\, A^{1/3} \tag{6.19}$$

where r_o is an empirical constant equal to about 1.5 times the diameter of a proton, or $r_o = 1.5\, R_p = 1.5 \times 0.8768(69)$ fm ~ 1.25 femtometers[1], and noting that Q = e Z and $Z^2 \sim (Z - 1)Z$. Substituting these values into the equation for the energy of a spherical charge, we find that

$$E = C_E\,(Z-1)\,Z/A^{1/3} \tag{6.20}$$

where $C_E = 3e^2/20\pi\varepsilon r_o$. This gives a value for C_E of 0.691 MeV, which is not far from the experimentally measured result.

6.12.4 The Asymmetry Energy Term

The fourth term $CA = (A - 2Z)^2/A$ is called the *Asymmetry Energy Term*. This term is included in the equation to represent the fact that there are certain combinations of protons and neutrons in the nucleus that have a different total energy than other combinations. Quantum mechanically it can be shown that the nucleus is in its lowest possible energy state when N = Z. In other words, when the number of neutrons is equal to the number of protons, this maximizes the binding energy because the overall mass of the nucleus is minimized. Conversely, when the number of neutrons N greatly exceeds the number of protons Z, then the binding energy is reduced, and the nucleus becomes progressively less stable. As we have seen, this is especially true for heavy elements where A > 200.

The asymmetry term can also be written as $(A - 2Z)^2/A = (N + Z - 2Z)^2/A = (N - Z)^2/A$. This form attempts to capture the asymmetry by comparing the number of neutrons N to the number of protons Z. If they are equal, then the term will be zero since $(N - Z)^2/A = 0$. Hence, the contribution of this term to the binding energy will be 0, rather than the usual negative number. The presence of A in the denominator also shows that the difference in the number of protons and neutrons $(N - Z)^2$ is less important for larger values of A than it is for the smaller ones. Using a number of quantum mechanical arguments, it can be shown that the coefficient C_A has a theoretical value of about 21 MeV. Again, this compares relatively favorably with the values obtained by experiment.

6.12.5 The Pairing Energy Term

The fifth term in the equation for the binding energy is called "*pairing energy term.*" Historically, this term was the last term to be added to the liquid drop model. This term attempts to account for the energy contained in the angular momentum, or the spin of the protons and the neutrons in the nucleus. Since the protons and neutrons are both matter particles, we know from Chapter 2 that they both have a spin of ½. However, depending on how their spins align—they can be parallel or anti-parallel—their spin energy in these two states can be different, since the spins can have values of 0 or ±1. The term $C_p(A,Z)$ attempts to account for this effect. The term $C_p(A,Z)$ can have only one of the following three values, depending upon the total number of protons and neutrons A in the nucleus, and whether Z, N, and A are even or odd. The possible values are

The Pairing Energy Term

$$\begin{aligned} C_P(A,Z) &= +\delta_o \quad \text{when Z and N are even (A even)} \\ C_P(A,Z) &= 0 \quad \text{when A is odd} \\ C_P(A,Z) &= -\delta_o \quad \text{when Z and N are odd (A even)} \end{aligned} \tag{6.21}$$

where $\delta_o = C'A^{-1/2}$ and C′ has a value of about 12 MeV. It can be seen that as the value of A gets larger, the value of δ_o is also reduced.

6.13 Interpreting the Results

In conclusion, the difference between the range of the electrical forces carried by the protons and the nuclear forces carried by the gluons ultimately determines the shape of the nuclear binding energy curve. The net binding energy of any atom can be thought of as the difference between the binding energy of the gluons, which is a positive number, and the repulsive energy of the electrical force, which is a negative number. When the binding energy becomes 0 or negative, the nucleus will fly apart because the strength of the electrical forces overwhelms the bonds that are carried by the gluons. This explains why heavy nuclei with atomic numbers greater than 200 are not very stable, while lighter elements with smaller atomic numbers are. When the nucleus becomes so large that the nuclear forces carried by the gluons can no longer reach across it efficiently, then certain spatial combinations of the protons will cause the electrical force to overwhelm the nuclear force, and the nucleus can temporarily become unstable. Under the right set of circumstances, the electric forces may become so destabilizing that entire chunks of the nucleus may have to be ejected, usually in combinations of two protons and two neutrons (or "alpha particles") before it can return to a stable state. *As we saw in Chapter 5, this force imbalance is the fundamental cause of alpha decay.*

In nuclei of an intermediate atomic weight, starting with magnesium (A = 55), and ending with Xenon (A = 131), there is very little change in the binding energy, as the atomic number A increases because the nuclei are of sufficient size that the nuclear binding force can reach across the entire nucleus, and the increase in the repulsive force due to the increase in the number of protons is almost exactly balanced by the reach of the nuclear force field itself. In this range of nuclear masses, the two opposing forces nearly balance each other out to create a state of temporal equilibrium.

This causes most of the nuclei in this region of the Periodic Table to be very stable, and rarely decay. Some of the better known examples of these nuclei are the isotopes of iron (Fe) and nickel (Ni). Finally, starting with hydrogen and continuing through sodium (Na) with an atomic number of Z = 11, the number of neutrons is not much greater than the number of protons, and the electrical force on a per nucleon basis begins to rise again. Since the force carried by the gluons does not distinguish between a neutron and a proton, the electrical forces again increase relative to the nuclear forces, and this causes the total binding energy, shown in Figure 6.7, to go down. Of course, corrections need to be made to account for the higher order terms in Equation 6.15, but the basic physics of the force balance/imbalance always remains the same. One of the interesting implications of Equation 6.15 is that it can be used to predict the number of protons needed to create the most stable nucleus of nuclear material for a given atomic weight A. By maximizing B_E (A, Z) with respect to Z, we can find the number of protons Z for the most stable nucleus having an atomic weight of A. The result is

Nuclei with the Highest Binding Energy

$$Z \approx \frac{1}{2}\left(\frac{A}{1+C_B A^{2/3}}\right) \tag{6.22}$$

where $C_B = C_E/4C_A$. This is extremely important because it allows us to determine the optimum proton-to-neutron ratio (Z/N) for any element as long as we know the total atomic weight A. It turns out that this number is roughly equal to A/2 for light nuclei, but for heavy nuclei there is even better agreement with experimental data.

By substituting the above value of Z back into B_E, one obtains the binding energy as a function of the atomic weight, $B_E(A)$. *Maximizing $B_E(A)/A$ with respect to A gives the nucleus that is the most strongly bound, or in layman's terms, the most stable*. The value we get when we perform this exercise is A = 63 (copper), which is close to the measured values of A = 62 (nickel) and A = 58 (iron). Hence, the binding energy equation does a relatively good job of predicting the binding energy accurately for very heavy nuclei, and its overall margin of error for these elements is less than 1%. The biggest drawback to this equation is that it is not very accurate when dealing with very light nuclei, such as Hydrogen and Helium. However, if you think about it, the surface area term is probably not the appropriate term to use in this case, because there are so few particles in the nucleus to begin with.

In this case, an alternative formulation would probably work better. Finally, we would like to mention that although the binding energy equation can be derived based on theoretical grounds alone, the actual values for the coupling coefficients in front of the five terms do not represent all of the physical complexities inside of the nucleus because some of them (such as surface area term and the electrical term) were based on purely Classical arguments. As a result, the most accurate forms of binding energy equation are usually based on fitting the five coupling coefficients to real experimental data. Table 6.8 lists the most currently used values for the coefficients that have been calculated in this way. They are presented in the table in units of MeV. You may feel free to use them in any problems involving the calculation of the nuclear binding energy. The values quoted by Rohlf are based on more modern instrumentation and are presumably more accurate than some of the others. The values quoted by Lamarsh are also much more contemporary in this regard.

TABLE 6.8
The Coefficients Used in the Liquid Drop Model of the Nucleus

Coupling Coefficient	Source	Least-Squares Fit	Wapstra	Lamarsh	Rohlf
C_V	Volume energy	15.8	14.1	15.56	15.75
C_S	Surface energy	17.3	13	17.23	17.8
C_C	Electrical energy	0.714	0.595	0.697	0.711
C_A	Asymmetry energy	23.2	19	23.28	23.7
C_P	Pairing energy	12	n/a	12	n/a
δ (even–even)	Pairing energy	n/a	−33.5	n/a	−11.18
δ (odd–odd)	Pairing energy	n/a	+33.5	n/a	+11.18
δ (even–odd)	Pairing energy	n/a	0	n/a	0

Wapstra: *Atomic Masses of Nuclides*, A. H. Wapstra, Springer, 1958.
Lamarsh: *Introduction to Nuclear Engineering*, Prentice Hall, 2001.
Rohlf: *Modern Physics from a to Z0*, James William Rohlf, Wiley, 1994.

One final model of the nucleus that we would like to bring to your attention is a variation of the liquid drop model that can be found in Rohlf (see Table 6.8). This model is called the *Weizsaecker model of nuclear structure*. This model is also referred to as the semi-empirical mass formula or the *Bethe–Weizsaecker formula*. This particular model attempts to express the binding energy curve using the following expression for E_B.

The Weizsaecker Formula

$$E_B(\text{MeV}) = 15.75A - 17.8\,A^{2/3} - 0.711\,Z^2/A^{1/3} - 23.7\,(A-2Z)^2/A + \delta(+,\,-,\,0) \qquad (6.23)$$

Notice that this formula again has five terms—a volume term, a surface term, a Coulomb term, an asymmetry term, and a pairing energy term δ. *The pairing energy term has the value of 11.18 MeV/$\sqrt{A}$ when there are even numbers of protons and neutrons, a value of −11.18 MeV/$\sqrt{A}$ when there are odd numbers of protons and neutrons, and a value of zero when the number of protons and neutrons is mixed (i.e., when there is one even and one odd).* Each formula attempts to use a slightly different approach to model the size of the mass defect, but they all result in a binding energy curve similar in shape to the one shown in Figure 6.7. *Notice when there are even–even groupings of protons or neutrons, the binding energy per nucleon is the highest (because the value of δ is positive), and this explains why these particular types of nuclei tend to be so stable.*

Example Problem 6.3

Estimate the average binding energy of the nucleons in the U-238 nucleus, which is commonly used as a nuclear fuel. Make this estimate using only the volume term, the surface term, and the Coulomb term in the Weizsaecker Formula.

Solution The volume, the surface, and the coulomb terms in the Weizsaecker formula are E_V (MeV) = 15.75A, E_S (MeV) = $-17.8\,A^{2/3}$, and E_C (MeV) = $-0.711\,Z^2/A^{1/3}$. Since Z = 92 and A = 238, E_V = 3748.5 MeV, E_S = −696 MeV, and E_C = −989 MeV. The total binding energy is therefore 3748.5 − 696 − 989 = 2063.5 MeV or 8.67 MeV per nucleon. [Ans.]

6.14 Shell Model of the Nucleus

Shell models of the nucleus have been around for a long time. These models assume that the protons and the neutrons inside of the nucleus occupy a number of preferred energy states or orbitals that are similar to the ones that the electrons occupy in the electron cloud. The nucleons in each orbital configuration, or "shell," are considered to be point particles moving in potential energy wells, or alternatively, probability waves moving through the same energy wells. In some modern forms of shell theory (such as the optical model), these probability waves are frictionless objects flying around the nucleus at very high speeds. *Inside the nucleus, protons and neutrons prefer to occupy these orbital configurations in pairs of two* (because this minimizes the total energy of each shell). However, the exact size and shape of these shells is different than the ones the electrons use. In some nuclei, especially very light ones, each neutron or proton pair fills a 1s orbital that is conceptually similar to the 1s orbital that was discussed earlier in the chapter. However, most studies of the nucleus also show that nuclear stability is a much more complex process than atomic stability is—particularly when the shells are only partially filled (i.e., when the number of nucleons is *ODD*). *In this case, some configurations can be stable and other configurations are not.*

When an atomic nucleus becomes much larger, the energy levels occupied by the protons and neutrons take on entirely different configurations than the electrons in the electron cloud do. However, there are still certain numbers of protons and neutrons (called *magic numbers*) that result in the shells being stable and completely filled. A closed shell is an unusually stable nuclear configuration that behaves in some ways like the closed electron shells in the noble gases do (see Section 6.3). This explains why some nuclei like Thorium-232 are very stable, and while other nuclei like U-233 are not. It is possible to gain some appreciation for what these energy levels look like by assuming that the nucleons move in a "*potential well*" similar to the potential wells that describe the motion of the electrons around the nucleus of a hydrogen atom. Just as in the atomic world, the use of these potentials leads to a quantization of the energy levels that depends on the shape of the potential well itself. For example, a *square well* will give a slightly different separation of the energy levels than the *harmonic oscillator* potential that is discussed in many elementary physics books. (See for example Reference 6 - *Eisberg R. Fundamentals of Modern Physics*, John Wiley & Sons, New York (1961).) Consequently, a great deal of work has gone into constructing potential wells that describe the state of the nucleus as a whole. Solving for the energies from these potential wells then gives the sequence of energy levels shown in Figure 6.7. The labels we have assigned to these energy levels are somewhat different than the symbols that are used in the atomic world. The energy levels increase with orbital angular momentum quantum l, and the symbols s, p, d, f, etc. are used for orbital configurations l = 0, 1, 2, 3, …. But there

is really no direct physical analog to the principal quantum number n. Because of this, the numbers we assign to each level just start at n = 1 for the lowest energy level associated with a given orbital quantum number, and this results in symbols such as 1g, which cannot occur in a description of the orbital levels in the Periodic Table.

Moreover, the quantum number for orbital angular momentum is not limited to just n as it is in the case of an electron. In addition, within the confines of the nucleus itself, there is a sizable *spin–orbit interaction* between the protons and neutrons, which splits the energy levels by an amount that increases with orbital quantum number. This leads to some overlapping energy levels, such as shown in Figure 6.7. In this figure, the subscript indicates the value of the total orbital angular momentum j, and the multiplicity of the state associated with this value of j is 2j + 1. The reader may wonder how the electronic charge of the protons fits into the picture. The contribution of a proton to these energy levels is somewhat different than it is for a neutron because of the coulomb repulsive force, but it makes little difference in the structure of the energy levels as a whole. This is an indication of the fact that the nuclear force completely overwhelms the Coulomb force even when the distances between the protons are on the order of 1×10^{-12} cm. With these quantum states and magic numbers, it is then possible to predict the net spin of the nucleus itself and to represent its nuclear state by the level of the odd nucleon in the order of the states shown in Figure 6.7. The parity of each state can also be predicted, so the shell model of the nucleus provides more insight into what is actually happening inside of the nucleus. *The primary weakness of the shell model is that it is not particularly good at predicting how stable a nucleus will become when some of the nuclear shells are only partially filled, that is, when A is ODD and the numbers of protons and neutrons (Z and N) are also odd*. This has caused some people to propose more realistic models of the forces between the protons and the neutrons involving *nucleon clusters* and to then devise a model for the entire nucleus based on adding new clusters to it one at a time. Two examples of popular clustering models are the Close-Packed Spheron Model of Linus Pauling and the 2D Ising Model of MacGregor. So in conclusion, both the Liquid Drop Model and the Shell Model can help to explain certain aspects of the behavior of the atomic nucleus as a whole. In particular, these models can be used to explain why some nuclei appear to be stable and other nuclei are not. They can also be used to gain additional insight into the process of nuclear fission, which we will discuss in more detail in a subsequent section.

Student Exercise 6.5

Calculate the size of the volume term and the surface area term for the element Carbon. Use the isotope Carbon-12 to perform your calculations.

6.15 How Nuclear Fission Is Related to Nuclear Structure

The binding energy per nucleon is an important parameter when attempting to understand how stable a particular nucleus can be. Nuclei where the binding energy per nucleon is high are relatively stable, and nuclei where the binding energy per nucleon is low are not as stable. The binding energy per nucleon is about 7.6 MeV for a heavy element like Uranium and about 8.5 MeV for elements of an intermediate atomic weight like Barium and Krypton. Hence, if a U-235 nucleus were to split apart into Barium-141 and Krypton-92 atoms, then we would release about 235 × (8.5 to 7.6 MeV) ≅ 210 MeV of useful energy. (However, only 200 MeV of this is actually recoverable.) Another implication of the nuclear binding energy curve is that some nuclei (particularly heavy ones) can split apart *without having to add additional energy to them. This can be quantified in terms of another variable called the critical energy for fission, E_{CRIT}*, which was first discussed in Chapter 3. The values of this critical energy for common isotopes of Thorium, Uranium, and Plutonium are shown in Table 6.9. If one of these nuclei happens to absorb a slow moving neutron, a compound nucleus will be formed with energy equal to the kinetic energy of the incident neutron plus the binding energy of the neutron in the compound nucleus. *If the binding energy alone is greater than the critical energy for fission, E_{CRIT}, then the compound nucleus will split apart even when it absorbs neutrons with essentially no kinetic energy.*

For example, when a U-235 nucleus absorbs a low-energy neutron, it immediately transforms itself into U-236, which is one of the compound nuclei shown in Table 6.9. According to Table 6.9, the U-236 nucleus is still produced with 1.1 MeV more energy than its critical energy—even if the neutron that it absorbs has no kinetic energy at all. Thus a fission reaction will immediately occur, and the U-236 nucleus will split apart. We simply add a neutron to the nucleus that causes it to deform and enter into an excited state. Then the only two options it has are to (1) to emit a gamma ray (which is known as radiative capture) or (2) to split apart and release approximately 200 MeV of recoverable energy in the process. This table also explains why Thorium cannot be used as the primary nuclear fuel in a thermal water reactor. *Absorbing a thermal neutron does not impart enough additional energy to the Thorium nucleus to cause it to split apart because the critical energy of fission is greater than the binding energy of the outermost nucleon in this case*.

TABLE 6.9
The Critical Energies That Are Required for the Nucleus of a Heavy Atom to Deform Enough to Undergo Nuclear Fission

Fissioning Nucleus	Compound Nucleus	Critical Energy (E_{CRIT})	Binding Energy of the Least Tightly Bound Neutron[a]
Th-232	No	5.9	[a]
Th-233	Yes	6.5	5.1
U-233	No	5.5	[a]
U-234	Yes	4.6	6.6
U-235	No	5.75	[a]
U-236	Yes	5.3	6.4
U-238	No	5.85	[a]
U-239	Yes	5.5	4.9
Pu-239	No	5.5	[a]
Pu-240	Yes	4.0	6.4

Source: Lamarsh, J.R. and Baratta, A.J. *Introduction to Nuclear Engineering,* Prentice Hall, Upper Saddle River, NJ, 2001.
The critical energies and the binding energies shown are in MeV.
[a] Neutron binding energies are not given for these nuclei because they cannot be formed by having the same element absorb another neutron.

Student Exercise 6.6

Compare the size of the pairing energy term to the asymmetry energy term for Uranium-238. Which of these terms do you think is more important in determining the stability of the U-238 nucleus?

6.16 Nuclear Fuels and Their Properties

Out of all of the elements in the Periodic Table, Uranium is the only naturally occurring element that can be used as a nuclear fuel. The term "naturally occurring" refers to the fact that uranium occurs naturally, and as such, it has not been created artificially or synthesized in significant quantities by man. The element uranium consists of several isotopes that are important to the production of nuclear power. It was first discovered by German chemist *Martin Heinrich Klaproth* in 1789, who found it in the mineral *pitchblende*, which is a combination of several uranium ores. It was originally believed to consist of only two isotopes—Uranium-235 and Uranium-238, which had a difference in mass of about 1%. Today we know that Uranium consists of *three stable isotopes—U-234, U-235, and U-238*. Each of these isotopes has a different half-life, and the relative abundance of these three isotopes is 0.0055%, 0.72%, and 97.275%, respectively. U-238 is by far the most common naturally occurring natural form of Uranium, and its half-life is about 4.47 Billion years—or about the same as the age of the Earth. Uranium-235 is the next most common form of Uranium, and its half-life is about 704 million years. Hence it decays at about 1/6th of the rate that U-238 does. The third naturally occurring isotope of Uranium is Uranium-234.

U-234 is the least common form of naturally occurring Uranium, and it has a half-life is about 245,000 years. Uranium-234 has a smaller number of neutrons than U-238 does, and it is created primarily by the alpha decay of U-238. This process begins when a uranium-238 nucleus emits an alpha particle to become Thorium-234 (Th-234). Thorium-234 immediately emits a beta particle to become protactinium-234 (Pa-234) and Pa-234 then emits another beta particle to become U-234. The U-234 that is produced in this way has a half-life of about 245,000 years, and when it decays, it does so by emitting another alpha particle to become Thorium-230. A small percentage of the uranium-234 nuclei that are found in nature also destroy themselves through an entirely different process called *spontaneous fission*. Here the atomic nucleus becomes unstable due to a temporary force imbalance, and it splits apart into two nearly equal fragments without absorbing an additional neutron. *Spontaneous fission* was first discovered by two Russian physicists by the name of *G.N. Flerov* and *K.A. Petrzhak* in 1941, and it can be found in many isotopes having an atomic mass number of 230 or more. Uranium-235 has an additional neutron, and its decay chain is shown in Figure 6.10. U-235 eventually decays only into Thorium-231 (which has an atomic number of 90). In about a day, the Thorium-231 decays into Protactinum-231 by emitting an energetic electron (or a Beta particle) in the process. Eventually, the decay chain ends when the by-products of the decay of Uranium turn into Lead (Pb-207). Lead-207 is a fundamentally stable isotope and does not decay any more.

It takes about 704 million years for half of the Uranium-235 that is present in nature to turn itself into Lead. Uranium-238, on the other hand, follows an entirely different decay chain (see Figure 6.11). It first decays into Thorium-234

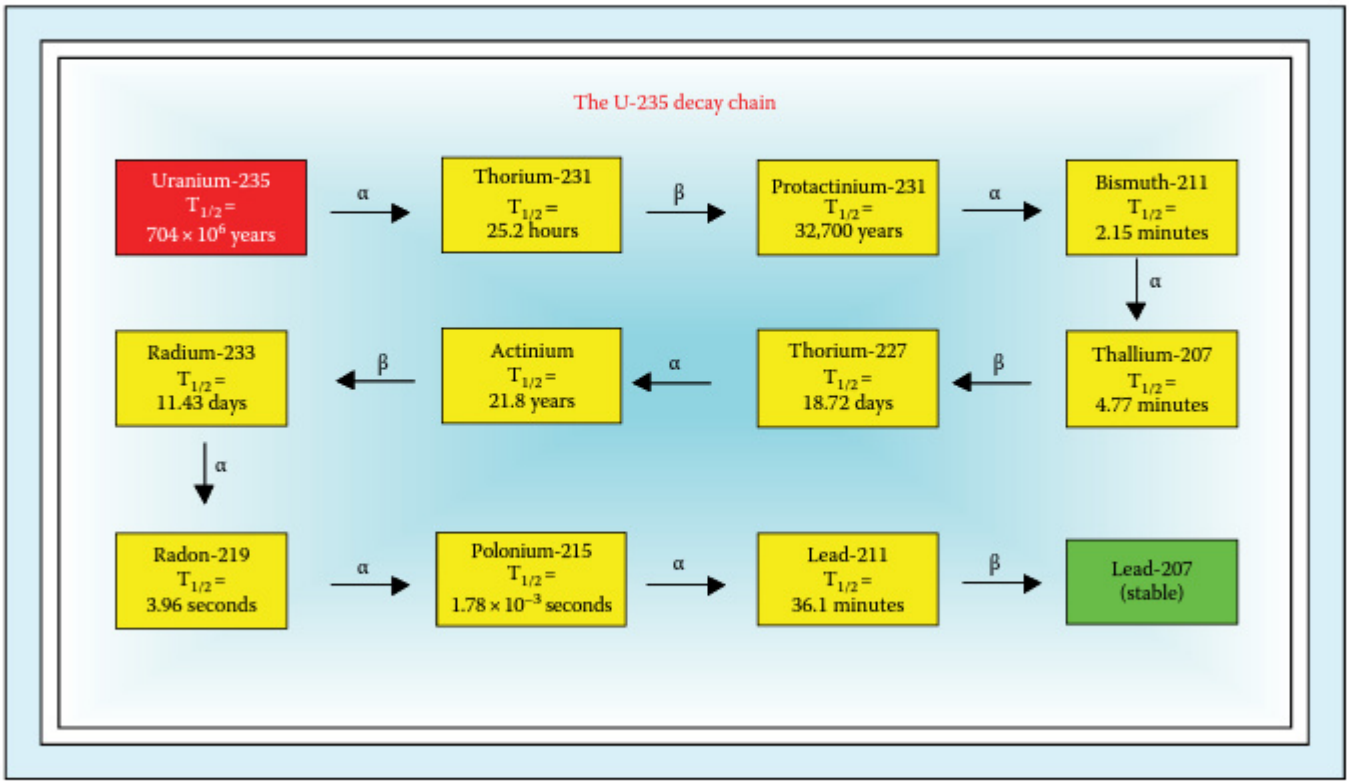

FIGURE 6.10 The main branches of the Uranium-235 decay chain.

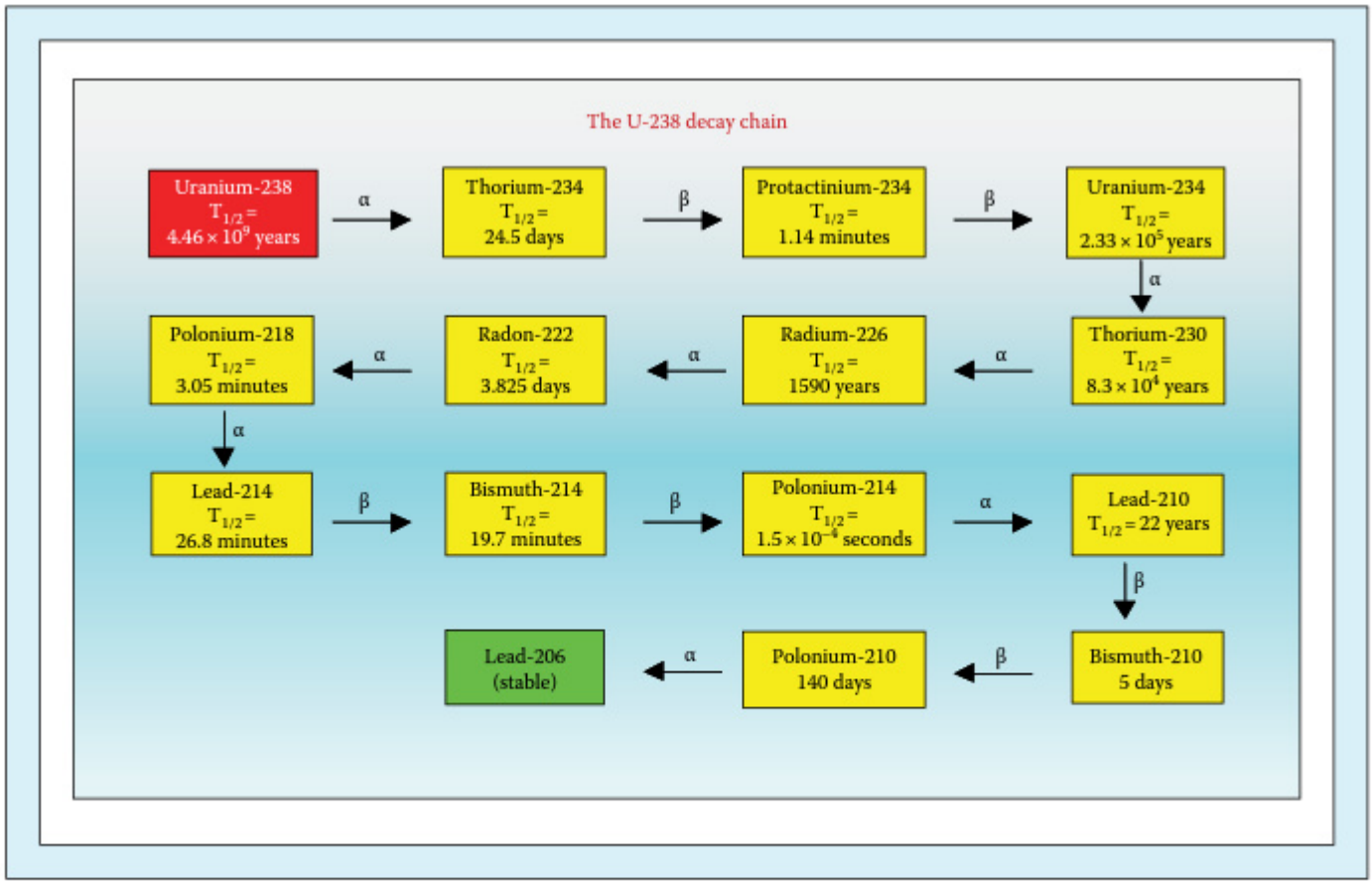

FIGURE 6.11 The main branches of the Uranium-238 decay chain.

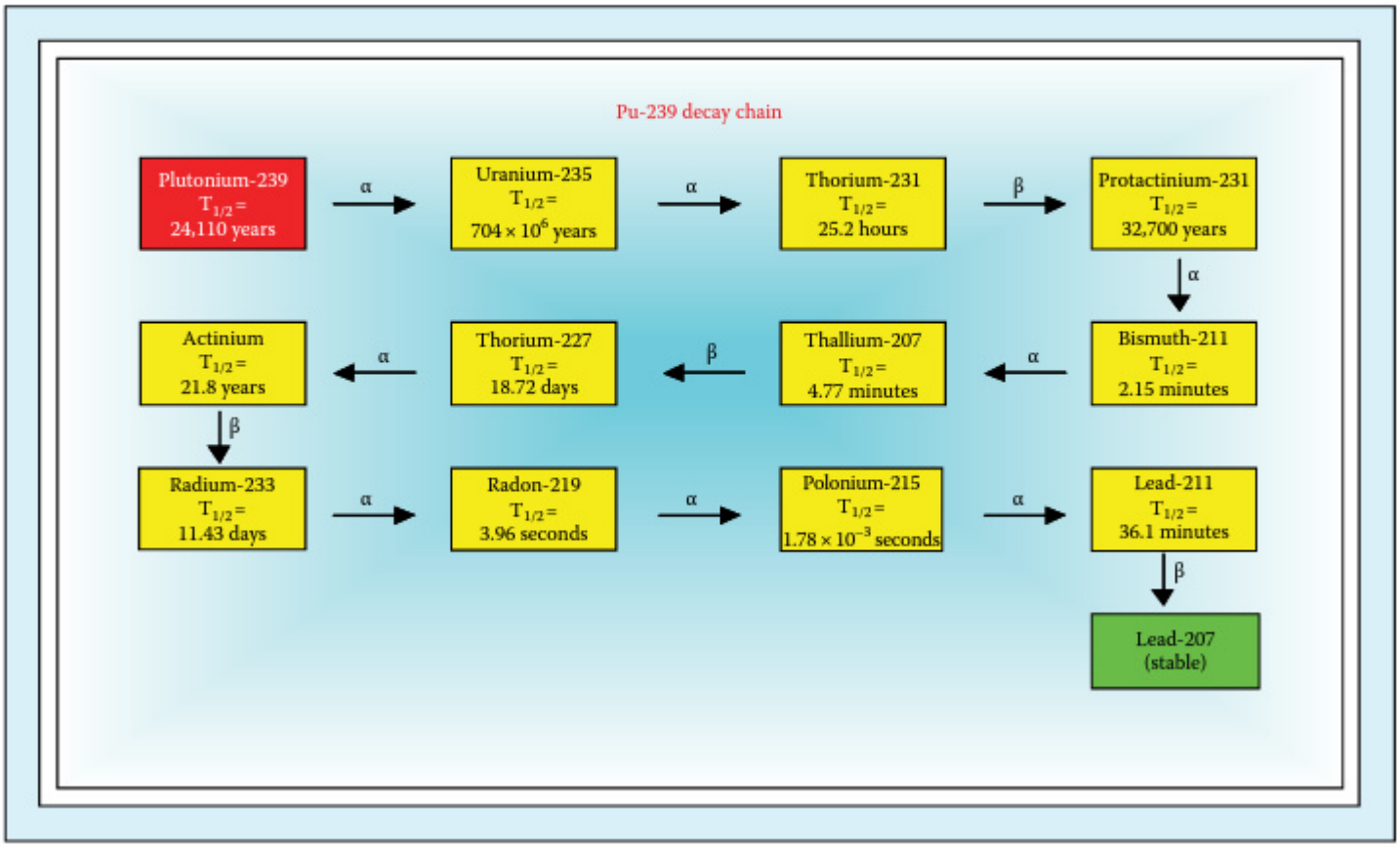

FIGURE 6.12 The main branches of the Plutonium-239 decay chain.

by emitting an energetic helium nucleus (or alpha particle). Thorium-234 decays into still lighter elements by emitting an energetic electron (or a Beta particle), until we finally end up with Lead-206, which is the end of the decay chain. Lead-206 is also fundamentally stable and does not decay any further. *From the time that a Uranium-238 nucleus decays into Thorium-234, it takes approximately 235,000 years for half of it to turn into Lead.*

As in the case of U-235, there are more than a dozen steps in the entire process (see Figure 6.12 for a complete description). *It is important to keep in mind that uranium-238 has a very low probability to split apart when it absorbs a thermal neutron, and because of this, it is not widely used to produce nuclear power directly*. However, it can be converted into Plutonium-239, which will split apart and release about 200 MeV in energy when it absorbs a thermal neutron. Consequently, Plutonium-239 is used to produce nuclear energy directly, while Uranium-238 is not. The Thorium-232 fuel cycle, which produces U-233, and the U-238 fuel cycle, which is used to produce Pu-239, are described in more detail in many fuel cycle books. The interested reader should feel free to refer to these books for more information about why U-233 and Pu-239 can be used to produce power through the process of nuclear fission, while Thorium-232 and Uranium-238 cannot. In order to produce Plutonium-239, atoms of Uranium-238 must first be exposed to a neutron source. The higher the average output of the neutron source, the greater the rate is that the U-238 will be converted to Pu-239. Uranium-239 can be created when uranium-238 absorbs a high-energy or a low-energy neutron. Uranium-239 has a half-life of about 23 minutes, and it will immediately decay into neptunium-239. Neptunium-239 has a half-life of about 2.4 days and it eventually decays into plutonium-239 by releasing an electron. Hence, we have just described the process as to how a breeder reactor converts Uranium-238 into Plutonium-239. Table 6.10 summarizes the properties of all of the known isotopes of uranium. The average atomic weight of naturally occurring Uranium is 238.02891. (See Table 6.10.) Again, this leads us to the conclusion that there must be more than one isotope present in natural uranium ore to account for the fact that the average weight is different than the weight of U-238 alone (238.050785).

6.17 Difference between Controlled and Uncontrolled Nuclear Reactions

Uranium is one of the few materials that can be used as a commercial nuclear fuel. (The other two are Thorium and Plutonium.) For reasons that we previously discussed, only materials that produce more neutrons than they absorb can be used to sustain the nuclear chain reaction. In an atomic bomb, the nuclear chain reaction only proceeds until the fertile

TABLE 6.10
Some Nuclear Data for the Isotopes of Uranium

Uranium Nuclear Data								
Isotope	Z	A	Atomic Mass (u)	Decay Rate λ (s^{-1})	Natural Abundance	Half-Life	Decay Mode	Q (MeV)
U-226	92	226	226.029170		—	0.5 s	a	7.56
U-231	92	231	231.036270		—	4.2 d	EC	0.36
U-232	92	232	232.037130		—	67.9 d	a	5.41
U-233	92	233	233.039628		5.5×10^{-5}	0.159 My	a	4.91
U-234	92	234	234.040947		—	0.245 My	a	4.86
U-235	92	235	235.043924		0.0072	0.704 Gy	a	4.68
U-236	92	236	236.045563		—	23.4 My	a	4.57
U-238	92	238	237.050785		0.99275	4.46 Gy	a	4.27
U-239	92	239	237.054290		—	23.54 m	b−	1.26

or fissile material that is used to construct the bomb begins to dissipate at the blast point. Then, as the explosion progresses, the uranium or plutonium atoms simply move too far apart from one another for the chain reaction to continue. This is sometimes called an *uncontrolled chain reaction* because it proceeds violently at first, and then as the uranium or plutonium atoms begin to separate, the material density ρ becomes too low for the process to continue any further. The neutron leakage rate L also increases the further away we move from the blast point. The combination of these two effects (increasing neutron leakage L and decreasing material density ρ) tends to shut down the reaction after its violent beginning. However, in a fission reactor, exactly the opposite situation occurs. In this type of reaction, it is desirable to sustain the chain reaction *for as long as possible*. This generally means that we must build up the chain reaction gradually and then maintain it by balancing the neutron production rate P and the neutron destruction rate D. If the material density ρ and the neutron leakage rate L are balanced very carefully, the reaction will continue until the uranium is burned long enough for the density of the uranium or plutonium atoms to decline. This type of chain reaction is often called a *controlled chain reaction*. A nuclear reactor relies on this type of reaction to generate electric power. Hence, we may express the difference between a controlled and an uncontrolled chain reaction in the following way:

Criteria for a Nuclear Chain Reaction

$$\text{Controlled chain reaction: } P(t) = D(t)$$
$$\text{Uncontrolled chain reaction: } P(t) > D(t) \qquad (6.24)$$

where

P(t) is the time-dependent neutron production rate (in neutrons per second)
D(t) is the time-dependent neutron destruction rate (in neutrons per second)

In the case of an atomic bomb, a great deal of energy can be released (trillions of Joules) very quickly when $P(t) \gg D(t)$ for a very short period of time T, which may be only a millionth of a second. The energy generation rate as a function of time for each of these reactions is compared in Figure 6.13.

6.18 The Process of Uranium Enrichment

Natural uranium is not a practical nuclear fuel except in CANDU* reactors because the U-235 concentration is too low to keep the reactor critical for long periods of time. In other types of reactors including PWRs, BWRs, and even LMFBRs, the ratio of the U-235 atoms to the U-238 atoms must be increased beyond 0.7% to provide enough fissile material to sustain the reaction over a longer period of time. For this reason, the U-235 concentration must be increased to at least 3% (and typically between 3% and 5% in conventional PWR and BWR fuel) to obtain the burnups required to minimize the

* The word CANDU is an acronym for a *CANada Deuterium Uranium* reactor. It is a Canadian-designed, pressurized heavy water reactor that can be fueled with natural uranium, enriched uranium, or a mixture of these two fuels and even plutonium in some cases (see Chapter 1 for more details).

FIGURE 6.13 Controlled and uncontrolled nuclear reactions. In a modern atomic bomb (a) about 10,000 terajoules (1 TJ = 10^{12} J) of energy is released in a fraction of a second, while in a modern nuclear reactor (b), the energy release is much more gradual, and less than a megajoule is typically released in the same period of time.

cost of generating electric power. In a LMFBR, this concentration must be increased to between 15% and 20%. Increasing the U-235 concentration can be achieved by the process of *uranium enrichment*.

In this process, the physical weight difference between the isotopes of U-235 and U-238 can be used to separate the lighter U-235 atoms from the heavier U-238 ones. On an industrial scale, three different processes are used to perform this isotopic separation:

1. *The Gaseous Diffusion Process*
2. *The Centrifugal Separation Process*
3. *The Laser Separation Process*

Each of these processes takes solid uranium yellowcake and converts it into a gaseous material known as *uranium hexafluoride* (UF_6). Uranium hexafluoride is then manipulated in various ways to increase the number of U235-F_6 molecules while reducing the number of ones that contain U238-F_6. The exact details of how this physical separation is achieved depend on the processing technology that is used, but the overall principle in each case is exactly the same. This principle is illustrated in Figure 6.14. Normally the outcome of the enrichment process is a UF_6 mixture with a U-235/U-238 weight ratio of between 3% and 5%. However, for military applications, the percentage of U-235 can be considerably greater because military reactors need more highly enriched uranium fuel. Here the average enrichment of the fuel can be between 90% and 95%.

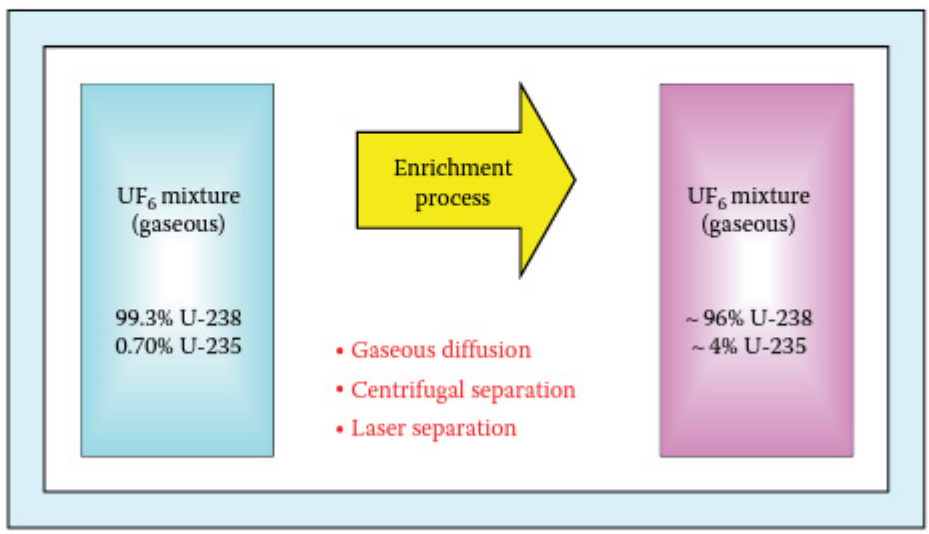

FIGURE 6.14 An illustration of the uranium enrichment process.

6.19 Man-Made Elements and Nuclear Fuels

The modern Periodic Table contains *approximately 120 elements, of which 92 elements occur naturally, and the other 26 are "man-made." Man-made elements* can be produced in nuclear reactors and in nuclear accelerators. The most well-known man-made elements have exotic names like as *Neptunium, Plutonium, Berkelium,* and *Californium*. They were discovered in the 1940s and the 1950s. Plutonium was named after the *Planet Pluto*, and Californium was named after the state of *California*, where it was initially discovered. Most man-made elements have very short half-lives and are not very stable. This explains why they do not occur in measurable quantities in nature. Man-made elements such as Plutonium are useful as power sources in space probes and certain types of medical instruments. A complete list of the man-made elements can be found in Table 6.11. On average, a new man-made element is discovered every 4–5 years. Of the 26 man-made elements that have been produced to date, the one that we will pay the most attention to is Plutonium. We will discuss how it can be produced, how it can be used, and how it decays. Another man-made element that is produced in nuclear reactors is *Neptunium*, which we will discuss in the next section. Neptunium has an atomic number of 97 and is positioned in the Periodic Table midway between the elements uranium and plutonium. It was discovered about a year before Plutonium was, and its half-life is many times shorter than the age of the earth. It is very difficult to detect in nature, and it only appears in negligible amounts (about 1 part per trillion) in common uranium ores.

6.20 The Element Neptunium

Neptunium is not as well known as uranium is because it has fewer commercial applications. It is the first element in the Periodic Table with more protons than uranium, and it is synthesized in reactors primarily by allowing U-235 to absorb a thermal neutron and convert itself into U-236. About 80% of the time, the U-236 nucleus splits apart, but about 20% of the time it does not, and instead it converts itself into a stable U-236 nucleus by emitting a gamma ray. If the

TABLE 6.11
Man-Made Elements

Element	Z	N	A	Symbol	λ	T½	Rest Mass (AMU)
Neptunium	93	—	—	Np	—	—	237.0482
Plutonium	94	—	—	Pu	—	—	244.0642
Americium	95	—	—	Am	—	—	243.0614
Curium	96	—	—	Cm	—	—	247.0704
Berkelium	97	—	—	Bk	—	—	247.0703
Californium	98	—	—	Cf	—	—	251.0796
Einsteinium	99	—	—	Es	—	—	252.0830
Fermium	100	—	—	Fm	—	—	257.0951
Mendelevium	101	—	—	Md	—	—	257.0984
Nobelium	102	—	—	No	—	—	257.1010
Lawrencium	103	—	—	Lr	—	—	262.1097
Rutherfordium	104	—	—	Rf	—	—	261.1088
Dubnium	105	—	—	Db	—	—	262
Seaborgium	106	—	—	Sg	—	—	266
Bohrium	107	—	—	Bh	—	—	264
Hassium	108	—	—	Hs	—	—	277
Meitnerium	109	—	—	Mt	—	—	268
Darmstadtium	110	—	—	Ds	—	—	271
Roentgenium	111	—	—	Rg	—	—	272
Ununbium	112	—	—	Uub	—	—	285
Ununtrium	113	—	—	Uut	—	—	284
Ununquadium	114	—	—	Uuq	—	—	289
Ununpentium	115	—	—	Uup	—	—	288
Ununhexium	116	—	—	Uuh	—	—	292
Ununseptium	117	—	—	Uus	—	—	—

Note: Elements in blue—Neptunium, Plutonium, Americium—are the only man-made elements with significant commercial applications.

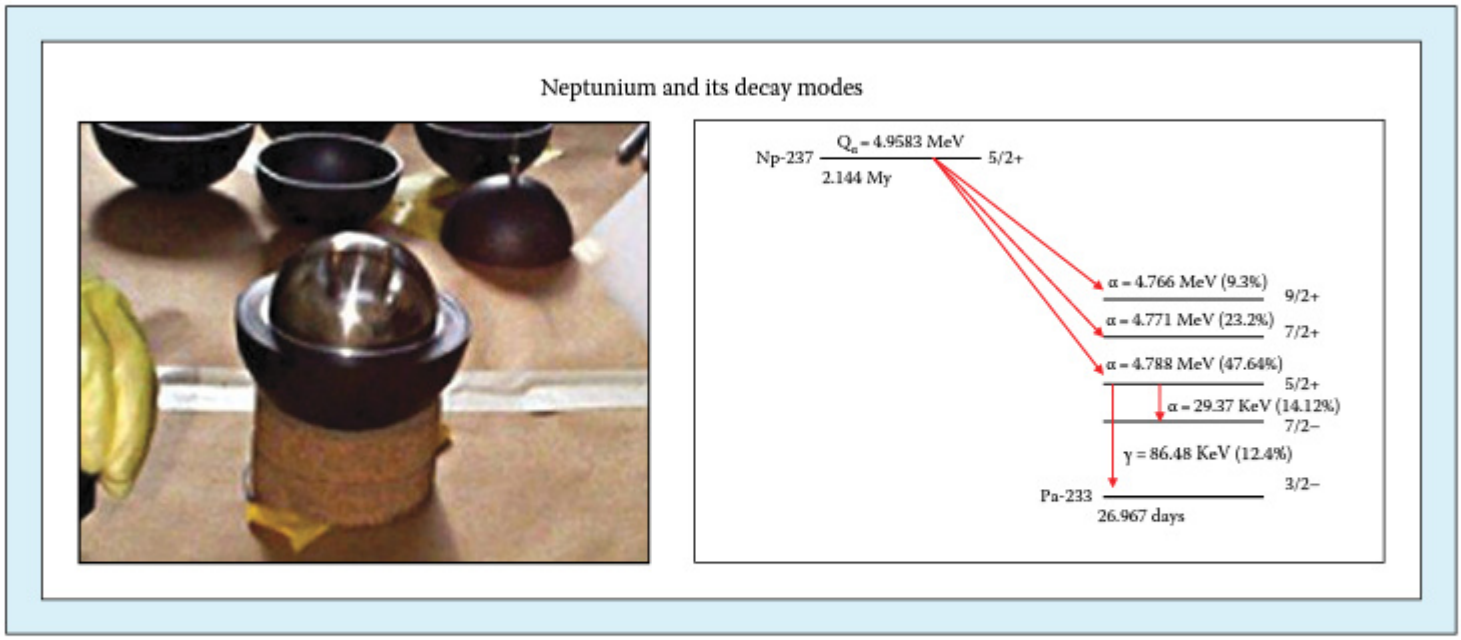

FIGURE 6.15 A picture of the element Neptunium in its metallic state, and an illustration of how it eventually decays into protactinium. (Pictures provided by Wikipedia.)

U-236 nucleus absorbs an additional neutron, it converts itself into U-237. U-237 then decays by emitting a beta ray into Neptunium-237. The entire process is illustrated below:

$$^{1}_{0}\mathrm{n} + {}^{235}_{92}\mathrm{U} \rightarrow {}^{236}_{92}\mathrm{U} + \gamma$$
$$^{1}_{0}\mathrm{n} + {}^{236}_{92}\mathrm{U} \rightarrow {}^{237}_{92}\mathrm{U} + \beta^{-} \rightarrow {}^{237}_{93}\mathrm{Np}$$

Thus *the production of Np-237 is a two-step process*. Neptunium has about 20 other isotopes, but only Np-237 has a long enough half-life (about 2.14 million years) to be useful commercially. Although many false claims of its discovery were made over the years, the first definitive proof of its existence was provided by *Edwin McMillan* and *Philip Abelson* at the University of California in 1940. In its natural state, Neptunium is a silvery metallic metal that looks a lot like uranium or plutonium (see Figure 6.15). It quickly oxidizes when exposed to air and is similar to uranium in terms of its physical workability. It is radioactive and can accumulate in bones and other types of human tissue. While Neptunium does not have many commercial applications, it is commonly used to produce Plutonium-238, which is used as a thermal radioisotope generator to power some types of spacecraft and interplanetary probes. Figure 6.16 shows a Plutonium-238 sphere generating its own heat and light. Plutonium-238 is an alpha emitter with a half-life of about 88 years (see Table 6.12).

6.21 The Element Plutonium

Plutonium was first discovered in 1940 by a team of researchers at the University of California, Berkeley, when U-238 was bombarded with a shower of slow-moving deuterons. This team was led by *Glenn Seaborg and Edwin McMillan*, who later won the Nobel Prize in Chemistry for their work. McMillan named this new element after the planet Pluto, and Seaborg later gave it the symbol Pu. Plutonium has an atomic number of 94 (meaning that it has 94 protons and 94 electrons) and approximately 20 isotopes with mass numbers ranging from 232 to well over 246. These isotopes are listed in Table 6.12.

6.22 Production of Plutonium-239

Of all of the isotopes of Plutonium, there are only two isotopes that are produced in large enough quantities to be useful as a nuclear fuel—Plutonium-239 and Plutonium-241. Because of their short half-lives, neither of these isotopes can be found in significant quantities in nature. However, we have seen that Plutonium-239 can be produced in a nuclear reactor by taking U-238 (which is very plentiful in nature) and bombarding it by either high-speed or low-speed neutron. The fast absorption cross section of U-238 is only about 0.12 barns, but the thermal absorption cross section is about 20 times

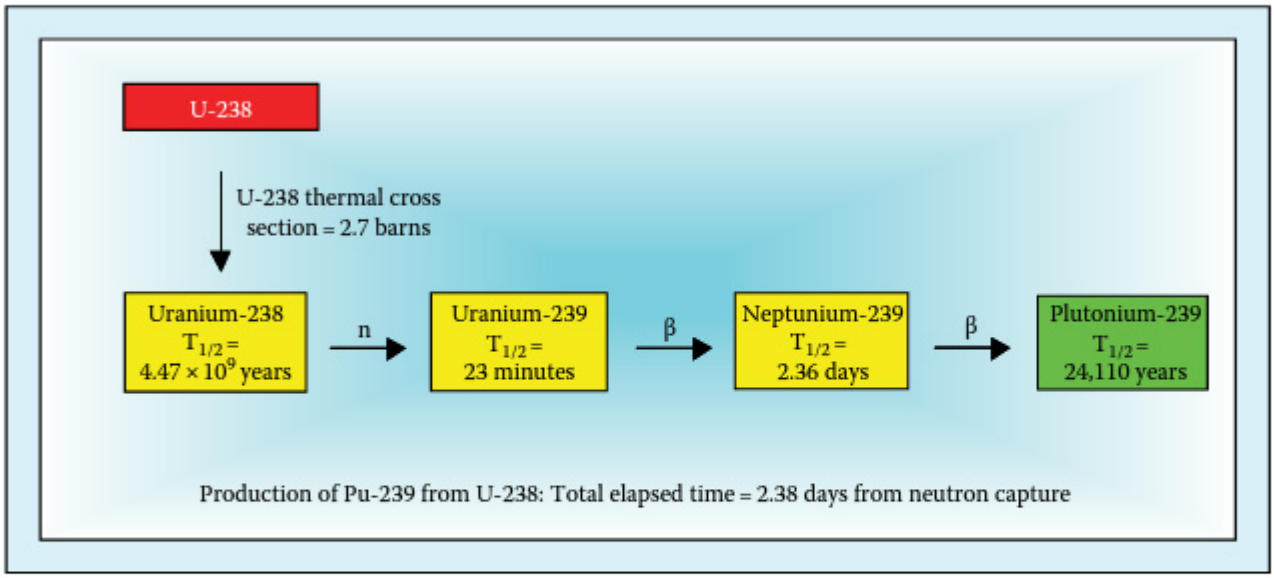
U-238
U-238 thermal cross section = 2.7 barns
Uranium-238 $T_{1/2}$ = 4.47 × 10^9 years
n
Uranium-239 $T_{1/2}$ = 23 minutes
β
Neptunium-239 $T_{1/2}$ = 2.36 days
β
Plutonium-239 $T_{1/2}$ = 24,110 years
Production of Pu-239 from U-238: Total elapsed time = 2.38 days from neutron capture

FIGURE 6.16 The Plutonium-239 production process.

TABLE 6.12
Isotopes of the Element Plutonium

Isotope	Z	A	Atomic Mass (AMUs)	N	Half-Life	Decay	Q (MeV)
Pu-228	94	228	227.03874	134	1.1 s		
Pu-229	94	229	227.04015	135	120 s		
Pu-230	94	230	230.039650	136	1.70 min		
Pu-231	94	231	231.041101	137	7.6 min		
Pu-232	94	232	232.041187	138	33.7 min		
Pu-233	94	233	233.04300	139	20.9 min		
Pu-234	94	234	234.043317	140	7.8 h		
Pu-235	94	235	235.045286	141	25.3 min		
Pu-236	94	236	236.0460580	142	2.858 y		
Pu-237	94	237	237.0484097	143	45.2(1) d		
Pu-238	94	238	237.0495599	144	87.74 y		
Pu-239	94	239	237.052158	145	24.11 Ky	b–	5.24
Pu-240	94	240	240.0538135	146	6,537 y		
Pu-241	94	241	241.0568515	147	14.40 y	b–	
Pu-242	94	242	242.058737	148	0.376 My	a	4.98
Pu-243	94	243	243.062003	149	4.956 h		
Pu-244	94	244	244.064198	150	82 My	a	4.67
Pu-245	94	245	245.067747	151	7.5 h		
Pu-246	94	246	246.070205	152	7.84 d		
Pu-247	94	247	247.074073	153	2.27 d		

Note: Only three of them (Pu-239, Pu-242, and Pu-244) are reasonably stable.

larger (about 2.7 barns). Hence, capturing either a high-speed neutron or a low-speed neutron will eventually allow U-238 to be converted into Plutonium-239. It takes about 2.38 days from the time a Uranium-238 nucleus absorbs a neutron until an atom of Plutonium-239 is produced. If U-238 is present, Plutonium-239 will be continuously produced as the less plentiful isotopes like U-235 are consumed. Since Plutonium-239 can also be split apart by absorbing low-speed neutrons, it also produces a significant portion of the energy that a thermal water reactor produces. In fact, *about 30% of the energy in a thermal water reactor can be produced in this way.*

TABLE 6.13
Stable Isotopes of the Element Lead

Chemical Symbol	Atomic Number	Natural Abundance (%)	Half-Life
Pb-204	204	1.4	≥1.4 × 10+17 years
Pb-206	206	24.1	~Infinite (stable)
Pb-207	207	22.1	~Infinite (stable)
Pb-208	208	52.4	~Infinite (stable)

Note: About 50% of naturally occurring Lead is Pb-208.

Next to U-235, Pu-239 is the most common fissile material to be used as a nuclear fuel. Some nuclear reactors such as *the N reactor* along the *Columbia River* in Eastern Washington State were built exclusively during World War II to produce Pu-239 from U-238. All you need is U-238, and some slow moving neutrons, to start making Plutonium-239. Plutonium-239 also has the interesting property that half of it will decay directly into Uranium-235 in about 25,000 years. The process of plutonium production is shown in Figure 6.16. Once it decays into Uranium-235, U-235 takes about 704 Million years to decay into Lead. Here the decay chain ends because the resulting isotope of Lead (Pb-207) is inherently stable, and will not decay into an element with a lower atomic number for a very long period of time. Isotopes of Lead that are produced through other decay chains include Lead-204, Lead-206, and Lead-207. The properties of these isotopes are summarized in Table 6.13. The isotopes of Lead are very heavy, and their outer electron shells are very good at absorbing high-energy photons or *γ-rays*. Hence, naturally occurring Lead and its isotopes are frequently used to build *radiation shields*.

6.23 Plutonium-239 Decay

Since Plutonium is not found in measurable quantities in nature, it should not be surprising to learn that it decays relatively quickly, at least when compared to geological time frames. Plutonium-239 has the interesting property that it will decay, at least initially into Uranium-235. The decay chain for Plutonium-239 is shown in Figure 6.12. Since it has a half-life of 24,110 years, it is stable enough to fabricate and use as a nuclear fuel. Plutonium-239 in higher concentrations is also used in a variety of nuclear weapons. Figure 6.17a shows a weapons-grade ring of electrorefined plutonium, which has a purity of 97.96%. This particular ring contains enough plutonium for one atomic bomb core. The geometry of the

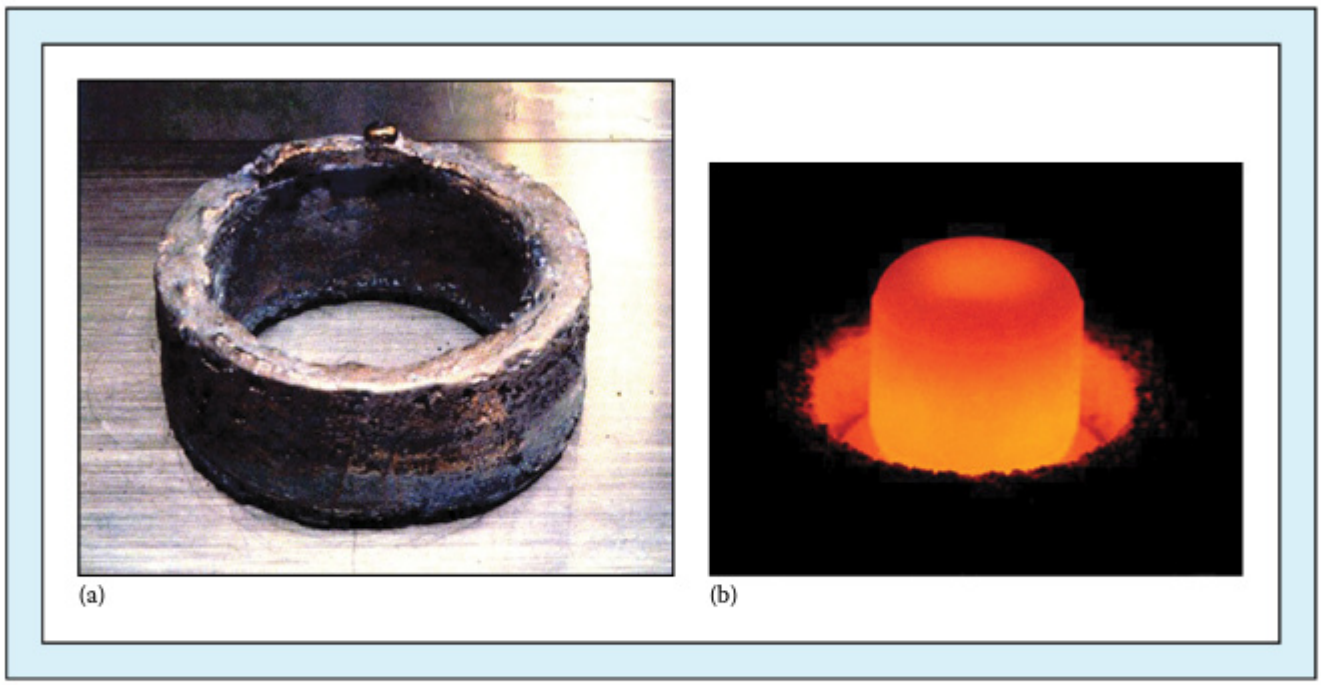
(a) (b)

FIGURE 6.17 (a) A weapons-grade ring of electrorefined plutonium, typical of the rings refined at Los Alamos and sent to Rocky Flats for fabrication. The ring has a purity of 97.96%, weighs 5.3 kg, and is approximately 11 cm in diameter. It is enough plutonium for one bomb core. The ring shape helps with criticality safety (less concentrated material). (b) A Plutonium-238 sphere generating its own heat and light. (Courtesy of Wikipedia.)

ring helps to keep the plutonium in a subcritical state while it is being shipped and assembled. Like Uranium-235 and Uranium-238, it is a dull and heavy metal in its natural state.

6.24 Other Isotopes of Plutonium

Besides Pu-239, the most commonly used isotopes of plutonium are Pu-238 and Pu-241. Plutonium-238 has a half-life of 88 years and is an abundant source of alpha particles (ionized helium nuclei). The process of alpha decay allows it to produce useful quantities of decay heat for about 100 years. Because the heat production can be maintained for so long, it is a popular energy source for small, portable electric generators called isotopic thermoelectric generators. *These generators have been used to power spaceships, satellites, and even some space probes built by NASA*. They are much more reliable than ordinary batteries over very long periods of time. A picture of a Plutonium-238 sphere generating its own heat and light is shown in Figure 6.17b. This particular sphere was used to power a satellite that was sent into orbit. The other commonly used isotope of Plutonium is Pu-241. Pu-241 has a radioactive half-life of 14.4 years, and decays quickly into Americium-241. *Americium-241 is a strong alpha emitter, and it is commonly used in household smoke detectors. Because Pu-241 has such a short half-life, it is not very practical to use as a conventional nuclear fuel*. These pellets are used for devices known as *radioisotope thermoelectric generators*. They are made of PuO_2. The image in Figure 6.17 was provided by the U.S. Department of Energy. (See Image ID 2006407 at *http://www.doedigitalarchive.doe.gov* and search for plutonium AND light.)

6.25 Radioactivity and Radioactive Decay

When discussing nuclear fuels and nuclear power production, one must account for the fact that not only the fuels but also the by-products of the fuels (the fission products) can be radioactive, and because the isotopes within these materials are usually unstable, the concentrations of these materials will also change with time—in other words, *they will decay away*. For this reason, it is important to know both the initial and final concentrations of each of these materials, as well as the rate at which they decay. The field of *radioactivity* attempts to explain this in a practical way.

6.26 Force Imbalances and the Origin of Radioactivity

In classical physics, *the fundamental cause of radioactivity is a temporary force imbalance* between the electrical forces in the nucleus that want to rip it apart and the nuclear forces carried by the gluons that want to hold it together. Occasionally, a W-boson (through a complex mechanism that we have only begun to understand) can transmute an *up quark* into a *down quark*, or a down quark into an up quark (see Chapter 2), and in the process, the nucleus can become destabilized. When this occurs, the nucleus must emit a number of particles (usually alpha particles, beta particles, gamma rays, or neutrinos) to return to a stable energy state. This force imbalance is the fundamental cause of what we perceive to be radioactive decay. It is interesting to explore the magnitude of these forces to get an idea of what it takes to cause the atomic nucleus to destabilize.

The electrical force F_e between a proton and an electron in a hydrogen atom is so strong that gravity and all other forces in nature (except the nuclear force field) are negligible by comparison. This force is only a couple of eV in the case of the binding energy between a proton and an electron in a hydrogen atom, but this only binds the electron to the atom and has nothing to do with the forces inside of the nucleus itself. However, inside of the nucleus, two protons that are very close together can exert a repulsive force on each other that is over one *Million times stronger* than the bond between a hydrogen atom and its electron because the strength of the electrical force increases as the inverse square of the distance between the protons. From classical physics, the magnitude of the electrical force is given by

The Electrical Nuclear Force

$$F_e = \frac{kq_1q_2}{r^2} \tag{6.25}$$

where

r is the distance between the protons

$q_1 = q_2 = q$ are the charges

k is called *Coulomb's constant*, which has the following units

$$k = 5.0 \times 10^9 \text{ N m}_2/\text{coul}^2 \tag{6.26}$$

Inside of the nucleus, r is so small (between 1×10^{-12} cm to 1×10^{-14} cm) that *the repulsive forces between two protons can approach several million electron volts*. The average energy, or the binding energy required to overcome this electrical repulsion, is almost 8 MeV (8 Million Electron Volts). So how can two protons in the nucleus stay in such close proximity? This may give you some appreciation for the enormity of the nuclear force that holds the nuclei together. We can also infer from this discussion that the strength of a typical nuclear bond is in the range of 5–10 MeV. Figure 6.18 shows how the forces are usually balanced and what happens when a force imbalance actually occurs. The net result is what we perceive to be radioactive decay!

There is an interesting *ratio of protons to neutrons* that determines whether or not a nucleus is inherently stable. For light elements like carbon and oxygen, this ratio is very close to one. If the ratio is close to this for elements lighter than iron, they will tend to be very stable, and they will very rarely be radioactive. On the other hand, the ideal ratio is about one proton to one and one-half neutrons for heavier elements like uranium and thorium. If there are more neutrons or less neutrons, the nucleus becomes unstable and will fly apart. *The Chart of the Nuclides* or a *Segre Chart* (see Figure 6.19) is a convenient way to visualize how many isotopes a given element in the Periodic Table can have. There are about 3000 independent dots on this chart, and each dot has a color to represent a specific isotope that can be found in nature. *In other words, the Chart of the Nuclides shows that there are about 3000 isotopes that make up the Periodic Table*. Notice that as the elements in the Periodic Table get heavier, more neutrons have to be added to the nucleus to create an atomic configuration that is stable. There are a number of reasons for this that we will subsequently discuss. For example, the element Carbon (with Z = 6 protons) has seven isotopes, but the most stable ones are when the N = 6 and N = 5. In this case, N/Z = 1.0 and N/Z = 1.16. The average neutron-to-proton ratio (N/Z) for carbon is 1.08. On the other hand, the only truly stable isotopes of Uranium, which are very heavy, are U-235 and U-238. In this case, Z = 92, and N/Z = 143/92 = 1.55 and N/Z = 146/92 = 1.55. The average N/Z ratio for a uranium atom is about 1.55. Isotopes that have more neutrons or less neutrons than these *magic numbers* are rarely stable for a long period of time. Practically speaking, the lower limit of the N/Z ratio that any isotope can have is 1.0 (for deuterium), and 1.6 for uranium. All other isotopes have N/Z ratios that fall somewhere between these two extremes. Notice that *some of the elements in the Periodic Table like tin (Z = 50) can have 30 or even 40 different isotopes, while lighter elements like carbon (Z = 6) can have only a few*. For example, carbon has seven different *isotopes* in all. Their atomic masses range from 9 to 15 AMU, but only carbon-12 and carbon-13, with N = 6 and N = 7, are truly stable. Not all isotopes in nature occur in the same proportions because their stability is a direct function of their neutron-to-proton ratio. The isotopes shown in pink, yellow, light blue, and white have very short half-lives and do not occur in appreciable quantities in nature. Only the isotopes that correspond to the black dots along the centerline of the chart have the correct number of neutrons to protons to be stable for a very long period of time. It turns out that these isotopes represent only about 10% (e.g., 0.10 × 3000) or about 300 of the total number of isotopes that actually exist. The remaining 90% of the isotopes, which correspond to the other 2700 yellow, green, and light blue dots, and nuclear combinations, do not.

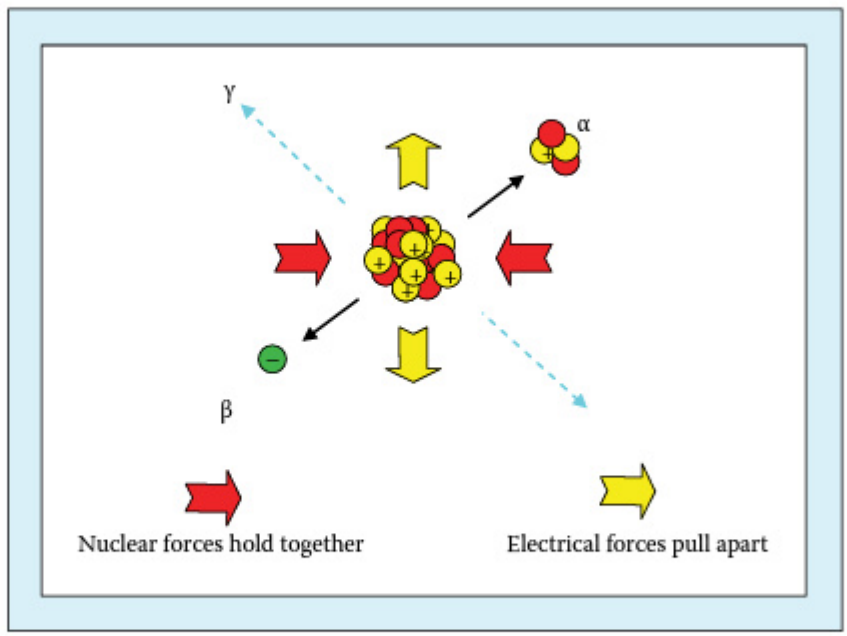

FIGURE 6.18 The force balance between the repulsive force of the protons and the attractive force of the Gluons. When the forces become temporarily imbalanced, the net result is radioactive decay.

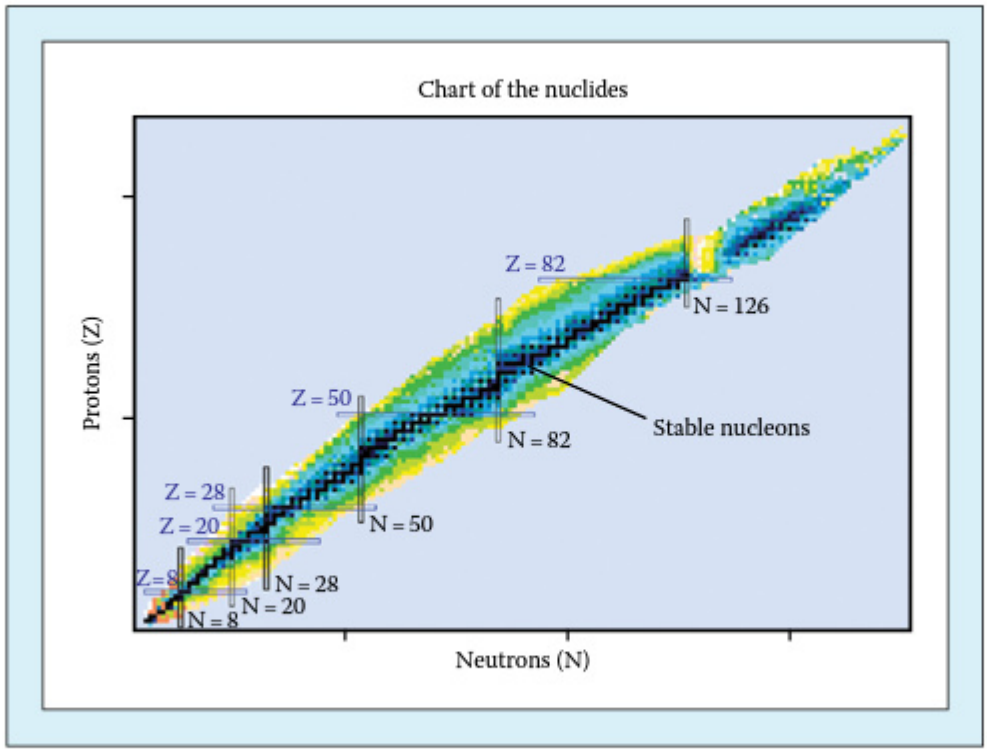

FIGURE 6.19 A *Chart of the Nuclides* from the National Nuclear Data Center (see *http://www.nndc.bnl.gov/chart/*). Interactive versions of this chart are also available at the following URLs: *http://www.nndc.bnl.gov/chart/* and also at *https://www-nds.iaea.org/relnsd/vcharthtml/VChartHTML.html*. The Chart of the Nuclides is sometimes called a *Segre chart* in honor of Italian physicist Emilio Segrè.

In other words, an isotope must have *exactly* the right combination of protons and neutrons to be stable. If it does not, the forces inside of the nucleus will tear it apart, and it will decay until exactly the correct ratio of neutrons to protons is reached. The element oxygen, which has eight protons (Z = 8), can be used to illustrate this point as well. In addition to having eight protons, oxygen has eight known isotopes—^{13}O, ^{14}O, ^{15}O, ^{16}O, ^{17}O, ^{18}O, ^{19}O, and ^{20}O—that have 5, 6, 7, 8, 9, 10, 11, and 12 neutrons, respectively. The following isotopes are unstable: the first three—^{13}O, ^{14}O, and ^{15}O (Z = 8, N = 5, 6, 7)—because they have too few neutrons and the heaviest two—^{19}O and ^{20}O (Z = 8, N = 11, 12)—because they have too many neutrons. These isotopes correspond to the orange, blue, and yellow dots on each side of the black dots shown in Figure 6.20. Only the middle three isotopes of oxygen are stable—^{16}O, ^{17}O, ^{18}O (with Z = 8 and N = 8, 9, 10)—because they have just the right number of neutrons to keep the nucleus in balance. Notice that only the three black dots in the middle (Z = 8, and N = 8, 9, 10) are physically stable, while the others decay away. Thus what is important to remember from this discussion is that the neutron-to-proton ratio (N/Z) inside of the nucleus is the major factor that determines what isotopes in nature are radioactive and what isotopes are not. One other interesting property of the nuclear force field (and radioactivity in general) is that the radioactive half-life is completely independent of what occurs outside of the nucleus as long as the effects of relativity do not come into play. The nucleus does not care whether the surrounding world is hot or cold, liquid or solid, or wet or dry—the nuclear binding forces are so strong that none of this matters. This means that the radioactive *half-life* of an isotope has almost no environmental sensitivity except when the effects of relativity come into play! To be clear, the half-life $T_{½}$ is not affected by the physical state of a material (solid, liquid, gas), its temperature, its pressure, its chemical composition, or any other outside influence. It is independent of the chemistry of the atomic surface, and independent of the ordinary physical factors of the outside world. The only two things that can alter how quickly a material will decay are a direct interaction between the nucleus and an outside particle such as a neutron or a proton, or a physical reaction where the nucleus is allowed to move at a very high speed for a very long period of time. In this case, the effects of *time dilation* due to the theory of relativity will begin to come into play (see Chapter 2), and the half-life will be increased from $T_{½}$ to

$$T'_{1/2} = \frac{T_{1/2}}{\gamma} \tag{6.27}$$

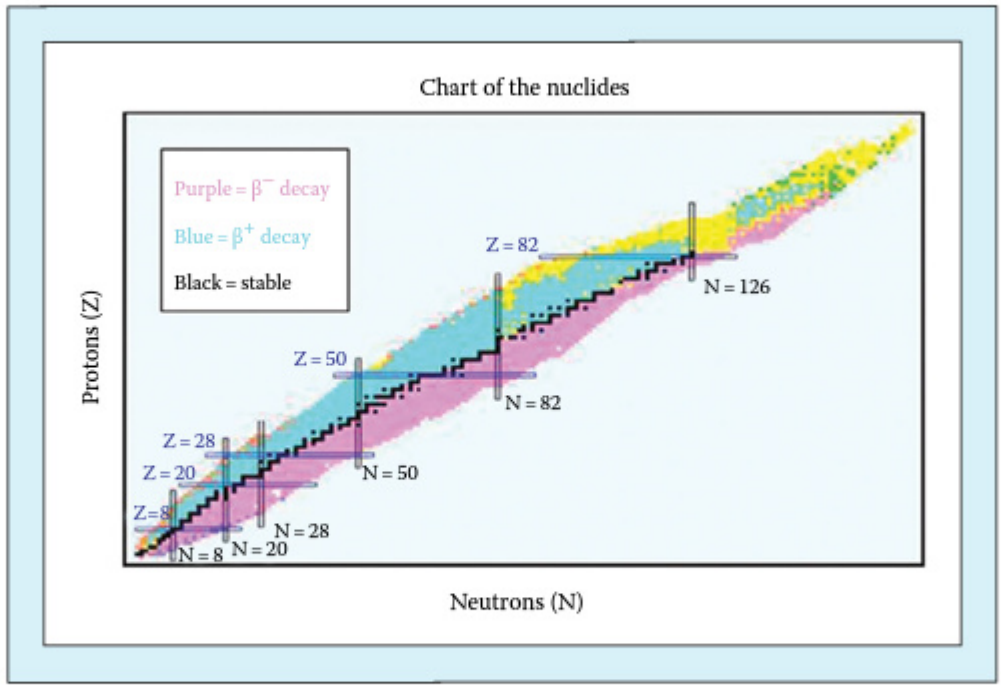

FIGURE 6.20 This Chart of the Nuclides shows which isotopes with an atomic number Z use β^- (electron) decay and which isotopes Z use β^+ (or positron) decay to achieve a stable N/Z ratio. (From http://www.nndc.bnl.gov/chart/.)

where $\gamma = \sqrt{1-(v/c)^2}$. The time dilation factor γ was discussed in Chapter 2. Since neither of these processes happens very frequently, one can usually use the radioactive half-life of an isotope to help measure and date the age of various organic and geological materials with great confidence and reliability because the decay of radioactive materials is so predictable.

6.27 Statistical Probability Distributions Associated with Radioactive Decay

The internal machinery of the nucleus is like a fine clock if its actions are viewed from a statistical point of view. A radioactive nucleus will decay in a predictable way as long as there are a large number of nuclei involved. The decay of a single nucleus cannot be predicted with any precision, but the decay pattern of a very large number of nuclei can be predicted almost exactly. When a large number of nuclei decay, their aggregate behavior is governed by what is known as a *statistical probability distribution*. We would now like to discuss some of the features of a typical statistical probability distribution. There are several types of statistical probability distributions, but radioactive materials obey what is called a *Poisson distribution* (named in honor of French mathematician *Siméon Denis Poisson*). This probability distribution is based on the fact that whatever an individual nucleus does is completely independent of what any other nucleus does. When a large number of nuclei are analyzed in this way, the entire population obeys a probability distribution of the form

The Poisson Probability Distribution

$$P(n, A) = \frac{A^n e^{-A}}{n} \tag{6.28}$$

where

A is the average number of decays per second averaged across the entire distribution
n is the number of probable outcomes or "bins" into which the distribution is divided

For example, if a sample of radioactive material is known to emit an average of 2.3 alpha particles per second for 1 million years, then the value of A is 2.3, and P(n, A) is the probability of having n alpha particles emitted in that 1-second interval, where n = 1, 2, 3, ... and so on.

For example, if we would like to know the probability that only one alpha particle will be emitted by the material per second, then we set n = 1, and A = 2.3. The result is

$$P(n, A) = \frac{A^n e^{-A}}{n!} = \frac{2.3^1 e^{-2.3}}{1!} = 0.23 = 23\% \tag{6.29}$$

So there is a 23% chance that only one alpha particle will be emitted per second. On the other hand, suppose that we would like to know the chance that two alpha particles are emitted per second. In this case, we set n = 2, and the result is

$$P(n, A) = \frac{A^n e^{-A}}{n!} = \frac{2.3^2 e^{-2.3}}{2!} = 0.265 = 26.5\% \tag{6.30}$$

So there is a 26.5% probability that two alpha particles will be emitted from the material in 1 second. A probability distribution like this with a finite number of "bins" is sometimes called a *histogram*, and the sum of the probabilities from all of the bins must always be equal to 1.0. Figure 6.21 shows the number of alpha particles emitted from the sample as well as the probability that n of them will be emitted per second. Notice that values close to the average (i.e., 2.3) have a much higher probability of occurring than values much further away from the average (say 8). Now let us see if we can repeat the same exercise again for another sample of radioactive material that emits an average of 11.5 electrons per second. We will learn later in this chapter that this can occur through the process of radioactive beta decay. In this case, we know that A = 11.5, and suppose that we calculate the probabilities for n from n = 4 to n = 20. In this case, we find that the probability distribution and the histogram look like the pictures shown in Figure 6.22. This distribution has several interesting properties. For large values of A (say A > 10), the distribution starts to look symmetric and takes on the appearance of a normal (or Gaussian) distribution with its characteristic bell-shaped curve. In fact, it can be shown that both the Poisson and *Gaussian probability distributions* are special limiting cases of another type of probability distribution called the *Binomial Distribution*. For small values of A, the distribution is asymmetric and has a *long tail* on the high side. For a large number of measurements, the uncertainty in the measurement of a nuclear property like the radioactive half-life can be shown to be equal to the width of the distribution. It can further be shown for many measurements of the decay rate that the uncertainty in the decay rate is approximately equal to the square root of the number of counts N, or σ (the uncertainty) ≈ $\sqrt{N}$. Fortunately, tabulated values for the decay rates

n	n!	2.3n	P (n, 2.3)
0	1	1.0	10.03%
1	1	2.3	23.06%
2	2	5.3	26.52%
3	6	12.2	20.33%
4	24	28	11.69%
5	120	64	5.38%
6	720	148	2.06%
7	5040	340	0.68%

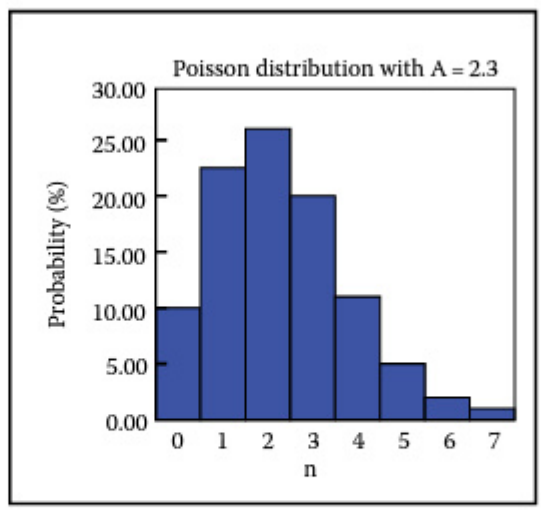

FIGURE 6.21 The emission probabilities for alpha particles emitted from a sample of radioactive material. The central peak in the probability distribution corresponds to the most probable number of particles that will be emitted. All radioactive elements obey a similar statistical distribution when it comes to the particle emission curve.

n	n!	11.5n	P (n, 11.5)
4	2.40×10^{1}	1.75×10^{4}	0.70%
5	1.20×10^{2}	2.01×10^{5}	1.70%
6	7.20×10^{2}	2.31×10^{6}	3.30%
7	5.04×10^{3}	2.66×10^{7}	5.30%
8	4.03×10^{4}	3.06×10^{8}	7.70%
9	3.63×10^{5}	3.52×10^{9}	9.80%
10	3.63×10^{6}	4.05×10^{10}	11.30%
11	3.99×10^{7}	4.65×10^{11}	11.80%
12	4.79×10^{8}	5.35×10^{12}	11.30%
13	6.23×10^{9}	6.15×10^{13}	10.00%
14	8.72×10^{10}	7.08×10^{14}	8.20%
15	1.31×10^{12}	8.14×10^{15}	6.30%
16	2.09×10^{13}	9.36×10^{16}	4.50%
17	3.56×10^{14}	1.08×10^{18}	3.10%
18	6.40×10^{15}	1.24×10^{19}	2.00%
19	1.22×10^{17}	1.42×10^{20}	1.20%

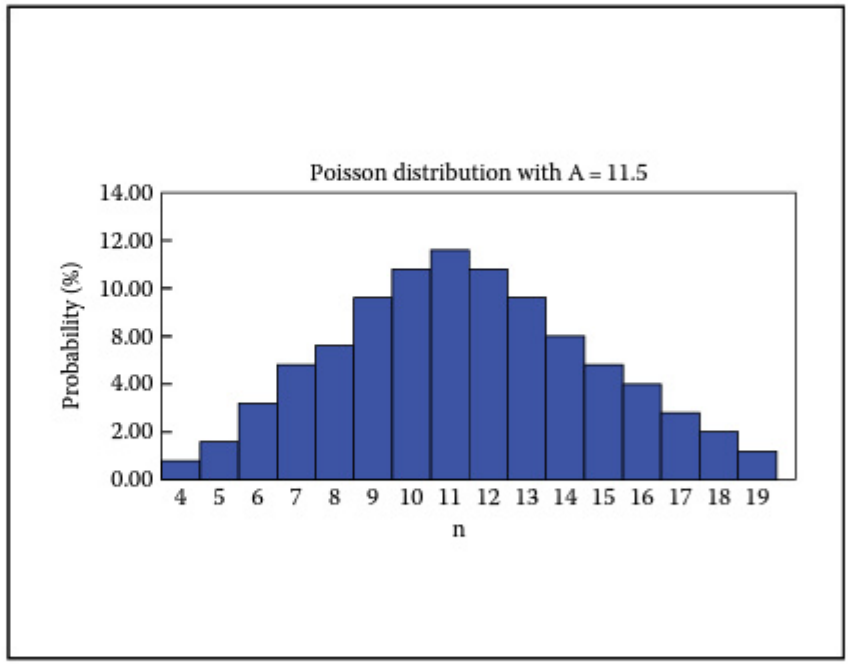

FIGURE 6.22 The emission probabilities for beta particles (electrons) emitted from a sample of radioactive material. The central peak in the probability distribution corresponds to the most probable number of particles that will be emitted. All radioactive elements obey a similar statistical distribution when it comes to the particle emission curve.

are based upon measurements involving the decay of millions and millions of particles. The value of the average decay rate A is A = nP where n is the number of atoms in a sample and P is the probability of a single atom decaying, which is determined from a very long time average of the counting rate. Therefore, the statistical error in the values of these tabulated parameters is very small. The statistical probability distributions that govern the decay rate of a radioactive material are also a direct by-product of the theory of *Quantum Mechanics*, which we also introduced in Chapter 2.

Example Problem 6.4

Suppose that a sample of radioactive material emits 10^8 alpha particles in 1 year (t = 3.16×10^7 seconds). What is the value of the decay rate A in this case, and what is the probability that only five alpha particles will be emitted from the sample per second?

Solution The value of the decay rate A is defined as the number of particles emitted in a given period of time. In this example, there are 1×10^8 particles emitted in 3.16×10^7 seconds, so there are A = $1 \times 10^8 / 3.16 \times 10^7 = 3.16$ particles emitted per second, and the probability P of five particles being emitted per second from the sample is given by

$$P(n, A) = P(5, 3.16) = 3.16^5 \, e^{-3.16}/5! = 315 \, e^{-3.16}/5! = 0.11 = 11\%$$

So there will be an average of 3.16 particles emitted per second, and there is an 11% chance that five particles will be emitted per second when we measure the decay rate. [Ans.]

6.28 Laws of Radioactive Decay

Shortly after radioactivity was discovered, people began to try to calculate the time it would take for a particular radioactive material to decay. All radioactive elements decay according to a simple, universal *exponential decay law* that we will study in great detail in this chapter, and in later sections of this book. We will even do a simple experiment to convince

you of the authenticity of this law. Mathematically speaking, an exponential decay law is one where the amount of material ΔN lost from a sample of N atoms after a period of time ΔT is proportional to the amount of material that existed before the time the decay occurred. In other words, the *fraction* of the atoms that decay is the same whether you have a pound of radioactive material or just an ounce. The decay fraction is independent of the amount of atoms in a sample. On the other hand, the *number* of atoms that decay is directly proportional to how many atoms you start with. The more atoms there are in the sample, the more atoms there are that will decay.

The constant of proportionality that expresses the relationship between the number of atoms you start with and the number of atoms that decay is called the *radioactive decay constant*. The radioactive decay constant has the units of inverse seconds (s^{-1}), or inverse time. Each element and its isotopes has a different radioactive decay constant. The radioactive decay constant is usually referred to in scientific literature by the symbol λ (lambda). The radioactive decay constant has the units of inverse seconds, or more generally, inverse time. If you are familiar with college math or calculus, you probably know that we can express the proportionality relationship between the amount of material we start with, N, and the amount of material that decays, ΔN, by a simple differential relationship of the form

An Expression for Radioactive Decay

$$\Delta N = -N\lambda\Delta t \tag{6.31}$$

where

λ is the radioactive decay constant that we previously discussed

Δt is the amount of elapsed time

This relationship can also be written as $dN = -N\lambda\, dt$. All radioactive decay is based on such a relationship. The radioactive decay constant λ for each element (and its individual isotopes) can be determined empirically with great precision. It is this precision that allows us to carbon date materials and thereby determine the age of various extinct animals, plants, and even ancient moon rocks.

6.29 Exponential Functions and Their Relationship to Radioactive Decay

As you are probably aware by now, Equation 6.31 is the differential representation of an exponential decay law. There are many examples of similar exponential laws in nature, and we would like to mention a few of them here. These laws constantly arise when dealing with very large quantities of atoms or molecules in a complex macroscopic system. For example, exponential laws seem to arise magically in the field of heat transfer and fluid flow when you try to measure the rate at which the atoms in a body of water (like your swimming pool) heat up or cool off. The temperature of many different materials, as they cool down, has also been found to follow a simple exponential relationship between the temperature of the material and the time they have cooled. Exponential decay laws also arise everywhere in the study of the science of radioactive decay. Moving N to the left-hand side of Equation 6.5 gives $dN/N = -\lambda dt$, and integrating both sides of the equation, we obtain the following exponential decay law as our final result:

The Radioactive Decay Law

$$N(t) = N_o\, e^{-\lambda t} \tag{6.32}$$

This equation says that the amount of material that decays in a given amount of time Δt is proportional to the amount of material N_o that we had to start with before the decay began, where e is the natural exponential function. If you have taken a nuclear physics, nuclear chemistry, or quantum mechanics course before, you probably know that every radioactive element has a different radioactive decay constant, or a unique rate at which it decays—and a unique value of λ. These unique values for λ are like a fingerprint or a chemical signature. They are unique for every element and isotope in the Periodic Table. If you have many different values for λ, then you will have many different types of isotopic behavior as well. The concentration as a function of the value of the decay constant is shown in Figure 6.23. Notice that as the decay constant increases, an isotope decays more quickly until it eventually disappears.

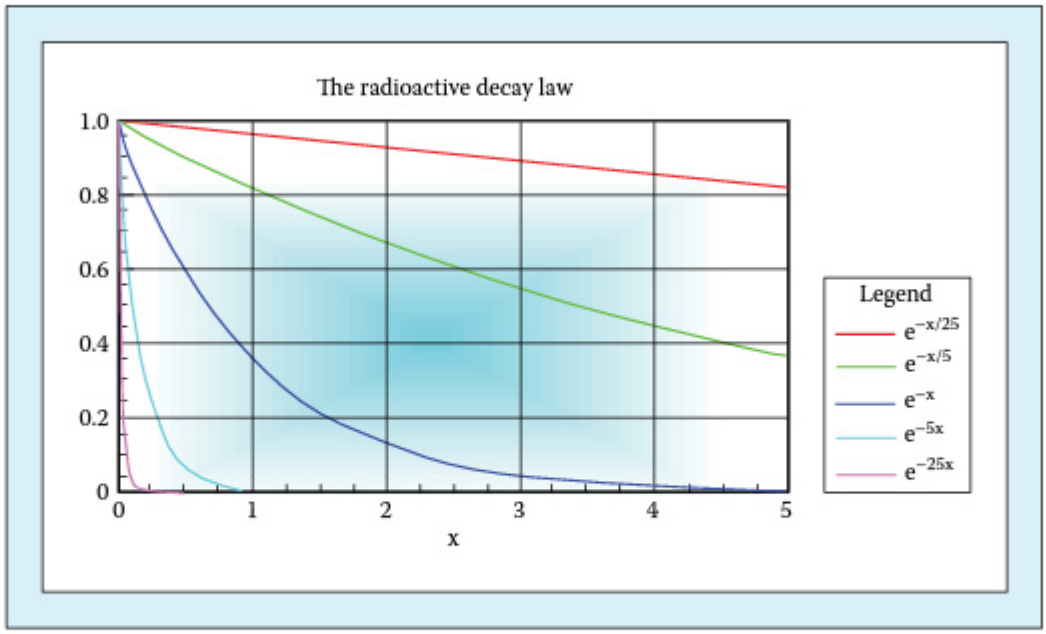

FIGURE 6.23 Some examples of an exponential decay law for different values of the decay constant λ.

6.30 Equations Governing a Sample of Several Radioactive Elements

It follows from our previous discussion that if there is a sample of material with multiple radioactive elements (say N of them) inside of it, then their individual concentrations of these elements over time will be given by

The Equations for Radioactive Decay

$$\begin{aligned} N_1(t) &= N_1(0)e^{-\lambda 1 * t} \\ N_2(t) &= N_2(0)e^{-\lambda 2 * t} \\ &\vdots \\ N_3(t) &= N_3(0)e^{-\lambda 3 * t} \\ N_4(t) &= N_4(0)e^{-\lambda 4 * t} \\ &\vdots \\ N_n(t) &= N_n(0)e^{-\lambda n * t} \end{aligned} \tag{6.33}$$

where there is a separate equation for the decay of each element. The half-lives for many common nuclear materials are shown in Table 6.14. The decay constants for these materials can then be deduced from the half-lives with the help of the equation

$$\lambda = \frac{0.693}{T_{1/2}} \tag{6.34}$$

which is derived later in the chapter. In Equation 6.34 the half-life is given the symbol $T_{1/2}$. Table 6.14 can be used to deduce the decay constants for all the isotopes of Thorium, Uranium, and Plutonium, as well as their six most common fission by-products, Cesium, Barium, Rubidium, Xenon, Krypton, and Iodine. Additional radioactive half-lives and other useful isotopic information can be found at the following URL:

http://hyperphysics.phy-astr.gsu.edu/hbase/hframe.html

If you are familiar with the process of nuclear decay, these equations and their decay constants should be very familiar to you. Each isotope, if it is not stable, has a predominant mode of radioactive decay that is indicated in column 8 by the symbols a, b−, or EC, where (a) stands for alpha decay, (b−) stands for beta decay, and (EC) stands for electron capture, which involves the emission of a photon, γ. We will have more to say about electron capture in another section.

TABLE 6.14
Radioactive Half-Lives and Other Important Properties of a Few Common Nuclear Materials

Z	A	Atomic Mass (u)	Nuclear Mass (GeV/c²)	Binding Energy (MeV)	Natural Abundance	Half-Life	Decay	Q (MeV)
				Thorium Nuclear Data				
90	227	225.027703	211.4307	1736.0	—	18.72 d	a	6.15
90	228	228.028715	212.3631	1743.0	—	1.912 y	a	5.52
90	229	225.031755	213.2975	1748.4	—	5.9 ky	a	5.17
90	230	230.033128	214.2302	1755.2	—	75.4 ky	a	4.77
90	231	231.036298	215.1647	1760.3	—	35.2 h	b−	0.39
90	232	232.038051	216.0978	1766.7	1.00	1.4×10^{10} y	a	4.08
90	234	234.043593	215.9660	1775.7	—	24.10 d	b−	0.27
				Uranium Nuclear Data				
92	226	226.029170	210.4995	1725.0	—	0.5 s	a	5.56
92	231	231.036270	215.1636	1758.7	—	4.2 d	EC	0.36
92	232	232.037130	216.0959	1766.0	—	68.9 d	a	5.41
92	233	233.039628	215.0298	1771.8	—	0.159 My	a	4.91
92	234	234.040947	215.9625	1778.6	5.5×10^{-5}	0.245 My	a	4.86
92	235	235.043924	218.8968	1783.9	0.0072	0.704 Gy	a	4.68
92	236	236.045563	215.8298	1790.4	—	23.4 My	a	4.57
92	238	238.050785	221.6977	1801.7	0.99275	4.46 Gy	a	4.27
92	239	235.054290	222.6324	1806.5	—	23.54 m	b−	1.26
				Plutonium Nuclear Data				
94	239	235.052158	222.6294	1806.9	—	24.11 ky	b−	5.24
94	242	242.058737	225.4301	1825.0	—	0.376 My	a	4.98
94	244	244.064198	225.2982	1836.1	—	82 My	a	4.67
				Cesium Nuclear Data				
55	133	132.905429	123.7735	1118.6	1.00	Stable	—	—
55	135	134.905885	125.6369	1134.3	—	2.3 My	b−	0.21
55	137	136.907074	125.5011	1145.3	—	30.17 y	b−	1.17
				Barium Nuclear Data				
56	130	125.906281	120.9793	1092.8	0.00106	Stable	—	—
56	132	131.905043	122.8411	1110.1	0.00101	Stable	—	—
56	133	132.905988	123.7735	1115.3	—	10.53 y	EC	0.52
56	134	133.904485	124.7036	1126.7	0.02417	Stable	—	—
56	135	134.905665	125.6362	1133.7	0.06592	Stable	—	—
56	136	135.904553	126.5667	1142.8	0.07854	Stable	—	—
56	137	136.905812	125.4994	1145.7	0.1123	Stable	—	—
56	138	135.905233	128.4303	1158.3	0.717	Stable	—	—
56	140	135.910581	130.2983	1165.5	—	12.76 d	b−	1.03
56	142	141.916361	132.1667	1180.2	—	10.7 m	b−	2.13
56	143	142.920483	133.1020	1184.5	—	15 s	b−	4.2
56	144	143.922845	134.0357	1190.3	—	11.5 s	b−	3.0
				Rubidium Nuclear Data				
37	83	82.915143	75.2167	720.03	—	86.2 d	EC	0.96
37	85	84.911794	75.0766	735.29	0.72165	Stable	—	—
37	87	86.909187	80.9371	755.86	0.27835	Stable	—	—
				Xenon Nuclear Data				
54	124	123.905894	115.3909	1046.3	0.001	Stable	—	—
54	126	125.904281	115.2524	1063.9	0.0009	Stable	—	—

(*Continued*)

TABLE 6.14 (*Continued*)
Radioactive Half-Lives and Other Important Properties of a Few Common Nuclear Materials

Z	A	Atomic Mass (u)	Nuclear Mass (GeV/c²)	Binding Energy (MeV)	Natural Abundance	Half-Life	Decay	Q (MeV)
54	127	126.905182	118.1848	1071.0	—	36.2 d	EC	0.66
54	128	125.903531	115.1147	1080.8	0.0191	Stable	—	—
54	129	128.904780	120.0474	1085.7	0.264	Stable	—	—
54	130	125.903509	120.9777	1096.9	0.041	Stable	—	—
54	131	130.905072	121.9107	1103.5	0.212	Stable	—	—
54	132	131.904144	122.8413	1112.5	0.269	Stable	—	—
54	133	132.905889	123.7745	1118.9	—	5.25 d	b–	0.43
54	134	133.905395	124.7055	1125.5	0.104	Stable	—	—
54	136	135.907213	126.5702	1141.9	0.089	Stable	—	—
				Krypton Nuclear Data				
36	78	75.920396	72.5646	675.56	0.0035	Stable	—	—
36	80	75.916380	74.4238	695.44	0.0225	Stable	—	—
36	81	80.916590	75.3555	703.32	—	0.21 My	EC	0.28
36	82	81.913483	76.2841	714.28	0.116	Stable	—	—
36	83	82.914135	75.2163	721.75	0.115	Stable	—	—
36	84	83.911507	78.1453	732.27	0.57	Stable	—	—
36	85	84.912532	75.0778	735.38	—	10.72 y	b–	0.69
36	86	85.910615	80.0075	745.24	0.173	Stable	—	—
36	90	85.919528	83.7418	773.23	—	32.3 s	b–	4.39
36	92	91.926270	85.6111	783.09	—	1.84 s	b–	6.06
				Iodine Nuclear Data				
53	125	124.904620	116.3218	1056.3	—	55.9 d	b–	0.18
53	127	126.904473	118.1846	1072.6	1.00	Stable	—	—
53	129	128.904986	120.0481	1088.3	—	17 My	b–	0.19

Table 6.14 shows that the average amount of kinetic energy Q released from the alpha decay of Thorium, Uranium, and Plutonium can vary from about 4 MeV to about 8 MeV, depending on the isotope involved, and that the average amount of kinetic energy Q released in the beta decay of the smaller and lighter radioactive by-products is 1–2 MeV, although the actual amounts can vary from about 0.2 MeV to about 6 MeV. This table shows very clearly that the *heavier elements prefer to decay through alpha emission, whereas the lighter and intermediate elements prefer to decay by emitting an electron*.

6.31 Measuring the Radioactive Decay Rate

Sometimes it is important to know how many alpha or beta particles a radioactive element emits in a given period of time. We can find this by simply taking the isotopic concentration N in atoms per cm³ and multiplying this by the decay constant λ for the isotope in question. For example, to find the number of alpha particles emitted by Polonium-218 per second, we would take the number of polonium-218 atoms, N^{Po-218}, and multiply this number by λ^{Po-218} to determine the decay rate

$$R = \lambda^{Po-218} N^{Po-218} \tag{6.35}$$

where R is the decay rate in particles emitted per cm³ per second. Notice that we can apply this logic to any isotope in a radioactive decay chain if we know the isotopic composition N. For example, if we know the initial concentrations for two materials X and Y, where X is the parent material and Y is the daughter, then the concentrations of these materials at any time t will be given by

$$X(t) = X_o\, e^{-\lambda_x t} \tag{6.36}$$

$$Y(t) = Y_o\, e^{-\lambda_y t} + X_o\, \lambda_x \Big/ (\lambda_x - \lambda_y)\left(e^{-\lambda_y t} - e^{-\lambda_x t}\right) \tag{6.37}$$

and the corresponding decay rates that would measure with a piece of test equipment would be

$$R_x(t) = \lambda_x\, X_o\, e^{-\lambda_x t} \tag{6.38}$$

$$R_y(t) = \lambda_y \left[Y_o\, e^{-\lambda_y t} + X_o\, \lambda_x \Big/ (\lambda_x - \lambda_y)\left(e^{-\lambda_y t} - e^{-\lambda_x t}\right) \right] \tag{6.39}$$

Now let us assume that the parent element X is an alpha emitter and the daughter element Y is a beta emitter. Then the rate of alpha decay that we would measure would be

$$R_\alpha(t) = \lambda_x X_o\, e^{-\lambda_x t} \tag{6.40}$$

and the rate of beta decay that we would measure would be

$$R_\beta(t) = \lambda_y \left[Y_o\, e^{-\lambda_y t} + X_o\, \lambda_x \Big/ (\lambda_x - \lambda_y)\left(e^{-\lambda_y t} - e^{-\lambda_x t}\right) \right] \tag{6.41}$$

We can illustrate the use of these equations with the following example.

Example Problem 6.5

Suppose that a sample of radioactive material consists of two isotopes that we will call X and Y. The number of atoms of isotope X in 1 cm^3 of the material is 1×10^{22} atoms/cm^3, and the number of atoms of isotope Y in one cubic centimeter of the same material is 2×10^{22} atoms/cm^3. Let us further assume that isotope X is the parent isotope and isotope Y is the daughter isotope. If isotope X is an alpha emitter with a decay constant of 1×10^{-6} per second, and isotope is a beta emitter with a decay constant of 5×10^{-7} per second, how many alpha particles and beta particles per second will 10 cm^3 of this material emit after a period of 1 year ($t = 3.16 \times 10^7$ seconds)?

Solution In this case, the equations of Section 6.31 apply. The rate of alpha decay is given by

$$R^\alpha(t) = \lambda_x X_o e^{-\lambda_x t}$$

and the rate of beta decay is given by

$$R^\beta(t) = \lambda_y \left[Y_o\, e^{-\lambda_y t} + X_o \lambda_x \Big/ (\lambda_x - \lambda_y)\left(e^{-\lambda_y t} - e^{-\lambda_x t}\right) \right]$$

Now when $t = 3.16 \times 10^7$ seconds, $R^\alpha(t) = \lambda_x\, X_o\, e^{-\lambda_x t} = 1 \times 10^{-6} \times 1 \times 10^{22} \times e^{-31.6} = 1 \times 10^{16} \times 1.89 \times 10^{-14} = 189$ alpha decays/cm^3/s and $R^\beta(t) = \lambda_y\, [Y_o\, e^{-\lambda_y t} + X_o\, \lambda_x/(\lambda_x - \lambda_y)\, (e^{-\lambda_y t} - e^{-\lambda_x t})] = 5 \times 10^{-7}\, [2 \times 10^{22}\, e^{-15.8} + 1 \times 10^{22} \times 1 \times 10^{-6} \times /(1 \times 10^{-6} - 5 \times 10^{-7})\, (e^{-15.8} - e^{-31.6})] = 5 \times 10^{-7}\, [2 \times 10^{22} \times 1.37 \times 10^{-7} + (1 \times 10^{16}/5 \times 10^{-7})(1.37 \times 10^{-7} - 1.89 \times 10^{-14}) = 5 \times 10^{-7} \times [2.74 \times 10^{15} + 2 \times 10^{10} \times 1.37 \times 10^{-7}] = 1.38 \times 10^7$ beta decays/cm^3/s. Since these are the number of alpha and beta particles emitted per second from 1 cm^3 of the material after 1 year, 10 cm^3 of the material will emit $R^\alpha(t) \times 10 = 1890$ alpha particles per second and $R^\beta(t) \times 10 = 1.38 \times 10^8$ beta particles per second. [Ans.]

Sometimes the quantities $R_x(t)$ and $R_y(t)$ that we have defined here are called the *radioactive activities* of the sample. The number of decays per second, or the *activity* of a sample of radioactive material, is currently measured in the units of *Becquerel* (Bq), after *Henri Becquerel*, who originally invented the term. In these units, one decay per second is equal to one Becquerel. An older unit for measuring the radioactive activity of a sample is the *Curie*, named after Pierre and Marie Curie. One curie is approximately the activity of 1 g of radium and equals exactly 3.7×10^{10} Becquerel, or 3.7×10^{10} decays per second. When the activity of a material is measured in this way, it is never dependent on the type of radioactive decay (alpha, beta, or gamma), but only on the total number of particles (alpha + beta + gamma) emitted from the sample per second. In some textbooks, the activities $R_x(t)$ and $R_y(t)$ are also written as $A_x(t)$ and $A_y(t)$. We will use these two notations interchangeably as we proceed further into this book.

6.32 Extensions to Radioactive Materials That Can Both Multiply and Decay

Sometimes a nuclear reactor will produce a radioactive material at a rate P that is determined by the concentration of the neutrons in the core as a whole. If the material that is produced also decays, the time-dependent concentration of the material will be given by

$$\frac{dC}{dt} = \text{Production rate} - \text{Destruction rate} \tag{6.42}$$

$$\Rightarrow \frac{dC}{dt} = P - \lambda C \tag{6.43}$$

where C is the material concentration. If the production rate P in atoms per second is known, this equation can be easily integrated to give

$$C(t) = C_o e^{-\lambda t} + \left(\frac{P}{\lambda}\right)\left(1 - e^{-\lambda t}\right) \tag{6.44}$$

where C_o is the initial concentration of radioactive atoms at t = 0. Every isotope that is produced directly by the fission of a uranium or plutonium nucleus will build up and decay according to this equation for C. This equation can also be used to find the equilibrium concentration of an isotope that is produced in this way. Notice that the time-dependent terms will eventually decay to 0 as $t \rightarrow \infty$. *When this happens, C will approach an equilibrium value of C = (P/λ).* This is the largest possible value of C that can be achieved when equilibrium is reached. Many isotopes that are produced by the process of nuclear fission behave in this way. The rate at which the maximum value (P/λ) is reached depends on only the production rate P and the size of the radioactive decay constant λ. However, the decay constant for a specific isotope is usually fixed, so the equilibrium concentration C_∞ in practice depends on only the production rate P. *The isotopes of Xenon and Samarium are classic examples of nuclides that behave in this way.* Notice that any isotope that obeys this equation will eventually reach an equilibrium concentration $C_\infty = (P/\lambda)$. The amount of time required to reach equilibrium is only a function of the decay constant λ. For a typical power reactor, the most important isotope of Xenon (Xe-135) will reach this equilibrium concentration in about 40 hours after startup, while the most important isotope of Samarium (Sm-149) will reach this concentration in about 300 hours (12½ days). The rate of reduction of the exponential decay term $e^{-\lambda t}$ is responsible for the behavior that is ultimately observed.

6.33 Time-Dependent Activity of a Radioactive Material

When a radioactive material decays, the rate R at which the atoms decay is given by

$$R(t) = \lambda C(t) \tag{6.45}$$

where

C(t) is the number of atoms that have not yet decayed
λ is the radioactive decay constant

Therefore, the value of R(t) is always measured in disintegrations per unit of elapsed time. This rate of decay R is sometimes called the *activity* of the material, and the activity at a particular time t is given by

The Equation for the Activity of a Radioactive Material

$$\text{Activity} = R(t) = \lambda C(t) \quad \text{(in disintegrations per second)} \tag{6.46}$$

As mentioned previously, the primary unit of the activity has historically been the *Curie*, where *1 curie, given by the symbol Ci, is defined as 3.7×10^{10} disintegrations per second.* Other measures of the activity include the millicurie (mCi), which is equal to 10^{-3} curies; the microcurie (μCi), which is equal to 10^{-6} curies; and the picocurie (pCi), which is equal to 10^{-12} curies. In modern times, the curie has been replaced by another unit of the activity called the *Becquerel*, or Bq, which is defined in the SI unit system as exactly equal to one disintegration per second.

1 curie = 1 Ci = 3.7×10^{10} disintegrations per second

1 Becquerel = 1 Bq = 1 disintegration per second

In other words, 1 Bq = 2.703×10^{-11} Ci ≈ 27 pCi. It also follows from our previous discussion that the time-dependent activity of a sample of radioactive material must be given by

$$R(t) = \lambda C(t) = \lambda C_o e^{-\lambda t} + P\left(1 - e^{-\lambda t}\right) \tag{6.47}$$

where P is the production rate. This latter equation is very helpful because it can be used to determine the activity of a radioactive material as a function of time. The example below helps to illustrate when this can be a useful thing.

Example Problem 6.6

Suppose that an unstable radioactive isotope U with a half-life of 100 hours can be produced by bombarding a stable isotope S with neutrons in a reactor core. Suppose that a foil containing 1 g of the stable isotope is placed in a reactor for 10 hours, and at the end of this period, its activity is 1 curie. What is the average life of this material, and what is its radioactive decay constant? What will its maximum theoretical activity be at the end of the 10-hour period? How long will it take to achieve 70% of this value?

Solution Its average life τ is equal to its half-life divided by 0.693, so τ = 144 hours, and its radioactive decay constant is $\lambda = 1/\tau = 0.00693\ h^{-1}$. Since $U_o = 0$, its time-dependent activity is given by Equation 6.47: $R(t) = \lambda U(t) = P(1 - e^{-\lambda t})$, where P is the production rate. Since R = 1 Ci and $\lambda = 0.00693\ h^{-1}$, $P = 1/(1 - e^{-0.00693 \cdot 10}) = 14.9$ curies. It will achieve 75% of its maximum value when the following equation is satisfied: $0.75P = P(1 - e^{-\lambda t})$. Solving this equation for t gives $t = \ln(0.25)/\lambda = 200$ hours. [Ans.]

6.34 Half-Life of a Radioactive Material

If you have ever worked in the nuclear power industry, you have probably heard of the "half-life" of a radioactive material. The "*half-life*" of a radioactive isotope is the amount of time required for exactly *half* of the original quantity of the isotope to decay. The half-life of a particular element, compound, or isotope can be easily found from Equation 6.32 by setting dN/N equal to one half, and solving for dt. If you do this, you will find that each element with a separate decay constant has a different half-life associated with it. Notice that the radioactive decay law (Equation 6.32) says nothing about the types of particles that a radioactive material can emit. It simply states that the material must emit *some* particles that we can measure or detect. When the radioactive decay chain becomes very long and complex, the activities are given by a general solution to the *Bateman equations*, which is specifically

$$A_i(t) = \lambda_i N_i(t) = N_1(0) \cdot \lambda_i \sum_{i=1,n} C_i e^{-\lambda i t} \tag{6.48}$$

where

n is the total number of isotopes in the decay chain

the coefficients C_i are given by

$$C_i = \lambda_1 \lambda_2 \lambda_3 \ldots \lambda_{i-1} / (\lambda_1 - \lambda_m)(\lambda_2 - \lambda_m) \ldots (\lambda_i - \lambda_m) \quad \text{when } m \neq i \tag{6.49}$$

The half-lives of several common elements used in the design and operation of a fission reactor are shown in Table 6.15. Today, the half-lives of all common radioactive elements and compounds have been measured with great precision, and they can be used for many purposes, including the carbon dating of objects such as dinosaur DNA and samples of ancient

TABLE 6.15
Radioactive Half-Lives of Common Nuclear Materials

Element	Z	A	Natural Abundance	Half-Life	Decay Mode
Thorium-232	90	232	1.00	1.4×10^{10} y	Alpha
Uranium-233	92	233	5.5×10^{-5}	0.159 My	Alpha
Uranium-235	92	235	0.0072	0.704 Gy	Alpha
Uranium-238	92	238	0.99275	4.46 Gy	Alpha
Plutonium-239	94	239	Man made	24.11 Ky	Beta

types of rocks, meteorites, plants, and bacteria. You can see from Table 6.14 that some radioactive by-products of the process of nuclear fission decay rather quickly, while others, which are at the end of the decay chains (like Lead), have half-lives of many *trillions* of years and are, for all purposes, completely stable. The Bateman equations are discussed in more detail in our companion book.*

Example Problem 6.7

A sample of radioactive material is found to emit 3.6×10^{12} particles per hour. What is the activity of this sample in Becquerels and Curies?

Solution There are 3600 seconds in 1 minute, so the number of particles emitted per second is $R(t) = 3.6 \times 10^{12}/3.6 \times 10^{2} = 1 \times 10^{10}$ particles per second. This is the activity of the sample in Becquerels. Since one Becquerel is the same as one particle emitted per second, the activity of the sample in curies is $1 \times 10^{10}/3.7 \times 10^{10} = 0.27$ curies. [Ans.]

6.35 Half-Lives, Average Lives, Decay Constants, and Doubling Times

As we saw in a previous section, the *half-life* of a radioactive isotope is the time required for exactly half the atoms to decay away. That is, if N_o is the number of the atoms of the isotope at time $t = 0$, then the half-life $T_{½}$ is defined by the relationship

$$N(t) = N_o 2^{-t/T_{1/2}} \tag{6.50}$$

so that when $t = T_{½}$

$$N(T_{½}) = N_o 2^{-1} = \frac{N_o}{2} \tag{6.51}$$

This relationship is based on writing the number of atoms present at any time t as a power of 2. It also defines the doubling time t_d as the time required for the concentration of a material (such as an isotope) to double, so that when $\mathbf{N = N_0 \times 2}$

$$2N_o = N_o 2^{Rt} \tag{6.52}$$

or after some cancellation of terms,

$$2^{Rt} = 2 \tag{6.53}$$

Taking the log of both sides to the base 2 gives

$$Rt = \log_2 2 = 0.693 \tag{6.54}$$

so the formula for the *doubling time*, t_d, is

A Formula for the Doubling Time

$$t_d = \frac{0.693}{R} \tag{6.55}$$

where R is the growth rate (which can be measured in seconds, minutes, or years). For example, if the growth rate of the world's population R is 2% per year, then the population will double in 0.693/0.02 = 34.5 years. Similarly, if the supply of depleted uranium increases at an average rate of 5% per year, then it will take about .693/.05 = 13.8 years for the supply of depleted uranium to double. You can also use this same equation to calculate how quickly an investment in a certificate of deposit will enable you to double your money if you know, for example, what the interest rate R is that the CD is paying. All these calculations have been based on the assumption of representing the behavior of a variable, such as the half-life, as a function of the number 2, for example, 2^n. However, most natural processes, such as radioactivity, are

* See *Nuclear Engineering Fundamentals: A Practical Perspective*, by R.E. Masterson, CRC Press (2017).

much more easily expressed as a power of the exponential function e, where e = 2.71828. We could therefore have just as easily written the doubling time as

$$2N_o = N_o\, e^{Rt} \quad \text{or} \quad e^{Rt} = 2 \tag{6.56}$$

Taking the natural logarithm (ln) of both sides, we would obtain

$$Rt = \ln 2 = 0.693 \tag{6.57}$$

so that t = 0.693/R. This is identical to the result we obtained previously (see Equation 6.55). Irrespective of the way in which we choose to represent variables like the half-life and the doubling time mathematically, it is important to be able to convert between one mathematical representation and the other. In our study of radioactivity, a number of frequently used variables such as the *radioactive half-life*, $T_{½}$, the *radioactive decay constant* λ, and the *average lifetime* of an element, τ, are often discussed interchangeably. It is therefore necessary to have a convenient way to convert from one representation to another. These three important variables are related to one another through the following equalities, where N is the population of a particle, compound, or isotope at time t, and N_o is the initial population at time = 0. It is always important to keep these equalities in mind when talking about radioactive decay. According to Equation 6.52, we can *define* the radioactive decay constant λ as $\lambda = 0.693/T_{½}$ where $T_{½}$ is the half-life of a radioactive material, and similarly, *we can define the average lifetime of a radioactive material τ as*

The Definition of the Average Life

$$\tau = \frac{T_{½}}{0.693} \tag{6.58}$$

where $T_{½}$ is again the half-life. Hence the average life of a radioactive material is always *longer* than the half-life. In particular, *it is a factor of (1/0.693) = longer*. Hence in conclusion, the half-life, the decay constant, and the average life are related to each other by the equation

Relating the Half-Life, the Average Life, and the Decay Constant

$$T_{½} = 0.693\tau = 0.693/\lambda \tag{6.59}$$

These definitions apply to *any* radioactive phenomena, irrespective of whether we are considering protons, neutrons, electrons, fission fragments, or alpha particles, where we must always remember that 0.693 = ln (2). Only the values of the half-lives, the average lives, and the decay constants will change from one particle type or isotope to the next. *Notice that the average life τ is always larger than the half-life T½, and this is due physically to the fact that the time-dependent concentration of a radioactive material has a very long tail* (refer again to Figure 6.23). Moreover, if the half-life of the material is known, the average life τ is always 1/0.693 or 1.443 times longer than the half-life. Thus if the half-life happens to be 1 million years, the average life of the same material will be 1.443 million years. *These relationships do not depend on the value of the radioactive decay constant λ because λ is defined as λ = 1/τ*.

The Relationship between λ and τ

$$\lambda = \frac{1}{\tau} \tag{6.60}$$

Consequently, when we later discuss the behavior of a time-dependent reactor (see Chapter 15), the time-dependent power level P(t) may also be written as

$$P(t) = P_o\, e^{\lambda t} = P_o\, e^{t/\tau} \tag{6.61}$$

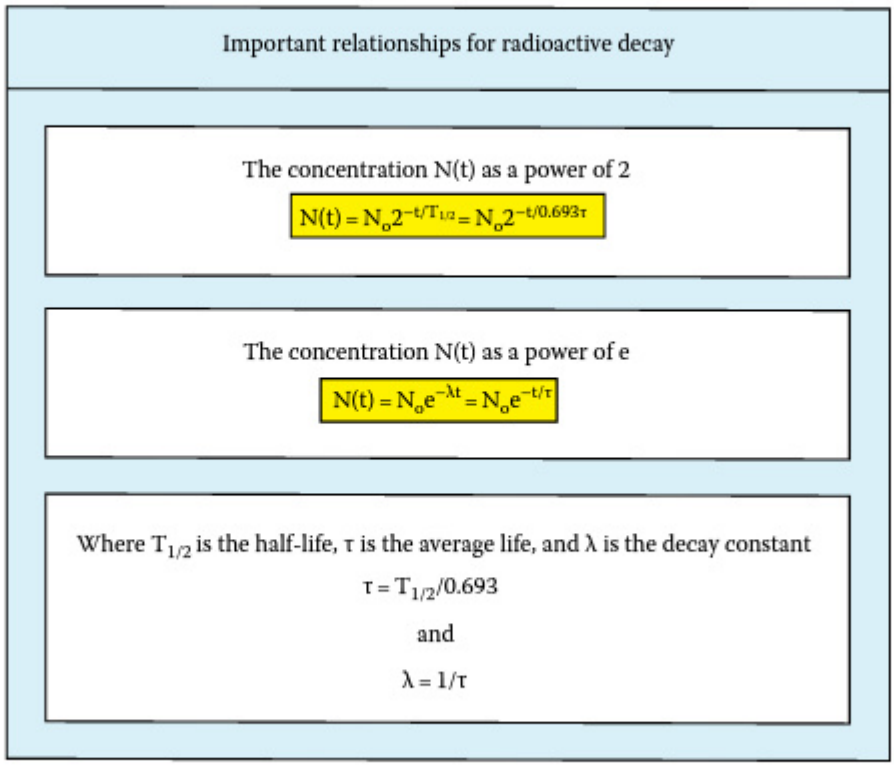
Important relationships for radioactive decay
The concentration N(t) as a power of 2
$N(t) = N_o 2^{-t/T_{1/2}} = N_o 2^{-t/0.693\tau}$
The concentration N(t) as a power of e
$N(t) = N_o e^{-\lambda t} = N_o e^{-t/\tau}$
Where $T_{1/2}$ is the half-life, τ is the average life, and λ is the decay constant
$\tau = T_{1/2}/0.693$
and
$\lambda = 1/\tau$

FIGURE 6.24 A summary of the relationships between some of the important parameters that can be found in the theory of radioactive decay.

where the value of τ is now known as the *reactor period*. Thus the reactor period τ is now defined as the amount of time required for the reactor power level to increase or decrease by a factor of e or 2.71828.

The value of τ is also very important when it comes to the study of *reactor kinetics* where the power level may change in a more complex way. Some of the important relationships we have just derived are shown in Figure 6.24. Notice that the half-life, the average life, and the radioactive decay constant λ are all related to each other in a simple way. Furthermore, if the initial concentration of a radioactive material is given by N_o, the final concentrations can be deduced from the equations presented in Figure 6.24. We will have occasion to use these equations in many different ways as we proceed further into the text.

Example Problem 6.8

Using your knowledge of first derivatives, show that when the concentration of a nuclear material C obeys an equation of the form $dC/dt = P - \lambda C$, where P is the production rate, the equilibrium concentration is given by C (equilibrium) = λ/P.

Solution Equilibrium is reached when the concentration C of a material no longer changes as a function of time. In this equation, equilibrium is achieved when $dC/dt = 0$. We then have $0 = P - \lambda C$, which then implies that C (equilibrium) = λ/P. [Ans.]

6.36 Understanding the Equations of Secular Equilibrium

Earlier in the chapter, we mentioned that some naturally occurring materials have very long and complex decay chains. One of the best known examples of a material like this is U-238, which has a half-life of 4.46 billion years (or about the age of the Earth itself). When a parent element like U-238 is very long lived compared to some of its daughters, then it is possible to infer the half-life of the parent from the behavior of the daughters. To illustrate this point, consider a very general radioactive decay chain of the form

$$N_1 \xrightarrow{\lambda_1} N_2 \xrightarrow{\lambda_2} N_3 \xrightarrow{\lambda_3} \cdots N_i \xrightarrow{\lambda_i} \cdots \xrightarrow{\lambda_{n-1}} N_n \quad (\text{stable}) \tag{6.62}$$

The time-dependent concentrations of the isotopes in this decay chain can be found from the equations

The Time-Dependent Concentrations in a General Radioactive Decay Chain

$$\begin{aligned}
\frac{dN_1(t)}{dt} &= -\lambda_1 N_1(t) \quad \text{(Parent)} \\
\frac{dN_2(t)}{dt} &= \lambda_1 N_1(t) - \lambda_2 N_2(t) \\
\frac{dN_3(t)}{dt} &= \lambda_2 N_2(t) - \lambda_3 N_3(t) \\
&\vdots \qquad\qquad \vdots \\
\frac{dN_{n-1}(t)}{dt} &= \lambda_{n-2} N_{n-2}(t) - \lambda_{n-1} N_{n-1}(t) \\
\frac{dN_n(t)}{dt} &= \lambda_{n-1} N_{n-1}(t) \quad \text{(Final daughter—stable)}
\end{aligned} \tag{6.63}$$

which were introduced to the reader in a previous section. However, if the parent isotope in the decay chain (N_1) is very stable, and does not decay appreciably over time, then the daughter elements can decay away no faster than they are produced by the decay of the parent. This implies that eventually all of the daughter elements will be produced and will decay at a constant rate, which can be correlated to the overall activity of the sample. Then one can set $dN_1/dt \approx 0$, $dN_2/dt \approx 0$, $dN_3/dt \approx 0$, etc., and a condition of *pseudo equilibrium* is reached for each successive daughter isotope in the decay chain. This condition of equilibrium is often referred to as *secular equilibrium*. In this case, the equations of secular equilibrium are

The Equations of Secular Equilibrium

$$\lambda_1 N_1 = \lambda_2 N_2 = \lambda_3 N_3 = \cdots = \lambda_n N_n \tag{6.64}$$

and it also follows that

The Activities of the Isotopes When Secular Equilibrium is Reached

$$A_1 = A_2 = A_3 = \cdots = A_n \tag{6.65}$$

In other words, *when secular equilibrium is reached in a long radioactive decay chain, each member of the decay chain has exactly the same activity!* We can use this fact to determine the decay constants for some of the longest-lived radionuclides. For example, suppose that we recover a sample of radioactive material from the moon where the ratio of the number to U-238 atoms to the number of Radium-226 atoms is 2.3×10^6 to one. Since Radium-226 is part of the U-238 decay chain, the half-lives of these two isotopes are related by

$$\lambda_{226} N_{226} = \lambda_{238} N_{238} \tag{6.66}$$

Since $\lambda = 0.693/T_{½}$, it also follows that

$$T_{238} = T_{226} \cdot (N_{238}/N_{226}) \tag{6.67}$$

Now the half-life of Radium-226 is 1620 years. Then the half-life of U-238 must be

$$T_{238} = 1620 \text{ years} \cdot 2.3 \times 10^6 = 4.5 \times 10^9 \text{ years}$$

The half-lives of other long-lived radioactive materials can be found in this way. For example, the exercise below illustrates how it is possible to determine the half-life of U-235 from one of the other radioisotopes in its decay chain. For this method to work, the half-lives of the daughter elements must be much shorter than the half-life of the parent. One other important point to keep in mind is that the activities $A_1 = A_2 = A_3 = \cdots = A_n$ described by Equation 6.65 *do not necessarily involve the same nuclear particles in each case*. For example, activities A_1, A_3, and A_4 may be the activities we measure

for alpha rays, while activities A_2, A_5, and A_6 may be the activities we measure for beta rays. The *type of activity* is determined by the individual radioisotope in the decay chain. *A state of secular equilibrium only guarantees that the overall activity and not the type of activity is the same.*

Example Problem 6.9

The half-life of Actinium-227, which is a key component of the U-235 decay chain, is known to be 21.78 years. Suppose that there are 3.23×10^7 atoms of U-235 to each atom of Actinium-227 in a sample of radioactive material that is recovered from the ocean floor. What is the projected half-life of U-235 using the atomic ratios in this sample?

Solution The half-life of U-235 can be found from the equation $T_{235} = T_{227} \cdot (N_{235}/N_{227})$. Plugging in the appropriate numbers, we find that $T_{235} = 21.78 \text{ years} \cdot 3.23 \times 10^7 = 7.04 \times 10^8$ years. [Ans.]

6.37 A Stable Daughter and a Radioactive Parent

Sometimes the opposite situation can occur where the daughter element in a decay chain is much more stable than the parent. When there are only two elements in a decay chain, the equations that have to be solved are

$$\frac{dN_1(t)}{dt} = -\lambda_1 N_1(t) \quad \text{(Parent)} \tag{6.68}$$

$$\frac{dN2(t)}{dt} = \lambda_1 N_1(t) - \lambda_2 N_2(t) \quad \text{(Final Daughter—Stable)} \tag{6.69}$$

If the daughter is very stable, then $\lambda_2 \to 0$, and these differential equations become

$$\frac{dN_1(t)}{dt} = -\lambda_1 N_1(t) \quad \text{(Parent)} \tag{6.70}$$

$$\frac{dN_2(t)}{dt} = \lambda_1 N_1(t) \quad \text{(Final Daughter—Stable)} \tag{6.71}$$

The concentration of the daughter element is therefore

$$N_2(t) = N_2(0) + N_1(0)\ (1 - e^{-\lambda_1 t}) \tag{6.72}$$

This result can also be obtained from the Bateman equations by setting $\lambda_2 = 0$. So in this case, the half-life of the daughter $T_{2½}$ is much larger than the half-life of the parent $T_{1½}$. ($T_{2½} \gg T_{1½}$).

6.38 Isotopic Stability and the Periodic Table

Nuclear energy production, and for that matter all of nuclear science and engineering, is based on the isotopic stability of the elements in the Periodic Table. Because of the fact that force imbalances can exist inside of the nucleus (see Section 6.4), the stability of the nucleus decreases as its atomic number increases (see Section 6.5), and at some point, the repulsive forces between the protons become strong enough that the nucleus can no longer remain stable under any conditions. The elements then return to a stable state through alpha or beta decay. It is possible to quantify this behavior by considering the interesting version of the Periodic Table shown in Figure 6.25. It differs from more conventional versions of the Periodic Table because it shows the elements ranked according to their half-lives. Below an atomic number of 82 (which happens to be the atomic number of lead), the orbitals or "shells" inside of the nucleus are arranged in such a way that at least some isotopes of an element can remain stable for a very long period of time. However, above an atomic number of 82, the shell structure of the nucleus changes, and only some isotopes of Bismuth, Thorium, Uranium, Neptunium, and Plutonium can remain stable for periods of time longer than 1 million years. Because of this, elements heavier than Plutonium have very short half-lives, and in general, their half-lives are limited to less than 1 day.

Eventually *Glenn Seaborg* (who also discovered the element Plutonium) suggested that some undiscovered elements (which were heavier than uranium) could be more stable than conventional elements that have atomic numbers closer to 92.

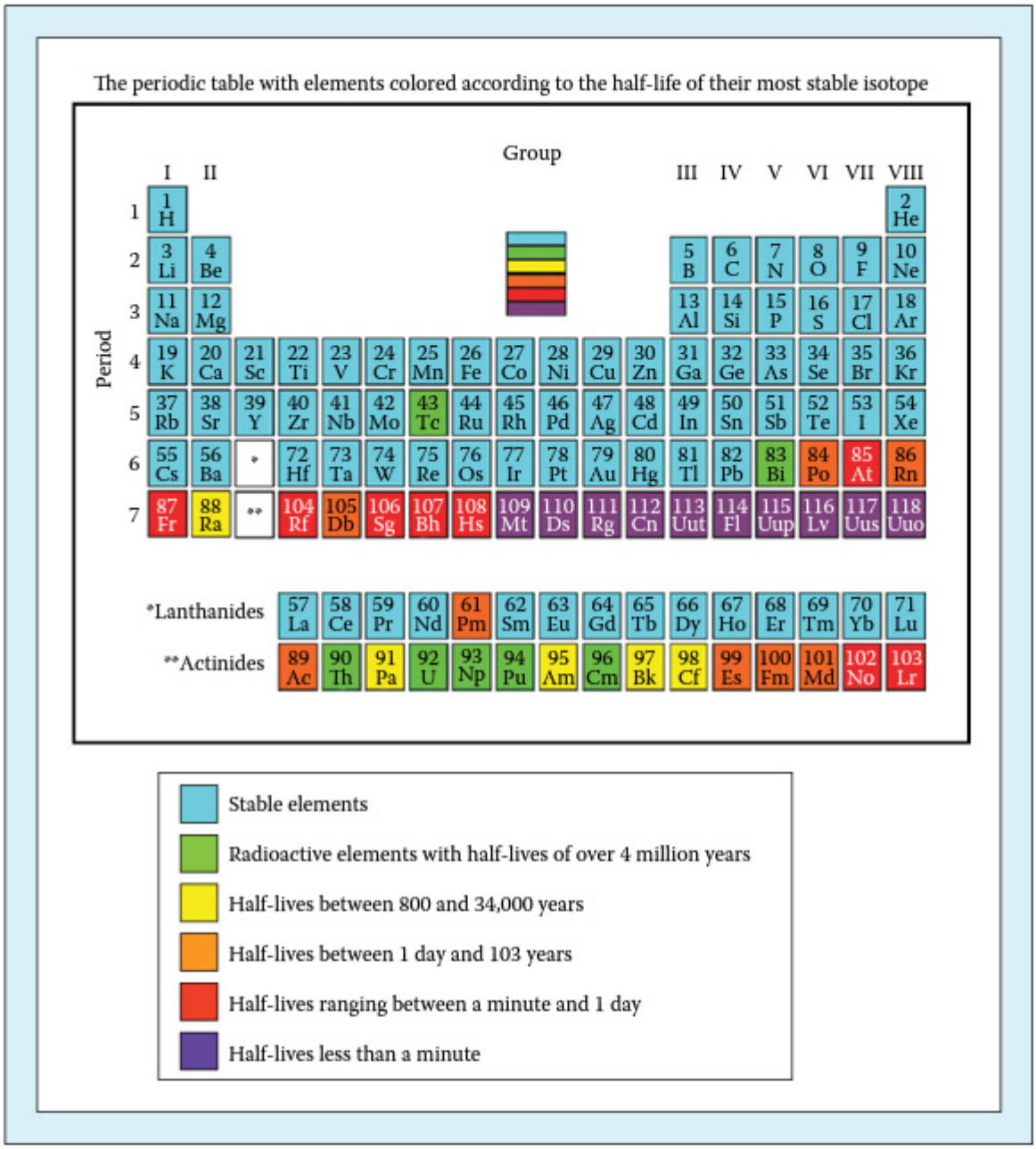
The periodic table with elements colored according to the half-life of their most stable isotope
Group
I II III IV V VI VII VIII
Period
1 H He
2 Li Be B C N O F Ne
3 Na Mg Al Si P S Cl Ar
4 K Ca Sc Ti V Cr Mn Fe Co Ni Cu Zn Ga Ge As Se Br Kr
5 Rb Sr Y Zr Nb Mo Tc Ru Rh Pd Ag Cd In Sn Sb Te I Xe
6 Cs Ba * Hf Ta W Re Os Ir Pt Au Hg Tl Pb Bi Po At Rn
7 Fr Ra ** Rf Db Sg Bh Hs Mt Ds Rg Cn Uut Fl Uup Lv Uus Uuo
*Lanthanides La Ce Pr Nd Pm Sm Eu Gd Tb Dy Ho Er Tm Yb Lu
**Actinides Ac Th Pa U Np Pu Am Cm Bk Cf Es Fm Md No Lr
Stable elements
Radioactive elements with half-lives of over 4 million years
Half-lives between 800 and 34,000 years
Half-lives between 1 day and 103 years
Half-lives ranging between a minute and 1 day
Half-lives less than a minute

FIGURE 6.25 The Periodic Table showing the elements in nature according to the half-lives of their most stable isotopes. (Adapted from *http://en.wikipedia.org/wiki/Island_of_stability*.)

These undiscovered elements would tend to cluster themselves around an "Island of Nuclear Stability" where some of the isotopes could have relatively long half-lives. Eventually it was discovered that this *Island of Nuclear Stability* (see Figure 6.26) appeared when the number of protons reached 118 and when the number of neutrons reached 178. In other words, some elements became stable again when the atomic mass number A = Z + N reached 296.

Student Exercise 6.7

We have mentioned on several occasions that free neutrons do not live for a very long time outside of the atomic nucleus. The average lifetime of a free neutron is about 14.8 minutes. Using the equations that we have just presented, calculate a free neutron's half-life $T_{½}$ and its radioactive decay constant λ if its average lifetime τ is 890 seconds (~14.8 minutes). Express all your results in units of seconds. Would you expect the half-life to be more than or less than the average lifetime? Present a reason to justify your results.

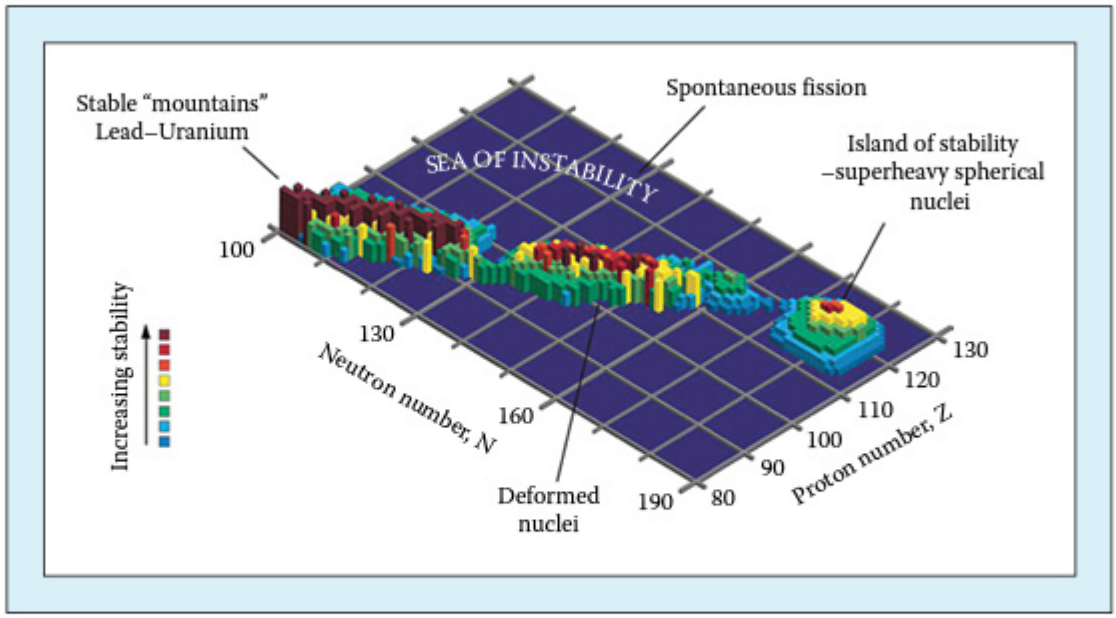

FIGURE 6.26 The island of nuclear stability that was first proposed by Glenn Seaborg in the late 1960s. The heavy nuclei at the tip of the island are stable because their nuclei are highly symmetrical. (Picture provided by Wikipedia.)

6.39 Radiation Released by Radioactive Materials

Nuclear radiation is released from radioactive materials through the process of *radioactive decay*, which occurs in nuclear fuel rods and in many naturally occurring elements. Radioactive decay is a function of the *isotopic stability* of the materials in the Periodic Table, which was discussed earlier in the chapter. When uranium or plutonium nuclei undergo nuclear fission, they split into two parts of roughly equal mass called *fission fragments* or *fission products*. In general, these fission products are highly radioactive and each fission product emits nuclear radiation at a different rate. Sometimes these fission products simply convert a neutron into a proton and an electron in order to become more energetically stable. They then emit an energetic electron from the nucleus called a *beta particle* or a *beta ray*. This process is called *beta decay*, and an example of beta decay involving the element Cesium is

An Example of the Process of Beta Decay

$$\text{Cs-137} \rightarrow \text{Ba-137} + e^{-} + \nu_e \tag{6.73}$$

In Equation 6.73, Cesium-137 is converted into Barium-137, and this shows that beta decay can be used to convert one element into another. Beta decay can occur in literally hundreds of different materials. *Beta decay is responsible for most of the decay heat produced in nuclear fuel rods.* Beta particles are also responsible for creating the *Cherenkov radiation* that is emitted from nuclear fuel assemblies in a spent fuel pool (Cherenkov radiation is discussed in Chapter 6 of our companion book,* where it is also famous for its characteristic light blue glow).

Extremely heavy atoms having an atomic weight greater than 110 can also become unstable and emit ionized helium nuclei to return to a stable state. These ionized helium nuclei are sometimes called *alpha particles*, and the corresponding radiation is then called *alpha radiation*. *Polonium* is an example of a heavy element that emits alpha particles. Another element that emits alpha particles is *Americium*, which is used in household smoke detectors. Alpha decay therefore requires two protons and two neutrons to be emitted from an unstable nucleus. Normally, alpha decay allows the resulting nucleus to become a more energetically stable structure.

An Example of the Process of Alpha Decay

$$\text{Ra-224} \rightarrow \text{Rn-220} + \text{He-4}$$
$$\text{Ra-224} \rightarrow \text{Rn-220} + \alpha \tag{6.74}$$

* See *Nuclear Engineering Fundamentals: A Practical Perspective*, by R.E. Masterson, CRC Press (2017).

As mentioned previously, alpha decay is normally restricted to heavy elements having atomic weights greater than about 110. Alpha decay does *NOT* occur in lighter elements such as Iron, Carbon, Oxygen, or Zirconium because these nuclei are too light and their average binding energy per nucleon is too high. The resulting alpha particles do not travel as far as photons, beta rays, or γ-rays do. They have kinetic energies between 2 and 6 MeV, and they are normally deposited in the nuclear fuel rods close to the atoms that created them. Alpha decay is frequently a by-product of the process of neutron capture. In a Segre Chart (see Figure 6.19), alpha decay normally occurs in the top right-hand quadrant of the chart.

6.40 Gamma Rays in Nuclear Power Plants

In addition to alpha particles and beta particles, an atomic nucleus can also emit energetic photons called *gamma rays*. *Gamma rays are only created in nuclear reactions and not in chemical ones*. Gamma rays are emitted whenever an atomic nucleus becomes energetically unstable. Gamma rays travel easily through ordinary matter, and heavy shielding materials such as concrete, lead, and steel are normally required to stop them. In nuclear power plants, gamma rays are produced in the reactor core with a distribution of energies from 100 KeV up to about 20 MeV. At these energies, gamma rays can easily penetrate the pressure vessel wall. Normally gamma rays do *NOT* deposit their energy at the location where they are produced—like alpha particles do. Instead, they deposit it according to an exponential attenuation law that is discussed in our companion book.

Gamma rays with energies higher than 20 MeV are considered to be extraterrestrial in nature, and these gamma rays are produced in the sun by the process of *nuclear fusion*. Sometimes these gamma rays are also called *cosmic rays*. The kinetic energies of gamma rays and X-rays are compared in Figure 6.27. In some cases, the energy of a gamma ray can be more than 100 times that of an X-ray. Thus gamma rays can do a great deal of structural damage to any materials that happen to be in their way. Like alpha particles and beta particles, their direction of emission is essentially random or *angularly isotropic*. That is, they are emitted with an equal probability into any solid angle from their parent nucleus. Gamma rays are also important in the study of *radiation protection*.

6.41 How Nuclear Decay Heat Is Produced

When alpha, beta, or gamma rays leave the confines of an atomic nucleus, they immediately interact with anything in their immediate vicinity. In nuclear science and engineering, this process is called the *interaction of radiation with matter*. Nuclear particles interact at an atomic level with other particles through a series of elastic and inelastic collisions in which they transfer some of their kinetic energy to the surrounding atoms. The rate of energy transfer depends on the type of particle, and it is different for alpha particles than it is for beta particles or gamma rays. In general, the rate of energy transfer is also material dependent. Alpha particles deposit their kinetic energy in nuclear fuel rods more quickly than beta particles or gamma rays do. *Hence, the effective range of alpha particles is much more limited than the range of other nuclear particles.* The kinetic energy carried by nuclear particles is deposited in the surrounding structural materials in the form of *heat*. This kinetic energy is also the source of the *decay heat* that is observed in nuclear fuel rods even after a reactor is shut down. Normally a spent fuel rod will continue to emit an appreciable amount of decay heat (in the form of beta radiation) for at least a month after shutdown. Then over time, a lot of the radioactive elements in the fuel rod disappear or are converted into more stable ones. However, the conversion process may take several thousand years to complete, and during this period time, the fuel rods will continue to emit at least a small amount of decay heat. The decay

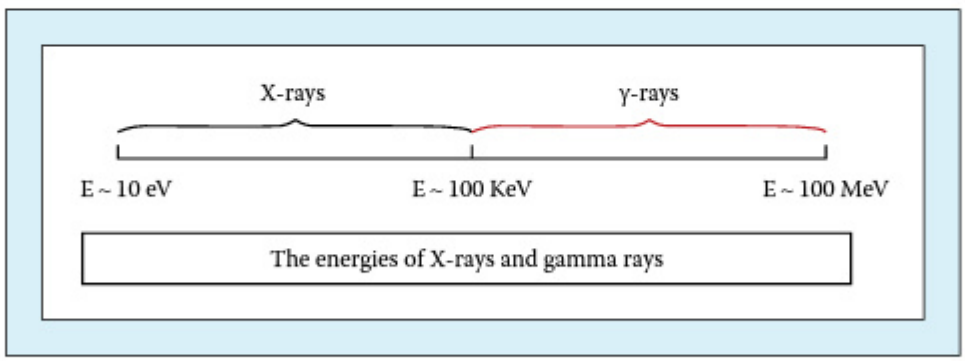

FIGURE 6.27 A picture comparing X-rays and gamma rays based on their kinetic energy alone. Gamma rays have much higher kinetic energies than dental X-rays, microwaves, and visible light waves do. Gamma rays can have kinetic energies between 100 KeV and 100 MeV, and at the higher end of this energy range their wavelength is about 1×10^{-10} m, which is about the size of an atomic nucleus.

heat production rate for the first 100 years is governed by a famous equation called the *Wigner–Way* equation, which is also discussed in our companion book—see Reference 8).

Finally, the amount of decay heat Q that these radioactive materials produce is equal to the difference between the masses of the individual atoms or particles before they decay and the masses of the individual atoms or particles after they decay. From Einstein's famous equation $E = mc^2$, the decay heat produced is

The Heat Produced by Radioactive Decay

$$Q = \left(\sum m_{before} - \sum m_{after}\right)c^2 \tag{6.75}$$

where c is the speed of light, and the summations in Equation 6.75 are to be performed over all the radioactive materials and their by-products. In the International System of Units, the speed of light is about 300,000,000 km/s. This implies that a very small amount of matter can be converted into a very large amount of heat. We will explore this process and its implications in more detail in Chapter 7. Decay heat must be taken very seriously when discussing nuclear power plants because it can continue to be produced by radioactive decay for days or even months after a reactor is shut down.

References

Books and Textbooks

1. Shultis, K. and Faw, R. *Fundamentals of Nuclear Science and Engineering*, 2nd edn., CRC Press, Boca Raton, FL (2008).
2. Lamarsh, J.R. *Introduction to Nuclear Reactor Theory*, Second printing, Addison-Wesley Publishing Company, Inc. New York, NY (1972).
3. Lamarsh, J.R. and Baratta, A.J. *Introduction to Nuclear Engineering*, Prentice Hall, Upper Saddle River, NJ (2001).
4. Duderstadt, J. and Hamilton, L. *Nuclear Reactor Analysis*, John Wiley & Sons, New York (1976).
5. Lewis, E. *Fundamentals of Nuclear Reactor Physics*, Academic Press, Boston, MA (2008).
6. Eisberg, R. *Fundamentals of Modern Physics*, John Wiley & Sons, New York (1961).
7. Kaplan, I. *Nuclear Physics*, Addison-Wesley, Reading, MA (1965).
8. Masterson, R.E. *Nuclear Engineering Fundamentals: A Practical Perspective*, CRC Press, Boca Raton, FL (2017).

Web References

1. *http://www.ptable.com/*.
2. *www.NNDC.gov.org*.
3. *http://www.webelements.com/*.
4. *http://www.doedigitalarchive.doe.gov*.
5. *http://en.wikipedia.org/wiki/Nuclear_density*.
6. *http://en.wikipedia.org/wiki/Big_Bang*.
7. *http://en.wikipedia.org/wiki/Andromeda_Galaxy*.
8. *http://hyperphysics.phy-astr.gsu.edu/hbase/nuclear/shell.html*.
9. *http://en.wikipedia.org/wiki/Natural_nuclear_fission_reactor*.
10. *http://hyperphysics.phy-astr.gsu.edu/hbase/astro/hydhel.html*.
11. *http://en.wikipedia.org/wiki/Natural_nuclear_fission_reactor*.
12. *http://www.americainwwii.com/articles/fat-man-and-little-boy/*.
13. *http://hyperphysics.phy-astr.gsu.edu/hbase/nuclear/liqdrop.html*.

Additional References

- Important physical constants used by nuclear scientists and engineers can be found in *Appendix A*.
- Unit systems and their conversion factors can be found in *Appendix B*.
- Nuclear cross sections for many important nuclear materials can be found in *Appendix C*.
- Physical properties of important nuclear materials can be found in *Appendix D*.
- Atomic masses, half-lives, and natural abundances can be found in *Appendix E*.

Questions for the Student

The following questions cover the material presented in this chapter, and in some cases, previous chapters as well. They are designed to test how well the student has acquired a working knowledge of the subject matter.

1. What is the definition of an isotope?
2. In nuclear engineering, what is the sum of the number of neutrons N and the number of protons Z in the nucleus of an atom called?
3. What is the difference between an element and an isotope?
4. Which element in nature has the most naturally occurring isotopes?
5. How many isotopes does the element uranium have?
6. How many naturally occurring elements have no stable isotopes at all?
7. What is the difference between a chemical reaction and a nuclear one? Approximately how many times more energy is released in a nuclear reaction than in a chemical one?
8. How many stable isotopes does the element uranium have and what are their names?
9. Name two naturally occurring elements that can be used as nuclear fuels.
10. What units are normally used to measure the activity of a sample of radioactive material?
11. Fill in the following sentence with the appropriate word or phrase: For a radioactive material, one disintegration per second is equal to one _____.
12. What is the purpose of the extra neutrons that the isotope of an atom contains?
13. Suppose you suddenly learned that the Earth was 9 billion years old instead of the 4.5 billion years old. How many times more U-235 would there have been 9 billion years ago than there is today?
14. If you compare the natural abundance of elements on earth to those in the universe as a whole, what does this tell you about the chemistry and the origin of our planet? Did we get more than our share or less than our share of natural uranium compared to the other planets in the Solar System?
15. Where did the uranium that we use today come from, and how was it created?
16. Is there enough naturally occurring plutonium in the earth's crust today to make an atomic bomb?
17. What is the purpose of an isotope, and why are there so many of them?
18. How many protons does the element uranium have?
19. Some elements of an intermediate atomic weight are produced by combining lighter elements together in the cores of stars. What is this process of element formation called?
20. Name three people who developed the liquid drop model of nuclear structure.
21. Who discovered the element uranium?
22. How many neutrons does uranium-238 have?
23. How many Becquerels are there in a Curie? Which unit of radioactivity is more commonly used in nuclear science and engineering today?
24. Who discovered the element Plutonium, and for which planet was it named?
25. What is the Big Bang, and how is it relevant to the nuclear power industry on the earth today?
26. Why do the elements in the Periodic Table have fractional atomic weights instead of integral ones?
27. How many stable isotopes does the element Uranium have?
28. Which element has the third largest number of stable isotopes, how many isotopes does it have, and how is it used in a nuclear power plant today?
29. For every atom of Uranium in the universe today, how many atoms of hydrogen are there?
30. How many protons and neutrons does Plutonium-239 have?
31. What is the half-life of Uranium-235?
32. What is the most stable isotope of the element Uranium, and what is its half-life?
33. If the average binding energy of each element in the Periodic Table was exactly the same, what would happen to the nuclear power industry in the world today?
34. What does the term "primordial" element refer to?
35. What is the mass defect and why is it so important?
36. What are the gases in the Periodic Table called that have all of their electron shells filled?
37. How many protons does the element uranium have?
38. What is the difference between the atomic number and the atomic weight?
39. If you could change one thing in the overall design of the elements to produce more energy, what would that be?
40. How many years from now do you think that significant amounts of Uranium will still be left on the earth for the nuclear power industry to use?

41. Approximately what percentage of the power produced by a thermal water reactor fueled with U-235 and U-238 is due to the buildup of Plutonium-239 in the core over time?
42. Approximately how old is the current version of the universe, and what relationship, if any, does this have to the production of nuclear power today?
43. How many naturally occurring elements are there in the Periodic Table?
44. How many man-made elements are there?
45. Approximately how many isotopes do all of the natural and man-made elements have?
46. What is the ratio of the half-life of U-235 to Pu-239?
47. What is the Periodic Table, and who discovered it originally?
48. How many different electron shell combinations can be found in the Periodic Table?
49. In the inner shell of an atom, how many orbital electrons can there be?
50. After the inner shell is filled, how many additional electrons can fit into the next shell?
51. If the first two electron shells were filled up, what would the chemical properties of the corresponding elements be?
52. What famous nuclear chemist is credited with the discovery of what is known as the "Island of Nuclear Stability"? What does the Island of Nuclear Stability represent?
53. What are the names of elements numbered 2–10 in the Periodic Table?
54. Name two different models of the nucleus that can be used to describe its internal structure.
55. What elements or isotopes in the Periodic Table are used for radiocarbon dating?
56. Some elements of an intermediate atomic weight are produced by combining lighter elements together in the cores of stars. At what heavy element does this process stop?
57. Which Russian scientist is most frequently credited with the discovery of the Periodic Table?
58. Why is the concentration of plutonium in the earth's crust much lower than the concentration of uranium?
59. What is the lightest element in the universe, and how many isotopes does it have?
60. What is the heaviest naturally occurring element in the Periodic Table, and how many protons does it have?
61. Suppose that isotope U-238, which can be found in nuclear fuel rods, begins to decay. At the end of its decay process, what stable element does it eventually become?
62. What is the most stable isotope of the element Lead?
63. What are the two most plentiful elements in the universe as a whole, which can also be used as nuclear fuels?
64. How can the isotope Pu-239 be produced in a nuclear power plant?
65. Which isotope of the element hydrogen is used to make the heavy water that is used as a moderator in some nuclear reactors?
66. What is the primary difference between the Liquid Drop Model and the Shell Model?
67. How many terms does the Liquid Drop Model have, and what are their names?
68. What is the average binding energy of a proton or neutron (in MeV)?
69. Why are very light elements and very heavy elements less stable than those with an intermediate atomic weight?
70. How many isotopes of the element plutonium can be used as a commercial nuclear fuel?
71. What is the largest of the five terms in the Liquid Drop Model of nuclear structure?
72. Name two elements that have the highest binding energy per nucleon.
73. Name the element that has the lowest binding energy per nucleon.
74. Approximately what percentage of the total mass of a nucleus is converted into energy to hold the nucleus together?
75. Is the nuclear force field attractive or repulsive?
76. What is the most common commercial use for Neptunium today?
77. Write a simple equation for the diameter of an atomic nucleus that is a function of only the number of nucleons it contains.
78. What is the Weizsaecker Formula and how can it be used?
79. Name four of the most common man-made elements.
80. When a radioactive material decays, it obeys a certain statistical probability distribution. What is the name of this statistical probability distribution?
81. If one AMU of nuclear matter was converted entirely into energy, how much energy would this produce?
82. What is the meaning of the fractional atomic weights that can be found in the Periodic Table?
83. What is the one element or isotope that does not have a fractional atomic weight?
84. How is the uranium-235, which is used in reactors, naturally produced?
85. What is the half-life of U-235?

86. How many naturally occurring isotopes does the element carbon have, and what are their names?
87. What is the half-life of a radioactive material?
88. How has the amount of uranium in the Earth's crust changed as a function of time?
89. If we were to add water to enriched uranium fuel, what would happen?
90. What is a common use for the radioactive isotope Americium-241?
91. What equation can be used to predict the orbital configuration of the electrons circling the nucleus of an atom?
92. What element that can be used as a nuclear fuel has only one stable isotope, and how many nucleons does it have?
93. What is the only stable isotope of Neptunium, and how is it produced?
94. How many stable isotopes does the element Lead have, and what is the chemical symbol for Lead?
95. What is the half-life of Uranium-238?
96. Write down an expression for the Weizsaecker Formula that uses the atomic number Z and the nucleon number A.
97. What is the least common form of naturally occurring uranium, and what is its half-life?
98. Who discovered the process of spontaneous fission, and how is it different than the process of conventional nuclear fission?
99. Is the average life of a radioactive material greater than or less than its half-life?
100. Write an equation for a sample of radioactive particles that obey a Poisson probability distribution.
101. When the decay of one radioactive isotope leads to the creation of another isotope, which in turn decays with a different decay constant, what is the relationship between these two isotopes called?
102. In what unit is the radioactive decay constant λ normally expressed?
103. Suppose that the production rate of a radioactive material is P and its decay constant is λ. Write an equation for the equilibrium concentration C of this material.
104. What is the relationship between the decay constant and the half-life of a radioactive material?
105. The field of reactor physics is based on the study of the neutron. Does the neutron ever decay?
106. Sometimes radioactive isotopes with very long half-lives decay into isotopes having much shorter half-lives. When the concentrations of these shorter lived isotopes stabilize, what is this condition called?
107. Write an equation that relates the half-life of a radioactive material to its average life.
108. Suppose that a condition of secular equilibrium between two radioactive materials is reached. If the concentrations of both materials are known, what is the relationship between the decay constant of the first material and the decay constant of the second material? Can this relationship be used to determine the half-life of the first material?
109. X-rays are sometimes released by energetic electrons, and gamma rays are sometimes released when an atomic nucleus decays. What is the kinetic energy of a typical X-ray, and at what energy is a photon normally considered to be a gamma ray?
110. What is the upper limit of the kinetic energy of a gamma ray? At energies above this, what does a gamma ray then become?
111. Write an expression for the activity A of a radioactive material as a function of its decay constant and its initial concentration C.
112. Write the same expression for the activity as a function of the half-life of the material and its initial concentration.
113. Fill in the following expression with the appropriate word or phrase: The process of increasing the U-235 concentration in a sample of natural uranium is called _____.
114. How is the mass defect of the atomic nucleus defined?
115. How many processes can be used today to commercially enrich uranium today?
116. For most elements, the mass defect is equal to approximately what percentage of the rest mass of the particles making up the nucleus?
117. What units are normally used to represent the nuclear binding energy that is shown on the nuclear binding energy curve?
118. What are the names of the processes that are used to enrich natural uranium ore today?
119. How many terms are there in the nuclear binding energy equation that is derived from the Liquid Drop model of nuclear structure?
120. What physical effects do each of these terms represent? Which of these terms was first proposed by physicist John Archibald Wheeler?
121. What is the fundamental cause of radioactive decay?
122. What is the difference between a controlled nuclear reaction and an uncontrolled one?

123. Fill in the following sentence with the appropriate word or phrase: A reactor used in a nuclear submarine is based on a _____ nuclear reaction.
124. Fill in the following sentence with the appropriate word or phrase: The atomic bomb dropped on Hiroshima was based on a _____ nuclear reaction.
125. What isotope of plutonium is used in some of the deep space probes built by NASA as a power source?
126. What particles does this particular isotope of plutonium emit?
127. What are the names of the equations that are used to describe the concentrations of the radioactive isotopes in a very complex decay chain?
128. What equation would you use to find the equilibrium concentrations of Xe-135 and Sm-149 in a reactor core if their decay constants and production rates were known?

Exercises for the Student

Exercise 6.1

Earlier in the chapter, we learned that it was possible to calculate the concentration of a radioactive material N(t) from a simple equation of the form. $N(t) = N_o e^{-\lambda t}$ where N_o is the current concentration at time = 0.

Part 1: Suppose that we would like to use this equation to estimate the amount of Uranium-238 that existed on the Earth 4.5 billion years ago—or about the time the Earth was first formed. If N_o^{238} is the concentration today, what was the concentration of U-238 on the Earth 4.5 billion years ago?

Part 2: Assuming that N_o^{235} is the concentration of U-235 today, what was the concentration of U-235 on the Earth 4.5 billion years ago?

Part 3: Based on the results of parts 1 and 2, what was the average natural "enrichment" of Uranium-235 in the uranium ore at the time (4.5 billion years ago)?

Exercise 6.2

An atomic nucleus has a radius of 5×10^{-13} cm. If the protons and neutrons inside of the nucleus have an average mass of 1.66×10^{-27} kg, what is its atomic density? Suppose that a neutron star created from this nuclear material is 1 km wide. How much heavier is it than the earth, which is 12,756 km wide?

Exercise 6.3

Using the Weizsaecker Formula, estimate the binding energy of the Uranium-235 nucleus using only the volume term and the surface term. Which term is larger, and what are their respective signs? When the binding energy of a nucleus becomes negative, what happens to the nucleus?

Exercise 6.4

Suppose that the mass defect of an element in the Periodic Table with 26 protons and 30 neutrons turns out to be equal to 1% of its total rest mass. How much energy (in MeV) is used to hold the nucleus of this isotope together, and what is the average binding energy per nucleon? What is the chemical symbol for this particular element?

Exercise 6.5

Suppose that an unknown element has 120 protons and 160 neutrons. What do you expect the radius of its nucleus to be? Do you think that it is theoretically possible for this element to exist in nature? What is its physical cross section?

Exercise 6.6

Estimate the binding energy of the most common isotope of Iron, which is called Iron-56. Make this estimate using only the volume term, the surface term, and the Coulomb term in the Weizsaecker Formula. How much error do you expect this estimate to have in it?

Exercise 6.7

Earlier in the chapter, we learned that Pu-239 is an excellent nuclear fuel. What is the ratio of the half-life of U-235 to the half-life of Pu-239? What is the primary mode by which both of these isotopes decay?

Exercise 6.8

Suppose that a nuclear reaction occurs where 5×10^{-27} kg of nuclear material is converted entirely into energy. How much energy is released from this reaction in MeV?

Exercise 6.9

People occasionally have difficulty understanding where the Earth's natural uranium came from. Exactly how was the Earth's natural uranium created, and how old do you think the Earth is? How many times higher was the concentration of U-235 and U-238 when the Earth was first formed than it is today?

Exercise 6.10

At the beginning of time, all of the elements in the physical universe were created in a colossal explosion of space and time called *The Big Bang*, which is discussed in great detail in our sister book. However, many of the heavy elements that we use to create our industrial society were not created directly in the Big Bang. Where do you think these heavy elements (like Iron) came from? What was the ratio of the amount of hydrogen to the amount of helium that was created as the result of the Big Bang?

Exercise 6.11

The element Lead, which is sometimes used as a shielding material, has four primary isotopes Pb-204, Pb-206, Pb-207, and Pb-208 with a relative abundance of 1.48%, 23.6%, 22.6%, and 52.3%, respectively. Using these percentages, determine the atomic weight of naturally occurring lead, which is sometimes used to build radiation shields.

Exercise 6.12

Suppose that someone comes to you and tells you that the Earth was created in 7 days. How old do you think the Earth actually is, and what fraction of the age of the universe is the age of the Earth as a whole? Do you think that you should take what this person says seriously?

Exercise 6.13

Approximately 2 billion years ago, the great natural nuclear reactors of Oklo (refer to Chapter 10 of this book or Chapter 9 of our sister book) produced nuclear energy without the need for human intervention for over 150,000 years before the U-235 in them began to run out. How many times longer did these reactors operate than the age of the great pyramids of Egypt?

Exercise 6.14

Earlier in this chapter, we spent a fair amount of time discussing the Periodic Table. Of the 92 naturally occurring elements that appear in the Periodic Table, how many of these elements can be found in the Earth's crust and are therefore stable over geologic time frames? Of the 3000 possible isotopes that all of these elements can have, how many of them are stable enough to be found in the Earth's crust today?

Exercise 6.15

Man-made elements and isotopes are created by bombarding heavy elements (like uranium-238) with protons in a nuclear accelerator. Approximately how many man-made elements have been created since the 1950s? Can you name at least five of them?

Exercise 6.16

One of the things that nuclear scientists worry about all the time is how to create Pu-239 from U-238. How do you think this process works, and what are the energies of the particles that are needed to make this reaction possible?

Exercise 6.17

Earlier in the chapter we talked about radioactive decay chains, and the Bateman equations (which are discussed in great detail in our sister book) are a general analytical solution to the isotopic concentrations in these decay chains. Suppose that there are three isotopes in a decay chain that we will call isotopes A, B, and C.

Part 1: Write down an explicit equation for their time-dependent concentrations assuming that their half-lives are 1 day, 3 days, and 2 days, respectively, and that the initial concentration of A at t = 0 is A_o. Assume that the concentrations of the other two isotopes (B and C) in the decay chain are 0 at t = 0.

Part 2: Do any of these three isotopes have a "bump" in their concentration curves as a function of time? If so, which one(s) have these bump(s), and when do these bump(s) occur?

Part 3: By what factor do we multiply the half-lives of each of these elements to get their average life?

Part 4: What are the decay constants (in inverse days) for each of the isotopes that we have used in this example?

Exercise 6.18

Carbon-14 (refer to our sister book) is produced in the Earth's upper atmosphere at a very predictable rate when atmospheric nitrogen molecules (N_2) are broken down by cosmic rays to produce an unstable isotope of Carbon called Carbon-14. This involves Nitrogen-14 absorbing a free neutron and converting itself into Carbon-14 in the process.

Part 1: Based on your knowledge of nuclear processes, write down the equation that governs this reaction.

Part 2: If the Baryon number is conserved, is the atomic number increased or decreased in this reaction, and what particle must be emitted by the Carbon-14 nucleus?

Part 3: Assuming that Carbon-14 has a half-life of 5730 years, what is *average life* of the Carbon-14 produced in this process?

Part 4: What is the value of the decay constant for Carbon-14, and what units does it have?

Exercise 6.19

Suppose that you were asked to calculate the concentration of Carbon-14 in the wood of the planks in the Royal Egyptian Barge that led to Dr. Willard Libby (see related Reference 1) being awarded the Nobel Prize in Chemistry in 1960.

Part 1: If the concentration of Carbon-14 in the Earth's atmosphere when the barge was built was C_o, what fraction of this concentration would exist in the wood in the Royal Egyptian Barge if we were able to conduct this experiment again today?

Part 2: Approximately how much would this concentration have to be corrected to account for variations in the concentration of Carbon-14 in the Earth's atmosphere over the last 5000 years?

Exercise 6.20

Suppose that we have a sample of a radioactive isotope A that has a current concentration of A_o atoms per cubic centimeter.

Part 1: If the half-life of this isotope $T_{½}$ is 1000 years, what was the concentration of this isotope 1000 years ago, and what will be the concentration of this isotope 1000 years from now?

Part 2: What is the ratio of the concentration of this isotope 1000 years ago to the concentration of this isotope 1000 years from now?

Part 3: Suppose that this isotope then decays into another isotope B, which then has a half-life of 2000 years. Write down *but do not solve* the equations for the time-dependent concentrations of isotopes A and B. Use the following terminology when writing out the equations

- ⊙ The concentration of isotope A is A.
- ⊙ The concentration of isotope B is B.
- ⊙ The initial concentration of isotope A is A_o.
- ⊙ The initial concentration of isotope B is B_o.
- ⊙ The decay constant for isotope A is λ_A.
- ⊙ The decay constant for isotope B is λ_B.

Part 4: Solve the equations in part 3, and write down their solutions here.

Part 5: Assuming that the concentrations of A_o and B_o are initially the same, draw a rough graph of how you would expect the concentration of isotope B to behave as a function of time. If the half-life of isotope B is reduced by 500 years, redraw the graph again. Has anything of importance between the two graphs changed? Explain the reason for any change or changes that you observe.

Exercise 6.21

A radioactive material used to treat brain tumors is produced in a nuclear accelerator (a cyclotron) at the rate of 1×10^{16} atoms per cubic centimeter per second.

Part 1: If the radioactive decay constant for the material has the value of 1×10^{-6} s^{-1}, what is the maximum amount of the material that can be produced?
Part 2: Approximately how long will it take to produce this amount of the material?
Part 3: If the material has a molecular weight of 60.22, how many grams of this material can be produced by the cyclotron?
Part 4: Based upon the knowledge you have acquired so far, is this material more likely to be an alpha emitter, a beta emitter, or a gamma emitter?
Part 5: What nuclear process was most likely used by the cyclotron to produce this radioisotope?

Exercise 6.22

A radioactive material has an average life of 1 million years. What is its half-life, and what is its radioactive decay constant?

Exercise 6.23

A radioactive material decays until only 1/8th of the original amount remains. How many half-lives does this take to occur? If the half-life of the material is 1 million years, when will only one-eighth of it remain?

Exercise 6.24

Theoretically speaking, it is possible to produce the element lead in a number of different ways. What are two possible ways to produce lead from the decay of uranium? What does the ratio of Lead-206 to Lead-207 that is produced in this way tell you?

Exercise 6.25

Part 1: Using the Wigner–Way equation, draw a curve showing the decay heat produced in a reactor core as a function of time. Assume that the reactor is shut down at $t = 0$.
Part 2: Approximately what percentage of the steady-state reactor power level is generated by decay heat in the nuclear fuel rods immediately after the reactor is shut down?
Part 3: What particles are responsible for generating most of this decay heat?

Exercise 6.26

Suppose that the concentration of the radioactive isotope Carbon-14 in a Woolly Mammoth bone is 1% of what it was when the Woolly Mammoth died. Approximately how long ago did the Woolly Mammoth roam the Earth?

Exercise 6.27

Suppose that the radiocarbon age for a wooden plank from an old ship wreck that was discovered in the Caribbean Sea is found to be 460 years. When did this ship first sink into the Caribbean Sea? Is it possible that this wooden plank was thrown overboard by Christopher Columbus in 1492?

Exercise 6.28

A nuclear accelerator produces a radioactive isotope that can be used to treat bone cancer at the rate of 1 million atoms per hour. The decay constant for this material is 1 hour. What is the maximum possible concentration of this material that can be produced by the nuclear accelerator?

Exercise 6.29

A new element is discovered with an atomic mass number of 300.

Part 1: If it has 180 neutrons, how many protons does it have?
Part 2: After some time, scientists are able to synthesize 1 g of this new element. After 6 months, only 80% of it remains. What is its half-life and its average life? What is its radioactive decay constant?

Exercise 6.30

The time-dependent concentration N(t) of a radioactive isotope, used to treat cancer patients, is given by the equation $N(t) = N_o\, e^{-0.01t}$, where t is the time in seconds. What is the activity of the isotope (i.e., the decay rate in disintegrations per second) after 10 minutes if the initial concentration N_o is 1,000,000?

Exercise 6.31

Part 1: Using the Bateman equations discussed in our sister book, show that the activity of the first parent isotope in a radioactive decay chain is given by $A(t) = A_o\, e^{-\lambda 1 t}$.

Part 2: Using the Bateman equations discussed in our sister book, show that the activity of the first daughter produced by the parent is given by $A_2(t) = A_2(0)\, e^{-\lambda 2 t} + A_1(0)\, (\lambda_2/(\lambda_2 - \lambda_1))\, [e^{-\lambda 1 t} - e^{-\lambda 2 t}]$.

Part 3: What is the equation for the activity of the first daughter isotope when the initial concentration of this daughter isotope is 0?

Exercise 6.32

When the earth was first formed from an enormous disk of gas and dust about 4.5 billion years ago, the concentration of U-235 was much higher in the Earth's crust than it is today. If the concentration of U-235 in the Earth's crust today is 1.5 parts per 100 million, what was the concentration of U-235 in the Earth's crust approximately 4.25 billion years ago?

Exercise 6.33

Suppose that a radioactive material that emits alpha particles has a concentration of 1 million atoms per cubic centimeter. If the radioactive decay constant for this material is 0.0001/second, how many atoms of this material will emit alpha particles after 1 second if the total volume of the material is 10 cm^3? What is the rate of decay sometimes called?

7

Nuclear Fission and Nuclear Energy Production

7.1 Converting Mass into Energy

Nuclear power has only been a commercial reality since the early 1950s. Out of all the possible elements in the universe, only four isotopes of Uranium and Plutonium (Uranium 233, Uranium-235, Uranium-238, and Plutonium-239) exist in sufficient quantities to produce nuclear energy on a commercial scale. *Uranium is relatively rare as far as other elements in the universe are concerned (see Chapter 6), and there is much less of it on the Earth today (due to radioactive decay) than there was several billion years ago*. However, it does not take much uranium to create a self-sustaining nuclear reaction, and as we will soon discover, several kilograms of natural uranium, when properly shaped and purified, can sustain a chain reaction for a very long period of time.

Most commercial nuclear power plants use *enriched uranium* to create a sustained nuclear chain reaction. The concentration of Uranium-235 in their fuel rods (i.e., the enrichment of the fuel) usually varies between about 2.5% and 5.0%, although other reactors (such as military reactors) use enrichments as high as 95% and the Canadian pressurized heavy water reactor (the CANDU reactor) does not require enriched uranium at all. In this chapter, we would like to study the process of nuclear fission and the nuclear reactions that are associated with it. We will illustrate how a nuclear chain reaction can be used to release tremendous amounts of energy, and in the process, what must be done to control such reactions to keep them in check. Our objective in this chapter will be to discuss the process of *nuclear fission*. We will only discuss the process of *nuclear fusion* on a superficial level, even though it generates *billions* of times more energy each day than fission does in the universe as a whole. Nuclear fusion is also the process that is responsible for creating the heat and light that are produced in stars such as our Sun.

Nuclear fission is based on the concept of inducing a heavy element (such as Uranium-233, Uranium-235, or Plutonium-239) to split apart into two or more parts. Practically speaking, this can be done by allowing one of these isotopes to absorb a slow-moving neutron and to transform themselves into an agitated state. The nucleus can only become stable again by releasing some of its excess energy and several photons and neutrons in the process. The difference between the mass of the nucleus before it splits apart and the mass of the nucleus after it splits apart (plus its by-products), when multiplied by the square of the speed of light c, is equal to the amount of kinetic energy E that is released. This kinetic energy is then converted into heat, which allows the blades of a steam turbine to spin, and for electrical energy to be produced. The key to all of this happening is to create what is known as a *controlled nuclear chain reaction* and to allow this chain reaction to occur for as long as possible without getting out of control. The length of time that this is possible is roughly proportional to the enrichment of the fuel. Commercial power reactors need to be partially refueled every 18 or 24 months, while military reactors can run for many years without the need for refueling. In this chapter, we would like to present the physical principles that allow the nuclear chain reaction to occur (see Figure 7.1).

7.2 Fission and Fusion: A Review of Fundamental Concepts

As opposed to the process of nuclear fission, nuclear fusion is defined as the process of fusing the nuclei of two very light elements together (such as hydrogen or helium) in order to create a heavier element—which in turn releases a significant amount of energy in the process. This process occurs in stars all of the time when the hydrogen and helium atoms within them are squeezed together under the enormous force and pressure of gravity. As the gravitational pressure increases, the nuclei of light elements, such as hydrogen and helium, fuse together, and enormous amounts of energy (in the form of light and heat) are released in the process. This is the basis of the nuclear furnace that fuels our Sun as well as all other stars that can be seen in the sky.

Because there is so much more hydrogen and helium in the universe than uranium and plutonium, an average star such as our Sun can continue to shine for 5 billion or even 10 billion years before all of its nuclear fuel is consumed. And there are at least 100 billion

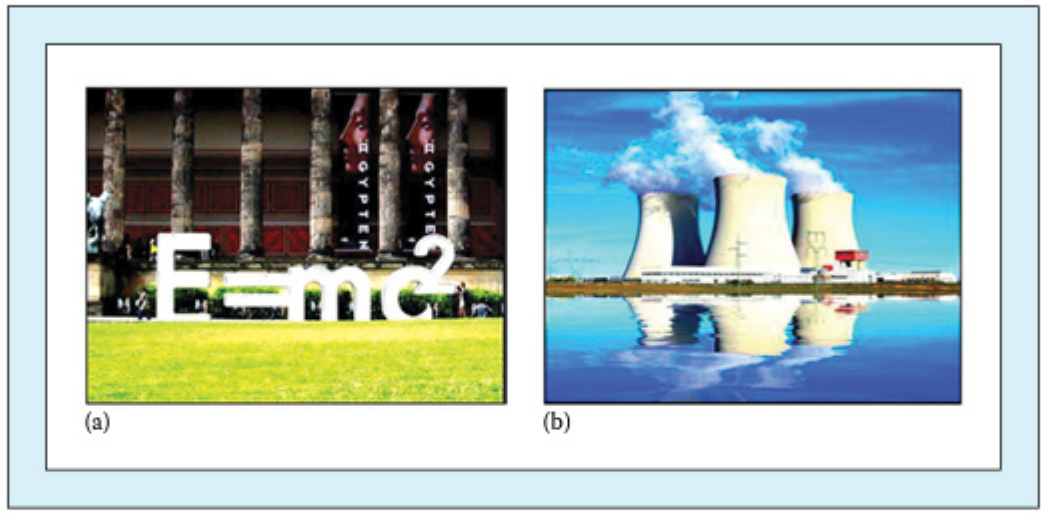

FIGURE 7.1 Two universal symbols of the nuclear power industry in the world today. (a) A 3-meter tall sculpture of Einstein's famous equation $E = mc^2$ at the Walk of Ideas in Berlin, Germany. (b) The cooling towers of a nuclear power plant releasing thermal energy produced by the plant.

stars in our galaxy alone—and 100 billion galaxies! The light elements that are needed for nuclear fusion to occur (mainly hydrogen, helium, and traces of deuterium and lithium) were created during the first few minutes of the *Big Bang*, whose evolution was described in Chapter 9 of our companion book.* These light elements are responsible for 98% of all of the nuclear material (or baryonic matter) that we observe in the universe today. While useful energy can be produced by combining two very light elements together into a single heavier element (see Figure 7.2), nuclear fission relies on exactly the opposite approach to create useful heat and power. In other words, *nuclear fission* is based on the idea of breaking the nucleus of a very heavy element into two or more parts to release the energy that is stored inside of it. This energy was put there by the gravitational collapse of very large stars called *supernovas* billions of years ago. The process that was used by these supernovas to produce the uranium that is found on the Earth today is also described in Reference 13.

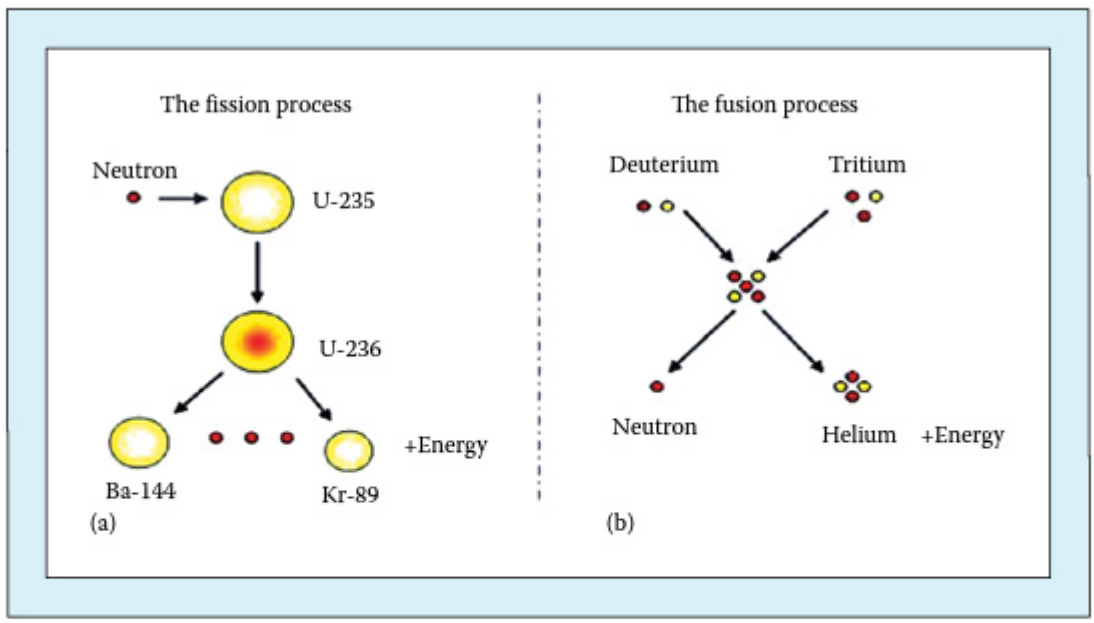

FIGURE 7.2 An illustration of the difference between fission and fusion. (a) Uranium-235 combines with a neutron to form an unstable intermediate, which quickly splits into Barium-144 and Krypton-89 plus three neutrons in the process of nuclear fission. (b) A deuterium and a tritium nucleus combine together through nuclear fusion to form a helium nucleus plus a neutron. About 20 MeV of kinetic energy is released in a fusion reaction, and about 200 MeV of kinetic energy is released in a fission reaction.

* See *Nuclear Engineering Fundamentals: A Practical Perspective*, by R.E. Masterson, CRC Press (2017).

7.3 Uranium and Its Characteristics

Unfortunately, very little uranium was produced when the universe first began because the universe cooled down too quickly for uranium and most of the other heavy elements to form. Most of the uranium that exists on the Earth today was created much later in the life cycle of the universe, per se. Its production occurred when very large and massive stars called *supernovas* exploded at the end of their useful life and ejected many heavier elements into the outer space. Almost all of the heavy elements in the universe with atomic numbers greater than iron (which has an atomic number of 26) were formed in this way. An example of a supernova that exploded in this way is shown in Figure 7.3. This picture shows the remains of a famous supernova called the *Crab Nebula*, which is discussed in many astronomy classes. The picture was taken in February 2008 by the *Hubble Space Telescope*. The star responsible for this beautiful stellar structure exploded in the year AD 1054. It created a temporary pulse of light that was brighter than the full moon, and its explosion was documented by a number of Chinese astronomers at the time. The Crab Nebula is located about 6500 light years from Earth and is about 10 light years across. By comparison, our entire solar system (the distance from the Sun to Pluto × 2) is less than 1 *light year* across. This corresponds to roughly the length of the word "nebula" in Figure 7.3. Today, we know that the clouds of nuclear material ejected from supernovas such as the Crab Nebula are responsible for most of the uranium that exists on the Earth today. The amount of uranium that is produced in this way is minimal compared to the amount of other materials in the universe as a whole, but it is enough to create a viable nuclear power industry for hundreds of thousands or even millions of years.

As we discovered in our companion book, uranium occurs in the Earth's crust at an average concentration of about 2.8 parts per million. *There is slightly more uranium in the Earth's crust than there is gold, silver, or mercury*. Traces of it can be found almost everywhere. It can also be found mixed with other materials in the world's oceans but in very low concentrations that are difficult to exploit commercially. *There are three naturally occurring isotopes of uranium that can be found in measurable quantities in nature, and we will spend a considerable amount of time discussing them in this chapter.* They are

1. *Uranium-234 (which has 92 protons and 142 neutrons)*
2. *Uranium-235 (which has 92 protons and 143 neutrons)*
3. *Uranium-238 (which has 92 protons and 146 neutrons)*

Uranium-233, which is not found in appreciable quantities in nature (because it has such a short half-life), is also an excellent nuclear fuel, and it can be produced commercially by bombarding Thorium-232 with fast or thermal neutrons. Uranium has 10 isotopes in all with atomic numbers from 226 to 239, but only three of them—U-234, U-235, and U-238—have long enough half-lives to occur in measurable quantities in nature.

Most of the other isotopes of uranium decay away soon after they are produced. The isotopic composition of the three most common isotopes of uranium is shown in Table 7.1. Notice that Table 7.1 is a subset of Table 7.2, which shows

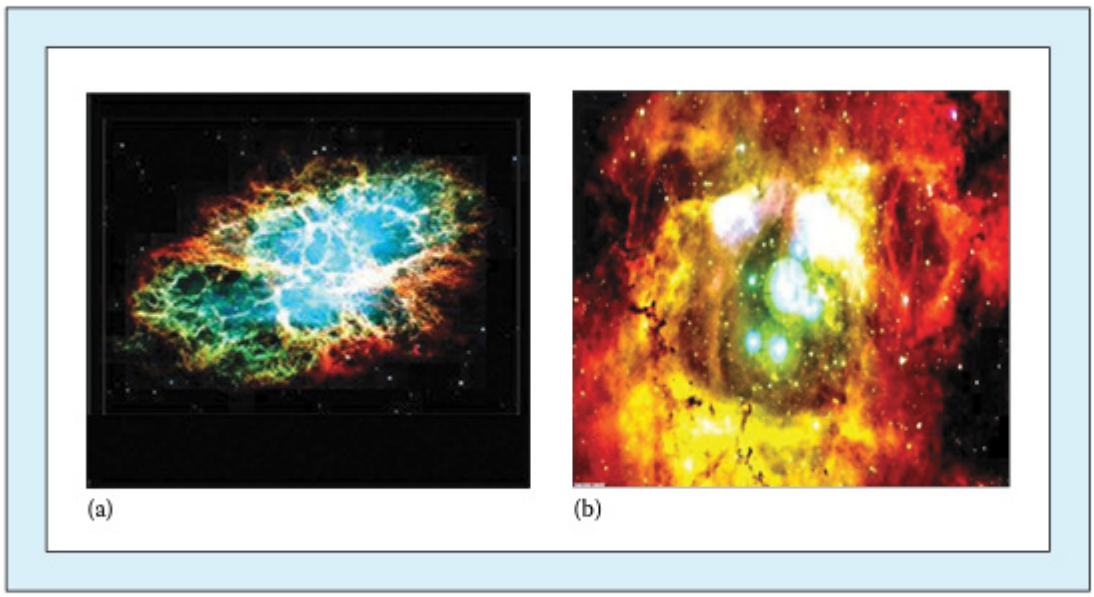

FIGURE 7.3 Supernova explosions are important for the process of uranium production. (a) A picture of the Crab Nebula taken by the Hubble Space Telescope where large amounts of Uranium-235 and Uranium-238 were produced when a massive star collapsed and then exploded. (b) The remnants of another supernova explosion where exactly the same process occurred. (Pictures provided by NASA.)

TABLE 7.1
Stable Isotopes of Uranium and Their Natural Abundance

Isotope	Type of Nuclear Material	Isotopic Rest Mass (AMU)	Natural Abundance	Half-Life (Years)
U-234	Fissile	233.040628	0.000057	0.159 My
U-235	Fissile	235.043924	0.007217	0.704 Gy
U-238	Fissionable	238.050785	0.992726	4.46 Gy
Natural uranium	Both	238.03	1.00	~4.45 Gy

TABLE 7.2
Nuclear Properties of the Common Elements of Uranium and Plutonium

Isotope	Number of Protons (Z)	Number of Neutrons (N)	Atomic Weight (A = Z + N)
U-226	92	134	226
U-231	92	139	231
U-232	92	140	232
U-233	92	141	233
U-234	92	142	234
U-235	92	143	235
U-236	92	144	236
U-238	92	146	238
U-239	92	147	239
Pu-239	94	145	239
Pu-240	94	146	240
Pu-241	94	147	241
Pu-242	94	148	242
Pu-244	94	150	244

some of the additional isotopes of uranium and plutonium. However, it is helpful to reproduce here because it gives some idea of how the natural abundance of each of these isotopes compares. As you can see by referring to Table 7.1, natural uranium consists of 99.27% U-238, 0.72% U-235, and 0.0057% U-234 by weight. Therefore, the *nuclear weight* of natural uranium that is presented in Table 7.1 is the *weighted average* of the atomic weights and the abundances of each of the individual isotopes. Because these quantities are normalized, the sum of all of these concentrations must add up to 1.00. Hence,

$$\mathrm{M}^{\text{Natural Uranium}} = \frac{\left(\mathrm{M}^{\mathrm{U238}} \times \mathrm{P}^{238} + \mathrm{M}^{\mathrm{U235}} \times \mathrm{P}^{235} + \mathrm{M}^{\mathrm{U234}} \times \mathrm{P}^{234}\right)}{\left(\mathrm{P}^{238} + \mathrm{P}^{235} + \mathrm{P}^{234}\right)} \tag{7.1}$$

where P is the *percentage abundance* of each of the naturally occurring isotopes of uranium. From our previous discussion, it immediately follows that $\mathrm{P}^{238} = 0.9927$, $\mathrm{P}^{235} = 0.0072$, $\mathrm{P}^{234} = 0.000057$, and $(\mathrm{P}^{238} + \mathrm{P}^{235} + \mathrm{P}^{234}) = 1.0$. The nuclear weight is also known as the *isotopic rest mass* M. Substituting the values of the nuclear weights for each of these isotopes into Equation 7.1 will yield the value of the weight of natural uranium that is shown in Table 7.1 or 238.03.

For those of you who have not yet had a chance to read Chapter 6, it is important to realize that *the isotopes of an element have the same number of protons and electrons Z. The isotopes of uranium only differ from one another in the number of neutrons N that they contain*. For example, all isotopes of uranium have a total of 92 protons. The number of protons in the nucleus is called the *atomic number*. Uranium-233 has a total of 92 protons and 233 − 92 = 141 neutrons, while Uranium-235 has a total of 92 protons and 235 − 92 = 143 neutrons. The total number of protons and neutrons in any isotope of uranium is then the sum of the number of protons and neutrons in the nucleus. The total number of protons and neutrons is also called the *atomic mass number* A. In some books, it is also called the *atomic weight*, for example,

Atomic Mass Number

$$\mathrm{A} = \mathrm{Z} + \mathrm{N} \tag{7.2}$$

TABLE 7.3
Summary of the Known Isotopes of Thorium and Their Relative Abundance

Isotope	Atomic Mass (AMU)	Binding Energy (MeV)	Spin	Natural Abundance	Half-Life	Decay Mode	Q (MeV)
Th-227	227.027703	1736.0	3/2	…	16.72 d	α	6.15
Th-228	226.028715	1743.0	0	…	1.912 y	α	5.52
Th-229	229.031755	1746.4	5/2	…	7.9 ky	α	5.17
Th-230	230.033128	1755.2	0	…	75.4 ky	α	4.77
Th-231	231.036298	1760.3	5/2	…	35.2 h	β–	0.39
Th-232	232.038051	1766.7	0	1.00	1.4×10^{10} y	α	4.08
Th-234	234.043593	1777.7	0	…	24.10 d	β–	0.27

The primary distinction between the atomic weight and the atomic mass number is that the atomic mass number can only be a *whole number*, while the atomic weight (with the exception of Carbon-12) is never a whole number. The numbers of protons and neutrons for the most common isotopes of uranium and plutonium are shown in Table 7.2. Notice that 150 neutrons are about the maximum number of neutrons that a nucleus can hold before it becomes unstable and begins to decay.

Student Exercise 7.1

The nuclear element thorium consists of eight isotopes, but only one of them is stable in nature. If the nuclear properties of all of the isotopes of thorium are shown in Table 7.3, calculate the atomic weight (in AMU) of naturally occurring thorium ore. Be prepared to explain how you arrived at your answer.

7.4 Energy Output: Fission versus Fusion

Compared to nuclear fusion reactions, nuclear fission produces about 12 times more energy per reaction. For example, a fission reaction releases about 210 million electron volts (MeV) of particle kinetic energy, while a fusion reaction involving the fusion of deuterium and tritium releases an average of about 17.6 MeV of particle kinetic energy. You can take a look at the link *http://www.mpoweruk.com/nuclear_theory.htm* for more details on how the energy output is calculated.

In nuclear science and engineering, the unit of 1 MeV is commonly used to compare the relative energy output from these two processes. You may recall from a previous chemistry or physics class that 1 MeV is equivalent to 1.60×10^{-13} J. This relationship between the value of an electron volt (eV) and a Joule was first introduced to the reader in Chapter 2. Essentially, an *electron volt* is the amount of energy (or Work = Force × distance) required to move an electron through an electric potential of 1 V. About 30 billion fissions per second are required to produce 1 W of *thermal power*. The procedure to calculate this number is explained in another section.

7.5 Splitting of the Uranium Atom: The Process of Induced Fission

In some previous chapters we mentioned that Uranium-235 is one of the few materials in nature that can be used as a commercial nuclear fuel. (The other primary materials are Uranium-233 and Plutonium-239.) If we take a sample of Uranium-235 atoms and observe them for some time, we would find that they would eventually decay into Thorium-231 atoms and then into Lead-206. We discussed the decay chains that governed this process in Chapter 6. The energy released by the radioactive decay of U-235 is carried away primarily by alpha particles. An alpha particle is an energetic helium nucleus with two protons and two neutrons and with both of the electrons removed. The alpha particle is usually ejected from the nucleus with an electrical charge of +2. Unfortunately, left to its own devices, U-235 has a half-life of about 710 million years—and so it does not decay rapidly enough on its own to be used as a nuclear fuel. For a fuel to be an effective nuclear fuel, we need to "kick start" the decay process to get larger quantities of it to split apart.

So the key question—which the founders of nuclear industry were faced with many years ago—was: How can the nucleus of a uranium atom be induced to split apart without waiting around 700 million years for it to do so? In the late 1930s, scientists found that U-235, in particular, was very sensitive to the presence of free neutrons in its immediate vicinity. If the nucleus actually managed to absorb one of these neutrons, it would immediately transform itself into U-236, which is highly unstable, and would either completely split apart (through nuclear fission) or release a gamma ray through the process of radioactive decay. They also discovered that the *slower* the neutrons were moving past the nucleus

(or the longer their wave functions were in the vicinity of the nucleus), the *higher* the probability was that one of these neutrons would be absorbed. Based on this observation alone, they concluded that *inducing* a sample of uranium-235 to split apart by exposing it to a *flux* of low-energy neutrons was the best way to create a viable nuclear reactor. In the sections that follow, we would like to describe how this can be done.

7.6 Understanding the Fission of Uranium-235

In order to understand how a nuclear power plant works, it is first necessary to understand how a Uranium-233, Uranium-235, or Plutonium-239 nucleus reacts to low-energy neutrons in its vicinity. In order to help visualize this behavior, we would like to construct a couple of simple pictures to illustrate how this process works. We can begin this process by referring to Figure 7.4. Uranium-235 is one of a small number of heavy elements in the universe (U-233, Pu-239, and Pu-241 being the other three) that can absorb a low-speed neutron and spontaneously split apart, or *fission*. As a matter of fact, the probability of absorption by a uranium nucleus is much greater for a low-speed neutron than it is for a high-speed one. This property was first discovered in the early 1940s and was discussed in Chapter 4. The probability of a fission or absorption reaction is measured in the units of *barns where 1 barn* $= 1 \times 10^{-24}$ *cm*^{2}.

A fast neutron has a very small chance of being absorbed by a U-235 nucleus—even when it collides directly with it. On the other hand, when something else gets in the way of a fast neutron and slows it down (see Chapter 3), then the neutron will have a much greater chance of being absorbed. Only when a neutron reaches speeds that are equivalent to what we call "thermal speeds" (which correspond to a kinetic energy of about 0.025 eV) does the probability of absorption become very high. A neutron with such a low kinetic energy is sometimes called a *thermal neutron*. In the discussion that follows, we will assume that we are dealing primarily with thermal neutrons. Later on, we will discover that the speed of a thermal neutron is about 2200 m/s or 1.35 miles/s. This corresponds to the speed of the first space plane, which is currently being tested by NASA. The speed of a thermal neutron is about 4850 miles/hour (see Figure 7.5).

7.7 Capture and Fission Channels for U-235

As we alluded to previously, there are many things that a U-235 nucleus can do when it absorbs a thermal neutron. When a U-235 nucleus first absorbs the neutron, it transforms itself into U-236. The U-236 nucleus starts to shake violently and acts as if it wants to split apart. Within about 10^{12} seconds, it decides to start down one of the two primary paths or *capture and fission channels*. Only one channel results in the nucleus splitting apart, and the other channel leads to the creation of a stable U-236 nucleus. Both processes are illustrated in Figure 7.6.

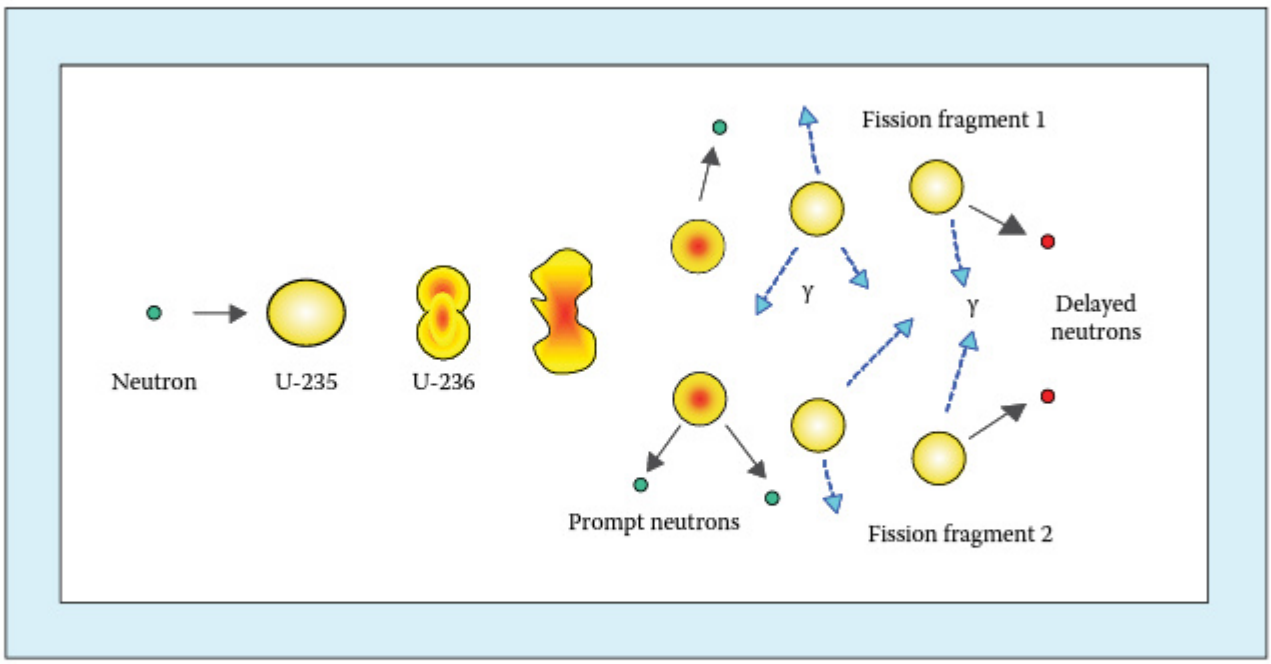

FIGURE 7.4 The induced fission of a uranium nucleus. The absorption of a thermal neutron by a Uranium-235 nucleus induces oscillations in the nucleus that deform it until it splits into fragments in the way a drop of liquid might break into smaller droplets. The irregularly shaped nucleus that is temporarily created in this case (see step 3) is called a *compound nucleus*.

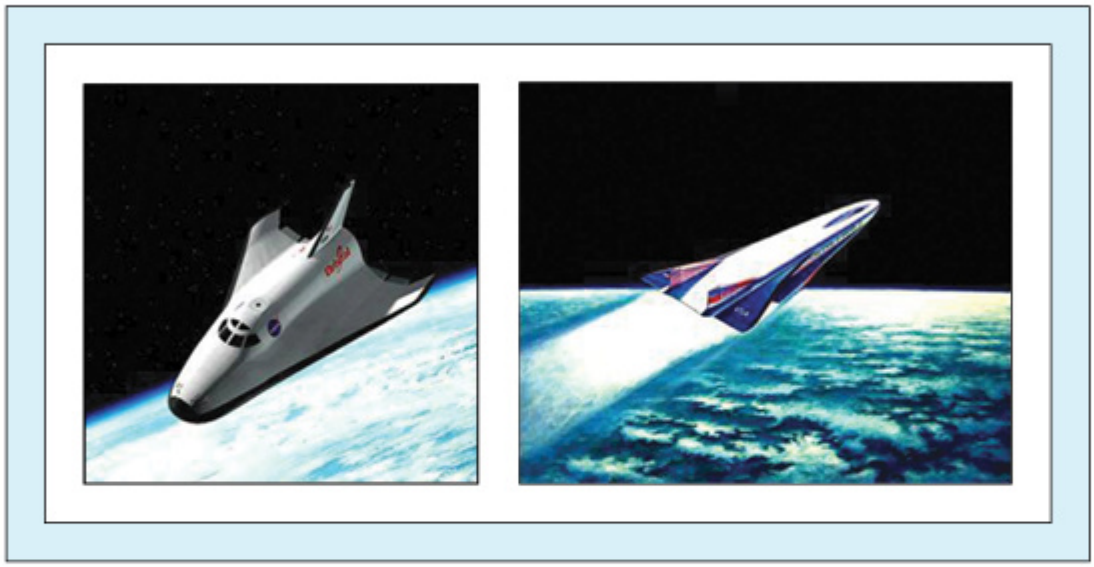

FIGURE 7.5 A *thermal neutron* in a reactor core travels at approximately the same speed as the space plane shown above. The space plane is a vehicle that operates as an aircraft while it is in Earth's atmosphere and as a spacecraft when it travels into the upper atmosphere and into the outer space. It combines the best features of an aircraft and a spacecraft. It can also land like an airplane. (Pictures provided by NASA.)

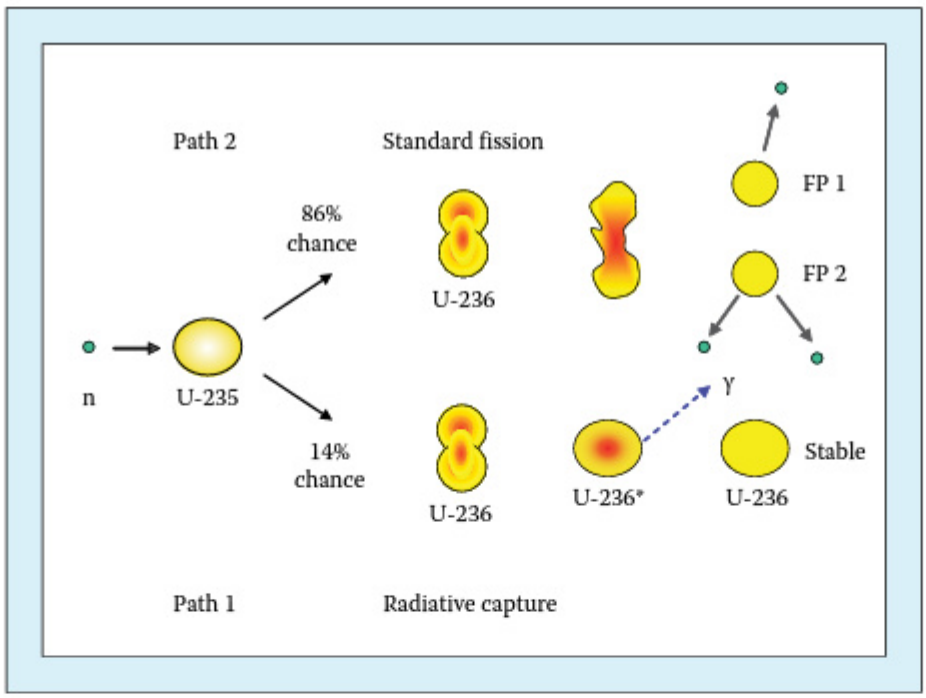

FIGURE 7.6 An example of what happens after the capture of a thermal neutron by a U-235 nucleus. About 86% of the time, the nucleus will split apart into two fission products and release two to three neutrons in the process. About 14% of the time, the nucleus will absorb a neutron, emit a gamma ray, and then become a stable version of U-236.

7.7.1 Channel 1: Capture

About 14% of the time, the U-236 nucleus continues to oscillate wildly until it releases a high-energy photon (which is also called a gamma ray). It then transforms itself into a lower energy state and becomes a "stable" U-236 atom. The resulting U-236 nucleus is stable and decays with a half-life of about 24 million years. There is a significant amount of energy released when the gamma ray is emitted (about 1 MeV), but after that, any further energy that is released only comes from the process of radioactive decay. This process is called *radiative capture* because the capture of a neutron causes the nucleus to emit a gamma ray. (See Chapter 3 for a detailed discussion of how radiative capture works.)

7.7.2 Channel 2: Fission

Conversely, about 86% of the time after the U-235 nucleus absorbs a thermal neutron, the U-236 nucleus that is created becomes unstable and splits into two smaller and more energetic parts. Each of these parts is called a *fission fragment*. There are over 60 known ways (or channels) that a U-236 nucleus can split apart in this way. Figure 7.4 depicts just one of them. The most common fission channels produce Strontium-94 and Xenon-150, with two fission neutrons, and Barium-141 and Krypton-92 with three fission neutrons. Frequently, a U-236 nucleus will also split into Barium-137 and Krypton-97. It may also split into Barium-141 and Krypton-92. It can split into Strontium-94 and Xenon-140. And finally, it can decay into Cesium-140 and Rubidium-93. The equations governing these reactions are

Some Fission Fragments (or Fission Products) from the Fission of Uranium-235

$$
\begin{aligned}
{}^{1}_{0}\mathrm{n} + {}^{235}_{92}\mathrm{U} &\rightarrow {}^{236}_{92}\mathrm{U} \rightarrow {}^{140}_{55}\mathrm{Cs} + {}^{93}_{37}\mathrm{Rb} + 3\,{}^{1}_{0}\mathrm{n} + \mathrm{Q}' \\
{}^{1}_{0}\mathrm{n} + {}^{235}_{92}\mathrm{U} &\rightarrow {}^{236}_{92}\mathrm{U} \rightarrow {}^{139}_{56}\mathrm{Ba} + {}^{94}_{36}\mathrm{Kr} + 3\,{}^{1}_{0}\mathrm{n} + \mathrm{Q}'' \\
{}^{1}_{0}\mathrm{n} + {}^{235}_{92}\mathrm{U} &\rightarrow {}^{236}_{92}\mathrm{U} \rightarrow {}^{142}_{54}\mathrm{Xe} + {}^{92}_{38}\mathrm{Sr} + 2\,{}^{1}_{0}\mathrm{n} + \mathrm{Q}''' \\
{}^{1}_{0}\mathrm{n} + {}^{235}_{92}\mathrm{U} &\rightarrow {}^{236}_{92}\mathrm{U} \rightarrow {}^{141}_{56}\mathrm{Ba} + {}^{92}_{36}\mathrm{Kr} + 3\,{}^{1}_{0}\mathrm{n} + \mathrm{Q}'''' \\
{}^{1}_{0}\mathrm{n} + {}^{235}_{92}\mathrm{U} &\rightarrow {}^{236}_{92}\mathrm{U} \rightarrow {}^{142}_{56}\mathrm{Ba} + {}^{92}_{36}\mathrm{Kr} + 2\,{}^{1}_{0}\mathrm{n} + \mathrm{Q}''''' \\
{}^{1}_{0}\mathrm{n} + {}^{235}_{92}\mathrm{U} &\rightarrow {}^{236}_{92}\mathrm{U} \rightarrow {}^{144}_{56}\mathrm{Ba} + {}^{90}_{36}\mathrm{Kr} + 2\,{}^{1}_{0}\mathrm{n} + \mathrm{Q}'''''' \\
{}^{1}_{0}\mathrm{n} + {}^{235}_{92}\mathrm{U} &\rightarrow {}^{236}_{92}\mathrm{U} \rightarrow {}^{134}_{54}\mathrm{Xe} + {}^{100}_{38}\mathrm{Sr} + 2\,{}^{1}_{0}\mathrm{n} + \mathrm{Q}'''''''
\end{aligned}
\tag{7.3}
$$

Here, the symbol Q represents the *quantity* of kinetic energy that is released, and the superscripts ′, ″, ..., ⁗ refer to the fact that the quantity of kinetic energy released is NOT the same in each case. Physicists have found that this energy is typically on the order of 210 MeV per fission. (However, only about 95% of this kinetic energy, or approximately 200 MeV per fission, is recoverable in the form of heat—see Chapter 2. The rest is simply carried away into outer space by strange ghost-like particles called *neutrinos*.)

It is also worth mentioning that the value of Q can depend on the composition of the fission products. This energy can be further subdivided into the kinetic energies of each of the fission products, the kinetic energy of the fission neutrons that are released, and the kinetic energy of the gamma rays that are released by the reaction. If you look at Equation 7.3, it is immediately obvious that all of these reactions have a number of things in common. This allows us to make the following observations about how the fission process works:

- First, the fission fragments (or fission products) released from the U-236 nucleus have very similar masses. This is not always the case, but statistically speaking, they are more likely to have similar masses than dissimilar ones. The distribution of their masses is shown in Figure 7.9. This distribution tends to be highly symmetrical, but the shape of the distribution can change depending on the energies of the neutrons that are absorbed. Above 10 MeV, the distribution of masses has a single hump (like the hump on a camel), and both sides have about an equal mass distribution around the center point. At thermal energies (~0.025 eV), the fission fragment mass distribution develops two distinct humps, with the peaks of the humps being centered at about 90 and 140 AMU, respectively. As Figure 7.9 shows, the center point in both cases is about 115 AMU.
- Second, the number of neutrons emitted is also not always the same, and it distributes itself according to a statistical probability distribution from *one to four*. The most common fission channels emit an average of about two neutrons per fission, while other fission channels emit an average of about three. Plutonium-239 emits the most fission neutrons, and on average, this number is about 20% greater than Uranium-235. The exact numbers are shown in Table 7.8.
- Third, the emitted and *recoverable energy*, which consists of the sum of the energy of all of the fission fragments, neutrons, and gamma rays, is not always the same, but on average, it adds up to about 200 MeV per fission. In addition to this, the kinetic energy of the neutrons that are emitted is not a constant. Rather, it follows a statistical distribution of kinetic energies from about 0.05 MeV up to about 10 MeV. (An additional 10 MeV of this energy is carried away by small, ghostlike particles called neutrinos. *However, this energy never appears in the form of heat, and so it is essentially unrecoverable. Therefore, the total energy released—both recoverable and unrecoverable—is approximately 210 MeV.*)

As shown in Figure 7.7, the "average" kinetic energy of a fission neutron is about 2 MeV, and the "most probable" energy is about 0.75 MeV. (The exact numbers are 1.98 MeV and 0.74 MeV, respectively, for the thermal fission of Uranium-235.)

- Fourth, the fission of U-236 takes place very quickly after the U-235 nucleus absorbs a free neutron. On average, this process takes about 10^{-12} seconds. The atomic masses of the by-products of the fission process will always add up to 236 (which is the original weight of the U-236 nucleus before it splits apart).

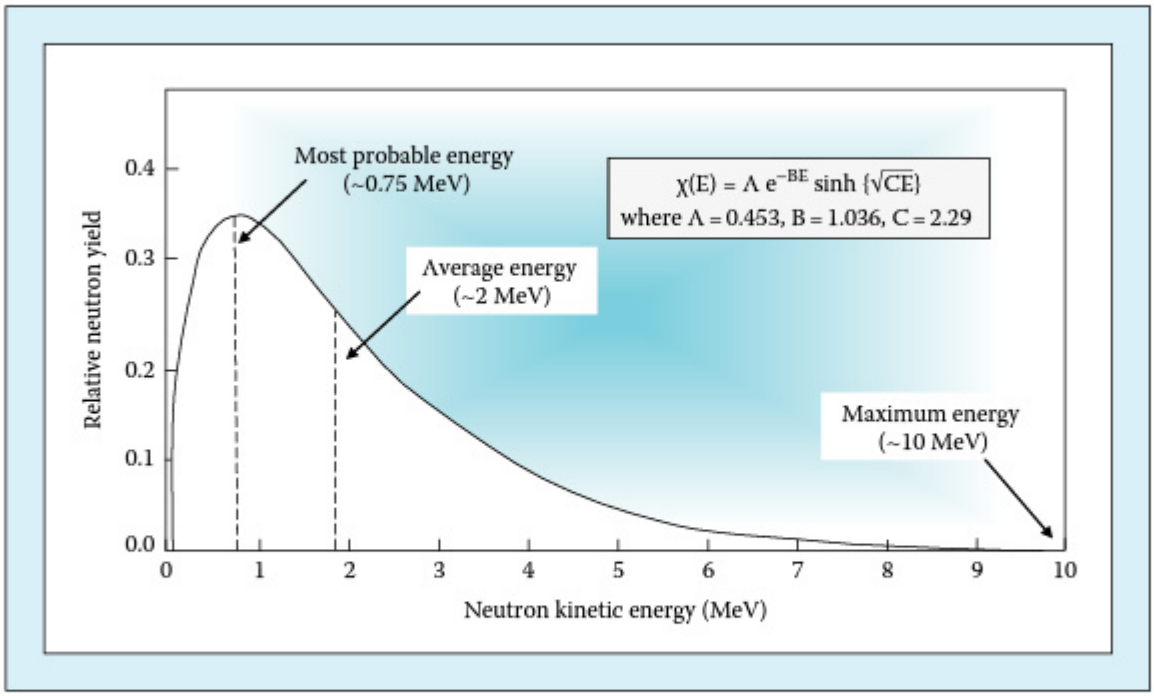

FIGURE 7.7 The kinetic energy spectrum of the neutrons emitted from the thermal fission of U-235.

TABLE 7.4
Probability of Fission and Capture due to the Absorption of a Thermal Neutron

Nuclear Fuel	Capture Cross Section σ_c (barns)	Fission Cross Section σ_f (barns)	Absorption Cross Section σ_a (barns) ($\sigma_a = \sigma_c + \sigma_f$)	Probability of Fission (σ_f/σ_a) (%)	Probability of Radiative Capture (σ_c/σ_a) (%)
U-233	45.800	528.45	574.25	92	8
U-235	96.685	585.086	681.77	86	14
Pu-239	270.000	747.401	1017.41	74	26
Pu-241	362.000	1012.0	1374.00	74	26

Note: Cross sections taken from Appendix C.

⊙ Fifth, at least two neutrons have to be produced for each neutron absorbed to sustain a nuclear chain reaction. This is because approximately 20% of the neutrons do not result in the U-236 nucleus fissioning. As we discussed earlier, sometimes the absorption of a neutron by a U-235 nucleus only results in the U-236 nucleus emitting a gamma ray. There are no further fission neutrons created in this case (see Table 7.4).

7.8 Fission Neutron Energy Spectrum

There is an empirical equation for the kinetic energy spectrum of the fission neutrons that are released from the thermal fission of Uranium-235. This equation was discovered in the early 1950s and is generally insensitive to the energy of the neutron causing the initial fission. The most common form of this equation is

Fission Neutron Energy Spectrum

$$\chi(E) = Ae^{-BE}\sinh\left\{\sqrt{CE}\right\} \quad \text{where} \quad \sinh(x) = \frac{\left(e^{x} - e^{-x}\right)}{2} \tag{7.4}$$

and

A = 0.453
B = 1.036
C = 2.29
E is the energy of the emitted neutron *in MeV*

The function sinh (x) that appears in this equation is called the *hyperbolic sine*, and it frequently appears in the study of nuclear energy systems. This equation for the fission neutron energy spectrum is also called the *Watt equation*, and it was originally developed by physicist B. E. Watt in 1952. (Watt's original paper can be found in the references at the end of the chapter.) Strictly speaking, $\chi(E)$ also depends on the energy of the neutron causing the fission to occur and on the specific isotope(s) involved. However, this dependence is usually very weak because the energy spectra for most isotopes are nearly identical, and this energy dependence can be accounted for by letting $\chi(E)$ depend on where one is actually situated in the reactor itself. Since $\chi(E)$ is a probability distribution, it follows that the integral of $\chi(E)$ from 0 to infinity must be equal to unity, for example,

$$\int \chi(E)\,dE = 1.0 \tag{7.5}$$

In other words, the Watt equation is *normalized* so that the sum of all the probable energies adds up to 1. Often times, the symbol $\chi(E)$ is replaced by the symbol P(E) to indicate that we are dealing with a probability distribution here.

Note in particular that the *most probable kinetic energy* of a neutron emitted from the thermal fission of U-235 is slightly less than 0.75 MeV and that the *average kinetic energy* of all the fission neutrons that are emitted is about 2.0 MeV. Figure 7.7 shows that very few neutrons are emitted with energies greater than 10 MeV. For this reason, we have arbitrarily chosen the upper energy cutoff in most of our energy integrals to be 10 MeV. (In some books, the upper limit is set to 15 MeV.) The neutrons that are emitted in accordance with Equation 7.4 emerge with equal probability in all directions. In other words, *the angular distribution of the fission neutrons is essentially random or isotropic*. This is very typical of reactions that involve the creation of a compound nucleus. *Atomic nuclei do not possess any memory of the angle that the "bullet" came from that destroyed them. In other words, they retain no knowledge of where the neutron came from that caused the nucleus to split apart!*

Example Problem 7.1

Show that the most probable energy of a neutron emitted from the probability distribution shown in Figure 7.7 is 0.74 MeV.

Solution Since the neutron energy spectrum $\chi(E) = Ae^{-BE}\sinh\{\sqrt{CE}\}$ describes the probability that a neutron will be emitted with an energy E, the most probable neutron energy will correspond to the peak of the curve shown in Figure 7.7. From college calculus, we know that this must correspond to the point on the curve where the slope is zero or where $d\chi(E)/dE = 0$. Therefore, to find the energy that corresponds to the maximum of the curve, we must take the first derivative of $\chi(E) = Ae^{-BE}\sinh\{\sqrt{CE}\}$, set it to zero, and solve for E. Performing the required math, we find that $d\chi(E)/dE = Ae^{-BE}\cosh\{\sqrt{CE}\}\sqrt{C/2 - ABe^{-BE}}\sinh\{\sqrt{CE}\} = 0$, and since $\cosh\{\sqrt{CE}\} = 1/2\left(e^{\sqrt{CE}} + e^{-\sqrt{CE}}\right)$ and $\sinh\{\sqrt{CE}\} = 1/2\left(e^{\sqrt{CE}} - e^{-\sqrt{CE}}\right)$, $d\chi(E)/dE = 1/2\left(e^{\sqrt{CE}} + e^{-\sqrt{CE}}\right)\sqrt{C/2} - 1/2\left(e^{\sqrt{CE}} - e^{-\sqrt{CE}}\right)B = 0$ and $\left(\sqrt{C/2B - 1}\right)\left\{e^{\sqrt{CE}} - e^{-\sqrt{CE}}\right\} = 0$. Multiplying through by $e^{\sqrt{CE}}$, we obtain $\left(\sqrt{C/2B - 1}\right)\left\{e^{2\sqrt{CE}} - 1\right\} = 0$ or $e^{2\sqrt{CE}} = 1/\left(\sqrt{C/2B - 1}\right)$. Finally, taking the natural log (ln) of both sides and solving for E, we obtain $E = \left(1/2\sqrt{C}\right)\ln\left(1/\left(\sqrt{C/2B - 1}\right)\right)$. Upon substituting the appropriate values for B and C into this expression, we find that E = 0.74 MeV. [Ans.]

Student Exercise 7.2

Using the same probability distribution, show by evaluating the integral

$$E_{avg} = \frac{\int \chi(E)\,E\,dE}{\int \chi(E)\,dE}$$

that the average energy E_{avg} of the neutrons produced immediately after the nucleus splits apart is 1.98 MeV.

7.9 Fast, Epithermal, and Thermal Energy Ranges for Nuclear Fission

Theoretically speaking, nuclear fuels like uranium and plutonium can absorb a neutron with *any kinetic energy*. However, nuclear materials are much better at absorbing low-energy neutrons than they are at absorbing high-energy ones. This means that *the probability of a neutron being absorbed increases as the neutron energy is decreased*. It is not always possible to define an exact relationship between the two, but it is easier to visualize why this is true by breaking the energy spectrum of the incoming neutrons into three distinct regions or "bands."

Region number I, which is called the *fast energy region (or the fission energy region)*, is the energy range where fission neutrons are produced and where they may exist for a short period of time before they lose their kinetic energy in collisions with other atoms. The fission energy range typically extends from about 100 keV to 10 MeV, and it corresponds to the right-hand side of the energy range shown in Figure 7.8. This is where the probability of being absorbed is very low and where the probability of being scattered is very high. Neutrons in this energy range are typically referred to as "fast" neutrons. Sometimes, this energy range is also called the *fission energy range*.

Between 1 eV and 10–100 keV, neutrons that are slowing down through collisions with other atoms behave entirely differently than they do at higher energies. This energy range is called the *epithermal energy range or the resonance energy range*, and we will refer to it in this chapter as Region number II. Here, the probability of a neutron being absorbed varies wildly as its kinetic energy is reduced because of the presence of what are known as "absorption resonances" in the fuel. As we learned in Chapter 4, these resonances are due to the formation of a *compound nucleus*, which may exist just long enough to increase the probability that the incoming neutron will be absorbed at a specific energy. Many neutrons get lost in these absorption resonances and do not make it down to thermal energies where they can cause additional fissions to occur. It is not uncommon for 10%–15% of the total number of neutrons that are produced to get absorbed in this way.

Finally, the neutrons that make it through the resonance energy range (Region number II) arrive at much lower energies where there are no more absorption resonances and where a neutron may be scattered many times by other nuclei before it is finally absorbed. A neutron at these energies is said to be in *the thermal energy range*, and the energy spectrum of the neutrons in this range is usually *Maxwellian* in shape. See Chapter 8 for a more detailed discussion of the characteristics of a Maxwellian energy spectrum. When these neutrons come into thermal equilibrium with their environment, this distribution of energies is known as a *Maxwell–Boltzmann probability distribution*.

Generally speaking, the thermal energy range is defined to extend from $E = 0$ *to* $E = 1$ *eV*. These definitions vary, but we will assume for the purpose of this discussion that the thermal energy range ends at about 1 eV. (In some books it is defined to end at 2 eV.) The thermal energy range will be called Region number III in our discussion. A neutron absorbed at thermal energies has a 91% chance of causing a U-233 nucleus to fission, a 86% chance of causing a U-235 nucleus to fission, and a 64% chance of causing a Pu-239 nucleus to fission. These probabilities are different because each material has a finite probability that the additional neutron will lead to a stable nucleus by emitting a gamma ray. The by-products

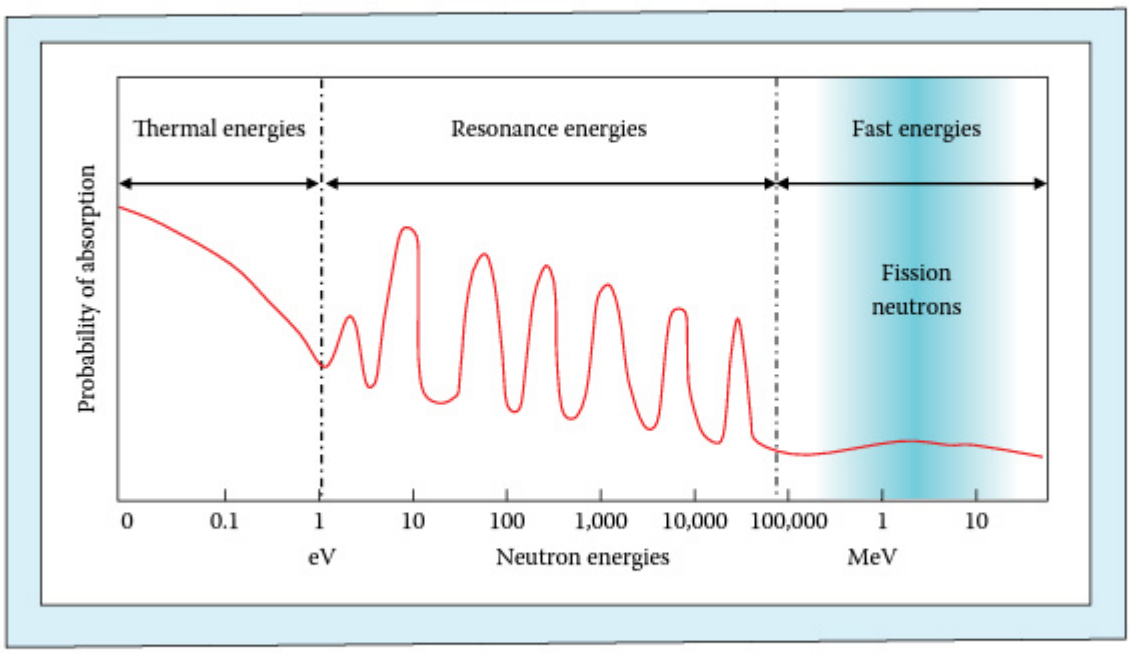

FIGURE 7.8 The three standard regions of the *neutron energy spectrum*—the thermal, the resonance or epithermal, and the fast energy regions.

of each fission reaction will vary slightly depending upon whether we are dealing with the fission of Uranium-233, Uranium-235, or Plutonium-239. However, *in any fission reaction, exactly two fission fragments are produced. The fission process never produces more than two fission fragments*.

7.10 Mass Distribution of the Fission Fragments

The fission fragments that are released when an atomic nucleus splits apart have very similar but not identical atomic masses. This is not always the case, but statistically speaking, they are more likely to have similar masses than dissimilar ones (see Figure 7.9). The distribution of these masses tends to be highly symmetrical in shape, but the shape of this distribution can change depending on the energies of the free neutrons that initiate the reaction. Above 10 MeV, the distribution of masses has a single hump (like the hump on a camel), and both sides have about an equal mass distribution around the center point. At thermal energies where E ≅ 0.025 eV, the fission fragment mass distribution develops two distinct humps, with the peaks of the humps being centered at about 90 AMU and 140 AMU, respectively. As Figure 7.9 shows, the center point in both cases is close to 115 AMU.

If you think about it, this is true because the sum of the two fragments, plus other particles, and the 2–3 neutrons released per fission (due to the conservation of mass) must always add up to between 236 and 240 AMU. Each fission fragment is produced from the fission of U-233, U-235, or Pu-239 with a predictable *probability of occurrence* or *yield*. Each fission reaction produces two fission fragments, and so in 100 nuclear fissions, 200 fission fragments are produced. The fission product yield is usually normalized per fission so that the sum of all the fission products produced equals 100%. The 20 most common fission products produced from the thermal fission of Uranium-235 are shown in Table 7.5. There are about 60 fission products produced in significant quantities in this way. Many of these fission products decay very rapidly and do not exist in the core for a protracted period of time. With the exception of Xenon-135 and Samarium-149, most of them do not have large enough cross sections to impact how a reactor behaves, and so their ability to influence the creation of future neutrons is limited. However, the delayed neutrons that they produce are of great practical importance because these neutrons are what allow a nuclear reactor to be controlled.

7.11 Amount of Energy Released from the Fission of Different Nuclear Materials

When an atomic nucleus splits apart, a predictable amount of kinetic energy is released in the process. This kinetic energy is manifested in the core in the form of *heat*. The quantity Q of kinetic energy produced depends on both the type of material involved and the kinetic energy of the incident neutron. Each fissile material will release a different number of neutrons per fission (see Table 7.8), and the distribution of the fission fragments will also vary slightly from one fissile

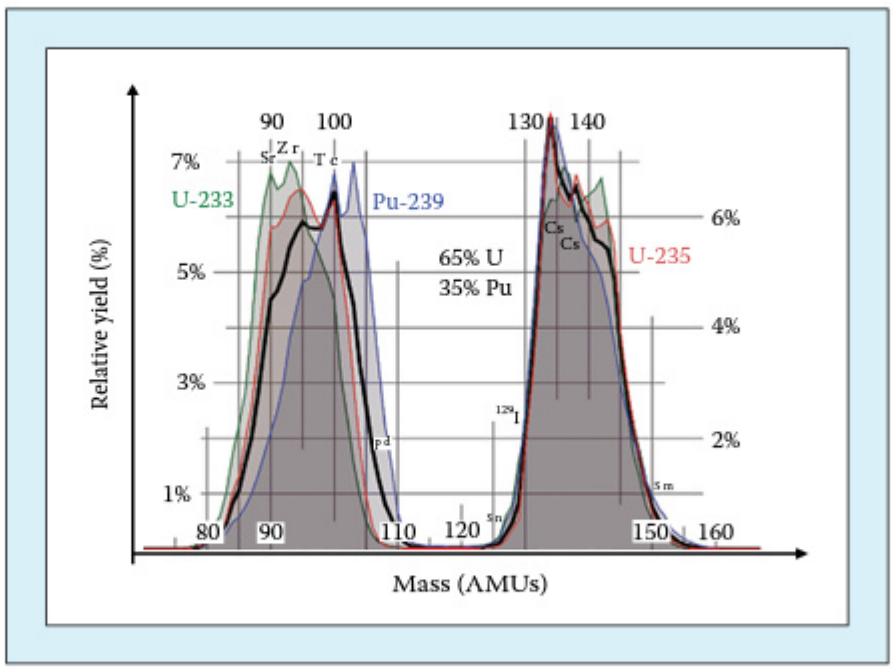

FIGURE 7.9 The distribution of fission fragments from the thermal fission of Uranium-233, Uranium-235, and Plutonium-239. (From Wikipedia.)

TABLE 7.5
Most Common Fission Products Produced from the Thermal Fission of U-235 and Their Yields

Fission Product	Relative Yield (Y) (%)	Half-Life	Information about the Fission Product
$^{133}Cs \rightarrow {}^{134}Cs$	6.7896	∞ 2.065 y	*Neutron capture* converts a few percent of nonradioactive ^{133}Cs to ^{134}Cs, which has very low direct yield because *beta decay* stops at ^{134}Xe; further capture will add to long-lived ^{135}Cs
$^{135}I \rightarrow {}^{135}Xe$	6.3333	6.57 h	Most important *neutron poison; neutron capture* rapidly converts ^{135}Xe to ^{136}Xe; remainder decays (9.14 h) to ^{135}Cs (2.3 my)
^{93}Zr	6.2956	1.53 my	Transmutation is impractical
^{137}Cs	6.0899	30.17 y	
^{99}Tc	6.0507	211 ky	Candidate for disposal by *nuclear transmutation*
^{90}Sr	5.7518	26.9 y	
^{131}I	2.8336	6.02 d	
^{147}Pm	2.2713	2.62 y	
^{149}Sm	1.0888	∞	Second most important *neutron poison*
^{129}I	0.6576	6.7 my	Candidate for disposal by *nuclear transmutation*
^{151}Sm	0.4203	90 y	Most will be destroyed by neutron capture
^{106}Ru	0.3912	373.6 d	
^{85}Kr	0.2717	10.78 y	
^{107}Pd	0.1629	6.5 my	
^{79}Se	0.0508	327 ky	
$^{155}Eu \rightarrow {}^{155}Gd$	0.0330	4.76 y	Both *neutron poisons*
^{125}Sb	0.0297	2.76 y	
^{126}Sn	0.0236	230 ky	
^{157}Gd	0.0065	∞	*Neutron poison*, but low yield
^{113m}Cd	0.0003	14.1 y	Most will be destroyed by neutron capture

Source: Lamarsh, J.R., *Introduction to Nuclear Reactor Theory*, second printing, Addison-Wesley Publishing Company, Inc., Reading, MA, 1972.

material to the next (see Figure 7.9). The kinetic energy of the fission fragments will not be the same for a uranium nucleus as it is for a plutonium one.

Table 7.6 shows the amount of energy that is released from the *thermal fission* of Uranium-235, and its sister table, Table 7.7, shows the amount of energy that is released from the thermal fission of Plutonium-239. As you can see, all of the by-products contribute to the total energy release. About 190 MeV of energy is released instantaneously; however, some of it can also be released over a much longer period of time. We will come back to these tables again when we

TABLE 7.6
Energy Released from the Thermal Fission of Uranium-235

Energy Released from the Fission of U-235	Average Energy Released (in MeV)
Instantaneously released energy	
Kinetic energy of fission fragments	169.10
Kinetic energy of prompt neutrons	4.8
Energy carried by prompt γ-rays	7.0
Energy from decaying fission products at a later time	
Energy of β-particles	6.5
Energy of delayed γ-rays	6.3
Energy released when those prompt neutrons that do not (re)produce fission are captured	6.8
Energy converted into heat in an operating thermal nuclear reactor	202.5
Energy of antineutrinos (unrecoverable energy)	6.8
Sum of all sources	209.3

TABLE 7.7
Energy Released from the Thermal Fission of Plutonium-239

Energy Released from the Fission of Pu-239	Average Energy Released (in MeV)
Instantaneously released energy	
Kinetic energy of fission fragments	175.8
Kinetic energy of prompt neutrons	5.9
Energy carried by prompt γ-rays	7.8
Energy from decaying fission products at a later time	
Energy of β-particles	5.3
Energy of delayed gamma rays	5.2
Energy released when those prompt neutrons that do not (re)produce fission are captured	7.1
Energy converted into heat in an operating thermal nuclear reactor	207.1
Energy of antineutrinos (unrecoverable)	7.1
Sum of all sources	214.2

discuss what happens when millions of these reactions occur at the same time. The important thing to keep in mind is that the fission of every U-235 or Pu-239 nucleus produces, on average, about 200 MeV of *useable* energy. By the term *useable energy*, we mean the amount of the energy released that is actually *recoverable* and can be used to generate useful heat or power. This energy is frequently given the symbol E_R to indicate that it is recoverable. Note that this is different from the total amount of energy produced, which is usually represented by the symbol E and sometimes by the symbol Q.

For a variety of reasons, it turns out that only about 95% of the energy that is produced from a fission reaction can be recovered. This energy can be recovered because it is eventually deposited in the core in the form of *thermal energy or heat*. This thermal energy causes the temperature of the materials in the core to rise. Oddly enough, the remaining 5% of this energy, which is not recoverable (about 10 MeV per fission), cannot be recovered by any technology or process known to man. As we first discussed in our companion book,* this energy is carried away by strange ghostlike particles called *neutrinos* and their corresponding antiparticles or *antineutrinos*. Because the probability of them interacting with matter is so low, the energy and momentum that they carry away simply go into space and are lost forever. It is simply distributed among the stars. Due to the conservation of energy, it is never really destroyed. Why the neutrinos carry away so much energy from a nuclear reactor remains a mystery. Their interaction cross sections are millions of times smaller than those of other nuclear particles such as the neutrons. In quantum mechanical terms, perhaps they simply contribute to the *expectation energy of the vacuum*.

Another important point to keep in mind is that about another 10% of the energy that is produced is not released immediately but shows up in the fuel through radioactive *beta decay* and through the emission of *delayed gamma rays*. This energy can be released anywhere from a couple of minutes to a couple of days after the original parent nucleus is destroyed. Depending upon how it is defined, *radioactive decay* can also contribute to between 6% and 7% of the total recoverable energy that is produced. To get the total amount of energy released, it is important to take the contributions from all of the by-products of the reaction (and their respective time frames) into account.

7.12 Neutrons Released per Fission

The number of fission neutrons that are released per fission is a function of the type of nuclear fuel that is used. This number can vary by as much as 30% between different types of uranium or plutonium fuel. The number of fission neutrons produced obeys a statistical probability distribution similar to the Watt equation that we discussed for Uranium-235. In general, the number that is produced varies from one to four. Table 7.8 shows the "average" number of fission neutrons released from the thermal fission of U-235, U-238, Pu-239, and Pu-241. The incoming neutron in this case is assumed to have a most probable energy of 0.025 eV.

The fissile isotopes of uranium produce an average of about 2.5 neutrons per fission, while the fissile isotopes of plutonium produce an average of about three neutrons per fission. Of course, the reason these numbers are not whole numbers is that some reactions produce two neutrons, while other reactions produce three or four. Table 7.8 shows the statistical average for the isotopes in question. In most textbooks, the quantity $\nu_j(E)$ is defined as the total number of neutrons released by the fission of an element having isotope j. It follows that the total number of neutrons released by the fission of isotope j due to thermal neutrons is

* See *Nuclear Engineering Fundamentals: A Practical Perspective*, by R.E. Masterson, CRC Press (2017).

TABLE 7.8
Number of Neutrons Released from the Thermal Fission of Uranium and Plutonium at 0.025 eV

Atomic Weight	Isotope Type	Isotope Name	Average Number of Neutrons Released (ν) per Fission
233	Fissile	Uranium-233	2.492
235	Fissile	Uranium-235	2.418
238	Fertile	Uranium-238	2.600
238	Mostly fertile	Natural uranium	1.353
239	Fissile	Plutonium-239	2.871
241	Fissile	Plutonium-241	2.927

Total Number of Neutrons Released per Fission

$$\nu^j = \int \nu^j(E)\,dE \tag{7.6}$$

where the limits of the integration are from E ~ 0 to E ~1 eV. We will make use of this definition again when the neutron diffusion equation is derived in Chapter 11.* You may also notice that Table 7.8 makes a distinction between what is a fissile isotope and what is a fertile one.

By definition, a *fissile material* is a heavy isotope with an *odd* atomic number A = Z + N that has a finite probability of absorbing a neutron and splitting apart, while a *fissionable or fertile material* is an isotope with an *even* atomic number that possesses the same capability. In general, fissile materials such as U-233, U-235, and Pu-239 have a much higher chance of absorbing a thermal neutron and splitting apart than fissionable or fertile materials (like U-238 and Thorium-232) do. The probability of a fertile material like U-238 and Th-232 splitting apart and releasing additional neutrons is generally insignificant at any neutron energy.†

7.13 Neutrons Released per Neutron Absorbed

The number of neutrons released per fission (see Table 7.8) is normally given the symbol ν. It is based on the assumption that every uranium or plutonium atom that absorbs a neutron causes a fission reaction to occur. In reality, this is not entirely true because about 14% of the time a Uranium-235 nucleus absorbs a low-speed neutron, the nucleus *does not split apart*. Instead, it captures the neutron and releases a gamma ray instead. When a single nucleus can undergo both neutron capture and fission, the ratio of the probability that the nucleus will emit a gamma ray to the probability that the nucleus will completely split apart is called the *capture-to-fission ratio*. The capture-to-fission ratio α is given by

The Capture-to-Fission Ratio (α)

$$\alpha = \frac{\text{Probability of capturing a neutron and emitting a gamma ray}}{\text{Probability of capturing a neutron and completely splitting apart}} \tag{7.7}$$

and it is usually represented by the symbol α. The capture-to-fission ratio is different for different nuclear fuels. It is also a function of the initial kinetic energy E of the incoming neutron that is absorbed. The values of α for a number of different nuclear fuels are shown in Table 7.9 for low-energy neutrons (i.e., what we have been calling thermal neutrons). In the case of Uranium-235, the capture-to-fission ratio is $\sigma_c/\sigma_f = (96.685\text{ b})/(585.086\text{ b}) = 0.169$. For Pu-239, it is about 0.362. Table 7.9 also shows the average number of neutrons ν (mu) released from the fission of several uranium and plutonium isotopes, as well as additional parameter that we would like to introduce. This additional parameter is called the η (eta) of the fuel, and it is defined in the following way:

The Eta of the Fuel (η)

$$\eta = \frac{\text{Number of neutrons produced by a nuclear fuel}}{\text{Number of neutrons absorbed by the same type of fuel}} \tag{7.8}$$

* See *Nuclear Engineering Fundamentals: A Practical Perspective*, by R.E. Masterson, CRC Press (2017).
† In the case of these isotopes, the neutron binding energy is not provided to the reader because they cannot be created by an isotope with a lower atomic number A by absorbing a free neutron.

TABLE 7.9
Nuclear Data for the Thermal Neutron Fission of Several Isotopes at E = 0.025 eV

Nuclear Fuel	Capture-to-Fission Ratio ($\alpha = \sigma_c/\sigma_f$)	Number of Neutrons Produced per Neutron Absorbed (η)	Number of Neutrons Produced per Fission (ν)
U-233	0.089	2.287	2.492
U-235	0.169	2.068	2.418
U-238	1.811	0.300	2.600
Pu-239	0.362	2.108	2.871
Pu-241	0.359	2.145	2.917

Source: Lamarsh, J.R., *Introduction to Nuclear Reactor Theory*, second printing, Addison-Wesley Publishing Company, Inc., Reading, MA, 1972.

In some textbooks, η (eta) is called the *neutron reproduction factor* because it *represents the number of neutrons produced per neutron absorbed in the fuel*. The total number of neutrons released per neutron absorbed η (eta) is therefore related to the total number of neutrons released per fission ν (mu) by the equation

The Relationship of η, α, and ν

$$\eta = \frac{\nu}{(1+\alpha)} \tag{7.9}$$

which is valid for any nuclear fuel that releases neutrons from a fission reaction. It is also interesting to observe that η is lowest for Uranium-235 and highest for Uranium-233, while ν is lowest for Uranium-235 and highest for Plutonium-239. (Pu-241 is not considered to be a credible nuclear fuel in this case.) So the correlation between their values differs from one isotope to the next, and isotopes that produce the most neutrons per fission ν do not necessarily have the highest value of η. If we rewrite the relationship between η and ν using the nuclear cross sections that we introduced in Chapter 4, then we can express the relationship between η and ν as

$$\eta(E) = \nu\left(\frac{\sigma_f(E)}{\sigma_a(E)}\right) \tag{7.10}$$

where
σ_a is now the neutron absorption cross section
σ_f is now the neutron fission cross section

If we suppress the energy dependence of the cross sections for the moment, then we may also write

$$\eta = \nu\left(\frac{\sigma_f}{\sigma_a}\right) \tag{7.11}$$

which may be easier to understand. In most nuclear engineering textbooks, Equation 7.11 is the definition that is most commonly used. Now we know from our previous discussion that when a fissile material absorbs a neutron, it will not necessarily cause a fission reaction to occur. The absorption cross section σ_a therefore consists of two parts—one part to represent the probability that the nucleus will fission σ_f and another part to represent the probability σ_c that the nucleus will capture the neutron and emit a gamma ray instead. We can represent this latter probability by the radiative capture cross section σ_c or σ_γ. So the total absorption cross section for an incoming neutron can be written as

The Definition of the Absorption Cross Section

$$\text{Absorption} = \text{Capture} + \text{Fission}$$

$$\sigma_a = \sigma_c + \sigma_f \tag{7.12}$$

and when we substitute this into the aforementioned equation, we obtain

$$\eta = \nu\left(\frac{\sigma_f}{(\sigma_c + \sigma_f)}\right) \tag{7.13}$$

or

$$\eta = \frac{\nu}{\left(1 + (\sigma_c/\sigma_f)\right)} = \frac{\nu}{(1+\alpha)} \tag{7.14}$$

where $\alpha = \sigma_c/\sigma_f$. Equation 7.14 is the fundamental link between the value of η and ν for any nuclear material at any neutron energy E.

Example Problem 7.2

Verify that if the value of ν for Plutonium-239 is 2.871, then the value of η for Plutonium-239 must be 2.106.

Solution From Table 7.9, the capture-to-fission ratio for Plutonium-239 or α is 0.362. Therefore, $\eta = \nu/(1 + \alpha) = 2.871/(1.362) = 2.108$. [Ans.]

7.14 The Value of Eta for Different Fuel Mixtures

Most of the time, fissile and fertile materials are mixed together to form composite compounds that are used as commercial nuclear fuels. In these compounds, the effective value of η (eta) can be considerably lower than the values of η quoted in Table 7.9. *Because of this, it is generally incorrect to use the values of η shown in Table 7.9 when attempting to determine if a particular mixture of fertile and fissile materials will cause a reactor to become critical.* In practice, the actual value of η may be considerably lower than the "absolute" values shown in the table. To calculate the correct neutron production rates in this case, it is necessary to go back to the original definition of η to determine the appropriate value to use. It should be recalled that η is defined as the number of neutrons produced per neutron absorbed *in the fuel*. Because of this, we must take the expression for eta that we just introduced

$$\eta = \nu\left(\frac{\sigma_f}{\sigma_a}\right) \tag{7.15}$$

and modify it to account for the fact that the absorption cross section σ_a is now the absorption cross section of more than one type of fuel. In most reactors, Uranium-235 is diluted with Uranium-238 to come up with the final mixture of materials that is used for the fuel rods. To find the correct value, we must recall that the percentage of Uranium-235 atoms to the percentage of Uranium-238 atoms is called *the enrichment* e of the fuel. Natural uranium has a U-235 concentration of about 0.72%, while enriched uranium has an average enrichment of about 3%. In light water reactors (LWRs), both isotopes of uranium are usually combined with two oxygen atoms to form *uranium dioxide* (UO_2) from which the actual fuel rods are made (see Chapter 1). However, the absorption probabilities for oxygen are so low in this case that they can usually be ignored in a direct calculation of η. So the correct equation to use for η whenever there is more than one type of fuel present in a fuel rod is

The Equation for η with Multiple Types of Fuel

$$\eta = \nu^j\left(\frac{e^j\sigma_f^j}{\sigma_a^j}\right) \tag{7.16}$$

where

j = 1, 2,…, N
e is now the *isotopic abundance* of isotope j
N is the number of isotopes in the mixture

Suppose for the moment that we consider natural uranium fuel with an isotopic composition of 0.72% U-235, 99.26% U-238, and 0.02% U-234. There are a total of three isotopes of uranium present in this case, so N = 3. Using the values for ν from

Table 7.9, $\nu^{U234} = 2.40$, $\nu^{U235} = 2.418$, and $\nu^{U238} = 0$, the values for e of $e^{U234} = 0.0002$, $e^{U235} = 0.0072$, and $e^{U238} = 0.9926$, and introducing the values for σ_f and σ_a from Appendix C of $\sigma_a^{U234} = 100.3$, $\sigma_a^{U235} = 680.8$, and $\sigma_a^{U238} = 2.7$ and $\sigma_f^{U234} = 0.0062$, $\sigma_f^{U235} = 585.08$, and $\sigma_f^{U238} = 0$, we find that the value of eta to be used for natural uranium fuel is

$$\eta = \nu^j \left(\frac{e^j \sigma_f^j}{\sigma_a^j} \right) \cong 1.35 \tag{7.17}$$

Notice that there is no contribution from U-238 in the numerator of this equation because the U-238 nucleus does not fission when it absorbs a low-energy neutron. So the presence of the Uranium-238 in the fuel has the effect of *reducing* the value of η shown in Table 7.9 from 2.068 for pure U-235 to a more realistic value of 1.35 for natural uranium. Notice that we are still talking about natural uranium here. If we increase the U-235 enrichment to about 3%, which is typical of the fuel that can be found in most LWRs, then the appropriate value of η would be 1.56. See the following example for more details. Of course, as the enrichment continues to increase, the value of eta will continue to increase as well. Figure 7.10 shows how the value of eta changes as a function of the enrichment e for various U-235 and U-238 mixtures. This figure is very important when the correct value of η is needed for a particular type of uranium fuel.

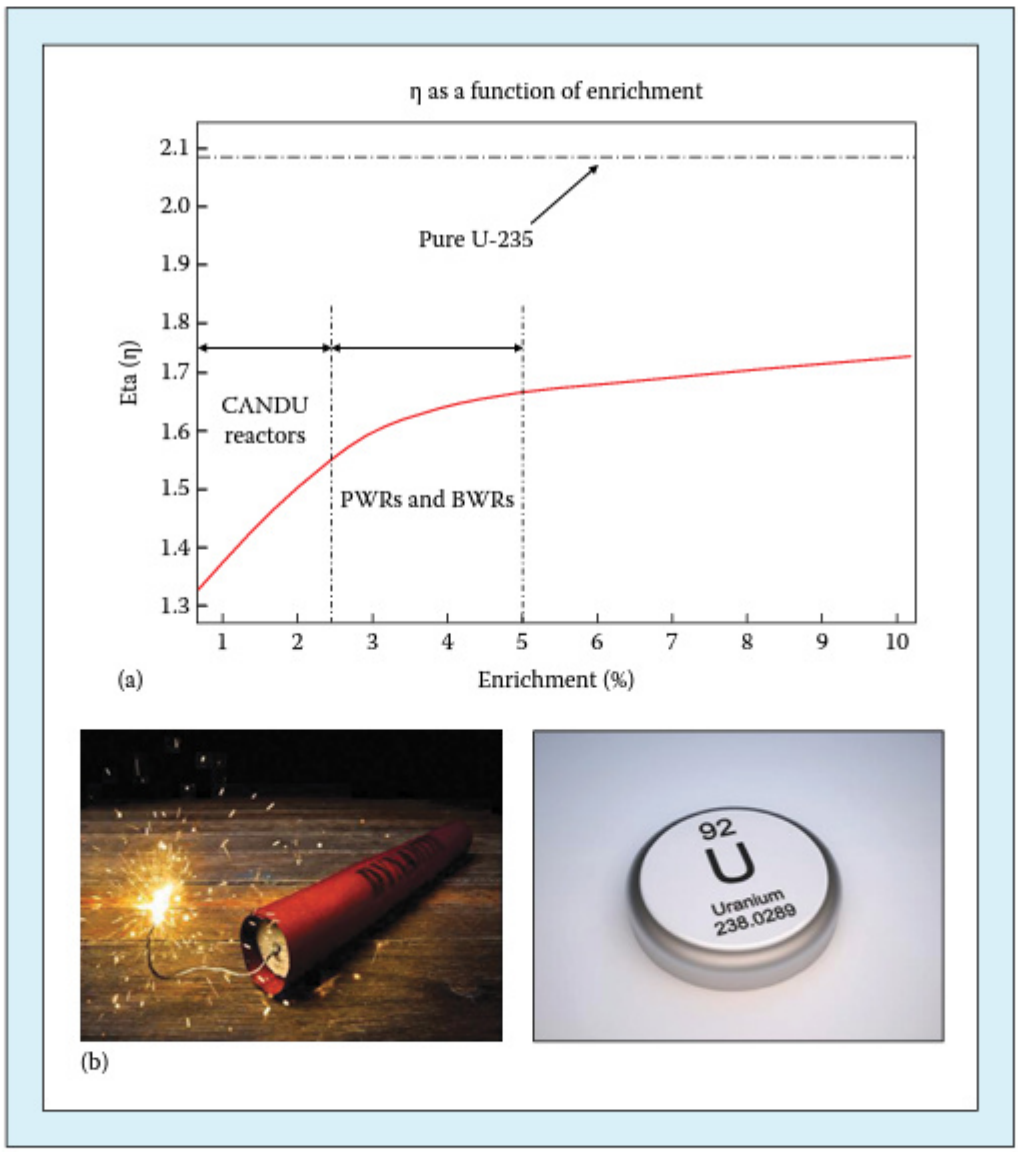

FIGURE 7.10 (a) The eta of a U-235/U-238 mixture as a function of the enrichment. (b) One kilogram of pure uranium can release as much energy as 20,000 metric tons of Hercules class C dynamite.

Example Problem 7.3

Suppose that a fuel rod in a thermal water reactor consists of 3% enriched UO_2. What is the eta of the fuel in this case?

Solution We know from our earlier discussion that we can ignore the presence of the oxygen atoms in the fuel in our calculation of the value for η and that this fuel is not likely to contain any significant amounts of U-234. So to perform our calculation, we can assume that the fuel consists of a mixture of 3% U-235 and 97% U-238. Ignoring for the moment the slight difference in the weight of U-235 and U-238, the eta in this case is

$$\eta = \frac{\nu^{U235} e^{U235} \sigma_f^{U235}}{\left(e^{U235}\sigma_a^{U235} + e^{U238}\sigma_a^{U238}\right)} = \frac{2.088 \times 0.03 \times 582.2}{\left(0.03 \times 680.8 + 0.97 \times 2.7\right)} = 1.58$$

Notice that we have ignored the contribution of U-238 in the numerator because this nuclide does not have a significant probability to fission with low-energy neutrons. A fuel rod containing fuel that is enriched to 4% would of course have a higher value of η. [Ans.]

Student Exercise 7.3

Using what you have just learned, calculate the value of η for a fuel rod that contains 4% enriched uranium and where the majority of the fissions are assumed to occur due to thermal neutrons.

7.15 Nuclear Energy Release versus Chemical Energy Release

Unlike the chemical reactions that most of us learned about in a high school chemistry class, nuclear reactions do not involve breaking the chemical bonds of atoms and rearranging the orbital configurations of the electrons. *Nuclear reactions involve breaking the bonds within the nucleus of the atom itself* (see Chapter 2). The energy released in this process is many times greater than the energy released in a typical chemical reaction. For example, even compared to a violent chemical reaction, such as one caused by exploding a stick of *dynamite*, the energy released by a nuclear reaction can be 1,000 or even 10,000 times as great. Nuclear energy is created by converting a small amount of the *mass* inside the nucleus of an atom *into kinetic energy or heat*. Different nuclear reactions can produce different amounts of energy, and this energy can be distributed in various ways between the particles that emerge from the reactions. Splitting a uranium or plutonium nucleus apart produces about 200 MeV of recoverable energy, while a radiative capture reaction produces about 1 MeV of energy (in the form of a photon or gamma ray), and alpha or beta decay produces between 4 and 10 MeV of recoverable energy (depending on the exact type of decay that occurs). Novices to the field of nuclear power are sometimes surprised to learn how the energy released by a chemical reaction compares to the energy released by a nuclear one. Consider the common exothermic chemical reactions whose energy output is shown in Table 7.10. Here, we have made use of the fact that

One Million Electron Volts

$$1\ \text{MeV} = \left(1.00 \times 10^{6}\ \text{eV}\right) \cdot \left(1.60 \times 10^{-19}\ \text{J/eV}\right)$$
$$= 1.60 \times 10^{-13}\ \text{J} \qquad (7.18)$$

TABLE 7.10
Typical Energy Conversion Values of Various Fuels

Fuel Source	Energy Equivalent
Dynamite	7.5 MJ/kg
Firewood	16 MJ/kg
Brown coal	9 MJ/kg
Black coal (low quality)	13–20 MJ/kg
Black coal (high quality)	24–30 MJ/kg
Natural gas	39 MJ/m^3
Crude oil	45–46 MJ/kg
Uranium[a]—in LWR	500,000 MJ/kg

[a] Natural uranium.

This relationship between the value of an MeV and a Joule was first introduced to the reader in Chapter 1. By comparing the numbers in this table, it is easy to see that 200 MeV of energy is equivalent to breaking over 10,000 hydrogen electron bonds. So 20,000 metric tons of TNT will release about much energy as we can release by converting about 1 kg of Uranium-235 (about half a pound) into pure energy. *In practical terms, this means that the fission of 1 kg (2.2 lb) of Uranium-235 releases about 16.7 million kWH of heat. So we may conclude from this simple exercise that nuclear reactions release much more energy than chemical ones.*

7.15.1 An Interesting Comparison

Suppose that we look at the rate of energy production from a slightly different perspective. The fission of a single uranium nucleus releases approximately 200 MeV of recoverable energy or about 3.2×10^{-11} J. In other words, 3.1×10^{10} fissions/s are required to produce 1 W of *thermal power*. The fission of 1 g of uranium or plutonium per day will liberate about 1 MW of thermal energy. This is the energy equivalent of about 3 tons of coal (or 600 gallons of fuel oil). *These fossil fuels produce about a quarter of a ton of carbon dioxide when they are burned, while the fission of 1 g of uranium or plutonium produces none.*

In practice, the *energy content* of a nuclear or fossil fuel can be measured by considering the amount of heat it generates. Using this definition of the energy content, a stick of Hercules dynamite contains roughly 2.1 MJ of thermal energy. The energy density (in joules/kilogram or J/kg) of dynamite is approximately 7.5 MJ/kg, compared to 4.7 MJ/kg for a comparable amount of TNT. Table 7.10 compares the energy potential of several common conventional fuels to the uranium used in an LWR. On average, the energy potential of uranium per kilogram is about 100,000 times as great. Other heat unit measurements include joules and kWH. One BTU is equal to 252 calories or 1055 J. One kWH is equal to 3,412 BTUs, 859,824 calories, or 3,599,660 J. Note that a 1″ thick × 8″ stick of *"Hercules C" class dynamite* weighs about 0.62 lb.

7.16 Energy Release per Fission

The amount of *thermal energy released per fission* depends on the type of fuel that is used. For thermal fission reactions, the average amount of *prompt energy* released per fission E_f (when measured in MeV) can be found from the equation

$$E_f = 1.29927 \times 10^{-3}\left(Z^2 \cdot \sqrt{A}\right) + 3.12 \quad (\text{MeV per fission}) \tag{7.19}$$

which was first proposed by *Unik and Gindler* in the early 1970s. Here, Z and A are the atomic number and the atomic mass number of the fissioning nucleus, and the energy released in Equation 7.19 is the *recoverable amount of prompt energy per fission*. On average, 20 MeV of additional kinetic energy is released after the fission products decay. This energy is called the *recoverable delayed energy per fission*, and it is gradually released within 100 seconds after the initial fission reaction. Finally, the total energy released per fission (which is the sum of the recoverable plus the unrecoverable energy) is about 5% higher, but in practice this additional 5% can be ignored because it escapes from the core entirely. In practice, Equation 7.19 applies to all fissionable isotopes from Uranium-233 to Plutonium-242. Hence, it is a useful tool when it comes to comparing the amount of energy released by different nuclear fuels.

Table 7.11 shows how the average amount of energy released per fission compares from one nuclear fuel to the next. This equation is used in many reactor physics calculations, and it has an overall accuracy of about 1%. As we discussed previously, the average energy released per fission is about 200 MeV (3.2×10^{-11} J) although this number can vary by about 5% depending on the type of nuclear fuel that is used. In a typical reactor fuel assembly, about 97.5% of this energy is deposited in the fuel, and the remaining 2.5% is deposited in the coolant and in the surrounding structural materials. The plutonium produced in an LWR core also participates in this energy release, and this *plutonium (which is produced when the U-238 atoms in the fuel absorb a thermal neutron) generates about one-third of the total energy output of the plant*. In some cases, this number may approach 50% of the total energy release near the end of a fuel cycle. Thus, the energy deposition rate varies as the Uranium-235 atoms are depleted, and additional Pu-239 atoms are produced.

7.17 The Origin of Nuclear Energy

When an atomic nucleus splits apart, about 200 MeV of *recoverable* energy is released. This energy is the result of a very small amount of the mass inside of the nucleus being converted into energy. One way to calculate this energy release is to add up the mass of all of the particles inside of the nucleus before it splits apart. We can do this by simply looking up the atomic mass of whatever isotope has absorbed the neutron in Table 7.11. We can call this mass M_i or the *initial mass*

TABLE 7.11
Amount of Prompt Recoverable Energy Released from the Thermal Fission of Uranium and Plutonium

Isotope	Z	A	$Z^2 \cdot \sqrt{A} \times 10^{-3}$	E_r (Recoverable) (MeV)
U-233	92	233	129.197	170.98
U-235	92	235	129.750	171.70
Pu-239	94	239	136.600	180.70
Pu-240	94	240	136.886	181.07
Pu-241	94	241	137.172	181.44
Pu-242	94	242	137.456	181.81

Notes: The numbers in this table include the kinetic energy of the fission fragments and prompt neutrons and gamma rays only. They do not include the energy from the delayed gamma rays, beta particles, and neutrinos in the total.

before the nucleus splits apart. We can then calculate the *final mass*, M_f, of all of the particles after the nucleus splits apart. The mass difference is then the amount of mass Δm that has been converted into energy by the nuclear reaction:

$$\Delta m = M_i - M_f \tag{7.20}$$

where Δm is the difference in mass between the mass that we started with, M_i, and the mass we ended up with, M_f.

Because the final mass M_f is always less than the initial mass M_i, this mass difference is always a positive number, and some useful energy will always be produced when the nucleus splits apart. There is a very specific relationship between the mass that has disappeared and the amount of energy that has been produced. You may recall from our previous discussion in Chapters 2 and 6 that the energy of a particle and its rest mass are essentially two manifestations of the same physical quantity—which is sometimes called the *mass energy*. These two quantities are related to each other by Einstein's famous equation

Einstein's Equation

$$\text{Energy released} = E = \Delta m c^2 \tag{7.21}$$

where
E is the energy of an object
m is the mass of an object
c is the speed of light

Since the speed of light is a very big number, 186,000 miles/s, or about 300 million m/s, *a small amount of mass can be equivalent to a very large amount of energy*. It turns out that it is relatively straightforward to determine how much energy is released by 1 AMU* of nuclear material (about the rest mass of a proton or a neutron) by using Einstein's equation with $m = 1\ \text{AMU} = 1 \times 10^{-13}$ kg. When we perform this calculation, we find that

Relationship of an AMU to an MeV

$$1\ \text{AMU} = 931.494\ \text{MeV}/c^2 \tag{7.22}$$

This formula applies to any nuclear particle that has a physical mass that we can measure—and not just to protons or neutrons. For example, it can be applied to electrons and quarks as well. So Equation 7.22 says that a mass difference Δm of only 0.1 AMU between the masses of the particles going into a reaction and the masses of the particles coming out of a reaction is equal to about 93.15 MeV/c^2, and this will result in the release of about 93.15 MeV of kinetic energy. Now let us apply Equation 7.22 to the fission of a typical uranium or a plutonium nucleus. Suppose that we would like to know how

* 1 AMU = atomic mass unit = 0.9915 the rest mass of the neutron.

nuclear mass must be converted into energy to release 200 MeV of *recoverable* thermal energy. Since fully 5% of this energy is not recoverable from a fission reaction (see Section 7.9), then we will assume that 210 MeV of energy must be produced so that 200 MeV of it will be recoverable. It therefore follows that $E = \Delta mc^2$ or $\Delta m = 210\ \text{MeV}/c^2$, and the result is that $\Delta m = 0.215$ AMU. *So about 1/5th of the mass of a proton or neutron must be converted into energy to create 200 MeV of recoverable energy in a typical fission reaction.* This is an astonishing amount of energy for such a small amount of mass.

In other words, we have answered the question of where the enormous energy released from the fission of an atomic nucleus comes from. It is produced by converting a very small amount of mass within the atomic nucleus itself (equivalent to about one-fifth of the rest mass of the proton or the neutron) directly into energy. This energy manifests itself as the kinetic energy of the fission products and the other nuclear particles that are produced. Over time, this kinetic energy is eventually converted into heat, which heats the coolant in the core, and therefore allows thermal power to be produced.

Proton and Neutron Rest Masses (in AMU and MeV)

$$\text{Proton: } 1.00728\ \text{AMU} = 938.28\ \text{MeV}/c^2 \tag{7.23a}$$

$$\text{Neutron: } 1.00866\ \text{AMU} = 939.57\ \text{MeV}/c^2 \tag{7.23b}$$

Equation 7.23 shows the rest masses of the proton and the neutron in AMUs and their equivalent energies in MeV. Notice that the neutron is slightly heavier than the proton. The difference in mass is slightly more than the rest mass of an electron (about 0.511 MeV).

Since the number of protons and neutrons going into the reaction (the value of $A = Z + N$) is always equal to the number of protons and neutrons coming out of the reaction (at least in the case of nuclear fission), this immediately begs the question of why only a fraction of a proton or a neutron does not come out. The reason is that free protons and the neutrons only exist as complete particles, and there is no such thing as a fractional proton or a neutron. *The energy that is released therefore comes from the binding energy that bonds the protons and neutrons together and not directly from the particles themselves.* Since the protons and the neutrons are in turn made out of quarks, this energy comes from the fact that a bound quark is part mass and part energy as we had first discussed in Chapter 2.

7.18 The Threshold Energy for Fission

We learned in Chapters 1 and 2 that all particles within the nucleus are bound together by force particles called *gluons*. Both the proton and the neutron are made up of three quarks, and the only difference between them is that *the proton consists of two up quarks and a down quark and the neutron consists of two down quarks and an up quark*. This slight difference in the mass of the third quark is responsible for the fact that the proton and the neutron have slightly different rest masses, and it is also responsible for the fact that the proton has an electrical charge of +1 and the neutron does not. A picture of the internal structure of the proton and the neutron is shown in Figure 7.11. Figure 7.12 also shows how each particle is built from these quarks and how the individual quarks are bound to each

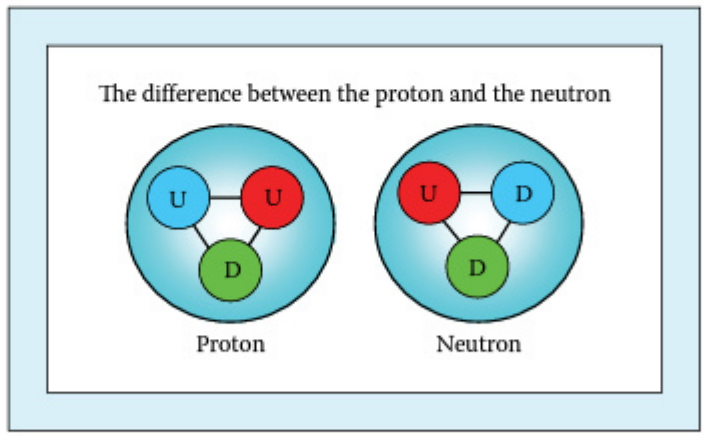

FIGURE 7.11 The quark composition of a proton and a neutron. Note that the interchange of one up quark U and one down quark D results in the proton having an electrical charge and the neutron having none.

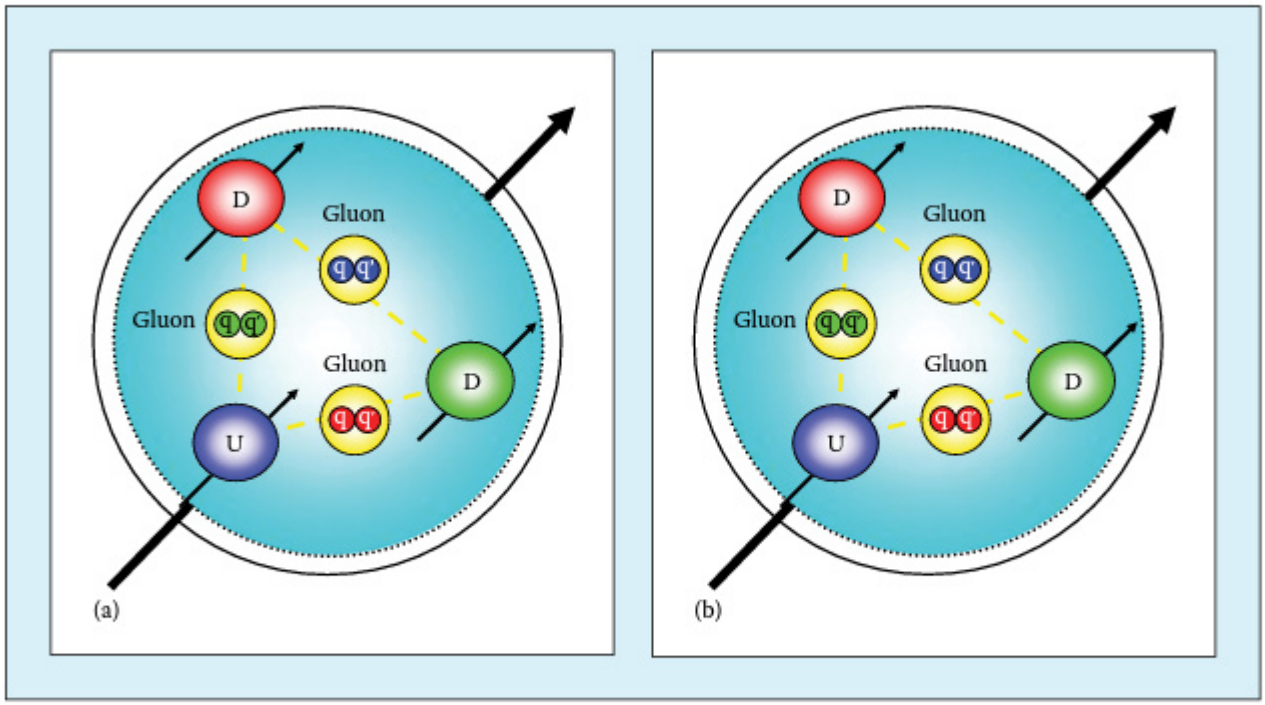

FIGURE 7.12 A picture of the internal structure of (a) the neutron and (b) the proton. (Notes: The gluons that hold these particles together are the small green, blue, and red balls that are shown in pairs of 2. This is to indicate that each gluon consists of a quark/antiquark pair.)

other by *gluons*, which in turn consist of quark/antiquark pairs that behave like the ends of a bar magnet. The gluons are then considered to be the carriers of the nuclear force field.

7.18.1 The Critical Energy of Fission

We also mentioned in Chapter 3 that there is a critical energy or threshold energy required for an atomic nucleus to split apart. This *critical energy of fission* is isotope dependent, and it is also a function of the number of protons Z and neutrons N that an isotope has. It is also called the *fission threshold energy*. This energy is represented by the symbol E_{crit}, and the values of E_{crit} are given in Table 7.12 for most common fertile and fissile materials. Because the binding energy for each successive fissile/fissionable pair (U-233 and U-234, U-235 and U-236, and Pu-239 and Pu-240) is always *lower* after the

TABLE 7.12
Fission Threshold Energy for the Most Common Heavy Elements in MeV

Isotope Name	Type of Nuclear Material	Isotopic Rest Mass (AMU)	Total Binding Energy of All Nucleons (MeV)	Fission Threshold Energy (MeV)	Binding Energy of Last Neutron (MeV)
Th-232	Fertile	232.038051		5.9	N/A[a]
Th-233	Fissionable			6.5	5.1
U-233	Fissile	233.039628	1771.8	5.5	N/A
U-234	Fissionable	234.040947	1776.6	4.6	6.6
U-235	Fissile	235.043924	1783.9	5.75	N/A
U-236	Fissionable	236.045563	1790.4	5.3	6.4
U-238	Fissionable	236.050785	1801.7	5.85	N/A
U-239	Fissionable	239.054290	1806.5	5.5	4.9
Pu-239	Fissile	239.052158	1806.9	5.5	N/A
Pu-240	Fissionable			4.0	6.4

Source: Lamarsh, J.R., *Introduction to Nuclear Reactor Theory*, second printing, Addison-Wesley Publishing Company, Inc., Reading, MA, 1972.

initial fissile material absorbs a free neutron than before it is absorbed, the incoming neutron does not necessarily have to have much energy for the nucleus of the resulting isotope to split apart. As a matter of fact, *this "design feature" of the universe means that adding an extra neutron to the nucleus of an isotope having an ODD atomic number will almost always result in the release of some energy by the resulting compound nucleus.*

In the case of U-233, U-235, and Pu-239, this happens when the nucleus splits apart. However, the resulting nucleus can also emit a gamma ray—which is the radiative capture process we discussed in Chapter 3. For example, it is easy to see from Table 7.12 that the binding energy of the last neutron in Uranium-234 is 6.6 MeV, while E_{crit} is only 4.6 MeV. So when a thermal neutron with virtually no kinetic energy is absorbed by a U-233 nucleus, the compound nucleus, U-234, is produced with 2.0 MeV more energy than its critical energy, and it is energetically possible for a fission reaction to occur. When we apply this same argument to the absorption of a thermal neutron by U-235, we find that the compound nucleus, U-236, is produced with 1.1 MeV *more* than its critical threshold energy.

Thus, the U-236 nucleus can either split apart by fissioning to remove this energy imbalance or it can release a gamma ray to get rid of the extra energy and to fall below the binding energy of the last neutron. In this case, the gamma ray is released with an energy of at least 1.1 MeV, and the resulting U-236 nucleus then becomes a stable nucleus with a half-life of about 25 million years. The exact probability of each of these events occurring is defined by the capture-to-fission ratio α that we discussed in a previous section. Notice that this does not tell us exactly how *much* energy will be released. It simply tells us that *some* energy will be released, and what the probability of each event will be. We would now like to show how different ways of splitting an atomic nucleus apart can result in slightly different amounts of kinetic energy being released. Some fission reactions will produce more than 200 MeV of recoverable energy, and some will produce less. (The exact number depends on how the mass of the by-products compares to the mass of the compound nucleus before the fission process occurs.)

7.19 Some Examples of the Amount of Energy Produced

A typical fission reaction can release about 210 MeV of kinetic energy, of which approximately 200 MeV, or 95%, of it is of the *recoverable kind*. However, not all fission reactions release exactly the same amount of energy (some will release less and some will release more). Depending on the mass of the fission products that are produced and how many neutrons are ejected, some reactions will release more than 200 MeV of energy, and some will release less. *Two hundred million electron volts of energy is therefore the average amount of recoverable kinetic energy per fission that is released.*

In the case of Uranium-235, we know that adding a neutron (with a mass of 1.00866 AMU) to a U-235 nucleus will convert a U-235 nucleus into a U-236 nucleus. This causes the U-236 nucleus, which has a rest mass of 236.0456 AMU, to become unstable, and it will break into two fission products and two or three neutrons about 86% of the time. The other 14% of the time, it will *NOT* break apart; however, it will release some additional energy by emitting an energetic photon or gamma ray. There are many common ways, or fission channels, that a U-236 nucleus can use to split apart. We would now like to illustrate two of these fission channels (out of about 60) that involve the production of barium and krypton. This process is by no means confined to the production of barium and krypton and their fission products. Many other fission products, such as Cs-133, I-135, Sr-88, Xe-136, Sr-90, and Zr-93, are also produced in similar reactions, and normally they lead to similar results. The goal of this discussion is to give a brief overview of the differences that the masses and the distribution of the fission products can have on the total energy release. Of course, the amount of energy released will always be given by Einstein's equation

$$E = \Delta mc^2 \quad \text{or} \quad \Delta m = 210 \ \text{Mev/c}^2 \tag{7.24}$$

where, on average, Δm = 0.225 AMU. The first example we would like to present involves splitting a U-235 nucleus into Barium-141 and Krypton-92 and releasing *three* fission neutrons in the process. The governing equation is

$$^{1}_{0}n + {}^{235}_{92}U \rightarrow {}^{236}_{92}U \rightarrow {}^{141}_{56}Ba + {}^{92}_{36}Kr + 3\,{}^{1}_{0}n \tag{7.25}$$

When the exact masses of the by-products are added together, the sum turns out to be less than the sum of the masses of a Uranium-235 nucleus and the original neutron. This mass difference Δm appears as the kinetic energy $\Delta E = \Delta mc^2$, of the by-products, where c is the speed of light. When a U-235 nucleus absorbs a neutron and splits apart, it can also produce Barium-142, Krypton-92, and *two* neutrons instead of three. In this case, the equation governing this process is

$$^{1}_{0}n + {}^{235}_{92}U \rightarrow {}^{236}_{92}U \rightarrow {}^{142}_{56}Ba + {}^{92}_{36}Kr + 2\,{}^{1}_{0}n \tag{7.26}$$

Now let us add up the differences in the atomic masses for each process. In the first case, where U-236 splits into Ba-141 and Kr-92 and three neutrons, the sum of the masses of the by-products (see Table 7.14) is

Fission Producing Three Neutrons

Ba-141 nuclear mass = 140.8833 AMU
Kr-92 nuclear mass = 91.9021 AMU
3 neutron rest masses = 3.0256 AMU
Total nuclear mass = 235.811 AMU (7.27)

And in the second case, where U-236 splits into Ba-142 and Kr-92 and two neutrons, the sum of the masses of the by-products (see Appendix E) is

Fission Producing Two Neutrons

Ba-142 nuclear mass = 141.9163 AMU
Kr-92 nuclear mass = 91.9021 AMU
2 neutron rest masses = 2.0171 AMU
Total nuclear mass = 235.835 AMU (7.28)

In the first case, the atomic mass difference is 236.0456 AMU − 235.811 AMU = 0.2346 AMU, and the energy released is therefore 218.53 MeV. In the second case, the atomic mass difference is 236.0456 AMU − 235.835 AMU = 0.2106 AMU, and the energy released is therefore 196.18 MeV. In each case the mass differences are slightly less than we would encounter in other reactions involving the production of Cs-133, I-135, Sr-88, Xe-136, Sr-90, and Zr-93. However, averaged over all possible combinations of these reactions, the mass difference Δm, on average, turns out to be about 0.225 AMU—or about 210 MeV (see Equation 7.24). If we were to repeat the same process with Pu-239 or U-233 instead of U-235, the results would be essentially the same. Thus the missing mass eventually shows up in the core in the form of light or heat.

7.20 Differences in Fission Product and Uranium and Plutonium Masses

As we have seen, uranium and plutonium atoms can split apart in many different ways and release different numbers of fission neutrons in the process. The mass difference between the nucleus before it splits apart and the sum of the atomic masses of the by-products after it splits apart determines how much kinetic energy is released in a particular reaction. Each combination of by-products will release a slightly different amount of kinetic energy. When we first studied this phenomenon in Section 7.5, we presented a few common ways in which a Uranium-235 nucleus could split apart. Among them were

Different Ways That a Uranium-235 Nucleus Can Split Apart

$$
\begin{aligned}
&{}^{1}_{0}\mathrm{n} + {}^{235}_{92}\mathrm{U} \rightarrow {}^{236}_{92}\mathrm{U} \rightarrow {}^{140}_{55}\mathrm{Cs} + {}^{93}_{37}\mathrm{Rb} + 3\,{}^{1}_{0}\mathrm{n} + \mathrm{Q}'\\
&{}^{1}_{0}\mathrm{n} + {}^{235}_{92}\mathrm{U} \rightarrow {}^{236}_{92}\mathrm{U} \rightarrow {}^{139}_{56}\mathrm{Ba} + {}^{94}_{36}\mathrm{Kr} + 3\,{}^{1}_{0}\mathrm{n} + \mathrm{Q}''\\
&{}^{1}_{0}\mathrm{n} + {}^{235}_{92}\mathrm{U} \rightarrow {}^{236}_{92}\mathrm{U} \rightarrow {}^{142}_{54}\mathrm{Xe} + {}^{92}_{38}\mathrm{Sr} + 2\,{}^{1}_{0}\mathrm{n} + \mathrm{Q}'''\\
&{}^{1}_{0}\mathrm{n} + {}^{235}_{92}\mathrm{U} \rightarrow {}^{236}_{92}\mathrm{U} \rightarrow {}^{141}_{56}\mathrm{Ba} + {}^{92}_{36}\mathrm{Kr} + 3\,{}^{1}_{0}\mathrm{n} + \mathrm{Q}''''\\
&{}^{1}_{0}\mathrm{n} + {}^{235}_{92}\mathrm{U} \rightarrow {}^{236}_{92}\mathrm{U} \rightarrow {}^{142}_{56}\mathrm{Ba} + {}^{92}_{36}\mathrm{Kr} + 2\,{}^{1}_{0}\mathrm{n} + \mathrm{Q}'''''\\
&{}^{1}_{0}\mathrm{n} + {}^{235}_{92}\mathrm{U} \rightarrow {}^{236}_{92}\mathrm{U} \rightarrow {}^{144}_{56}\mathrm{Ba} + {}^{90}_{36}\mathrm{Kr} + 2\,{}^{1}_{0}\mathrm{n} + \mathrm{Q}''''''\\
&{}^{1}_{0}\mathrm{n} + {}^{235}_{92}\mathrm{U} \rightarrow {}^{236}_{92}\mathrm{U} \rightarrow {}^{134}_{54}\mathrm{Xe} + {}^{100}_{38}\mathrm{Sr} + 2\,{}^{1}_{0}\mathrm{n} + \mathrm{Q}'''''''
\end{aligned}
\tag{7.29}
$$

Here, the symbol Q refers to the amount of kinetic energy that is released. Notice that the value of Q can vary from one reaction to the next. In order to be able to determine each of these values for Q with absolute precision, we need to know the atomic mass of each uranium and plutonium isotope that forms a compound nucleus, and we also need to know the atomic masses of each fission product that comes out of the reaction. Since each different fission product can have many different isotopes, it is necessary to know the exact atomic mass (in AMU) of each isotope as well.

TABLE 7.13
Atomic Masses of All of the Common Isotopes of Uranium and Plutonium

Isotope	Z	A	Atomic Mass (AMU)	Binding Energy (MeV)	Spin	Natural Abundance	Half-Life	Decay Mode[a]	Q (MeV)
U-226	92	226	226.029170	1725.0	0	…	0.5 s	a	7.56
U-231	92	231	231.036270	1756.7	5/2	…	4.2 d	EC	0.36
U-232	92	232	232.037130	1766.0	0	…	66.9 d	A	5.41
U-233	92	233	233.039628	1771.8	5/2	0.000055	0.159 My	A	4.91
U-234	92	234	234.040947	1776.6	0	…	0.245 My	A	4.86
U-235	92	235	235.043924	1783.9	7/2	0.00720	0.704 Gy	A	4.68
U-236	92	236	236.045563	1790.4	0	…	23.4 My	A	4.57
U-238	92	238	236.050785	1801.7	0	0.99275	4.46 Gy	A	4.27
U-239	92	239	239.054290	1806.5	5/2	…	23.54 m	b-	1.26
Pu-239	94	239	239.052158	1806.9	1/2	…	24.11 ky	b-	5.24
Pu-241	94	241							
Pu-242	94	242	242.058737	1825.0	0	…	0.376 My	A	4.98
Pu-244	94	244	244.064198	1836.1	0	…	82 My	A	4.67

[a] EC, electron capture.

Table 7.14 presents an accurate list of the atomic masses of the isotopes of all of the major fission products, and Table 7.13 presents the atomic masses of each isotope of uranium and plutonium. With this information, it is possible in principle to calculate the energy release Q from *any* common fission process involving the fission of U-233, U-235, or Pu-239. All that is required is a knowledge of the rest masses of these fission fragments and the equation that governs a specific reaction. Of course, *a mass difference Δm of 1 AMU is equivalent to exactly 931.494 MeV of kinetic energy*.

Several sources of nuclear data were used in the preparation of these tables. The first is an interactive version of the Periodic Table that can be found at the following URL:

http://hyperphysics.phy-astr.gsu.edu/hbase/pertab/pertab.html#c1

If you click on a specific element that is shown in the table (such as krypton or Kr), you will be presented with an additional set of tables that contains additional information on the properties of that element. If you click on the nuclear properties table, the properties of all the stable isotopes of each isotope can be found. The second source of data that was used to produce this table is a computational knowledge engine that can be accessed at the following URL:

http://www.wolframalpha.com

To use this engine, simply type in the name of an element, followed by a dash and its atomic weight. For example, to get the properties of Uranium-235 or the properties of Strontium-100, type in the name and the atomic weight exactly as shown. The dash (–) that separates the name and the atomic weight must always be used to obtain the correct result. The Wolfram Alpha knowledge engine is an outstanding attempt to make a large amount of basic information available to anyone who can access the Internet. It can be used to find the nuclear properties of any isotope that is not stable enough to be listed in the HyperPhysics URL. With the isotopic rest masses that are shown in Table 7.14 or that can be found at the previous URLs, it is possible to calculate the amount of matter that is converted into energy in any of the reactions we have discussed so far. To do so, simply apply Einstein's equation $E = mc^2$ to any reaction that involves splitting the U-235 nucleus apart.

7.21 Types of Nuclear Chain Reactions

In principle, there are two types of chain reactions that can occur in nuclear systems. The first is called a controlled chain reaction and the other is called an uncontrolled chain reaction. In a *controlled chain reaction*, the number of neutrons that are produced by the fission process are balanced by the number of neutrons that are destroyed due to leakage and absorption. As long as this balance is maintained, useful energy can be produced. In an *uncontrolled chain reaction*, the goal is to have as many neutrons as possible produced in the shortest possible time. The intent of this type of chain reaction is to release a great deal of energy very quickly. In other words, the intent of this reaction is to create an atomic *bomb*.

TABLE 7.14
Atomic Masses of All of the Common Fission Products of Uranium and Plutonium

Isotope	Z	A	Atomic Mass (AMU)	Binding Energy (MeV)	Spin	Natural Abundance	Half-Life	Decay Mode	Q (MeV)
Br-77	35	77	76.921377	667.36	3/2	…	57.0 h	b+	1.37
Br-79	35	79	76.918336	686.33	3/2	0.5069	Stable	…	…
Br-81	35	81	80.916289	704.38	3/2	0.4931	Stable	…	…
Br-82	35	82	81.916802	76.98	5	…	35.30 h	b–	3.09
Kr-78	36	78	77.920396	675.56	0	0.0035	Stable	…	…
Kr-80	36	80	79.916380	695.44	0	0.0225	Stable	…	…
Kr-81	36	81	80.916590	703.32	7/2	…	0.21 My	EC	0.28
Kr-82	36	82	81.913483	714.28	0	0.116	Stable	…	…
Kr-83	36	83	82.914135	721.75	9/2	0.115	Stable	…	…
Kr-84	36	84	83.911507	732.27	0	0.57	Stable	…	…
Kr-85	36	85	84.912532	739.38	9/2	…	10.72 y	b–	0.69
Kr-86	36	86	85.910615	749.24	0	0.173	Stable	…	…
Kr-90	36	90	89.919528	773.23	0	…	32.3 s	b–	4.39
Kr-92	36	92	91.926270	783.09	0	…	1.84 s	b–	6.06
Rb-83	37	83	82.915143	720.03	5/2	…	86.2 d	EC	0.96
Rb-85	37	85	84.911794	739.29	5/2	0.72165	Stable	…	…
Rb-87	37	87	86.909187	757.86	3/2	0.27835	Stable	…	…
Rb-93	37	93	92.922042				5.84 s		
Sr-84	38	84	83.913430	726.91	0	0.0056	Stable	…	…
Sr-85	38	85	84.912937	737.44	9/2	…	64.8 d	b+	1.08
Sr-86	38	86	85.909267	746.93	0	0.0986	Stable	…	…
Sr-87	38	87	86.908884	757.36	9/2	0.07	Stable	…	…
Sr-88	38	88	87.905619	766.47	0	0.8258	Stable	…	…
Sr-90	38	90	89.907738	782.64	0	…	29 y	b–	0.55
Sr-100	38	100	99.935352				200 ms		
I-125	53	125	124.904620	1056.3	5/2	…	59.9 d	b–	0.18
I-127	53	127	126.904473	1072.6	5/2	1.00	Stable	…	…
I-129	53	129	126.904986	1086.3	7/2	…	17 My	b–	0.19
Xe-124	54	124	123.905894	1046.3	0	0.001	Stable	…	…
Xe-126	54	126	125.904281	1063.9	0	0.0009	Stable	…	…
Xe-127	54	127	126.905182	1071.0	1/2	…	36.2 d	EC	0.66
Xe-128	54	128	127.903531	1080.8	0	0.0191	Stable	…	…
Xe-129	54	129	126.904780	1087.7	1/2	0.264	Stable	…	…
Xe-130	54	130	129.903509	1096.9	0	0.041	Stable	…	…
Xe-131	54	131	130.905072	1103.5	3/2	0.212	Stable	…	…
Xe-132	54	132	131.904144	116.5	0	0.269	Stable	…	…
Xe-133	54	133	132.905889	1116.9	3/2	…	5.25d	b–	0.43
Xe-134	54	134	133.905395	1127.5	0	0.104	Stable	…	…
Xe-135	54	135	134.907227				9.14 h	b–	
Xe-136	54	136	135.907213	1141.9	0	0.089	Stable	…	…
Cs-133	55	133	132.905429	1116.6	7/2	1.00	Stable	…	…
Cs-135	55	135	134.905885	1134.3	7/2	…	2.3 My	b–	0.21
Cs-137	55	137	136.907074	1149.3	7/2	…	30.17 y	b–	1.17
Cs-140	55	140	139.917282				63.7 s	b–	
Ba-130	56	130	129.906281	1092.8	0	0.00106	Stable	…	…
Ba-132	56	132	131.905043	1110.1	0	0.00101	Stable	…	…
Ba-133	56	133	132.905988	1117.3	1/2	…	10.53 y	EC	0.52
Ba-134	56	134	133.904485	1126.7	0	0.02417	Stable	…	…

(*Continued*)

TABLE 7.14 (*Continued*)
Atomic Masses of All of the Common Fission Products of Uranium and Plutonium

Isotope	Z	A	Atomic Mass (AMU)	Binding Energy (MeV)	Spin	Natural Abundance	Half-Life	Decay Mode	Q (MeV)
Ba-135	56	135	134.905665	1133.7	3/2	0.06592	Stable	…	…
Ba-136	56	136	135.904553	1142.8	0	0.07854	Stable	…	…
Ba-137	56	137	136.905812	1149.7	3/2	0.1123	Stable	…	…
Ba-138	56	138	137.905233	1156.3	0	0.717	Stable	…	…
Ba-139	56	139	136.908841						
Ba-140	56	140	139.910581	1169.5	0	…	6.76 d	b–	1.03
Ba-141	56	141	140.914411						
Ba-142	56	142	141.916361	1180.2	0	…	10.7 m	b–	2.13
Ba-143	56	143	142.920483	1184.5	5/2	…	15 s	b–	4.2
Ba-144	56	144	143.922845	1190.3	0	…	6.5 s	b–	3.0

Both types of reactions have certain characteristics associated with them, and they also have certain challenges that we would like to discuss in this section. The idea of any chain reaction is to create an environment where more *free neutrons* are initially produced than are absorbed. These additional neutrons can be used to induce U-235 nuclei to become unstable, to split into a number of fission fragments, and to release more additional free neutrons in the process. For every thermal neutron a U-235 nucleus absorbs, it emits on average 2.068 additional neutrons. You may recall that this number comes from the fact that 2.418 neutrons are produced whenever the resulting U-236 nucleus splits apart and that no additional neutrons are produced when the U-236 nucleus emits a gamma ray.

These 2.068 neutrons can go on to hit other U-235 nuclei—inducing them to fission and to create more fission products, gamma rays, and additional neutrons (in quantities of 1, 2, 3, or 4). Every time this happens, an extra 210 MeV of energy is produced. After a few cycles of neutron absorption and emission, the neutron population begins to increase dramatically. (Refer to Figure 7.13 to get an idea of what the neutron population looks like after several neutron reproduction cycles.) To keep the picture simple, only three generations of neutrons (from left to right) are assumed. A *nuclear chain reaction* can only occur when the energy of the emitted neutrons is just right and when there is a "critical mass" of

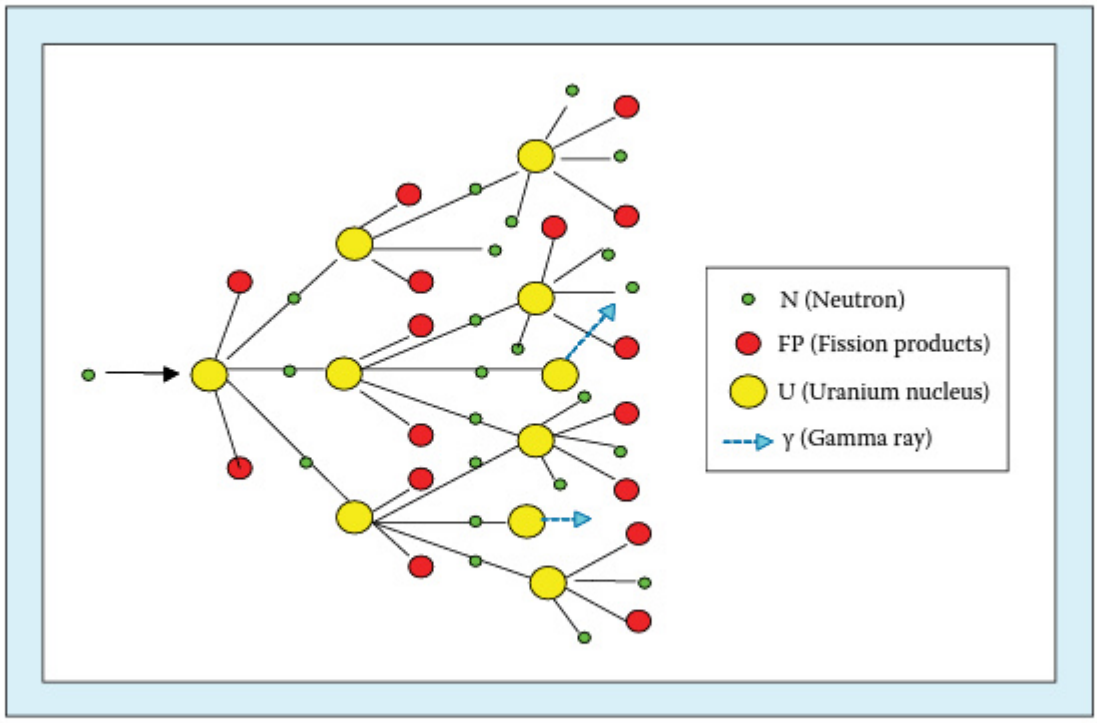

FIGURE 7.13 A visual depiction of the nuclear chain reaction.

fissionable material present to absorb them. Back in the days of the *Manhattan Project*, scientists were not exactly sure what this critical mass would be.

After some lengthy experiments, it was determined that the concentration of U-235 (that we call the enrichment today) had to be somewhere between 3% and 5% to sustain this type of reaction in a reactor cooled with ordinary water. This number depended critically on the speed of the neutrons as well as their density. These scientists also discovered that if they used water to cool the reactor (which was a very logical coolant to use at the time), then the neutrons would bounce off of the water molecules and give up some of their kinetic energy in the process. Eventually, they would slow down to a point where their most probable kinetic energy was about 0.025 eV. At that point, they eventually reached thermal equilibrium with their environment, and they were henceforth referred to "thermal" neutrons.

When a large number of thermal neutrons achieve this energy, it can be shown that they obey a statistical probability distribution (see Chapter 8) called a *Maxwell–Boltzmann probability distribution. The Maxwell–Boltzmann probability distribution* is named in honor of *James Maxwell* and *Ludwig Boltzmann* (see Figure 7.14), who originally discovered its properties in 1869. The shape of this distribution is shown in Figure 7.15 and its shape changes as the absolute temperature T of the neutrons changes. The interesting thing about this distribution is that it predicts that some neutrons in thermal equilibrium with their environment will actually *gain* energy in collisions with other neutrons and atomic nuclei, while other neutrons will *lose* it. However, because this probability distribution represents a true equilibrium condition, the *average value* of the energy of all of the neutrons, as well as the *most probable value*, will always remain the same for a given value of the absolute temperature T.

If there is slightly more U-235 present than is required to achieve a "critical mass," then there is enough fissionable material to produce a sustained chain reaction. If the chain reaction continues to proceed at an uncontrolled rate, then the result will be an atomic bomb. If the chain reaction is carefully controlled with control rods and other nuclear materials, then the reaction is called a "controlled" nuclear reaction and useful power can be produced in this way.

The Maxwell–Boltzmann probability distribution does not apply to just neutrons. It applies to any system of molecules or uncharged nuclear particles in thermal equilibrium with their environment where the thermal equilibrium temperature T is known. It also applies to the molecules of most liquids and gases. In particular, the average velocity V_{AVG} is equal to $\sqrt{(3/2)}$ times the most probable molecular velocity V_{MP} for any system of particles to which the distribution applies. For example, if V_{MP} for a nitrogen molecule at 300 K (room temperature) $\approx$ 360 m/s, the average velocity will be $\sqrt{3/2} \times 360$ m/s $\approx$ 440 m/s for all of the nitrogen molecules in the room. Both numbers will increase as the temperature is increased. This distribution is discussed in more detail in Chapter 8 (refer to Figure 7.14).

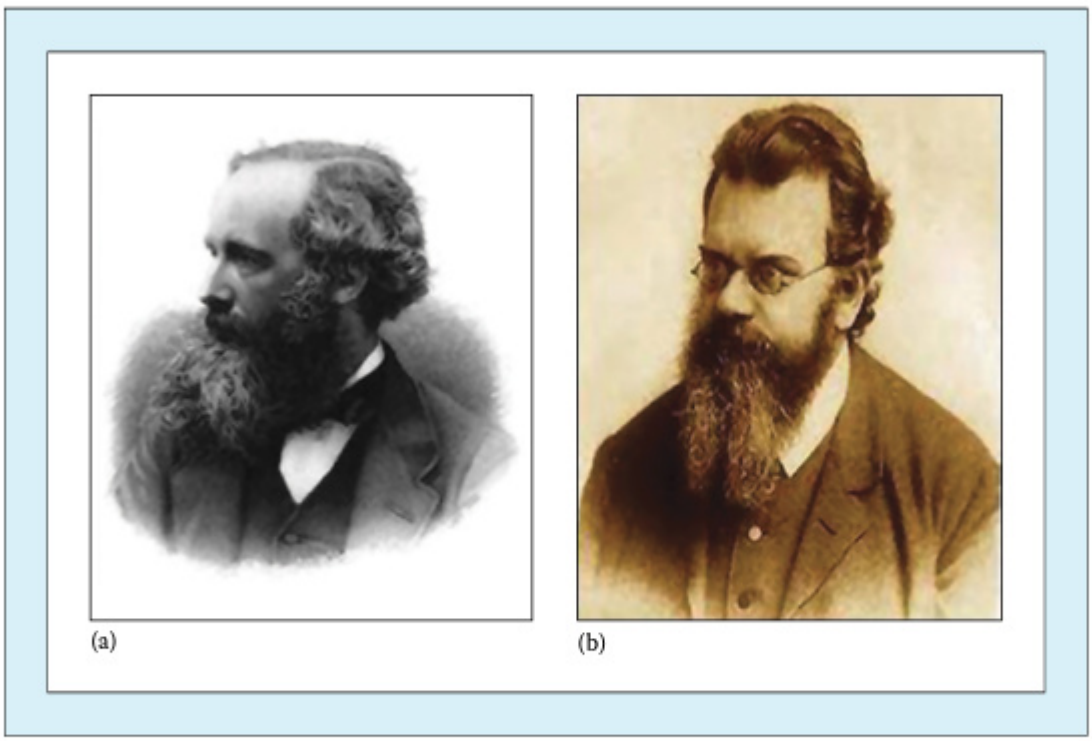

FIGURE 7.14 James C. Maxwell (a) and Ludwig Boltzmann (b). The inventors of the Maxwell–Boltzmann particle energy distribution. (Pictures provided by Wikipedia.)

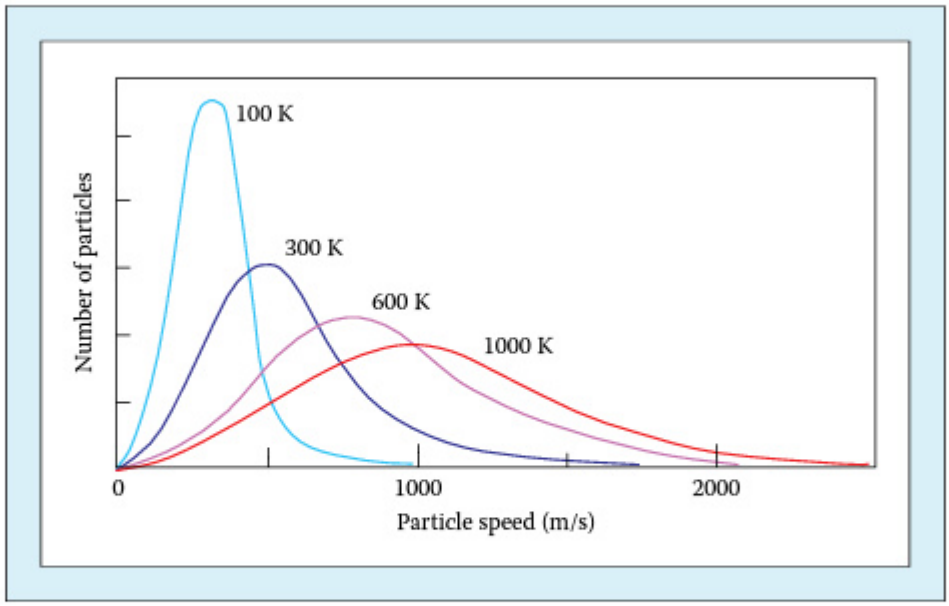

FIGURE 7.15 An example of a Maxwell–Boltzmann energy distribution. Notice that the shape of the distribution changes as a function of the temperature of the medium that the neutrons are in thermal equilibrium with.

Student Exercise 7.4

Part 1: Calculate the nuclear masses of the by-products for the seven nuclear reactions discussed in Section 7.16.

Part 2: Using these data, apply Einstein's equation $E = mc^2$ to calculate the missing values of Q′ (e.g., Q′, Q″, Q‴, etc.) and therefore the total kinetic energy released for each of the seven reactions shown earlier. Also calculate the average energy released by these seven distinct reactions.

Part 3: Can you make any general observations about these reactions from your answers in parts 1 and 2?

7.22 The Speed of a Nuclear Chain Reaction

In an operating reactor, the underlying physical processes can be quite fast and furious. We would like to take a few paragraphs to give you some appreciation for how quickly things can change under some conditions. In a commercial nuclear power plant, which is fueled with uranium dioxide (UO_2) with a U-235 concentration between 3% and 5%, the mean free path of a neutron emitted by the fission of a Uranium-235 nucleus is about 3 cm. When neutrons are first produced due to the fission of a uranium or plutonium nucleus, they have a very high speed (or distribution of speeds) that averages about 20 million m/s, or about 7% of the speed of light, and their most probable speed is about 63% of their average speed, or about 12.6 million m/s. By any objective measure, these are very high speeds. Because these high-speed neutrons are produced immediately after the nucleus splits apart (in 10^{-12} seconds or less), they are also known as *prompt neutrons*.

After a prompt neutron leaves the nucleus. It continually bounces around between the fuel atoms, the structural materials, and the coolant. After many elastic and inelastic collisions with these materials, its mean free path starts to change. Eventually, it reaches a much lower speed (about 2200 m/s), where, on average, it does not slow down any further and where the probability of being absorbed increases substantially. In a thermal water reactor, this entire process takes about 10^{-3} seconds or about 1 ms to complete. Hence the average time for a neutron to be emitted and reabsorbed by a U-235 nucleus is about one millisecond (or 1×10^{-3} seconds). *Therefore, it is possible that 1000 absorptions and reemissions can occur in a single second.*

Now let us consider what this means in terms of the total number of additional neutrons that are produced. Assume that the value of η (see Table 7.9) is exactly equal to 2.0 to simplify the math. Different values of eta will cause the neutron population to increase at different rates because this determines the number of free neutrons that are created per neutron absorbed. Figure 7.16 shows how the neutron population changes for different values of η. To illustrate this point, suppose that we start out with one free neutron at T = 0 ms.

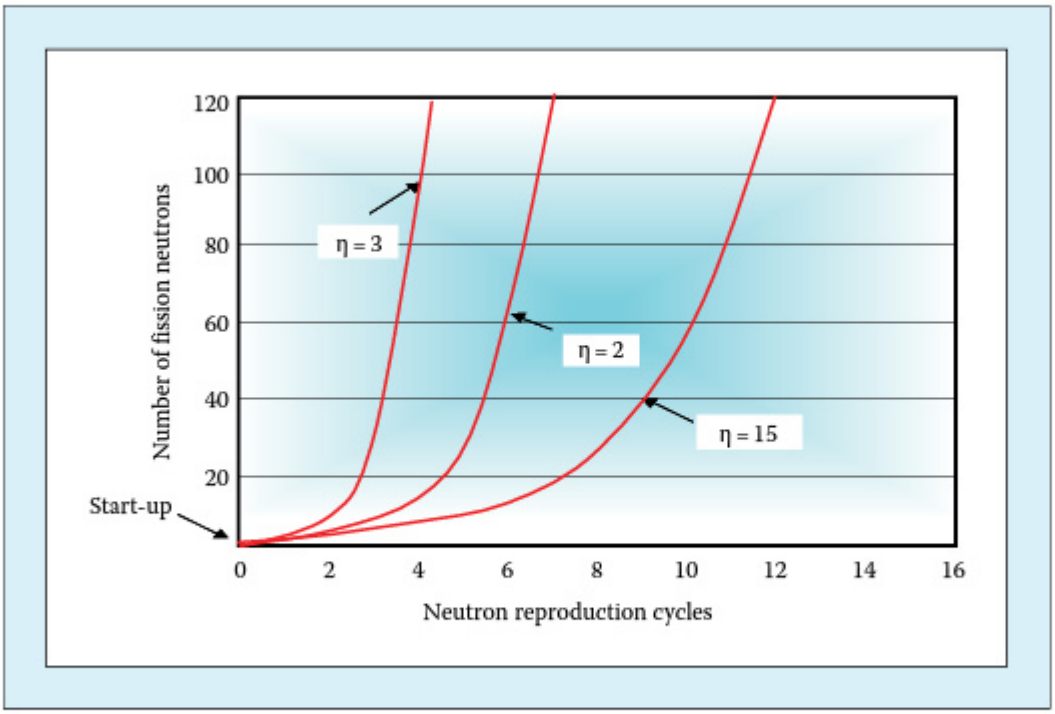

FIGURE 7.16 The relative change in the prompt neutron population for different values of η. A neutron production and absorption cycle of approximately 1 ms is assumed.

$$\text{At T} = 1 \text{ ms, we have 2 free neutrons}$$

$$\text{At T} = 2 \text{ ms, we have } 2 * 2 = (2)^2 = 4 \text{ free neutrons}$$

$$\text{At T} = 3 \text{ ms, we have } 2 * 2 * 2 = (2)^3 = 8 \text{ free neutrons}$$

$$\text{At T} = 4 \text{ ms, we have } 2 * 2 * 2 * 2 = (2)^4 = 16 \text{ free neutrons}$$

$$\text{At T} = 5 \text{ ms, we have } 2 * 2 * 2 * 2 * 2 = (2)^5 = 32 \text{ free neutrons}$$

and so on. The reader may have seen this type of mathematical pattern before. The free neutrons are increasing at an *exponential rate*! If it were not for the presence of another kind of neutron—that we will introduce to you in Section 7.27—which is called a *delayed neutron*, it would simply not be possible to control this type of chain reaction. We would have literally billions of free neutrons flying around in a single second! Fortunately, because of delayed neutrons, commercial reactors are able to maintain a very delicate balance between having too few free neutrons (and being subcritical) and having too many free neutrons, and being out of control. The goal of a commercial power reactor is therefore to sustain a controlled chain reaction as long as possible. This depends on a number of factors that we will subsequently discuss.

A coolant like water can be very helpful in maintaining the proper neutron balance under these conditions. As more neutrons are produced, the water heats up, and it begins to expand and turn to steam. When this happens, the number of water molecules available to slow down the newly emitted neutrons diminishes rapidly (since the molecular density of the water goes down). The energy spectrum of the emitted neutrons shifts to higher energies so that more neutrons, statistically speaking, stay at the upper end of their energy range, and because the reaction cross sections are lower there, fewer neutron absorptions occur. So in a sense, a controlled chain reaction is a self-correcting process. Any significant concentration of Uranium-235 or Plutonium-239 atoms will eventually expand to the point that the thermal expansion (or the release of heat and energy) will eventually overtake the process of neutron production, and the end result will be that fewer neutrons will be produced. However, this process can happen much faster than we can move a control rod (it can occur in much less than a tenth of a millisecond), and so there is very little chance that a properly designed and cooled nuclear reactor will simply "blow up" or run out of control. A reactor with this characteristic behavior is said to have *a negative temperature coefficient*.

We will explore the meaning of this coefficient and other coefficients in Chapter 17 where other types of temperature feedback are discussed.* As long as the number of neutrons that are produced is exactly equal to the number of neutrons that are destroyed, a nuclear chain reaction can continue forever. In principle, a chain reaction does not need many neutrons to be self-sustaining. As a matter of fact, it can be shown under certain conditions that it only needs one! However, a chain reaction that involves creating and destroying 1 neutron per second, or even 1 neutron per millisecond, will not produce much power. In order to produce a useful amount of power, *many billions of neutrons must be created and destroyed each second*.

The easiest way to do this is to simply increase the enrichment e of the fuel. This makes more fissile material available to be fissioned, and therefore, more fission reactions can occur. So in conclusion, a nuclear chain reaction can produce a lot of useful power as long as it is properly designed and *controlled*. Today, computers are used extensively to simulate these reactions and to ensure that this is always the case. We will come back to this subject again when we discuss the behavior of time-dependent reactors in Chapters 15 and 16, where the *Inhour Equation* is also presented. Here, the exact rate at which neutrons are produced and destroyed becomes very important to a reactor operator who must always keep these two opposing forces precisely balanced.

7.23 Neutron Velocities at Different Neutron Energies

Before moving on to other topics, we would like to take a moment to understand the speed with which the fission neutrons are initially emitted and how their initial ejection velocity corresponds to their final thermal one. When they are initially emitted from the nucleus of an atom, prompt neutrons have a *most probable* energy of about 0.74 MeV and an *average energy* of about 1.98 MeV. When they finally reach thermal equilibrium (about 10^{-3} to 10^{-4} seconds later), their energy has been reduced to a most probable energy of about 0.025 eV.

This corresponds to a reduction in the most probable energy of a factor of 28,800,000 and a reduction in the average energy of a factor of 79,200,000! We also know from Chapters 2 and 3 that as long as their velocity is less than about 10% of the speed of light, their kinetic energy E and their velocity v are related to each other by the simple classical equation $E = 1/2\ mv^2$, where m is the rest mass of the particle involved. The ratio of the average emitted energy to the average thermal energy is therefore $E/E_T = (v/v_T)^2$ so that we may write

Comparing the Speed of a Thermal Neutron to a Fission Neutron

$$v = v_T\sqrt{\left(\frac{E}{E_T}\right)} \tag{7.30}$$

This simple equation gives the value of the average emitted velocity and the most probable emitted velocity v as a function of the thermal neutron velocity v_T. Now let us assume that E = 1.98 MeV for the average energy when a neutron is born (see Section 7.6) and $E_T = 0.025$ eV when the neutron has reached thermal equilibrium. Solving the aforementioned equation for v_{AVG}, we find that

$$v_{AVG} \cong 9000\ v_T \tag{7.31}$$

So *the average velocity of a prompt neutron in a fission reaction is almost 9000 times greater than the final velocity of the neutron when it reaches thermal equilibrium* and can create another neutron in a thermal water reactor by being absorbed. Based on this observation alone, we can conclude that many violent collisions must occur between the time a neutron is first produced and the time a neutron is absorbed. In the process of slowing down, its kinetic energy is then transferred to the reactor lattice in the form of heat.

Example Problem 7.4

In the earlier discussion, we discovered that the average velocity of a prompt neutron when it is initially emitted from a uranium nucleus is 9000 times greater than the velocity of the same neutron when it reaches thermal equilibrium. If the most probable energy that a prompt neutron is emitted from a Uranium-235 nucleus is 0.72 MeV, how many times greater is this than the velocity of the neutron when it becomes a thermal neutron?

Solution Since $E/E_T = (v/v_T)^2$, we know that $v/v_T = \sqrt{(E/E_T)}$. If the most probable energy of the neutron when it is emitted is E = 0.72 MeV and the energy of the neutron at thermal equilibrium is 0.025 eV, then $E/E_T = 28,800,000$, and $v_{MP} = \sqrt{28,800,000}v_T = 5,366v_T$. So the most probable velocity that the neutron is emitted with v_{MP} is about *5366 times* the final thermal equilibrium velocity v_T. By any objective measure, this is an enormous difference in the speed. [Ans.]

* Refer to Masterson [13].

7.24 The Total Energy Released by a Fission Reaction

We also know that the amount of *recoverable* energy per fission is about 200 MeV and that the majority of this energy (~180 MeV) is released immediately after the nucleus splits apart. The heat output of most commercial power reactors is measured in megawatts of thermal energy (MWT), and so it is important to be able to understand how many fissions per second are required to create a megawatt of thermal power. A megawatt of thermal power can be found by multiplying the number of fissions per second required to create 1 W of power by 1 million, where a megawatt is equal to 1 million or 1×10^6 W. To convert 200 MeV per fission per second to the unit of a watt, we must realize that 1 MeV is equal to 1.60×10^{-13} J of energy. Therefore, 1 fission/s will release a total of

$$200 \text{ MeV/fission/s} \times 1.60 \times 10^{-13} \text{ J/MeV} = 3.2 \times 10^{-11} \text{ J/fission/s} \tag{7.32}$$

Nuclear Fissions Required to Produce 1 W of Recoverable Power

$$1 \text{ W} = 3.12 \times 10^{10} \text{ fissions/s} \tag{7.33}$$

And if 1 W = 1 J/s, then 1 W = 1 J/s/(3.2×10^{-11} J/s/fission) = 3.12×10^{10} fissions/s. *So roughly 30 billion fissions per second are required to produce 1 J/s or 1 W of recoverable thermal power.*

Since 1 MW is 1 million watts, or 1×10^6 W, 1 MW of continuous thermal power requires a total fission rate of 3.12×10^{16} fissions/s. A 1000 MWT* reactor would then require a total fission rate of 3.12×10^{19} fissions/s, or 3.12×10^{19} fissions/s × 86,400 s/day = 2.70×10^{24} fissions/day. Sometimes, it is helpful to be able to calculate how many grams of nuclear fuel must be consumed per day to generate 1 MWT of power. In the case of Uranium-235, this can be found (see Chapter 4) by multiplying the number of fissions per second by 1 million, then multiplying this by the molecular weight of Uranium-235 (which is 235.0), and then dividing by Avogadro's number, which is 6.022×10^{23} atoms/mol. The result is

Grams of U-235 Required to Produce 1 MW of Power

$$1 \text{ MW/day} = 1.05 \text{ g of U-235 consumed per day} \tag{7.34}$$

The number of grams fissioned per day is also called the *burnup rate*. In other words, if a commercial nuclear reactor produces 1 MW of thermal power in 1 day, it requires approximately 1 g of Uranium-235 to be consumed per day. Of course, this number assumes that every thermal neutron that is absorbed by a Uranium-235 nucleus results in 200 MeV of recoverable energy being produced. However, as we learned in an earlier section, a Uranium-235 nucleus that absorbs a thermal neutron will only split apart 86% of the time. The rest of the time, it will absorb the neutron and emit a gamma ray instead. So the actual consumption rate of U-235 must be adjusted for the fact that not every thermal neutron captured will result in the nucleus splitting apart. The other 14% of the time, only about 1 MeV of recoverable energy will be produced from a gamma ray. We can make this adjustment by realizing that the total absorption rate σ_a/σ_f is simply $(1 + \alpha)$ times the fission rate, where α is the capture-to-fission ratio that we defined previously:

$$\alpha = \frac{\sigma_c}{\sigma_f} \tag{7.35}$$

With these adjustments, the true consumption rate of U-235 is given by

True Rate of Uranium Consumption

$$1 \text{ MW} = 1.05(1 + \alpha) \text{ g/day of U-235} \tag{7.36}$$

where $\alpha = 0.169$ for the thermal fission of U-235 (see Table 7.9). Since U-233 and Pu-239 have different values of α, it should be clear by now that each fissile isotope requires a slightly different daily consumption rate to generate an MWT of useful power. The following exercise should help to illustrate this point.

* Throughout this book, we will use the abbreviation *MWT* to refer to the total recoverable energy in mega watts of *thermal* energy. The total electrical power output MWE will of course be about 66% less than this because of the efficiency of the thermal cycle that allows the heat to be converted into electricity. So, for most thermal power reactors, 1 MWE, which is 1 MW of electrical energy produced, is given by MWE ≈ 1/3 × MWT. A 3000 MWT power plant is therefore needed to generate about 1000 MW of electricity.

Example Problem 7.5

Using the equations presented previously and assuming that the nuclear fuel is Uranium-233 instead of Uranium-235, estimate the number of grams of U-233 that must be consumed per day to produce 1000 MWT of recoverable power.

Solution From the equations presented previously, it can be seen that a 1000 MWT reactor will require a daily consumption rate of $1000 \times 1.05(1 + \alpha) = 1050(1 + \alpha)$ g/day of whatever fissile material it uses. In the case of Uranium-233, the value for α (from Table 7.12) is 0.089, and therefore, $1050\,(1 + 0.089) = 1143.45$ g of Uranium-233 must be consumed to generate this amount of power for 1 day. This is equivalent to about 2.5 lbs of Uranium-233 consumed per day. [Ans.]

7.25 Electrical versus Thermal Energy Production

The energy that we have been referring to up to this time is the *thermal energy* that is deposited in the core in the form of heat. In order to find out how much electricity a power plant can produce (see Chapter 1), it is necessary to convert this heat into electrical energy using the *thermal cycle* of the power plant. LWRs (PWRs and BWRs) use slightly different forms of the Rankine thermal cycle to do this. In a PWR, two thermal loops are used to convert the heat from the core into steam, while a BWR uses only a single loop to send the energy that is produced (in the form of steam) to the steam turbines.

The *thermal efficiency* (TE) of these designs is also different because of the differences in the temperatures and pressures involved. However, as a rule of thumb, a modern nuclear power plant will operate with a TE of about 33%. This means that approximately 1/3 of the energy released in the form of heat Q is eventually converted into electric power. In symbolic form, this relationship can be written as

Converting Thermal Power to Electrical Power

$$\mathrm{MWE} = \mathrm{TE} \times \mathrm{MWT} \tag{7.37}$$

where TE is the efficiency of the thermal cycle. In some books, the TE is also given the symbol η. So for a standard LWR, it is reasonable to assume that

Important Rule of Thumb for Nuclear Power Plants

$$1\,\mathrm{MW(Electric)} \approx 3\,\mathrm{MW(Thermal)} \tag{7.38}$$

Of course, this relationship is just an approximation, but we will find it to be very useful when we attempt to understand how much uranium must be burned to generate a specific amount of electrical power over the course of a year.

7.26 Finding the Uranium Consumption Rate over Time

A reactor fueled with U-235 will consume about 1.23 g of U-235 per day for each 1 MWT of recoverable energy produced (assuming that $\alpha = 0.169$). It is instructive to see what this means in terms of the amount of fuel that is required for a 1000 MWE or a 3000 MWT reactor to operate for a much longer period of time. A 3000 MWT (~1000 MWE) power plant will consume about 1.23 kg × 3 = 3.69 kg (about 6.12 lbs) of U-235 per day for every full day that it operates. In 1 year, this corresponds to 365 days × 3.69 kg/day = 1350 kg/year (about 1.35 metric tons).[1] However, the Uranium-235 in a thermal water reactor usually makes up only about 3% of the total weight of the fuel (the remaining 97% is U-238). So the total amount of uranium burned per year (assuming an enrichment of 3%) is 33.3 × 1.35 kg/year = 44,955 kg/year, or ~45 metric tons/year. If the fuel is UO_2, and the enrichment is about 4%, then this number falls to about 33 metric tons, and if the average availability of the reactor is about 85% due to the fact that the reactor needs to be refueled, then the total uranium consumption (U-235 + U-238) is about 27 metric tons/year. This relationship can be expressed very simply as

Amount of Uranium Required to Run a 1000 MWE Power Plant for 1 Year

$$1000\ \mathrm{MWE\ for\ 1\ year} \approx 35\ \mathrm{metric\ tons\ of\ enriched\ uranium\ burned} \tag{7.39}$$

This is the same amount of energy that would be produced by burning about *3.1 million metric tons* of high-quality coal. So *a nuclear power plant fueled with slightly enriched uranium will require about 100,000 times less fuel than a coal-fired plant with the same thermal cycle to generate the same amount of electric power*. This is fairly typical of the reduction in the volume of the fuel that can be obtained by burning uranium as opposed to burning conventional fossil fuels.

7.27 Prompt Neutrons and Their Origin

In addition to fast and thermal neutrons, there are other ways that we can distinguish the neutrons from one another based on how they are born and when they appear—as opposed to what their respective kinetic energies are (fast or thermal). These neutrons are called prompt neutrons and delayed neutrons. *Prompt neutrons* are fission neutrons that are produced in a very short period of time (usually within 10^{-12} seconds) after a uranium nucleus splits apart. They carry away about 2 MeV of kinetic energy per fission, and the shape of their energy spectrum is relatively insensitive to the type of nuclear material involved. *They are the immediate by-products of a fission reaction.* The majority of the neutrons in a reactor core are produced in this way. On average, they "live" between 10^{-4} and 10^{-7} seconds before they either leak out of the core or are absorbed by another nucleus. For thermal water reactors (like PWRs and BWRs), the typical prompt neutron lifetime is on the order of 10^{-4} seconds. This is because it takes a while for a fast neutron to transfer its kinetic energy to the environment and slow down to become a thermal neutron ($v \cong 2200$ m/s). *The prompt fission neutron population dominates the steady-state behavior of a reactor, because approximately 99% of the neutrons in the core are prompt neutrons.* In fast reactors, the prompt neutron lifetime is much less (about 1000 times less) than it is in thermal reactors because most neutrons are absorbed before they reach the thermal energy range.

7.28 Delayed Neutrons and Their Origin

In addition to prompt neutrons, there is another type of neutron that is also produced. These neutrons are called *delayed neutrons*. Delayed neutrons are produced in much smaller numbers than prompt neutrons are, but they can play a very important role in the control of a reactor—particularly as the power level changes. As the name implies, delayed neutrons are *not* produced immediately after a fission reaction occurs. On a nuclear time scale, they are produced long after the parent nucleus has been destroyed. Delayed neutrons come from the fission fragments that are left over from the fission of the parent nucleus. These fission fragments are usually "neutron rich" and they have to eject one or more neutrons to return to a stable energy state. The normal progression of events is shown in Figure 7.17.

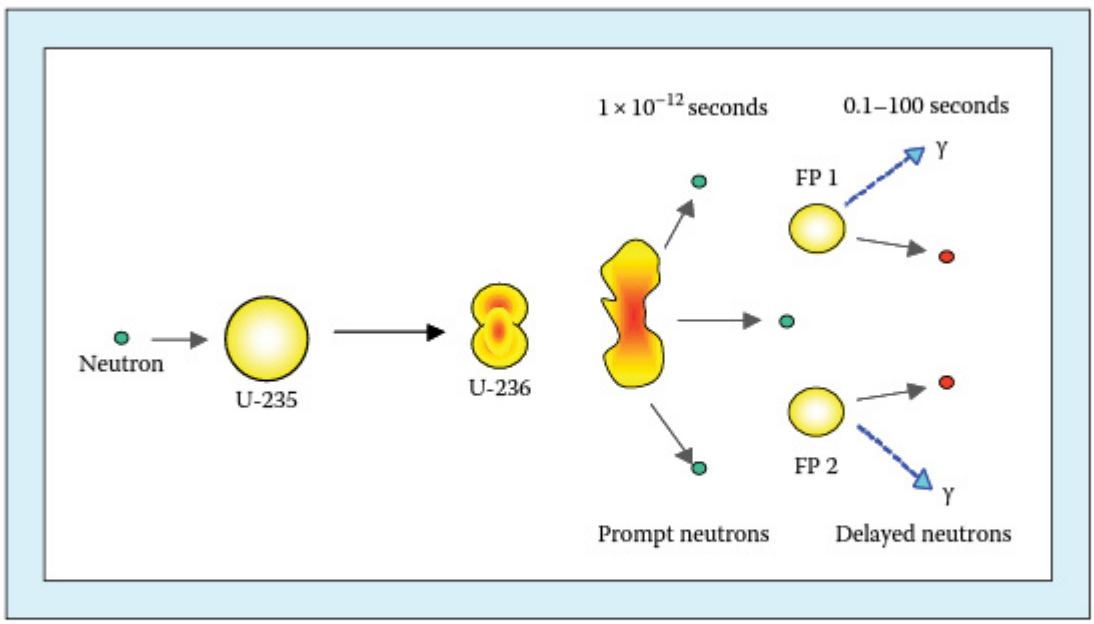

FIGURE 7.17 An example of the emission of prompt neutrons from the parent nucleus and delayed neutrons from the fission fragments that are subsequently produced.

Under steady-state conditions, delayed neutrons account for slightly less than 1% of the total neutron population. On average, a delayed neutron will appear about 12 seconds after the parent nucleus is destroyed, although their appearance is governed by a probability distribution that can be correlated to the decay chains of the fission products themselves. Some delayed neutrons can appear as soon as a tenth of a second after the parent nucleus decays, while others may not appear until 50 or even 100 seconds later. Delayed neutrons are also emitted with slightly lower energies than their prompt neutron cousins (approximately 0.62 MeV vs. 2 MeV). The energy spectrum for both types of neutrons is shown in Figure 7.18. Delayed neutrons allow a reactor to respond several orders of magnitude more slowly than if the only neutrons available were prompt neutrons. *Without delayed neutrons, changes in the reaction rates would simply be too fast for human beings to control!*

There are about 60 decay chains in a thermal water reactor that produce delayed neutrons, but these decay chains can be reduced to only six primary decay chains per fuel type through appropriate statistical analysis. These decay chains have different yields and different time constants associated with them. Almost all delayed neutrons are emitted through the process of radioactive *beta decay*. The process by which a delayed neutron is produced is much more complex than it may initially seem. To begin with, not all fission products are capable of producing delayed neutrons, and as a rule of thumb, less than 1% of them actually do. When a fission product capable of producing a delayed neutron is born, a prerequisite for the appearance of a delayed neutron is that the fission product must be "neutron rich" in a nuclear sense. In other words, the fission product that is produced must lie to the right of the centerline of the *Chart of the Nuclides* or the *Segre chart* shown in Figure 7.19. Specifically, it must correspond to a combination of the atomic weight A and the atomic number Z that lies in the pink area to the right of the centerline. We can represent a fission product with these properties by the symbol FP (A, Z). Because the fission product is "neutron rich," it first converts one of the neutrons inside of the nucleus into a proton and releases an electron and a neutrino in the process. This transforms the fission product, which is initially an element with an atomic number of Z, into a "heavier" element with an atomic number of Z + 1. The resulting "heavier" element then releases an additional neutron, which is the delayed neutron that we finally see. In other words, *the creation of the delayed neutron is always a two-step process*. The two steps are

The Two Steps to Create a Delayed Neutron

$$\text{Step 1: } \mathrm{FP}(\mathrm{A}, \mathrm{Z}) \rightarrow \mathrm{FP}(\mathrm{A}, \mathrm{Z}+1) + 1\,\text{electron and 1 neutrino}$$
$$\text{Step 2: } \mathrm{FP}(\mathrm{A}, \mathrm{Z}+1) \rightarrow \mathrm{FP}(\mathrm{A}-1, \mathrm{Z}+1) + 1\,\text{delayed neutron} \qquad (7.40)$$

On average, this process can take anywhere from 12 to 18 seconds. *Our ability to control a reactor without the need for a sophisticated control system is entirely dependent upon this.* The concentrations and yields of each fission product decay chain have been measured with great accuracy, and their time constants have been measured with great accuracy as well.

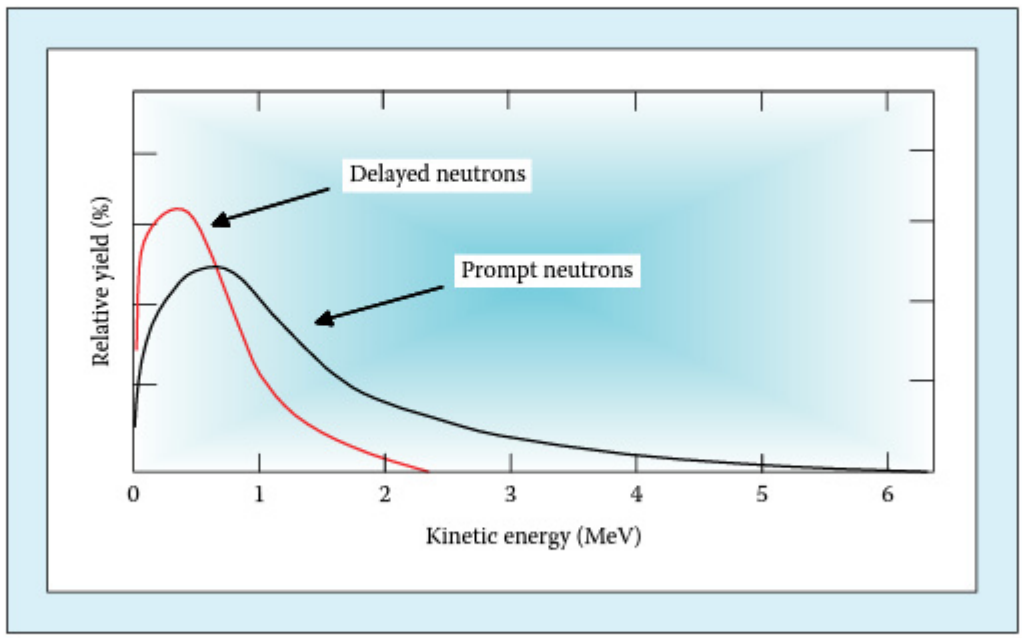

FIGURE 7.18 The energy spectrum of prompt and delayed neutrons from the thermal fission of U-235.

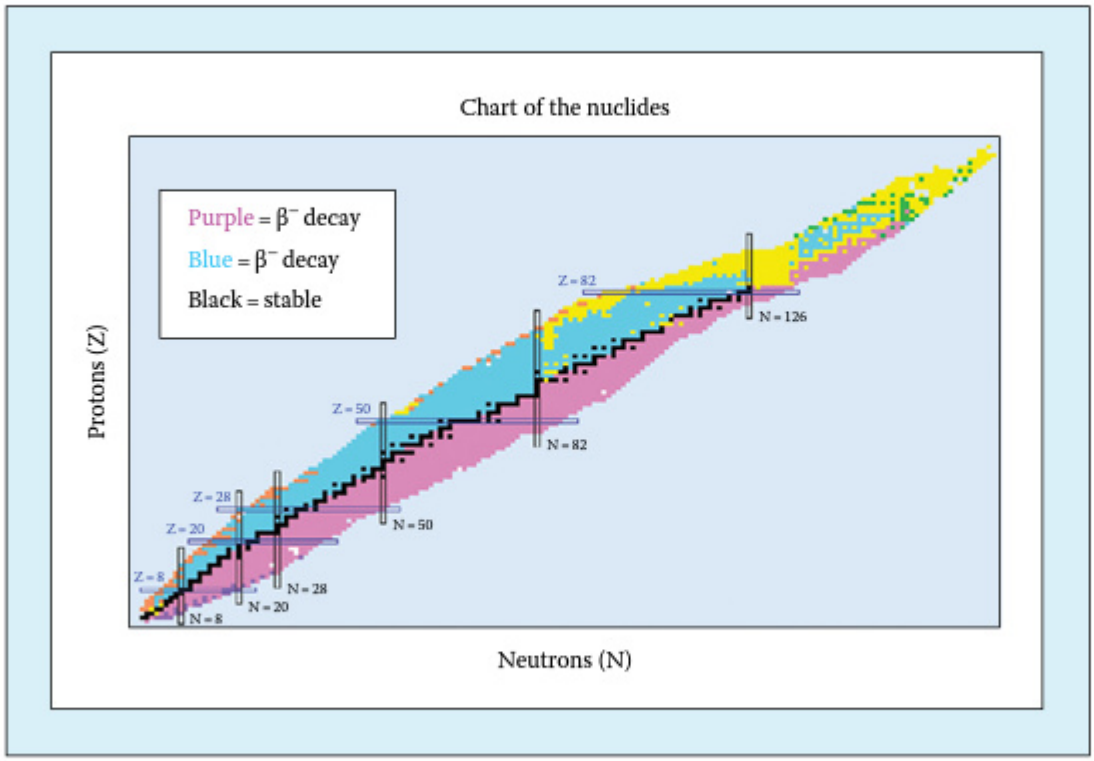

FIGURE 7.19 The chart of the nuclides that helps to determine the production of delayed neutrons.

The yield for an individual decay chain is usually represented by the symbol C_i, and the time constant for emitting a delayed neutron from that decay chain is usually given the symbol λ_i. Their contributions to the neutron population at any instant in time can be found by summing up the six fission fragment populations multiplied by their specific decay constants for beta decay. In other words, the percentage of delayed neutrons P_d emitted per cc per second at point r and time t is given by

$$P_d = \text{SUM}\left\{\lambda_i C_i(t)\right\} \quad (i = 1 \text{ to } 6) \tag{7.41}$$

where

$C_i(t)$ is the percentage of the fission product population at time t for decay chain i

λ_i is the decay constant (in units of s^{-1}) for fission fragment decay chain i for the production of a delayed neutron due to beta decay

The sum i is over all the fission fragments that are delayed neutron emitters. The concentration of delayed neutrons from decay chain i (in neutrons per cc) produced per second can be found by taking the normal fission rate R (in fissions per cc per second)

$$R = \phi\Sigma_f \tag{7.42}$$

and multiplying by P_d (in delayed neutrons per fission), where P_d is again the average percentage of *delayed* neutrons produced per fission, as defined by Equation 7.41. Hence, $R_d = P_d\phi\Sigma_f$, or

$$R_d = \phi\Sigma_f \cdot \sum_i \left\{\lambda_i C_i(t)\right\} \quad (i = 1 \text{ to } 6) \tag{7.43}$$

where R_d is now the total delayed neutron production rate (in delayed neutrons per cc per second). For most applications, the number of *delayed neutron emitters* will be 6; that is, the sum will be from i = 1 to i = 6. For Uranium-235, the resulting emission rate is shown in Figure 7.20. In general, the emission rate always declines as a function of time.

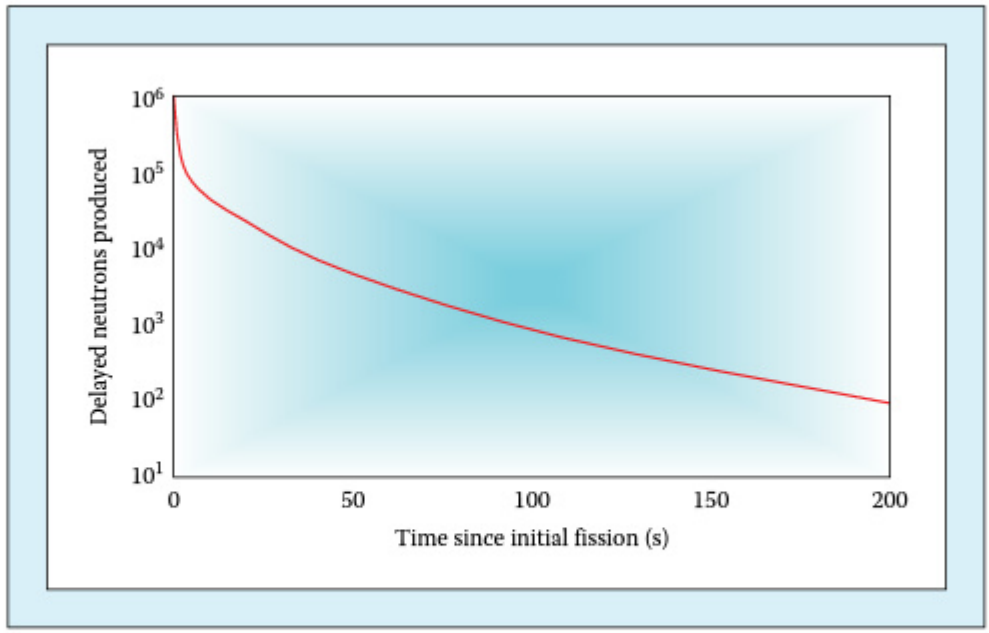

FIGURE 7.20 The delayed neutron production rate from a Uranium-235. (From Robert Keepin.)

TABLE 7.15
Delayed Neutron Fractions and Yields for Various Reactor Fuels

Delayed Neutron Group (i)	Fission Fragments	Average Neutron Energy (MeV)	Half-Life of Fission Fragments (seconds) $T_{1/2}$			Delayed Neutron Fraction (β)		
			U-235	Pu-239	U-233	U-235	Pu-239	U-233
1	^{87}Br, ^{142}Cs	0.25	55.72	54.28	55.0	0.021	0.0072	0.0226
2	^{137}I, ^{88}Br	0.56	22.72	23.04	20.57	0.140	0.0626	0.0786
3	^{138}I, ^{89}Br, $^{(93,94)}$Rb	0.43	6.22	5.60	5.00	0.126	0.0444	0.0658
4	^{139}I, $^{(93,94)}$Kr_σπι_βρ_^{143}Xe, $^{(90,92)}$Br	0.62	2.3	2.13	2.13	0.252	0.0685	0.0730
5	^{140}I, ^{145}Cs	0.42	0.61	0.618	0.615	0.074	0.018	0.0135
6	(As, Br, Rb, etc.)	0.42	0.23	0.257	0.277	0.027	0.0093	0.0087
Total yield						0.65	0.20	0.26

Source: Henry, A.F., *Nuclear Reactor Analysis*, MIT Press, Cambridge, MA, 1975.

Table 7.15 shows the delayed neutron emitters and their yields for U-233, U-235, U-238, and Pu-239. Their decay constants are shown in Table 7.16.

When several of these isotopes are present, then the numbers must be appropriately averaged to calculate the delayed neutron population as a function of time. It is also important to realize that there are significant differences in the yields of delayed neutrons depending upon the type of nuclear fuel involved.

U-235 has by far the greatest delayed neutron yield with 0.65% per fission, while U-233 and Pu-239 have yields of only 0.26% and 0.20%, respectively. The delayed neutron fraction, or yield, is typically represented by the symbol beta, β, since most delayed neutrons are produced from beta decay. *Using this terminology, the delayed neutron fractions for U-233, U-235, and Pu-239 are* $\beta_{U233} = 0.0026$, $\beta_{U235} = 0.0064$, and $\beta_{Pu239} = 0.0020$. The most common delayed neutron emitters, starting with the largest decay constants and continuing down to the smallest decay constants, are ^{87}Br, ^{142}Cs, ^{137}I, ^{88}Br, ^{138}I, ^{89}Br, $^{(93,94)}$Rb, ^{139}I, $^{(93,94)}$Kr ^{143}Xe, $^{(90,92)}$Br ^{140}I, ^{145}Cs and Br, Rb, As, where $\lambda = 0.693/T_{1/2}$ and $\tau = T_{1/2}/.693$ with *average value = straight average—not weighted by C_i, and $T_{1/2}$ is again the half-life (see Chapter 6).

TABLE 7.16
Average Lifetime of Delayed Neutron Fractions by Group of Various Reactor Fuels

Delayed Neutron Group (i)	Fission Fragments	Average Neutron Energy (MeV)	Average Lifetime of Fission Fragments (seconds) τ			Decay Constant (s^{-1}) λ		
			U-235	Pu-239	U-233	U-235	Pu-239	U-233
1	^{87}Br, ^{142}Cs	0.25	80.40	76.32	79.36	0.0124	0.0127	0.0126
2	^{137}I, ^{88}Br	0.56	32.78	33.24	29.68	0.0305	0.0300	0.0337
3	^{138}I, ^{89}Br, $^{(93,94)}$Rb	0.43	6.97	6.08	7.21	0.1114	0.1237	0.1386
4	^{139}I, $^{(93,94)}$Kr_σπι_βρ_^{143}Xe, $^{(90,92)}$Br	0.62	3.31	3.07	3.07	0.3013	0.3253	0.3253
5	^{140}I, ^{145}Cs	0.42	0.88	0.89	0.88	1.136	1.121	1.127
6	(As, Br, Rb, etc.)	0.42	0.33	0.37	0.40	3.013	2.696	2.502
Average value*		0.45	21.11	20.66	20.10	0.767	0.718	0.690

Source: Henry, A.F., *Nuclear Reactor Analysis*, MIT Press, Cambridge, MA, 1975.

Of all of the delayed neutron emitters, Xe^{143} plays the most important role in reactor control because it has the highest delayed neutron fraction, or beta (β). It also has a relatively short average half-life (about 2 seconds) before it emits its delayed neutron through beta decay. For transient power conditions, the average delayed neutron lifetime is not fixed and can change depending on the mix of precursor atoms in the precursor inventory. Several books have been written just to explain how the change in the mean neutron lifetime can affect how a reactor behaves. We will have more to say about this when we explore the time-dependent behavior of a reactor again in Chapters 15 and 16.

What is important to keep in mind is that this small number of delayed neutrons is the key to being able to control a nuclear reactor and to allow it to produce useful power on a continuous basis. In other words, delayed neutrons are the "lever" that controls the rate at which the nuclear chain reaction can occur. Without delayed neutrons, reactors would be almost impossible to control, and the technology to control them would probably not exist for another 100 years.

7.29 Buildup of Xenon and Samarium

When a reactor is operating normally, radioactive fission product poisons build up at different rates, and the buildup of each fission product is governed by a different decay chain. *Xenon-135 and Samarium-149 are by far the most important fission product poisons that can directly affect the operation of a nuclear power plant.* In this section, we would like to briefly discuss the rate at which these two fission products can build up and decay. A more comprehensive discussion of this topic is presented in Chapter 21.

Xenon-135 is important in the reactor control theory because it has the highest thermal neutron absorption cross section of any nuclear material known. In other words, it literally soaks up thermal neutrons like a sponge (see Chapter 5). The amount of each fission product produced from the fission of a heavy nucleus is called its yield, and the yield is represented in most nuclear engineering books by the symbol Y. (In other books, the fission product yield is represented by the Greek symbol γ.)

The *yields* or percentages of the 20 most important fission products produced from the thermal fission of U-235 are summarized in Table 7.17. The "*relative importance*" in column 3 is the product of the microscopic cross section and the total yield (column 1 × column 2). It is apparent from inspecting this table that *xenon, samarium, and cesium (sometimes spelled caesium) are by far the most important fission products from the viewpoint of their neutron-absorbing potential*. Some isotopes of cadmium, europium, and gadolinium also have very high thermal cross sections, but they have such low yields that their impact on the normal operation of a nuclear power plant is much more limited. Usually, the fission product yield Y is a small dimensionless number that can vary from close to zero to about 7%. During normal operation, there are about 40 fission product decay chains that must be accounted for to track changes in the isotopic composition of the core. By convention, the sum of the yields of all these fission product decay chains is equal to 1.0:

$$\text{Total yield} = 1.0 = \sum_n Y_n \quad (n = 1, 2, \ldots, 40) \tag{7.44}$$

TABLE 7.17
Fission Products Produced from the Fission of Uranium-235 and Their Relative Yield

Cross Section (σ in Barns)	Yield (%)	Relative Importance (σ · Yield)	Isotope	Half-Life ($T_{1/2}$)	Observations regarding the Fission Product(s)
29,140	6.7896	1,975	$^{133}Cs \rightarrow {}^{134}Cs$	∞ 2.065 y	Neutron capture converts a few percent of nonradioactive ^{133}Cs to ^{134}Cs, which has very low direct yield because beta decay stops at ^{134}Xe; further capture will add to long-lived ^{135}Cs
2,650,000	6.3333	167,750	^{135}Xe	6.57 h	Most important neutron poison; neutron capture rapidly converts ^{135}Xe to ^{136}Xe; remainder decays (9.14 h) to ^{135}Cs (2.3 my)
2.7	6.2956	0.17	^{93}Zr	1.53 my	Transmutation impractical
0.11	6.0899	<1	^{137}Cs	30.17 y	
20	6.0507	1.20	^{99}Tc	211 ky	Candidate for disposal by nuclear transmutation
0.90	5.7518	0.05	^{90}Sr	28.9 y	
80	2.8336	2.30	^{131}I	8.02 d	
96	2.2713	2.18	^{147}Pm	2.62 y	
40,140	1.0888	442	^{149}Sm	∞	Second most important neutron poison
18	0.6576	<1	^{129}I	15.7 my	Candidate for disposal by nuclear transmutation
15,200	0.4203	63	^{151}Sm	90 y	Most will be destroyed by neutron capture
0.15	0.3912	<1	^{106}Ru	373.6 d	
1.66	0.2717	<1	^{85}Kr	10.78 y	
1.8	0.1629	<1	^{107}Pd	6.5 my	
	0.0508	<1	^{79}Se	327 ky	
3,950	0.0330	1.30	$^{155}Eu \rightarrow {}^{155}Gd$	4.76 y	Both neutron poisons
	0.0297	<1	^{125}Sb	2.76 y	
	0.0236	<1	^{126}Sn	230 ky	
254,000	0.0065	18.50	^{157}Gd	∞	Neutron poison, but low yield
20,600	0.0003	<1	^{113m}Cd	14.1y	Most will be destroyed by neutron capture

Source: Wikipedia—see *https://en.wikipedia.org/wiki/Fission_product_yield.*

7.30 Cumulative Effect of the Buildup of Fission Product Poisons

Over time, radioactive by-products can be built up through the process of nuclear fission. It is possible to represent the combined effect of the buildup of these fission product poisons by a hypothetical radionuclide that represents the average absorption cross section of all of the fission products. The absorption cross sections for this hypothetical nuclide for a U-235-fueled thermal water reactor are shown in Figure 7.21.

After several weeks of normal operation, these radioactive by-products usually approach an equilibrium concentration in the core that is dependent on the reactor's previous power history. As the power level P is increased, more fission products will be produced. Some fission products can build up to the extent that they can completely dominate the behavior of the core when the power level abruptly changes. This is because some of the radioactive by-products, like Xenon-135 and Samarium-149, can absorb vast numbers of neutrons and alter the reactor power level as they decay. This ability to absorb thermal neutrons easily exceeds that of any other known nuclear material, including the carefully concocted molecular mixtures of cadmium, boron, and hafnium that are used in a reactor's control rods. The presence of these fission products can sometimes bring the nuclear chain reaction to a complete standstill.

Figure 7.21 shows that a "typical" fission product can produce an average absorption cross section of between 50 barns and 100 barns over the life of the core. While this may not seem like a particularly large number, there can be nearly as many fission products after 1 year of full power operation as there are U-235 atoms left in the fuel rods! The net effect of all of these fission products is nearly as great as that of the control rods. Hence, great care must be taken to ensure that the core can stay critical in spite of their continued buildup.

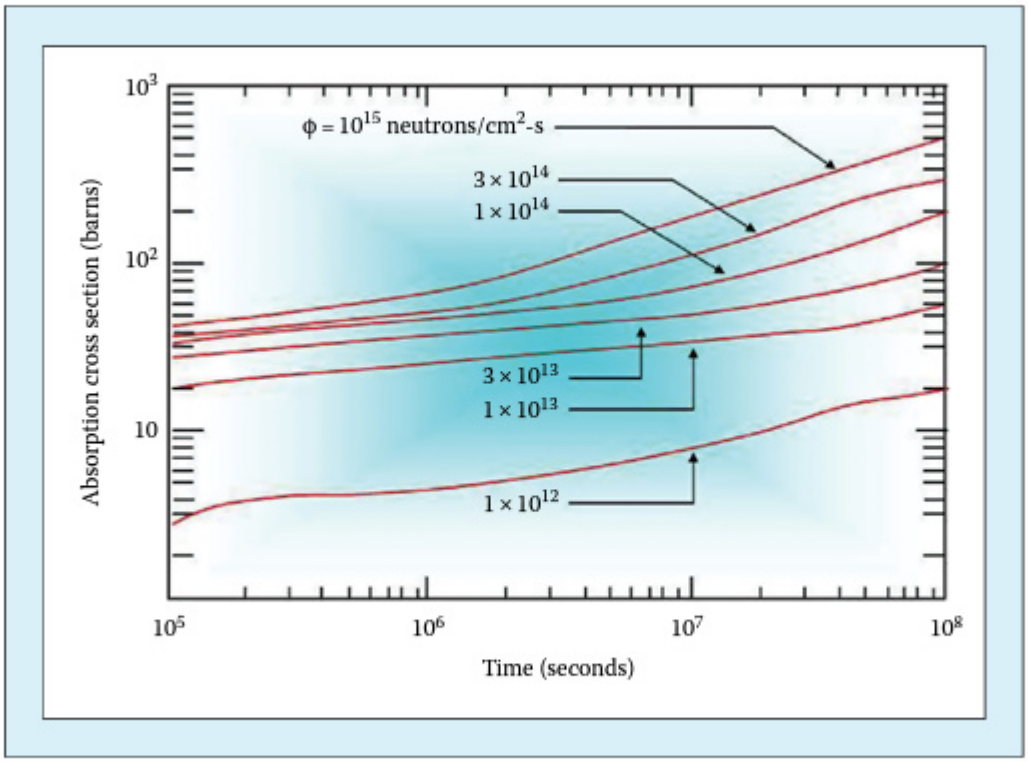

FIGURE 7.21 The cumulative buildup of fission product poisons as a function of flux and time. (Adapted from Lamarsh, J.R. and Baratta, A.J., *Introduction to Nuclear Engineering*, Prentice Hall, Upper Saddle River, NJ, 2001.)

Example Problem 7.6

Earlier in this chapter we learned that when a uranium or plutonium nucleus absorbs a low-speed neutron, it does not necessarily split apart. What percentage of the time does this happen for U-233 and Pu-239? If 30 billion U-233 and Pu-239 atoms absorb a thermal neutron, how much thermal energy is produced?

Solution The probability of a uranium or plutonium nucleus absorbing a low-speed neutron and *not* splitting apart is given by σ_c/σ_a, where $\sigma_a = \sigma_c + \sigma_f$. From Table 7.4, we see that a U-233 nucleus does *not* fission about 8% of the time it absorbs a thermal neutron and a Pu-239 nucleus does *not* fission about 26% of the time. In this case, they simply emit a gamma ray to return to a stable state.

Thirty billion fissions are required to produce 1 J of thermal energy. If each of these isotopes absorbs 30 billion neutrons, the fission of U-233 will produce $0.92 \times 1 = 0.92$ J and the fission of Pu-239 will produce $0.74 \times 1 = 0.74$ J. [Ans.]

References

Books and Textbooks

1. Shultis, K. and Faw, R. *Fundamentals of Nuclear Science and Engineering*, 2nd edn., CRC Press, Boca Raton, FL (2008).
2. Glasstone, S. and Eedlund, M.C. *The Elements of Nuclear Reactor Theory,* Second Printing, *D*, Van Nostrand Company, Inc., New York (1952).
3. Watt, B.E. Energy spectrum of neutron from thermal fission of 235U, *Physical Review*, 87, 6 (1952).
4. Lamarsh, J.R. *Introduction to Nuclear Reactor Theory*, Second Printing, Addison-Wesley Publishing Company, Inc., Reading, MA (1972).
5. Glasstone, S. and Sesonske, A. *Nuclear Reactor Engineering*, 3rd edn., Van Nostrand Reinhold Company, New York (1981).
6. Kaplan, I. *Nuclear Physics*, Addison-Wesley, Reading, MA (1965).
7. Lamarsh, J.R. and Baratta, A.J. *Introduction to Nuclear Engineering*, Prentice Hall, Upper Saddle River, NJ (2001).
8. Stacey, W.M. *Nuclear Reactor Physics*, 2nd edn., John Wiley & Sons, New York (2007).
9. Duderstadt, J. and Hamilton, L. *Nuclear Reactor Analysis*, John Wiley & Sons, New York (1976).
10. Lewis, E. *Fundamentals of Nuclear Reactor Physics*, Academic Press, Boston, MA (2008).
11. Schultz, M.A. *Control of Nuclear Reactors and Power Plants*, 2nd edn., McGraw-Hill, New York (1961).
12. Henry, A.F. *Nuclear Reactor Analysis*, MIT Press, Cambridge, MA (1975).
13. Masterson, R.E. *Nuclear Engineering Fundamentals: A Practical Perspective*, 1st edn., CRC Press, Boca Raton, FL (2017).

Web References

1. *http://www.wolframalpha.com.*
2. *http://en.wikipedia.org/wiki/Nuclear_fission.*
3. *http://en.wikipedia.org/wiki/Nuclear_chain_reaction.*
4. *http://www.atomicarchive.com/Fission/Fission2.shtml.*
5. *http://energy.gov/sites/prod/files/2013/06/f2/h1019v1.pdf.*
6. *http://hyperphysics.phy-astr.gsu.edu/hbase/nucene/fission.html.*
7. *http://hyperphysics.phy-astr.gsu.edu/hbase/pertab/pertab.html#c1.*
8. *http://www.britannica.com/EBchecked/topic/421629/nuclear-fission.*
9. *http://www.world-nuclear.org/info/Nuclear-Fuel-Cycle/Introduction/Physics-of-Nuclear-Energy/.*
10. *http://chemwiki.ucdavis.edu/Physical_Chemistry/Nuclear_Chemistry/Fission_and_Fusion/Nuclear_Chain_Reactions.*

Additional References

- Important physical constants used by nuclear scientists and engineers can be found in *Appendix A*.
- Unit systems and their conversion factors can be found in *Appendix B*.
- Nuclear cross sections for many important nuclear materials can be found in *Appendix C*.
- Physical properties of important nuclear materials can be found in *Appendix D*.
- Atomic masses, half-lives, and natural abundances can be found in *Appendix E*.
- Delayed neutron emitters and their properties are discussed in *Appendix F*.

Questions for the Student

The following questions cover the material presented in this chapter, and in some cases, previous chapters as well. They are designed to test how well the student has acquired a working knowledge of the subject matter.

1. What is the fundamental difference between nuclear fission and nuclear fusion?
2. What is the difference between the atomic weight of an element (its number of nucleons) and its nuclear or isotopic weight?
3. How many neutrons does a Uranium-235 nucleus release when it splits apart through the capture of a thermal neutron?
4. What is the minimum number of neutrons that are needed to sustain a nuclear chain reaction (per fission)? Assume that the absorption cross sections of the surrounding materials can be ignored when making this estimate.
5. How much energy is released in an "average" fission reaction involving the use of Uranium-235?
6. What percentage of this energy can be recovered as useful energy, and where does the remaining energy go?
7. What is the difference between a fast neutron and a thermal neutron?
8. Where does the energy to power a nuclear power plant come from?
9. How much mass must be converted into energy each day to power a 3000 MWT power plant?
10. What particle is responsible for creating the nuclear bonds that hold together the nucleus of an atom?
11. According to Einstein, what is the constant of proportionality between the mass m of a particle and its energy E?
12. How big is this constant of proportionality in metric units?
13. What percentage of the time does a Uranium-235 nucleus absorb a thermal neutron to actually split apart and undergo nuclear fission?
14. How much energy is released in an "average" fission reaction involving the use of Plutonium-239?
15. What percentage of the time does a U-235 nucleus absorb a thermal neutron and not split apart?
16. When it does split apart, what does it normally do?
17. When it comes to the nuclear fission of U-235 or Pu-239, what is a nuclear decay channel?
18. How much energy is carried away by the fission fragments when a Uranium-235 nucleus splits apart?
19. What is the minimum number of neutrons and the maximum number of neutrons that the thermal fission of Uranium-235 can produce?
20. How many decay channels are there for a typical Uranium-235 nucleus?
21. What are the most common by-products of the fission of Uranium-235?
22. What percentage of Uranium-235 do we need to have in the fuel to create a self-sustaining nuclear chain reaction in a reactor moderated by heavy water?
23. What is the most probable energy of a neutron that is released when the nucleus of a uranium atom splits apart?
24. What is the average kinetic energy of a neutron released by the fission of a uranium atom?
25. If we were able to split 100 uranium and plutonium atoms apart, how much energy would we be able to produce?
26. What are some common materials that can be used for reactor control rods?
27. What is the primary difference between an induced fission reaction and a naturally occurring one?
28. How can we "kick start" a nuclear chain reaction?
29. What isotopes of uranium and plutonium are normally fissionable?
30. How many isotopes does naturally occurring uranium have, and what are their names?
31. Which of these isotopes (if they existed in sufficient quantities) could be used to build a nuclear reactor?
32. How long can a sample of 100 free neutrons exist outside of the nucleus of an atom before half of them decay into protons and electrons?
33. In what unusual unit are most nuclear cross sections measured, and in terms of cross sectional area, how large is this unit?
34. What percentage of the neutrons that are produced by the thermal fission of Uranium-235 are prompt neutrons?
35. Why do we say that a nuclear chain reaction is a self-correcting process?
36. Where do the delayed neutrons that we observe in a reactor core come from?
37. Do delayed neutrons that are released have a higher or lower initial energy than the prompt neutrons that the fission process produces?
38. Who was Ludwig Boltzmann?
39. Approximately what percent of the energy from the fission of an atomic nucleus is released immediately?
40. Suppose that during the steady-state operation of a commercial nuclear reactor approximately 10^9 delayed neutrons are emitted by the fuel rods per second. Approximately how many prompt neutrons are emitted during this same period of time?

41. What is a joule/second called?
42. Describe what is meant by the term "compound nucleus," and give at least one example of an isotope that produces one.
43. What does the term MWT refer to, and how is it different from the term MWE?
44. Approximately what percentage of the energy that is released from the fission of a uranium or plutonium nucleus is ultimately recoverable?
45. What is the difference between a joule and a watt?
46. What percent of the time does a Uranium-235 nucleus split apart when it absorbs a thermal neutron?
47. What percent of the time does a plutonium-239 nucleus emit a gamma ray when it absorbs a thermal neutron?
48. How many nuclear fissions per second are required to produce 1 W of useful power?
49. How much Uranium-235 (by weight) is there in a fuel of a typical thermal water reactor that is moderated by light water?
50. How many decay chains are typically required to describe the behavior of the delayed neutrons in a thermal water reactor?
51. How much energy does an atomic mass of 1 AMU represent?
52. What is the name of a famous equation for the fission neutron energy spectrum, and what is the explicit form of this equation?
53. What is the formula for the neutron capture-to-fission ratio?
54. What is the average number of prompt neutrons that are produced when a Uranium-235 or a Plutonium-239 nucleus splits apart?
55. Name at least three common fission products that can be found in a nuclear fuel rod.
56. What is a fissile material, and what is a fertile one?
57. What is the average value of the energy of a prompt neutron when it is released?
58. What is its most probable value?
59. What is the maximum energy that a prompt neutron can be released from the fission of a uranium or plutonium nucleus?
60. How much U-235 is there in naturally occurring uranium?
61. In addition to some additional neutrons, what else is produced when the nucleus of an atom splits apart?
62. What is the binding energy of the last nucleon in a typical fissionable material?
63. What is the difference between the eta η of a nuclear fuel and the mu ν?
64. For a typical nuclear fuel, which is larger—the value of η or the value of ν?
65. What is the amount of time that it takes for a typical delayed neutron to be produced?
66. What equation can be used to calculate the energy released by converting the mass of a nuclear particle to pure energy?
67. What is a gamma ray and what nuclear particle carries its energy?
68. What is the approximate value for the speed of light in a vacuum?
69. What do a neutron and a molecule of ordinary unionized hydrogen gas have in common?
70. Compared to a prompt neutron, is the average initial energy of a delayed neutron higher or lower?
71. An atomic nucleus with a mass of 240 AMU splits apart and releases three neutrons. If one of the fission products has a mass of 170 AMU, what is the mass of the other?
72. When a neutron in a reactor reaches thermal equilibrium with its environment, what is the most likely energy that it will have?
73. What isotope of uranium has a natural abundance of about 0.02%?
74. How many regions or energy ranges does a typical neutron move through between the time it is produced and the time it is absorbed?
75. What is the velocity of a normal neutron when it reaches the thermal energy range?
76. Name three examples of fissile materials and two examples of fertile ones.
77. What is a microscopic nuclear cross section, and what is its purpose?
78. If a thermal water reactor produces 1000 MW of recoverable thermal power, approximately how much electricity does it produce?
79. In what units is this power of a reactor usually measured?
80. What nuclear process is responsible for the production of heat and light in stars?
81. What particle carries away most of the energy from a nuclear reaction that is not recoverable?
82. What material in a thermal reactor is most likely responsible for changing a fast neutron into a thermal one?
83. What isotope of uranium has the highest natural abundance?
84. What is an epithermal neutron likely to see in the epithermal energy range?

85. Where does the kinetic energy go when the by-products of a fission reaction begin to slow down?
86. In what form is this energy usually manifested in a thermal reactor?
87. U-233, U-235, and Pu-239 are three common fissile materials. Can you name the fourth one?
88. How many joules are there in an electron volt?
89. At what energy does the epithermal or resonance energy range in a typical nuclear material begin and end?
90. If a U-233 nucleus absorbs a thermal neutron and splits apart, what is the value of ν?
91. What is radioactive beta decay, and what particles does it involve?
92. What is the delayed neutron fraction for U-235?
93. On average, how many prompt neutrons are released when 50 Uranium-235 nuclei split apart?
94. Suppose that a nuclear reaction produces 3.6 MJ of electricity in 1 hour. How many kilowatt hours of electricity on your electric meter is this equivalent to?
95. On average, what material produces more prompt neutrons if it absorbs a thermal neutron—U-235 or Pu-239?
96. How long does it take a fast neutron in a thermal reactor to be absorbed?
97. How many fission products are created when 200 Pu-239 nuclei split apart?
98. When studying the time-dependent behavior of the neutron population in a reactor core, what does the symbol β refer to?
99. If an isotope has a λ of -0.1 seconds, how much of it will remain after 10 seconds?
100. Suppose that the fission products in a nuclear reactor have the following delayed neutron yields: $\beta_1 = 0.00022$, $\beta_2 = 0.00142$, $\beta_3 = 0.00127$, $\beta_4 = 0.00257$, $\beta_5 = 0.00075$, and $\beta_6 = 0.00027$. What is the total delayed neutron fraction for this material, and what nuclear fuel are the fission product decay chains most likely to represent?
101. What is the nuclear process that is responsible for creating the energy produced by stars?
102. What was the first example of a known terrestrial-based nuclear reactor?
103. Suppose that we convert some matter into energy using Einstein's famous equation and we find that the result of this conversion process is 100,000 kg m^2/s^2. How many megajoules of energy does this correspond to?
104. How many fission product decay chains are normally required to predict the time-dependent release of the delayed neutrons in a nuclear reactor with a reasonable degree of accuracy?
105. For a specific nuclear fuel, what is the key parameter that determines how fast a nuclear chain reaction will proceed?
106. If 1 g of nuclear fuel is converted entirely into energy, how much energy is released?
107. Where in the city of Berlin, Germany, can Einstein's famous equation $E = mc^2$ be found on a 3 m tall sculpture?
108. Write an expression for the eta (η) of the fuel when an arbitrary number N of different fissionable materials are present in a nuclear fuel rod.

Exercises for the Student

Exercise 7.1

Suppose that a reactor consists of two materials—the first material has an absorption cross section of 1 cm^{-1} and a fission cross section of 0.5 cm^{-1}. The second material has an absorption cross section of 0.25 cm^{-1} and a fission cross section of 0. If half of the reactor consists of material 1 and half of the reactor consists of material 2, what must be the minimum value of ν for the reactor to be exactly critical? Assume that no neutrons leak out of the core.

Exercise 7.2

A specific type of nuclear fuel has a capture-to-fission ratio of 0.169 and, on average, produces 2.418 neutrons per thermal fission. What is the number of fission neutrons produced per neutron absorbed?

Exercise 7.3

Suppose that a thermal water reactor is designed to run on Pu-239 instead of U-235. Estimate the amount of plutonium that must be burned each day to produce 3000 MW of thermal power.

Exercise 7.4

Thermal water reactors can be designed to run on either U-235 or Pu-239. To produce 1000 MW of electricity, does a thermal water reactor have to consume more U-235 or Pu-239? What is the ratio of the masses of these materials required to produce the same amount of power?

Exercise 7.5

Nuclear fuel rods are made out of hundreds of smaller fuel pins that contain enriched uranium. When a thermal water reactor is operating normally, several trillion uranium atoms can split apart in each of these fuel pins each second. Assume that each fuel rod consists of 500 fuel pins and that there are 3 trillion fissions/s in each fuel pin. How much thermal energy does a fuel rod consisting of 500 of these fuel pins produce in 1 second?

Exercise 7.6

Suppose that a reactor fuel assembly is capable of producing 16 MW of energy every second. How much of this energy is not recoverable and does not show up in the form of heat? Where does this additional energy go?

Exercise 7.7

Suppose that a nuclear chain reaction takes place where 500 AMU of nuclear material is converted into pure energy. Using Einstein's equation of mass and energy equivalence, estimate the total amount of energy that is released in MeV.

Exercise 7.8

A commercial power reactor is capable of generating between 3000 and 4000 MW of thermal energy. Suppose that it is possible to convert 35% of this energy directly into electricity. How much electricity does a 3500 MWT reactor produce, and how much waste heat does the reactor produce?

Exercise 7.9

Delayed neutrons are produced when the radioactive fission products produced by the process of nuclear fission become neutron rich and decide to emit a neutron to return to a more stable state.

Part 1: Compared to the prompt neutrons, which are produced about 10^{-12} seconds after the nucleus is split apart, how long does it take on average for these "delayed" neutrons to appear?

Part 2: Relative to the prompt neutrons, how many delayed neutrons are produced for every 1000 prompt neutrons from a typical U-235 fuel rod?

Part 3: How many steps are there in the process that allows a fission product to produce a delayed neutron?

Part 4: Write down each of these steps, and show each of the reactions involved, assuming that we start with a "neutron-rich" fission product having the following composition: FP (A, Z).

Exercise 7.10

An exercise on reactor energetics:

Part 1: Using Einstein's famous equation $E = mc^2$, calculate Q, the amount of energy released in MeV, for the following fission reaction:

$$ {}^{1}_{0}\mathrm{n} + {}^{235}_{92}\mathrm{U} \rightarrow {}^{236}_{92}\mathrm{U} \rightarrow {}^{139}_{56}\mathrm{Ba} + {}^{94}_{36}\mathrm{Kr} + 3\,{}^{1}_{0}\mathrm{n} + \mathrm{Q} $$

Part 2: What is the average amount of energy released from the thermal fission of a Uranium-235 nucleus, and how does this number compare to the amount you just calculated in part 1?

Part 3: Approximately how much of this energy is recoverable, and how much is not? Where does the rest of this energy go?

Part 4: Suppose that a reactor has been operating at steady-state conditions for some period of time and that it is decided to shut the reactor down. Immediately after the reactor is shut down, how much of the remaining energy (compared to when the reactor was operating at a steady-state power level P) does the radioactive decay of the fuel rods produce?

Exercise 7.11

In a previous section, we learned that the neutron absorption probability increases as the energy of the incoming neutron decreases.

Part 1: What are the two fundamental reasons why this is true?

Part 2: Suppose that a U-235 nucleus absorbs one of these neutrons and we are then asked to predict what will happen next. If the neutron is a thermal neutron, what is the chance that the neutron will cause the U-235 nucleus to split apart, and what is the chance that it will not?

Part 3: Suppose that a particular type of nuclear fuel emits an average of 2.8 neutrons per fission. Suppose that there is a 30% chance that it will undergo radiative capture instead and not cause any neutrons to be released. What is the value of η (eta) for this nuclear fuel in this case?

Part 4: What are the minimum and the maximum number of neutrons that you would expect this fuel to emit? You may ignore the contributions of the delayed neutrons to this total when giving your answer.

Exercise 7.12

In the early days of the nuclear business, people struggled to understand how often a U-235 nucleus would split apart and how often it would not. Eventually, they found that the best way for the nucleus to split apart was for it to absorb a thermal neutron. Using the values for the fission and capture cross sections that we presented in Chapter 5, estimate the probability that a thermal neutron will cause a U-235 nucleus to split apart. If the nucleus happens to absorb a fast neutron, is the probability of the nucleus splitting apart exactly the same?

8

Neutron Slowing Down Theory, Neutron Moderators, and Reactor Coolants

8.1 Introduction

In this chapter, we would like to discuss how *fission neutrons*, which are initially produced with an average kinetic energy of about 2 MeV, are converted into *thermal neutrons* (with an energy less than 1 eV) or *epithermal neutrons* (with an energy between 10 keV and 1 eV). This process occurs through a series of elastic collisions in which the energy loss per collision depends on the mass of the target nucleus. Neutrons lose more energy per collision in elastic collisions with lighter nuclei than they do in similar collisions with heavier and more massive ones. In Chapter 3, we learned that if we know the energy and the momentum of two particles going into a collision, then we can predict the energy and the momentum of the same particles coming out of the collision. The process by which this occurs can be described by an elegant mathematical framework called *neutron slowing down theory*. Within this framework, the average energy loss per collision becomes a function of the neutron scattering angle θ. Slowing down theory usually concerns itself with elastic collisions, although inelastic scattering collisions can also occur.

Once neutrons reach thermal energies and cannot slow down any further, their distribution of kinetic energies is governed by a famous statistical probability distribution called the *Maxwell–Boltzmann probability distribution*. Neutrons that obey this distribution are called *thermal neutrons*, and their most probable kinetic energy (corresponding to the peak of this distribution) in a thermal water reactor is about 0.025 eV. A gas of neutrons (or a flux of neutrons for that matter) that obeys this probability distribution is then said to be in *thermal equilibrium* with its environment, and when a state of thermal equilibrium is reached, the kinetic energy of an average neutron can neither increase nor decrease. (However, individual neutrons within the distribution *can* gain or lose energy.) From the viewpoint of a reactor designer, this process is extremely important because it determines the dynamics of the nuclear chain reaction. It determines not only the power generation rate but also where the power is generated. In fast reactors, reactor design is predicated on the fact that most fission neutrons are absorbed before they reach kinetic energies below 10 keV. Hence, the majority of the neutrons are "fast," and the coolant must be selected so that very few neutrons enter the thermal energy range.

Conversely, thermal water reactors such as PWRs and BWRs require large numbers of thermal neutrons to function properly. Because of this, fast neutrons have to be converted into thermal neutrons, and another material, normally called *the moderator*, must be used for this purpose. In most of these reactors, the coolant is also used as the moderator, but this does not necessarily have to be the case. For example, in gas-cooled reactors, graphite or beryllium is used to convert fast neutrons into thermal ones, and carbon dioxide (CO_2), hydrogen, or helium is used as the coolant. Hence, the choice of the coolant or the moderator plays an important role in the overall design of a nuclear power plant. It also affects the neutronic behavior of the core, which we will subsequently discuss.

8.2 Neutron Moderators and Their Function

As neutrons slow down in elastic and inelastic collisions, a percentage of their kinetic energy is transferred from the neutron to the target nucleus. *In thermal reactors, it is the role of the moderating material—or the moderator—to allow this to occur*. Many materials can serve as neutron moderators, and ideally, the moderator should be the same as the coolant. However, not all coolants are suitable for use in all reactor types, and so the moderating material can vary from one type of reactor to the next. For many reasons, the most common moderating material in use today is ordinary water. We will have more to say about the moderating properties of ordinary water in another section. However, before descending into the topic of neutron moderation, we would first like to classify the types of coolants that are used in reactors today. The coolants are in turn a function of the design of the plant, and the choice of the correct coolant to use is strongly dependent on the goals of a particular design.

8.3 Reactor Coolant Comparisons

Nuclear reactors can use a wide variety of coolants, but not all coolants are suitable for all reactor types. Reactor coolants can be classified as fluids, liquid metals, and gases. By far, the most common reactor coolant is ordinary water (H_2O). Sometimes, ordinary water is also called *light water*. PWRs and BWRs use light water to cool the core, and the only difference is that BWRs allow the coolant to boil, while PWRs do not. CANDU reactors use water in their secondary loops, but their cores also moderated by another form of water called *heavy water*. Heavy water has an additional neutron attached to the hydrogen atoms in the water molecule. Sometimes, this modified hydrogen atom is called a *deuterium atom*. A picture of an ordinary water molecule and a heavy water molecule is shown in Figure 8.1. *Except for the presence of the heavier hydrogen atom (deuterium), the structure of the two water molecules is identical. However, their nuclear properties are considerably different.*

Light water is used in reactors primarily because of its availability and because its thermodynamic properties are well known and well understood. The only problem with light water is that it cannot be used in fast reactors because it contains a high concentration of the element hydrogen. It can also be somewhat corrosive at times. *The hydrogen in the water molecules slows down the neutrons that are produced in the core.* This process works very well in a thermal water reactor because the coolant also serves as the moderator. However, it does not work well in fast reactors because the neutrons cannot be allowed to slow down to the thermal energy range. Consequently, fast reactors are limited to liquid metal coolants (such as liquid sodium, potassium, and sometimes mercury). These liquid metals have excellent heat conduction and retention capabilities, and they can more easily remove the heat that the fast reactors produce.

Particle economy is also an important factor to consider when deciding the best type of reactor coolant to use. CANDU reactors are powered by natural uranium and cannot use coolants that have high particle absorption cross sections because there are simply not enough neutrons to go around. They are limited to using heavy water as a moderator and a coolant because the neutron absorption cross sections are much lower than they are for ordinary water (about a factor of 500 less).* Gas-cooled reactors, on the other hand, use fuel with a higher enrichment than CANDU reactors do, and they need gases in conjunction with a solid moderator to function properly. Usually, this moderator is some form of the element carbon. Normally, the element carbon is compacted into a *graphite block*. However, gas reactors have the advantage that they can use the *Brayton thermal cycle* instead of the *Rankine thermal cycle* to extract heat from the core, and if the temperature of the gas is high enough, the thermal efficiency can exceed that of

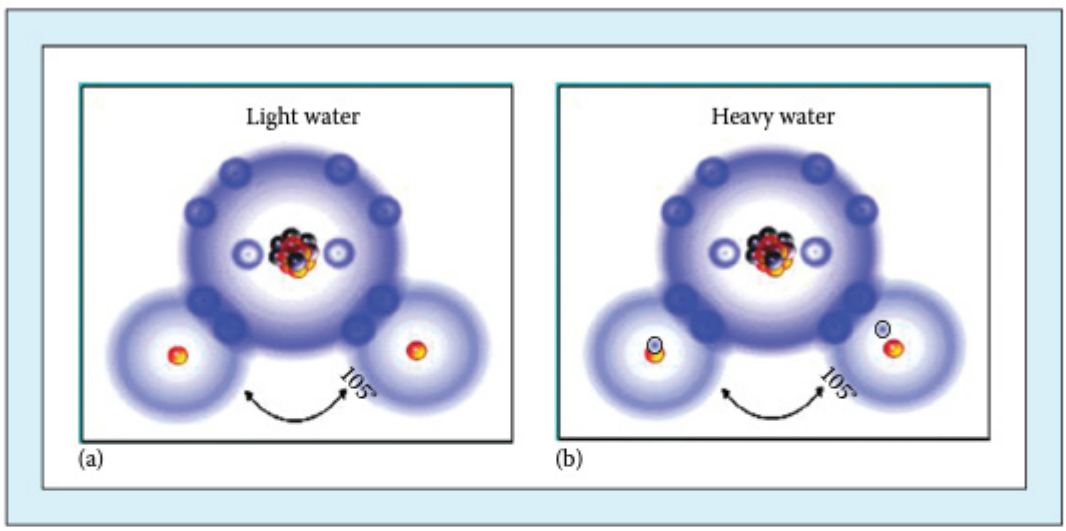

FIGURE 8.1 Ordinary water (a) and heavy water (b) can both be used as reactor coolants. The extra neutron in the nucleus of the hydrogen atoms converts light water into heavy water. The structure of the two molecules is identical. However, their nuclear properties are considerably different because heavy water absorbs fewer neutrons than light water does. (Adapted from a public domain picture provided by Wikipedia.)

* The thermal absorption cross section of light water is about 0.644 barns, and the thermal absorption cross section of heavy water is about 0.00133 barns (see Appendix C). Hence, light water is approximately 0.644/0.00133 = 485 times more likely than heavy water to absorb a thermal neutron.

TABLE 8.1
Properties of Common Reactor Coolants in Use Today

Common Reactor Coolants					
Reactor Coolant	Used In	Availability	Cost	Heat Transfer Coefficient	Neutron Absorption Cross Section
Light water	PWR, BWR	High	Low	High	Moderate
Heavy water	CANDU	Low	High	High	Very low
Liquid sodium	LMFBR	Moderate	Moderate	Very high	Moderate
Carbon dioxide	Gas reactors	High	Low	Low	Low
Helium	Gas reactors	High	Low	Low	Low

a comparable PWR or BWR. CO_2 is the most popular coolant to use, although other industrial gases such as hydrogen and helium have also been used. In selecting which coolant to use, several important factors come into play. These factors include

- The availability of the coolant
- The cost of the coolant
- The heat transfer coefficient of the coolant
- The particle absorption cross section of the coolant
- The scattering cross section of the coolant
- The pumping power required to pump the coolant through the core and the nuclear steam supply system (NSSS)

Needless to say, no single reactor coolant possesses an optimum value for all of these characteristics all of the time. Hence, the selection of which coolant to use becomes an engineering trade-off between several different and often competing factors.

Some of these properties are compared in Table 8.1. Notice that each reactor type has a preferred coolant that satisfies the majority of its requirements. However, in many cases, a slightly less desirable coolant can also be used.

8.4 Common Reactor Coolants and Their Properties

A suitable *reactor coolant* is one that has a low neutron absorption cross section, low pumping power requirements, a high heat transfer coefficient, good thermal stability, good industrial availability, and low initial cost. For a variety of reasons, fast reactors use different coolants than thermal reactors do, and in general, most reactor coolants tend to fall into three broad categories. We would next like to discuss these categories in more detail.

8.4.1 Category I: Thermal Water Reactor Coolants

The two coolants used in thermal water reactors are *light water* and *heavy water*. Light water is the same as ordinary water, but it is more highly purified to remove any minerals that can corrode the components of the NSSS. Heavy water is the same as light water except that each hydrogen atom in the water molecule is replaced by a heavier hydrogen atom that has an additional neutron attached to it. Heavy water has the symbol D_2O, and light water has the symbol H_2O. The "D" in this case refers to a specific isotope of hydrogen called *deuterium*. The nuclear properties of deuterium are discussed in Appendix C, and its physical properties are discussed in Section 8.20. We will have more to say about the process of heavy water production at the end of the chapter. Reactors that use heavy water to moderate fission neutrons are extremely attractive in less technologically developed countries because one does not need a uranium enrichment plant to build a commercial power reactor. Reactors that are moderated by heavy water can run on *natural uranium* alone. Neutronically, this is possible because heavy water absorbs fewer thermal neutrons than light water does. Hence, *neutron economy* in a heavy water reactor is generally better than it is in a light water reactor that uses natural uranium fuel.

Sometimes, heavy water is referred to as *deuterium oxide* or D_2O. PWRs and BWRs use light water, while Canadian reactors, called CANDU reactors, use heavy water. The physical properties of light water and heavy water are very similar to each other (except for their atomic weight), but their nuclear properties are considerably different. Heavy water absorbs fewer neutrons than light water does. It also takes longer to slow down a neutron from fast energies to thermal ones. Hence, heavy water reactors that run on natural uranium tend to be larger than light water reactors that use enriched uranium. Military reactors (see Chapter 1), which use highly enriched uranium with an average enrichment of about 95%, tend to be even smaller and more compact.

Student Exercise 8.1

Using the values of the neutron absorption cross sections for light water and heavy water given in Appendix C, estimate how many times more likely it is for a thermal neutron to be absorbed by a molecule of light water than it is for the same neutron to be absorbed by a molecule of heavy water.

Assuming that the volume of the fuel and the volume of the coolant in the core are essentially the same (see Chapter 1), approximately how many times more thermal neutrons would be available to be absorbed by the fuel when the coolant is heavy water than when the coolant is light water? Assume that the fuel consists of uranium dioxide with an average enrichment of 3%.

8.4.2 Category II: Gas Reactor Coolants

As the name implies, gas reactors are cooled by gases that do not undergo a phase change. *The most common gas reactor coolants used are He and CO_2*. As we will see in a future chapter, these reactors are capable of using the Brayton thermal cycle, and one of the great advantages of gas-cooled reactors is that they have a very high thermal efficiency (on the order of 40%). Outside of the United States, gas reactors use CO_2 as their primary coolant. In England and most of Europe, these gas reactors are called *advanced gas reactors or AGRs* for short. The actual flow of gas through a gas reactor is somewhat complicated, and we will not discuss it here. The core inlet temperatures range from about 400°C to 500°C, and the core outlet temperatures range between 700°C and 850°C. CO_2 is not a strong neutron absorber, and so it does not become excessively radioactive. It also has good chemical stability and does not react with the fuel or the structural materials in the core. It is also much less corrosive than ordinary water.

In the United States, gas-cooled reactor technology has been centered around the development of the *high-temperature gas reactor, or HTGR*. It is a graphite-moderated thermal reactor. HTGRs are cooled with helium gas, and in general, helium is an excellent coolant. It is far more inert than CO_2 is and does not absorb as many neutrons. Therefore, it does not become radioactive. A HTGR has a core inlet temperature of about 750°C and a core outlet temperature of about 850°C. The primary provider of HTGRs in the United States is the General Atomics Company located in San Diego, California. In spite of these technical advantages, HTGRs evidently do not produce electricity as cheaply as PWRs do, and while much interest in them remains, their world market share has not been very large.

8.4.3 Category III: Fast Reactor or Liquid Metal Coolants

Fast reactors are fundamentally different than thermal reactors because they are designed to create large quantities of heat based on the use of fast neutrons rather than thermal neutrons. Technically speaking, fast reactors do not need a moderator, and so the core and the blanket contain only three types of materials: the fuel, the structure, and the coolant (to take away the heat). In the early days of the nuclear power business, a number of different materials were used to cool fast reactors. Over a period of time, it became apparent that *liquid metals* were the best type of coolant to use because they did not slow down the fast neutrons that were produced. They were also very good at conducting and removing heat from the core because of their high thermal conductivity and heat capacity. Early on, three liquid metals were considered as fast reactor coolants; they were *liquid sodium, liquid potassium, and liquid mercury*. However, for a variety of reasons, liquid sodium eventually became the coolant of choice. Hence, virtually all modern fast reactors use liquid sodium as their coolant, and these reactors are referred to as liquid metal fast breeder reactors, or *LMFBRs*. Sometimes, they are also called sodium-cooled reactors.

Liquid metal coolants have a lot of positive attributes compared to other reactor coolants, but they also have a few shortcomings. They are excellent heat transfer agents, and so LMFBRs that use them can be operated at very high power densities. This in turn means that LMFBR cores can be relatively small and compact compared to their water reactor counterparts. Liquid sodium has a very high boiling point (about 880°C at atmospheric pressure), and so reactor coolant loops can be operated at very high temperatures and low pressures without boiling the coolant. This means that large, heavy, and expensive pressure vessels are not required to hold the liquid metal. Sodium is also not as corrosive as water is, and so components immersed in liquid sodium can look almost new after many years. However, the same components exposed to liquid water can become corroded due to the buildup of a mineral film on the surface. If the water happens to boil, even more minerals can be deposited on the surface. All LMFBRs tend to operate close to atmospheric pressure (about 0.3 MPa or 50 PSI).

The major drawback of using liquid sodium to cool these reactors is that it is highly reactive chemically. It reacts violently with water and catches fire when it comes in contact with ordinary air. It also has a high melting point (about 100°C), so the entire cooling system must be heated at all times to keep the sodium from solidifying. Finally, liquid sodium can absorb some fast neutrons, and this can cause it to become radioactive. Therefore, *all LMFBRs use two sodium cooling loops*—a primary coolant loop containing the radioactive sodium and an intermediate coolant loop

containing sodium that is not radioactive before the heat is passed onto a steam generator. Sometimes, the intermediate loop is called an *intermediate heat exchanger* because it transfers heat from the primary loop (which includes the core) to the NSSS. The steam-producing side of the NSSS is normally cooled with light water.

8.5 Fast Reactors versus Thermal Reactors

Neutron moderation is not an important factor in fast reactors because fast reactors use high-energy neutrons rather than low-energy ones. The neutron energy spectrum of a fast reactor is compared to that of a thermal reactor in Figure 8.2 and the fission process is illustrated again in Figure 8.3. Figure 8.4 demonstrates the difference between fission and fusion. As of the writing of this book, a commercial fusion reactor has *not* been built. Notice that the energy of a neutron in a fast reactor rarely falls below 10 keV, while in a thermal reactor, about half the neutrons have energies below 10 keV. Because the average energy loss per collision depends on the atomic weight of the moderating material, some materials are more effective than others as a neutron moderator. In head-on elastic collisions, we learned from our previous discussion in Chapter 3 that the energy loss per collision ΔE is given by

$$\Delta E = E - E' = E(1-\alpha) \tag{8.1}$$

where

E is the initial neutron energy

E′ is the final neutron energy

$\alpha = (A-1)^2/(A+1)^2$ is a constant that depends on only the *atomic weight* or the *atomic mass number* of the target nucleus A

It follows directly from this equation that the lighter the target nucleus is, the smaller the value of α will be, and the greater the energy loss ΔE per collision will be. In glancing collisions, which are a much more common process because the nucleus is so small, we also found that the energy loss per collision is given by

$$\Delta E = E - E' = E\left(1 - \left\{\frac{(1+\alpha)}{2} + \frac{(1-\alpha)}{2}\cdot\cos\theta\right\}\right) \tag{8.2}$$

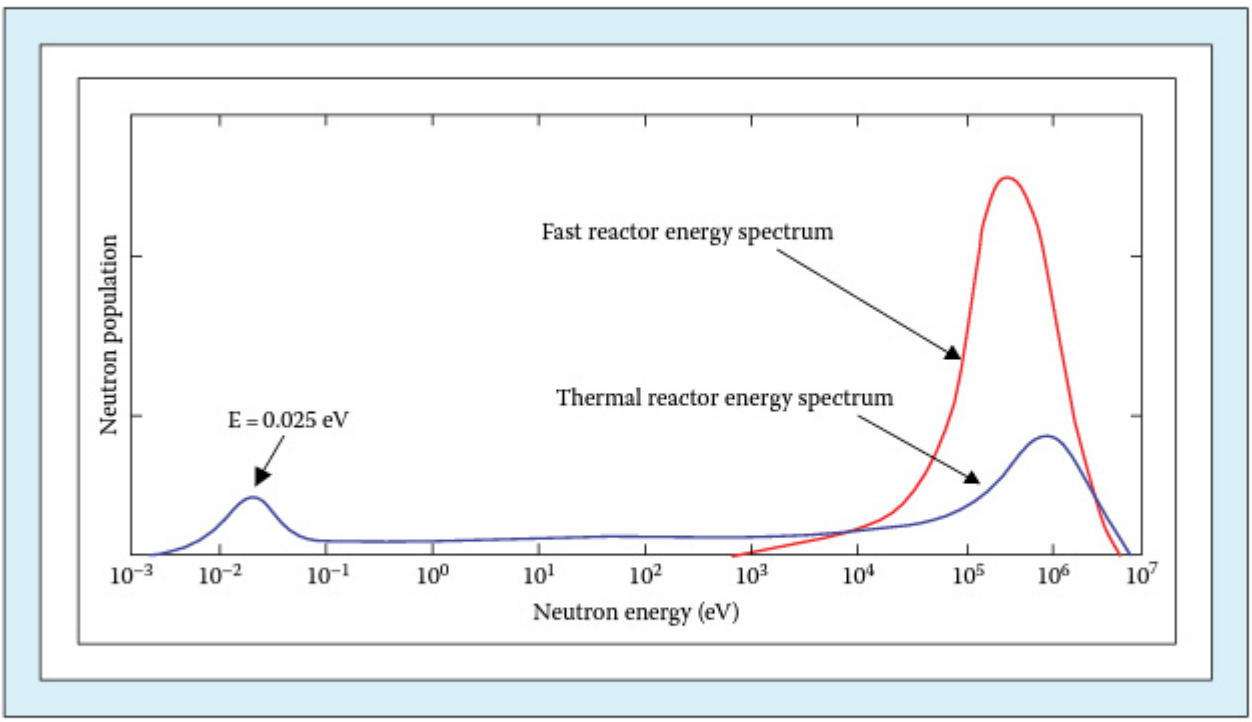
Fast reactor energy spectrum
Thermal reactor energy spectrum
E = 0.025 eV
Neutron population
10⁻³ 10⁻² 10⁻¹ 10⁰ 10¹ 10² 10³ 10⁴ 10⁵ 10⁶ 10⁷
Neutron energy (eV)

FIGURE 8.2 A fast reactor energy spectrum compared to a thermal reactor energy spectrum. Note that the energy of a neutron in a fast reactor rarely falls below 10 keV, while in a thermal reactor, approximately half of the neutrons have an energy less than this.

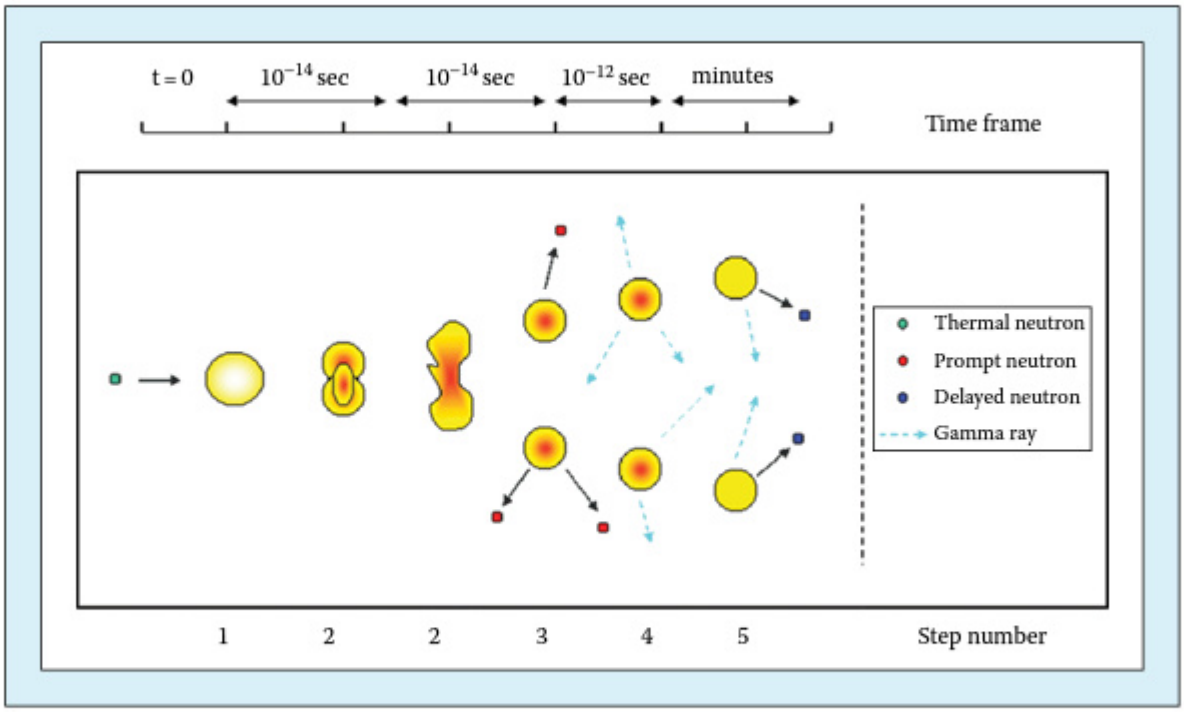

FIGURE 8.3 The evolution of the nuclear fission process as a function of time.

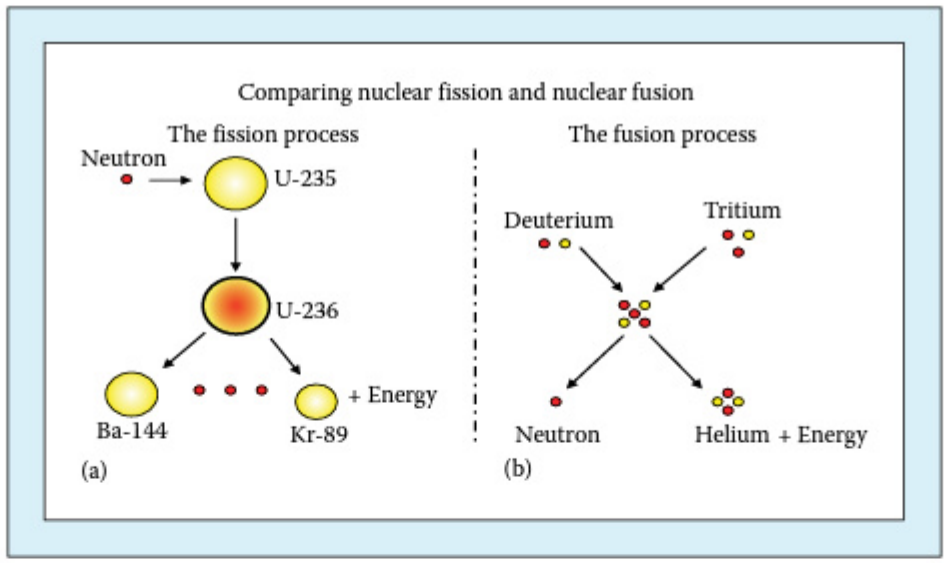

FIGURE 8.4 How the process of (a) nuclear fission and (b) nuclear fusion compare when it comes to the process of neutron generation.

which means that the energy loss is a function of the *neutron scattering angle* θ. Assuming a random distribution of glancing collisions, the energy loss per collision is given by

$$\Delta E = \left(1 - \left[\frac{1}{2} + \frac{\alpha}{2} + \frac{(1-\alpha)}{3A}\right]\right)E \tag{8.3}$$

or finally,

$$\Delta E = \left(\frac{1}{2} - \frac{\alpha}{2} - \frac{(1-\alpha)}{3A}\right)E \tag{8.4}$$

Using a related equation, we can also show that the average cosine of the scattering angle $\mu = \langle\cos\theta\rangle$ is related to the atomic mass of the target nucleus by $\mu = \langle\cos\theta\rangle = 2/3A$. In other words, we can write

$$E' = E - \Delta E = E - \left(\frac{1}{2} - \frac{\alpha}{2} - \frac{(1-\alpha)}{3A}\right)E \tag{8.5}$$

or

$$E' = \left(\frac{1}{2} + \frac{\alpha}{2} - \frac{(1-\alpha)}{3A}\right)E \tag{8.6}$$

and finally,

$$E' = \alpha' E \tag{8.7}$$

where now

$$\alpha' = \frac{1}{2} + \frac{\alpha}{2} - \frac{(1-\alpha)}{3A} \tag{8.8}$$

and A is the atomic mass number of the moderating material. If we ignore the last term because it is very small for most materials (which is typically the case when A is large), then Equation 8.8 becomes

$$\alpha' = \frac{(1+\alpha)}{2} \tag{8.9}$$

The average energy loss per collision $\Delta E = E - E' = E - \alpha' E = E(1-\alpha') = E(1-\alpha)/2$ *is then given by the very simple relationship*

The Average Energy Loss per Collision

$$\Delta E = \frac{(1-\alpha)}{2} \tag{8.10}$$

This equation can be used to find the energy loss for both head-on and glancing collisions. Now, let us see what this relationship can tell us about how a neutron behaves when it collides with atoms of different atomic weights. In the case of hydrogen, which is the lightest element, $\alpha = 0$ and $\alpha' = 0.5$, so on average, a neutron loses one-half of its energy in a collision with a hydrogen nucleus. Similarly, when a neutron is scattered by a carbon nucleus, which has an intermediate atomic weight, then $\alpha = 0.716$ and $\alpha' = 0.853$, so the energy loss per collision, ΔE, is about 15%. Finally, if we were to extrapolate these results to a very heavy nucleus like U-238, then we would find that $\alpha = 0.983$ and $\alpha' = 0.0085$, so the energy loss per collision, ΔE, would be less than 1%. From our previous analysis, it also follows from Equation 8.10 that

$$E'' = \alpha' E' = \alpha'\alpha' E \tag{8.11}$$

and

$$E''' = \alpha'\alpha'\alpha' E \quad \text{and so on.} \tag{8.12}$$

We can generalize this to the case of n successive collisions, or scattering events, by writing

The Final Neutron Energy after N Collisions

$$E'_n = (\alpha')^n E \tag{8.13}$$

where

E'_n is the energy of the neutron after the *n*th successive collision
E is the initial energy of the neutron before any collisions occur

TABLE 8.2
Comparison of the Moderating Properties of Common Nuclear Materials

Material	A	α	α′	Average Energy Loss in an Elastic Collision $\Delta E = 0.5\,(1-\alpha)$ (%)	Average Number of Collisions Required to Thermalize a 2 MeV Neutron to 0.025 eV
H	1	0.0	0.50	50.0	26
D	2	0.11	0.55	44.5	30
Be	8	0.61	0.80	19.5	80
C	12	0.72	0.85	14.0	112
O	16	0.78	0.89	11.0	155
U-238	238	0.98	0.99	1.00	1805

If we would like to know how many collisions it takes to go from an initial energy E of ~2 MeV to a final energy E′ of ~0.025 eV, we simply substitute these values into Equation 8.13 and solve for n. The value of n can be found from a lookup table or by solving Equation 8.13 directly. The exact value of n is

Number of Collisions for a Particle to Go from an Initial Energy E to a Final Energy E′

$$n = \log_{\alpha'}\left(E'/E\right) \tag{8.14}$$

where $\alpha' = (1 + \alpha)/2$. This equation can be used to calculate how many collisions it takes for a neutron to go from an initial energy E to a final energy E′. Notice that the base of the logarithm in Equation 8.14 is α′. In Section 8.12, we will derive a more convenient way to find the value of n, which is based on the use of the natural logarithm (ln). In general, E and E′ can be any energies at all. Table 8.2 shows the value for α and the number of collisions that are required to reduce the energy of a fission neutron from an initial energy E of approximately 2 MeV to a final energy E′ of approximately 0.025 eV. *Obviously, lighter elements are preferable to heavy elements when it is important to reduce the kinetic energy of a fission neutron as quickly as possible.*

Now, let us see if we can compare the hydrogen atoms in heavy water and light water from a slightly different perspective. For ordinary hydrogen, it takes an average of 26 collisions to thermalize a 2 MeV fission neutron. The energy of the neutron after each successive collision is calculated in Table 8.3. If we plot the final neutron energies $E'_n = E(\alpha')^n$ for hydrogen, which has a value of $\alpha' = 0.50$, and for deuterium, which has a value of $\alpha' = 0.55$, we get the curves shown in Figure 8.5. Since the energy decrement α is a constant that is independent of the initial energy E, the final energy E′ decays exponentially from its initial value (see Figure 8.5) with each successive value of n. Hence, the important point to take away from this discussion is that only certain materials are suitable to use for slowing down neutrons quickly, and the lighter the material is, the better chance it has to be an effective neutron moderator.

Example Problem 8.1

A neutron collides with a material with an atomic number of 8 and with an equal number of protons and neutrons in its nucleus. Assuming that glancing collisions and head-on collisions are equally probable, what is the percentage energy loss per collision?

Solution The energy loss per collision is given by $\Delta E = (1 - \alpha)/2$, where $\alpha = (A - 1)^2/(A + 1)^2$. For this particular material, $A = Z + N = 16$. Therefore, $\alpha = (15/17)^2 = 0.778$ and $\Delta E = (1 - \alpha)/2 = 0.11$. The average energy loss per collision is therefore 11%. [Ans.]

8.6 Advantages to Moderating a Neutron

Light water reactors such as PWRs and BWRs are inherently safe to operate because the nuclear chain can no longer be sustained when there is no more water left in the core to moderate the high-energy fission neutrons that the fission of Uranium-235 or Plutonium-239 produces. The water that cools the fuel rods contains a large number of hydrogen atoms that can help to slow down the fast neutrons. If these hydrogen atoms are taken away, or the water boils and is converted to steam, then the process of nuclear fission stops because there are not enough hydrogen atoms to slow down the fast neutrons to thermal speeds and split apart another generation of uranium or plutonium atoms. *This is one way in which a normal power reactor is different than the atomic bomb*. A power reactor uses a moderator to control the nuclear chain

TABLE 8.3
Comparison of the Average Number of Collisions to Thermalize a Fission Neutron for Deuterium and Hydrogen

Number of Collisions (n)	Deuterium ($\alpha' = 0.55$)		Hydrogen ($\alpha' = 0.50$)	
n	$(\alpha')^n$	$E'_n = (\alpha')^n E$	$(\alpha')^n$	$E'_n = (\alpha')^n E$
0	1	2,000,000	1	2,000,000
1	0.550		0.500	
2	0.302		0.250	
3	0.166		0.125	
4	0.135		0.0625	
5	0.091		0.03125	
6	0.050		0.015625	
7	0.027		0.007825	
8	0.015		0.003906	
9	0.008		0.001953	
10	0.004		0.000976	
11	0.002		0.000488	1,000
12	0.0014		0.000244	
13	0.00076	1,000	0.000122	
14	0.00042		0.000061	
15	0.00023		0.0000305	
16	0.00012		0.0000152	
17	0.00007		0.0000076	
18	0.000038		0.0000038	7.6
19	0.000021		0.0000019	
20	0.000017		0.00000095	
21	0.0000064		0.000000475	
22	0.0000035		0.0000002375	
23	0.0000019		0.00000011875	
24	0.0000011		0.000000059375	
25	0.000000587		0.0000000296875	
26	0.000000323		0.00000001484375	.0296875
27	0.000000178		0.00000000742175	
28	0.000000098		0.00000000371093	

Note: This table assumes an average fission energy of 2 MeV.

reaction, while an atomic bomb does not. *As long as there is an efficient way to remove the decay heat from the core, light water reactors are very safe and reliable devices to operate*.

As such, their safety record has been exceptional since they were first introduced in the early 1950s. When you think about it, water is an obvious choice as a reactor coolant because it is a highly effective moderating material. It is also cheap and plentiful. Today, carbon (graphite), light water, and heavy water (deuterium) are the most common moderating materials for thermal reactors. Fast reactors do not require a moderating material because most of the neutrons are absorbed at energies above 10 keV. Because of this, these reactors are cooled with *liquid metals*. We explored the design of fast reactors and the fuels they required in Chapter 1. A much more extensive discussion of fast reactors can also be found in Chapter 15 of our companion book.*

Example Problem 8.2

Suppose that a material to be used in a nuclear power plant has an atomic mass of about 27. What is this material most likely to be, and how many elastic collisions with this material are required for a neutron to slow down from an energy of 10 MeV to an energy of 0.025 eV?

* See *Nuclear Engineering Fundamentals: A Practical Perspective*, by R.E. Masterson, CRC Press (2017).

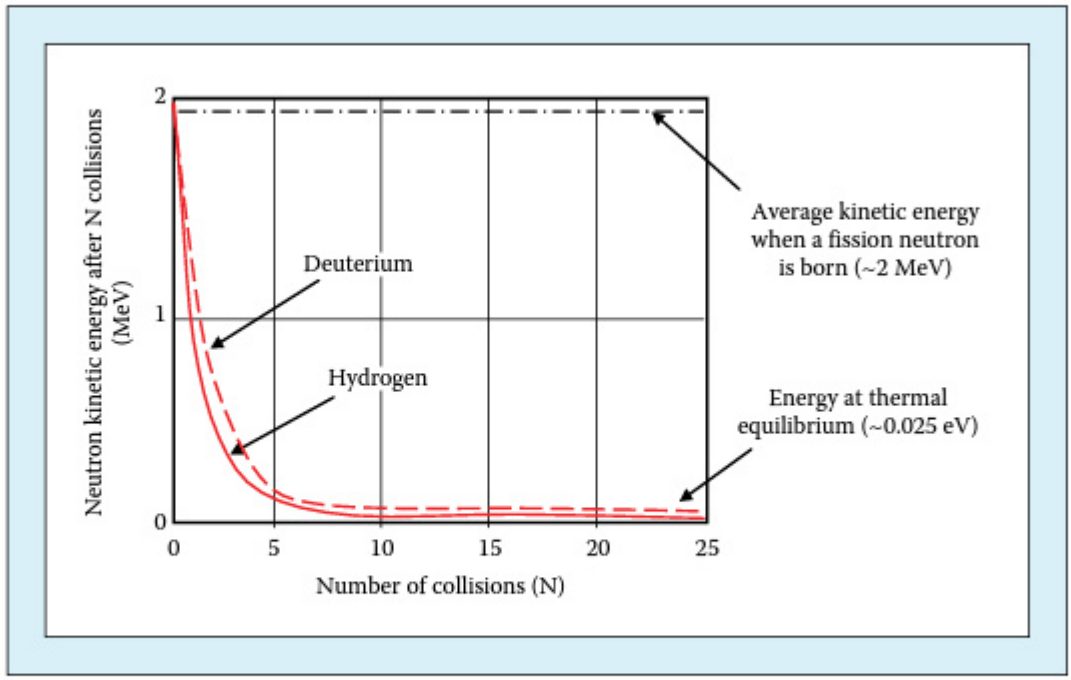

FIGURE 8.5 The average neutron kinetic energy after N successive collisions with hydrogen and deuterium atoms.

Solution Based on its atomic weight (see Appendix D), this material is most likely to be aluminum, which has a value of $\alpha = (A-1)^2/(A+1)^2 = 0.86$, and a value for α' of $\alpha' = (1+\alpha)/2 = 0.93$. The number of collisions required for the neutron to slow down from an energy of 10 MeV to an energy of 0.025 eV can be found from the equation $n = \log \alpha' (E'/E)$, where E = 10 MeV and E′ = 0.025 eV. Plugging in the appropriate values, we find that n = 73 collisions. [Ans.]

8.7 The Relationship between the Temperature, the Energy, and the Velocity of a Moderated Neutron

When a uranium nucleus splits apart, it is important to understand the relationship between the velocities and the temperatures of the neutrons that are produced and the velocities and the temperatures of the neutrons that are absorbed. *Normally, a prompt neutron is released from a uranium or plutonium nucleus with an average kinetic energy of about 2 MeV and a most probable kinetic energy of about 0.75 MeV. This corresponds to an initial velocity of 14,000,000 m/s and 5,250,000 m/s, respectively.* All neutrons have the same rest mass and they also have no electrical charge, so statistically speaking, they behave no differently than the molecules of an ideal gas. After repeatedly colliding with other atoms and the moderator, they eventually come into *thermal equilibrium* with their environment. When they do so, they do not have just a single velocity, but they have a *distribution of velocities*, and some of them are moving very fast, while others are moving very slow.

As long as we can ignore the details of how they interact with each other, we can correlate their average velocity v to their average kinetic energy E. When we do so, we find that their average kinetic energy when they reach thermal equilibrium is about 0.025 eV and their average velocity is about 2200 m/s. However, not all of the neutrons have this velocity, and depending on their average temperature T or average kinetic energy E, *they will have a distribution of velocities that can be represented by a Maxwell–Boltzmann probability distribution*. If a particle happens to follow this distribution, it can be shown that the probability P of the particle having a velocity v is related to its absolute temperature T in the following way:

The Velocities in a Maxwell–Boltzmann Probability Distribution

$$P(v) = Av^2 e^{-(mv^2)/2kT} \tag{8.15}$$

where

m is the mass of the particle
v is the velocity
T is its temperature in degrees Kelvin
k is Boltzmann's constant in joules/K
A is a constant given by

$$A = \sqrt{\left\{\left(\frac{2}{\pi}\right)\left(\frac{m}{kT}\right)^3\right\}} \tag{8.16}$$

Notice that the kinetic energy $E = 1/2\ mv^2$ of the particle appears explicitly in the exponent, and by inference, indirectly in the term Av^2 in front of the exponent. Starting with the original definition of A, we can also rewrite Av^2 as

$$Av^2 = v^2\sqrt{\left\{\left(\frac{2}{\pi}\right)\left(\frac{m}{kT}\right)^3\right\}} \tag{8.17}$$

or

$$mv^2\sqrt{\left\{\left(\frac{2m}{\pi}\right)\left(\frac{1}{kT}\right)^3\right\}} = \frac{1}{2}mv^2\sqrt{\left\{\left(\frac{8m}{\pi}\right)\left(\frac{1}{kT}\right)^3\right\}} = \frac{1}{2}mv^2\sqrt{\left\{\left(\frac{m}{\pi}\right)\left(\frac{2}{kT}\right)^3\right\}}. \tag{8.18}$$

Since $E = 1/2\ mv^2$, the Maxwell–Boltzmann probability distribution can also be written as a function of the kinetic energy as

The Energies in a Maxwell–Boltzmann Probability Distribution

$$P(E) = \sqrt{\left\{\left(\frac{m}{\pi}\right)\left(\frac{2}{kT}\right)^3\right\}}E^{1/2}e^{-E/kT} \tag{8.19}$$

So, in general, the Maxwell–Boltzmann probability distribution is a function of both the kinetic energy E of the particle and its absolute temperature T. Once the absolute temperature is specified, we can draw the probability distribution for the number of neutrons as a function of either the velocity v (Equation 8.15) or the kinetic energy E (see Equation 8.19). Figure 8.6 shows what this velocity distribution looks like at temperatures of 100°K, 300°K, 600°K, and 1000°K. Here, 300°K is

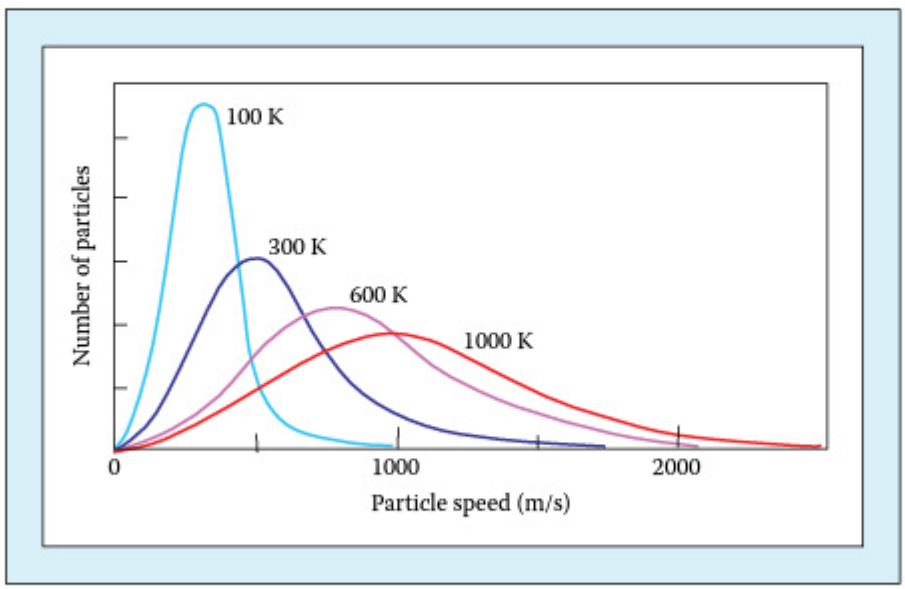

FIGURE 8.6 The shape of a Maxwell–Boltzmann distribution as a function of a particle's average temperature T. (Adapted from a picture in Wikipedia.)

close to room temperature and 600°K is close to the temperature of the coolant in a PWR core. As the absolute temperature rises, the shape of the distribution shifts to the right and the average velocity of the particles increases as well. We can also use this distribution to derive a relationship between a neutron's kinetic energy E, its velocity v, and its absolute temperature T.

If we attempt to find the average neutron energy <E> using P(E) as our guide, it is relatively easy to show that *the average kinetic energy <E> can be related to the average velocity v and the average temperature T in the following way*:

The Average Energy of a Particle That Follows a Maxwell–Boltzmann Probability Distribution

$$<E> = \frac{1}{2}mv^2 = \frac{3}{2}kT \tag{8.20}$$

where

v is the velocity in meters per second
k is Boltzmann's constant = 1.38×10^{-23} J/K
m is the mass in kilograms
T is the temperature in Kelvin

In other words, when a state of thermodynamic equilibrium is reached, the average kinetic energy <E> of a neutron is proportional to its absolute temperature T! The constant of proportionality turns out to be *Boltzmann's constant k*, multiplied by 3/2.

Similarly, it can also be shown that the *most probable energy E_{MP} of any particle that obeys the Maxwell–Boltzmann distribution can be found by taking the derivative of the probability distribution function P(E) with respect to the kinetic energy E and then by setting the derivative to zero*. This corresponds to the energy where the curve reaches its maximum value. The most probable energy E_{MP} is easily found to be

Most Probable Energy of a Particle That Follows a Maxwell–Boltzmann Probability Distribution

$$E_{MP} = \frac{1}{2}kT \tag{8.21}$$

which means that the most probable kinetic energy E_{MP} in a Maxwell–Boltzmann distribution is 1/3 of the average kinetic energy <E>. Thus,

Relationship between the Most Probable Energy and the Average Energy

$$E_{MP} = \frac{1}{3}<E> \tag{8.22}$$

Notice that the average kinetic energy of a particle that follows a Maxwell–Boltzmann probability distribution has nothing to do with the mass of the particle inside of the distribution! In other words, it only depends on the temperature T of the environment in which the particle is placed. This implies that the average kinetic energy of a uranium nucleus and a neutron passing alongside of it inside of a fuel rod is exactly the same when thermal equilibrium is reached.

The velocities may be different (because the masses are different), but their average kinetic energies are exactly the same. In other words, this is what a state of thermodynamic equilibrium in a reactor implies. The astute reader may have also noticed that the value of kT must have a great deal to do with the behavior of a reactor as a whole because the average energy of the neutrons in the core is determined solely by the product of k and T. In other words, this term must have some fundamental significance that goes beyond the other terms we have encountered before. We would now like to explain this significance.

8.8 The Origin of the Term Thermal Neutron

Eventually, a fast neutron loses enough energy to come into thermal equilibrium with its environment, and when it does so, it becomes what is known as a thermal neutron. When this happens, its most probable energy and its average energy are given by Equations 8.20 and 8.21. However, it is important to realize that the term kT in both equations has the units of energy, and so the kinetic energy of an average neutron is related to its absolute temperature when it reaches a state of thermal equilibrium. Now, let us look at what the specific values of kT can be when a neutron is at room temperature and

then when the same neutron reaches a state of thermal equilibrium in a nuclear reactor core. At room temperature, which is equal to $T_o = 273\ K + 27°C \approx 300°K$, the quantity kT_o has a value of $kT_o = 0.025\ eV = 1/40\ eV$. *This particular energy is then referred to as the "thermal energy" of the neutron.*

However, most reactors operate at approximately twice this temperature (600 K on the Kelvin scale), and so the value of kT in this case is twice as large ($kT = 2\ kT_o$). However, the most probable energy E_p (from Equation 8.24) is also half this amount. Then, the factors 1/2 and 2 cancel, and the most probable kinetic energy of a neutron in this case is $E_{MP} = 1/2 \cdot (2\ kT_o) = kT_o$. So, the outcome of this simple exercise is that *a neutron in an operating reactor (if it is not absorbed) eventually reaches a most probable kinetic energy of kT_o (0.025 eV), and this is the origin of the term thermal neutron that can be found in most nuclear science and engineering textbooks.*

Example Problem 8.3

Suppose that you are riding a subway train in New York City during the month of August where the average air temperature is about 100°F (~38°C). What is the average energy of the air molecules in a subway station at rush hour?

Solution The average energy <E> of an air molecule is given by the equation $\langle E \rangle = 1.5\ kT$, where T is the absolute temperature and k is Boltzmann's constant. Since $T \approx 38°C$, the absolute temperature of the air molecules is 38°C + 273 K = 311°C. The average energy of an air molecule is therefore 0.040 eV. [Ans.]

8.9 The Apparent Temperature of a Fission Neutron

Now, let us see if we can use what we have just learned to find the *apparent temperature of a free neutron* when it is first released from a uranium or plutonium nucleus. We would then like to show how this compares to the apparent temperature of a thermal neutron, which has reached thermal equilibrium with its surroundings. A thermal neutron that has reached thermal equilibrium can no longer gain or lose energy (in an average sense) because its average and most probable energies are determined by a Maxwell–Boltzmann distribution. So, in some cases, neutrons that reach the thermal energy range will continue to lose energy, while other neutrons will continue to gain it. However, on average, the average energy and the most probable energy will not change unless the ambient temperature changes as well. So, there are two cases that we would like to use to make a comparison at this time:

Case I: $E_p = 1$ MeV, which applies to a *fission neutron*
Case II: $E_p = 0.025$ eV, which applies to a *thermal neutron*
(after it has slowed down)

Performing the required math and noting that $E_p = 1$ MeV, we find that the temperature that a fast neutron is released at is

$$T = 2.4 \times 10^{10}\ K \tag{8.23}$$

So, when a fission neutron is first released, its apparent temperature is about *24 Billion degrees Kelvin*. This is hotter than the temperature of an average particle on the surface of the sun—so this is a very high number indeed!

Example Problem 8.4

Deuterium, a form of hydrogen used in fusion reactors and a key component of heavy water, has an extra neutron attached to its atomic nucleus. At sufficiently high temperatures, deuterium can become energetically unstable and can disassociate into a proton and a free neutron. Estimate the temperature at which this reaction can occur for a gas of high-temperature deuterium nuclei where the deuterium atoms in the gas obey a Maxwell–Boltzmann probability distribution. The governing equation for this reaction is

$$m_d c^2 + \frac{1}{2}\ kT > m_P c^2 + m_n c^2 \quad \text{(for deuterium to become unstable)}$$

Assume the rest masses of the proton, the neutron, and the deuterium nucleus are

$$m_p = 938.27\ MeV/c^2$$

$$m_n = 939.565\ MeV/c^2$$

$$m_d = 1875.613\ MeV/c^2$$

Solution Using the rest masses provided earlier, we find that this reaction can occur when $1/2\ kT \geq m_p c^2 + m_n c^2 - m_d c^2 = 2.2$ MeV. Since the value of Boltzmann's constant is $k = 8.617 \times 10^{-5}$ eV/K, the deuterium nucleus can split apart when $T \geq 5.16 \times 10^{10}$ K. Note that this corresponds to the same apparent temperature as a 2.2 MeV fission neutron. [Ans.]

8.10 Neutron Slowing Down Theory

Most of the neutrons that are created in the fission process have an average kinetic energy of 2 MeV and a most probable kinetic energy of about 0.75 MeV. Of course, these energies only apply to "prompt" neutrons. However, for most nuclear reactors to function successfully, these neutrons must be converted by collisions with the moderator from "fast" neutrons or high-speed neutrons to "slow" neutrons or low-speed neutrons. Only when this process occurs continuously and in very large numbers does a thermal reactor have enough neutrons to keep the nuclear chain reaction going. It is therefore appropriate to spend some time to review the process by which the fast neutrons are converted into thermal ones. In reactor physics books, this process is known as *neutron slowing down theory*. In the following section, we would like to discuss the process of neutron slowing down theory at an elementary level.

8.11 The Energy Staircase

When a fission neutron is born, it undergoes a series of successive elastic collisions, where it collides with another object such as a stationary atomic nucleus, and it loses a small amount of energy in each collision. If this process is repeated over and over again in the presence of a moderator, and if it is not absorbed, a fast neutron will eventually convert itself into a thermal or epithermal neutron.

This process is analogous to a fast neutron with a high initial energy E (see Figure 8.7) falling down an energy staircase and converting itself into a thermal neutron with a lower energy E′. If all of the nuclei that the neutron hits have the same rest mass A, then the fractional energy loss ΔE will be the same per collision. Then, all of the stairs in the staircase will have exactly the same height. The kinetic energy of the neutron will then fall in a simple and predictable manner that is proportional to the number of collisions involved. The exact relationship that controls the final energy is

The Relationship between the Tops of the Steps in the Energy Staircase

$$E'_n = (\alpha')^n E \tag{8.24}$$

where

E'_n is the energy of the neutron after the nth successive collision
E is the initial energy of the neutron before it hits anything

The slowing down parameters for different nuclear materials, as well as their values for α and α', are shown in Table 8.4. *As long as the fission neutron does not get absorbed (by falling through the "holes" in the floorboards), it will eventually be converted from a "fast" neutron at the top of the staircase—with an average energy of about 2 MeV—to a "slow" neutron at the bottom of the staircase with an average energy of about 0.025 eV*. If, on the other hand, the incoming neutron is able to collide with a variety of different target nuclei that have more than one size (or mass), then the fractional energy loss per collision ΔE will vary depending upon the ratio of the mass of the incoming neutron to that of the target nucleus.

If the target nucleus is very heavy (like a zirconium or uranium nucleus), then the fractional energy loss per collision will be small, and if the target nucleus is very light (like a hydrogen nucleus), then the fractional energy loss per collision will be large. Sometimes, the neutron will hit a heavy nucleus, and sometimes, it will hit a lighter one. Depending upon the exact combination of materials that are present in the core, it can take anywhere from 1 collision (in the case of a simple nucleus like hydrogen) to several hundred collisions (with a uranium nucleus) for a fission neutron to be converted into a thermal one.

In this case, not all of the stairs in the energy staircase will be the same height, and some (corresponding to collisions with lighter nuclei) will be large, while others (corresponding to collisions with heavier nuclei) will be small. The fast neutron will eventually lose enough energy to become a thermal neutron, but the path it will take will be different. The number of collisions it requires to do so will also be different. The process we have just outlined can be described by an elegant mathematical framework that has become known as "*neutron slowing down theory,*" and several books have

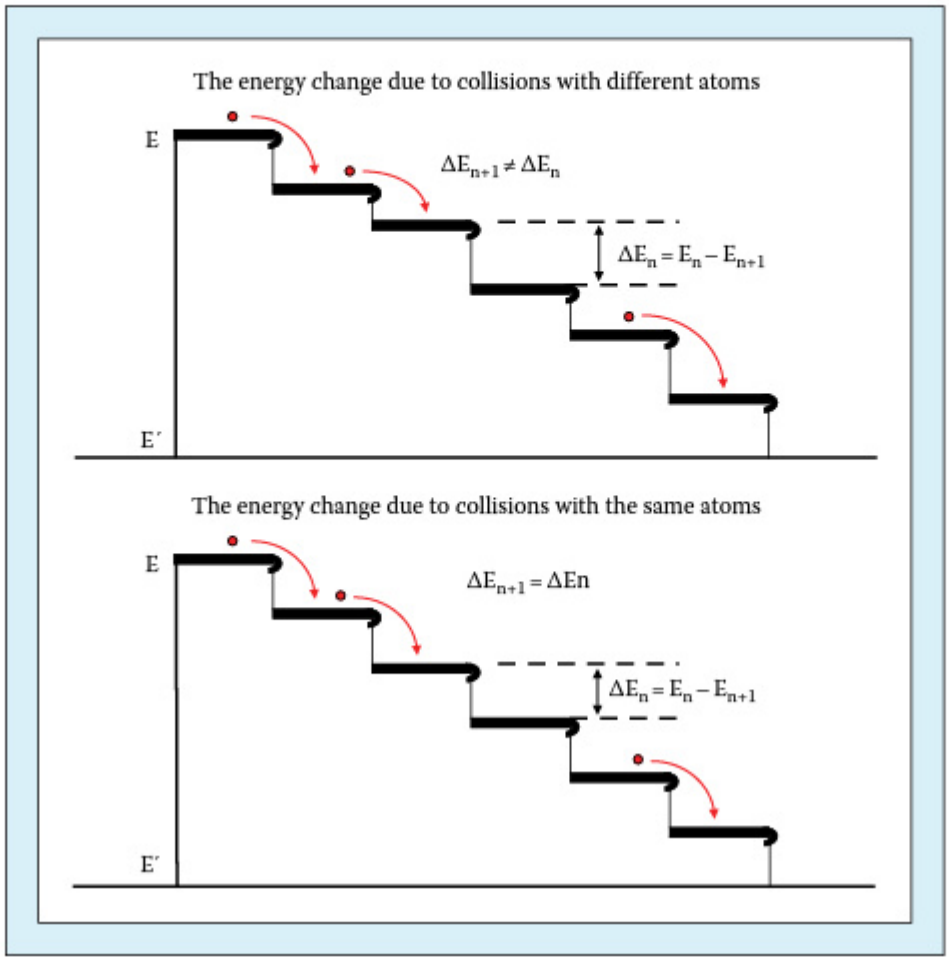
The energy change due to collisions with different atoms
E
$\Delta E_{n+1} \neq \Delta E_n$
$\Delta E_n = E_n - E_{n+1}$
E′
The energy change due to collisions with the same atoms
E
$\Delta E_{n+1} = \Delta En$
$\Delta E_n = E_n - E_{n+1}$
E′

FIGURE 8.7 An "energy staircase" can be used to model a set of elastic scattering collisions. In the staircase at the bottom of the figure, all of the collisions are with light nuclei of approximately the same atomic weight, and ΔE is larger, on average, than it is for the staircase at the top. In the upper staircase, some of the collisions are with light nuclei (i.e., hydrogen), but others are with heavier nuclei. Very heavy elements like uranium are very poor at slowing down fast neutrons, and fast neutrons generally lose no more than 1/100th of their kinetic energy E in a single collision.

TABLE 8.4
Slowing Down Parameters for Different Nuclear Materials

Material	Atomic Mass	α	$\alpha' = (1-\alpha)/2$	$(1-\alpha')$	$\xi = \Delta L$
Hydrogen	1	0	0.500	0.500	1.000
Deuterium	2	0.111	0.444	0.556	0.725
Helium	4	0.360	0.320	0.680	0.425
Beryllium	9	0.640	0.180	0.820	0.209
Carbon	12	0.716	0.142	0.858	0.158
Oxygen	16	0.779	0.110	0.890	0.120
Light water (H_2O)	18	~	~	~	0.920[a]
Heavy water (D_2O)	20	~	~	~	0.510[a]
Sodium	23	0.840	0.080	0.920	0.083
Iron	56	0.931	0.035	0.965	0.036
Uranium	238	0.983	0.008	0.992	0.008

[a] Average molecular value.
~only defined for a single nucleus.

been written to describe the physics of this theory in great detail. *Weston Stacy's* book in the references at the end of the chapter (see Reference 6) does a particularly good job of explaining how the slowing down process works. However, it is quite advanced and contains many additional equations that we have not presented here. It also discusses what are known as neutron *scattering kernels*.

8.12 The Lethargy and Its Application to Neutron Slowing Down Theory

Earlier we learned that the largest fractional neutron energy loss α′ that a neutron can have occurs in a head-on collision. The value of α′ in this case is given by

The Fractional Energy Loss in a Head-On Elastic Collision

$$\alpha' = (1-\alpha)$$

where

$$\alpha = \frac{(A-1)^2}{(A+1)^2} \tag{8.25}$$

However, it is much more likely that a neutron will hit the nucleus in a glancing collision (rather than a direct one), and the average fractional energy loss from all types of collisions (both glancing and direct) is given by

$$\alpha' = \frac{(1-\alpha)}{2} \tag{8.26}$$

In many practical calculations, especially those related to the conversion of fast neutrons into thermal ones, it is convenient to describe the number of neutron collisions required to achieve a specific final energy E′ in terms of a new variable called the *neutron lethargy L*. The neutron lethargy is given the symbol L or ξ and is defined in the following way:

The Definition of the Lethargy

$$L = \ln\left(\frac{E}{E'}\right) \tag{8.27}$$

where

E is the energy at which a fission neutron is "born"
E′ is the energy at which it becomes a thermal neutron

Notice that these energies can be any energy at all, although in a reactor core E will have a value of about 2 MeV and E′ will have a value of about 0.025 eV. It can be easily shown from the way the lethargy is defined that a neutron's lethargy is "low" when its energy is high, and as it slows down, and the value of E′ decreases, its lethargy starts to grow. Using this definition and the previous equations, it is possible to calculate the average change in the lethargy of a neutron in an elastic scattering collision with the nucleus of hydrogen or uranium atom. This quantity $\zeta = \langle \ln(E/E') \rangle$ is sometimes called *the slowing down decrement* and can be calculated in the following way:

$$\zeta = \left\langle \ln\left(\frac{E}{E'}\right) \right\rangle = \langle L \rangle = \int \ln\left(\frac{E'}{E}\right) P(E \rightarrow E')\, dE' \tag{8.28}$$

where

$$P(E \rightarrow E') = \frac{1}{(1-\alpha)E} \tag{8.29}$$

is the probability that a neutron will slow down in an elastic scattering collision from energy E to energy E′. The solution to Equation 8.28 is

$$\zeta = \left\langle \ln\left(\frac{E}{E'}\right)\right\rangle = 1 + \ln(\alpha)\left(\frac{\alpha}{(1-\alpha)}\right) \tag{8.30}$$

Defined in this way, the slowing down decrement is independent of the energy of the incident and the scattered neutron. It is therefore a "normalized" and independent measure of the energy loss in an elastic slowing down collision. Thus, the scattered neutron always loses the same logarithmic fraction of its total energy, since ζ is dependent upon only the atomic mass A of the nucleus that it collides with.

Returning to the original definition of α, we can also write ζ as

$$\zeta = \left\langle \ln\left(\frac{E}{E'}\right)\right\rangle = \frac{1-(A-1)^2}{2A}\left\{\ln\left(\frac{(A+1)}{(A-1)}\right)\right\} \tag{8.31}$$

where A is the mass number of the scattering nucleus. Except for small values of A, it can be shown that this expression for ζ reduces to

Slowing Down Decrement

$$\zeta = \frac{2}{(A+2/3)} \tag{8.32}$$

Even for A = 2, the total error in Equation 8.32 is only about 3%. For larger values of A, the total error becomes progressively smaller. Therefore, the expression ζ = 2/(A + 2/3) can be used with little error when dealing with the composition of the reactor as a whole. Using the aforementioned definition for ζ, it then becomes a rather simple exercise to find the number of elastic collisions required to slow down a neutron from fast energies to thermal energies. To do so, we simply need to define E_1, E_2, E_3, E_4, …, E_n as the energies of the neutron after the first, second, third, fourth, and the *n*th collisions. Because of the way that natural logarithms work, we can then write the energy loss from an initial energy E to a final energy E′ as

$$\ln\left(\frac{E}{E'}\right) = \ln\left(\frac{E}{E_i}\right) + \ln\left(\frac{E_1}{E_2}\right) + \ln\left(\frac{E_2}{E_3}\right) + \ln\left(\frac{E_3}{E_4}\right) + \cdots + \ln\left(\frac{E'-1}{E'}\right) \tag{8.33}$$

Assuming that each of these terms can then be replaced by our previous definition for ζ, we can then rewrite this equation as

Number of Collisions Required to Transition from an Energy E to an Energy E′

$$n = \ln\frac{(E/E')}{\zeta}$$

or

$$n = \frac{L}{\zeta} \tag{8.34}$$

Notice that this result establishes a unique relationship between ζ, which depends on only the atomic weight A of the target nucleus, and the number of head-on and glancing collisions required for the neutron to transition from an energetic neutron of energy E to a lower energy neutron of energy E′. We simply need to specify the values of E and E′, and the value for ζ, which is a function of the atomic weight A, or ζ(A). With this equation, we can calculate the number of elastic collisions required for *any element* to slow down a neutron from fast to thermal speeds. The following example illustrates how this can be done.

Example Problem 8.5

Using what you have just learned, calculate the average number of elastic collisions required for a fast neutron, born with an average energy of about 2 MeV to slow down to a thermal neutron, with an average energy of about 0.025 eV for deuterium, which is a heavy form of hydrogen with one proton and one neutron.

Solution For this problem, we will assume that the neutron starts with an average energy E = 2 MeV and that the slowing down process concludes when the neutron reaches an average energy of E′ = 0.025 eV. Therefore, from Equation 8.27, L = ln(E/E′) = ln(2,000,000/0.025) = ln(80,000,000) = 18.2. We also know from the atomic mass numbers of the materials involved that

$$\zeta(\text{for deuterium}) = \frac{2}{(A + 2/3)} = \frac{2}{(2 + 2/3)} = 0.75$$

Therefore, we know from the equation n = ln(E/E′)/ζ that the total number of collisions n required for the neutron to slow down from E = 2 MeV to E′ = 0.025 eV will be

$$n(\text{for deuterium}) = \frac{18.2}{0.75} = 24$$

Because of their low rest masses, it should come as no surprise to the interested reader that hydrogen (A = 1) and deuterium (A = 2) are the most efficient materials at converting high-speed neutrons into low-speed ones. [Ans.]

8.13 Collisions between Neutrons and More Complex Materials

Obviously, one of the things that this example shows is that elements with a low atomic weight (such as hydrogen) are much more effective at slowing down fission neutrons than heavier materials are. All scattering reactions—as long as they do not involve the creation of a compound nucleus—follow this same basic rule. However, materials with a light atomic weight are not always the most effective reactor coolants to use, and when the need arises to remove heat from a reactor core, it is usually better to use another coolant that contains a couple of hydrogen atoms rather than pure hydrogen itself. From a practical point of view, evaluating the slowing down power of these materials involves being able to calculate the *slowing down decrement* ζ in situations where more than 1 element or isotope may be present. For example, in the case of light water or heavy water, some of the neutrons will collide with hydrogen atoms, and other neutrons will collide with oxygen atoms. In this case, the slowing down decrement must be replaced by a more general equation of the form

Slowing Down Decrement Based on a Scattering Kernel

$$\zeta = \left\langle \ln\left(\frac{E}{E'}\right)\right\rangle = \frac{1}{\Sigma_s(E)}\int_i \Sigma_{si}(E)\ln\left(\frac{E'}{E}\right)P_i(E \to E')dE'$$

where

$$P(E \to E') = \frac{1}{(1-\alpha_i)}E \qquad (8.35)$$

When this is done, the average slowing down decrement of a substance containing more than one material can be shown to be the solution of the following equation:

$$\langle\zeta\rangle = \left(\frac{1}{\Sigma_s}\right)\text{SUM}_i(\zeta_i \Sigma_{si}) \qquad (8.36)$$

which is *the definition of the weighted average for the logarithmic energy decrement*—with the energy dependence removed—as we might expect. For cross sections with only one energy group, the process of evaluating <ζ> becomes very straightforward, because it involves just substituting the number of atoms for each molecule into the equation given earlier and canceling everything but the remaining cross sections and the values for ζ_i. The result of this operation is

then the average slowing down decrement for the nuclear material in question. The total number of collisions required to thermalize a neutron in collisions with a complex material can then be found from the simple expression

Finding the Number of Collisions from the Average Logarithmic Energy Decrement

$$n = \frac{\ln(E/E')}{\langle\zeta\rangle} \tag{8.37}$$

where $\langle\zeta\rangle$ is now the *average logarithmic energy decrement*. The following example should help to clarify some of the key points. It also shows how the contributions of the individual atoms to the overall properties of a material may be found.

Example Problem 8.6

Using the following values for the microscopic scattering cross sections for hydrogen and oxygen, $\sigma_s^H = 20.1$ barns and $\sigma_s^O = 3.8$ barns, and using the following values for the logarithmic energy decrements, $\zeta^H = 1.0$ and $\zeta^O = 0.12$, calculate $\langle\zeta\rangle_{H_2O}$ and then the average number of collisions that a fast neutron with an average energy of 2 MeV must have with a water molecule before it can become a thermal neutron.

Solution The slowing down decrement for a complex molecule like H_2O is simply the weighted average of the microscopic scattering cross sections for the hydrogen and oxygen atoms it contains, where the "weighting factor" in this case is the slowing down decrement ζ for each individual atom, multiplied by the number of atoms that are present.

In this case, we have $\zeta^H = 1.0$ and $\zeta^O = 0.12$, so it is a simple matter to see that

$$\langle\zeta\rangle_{H_2O} = \frac{\left(2\zeta^H\sigma_s^H + \zeta^O\sigma_s^O\right)}{\left(2\zeta^H + \zeta^O\right)}$$

Plugging in the numbers gives $\langle\zeta\rangle_{H_2O} = 0.92$, and from the equation $n = \ln(E/E')/\langle\zeta\rangle$, the number of collisions required is $n = \ln(2{,}000{,}000/0.025)/\langle\zeta\rangle = 18.2/0.92 = 19.8$ collisions. [Ans.]

Notice that the complexity of the material used for the moderator makes absolutely no difference in the basic approach we have just described. Materials containing any number of different atoms and molecules can be handled in this way. As long as the heat can be safely removed and the neutron absorption cross sections are small, it is generally better to use a lighter nuclear material for the moderator than a heavier one. The problems at the end of the chapter will provide additional examples of how these equations can be used. The fewer the number of collisions that are required to achieve a final neutron energy E′, the more effective a moderator will generally be. Of course, other materials may remove neutrons from the neutron population as they are slowing down, and these losses must be taken into account when considering whether or not a particular combination of materials will result in a critical mass.

To be an effective moderator, a reactor coolant must not only be able to remove large amounts of heat from the core, but it must also be cheap and plentiful. For this reason, light water and heavy water are the most commonly used coolants or moderators in thermal reactors today. Graphite (or crystalline carbon) is used as a moderator in gas-cooled reactors, but the cooling is provided using a CO_2 or helium gas because this is the best way to remove the heat.

8.14 The Moderating Ratio

The *moderating ratio*, or the MR for short, is another way to determine how good or bad a particular moderator can be. The MR is the product of slowing down decrement ξ (the average lethargy gain in an elastic collision) times the probability that a neutron will scatter from a nucleus divided by the probability that a neutron will be absorbed by the nucleus. In other words, the MR can be written as

Definition of the Moderating Ratio

$$MR = \xi \cdot \left(\frac{P_s}{P_a}\right) \tag{8.38}$$

where

P_s is the probability of a neutron scattering to thermal energies

P_a is the probability of the neutron being absorbed before reaching thermal energies

TABLE 8.5
Microscopic and Macroscopic Scattering and Absorption Cross Sections for Some Common Moderating Materials at Thermal Energies

Cross Sections for Common Moderators near E = 0.025 eV				
Material	σ_a (barns)	σ_s (barns)	Σ_a (cm^{-1})	Σ_s (cm^{-1})
Light water	0.644	66.06	0.022	3.443
Heavy water	0.001	20.03	0.0000442	0.4519
Beryllium	0.009	6.140	0.001240	0.7589
Carbon	0.00038	4.942	0.0003	0.3952

Note: A more comprehensive listing can be found in Appendix C.

TABLE 8.6
Comparison of the Moderating Properties of Common Nuclear Materials

Material	Symbol	A	α	$\xi = \Delta L$	$\sum_a$ (cm^{-1})	$\sum_s$ (cm^{-1})	MR = $\xi(\sum_s/\sum_a)$
Hydrogen	H	1	0.0	1	1.7×10^{-4}	1.5×10^{-3}	9
Deuterium	D	2	0.11	0.725	1.35×10^{-7}	0.00056	3007
Helium	He	4	0.36	0.425	0.001240	0.7589	83
Beryllium	Be	8	0.61	0.209	0.0011	0.7589	143
Carbon	C	12	0.72	0.158	0.00027	0.3952	208
Oxygen	O	16	0.78	0.120	1.4×10^{-8}	2.08×10^{-4}	1782
Light water	H_2O	—	—	0.920	0.022	3.443	144
Heavy water	D_2O	—	—	0.509	0.0000442	0.4519	5204
Uranium	U-238	238	0.98	0.008	0.130	0.4239	0.03

It follows from this expression that the perfect moderating material is one that has a very low mass, a high scattering cross section, and a very low absorption cross section. In this regard, deuterium D_2O, or *heavy water, is an absolutely superb moderator*. However, because it is very costly to make, most thermal reactors today are built using either graphite (carbon) or ordinary light water (H_2O) as the moderating material. Sometimes, the probabilities in Equation 8.38 are replaced by the macroscopic scattering and absorption cross sections $\sum_s$ and $\sum_a$. Then, 8.38 can be written as

Another Definition of the MR

$$MR = \xi \cdot \left(\frac{\sum_s}{\sum_a} \right) \tag{8.39}$$

and this is the most common definition that most nuclear engineers use. The specific values for $\sum_s$ and $\sum_a$ for light water, heavy water, carbon, and beryllium are shown in Table 8.5. Clearly, heavy water with an MR of 5204 is better than light water with an MR of 144. Again, most of this difference is due to the fact that heavy water absorbs fewer thermal neutrons than light water does. Heavy water is used as a moderating material in CANDU reactors (see Chapters 12 and 13), and because heavy water has such a low absorption cross section, reactors that use it can be run on natural uranium alone. In other words, *one does not need enriched uranium to build a reactor that uses heavy water as its moderating material* (Table 8.6).

Example Problem 8.7

How many fewer thermal neutrons does a molecule of heavy water absorb than a molecule of light water?

Solution From Table 8.2, it can be seen that heavy water absorbs 660 times fewer thermal neutrons than a molecule of light water does. This is one of the reasons why its MR is so high and why it is such a superb neutron moderator. [Ans.]

Example Problem 8.8

As the reader may have inferred from our previous discussion, the ratio of the scattering cross section of a material to its absorption cross section is a good measure of how good a neutron moderator can be. For the four materials listed in Table 8.5, rank them from best to worse according to their values of $\sum_s/\sum_a$.

Solution From Table 8.5, it can be seen that the values of these ratios are 10,225 for D_2O, 1,300 for carbon, 700 for beryllium, and 156 for H_2O. [Ans.]

Student Exercise 8.2

Using the results presented in the previous chapter, estimate the total number of collisions required for a 2 MeV neutron to come into thermal equilibrium with its environment if the moderating material is graphite (carbon with an atomic weight of 12) instead of hydrogen.

What is the approximate ratio of the number of collisions required for the neutron to slow down to thermal energies for a carbon atom than it is for a hydrogen atom? Be prepared to explain why more collisions are needed when the moderator material is hydrogen than when the moderating material is hydrogen.

8.15 The Maxwell–Boltzmann Probability Distribution

The *Maxwell–Boltzmann probability distribution* is the key to understanding how a thermal water reactor works. It appears so frequently in the study of nuclear science and engineering that it is important to understand its underlying assumptions. The distribution itself was not discovered until the mid-1860s when James Clerk Maxwell and Ludwig Boltzmann (see Figure 8.8) independently deduced its analytical form and showed how it could be applied. In this section, we would like to repeat their initial derivation of this famous distribution and show the assumptions that were used to create it. If you are already familiar with this distribution and its implications, then you may want to proceed directly to Chapter 9. Otherwise, the derivation that we will present later should be studied carefully because it shows how large populations of thermal neutrons and other electrically neutral particles behave.

The major implication of this distribution is that the particles of any material substance (including those in a nuclear reactor core) do not all have the same energy or velocity even when they have the same temperature T! It does not really matter whether the particles are atoms, molecules, or elementary particles such as neutrons. As long as these particles are electrically neutral, the Maxwell–Boltzmann probability distribution applies equally well to all of them.

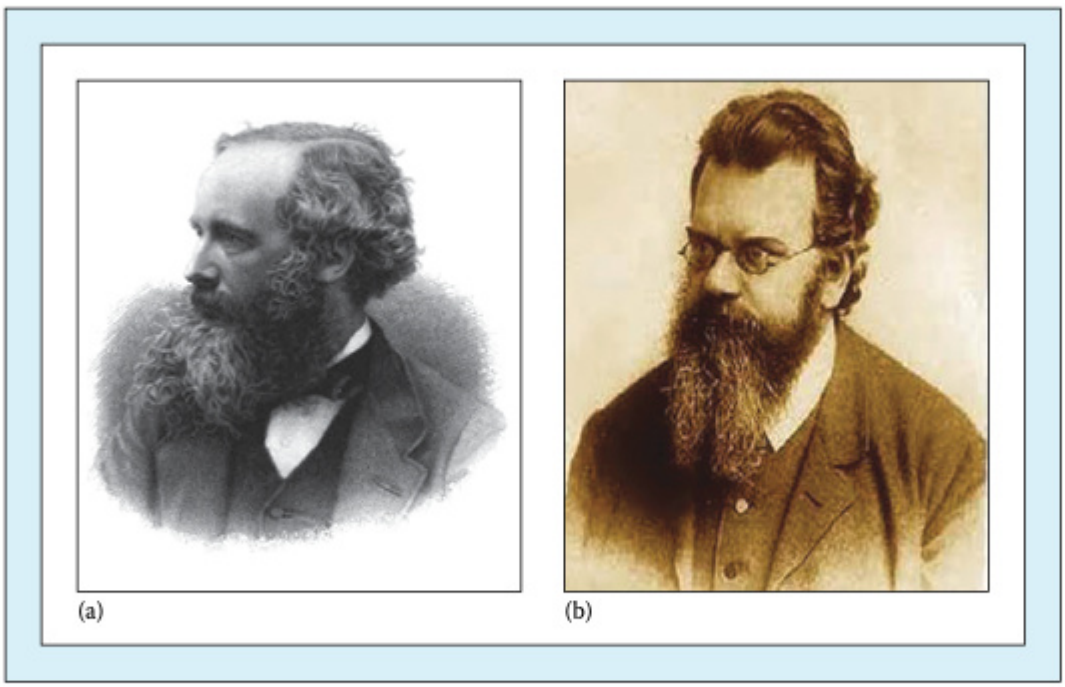

FIGURE 8.8 (a) James C. Maxwell and (b) Ludwig Boltzmann. The inventors of the Maxwell–Boltzmann particle energy distribution.

8.16 The Origin of the Maxwell–Boltzmann Probability Distribution

Around 1860, James Clerk Maxwell and Ludwig Boltzmann wondered whether a distribution of independent particles, such as those in an ideal gas, obeyed a *Gaussian probability distribution*, such as the one that we discussed in Chapter 6. It was known at the time that other objects that followed a distribution of this type could be represented by an equation of the form

$$P(n, A) = A(n)e^{-A\lambda} \tag{8.40}$$

where

P was the probability of finding them with a property A
n was the number of objects in a specific part of the distribution
λ was a "decay factor" associated with the distribution

Since gases are composed of atoms and molecules, these objects only interact with each other through sets of elastic collisions. In other words, a gas can be thought of as a collection of billiard balls flying around in empty space and hitting one another as they move. Even if they all start out with exactly the same speed (which they do not), the constant collisions between them eventually result in a spread of many different velocities and energies. In other words, some of the particles in the distribution can have very high speeds, and other particles in the distribution can have very low ones. Maxwell wondered how these velocities distributed themselves among the particles. He proposed that the velocities of the particles were completely independent of one another and that they followed a number of rules that have since become known as *Maxwell's rules*. The rules Maxwell proposed were as follows:

Maxwell's Particle Collision Rules

- The diameter of the particles is much smaller than the distance between them.
- The collisions between the particles conserve kinetic and potential energy. In other words, the collisions can be considered to be elastic collisions.
- Between collisions, the particles move according to Newton's laws; that is, they move at a constant speed along straight lines.
- The velocities and the positions of the particles are completely random (at least initially).

This implies that the velocities of the particles are completely uncorrelated along each coordinate direction—x, y, and z or r, θ, and ϕ. These rules then became known as "Maxwell's collision rules."

8.17 Maxwell's Derivation of the Maxwell–Boltzmann Probability Distribution

The most important assumption that flows from these rules is that the three components of the particle velocity vector v_x, v_y, and v_z are statistically independent of each other in a Cartesian coordinate system. This allowed Maxwell to write

$$P(v_x, v_y, v_z) = p(v_x) \cdot p(v_y) \cdot p(v_z) \tag{8.41}$$

where $p(v_x)$, $p(v_y)$, and $p(v_z)$ are the probability distributions of the individual velocity components. In other words, Maxwell assumed that the total probability P of a particle having a particular velocity $V = iv_x + jv_y + kv_z$ was equal to the product of the individual probability distributions along each of the three coordinate directions. Taking the logarithm of each side of the given distribution yields

$$\ln P(v) = \ln\left[p(v_x) \cdot p(v_y) \cdot p(vz)\right] = \ln p(v_x) + \ln p(v_y) + \ln p(v_z) \tag{8.42}$$

Now suppose that $P(v_x, v_y, v_z)\, dv_x\, dv_y\, dv_z$ is the fraction of the molecules (or other nuclear particles) that have velocity components between v_x and $v_x + dv_x$, v_y and $v_y + dv_y$, and v_z and $v_z + dv_z$. Differentiating the given expression with respect to v_x gives

$$\left(\frac{\partial \ln P(v)}{\partial v_x}\right) = \frac{\partial \ln P(v_x)}{\partial v_x} \tag{8.43}$$

Because the function P(v) depends on v, we can rewrite the derivative as a function of v. The result is

$$\frac{\partial \ln P(v)}{\partial v_x} = \left(\frac{\partial \ln P(v)}{\partial v}\right)\left(\frac{\partial v}{\partial v_x}\right) = \frac{v_x}{v}\left[\frac{\partial \ln P(v)}{\partial v}\right] \tag{8.44}$$

We therefore have

$$\frac{1}{v}\frac{d\left(\ln P(v)\right)}{dv} = \frac{1}{v_x}\frac{d(\ln(f(v_x))}{dv_x} = \frac{1}{v_y}\frac{d(\ln(f(v_y))}{dv_y} = \frac{1}{v_z}\frac{d(\ln(f(v_z))}{dv_z} \tag{8.45}$$

Because v_x, v_y, and v_z are statistically independent of each other, the previous equation must be equal to a constant that we will call $-\gamma$. This allows us to write

$$\frac{1}{v_j}\frac{d\left(\ln f(v_j)\right)}{dv_j} = -\gamma \tag{8.46}$$

And integrating this equation gives

$$f(v_j) = Ae^{-\gamma v_j^2} \quad \text{where } j = x,y,z \tag{8.47}$$

Note the similarity between this equation and the Gaussian probability distribution function that we discussed in Chapter 6. Since $f(v_j)$ is the probability distribution that we seek, it must be subject to a standard normalization condition, which requires that

$$\int f(v_j)dv_j = \int Ae^{-\gamma v_j^2}dv_j = 1 \tag{8.48}$$

for each of the three coordinate directions. Here, the limits of integration are from $-\infty$ and $+\infty$. Evaluating the aforementioned expression for the probability distribution, we find that the value of A required to normalize the distribution is $A = (\gamma/\pi)^{1/2}$. The normalized form of the probability distribution is then

$$f(v_j) = (\gamma/\pi)^{1/2} e^{-\gamma v_j^2} \quad \text{where } j = x,y,z \tag{8.49}$$

Next, we would like to determine the value of γ that appears in the probability distribution for the velocities. Maxwell used the expression

$$\langle v_x^2 \rangle = \frac{RT}{M} \tag{8.50}$$

from the kinetic theory of gases to help find the value of γ. Here, R is the universal gas constant, T is the temperature of the gas in degrees Kelvin, and M is the molar mass of the gas. Using the fact that $\langle v_x^2 \rangle = 1/3 \langle v^2 \rangle$, it follows that $\langle v^2 \rangle = 3 \langle v_x^2 \rangle$ and $\langle v^2 \rangle = 3RT/M$. In just one coordinate direction, the mean square velocity is

$$\langle v_j^2 \rangle = (\gamma/\pi)^{1/2} \int v_j^2 e^{-\gamma v_j^2} dv_j \tag{8.51}$$

where the limits of integration are again from $-\infty$ and $+\infty$. The result of evaluating this messy integral is $1/(2\gamma)$. Hence, we eventually find that $\langle v_j^2 \rangle = 1/(2\gamma)$ and $\gamma = M/2RT$. Using exactly the same argument, it can be shown that the Maxwell–Boltzmann probability distribution function for the velocity alone in one dimension is

$$p(v_j) = \left(\frac{M}{2\pi RT}\right)^{1/2} v_j e^{-Mv_j^2/2RT} \quad \text{where } j = x, y, z \tag{8.52}$$

This is the distribution that Maxwell first derived about 150 years ago. Notice that since each of the velocities is independent of each other, the probability distribution in three dimensions becomes

$$p(v) = \left(\frac{M}{2\pi RT}\right)^{3/2} v e^{-M\left(v^2x+v^2y+v^2z\right)/2RT} \tag{8.53}$$

or

$$p(v) = \left(\frac{M}{2\pi RT}\right)^{3/2} v e^{-M\left(v^2\right)/2RT} \tag{8.54}$$

where $v^2 = v_x^2 + v_y^2 + v_z^2$. The factor $\gamma = M/2RT$ is called the *Maxwell distribution factor*. This is the classical form of the Maxwell–Boltzmann probability distribution. In practice, the distribution is frequently written in terms of the particle energy E instead of the particle velocity. The most appropriate form of the distribution to use in this case is

$$p(E) = \frac{2\pi}{(pkT)^{3/2}} E^{1/2} e^{-E/kT} \tag{8.55}$$

where we have used the fact that $E = 1/2\ mv^2$. This is the form that is most commonly used when discussing the behavior of neutrons and other elementary particles. Since we used the ideal gas law to perform this derivation, it is easy to see that the Maxwell–Boltzmann probability distribution can be used to describe any gas of particles where all of the particles are in thermal equilibrium.

8.18 Boltzmann's Constant and Its Relationship to the Maxwell–Boltzmann Probability Distribution

Sometimes, Boltzmann's constant $k = Rm/M$ also appears explicitly in other forms of the distribution. Here, R is the *universal gas constant*, $M = A_o\ m$ is the molar mass of the gas, A_o is *Avogadro's number* (see Chapter 4), and m is the molecular weight. The value of Boltzmann's constant is $k = 8.6173324(78) \times 10^{-5}$ eV/K, and the value of the universal gas constant is $R = 8.3144621\ J\ K^{-1}\ mol^{-1}$. For neutrons, $m = 1$, so $k = R/A_o$. In this case, the distribution can be written as

$$p(E) = \frac{2\pi}{(\pi kT)^{3/2}} E^{1/2} e^{-E/kT} \tag{8.56}$$

and this form is the gas dynamists' best friend. Many popular books use this form of the distribution to introduce the concept of the *Maxwellian flux*, which we will discuss in detail in a future chapter. In any event, the thermal neutrons in a nuclear reactor religiously obey this distribution, and Maxwellian distributions are commonly used to create neutron cross-section libraries (see Chapter 5). In multiple dimensions, the fraction of the particles having a velocity between v and v + dv is given by

$$p(v)dv = \left(\frac{M}{2\pi RT}\right)^{3/2} v e^{-M\left(v_x^2+v_y^2+v_z^2\right)/2RT} dv_x dv_y dv_z \tag{8.57}$$

In three dimensions, we can replace the infinitesimal velocity volume $dv_x dv_y dv_z$ with $4\pi v^2 dv$. The fraction of the particles having a velocity between v and v + dv is then

$$p(v)dv = 4\pi\left(\frac{M}{2\pi RT}\right)^{3/2} v e^{-Mv^2/2RT} dv \tag{8.58}$$

and this is a form that is commonly used in problems involving a spherical coordinate system. One simply has to specify the limits of integration (i.e., the starting and the ending values of v) in order to determine the fraction of the

neutrons that will lie between $v = v_1$ and $v = v_2$. Obviously, when $v_1 = 0$ and $v_2 = \infty$, the sum of the probabilities will equal 1.0, and 100% of the neutrons will be contained within these limits. When James Maxwell originally derived his distribution, he assumed that all of the particles in the distribution were identical. Later, Ludwig Boltzmann generalized his derivation to include multiple particle types and removed some of the more restrictive assumptions that Maxwell made. For this reason, this probability distribution is known as the Maxwell–Boltzmann probability distribution today. When the Maxwell–Boltzmann probability distribution is extended to a gas of relativistic particles, it is known as a Maxwell–*Jüttner probability distribution*. This distribution is discussed in more detail at the following URL:

http://en.wikipedia.org/wiki/Maxwell%E2%80%93J%C3%BCttner_distribution.

One of the key features of this distribution is the fact that the energy of the distribution is now expressed in terms of the *Lorentz scale factor*

$$\gamma = \sqrt{\left(1 - \left(\frac{v}{c}\right)^2\right)} \tag{8.59}$$

which was introduced to the reader in Chapter 2. This factor also appears in Einstein's great equation of mass and energy equivalence:

$$E(v) = mc^2 = \frac{m_o c^2}{\sqrt{\left(1 - (v/c)^2\right)}} = \frac{m_o c^2}{\gamma} \tag{8.60}$$

which forms the foundation of the theory of *special relativity*. In other words, when a gas of particles becomes very hot and the value of kT approaches the value of $E = mc^2$, the probability distribution for the gas can be written as

$$p(\gamma) = \left[\frac{\beta\gamma^2}{\alpha K_2(1/\alpha)}\right] \cdot e^{-\gamma/\alpha} \tag{8.61}$$

where K_2 is a *modified Bessel function of the second kind*, $\beta = v/c$, and $\alpha = kT/mc^2$.

In the limit of low particle temperatures where $T \ll m_o c^2/k$, the Maxwell–Jüttner probability distribution reduces to the Maxwell–Boltzmann probability distribution. This can be seen by comparing the shape of the distributions shown in Figure 8.9. When $kT/m_o c^2 \approx 0.1$, the Maxwell–Jüttner probability distribution begins to look like the Maxwell–Boltzmann probability distribution, and when the energy becomes even lower, the two shapes become identical.

The Maxwell–Jüttner probability distribution is commonly used in the study of *nuclear fusion*, and the Maxwell–Boltzmann probability distribution is normally used in the study of *nuclear fission*. The Maxwell–Jüttner probability distribution is important in fusion reactors because the particle temperature in plasmas is high enough for *relativistic effects* to become important. Plasmas that have this general behavior can be found in stars, on the surface of the sun, and in modern fusion devices. A common application of the Maxwell–Boltzmann probability distribution is illustrated in the following example. The thermal neutrons in a fission reactor religiously obey this distribution as long as they have enough time to reach thermal equilibrium with their environment.

Example Problem 8.9

Using the equations presented earlier in the chapter, find the most probable speed, v_{MP}, of a particle that obeys a Maxwell–Boltzmann probability distribution.

Solution The most probable speed is defined by the peak of the distribution shown in Figure 8.6. Notice that the peak of the distribution is temperature dependent, and it moves to the right or the left as the temperature T is changed. The most probable speed of a particle can be found by simply taking the derivative of p(v) with respect to v and setting the derivative equal to zero. When we set $dp/dv = 0$, we find that $v = (2kT/m)^{1/2}$ or $v = (2RT/M)^{1/2}$, and this is the most probable velocity v_{MP} of one of the particles. [Ans.]

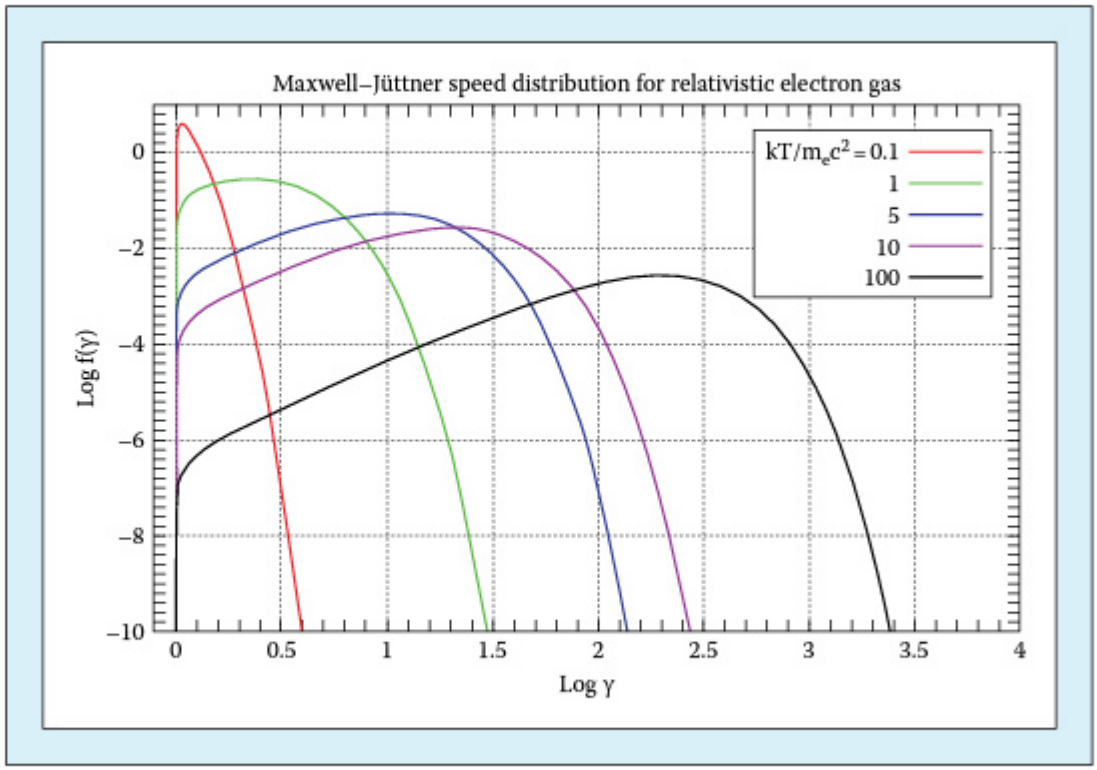

FIGURE 8.9 A picture of Maxwell–Jüttner probability distribution for different particle energies. Notice that the particle energy E is now represented by the *Lorentz scale factor* γ in this case. (Picture provided by Wikipedia.)

As a point of comparison, a molecule of air at room temperature (which is 300 K) consists primarily of diatomic nitrogen or N_2, and the most probable speed of this molecule is about 420 m/s. This is about 1/5th the speed of a thermal neutron in a power reactor core. The difference in speed is primarily due to the square root of the ratio of their respective masses since the energy E is set by the ambient temperature T.

8.19 Heavy Water and Some of Its Uses

In previous sections, we mentioned that heavy water is an excellent neutron moderator and reactor coolant. *Heavy water* is the same as ordinary water except that the hydrogen atoms have an additional neutron attached to their atomic nuclei. Because of this, "heavy hydrogen" weighs twice as much as ordinary hydrogen does, and so it is considerably less common in nature. Heavy hydrogen gas (represented by the symbol D_2) is also known as *deuterium*. Heavy water, which is made from deuterium, has a natural abundance in the earth's oceans of about one part in 6420. Heavy water absorbs fewer neutrons than light water does, and so any reactor cooled with heavy water does not require enriched uranium to operate initially. The CANDU pressurized heavy water reactor is an example of a reactor that uses heavy water in this way. However, reactors that use enriched uranium and plutonium can also be cooled with heavy water, and when properly used, the use of heavy water can increase the conversion ratio. The properties of heavy water and light water are compared to each other in the following example and also in Table 8.7.

Example Problem 8.10

For a thermal neutron, how much more likely is it for the neutron to be absorbed by H_2O than by D_2O? What is the MR of heavy water compared to that of light water?

Solution From Appendix C, it can be seen that the thermal absorption cross section of ordinary water is 0.644 barns and the thermal absorption cross section of heavy water is 0.00133 barns. Therefore, a molecule of ordinary water is 484 times more likely to absorb a thermal neutron than a molecule of heavy water is. The MR is defined by $MR = \xi \cdot (\sum_s / \sum_a)$, where $\zeta = \langle \ln(E/E') \rangle$ is the slowing down decrement. The MR for heavy water is 5204 and the MR for light water is 144. Therefore, by this measure, heavy water or D_2O is approximately 36 times more effective as a neutron moderator than light water or H_2O is. [Ans.]

TABLE 8.7
Comparison of the Nuclear Properties of Light Water (H_2O) and Heavy Water (D_2O)

Substance	Symbol	Capture σ_c	Fission σ_f	Scattering σ_s	Total σ_t	Density (10^{24}/cm^3)	Capture Σ_c	Fission Σ_f	Scattering Σ_s	Total Σ_t
Water (light)	H_2O	0.644	0	103	103.644	0.03343	0.02220	0.0	3.443	3.465
Water (heavy)	D_2O	0.00133	0	13.6	13.6	0.03323	0.0000442	0.0	0.4519	0.4519

Note: The microscopic cross sections are given in barns and the macroscopic cross sections are given in cm^{-1}.
See Appendix C for a more comprehensive listing.

One of the interesting features of heavy water is that it can be used to create a reactor in which plutonium can be bred from natural uranium alone. Because of this, facilities to separate heavy water from ordinary water have always been a subject of great concern to the nuclear community as a whole. In fact, Nazi Germany attempted to build a heavy water–moderated reactor during the Second World War to produce weapons-grade plutonium. In addition, heavy water–moderated reactors can also be used to make *tritium*, which is a key component of some thermonuclear weapons. For this reason, the production of heavy water in the world today is carefully monitored and controlled.

8.20 The Process of Heavy Water Production

Separating heavy water from ordinary water is not as technically difficult or challenging as enriching uranium, but it does require a fair amount of technical infrastructure. This process has many similarities to the process of ammonia production or *alcohol distillation*. Heavy water can be separated directly from ordinary water because of the difference in their boiling points (101.4°C vs. 100°C) or because of the difference in the boiling points of deuterium and hydrogen gas (−249.7°C and −252.5°C). However, because there is only one deuterium atom for every 6420 hydrogen atoms in the earth's oceans, a vast amount of ordinary water must be boiled to produce a small amount of heavy water.

Because the heat of vaporization of ordinary water is very high relative to most liquids (about 2256 kJ/kg), the process of deuterium production requires an enormous amount of electrical power. Alternatively, ordinary water can be electrolyzed to make oxygen and hydrogen containing normal hydrogen and deuterium gas. The hydrogen gas can then be liquefied and distilled to separate the deuterium from the hydrogen. The deuterium can then be combined with oxygen to form heavy water. Today, heavy water is produced commercially in a number of different countries. The first commercial heavy water plant was the *Norsk Hydro facility* in Norsk, Norway, which was attacked by the Allies during the Second World War to prevent Nazi Germany from producing enough heavy water to make an atomic bomb (Figure 8.10).

The *Bruce Heavy Water Plant* in Ontario, Canada, is currently the world's largest producer of heavy water. It uses a process called the *Girdler sulfide process* to separate the deuterium atoms from ordinary hydrogen. In the first stage of this process, the deuterium content of the hydrogen gas is increased to between 0.015% and 0.07%. In the second stage of this process, the deuterium content is increased to 0.35%, and in the third stage, a concentration of between 10% and 30% deuterium is obtained. The deuterium is then combined with oxygen to form heavy water or D_2O. The production of a single kilogram of heavy water requires about 340,000 kg of ordinary water. Thus, the production of heavy water is similar in many respects to the process of uranium enrichment, which we will discuss in another chapter. The production of heavy water is a strategic necessity to any country that does not possess a uranium enrichment plant. Heavy water is about 10% heavier than ordinary water is and has a density of about 1.10 g/cm^3. The density of ordinary water at atmospheric pressure is about 1.00 g/cm^3. However, their thermodynamic properties, such as their specific heats and thermal conductivities, are nearly the same.

Example Problem 8.11

A tank of ordinary water to be used in a pressurized water reactor weighs 300,000 kg. How much does the same tank of heavy water weigh? At atmospheric pressure, what is the boiling point of heavy water?

Solution Since heavy water weighs 10% more than light water, the tank will weigh 330,000 kg when it is filled with heavy water. The boiling point of heavy water is 101.4°C, which is about 1.5% higher than that of ordinary water at atmospheric pressure. [Ans.]

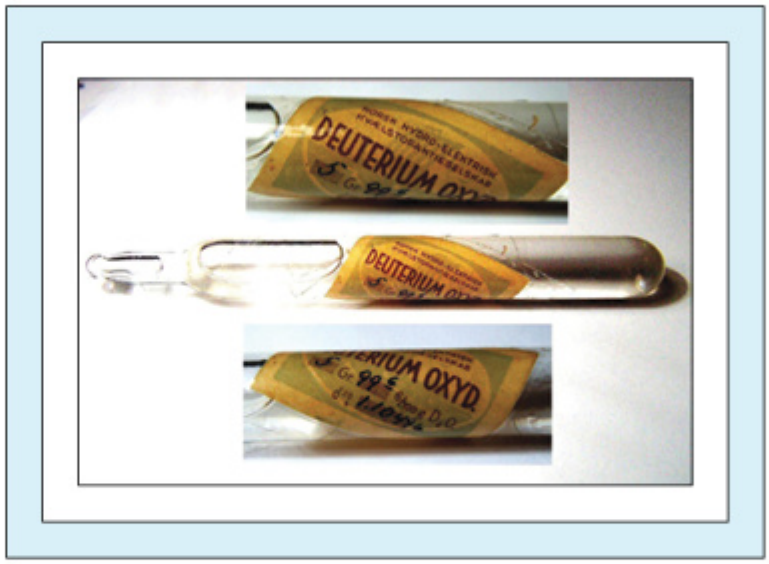

FIGURE 8.10 A vial of heavy water produced by the Norsk hydroelectric plant in Norway. In small quantities, heavy water is not toxic and tastes nearly the same as natural water does. (Picture taken from Wikipedia.)

Example Problem 8.12

A neutron is born with an average energy of 4 MeV and is absorbed by a Uranium-235 nucleus when its energy reaches to 0.10 eV. What is the total lethargy gain of the neutron in this process?

Solution The lethargy gain L is given by the equation $L = \ln(E/E')$, where E is the energy at which it is born and E′ is the energy at which it dies. Since E = 4 MeV and E′ = 0.10 eV, the lethargy gain is $L = \ln(E/E') = \ln(40{,}000{,}000) = 17.5$. Notice that if the neutron had been absorbed at the same energy at which it was created, then E′ = E and $L = \ln(1) = 0$. [Ans.]

Example Problem 8.13

Suppose that a fission neutron is born with an average energy of 1 MeV and is absorbed by a U-238 nucleus at exactly the same energy. What is the lethargy change of the fission neutron?

Solution The lethargy change L is given by the equation $L = \ln(E/E')$, where E is the energy at which it is born and E′ is the energy at which it dies. Since E′ = E, the lethargy change is $L = \ln(E/E') = \ln(1) = 0$! In other words, the neutron does not become more lethargic in this process. [Ans.]

References

Books and Textbooks

1. Shultis, K. and Faw, R. *Fundamentals of Nuclear Science and Engineering*, 2nd edn., CRC Press, Boca Raton, FL (2008).
2. Glasstone, S. and Eedlund, M.C. *The Elements of Nuclear Reactor Theory*, D. Van Nostrand Company, Inc., New York (1952).
3. Lamarsh, J.R. *Introduction to Nuclear Reactor Theory*, second printing, Addison-Wesley Publishing Company, Inc., Reading, MA (1972).
4. Glasstone, S. and Sesonske, A. *Nuclear Reactor Engineering*, 3rd edn., Van Nostrand Reinhold Company, New York (1981).
5. Lamarsh, J.R. and Baratta, A.J. *Introduction to Nuclear Engineering*, Prentice Hall, Upper Saddle River, NJ (2001).
6. Stacey, W.M. *Nuclear Reactor Physics*, 2nd edn., John Wiley & Sons, New York (2007).
7. El-Wakil, M.M. *Nuclear Heat Transport*, American Nuclear Society, La Grange Park, IL (1981).
8. Todreas, N. and Kazimi, M.S. *Nuclear Systems,* Vol. 1, CRC Press, Boca Raton, FL (2012).
9. Duderstadt, J. and Hamilton, L. *Nuclear Reactor Analysis*, John Wiley & Sons, New York (1976).
10. Lewis, E. *Fundamentals of Nuclear Reactor Physics*, Academic Press, Boston, MA (2008).
11. Masterson, R.E. *Nuclear Engineering Fundamentals: A Practical Perspective*, 1st edn., CRC Press, Boca Raton, FL (2017).

Web References

For the Maxwell–Boltzmann probability distribution: http://en.wikipedia.org/wiki/Maxwell%E2%80%93Boltzmann_distribution.
For the Maxwell–Jüttner probability distribution: http://en.wikipedia.org/wiki/Maxwell-Juttner_distribution.
For the process of heavy water production: http://fas.org/nuke/intro/nuke/heavy.htm.
For the history of heavy water use during the Second World War: http://www.jcs-group.com/military/war1941allies/norway.html.

Additional References

- Important physical constants used by nuclear scientists and engineers can be found in *Appendix A*.
- Unit systems and their conversion factors can be found in *Appendix B*.
- Nuclear cross sections for many important nuclear materials can be found in *Appendix C*.
- Physical properties of important nuclear materials can be found in *Appendix D*.
- Atomic masses, half-lives, and natural abundances can be found in *Appendix E*.

Questions for the Student

The following questions cover the material presented in this chapter, and in some cases, previous chapters as well. They are designed to test how well the student has acquired a working knowledge of the subject matter.

1. What is the sole parameter that determines the average energy of a thermal neutron in a water reactor core?
2. Is the value of Boltzmann's constant different for a neutron than it is for a molecule of air?
3. Name two liquids, two gases, and a solid that are commonly used as neutron moderators.
4. On an atomic level, what is the difference between light water and heavy water?
5. What is the chemical formula for heavy water?
6. What units does the lethargy have?
7. Name three metals that can be used as fast reactor coolants.
8. Why is a neutron moderator not required for a fast reactor?
9. What is the one fundamental assumption that James Clerk Maxwell made regarding the particle velocities when he first derived his famous Maxwell–Boltzmann probability distribution?
10. According to a Maxwell–Boltzmann probability distribution, how many times greater is the average energy of a particle than its most probable energy?
11. Name Maxwell's four particle collision rules.
12. If the temperature of a neutron that is in thermal equilibrium with its environment increases by a factor of two, how much does its average energy increase?
13. When the Maxwell–Boltzmann probability distribution is extended to a gas of relativistic particles, what is it called?
14. What are the primary advantages of light water as a reactor coolant?
15. Which reactor coolant has a higher heat transfer coefficient—liquid sodium or liquid water?
16. Name the six factors that normally go into the selection of a reactor coolant.
17. Which reactor coolant absorbs fewer neutrons—light water or heavy water?
18. Which reactor coolant has a higher heat transfer coefficient—liquid water or helium gas?
19. What is the lower limit of the neutron energies in a fast reactor?
20. How many coolant loops does a loop-type LMFBR have?
21. Consider the quantity kT that occurs in a Maxwell–Boltzmann probability distribution. What units does this quantity normally have?
22. Approximately how much heavier is heavy water than light water?
23. Write an equation for the average energy loss per collision ΔE of a neutron that is involved in both head-on and glancing scattering collisions.
24. Suppose that a neutron has a head-on elastic collision with a helium atom. If the initial energy of the neutron is 1 MeV, what is the final energy of the neutron after the collision?
25. Write an expression for the velocities of the neutrons that follow a Maxwell–Boltzmann probability distribution.
26. What is the value of Boltzmann's constant, which appears in the Maxwell–Boltzmann probability distribution?
27. Write a mathematical expression that defines the neutron lethargy L.
28. Write down the mathematical definition for the slowing down decrement ξ.
29. From the viewpoint of a reactor moderator, is it better for a reactor moderator to have a large slowing down decrement or a small one?
30. Suppose that a reactor goes on a slow transient where the power level gradually increases by 10%. If the average energy of a thermal neutron at the beginning of the transient is 0.075 eV, what is the average energy of a thermal neutron at the end of the transient?
31. Suppose that the energy of a thermal neutron in a reactor core happens to be exactly 0.025 eV. Is this the average energy of the neutron or its most probable energy?
32. Assuming an elastic scattering kernel, write down an expression that gives the probability P that a neutron with an initial energy E will have a final energy E′.
33. Write an expression for the number of elastic collisions required for a neutron having an initial energy E to acquire a final energy E′.
34. Write an expression for Boltzmann's constant as a function of the ideal gas constant R and Avogadro's number A_o.
35. What is the name of the process by which fast neutrons are converted into thermal neutrons sometimes called?
36. If a gas of fast fission neutrons could somehow be created with an average energy of 1 MeV, what would be the apparent temperature of this gas if all of the fission neutrons were assumed to be in thermal equilibrium with each other?

Exercises for the Student

Exercise 8.1

Suppose that approximately 30 trillion neutrons per second are successfully able to slow down and cause a fission reaction to occur in one of the fuel rods in a thermal water reactor. If the reactor is fueled with Uranium-235, what is the average power output of the fuel rod?

Exercise 8.2

Suppose that 1 billion neutrons per second (1×10^9 neutrons/s) are able to reach thermal equilibrium each second in the fuel rods of a small research reactor. Write down an expression for how many of these neutrons will reach an average velocity of less than 2200 m/s after the reactor has been operating for 1 hour.

Exercise 8.3

A scattering material has a logarithmic energy decrement ξ of 0.05 per collision. What is the atomic mass of this material, and if it has an equal number of protons and neutrons, what would this material be?

Exercise 8.4

A fission neutron collides with a material with an atomic number of 11 and with an equal number of protons and neutrons in its nucleus. Assuming that glancing collisions and head-on collisions are equally probable, what is the percentage energy loss per collision?

Exercise 8.5

Suppose that N(E) is the number of neutrons in a volume of space where a Maxwell–Boltzmann probability distribution applies. Write down an expression for the total number of neutrons in the distribution having an energy between E and E + dE.

Exercise 8.6

Using the probability distribution you derived in Exercise 8.5, write an expression for the number of neutrons N having an energy greater than 0.025 eV with an average temperature of 600 K.

Exercise 8.7

Using the probability distribution in Exercise 8.6, write down an expression for the average energy <E> of the neutrons in the distribution. How does the average energy compare to the most probable energy E_{MP}?

Exercise 8.8

Calculate the ratio of the average velocity of a neutron to a U-238 atom in a nuclear fuel rod after thermal equilibrium has been reached.

Exercise 8.9

Approximately how many times greater is the average kinetic energy of a thermal neutron in a reactor core that is operating at 1200 K than it is in a reactor core operating at 600 K?

Exercise 8.10

What is the ratio of the velocities of the uranium atoms in a reactor core that is operating at 1200 K to the velocities of the uranium atoms in a reactor core that is operating at 600 K?

Exercise 8.11

If the average energy of a gas of fission neutrons is 3 MeV, what would the most probable energy of a fission neutron be?

Exercise 8.12

Using your handheld calculator, or an Excel spreadsheet, show what the Maxwell–Boltzmann distribution looks like for an average neutron energy of 3 keV or a temperature of approximately 24,000,000 K.

Exercise 8.13

Suppose that you are on a desert island where the average air temperature in the summer is 100°F (about 38°C). What are the average and most probable energies of the air molecules? How does the average energy of these air molecules compare to the energy of the air molecules in the New York City subway system in the summer?

Exercise 8.14

Show that by integrating the Maxwell–Boltzmann probability distribution $N(E) = N\sqrt{\left\{(m/\pi)(2/kT)^3\right\}}\, Ee^{-E/kT}$ where the average energy $\langle E \rangle$ is defined by $\langle E \rangle = \int N(E)EdE/N$, N is the total number of particles, and the limits of integration are from $E = 0$ to $E = \infty$ that the average energy $\langle E \rangle$ of a particle that follows this distribution is $\langle E \rangle = 3/2\ kT$.

Exercise 8.15

Show by taking the derivative of the Maxwell–Boltzmann probability distribution $P(E) = \sqrt{\left\{(m/\pi)(2/kT)^3\right\}}\, Ee^{-E/kT}$ with respect to the energy E, and setting the derivative equal to 0, that the most probable energy E_p of a particle in the distribution, which corresponds to the maximum of the curve, is given by $E_p = 1/2\ kT$.

Exercise 8.16

The cooling water in the primary loop of a large Westinghouse PWR weighs 350,000 kg. If the light water is replaced by heavy water to reduce the neutron absorption rate in the core, how much will an equivalent volume of heavy water weigh?

Exercise 8.17

A hypothetical nuclear material has an average lethargy gain ξ of 0.25 per collision. If the scattering cross section of the material is 100 times the absorption cross section, what is the moderating ratio for this material?

Exercise 8.18

Beryllium, which is a common neutron scattering material, has an atomic mass number of 9. What is the mean lethargy gain ξ per collision?

Exercise 8.19

A neutron is born with an average energy of 2 MeV and is absorbed by a uranium nucleus at an average energy of 0.025 eV. What is the lethargy gain in the process?

Exercise 8.20

A scattering material used in a nuclear power plant has an average lethargy gain ξ of 0.22 per collision. What is the percentage energy loss per collision if a neutron has an elastic collision with this material?

Exercise 8.21

Under certain conditions, it is energetically possible for free protons and electrons in a high-temperature plasma to combine together to form neutrons. Using the following rest masses for the proton, the neutron, and the electron, estimate the absolute temperature at which this reaction can occur.

$$m_p = 938.27\ \text{MeV}/c^2$$
$$m_n = 939.565\ \text{MeV}/c^2$$
$$m_e = 0.511\ \text{MeV}/c^2$$

Assume that the particles in the plasma are in thermal equilibrium with one another.

9

The Neutron Multiplication Factor, the Reactivity, and the Four-Factor Formula

9.1 Uses for the Macroscopic Fission and Absorption Cross Sections

In Chapter 4 we learned that two of the most important variables in nuclear science and engineering are the neutron absorption cross section, Σ_a, and the neutron fission cross section, Σ_f. Because neutrons are produced by the process of nuclear fission, the neutron fission cross section is sometimes called the *neutron production cross section*. Armed with the values of these two cross sections and the value of the neutron flux, it is possible to predict whether the neutron population will increase, decrease, or stay the same as a function of time. If the neutron population increases, then the power level P will increase as well (since there are more fission reactions than absorption reactions). Conversely, if there are more absorptions than fissions, the power level will fall over time because there are fewer neutrons available to split the nuclear fuel apart. *In other words, the difference between these two numbers determines how a nuclear reactor behaves*. In practice, commercial nuclear power plants operate in a state where the neutron production rate P is almost always balanced by the neutron destruction rate D. In other words, a reactor remains critical and stable when

The Condition for a Critical Reactor

$$\text{Neutron production rate}\,(\mathrm{P}) \cong \text{Neutron destruction rate}\,(\mathrm{D}) \tag{9.1}$$

When calculating the neutron production and destruction rates, the fission and absorption cross sections are used to represent the sum of the individual cross sections for many different materials. For example, when many neutron absorbers are present, we can write

$$\Sigma_a = \Sigma_{a1} + \Sigma_{a2} + \Sigma_{a3} + \Sigma_{a4} + \Sigma_{a5} + \cdots \Sigma_{aN} \quad (\text{N is the number of elements involved}) \tag{9.2}$$

and similarly, when many fissionable materials are present, we can write

$$\Sigma_f = \Sigma_{f1} + \Sigma_{f2} + \Sigma_{f3} + \Sigma_{f4} + \Sigma_{f5} + \cdots \Sigma_{fN} \quad (\text{N is the number of elements involved}) \tag{9.3}$$

where N is the number of elements that will be participating in each of these reactions. For instance, suppose that a nuclear fuel assembly consists of only four materials: the Uranium fuel, the cladding (which is made primarily of Zirconium), Boron (which is used in the control rods), and water (which is used for the coolant). This is of course a gross simplification, but it can have many helpful benefits as we will shortly see. Then the value of N in this example is 4, and the total absorption cross section Σ_a would represent the sum of the absorption cross sections of each of these individual elements; for example,

$$\Sigma_a = \Sigma_{au} + \Sigma_{ac} + \Sigma_{ab} + \Sigma_{aw} \quad (\text{For a typical fuel assembly}) \tag{9.4}$$

Similarly, the total fission cross section could be written as

$$\Sigma_f = \Sigma_{fu} + \Sigma_{fc} + \Sigma_{fb} + \Sigma_{fw} \quad \text{(For a typical fuel assembly)} \tag{9.5}$$

Here the subscripts u, c, b, and w refer to the cross sections for uranium, the zirconium cladding, the boron in the control rods, and cooling water, respectively. Before we attach any specific numerical values to these cross sections, let's see if we can use some common sense to simplify these equations a bit—using rough order of magnitude approximations. In the first equation, the largest contribution to the neutron absorption cross section comes from the uranium in the fuel rods, and from the boron in the control rods. The contributions to the absorption cross section from the zirconium cladding and the coolant are minimal. We can therefore rewrite Equation 9.4 as

$$\Sigma_a \cong \Sigma_{au} + \Sigma_{ab} \quad \text{(For a typical fuel assembly)} \tag{9.6}$$

by ignoring the contributions from the Zirconium cladding and the water. Similarly, of the four terms in Equation 9.4, the only one that is truly significant is the first term, which represents the fission cross section for the uranium fuel. None of the other elements are able to produce fission neutrons, except through the process of radioactive decay, which we are ignoring here.

We can therefore rewrite Equation 9.3 as $\Sigma_f \cong \Sigma_{fu}$. The ratio of the fission cross section to the absorption cross section cannot be used to represent the behavior of the neutron population entirely. To do so, we must multiply the fission cross section Σ_f by the number of neutrons produced per fission. In reactor physics, the number of neutrons produced per fission is normally given the symbol ν (mu). Then the neutron production rate at a particular location in the core is given by $\nu\Sigma_f\phi$, where ϕ is the neutron flux. The value of $\nu\Sigma_f\phi$ divided by the value of $\Sigma_a\phi$ then determines whether the neutron population is increasing, decreasing, or remaining the same. *The ratio of these terms is also called the location dependent neutron multiplication factor for a particular point in the core*:

The Location Dependent Neutron Multiplication Factor

$$\text{Multiplication factor}\,(x,y,z) = \frac{\nu \cdot \Sigma_f(x,y,z) \cdot \phi(x,y,z)}{\Sigma_a(x,y,z) \cdot \phi(x,y,z)} \tag{9.7}$$

Since the value of the neutron flux in the numerator and the denominator of Equation 9.7 cancels, Equation 9.7 can be further simplified to read

$$\text{Neutron multiplication factor}\,(x,y,z) = \frac{\nu\Sigma_f(x,y,z)}{\Sigma_a(x,y,z)} \tag{9.8}$$

Here we have retained the spatial dependence of the multiplication factor to indicate that it may be different from one location in the core to another. Hence the *total multiplication factor* can be obtained by integrating the position dependent multiplication factors (and therefore the fission and absorption rates) over the entire volume of the core. If there are I points in the x direction, J points in the y direction, and K points in the z direction, and each of them is centered around a *control volume* of size $V = \Delta x \Delta y \Delta z$, then it is possible to write the total multiplication factor as

The Total Multiplication Factor

$$\text{Total multiplication} = \frac{\sum_i \sum_j \sum_k \left(\nu\Sigma_f(i,j,k) \cdot \phi(i,j,k) \cdot V(i,j,k)\right)}{\sum_i \sum_j \sum_k \left(\Sigma_a(i,j,k) \cdot \phi(i,j,k) \cdot V(i,j,k)\right)} \tag{9.9a}$$

where V_{CORE} is the volume of the core where nuclear fuel is present. In terms of a continuous integral, Equation 9.9(a) can also be written as

The Total Multiplication Factor in Integral Form

$$\text{Total multiplication} = \frac{\int_{VCORE} \nu\Sigma_f(x,y,z) \cdot \phi(x,y,z)\, dV}{\int_{VCORE} \Sigma_a(x,y,z) \cdot \phi(x,y,z)\, dV} \tag{9.9b}$$

where dV = dxdydz. Thus each control volume can be thought of as a *computational cell* when a *nodal approach* is used to represent the shape of the flux and the geometrical composition of the core. Finally, the approach we have outlined above can be extended to more than one energy group using what is called *multi-group theory* (Multi-group theory is discussed in Chapter 12). Hence *the total multiplication factor can be thought of as a measure of the behavior of the neutron population in the reactor as a whole*. In the discussion that follows, we will explore the meaning of this important parameter in more detail.

9.2 Meaning of the Effective Multiplication Factor

Sometimes it is helpful to understand the behavior of the neutron population in more holistic terms. Suppose that we would like to determine whether the neutron population is increasing, decreasing, or staying the same at a particular location in the core. This location could represent an entire fuel assembly or just an individual fuel rod. If we know the neutron production rate P and the neutron destruction rate D at this location, then it is possible to write

Total Neutron Production Rate

$$P = \nu\Sigma_f\phi \text{ (in neutrons per cm}^3\text{ per second)} \tag{9.10}$$

and

Total Neutron Destruction Rate

$$D = \Sigma_a\phi \text{ (in neutrons per cm}^3\text{ per second)} \tag{9.11}$$

Normally ν has a value of about 2.5; however, its exact value can vary depending on the type of nuclear fuel that is used (see Chapter 7). Here, we have again suppressed the energy dependence of the cross sections to keep the notation simple. Then the ratio of the neutron production rate to the neutron destruction rate at a particular location is

$$\frac{P}{D} = \nu\frac{\Sigma_f\phi}{\Sigma_a\phi} \tag{9.12}$$

where it is understood that all of the terms in Equation 9.12 have *some* spatial dependence. If we cancel the value of the neutron flux from the numerator and the denominator, we obtain

$$K_{effective} = \nu\left(\frac{\Sigma_f}{\Sigma_a}\right) \tag{9.13}$$

where $K_{effective}$ is an important parameter called the effective multiplication factor for the core. For an infinite reactor lattice, the effective multiplication factor can also be written as

The Infinite Multiplication Factor

$$K_\infty = \nu\left(\frac{\Sigma_f}{\Sigma_a}\right) \tag{9.14}$$

because there is no neutron leakage at the location where Equation 9.14 applies. For an infinite reactor lattice (or core), the effective multiplication factor then becomes what is known as the *infinite multiplication factor* K_∞. The infinite multiplication factor is one of the most important parameters in all of nuclear science and engineering. In particular, it is frequently used to determine whether the neutron population is increasing, decreasing, or staying the same as a function of time. If we decide to include the neutron leakage rate L (in neutrons per second) in the definition of the effective multiplication factor, then neutron destruction term D in the denominator of Equation 9.14 becomes larger, and the effective multiplication factor for a core of finite size can be written as

The Effective Multiplication Factor

$$K_{effective} = \frac{P}{D+L} = \frac{\nu\Sigma_f}{\Sigma_a + C} \tag{9.15}$$

where it is understood that this is just the location dependent multiplication factor, and the neutron leakage rate $L = C \cdot \phi$ in the denominator is usually just a small fraction C of the total neutron flux ϕ (normally between 1% and 10%). In a reactor fuel assembly, the value of L is typically a few percent of $\nu\Sigma_{f\phi}$. *Hence, the primary difference between the infinite multiplication factor, which applies to an infinite lattice, and the effective multiplication factor, which applies to a finite lattice, is that the effective multiplication factor includes the effects of neutron leakage while the infinite multiplication factor does not.* The values of these parameters for an actual core (which may consist of hundreds of fuel assemblies) are then obtained by integrating equations 9.14 and 9.15 over the entire volume of the core, which we previously defined to be V_{CoRe}. Normally this process is done numerically, but in this chapter, we will show how it can be done analytically.

9.3 Relationship between the Effective Multiplication Factor and the Neutron Life Cycle

The effective multiplication factor $K_{effective}$ and the infinite multiplication factor K_{∞} were originally conceived during the Second World War, by scientists such as *J. Robert Oppenheimer, Enrico Fermi* (see Figure 9.1), and *Richard Feynman* (see Chapter 3) because they needed to develop a simple and reliable method for predicting how the neutron population in a reactor lattice (or an atomic bomb for that matter) would behave as a function of time. Computers were just in their infancy when the war began, and so it became necessary to develop an alternative approach to determine what combinations of materials would be able to make a reactor critical and what combinations would not. Thus the concept of the effective multiplication factor was developed to simplify these calculations. When thought of in a slightly different way, the value of $K_{effective}$ was actually defined to represent the ratio of the number of neutrons produced in generation n + 1 to the number of neutrons produced in generation n. Therefore, the effective multiplication factor was also intended to mean

Effective Multiplication Factor

$$K_{effective}(n) = \frac{\text{Number of free neutrons produced in generation } n+1}{\text{Number of free neutrons produced in generation } n} \tag{9.16}$$

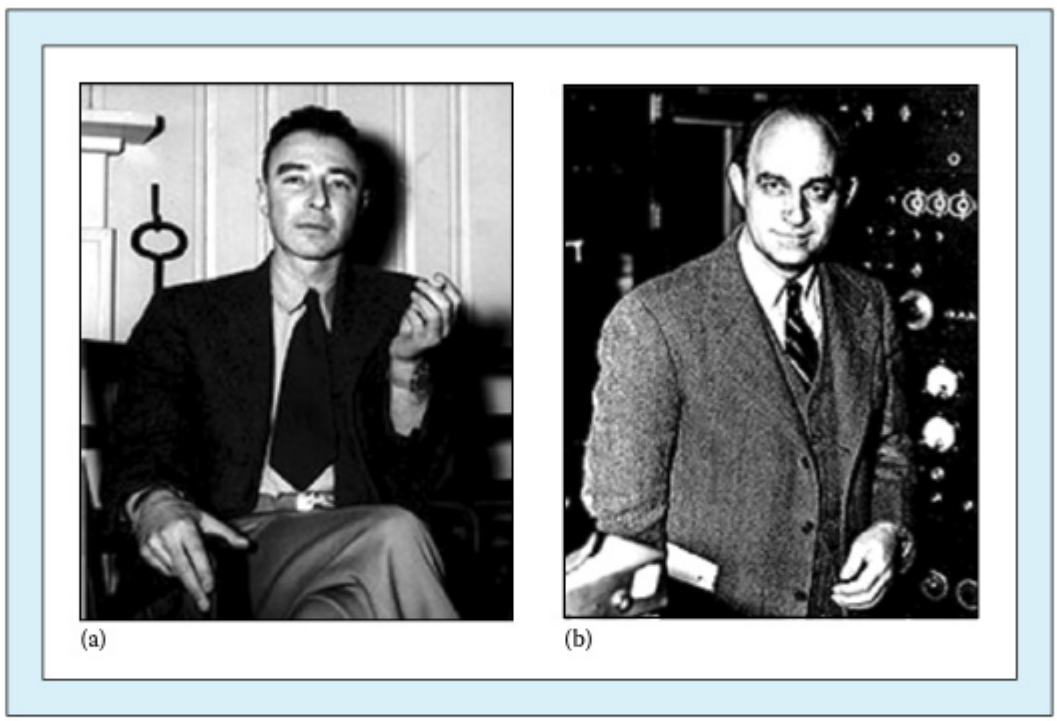

FIGURE 9.1 A picture of Robert Oppenheimer (a) and Enrico Fermi (b)—two of the founders of the modern nuclear industry as we know it today. (These public domain pictures were provided by Google Images.)

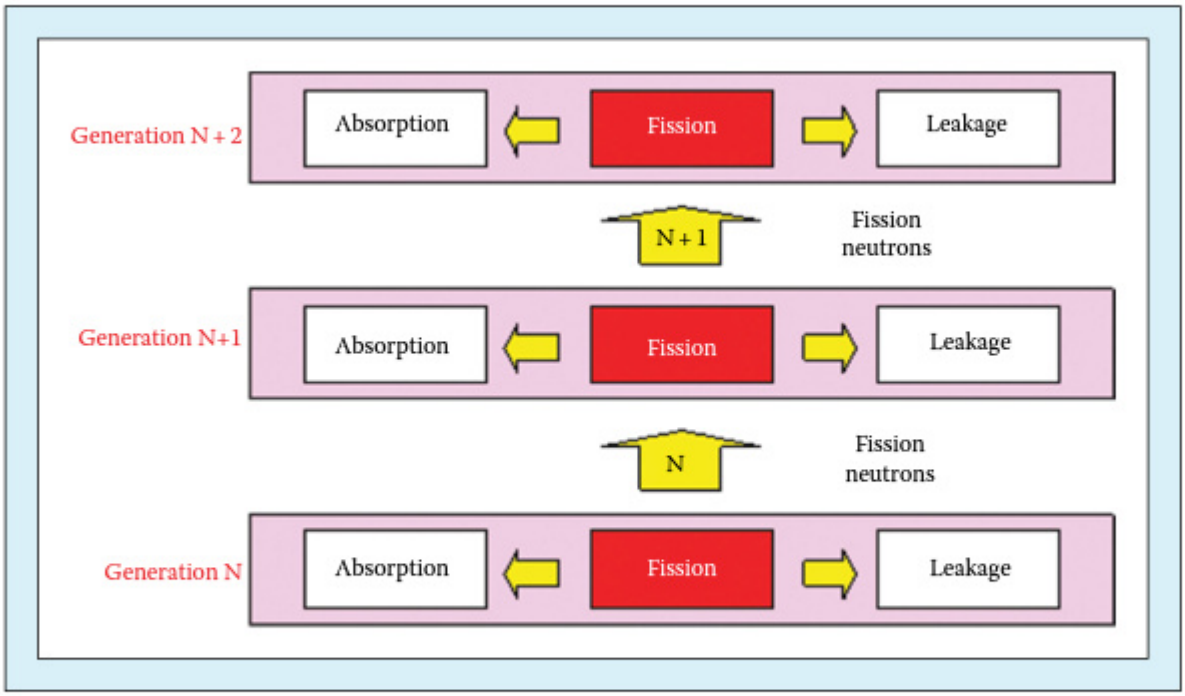

FIGURE 9.2 An illustration of the neutron life cycle in a typical fast or thermal reactor.

where n is an arbitrary number, representing the generation of neutrons produced, between 1 and infinity. Here the neutrons in generation n are considered to be born in a fission reaction when the nucleus splits apart, and they are considered to be destroyed when they are either absorbed by another nucleus or when they cause new fission neutrons to be produced in generation n + 1. The neutron life cycle represented by Equation 9.16 is shown in Figure 9.2. Statistically speaking, the neutrons in a reactor core behave in exactly the same way. Notice that it is not necessary to specify how many neutrons belong to generation n and how many neutrons belong to generation n + 1. This number is determined by the geometry and the composition of the core.

In an extreme case, this number of neutrons can be as small as 1, although in any real reactor, it is normally measured in billions or even trillions of neutrons. It also follows from our earlier discussion that each material region in the core can have its own unique composition; and therefore, it can also have its own unique values for Σ_f and Σ_a. For example, some fuel assemblies may not produce enough neutrons to sustain a nuclear chain reaction (e.g., $\nu\Sigma_f \ll \Sigma_a$), while other fuel assemblies may be able to produce more than enough neutrons to sustain it indefinitely (e.g., $\nu\Sigma_f \gg \Sigma_a$). Let us call the value of $K_{effective}$ for fuel assembly i $K_{effective}$ (i), where i is the index of the assembly. Clearly some fuel assemblies will have $K_{effective}$ (i) < 1, other fuel assemblies will have $K_{effective}$ (i) ~ 1, and still other fuel assemblies may have $K_{effective}$ (i) > 1. In order to create a value for $K_{effective}$ that can be used to predict the criticality of the core the effective multiplication factors for all of the material regions must be averaged together to produce a value that is a meaningful representation of the behavior of the core as a whole.

This then leads us to define a system-wide value for $K_{effective}$ that provides a simple and reliable way to determine how close an entire reactor is to becoming critical. *It then follows that if $K_{effective}$ is greater than 1.0, the neutron population will continue to increase with time, and if $K_{effective}$ is less than 1.0, the neutron population will continue to decrease with time. Only when its value is exactly equal to one will the neutron population remain the same*. Since the values of Σ_f and Σ_a inside of a fuel assembly are generally fixed by the design of the assembly (because the uranium in the fuel rods does not move), the value of Σ_a in the denominator of Equation 9.12 will determine how the neutron population behaves. If we move the control rods into a fuel assembly, the value of Σ_a in the denominator will increase. If we move them just far enough out, then the denominator will have the same value as the numerator. When this happens, there will be a stable neutron population—and therefore, a sustained chain reaction! It is sometimes convenient to consider an alternative formulation for the neutron cross sections that allows us to see whether the net neutron creation rate is positive or negative. This will then lead us to a discussion of a new parameter called the *reactivity*, which we will introduce in Section 9.5. *In general, the reactivity is used to determine the time-dependent behavior of a reactor. If we know the value of the reactivity, then it is possible to determine how the power level changes as a function of time.*

9.4 Finding the Effective Multiplication Factor and the Infinite Multiplication Factor with More than One Energy Group

For a single energy group, the expressions for the effective multiplication factor and the infinite multiplication factor are relatively simple because the values of the neutron flux cancel from the numerator and the denominator of Equation 9.8. Then all we are left with (when neutron leakage can be ignored) is the ratio of the macroscopic fission cross section to the macroscopic absorption cross section ($\sum_f$ and $\sum_a$) multiplied by ν. However, it is often necessary to find a more accurate way of finding $K_{effective}$ and K_∞ that involves more than one energy group. In this case, the expressions for the neutron production and the destruction rates become

Neutron Production Rate with More than One Energy Group

$$P = \sum_g \nu_g \Sigma_{fg} \phi_g \tag{9.17}$$

and

Neutron Destruction Rate with More than One Energy Group

$$D = \sum_g \Sigma_{ag} \phi_g \tag{9.18}$$

where the summations in Equations 9.17 and 9.18 must be performed over all energy groups from g = 1 to g = G. Similarly for the neutron leakage rate, we obtain

Neutron Leakage Rate with More than One Energy Group

$$L = \sum_g L_g = \sum_g C_g \phi_g \tag{9.19}$$

The corresponding expressions for $K_{effective}$ and K_∞ then become

The Equation for $K_{effective}$

$$K_{effective} = \frac{P}{D+L} = \frac{\sum_g \nu_g \Sigma_{fg} \phi_g}{\sum_g \Sigma_{ag} \phi_g + \sum_g L_g} \tag{9.20}$$

and

The Equation for K_∞

$$K_\infty = \frac{P}{D} = \frac{\sum_g \nu_g \Sigma_{fg} \phi_g}{\sum_g \Sigma_{ag} \phi_g} \tag{9.21}$$

where C_g is the fraction of neutrons leaking out of the core within energy group g. Here the group fluxes in the numerator and denominator do NOT cancel and therefore the neutron energy spectrum must be known to calculate the values of $K_{effective}$ and K_∞ accurately. Now let us make some additional comments about the size of the neutron leakage rate in a representative reactor core. In a typical thermal water reactor, the neutron leakage rate for the fast energy group is about 3% of the total neutron production rate and the value of L for the thermal energy group is about 1% of total neutron production rate. Therefore, when the effects of neutron leakage are taken into account, the effective multiplication factor is typically 3% to 4% *smaller* than the infinite multiplication factor for the same reactor geometry because the value of L in the denominator of Equation 9.20 is approximately 3% to 4% greater.

9.5 Defining the Reactivity

Now suppose that we would like to invent another way of determining whether or not a reactor is critical. If we take the total fission cross section multiplied by ν, that is, $\nu\Sigma_f$, and subtract the total absorption cross section Σ_a from it, we have a simple measure of whether a representative neutron will be created or destroyed. If we multiply the difference between these two macroscopic cross sections by the neutron flux ϕ, then we have the total number of neutrons being created or destroyed per second:

$$R = \phi\left(\nu\Sigma_f - \Sigma_a\right) \quad \text{(in neutrons/cm}^3\text{/sec)} \tag{9.22}$$

where

R is the reaction rate

ν is the average number of neutrons released per fission

The total number of neutrons created or destroyed per second in a volume of space V measured in cubic centimeters can then be found my multiplying Equation 9.22 by V. If we divide Equation 9.22 by the total neutron production rate $\nu\Sigma_{f\phi}$, we can create another extremely useful parameter called *the reactivity*. In nuclear science and engineering, the reactivity is represented by the symbol ρ (rho), which is not to be confused with the physical density ρ of the fuel or the moderator. For a representative reactor core, the reactivity is defined by

An Expression for the Reactivity

$$\rho = \frac{(\nu\Sigma_f - \Sigma_a)\phi}{(\nu\Sigma_f)\phi} = \frac{\nu\Sigma_f - \Sigma_a}{\nu\Sigma_f} \tag{9.23}$$

Equation 9.23 can be further simplified to produce the following relationship between $K_{effective}$ and the reactivity ρ:

Definition of the Reactivity

$$\rho = \frac{K_{effective} - 1}{K_{effective}} \tag{9.24}$$

Hence, the reactivity can be thought of as the ratio of the net neutron production rate to the neutron production rate due to fission alone. Like the effective multiplication factor, the reactivity is a property of the reactor as a whole—and not just the property of an individual fuel assembly—although it can be quantitatively useful in determining how close a fuel assembly is to becoming critical. *Depending on the size of Σ_f and Σ_a, the value of the reactivity can be either zero, positive, or negative. The sign of the reactivity then determines how the neutron population behaves. Moreover, Equation 9.24 implies that the reactivity is zero for an exactly critical reactor because $\rho = 0$ when $K_{effective} = 1$. In Chapter 15, we will also learn that the reactivity of an operating reactor usually falls between 0.05 and –0.05. Larger values of the reactivity are rarely encountered in practice because they cause the power level to rise or fall too quickly*. In general, there are three cases to consider when discussing how the reactor power level changes as a function of time:

Case 1: If $K_{effective} < 1$, a reactor is said to be *subcritical*. The reactor cannot sustain a nuclear chain reaction, and any new chain reaction which begins will die out over time. For every fission that is induced in the system, less than one new fission will occur. According to Equation 9.24 *this results in a negative value of the reactivity* ρ.

Case 2: If $K_{effective} = 1$, a reactor is said to be exactly *critical*. Every fission causes an average of just one more fission, leading to a power level that is independent of time. Nuclear power plants operate with a $K_{effective}$ very close to 1 unless the power level is being increased or decreased rapidly. *The reactivity ρ in this case is zero*.

Case 3: *If $K_{effective} > 1$*, a reactor is said to be *supercritical*. For every fission reaction that occurs on average, there will be "K" fissions after the next *mean generation time*. The result is that the number of fission reactions increases exponentially, unless some other action is taken to prevent it. *The reactivity ρ in this case is therefore a positive number*.

In Chapter 15, we will learn that the prompt neutron population N(t) at any time t (ignoring spatial effects and the delayed neutrons produced by the fission products) can be approximated (to first order) by an exponential relationship of the form

$$N(t) = N(0)e^{(k-1)t/\Lambda} \tag{9.25}$$

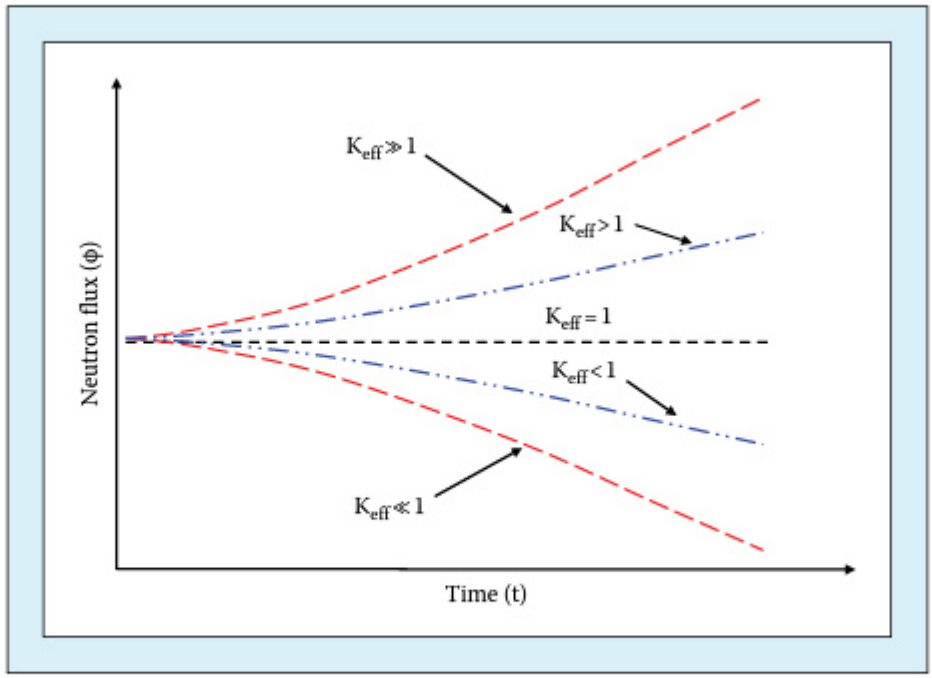

FIGURE 9.3 The behavior of the neutron population as a function of time when $K_{eff} > 1.0$, $K_{eff} = 1.0$, and $K_{eff} < 1.0$.

where N(0) is the initial neutron population at time = 0 and Λ is a parameter called the *mean neutron generation time*. This harmless-ooking equation establishes a unique relationship between the value of $K_{effective}$ (shown here as k), and how the prompt neutron population in the "object" that k represents changes as a function of time. Now let us see if we can understand what Equation 9.25 means. Consider three different reactor configurations: one where k is >1, one where k is <1, and the third one where k is exactly equal to 1. Figure 9.3 shows how the neutron population behaves in each case. No matter how many fuel assemblies a reactor contains, Equation 9.25 implies

- If k > 1.0, the neutron population will increase, and the reactor will be *supercritical*.
- If k = 1.0, the neutron population will remain essentially constant, and the reactor will be *critical*.
- If k < 1.0, the neutron population will decrease, and the reactor will be *subcritical*.

It also follows from this simple example that when k = 1, $N(t) = N(0)\, e^0 = N(0)$, and the time-dependent neutron population remains the same as the initial population. Therefore, in practice, reactors are designed to be operated with a value of $K_{effective}$ very close to 1. There are a number of factors that come into play when trying to keep a reactor "exactly critical" under these conditions. *In practice, the value of $K_{effective}$ will usually oscillate from slightly less than unity to slightly more than unity, primarily due to thermal feedback effects*. As the reactor power level is increased, the fuel rods and the coolant begin to heat up and expand, and this reduces the fission to capture ratio Σ_f/Σ_a and drives $K_{effective}$ lower. This leaves the average value of $K_{effective}$ almost exactly equal to unity. Figure 9.3 shows how the neutron population will behave when this is true. Notice that as the value of $K_{effective}$ departs from 1.0, the neutron population grows or shrinks in direct proportion to the difference between $K_{effective}$ and unity. For example, the neutron population grows much faster when $K_{effective} \gg 1$ than when $K_{effective} > 1$. Similarly, when $K_{effective} \ll 1$ the neutron population declines much faster than when $K_{effective} < 1$. We will discuss how quickly this happens in Chapter 15, when we derive the *prompt jump* and the *prompt drop* approximations for the time-dependent neutron populations.

Although the reactivity is normally found from the effective multiplication factor, it is possible to invert Equation 9.24 and to find the value of the $K_{effective}$ directly from the reactivity as well. When we do so, we find that

Finding $K_{effective}$ from the Reactivity

$$K_{effective} = \frac{1}{1-\rho} \tag{9.26}$$

Notice that when ρ = 0, Equation 9.26 says that $K_{effective} = 1$. Intuitively this implies that the neutron population stays the same when ρ = 0. In other words, it neither increases nor decreases, and in this case, the neutron population is said to be *time independent*. The implications of this behavior are explored in the sample problems that follow.

Example Problem 9.1

A thermal water reactor has been operating for some time with a net reactivity of zero, and then the reactivity is suddenly changed to 0.00001. What is the effective multiplication factor for the core before and after this change is made?

Solution From Equation 9.26, the effective multiplication factor when $\rho = 0$ is 1.0 and the effective multiplication factor when $\rho = 0.00001$ is $K_{effective} = 1/(1 - 0.00001) = 1.00001$. [Ans.]

9.6 Units for the Reactivity

In many reactor physics books, the reactivity is expressed in the units of dollars and cents. The *dollar* is a dimensionless unit for measuring the reactivity that is a function of the delayed neutron fraction β (see Chapter 7). When the reactivity increases or decreases from its steady-state value ($\rho = 0$), it is normally measured by how close the reactivity approaches the value of the delayed neutron fraction β. *A value of $\rho = \beta$ corresponds to a reactivity of one dollar, and a value of $\rho = 0.01\ \beta$ corresponds to a reactivity of one cent*. The value of the delayed neutron fraction is also a function of the type of nuclear fuel that is used. In thermal water reactors, the value of β is 0.0065 for U-235, 0.0026 for U-233, and 0.0020 for Pu-239. We will have more to say about these relationships in Chapters 15 and 16.

9.7 Effect of Delayed Neutrons on the Value of the Reactivity

In Chapter 7 we briefly discussed the role that delayed neutrons play in the process of reactor control. *Delayed neutrons play an important role in controlling the magnitude of the oscillations in the reactor power level.* The reader may recall from our previous discussion that neutrons produced directly from the fission of Uranium or Plutonium are called "prompt neutrons," while neutrons produced from the radioactive decay of fission fragments are called "delayed neutrons." Under steady-state operation, more than 99% of the neutron population is considered to be "prompt." Thus the fraction of neutrons that are delayed neutrons is normally less than 1% of the total neutron population (the exact percentage depends on the type of fuel). The average creation time of a delayed neutron (for a reactor fueled with U-235) is about 12 seconds. *In Chapter 15 we will also learn that delayed neutrons allow a nuclear reactor to respond several orders of magnitude more slowly than if the only neutrons available are prompt neutrons. Without delayed neutrons, changes in the reaction rates would simply be too fast for human beings to control!*

The region of supercritical operation between $K_{effective} = 1$ and $K_{effective} = 1/(1 - \beta)$ is known as the region of operational criticality. This is the region where all nuclear power plants are designed to operate. The change in the value of $K_{effective}$ needed to go from a prompt critical state to prompt super critical condition is defined as a "dollar" of reactivity. There are six major groups of radioactive decay chains consisting of about 50 fission products that create most of the delayed neutrons that are observed in practice. The fission products with these decay chains have their own individual yields, or concentrations, C_i, associated with them as well as their own decay constants, which are represented in this book by the symbol λ_i. Their contributions to the neutron population can be expressed by summing over the six fission fragment populations multiplied by their respective decay constants. In other words, the change in the number of delayed neutrons, n, per second is given by

The Change in the Number of Delayed Neutrons

$$\frac{dn}{dt} = \sum_i \lambda_i C_i(t) \tag{9.27}$$

where

n is the number of delayed neutrons produced per cubic centimeter per second (i.e, the neutron density)

λ_i is the decay constant for fission fragment decay chain i for the production of delayed neutrons due to radioactive Beta decay

$C_i(t)$ is the concentration of the fission product population i, and the sum is over six groups of delayed neutron precursors from i = 1 to 6

It is important keep in mind that delayed neutrons (see Chapter 7) are primarily produced by the process of beta decay, and very few, if any, delayed neutrons are produced by alpha or gamma decay.

9.8 Using the Four-Factor and Six-Factor Formulas to Determine When a Reactor Becomes Critical

Before high-speed computers were invented, it was hard to predict when a reactor or *nuclear pile* would produce enough neutrons to become critical. The reactor designers in the early days of the nuclear industry realized that some of the neutrons produced would simply leak out of the core before participating in a chain reaction, while others would stay in the core to generate additional neutrons. To understand what geometries and combinations of materials allowed a reactor to become critical, they devised two relatively simple but relatively accurate formulas to calculate a "system-wide" value for the neutron multiplication factor K. These formulas eventually became known as the *four-factor formula* and the *six-factor formula*. *The four-factor formula was designed to predict the value of the infinite multiplication factor in reactor cores with no neutron leakage*. In other words, it was devised to predict the value of the neutron multiplication factor for an *infinite repetitive medium. The six-factor formula, on the other hand, was devised to find the neutron multiplication factor for a finite medium, that is, one where the effects of neutron leakage and spatial heterogeneity become important.* These two formulas are then related to each other by two simple geometric parameters called *the fast and thermal nonleakage probabilities*. In Chapter 10, we will show how these parameters are related to each other for an exactly critical reactor. However, we would first like to show how the four-factor formula can be derived for an infinite reactor lattice consisting of a large number of repetitive unit cells. Derivations of the four factor formula are normally not presented in elementary reactor physics books. Before proceeding with this derivation, we would first like to make some observations about the composition of a typical reactor core. A more extensive discussion of core composition is provided in our companion book.*

Example Problem 9.2

Calculate the neutron density in a reactor 10 seconds after the reactivity has been changed from $\rho = 0$ to $\rho = 0.00001$. Assume the steady-state neutron density is 1×10^{14} neutrons/cm^3. Also assume that the mean neutron generation time is 10^{-4} seconds and that there are no delayed neutrons in the core.

Solution From Equation 9.25, the neutron density 10 seconds after the change is made is $N = 10^{14}\, e^{(0.00001)t/\Lambda} = 2.718 \times 10^{14}$ n/cm^4. [Ans.]

9.9 Unit Cells

Sometimes, it is convenient to represent a fuel pin and the surrounding coolant by what is called a *unit cell*. A unit cell allows the design features of different fuel assemblies to be compared on an "apples to apples" basis. A unit cell is basically a simple way to compare the material ratios that a fuel assembly contains on a geometry-independent basis. A square and hexagonal lattice and their equivalent unit cells are shown in Figures 9.4 and 9.5. Notice that we can define the unit cells to be either square, hexagonal, or cylindrical in shape.

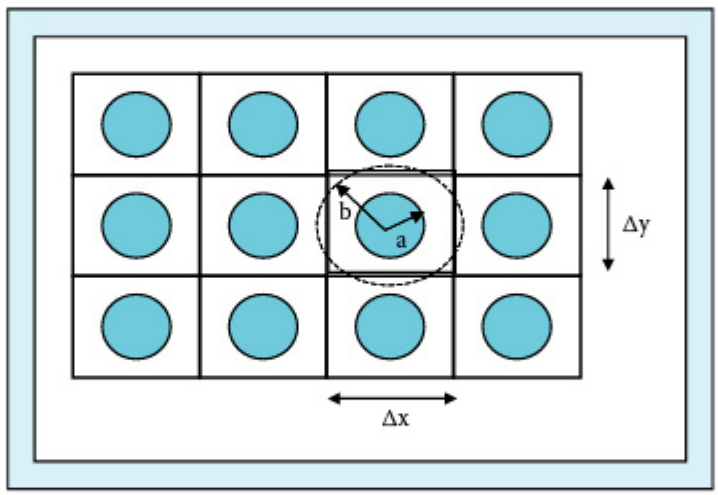

FIGURE 9.4 An equivalent cylindrical unit cell in a standard reactor lattice.

* See *Nuclear Engineering Fundamentals: A Practical Perspective*, by R.E. Masterson, CRC Press (2017).

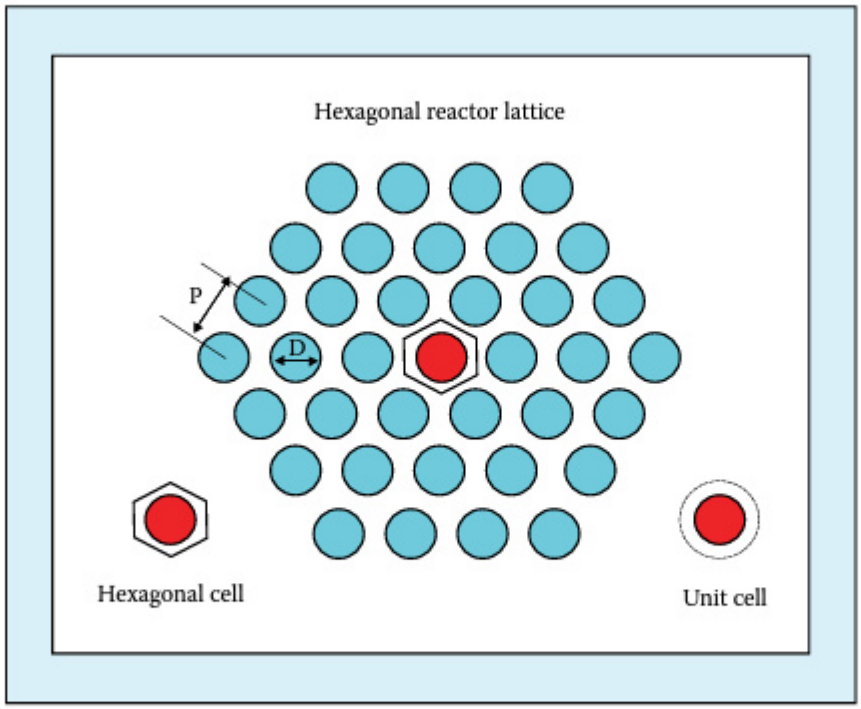

FIGURE 9.5 A hexagonal reactor lattice and its equivalent cylindrical unit cell (s).

To calculate the outer radius of a cylindrical unit cell, one simply calculates the area of the square unit cell in the reactor lattice and then equates the two areas to find the radius of the equivalent cell if it were cylindrical in shape. This can be achieved by using the following relationship to find the radius of the unit cell:

$$\pi R_{cell}^2 = \Delta x^2 \tag{9.28}$$

in which case it is easy to see that

$$R_{cell} = \frac{\Delta x}{\sqrt{\pi}} \tag{9.29}$$

or $R_{cell} = P/\sqrt{\pi}$, since the pitch P of the lattice is equal to Δx in this case. The radius of the fuel R_{fuel} and the radius of the cladding R_{clad} within an individual fuel rod are then the same as earlier. The total volume of the fuel, the cladding, and the moderator (or coolant) in the unit cell can then be found from

$$V_{fuel} = \pi R_{fuel}^2 \Delta z \tag{9.30}$$

$$V_{clad} = \pi R_{clad}^2 \Delta z - \pi R_{fuel}^2 \Delta z \tag{9.31}$$

and

$$V_{mod} = \pi R_{cell}^2 \Delta z - \pi R_{clad}^2 \Delta z \tag{9.32}$$

where Δz is the length in the axial direction.

Student Exercise 9.1

In a modern-day PWR, the spacing between the centers of the adjacent fuel rods is about 2 cm, and a typical fuel rod is about 1.2 cm in diameter. Assuming that the gap between the cladding and the fuel is about 0.3 mm and that the cladding is about 1 mm thick, what is the percentage of fuel, moderator, and structural material (i.e., the cladding) in this configuration?

9.10 Representing the Fuel to Cladding Gap

Moreover, this approach can be extended to handle the small gap between the fuel and the cladding as well. In light water reactors, this gap normally has a thickness Δr between 0.08 and 0.12 mm. The gap allows the fuel pellets to expand and contract slightly as the temperature of the fuel is raised or lowered. *The purpose of this gap is similar in principle to the expansion joints between the sections of the road surface on a bridge*. It allows the fuel to expand and contract without allowing it to buckle or crack. Another important advantage of creating a cylindrical unit cell is that it makes it easy to calculate the ratios of the fuel, the moderator, and the cladding volumes because the values of π and Δz always cancel whenever a ratio is taken. It then follows that

$$V_{mod}/V_{fuel} = \left(\pi R_{cell}^2 \Delta z - \pi R_{clad}^2 \Delta z\right)/\pi R_{fuel}^2 \Delta z = \left(R_{cell}^2 - R_{clad}^2\right)/R_{fuel} \tag{9.33}$$

$$V_{clad}/V_{fuel} = \left(\pi R_{clad}^2 \Delta z - \pi R_{fuel}^2 \Delta z\right)/\pi R_{fuel}^2 \Delta z = \left(R_{clad}/R_{clad}\right)^2 - 1 \tag{9.34}$$

and

$$V_{cell}/V_{fuel} = \pi R_{cell}^2 \Delta z/\pi R_{fuel}^2 \Delta z = R_{cell}^2/R_{fuel}^2 \tag{9.35}$$

The mathematics required to do so is straightforward. While we have only decided to do so here for a rectangular lattice, extending this same approach to a hexagonal fuel assembly is straightforward as well. When this is done, the ratio V_{clad}/V_{fuel} remains the same, but the values of V_{mod}/V_{fuel} and V_{cell}/V_{fuel} are approximately 1/1.16 = 0.86 or about 14% lower. This also means that the average volume of the fuel in a hexagonal fuel assembly is about 16% *higher* than it is in rectangular fuel assembly having the same *fuel rod pitch* P, or centerline to centerline spacing.

In LMFBRs, this tends to reduce the amount of coolant required by about 20% because the additional coolant is not required to serve as a moderator and create thermal neutrons. As a matter of fact, in fast reactors, most fuel assemblies are also surrounded by metal "cans" to keep the coolant from expanding into other fuel assemblies that may have a lower power rating. This causes the overall composition of a fast reactor core to be considerably different from that of a thermal reactor core. A typical breakdown of the materials by category (fuel, structure, and coolant) for a LMFBR core is summarized in Figure 9.6. In most designs, between 35% and 40% of the core is uranium dioxide fuel, about 1/3 of the core is structural material, and the remainder of the core is occupied by the coolant. Notice that the coolant is not called a moderator in this case because moderation of the fission neutrons is no longer required. Sometimes the uranium dioxide in the fuel rods is replaced by plutonium dioxide as well.

Student Exercise 9.2

Suppose that the fuel assemblies in the same PWR contain control rods, burnable poisons, and additional structural materials that are equal in volume to approximately five times the volume of the cladding above. What is the total percentage of fuel, moderator, and structural materials (including the cladding, the control rods, the burnable poisons, and the other structural materials) in this design?

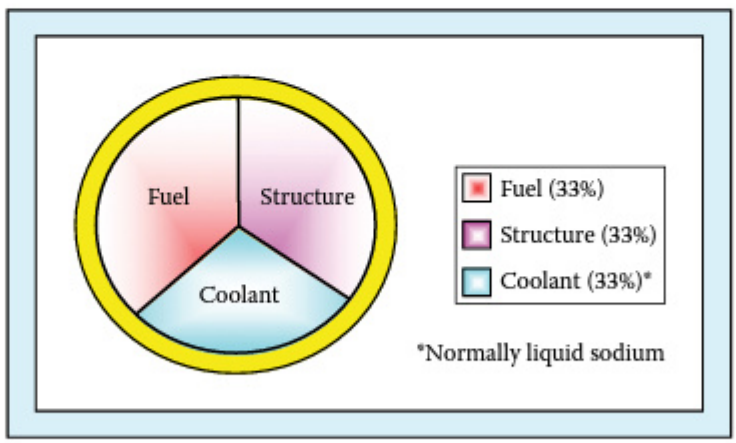

FIGURE 9.6 The core composition of a typical LMFBR with a fuel rod pitch of about 1.5.

9.11 The Infinite Lattice Approximation

Most calculations of the infinite multiplication factor are based on the premise that each fuel assembly is built from an infinite array of identical fuel rods, which in turn implies that all of the surrounding unit cells must be the same. In nuclear science and engineering, this assumption is called *the infinite lattice approximation*. An infinite lattice of identical unit cells is shown in Figure 9.7. The *neutron flux* is also shown within each of these cells. In thermal water reactors, the fast flux tends to peak in the fuel (where the neutrons are born) and the thermal flux tends to peak in the moderator. Normally there are about two fast neutrons for every thermal neutron in a BWR or PWR core. Because the fuel assemblies consist of large arrays of identical unit cells, it is easy to calculate the shape of the power distribution in these geometries because the shape of the neutron flux does not really change from one unit cell to the next. In practice, this assumption turns out to be appropriate as long as the number of fuel rods in a fuel assembly is quite large (say > 100).

For example, a modern PWR fuel assembly is usually designed with about 17 rods per side. This is a total of $17 \times 17 = 289$ slots for the fuel rods and control rods. Consequently, 25 of these slots—or about 8% of the total—are reserved for other purposes such as instrumentation and control. This means that even if a fuel assembly is very large, the moderator to fuel ratio (MFR) can vary by about ±10% depending upon whether the control rods are fully inserted or fully withdrawn. However, as long as we keep this in mind, and a fuel assembly has more than 100 fuel rods, the infinite lattice approximation is a good one. There is no difference in principle between a unit cell in a hexagonal lattice and a unit cell in a square one. In a hexagonal lattice, a unit cell (see Figure 9.5) is simply a hexagon. Irrespective of the shape, there are certain combinations of materials within a unit cell that are more effective in achieving a critical configuration than others. We will be able to quantify these material combinations when we discuss the *4-factor formula* next. As we shall soon see, the four factor formula is one of the most important equations in all of nuclear science and engineering. It has a great deal of both historical and practical significance.

Student Exercise 9.3

Part 1: Suppose that we would like to build a reactor fuel assembly out of nuclear fuel pellets having a diameter of 1 cm with a fuel to cladding gap of 0.5 mm and surrounded by a tube of zirconium cladding having a thickness of approximately 1 mm.

If the fuel rods built from these parts are deployed in a rectangular array with a pitch P (centerline to centerline spacing) of 2 cm, calculate the MFR (thew moderator to fuel ratio), the cladding to fuel ratio, and the unit cell to fuel ratio for this configuration.

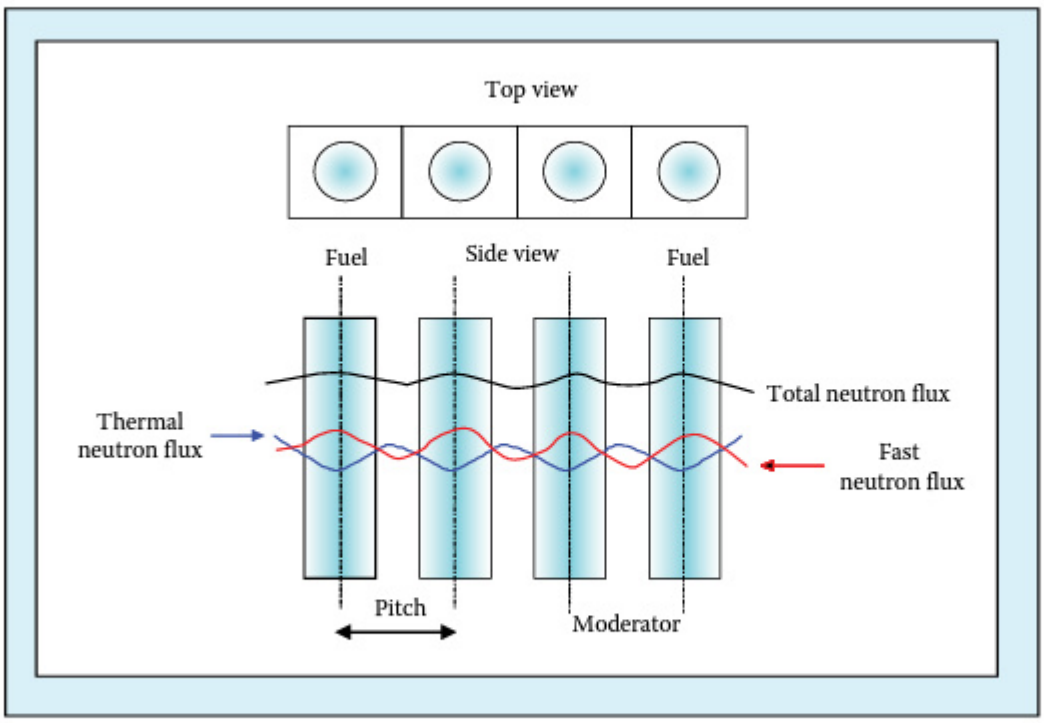

FIGURE 9.7 The neutron population in an infinite lattice of identical fuel rods (or unit cells).

Part 2: Moreover, on a per volume basis, calculate the percentage of the fuel assembly that consists of fuel, moderator, and cladding. You may ignore the presence of the control rods and other structural materials in the assembly when doing your calculations.

Part 3: Repeat your calculations for a similar fuel assembly in which the pitch P has been reduced to 1.75 but all other parameters remain the same. By what percentage has the volume of the fuel increased in this case?

9.12 Four-Factor Formula for an Infinite Reactor Lattice

To begin our discussion of the four-factor formula, we would first like to take a moment to explain how reactors were designed before high-speed computers became commonplace. During the *Second World War*, modern computers were just in their infancy, and the most powerful computers on the planet at the time were *IBM mainframes*, which had about 1/1000th of the processing power of an average smartphone today. The physicists and engineers who were asked to design the first nuclear reactors had to rely on simple analytical methods to get the job done. Realizing the complexity of the task at hand, they devised several simple but elegant methods to determine when an assembly of nuclear materials would become critical and when it would not. Collectively they decided that the best way to approach the problem would be to consider an idealized reactor of infinite size, in which the same basic physical structure of the core was repeated over and over again. In other words, *the first criticality calculations were performed on large reactor lattices consisting of many identical fuel assemblies in which the fuel rods were imbedded in periodic arrays of moderating material or coolant*. Under these conditions, it it could then be assumed that the lattice was large enough to neglect the effects of neutron leakage. In other words, the first criticality experiments were conducted on what was assumed to be an *infinite lattice*. Of course, this assumption was equivalent to assuming that the value of the neutron leakage rate L could be neglected in the calculation of $K_{effective}$ (see Equation 9.15). Hence for an infinite reactor lattice, the value of $K_{effective}$ would be the same as the value of K_∞, and with no loss of generality one can write

$$K_\infty = \nu\left(\frac{\Sigma_{f\infty}}{\Sigma_{a\infty}}\right) \tag{9.36}$$

or

$$\rho = \frac{K_\infty - 1}{K_\infty} \tag{9.37}$$

where

ν is the average number of neutrons released per fission—averaged over all energies and all nuclear materials present
ρ is the corresponding value of the reactivity

The repetitive geometric unit of the lattice that was used to preform these criticality calculations then became a fuel rod surrounded by a layer of moderating material. Eventually this geometric combination of fuel and moderator became known as a *unit cell*, and several examples of representative "unit cells" are shown in Figure 9.8. It should be clear to anyone who is familiar with reactor design that the neutron flux in such an array of unit cells is spatially periodic. That is, if the shape of the flux is known in one cell, then the shape of the neutron flux is known in all unit cells. Thus the ratio of the neutron production rate in the fuel to the neutron absorption rate in the entire cell (no matter how the cell is defined geometrically) should be equal to the value of K_∞ for a lattice consisting of a large number of these identical cells. In other words, for an infinite lattice consisting of identical unit cells

$$K_\infty = \frac{\nu\Sigma_{f\,fuel}}{\Sigma_{a\,cell}} \tag{9.38}$$

or after incorporating the energy dependence of the neutron cross sections back into Equation 9.38, we have

$$K_\infty = \frac{\nu\int \Sigma_f(E)_{fuel}\,\phi(E)_{fuel}\,dE}{\int \Sigma_a(E)_{cell}\,\phi(E)_{cell}\,dE} \times \frac{\int \phi(E)_{cell}\,dE}{\int \phi(E)_{fuel}\,dE} \tag{9.39}$$

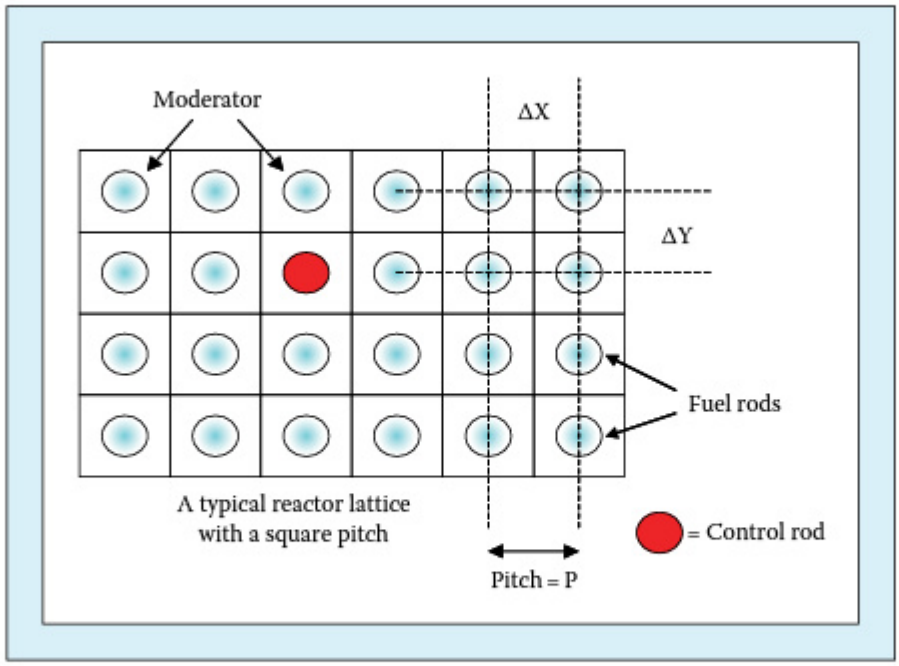

FIGURE 9.8 A simple reactor lattice consisting of an infinite number of unit cells arranged in a square array.

Equation 9.39 can then be thought of as the defining equation for the infinite multiplication factor an infinite reactor lattice. To derive the four-factor formula from this equation, suppose that we write Equation 9.39 in a slightly different form as

$$K_\infty = \frac{\nu \int \Sigma_f(E)_{fuel}\,\phi(E)_{fuel}\,dE}{\int \Sigma_a(E)_{cell}\,\phi(E)_{cell}\,dE} \times \frac{\phi_{cE}}{\phi_{fE}} \tag{9.40}$$

where the limits of the energy integrals are from E = 0 to E = ∞, and the average flux in the fuel and in the cell across all neutron energies are defined by

$$\phi_{fE} = \frac{\int \phi(E)_{fuel}\,dE}{\int dE} \quad \text{(for all neutron energies)} \tag{9.41}$$

$$\phi_{cE} = \frac{\int \phi(E)_{cell}\,dE}{\int dE} \quad \text{(for all neutron energies)} \tag{9.42}$$

and similarly

$$\phi_{fE'} = \frac{\int \phi(E')_{fuel}\,dE'}{\int dE'} \quad \text{(for the energies of thermal neutrons only)} \tag{9.43}$$

$$\phi_{cE'} = \frac{\int \phi(E')_{cell}\,dE'}{\int dE'} \quad \text{(for the energies of thermal neutrons only)} \tag{9.44}$$

Now let us take a minute to consider the implications of Equation 9.40 in more detail. Suppose that we rewrite the right-hand side of Equation 9.40 as the product of the following four terms:

The Origin of the Four-Factor Formula

Expressing the Value of K_∞ as a Function of Four Separate Factors

$$K_\infty = \left(\frac{\nu\int \Sigma_f(E)_{fuel}\,\phi(E)_{fuel}\,dE}{\int \Sigma_a(E)_{cell}\,\phi(E)_{cell}\,dE)}\right)\left(\frac{\phi_{cE}}{\phi_{fE}}\right)$$
$$= (\nu)\left(\frac{\int \Sigma_f(E')_{fuel}\,\phi(E')_{fuel}\,dE'}{\int \Sigma_a(E')_{fuel}\,\phi(E')_{fuel}\,dE'}\right)\left(\frac{\phi_{fE'}}{\phi_{fE'}}\right)\cdot\left(\frac{\int \Sigma_f(E)_{fuel}\,\phi(E)_{fuel}\,dE}{\int \Sigma_f(E')_{fuel}\,\phi(E')_{fuel}\,dE'}\right)\left(\frac{\phi_{fE'}}{\phi_{fE}}\right)$$
$$\cdot\left(\frac{\int \Sigma_a(E')_{fuel}\,\phi(E')_{fuel}\,dE'}{\int \Sigma_a(E')_{cell}\,\phi(E')_{cell}\,dE'}\right)\left(\frac{\phi_{cE'}}{\phi_{fE'}}\right)\cdot\left(\frac{\int \Sigma_a(E')_{cell}\,\phi(E')_{cell}\,dE'}{\int \Sigma_a(E)_{cell}\,\phi(E)_{cell}\,dE}\right)\left(\frac{\phi_{cE}}{\phi_{cE'}}\right) \qquad (9.45)$$

where the limits of integration for the integrals with energy E′ are from E′ = 0 to E′ = E_1 and the limits of integration for the integrals with energy E are from E = 0 to E = ∞. Here, E_1 is the fast to thermal cutoff energy, specifically defined as the energy between the thermal energy region, where up-scattering is important, from the slowing down region, where it is not. Historically, E_1 has been defined to be about 1.0 eV (see Chapter 4).

Each of the four terms or factors in Equation 9.45 then has a simple physical interpretation, and the product of these four terms, or factors, defines what is known as *the four-factor formula*. Thus the four-factor formula represents a simple way to find the value of the infinite multiplication factor K_∞ for an infinite reactor lattice. Because high-speed computers were not available when the first reactors were being designed, simple analytical methods like the four-factor formula were commonly used to predict when a lattice of identical unit cells would first become critical. Historically, the four terms in the four-factor formula (Equation 9.45) were then given the following names and definitions:

Term 1 (The Eta of the Fuel)

$$(\nu)\left(\frac{\int \Sigma_f(E')_{fuel}\,\phi(E')_{fuel}\,dE'}{\int \Sigma_a(E')_{fuel}\,\phi(E')_{fuel}\,dE'}\right)\left(\frac{\phi_{fE'}}{\phi_{fE'}}\right)$$

Term 2 (The Fast Fission Factor)

$$\left(\frac{\int \Sigma_f(E)_{fuel}\,\phi(E)_{fuel}\,dE}{\int \Sigma_f(E')_{fuel}\,\phi(E')_{fuel}\,dE'}\right)\left(\frac{\phi_{fE'}}{\phi_{fE}}\right)$$

Term 3 (The Thermal Utilization)

$$\left(\frac{\int \Sigma_a(E')_{fuel}\,\phi(E')_{fuel}\,dE'}{\int \Sigma_a(E')_{cell}\,\phi(E')_{cell}\,dE'}\right)\left(\frac{\phi_{cE'}}{\phi_{fE'}}\right)$$

Term 4 (The Resonance Escape Probability)

$$\left(\frac{\int \Sigma_a(E')_{cell}\,\phi(E')_{cell}\,dE'}{\int \Sigma_a(E)_{cell}\,\phi(E)_{cell}\,dE}\right)\left(\frac{\phi_{cE}}{\phi_{cE'}}\right)$$

In the next few sections, we would like to explore the meaning of these terms, and discuss their historical significance.

9.13 The First Factor: The Eta of the Fuel

The first of the factors in the four-factor formula (see Equation 9.37) represents the ratio of the rate at which fission neutrons are created by thermal fission in the fuel to the rate that thermal neutrons are absorbed in the fuel. This ratio is simply called the "*eta*" of the fuel and in most reactor physics books, it is given the symbol η. According to Equation 9.37, we can write eta as

The Definition of the Eta of the Fuel (η)

$$\eta = \frac{\int \nu(E')\Sigma_f(E')_{fuel}\,\phi(E')_{fuel}\,dE'}{\int \Sigma_a(E')_{fuel}\,\phi(E')_{fuel}\,dE'} \times \frac{\phi_{fE'}}{\phi_{fE'}} \tag{9.46}$$

where the limits of integration are from E′ = 0 to E′ = 1 eV, and obviously $(\phi_{fE'}/\phi_{fE'}) = 1$. *This implies that the value of eta is a measure of the neutron production rate to the neutron absorption rate in the thermal energy range.* The primary purpose of defining the "eta" of the fuel in this way is that its value can be correlated to the isotopic composition of the fuel. Moreover, because it has only a weak dependence on the neutron energy spectrum, the value of η in any thermal reactor will be a good approximation to the value of eta in any other thermal reactor. Because η *is defined to be the average number of neutrons emitted per thermal neutron absorbed in the fuel*, it is natural to define ν (the average number of neutrons emitted per thermal fission) as

$$\nu = \frac{\int \nu(E')\Sigma_f(E')_{fuel}\,\phi(E')_{fuel}\,dE'}{\Sigma_f(E')_{fuel}\,\phi(E')_{fuel}\,dE'} \times \frac{\phi_{fE'}}{\phi_{fE'}} \tag{9.47}$$

where the denominator is now written in terms of the fission cross section rather than the absorption cross section.

When defined in this way, the fast to the thermal flux ratio $(\phi_{fE'}/\phi_{fE'})$ is still equal to unity and we have replaced n(E′), the number of neutrons emitted *per fission* by η(E′), and the number of neutrons emitted *per neutron absorbed*. As we saw in Chapter 7, there is approximately a 17% chance that when a U-235 nucleus absorbs a thermal neutron, it will *not* split apart, but instead it will emit a gamma ray with an average energy of about 1 MeV. The microscopic cross section for this process is called the "radiative capture" cross section and is it represented by the symbol σ_c. Consequently, the absorption cross section $\Sigma_a(E)$ for U-235 is approximately 20% *larger* than the fission cross section and

$$\Sigma_a(E) = \Sigma_f(E) + \Sigma_c(E) \tag{9.48}$$

So η(E′) in this case is the same as ν(E′) when we were discussing the number of neutrons produced by the fission of a U-235 nucleus, except that η(E′) must be reduced by about 17% to account for the radiative capture. It then follows for any pure material (e.g., a single nuclide) that η and ν are related to each other by

$$\eta = \nu\left(\frac{\sigma_f}{\sigma_a}\right) \tag{9.49}$$

where the constant of proportionality for the thermal energy group (σ_f/σ_a) is called the *fission to absorption ratio* α. According to Equation 9.49, this ratio is always less than unity, and it typically has a value of about 0.8 for most nuclear fuels. So if we decide to define eta as

$$\eta = \frac{\nu(E')\Sigma_f(E')_{fuel}\,\phi(E')_{fuel}\,dE'}{\int \Sigma_a(E')_{fuel}\,\phi(E')_{fuel}\,dE'} \tag{9.50}$$

then we simply need to know the shape of the *Maxwellian flux* ϕ(E′) in the thermal energy range (see Chapter 8) to calculate the values for η (eta) and ν (mu). The reader may recall from Chapter 8 that the value ϕ(E′) for the Maxwellian flux can be written as

$$\phi(E') = P(E')\nu(E') = \sqrt{\left\{\left(\frac{m}{\pi}\right)\left(\frac{2}{kT}\right)^3\right\}} E'^{1/2} e^{-E'/kT} \cdot \nu(E') \tag{9.51}$$

TABLE 9.1
Values of η and ν for Three Fissile Materials Exposed to a Thermal Neutron Flux at Various Ambient Temperatures T

Fuel Temperature (°C)	η for U-233	η for U-235	η for Pu-239	ν for U-233	ν for U-235	ν for Pu-239
20	2.284	2.065	2.035	2.492	2.418	2.871
100	2.288	2.063	1.998	2.496	2.416	2.819
200	2.291	2.060	1.947	2.499	2.414	2.747
400	2.292	2.050	1.860	2.499	2.399	2.624
600	2.292	2.042	1.811	2.499	2.391	2.555
800	2.292	2.037	1.785	2.499	2.385	2.518
1000	2.292	2.033	1.770	2.499	2.380	2.497

Source: Lamarsh, J.R., *Introduction to Nuclear Reactor Theory*, Second Printing, Addison-Wesley Publishing Company, Inc., Reading, MA, 1972.

Note: η is defined as the average number of fission neutrons emitted per neutron absorbed.

where v is the neutron velocity. Since $v(E') = (2E'/m)^{1/2}$,

$$\phi(E') = P(E')v(E') = \sqrt{\left\{\left(\frac{m}{\pi}\right)\left(\frac{2}{kT}\right)^3\right\}}\sqrt{\left(\frac{2}{m}\right)}E'e^{-E'/kT} \tag{9.52}$$

In thermal reactors this value for the neutron flux $\phi(E')$ is used to calculate the value of η. When we perform this calculation for most common nuclear fuels (U-233, U-235, and Pu-239), we obtain the results shown in Table 9.1. Here, the values of η and ν for thermal neutrons can be seen to be a slowly varying function of the absolute temperature of the fuel T. This is because the temperature in the integrals for the Maxwellian flux never fully cancels out in the calculation of η and ν. Therefore both η and ν retain the temperature dependence illustrated in Table 9.1. *η is generally the largest of the four factors in the four-factor formula, and it is the "source" of most of the neutrons that allow* a reactor to become critical. In other words, it is a *neutron production term* having a value between 1.8 and 2.3 for most nuclear fuels.

It can also be inferred from what we have just said that the value of "eta" for U-235 is different than the value of eta for U-233 or Pu-239. Moreover, the value of eta is a function of the enrichment - it is about 1.65 for a Westinghouse pressurized water reactor (PWR) and about 1.33 for a natural uranium-fueled reactor like the Canadian Deuterium Uranium (or CANDU) reactor. Hence the Uranium-238 in the fuel "dilutes" the value of η from the actual values presented in Table 9.1 for "pure" U-233, U-235, and Pu-239 fuel. Thus the value of η becomes smaller as the fuel is burned. For fresh uranium-dioxide fuel, it has a value of about 1.9.

9.14 The Second Factor: The Fast Fission Factor

Now let us consider the second factor in Equation 9.45, which is called *the fast fission factor.* This term is defined as

The Definition of the Fast Fission Factor (ε)

$$\varepsilon = \frac{\int \Sigma_f(E)_{fuel}\,\phi(E)_{fuel}\,dE}{\int \Sigma_f(E')_{fuel}\,\phi(E')_{fuel}\,dE'} \times \left(\frac{\phi_{fE'}}{\phi_{fE}}\right) \tag{9.53}$$

where the limits of integration for the denominator are from E′ = 0 to E′ = 1 eV, the limits of integration for the numerator are from E = 0 to E = ∞, and $(\phi_{fE'}/\phi_{fE})$ is the ratio of the neutron flux in the fuel at thermal energies to the neutron flux in the fuel at all energies. Sometimes the fast fission factor is also called *the epsilon ε of the fuel.*

Physically, the fast fission factor represents the ratio of the neutron production rate at all energies to the neutron production rate at thermal energies (E ≤ 1 eV) alone. The type of fuel affects the value of the fast fission factor the most. For example, changing the enrichment of a fuel rod will change the value of ε. This is because the fission cross section for a U-235/U-238 mixture is a function of the enrichment (see Appendix C), and for pure U-235, its value is about 1.08. The fast fission factor is also affected by how the fuel and the moderator are distributed in the cell. If the fuel and the moderator are combined into a homogeneous mixture, then the fast fission factor will almost always be equal to 1.00. However, if the fuel and the moderator are physically separated from one another by putting the fuel into fuel rods and the coolant into the coolant channels, the fast fission factor will be much larger.

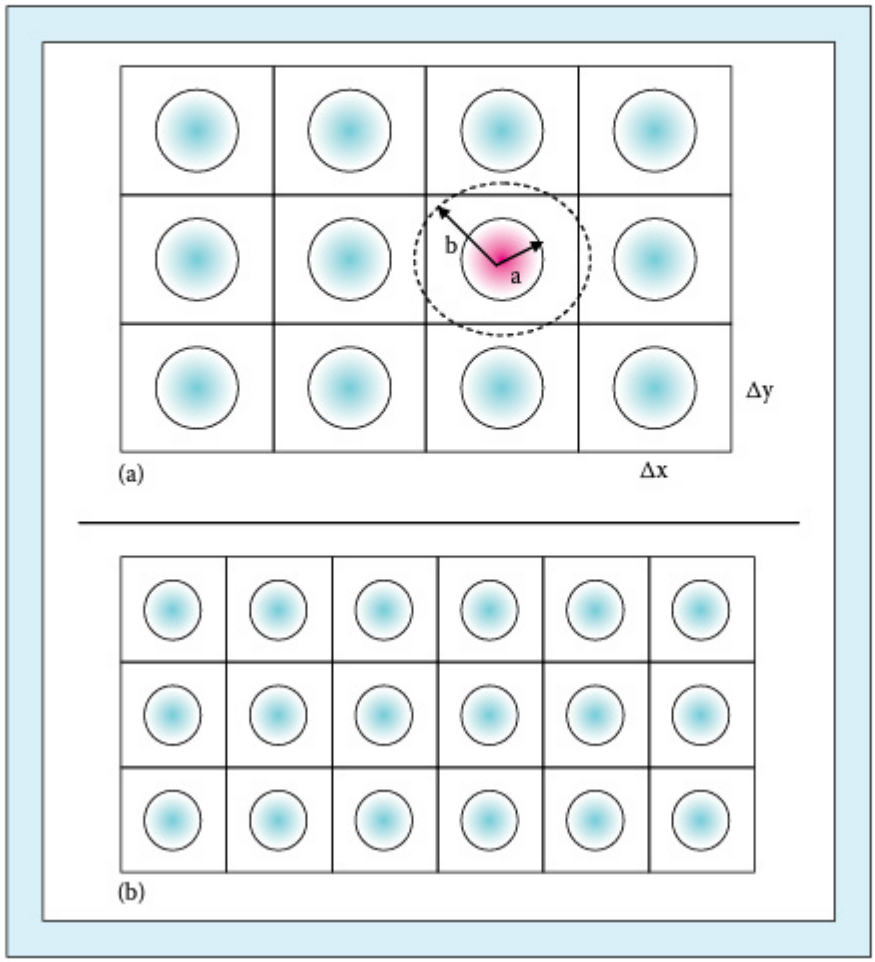

FIGURE 9.9 The fast fission factor is always somewhat higher for thicker fuel rods (a) than for thinner fuel rods (b) that have exactly the same enrichment.

Thus *the value of the fast fission factor is always higher for a heterogeneous mixture of fuel and moderating material than it is for a homogeneous one*. Thus the fast fission factor is a function of the diameter of the fuel rods one chooses to use. Hence a fuel assembly with very large fuel rods, such as that shown on the top of Figure 9.9a, will have a larger fast fission factor than a fuel assembly with smaller fuel rods such as those shown on the bottom of Figure 9.9b. After the geometry of the fuel rods is determined, the fast fission factor is relatively insensitive to the way that the fuel rods are distributed through the core. In uranium-fueled light water reactors, values for ε range from about 1.02 to 1.08. If the fuel and the moderator are physically lumped together to create a fuel assembly, an average value of the fast fission factor for a light water reactor with an enrichment of 3% to 4% is about 1.03.

9.15 The Third Factor: The Thermal Utilization

The third factor in the four-factor formula is called the thermal utilization of the fuel, and the thermal utilization is usually given the symbol f. The thermal utilization is the probability that a thermal neutron will be absorbed in the fuel. The formal definition of the thermal utilization is

The Definition of the Thermal Utilization (f)

$$f = \frac{\int \Sigma_a(E')_{fuel}\,\phi(E')_{fuel}\,dE'}{\int \Sigma_a(E')_{cell}\,\phi(E')_{cell}\,dE'} \times \frac{\phi_{cE'}}{\phi_{fE'}} \tag{9.54}$$

where the limits of integration of both integrals are from $E' = 0$ to $E' = 1$ eV, and $(\phi_{cE'}/\phi_{fE'})$ is the ratio of the neutron flux in the cell to the neutron flux in the fuel at thermal energies. *Of all of the factors in the 4-factor formula, the thermal*

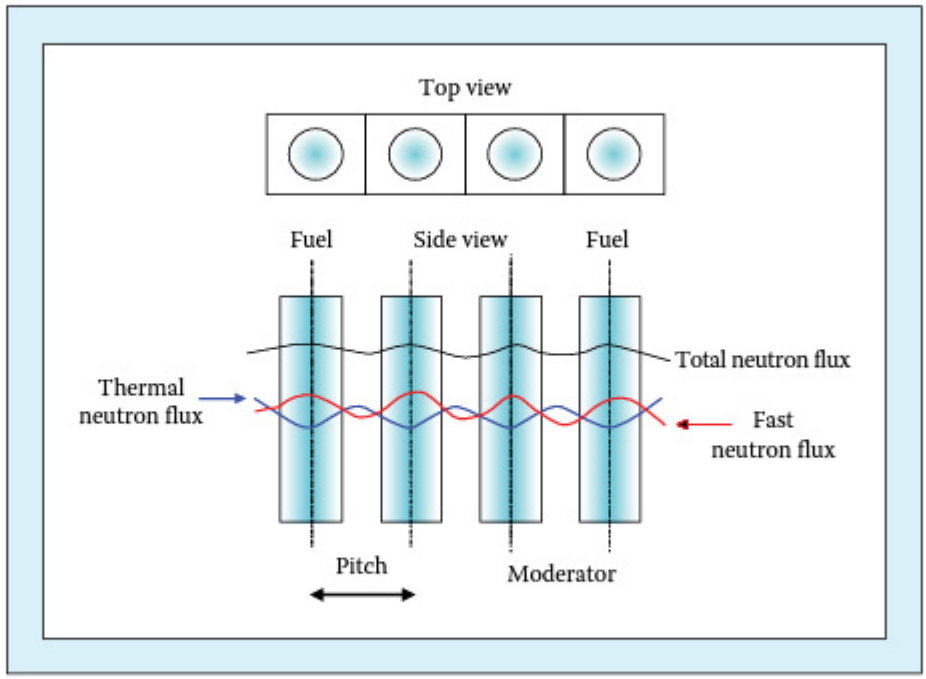

FIGURE 9.10 The neutron flux in and around an array of nuclear fuel rods.

utilization is the one that is most sensitive to the spatial shape of the neutron flux. In general, the average thermal flux is always *lower* in the center of a fuel rod than it is in the surrounding coolant or moderator because the absorption cross section of the fuel is many times larger. The flux also assumes a periodic, or predictable, shape if a fuel assembly consists of regular arrays of unit cells.The shape for a representative PWR fuel assembly is shown in Figure 9.10.

The pitch P of the reactor lattice, which is the centerline to centerline spacing between adjacent fuel rods, determines the periodicity of the flux, and again its shape is very similar to that shown in Figure 9.10. In other words, the ratio of the thermal flux in the fuel and to the thermal flux in the rest of the cell matters. For this reason, measurements of the thermal utilization are usually made for a specific pitch to diameter ration (P/D) when a value of K_∞ is required for a lattice with that ratio. Values of the thermal utilization range from a low of about 0.90 for a thermal water reactor to a high of about 0.95 for a natural uranium reactor. In practice, it is important to keep the value of the thermal utilization as large as possible to sustain a nuclear chain reaction. *Without the use of high-speed computers, it is not possible to obtain an exact value for f in most reactor unit cells.* However, it is possible to develop an analytical approximation for its value by replacing one of the square or rectangular cells shown in Figure 9.11 with an equivalent cylindrical cell having an identical internal volume. As long as the array of unit cells is infinitely long in both directions, and the radius of the fuel rod is much less than the radius of the cell, a reasonably accurate value for *f* can be found. To determine the radius of the equivalent cylindrical cell, r, we simply equate the areas, where the area of the square cell is determined by the pitch of the lattice in the x and y directions, for example, $A = \Delta x \Delta y$, and solve for r, where

The Radius of an Equivalent Unit Cell

$$\pi r^2 = \Delta x \Delta y$$

or

$$r = \sqrt{(\Delta x \Delta y / \pi)} \tag{9.55}$$

The rate at which the neutrons are absorbed in various regions of the cell are then calculated in the equivalent cylindrical cell using a method called the *Wigner-Seitz* method, in which "a" is defined as the radius of the fuel rod and "b" is defined as the radius of the equivalent cylindrical cell. The equations for the thermal utilization turn out to be a set of *Bessel functions* of the first kind, and the absorption rate in both the fuel and moderator can be calculated as a function of r. We will not present a detailed derivation of these functions except to say that this was how the value of the thermal utilization was calculated before the neutron diffusion equation could be solved numerically. If the Wigner–Seitz method is

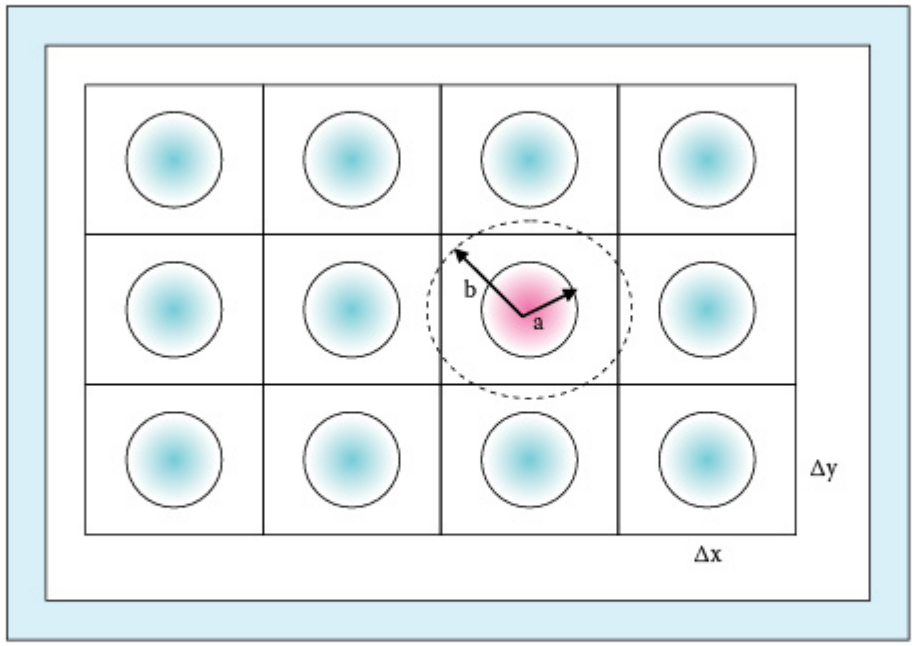

FIGURE 9.11 The conversion of a square fuel cell to an equivalent cylindrical one. The dashed lines show the equivalent cylindrical cell.

applied to a lattice of natural uranium fuel rods imbedded in a graphite moderator with an average pitch of about 10 inches (25 cm), and with an average fuel rod diameter of about 0.8 inches (2 cm), the Wigner–Seitz method predicts a value for f of about 0.83. This happens to be very close to the actual value that is found by solving the neutron diffusion equation directly. Thus the thermal utilization is very sensitive to the geometry of the lattice, but it is not particularly sensitive to the material composition of the fuel.

Other factors like the spacing of the fuel rods, the pitch of the lattice, and the moderator to fuel ratio also have a significant effect on the value of *f*. *The highest value of the thermal utilization is always obtained by mixing the fuel and the moderator together. In other words, the value of f is largest when the fuel and the moderator become a homogeneous mixture.* Unfortunately, this does not optimize the value of K_∞ when the effects of resonance capture and reactor heat removal are taken into account.

Example Problem 9.3

Find the thermal utilization for a homogeneous thermal reactor that has a value of $\Sigma_u = 0.16\ \text{cm}^{-1}$ for the fuel and a value of $\Sigma_a = 0.020\ \text{cm}^{-1}$ for the moderator. Assume that the reactor is designed so that each fuel assembly has a moderator to fuel ratio (the volume of the moderator V_m to the volume of the fuel V_f) of 2:1.

Solution The thermal utilization factor is defined as the number of neutrons absorbed by the fuel to the number absorbed by the fuel and the moderator. Since $V_m = 2V_f$, we have $f = 0.16V_f/(0.16V_f + 0.02V_m) = 0.16V_f/(0.16V_f + 0.04V_f) = 0.16/0.20 = 0.80$. So the thermal utilization factor in this case is 0.80 = 80%. [Ans.]

Student Exercise 9.4

Suppose that we want to modify the design of the reactor in the previous example by changing the moderator to fuel ratio to 1 to 1—so there is now less moderator and more fuel. If all other factors remain the same, what is the thermal utilization of the fuel in this case?

9.16 The Fourth Factor: The Resonance Escape Probability

The fourth and final factor in the four-factor formula is the *resonance escape probability p*. In some books, the resonance escape probability is italicized, and in other books, it is not. As the name implies, *the resonance escape probability is the percentage of the neutrons that are able to slow down from fast energies to thermal energies without being absorbed*

in the absorption resonances in the fuel above the thermal energy range. Hence, the resonance escape probability is the probability that a neutron will escape capture at energies just above thermal. The resonance escape probability p is defined by the equation

The Definition of the Resonance Escape Probability (p)

$$p = \frac{\int \Sigma_a(E')_{cell}\,\phi(E')_{cell}\,dE'}{\int \Sigma_a(E)_{cell}\,\phi(E)_{cell}\,dE} \times \frac{\phi_{cE}}{\phi_{cE'}} \tag{9.56}$$

where the limits of integration in the numerator are from $E' = 0$ to $E' = 1$ eV, the limits of integration in the denominator are from $E = 0$ to $E = \infty$, and $(\phi_{cE}/\phi_{cE'})$ is the ratio of the flux in the cell at all energies to the flux in the cell at thermal energies alone. Values of the resonance escape probability range from a low of about 0.87 in a modern PWR to a high of about 0.95 for a natural uranium-fueled reactor (such as the Canadian CANDU reactor). It is hard to calculate the resonance escape probability in a heterogeneous reactor lattice because the neutron density dips significantly in both position and energy in the vicinity of the absorption resonances. However, for relatively homogeneous geometries, analytical methods can be developed for calculating its value.

Unfortunately, a detailed discussion of these methods is beyond the scope of this book. The approximate form of the analytical expressions these methods use for a spatially homogeneous medium is

$$p = A\,e^{-\Sigma_i I_j/B} \tag{9.57}$$

where A and B are experimentally determined constants, and the summation $\sum_i$ in the exponent is over all resonance integrals for all isotopes from $j = 1$ to $j = J$ and for all resonances within a given isotope j from $i = 1$ to $i = N$. The tabulated values for these resonance integrals can be found in many data repositories. For example, values of these integrals can be found at *www.nndc.bnl.gov* and *http://www-nds.iaea.org/*. There is, however, an alternative way to calculate the resonance escape probability that avoids the need to sum over all of the individual absorption resonances independently. This method lumps most of the physics into the macroscopic scattering cross section for the moderator at resonance energies and introduces a new parameter into the equations called the *resonance integral* I. The resonance integral I has been measured experimentally in different reactor geometries, and it is usually tabulated for cylindrical fuel rods having different radii. It is also a function of the density of the fuel ρ, and the particular moderating material that is used. The general form of an empirical expression for the resonance integral is

An Empirical Expression for the Resonance Integral

$$I = \frac{C1 + C2}{\sqrt{r\rho}} \tag{9.58}$$

where

C1 and C2 are constants to be determined experimentally
ρ is the density of the fuel

If N_{fuel} is the atomic density of the fuel, V_{fuel} is the volume of the fuel, V_{mod} is the volume of the moderator, Σ_s^{mod} is the macroscopic cross section of the moderator at resonance energies, and L_{mod} is the *neutron lethargy* for the moderator (see Chapter 8), then the resonance escape probability p can be written as

A General Expression for the Resonance Escape Probability

$$p = e^{-IQ} \tag{9.59}$$

where the quantity Q (not to be confused with the value of A in Equation 9.57) is now

$$Q = \frac{N_{fuel} V_{fuel}}{\left(V_{mod} \Sigma_s^{mod} L_{mod}\right)} \tag{9.60}$$

Here the resonance integral I has the dimensions of barns, where 1 barn = 1×10^{-24} cm^2. Therefore, N_{fuel}, which is the atomic density of the fuel, must also have the units of 10^{24}/cm^3. We can simplify this expression a bit by introducing an

TABLE 9.2
Constants for Calculating the Resonance Escape Probability for Different Nuclear Fuels

Fuel Type	Chemical Symbol	Density (g/cm^3)	C1	C2
Uranium dioxide	UO_2	10.0	30.0	39.6
Thorium dioxide	ThO_2	10.0	30.4	24.5
U (metallic)	U-238	19.1	20.8	38.3
Th (metallic)	Th-232	11.7	30.9	20.9

TABLE 9.3
Constants for Calculating the Resonance Escape Probability for Different Moderators

Moderator	Chemical Symbol	σ_s (cm^2)	L_{mod}	$\sigma_s L_{mod}$
Light water	H_2O	5.60×10^{-23}	00.920	5.15×10^{-23}
Heavy water	D_2O	2.60×10^{-23}	00.509	1.32×10^{-23}
Beryllium	Be	6.14×10^{-24}	00.209	1.28×10^{-24}
Graphite	C	4.75×10^{-24}	00.158	7.50×10^{-25}

another quantity into the equations called the *moderator to fuel ratio*, or *MFR*, that we will study in great detail in Chapter 10. For a unit cell similar to the ones shown in Figure 9.11, the moderator to fuel ratio is simply the ratio of the volume of the moderator V_{mod} to the volume of the fuel V_{fuel}:

The Moderator to Fuel Ratio (MFR)

$$MFR = \frac{V_{mod}}{V_{fuel}} \tag{9.61}$$

The expression for the empirical constant Q then becomes

$$Q = \frac{N_{fuel}}{N_{mod}} \left[\frac{\sigma_s^{mod} L_{mod}}{MFR} \right] \tag{9.62}$$

Table 9.2 shows some representative values of C1 and C2 for different types of fuels, and Table 9.3 shows the values of σ_s^{mod}, L_{mod}, and σ_s^{mod} for different types of moderators. Knowing the pitch of the reactor lattice (from which the moderator to fuel ratio can be deduced), the radius of the fuel rods r, the composition of the fuel, and the type of moderator used, it is possible to use Equation 9.54 to calculate the resonance escape probability. The values presented in Table 9.2 can also be used for fuel rods containing slightly enriched uranium because the presence of small amounts of U-235 or U-233 in the fuel do not significantly alter the amount of resonance absorption in Uranium-238. It also does not matter if U-235 or U-233 is mixed with Thorium instead of U-238 in this case because the absorption resonances in Th-232 still control the overall resonance absorption rate.

Generally speaking, the fuel rod radius r must be given in cm, and the density of the fuel ρ must be given in grams/cm^3. In particular, the resonances that are responsible for this resonance capture are shown in Figure 9.12 for neutron energies between 0 and 5 eV. The U-238 resonances are shown in red, and the Thorium-232 resonances are shown in green. *Notice that the U-238 resonances have a spacing of about 1.5 eV, and they are almost 10,000 barns high! Because they are very large, they completely dominate the behavior of p above the thermal energy range.*

Example Problem 9.4

Suppose that you decide to build a fuel assembly for a thermal water reactor with a moderator to fuel ratio of 4. If the fuel rods are made out of pure uranium metal and have a diameter of 2 cm, what is the value of the resonance integral I and what is the value of the resonance escape probability p if the fuel rods are to be cooled and moderated by light water (H_2O)? Assume the geometry of the fuel assembly is square.

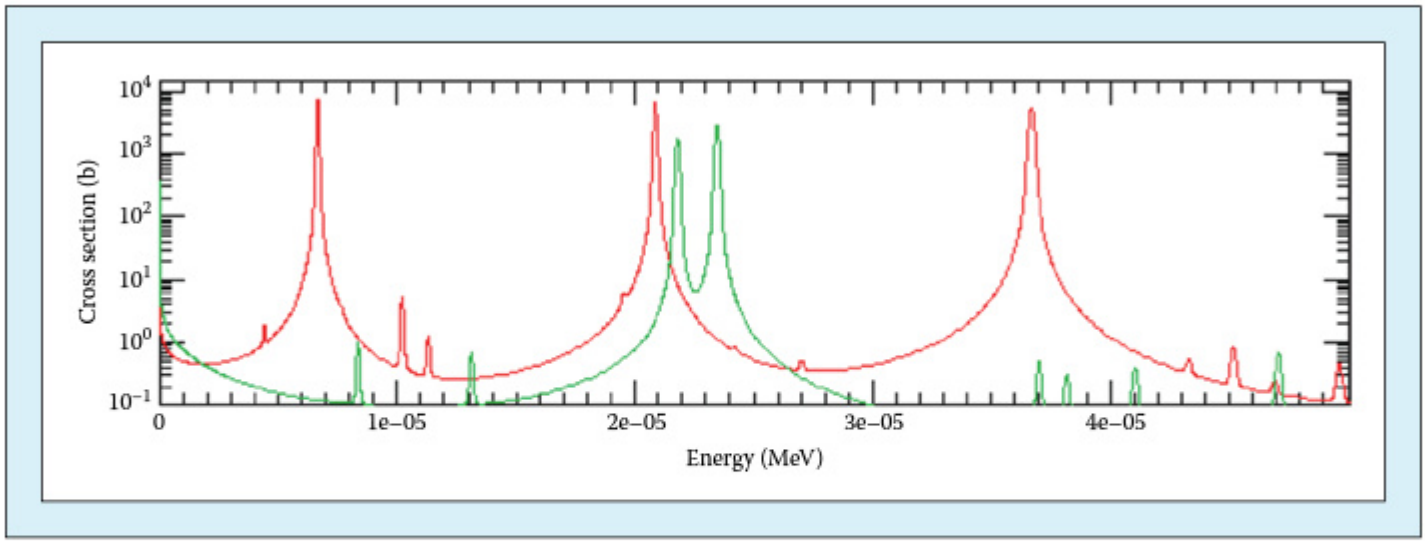

FIGURE 9.12 The absorption resonances for U-238 (in red) and Thorium-232 (in green) that dominate the value of resonance escape probability P just above the thermal energy range. (Picture generated by ENDFPLOT—see Chapter 4.)

Solution The resonance integral I is given by $= C_1 + C_2/\sqrt{r\rho}$, so for a radius of 1 cm and a density (from Table 9.2) for the fuel of $\rho = 19.1$ g/cm^4, $I = 2.8 + 38.3/\sqrt{19.1} = 8.76$ barns $= 8.76 \times 10^{-24}$ cm^3. The empirical constant A is given by $A = N_{fuel}/N_{fuel}\ [\sigma_s^{mod}\ L_{mod}/MFR]$. From the values in Tables 9.2 and 9.3 we obtain $A = (0.0483/0.0334) \times 5.15 \times 10^{-23}/4 = 1.70 \times 10^{-23}$ cm^3. The resonance escape probability $p = e^{-IA}$ is therefore $p = e^{-(0.147)} = 86.3\%$. This value is quite typical for a thermal water reactor where the lattice has this pitch. [Ans.]

9.17 Effects of Resonance Self-Shielding on the Resonance Escape Probability

When scientists first tried to use the four-factor formula to find the value of K_∞ in an actual reactor lattice, they found that mixing the fuel and the moderator together caused the resonance escape probability to fall to about 70%. This was because mixing the fuel and moderator together actually *increased* the probability that a fission neutron would be absorbed. *So even though this caused the thermal utilization of the fuel to increase, it did NOT optimize the product of the thermal utilization and the resonance escape probability, which effectively determines the size of K_∞ for a reactor core.*

No matter how hard they tried, they found that it was nearly impossible to create an infinite multiplication factor greater than 1.0 for a homogeneous natural uranium-fueled reactor. Eventually they discovered that this was due to an important effect that is called *resonance self-shielding* today. *Eventually they discovered that only way to achieve a value of $K_\infty \geq 1.0$ for a reactor fueled with natural uranium was to lump the fuel and the moderator into separate regions of the core to reduce the effects of resonance self-shielding*. That is, they were able to *increase* the value of the resonance escape probability by separating the fuel from the moderator, and this became the reason why most nuclear reactors employ heterogeneous fuel assemblies today. Today, modern reactors can achieve a resonance escape probability p between 0.75 and 0.85, and for many fuel assemblies, the thermal utilization can also be designed to have a comparable value. *Thus the importance of physically separating the fuel from the moderator was one of the major historical insights gained from the four-factor formula*. Its application eventually steered engineers toward the highly optimized reactor fuel assemblies that are used today. *Thus, it is the product of f and p that determines how large the neutron multiplication factor can become, and the other factors in the four-factor formula (the eta of the fuel and the fast fission factor) are used primarily to generate the fission neutrons that p and f then act upon. Hence, in the early stages of a reactor design, most designers attempt to make the product of the resonance escape probability and the thermal utilization as large as possible. In Chapter 10, we will present some practical examples of how this can be done.*

Student Exercise 9.5

Explain how you would optimize the effective multiplication factor for a large water reactor by changing the pitch to diameter ratio of the lattice. What set of parameters associated with the pitch to diameter ratio would you attempt to collectively optimize?

9.18 Classical Form of the Four-Factor Formula

In this section, we would like to summarize what we have learned about the four-factor formula so far. Earlier we found that the expression

An Expression for the Infinite Multiplication Factor

$$K_\infty = \nu\left(\frac{\int \Sigma_f(E)_{fuel}\,\phi(E)_{fuel}\,dE}{\int \Sigma_a(E)_{call}\,\phi(E)_{cell}\,dE}\right)\left(\frac{\phi_{cE}}{\phi_{fE}}\right)$$

$$= (\nu)\left(\frac{\int \Sigma_f(E')_{fuel}\,\phi(E')_{fuel}\,dE'}{\int \Sigma_a(E')_{fuel}\,\phi(E')_{fuel}\,dE'}\right)\cdot\left(\frac{\phi_{fE'}}{\phi_{fE'}}\right)\left(\frac{\int \Sigma_f(E)_{fuel}\,\phi(E)_{fuel}\,dE}{\int \Sigma_f(E')_{fuel}\,\phi(E')_{fuel}\,dE'}\right)\left(\frac{\phi_{fE'}}{\phi_{fE}}\right)$$

$$\cdot\left(\frac{\int \Sigma_a(E')_{fuel}\,\phi(E')_{fuel}\,dE'}{\int \Sigma_a(E')_{cell}\,\phi(E')_{cell}\,dE'}\right)\cdot\left(\frac{\phi_{cE'}}{\phi_{fE'}}\right)\left(\frac{\int \Sigma_a(E')_{cell}\,\phi(E')_{cell}\,dE'}{\int \Sigma_a(E)_{cell}\,\phi(E)_{cell}\,dE}\right)\left(\frac{\phi_{cE}}{\phi_{cE'}}\right) \qquad (9.63)$$

for the infinite multiplication factor could be written as the product of four terms or factors that are referred to today as

1. The neutron reproduction factor η (eta)
2. The fast fission factor of the fuel ε (epsilon)
3. The thermal utilization of the fuel *f*
4. The resonance escape probability *p*

Each of these factors can be determined analytically or experimentally for an infinite lattice. They can then be multiplied together to find the infinite multiplication factor K_∞ for that particular lattice. Thus the four-factor formula can be used to predict how close certain repetitive lattice configurations are to achieving a critical mass. Using the aforementioned definitions, the four-factor formula can be written as

The Classic Form of the Four-Factor Formula

$$K_\infty = \eta\varepsilon f p \qquad (9.64)$$

This form of the formula can be found in many reactor physics books, and it is a very simple way to find the infinite multiplication factor for a large, repetitive lattice. Representative values of these factors are discussed in the next section.

9.19 Representative Values of the Four Factors for a Reactor Lattice

To find the value of K_∞ for a large repetitive lattice, one simply measures the values of η, ε, *f*, and *p* for a number of representative configurations based on the type of fuel that is used and the pitch to diameter ratio (P/D) of the lattice, and then multiplies these values together to find an initial estimate for K_∞. Representative values of each of these factors are presented in Table 9.4. *The values in Table 9.4. are only applicable to fresh fuel rods*. When fission products and other neutron poisons begin to build up in the fuel, then the values of some of the factors such as η and *f* become smaller, while the values of some of the other factors such as the resonance escape probability become larger. In this case, the values discussed in future chapters should be used to determine whether or not a reactor lattice has achieved a critical configuration.

9.20 Understanding the Neutron Life Cycle in a CANDU Reactor Unit Cell

Sometimes the four-factor formula can be used to perform a *neutron balance* calculation to understand how the neutron population behaves under steady state conditions; that is, when $K_\infty = 1.0$. If there is no neutron leakage, the four-factor formula can be used to construct a neutron life cycle diagram similar to the one shown in Figure 9.13. This particular diagram is used to describe the neutron life cycle in a Canadian CANDU reactor fueled with natural uranium. The neutrons produced in the fuel escape from the fuel rods and are moderated by the heavy water which surrounds the rods. The water flowing over the rods also serves as the coolant.

TABLE 9.4
Representative Values for the Terms in the Four-Factor Formula for Thermal Water Reactors

Factor Name	PWR (Typical)	BWR (Typical)	CANDU Reactor (Typical)
η	1.89	1.89	1.25
ε	1.08	1.08	1.03
f	0.94	0.93	0.94
p	0.74	0.74	0.91
K_∞	1.41	1.40	1.09

Source: Values provided by the Argonne National Laboratory.

Note: These values pertain to fresh fuel only; that is, fuel containing no neutron poisons. They also neglect the presence of other neutron absorbing materials such as control rods, burnable poisons, and chemical shim.

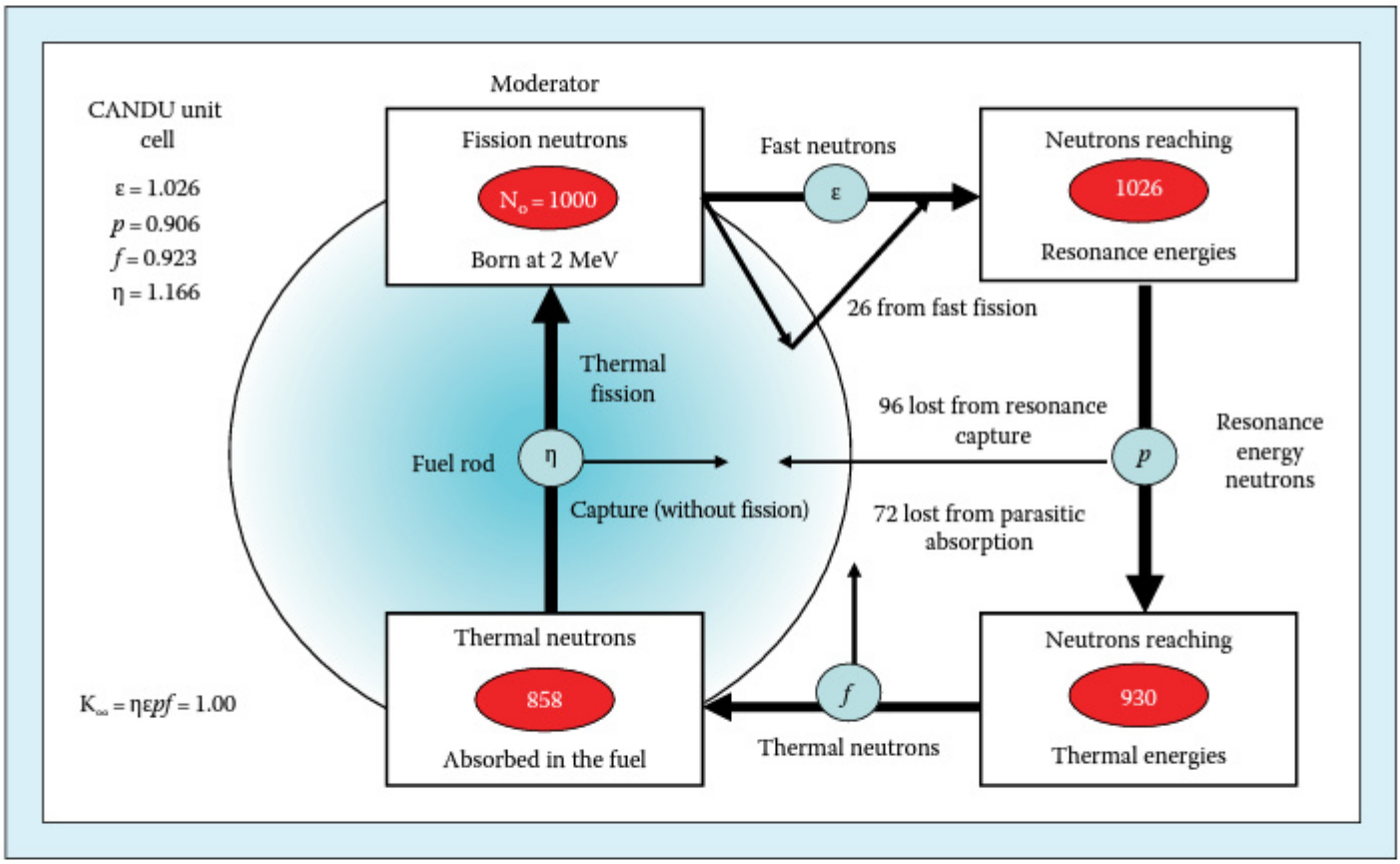

FIGURE 9.13 The life cycle of 1000 neutrons in a CANDU reactor unit cell. (Adapted from *https://canteach.candu.org/Content%20Library/20030101.pdf*.)

If 1000 neutrons are produced from the thermal fission of U-235, 1026 fission neutrons are actually produced in the fuel because the fast fission factor is $\varepsilon = 1.026$. Since the coolant does not boil, the fast fission factor does not change significantly during normal reactor operation.

Now let us see if we can determine the value of the resonance escape probability for this reactor. The capture of neutrons in the U-238 absorption resonances (see Figure 9.12) accounts for the largest neutron loss rate in the core. Collisions with the heavy water molecules slow down any neutrons that enter the coolant. These neutrons are not immune to resonance capture because they can diffuse back into the fuel before the thermalization process is complete. The resonance escape probability is then the probability that a fission neutron will escape capture in one of these absorption resonances.

From the neutron balance shown in Figure 9.13, the resonance escape probability is found to be 90.6%, so the number of neutrons that actually become thermal neutrons is 0.906 × 1026 = 930. The resonance escape probability is optimized in this type of reactor by separating the fuel atoms from the moderator atoms (see the discussion of resonance "self-shielding" in Section 9.17).

The neutrons that escape the U-238 resonances become thermal neutrons that are more easily absorbed by the fuel. The ratio of the number of thermal neutrons that are absorbed by the fuel to the number of thermal neutrons that are absorbed by the fuel and by everything else then becomes the *thermal utilization factor f* for the fuel. Strictly speaking, the value of *f* depends on the flux shape $\phi(x, y)$ because

$$f = \frac{\phi_{\text{fuel}}\Sigma_{\text{a fuel}}}{\phi_{\text{fuel}}\Sigma_{\text{a fuel}} + \phi_{\text{non-fuel}}\Sigma_{\text{a non-fuel}}} \tag{9.65}$$

However, if we do not know the shape of the flux we can assume that $\phi_{\text{fuel}} = \phi_{\text{non-fuel}}$ to simplify our analysis. This allows us to cancel the neutron flux in the numerator and the denominator, and the equation for the thermal utilization becomes

$$f = \frac{\Sigma_{\text{a fuel}}}{\Sigma_{\text{a fuel}} + \Sigma_{\text{a non-fuel}}} \tag{9.66}$$

From the numbers shown in Figure 9.13, the thermal utilization is then *f* = 92.3%, and the number of thermal neutrons absorbed by the fuel is 0.923 × 930 = 858.

Finally, if 858 thermal neutrons are absorbed by the fuel, many (but not all) of these neutrons are absorbed by the U-235 atoms. This absorption causes additional fission neutrons to be produced. Now let us assume that the value of η (the neutron reproduction factor) for a hypothetical unit cell in this lattice is η = 1.166. Using this value for eta, the number of fission neutrons that are created to start the next neutron reproductive cycle is N = 858 × 1.166 = 1000. Thus, the neutron life cycle repeats itself, and the reactor remains critical as long as the number of neutrons created is equal to the number of neutrons destroyed. In practice, the value of η required for a CANDU reactor to achieve criticality is about 1.2, and for a Westinghouse PWR it can be even higher. This offsets the effects of neutron leakage on the multiplication factor, which we will expound upon in Chapter 10.

9.21 Understanding the Neutron Life Cycle in a Westinghouse PWR Unit Cell

It is interesting to compare the neutron lifecycle in a Westinghouse PWR to the neutron lifecycle in a CANDU PHWR. The neutron life cycle is somewhat different in this case because the enrichment of the fuel is higher (about 4.5% vs. 0.072%) and because light water (H_2O) rather than heavy water (D_2O) is used as the moderator. Light water absorbs more thermal neutrons than heavy water does (about a factor of 500 more when the flux becomes Maxwellian), and therefore the value of η must be higher to account for this additional parasitic absorption. When representative values for the fast fission factor ε, the thermal utilization *f*, and the resonance escape probability *p* are used, we find that a unit cell with no neutron leakage requires a neutron reproduction factor η of about 1.33 to become critical. If we start again with 1000 neutrons in a fuel rod, 1080 fast neutrons will reach the resonance energy range, and 800 of these will escape the absorption resonances entirely. The thermal utilization for the fuel is similar to that for the CANDU reactor, so 762 neutrons will reach the fuel rods and become thermal neutrons again. The neutron life cycle is shown in Figure 9.14. Notice that the flow of neutrons is essentially the same as it is in a CANDU PHWR. Only the actual values at each step in the process are different. Normally the value of η for a fresh PWR core is about 1.90. This is due primarily to the higher enrichment of the fuel. If the fuel were even more highly enriched (say 95% as it is in some military reactors), then the value of η would be closer to 2.0. In fact, for pure U-235, the neutron reproduction factor becomes η = 2.068 (see Chapter 7).

Example Problem 9.5

Suppose that a representative unit cell in a thermal water reactor has a fast fission factor of 1.06, a resonance escape probability of 0.74, a thermal utilization factor of 0.94, and a neutron reproduction factor of 1.88. Neglecting the effects of neutron leakage, what is the infinite multiplication factor for this unit cell? What sort of reactor would most likely contain a unit cell of this type?

Solution To answer this question, we must use the four-factor formula $K_\infty = \eta\varepsilon fp$ with the values provided. When we do so, we find that $K_\infty = 1.88 \times 1.06 \times 0.94 \times 0.74 = 1.38$. Based on the characteristics of this unit cell, the reactor is most likely to be a PWR or a BWR. [Ans].

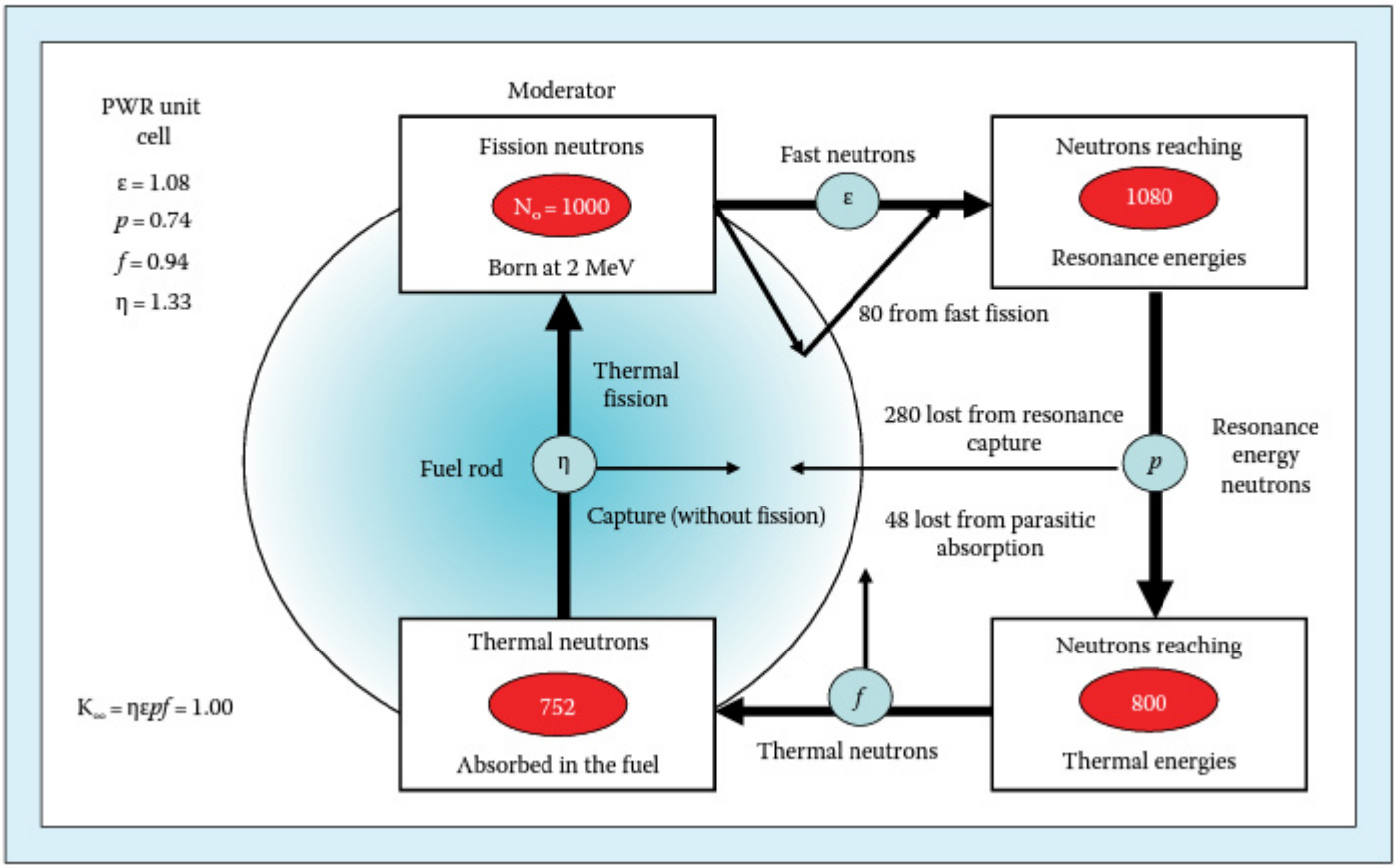

FIGURE 9.14 The life cycle of 1000 neutron in a Westinghouse PWR unit cell.

9.22 Understanding the Behavior of the Neutron Population in a Typical Reactor Unit Cell

Now let us reflect upon what we just learned. In our previous discussion of the neutron life cycle, we began with a neutron population of neutrons (N_o = 1000) in a representative unit cell. The total number of neutrons N_1 that there were in the unit cell at the end of one neutron life cycle was

$$N_1 = \eta\varepsilon f p N_o \tag{9.67}$$

Since we defined $K_\infty = \eta\varepsilon fp$, we could also write the number of prompt neutrons after one life cycle as

$$N_1 = K_\infty N_o \tag{9.68}$$

After two life cycles, the number of prompt neutrons becomes

$$N_2 = K_\infty N_1 = K_\infty \times K_\infty N_o \tag{9.69}$$

and after three life cycles, the number is

$$N_3 = K_\infty N_2 = K_\infty \times K_\infty \times K_\infty N_o \tag{9.70}$$

and so on. Obviously, the number of prompt neutrons after N cycles can be represented by

The Neutron Population after N Reproductive Cycles

$$N_N = (K_\infty)^N \times N_o \tag{9.71}$$

Notice that if $K_\infty = 1.0$, the neutron population remains stable, and the number of neutrons stays the same from one reproductive cycle to cycle. However, if $K_\infty \neq 1.0$, the neutron population will either increase or decrease *exponentially* with time (see Figure 9.3), and the power level P will increase or decrease with the number of neutrons as well. In other words, *the power production rate is very sensitive to the value of* K_∞. Next, if the value of K_∞ is slightly greater than 1.0, the power level and the neutron population will *increase* very quickly. Conversely, if the value of K_∞ is slightly less than 1.0, the power level and the neutron population will *decrease* very quickly. This change in the power level is normally *exponential* in nature, and in the absence of delayed neutrons and temperature feedback effects (which we will discuss in Chapters 15 and 16), the power level can increase or decrease by a factor of 1000 or more in a very short period of time. Hence we can see from Equation 9.71 that any value of K_∞ other than unity will immediately cause the prompt neutron population to rise or fall.

9.23 How the Factors in the Four-Factor Formula Are Affected by Burnup

To understand how each of the factors in the four-factor formula change with time, consider what happens to a unit cell in a CANDU reactor when the fuel is burned. Because the CANDU reactor is moderated by heavy water (D_2O) and fueled with natural uranium, its reactivity swing is much less than that of a conventional PWR. Practically speaking, this limits the burnup of the fuel to between 6000 and 8000 MWD/Ton. (At higher burnups the multiplication factor falls below unity, and the reactor becomes subcritical). Representative values for each of the four factors are shown in Table 9.4 for a fresh CANDU reactor core. Now let us consider how they behave when the fuel is burned.

The fast fission factor ε has an initial value of about 1.03 and the resonance escape probability has an initial value of about 0.91. The values of these parameters change very little (less than one part per thousand) as the uranium atoms are consumed. Now let us consider how the thermal utilization changes over time. The initial value of f is about 0.94, and it initially increases a few parts per thousand as the fuel is burned; however, it does not increase any further.

The only one of the four factors that changes significantly with burnup is the neutron reproduction factor η *(eta).* The value of η starts out at about 1.24 for fresh fuel and then declines to about 1.11 at a burnup of 8000 MWD/Ton. At first (up to the point where some Pu-239 is produced) it increases a bit. Then it decreases with burnup because the rate that U-235 is burned in the fuel rods is greater than the rate that Pu-239 is produced by the capture of thermal neutrons by U-238. The net effect is for η to decrease from about 1.24 to about 1.11 when the burnup reaches 8000 MWD/Ton. This drives down the value of K_∞, and the reactor is no longer able to remain critical again. The behavior of the infinite multiplication factor in this case is shown in Figure 9.15. It should come as no surprise that the values of p and ε are relatively insensitive to the burnup of the fuel and do not have much effect on the value of K_∞.

Example Problem 9.6

Suppose that the infinite multiplication factor for a representative unit cell in a thermal water reactor lattice is 1.01. If the unit cell starts out with 1 million prompt neutrons in it, and it takes one tenth of a millisecond (0.0001 seconds) to complete a representative neutron lifecycle, how many prompt neutrons will there be in the unit cell after 10 milliseconds?

Solution In this problem, we want to know how many prompt neutrons there will be in the unit cell after 100 neutron life cycles. From Equation 9.71, the number of prompt neutrons remaining after 100 neutron life cycles will be $N_{100} = (K_\infty)^{100} \times N_o = (1.01)^{100} \times 1{,}000{,}000 = 2{,}700{,}000$ prompt neutrons. In other words, the prompt neutron population has nearly tripled in 10 milliseconds, which is a very short period of time [Ans.]

9.24 Understanding the Limitations of the Four-Factor Formula

Sometimes nuclear engineers are surprised to learn that the four-factor formula *cannot* be applied to fast reactors. When the four-factor formula was originally invented, it was designed to be used for reactors that followed the *thermal neutron life cycle*. Since fast reactors do not follow this life cycle, many of the terms in the four-factor formula do *not* apply to fast breeder reactors. Now let us make some observations about the limitations of the four-factor formula.

The four-factor formula is based on the assumption that no neutrons can leak out of a unit cell. For a large reactor lattice containing many identical unit cells, this is a very good assumption. *However, for real reactors, one cannot use the four-factor formula (without making some significant modifications)* because some neutrons will leak out of the core—especially around the periphery. Thus to predict the value of $K_{effective}$ in this case, a mechanism must be devised to account for the leakage of both fast and thermal neutrons from the peripheral cells. Finally, it should come as no surprise

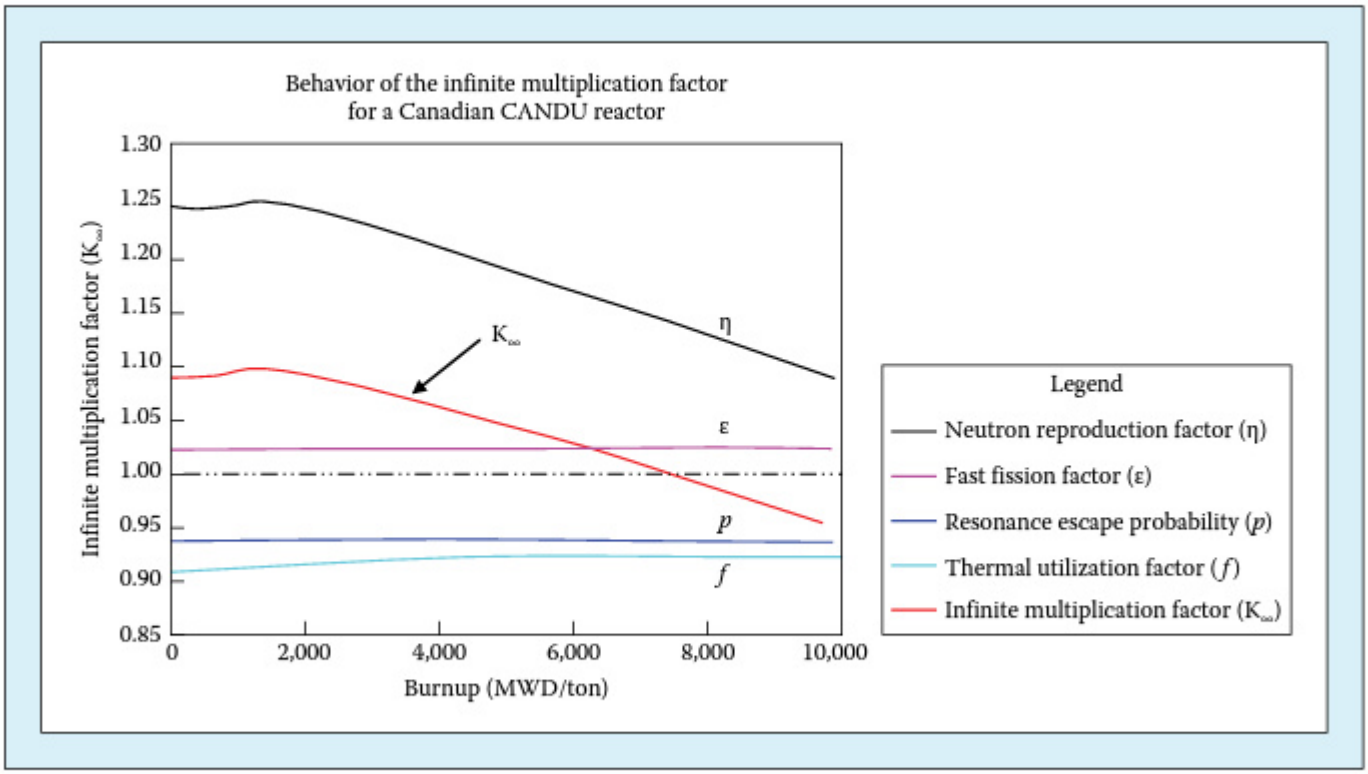

FIGURE 9.15 The behavior of the four factors in the four-factor formula as a function of burnup in a CANDU reactor fuel assembly. Notice that the values of the fast fission factor (ε) and the resonance escape probability (p) barely change as a function of time. The thermal utilization factor f increases by about 1% (due to fission product buildup in the fuel rods), and the only factor that changes significantly is the η (eta) of the fuel, which declines from 1.25 to about 1.11. The same trend applies to all thermal water reactors fueled with U-235. The small "peak" in the value of η at about 1200 MWD/Ton is caused by the buildup of Pu-239 in the fuel rods.

that the value of $K_{effective}$ will always be less than the value K_∞ when neutron leakage is taken into account. (Normally the effective multiplication factor happens to be three or four percent less). If we retain the previous definitions for all of the terms, we have

The Four Terms in the Four-Factor Formula

$$\text{Term 1. } \eta = (\nu)\left(\frac{\int \Sigma_f(E')_{fuel}\,\phi(E')_{fuel}\,dE'}{\int \Sigma_a(E')_{fuel}\,\phi(E')_{fuel}\,dE'}\right)\left(\frac{\phi_{fE'}}{\phi_{fE'}}\right) \quad \text{(the eta of the fuel)} \tag{9.72}$$

$$\text{Term 2. } \varepsilon = \frac{\int \Sigma_f(E)_{fuel}\,\phi(E)_{fuel}\,dE}{\int \Sigma_f(E')_{fuel}\,\phi(E')_{fuel}\,dE'} \times \left(\frac{\phi_{fE'}}{\phi_{fE}}\right) \quad \text{(the fast fission factor—epsilon)} \tag{9.73}$$

$$\text{Term 3. } f = \frac{\int \Sigma_a(E')_{fuel}\,\phi(E')_{fuel}\,dE'}{\int \Sigma_a(E')_{cell}\,\phi(E')_{cell}\,dE'} \times \left(\frac{\phi_{cE'}}{\phi_{fE'}}\right) \quad \text{(the thermal utilization)} \tag{9.74}$$

$$\text{Term 4. } p = \frac{\int \Sigma_a(E')_{cell}\,\phi(E')_{cell}\,dE'}{\int \Sigma_a(E)_{cell}\,\phi(E)_{cell}\,dE} \times \left(\frac{\phi_{cE}}{\phi_{cE'}}\right) \quad \text{(the resonance escape probability)} \tag{9.75}$$

and additional terms must be added to the four-factor formula to account for these effects. This gives rise to another famous equation of reactor physics called the *six-factor formula, which we will discuss in Chapter 10. There we will discover that additional terms must be added to the four-factor formula to account for the effects of neutron leakage.*

Normally there is one term to account for the leakage of thermal neutrons and another term to account for the leakage of fast neutrons. These terms are usually expressed as *non-leakage probabilities*, and consequently, there is a different non-leakage probability for fast neutrons than there is for thermal neutrons. *Then and only then can the true multiplication factor be estimated with a reasonable degree of certainty.*

9.25 Definitions of the Instantaneous Reactivity and the Net Reactivity

In Chapter 7 we provided several examples of how the burnup of the fuel could be measured. However, we never discussed how the reactivity ρ was related to the burnup B. The relationship of the reactivity to the burnup is an important design parameter because it can be used to determine when a reactor needs to be refueled. In the following sections, we would like to derive an explicit relationship between the burnup B and the reactivity ρ_{NET} of the core. However, first we need to draw an important distinction between the net reactivity of the core and the instantaneous reactivity. *The net reactivity of the core ρ_{NET} is not the same as the instantaneous reactivity ρ.* The *instantaneous reactivity* describes how close a reactor is being operated to a neutron multiplication factor of unity. In BWRs, the instantaneous reactivity of the core is controlled by moving large cruciform-shaped control rods into and out of the core, and in PWRs, control rods are also used to keep the reactivity (as defined by Equation 9.32) as close as possible to zero. *In other words, the instantaneous reactivity is adjusted to keep the reactor critical.*

On the other hand, *the net reactivity is used to measure how long a reactor core can remain in a critical state when its instantaneous reactivity is 0.* When a reactor is first started up, control rods are used to absorb the extra neutrons that are generated by the fuel. These fuel assemblies have a great deal of excess reactivity built into them (as much as thirty or forty dollars when the core is fresh), and *this excess reactivity is what allows a reactor to be operated for long periods of time before it needs to be refueled.* When a reactor is first started up, and some of the fuel atoms are burned, the net reactivity of the core starts to decline. To compensate for this reduction in the net reactivity (which usually is a large positive number), the control rods are withdrawn from the core. The large negative reactivity of the control rods is used to balance the large positive reactivity of the fuel rods, and this allows the instantaneous reactivity of the core to remain close to zero. Normally this delicate balancing act is maintained until the reactor needs to be refueled. In many cases, a reactor can be operated for several years before it needs to be refueled. During this time, the net reactivity falls from a very large number (usually 30 or 40 dollars) to a very small number (usually quite close to zero). At the same time, the instantaneous reactivity is maintained close to zero (within a couple of decimal places) to keep the fission process under control. Hence, *the instantaneous reactivity is not the same as the net reactivity*, although they are both defined by the same equation

Definition of the Reactivity

$$\rho = \frac{(k-1)}{k} \tag{9.76}$$

In other words, one generally equates the net reactivity of the core to the net reactivity of the fuel and the instantaneous reactivity of the core to the sum of the negative reactivity of the control rods and the positive reactivity of the fuel. Sometimes these differences can be highlighted more clearly by writing them as

$\rho_{NET} = \rho_{FUEL}$ = Net reactivity = The reactivity of the fuel in the core (Normally a large positive number)
ρ_{CR} = Control rod reactivity = The reactivity of the control rods in the core (Normally a large negative number)

Then we can write the instantaneous reactivity as

ρ = Instantaneous reactivity of the core (Normally a number very close to zero)
= Net reactivity of the fuel – Control rod reactivity

Then it is easy to see that

$$\rho(t) = \rho_{FUEL}(t) - \rho_{CR}(t) \tag{9.77}$$

or

$$\rho(t) = \rho_{NET}(t) - \rho_{CR}(t) \tag{9.78}$$

Now, we would like to discuss how $\rho_{NET}(t)$ changes as a function of burnup. We will then explore how fission products and burnable poisons effect the equations we have just written.

9.26 How Fuel Burnup Affects the Net Reactivity

In reactor design, the burnup of the fuel is defined as the fraction of the initial heavy metal atoms that have undergone nuclear fission. In other words, if the fraction of the U-233, U-235, or Pu-239 heavy metal atoms after some period of time is N(t), then the fraction f of the heavy metal atoms burned is

$$f = \frac{N_o - N(t)}{N_o} \tag{9.79}$$

where N_o is the initial inventory of heavy metal atoms (at t = 0) when the core is fresh. We can express the burnup B as the percentage of the heavy metal atoms that undergo fission by multiplying Equation 9.79 by 100. Then the percentage of heavy metal atoms burned is

$$B = 100 \times \frac{N_o - N(t)}{N_o} \tag{9.80}$$

and this is the definition of the burnup that most nuclear engineers use. In other words, if 5% of initial heavy metal atoms are burned to produce electric power, then the burnup of the fuel is 5%. This is a very simple definition, but it has many practical applications. Moreover, Equation 9.79 says that when the fuel is fresh, B is 0, and when all of the heavy metal atoms are burned, B is 100%. In practice, we can derive an analytical expression for N(t) by realizing that the rate of change of the number of heavy metal atoms is proportional to the neutron flux ϕ. The exact relationship is

$$\frac{\Delta N}{N} = -\sigma\phi\Delta t \tag{9.81}$$

If we integrate this equation, we obtain

$$N(t) = N_o e^{-\sigma\phi t} \tag{9.82}$$

Here σ is the microscopic fission cross section for the heavy metal atoms (see Chapter 4), N_o is the initial number of heavy metal atoms, ϕ is the neutron flux (in neutrons/cm^2/s), and t is the time (in seconds). If we substitute this equation into the previous definition for the burnup, we obtain

$$B = 100 \times \frac{N_o - N(t)}{N_o} \tag{9.83}$$

or

The Burnup Equation

$$B(t) = 100 \times \left(1 - e^{-\sigma\phi t}\right) \tag{9.84}$$

Notice that when a reactor is just starting up (at t = 0), then B = 0%, and when t and ϕ are very large, $e^{-\sigma\phi t} \rightarrow 0$, and B(t) $\rightarrow$ 100%. This latter equation can be used to find the burnup of the fuel whenever the magnitude of the neutron flux within an individual fuel assembly is known. The implications of Equation 9.84 are shown in Figure 9.16 for various values of the flux. Notice that as the neutron flux is increased, the fuel tends to burn more quickly. Now let us see if we can find a relationship between the burnup of the fuel B(t) and the net reactivity of the core $\rho_{NET}(t)$. When the net reactivity of the core falls to 0, the core has to be refueled. The reader may recall from Section 9.5 that the definition of the net reactivity is

An Expression for the Reactivity

$$\rho_{NET} = \frac{\phi(\nu\Sigma_f - \Sigma_a)}{\phi\nu\Sigma_f} = \frac{\nu\Sigma_f - \Sigma_a}{\nu\Sigma_f} \tag{9.85}$$

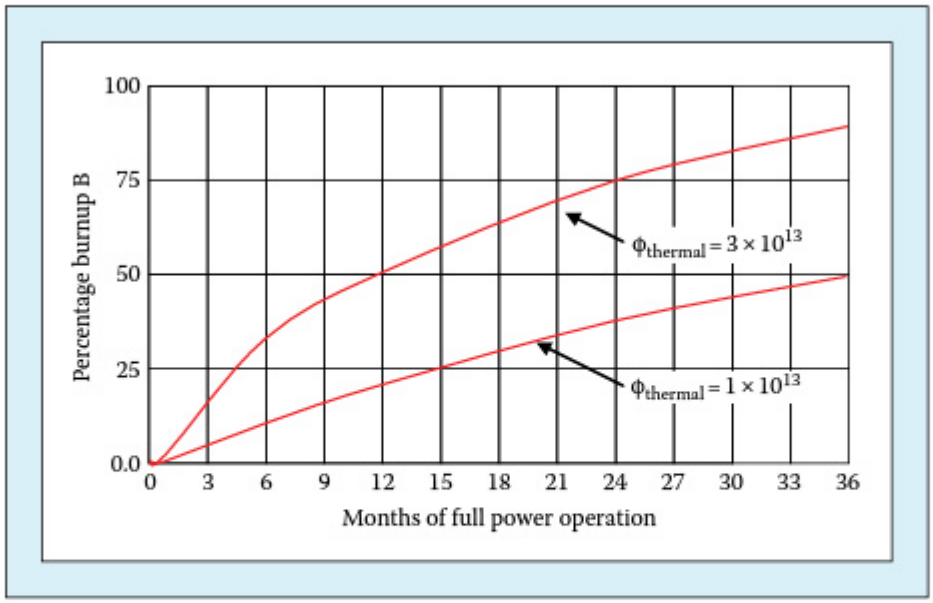

FIGURE 9.16 The burnup B as a function of the neutron flux for a thermal water reactor fueled with U-235. Recall that the thermal flux in a thermal water reactor is only about 1/3 of the total flux (fast + thermal). *For this reason, we can always assume that the burnup is a linear function of time as long as the thermal flux is low (say $\phi \approx 1 \times 10^{13}$ neutrons/cm^2/s).*

Now if the neutron multiplication factor is defined as

$$k = \frac{\text{Total neutron production rate}}{\text{Total neutron destruction rate}} \tag{9.86}$$

we can write

$$k = \frac{\nu\phi\Sigma_f}{\phi\Sigma_a} \tag{9.87}$$

Then, if we divide both the numerator and the denominator of the expression for the reactivity by Σ_a, we obtain

$$\rho_{NET} = \frac{(k-1)}{k} \tag{9.88}$$

Notice that k is directly proportional to the number of heavy metal atoms in the fuel, since $\Sigma_f = N\sigma_f$. This means that the time-dependent reactivity can also be written as

$$\rho_{NET}(t) = 1 - \frac{1}{N(t)\nu\sigma_f/\Sigma_a} \tag{9.89}$$

The values of ν, σ_f, and Σ_a in Equation 9.80 do not change very much as a function of time because there are normally many more U-238 atoms than there are U-235 or Pu-239 atoms. Therefore, we can replace the term $\nu\sigma_f/\Sigma_a$ with a simple constant C. The net reactivity is then related to the heavy metal atom concentration N(t) by

$$\rho_{NET}(t) = 1 - \frac{1}{CN(t)} \tag{9.90}$$

Notice that the reactivity is inversely proportional to the heavy metal concentration unless the burnup is very high. Thus as N(t) becomes smaller, the reactivity must also decline. However, we learned earlier that N(t) is related to the burnup B(t) by

$$B = 100 \times \frac{N_o - N(t)}{N_o} \tag{9.91}$$

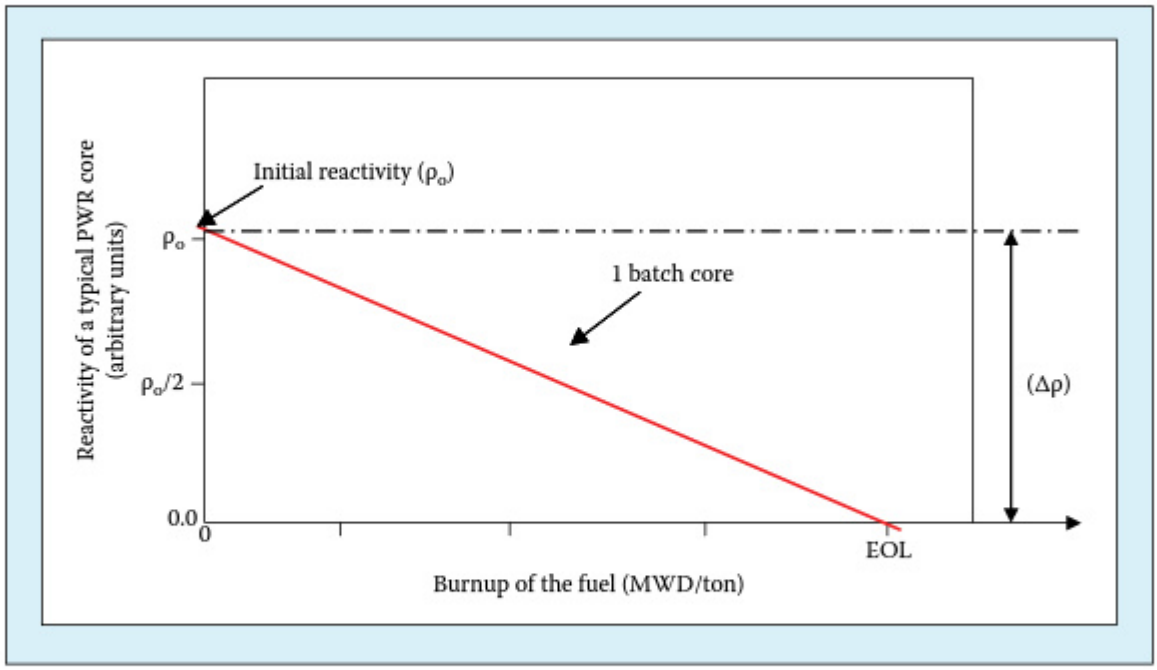

FIGURE 9.17 The behavior of the reactivity as a function of the burnup B in a typical water reactor core.

Solving this equation for N(t) gives

$$N(t) = N_o\left(\frac{1 - B(t)}{100}\right) \tag{9.92}$$

hence we discover that the net reactivity is related to the percentage burnup B by

The Relationship between the Reactivity and the Percentage Burnup B

$$\rho_{NET}(t) = 1 - \frac{1}{C\,N_o\left(1 - 0.01\,B(t)\right)} \tag{9.93}$$

where $C = \nu\sigma_f/\Sigma_a$. In other words, as the burnup increases, the denominator becomes smaller, and $\rho_{NET}(t)$ starts to decline. Moreover, Equation 9.93 shows that *the relationship between the burnup and the reactivity is approximately a linear one. Therefore, the net reactivity always falls as the burnup of the fuel increases*. In Chapter 18, we will use this relationship to determine when a reactor core needs to be refueled. The general trend implied by Equation 9.93 is also shown in Figure 9.17. Clearly, this is an important result because it establishes a unique relationship between the amount of fuel that remains in the core and the net reactivity of the system. The implications of this equation are explored in more detail in Chapter 18 where various methods for refueling a commercial power reactor are discussed.

Example Problem 9.7

Earlier in the chapter, we learned that the net reactivity of the core was related to the burnup of the fuel by an equation of the form $\rho_{NET}(t) = 1 - 1/[C\,N_o(1 - 0.01\,B(t)]$. Use this equation to derive an expression for when the core needs to be refueled.

Solution The core needs to be refueled when $\rho_{NET}(t) = 0$. Setting $\rho_{NET}(t) = 0$, we find that the core must be refueled when $C\,N_o\,(1 - 0.01\,B(t)) = 1$. For a light water reactor, this normally corresponds to a burnup of about 30% of initial inventory of heavy metal atoms. (By this we mean the U-235 atoms.) Notice that when the value of B(t) is known when the reactor first becomes subcritical, we can use the equation $B(t) = 100 \times (1 - e^{-\sigma\phi t})$ to determine the time t when sub criticality first occurs. In a commercial power reactor, this tends to happen every 1 or 2 years. [Ans.]

9.27 Cross Sections Used to Calculate the Infinite Multiplication Factor and the Reactivity in Thermal Water Reactors

In practice, the infinite multiplication factor, the net reactivity, and the instantaneous reactivity can be deduced from the macroscopic cross sections of the fuel, the moderator, and the control rods. The values of the macroscopic fission cross sections are determined primarily by the enrichment of the fuel (i.e., the U-235 to U-238 ratio), and in many cases, fairly accurate estimates for the reactivity can be made using the cross sections we have presented for the thermal energy group (see Appendix C). In thermal water reactors, we can also make parametric estimates of the infinite multiplication factor if we decide to ignore the effects of the fast neutrons entirely. Table 9.5 shows the macroscopic absorption and fission cross sections that can be used to perform these calculations. The macroscopic absorption cross sections for some materials used in reactor control rods (boron and cadmium) are also shown. If we know the enrichment of the fuel (i.e., the U-235 to U-238 ratio), and the effects of neutron leakage can be ignored, the cross sections in Table 9.5 can be used to find reasonably accurate values for K_∞ and ρ. We simply use the equations presented earlier in the chapter to do so. For example, we can use Equation 9.14 to find K_∞, and for the reactivity, we can use Equation 9.23. In future chapters, we will attempt to develop a more accurate method of estimating these parameters by considering how the neutron flux $\phi(x, y, z)$ behaves as a function of position. However, before doing so, we would first like to give an example of how Equations 9.14 and 9.23 are used.

Example Problem 9.8

A reactor core is built out of fuel assemblies using 4% enriched uranium. Neglecting the effects of neutron leakage, what is the infinite multiplication factor for the core if the core is cooled with light water? Assume the number of fuel atoms and the number of moderator atoms are approximately the same and that the value for ν is 2.5.

Solution In this case, we can find the infinite multiplication factor from Equation 9.14. Since the core contains 4% U-235 and 96% U-238, the total macroscopic fission cross section for the core is $0.04 \times 27.56 + 0.96 \times 0.2025 = 1.3$, and the value of $\nu\sum_f$ is $2.5 \times 1.3 = 3.25$. The total absorption cross section for the fuel is $0.04 \times 35.58 + 0.96 \times 0.3668 = 1.77$. The total absorption cross section for the moderator is 0.022. The sum of the absorption cross sections for the fuel and the moderator is $\sum_a = 1.792$. The infinite multiplication factor K_∞ is given by the ratio of these two numbers. Thus $K_\infty = \nu\sum_f/\sum_a = 3.25/1.792 = 1.81$. Clearly, the core in this case has more than enough fuel to stay critical. [Ans.]

Notice that the four-factor formula could have also been used to find the value of K_∞. However, then we would have needed to know the values of η, ε, f, and p for this particular core. If we had done so, the effects of the neutron flux shape would have been included in the values of p and f. Conversely, the values of η and ε would have been relatively insensitive to the geometry of the fuel rods, and to a first approximation, they would only be dependent on the isotopic composition of the core. Now let us consider what happens when we add some control rods to the core. (Control rods were first introduced to the reader in Chapter 1.) Control rods help to absorb the excess reactivity of the fuel and keep a reactor critical even when there is 30% or 40% more fuel in the core than is needed to obtain an effective multiplication factor of 1.0.

TABLE 9.5
Thermal Neutron Cross Sections (in Barns) Required to Calculate the Effective Multiplication Factor for an Infinite Lattice

Thermal Group Macroscopic Cross Sections for Some Important Nuclear Materials				
Name	Usage	$\sum_a$ (cm^{-1})	$\sum_f$ (cm^{-1})	$\sum_s$ (cm^{-1})
Light water (H_2O)	Coolant/moderator	0.02220	0.0	3.443
Heavy water (D_2O)	Coolant/moderator	0.0000442	0.0	0.4519
U-233	Fuel	27.449	25.26	0.999
U-235	Fuel	32.58	27.56	0.669
U-238	Fuel	0.130	5.25×10^{-7}	0.4239
Pu-239	Fuel	50.666	37.220	0.3835
Boron-10	Control rods	491.14	0	0.2880
Cadmium-112	Control rods	114	0.0	0.325

Source: Duderstadt, J. and Hamilton, L., Nuclear Reactor Analysis, John Wiley & Sons, New York, 1976; Lamarsh, J.R., Introduction to Nuclear Reactor Theory, Second Printing, Addison-Wesley Publishing Company, Inc., Reading, MA, 1972.

Example Problem 9.9

What is the reactivity of the core in Example Problem 9.8, and what percentage of the core must consist of control rods made out of Boron-10 for the reactor to be exactly critical?

Solution Since $K_\infty = 1.81$, the reactivity ρ is given by $\rho = (K_\infty - 1)/K_\infty = 0.44$. For the reactor to be exactly critical, $K_\infty = 1$. For this to occur, the following equation must be true: $1 = \nu\sum_f/(\sum_{af} + \sum_{am} + R\sum_{ab})$, where R is the ratio of boron to fuel in the core. Solving this equation for R gives

$$R = \left(\frac{1}{\Sigma_{ab}}\right)\cdot\left(\nu\Sigma_f - \Sigma_{af} - \Sigma_{am}\right)$$

Substituting the appropriate values into this expression, we then find that $R = (1/342)\cdot(3.25 - 1.77 - 0.022) = 0.00426$. Since the volume of the moderator is assumed to be the same as the volume of the fuel, the actual percentage of the core that must be occupied by the boron is half of this or $P = R/2 = 0.00213$ (about two-tenths of one percent). [Ans.]

Clearly, the control rods have to take up less than 1% of the total volume of the core to keep the reactor critical. This example is indicative of the amount of space they require in an actual thermal water reactor. However, as we will subsequently see, the actual space requirement varies depending upon whether the reactor is a PWR or a BWR. In general, the volume of the control rods in a BWR is *greater* than the volume of the control rods in a PWR.

References

Books and Textbooks

1. Reactor Theory (Nuclear Parameters) DOE-HDBK-1019/2-93.
2. Zweifel, P.F. *Reactor Physics*, McGraw-Hill, New York (1973).
3. Henry, A.F. *Nuclear Reactor Analysis*, MIT Press, Cambridge, MA (1975).
4. Stacey, W.M. *Nuclear Reactor Physics*, 2nd edn., John Wiley & Sons, New York (2007).
5. Duderstadt, J. and Hamilton, L. *Nuclear Reactor Analysis*, John Wiley & Sons, New York (1976).
6. Lewis, E. *Fundamentals of Nuclear Reactor Physics*, Academic Press, Boston, MA (2008).
7. Rydin, R.A. *Nuclear Reactor Theory and Design*, University Publications, Blacksburg, VA (1977).
8. Lamarsh, J.R. and Baratta, A.J. *Introduction to Nuclear Engineering*, Prentice Hall, Upper Saddle River, NJ (2001).
9. Lamarsh, J.R. *Introduction to Nuclear Reactor Theory,* second printing, Addison-Wesley Publishing Company, Inc. (1972).
10. Glasstone, S. and Eedlund, M.C. *The Elements of Nuclear Reactor Theory*, D Van Nostrand Company, Inc., New York (1952).
11. Glasstone, S. and Sesonske, A. *Nuclear Reactor Engineering*, 3rd edn., Van Nostrand Reinhold Company, New York (1981).
12. Shultis, K. and Faw, R. *Fundamentals of Nuclear Science and Engineering*, 2nd edn., CRC Press, Boca Raton, FL (2008).
13. Masterson, R.E. *Nuclear Engineering Fundamentals: A Practical Perspective*, CRC Press, Boca Raton, FL (2017).
14. Cochran, R.G. and Toulfanidis, N. *The Nuclear Fuel Cycle: Analysis and Management*, American Nuclear Society, La Grange Park, IL (1999).

Web References

1. *www.nndc.bnl.gov.*
2. *http://www-nds.iaea.org/.*
3. *http://en.wikipedia.org/wiki/Enrico_Fermi.*
4. *http://en.wikipedia.org/wiki/Prompt_neutron.*
5. *http://en.wikipedia.org/wiki/Four_factor_formula.*
6. *http://en.wikipedia.org/wiki/J._Robert_Oppenheimer.*
7. *http://en.wikipedia.org/wiki/Nuclear_reactor_physics.*
8. *http://energy.gov/sites/prod/files/2013/06/f2/h1019v1.pdf.*
9. *https://canteach.candu.org/Content%20Library/20030101.pdf.*
10. *http://nuclearpowertraining.tpub.com/h1019v2/css/h1019v2_43.htm.*
11. *http://www.nuceng.ca/br_space/ep4d03/learning_modules/9_4-factor_formula_for_k-inf.ppt.*

Additional References

- Important physical constants used by nuclear scientists and engineers can be found in *Appendix A.*
- Unit systems and their conversion factors can be found in *Appendix B.*
- Nuclear cross sections for many important nuclear materials can be found in *Appendix C.*
- Physical properties of important nuclear materials can be found in *Appendix D.*
- Atomic masses, half-lives, and natural abundances can be found in *Appendix E.*
- Delayed neutron emitters and their properties are discussed in *Appendix F.*

Questions for the Student

The following questions cover the material presented in this chapter, and in some cases, previous chapters as well. They are designed to test how well the student has acquired a working knowledge of the subject matter.

1. Name two men who helped to develop the four-factor formula.
2. What famous measure of reactor behavior is the four-factor formula used to determine?
3. Is the four-factor formula appropriate to use for an infinite lattice or a finite one?
4. Name each of the four factors that can be found in the four-factor formula.
5. Which of these factors are net producers of neutrons (i.e., have values greater than 1.0), and which of these factors are net destroyers of neutrons (i.e., have values less than 1.0)?
6. Can the four-factor formula be used to determine the infinite multiplication factor for a fast reactor?
7. Write an expression which shows how the reactivity is related to the neutron multiplication factor.
8. Why do you think that the four-factor formula was initially invented?
9. What is the difference between the instantaneous reactivity and the net reactivity?
10. Fill in the following sentence with the appropriate word or phrase: A reactivity of _____ is equivalent to a reactivity of $\rho = 2\beta$.
11. Write an equation which relates the net reactivity of the fuel to the burnup.
12. How is the pitch P of a reactor lattice defined?
13. Which factor(s) in the four-factor formula are most sensitive to the pitch of a reactor lattice?
14. Which factor(s) in the four-factor formula are most sensitive to the material composition of the fuel?
15. Write an equation for the definition of the moderator to fuel ratio?
16. If the absorption cross section of the fuel increases, does the thermal utilization increase or decrease?
17. Write an equation that relates the resonance escape probability to the value of the resonance integral I.
18. What is the value of the infinite multiplication factor for a PWR lattice when all of the control rods are removed?
19. What does a value of the reactivity greater than zero imply?
20. What is the infinite multiplication factor for the lattice of a CANDU heavy-water reactor if all of the control rods are removed from the core?
21. What does a value of the neutron multiplication factor equal to one imply?
22. What is a typical value of the thermal utilization factor for a well-designed thermal water reactor lattice?
23. How does the value of eta (η) change as the ratio of U-235 to U-238 atoms in the fuel is decreased?
24. What range of values for $K_{effective}$ are used to represent the region of delayed criticality in an operating nuclear reactor?
25. What is a typical value for the fast fission factor?
26. What is the definition of a reactivity of one dollar?
27. What is the difference between the infinite multiplication factor and the effective multiplication factor?
28. What does a value of the reactivity less than zero imply?
29. If the total flux in a thermal water reactor is $\phi = 3 \times 10^{13}$ neutrons/cm^3/s, what is the flux of fast neutrons, and what is the flux of thermal neutrons?
30. Suppose that you insert some control rods into a reactor core and the reactivity becomes negative, reaching a value of −0.001. For a U-235-fueled thermal water reactor, how many cents of negative reactivity have you created?
31. What is the value of the infinite multiplication factor for a BWR lattice when all of the control rods are removed from the core?
32. What is a typical value of the resonance escape probability for a well-designed thermal water reactor fuel rod?
33. What nuclear process is responsible for creating the delayed neutrons that appear in a thermal water reactor?
34. Fill in the following sentence with the appropriate word or phrase: In a thermal water reactor, the value of eta is a measure of the neutron fission rate to the neutron absorption rate in the _____.
35. Is the value of the resonance escape probability greatest when the fuel is separated from the moderator or when it is mixed with it?
36. Fill in the following sentence with the appropriate word or phrase: In monetary terms, a reactivity of _____ is equivalent to a reactivity of $\rho = 0.05\beta$.
37. Write an empirical expression for the resonance integral I that can be used for a thermal water reactor lattice if the radius and the density of a cylindrical fuel rod are known.
38. Fill in the following sentence with the appropriate word or phrase: The rate at which the neutrons are absorbed in the fuel and the moderator can be calculated in an equivalent cylindrical cell using a procedure called the _____.

39. What is the role of the delayed neutrons in a thermal water reactor?
40. What does a value of $\rho = \beta$ imply?
41. Under what condition(s) does the thermal utilization of the fuel achieve its maximum possible value?
42. In a U-235-fueled thermal water reactor, how long on average does it take for a delayed neutron to be produced?
43. What is the nominal density of the uranium dioxide fuel that should be used in the calculation of the resonance integral?
44. In a thermal water reactor, write a simple expression for the spatially dependent neutron production rate.
45. In a thermal water reactor, write a simple expression for the spatially dependent neutron destruction rate when the effects of neutron leakage can be ignored.
46. Using the answers to the two previous questions, write an expression for the neutron multiplication factor that does not rely on the use of the four-factor formula.
47. At normal reactor operating temperatures (about 300°C) does Pu-239 or U-235 have a higher value of eta?
48. Suppose that you withdraw some control rods from a thermal water reactor lattice and the reactivity reaches a value of +0.001. What do you do?
49. What are the dimensions of the reactivity?
50. Write an equation for the four-factor formula showing all of its important terms.
51. Why does the eta (η) of the fuel have some temperature dependence?
52. When does the phenomenon of energy self-shielding become a problem in a reactor lattice?
53. If you were to design a thermal water reactor, what moderator to fuel ratio would you use?
54. If you were a reactor designer, which fuel would you use based on the value of eta (η) alone to optimize the reactivity of the core, U-233, U-235, or Pu-239?
55. Write an expression for the reactivity involving the macroscopic neutron fission and absorption cross sections. Why was this expression not used instead of the four-factor formula at the time?
56. As the fuel in a reactor core is burned to create useful power, how is the instantaneous reactivity maintained close to zero?

Exercises for the Student

Exercise 9.1

Calculate the reactivity when k_{eff} is equal to 1.002 and 0.998. Is the reactivity positive for both values of k_{eff}?

Exercise 9.2

According to Equation 9.24, what is the only time when the reactivity of a reactor core can be equal to 0? What happens to the neutron population in this case?

Exercise 9.3

Consider a reactor with no delayed neutrons. Initially the core is stable with an effective multiplication factor of 1.0. Then a control rod is dropped into the core and the reactivity falls to −0.001. What is the change in the neutron population 1 minute after the rod is dropped into the core if the mean neutron generation time is 10^{-4} seconds and the initial neutron population is 1013 neutrons/cm^3?

Exercise 9.4

The reactivity of a light-water reactor is reduced by 0.015 after the fuel has been burned for 18 months. What is the reactivity change in dollars and cents if the reactor is fueled with U-235? The fuel rods are then replaced by fuel rods containing U-233 and eventually by fuel rods containing Pu-239 and the same cycle is repeated again. What is the reactivity change in dollars and cents in these other two cases?

Exercise 9.5

Assume that the neutron multiplication factor before the fuel in a reactor core is burned is 1.3. If the fuel is replaced after the neutron multiplication factor falls to 1.0, what is the change in the overall reactivity of the core?

Exercise 9.6

Suppose that the reactivity of a control rod is 0.0001. If the reactor is fueled with U-235, what is the reactivity of the control rod in dollars and cents? If the U-235 is replaced by the same amount of Pu-239, what is the reactivity of the same control rod in dollars and cents?

Exercise 9.7

The control rods of a thermal reactor have a reactivity of $20 when they are fully inserted and a reactivity of 0 when they are fully withdrawn. After the fuel is burned for 2 years, the value of k_{eff} falls from 1.3 to 1.15. Assuming that the reactivity of the control rods is a linear function of their position, by what percentage of their total insertion distance do they have to be withdrawn from the core to keep the reactor critical? Assume the core is fueled with U-235.

Exercise 9.8

The neutron leakage rate out of the core of a thermal water reactor is 4% of the neutron absorption rate when the reactor is exactly critical. After some design changes are made, the neutron leakage rate is reduced to 1%. What is the change in the effective multiplication factor of the core in this case? What is the change in the overall reactivity?

Exercise 9.9

The fuel assemblies in a PWR use 4% enriched uranium. Neglecting the effects of neutron leakage, what is the infinite multiplication factor for the core when the fuel assemblies are cooled with light water? Assume the number of moderator atoms is twice the number of fuel atoms and that the value for ν is 2.4. Assume that the fuel rods are made of uranium dioxide.

Exercise 9.10

A thermal water reactor is to be designed with the following values for η, ε, f, and p when the fuel is fresh:

η 1.89
ε 1.08
f 0.94
p 0.74

What is the reactivity of the core at the beginning of life (BOL) and what is the infinite multiplication factor? If the fissile material in the core is primarily U-235, what is the reactivity in dollars and cents?

Exercise 9.11

The reactor in Exercise 9.9 has a neutron leakage rate that is 4% of the neutron absorption rate. What is the reactivity of the core at the beginning of life (BOL) and what is the infinite multiplication factor? If the fissile material in the core is primarily U-235, what is the reactivity in dollars and cents?

Exercise 9.12

A wise man comes to you and claims that the effective multiplication factor for a PWR can be increased by removing the U-235 from the core and replacing it with an equivalent amount of Pu-239. When the fuel is replaced, what is the reactivity of the core at the beginning of life (BOL) if all of the fuel assemblies now contain Pu-239? What is the new multiplication factor? Has the effective multiplication factor increased or decreased? Assume that the geometry of the fuel assemblies and the other core parameters have not changed. Use the values in Table 9.4 for your estimate.

Exercise 9.13

A thermal water reactor is designed with the following parameters:

η 1.31
ε 1.06
f 0.97
p 0.84

What type of reactor is this likely to be? What type of fuel does it use, and what sort of material should be used for its moderator?

Exercise 9.14

A member of your nuclear design team calls a meeting in which you are informed that the reactivity of your reactor will be increased by 0.20 at EOL (End of Life) if the enrichment of the fuel is increased from 4% to 5%. Do you think this is a credible claim for this person to make? How can you verify that this claim is correct?

Exercise 9.15

Find the thermal utilization factor for a homogeneous thermal reactor that has a value of $\Sigma_a = 0.16\ cm^{-1}$ for the fuel and a value of $\Sigma_a = 0.020\ cm^{-1}$ for the moderator. Assume that the reactor is designed so that each fuel assembly has a moderator to fuel ratio (the volume of the moderator VM to the volume of the fuel VF) of 4:1.

Exercise 9.16

Suppose that someone comes to you and tells you that they have been able to design a fast breeder reactor using the four-factor formula. Do you trust the values for the infinite multiplication factor they have been able to obtain under these circumstances? Can you suggest an alternative way to determine the value for the neutron multiplication factor under these conditions?

Exercise 9.17

Suppose that the infinite multiplication factor for a representative unit cell in a thermal water reactor is 0.99. If the unit cell starts out with 1 million prompt neutrons in it and it takes one tenth of a millisecond (0.0001 seconds) to complete a representative neutron life cycle, how many prompt neutrons will there be in the unit cell after 1 millisecond?

10

Neutron Leakage, Reactor Criticality, and the Six-Factor Formula

10.1 Understanding the Purpose of the Six-Factor Formula

One obvious way to extend the four-factor formula to more realistic situations is to take the four-factor formula and add additional terms to it to account for the percentage of neutrons that leak out of the core through the process of diffusion alone. In making these modifications, there is a rigorous process that must be followed to deduce the neutron leakage rates. Essentially, the idea is to quantify the number of fast neutrons and thermal neutrons that escape from the core, and to use these numbers to calculate the value of $K_{effective}$ from K_{∞}. Sometimes the percentage of neutrons that escape from the core is called the *neutron leakage probability* L′ (not to be confused with the neutron leakage rate L, which is measured in neutrons/s). The leakage rate is slightly different for thermal neutrons than it is for fast neutrons. Fast neutrons have longer mean free paths than thermal neutrons do ($\lambda_{FAST} \cong 10\,\lambda_{THERMAL}$) and at the typical kinetic energies of fission neutrons and thermal neutrons (2 MeV and 0.025 eV, respectively), the ratio of λ_{FAST} to $\lambda_{THERMAL}$ is about a factor of 10. Because of this, we can *define* two additional terms, or factors, that can be added to the four-factor formula to account for the effects of neutron leakage.

These factors are called the *fast nonleakage probability*, P_{FNL}, and the *thermal nonleakage probability*, P_{TNL}. As the names imply, these probabilities are the probabilities that fast and thermal neutrons will *NOT* leak out of the core. Since fast and thermal neutrons have different cross sections (see Figure 10.1) and different spatial sensitivities, it is reasonable to assume that their nonleakage probabilities are statistically independent of each other. In most cases, this turns out to be the case.

10.2 Finding the Value of $K_{effective}$ from K_{∞} in a Finite Reactor Lattice

If the nonleakage probabilities are truly *independent variables*, then we know from our study of probability and statistics that the probabilities of them affecting the reaction rates, and therefore the value of K_{∞}, will be multiplicative. We can then multiply the four-factor formula by these additional terms to obtain the following set of equations:

Six-Factor Formula

$$K_{effective} = P_{FNL} P_{TNL} K_{\infty} = P_{FNL} P_{TNL} (\eta \varepsilon f p) \tag{10.1a}$$

or equivalently

$$K_{effective} = (1 - L') \cdot K_{\infty} = (1 - L') \cdot (\eta \varepsilon f p) \tag{10.1b}$$

where L′ is the neutron leakage probability (the fraction of neutrons that leak out of the core from both energy groups) and it is related to the thermal and fast nonleakage probabilities by

$$L' = 1 - P_{FNL} \cdot P_{TNL} \tag{10.2}$$

Equation 10.1(a) is the famous six-factor formula. It is one of the most important equations in all of nuclear science and engineering. All that is required to find a realisitc value of $K_{effective}$ is to determine the values for η, ε, *f*, and *p* (which we already

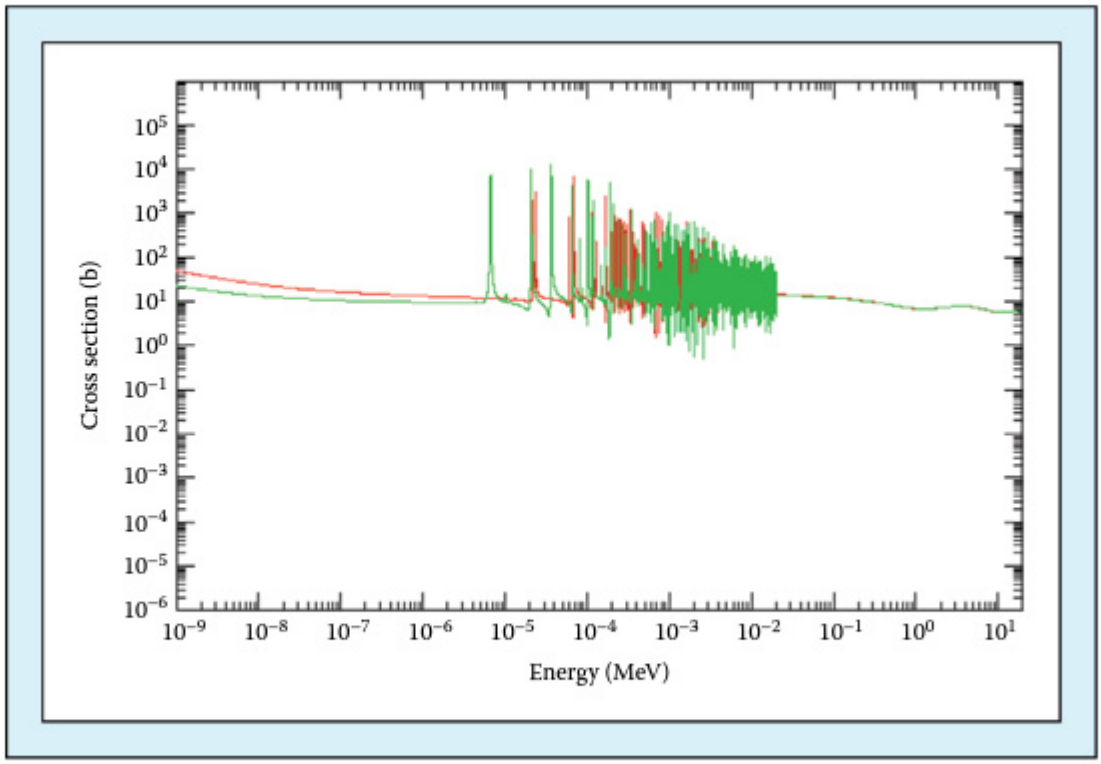

FIGURE 10.1 The absorption resonances for U-238 (in green) and Thorium-232 (in red) that dominate the value of resonance escape probability P just above the thermal energy range. (Courtesy of Kaere.)

tabulated in Chapter 9) and then obtain reliable estimates for P_{FNL} and P_{TNL}. The values of P_{FNL} and P_{TNL}, when defined in this way, are geometry dependent. For example, a modern pressurized water reactor (PWR) or boiling water reactor (BWR) has a typical value for P_{FNL} about 0.97, and a typical value for P_{TNL} about 0.99. Thus, *the nonleakage probability is higher for thermal neutrons than it is for fast neutrons because thermal neutrons are much more likely to be absorbed in the fuel and the control rods than fast neutrons are*. Hence, thermal neutrons are more likely to remain in the core.

If we take the product of P_{FNL} and P_{TNL} we obtain $P_{FNL}P_{TNL} = 0.97 \times 0.99 \cong 0.96$. In other words, about 4% of the neutrons in a commercial thermal water reactor leak out of the core without being absorbed by the fuel assemblies or the control rods. This means that whatever value we calculate for K_∞, the value of $K_{effective}$ for a real reactor must be about 4% *lower*. In other words, the value of K_∞ must be at least 4% higher in order to achieve a critical mass! As we will soon discover, this is one of the primary reasons why the fuel assemblies in commercial water reactors have enrichments between 3% and 5%. Hence, if we know the value of K_∞, the value of $K_{effective}$ is simply

$$K_{effective} = P_{FNL}P_{TNL}K_\infty \tag{10.3}$$

where P_{FNL} and P_{TNL} are the aforementioned nonleakage probabilities. Naturally, the neutron leakage rates for both fast and thermal neutrons become smaller when either the width or the height of the core is increased.

Example Problem 10.1

A thermal water reactor lattice is found to have an infinite multiplication factor of 1.10. If the thermal nonleakage probability is 0.99 and the fast nonleakage probability is 0.97, what is the effective multiplication factor and what is the net reactivity with the control rods inserted into the core?

Solution According to Equation 10.3, the effective multiplication factor is $K_{effective} = P_{FNL}P_{TNL}K_\infty = 0.97 \times 0.99 \times 1.10 = 1.056$. The net reactivity is $\rho = (K_{effective} - 1)/K_{effective} = 0.056/1.056 = 0.053$. This means that the reactor has enough excess reactivity to remain critical for some time. [Ans.]

10.3 Calculating the Fast and Thermal Nonleakage Probabilities

For a bare homogeneous core, the thermal nonleakage probability and the fast nonleakage probability are given by two equations that have an almost identical form. These equations can be derived from simple two-group neutron diffusion theory (see Chapter 12), and later we will demonstrate how they are affected by a neutron reflector that surrounds the core. The explicit expressions for the fast and thermal nonleakage probabilities are

The Thermal Nonleakage Probability

$$P_{TNL} = \frac{1}{1 + B^2 L_T^2} \tag{10.4}$$

and

The Fast Nonleakage Probability

$$P_{FNL} = 1\left(1 + B^2 \tau_T\right) \tag{10.5}$$

where

L_T is the *thermal diffusion length* having the units of cm
τ_T is the *neutron age* having the units of square cm
B^2 is a constant called the *geometric buckling* of the flux, which depends on the geometrical characteristics of the core

In Equations 10.4 and 10.5 the buckling represents the *curvature* of the neutron flux as one moves from the center of the core to the edge. Reactors that have very large neutron leakage rates have very large values for the buckling, and reactors that have very small neutron leakage rates have very small values for the buckling. Hence there is a direct relationship between the size of the geometric buckling B^2 and the neutron leakage rate, which is given by $-D\nabla^2\phi$. This should also be apparent from the flux shapes shown in Figure 10.2.

In general, the geometric buckling decreases in a manner that is inversely proportional to the physical size of the core. Hence for a simple cylindrical reactor or sphere, $B^2 \sim (A/R)^2$, where R is the radius, and A is a dimensionless constant that is shape specific. The same pattern also holds for rectangular and slab-shaped reactors as well. Notice that the buckling is defined as the *square* of B and not just the value of B itself. Physically, this is because it corresponds to the square of the lowest eigenvalue of the neutron diffusion equation, whose solutions we will discuss in Chapter 13. The neutron

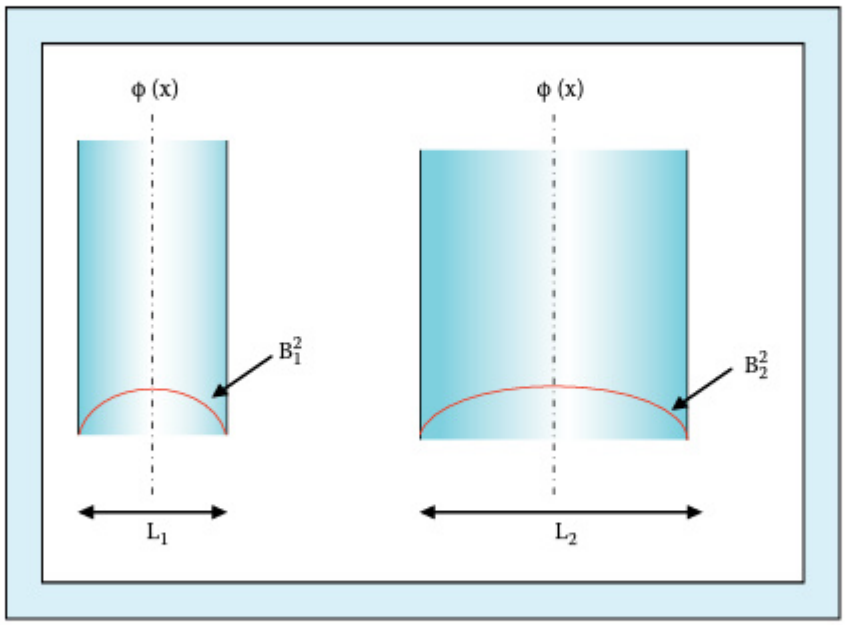

FIGURE 10.2 The geometric buckling and the flux shape in a small reactor and a larger one. Notice that the curvature of the flux, and therefore the buckling, become smaller as the core becomes larger.

TABLE 10.1
Thermal Diffusion Length and the Neutron Age for Several Materials at Room Temperature

Material	L_T (cm)	L_T^2 (cm^2)	τ_T (cm^2)
Water H_2O	2.85	8.12	27
Heavy water D_2O	97.0	9410	131
Beryllium	22.0	480	102
Graphite	59.1	3500	368

leakage rates are also affected by the choice of the moderator that is used. Different moderators have different values of the variables we have called the thermal diffusion length and the neutron age. The thermal diffusion length L_T can have a value between about 3 cm for ordinary water and a value of about 100 cm for heavy water D_2O, while the values for the neutron age τ_T typically range from about 30 cm^2 for ordinary water to over 350 cm^2 for solid graphite. Values for several of these parameters are shown in Table 10.1 at room temperature (300 Kelvin). In some calculations of the neutron leakage rate, the fast and thermal nonleakage probabilities can be combined together into a single nonleakage probability that is consistent with the predictions of one diffusion group theory. In this case, the neutron leakage rate is given by

$$P_{NL} = P_{FNL} P_{TNL} \tag{10.6}$$

where P_{NL} may be calculated from the simple equation

$$P_{NL} = \frac{1}{1 + B^2 M_T^2} \tag{10.7}$$

and the parameter

$$M_T^2 = L_T^2 + \tau_T \tag{10.8}$$

is called the *thermal migration area*. It is worth noting that if τ_T is much less than L_T^2, then the overall neutron leakage rate reduces to

$$P_{NL} = \frac{1}{1 + B^2 L_T^2} \tag{10.9}$$

which is an important finding of one-group theory. In general, *fast neutrons leak out of the core much more readily than thermal neutrons do*, as can be easily seen from the following example. It is also possible to show that this is true (see Chapter 11) because the neutron mean free path λ is much longer at fast energies than it is at thermal ones. Again, *the effect of increasing the size of the core is to increase the size of P_{FNL} and P_{TNL}*.

Example Problem 10.2

Using the values for the thermal diffusion length and the neutron age given in Table 10.1 and assuming that we are dealing with a heavy water reactor with a geometric buckling of $B^2 = 0.0001$ cm^{-2}, determine the nonleakage probabilities from the core for both the fast and thermal neutrons.

Solution The fast nonleakage probability is given by Equation 10.5, and the thermal nonleakage probability is given by Equation 10.4. In the case of the fast nonleakage probability, the neutron age is equal to $\tau_T = 131$ cm^2, and in the case of the thermal nonleakage probability, the square of the thermal diffusion length is $L_T^2 = 9410$ cm^2. So if $B^2 = 0.0001$ cm^{-2},

$$P_{TNL} = \frac{1}{1 + B^2 L_T^2} = \frac{1}{1 + 0.0001 \times 131} = 98.7\% \text{ [Ans.]}$$

and

$$P_{FNL} = 1\left(1 + B^2 \tau_T\right) = \frac{1}{1 + 0.0001 \times 9410} = 52.5\% \text{ [Ans.]}$$

10.4 Physical Significance of the Six Factors

Before discussing the six factor formula in more detail, we would like to take a moment to review the physical significance of each of the six factors. When the nuclear power industry was founded in the early 1940s, each of the factors had to be measured experimentally in order to understand the cumulative effect they would have on the criticality of the core. Therefore, all of the factors were designed to be *experimentally measureable variables* which could be used to assist in the design of the core as a whole. Accordingly,

- The *eta* η of the fuel was intended to understand how the neutron production rate was affected by the isotopic composition of the fuel.
- The *resonance escape probability p* was intended to understand how separating and lumping the fuel and the moderator into distinct physical regions of the lattice could enhance the ability of the lattice to become critical.
- The *thermal utilization factor f* was intended to understand how different fuel rod geometries would effect the value of the effective multiplication factor.
- The *fast fission factor* ε was intended to account for the affect of the neutron energy spectrum on the neutron production rate.
- The *fast and thermal nonleakage probabilities* P_{FNL} *and* P_{TNL} were intended to understand how many neutrons would leak out of core as a function of their average kinetic energies.

Hence, each of these factors contributed to the design of the nuclear reactors that were built at the time. Table 10.2 summarizes the definitions of each of these factors and shows the contributions they can individually make to the effective multiplication factor. Finally, we would like to review how of each of these factors can be calculated or determined experimentally. The appropriate equations to use for the individual factors are shown in Table 10.3. In the case of the resonance escape probability, we have simplified the resonance integrals to make them easier to understand. In these formulas, B^2 is the geometric buckling of the flux, L_{th}^2 is the diffusion length of the thermal neutrons, and τ_{th} is the neutron age (see a more extensive discussion of the age in Chapter 13). Again the values of the flux in the fuel and in a unit cell containing the fuel at thermal energies are represented by the equations

$$\phi_{fE'} = \frac{\int \phi(E')_{fuel}\, dE'}{\int dE'} \tag{10.10}$$

TABLE 10.2
Definition of the Factors in the Six-Factor Formula

Factor	Name	Purpose of the Factor	Typical Water Reactor Values[a]	Definition or Method of Calculation
η (eta)	Eta of the fuel	Determines the effect of different isotopic fuel concentrations on the value of $K_{effective}$	1.60–1.70	The number of neutrons produced per neutron absorbed in the fuel
f	Thermal utilization factor	Determines the effect of the spatial flux shape on $K_{effective}$	0.85–0.95	The probability that a neutron that gets absorbed does so in the fuel
p	Resonance escape probability	Determines the effect of resonance self-shielding on the number of neutrons available for thermal fission	0.75–0.85	The fraction of fission neutrons that manage to slow down from fast to thermal energies without being absorbed
ε (Epsilon)	Fast fission factor	Determines the effect of the neutron energy spectrum on the fission process	1.02–1.08	The total number of fission neutrons to the number of neutrons from thermal fissions
P_{FNL}	Fast nonleakage probability	Determines how many fast neutrons will not leak out of a fuel assembly	0.95–0.97	The probability that a fast neutron will not leak out of the core
P_{TNL}	Thermal nonleakage probability	Determines how many thermal neutrons will not leak out of a fuel assembly	0.98–0.99	The probability that a thermal neutron will not leak out of the core

[a] For partially burned fuel.

TABLE 10.3
Appropriate Formulas to Use to Calculate the Factors in the Six-Factor Formula

Factor	Name	Simple One-Group Formula	Equivalent Energy Integral
η (eta)	Eta of the fuel	$\nu\Sigma_{f\,fuel}/\Sigma_{a\,fuel}$	$\nu\Sigma_f(E')_{fuel}\,dE' \Big/ \int \Sigma_a(E')_{fuel}\,dE'$
f	Thermal utilization factor	$\Sigma_{a\,fuel}/\Sigma_{a\,cell}$	$\int \Sigma_a(E')_{fuel}\,\phi(E')_{fuel}\,dE' \Big/ \int \Sigma_a(E')_{cell}\,\phi(E')_{cell}\,dE' \times (\phi_{cE'}/\phi_{fE'})$
p	Resonance escape probability	N/A	$p = Ae^{-\Sigma I/B}$
ε (Epsilon)	Fast fission factor	N/A	$\int \Sigma_f(E)_{fuel}\,dE \Big/ \int \Sigma_f(E')_{fuel}\,dE' \times (\phi_{fE'}/\phi_{fE})$
P_{FNL}	Fast nonleakage probability	N/A	$P_{FNL} = e^{-B\times B/\tau_{th}}$
P_{TNL}	Thermal nonleakage probability	N/A	$P_{TNL} = 1/\left(1 + L_{th}^2 B^2\right)$

and

$$\phi_{cE'} = \frac{\int \phi(E')_{cell}\,dE'}{\int dE'} \tag{10.11}$$

Similarly, the total flux in the fuel and the unit cell from the existing neutrons having all possible kinetic energies are

$$\phi_{fE} = \frac{\int \phi(E)_{fuel}\,dE}{\int dE} \tag{10.12}$$

and

$$\phi_{cE} = \frac{\int \phi(E)_{cell}\,dE}{\int dE} \tag{10.13}$$

Again, A and B are empirically determined constants used to find the resonance escape probability p, and the summation $\sum$ in the definition of the resonance escape probability (not to be confused with the neutron cross section) is the sum over the resonance integrals for all isotopes from j = 1 to j = J and for all resonances within a given isotope j from i = 1 to i = N. The terms in the other formulas are relatively straightforward, and so we will not discuss their definitions further.

Student Exercise 10.1

Suppose that we were to double the size of the core used in the previous example. If the geometric buckling B^2 was related to the core radius R by the following equation $B^2 = (2.405/R)^2$, what would the fast and thermal nonleakage probabilities be in this case?

Is the observed change in the neutron leakage rate with core size linear or more than linear in this particular case? Moreover, how does this change affect the value of $K_{effective}$ if the core happened to be exactly critical before the size was doubled?

10.5 Criticality and Core Composition

In most light water reactors, between 20% and 25% of the total core volume is reserved for the fuel. The uranium atoms are bonded together with two oxygen atoms to form a ubiquitous and very popular compound called *uranium dioxide* (UO_2), which can be found in about 95% of the nuclear reactors in the world today. As we explained in our companions book,* uranium dioxide is a complex ceramic material that is generally dark gray or black in color. It has excellent dimensional stability and it does not swell when fission products produced by the fission process enter the fuel. Figure 10.3 shows the composition of a typical light water reactor core when it is fresh. Here, the word "fuel" refers to the uranium dioxide fuel

* *See Nuclear Engineering Fundamentals: A Practical Perspective*, by R.E. Masterson, CRC Press (2017).

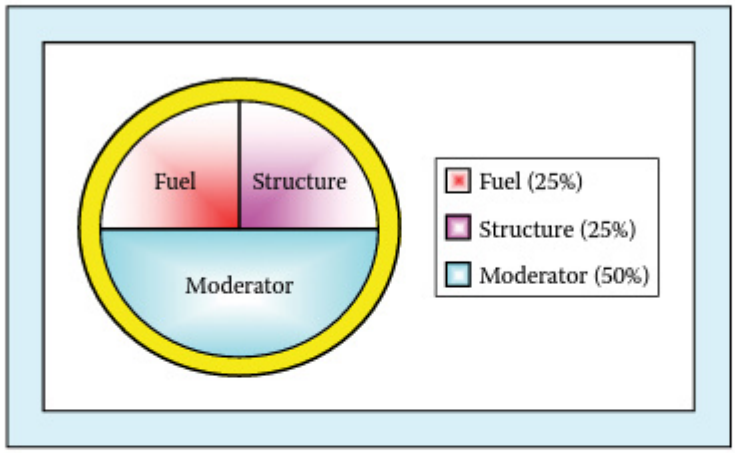

FIGURE 10.3 The core composition in a typical light water reactor with a fuel rod pitch of about 1.5.

pellets in the fuel rods, and the word "structure" refers to the cladding surrounding the fuel rods as well as the control rods and all of other structural materials (grid spacers), inlet and outlet plenums, etc., needed to hold the core together. The remainder of the core is then cooled by the moderator or reactor coolant, which is shown in Figure 10.3 as the *moderator*.

In conventional PWRs and BWRs, the coolant is ordinary water (H_2O), while in pressurized heavy water reactors (PHWRs), the coolant is replaced by heavy water or D_2O. In each of these designs, there are many reasons why the material composition of the core has these specific ratios. First and foremost, these ratios are required to achieve the highest possible reaction rates and allow the most fuel atoms to be burned over long periods of time. Secondly, enough coolant must be available to remove the heat from the core and also to slow down the fission neutrons so that they can be absorbed. Finally, about one quarter of the total core volume must be reserved for the structural materials required to hold the other components of the core together (see Figure 10.3).

The ratio of the amount of moderator to the amount of fuel is affected by both safety and performance considerations, and because of this, most LWRs require a *moderator to fuel ratio* (or MFR) between 2.00 to 1 and 4.00 to 1. The value of the MFR for a reactor lattice is determined primarily by the fuel *rod pitch* P, or the centerline to centerline spacing of the rods in the core. A low MFR requires a very tightly packed lattice with the fuel rods very close together, while a high MFR allows the fuel rods to be spaced further apart. The volumetric power density, or the power output per liter of fuel assembly volume, is also inversely proportional to the MFR. For MFRs close to 2, the amount of structural material in the core (including the fuel rod cladding) is approximately equal to the volume for the fuel. This fuel to structure ratio (1 to 1) is highly sought after by the designers of light water reactors today. Figure 10.4 shows how the pitch is defined

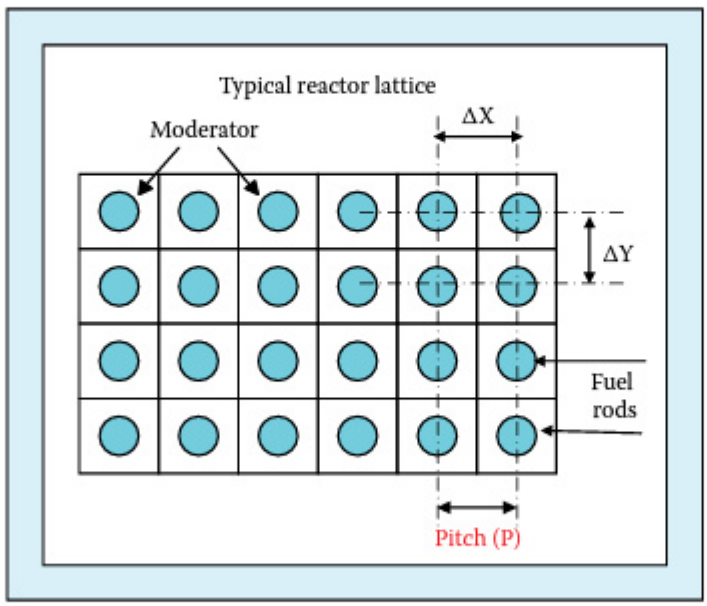

FIGURE 10.4 A simple reactor lattice with the fuel rods arranged in a square array.

for a square reactor lattice. Assuming the fuel rods are cylindrical in shape and the lattice is rectangular or square, it can be shown that the pitch P of the lattice is related to the diameter D of the fuel rods by

Relationship between the Rod Pitch, the Rod Diameter, and the MFR

$$P^2 = \frac{\pi D^2}{4} \times (MFR + 1) \tag{10.14}$$

or equivalently,

$$P^2 = \pi R^2 \times (MFR + 1) \tag{10.15}$$

where MFR is the moderator to fuel ratio, expressed as the ratio of the volume of the moderator V_M to the volume of the fuel V_F or

$$MFR = \frac{V_M}{V_F} \tag{10.16}$$

In this case, the *MFR is a dimensionless number*. Hence, any two of the three variables in Equation 10.15 (MFR, P or D) may be used to determine the third. For example, if the MFR is 3, then Equation 10.14 requires the pitch of the lattice must be $P = D\sqrt{\pi}$. Conversely, if two adjacent fuel rods are allowed to just touch each other so that P = D, then this would correspond to an MFR of $MFR = (P^2 - \pi R^2)/\pi R^2 = (4 - \pi)/\pi = 0.273$. This is the smallest possible value for the MFR when a reactor lattice is square. *Most light water reactor fuel assemblies today have a pitch to diameter ratio of about 1.5*. In the Western world, the optimum MFR is affected by safety considerations and even by local regulations that can change from country to country or even from region to region. In some countries, the "optimal" value of the MFR depends on a specific reactor design or even an entire "class" of designs. Some of the reasons for this are explained in the next section.

Student Exercise 10.2

For the reactor lattice shown in Figure 11.16, show that $P^2 = \pi R^2 \times (MFR + 1)$ where P is the pitch of the lattice and R is the diameter of a fuel rod. *Hint*: Start with the basic equation $MFR = V_M/V_F$ to begin your derivation.

10.6 Moderator to Fuel Ratio and the Four-Factor Formula

Another key design parameter that is related to the six-factor formula is the *moderator to fuel ratio, or the MFR*. Once the fuel (i.e., U-233, U-235, or Pu-239) has been selected, the MFR can almost single-handedly determine the value of $K_{effective}$ for a reactor core. *As we alluded to previously, the MFR is generally defined as the ratio of the number of moderator atoms in a volume of material V to the ratio of the number of fuel atoms in the same volume of material.*

A small MFR means that there are a lot of fuel atoms for every moderator atom, and a large MFR means that there are many more moderator atoms than fuel atoms. From a statistical point of view, it turns out that the thermal utilization *f* of the fuel and the resonance escape probability *p* change in exactly the opposite way as the MFR of the lattice is changed. This can be seen quite clearly in Figure 10.5, when the product of these parameters is calculated for different values of the MFR. Notice that as the MFR is decreased, many more thermal neutrons are absorbed by the fuel (since there are fewer moderator atoms available), and the thermal utilization increases. Eventually a point is reached where there are no more moderator atoms left, and the thermal utilization becomes equal to 1.0. In other words, at this point, all of the thermal neutrons are absorbed by the fuel. Hence, the thermal utilization can never have a value greater than unity.

Now let us discuss what happens to the resonance escape probability *p* when we change the MFR under the same conditions. If there is a lot of fuel and very little moderator present, which corresponds to a very low MFR, the fuel atoms are so tightly packed together that very few neutrons are able to escape the absorption resonances of U-238 and Th-232 shown in Figure 10.1. So a low MFR also causes the resonance escape probability to be low. As the number of moderator atoms is increased, neutron moderation increases, and there are fewer fuel atoms available to absorb neutrons in the resonance energy range. So as the MFR increases, the resonance escape probability increases as well. Since the *value of $K_{effective}$ is proportional to the product of these two factors*, let us see how the value of $K_{effective}$ is affected when we multiply them together. The result is shown in Figure 10.5. Clearly, the product of these two factors

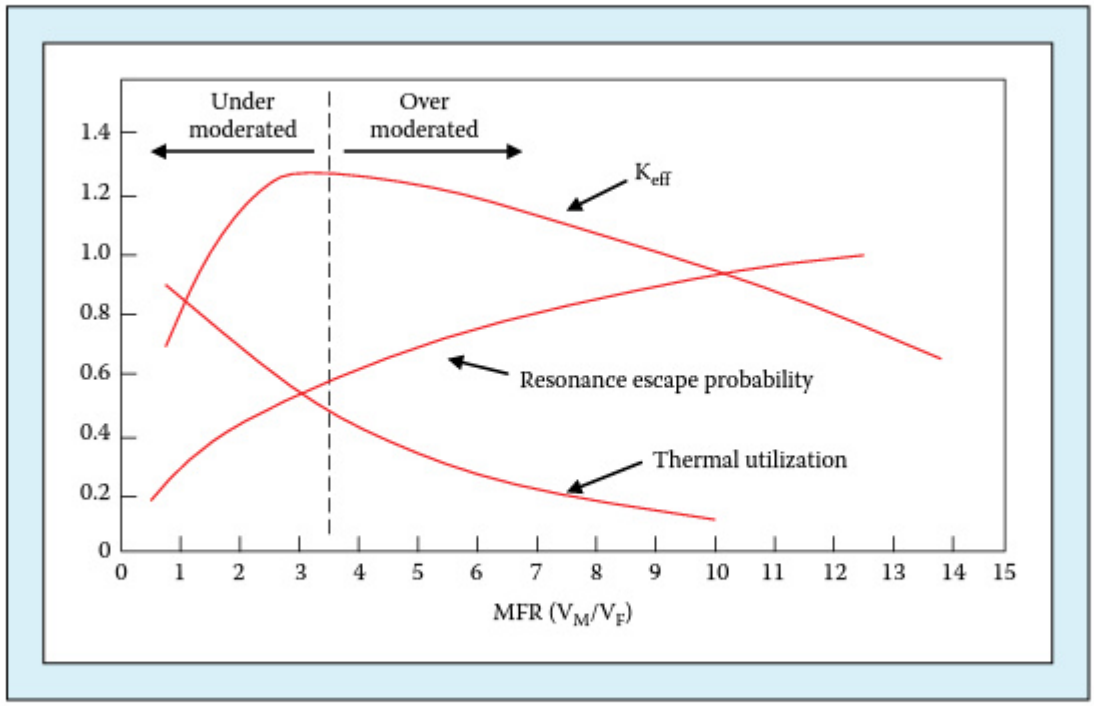

FIGURE 10.5 The value of $K_{effective}$ as a function of the MFR. *Note*: the values of the effective multiplication factor in the graph are based on an eta η of about 1.9 and a fast fission factor ε of 1.0 (unity).

reaches its maximum value at a MFR that is fuel- and coolant-dependent, and then begins to fall off on either side of this optimum value. The MFR, which results in this optimum value for $K_{effective}$, is the value that most reactor designers try to use in practice, because it is here that the greatest possible reactivity can be obtained for a given amount of fuel. It is worth mentioning that the MFR can be expressed as either the ratio of the volume of the moderator to the volume of the fuel (V_M/V_F) or as the ratio of the number of moderator atoms to the number of fuel atoms (N_M/N_F). Either definition is acceptable as long as it is used consistently. A reactor having a MFR less than this ideal value is said to be "under-moderated," and a reactor having a MFR greater than this ideal value is said to be "over-moderated." While neither of these conditions is completely ideal, it is better in practice to be slightly under-moderated than slightly over-moderated because this achieves the highest value for the thermal utilization. *If a reactor is under moderated, the temperature coefficient of the moderator will also be slightly negative (see Chapter 17), and the reactor will be easier to control.** Hence, thermal reactors tend to be slightly under-moderated rather than slightly over-moderated because this makes them much safer to operate.

Example Problem 10.3

A U-235-fueled light water reactor has an MFR of 2:1 (by volume). If the fuel rods are 1 cm in diameter and they are placed on a rectangular grid, what is the pitch P of the lattice (e.g., the centerline to centerline spacing) between adjacent fuel rods in this configuration?

Solution If the MFR is 2, there must be two times more coolant by volume than there is fuel by volume, so it follows from this that $V_M = 2V_F$, or in a regular reactor lattice, $A_M = 2A_F$. Now $A_f = \pi D^2/4 = 0.785\ cm^2$, so $Ac = 2 \times 0.785 = 1.57\ cm^2$. If the fuel rods are equally spaced in the x and y directions, then $\Delta x = \Delta y = \Delta p^2 = 1.57\ cm^2 + 0.785\ cm^2$, so the rod to rod spacing, or the pitch P is given by $P = \sqrt{(2.35\ cm^2)} \approx 1.50$ cm. [Ans.]

* In recent years the NRC has adopted the position that it will *NOT* license a commercial power plant in the United States unless it is slightly under-moderated because only then will the moderator temperature coefficient of the reactivity be negative over its entire operating range. As the temperature of the moderator is increased, fewer fast neutrons will be converted into thermal neutrons because the coolant density falls, and therefore the fission process can be self-regulated by increasing the temperature of the coolant. *Therefore, a slightly under-moderated reactor is better than a slightly over-moderated one at controlling a power surge in the event of a rapid increase in the level of the flux or the power.*

Student Exercise 10.3

In Example Problem 10.3, the MFR was specified in the units of absolute volume, that is, as the ratio of the volume of the moderator to the volume of the fuel. If the MFR for the same reactor lattice is 10:1 but it is measured on a per molecule basis (e.g., N_m/N_f) rather than as an absolute volume ratio, what will be the pitch of the lattice in this case? Hint: Use Table 10.3 to get the information you need.

10.7 Optimal Moderator to Fuel Ratios and the Effect of the Pitch on the Value of K

As we mentioned earlier, *the value of K_∞ in a thermal water* reactor *is very sensitive to the moderator to fuel ratio, and this ratio is one of the key parameters that a reactor designer attempts to optimize to create a successful design*. Table 10.4 shows how the infinite multiplication factor behaves as a function of the MFR for a square reactor lattice. Note in particular that increasing the MFR up to a certain point has the effect of decreasing the thermal utilization, but it also has the effect of increasing the resonance escape probability at the same time. Since the multiplication factor is a product of these two competing factors, the multiplication factor reaches its maximum value in a U-235-fueled PWR at a MFR of about 5.0. *Because of some regulatory and safety requirements that we will discuss in at a later time, most commercial power reactors are designed to have a MFR between 2.00 and 4.00. The exact value depends on the regulatory requirements governing the moderator coefficient of the reactivity* in the country in which the reactor is to be operated. The MFR has a direct bearing on the fuel rod spacing and by inference, the pitch of the lattice in a PWR or BWR. Low MFRs require a very tightly packed lattice with the fuel rods very close together, while higher MFRs allow the fuel rods to be spaced further apart. Figure 10.6 shows the behavior of this relationship for a square reactor lattice. For a 1 cm diameter fuel rod, notice that the optimal pitch of the lattice P corresponding to a MFR between 2.0 and 4.0 is about 1.5 cm to 2.0 cm. Assuming that the fuel rods are cylindrical in shape, the pitch P related to the diameter D of the fuel rods by

The Relationship of the Pitch P to the MFR

$$P^2 = \frac{\pi D^2 \times (MFR + 1)}{4} \tag{10.17}$$

where the MFR is expressed as the ratio of the volume of the moderator V_M to the volume of the fuel V_F:

$$MFR = \frac{V_M}{V_F} \tag{10.18}$$

We can also write the MFR in terms of the ratio of the number of atoms or molecules in the moderator to the number of atoms or molecules in the fuel. We can do this by realizing that the molecular weight of the moderator is given by $W_M = N_M V_M M_M$, and the molecular weight of the fuel is given by $W_F = N_F V_F M_F$. Hence if we know the ratio of the weight of the moderator to the weight of the fuel, W_M/W_F, we can express the ratio of the number of moderator atoms to the number

TABLE 10.4
Values of K Infinity for Different Moderator to Fuel Ratios in a Thermal Water Reactor

K_∞	Moderator to Fuel Ratio (H_2O/U-235)	Resonance Escape Probability *p*	Thermal Utilization of the Fuel *f*	Product of *p* and *f*
0.55	0.25	0.29	0.99	0.29
0.88	0.50	0/47	0.98	0.46
1.15	1.00	0.62	0.97	0.60
1.34	2.00	0.74	0.95	0.70
1.40	3.00	0.79	0.93	0.73
1.42	4.00	0.82	0.91	0.75
1.43	5.00	0.84	0.89	0.75
1.33	10.00	0.86	0.81	0.69

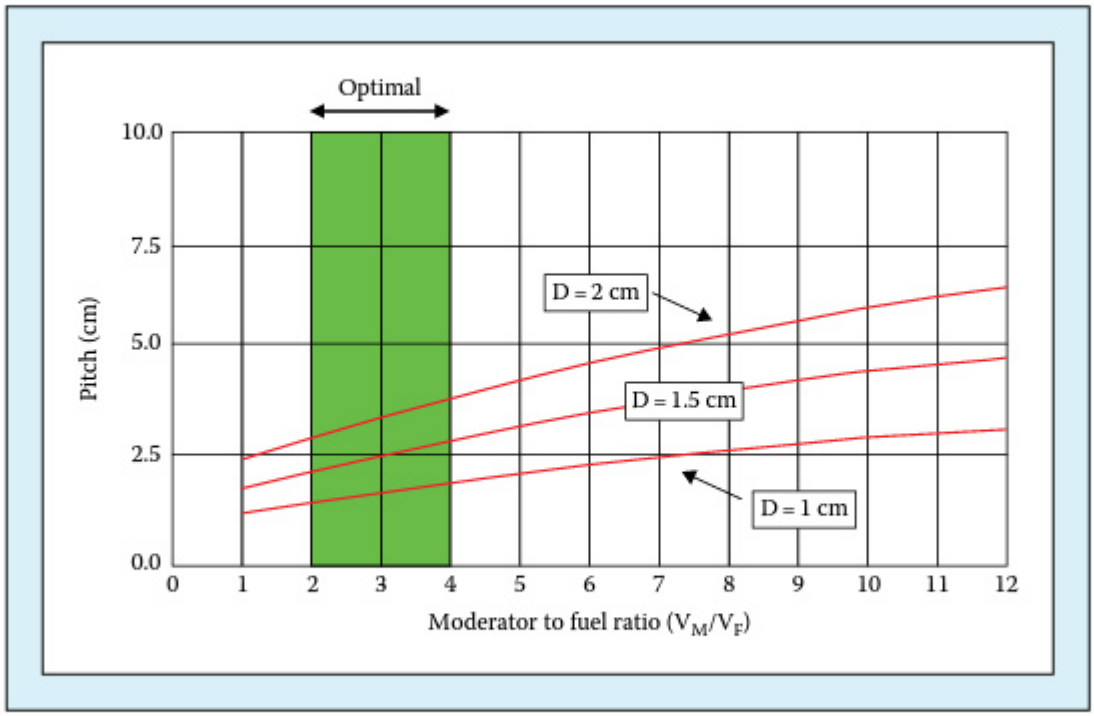

FIGURE 10.6 The pitch of a rectangular lattice for different MFRs for a cylindrical fuel rod.

of fuel atoms by writing this ratio as

$$\frac{W_M}{W_F} = \frac{N_M V_M M_M}{N_F V_F M_F} \tag{10.19}$$

where

M_F is the molecular weight of the fuel
M_M is the molecular weight of the moderator

It is easy to see that Equation 10.16 can be solved for N_M/N_F in which case we obtain

$$MFR' = \frac{N_M}{N_F} = \frac{W_M}{W_F}\frac{V_F}{V_M}\frac{M_F}{M_M} \tag{10.20}$$

Equation 10.17 is the fundamental link between (N_M/N_F) and (V_M/V_F) that allows us to interchange these two definitions. If we know the MFR as a function of the ratio of these volumes, then we can use Equation 10.17 to express the MFR as a function of the ratio of the number of atoms present. In either case, the physics is unchanged as long as Equation 10.17 is used, that is, as long as we require the following equality be true:

$$MFR' \times MFR = \left(\frac{W_M}{W_F}\right) \times \left(\frac{M_F}{M_M}\right) \tag{10.21}$$

Relationships of this type can sometimes be helpful when converting between alternative points of view. Elmer Lewis[1] in his book *The Fundamentals of Nuclear Reactor Physics* (p. 109, 1st edn.) presents an interesting graph showing the combined effects of the fuel rod enrichment, the fuel rod radius, and the soluble boron concentration on the infinite multiplication factor for a representative PWR. This figure, which is reproduced in a slightly different form here, is shown in Figure 10.7. Notice that the largest multiplication factors can be achieved for volume-based MFRs between 2 and 4. Fuel rods with larger diameters tend to increase the value of the multiplication factor slightly, but then it is more difficult to remove the heat from the fuel.

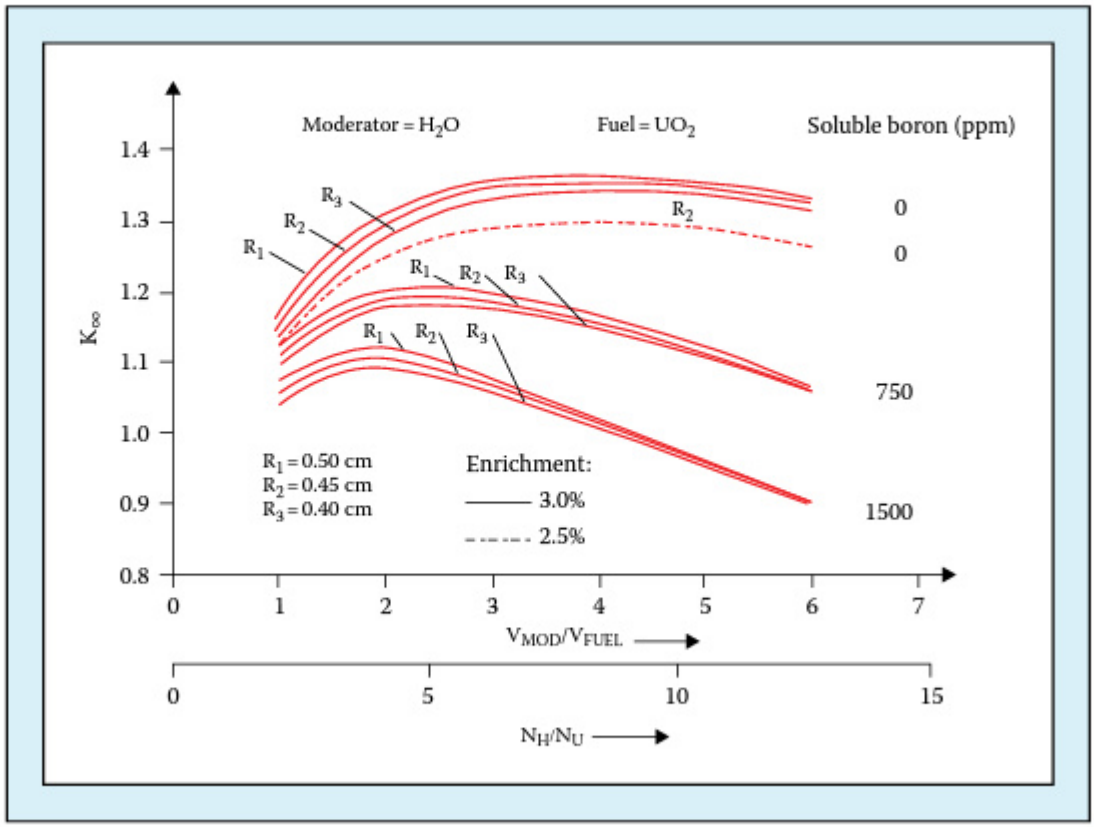

FIGURE 10.7 Various values of K_∞ for a pressurized water reactor lattice as a function of the fuel rod radius R, the MFR (V_M/V_F), the enrichment of the fuel e, and the soluble boron concentration in the coolant (in PPM). (Adapted from Lewis, E., *Fundamentals of Nuclear Reactor Physics*, Academic Press, Boston, MA, 2008.)

For a variety of reasons (mostly related to reactor safety and the transient response of the core), the multiplication factor is generally optimized for a fresh PWR core at a MFR of about 2, and the fuel rods in this case have a diameter of about 1 cm. Later in life, the optimum value of the MFR is about 3.5, but this requires virtually all of the soluble boron to be removed from the core. Hence, a multiplication factor of 1.4 is about the maximum value that can be achieved when the moderator is separated from the fuel. In some cases (see Table 10.4), this can be extended to about 1.43, but in both PWRs and BWRs, this is the practical upper limit of the multiplication factor—assuming that the fuel assemblies are square.

Example Problem 10.4

Using what you have just learned about the relationship between the MFR and K_∞, we would like you to be able to solve the problem described below.

If the MFR in a thermal water reactor is 2 to 1, what is the thermal utilization and the resonance escape probability in this reactor if it uses uranium fuel enriched to a concentration of about 2.5%? How many neutrons that make it to thermal energies in this reactor are *not absorbed in the fuel*?

Solution From Table 10.4, it can be seen that a MFR of 2 corresponds to a value for f of 0.95 and p of 0.74. Since the thermal utilization is defined as the fraction of the neutrons that reach thermal energies and are absorbed by the fuel, 100% − 95% = 5% of these neutrons are *not* absorbed by the fuel in this case. [Ans.]

10.8 Comparing Hexagonal Fuel Assemblies to Square Ones

Certain types of reactors such as Liquid Metal Fast Breeder Reactors (or *LMFBRs* for short) use a hexagonal lattice rather than a rectangular one to increase the power density of the core. An example of this type of lattice is shown in Figure 10.8. The hexagons can be further subdivided into equilateral triangles that define the centerline to centerline rod spacing, or the overall pitch P of the lattice. Relative to a square lattice with the same fuel rods, a hexagonal lattice will have a power

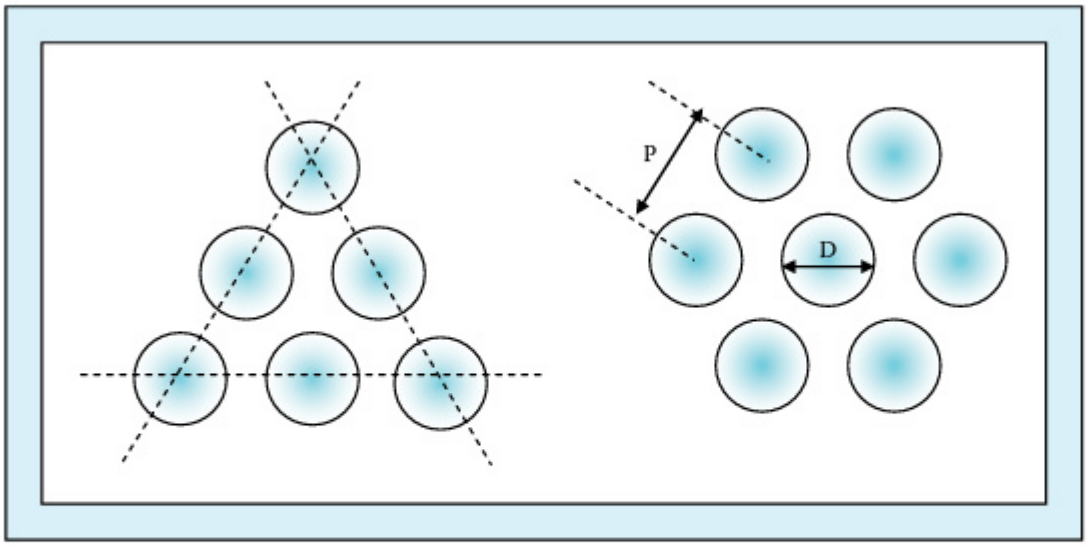

FIGURE 10.8 Two views of the fuel pins in a hexagonal reactor fuel assembly.

density about 16% higher than its rectangular equivalent. *Military and space-bound reactors tend to use hexagonal lattices because the reactor vessel can be made smaller and because space in these applications is usually at a premium.*

However, each type of lattice offers its own unique advantages, and when more moderator is required to increase the thermal neutron population, it is usually easier to simply increase the enrichment of the fuel than it is to move to a hexagonal arrangement of pins with a reduced pitch. Fast reactors do not require any moderator to slow down the neutrons and so the additional volume needed to house the extra moderator is not required in this case.

Example Problem 10.5

Relative to a rectangular lattice with a square pitch, show that density of the fuel, and hence the theoretical power density is approximately 16% greater for a triangular or hexagonal lattice having the same size fuel rods.

Solution Assume that both lattices consist of fuel rods having a diameter D. When the fuel rods exactly touch each other in a rectangular lattice, the area A_F occupied by the fuel is $\pi D^2/4$ and the area A_M occupied by the moderator is $D^2 - \pi D^2/4$. The ratio of the area occupied by the moderator to the area occupied by the fuel is therefore $A_M/A_F = (4 - \pi)\,\pi = 0.273$.

When the same type of fuel rods exactly touch each other in a hexagonal lattice, the area A_F occupied by the fuel is $\pi D^2/8$ and the area A_M occupied by the moderator is $2\sqrt{3D^2/8 - \pi D^2/8}$. The ratio of the area occupied by the moderator to the area occupied by the fuel in a hexagonal lattice is therefore $A_M/A_F = \left(2\sqrt{3-\pi}\right)\pi = 0.102$. The difference between these two ratios is $0.273 - 0.102 = 0.17$ or about 17%. In this simple example, we did not account for the thickness of the cladding. When the thickness of the cladding is factored into these numbers, the difference in these ratios is about 16%. So, a hexagonal lattice can contain about 16% more fuel for the same diameter fuel rods than an equivalent rectangular lattice can. [Ans.]

10.9 Using the Six-Factor Formula to Predict When a System Becomes Critical

Before moving on, we would like to take a moment to describe the neutron life cycle in a thermal water reactor using the six-factor formula, which we introduced earlier in the chapter. This can sometimes be helpful when attempting to understand the parameters in the six factor formula that need to be adjusted to force a reactor into a critical state. Of course, *the four-factor formula and the six-factor formula CANNOT be applied to fast reactors because there are very few thermal neutrons in a fast reactor, and there is no thermal neutron life cycle corresponding to the process that the four-factor formula attempts to represent.*

When one looks at the six-factor formula from the perspective of a reactor designer, it is obvious that there are only two terms in the formula that serve to "create" neutrons. These terms are the fast fission factor ε (epsilon), which has a value between 1.02 and 1.08, and the eta of the fuel η, which has a value for pure fissile materials between 1.8 and 2.3.

TABLE 10.5
Typical Values of f and p for a Modern Thermal Water Reactor

Typical Values for f and p	
Thermal utilization factor f	0.85–0.95
Resonance escape probability p	0.75–0.85

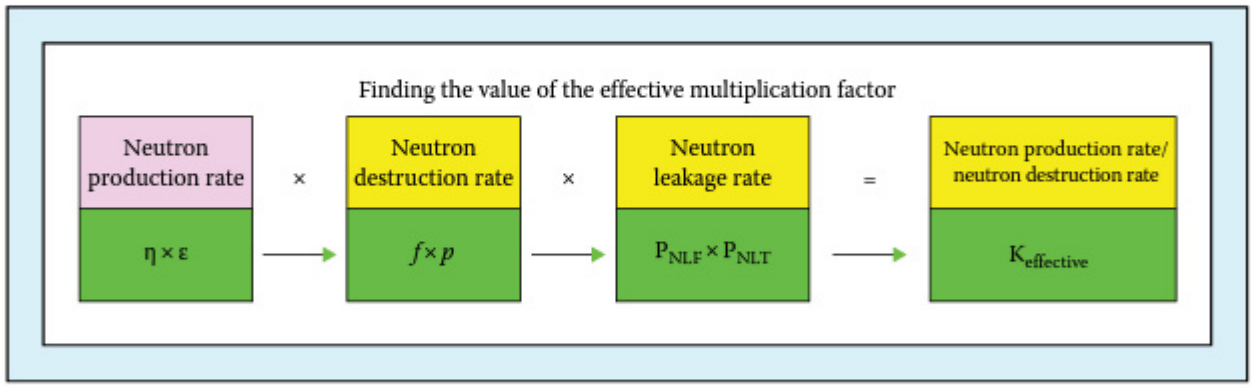

FIGURE 10.9 The neutron life cycle and its relationship to the six-factor formula.

(However, η will normally have a value between 1.3 and 1.7 when U-235 is mixed with other materials such as U-238 and Th-232.) So the largest value that the product of these two factors can have for a typical thermal water reactor is about 1.8, and the lowest value the product can have is about 1.35. This value of ηε then represents the size of the neutron production rate from all sources in the six-factor formula. So to achieve a $K_{effective}$ greater than or equal to 1.0, the product of the remaining four terms *must* be greater than 0.75 and slightly larger if possible unless we want the enrichment to exceed 3%. Now let us see how this can be done. Assume for the moment that the total fast and thermal leakage is about 4% of the total neutron population since $P_{FNL}P_{TNL} = 0.97 \times 0.99 = 0.96$. *It follows directly from this assumption that the product of the thermal utilization and the resonance escape probability, that is, fp must always be at least 0.96 × 0.75 = 0.72 to keep a reactor critical.* Now let us see when this can occur. From the values in Table 10.4, we see that the thermal utilization typically varies for a water reactor from about 0.93 to 0.94. So ideally, we need a resonance escape probability of about 0.77 for a natural uranium-fueled reactor to achieve this level of criticality. Here the U-235 concentration in the fuel is only about 0.7%.

However, if we increase the enrichment to about 3% so that product of epsilon and eta is closer to 1.7 (which is typical of a modern day PWR), then we only need the product of *f* and *p* to be about $1.7 \times 0.96 \times fp = 1.0$ or 0.61 for the reactor to be critical. Thus we can see that even when the thermal utilization of the fuel is 0.85 and the resonance escape probability is 0.75, the product of the two is $0.75 \times 0.85 = 0.64$, so in most cases, we can maintain criticality even with a very poor design when the values of *f* and *p* are low. Table 10.5 shows some typical values of *f* and *p* for a modern PWR. In these reactors, a good design can have a total $K_{effective}$ of about 1.35 even with the control rods withdrawn. The neutron production, destruction, and loss cycle for a reactor of this type is shown in Figure 10.9.

The first two terms, the eta of the fuel η and the fast fission factor ε (Epsilon), create fast neutrons and put them into the neutron life cycle. The last two terms—the fast and thermal neutron nonleakage probabilities—remove other neutrons in the reactor before they enter the absorption resonances and after they achieve thermal equilibrium with a most probable energy of 0.025 eV. The second two terms, the thermal utilization *f* and the resonance escape probability *p* remove them from the neutron life cycle because they are either absorbed before they can create another neutron or they are absorbed by a material other than the fuel that is not capable of producing any additional neutrons. The product of what is left, $K_{effective}$, is simply the ratio of the number of neutrons produced per fission to the number of neutrons removed per fission after taking all of these factors into account.

10.10 Some Limitations of the Four-Factor Formula and the Six-Factor Formula

The four-factor formula and the six-factor formulas are only designed to work for thermal reactors because the terms inside of these formulas attempt to emulate the thermal neutron life cycle. Fast reactors do not have many thermal neutrons, and so using these formulas to predict the effective multiplication factor of a fast reactor can result in significant

errors and can even lead to completely erroneous results. The most reliable way to find the value of $K_{effective}$ when moving from one type of reactor to the next is to simply use the equations for the neutron production rate P and the neutron destruction rate D that we presented in Chapter 9. However, to use these equations, we must know the neutron energy spectrum and for more detailed calculations, the shape of the neutron flux. In Chapter 13, we will demonstrate how this can be done for simple reactor geometries where the Laplacian operator (which defines the neutron leakage rate L) can be used. *Other reactor geometries can be handled by replacing the Laplacian operator ∇^2 by its finite difference equivalent*.

Thus, although the four-factor formula and the six-factor formula can be useful for performing parametric studies, they are almost never used exclusively to design reactors today. In the sections that follow, we would like to demonstrate how the six-factor formula can be used to estimate the size and the material composition of a reactor that is *not man-made*. In other words, although these formulas can be thought of as a simple set of design rules that can be used to estimate the behavior of a thermal water reactor, they should never be thought of as real design tools when more accurate calculations are required. Under these conditions, solving the neutron diffusion equation with a digital computer is a much more reliable way to proceed. Moreover, *this approach has the advantage that it can be used to predict the behavior of both fast and thermal reactors.*

10.11 Applying the Six-Factor Formula to the Great Natural Nuclear Reactors of Oklo

We would now like to turn out attention to how the six-factor formula can be applied to *natural nuclear reactors* as well. In our companion book*, we discussed how the concentrations of U-235 and U-238 in the Earth's crust have changed over time. In particular, we presented a detailed account of how the relative concentrations of these two isotopes have changed over geologic time frames through the process of radioactive decay. Because their radioactive half-lives are different, the U-235 used as fuel in nuclear reactors today decays about *four times* more rapidly than its sister isotope, U-238, which is also used as a nuclear fuel. To put all of this into perspective, we would like to discuss how *natural nuclear reactors* once covered the Earth long before humans appeared to build the nuclear power plants of today. The best known examples of these natural nuclear reactors are the *great natural nuclear reactors of Oklo* (see Figure 10.10), which once covered the Earth billions of years ago. About 2 billion years ago when the Earth was very young, one of the strangest events in the history of the Earth, geologically speaking, occurred in a region of West Africa that has become known as the country of Gabon today. The concentration of U-235 in the Earth's crust became so high that it actually triggered a sustained nuclear chain reaction in the rocks at *Oklo*.

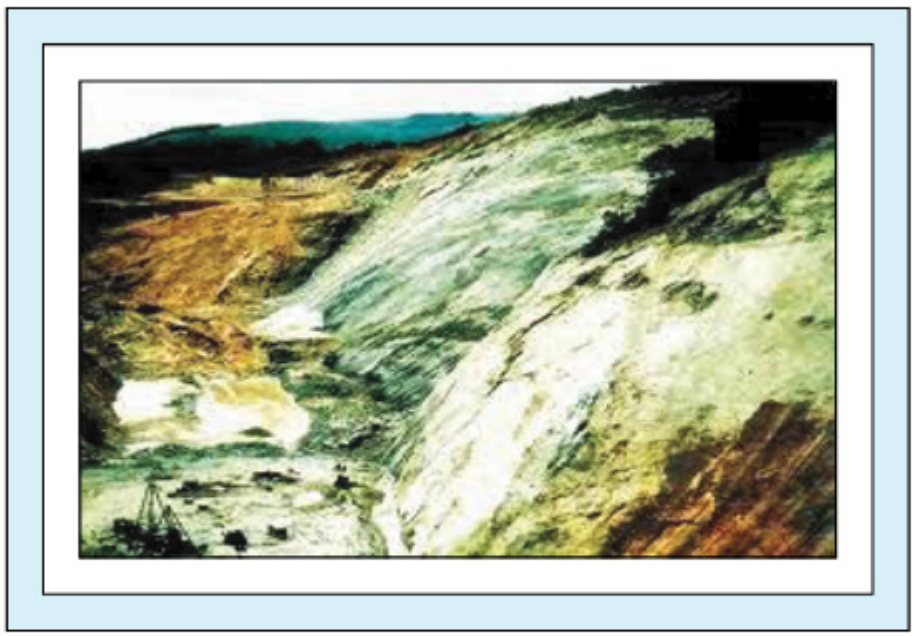

FIGURE 10.10 The site of some of the great natural nuclear reactors of Oklo, which burned vigorously on the surface of the Earth about 2 billion years ago. (This public domain image was obtained from Google Images.)

* See *Nuclear Engineering Fundamentals: A Practical Perspective*, by R.E. Masterson, CRC Press (2017).

But rather than exploding like an atomic bomb does, it produced *a sustained nuclear chain reaction* that continued gently for over 100 millennia, generating more energy in the process than a large research reactor (about 100 kilowatts) does today. This remarkable event did not occur at just one location at Oklo, but instead it occurred at 16 separate locations where self-sustaining nuclear reactions have been found. The Oklo reactors, built entirely out of natural uranium, ran for over 150,000 years, and during that period of time, they produced more energy than 100 Megaton bombs. (In comparison, the atomic bombs that were dropped on Japan near the end of the Second World War had an explosive yield of only 20 Kilotons) Groundwater mixed with uranium ore at these locations to make these reactions possible. The water acted as a neutron moderator and coolant—just like the moderators in commercial nuclear reactors do today. The water slowed down, or "moderated," the neutrons produced by the U-235 so additional fission reactions could occur in the uranium ore. The heat generated by these reactions caused the groundwater to boil away, which slowed down or stopped the reactions entirely. Then after the uranium cooled, and the short-lived fission product poisons decayed, the ground water returned, more neutrons were moderated, and the reactions started over again. *This is exactly the same principle that a BWR uses to operate today*.

The concentrations of the fission products in the rocks at Oklo suggest the reactors would turn themselves on for about 30 minutes when the ground water was present, and then after the water boiled away, they would shut down for about 2.5 hours before coming to life again (see *Physical Review Letters*, Volume 93, paper 182302). In other words, these natural nuclear reactors acted as a power source for a geyser like "Old Faithful," which still erupts in Yellowstone National Park today with a period of about 1 hour. Just like the modern nuclear reactors of today, the great natural nuclear reactors of Oklo had a negative temperature coefficient (due to the boiling and thermal expansion of the ground water), and the neutron poisons that were generated from the short-lived fission products controlled the size of any nuclear transients that occurred. We would like to apply the six-factor formula to these ancient reactors to show exactly what made a value of $K_{effective}$ greater than 1.0 possible for not just a few years, but for more than 100 millennia. *No man-made structure or machine ever built (including the Great Pyramids of Egypt—see Figure 10.11) has even remotely approached the longevity that these natural reactors achieved as they operated peacefully for over 150,000 years*. The remains of these reactors can be seen in Figure 10.10, and other pictures of these reactors can be found in Chapter 9 of our companion book.* Therefore, we can learn a great deal about how to design a modern nuclear reactor from the natural nuclear reactors that nature decided to build on its own about 2 billion years ago. Some conspiracy theorists have suggested that the Oklo reactors were built by aliens from another world, but there is no credible evidence to suggest that this is the case.

Now we would like to take a moment to analyze the behavior of these reactors in more detail. At the time the Oklo reactors existed, the concentration of U-235 in the Earth's crust was about four times higher than it is today, or about 2.8% (see Chapter 9 of our companion book*), and the U-238 concentration was about 97%. This is equivalent to the enrichment of the fuel rods in a modern thermal water reactor today. So the eta of the fuel η had a value between 1.3 and 1.7, which is very comparable to what we observe in modern thermal water reactors today. Because U-238 was intermixed with U-235 in the uranium ore, the value of the fast fission factor Epsilon, or ε, was also comparable to what is used in

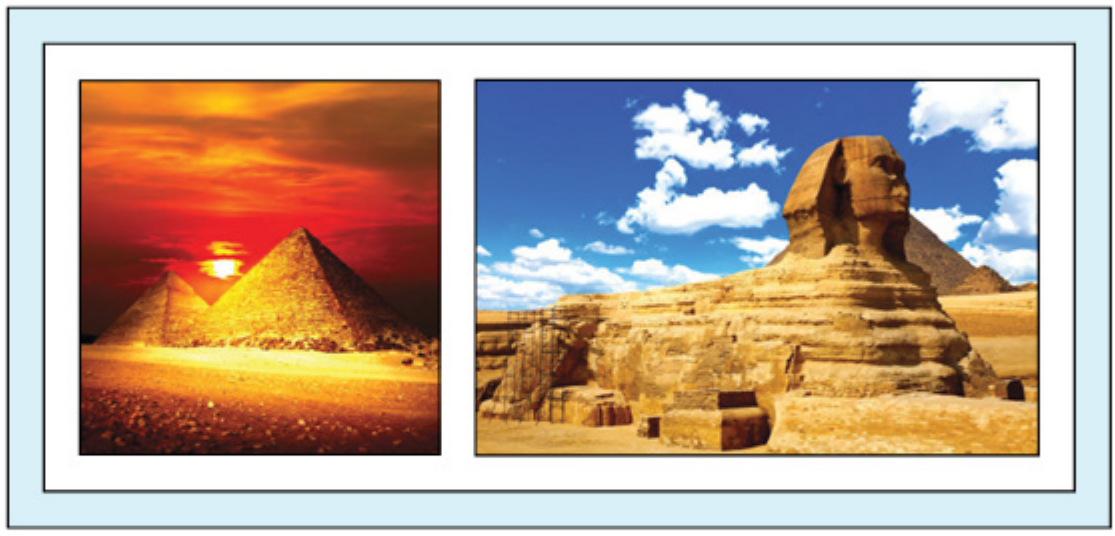

FIGURE 10.11 The great natural nuclear reactors of Oklo operated peacefully for over 150,000 years, which happens to be over 30 times the age of the great pyramids of Egypt including the great pyramid of Khufu, which can still be seen on the Giza plateau. The amount of time they remained critical can be predicted quite accurately with the six-factor formula.

* *See Nuclear Engineering Fundamentals: A Practical Perspective*, by R.E. Masterson, CRC Press (2017).

thermal water reactors today. Hence, it had a value between 1.02 and 1.08. So it is obvious from these initial observations that the neutron production terms in the six-factor formula were very comparable to those that we find in modern reactors today. The reader must also recall from our previous discussion that the infinite multiplication factor (in the absence of neutron leakage) exceeds unity in a thermal water reactor when the MFR is greater than about 0.80. So a self-sustaining chain reaction can be achieved if the MFR is properly chosen. A study of the geology of Oklo suggests that the MFR at the time was about 10 to 1. This is about the same ratio we see in light water reactors today. *So again the data suggests that there are many similarities between the way modern reactors are designed, and the way the Oklo natural nuclear reactors operated about 2 billion years ago.*

10.12 Estimating the Critical Size of the Oklo Reactors

For the Oklo reactors to achieve a self-sustaining nuclear chain reaction, the leakage rate from the surface of the water–uranium mixture would have had to be *less* than the leakage rate required to drive the effective multiplication factor below 1.0. Since the neutron leakage rate is proportional to the surface area S of the mixture, and the fission process must have occurred in an ore deposit having volume V, the surface to volume ratio (S/V) was apparently small enough to keep the Oklo reactors critical for a significant period of time (see Figure 10.12).

Hence, many of the uranium ore deposits that became critical were eventually found to be spherical in shape. If the shape of these deposits could be approximated by a sphere of radius R, then the surface to volume ratio would be $S/V = 4\pi R^2/4/3\pi R^3 = 3/R$. Thus the surface to volume ratio is inversely proportional to the radius of the sphere, and the nonleakage probability decreases when the radius of the ore deposits increases. A large sphere will simply absorb more neutrons within its volume than a small sphere, and so a large sphere will have more neutrons available to participate in another fission reaction. When a sphere of enriched uranium is very small, the neutrons leaking from its surface are not balanced by the fission reactions occurring in the interior. But as R increases, the surface to volume ratio S/V decreases, and the nonleakage probability P_{NL} increases accordingly. At some point, the radius becomes large enough that the neutron production rate and the neutron leakage rate come into balance, and a critical size is reached where a nuclear chain reaction can be sustained. For the Oklo reactors, the uranium deposits were just large enough (about a meter in diameter), and the enrichment of the ore was just high enough (about 3%) that the nonleakage probability stayed above 0.75 (75%) for a long period of time. Using the six-factor formula as our guide, the Oklo reactors could be modeled by requiring that

Modeling the Oklo Reactors with the Effective Multiplication Factor

$$K_{effective} = P_{FNL}P_{TNL}K_{\infty} = P_{FNL}P_{TNL}(\eta\varepsilon fp) \qquad (10.22)$$

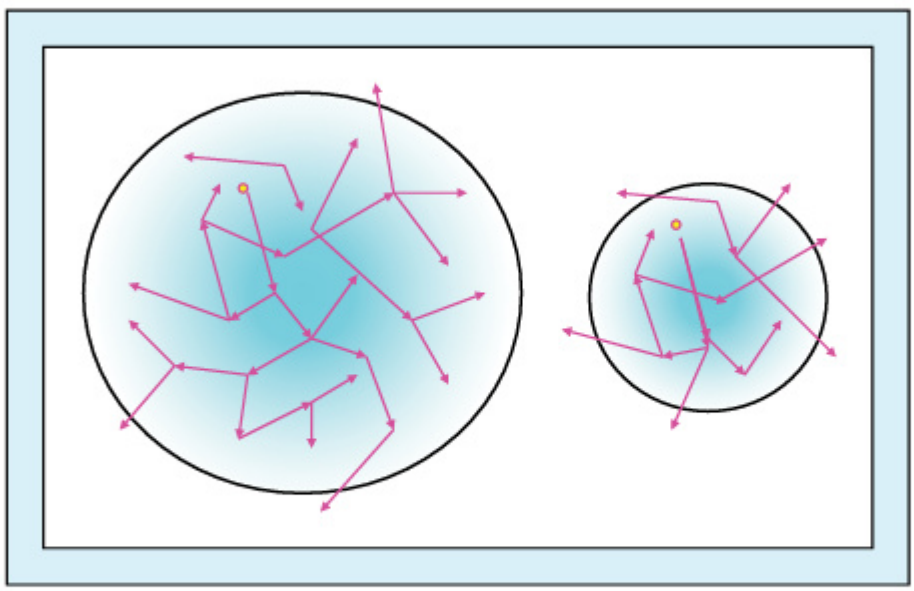

FIGURE 10.12 An illustration of why the nuclear reactors of Oklo worked so well. A large sphere will trap more neutrons and lead to more fissions than a smaller sphere of the same material. As the sphere becomes larger, more neutrons are trapped within its volume, and it will have a lower leakage rate than a smaller sphere. The Oklo reactors were just large enough to strike a balance between the neutron production and leakage rates and stay critical for a very long period of time.

where $\eta\varepsilon \approx 1.9$, $fp \approx 0.75$, and $P_{NL} = P_{FNL}P_{TNL} = 0.72–0.75$. This results in a value for $K_{effective}$ between 1.02 and 1.07 when ground water flowed through the deposits. Hence, the Oklo reactors were able to stay critical for a very long period of time without exploding or forcing the uranium ore apart.

In fact, this remarkable balance between the fission rate and the leakage rate was achieved in at least 16 separate locations across the Oklo site. So, in hindsight, the natural nuclear reactors of Oklo actually provided a good engineering blueprint for how to build a nuclear reactor from scratch without becoming too energetic in the process. It is truly remarkable that these blueprints for how to build a successful nuclear reactor existed for almost 2 billion years before they were first discovered by the French, and later published by George Cowan in a Scientific American article in 1976.† This was approximately 30 years after the first man-made reactor was built as part of the Manhattan project during the Second World War.*

10.13 Other Applications of the Six-Factor Formula

We can also use the six-factor formula to understand how to build a reactor that will "go critical" and thereby produce useful amounts of electrical power. Critical mass experiments have shown that a uranium sphere with a 3% enrichment that is water reflected will have a minimum critical mass of about 2 kg in a heterogeneous medium and nearly 3 kg in a homogeneous one. This minimum critical volume will be just large enough to go critical initially and will not sustain a chain reaction for a prolonged period of time. A larger reactor will have a higher power output, and will be able to operate for a longer period of time as well. The presence of a reflector reduces the geometric buckling, as does increasing the size of the fuel-bearing region. Both of these observations, if properly implemented, then increase the probability that a reactor will be able to remain critical for at least a very short period of time. A critical reactor is also very sensitive to the MFR. MFRs between 2 to 1 and 4 to 1 provide very large values of the effective multiplication factor and still produce a negative moderator temperature coefficient—which is required to obtain an operating license if the reactor happens to be located in the United States. Other guidelines that most commercial nuclear reactors tend to follow include

- Minimizing the number of nonfissionable atoms with high neutron capture cross sections (poisons)
- Providing a reflector to further reduce the geometric buckling of the flux because this reduces the neutron leakage rate
- Using a moderator which is close to the mass of a neutron in order to have the maximum energy transfer per collision, reducing the chance for resonance absorption of the neutrons
- Using fuels with higher enrichments to compensate for increased neutron leakage when attempting to achieve a critical mass in a very small reactor, such as those developed for aircraft carriers and nuclear submarines.

We can also use these guidelines to compare a research reactor to one that is designed to produce electric power.

10.14 Reactor Characteristics and Some Typical Values of the Neutron Flux

Reactors can be designed to have many different sizes and shapes. The primary utility of the six-factor formula is that it can be used to quickly estimate the effective multiplication factor of any thermal reactor as long as the isotopic composition of the fuel and the geometry of the core are known. Commercial power reactors tend to operate at high temperatures and pressures (usually in excess of 2000 PSI and 500°F), while some research reactors operate at atmospheric pressures to avoid the cost of an expensive containment system. Fuel loading schemes can also vary from one reactor type to the next. Neutron fluxes can vary too based on the enrichment of the fuel, the core size, the moderator type, and other core characteristics, but for water reactors, their values are typically in the range of 1×10^{13} to 5×10^{15} neutrons/cm^2/s. On the other hand, *military reactors* are much smaller due to their more highly enriched fuel, and *research reactors* are also much smaller because of their lower power output. The six-factor formula is useful for calculating the value of $K_{effective}$ for any of these reactors. Without the fuel rods inserted, well-designed thermal reactors have a value for $K_{effective}$ between 1.35 and 1.40 at startup. This is quite common for modern PWRs and BWRs. The reactor power level is also proportional to the neutron flux, and reactors with higher enrichments tend to have higher values of ϕ as well.

10.15 Understanding the Relationship between the Flux and Power

Once the enrichment of the fuel is specified, the power generated in the core is directly proportional to the value of the neutron flux $\phi(x, y, z)$. As the value of the flux increases, more heat is generated in the core, and more nuclear chain reactions occur. Conversely, if the flux is lower, fewer chain reactions will occur, and less heat will be produced. This trend

* See Reference 11.

† See Reference 12.

remains the same if one uses one energy group or more than one energy group to describe the neutron flux. However, using more than one energy group can give more accurate estimates of the power level as well as where the power is produced. We can express the relationship between the power P and the flux ϕ as

$$P = c\phi\Sigma_f \tag{10.23}$$

where c is an empirical constant (not to be confused with the speed of light) on the order of 3.205×10^{-11}/fission/W s, and

$$R_f = \phi\Sigma_f \tag{10.24}$$

is the total fission reaction rate in fissions per cm^3 per second. These equations can be generalized to account for both thermal neutrons and fast neutrons by writing the fission rate as

$$R_f = \phi_f\Sigma_{ff} + \phi_t\Sigma_{ft} \tag{10.25}$$

where Σ_{ff} and Σ_{ft} are the fast and thermal fission cross sections. Multiplying the fission rate R_f by the volume of the core V then gives the total fission rate R_{total} for the entire reactor. Multiplying by the constant c then gives the total power produced in watts. From these equations, it is easy to see that about 3×10^{10} fissions, *or about 30 billion fissions, per second are required to produce one Watt of thermal power*. This is because each fission, on average, generates about 200 MeV of thermal energy, or in more conventional units, 3.2×10^{-9} J. To calculate the total power produced P (in watts), the following unit conversions are required:

Converting the Number of Fissions per Second to Useful Power in Watts

$$\begin{aligned}\text{Thermal power (in watts)} = {} & \text{Total neutron flux } \phi \text{ (in neutrons/cm}^2\text{ s)} \\ & \times \text{the macroscopic fission cross section } \Sigma_f \text{ (in cm}^{-1}\text{)} \\ & \times \text{the total volume of the core V (in cm}^3\text{)} \\ & \times 1/\text{(number of fissions/W/s)}\end{aligned} \tag{10.26}$$

Of course, these relationships do not account for the fact that only about 1/3 of the thermal power generated in the core is converted into electricity because the remaining thermal power is simply discarded in the form of *waste heat*. There are four additional points we would like to make at this time:

1. For a given value of the neutron flux ϕ, the power output, or the power density, will be greater in regions of the core having a higher enrichment than in regions of the core having a lower enrichment.
2. The value of the neutron flux $\phi(x, y, z)$ is not the same everywhere in the core, and this means that some regions of the core may run hotter or colder than others.
3. As the fuel atoms are burned and the enrichment of the fuel falls, the neutron flux must be increased very slowly (usually over a time period of several months) to keep the power level constant. This is normally done by removing control rods from the core.
4. As the fuel is burned, fission products build up in the fuel rods, and the concentration of these fission products will increase over time. To compensate for the neutrons that some of these fission products absorb, the control rods must be removed from the core even further. This reduces the effective multiplication factor, and eventually some of the fuel assemblies have to be replaced.

If there is less fuel to consume, a reactor fuel assembly will also produce less power for the same value of the neutron flux. Over time, the effective multiplication factor will decline from about 1.4 to 1.0. Then, the reactor will have to be shut down for refueling. The refueling period normally lasts between 30 and 45 days, although shorter refueling periods are more common than longer ones these days (see Chapter 18).

10.16 Representative Values of the Flux and the Enrichment

There are a variety of ways that the value of the neutron flux can be increased to obtain more power from a given amount of fuel. Using simple neutron diffusion theory (see Chapter 13), it can be shown that the most straightforward way to do this is to simply increase the enrichment of the fuel. Many *military reactors use this approach, where the average enrichment of the fuel can approach 95%*. Hence more fissionable material in a given volume of space means that more neutrons

can be produced from the fission of this material. In addition, if we increase the enrichment of the fuel to increase the core power density, then it is possible to reduce the size of the core required to produce this power. Fuel assemblies with an enrichment between 6% and 10% create a neutron flux of approximately 10^{16} neutrons/cm^2/s. This is a very high value for the enrichment and the flux in a commercial power reactor. A modern PWR will have an average fuel enrichment between 3.5% and 4.0%, and even a fresh core having several fuel assemblies with an enrichment of 5% will not have a neutron flux much greater than about 5×10^{15} neutrons/cm^2/s.

The neutron flux in a modern PWR today varies between about 1×10^{15} neutrons/cm^2/s and 5×10^{15} neutrons/cm^2/s. Higher flux levels will either cause the fuel rods to overheat or they will shorten the life of the reactor pressure vessel because of increased radiation levels. Normally the core is configured in order to reduce the number of high energy neutrons that strike the reactor pressure vessel wall. This prolongs the life of the pressure vessel and also has a number of other desirable benefits that we will discuss in Chapter 17.

10.17 Thermal to Fast Neutron Flux Ratios in Thermal Water Reactors

At any given point in time, modern *thermal water reactors are designed so that between 33% and 40% of the neutron population in the core is in the thermal energy range (<1 eV), and the remaining neutrons (60%–67% of them) are in the epithermal or fast energy range.* These epithermal and fast neutrons have energies between about 1 eV and 10 MeV. If we consider the shape of the neutron energy spectrum in these reactors, it is apparent that approximately 60% of the neutrons that are created every second (see Figure 10.13) never make it down to the thermal energy range because of the interdependence between the resonance escape probability p and the thermal utilization f. *Fast reactors, on the other hand, do not need as many thermal neutrons to function effectively, so between 95% and 99% of the neutrons in the core can be considered to be fast.* Therefore, it should come as no surprise that the four-factor formula and the six-factor formula *DO NOT APPLY to fast reactors* because the values of the thermal utilization and the resonance escape probability are completely different in this case. The fast and thermal flux distributions in a typical thermal water reactor surrounded by a neutron reflector are shown in Figure 10.14. *Notice that the only place where the number of fast neutrons and thermal neutrons is approximately the same is in the reflector. In the core, there are approximately two fast neutrons for every thermal neutron*. In recent years, there has been considerable interest in developing new materials to increase the *volumetric power density* P/V as well. Again, P refers to the total recoverable power that is generated, and V refers to the volume of the core where the power is generated.

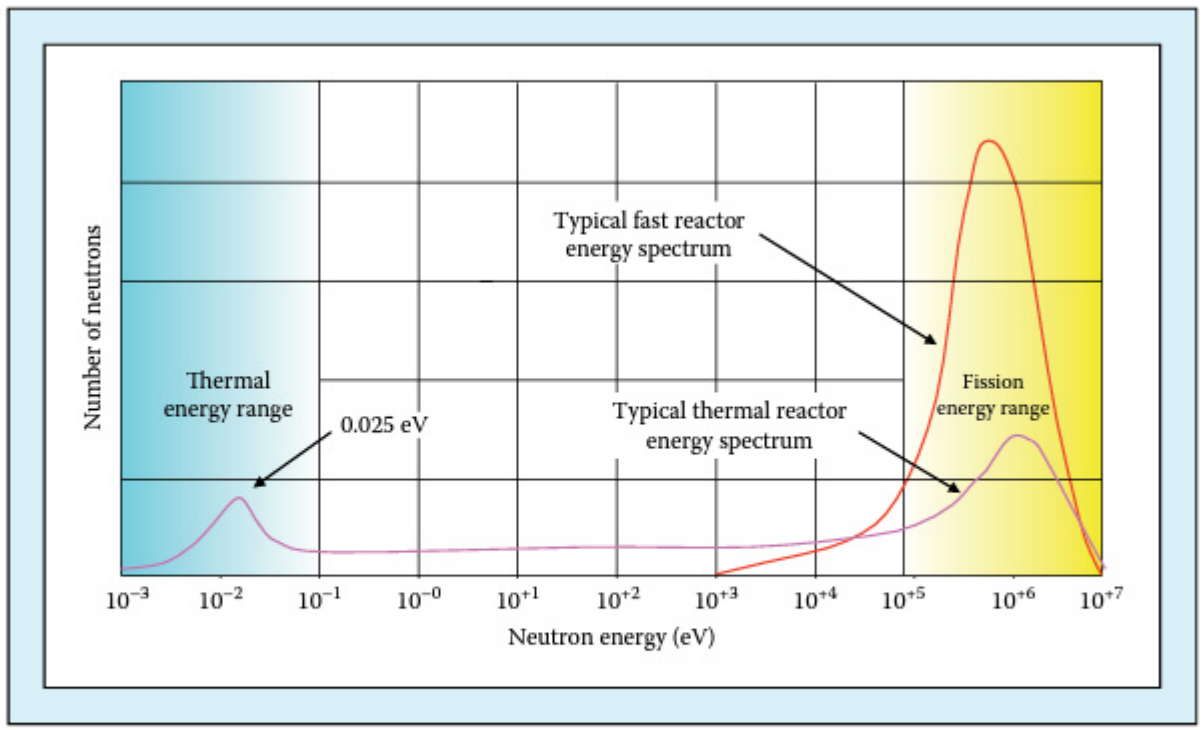

FIGURE 10.13 A picture of the neutron energy spectrum of a fast and thermal reactor. Notice that even when a reactor is referred to as a "thermal reactor," only about 1/3 of the neutrons are in the thermal energy range.

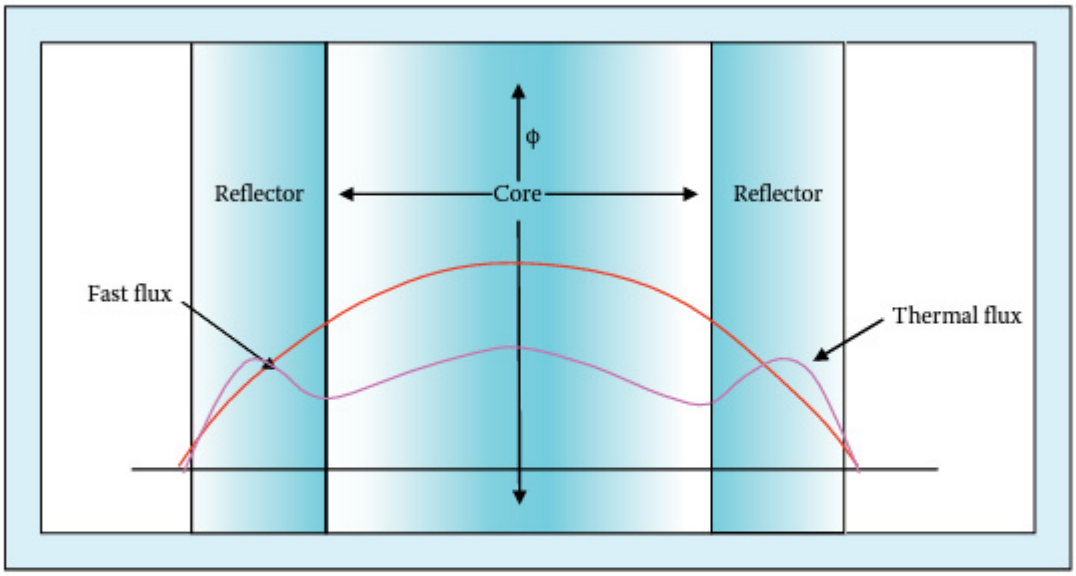

FIGURE 10.14 A picture illustrating the fast and thermal flux levels in a typical PWR or BWR with a reflector around the core.

Example Problem 10.6

Suppose that the neutron flux in a PWR is 2×10^{15} neutrons/cm^2/s. If the average enrichment of the fuel is 3.12%, how much power is generated from 1 cm^3 of the fuel? Assume that Σ_f for U-235 with only a single energy group is about 0.05 cm^{-1}.

Solution If the fuel has an enrichment of 3.12%, then the fission cross section for the fuel is approximately $0.0312 \times 0.05\ \text{cm}^{-1} = 0.00156\ \text{cm}^{-1}$. The total power generated from a cubic centimeter of the fuel is therefore $P = c\phi\Sigma_f = 2 \times 10^{15}$ neutrons/cm^2/s $\times$ 0.00156/cm/3.12×10^{10} fissions/watt/s = 100 watts/cm^3 where c (not to be confused with the speed of light) = $1/(3.12 \times 10^{10}$ fissions watts). [Ans.]

10.18 Comparing the Shape of the Fast and Thermal Buckling

Simple prescriptions such as the six-factor formula are based on the premise that the geometrical buckling of the fast and thermal flux is similar—at least in a bare homogeneous core without a reflector. However, the curvature of the fast flux is normally *greater* than that of the thermal flux because more fast neutrons will leak out of the core than thermal neutrons. In practice, this means that *there are actually two values for the geometric buckling in a thermal water reactor, and the buckling for the fast group $(B_1)^2$ will normally be greater than the buckling for the thermal group $(B_2)^2$*. When we study two-group diffusion theory in Chapter 12, we will see that it is possible to derive separate formulas for the geometric buckling for the fast and thermal neutrons from the two-group neutron diffusion equations. Using two-group diffusion theory as our guide, it can be shown that the effective multiplication factor of the core is then

$$k_{\text{eff}} = p\varepsilon\eta_2 f_2 \cdot P_{NL1}P_{NL2} \tag{10.27}$$

where

η_2 is the eta of the fuel for the thermal energy range
f_2 is the thermal utilization factor for the thermal neutrons (which are also in the thermal energy range)
P_{NL1} is the fast nonleakage probability
P_{NL2} is the thermal nonleakage probability

In general, $P_{NL1} < P_{NL2}$ because $B_1^2 > B_2^2$. We can see this more clearly by realizing that the fast and thermal nonleakage probabilities (see Chapter 12) can be written as

$$P_{NL1} = \frac{1}{1 + L_1^2 B_1^2} \quad \text{and} \quad P_{NL2} = \frac{1}{1 + L_2^2 B_2^2} \tag{10.28}$$

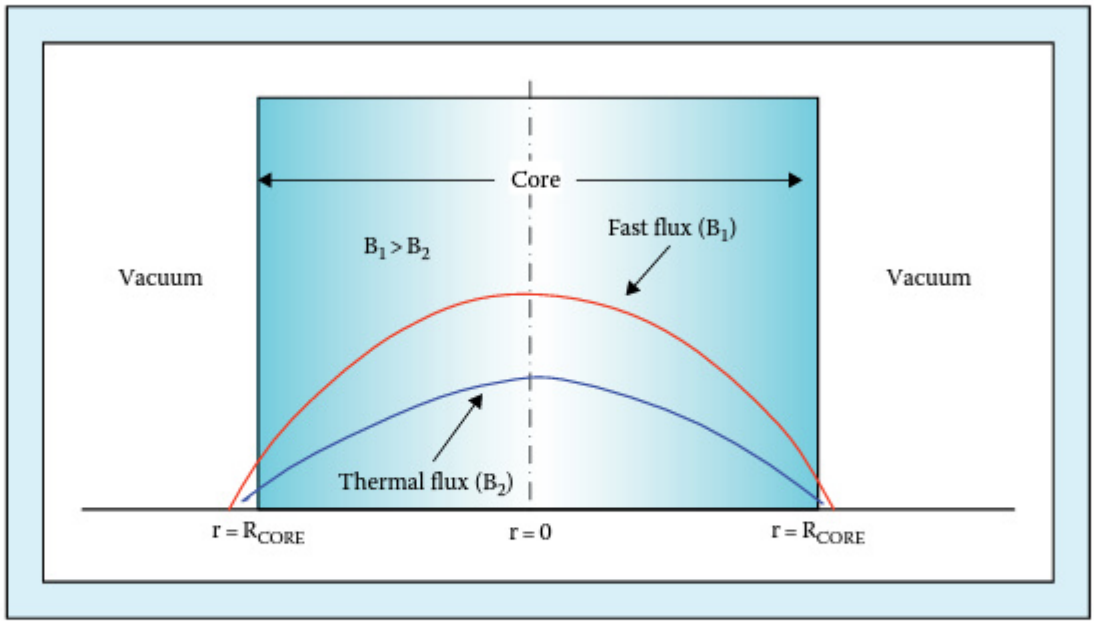

FIGURE 10.15 The fast and thermal flux shapes in a bare homogeneous reactor without a reflector. Notice that the geometric buckling of the fast flux $(B_1)^2$ is greater than the geometric buckling of the thermal flux $(B_2)^2$. This means that a greater percentage of the fast neutrons leak out of the core. In addition, in a thermal water reactor, there are about two fast neutrons for every thermal neutron.

where $B_1 \neq B_2$. However, in this case the diffusion length L_1 for the fast energy group is defined as

$$L_1^2 = \frac{D_1}{\Sigma_{R1}} \tag{10.29}$$

which is slightly different than $L_1 = D_1/\Sigma_{a1}$ because this alternative definition contains *both the absorption cross section and the scattering cross section in the denominator* (e.g., $\Sigma_{R1} = \Sigma_{a1} + \Sigma_{12}$). However, this is essentially the same as the standard definition of the diffusion length (see Chapter 11) because both terms serve to remove neutrons from the fast energy group. Upon further reflection, it is easy to see that Σ_{s12}/Σ_{R1} for a homogeneous reactor is essentially the probability that neutrons born in the fast energy group are able to escape down to the thermal energy group. In other words, the ratio Σ_{s12}/Σ_{R1} is the *resonance escape probability* p for a thermal water reactor:

$$p = \Sigma_{s12}/\Sigma_{R1} \tag{10.30}$$

In general, the fast and thermal nonleakage probabilities given by Equation 10.25 are more accurate than those given by Equations 10.4 and 10.5 because they are based on a more solid theoretical foundation. In addition, the geometric buckling of the fast flux can be different than the geometric buckling of the thermal flux ($B_1^2 \neq B_2^2$), and this is exactly what we observe in practice (see Figure 10.15).

Student Exercise 10.4

Explain in general terms why the geometric buckling for the fast neutrons is normally larger than the geometric buckling for the thermal neutrons. Hint: Consider the ratio of the neutron mean free path λ.

10.19 Comparing Core Power Densities

Modern PWRs have a core power density of about 100 kW/L and modern BWRs have a core power density of about 55 kW/L (see Figure 10.16). LMFBRs have an even higher power density (~ 400 kW/L) although some designs such as the Russian BM 600 have reported core power densities as high as 550 kW/L. These numbers have gradually increased

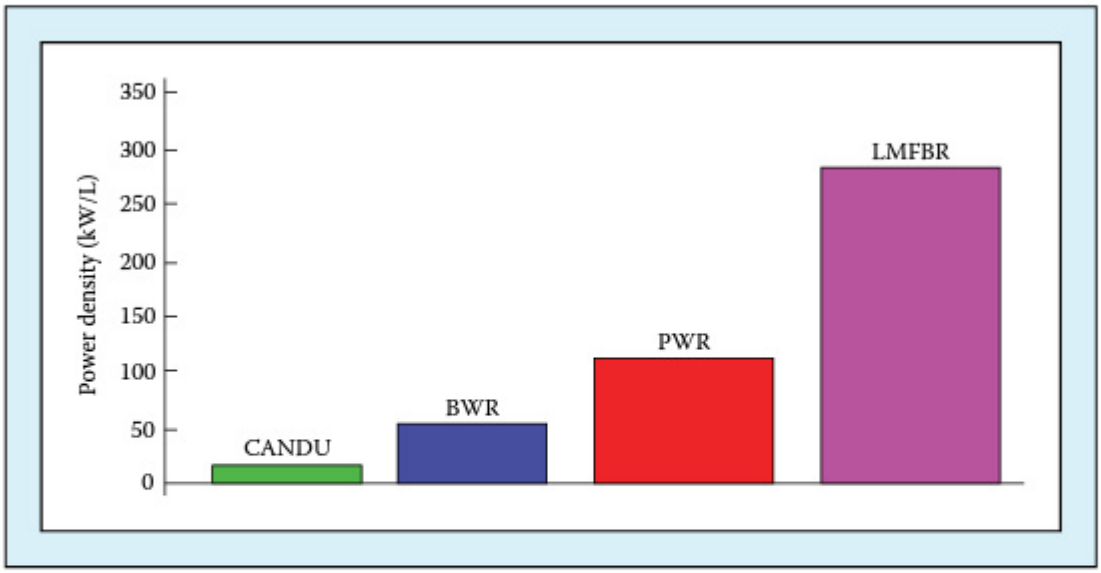

FIGURE 10.16 A comparison of the volumetric power densities in modern nuclear reactor cores. As the figure indicates, the power density is roughly proportional to the enrichment of the fuel. Fast reactors have the highest average power density, and CANDU reactors, which use natural uranium, have the lowest.

as newer and more efficient designs have come on line. If both the neutron flux and the enrichment are known, the power density can be calculated for a liter of fuel from the following equation:

The Core Power Density

$$PD = \frac{c\phi\Sigma_f}{1000} \text{ in kW/L} \tag{10.31}$$

where c (not to be confused with the speed of light) is 3.205×10^{-9}/fission/W s. Notice that this is the power density per liter of fuel only. To convert the power density to a number that is representative of the entire core, we need to know the MFR expressed as a function of (V_M/V_F). The power density expressed in terms of the actual core volume can then be found by multiplying the power density calculated per unit volume of the fuel by (V_M/V_F) or 1/MFR expressed in terms of the volume ratio of moderator to the fuel only. The average power density PD per liter of core volume is then

Average Power Density as a Function of the Moderator to Fuel Ratio

$$PD = \frac{P}{MFR} = P = \frac{c\phi\Sigma_f}{1000 \times MFR} \text{ in kW/L} \tag{10.32}$$

where

ϕ is the average value of the neutron flux

Σ_f is the average fission cross section

Of course, this equation is only valid for one energy group. The power density expressed in this way can easily be converted into the total power output of the core by simply multiplying the power density per liter by the total core volume V. The result is

$$P = PD \times V = \frac{cV\phi\Sigma_f}{1000 \times MFR} \text{ in kW} \tag{10.33}$$

where V is the total core volume in liters, and 1 L = 1000 cm^3. If there are two energy groups, the correct and more accurate form of Equation 10.30 to use is

$$P = PD \times V = \frac{c\left(\phi_f \Sigma_{ff} + \phi_t \Sigma_{ft}\right) V}{1000 \times MFR} \text{ in kW} \tag{10.34}$$

where the double subscripts f and t refer to the fast and thermal fluxes and cross sections. *Since thermal water reactors have a thermal efficiency of about 33%, multiplying this number by the thermal efficiency TE gives the total electrical output of the plant:*

Converting the Thermal Power to Electrical Power

$$P(MWE) = TE \times P(MWT) \tag{10.35}$$

Sometimes the thermal efficiency is also represented by the symbol η *(not to be confused with the eta for the fuel).* Then the equation to convert the thermal power to the electrical power becomes

$$P(MWE) = \eta \times P(MWT) \tag{10.36}$$

Now let us attempt to illustrate what Equation 10.33 implies.

Example Problem 10.7

Suppose that a thermal water reactor has a thermal efficiency of 30% and operates at a rated power of 900 MWE. How much power must the reactor generate to allow the reactor to achieve this electrical output?

Solution The actual thermal power and the rated power are related to each other by

$$P(MWE) = \eta \times P(MWT), \quad \text{so if } \eta = 0.30 \text{ and } P(MWE) = 900 \text{ MW, then}$$

$$P(MWT) = \frac{900 \text{ MW}}{0.30} = 3000 \text{ MWT} \left[\text{Ans.}\right]$$

Clearly there is an economic incentive to increase the power density because this means that the reactor pressure vessel can be smaller, lighter, and less expensive to construct. In recent years, there has also been a trend to increase both the power density and the average enrichment of the fuel. This increases the time between subsequent refuelings and it also minimizes the amount of reactor down time as well. *Today many commercial power reactors have gone to 24- or 36-month refueling cycles to get the maximum amount of energy out of the fuel before it has to be replaced. Some military reactors (because they use highly enriched uranium) can run for as long as 40 or 50 years before they have to be refueled*. These reactors are commonly found on aircraft carriers and nuclear submarines. As we mentioned in Chapter 1, the cores of these reactors have an average U-235 concentration between 90% and 95%. As a point of comparison, the CANDU heavy water reactor uses natural uranium fuel with a U-235 content of only 0.711% (about 135 times lower). Hence, the core must be at least 100 times larger to produce the same amount of thermal energy.

Student Exercise 10.5

Suppose that the same reactor we discussed in Example Problem 10.6 has a core that contains 200 fuel assemblies. What is the average power density of a fuel assembly if each fuel assembly has a cross sectional area of 30 cm^2 and is 300 cm in length? Express the power density in units of kW/L. What type of reactor do you think this is most likely to be?

References

Books and Textbooks

1. Shultis, K. and Faw, R. *Fundamentals of Nuclear Science and Engineering*, 2nd edn., CRC Press, Boca Raton, FL (2008).
2. Glasstone, S. and Eedlund, M.C. *The Elements of Nuclear Reactor Theory,* D Van Nostrand Company, Inc., New York (1952).
3. Lamarsh, J.R. *Introduction to Nuclear Reactor Theory*, 2nd printing, Addison-Wesley Publishing Company Inc. (1972).
4. Lamarsh, J.R. and Baratta, A.J. *Introduction to Nuclear Engineering*, Prentice Hall, Upper Saddle River, NJ (2001).

5. Lewis, E. *Fundamentals of Nuclear Reactor Physics*, Academic Press, Boston, MA (2008).
6. Duderstadt, J. and Hamilton, L. *Nuclear Reactor Analysis*, John Wiley & Sons, New York (1976).
7. Stacey, W.M. *Nuclear Reactor Physics*, 2nd edn., John Wiley & Sons, New York (2007).
8. Todreas, N. and Kazimi, M.S. *Nuclear Systems*, Vol. 1, CRC Press, Boca Raton, FL.
9. Henry, A.F. *Nuclear Reactor Analysis*, MIT Press, Cambridge, MA (1975).
10. Masterson, R.E. *Nuclear Engineering Fundamentals: A Practical Perspective*, CRC Press, Boca Raton, FL (2017).
11. Neuilly et al. Analysis of ore samples from the Oklo Mines in Gabon, Africa, *C.R. Acad. Sci. Paris*, 275, Ser. D:1847 (1972).
12. Cowan, G.A. A natural fission reactor, *Sci. Am.*, 235(1), 36–47 (July 1976).

Web References

1. *http://en.wikipedia.org/wiki/Prompt_neutron.*
2. *http://en.wikipedia.org/wiki/Four_factor_formula.*
3. *http://en.wikipedia.org/wiki/Nuclear_reactor_physics.*
4. *http://energy.gov/sites/prod/files/2013/06/f2/h1019v1.pdf.*
5. *http://en.wikipedia.org/wiki/Natural_nuclear_fission_reactor.*
6. *https://canteach.candu.org/Content%20Library/20030101.pdf.*
7. *http://nuclearpowertraining.tpub.com/h1019v2/css/h1019v2_43.htm.*
8. *http://www.nuceng.ca/br_space/ep4d03/learning_modules/9_4-factor_formula_for_k-inf.ppt.*
9. *http://www.nrc.gov/reactors/operator-licensing/generic-fundamentals-examinations/bwr/bwr-files/292004.pdf.*
10. *http://ocw.mit.edu/courses/nuclear-engineering/22-091-nuclear-reactor-safety-spring-2008/lecture-notes/MIT22_091S08_lec02.pdf.*

Additional References

- Important physical constants used by nuclear scientists and engineers can be found in *Appendix A*.
- Unit systems and their conversion factors can be found in *Appendix B*.
- Nuclear cross sections for many important nuclear materials can be found in *Appendix C*.
- Physical properties of important nuclear materials can be found in *Appendix D*.
- Atomic masses, half-lives, and natural abundances can be found in *Appendix E*.

Questions for the Student

The following questions cover the material presented in this chapter, and in some cases, previous chapters as well. They are designed to test how well the student has acquired a working knowledge of the subject matter.

1. What is the difference between the effective multiplication factor and the infinite multiplication factor?
2. What is the fundamental difference between the four-factor formula and the six-factor formula?
3. Approximately what percentage of the neutrons leak out of the core of a well-designed commercial thermal water reactor under steady-state conditions?
4. Write down an explicit expression for the six-factor formula.
5. What does the eta (η) of the fuel refer to in the six-factor formula?
6. What is the epsilon (ε) of the fuel that appears in the six-factor formula called, and what is its physical interpretation?
7. In a thermal water reactor, which neutrons are most likely to leak out of the core, fast neutrons or thermal neutrons?
8. Which terms in the four- and six-factor formulas are responsible for the creation of neutrons (i.e., they have a value greater than 1.0)?
9. Which terms in the four- and six-factor formulas are responsible for the destruction or leakage of neutrons (i.e., they have a value less than 1.0)?
10. What are the names of the two additional terms in the six-factor formula and what do they represent?
11. In a commercial thermal water reactor, does a fast neutron or a thermal neutron have a shorter mean free?
12. Explain why it is it not possible to use the four-factor formula to predict the infinite multiplication factor for a fast breeder reactor.
13. What does the thermal utilization of the fuel in the six-factor formula represent? Ans: The thermal utilization of the fuel f represents the fraction of neutrons that are produced in the fuel that are absorbed by the fuel.
14. What do the fast and thermal nonleakage probabilities in the six-factor formula represent?
15. In general, in a thermal water reactor, is the fast nonleakage probability or the thermal nonleakage probability higher?
16. If you had to calculate the effective multiplication factor for a fast reactor core with a single energy group, what equation would you use to calculate the effective multiplication factor if the six-factor formula was not applicable to this problem?
17. Write two equations for the fast and thermal nonleakage probabilities that depend upon the geometric buckling of the flux.
18. If the buckling of the fast and thermal flux is equal to zero, what do the values for the fast and thermal nonleakage probabilities in the previous problem become?
19. To a first approximation, are the fast and thermal nonleakage probabilities inversely proportional to the neutron mean free path λ?
20. Suppose that we divide the effective multiplication factor for a nuclear reactor core by the infinite multiplication factor. What two terms in the six-factor formula represent the specific ratio of these two values?
21. What are some typical values for the fast and thermal nonleakage probabilities in a commercial thermal water reactor?
22. If you had to calculate the effective multiplication factor in a thermal water reactor using two energy groups, what equation would you use to calculate the effective multiplication factor if the six-factor formula was not available?
23. What is the meaning of the resonance escape probability p that appears in the six-factor formula?
24. In the equation $P_{FNL} = 1(1 + B^2 \tau_T)$ for the fast nonleakage probability, what is the term τ_T sometimes called?
25. Theoretically speaking, in an unreflected reactor, should the geometric buckling of the fast flux be larger than, smaller than, or the same as the geometric buckling for the thermal flux?
26. What are some typical values for the moderator to fuel ratio (or MFR) for a pressurized water reactor?
27. Name at least one reason why the value of the MFR never exceeds a value of about five in a thermal water reactor.
28. Why are most modern reactor designed with an MFR of about three?
29. Is the value of the resonance escape probability higher or lower when the fuel is physically separated from the moderator?
30. What units does the neutron age, which sometimes appears in the calculation of the fast nonleakage probability, usually have?
31. Suppose that the total nonleakage probability for both the fast and thermal neutrons in a reactor core can be represented by an equation of the form $P_{NL} = 1/\left(1 + B^2 M_T^2\right)$, which can be easily deduced from two-group theory. What is the term M_T^2 in this equation usually called, and under what conditions does the total nonleakage probability reduce to $P_{NL} = 1/\left(1 + B^2 L_T^2\right)$, which is the expected result from one-group theory?

32. Write an expression that shows the relationship between the MFR and the pitch P of the fuel rods in a nuclear reactor fuel assembly.
33. Suppose that the ratio of the volume of the moderator to the volume of the fuel in a thermal water reactor happens to be about 4.75. Approximately how many hydrogen atoms are there for every uranium atom in the reactor lattice?
34. Write an equation for the percentage of the neutrons that leak out of the core as a function of the fast and thermal nonleakage probabilities.
35. If the pitch of a reactor lattice becomes smaller, what happens to the MFR?
36. Fill in the following sentence with the appropriate word or phrase: In a thermal water reactor, criticality can be achieved with _____ fuel when the core is _____ rather than homogeneous.
37. Suppose that we would like to express the MFR as a function of the number of moderator atoms to the number of fuel atoms instead of as the ratio of the volume of the moderator to the volume of the fuel. What equation can be used to do this?
38. For the same pitch and fuel rod diameter, is the MFR higher or lower in a thermal breeder reactor that utilizes hexagonal fuel assemblies?
39. What is a representative value for the average power density in a modern PWR core?
40. How high can the average core power density in a modern fast reactor become?
41. What is a representative value for the average power density in a modern BWR core?
42. How long did the great natural nuclear reactors of Oklo operate before they eventually shut down? Was the time that these reactors operated greater than or less than the age of the great pyramids of Egypt?
43. What is a typical percentage value for the fast neutron leakage rate, the thermal neutron leakage rate, and the total neutron leakage rate in a well-designed thermal water reactor?
44. In a thermal water reactor, approximately how many fissions per second are required to produce one watt of electrical power?
45. How is it simultaneously possible for the infinite multiplication factor to be greater than one when the effective multiplication factor is less than one?
46. How long did the blueprints to build a successful nuclear reactor exist on the Earth before the first commercial nuclear reactor was made by man?
47. Write down an expression for the effective multiplication factor when we know the values of the neutron flux and the neutron cross sections for more than one energy group.
48. At what value of the MFR does the product of the resonance escape probability and the thermal utilization achieve its maximum value in a thermal water reactor?
49. What causes the product of these two factors to achieve their maximum possible value in this case?
50. Explain why the four- and six-factor formulas are not used to design commercial power reactors today.
51. Write an equation that can be used to find the effective multiplication factor for a fast breeder reactor having ten energy groups when the neutron life cycle cannot be described using the six-factor formula.
52. In what units is the power density of most modern reactor cores measured?
53. What is a representative value for the neutron age τ in a heavy water reactor, and is it smaller or larger than it is in a light water reactor?
54. Do military reactors have higher enrichments and higher levels of the neutron flux than conventional thermal water reactors do?
55. Suppose that a thermal water reactor has a thermal power output of 2000 MW. What is the electrical power output likely to be from the nuclear power plant in which this reactor is located?
56. What is the average enrichment of the fuel in a reactor to be used in a nuclear submarine when it is first put in service? What type of reactor is this expected to be?
57. For the same MFR, does a fuel rod with a larger radius have a higher or lower effective multiplication factor than a fuel rod with a smaller radius?
58. In the six-factor formula, what does the geometric buckling B^2 that appears in the fast and thermal nonleakage probabilities represent?
59. Describe an alternative way to find the reactivity of a thermal water reactor without having to use the six-factor formula. Assume that we have only one energy group and that neutron cross sections for this energy group are known.
60. Under steady-state conditions, approximately what percentage of the neutrons in a thermal water reactor are in the fast or epithermal energy range, and what percentage of the neutrons remain thermal neutrons with an energy less than 1 eV?
61. Approximately what percentage of the neutrons in a fast breeder reactor have an energy below about 1 keV?
62. In a conventional reactor, approximately how many fissions per second are required to produce one watt of thermal power?
63. What is a representative value for the neutron age τ in a light water reactor fuel assembly?

64. How much uranium with an average enrichment of 3% is required in a heterogeneous, spherical, reflected reactor to achieve a minimum critical mass?
65. What is the value of the neutron flux in a typical PWR today?
66. Why does a spherical shape generally require the least uranium or plutonium to become critical?
67. What was one of the primary reasons why the factors in the six-factor formula were defined the way they were?
68. How many joules of recoverable energy does a single nuclear fission release?

Exercises for the Student

Exercise 10.1

Develop a simple expression for the macroscopic fission cross section of uranium dioxide as a function of the enrichment. What is the macroscopic fission cross section for thermal neutrons when the enrichment of the fuel is 3%, 4%, and 5%?

Exercise 10.2

Develop a simple expression for the macroscopic fission cross section of plutonium dioxide as a function of the Plutonium-239 content. What is the macroscopic fission cross section for thermal neutrons when the Pu-239 content is 15%, 20%, and 25%?

Exercise 10.3

A thermal water reactor contains 30% uranium dioxide and 70% light water. If no thermal neutrons leak out of the core, what is the effective multiplication factor when the enrichment of the fuel is 4%?

Exercise 10.4

A thermal water reactor contains 30% uranium dioxide and 70% heavy water. If no thermal neutrons leak out of the core, what is the effective multiplication factor when the enrichment of the fuel is 2%?

Exercise 10.5

A thermal water reactor contains 30% uranium dioxide and 70% heavy water. If no thermal neutrons leak out of the core, what is the effective multiplication factor when the reactor uses natural uranium dioxide instead of enriched uranium dioxide?

Exercise 10.6

Suppose that the thermal neutron leakage rate in Exercise 10.3 is 5% of the neutron absorption rate. What are the effective multiplication factor and the reactivity of the core?

Exercise 10.7

Suppose that the thermal neutron leakage rate in Exercise 10.4 is 3% of the neutron absorption rate. What are the effective multiplication factor and the reactivity of the core?

Exercise 10.8

A fast reactor contains 50% plutonium dioxide by volume and 50% liquid sodium, which is also used as the coolant. Suppose that the fast neutron leakage rate is 5% of the neutron absorption rate. What are the effective multiplication factor and the reactivity of the core if the plutonium content of the fuel is 20%?

Exercise 10.9

The fuel rods in a pressurized water reactor have a pitch of 12.6 mm and a diameter of 8.2 mm. Part 1: Neglecting the presence of the cladding, what is the moderator to fuel ratio (MFR) for this PWR? Part 2: Show that when the MFR is 3, the pitch of the reactor lattice must be $\sqrt{\pi} \cdot D$.

Exercise 10.10

Suppose that a fuel assembly in a commercial PWR contains uranium dioxide fuel pellets with an average enrichment of 5%. If the total neutron flux in the fuel assembly (fast plus thermal) is 3×10^{15} neutrons/cm^2/s, what is the total fission rate in 1 cm^3 of the uranium dioxide fuel? How many joules of thermal energy does this 1 cm^3 of uranium dioxide fuel produce every second?

Exercise 10.11

Suppose that the fuel assembly in Exercise 10.10 contains one million cubic centimeters of uranium dioxide fuel. How much electrical power does the fuel assembly produce per second?

Exercise 10.12

The thermal diffusion length in a light water reactor core is 3 cm. If the geometric buckling of the thermal flux is 0.015/cm, what percentage of the thermal neutrons leak out of the core? What can you do to reduce the neutron leakage rate in this case?

Exercise 10.13

The neutron age in a fast reactor core is 130 cm^2. If the geometrical buckling of the flux is 0.02/cm, what percentage of the fast neutrons leak out of the core? What percentage of the total number of neutrons in the core is likely to have energies below 1 KeV.

Exercise 10.14

A liquid-metal-cooled fast breeder reactor has a thermal efficiency of 42%. If the core contains 100 fuel assemblies and each fuel assembly produces 20 MW of thermal power, what is the total electrical output of this plant?

11

An Introduction to Neutron Diffusion Theory and Fick's Law of Diffusion

11.1 Neutrons and Their Flow through Matter

In previous chapters, we discussed neutron cross sections and reaction rates. We discussed the physics of the nuclear chain reaction, and we briefly discussed how alpha particles, beta particles, and gamma rays interact with matter. However, we purposely did not include free neutrons in our discussion, except to demonstrate how their macroscopic cross sections behave. In this context, *free neutrons are defined as neutrons that escape the nucleus of an atom and are therefore free to roam outside of it*.

In a reactor, free neutrons are the by-products of the fission chain reaction—whether they come in the form of "*prompt*" neutrons, which appear immediately after an atomic nucleus splits apart, or "*delayed*" neutrons, which appear later as the radioactive fission products produced by the fission process decay away. For a variety of reasons buried deep in the theory of nuclear structure, free neutrons are confronted with an interesting dilemma that is not always apparent to the casual reader. Once they leave the friendly confines of the nucleus, they are much more vulnerable to being destroyed, or decaying into something else. *Inside of the nucleus, they are essentially immortal, and they have a half-life of at least 20 billion years. However, outside of the nucleus, their half-life is suddenly reduced to about 15 minutes. In other words, they must either find another nucleus to hide inside of or decay into something else.* In this chapter, we would like to turn our attention to how free neutrons behave after they are released from an atomic nucleus. We would like to begin our discussion by initially ignoring the fact that there may be another nucleus that would like to absorb the neutron. This is equivalent to assuming that the neutron absorption and fission cross sections Σ_a and Σ_f we discussed in Chapter 4 are zero. For many materials, this is in fact quite close to the truth, because at the average energy with which a free neutron is initially produced (about 2 MeV), its reaction cross sections for fission and absorption are quite small—typically on the order of a single "barn." By any standard, this is a very small number—about 10^{-24} cm^2. A neutron traveling at these energies also has a large mean free path, and for all intents and purposes, it cannot "see" any of the details of the physical environment that it is moving through. It simply moves too fast to see what its surrounding environment looks like.

Its perspective is not much different than a human being would have looking out of the window of a *bullet train* that is traveling down the track at a couple of hundred miles an hour (see Figure 11.1). Everything outside of the window is simply a blur. It is hard to see the individual details of the objects that are passing by. In the case of the bullet train, the person on the train just continues to move down the track (because it is designed not to hit anything as it moves). Fast neutrons, on the other hand, do not have that luxury. When they are initially ejected from an atomic nucleus, they behave like a swarm of billiard balls randomly bouncing around on a pool table. They crash into other objects and themselves, and mindlessly bounce around, because they are rarely absorbed. Their kinetic energy is transferred to the objects in their path (in this case other protons, neutrons, and electrons through the process of elastic scattering) as they go, and as they heat up the objects around them, they begin to slow down. Because neutrons have no electric charge, they will simply continue moving in a straight line unless an atomic nucleus or another object gets in their way. At very high speeds, neutrons have an extremely low probability of being absorbed, and so initially, a neutron will just continue to penetrate the object that it is pointed at. Neutrons also cannot be easily focused, concentrated, or directed into narrow beams (see Chapter 3) because they do not have an electric charge. Neutrons are also not very good at ionizing the objects they come in contact with because they have no net electric charge to convey.

When a free neutron is released, it begins to slow down by randomly colliding with other particles in its way, and its probability of capture begins to increase as its speed decreases. Relative to alpha particles and electrons of comparable energy, this slowing down process takes some time. Eventually, a neutron loses enough energy that it begins to come into thermal equilibrium with its environment (at about 0.025 eV). At these energies, its mean free path becomes only a few centimeters, and the probability that it will be absorbed by another nucleus begins to increase. The neutron begins to see the structure of the material world around it! Because neutrons are electrically neutral particles, they behave in many respects like the molecules of a diffuse gas. Their individual motions can be modeled by doing a *Monte Carlo calculation*, which is essentially the simulation of the *random walk* (see Chapter 23) of a nuclear particle.

FIGURE 11.1 It is very hard to see what is around you when you are traveling at a very high speed. If you look out the window of a bullet train, everything appears to be a blur. However, as the train begins to slow down, the structure of the world becomes more apparent, and it is easier to "see" an individual object from the window. Neutrons behave in a similar way as their speed is increased. At high speeds, they have a difficult time "seeing" the structure around them, and at lower speeds, the structure becomes more apparent. This analogy helps to explain the difference between a "fast" neutron and a "slow" or thermal neutron.

However, in aggregate, their motion is still governed by a *diffusion equation*. In this chapter, we would like to derive the neutron diffusion equation and discuss some of its limitations. This will serve as an introduction to neutron diffusion theory and its application to nuclear systems. In future chapters, we will then discuss how the neutron diffusion equation can be solved both analytically and numerically. The field of *reactor physics* is based on solving the neutron diffusion equation under these conditions.

11.2 Definition of the Neutron Density

Before deriving the neutron diffusion equation, we would first like to introduce some additional terms to describe how the neutron population behaves. We will begin our discussion of neutron diffusion theory by introducing the concept of the *neutron density*, which represents the number of neutrons that can be found in a small volume of space. The neutron density is illustrated schematically in Figure 11.2. Notice that neutrons always move from a region of high density (which is shown on the left) to a region of low density (which is shown on the right). The rate of diffusion is proportional to something that is called the *concentration gradient*, and the diffusion of other electrically neutral particles (and molecules) follows a similar trend.

In a reactor core, neutrons are emitted and absorbed by the fuel all of the time. The total number of free neutrons N in a volume of space V having dimensions Δx, Δy, and Δz is given by

$$N(x, y, z, t) = \rho(x, y, z, t) \cdot V = \rho(x, y, z, t)\Delta x \Delta y \Delta z \tag{11.1}$$

where $\rho(x, y, z, t)$ is the *neutron density* per unit volume at point x, y, and z. Here we have temporarily suppressed the energy dependence E of the neutrons to simplify the notation. According to Equation 11.1, *the neutron density is the number of neutrons N that exist at a particular location (x, y, z) and at a particular time t, divided by the volume of space V* that the neutrons occupy. *In the field of reactor physics, the neutron density is represented by the symbol* ρ. However, it should not be confused with the physical density ρ_F of the fuel, which is also an important nuclear parameter. As we move around the core, some locations will have more neutrons in them than other locations will. (This is normally the case in all reactor fuel assemblies.) We can represent this dependency by writing the neutron density as

Neutron Density

$$\rho(x, y, z, t) = \frac{N(x, y, z, t)}{\Delta x \Delta y \Delta z} = \frac{N(x, y, z, t)}{V} \tag{11.2}$$

where

x, y, and z are the coordinates where the density is measured

t is the time at which the measurement is made

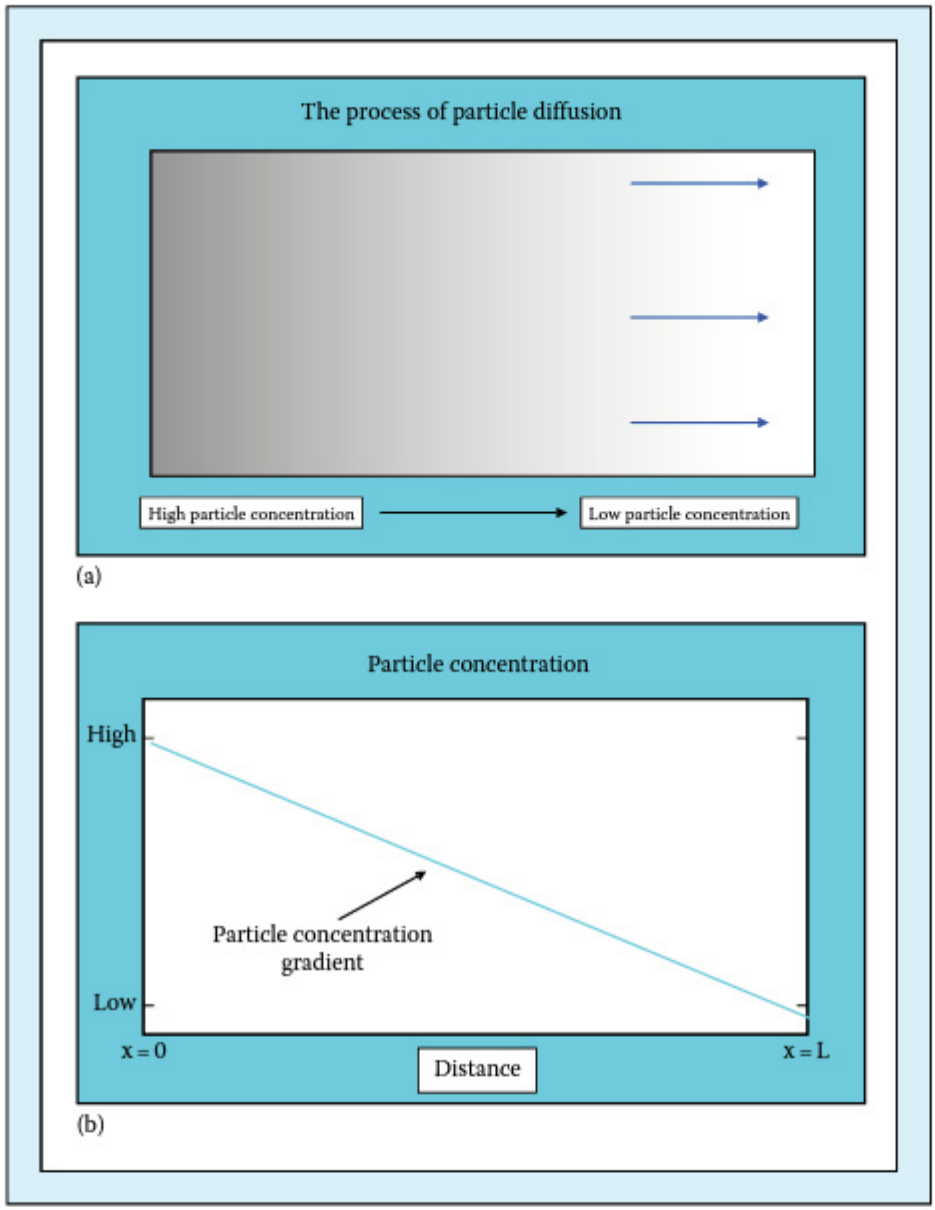

FIGURE 11.2 Diffusion can be considered to be the random molecular movement of particles from the left to the right. In this case, the movement of the particles is proportional to the concentration gradient dC/dx at a molecular level. Most of the time, the same process applies to the diffusion of neutrons as well.

If the energy dependence of the neutrons is added back into Equation 11.3, then the neutron density becomes ρ(x, y, z, E, t). In other words, in its most general form, the neutron density is a function of five independent variables: x, y, z, E, and t. The neutron density is no different than the density of a gallon of water or a piece of steel. It is simply a measure of the number of particles (in this case the number of neutrons) in a volume of space divided by the volume. In other words, it is just a simple number (i.e., a *scalar*). *In practice, the neutron density is measured in neutrons per cubic centimeter*. We can physically visualize where the neutrons can be found by building a small cube with dimensions Δx, Δy, and Δz around a point in space with coordinates (x, y, z). A typical cube of this type is shown in Figure 11.3. Because the cube is centered about point (x, y, z), the distance from the center of the cube to each of the faces is Δx/2, Δy/2, and Δz/2.

11.3 Definition of the Neutron Flux

While the neutron density ρ is the best way to measure the number of neutrons in a particular volume of space, the *neutron flux* ϕ(E) is the best way to measure the number of neutrons on the surfaces S of that control volume. *The neutron flux does not tell us anything about how the neutrons are moving across these surfaces*; *it simply tells us how many neutrons*

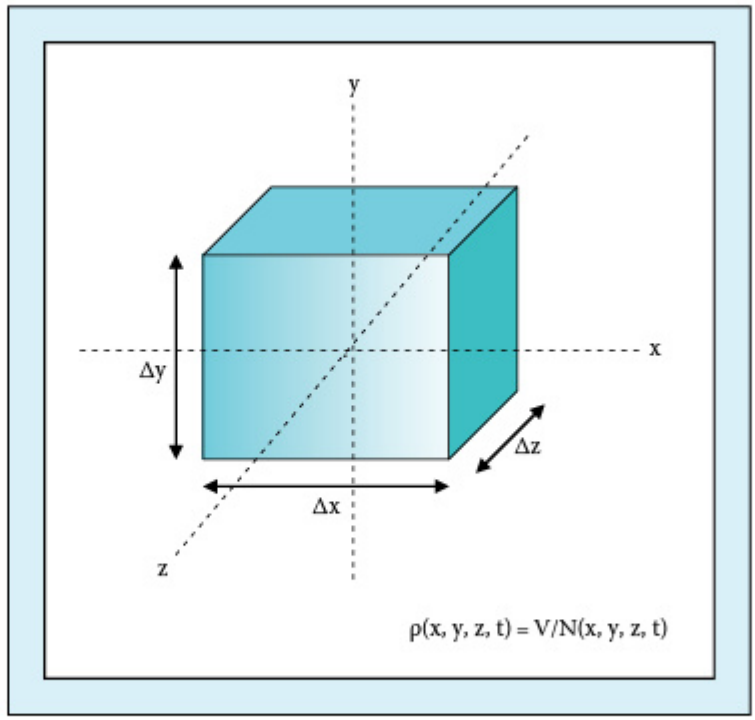

FIGURE 11.3 A simple three-dimensional cube used to define the neutron density ρ.

there are on a particular surface. This is precisely what we need to know to calculate the reaction rates because the number of free neutrons absorbed per cm^3/s is given by

$$R_a = \int_E \phi(E) \cdot \Sigma_a(E) dE \tag{11.3}$$

and the number of scattering collisions per cm^3/s is given by

$$R_s = \int_E \phi(E) \cdot \Sigma_s(E) dE \tag{11.4}$$

The reaction rate for an arbitrary reaction type x per cm^3/s is then

$$R_x = \int_E \phi(E) \cdot \Sigma_x(E) dE \tag{11.5}$$

where x = a, c, f, s, and so on. Notice that we do not require any specific knowledge of the direction that the neutrons are traveling to calculate the reaction rates. All we need to know is that there are ϕ(E) of them on a surface with an energy E. In most nuclear engineering textbooks, the *neutron flux* is defined as the number of neutrons passing through a region of space having an area A over a span of time t. In other words, it is a measure of the number of neutrons per second that cross a particular *surface area* without regard to their direction of motion. It is usually measured in the units of neutrons/$cm^2 \cdot s$. According to the U.S. NRC, the formal definition of the neutron flux is

The NRC's Definition of the Neutron Flux

The number of neutrons passing through 1 square centimeter of a given target in 1 second.

It may also be expressed as ρv, where ρ is the neutron density, or the number of neutrons per cubic centimeter, and v is the average velocity of the neutrons in centimeters per second.

In other words, an alternative and equally valid definition of the neutron flux is

$$\phi(E) = \rho(E) \cdot v(E) \tag{11.6}$$

where v(E) is a velocity distribution that the neutrons obey. If we suppress the energy dependence of the neutron flux, then this definition requires a knowledge of their *average velocity* v:

$$v = \frac{\int_E v(E)\, dE}{\int_E dE} \tag{11.7}$$

Similarly, we may define the *average neutron density* ρ as

$$\rho = \frac{\int_E \rho(E)\, dE}{\int_E dE} \tag{11.8}$$

and the total flux is therefore

$$\phi = \int_E \rho(E) \cdot v(E)\, dE \tag{11.9}$$

or simply $\phi = \rho v$. In some textbooks, *the neutron density is also represented by the symbol n.* In this case, Equation 11.9 becomes

$$\phi = \int_E n(E) \cdot v(E)\, dE \tag{11.10}$$

where the subscript E represents the energy range over which the integrals are to be performed. Normally, this is taken to be $E_1 \sim 0$ eV to $E_2 \sim 10$ MeV, although the upper limit of this range can be as high as 15 MeV.

11.4 Definition of the Neutron Current

While the neutron flux is a particularly good measure of how many neutrons are moving across an arbitrary surface S surrounding a volume of space V, it does not tell us anything about *the direction* that the neutrons are traveling. Because of this, the neutron flux is a *scalar quantity* that does not have any directional content (it is simply a number). *If we want to know which way the neutrons are moving across one of the surfaces of the control volume, then this requires us to define another variable called the neutron current J.* The *neutron current* is just like the flow of electricity through a wire in your house. It measures how many electrons are moving through a cross-sectional area of the wire in a certain direction **r**. See Figure 11.4 to visualize the direction of particle flow. By convention, the neutron current is given the symbol **J**. Just like the neutron flux, the neutron current has the units of neutrons/cm²-s. *However, because it is a vector, it has both magnitude and direction*. In other words, we can *define* the neutron current **J** in three-dimensional space as

$$\mathbf{J} = \mathbf{i} \cdot (J_x) + \mathbf{j} \cdot (J_y) + \mathbf{k} \cdot (J_z) \tag{11.11}$$

where

J_x is the net current (in neutrons/cm²-s) flowing in the x direction
J_y is the net current (in neutrons/cm²-s) flowing in the y direction
J_z is the net current (in neutrons/cm²-s) flowing in the z direction
i, **j**, and **k** are the unit vectors along the x, y, and z directions, respectively

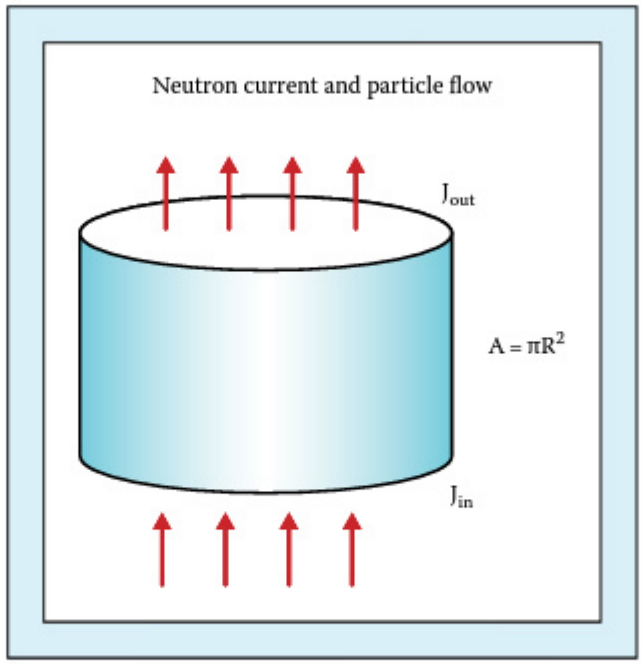

FIGURE 11.4 Visualizing the flow of current through a wire.

Equivalently, in a cylindrical coordinate system, we can also write the neutron current **J** as

$$\mathbf{J} = \mathbf{i}_r \cdot (J_r) + \mathbf{i}_z \cdot (J_z) \tag{11.12}$$

where

J_r is the current flowing in the radial direction
J_z is the current flowing in the axial direction
$\mathbf{i}_r$ is the unit vector along the radial direction
$\mathbf{i}_z$ is the unit vector along the axial (or z) direction

Using the *Pythagorean Theorem*, it immediately follows that the magnitude of the neutron current is

$$J = \sqrt{(J_x)^2 + (J_y)^2 + (J_z)^2} \tag{11.13}$$

for rectangular coordinates and

$$J = \sqrt{(J_r)^2 + (J_z)^2} \tag{11.14}$$

for cylindrical ones (where the flux is a function of r and z). Similarly, we can also define the neutron current for a spherical coordinate system if the need arises.

11.5 Fick's Law of Diffusion

When the process of particle diffusion was first discovered in the 1800s, scientists found that electrically neutral particles moved from a region of a high particle density ρ^H *to a region of a low particle density* ρ^L. They wondered how the particles "knew" which way to move. Was there an underlying physical principle or "law" that told them which way to go, or was their motion just the result of some truly random process? What was the underlying mechanism that nature had put in place to govern the behavior of such things?

The first correct interpretation of the process of molecular diffusion was made by a German chemist by the name of *Adolf Fick* in 1855 (see Figure 11.5). In that year, Fick introduced *Fick's Law of Diffusion*, which governed the diffusion

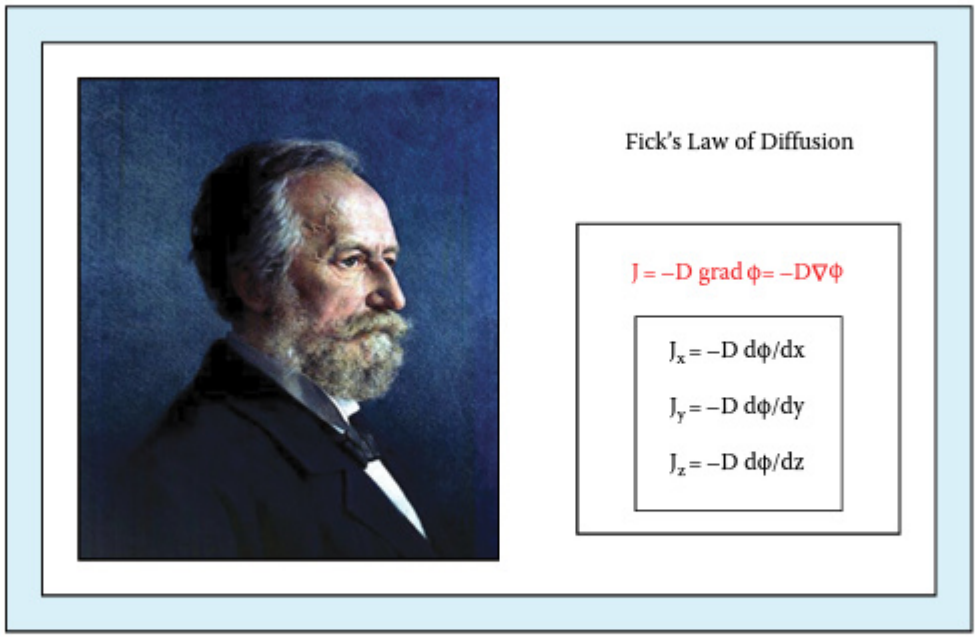

FIGURE 11.5 Adolf Fick, who formulated the Law of Particle Diffusion—circa 1850. (Courtesy of Google Images.)

of a gas across a fluid membrane. Several years later, his law was eventually generalized to molecular particle flow, to the flow of dyes and solvents, and eventually to the flow of neutrons through a reactor core. His nephew (of the same name) was also the inventor of the modern *contact lens*. In this section, we would like to briefly explain Fick's Law of diffusion and describe how it can be applied to electrically neutral particles such as neutrons. This will lead to a simple formula that can be used to determine the *magnitude and the direction* of the neutron current **J**. We will begin our discussion by referring to Figure 11.6, which shows a large number of neutrons whose density varies as a function of position along the x-axis. The neutron population in Figure 11.6 has a different molecular density ρ(x) at every point

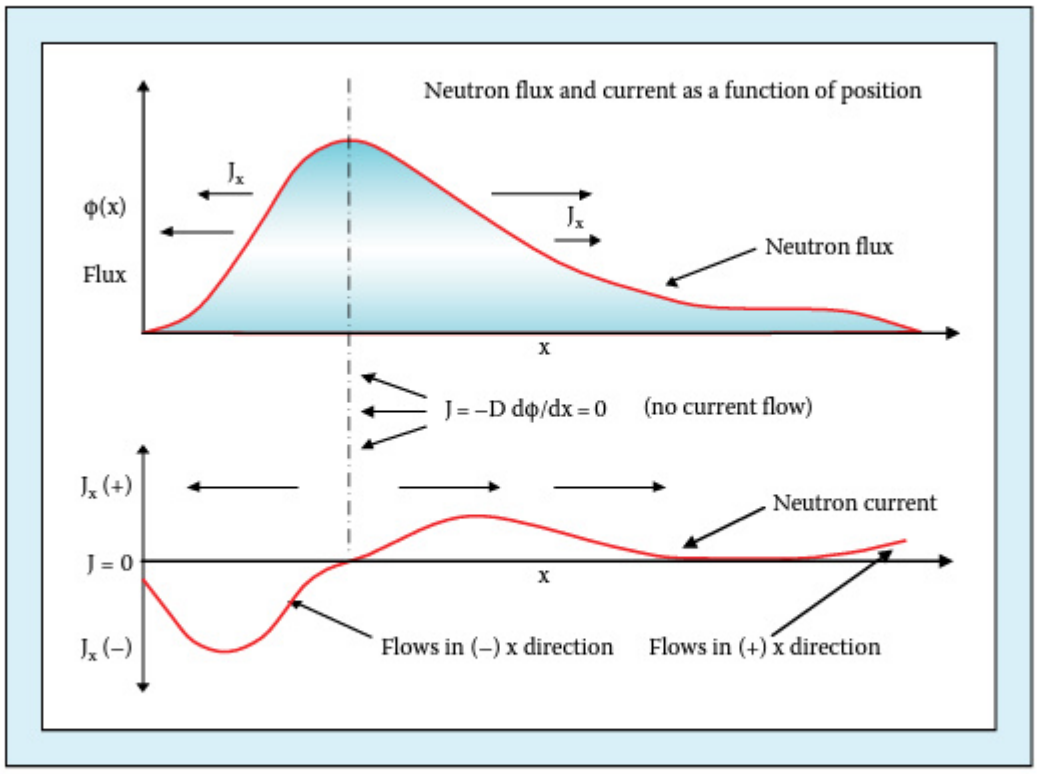

FIGURE 11.6 Relationship between the neutron current and the neutron flux.

along the x-axis, and hence the neutron flux, which is related to the neutron density by $\phi(x) = \rho(x)v$, is also position dependent. To simplify our discussion, assume for the moment that all of the neutrons have exactly the same speed so that the neutron flux $\phi(x)$ is directly proportional to the density $\rho(x)$ at every point x. Sometimes this is called the *constant velocity approximation*. In a future chapter, we will find that this assumption gives rise to what is known as *one-group diffusion theory* (see Chapter 12).

There is also no particular reason why we have chosen to draw the shape of the neutron flux the way we have, except that it can help to understand how the current **J** and the flux ϕ are related to each other. From Figure 11.6, it is easy to see that the magnitude and the direction of the neutron current **J** depend on where we are. In particular, since the neutron current **J** is a vector, and the neutron flux ϕ is not, the neutrons to the left of the peak flow "downhill" in the negative x direction, and the neutrons to the right of the peak flow "downhill" in the positive x direction. This creates a net current in the positive x direction **J(+)** and another net current in the negative x direction **J(−)**.

It is only when we are directly on top of the flux peak in Figure 11.6 (where $d\phi/dx = 0$) that there is no net flow of neutrons in either direction. Here the number of neutrons flowing in the positive direction is exactly balanced by the number of neutrons flowing in the negative direction. Therefore, at the point of maximum flux, the neutron current is

$$\mathbf{J} = \mathbf{J}(+) + \mathbf{J}(-) = 0 \tag{11.15}$$

A large number of neutrons may be flowing to the left, and a large number of neutrons may be flowing to the right. *However, there is no net flow of neutrons at the flux peak because the gradient of the flux $\nabla\phi$ is zero*. Based on this observation alone, it should be apparent that the neutron flux and the neutron current must be related to each other in some fundamental way that involves the gradient of the flux. Furthermore, by inspecting the direction that the neutron current flows, we must conclude that *the direction of the neutron current must have the opposite sign as the gradient of the neutron concentration*. When scientists first began to study the motion of large ensembles of particles in the 1800s, they found that many chemical processes, as well as most nuclear ones, seemed to follow a similar pattern. It did not seem to matter whether they were dealing with the flow of heat through a solid object or the flow of air molecules through a room filled with air. As long as the particles did not possess an electric charge (like the particles in a plasma do), they all behaved in essentially the same way. In particular, Adolf Fick hypothesized that *uncharged particles always flow from the area of the highest particle concentration to the area of the lowest particle concentration. Furthermore, he found that the rate of particle flow (which is represented by the particle current J) was directly proportional to the difference between the particle fluxes, ϕ_1 and ϕ_2, and inversely proportional to the distance over which the fluxes were measured. In other words, the neutron current gets stronger as the slope of the flux gets greater. In mathematical terms, this can be expressed by saying that the net flow of the particles, and therefore their direction, is proportional to the negative gradient of the particle flux ϕ*:

Relationship between the Neutron Current and the Particle Flux

$$J_x = -D\frac{\Delta\phi}{\Delta x} \tag{11.16}$$

where $\Delta\phi = (\phi_2 - \phi_1)$ and $\Delta x = (x_2 - x_1)$. In Equation 11.16, D is an empirically determined constant of proportionality called the *diffusion coefficient*. This simple mathematical expression that relates the particle current to the negative gradient of the particle flux is called *Fick's Law of Diffusion*. We can extend our initial statement of Fick's Law to multiple dimensions by realizing that $d\phi/dx = \Delta\phi/\Delta x$, so the neutron current along each coordinate direction is

$$J_x = -D\frac{d\phi}{dx} \tag{11.17}$$

$$J_y = -D\frac{d\phi}{dy} \tag{11.18}$$

$$J_z = -D\frac{d\phi}{dz} \tag{11.19}$$

Since the neutron current is a vector, this also allows us to write the total current **J** as the sum of the individual components:

$$\mathbf{J} = \mathrm{i}\cdot\left(\mathrm{J_x}\right) + \mathrm{j}\cdot\left(\mathrm{J_y}\right) + \mathrm{k}\cdot\left(\mathrm{J_z}\right) = -\mathrm{D}\left(\frac{\mathrm{d}\phi}{\mathrm{dx}} + \frac{\mathrm{d}\phi}{\mathrm{dy}} + \frac{\mathrm{d}\phi}{\mathrm{dz}}\right) \tag{11.20}$$

Upon introducing the *gradient operator* ∇, we also see that Fick's Law can be written as

Fick's Law of Diffusion

$$\mathbf{J} = -\mathrm{D}\,\mathbf{grad}\,\phi = -\mathrm{D}\nabla\phi \tag{11.21}$$

which is Fick's Law in its more complete differential form. The exact expression for the calculation of the neutron current is then

$$\mathbf{J}(\mathrm{x},\mathrm{y},\mathrm{z}) = -\mathbf{grad}\left[\mathrm{D}(\mathrm{x},\mathrm{y},\mathrm{x})\phi(\mathrm{x},\mathrm{y},\mathrm{z})\right] = -\nabla\left[\mathrm{D}(\mathrm{x},\mathrm{y},\mathrm{z})\phi(\mathrm{x},\mathrm{y},\mathrm{z})\right] \tag{11.22}$$

For a spatially homogeneous medium, this reduces to the simpler expression we discussed earlier. In some derivations of Fick's Law, the diffusion coefficient D also has a spatial dependence. When this occurs, a more accurate expression for the neutron current is

$$\mathrm{J}(\mathrm{x}) = -\frac{\mathrm{d}\left(\mathrm{D}(\mathrm{x})\phi(\mathrm{x})\right)}{\mathrm{dx}} = -\mathrm{D_x}\frac{\mathrm{d}\phi}{\mathrm{dx}} - \phi\frac{\mathrm{dD_x}}{\mathrm{dx}} \tag{11.23}$$

Note that when D is independent of x, this reduces to our previous definition:

$$\mathrm{J}(\mathrm{x}) = -\frac{\mathrm{d}(\mathrm{D}(\mathrm{x})\phi(\mathrm{x})}{\mathrm{dx}} = -\mathrm{D}\frac{\mathrm{d}\phi}{\mathrm{dx}} \tag{11.24}$$

which is the more commonly used form of Fick's Law. In three dimensions, Equations 11.23 and 11.24 can be generalized to

$$\mathbf{J}(\mathrm{x},\mathrm{y},\mathrm{z}) = -\left[\frac{\mathrm{d}\left(\mathrm{D}(\mathrm{x})\phi(\mathrm{x})\right)}{\mathrm{dx}} + \frac{\mathrm{d}\left(\mathrm{D}(\mathrm{y})\phi(\mathrm{y})\right)}{\mathrm{dy}} + \frac{\mathrm{d}\left(\mathrm{D}(\mathrm{z})\phi(\mathrm{z})\right)}{\mathrm{dz}}\right] \tag{11.25}$$

or

$$\mathbf{J}(\mathrm{x},\mathrm{y},\mathrm{z}) = \mathbf{i}\cdot\left(\mathrm{J_x}\right) + \mathbf{j}\cdot\left(\mathrm{J_y}\right) + \mathbf{k}\cdot\left(\mathrm{J_z}\right) \tag{11.26}$$

where

$$\mathbf{J_x} = -\frac{\mathrm{d}\left(\mathrm{D}(\mathrm{x})\phi(\mathrm{x})\right)}{\mathrm{dx}} \tag{11.27}$$

$$\mathbf{J_y} = -\frac{\mathrm{d}\left(\mathrm{D}(\mathrm{y})\phi(\mathrm{y})\right)}{\mathrm{dy}} \tag{11.28}$$

$$\mathbf{J_z} = -\frac{\mathrm{d}\left(\mathrm{D}(\mathrm{z})\phi(\mathrm{z})\right)}{\mathrm{dz}} \tag{11.29}$$

In practice, one rarely encounters a situation where the material composition of the core varies in the same way along each coordinate direction. Hence, Equation 11.25 is actually more useful in situations where it is not possible to spatially

homogenize the core over a large volume of space. In this case, the more fundamentally correct version of Fick's Law, Equation 11.25, gives a more accurate picture of the spatial reaction rates. Notice that Equation 11.25 reduces to the standard form of Fick's Law when the spatial dependence of D(x), D(y), and D(z) is removed. A region of space where the diffusion coefficient has an explicit spatial dependence is called a *heterogeneous region*, and a region of space where it does not is called a *homogeneous one*. In practice, most reactor fuel assemblies appear to be heterogeneous to thermal neutrons because their mean free paths are on the order of 1 cm or less. If the level of spatial heterogeneity exceeds the threshold where diffusion theory is valid, then neutron transport theory must be used to describe the behavior of the neutron population. In this case, the spatial distribution of the neutrons can be found by solving what is known as the *neutron transport equation*. In Chapter 22, we will explore the relationship between the neutron transport equation and the neutron diffusion equation. This will lead to what is known as the *diffusion theory approximation*.

11.6 Neutron Diffusion Coefficient and Its Meaning

Now let us turn our attention to the distribution of neutrons shown in Figure 11.6 and ask ourselves the following questions: Why does the neutron current always flow from a region of high flux (or a high particle concentration) to a region of low flux (or a lower particle concentration)? What is the physical principle or "force" that drives this particular behavior? The answer is that there are simply more neutrons to collide with in regions of high neutron density than there are in regions of low neutron density. These random molecular collisions tend to exert more pressure on the neutrons when they are more densely packed together than when they are less densely packed together.

The *net* effect of this momentum transfer due to random collisions between the particles is to create a kind of particle flow, or a "*current*" from a "high-pressure" region of space to a "low-pressure" region of space (see Figure 11.7). In other words, the neutrons do not flow from point A to point B because they "think" that is what they are supposed to do! They are not programmed internally to think that way! They simply bounce around like mindless objects in many different directions, and in the process of doing so, the statistical force imbalances between them push more than 50% of the neutrons to the low-density side. There are simply more neutrons scattered in one direction than there are scattered in the other. On the other hand, when the situation is reversed, and there is a trough in the shape of the neutron flux (see Figure 11.8), then the neutrons will flow into the trough to try to equalize the number of collisions at each location along the x-axis. In other words, they will flow again from a region of "high" pressure, where there are a lot of neutrons, to a region of "low" pressure, where there are fewer of them. Only in this case, the low-pressure area is the "trough."

The rate of particle flow into the trough depends on the value of the diffusion coefficient D. *In Fick's Law (Equation 11.21), the diffusion coefficient D is an empirical constant of proportionality that relates the magnitude and the direction of the neutron current J to the negative gradient of the neutron flux*. The diffusion coefficient can also vary

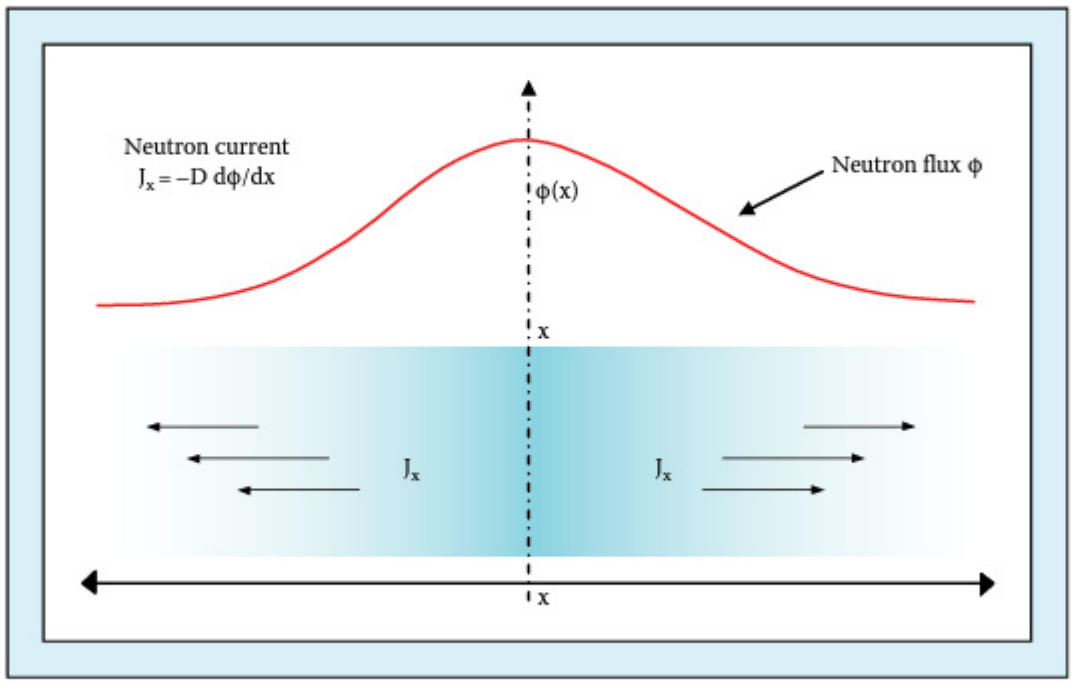

FIGURE 11.7 The particle flow away from a peak in the neutron flux.

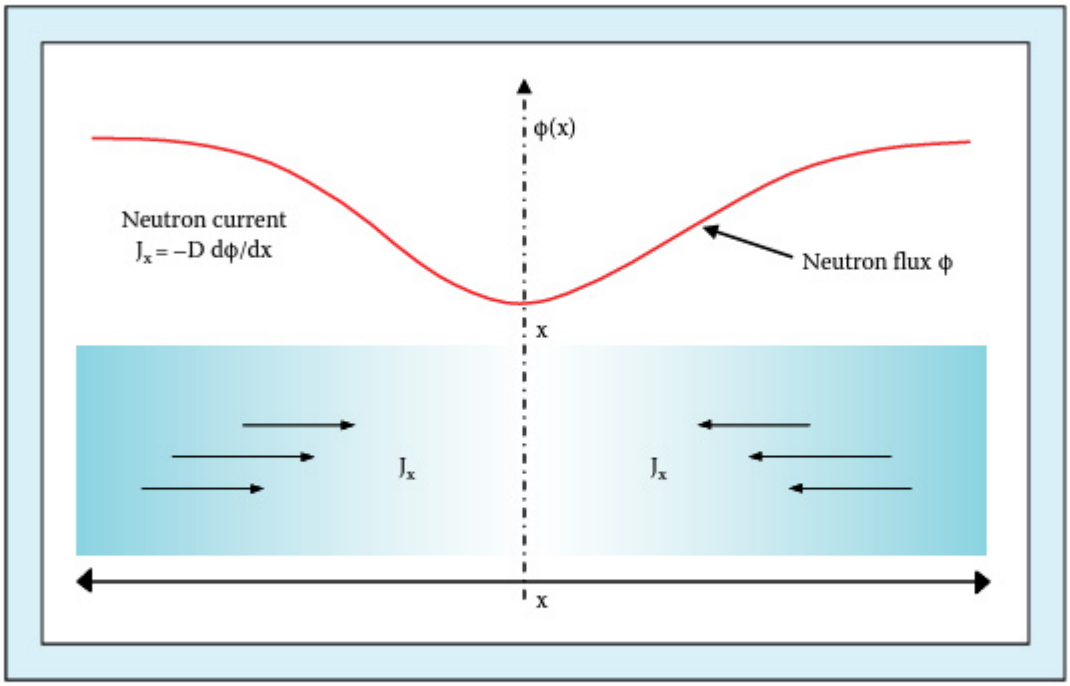

FIGURE 11.8 The particle flow toward a trough in the neutron flux.

from one material to another, but for a given density of the material at a given temperature T and pressure P, it always has the same value. It is a characteristic of the internal structure of the material. In other words, it is related to the molecular structure through which the neutrons are flowing. The diffusion coefficient can be spatially dependent, but it will always have the units of length (cm). This observation implies that there must be a relationship between the size of the diffusion coefficient D and the rate at which the neutrons are being scattered as they move. In fact, there is a simple relationship between these processes that we would like to present to you now. Before we present this relationship, we would first like to provide a simple physical argument that explains how the flow of neutrons is related to a material's internal molecular structure.

The diffusion coefficient D can be thought of as a measure of the physical resistance that a material presents to the flow of neutrons. A large diffusion coefficient implies that it is easy for a neutron to move through a material, and a small diffusion coefficient implies that it is hard. Materials that neutrons move through easily have two characteristics in common:

- First, they have fewer collisions between their atoms and the neutrons as they move.
- Second, they have a lower probability of scattering or absorbing the neutrons.

In other words, they have either a low material density or a low scattering cross section. From Chapter 4, we know that both of these effects are contained within the value of the *macroscopic scattering cross section* Σ_s, which is defined by the equation

$$\Sigma_s = N\sigma_s \tag{11.30}$$

Thus, the size of the macroscopic scattering cross section determines the resistance to the neutron flow. If Σ_s is small, neutrons will flow through a material easily, and if Σ_s is large, they will not. To a first approximation, we can then conclude that the diffusion coefficient D is inversely proportional to the macroscopic scattering cross section:

$$D \sim \frac{1}{\Sigma_s} \sim \frac{1}{N\sigma_s} \tag{11.31}$$

where

N is the number of atoms per cubic centimeter
σ_s is the microscopic scattering cross section

Using a more comprehensive analysis, it can be shown that the actual relationship between these two quantities is

Relationship of the Diffusion Coefficient and the Scattering Angle

$$D = \frac{1}{3\Sigma_s(1-\cos\theta)} = \frac{1}{3\Sigma_{tr}} \tag{11.32}$$

in any material where the macroscopic absorption cross section is small ($\Sigma_a \approx 0$). Here θ is the *average angle* that the neutrons are scattered in the material. In other words, *the diffusion coefficient D is inversely proportional to the scattering cross section Σ_s of the material in which the neutrons are flowing*. The quantity $\Sigma_s(1 - \cos\theta)$ is sometimes given a special name to represent the fact that neutron scattering can be anisotropic for light elements. In this case, the value of $\Sigma_s(1 - \cos\theta)$ is called the *transport cross section* Σ_{tr}, and the transport cross section can be derived from the neutron transport equation (see Chapter 21). We will have more to say about the actual form of the transport cross section in a future section. However, when the scattering process completely dominates the absorption process in a particular material (i.e., when $\Sigma_s \gg \Sigma_a$), the transport cross section $\Sigma_{tr} = \Sigma_s(1 - \cos\theta)$ is the more accurate expression to use. The larger the scattering cross section Σ_s is, the shorter the distance is that a neutron must travel before it is scattered, and the smaller the diffusion coefficient D will be. Conversely, the smaller the scattering cross section Σ_s is, the further the neutrons will travel before they are scattered, and the larger the diffusion coefficient will be. When a material becomes a gas, the number of atoms N in a cubic centimeter of the material can become very low. In this case, the scattering cross sections may become very small, and the diffusion coefficient D may become very large. This is particularly true when neutrons are scattered in gaseous materials and in conditions that may approach a partial vacuum. At most energies of interest to nuclear engineers, there is a simple relationship between the cosine of the scattering angle, $\cos\theta$, and the atomic weight A of the atom that the neutron hits. This relationship is

Relationship of the Scattering Angle θ to the Atomic Weight A

$$\cos\theta = \frac{2}{3A} \tag{11.33}$$

where A is the atomic weight of an atom in AMUs and to a first approximation, it is simply equal to the sum of the number of protons and neutrons. *This means that as the nucleus of an atom gets heavier, the neutron colliding with it has a larger average scattering angle than when the nucleus is lighter*. Now consider what this implies in terms of the elastic scattering of a neutron from a Uranium-238 nucleus or a Hydrogen nucleus. In the case of the Uranium nucleus, A = 238, so $\cos\theta = 2/(3 \times 238) = 0.0028$ and $\theta = \cos^{-1}(0.0028) \approx 90°$, and in the case of the Hydrogen nucleus, A = 1, so $\cos\theta = 2/(3) = 0.67$ and $\theta = \cos^{-1}(0.67) \approx 48°$. In other words, a uranium nucleus will deflect an incoming neutron by an average of 90° if it is not absorbed, while a collision with a lighter element like hydrogen will scatter it by an average of only 48°.

In other words, if a heavy element is hit by a neutron, any scattering angle between 0° and 180° is equally possible, while if a light element is hit by the same neutron, the scattering angle will usually be between 0° and 90°. For light elements, this behavior is called *forward scattering*, and it is illustrated schematically in Figure 11.9. Notice that although both collisions are elastic, the difference in the distribution of the scattered neutrons is dramatic. When an element becomes heavier than Carbon (A = 12), $\cos\theta \to 0$, the equation for the diffusion coefficient D becomes

Simplified Equation for the Diffusion Coefficient

$$D = \frac{1}{3\Sigma_s} \tag{11.34}$$

(The scattering cross section of Carbon is shown in Figure 11.10.) This equation establishes a simple relationship between D and Σ_s that can be used for almost any heavy element where A is large. In a material like water, where the scattering cross section is many times larger than the absorption cross section, there also simple relationship between the diffusion coefficient and the neutron's *mean free path*, λ. We learned in an earlier chapter that

$$\lambda_x = \frac{1}{\Sigma_x} \tag{11.35}$$

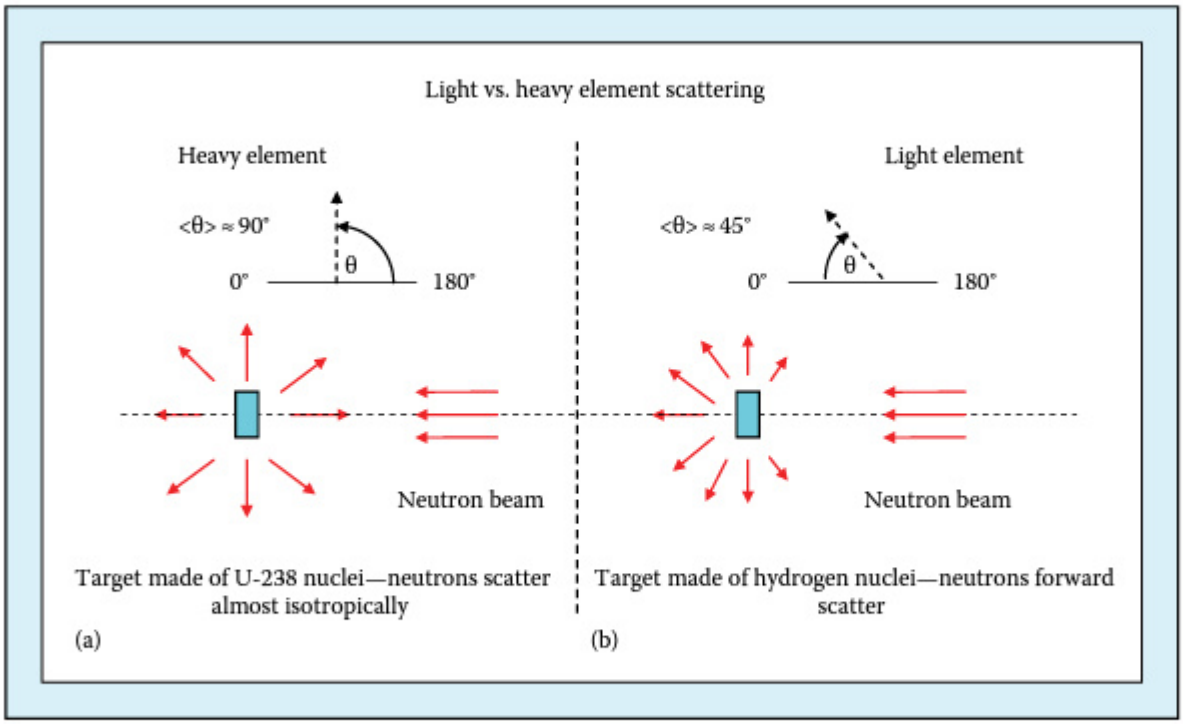

FIGURE 11.9 The scattering angles of a neutron bouncing off a heavy nucleus (uranium-238—(a)) and off a light nucleus (hydrogen—(b)). Notice that the heavy nucleus scatters the neutron more isotropically than the light nucleus does.

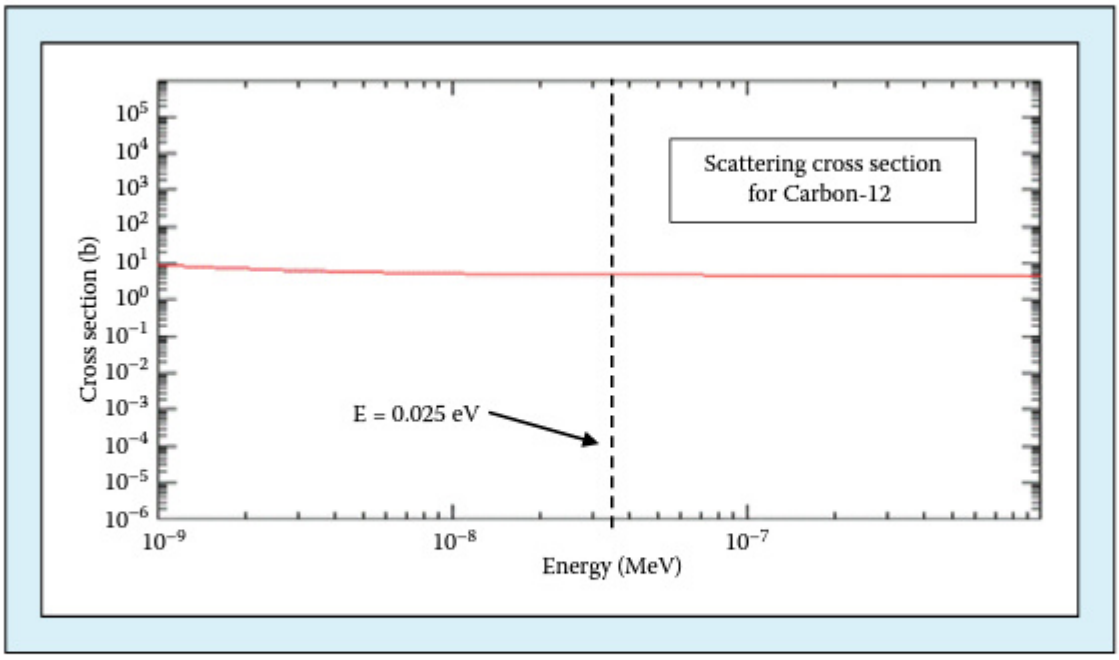

FIGURE 11.10 Scattering cross section for Carbon-12 in the thermal energy range. (Courtesy of KAERE.)

TABLE 11.1
Neutron Diffusion Coefficients for Several Important Nuclear Materials

Material	Function	Thermal Diffusion Coefficient D (cm)	Thermal Scattering Cross Section Σ_s (cm^{-1})	Thermal Diffusion Length $L = \sqrt{D}/\Sigma_a$ (cm)	Scattering Mean Free Path $\lambda_s = 1/\Sigma_s$ (cm)	Absorption Mean Free Path $\lambda_a = 1/\Sigma_a$ (cm)
U-233	Fuel	0.303	1.10	0.14	1.61	0.03
U-235	Fuel	0.498	0.67	0.12	1.49	0.03
U-238	Fuel	0.833	0.40	2.45	2.34	7.69
H_2O	Moderator	0.160	3.45	2.85	0.46	50.76
D_2O	Moderator	0.870	0.45	169.5	2.00	10752
Graphite	Moderator	0.840	0.38	58.8	0.18	962
Pu-239	Fuel	0.883	0.48	0.13	2.65	0.02

where x is the reaction type. Now in the case of water, one can normally write $\Sigma_s \approx \Sigma_t$. In this case, we know to a fair degree of accuracy that $\lambda \approx 1/\Sigma_s$. Substituting this expression into Equation 11.32 and rearranging terms, we find that

$$D = \frac{\lambda}{\{3(1-2/3A)\}} \tag{11.36}$$

In other words, *the diffusion coefficient is directly proportional to the neutron mean free path* λ. The longer the neutron mean free path, the larger the diffusion coefficient will be (e.g., the longer "reach" it has). Conversely, the smaller the mean free path, the smaller the diffusion coefficient will be. Virtually all nuclear materials exhibit this behavior when large numbers of uncharged particles are involved. Table 11.1 lists the values of the diffusion coefficients for a number of different nuclear materials. We will come back to this table again when we are in a position to solve the neutron diffusion equation. Finally, when A becomes large, the neutron mean free path is related to the diffusion coefficient D by the following relationship:

Relationship of the Mean Free Path λ and the Neutron Diffusion Coefficient D

$$\lambda = 3D \tag{11.37}$$

so if the diffusion coefficient for a material is 10 cm, then the mean free path of a neutron in that same material will be $\lambda = 3 \times 10 = 30$ cm. One may ask where the number 3 comes from in this case. It is simply there because it represents the diffusion of particles in three-dimensional space. If we were to derive the same relationship for only one or two spatial dimensions, then the number 3 would be replaced by a 1 or a 2. Hence, the constant of proportionality between the mean free path λ and the diffusion coefficient D is simply a measure of the number of dimensions in the diffusing medium itself. Several proofs of this statement can be found in more advanced texts. Finally, when the atomic weight of the target nucleus becomes relatively small (say, A < 12), the neutron scattering becomes anisotropic, and we may write

$$\lambda_{tr} = \frac{1}{\Sigma_{tr}} \tag{11.38}$$

where λ_{tr} is now called the *transport mean free path*. The *transport cross section* is then given by $\Sigma_{tr} = \Sigma_s(1-\mu)$, where μ can be thought of as *the average value of the cosine of the scattering angle*. Slightly different definitions for the transport cross section can be found in the literature, and we will present a more rigorous definition of this parameter at the end of the chapter. In any event, regardless of how the transport cross section is defined, the mean free path of a neutron is inversely proportional to it in a scattering reaction.

Example Problem 11.1

The scattering cross section for a Carbon-12 nucleus in the thermal energy range (<1 eV) is shown in the following. If the atomic density of carbon in a graphite-moderated reactor is known to be about 8×10^{22} atoms per cubic centimeter, find the diffusion coefficient of graphite at 0.1 eV.

Solution The diffusion coefficient D of graphite (a common reactor moderator) can be found from the following equation:

$$D = \frac{1}{\{3\Sigma_s(1-2/3A)\}}$$

when the neutron energy is low. Using this equation with A = 12 gives $\cos\theta = 2/3A = 2/36 = 0.055$, and upon introducing these values into the equation for D with $\sigma_s \approx 5$ barns gives $D = 1/[3 \times 8 \times 10^{22} \times 5 \times 10^{-24}(1 - 0.055)] = 0.88$ cm. As the reader can see, this value will be relatively constant throughout the entire thermal energy range. [Ans.]

11.7 Some Limitations of Fick's Law

In our initial derivation of Fick's Law, we assumed that the value of the diffusion coefficient D was the same along each coordinate direction. This allowed us to establish a simple relationship between the neutron current and the neutron flux:

$$\mathbf{J}(x, y, z) = -\mathbf{grad}\left[D(x, y, x)\phi(x, y, z)\right] = -D\,\mathbf{grad}\,\phi(x, y, z) = -D\nabla\phi(x, y, z) \tag{11.39}$$

We also assumed that the material medium was large enough that we did not have to worry about what happened to the neutron flux near the boundaries. Unfortunately, in the real world, there are a number of limitations to this approach because reactors tend to be more heterogeneous than homogeneous. In practice, it is normally possible to compensate for this behavior by making the diffusion coefficient D spatially dependent. Then the appropriate version of Fick's Law becomes

Fick's Law with a Spatially Dependent Diffusion Coefficient

$$\mathbf{J}(x, y, z) = -\left[\frac{d(D(x)\phi(x))}{dx} + \frac{d(D(y)\phi(y))}{dy} + \frac{d(D(z)\phi(z))}{dz}\right]$$

or

$$\mathbf{J}(x, y, z) = i\cdot(J_x) + j\cdot(J_y) + k\cdot(J_z)$$

where

$$J_x = -\frac{d(D(x)\phi(x))}{dx}$$

$$J_y = -\frac{d(D(y)\phi(y))}{dy}$$

$$J_z = -\frac{d(D(z)\phi(z))}{dz} \tag{11.40}$$

Notice that each of the components of J then depends on the derivatives of $D\phi$. Furthermore, when the degree of spatial heterogeneity becomes even higher, the neutron current may no longer be simply related to the gradient of the neutron flux. In particular, the flux may acquire an angular dependence, and when this happens, it becomes a function of *six independent variables* rather than just five. Then we must express the neutron flux as $\phi(x, y, z, E, \mathbf{\Omega}, t)$, where now $\mathbf{\Omega}$ is the *solid angle* through which the neutrons are flowing. Of course, *when this occurs, it is no longer possible to use diffusion theory because neutron diffusion theory assumes that the neutron flux has no angular dependence (i.e., the flux is angularly isotropic). Consequently, as soon as the neutron flux acquires a strong angular dependence (which is represented by the variable Ω), Fick's Law becomes invalid and neutron transport theory may have to be used instead.*

In practice, there are four specific scenarios where Fick's Law may become invalid:

- First, Fick's Law does not apply to ensembles of charged particles, where strong forces like electricity and magnetism come into play. These forces simply overwhelm the randomness that is implied by the diffusion process.
- Second, Fick's Law cannot be used when the scattering process is highly anisotropic. This means that it does *not* apply to particles like high-energy x-rays and gamma rays. In this case, their energies are so high that the *angular isotropy* of the scattering process is lost. These particles stream through matter rather than diffusing through it.
- Third, Fick's Law cannot be used in the vicinity of very strong neutron sources and sinks. In the presence of these sources and sinks (such as reactor control rods), the neutron flux becomes anisotropic, and it acquires a

strong angular dependence. In practice, this angular dependence is represented by what is called the *angular unit vector* **Ω**. The definition of **Ω** is

$$\Omega = \mathbf{i}\sin\theta\cos\varphi + \mathbf{j}\sin\theta\sin\varphi + \mathbf{k}\cos\theta$$

and we will formally explain how it is used in Chapter 22. The angles θ and φ that appear in the definition of **Ω** are the angles of neutron flow with respect to the x- and z-axes.

⊙ Fourth, the flow of neutrons through matter is determined by the mean free path of a neutron in relation to the physical structures around it. If the mean free path λ becomes too small in relation to these structures, then the physical structure will affect both the angular distribution of the neutrons and the way in which they scatter. It turns out that this distance is equal to about *3 mean free paths* for a typical neutron. So we must maintain this distance from a neutron source, a neutron sink (like a burnable poison or a control rod), or an abrupt material boundary (such as the fuel to moderator transition) in order for Fick's Law to give acceptable results. If we get any closer than this, then Fick's Law is just not accurate enough to predict the correct spatial distribution and reaction rates, and neutron transport theory must be used. To a certain extent, this problem can be corrected by spatially homogenizing the region in which these sources and sinks occur (see Chapter 19), but this can cause us to underpredict or overpredict the reactivity under certain conditions.

Although we will not formally discuss what modifications must be made to the diffusion equation to account for these anomalies, any nonuniformity in the shape of the neutron flux requires us to derive a different equation to handle the angular dependence of the neutrons. In practice, this equation has become known as the *neutron transport equation*. The problem of particle transport is then reduced to the problem of solving the neutron transport equation (see Chapter 22) in different reactor geometries. Unfortunately, this is a much more difficult equation to solve than the neutron diffusion equation. For this reason, neutron transport theory is usually discussed in more advanced textbooks. For example, an excellent discussion of the transport equation presented in Duderstadt and Hamilton (see Reference 4).

The neutron diffusion equation is then nothing more than a special case of the neutron transport equation where the angular dependence of the neutron flux and the nuclear cross sections can be suppressed. (This corresponds to a case where the flux and scattering cross sections are angularly isotropic, and the dependence on Ω can be ignored.) Then the *directional neutron flux* $\phi(x, y, z, E, \mathbf{\Omega}, t)$ reduces to the *conventional neutron flux* $\phi(x, y, z, E, t)$, and the transport equation, which is an integrodifferential equation, reduces to a standard second-order partial differential equation. The neutron diffusion equation, which we will discuss shortly, is an example of such a second-order differential equation. In general, the neutron diffusion equation can be written in two different forms—the *time-dependent neutron diffusion equation* and the steady-state or *time-independent neutron diffusion equation*. We will derive both of these equations in this chapter. In Chapters 13 and 14, we will discuss solutions to the steady-state neutron diffusion equation, and in Chapters 15 and 16, we will discuss its time-dependent solutions. Steady-state solutions are helpful for doing the preliminary design of a reactor, and time-dependent solutions are helpful for understanding how the core behaves when the neutron population changes very rapidly. Additional isotopes, such as Xenon and Samarium, may also affect the behavior of the core as a function of time. As we will soon discover, the neutron diffusion equation is also an *eigenvalue equation*. This means that the eigenvalues represent both the time-dependent and steady-state behavior of the core. The first eigenvalue, which is discussed in Chapter 13, represents the effective multiplication factor k of the core. The higher order eigenvalues (and their associated eigenfunctions) then determine how the core behaves as a function of time. This topic is discussed more extensively in our companion book,* where the numerical implications of these eigenvalues are also explored.

11.8 Introduction to the Neutron Diffusion Equation

The neutron diffusion equation is probably the most important equation in nuclear science and engineering. In general, the neutrons move in complicated paths through the core as the result of repeated collisions with themselves and with other atoms in the lattice. However, the overall effect of these collisions is to create a kind of particle flow, which is analogous to the diffusion of one gas or solute into another. In other words, the neutrons, on average, move like the molecules in a room filled full of gas. *The approximate value and shape of the neutron distribution (e.g., the neutron flux) can then be described by a neutron diffusion equation*. We discovered earlier that the diffusion equation has some important limitations because it is based in part on Fick's Law. When the physical principles embodied by Fick's Law no longer apply, we must resort to *neutron transport theory* to find the shape of the flux, and this involves solving the *neutron transport equation*, which we will discuss in Chapter 22.

However, for many materials and geometric configurations that we will encounter, the neutron diffusion equation can help us find both the magnitude and the shape of the neutron flux. In other words, it can help us calculate the

* See *Contemporary Nuclear Reactor Physics with an Introduction to Reactor Dynamics, Computational Methods, and Nuclear Particle Transport*, by R.E. Masterson, CRC Press (2019).

nuclear reaction rates—and determine if the effective multiplication factor is greater than, less than, or equal to one. Unfortunately, except in very simple reactor geometries (such as a homogeneous slab, sphere, or cylinder), exact analytical solutions to the neutron diffusion equation do not exist. This means that the only practical way to solve the neutron diffusion equation is to use a computer. In later chapters, we will show how this can be done. However, we will start by first deriving the neutron diffusion equation. In Chapters 12 and 13, we will then show what some simple analytical solutions look like. There are a number of important simplifying assumptions that make these solutions possible. If these assumptions do not apply, then writing a software program to solve the diffusion equation is usually the best way to proceed. If you have not taken a course in differential equations yet, then this would be a good time to do so.

11.9 Writing an Equation to Conserve Neutrons

In order to gain some appreciation for how the neutrons in a reactor behave, it is customary to write down an expression for their behavior in the form of a conservation principle. In Chapter 2, we discussed *the Conservation of Mass and Energy*. We would now like to apply this principle to a swarm of neutrons moving around within the confines of a reactor fuel assembly. Since neutrons do not have an electric charge (see Chapter 2), this is the correct conservation principle to describe them. To get started, assume for the moment that the density ρ of neutrons in the volume of space V we are considering is reasonably uniform. This is a reasonable assumption to make under most conditions. However, in this case, it will allow us to simplify our derivation slightly. Simply stated, the conservation of mass requires that

The Conservation of Mass for a Population of Neutrons

"The rate of change of the number of neutrons in a volume of space V is equal to the number that go into the volume from all sides minus the number that go out of the volume from all sides."

Now let us ask the following question: If we were able to express this principle as a mathematical equation, what would the equation look like? To find out, consider a small volume of space $V = \Delta x \Delta y \Delta z$, centered about a point p with dimensions Δx, Δy, and Δz. The coordinates of the point are x, y, and z. You can think of this volume of space as a small square or rectangle with each of the six faces having an area equal to ΔxΔy, ΔxΔz, or ΔyΔz. This volume is shown in Figure 11.11. Sometimes this volume is also called a *control volume*.

Neutrons can travel across each of the six faces of this control volume at different rates. On some faces, the neutron current **J** will be positive, or into the volume. On other faces, the neutron current **J** will be negative, or out of the volume. The number of neutrons moving across any face is then the product of the neutron current and the area of the face

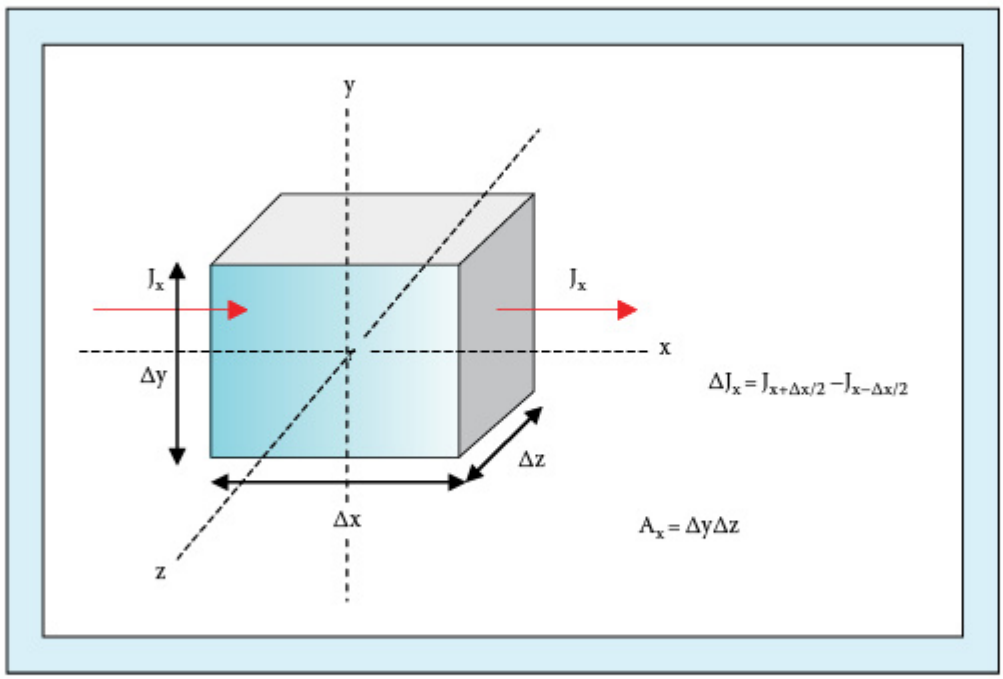

FIGURE 11.11 A cube with a particle current flowing through it.

itself (which can be either $\Delta x\Delta y$, $\Delta x\Delta z$, or $\Delta y\Delta z$). Therefore, the number of neutrons moving across each face is $\mathbf{J}\cdot\Delta A$, where $\Delta A = \Delta x\Delta y$, $\Delta x\Delta z$, or $\Delta y\Delta z$ and J is the component of the current normal to the surface. Referring to Figure 11.11 again, we can conserve the total number of neutrons by requiring that

$$V\cdot\frac{\Delta\rho}{\Delta t} = A_x\Delta\mathbf{J}_x + A_y\Delta\mathbf{J}_y + A_z\Delta\mathbf{J}_z \tag{11.41}$$

where

A_x is the area of the face in the x direction
A_y is the area of the face in the y direction
A_z is the area of the face in the z direction

Here ΔJ_x is the difference between the neutron current at point $x_1 = x + \Delta x/2$ and the neutron current at point $x_2 = x - \Delta x/2$. Similarly, ΔJ_y is the difference between the neutron current at point $y_1 = y + \Delta y/2$ and the neutron current at point $y_2 = y - \Delta y/2$, and ΔJ_z is the difference between the neutron current at point $z_1 = z + \Delta z/2$ and the neutron current at point $z_2 = z - \Delta z/2$. It is also worth noting that $A_x = \Delta y\Delta z$, $A_y = \Delta x\Delta z$, and $A_z = \Delta x\Delta y$. Since $A_x = \Delta y\Delta z$, $A_y = \Delta x\Delta z$, and $A_z = \Delta x\Delta y$ and $V = \Delta x\Delta y\Delta z$, we can rewrite Equation 11.41 as

$$\Delta x\Delta y\Delta z\cdot\Delta(pv)/\Delta t = \Delta y\Delta z\Delta J_x + \Delta x\Delta z\Delta J_y + \Delta x\Delta y\Delta J_z \tag{11.42}$$

After dividing both sides by $\Delta x\Delta y\Delta z$, we obtain

$$\frac{\Delta\rho}{\Delta t} = \frac{\Delta J_x}{\Delta x} + \frac{\Delta J_y}{\Delta y} + \frac{\Delta J_z}{\Delta z} \tag{11.43}$$

Upon realizing that $d\rho/dt = \Delta\rho/\Delta t$, $dJ_x/dx = \Delta J_x/\Delta x$, $dJ_y/dy = \Delta J_y/\Delta y$, and $dJ_z/dz = \Delta J_z/\Delta z$, Equation 11.43 can be written as

$$\frac{d\rho}{dt} = \frac{dJ_x}{dx} + \frac{dJ_y}{dy} + \frac{dJ_z}{dz} \tag{11.44}$$

Finally, because $\mathbf{J}$ is a vector, Equation 11.44 becomes

$$\frac{\partial\rho}{\partial t} = \frac{\partial\mathbf{J}}{\partial x} + \frac{\partial\mathbf{J}}{\partial y} + \frac{\partial\mathbf{J}}{\partial z} \tag{11.45}$$

where $\mathbf{J} = \mathbf{i}\cdot(J_x) + \mathbf{j}\cdot(J_y) + \mathbf{k}\cdot(J_z)$. In other words, we have just learned a great truth! We have found that the saying "The rate of change of the number of neutrons in a volume of space V is equal to the number that go into the volume from all sides minus the number that go out of the volume from all sides" is equivalent to the following conservation equation for the neutron current:

A Conservation Equation for the Neutron Current

$$\frac{\partial\rho}{\partial t} = \frac{\partial\mathbf{J}}{\partial x} + \frac{\partial\mathbf{J}}{\partial y} + \frac{\partial\mathbf{J}}{\partial z} \tag{11.46}$$

This conservation equation can also be written as

An Alternative Form of the Neutron Conservation Equation

$$\frac{\partial\rho}{\partial t} = \text{div}\,\mathbf{J} = \nabla\cdot\mathbf{J} \tag{11.47}$$

where $\nabla\cdot$ is a *vector operator* that frequently appears in the study of differential equations. This particular vector operator $\nabla\cdot$ is called the *divergence operator*, and physically, it represents the magnitude of the outwardly directed neutron current $\mathbf{J}$ from the control volume shown in Figure 11.11. In particular, the total neutron leakage rate is given by

$$\text{Total neutron leakage rate} = \int_V \nabla\cdot\mathbf{J}\,dV \tag{11.48}$$

where $V = \Delta x \Delta y \Delta z$ is the volume of the cube. Thus, the divergence operator is a convenient way to write Equation 11.46 in a more elegant form. We can extend Equation 11.37 to other simple geometries, such as cylindrical or circular ones, by simply substituting the appropriate form of the divergence operator for the *Cartesian* version that we have used up to this time. Various forms of the divergence operator are described at

http://en.wikipedia.org/wiki/Divergence

A discussion of the *gradient operator*, which is related to the divergence operator and appears in Fick's Law (see Equation 11.22), can be found at

http://en.wikipedia.org/wiki/Gradient

The reader should attempt to understand the difference between these two operators because they represent very different things when applied to the diffusion equation.

Example Problem 11.2

Based on the information presented in Table 11.1, what would be one reason why heavy water (D_2O) would be a better material to use than light water (H_2O) in a thermal water reactor? Also, which material would allow more thermal neutrons to leak out of a reactor core of a constant size?

Solution Based on the information presented, we can see that heavy water has a much lower absorption cross section than light water. This is one of the reasons why heavy water was so sought after during the World War II when enriched uranium was in short supply. Heavy water, however, has a much larger thermal neutron diffusion coefficient than light water does (see Table 11.1). This means that the neutron leakage rate $J = -D\nabla\phi$ is always higher in a reactor moderated by heavy water than a reactor moderated by light water. So more thermal neutrons would leak out of a heavy water reactor than an identical light water reactor of the same size. [Ans.]

11.10 Adding Sources and Sinks to the Neutron Conservation Equation

Earlier we derived the neutron conservation equation by simply counting the number of neutrons entering and leaving an arbitrary control volume. We would now like to extend our derivation to include problems where neutrons are being created all the time (by the process of nuclear fission) and are being destroyed all the time (through the process of capture and absorption). In other words, we would like to extend the neutron conservation equation to problems with both *sources* and *sinks*. To do so, let us return to Equations 11.46 and 11.47 for the moment and attempt to modify them to account for these additional effects. Equations 11.46 and 11.47 simply state that the rate of change of the neutron population is equal to the number of neutrons that flow into the control volume minus the number that flow out of the control volume. When there are additional processes at work (like neutron creation and absorption), it is essential to add another term to our original equations to account for these additional sources and sinks. In Chapter 4, we were first introduced to nuclear cross sections, where we learned that the number of neutrons being created or destroyed per second (e.g., the reaction rate R) could be written as

$$R = \left(\nu\Sigma_f - \Sigma_a\right)\phi V \tag{11.49}$$

where

Σ_f and Σ_a were the macroscopic fission and absorption cross sections
ν was the average number of neutrons released per fission
V was the volume of material in which the reactions were occurring

For most fissile materials value for ν is about 2.5. Ignoring the energy dependence of ϕ, ν, Σ_f, and Σ_a for the moment, Equation 11.49 defines the number of neutrons being created or destroyed per second in the presence of the neutron flux ϕ. In other words, this expression represents the net number of neutrons being created or destroyed per second. If we reflect on this, the expression for the conservation of neutrons, which we discussed previously, should have been written as

An Expression for the Conservation of Neutrons with Internal Sources and Sinks

"The rate of change of the number of neutrons in a volume of space V is equal to the number that go into the volume from all sides minus the number that go out of the volume from all sides *plus the number of neutrons in the volume that are created or destroyed by interactions with other atoms*."

In other words, we can produce the correct and more general form of the neutron balance equation by simply taking Equations 11.46 and 11.47 and adding another term to them, which is defined by Equation 11.49. The final result of this operation is

A More General Form of the Neutron Conservation Equation

$$\frac{\partial \rho}{\partial t} = \frac{\partial \mathbf{J}}{\partial x} + \frac{\partial \mathbf{J}}{\partial y} + \frac{\partial \mathbf{J}}{\partial z} + \left(\nu\Sigma_f - \Sigma_a\right)\phi$$

or

$$\frac{\partial \rho}{\partial t} = \nabla \cdot \mathbf{J} + \left(\nu\Sigma_f - \Sigma_a\right)\phi \tag{11.50}$$

where Σ_f and Σ_a are the *macroscopic fission and absorption cross sections*, and the energy dependence of all of the variables has been temporarily suppressed to simplify the notation. So by simply counting neutrons, we have come to the conclusion that the neutrons in a nuclear reactor must obey equation 11.50 in order for the actual number of neutrons to be conserved. Assuming that the composition of the materials in the control volume is known (or can be inferred from their atomic densities), the remaining unknowns in Equation 11.50 are the neutron current J, the neutron flux ϕ, and the neutron density ρ. If we want to solve this equation for the neutron flux ϕ, then we need to reduce the number of unknowns to one. This involves understanding how the neutron flux ϕ is related to the neutron current $\mathbf{J}$, and how the neutron flux is related to the neutron density ρ. Now let us discuss how these additional relationships can be used.

11.11 Derivation of the Time-Dependent Neutron Diffusion Equation

If the conditions specified in Section 11.7 apply, then there is a relatively straightforward relationship between the neutron current J and the neutron flux ϕ, Then Fick's Law of Diffusion can be used, and when the flux is angularly isotropic, we can write

$$\mathbf{J}_x = -D\frac{d\phi}{dx} \tag{11.51}$$

or more generally,

$$\mathbf{J} = -D\nabla\phi \tag{11.52}$$

where the gradient operator ∇ is defined by

$$\nabla = \mathbf{i}\cdot\frac{\partial}{\partial x} + \mathbf{j}\cdot\frac{\partial}{\partial y} + \mathbf{k}\cdot\frac{\partial}{\partial z} \tag{11.53}$$

and the constant of proportionality D between the flux and the current is the *diffusion coefficient*. Assuming for the moment that D is independent of position, we can substitute Equation 11.52 into Equation 11.50 to eliminate the neutron current. When we do so, we find that

Time-Dependent Neutron Balance

$$\frac{\partial \rho}{\partial t} = D\nabla^2\phi + \left(\nu\Sigma_f - \Sigma_a\right)\phi \tag{11.54}$$

where the diffusion coefficient is multiplied by the familiar *Laplacian operator* ∇^2. The product of the diffusion coefficient and the Laplacian operator then defines the neutron leakage rate from a small control volume at a particular point in space. Expressions for the Laplacian operator and the *Gradient operator* are given in Table 11.2 for Cartesian, cylindrical, and spherical geometries for a hypothetical F. We will use this table later to illustrate how the flux behaves in geometries

TABLE 11.2
Expressions for the Gradient and the Laplacian Operators in Common Coordinate Systems

Coordinate System	Coordinates	Gradient Operator ∇	Laplacian Operator ∇^2
Cartesian	x, y, z	$\partial F/\partial x + \partial F/\partial y + \partial F/\partial z$	$\partial^2 F/\partial x^2 + \partial^2 F/\partial y^2 + \partial^2 F/\partial z^2$
Cylindrical	r, θ, z	$(1/r)\,\partial(rF)/\partial r + (1/r)\,\partial F/\partial\theta + \partial F/\partial z$	$(1/r)\,\partial/\partial r\,(r\partial F/\partial r) + (1/r^2)\,\partial^2 F/\partial\theta^2 + \partial^2 F/\partial z^2$
Spherical	r, θ, φ	$(1/r^2)\,\partial/\partial r\,(r^2 F) + (1/r\sin\theta)\,\partial/\partial\theta$ $(\sin\theta \cdot F) + (1/r\sin\varphi)\,\partial F/\partial\varphi$	$(1/r^2)\,\partial/\partial r\,(r^2\partial F/\partial r) + (1/r^2\sin\theta)\,\partial/\partial\theta$ $(\sin\theta \cdot \partial F/\partial\theta) + (1/r^2\sin^2\varphi)\,\partial^2 F/\partial\varphi^2$

other than Cartesian ones. Depending on the coordinate system used, F can be a function of x, y, z, or r, θ, z, or r, θ, φ, that is, F(x, y, z) or F(r, θ, z) or F(r, θ, φ). The choice of which coordinate system to use is arbitrary. Now let us discuss how to find the neutron flux from Equation 11.54.

Now that we have eliminated the neutron current from Equation 11.33, all we need to do is to establish a relationship between the neutron density ρ and the neutron flux ϕ. You may recall from our previous discussion in Section 11.3 that this relationship is

$$\phi = \rho v \tag{11.55}$$

where v is the neutron velocity and specifically, the *average neutron velocity*. Solving for ρ, we get

$$\rho = \frac{\phi}{v} \tag{11.56}$$

and substituting $\rho = \phi/v$ into Equation 11.54, we obtain

$$(1/v)\partial\phi/\partial t = D\nabla^2\phi + (\nu\Sigma_f - \Sigma_a)\phi \tag{11.57}$$

After rearranging the terms slightly, Equation 11.57 becomes

Time-Dependent Neutron Diffusion Equation

$$D\nabla^2\phi + (\nu\Sigma_f - \Sigma_a)\phi = \left(\frac{1}{v}\right)\frac{\partial\phi}{\partial t} \tag{11.58}$$

This is the famous *time-dependent neutron diffusion equation* of reactor physics. Because it involves only one value for the neutron velocity v, it is sometimes called the "*one-speed*" or "*one-group*" neutron diffusion equation, and it is the basis of "*one-speed*" or "*one-group*" neutron diffusion theory. For a medium in which the macroscopic cross sections and the diffusion coefficient D can be suitably homogenized, Equation 11.58 is the equation that can be used to predict the time-dependent neutron population. In other words, this equation allows up to predict how the flux *changes* with time. *It is perhaps the most important equation in all of reactor kinetics*. In Chapter 12, we will show how this equation can be extended to handle multiple energy groups as well.

11.12 Steady-State Neutron Diffusion Equation

When the neutron flux does not change with time, we can set $\partial\phi/\partial t = 0$ and Equation 11.58 becomes

Steady-State Neutron Diffusion Equation

$$D\nabla^2\phi + (\nu\Sigma_f - \Sigma_a)\phi = 0 \tag{11.59}$$

This equation is called *the steady-state neutron diffusion equation*. Note that the only unknown variable in this equation is the neutron flux. The steady-state neutron diffusion equation is appropriate for finding the flux shape in a reactor that is operating very close to steady-state conditions—that is, in situations where the flux and the power do not change rapidly as a function of time. It is also helpful in determining what needs to be done to maintain a reactor in a critical state, that is, a reactor in which the neutron production, leakage, and destruction rates exactly cancel.

11.13 Steady-State Neutron Diffusion Equation with an External Neutron Source

Up to this time, we have assumed that the neutrons represented by the diffusion equation are created through the process of nuclear fission alone. However, neutrons can be created in nuclear materials in other ways. For example, they can be introduced into a material through a radioactive neutron emitter of arbitrary strength S. The total number of neutrons S emitted from this neutron source s(r) is then

$$S = \int_V s(r)dV \tag{11.60}$$

where s(r) is the number of neutrons emitted per cubic centimeter per second, and the integration is performed over the entire volume of space V in which the neutron emitter can be found. Because this source is independent of the neutron flux, it appears in the neutron diffusion equation *as a constant* with the units of neutrons/s. If the source s(r) is concentrated at a single point in space, it appears in the diffusion equation as what is known as a *point source*. The behavior of this point source can be described by the *Dirac Delta Function* δ, which is defined in the following way:

$$\delta(r - r_o) = 0 \quad \text{if } r \neq r_0 \quad \text{and} \quad \delta(r - r_o) = \infty \quad \text{if } r = r_0 \tag{11.61}$$

It also follows from Equation 11.61 that

$$\int \delta(r - r_o)dr = 1 \quad \text{where the limits of integration are from } r = -\infty \text{ to } r = +\infty \tag{11.62}$$

Notice that this definition *does not say* exactly what the shape of s(r) must be as long as s(r) is very small. It simply says that it must add up to some finite number S that we can interpret as

$$S = \int \delta(r - r_o)s(r)dr \tag{11.63}$$

If a number of point sources are connected together to form a line, then the neutron source becomes what is known as a *line source*. Finally, if all of the sources are connected together to form a plane, the resulting source is sometimes called a *planar source*. A neutron source can be distributed across a large volume $V = \Delta x \Delta y \Delta z$ of space as well. Such a neutron source is appropriately called a *distributed source*. Examples of these types of neutron source are shown in Figure 11.12. In any event, the resulting neutron source can be modeled by the simple neutron source term S, which may or may not have an explicit temporal dependence. When an external source is present, the neutron diffusion equation needs to be written as

The Neutron Diffusion Equation with an External Neutron Source

$$D\nabla^2\phi + (\nu\Sigma_f - \Sigma_a)\phi + S = 0 \quad (\text{where S is an external source}) \tag{11.64}$$

or since S is a positive constant,

$$D\nabla^2\phi + (\nu\Sigma_f - \Sigma_a)\phi = -S \tag{11.65}$$

Equation 11.65 can be solved just like any other diffusion equation if we know the value for S. When there is no fuel present, then the production term $P = \nu\Sigma_f\phi$ can be set to zero, and the steady-state diffusion equation becomes

The Neutron Diffusion Equation with No Fissionable Material

$$D\nabla^2\phi - \Sigma_a\phi = -S \tag{11.66}$$

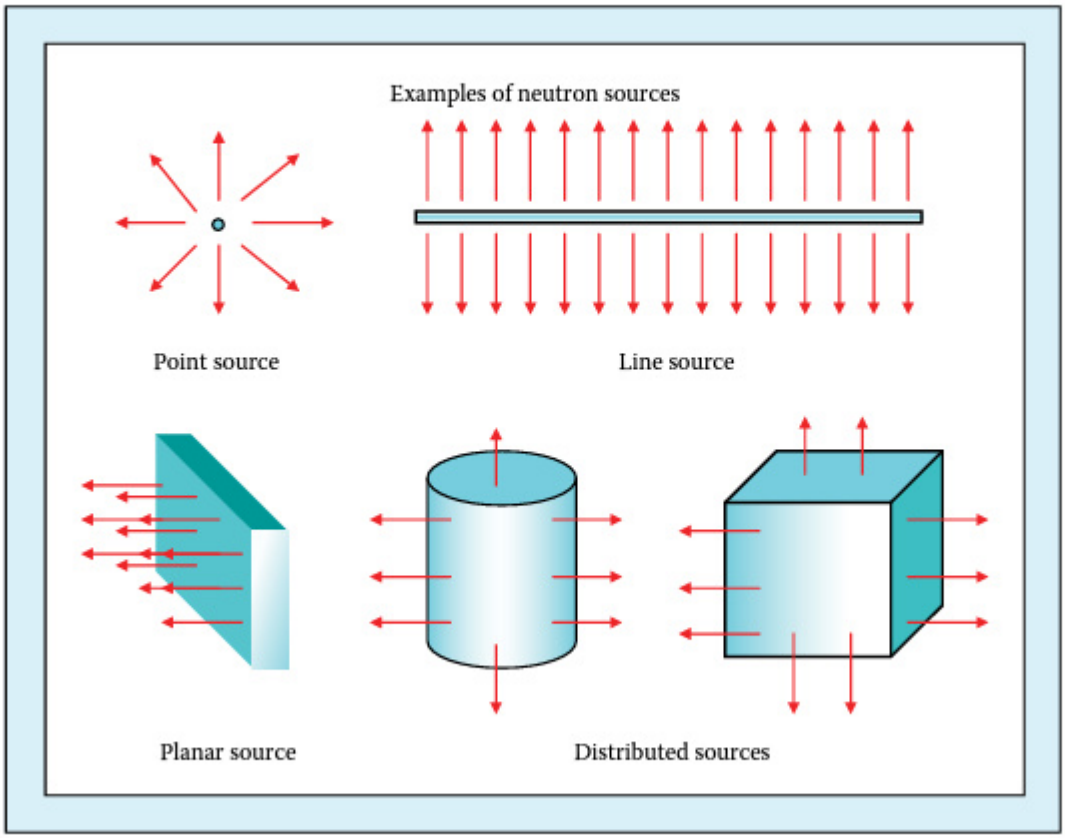

FIGURE 11.12 Some examples of neutron sources—both concentrated and distributed.

In practice, it is often convenient to remove the diffusion coefficient D from this equation entirely by writing it as

$$\nabla^2\phi - \left(\frac{\Sigma_a}{D}\right)\phi = -\frac{S}{D} \tag{11.67}$$

or

The Classic Form of the Neutron Diffusion Equation with No Fissionable Material and an External Neutron Source

$$D\nabla^2\phi - \left(\frac{1}{L^2}\right)\phi = -S' \tag{11.68}$$

where $L^2 = D/\Sigma_a$ is a quantity known as *the neutron diffusion area* and $S' = S/D$. The square root of the diffusion area $L = \sqrt{L^2}$ appears in many practical problems and is sometimes called *the diffusion length*. We will have more to say about this in Section 11.16, where we will also offer a physical interpretation for what each of these terms means. For the special case where $S = 0$ and $\Sigma_f \neq 0$, the remaining terms can be written in a more common form that we will discuss next. This form is sometimes called the *standard form* of the steady-state neutron diffusion equation.

11.14 Standard Form of the Steady-State Neutron Diffusion Equation

In neutron producing regions of space (such as a reactor core) it is often convenient to write the steady state diffusion equation in what has become known as its *standard form*. There is also some physical insight to be gained by writing it in this way. If we divide both sides of Equation 11.68 by the diffusion coefficient, and assume for the moment that D has no spatial dependence, then we obtain

$$\nabla^2\phi + \frac{(\nu\Sigma_f - \Sigma_a)\phi}{D} = 0 \tag{11.69}$$

Equation 11.69 can also be written as

$$\nabla^2\phi + B^2\phi = 0 \tag{11.70}$$

where B^2 is a new parameter called *the material buckling*. The material buckling therefore has a value of $B^2 = (\nu\Sigma_f - \Sigma_a)/D$, and its value can be either positive or negative depending on the sign of the numerator.

Notice that when $(\nu\Sigma_f - \Sigma_a) > 0$, the value for B^2 is positive, and this corresponds to a region of space in which more neutrons are produced than are destroyed. Suppose that we call this Region 1. This region normally corresponds to a fuel assembly or even a set of fuel assemblies within the reactor pressure vessel. This region is commonly called *the core*. Conversely, when $(\nu\Sigma_f - \Sigma_a) < 0$, the value for B^2 becomes negative, and this corresponds to a region of space in which more neutrons are destroyed (by absorption and leakage) than are created by the fission process itself. Suppose that we call this Region 2. Similarly, additional regions of space may exist where the material buckling will have a different value than in Region 2. We will call this region in which we wish to find the value of the flux Region 3. In most reactors, Regions 2 and 3 correspond to what is known as *the reflector*. The makeup of these three regions is illustrated for the case of a simple slab reactor in Figure 11.13. For Region 1, we may write the diffusion equation as

$$\text{Region 1}: \quad \nabla^2\phi + B_1^2\phi = 0 \tag{11.71}$$

and similarly in Regions 2 and 3

$$\text{Region 2}: \quad \nabla^2\phi + B_2^2\phi = 0 \tag{11.72}$$

$$\text{Region 3}: \quad \nabla^2\phi + B_3^2\phi = 0 \tag{11.73}$$

where the subscripts on the buckling refer to the value of the material buckling B^2 in each of these regions individually.

Student Exercise 11.1

Based on the discussion in Section 11.13, provide a qualitative explanation for why the shape of the neutron flux $\phi(r)$ peaks in regions where $B^2 > 0$, falls in regions where $B^2 < 0$, and is relatively flat in regions where $B^2 = 0$. If the macroscopic cross sections and the diffusion coefficient are measured in centimeters, what units does the material buckling have?

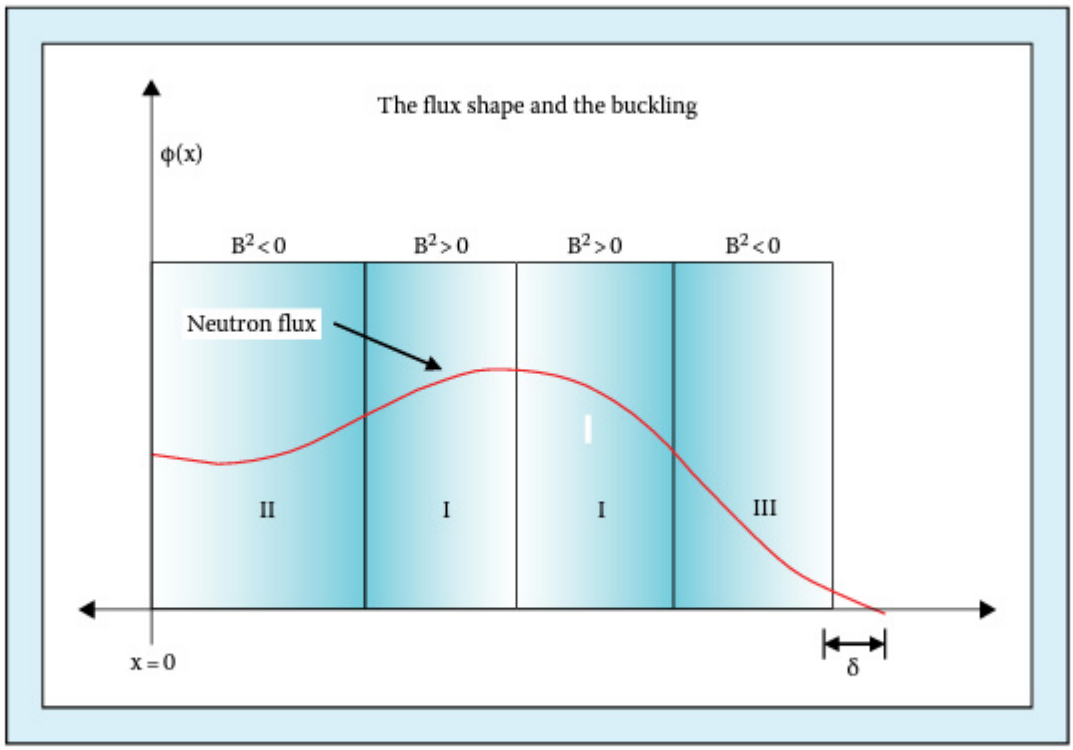

FIGURE 11.13 The neutron flux shape $\phi(x)$ in a multiregion reactor.

11.15 Boundary Conditions for the Neutron Diffusion Equation

We are now very close to having everything that we need to solve the steady-state neutron diffusion equation in any coordinate system and corresponding reactor geometry we want. All we need to do is to specify the coordinate system (Cartesian, cylindrical, or spherical), apply the boundary conditions governing the flux and the current, and select the appropriate values to use for the materials. The *boundary conditions* are simply the values of the neutron flux or the neutron current on the boundaries of the regions in which we would like to solve the diffusion equation. To see why these boundary conditions are important, consider the infinite slab of material shown in Figure 11.14.

Assume for the moment that there are neutrons being produced inside of the slab so that $\nu\Sigma_f > 0$ and that the slab is homogeneous, so that we can neglect the effects of position on D, Σ_a, and Σ_f. If we tell the neutron diffusion equation that the flux on both of the outer boundaries (x = 0 and x = a) is 0, then the diffusion equation will give us a solution similar to the one shown in Figure 11.14 *in red*. However, if we tell the diffusion equation that the flux on one boundary (x = 0) is 0 and that the current on the other boundary (x = a) is 0, then we get the result shown *in blue*. In other words, *the shape of the neutron flux depends on what the boundary conditions are!*

In addition to these simple boundary conditions, consider the more practical problem posed by the material configuration shown in Figure 11.15. This configuration consists of three regions: a central homogeneous region where we would like to predict the flux, surrounded by two regions consisting of entirely different materials than the central region. These two regions can consist of any combination of materials that we want. For the sake of this discussion, we will assume that the two outer regions, Regions 2 and 3, contain materials with nontrivial macroscopic scattering cross sections Σ_{s1} and Σ_{s2} but that their macroscopic fission cross sections are zero. This is equivalent to saying that region 1 in the center is the reactor core and that the material regions on each side of it correspond to what we shall call the "reflector." Many studies have been done to determine what boundary conditions should be used to handle situations like this. Although there may be slight variations with respect to the recommendations of these studies (such as when the surrounding regions do not have any material in them at all), it is generally agreed that *both the neutron flux and the neutron current must be physically continuous across the boundaries of these material regions in order to give correct and physically meaningful results*.

The dimensions of each of the regions are not drawn to scale. In practice, the reflector can be either a large volume of water or a thick piece of steel, like the reactor pressure vessel. In some reactors, it can even be filled with a gas such as carbon dioxide or air. The important thing to keep in mind is that we must tell the diffusion equation what the behavior of the neutron flux and the current is on each of the material boundaries. Otherwise, it will not

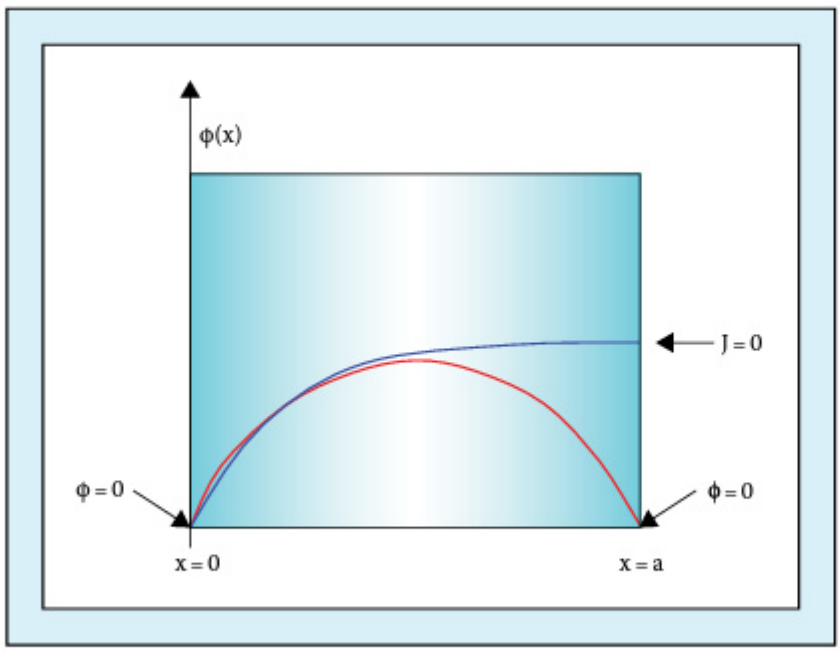

FIGURE 11.14 How different boundary conditions can affect the flux shape.

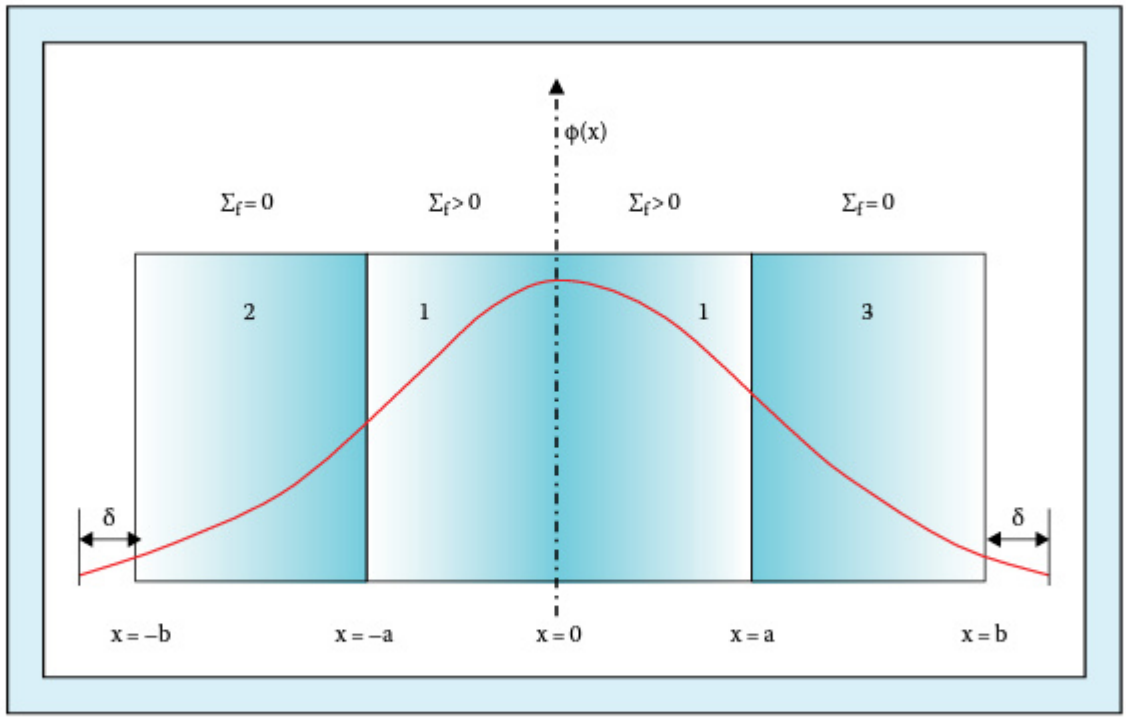

FIGURE 11.15 The neutron flux in a three-region reactor.

give us a physically realistic result. Thus, at each material interface I in Figure 11.15, the following conditions must be satisfied:

Boundary Conditions for the Neutron Flux and the Neutron Current (with 1 Energy Group)

$$\text{For the flux } \phi_{i(+)} = \phi_{i(-)} \tag{11.74}$$

and

$$\text{For the current } J_{i(+)} = J_{i(-)} \tag{11.75}$$

where the symbols (+) and (−) refer to the right- and left-hand sides of each interface i. Since there are four material interfaces in our example (two on the inside and two on the outside), these boundary conditions must be satisfied at all four interfaces (x = −b, x = −a, x = a, and x = b). If the neutron flux and the neutron current are further decomposed into a number of different energy groups (such as the fast and thermal energy groups), then each energy group in turn must respect these boundary conditions as well.

11.16 Boundary Conditions for More than One Energy Group

It may have occurred to you if you look at Equation 11.16 that the continuity of the neutron current at a material interface i implies that

$$\mathbf{J}_x = -D\frac{d\phi}{dx}, \quad \mathbf{J}_y = -D\frac{d\phi}{dy}, \quad \text{and} \quad \mathbf{J}_z = -D\frac{d\phi}{dz} \tag{11.76}$$

for each coordinate direction (x, y, and z). If the neutron flux and the neutron current consist of G energy groups, then each energy group must respect these boundary conditions as well. Thus, in a *multigroup model* of neutron behavior where the neutron current in the x direction is given by

$$\mathbf{J}_g(x) = -D_g d\phi_g(x)/dx \tag{11.77}$$

the following conditions must always be satisfied at each material interface as well:

Boundary Conditions for the Neutron Flux and the Neutron Current (with More than One Energy Group)

$$\text{For the flux } \phi_g i_{(+)} = \phi_g i_{(-)}$$

and

$$\text{For the current } \mathbf{J}_g i_{(+)} = \mathbf{J}_g i_{(-)}$$

$$\text{for } g = 1 \text{ to } G \tag{11.78}$$

Here G is the total number of *energy groups*. Thus this relationship must be imposed at every interface if the neutron current is to be continuous across the material boundaries.

11.17 Defining the Neutron Diffusion Length

So far, we have lumped most of the physics into the value of a constant that we have decided to call the *material buckling* B^2. When dealing with large homogeneous reactors, this is what most nuclear engineers tend to do. In general, the values of the material buckling B^2 will be different for each material region for which the value of the neutron flux is to be found. In Chapter 9, we learned that the value of the neutron multiplication factor for an infinite reactor lattice could be written as

$$K_\infty = \nu\left(\frac{\Sigma_f}{\Sigma_a}\right) \tag{11.79}$$

where ν was the average number of neutrons released per fission (normally a number between $\nu = 2.4$ and $\nu = 2.9$ for a common fissile material). If we substitute this into the diffusion equation and rearrange terms, we find that

$$B^2\phi = \frac{(K_\infty - 1)\phi}{L^2} \tag{11.80}$$

Upon solving this equation for B^2, we obtain

$$B^2 = \frac{K_\infty - 1}{L^2} \tag{11.81}$$

In Equation 11.81, the parameter L^2 can be written as

$$L^2 = \frac{D}{\Sigma_a} \tag{11.82}$$

and it is easy to see that the value of this parameter depends on only the material composition of each homogeneous region. *This is another way of saying that the geometric buckling B^2 of the flux will be positive in a region where $K_\infty > 0$, it will be negative in a region where $K_\infty < 0$, and it will be flat in a region where $K_\infty = 0$.* Hence, Equation 11.81 establishes an important relationship between the geometric bucking of the flux B^2 and the infinite multiplication factor for a homogeneous and exactly critical system. *The parameter L that appears in Equation 11.82 is our old friend, the neutron diffusion length.* It is defined by $L = \sqrt{D/\Sigma_a}$, and it is easy to see that it has the units of length (usually cm). Physically, the diffusion length is related to the distance a free neutron must travel from the time it is emitted from an atomic nucleus to the time it is absorbed. As such, it is a measure of the strength of the absorbing medium. Tables 11.3 and 11.4 show the values of the diffusion length for several important nuclear materials. Note that the diffusion length is different for fast neutrons than it is for thermal neutrons.

Here we have used the convention that D_F is the diffusion coefficient for fast neutrons and D_T is the diffusion coefficient for thermal neutrons. For the same material, it is almost always true that $D_F > D_T$. Hence, thermal neutrons do not have to travel very far before they are absorbed. Fast neutrons, on the other hand, can travel right through a typical fuel rod (which is about 1 cm in diameter) before they are either scattered or absorbed. This also implies that the

TABLE 11.3
Some Representative Diffusion Parameters for Thermal Neutrons

Nuclear Fuel	Thermal Scattering Cross Section ($\times 10^{-24}$ cm^2)	Thermal Neutron Diffusion Coefficient $D = 1/(3\Sigma_s)$	Thermal Absorption Cross Section (cm^{-1}) Σ_a	Thermal Neutron Diffusion Length (cm) $L = \sqrt{D/\Sigma_a}$	Scattering Mean Free Path (cm) $\lambda_s = 1/\Sigma_s$	Absorption Mean Free Path (cm) $\lambda_a = 1/\Sigma_a$
U-233	12.9	0.538	27.6	0.14	1.61	0.03
U-235	18.0	0.498	32.8	0.12	1.49	0.03
U-238	8.9	0.780	0.13	2.45	2.34	7.69
Pu-239	7.7	0.883	50.3	0.13	2.65	0.02

TABLE 11.4
Some Representative Diffusion Parameters for Fast Neutrons

Type of Fuel	Fast Scattering Cross Section ($\times 10^{-24}$ cm^2)	Fast Neutron Diffusion Coefficient $D = 1/(3\Sigma_s)$	Fast Absorption Cross Section (cm^{-1}) Σ_a	Fast Neutron Diffusion Length (cm) $\sqrt{D/\Sigma_a}$	Scattering Mean Free Path (cm) $\lambda_s = 1/\Sigma_s$	Absorption Mean Free Path (cm) $\lambda_a = 1/\Sigma_a$
U-233	6.71	1.03	0.145	2.66	3.09	6.90
U-235	6.73	1.02	0.117	2.95	3.06	8.55
U-238	6.87	1.00	0.018	7.45	3.00	55.55
Pu-239	6.98	0.98	0.113	2.95	2.94	8.85

shape of the fast flux will change more slowly than the shape of the thermal flux. For the fissile materials, Pu-239 has the largest thermal absorption cross section, and therefore the smallest mean free path, followed by U-235 and U-233, respectively.

11.18 Neutron Diffusion Distance

Sometimes one would like to know how far a neutron can theoretically travel before it is absorbed. If a neutron is emitted from an atomic nucleus, it is emitted with the same probability into any solid angle Ω centered about the source of emission S. In other words, wherever the neutron is emitted, the probability is the same that it will be emitted to the right as it will be emitted to the left. *There is no way to predict a priori which way it will go*. However, after it is emitted, it is possible to predict the *average distance* that it will travel before it is absorbed. This distance is called the *average diffusion distance* $<r>$, and later in the chapter, we will show that it is related to the diffusion length L by the following equation:

$$<r> = \sqrt{6}L = 2.45L \tag{11.83}$$

where the parameter L^2 is given by

$$L^2 = \frac{D}{\Sigma_a} \tag{11.84}$$

and L^2 for a homogeneous medium is known as the *diffusion area*.

Since the diffusion coefficient D has the units of cm and the absorption cross section Σ_a has the units of cm^{-1}, it is easy to see that the diffusion area L^2 has the units of cm^2 and the diffusion length L has the units of cm. It is sometimes easier to illustrate the average diffusion distance $<r>$ by considering the trajectory of the neutron shown in Figure 11.16. The neutron is emitted by an atomic nucleus in a random direction and then undergoes a series of elastic scattering collisions as it moves through the lattice. Sometimes it will move a short distance before it collides with an atomic nucleus, and

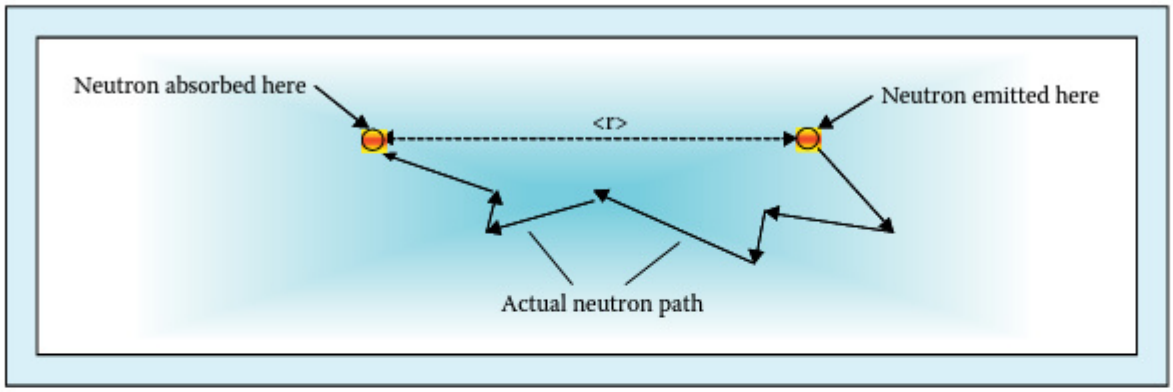

FIGURE 11.16 The diffusion distance for a neutron in a homogeneous material.

sometimes it will not. *The average distance between successive collisions is called the mean free path* λ of the neutron, and the mean free path is related to the macroscopic scattering cross section Σ_s by

$$\lambda = \frac{1}{\Sigma_s} \tag{11.85}$$

The greater the value of L, the further the neutron will move before it is absorbed. *This equation does not allow us to predict exactly where the neutron will be absorbed. However, it does allow us to predict the average distance <r> the neutron will travel from its point of origin (as the crow flies) until it is absorbed.*

It is important to realize that the average distance <r> a neutron travels represents the *statistical average* of the case histories of many individual neutrons. Some neutrons will not travel as far as the average distance <r> and some neutrons will travel further. In general, the paths of these neutrons tend to follow a statistical probability distribution similar to the distribution shown in Figure 11.17. This distribution is sometimes called a *Gaussian probability distribution*, although in this case it is not a symmetrical one. In this type of distribution, 50% of the neutrons will travel less than the average

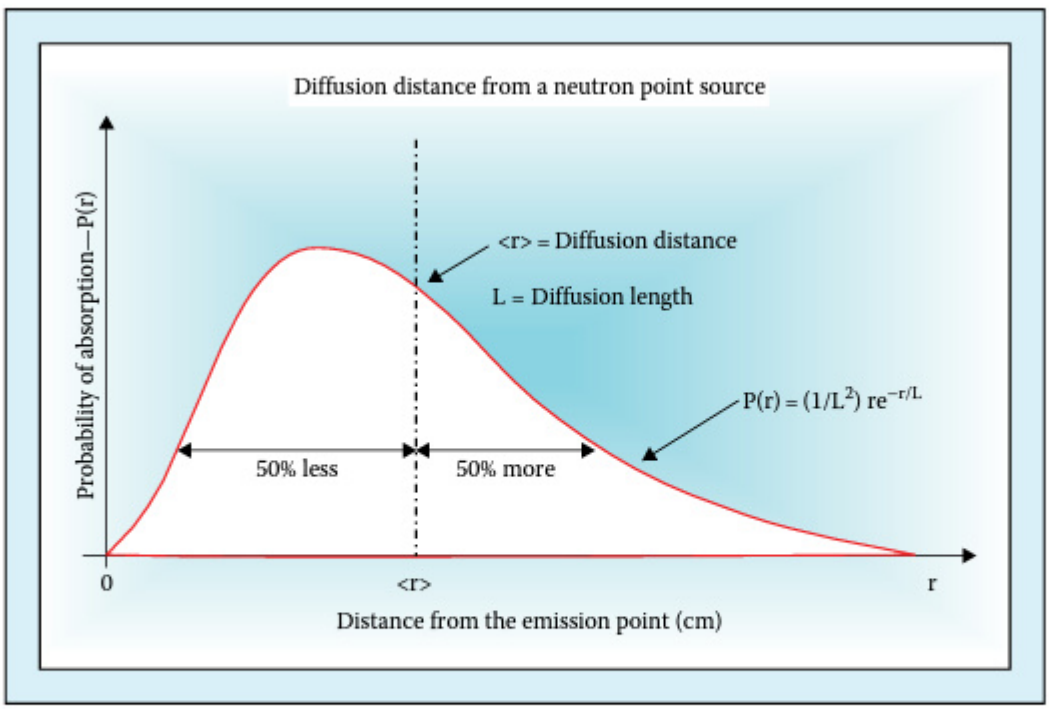

FIGURE 11.17 A probability distribution showing where a fission neutron will be absorbed.

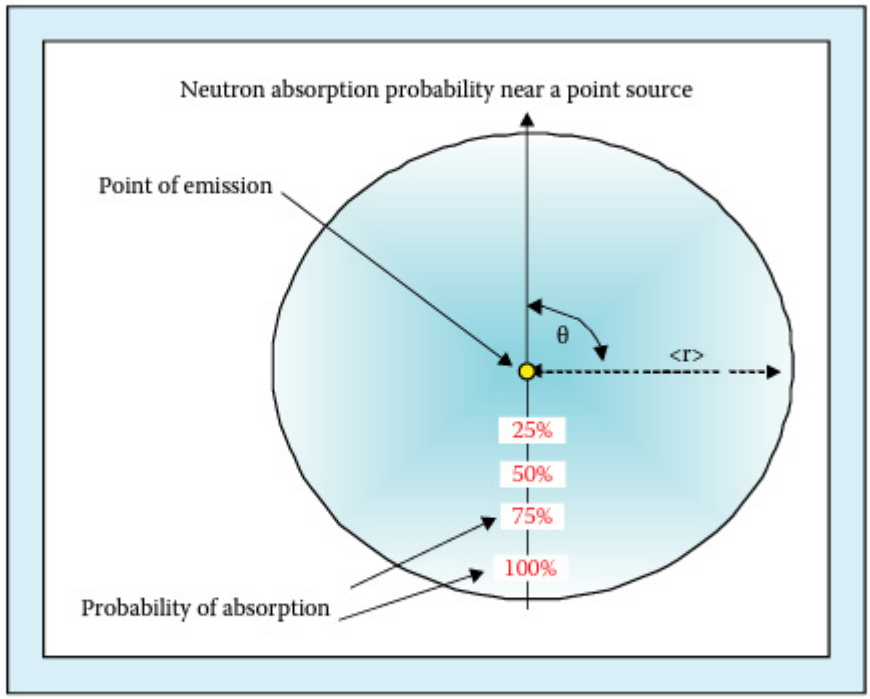

FIGURE 11.18 The probability that a neutron will be absorbed as a function of its distance from its emission point.

distance, and 50% will travel more. The characteristics of these distributions can be found in many probability and statistics books. Similarly, we can apply the same logic to estimate how far a fission neutron will travel on average before it is absorbed in the fuel. To find the average distance, we simply use the relationship $\langle r \rangle = \sqrt{6}L$, where the values for the diffusion length for a typical pressurized water reactor (PWR) fuel rod are shown in Table 11.4.

Notice that the *Equation 11.83 does not contain any information about the angle where the neutron is absorbed*. (Thus in spherical coordinates, the equation for <r> has no dependence on θ or φ.) For this reason, fission neutrons are normally considered to be absorbed within a spherical region of space a distance <r> from the source S itself. In two dimensions, this reduces to a cylinder of radius <r> where the nucleus that emits the neutron is now on the axis of a cylinder (see Figure 11.17). In two dimensions, each concentric ring emanating from the cylinder represents a different probability of absorption. However, when the neutron reaches a distance equivalent to $\langle r \rangle = \sqrt{6}L$ from the center, then the probability of absorption will equal to 100% or 1.0. An analogous equation also exists for the probability P(r) that a neutron is absorbed in a concentric shell of thickness dr located a distance r from the point of emission shown in (Figure 11.18). This equation, which was originally derived by James Maxwell (the father of the Maxwell–Boltzmann probability distribution), says that

$$P(r)dr = \left(1/L^2\right) r e^{-r/L} dr \tag{11.86}$$

where P(r) is the probability of absorption. The reader will find by integrating this probability distribution P(r) that the average value of <r> is given by $\langle r \rangle = \sqrt{6}L$. We will also show how this probability distribution is derived later in the chapter.

Example Problem 11.3

Calculate how far a neutron will go through a scattering material like water (H_2O) in the thermal energy range before it is absorbed.

Solution We know from Table 11.1 that L = 2.85 cm. The average diffusion distance is <r>, and it is related to the average diffusion length L by the following relationship: $\langle r \rangle = \sqrt{6}L = 2.45L$, so in this case where L = 2.85 cm, <r> = 2.45 × 2.85 = 6.98 cm. [Ans.]

11.19 Neutron Mean Free Path and Its Relationship to Diffusion Theory

There is a rather interesting relationship between the macroscopic cross section Σ and the mean free path of a free neutron. This relationship applies to *any nuclear particle* that moves through a material—irrespective of the nature of the material itself. In other words, it applies to protons, electrons, and neutrons as well as any other particles whose cross sections we can measure. *This relationship states that the mean free path of a nuclear particle λ (not to be confused with the radioactive decay constant) is inversely proportional to the macroscopic cross section Σ for whatever reaction type we can measure*. In other words, the larger the total cross section is, the shorter a particle has to travel before it interacts with something. This can be expressed mathematically by writing

$$\lambda_x = \frac{1}{\Sigma_x} \tag{11.87}$$

where x refers to the reaction type. Let us illustrate how this relationship can be applied to estimate the mean free path of a neutron in a typical radiation shield. Suppose that the shield consists of a material with a macroscopic absorption cross section of 0.01345 cm^{-1} and a macroscopic scattering cross section of 0.0903 cm^{-1}. According to Equation 11.87, a neutron traveling through this material will have a mean free path of $\lambda_a = 1/0.01345\ cm^{-1} = 74.3$ cm before it is absorbed and a mean free path of $\lambda_s = 1/0.0903\ cm^{-1} = 11.1$ cm before it is scattered. Figure 11.19 illustrates how the particle behaves. From a statistical perspective, there is very little difference between how an air molecule behaves and how a neutron behaves. They both bounce around (primarily through elastic collisions with other atoms) until they are either absorbed, combine with another atom, or eventually leak out of the box. The mean free path is simply the sum of the distances between where the particle begins its journey (Point P_1) and where the particle ends its journey (Point P_2), divided by the number of collisions n it had along the way. In this case, the size of the mean free path is

A Simple Definition for the Mean Free Path

$$\lambda = \frac{(L_1 + L_2 + L_3 + L_4 + \cdots + L_N)}{N} \tag{11.88}$$

where

N is the number of collisions that occurred on its journey between P_1 and P_2

L_n is the distance traveled in a specific collision n

This definition does not say anything about *where* a specific reaction will occur. The reaction can occur *anywhere* in the material. All the mean free path can tell us is the *average distance* λ from the site of the previous collision to the

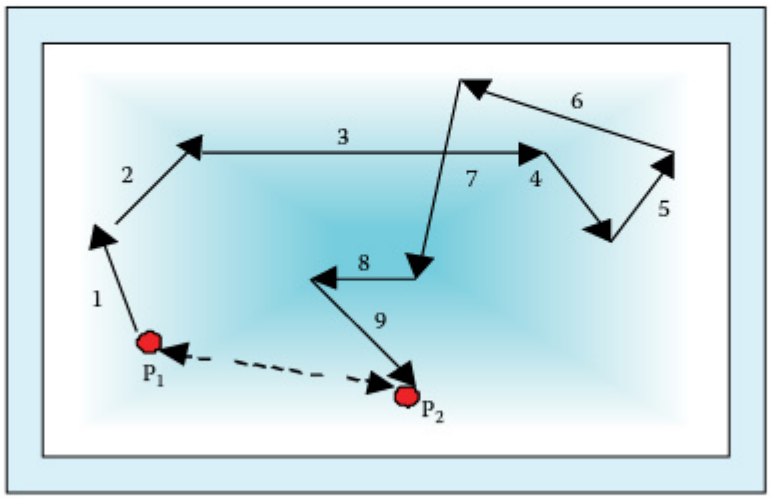

FIGURE 11.19 A figure illustrating the concept of the neutron mean free path.

TABLE 11.5
Value of C as a Function of the Atomic Weight A

Atomic Weight A	Material	Value of C
A = 1	Hydrogen	C = 1
A = 7	Beryllium	C = 0.37
A = 12	Carbon	C = 0.35
A = 235	Uranium	C = 0.33

next one. When a material has a very large scattering cross section and a very small absorption cross section, there is a direct relationship between the mean free path λ and the diffusion coefficient D. This relationship is given by

The Diffusion Coefficient and the Mean Free Path

$$D = \frac{\lambda}{3\left(1-\left(2/3A\right)\right)}$$

or

$$D = C\lambda \tag{11.89}$$

where

C is a constant of proportionality that is equal to C = 1/[3(1 − 2/A3)]

A is the atomic weight of the material in AMUs (see Chapter 2)

The value of C is shown as a function of the atomic weight of the target nucleus in Table 11.5. Notice that the value of C asymptotically approaches 1/3 as the weight of the target nucleus becomes large. This means that for very heavy materials (say, where A > 100), the diffusion coefficient is just 1/3 of the neutron mean free path. In other words, *the diffusion coefficient is directly proportional to the value of the free path*. The longer the mean free path, the larger the diffusion coefficient will be (e.g., the longer "reach" it will have). Conversely, the smaller the mean free path, the smaller the diffusion coefficient will be. Virtually all nuclear materials exhibit this behavior when large numbers of neutrons are involved. The mean free path also varies with the kinetic energy E of the neutron. In a good moderating material like water, the *scattering mean free path* λ_s is about 0.45 cm for thermal neutrons, while it is about 1.8 cm for fast neutrons. In natural uranium, it is about 50 cm for thermal neutrons and over 1000 cm for fast neutrons. (See Figure 11.20 for a direct comparison of their respective mean free paths.)

The *absorption mean free paths* λ_a are different, but they follow a similar trend as the energy of the particle is increased. For ordinary water, the absorption mean free path is about 50 cm for thermal neutrons and over 1000 cm for fast neutrons. Similarly, in natural uranium (99.3% U-238 and 0.7% U-235), the absorption mean free path is 6.1 cm at thermal energies and about 170 cm at fast energies. The fact that the mean free path increases as the neutron energy increases means that high-energy neutrons (which belong to the fast energy group) will generally have a smoother flux shape than low-energy neutrons (which belong to the thermal energy group).

Physically, their mean free paths are just long enough to obscure most of the underlying physical structure of the lattice. However, if their mean free paths get shorter, the physical structure of the lattice becomes more apparent and more peaks and valleys develop in the shape of the flux. This is particularly true if we look at the flux shape ϕ(x, y, z) in the vicinity of a fuel rod or a control rod. *The fast flux will always be smoother than the thermal flux* when looked upon in this way. The values of λ for fast and thermal neutrons traveling through uranium and water are compared in Figure 11.20. Again, the difference in the mean free path is primarily due to the energy dependence of the scattering and absorption cross sections.

11.20 Monte Carlo Method: An Alternative to Neutron Diffusion Theory

While neutron diffusion theory is good at predicting which way a large number of particles will flow when their mean free paths are much longer than the size of the individual structures around them, it does not say anything about *where* an individual neutron or a group of neutrons will go. If we want to know exactly where an *individual neutron* may go, then we would have to perform what is known as a *Monte Carlo calculation*.

In a Monte Carlo calculation, the motions (or *case histories*) of millions of individual neutrons are tracked to understand how they interact with matter. At each interaction point, the neutron speeds, cross sections, and directions of travel are evaluated. Eventually, a picture emerges of what the overall flow of neutrons looks like and what attenuation or amplification of the neutron population occurs as a function of position. Figure 11.21 shows the predictions of a

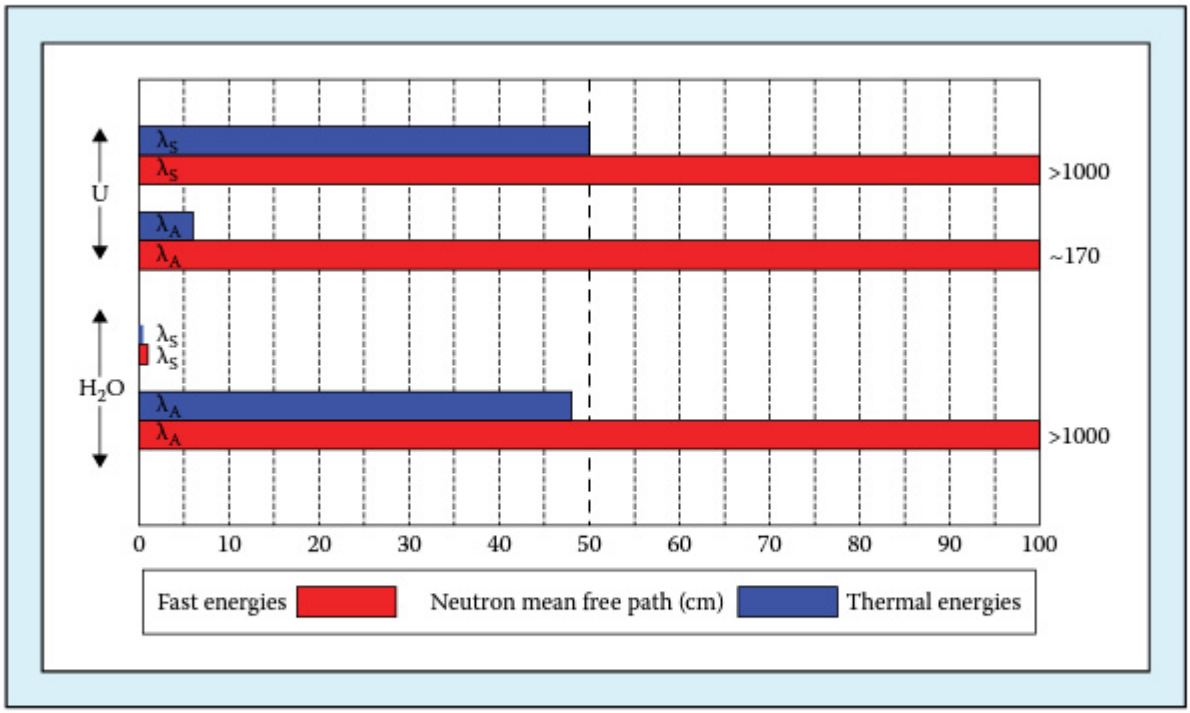

FIGURE 11.20 Neutron mean free paths for natural uranium and water at various neutron energies.

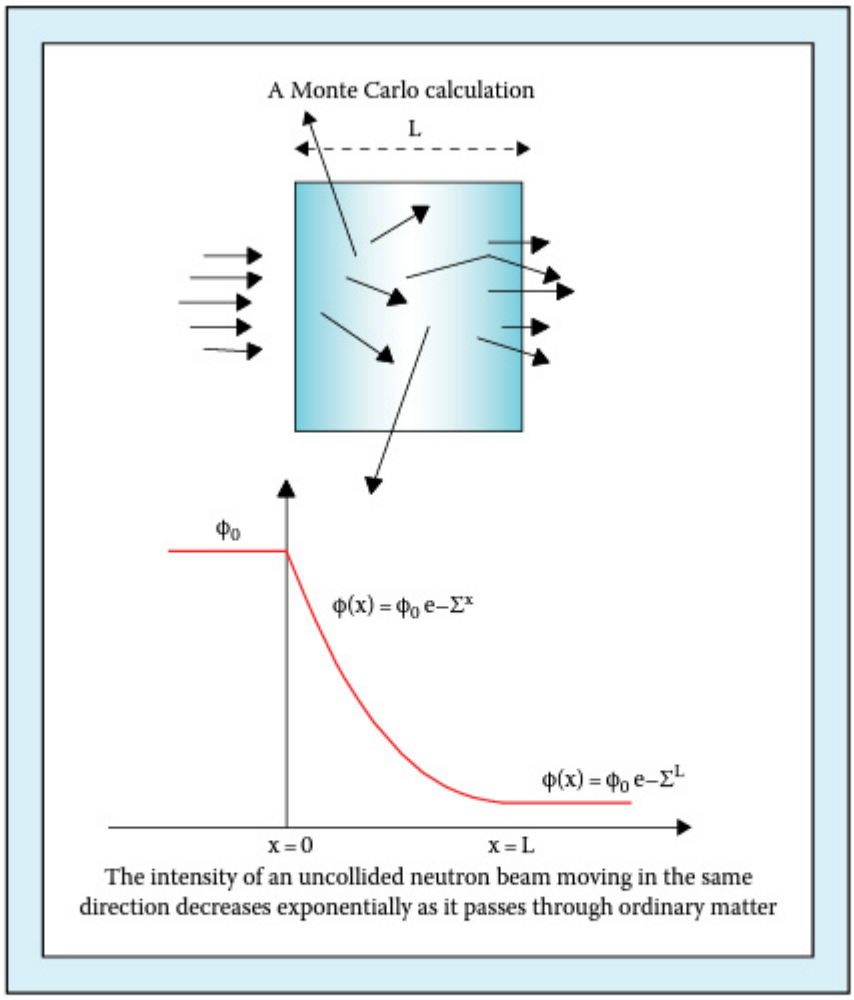
A Monte Carlo calculation
L
ϕ0
ϕ(x) = ϕ0 e−Σx
ϕ(x) = ϕ0 e−ΣL
x = 0
x = L
The intensity of an uncollided neutron beam moving in the same direction decreases exponentially as it passes through ordinary matter

FIGURE 11.21 A simple Monte Carlo calculation of the neutron flux.

Monte Carlo simulation that is used to track the motion of a beam of monoenergetic neutrons through a Lead plate. Some of the neutrons go right through the Lead plate without hitting anything, while other neutrons are scattered off of it in rather surprising directions. Monte Carlo simulations of this type are commonly used to determine the intensity of the neutron flux as a function of the distance of penetration, d, into oddly shaped materials. Monte Carlo calculations are also used to find the paths of the neutrons at energies where neutron diffusion theory no longer applies. At thermal neutron energies in materials like water, this tends to be about 1 cm. Monte Carlo simulations are also used to validate the results of more complex solutions to the neutron diffusion equation. We will examine some of these solutions in Chapter 23. A Monte Carlo method can be used to solve the same kinds of problems as the neutron transport equation. However, as its name implies, *it is a statistically based method rather than a deterministic one*. This means that there is no deterministic equation (such as the transport equation) that needs to be solved when a Monte Carlo method is used. Instead, the Monte Carlo method simply simulates the case histories of thousands or even millions of individual neutrons using *Newton's Laws* of Motion as its guide. In principle, this is no different than simulating the motion of a large number of ping-pong balls in a video game. (The only difference is that the interaction rules are more complex because we are dealing with neutrons.)

11.21 Diffusion Theory versus Transport Theory

There is an interesting relationship between the mean free path of a neutron and the accuracy of a solution to the neutron diffusion equation. In general, *neutron diffusion theory works properly when the mean free path of a neutron is large compared to the geometric arrangement of the materials through which it is traveling*. In other words, diffusion theory works well when the diffusion coefficient is *large*.

If a neutron is traveling through a material heavier than Carbon, the scattering process also becomes isotropic, and the diffusion coefficient is related to the mean free path by $\lambda = 3D$. However, if the neutrons happen to move through a lighter material, then transport effects (and angular anisotropy) may come into play (see Section 11.6). There are a number of empirical correlations that are widely used to determine when neutron diffusion theory can be used and when it cannot. We discussed some of these conditions in Section 11.7. *In general, the neutron diffusion equation gives acceptable results when the neutron mean free path λ is greater than about three times the size of the smallest geometrical structure* through which the neutrons are passing. Simply put, this guideline becomes

Distinguishing Transport Theory from Diffusion Theory

$$\lambda \geq 3\,\mathrm{L}\,(\text{Diffusion theory applies})$$
$$\lambda < 3\,\mathrm{L}\,(\text{Transport theory applies}) \qquad (11.90)$$

where L is a representative length (in cm) not to be confused with the average diffusion length. Now let us see if we can apply this guideline to the fuel rods in a thermal water reactor such as the one shown in Figure 11.22. In most thermal water reactors, the fuel rods have a diameter of about 1 cm, although sometimes the fuel rods may be smaller (see Chapter 1). The scattering mean free path λ_s of a thermal neutron in one of these fuel rods is about 2.34 cm, and the scattering mean free path of a fast neutron in one of these fuel rods is about 3.0 cm. (However, it is larger in the surrounding water.) In other words, *a fuel rod in a thermal water reactor is just small enough that the neutron diffusion equation can be used to find the shape of the neutron flux without incurring significant errors*. Now let us examine how this same guideline applies to a fast reactor. In a fast reactor, the fuel rods are even smaller (the average diameter is about 0.66 cm) and the neutron mean free paths are larger. *Thus, our guideline says that neutron diffusion theory works better in a fast reactor than it does in a thermal one*. In particular, it works better for fast neutrons than it does for thermal neutrons. (Again, this is due to the fact that the mean free path of a fast neutron is always larger.) Now let us see if we can quantify these statements a bit further.

Example Problem 11.4

Suppose that the mean free path of a neutron is 100 cm and that it has five collisions with the material it is traveling through before it is absorbed. How far does it travel in these five collisions with other nuclei in the lattice?

Solution In this case, the total distance traveled between the five collisions is $5 \times 100 = 500$ cm. [Ans.]

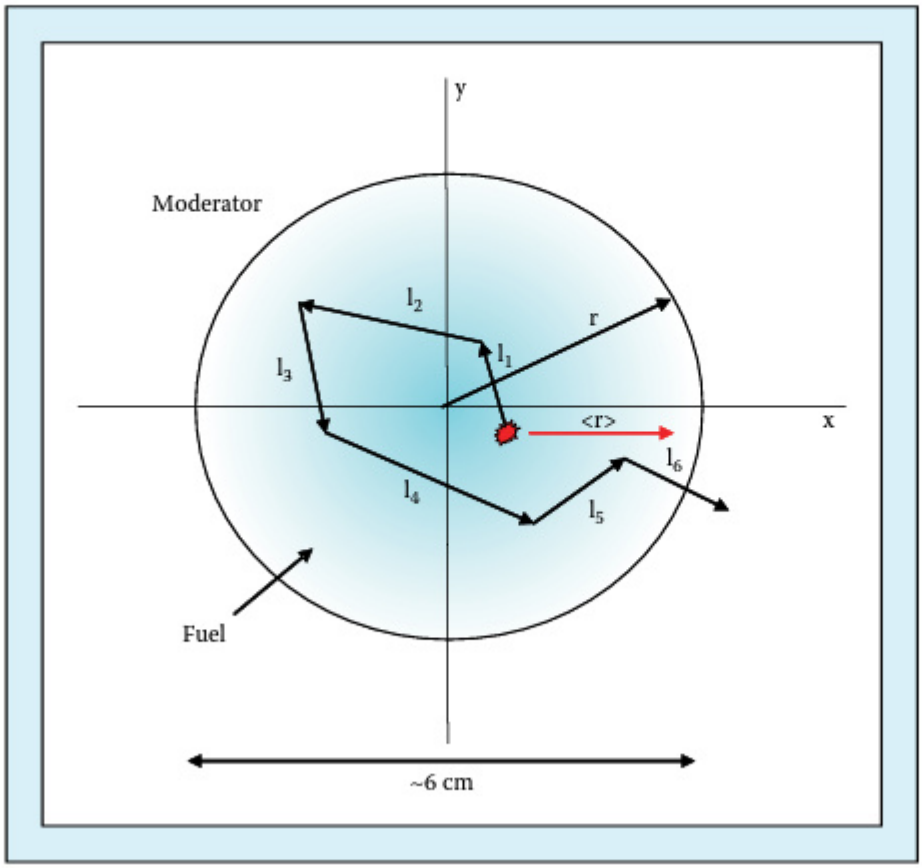

FIGURE 11.22 An example of how the diffusion distance <r> and the mean free path λ of a thermal neutron compare in a large uranium fuel rod.

11.22 Use of Neutron Diffusion Theory with Control Rods

The guideline mentioned earlier is only valid when the materials through which the neutrons are traveling have a weak absorption cross section. Water happens to be a good example of this type of material because the absorption mean free path of a neutron in water is about 50 cm. However, *if the absorption mean free path in λ_a is less than about 3L, the material becomes a strong neutron absorber, and in the vicinity of these materials, the neutron diffusion equation may no longer be able to give accurate results.* The control rods in PWRs and boiling water reactors (BWRs) are a good example of when this happens to be true. For example, at thermal energies, the absorption cross section of a Boron-10 control rod is $\Sigma_a = 532\ \text{cm}^{-1}$, and the absorption mean free path $\lambda_a = 1/\Sigma_a = 0.0018$ cm. In this case, the neutron diffusion equation *CANNOT* be used to find the flux shape in the vicinity of the control rod because the control rod appears to be *black* to the neutrons falling into it. (In other words, it behaves like a *black hole*—see Figure 11.23.) Furthermore, this violates our previous condition regarding the suitability of diffusion theory because λ is about 1000 times smaller than L.

In BWRs, the shortened mean free paths cause the cruciform-shaped control rods to behave like *black bodies* or "*black surfaces*." A neutron that happens to fall into one of these control rods will simply not escape from it. It must go a very short distance into the rod before it is absorbed. Thus, beyond this short distance d, the rod will behave as if it is entirely "black." When we study the solutions to the neutron diffusion equation in future chapters, we will learn that the neutron flux falls to zero a short distance beyond the edge of a material boundary that is a strong absorber. This distance is called *the extrapolation distance* δ, and it is generally measured in the units of centimeters. (The extrapolation distance can also be predicted directly from neutron transport theory.) A picture of the extrapolation distance near the edge of a reactor core is shown in Figure 11.23. Notice that the flux shape falls to zero more quickly than diffusion theory predicts. (A similar situation may also exist in the vicinity of a control rod.)

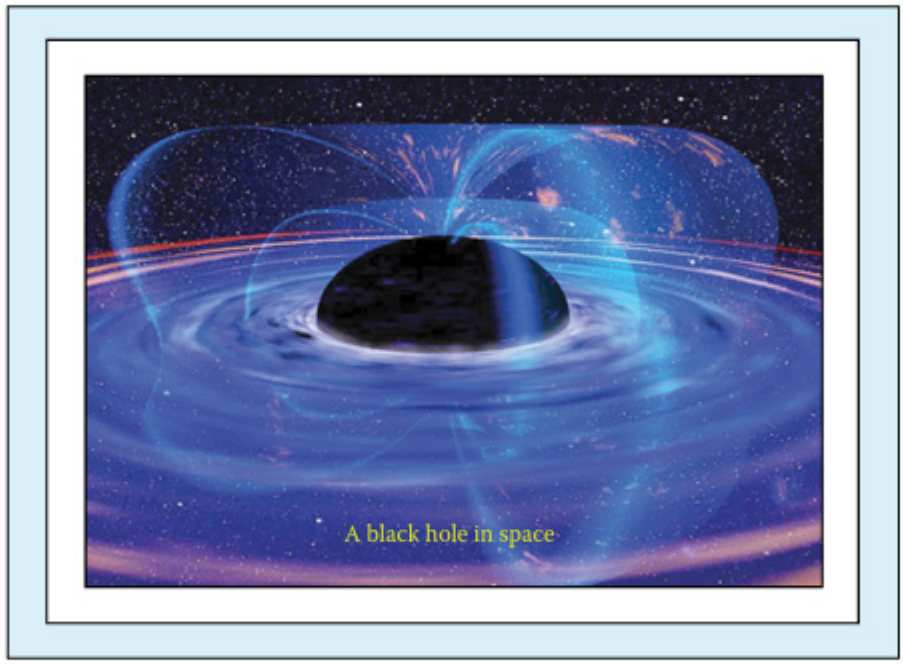

FIGURE 11.23 A neutron falling into a control rod is conceptually no different than a person falling into a black hole. Once the neutron falls into the control rod, it has essentially no chance of escaping from the rod again. (Image provided by NASA—see *www.nasa.gov*.)

11.23 Assumptions about Neutron Diffusion Theory near a Cylindrical Control Rod

Even if diffusion theory is not entirely accurate near a control rod because the neutron flux becomes so depressed, the diffusion equation can still be used to determine the overall reaction rates if the thermal flux is required to satisfy the following boundary condition at the surface of the rod:

The Extrapolated Boundary Condition Defined by Neutron Transport Theory

$$\frac{1}{\phi_T}\frac{d\phi_T}{dr} = \frac{1}{\delta}$$

or

$$\delta = \frac{\phi_T}{d\phi_T/dr} \tag{11.91}$$

where the value of δ can be found by solving the neutron transport equation and δ is defined as the distance into the rod where the thermal flux falls to 0 ($\phi_T = 0$). (The reader may note that this is just another application of the *extrapolation distance*, which we discussed previously.) In the case of a cylindrical control rod, the control rod can be thought of as a *"black" neutron absorber*, and the value of δ can be found from the following empirical formula:

$$\delta = 2.131 D_T \cdot f \tag{11.92}$$

where R is the radius of the control rod, D_T is the thermal diffusion coefficient, and the *rod correction factor* f (similar to the thermal utilization) is defined by

$$f = \frac{R\Sigma_t + 0.9354}{R\Sigma_t + 0.5098} \tag{11.93}$$

All of the parameters presented here are given in cm. Hence, even though a control rod can distort the thermal neutron flux to the extent that neutron diffusion theory no longer applies, the *extrapolated boundary condition* (see the discussion

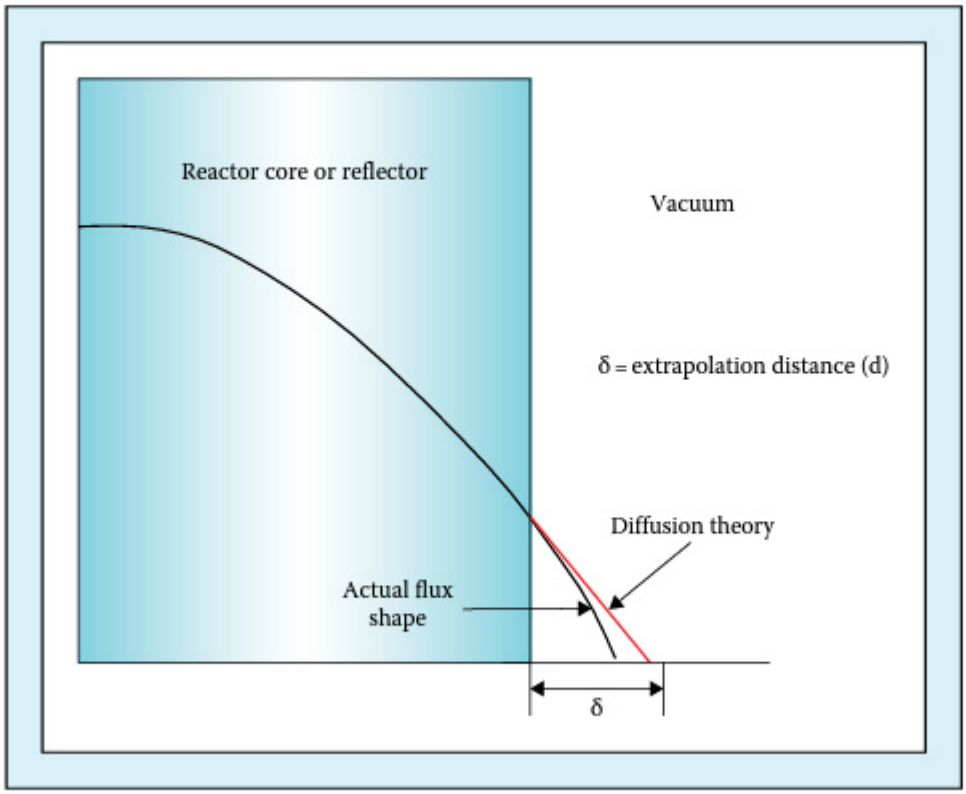

FIGURE 11.24 The extrapolation distance δ near the outer surface of a bare homogeneous core.

above) still allows us to use the neutron diffusion equation under certain conditions. (The shape of the neutron flux can then be found with some accuracy just outside of the control rod.) However, because the equation for f assumes we are dealing with a cylindrical control rod, the diffusion equation must be solved in cylindrical coordinates (r, θ, and z), rather than Cartesian coordinates, and the Laplacian operator for a cylindrical coordinate system must be used.

Notice that when the rod becomes very thick and $R \rightarrow \infty$, the extrapolation distance reduces to just $\delta = 2.131D_T$. When this occurs, the last remaining neutron has been "swallowed up" by the control rod. This corresponds to a condition where the rod has become *completely black. Making the rod thicker (or in layman's terms making the black hole bigger) will not cause any additional neutrons to be absorbed by the rod.* From the equation for f, the point at which this occurs is also determined by the value for Σ_t. For example, in the case of a control rod made from pure Boron-10 (a strong neutron absorber), $\Sigma_t = 532\ cm^{-1}$ for thermal neutrons, and the extrapolation distance δ rapidly approaches $\delta = 2.131D_T \cdot f$. The following example illustrates how quickly this can occur.

Example Problem 11.5

A cylindrical control rod 10 cm in diameter is made out of pure boron-10. Assume that the thermal neutron diffusion coefficient for boron-10 is 0.333 cm. What is the distance into the rod where the thermal neutron flux ϕ_T goes to 0 in this case?

Solution According to the equation for f, $f = (R\Sigma_t + 0.9354)/(R\Sigma_t + 0.5098) = 5320.93/5320.51 = 1.00008$. In this case, $\delta = 2.131D_T \cdot f = 2.131 \times 0.333 = 0.71$ cm. [Ans.]

The extrapolation distance can also be used to estimate the location where the flux falls to zero at the edge of a bare homogeneous core. An example of how the extrapolation distance is used in this case is shown in Figure 11.24.

11.24 Other Uses for the Extrapolation Distance

If one is willing to accept a small amount of error in the neutron flux shape, the equation for the extrapolation distance δ can also be applied to a "*gray surface*" such as a nuclear fuel rod. In this case, it can be used to predict the amount that the thermal flux ϕ_T falls as we move inward from the surface of the rod. Suppose that we have an ordinary UO_2 fuel rod in which the fuel pellets are 1 cm in diameter. Assume that the fuel rod consists of natural uranium (~99% U-238) to

simplify the calculations. From the definition of the rod factor f, this corresponds to a radius for the fuel rod R of 0.5 cm. At thermal energies, the thermal diffusion coefficient for U-238 is $D_T = 0.780$ cm, and the total cross section Σ_t is about 0.80 cm^{-1}. From the previous equation for the rod factor, we have

Extrapolation Distance in a Cylindrical Fuel Rod

$$f = \frac{R\Sigma_t + 0.9354}{R\Sigma_t + 0.5098}\,(\text{cm}) \tag{11.94}$$

or

$$f = \frac{0.5 \times 0.80 + 0.9354}{0.5 \times 0.80 + 0.5098} = 1.46$$

and

$$\delta = 2.131 D_T \cdot f$$

$$\text{so } \delta = 2.42 \text{ cm}$$

Assuming that the flux falls off as R/δ, then the thermal flux ϕ_T will be reduced by a factor of 0.5/2.42 or about 20% between the surface of the fuel rod and the center of the rod in this case. This is almost exactly what we portrayed when we drew the shape of the thermal flux in a lattice of identical unit cells in Chapter 9. Recall that the unit cells were assumed to have an infinite multiplication factor of 1.0 and that the reactor was assumed to be a thermal water reactor.

11.25 Using Diffusion Theory near a BWR Control Rod

A similar expression for f can be found for a *cruciform-shaped control rod* if one is willing to accept a small amount of error in the location where the flux falls to zero. See Reference 6 (Lamarsh) for a description of how this expression for a BWR control rod can be derived. Only in this case, the extrapolation distance δ—using an entirely different equation to arrive at it—turns out to be about 0.75 cm for the thermal neutron flux. *Thus, the neutron diffusion equation can be used in the vicinity of the control rod if we set the neutron flux equal to zero (ϕ = 0) at the extrapolation distance δ. The extrapolation distance then becomes the boundary condition to use for the rod.* Typical NWR control rods (see Figure 11.25) tend to be 1–2 cm thick, and so they are again optimized so that virtually all of the thermal neutrons that fall into them are absorbed. However, because the geometry is different, the rods appear to be a set of *black planar surfaces*, where corrections are to be applied to the center of the rods where the two planar surfaces join. To solve the neutron diffusion equation in this case, the diffusion equation must be solved in a Cartesian coordinate system with coordinates (x, y, z), and Laplacian operator for a Cartesian coordinate system must be used. Since the control blades are about 10 times wider than their average thickness, and they are several meters long, the diffusion equation in this case generally needs to be solved in only the x direction. This is equivalent to a simple infinite slab reactor in which the central slab is made entirely out of Boron-10, and there is a source of thermal neutrons of strength S on each of the outer surfaces. Other materials may also be used to construct these control rods.

Finally, it is possible to find the flux shape in both the x and y directions if the thermal flux is needed at the point where the two planar surfaces join. In the 1970s, many technical papers were written to address this subject when the BWRs were first developed. Today, most of this work is done by solving the *neutron transport equation* with a high-speed computer.

Example Problem 11.6

Based on the answer in Example Problem 11.5, what is the optimum diameter for a cylindrical PWR fuel rod made out of pure Boron-10?

Solution It is apparent from part 1 that all of the thermal neutrons entering the rod will be completely absorbed when $\delta \approx 0.75$ cm. Therefore, the optimal diameter of a cylindrical fuel rod D in a PWR is $D = 2 \times \delta = 1.50$ cm. [Ans.] Notice that this is roughly the size of the control rods in a PWR that are actually used.

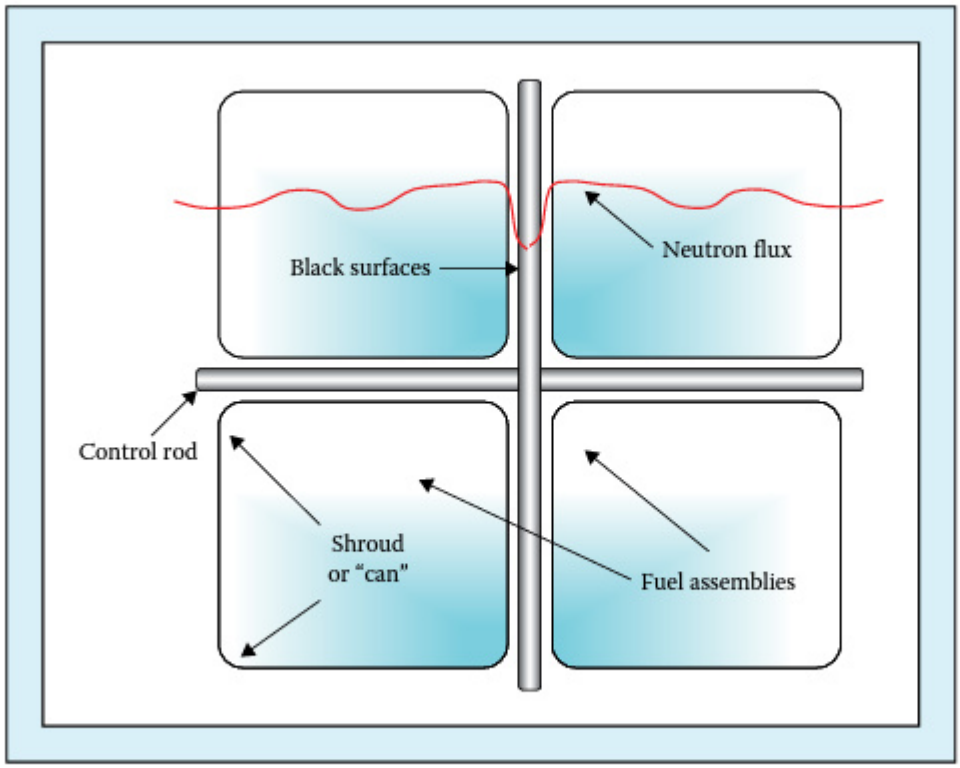

FIGURE 11.25 A cruciform-shaped control rod from a BWR and its effect on the global neutron flux in a fuel assembly.

11.26 How the Diffusion Distance Is Derived

In an earlier section, we mentioned that a neutron traveling through an absorbing material will travel an average distance of $\langle r \rangle = \sqrt{6}L$ or $\langle r \rangle = 2.45\sqrt{D/\Sigma_a}$ before it is absorbed. This allowed us to formally define the *diffusion distance* as

Definition of the Diffusion Distance

$$\text{Diffusion distance} = \langle r \rangle = \sqrt{6}L = 2.45\sqrt{\frac{D}{\Sigma_a}} \tag{11.95}$$

and the *diffusion area* as

Definition of the Diffusion Area

$$\text{Diffusion area} = L^2 = \frac{D}{\Sigma_a} \tag{11.96}$$

In this section, we would like to discuss how this expression was derived and how it can be applied to *any* nuclear particle that has a finite absorption cross section Σ_a. In our companion book,* we also used this expression to determine how thick a radiation shield needed to be to shield a person from the harmful effects of nuclear radiation. Since this radiation consists of individual particles, its attenuation rate is represented by the value of $\langle r \rangle$.

In general, the values for D and Σ_a that define the diffusion distance are energy dependent, and so the diffusion distance $\langle r \rangle$ for a neutron is energy dependent as well. To appreciate this distinction, suppose that we have a source of monoenergetic neutrons that are emanating from a single point in space. (This point in space is sometimes called a *point source*.) The neutrons that emanate from this source diffuse into an infinite, homogeneous medium at a rate of S neutrons per second. The medium has a constant absorption cross section of Σ_a. (In a reactor, this medium can

* See *Nuclear Engineering Fundamentals: A Practical Perspective*, by R.E. Masterson, CRC Press (2017).

sometimes be equated to the *moderator*.) In any event, let us assume that the diffusing medium is effectively an infinite one—at least in the radial direction. As neutrons move through the medium, they collide with individual atoms in their path, and they move in complicated zigzag paths similar to those shown in Figure 11.19. Eventually, they hit an atomic nucleus and are absorbed rather than being scattered. The exact probability of this occurring is given by the ratio of the absorption cross section to the total cross section (see Chapter 4). Now let us see if we can calculate the rate at which they are absorbed.

Example Problem 11.7

Suppose that the diffusion equation tells us that the thermal neutron flux at a particular location in a reactor core is 1×10^{14} neutrons/cm^2/s. What is the average density (in neutrons per cubic centimeter) of the thermal neutrons at the same location in the core?

Solution The neutron flux ϕ is related to the neutron density n by the equation $\phi = nv$. Since the average velocity of a thermal neutron v is 2.2×10^3 m/s $= 2.2 \times 10^5$ cm/s, the value of the neutron density n at the same location is $n(x, y, z) = \phi(x, y, z)/v = 1 \times 10^{14}/2.2 \times 10^5 = 4.55 \times 10^8$ neutrons/cm^3. [Ans.]

11.27 Finding the Diffusion Distance from a Point Source

Consider a point source of strength S that is emitting S neutrons per second into a diffusive medium in which both the scattering and absorption occur (see Figure 11.26). We know from our discussion in Chapter 2 that the number of neutrons dn that are absorbed per second within a spherical shell having a volume dV located a distance r from the point source and having a thickness dr is

$$dn = \Sigma_a \phi(r) dV \tag{11.97}$$

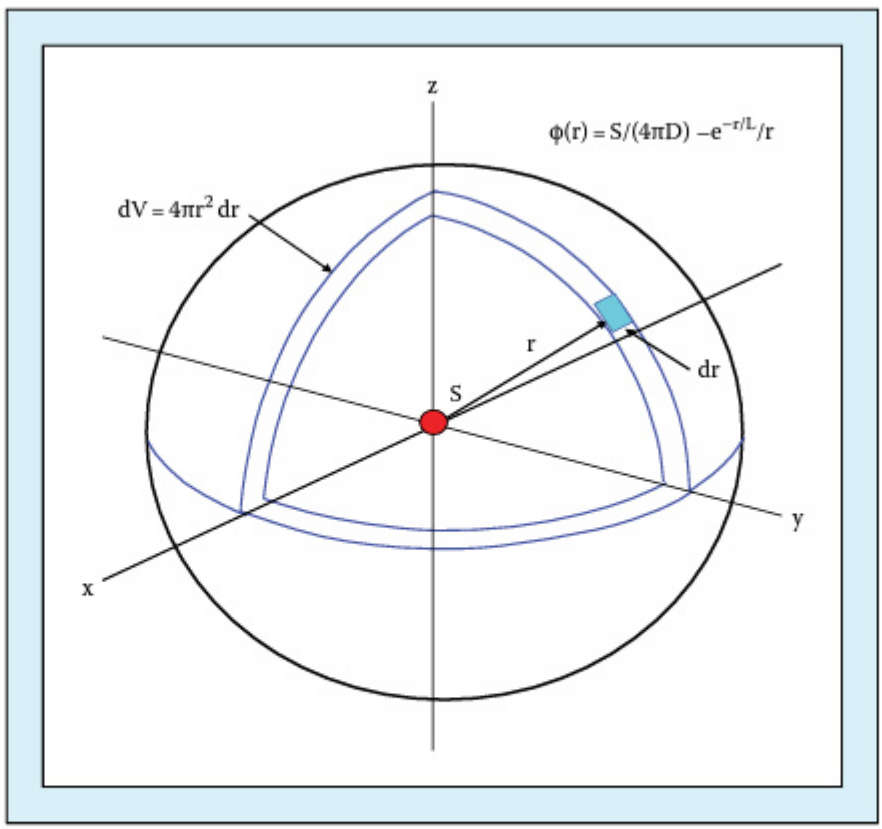

FIGURE 11.26 A picture illustrating how the diffusion distance can be derived for a point source S.

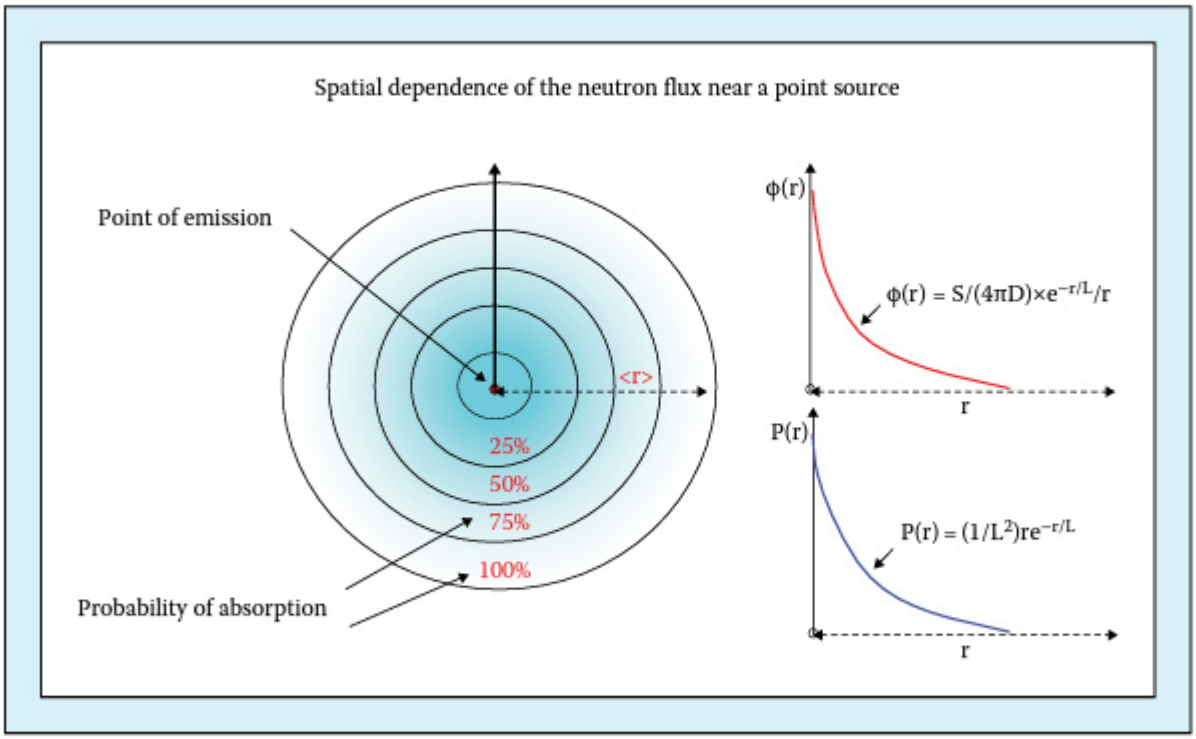

FIGURE 11.27 The spatial dependence of the neutron flux $\phi(r)$ and the neutron absorption probability $P(r)$ in a diffusive medium involving a neutron point source of strength S.

where ϕ is the neutron flux and $dV = 4\pi r^2 dr$ is the volume of the spherical shell surrounding the point source at a distance r. However, we also know from our companion book that the neutron flux in the vicinity of the point source (see Figure 11.27) is attenuated as

$$\phi(r) = \frac{S}{4\pi D} \cdot \frac{e^{-r/L}}{r} \tag{11.98}$$

where

D is the diffusion coefficient

L is the diffusion length

The neutron attenuation rate is therefore

$$dn = \Sigma_a \phi(r) dV = 4\pi r^2 \Sigma_a \phi(r) dr \tag{11.99}$$

Since $\phi(r)$ is given by $\phi(r) = S/(4\pi D) \cdot e^{-r/L}/r$, we can also rewrite Equation 11.99 as

$$dn = \frac{S\Sigma_a}{D} re^{-r/L} dr = \frac{S}{L^2} re^{-r/L} dr \tag{11.100}$$

Since the point source emits S neutrons per second, the probability $P(r)dr$ that a neutron is absorbed between r and r + dr is dn/S or

$$P(r)dr = \frac{1}{L^2} re^{-r/L} dr \tag{11.101}$$

We can then use Equation 11.101 to estimate the average distance <r> that a neutron will travel before it is absorbed. The average distance is simply given by

$$\langle r \rangle = \int_0^\infty rP(r)dr = \sqrt{6}L = 2.45L \tag{11.102}$$

which corresponds to our previously quoted result. Finally, it is easy to see that the diffusion area L^2 must be given by

$$L^2 = \frac{1}{6}\langle r \rangle^2 \tag{11.103}$$

which is consistent with our earlier discussion as well. *Thus, the diffusion area is equal to 1/6th of the average distance <r> that a neutron travels (as the crow flies) from point 1 (where it is created) to point 2 (where it is destroyed).* It is relatively easy to generalize our discussion to more than one energy group by considering the energy dependence of L. If L is energy dependent, then we can write

$$\langle r(E) \rangle = \sqrt{6L(E)} \tag{11.104}$$

The same result can be obtained by doing a Monte Carlo calculation (see Chapter 23).

Student Exercise 11.2

Suppose that you were asked to make a recommendation for the cutoff point (in eV) where neutron up-scattering could be neglected when solving the two-group neutron equations in a high-temperature gas reactor. If the average temperature T of the scattering material is approximately twice what it is in a light water reactor, and carbon dioxide gas (rather than water) is used for the coolant, estimate how high the cutoff point (in eV) between the fast and thermal energy groups can be chosen in this case.

Hint: You may want to refer to Chapter 4 for additional details.

11.28 Neutron Scattering and the Size of the Neutron Diffusion Coefficient

In earlier sections, we discussed the diffusion coefficient and showed how it could be used. However, the diffusion coefficient D for a *pure scatterer* does not necessarily follow a relationship of the form

$$D = \frac{1}{\{3\Sigma_s(1-\cos\theta)\}} = \frac{1}{3\Sigma_{tr}} \tag{11.105}$$

because at thermal energies, the molecular bonds surrounding the target nucleus can affect the scattering cross sections and the angular dependence of the scattered neutrons. Moreover, these bonds can affect the value of D irrespective of whether the material is a solid, a liquid, or a gas. For example, the diffusion coefficient for light water (H_2O) at room temperature is 0.160 cm, while Equation 11.105 tells us that it is only 0.096 cm when the neutron scattering angle is 90° (see Table 11.1)—a 40% difference. A similar situation occurs when we try to calculate the diffusion coefficient for heavy water (D_2O) at thermal energies. In this case, Equation 11.105 predicts a thermal diffusion coefficient of 0.740 cm, while the actual value is 0.870 cm (a 15% difference). Finally, consider another common moderating material such as graphite, which is made from Carbon-12 atoms. Equation 11.105 predicts a value of 0.88 cm, while the actual value is 0.84 cm (a 5% difference).

Thus we can infer from these three examples that as the target nucleus gets heavier, Equation 11.105 becomes more accurate because the molecular bonds have a smaller effect on how the nucleus behaves when it is hit by a thermal neutron. So the lesson to be learned from this simple exercise is that we must always *verify* the actual value of the diffusion coefficient before we use it in the neutron diffusion equation. This is the only way to get the correct results when we are dealing with an actual reactor lattice. The values of θ, cos θ, (1 – cos θ), and ξ (the average lethargy gain per collision) are shown in Table 11.6 for a number of nuclear materials. Here the *average lethargy gain per collision* (see Chapter 8) is defined by

$$\xi = 1 + \frac{\alpha}{1-\alpha}\cdot\ln\alpha = 1 - \frac{(A-1)^2}{2A}\cdot\ln\left(\frac{A+1}{A-1}\right) \tag{11.106}$$

TABLE 11.6
Values of θ, cos θ, (1 − cos θ), and ξ for Some Important Nuclear Materials

Material	Average Neutron Scattering Angle θ (degrees)	cos θ	(1 − cos θ)	ξ
Hydrogen (H)	48.5	0.662	0.338	1.000
Helium (He)	80.4	0.167	0.833	0.425
Light water (H_2O)	71.1	0.324	0.676	0.948
Heavy water (D_2O)	83.3	0.116	0.884	0.570
Beryllium (Be)	85.8	0.074	0.926	0.209
Graphite (C)	86.8	0.056	0.944	0.158

where $\alpha = (A - 1)/(A + 1)$. Thus, α can possess a range of values between 0 and approximately 0.99, and ξ can possess a range of values between approximately 1 and 0.01. The *transport cross section* $\sum_{tr}$ is simply

$$\Sigma_{tr} = \Sigma_t - \cos\theta\Sigma_s \tag{11.107}$$

where it is understood that *cos θ is the average value of the cosine of the scattering angle* in Equation 11.107. In Chapter 22, we will see that the average value of cos θ is sometimes written as μ when we are trying to solve the neutron transport equation. Hence, strictly speaking, the value of the diffusion coefficient is given by

The Diffusion Coefficient when the Absorption Cross Section Is High

$$D = \frac{1}{3\Sigma_{tr}} = \frac{1}{\left\{3\left(\Sigma_t - \cos\theta\Sigma_s\right)\right\}} \tag{11.108}$$

and *only when the neutron absorption cross section is very low* can we replace Equation 11.107 by

$$\Sigma_{tr} = \Sigma_t - \cos\theta\Sigma_s \tag{11.109}$$

which leads to the expression for D that we used earlier in the chapter:

Diffusion Coefficient when the Absorption Cross Section Is Low

$$D = \frac{1}{3\Sigma_{tr}} = \frac{1}{\left\{3\Sigma_s\left(1 - \cos\theta\right)\right\}} \tag{11.110}$$

This result is a consequence of what is known as the *P_1 approximation*, which we will derive in Chapter 22. Now suppose that we repeat our previous analysis with the more rigorous definition of the diffusion coefficient D (and the transport cross section Σ_{tr}) that we just presented. In this case, the values for the diffusion coefficient we get by applying Equation 11.108 are shown in Table 11.7. In the first case, the absorption cross section is assumed to be negligible compared to the scattering cross section ($\sum_a \approx 0$), and in the second case, it is not.

Example Problem 11.8

Suppose that a region in an exactly critical reactor has a value for $\nu\sum_f$ of 2.2 cm^{-1} and a value for $\sum_a$ of 2.0 cm^{-1}. Is the flux shape in this region of the reactor concave or convex?

Solution Since $\nu\sum_f > \sum_a$, the neutron flux shape (see Section 11.13) will be convex in this case. [Ans.]

TABLE 11.7
Values of the Neutron Diffusion Coefficient for Two Slightly Different Definitions of the Diffusion Coefficient in the Thermal Energy Range

Material	$\sum_a$ (cm^{-1})	$\sum_s$ (cm^{-1})	D (cm)[a]	D (cm)[b]	D (cm)[c]
Hydrogen (H)	0.000017	0.002	493.1	493.1	
Helium (He)	0.0000002	0.000021	>1000	>1000	
Light water (H_2O)	0.0000002	3.450	0.096	0.096	0.160
Heavy water (D_2O)	0.000033	0.449	0.742	0.742	0.870
Beryllium (Be)	0.00124	0.865	0.385	0.385	
Graphite (C)	0.00103	0.385	0.865	0.865	0.840
Uranium (U-238)	0.367	0.397	0.840	1.310	1.312
Uranium dioxide (UO_2)	0.169	0.372	0.896	0.620	
Plutonium (Pu-239)	51.1	0.478	0.697	0.0065	

[a] Definition 1: $D = 1/\{3\Sigma_s(1 - \cos\theta)\}$.
[b] Definition 2: $D = 1/\{3(\Sigma_t - \cos\theta\Sigma_s)\}$.
[c] D = experimentally determined value.

The correct values of the diffusion coefficient D are then shown in the final column. Note that this new "definition" does not fix the accuracy problem entirely, but it does help. The molecular bonds at thermal energies still have a major impact on the value of the diffusion coefficient when the neutron energy is low (0 eV $\leq$ E $\leq$ 1 eV). However, for heavy water, light water, graphite, and beryllium, the results of the two formulas (Equations 11.108 and 11.109) appear to be nearly identical. It is only when we have to deal with heavier nuclear materials with very large neutron absorption cross sections (like uranium and plutonium) where the differences between these two approaches become apparent. *Hence, when it comes to the diffusion coefficient D, the main differences apply to the fuel and not to the moderator*. In the next chapter, we will extend what we have just discussed to more than one energy group.

Example Problem 11.9

Suppose the neutron flux in a thermal water reactor consists of two energy groups. The neutron flux in the core for the fast energy group is given by the equation $\phi_1(x) = 100\sin(10x)$, and the neutron flux in the core for the thermal energy group is given by the equation $\phi_2(x) = 50\sin(10x)$. The core has a thermal diffusion coefficient of $D_2 = 4$ cm and a fast diffusion coefficient of $D_1 = 10$ cm. What is the ratio of the fast neutron current to the thermal neutron current (J_1/J_2) at x = 0?

Solution The fast neutron current is given by $J_1 = -D_1 d\phi_1/dx$, and the thermal neutron current is given by $J_2 = -D_2 d\phi_2/dx$. Taking the derivatives, we find that $J_1 = -D_1 d\phi_1/dx = -10{,}000\cos(10x)$ and $J_2 = -D_2 d\phi_2/dx = -2{,}000\cos(10x)$. The ratio is $(J_1/J_2) = 5$. [Ans.]

This will then lead us to what is known as the *multigroup approximation*.

References

Books and Textbooks

1. Zweifel, P.F. *Reactor Physics*, McGraw-Hill, New York (1973).
2. Henry, A.F. *Nuclear Reactor Analysis*, MIT Press, Cambridge, MA (1975).
3. Stacey, W.M. *Nuclear Reactor Physics*, 2nd edn, John Wiley & Sons, New York (2007).
4. Duderstadt, J. and Hamilton, L. *Nuclear Reactor Analysis*, John Wiley & Sons, New York (1976).
5. Lewis, E. *Fundamentals of Nuclear Reactor Physics*, Academic Press, Boston, MA (2008).
6. Lamarsh, J.R. and Baratta, A.J. *Introduction to Nuclear Engineering*, Prentice Hall, Upper Saddle River, NJ (2001).
7. Glasstone, S. and Sesonske, A. *Nuclear Reactor Engineering*, 3rd edn., Van Nostrand Reinhold Company, New York (1981).
8. Lamarsh, J.R. *Introduction to Nuclear Reactor Theory*, Second Printing, Addison-Wesley Publishing Company, Inc., Reading, MA (1972).
9. Shultis, K. and Faw, R. *Fundamentals of Nuclear Science and Engineering*, 2nd edn., CRC Press, Boca Raton, FL (2008).
10. Glasstone, S. and Eedlund, M.C. *The Elements of Nuclear Reactor Theory*, D. Van Nostrand Company, Inc., New York (1952).
11. Masterson, R.E. *Nuclear Engineering Fundamentals: A Practical Perspective*, CRC Press, Boca Raton, FL (2017).

Web References

1. *http://en.wikipedia.org/wiki/Gradient.*
2. *http://en.wikipedia.org/wiki/Divergence.*
3. *http://en.wikipedia.org/wiki/Mean_free_path.*
4. *http://en.wikipedia.org/wiki/Neutron_transport.*
5. *http://web.mit.edu/11.54/ClassNotes/Lec14.pdf.*
6. *http://en.wikipedia.org/wiki/Fick's_laws_of_diffusion.*
7. *mragheb.com/.../Neutron%20Diffusion%20Theory.pdf.*
8. *encyclopedia2.thefreedictionary.com/Diffusion+of+Neutrons.*
9. *http://en.wikipedia.org/wiki/Geometric_and_material_buckling.*
10. *neutron.kth.se/courses/reactor_physics/.../102_DiffusionEquation.pdf.*
11. *http://encyclopedia2.thefreedictionary.com/Diffusion+of+Neutrons.*
12. *https://moodle.polymtl.ca/pluginfile.php/49389/mod_resource/content/0/week2.pdf.*

Additional References

- Important physical constants used by nuclear scientists and engineers can be found in *Appendix A*.
- Unit systems and their conversion factors can be found in *Appendix B*.
- Nuclear cross sections for many important nuclear materials can be found in *Appendix C*.
- Physical properties of important nuclear materials can be found in *Appendix D*.
- Atomic masses, half-lives, and natural abundances can be found in *Appendix E*.
- Neutron diffusion coefficients and neutron mean free paths are discussed in *Appendix H*.
- Diffusion parameters for common nuclear materials are presented in *Appendix I*.

Questions for the Student

The following questions cover the material presented in this chapter and, in some cases, previous chapters as well. They are designed to test how well the student has acquired a working knowledge of the subject matter.

1. Who is Adolf Fick and what important equation was he responsible for discovering?
2. What is the physical distinction between the absorption mean free path and the scattering mean free path?
3. In the case of ordinary water, which one of these mean free paths is longer?
4. In the case of uranium dioxide, which one of these mean free paths is shorter?
5. What is the physical distinction between the neutron mean free path and the neutron diffusion distance?
6. Name an example of a material where the diffusion distance is larger than the scattering mean free path.
7. When we are dealing with the diffusion of neutrons through a reactor lattice, what is the constant of proportionality that relates the neutron current J and the gradient of the particle flux ϕ?
8. Is the neutron current a scalar or vector quantity?
9. Name three examples of situations where neutron diffusion theory can be used.
10. Suppose that the fuel rods in a reactor lattice are 1 cm in diameter and that the mean free path of the neutrons in these fuel rods is 5 cm. Can neutron diffusion theory be used to find the shape of the neutron flux in this case?
11. Now consider exactly the same fuel rods but one where the neutron mean free path is 0.25 cm. Can neutron diffusion theory be used in this case?
12. What is the fundamental difference between the neutron transport equation and the neutron diffusion equation?
13. What units does the scattering mean free path have?
14. Suppose that the neutron flux at a particular position in a reactor lattice is given by $\phi(x, y, z)$. If the average velocity of the neutrons at that location is v, write an expression for the neutron density $\rho(x, y, z)$ at that location in space.
15. In neutron diffusion theory, the steady-state neutron flux ϕ is a function of the neutron energy E and three spatial variables (x, y, z). How many variables are needed to describe the angular dependence of the flux in neutron transport theory?
16. Starting with Fick's Law of Diffusion, write an expression for the neutron current $\mathbf{J}(\mathbf{r})$ in three dimensions in a Cartesian coordinate system using the neutron flux as the independent variable.
17. What units does the neutron diffusion coefficient have?
18. What is the fundamental equation that relates the diffusion distance <r> to the average diffusion length L?
19. What is a better neutron scattering material—heavy water or light water?
20. Suppose that the absorption cross section of a material is increased by a factor of four, while the diffusion coefficient D remains the same. By how much is the diffusion length L decreased in this case?
21. When the diffusion coefficient is spatially dependent, write an expression relating the neutron current to the neutron flux in three dimensions in a Cartesian coordinate system.
22. What is the half-life of a free neutron outside of the nucleus of an atom?
23. What material has a larger value of the thermal diffusion coefficient—light water or heavy water?
24. If you were asked to decide whether graphite or heavy water is a better neutron moderating material based on its macroscopic scattering cross section alone, what would you conclude?
25. Write an expression for the steady-state neutron diffusion equation in a cylindrical coordinate system when the angular dependence of the flux can be neglected.
26. Write an expression for the neutron diffusion equation in a spherical coordinate system when the angular dependence of the flux can be neglected.
27. What is the form of the neutron leakage operator in the neutron diffusion equation in each case?
28. What does the material buckling of the flux refer to in the neutron diffusion equation?
29. What is the half-life of a neutron inside of the nucleus of Thorium-232 atom?
30. Write an exact expression for the material bucking with just a single energy group.
31. Suppose that the diffusion coefficient in an exactly critical reactor is reduced by a factor of two, while the fission and absorption cross sections remain unchanged. By how much is the material buckling of the flux reduced in this case?
32. Name three examples of situations where neutron diffusion theory cannot be used, or where its use will result in significant errors in the calculation of the neutron flux shape.
33. Can the definition of the neutron flux be extended to other types of particles such as alpha particles, x-rays, and gamma rays? What would be the units of the particle flux in this case?
34. Write an equation that can be used to calculate the number of neutrons emitted from a distributed source s(r) if the region of space V in which the source is contained is known.

35. In neutron diffusion theory, under what set of conditions is the geometric buckling of the flux exactly equal to the material buckling?
36. If the polar plot of the neutron flux at a particular location in a reactor core is completely symmetrical, can the neutron diffusion equation be used in this case?
37. Now suppose that the same polar plot reveals an asymmetry of 5% in the shape of the angular flux. Do you think that neutron diffusion theory can still be used in this case?
38. Write down Fick's Law in the radial direction in a homogeneous cylindrical reactor.
39. What does the term "case history" refer to in a Monte Carlo method?
40. Write an equation describing the relationship between the diffusion coefficient and the neutron mean free path in an environment where at least one light element is present.
41. In neutron diffusion theory, what are the units of the neutron current?
42. Write an equation describing the relationship between the diffusion coefficient and the neutron mean free path in an environment where only very heavy elements are present.
43. What is the value of the diffusion coefficient in outer space (i.e., in a vacuum)?
44. In general, is the diffusion coefficient larger in uranium dioxide or in light water?
45. When is the following equation for the diffusion coefficient $D = 1/\{3\Sigma_s(1 - \cos\theta)\} = 1/3\Sigma_{tr}$ more accurate? For a heavy material such as uranium or for a lighter material such as hydrogen?
46. Write an expression for the neutron diffusion area for a homogeneous material.
47. In neutron diffusion theory, how many times larger is the diffusion distance than the diffusion length?
48. What is the physical interpretation of the diffusion distance <r>?
49. What two fundamental assumptions are required to derive the standard form of the neutron diffusion equation?
50. Suppose that a particle collides six times with different uranium atoms before it is absorbed. If the distance between successive collision is 1, 2, 3, 4, 5, and 6 cm, what is the mean free path of the neutron in this case?
51. Write an equation for the relationship between the diffusion distance from the mean free path in this case.
52. How is a control rod in a nuclear reactor similar to a black hole?
53. Is the diffusion equation also an eigenvalue equation? If so, what does the first eigenvalue of the diffusion equation represent?
54. Write the neutron diffusion equation for a homogeneous material in what is known as its standard form.
55. In neutron diffusion theory, what are the units of the neutron flux ϕ?
56. Is the neutron flux a scalar or a vector quantity?
57. How long does a neutron live inside of the nucleus of an atom before it decays into a proton and an electron?
58. Write down an expression for Fick's Law in one dimension when the diffusion coefficient becomes a function of axial position z.
59. How is the scattering angle of a neutron related to the atomic weight of the target nucleus in the laboratory coordinate system?
60. What is the definition of the transport mean free path Σ_{tr} of a neutron?
61. Under what condition(s) does the transport mean free path reduce to the scattering mean free path?
62. Write an expression for the one-group neutron diffusion equation in a region that contains no fissionable material and no sources of external neutrons.
63. What is the difference between a point source and a distributed source?
64. What is the underlying principle that causes the neutron current to flow from a region of high particle flux to a region of low particle flux?
65. Write down the time-dependent neutron diffusion equation with an external neutron source S.
66. Under what conditions does the steady-state form of this diffusion equation reduce to what is known as Laplace's equation: $\nabla^2\phi = 0$?
67. How does the diffusion coefficient behave when one moves from the bottom of a BWR core to the top of the core?
68. What is the physical interpretation of the extrapolation distance d that sometimes appears in neutron diffusion theory?
69. Can the cruciform-shaped control rods in the core of a BWR be considered to be black surfaces?
70. Write down an equation that relates the extrapolation distance to the gradient of the thermal flux in the vicinity of a cylindrical control rod.
71. What boundary condition is normally used at the interface between two material regions (Regions 1 and 2) to guarantee the continuity of the neutron flux?
72. What is the average energy of a fission neutron?
73. In the time-dependent neutron diffusion equation, what does the value of v represent?

74. When a single neutron energy group is used, write an equation that guarantees the continuity of the neutron current across a material boundary between two regions (called Region 1 and Region 2) that have different values of the neutron diffusion coefficient D.
75. What is the U.S. NRC's definition of the neutron flux?
76. Fill in the following sentence with the appropriate word or phrase: In general, the neutron diffusion equation gives accurate results when the neutron mean free path is greater than about _____ the size of the smallest geometrical structure through which the neutrons are traveling.
77. If the macroscopic cross sections and the diffusion coefficient in a reactor core are measured in centimeters, what units does the material buckling have?
78. In a reactor fuel assembly where the value of $\nu\sum_f$ is less than the value of $\sum_a$, is the neutron flux concave or convex in shape?
79. In some reactor physics books, the steady-state neutron diffusion equation in one dimension is written as $d^2\phi(x)/dx^2 - 1/L^2\phi(x) = 0$. What exactly does the value of L^2 represent in this case, and is there any fissionable material present in the region of the core where this equation is to be applied?
80. Write an equation for the probability p(r)dr that a neutron emitted by a point source is absorbed within a distance between r and r + dr from the point at which it is created.

Exercises for the Student

Exercise 11.1

Plot the shape of the rod factor f and the extrapolation distance d for a cylindrical control rod in a PWR and a cylindrical fuel rod in a PWR having the following values for the rod radius R: R = 0.10 cm, R = 0.25 cm, R = 0.5 cm, R = 1.0 cm, R = 1.25 cm, R = 1.50 cm, R = 5.0 cm, R = 10 cm. Assume the control rods are made out of pure Boron-10 and that the fuel rods are made out of uranium dioxide with an average enrichment of 3%. What do these plots tell you about the size of the fuel rods and control rods that are used in PWRs today?

Exercise 11.2

A neutron undergoes collisions with six different atoms in a homogeneous material before it is absorbed. If these collisions occur at distances of 20, 15, 10, 14, 9, and 22 cm from the previous collision, what is the absorption mean free path of the neutron in this material?

Exercise 11.3

Suppose that a neutron undergoes a number of elastic scattering collisions as it travels through a large iron brick. Based upon the equation $D = \lambda/\{3(1 - 2/A3)\}$ and the fact that $\lambda = 1/\Sigma_s$, estimate the value of the diffusion coefficient for Iron-56 in this case.

Exercise 11.4

The largest spatial structures in a heterogeneous material have a width of about 5 cm. If a random assortment of neutrons having a kinetic energy greater than E are traveling through the medium in all directions, and the medium is very large, what must be the minimum mean free path of these neutrons so that the predictions of diffusion theory are accurate in this case?

Exercise 11.5

In Example Problem 11.4, how large would you estimate that the diffusion coefficient D for this medium should be (in cm) for the neutron diffusion equation to give accurate results in this case?

Exercise 11.6

The diffusion length of a neutron in Uranium-238 is approximately 7.45 cm. How far must this neutron travel on average in a large block of U-238 before it is absorbed?

Exercise 11.7

Suppose that two points in a homogeneous medium, which are separated by a distance of 10 cm, have a neutron current between them of 1000 neutrons/cm^2 s. If the neutron flux at one point is 10,000 neutrons/cm^2 s, and the neutron flux at the other point is 20,000 neutrons/cm^2 s, what is the value of the diffusion coefficient for the medium?

Exercise 11.8

A neutron-producing material has an average one-group diffusion coefficient of 100 cm. If the average macroscopic fission cross section for the material is 5 cm^{-1}, and the average macroscopic absorption cross section for the material is 10 cm^{-1}, what is the value of the geometric buckling B^2 for the material if it is exactly critical and if the fuel inside of it emits an average of 2.5 neutrons per fission? Is the buckling of the flux positive or negative in this case?

Exercise 11.9

The shape of the neutron flux in a simple one-dimensional reactor is given by the following equation: $\phi(x) = 10\sin(10x)$. The core has a diffusion coefficient of D = 5 cm. What is the value of the neutron current at x = 0, and which way are the neutrons flowing at this point?

Exercise 11.10

Suppose that a reactor consists of a core surrounded by a reflector. The neutron current J on one side of the core–reflector boundary is 1000 neutrons/cm^2 s. If the diffusion coefficient on the other side of the boundary is 10 cm, what is the gradient of the flux at this point?

Exercise 11.11

Suppose the neutron flux in a reactor consists of two energy groups. The neutron flux in the core for the fast energy group is given by the equation $\phi_1(x) = 50\sin(10x)$, and the neutron flux in the core for the thermal energy group is given by the equation $\phi_2(x) = 25\sin(10x)$. The core has a thermal diffusion coefficient of $D_2 = 5$ cm and a fast diffusion coefficient of $D_1 = 10$ cm. What is the ratio of the fast neutron current to the thermal neutron current (J_1/J_2) at x = 0?

Exercise 11.12

Calculate the values of the neutron diffusion coefficient for thermal neutrons in light water at room temperature (~30°C) and at a reactor operating temperature of 300°C. In which case is the value of the diffusion coefficient higher? What is the physical reason for the apparent difference in their values?

Exercise 11.13

Calculate the value of the neutron diffusion coefficient for fast neutrons in light water at a reactor operating temperature of 300°C. Is the value of the diffusion coefficient higher or lower than it is for thermal neutrons at the same operating temperature? See Appendix H to get the cross sections you need.

Exercise 11.14

The coolant in a CANDU reactor flows through the core horizontally at an operating temperature of 300°C and the moderator surrounding the core is heavy water (D_2O). Is the value of the diffusion coefficient D for heavy water higher or lower than it is for thermal neutrons in light water at the same operating temperature? Although heavy water is more expensive, what is the practical advantage of using heavy water instead of light water in this case?

Exercise 11.15

Using the information provided in Exercises 11.12 and 11.14, estimate the value of the mean free path λ of a thermal neutron in heavy water and in light water at a typical reactor operating temperature of 300°C. What is the ratio of their mean free paths in this case? In what units is the mean free path usually measured?

Exercise 11.16

Suppose that the coolant enters the core of a pressurized water reactor at a temperature of 270°C and leaves the core at a temperature of 310°C. Assume for the moment that the pressure in the core is 2250 PSI. What is the ratio of the mean free path of a thermal neutron at the top of the core to the mean free path of a thermal neutron at the bottom of the core? At which location is the neutron mean free path larger?

Exercise 11.17

Earlier in the chapter, we asserted that the average scattering angle of a neutron in an elastic scattering collision is given by $\cos\theta = 2/(3A)$. Using this expression, compare the values of the scattering angles θ for a uranium-238 atom and a hydrogen one. What is the physical reason why the scattering angles are so different in this case? Does the scattering angle have any effect on the neutron energy loss in an elastic collision?

Exercise 11.18

Suppose that a thermal neutron has an absorption mean free path of 40 cm. If the neutron is traveling through light water at a temperature of 300°C and a pressure of 2250 PSI, what is the average diffusion distance and what is the average diffusion length? What is the physical difference between these two quantities, and why is this distinction important in this case?

Exercise 11.19

What is the average scattering angle θ of a thermal neutron that bounces off a beryllium atom in a thermal water reactor? Is it higher or lower than the scattering angle of the same neutron bouncing off a hydrogen atom in an adjacent water molecule?

Exercise 11.20

Suppose that at a particular location in a reactor fuel rod, the gradient of the neutron flux is found to have a value of 10 million neutrons/cm^3/s. If the fuel rod consists primarily of U-238, what is the value of the neutron current J in the fuel rod at this same location?

Exercise 11.21

Now consider the same fuel rod that was used in Exercise 11.20. Assume that the fuel rod is now loaded into a PWR core. Are the thermal neutrons at the location where the neutron current is being measured more likely to be entering or leaving the rod? Are the fast neutrons at the same location more likely to be entering or leaving the rod? Be prepared to justify the reason(s) for your answer.

Exercise 11.22

Find the material buckling of the flux in a thermal water reactor where the value of the diffusion coefficient is D = 1 cm, the value of the macroscopic fission cross section is $\Sigma_f = 1\ \text{cm}^{-1}$, and the value of the macroscopic absorption cross section is $\Sigma_a = 2\ \text{cm}^{-1}$. Assume that the reactor is fueled with a material where the value of ν is 2.5.

Exercise 11.23

Consider the exercise that was initially posed in Example Problem 11.7. If the reactor in question is a commercial thermal water reactor, what is the total neutron flux and the total neutron density (the total number of fast neutrons and thermal neutrons) at the same location in the core?

Exercise 11.24

Suppose that the region of the reactor core described in Example Problem 11.8 has a diffusion coefficient of 1 cm. What is the value of the material buckling of the flux in this region of the core? Is the flux shape in this region of the core concave or convex?

Exercise 11.25

The geometric buckling B^2 in an exactly critical reactor has a value of 100/cm^2. If the shape of the neutron flux is given by the equation $\phi(x) = 1000\cos(\pi x/B)$, what is the neutron flux and the neutron current at x = 5 cm if the diffusion coefficient is 1.0 cm?

12

Multigroup Neutron Diffusion Theory

12.1 Multigroup Neutron Diffusion Theory and Its Applications

In Chapter 11, we derived the energy dependent neutron diffusion equation from first principles. In this chapter, we would like to extend our discussion of this equation to more than one energy group using what is called *a multigroup approach*. After discussing the *multigroup neutron diffusion equation*, we will then turn our attention to how to solve it in Chapters 13, 14, and 15. There solutions to the diffusion equation will be presented with a single energy group, and the behavior of the neutron flux will be discussed for both steady state and transient conditions. *Using more than one energy group is always better than using a single energy group because the reaction rates can be calculated more accurately*. In addition, multigroup diffusion theory allows the shape of the fast flux to be different than the shape of the thermal flux, and in a thermal water reactor, this can make a significant difference in the value of the effective multiplication factor. (It does not make such a large difference in fast reactors where there are fewer thermal neutrons.) In this chapter, we would like to show how the neutron diffusion equation can be written with more than one energy group. The resulting diffusion equation is then called the *multigroup diffusion equation*.

12.2 Introduction to Multigroup Theory

In Chapter 11, we based our discussion of diffusion theory on the premise that all of the neutrons had a *single energy or speed*. The principal drawback to this approach is that thermal neutrons behave differently than fast neutrons do, and because of this, a one-group model of neutron behavior is simply not accurate enough to predict the reaction rates in a real reactor. Moreover, because the mean free paths of fast neutrons are longer than those of thermal neutrons (see Chapter 11), the thermal flux may have a different shape than the fast flux. Hence using only a single energy group makes it impossible to model the behavior of the neutron population correctly. Thus multigroup theory is required to understand the differences between how fast neutrons and thermal neutrons behave.

12.3 Energy-Dependent Diffusion Equation

In thermal water reactors, neutron kinetic energies can range from about 0.001 eV to about 10 MeV. This is an incredibly wide range of kinetic energies to model with a single neutron energy or speed. In particular, this energy range spans almost *ten orders of magnitude*. Finally, most neutron cross sections have a strong energy dependence, and generally speaking, they are much larger at thermal energies than they are at fast energies. For this reason, their energy dependence must be taken into account when we write the diffusion equation (see Chapter 11) in its true energy-dependent form:

$$D\nabla^2\phi(E,\mathbf{r},t)+\nu(E)\Sigma_f(E,\mathbf{r},t)\phi(E,\mathbf{r},t)-\Sigma_a(E,\mathbf{r},t)\phi(E,\mathbf{r},t)=\frac{1}{v(E)}\frac{\partial\phi(E,\mathbf{r},t)}{\partial t} \tag{12.1}$$

where

$v(E)$ is the velocity of the neutrons

$\nu(E)$ is the average number of neutrons released per fission (which is also called the "mu" of the fuel)

In general, most fission and absorption cross sections have a strong spatial dependence as well (see Chapter 11) because they depend on the temperature of the fuel and the moderator. However, if we suppress this dependence for the moment, we can write

$$D\nabla^2\phi(E,t)+\nu(E)\Sigma_f(E,t)\phi(E,t)-\Sigma_a(E,t)\phi(E,t)=\frac{1}{v(E)}\frac{\partial\phi(E,t)}{\partial t} \tag{12.2}$$

If we are further interested in solving for only the steady-state neutron flux, then we can eliminate the time-dependent terms, and the neutron diffusion equation becomes

$$D\nabla^2\phi(E) + \nu(E)\Sigma_f(E)\phi(E) - \Sigma_a(E)\phi(E) = 0 \tag{12.3}$$

or

$$D\nabla^2\phi(E) + [\nu(E)\Sigma_f(E) - \Sigma_a(E)]\phi(E) = 0 \tag{12.4}$$

where the value of ν depends on the type of fuel. Even in this very simple form the neutron diffusion equation cannot be solved exactly in most reactor geometries because the neutron flux and the neutron cross sections are energy dependent. However, we can obtain approximate solutions to the energy-dependent diffusion equation by subdividing the neutron cross sections into a number of distinct *energy groups* using the approach that was outlined in Chapters 4 and 5. *In this case, the energy-dependent diffusion equation becomes a set of G coupled differential equations* where there is one second-order differential equation for each energy group (from g = 1 to G). Using finite difference methods, each equation can then be written as an equivalent set of algebraic equations with constant coefficients. The resulting equations can then be solved with a digital computer. The underlying mathematical and physical framework that allows us to perform this transformation is called "*multigroup diffusion theory*," and the neutron flux and the neutron cross sections that are used in this approach are called the "*multigroup flux*" and the "*multigroup cross sections*." (Refer to Chapter 4, for a discussion of how they are defined). In principle, it really does not matter whether we use two energy groups or more than two energy groups to describe the core. However, fast neutrons and thermal neutrons behave so differently that many problems in nuclear science and engineering can be naturally segmented in this way. Hence, we will start our discussion with two energy groups and then add additional energy groups to the diffusion equation as they are needed. Of course, when the two energy groups are lumped together, we should be able to recover the one-group neutron diffusion equation that we initially introduced in Chapter 11.

12.4 Introducing the Two-Group Approximation

The neutron flux and the neutron cross sections behave differently at fast energies than they do at thermal energies. While there is no exact line of demarcation between what constitutes a "fast" neutron and what constitutes a "thermal" neutron (see Chapter 4), most cross section libraries arbitrarily define this line of demarcation to be between 1 eV and 2 eV. So the fast energy group is defined to contain any neutron that has a kinetic energy greater than about 1 eV, and the thermal energy group is defined to contain any neutron that has a kinetic energy of less than about 1 eV. Defined in this way, the neutron flux for both the thermal and the fast energy groups can be written as

$$\phi_2 = \int_E \phi(E)dE \quad \text{where } E_o = 0 \text{ and } E_1 \sim 1\text{ eV} \quad \text{(For the thermal energy group)} \tag{12.5}$$

$$\phi_1 = \int_E \phi(E)dE \quad \text{where } E_1 \sim 1\text{ eV and } E_2 \sim 10\text{ MeV} \quad \text{(For the fast energy group)} \tag{12.6}$$

where, by convention, the fast energy group (group 1) has the higher index and the thermal energy group (group 2) has the lower index. Similarly, we can define the fast and thermal cross sections for fission, absorption, radiative capture, and scattering in the following way:

Fast and Thermal Fission Cross Sections

Thermal

$$\Sigma_{f2} = \frac{\int_E \Sigma_f(E)\phi(E)dE}{\int_E \phi(E)dE} \quad \text{where } E_o = 0 \text{ and } E_1 \sim 1\text{ eV} \tag{12.7}$$

Fast

$$\Sigma_{f1} = \frac{\int_E \Sigma_f(E)\phi(E)dE}{\int_E \phi(E)dE} \quad \text{where } E_1 \sim 1\text{ eV and } E_2 \sim 10\text{ MeV} \tag{12.8}$$

and

Fast and Thermal Absorption Cross Sections

Thermal

$$\Sigma_{a2} = \frac{\int_E \Sigma_a(E)\phi(E)\,dE}{\int_E \phi(E)dE} \quad \text{where } E_o = 0 \text{ and } E_1 \sim 1 \text{ eV} \tag{12.9}$$

Fast

$$\Sigma_{a1} = \frac{\int_E \Sigma_{fa}(E)\phi(E)dE}{\int_E \phi(E)dE} \quad \text{where } E_1 \sim 1 \text{ eV and } E_2 \sim 10 \text{ MeV} \tag{12.10}$$

and

Fast and Thermal Capture Cross Sections

Thermal

$$\Sigma_{c2} = \frac{\int_E \Sigma_c(E)\phi(E)dE}{\int_E \phi(E)dE} \quad \text{where } E_o = 0 \text{ and } E_1 \sim 1 \text{ eV} \tag{12.11}$$

Fast

$$\Sigma_{c1} = \frac{\int_E \Sigma_c(E)\phi(E)dE}{\int_E \phi(E)dE} \quad \text{where } E_1 \sim 1 \text{ eV and } E_2 \sim 10 \text{ MeV} \tag{12.12}$$

and

Fast and Thermal Scattering Cross Sections

Thermal

$$\Sigma_{s2} = \frac{\int_E \Sigma_s(E)\phi(E)dE}{\int_E \phi(E)dE} \quad \text{where } E_o = 0 \text{ and } E_1 \sim 1 \text{ eV} \tag{12.13}$$

Fast

$$\Sigma_{s1} = \frac{\int_E \Sigma_s(E)\phi(E)dE}{\int_E \phi(E)dE} \quad \text{where } E_1 \sim 1 \text{ eV and } E_2 \sim 10 \text{ MeV} \tag{12.14}$$

where it is again understood in the case of a fissile material that

$$\Sigma_{a1} = \Sigma_{c1} + \Sigma_{f1} \quad \text{(for the fast group)} \tag{12.15}$$

and

$$\Sigma_{a2} = \Sigma_{c2} + \Sigma_{f2} \quad \text{(for the thermal group)} \tag{12.16}$$

In some textbooks, the index 1 is replaced by the index f (for fast), and index 2 is replaced by the index t (for thermal). However, both formulations are equivalent to each other and they are sometimes used interchangeably at the same time. Notice that because of the way the cross sections are defined (e.g., by integrating *the product* of the energy-dependent cross sections and the energy-dependent flux), the multigroup cross sections do in fact conserve the reaction rates. Consequently, this approach is sometimes referred to as the *two-group approach*.

12.5 Multigroup Cross Sections

In practice, there is no reason to arbitrarily restrict the number of energy groups to just two. In principle, any number of energy groups, and any number of cross sections, differentiated by different energy ranges, can be used to find the neutron flux. For example, we could break the neutron energy spectrum into 3 energy groups instead of just 2. Energy group 1 (the fast group) could be defined to begin at 10 keV and end at 10 MeV, energy group 2 (the epithermal or resonance energy group) could be defined to begin at 1 eV and end at about 10 keV (where the resonances in the absorption and fission cross sections usually stop), and energy group 3 (the thermal group) could be defined to start at 0 eV and end at 1 eV. In this case, group 3 contains all of the thermal neutrons. Knowing the energy dependence of each cross section allows us to write

$$\Sigma_{x3} = \frac{\int_E \Sigma_x(E)\phi(E)dE}{\int_E \phi(E)dE} \quad \text{where } E = 0 \text{ to } E' = 1 \text{ eV} \tag{12.17}$$

$$\Sigma_{x2} = \frac{\int_E \Sigma_x(E)\phi(E)dE}{\int_E \phi(E)dE} \quad \text{where } E = 1 \text{ eV to } E' = 10 \text{ keV} \tag{12.18}$$

$$\Sigma_{x1} = \frac{\int_E \Sigma_x(E)\phi(E)dE}{\int_E \phi(E)dE} \quad \text{where } E = 10 \text{ keV to } E' = 10 \text{ MeV} \tag{12.19}$$

and x is the cross section for an arbitrary reaction type—a, c, f, and so on. Using this approach, the neutron flux can also be subdivided into three energy groups, so that the neutron flux for the thermal, the intermediate or epithermal, and the fast energy groups can be defined as

$$\phi_3 = \int_E \phi(E)dE \quad \text{where } E = 0 \text{ and } E' \sim 1 \text{ eV } (\text{For the thermal energy group}) \tag{12.20}$$

$$\phi_2 = \int_E \phi(E)dE \quad \text{where } E \sim 1 \text{ eV and } E' \sim 10 \text{ keV } (\text{For the intermediate or epithermal energy group}) \tag{12.21}$$

$$\phi_1 = \int_E \phi(E)dE \quad \text{where } E \sim 10 \text{ keV and } E' \sim 10 \text{ MeV } (\text{For the fast energy group}) \tag{12.22}$$

Again, *by convention*, the fast energy group (group 1) has the *highest* index, and the thermal energy group (group 3) has the *lowest index*. It also follows from the fact that the neutrons are conserved that

$$\phi = \phi_1 + \phi_2 + \phi_3 \tag{12.23}$$

where each energy interval so defined is called an energy "group." We have not introduced any new concepts so far that we have not at least peripherally discussed before. Therefore, the neutron flux ϕ_g would be the total flux of neutrons in energy group g (g = 1, 2, 3, …, G), and the reaction cross section Σ_g would be the total cross section for the neutrons in energy group g (g = 1, 2, 3, …, G).

12.6 Deriving the Multigroup Approximation

It is easy to extend this logic to as many energy groups as we want. In practice, these energy groups do *not* have to have the same width or spacing. In fact, most of the time, they do not. (Refer to Figure 12.1 to see how they can be partitioned when the spacing varies). *By convention, neutrons with the highest energies are put in group 1 (g = 1), and neutrons with the lowest energies are put in group G (g = G).* There is a practical advantage to this convention because we can write the transitions between the higher energy groups and the lower energy groups in the following way: $E_{1\to2}$ or $E_{2\to3}$ (and more generally $\Sigma_{Sgg'}$, where Σ_S is the macroscopic scattering cross section between group g and group g′ (g being less than g′).

This convention can be helpful when working with the scattering cross sections because it also allows us to account for both the *up-scattering* of neutrons between energy groups as well as the more common phenomenon of neutron *down-scattering*. Using this convention, we can write the width of an energy group as $\Delta E_g = E_{g-1} - E_g$ (where g = 1, 2, 3, …, G). The energy intervals ΔE_g do not have to all be the same size. In fact, they usually are not. Similarly, this allows us to define the *group flux* ϕ_g as

Definition of the Group Flux

$$\phi_g = \int_E \phi(E)\,dE$$

or

$$\phi_g = \int_E n(E)v(E)\,dE \tag{12.24}$$

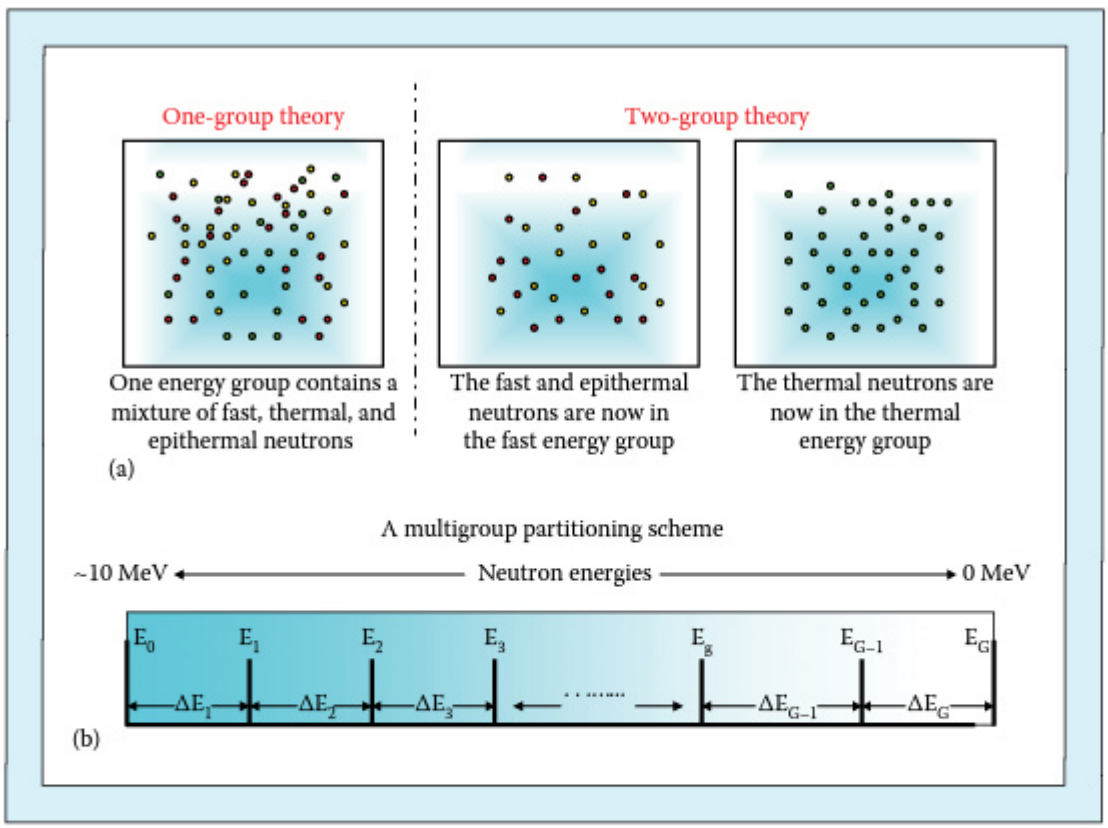

FIGURE 12.1 (a) A picture illustrating the difference between one-group theory and multigroup theory. In multigroup theory, fast neutrons are represented by the color red, epithermal neutrons are represented by the color yellow, and thermal neutrons are represented by the color green. In one-group theory, all of these neutrons are lumped into a single energy group. (b) A multigroup neutron energy partitioning scheme in which the fast, thermal, and epithermal neutrons may be placed in different energy groups.

where v is the neutron velocity, n is the neutron density, and the integral is to be evaluated from $E = E_g$ to $E = E_{g-1}$. *Thus, the neutron flux within energy group ϕ_g can be thought of as the neutron density within an energy group n(E), multiplied by the respective neutron velocities v(E) (between $E = E_g$ and $E = E_{g-1}$).* Under these conditions, the neutron density n(E) is usually given the units of neutrons/cm^3, the neutron velocity v(E) is usually given the units of cm/sec, and the neutron flux ϕ(E) is usually given the units of neutrons/cm^2-sec. The resulting approach is then referred to as "multigroup" theory—because the neutron energy spectrum is now subdivided into multiple energy groups and the reaction rates can then be found for each energy group. The sum of the reaction rates from all of the individual energy groups must then be equal to the total reaction rate R. Hence, *a fundamental premise of multigroup theory is that the reaction rates must be conserved as well*:

$$R = R_{x1} + R_{x2} + R_{x3} + \cdots + R_{xG} \tag{12.25}$$

Here

x is the index of the reaction type (a, s, c, f, or t)

G is the number of energy groups into which the neutrons have been partitioned

Today, cross section libraries with up to 50 energy groups are commonly used to calculate these reaction rates, and some nuclear scientists and engineers have attempted to create cross section libraries with as many as 1000 energy groups (see Chapter 5).

12.7 Defining Scattering Cross Sections between Energy Groups

In a multigroup method, scattering cross sections between energy groups are usually written as $\Sigma_{gg'}$, where the most energetic neutrons are in energy group g and the least energetic neutrons are in energy group g'. In other words, Σ_{12} refers to the scattering cross section for neutrons from energy group 1 to energy group 2, and Σ_{23} refers to the scattering cross section for neutrons from energy group 2 to energy group 3. Any time g′ is greater than g, a group scattering cross section will have a finite value. This is because "down-scattering" (e.g., scattering from a higher energy group to a lower energy group) always occurs when neutrons lose energy as they collide with other atoms. Similarly, scattering within the same energy group (g′ = g) is allowed as well. This type of "self-scattering" can sometimes occur—particularly in the thermal energy range—when a neutron actually has a chance of *gaining* energy within the group as well as losing it. The only time when $\Sigma_{gg'}$ is 0 is when g′ < g. As a rule of thumb, only the cross sections for "up-scattering" between energy groups are zero. The nomenclature above remains consistent no matter how many energy groups are used. An example of the multigroup scattering process is shown in Figure 12.2. Sometimes it is permissible to simplify the notation used in the scattering cross sections by casting them into a more intuitive and easily understandable form. Previously, we learned that Σ_{12} refers to the scattering cross section from energy group 1 to energy group 2 and Σ_{23} refers to the scattering cross section from energy group 2 to energy group 3. *Sometimes the scattering cross sections are also written as $\Sigma_{1\to2} = \Sigma_{12}$ and $\Sigma_{2\to3} = \Sigma_{23}$, but this is primarily a matter of taste rather than substance, and the underlying physical processes are exactly the same.*

Before moving on, we would like to make a few additional comments about the size of the scattering cross sections that appear in the diffusion equation. The microscopic scattering cross sections for most common materials that interact with low-energy neutrons are relatively small (about 10 barns—see Appendix C) compared to the fission and absorption cross sections, and they are relatively constant as a function of the neutron's kinetic energy E. The scattering process is usually elastic and it is not much different than a collection of marbles with different sizes and speeds bouncing around on a billiard table. *The one important exception to this rule is the scattering cross section for the hydrogen atoms in a water molecule*. Their scattering cross sections can rise significantly at thermal energies rather than remaining constant. Naturally, the scattering cross sections for fast neutrons are even lower, (see Chapter 4), and most of the time, their values tend to average about 1 barn. Now let us turn our attention to how the diffusion coefficients behave.

Example Problem 12.1

Suppose that some measurements of a thermal water reactor operating under steady-state conditions reveal that the total neutron flux is 1×10^{15} neutrons/cm^2/s. Upon further study, it is found that there are approximately half as many neutrons in the core with an energy less than 1 eV as there are with an energy greater than 1 eV. If the scattering cross section for water for the fast energy group is $\sigma_s = 1.67$ barns, and the scattering cross section for water for the thermal energy group is $\sigma_s = 11.27$ barns, what is the total number of neutrons per second being down-scattered from the fast energy group to the thermal energy group? Assume that there are $N = 3.343 \times 10^{22}$ molecules of water in a cubic centimeter of the coolant.

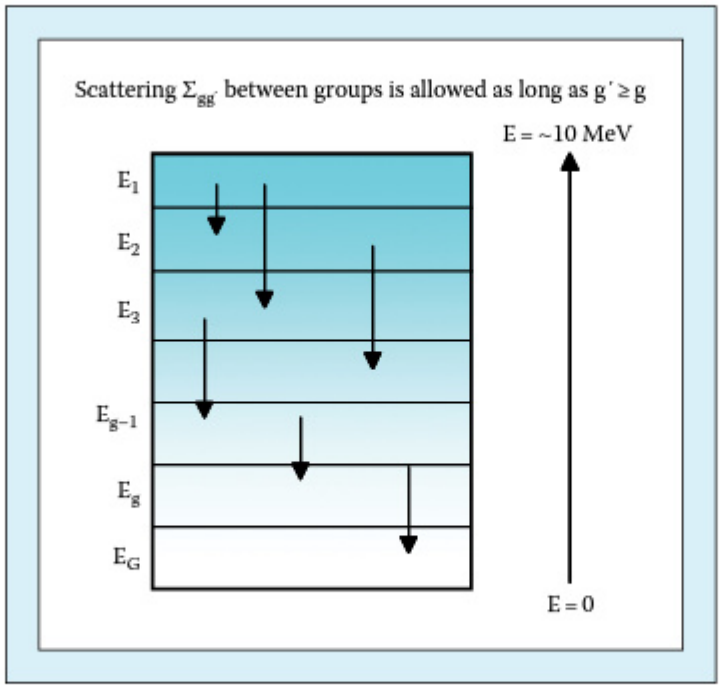

FIGURE 12.2 An example of the process of multigroup scattering from higher energy groups to lower energy ones.

Solution Based on the information provided, we can assume that the line of demarcation between the fast energy group and the thermal energy group is about 1 eV. Since there are about half as many thermal neutrons in the reactor as there are fast neutrons on average, the fast flux is $2/3 \times 1 \times 10^{15}$ neutrons/cm^2/s, and the thermal flux is $1/3 \times 10^{15}$ neutrons/cm^2/s. Therefore,

$$\phi_2 = \int_E \phi(E)dE = 0.33 \times 10^{15} \text{ neutrons/cm}^2\text{/s}, \quad \text{where } E = 0 \text{ and } E \sim 1 \text{ eV} \quad \text{and}$$

$$\phi_1 = \int_E \phi(E)dE = 0.66 \times 10^{15} \text{ neutrons/cm}^2\text{/s}, \quad \text{where } E \sim 1 \text{ eV and } E \sim 10 \text{ MeV}$$

Now the microscopic scattering cross section for the fast energy group (see Appendix C) is $\sigma s = 1.67$ barns $= 1.67 \times 10^{-24}$ cm^2, so the macroscopic scattering cross section from the fast group to the thermal group is $\Sigma_{1\to2} = N \times \sigma_{1\to2} = (3.343 \times 10^{22}) \times (1.67 \times 10^{-24}) = 0.58$/cm, and the total scattering rate R from group 1 to group 2 is $R_{1\to2} = \Sigma_{1\to2}\,\phi_1 = 0.58 \times 0.66 \times 10^{15}$ neutrons/cm^2/s $= 0.38 \times 10^{15}$ neutrons/cm^3/s. [Ans.] So approximately 2 out of every 5 neutrons in the reactor is continually being down-scattered from energies above 1 eV into the thermal energy group, where they can either leak out of the core, be absorbed, or cause another uranium-235 atom to fission.

12.8 Multigroup Diffusion Coefficients

Earlier, we learned that the diffusion coefficient for a single energy group could be written as

$$D = \frac{\lambda_{tr}}{3} \tag{12.26}$$

where λ_{tr} was the *transport mean free path*, which was in turn given by

$$\lambda_{tr} = \frac{1}{\Sigma_{tr}} \tag{12.27}$$

In Equation 12.27, Σ_{tr} is called the *transport scattering cross section* and in practice, this scattering cross section is energy dependent. The transport cross section is also related to the actual macroscopic scattering cross section Σ_s by the simple prescription (see Chapter 22 for the actual derivation)

$$\Sigma_{tr} = \Sigma_s (1 - \mu) \tag{12.28}$$

where μ *is the average cosine of the scattering angle* for the material in question (i.e., $\mu = \cos\theta$). The material in question may consist of only one compound, or it may consist of many materials having different properties and atomic weights. It immediately follows that the diffusion coefficient for the fast and thermal energy groups is given by

Fast and Thermal Diffusion Coefficients

Thermal

$$D_2 = \frac{\int_E D(E)\phi(E)dE}{\int_E \phi(E)dE} \quad \text{where } E_o = 0 \text{ and } E_1 \sim 1 \text{ eV} \tag{12.29}$$

Fast

$$D_1 = \frac{\int_E D(E)\phi(E)dE}{\int_E \phi(E)dE} \quad \text{where } E_1 \sim 1 \text{ eV and } E_2 \sim 10 \text{ MeV} \tag{12.30}$$

where the group flux ϕ_g is

$$\phi_g = \int_E \phi(E)dE \tag{12.31}$$

The *diffusion coefficient* D_g for energy group g is therefore based on the assumption that

$$D_g = \frac{1}{\phi_g}\int_g D(E)\phi(E)dE = \frac{1}{3\phi_g}\int_g \frac{1}{\Sigma_{tr}(E)}\phi(E)dE \tag{12.32}$$

and this is in fact how the diffusion coefficients we have been using can be found.

12.8.1 Alternative Definitions for the Diffusion Coefficient

Sometimes the diffusion coefficient D_g for energy group g = 1, 2, 3, …, G is calculated using a slightly different approach than the one we have outlined above. In particular, an alternate definition that is provided by neutron transport theory (see Chapter 22 and Reference 4) is

$$D_g = \frac{\int_g D(E)\nabla\phi(\mathbf{r},E)dE}{\int_g \nabla\phi(\mathbf{r},E)dE} \tag{12.33}$$

where $\nabla\phi(\mathbf{r}, E)$ represents the *spatial gradient* of the energy-dependent flux. Unfortunately, this definition requires us to know *the shape* of the neutron flux in advance in addition to its energy dependence, and the flux shape is generally not available when the diffusion coefficient is being found.

12.9 Neutron Diffusion Equation with Two Energy Groups

Now that we have discussed the fundamentals of multigroup theory, we would like to write down the neutron diffusion equation with more than one energy group. Holistically speaking, it really does not matter whether we write it with two energy groups or more than two energy groups. The physical principles and the underlying logic are exactly the same.

However, to keep the notation simple, we would like to start with two groups and then add more energy groups as they are required. Let us again start with the steady-state diffusion equation, and using the definitions for the group cross sections and the group flux that we just developed, see what the neutron diffusion equation looks when we write it with more than a single energy group. To begin, assume that we can subdivide the neutron flux into two energy groups (fast and thermal), where the fast flux refers to energy group 1 and the thermal flux refers to energy group 2. (We will use this same basic notation for all of the neutron cross sections as well.)

Let us further assume that the number of neutrons created in each energy group is equal to the number of neutrons that are destroyed in that energy group. That is, for the fast energy group, the fast neutron production rate must equal the fast neutron destruction rate, and for the thermal energy group, the thermal neutron production rate must equal the thermal neutron destruction rate. This is again equivalent to requiring that $d\phi_1/dt = 0$ and $d\phi_2/dt = 0$. *In other words, this condition is equivalent to assuming that we have an exactly critical reactor. Perhaps the easiest way to derive the two-group diffusion equation is to write a neutron balance equation for each energy group by balancing the ways that a neutron can enter or leave a group*. In this case, we have two groups to consider—the fast group (group 1) and the thermal group (group 2). However, before beginning this process, we would like to review a number of topics that we discussed in an earlier section. The reader may recall from Chapter 7 that the number of neutrons produced per fission ν varies slightly from one energy group to the next. We can represent this fact by defining the value of ν (or mu) for each energy group in the following way:

$$\nu_1 = \frac{\int_E \nu(E)\phi(E)dE}{\int_E \phi(E)dE} \quad \text{where } E \sim 1 \text{ eV and } E' \sim 10 \text{ MeV (Fast)} \tag{12.34}$$

$$\nu_2 = \frac{\int_E \nu(E)\phi(E)dE}{\int_E \phi(E)dE} \quad \text{where } E = 0 \text{ and } E \sim 1 \text{ eV (Thermal)} \tag{12.35}$$

In general, these values will be very similar, and so in our derivation we will make the assumption that

$$\nu_1 \approx \nu_2 \approx \nu \tag{12.36}$$

This may introduce a small error into our calculations but generally this error is small enough to be ignored. The reader may also recall from Chapter 9 that not all fissions are due to thermal neutrons alone. In fact, *in a thermal water reactor, between 2% and 8% of the fissions are produced by neutrons having energies above the thermal energy range*. This means that we must write the neutron production rate in a two-group model as

$$P = \{\nu_1 \Sigma_{f1} \phi_1 + \nu_2 \Sigma_{f2} \phi_2\} \tag{12.37}$$

or

$$P = \{\nu \Sigma_{f1} \phi_1 + \nu \Sigma_{f2} \phi_2\} \tag{12.38}$$

when $\nu_1 \approx \nu_2 \approx \nu$. Finally, the reader may recall from Chapter 7 that the fission neutrons in a thermal reactor are produced with a continuous distribution of energies $\chi(E)$ from about 10 MeV down to a couple of keV. In other words, the neutron production rate in a two-group model must be found from the equations

$$\chi_1 = \frac{\int_E \chi(E)\phi(E)dE}{\int_E \phi(E)dE} \quad \text{where } E \sim 1 \text{ eV and } E \sim 10 \text{ MeV (Fast)} \tag{12.39}$$

$$\chi_2 = \frac{\int_E \chi(E)\phi(E)dE}{\int_E \phi(E)dE} \quad \text{where } E = 0 \text{ and } E \sim 1 \text{ eV (Thermal)} \tag{12.40}$$

where $\chi(E)$ is a distribution function that is normalized to have a value of 1.0. In most reactors, the cutoff point between the fast and the thermal energy groups is low enough that we can set $\chi_1 = 1$ and $\chi_2 = 0$. (Incidentally, if we had more than two energy groups, this would not necessarily be the case, and our equations would be much more complex). So for the fast energy group, we can write

$$-D_1\nabla^2\phi_1 + \Sigma_{a1}\phi_1 + \Sigma_{12}\phi_1 = \frac{1}{k}\chi_1\{\nu_1\Sigma_{f1}\phi_1 + \nu_2\Sigma_{f2}\phi_2\} \tag{12.41}$$

and we will assume that $\chi_1 = 1$ if only two energy groups are used. Here we have inserted a multiplication factor equal to 1/k in front of the fission producing term because we are eventually going to want to know what combinations of materials will result in a critical system. In other words, Equation 12.41 simply says that

Fast Neutron Destruction Rate = Fast Neutron Production Rate

Fast neutron leakage + Fast absorption + Fast down-scattering (out of the group)
= Fast neutrons produced by fast fission + Fast neutrons produced by thermal fission

Now let us turn our attention to the thermal energy group, which we have called group 2. For the thermal energy group, we can also write the neutron balance equation as

$$-D_2\nabla^2\phi_2 + \Sigma_{a2}\phi_2 = \frac{1}{k}\chi_2\{\nu_1\Sigma_{f1}\phi_1 + \nu_2\Sigma_{f2}\phi_2\} + \Sigma_{12}\phi_1 \tag{12.42}$$

with the understanding that

Thermal Neutron Destruction Rate = Thermal Neutron Production Rate

Thermal leakage + Thermal absorption = Thermal neutrons created by down-scattering from the fast group

Thus fast neutrons can be produced either from other fast neutrons (by fast fission) or from thermal neutrons (through the process of thermal fission), and thermal neutrons can only be produced when fast neutrons scatter out of the fast energy group into the thermal energy group. Thus we can set the value of $\chi_2 = 0$ for the thermal energy group, in which case the balance equation for the thermal neutrons becomes

$$-D_2\nabla^2\phi_2 + \Sigma_{a2}\phi_2 = \Sigma_{12}\phi_1 \tag{12.43}$$

For a steady-state reactor, the flow of the neutrons between each energy group is shown in Figure 12.3. This figure, of course, is just an illustration of what is called the *thermal neutron life cycle*. The scattering rate from the fast energy group to the thermal energy group is given by $\Sigma_{12}\phi_1$, where Σ_{12} is the scattering cross section from the fast energy group (group 1) to the thermal energy group (group 2). Again, we are assuming that neutrons can only "down-scatter" from higher energies to lower ones.

So with fast and thermal neutron leakage included, the steady-state two-group neutron diffusion equations become

Two-Group Neutron Diffusion Equations

$$-D_1\nabla^2\phi_1 + \Sigma_{a1}\phi_1 + \Sigma_{12}\phi_1 = \frac{1}{k}\{\nu_1\Sigma_{f1}\phi_1 + \nu_2\Sigma_{f2}\phi_2\} \text{ (for the fast group)}$$
$$-D_2\nabla^2\phi_2 + \Sigma_{a2}\phi_2 - \Sigma_{12}\phi_1 = 0 \text{ (for the thermal group)} \tag{12.44}$$

These are the equations that we must ultimately solve for ϕ_1 and ϕ_2. Notice that we have replaced the energy-dependent diffusion equation (Equation 12.4) by two separate diffusion equations—one for each energy group—and that we have added a scattering term $\Sigma_{12}\phi_1$ to account for the fact that neutrons are down-scattered from the fast energy group (group 1) to the thermal energy group (group 2). *These simple-looking equations are called the two-group diffusion equations, and they are the "workhorses" that nuclear engineers use to design real reactors.* Incidentally, it can be shown that a

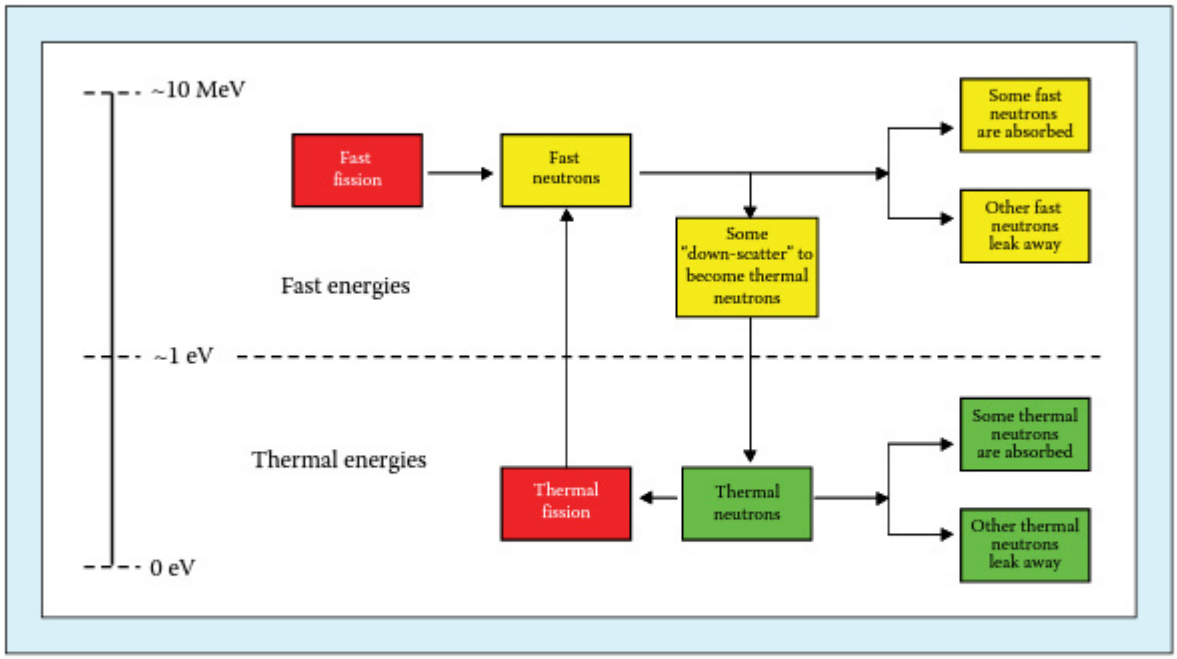

FIGURE 12.3 The fast and thermal neutron life cycles in a two-group model.

unique solution to these equations exists when the group fluxes are positive everywhere and that there is a single positive eigenvalue or value of k for which this occurs. Of course, for a critical reactor, this requires a value for k that is exactly equal to 1.0. Now let us discuss how the reaction rates behave in this case. If we decide to add the two-group equations together, we obtain

Sum of the Two-Group Equations

$$-\left[D_1\nabla^2\phi_1 + D_2\nabla^2\phi_2\right] + \left[\Sigma_{a1}\phi_1 + \Sigma_{a2}\phi_2\right] = \frac{1}{k}\left[\nu_1\Sigma_{f1}\phi_1 + \nu_2\Sigma_{f2}\phi_2\right] \tag{12.45}$$

Leakage + Absorption = Fission

since the scattering cross sections cancel. In two-group theory, the fast and thermal neutron leakage rates ($-D_1\nabla^2\phi_1$ and $-D_2\nabla^2\phi_2$) can be combined into a single neutron leakage rate $-D\nabla^2\phi$. Similarly, the fast and thermal neutron absorption rates ($\Sigma_{a1}\phi_1 + \Sigma_{a2}\phi_2$) can be combined into a single neutron absorption rate $\Sigma_a\phi$, and the fast and thermal neutron production rates ($\nu_1\Sigma_{f1}\phi_1 + \nu_2\Sigma_{f2}\phi_2$) can be combined into a single neutron production rate $\nu\Sigma_f\phi$. Hence, *in a two-group model of neutron behavior, the reaction rates are conserved when we require that*

$$\Sigma_a\phi = (\Sigma_{a1}\phi_1 + \Sigma_{a2}\phi_2) \tag{12.46}$$

and

$$\nu\Sigma_f\phi = (\nu_1\Sigma_{f1}\phi_1 + \nu_2\Sigma_{f2}\phi_2) \tag{12.47}$$

Using Equations 12.46 and 12.47, it is easy to see that Equation 12.44 then reduces to the one-group neutron diffusion equation that we discussed previously:

$$-D\nabla^2\phi + \Sigma_a\phi = \frac{1}{k}\nu\Sigma_f\phi \tag{12.48}$$

Thus, *the two-group neutron diffusion equations are a set of coupled differential equations because neutrons from the higher energy group (group 1) are scattered down into the lower energy group (group 2) through the term $\Sigma_{12}\phi_1$, and the thermal flux ϕ_2 creates fast neutrons to add to the fast energy group (group 1).*

Now suppose that we ignore the *neutron leakage terms $D_1\nabla^2\phi_1$ and $D_2\nabla^2\phi_2$* in Equation 12.44. Then the two-group neutron diffusion equations become a set of simple algebraic equations, and if we are dealing with an exactly critical reactor, we can write

The Two-Group Equations for an Infinite, Homogeneous, and Exactly Critical Reactor

$$(\Sigma_{a1}+\Sigma_{12}-\nu_1\Sigma_{f1})\phi_1-\nu_2\Sigma_{f2}\phi_2=0 \quad \text{(For the fast group)}$$
$$\Sigma_{12}\phi_1-\Sigma_{a2}\phi_2=0 \quad \text{(For the thermal group)} \tag{12.49}$$

and we can repeat the same logic we used previously to find the values of ϕ_1 and ϕ_2. Notice that we have done so by ignoring the fast and thermal neutron leakage terms in Equation 12.44, but in doing so, we have gained a great deal of physical insight because we have transformed the two-group neutron diffusion equations into two linear algebraic equations with constant coefficients. Moreover, these equations are now a set of *homogeneous linear equations* because they do not contain any neutron source terms (such as S_1 or S_2) on the right-hand side. Now let us explore what the solutions to these equations look like for an infinite, homogeneous reactor. To begin our discussion, we must first discuss what is known as *Cramer's Rule.**

12.10 Cramer's Rule

In elementary algebra, one quickly learns that *any system of homogeneous algebraic equations (where the terms on the right-hand side are zero) can only have a physical solution when the determinant of the coefficients vanishes*. Thus if we write the two-group diffusion equations in matrix form as

$$[\mathbf{M}]\{\phi\}=0 \tag{12.50}$$

where M is the coefficient matrix, a meaningful (or nontrivial) solution is only possible when

$$\begin{pmatrix}\mathbf{A} & \mathbf{B}\\ \mathbf{C} & \mathbf{D}\end{pmatrix}\begin{Bmatrix}\phi_1\\ \phi_2\end{Bmatrix}=\mathbf{0} \tag{12.51}$$

or when

A Simple Statement of Cramer's Rule

$$|\mathbf{M}|=0 \quad \text{and} \quad AD-BC=0 \tag{12.52}$$

Equation 12.52 is called *Cramer's rule*, and it states that a physically meaningful (i.e., nontrivial) solution to the two-group equations is only possible when AD = BC. Since the values of A, B, C, and D are given by

$$A=\Sigma_{a1}+\Sigma_{12}-\nu_1\Sigma_{f1} \quad B=-\nu_2\Sigma_{f2} \quad \textit{(Values for Row 1)} \tag{12.53}$$

$$C=\Sigma_{12} \quad D=-\Sigma_{a2} \quad \textit{(Values for Row 2)} \tag{12.54}$$

* A good introduction to *Cramer's rule* is available at the following URLs, which the reader is encouraged to read:
http://en.wikipedia.org/wiki/Cramer's_rule.
http://mathworld.wolfram.com/CramersRule.html.

Gabriel Cramer is the inventor of Cramer's rule

Cramer deduced that any set of linear equations

$ax + by = e$

$cx + dy = f$

Must have the solution:

$x = (ed - bf)/(ad - bc)$

$y = (af - ce)/(ad - bc)$

When $ad - bc \neq 0$

And that there is no unique solution when $ad - bc = 0$

FIGURE 12.4 Cramer's rule was named after Swiss mathematician Gabriel Cramer who invented it around 1750. His rule is an explicit formula for the solution of a system of linear equations where there are as many equations as there are unknowns. It is valid when a system of equations has a unique solution, or when the determinant of the coefficients vanished, and no unique solution to the equations is possible. (The picture of Gabriel Cramer was provided by Wikipedia.)

we can solve these two equations for the ratio of ϕ_1 to ϕ_2 by realizing that a meaningful solution is only possible when AD = BC, or when A = BC/D. This allows us to write $A\phi_1 = -B\phi_2$ or $(BC/D)\phi_1 = -B\phi_2$. Therefore, the ratio ϕ_2 to ϕ_1 for an exactly critical reactor must be

$$\phi_2 = \frac{-C\phi_1}{D} \quad \text{or} \quad \phi_2 = \frac{\Sigma_{12}}{\Sigma_{a2}} \cdot \phi_1 \tag{12.55}$$

Now let us reflect upon what we have just done. Using Cramer's rule, we can now use our knowledge of Σ_{12} and Σ_{a2} to determine the ratio of the fast flux to thermal flux in a critical reactor with no neutron leakage (see Figure 12.4). Normally the ratio of the fast flux to the thermal flux is about 2 to 1 in a thermal water reactor core. Thus we have produced an extremely useful result because we can apply Equation 12.55 to predict the neutron flux splits for a very large core. Since Equation 12.48 is a homogeneous set of linear equations, we can only find a solution to these equations within a multiplicative constant, and so we are free to set one of the group fluxes equal to an arbitrary value, and find the other fluxes in terms of that value. A related situation occurs when there are external source terms on the right-hand side of Equation 12.49. If these neutron sources exist, then, either S_1 or S_2 can be nonzero, and there may be a different external source S_1 for the fast flux than there is for the thermal flux S_2. Then the equations we must solve for ϕ_1 and ϕ_2 are

$$(\Sigma_{a1} + \Sigma_{12} - \nu_1 \Sigma_{f1})\phi_1 - \nu_2 \Sigma_{f2} \phi_2 = S_1 \tag{12.56}$$

and

$$\Sigma_{12} \phi_1 - \Sigma_{a2} \phi_2 = S_2 \tag{12.57}$$

where in general, $S_1 \neq S_2$. In matrix form, Equations 12.56 and 12.57 can be written as

$$[M]\{\phi\} = \{S\} \tag{12.58}$$

where

$$\{\phi\} = \text{col}(\phi_1, \phi_2, \phi_3, \ldots, \phi_G) \quad (g = 1,2,3,\ldots,G) \tag{12.59}$$

and

$$\{S\} = \text{col}(S_1, S_2, S_3, \ldots, S_G) \quad (g = 1,2,3,\ldots,G) \tag{12.60}$$

Obviously, because we are concerned with only two energy groups, the value of G is equal to 2. However, when there is a problem with more than two energy groups, the same basic methodology applies. Now we would like to examine some additional solutions to Equation 12.58 when the external neutron sources are finite.

12.11 Solving the Inhomogeneous Neutron Diffusion Equation with Two Energy Groups

Now let us turn our attention to a related problem where the source vector {S} on the right-hand side of Equation 12.58 is finite. Then the value of the neutron flux on at least one of the boundary nodes must be finite and positive, and this will cause the values of S_1 or S_2 to become finite as well. However, when $S_1 \neq 0$ or $S_2 \neq 0$ Equation 12.58 becomes what is known as a set of *inhomogeneous linear equations*. The values of the fast and thermal fluxes then become

$$\phi_1 = \frac{ED - BF}{AD - BC} = \frac{\nu_2 \Sigma_{f2} S_2 - \Sigma_{a2} S_1}{\nu_1 \Sigma_{f1} \Sigma_{a2} - \Sigma_{a1} \Sigma_{a2} - \Sigma_{a1} \Sigma_{12} + \nu_2 \Sigma_{f2} \Sigma_{12}} \tag{12.61}$$

$$\phi_2 = \frac{AF - CE}{AD - BC} = \frac{S_2 \cdot (\Sigma_{a1} + \Sigma_{12} - \nu_1 \Sigma_{f1}) - S_1 \Sigma_{12}}{\nu_1 \Sigma_{f1} \Sigma_{a2} - \Sigma_{a1} \Sigma_{a2} - \Sigma_{a1} \Sigma_{12} + \nu_2 \Sigma_{f2} \Sigma_{12}} \tag{12.62}$$

and the only time a unique solution is *not* possible is when AD = BC. Then the ratio of the fast to the thermal flux becomes

$$\frac{\phi_1}{\phi_2} = \frac{ED - BF}{AF - CE} = \frac{\nu_2 \Sigma_{f2} S_2 - \Sigma_{a2} S_1}{S_2 \cdot (\Sigma_{a1} + \Sigma_{12} - \nu_1 \Sigma_{f1}) - S_1 \Sigma_{12}} \tag{12.63}$$

Their absolute levels must then be determined from the reactor power level or from a similar normalization condition. Hence this is as much as we can say about the values of ϕ_1 and ϕ_2 unless we have explicit knowledge of the shape of the fast and thermal flux. In the next section, we would like to extend this approach to a real reactor with realistic values for the fast and thermal buckling.

12.12 Solving the Two-Group Diffusion Equations in a Finite Reactor Core

When we extend what we have just done to a finite reactor core, we can show how the geometric buckling B^2 of the flux is related to the neutron leakage rate. Consider for the moment the two-group neutron diffusion equations in their general form:

$$-D_1 \nabla^2 \phi_1 + \Sigma_{a1} \phi_1 + \Sigma_{12} \phi_1 = \frac{1}{k} \{\nu_1 \Sigma_{f1} \phi_1 + \nu_2 \Sigma_{f2} \phi_2\} \tag{12.64}$$

$$-D_2 \nabla^2 \phi_2 + \Sigma_{a2} \phi_2 = \Sigma_{12} \phi_1 \tag{12.65}$$

If we define $\Sigma_{a1} + \Sigma_{12} = \Sigma_{R1}$ as the total removal cross section from the fast energy group, then these two-group equations can be written as

$$-D_1 \nabla^2 \phi_1 + \Sigma_{R1} \phi_1 = \frac{1}{k} \{\nu_1 \Sigma_{f1} \phi_1 + \nu_2 \Sigma_{f2} \phi_2\} \quad \text{(for the fast group)} \tag{12.66}$$

and

$$-D_2 \nabla^2 \phi_2 + \Sigma_{a2} \phi_2 = \Sigma_{12} \phi_1 \quad \text{(for the thermal group)} \tag{12.67}$$

where we have inserted the effective multiplication factor 1/k in front of the fission producing terms because we are eventually going to know what combinations of materials will result in a critical system. If we replace the neutron leakage terms $\nabla^2\phi_1$ and $\nabla^2\phi_2$ with the appropriate values for the fast and thermal buckling B_1^2 and B_2^2 (see Chapters 10 and 11 for an explanation of what the buckling represents), then the two-group neutron diffusion equations become

$$D_1B_1^2\phi_1 + \Sigma_{R1}\phi_1 = \frac{1}{k}\{\nu_1\Sigma_{f1}\phi_1 + \nu_2\Sigma_{f2}\phi_2\} \quad \text{(for the fast group)} \tag{12.68}$$

$$D_2B_2^2\phi_2 + \Sigma_{a2}\phi_2 = \Sigma_{12}\phi_1 \quad \text{(for the thermal group)} \tag{12.69}$$

These equations then become a set of algebraic equations because the values of B_1^2 and B_2^2 are just *numbers*. Thus we can write Equations 12.68 and 12.69 as

$$\left[D_1B_1^2 + \Sigma_{R1} - \frac{1}{k}\nu_1\Sigma_{f1}\right]\phi_1 - \left[\frac{1}{k}\nu_2\Sigma_{f2}\right]\phi_2 = 0 \tag{12.70}$$

$$\left[-\Sigma_{12}\right]\phi_1 + \left[D_2B_2^2 + \Sigma_{a2}\right]\phi_2 = 0 \tag{12.71}$$

where the first terms refer to the fast flux and the second terms refer to the thermal flux. From our previous discussion of Cramer's rule, this system of algebraic equations will have a nontrivial solution when and only when

$$\left[D_1B_1^2 + \Sigma_{R1} - \frac{1}{k}\nu_1\Sigma_{f1}\right]\cdot\left[D_2B_2^2 + \Sigma_{a2}\right] = \left[\Sigma_{12}\right]\cdot\left[\frac{1}{k}\nu_2\Sigma_{f2}\right] \tag{12.72}$$

In other words, Equation 12.72 can be solved for the effective multiplication factor when the neutron leakage rates are a function of B_1 and B_2. Solving directly for k gives

$$k = \frac{\nu_1\Sigma_{f1}}{D_1B_1^2 + \Sigma_{R1}} + \frac{\Sigma_{12}}{D_1B_1^2 + \Sigma_{R1}}\cdot\frac{\nu_2\Sigma_{f2}}{D_2B_2^2 + \Sigma_{a2}} \tag{12.73}$$

Now let us see if we can understand what we have just done. The first term in Equation 12.73 represents the contributions to the effective multiplication factor from fast fissions, and the second term represents the contributions to the effective multiplication factor from thermal fissions. Since we expect the thermal fission rate to be many times greater than the fast fission rate (e.g., $\nu_2\Sigma_{f2} \gg \nu_1\Sigma_{f1}$), we can temporarily ignore the fast fission term and consider the effect that the second term has on the effective multiplication factor. We can also rewrite the remaining terms as

$$k = \left[\frac{\Sigma_{12}}{\Sigma_{R1}}\right]\left[1 + \left(\frac{D_1}{\Sigma_{R1}}\right)B_1^2\right]\cdot\frac{\left[\nu_2\Sigma_{f2}/\Sigma_{a2}\right]}{\left[1 + (D_2/\Sigma_{a2})B_2^2\right]} \tag{12.74}$$

or expressed somewhat differently, the value for the effective multiplication factor becomes

$$k = \left[\frac{\Sigma_{12}}{\Sigma_{R1}}\right]\frac{1}{\left[1 + L_1^2B_1^2\right]}\cdot\frac{\left[\nu_2\Sigma_{f2}/\Sigma_{a2}\right]}{\left[1 + L_2^2B_2^2\right]} \tag{12.75}$$

12.13 Deriving the Six-Factor Formula from the Neutron Diffusion Equation

Now we would like to use the equations we have just derived to make some additional observations about the six-factor formula, which we discussed previously in Chapter 10. From our earlier discussion it is easy to see from Equation 12.75 that

$$P_{NL1} = \frac{1}{1 + L_1^2B_1^2} \quad \text{and} \quad P_{NL2} = \frac{1}{1 + L_2^2B_2^2} \tag{12.76}$$

are just the *fast and thermal nonleakage probabilities*—P_{NLF} and P_{NLT}. However, in this case, the diffusion length L for the fast energy group is defined somewhat differently as

$$L^2 = \frac{D_1}{\Sigma_{R1}} \tag{12.77}$$

which departs from the standard definition for $L^2 = D_1/\Sigma_{a1}$ because the new definition contains *both the absorption cross section and the scattering cross section in the denominator* (e.g., $\Sigma_{R1} = \Sigma_{a1} + \Sigma_{12}$). Upon further reflection, one can also see that Σ_{12}/Σ_{R1} represents the probability that neutrons born into the fast energy group are able to escape to the thermal energy group without being absorbed. In other words, the ratio Σ_{12}/Σ_{R1} represents the *resonance escape probability* p for a homogeneous reactor:

$$p = \frac{\Sigma_{12}}{\Sigma_{R1}} \tag{12.78}$$

Thus we have been able to deduce three of the six terms in the six-factor formula by simply manipulating the two-group diffusion equations. Similarly, the term $\nu_1\Sigma_{f1}/\Sigma_{R1}$ can be recognized as the *fast neutron multiplication factor* (see Chapter 9) because it can be written as

$$\frac{\nu_1 \Sigma_{f1}}{\Sigma_{R1}} = \frac{\nu_1 \Sigma_{f1}}{\Sigma_{a1}} \frac{\Sigma_{a1}}{\Sigma_{R1}} = \eta_1 \cdot f_1 \tag{12.79}$$

where f_1 is the *fast utilization factor*. Finally, if we define the *fast fission factor* ε (epsilon) as

$$\varepsilon = 1 + \left(\frac{\nu_1 \Sigma_{f1}}{\nu_1 \Sigma_{f1}} \right) \frac{D_2 B^2}{\Sigma_{12}} \tag{12.80}$$

we soon discover that

The Six-Factor Formula Derived from Two-Group Neutron Diffusion Theory

$$k = p\varepsilon\eta_2 f_2 \cdot P_{NL1} P_{NL2} \tag{12.81}$$

Thus, *we have been able to derive the six-factor formula for a thermal reactor by simply manipulating some of the terms in the two-group neutron diffusion equations. This process was relatively straightforward, and we simply had to replace the neutron leakage terms with the appropriate values of the geometric buckling B^2 for each energy group. When we did so, the six-factor formula simply "fell out" of the neutron diffusion equation*. Of course, this new definition for the effective multiplication factor is somewhat different than our previous definition (see Chapter 10), and so it must be used with caution because the values for the thermal utilization and the neutron reproduction factor are different. Consequently, casting some of the components of the six-factor formula in terms of the two-group parameters has created an additional ambiguity when it comes to selecting the correct version to use. This arbitrariness is not unique to just the six-factor formula, and similar inconsistencies can be found in the treatment of the two-group constants in the literature (see Reference 3). For this reason and others, the utility of the six-factor formula is rather limited when it comes to designing real reactors. Next, we would like to explore an alternative version of neutron diffusion theory called *modified one group theory*. In this version of the theory, the thermal neutron leakage rates are assumed to be very small.

12.14 Modified One-Group Neutron Diffusion Theory

Equation 12.81 does not make any new assumptions about the neutron reproductive cycle, except that the neutron life cycle must be representative of the neutron life cycle in a thermal water reactor. In many situations (particularly those involving large, loosely coupled thermal water reactor cores) it is possible to simplify the two-group diffusion equations even further by ignoring the leakage of the thermal neutrons entirely. This can be done by setting the term $-D_2\nabla^2\phi_2$ to

zero in Equation 12.67 since the thermal neutron leakage rate is usually 5 or 10 times smaller than the fast neutron leakage rate. When we do this, the fast and thermal neutrons are then related by the equation

$$\Sigma_{a2}\,\phi_2 = \Sigma_{12}\,\phi_1 \tag{12.82}$$

and if we plug this value for ϕ_2 into the equation for the fast energy group, we obtain

$$-D_1\nabla^2\phi_1 + \Sigma_{a1}\,\phi_1 + \Sigma_{12}\,\phi_1 = \nu_1\,\Sigma_{f1}\,\phi_1 + \nu_2\,\Sigma_{12}\left(\frac{\Sigma_{12}}{\Sigma_{a2}}\right)\phi_1 \tag{12.83}$$

For a homogeneous core, we can also write Equation 12.83 as

$$\nabla^2\phi_1 + B^2\phi_1 = 0 \tag{12.84}$$

where now the buckling of the flux is given by $B^2 = \left(k_\infty - 1\right)/L_1^2)$ and $L_1^2 = D_1/\Sigma_{R1}$. This model of neutron behavior is sometimes called *modified one-group diffusion theory* because it accounts for the behavior of the fast and thermal neutrons at the same time, but it does so in a slightly different way. A more comprehensive analysis would then show that when both the fast and thermal leakage rates are taken into account, the value of L_1^2 would need to be replaced by the value of $M^2 = L_1^2 + L_2^2$, where $L_1^2 = D_1/\Sigma_{R1}$ and $L_2^2 = D_2/\Sigma_{R2}$ (again refer to our discussion in Chapter 11). Here M^2 is defined as the *thermal migration area*, and it can be shown that the thermal diffusion area L^2 is equal to 1/6th of the distance that a neutron must travel (as the crow flies) from the time that it is created until the time that it is destroyed. The model we have just presented is also referred to as *one-and-one-half-group theory* because its predictions are midway between those of one group theory and two-group theory.

Student Exercise 12.1

Suppose that the thermal flux source term S_2 was inserted back into the two-group neutron diffusion equations and that $S_1 = 0$. If the neutron leakage rates for the fast and thermal energy groups can be neglected, derive a relationship between the value of the fast flux ϕ_1 and the thermal flux ϕ_2 for a system that is exactly critical.

12.15 Working with the N-Speed Neutron Diffusion Equation

It is easily possible to generalize what we have said to more than two energy groups by expanding the terms in the neutron diffusion equation. *In most reactor designs, breaking the neutron energy spectrum into fast and thermal components is usually sufficient to obtain a good value for k. However, in some cases (like in the region between a fuel rod and a control rod), two energy groups may not be sufficient to predict how the neutron population behaves.* In this case, it may be necessary to rewrite the neutron diffusion equation in a form that can simultaneously handle more than two energy groups. The easiest way to do this is to simply write a neutron balance equation for each energy group. This can be done by putting all of the terms that add neutrons to each group g on the right-hand side and all the terms that remove neutrons from the same energy group on the left-hand side. In a steady-state system, the two sides of each equation must be in perfect balance, and we can ensure that this is true by inserting an effective multiplication factor 1/k in front of the fission producing terms in each energy group. When we do this for a four group or a four speed model, we obtain

The Four-Group Neutron Diffusion Equations

$$\begin{aligned}
-D_1\nabla^2\phi_1 + \Sigma_{a1}\,\phi_1 + \Sigma_{12}\phi_1 + \Sigma_{13}\phi_1 + \Sigma_{14}\,\phi_1 &= \frac{1}{k}\chi_1\{\nu\Sigma_{f1}\,\phi_1 + \nu\Sigma_{f2}\,\phi_2 + \nu\Sigma_{f3}\,\phi_3 + \nu\Sigma_{f4}\,\phi_4\}\\
-D_2\nabla^2\phi_2 + \Sigma_{a2}\,\phi_2 + \Sigma_{23}\,\phi_2 + \Sigma_{24}\,\phi_2 &= \frac{1}{k}\chi_2\{\nu\Sigma_{f1}\,\phi_1 + \nu\Sigma_{f2}\,\phi_2 + \nu\Sigma_{f3}\,\phi_3 + \nu\Sigma_{f4}\,\phi_4\} + \Sigma_{12}\,\phi_1\\
-D_3\nabla^2\phi_3 + \Sigma_{a3}\,\phi_3 + \Sigma_{34}\,\phi_3 &= \frac{1}{k}\chi_3\{\nu\Sigma_{f1}\,\phi_1 + \nu\Sigma_{f2}\,\phi_2 + \nu\Sigma_{f3}\,\phi_3 + \nu\Sigma_{f4}\,\phi_4\} + \Sigma_{13}\,\phi_1 + \Sigma_{23}\,\phi_2\\
-D_4\nabla^2\phi_4 + \Sigma_{a4}\,\phi_4 &= \frac{1}{k}\chi_4\{\nu\Sigma_{f1}\,\phi_1 + \nu\Sigma_{f2}\,\phi_2 + \nu\Sigma_{f3}\,\phi_3 + \nu\Sigma_{f4}\,\phi_4\} + \Sigma_{14}\,\phi_1 + \Sigma_{24}\,\phi_2 + \Sigma_{34}\,\phi_3
\end{aligned} \tag{12.85}$$

where χ_g is the fraction of the fission neutrons that are produced in energy group g. In practice, the number of fission neutrons produced in the lowest energy group is usually a very small number, and if the group boundary starts at a low enough energy (say, 1 eV), then we can set $\chi_4 = 0$. Equation 12.85 then becomes a system of four coupled differential equations for the neutron flux, and there is a separate equation for the neutrons in each energy group. Sometimes it is easier to visualize the form of these equations by writing out the first few of them explicitly. In the case of G energy groups, we have

Multigroup Diffusion Equations

$$-D_g\nabla^2\phi_g + \Sigma_{ag}\phi_g + \sum_{g'>g}\Sigma_{gg'}\phi_g = \frac{1}{k}\sum_{g=1,G}\chi_g\{\nu\Sigma_{fg}\phi_g\} + \sum_{g'<g}\Sigma_{g'g}\phi_g, \tag{12.86}$$

Notice that each equation (except the first equation) is coupled to the equations immediately above it because the neutrons can always down-scatter from a higher energy group to a lower one (e.g., from group g to groups g + 1, g + 2, g + 3, g + N, etc.). However, in most cases, the neutrons do not up-scatter from a lower energy group to a higher one. Thus we can set the up-scattering terms $\Sigma_{gg'}$ to zero when $g' > g$ because a neutron will not generally gain enough energy in a collision with another nucleus. This has the effect of forcing the coefficient matrix into a *lower triangular form* that is much easier to solve with a computer. We can visualize this by writing the first few equations with the up-scattering terms removed. The result is

$$\begin{aligned}
-D_1\nabla^2\phi_1 &+ \Sigma_{a1}\phi_1 + \Sigma_{12}\phi_1 + \Sigma_{13}\phi_1 + \Sigma_{14}\phi_1 &&= \frac{1}{k}\chi_1 P \\
-D_2\nabla^2\phi_2 &+ \Sigma_{a2}\phi_2 + \Sigma_{23}\phi_2 + \Sigma_{24}\phi_2 &&= \frac{1}{k}\chi_2 P &&+ \Sigma_{12}\phi_1 \\
-D_3\nabla^2\phi_3 &+ \Sigma_{a3}\phi_3 + \Sigma_{34}\phi_3 &&= \frac{1}{k}\chi_3 P &&+ \Sigma_{13}\phi_1 + \Sigma_{23}\phi_2 \\
-D_4\nabla^2\phi_4 &+ \Sigma_{a4}\phi_4 &&= \frac{1}{k}\chi_4 P &&+ \Sigma_{14}\phi_1 + \Sigma_{24}\phi_2 + + \Sigma_{34}\phi_3 \\
\textbf{Leakage} &\textbf{ + Out-scattering} &&\textbf{= Production} &&\textbf{+ In-scattering}
\end{aligned}$$

where P is the neutron production term, and it is given by

$$P = \text{Production} = \nu\Sigma_{f1}\phi_1 + \nu\Sigma_{f2}\phi_2 + \nu\Sigma_{f3}\phi_3 + \nu\Sigma_{f4}\phi_4 \tag{12.87}$$

Here again we have made the assumption that $\nu_1 \approx \nu_2 \approx \nu_3 \approx \nu_4 \approx \nu$. Of course, this assumption can be normally justified based on physical grounds alone. So what we have just done is to replace the energy dependent diffusion equation by G separate diffusion equations, which are coupled together through the energy-dependent neutron fission and absorption cross sections—as well as through in-scattering and out-scattering between the various energy groups. There is one differential equation for each energy group (fast, slow, and intermediate, etc.). This means that if we would like to know the neutron flux in G separate energy ranges ($\phi_1, \phi_2, \phi_3, \ldots, \phi_G$), then we will have to solve G coupled differential equations to find it. Notice that solving these equations allows us to find both the *magnitude* and the *shape* of the neutron flux in each energy group. Generally speaking, the shape of the flux is different for each energy group, and for thermal water reactors, it is considerably different for neutrons in the core and in the reflector.

12.16 Matrix Form of the Multigroup Diffusion Equations

For those of you who are mathematically inclined, it is easy to deduce from our earlier discussion that we can rewrite the multigroup diffusion equations in matrix form as

$$[\mathbf{M}]\{\{\phi\} = \frac{1}{k}[\mathbf{F}]\{\phi\} \tag{12.88}$$

where [**M**] is the coefficient matrix containing neutron leakage, absorption, and scattering terms, $\{\phi\}$is a vector containing the group fluxes

$$\{\phi\} = \{\phi_1 + \phi_2 + \phi_3 + \phi_4 + \phi_5 + \cdots + \phi_G\} \tag{12.89}$$

and [**F**] is a "*fission matrix*" containing the neutron production terms. The structure of this set of equations (one for each energy group) can be seen more clearly if we write all of the equations in the following format. The result is

$$\underbrace{\begin{pmatrix} -D_1\nabla^2+\Sigma_{R1} & 0 & 0 & 0 & \cdots \\ -\Sigma_{12} & -D_2\nabla^2+\Sigma_{R2} & 0 & 0 & \cdots \\ -\Sigma_{13} & -\Sigma_{23} & -D_3\nabla^2+\Sigma_{R3} & 0 & \cdots \\ -\Sigma_{14} & -\Sigma_{24} & -\Sigma_{34} & -D_4\nabla^2+\Sigma_{R4} & \cdots \\ \cdot & \cdot & \cdot & \cdot & \cdots \\ \cdot & \cdot & \cdot & \cdot & \cdots \\ \cdot & \cdot & \cdot & \cdot & \cdots \end{pmatrix}}_{[M]} \underbrace{\begin{Bmatrix} \phi_1 \\ \phi_2 \\ \phi_3 \\ \phi_4 \\ \cdot \\ \cdot \\ \cdot \end{Bmatrix}}_{\phi} = \frac{1}{k} \underbrace{\begin{pmatrix} \nu\chi_1\Sigma_{f1} & \nu\chi_1\Sigma_{f2} & \cdots \\ \nu\chi_2\Sigma_{f1} & \nu\chi_2\Sigma_{f2} & \cdots \\ \nu\chi_3\Sigma_{f1} & \nu\chi_3\Sigma_{f2} & \cdots \\ \nu\chi_4\Sigma_{f1} & \nu\chi_4\Sigma_{f2} & \cdots \\ \cdot & \cdot & \cdots \\ \cdot & \cdot & \cdots \\ \cdot & \cdot & \cdots \end{pmatrix}}_{[F]} \underbrace{\begin{Bmatrix} \phi_1 \\ \phi_2 \\ \phi_3 \\ \phi_4 \\ \cdot \\ \cdot \\ \cdot \end{Bmatrix}}_{\phi} \tag{12.90}$$

where k is the *eigenvalue* that tells us whether or not this system of equations represents an exactly critical system. Note in particular that many of the scattering terms in the coefficient matrix [M] are zero because most of the time, neutrons cannot gain energy as they scatter from a lower energy group to a higher energy group. (The one exception to this rule is when we choose to have a lot of closely spaced energy groups in the thermal energy range.) The absence of this *up-scattering* means that all of the upper triangular terms in the coefficient matrix will be zero, and what we are left with is only the terms below the diagonal (which represent the down-scattering of neutrons from a higher energy group to a lower energy group). Hence, as long as we do not have a lot of energy groups where the thermal neutrons reside, the coefficient matrix [M] will always be *lower triangular*, and the methods to invert it must take this general structure into account. However, the fission matrix [F] that is responsible for producing the neutrons is completely full because the fission neutrons produced by neutron absorption in a lower energy group will distribute themselves among all of the higher energy groups in some way. Hence, *all of the fission producing terms will have small but finite contributions to the fission production rate in a multigroup approximation*.

Student Exercise 12.2

Suppose that the fission neutrons are released with a continuous distribution of energies that is given by the probability distribution function

$$\chi(E) = X(E) = Ae^{-BE}\sinh\left\{\sqrt{CE}\right\}$$

where A = 0.453, B = 1.036, C = 2.29, and E is the energy of the emitted neutron in MeV. If we break the neutron energy spectrum into four energy groups (1, 2, 3, and 4), and the boundaries between each of these energy groups are as follows

Group #	Start	Stop
Group 1	100 keV	10 MeV
Group 2	10 keV	100 keV
Group 3	1 eV	10 keV
Group 4	0 eV	1 eV

what are the corresponding values of χ_1, χ_2, χ_3, and χ_4 that should be used in Equation 12.85 in this case?

12.17 Fast and Thermal Flux Shapes Predicted by Two-Group Theory

In order to validate the results of two-group theory, the shape of the neutron flux ϕ in a unit cell can be measured experimentally, or it can be found by solving the diffusion equation directly. (The transport equation provides a slightly more accurate result.) However, for a light-water reactor fuel assembly, the shape of the neutron flux is quite predictable as long as the presence of the control rods can be ignored. In this case, Figure 12.5 shows what the flux shape looks like in an infinite reactor lattice consisting of many identical unit cells.

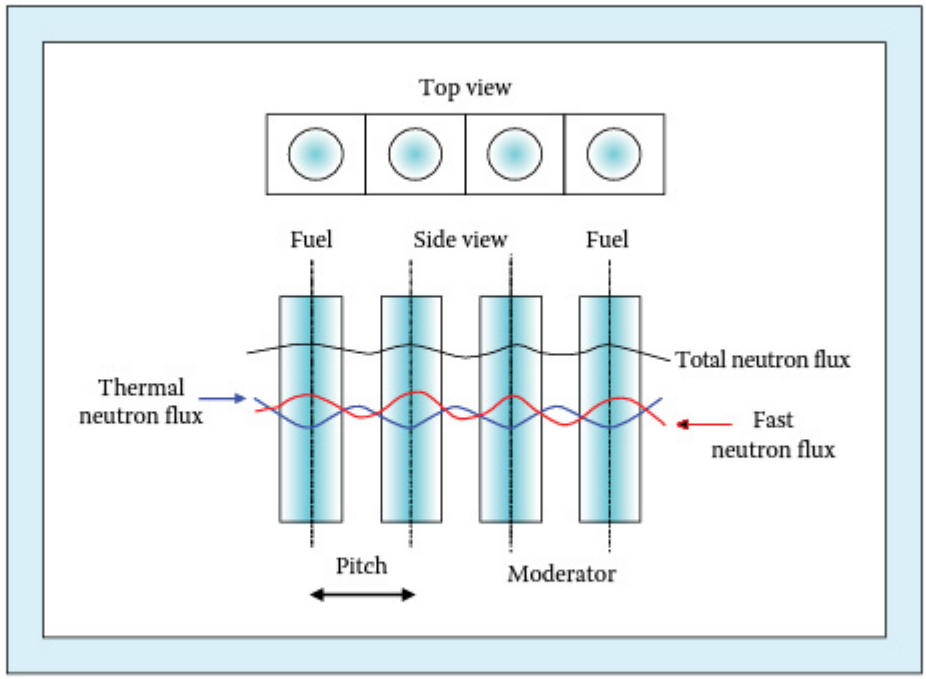

FIGURE 12.5 The shape of the fast and thermal neutron fluxes in a thermal water reactor. Notice that the fast flux peaks in the fuel and the thermal flux peaks in the moderator. The total flux also peaks in the fuel because there are approximately twice as many fast neutrons as there are thermal neutrons.

Here the shape of the fast neutron flux is shown in ***red***, and the shape of the thermal neutron flux is shown in ***blue***. The total neutron flux, which represents the sum of the thermal neutron flux and the fast neutron flux, is shown in ***black***. From our previous discussion, the reader may recall that

$$\phi(x, y, z) = \phi_1(x, y, z) + \phi_2(x, y, z) \tag{12.91}$$

where we have inserted the explicit spatial dependence of the flux back into Equation 12.91 to emphasize this point. Notice that the thermal neutron flux and the fast neutron flux in a light-water reactor behave in entirely different ways. *The fast neutron flux (group 1) in a reactor fuel assembly peaks in the fuel rods where the fast fission neutrons are born. On the other hand, the thermal neutron flux (group 2) peaks in the moderator, where there are lighter materials such as hydrogen and oxygen to slow the fission neutrons down.* In other words, one can see that the spatial distributions of the fast and thermal neutrons in a light-water reactor behave in exactly the opposite way. By inspecting Figure 12.5, we can also deduce that the total neutron flux is not the same everywhere, although it is relatively uniform in the lattice as a whole. One can see that it is slightly *higher* in the center of the fuel than it is in the moderator. *This is true in general because a thermal water reactor has about two fast neutrons for every thermal one*. However, the total flux $\phi = \phi_1 + \phi_2$ is much flatter than either the fast or thermal neutron flux. Hence we have learned a great deal about how to calculate the reaction rates in a real reactor, and in any reactor fuel assembly, by simply reducing the problem to one of finding the reaction rates in a lattice composed of identical unit cells.

When the same calculation is performed for a homogeneous core surrounded by a reflector, the fast and thermal fluxes behave in a similar way. The thermal flux peaks in the reflector, and the fast flux peaks in the core. However, the sum of the fast and thermal fluxes is the same as the total flux $\phi(x) = \phi_1(x) + \phi_2(x)$, which we would predict from one-group theory. (The exact flux shapes are shown in Figure 12.6.) It should be obvious from this diagram that *using three or four energy groups will always be more accurate than using just one or two. For this reason, most reactor vendors use one or two group models for parametric studies, and they resort to using at least four energy groups when more detailed calculations are required*. The extra energy groups mean that the reaction rates can be calculated more accurately and that the change in the flux shape between adjacent fuel rods and control rods is much easier to see. The main drawback to this approach is that we must increase the number of finite difference equations we must solve, and this increases the complexity of the computational model required to achieve the greater accuracy we desire.

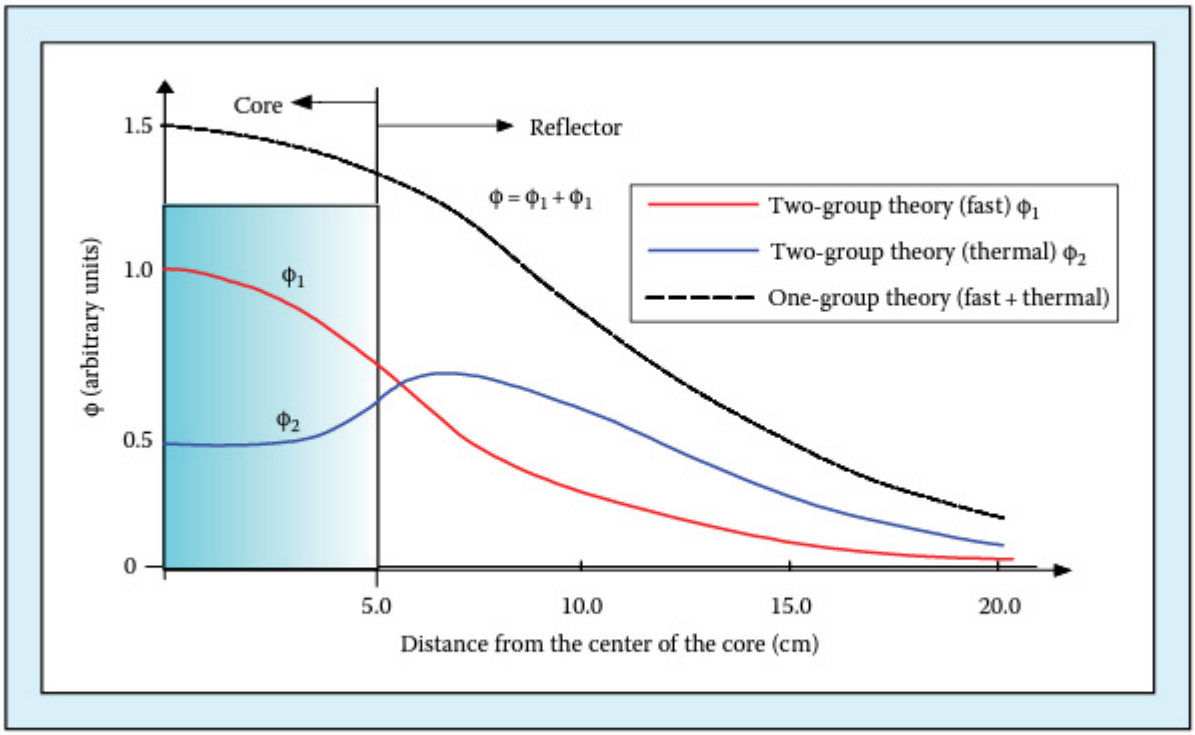

FIGURE 12.6 The one-group flux and the two-group flux in a simple homogeneous water reactor core with a light-water reflector.

12.18 Popular Multigroup Neutron Diffusion Theory Programs

There are many publicly available computer programs that can be used to find the multigroup flux shape $\phi_g(x, y, z)$ in a reactor core. Some of the most popular programs are listed in Table 12.1. In nuclear science and engineering, these programs are also referred to as *computer codes*. In general, reactor vendors prefer to use two- and three-dimensional computer programs rather than the one-dimensional ones to perform a parametric analysis of a large region of the core. Two- and three-dimensional codes allow the fast and thermal flux shapes to be calculated with more precision, and consequently, the reaction rates can be calculated with greater precision as well. They also allow each fuel assembly in the core (see Figure 12.7) to be simulated numerically with a separate *node* or *computational cell*. Methods that allow the neutron flux to be found in this way are therefore called *nodal methods*, and nodal methods are extremely popular in the design and analysis of large reactor cores. Thus, the power generation rates can be different in different fuel assemblies, and nodal methods (with the appropriate boundary conditions) can be used to predict both the power shape and the flux shape under these conditions.

Some of the more popular diffusion theory codes in widespread use today are *DIFF, PDQ, CITATION, and SIMULATE.* (Refer to Table 12.1 again.) Thus, a reactor core can be simulated by these programs in a variety of different ways. Some of the more obvious ways are illustrated in Figure 12.8, where the computational cells that are required by a nodal method are shown. *In practice, virtually any reactor geometry can be simulated properly if enough computational cells are used.* Increasing the number of computational cells and the number of energy groups increases the accuracy of the solution. However, it also makes the coefficient matrix [M] that we presented in Section 12.16 more difficult and time consuming to invert. Hence, larger and more complex problems require additional computer time but the trade off is usually well worthwhile because the solutions are more accurate. Reducing the size of the computational cells makes the solutions more accurate as well.

12.19 Reactor Licensing Applications

Some of the computer programs listed in Table 12.1 are also used to support the licensing and design of thermal water reactors in the United States. Computer programs such as SIMULATE, DIFF, and CITATION have been used by nuclear utilities in many countries to perform burnup and depletion calculations. PDQ is used by some reactor vendors to design fuel assemblies, although its use has declined in recent years as more sophisticated computer programs such as TRACE (see Section 12.20) have become available.

TABLE 12.1
Some Popular Multigroup Diffusion Theory Codes in Widespread Use Today

Diffusion Theory Code	Primary Developer	Programming Language or O/S	Function or Purpose
CITATION 2D/3D	Oak Ridge National Laboratory, Oak Ridge, TA	Fortran-IV; runs on IBM mainframes, CDC machines, Micro VAXs, and IBM PCs	CITATION is a very sophisticated and flexible computer program designed to solve the neutron diffusion equation in 1, 2, or 3 spatial dimensions with arbitrary group-to-group scattering cross sections. It can be used for x-y-z, θ-r-z, hexagonal-z, and triagonal-z geometries and has no limit on the number of energy groups that can be used.
DIFF3D	Nuclear Engineering Division, Argonne National Laboratory, Argonne, IL	Fortran 90 and C source code for Linux PCs, Mac OS, and SUN	DIFF3D is a widely used neutron diffusion theory program that uses variational nodal methods and finite difference methods to solve the neutron diffusion equation in one-, two-, and three-dimensional geometries.
PDQ-7	Bettis Atomic Power Laboratory, Pittsburgh, PA	FORTRAN-IV and FORTRAN-77; IBM mainframes and IBM PCs	PDQ-7 is a few-group neutron diffusion theory code that can be used to predict the flux shape in light-water reactor fuel assemblies for individual fuel pins. It uses the few-group cross sections generated by the GAM computer program, which in turn uses the data provided by the ENDF-B database.
SIMULATE-2 and SIMULATE 3	Studsvik Scandpower AB, Hantverkargatan 2A, SE-72212 Västerås, Sweden	FORTRAN-77, IBM, and UNIX	The SIMULATE coarse-mesh nodal code and the PDQ-7 fine-mesh diffusion theory code have been used for any years to synthesize three-dimensional power distributions and flux shapes in pressurized water reactors. SIMULATE takes the few-group cross sections generated by the PDQ-7 code and uses them to perform burnup and depletion calculations.
QUANDF	Originally developed at MIT and modified by several European groups to meet the needs of the U.S. DOE	Fortran 77; runs on PCs, UNIX workstations, and IBM mainframes	The QUANDF code is based on the analytical nodal method for the two-group neutron diffusion equation in three-dimensional Cartesian geometries, developed by A.F. Henry and his coworkers at MIT. It has undergone major revisions since its initial introduction.

12.20 Performing a Reactor Licensing Analysis with TRACE

Perhaps the most famous of all computer codes used to license commercial nuclear power plants in the United States is a new and highly advanced computer program called *TRACE*. TRACE is used by the U.S. NRC to license commercial nuclear power plants in the United States, and several other countries have expressed an interest in using it for their reactor licensing work as well. The neutronic modules used in TRACE are based on a powerful computer program called *QUANDF*, which solves the multigroup neutron diffusion equations in one, two, or three dimensions. QUANDF can be used for steady-state as well as transient reactor analysis. It was originally developed by *Alan Henry* and his team at MIT in the late 1980s to simulate large reactor cores, and it uses cross sections supplied by the ENDF-B 7 database. It differs from many of the other computer programs listed in Table 12.1 because it can be used to solve time-dependent problems as well as steady-state ones. Time-dependent reactor behavior is an important part of any licensing process. Hence, nuclear utilities are often required to use TRACE to model the transient behavior of an entire nuclear power plant, such as the *Maanshan PWR* shown in Figure 12.9. In future chapters, we will discuss exactly how the multigroup neutron diffusion equations can be solved when the neutron leakage terms can no longer be neglected or replaced by a simple constant to represent the geometric buckling. The solutions can be used to determine the shape of the neutron flux in a variety of different configurations. We will discuss some of these configurations and their attributes in the next chapter. In general, the diffusion equation can only be solved exactly in a few idealized reactor geometries.

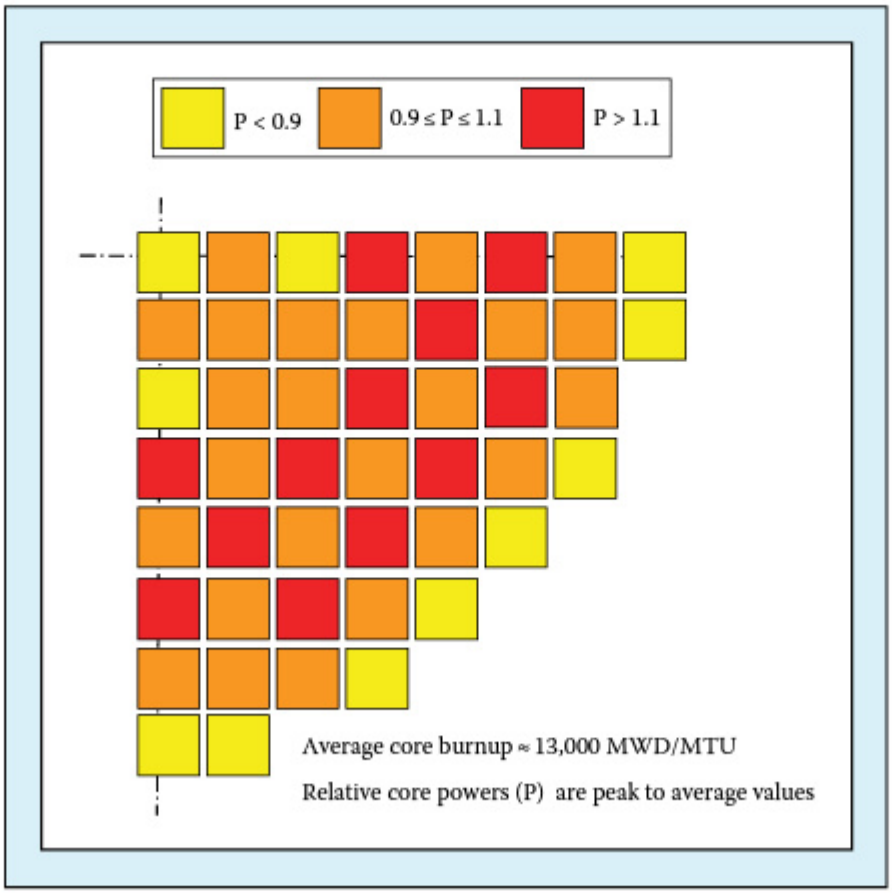

FIGURE 12.7 An example of a symmetry section that can be used to calculate the global flux shape when the fuel assemblies are loaded symmetrically.

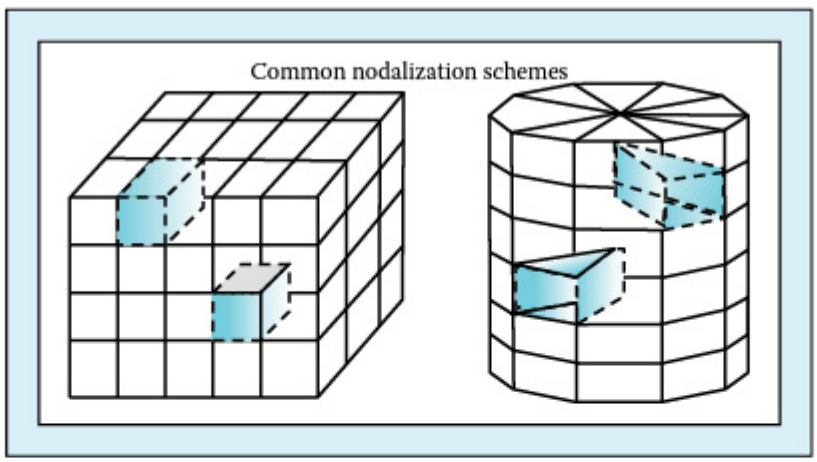

FIGURE 12.8 Some ways in which a nodal method can be used to perform a simple parametric analysis of a nuclear reactor core. Here the "nodes" or computational cells are shown in white and blue.

Student Exercise 12.3

Suppose that you were asked to make a recommendation for the cutoff point (in eV) where neutron up-scattering could be neglected when solving the two-group neutron equations in a high-temperature gas reactor. If the average temperature T of the scattering material is approximately twice what it is in a light-water reactor, and carbon dioxide gas (rather than water) is used for the coolant, estimate how high the cutoff point (in eV) between the fast and thermal energy groups can be chosen in this case.

Hint: You may want to refer to Chapter 4 for additional details.

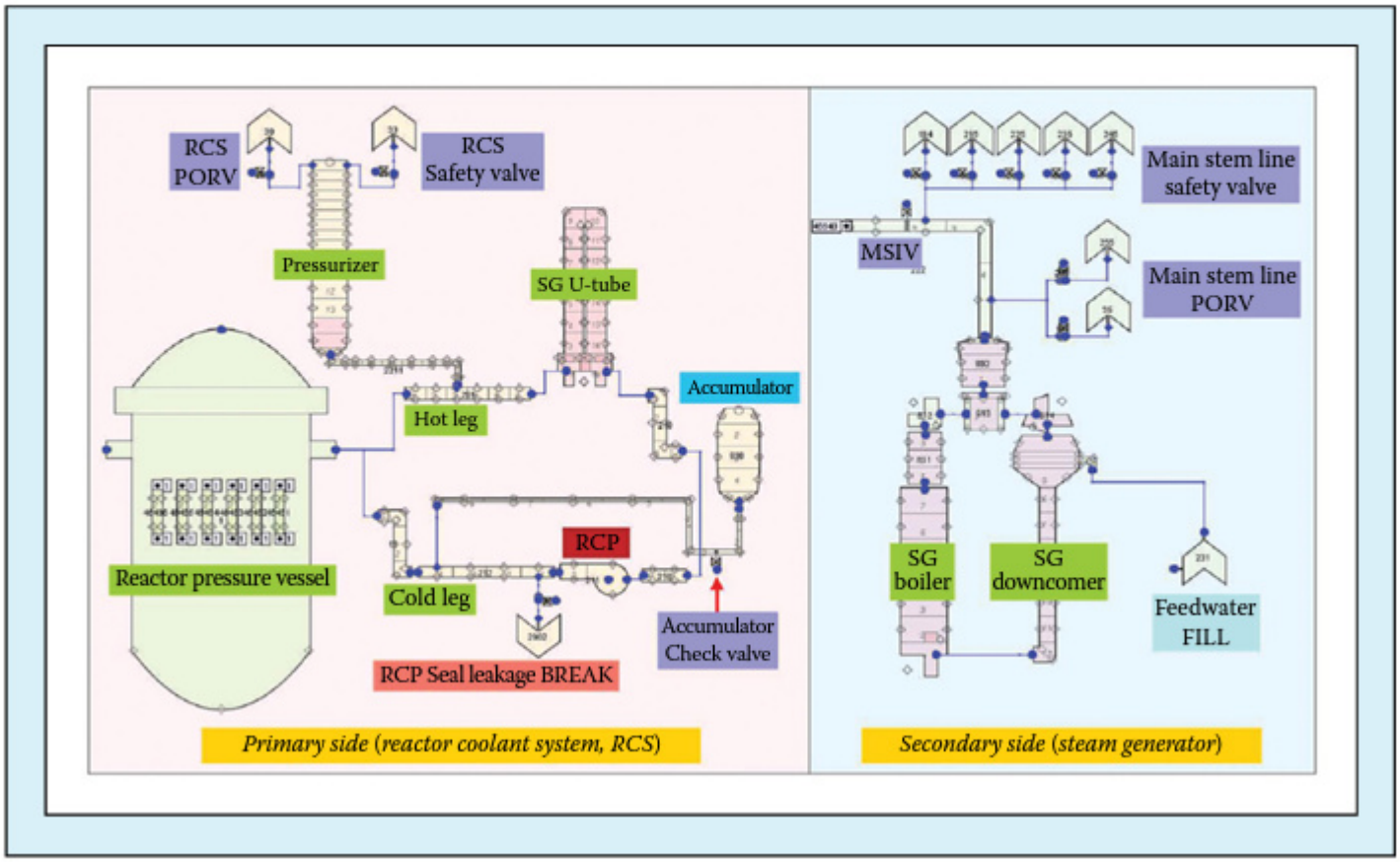

FIGURE 12.9 A TRACE simulation of the Maanshan PWR that was ultimately used to license the plant in Taiwan. (Picture taken from https://www.nrc.gov/docs.)

12.21 Parameters to Use with the Multigroup Equations

When the neutron diffusion equation is used to predict the flux shapes in an actual reactor lattice, it is important to have physically reliable values for the macroscopic fission and absorption cross sections for the fuel, the moderator, and the cladding. When two energy groups are used, some of these values can be found in Tables 12.2 and 12.3. (A more comprehensive listing can be found in Appendix C.) Notice that the fast fission cross sections for many nuclear fuels are about 100 times smaller than the thermal fission cross sections for exactly the same materials. *The one notable exception to this rule is U-238, which actually has a fast fission cross section that is slightly higher than its thermal fission cross section*

TABLE 12.2
Thermal Cross Sections Required to Calculate the Effective Multiplication Factor in Neutron Diffusion Theory

Thermal Group Macroscopic Cross Sections for Some Important Nuclear Materials						
Name	Use	$\sum_c$ (cm^{-1})	$\sum_f$ (cm^{-1})	$\nu\sum_f$ (cm^{-1})	$\sum_s$ (cm^{-1})	D (cm)
Light water (H_2O)	Coolant/moderator	0.02220	0.0	0.0	3.334	0.160
Heavy water (D_2O)	Coolant/moderator	0.0000442	0.0	0.0	0.452	0.870
Liquid sodium (Na)	Coolant	0.0135	0.0	0.0	0.081	4.115
Zirconium	Fuel rod cladding	0.008	0.0	0.0	0.338	0.986
Stainless steel	Fuel rod cladding	0.222	0.0	0.0	0.933	0.357
U-233	Fuel	2.189	25.26	62.95	0.999	0.329
U-235	Fuel	4.621	27.96	67.61	0.669	0.490
U-238	Fuel	0.130	5.25×10^{-7}	1.365×10^{-6}	0.4239	0.775
Pu-239	Fuel	13.446	37.220	106.86	0.3835	0.855

Source: Duderstadt, J. and Hamilton, L., *Nuclear Reactor Analysis*, John Wiley & Sons, New York, 1976.

TABLE 12.3
Fast Cross Sections Required to Calculate the Effective Multiplication Factor in Neutron Diffusion Theory

Fast Group Macroscopic Cross Sections for Some Important Nuclear Materials						
Name	Use	$\sum_c$ (cm^{-1})	$\sum_f$ (cm^{-1})	$\nu\sum_f$ (cm^{-1})	$\sum_s$ (cm^{-1})	D (cm)
Light water (H_2O)	Coolant/moderator	0.0000037	0.0	0.0	0.853	1.130
Heavy water (D_2O)	Coolant/moderator	0.0000039	0.0	0.0	0.460	1.290
Liquid sodium (Na)	Coolant	0.0000703	0.0	0.0	0.078	4.273
Zirconium	Fuel rod cladding	0.008	0.0	0.0	0.338	0.986
Stainless steel	Fuel rod cladding	0.00033	0.0	0.0	1.865	0.179
U-233	Fuel	0.0367	0.1285	0.320	0.325	1.025
U-235	Fuel	0.2000	0.0895	0.216	0.326	1.025
U-238	Fuel	0.0158	0.00204	0.0053	0.328	1.000
Pu-239	Fuel	0.0247	0.0894	0.257	0.3377	0.942

Source: Duderstadt, J. and Hamilton, L., *Nuclear Reactor Analysis*, John Wiley & Sons, New York, 1976.

(see Tables 12.2 and 12.3). This explains why U-238 is such a popular nuclear fuel in fast breeder reactors (see Chapter 1) in which virtually all of the neutrons are fast.

Finally, *the diffusion coefficients, which are inversely proportional to the neutron scattering cross sections, are about seven times higher for fast neutrons in a thermal water reactor than they are for thermal neutrons. This means that their mean free paths are about seven times longer as well*. However, for other coolants such as heavy water and liquid sodium, the fast and thermal diffusion coefficients are about the same. The cross sections for up-scattering are effectively zero in two-group theory because very few neutrons up-scatter to energies above 1 eV after they have reached the thermal energy range. In the next chapter, we would like to present some solutions to the neutron diffusion equation that rely upon the values of these cross sections.

References

Books and Textbooks

1. Henry, A.F. *Nuclear Reactor Analysis*, MIT Press, Cambridge, MA (1975).
2. Stacey, W.M. *Nuclear Reactor Physics*, 2nd edn., John Wiley & Sons, New York (2007).
3. Duderstadt, J. and Hamilton, L. *Nuclear Reactor Analysis*, John Wiley & Sons, New York (1976).
4. Lewis, E. *Fundamentals of Nuclear Reactor Physics*, Academic Press, Boston, MA (2008).
5. Clark, M. and Hansen, K. *Numerical Methods of Reactor Analysis*, Academic Press, New York (1964).
6. Lamarsh, J.R. and Baratta, A.J. *Introduction to Nuclear Engineering*, Prentice Hall, Upper Saddle River, NJ (2001).
7. Lamarsh, J.R. *Introduction to Nuclear Reactor Theory*, second printing, Addison-Wesley Publishing Company, Inc., Reading, MA (1972).
8. Shultis, K. and Faw, R. *Fundamentals of Nuclear Science and Engineering*, 2nd edn., CRC Press, Boca Raton, FL (2008).
9. Masterson, R.E. *Nuclear Engineering Fundamentals: A Practical Perspective*, CRC Press, Boca Raton, FL (2017).

Web References

1. *http://en.wikipedia.org/wiki/Cramer's_rule.*
2. *http://en.wikipedia.org/wiki/Mean_free_path.*
3. *www.nuceng.ca/ep4d3/text/9-multigroup.pdf.*
4. *http://en.wikipedia.org/wiki/Neutron_transport.*
5. *http://web.mit.edu/22.54/ClassNotes/Lec14.pdf.*
6. *http://mathworld.wolfram.com/CramersRule.html.*
7. *http://en.wikipedia.org/wiki/Fick's_laws_of_diffusion.*
8. *mragheb.com/.../Neutron%20Diffusion%20Theory.pdf.*
9. *encyclopedia2.thefreedictionary.com/Diffusion+of+Neutrons.*
10. *http://en.wikipedia.org/wiki/Geometric_and_material_buckling.*
11. *neutron.kth.se/courses/reactor_physics/.../102_DiffusionEquation.pdf.*
12. *neutron.kthttp://encyclopedia2.thefreedictionary.com/Diffusion+of+Neutrons.*
13. *http://www.engr.psu.edu/cde/courses/nuce521/nuce521_chapter1_reading.pdf.*
14. *https://moodle.polymtl.ca/pluginfile.php/49389/mod_resource/content/0/week2.pdf.*
15. *https://www.nrc.gov/docs/ML1326/ML13262A068.pdf.*

Additional References

- Important physical constants used by nuclear scientists and engineers can be found in *Appendix A*.
- Unit systems and their conversion factors can be found in *Appendix B*.
- Nuclear cross sections for many important nuclear materials can be found in *Appendix C*.
- Physical properties of important nuclear materials can be found in *Appendix D*.
- Atomic masses, half-lives, and natural abundances can be found in *Appendix E*.
- Neutron diffusion coefficients and neutron mean free paths are discussed in *Appendix H*.
- Diffusion parameters for common nuclear materials are discussed in *Appendix I*.

Questions for the Student

The following questions cover the material presented in this chapter and, in some cases, previous chapters as well. They are designed to test how well the student has acquired a working knowledge of the subject matter.

1. What is the primary difference between one-group theory and multigroup theory?
2. In general, is a four-group model of neutron behavior less accurate, more accurate, or equally accurate to a two-group model?
3. What is the primary difference between two-group theory and one-and-one-half-group theory?
4. In general, is it legitimate to ignore the presence of the up-scattering terms in the coefficient matrix of the diffusion equations for a multigroup model?
5. In a four-group model of neutron behavior, what does the term ϕ_1 refer to and what does the term ϕ_4 refer to?
6. What values for the fast and thermal nonleakage probabilities can be deduced from traditional two-group neutron diffusion theory?
7. What is the ratio of the fast flux to the thermal flux in a typical light-water reactor fuel assembly?
8. In traditional two-group theory, where does the fast energy group stop and the thermal energy group begin?
9. Fill in the following sentence with the appropriate word or phrase: In the United States, the U.S. NRC used an advanced computer program called _____ to support the licensing of commercial nuclear power plants.
10. For an exactly critical homogeneous reactor of infinite size, write an expression for the ratio of the fast neutron flux to the thermal neutron flux.
11. Write the two-group neutron equations for an infinite homogeneous core where the effects of neutron leakage can be neglected.
12. How is the flux within an energy group different than the group flux?
13. In multigroup neutron diffusion theory, what does the term "down-scattering" refer to?
14. Why is using more than one energy group preferable to using just a single energy group?
15. What is a typical value for the scattering cross section $\sum_{s2\to1}$ in a two-group model?
16. What is the typical energy range for a thermal neutron in a multigroup model?
17. Suppose that the term $D_2\nabla^2\phi_2$ is set to zero in a two-group model. What does this imply?
18. Fill in the following sentence with the appropriate word or phrase: Within the nuclear business, computer programs used to analyze the behavior of nuclear reactors are sometimes called _____.
19. In a two-group model of neutron behavior, where do the fast flux and the thermal flux peak in a thermal reactor fuel assembly?
20. Suppose that we would like to find the value of the total neutron flux ϕ in a six-group model of neutron behavior. If the individual group fluxes are known, write an expression for the total neutron flux.
21. In two-group model, which version of the neutron flux peaks in the reflector?
22. For the same reactor material, which diffusion coefficient is larger in a two-group model—D_1 or D_2?
23. Which common moderating material is a more isotropic neutron scatterer—hydrogen or carbon?
24. Fill in the following sentence with the appropriate word or phrase: In high school algebra, one learns that two homogeneous algebraic equations will only have a nontrivial solution when the determinant of the coefficients _____. In matrix form, this is often expressed by invoking _____ rule.
25. Suppose that we would like to build a homogeneous, unreflected cylindrical reactor of radius R. When the reactor is exactly critical, write an expression for the material buckling for the fast energy group and an expression for the material buckling for the thermal energy group.
26. What is the fundamental assumption that is used to derive the two-group neutron diffusion equation?
27. Write down the neutron diffusion equations that describe the behavior of the neutron flux with two energy groups.
28. Does the value of ν (the number of neutrons released per fission) differ very much between the different energy groups in a multigroup model?
29. What is the typical energy range for a fast neutron in a two-group model of neutron behavior?
30. Write an expression for the thermal migration area M^2 that is valid for one-and-one-half-group neutron diffusion theory.
31. Fill in the following sentence with the appropriate word or phrase: If we can temporarily neglect the up-scattering of neutrons from the lower energy groups to the higher energy groups when we write the multigroup neutron diffusion equations in matrix form, then coefficient matrix [M] becomes _____ in shape.
32. Where does the thermal flux peak in a reactor fuel assembly?
33. What is the average cosine of the scattering angle for a fast neutron in a reactor fuel rod?

34. Write down the multigroup neutron diffusion equations in matrix form. What do the fission matrix and the scattering matrix look like?
35. What does the removal cross section Σ_{Rg} in the matrix form of the multigroup neutron diffusion equations consist of?
36. How many coupled differential equations are required to describe the neutron flux if it is subdivided into three energy groups?
37. Suppose that the neutron diffusion equations for the fast and thermal fluxes can be written as $A\phi_1 + B\phi_2 = 0$ and $C\phi_1 + D\phi_2 = 0$, where A, B, C, and D are previously known constants. Under what conditions does this set of equations have a nontrivial solution?
38. Write a mathematical expression for the neutron flux for energy group g in a multigroup model of neutron behavior.
39. In a three-group model of neutron behavior, what is the middle energy group sometimes called?
40. Fill in the following sentence with the appropriate word or phrase: In a multigroup model, the fast energy group has the _____ index, and the thermal energy group has the _____ index.
41. Name four common computer programs in widespread use today that can be used to solve the neutron diffusion equation with more than one energy group.
42. Suppose that you were put in charge of solving the neutron diffusion equations in a very large thermal water reactor. If you decided to use a two-group model to do this, which energy group would have a higher nonleakage probability—the fast group or the thermal group?
43. Write an expression for the transport scattering cross section $\sum_{trg}$ for energy group g in a multigroup model of neutron behavior.
44. In multigroup neutron diffusion theory, it is sometimes convenient to replace a reactor fuel assembly with a computational cell or a set of computational cells. In the nuclear business, what is another common name for these computational cells?
45. Fill in the following sentence with the appropriate word or phrase: Fundamentally speaking, the neutron diffusion equation is a _____ partial differential equation where the neutron leakage terms are represented by a mathematical operator called the _____ operator.
46. In a four-group model of neutron behavior, what does the fission source term F_1 look like for just the first energy group?
47. When it comes to solving the neutron diffusion equation with multiple energy groups, what is the fundamental difference between one-and-one-half-group neutron diffusion theory and two-group neutron diffusion theory?
48. Write an analytical expression that can be used to find the value of the material buckling B^2 in a modified one-group model of neutron behavior.
49. Fill in the following sentence with the appropriate word or phrase: In a _____ model of neutron behavior, all of the neutrons can be characterized by a single neutron energy or _____.
50. In multigroup theory, what is another name for the effective multiplication factor k that sometimes appears in the matrix form of the multigroup equations?
51. Fill in the following sentence with the appropriate word or phrase: Suppose that we add a fast neutron source term S_1 and a thermal neutron source term S_2 to the standard form of the two-group diffusion equations. In this case, the diffusion equations are no longer homogeneous differential equations. Instead they are called _____?
52. How many energy groups are normally used to design a fast reactor?
53. In a two-group model of neutron behavior, the fast flux peaks in the fuel and the thermal flux peaks in the moderator. In a typical thermal water reactor fuel assembly, where does the total neutron flux peak?
54. Why is a two-group model of neutron behavior so important to a reactor designer?
55. If you were asked to design a thermal water reactor using multigroup neutron diffusion theory, how many energy groups would you use?
56. In multigroup theory, what term(s) in the neutron diffusion equation represents the spatial leakage of neutrons out of each energy group?

Exercises for the Student

The following exercises are left for the student to perform.

Exercise 12.1

In multigroup neutron diffusion theory, the fast flux and the thermal flux normally have different shapes. However, in a bare homogeneous core that is not surrounded by a reflector, the shapes of the fast and the thermal flux are similar.

Suppose that the shapes of the fast and thermal fluxes in a thermal water reactor are given by the equations, where the core centerline is assumed to be at x = 0. What is the ratio of the fast to thermal flux at the center of the core? What is the ratio of the fast to thermal neutron current halfway between the center of the core and its outer boundary? From the equations given earlier, what do you think is the diameter of the core?

Exercise 12.2

In a fast reactor, the neutron diffusion coefficient in the fuel is about 10 cm, and in a thermal water reactor, the neutron diffusion coefficient in the fuel is about 1 cm. What are the mean free paths of the neutrons in the fuel rods in each case?

Exercise 12.3

In a two-group model of neutron behavior, approximately 80% of the neutrons are scattered down from the fast group to the thermal group without being absorbed. Suppose that the macroscopic scattering cross section before resonance absorption is 0.328/cm and the macroscopic thermal absorption cross section for neutrons in the thermal energy group is 0.20/cm. If the average fast neutron flux is 5×10^{13} neutrons/cm^2/s, what is the thermal neutron flux near the center of the core where the effects of neutron leakage can be neglected?

Exercise 12.4

Suppose that the fast and thermal nonleakage probabilities are given by the equations $P_{NL1} = 1/\left[1 + L_1^2 B_1^2\right]$ and $P_{NL2} = 1/\left[1 + L_2^2 B_2^2\right]$. Using typical values for these parameters, estimate the fast and thermal nonleakage probabilities for a thermal water reactor core that is 400 cm in diameter.

Exercise 12.5

Neglecting the effects of neutron leakage, it can be shown that the two-group neutron diffusion equations for an exactly critical system are

$$(\Sigma_{a1} + \Sigma_{12} - \nu_1 \Sigma_{f1})\phi_1 - \nu_2 \Sigma_{f2} \phi_2 = 0 \quad \text{(fast group)}$$

$$\Sigma_{12} \phi_1 - \Sigma_{a2} \phi_2 = 0 \quad \text{(thermal group)}$$

For these equations to hold for a critical reactor, what should the ratio of the fast flux to the thermal flux be?

Exercise 12.6

The fast flux in a thermal water reactor is 6×10^{13} neutrons/cm^2/s, and the thermal neutron flux in the same reactor core is 3×10^{13} neutrons/cm^2/s. If the macroscopic fission cross sections for a U-235 fuel rod are 0.0895 and 27.96 cm^{-1} for the fast and thermal energy groups, how many fissions occur per second in one cubic centimeter of the fuel? How many fission neutrons are released per second in this process?

Exercise 12.7

Suppose that each of the fuel rods in Exercise 12.6 contains 500 fuel pins with a total volume of 400 cm^3. If there are 200 fuel rods in a reactor fuel assembly, and it takes 30 billion fissions per second to produce one watt of thermal power, what is the thermal power output of a typical fuel assembly in this case?

Exercise 12.8

Suppose that a one-group model of neutron behavior uses a macroscopic fission cross section of 27.5 cm^{-1} and a neutron flux of 9×10^{13} neutrons/cm^2/s to calculate the reactor power level. Now suppose that we would like to use a two-group model to calculate the reactor power level where the fast neutron flux is 6×10^{13} neutrons/cm^2/s, and the thermal neutron flux is 3×10^{13} neutrons/cm^2/s. If the macroscopic fission cross sections for a U-235 fuel rod are 0.0895/cm and 27.96 cm^{-1} for the fast and thermal energy groups, what is the percentage difference in the power generation rate between the one-group model and the two-group model under these conditions?

Exercise 12.9

The smallest spatial structures in a thermal water reactor typically have a width of about 1 cm. Calculate the mean free path of a thermal neutron in a thermal water reactor fuel assembly that is similar to a PWR fuel assembly. Is the mean free path long enough for neutron diffusion theory to be used in this case?

Exercise 12.10

For a variety of reasons, fuel assemblies in fast breeder reactors are hexagonal in shape. The smallest spatial structures in these fuel assemblies tend to be the fuel rods, which have an average diameter of about 0.70 cm. Calculate the mean free path of a fast neutron in one of these fuel assemblies. Is the mean free path large enough for diffusion theory to be used in the entire fuel assembly?

13

Solutions to the Steady-State Neutron Diffusion Equation

13.1 Solutions to the Steady-State Neutron Diffusion Equation for Slab Reactor

In Chapters 11 and 12, we derived the neutron diffusion equation from first principles. We learned that it was a second order differential equation, and in general, we learned that it could be applied to problems where the neutron flux was angularly isotropic. In this chapter, we would like to apply it to several reactor geometries that are idealizations or simplifications to real reactors. These reactor geometries include rectangles, cylinders, and spheres. We will then find that exact solutions are possible for bare reactor cores that are spatially homogeneous; in other words, for cores where the material composition is independent of position. Time dependent reactors behave differently than steady state reactors do, and we will discuss their behavior in Chapters 15 and 16. When a reactor is exactly critical, the neutron population neither increases nor decreases with time, and we can set $\partial\phi/\partial t = 0$. The neutron diffusion equation then becomes

The Steady-State Neutron Diffusion Equation with a Single Energy Group

$$\nabla^2\phi(\mathbf{r}) + B_M^2\phi(\mathbf{r}) = 0 \tag{13.1}$$

This equation is called the *steady state neutron diffusion equation*. In Equation 13.1, B_M^2 is a parameter that we defined in Chapter 10 as the *material buckling* of the flux. For a single energy group, the material buckling can be written as

The Definition of the Material Buckling

$$B_M^2 = \frac{\nu\Sigma_f - \Sigma_a}{D} \tag{13.2a}$$

where Σ_f, Σ_a, and D are the *one-group* cross sections and diffusion coefficients for the material in which the neutron diffusion equation is to be solved. For a critical reactor it can then be shown that the material buckling becomes equivalent to the geometric buckling (which determines the curvature of the flux) and this allows up to write

$$\textit{Geometric Buckling} = \textit{Material Buckling}$$

$$\textit{or} \tag{13.2b}$$

$$B_G^2 = B_M^2$$

Again, it is worth mentioning that *Equation 13.2 only applies to reactors that are exactly critical and have an effective multiplication factor* of one. Time dependent reactors do not have these properties, and so for these reactors, the geometric buckling can be less than or greater than the material buckling. A reactor where the material buckling is greater than the geometric buckling is said to be a *supercritical reactor*, and a reactor where the material buckling is less than the geometric buckling is said to be a *subcritical reactor*. Both types of reactors are discussed in Chapter 15.

Now suppose that we would like to find the shape of the neutron flux in the one dimensional reactor shown in Figure 13.1. This reactor is called a "*slab reactor*" because it is an idealization of a real reactor in which all the fuel assemblies are assumed to be the same. Moreover, if the reactor is assumed to be infinitely long in the y and z directions, and has a thickness L (in cm) in the x direction, it is sometimes called an *infinite slab reactor*. If the core is spatially uniform, the values of Σ_f, Σ_a, and D become independent of position, and the material buckling becomes constant between x = –L/2 and x = +L/2. Of course, these assumptions result in a reactor that is just an idealization of a real reactor, but in reactors such as this, the neutron diffusion equation is much easier to solve. In fact,

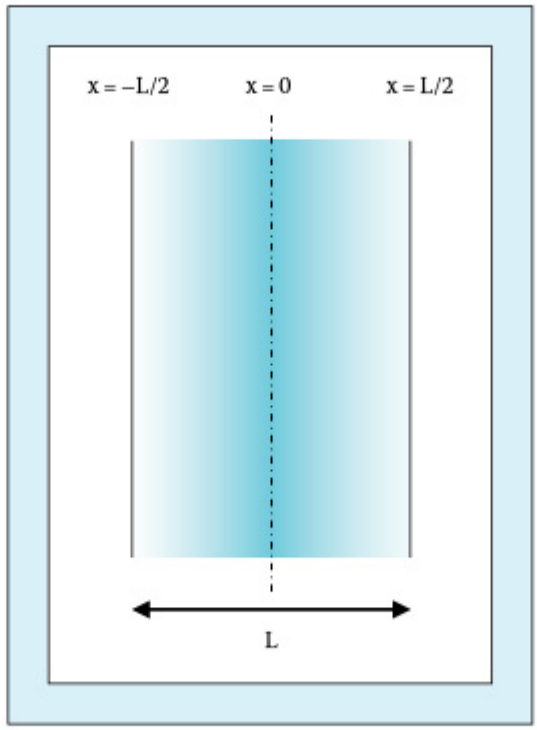

FIGURE 13.1 An infinite slab reactor of thickness L.

exact solutions can be obtained for several hypothetical reactors that meet these conditions. For such a reactor, the neutron diffusion equation becomes a second order differential equation with constant coefficients. In one dimension, we can then write the diffusion equation as

$$\frac{d^2\phi(x)}{dx^2} + B^2\phi(x) = 0 \tag{13.3}$$

where the buckling in Equation 13.3 now refers to the material buckling, and we have suppressed both subscripts to keep the notation simple. The center of the core is located at x = 0 (see Figure 13.1). To find a unique solution to Equation 13.3, we must supply it with an appropriate set of *boundary conditions*. Because Equation 13.3 is a second-order differential equation with constant coefficients, only two boundary conditions are required in this case. Assuming for the moment that the flux falls to zero at the edges of the core (where x = −L/2 and x = L/2), the first boundary condition that we need to use is

$$\textit{Boundary Condition 1} \quad \phi\left(\frac{-L}{2}\right) \text{ then } = \phi\left(\frac{L}{2}\right) = 0 \quad \text{(for the neutron flux)} \tag{13.4}$$

Furthermore, since the core is symmetrical about the origin, the neutron current can assumed to be zero at x = 0, and the second boundary condition that is required is

$$\textit{Boundary Condition 2} \quad \mathbf{J}(x=0) = \frac{d\phi}{dx} = 0 \quad \left(\text{for the neutron current}\right) \tag{13.5}$$

These two boundary conditions can then be used to guarantee that the neutron flux and the neutron current will remain continuous everywhere between x = −L/2 and x = +L/2. The general solution to Equation 13.3 is then

$$\phi(x) = A1\sin(Bx) + A2\cos(Bx) \tag{13.6}$$

where $B^2 > 0$, and A1 and A2 are constants to be determined from the boundary conditions. Since dϕ/dx = 0 at x = 0, one can quickly deduce that A1 = 0. We can therefore write the neutron flux as

$$\phi(x) = A2\cos(Bx) \tag{13.7}$$

To find the value of the second coefficient, A2, we need to apply another boundary condition on the outside surface of the reactor, which states that, $\phi(-L/2) = \phi(L/2) = 0$. Since the cosine is an even trigonometric function, it does not matter which side of the reactor is used. We can therefore conclude that

$$\phi\left(\frac{L}{2}\right) = A2\cos\left(\frac{BL}{2}\right) = 0 \tag{13.8}$$

Notice that there are two possible solutions to this equation—one where $A2 = 0$ and the other where $\cos(BL/2) = 0$. Since the former solution is the trivial one, we must conclude that

$$\cos\left(\frac{BL}{2}\right) = 0 \tag{13.9}$$

The exact value of A2 is then determined by the reactor power level (see Section 13.2). Since the cosine is a periodic function, Equation 13.9 can only be satisfied when B assumes one of the following values

$$B_n = \frac{n\pi}{L} \tag{13.10}$$

where n = 1, 3, 5, 7, etc. These discrete values for B_n are sometimes called *eigenvalues*, and the corresponding solutions of Equation 13.7 are then called *eigenfunctions*. Sometimes an eigenvalue can be used to represent the physical state of a core, and sometimes it cannot. For example, the lowest eigenvalue, n = 1, corresponds to a condition when the reactor is exactly critical and higher order eigenvalues correspond to conditions when the reactor is not (e.g., where the flux may be time dependent). Hence, it is easy to see that the one dimensional flux shape is given by

The Flux Shape for an Exactly Critical One-Dimensional Reactor

$$\phi(x) = A2\cos\left(\frac{\pi x}{L}\right) \tag{13.11}$$

This equation represents the flux shape when the reactor is exactly critical (that is, when $K_{effective} = 1$). In Chapter 15, we will then discuss how to obtain the time dependent flux shape from the time-dependent diffusion equation

Time-Dependent Diffusion Equation

$$D\nabla^2\phi + (\nu\Sigma_f - \Sigma_a)\phi = \frac{1}{v}\frac{\partial\phi}{\partial t} \tag{13.12a}$$

with and without delayed neutrons. In this case all of the other eigenfunctions, except the one corresponding to $B_n = B_1$ are time dependent, and they decay or grow at different rates depending on the value of K. The flux, which is the sum of these time dependent eigenfunctions is then

$$\phi(x) = \sum_n A_n \cos(B_n x)e^{-\lambda_n t} \tag{13.12b}$$

and it converges to the steady-state solution $\phi(x) = A2\cos(\pi x/L)$ for large values of t. The *time-dependent terms* $-\lambda_1 t$, $-\lambda_2 t$, $-\lambda_3 t$, …, $-\lambda_n t$ in Equation 13.12(b) vary in magnitude and the eigenvalues are ordered such that $\lambda_1 < \lambda_2 < \lambda_3 < \cdots < \lambda_n$, which means that only $e^{-\lambda_1 t}$ remains as $t \to \infty$, and for very large values of t, it is simply equal to 1.

Hence for steady-state problems the higher order eigenfunctions disappear, and all that we are left with is the "fundamental" eigenvalue and eigenfunction which correspond to the case where n = 1. This eigenfunction is compared to some of the higher order eigenfunctions in Figure 13.2. *Notice that the fundamental eigenfunction - $\cos(B_1 x)$ is the only eigenfunction where the flux is positive everywhere within our one-dimensional reactor*. The reader may also observe that the odd-numbered eigenfunctions are symmetrical about the center of the reactor (x = 0) while the even-numbered eigenfunctions are not. This is a consequence of what is called the *orthogonality* of the eigenfunctions, and the orthogonality

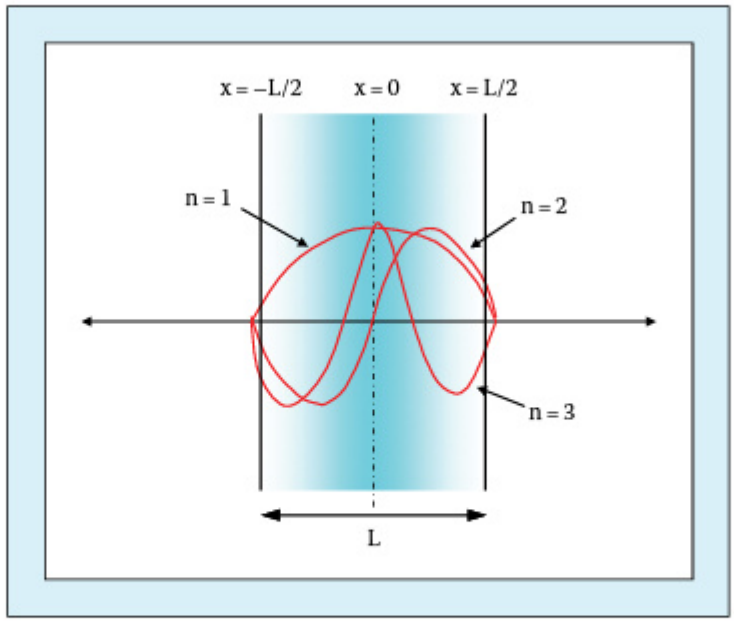

FIGURE 13.2 The eigen-functions for the solution of the neutron diffusion equation for a simple slab.

requires that the product of any two eigenfunctions will vanish when integrated over the volume of the slab, except for identical functions, in which case the result of the integral will be L/2. This requirement is embodied by the following orthogonality conditions:

The Orthogonality Condition for the Eigenfunctions

$$\int \phi_n(x)\phi_m(x)dx = 0, \quad \text{if } m \neq n$$

and (13.13)

$$\int \phi_n(x)\phi_m(x)dx = \frac{L}{2}, \quad \text{if } m = n$$

and any linear combination of the terms $\phi(x) = \sum_n A_n\phi_n(x)$ will have a similar outcome. Here the limits of integration are between x = –L/2 to x = +L/2. Finally, the reader may have noticed that we have not yet found the value of A2—which is the *magnitude of the flux* in the reactor. This is because *any* value of A2 is acceptable because of the boundary conditions we have imposed on it. To find the true value of A2 we need to know the *reactor power level*, and that is the next topic we would like to discuss.

13.2 Correlating the Power Level to the Neutron Flux

In several previous chapters (notably Chapter 7) we learned that there is a direct relationship between the neutron flux ϕ and the power level P. In other words, this relationship can be written as

$$P = c\phi\Sigma_f \tag{13.14}$$

where

P is the *thermal power* in watts

Σ_f is the macroscopic fission cross section

$c = 1/(3.12 \times 10^{10}$ fissions/watt) is the constant of proportionality (not to be confused with the speed of light) relating the flux to the power

According to Equation 13.14, about *30 billion fissions per second* are required to generate *one watt* of recoverable power. This allows us to write the spatially dependent power profile as

$$P(x) = c\phi(x)\Sigma_f(x) \tag{13.15}$$

where

$$\phi(x) = A2\cos\left(\frac{\pi x}{L}\right) \tag{13.16}$$

is the steady state flux shape. The total core power P can then be found by integrating Equation 13.15 from the left side of the slab, where x = −L/2 to the right side of the slab, where x = L/2

$$P = c\Sigma_f \int_v \phi(x)dx \tag{13.17a}$$

Upon performing the integration, we find that the value of A2 is then

$$A2 = \pi P/2cL\Sigma_f \tag{13.17b}$$

The neutron flux as a function of the power level is then

The Neutron Flux as a Function of the Power Level

$$\phi(x) = \frac{\pi P}{2cL\Sigma_f}\cos\left(\frac{\pi x}{L}\right) \tag{13.18}$$

Thus the power level is directly proportional to the flux. Since our reactor is homogeneous and symmetrical, we now know the value of the flux at any point x for a given reactor power level P. Thus we have just found our first successful solution to the neutron diffusion equation!

13.3 A Physical Interpretation for the Geometric Buckling

Earlier we promised to provide a physical explanation of what the geometric buckling represents. In an exactly critical reactor, the square of the lowest eigenvalue B_l^2 of the solution to Equation 13.1 is called the *geometric buckling* of the flux, and according to Equation 13.10, it is given by

$$B_l^2 = \left(\frac{\pi}{L}\right)^2 \tag{13.19}$$

For our hypothetical reactor (see Figure 13.3), the buckling decreases as the thickness L increases, and so as the reactor gets larger (see Figure 13.3), the buckling gets smaller. When the reactor becomes very large and L approaches infinity, B_l approaches 0, and the flux

$$\phi(x) = A2\cos(B_l x) \tag{13.20}$$

becomes uniform everywhere. In this case, it is said to have *no buckle*. *The buckling is therefore a measure of the curvature of the neutron flux*, and more the neutrons that leak out of the core, the larger the curvature will be (see Figure 13.3). Another way to deduce this relationship is to consider the one-dimensional diffusion equation

$$\frac{d^2\phi}{dx^2} + B_l^2\phi = 0 \tag{13.21}$$

and write it as

$$B_l^2 = -\frac{1}{\phi}\frac{d^2\phi}{dx^2} \tag{13.22}$$

Then Equation 13.22 represents the local *curvature*, since the curvature is proportional to the second derivative. That is,

$$Curvature = d^2\phi/dx^2/\phi$$

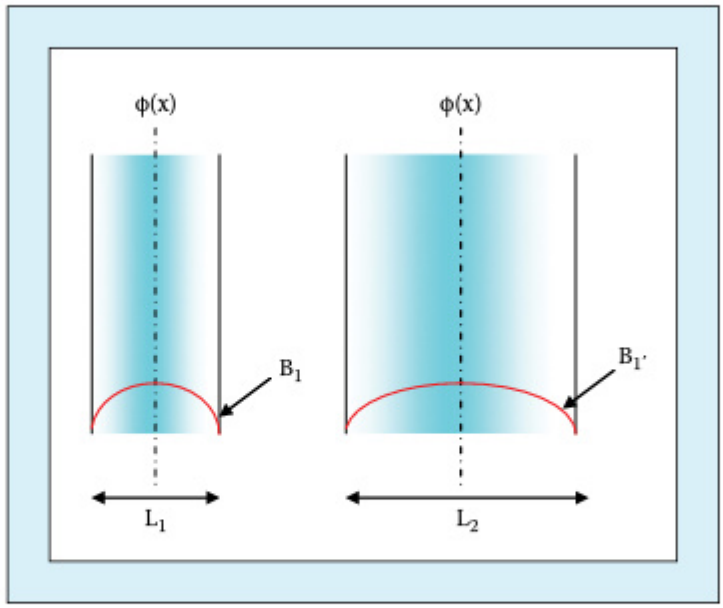

FIGURE 13.3 A physical interpretation of the geometric buckling. Notice that as the buckling of the flux increases, the curvature of the flux increases too. The neutron leakage rate can also be shown to be proportional to the size of the geometric buckling (see Equation 13.22).

Using Fick's Law to take this observation a little further

$$J = -D\frac{d\phi}{dx} \tag{13.23}$$

it is also possible to see that Equation 13.22 can be written as

$$B_1^2 = -\frac{1}{\phi D}\frac{dJ}{dx} \tag{13.24}$$

Thus the curvature of the flux is proportional to the second derivative and the first derivative of the current J. Hence the current can be finite, but this does not necessarily mean that the flux has any curvature.

Now let us explore some additional relationships between the composition of the core and the size of the core using the geometric buckling and the material buckling as our guide. For an exactly critical core, the material buckling is

Material Buckling

$$B_M^2 = \frac{\nu\Sigma_f - \Sigma_a}{D} \tag{13.25}$$

and our old friend, the geometric buckling becomes

Geometric Buckling

$$B_G^2 = \left(\frac{\pi}{L}\right)^2 \tag{13.26}$$

Equating (Equations 13.25 and 13.26) then allows us to determine what the composition of the core must be for a slab reactor of thickness L to be exactly critical. The result is

$$\left(\frac{\pi}{L}\right)^2 = \frac{\nu\Sigma_f - \Sigma_a}{D} \tag{13.27}$$

Thus Equation 13.27 leads us to conclude that a necessary and sufficient condition for our idealized reactor to be critical is

A Necessary and Sufficient Condition for the Width of a Critical Slab Reactor

$$L = \frac{\pi}{\sqrt{(\nu\Sigma_f - \Sigma_a)/D}} \tag{13.28}$$

when the material composition of the core is fixed by the values of Σ_f, Σ_a, and D. *In other words, by varying the material composition of the core, we can affect how large or small a particular reactor needs to be*. In general, the more enriched the fuel is the larger the value of $\nu\Sigma_f$ becomes in the denominator, and the smaller the core can be and still remain critical. This implies that more highly enriched cores can be smaller than more lowly enriched ones.

13.4 Design Parameters for Different Reactors

For example, Equation 13.27 can also be used to design very specialized reactors that are different than the ones that are used to produce commercial electric power. The most common example of a reactor of this type is a *military reactor*. In military reactors (and also for reactors used on space probes), physical space is at a premium and reactors can only be refueled once every 30 or 40 years. By increasing the initial enrichment of the fuel inside the core to about 95% (vs. 3% or 4% for conventional power reactors), the core of a military reactor can be made to be extremely small. (As a matter of fact, the cores of most military reactors on nuclear submarines are less than 1 m in diameter.) Hence, we have used the relationship between the geometric buckling and the material buckling to derive a very useful equation (see Equation 13.27) that can be used to determine the *critical size* of a simple, unreflected reactor. Thus as the amount of fissionable material in the denominator of Equation 13.28 gets larger, the size of the core required to achieve a critical mass gets *smaller*. Later in the chapter, we will learn that this concept can be extended to other reactors such as cylindrical and spherical ones. Thus the relationship between the geometric buckling and the material buckling (Equation 13.2(b)) determines not only how much fuel a reactor must have, but also how large it needs to be for the same amount of fuel.

Example Problem 13.1

Suppose that we would like to reduce the size of the infinite slab reactor discussed earlier by a factor of four, and still be able to remain critical. To a first approximation, how many times would we have to increase the enrichment of the fuel to obtain this effect?

Solution From the equation $L = \pi/\sqrt{(\nu\Sigma_f - \Sigma_a)/D}$, it is easy to see that $\nu\Sigma_f$ is directly proportional to the enrichment e, while the other terms have a much weaker dependence on the U-235 content of the fuel. So to a first approximation $L = \pi D/\sqrt{(\nu\Sigma_f - \Sigma_a)}$ or $L \sim 1/\sqrt{e}$, where e is the total enichment of the fuel. To reduce the value of L by a factor of 4, the enrichment must therefore be increased by a factor of 16. Of course, this assumes that $\nu\Sigma_f \gg \Sigma_a$. [Ans.]

13.5 Boundary Conditions for the Neutron Flux

Up to this time, we assumed that the neutron flux could be set equal to 0 at the edges of the core, that is, for our hypothetical reactor where $x = -L/2$ and $x = L/2$. However there are always a few neutrons that manage to leak beyond the outer boundary of the core. This means that while it is a good approximation to set the flux to zero at the edges of the core, it is not entirely correct to assume that the flux drops to 0 exactly at that point. If we were to look more closely into its behavior, we would find that diffusion theory *under-predicts* the reaction rates on both sides of the core. This can be most easily seen by plotting the real value of the neutron flux (i.e., the value that is experimentally measured) against the results predicted by diffusion theory at the reactor boundary. When we do so, we find that the flux actually continues beyond the outer surface a small distance δ, which is sometimes called the *extrapolation length* (see Figure 13.4).

This distance is generally on the order of one neutron mean free path, or in most reactors, about the length of the diffusion coefficient D. In other words, $\delta \sim D$. Measured values of D for most nuclear materials are frequently on the order of the diameter of a fuel rod (about 1 cm), and in some nongaseous materials, they can be considerably less. In a reactor core about 4 meters in diameter, this would result in an error of about one part in 365, or less than one-third of a percent. For this reason, there is very little difference between assuming that $\phi = 0$ at $x = -L/2$ and $x = L/2$, and assuming that $\phi = 0$ at $x = -(L/2 + \delta)$ and $x = (L/2 + \delta)$. In some texts, the flux offset we have just described is called *the extrapolation length*, and the boundary condition associated with it is called *the extrapolated boundary condition*. This boundary condition is

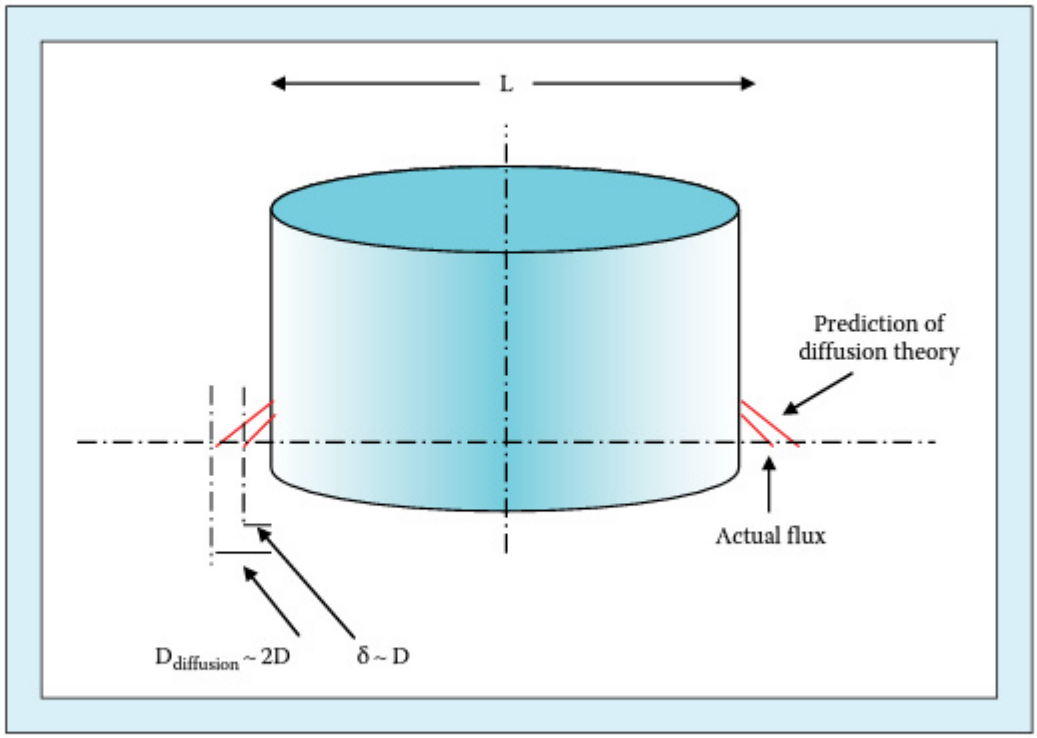

FIGURE 13.4 Various flux extrapolation schemes at a material boundary.

not to be confused with the value of δ that is predicted by neutron transport theory. The value of δ in this case is about 2.13 D. Sometimes δ is also referred to as $d_{diffusion}$.

Both cases are shown in Figure 13.4. In the remainder of this book, we will assume that the values of δ and $d_{diffusion}$ are so small that the extrapolated boundary condition can be ignored when solving the neutron diffusion equation. The sole exception to this rule is when we would like to find the thermal neutron flux ϕ_T inside of a control rod. In this case (see Chapter 11), the *extrapolation distance* δ is about $2.13D_T$ for thermal neutrons, and D_T is the *thermal diffusion coefficient* for the materials inside of the rod. Under these conditions, the rod behaves as if it is completely "black" (i.e., a *black hole*). Thus if a neutron happened to fall into it, it would have no chance that it would ever escape. Hence the extrapolation distance can be used to estimate where the flux falls to zero under these conditions.

13.6 Solutions to the Neutron Diffusion Equation in Common Reactor Geometries

Some idealized reactor geometries, such as those shown in Figure 13.5, can also be modeled using a similar approach. In each of these geometries, an exact or analytical solution to the neutron diffusion equation can be found - provided that the core is bare and homogeneous. In other words, the diffusion equation can be solved in each of these geometries to find the flux and power shape, as long as the core is spatially homogeneous. In this section, we would like to obtain some of these solutions, and show how they can be found from simple one group theory.

To keep the math as straightforward as possible, we will use the same boundary conditions that we used previously for our hypothetical slab reactor; namely, that the neutron flux ϕ falls to zero at the boundary of the core, and that the neutron current J is zero at the center the core because the flux is symmetrical about the centerline. Our solutions will only show what the neutron flux looks like in a *"bare" reactor*— that is, in one without a neutron reflector. Then in a future section, we will discuss reflected reactors, and we will show how the reflector affects the shape of the fast and thermal flux.

13.7 Understanding the Neutron Flux in a Three-Dimensional Rectangular Reactor

A *three-dimensional rectangular reactor* is similar to the infinite slab reactor we discussed earlier, except that the same procedure must be applied to the y and z directions. In this reactor, the neutron flux is a function of x, y, and z. In other words, ϕ(x, y, z). Here the neutron diffusion equation can be written as

$$\frac{\partial^2\phi(x,y,z)}{\partial x^2}+\frac{\partial^2\phi(x,y,z)}{\partial y^2}+\frac{\partial^2\phi(x,y,z)}{\partial z^2}+B^2\phi(x,y,z)=0 \tag{13.29}$$

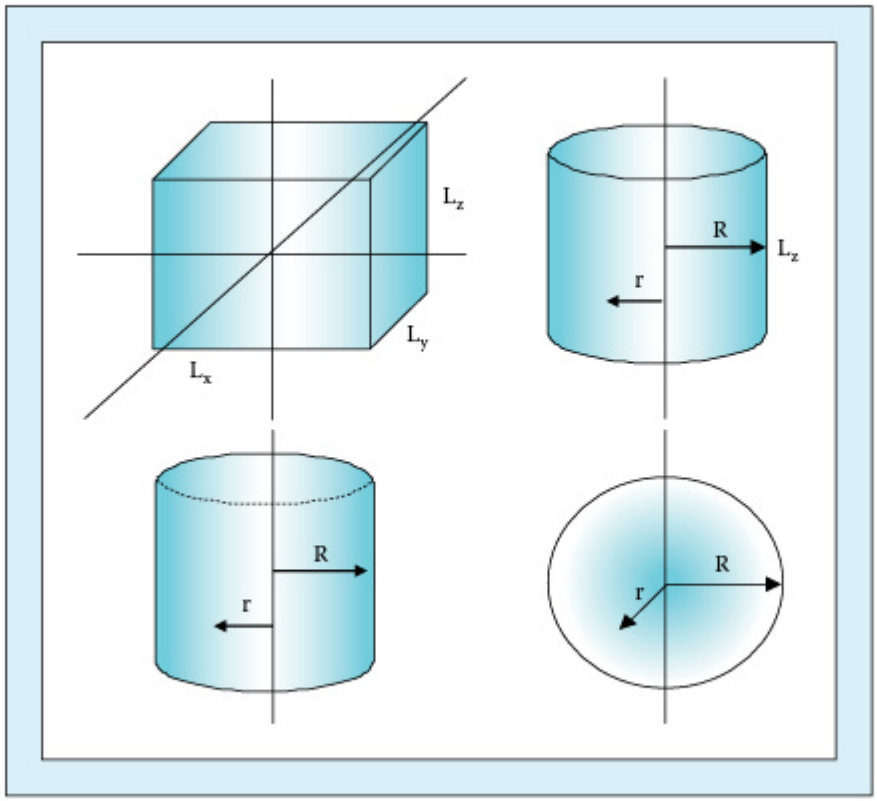

FIGURE 13.5 A few simple reactor geometries where the neutron diffusion equation can be solved in closed form.

The correct solution for the flux is then given by the product of the fluxes along each of the coordinate directions, or

$$\phi(x, y, z) = \phi_x(x)\,\phi_y(y)\,\phi_z(z) \tag{13.30}$$

where

$$\phi_x(x) = A_x \cos\left(\frac{\pi x}{L_x}\right) \tag{13.31}$$

$$\phi_y(x) = A_x \cos\left(\frac{\pi y}{L_y}\right) \tag{13.32}$$

$$\phi_z(x) = A_z \cos\left(\frac{\pi z}{L_z}\right) \tag{13.33}$$

Here again A_x, A_y, and A_z are constants that must be determined by the reactor power level, and L_x, L_y, and L_z are the dimensions of the core in the x, y, and z directions. Normally these dimensions are given in cm. This immediately leads us to conclude that the equation for the *three-dimensional flux* $\phi(x, y, z)$ is

Flux Shape in a Rectangular Reactor

$$\phi(x,y,z) = A \cos\left(\frac{\pi x}{L_x}\right)\cos\left(\frac{\pi y}{L_y}\right)\cos\left(\frac{\pi z}{L_z}\right) \tag{13.34}$$

where, as before, $A = P/(0.26c\Sigma_f L_x L_y L_z)$, and P is the total reactor power.

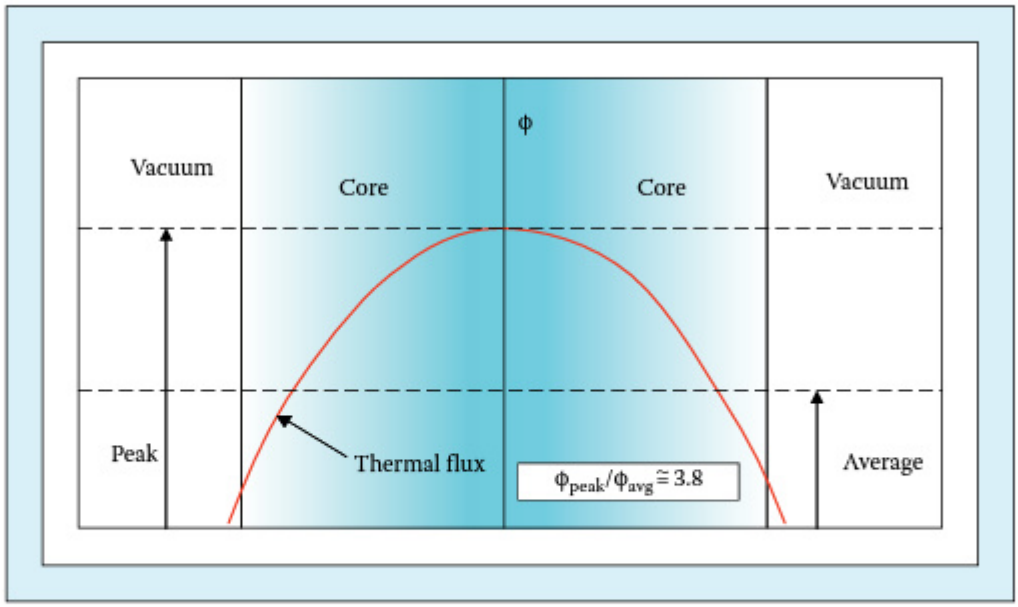

FIGURE 13.6 The flux shape in a bare rectangular reactor. The peak-to-average flux in a bare reactor that is the same size on all three sides and has no reflector is about 3.8 to 1.

Hence the key assumption we used to derive this result was that the three dimensional flux could be written as the product of the individual fluxes along each coordinate direction. This also means that the buckling of the flux is different along each coordinate direction and we can write

$$B_x^2 = \left(\frac{\pi}{L_x}\right)^2 \tag{13.35}$$

$$B_y^2 = \left(\frac{\pi}{L_y}\right)^2 \tag{13.36}$$

$$B_z^2 = \left(\frac{\pi}{L_z}\right)^2 \tag{13.37}$$

The *total buckling* B^2 is then $B^2 = B_x^2 + B_y^2 + B_z^2$. Again, all that is required is that the critical "reactor" we are attempting to model is spatially homogeneous so that the values of Σ_f, Σ_a, and D are independent of position. The shape of the neutron flux predicted by Equation 13.29 is shown in Figure 13.6. It is easy to see how this method can be generalized to other shapes and sizes by simply applying the same procedures that were used for Equation 13.30. The mathematical "trick" of decomposing the neutron flux into the product of three separate and independent functions is called the *separation of variables method.* Every multidimensional solution to the neutron diffusion equation uses some variation of it. It is also frequently applied to homogeneous reactors where the neutron flux changes with time. This then gives rise to what is known as the *point kinetics approximation*. We will explore how this process works for a time-dependent reactor in Chapter 15. Then, the general solution for the time-dependent flux is given by

$$\phi(x, y, z, t) = \left\{\phi_x(x)\,\phi_y(y)\,\phi_z(z)\right\} \cdot \phi_t(t) \tag{13.38}$$

where $\phi_t(t)$ is the expression for the time-dependent part. For a three-dimensional rectangular reactor, this then becomes

$$\phi(x, y, z, t) = \left\{A\cos\left(\frac{\pi x}{L_x}\right)\cos\left(\frac{\pi y}{L_y}\right)\cos\left(\frac{\pi z}{L_z}\right)\right\} \cdot \phi_t(t) \tag{13.39}$$

which is obviously consistent with our previous solution. A meaningful expression for the time dependent part - $\phi_t(t)$ is presented in Chapter 15. There we will use the separation of variables method to attack the time dependent diffusion equation directly.

13.8 Understanding the Flux Shape in a Three-Dimensional Spherical Reactor

A *spherical reactor* is similar to a rectangular reactor when the core is spatially homogeneous. For a completely symmetrical core without a reflector, the neutron flux is a function of the radius only, and we can write $\phi(x, y, z) = \phi(r)$. Then the steady-state neutron diffusion equation becomes

$$\nabla^2\phi(\mathbf{r}) + B^2\phi(\mathbf{r}) = 0 \tag{13.40}$$

and the only difference is that the Laplacian operator is a function r (and not θ or φ) because the core is spatially uniform. Then Equation 13.40 can be written as

$$\frac{1}{r^2}\frac{d}{dr}\left(\frac{r^2 d\phi}{dr}\right) + B^2\phi = 0 \tag{13.41}$$

or after further differentiating the first term,

$$\frac{d^2\phi}{dr^2} + \frac{2}{r}\frac{d\phi}{dr} + B^2\phi = 0 \tag{13.42}$$

Applying the same boundary conditions as we did before, namely, that $J_r = 0$ at $r = 0$, and $\phi_r = 0$ at $r = R$, we obtain the general solution

$$\phi(r) = \frac{A\sin(Br)}{r} \tag{13.43}$$

where

A is a *constant of integration*
$B = \pi/R$
R is the radius of the core

This is the general solution to the neutron diffusion equation for a spherical reactor. The shape of the flux is therefore given by

$$\phi(r) = \frac{A\sin(\pi r/R)}{r} \tag{13.44}$$

where A is another constant that is determined by the reactor power level (see Section 13.2). Using the same procedure we applied previously to find the value of A (or A2 in Equation 13.17b), we obtain

Flux Shape in a Spherical Reactor

$$\phi(r) = \frac{A\sin(\pi r/R)}{r} \tag{13.45}$$

where

$A = P/(4c\Sigma_f R^2)$
P is the total reactor power

Now let us see if we can determine the magnitude of the neutron flux

$$\phi(r) = \frac{\sin(\pi r/R)}{r} \tag{13.46}$$

at the center of the reactor, where $r = 0$. The answer, which we will simply quote here, is $\phi(0) = \pi/R$.* Therefore, the maximum value of the neutron flux (which is reached at $r = 0$) is $\pi P/(4c\Sigma_f R^3)$, where as before, P is the reactor power level (in Watts or Megawatts). Thus the maximum flux is directly proportional to the power and inversely proportional to the *cube* of the radius. The flux shape is shown in Figure 13.7. Again, there are some similarities between its shape and the shape of the flux in a rectangular core. Again we have assumed that the flux is symmetric.

* Note: This result can be easily verified by expanding the general solution $\sin(\pi r/R)$ in a Taylor series about the origin, dividing by r, and taking the limit as $r \to 0$.

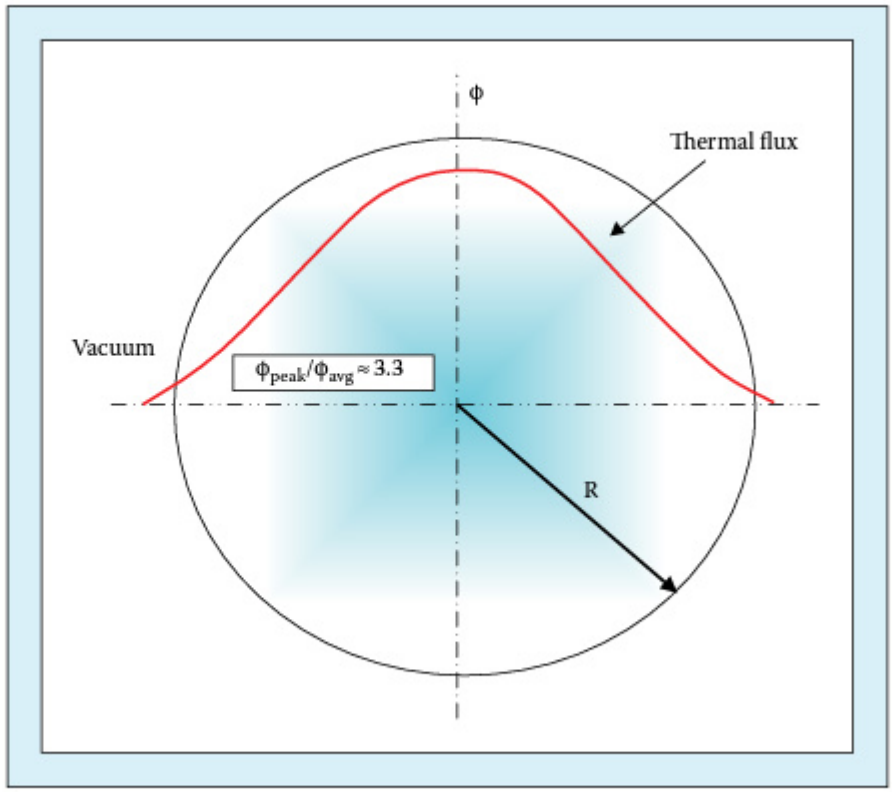

FIGURE 13.7 The flux shape in a bare spherical reactor. The peak-to-average flux ratio in this case is about 3.3 to 1.

13.9 Understanding the Flux Shape in a Three-Dimensional Cylindrical Reactor

Cylindrical reactor cores are more common than either rectangular or spherical ones. Hence, we would like to continue our study of the neutron diffusion equation by solving it for a core that is cylindrical in shape. We would first like to start out with a core of finite size, and then we would like to extend the solution to a core which is extremely long (or effectively infinite) in the axial direction. For a semi-infinite core, the geometric buckling B_z^2 is then zero in the axial direction. The easiest way to attack this problem is to solve the neutron diffusion equation for a finite cylinder of height L_z and radius R (see Figure 13.5), and to then illustrate what happens to the solution as L_z approaches infinity. Again we will assume that we are only dealing with a spatially uniform core. Substituting the appropriate form of the Laplacian into neutron diffusion equation, and differentiating the first term, we obtain the following equation for ϕ:

$$\frac{d^2\phi}{dr^2}+\frac{1}{r}\frac{d\phi}{dr}+\frac{d^2\phi}{dz^2}+B^2\phi=0 \tag{13.47}$$

Again, this is a second order differential equation with constant coefficients. Besides satisfying this equation, the neutron flux must also satisfy the usual boundary conditions; namely that $J_r = 0$ at $r = 0$, $\phi_r = 0$ at $R = 0$, and $\phi_z = 0$ at $z = L_z/2$ and $z = -L_z/2$. We will also assume that the core is spatially homogeneous so that the Laplacian has no dependence on θ.

In this case, the flux is a function of only r and z, and we can write $\phi = \phi(r, z)$. Then the diffusion equation becomes

$$\frac{\partial^2\phi(r,z)}{\partial r^2}+\frac{1}{r}\frac{\partial^2\phi(r,z)}{\partial r^2}+\frac{\partial^2\phi(r,z)}{\partial z^2}+B^2\phi=0 \tag{13.48}$$

The correct solution for the three dimensional flux can again be obtained by assuming that the flux can be written as the product of the fluxes along the r and z directions. After doing this, and applying the separation of variables method, the reader can verify that the exact solution is

$$\phi(r,z)=\phi_r(r)\,\phi_z(z) \tag{13.49}$$

where

$$\phi_r(r) = A_r J_o\left(\frac{2.405r}{R}\right) \tag{13.50}$$

$$\phi_z(x) = A_z \cos\left(\frac{\pi z}{L_z}\right) \tag{13.51}$$

and

A_r and A_z are constants determined by the reactor power level

J_o is an important new function called a *Bessel function of the first kind* (see Figure 13.8)

Bessel functions are oscillating and slightly damped functions of the argument x_o. They appear (in a slightly different form) in the *Feynman propagator* of quantum field theory and in any solution to the diffusion equation in a cylindrical coordinate system involving the Laplacian operator. They were the original brainchild of German astronomer, mathematician, and physicist

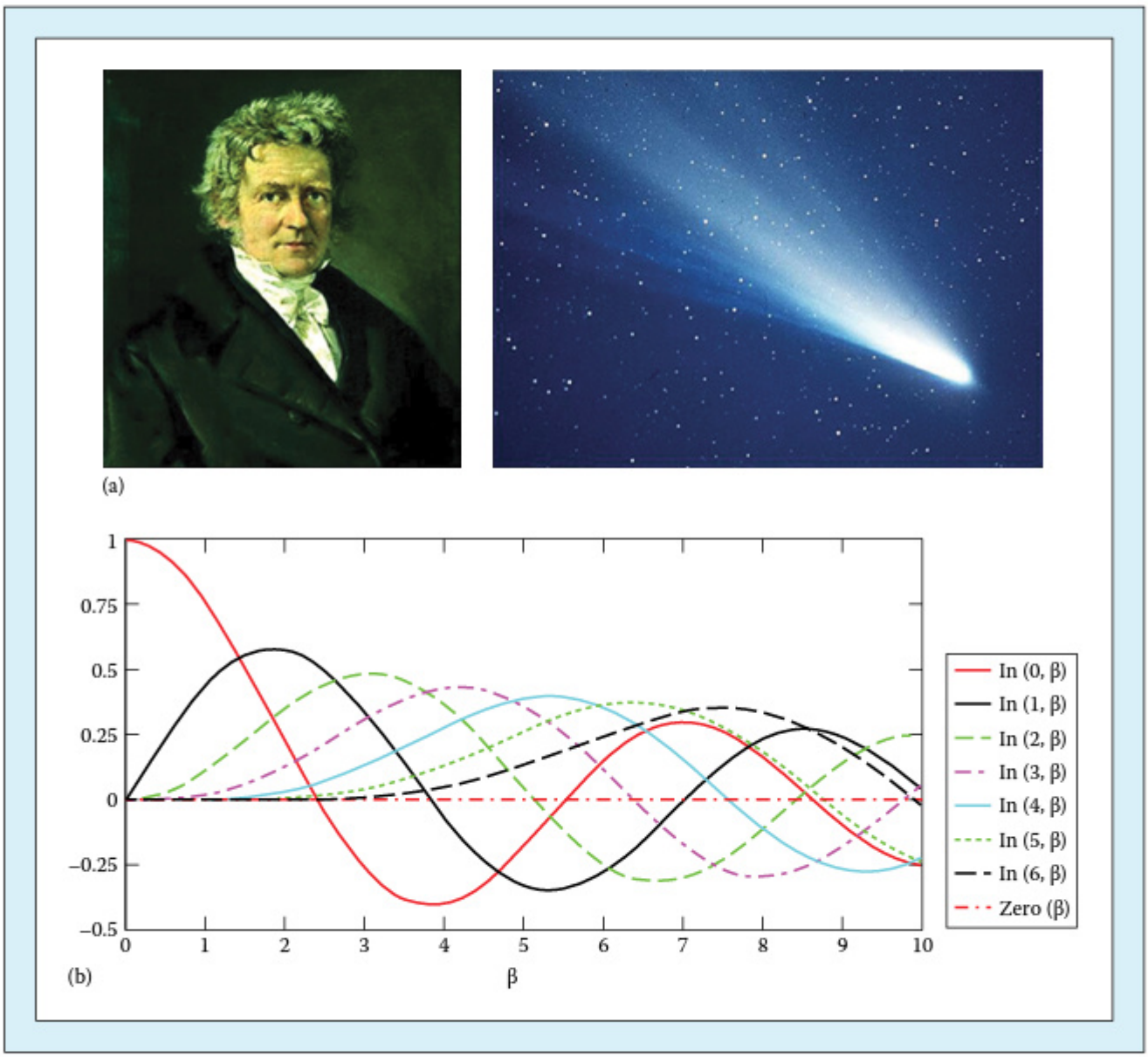

FIGURE 13.8 (a) A portrait of *Friedrich Wilhelm Bessel* on the left, and a picture of Halley's comet on the right, whose orbital path he predicted using Bessel functions of the first kind over 200 years ago. (The picture of Bessel was provided by Wikipedia and the picture of Halley's comet was provided by NASA—see NASA.gov.) (b) The shape of various Bessel functions as a function of the Parameter x_o. Note that a Bessel function of the first kind, J_o, is shown in red. Its first root is at $x_o = 2.405$. (Picture provided by Wikipedia.)

TABLE 13.1
Shape of Various Bessel Functions as a Function of the Parameter x_o

x_o	$J_o(x_o)$	x_o	$J_o(x_o)$
0.0	1	2.1	0.166607
0.1	0.997502	2.2	0.110362
0.2	0.990025	2.3	0.05554
0.3	0.977626	2.4	0.002508
0.4	0.960398	2.5	−0.04838
0.5	0.93847	2.6	−0.0968
0.6	0.912005	2.7	−0.14245
0.7	0.881201	2.8	−0.18504
0.8	0.846287	2.9	−0.22431
0.9	0.807524	3.0	−0.26005
1.0	0.765198	3.1	−0.29206
1.1	0.719622	3.2	−0.32019
1.2	0.671133	3.3	−0.3443
1.3	0.620086	3.4	−0.3643
1.4	0.566855	3.5	−0.38013
1.5	0.511828	3.6	−0.39177
1.6	0.455402	3.7	−0.39923
1.7	0.397985	3.8	−0.40256
1.8	0.339986	3.9	−0.40183
1.9	0.281819	4.0	−0.39715
2.0	0.223891		

Note: The first-order Bessel function, J_o, is shown in red in Figure 13.8. Its first root is at $x_o = 2.405$.

Friedrich Wilhelm Bessel, who first introduced them in the 1800s to make orbital predictions of the path of *Halley's comet*, which returns to the earth's vicinity about once every 75 years. Bessel's portrait, together with a picture of Halley's comet taken by the *Hubble Space Telescope*, is shown in Figure 13.8(a). Bessel functions are normally tabulated as a function of the argument x_o (not to be confused with the value of x), and* Table 13.1 shows their values for various values of x_o for a Bessel function of the first kind. Figure 13.8(b) then shows the shape of the same Bessel function from $x_o = 0$ to 4. Higher order Bessel functions called Bessel functions of the second, third, fourth, fifth, and sixth kinds are also shown in Figure 13.8(b). Notice that when $x_o = 0$, $J_o = 1$, and when $x_o = 2.405$ (which in our case corresponds to the edge of our cylindrical reactor), $J_o = 0$. This easily leads us to conclude that the equation for the neutron flux $\phi(r, z)$ in a cylindrical reactor of radius R and height L_z is

The Neutron Flux Shape in a Cylindrical Reactor of Finite Size

$$\phi(r, z) = \phi_o \cdot J_o\left(\frac{2.405r}{R}\right) \cdot \cos\left(\frac{\pi z}{L_z}\right) \tag{13.52}$$

where in this case, the magnitude ϕ_o of the flux at the origin is given by $\phi_o = P/(0.275c\Sigma_f L_z R^2)$, and as before, P is the total reactor power (in watts) and c is a conversion factor from fissions per second to watts. Hence the flux at the center of the core is directly proportional to the reactor power P and inversely proportional to the square of the radius. The *separation of variables* method also leads us to conclude that the geometric buckling is different along each coordinate direction, and as a consequence of Equation 13.52, it becomes

$$\text{For the radial direction: } B_r^2 = \left(\frac{2.405}{R}\right)^2 \tag{13.53}$$

* Bessel functions were originally used by Wilhelm Bessel to solve *Kepler's Three Laws* of planetary motion, but since then, they have been applied to many other problems in physics, mathematics, and astronomy including vibrating membranes on the surface of a drum and cylindrical heat flow. They appear almost magically when the Laplacian operator is used in a cylindrical coordinate system.

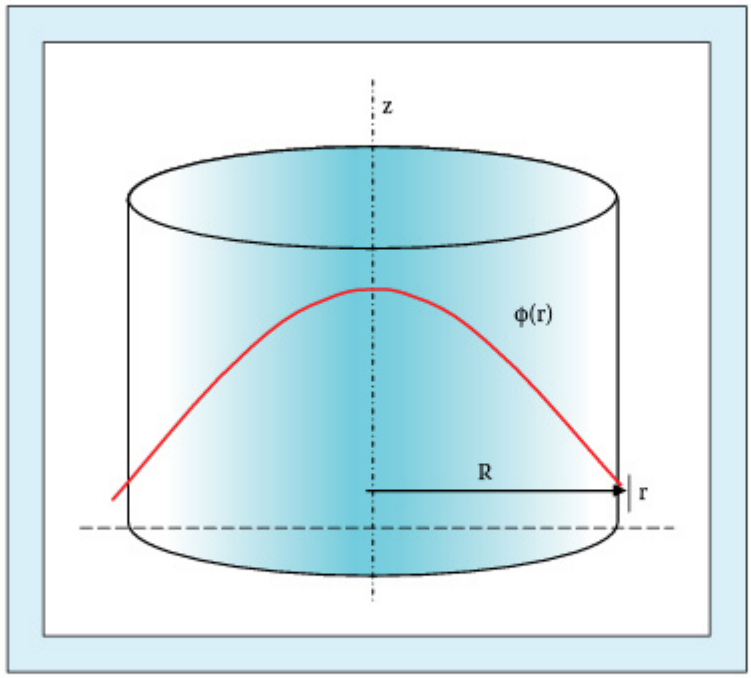

FIGURE 13.9 The flux shape in a bare homogeneous cylindrical reactor of radius R. The flux shape in the radial direction is governed by a Bessel function of the first kind, and the flux shape in the axial direction is a cosine.

and

$$\text{For the axial direction: } B_z^2 = \left(\frac{\pi}{L_z}\right)^2 \tag{13.54}$$

Then the total buckling of the core B^2 is given by

$$B^2 = B_r^2 + B_z^2 \tag{13.55}$$

The shape of the flux predicted by the Equation 13.52 is shown in Figure 13.9. If we use this same approach for a time dependent reactor, we obtain

$$\phi(r, z, t) = \phi(r, z) \cdot \phi(t) \tag{13.56}$$

where $\phi_t(t)$ is the expression for the time-dependent part.

13.10 Understanding the Flux Shape in an Infinite Cylindrical Reactor

Now suppose that we take the solution we just derived and see what happens to the neutron flux when the axial dimension L_z becomes very large, or essentially infinite. When $L_z \to \infty$, $\cos(\pi z/L_z) \to 1$, and the equation for the neutron flux becomes

The Flux Shape in an Infinite Cylindrical Reactor

$$\phi(r) = A J_o \frac{2.405r}{R} \tag{13.57}$$

Hence Equation 13.57 can be used to find the shape of the flux in an infinite cylindrical reactor of radius R. It is essentially the same as the flux shape predicted in our previous analysis, except that the axial term has now vanished and the overall buckling is different. Notice that the flux shape in the radial direction $\phi(r)$ is still given by a Bessel function of

the first kind, and that the value of the flux approaches 0 as the argument x_o approaches 2.405. Finally, it can be seen that the geometric buckling of the flux in the radial direction is now

$$B_r^2 = \left(\frac{2.405}{R}\right)^2 \tag{13.58}$$

because there is no axial component. Thus the magnitude of the flux is now given by $A = P/(1.355c\Sigma_f R^2)$, which is a different result than we obtained previously. With this expression we have basically exhausted the number of "bare" reactor configurations where an exact solution to the neutron diffusion equation can be found. In later sections, we would then like to turn our attention to how these solutions are affected by surrounding the core by a reflector.

13.11 Finding the Peak-to-Average Power Ratio in a Bare Core

It is interesting to compare the *peak-to-average power ratios* for each of the configurations we have already discussed. In these geometries, the flux reaches its maximum value at the center of the core because this is where the neutron leakage is least ($\mathbf{J} = 0$). Since we have restricted ourselves exclusively to homogeneous cores, the point where the flux is highest is also the point where the power is highest. In each of these geometries, the average power P_{avg} is equal to the total power P divided by the total core volume V_{CORE}

$$P_{avg} = \frac{P}{V_{CORE}} = c\Sigma_f \int_{V_{CORE}} \phi dV / V_{CORE} \tag{13.59}$$

where V_{CORE} is the volume of the core. The maximum power P_{max} is also given by

$$P_{max} = \phi_{max} c\Sigma_f \tag{13.60}$$

The ratio of the peak-to-average power, $R_{power} = P_{max}/P_{avg}$ is then

$$R_{power} = \frac{\{\phi_{max} c\Sigma_f\}}{\left\{c\Sigma_f \int_{V_{CORE}} \phi dV / V_{CORE}\right\}} \tag{13.61}$$

or

$$R_p = \frac{\phi_{max}}{\phi_{avg}} \tag{13.62}$$

$$\text{where } \phi_{avg} = (1/V_{CORE}) \int_{V_{CORE}} \phi \, dV \tag{13.63}$$

Recalling from our previous discussion that ϕ_{max} for a spherical reactor is $\phi_{max} = \pi P/(4c\Sigma_f R^3)$ and evaluating the appropriate integrals to find the value of ϕ_{avg} for all of the other shapes, we obtain the results shown in Table 13.2. These results are applicable to any bare homogeneous core that is not surrounded by a reflector. Notice that bare three-dimensional cores that are rectangular and cylindrical in shape have the worst peak-to-average power ratios (3.88 and 3.64, respectively), while the infinite slab and the infinite cylinder have the best. Not surprisingly, it is essential to minimize the peak-to-average power ratio to make these configurations as economically attractive as possible. Naturally, this is the next topic that we would like to discuss.

TABLE 13.2
Peak-to-Average Power Ratios for Bare Homogeneous Reactors with Different Shapes

Reactor Shape	Dimensions	Volume	Maximum Flux (ϕ_{max})	Power Ratio[1] (Peak/Average)
Infinite slab	Thickness L_x	L_x	$1.58P/(c\Sigma_f V)$	1.57
Three-dimensional rectangle	L_x, L_y, L_z	$L_x \times L_y \times L_z$	$3.88P/(c\Sigma_f V)$	3.88
Finite cylinder	R, L_z	$\pi R^2 \times L_z$	$3.63P/(c\Sigma_f V)$	3.64
Infinite cylinder	R	πR^2	$0.74P/(c\Sigma_f R^2)$	2.32
Simple sphere	R	$1.33\,\pi R^3$	$0.78P/(c\Sigma_f R^3)$	3.29

Here the constant c has the value of $c = 1/(3.12 \times 10^{10}$ fissions/watt).

13.12 Flux and Power Shaping

For several reasons, the *peak-to-average power ratios* shown in Table 13.2 are completely unacceptable for commercial power reactors. (However, they may be marginally acceptable for small research reactors.) The primary reason for this is that large values of the peak to average power ratio make it very difficult to get all of the heat out of the core, and also to burn the fuel uniformly because the fuel tends to burn faster near the center of the core than it does along the periphery. *In other words, some parts of the core run too hot, and other parts of the core run too cold.* The flux shapes for these cores are shown in Table 13.3. Thus, the power level at any point can then be found by multiplying these flux shapes by the appropriate constants in Equation 13.60. So when the burnup of the fuel is taken into account, the most economical operation of a reactor can normally be achieved when the flux within a fuel assembly, and between fuel assemblies, *is as uniform as possible*. In practice, there are three practical ways to achieve this goal of *flatness* or uniformity:

1. The first way is to *add a reflector* around the outside of the core. This has the effect of flattening the neutron flux considerably, and bringing the peak-to average-power ratios much closer to unity. In the case of a well-designed and reflected core, the flux does not fall as sharply at the fuel-reflector interface, and therefore not as much fuel is required to keep the reactor critical. This may also allow the reactor to be made smaller because the neutron leakage rate (which is proportional to the curvature of the flux) is lower in a reflected core than in an unreflected one.
2. The second way in which the power can be flattened is to *distribute the fuel nonuniformly* across the core. In other words, the concentration of fuel must be reduced in areas of high flux, and increased in areas of low flux. This allows most of the fuel assemblies to be operated at essentially the same temperature, and therefore the fuel can be burned at essentially the same rate. This contributes to improving both reactor stability and *neutron economy*.
3. Finally, the flux and power peaks can be reduced by carefully placing *burnable poisons or neutron-absorbing materials* in the core where a flux peak may occur. This again makes it possible to maximize the product of the neutron flux and the amount of fissionable material that is available locally, and thus, it makes it possible to keep the radial power profile as uniform as possible (see Figure 13.10).

In general, a flatter power distribution can almost always be obtained by placing lower enriched fuel in the center of the core and higher enriched fuel along the periphery. As we will soon discover, this implies that a reactor designer must strive to develop a reactor configuration that is not only critical but also distributes the flux and the fuel so that the power distribution is as uniform as possible. As a result, the reactor becomes easier to control, and it is also easier to remove the heat. Finally, this promotes a more uniform burnup of the fuel, which means that more energy can be extracted from each fuel assembly before it has to be replaced.

Consequently, although the solutions to the diffusion equation we have presented so far can be helpful in understanding how real reactors behave, the reader should not be fooled into thinking that real reactors can be designed in this way. In practice, reactor fuel assemblies can be very heterogeneous to thermal neutrons and reactor cores are normally surrounded by a layer of neutron reflecting material called the *reflector*. A reflector reduces the neutron leakage rate and also allows the core to remain critical with a much smaller amount of fuel. For these reasons and others, virtually all commercial thermal water reactors are surrounded by a reflector. Unfortunately, the presence of the reflector makes it harder to obtain an exact solution to the neutron diffusion equation, and even when an exact solution exists, the solution can generally not be used to perform an accurate criticality calculation.

TABLE 13.3
Neutron Flux Shapes for Different Types of Bare Homogeneous Reactors

Reactor Shape	Dimensions	Flux Shape	Value of A[a]	Geo. Buckling (B^2)
Infinite slab	Thickness L_x	$A\cos(\pi x/L_x)$	$1.58P/(c\Sigma_f V)$	$(\pi/L_x)^2$
Three-dimensional rectangle	L_x, L_y, L_z	$A\cos(\pi x/L_x)\cos(\pi y/L_y)\cos(\pi z/L_z)$	$3.88P/(c\Sigma_f V)$	$(\pi/L_x)^2 + (\pi/L_y)^2 + (\pi/L_z)^2$
Finite cylinder	R, L_z	$A\cos(\pi z/L_z)J_o(2.405r/R)$	$3.63P/(c\Sigma_f V)$	$(\pi/L_z)^2 + (2.405/R)^2$
Infinite cylinder	R	$AJ_o(2.405r/R)$	$0.74P/(c\Sigma_f R^2)$	$(2.405/R)^2$
Simple sphere	R	$A\sin(\pi r/R)/r$	$0.78P/(c\Sigma_f R^3)$	$(\pi/R)^2$

Here the constant c has the value of $c = 1/(3.12 \times 10^{10}$ fissions/watt).

[a] Peak-to-average power ratio.

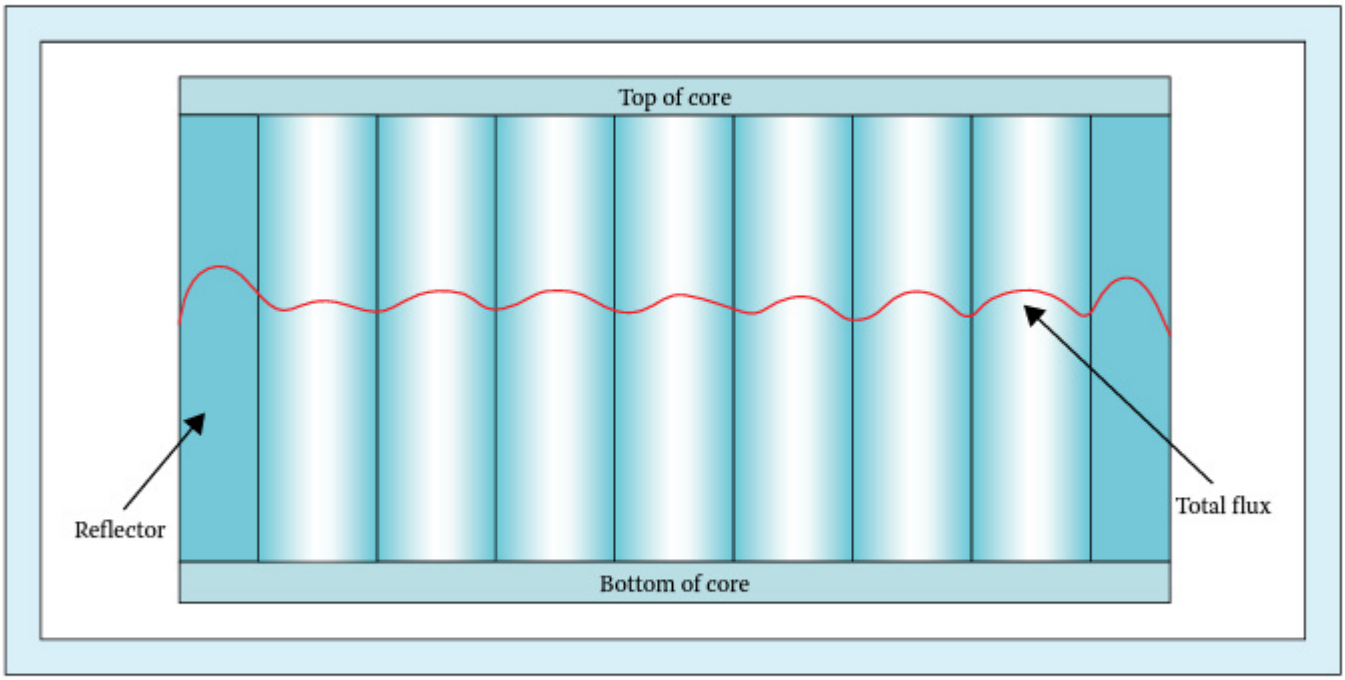

FIGURE 13.10 By nonuniformly distributing the fuel from one side of a reactor to another, one can reduce the peak-to-average power ratio and also flatten the shape of the flux. Each zone in the reactor shown here has a different enrichment, with the lighter zones being more highly enriched than the darker ones. The "handles" or peaks of the thermal neutron flux are also clearly seen in this picture as soon as one enters the reflector.

13.13 Benefits of Reflected Reactors

We mentioned briefly in the previous section that there are many benefits to having a reflected reactor core. In this section, we would like to explore some of these benefits in more detail. In addition to the fact that less radiation escapes from a reflected reactor (which is obviously quite desirable) there are three basic reasons why a reflected reactor is preferable to an unreflected one. We alluded to some of these reasons in the previous section, but we would like to expand upon them here.

First, *a reflected reactor does not have to be as large as an unreflected reactor to generate the same amount of power*. This means that a reflected reactor can be *smaller* than its nonreflected cousin if it is asked to generate the same amount of thermal energy. Of course, this means that it is less expensive to build, and even possibly to operate. Secondly, because the neutrons do not drop off as sharply at the fuel-reflector interface as they would in the case of a bare core, the peak-to-average power ratio is *lower* in a reflected reactor, and the flux shape from the middle of the core to the edge is *flatter*. *Hence the curvature of the flux in a reflected reactor is generally lower, and if the core is homogeneous, the buckling is lower as well.*

Finally, *a reflected reactor requires less fuel to achieve a critical mass than its nonreflected counterpart*. Of course, this means that less fuel is required to keep the plant running. In everyday life, this would be like saying that a smaller and more smartly designed engine would get better fuel economy than a larger, but less intelligently designed one. The same is true for reactors as well. Unfortunately, there are only three reactor geometries where analytical solutions to the neutron diffusion exist when the core is surrounded by a reflector. Naturally, they are

1. The fully reflected three-dimensional rectangular reactor (see Section 13.7)
2. The fully reflected spherical reactor (see Section 13.8)
3. The fully reflected cylindrical reactor (see Section 13.9)

In other reactor geometries, a set of transcendental equations must be solved to find the shape of the flux and the critical composition of the core. As one can imagine, these solutions can quickly become cumbersome, and it is easy to get bogged down in many unessential mathematical details. Hence, we would like to concentrate on what the corresponding solutions look like for a three-dimensional rectangular reactor and for a three-dimensional cylindrical one. We will then try to discuss the difference a reflector makes on their overall design and operation.

13.14 Flux Shapes for Fast and Thermal Neutrons in a Reflected Thermal Reactor

In reality, the solutions to the diffusion equation we have presented so far are not entirely accurate in the presence of a reflector because at least one-third of the neutrons in the core and most of the neutrons in the reflector are thermal neutrons. Moreover, the fast neutrons that diffuse into the reflector have an entirely different spatial distribution than thermal ones.

It is therefore important to find the fast and thermal flux in the core and the reflector although we will not have the analytical tools to do so until a later chapter. For a representative picture of what the fast and thermal flux look like in a reactor with a reflector, the reader should refer to Figure 13.11. One of the salient features of the flux in this figure is that *the thermal flux rises beyond the core reflector interface*, and peaks several centimeters into the reflector, while the fast flux does not. A simple one-group diffusion theory model would never allow this to occur. In other words, the rate at which thermal neutrons are absorbed in the reflector is much lower than the rate at which fast neutrons leak out of the core and become *thermalized*.

This behavior eventually causes the thermal flux near the core reflector interface to peak because the thermal neutrons have no other place to go. Thus the "reflected" neutrons must either flow back into the core where they will be absorbed by the fuel, or they must permanently stay in the reflector (or be removed from it). The thermal flux peaks in the reflector in this case are sometimes referred to as *handles*. The net effect of this thermal *"backflow"* is to flatten the thermal flux and the power distribution in the core. In order to find out how much smaller a reactor core has to be as a result of this backflow, we must again go back to our initial derivation of neutron diffusion theory and broaden our discussion to account for the backflow of these neutrons. We will begin where we left off with our original discussion of the diffusion length L, and the diffusion coefficient D in Chapter 11. Only this time, we must broaden these definitions to account for the fact that we are dealing with both thermal and fast neutrons.

13.15 Defining the Reflector Savings and the Albedo

Simply put, the *reflector savings* is a measure of how much the size of a reactor core can be reduced *in each dimension* if it is surrounded by a neutron reflecting material. The fraction of the neutrons that are reflected back into the core by the reflecting material is called the *reflection coefficient* or the *albedo*.

In particular, the *albedo* α is defined as the ratio of the neutron current flowing out of the reflecting region to the neutron current flowing into the reflecting region:

Definition of the Albedo

$$\alpha = J_{out}/J_{in} \tag{13.64}$$

If we know the current J_{in} entering a planar reflecting surface, we can solve the neutron diffusion equation within the reflecting region

$$d^2\phi/dx^2 - \left(1/L^2\right)\phi(x) = 0 \tag{13.65}$$

subject to the condition that $J = J_{in}$ at the inner surface and $\phi = 0$ at the outer surface. We can then solve for the neutron flux shape in the reflector and use this solution to compute the albedo as a function of the reflector's thickness W. A hypothetical reflector is shown on the left hand side of Figure 13.12 and the value of the albedo is shown on the right. The equation for the albedo is

$$\alpha(x) = \left[1 - (2D/L)\coth(x/L)\right]/\left[1 + (2D/L)\coth(x/L)\right] \tag{13.66}$$

where D is the diffusion coefficient and coth is the *hyperbolic cotangent* function. If the width of the reflector is W, the value of the albedo becomes

$$\alpha = \left[1 - (2D/L)\coth(W/L)\right]/\left[1 + (2D/L)\coth(W/L)\right] \tag{13.67}$$

Next suppose that we plot the albedo as a function of the thickness W of the reflector. The result is shown on the right hand side of Figure 13.12. For thin reflectors, only a few of the neutrons are reflected back into the core, and the albedo is small. However, as the reflector becomes thicker, the albedo approaches an *asymptotic limit* that depends on only the value of the diffusion coefficient D and the diffusion length L:

$$\alpha = \left[1 - (2D/L)\right]/\left[1 + (2D/L)\right] \tag{13.68}$$

Using representative one group values for D and L, the asymptotic albedos for light water, heavy water, and graphite are 0.82, 0.97, and 0.93, respectively. These values are normally reached when the reflector becomes 6–9 inches, or 15–23 cm thick. It is also possible to use the albedo to create an *effective boundary condition* for the reflected flux at the edge of the core (where x = 0). This boundary condition is

$$(D/\phi)\,d\phi/dx = -(1/2)\left[(1-\alpha)/(1+\alpha)\right] \quad (\text{at } x = 0) \tag{13.69}$$

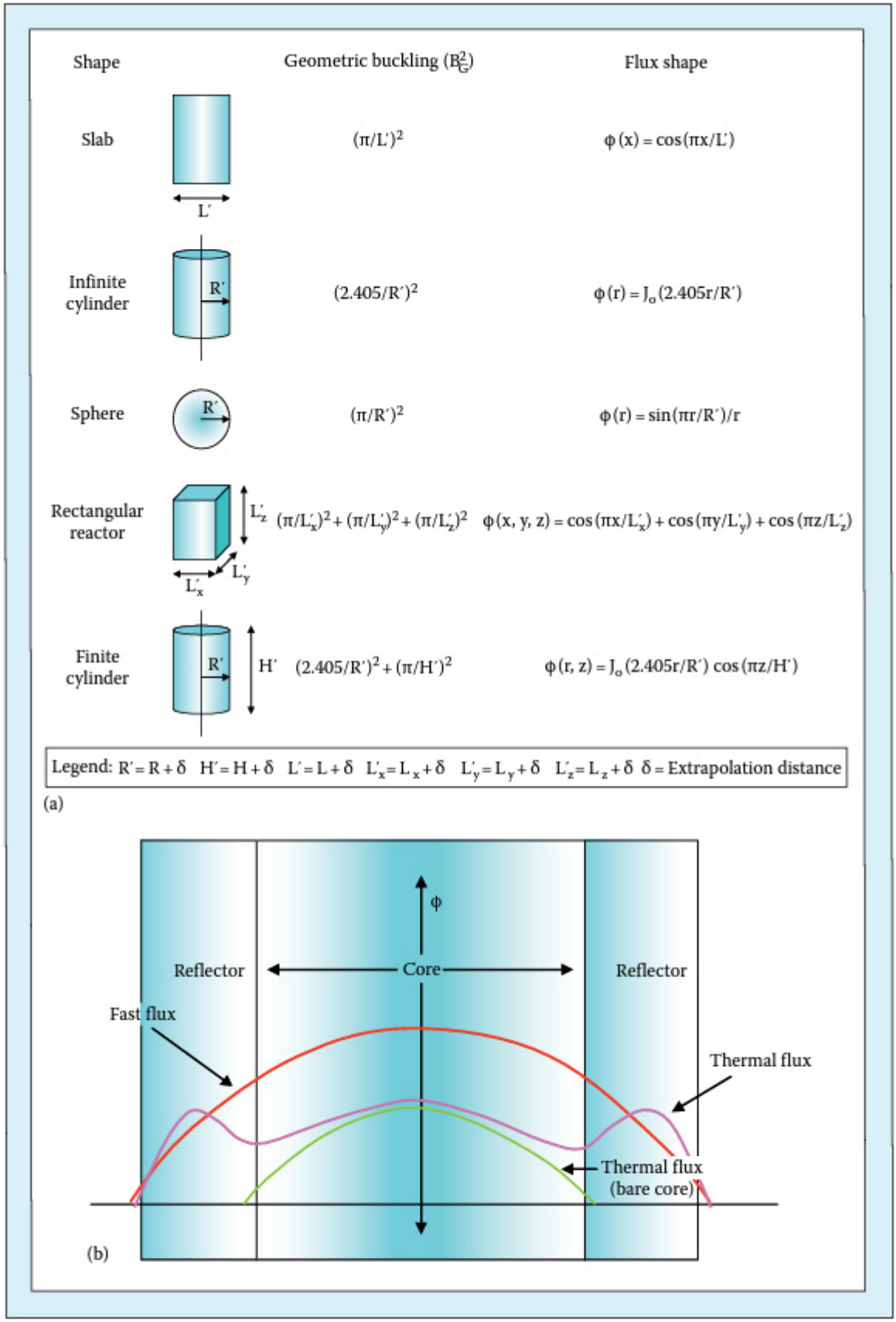

FIGURE 13.11 (a) The flux shapes and the values of the geometrical buckling in a number of different bare homogeneous reactors without a reflector. (b) The fast and thermal neutron flux in the vicinity of a neutron reflector. In this case, the fast flux peaks in the core and the thermal flux peaks in the reflector.

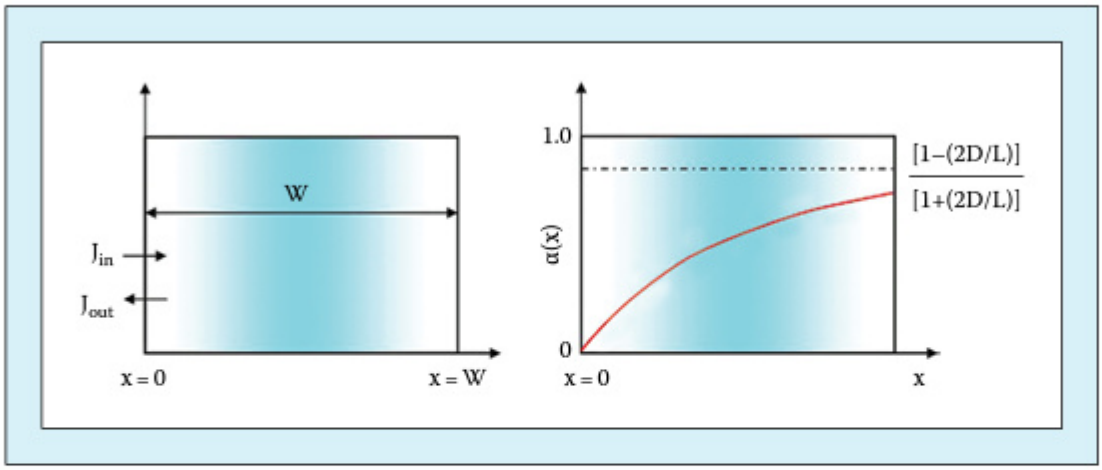

FIGURE 13.12 A reflecting material of width W (on the left), and the albedo α as a function of the thickness of the material on the right. Notice how the albedo approaches an asymptotic limit that is dependent on the material properties of the reflector (D and L) when the reflector becomes very thick. *This phenomenon is used reduce the size of many commercial reactor cores* by reducing the neutron leakage rate, and hence improving overall neutron economy.

Thus the value of the albedo can be used to obtain a boundary condition that can be applied to the edge of the core. The reader may recall that this is similar to using the extrapolated boundary condition for the neutron flux in the vicinity of a control rod (see Chapter 11). Only in this case, most of the neutrons are reflected back into the core.

There are several empirical expressions that can be used to calculate the reflector savings if we know both the material composition and the geometry of the core and the reflector. In our initial study of neutron diffusion theory (see Section 11.6), we learned that the *diffusion length* L could be written as $L = \sqrt{D/\Sigma_a}$, and the *diffusion area* L^2 could be written as $= D/\Sigma_a$, where D and Σ_a were the one-group neutron diffusion coefficient and the one-group neutron absorption cross section respectively. However, when it comes to reflected reactors it is necessary to separate the neutron flux into at least two energy groups (fast and thermal) to get the correct reaction rates.

It should come as no surprise from our initial discussion of diffusion theory for a reflected reactor (see Figure 13.11) that the predictions of two-group theory are considerably different than the predictions of one-group theory. In particular, it is necessary to use different diffusion coefficients for each energy group—D_f for fast neutrons, and D_t for thermal neutrons to obtain really accurate results. Moreover, this means that the diffusion length and the diffusion area for fast neutrons are different than they are for thermal neutrons. However, the fast to thermal diffusion area $D_f/\Sigma^s_{f->t}$ has an additional physical significance because it can be shown that it is related to the distance $L_{f->t}$ required for a neutron to slow down from fast energies to thermal energies. Historically, this parameter has become known as the *neutron age* τ because it can be shown to be a function of how long it takes a fast neutron to slow down. Hence, the neutron age can be defined as

Definition of the Neutron age

$$L^2_{f->t} = D_f/\Sigma^s_{f->t} \tag{13.70}$$

and the age has the units of area or length squared. Normally the neutron age is expressed in square centimeters. Thus the fundamental relationships between fast and thermal neutrons as they slow down are

Defining the Diffusion Length for Fast and Thermal Neutrons

$$L_f = \sqrt{\frac{D_f}{\Sigma_{af}}} \quad \text{and} \quad L^2_f = \frac{D_f}{\Sigma_{af}} \quad \text{(for fast neutrons)}$$

and

$$L_t = \sqrt{\frac{D_t}{\Sigma_{at}}} \quad \text{and} \quad L^2_t = \frac{D_t}{\Sigma_{at}} \quad \text{(for thermal neutrons)} \tag{13.71}$$

and

$$L_{f->t} = \sqrt{\frac{D_f}{\Sigma^s_{f->t}}} \quad \text{and} \quad L^2_{f->t} = \frac{D_f}{\Sigma^s_{f->t}} \quad \text{(for neutrons in transition)}$$

TABLE 13.4
Neutron Diffusion Parameters for Several Common Moderators

Moderating Material	Thermal Diffusion Coefficient D (cm)	Thermal Diffusion Length $L_t = \sqrt{D_t/\Sigma_a}$ (cm)	Fast to Thermal Diffusion Length $L_{f->t} = \sqrt{D_f/\Sigma^s_{f->t}}$ (cm)	Thermal Diffusion Area L_t^2 (cm²)	Fast to Thermal Diffusion Area (The Neutron Age τ) $L^2_{f->t}$ (cm²)	Modified Thermal Migration Area $M^2 = L_t^2 + L^2_{f->t}$
H_2O	0.160	2.85	5.20	8.10	27	35.1
D_2O	0.870	96.9	11.45	9409	131	9540
Graphite	0.840	58.9	19.18	3480	368	3848
Beryllium						582

Table 13.4 shows the values of these parameters for light water, heavy water, and graphite in the thermal energy range, as well as the corresponding values for the neutron age τ. Armed with these values, many routine calculations concerning the behavior of thermal neutrons can be performed. Moreover, it can be seen (with the notable exception of water) that the neutron age is less than L_t^2 for most other moderators. In fact, it is much less than L_t^2 for D_2O or graphite.

Now let us see if we can use these parameters to show how a reflector can affect the size of a critical core. You may recall from our previous discussion that *reflected reactors are always smaller than nonreflected ones*. This is because fewer neutrons leak out of the core when it is surrounded by a reflector, and more neutrons are therefore available to be absorbed by the fuel. For any common geometric shape, we can call the unreflected critical core size L, R, or H, and the reflected critical core size L′, R′, or H′. The *reflector savings* for a rectangular reactor along any side of the reactor L = L_x, L_y, L_z is then

$$\Delta L = L - L' \quad (\text{per side for a rectangular reactor}) \tag{13.72}$$

and similarly for cylindrical reactors

$$\Delta R = R - R' \quad (\text{per side for a cylindrical reactor}) \tag{13.73}$$

and

$$\Delta H = H - H' \quad (\text{per side for a cylindrical reactor}) \tag{13.74}$$

and finally for spherical ones

$$\Delta R = R - R' \quad (\text{from the center point of a spherical reactor}) \tag{13.75}$$

In Equation 13.74, H refers to the *core height*. When neutron diffusion theory was first devised, several empirical expressions were developed to calculate the reflector savings. In the 1960s, *R.W. Deutsch* developed the most famous empirical expression for the reflector savings, and it is particularly suitable for finding the reflector savings in water and water-moderated reactors. The exact expression for the reflector savings (per side) is

The Deutsch Equation for the Reflector Savings (for Light-Water Reactors)

$$\Delta L = 7.2 + 0.1\left(M^2 - 40\right)\ (\text{cm}) \tag{13.76}$$

where M^2 is called the modified *thermal migration area*. The modified thermal migration area is defined by

$$M^2 = L^2_{f->t} + L_t^2 \tag{13.77}$$

which of course uses the definitions we presented previously. The extent that the core size can be reduced depends on the materials used in the reflector. If the reflector is made from a material other than light water, then a different expression is needed to calculate the reflector savings. The reflector savings for heavy-water, beryllium, and graphite can be found using the following equation:

Reflector Savings (for Other Reactors)

$$\Delta L = \frac{D_{CORE}}{D_{REFLECTOR}} \times L_{T\ REFLECTOR} \tag{13.78}$$

TABLE 13.5
Reflector Savings for Four Common Reflector Materials

Thermal Diffusion Coefficient D Core (cm)	Thermal Diffusion Coefficient D Reflector (cm)	Thermal Diffusion Length (Moderator in Reflector) L_T (cm)	Reflector Savings Equation 13.71 ΔL (cm)	Reflector Savings (Deutsch) ΔL (cm)
0.538 (U-233)	0.160 H_2O	2.85 H_2O	9.44	6.7
0.498 (U-235)	0.870 D_2O	96.9 D_2O	55.69	N/A
0.780 (U-238)	0.840 Graphite	58.9 Graphite	54.78	N/A
0.883 (Pu-239)	0.562 Beryllium	21 Beryllium	33.00	N/A

where

D_{CORE} is the average diffusion coefficient of the core
$D_{REFLECTOR}$ is the average diffusion coefficient of the reflector
$L_{T\,REFLECTOR}$ is the *thermal diffusion length of the reflector*

Equation 13.78 can also be used if the reflector is made out of a material like stainless steel, zirconium, or lead. For this equation to be used with confidence, the reflector must be at least a few diffusion lengths (or mean free paths) thick. Obviously, reflectors are most efficient when they are made from materials with a low atomic weight. However, it is not absolutely necessary that they should be so. The reflector savings ΔL for four common moderator-fuel combinations is shown in Table 13.5.

Notice that there is a considerable difference in the reflector savings that each equation implies. In practice, the most accurate results can be obtained by solving the two-group neutron diffusion equation in the reflector geometry of interest, and then validating the results by performing an experiment. Depending on the type of moderating material, the reflector savings can be significant. For example, plugging in the values of $L_{f->t}$ and L_t for a water-moderated reactor from Table 13.3, the reflector savings turns out to be about 6 cm (per side). In the case of graphite-moderated reactors, the reflector savings is about 55 cm, or about 1.5 feet (per side). Of course, in order for Equation 13.78 to be used, the reflector surrounding the core must be at least several diffusion lengths thick. For all practical purposes, commercial power reactors have reflectors several times thicker than this, and it can therefore be assumed that their reflectors are effectively infinitely deep. The values of the albedo presented earlier in the section can then be used.

13.16 Deriving the Reflector Savings from the Diffusion Equation

Most reactors have both radial and axial reflectors. In light-water reactors, each of these reflectors is between 15 and 25 cm thick. When the thickness of a reflector increases beyond this point, it tends to have almost no additional effect on the value of the reflector savings ΔL because the neutrons simply do not diffuse any further into the reflector to be redirected. In other words, beyond a certain point, the increase in $K_{effective}$ of the core is no longer linear with a corresponding increase in the thickness of the reflector. We can estimate the size of this effect by solving the neutron diffusion equation in the materials shown in Figure 13.13. Let us assume again that we are dealing with a simple planar reactor, but in this case, we have decided to surround the core with a reflector of width T on both sides. Again, the reflector does not contain any neutron multiplying material. The relevant diffusion equations we must solve are

Diffusion Equations for the Core and the Reflector

$$\textbf{Core:}\quad \frac{D^C d^2\phi^C}{dx^2} + (\nu\Sigma_f^C - \Sigma_a^C)\phi^C = 0 \quad 0 \le x \le \frac{L}{2}$$

$$\textbf{Reflector:}\quad \frac{D^R d^2\phi^R}{dx^2} - \Sigma_a^R\phi^R = 0 \quad \frac{L}{2} \le x \le \frac{L}{2} + T + \delta \tag{13.79}$$

where δ is the extrapolation length (where the flux falls to zero) in cm. To keep the terminology simple, we will refer to all of the materials in the core with the superscript "C" and all of the materials in the reflector with the superscript "R." We will again suppress the time-dependent terms because we are dealing with an exactly critical system. Just as we have done before, we seek a solution to the neutron diffusion equation in each region of the reactor that has a different material composition. We will then use the boundary conditions to stitch together the solutions for each region. Notice that we only have to solve the

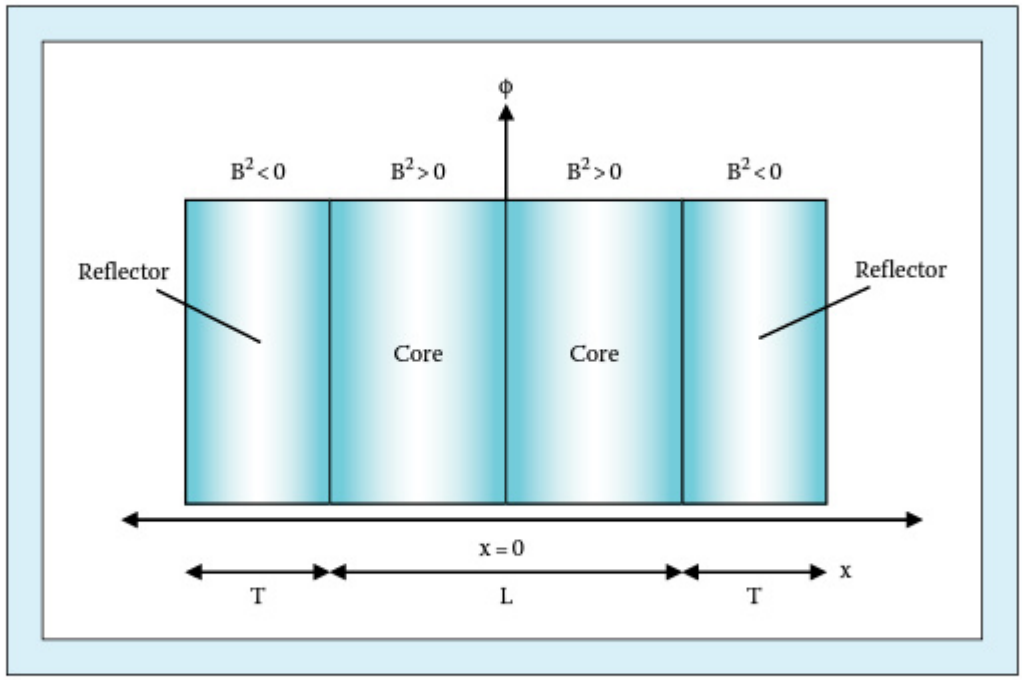

FIGURE 13.13 A simple homogeneous reactor core surrounded by a reflector.

diffusion equation to the right of the origin (x = 0) because the reactor is symmetrical. Based on our previous experience, we must then solve the diffusion equations subject to the following requirements that are imposed by the boundary conditions:

$$\text{(I)} \quad \phi^C\left(\frac{L}{2}\right) = \phi^R\left(\frac{L}{2}\right) \tag{13.80}$$

$$\text{(II)} \quad J^C\left(\frac{L}{2}\right) = J^R\left(\frac{L}{2}\right) \tag{13.81}$$

$$\text{(III)} \quad \phi^R\left(\frac{L}{2} + T + \delta\right) = 0 \tag{13.82}$$

In this case, we have assumed that the flux falls to zero a short distance δ beyond the outer boundary of the reflector; hence the flux ϕ^R falls to 0 at $x = L/2 + T + \delta$. In many reactor physics books, this distance is called the *vacuum boundary condition* because it stipulates where the flux falls to zero in a reflected or unreflected reactor surrounded by a vacuum.

Because the reactor is exactly critical, we will assume that we have chosen the correct combination of core composition and size to avoid any of the higher order eigenvalues in the solution to the diffusion equation (see Section 13.1). We will then assume that the neutron flux in the core has the following shape:

$$\phi^C(x) = A^C \cos B^C x \tag{13.83}$$

where the material buckling is given by

$$(B^C)^2 = \frac{\nu\Sigma_f^C - \Sigma_a^C}{D^C} \tag{13.84}$$

Moreover, we will assume that the shape of the flux in the reflector is given by

$$\phi^R(x) = A^R \sinh\left[\frac{L/2 + T + \delta - x}{L^R}\right] \tag{13.85}$$

where again $L^R = \sqrt{\left(D^R/\Sigma_a^R\right)}$ is the neutron diffusion length in the reflector. When we apply the boundary conditions at x = L/2, we obtain the following equations for the neutron flux and current:

$$\text{Flux:} \quad A^C \cos\left(B^C \frac{L}{2}\right) = A^R \sinh\left[\frac{T+\delta}{L^R}\right] \tag{13.86}$$

$$\text{Current:} \quad D^C B^C A^C \sin\left(B^C \frac{L}{2}\right) = \frac{D^R A^R}{L^R \cosh[(T+\delta)/L^R]} \tag{13.87}$$

After dividing the first equation by the second, we can cancel both A^C and A^R to obtain

$$D^C B^C \tan\left(B^C \frac{L}{2}\right) = \frac{D^R}{L^R \coth[(T+\delta)/L^R]} \tag{13.88}$$

This is a *transcendental equation* that represents a mathematical relationship between the size of the reactor (L, T) and the composition of the core (D^C, B^C, D^R, L^R), which must always be satisfied if a solution to the steady-state neutron diffusion equation is to be obtained. This equation can also be written as

$$L = \frac{1}{B^C} \tan^{-1}\left\{\frac{D^C B^C L^R}{D^R \tanh[(T+\delta)/L^R]}\right\} \tag{13.89}$$

which after some work can be solved to find the value of L when $T \approx 0$, and when $T \to \infty$. The difference in ΔL between these two extremes then becomes the analytical expression for the reflector savings:

$$\Delta L = L - L' \tag{13.90}$$

where L is the thickness of the core when $T \approx 0$, and L′ is the thickness of the core when $T \to \infty$. Notice that the core will always be *smaller* and still remain critical when $T \to \infty$ than when $T \approx 0$. *In other words, a reflected core will always be smaller than an unreflected one having the same composition*. *For a very thick reflector* $T \gg L^R$ and the expression for the reflector savings reduces to

$$\Delta L \approx \frac{D^C}{D^R} L^R \tag{13.91}$$

which is consistent with the expression we presented earlier in the chapter. Equation 13.91 represents the *maximum reflector savings* ΔL_{MAX} that is possible as long as the reactor (which is now defined as the core + the reflector) is in a critical state. Notice that the reflector savings depends on only the ratio of the diffusion coefficients in the core and the reflector, which are then multiplied by the diffusion length L^R for the neutrons in the reflector. As we have seen, the diffusion length is the *thermal diffusion length* shown in Table 13.5. Let us examine the implications of Equation 13.91 to see how important the reflector savings can be.

Suppose that we have a uranium-fueled light-water reactor with $D^C \approx 0.780$ cm (for U-238), and a reflector made out of ordinary water where $D^R \approx 0.160$ cm. Since the thermal neutron diffusion length in light water is $L^R \approx 2.85$ cm, the maximum possible value of the reflector savings that can be achieved from Equation 13.91 is about $\Delta L \approx (D^C/D^R)L^R = (0.780/0.160) \times 2.85 = 13.9$ cm (or about 6 inches). Notice that this is roughly twice the value of 6.7 cm implied by the *Deutsch* equation (Equation 13.76). The reason for this is that *the Deutsch equation applies to only a single side of a reactor*, while the equation we have derived for ΔL, that is,

$$\Delta L = \frac{D^C}{D^R} L^R \tag{13.92}$$

applies to both sides of a reactor (e.g., the entire core). Multiplying the result presented by Deutsch by 2, we obtain $\Delta L = 2 \times 6.7$ cm = 13.4 cm. This compares favorably with the value of 13.9 cm. we just derived from Equation 13.91. However, the equation we derived for the reflector savings $\Delta L = (D^C/D^R)\, L^R$ is more general because it can be applied to *any* critical system where the material composition of the core and reflector known. For example, it can be applied to

light-water reactors as well as reactors where the reflector is made out of heavy water, beryllium, or graphite. All that we need to know are the values of D^C, D^R, and L^R. *Thus, this exercise has shown us that a reactor surrounded by a reflector will always be smaller and will always require less fuel than a reactor with a bare core*. In future sections, we would like to explore the amount of fuel that can be saved, or the *fuel savings* when a neutron reflector is used. It is not unusual for the amount of fuel required for a reactor to become critical can be reduced by 40% to 60%. Because uranium and other nuclear fuels are relatively expensive, surrounding the core by a reflector made out of a ubiquitous material like water is a very prudent thing to do. That is why virtually all light-water reactors today use water-based reflectors.

13.17 Predicting the Size of a Critical Reactor

Furthermore, it turns out that there is a rather remarkable relationship between the value of the buckling and the size of a critical reactor. If we know the material composition of the core (from our knowledge of the diffusion coefficient and the cross sections), then the buckling will enable us to determine how large a reactor must be in order to achieve a critical mass. For example, in the case of a spherical reactor, the geometric buckling is

$$B_G^2 = \left(\frac{\pi}{R}\right)^2 \tag{13.93}$$

We also know that the material buckling is given by

$$B_M^2 = \frac{(\nu\Sigma_f - \Sigma_a)}{D} \tag{13.94}$$

From our previous knowledge of diffusion theory, we also know that the one condition for which $K_{effective} = 1$ is always true is when the material buckling of a homogeneous core is equal to the geometric buckling. So equating Equations 13.93 and 13.94, we obtain

$$\left(\frac{\pi}{R}\right)^2 = \frac{\nu\Sigma_f - \Sigma_a}{D} \tag{13.95}$$

or solving for the critical radius R,

$$R = \frac{\pi}{\sqrt{(\nu\Sigma_f - \Sigma_a)/D}} \tag{13.96}$$

Equation 13.96 implies that if we know the values of the macroscopic cross sections (and therefore the material composition), then we also know the value of the critical radius R. Moreover, different materials will have different values for their cross sections, so an entire distribution of *critical sizes* (and hence *critical masses*) is theoretically possible. Now we would like to explore the consequences of this for one-group theory. Using a similar approach to the one we just presented, it can also be shown that the critical dimensions for a bare homogeneous sphere and a bare homogeneous cube are

Critical Dimensions for a Sphere and a Cube

$$R = \frac{\pi}{B_G} \quad \text{(for a sphere)}$$

$$L = \frac{\pi\sqrt{3}}{B_G} \quad \text{(for a cube)} \tag{13.97}$$

where B_G^2 is the geometric buckling for the one-group flux. Now let us discuss how these equations work when two energy groups are used. The primary implication of adding a second energy group is that the value of the buckling changes because we now have to deal with the buckling of the fast neutrons B_F^2, as well as the buckling of the thermal neutrons B_T^2. Conceptually, these two values can be very different from one another, especially when we are dealing with a thermal reactor with a reflector. Consequently, the flux shape for each energy group diverges at the reflector (see Figure 13.11), and the fast and thermal neutron leakage rates become different as well. However, if a reactor core is homogeneous and unreflected, then the fast and thermal energy groups will have approximately the same shape, and it is reasonable to

assume that $B_F^2 \approx B_T^2$. In this case and this case only, it can be shown that the value of the infinite multiplication factor K_∞ is related to the value of the "combined" one-group buckling B^2 by the equation:

$$K_\infty = \left(1 + B^2 L_t^2\right)\left(1 + B^2 L_{f->t}^2\right) \tag{13.98}$$

or

$$\frac{K_\infty}{\left\{\left(1 + B^2 L_t^2\right)\left(1 + B^2 L_{f->t}^2\right)\right\}} = 1 \tag{13.99}$$

where all of the physics that separates the predictions of one-group theory and two-group theory is lumped into the thermal diffusion area L_t^2 and the fast to thermal diffusion area $L_{f->t}^2$, or the *neutron age*. If one thinks about it, it is quite remarkable that this symmetry between the energy groups continues to persist at this level; but the symmetry is maintained because it is directly attributable to the structure of the two-group equations. In an earlier chapter (see Chapter 10) we learned that the term

$$\frac{1}{1 + B^2 L_t^2} \tag{13.100}$$

represents the *thermal nonleakage probability* P_{NLT} and the term

$$\frac{1}{1 + B^2 L_{f->t}^2} \tag{13.101}$$

represents the *fast nonleakage probability* P_{NLF}, so what we have found is simply a more general case of

$$K_{effective} = K_\infty \left(P_{NLF} \times P_{NLT}\right) \tag{13.102}$$

which we first discussed in Chapter 10. However, we would like to make an additional refinement to Equation 13.99 when the values of both $B^2 L_t^2$ and $B^2 L_{f->t}^2$ are small. As long as a reactor is designed so that the nonleakage probabilities are very close to 1.0, then neither $B^2 L_t^2$ nor $B^2 L_{f->t}^2$ can be much larger than about 0.04. In this case the two terms $\left\{\left(1 + B^2 L_t^2\right)\left(1 + B^2 L_{f->t}^2\right)\right\}$ can be multiplied out, and the term $B^4 L_t^2 L_{f->t}^2$ is so small (about 1 part in 1000) that it can usually be ignored. In this case, the equation for the infinite multiplication factor becomes

$$K_\infty = 1 + B^2\left(L_t^2 + L_{f->t}^2\right) \tag{13.103}$$

or

$$K_\infty = \left(1 + B^2 M^2\right) \tag{13.104}$$

where

$$M^2 = L_t^2 + L_{f->t}^2 \tag{13.105}$$

is again the *thermal migration area*, representing the slowing down and eventual capture of a fission neutron. We have therefore shown that the buckling of the flux when we know the two-group cross sections is

$$B^2 = \frac{K_\infty - 1}{M^2} \tag{13.106}$$

and if we take the square roots of both sides, we arrive at the very simple expression for B as a function of K_∞ and M:

$$B = \frac{\sqrt{(K_\infty - 1)}}{M} \tag{13.107}$$

Plugging in the appropriate values for M, and knowing the value of K_∞ from the four-factor formula, it is a relatively straightforward to calculate what the critical size of bare core must be for any geometrical shape. For example, in the case of a spherical reactor, the buckling is given by

$$B^2 = \left(\frac{\pi}{R}\right)^2 \tag{13.108}$$

and so the *critical radius* becomes

$$R = \frac{\pi}{B} = \frac{\pi M}{\sqrt{(K_\infty - 1)}} \tag{13.109}$$

or more succinctly,

$$R = \frac{\pi M}{\sqrt{(K_\infty - 1)}} = \frac{\pi M}{\sqrt{(\eta \varepsilon f p - 1)}} \tag{13.110}$$

where the four factors have their usual meaning (see Chapter 9 for details).

The same logic can be extended to a rectangular reactor or a cylindrical one. So what we have just done is to relate the factors in the *four-factor formula*, which we can measure and tabulate, to the critical size (and shape) of an unreflected reactor. This is how the size (and the shape) of the cores in some of the first nuclear reactors were determined. In other words, it is possible to estimate the properties of a critical system (within a couple of tenths of one percent) without the need for a calculator or modern computer. Obviously, things have changed dramatically since the first nuclear reactors were built, but the equations we have just presented are indicative of what can be accomplished if the computing power at our disposal is limited.

Example Problem 13.2

Suppose that you are asked to analyze a perfect sphere consisting of a mixture of light water and plutonium with a value of $M^2 = 25\ cm^2$. If the sphere contains enough plutonium so that its infinite multiplication factor is 1.10, what should the diameter of the sphere be so that it will be exactly critical?

Solution From Equation 13.102, we know that $R = \pi/B = \pi M/\sqrt{(K_\infty - 1)}$. So the plutonium sphere must have a diameter of $D = 2R = (3)(3.14)(6)/0.31 = 100$ cm to be exactly critical. [Ans.] Notice that we did not have to know the thermal or fast nonleakage probabilities to perform this calculation. The value of K_∞, which was related to the buckling, took care of all of these details for us for these simple homogeneous shapes.

13.18 Differences between the Geometric Buckling with One and Two Energy Groups

You may recall from our previous discussion of the one group diffusion equation

The One-Group Neutron Diffusion Equation

$$\nabla^2 \phi(\mathbf{r}) + B_M^2 \phi(\mathbf{r}) = 0 \tag{13.111}$$

that the *material buckling* B_M^2 for a bare critical core was a function of only the material composition:

The Material Buckling

$$B_M^2 = \frac{(\nu \Sigma_f - \Sigma_a)}{D} \tag{13.112}$$

Here ν was the average number of neutrons produced per fission (the "mu" of the fuel), Σ_f was the macroscopic fission cross section, Σ_a was the macroscopic absorption cross section, and D was the diffusion coefficient for just a single energy group. If we take this innocent equation and divide both the numerator and the denominator by Σ_a, we get

$$B_M^2 = \frac{(\nu \Sigma_f/\Sigma_a - 1)}{D/\Sigma_a} \tag{13.113}$$

Since $\nu\Sigma_f/\Sigma_a$ is the definition of the infinite multiplication factor and $(D/\Sigma_a) = L^2$ is just the diffusion area, then the buckling for a single energy group was just a different way of saying

$$B^2 = \frac{K_\infty - 1}{L^2} \tag{13.114}$$

which can also be written as

$$K_\infty = \left(1 + B^2L^2\right) \tag{13.115}$$

when $K_{effective} = 1$. If we compare the buckling with one energy group $B^2 = (K_\infty - 1)/L^2$ to the buckling with two energy groups $B^2 = \left(K_\infty - 1\right)/\left(L_t^2 + L_{f->t}^2\right)$, we can immediately see that the only difference between them is that the one-group buckling uses the one-group diffusion area L^2, and that two-group buckling uses the sum of the thermal diffusion area L_t^2 and the fast to thermal diffusion area $L_{f->t}^2$ (*or the neutron age*). Obviously, if we have two-group cross section data available, then the expression for the two-group buckling will give more accurate results than the expression for the one-group buckling. Otherwise, they are both conceptually identical except for the number of energy groups.

Before moving on to other topics, there is an additional way to look at the equations we have just presented. With just one energy group, the infinite multiplication factor and the effective multiplication factor are related to each other by

$$K_{effective} = K_\infty \times P_{NL} \tag{13.116}$$

where the *nonleakage probability* is given by

$$P_{NL} = \frac{1}{\left(1 + B^2L^2\right)} \tag{13.117}$$

However, if we are dealing with two energy groups, the infinite multiplication factor and the effective multiplication factor are related to each other by the slightly more complicated equation:

$$K_{effective} = K_\infty P_{NLF} \times P_{NLT} \tag{13.118}$$

where

Expression for the Fast Nonleakage Probability

$$P_{NLF} = \frac{1}{1 + B^2L_{f->t}^2} \tag{13.119}$$

is the *fast nonleakage probability* P_{NLF}, and

Expression for the Thermal Nonleakage Probability

$$P_{NLT} = \frac{1}{1 + B^2L_t^2} \tag{13.120}$$

is the *thermal nonleakage probability*. It therefore follows that the leakage rates from one-group theory and the leakage rates from two-group theory are related to the total leakage rate by

$$P_{NL} = \left(P_{NLF} \times P_{NLT}\right) \tag{13.121}$$

Hence *the total nonleakage probability is the product of the nonleakage probabilities for the fast and the thermal energy groups*. This is illustrated for an unreflected reactor in Example Problem 13.3 below.

Example Problem 13.3

Suppose that we use the two-group cross sections available from the ENDFB database to find the fast and thermal nonleakage probabilities for a low power research reactor that is operating at 200°F (just below the boiling point of water). If the thermal nonleakage probability is $P_{NLT} = 0.95$ (95%), and the fast nonleakage probability is $P_{NLF} = 0.90$ (90%), what is the total nonleakage probability for the entire system?

Solution If we assume that the reactor is unreflected, then we can write

$$P_{NL} = \left(P_{NLF} \times P_{NLT}\right)$$

and since $P_{NLT} = 0.95$ and $P_{NLF} = 0.90$ the total nonleakage probability is $P_{NL} = (0.90 \times 0.95) = 0.85 = 85\%$. So 85% of the neutrons produced in this reactor *will not leak* out of the core. [Ans.]

13.19 Optimum Sizes and Shapes for Reactor Cores

You may recall that when we first discussed the dimensions of a critical three dimensional reactor that we did not present an equation for the critical size for either a cylindrical reactor or a rectangular one where $L_x \neq L_y \neq L_z$. Although we did not explain the reason for this, it is actually quite simple to understand if you think about it. *There is no unique solution for the size of a critical reactor under these conditions*. For a finite cylinder, the geometric buckling only provides us with *a relationship* between the height H of the cylinder and the radius R of the cylinder that must be satisfied for the core to remain critical. Each unique combination of H and R therefore leads to a different reactor volume and therefore a different critical mass. Similarly, for the three-dimensional rectangle, the geometric buckling only provides us with a relationship between L_x, L_y, and L_z.

There is no unique solution that results in a critical system in this case. However, if two of the three spatial dimensions are specified, then the third spatial dimension can be inferred from the other two. What we did not say initially is that it is possible to find what *the ratio* of these critical dimensions must be in order to find the smallest possible core. This ratio can be determined by calculating the surface area S for each geometrical shape, and then attempting to minimize the surface-to-volume ratio (S/V) for that shape. If we minimize the surface to volume ratio, the neutron leakage rates will be minimized as well. Thus minimizing the surface-to-volume ratio (S/V) allows us to minimize the volume of the core that is required to achieve a *critical mass*. Now let us illustrate how this can be done for a bare cylindrical core. Consider a cylinder of height H and radius R. The total surface area S of the cylinder is

$$S = 2\pi R^2 + 2\pi RH \tag{13.122}$$

The volume V of the cylinder is

$$V = \pi R^2 H \tag{13.123}$$

The surface-to-volume ratio (S/V) is then

$$\frac{S}{V} = \frac{2\pi R^2 + 2\pi RH}{\pi R^2 H} \tag{13.124}$$

The πs and the Rs in the numerator and the denominator cancel, and what remains is

$$\frac{S}{V} = \frac{2(R+H)}{RH} \tag{13.125}$$

To obtain the radius R for which the surface-to-volume ratio (S/V) is minimized, we must differentiate Equation 13.125 with respect to R, and then set the result to 0. This will be the point on the curve of S versus R where the surface area is minimized for a given value of H. The result is

$$\frac{d(S/V)}{dR} = \frac{-(R+H)}{R^2 H} - \frac{2}{RH} = 0 \tag{13.126}$$

or

$$H = 2R \tag{13.127}$$

Consequently, when the height of a cylindrical core is the same as its diameter, or twice the radius, *the surface to volume ratio (and therefore the neutron leakage rate) is minimized* as well. Moreover, we could have inferred the same

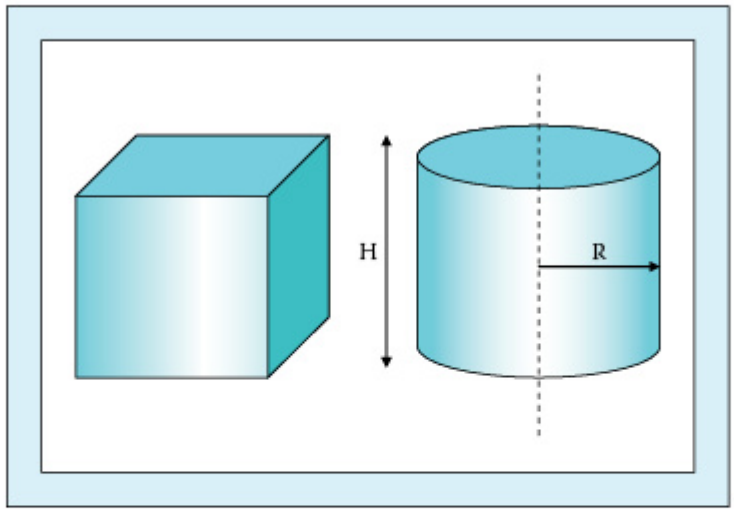

FIGURE 13.14 The surface-to-volume ratio (S/V) is minimized when each side of a rectangle is exactly the same size, or when the diameter of a cylinder is the same as its height.

result by approximating the cylindrical core with a perfect cube, where the edges were rounded off at the corners (see Figure 13.14). Now, let us determine the relationship between the buckling and the radius is in this case. Since

$$B^2 = \left(\frac{\pi}{H}\right)^2 + \left(\frac{2.405}{R}\right)^2 \tag{13.128}$$

it follows that

$$B^2 = \left(\frac{\pi}{2R}\right)^2 + \left(\frac{2.405}{R}\right)^2 = \frac{1}{R^2}\left[\left(\frac{\pi}{2}\right)^2 + (2.405)^2\right] = \left(\frac{2.86}{R}\right)^2 \tag{13.129}$$

So the minimum size and mass of the cylinder are obtained when BR = 2.86. Thus the critical mass will be minimized when

Dimensions to Minimize the Critical Mass of a Cylindrical Core

$$H = 1.82R \quad \text{or} \quad H = 0.91D \tag{13.130}$$

Notice that the value of H in this case is slightly less than 2R because the effects of fast neutrons were not included in our previous analysis. A similar exercise can also be performed to find the dimensions of a rectangular core that results in the smallest critical mass. When we do so, the shape of the core in this case happens to be a *cube*.

Student Exercise 13.1

Suppose that we build a very low-power test reactor in the form of a perfect cube. We decide to make the core out of a mixture of ordinary water and plutonium with a fuel-to-water ratio of 2% by weight. Due to its low power, we believe that the room temperature ENDFB libraries can be used to obtain the thermal cross section data. We know that this mixture has an eta of $\eta = 2.03$, a fast fission factor $\varepsilon = 1.04$, and a resonance escape probability $p = 0.90$. Assume that the thermal migration length of the mixture is 10% less than the thermal migration length of ordinary water alone.

Part 1: Calculate the thermal utilization factor f for the fuel in this homogeneous mixture.

Part 2: Calculate the value of the infinite multiplication factor for this mixture.

Part 3: With this data, calculate the minimum critical size Δx of each face of the cube.

Part 4: Finally, calculate the total volume of the cube and the minimum amount of fuel required to go critical assuming that the plutonium has a density at room temperature of 13.6 g/cm^3.

It is also possible to use the information we have acquired from this example to gain more insight into the behavior of different materials when we choose to use them as reflectors. Several important conclusions can be drawn about these materials by completing the simple student exercise in the following. Note that as long as the reflector is more than a few diffusion lengths thick, $L_t^2 + L_{f->t}^2$, and ordinary one-group diffusion theory can still apply, then estimates of the total reflector savings can be made by using ΔL = (D core/D reflector) × L_T reflector.

Student Exercise 13.2

Suppose that, as a class project, we wish to build a reflector out of ordinary water around the core to reduce the amount of plutonium that we need.

Part 1: Calculate the expected reflector savings (per side) for this case.

Part 2: How much less Plutonium can we use if the reactor is surrounded by a light-water reflector?

Part 3: In our prior discussion of reflected reactors (see Section 13.13), we learned that the Deutsch equation, equation XYZ, works well for cases where one-group diffusion theory breaks down, and where $L_t^2 + L_{f->t}^2$ (the neutron age).

Suppose that we consider the opposite case where one-group diffusion theory is still valid so that $L_t^2 + L_{f->t}^2$, and we want to build the reflector out of lead. Assuming that the reflector savings can be found from the following equation ΔL = (D core/D reflector) × L_T reflector (Equation 13.85), what is the reflector savings and how thick does the reflector have to be?

13.20 Calculating the Critical Mass for Bare Reactors Having Different Sizes and Shapes

Now that we know how to find the critical dimensions of an unreflected core, it is relatively easy to find the *minimum amount* of the uranium or plutonium that is required to bring the core into a critical state. In nuclear science and engineering, the quantity of uranium or plutonium is called the *minimum critical mass*. To find the critical mass of the fuel M_f, we simply take the density of the fuel ρ_f (in g/cm^3) and multiply by the critical size V (in cm^3):

$$M_f = \rho_f V \tag{13.131}$$

For a spherical core, the volume of the core is the volume of a sphere ($V = 4/3\pi R^3$), and the critical radius, R (see Section 13.17) is $R = \pi/B$, so the critical mass is

$$M_f = \rho_f(4/3\pi R^3) = \rho_f(4/3\pi(\pi/B)^3) = 4\rho_f\pi^4/3B^3 \tag{13.132}$$

or

Critical Mass for a Bare Spherical Reactor

$$M_f = \frac{4\rho_f\pi^4}{3B^3} \tag{13.133}$$

and in the case of a cube, the volume of the cube is $V = R^3$, and the critical dimension R from Section 13.17 is $R = \pi\sqrt{3/B}$, so the critical mass is

$$M_f = \rho_f(R^3) = \rho_f\left(\frac{\pi\sqrt{3}}{B}\right)^3 = \frac{3\rho_f\pi^3}{B^3} \tag{13.134}$$

Hence we may write

Critical Mass for a Bare Cubical Reactor

$$M_f = \frac{3\rho_f\pi^3}{B^3} \tag{13.135}$$

The critical mass for other reactor configurations can be estimated in a similar way. Note that Equations 13.133 and 13.135 assume that we are dealing with a *bare core*, that is, one without a reflector. If the core is surrounded by a neutron reflector, the critical mass will be *less*, and in many cases, it will be as much as 30% to 50% less.

Student Exercise 13.3

Using what you have already learned, find the minimum critical mass in kg for the same fuel assembly. *Hint*: Assume that the height is H = 1.82 R in this case.

13.21 Estimating the Effect of a Reflector on the Critical Mass

For simple reactor geometries, it is easy to see why reflectors are so good at reducing the amount of fuel that is required for a core to become critical. *Adding a reflector to any of these geometries will always reduce the critical mass.* To estimate this reduction in mass, we need to calculate the reflector savings ΔL (per side) from Equations 13.76 or 13.78, and subtract this from the bare critical size. When we do so, the critical dimensions for a spherical core will be reduced from R cm to $R' = (R - \Delta R)$ cm, the dimensions for a core in the shape of a cube will be reduced from L cm to $L' = (L - 2\Delta L)$ cm, and the dimensions for a cylindrical core will be reduced from R cm to $R' = (R - \Delta R)$ cm, and H cm to $H' = (H - 2\Delta H)$ cm. We can then take the initial critical volume V, and subtract the final critical volume V' from it to get the reduction in the total volume of the fuel, $\Delta V = V - V'$. When we multiply this by the density of the fuel ρ_f (in g/cm^3) we get the reduction in the critical mass required:

Effect of a Reflector on the Critical Mass

$$\Delta M_{fuel} = \rho_f \Delta V \tag{13.136}$$

where ΔM_f is the *mass reduction* for the fuel. It should be obvious that the fuel savings can be very significant when a core is surrounded by a properly designed reflector. Since fresh water is free, and uranium is very expensive, it should not be surprising that almost every reactor in operation today uses a neutron reflector to minimize the amount of fuel that is required.

Example Problem 13.4

Using one-group diffusion theory, find the minimum critical volume for a bare homogeneous core in the shape of a cylinder. What must the ratio of the height of the cylinder to its radius be to achieve a minimum critical mass? What is the buckling of the flux in the radial and axial directions if the radius of the cylinder is 100 cm? What is the thermal non-leakage probability if the thermal neutron diffusion length is 3 cm?

Solution From Equation 13.123, the height H of the cylinder must be 1.82 times its radius R to achieve a minimum critical mass. Since R = 100 cm, the minimum critical volume is $V = \pi R^2 H = 1.82\,\pi R^3 = 5.717 \times 10^6$ cm^3. The radial and axial components of the geometrical buckling are $B_r^2 = (2.405/R)^2$ and $B_z^2 = (\pi/H)^2$. The total buckling B^2 is therefore $B^2 = B_r^2 + B_z^2 = (2.405/R)^2 + (\pi/H)^2$. Since H = 1.82 R, the total buckling is $B^2 = B_r^2 + B_z^2 = (2.405/R)^2 + (\pi/1.82R)^2$. The radial buckling is $B_r^2 = 0.00058$, the axial buckling is $B_z^2 = 0.00030$, and the total buckling is $B^2 = B_r^2 + B_z^2 = 0.00088$. If L = 3 cm, the thermal nonleakage probability is $P_{NLT} = 1/(1 + B^2 L_t^2) = 1/(1 + 0.00088 \times 9) = 1/1.0079 = 99.2\%$. [Ans.]

13.22 Saving Fuel with a Neutron Reflector

It should be obvious from our previous discussion that using a reflector allows a reactor designer to reduce the amount of fuel that is required to keep a reactor in a critical state. Although reflectors are normally associated with just thermal reactors, *fast reactors* can benefit from the use of reflectors too. Only in fast reactors, the reflectors are called "*blankets*," and it is not unusual for there to be a radial blanket and an axial blanket to breed additional nuclear fuel. The following example illustrates how much fuel can be saved by surrounding a bare core with a reflector.

Example Problem 13.5

Suppose that a bare sphere of 40 cm in diameter is able to achieve a critical mass with only 20 kg of Uranium-235. If the same sphere is surrounded by a reflector made out of ordinary water, how much Uranium-235 can be saved in the process?

Solution We know from our previous discussion of the Deutsch equation (see Equation 13.76) that a reflector made out of ordinary water will have a reflector savings ΔR of about 6.5 cm. So when the sphere is surrounded by a

reflector, the critical radius will be reduced from R = 20 cm to R′ = R − ΔR = 19.0 − 6.5 = 13.5 cm. The volume of the sphere before adding the reflector is V = $(4/3\pi R^3) = 4.18 \times (20)^3 = 33{,}440$ cm^3, and the volume of the sphere after adding the reflector is V′ = $(4/3\pi R'^3) = 4.18 \times (13.5)^3 = 10{,}284$ cm^3. So the amount of uranium required is reduced by (33,440 − 10,284)/33,440 × 20 kg = 0.6925 × 20 kg = 13.85 kg. This is a savings in the amount of fuel required of about 70%. [Ans.]

13.23 Dependence of the Buckling and Diffusion Coefficient on Temperature

The properties of all reactor materials have some dependence on the temperature at which they are operated. For this reason, when we first defined the neutron diffusion coefficient D and the geometric buckling B^2, we did not discuss their temperature dependence. Consequently, certain *reference temperatures* are usually defined where the values of the density and other nuclear parameters are measured experimentally. Any deviation from these reference temperatures can then be used to calculate the effect of the temperature change on the reaction rates.

For example, the cross section libraries that can be found in the ENDF/B database are usually measured at *room temperature* (300°K). When values for the cross sections (or the densities) are required at other temperatures, then *temperature correction factors* must be applied. Reactors as a whole do not operate at room temperatures or at atmospheric pressures. For example, in pressurized water reactors (see Figure 13.15), the water enters the core at a temperature of about 290°C (555°F) and leaves the core at a temperature of about 325°C (615°F). The average water temperature in the core is about 310°C (590°F), and the average pressure in the reactor vessel is about 2250 PSI (15.5 MPa). In boiling water reactors, the water enters the core at a temperature of about 275°C (527°F) and leaves the core at a temperature of about 285°C (546°F). The water begins to boil at about 545°F, and the average pressure in the reactor vessel is about 1050 PSI (7.15 MPa). The actual fuel temperature varies both radially and axially depending on the power distribution and the shape of the flux. *The maximum fuel pin temperature in a PWR under normal operating conditions is about 1800°C with standard deviation of about 120°C, and the maximum fuel pin temperature in a BWR is about 1700°C with a standard deviation of about 50°C.* These values are based on the analysis of many reactors at different points in their operating cycles. Most of the time, the maximum fuel temperature $TFUEL_{MAX}$ is limited by a

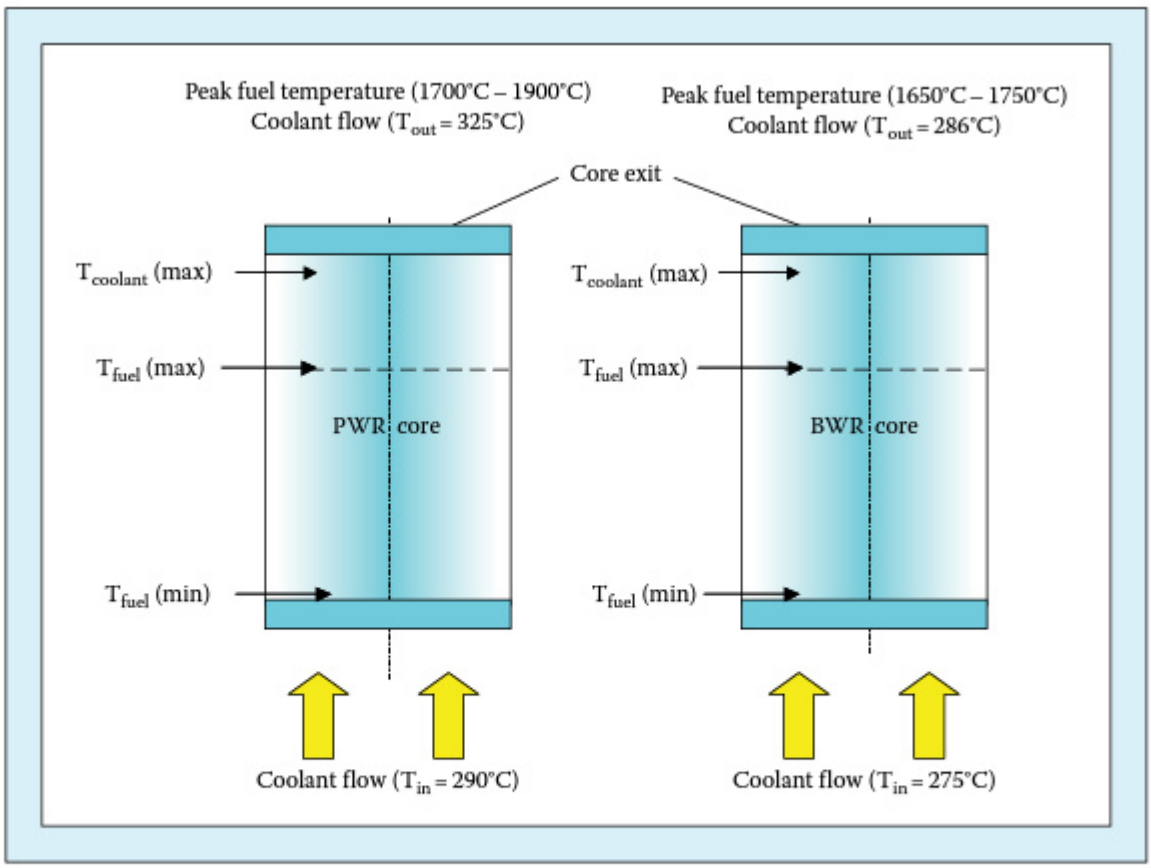

FIGURE 13.15 A comparison of fuel temperatures and coolant temperatures in a PWR and a BWR.

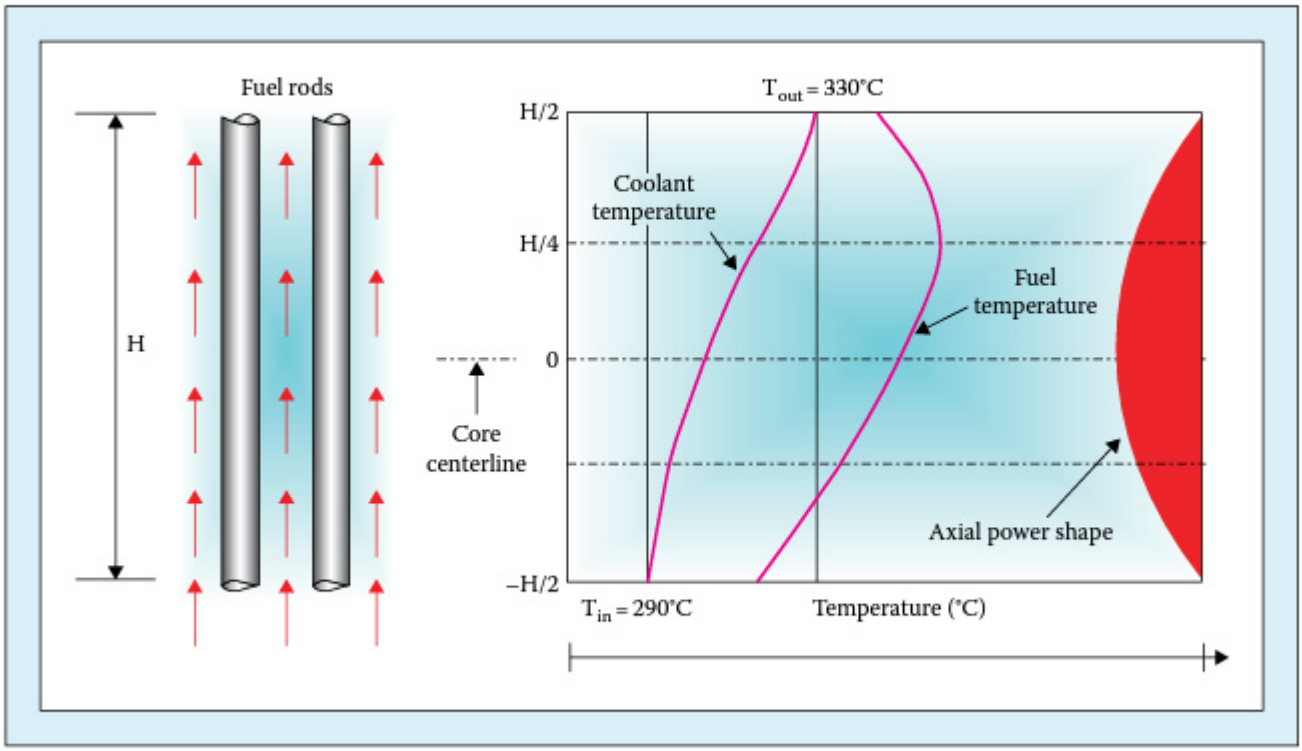

FIGURE 13.16 Normal reactor temperature profiles as a function of axial elevation, assuming no bulk boiling in the core.

desire to prevent the release of fission gases from the fuel (see Chapter 11 of our companion book for a more complete discussion of this subject*). Both of these scenarios are illustrated in Figure 13.16. *For an axially symmetric power distribution, the fuel temperature peaks about 3/4 of the way between the bottom of the core and the top*. As long as the coolant continues to flow, *the highest coolant temperature is always reached at the top of the core*. In PWRs, the density of the water also falls as the temperature of the coolant is increased, and in the case of a BWR, the density falls dramatically when the water begins to boil. Since the multi-group cross sections and the diffusion coefficient depend on the density of the coolant, all of these parameters are temperature dependent as well.

Table 13.6 shows the values of important reactor parameters at *Standard Temperature and Pressure* (STP = 300°K and 14.7 PSI). For a variety of reasons it turns out that the diffusion coefficient has almost no dependence on the pressure

TABLE 13.6
Some Helpful Constants to Be Used When Calculating the Critical Mass

Name	Atomic Number (Z)	Chemical Symbol	Density at Room Temperature (g/cm³)	Atoms or Molecules per cm³ (1 × 10²⁴)	Atomic or Molecular Weight	Percent Fuel by Weight
Water (light)	—	H_2O	1.00	0.0334	19.015	
Water (heavy)	—	D_2O	1.105	0.0332	19.028	
Plutonium	94	Pu	19.60	0.0494	239.052	100
Plutonium dioxide	—	PuO_2			271.042	88.2
Thorium	90	Th	11.71	0.0304	232.038	100
Thorium dioxide	—	ThO_2			264.028	87.8
Uranium	92	U	19.10	0.0483	238.030	100
Uranium dioxide	—	UO_2			270.020	88.1

* See *Nuclear Engineering Fundamentals: A Practical Perspective*, by R.E. Masterson, CRC Press (2017).

P as long as the moderator is solid. But at thermal energies, it *does* have a significant dependence on the density ρ and the temperature T. You may recall from our earlier discussion of neutron diffusion theory in Chapter 11 that the diffusion coefficient D is inversely proportional to the macroscopic scattering cross section Σ_s when $\Sigma_s \gg \Sigma_a$.

Relating the Diffusion Coefficient to the Macroscopic Scattering Cross Section

$$D = \frac{1}{3\Sigma_s(1-(2/3A))} \tag{13.137}$$

Here again, A is the atomic weight measured in AMUs. This implies that the diffusion coefficient is inversely proportional to the physical density of the material since $\Sigma_s = \sigma_s\rho$. Therefore, at thermal energies, we may write

$$D_t \sim \frac{C}{\rho} \tag{13.138}$$

where C is a constant that varies from one material to the next. It immediately follows from Equation 13.138 that if we know the diffusion coefficient at a reference density ρ_{ref}, then we can compute it at any other material density ρ by taking the ratio

$$D_t(\rho) = D_t(\rho_{ref})\left\{\frac{\rho_{ref}}{\rho}\right\} \tag{13.139}$$

The temperature dependence of the density is also a function of whether we are dealing with a liquid or a solid. For solid materials like graphite, there is almost no change in D as a function of T. Hence if we write Equation 13.139 as

$$D_t(\rho, T) = D_t(\rho_{ref}, T_{ref})\left\{\frac{\rho_{ref}}{\rho}\right\}\left\{\frac{T}{T_{ref}}\right\}^n \tag{13.140}$$

then for a solid material like graphite or beryllium, n would obviously be 0, and Equation 13.140 would become

Temperature Dependence of the Diffusion Coefficient for a Solid Moderator

$$D_t(\rho, T) = D_t(\rho_{ref}, T_{ref})\left\{\frac{\rho_{ref}}{\rho}\right\} \quad \text{(for all solid moderators)} \tag{13.141}$$

where

T_{ref} is the reference temperature
ρ_{ref} is the density at the reference temperature

However, for liquids like water, D_t varies as $T^{0.470}$ and in the case of heavy water (D_2O), it varies as $T^{0.112}$. We can therefore write Equation 13.141 as

Temperature Dependence of the Diffusion Coefficient for a Liquid Moderator

$$D_t(\rho, T) = D_t(\rho_{ref}, T_{ref})\left\{\frac{\rho_{ref}}{\rho}\right\}\left\{\frac{T}{T_{ref}}\right\}^n \quad \text{(for any liquid moderator)} \tag{13.142}$$

where n = 0 for graphite and beryllium, n = 0.470 for water, and n = 0.112 for heavy water (D_2O). Hence Equation 13.142 can be used to find the value of the thermal diffusion coefficient at any density or temperature T. However, the temperature T in Equation 13.142 must be measured in degrees *Kelvin*. To convert from degrees *Centigrade* to degrees Kelvin, we must apply the relationship

$$K° = C° + 273 \tag{13.143}$$

and to convert from degrees *Fahrenheit* to degrees Centigrade we must perform the additional conversion

$$C° = \frac{5}{9}(F° - 32) \tag{13.144}$$

so that

$$K^\circ = \frac{5}{9}\cdot(F^\circ - 32) + 273 \tag{13.145}$$

It follows from Equation 13.142 that the thermal diffusion length $L_t = \sqrt{D/\Sigma_a}$ can also be written as

The Thermal Diffusion Length as a Function of Temperature

$$L_t(\rho, T) = L_t(\rho_{ref}, T_{ref})\left\{\frac{\rho_{ref}}{\rho}\right\}\sqrt{\left\{\frac{T}{T_{ref}}\right\}^n} \tag{13.146}$$

where the values of the exponent n are the same as before, and *the temperature T is in K°*.

Armed with these simple equations, it is possible to calculate the values of L_t and D_t at any temperature and density if we know their values at a standard temperature T_{ref} and a standard density ρ_{ref}. Thus we simply look up the standard values of these parameters in Table 13.7, and evaluate the ratios in Equation 13.146 at the appropriate temperatures and densities. The three primary temperature scales that are used to do this today (Fahrenheit, Centigrade, and Kelvin) are compared at important temperatures such as the boiling point of water, the freezing point of water, and *absolute zero (the point of minimum entropy)* in Figure 13.17.

TABLE 13.7
Melting Points of Common Nuclear Materials in Degrees Fahrenheit and Centigrade

Nuclear Material	Used for	Melting Point (°F)	Melting Point (°C)
Uranium dioxide (UO_2)	Fuel	5190	2865
Zircaloy-2	Cladding in BWRs	3362	1850
Zircaloy-4	Cladding in PWRs	3362	1850

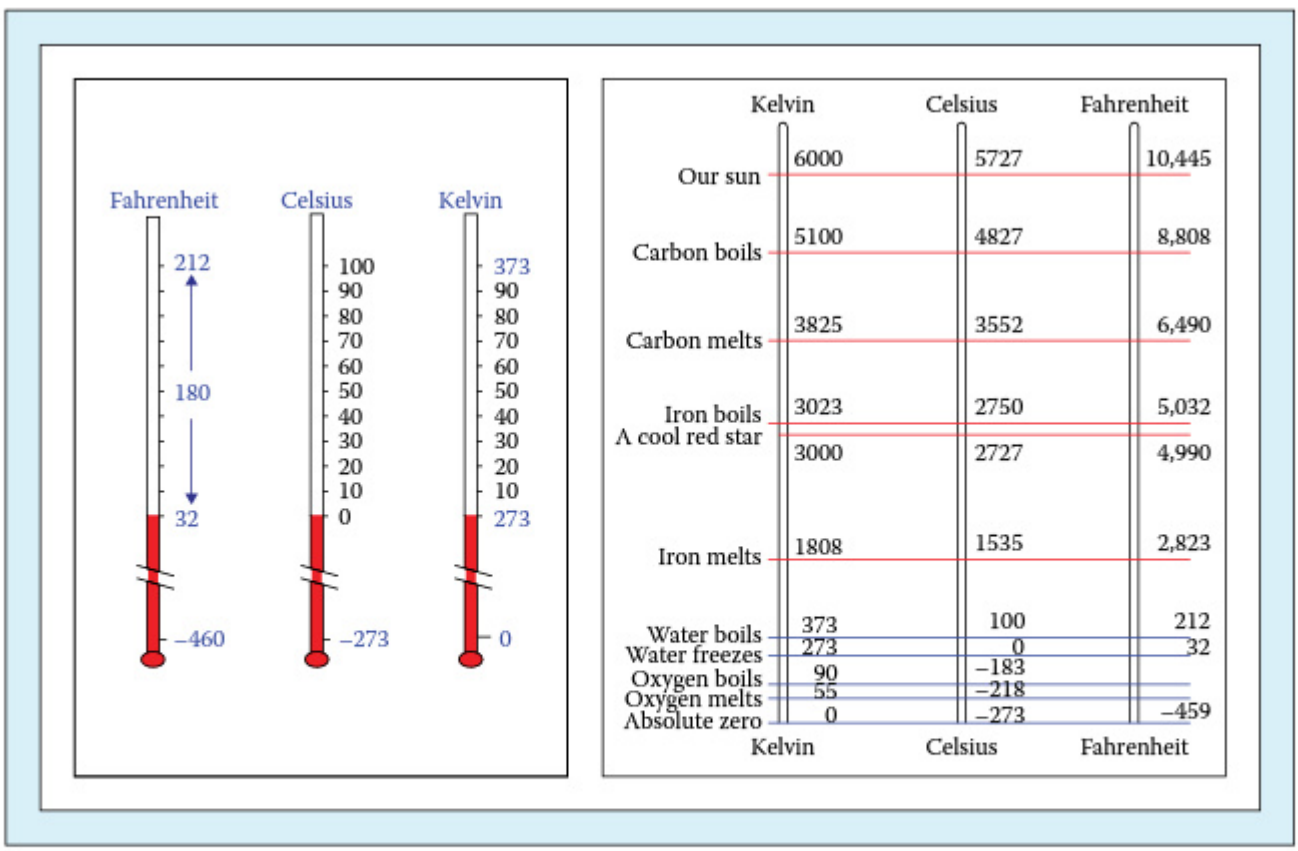

FIGURE 13.17 The three primary temperature scales in use in the world today and their respective ranges. (Courtesy of Wikipedia.)

In the United States, the Fahrenheit scale is still commonly used, and in most of Europe, temperatures are now measured in °C. Absolute temperatures are measured in °K but these are normally reserved for applications involving low-temperature physics, chemistry, and power plant thermal cycles. For example, the absolute temperature scale is also required to find the thermal efficiency of a nuclear power plant, and *these absolute temperatures appear in the calculation of the thermal efficiency for both the Rankine and Brayton thermal cycles.** Finally, the absolute temperature scale is also quite popular in the fields of astronomy and astrophysics.

Again, the equations we have presented so far only apply to liquids and solids that no not change phase. For uranium dioxide (UO_2) this occurs at a temperature of about 2865°C or 5190°F, where UO_2 begins to melt, and in the case of Zircaloy-2 and Zircaloy-4, which are common cladding materials, the corresponding melting points occur at a temperature of about 1850°C (3362°F). As you can imagine, these temperatures are rarely approached during normal reactor operation. Example Problem 13.6 shows how the diffusion coefficient is affected by the elevated temperatures in a PWR.

Example Problem 13.6

Suppose that we know that the diffusion coefficient for ordinary water at room temperature (300°K) is 0.16 cm. What is the diffusion coefficient for the water in a PWR core that is operating at normal pressures and temperatures? Assume that the density of the water in the center of the core is about 0.8 g/cm^3.

Solution We know from our previous discussion that water enters the core of a PWR at a temperature of about 300°C (570°F) and leaves the core at a temperature of about 330°C (625°F). We will assume the average operating temperature is 315°C (about 590°K). We also know that the density of water at room temperature (300°K) is 1.0 g/cm^3. Therefore, the diffusion coefficient of the water in the center of the reactor is

$$D_{H_2O}(590) = 0.16 \times \frac{1.0}{0.8} \times \left(\frac{590}{300}\right)^{0.47} = 0.282 \text{ cm}.$$

The diffusion coefficient is almost twice as large in this case. This is why it is so important to always include the effects of temperature and pressure when making such a calculation. [Ans.]

As this example indicates, the diffusion coefficient D_{H_2O} for water is much larger when the water is heated than when it is cold. A neutron simply needs to travel a larger distance to collide with an H_2O nucleus when the density of the water is reduced due to thermal expansion. This implies that the thermal diffusion length L_T also varies with the temperature of the coolant, and that it must be much *larger* when the coolant is hot than when the coolant is cold. Using simple one-group theory, it is then possible to calculate the difference this makes in the value of the geometric buckling B^2 when a reactor is hot and when a reactor is cold. When a reactor is exactly critical and $K_{effective} = 1$, the buckling for a cold core is given by

$$B^2_{COLD} = \frac{(K_\infty - 1)}{L^2_{COLD}} \tag{13.147}$$

and the buckling for a hot core is given by

$$B^2_{HOT} = \frac{(K_\infty - 1)}{L^2_{HOT}} \tag{13.148}$$

The value

$$\Delta B^2 = \frac{B^2_{COLD} - B^2_{HOT}}{B^2_{COLD}} = 1 - \frac{B^2_{HOT}}{B^2_{COLD}} \tag{13.149}$$

or

$$\Delta B^2 = 1 - \frac{L^2_{COLD}}{L^2_{HOT}} \tag{13.150}$$

therefore determines the incremental change in the buckling due to temperature changes in the diffusion length alone.

* See *Nuclear Engineering Fundamentals: A Practical Perspective*, by R.E. Masterson, CRC Press (2017).

Example Problem 13.7

Using the information provided in the previous example, estimate the percentage change in the buckling of the one-group flux between a cold PWR core and a hot one. The reactors can be assumed to be exactly critical in both cases. In which case is the buckling, and therefore the neutron leakage, greater?

Solution We know from Appendix I that the diffusion length L_{COLD} for a thermal neutron at STP is about 2.9 cm. From Equation 13.146, the diffusion length in water at the center of the core when the reactor is operating normally is

$$L_{HOT} = 2.8 \times (1.0/0.8) \times (600/300)^{0.235} = 4.12 \text{ cm}.$$

Therefore, the incremental change in the buckling (from Equation 13.150) is $\Delta B^2 = 1 - (L^2_{COLD}/L^2_{HOT}) = 1 - (2.9/4.12)^2 = 0.50 = 50\%$ and the buckling is *50% larger* when the reactor is hot than when the reactor is cold. Of course, this does not account for any changes the temperature has on the value of K_∞. So the neutron leakage rate increases as the reactor is heated up, and this is due primarily to an increase in the value of the diffusion coefficient D. [Ans.]

Thus we see that the neutron leakage rate *increases* as the coolant temperature increases because the geometric buckling increases as well. This conclusion applies to both fast neutrons and thermal neutrons, but the effects are generally more pronounced for thermal neutrons because their diffusion coefficients change more dramatically with temperature up to the boiling point.

13.24 Temperature Dependence of the Neutron Mean Free Path

A final consequence of Equation 13.142 is that we can use this equation to predict how the mean free path of a thermal neutron changes between the top and the bottom of the core. If the moderator does not boil, then for modest temperature changes we can write

$$D(T_2) = D(T_1) \cdot \left(\frac{T_2}{T_1} \right)^{0.470} \tag{13.151}$$

because the density of water will not change much with respect to its reference density. Since the mean free path λ is directly proportional to the diffusion coefficient D, we can also write Equation 13.151 as

$$\lambda(T_2) = \lambda(T_1) \cdot \left\{ \frac{T_2}{T_1} \right\}^{0.47} \tag{13.152}$$

This final equation implies that as the temperature of the water rises, and T_2 becomes greater than T_1, the mean free paths of the fast and thermal neutrons become longer. Now let us apply this equation to a PWR where the water enters the core at 290°C and leaves the core at 320°C. This temperature change is typical of the water in the core of a Westinghouse AP-1000 (see Chapter 13 of our companion book*). So for this PWR, T_1 = 290°C = 563°K and T_2 = 320°C = 593°K. The ratio of the mean free paths is therefore $\lambda(T_2)/(T_1) = (T_2/T_1\}^{0.47} = 1.025$. So the mean free path at the top of the core is about 2.5% longer than it is at the bottom of the core. The material buckling is effected in a similar way. While these temperature induced effects are normally small, the reactivity can still be affected by a meaningful amount. We will have more to say about this when we examine the effects of burnup and temperature feedback on the multiplication factor of the core in Chapter 17. However, it is important to take these changes into account when designing an actual reactor core because the reaction rates are so sensitive to them.

13.25 Solutions to the Neutron Diffusion Equation with More than One Homogeneous Region

Assuming that we understand the temperature dependence of the materials in the core, it is possible to solve the steady-state diffusion equation in more complicated reactor geometries where each of the material regions is spatially homogeneous. Under these conditions the neutron diffusion equation for a reactor consisting of three homogeneous material

* See *Nuclear Engineering Fundamentals: A Practical Perspective*, by R.E. Masterson, CRC Press (2017).

regions may be written as the sum of three separate diffusion equations, which are in turn related to each other through the boundary conditions. In region #1, we may write the diffusion equation as

$$\nabla^2\phi(x) + B_1^2\phi(x) = 0 \tag{13.153}$$

and similarly for regions 2 and 3, we have

$$\nabla^2\phi(x) + B_2^2\phi(x) = 0 \tag{13.154}$$

$$\nabla^2\phi(x) + B_3^2\phi(x) = 0 \tag{13.155}$$

where, in principle, the value of the diffusion coefficient D is also different from one region to the next. Here the value of the material buckling $B^2 = (\nu\Sigma_f - \Sigma_a)/D$ may be region dependent, and in general, for the ith region, it is defined as

$$B_i^2 = \frac{(\nu\Sigma_f - \Sigma_a)_i}{D_i} \tag{13.156}$$

where the subscript i refers to the ith region only. When $B_i^2 > 0$, the general solution for each material region is

$$\phi(x) = A1_i \sin(B_i x) + A2_i \cos(B_i x) \tag{13.157}$$

where $A1_i$ and $A2_i$ are coefficients that depend on the boundary conditions. This assumes that each of the regions is a spatially uniform slab that is many times longer than it is wide. Because of this, it is possible to neglect the spatial variation of the flux in the y and z directions and set the axial buckling to zero. When $B_i^2 < 0$, the general solution for each region is

$$\phi(x) = A1_i\, e^{+B_i x} + A2_i\, e^{-B_i x} \tag{13.158}$$

where $A1_i$ and $A2_i$ are again coefficients to be determined from the boundary conditions. The most common case where $B_i^2 < 0$ corresponds to one where there is no nuclear fuel present. This corresponds to a situation where $\Sigma_f = 0$. In this case, the value of B_i^2 becomes

$$B_i^2 = \frac{\Sigma_{a_i}}{D_i} \tag{13.159}$$

which is essentially the same as the inverse of the diffusion length squared. In the case of three regions, each having different values for the material buckling B_i^2, the general solutions are

$$\phi(x) = A1_1 \sin(B_1 x) + A2_1 \cos(B_1 x) \quad \text{for region 1} \tag{13.160}$$

$$\phi(x) = A1_2 \sin(B_2 x) + A2_2 \cos(B_2 x) \quad \text{for region 2} \tag{13.161}$$

$$\phi(x) = A1_3 \sin(B_3 x) + A2_3 \cos(B_3 x) \quad \text{for region 3} \tag{13.162}$$

and so on, when $B_i^2 > 0$. Conversely, when $B_i^2 < 0$, the general solutions for each of the three regions are

$$\phi(x) = A1_1 e^{+B_1 x} + A2_1 e^{-B_1 x} \quad \text{for region 1} \tag{13.163}$$

$$\phi(x) = A1_2 e^{+B_2 x} + A2_2 e^{-B_2 x} \quad \text{for region 2} \tag{13.164}$$

$$\phi(x) = A1_3 e^{+B_3 x} + A2_3 e^{-B_3 x} \quad \text{for region 3} \tag{13.165}$$

To simplify our discussion of these equations, assume that the LHS of region 1 is located on the x axis where x = 0. Similarly, we will assume that all three regions are of equal width W and are spatially homogeneous. Therefore, region 1 extends from x = 0 to W, region 2 extends from x = W to x = 2W, and region 3 extends from x = 2W to x = 3W. Refer to

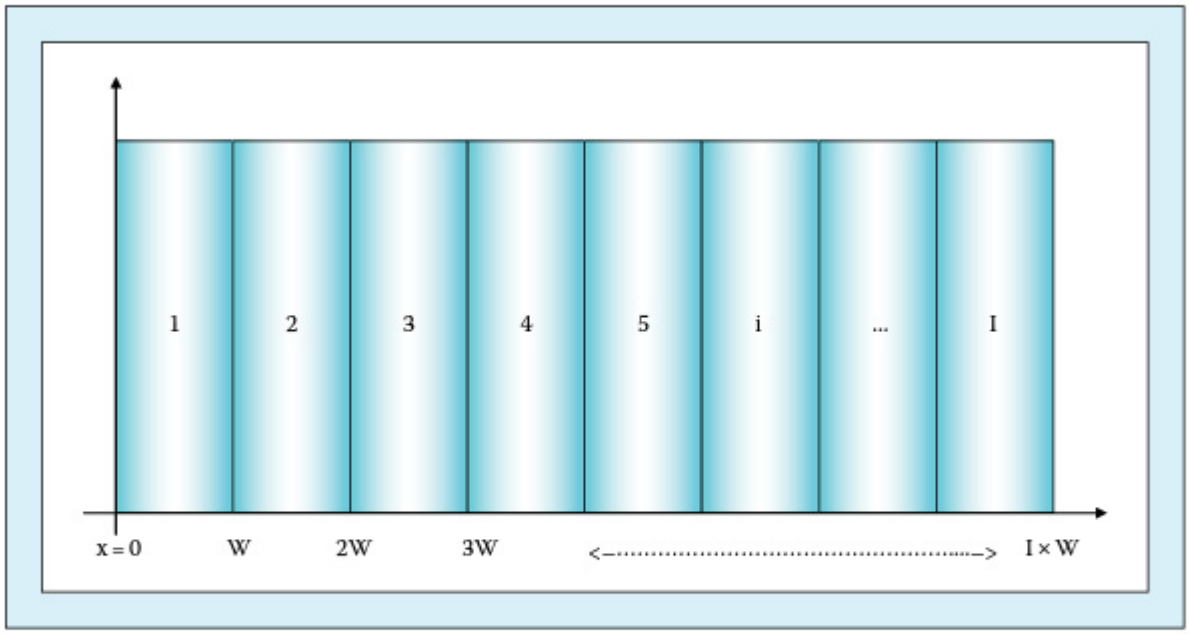

FIGURE 13.18 A multiregion reactor with I homogeneous regions in which to solve the neutron diffusion equation.

Figure 13.18 to visualize how these regions are positioned spatially. At each material interface (between regions 1 and 2 and regions 2 and 3) we also require that

$$\phi(x_{12}) = \phi(x_{21}) \tag{13.166}$$

and

$$\phi(x_{23}) = \phi(x_{32}) \tag{13.167}$$

These interfaces occur where x = W and x = 2W. First let us consider the case where $B_i^2 > 0$. Applying these boundary conditions to the fluxes between each material region, we find that

$$A1_1 \sin(B_1 W) + A2_1 \cos(B_1 W) = A1_2 \sin(B_2 W) + A2_2 \cos(B_2 W) \quad \text{for regions 1 and 2} \tag{13.168}$$

$$A1_2 \sin(2B_2 W) + A2_2 \cos(2B_2 W) = A1_3 \sin(2B_3 W) + A2_3 \cos(2B_3 W) \quad \text{for regions 2 and 3} \tag{13.169}$$

This is a set of two simultaneous equations with six unknowns—$A1_1$, $A1_2$, $A2_1$, $A2_2$, $A1_3$, and $A2_3$. We can obtain two additional equations for the six unknowns by specifying a value for the flux at the outer boundaries of regions 1 and 3. Let us assume for the sake of simplicity that the flux has a value of $\phi = \phi_o$ on each of these boundaries. However, the reader should bear in mind that does not always have to be the case. In fact the flux at the boundaries can have any value we want, and in general we will find that $\phi(0) \neq \phi(3W)$. However, to simplify our calculations and preserve the symmetry of the results, we will use the fact that $\phi(0) = \phi(3W) = \phi_o$. This then implies that

$$\phi = \phi_o \quad \text{at } x = 0 \tag{13.170}$$

and

$$\phi = \phi_o \quad \text{at } x = 3W \tag{13.171}$$

Of course, Figure 13.18 does not have a physical boundary except at x = 0 and x = I × W, but we can still use these boundary conditions to illustrate how a more general solution can be found. Applying these boundary conditions to the fluxes on the edges of regions 1 and 3, we obtain

$$A1_1 \sin(0) + A2_1 \cos(0) = \phi_o \quad \text{for region 1} \tag{13.172}$$

$$A1_3 \sin(3B_3 W) + A2_3 \cos(3B_3 W) = \phi_o \quad \text{for region 3} \tag{13.173}$$

Finally, in order to obtain the final two equations for ϕ (so that we will now have a total of six equations and 6 unknowns), we must require the neutron currents to be continuous across the boundaries between regions 1 and 2 and 2 and 3. At each material interface (between regions 1 and 2 and regions 2 and 3) we therefore require that

$$J(x_{12}) = J(x_{21}) \tag{13.174}$$

and

$$J(x_{23}) = J(x_{32}) \tag{13.175}$$

Because of Fick's Law, we also know that

$$-D_1 \frac{d\phi_1}{dx} = -D_2 \frac{d\phi_2}{dx} \quad \text{when } x = W \tag{13.176}$$

and

$$-D_2 \frac{d\phi_2}{dx} = -D_3 \frac{d\phi_3}{dx} \quad \text{when } x = 2W \tag{13.177}$$

So this then gives the final 2 equations that we need to solve for coefficients

$$D_1\left(A1_1 B_1 \cos(B_1 W) - A2_1 B_1 \cos(B_1 W)\right) = D_2\left(A1_2 B_2 \cos(B_2 W) - A2_2 B_2 \cos(B_2 W)\right) \quad \text{for regions 1 and 2} \tag{13.178}$$

$$D_2\left(A1_2 B_2 \cos(2B_2 W) - A2_2 B_2 \cos(2B_2 W)\right) = D_3\left(A1_3 B_3 \cos(2B_3 W) - A2_3 B_3 \cos(2B_3 W)\right) \quad \text{for regions 2 and 3} \tag{13.179}$$

We then have a set of 6 simultaneous equations with 6 unknowns.

$$A1_1,\ A2_1,\ A1_2,\ A2_2, \text{ and } A1_3,\ A2_3 \tag{13.180}$$

These equations can be solved using any standard numerical technique to find the values of the six coefficients multiplying the sines and cosines. Alternatively, they can be solved graphically to establish the relationships between the fluxes in each region that are required. So to summarize what we have just said, the continuity of the flux at the interfaces

$$\phi(x_{12}) = \phi(x_{21}) \tag{13.181}$$

and

$$\phi(x_{23}) = \phi(x_{32}) \tag{13.182}$$

provides 2 equations for relationships between

$$A1_1,\ A2_1 \quad \text{and} \quad A1_2,\ A2_2 \tag{13.183}$$

and

$$A1_2,\ A2_2 \quad \text{and} \quad A1_3,\ A2_3 \tag{13.184}$$

The continuity of the current across each of the material boundaries requires that

$$J(x_{12}) = J(x_{21}) \tag{13.185}$$

and

$$J(x_{23}) = J(x_{32}) \tag{13.186}$$

which also implies that

$$D_1 \frac{d\phi}{dx} = D_2 \frac{d\phi}{dx} \quad \text{at } x_{12} \tag{13.187}$$

and

$$D_2 \frac{d\phi}{dx} = D_3 \frac{d\phi}{dx} \quad \text{at } x_{23} \tag{13.188}$$

This provides us with two more equations for the relationships between

$$A1_1,\ A2_1 \quad \text{and} \quad A1_2,\ A2_2 \tag{13.189}$$

and

$$A1_2,\ A2_2 \quad \text{and} \quad A1_3,\ A2_3 \tag{13.190}$$

Finally, the values of the neutron flux at x = 0 and x = 3W provides us with the final set of relationships between

$$A1_1,\ A2_1 \quad \text{and} \quad A1_3,\ A2_3 \tag{13.191}$$

This is a total of six equations in all that can be solved for $A1_1$, $A2_1$, $A1_2$, $A2_2$, $A1_3$, and $A2_3$. This provides a unique set of solutions for the shape of the neutron flux $\phi(x)$ in regions 1, 2, and 3. The same approach can easily be extended to i independent spatially homogeneous regions as long as the continuity of the flux and the current across each material boundary is preserved. Every time we add another material region, the number of equations that need to be solved simply increases by 2. So four regions will require a total of $4 \times 2 = 8$ simultaneous equations, and five regions will require a total of $5 \times 2 = 10$ simultaneous equations, and so on. Thus this approach can be extended to as many different material regions as we want. The only caveat is that each material region must be spatially homogeneous and relatively long in comparison to its overall width W. Finally, it is possible to mix the solutions between the regions so that some regions have a general solution of the form

$$\phi(x) = A1_i \sin(B_i x) + A2_i \cos(B_i x) \tag{13.192}$$

when $B_i^2 > 0$, and other regions will have another solution of the form

$$\phi(x) = A1_i e^{+B_i x} + A2_i e^{-B_i x} \tag{13.193}$$

when $B_i^2 < 0$. For example, if we were interested in modeling the RHS or the LHS of a reactor with three material regions, then the central region would probably be a neutron-producing region where $B_i^2 > 0$, and the first and third regions would probably be regions with no net neutron production (such as a reflector) where $B_i^2 < 0$. As long as we are able to find 2 boundary conditions for each material region, the end result will be a set of $2 \times N$ linear equations to solve for $A1_i$ and $A2_i$, when there are a total of N material regions in all.

Student Exercise 13.4

Based on the results presented earlier, are there any similar geometries where it is possible to solve the steady-state neutron diffusion equation to predict the shape of the flux throughout a series of contiguous but spatially homogeneous regions?

If so, sketch out the process that you would use to solve the neutron diffusion equation in this case.

13.26 How to Model a Fuel Assembly next to a Reflector

To extend this model further, suppose that we would like to show what the solutions to the diffusion equation look like when we have two arbitrary material regions—one of which produces neutrons and has a value of $B_i^2 > 0$ (such as a fuel assembly) and the other which absorbs or scatters neutrons and has a value of $B_i^2 < 0$ (such as a reflector). Clearly, this is just another example of the problem we just solved, so we would like to present a solution for the case where both material regions can be thought of as long, narrow slabs.

Consider the two identical slabs of material shown in Figure 13.19, which are assumed to be infinitely long in the y and z directions and are positioned on the x axis starting at x = 0. Both material regions have identical widths W, and the first material region extends from x = 0 to W, while the second material region extends from x = W to 2W. Let us further assume that the first slab contains enough fissionable material to have a *positive buckling* where $B_i^2 > 0$, and the other slab has no fissionable material so that it has a *negative buckling* with $B_2^2 < 0$. Refer to Figure 13.19 to see how the two slabs are connected. Now let us assume that the neutron current on the LHS of region #1 (at x = 0) is equal to 0. This is equivalent to assuming that the LHS of region #1 corresponds to the centerline of the neutron-producing region (which happens to be the centerline of the core). Since this problem is symmetrical, setting J = 0 at the center of the core is a reasonable thing to do. Furthermore, let us assume that the neutron flux drops to 0 at x = 2W, which is the right-hand boundary of region 2. This boundary can be thought of as the edge of the reflector. The general solution of the neutron diffusion equation in region #1 is

$$\phi(x) = A1_1 \sin(B_1 x) + A2_1 \cos(B_1 x) \tag{13.194}$$

and the general solution of the neutron diffusion equation in region #2 is

$$\phi(x) = A1_2 e^{+B_2 x} + A2_2 e^{-B_2 x} \tag{13.195}$$

Now let us apply the two boundary conditions that we just discussed. First, consider the boundary condition on the outside of region #2, namely, that $\phi = 0$ at x = 2W. Since no neutrons are produced in this region, this leads us to conclude that the value of $A1_2$ must be 0 for x > 0. The equation for the neutron flux in region # 2 then becomes

$$\phi(x) = A2_2 e^{-B_2 x} \tag{13.196}$$

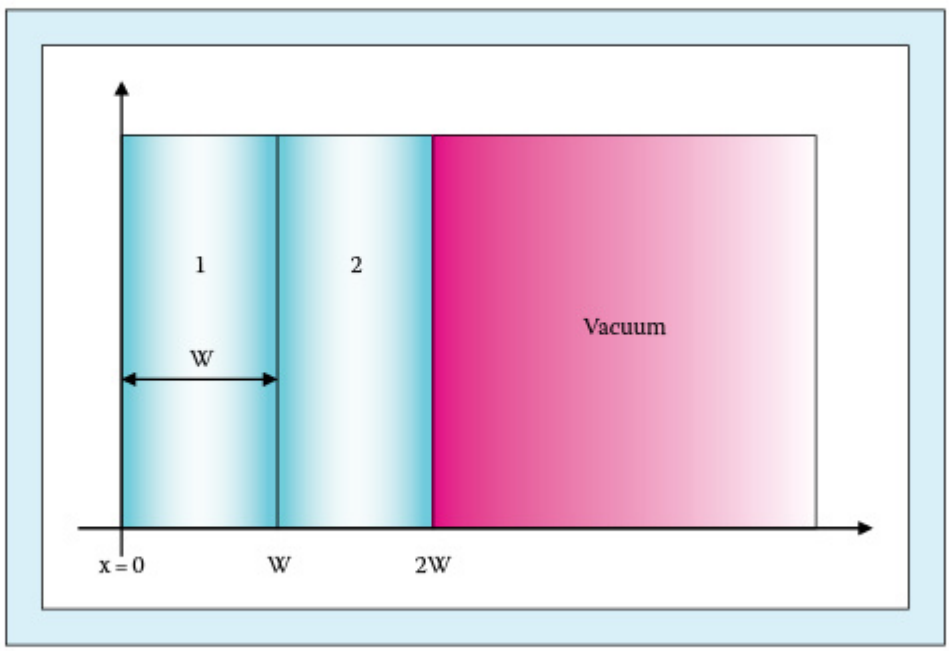

FIGURE 13.19 A two-region reactor in which a solution to the neutron diffusion equation is required.

Now let us apply one of the other assumptions we made regarding the neutron current to provide an additional boundary condition for region #1. On the LHS of region #1, setting J = 0 implies that J = −D dϕ/dx = 0 at x = 0, and this leads us to conclude that

$$A1_1 B_1 \cos(0) - A2_1 B_1 \sin(0) = 0 \tag{13.197}$$

which can only be true if $A1_1 = 0$. Therefore the equations for region #1 reduce to

$$\phi(x) = A2_1 \cos(B_1 x) \tag{13.198}$$

and the equations for region #2 reduce to

$$\phi(x) = A2_2 e^{-B_2 x} \tag{13.199}$$

We can now use the boundary conditions at the interface between regions 1 and 2 to give us the remaining values for $A2_1$ and $A1_2$. Now let us consider what happens to the neutron flux at the boundary between region #1 and region #2. We learned in Chapter 11 that the value of the neutron flux must be continuous across this interface. This implies that

$$A1_1 \sin(B_1 W) + A2_1 \cos(B_1 W) = A2_2 e^{-W B_2} \tag{13.200}$$

at x = W. But since $A1_1 = 0$, this becomes

$$A2_1 \cos(B_1 W) = A2_2 e^{-B_2 W} \tag{13.201}$$

or

$$A2_2 = A2_1 \cos(B_1 W) e^{+B_2 W} \tag{13.202}$$

Substituting this expression for $A2_2$ into the equation for the neutron flux in region #2, we obtain

$$\phi(x) = A2_1 \cos(B_1 W) e^{+B_2 W} e^{-B_2 x} \tag{13.203}$$

The equations for the shape of the flux in each region are then

$$\phi(x) = A2_1 \cos(B_1 x) \quad \text{(for Region I)} \tag{13.204}$$

$$\phi(x) = A2_1 \cos(B_1 W) e^{+B_2 W} e^{-B_2 x} \quad \text{(for Region II)} \tag{13.205}$$

where the constant $A2_1$ that appears in these equations is the same in both cases. So apparently requiring the flux to be continuous across the interface between regions 1 and 2 means that *any value* of $A2_1$ is a legitimate solution for the shape of the neutron flux. As before, the exact value of $A2_1$ must be determined by the power level P of the reactor itself:

$$P = c \int_V \Sigma_f \phi(x) dV \tag{13.206}$$

where c is the average energy released per fission (~210 MeV) and the integration is to be performed over all of region #1 where the power is produced. As we learned in Chapter 2, only about 95% of this power is actually recoverable, so the reactor power level P that determines the value of $A2_1$ is

$$P = 0.95 c \int_V \Sigma_f \phi(x) dV \tag{13.207}$$

Furthermore, because we are dealing with a slab reactor,

$$P = 0.95 c \int_V \Sigma_f \phi(x) dx \tag{13.208}$$

or

$$P = 0.95c \int_V \Sigma_f A2_1 \cos(B_1 x) dx \tag{13.209}$$

Finally, solving for $A2_1$, we obtain

$$A2_1 = \frac{P}{0.95c \int_V \Sigma_f \cos(B_1 x) dx} \tag{13.210}$$

which can be used to determine the ultimate value of $A2_1$. Hence, this is the equation we must solve for $A2_1$, where the limits of integration are now from x = 0 to W (because this is where the neutron-producing material is located). The remarkable thing about this equation is that it implies *that the neutron diffusion equation for an exactly critical reactor does not tell us anything about the number of neutrons that are needed to sustain a nuclear chain reaction.*

As long as the rate at which the neutrons are being produced is exactly balanced by the rate at which the neutrons are being destroyed, then *any number of neutrons is an acceptable solution to the steady-state diffusion equation*. The solution can be either one million neutrons per second, one billion neutrons per second, one trillion neutrons per second, or even 10 neutrons per second. The mathematics that we have just presented does not really care. Thus any value for $A2_1$ can be used until the reactor power level P is specified.

Student Exercise 13.5

Suppose that the reactor power level P in our previous discussion (see Section 13.26) turned out to be just 10 W, or 10 J/s. This would correspond to a very low-power research reactor in the shape of a semi-infinite slab.

Using typical values for Σ_f, B_1, B_2, and D, and assuming that the homogeneous fuel assembly in region 1 is made out of natural uranium, and that the homogeneous reflector in region 2 is made out of light water, calculate the neutron flux ϕ at the boundary between regions 1 and 2. Calculate the neutron current across the same boundary as well.

13.27 Other Topics

Next we would like to extend our discussion of neutron diffusion theory to problems where a *radioactive source term* $S(\mathbf{r})$ is added to the left hand side of the neutron diffusion equation. This source term is usually an *external neutron source* that has nothing to do with the fissionable material that is already present. In this case, the general solutions to the diffusion equation are slightly different, and the diffusion equation needs to be written as

Steady-State Diffusion Equation with a Radioactive Source

$$\nabla^2 \phi(\mathbf{r}) + B^2 \phi(\mathbf{r}) + S(\mathbf{r})/D = 0 \tag{13.211}$$

Here the buckling of the flux B^2 can be either positive or negative. In particular, when we try to design a *radiation shield* using Equation 13.211 as our guide, we soon find that B^2 can have a *negative* value at the same time that the value of $S(\mathbf{r})$ is positive. *When this occurs, solutions to the diffusion equation are more likely to contain exponentially increasing or decreasing terms than sinusoidally varying ones*. The net flow of neutrons through the shield is then simulated by providing an appropriate value for the neutron current on one of the boundaries. In other words, this approach is equivalent to applying a *current boundary condition* to the shield. Then the neutron current is assumed to flow directly *into* the shield from the outer boundary. This is one of the first topics we would like to discuss in Chapter 14, where additional solutions to the neutron diffusion equation are explored.

References

Books and Textbooks

1. Henry, A.F. *Nuclear Reactor Analysis*, MIT Press, Cambridge, MA (1975).
2. Todreas, N. and Kazimi, M.S. *Nuclear Systems*, Vol. 1, CRC Press, Boca Raton, FL.
3. Stacey, W.M. *Nuclear Reactor Physics*, 2nd edn., John Wiley & Sons, New York (2007).
4. Duderstadt, J. and Hamilton, L. *Nuclear Reactor Analysis*, John Wiley & Sons, New York (1976).

5. El-Wakil, M.M. *Nuclear Heat Transport*, American Nuclear Society, La Grange Park, IL (1981).
6. Lewis, E. *Fundamentals of Nuclear Reactor Physics*, Academic Press, Boston, MA (2008).
7. Lamarsh, J.R. and Baratta, A.J. *Introduction to Nuclear Engineering*, Prentice Hall, Upper Saddle River, NJ (2001).
8. Lamarsh, J.R. *Introduction to Nuclear Reactor Theory*, second printing, Addison-Wesley Publishing Company Inc. (1972).
9. Shultis, K. and Faw, R. *Fundamentals of Nuclear Science and Engineering*, 2nd edn., CRC Press, Boca Raton, FL (2008).
10. Masterson, R.E. *Nuclear Engineering Fundamentals: A Practical Perspective*, CRC Press, Boca Raton, FL (2017).

Web References

1. *www.nuceng.ca/ep4d3/text/9-multigroup.pdf.*
2. *http://en.wikipedia.org/wiki/Neutron_transport.*
3. *http://web.mit.edu/22.54/ClassNotes/Lec14.pdf.*
4. *mragheb.com/.../Neutron%20Diffusion%20Theory.pdf.*
5. *http://web.mit.edu/6.013_book/www/chapter5/5.4.html.*
6. *http://en.wikipedia.org/wiki/Geometric_and_material_buckling.*
7. *neutron.kth.se/courses/reactor_physics/.../102_DiffusionEquation.pdf.*
8. *neutron.kthttp://encyclopedia2.thefreedictionary.com/Diffusion+of+Neutrons.*
9. *http://www.engr.psu.edu/cde/courses/nuce521/nuce521_chapter1_reading.pdf.*
10. *http://dspace.mit.edu/bitstream/handle/1721.1/74136/22-05-fall-2006/contents/lecture-notes/lecture22.pdf.*

Additional References

- Important physical constants used by nuclear scientists and engineers can be found in *Appendix A*.
- Unit systems and their conversion factors can be found in *Appendix B*.
- Nuclear cross sections for many important nuclear materials can be found in *Appendix C*.
- Physical properties of important nuclear materials can be found in *Appendix D*.
- Atomic masses, half-lives, and natural abundances can be found in *Appendix E*.
- Neutron diffusion coefficients and neutron mean free paths are discussed in *Appendix H*.
- Diffusion parameters for common nuclear materials are discussed in *Appendix I*.
- Bessel functions that appear in solutions to the neutron diffusion equations are discussed in *Appendix K*.

Questions for the Student

The following questions cover the material presented in this chapter, and in some cases, previous chapters as well. They are designed to test how well the student has acquired a working knowledge of the subject matter.

1. Suppose that we encounter a problem where the neutron diffusion equation can be written in the following form, that is, $\nabla^2\phi(\mathbf{r}) + B^2\phi(\mathbf{r}) = 0$. What other famous equation that frequently appears in the field of nuclear science and engineering has exactly the same form?
2. Suppose that we would like to obtain a general solution to the neutron diffusion equation for a bare homogeneous core having a width of L where the neutron flux is allowed to change as a function of time. Write down a general solution to the time-dependent neutron diffusion equation in this case.
3. Assume that the reactor core in the previous problem is exactly critical, and that the neutron flux is no longer a function of time. When this occurs, what does the term $\cos(B_1 x)$ that appears in the steady-state solution refer to?
4. Suppose that the neutron diffusion equation is written in the following form: $\nabla^2\phi(\mathbf{r}) = -S(\mathbf{r})/D$, where $S(\mathbf{r})$ is a radioactive source term. What other famous equation that frequently appears in the field of nuclear science and engineering has exactly the same form, and also has very similar solutions?
5. For a one-dimensional bare homogeneous reactor of width L, write an expression for the value of the geometric buckling when the reactor is exactly critical.
6. Fill in the following sentence with the appropriate word or phrase: For a bare homogeneous core, the neutron diffusion equation is a _____ _____ partial differential equation and its solutions are sometimes called _____ and _____.
7. Suppose that a general solution to the neutron diffusion equation reveals that the neutron flux $\phi(x, t)$ can be written as $\phi(x, t) \cong A_1 e^{-t/T}\cos(B_1 x)$. What does the value of T that appears in this equation refer to, and what units does it normally have?
8. In one-group neutron diffusion theory, what fundamental *nuclear* property does the term $B^2 = -d^2\phi(x)/dx^2/\phi(x)$, which can be derived from the neutron diffusion equation, represent?
9. In one-group neutron diffusion theory, what fundamental *geometric* property of the core does the term $B^2 = -d^2\phi(x)/dx^2/\phi(x)$, which can also be derived from the neutron diffusion equation, represent?
10. Assume that you are asked to examine a situation where $B_M^2 > B_G^2$. In the reactor where this occurs, is the neutron flux increasing, decreasing, or staying the same as a function of time?
11. For an exactly critical, bare homogeneous reactor, what equation establishes a fundamental mathematical relationship between the material composition of the core and the critical size of the core?
12. Suppose that the neutron flux in a bare homogeneous reactor is found to obey the following equation: $\phi(x) = A_1 \cos(B_1 x)$. If the thickness of the reactor core is increased by a factor of three, by what factor does the value of B_1 increase or decrease?
13. Fill in the following sentence with the appropriate word or phrase: In a _____, the neutron diffusion equation is mathematically equivalent to _____'s equation.
14. Suppose that you are asked to examine a situation where $B_M^2 = B_G^2$. In the reactor where this occurs, is the neutron flux increasing, decreasing, or staying the same as a function of time?
15. A research reactor is made out of 30 identical fuel assemblies which are grouped together to form a core in the shape of a cylinder. If the fuel rods in each fuel assembly generate one million billion fissions per second, what is the energy output of the entire reactor per second? In what form does this energy ultimately appear?
16. Suppose that you were asked to build a reactor where $B_M^2 \gg B_G^2$. What would be a typical value for the reactor period under these conditions?
17. The radius of the core of the research reactor described in problem 1 is 50 cm. Approximately how high must the fuel assemblies in the core be to generate the minimum critical mass required to operate this reactor?
18. Fill in the following sentence with the appropriate word or phrase: The key requirement in any spatial homogenization scheme is that the cross sections used in the process must guarantee the conservation of _____ within the region of the core to be homogenized.
19. Suppose that the neutron flux in a bare homogeneous reactor is found to obey the following equation: $\phi(x) = A_1 \cos(B_1 x)$. What additional piece of information is required to determine the value of A_1?
20. Fill in the following sentence with the appropriate word or phrase: When the neutron flux is changing as a function of time, the value of the neutron flux obeys a neutron diffusion equation that is nearly identical in form to _____'s equation.
21. Suppose that you are asked to examine a reactor core where $B_M^2 < B_G^2$. When this condition occurs, is the neutron flux increasing, decreasing, or staying the same as a function of time?
22. Using a very simple geometric argument, explain why a spherical reactor has the lowest peak-to-average power ratio of any common three-dimensional shape.

23. Assume that the reactor in Problem 13.1 is centered about a cylindrical coordinate system whose origin is at the center of the core. At what point does the neutron flux achieve its maximum possible value?
24. In multigroup neutron diffusion theory, how is the transport cross section related to the total cross section?
25. Fill in the following sentence with the appropriate word or phrase: When a reactor becomes subcritical or supercritical, the value of the neutron flux increases or decreases _____ as a function of time.
26. Write an expression that can be used to find the neutron flux shape in a bare spherical reactor having a radius R during steady-state conditions. Where does the neutron flux shape attain its maximum value in this case?
27. Suppose that you withdraw some control rods from the core of an exactly critical reactor where the power level is assumed to be constant. If the reactor period soon becomes 10 seconds, by how much will the steady-state power level increase in 10 seconds?
28. Assume that a reactor fuel assembly is to be spatially homogenized by volume weighting the cross sections within the fuel assembly. If only volume weighting of the cross sections is used, will this spatial homogenization process produce the correct value for the reaction rates?
29. Suppose that a reactor operator inserts some control rods into the core of an exactly critical reactor. After a short period of time, the reactor becomes subcritical, and the asymptotic reactor period becomes 10 seconds. By how much will the steady-state power level decrease 10 seconds after the asymptotic period has been established?
30. Fill in the following sentence with the appropriate word or phrase: For a bare homogeneous core, the only time that the neutron flux has a positive value everywhere is when the neutron flux shape corresponds to the first _____ and _____ of the neutron diffusion equation.
31. What geometric function(s) can be best used to describe the shape of the neutron flux in the radial and axial directions of a bare homogeneous cylindrical reactor?
32. In an earlier section, we learned that the material composition of a reactor core determines the value of the material buckling B_M^2. What equation can be used to determine the value of the material buckling when the material composition of the core is already known?
33. Assume that a bare homogeneous reactor can be constructed from the same fuel assemblies that we discussed in Problem 1 but the core is now in the shape of a rectangle. If the width of the core is W, the height of the core is H, and the depth of the core is D, write an analytical expression for the shape of the steady-state neutron flux in this specific configuration.
34. Suppose that a solution to the neutron diffusion equation can be written as $\phi_n(x, t) = \phi_n(t) \cdot \phi_n(x) = A_n e^{-\lambda_n t} \cos(B_n x)$. What do the terms corresponding to n = 3 and 5 refer to in this equation?
35. Write down the steady-state neutron diffusion equation in what is known as its standard form. Under what conditions is the value of B^2 in this equation negative when only a single energy group is used?
36. Suppose that we find a way to increase the value of the neutron diffusion coefficient D that appears in the diffusion equation by a factor of two in a bare homogeneous core without changing any of the other material properties. Does this increase or decrease the value of the material buckling for the core?
37. In neutron diffusion theory, Bessel functions of the first kind are sometimes used. In what reactor geometries are these functions normally found, and what is the value of the neutron flux when r = 2.405 in an expression for a Bessel function of the first kind?
38. When the neutron diffusion equation is to be solved in a three-dimensional Cartesian geometry, exactly how many boundary conditions are required to find the shape of the flux when the fuel assemblies in Problem 13.5 are arranged in the shape of a rectangle? Assume that one-group diffusion theory can be used in this case.
39. Now suppose that we would like to find the shape of *both* the fast and the thermal flux in the bare homogeneous rectangular reactor discussed in Problem 13.5. How many boundary conditions are required to find the two-group flux shape in this case?
40. Assume that the bare reactor core in Problem 13.5 is surrounded by a reflector that is made of light water which is approximately 20 cm thick. By how much can the thickness of the core be reduced in this case if the fuel assemblies are arranged in the shape of a simple cube?
41. In general, how many boundary conditions are required to find the shape of the neutron flux in each dimension when a bare core is surrounded by a water reflector on each side?
42. Suppose that the concentration of U-235 in the fuel rods of a bare homogeneous reactor is to be doubled from 2% to 4% to allow the reactor to be operated for a longer period of time before it has to be refueled. If none of the other material properties of the core are affected by this design change, does the material buckling B_M^2 of the core increase or decrease in this case?
43. If a symmetry condition can be used to describe the flux shape in Problem 8, how many boundary conditions are required in one dimension with only one energy group?

44. A reactor having a homogeneous core is to be constructed in the shape of a simple unreflected sphere. If the core is not surrounded by a reflector, write an expression for the critical radius of the sphere when the material composition of the core is known.
45. Suppose that the value of the neutron diffusion coefficient in the thermal energy range is known. In a bare homogeneous core, what is the approximate size of the extrapolation distance d if the value of the diffusion coefficient is D_T?
46. In neutron diffusion theory, under what specific conditions does Poisson's equation reduce to Laplace's equation?
47. Why does a three-dimensional rectangular reactor have the highest peak-to-average power ratio of any common geometric shape?
48. Using only the value of B_M, write an analytical expression for the minimum critical mass of a bare homogeneous sphere.
49. How is the value of the extrapolation distance d normally determined for a bare reactor core?
50. When a reactor core is *not* surrounded by a reflector, which geometrical configuration has the lowest peak-to-average power ratio, and which geometric configuration has the highest?
51. Under what specific set of conditions does the geometric buckling B_G^2 have exactly the same value as the material buckling B_M^2?
52. In most reactor designs, the coolant enters the core from below and exits the core from above. If the height of the core is H, and the core is either rectangular or cylindrical in shape, at what fraction of the total core height H does the temperature of the fuel usually peak? Does the fuel and the coolant temperature have to be taken into account when determining the correct value of the diffusion coefficient D to be used in this case?
53. Name two boundary conditions that can be used for the neutron flux $\phi(x)$ at an interface between two different material regions having a different molecular composition.
54. Suppose that you were put in charge of designing a BWR core. At what temperature would you expect the water in the core to begin boiling?
55. For a homogeneous reactor core surrounded by a water reflector, does the value of the thermal neutron flux tend to be higher in the center of the core or in the reflector?
56. Approximately how much smaller is the peak-to-average power ratio for spherical reactor than it is in one that resembles a cube?
57. Suppose that we would like to design a cylindrical reactor of height H and radius R to have a minimum critical mass. What should the ratio of the height to the radius be to allow the reactor to become critical with the least possible amount of nuclear fuel?
58. In a CANDU heavy-water reactor, the reactor coolant enters the core from right to left through a series of horizontal pressure tubes. For thermal neutrons, is the neutron diffusion coefficient lower on the right-hand side of the core or on the left-hand side?
59. In a thermal water reactor core, at what temperature does the uranium dioxide fuel begin to melt, and at what temperature does the zirconium cladding surrounding the fuel (in the form of Zircaloy-II or Zircaloy-IV) begin to melt as well?
60. In general, in a thermal water reactor, is the value of the fast neutron flux higher in the fuel or in the surrounding reactor coolant?
61. Suppose that you were put in charge of designing a PWR core. At what temperature would you expect the water in the core to begin boiling?
62. Draw the shape of the fast and the thermal neutron flux when a homogeneous reactor core is NOT surrounded by a reflector.
63. Suppose that you were asked to design a reactor core which is 4 m high, and where the coolant enters the core from below. If the coolant is ordinary water, is the neutron diffusion coefficient higher at the bottom of the core, at the center of the core, or at the top of the core?
64. As we have seen, reactors can be designed with both radial and axial reflectors. However, when the thickness of one of these reflector increases beyond a certain point, it tends to have almost no additional effect of the value of the reflector savings because the neutrons simply do not diffuse any further into the reflector under these conditions. In a light-water reactor, how thick does a reflector have to be before this occurs?
65. Draw the shape of the fast and the thermal neutron flux when a homogeneous reactor core is surrounded by a reflector.
66. Is a reflected reactor core always smaller than an unreflected one which contains the same type of fissionable material? Can you think of any condition where this restriction does not apply?
67. In a normal light-water reactor fuel assembly, is the diffusion coefficient higher in the fuel or in the moderator?
68. Suppose that a thermal water reactor is surrounded by a reflector, and that the diffusion coefficients in both the core and the reflector are known. What additional piece of information is required to calculate the size of the reflector savings in this case?

69. Sometimes the reflector savings is calculated using the Deutsch equation. However, the Deutsch equation is normally used for just thermal water reactors. If a reflector is designed using a different material, what equation should be used instead of the Deutsch equation?
70. What are the three primary temperature scales that are used to measure the properties of nuclear materials in the world today?
71. Suppose that the material buckling of the flux is a function of temperature, and that the material buckling happens to be measured at a temperature of 300°C. On the Kelvin or absolute temperature scale, what temperature does this happen to correspond to?
72. In a well-designed thermal water reactor, approximately how much fuel can be saved (on a percentage basis) by surrounding the core with a reflector?

Exercises for the Student

Exercise 13.1

A bare homogeneous reactor in the shape of an infinite slab is 200 cm wide. If the neutron flux at the core center point is 1×10^{14} neutrons/cm^2/s when the reactor is exactly critical, what is the value of the neutron flux halfway between the center of the reactor and the edge? If the diffusion coefficient D is 1 cm, what is the value of the neutron current at the same location?

Exercise 13.2

A bare homogeneous reactor in the shape of a right circular cylinder has a height of 200 cm and a radius of 100 cm. If the neutron flux at the center point is 5×10^{13} neutrons/cm^2/s when the reactor is exactly critical, what is the value of the neutron flux halfway between the center of the reactor and the edge in the radial direction? If the diffusion coefficient D has a value of 2 cm, what is the value of the neutron current halfway between the core center point and the top of the core?

Exercise 13.3

Assume that an exactly critical reactor in the shape of a perfect cube is cooled by light water and is fueled with enriched uranium. If the neutron flux at the center of the reactor is 6×10^{13} neutrons/cm^2/s when the reactor is exactly critical, what is the value of the fast neutron flux and the thermal neutron flux at the same location?

Exercise 13.4

Suppose that you are put in charge of increasing the power density of an existing thermal water reactor by 20%. The reactor is surrounded by a water reflector 10 cm thick, and has an average enrichment of 3%. What enrichment should you use in the core instead to increase the average power density by 20%?

Exercise 13.5

A bare unreflected reactor in the shape of a perfect cube 100 cm on a side requires 100 kg of enriched uranium to achieve a critical mass. If the core is surrounded by a water reflector 20 cm thick, how much can the critical mass of the reactor be reduced in this case?

Exercise 13.6

What is the reflector savings for a square thermal water reactor surrounded by a reflector made out of heavy water when the average diffusion coefficient of the core is 1 cm, the average diffusion coefficient of the reflector is 4 cm, and the thermal diffusion length in the reflector is 170 cm?

Exercise 13.7

A reactor core is to be built in the shape of a right circular cylinder. If the radius of the core is 100 cm, how high long should the active length of the fuel rods be to achieve a critical core with the least amount of uranium?

Exercise 13.8

A cylindrical reactor core is initially unreflected, and has a thermal diffusion coefficient of about 1 cm. If the core has a diameter of 200 cm, at what distance beyond the centerline of the core does the neutron flux fall to zero?

Exercise 13.9

A spherical research reactor contains an unreflected core, and has a thermal diffusion coefficient of about 1 cm. If the core has a diameter of 100 cm, what must the value of the quantity $\nu\Sigma_f - \Sigma_a$ be in order for the reactor to achieve a critical mass?

Exercise 13.10

Before a cylindrical reactor core is surrounded by a water reflector, the thermal flux in the center of the core is found to have a value of 5×10^{13} neutrons/cm^2/s. When a 12 cm thick water reflector is added to the core, the thermal flux is also found to peak in the reflector. What do you expect the maximum value of the thermal flux to be in the reflector under these conditions?

Exercise 13.11

Suppose that you are asked to evaluate three different reactor core configurations to determine the maximum volumetric heat generation rate q''' at the center of the core. Suppose that the average volumetric heat generation rate in each of these configurations is 100 kW/L. If the core shapes to be evaluated are a cube, a cylinder, and a sphere, what is the maximum volumetric heat generation rate q'''_{MAX} for each of these three geometries if the cores are assumed to be spatially homogeneous? To simplify your analysis, assume that you can neglect the presence of the radial and axial reflectors.

Exercise 13.12

Suppose the neutron flux in a reactor consists of two energy groups. The neutron flux in the core for the fast energy group is given by the equation $\phi_1(x) = 50 \sin(10x)$, and the neutron flux in the core for the thermal energy group is given by the equation $\phi_2(x) = 25 \sin(10x)$. The core has a thermal diffusion coefficient of $D_2 = 5$ cm, and a fast diffusion coefficient of $D_1 = 10$ cm. What is the ratio of the fast neutron current to the thermal neutron current (J_1/J_2) when $x = 0$?

Exercise 13.13

Suppose that you are asked to homogenize a reactor fuel assembly where the moderator-to-fuel ratio is 4 to 1. If the thermal flux in the moderator is twice the thermal flux in the fuel, what is the average macroscopic absorption cross section for the fuel assembly if the average macroscopic absorption cross section for the fuel is 0.17 cm^{-1}, and the average macroscopic absorption cross section for the moderator is 0.02 cm^{-1}?

Exercise 13.14

A reactor is to be built in the shape of a right circular cylinder using the least amount of uranium possible. If the radius of the core is 100 cm, and the core is to be unreflected, what must the total volume of the core be?

Exercise 13.15

After doing a design review, it is decided to replace the bare homogeneous reactor core in the previous exercise (Exercise 13.14) with a new core surrounded by a water reflector 25 cm thick. If the reflector reflects essentially all of the thermal neutrons back into the core, how much fuel will the reflected core use if the bare core uses 100 kg?

Exercise 13.16

The infinite multiplication factor for a homogeneous material is 1.1 and the effective multiplication factor is 1.0. If the thermal diffusion length of the neutrons in this material is 5 cm, what is the geometric buckling of the flux in this material if the material is in the shape of a cylinder? If the cylinder has a radius of 100 cm and a height of 200 cm, do more neutrons leak out of the sides of the cylinder or the top and the bottom?

14

Solving the Neutron Diffusion Equation with a Radioactive Source Term

14.1 Solutions to the Diffusion Equation with No Fissionable Materials

In Chapter 13, we provided solutions to the neutron diffusion equation in what could be considered to be *conventional reactor geometries*. *In this chapter, we would like to extend our discussion of the neutron diffusion equation to other geometries where an external neutron source denoted by the symbol S(r)* is either imbedded in a material or is allowed to interact with a material (such as a radiation shield) that does not produce any additional neutrons. In this case, we can set $\phi\sum_f = 0$ and any fast or thermal neutrons that appear in the material must be due exclusively to the presence of the source. These neutrons can be produced by a radioactive source that is injected directly into the material, or they can also be produced by another external device such as a *neutron beam generator.* When neutrons are intentionally injected into a material, the additional neutrons are usually simulated by adding an additional *boundary condition* to the neutron diffusion equation. Normally this boundary condition requires a *neutron current* to enter the material from one or both sides. The best way to understand how this works is to go back to the neutron diffusion equation (see Chapter 13) and add a radioactive source term to it to track these additional neutrons. The most general form of the diffusion equation when this source is independent of time is

Steady-State Diffusion Equation with a Radioactive Source

$$\nabla^2\phi(\mathbf{r}) + B^2\phi(\mathbf{r}) + \frac{S}{D} = 0 \tag{14.1}$$

where S is usually measured in neutrons/sec (or n/s). For line sources, it is also measured in n/cm/s, for planar sources it is measured in n/cm^2/s, and for distributed sources, it is measured in n/cm^3/s. Examples of these sources are provided in Section 14.2. The material buckling in Equation 14.1 is in turn defined by

Definition of the Material Buckling

$$B^2 = \frac{\nu\Sigma_f - \Sigma_a}{D} \tag{14.2}$$

For the special case where there is no nuclear fuel present, we can set the local neutron production rate $P = \nu\Sigma_f\phi$ to zero, and the steady-state neutron diffusion equation becomes

The Steady-State Diffusion Equation with No Fissile Materials

$$\nabla^2\phi(\mathbf{r}) - \Sigma_a\frac{\phi(\mathbf{r})}{D} = -\frac{S}{D} \tag{14.3}$$

In general, Equation 14.3 has a different set of solutions when S is present than when S is not. In some problems, S is also a function of position in which case it must be written as $S(\mathbf{r})$. However, if we can neglect this positional dependence for the moment, then the diffusion equation when no nuclear fuel is present material can be written as

$$\nabla^2\phi(\mathbf{r}) - \left(\frac{\Sigma_a}{D}\right)\phi(\mathbf{r}) = -\frac{S}{D} \tag{14.4}$$

or

The Diffusion Equation with No Nuclear Fuel

$$\nabla^2\phi(\mathbf{r}) - \left(\frac{1}{L^2}\right)\phi(\mathbf{r}) = -\frac{S}{D} \tag{14.5}$$

where

$$L^2 = \frac{D}{\Sigma_a} \tag{14.6}$$

is our old friend *the neutron diffusion area* and L is a related parameter called *the neutron diffusion length*. The physical meanings of both of these parameters were presented in Chapter 11.

14.2 Types of Neutron Sources

The neutron source S that appears in the diffusion equation (Equation 14.5) can assume a number of different configurations depending upon the way the source is deployed. If the neutrons emanate from a single point, it appears in the diffusion equation as *a point source*. If a number of point sources are connected together to form a line, then the source becomes what is known as *a line source*. Finally, if all of the sources are connected together to form a plane, the resulting source is called *a planar source*. Examples of these sources are shown in Figure 14.1. In most cases, the source term S can be replaced by a boundary condition involving the neutron current J(**r**). It is legitimate to do this as long as the source is very thin, and it is placed next to another material that does not produce any additional neutrons.

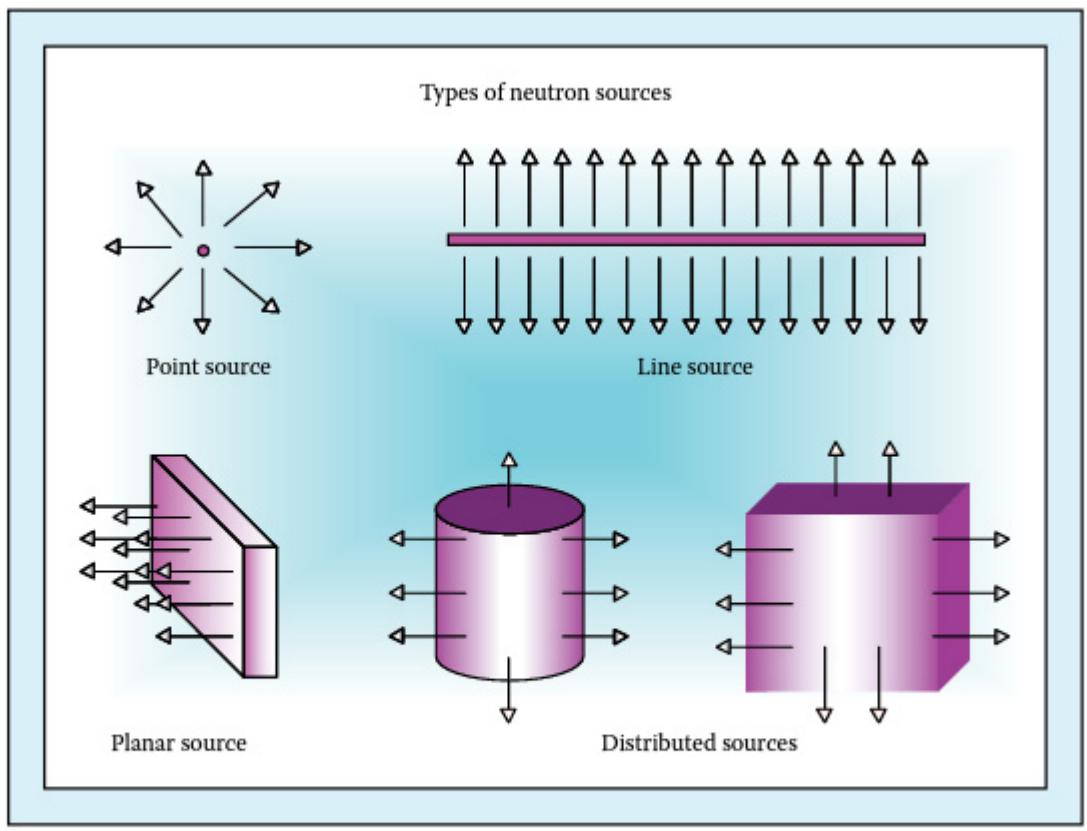

FIGURE 14.1 Examples of some common neutron sources that are either distributed or nondistributed.

TABLE 14.1
Expressions for the Laplacian Operator in Popular Coordinate Systems

Coordinate System	Coordinates	Form of the Laplacian Operator $\nabla^2\phi$
Cartesian	x, y, z	$\partial^2\phi/\partial x^2 + \partial^2\phi/\partial y^2 + \partial^2\phi/\partial z^2$
Cylindrical	r, θ, z	$(1/r)\partial/\partial r(r\partial\phi/\partial r) + (1/r^2)\partial^2\phi/\partial\theta^2 + \partial^2\phi/\partial z^2$
Spherical	r, θ, φ	$(1/r^2)\partial/\partial r(r^2\partial\phi/\partial r)) + (1/r^2\sin\theta)\partial/\partial\theta(\sin\theta\cdot\partial\phi/\partial\theta) + (1/r^2\sin^2\varphi)\partial^2\phi/\partial\varphi^2$

Fortunately, many problems that we encounter in nuclear science and engineering tend to fall into one of these categories. If this is not the case, then the source term is said to be *distributed*, and the neutron source may be distributed throughout the material instead of being concentrated at just one location. For example, this can occur when a neutron emitting material is dissolved in a tank of water. If the water does not have any fissionable material in it, then we can set $\nu\Sigma_f\phi = 0$ and the diffusion equation becomes

The Diffusion Equation with a Source Implemented as a Boundary Condition

$$\nabla^2\phi(\mathbf{r}) - \left(\frac{1}{L^2}\right)\phi(\mathbf{r}) = 0 \tag{14.7}$$

where the source term S has been replaced by a simple boundary condition. We then need to use the appropriate form of the Laplacian operator ∇^2, which varies depending upon whether the neutron source S is in the shape of a point, a line, or a plane. The exact expressions for this operator are shown in Table 14.1. Depending on the coordinate system that is used, ϕ can be a function of (x, y, z), (r, θ, z), or (r, θ, φ); that is, it can be written as $\phi(x, y, z)$, $\phi(r, \theta, z)$, or $\phi(r, \theta, \varphi)$.

The choice of which coordinate system to use is purely arbitrary. It depends on what coordinate system best fits the geometry of the problem at hand. However, once this is determined, finding the shape of the flux is a relatively simple process, and this is the next subject that we would like to discuss.

14.3 General Solutions to the Neutron Diffusion Equation

We learned in Chapter 13 that the neutron diffusion equation in a spatially homogeneous material can be thought of as a second-order differential equation with constant coefficients:

$$\nabla^2\phi(\mathbf{r}) \pm B^2\phi(\mathbf{r}) = -S \tag{14.8}$$

because the values of the cross sections and the diffusion coefficient are independent of position. In this case, the solutions to the diffusion equation depend almost entirely on the sign of B^2. If $B^2 > 0$, then the general solution for a one-dimensional planar slab is

The General Solution with $B^2 > 0$

$$\phi(x) = A1\sin Bx + A2\cos Bx - \frac{S}{B^2} \tag{14.9}$$

and if $B^2 < 0$, then the general solution is

The General Solution with $B^2 < 0$

$$\phi(x) = A1\,e^{+Bx} + A2\,e^{-Bx} + \frac{S}{B^2} \tag{14.10}$$

where both B and S are considered to be constants. In a uniform material, B and S will be the same everywhere, and all that is required to solve Equations 14.9 or 14.10 are two boundary conditions. One boundary condition determines the

value of A_1 and the other boundary condition determines the value of A_2. Now let us show how these boundary conditions can be implemented.

14.4 Solutions to the Diffusion Equation with a Neutron Source on the Boundaries

Consider a problem where there is a well-defined neutron source S on the boundary of a homogeneous material, but there is no fissile material present within the material itself. This corresponds to a situation where $\Sigma_f = 0$ and $\Sigma_a > 0$. In this case, $B^2 < 0$, and the general solution to the diffusion equation is

$$\phi(x) = A_1 e^{+Bx} + A_2 e^{-Bx} + \frac{S}{B^2} \tag{14.11}$$

Since the neutron source is located on the boundary, and it is not located inside the material, we can set S = 0, and the general solution becomes

$$\phi(x) = A_1 e^{+Bx} + A_2 e^{-Bx} \tag{14.12}$$

Notice that when there is no fissile material present, the buckling of the flux becomes negative, and the general solutions contain exponentially decaying terms, rather than those involving sines and cosines. In general, there can be many different situations where this can occur. For example, consider a tank of water that is adjacent to a source of incoming neutrons. The same region can also consist of a stack of lead bricks or a concrete block with a radiation source close to one side. In any event, as long as the dimensions of the materials remain the same (see Figure 14.2), the only thing that is different as far as the diffusion equation is concerned is the value of B. Large values of B cause the flux to be attenuated faster than small values do, but other than the rate of attenuation, the overall shape of the flux is the same.

In other words, *the same general solutions can be used for many different materials—as long as* $\Sigma_f = 0$. The diffusion equation simply requires a different value of B for each material type. When $\Sigma_f = 0$ and $\Sigma_a > 0$, the diffusion equation becomes

$$\nabla^2\phi(x) - \left(\frac{\Sigma_a}{D}\right)\phi(x) = 0 \tag{14.13}$$

which can also be written as

$$\nabla^2\phi(x) - \left(\frac{1}{L^2}\right)\phi(x) = 0 \tag{14.14}$$

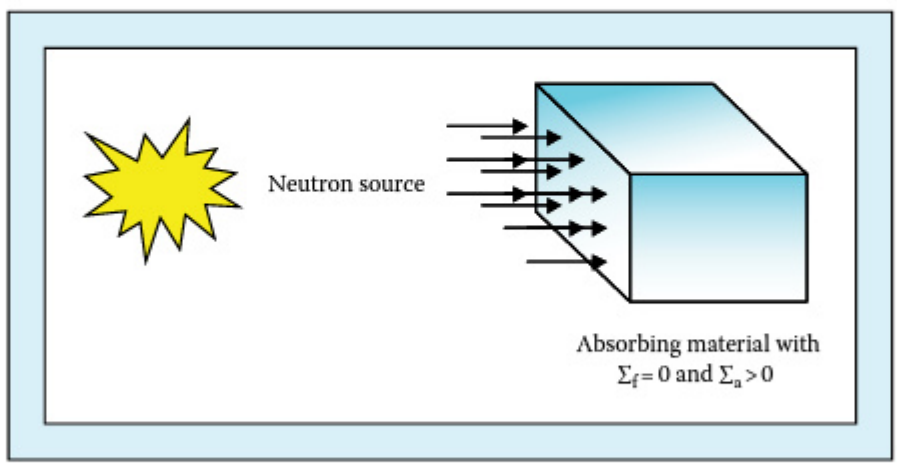

FIGURE 14.2 A neutron source of strength S that can be represented by a boundary condition from a distance.

where

$$L^2 = \frac{D}{\Sigma_a} \tag{14.15}$$

In other words, the solution remains the same and the only difference is that $L^{H_2O} \neq L^{Pb} \neq L^{C}$. The neutron flux may attenuate as we move away from the source at different rates because the values of the diffusion length L are different. However, the pattern of the attenuation remains the same. Now let us illustrate what the solutions look like for a few simple geometries.

14.5 Simple Planar Neutron Source

The first case we would like to examine is a neutron absorbing material next to a planar neutron source. Refer to Figure 14.3 to visualize the layout of the material and the source. If we assume that the planar source is very large or effectively infinite in the y and z directions, then the problem of solving the neutron diffusion equation reduces to finding the neutron flux in the x direction. The neutron flux in this case is a function of x only, and the appropriate version of the Laplacian operator to use is $d^2\phi/dx^2$. The version of the diffusion equation to be solved is then

The Diffusion Equation Next to a Planar Neutron Source

$$\frac{d^2\phi(x)}{dx^2} - \left(\frac{1}{L^2}\right)\phi(x) = 0 \tag{14.16}$$

Since $B^2 = -1/L^2$ is negative, Equation 14.16 has the following general solution:

$$\phi(x) = A_1 e^{-x/L} + A_2 e^{+x/L} \tag{14.17}$$

This solution applies to the entire material except at x = 0, where the neutron source is located. Because the source has been positioned at the origin, this problem possesses a high degree of symmetry, and we only have to solve the diffusion

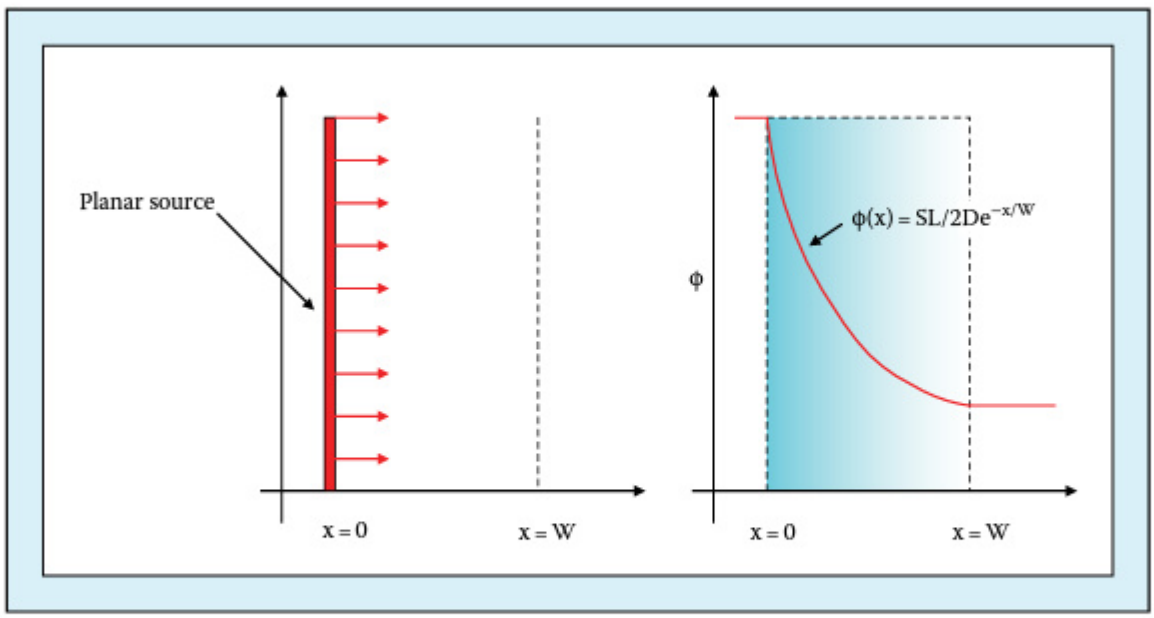

FIGURE 14.3 The shape of the neutron flux in a homogeneous region filled with water, lead, or concrete. Here, an external neutron source of strength S can be found where x = 0.

equation to the right of the origin or to the left of it. Suppose we would like to find the flux shape for $x > 0$. Under these conditions it follows that $A_2 = 0$ because the flux cannot increase indefinitely with increasing x. The equation for the neutron flux then becomes

$$\phi(x) = A_1 e^{-x/L} \tag{14.18}$$

where the value of A_1 is a function of the boundary conditions. Since the planar source emits a total of S neutrons per second, it must emit a neutron current **J** equal to S/2 in each direction. That is to say, *the neutron source S creates a current* $J = S/2$ along both the positive and negative directions when $x = 0$. The sum of these two currents then equals the value of S itself. We also know from Fick's Law of Diffusion (see Chapter 11) that

$$\mathbf{J}(x) = -D\frac{d\phi}{dx} \tag{14.19}$$

or from Equation 14.18,

$$\mathbf{J}(x) = A_1\frac{D}{L}e^{-x/L} \tag{14.20}$$

Since $\mathbf{J} = S/2$, it follows from this equality that

$$A_1 = \frac{SL}{2D} \tag{14.21}$$

at $x = 0$, and the exact solution for $x > 0$ is

$$\phi(x) = \frac{SL}{2D}e^{-x/L} \tag{14.22}$$

Hence the same solution must also apply for $x < 0$. In this case, a solution that is valid for all values of x can be obtained by replacing x by its absolute value $|x|$. Then the equation for the neutron flux becomes

The Neutron Flux near a Planar Source

$$\phi(x) = \frac{SL}{2D}e^{-|x|/L} \tag{14.23}$$

Equation 14.23 indicates that the value of the flux falls off *exponentially* with distance from the planar neutron source and achieves its maximum value at the origin where $\phi = SL/2D$ (see Figure 14.3). As the reader may recall, this is exactly the same behavior that occurs when a reactor core is surrounded by a neutron reflector (see Chapter 13). Only in this case, the reflector tends to scatter neutrons rather than just absorbing them.

Student Exercise 14.1

Using representative values for D and Σ_a, calculate the diffusion lengths for water, lead, and concrete, L^{H_2O}, L^{Pb}, and L^{C}, and plot the attenuation of the neutron flux through a solid block of water, lead, and concrete assuming that the general solution to the flux shape in each case is given by

$$\phi = \phi_o e^{-x/L}$$

where ϕ_o is the intensity at the left-hand surface of the block, and the LHS of the block is located at $x = 0$. Which material attenuates the neutron flux the most and which material attenuates the neutron flux the least? Why do you think that this is the case?

14.6 Point Sources of Neutrons

Now consider for the moment a related problem with a *neutron point source*. Assume that the source is imbedded in a large homogeneous medium that can be considered to be spherical in shape. The point source emits S neutrons per second isotropically in all directions. In other words, the neutron emission rate into every solid angle **Ω** surrounding the point source is identical. Finally, assume that the point source is located at the origin of the spherical coordinate system shown in Figure 14.4. Hence the value of ϕ depends on only the distance from the origin r. Because we are dealing with a spherical coordinate system, we must write the diffusion equation in spherical coordinates and apply the appropriate version of the Laplacian operator ∇^2 to the diffusion equation (see Table 14.1). When we do so, we find that

$$\frac{1}{r^2}\frac{d}{dr}\left(\frac{r^2 d\phi(r)}{dr}\right) + B^2\phi(r) = 0 \tag{14.24}$$

and after differentiating the first term, we obtain

The Diffusion Equation for a Neutron Point Source

$$\frac{d^2\phi(r)}{dr^2} + \left(\frac{2}{r}\right)\frac{d\phi(r)}{dr} + B^2\phi(r) = 0 \tag{14.25}$$

where $B^2 = 1/L^2$. The general solution to Equation 14.25 is

$$\phi(r) = \frac{A_1 e^{-r/L}}{r} + \frac{A_2 e^{+r/L}}{r} \tag{14.26}$$

Not surprisingly, this solution is nearly identical to the solution we obtained previously for a planar source except that the term 1/r appears in the denominator because the coordinate system is spherical. Again, A_1 and A_2 are constants of integration that depend on the boundary conditions. We can use the same approach we used for the planar neutron source to evaluate A_1 and A_2. Obviously, A_2 must be equal to zero because the flux must always decline as we move further away from the origin. Then the general solution to this problem is

$$\phi(r) = \frac{A_1 e^{-r/L}}{r} \tag{14.27}$$

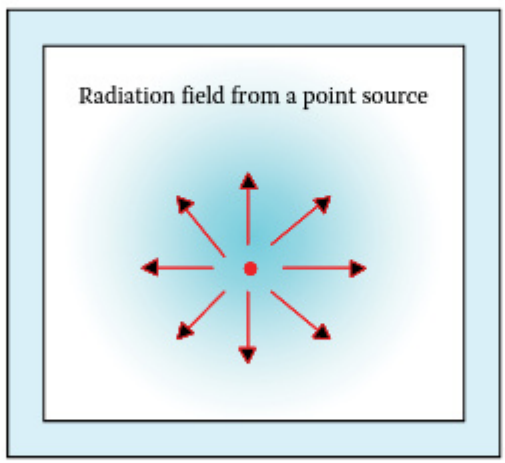

FIGURE 14.4 A point source emitting neutrons into a homogeneous medium.

To find the value of A_1, we must again evaluate the neutron current **J** at the origin. From Fick's Law of Diffusion, we know that

$$\mathbf{J}(r) = -D\frac{d\phi(r)}{dr} = A_1 D\left(\frac{1}{rL} + \frac{1}{r^2}\right)e^{-r/L} \tag{14.28}$$

Since the current emanating from the point source is $J = S/4\pi$, the value for A_1 becomes

$$A_1 = \frac{S}{4\pi D} \tag{14.29}$$

and the equation for the neutron flux is

The Neutron Flux near a Point Source in an Isotropic Medium

$$\phi(r) = \frac{S}{4\pi D}\frac{e^{-r/L}}{r} \tag{14.30}$$

Again the flux falls off exponentially with distance from the point source. Only in this case, the exponential attenuation is further enhanced by the presence of the 1/r term. Ironically, this behavior is also observed when a neutron source is surrounded by a radiation shield.* Thus a similar level of attenuation can be expected in any large, homogeneous material where *both scattering and absorption* occur. However, Equation 14.30 is based on the assumption that the material through which the neutrons are travelling absorbs at least *some* of the neutrons. If the material scatters the neutrons instead of absorbing them, then the rate of attenuation obeys an entirely different equation.

14.7 Radiation Field from a Point Source in a Vacuum

Now consider what would happen to the flux if the material through which the neutrons were travelling was a *vacuum*. In this case, there would be no absorption or scattering, and the diffusion equation would become

The Neutron Diffusion Equation in a Complete Vacuum

$$\nabla^2\phi(\mathbf{r}) = 0 \tag{14.31}$$

The reader may also recognize Equation 14.31 as *Laplace's equation*. In spherical coordinates, Laplace's equation can be written as

$$\frac{1}{r^2}\frac{d}{dr}\left(\frac{r^2 d\phi}{dr}\right) = 0 \tag{14.32}$$

or more concisely,

$$\frac{d}{dr}\left(\frac{r^2 d\phi}{dr}\right) = 0 \tag{14.33}$$

Since a vacuum does not contain any atoms for the neutrons to "interact" with, the scattering and absorption cross sections are zero and the diffusion length L is effectively infinite. For a point source of strength S, the flux then attenuates according to the well-known *Inverse Square Law*:

The Inverse Square Law

$$\phi(r) = \frac{S}{4\pi r^2} \tag{14.34}$$

* See *Nuclear Engineering Fundamentals: A Practical Perspective*, by R.E. Masterson, CRC Press (2017).

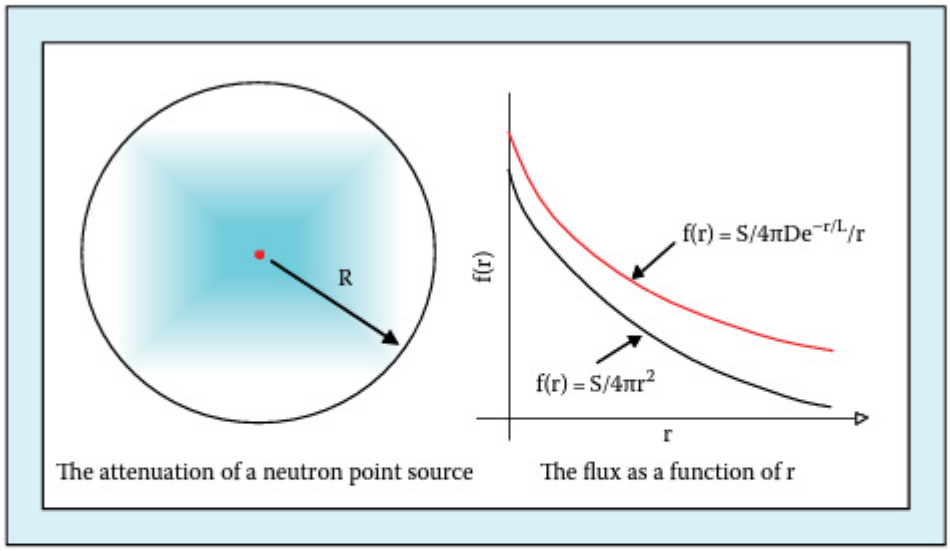

FIGURE 14.5 The flux as a function of distance from a neutron point source.

Many other applications of the inverse square law are also discussed in our companion book.* *In other words, the attenuation of the neutron flux depends on whether or not the neutrons are hitting anything!* If they are moving through a vacuum, the flux shape is given by $\phi(r) = S/4\pi r^2$, and if they are *not* moving through a vacuum, the flux shape is given by $\phi(r) = (S/4\pi D)\, e^{-r/L}/r$, where D is the diffusion coefficient. Both scenarios are compared in Figure 14.5. *Notice that the attenuation of a neutron beam in a diffusive medium is less than the attenuation predicted by the inverse square law* because the neutrons are colliding with other objects as they move. In general, Equations 14.30 and 14.34 can be applied to other electrically neutral particles, and not just neutrons. If other particles are produced by atoms scattering or absorbing these particles then Equations 14.30 and 14.34 can be applied to these particles as well, but the particle flux must now be multiplied by a *buildup factor* B to account for the additional particles that are produced. The particle flux in this case becomes

The Particle Flux in an Isotropic Medium with Additional Particle Production

$$\phi(r) = \frac{SB}{4\pi D}\frac{e^{-r/L}}{r} \tag{14.35}$$

Normally, the buildup factor is a dimensionless number greater than unity but less than ten. The buildup factor is also a function of the initial particle energy E. An analogous equation can also be derived to predict the behavior of photons.* However, for gamma rays, the form of Equation 14.35 is different, and if it is applied to an isotropic point source emitting S gamma rays per second surrounded by a radiation shield of radius R, the value of 1/L must replaced by a linear *attenuation coefficient* μ and the value of r in the denominator must be squared. The diffusion coefficient that appears in the denominator must also be removed.

Example Problem 14.1

In an earlier section, we learned that the neutron diffusion length L is an important parameter that appears in many different forms of the neutron diffusion equation. Suppose that a material is able to scatter neutrons but not absorb them. What is the value of the neutron diffusion length in this case?

Solution The diffusion length is given by the equation, $L = \sqrt{(D/\Sigma_a)}$. If the material is a pure scatterer, D will always be greater than zero, while $\Sigma_a = 0$. Thus, the diffusion length L must be effectively infinite in this case. [Ans.]

* See *Nuclear Engineering Fundamentals: A Practical Perspective*, by R.E. Masterson, CRC Press (2017).

14.8 Understanding the Principle of Superposition

When particles emanate simultaneously from more than one point source, the particle flux $\phi(r)$ is simply equal to the sum of the contributions from all of the point sources. In classical physics, this effect is called *superposition* and in addition to particles, it also applies to sound waves, light waves, and even ocean waves. However, when it comes to neutrons or other electrically neutral particles, phase effects (including constructive or destructive interference) are not important—at least when it comes to determining their density distribution as a function of space and time. Thus to find the neutron concentration at a specific point in space and time, we simply add the contributions from each point source S_i and sum these contributions over as many point sources as there are present, that is, from i = 1 to N. Since the number of neutrons (and hence the neutron flux) is proportional to the particle density ρ, it also follows that

$$\phi(\mathbf{r}) = \rho(r)\, v(r, E) \tag{14.36}$$

where v is the neutron velocity. In one group theory, the velocity distribution v(E) shown in Equation 14.36 is then replaced by the average neutron velocity <v>

$$<v> = \frac{\int_E v(E)\,dE}{\int_E dE} \tag{14.37}$$

and so it is easy to see that the neutron fluxes can also be summed at a distance to find the total flux. In Section 14.6, we derived an expression for the particle flux $\phi(r)$ at a distance from a spherical point source in an isotropic diffusing medium. The equation for the intensity of the flux was

$$\phi(r) = \frac{S\, e^{-r/L}}{4\pi D r} \tag{14.38}$$

where

D is the diffusion coefficient (in cm)
L is the diffusion length (in cm)
S is the source strength or intensity (in neutrons per second)

However, if $\mathbf{r}$ is a vector, Equation 14.38 can also be written as

$$\phi(\mathbf{r}) = \frac{S e^{-|\mathbf{r}-\mathbf{r}'|/L}}{4\pi D|\mathbf{r}-\mathbf{r}'|} \tag{14.39}$$

and the point source is now located at an arbitrary point $\mathbf{r}'$ instead of at the origin itself. If we have several point sources, each of which has a different spatial location $\mathbf{r}_i$, and a different source strength S_i, then the *Principle of Superposition* can be used to obtain the total neutron density or the total neutron flux ϕ at a point. The result is

$$\phi(\mathbf{r}) = \sum_i \frac{S_i e^{-|\mathbf{r}-\mathbf{r}_i'|/L}}{4\pi D|\mathbf{r}-\mathbf{r}_i'|} \tag{14.40}$$

Equation 14.40 can be applied to any homogeneous material through which the neutrons are moving. Moreover, Equation 14.40 makes it possible to bridge the gap between what exists at a point (which has no volume), and a distributed source, which has a finite volume, size, and shape (see Figure 14.6).

14.9 Some Additional Observations regarding the Principle of Superposition

The principle of superposition is a universal principle that is manifested in nuclear power plants in many different ways. In fact, it can be applied to *both* neutrons and photons. However, its application to photons requires a slightly different

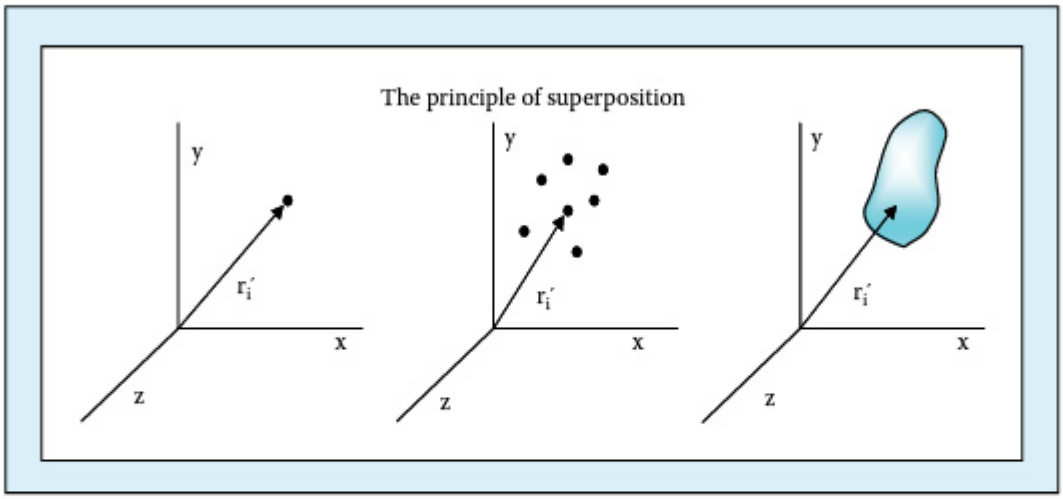

FIGURE 14.6 The superposition of point sources to create a distributed source.

approach because photons can interfere with each other either constructively or destructively. Thus the *phase* of the photons becomes important when determining the behavior of photon population as a whole.

In electricity and magnetism, the principle of superposition is sometimes applied to add together (or subtract) waves that emanate from different physical sources. Each of these sources can be thought of as a point source, and a common example of two point sources emanating from a single object is an electric or magnetic *dipole*. The properties of the dipole are determined by the *phases* of the individual waves that emanate from points on each of the poles. If the waves have the same frequency and phase, then the point sources add constructively, and if they do not, then they may interfere destructively as well. The principle of superposition therefore guarantees that any solution to a single point source can also be applied to any distribution of point sources such as the ones shown in Figure 14.6. This principle can easily be generalized to any distribution of point sources $S_i(\mathbf{r}')$ by replacing the summation in Equation 14.40 by an integral over the entire volume of space that contains the point sources. The result of this operation is

$$\phi(\mathbf{r}) = \int_V \frac{S_i(\mathbf{r}')e^{-|\mathbf{r}-\mathbf{r}'|/L}}{4\pi D|\mathbf{r}-\mathbf{r}'|} dV \tag{14.41}$$

or

$$\phi(\mathbf{r}) = \int_V \mathbf{K}(\mathbf{r}, \mathbf{r}') S_i(\mathbf{r}') dV \tag{14.42}$$

where the function

$$\mathbf{K}(\mathbf{r}, \mathbf{r}') = \frac{e^{-|\mathbf{r}-\mathbf{r}'|/L}}{4\pi D|\mathbf{r}-\mathbf{r}'|} \tag{14.43}$$

is sometimes called the *point diffusion kernel* for an infinite medium. Now let us apply these concepts to a very simple problem that you are probably familiar with. Suppose that two point sources having different strengths S_1 and S_2 are located along the y-axis of an infinite diffusing medium such as the one shown in Figure 14.7. One point source is located a distance r_1 from the origin and the other point source is located a distance r_2 from the origin. Because of the principle of superposition, the value of the flux at the origin is

$$\phi(0) = \phi_1(r_1) + \phi_2(r_2) \tag{14.44}$$

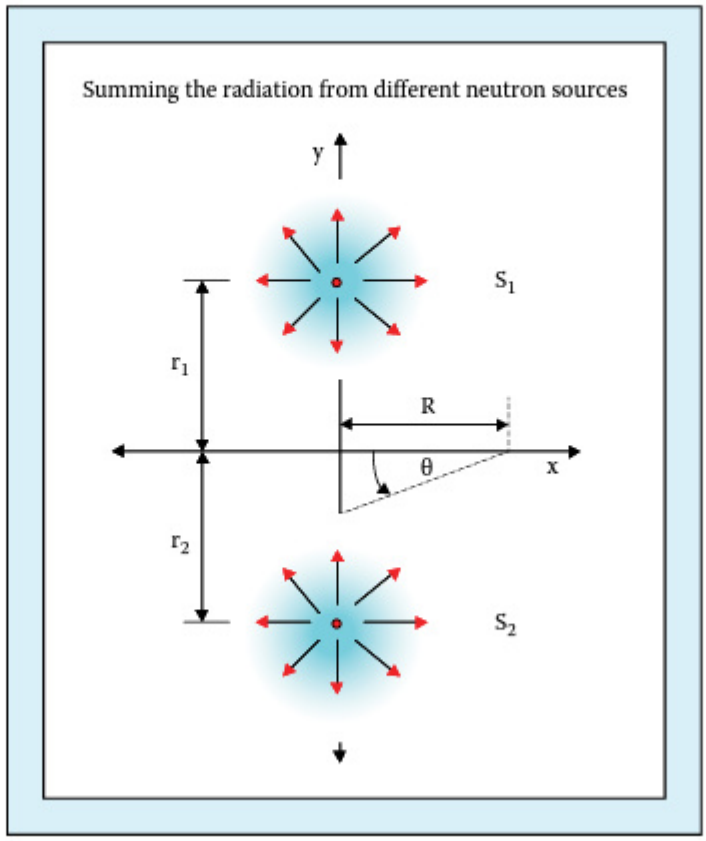

FIGURE 14.7 Two point sources S_1 and S_2 that emit neutrons isotropically.

or

$$\phi(0) = \frac{S_1 e^{-r_1/L}}{4\pi D r_1} + \frac{S_2 e^{-r_2/L}}{4\pi D r_2} \tag{14.45}$$

Notice that when $r_1 = r_2 = R$ and $S_1 = S_2 = S$, Equation 14.45 becomes

$$\phi(0) = \frac{S e^{-R/L}}{4\pi D R} + \frac{S e^{-R/L}}{4\pi D R} \tag{14.46}$$

which then leads to

$$\phi(0) = \frac{S e^{-R/L}}{2\pi D R} \tag{14.47}$$

The neutron current **J** at the origin is zero when the two point sources are identical and equidistant because the current vectors $\mathbf{J}_1$ and $\mathbf{J}_2$ from each of the sources are equal and oppositely directed at this point so that

$$\mathbf{J} = \mathbf{J}_1 + \mathbf{J}_2 = 0 \tag{14.48}$$

Again, this is a simple illustration of how the principle of superposition works. The neutron current **J** and the neutron flux $\phi(\mathbf{r})$ are shown in Figure 14.8 as a function of axial position for the case where both point sources are located a distance R from the origin and both sources have exactly the same strength. Note the interesting symmetry that this problem displays. The only place where the neutron current does *not* flow is at the origin. However, depending on the value of r, the flux can peak at *two* different points along the y-axis.

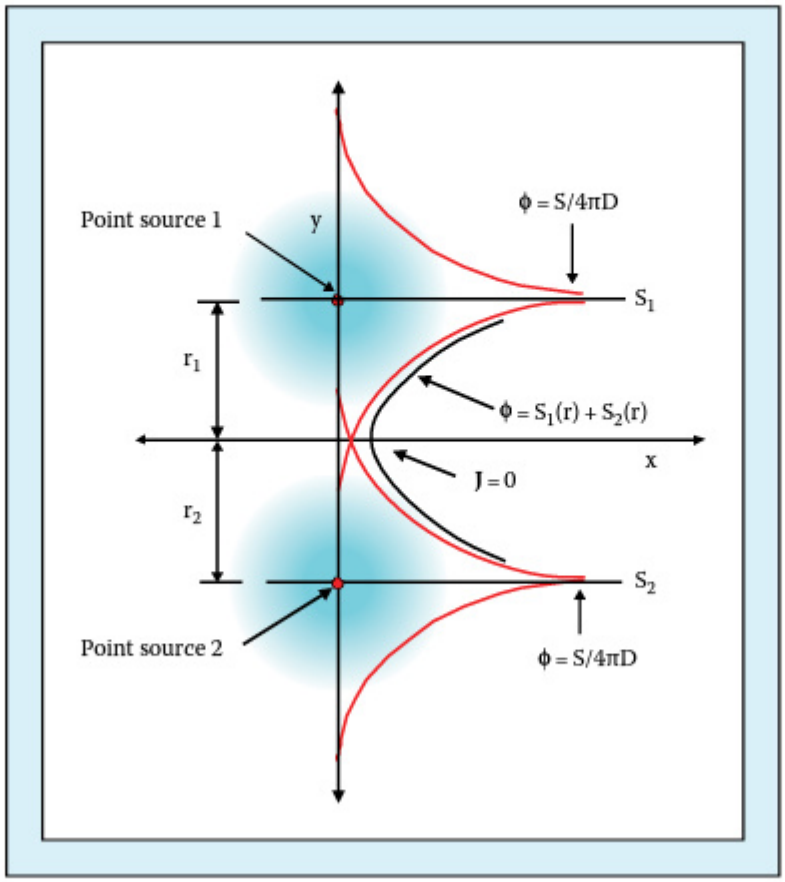

FIGURE 14.8 The shape of the neutron flux ϕ in the vicinity of the two point sources shown in Figure 14.7.

Student Exercise 14.2

Based on the information provided in Section 14.9, derive an equation for the shape of the neutron flux at any point x along the positive x-axis and for all values of y. Also derive an expression for the neutron current **J** as a function of x and y. You may assume that both neutron sources are identical in strength and the sources are located at exactly the same distance R from the origin of the coordinate system along the y-axis. Use symmetry arguments to simplify your derivation as much as possible.

14.10 Finding the Neutron Flux from Multiple Point Sources

Our previous analysis can be extended to other geometries by summing Equation 14.40 over multiple point sources. Now let us attempt to illustrate this for the problem shown in Figure 14.11 where a point on the x-axis is located a distance R from a vertical array of identical point sources each of which located a distance r_i from the point where we wish to know the value of the flux. In this case, the flux at a specific location is given by

$$\phi(\mathbf{r}) = \sum_i \frac{S_i e^{-|\mathbf{R}/\cos\theta_i|/L}}{4\pi D\,|\mathbf{R}/\cos\theta_i|} \tag{14.49}$$

where the closest point source is located a distance R away. Here we have used the helpful trigonometric identity, since the problem is symmetric about the y axis.

$$\sec\theta_i = 1/\cos\theta_i \tag{14.50}$$

We will leave it up to the reader to show that the Principle of Superposition will lead to an exponentially declining particle density that has the same form as one of the *modified Bessel functions of the second kind* that we will introduce to

the reader in Section 14.13. Hence the neutron density declines exponentially as a function of distance from the y-axis. Again, this exponential attenuation is characteristic of any large diffusive medium.

14.11 Applying the Principle of Superposition to Neutrons in a Vacuum

Up to this time, we have taken the liberty to assume that the source term $S(\mathbf{r})$ in the neutron diffusion equation is surrounded by a material object (such as a radiation shield) that has a finite value for the diffusion coefficient D and the diffusion length L. In other words, we have assumed that the neutrons are surrounded by a *diffusing material* where Equation 14.40 can be used:

$$\phi(\mathbf{r}) = \sum_i \frac{S_i e^{-|\mathbf{r}-\mathbf{r}_i'|/L}}{4\pi D|\mathbf{r}-\mathbf{r}_i'|} \quad \text{(for neutrons in a diffusing medium)} \tag{14.51}$$

However, if the diffusing material is replaced by a vacuum, then the neutrons behave differently because the values of L and D are *infinite* and a neutron can move in a straight line essentially forever. Consequently, neutrons in a vacuum follow the *Inverse Square Law*, rather than Equation 14.51, and to describe this behavior, the following form of the Inverse Square Law should be used:

$$\phi(\mathbf{r}) = \sum_i \frac{S_i}{4\pi|\mathbf{r}-\mathbf{r}_i'|^2} \quad \text{(for neutrons in a vacuum)} \tag{14.52}$$

In the summation in Equation 14.52, there can be up to N separate point sources. It then follows from Equation 14.52 that the neutron flux at the same distance R from N identical point sources will be $\phi(\mathbf{R}) = NS/4\pi R^2$. In other words, Equation 14.52 can be used to find the neutron flux at the center of a hollow sphere coated with a thin layer of radioactive material having an output of $N \times S_i$ particles per second. If two point sources are located at a distance R from a point that is located midway between them and they are located in a vacuum, then the corresponding equation for the value of the flux is simply

$$\phi(\mathbf{R}) = \frac{S_1 + S_2}{4\pi R^2} \tag{14.53}$$

Again, Equation 14.53 assumes *no destructive interference* between the individual particles.

14.12 Applying the Principle of Superposition to Light Waves

While phase effects are not important for neutrons, they can be very important for x-rays and gamma rays. In Chapter 2, we learned that x-rays and gamma rays are simply energetic photons of light. Their kinetic energy E is proportional to their frequency f, and the constant of proportionality between their energy and their frequency is *Planck's constant* h, which in the SI system has a value of $h = 6.6 \times 10^{-34}$ kg · m²/s. Their wavelength λ is also inversely proportional to their frequency f. In a vacuum, this relationship is given by $\lambda = c/f$ or since $E = hf$, the wavelength may also be written as $\lambda = hc/E$, where c is the speed of light (~300,000,000 m/s). Notice that increasing the energy E of a photon always reduces its wavelength λ. Hence, light waves tend to become more localized as their energy and their frequency are increased.

Industrial lasers and other devices make use constructive and destructive interference to increase the intensity of the light that the device emits. Thus, the extent to which two light waves interact with one another constructively or destructively is a function of their frequency (or equivalently their wavelength) and also their phase. In college physics, one learns that if one photon has a frequency f_1 and the other photon has a frequency f_2, then each photon has an electric field **E** that oscillates perpendicular to the direction of propagation with an amplitude that is given by A_1 and A_2 (see Figure 14.9). We can describe the time dependence of this field by writing

$$A_1(t) = A_1 \cos 2\pi f_1 t \ \text{(for photon 1)} \quad \text{and} \quad A_2(t) = A_2 \cos 2\pi f_2 t \ \text{(for photon 2)} \tag{14.54}$$

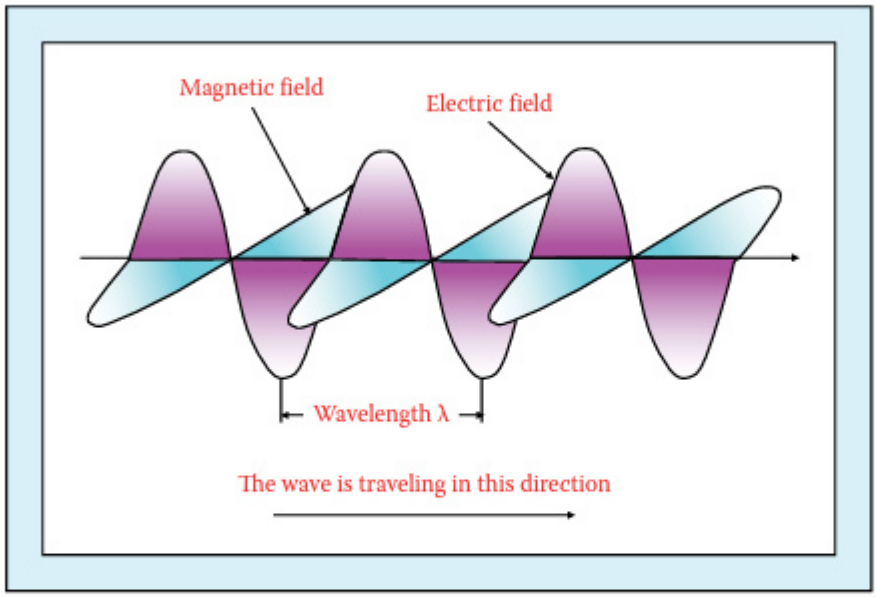

FIGURE 14.9 A photon is a very complex particle that generates an electric and a magnetic field as it moves. The fields are at right angles to its direction of propagation, and when the electric field interacts with an atom, it causes the electrons to vibrate and emit additional photons.

In other words, the principle of superposition also applies to photons, but their phase differences must be taken into account when determining how they affect the particles in their path. The total energy each photon carries through space is proportional to the square of these amplitudes, so the kinetic energy of each particle is simply

$$E_1 = \left|A_1 \cos 2\pi f_1 t\right|^2 = A_1^2 \quad \text{and} \quad E_2 = \left|A_2 \cos 2\pi f_2 t\right|^2 = A_2^2 \tag{14.55}$$

These equations assume that the photons (like other point particles) do not interfere with one another unless their wave functions overlap so that the total energy E of the two photons is simply

$$E = E_1 + E_2 = A_1^2 + A_2^2 \tag{14.56}$$

Of course, this is exactly what one would expect if the photons do not overlap or interact in any way. However, as we discovered earlier, photons have an entirely different side to their behavior because they can also act as waves. This *wave/particle duality* means that photons can also behave like water waves and constructively or destructively interfere if they happen to travel in exactly the same direction with exactly the same frequency and speed. This interaction between their wave patterns is also known as *interference*. If the wave patterns have exactly the same frequency and phase angle, and if they are traveling in exactly the same direction, then they can add together just like water waves do to produce a larger wave. This is an example of what is known as *constructive interference*. However, if the wave patterns overlap in exactly the opposite way, then the resulting wave patterns will cancel each other out, and this interaction is known as *destructive interference*. In this case, the time-dependent amplitude A(t) of the two waves is given by

$$A = A_1(t) + A_1(t) \tag{14.57}$$

or

$$A(t) = A_1 \cos 2\pi f_1 t + A_2 \cos 2\pi f_2 t \tag{14.58}$$

Hence, *the total energy E of the combined wave function* of the two photons is

$$E = A^2 = \left|A_1(t) + A_1(t)\right|^2 \tag{14.59}$$

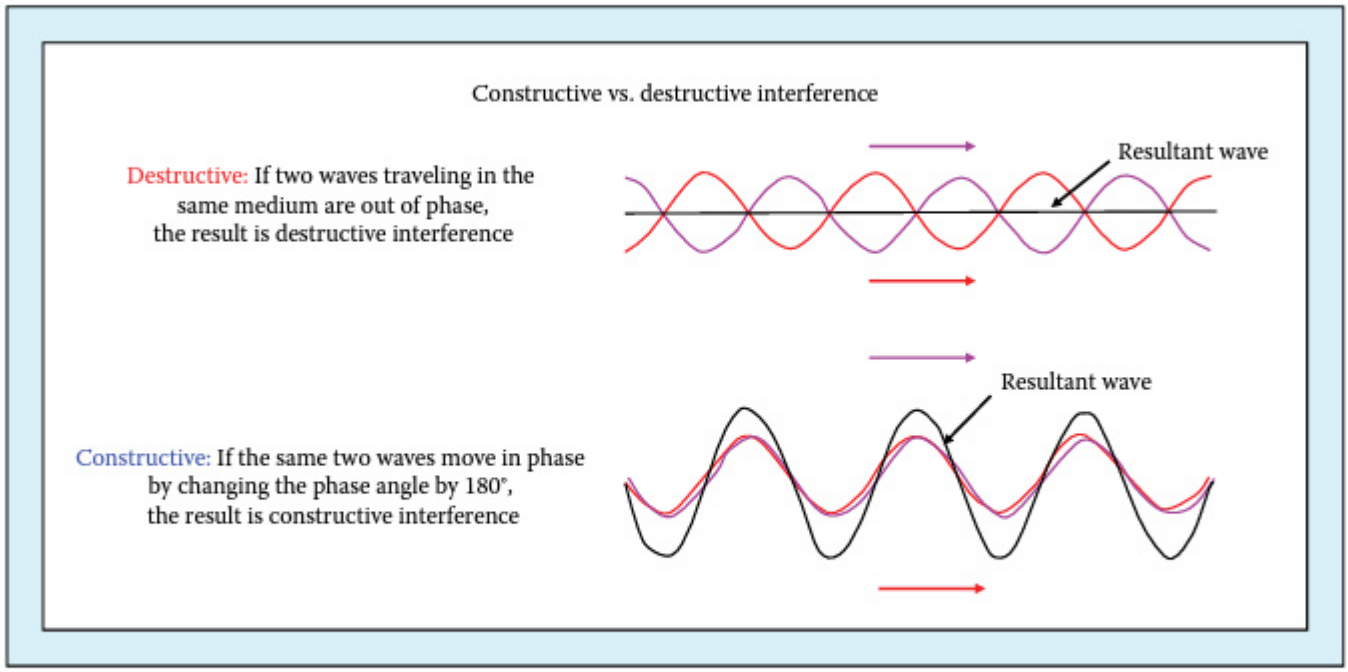
Constructive vs. destructive interference
Destructive: If two waves traveling in the same medium are out of phase, the result is destructive interference
Resultant wave
Constructive: If the same two waves move in phase by changing the phase angle by 180°, the result is constructive interference
Resultant wave

FIGURE 14.10 An example of two photons having the same frequency, but interacting with each other in different ways (due to a phase difference) to demonstrate the phenomenon of constructive and destructive interference.

or

$$E = A^2 = A_1^2 + A_2^2 + 2A_1 A_2 \cos(\phi) \tag{14.60}$$

where $\phi = \phi_1 - \phi_2$ is the *phase angle* between them (see Figure 14.10). *The phase angle can be thought of as the fraction of a wavelength λ that one vibrating photon happens to be offset from another*. We can simplify Equation 14.60 slightly by realizing that each individual photon must satisfy the following equalities: $E_1 = A_1^2$ and $E_2 = A_2^2$. In this case, the result is

The Equation for the Energy of a Photon Beam

$$E = E_1 + E_2 + 2\sqrt{E_1}\sqrt{E_2}\cos(\phi) \tag{14.61}$$

Note in particular that there is now a new term $2\sqrt{E_1}\sqrt{E_2}\cos(\phi)$ to account for the fact that photons can interfere with each other constructively or destructively (like water waves do). Most of the time, the photons that are produced in a reactor core are emitted with a random distribution of phase angles so that the average phase angle between any two photons is $\phi = 90°$ or $\phi = \pi/2$. In other words, most of the time, these photons do not interfere with each other constructively or destructively, and the average value of the interference term $2\sqrt{E_1}\sqrt{E_2}\cos(\pi/2)$ is 0. However, in industrial lasers and similar devices, the wavelengths of the photons are designed to be similar enough that the interference term $2\sqrt{E_1}\sqrt{E_2}\cos(\phi)$ can be used to reinforce the wave patterns of the individual photons to produce what is known as *constructive interference*. In this case, $\sqrt{E_1} = \sqrt{E_2}$, and the value of the interference term is $2E_1\cos(\phi = 0) = 2E_1$. Hence, the combined energy of the two photons in this case is not just $E = E_1 + E_2$ but rather

$$E = E_1\,(\text{from photon 1}) + E_1\,(\text{from photon 2}) + 2E_1\,(\text{from the interference term}) = 4E_1 \tag{14.62}$$

Thus, Equation 14.62 shows that the constructive interference of two photons can *double the energy* that each of the photons can deliver to a material individually. This is purely a quantum mechanical effect that can be used to increase the energy of a beam of photons beyond what would be possible if the wavelengths and phases of each of the photons were completely random. Today virtually all industrial lasers use this simple principle to enhance the energy of the photons that

they can deliver to a piece of material in their path. Because the energies and the wavelengths of the individual photons are also nearly identical, the light a laser emits is very pure and can be used for many practical purposes, including cutting materials, carrying information, and even enriching uranium if the frequency of the photons happens to be exactly right (This topic is discussed in more detaill in our companion book*).

Example Problem 14.2

Suppose that two light beams are pointed in the same direction and originate from exactly the same point. If the two beams happen to be 180° out of phase with each other and have the same intensity I, what is the intensity of the two beams at a distance r from the source?

Solution The intensity of the two beams is given by the equation $I = I_1 + I_2 + 2\sqrt{I_1}\sqrt{I_2}\cos(\phi)$, where ϕ is the phase angle. If $\phi = 180° = \pi$, then $\cos(\phi) = -1$, and $I = 2I - 2I = 0$! So the beams interfere with each other destructively, and the aggregate intensity of the combined beam is zero. [Ans.]

14.13 Simulating Line Sources of Neutrons

Using the principle of superposition, we can derive an equation for the neutron flux when a large number of neutrons are emitted isotropically from an infinite line source. A line source S can be thought of as a thin filament of material that emits neutrons outward in all directions. To understand how the neutron population behaves in this case, the diffusion equation must be solved in cylindrical coordinates with the line source located at the origin where r = 0. The line source can be placed on the y-axis in the manner shown in Figure 14.11. Because the line source can be thought of as an infinite neutron emitter, the appropriate version of the Laplacian to use is

$$\nabla^2 = \frac{1}{r}\frac{d}{dr}\frac{r\,d\phi(r)}{dr} = \frac{d^2\phi(r)}{dr^2} + \frac{1}{r}\frac{d\phi(r)}{dr} \tag{14.63}$$

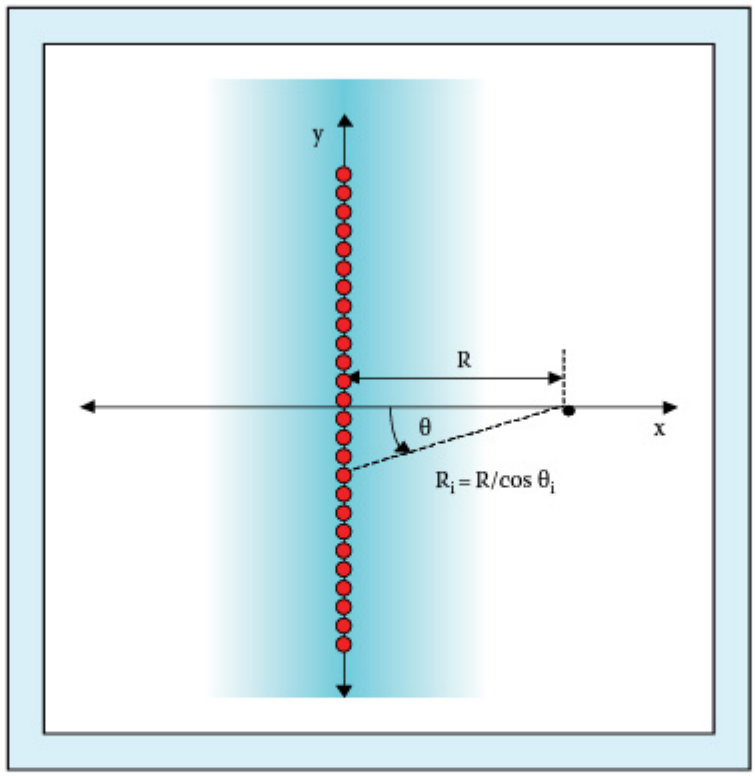

FIGURE 14.11 A line array built from multiple point sources.

* See *Nuclear Engineering Fundamentals: A Practical Perspective*, by R.E. Masterson, CRC Press (2017).

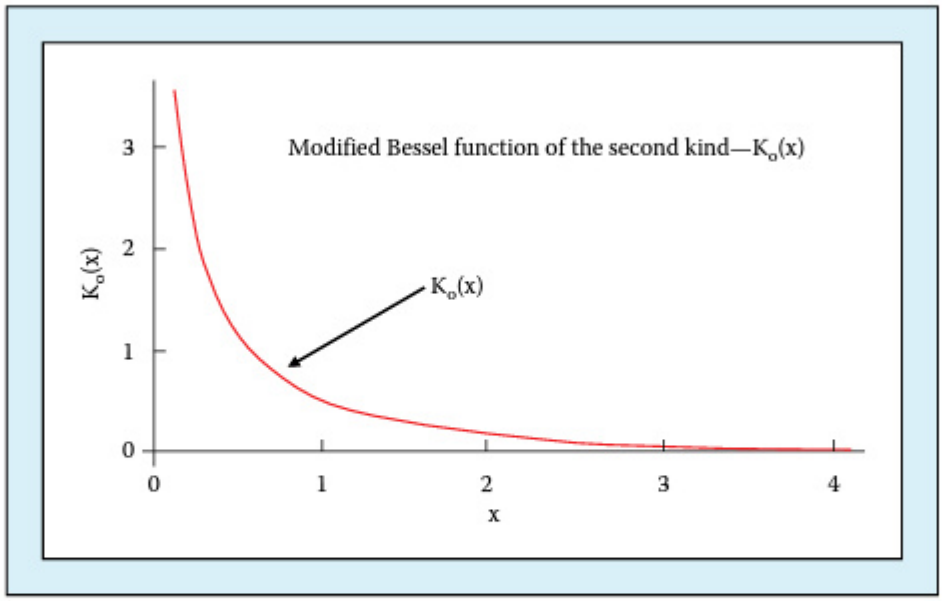

FIGURE 14.12 The behavior of $K_o(x)$, which is a modified Bessel function of the second kind.

because there is no variation of the line source in the z direction. In a diffusive material (i.e., one where the value of L is finite) the diffusion equation becomes

$$\frac{d^2\phi(r)}{dr^2}+\frac{1}{r}\frac{d\phi(r)}{dr}-\frac{1}{L^2}\phi(r)=0 \tag{14.64}$$

The neutron flux in this case is only a function of r. The general solution to Equation 14.64 is then

$$\phi_r(r)=A_1K_o\left(\frac{r}{L}\right)+A2I_o\left(\frac{r}{L}\right) \tag{14.65}$$

where $K_o(x)$ and $I_o(x)$ are called *modified Bessel functions of the first and second kind.* Unlike ordinary Bessel functions, which are oscillating as functions of a real argument (see Chapter 13), I_o and K_o are *exponentially growing* and *decaying functions*, of the argument x = r/L. The shape of K_o is shown in Figure 14.12 and the shape of I_o can be found in the references at the end of the chapter.

Thus value of A_2 is 0 because I_o increases exponentially as the value of the radius r is increased. Since the neutron current emanating in all directions from the line source is $J = S/2\pi$, the value of A_1 when $r \rightarrow 0$ is $A_1 = S/2\pi D$. Hence, the shape of the neutron flux is given by

$$\phi(r)=\frac{S}{2\pi D}K_o\left(\frac{r}{L}\right) \tag{14.66}$$

When the modified Bessel functions are evaluated, it can be shown that when r = L, the flux is about 10% as high as it is at r = 0 and when r = 2L, it is about 2% as high. Modified Bessel functions such as $K_o(x)$ also appear in the *Feynman propagator* of *quantum field theory*, so they are considerably more common than most people think. Now let us turn our attention to problems where a neutron source can no longer be placed on a boundary and treated as boundary condition involving the magnitude and direction of the neutron current **J**.

14.14 Solutions to the Neutron Diffusion Equation in a Diffusive Medium with a Distributed Source

Earlier in the chapter, we showed how the neutron diffusion equation could be solved when a neutron source S could be implemented as a boundary condition involving the neutron current **J**. We then extended the external neutron source to include problems where the flux could be described by the equation

$$\phi(\mathbf{r})=\sum_i\frac{S_ie^{-|\mathbf{r}-\mathbf{r}_i'|/L}}{4\pi D|\mathbf{r}-\mathbf{r}_i'|} \tag{14.67}$$

We would now like to turn our attention to how the diffusion equation can be solved when an external boundary condition can no longer be used to represent the neutron source. For example, a fuel rod or an entire fuel assembly may be too large to model accurately using a simple boundary condition involving the neutron current. When this occurs, we must modify our approach and explicitly include the value of S on the right-hand side of Equation 14.68. This approach is called solving the neutron diffusion equation *with a distributed source* term. In the next section, we would like to describe how this can be done.

14.15 Solving the Neutron Diffusion Equation with a Distributed Source

As we discussed previously, the appropriate form of the diffusion equation to use with a distributed source is

Diffusion Equation with a Distributed Source

$$\nabla^2\phi(\mathbf{r}) - \left(\frac{1}{L^2}\right)\phi(\mathbf{r}) = -\frac{S}{D} \tag{14.68}$$

where the source S is assumed to be distributed throughout an entire *region of space*. Equation 14.68 can be solved just like any other diffusion equation if we know the value for S. Specifically, this equation has the same form as another famous equation of classical physics called *Helmholtz's equation*, which appears frequently in the study of nuclear heat transfer and fluid flow. The general solution to Equation 14.68 is

$$\phi(x) = A_1 e^{+Bx} + A_2 e^{-Bx} - \frac{S}{B^2} \tag{14.69}$$

or equivalently,

$$\phi(x) = A_1 e^{x/L} + A_2 e^{-x/L} - \frac{SL^2}{D} \tag{14.70}$$

since B = 1/L. Notice that the sign of S has been reversed in each case.

Now suppose that the region of space that contains S is centered about the y-axis and has its centerline at x = 0. Moreover assume that the region has a total width 2W. What does the shape of the neutron flux look like in this case? To find out, we must apply the appropriate boundary conditions to find the values of A_1 and A_2. However, from our earlier discussion in Chapter 13, we know that two boundary conditions are required to determine these coefficients. (First-order differential equations require only one). If we assume that $\phi = 0$ at x = W and $\phi = 0$ at x = −W, then

$$A_1 e^{W/L} + A_2 e^{-W/L} + \frac{SL^2}{D} = 0 \tag{14.71}$$

at x = W. Because the problem is symmetrical, we can also assume that $J = -D d\phi/dx = 0$ at x = 0. This implies that $A_1 D/L - A_2 D/L = 0$, which means that $A_1 = A_2$. Therefore, we can conclude that

$$A_1 = A_2 = -\frac{SL^2}{D}\left(e^{W/L} + e^{-W/L}\right)^{-1} \tag{14.72}$$

which leads to the particular solution for a planar neutron source:

A Solution to the Neutron Diffusion Equation with a Planar-Distributed Source

$$\phi(x) = \frac{SL^2}{D}\left(1 - \frac{e^{x/L} + e^{-x/L}}{e^{W/L} + e^{-W/L}}\right) \tag{14.73}$$

Notice that when x = W, $\phi = 0$ and that we could have come to the same conclusion by requiring that $\phi = 0$ at x = −W, in which case

$$A_1 e^{-W/L} + A_2 e^{W/L} + \frac{SL^2}{D} = 0 \tag{14.74}$$

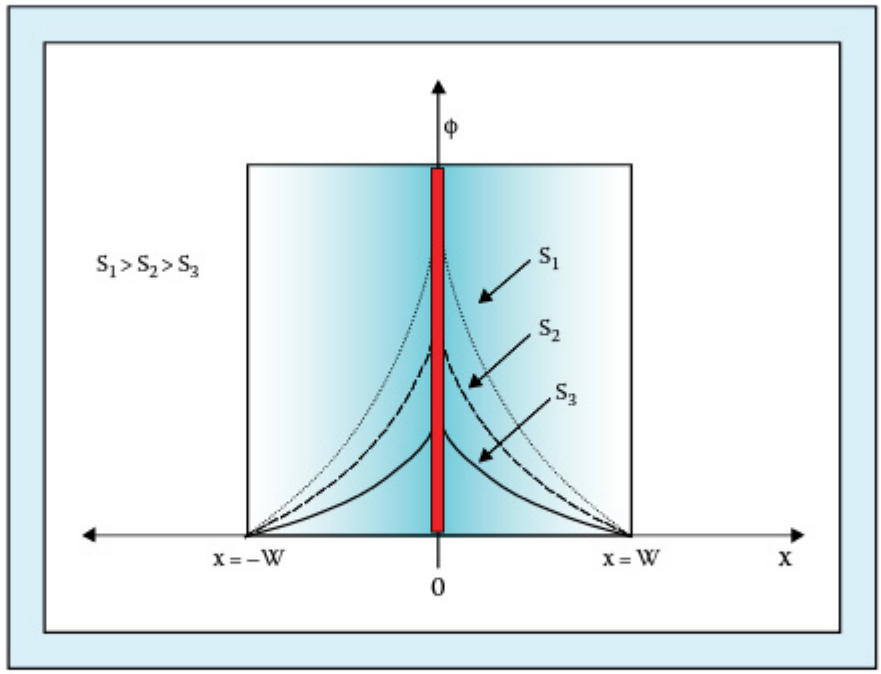

FIGURE 14.13 A symmetric region with a distributed neutron source.

Since $\phi = 0$ at $x = W$, we also know that

$$A_1 e^{W/L} + A_2 e^{-W/L} + \frac{SL^2}{D} = 0 \tag{14.75}$$

Again, this can only be true if $A_1 = A_2$. Thus the presence of the distributed neutron source S elevates the level of the neutron flux everywhere inside of the material. It therefore appears as a *scalar multiplier* of the total intensity S. In other words, *in the problem we have just solved, the value of the flux increases in direct proportion to the strength of the neutron source*. It increases the value of the flux everywhere except at the boundaries where $\phi = 0$. In other words, away from the boundaries, it does *not* change the shape of the flux. It simply changes its value. We have attempted to illustrate this for the interested reader in Figure 14.13. Now let us consider a related problem where the neutron flux is allowed to "float" on each of the boundaries in direct proportion to the strength of the source S. We can do this by changing the value of ϕ to ϕ_o, and then at the boundaries the value of ϕ_o can be anything we want. Then if the flux on the boundaries had a value of, say, $\phi = \phi_o$ instead of just 0, the boundary conditions at the surface would become

$$A_1 e^{-W/L} + A_2 e^{W/L} + \frac{SL^2}{D} = \phi_o \tag{14.76}$$

and

$$A_1 e^{W/L} + A_2 e^{-W/L} + \frac{SL^2}{D} = \phi_o \tag{14.77}$$

Again, this is only possible when $A_1 = A_2$, so this leads to

$$A_1 = A_2 = \phi_o - \frac{SL^2}{D} \cdot \left(e^{W/L} + e^{-W/L}\right)^{-1} \tag{14.78}$$

The specific solution then becomes

$$\phi = \left(\phi_b - \frac{SL^2}{D}\right) \frac{e^{x/L} + e^{-x/L}}{e^{W/L} + e^{-W/L}} + \frac{SL^2}{D} \tag{14.79}$$

Thus, we have obtained a general solution to the diffusion equation for a homogeneous material region that contains a uniformly distributed neutron source having strength S. In one dimension, this region could be a tank of radioactive liquid or a fuel assembly that has just been removed from the core and is in the process of cooling down. As long as the region of space can be spatially homogenized (see Chapter 19), then the solution we have found can be used. We would now like to extend our discussion to two material regions where a distributed neutron source is present in the innermost one. This increases the number of boundary conditions that must be used, and we must now solve two diffusion equations instead of just one.

14.16 Two Diffusive Regions with a Distributed Neutron Source in the Interior One

Before attempting to find the appropriate value for the neutron flux on an external boundary, we would first like to demonstrate what the flux shape looks like when the external boundary is far enough away from a distributed source that the neutron flux approaches an asymptotic value for very large values of r. In order to illustrate how the flux behaves under these conditions we would like to solve a slightly more complicated problem that allows us to see the behavior far away from a distributed source. To begin with, we would like to select a geometry where the solution is relatively easy to obtain.

Consider a sphere having two concentric regions—an inner region of reasonable size that contains a distributed neutron source S and an outer region surrounding the inner region that is source free. To simplify the arithmetic, assume that the inner region has radius R with a diffusion coefficient and an absorption coefficient of D and Σ_a and a uniform neutron source S. The source emits S neutrons per second. Suppose that the sphere is surrounded by a second source free region of much larger size that has the same material properties but extends to $r = \infty$. The sphere is again centered about the origin of a coordinate system where r = 0. Refer to Figure 14.14 to visualize how the two regions are aligned. To simplify our analysis, the values for D and Σ_a are assumed to be the same in both material regions. This implies that the values of $1/L^2 = \Sigma_a/D$ for both regions will be the same. To find the neutron flux, we must find solutions to the following two neutron diffusion equations:

For Region 1:

$$\frac{d^2\phi(r)}{dr^2} + \frac{2}{r}\frac{d\phi(r)}{dr} - \frac{\phi(r)}{L^2} = \frac{S}{D} \quad \text{for } 0 \le r \le R \tag{14.80}$$

For Region 2:

$$\frac{d^2\phi(r)}{dr^2} + \frac{2}{r}\frac{d\phi(r)}{dr} - \frac{\phi(r)}{L^2} = 0 \quad \text{for } R < r \le \infty \tag{14.81}$$

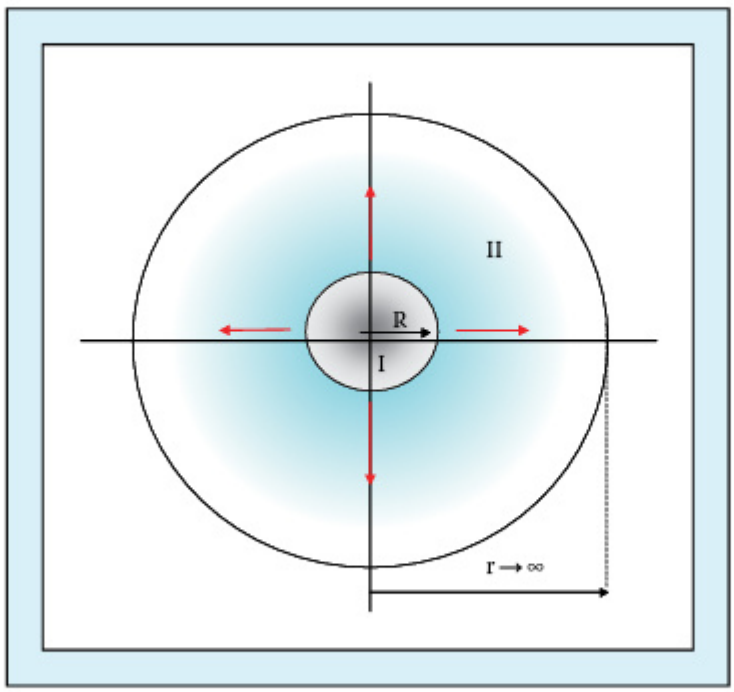

FIGURE 14.14 Two regions with a neutron source in the interior one.

Here, we have already consolidated the derivatives in the Laplacian that are shown in Table 14.1. Because the spherical regions are spatially uniform, the derivatives of θ and φ can be ignored. The general solutions for the neutron flux ϕ(r) in each region are

Region I:

$$\phi(r) = (A_1/r)\exp(r/L) + (A_2/r)\exp(-r/L) + SL^2/D \tag{14.82}$$

or

$$\phi(r) = (A_1/r)\exp(r/L) + (A_2/r)\exp(-r/L) + S/\Sigma_a \tag{14.83}$$

since

$$L^2 = \frac{D}{\Sigma_a} \tag{14.84}$$

Region II:

$$\phi(r) = (A_3/r)\exp(r/L) + (A_4/r)\exp(-r/L) \tag{14.85}$$

where A_1, A_2, A_3, and A_4 are constants of integration to be determined from the boundary conditions. Because the geometry is spherically symmetric there are four boundary conditions that must be applied to these equations:

For Region I:

1. ϕ(r) must be finite as $r \to 0$
2. This implies that $A_2 = -A_1$
3. ϕ(r) must be continuous across the interface where $r = R$
4. This establishes a relationship between A_1 and A_4

For Region II:

1. ϕ(r) must be 0 when $r \to \infty$
2. This implies that $A_3 = 0$
3. J(r) must be continuous across the interface where $r = R$
4. This establishes another relationship between A_1 and A_4

It is somewhat messy to go through each boundary condition separately, so we will simply present the final results. In region I, the solution is

Region I:

$$\phi(r) = \frac{S}{\Sigma_a}\cdot\left(1 - f\frac{R\sinh(r/L)}{r\sinh(R/L)}\right) \tag{14.86}$$

and in region II, the solution is

Region II:

$$\phi(r) = \frac{S}{\Sigma_a}\cdot(1-f)\frac{R}{r}e^{-(r-R)/L} \tag{14.87}$$

where the variable f is sometimes called a *form factor*, which is defined in the following way:

$$f = \left(1 + R/(R+L)\coth(R/L) - 1\right)^{-1} \tag{14.88}$$

Notice that the solution requires us to evaluate the hyperbolic cotangent coth(R/L). To see how this can be done, first consider the definitions of sinh(x), cosh(x), and coth(x):

Definitions of the Hyperbolic Sine, Cosine, and Tangent

$$\coth(x) = \frac{e^{x} + e^{-x}}{e^{x} - e^{-x}}$$

and

$$\sinh(x) = \frac{1}{2}\left(e^{x} - e^{-x}\right) \tag{14.89}$$

and

$$\cosh(x) = \frac{1}{2}\left(e^{x} + e^{-x}\right)$$

Notice that the *hyperbolic cotangent* coth(x) is defined in a similar way as the cotangent function that is used with normal sines and cosines. So by analogy with the definition of cot(x)

$$\cot(x) = \frac{\cos(x)}{\sin(x)} \tag{14.90}$$

the expression for the hyperbolic cotangent is

$$\coth(x) = \frac{\cosh(x)}{\sinh(x)} \tag{14.91}$$

Equations 14.86 and 14.87 are appropriate to use when the second material region is very large. Notice that there was no need to "float" the neutron flux on the outer boundary to obtain these results. It simply fell off naturally as the distance r from the neutron source increases. However, one must be a considerable distance away from the neutron source before it finally approaches zero.

14.17 Vacuum Boundary Conditions for the Diffusion Equation

When neutrons encounter a material region with a sharp outer boundary, it is necessary to use an alternative boundary condition to account for the fact that the neutron flux does not fall to 0 exactly where the boundary ends. For example, if there is a *vacuum* on one side of the boundary, then we must be able to estimate the value of r or x where the neutron flux falls to zero. Presumably this location must lie a short distance δ beyond the boundary itself. Otherwise, we are faced with the task of simply guessing what the value of the flux ϕ_o on the boundary must be. To determine the distance δ beyond the boundary where the flux falls to zero, we must resort to invoking what is known as the *extrapolated boundary condition*. The *extrapolation distance* δ where this occurs can be derived from transport theory under certain conditions (see Chapter 22). The vacuum boundary condition is implemented by observing that any neutrons that leave the surface of the neutron-rich region do not reenter it. This implies that the angular neutron flux $\phi(r, E, \mathbf{\Omega})$ that appears in the transport equation is zero for any solid angle that causes neutrons to be reflected back into the core. Mathematically, this is equivalent to requiring that

$$\phi(\mathbf{r}, E, \Omega, t) = 0 \quad \text{for } \mathbf{\Omega} \cdot \mathbf{dS} < 0 \tag{14.92}$$

This relationship applies to all points on the surface S of the neutron-rich area A. As such, this boundary condition is sometimes referred to as the *vacuum boundary condition*. Obviously, the value of the neutron diffusion length L will also change across the boundary. If the materials on both sides of the boundary have completely different densities, then this change can be quite dramatic. We can then use the results of neutron transport theory to provide us with an exact estimate of the distance δ where the value of the neutron flux ϕ will fall to zero by providing a curve fit to the predictions of diffusion theory. Alternatively, we can just guess a value for ϕ at the boundary and hope for the best. This distance is sometimes known as the *extrapolation distance*, and we will discuss its properties in more detail next.

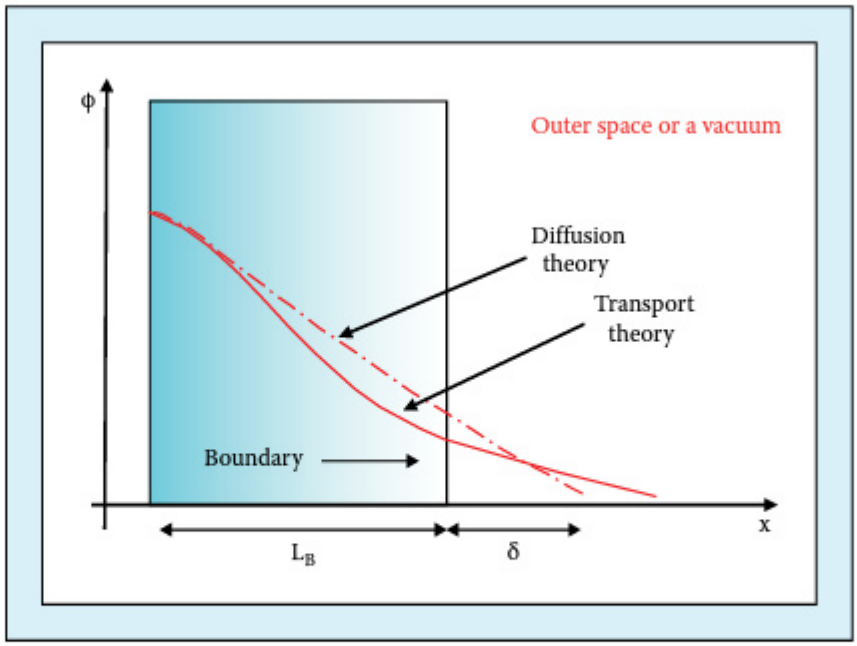

FIGURE 14.15 A picture illustrating the extrapolated boundary condition for an infinite slab.

It turns out that the extrapolation distance δ (where the flux falls to zero on the other side of the boundary) can be inferred from the simple formula

Equation for the Extrapolation Distance

$$\delta = 0.71\lambda_{tr} \tag{14.93}$$

where λ_{tr} is the *transport mean free path* that we discussed in Chapter 11 (refere to Figure 14.15). We also know that the transport mean free path is related to the diffusion coefficient D by

$$\lambda_{tr} = 3D \tag{14.94}$$

where the diffusion coefficient D is now the diffusion coefficient of the material immediately preceding the vacuum. In any event, *the extrapolation distance* δ can be found from the equation

Relationship between the Extrapolation Distance and the Diffusion Coefficient

$$\delta = 0.71\lambda_{tr} = 0.71 \times 3D = 2.13D \tag{14.95}$$

and this is the boundary condition that we must use for the flux whenever a vacuum exists beyond the outer boundary. Reactor cores that are surrounded by a vacuum are then referred to as *bare cores*. As we learned in Chapter 13, they are also called *unreflected cores*. In other words, the extrapolated boundary condition requires that

$$\phi = 0 \quad \text{when } x = \delta + L_B \text{ or } r = \delta + L_B \tag{14.96}$$

where L_B *is the physical location of the outer boundary.* In many text books, the extrapolation distance δ is also energy dependent. To help the reader visualize why this is so important, consider the bare, homogeneous reactor core shown in Figure 14.16. The core has a physical height of H and a physical width of W. In the radial direction, the flux falls to zero at $x = -W/2 - \delta$ and $x = W/2 + \delta$. In the axial direction, the flux falls to zero at $y = -H/2 - \delta$ and $y = H/2 + \delta$. The value of the extrapolation distance δ is therefore seen to be directly proportional to the value of the neutron diffusion coefficient D immediately preceding the boundary. When the inner region contains a relatively dense material (such as a nuclear fuel rod), then the value of D will be small and the value of δ will be correspondingly small as well. In the case of a fuel assembly surrounded by a water reflector, this distance is on the order of a few centimeters. However, when the

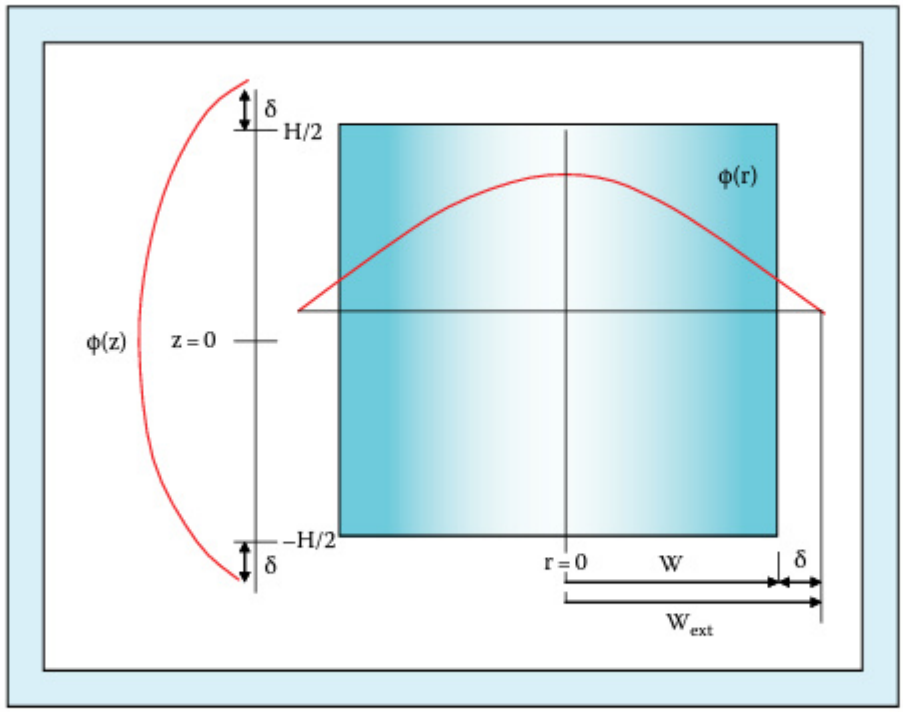

FIGURE 14.16 An illustration of how the extrapolation distance δ may be used in the x and y directions.

inner region contains a less dense material such as a gas, then the opposite behavior occurs, and the diffusion coefficient D becomes very large (because there are fewer atoms for the neutrons to collide with). Then the extrapolation distance δ becomes much larger as well.

14.18 Defining an Energy-Dependent Extrapolation Distance

Strictly speaking, the diffusion coefficient D is a continuous function of the neutron kinetic energy E. This is because the absorption and scattering cross sections Σ_a and Σ_s are energy dependent. Therefore, the extrapolation distance δ in our previous analysis should have been written as

The Energy-Dependent Extrapolation Distance

$$\delta(E) = 0.71\lambda_{tr} = 0.71 \times 3D(E) = 2.13D(E) \tag{14.97}$$

where the energy dependence of the diffusion coefficient D(E) is now evident. Because of this dependence, the diffusion coefficient D(E) may be larger at higher energies than it is at lower ones. This is even true for simple neutron moderators such as light and heavy water. This means that the extrapolation distance δ may be different for fast neutrons than it is for thermal neutrons, and in general, the extrapolation distance for fast neutrons will be much greater (between a factor of 3 and 10 greater than thermal neutrons depending upon the material). To be more specific, the diffusion coefficient for thermal neutrons in ordinary water is only 0.160 cm, while for 1 MeV fast neutrons, it is about four times greater or about 0.623 cm. This means that the extrapolation distance for thermal neutrons in water is about

$$\delta_T = 2.13D_T = 0.34 \text{ cm} \tag{14.98}$$

and the extrapolation distance for fast neutrons in water is about

$$\delta_F = 2.13D_F = 1.33 \text{ cm} \tag{14.99}$$

The differences between the extrapolation distances for fast and thermal neutrons are shown in Figure 14.17. As one might expect, as the neutrons become more energetic, they diffuse further away from the boundary before they are scattered or absorbed. Clearly, as the neutron energy E is increased, the further the neutron flux ϕ(E) will extend beyond the outer boundary before it falls to 0. Obviously, the extrapolation distance can be extended to more than two energy groups

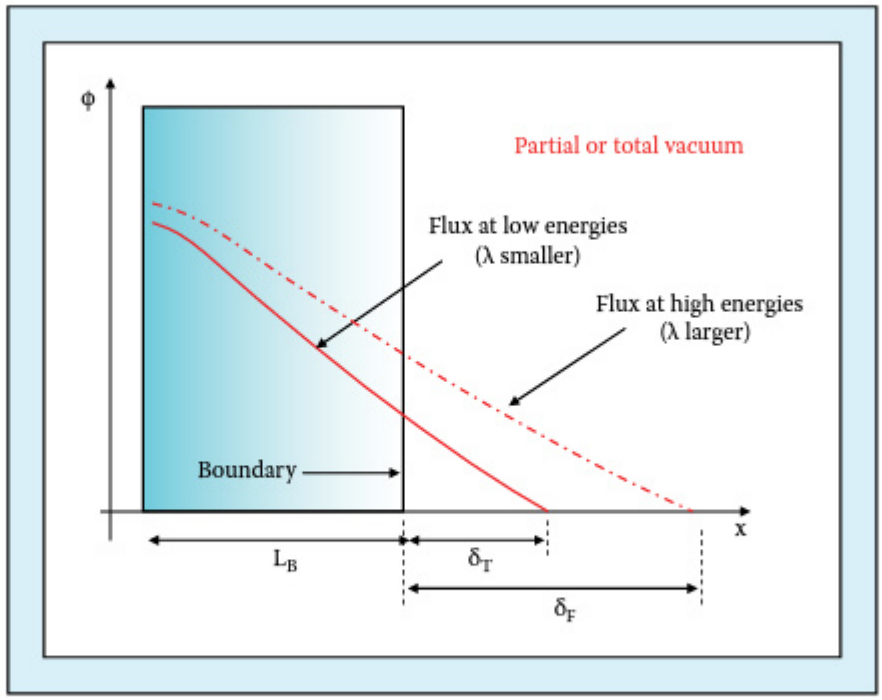

FIGURE 14.17 Differences between the fast and thermal flux with the extrapolated boundary condition.

as well. In fact, this is essential to obtaining the correct shape for the fast neutron flux when more than one energy group is used. It also comes as no surprise that the extrapolated boundary condition can be helpful when finding the flux shape in reactors that are surrounded by a reflector. This was discussed in some detail in Chapter 13 when the reader was introduced to the concept of the *reflector savings.*

Establishing a point at which the flux falls to zero with the extrapolated boundary condition is often better than just assuming it falls to zero at the boundary. It is also preferable to averaging the diffusion coefficients and the absorption or scattering cross sections between two different material regions as well. Notice that we have not said anything about what the neutron current **J** must be at the outer boundary for diffusion theory to apply. All that we have assumed so far is that the neutron current across the boundary must be finite and continuous.

Example Problem 14.3

Suppose that a distributed neutron source is surrounded by a region of space where the diffusion coefficient is effectively infinite (i.e., it is surrounded by a vacuum). If the average diffusion coefficient in the source material is 1 cm, approximately how far away from the edge of the material will the neutron flux fall to zero?

Solution According to our previous discussion the neutron flux falls to zero at a distance of $\delta = 2.13D$ cm. from the edge of the material. In this case, the value of D is 1 cm, so the neutron flux falls to zero approximately 2.13 cm from the material boundary. Not surprisingly, this is known as the *vacuum boundary condition.* [Ans.]

14.19 A Planar Neutron Source with the Extrapolated Boundary Condition

Before moving on to other topics, we would like to present one additional problem that illustrates how to solve the neutron diffusion equation when the extrapolated boundary condition is used. This problem also illustrates how the neutron flux behaves when there is a thin planar source in the middle of a large region of spatially homogeneous material. This source could be constructed from two plates of a material coated with a neutron source on just one side and then glued together. A thin plate-type fuel rod immersed in a large tank of water can also be modeled in this way. Suppose that the regions of material on each side of the neutron source are of thickness W and that the planar neutron source is negligible in thickness compared to them.

The neutron source (see Figure 14.18) is assumed to emit S neutrons per second isotropically in all directions. Half of the neutrons flow into the material on the right, and half of the neutrons flow into the material on the left. The planar source S is again located at the origin of the coordinate system shown in Figure 14.18 where we can set $x = 0$. Because each

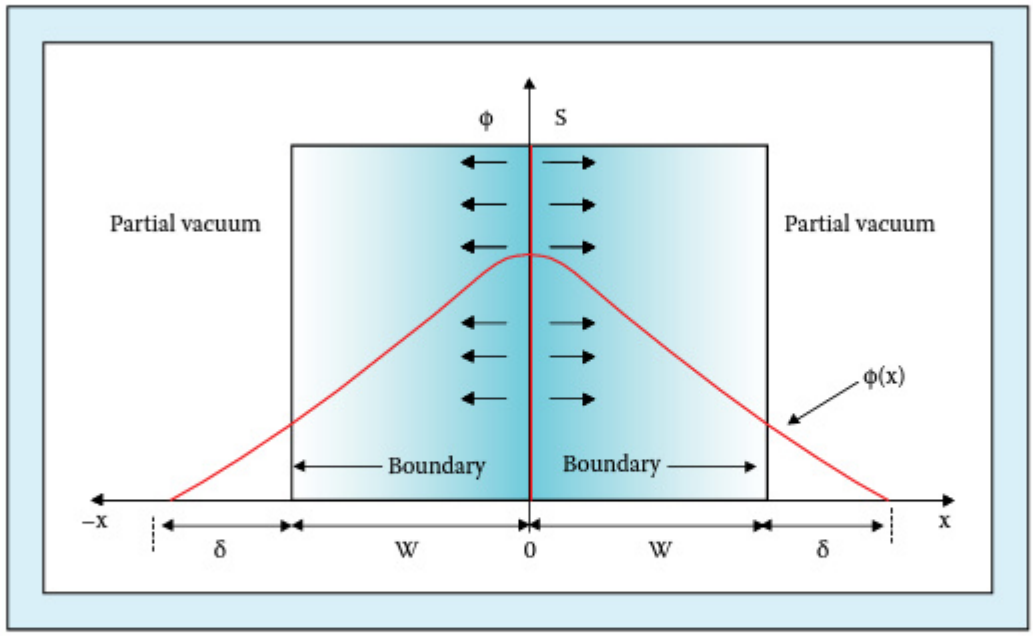

FIGURE 14.18 The extrapolated boundary condition on both sides of a symmetric slab.

region is effective infinite in the y and z directions, the value of the flux does not change as a function of y or z. Hence, we may assume that the flux changes in only the x direction, and we can also assume that the neutron current in each direction has a magnitude at the origin of J = S/2. However, because we will be using the extrapolated boundary condition, the flux vanishes just beyond the boundary of each material region where x = W + δ and x = −W − δ. In mathematical terms, this means that

$$\phi(W+\delta)=0 \quad \text{and} \quad \phi(-W-\delta)=0 \tag{14.100}$$

Because the problem is symmetrical, the general solution to the diffusion equation on the right-hand side is

$$\phi = A_1 e^{-x/L} + A_2 e^{+x/L} \tag{14.101}$$

This solution applies to all x except where the neutron source is located. In view of the fact that ϕ = 0 at x = W + δ, we can write,

$$\phi(W+\delta) = A_1 e^{-(W+\delta)/L} + A_2 e^{+(W+\delta)/L} = 0 \tag{14.102}$$

which implies that

$$A_2 = -A_1 e^{-2(W+\delta)/L} \tag{14.103}$$

Taking this result and substituting it into the general solution gives

$$\phi = A_1\left[e^{-x/L} - e^{+x/L}\cdot e^{-2(W+\delta)/L}\right] \tag{14.104}$$

All that remains now is to find the value for A_1. The value of A_1 is again obtained by requiring that J = S/2 as x → 0. The result is

$$A_1 = \frac{SL}{2D}\cdot\left[\frac{1}{1+e^{-2(W+\delta)/L}}\right] \tag{14.105}$$

For the slab to the right of the point source, where x > 0, the solution is

$$\phi(x) = \frac{SL}{2D} \cdot \left[\frac{1}{1 + e^{-2(W+\delta)/L}} \right] [e^{-x/L} - e^{+x/L} \cdot e^{-2(W+\delta)/L}] \tag{14.106}$$

This solution can be written more elegantly by multiplying the numerator and the denominator by $e^{(W+\delta)/L}$. For x > 0, the result is

$$\phi(x) = \frac{SL}{2D} \cdot \frac{\sinh(W + \delta - x)/L}{\cosh(W + \delta)/L} \tag{14.107}$$

Since the problem is symmetrical, a solution that is valid for any value of x (either positive or negative) is

$$\phi(x) = \frac{SL}{2D} \cdot \frac{\sinh(W + \delta - |x|)/L}{\cosh(W + \delta)/L} \tag{14.108}$$

where |x| is the absolute value of x. Here, we have used the fact that the *hyperbolic functions* for the sine and cosine are

$$\sinh(x) = \frac{1}{2}(e^{x} - e^{-x}) \quad \text{and} \quad \cosh(x) = \frac{1}{2}(e^{x} + e^{-x}) \tag{14.109}$$

Unlike the sine and cosine functions, which are periodic functions of the real argument x, *sinh(x)* and *cosh(x)* are exponentially growing or decaying functions of the argument x. The behavior of these functions is shown in Figure 14.19. Notice that when δ = 0, the solution becomes

$$\phi(x) = \frac{SL}{2D} \cdot \frac{\sinh(W - |x|)/L}{\cosh(W/L)} \tag{14.110}$$

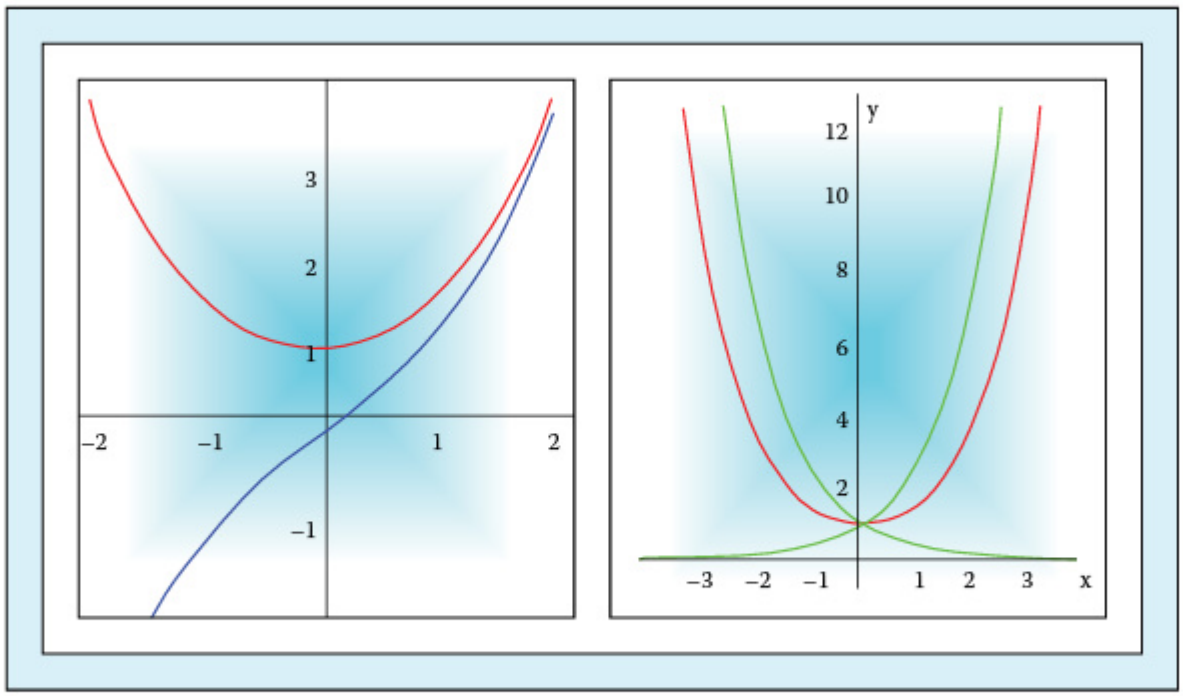

FIGURE 14.19 The cosh(x) function, which is the average of e^{x} and e^{-x}, is shown in red, and the sinh(x) function, which is the difference between e^{x} and e^{-x}, is shown in blue.

If we compare this solution to the case where $\delta > 0$, it can be seen that the shape of the flux is only different when one approaches the outer boundary itself. In the center of the slab, the shape of the flux is essentially the same. It is also worth remembering that

Other Identities for the Hyperbolic Sine and Cosine

$$e^{x} = \cosh(x) + \sinh(x)$$
and
$$e^{-x} = \cosh(x) - \sinh(x) \tag{14.111}$$
and
$$\cosh^2(x) - \sinh^2(x) = 1$$

Now we would like to make some additional observations about how the flux behaves in problems with more than one material region.

14.20 Solutions to the Neutron Diffusion Equation with More than One Material Region

When there is more than one material region, the value of B^2 (see Equation 14.8) in one region may be positive, while the value of B^2 in another region may be negative. Because of the boundary conditions, this places certain constraints on the final solution. For example, recall that the general solution to the diffusion equation

$$\nabla^2\phi(x) \pm B^2\phi(x) = -S/D \tag{14.112}$$

has two basic forms—depending on the sign of B^2. If $B^2 > 0$, then the general solution is

$$\phi(x) = A_1 \sin Bx + A_2 \cos Bx - \frac{S}{D} \tag{14.113}$$

and if $B^2 < 0$, then the general solution to the equation is

$$\phi(x) = A_1 e^{+Nx} + A_2 e^{-Bx} + \frac{S}{D} \tag{14.114}$$

When dealing with neutrons, a positive value of B^2 implies that there is a net production of neutrons in the region and a negative value of B^2 implies that there is no net production of neutrons in the region (unless an external source term is present).

When neutrons are being produced in a region of space, the shape of the flux in that region will be generally *convex*. Conversely, when neutrons are not being produced, or when more neutrons are leaking out of the region than are leaking into it, then the shape of the flux in that region will be generally *concave*. Figure 14.20 illustrates what the flux looks like in each case. Areas 1 and 3 correspond to areas in which neutrons are being produced, and area 2 corresponds to an area where they are not. Each region therefore requires one of the two general solutions we have already presented. Thus in principle, it is possible to "stitch together" as many solutions as possible as long as we know whether $B^2 > 0$ or if $B^2 < 0$. The boundary conditions must then be used to provide the thread we need. In general, two boundary conditions are required for each material region to find the values of A_1 and A_2. As we have seen, these boundary conditions can fall into three distinct categories:

Category 1: In this case, the values for the neutron flux ϕ must be provided at each material boundary. If there is more than one energy group, then different values must be provided for each energy group as well. At the edge of the reactor, the extrapolated boundary condition $\delta = 0.71\lambda_{tr} = 2.13D$ can be used.

Category 2: In this case, the values for the neutron current J must be provided at each material boundary. If there is more than one energy group, then different values must be provided for each energy group as well.

Category 3: In this case, the value for the neutron current J must be provided at one boundary, and the value for the neutron flux must be provided at the other. If there is more than one energy group, then different values must be provided for each energy group as well. This set of boundary conditions is generally used when some type of geometrical symmetry exists, such as the condition that $J = 0$ at the center of a symmetrical reactor core. If one has enough intestinal fortitude, it is simply a matter of writing down all of the boundary conditions, with the appropriate solutions for each region, and evaluating the constants A1, A2, …, AN, etc., until the final solution is found.

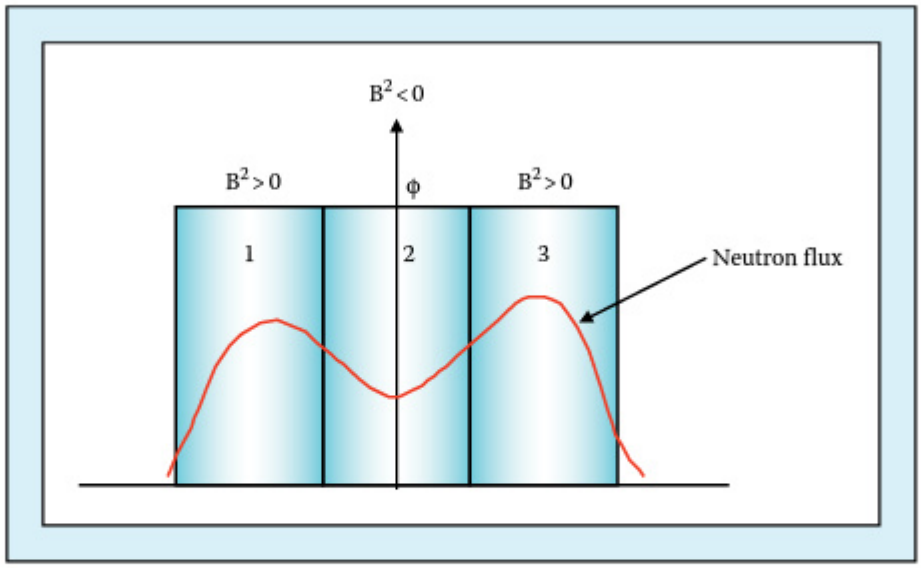

FIGURE 14.20 The flux shape with distributed sources with different values of the buckling.

There is certainly a lot of work involved. However, if the values of D, Σ_f, and Σ_a are known for each material region, then a general solution can certainly be found for N material regions. This is about as far as we can take conventional neutron diffusion theory without resorting to a computer program to find the shape of the flux. When more than one energy group is used, a numerical approach is preferable to an analytical one.

14.21 Introduction to the Iterative Power Method

Neutron sources can also be used in other ways. Earlier in the chapter, we assumed we were dealing with a critical reactor where the effective multiplication factor could be set equal to one. This allowed us to define the geometric buckling and the material buckling B_g^2 and B_m^2 and examine their properties for an exactly critical system. Unfortunately, one does not always know in advance what core compositions and geometric configurations will result in an exactly critical system. In the early stages of reactor design, it is often necessary to "guess" the combinations of these parameters that must be used to create an exactly critical configuration. At each stage in the design process, whatever is "learned" from the previous stage can then be used to improve the estimates of the effective multiplication factor. The better we are at guessing these ratios, the quicker we will be able to obtain the value of $K_{effective}$ we require. The value of

$$K_{effective} = \frac{\text{Production}}{\text{Destruction} + \text{Leakage}} = \frac{P}{D + L} \tag{14.115}$$

is one way to determine how close we are to achieving this goal. In homogeneous systems where the shape of the neutron flux is the same everywhere and there is no neutron leakage, the fluxes in the numerator and the denominator of Equation 14.115 cancel, and we are left with the simple ratio

$$K = \frac{\nu\Sigma_a\phi}{\Sigma_a\phi} = \frac{\nu\Sigma_a}{\Sigma_a} \tag{14.116}$$

to decide how to proceed. Many reactor physics books define the effective multiplication factor in this way. However, when we can no longer neglect the effects of neutron leakage, then balancing the neutron production rate and the neutron destruction rate becomes harder to do. Then the question becomes how to manipulate the diffusion equation to obtain the

appropriate value for K without having to deal with the time-dependent terms. With one energy group, this requires us to use the definition of K

$$K = \frac{P}{D + L} \tag{14.117}$$

to write the diffusion equation as

$$K = \frac{\nu\Sigma_f\phi(\mathbf{r})}{-D\nabla^2\phi(\mathbf{r}) + \Sigma_a\phi(\mathbf{r})} \tag{14.118}$$

or

$$-D\nabla^2\phi(\mathbf{r}) + \Sigma_a\phi(\mathbf{r}) = \frac{1}{K}\nu\Sigma_f\phi(\mathbf{r}) \tag{14.119}$$

where D is the one group diffusion coefficient and K is the *eigenvalue* that causes both sides of Equation 14.119 to balance.

There are literally thousands of combinations of these terms that will give us the correct value for K. But how do we find the value for K under these conditions? The answer is that we can treat the term $(1/K)\nu\Sigma_f\phi(\mathbf{r})$ as a *distributed neutron source* $S(\mathbf{r})/K$ and rewrite the diffusion equation as

$$-D\nabla^2\phi\ (\mathbf{r}) + \Sigma_a\phi(\mathbf{r}) = \frac{1}{K}S(\mathbf{r}) \tag{14.120}$$

where $S(\mathbf{r}) = \nu\Sigma_f\phi(\mathbf{r})$. We can then use some of the techniques we discussed previously to manipulate the neutron source term. If we know the shape of the flux ϕ^n when the system is close to being critical, then we can use it to estimate the value of S^n and therefore find a new value for ϕ^{n+1} and K^{n+1}. We can repeat this process with new values of D^{n+1} and $\sum_a^{n+1}$ until the appropriate value of K^{n+1} is found. In other words, we can use the diffusion equation, when it is written as an eigenvalue equation to *iteratively converge* the value of K^{n+1} we want. If the value of K^{n+1} is too small, we can increase the value of Σ_f to make it larger; conversely, if the value of K^{n+1} is too large, we can decrease the value of Σ_f to make it smaller. In most cases, just changing the enrichment is enough to obtain a critical configuration. This method of obtaining increasingly accurate estimates of ϕ^{n+1} and K^{n+1} by varying the values of D and Σ_a is called *the iterative power method*, and this method is widely used by reactor designers to find the value of K when the shape of the flux is known (or even guessed).

For simple geometries, this method converges very rapidly if the initial estimate of the flux shape is a good one. Mathematically speaking, this is because the only eigenvalue that survives is the largest one, and moreover, this eigenvalue corresponds to the only one where the neutron flux $\phi(r)$ is positive everywhere. This eigenvalue then becomes the *fundamental mode* of the system. The shape of the flux converges to align itself with this eigenvalue very quickly. The other eigenvalues disappear as more iterations are performed. An overview of this process is shown in Figure 14.21. In practice, the power method consists of an *outer iteration* where the values of D, Σ_f, and Σ_a, the boundary conditions, and the size of the core are specified by the reactor designer. Then a guess is made concerning the initial value of where S^n, which is in turn given by $S^n(\mathbf{r}) = \nu\Sigma_f\phi(\mathbf{r})$. Using this value for $S^n(\mathbf{r})$, the steady-state neutron diffusion equation is solved for the neutron flux shape $\phi^{n+1}(\mathbf{r})$. This flux shape is then used to generate a new value for $S^{n+1}(\mathbf{r})$, and the process is repeated again. The process of solving the diffusion equation and generating a new value for $S^{n+1}(\mathbf{r})$ is called the *inner iteration*. The value of K^n is then updated as the process proceeds. Thus the three "steps" required to implement the inner iteration include

1. Updating the value of $S^{n+1}(\mathbf{r})$
2. Solving the diffusion equation for a new value of $\phi^{n+1}(\mathbf{r})$ given the updated value of $S^{n+1}(\mathbf{r})$
3. Updating the value of K^{n+1} using the new value of $\phi^{n+1}(\mathbf{r})$ until an acceptable value of K can be found.

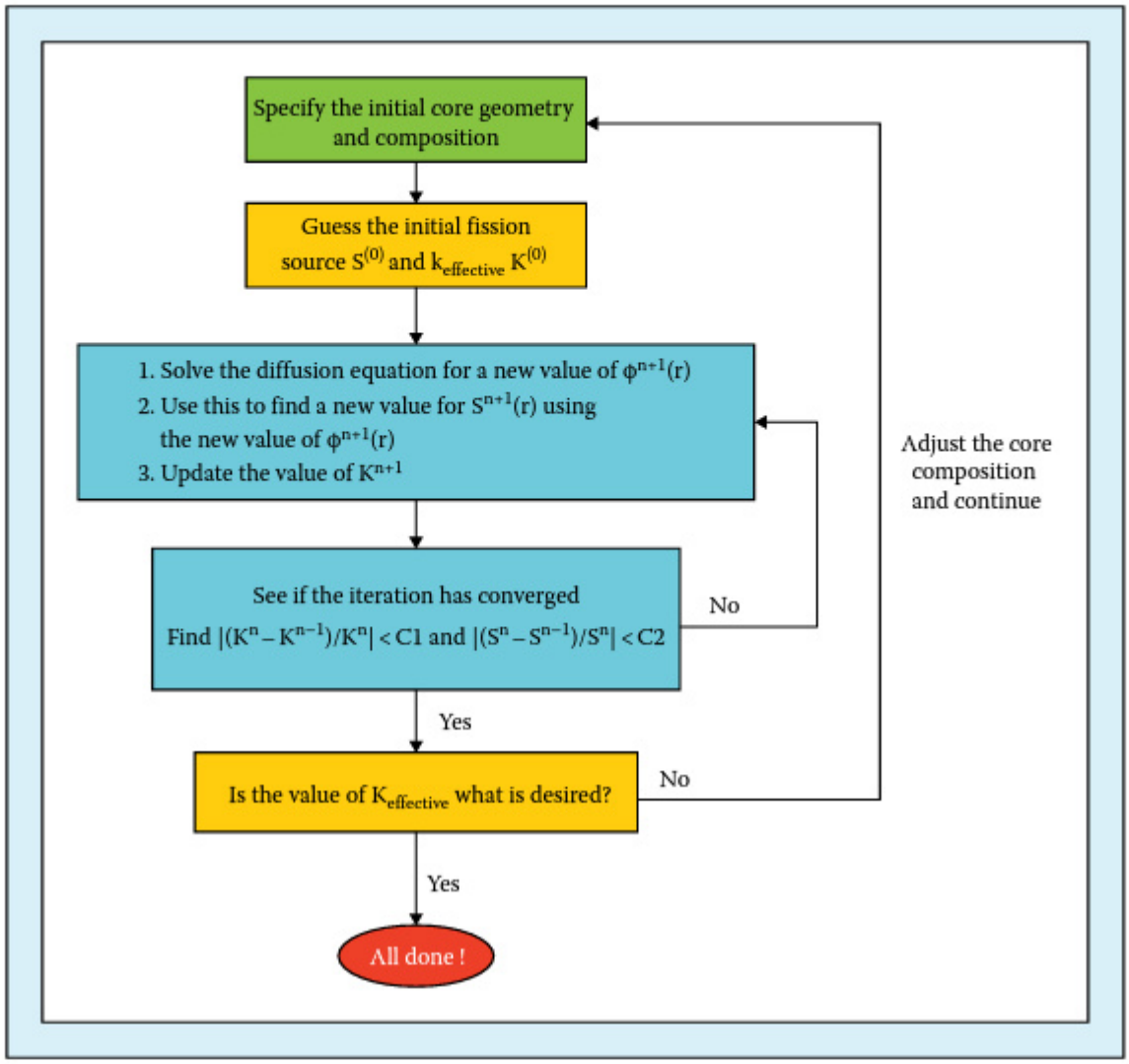
Specify the initial core geometry and composition
Guess the initial fission source $S^{(0)}$ and $k_{effective}$ $K^{(0)}$
1. Solve the diffusion equation for a new value of $\phi^{n+1}(r)$
2. Use this to find a new value for $S^{n+1}(r)$ using the new value of $\phi^{n+1}(r)$
3. Update the value of K^{n+1}
See if the iteration has converged
Find $|(K^n - K^{n-1})/K^n| < C1$ and $|(S^n - S^{n-1})/S^n| < C2$
No
Yes
Is the value of $K_{effective}$ what is desired?
No
Yes
All done !
Adjust the core composition and continue

FIGURE 14.21 An iterative strategy for designing an exactly critical reactor based on a neutron source.

14.22 Convergence Criteria and Numerical Errors

Eventually, a point is reached where the change in the values of S and K falls below a specific limit, which is usually referred to as the *convergence criterion*. Most of the time, different convergence criteria are used for S and K. Typical values for these convergence criteria are

$$\left|\left(\frac{K^n - K^{n-1}}{K^n}\right)\right| < c_1 \quad \text{and/or} \quad \left|\frac{S^n - S^{n-1}}{S^n}\right| < c_2 \tag{14.121}$$

where c_1 and c_2 are constants on the order of about 0.0001. If the resulting value of K^n is too small (i.e. $\ll 1$), the geometry or the core composition is adjusted, and the outer iterations are repeated again. Figure 14.22 shows how the value of $\left|(K^n - K^{n-1})/K^n\right|$ behaves as more iterations are performed. Normally, it takes between 10 and 20 outer iterations to find a good value for K, which is of course the value that meets the convergence criteria the user has specified. In one dimension, the process is easy to implement, and the diffusion equation can be solved either analytically or numerically. However, for two and three-dimensional problems, a numerical method must be used.

In most cases, the number of "inner iterations" required to converge the neutron flux is greater than the number of outer iterations required to adjust the material composition of the core. For typical PWRs with several material regions, it is not unusual to require several hundred inner iterations to converge the flux shape accurately enough. The number

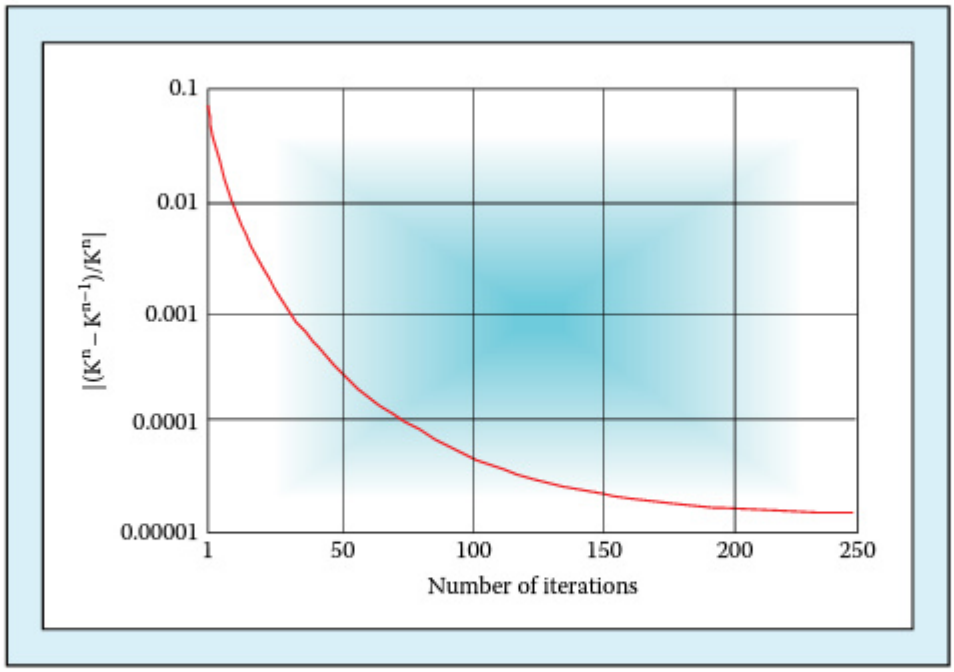

FIGURE 14.22 The behavior of the convergence criterion $|(K^n - K^{n-1})/K^n|$ for the eigenvalue of K as a function of the iteration count.

of inner iterations required for a specified value of c_1 or c_2 increases as the number of dimensions is increased, and it also increases with the geometric complexity of the core. Occasionally, numerical techniques called *accelerators* are used to converge the process more quickly.

Adding additional energy groups to the power method may also increase its computational complexity. This is because each energy group may have its own eigenvalue that converges at a slightly different rate than the eigenvalues for the other energy groups. The power method will work for *any* reactor geometry and the reactor itself does not have to be spatially homogeneous. However, the solution will converge more quickly if the system is spatially homogenized in advance. Now we would like to turn our attention to how to solve the diffusion equation in the presence of a burnable poison. In many cases, a burnable poison can be modeled as a *neutron sink* instead of a neutron source.

14.23 Solutions to the Neutron Diffusion Equation near a Burnable Poison

As we mentioned earlier, *burnable poisons* are added to the fuel to reduce local power peaks between adjacent fuel rods within an assembly. These poisons act as a strong absorber for thermal neutrons and tend to make the fuel rod appear to be "black" to the thermal neutrons in their vicinity. In other words, they act as *neutron "sinks"* (as opposed to neutron sources). The effects of burnable poisons are strongest when the fuel is fresh and when the concentration of the burnable poison is high. Then as the poison is "burned away" the concentration declines, and the thermal flux becomes less depressed. This depression in the flux shape rarely extends more than a few diffusion lengths (or 2–4 cm) away from the surface of the fuel itself, so its effects are quite localized and they are usually restricted to only the individual fuel assemblies in which burnable poisons are used. The influence of a burnable poison as a function of time is shown in Figure 14.23. *Thus, burnable poisons can be used to reduce the amount of radial power peaking when the fuel is fresh.*

The effects of burnable poisons can be modeled in two ways. First, the poisons can be considered to be neutron "sinks" that absorb all of the neutrons that fall into them. We can represent this as a boundary condition if we require that any neutron that falls into the "sink" does not return. In other words, if the poison is strong enough, it can be considered to be a *black surface*, and we can use the extrapolated boundary condition (see Section 14.17) to determine where the thermal flux falls to zero. Unfortunately, the extrapolation distance changes as the poison is burned, and we can only assume that a burnable poison behaves like a black surface when the fuel is fresh. (Over time, the surface becomes progressively gray).

The second and more common way to model a burnable poison is to consider it to be a separate region of a unit cell in which the neutron absorption cross section Σ_a is high. If we are willing to do this, we can determine the shape of the neutron flux by solving the diffusion equation in a homogeneous fuel rod surrounded on both sides by identical regions containing only moderator and no fuel. In other words, we can model the effects of the burnable poison by solving the neutron diffusion equation in a unit cell consisting of two separate regions. Only in this case, instead of assuming the central region is a reactor

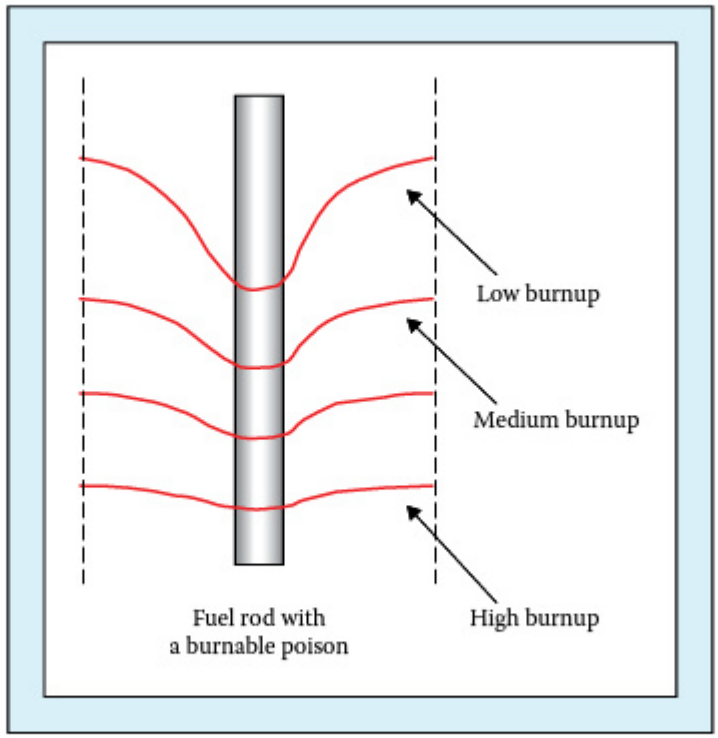

FIGURE 14.23 The flux shape as a function of time for a fuel rod that contains a burnable poison.

core, we can assume that it is a fuel rod in which the burnable poison resides. Mathematically, the burnable poison appears as just another macroscopic absorption cross section to be added to the fuel rod. Thus the absorption cross section of the fuel consists of two parts—the first part which is relatively constant over the life of the fuel and the second part that changes as the poison is burned. The total absorption cross section Σ_a^F of the fuel is then the sum of these parts:

$$\Sigma_a^F = \Sigma_a^{FO} + \Sigma_a^{BP}(t) \tag{14.122}$$

where

Σ_a^{FO} is the macroscopic absorption cross section of the fuel only
$\Sigma_a^{BP}(t)$ is the time-dependent cross section due to the presence of the burnable poison

Since the poison burns very slowly (usually over the course of weeks or even months), the value of $\Sigma_a^{BP}(t)$ is essentially constant for several weeks at a time, and the equation for the total absorption cross section reduces to

$$\Sigma_a^F = \Sigma_a^{FO} + \Sigma_a^{BP} \tag{14.123}$$

A similar situation exists in the case of the diffusion coefficient for the D^F for the fuel rod as well, where D^F is defined as

$$D^F = D^{FO} + D^{BP} \tag{14.124}$$

where

D^{FO} is the diffusion coefficient for the fuel only
$D^{BP}(t)$ is the time-dependent diffusion coefficient due to the presence of the burnable poison alone

With these two assumptions, it then becomes possible to predict the flux shape in the vicinity of the fuel rod by simply solving the neutron diffusion equation in three homogeneous regions—in the central fuel rod and then in the surrounding moderator—using the same basic approach that we previously outlined to find the flux shape in the vicinity of a reflector. We will repeat this exercise here with only minor changes in order to illustrate the overall approach. However, the final solution is a little messier than we might initially expect because of the boundary conditions between the poison and the moderator. The reader may wish to refer to Chapter 13 if additional background information is required. To begin our discussion, consider the unit cell shown in Figure 14.24, which consists of three homogeneous material regions. Due to symmetry, we can easily reduce the problem from three material regions down to just two—the first one being the central

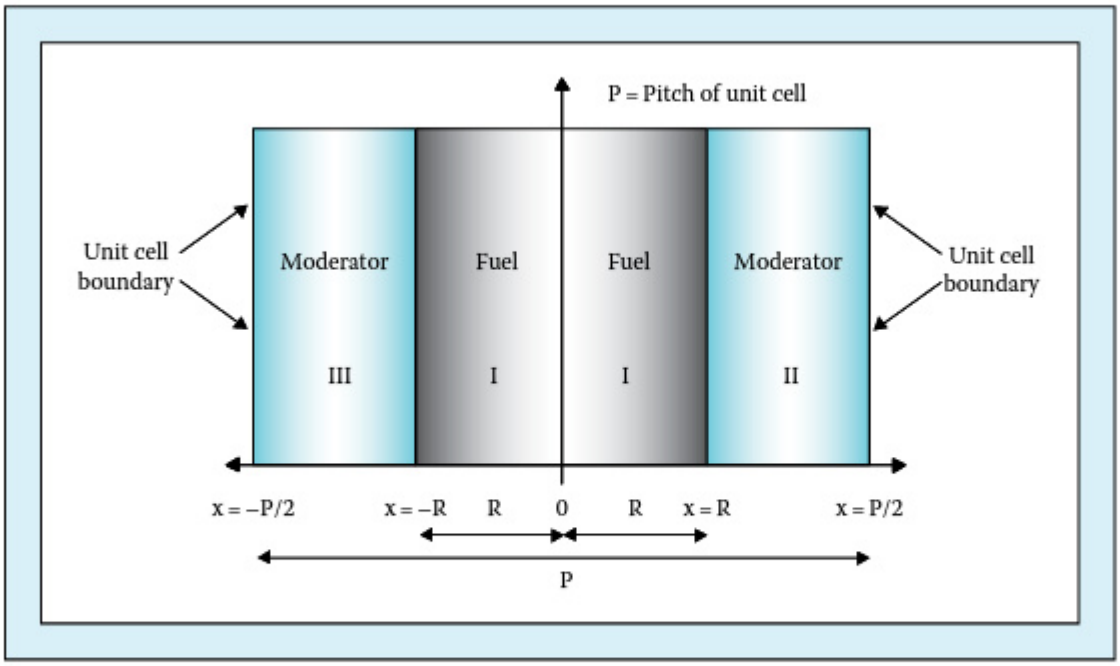

FIGURE 14.24 A fuel rod with a burnable poison represented by a unit cell.

fuel rod, that we will call region "F," and the second one being the surrounding moderator, that we will call region "M." The fuel rod is again centered along the y-axis at x = 0, and the unit cell has a width that is equal to the pitch P of the reactor lattice. The fuel rod has a radius R which is also measured from its centerline. Refer to Figure 14.24 to visualize the geometrical layout that is used. Using the same symmetry arguments that we used previously, we would like to find a solution to the steady-state neutron diffusion equation for $x \geq 0$. The flux shape will then be exactly the same for $x \leq 0$ as long as we reverse the signs of x and R in our solution.

Depending on the size of Σ_a^F relative to the value of $\nu\Sigma_f^F$, the material buckling for the fuel may be greater than 0 or less than 0. We will assume that it is greater than 0 in this case. We will again suppress any time dependence so that we are again dealing with an exactly critical system. Just as we have done in the past, we seek a solution to the neutron diffusion equation in each region of the unit cell that corresponds to the material properties that the individual regions possess. We will then use a flux or current boundary condition to "stitch together" the solutions for the two regions. Based upon our previous experience with how the solutions behave, we must solve the following equations in the fuel and the moderator:

$$\text{Fuel:} \quad D^F \frac{d^2\phi^F}{dx^2} + \left(\nu\Sigma_f^F - \Sigma_a^F\right)\phi^F = 0 \quad 0 \leq x \leq R \tag{14.125}$$

$$\text{Moderator:} \quad D^M \frac{d^2\phi^M}{dx^2} - \Sigma_a^M \phi^M = 0 \quad R \leq \times \leq \frac{P}{2} \tag{14.126}$$

subject to the requirements that are imposed by the boundary conditions for the unit cell:

$$\phi^F(R) = \phi^M(R)$$

$$J^F(R) = J^M(R)$$

$$J^F(0) = 0$$

$$J^M(P/2) = 0$$

where

R is the radius of the fuel rod inside of the unit cell

P is the pitch of the reactor lattice

Notice that the neutron current goes to zero at both the center of the fuel rod and the edge of the moderator (i.e., at x = 0 and x = P/2). Furthermore, we can make use of the symmetry of the problem to narrow our solution down to only the region where x > 0. We will then assume that the flux in the fuel rod has the following shape:

$$\phi^F(x) = A^F \cos B^F x \tag{14.127}$$

where the material buckling is given by

$$\left(B^F\right)^2 = \frac{\nu\Sigma_f^F - \Sigma_a^F}{D^F} \tag{14.128}$$

Moreover, we will assume that the shape of the flux in the moderator is given by a general solution of the form

$$\phi^M(x) = A^M \cosh\left[\frac{|(x - P/2)|}{L^M}\right] \tag{14.129}$$

where once again $L^M = \sqrt{\left(D^M/\Sigma_a^M\right)}$ is the neutron diffusion length in the reflector. Only in this case, because of the symmetry of the unit cell, the one group current J will be 0 at the center of the cell (x = 0) and at both of its outer boundaries (x = P/2 and x = −P/2). This can be verified by taking the derivatives of Equation 14.127 and 14.129 , respectively. When we now apply the boundary conditions at x = R, we obtain

$$\text{Flux:} \quad A^F \cos\left(B^F R\right) = A^M \cosh\left(R/L^M\right) \tag{14.130}$$

$$\text{Current:} \quad D^F B^F A^F \sin(B^F R) = \frac{D^M A^M P}{2L^M \sinh[(R - P/2)/L^M]} \tag{14.131}$$

These two equations can then be solved to find the relationship between A^F and A^M. When this is done, what remains are the two general solutions for $\phi^F(x)$ and $\phi^M(x)$ multiplied by the constant A^F. *The value of the constant A^F is then determined by the amount of power generated in the unit cell.* The procedure to find A^F in this case is presented in Chapter 13. However, we would like to show you graphically how the flux profile in the unit cell changes as the poison is burned. When the fuel is fresh (see Figure 14.25) the value of Σ_a^{BP} is greatest and therefore the value of $\Sigma_a^F = \Sigma_a^{FO} + \Sigma_a^{BP}$ is greatest as well. This causes a large depression in the value of the flux in the fuel. The value of the flux barely recovers when we reach the boundaries of the cell. Then as the poison is burned, the value of $\Sigma_a^F = \Sigma_a^{FO} + \Sigma_a^{BP}$ falls, and the flux begins to recover. Finally, when all of the poison is burned away, $\nu\Sigma_f^F$ becomes greater than Σ_a^F and the neutron flux in the fuel again recovers its familiar bump. Of course, the flux may take some time to flatten out completely, and this in turn depends on the concentration of the burnable poison in the fuel when it was fresh. In most reactors, a burnable poison will take at least a year to completely disappear. Different types of burnable poisons will also dissipate at different rates. These poisons are essential in flattening the power profile and maximizing the burnup of the fuel.

14.24 Time-Dependent Effects

Up to this time, we have only discussed solutions to the steady-state neutron diffusion equation. We would now like to turn our attention to the time-dependent diffusion equation, Equation 14.132. Solutions to the time-dependent diffusion equation are discussed in Chapters 15 and 16, so we will only illustrate some of the basic principles involved. This means that we can no longer neglect the term $(1/v)\partial\phi/\partial t$ when the effective multiplication factor is no longer equal to 1.0. This adds an additional level of complexity to the diffusion equation because the one-group flux is now a function of *four independent variables* (x, y, z, t), instead of just three (x, y, and z).

Time-Dependent Neutron Diffusion Equation

$$D\nabla^2\phi(\mathbf{r}, t) + (\nu\Sigma_f - \Sigma_a)\phi(\mathbf{r}, t) + S(\mathbf{r}, t) = \frac{1}{v}\frac{\partial\phi(\mathbf{r}, t)}{\partial t} \tag{14.132}$$

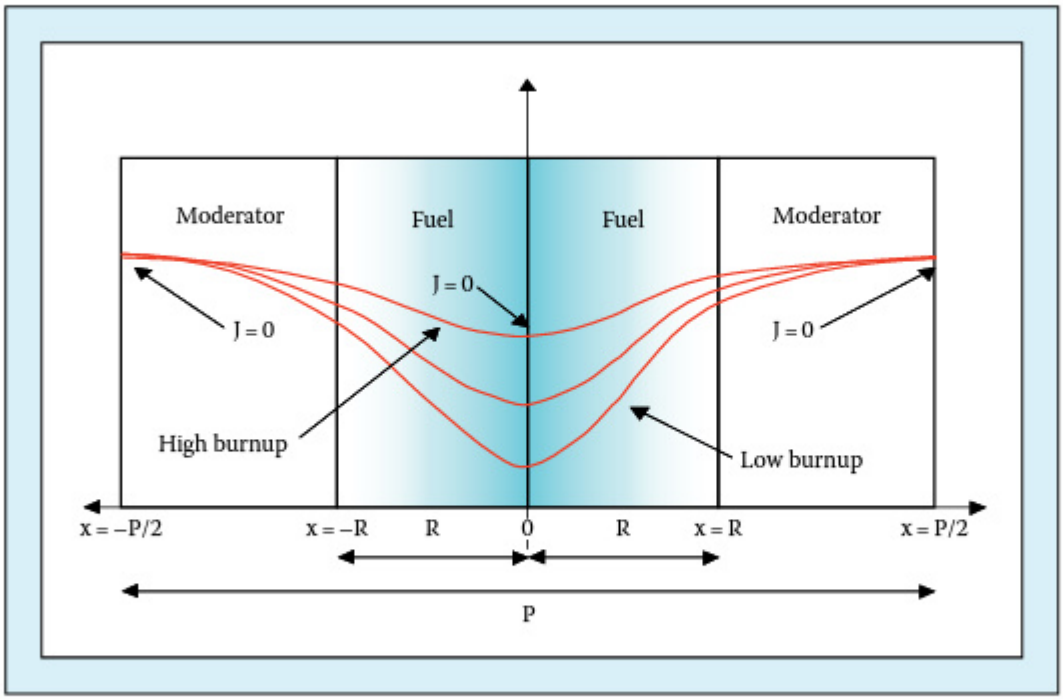

FIGURE 14.25 The flux shapes and boundary conditions for a unit cell with a burnable poison.

This also means that the neutron source term $S(\mathbf{r}, t)$ that appears in the diffusion equation can be *time dependent*. For most problems, this requires us to resort to a numerical method rather than an analytical one to obtain a solution. However, if we can ignore the time dependence of S and replace it by a simple constant, then an analytical solution may be possible in some cases. In the next few chapters, we would like to explore how the neutron flux behaves when the effective multiplication factor is no longer unity. This will then lead to what is known as the *point kinetics approximation*.

14.25 Comparing the Neutron Diffusion Equation to Laplace's Equation, Poisson's Equation, and Helmholtz's Equation

Finally, anyone who has worked with differential equations knows that there are many similarities between the neutron diffusion equation and other differential equations of classical physics. Before delving into the topic of time-dependent reactor behavior, we would first like to take a moment to review some of these similarities. Suppose that we would like to find a solution to the neutron diffusion equation in a region of empty space (i.e., in a region where a vacuum exists). In this case, the value of the material buckling B^2 is zero and *in empty space, the value of the diffusion coefficient D is infinite*. Then the steady state diffusion equation becomes

The Diffusion Equation in a Vacuum

$$\nabla^2\phi(\mathbf{r}) = 0 \tag{14.133}$$

and the astute reader may recognize as *Laplace's equation*. Next, suppose that we would like to apply the diffusion equation to a *pure scattering material* where there is no fission or absorption, but where a significant amount of scattering may occur. In this case, the neutron diffusion equation becomes

Poisson's Equation

$$\nabla^2\phi(\mathbf{r}) = \frac{-S(\mathbf{r})}{D} \tag{14.134}$$

which the astute reader may recognize as *Poisson's equation*. Solutions to Poisson's equation are different than the solutions to Laplace's equation, and some of these differences were highlighted in Chapter 13. Finally, consider the steady-state neutron diffusion equation in its conventional form. It turns out that this version of the diffusion equation is equivalent to another famous second-order differential equation called the *Helmholtz equation*, which was analyzed in great detail by Hermann von Helmholtz (see Figure 14.26) over 100 years ago.

The Steady-State Helmholtz Equation

$$\nabla^2\phi(\mathbf{r}) + B^2\phi(\mathbf{r}) = 0 \tag{14.135}$$

FIGURE 14.26 In this figure, we present some of the mathematicians, scientists, and engineers and who solved differential equations similar to the modern-day neutron diffusion equation. Hermann von Helmholtz is shown in the upper left, Joseph Fourier is shown in the upper right, Simeon Poisson is shown in the lower left, and Pierre Laplace is shown in the lower right. Today, the names of these great men are carved into the walls of the Great Court and the Great Dome of MIT (see Figure 14.27). (Pictures are again provided by Wikipedia.)

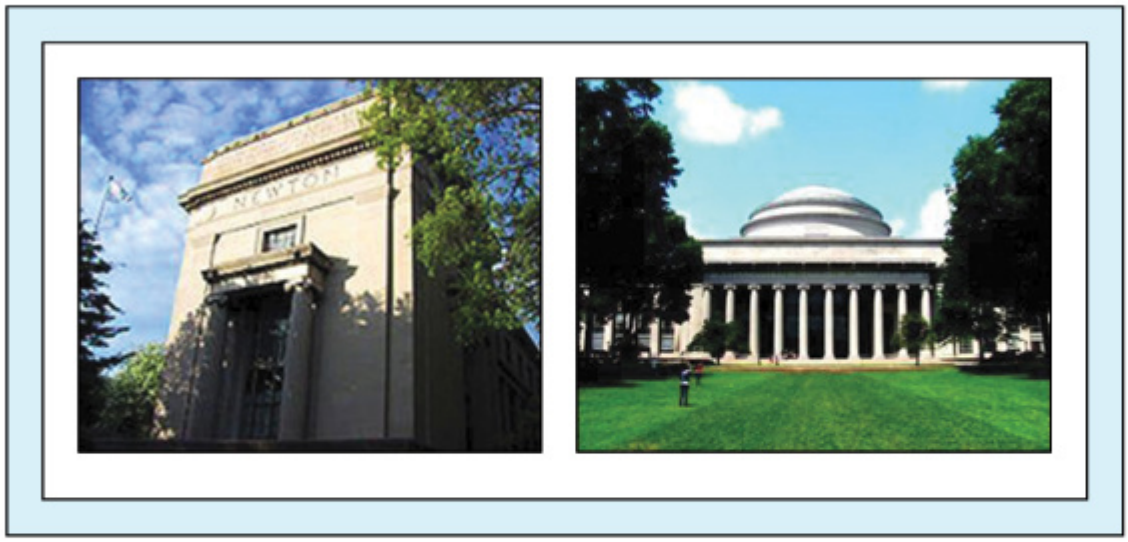

FIGURE 14.27 A picture of the walls surrounding Killian Court and the Great Dome of MIT where the names of great men such as Newton, Einstein, Laplace, Poisson, and Fourier are inscribed. The solutions to the neutron diffusion equation are based in part on the work of these great men. (Pictures of Killian Court and the Great Dome were provided by the Massachusetts Institute of Technology.)

The *Schrödinger Wave Equation*, which we briefly mentioned in Chapter 1 of our companion book*, is one of the best-known examples of the Helmholtz equation. However, if one looks more closely into the subject there are many others. For example, the Helmholtz equation can also be used to predict the flow of heat through a nuclear fuel rod.† This thermal heat conduction process is discussed in reactor thermal hydraulic books and it is very important to the field of nuclear science and engineering as a whole.

14.26 Time-Dependent Neutron Diffusion Theory

Hence, our discussion of the neutron diffusion equation up to this time has amounted to finding solutions to what is known as the steady-state version of Helmholtz's equation. Finally, consider what would happen if we took the neutron diffusion equation in outer space (see Equation 14.133) and added a time-dependent term to it. Then the diffusion equation would become another famous equation of classical physics called *Fourier's equation*:

Fourier's Equation

$$\nabla^2\phi(\mathbf{r}) = \frac{1}{v}\frac{\partial\phi}{\partial t} \tag{14.136}$$

where v is the average velocity of the neutrons (see Chapter 12). Solutions to Fourier's equation (when it applied to nuclear reactors) are discussed in Chapter 15, and they introduce the concept of *time-dependent behavior* into the study of nuclear systems. Thus, when we look at the diffusion equation holistically, we find that specific versions of it are in fact equivalent to

1. Laplace's equation
2. Poisson's equation
3. Fourier's equation
4. Helmholtz's equation

* See, for example, *Nuclear Engineering Fundamentals: A Practical Perspective*, by R.E. Masterson, CRC Press (2017).
† See, for example, *Nuclear Heat Transport,* by M.M. El-Wakil (Reference 3).

TABLE 14.2
Various Forms of the Neutron Diffusion Equation and Their Classical Equivalents

Neutron Diffusion Equation	Closest Classical Equivalent	Common Classical Application(s)	Most Common Classical Form
$\nabla^2\phi(\mathbf{r})=0$	Laplace's equation	Steady-state heat transfer with no heat generation	$\nabla^2\phi=0$
$\nabla^2\phi(\mathbf{r})=-S(\mathbf{r})/D$	Poisson's equation	Steady-state heat transfer with heat generation	$\nabla^2\phi+\lambda^2=0$
$\nabla^2\phi(\mathbf{r})+B^2\phi(\mathbf{r})=0$	Helmholtz's equation	Steady-state heat transfer with a term that is a linear function of temperature	$\nabla^2\phi+B^2\phi=0$
$\nabla^2\phi(\mathbf{r})=1/v\partial\phi/\partial t$	Fourier's equation	Time-dependent heat transfer with no heat generation	$\nabla^2\phi=1/\alpha\partial\phi/\partial t$
$\nabla^2\phi(\mathbf{r})+S(\mathbf{r})/D=(1/v)\partial\phi/\partial t$	General heat conduction equation	Time-dependent heat transfer with internal heat generation	$\nabla^2\phi+\lambda^2=(1/\alpha)\partial\phi/\partial t$

Moreover, the most general form of the neutron diffusion equation is equivalent to the time-dependent Helmholtz equation which appears below:

The Time-Dependent Helmholtz Equation

$$\nabla^2\phi(\mathbf{r})+B^2\phi(\mathbf{r})=\frac{1}{\alpha}\frac{\partial\phi}{\partial t} \tag{14.137}$$

where α is a constant that appears in the study of nuclear heat transfer and fluid flow. Specifically, in a nuclear fuel rod, it can be shown that this constant is equal to $\alpha = q'''/k$, where q''' is the *volumetric heat generation rate* and k is the thermal conductivity of the fuel (see References 2 and 3). All of these forms of the diffusion equation are compared in Table 14.2, where they are also compared to their classical equivalents. *Therefore, although solutions to the neutron diffusion equation have only been the subject of great academic and commercial interest since the 1940s, they are no different than the solutions to other related equations in the fields of mechanical engineering, quantum mechanics, and heat transfer that have been used for hundreds of years. With this in mind, we would then like to move on to the subject of time dependent reactor behavior.*

References

Books and Textbooks

1. Stacey, W.M. *Nuclear Reactor Physics*, 2nd edn. John Wiley & Sons, New York (2007).
2. Todreas, N. and Kazimi, M.S. *Nuclear Systems*, Vol. 1, CRC Press, Boca Raton, FL (2012).
3. El-Wakil, M.M. *Nuclear Heat Transport*, American Nuclear Society, La Grange Park, IL (1981).
4. Duderstadt, J. and Hamilton, L. *Nuclear Reactor Analysis*, John Wiley & Sons, New York (1976).
5. Lewis, E. *Fundamentals of Nuclear Reactor Physics*, Academic Press, Boston, MA (2008).
6. Lamarsh, J.R. and Baratta, A.J. *Introduction to Nuclear Engineering*, Prentice Hall, Upper Saddle River, NJ (2001).
7. Lamarsh, J.R. *Introduction to Nuclear Reactor Theory*, second printing, Addison-Wesley Publishing Company Inc., Reading, MA (1972).
8. Shultis, K. and Faw, R. *Fundamentals of Nuclear Science and Engineering*, 2nd edn., CRC Press, Boca Raton, FL (2008).
9. Masterson, R.E. *Nuclear Engineering Fundamentals: A Practical Perspective*, CRC Press, Boca Raton, FL (2017).

Web References

1. *www.nuceng.ca/ep4d3/text/9-multigroup.pdf.*
2. *http://en.wikipedia.org/wiki/Neutron_transport.*
3. *http://web.mit.edu/22.54/ClassNotes/Lec14.pdf.*
4. *http://en.wikipedia.org/wiki/Poisson's_equation.*
5. *http://en.wikipedia.org/wiki/Helmholtz_equation.*
6. *http://en.wikipedia.org/wiki/Superposition_principle.*
7. *http://web.mit.edu/6.013_book/www/chapter5/5.4.html.*

8. *http://en.wikipedia.org/wiki/Geometric_and_material_buckling.*
9. *neutron.kth.se/courses/reactor_physics/.../102_DiffusionEquation.pdf.*
10. *neutron.kthttp://encyclopedia2.thefreedictionary.com/Diffusion+of+Neutrons.*
11. *http://www.sparknotes.com/testprep/books/sat2/physics/chapter17section4.rhtml.*

Additional References

- Important physical constants used by nuclear scientists and engineers can be found in *Appendix A.*
- Unit systems and their conversion factors can be found in *Appendix B.*
- Nuclear cross sections for many important nuclear materials can be found in *Appendix C.*
- Physical properties of important nuclear materials can be found in *Appendix D.*
- Atomic masses, half-lives, and natural abundances can be found in *Appendix E*
- Neutron diffusion coefficients and neutron mean free paths are discussed in *Appendix H.*
- Diffusion parameters for common nuclear materials are discussed in *Appendix I.*
- Bessel functions that appear in solutions to the neutron diffusion equation are discussed in *Appendix K.*

Questions for the Student

The following questions cover the material presented in this chapter and, in some cases, previous chapters as well. They are designed to test how well the student has acquired a working knowledge of the subject matter.

1. Write an explicit expression for the term L^2 which appears in the modified form of the neutron diffusion equation $\nabla^2\phi - (1/L^2)\,\phi = -S/D$. What is the name for this term and also the name for the value for L?
2. Name three common types of radiation sources that can be implemented using a neutron current boundary condition.
3. What common type for a radiation source has a steady-state flux shape that must be described by a modified Bessel function of the second kind, which also appears in the Feynman propagator of quantum field theory?
4. Write a general expression that can be used to find the value of the neutron flux $\phi(\mathbf{r})$ at a distance r from a large number of point sources in a diffusing medium.
5. In the SI unit system, what units do the terms L and L^2 that appear in the neutron diffusion equation have?
6. Fill in the following sentence with the appropriate word or phrase: Unlike ordinary Bessel functions, which are oscillating functions of a real argument like $J_\alpha(x)$, Bessel functions of the second kind, like $I_\alpha(x)$ and $K_\alpha(x)$ are _____ functions of the same argument, and are therefore likely to be found when a radiation source S is present.
7. What is the name that is normally given to the term L^2 which appears in the neutron diffusion equation?
8. Write an expression that can be used to find the particle flux shape at a distance r from a point source in a material medium where secondary particle buildup, due to photon interaction and scattering, can occur.
9. Propose four examples of how a set of point sources can be connected together to form another type of radiation source.
10. Under what conditions can Laplace's equation $\nabla^2\phi(\mathbf{r}) = 0$ be used to determine the intensity of a particle beam at a distance r from a point source?
11. Suppose that the amplitude of one light wave is given by $A_1(t) = A_1\cos(2\pi f_1 + \phi_1)t$ and the amplitude of a second light wave is given by $A_2(t) = A_2\cos(2\pi f_2 + \phi_2)t$. If $\phi_2 = \phi_1 + \pi$, and $f_1 = f_2$, will they interfere constructively or destructively if they originate from the same point?
12. Write down an explicit equation for the particle flux $\phi(x)$ as a function of distance from a line source of strength S in a diffusive medium where the values of the diffusion coefficient and the diffusion length are known.
13. Consider the standard form of the diffusion equation $\nabla^2\phi + B^2\phi + S = 0$ where S is a neutron source of strength S. From the viewpoint of a college course in differential equations, what is the difference between a set of equations where $S = 0$ and $S \neq 0$?
14. Write an equation for the spatial dependence of the neutron flux $\phi(\mathbf{r})$ at a distance r from a point source in an isotropic medium which has a finite absorption cross section and which both absorbs and scatters neutrons. Why is the neutron flux in the denominator not attenuated as $1/r^2$?
15. Suppose that the amplitude of one light wave is given by $A_1(t) = A_1\cos(2\pi f_1 + \phi_1)t$ and the amplitude of a second light wave is given by $A_2(t) = A_2\cos(2\pi f_1 + \phi_1 + \pi/2)t$. What is the phase angle between these two light waves?
16. Fill in the following sentence with the appropriate word or phrase: When more neutrons are being produced in a region than are being destroyed, the flux shape in the region is normally _____ and the equation for the flux shape will contain a ____ or _____.
17. If no material is present in the vicinity of the point source, and no scattering or absorption occurs, then what law does the particle flux follow?
18. What does the principle of superposition say when it is applied to the flow of neutrons though a diffusive medium? How is the principle of superposition different than when it is applied to the flow of photons?
19. Write an equation for the neutron flux $\phi(\mathbf{r})$ at a distance r from an infinite line source in a diffusing medium.
20. Suppose that we would like to use the principle of superposition to determine the intensity of two light waves which have exactly the same frequency and are emitted from exactly the same location, but are out of phase with one another by 180°. What will the intensity I(r) of these light waves be at a distance r from a point source?
21. What is the relationship between the extrapolation distance d and the neutron diffusion coefficient D at the outer boundary of a reactor core?
22. Write a general expression that can be used to find the value of the neutron flux $\phi(\mathbf{r})$ at a distance r from a large number of point sources in a vacuum.
23. What are the explicit analytical expressions for the hyperbolic sine and cosine functions sinh(x) and cosh(x) which sometimes appear in solutions to the neutron diffusion equation in the presence of a radioactive source?
24. In the iterative power method, which is sometimes used to perform a reactor criticality calculation, what is the process of solving the neutron diffusion equation and then generating a new value for the source term $S^{n+1}(\mathbf{r})$ called?

25. Fill in the following sentence with the appropriate word or phrase: When more neutrons are leaking out of a region than are leaking into it, then the shape of the flux in the region will generally be _____.
26. When the diffusion length becomes effectively infinite in a material that contains a radioactive source S(r), what classic second-order differential equation acquires the same form as the neutron diffusion equation?
27. In the equation for the amplitude A of a photon beam $A(t) = A\cos(2\pi f_1 + \phi_1)t$, what does the amplitude A physically represent in this case?
28. Suppose that a thermal water reactor is core surrounded by vacuum rather than by a water reflector. What boundary condition would you use to determine where the flux falls to zero beyond the edge of the core?
29. If the number of photons in a beam of x-rays is doubled, what happens to the intensity of the x-ray beam in this case?
30. Suppose that the neutron flux in a fast reactor is being modeled with 10 energy groups. The reactor is sent into orbit to power the International Space Station. Because it is designed to operate in empty space, it is not surrounded by a reflector. Which energy group—energy group 1, 5, or 10—falls off fastest at the edge of the core?
31. What is the name that is normally given to the term L which appears in the neutron diffusion equation?
32. Suppose that we would like to determine the amount of energy E that a photon beam deposits in a radiation shield. If all of the photons that are hitting the shield are in phase with one other, and the amplitude of the beam is doubled, how does this affect the amount of energy that is deposited in the shield?
33. Why is the material buckling always a negative number in a substance that contains no fissile material?
34. Suppose that the amplitude of one light wave is given by $A_1(t) = A_1\cos(2\pi f_1 + \phi_1)t$ and the amplitude of a second light wave is given by $A_2(t) = A_2\cos(2\pi f_2 + \phi_2)t$. If $\phi_1 = \phi_2$ and $f_1 = f_2$, will they interfere constructively or destructively if they originate from the same point?
35. Fill in the following sentence with the appropriate word or phrase: When a light wave is traveling through a vacuum, the electric and magnetic fields generated by the wave are at _____ angles to each other.
36. Suppose that you are asked to solve the neutron diffusion equation in a region of space where a radioactive material of strength S has been dissolved into a large tank of water. What form of the neutron diffusion equation do you have to solve to determine the shape of the neutron flux in this water tank?
37. Draw the neutron flux shape in a reactor unit cell that contains a burnable poison when the burnup is very high and very low. In which case is the neutron flux shape flatter?
38. In practice, is the diffusion coefficient D larger for high energy neutrons or low energy neutrons?
39. Suppose that a bare reactor core has a width W and a height H. If the center of the core is located at $x = 0$ and $y = 0$, write an expression showing where the neutron flux falls to zero in the x and y directions if the extrapolation distance is represented by the symbol δ.
40. Write an expression for the value of the neutron flux $\phi(x)$ in a distributed neutron source having the shape of a long, narrow slab where the width of the slab is W, the diffusion coefficient for the slab is D, and the volumetric source strength is S.
41. What do the values of the neutron diffusion coefficient D and the diffusion length L become for a neutron travelling through a vacuum?
42. Suppose that a reactor has a radial and axial reflector. If the reflectors are made out of exactly the same material, is the extrapolation distance d_{EXT} any different in the radial and axial directions in this case?
43. Write an explicit expression for the material buckling B_M^2 in a homogeneous material where neutron diffusion theory applies. When does the material buckling become a negative number?
44. When the diffusion length becomes effectively infinite in a material that has a beam of neutrons entering from one side, but does not contain a radioactive source S(r), what classic second-order differential equation acquires the same form as the neutron diffusion equation?
45. Suppose that a neutron scattering material has a diffusion coefficient of 10 cm and an absorption cross section of zero. What is the value of the neutron diffusion length L for this material?
46. Write an equation for the neutron flux shape $\phi(\mathbf{r})$ at a distance r from a point source of strength S in a diffusive medium where the diffusion coefficient and the diffusion length are known.
47. Suppose that the neutron flux in a radiation shield is given by $\phi(r) = Se^{-r/L}/4\pi Dr$. What is the neutron current J at a distance R from the location of the radioactive source S?
48. Suppose that a bare homogeneous reactor core is surrounded by a region of space where the diffusion coefficient is effectively infinite (i.e., it is surrounded by a vacuum). If the average diffusion coefficient in the core is 2 cm, approximately how far from the edge of the core will the neutron flux fall to zero?
49. What is the neutron current a distance r from an infinite line source in a diffusive medium?
50. What is the diffusion coefficient for the neutron flux in outer space?

51. A research reactor core is 100 cm high and 100 cm wide, and it is placed in a pressure vessel containing helium gas. If the extrapolation distance for the core is 1 cm, what is the percentage error in the shape of the neutron flux if we erroneously assume that the neutron flux falls to zero at the physical boundary of the core rather than at the width and height implied by the extrapolated boundary condition?
52. In neutron transport theory, what fundamental assumption is used to derive the equation for the extrapolated boundary condition $\delta(E) = 0.71\lambda_{tr}$?

Exercises for the Student

Exercise 14.1

Calculate the diffusion coefficient D and the extrapolation distance δ for a beam of thermal neutrons traveling through a tank of water, which is surrounded by a vacuum. Repeat the same exercise with a beam of fast neutrons. What is the ratio of the diffusion coefficient of the fast neutrons to the diffusion coefficient of the thermal neutrons? What is the ratio of their mean free paths?

Exercise 14.2

A point source of neutrons of strength S is located at the center of a spherical tank of radius R in which all of the air has been removed. The tank is then filled with water and the strength of the radiation is measured again at a distance r from the center. What is the ratio of the neutron flux at a distance r from the center when the tank has no air in it and when it is filled with water?

Exercise 14.3

A man is located a distance d_1 from a radiation source of strength S_1 and a distance d_2 from a radiation source of strength S_2. If there is no material between the man and these two radiation sources, write an equation for the intensity of the radiation that the man receives.

Exercise 14.4

A man is located a distance d_1 from a radiation source of strength S_1 and a distance d_2 from a radiation source of strength S_2. If the diffusion coefficient for the material through which the radiation is traveling is D, and the diffusion length is L, write an expression for the intensity of the radiation that the man receives.

Exercise 14.5

The neutron diffusion equation in a region of space where there is no nuclear fuel can be written as $\nabla^2\phi(\mathbf{r}) - (1/L^2)\phi(\mathbf{r}) = -S/D$. If this region of space is filled with ordinary water at room temperature, what are the values of L and D that should be used in this case? Do you expect the neutron flux shape in this region to be concave or convex?

Exercise 14.6

Write an equation for the neutron flux ϕ at a distance z from a planar radiation source of strength S if the source is surrounded by a diffusive medium with a diffusion coefficient of D and a diffusion length of L.

Exercise 14.7

The hyperbolic sine and the hyperbolic cosine are defined by functions of the form $\sinh(x) = \frac{1}{2}(e^x - e^{-x})$ and $\cosh(x) = \frac{1}{2}(e^x + e^{-x})$ which appear in solutions to the neutron diffusion equation when a point source emits a neutron beam through several nested material regions. What is the value of the hyperbolic cotangent function coth(x) which is derived from these functions when the value of x is 0.5?

Exercise 14.8

Two photon beams with amplitudes A_1 and A_2 are emitted in the same direction with a phase difference of 60°. If the energy of the radiation from the first beam is E_1 and the energy of the radiation from the second beam is E_2, and $E_1 = E_2 = E$ what is the total energy of the radiation a large distance from the emission point?

Exercise 14.9

A neutron source having an emission rate of S is pounded into the shape of a round circular disk having a radius R. Half of the neutrons are emitted from the top of the disk and the other half of the neutrons are emitted from the bottom. Derive an expression for the neutron flux at a distance of z from the center of the disk along the symmetry axis. What does this expression reduce to when $z \gg R$?

Exercise 14.10

A large spherical object having radius R is coated with a thin layer of radioactive material having thickness T. What is the volume of the radioactive material surrounding the sphere? If the radioactive material emits N neutrons/cm^3/s, what is the total source strength S of the radioactive material surrounding the sphere?

Exercise 14.11

Suppose that a hollow sphere of radius R is coated with a layer of radioactive material having a neutron emission rate of S. In a vacuum, what is the neutron flux at a distance r from the center of the sphere, where $r \gg R$.

Exercise 14.12

A hollow spherical object of radius R is coated with a layer of radioactive material having a neutron emission rate of S. The sphere is placed in a tank of water with a diffusion coefficient D and an extrapolation length L. What is the neutron flux at a distance r from the center of the sphere, where $r \gg R$.

Exercise 14.13

A beam of thermal neutrons is traveling through a tank filled with light water. The tank is sent into outer space for use on the International Space Station. How far from the edge of the tank does the thermal neutron flux fall to zero if the tank is attached to one of the antennas on the space station?

Exercise 14.14

Suppose that we write the neutron diffusion equation as $\nabla^2\phi(\mathbf{r}) + B^2\phi(\mathbf{r}) = 0$ when $\sum_f > 0$ and $\nabla^2\phi(\mathbf{r}) = -S(\mathbf{r})/D$ where there is a radioactive neutron source S in a material in which the neutrons can be scattered but not absorbed. What famous classical differential equations are equivalent to these two forms of the neutron diffusion equation? When the scattering material is removed from the second equation and the diffusion coefficient D becomes infinite, what famous differential equation does this equation reduce to?

15

Time-Dependent Reactors and Their Behavior

15.1 Time-Dependent Reactor Behavior

Real reactors are very complex and dynamic machines that very rarely, if ever, operate for more than a few seconds at exactly the same flux or power level. This is because the time-dependent neutron production and destruction rates are very rarely, if ever, precisely balanced, and so even a well-designed reactor will not be exactly critical all of the time. When a reactor first starts up, it must be forced into a situation where it is supercritical for at least a few seconds for the neutron inventory to build up, and when a reactor shuts down, it must be forced into a subcritical state so that its power level can be reduced. *Hence, all real reactors operate between being slightly supercritical, critical, and slightly subcritical all of the time*. The study of how a reactor behaves when it is not exactly critical, and the neutron population is increasing or decreasing, is called the study of *reactor kinetics*. When both the time-dependent behavior and the spatial behavior are modeled at the same time, the study of this behavior is called *space–time kinetics*. In the sections that follow, we will concentrate on the equations that are used to predict this behavior. When the flux (and hence the power) are time dependent, the reactivity ρ, which we previously defined as

Definition of the Time-Dependent Reactivity

$$\rho(t) = \frac{K_{effective}(t) - 1}{K_{effective}(t)} \tag{15.1}$$

is also time dependent. In general, it usually fluctuates between about 0% and ±20% of the delayed neutron fraction β. During normal operation the reactivity (and therefore the power level) is changed by inserting or withdrawing the control rods from the core, and in the case of a pressurized water reactor (or PWR), the reactivity is also changed by varying the concentration of the boric acid in the coolant. The stability of a reactor under these conditions is determined by the number of delayed neutrons the fuel emits, as well as how the temperature of the fuel and the moderator change as a function of time.

If the reactivity falls below zero, the power level falls and the neutron production rate P must then be increased by withdrawing a control rod from the core to force the reactor back into a critical state. Conversely, if the power level rises, the reactivity must be reduced by inserting a control rod back into the core. This delicate balancing act is repeated over and over again until all of the fuel is burned, or until it is necessary to shut the reactor down for refueling. Finally, the value of the reactivity is affected by how much fuel is available to be burned. As long as a reactor contains enough fresh fuel, it is possible to maintain the core in a critical state for a very long period of time. In practice, there is usually enough excess reactivity built into a commercial power reactor to keep it critical for at least a year or two with a fresh batch of fuel. After that, it must be shut down, and the depleted fuel must be replaced.

15.2 Time-Dependent Neutron Production

The time-dependent behavior of a reactor can be predicted by solving the time-dependent neutron diffusion equation which was introduced to the reader in Chapter 11. Not accounting for the effects of delayed neutrons, this equation can be written as

Time-Dependent Neutron Diffusion Equation

$$D\nabla^2\phi + \left(\nu\Sigma_f - \Sigma_a\right)\phi + S(t) = \frac{1}{v}\frac{\partial\phi}{\partial t} \quad \text{(with No Delayed Neutrons)} \tag{15.2}$$

where

D is the neutron diffusion coefficient having the units of length (usually cm)
S is an *additional source* of neutrons having the units of neutrons/second
v is the average velocity of these neutrons, and the other parameters have their usual meanings

Notice that in a time-dependent reactor, the value of $\partial\phi/\partial t$ is always greater than or less than zero. Moreover, Equation 15.2 assumes that all of the neutrons (both prompt neutrons and delayed neutrons) are produced at the same time. However, they are *NOT* produced at exactly the same time, and consequently, there can be a delay of a couple of seconds (or even a couple of minutes) between the time the prompt neutrons are produced and the delayed neutrons are produced. To understand the effects of this delay, we must modify Equation 15.2 to account for the fact that most of them, which we will represent by the term $(1 - \beta)$ are produced instantaneously, while a small fraction of them β may not appear for 5, 10, 20, or even 100 seconds after the prompt neutrons are produced. Thus the term β can be considered to be the *delayed neutron fraction*, and the term $(1 - \beta)$ can be considered to be the *prompt neutron fraction*. In practice, *less than one percent of the neutrons that are produced are delayed*.

The easiest way to represent this process mathematically is to partition the neutron production terms into two parts so that the prompt neutron production rate is given by $(1 - \beta)\ (\nu\Sigma_f)\ \phi$ *and the delayed neutron production rate* $S_d(t)$ *is written as some other factor that is proportional to the fission product concentration C*. Usually, the delayed neutron production rate $S_d(t)$ is equal to λC, so if we subdivide the neutron production term S(t) into both prompt and delayed components, we obtain

$$S(t) = S_p(t) + S_d(t) \tag{15.3}$$

where

λ is the decay constant governing how fast the fission products decay and produce delayed neutrons
$S_p(t)$ = prompt neutrons introduced from an external source
C is the concentration of fission products that produce delayed neutrons, measured in fission products per cubic centimeter; i.e., $S_d(t) = \lambda C(t)$

The term $(1 - \beta)\ (\nu\ \Sigma_f)\ \phi$ is then retained independently because of its dependence on ϕ. Hence, the "real" form of the diffusion equation that governs the time-dependent neutron population is

Time-Dependent Neutron Diffusion Equation

$$D\nabla^2\phi(\mathbf{r}) + (1-\beta)\nu\Sigma_f\phi(\mathbf{r}) - \Sigma_a\phi(\mathbf{r}) + S(t) = \frac{1}{v}\frac{\partial\phi(\mathbf{r})}{\partial t} \quad \text{(with Delayed Neutrons)} \tag{15.4}$$

where

$$S(t) = S_p(t) + \lambda C(t) \tag{15.5}$$

The total fraction of the neutrons produced in this way (which is equal to the sum of the delayed neutrons from all of the fission products) is sometimes called the *delayed neutron fraction* β. *The delayed neutron fraction is generally expressed as the number of delayed neutrons that are produced from the fission of 100 uranium or plutonium nuclei.*

This number is also normalized so that even if every nuclear fission reaction produces two fission fragments, the delayed neutron fraction is the number of fission fragments *per fission* that will produce a delayed neutron at some point in time. Therefore, if the delayed neutron fraction is 0.0065 (which it happens to be in the case for U-235), then only 1 out of 2/0.0065 = 308 fission products will produce a delayed neutron. Therefore, we need to understand why the delayed neutrons take so long to appear, and how they can be added to the diffusion equation without violating the laws of mass

or energy conservation. This will require us to take a brief detour into how prompt and delayed neutrons are produced so that we will be able to draw the distinction between what makes a neutron "prompt" and what makes a neutron "delayed." This will also allow us to correctly add a prompt neutron to the diffusion equation, which we will also find is different in principle from adding a delayed neutron to the same equation. However, these two source terms (one due to prompt neutrons S_p and the other due to delayed neutrons S_d) then determine how a reactor as a whole will behave.

15.3 Delayed Neutrons and Their Importance

In Chapter 7, we learned that when a uranium or plutonium nucleus splits apart, a number of "prompt" neutrons are produced immediately, and the exact number of prompt neutrons varies from about 2.5 to 3.0 depending upon whether they are released from the fission of Uranium-233, Uranium-235, or Plutonium-239. The average energy of these prompt neutrons is about 2 MeV, and on average, they are released about 1×10^{-10} seconds after the fission process begins. In addition to these prompt neutrons, each nucleus splits into two smaller parts of approximately the same size and weight called *fission products* or *fission fragments*. Initially, these parts are called *fission fragments*, and then when they slow down and acquire additional free electrons, they become *fission products*. Fission products usually have an extra neutron in their nucleus, and some of them will decay into more stable elements or isotopes within a reasonably short period of time. In addition, a very small fraction of them (typically 1% or less) decay by emitting an extra neutron in the process. This extra neutron can take anywhere from a few hundredths of a second to about 100 seconds to appear. Since this neutron appears much later than the prompt neutrons do, it is sometimes referred to as a "*delayed neutron*." *Some of the fission products that produce delayed neutrons are Br-87, Br-88, Br-89, Br-90, Br-92, Kr-93, Kr-94, Rb-93, Rb-94, I-137, I-138, I-139, I-140, Cs-142, Cs-145, and Xe-143*. We can elaborate upon these observations by defining the average number of neutrons produced per fission (the total neutron yield), the number of delayed neutrons, and the delayed neutron fraction in the following way:

1. The *total number of fission neutrons* produced after an atomic nucleus splits apart (ν) is always equal to the sum of the yields of the prompt and delayed neutrons (ν_p and ν_d) from that nucleus. Hence, the value of ν (see Chapter 7) is defined by

The Total Neutron Yield

$$\nu = \nu_p + \nu_d \tag{15.6}$$

where the subscript p means that the neutron is "prompt" and the subscript d means that the neutron is "delayed".

2. The *number of delayed neutrons* produced per fission is then

Number of Delayed Neutrons

$$\nu_d = \nu - \nu_p \tag{15.7}$$

3. The delayed neutron fraction β may then be written as

Definition of the Delayed Neutron Fraction

$$\beta = \frac{\nu_d}{\nu} = \frac{\nu_d}{\nu_p + \nu_d} \tag{15.8}$$

Notice that the delayed neutron fraction β is always a number less than 1.0. It turns out that there are about 66 different fission products that can produce delayed neutrons at some time in their life cycle. Each of these radioactive fission products can be further subdivided into about 20 fission product decay chains, which each have their own decay constants λ_i and their delayed neutron yields β_i.

When the nuclear industry was first being founded, the decay constants and the yields for these 66 fission products were not accurately known, and so it was generally believed that it was not practical to solve the equations for all of the delayed neutron decay chains at the same time to determine the effect this would have on a reactor's behavior. Then as the industry became more mature, these 20 fission product decay chains were collapsed down to six or eight, and most time-dependent reactor behavior is determined by these collapsed fission product decay chains today. In the next sections, we would like to briefly describe how this process evolved and show how each of these decay chains contributes to the time-dependent behavior of a reactor as a whole.

TABLE 15.1
Nuclear Properties of Uranium and Plutonium at a Thermal Energy of 0.025 eV

Isotope	Prompt Neutrons Produced per Thermal Fission (ν)	Delayed Neutron Fraction per Thermal Fission ($\beta = \nu_d/\nu$)	Average Delayed Neutron Production Time T (s)	Thermal Absorption Cross Section (barns)	Thermal Fission Cross Section (barns)
U-233	2.49	0.0026	25.44	578.8	531.1
U-235	2.42	0.0065	13.04	680.8	582.2
Pu-239	2.87	0.0020	14.65	1011.3	742.5
Pu-241	2.92	—	—	1377.1	1008.9

Note that $\sigma_a = \sigma_f + \sigma_c$.

On average, it takes between 13 and 20 seconds for a delayed neutron to appear. This does not mean that all of the delayed neutrons will appear at exactly the same time. As a matter of fact, they can appear *anytime* between about one-tenth a second and 2 minutes after a nucleus splits apart. The actual production time also depends on the isotope of uranium or plutonium that is being used. For example, a fission product that is produced from the thermal fission of U-235 will emit a delayed neutron with an average period (T = 1/λ) of 13.04 seconds. A fission product produced from the thermal fission of U-233 will emit a delayed neutron with an *average period* (T = 1/λ) of 25.44 seconds, and a fission product produced from the thermal fission of Pu-239 will emit a delayed neutron with an average period (T = 1/λ) of 14.65 seconds. Hence, on average, atoms of U-235 produce delayed neutrons the fastest, and atoms of U-233 produce delayed neutrons the slowest. Atoms of Pu-239 produce delayed neutrons at a rate midway between these two extremes.

Example Problem 15.1

From Table 15.1, it can be easily seen that the delayed neutron fraction for the thermal fission of Plutonium-239 is 0.0026. How many fission products have to be produced from the thermal fission of Plutonium-239 to produce a single delayed neutron?

Solution Since two fission fragments are produced from the fission of every Pu-239 nucleus, 2/0.0026 = 700 fission products have to be created to produce a single delayed neutron. [Ans.]

In the late 1940s, an American physicist by the name of George *Robert Keepin*, who worked at the Los Alamos Scientific Laboratory at the time (see Figure 15.1), suggested that all of the fission products that produce delayed neutrons could be replaced by a single hypothetical "delayed neutron source" S_d, which could describe the decay of all of the precursor nuclei, and also the delayed neutron energy spectrum. By applying some simple statistical methods, he showed that the number of delayed neutrons emitted from a hypothetical neutron precursor could be predicted using only *six radioactive decay chains* with different decay constants and yields for U-233, U-235, Pu-239, and Pu-241. This became the basis for modifying the neutron diffusion equation to predict the time-dependent behavior of nuclear reactors today. In Keepin's original work, he irradiated a sample of Uranium-235 and then measured the delayed neutrons that were emitted from the sample. The delayed neutron production rate followed the curve shown in Figure 15.2. *He then attempted to "curve fit" the resulting curve with six separate exponential decay chains*.

Later he found that different types of nuclear fuels produced delayed neutrons at different rates, and generally speaking, fuels that produced more delayed neutrons resulted in nuclear systems that were easier to control. In the next few sections, we would like to explain the implications of what these differences mean and then illustrate how they can affect the way that a reactor (and its control system) must be designed. Keepin also showed that the composite decay curve to describe the delayed neutrons emitted in Figure 15.2 could be represented by the sum of exponential functions:

$$S_d(t) = \beta_1\lambda_1 e^{-\lambda_1 t} + \beta_2\lambda_2 e^{-\lambda_2 t} + \beta_3\lambda_3 e^{-\lambda_3 t} + \beta_4\lambda_4 e^{-\lambda_4 t} + \beta_5\lambda_5 e^{-\lambda_5 t} + \beta_6\lambda_6 e^{-\lambda_6 t} \tag{15.9}$$

where

$S_d(t)$ was the time-dependent source of the delayed neutrons
β_1, β_2, β_3, β_4, β_5, and β_6 were the yields for each of the six decay chains
λ_1, λ_2, λ_3, λ_4, λ_5, and λ_6 were the decay constants for decay chains from N = 1 to 6

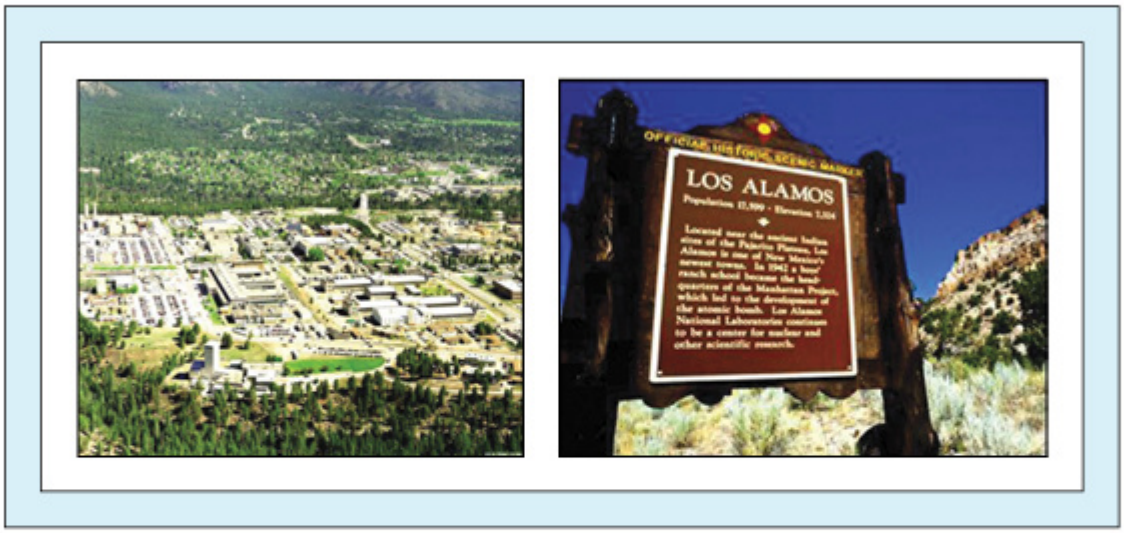

FIGURE 15.1 A sign near the Los Alamos National Laboratory in Los Alamos, New Mexico, where the delayed neutron fractions for the thermal fission of U-235 were first accurately measured by American physicist G. Robert Keepin.

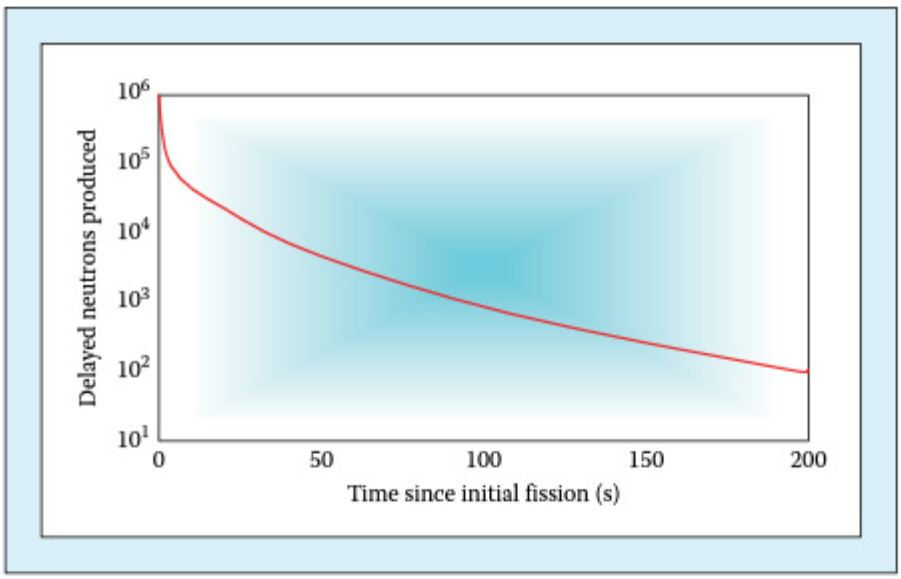

FIGURE 15.2 Keepin's original curve for the delayed neutron production rate from a Uranium-235 source. (Courtesy of Robert Keepin.)

By convention, delayed neutron precursor group 1 has the longest time constant for delayed neutron production, and delayed neutron precursor group 6 has the shortest. Hence, the *shape* of the $S_d(t)$ curve can be represented by the sum of the six delayed neutron precursors decay curves. The values of β and λ could then be found for each decay chain by statistical analysis of the resulting experimental data (see Figure 15.2). Eventually, Keepin discovered that a different set of β's and λ's were needed for each fissile material (U-233, U-235, Pu-239, and Pu-241) because the shape of the source curve varied from one type of fuel to another. Today, we know that these six decay chains are good enough to provide a reasonably accurate picture of how the delayed neutron population behaves. The values of the time constants for the delayed neutrons produced from U-235 are shown in Table 15.2. For the thermal fission of Uranium-235, these six decay chains have a total delayed neutron fraction β that sums to 0.0065 (0.65%). In other words, the total delayed neutron fraction for U-235 from the sum of these six decay chains is

$$\beta^{U235} = \beta_1 + \beta_2 + \beta_3 + \beta_4 + \beta_5 + \beta_6 = 0.00022 + 0.00142 + 0.00127 + 0.00257 + 0.00075 + 0.00027 = 0.0065$$

TABLE 15.2
Delayed Neutron Data for Uranium-235 (Total $\beta = 0.0065$)

Decay Group i	Decay Constant λ_i (s^{-1})	Period $T_i = 1/\lambda_i$ (s)	Yield β_i (in Delayed Neutrons per Fission)
1	0.0124	80.65	0.00022
2	0.0305	32.79	0.00142
3	0.111	9.01	0.00127
4	0.301	3.22	0.00257
5	1.14	0.88	0.00075
6	3.01	0.33	0.00027
Average	0.077	13.04	0.00108

Source: Courtesy of Alan Henry.

The corresponding decay constants for each of the six decay chains are

$$\lambda_1 = 0.0124\,s^{-1},\quad \lambda_2 = 0.0305\,s^{-1},\quad \lambda_3 = 0.111\,s^{-1},\quad \lambda_4 = 0.301\,s^{-1},\quad \lambda_5 = 1.14\,s^{-1},\quad \text{and}\quad \lambda_6 = 3.01\,s^{-1}$$

which gives an average decay constant of

Average Decay Constant for Delayed Neutrons

$$\lambda = \frac{\lambda_1 + \lambda_2 + \lambda_3 + \lambda_4 + \lambda_5 + \lambda_6}{6} = 0.0767\,s^{-1} \tag{15.10}$$

Notice that if the decay constants are weighted by the individual fission product yields, β_i, where i = 1 to 6, then the weighted average of the decay constants results in the slightly more accurate value of

$$\lambda = \frac{\lambda_1\beta_1 + \lambda_2\beta_2 + \lambda_3\beta_3 + \lambda_4\beta_4 + \lambda_5\beta_5 + \lambda_6\beta_6}{\beta^{U235}} = 0.0404\,s^{-1}$$

Sometimes these values are quoted in the literature, but almost everyone forgets to mention that one value is the *weighted average* of the decay chains and the other value is not. Of course, the decay constants are the *average values* that determine when a delayed neutron will be emitted. To compute the average time τ before a delayed neutron is emitted, we must then remember that the *half-life* $T_{1/2}$, the decay constant λ, and the *average life* τ are related to one another by

Important Relationships for Delayed Neutrons

$$T_{1/2} = 0.693\tau = \frac{0.693}{\lambda} \tag{15.11}$$

We derived this relationship from our earlier study of radioactive decay in Chapter 6.

In the case of U-235, it then follows that $\tau = 1/\lambda = 13.04$ seconds. As Keepin later found, *the shape of the delayed neutron production curve S (t) is NOT the same for all fissile materials. In fact, the delayed neutron fraction is also not the same for all fissile materials.* The number of delayed neutrons, and therefore the size of the delayed neutron fraction β, also depends on whether one is working with a thermal reactor or a fast reactor energy spectrum. The delayed neutron fractions, or yields, for a variety of fissile materials are shown in Table 15.3. This table also takes the presence of a fast or thermal neutron energy spectrum into account in the calculation of β. In subsequent chapters we will have an opportunity to use these values to understand how easy (or difficult) it is for a reactor to be controlled. *Delayed neutrons are also produced with slightly lower kinetic energies than prompt neutrons are.* This can be seen by examining the kinetic energy spectrum of the prompt neutrons and the delayed neutrons produced from the thermal fission of Uranium-235 in Figure 15.3. Now we would like to shift our attention to a detailed discussion of the processes that affect how prompt and delayed neutrons are produced.

TABLE 15.3
Delayed Neutron Fractions for Fast and Thermal Reactors

Material	Thermal Neutron Delayed Neutron Fraction (β)	Fast Neutron Delayed Neutron Fraction (β)
Th-232	0.0000	0.0203
U-233	0.0026	0.0026
U-235	0.0065	0.0064
U-238	0.0000	0.0148
Pu-239	0.0020	0.0020

Source: Courtesy of Alan Henry.

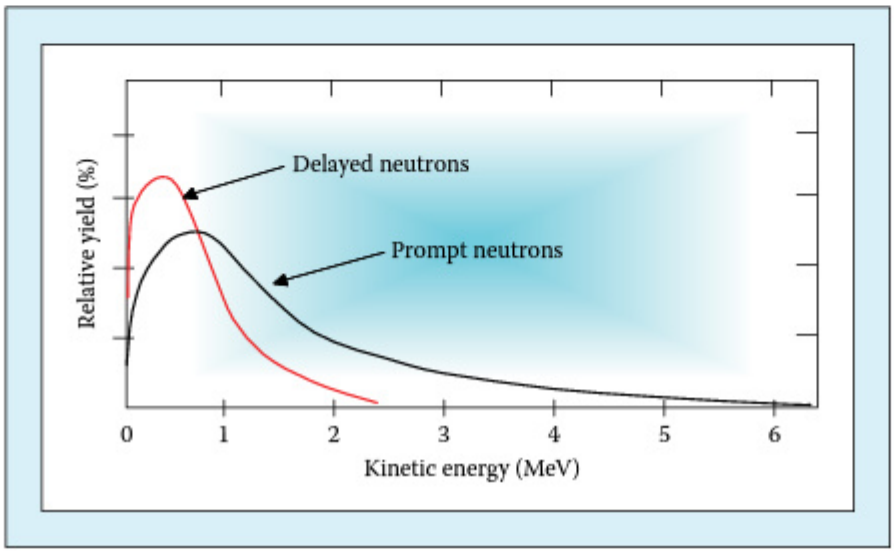

FIGURE 15.3 The energy spectrum of prompt and delayed neutrons from the thermal fission of U-235.

Example Problem 15.2

Using the previous equations, calculate the average amount of time τ before a delayed neutron will be emitted by the radioactive fission products from the third of the six radioactive decay chains produced by the fission of Uranium-235.

Solution For the third decay chain, the value of λ is 0.111 s^{-1}. Since $\tau = 0.693/\lambda$ and $\lambda_3 = 0.111\ s^{-1}$, $\tau = 0.693/0.111 = 6.24$ s in this case. [Ans.]

Example Problem 15.3

What percentage of the total delayed neutrons produced from the thermal fission of Uranium-235 are produced by the third decay chain?

Solution The delayed neutron faction (yield) for the third decay chain is $\beta_3 = 0.00127$. Since the total value of β for all six decay chains is $\beta = 0.0065$, the percentage of the delayed neutrons produced by the third decay chain is 0.00127/0.0065 = 0.195 = 19.5%. So, 19.5% of all of the delayed neutrons are produced from the fission of Uranium-235 with an average emission time of about 6.24 seconds. Also half of them will be emitted within a period of $T = 1/\lambda_3 = 9.01$ seconds. [Ans.]

15.4 Isotopes That Produce Delayed Neutrons

Table 15.4 shows the fission products that produce the most delayed neutrons, and the timing with which these delayed neutrons are produced. Almost all the delayed neutrons are produced by the process of beta decay (β^- decay), which we discussed in Chapter 6. This means that some fission products with an atomic number of Z transform themselves into fission

TABLE 15.4
Most Common Emitters of Delayed Neutrons in a Reactor Core Fueled with U-235

Delayed Neutron Precursor Group	Delayed Neutron Precursor	Chemical Symbol	Decay Mode	Average Delayed Neutron Energy (MeV)	Delayed Neutron Precursor Half-Life (T ½) (s)	Decay Constant for Delayed Neutron Production (λ)
1	Bromine-87	Br-87	β^-	0.25	55.7	0.0179 s^{-1}
2	Iodine-137	I-137	β^-	0.56	24.5	0.0408 s^{-1}
	Bromine-88	Br-88	β^-		16.3	0.0613 s^{-1}
3	Iodine-138	I-138	β^-	0.43	6.5	0.1538 s^{-1}
	Rubidium-93	Rb-93	β^-		5.9	0.1685 s^{-1}
	Bromine-89	Br-89	β^-		4.4	0.2273 s^{-1}
4	Iodine-139	I-139	β^-	0.45 MeV	2.4	0.4167 s^{-1}
	Cesium-144	Cs-144	β^-		1.0	1.0000 s^{-1}
	Tellurium-137	Te-137	β^-		3.5	0.2857 s^{-1}
	Bromine-90	Br-90	β^-		1.8	0.5555 s^{-1}
	Krypton-92	Kr-92	β^-		1.8	0.5555 s^{-1}
	Krypton-93	Kr-93	β^-		1.3	0.7692 s^{-1}
5	Krypton-95	Kr-95	β^-	0.42	0.8	1.2500 s^{-1}
	Iodine-140	I-140	β^-		0.9	1.1111 s^{-1}
	Iodine-141	I-141	β^-		0.5	2.0000 s^{-1}
6	Iodine-142	I-142	β^-	0.42	0.2	5.0000 s^{-1}
	Bromine-92	Br-92	β^-		0.4	2.5000 s^{-1}
	Rubidium-95	Rb-95	β^-		0.4	2.5000 s^{-1}
	Rubidium-97	Rb-97	β^-		0.2	5.0000 s^{-1}

Source: Courtesy of Robert Keepin.
Note that they are arbitrarily lumped into six delayed neutron precursor groups according to their half-lives. Several fewer or several more delayed neutron precursor groups could have also been used to represent the same source data.

products with an atomic number of Z + 1. The additional proton that is created in this way changes the stability of the nucleus, and the easiest way for the nucleus to become energetically stable again is to release an additional neutron, which is referred to in the field of reactor physics as a *delayed neutron*.

This process is depicted in Equation 15.12, which is repeated from Chapter 7 for the interested reader.

The Steps to Create a Delayed Neutron

Step 1:

$$\mathrm{FP}(A, Z) \rightarrow \mathrm{FP}(A, Z+1) + 1\,\text{electron and}\,1\,\text{neutrino}$$

Step 2:

$$\mathrm{FP}(A, Z+1) \rightarrow \mathrm{FP}(A-1, Z+1) + 1\,\text{delayed neutron} \qquad (15.12)$$

Notice that *the creation of a delayed neutron is a two-step process*. The first step creates an additional proton, and the second step ejects a delayed neutron from the nucleus to make it stable again. The reasons why the nucleus chooses to emit a delayed neutron were discussed in Chapters 6 and 7 of our companion book.* Thus, *delayed neutrons are produced primarily through the process of β^- decay rather than through the process of β^+ decay*. For historical reasons, the symbol β was then chosen to represent the delayed neutron fraction in order to remind reactor physicists of the source of these neutrons.

* See *Nuclear Engineering Fundamentals: A Practical Perspective*, by R.E. Masterson, CRC Press (2017).

15.5 Visualizing How Delayed Neutrons Are Produced

Figure 15.4 depicts how both prompt neutrons and delayed neutrons are created from the process of nuclear fission. Prompt neutrons are produced almost immediately (within ~10^{-12} seconds) after the nucleus splits apart, while delayed neutrons may not be produced for several seconds (or even several minutes) after the fission products have been created. *Prompt neutrons are created directly from a uranium or plutonium nucleus while delayed neutrons are not.* The kinetic energy E of the delayed neutrons is almost always less than that of their prompt counterparts, and the number of them that are produced per fission is also much smaller by comparison (~2.5 per fission vs. ~0.01 per fission). Yet, the production of these delayed neutrons on a much longer time frame is what allows a reactor to be operated safely without the need for exotic control systems. The larger the delayed neutron fraction β, the longer it will take for the power level to increase before a reactor enters a super critical state. *In other words, the larger the value of β, the easier it is—with all other factors being equal—to control how a reactor behaves.*

Once created, both prompt and delayed neutrons take approximately the same amount of time to reach the thermal energy range (E < 1 eV). Therefore, they take about the same amount of time to come into thermal equilibrium with their environment. The only difference is that the delayed neutrons are a direct by-product of the beta decay of one of the radioactive fission fragments (see Figure 15.4 again), while the prompt neutrons are not. In recent years, there have been various proposals to increase the accuracy of Keepin's original equations by curve fitting the delayed neutron fractions to *eight decay chains* instead of just six. While this has not become universally accepted, it is likely that using eight delayed precursor groups rather than six will become more popular as reactor design becomes increasingly more sophisticated.

Example Problem 15.4

As we mentioned previously, U-233 has a different source curve S(t) for creating delayed neutrons. Using the values given in Table 15.6 at the end of the chapter, show what the explicit shape of the source curve is for Uranium-233.

Solution From Table 15.6, we know that $\lambda_1 = 0.0126\ s^{-1}$, $\lambda_2 = 0.0337\ s^{-1}$, $\lambda_3 = 0.139\ s^{-1}$, $\lambda_4 = 0.305\ s^{-1}$, $\lambda_5 = 1.13\ s^{-1}$, and $\lambda_6 = 2.50\ s^{-1}$, and $\beta_1 = 0.00023$, $\beta_2 = 0.00081$, $\beta_3 = 0.00068$, $\beta_4 = 0.00075$, $\beta_5 = 0.00014$, and $\beta_6 = 0.00009$. Therefore, $S(t) = \beta_1\lambda_1 e^{-\lambda 1t} + \beta_2\lambda_2 e^{-\lambda 2t} + \beta_3\lambda_3 e^{-\lambda 3t} + \beta_4\lambda_4 e^{-\lambda 4t} + \beta_5\lambda_5 e^{-\lambda 5t} + \beta_6\lambda_6 e^{-\lambda 6t}$ where the values of the constants are those given above. [Ans.]

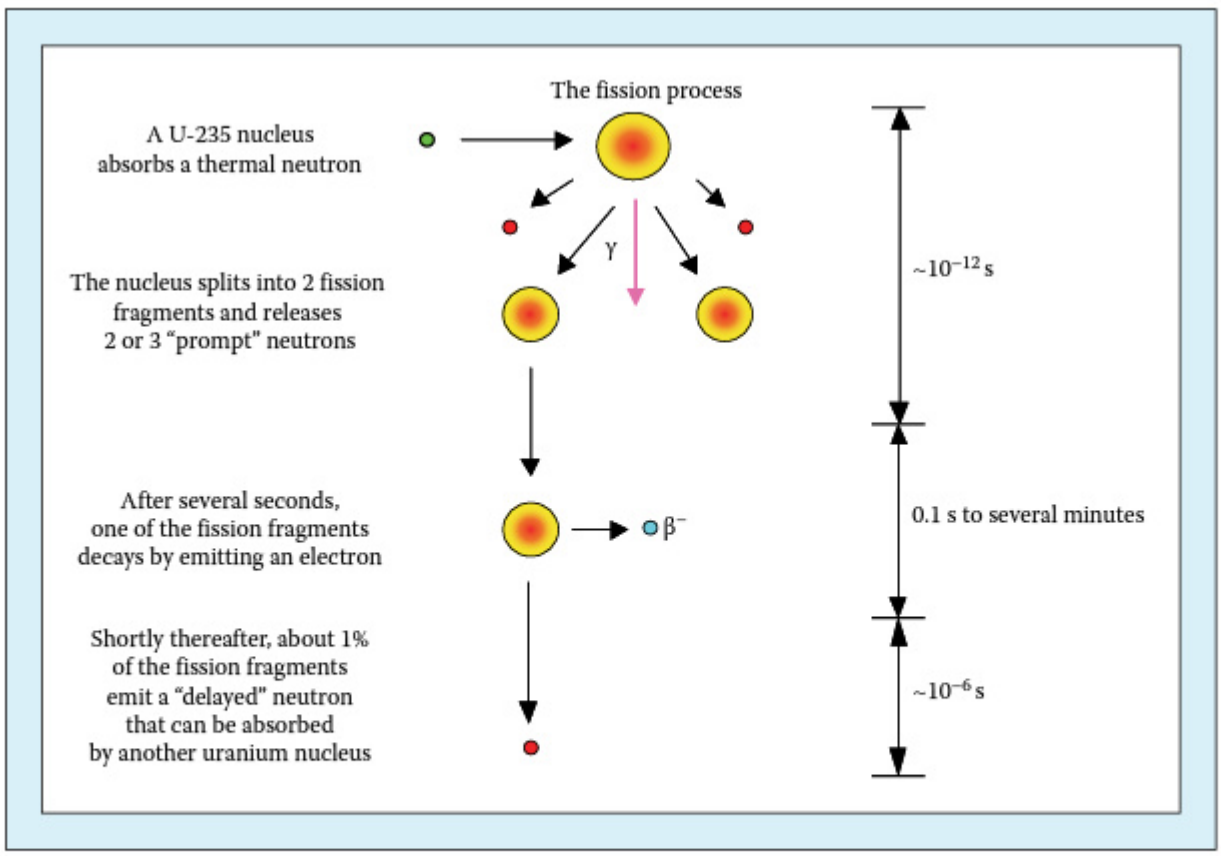
The fission process
A U-235 nucleus absorbs a thermal neutron
The nucleus splits into 2 fission fragments and releases 2 or 3 "prompt" neutrons
After several seconds, one of the fission fragments decays by emitting an electron
Shortly thereafter, about 1% of the fission fragments emit a "delayed" neutron that can be absorbed by another uranium nucleus
γ
β⁻
~10⁻¹² s
0.1 s to several minutes
~10⁻⁶ s

FIGURE 15.4 The process of creating prompt neutrons and delayed ones.

15.6 Time-Dependent Diffusion Equation without Delayed Neutrons

To understand how a time-dependent reactor behaves, it is necessary to understand how the neutron population changes as a function of time. When the value of the neutron flux is time dependent, it is no longer possible to set $\partial\phi/\partial t = 0$ and to assume that ϕ is a function of position alone. To understand this behavior we must find a way to solve the time-dependent neutron diffusion equation

The Time-Dependent Neutron Diffusion Equation with a Source Term

$$D\nabla^2\phi(\mathbf{r}, t) + ((1-\beta)\nu\Sigma_f - \Sigma_a)\phi(\mathbf{r}, t) + S(\mathbf{r}, t) = \frac{1}{v}\frac{\partial\phi(\mathbf{r}, t)}{\partial t} \tag{15.13}$$

to find ϕ as a function of position and time. To begin this process, we would like to first assume that there are no source terms in the diffusion equation to represent the delayed neutrons and that all of the neutrons that are produced are initially prompt ($\beta = 0$). This never occurs in practice, but if we are willing to make this single assumption, we can then show how a reactor behaves when there are no delayed neutrons or external neutron sources present. Depending on your point of view, the results may surprise you or even shock you when you find out how sensitive a time-dependent reactor becomes in this case. Hence, we will begin by setting $S(t) = 0$ and $\beta = 0$ with the understanding that we will add the source term containing the delayed neutrons back into the diffusion equation at a later time.

15.7 Finding Simple Solutions to the Time-Dependent Diffusion Equation Using the Separation of Variables Method

Even when the cross sections are temperature dependent, we can still solve the time-dependent diffusion equation as long as the macroscopic cross sections and the diffusion coefficient D do not also have an explicit spatial dependence, that is, that if we can assume for all r that D, Σ_f, and Σ_a are constant, and we are dealing with only a homogeneous system. If the neutron flux ϕ (r, t) changes rapidly with time (on the order of a couple of milliseconds), then the neutrons simply do not have enough time to diffuse more than a few diffusion lengths and change the shape of the flux. Because of this, reactors as a whole are loosely coupled time-dependent devices where the spatial behavior of the neutron population tends to be very localized rather than globally interconnected.

In general, the cores of most power reactors are between 150 and 250 diffusion lengths in diameter. Moving a single control rod in an attempt to control the power level will generally not change the overall shape of the neutron flux except in the vicinity of the rod. Because of this, there are certain situations where it is actually legitimate to assume that the global flux shape $\phi(r)$ stays exactly the same for a short period of time, while the overall level of the flux moves up and down in response to the multiplication factor of the core. In these cases, the physical coupling of the spatial flux shape and its time-dependent behavior is loose enough that it is possible to assume to a fair degree of accuracy that

The Point Kinetics Approximation

$$\phi(\mathbf{r}, t) = \phi(\mathbf{r}) \cdot \phi(t) \tag{15.14}$$

In other words, *the spatial dependence of the neutron flux, which is represented by $\phi(r)$, is relatively independent of the time dependence of the flux, which is represented by $\phi(t)$*. This means that if we already know what the spatial flux shape looks like, for example, we know the value of $\phi(r)$, then we can find $\phi(r, t)$ by simply multiplying this known shape by the time-dependent component, which represented by the function $\phi(t)$. Under these conditions, the time-dependent neutron diffusion equation can be solved by what is known as "*the point kinetics method*."

The general principle that the point kinetics method employs is illustrated in Figure 15.5, where the flux shape simply moves up and down in response to global changes in the value of the reactivity. Of course, there are certain situations where using a point kinetics method will introduce additional errors into our calculations, and these situations must be handled with additional care. For example, a situation where changes to the global flux shape *cannot* be ignored is when the reactor power begins to "tilt" due to the nonuniform buildup of fission products in the core. Another example of a related situation is when changes in the coolant flow across the core cause the diffusion coefficient D to be different on the RHS of the core than it is on the LHS. In any event, the spatial distribution of the flux becomes more tightly coupled to temporal changes in the neutron flux, and one may be forced to use a brute force approach to solve the time-dependent neutron diffusion equation and the associated precursor equations for the spatial and temporal behavior.

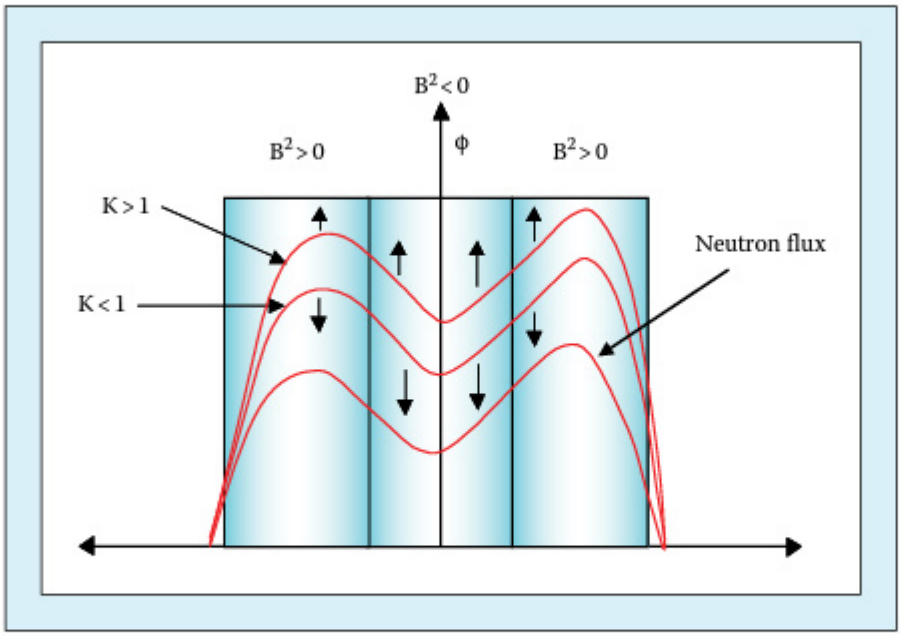

FIGURE 15.5 The time-dependent flux shape in the point kinetics approximation.

However, putting aside for the moment the possibility that the global flux shape will change appreciably during a specific transient, we can proceed with our description of the point kinetics method. *Thus decoupling the time-dependent behavior of the flux from its spatial shape allows us to take the time-dependent neutron diffusion equation, which is a very difficult equation to solve, and replace it by two simpler differential equations, which are much easier to solve*. Now suppose we begin this process by substituting $\phi(r, t) = \phi(r) \cdot \phi(t)$ into the time-dependent diffusion equation with no delayed neutrons to illustrate how the point kinetics method works. The result is

Implementing the Separation of Variables Method

$$D\nabla^2\phi(\mathbf{r}) + (\nu\Sigma_f - \Sigma_a)\phi(\mathbf{r}) = \frac{1}{v}\frac{d\phi(t)}{dt} = C_o \tag{15.15}$$

where we have now put all of the spatially dependent terms on the left-hand side and all of the temporally dependent terms on the right-hand side. By now it should be obvious that at any given point in time, both sides of Equation 15.15 must be equal to the same value C_o. For the sake of this derivation, we will assume that this value is a constant and that C_o have any value that we want. But if we are very close to being exactly critical, then it will have a very small value that can be either positive or negative. In any event, as long as this constant has *some value*, then we can replace the time-dependent diffusion equation by the following two differential equations:

The Equations for the Flux Shape and the Time-Dependent Flux

$$D\nabla^2\phi(\mathbf{r}) + (\nu\Sigma_f - \Sigma_a)\phi(\mathbf{r}) = C_o \tag{15.16}$$

$$\frac{1}{v}\frac{d\phi(t)}{dt} = C_o \tag{15.17}$$

This means that instead of having one extremely difficult differential equation to solve (Equation 15.13), we can now solve two simpler differential equations (Equations 15.16 and 15.17). We also know from our previous definition of the neutron flux ϕ (see Chapter 11) that $\phi(t) = n(t)v$, so the left-hand side of Equation 15.17 can simply be written as

$$\frac{d\phi(t)}{\phi(t)} = (C_o/n)dt \tag{15.18}$$

Integrating both sides, and defining a new constant $\omega = C_o/n$, we obtain

$$\phi(t) = Ae^{\omega t} \tag{15.19}$$

where A is now a constant of integration to be determined from the boundary conditions. The references at the end of the chapter explain how the actual value of A can be found. Thus we can take our previous expression for the time-dependent neutron flux $\phi(r, t)$ and write it as

The Equation for the Total Flux

$$\phi(\mathbf{r}, t) = A\,\phi(\mathbf{r})e^{\omega t} \tag{15.20}$$

where $\phi(r)$ is the solution to the steady-state neutron diffusion equation that contains the overall shape. In Chapter 13, we solved the steady-state neutron diffusion equation for a few hypothetical problems, including a three-dimensional rectangle, a three-dimensional cylinder, and a completely symmetrical sphere. The neutron flux shapes for these particular geometries were

Solutions to the Steady-State Diffusion Equation for a Few Simple Geometries

For a rectangular core:

$$\phi(x, y, z) = A\cos(\pi x/L_x)\cos(\pi y/L_y)\cos(\pi z/L_z)$$

For a cylindrical core:

$$\phi(r, z) = A\,J_o\left(2.405\frac{r}{R}\right)\cdot\cos\left(\pi\frac{z}{H}\right)$$

For a spherical core:

$$\phi(r) = \frac{A\sin(\pi r/R)}{r} \tag{15.21}$$

where it was assumed that the cores were bare and unreflected. It therefore follows that the general solutions to the time-dependent neutron diffusion equation can be written as

Solutions to the Time-Dependent Diffusion Equation for a Few Simple Geometries

For a rectangular core:

$$\phi(x, y, z, t) = A\cos(\pi x/L_x)\cos(\pi y/L_y)\cos(\pi z/L_z)e^{\omega t}$$

For a cylindrical core:

$$\phi(r, z, t) = A\,J_o\left(2.405\frac{r}{R}\right)\cdot\cos\left(\pi\frac{z}{H}\right)e^{\omega t}$$

For a spherical core:

$$\phi(r,t) = \frac{A\sin(\pi r/R)e^{\omega t}}{r} \tag{15.22}$$

in situations where the shape of the neutron flux does not change appreciably as a function of time (i.e., *where the point kinetics approximation applies*). Here A is the aforementioned *constant of integration* that depends on the boundary conditions or the initial reactor power. We will now demonstrate how the value of ω can be found. We will also learn that it represents the inverse of the reactor period T.

15.8 Defining the Reactor Period

For very large reactors, the neutron leakage term $-DV^2\phi(r)$ tends to be small in comparison to the neutron production and absorption terms $\nu\Sigma_f\phi$ and $\Sigma_a\phi$. Under these conditions, the value of ω depends primarily on the fission and absorption cross sections and therefore on the value of $k = \nu\Sigma_f - \Sigma_a$, or equivalently, $\rho = (\nu\Sigma_f - \Sigma_a)/\nu\Sigma_f$ where we have taken the liberty of canceling the neutron flux from both the numerator and the denominator. If $\rho > 0$, ω will be positive and the neutron flux will *increase* as a function of time. If $\rho < 0$, ω will be negative, and the neutron flux will *decrease* as a function of time. Finally, if $\rho = 0$, ω will be zero and $e^{\omega t} = 1$. Thus, the time-dependent neutron flux, based on just prompt neutrons alone, will either

- Increase exponentially
- Decrease exponentially
- Stay the same

In most text books, the term $T = 1/\omega$ is also called the reactor period, and it is a measure of how long it takes for the neutron flux (and therefore the reactor power level) to increase by a factor of e or decrease by a factor of 1/e. It is important to realize that this definition applies to *any* reactor whether or not the delayed neutrons are taken into account. The time-dependent neutron flux can therefore be written as a function of the reactor period T:

The Equation for the Time-Dependent Flux

$$\phi(t) = \phi(0)e^{t/T} = \phi_o\, e^{t/\tau} \tag{15.23}$$

and this expression is equivalent to saying that

An Alternative Equation for the Time-Dependent Flux

$$\phi(t) = \phi(0)e^{\omega t} \tag{15.24}$$

since $\omega = 1/T = 1/\tau$. Here again, t is the elapsed time in seconds, and the reactor period T is sometimes given the Greek letter τ (tau). The behavior of the neutron flux under these conditions is shown in Figure 15.6. In the absence of delayed neutrons, it can also be shown that the value of ω is given by

$$\omega = \frac{1}{T} = \frac{K_\infty - 1}{\Lambda} \tag{15.25}$$

where

K_∞ is the infinite multiplication factor

Λ is the *prompt neutron lifetime* that we first introduced to the reader in Chapter 7

So when a prompt neutron is initially produced, it slows down through a series of elastic and inelastic collisions with other nuclei in the lattice. In fast reactors, prompt neutrons do not have to slow down as much as they do in thermal reactors before they are either captured or absorbed. Depending upon the type of fuel that is used, the majority of them are absorbed at energies between 50 keV and 250 keV.

In thermal reactors, however, the material mix is different and most prompt neutrons escape resonance capture and reach thermal energies (~0.025 eV) before they either leak out of the core or are absorbed. Consequently, *the prompt neutron lifetime is usually defined as the average amount of time between the emission of a prompt neutron and its subsequent absorption or destruction somewhere in the core. Notice that the definition of the prompt neutron lifetime is reactor independent (e.g., it does not depend on whether or not we have a fast or a thermal reactor).* For thermal reactors, the time a prompt neutron exists can further be subdivided into the time τ it takes for the neutron to slow down from fast energies to thermal energies (not to be confused with the reactor period), and the time it takes for a thermal neutron to be captured after it has already slowed down to the thermal energy range, which is called the *thermal diffusion time* τ_d. In other words, to a first approximation, the prompt neutron lifetime Λ can be written as

The Prompt Neutron Lifetime in a Thermal Reactor

$$\Lambda = \tau + \tau_d \tag{15.26}$$

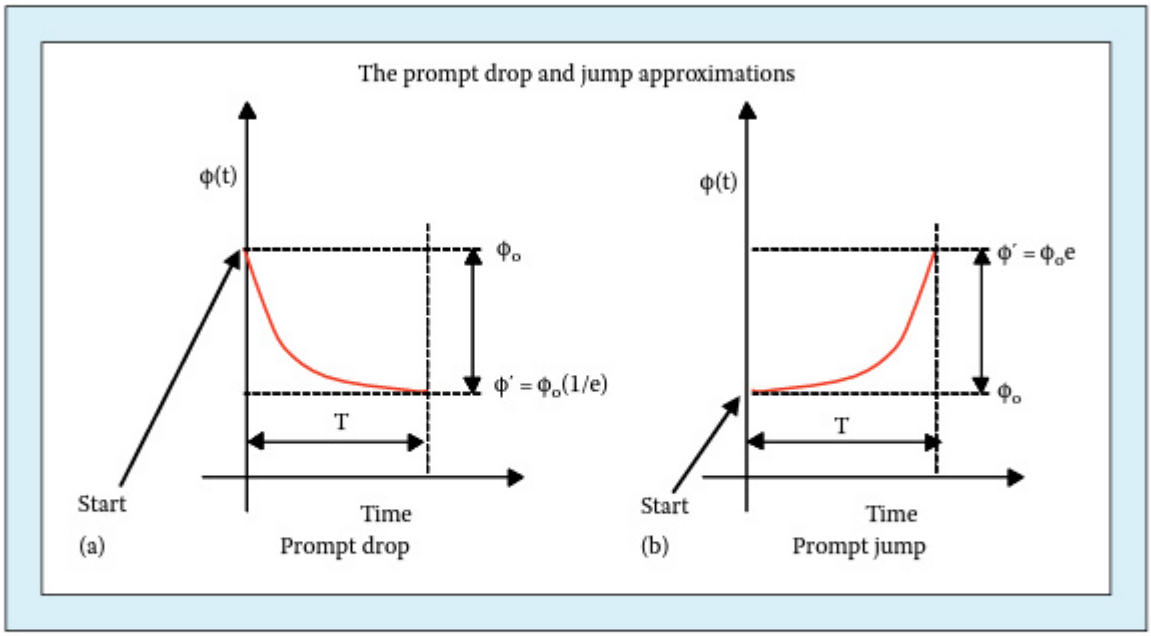

FIGURE 15.6 How the reactor period T is defined when the neutron flux decreases (a) and the neutron flux increases (b).

TABLE 15.5
Thermal Diffusion Lengths and Diffusion Times for Several Common Moderators

Material	Thermal Diffusion Length (cm)	Thermal Diffusion Time τ_d (s)
Water (H_2O)	~2.85	~2.0×10^{-4}
Graphite (C)	~59.5	~1.7×10^{-2}
Heavy water (D_2O)	~96.8	~4.3×10^{-2}

which is the sum of the slowing down time and the thermal diffusion time. Most of the time, it takes much longer for a neutron to be absorbed at thermal energies than it takes for a fast neutron to become a thermal one. Because it takes much less time to slow down than it does to be absorbed, it is appropriate to assume in most thermal reactors that $\tau \ll \tau_d$, so $\Lambda \approx \tau_d$. Now we can use this fact to estimate the value of ω in Equation 15.25.

The prompt neutron lifetime for a thermal reactor is on the order of 10^{-4} seconds, and for a fast reactor, the prompt neutron lifetime is on the order of 10^{-7} seconds. The difference in these values is attributable primarily to the difference in the value of τ_d. (For a fast reactor, the value of τ_d is essentially 0.) The value of τ_d for a number of common moderating materials is shown in Table 15.5. These values are for the moderator alone. When there is fuel present, the mean diffusion time τ_d depends on the value of the thermal utilization f, which also takes the macroscopic absorption cross section Σ_a of the fuel into account. The actual value of the thermal diffusion time is then given by

An Expression for the Thermal Diffusion Time

$$\tau_d = (1 - f)\,\tau_{dm} \tag{15.27}$$

where τ_{dm} is the thermal diffusion time for the moderator alone. So for a thermal reactor where we know what the moderator is, and we know the thermal utilization of the fuel, we can find the value of τ_d directly from Equation 15.27. It turns out for a homogeneous, critical thermal water reactor that $f = 1/\eta$ is about 0.50, so the prompt neutron lifetime Λ is $\Lambda \approx \tau_d \approx 1.0 \times 10^{-4}$ s.* So if one of the homogeneous reactors we discussed previously was just critical at t = 0, (with $K_\infty = 1.000$) and K_∞ was increased from 1.000 to 1.001 (or just 1 part in 1000) by withdrawing a control rod,

* It is important to bear in mind that the prompt neutron lifetimes we have discussed so far pertain to only thermal reactors. In fast reactors, the prompt neutron lifetimes are considerably shorter, since the prompt neutrons are absorbed much earlier in their life cycle—and rarely, if ever, reach thermal energies. In fast reactors, the prompt neutron lifetime is about 1000 times shorter, or on the order of 10^{-7} s. So, the delayed neutrons are even more essential to the control of such a design.

then reactor period (from Equation 15.25) would be equal to $T = 1.0 \times 10^{-4}/(1.001 - 1.000)$, or $T \approx 0.1$ second, and the time-dependent neutron flux would be

The Behavior of the Neutron Flux without Delayed Neutrons

$$\phi(t) = \phi(0)e^{10t} \tag{15.28}$$

where now t is the time in seconds. These numbers are quite typical for commercial light-water reactors. *Thus if we ignore the contributions of the delayed neutrons for the moment, we find that the reactor period T due to the prompt neutrons alone is quite short.* This means that if we had started out with a steady-state power level of 100 Megawatts, the power level would increase exponentially to $e^{10} = 22{,}000$ times the initial power level in just 1 second!

Obviously, this would completely destroy the reactor and everything else around it. (It could also send the reactor into orbit.) Fortunately, the example that we have just presented does not accurately describe the way that a real reactor behaves because we have ignored the effects of the delayed neutrons. *When the delayed neutrons are put back into the point kinetics equations the reactor period becomes much longer (on the order of 5 seconds to several hundred seconds), and the reactor becomes much easier to control*. As such, Equation 15.25, while it is reasonably accurate and instructive, does not accurately describe the kinetics of a real operating reactor. To do so, we must take the contributions of the delayed neutrons and the fission product poisons into account. Before showing how this can be done, we would first like to review a number of important concepts that we introduced to the reader in Chapters 11, 12, and 13. These concepts will help to prepare us for the important physical and analytical discussions that will follow. The effects of temperature feedback are then added to this discussion in Chapter 17.

15.9 Understanding the Life Cycle of a Prompt Neutron

Physically, the value of the *prompt neutron lifetime* can be represented by

The Prompt Neutron Lifetime

$$\Lambda = \tau + \tau_d \tag{15.29}$$

and so its value is ultimately related to the chain of events that occurs from the time a prompt fission neutron is first emitted until the time it is finally absorbed. We would like to illustrate this process again because it has such as profound effect on what the length of the reactor period T will be. Figure 15.7 shows a picture of how the entire process works. Thus it illustrates the life cycle of a prompt neutron. When a prompt neutron is initially emitted from the nucleus of a uranium atom, it starts an interesting journey from fast to thermal energies. The actual emission process itself is very fast and generally occurs in less than 1×10^{-10} seconds. After being emitted, the neutron immediately begins to collide with other atomic nuclei, and through a series of elastic and inelastic collisions, it eventually reaches the neutron absorption resonances, which can lie anywhere from about 1 eV to about 100 keV, depending on the material mix. It takes about 10^{-7} seconds to reach this point. If it is successful in avoiding the absorption resonances, which is determined by the resonance escape probability p, then it makes some more collisions before entering the thermal energy range ($E < 1$ eV). At this point, the entire process has taken about 10^{-7} seconds. Now let us illustrate the relationship between K_∞, the prompt neutron lifetime Λ, and the reactor period T with a simple example.

Example Problem 15.5

A reactor operator is operating a reactor with a prompt neutron lifetime of approximately 10^{-3} seconds. If the reactivity is 0.0001, what is the time period of the reactor in this case?

Solution We know that the reactor period T is given by $1/T = (K_\infty - 1)/\Lambda$, where K_∞ is the infinite multiplication factor. It therefore follows that $T = \Lambda/(K_\infty - 1)$. We also know for an infinite reactor that K_∞ is related to the reactivity by $K_\infty = 1/(1 - p)$. So, a reactivity of 0.0001 corresponds to a value of K_∞ of 1.0001. This then corresponds to a reactor period T of $T = \Lambda/(K_\infty - 1)\ 10^{-3}$ seconds$/0.0001 \approx 10$ seconds. [Ans.]

It should be clear from this example that the prompt neutron lifetime completely dominates the time-dependent behavior of a reactor when there are no delayed neutrons present. Once a neutron has reached the thermal energy range, it continues to collide with the nuclei of other atoms, and in some collisions, it will lose energy, while in other collisions, it may gain energy as well. Its most probable energy is about 0.025 eV, and its average energy, if it follows a *Maxwell–Boltzmann distribution* (see Chapter 8), is about three times higher, or 0.075 eV. At these energies, it takes about 1000 times longer, or about

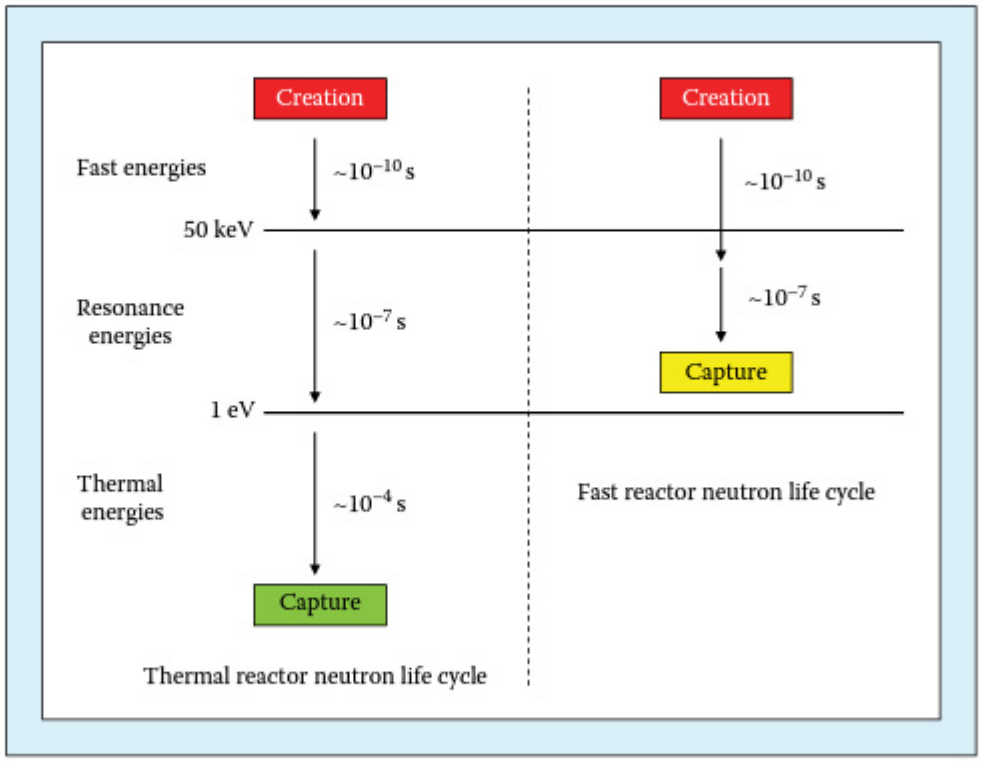

FIGURE 15.7 An illustration of the prompt neutron life cycle.

10^{-4} seconds, before it is either absorbed by another nucleus or until it leaks out of the core. This is the chain of events in the life of a prompt neutron in a thermal reactor. However, in fast reactors, the chain of events can be considerably different.

Fast reactors are designed so that very few neutrons reach the thermal energy range, and in fact, most of them are captured at energies above about 50 keV. This means that most fast neutrons do not have to slow down appreciably before they are absorbed. *As a result, the prompt neutron lifetime in a fast reactor is about 10^{-7} seconds. There are simply fewer collisions that have to occur before absorption occurs*. The prompt neutron life cycle in this case is illustrated on the right-hand side of Figure 15.7. This is what allows us to eliminate the thermal diffusion time τ_d from the calculation of the prompt neutron lifetime and write

$$\Lambda \approx \tau \tag{15.30}$$

By inspection, the value of the reactor period T, and therefore the reactor time constant, follows directly from this observation since

$$\omega \cong \frac{K_\infty - 1}{\Lambda} \tag{15.31}$$

Moreover, since $\omega = 1/T$

$$T \cong \frac{\Lambda}{K_\infty - 1} \tag{15.32}$$

This final equation is a particularly important result because it relates the reactor period to the reactivity. Again, some actual numbers are presented for a thermal water reactor in Example 5.5.

15.10 Time-Dependent Diffusion Equation with Delayed Neutrons

To understand how a reactor behaves when fission products are present, the best way to proceed is to modify the neutron diffusion equation to see what happens when a fission product emits a delayed neutron. As we saw at the beginning of the chapter, this involves tracking the number of delayed neutrons to be added to the diffusion equation from six different *fission product decay chains*. *There are actually about 20 decay chains in all, but through appropriate statistical analysis, they can be reduced to between 6 and 8 practical ones*. Most reactor physics books assume that six delayed neutron

groups are used, so we will abide by this convention for now and solve the time-dependent neutron equation when only six delayed neutron groups (each represented by a different decay chain) are used. The exercises at the end of the chapter then ask the reader to repeat this exercise when eight delayed neutron groups are used. When this is done, the results are quantitatively similar. However, they are much more accurate under certain conditions.

By convention (see Table 15.6), the first delayed neutron group has the longest average time before a delayed neutron is produced (about 80 seconds), and the sixth delayed neutron group has the shortest average time (about 0.33 seconds). Each decay chain from i = 1 to 6 will also make a contribution β_i to the total number β of delayed neutrons that are produced. For a thermal water reactor fueled with Uranium-235, the total number of delayed neutrons produced, β, is equal to about 0.65% of the total neutron population. This particular number, which is called the *delayed neutron fraction*, assumes that the reactor is being operated close to a critical state (where K = 1.000). During some types of transients, the delayed neutron fraction can temporarily rise as high as 1% of the total neutron population before returning to its steady-state value, but on average, the delayed neutron fraction always stays below 1%. We can model this behavior using the time-dependent diffusion equation by assuming that $(1 - \beta)$ percent of the neutrons are prompt neutrons and that β percent of the neutrons are delayed neutrons. We will call the production rate of prompt neutrons per second P_p and the production rate of delayed neutrons per second P_d. Therefore, we must modify the neutron production term $P = \nu\Sigma_f \phi$ in the diffusion equation to account for the fact that these delayed neutrons exist. We can therefore write the total neutron production rate P as

The Total Neutron Production Rate (due to Prompt and Delayed Neutrons)

$$P = P_p + P_d$$

or

$$P = (1-\beta)\,\nu\,\Sigma_f\,\phi + \Sigma_i\,\lambda_i\,C_i(t) \tag{15.33}$$

TABLE 15.6
Delayed Thermal Neutron Parameters for Uranium-233, Uranium-235, and Plutonium-238 Fuel

Decay Group i	Decay Constant λ_i (s^{-1})	Period $T_i = 1/\lambda_i$ (s)	Yield β_i (in Delayed Neutrons per Fission)
	Delayed neutron data for U-233 (total $\beta = 0.0026$)		
1	0.0126	79.36	0.00023
2	0.0337	29.67	0.00081
3	0.139	7.19	0.00068
4	0.305	3.28	0.00075
5	1.13	0.88	0.00014
6	2.50	0.40	0.00009
Average	0.054	25.44	0.00045
	Delayed neutron data for U-235 (total $\beta = 0.0065$)		
1	0.0124	80.65	0.00022
2	0.0305	32.79	0.00142
3	0.111	9.01	0.00127
4	0.301	3.22	0.00257
5	1.14	0.88	0.00075
6	3.01	0.33	0.00027
Average	0.077	13.04	0.00108
	Delayed neutron data for Pu-239 (total $\beta = 0.0020$)		
1	0.0129	77.52	0.000076
2	0.0311	32.15	0.000560
3	0.134	7.46	0.000432
4	0.331	3.02	0.000656
5	1.26	0.79	0.000206
6	3.21	0.31	0.000070
Average	0.068	14.65	0.00033

Source: Courtesy of Robert Keepin.

where λ_i is the decay constant for fission product group i and $C_i(t)$ is the fission product concentration in fission product group i in atoms/cm^3, and the summation is to be performed over all delayed neutron groups from i = 1 to 6. It is important to understand how the term, $\Sigma_i \lambda_i C_i(t)$ actually works when it is used in this context. In earlier sections, we learned that delayed neutrons are produced when certain fission fragments, which after emitting an electron in the process of β^- decay, happen to become unstable with respect to the number of neutrons that they contain. Once the beta decay occurs, a delayed neutron appears almost immediately. To determine the rate of delayed neutron emission, it is necessary to track the concentrations of these *delayed neutron precursors*, which are created at a rate proportional to $\beta_i \Sigma_f \phi(t)$. That is, $C_i(t) = \beta_i \Sigma_f \phi(t)$. So, the delayed neutron precursor production rate is actually $C_i(t) = \beta_i \Sigma_f \phi(t)$ for the *i*th group. If the concentration of the *i*th precursor groups is $C_i(t)$, and if the fission products emit a delayed neutron almost immediately after they decay, then the total number of delayed neutrons emitted per cc per second at point r and time t from the decay of these fission products is

The Total Number of Delayed Neutrons Produced per Second

$$P_d = \sum_i \lambda_i C_i(r, t) \tag{15.34}$$

If we suppress the spatial dependence of the delayed neutron emitters, then this becomes the term $\Sigma_i \lambda_i C_i(t)$, which was presented earlier. Bearing this in mind, we can write the time-dependent diffusion equation for the neutron flux ϕ as

The Time-Dependent Diffusion Equation with Prompt and Delayed Neutrons

$$D\nabla^2\phi + (1-\beta)\nu\Sigma_f \phi + \sum_i \lambda_i C_i(t) - \Sigma_a \phi = \frac{1}{v}\frac{\partial \phi}{\partial t} \quad \text{where } (i = 1 \text{ to } 6) \tag{15.35}$$

The unknowns in this equation are the neutron flux ϕ and concentrations of the six time-dependent fission product groups, C_1, C_2, C_3, C_4, C_5, and C_6. Notice that the delayed neutron fraction β is imbedded in the values of $C_i(t)$, and for this reason, it does not explicitly appear as a multiplier in front of each of the C_i's. If we were to explicitly include the true spatial and temporal dependence of the neutron flux $\phi(r, t)$ in Equation 15.35, then it would be written more voluminously as

The Time-Dependent Diffusion Equation Written Out Explicitly

$$D\nabla^2\phi(\mathbf{r}, t) + (1-\beta)\nu\Sigma_f \phi(\mathbf{r}, t) + \Sigma_i \lambda_i C_i(t) - \Sigma_a \phi(\mathbf{r}, t) = \frac{1}{v}\frac{\partial \phi}{\partial t}, \tag{15.36}$$

where i = 1 to 6, and we are again assuming a homogeneous medium so that D, Σ_f, and Σ_a have no spatial dependence.

Example Problem 15.6

Suppose that a reactor fuel assembly contains three dominant delayed neutron precursor groups with decay constants of 0.02 per second, 0.10 per second, and 0.20 per second. If the concentrations of the delayed neutron precursors within each of these three groups are 1 million atoms/cm^3, 2 million atoms/cm^3, and 4 million atoms/cm^3, respectively, what is the total delayed neutron production rate in 1 cm^3 of the fuel assembly?

Solution From Equation 15.34, the total number of delayed neutrons produced per second is $P_d = \lambda_1 C_1 + \lambda_2 C_2 + \lambda_3 C_3$. Since the values of λ_1, λ_2, and λ_3 are 0.02 per second, 0.10 per second, and 0.20 per second, and the values of C_1, C_2, and C_3 are 1 million atoms/cm^3, 2 million atoms/cm^3, and 4 million atoms/cm^3, the total delayed neutron production rate is $0.02 \times 1{,}000{,}000 + 0.10 \times 2{,}000{,}000 + 0.20 \times 4{,}000{,}000 = 1{,}020{,}000$ delayed neutrons/cm^3/s. [Ans.]

15.11 Finding the Time-Dependent Neutron Flux and Fission Product Concentrations

The fission products in a reactor core are produced at a rate that is proportional to the product of the neutron flux and the macroscopic fission cross section Σ_f

$$R_p = \Sigma_f \phi(t) \tag{15.37}$$

where R_p is the total fission product production rate. Of these fission products, only a small fraction, β, produces delayed neutrons because they are unstable. *The total number of delayed neutrons produced per cubic centimeter per second is therefore equal to the total number of fission neutrons produced, $\nu\Sigma_f\,\phi(t)$, multiplied by the delayed neutron fraction* β:

Delayed Neutron Production Rate

$$P_d = \nu_d\Sigma_f\phi(t) = \beta\,\nu\Sigma_f\phi(t)$$

Delayed neutrons = the delayed neutron fraction × fission neutrons (15.38)

In the case of the *i*th fission product group, C_i, the rate of change of its concentration with time is equal to the production rate, $\beta_i\nu\Sigma_f\phi(t)$, minus the decay rate $\lambda_i C_i(t)$. In other words, the rate equation for the concentration $C_i(t)$ of the *i*th fission product group is

Delayed Neutron Precursor Concentration for the *i*th Precursor Group

$$\frac{dC_i}{dt} = \beta_i\nu\Sigma_f\phi(t) - \lambda_i C_i(t) \quad i = 1,2,\ldots,6 \tag{15.39}$$

where there are six groups of fission products in all. If we were to write them out explicitly, we would obtain the equations shown below:

The Precursor Equations for All Six Delayed Neutron Groups

$$\begin{aligned}
\frac{dC_1}{dt} &= \beta_1\nu\Sigma_f\phi(t) - \lambda_1 C_1(t)\\
\frac{dC_2}{dt} &= \beta_2\nu\Sigma_f\phi(t) - \lambda_2 C_1(t)\\
\frac{dC_3}{dt} &= \beta_3\nu\Sigma_f\phi(t) - \lambda_3 C_3(t)\\
\frac{dC_4}{dt} &= \beta_4\nu\Sigma_f\phi(t) - \lambda_4 C_1(t)\\
\frac{dC_5}{dt} &= \beta_5\nu\Sigma_f\phi(t) - \lambda_5 C_1(t)\\
\frac{dC_6}{dt} &= \beta_6\nu\Sigma_f\phi(t) - \lambda_6 C_1(t)
\end{aligned} \tag{15.40}$$

These are the time-dependent precursor concentrations when the fuel is stationary. Each type of fuel—U-233, U-235, or Pu-239—then has its own fission product distribution and therefore its own unique values for β_i and λ_i. The values of β_i and λ_i are fuel dependent, and fast reactors can have different values for β_i and λ_i than thermal reactors do. Table 15.6 shows these values for a representative thermal water reactor fueled with Uranium-233, Uranium-235, and Plutonium-239. *The smallest decay constant, λ_1, has a period $T_1 = 1/\lambda_1$ of about 80 seconds and it dominates the behavior of the core when t is large. The largest decay constant, λ_6, has a period $T_6 = 1/\lambda_6$ of about 0.33 seconds and it dominates the behavior of the core when t is small. The other decay constants, λ_2 to λ_5, have intermediate values that fall somewhere between these two extremes.*

In general, the behavior of a reactor when the power level falls is governed by the behavior of the longest-lived decay chain, which in this case is decay chain #1 (see Table 15.4). In this decay chain, the primary delayed neutron precursor is Bromine-87, which has a half-life of 55.7 seconds. *Bromine-87* is extremely important to the operation of a nuclear power plant because when it is shut down suddenly and the shorter-lived delayed neutron percursors have decayed away, the neutron population is determined by the number of delayed neutrons produced from Bromine-87. In other words, *the asymptotic reactor period in the event of a rapid core shutdown is determined primarily by the Bromine-87 concentration in the core*. No other radioisotope produced from the fission of uranium or plutonium has such an important impact on the time-dependent behavior of the core.

The expressions for the delayed neutron precursor concentrations (again refer to Equation 15.40) are coupled to the time-dependent neutron diffusion equation through the fission product concentrations $C_i(t)$, which are in turn dependent on the neutron flux $\phi(r, t)$. This means that if we are interested in predicting how the flux behaves with time, we must, in principle, solve seven coupled differential equations simultaneously. This is a rather laborious task that we will not repeat here. However, it is possible to obtain a great deal of information about the time-dependent behavior of the flux by assuming that these six distinct groups of fission products can be replaced by a single hypothetical fission product group, C(t), which has a single average decay constant λ. This decay constant can be found by simply averaging the individual decay constants, weighted by their respective yields:

The Decay Constant for a Single Delayed Neutron Group

$$T = \frac{1}{\lambda} = \frac{1}{\beta}\sum_i\left(\frac{\beta_i}{\lambda_i}\right) \quad i = 1, 2, ..., 6 \tag{15.41}$$

For U-233, the average value of λ is 0.054 s^{-1}; for U-235, the average value of λ is 0.077 s^{-1}; and for Pu-239, the average value of λ is 0.068 s^{-1}. These correspond to a period T of 25.44 seconds for U-233, 13.04 seconds for U-235, and 14.65 seconds for Pu-239. The total yields or β's for U-233, U-235, and Pu-239 are 0.0027, 0.0065, and 0.0020, respectively. Lumping all the fission product precursors together, the rate equation for the concentration C(t) of the fission products becomes

The Rate Equation for the Concentration of the Fission Products

$$\frac{dC}{dt} = \beta\nu\Sigma_f\phi(t) - \lambda C(t) \tag{15.42}$$

and together with the time-dependent neutron diffusion equation, we only have two coupled differential equations left to solve:

The Two Equations We Have to Solve to Find the Time-Dependent Flux

$$D\nabla^2\phi(r,t) + (1-\beta)\nu\Sigma_f\phi(r,t) + \lambda C(t) - \Sigma_a\phi(r,t) = \frac{1}{v}\frac{\partial\phi(r,t)}{\partial t}$$

$$\frac{dC}{dt} = \beta\nu\Sigma_f\phi(r,t) - \lambda C(t) \tag{15.43}$$

While it is by no means a trivial exercise to solve these equations, it can be done without a computer both graphically and analytically if we are willing to make certain simplifying assumptions about how the reactivity ρ changes with time. In the next few chapters, we would like to explore exactly how this can be done. The specific analytical procedures for doing so are discussed in Chapter 16. Chapters 17 and 18 then provide additional information to show how the reactivity changes as a function of time. Sometimes, the solutions to the point kinetics equations (see the discussion in Chapter 16) are also written in terms of the reactivity ρ to show the relationship between the value of ρ and the reactor period T. Generally speaking, the larger the reactivity is (and the more positive it is), the shorter the reactor period will be; conversely, the smaller the reactivity is (and the more negative it is), the longer the reactor period will be. *In the meantime, the reader should keep in mind that it is desirable to keep the reactivity as close as possible to 0 because this causes the reactor power P and the neutron flux ϕ to be as stable as possible for as long as possible. For this reason, all commercial power reactors are designed to operate with the reactivity between ρ = 0 and ρ ~ ± 0.05 β. This reactivity range keeps the reactor period between 100 and 300 seconds, and this makes the reactor easy to control.* Larger values of the instantaneous reactivity are normally not allowed during normal operation because they can make the power level change more rapidly. Reactors must also be operated in such a way that the fuel temperature T_{FUEL} never exceeds its maximum possible design temperature T_{MAX}, which is normally about 1800°C.

Example Problem 15.7

In reactor design, one quickly learns that there is a strong relationship between the effective multiplication factor $K_{effective}$ and the reactivity ρ. What is the value of the reactivity that corresponds to a change in $K_{effective}$ from 1.000 to 1.001?

Solution From Equation 15.1,

$$\rho = \frac{K_{effective} - 1}{K_{effective}} = \frac{1.001 - 1}{1.001} \approx 0.001$$

Normally, for small changes to the effective multiplication factor, the denominator has a numerical value close to 1.0. In this case, the change in the reactivity $\Delta\rho$ is related to the change in the effective multiplication factor Δk by

$$\Delta\rho \approx \Delta k$$

where $\Delta k = (k - 1)$. This relationship is particularly useful when small changes to the reactivity are involved. [Ans.]

15.12 The Reactor Period and the Reactor Power

Earlier we mentioned that the reactor period τ was defined as the amount of time required for the neutron population to increase by a factor of e (2.71828) or decrease by a factor of 1/e (0.3678). Since the power level P is directly proportional to the neutron flux ϕ, the reactor period can also be thought of as the amount of time required for the power level to increase by 271% (2.71828) or decrease by 63.3% (to 0.3678). In practice, reactor operators are more interested in knowing how long it takes for the power level to increase by a factor of two (i.e., to double) or decrease by a factor of two (i.e., to be cut in half). We can find this time by realizing that if the time-dependent flux is given by Equation 15.23, then the time-dependent power level must obey an analogous equation:

The Equation for the Time-Dependent Power

$$P(t) = P(0)e^{t/T} = P_o e^{t/\tau} \tag{15.44}$$

where P_o is the steady-state power level. Thus, we can write Equation 15.44 as

$$\frac{P}{P_o} = e^{t/\tau} \tag{15.45}$$

and taking the natural logarithm of both sides, we obtain

The Relationship between the Reactor Power Level, the Reactor Period, and the Time

$$\tau = \frac{t}{\ln(P/P_o)} \tag{15.46}$$

Equation 15.46 allows us to establish a unique relationship between the reactor power level P, the reactor period τ, and the time required to achieve a specific power level P. Now suppose that we would like to estimate how long it takes for the reactor power level to increase by a factor of two (i.e., to double) or decrease by a factor of two (i.e., to be cut in half). The *doubling time* can be found by setting $P = 2P_o$, in which case the reactor period and the doubling time are related by

$$\tau = \frac{t}{\ln(2)} = \frac{t}{0.693} \tag{15.47}$$

Similarly, the *halving time* can be found by setting $P = \frac{1}{2} P_o$, in which case the reactor period and the halving time are related by

$$\tau = -\frac{t}{\ln(0.5)} = \frac{t}{0.693} \tag{15.48}$$

In either case, it should come as no surprise that both the halving time and the doubling time are the same. In other words, if the reactor power level increases by a factor of two or decreases by a factor of two in 1000 seconds, then the reactor period must be $\tau = 1000/0.693 = 1443$ seconds, and if the reactor period is 300 seconds, then the time it takes to double

the power or to be cut in half is $t = 300 \times 0.693 = 208$ seconds. In fact, Equation 15.46 can be used to determine the relationship between t and τ for *any arbitrary change in the power level* (up or down) as long as the steady-state power level P_o is known. The utility of this approach is illustrated in Examples 15.8 and 15.9.

Example Problem 15.8

The control rods in a research reactor are configured so that moving the control rods up or down will increase or decrease the power level very gradually. Suppose that it is desired to double the power level of the core in 20 minutes. What does the reactor period τ have to be in this case?

Solution To double the power level of the core in 20 minutes (or 1200 seconds), the reactor period must be $\tau = t/\ln(2) = 1200/0.693 = 1732$ seconds. This can be achieved by simply withdrawing one of the control rods from the core. [Ans.]

Example Problem 15.9

A research reactor in Cambridge, Massachusetts which is run by the Massachusetts Institute of Technology, produces 10 MW of electric power while it is operating normally. When the reactor is suddenly scrammed during a safety test required by the Cambridge City Council, it is observed that the power level drops to 100 watts in 10 minutes. What is the reactor period for this particular transient?

Solution If the power level drops to 100 watts in 10 minutes (or 600 seconds), the reactor period must be $\tau = -t/\ln(P/P_o)$. Since P = 100 watts, P_o = 10 MW, and t = 600 seconds, $\tau = -600/\ln(0.00001) = 52.1$ seconds. [Ans.]

Many other examples of this fundamental relationship between the power level and the reactor period can be seen in everyday life. In future chapters, we will explore the relationship between the reactor period τ and the reactivity change $\Delta\rho$ required to increase or decrease the power level by a specific amount. In practice, the reactivity can be increased or decreased by simply moving a control rod into or out of the core. As long as the point kinetics approximation can be used, the approach we have just outlined can be used to obtain reliable results. We would now like to consider how the effects of temperature feedback can affect the reactor power level. To understand the magnitude of these effects, please refer to the discussion in Chapter 17.

References

Books and Textbooks

1. Ash, M. *Nuclear Reactor Kinetics*, McGraw-Hill, New York (1965).
2. Henry, A.F. *Nuclear Reactor Analysis*, MIT Press, Cambridge, MA (1975).
3. Keepin, G.R. *Physics of Nuclear Kinetics*, Addison-Wesley, Reading, MA (1965).
4. Stacey, W.M. *Nuclear Reactor Physics*, 2nd edn., John Wiley & Sons, New York (2007).
5. Duderstadt, J. and Hamilton, L. *Nuclear Reactor Analysis*, John Wiley & Sons, New York (1976).
6. Lewis, E. *Fundamentals of Nuclear Reactor Physics*, Academic Press, Boston, MA (2008).
7. Hetrick, D.L. *Dynamics of Nuclear Reactors*, American Nuclear Society, La Grange Park, IL (1993).
8. Schultz, M.A. *Control of Nuclear Reactors and Power Plants*, 2nd edn., McGraw-Hill, New York (1961).
9. Lamarsh, J.R. and Baratta, A.J. *Introduction to Nuclear Engineering*, Prentice Hall, Upper Saddle River, NJ (2001).
10. Lamarsh, J.R. *Introduction to Nuclear Reactor Theory*, second printing, Addison-Wesley Publishing Company Inc., Reading, MA (1972).
11. Shultis, K. and Faw, R. *Fundamentals of Nuclear Science and Engineering*, 2nd edn., CRC Press, Boca Raton, FL (2008).
12. Masterson, R.E. *Nuclear Engineering Fundamentals: A Practical Perspective*, CRC Press, Boca Raton, FL (2017).

Web References

1. *http://en.wikipedia.org/wiki/Delayed_neutron.*
2. *https://www.euronuclear.org/e-news/e-news-14/pwr.htm.*
3. *https://canteach.candu.org/Content%20Library/20043611.pdf.*
4. *http://tutorial.math.lamar.edu/Classes/DE/SeparationofVariables.aspx.*
5. *http://ansn.iaea.org/Common/documents/Training/TRIGA%20Reactors%20(Safety%20and%20Technology)/chapter2/physics213.htm.*

Additional References

- Important physical constants used by nuclear scientists and engineers can be found in *Appendix A*.
- Unit systems and their conversion factors can be found in *Appendix B*.
- Nuclear cross sections for many important nuclear materials can be found in *Appendix C*.
- Physical properties of important nuclear materials can be found in *Appendix D*.
- Atomic masses, half-lives, and natural abundances can be found in *Appendix E*.
- Delayed neutron emitters and their properties are discussed in *Appendix F*.

Questions for the Student

The following questions cover the material presented in this chapter and, in some cases, previous chapters as well. They are designed to test how well the student has acquired a working knowledge of the subject matter.

1. What specific variables in the neutron diffusion equation does the point kinetics approximation attempt to separate?
2. Name four methods that can be used to determine the worth of a control rod.
3. What delayed neutron precursor is primarily responsible for controlling the long-term power level of a reactor core following an emergency shutdown or "scram"? What is its approximate half-life?
4. Which of the following isotopes (U-233, U-235, or Pu-239) produces the most delayed neutrons and which one produces the least?
5. Earlier in the chapter, we learned that the asymptotic period T∞ of a fast reactor is entirely different than it is for a thermal reactor for exactly the same change in the reactivity when the change in the reactivity $\rho = \Delta\rho$ is small. Suppose that a thermal water reactor is fueled with U-235 and a fast reactor is fueled with Pu-239. For small positive values of the reactivity, approximately how many times longer is the asymptotic period in the thermal reactor? What is the reason for such a large difference?
6. What is the name of the radioactive decay process that eventually leads to the production of the delayed neutrons that are used to control a reactor core?
7. Name at least six fission products that will eventually produce delayed neutrons.
8. How long does it take for a typical delayed neutron to be produced after a uranium or plutonium nucleus splits apart? In most common models of time-dependent rector behavior, what is the range of times between the minimum time when a delayed neutron may first appear and the maximum time when a delayed neutron may first appear?
9. How quickly does a prompt neutron appear from the same atomic nucleus after it splits apart?
10. On average, how many prompt neutrons are released from the thermal fission of Uranium-235?
11. If a fissionable material has an average neutron yield of 2.5 neutrons, and the delayed neutron fraction is 0.006, how many delayed neutrons does it produce per fission?
12. On average, is the delayed neutron fraction higher in a fast reactor or a thermal reactor?
13. Because of differences in the delayed neutron fraction, which type of reactor is easier to control? A fast reactor or a thermal one?
14. In the point kinetics equations, what does the symbol Λ refer to? What is the difference in the size of the prompt neutron lifetime between a fast reactor and a thermal reactor?
15. What contribution did Robert Keepin make to the field of time-dependent reactor behavior?
16. Approximately how long after a thermal reactor is shut down does the level of Xenon-135 reach its maximum value?
17. Approximately how long after a thermal reactor is started up with a fresh load of fuel does the Xenon-135 level reach its equilibrium concentration?
18. Is the buildup of xenon or samarium of any particular importance in the operation of a fast reactor? If so, why?
19. What is the thermal absorption cross section of the neutron poison Xenon-135?
20. Approximately how many more times negativity reactivity does the buildup of Xenon-135 introduce into a thermal water reactor than the buildup of Samarium-149 does?
21. What is the formal definition of the inhour?
22. Write down an expression for the inhour equation for a reactor with only one delayed neutron group. In the limit of very small values of the reactivity (i.e., large reactor periods), write down a simplified expression for the inhour equation that is less complicated than the original one.
23. Approximately how much reactivity does a dollar of reactivity refer to, and how much reactivity is equivalent to one nile?
24. Why are almost all commercial power reactors operated in a base-loading mode?
25. What are the two basic assumptions that are used to derive the prompt jump approximation?
26. Under what set of conditions does a reactor become prompt critical?
27. Why does the delayed neutron fraction β change from one type of reactor to the next?
28. Which type of nuclear fuel has the highest delayed neutron fraction and what type has the lowest?
29. During a very fast reactor transient, what assumption can we generally make about the delayed neutron precursor concentration C?
30. What is the definition of the reactor period T?
31. Which nuclear scientist originally proposed representing the delayed neutron production rate $S_d(t)$ from the fission of U-235 as the sum of six decaying exponential terms? Why was the production rate based on an exponential series instead of a polynomial curve fit of the form $S_d(t) = a + bt + ct^3 + dt^4 + et^5$?

32. Write an expression for the total neutron yield ν, and use this to derive an expression for the delayed neutron fraction β.
33. Generally speaking, what is the only time when the delayed neutron fraction can exceed a value of about 0.0065? What type of fuel must be used for this to happen?
34. Illustrate how the separation of variables method can be used to derive the time-dependent reactor kinetics equations.
35. Approximately how many delayed neutron precursors are contained within the six delayed neutron precursor groups that determine the time-dependent production rate of delayed neutrons? Can you name at least six of these delayed neutron precursors?
36. In principle, can more than six delayed neutron precursor groups be used to describe the time-dependent delayed neutron population, and if so, how many groups represent a significant improvement over the standard model in this area?
37. What is the average energy of a delayed neutron produced from the thermal fission of U-235? Is this higher or lower than the average energy of one of the prompt neutrons?
38. Approximately what percentage of the neutrons emitted from the fission of Pu-239 are prompt neutrons, and what percentage of the neutrons are delayed neutrons?
39. Suppose that the delayed neutron fraction β is given by the expression $\beta = \nu_d/\nu = \nu_d/(\nu_p + \nu_d)$. What is the prompt neutron fraction as a function of β, and what is an analytical expression for the prompt neutron fraction as a function of ν?
40. Write down an equation for the time-dependent neutron flux shape $\phi(x, t)$ in a bare homogeneous slab reactor of width L.
41. Write down an expression for the prompt jump approximation J. Up to what value of ρ is the prompt jump approximation generally considered to be valid?
42. Why are most important measurements of the asymptotic reactor period made by withdrawing a control rod from the core rather than inserting one?
43. What is the highest value that the delayed neutron fraction β can attain in a thermal water reactor during a very severe transient?
44. Suppose that a delayed neutron precursor has a concentration of 1 million atoms/cm^3 in a nuclear fuel rod. If its decay constant λ is 0.3 s^{-1}, how many delayed neutrons does it produce per second?
45. What isotope is primarily responsible for controlling the behavior of the longest-lived delayed neutron precursor group in a thermal water reactor? What is its half-life and its average life?
46. What fraction of the total number of delayed neutrons in a U-235-fueled thermal water reactor is produced by the radioactive fission products in delayed neutron precursor groups 3 and 4?

Exercises for the Student

Exercise 15.1

Suppose that the delayed neutron precursor concentration C(t) in a reactor fuel assembly is 1×10^{10} precursors/cm^3. If the primary fissile material in the reactor fuel rods is enriched uranium, how many delayed neutrons will be created by the delayed neutron precursors each second?

Exercise 15.2

In Chapter 16, we will show that the two roots to the point kinetics equations (Equation 15.43) with one delayed neutron precursor group are $\omega_1 \approx \lambda\rho/(\beta - \rho)$ and $\omega_2 \approx -(\beta - \rho)/\Lambda$. If the prompt neutron lifetime is $\Lambda = 6 \times 10^{-5}$ seconds, write these two roots as a function of the reactivity only for a thermal water reactor fueled with U-235.

Exercise 15.3

Using the results presented in the previous exercise, find the numerical values for the two roots ω_1 and ω_2 of the point kinetics equations if a reactor is exactly critical, and then two control rods are withdrawn from the core to increase the reactivity by 5 cents (0.05 β). What is the asymptotic reactor period in this case?

Exercise 15.4

Using the results presented in the previous exercise, write an expression for the time-dependent reactor power level P(t) with a single delayed neutron precursor group.

Exercise 15.5

Suppose that the asymptotic reactor period for a light-water reactor after one control rod is withdrawn from the core is 1000 seconds. How long does it take the power level to double in this case?

Exercise 15.6

Suppose that the average number of neutrons ν produced from the thermal fission of a mixture of uranium and plutonium atoms is 2.5. If the delayed neutron fraction β is 0.005, how many prompt neutrons and delayed neutrons are produced per fission?

Exercise 15.7

Calculate the average value of the decay constant λ for the delayed neutrons that are produced from the thermal fission of Uranium-235. Show that when the decay constant is found using a weighted average rather than a linear average that the value of the decay constant is reduced by approximately 52%. Which value of the decay constant do you believe is more accurate in this case?

Exercise 15.8

A commercial thermal water reactor is fueled with a 50% mixture of Uranium-235 and Plutonium-239. What is the value of the delayed neutron fraction for the reactor? What is the value of the decay constant λ for the delayed neutrons in this case? What is the average amount of time before a delayed neutron appears?

Exercise 15.9

The thermal water reactor in Exercise 15.8 is exactly critical before three banks of control rods are withdrawn from the core to increase the reactor power level. If the reactivity of each of the control rods is two cents, what is the absolute value of the reactivity change in this case?

Exercise 15.10

In Chapter 20, we will learn that a common unit for measuring the absolute reactivity is the pcm (or percent milli-rho). If 1 pcm = 0.00001, what is the absolute reactivity change in pcm a thermal water reactor fueled with U-235 if the reactivity is increased by 5 cents?

Exercise 15.11

A small 100 MW research reactor built in the United States has a reactor period of 10 minutes when the reactor is exactly critical and when one bank of control rods is subsequently withdrawn from the core. If the reactor is initially operating at a power level of 25 MW before the control rod bank was withdrawn, what is the power level of the reactor 10 minutes later?

Exercise 15.12

Using the data presented in Table 15.4, how could the delayed neutron precursors be partitioned into eight delayed neutron precursor groups to obtain a more accurate representation of the total delayed neutron production rate $S_d(t)$?

16

The Point Kinetics Approximation and the Inhour Equation

16.1 Deriving the Inhour Equation

In this chapter, we would like to derive the *Inhour equation* and discuss the implications of the *point kinetics approximation*, which was introduced to the reader in Chapter 15. The behavior of almost all time-dependent reactors can be analyzed in this way. When a reactor is homogeneous and the spatial dependence of the neutron flux can be neglected, then $\nabla^2\phi(\mathbf{r}, t) = 0$ and the time-dependent diffusion equation (see Chapter 15) can be written as

$$(1-\beta)\nu\Sigma_f\phi(t) + \lambda C(t) - \Sigma_a\phi(t) = \left(\frac{1}{v}\right)\frac{d\phi(t)}{dt} \tag{16.1}$$

If we divide both sides of the diffusion equation by Σ_a and use the fact that the prompt neutron lifetime Λ is equal to $\Lambda = 1/(v\Sigma_a)$, $K_\infty = \nu\Sigma_f/\Sigma_a$, and $\rho \approx 1$, the time-dependent diffusion equation becomes

Time-Dependent Diffusion Equation with No Neutron Leakage

$$\left[(1-\beta)K_\infty - 1\right]\phi(t) + \frac{\lambda C(t)}{\Sigma_a} = \frac{\Lambda d\phi(t)}{dt} \tag{16.2}$$

The time-dependent equation for the neutron precursor concentration C(t) can also be written as

Time-Dependent Precursor Equation

$$\frac{dC(t)}{dt} + \lambda C(t) = \beta K_\infty \Sigma_a \phi(t) \tag{16.3}$$

where

the precursor concentration C(t) is assumed to be in atoms per cubic centimeter
λ is the decay constant for fission products that produce delayed neutrons

Thus, we have reduced the problem of how the neutron flux behaves in the presence of delayed neutrons to just two coupled differential equations (Equations 16.2 and 16.3) that must be solved simultaneously to determine the values of ϕ and C. Now suppose that we would like to see how the reactor period T behaves when we add delayed neutrons to the prompt neutron population. To begin our discussion, we can assume that these coupled differential equations have general solutions of the form

General Solutions for the Neutron Flux and Precursor Concentrations

$$\phi(t) = Ae^{t/T} \quad \text{and} \quad C(t) = Ce^{t/T} \tag{16.4}$$

where

A and C are arbitrary constants
T is the reactor period (usually expressed in seconds)

When we substitute these general solutions into the equation for the time-dependent precursor population (Equation 16.3), we obtain

$$(C/T)e^{t/T} = A(\beta K_\infty \Sigma_a)e^{t/T} - \lambda C e^{t/T} \tag{16.5}$$

Dividing both sides by $e^{t/T}$ and solving for C, we find that

$$C = \frac{AX}{1/T + \lambda} \tag{16.6}$$

where $X = \beta K_\infty \Sigma_a$. If we then substitute $\phi(t) = Ae^{t/T}$ and $C(t) = AX(1/T + \lambda)e^{t/T}$ back into Equation 16.2, we finally obtain

$$Ae^{t/T}(1-\beta)K_\infty + \frac{Ae^{t/T}\lambda X}{(1/T + \lambda)\Sigma_a} - Ae^{t/T} = \frac{Ae^{t/T}\Lambda}{T} \tag{16.7}$$

The terms containing $Ae^{t/T}$ cancel, and all that we are left with is

$$K_\infty = \frac{1}{1-\beta}\left(1 + \frac{\Lambda}{T} - \frac{\lambda\beta K_\infty}{(1/T + \lambda)}\right) \tag{16.8}$$

After some further rearrangement, we arrive at the following equation for the reactor period T:

Initial Solution for the Reactor Period

$$\frac{K_\infty - 1}{K_\infty} = \frac{\Lambda}{\Lambda + T} + \frac{T}{\Lambda + T}\cdot\frac{\beta}{1 + \lambda T} \tag{16.9}$$

The term on the left-hand side, $(K_\infty - 1)/K_\infty$, is the classic expression for the reactivity ρ when the effects of neutron leakage, which are represented by $\nabla^2\phi(\mathbf{r}, t)$, can be ignored. (Neglecting neutron leakage is equivalent to assuming that $D\nabla^2\phi(\mathbf{r}, t) = 0$). If we use the fact that the reactivity $\rho = (K_\infty - 1)/K_\infty$, then we are left with the following fundamental relationship between the reactivity and the reactor period T for a homogeneous reactor with one group of delayed neutrons:

Equation for the Reactivity ρ and the Reactor Period T with One Delayed Neutron Group

$$\rho = \frac{\Lambda}{\Lambda + T} + \frac{T}{\Lambda + T}\cdot\frac{\beta}{1 + \lambda T} \tag{16.10}$$

Notice that if there are no delayed neutrons present, then $\beta = 0$ and that the reactor period T becomes

$$T = \frac{\Lambda K_\infty}{(K_\infty - 1)} - \Lambda \tag{16.11}$$

or

$$T = \frac{\Lambda K_\infty}{K_\infty - 1} - \frac{\Lambda(K_\infty - 1)}{K_\infty - 1} = \frac{\Lambda}{K_\infty - 1} \quad \text{(with no delayed neutrons)} \tag{16.12}$$

which is exactly the result we presented in Chapter 15. If we were to repeat the same derivation with six delayed neutron decay chains instead of just one, then the appropriate form of Equation 16.10 would be

Inhour Equation

$$\rho = \frac{\Lambda}{\Lambda + T} + \frac{T}{\Lambda + T}\cdot\sum_i\left(\frac{\beta_i}{1 + \lambda_i T}\right), \quad \text{where } i = 1,2,\ldots,6 \tag{16.13}$$

where all of the terms have their usual meaning. This equation is the famous *Inhour equation* that shows how the reactor period T is related to the value of the reactivity ρ. If the reactor period T is long compared to the prompt neutron lifetime Λ (i.e., if $T \gg \Lambda$), then the Inhour equation can be reduced to the much simpler form that is shown below:

Simplified Inhour Equation

$$\rho = \frac{\Lambda}{T} + \sum_i \frac{\beta_i}{1+\lambda_i T}, \quad \text{where } i = 1,2,\ldots,6 \tag{16.14}$$

If only a single delayed neutron precursor group is used, then the Inhour equation can be reduced even further to read

The Inhour Equation with One Delayed Neutron Precursor Group

$$\rho = \frac{\Lambda}{T} + \frac{\beta}{1+\lambda T} \tag{16.15}$$

where the average delayed neutron group lifetime is

$$\tau = 1/\lambda = (1/\beta)\sum_i \beta_i/\lambda_i \approx 13 \text{ seconds}$$

for a Uranium-235-fueled thermal water reactor. Notice that Equation 16.15 shows that as long as the reactor period T increases, the reactivity ρ decreases, and in the limit where $T \to \infty$, $\rho \to 0$. Conversely, when the reactivity is increased very quickly, such as when a control rod is quickly withdrawn from the core, then the reactor period T must become much smaller for both sides to balance.

This later case corresponds to an exponentially increasing neutron population with time. Notice that when the reactor period T is very large, then $\lambda T \gg 1$, and the relationship between the reactivity and the reactor period becomes even simpler because we can write

Relationship between T and ρ for Long Reactor Periods

$$\rho \approx \frac{\Lambda}{T} + \frac{\beta}{\lambda T}$$

or

$$T \approx \frac{M}{\rho} \tag{16.16a}$$

where $M = (\Lambda + \beta/\lambda)$. So with only one delayed neutron group, the reactor period T is inversely proportional to the size of ρ. Small values of ρ cause the reactor period to be very large, and large values of ρ cause the reactor period to be very small. As long as T is on the order of about 1 minute, this inverse relationship is reasonably accurate (to about 2%). Now suppose that we would like to expound upon what we have just said in more detail. Most of the time, it turns out that $\beta/\lambda \gg \Lambda$. When this is true, $M \approx \beta/\lambda$, and the reactor period T when the period is long enough can be written as

$$T \approx \frac{(\beta/\lambda)}{\rho} \tag{16.16b}$$

This implies that once the values of β and λ are set by the type of nuclear fuel used in the core, the asymptotic reactor period (for very large values of T) is given by

The Asymptotic Reactor Period

$$T \approx \frac{(\beta/\lambda)}{\rho} \quad (\text{for very large values of } T) \tag{16.17}$$

which is inversely proportional to the reactivity ρ. Now let us examine the opposite case where we would like to determine the reactor period T when the reactor period is *very short* (say a few seconds or less) and, in particular, when the

reactor period T is short enough so that $\lambda T \ll 1$. Under these conditions, Equation 16.15 reduces to $T \approx \Lambda/(\rho - \beta)$, and so the instantaneous reactor period during a very fast transient (where $\rho \approx \beta$) is given by

The Instantaneous Reactor Period

$$T \approx \frac{\Lambda}{(\rho - \beta)} \quad (\text{for very small values of } T) \tag{16.18}$$

We can use Equations 16.17 and 16.18 to determine the limiting dynamic behavior of *any power reactor* if we know the type of nuclear fuel that is used. For example, suppose that we use the values for Λ, β, and λ that are shown in Table 16.1 for U-233, U-235, and Pu-239. *In a thermal water reactor, the value of Λ (the prompt neutron lifetime) is about 1×10^{-4} seconds, while for a fast reactor, it is about 1×10^{-7} seconds. This means that the asymptotic reactor period for both thermal and fast reactors is independent of Λ and depends on only the value of (β/λ).*

In other words, for very long time periods, the value of T depends on only the reactivity ρ and the value of (β/λ). However, for very short transients (or nearly instantaneous ones), the instantaneous reactor period is determined by the values of Λ, β, and ρ and because the prompt neutron lifetime Λ in a fast reactor is 1000 times smaller than it is in a thermal water reactor, the reactor period for fast reactor with the same value of ρ will be 1000 times as short! This means that the designer of a fast reactor must always ensure that the reactor never approaches a prompt critical condition where $\rho \approx \beta$. If this were to occur, the reactor power level would escalate exponentially and the reactor would go into orbit or would be otherwise destroyed! Hence, a control system for a fast reactor must be considerably more sensitive to changes in the reactivity than in the corresponding control system of a thermal water reactor for the same value of ρ.

The total reactivity that corresponds to a reactor period of 1 hour (3600 seconds) is sometimes called an "Inhour" (which is an acronym for inverse hours). So in the case of a Uranium-235-fueled thermal water reactor with one delayed neutron group, $\beta = 0.0065$, $\lambda = 0.077$ seconds^{-1}, and $\Lambda \approx 1 \times 10^{-4}$ seconds. Then $M = (0.0001 + 0.0065/0.077) = 0.085$ seconds, and the value of *the reactivity required for the reactor to have a reactor period of 1 hour is $\rho = M/T = 0.085/3600 = 0.000020$*. Thus,

Reactivity Required to Have a Reactor Period of 1 Hour

$$\rho = 0.000020 \, (\text{with U-235 fuel only}) \tag{16.19}$$

So for this particular case, the value of the reactivity is in fact 1 inverse hour, or "Inhour." In the exercises near the end of this section, we will ask the reader to determine the amount of positive reactivity that is required to produce a reactor period of 1 hour when the U-235 in the fuel rods is replaced by U-233 or Pu-239. *In general, we will find that the value of the Inhour is much smaller in this case.* As long as the values of Λ and β are not time dependent, we can actually solve the Inhour equation with one delayed precursor group to obtain some useful information about how changes in the reactivity ρ affect the reactor period T and the time-dependent flux $\phi(t)$. *The Inhour equation allows us to write an*

TABLE 16.1
Approximate Asymptotic and Instantaneous Reactor Periods for Various Nuclear Fuels Used in Fast and Thermal Reactors

Fuel	β	λ (Seconds^{-1})	T Thermal Asymptotic[a] (Seconds)	T Fast Asymptotic[a] (Seconds)	T Thermal Instantaneous[b] (Seconds)	T Fast Instantaneous[b] (Seconds)
U-233	0.0026	0.054	$T = 0.048/\rho$	$T = 0.048/\rho$	$T \approx 10^{-4}/(\rho - 0.0026)$	$T \approx 10^{-7}/(\rho - 0.0026)$
U-235	0.0065	0.077	$T = 0.084/\rho$	$T = 0.084/\rho$	$T \approx 10^{-4}/(\rho - 0.0065)$	$T \approx 10^{-7}/(\rho - 0.0065)$
Pu-239	0.0020	0.068	$T = 0.030/\rho$	$T = 0.030/\rho$	$T \approx 10^{-4}/(\rho - 0.0020)$	$T \approx 10^{-7}/(\rho - 0.0020)$

Note: These values are dependent on the values for Λ, β, and λ.

[a] The asymptotic reactor period is nearly independent of the value of the prompt neutron lifetime Λ.

[b] The instantaneous reactor period is crucially dependent on the value of the prompt neutron lifetime Λ. For a thermal reactor, $\Lambda \approx 1 \times 10^{-4}$ seconds, and for a fast reactor, $\Lambda \approx 1 \times 10^{-7}$ seconds. However, these values can vary slightly depending on the details of a particular design.

explicit relationship between the reactivity and those values of the reactor period T that correspond to solutions of the time-dependent diffusion equation and the precursor equation for which the functions

$$\phi(t) = Ae^{t/T} \tag{16.20}$$

and

$$C(t) = Ce^{t/T} \tag{16.21}$$

are used. In other words, the problem of solving the time-dependent neutron diffusion equation for the flux $\phi(t)$ and the delayed neutron precursor concentration C(t) has been reduced to the much simpler problem of finding the roots of Equation 16.15 with one delayed precursor group and finding the roots of Equation 16.16 with six delayed precursor groups. We would now like to illustrate what these solutions look like. These solutions can be found graphically, or they can be found by direct analytical means. However, the graphical methods are easier to illustrate and understand, and so we will start with them first.

Example Problem 16.1

When a reactor is exactly critical, how much excess reactivity (in pcm) is required to produce a period of 1 hour when the U-235 in the fuel rods is replaced by U-233 or Pu-239?

Solution From Table 15.6 (see Chapter 15) we know that $\beta = 0.0025$ and $\lambda = 0.054$ seconds^{-1} for U-233 and $\beta = 0.0020$ and $\lambda = 0.068$ seconds^{-1} for Pu-239. Therefore, $M_{U233} = (0.0001 + 0.0025/0.054) = 0.046$ seconds for U-233 and $M_{Pu239} = (0.0001 + 0.0020/0.068) = 0.029$ seconds for Pu-239. So, the reactivity required for the reactor to have a reactor period of 1 hour is $\rho = M/T = 0.046/3600 = 0.0000127$ for U-233 and $\rho = M/T = 0.029/3600 = 0.000008$ for Pu-239. So in the case of U-233, the reactivity is 1.27 pcm, and in the case of Pu-239, the reactivity is 0.8 pcm. [Ans.]

16.2 Graphical Solutions to the Inhour Equation

One of the most straightforward ways to appreciate how a time-dependent reactor behaves is to plot the right-hand side of the Inhour equation (Equation 16.15) as a function of T, showing ρ on one axis and T on another. When we do so, we obtain the graph shown in Figure 16.1, where, for convenience, we have defined $\omega = 1/T$. The results are rather interesting because there are three distinct branches to the curve, but only two of them are physically relevant because reactors are never operated with $\rho \approx 1$. These are the middle curve and the curve on the right. The roots of the equation are located where the curves cross the horizontal lines, which correspond to specific values of ρ, which, in the most general case, can be either positive or negative. If ρ is negative, or if ρ is positive, but less than 1, there are only two roots for any value of ρ, which we will call ω_1 and ω_2. These are the two roots of equation $\phi(t) = Ae^{t/T}$, where $T_1 = 1/\omega_1$ and $T_2 = 1/\omega_2$. So if we start at $\rho = 0$, when a system is exactly critical, and change the reactivity in a *stepwise manner* either positively or negatively to a finite value that corresponds to one of the horizontal lines shown in Figure 16.1, then the neutron flux behaves as

The Time-Dependent Neutron Flux with Just Two Roots

$$\phi(t) = A_1e^{\omega_1 t} + A_2e^{\omega_2 t}$$

or

$$\phi(t) = A_1e^{t/T_1} + A_2e^{t/T_2} \tag{16.22}$$

In general, for a given value of ρ, $\omega_1 \neq \omega_2$ and $T_1 \neq T_2$. If $\rho > 0$, then ω_1 will be positive and ω_2 will be negative. So over time, the second term ω_2 decays away, and the flux increases exponentially as $\phi(t) = A_1e^{t/T_1}$. In other words, it ramps up slowly and then takes off! Conversely, when $\rho < 0$, then both ω_1 and ω_2 are negative, but ω_1 is less negative than ω_2. So over time, the second term ω_2 dies out more rapidly than the first term, and the flux *decreases exponentially* at a rate determined by $\phi(t) = A_1e^{t/T_1}$. In the first case, $\rho > 0$, the first term completely dominates the second, and the flux increases almost immediately in the form of a single abrupt step (see the LHS of Figure 16.2). In the second case, the second term completely dominates the first, and the flux decreases immediately, also in the form of a single abrupt step (see the RHS of Figure 16.2).

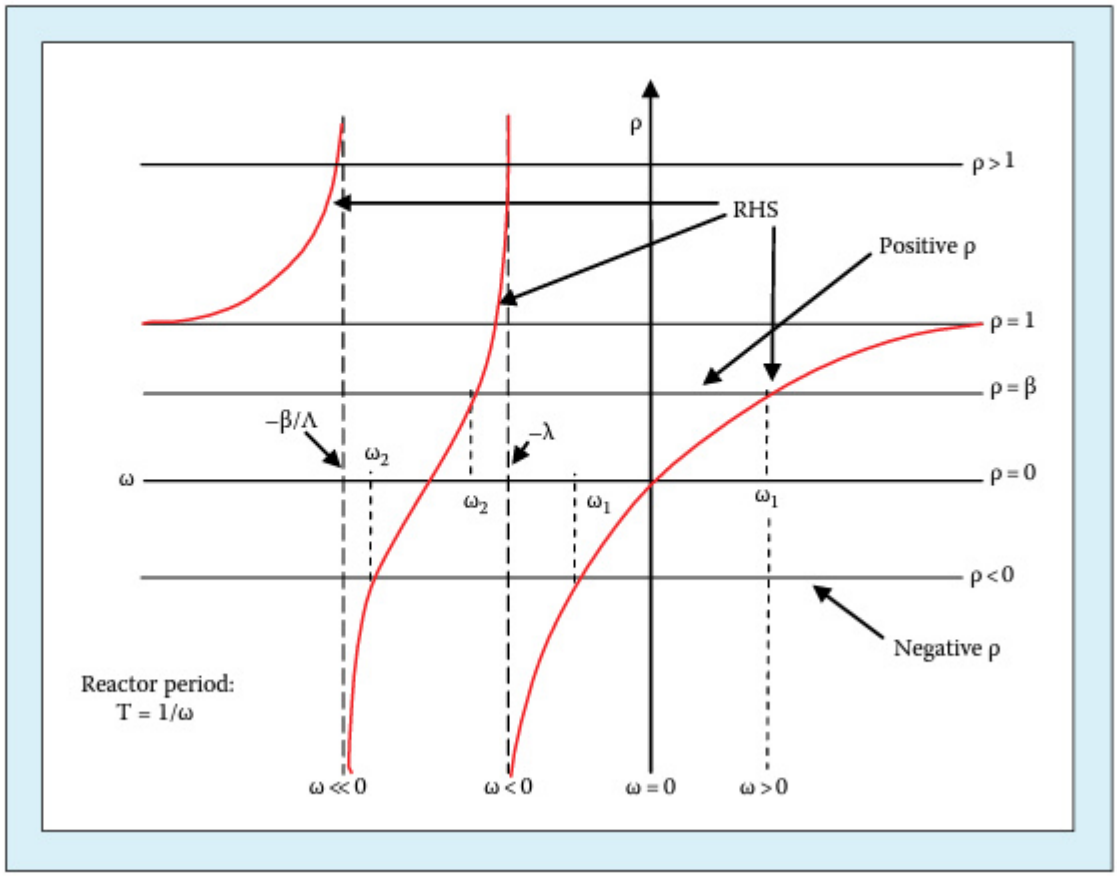

FIGURE 16.1 A plot of the roots of the Inhour equation with one delayed neutron group.

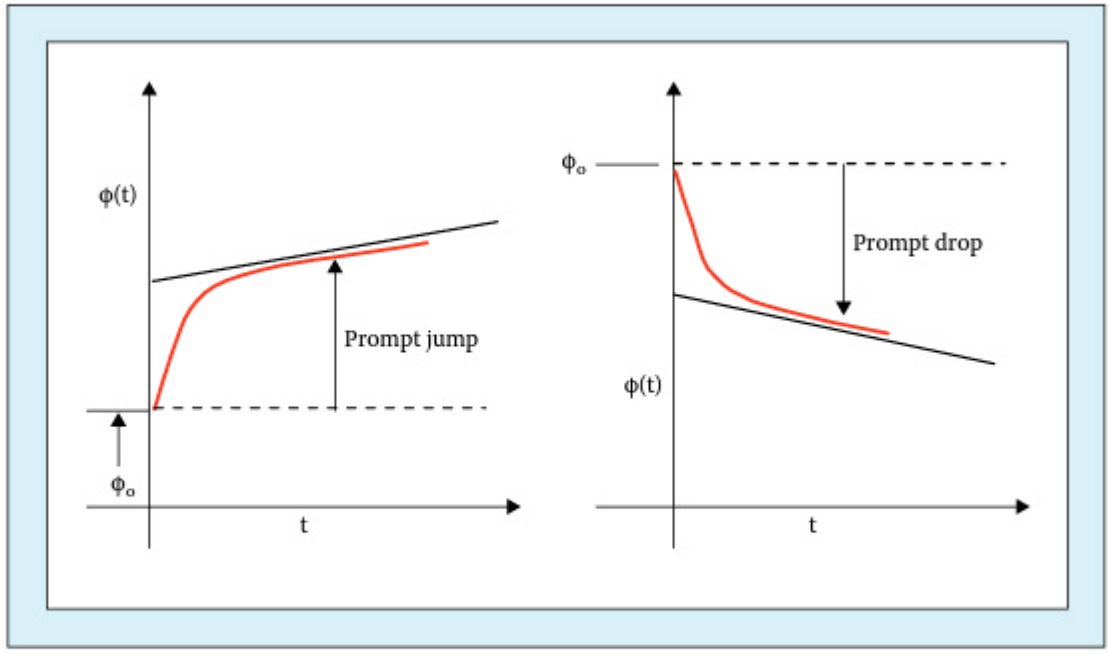

FIGURE 16.2 An illustration of how quickly the neutron flux (and hence the reactor power level) rises and falls with a rapid reactivity reduction or a rapid reactivity insertion. A rapid stepwise increase in the reactivity will lead to what is known as the "prompt jump," and a rapid stepwise reduction in the reactivity will lead to what is known as the "prompt drop."

When the reactivity is increased suddenly, the resulting change in the level of the neutron flux is called the "*prompt jump*," and when the reactivity is decreased suddenly, the resulting change in the level of the flux is called the "*prompt drop*." Both of these terms are commonly used in the nuclear industry to describe abrupt changes in the flux and power that can be attributed to the rapid insertion or ejection of a control rod. This curious symmetry prevails for both positive and negative reactivity insertions as long as the amount of time in question from the original reactivity change at t = 0 is large. Of course, this is somewhat of an idealized situation, but it clearly reflects the way that most reactors behave as long as we can ignore the reduction of the reactivity due to time-dependent fission product poisoning.

16.3 Exact Solutions to the Inhour Equation

Before moving on to other topics, we would like to mention that it is possible to solve Equation 16.15 analytically as well. While we will not show how this is done here, we will present the results and explain what the exact solutions imply. Before doing so, we must establish a reference point from which the time-dependent solutions apply. We will therefore assume that the exact equations we will present are valid for times > 0, where the reactivity at t = 0 is $\rho = 0$, and the flux at t = 0 is ϕ_o. In this case, it can be shown that the exact time-dependent flux and the precursor concentrations for one delayed neutron group become

The Trial Solutions to the Point Kinetics Equations with One Delayed Neutron Group

$$\phi(t) = A_1 e^{\omega_1 t} + A_2 e^{\omega_2 t}$$

and

$$C(t) = C_1 e^{\omega_1 t} + C_2 e^{\omega_2 t} \tag{16.23}$$

where the coefficients A_1, A_2, C_1, and C_2 are given by

Coefficients Found by Solving the Point Kinetics Equation

$$A_1 = \frac{-\rho}{\beta - \rho}, \quad A_2 = \frac{\beta}{\beta - \rho}, \quad C_1 = \frac{\rho\beta}{(\beta - \rho)^2}, \quad C_2 = \frac{\beta}{\Lambda\lambda}$$

and

$$\omega_1 = -\frac{\beta - \rho}{\Lambda} \quad \text{and} \quad \omega_2 = \frac{\lambda\rho}{\beta - \rho} \tag{16.24}$$

and where ρ, β, Λ, and λ have their usual meanings, and the time t is normally quoted in seconds. The expressions for these coefficients were first derived at the *Bettis Atomic Power Laboratory* and at the *Los Alamos National Laboratory* in the 1940s to support the development of the first atomic bomb. They were also used to describe the dynamic behavior of early nuclear reactors before the time dependent diffusion equation could be solved using high speed computers.

16.4 Reactor Period with Delayed Neutrons

In Chapter 15, we discovered that a reactor operating on prompt neutrons alone has a very short time constant and for all intents and purposes, the neutron population changes too quickly to be able to control without an exotic control system. For a thermal water reactor, the reactor period T without delayed neutrons is approximately 1/10th of a second, so that if the neutron flux under steady-state conditions is given by $\phi(t) = \phi(0)$, then the time-dependent flux would be

$$\phi(t) = \phi(0) e^{t/T} \tag{16.25}$$

and for a reactor period of only $T \approx 0.1$ second, the time-dependent flux would be given by

$$\phi(t) = \phi(0) e^{10t} \tag{16.26}$$

Hence, when the contributions of the delayed neutrons to the neutron population are ignored, the flux and power levels increase exponentially to $e^{10} = 22{,}000$ times their initial values in just a single second! Obviously, this would completely destroy the reactor and everything around it. *We subsequently learned that real reactors rely on the existence of delayed neutrons to slow down the rate of the flux and power changes to much more manageable levels by increasing the reactor period substantially*. Consequently, we would like to repeat the exercise we presented in Chapter 15 to illustrate the difference that the presence of these delayed neutrons makes. Without delayed neutrons, we found that a change in K_∞ from $K_\infty = 1.000 - 1.001$, or just 1 part in 1000, would result in a reactor period T of approximately 0.1 seconds. This is only a change in the reactivity of $\rho = (K_\infty - 1)/K_\infty = 0.001/1.000 = 0.001$, or just a 10th of 1%. When we include the presence of the delayed neutrons in the same problem, then we obtain the physically correct reactor period shown in Figure 16.3, where the period is presented for both positive and negative reactivity changes. Since we are again dealing with a U-235-fueled water reactor, this is a true "apples-to-apples" comparison of how the reactor period changes with and without delayed neutrons.

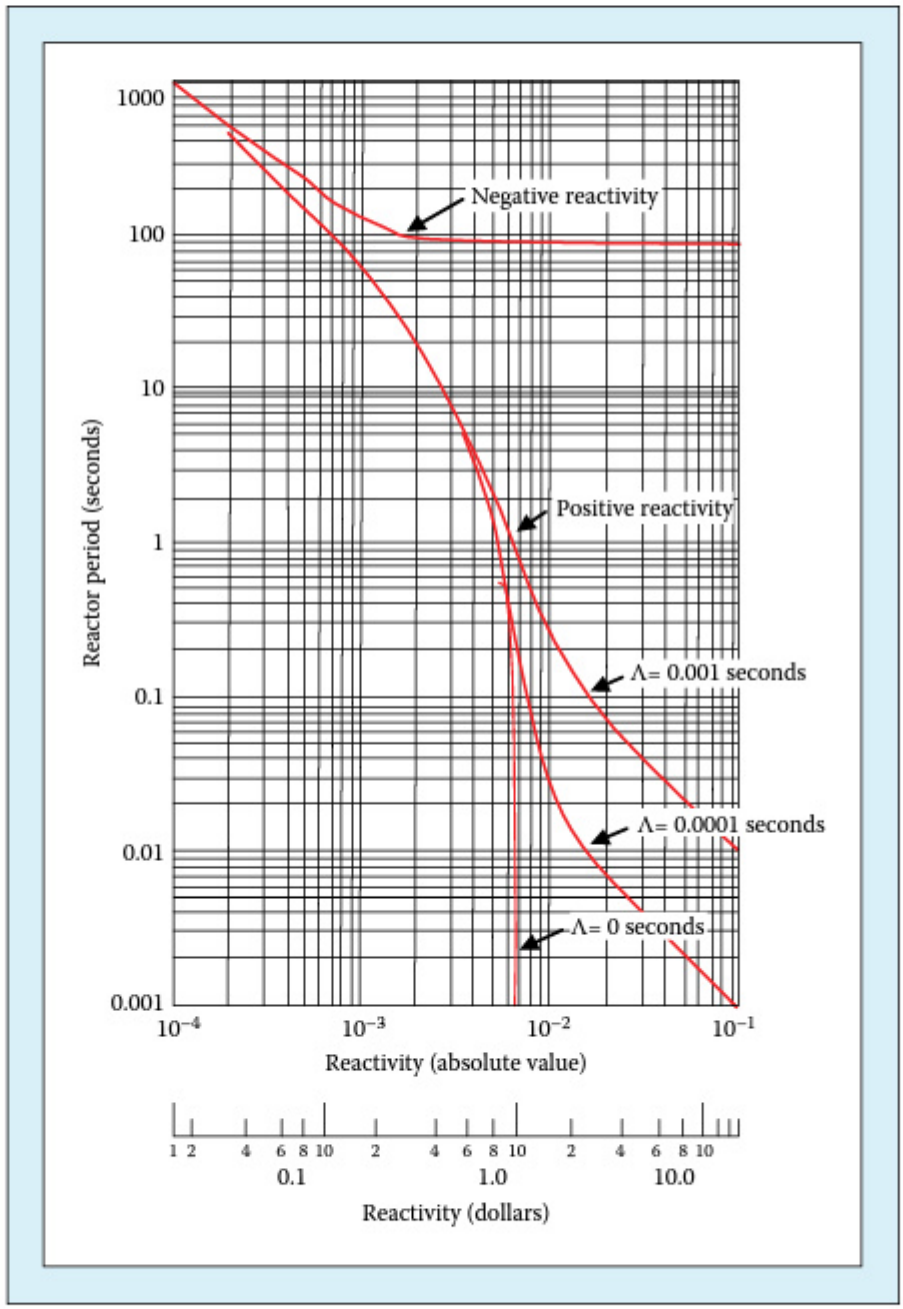

FIGURE 16.3 The reactor period T for positive and negative values of the reactivity ρ. Here, the symbol Λ refers to the prompt neutron lifetime. (Adapted from Lamarsh, J.R. and Baratta, A.J., *Introduction to Nuclear Engineering*, Prentice Hall, Upper Saddle River, NJ, 2001—with notational changes.)

Example Problem 16.2

Using Equation 16.24, derive an expression for the reactor period T for a Uranium-235-fueled thermal water reactor with one delayed neutron precursor group.

Solution Equation 16.24 says that the two roots of the Inhour equation for a reactor with one delayed neutron group are $\omega_1 = -(\beta - \rho)/\Lambda$ and $\omega_2 = \lambda\rho/(\beta - \rho)$. Since $T_1 = 1/\omega_1$ and $T_2 = 1/\omega_2$, we can also write the two values for the reactor period as

$$T_1 = -\Lambda/(\beta - \rho) \quad \text{and} \quad T_2 = (\beta - \rho)/\lambda\rho$$

For a Uranium-235-fueled reactor, $\beta = 0.0065$, $\lambda = 0.077$ seconds^{-1}, and $\Lambda \approx 1 \times 10^{-4}$ seconds. So, $T_1 = -0.0001/(0.0065 - \rho)$ and $T_2 = (0.0065 - \rho)/0.0005$. [Ans.]

From Figure 16.3, it can also be seen that the reactor period T is about 56 seconds, or over 550 times *longer* when the effects of the delayed neutrons are included! In other words, we now have about a minute after a reactivity insertion of 0.1% before the flux (and hence the power level) increases by a factor of e. By comparison, if we *decrease* the reactivity by 0.1%, the reactor period is now −150 seconds, and it takes 2½ minutes for the power level to decline a factor of 1/e. Hence, delayed neutrons are truly remarkable in their ability to affect the time-dependent behavior of a nuclear power plant. They are even more important when we would like to control a fast reactor, where the prompt neutron lifetime is about 1000 times shorter (10^{-7} vs. 10^{-4} seconds for a water reactor). We can demonstrate this fact by considering what happens to the reactor period T in Figure 16.3 when $\Lambda \approx 0$. In this case, a reactivity insertion greater than about 0.003 would have a disastrous effect on the reactor period by reducing it to approximately 2 seconds, and a reactivity increase of only about 0.005 would further reduce it to about 0.2 seconds. In other words, Figure 16.3 implies that any planned reactivity changes to a fast reactor must normally be limited to much smaller values of the reactivity, say $\rho < 0.002$, or 0.2%.

16.5 Understanding Time-Dependent Reactor Behavior

To illustrate how changes to the reactivity affect the power level, there are five classic examples of time-dependent reactor behavior we would like to discuss. These examples of reactor behavior include:

- The gradual or planned shutdown of a reactor from a previous critical state where $\rho \approx 0$
- The emergency shutdown of a reactor from a previous critical state where $\rho \approx 0$, by scramming the control rods and reducing the reactivity substantially
- The behavior of a reactor when it enters a "*prompt critical*" state, where it has achieved criticality based on the presence of prompt neutrons alone
- The behavior of a reactor when it starts a supercritical transient
- The behavior of a reactor when it starts a prompt supercritical transient

Each of these scenarios offers considerable insight into the way real reactors behave. Consequently, let us start with the first scenario and then move on to the other four.

Example Problem 16.3

What is the reactor period for the reactor in Example Problem 16.2 when we suddenly increase the reactivity by 0.1%?

Solution In this case, $\rho = 0.001$, and substituting into our previous equations for T_1 and T_2, we obtain $T_1 = -0.018$ seconds and $T_2 = 11$ seconds. The first root, T_1, decays away very quickly, and the flux therefore increases asymptotically with a period given by $e^{t/T_2} = e^{t/11}$. So, the presence of one group of delayed neutrons has caused the amount of time it takes for the reactor power level to increase by a factor of e to increase from 0.1 to 11 seconds—or a factor of about 100. Finally, if we had used six delayed neutron groups instead of just one, then the reactor period would have increased to about 56 seconds. Figure 16.3 provides the exact answer to the problem in this situation. [Ans.]

16.5.1 Normal or Planned Shutdown

Suppose that we start with the planned shutdown of a reactor first, in which case the reactivity changes from $\rho \approx 0$ to $\rho = -0.0005$ (a change of about 8 cents when the fuel is U=235) in a mostly stepwise manner by partially inserting a control rod into the core. This mode of reactor shutdown is very common, and the behavior of the reactor is generally quite benign. There are no unexpected "surprises" under these conditions, and the power gradually declines after the control

rod has been inserted. Assume that Figure 16.3 can be used to estimate the reactor period in this case. Hence, the reactor period becomes about 85 seconds, and the flux decays exponentially according to the equation.

Time-Dependent Flux during a Planned Shutdown

$$\phi(t) = \phi(0)e^{-t/85} \tag{16.27}$$

which means that the flux, and hence the power level, decreases to 37% or a factor of 1/e in 85 seconds (about 1½ minutes). This is a scenario that any utility would be happy with, since there are no sudden power increases or decreases in the reactor core.

16.5.2 Emergency Shutdown

In this case, a reactor is "*scrammed*," by dropping several control rods into the core. The reactivity falls rapidly because the control rods immediately begin to absorb the excess thermal neutrons. Under most conditions, this scenario can be modeled by a stepwise reduction in the reactivity ρ. For this scenario, we will assume that the reactivity reduction is approximately 10 times greater what it was in the previous example. In other words, the reactivity falls from $\rho \approx 0$ to $\rho = -0.05$ in a very short period of time. Events such as this do not occur every day, but when they do occur, the power level declines very rapidly. Assuming that $\rho = -0.05$, we obtain

The Neutron Flux and Precursor Concentrations during an Emergency Shutdown

$$\phi(t) = 0.87e^{-958t} + 0.130e^{-0.068t}$$

$$C(t) = 0.01e^{-958t} + 1563e^{-0.068t} \tag{16.28}$$

This scenario corresponds to a change in the reactivity of about $-0.05/0.0065 = -\$7.7$. Under these conditions the first terms in Equation 16.28 decay very rapidly, and after a few milliseconds, all we are left with is

$$\phi(t) = 0.130e^{-0.068t} \tag{16.29}$$

$$C(t) = 1563e^{-0.068t} \tag{16.30}$$

Thus the flux (and hence the power level) drops almost instantaneously to 13% of its steady state value, and if we plot the results on the right hand side of Figure 16.2, it appears that both the flux and the power level have "fallen off of a cliff". The precursor concentration C barely changes initially, and then after the flux recovers from this initial step decrease, the remaining neutrons gradually decay at a rate proportional to $\omega_2 = -0.068$ seconds^{-1}, which corresponds to a reactor period T of $T = 1/\omega_2 = 14.7$ seconds. The remaining neutrons hang around for a while because the precursors, which were barely affected initially, take a while to decay. Eventually, in about 30 seconds, the flux declines to $\phi(30) = 0.130\ e^{-0.068 \cdot 30} = 0.13/e^2 \approx 2\%$ of its original value and the heat generated by simple radioactive decay exceeds the heat generated by the fission process alone. This is the classic behavior of a reactor after the core has been scrammed.

16.5.3 Prompt Critical Behavior

Obviously, there is only a certain range of conditions where a reactor can be operated safely before the reactor period T becomes too short to control. A reactor that is exactly critical has a value of $K_{effective} = 1$, and a reactivity ρ of 0, so using either prompt neutrons alone or both prompt and delayed neutrons, the reactor period is infinite as long as the reactivity is zero. This condition does not present a problem from a control perspective or a safety perspective. However, as soon as we begin to change the reactivity by about a hundredth of one percent, the period for a water reactor falls to about 1 second, and it is no longer practical to continue to operate it on prompt neutrons alone. Therefore, from purely a design perspective, it is important that a reactor is never operated at a reactivity where it is allowed to become critical based on just prompt neutrons alone. A scenario of this type would create a disastrous and unsafe power excursion. A reactor that can become critical on prompt neutrons alone is said to be in a *prompt critical state*. Now let us examine how the core behaves when such a state is reached.

16.6 Conventional Units for Measuring the Reactivity-Dollars and Cents

Earlier we learned that the $K_{effective}$ is proportional to the total number of neutrons produced per fission, both prompt and delayed. However, if we temporarily take the delayed neutrons out of this scenario, then the effective multiplication factor due to prompt neutrons alone is $(1 - \beta)K_{eff}$. Therefore, we can assume that the following relationship applies to a reactor that is critical on prompt neutrons alone:

$$(1-\beta)K_{eff} = 1 \tag{16.31}$$

Using the fact that $\rho = (K_{eff} - 1)/K_{eff}$, $\rho K_{eff} = (K_{eff} - 1)$, $\rho K_{eff} - K_{eff} = -1$, and $K_{eff}(\rho - 1) = -1$, we can also establish the following set of useful relationships between the effective multiplication factor, the delayed neutron fraction, and the reactivity:

Important Relationships between $K_{effective}$, β, and ρ

$$K_{eff} = \frac{1}{(1-\rho)}$$

and (16.32)

$$K_{eff} = \frac{1}{(1-\beta)}$$

These relationships apply to any reactor that is critical, supercritical, or subcritical. Thus, when a reactor is critical based on prompt neutrons alone, the relationship of the reactivity to the delayed neutron fraction (which can be obtained by combining Equation 16.32 together) is given by

$$\frac{(1-\beta)}{(1-\rho)} = 1 \tag{16.33}$$

It is easy to see from this latter equation that the condition for a reactor to achieve a prompt critical condition is

The Condition for a Reactor to Become Prompt Critical

$$\rho = \beta \tag{16.34}$$

For example, for a thermal water reactor fueled with U-235 (see Table 16.1) Equation 16.34 implies that a prompt critical condition will be attained when there is a reactivity insertion of $\rho = \beta = 0.0065$, or 0.65%. Commercial power reactors are therefore restricted to smaller reactivity insertions (on the order of about 20% of the value of β) to keep changes to the core power level (i.e., the reactor period T) to a manageable level. A convenient unit of the reactivity that is used to describe any reactor that has both prompt and delayed neutrons is

The Definition of a Dollar of Reactivity

The amount of reactivity needed to make a reactor critical on prompt neutrons alone ($\rho = \beta$) is called a dollar of reactivity.

We can therefore express the system-wide reactivity in terms of the delayed neutron fraction as

A Dollar of Reactivity

$$\beta = (\$1) = \$1.00 \text{ of reactivity}$$

In the early 1950s, this nomenclature became embedded in the nuclear industry, and now virtually every reactor vendor uses the *dollar* to define the amount of excess reactivity that is required to force a reactor into a prompt supercritical state. *Another common unit of the reactivity that is encountered in nuclear science and engineering is one-hundredth of a dollar, which is also referred to as "the cent."* Naturally, this allows us to write,

\$1.00 of reactivity = 100 cents of reactivity

and by inference,

1 cent = 1/100th of $1.00 of reactivity

Other less commonly used units for the reactivity are called the *milli-k* and the *pcm*. Since the reactivity is represented by the symbol rho (ρ), *1/1000th of a rho is called a "milli rho" or mrho, and one percent of a milli rho is called a pcm (percent of a milli-rho)*. The reactivity can also be expressed as a function of Δk/k. Thus, if Δk/k = 0.001 is defined as 1 milli-rho, then 1 pcm = 1% of a milli rho = 0.00001 = 10^{-5}. Consequently, the reactivity is always designed to be a dimensionless number, and these different units are just different ways to measure its magnitude. Other definitions for the reactivity such as the *nile* can also be found in the literature, but these definitions are not as common as the ones we presented earlier. Figures 16.4 and 16.5 illustrate the different ways that can be used to measure the system-wide reactivity.

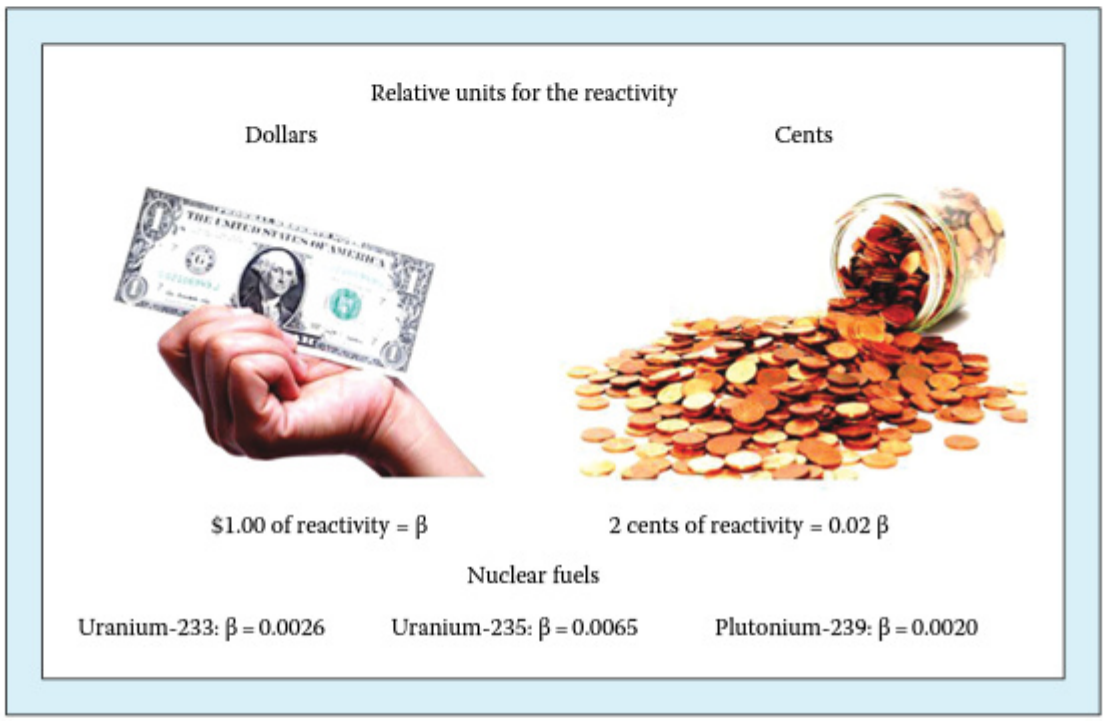

FIGURE 16.4 Some relative units for measuring the reactivity that are a function of the delayed neutron fraction β.

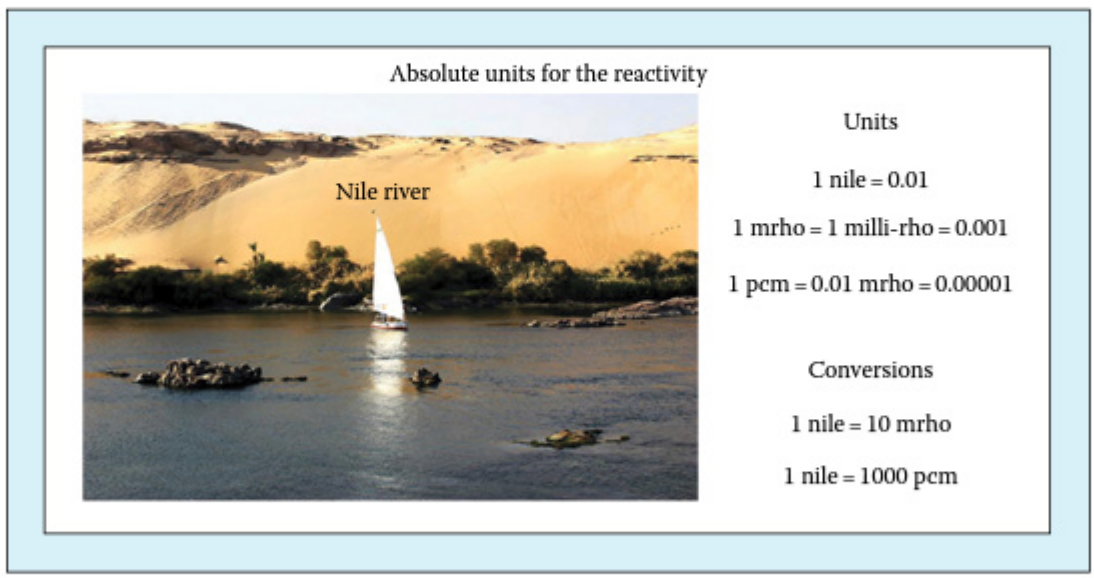
Absolute units for the reactivity
Nile river
Units
1 nile = 0.01
1 mrho = 1 milli-rho = 0.001
1 pcm = 0.01 mrho = 0.00001
Conversions
1 nile = 10 mrho
1 nile = 1000 pcm

FIGURE 16.5 Some absolute units for measuring the reactivity that do not depend on the delayed neutron fraction β.

TABLE 16.2
Reactivity in PCM and Dollars and Cents for Different Nuclear Fuels

Absolute Reactivity	Reactivity in PCM	U-233 ($)	U-235 ($)	Pu-239 ($)
0.00001	1	0.0038	0.0015	0.0050
0.00005	5	0.0192	0.0077	0.0250
0.00010	10	0.0384	0.0154	0.0500
0.00020	20	0.0769	0.0308	0.1000
0.00050	50	0.1923	0.0769	0.2500
0.00100	100	0.3846	0.1538	0.5000

TABLE 16.3
Delayed Neutron Fractions for Fast and Thermal Reactors as a Function of the Fuel Type

Fuel Type	Thermal Neutron β	Fast Neutron β
Thorium-232	0.0000	0.0203
Uranium-233	0.0026	0.0026
Uranium-235	0.0065	0.0064
Uranium-238	0.0000	0.0148
Plutonium-239	0.0020	0.0020

Notice that the reactivity can be measured in either *absolute or relative units*. The dollar and the cent are *relative units* that depend on the value of the delayed neutron fraction, while the nile, the milli-rho, and the pcm (percent milli-rho) are absolute units that do not.

In other words, the milli-rho, the nile (which is equal to 10 milli-rho) or 0.01, and the pcm (percent milli-rho) are *absolute units* that have nothing to do with the delayed neutron fraction β. Some relationships between the pcm and the dollar are illustrated in Table 16.2. The delayed neutron fraction as a function of the type of fuel is shown in Table 16.3. *Normally, changes in the reactivity in either a positive or negative direction are limited to about ±20 cents (±0.20β) during normal reactor operation* (in some reactors, the changes that are allowed can be considerably less). Larger changes in the reactivity will cause the power level to change rather dramatically, and these changes will lead in turn to what are known as the "prompt drop" or the "prompt jump." We will discuss the conditions required for this to occur in subsequent sections. Thus the amount of reactivity required to make a reactor prompt critical depends on the value of the delayed neutron fraction. Since the value of the delayed neutron fraction depends on the type of fuel that is used, thermal reactors fueled with Pu-239 have a value of β as low as 0.0020, while other reactors fueled with U-235 have a value of β as high as 0.0065. Finally, the other point to remember is that *the delayed neutron fraction is not an absolute number* (like π, e, or some other immutable constant of nature). It is simply a way to measure the number of delayed neutrons that are released by a particular type of fuel.

Consequently, *a dollar of reactivity, which is a function of the reactor fuel type (U-233, U-235, Pu-239), is not an absolute number as well. It varies from one type of reactor to the next and from one type of fuel to the next.* For example, one dollar of reactivity in a U-233-fueled thermal water reactor (where $\beta = 0.0026$) is only equivalent to about 40 cents in a Uranium-235-fueled thermal water reactor, where the value of β is $\beta = 0.0065$. Table 16.3 shows the delayed neutron fractions for several common nuclear fuels (U-233, U-235, Pu-239) and for both fast and thermal reactors. Notice that the practical lower limit to the delayed neutron fraction is about 0.002, or about 2 delayed neutrons per 1000 prompt neutrons released. *No practical reactor fuel has a lower value of β than this.*

16.7 Deriving the Prompt Jump and the Prompt Drop Approximations

Based on our prior discussion, a sharp increase in the reactivity will cause the neutron flux $\phi(t)$ and the power $P(t)$ to increase very rapidly as well, but at least during this initial period of time, which may be on the order of 10–100 milliseconds, the concentration of the fission product precursors may barely change. Before high-speed computers were invented, this observation caused a considerable stir in the nuclear industry because it meant that one could set $dC/dt = 0$ during the initial stages of a reactor transient, and therefore the solution of the time-dependent diffusion equation (Equation 16.2) could be accomplished by manual methods alone.

The mathematical solution to the time-dependent neutron diffusion equation under the assumption that the neutron precursor concentration C is constant for a very short period of time, which in practice can be up to about 0.1 seconds, is called the *prompt jump approximation*. Now we would like to discuss what this implies physically, because at least with one delayed neutron group, it makes it possible to predict the time-dependent behavior of the core when the reactivity is suddenly changed in either a positive or negative direction. As one can imagine, this has enormous practical importance when sudden changes in the reactivity (due to control rod insertions and withdrawals or temperature-related effects) must be taken into account. We learned earlier in the chapter that the time-dependent flux could be described by the equation

$$\phi(t) = A_1 e^{t/T_1} + A_2 e^{t/T_2} \tag{16.35}$$

when there is a sudden change to the reactivity, the reactor is initially critical, and only one delayed neutron precursor group is used. If this were to be extended to the more realistic case of six delayed neutron precursor groups, then the time-dependent flux would consequently be described by the sum of the following seven exponential functions rather than just two:

$$\phi(t) = A_1 e^{t/T_1} + A_2 e^{t/T_2} + A_3 e^{t/T_3} + \cdots + A_7 e^{t/T_7} \tag{16.36}$$

Obviously, it becomes harder to understand what Equation 16.36 implies, and physical insight into the dependence of the point kinetics parameters on $\phi(t)$ is sometimes lost. The *prompt jump approximation* overcomes this objection by making it very simple, at least in principle, to understand the parameters that actually drive sudden changes to the reactor power and the neutron flux. To derive the prompt jump approximation, let us return to Equations 16.2 and 16.3 and make the same approximations that we did before. The result is that the time-dependent diffusion equation can be written as

$$(1-\beta)K_\infty \phi(t) + \frac{\lambda C(t)}{\Sigma_a} - \phi(t) = \frac{\Lambda d\phi(t)}{dt} \tag{16.37}$$

and the time-dependent equation for the precursor concentration C(t) can be written as

$$\frac{dC(t)}{dt} = (\beta\ K_\infty \Sigma_a)\phi(t) - \lambda C(t) \tag{16.38}$$

The prompt jump approximation assumes that dC(t)/dt in Equation 16.38 is 0 during the early stages of a reactor transient and that $K_\infty = 1$ at $t = 0$. Notice that it does not make the same assumption regarding the time-dependent diffusion equation or the level of the neutron flux. We can therefore write Equation 16.38 as

$$C(t) = \left(\frac{\beta}{\lambda}\right)\Sigma_a \phi(0) \tag{16.39}$$

where $\phi(0)$ is the flux at t = 0. If we substitute this result into Equation 16.37, we obtain

$$(1-\beta)K_\infty \phi(t) + (\beta)\phi(0) - \phi(t) = \frac{\Lambda d\phi(t)}{dt} \tag{16.40}$$

or more after some further manipulation,

$$\left[(1-\beta)K_\infty - 1\right]\phi(t) + (\beta)\phi(0) = \frac{\Lambda d\phi(t)}{dt} \tag{16.41}$$

Equation 16.41 can be easily solved for $\phi(t)$ based on the assumption that $\phi(0) = \phi_o(t)$ when t = 0. The result is

$$\phi(t) = \phi_o\left[e^{t/T} e^{-K_\infty(\beta/\Lambda)t} + A\left[1 - e^{t/T} e^{-K_\infty(\beta/\Lambda)t}\right]\right] \tag{16.42}$$

where

$$T = \frac{\Lambda}{K_\infty - 1} \quad \text{and} \quad A = \frac{\beta}{(1-\beta)K_\infty - 1} \tag{16.43}$$

Both of the exponential terms decay very quickly when $\rho \ll \beta$, and all that remains is

$$\phi(t) = A\phi_o = \frac{\beta\phi_o}{\left((1-\beta)K_\infty - 1\right)} \tag{16.44}$$

Since we know from our earlier definition of the reactivity that $K_\infty = 1/(1 - p)$, we finally obtain

$$\phi = \frac{\beta(1-\rho)\phi_o}{(\beta-\rho)} \tag{16.45}$$

when $t \to \infty$. This also allows us to write

The Prompt Jump Equation

$$\phi = J\phi_o \tag{16.46}$$

where J is the *prompt jump (or drop) factor* given by

The Prompt Jump Factor

$$J = \frac{P}{P_o} = \frac{\phi}{\phi_o} \tag{16.47}$$

Thus, we may infer that

The Relationship between the Initial Power Level and the Final Power Level when the Prompt Jump Approximation Is Used

$$P = \frac{\beta(1-\rho)\cdot P_o}{(\beta-\rho)} \tag{16.48}$$

There is an enormous amount of physics imbedded in this simple equation that we would like to illustrate for you now. Using Equation 16.48, we can calculate the flux and power levels immediately after the reactivity has been changed from its initial value of $\rho = 0$ to a different value of ρ'. The reactivity change is therefore given by the difference between its initial value, ρ, and its final value, ρ':

$$\Delta\rho = \rho - \rho' \tag{16.49}$$

If the initial flux or power is given by ϕ_o or P_o, then the final flux or power will be given by ϕ or P. The normalized flux and power ratios are shown in Table 16.4, and the corresponding reactor periods in seconds are shown in Table 16.5. The ratio of the final flux or power to the initial flux or power is the *prompt jump factor J.* The prompt jump approximation can be used whenever $\rho \ll \beta$, and even in the case when $\rho \sim \beta$, a great deal of insight can still be gained by using it judiciously with smaller values of t. For example, suppose that $\beta = 0.0065$, and the change in the reactivity is 20% of β (i.e., we change the reactivity from $\rho = 0$ to $\rho = 0.20\ \beta$). The change in the power level P of the core is then

$$\frac{P}{P_o} = \frac{\phi}{\phi_o} = J \tag{16.50}$$

Inserting the appropriate values for β and ρ into Equation 16.47 for J, we find that the power level P immediately increases from $P_o(100\%)$ to a value of $1.25\ P_o(125\%)$. Clearly, this is a dramatic increase in the power level for such a small change in the reactivity.

TABLE 16.4
Values of the Prompt Jump Factor J for Various Reactivity Changes[a]

Positive Reactivity Changes			Negative Reactivity Changes		
Δρ (Cents)	Δρ (Actual)	Flux or Power (Normalized)[b]	Δρ (Cents)	Δρ (Actual)	Flux or Power (Normalized)
0	0	1.00	0	0	1.00
5¢	0.00032	1.05	−5¢	−0.00032	0.95
10¢	0.00065	1.11	−10¢	−0.00065	0.91
20¢	0.00130	1.25	−20¢	−0.00130	0.83
30¢	0.00195	1.43	−30¢	−0.00195	0.77
40¢	0.00260	1.66	−40¢	−0.00260	0.71
50¢	0.00325	2.00	−50¢	−0.00325	0.67
60¢	0.00390	2.50	−60¢	−0.00390	0.62
70¢	0.00455	3.33	−70¢	−0.00455	0.59
80¢	0.00520	5.00	−80¢	−0.00520	0.55
90¢	0.00858	10	−90¢	−0.00858	0.52
$1.00	0.00650	∞	−$1.00	−0.00650	0.50
			−$2.00	−0.01300	0.33
			−$3.00	−0.01950	0.25
			−$4.00	−0.02600	0.20
			−$5.00	−0.03250	0.16
			−$10.00	−0.06500	0.09
			−$20.00	−0.13000	0.05

[a] Assumes a Uranium-235-fueled reactor with a delayed neutron fraction $\beta = 0.0065$ that is initially critical.
[b] Normalized to a pre jump value of 1.0.

In practice, the prompt jump approximation becomes very accurate for relatively small changes to the reactivity. For example, numerical solutions to the point kinetics equations have shown that it has an average error of less than 1% up to reactivity insertions of about 50 cents ($\rho = 0.50\ \beta$)—either positive or negative. For larger changes to the reactivity, it can still be used to predict the general behavior of the power level, but the results should be viewed with caution because the errors introduced by the prompt jump approximation can become larger. One of the interesting things about Table 16.5 is that it implies that whenever the reactivity is reduced by more than $1.00 in a thermal water reactor fueled with enriched uranium (i.e., U-235), *adding more negative reactivity does not necessarily reduce the reactor period any further*. In other words, after one dollar's worth of control rods are inserted into the core, inserting more control rods into the core will not cause the reactor to shut down any faster!

This effect can be clearly seen in Figure 16.3, which is a slightly more accurate depiction of the time dependent power level than that given by the prompt jump approximation. The reason for this novel time-dependent behavior is that the *Bromine-87 decay chain* (which is normally in delayed neutron precursor group 1) completely dominates the long-term behavior of the core after a certain period of time, and reducing the reactivity any further does not change the asymptotic period τ (although it may change the instantaneous power level P' immediately after the control rods are inserted). The following example illustrates how this affects a thermal water reactor that is scrammed during a routine safety test. Obviously, if one wants to know exactly how much reactivity there is in a control rod, one needs to understand how quickly the power level changes immediately after the rod is inserted or withdrawn. For example, if one does a routine safety test where the power level drops by 50% a few seconds after the rod is inserted, then the control rod must have a worth of $1.00 (see Table 16.4). Similarly, if the power level drops immediately by 17%, then the worth of the control rod must be 20 cents.

Example Problem 16.4

A research reactor in Los Alamos, New Mexico, is to be given an annual performance test. The reactor produces 10 MW of electrical power when it is operating normally. When all of the control rods are dropped into the core, the power level falls to 10 kW in 10 minutes. When 1/3 of the control rods are dropped into the core, the same thing happens. How much negative reactivity was inserted into the core in the second test?

Solution If the power level drops to 10 kW in 10 minutes (or 600 seconds), the reactor period must be $\tau = -t/\ln(P/P_o)$. Since P = 10 kW, P_o = 10 MW, and t = 600 seconds, $\tau = -600/\ln(0.001) = 87$ seconds. From Table 16.5, it can be seen that

TABLE 16.5
Values of the Reactor Period T for Various Values of the Reactivity[a]

Positive Reactivities			Negative Reactivities		
ρ (Cents)	ρ (Actual)	Reactor Period (Seconds)	ρ (Cents)	ρ (Actual)	Reactor Period (Seconds)
0	0	∞	0	0	∞
5¢	0.00003	250	−5¢	−0.00003	300
10¢	0.00065	100	−10¢	−0.00065	185
20¢	0.00130	32	−20¢	−0.00130	110
30¢	0.00195	20	−30¢	−0.00195	91
40¢	0.00260	10	−40¢	−0.00260	91
50¢	0.00325	5	−50¢	−0.00325	90
60¢	0.00390	3	−60¢	−0.00390	89
70¢	0.00455	1.5	−70¢	−0.00455	88
80¢	0.00520	0.8	−80¢	−0.00520	88
90¢	0.00585	0.4	−90¢	−0.00585	87
$1.00	0.00650	0.1	−$1.00	−0.00650	87
			−$2.00	−0.01300	85
			−$3.00	−0.01950	85
			−$4.00	−0.02600	85
			−$5.00	−0.03250	85
			−$10.00	−0.06500	85
			−$20.00	−0.13000	85

Note: The values shown here are approximately correct for ρ < 50 cents. Consult Figure 16.3 for the appropriate reactor period for larger changes in ρ.

Larger power changes assume an initially critical system (ρ = 0), with a reactor period T deduced from Figure 16.1.

[a] Assumes a Uranium-235-fueled reactor with a delayed neutron fraction $\beta = 0.0065$, and $\Lambda = 1.0 \times 10^{-4}$.

the period does not change when the reactivity falls by more than about $1.00. Therefore, the control rods in the second test must have had at least $1.00 of negative reactivity. The only way to determine the exact amount of reactivity is to measure the percentage reduction in the power level (P′/P) a couple of seconds after the test begins. [Ans.]

Later in the chapter, we will learn that *most measurements of the reactor period T (and therefore the value of ρ) are performed by withdrawing a control rod from the core (instead of inserting it), because the size of the reactor period is not obscured by the presence of Bromine-87 in the longest-lived delayed neutron precursor group (which is generally referred to as group 1).* (The effects of Bromine-87 are discussed in more detail in Chapter 15).

16.8 Normal Reactor Behavior and Normal Reactivity Swings

One of the first things one notices in Table 16.4 is that very small changes to the reactivity, on the order of ±5 cents, have very little effect on the total flux or power level in either direction (positive or negative). The reactor period T remains between 100 and 300 seconds, and the core is relatively easy to control. It therefore follows that the magnitude of the prompt jump (or drop) is usually small for small reactivity insertions or reductions and that the power level will increase or decrease from its initial value at a very stable rate, corresponding to an exponential curve with a constant period T. However, larger changes to the reactivity can affect the power level in a more dramatic way. Example Problem 16.5 shows how the power level changes when the reactivity change is larger and more pronounced.

Example Problem 16.5

Suppose that we would like to determine how much reactivity we would have to suddenly add to a U-235-fueled thermal water reactor (by withdrawing one or more of the control rods) to cause the power to suddenly jump by 20% (from 100% to 120%). Using the prompt jump approximation, estimate how much reactivity in dollars (or cents) would have to be added to the core in order to cause this to happen.

Solution From the equation given earlier for the prompt jump J, we know that this corresponds to a situation where J = 1.20. If the value of β is 0.0065, then the amount of reactivity required for this to happen is ρ = 0.17β. So for J = 1.20 and β = 0.0065, the value of ρ is ρ = 0.0011 (or about 17 cents of positive reactivity). [Ans.]

Notice that small positive changes to the reactivity affect the reactor period T quite differently than small negative changes do. Again, this is an important distinction that the reader needs to keep in mind.

16.8.1 Large Positive Reactivity Changes (Increases)

Notice that as soon as changes to the reactivity begin to depart from this range, the power and the flux tend to change very rapidly, and great care must be exercised to ensure that the reactivity returns to zero very quickly. For example, a reactivity increase of just 50¢ will double the power level in just a few hundredths of a second, and after the new power level is reached, the reactor period is reduced to only 5 seconds after that (when thermal feedback effects are ignored). So if we ignore the effects that neutron poisons and changes in the operating temperature can have on the reactivity, it is only a matter of several seconds (5–6 to be exact) after a control rod is withdrawn before the reactor reaches a prompt critical state and goes on an uncontrolled power excursion. This is a very dangerous condition that needs to be avoided at all costs. For this reason, routine changes to the reactivity are usually restricted to about ±5 cents in either direction. Reactor operators must constantly ensure that these limits are adhered to if a reactor is to be operated safely. This allows the reactor power level to be gradually increased for about 2 or 3 minutes at a time, and then the reactivity can be reduced by partially inserting a control rod, which causes the power level to slowly decline at a similar rate.

In commercial power reactors, this cycle is repeated over and over again as the nuclear fuel is burned. In other words, *the reactor power level constantly oscillates in a very narrow range*. An example of this behavior is shown in Figure 16.6. So, one of the most important observations that we can immediately make is that the power level in a real reactor is never really constant. It is designed to oscillate between a slightly supercritical state, which corresponds to $\rho < 0.0003$ with U-235 fuel assemblies, and one that it is just critical, which corresponds to $\rho \approx 0$. The nominal power output is just the average of the power levels between these two bipolar states. Thus, an operating reactor is an incredibly complex and dynamic machine that must walk a fine line between becoming too supercritical (and therefore getting out of control), and not being critical enough (and therefore shutting down). To be even more specific, the control systems in a nuclear

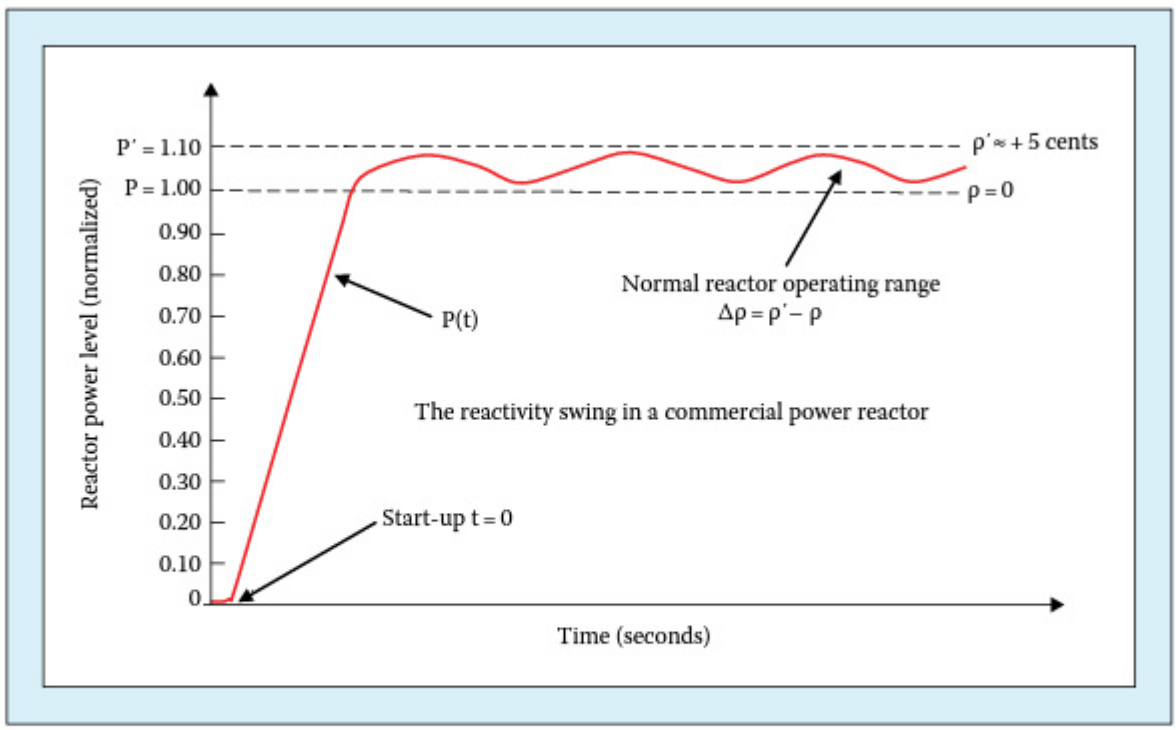

FIGURE 16.6 A normal reactor operating range for the reactivity ρ and the power P.

power plant must be designed to restrict the value of the reactivity so that it never gets larger than about 15 cents (0.001), or about 15% of the prompt supercritical limit. At the same time, it must never go below 0 if the reactor is to remain critical.

Thus, the allowable reactivity range in which a commercial power reactor can be operated without causing undue power oscillations is extremely limited. In thermal Uranium-235-fueled reactors, this range is about $0 \leq \Delta\rho \leq 0.0003$, or about 2 delayed neutrons per 1000. We have attempted to illustrate this in Figure 16.6. Between the reactivity limits shown, the power level simply oscillates back and forth, over and over again. Eventually, the fuel becomes depleted, and the reactor needs to be refueled. In fast reactors, controlling swings in the power level becomes even more difficult because the delayed neutron fraction β for a Plutonium-239-fueled reactor is only about 1/3 of what it is for a Uranium-235-fueled reactor (0.0021 vs. 0.0065). In addition, the prompt neutron lifetime Λ may be between 100 and 1000 times smaller, so the reactor period T associated with a runaway is between 100 and 1000 times shorter. Because of this small margin for error, reactors are always designed so that the immediate consequence of any increase in the power level is a decrease in the criticality through a corresponding reduction in the reactivity. Consequently, the control systems are very complex, very intelligent, and very redundant.

16.8.2 Large Negative Reactivity Changes (Decreases)

As we have found, reactors do not respond as violently to reductions in the reactivity as they do to reactivity increases. For example, a reactivity decrease of 90¢ will only reduce the power level in a Uranium-235-fueled thermal water reactor by about 50% (see Table 16.4), while a reactivity increase of 90¢ will increase the power level in exactly the same reactor by a factor of 10 (1000%). Physically, the reason for this is that negative changes to the reactivity result in a much longer reactor period than positive changes to the reactivity do. For example, a 30¢ increase to the reactivity, which is about the upper limit of what a reactor is normally designed to handle, will increase the power level immediately by about 43%, and the reactor period thereafter will be about 20 seconds. In contrast, a 30¢ decrease to the reactivity will reduce the power level immediately by 23%, after which the reactor period will fall to about 90 seconds. Hence, we can conclude that

Reactors are much more forgiving when it comes to shutting them down than when it comes to ramping them up. Large negative reactivities can usually be introduced into the system without any adverse side effects.

For example, during a scram, several control rods are quickly inserted into the core. When this occurs, it is not uncommon for the system to receive an immediate reactivity reduction of \$10–\$20. To be more specific, suppose that the scram results in a negative reactivity insertion of \$20 in about half a second. This will cause a very large reduction in the number of free neutrons that are available to the fuel rods. As soon as the control rods are inserted into the core, prompt neutron production immediately drops by about 95% in less than 0.01 seconds. In this case (see Table 16.4), the neutron flux (and therefore the power level) immediately declines to about 5% of its initial value before the reactor goes on a new but stable period of about 80 seconds. This is a drastic change in the behavior of the core to say the least. With a large negative reactivity insertion and only one delayed neutron precursor group, the first root of the Inhour equation ω_1 (see Figure 16.1) approaches the value of $-\lambda$, which is the aggregate decay constant for the delayed neutrons. If this is extended to include additional delayed neutron precursor groups, it can also be shown that the value of ω_1 approaches the decay constant for the longest-lived delayed neutron group, λ_1 (see Chapter 15), which happens to have a value of 0.0124 seconds^{-1} in this case. The new reactor period then becomes

$$T = 1/\omega_1 = 1/\lambda_1 \approx 81 \text{ seconds}$$

So, the reactor goes on this period even with a negative reactivity insertion of \$20. We can illustrate the same behavior analytically by going back to the exact solutions to Equations 16.1 and 16.3, and showing what they predict for a slightly more modest reactivity reduction. A step change in the reactivity from $\rho = 0$ to $\rho = -0.05$ (a slightly less severe scram equal to about—\$8.00) results in the following equations for $\phi(t)$ and C(t):

The Neutron Flux and Precursor Populations during a Reactor Scram

$$\phi(t) = 0.87e^{-958t} + 0.13e^{-0.068t}$$

$$C(t) = 0.01e^{-958t} + 1563e^{-0.068t} \qquad (16.51)$$

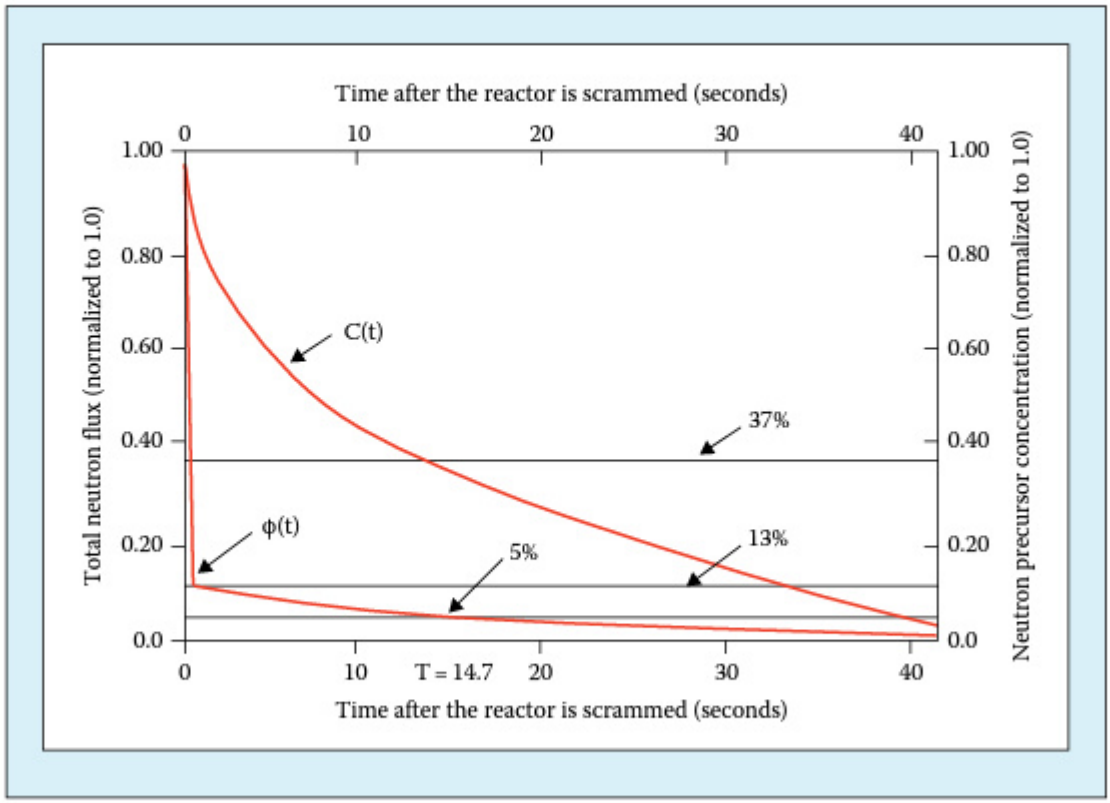

FIGURE 16.7 A plot of the neutron flux and the delayed neutron precursor concentrations during a reactor scram.

A plot of the reactor behavior implied by these equations is shown in Figure 16.7. The value of C(t) represents the number of delayed neutron precursors relative to the total number of neutrons (the neutron flux in the core) for representative values of β, Λ, and λ. In other words, for steady-state operation, corresponding to t = 0, Equation 16.51 shows that the precursor population outweighs the neutron population by a factor of about 1600 to 1. In this case, the exact roots to the Inhour equation with one delayed neutron group are $\omega_1 = -958.0$ and $\omega_2 = -0.068$. The first root means that 87% of the total neutron population ϕ(t) dies off in less than 0.01 seconds, since $\omega_1 t = -958.0 \times 0.01 = -9.58t$ and

$$\phi(t) = 0.87e^{-9.58t} + 0.13e^{-0.068t} \tag{16.52}$$

However, only a very small fraction of the precursors have a chance to decay in such a short period of time, since

$$C(t) = 0.011e^{-9.58t} + 1563e^{-0.068t} \tag{16.53}$$

This means that the remaining 13% of the neutron population (and hence the power that is proportional to these neutrons) falls with a time constant that is inversely proportional to the second root ω_2 which leads us to conclude that

$$T = 1/\omega_2 = 1/0.068 \approx 14.7 \text{ seconds}$$

Since the precursor population changes by only one part in 1000, while the power level falls by 87%, it is easy to see that the assumption upon which the prompt jump (or drop) approximation is based, namely, that $dC/dt \approx 0$ at t = 0, is indeed a very good one. The value of the neutron precursor population (shown on the right) is normalized to 1.0 just before the scram begins (at t = 0) in Figure 16.7. At t = 14.7 seconds, the precursor population declines by approximately 63%. There are two other scenarios we would like to discuss before moving on to other topics. These scenarios, which are very important to the field of reactor safety as a whole, are

- The behavior of a reactor during a supercritical transient
- The behavior of a reactor during a prompt supercritical transient

Although this second scenario is not very likely to occur over the life of a nuclear power plant, it can be helpful in mathematically quantifying how the neutron population behaves when the reactivity is a large positive number. In practice, the control systems are designed to ensure that this second scenario never occurs.

Student Exercise 16.1

In Chapter 15, we learned that the delayed neutrons which are created after the fission process can be represented by the sum of six exponential functions:

$$S_d(t) = \beta_1\lambda_1 e^{-\lambda_1 t} + \beta_2\lambda_2 e^{-\lambda_2 t} + \beta_3\lambda_3 e^{-\lambda_3 t} + \beta_4\lambda_4 e^{-\lambda_4 t} + \beta_5\lambda_5 e^{-\lambda_5 t} + \beta_6\lambda_6 e^{-\lambda_6 t}$$

where

β_1, β_2, β_3, β_4, β_5, and β_6 are the yields for each of the six delayed neutron precursor decay chains
λ_1, λ_2, λ_3, λ_4, λ_5, and λ_6 are their corresponding decay constants

However, it would have been just as easy (or even easier) to represent the number of delayed neutrons produced by an equation of the form

$$S_d(t) = at + bt^2 + ct^3 + dt^4$$

where a, b, c, and d are constants that depend on the type of fuel used. Why do you think that the first equation ended up being the nuclear industry standard instead of the second? Be prepared to justify the reasons for your answer.

16.8.3 Supercritical Transients

If an initially critical U-235-fueled thermal water reactor is subject to a step increase in the reactivity of 0.0015 (about 20¢), then according to Equations 16.23 and 16.24, the time-dependent flux and precursor concentrations become

The Neutron Flux and Precursor Populations during a Supercritical Transient

$$\phi(t) = -0.25e^{-100t} + 1.25e^{0.02t}$$

$$C(t) = 0.31e^{-100t} + 1563e^{0.02t} \qquad (16.54)$$

In this case, the two roots of the Inhour equation are $\omega_1 = -100$ and $\omega_2 = 0.02$. As far as the flux is concerned, the first term decays immediately, and the flux instantaneously jumps in the first few milliseconds to 1.25 times its initial value. So, the power increases instantaneously in a single step by 25% before we can even react to it. Just as in our previous example, the neutron precursor population changes negligibly during the same period of time. After the first term decays, the remaining terms continue to rise with a time constant that is inversely proportional to the second root ω_2 or

$$T = 1/\omega_2 = 1/0.02 \approx 50 \text{ seconds}$$

This gives us some time to return the reactor to its initial power level before the fuel rods begin to melt.

16.8.4 Prompt Supercritical Transient

We would now like to discuss our final and most interesting example of time-dependent reactor behavior—the dreaded *prompt supercritical transient*. This transient has been the subject of literally millions of hours of analysis by nuclear scientists and engineers, and many models have been built, both experimentally and computationally, to understand its consequences in excruciating detail. Later in the chapter, we will discover that several computer programs such as TRAC and TRACE were written specifically to understand the consequences of a reactor entering into this state. *A prompt supercritical transient can only occur when a step increase in the reactivity ρ exceeds the delayed neutron fraction β, In other words, such a transient can only occur when the reactivity is instantaneously increased to a value that is at least $1.00 greater than the reactivity that was initially required to keep the reactor in a critical state.*

Normally such a scenario can only occur as the result of the complete mismanagement of the control rods by a reactor operator. Even then, the reactor's control systems would try to prevent the reactor from entering this state. In the example that

follows, we would like to assume an instantaneous or stepwise reactivity increase of $\Delta\rho = 0.0115$, or about twice the prompt supercritical limit (~\$2.00). In this case, using typical values for Λ, β, and λ, the time-dependent flux and precursor concentrations become

The Neutron Flux and Precursor Populations during a Prompt Supercritical Transient

$$\phi(t) = 2.9e^{66.7t} - 1.9e^{-0.23t}$$

$$C(t) = 5.4e^{66.7t} + 1563e^{-0.23t} \qquad (16.55)$$

Thus the exact roots of the Inhour equation are $\omega_1 = 66.7$ and $\omega_2 = -0.20$. Under these conditions, the first term completely dominates the second, and the reactor *runs away. In other words, the neutron flux rises by a factor of almost 700 in just a tenth of a second*, and even if the reactor is still intact after the initial power surge, it goes on a 1.5 millisecond period where the power level continues to increase without limit. The delayed neutron precursor population also explodes exponentially. *In other words, the reactor goes into orbit!* A scenario of this type would obviously be a disaster in the making. There are a number of additional factors that we will discuss in Chapter 17 to help mitigate the efects of this depressing scenario. They include various forms of temperature and thermal feedback to reduce the growth rate of the neutron population, as well as the Doppler broadening of the absorption resonances in the fuel as the fuel temperature rises rapidly. Both of these effects tend to create a form of *negative feedback* in which temperature increases limit the neutron production rate to much lower levels than those implied by the two root or seven root Inhour equation.

The inclusion of these effects would result in a slightly less severe reactor transient. However, even when all of these factors are taken into account, the best way to avoid such a transient is to prevent it from occurring in the first place. As such, reactor control systems have become increasingly sophisticated over the years—especially when large reactivity increases are initiated by reactor operators after the concentrations of xenon and samarium have built up to very high levels (see the additional discussion of this topic in Chapter 21). When these fission product poisons start to decay, they can add several dollars of positive reactivity to the core, and if their behavior is not properly anticipated, especially in conjunction with withdrawing a couple of control rods, a prompt supercritical transient can occur.

Student Exercise 16.2

The reactivity of a single control rod in a gas-cooled reactor is 0.1 niles. What is its reactivity in PCM, and if 10 of these control rods are withdrawn from the core during a rod ejection accident, by how much will the power level immediately jump after the rods are withdrawn? How long will it take for the power level in the core to double? Assume the reactor is fueled with enriched uranium.

16.9 Solutions to the Inhour Equation with Six Delayed Neutron Groups

To solve the Inhour equation in its most general form, it is necessary to find all *seven roots* of the equation for each value of the reactivity ρ, which would correspond to the sum of the seven exponential functions for ϕ and C. When we extend our analysis using six delayed neutron precursor groups, then the time-dependent flux must be described by the sum of the seven exponentials instead of just two:

$$\phi(t) = A_1e^{t/T_1} + A_2e^{t/T_2} + A_3e^{t/T_3} + \cdots + A_7e^{t/T_7} \qquad (16.56)$$

and the precursor concentrations would have to follow a similar trend:

$$C(t) = C_1e^{t/T_1} + C_2e^{t/T_2} + C_3e^{t/T_3} + \cdots + C_7e^{t/T_7} \qquad (16.57)$$

Under these conditions, the Inhour equation can be solved numerically, or its solutions can be plotted graphically to find each of the seven roots. After doing so, we obtain the graph shown in Figure 16.8 where, for the sake of convenience, we have again defined $\omega = 1/T$. This particular graph is based on writing the Inhour equation as

The Classic Form of the Inhour Equation

$$\rho = \frac{\omega\Lambda}{1+\omega\Lambda} + \frac{\omega}{1+\omega\Lambda}\sum_i \frac{\beta_i}{\omega+\lambda_i}, \quad \text{where } i = 1,2,\ldots,6 \qquad (16.58)$$

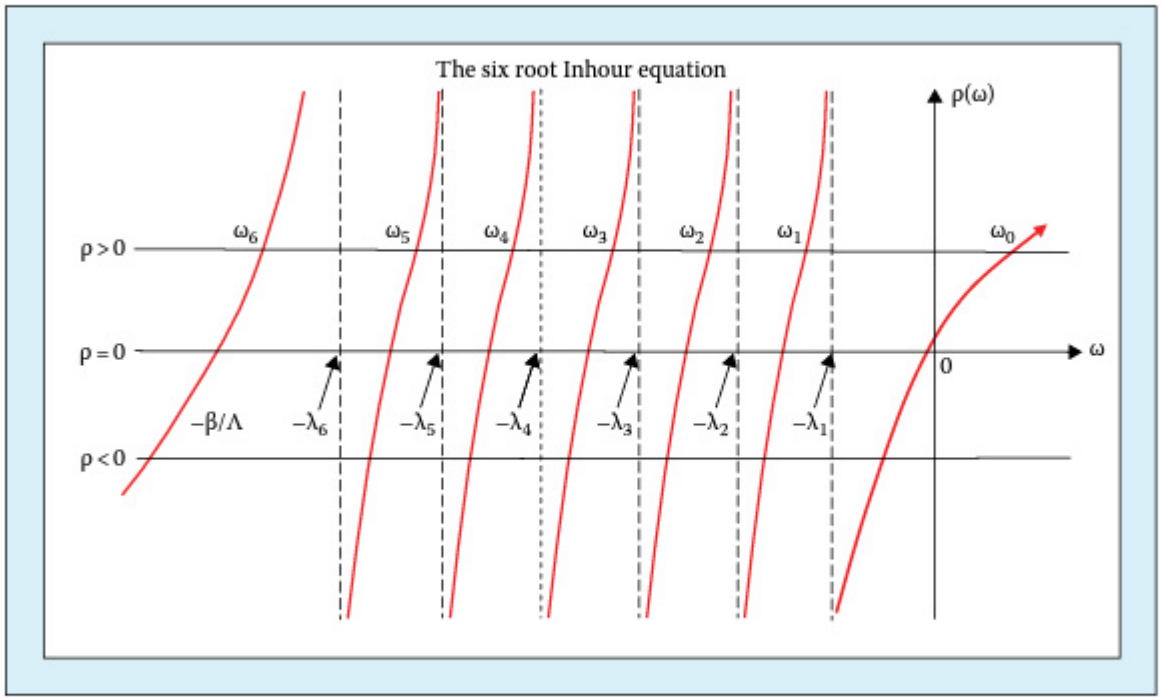

FIGURE 16.8 A plot of the Inhour equation with all six delayed neutron groups.

where $\omega = 1/T$. To get some feeling for the behavior of these roots, suppose that we plot the function

$$\rho(\omega) = \frac{\omega\Lambda}{1+\omega\Lambda} + \frac{\omega}{1+\omega\Lambda}\sum_i \frac{\beta_i\omega}{\omega+\lambda_i} \quad \text{where } i = 1,2,\ldots,6 \tag{16.59}$$

for different values of ρ. To see what happens next, suppose that we multiply both sides of Equation 16.59 by $(1 + \omega\Lambda)$ and expand the resulting expression a bit. Initially, we find that

$$\rho\cdot(1+\omega\Lambda) = \omega\Lambda + \omega\sum_i \frac{\beta_i\omega}{\omega+\lambda_i} \quad \text{where } i = 1,2,\ldots,6 \tag{16.60}$$

and after some rearrangement, we obtain

$$\rho = \Lambda(1-\rho)\omega + \omega\sum_i \frac{\beta_i\omega}{\omega+\lambda_i} \tag{16.61}$$

or

$$\rho = \omega\Lambda(1-\rho) + \omega\left[\frac{\beta_1\omega}{\omega+\lambda_1} + \frac{\beta_2\omega}{\omega+\lambda_2} + \frac{\beta_3\omega}{\omega+\lambda_3} + \frac{\beta_4\omega}{\omega+\lambda_4} + \frac{\beta_5\omega}{\omega+\lambda_5} + \frac{\beta_6\omega}{\omega+\lambda_6}\right] \tag{16.62}$$

Thus, the Inhour equation in its most general form is a seventh-order equation with seven unknowns—which correspond to the roots of ω. As before, the scale shown in Figure 16.8 is logarithmic, so if $-\omega_6 = -3$ seconds^{-1}, the value of β/Λ might be −125. The *seven roots - $\omega_0, \omega_1, \ldots, \omega_6$ - then correspond to the intersection points of each horizontal line with the seven branches of the curve*. In this scenario, all seven roots are real, and five of them lie between $-\lambda_6$ and $-\lambda_1$. At most, only one of the roots is positive, and from Figure 16.8, it can readily be seen that this only occurs when $\rho > 0$. Furthermore, we see from Equation 16.62 that when the $\omega \gg \lambda_i$ and $\Lambda \ll \omega$, $\rho \approx \omega\sum_i\beta_i$, so

$$\omega \approx \frac{\rho}{\beta} \quad \text{and} \quad T = \frac{1}{\omega} \approx \frac{\beta}{\rho} \tag{16.63}$$

Consequently, the asymptotic reactor period T becomes inversely proportional to the value of the reactivity ρ and directly proportional to the value of the delayed neutron fraction β. This result applies to both fast and thermal reactors in the limit of small reactivity changes. Finally, when $\beta/\Lambda \gg \lambda_i$, there is always at least one large negative root when $\rho \leq 0$.

Hence the qualitative behavior we were able to obtain with just one delayed neutron group is remarkably similar to the behavior that we actually observe when all six delayed precursor groups are taken into account.

16.10 Time-Dependent Behavior of Fast Reactors

Now let us turn our attention to how fast reactors behave under these conditions. *Fast reactors are different than thermal reactors in two fundamental ways*:

1. First, because they are usually fueled with Pu-239, their delayed neutron fractions are much smaller than those of thermal water reactors fueled with U-235. (Hence, the value of β for a Pu-239-fueled core is about three times *smaller* than the value of β for a U-235-fueled core.)
2. Secondly, the prompt neutron lifetime Λ in a fast reactor is about 10^{-7} seconds, which is about 1000 times *less* than the prompt neutron lifetime of a thermal water reactor (where $\Lambda \approx 10^{-4}$). Therefore, except for very large reactivity insertions where the reactor period T is very short and ω is very large, we can neglect the value of ωΛ when the Inhour equation is used to estimate the reactor period.

This means that the time-dependent behavior of a fast reactor can be predicted from the simplified form of the Inhour equation shown below:

The Inhour Equation for Fast Reactors

$$\rho = \omega \cdot \sum_i \frac{\beta_i}{\omega + \lambda_i}, \quad \text{where } i = 1,2,\ldots,6 \tag{16.64}$$

Notice that Equation 16.64 does not contain the prompt neutron lifetime Λ. Hence the period for a fast reactor can be found from Figure 16.3 by setting Λ = 0. *Since fast reactors have fewer delayed neutrons per fission, they are also more difficult to control. For a given change in the reactivity, the margin for error is only about 1/3 as large as it is in a thermal water reactor fueled with U-235. Now let us make some additional observations about the graph shown in Figure 16.7.* If the reactivity is zero (ρ = 0), the values of ω_o, ω_1, ω_2, ω_3, ω_4, ω_5, and ω_6 are simply where the roots intersect the x-axis. If the reactivity is greater (ρ > 0), the roots shift to the right, and the largest root (ω_o or the first root) becomes positive. If the reactivity is less than zero (ρ < 0), then all of the roots shift to the left, and all seven roots become negative. *Hence a reactor with a positive value of the reactivity has one positive root, while a reactor with a negative value of the reactivity has 7 negative roots.* Now let us see how this affects the time-dependent power level P(t). In general, the power level is given by the sum of seven different exponentials, and at least six of these terms are due to the delayed neutron precursor groups. Thus, when all of the delayed neutron precursors are taken into account, the time-dependent power level is given by

Time-Dependent Reactor Power Level Predicted by the Inhour Equation

$$P(t) = \sum_i P_i e^{\omega_i t} \left(\text{for } i = 0, \ldots, 6\right)$$

or more explicitly,

$$P(t) = P_o\, e^{\omega_0 t} + P_1\, e^{\omega_1 t} + P_2\, e^{\omega_2 t} + P_3\, e^{\omega_3 t} + P_4\, e^{\omega_4 t} + P_5\, e^{\omega_5 t} + P_6\, e^{\omega_6 t} \tag{16.65}$$

In this case, the root lying furthest to the right (ω_o) turns out to be the reciprocal of the reactor period T. In other words, the asymptotic period is given by T = 1/(ω_o). *Moreover, it should also be apparent from Figure 16.7 that this root is the only root that will ever be positive.* The other roots, corresponding to ω_1, ω_2, ω_3, ω_4, ω_5, and ω_6, are simply transient components of the time dependent solution (with different phases than the primary root). As we discussed before, these additional roots die out rapidly when the system reactivity is changed.

16.11 Finding the Asymptotic Reactor Period

Now we would like to make some additional observations about how the asymptotic reactor period can be deduced from the Inhour equation:

$$\rho_o = \frac{\Lambda}{\Lambda + T} + \frac{T}{\Lambda + T} \cdot \sum_i \frac{\beta_i}{1 + \lambda i T} \tag{16.66}$$

If we expand the final term on the right hand side, we see that the Inhour equation becomes

$$\rho_o = \frac{\Lambda}{\Lambda+T} + \frac{T}{\Lambda+T}\cdot\left[\frac{\beta_1}{1+\lambda_1 T} + \frac{\beta_2}{1+\lambda_2 T} + \frac{\beta_3}{1+\lambda_3 T} + \frac{\beta_4}{1+\lambda_4 T} + \frac{\beta_5}{1+\lambda_5 T} + \frac{\beta_6}{1+\lambda_6 T} + \frac{\beta_7}{1+\lambda_7 T}\right] \tag{16.67}$$

where the values of β_i and λ_i depend on the type of fuel (U-233, U-235, or Pu-239) that is used. If the left-hand side is a constant, the resulting equation, no matter how complex, is still an algebraic one. Thus, we have a seventh-order algebraic equation to solve for the reactor period T. The roots of this equation are T_1, T_2, T_3, T_4, T_5, T_6, and T_7. In the language of Laplace transforms, these roots are simply the *poles* of the solution. However, the solutions we have just presented are only valid for a step change in the reactivity $\pm\rho_o$, which is assumed to occur at t = 0. Any other behavior for ρ will result in an entirely different expression for the reactor period T, and the roots will be different as well. The consequences of this are discussed in our follow-on book.*

Now let us discuss how the dynamic behavior is affected by the value of ω_1. Since the value of $\rho_o = (k-1)/k$ is always bounded by unity (1.0), we can write

$$-\infty < \rho_o < 1 \tag{16.68}$$

and the seven roots ω in the limit where $\rho_o = 0$, $\rho_o \to 1$, and $\rho_o \to -\infty$ become

$$\frac{1}{\omega_1} = 0 \quad \rho_o = 0 \quad \text{(critical)} \tag{16.69}$$

$$\frac{1}{\omega_1} \to \infty \quad \rho_o \to 1 \quad \text{(supercritical)} \tag{16.70}$$

$$\frac{1}{\omega_1} \to -\lambda_1 \quad \rho_o \to -\infty \quad \text{(subcritical)} \tag{16.71}$$

In other words, each of these roots corresponds to a critical, supercritical, or subcritical state. Equation 16.71 is particularly interesting because it implies that no matter how much negative reactivity is introduced into the core by a step function, the reactor period following the prompt drop will decline at a rate given by the time constant of the longest-lived delayed neutron group, $T = 1/\omega_1$, which in the case of Uranium-235 is about 80 seconds. So if we reduce the reactivity of the entire core by between about \$5 and \$10 in a step-wise manner, the reactor power will immediately fall to about 13% of its initial value, and the remaining power will decay with an asymptotic time constant of $\omega = 1/T$ or about 1/80 = 0.0125/s.

Figure 16.9 attempts to illustrate how the asymptotic reactor period $T = 1/\omega_1$ behaves as a function of a step-wise change in the reactivity ρ_o for U-233, U-235, and Pu-239 fueled cores. Note in particular how quickly the reactor period T falls as ρ approaches the value of β. When the prompt critical limit is reached, ρ = β, and the reactor becomes critical based on prompt neutrons alone. Then the reactor period T is driven primarily by the value of the prompt neutron lifetime Λ. It is easy to see that this will correspond to an asymptotic reactor period of no more than 10^{-3} seconds depending on the value of Λ that is used. Except for a step-wise change in the reactivity ρ_o at t = 0, it is nearly impossible to solve the seven root Inhour equation without resorting to Laplace transforms or more sophisticated numerical techniques. In fact, it is easier to simply go back to the time-dependent point kinetics equations for the power and the precursor concentrations, and apply Laplace transforms to them directly for the case where we know the explicit form of ρ(t). In fact, many examples of this approach are presented in our follow-on book,* where the role of Laplace transforms in solutions to the point kinetics equations is discussed in more detail.

In practice, reactor designers usually design a core with just a single value for ω that is obtained by averaging the individual values of β_i and λ_i (see Chapter 15)

$$\beta = (1/N)\sum_i \beta_i \quad (i = 1,2,3,4,5,N) \tag{16.72}$$

* See *Contemporary Nuclear Reactor Physics with an Introduction to Reactor Dynamics, Computational Methods, and Nuclear Particle Transport*, by R.E. Masterson, CRC Press (2019).

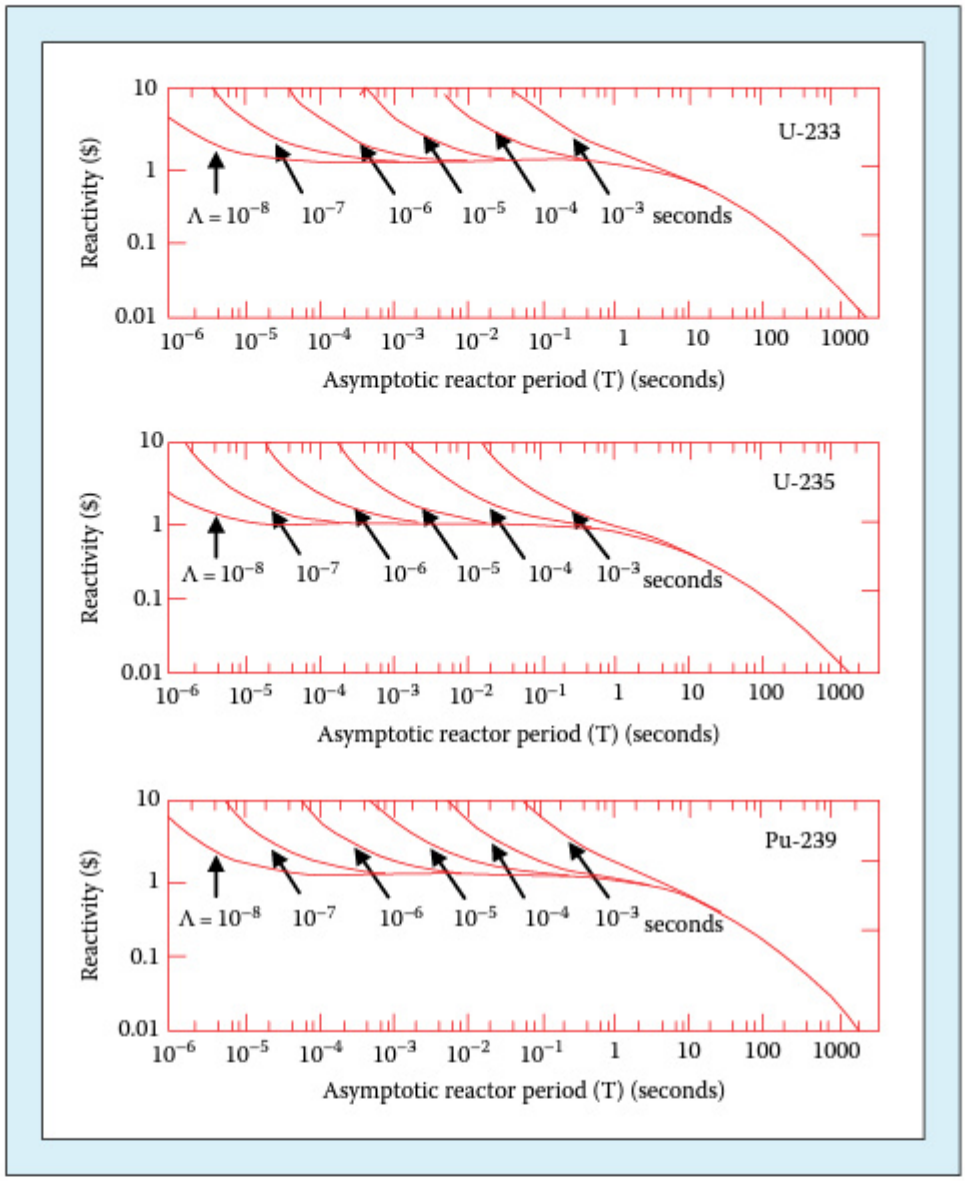

FIGURE 16.9 The asymptotic reactor period T as a function of the reactivity for U-233-, U-235-, and Pu-239-fueled cores. (Adapted from a figure in Duderstadt, J. and Hamilton, L., *Nuclear Reactor Analysis*, John Wiley & Sons, New York, 1976.)

and

$$\lambda = \left[\frac{1}{\beta}\sum_i \frac{\beta_i}{\lambda_i}\right]^{-1} \quad (i = 1,2,3,4,5,N) \tag{16.73}$$

and then they extend their analysis to the seven root Inhour equation (Equation 16.67). The motion of the individual control rods may then be programmed into the reactor control system to simulate the dynamic behavior of the core. Normally, this process is completely transparent to the reactor operator.

16.12 Flux and Power Changes Starting from an Arbitrary State

In our earlier discussion, we assumed that all transients were initiated from an initially critical reactor with $\rho = 0$. This allowed us to solve the time-dependent diffusion equation with the prompt jump approximation:

$$J = \frac{\beta(1-\rho)}{(\beta-\rho)} \tag{16.74}$$

where $J = \phi/\phi_o$, and $J = P/P_o$ (since the power P is proportional to the flux ϕ). *There is, however, a more general form of the prompt jump approximation that can be used to predict the flux and power levels even when a reactor is not initially in a critical state*, that is, when $\rho \neq 0$. To derive the prompt jump approximation under these conditions, we can again begin with the time-dependent neutron diffusion equation, and assume that $K_\infty \neq 1$. It is also necessary to assume that the prompt neutron lifetime Λ is very short, so that the flux can jump to a new level (either higher or lower) without the neutron precursor concentration C changing. Under these conditions, we can write the neutron diffusion equation as

$$(1-\beta)K_\infty\phi(t) + \frac{\lambda C}{\Sigma_a} - \phi(t) = \frac{\Lambda d\phi}{dt} \tag{16.75}$$

If the prompt neutron lifetime Λ is small relative to λC, then we can neglect the value of $\Lambda\, d\phi(t)/dt$ for reactivity changes (typically less than 50¢). Under these conditions it is possible to show that the neutron flux ϕ immediately before a reactivity change is related to the neutron flux ϕ' immediately after the reactivity change by

Neutron Flux vs. Reactivity

$$\phi' = \phi\frac{(1-\rho)}{(1-\rho')} \tag{16.76}$$

where

ρ is the reactivity before the change is made
ρ' is the reactivity after the change is made

Since the power level P is proportional to the flux, the power P′ after the reactivity changes is also given by

Reactor Power vs. Reactivity

$$P' = P\frac{(1-\rho)}{(1-\rho')} \tag{16.77}$$

These two deceptively simple equations can be thought of as a more general form of the prompt jump approximation, and they are appropriate to use for reactivity changes (both positive and negative) in homogeneous Uranium-235-fueled reactors of less than about 50¢. Under these conditions, they can predict the final flux and power levels to within about 1%.

16.13 Understanding the Origin of the Term "Inhour"

Before leaving this chapter entirely, we would like to take a moment to explain how the Inhour and the Inhour equation acquired their names. Normally, this is not discussed in most nuclear engineering textbooks, but the Inhour plays such an important role in the history of the nuclear power industry that its historical origins require some additional discussion. In the next chapter, we will then discuss how thermal feedback affects the way in which a reactor behaves. However, for now, we hope that you will enjoy the discussion that follows, and remember it whenever the subject of time-dependent reactor behavior arises (see Table 16.6).

TABLE 16.6
Fission Product Yields and Decay Constants for Important Nuclear Fission Products

Isotope	Yield Y from U-235 (Atoms/Fission)[b]	Yield Y from Pu-239 (Atoms/Fission)[b]	Decay Constant λ (Seconds^{-1})	Decay Constant λ (Hour^{-1})
I-135	0.0639	0.0604	0.0000287	0.1035
Xe-135	0.0028	0.0105	0.0000209	0.0753
Pm-149	0.0107	0.0121	0.0000036	0.0131
Sm-149[a]	0.0188	0.0123	0.0000000	0.0000

[a] Stable under normal conditions.
[b] Thermal fission only.

Example Problem 16.6

Suppose that a Uranium-235-fueled thermal water reactor is operating between a reactivity of $\rho = 0$ and $\rho < 0.001$, with the power oscillating normally between these two limits, which correspond to a reactivity of 0 and a reactivity of about 20¢. The reactor senses that the power has reached the upper limit of its allowable range, and it would like to return to an exactly critical state, corresponding to a value of $\rho = 0$ to begin another power cycle. If the power level at $\rho = 0.001$ is 1000 MW, what is the power level at $\rho = 0$?

Solution From Equation 16.77, we know that $\rho = 0.001$ and $\rho' = 0$. We also know that P = 1000 MW. We can therefore use Equation 16.37 to solve for P′. The result is $P' = 1000 \text{ MW } (1 - 0.001)/(1 - 0) = 0.999 \text{ P} = 999 \text{ MW}$. [Ans.]

16.14 History of the Inhour Equation and the Unit of the Inhour

In earlier sections, we learned that *the Inhour is a method of determining the amount of reactivity required to increase or decrease the neutron flux in a critical reactor by a factor of e or 1/e in 1 hour.* When viewed in this way, *the reactivity in Inhours is the same as the reciprocal of the reactor period* T, but this is only true under certain conditions that we would now like to discuss. When *Enrico Fermi* and his colleagues first proposed the modern definition of the Inhour in 1947, they were in the process of investigating how reactor control rods affected the period T of a critical reactor pile. At that time, they considered the Inhour to be a measurement of how far a control rod had to be moved to produce a defined increase or decrease in the reactivity. The other men who worked on this rod calibration project were *Walter Zinn*, *Albert Wattenberg*, and *Herbert Anderson*, whose pictures are shown in Figure 16.10 (in the front row from left to right).

Fermi had previously discovered experimentally that the period of the pile T was proportional to $1/(k - 1)$, and in the limit of very long periods, he found that the exact relationship between the period and the reactivity ρ could be written as

$$T = \frac{l}{C(k-1)} = \frac{l}{C\rho} \text{ as } k \to 1 \tag{16.78}$$

FIGURE 16.10 A picture of some of the original developers of the idea of the Inhour. Enrico Fermi is the person in the first row on the far left. (From Google Images.)

where C was a constant of proportionality that depended on the composition of the pile. Thus, for extremely long reactor periods, the Inhour was defined as

The Original Definition of the Inhour

$$\text{Inhour} = \frac{C(k-1)}{k} = C\rho \tag{16.79}$$

which as the reader can clearly see has the units of *inverse hours*. For a Uranium-235 graphite-moderated pile, Fermi and his colleagues subsequently found that the amount of reactivity that gave the pile a period of 1 hour (3600 seconds) was approximately 0.000025 or 2.5×10^{-5}. So this is how the original definition of the Inhour was born. About a year later, *Anderson* and *Nordheim*, who were working on another related project, found that the reactivity (in Inhours) for a similar pile could be written as

Expression for the Reactivity of a Critical Uranium-235 Pile

$$\rho\,(\text{in Inhours}) = \frac{54}{T} + \frac{20.3}{T+0.62} + \frac{204}{T+2.19} + \frac{535}{T+6.5} + \frac{2036}{T+31.7} + \frac{787}{T+80.3} \tag{16.80}$$

where T was again the period of the pile in seconds. Notice that for very large values of the reactor period T, Equation 16.80 reduces to

$$\rho\,(\text{in Inhours}) = \frac{3636}{T} \cong \frac{3600}{T} \tag{16.81}$$

which has a margin of error of about 1%. Hence, it is easy to see that the reactivity ρ can be related to the reactor period T using the following expression:

$$\rho = \frac{\omega}{k} + \sum_i \frac{\omega\beta_i}{\omega + \lambda_i} \tag{16.82}$$

or

$$\rho \cong \frac{1}{T} + \sum_i \frac{\beta_i}{1 + \lambda_i T} \tag{16.83}$$

where β is the delayed neutron fraction, and the summations are performed over all delayed neutron precursor groups from 1 to 6. Hence, for small reactivity changes and long reactor periods, the denominator reduces to $\beta_i/(1 + \lambda_i T) \rightarrow \beta_i/\lambda_i T$, and $\rho \cong 3600/T$. *In other words, the reactivity in Inhours becomes inversely proportional to the reactor period T*, and we can write

$$T \cong \frac{1}{C\rho} \tag{16.84}$$

where C = 1/3600 for a Uranium-235-fueled core. Obviously, the value of C is different for Pu-239 fuel than it is for U-235 fuel but the same basic equation applies as long as $\rho \cong 0$ and $k \cong 1$. *So, the definition of the reactivity depends on the type of fuel that is used, and because of this, the reactivity is not an immutable constant of nature like e, π, or even the natural logarithm ln is*.

Example Problem 16.7

Using the information presented in Example problem 16.6, what is the reactor period when ρ = 100 pcm?

Solution Since 1 pcm = 0.00001, 100 pcm corresponds to a reactivity of ρ = 0.001. From Table 16.5, the maximum positive reactivity is about 20¢, which means that the reactor period T (from Table 16.5) is 32 seconds. [Ans.]

16.15 Using the Reactor Period to Measure the Worth of a Control Rod

In any reactor it is important to understand the effect that the motion of a control rod has on the reactor period T. If we drop a control rod into the core, it absorbs excess neutrons, and if the reactor is initially critical with a power level P, the power level will be reduced after several prompt neutron lifetimes to new value of P′. Knowing the values of P and P′, we can then use the prompt jump or prompt drop approximations to infer the reactivity change Δρ that the control rod has induced. This reactivity change can then be used to infer the final reactor period T′. Normally, a perturbation of this type only disturbs the flux shape in the vicinity of where the control rod has been moved. If a control rod bank has a total of N individual rods, then the reactivity change *per rod* caused by dropping the entire bank into the core is −Δρ/N. *The control rod worth of an individual rod (see Chapter 20) is then seen to be*

$$W = \frac{\left|K'_{effective} - K_{effective}\right|}{K'_{effective}} \tag{16.85}$$

where $\rho' = \rho - \Delta\rho/N$. Notice that it is very simple to determine the worth of an individual rod in this case. We can illustrate how the process works by recalling that the initial power level P and the final power level P′ are related to each other by

$$P' = \frac{\beta(1-\rho')}{(\beta-\rho')} \cdot P \tag{16.86}$$

where ρ′ is the final reactivity (ρ′ = ρ + Δρ). If we solve for the reactivity insertion in terms of the initial and final power levels, we obtain

Relating the Change in the Reactivity Δρ to the Change in the Power Level ΔP

$$\Delta\rho = \beta\left(\frac{P}{P'-1}\right) \tag{16.87}$$

where ΔP = P′ − P. *The asymptotic period T can then be inferred by extrapolating how long it takes for P to become P′.* This prescription is sometimes called the "*rod drop method*," and it is commonly used to validate the theoretical predictions of more deterministic solutions to the point kinetics equations.

In practice, most measurements of the reactor period are performed by withdrawing a control rod from the core (instead of inserting it) and determining the effect that the withdrawal has on the value of ω = 1/T. Normally, the asymptotic period can be determined more accurately in this way because the value of the reactor period is not obscured by the presence of the longest-lived delayed neutron precursor decay chain (which contains the isotope Bromine-87). In other words, the accuracy of this process is greater when we try to measure a positive period instead of a negative one. Of course, it is very important for these experiments to be performed with reactivity changes well below the prompt critical limit (where ρ = β). These longer periods can then lead to very accurate estimates of ω_o since T = 1/ω when ω → ω_o.

Student Exercise 16.3

In the previous section, we learned that the reactor period T was related to the reactivity ρ for very small reactivity changes in an exactly critical system by an equation of the form T ≅ 1/cρ, where c = 1/3600. Using the knowledge you have just acquired, and the tables presented earlier in the chapter, calculate the value of c for (1) a Plutonium-239-fueled core and (2) for a Uranium-233-fueled core. Is the reactor period larger or smaller in each case? What would you propose to use to account for these changes if you were designing one of these reactors so that the reactivity could still be expressed in the units of dollars and cents?

16.16 Measuring the Point Kinetics Parameters

There are several methods for measuring the point kinetics parameters in Equation 16.24. These methods include (1) the *pulsed neutron source method*, (2) the *source jerk method* (the inverse of the rod drop method), and (3) the *rod oscillator method*. All three methods give acceptable results when a small change is made to the isotopic composition of the core. In addition, the pulsed source method can be used to find values for ρ/Λ. However, to take full advantage of its capabilities, we must know the value of β/Λ and the smallest root of the Inhour equation (ω_6). In particular, Duderstadt and Henry (refer again to the references at the end of the chapter) discuss the applications of the pulsed source method at a more detailed level. Each of these methods is also discussed in Sections 16.20, 16.21, 16.22, and 16.23.

Example Problem 16.8

During a rod calibration experiment, a bank of control rods is completely withdrawn from the core of a large thermal water reactor, and this results in a change in the core power level of 2%. If the reactor in which the control rod bank is withdrawn is fueled with Uranium-235, what is the overall change in the reactivity of the core? If the control rod bank contains 20 control rods, what is the worth of an individual rod?

Solution The reactivity increase may be found from the equation $\Delta\rho = \beta(\Delta P/P')$. For $\beta = 0.0065$ and $\Delta P/P' = 0.02$, the reactivity increase is $\Delta\rho = 0.0065 \times 0.02 = 0.00013$ (about 2 cents). The worth of an individual control rod is then 2 cents/20 or 1/10th of a cent. These values are relatively typical of the control rods that are used in pressurized water reactors (PWRs). [Ans.]

16.17 Other Applications of the Point Kinetics Equations

Earlier we explained how withdrawing a control rod from the core could be used to determine its worth from the asymptotic reactor period T. However, on may occasions, the worth of a control rod is known in advance, and so the role of the Inhour equation is to determine the reactor period from the change in the axial position of the rod. *In practice, most reactor transients happen very slowly because the maximum reactivity change (due to the motion of a single rod or even a bank of rods) is restricted by the control system to between 5 and 10 cents.*

For these particular transients, the power level changes by only a few percent per minute, and the prompt jump approximation can predict the incremental changes to the power level. Moreover, in most of these transients, the neutron flux shape $\phi(x, y, z, t)$ barely changes as a function of position through the core. Hence, we can often assume that the point kinetics equations can be used to find changes to the power level P(t) because the spatial flux shape $\phi(x, y, z)$ is effectively decoupled from the time-dependent behavior of the flux $\phi(t)$; that is, $\phi(x, y, z, t) = \phi(x, y, z) \cdot \phi(t)$. *The neutron flux shape simply stays in its fundamental mode which is determined by the lowest root of the Inhour equation*. Of course, this does not account for the effects of *temperature feedback*, which we will discuss in Chapter 17.

16.18 Examining the Validity of the Point Kinetics Approximation

In practice, the only time the accuracy of the point kinetics approximation comes into question is when a reactivity insertion exceeds the prompt critical limit ($\Delta\rho > \beta$). When this occurs the point kinetics equations can still be used to predict the overall behavior of the core, but the spatially dependent kinetics equations must then be solved to understand the behavior of the core on a more detailed level. For the most severe reactor transients (i.e., those caused by reactivity insertions on the order of \$5 or more), the power level changes so abruptly that some portions of the core may melt and lose their structural integrity more quickly than others. The molten portions may then reconfigure themselves into a different configuration than the original configuration.

These different internal configurations of the materials inside of the core can sometimes lead to what are known as *Hypothetical Core Disruptive Accidents* or *HCDAs*. In general, HCDAs are accompanied by very large temporary energy increases, which can be accompanied by an energetic disassembly of part of the core itself. Such hypothetical transients are usually classified as *class seven transients* on the *INES scale* of accident severity (see Chapter 21). Such severe transients, although their probability of occurrence is quite small (on the order of less than 1×10^{-6} per reactor operating year), must still be considered as part of any plant safety or regulatory analysis.

Today, the U.S. NRC uses a sophisticated computer program called *TRACE* to perform this type of analysis, although other accident analysis codes such as MAAP (see below) can be used to perform a similar function. For example, the Electric Power Research Institute (or EPRI) uses MAAP (which is an acronym for a Modular Accident Analysis Program) to simulate a severe reactor accident where the structural integrity of the core is compromised. In some of these scenarios, the molten material at the bottom of the pressure vessel becomes a simmering mass of fuel, metal, and other structural debris known as *Corium*. A picture of the corium pool in the lower plenum of the pressure vessel following the complete meltdown of a large PWR core is shown in Figure 16.11. The temperature profiles in the pool are also shown. Notice that the temperatures near the bottom of the pool approach 2500°C. If this material is ejected from the reactor pressure vessel or the Nuclear Steam Supply System, the results of a MAAP analysis can be supplemented by running another safety analysis program called *GOTHIC*. The combination of these three computer programs—TRACE, MAAP, and GOTHIC—then provides a reactor vendor with all the information that is required to simulate most HCDAs.

It is important to point out that HDCAs are not restricted to just thermal reactors or thermal water reactors. In fact, in many fast reactors, the liquid sodium coolant can boil during very fast and severe transients, and this boiling can sometimes lead to an energetic disassembly of the core. Obviously, analyzing these transients can be a very complicated business. The results of these simulations are then fed into other computer programs that turn the raw data into computer-generated movies (which are similar to the CGI videos that can be found on the Internet). Several of these movies are

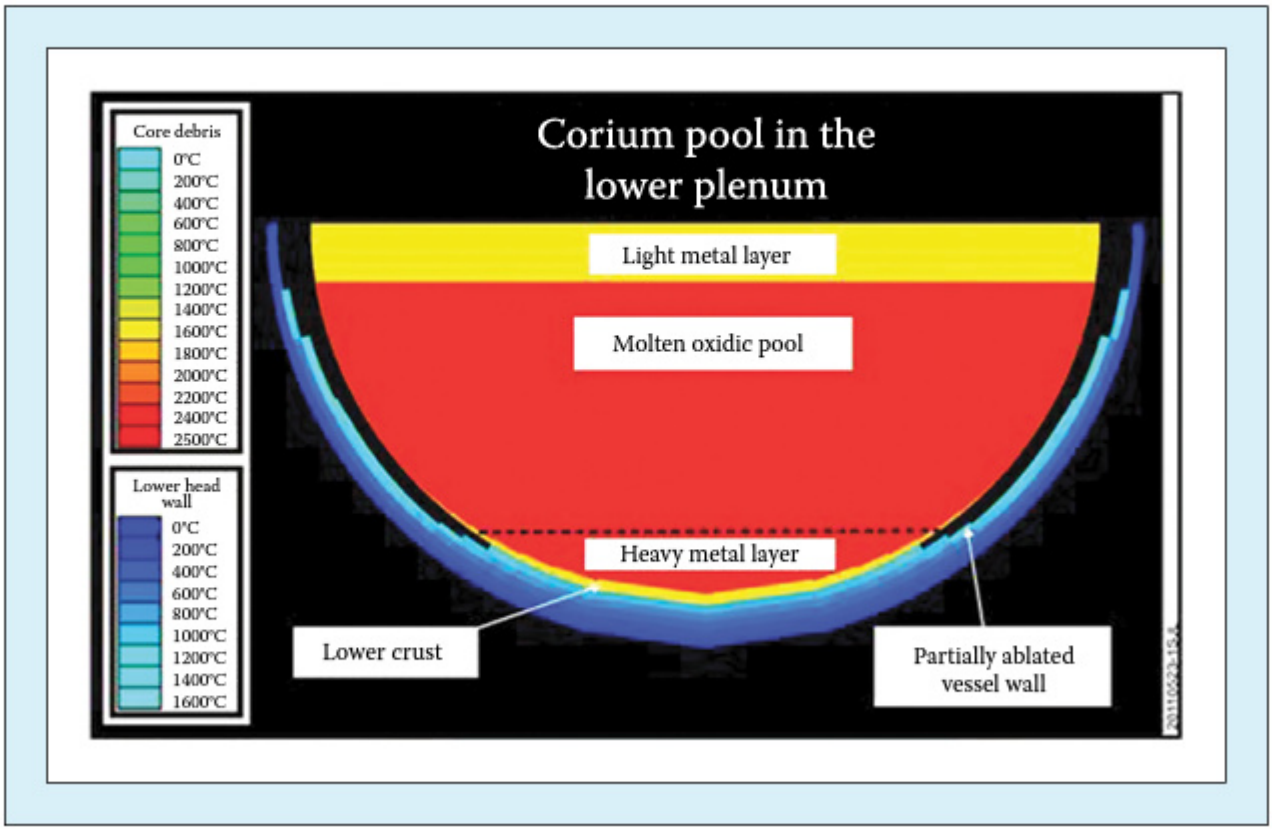

FIGURE 16.11 The corium pool at the bottom of a PWR pressure vessel following an HCDA in which all of the cooling to the core is lost. This HCDA was simulated using the MAAP computer program, which is owned, licensed, and administered by the Electric Power Research Institute. The MAAP program is available to nuclear utilities and other interested institutions on request. (The simulation above was provided by Fauske and Associates—see *http://www.fauske.com*.)

available from the NRC and from other National Laboratories and academic institutions. The *TRACE postprocessor* is also capable of generating some very nice interactive videos.

16.19 Estimating the Instantaneous Reactor Power Level as a Function of Time

Now let us turn out attention to how the power level responds to step changes in the reactivity (±). From our earlier discussion, there are several cases we would like to consider:

- Planned shutdown
- Emergency shutdown
- A reactor scram
- A supercritical transient
- A prompt supercritical transient

Each of these scenarios leads to a different expression for the reactor power level because the value of ρ that is used to model these transients is different. Since the time dependent power level P(t) is proportional to the neutron flux ϕ(t), we can determine the *instantaneous power level P due to fission alone* by replacing the value of the neutron flux in Equations 16.27, 16.28, 16.51, and 16.54 with the reactor power P. In this case, the instantaneous power level is

Instantaneous Power Level (due to Fission Alone) for a U-235-Fueled Thermal Water Reactor

$$
\begin{aligned}
&P(t) = e^{-t/85} && \text{(during a planned shutdown)} && \Delta\rho = -8 \text{ cents} \\
&P(t) = 0.87e^{-958t} + 0.130e^{-0.068t} && \text{(during an emergency shutdown)} && \Delta\rho = -\$7.7 \\
&P(t) = 0.87e^{-958t} + 0.13e^{-0.068t} && \text{(after a scram)} && \Delta\rho = -\$20 \\
&P(t) = -0.25e^{-100t} + 1.25e^{0.02t} && \text{(during a supercritical transient)} && \Delta\rho = +20 \text{ cents} \\
&P(t) = -2.9e^{-66.7t} - 1.9e^{-0.23t} && \text{(during a prompt supercritical transient)} && \Delta\rho = +\$2
\end{aligned}
\qquad (16.88)
$$

where the power level during steady-state operation is normalized to a value of 1.0. Then after the reactor has been operating for a while, radioactive fission products build up in the fuel rods, and they also produce a significant amount of *decay heat*.

Under normal conditions, this decay heat is equal to about 7% of the total heat that is generated in the core (see Chapter 6). The total time-dependent power level in each of these five cases is then the sum of the instantaneous power level (which is 93% of the total power level and can change rapidly with time) and the additional decay heat (which is 7% of the total power level and changes much more slowly). The total time-dependent power level P_{TOTAL} is then

$$P_{TOTAL}(t) = P_{FISSION}(t) + P_{DECAY}(t) \tag{16.89}$$

Plugging these values into the appropriate expressions given earlier, we find that the total time-dependent reactor power in each of these five scenarios is

Total Time-Dependent Power Level for a U-235-Fueled Thermal Water Reactor

$P(t) = 0.07 + 0.93e^{-t/85}$	(during a planned shutdown)	$\Delta\rho = -8$ cents
$P(t) = 0.07 + 0.93\left(0.87e^{-958t} + 0.130e^{-0.068t}\right)$	(during an emergency shutdown)	$\Delta\rho = -\$7.7$
$P(t) = 0.07 + 0.93\left(0.87e^{-958t} + 0.13e^{-0.068t}\right)$	(after a scram)	$\Delta\rho = -\$20$
$P(t) = 0.07 + 0.93\left(-0.25e^{-100t} + 1.25e^{0.02t}\right)$	(during a supercritical transient)	$\Delta\rho = +20$ cents
$P(t) = 0.07 + 0.93\left(2.9e^{66.7t} - 1.9e^{-0.23t}\right)$	(during a prompt supercritical transient)	$\Delta\rho = +\$2$

(16.90)

where the transients are assumed to begin at t = 0. The decay heat level only stays at about 7% for a short period of time, but during the first few minutes of a reactor transient, this is a reasonable assumption to make.

These equations can also be used to determine the power level for the first minute or so after a transient begins because the decay heat remains effectively constant during this period of time. After about a minute, the value of 0.07 becomes slightly smaller, and its actual value must be determined from what is known as the *Wigner–Way equation*, which is discussed in Chapter 11 of our companion book*:

The Wigner–Way Equation

$$\text{Decay heat}(t) = 0.0666P_o\left[t^{-0.2} - (t_o + t)^{-0.2}\right] \tag{16.91}$$

Here

P_o is the reactor power before shutdown

t_o is the time of operation (in seconds) before shutdown

Similar expressions can be derived for a reactor fueled with U-233 or Pu-239. In this case, we simply substitute the appropriate values of β into Equation 16.24. The values of A_1, A_2, ω_1, and ω_2 then become

$$A_1 = \frac{-\rho}{\beta - \rho} \quad \text{and} \quad A_2 = \frac{\beta}{\beta - \rho} \tag{16.92a}$$

and

$$\omega_1 = -\frac{\beta - \rho}{\Lambda} \quad \text{and} \quad \omega_2 = \frac{\lambda\rho}{\beta - \rho} \tag{16.92b}$$

The values of β to be used in these equations are found from Table 16.7. Thus, the value of β for U-233 is $\beta_{U\text{-}233} = 0.0026$ and the value of β for Pu-239 is $\beta_{Pu\text{-}239} = 0.0020$. *This implies that the number of delayed neutrons is only about one third*

* See *Nuclear Engineering Fundamentals: A Practical Perspective*, by R.E. Masterson, CRC Press (2017).

TABLE 16.7
Nuclear Properties of Uranium and Plutonium Fuel at a Thermal Energy of 0.025 eV

Isotope	Prompt Neutrons Produced per Thermal Fission (ν)	Delayed Neutron Fraction per Thermal Fission ($\beta = \nu_d/\nu$)	Decay Constant (λ = seconds^{-1})	Prompt Neutron Lifetime Λ (seconds)
U-233	2.49	0.0026	0.0690	~0.0001
U-235	2.42	0.0065	0.0767	~0.0001
Pu-239	2.87	0.0020	0.0718	~0.0001
Pu-241	2.92	—	—	

Note: Values of the prompt neutron lifetime Λ range from about 1×10^{-4} for very thermal reactors to 1×10^{-7} for very fast reactors. In computing the time-dependent power levels shown in Equations 16.88 and 16.89, a value of $\Lambda = 6 \times 10^{-5}$ seconds was used.

as great for Uranium-233 and Pu-239 as it is for U-235. Moreover, assume for the moment that we can use the same value for the prompt neutron lifetime Λ that designers use for commercial PWRs (about 0.00006 or $\Lambda = 6 \times 10^{-5}$ seconds).*

After doing so, we find that the values of A_1, A_2, ω_1, and ω_2 for a U-235-fueled thermal water reactor are

For a Thermal Water Reactor Fueled with U-235

$$A_1 = -\frac{\rho}{0.0065 - \rho} \quad \text{and} \quad A_2 = \frac{0.0065}{0.0065 - \rho}$$

and

$$\omega_1 = -\frac{0.0065 - \rho}{0.00006} \quad \text{and} \quad \omega_2 = \frac{0.0767\rho}{0.0065 - \rho} \tag{16.93}$$

Moreover, we find that the values of A_1, A_2, ω_1, and ω_2 for a U-233-fueled thermal water reactor are

For a Thermal Water Reactor Fueled with U-233

$$A_1 = -\rho/(0.0026 - \rho) \quad \text{and} \quad A_2 = 0.0026/(0.0026 - \rho),$$

and

$$\omega_1 = -(0.0026 - \rho)/0.00006 \quad \text{and} \quad \omega_2 = 0.0690\,\rho/(0.0026 - \rho) \tag{16.94}$$

and the comparable values for a Pu-239-fueled thermal water reactor are

For a Thermal Water Reactor Fueled with Pu-239

$$A_1 = -\frac{\rho}{0.0020 - \rho} \quad \text{and} \quad A_2 = \frac{0.0020}{0.0020 - \rho}$$

and

$$\omega_1 = -\frac{0.0020 - \rho}{0.00006} \quad \text{and} \quad \omega_2 = \frac{0.0718\rho}{0.0020 - \rho} \tag{16.95}$$

Thus the values of the delayed neutron fraction β and the reactivity ρ determine the magnitude of A_1 and A_2, while the delayed neutron fraction β and the prompt neutron lifetime Λ determine the value of ω_1. The value of the second root, ω_2, is determined by the delayed neutron fraction β and the value of the delayed neutron time constant λ. *Now suppose we apply the same logic to a fast reactor fueled with Pu-239. In this case, the prompt neutron lifetime is about 1000 times*

* From Henry, A.F., *Nuclear Reactor Analysis*, MIT Press, Cambridge, MA, 1975.

shorter, and so an appropriate value to use is $\Lambda = 1 \times 10^{-7}$ *seconds*. So, the values of A_1, A_2, ω_1, and ω_2 for a typical sodium-cooled fast breeder reactor are

For a Fast Reactor Fueled with Pu-239

$$A_1 = -\frac{\rho}{0.0020 - \rho} \quad \text{and} \quad A_2 = \frac{0.0020}{0.0020 - \rho}$$

and

$$\omega_1 = -\frac{0.0020 - \rho}{0.0000001} \quad \text{and} \quad \omega_2 = \frac{0.0718\rho}{0.0020 - \rho} \tag{16.96}$$

Clearly, this reactor is more difficult to control because the value of the first root, ω_1, is larger. The equations we have presented can be used to simulate any reactor transient where the shape of the neutron flux does not change rapidly with time. In other words, they can be used to find the time-dependent power level whenever the *point kinetics approximation* is valid. As we discussed in Section 16.17, the only time that the accuracy of the point kinetics equations comes into question is when a reactivity insertion exceeds the prompt critical limit ($\Delta\rho > \beta$). Then the point kinetics equations can still be used to perform a parametric analysis, but the spatially dependent kinetics equations must ultimately be solved to validate the results of the simpler point kinetics models.

Example Problem 16.9

Earlier in the chapter, we discussed a prompt critical transient for a U-235-fueled thermal water reactor with a reactivity insertion of 20 cents (+0.20 β). We found that the time-dependent neutron flux and the delayed precursor concentrations obeyed the equations:

$$\phi(t) = -0.25e^{-100t} + 1.25e^{0.02t}$$

$$C(t) = 0.31e^{-100t} + 1563e^{0.02t}$$

Part 1: What is the value of the $\phi(t)$ and $C(t)$ immediately after the transient begins?

Part 2: Suppose that we conduct a nearly identical experiment in which the reactivity of the system is increased in a stepwise manner by 5 cents (+0.05 β) rather than by 20 cents. What do the corresponding equations for $\phi(t)$ and $C(t)$ look like in this case?

Part 3: Plot the neutron flux for each case for the first 100 seconds after the transient begins. What is the value of the reactor period T in each case?

Solution Part 1: A few milliseconds after the transient begins, the neutron flux jumps by 25% to a value of 1.25, while the delayed precursor concentration is approximately 1563.

Part 2: When the reactivity insertion is +5 cents instead of +20 cents, the equations for the time-dependent flux and precursor concentrations become

$$\phi(t) = -0.05e^{-36t} + 1.05e^{0.004t}$$

$$C(t) = 0.05e^{-36t} + 1412e^{0.004t}$$

Notice that the value of C(t) barely changes (it goes from 1563 to 1412) while the neutron flux jumps by 5% during the first few milliseconds.

Part 3: In this case, the reactor period increases from 50 seconds to about 250 seconds. (It takes about a minute for the power level to increase by 20%.) A plot of the neutron flux for each transient is shown in Figure 16.12. Clearly, for a thermal water reactor, there is a strong incentive to limit any reactivity increases to five cents or less. [Ans.]

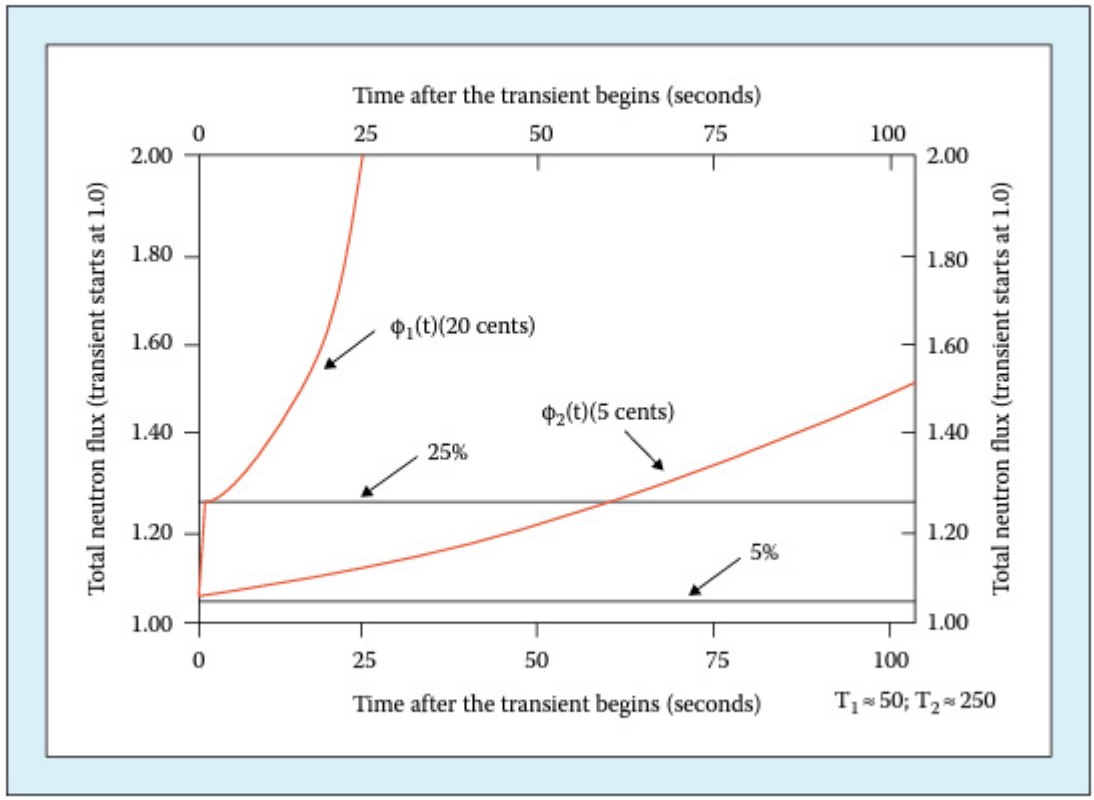

FIGURE 16.12 Comparing the behavior of the neutron flux during a transient where the reactivity is increased by 20 cents to a transient where the reactivity is increased by 5 cents. The first transient has a reactor period T of about 50 seconds, while the second transient has a reactor period T of about 250 seconds. If the reactivity was increased by 1 cent, the neutron flux (not shown) would slowly increase to about 110% of its steady-state value in about 2 minutes (~120 seconds). In the absence of thermal feedback (see Chapter 17), the reactor power level would follow almost exactly the same trend.

Example Problem 16.10

Suppose that a thermal water reactor is fueled with a mixture of U-235 and U-238. Using the information presented earlier in the chapter, estimate the asymptotic period for this reactor when the system-wide reactivity is increased from $\rho = 0$ to $\rho = 0.001$ (i.e., by an amount equal to one milli-rho) for a fresh core.

Solution According to Table 16.1, the asymptotic reactor period for a U-235-fueled reactor is given by $T = 0.084/\rho$. When $\rho = +0.001$, the asymptotic period will be $T = 0.084/0.001 = 84$ seconds. [Ans.]

16.20 Ways to Measure the Point Kinetics Parameters

When a reactor core contains several different types of nuclear fuel is not always obvious what the correct values for Λ, β, and λ should be. These values can either be guesstimated, or they can be determined experimentally. Normally they are measured experimentally using one of the three methods we discussed previously. These methods are

1. The rod drop method
2. The rod oscillator method
3. The pulsed neutron method

In this section, we would like to briefly discuss each of these methods and show how they can be used. Let us first consider the rod drop method.

16.21 The Rod Drop Method

The *rod drop method* is perhaps the oldest and most widely used method for estimating the reactivity of a control rod. Like the other methods we will discuss, it involves making a small perturbation to the material composition of the core. If we start with an initially critical core, we can measure the stable or asymptotic reactor period T after this perturbation occurs. This then provides us with a relationship between the reactivity ρ and the reactor period T.

The most straightforward way to perform a rod drop experiment is to simply drop a control rod into the center of the core. Using the Inhour equation, we can then infer the *worth* of the rod by measuring the asymptotic reactor period T. Normally the worth of the rod corresponds to the observed reactivity change. Usually this is done by dropping a single control rod, but it can also be done by dropping a bank of control rods as well. In commercial power reactors, these control rods are sometimes called *shutdown rods*. The reactor period is then determined by the longest-lived delayed neutron precursor group (group 1), which happens to contain Bromine-87. In principle, we can also measure the reactor period by withdrawing the same rod suddenly (see Chapter 20), and watching the power level rise. This approach is sometimes called a *rod ejection event*. Normally, this second approach is more accurate than the first because the reactor period is determined by the shortest delayed neutron precursor group (group 6). Since this group contains short-lived radioactive isotopes such as Iodine-142, Bromine-92, Rubidium-95, and Rubidium-97, the overall error is less when we withdraw a control rod than when we insert one. The reactor period in this case is called a *positive period*. Conversely, inserting a control rod results in what is called a *negative period*. Thus the rod drop method always causes the reactor period to be negative.

Consider a hypothetical reactor that has been operating at constant power for several days. The reactor is in a stable state with a reactivity of $\rho = 0$ and an equilibrium power of $P = P_0$. Suppose that some negative reactivity $-\Delta\rho$ is suddenly introduced into the core by dropping a control rod. After a few neutron lifetimes, the power level will drop from P_0 to a lower power P_1, and it will continue to remain at this reduced level until it is ultimately decreased by more delayed neutron precursor decay. If the initial reactivity is zero, we can use the prompt jump (and drop) approximations to write

$$\frac{P_1}{P_0} = \frac{\beta}{\beta + \Delta\rho} \tag{16.97}$$

If we rearrange Equation 16.97 slightly, we discover that

The Control Rod Worth

$$w = \frac{\Delta\rho}{\beta} = \frac{P_0}{P_1} - 1 \tag{16.98}$$

where now w is the *worth* of the control rod. Hence we can infer the reactivity insertion in dollars and cents from the value of $\Delta\rho/\beta$. To determine the value for P_1, we simply need to know the power level a short time after the rod has been dropped into the core. Normally this is between half a second and one second after the rod has reached its final position.

Example Problem 16.11

Suppose that we drop an isolated control rod into the core of a light water reactor in order to determine the worth of the rod. If the power level immediately before dropping the rod is 100 MW and the power level immediately after dropping the rod is 99 MW, what is the worth of the rod in dollars and cents?

Solution According to Equation 16.98, the worth of the rod is $|w| = \Delta\rho/\beta = (P_0/P_1) - 1 = (100/99) - 1 = 1.01 - 1 = 0.01$. Hence the control rod has an overall worth of about 1 cent. [Ans.]

16.22 The Rod Oscillator Method

The *rod oscillator method* is an alternative method that is often used to measure the *prompt neutron lifetime* Λ, or the worth w of an oscillating rod. In future chapters we will learn that when we move a control rod up and down with a periodic frequency ω, the prompt neutron lifetime and the rod worth $|w| = \Delta\rho$ are related by

$$|w| = \Delta\rho = \omega\Lambda\left(\frac{\Delta P}{P_0}\right) \tag{16.99}$$

Thus if we know the value of Λ and the frequency of oscillation ω, we can solve Equation 16.99 for the rod worth $|w| = \Delta\rho$. Conversely, if the worth of the rod is known, we can solve Equation 16.99 for the prompt neutron lifetime Λ. The rod oscillator method can also be used to determine the stability of a reactor.

16.23 The Pulsed Neutron Source Method

One final way to measure the point kinetics parameters is to use what is known as the *pulsed neutron source method*. Using this method, the transient behavior of the neutron population is measured immediately after injecting a burst of neutrons into the core. These neutrons are usually provided by an *external neutron source*. The resulting neutrons can be either fast neutrons or thermal neutrons, and the fuel assembly into which they are injected can be either a multiplying or non-multiplying one. If all of the neutrons have the same speed, we can write the one group neutron diffusion equation as

$$\left(\frac{1}{v}\right)d\phi/dt = D\nabla^2\phi(\mathbf{r},t) + (v\Sigma_f - \Sigma_a)\phi(\mathbf{r},t) \tag{16.100}$$

where the neutron velocity v is not to be confused with the average number of neutrons released per fission ν (mu). At $t = 0$ assume that the neutron flux is given by $\phi(\mathbf{r}, 0) = \phi_0(\mathbf{r})$. Then for very long time frames, it can be shown that the neutron flux $\phi(\mathbf{r}, t)$ in the fuel assembly will approach an asymptotic value of the form

$$\phi(\mathbf{r},t) = a_1\phi_1(\mathbf{r})e^{-\alpha t} \tag{16.101}$$

where $\phi_1(\mathbf{r})$ is the *fundamental mode* of the fuel assembly (which is geometry dependent), and

$$\alpha = v\left(v\Sigma_f - \Sigma_a + DB_G^2\right) \tag{16.102}$$

Here B_G^2 is the geometric buckling of the flux, and $\phi_1(\mathbf{r})$ is the flux shape corresponding to the *fundamental mode* (see Chapter 13). If we plot the value of α against the geometric buckling, we can produce the curves shown in Figure 16.13.

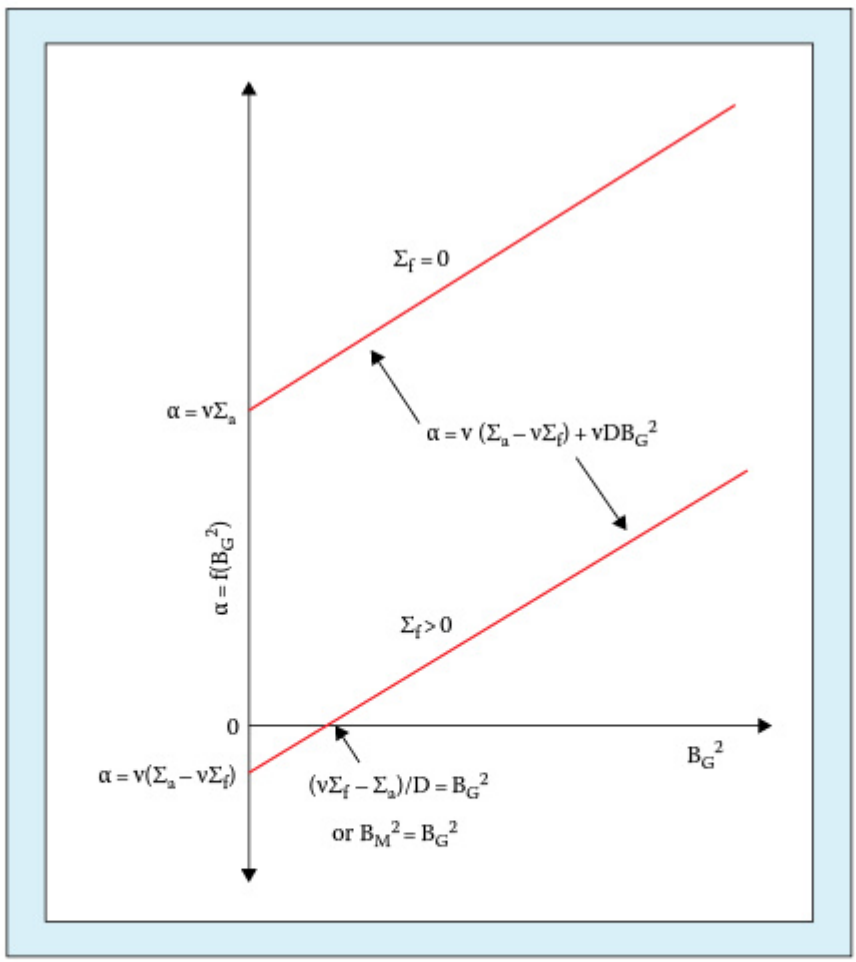

FIGURE 16.13 The decay constant α as a function of the geometric buckling in a pulsed neutron source experiment for both multiplying and non-multiplying fuel assemblies.

This technique can be used to obtain accurate results as long as the neutron injection process is performed over a time frame that is short compared to the lifetimes of the delayed neutrons. Moreover, we know that when the pulse is extremely short, the value of α is related to the values of the one group flux and the reactor power level by

$$\alpha = \left(\frac{1}{\phi}\right) d\phi/dt = \left(\frac{1}{P}\right) dP/dt = \frac{\rho - \beta}{\Lambda} \tag{16.103}$$

Hence the value of α can be used to infer the value of ρ, provided that the values of Λ and β are known. Conversely, if we maintain the core in a critical state (with $\rho = 0$), the pulsed neutron source method can also be used to measure the value of β/Λ since

$$\alpha = -\frac{\beta}{\Lambda} \tag{16.104}$$

Note that we require only the material composition of the core and the geometric buckling of the flux to arrive at this ratio.

16.24 Reactor Noise Analysis

Finally, all reactors make a great deal of statistical "noise" when they are operating. This noise can take the form of small random fluctuations in the power level, the neutron flux, or even the flow rate about a statistical average or *mean*. This *random noise* is no different than the random velocity fluctuations in a turbulent flow field. These random fluctuations are shown in Figure 16.14. In this section, we would like to discuss some of the sources of this noise, and illustrate how this noise can be used statistically to obtain additional information about the state of a reactor. This will require us to introduce some additional concepts that we have not encountered before, but these will be covered in more detail in our follow-on book.*

Earlier, we treated the process of neutron diffusion as a deterministic one when in fact it is a statistical one. By this we mean that we cannot predict exactly where an individual neutron will go. We can only predict the *probability* that a neutron will go in a particular direction with a particular speed. Similarly, we find that the reactor power level fluctuates randomly about the values implied by the point kinetics equations. However, at very low power levels, these statistical fluctuations become even more significant than they do at higher power levels because of the mechanical vibrations of the fuel rods, the boiling of the coolant, and random instabilities in the flow field that are induced by turbulent eddies and other stochastic effects. Regardless of the source of this noise, reactor noise is important to the study of reactor dynamics for a number of reasons.

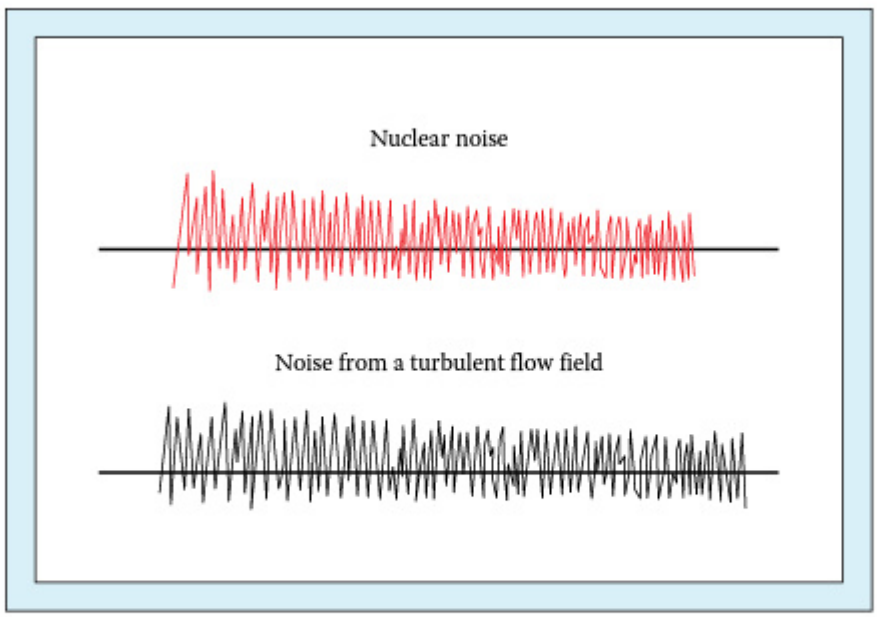

FIGURE 16.14 The noise in a turbulent flow field and the "noise" that can occur in a reactor while it is being operated.

* See *Contemporary Nuclear Reactor Physics with an Introduction to Reactor Dynamics, Computational Methods, and Nuclear Particle Transport,* by R.E. Masterson, CRC Press (2020).

First, it affects the precision that we can measure the flux or power levels because must extract these values out of the background noise. Secondly, the level of this noise (and its frequency) tells us something about how the core is behaving as a whole. For example, if the amount of noise increases but the frequency of the noise remains the same, this usually implies that the reactor power level is increasing and the flow rate is increasing as well. However, if the frequency of the noise starts to change and develops an unusual number of harmonics, the flow field may be starting to oscillate or become unstable. In BWRs, this occurs when the power level stays the same but the flow rate is reduced. In other words, these oscillations begin to develop when the power to flow ratio becomes higher than it should, and the coolant begins to boil. These undesirable power to flow ratios are sometimes quantified using what are known as *operating maps*. Operating maps are discussed in Chapter 14 of our companion book.*

For these reasons and others, instruments inside the core must measure the *average* values of certain reactor parameters (such as the temperature, the flow rate, the flux, and the power), and the deviation of these parameters from a statistical average or mean. If the variance or standard deviation of this high level noise exceeds the expected values that are programmed into the control system, then this is an indication that the reactor is behaving abnormally or that the power and flow fields are about to change. *In other words, by sampling changes in the magnitude and the frequency of this noise, we can predict what the reactor is likely to do next.*

Similarly, one can vary the reactivity in a random manner about an average value or mean and measure the corresponding fluctuations in the power level or the flux. With these measurements, one can then infer both the *gain* and the *phase* of the *closed loop transfer function* that the control system uses to link changes in the power level to changes in the reactivity. Similarly, an additional closed loop transfer function can be developed to link changes in the level of the neutron flux to changes in the flow rate. Normally this requires a form of *signal processing* that involves the use of an auto correlation function and a cross correlation function.

The autocorrelation function F_{xx} of a time-dependent variable such as x(t) is defined as one which obeys the following equation

$$F_{xx}(\Delta t) = \left(\frac{1}{2T}\right)\int_{-T}^{T} x(t)x(t+\Delta t)dt \quad \lim T \to \infty \tag{16.105}$$

where

Δt is a small time increment that is essentially an offset from the original time t

T is the interval over which the correlation is to be performed

Similarly, we can define the *cross-correlation* between two time dependent functions x(t) and y(t) with the equation

$$F_{xy}(\Delta t) = \left(\frac{1}{2T}\right)\int_{-T}^{T} x(t)y(t+\Delta t)dt \quad \lim T \to \infty \tag{16.106}$$

where the same terminology applies. For example, if x(t) happens to be the reactivity $\rho(t)$, and y(t) happens to be the power P(t), we can use the character of the reactor noise to establish a practical relationship between them. From this relationship we can then obtain the gain G and the phase φ of the transfer function that links changes in the time dependent reactivity $\rho(t)$ to changes in the time dependent power level P(t). Similar transfer functions can be developed to correlate changes in the time dependent reactor power level P(t) to changes in the time dependent mass flow rate $\dot{m} = dm/dt$. In other words, all of these correlations can be inferred from the noise that is naturally present in an operating reactor. References 5 and 8 at the end of the chapter discuss how these correlations can be developed from a signal processing perspective. This subject is also discussed in more detail in our follow-on book.†

References

Books and Textbooks

1. Ash, M. *Nuclear Reactor Kinetics*, McGraw-Hill, New York (1965).
2. Henry, A.F. *Nuclear Reactor Analysis*, MIT Press, Cambridge, MA (1975).

* See *Nuclear Engineering Fundamentals: A Practical Perspective,* by R.E. Masterson, CRC Press (2017).

† See *Contemporary Nuclear Reactor Physics with an Introduction to Reactor Dynamics, Computational Methods, and Nuclear Particle Transport*, by R.E. Masterson, CRC Press (2020).

3. Keepin, G.R. *Physics of Nuclear Kinetics*, Addison-Wesley, Reading, MA (1965).
4. Stacey, W.M. *Nuclear Reactor Physics*, 2nd edn., John Wiley & Sons, New York (2007).
5. Duderstadt, J. and Hamilton, L. *Nuclear Reactor Analysis*, John Wiley & Sons, New York (1976).
6. Lewis, E. *Fundamentals of Nuclear Reactor Physics*, Academic Press, Boston, MA (2008).
7. Clark, M. and Hansen, K. *Numerical Methods of Reactor Analysis*, Academic Press, New York (1964).
8. Hetrick, D.L. *Dynamics of Nuclear Reactors*, American Nuclear Society, La Grange Park, IL (1993).
9. Schultz, M.A. *Control of Nuclear Reactors and Power Plants*, 2nd edn., McGraw-Hill, New York (1961).
10. Lamarsh, J.R. and Baratta, A.J. *Introduction to Nuclear Engineering*, Prentice Hall, Upper Saddle River, NJ (2001).
11. Glasstone, S. and Sesonske, A. *Nuclear Reactor Engineering*, 3rd edn., Van Nostrand Reinhold, New York (1981).
12. Lamarsh, J.R. *Introduction to Nuclear Reactor Theory*, second printing, Addison-Wesley Publishing Company, Inc., Reading, MA (1972).
13. Glasstone, S. and Eedlund, M. *The Elements of Nuclear Reactor Theory D*, Van Nostrand Company, Inc., New York (1952).
14. Shultis, K. and Faw, R. *Fundamentals of Nuclear Science and Engineering*, 2nd edn., CRC Press, Boca Raton, FL (2008).
15. Masterson, R.E. *Nuclear Engineering Fundamentals: A Practical Perspective*, CRC Press, Boca Raton, FL (2017).

Web References

1. *http://sizes.com/units/inhour.htm*.
2. *http://www.hindawi.com/journals/stni/2013/261327/*.
3. *https://www.euronuclear.org/e-news/e-news-14/pwr.htm*.
4. *https://canteach.candu.org/Content%20Library/19750105.pdf*.
5. *http://ocw.mit.edu/courses/nuclear-engineering/22-091-nuclear-reactor-safety-spring-2008/lecture-notes/MIT22_091S08_lec03.pdf*.
6. *http://ansn.iaea.org/Common/documents/Training/TRIGA%20Reactors%20(Safety%20and%20Technology)/chapter2/physics221.htm*.

Additional References

- Important physical constants used by nuclear scientists and engineers can be found in *Appendix A*.
- Unit systems and their conversion factors can be found in *Appendix B*.
- Nuclear cross sections for many important nuclear materials can be found in *Appendix C*.
- Physical properties of important nuclear materials can be found in *Appendix D*.
- Atomic masses, half-lives, and natural abundances can be found in *Appendix E*.
- Delayed neutron emitters are their properties are discussed in *Appendix F*.

Questions for the Student

The following questions cover the material presented in this chapter and, in some cases, previous chapters as well. They are designed to test how well the student has acquired a working knowledge of the subject matter.

1. The reactivity of a control rod in a thermal water reactor is 100 pcm. What is its reactivity in dollars and cents when the reactor is fueled with enriched uranium?
2. What specific set of assumptions is needed to derive the Inhour equation for a time-dependent reactor?
3. Write an expression for the reactor period T when a reactor does not contain any delayed neutrons. Is the reactor period longer or shorter in this case?
4. What specific variables in the neutron diffusion equation does the point kinetics approximation attempt to separate?
5. Under what specific set of conditions is an analytical solution to the Inhour equation with one delayed neutron group possible?
6. Name four methods that can be used to determine the worth of a control rod.
7. Which of the following isotopes (U-233, U-235, or Pu-239) produces the most delayed neutrons and which one produces the least?
8. Earlier in the chapter we learned that the asymptotic period $T\infty$ of a fast reactor is entirely different than it is for a thermal reactor for exactly the same change in the reactivity when the change in the reactivity $\rho = \Delta\rho$ is small. Suppose that a thermal water reactor is fueled with U-235 and a fast reactor is fueled with Pu-239. For a small positive values of the reactivity, approximately how many times longer is the asymptotic period in the thermal reactor? What is the reason for such a large difference?
9. What is the name of the radioactive decay process that eventually leads to the production of the delayed neutrons that are used to control a reactor core?
10. Name at least six fission products that will eventually produce the delayed neutrons that are needed to make a reactor more stable.
11. How long does it take for a typical delayed neutron to appear after a uranium or plutonium nucleus splits apart? In most common models of time-dependent rector behavior, what is the range of times between the minimum time when a delayed neutron may first appear and the maximum time when a delayed neutron may first appear?
12. How quickly does a prompt neutron appear from the same atomic nucleus after it splits apart?
13. The exponential constant e can be found in the solutions to many partial differential equations, and it frequently appears in the solutions to the point kinetics equations. What is the numerical value of this constant to five decimal places? Is it greater than or less than π?
14. The reactor power level declines by a factor of 1/e after a control rod is inserted into the core. If it takes 200 seconds for the reactor power to reach this level, what is the reactor period T?
15. When measuring the point kinetics parameters experimentally, what method can be used to determine an accurate value for ρ/Λ?
16. What root in the solution to the point kinetics equations is extremely sensitive to the value of the prompt neutron lifetime Λ?
17. On average, how many prompt neutrons are released from the thermal fission of Uranium-235?
18. If a fissionable material has an average neutron yield of 2.5 neutrons, and the delayed neutron fraction is 0.006, how many delayed neutrons does it produce per fission?
19. On average, is the delayed neutron fraction higher in a fast reactor or a thermal reactor?
20. Suppose that a nuclear scientist decides to introduce 1 Inhour of additional reactivity into a reactor lattice that is exactly critical. After this additional reactivity is added to the lattice, what will the period T of the lattice be?
21. In practice, what is the only time that the accuracy of the point kinetics equations comes into question?
22. Because of differences in the delayed neutron fraction, which type of reactor is easier to control? A fast reactor or a thermal one?
23. What root in the solution to the point kinetics equations is extremely sensitive to the value of the decay constant λ for the delayed neutron precursors?
24. The period of a thermal water reactor with delayed neutrons is 120 seconds. If a control rod is inserted into the core, and the core is exactly critical, what will the power level be 120 seconds after the control rod reaches the bottom of the core? Assume that the reactor power level before the control rod is inserted is 2000 MW thermal.
25. What important physical parameters determine the value of the coefficients A1 and A2 that appear in the point kinetics equations for the time-dependent reactor power P(t) and the time-dependent neutron flux $\phi(t)$?
26. In the point kinetics equations, what does the symbol Λ refer to? What is the difference in the size of the prompt neutron lifetime between a fast reactor and thermal reactor?
27. What contribution did Robert Keepin make to the field of time-dependent reactor behavior?

28. What important physical parameters determine the size of the roots ω_1 and ω_2 that appear in the point kinetics equations for the time-dependent reactor power P(t) and the time-dependent neutron flux $\phi(t)$?
29. An engineer decides to perform a rod drop experiment where the initial and final power levels are 10 and 8 MW, respectively. If the reactor is fueled with U-235, what is the value of the reactivity change caused by dropping the control rod into the core?
30. What is the formal definition of the Inhour?
31. Write down the Inhour equation for a thermal water reactor with only one delayed neutron group. In the limit of very small values of the reactivity (i.e., large reactor periods), write down a simplified expression for the Inhour equation that is less complicated than the original one.
32. Approximately how much reactivity does a dollar of reactivity refer to, and how much reactivity is equivalent to one nile?
33. The decay heat that is produced in a reactor's fuel rods (and in spent nuclear fuel) is caused by a very specific type of decay process. What is this decay process called?
34. Suppose that the period T of a thermal water reactor with delayed neutrons is 90 seconds. If a control rod is withdrawn from the core, and the core is exactly critical, what will the power level be 90 seconds after the control rod is withdrawn? Assume that the reactor power level before the control rod is withdrawn is 1000 MW thermal.
35. While certain forms of beta decay are very common in spent nuclear fuel, another type of radioactive beta decay is very common in the cores of very large stars. What is this second type of beta decay called? Does it occur very frequently in nuclear fuel rods so that it can be used to release additional delayed neutrons?
36. What are the two basic assumptions that are used to derive the prompt jump approximation?
37. Under what set of conditions does a reactor become prompt critical?
38. Does the asymptotic reactor period T depend on the value of Λ—the prompt neutron lifetime?
39. What is the appropriate value of the prompt neutron lifetime Λ to use when designing a fast breeder reactor?
40. A control rod is withdrawn from a reactor core that is initially critical. If the reactor core is fueled with U-233, and the worth of the control rod is 1 cent, what is the power level after the rod is fully withdrawn if the power level before the rod is withdrawn is 100 MW?
41. Why does the delayed neutron fraction β change from one type of reactor to the next?
42. Which type of nuclear fuel has the highest delayed neutron fraction and what type has the lowest?
43. A reactor operator decides to withdraw a control rod from a commercial power reactor that is exactly critical. If the reactor period is 100 seconds, and the initial power level is 1000 MWE, what will the power level be after 50 seconds?
44. During a very fast reactor transient, what assumption can we generally make about the delayed neutron precursor concentration C?
45. Write down an expression for the asymptotic reactor period T using the point kinetics parameters β, λ, and ρ.
46. Does the instantaneous reactor period T depend on the value of λ—the decay constant for the delayed neutron precursors?
47. Write down an expression for the time-dependent neutron flux shape $\phi(x,t)$ in a bare homogeneous slab reactor of width L.
48. What is the relationship between the smallest root ωMIN of the Inhour equation and the reactor period T?
49. A thermal water reactor and a fast breeder reactor are to be both fueled with plutonium dioxide fuel, which consists primarily of Pu-239. For the same concentration of the Pu-239, and the same value of ρ, approximately how many times larger is the first root $\omega 1$ in the point kinetics equations for the fast reactor than it is for the thermal reactor?
50. What is the definition of the reactor period T?
51. Write down the Inhour equation for a fast reactor with six delayed neutron groups. Is the reactor period T a function of the prompt neutron lifetime Λ in this case?
52. A thermal water reactor fueled with U-235 undergoes a sudden reactor scram. If the power level before the scram is 1000 MWT, what is the power level 1/10th of 1 second after the scram? Neglect the decay heat in the fuel rods when estimating the final power level.
53. Estimate the amount of time it takes for the power level in a thermal water reactor with a period of 1000 seconds to increase by 10%.
54. Using the point kinetics equations with a single delayed neutron precursor group, estimate the reactor period T for positive reactivity insertions of +1 cent, +2 cents, +3 cents, +4 cents, and +5 cents. Assume that the reactor is a U-235-fueled thermal water reactor.
55. Using the point kinetics equations with a single delayed neutron precursor group, estimate the reactor period T for negative reactivity changes of −1 cent, −2 cents, −3 cents, −4 cents, and −5 cents. Assume that the reactor is a U-235-fueled thermal water reactor.
56. Suppose that you were put in charge of designing a fast reactor where the delayed neutron fraction was 0 (i.e., $\beta = 0$). What would be the value of the two roots that appear in the point kinetics equations under these conditions?

57. Write an expression for the total neutron yield ν, and use this to derive an expression for the delayed neutron fraction β.
58. Generally speaking, what is the only time when the delayed neutron fraction can exceed a value of about 0.0065? What type of fuel must be used for this to happen?
59. Illustrate how the separation of variables method can be used to derive the time-dependent reactor kinetics equations.
60. Suppose that a thermal water reactor that uses enriched uranium is scheduled to be shutdown for routine refueling. A reactor operator inserts a control rod bank into the core to reduce the reactivity by 7.7 cents. Approximately how long will it take for the reactor power level to decrease by a factor of 1/e?
61. In principle, can more than six delayed neutron precursor groups be used to describe the time-dependent delayed neutron population, and if so, how many groups represent a significant improvement over the standard model in this area?
62. A research reactor has been in operation for 100 days. Immediately before the reactor is scrammed, what percentage of the power in the core is being produced by the process of radioactive decay?
63. Write down an expression for the instantaneous reactor period T using the point kinetics parameters β, λ, Λ, and ρ.
64. How long does it take for the power level in a thermal water reactor with a period of 250 seconds to increase by 20%?
65. When delayed neutrons were first discovered, a decision was made to represent the production rate of the delayed neutrons $S_d(t)$ by the sum of seven exponential terms (see Chapter 15) rather than by a polynomial of the form $S_d(t) = at + bt_2 + ct_3 + dt_4$. Why do you think that this particular decision was made?
66. A bank of control rods contains 25 individual control rods, and each control rod has a maximum worth of 0.2 cents. In a rod drop experiment, the reactor power level declines by 83% in 100 seconds. If the same bank of control rods was withdrawn from an exactly critical core, by what percentage would the reactor power level increase in 50 seconds?
67. Suppose that you are suddenly put in charge of designing a commercial pressurized water reactor. What value would you use for the prompt neutron lifetime Λ to obtain the correct values for the other terms in the point kinetic equations?
68. Fill in the following expression with the appropriate word or phrase: The reactor period T is defined as the amount of time required for the neutron flux to increase by a factor of _____ or decrease by a factor of _____.
69. Write down an expression for the prompt jump approximation J. Up to what value of ρ is the prompt jump approximation generally considered to be valid?
70. Suppose that the reactivity of a critical reactor core is changed from $\rho \approx 0$ to $\rho = -0.0005$ (a change of about 8 cents) in a mostly stepwise manner by inserting several control rods into the core. What type of nuclear fuel must be used to create this particular effect?
71. Approximately what percentage of the total power P(t) that is generated in a nuclear power plant can be described by the point kinetics equations alone?
72. If you were put in charge of operating a commercial nuclear power plant, what would be the allowable values for the reactivity that you would want to use to operate the plant?
73. What is the reactor period T when the reactivity is +5 cents, and what is the reactor period when the reactivity is +1 cents. Assume the reactor is a U-235-fueled thermal water reactor.
74. Why are most important measurements of the asymptotic reactor period made by withdrawing a control rod from the core rather than inserting one?
75. Using the prompt jump approximation, compare and contrast the size of the prompt jump for positive reactivity insertions of +1 cent, +2 cents, +3 cents, +4 cents, and +5 cents. Assume that the reactor is a U-235-fueled thermal water reactor.
76. A control rod in a gas-cooled reactor has a reactivity of 0.001 niles. What is the reactivity of 20 of these control rods in pcm? What is a cluster of 10 or 20 of these control rods sometimes called?

Exercises for the Student

Exercise 16.1

Many times the point kinetics equations are written in terms of the neutron density n(t) instead of in terms of the neutron flux $\phi(t)$. Using the fact that $\phi(t) = v \cdot n(t)$ for just a single energy group, prove that the point kinetics equations can also be written as

$$dn/dt = \left[\left(\rho - \beta\right)/\Lambda\right] \cdot n + \sum_i \lambda_i C_i(t) \quad (\text{for } i = 1, \ldots, 6)$$

and

$$dC_i/dt = \beta_i/\Lambda \cdot n - \lambda_i C_i(t)$$

Is it theoretically possible to use the same approach to understand the behavior of the neutron population for more than one energy group?

Exercise 16.2

Earlier in the chapter we derived the Inhour equation with a single delayed neutron precursor group. Suppose that we write the point kinetics equations as

$$dn/dt = \left[\left(\rho - \beta\right)/\Lambda\right] \cdot n + \sum_i \lambda_i C_i\left(t\right) \quad \left(\text{for } i = 1, \ldots, 6\right)$$

and

$$dC_i/dt = \beta_i/\Lambda \cdot n - \lambda_i C_i\left(t\right)$$

where $n = \phi/v$. Assuming that $n(t) \approx e^{\omega t}$ and $C(t) \approx e^{\omega t}$, show that the final result is $\rho = \omega\Lambda + \Sigma_i \beta_i \omega/(\omega + \lambda_i)$ (for $i = 1, \ldots, 6$) when six delayed neutron groups are used. How many roots does this particular version of the Inhour equation have?

Exercise 16.3

In many text books, the seven root Inhour equation is derived based on the assumption that all of the delayed neutron groups and the neutron density all have the same basic time dependence, that is, $n(t) \approx e^{\omega t}$ and $C(t) \approx e^{\omega t}$. Suppose that this is not the case and each of the delayed neutron precursor groups had its own individual time dependence. In this case, what would the final solution to the neutron density n(t) look like?

Exercise 16.4

Suppose that we write the point kinetic equations for the reactor power P with one delayed neutron group as

$$dP/dt = \left[\left(\rho_o - \beta\right)/\Lambda\right] \cdot P + \lambda C\left(t\right)$$

and

$$dC/dt = \beta/\Lambda \cdot P - \lambda C\left(t\right)$$

If we assume that a possible solution to this set of coupled differential equations is $P(t) = Pe^{\omega t}$ and $C(t) = Ce^{\omega t}$, show that this implies that both equations will have a solution if and only if $[\omega - (\rho_o - \beta)/\Lambda][\omega + \lambda] - \lambda\beta/\Lambda = 0$ or $\Lambda\omega^2 + (\lambda\Lambda + \beta - \rho_o)\omega - \rho_o\lambda = 0$.

Exercise 16.5

Use the quadratic formula to prove that in most reasonable cases where $\lambda\Lambda/\beta \ll 1$ and $|\rho_o| \ll \beta$, that the general solution to the point kinetics equation, as defined in Exercise 16.4, will be $P(t) = P_1 e^{\omega 1 t} + P_2 e^{\omega 2 t}$ and $C(t) = C_1 e^{\omega 1 t} + C_2 e^{\omega 2 t}$ and that the two roots ω_1 and ω_2 will be $\omega_1 \approx \lambda\rho_o/(\beta - \rho_o)$ and $\omega_2 \approx -(\beta - \rho_o)/\Lambda$.

Exercise 16.6

Prove that when the reactivity is 0, the only credible solution to the Inhour equation is one where the reactor period is infinite (i.e., $T = \infty$).

Exercise 16.7

Prove that when the Inhour equation is used with six delayed neutron precursor groups that six of the roots must always be negative and only the largest root can be either 0 or positive.

Exercise 16.8

Calculate the average value of the decay constant λ for the delayed neutrons that are produced from the thermal fission of Uranium-235. Show that when the decay constant is found using a weighted average rather than a linear average that the value of the decay constant is reduced by approximately 52%. Which value of the decay constant do you believe is more accurate in this case?

Exercise 16.9

A commercial thermal water reactor is fueled with a 50% mixture of Uranium-235 and Plutonium-239. When the reactor is exactly critical, five banks of control rods are suddenly withdrawn from the core, and each bank of control rods has an average reactivity of 2 cents. What is the asymptotic period of the reactor T_∞ after the control rods have been completely withdrawn?

Exercise 16.10

The thermal water reactor in Exercise 16.9 is then shut down for refueling and the fuel assemblies are replaced with new fuel assemblies containing Uranium-233. If three banks of control rods are withdrawn from the core when the reactor is exactly critical, and the reactivity of the control rods is the same as before, calculate the asymptotic period of the reactor $T\infty$ after the control rods have been withdrawn.

Exercise 16.11

A small 100 MW research reactor built in the United States has a reactor period of 10 minutes when the reactor is exactly critical and when one bank of control rods is subsequently withdrawn from the core. If the reactor is initially operating at power level of 25 MW before the control rod bank was withdrawn, what is the power level of the reactor 10 minutes later?

Exercise 16.12

When one delayed neutron precursor group is used, it is reasonable to assume that the solutions to the point kinetics equations are $\phi(t) = A_1e^{\omega 1t} + A_2e^{\omega 2t}$ and $C(t) = C_1e^{\omega 1t} + C_2e^{\omega 2t}$. Assuming that these are in fact the correct solutions, write down explicit expressions for the values of A_1, A_2, C_1, C_2, ω_1, and ω_2 that appear in the proposed solutions. What does the value of C(t) in the trial solutions represent in this case? Write down the corresponding expression for the time-dependent power in this case.

Exercise 16.13

For the case where the Inhour can be written as $\rho = \Lambda/T + \beta/(1 + \lambda T)$, that is, when $T \gg \Lambda$ use the quadratic formula to show that the two primary roots for the reactor period are given by $T = [(\rho - \beta)/\Lambda - \lambda) + \sqrt{(((\rho - \beta)/\Lambda - \lambda)^2 + 4\lambda\rho/\Lambda)}/(2\lambda\rho/\Lambda)]$ and $T = [(\rho - \beta)/\Lambda - \lambda) - \sqrt{(((\rho - \beta)/\Lambda - \lambda)^2 + 4\lambda\rho/\Lambda)}/(2\lambda\rho/\Lambda)]$.

Exercise 16.14

The reactivity of a control rod in a gas-cooled reactor near Manchester, England is 0.1 niles. During a rod ejection addident, 20 of these control rods are ejected from the core. By how much will the power level jump immediately after the rods are withdrawn? How long will it take for the power level in the core to double? Assume the reactor is fueled with a mixture of 50% enriched uranium and 50% plutonium.

Exercise 16.15

A BWR and a LMFBR are both to be fueled with recycled Pu-239. For a positive reactivity insertion of 1 cent, what is the asymptotic reactor period for the BWR and what is the asymptotic reactor period for the LMFBR? How do the two reactor periods compare?

Exercise 16.16

A PWR and a LMFBR are both to be fueled with U-233. For a positive reactivity insertion of 1 pcm, what is the asymptotic reactor period for the PWR and what is the asymptotic reactor period for the LMFBR? How do the two reactor periods compare?

Exercise 16.17

A PWR and a LMFBR are both to be fueled with a U-235/U-238 mixture. For a positive reactivity insertion of $\rho = 0.99\beta$, what is the instantaneous reactor period for the PWR and what is the instantaneous reactor period for the LMFBR? How do the two reactor periods compare?

Exercise 16.18

A PWR and a LMFBR are both to be fueled with a U-233. At the beginning of life for a positive reactivity insertion of $\rho = 0.99\beta$, what is the instantaneous reactor period for the PWR and what is the instantaneous reactor period for the LMFBR? How do the two reactor periods compare?

17

Burnup, Depletion, and Temperature Feedback

17.1 Tracking the Burnup of Nuclear Fuel

Once steady-state operation has been achieved, the amount of fuel in a reactor core starts to decline as a function of time. *So although a reactor may initially start its life with more fuel than it needs to remain critical, this excess fuel is what allows it to operate for long periods of time after initial criticality has been achieved*. In this chapter, we would like to explore exactly how this process works. The amount of fuel that is burned depends on the level of the thermal neutron flux ϕ and the period of time t that the fuel is exposed to this flux. For a reactor fueled with Uranium-235, the concentration of the fuel (in atoms/cm^3) is time dependent and can be determined from the equation

The U-235 Rate Equation

$$\frac{dU}{dt} = -U\sigma_{aU}\phi \tag{17.1}$$

where U is the number of atoms of U-235 per cubic centimeter. The solution to this equation is of course

Solution to the U-235 Rate Equation

$$U(t) = U_o e^{-\sigma_{aU}\phi t} \tag{17.2}$$

where U_o is the concentration of U-235 atoms (per cm^3) in the core at start-up. A small amount of Plutonium-239 is subsequently produced from the Uranium-238 in the fuel rods. However, over time, this additional plutonium can generate nearly *one-third of the total power* in a light-water reactor at the end of a refueling cycle. Depending on the level of the neutron flux, the reduction in the concentration of U-235 and U-238 can occur at different rates. To illustrate this point, suppose that we would like to simulate a thermal water reactor with an average neutron flux of 1×10^{14} neutrons/cm^2/s.

If the energy spectrum is typical of a thermal water reactor, about two-thirds of the neutrons will be fast neutrons and the remaining one-third of the neutrons will be thermal neutrons. The energy spectrum in the thermal energy range is Maxwellian in shape. Under these conditions, we can assume that the thermal neutron flux is approximately $\phi_T = 3.3 \times 10^{13}$ neutrons/cm^2/s, and the fast neutron flux is approximately $\phi_F = 6.7 \times 10^{13}$ neutrons/cm^2/s. Depending on the way in which the core is configured, the thermal utilization factor will be about 90% (f = 0.90) so the number of thermal neutrons in the fuel ϕ_T should be approximately $0.90 \times 3.3 \times 10^{13}$ neutrons/cm^2/s = 3×10^{13} neutrons/cm^2/s. At thermal energies (see Chapter 5), $\sigma_{aU} \approx 700$ barns = 700×10^{-24} cm^2. Moreover, the time constant $\lambda = \sigma_{aU}\,\phi_T$ that appears in Equation 17.2 is a function of the level of the thermal flux ϕ_T. In our specific example, it is easy to show that $\lambda = -0.33$ after 6 months of full power operation and $\lambda = -0.66$ after 1 year of continuous operation. So after 6 months of full power operation, the amount of U-235 in the core will be reduced by $U_o - U = U_o - U_o e^{-0.33} = 0.28U_o$ (28%), and after 1 year of full power operation, the amount of U-235 in the fuel will be $U = U_o e^{-0.66} = 0.52U_o$ (52%). Higher levels of the neutron flux will of course cause the fuel to burn more quickly. Uranium-238, which also exists in the fuel in much larger quantities, has a much smaller absorption cross section than Uranium-235 does (2.7 barns vs. approximately 575 barns), so it burns off at a much lower rate.

In fact, for a typical thermal neutron, the total absorption cross section (fission plus capture) for U-238 is about 210 times smaller than it is for U-235. So in a thermal water reactor, Uranium-238 burns about 200 times more slowly than Uranium-235 does. Figure 17.1 shows the concentration of U-235 as a function of time in a thermal water reactor for several different values of the thermal neutron flux, and Figure 17.2 shows the change in the concentration of U-238 with time for the same values of the thermal neutron flux. It should be apparent that more than half of the Uranium-235 can be burned away in a single year, while in the case of Uranium-238, barely 1% of the initial inventory is burned in that time. Yet, it is this very small percentage of Uranium-235 in the fuel rods that completely dominates the isotopic composition of the core.

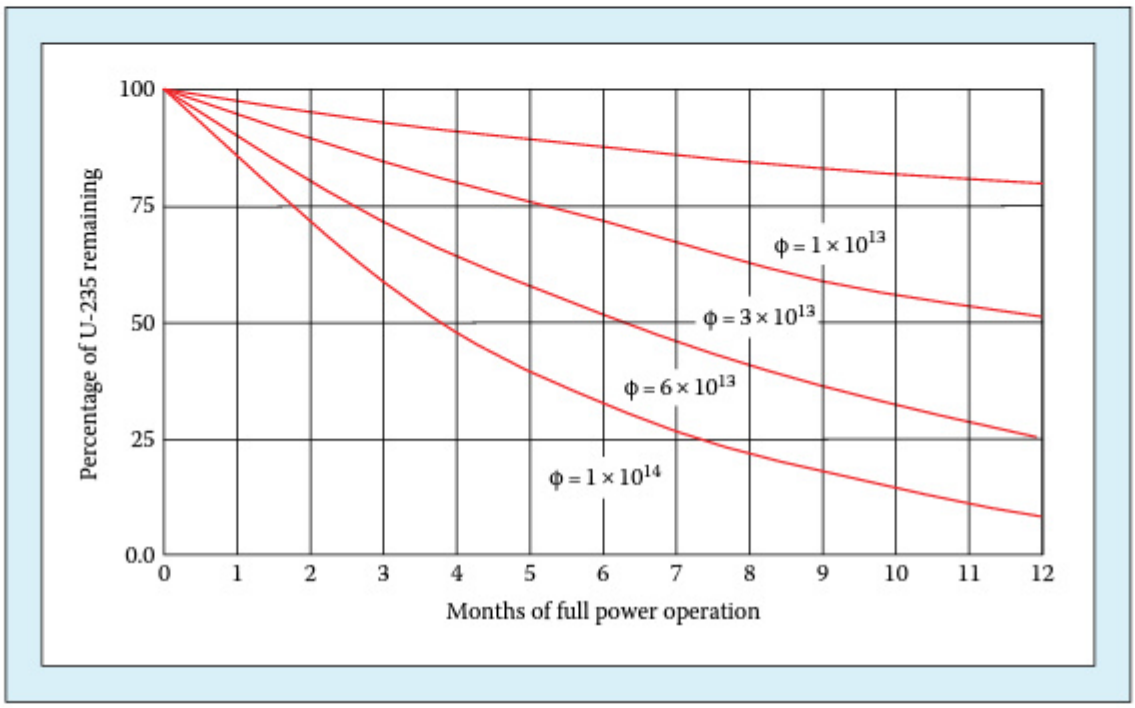

FIGURE 17.1 The amount of U-235 remaining in the fuel as a function of time for different values of the thermal neutron flux.

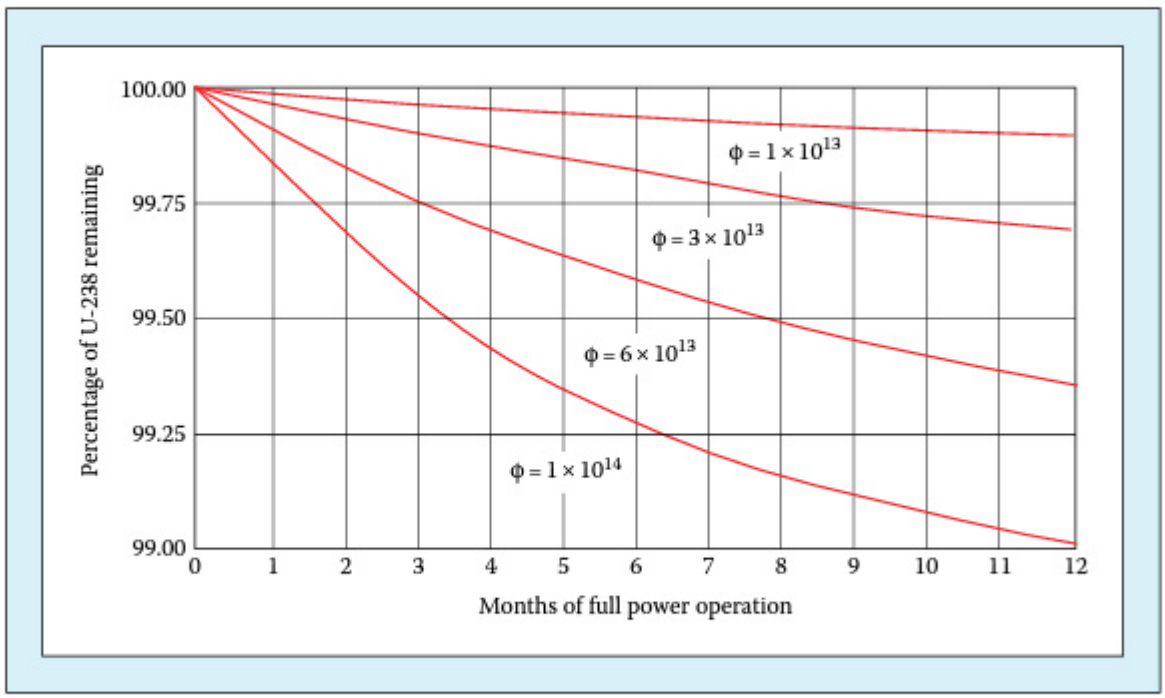

FIGURE 17.2 The amount of U-238 remaining in the fuel as a function of time for different values of the thermal neutron flux.

17.2 Factors That Affect the Life of the Fuel

It is relatively easy to estimate how long the fuel can be burned in a thermal water reactor before the reactor will no longer be able to stay critical based on the presence of the fuel alone. Although we will defer a detailed discussion of this topic until Chapter 18, there are a number of important points that we would like to make at this time. *The length of time that a reactor can stay critical before it runs out of fuel depends primarily on the enrichment of the fuel e and the value of the thermal flux* ϕ_T. If the flux is increased, the fuel will burn faster, and it will take less time for the reactor to go subcritical. So, a higher power level means that the refueling interval must be shortened for a given enrichment of the fuel. Also, we can prolong the life of the core by simply increasing its enrichment, since there are more Uranium-235 atoms to burn.

A simple graph showing how the Uranium-235 concentration behaves as a function of time is shown in Figure 17.1. There are several important lessons that can be learned from these curves. First, for a given value of the flux or the power, the *burnable lifetime* (BL) of the fuel increases with e. The higher the enrichment is, the longer its burnable life will be. Secondly, the lifetime of the fuel is *inversely proportional* to the level of the flux or the power. This implies that BL ~ 1/ϕ. Therefore, the more power that is produced in a given period of time, the shorter the lifetime of the fuel will be because the value of ϕ will be higher. Example Problem 17.1 illustrates how the concentrations of U-235 and U-238 change as a function of time. The buildup of another important isotope (Plutonium-239) can also affect the thermal energy output of the core.

17.3 Buildup of Plutonium in the Core

As we mentioned previously, various isotopes of plutonium are produced in thermal water reactors from the burnup of Uranium-238. The U-238 in the fuel is generally bonded together with two oxygen atoms to form a ceramic fuel pellet consisting of about 97% U-238 and 3% U-235. The pellet consists of UO_2, which has a composition of 3% U-235 and 97% U-238. In most thermal water reactors, the fuel contains enriched uranium, but no plutonium initially. Plutonium atoms (in the form of Pu-239, Pu-240, and Pu-241) are then produced from U-238 as the fuel is burned. *In fast reactors, the initial plutonium concentration is much higher—even in the fresh fuel assemblies—and the percentage of Pu-239 can approach 18% to 22%*. As we learned previously, U-238 has a thermal absorption cross section of about 2.7 barns. The capture of a thermal neutron eventually converts it to Plutonium-239. The entire process takes about 2.38 days. The steps in this process are shown in Figure 17.3. Notice that U-238 must first be converted into U-239 and then into Np-239 before it can become Pu-239.

Example Problem 17.1

Suppose that a fuel assembly in a thermal water reactor contains 50 lb (18.7 kg) of Uranium-235 when it is first started up and that the enrichment of the fuel at start-up is 4%. If the remaining fuel is Uranium-238, and the reactor operates at an average flux of 2×10^{13} neutrons/cm^2/s for 400 days, how much U-235 and U-238 will remain in the assembly when it is shut down for refueling after 400 days?

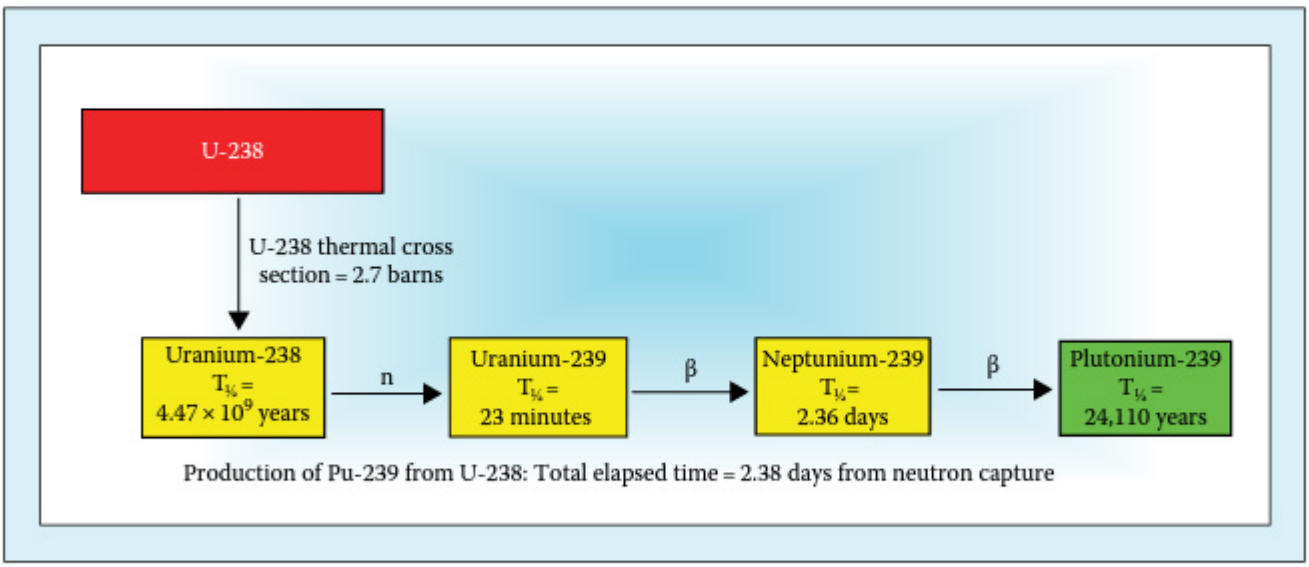
U-238
U-238 thermal cross section = 2.7 barns
Uranium-238 T½ = 4.47 × 10^9 years
n
Uranium-239 T½ = 23 minutes
β
Neptunium-239 T½ = 2.36 days
β
Plutonium-239 T½ = 24,110 years
Production of Pu-239 from U-238: Total elapsed time = 2.38 days from neutron capture

FIGURE 17.3 The Plutonium-239 production cycle in a thermal water reactor fueled with a mixture of U-235 and U-238.

Solution Since the fuel contains 50 lb of Uranium-235, it must contain (96%/4%) ≈ 24 times more U-238 by weight than U-235. Therefore, the amount of U-238 present in the fuel at start-up is 24 × 50 lb = 1200 lb. Since U-235 and U-238 both obey the same rate equation:

$$U(t) = U_o e^{-\sigma_{au}\phi t}$$

the time-dependent U-235 concentration is

$$U^{235}(t) = U_o^{235} e^{-\sigma_{au}235\phi t}$$

and time-dependent U-238 concentration is

$$U^{238}(t) = U_o^{238} e^{-\sigma_{au}238\phi t}$$

where U_o^{235} and U_o^{238} are the initial concentrations, in atoms/cm^3, at start-up. In the case of U-235, $\sigma_{au}235 \approx 700$ barns, and in the case of U-238, $\sigma_{au}238 \approx 2.7$ barns. After 400 days (or 3.45×10^7 seconds) of full-power operation with an average flux of 2×10^{13} neutrons/cm^2/s, the concentration of U-235 is

$$U^{235}(t) = U_o^{235} e^{-\sigma_{au}235\phi t} = U_o^{235} e^{-0.483} = 0.617 U_o^{235}$$

and the U-238 concentration is $U^{238}(t) = U_o^{238} e^{-\sigma_{au}238\phi t} = e^{-0..00186} = 0.998\, U_o^{238}$. Since $U_o^{235} = 50$ lb, and $U_o^{238} = 1200$ lb, the remaining amounts of U-235 and U-238 after 400 days are U^{235} = 50 lb × 0.617 = 30.85 lb of U-235 and U^{238} = 1200 lb × 0.998 = 1197.6 lb of U-238. So roughly 40% of the U-235 will be burned up, and over 99% of the U-238 will still remain. These results are quite typical of the behavior of a thermal water reactor under normal operating conditions. [Ans.]

In order to determine how much Plutonium-238 is produced as a function of time, we can ignore the intermediate steps that involve the production of Uranium-239 and Neptunium-239 and assume that all of the Uranium-238 is converted directly into Plutonium-239. Notice that this only changes the *rate* at which Plutonium-239 is produced by about 2½ days. It does *not* change the *amount* of Plutonium-239 that is produced in the core. With these simplifications, the rate equations for the change in the concentration of Uranium-238 and the production of Plutonium-239 are

The U-238 and Plutonium-239 Rate Equations

$$\frac{dU}{dt} = -U\sigma_{au}\phi$$
$$\frac{dP}{dt} = U\sigma_{au}\phi - P\sigma_{ap}\phi \qquad (17.3)$$

where U and P are the number of atoms of U-238 and Plutonium-239 per cubic centimeter and σ_{aU} is the thermal neutron absorption cross section of U-238 (about 2.7 barns) and σ_{aP} is the total thermal neutron absorption cross section of Pu-239 (about 1015 barns, including both fission and capture). The solution to the first rate equation is of course

Solution to the U-238 Rate Equation

$$U_{238}(t) = U_o e^{-\sigma_{au}\phi t} \qquad (17.4)$$

where U_o is the concentration of U-238, in atoms/cm^3, at start-up. The solution to the second rate equation is

Solution to the Pu-239 Rate Equation

$$P_{239}(t) = \frac{U_o\sigma_{au}}{\sigma_{ap} - \sigma_{au}}\left[e^{-\sigma_{au}\phi t} - e^{-\sigma_{ap}\phi t}\right] \qquad (17.5)$$

where again we have assumed that the neutron flux is constant during the period of time where the Plutonium production is taking place. Now let us see what this means when we operate a reactor for 1 year (3.15×10^7 seconds) at an average thermal flux of 1×10^{13} neutrons/cm²/s. The amount of U-238 remaining is

$$\frac{U_{238}\left(3.15\times10^{7}\right)}{U_o} = e^{-\left(2.7\times10^{-24}\times3.15\times10^{7}\times1\times10^{13}\right)} = e^{-0.00085} = 0.99915 = 99.915\%$$

So, 0.00085 or 0.085% of the Uranium-238 is converted into a variety of different elements and isotopes during this time. If we started out with a metric ton (1000 kg) of Uranium-238, burning Uranium-238 for a year will produce about 0.850 kg (or 1.9 lb) of some other combination of materials. Now let us see how much Pu-239 is produced in the process. Substituting the same numbers into Equation 17.5, we get

$$P_{239}(t) = 0.00267\,U_o\left[e^{-.00085} - e^{-.32}\right] = 0.00267\,U_o\left[0.99915 - 0.72610\right] = 0.00267\times U_o \times 0.27305 = 0.00073\,U_o$$

So, 0.00073 or 0.073% of Uranium-238 is converted into Plutonium-239 in the same amount of time. Now let us see how this additional plutonium affects the power production in the core.

17.4 Plutonium Production Rate in a Typical Thermal Water Reactor

Suppose that a reactor is loaded with one ton (2000 lb) of Uranium-238. Then, according to the calculations presented earlier, burning this Uranium-238 for a year will produce about 1.46 lb (or 0.66 kg) of Plutonium-239. Note that increasing the thermal flux by a factor of 10 would only increase the Plutonium-239 production by a factor of about 0.969/0.273 = 3½. So, this would produce about 5 lb of Plutonium-239 in 1 year from one ton (2000 lb) of pure Uranium-238. In the same amount of time, and at the same initial flux level of 1×10^{13} neutrons/cm²/s, we would find that $U^{235}(t) = U_o^{335}e^{-\sigma_{a5}\phi t} == e^{-.2205} = 0.8022\,U_o^{235}$ of the Uranium-235 would remain, so about 20% of it would be burned. At a Uranium-235 to Uranium-238 ratio of about 3%, which would correspond to a fuel with an initial enrichment of about 3%, this would mean that about $0.03 \times 0.20 = 0.6\%$ of the total weight of the fresh fuel would be burned in 1 year from the burnup of Uranium-235.

So if the reactor starts out with one ton of uranium with an initial enrichment of about 3%, then we have to burn up about 12 lb of Uranium-235 to produce about 1½ lb of Plutonium-239. Superficially, this does not seem like a good trade-off, but we must remember that we have produced a great deal of power for an entire year to make this happen. The concentrations of Plutonium-240 and Plutonium-241 produced in this process are much smaller, and except for very special applications, their presence can generally be ignored when calculating the amount of fissile material available.

17.5 Estimating the Amount of Energy Produced from Plutonium in a Thermal Water Reactor Core

At the end of a refueling cycle, pressurized water reactor (PWR) or boiling water reactor (BWR) fuel will contain about 0.8% Plutonium-239 by weight. Virtually, all of this plutonium is produced when the surrounding Uranium-238 atoms are converted into Pu-239. Because Plutonium-239 is a true fissile material, it can absorb a thermal neutron and produce additional fission neutrons just like Uranium-235 can. Since Plutonium-239 is constantly being created from U-238 in the fuel rods, the nuclear fission of Plutonium-239 produces about *one-third* of the total energy output of a conventional power plant over the life of the core. Commercial reactor fuel would contain even more plutonium than this, but some of the plutonium is burned away while the reactor is being operated. Finally, this plutonium can be recycled or reused in a thermal water reactor. However, it can also be used in the core of a fast breeder reactor to breed additional nuclear fuel (see Chapter 1). In this case, it is mixed with uranium to create what is known as mixed oxide or *MOX fuel*. MOX fuel is discussed more extensively in our companion book.*

Example Problem 17.2

Suppose that a thermal water reactor is fueled with Plutonium-239 instead of Uranium-235, that the thermal utilization of the fuel is 0.90, and that the average neutron flux is 3×10^{14} neutrons/cm²/s. If one-third of the neutrons in the reactor are thermal neutrons, how much of the Pu-239 will be left in the core after 6 months, based on the presence of the thermal neutrons alone?

* See *Nuclear Engineering Fundamentals: A Practical Perspective*, by R.E. Masterson, CRC Press (2017).

Solution From Appendix C, we know that the thermal fission cross section of Plutonium-239 is 747 barns and that the thermal capture cross section of Plutonium-239 is 270 barns, so the total absorption cross section is $\sigma_a = \sigma_c + \sigma_f = 270$ barns + 747 barns = 1017 barns. We also know that the average thermal flux is 0.33 × is 3×10^{14} neutrons/cm^2/s = 1×10^{14} neutrons/cm^2/s and that there are 1.56×10^7 seconds in 6 months. Since the thermal utilization of the fuel is 0.90, the plutonium in the fuel can absorb 90% of these thermal neutrons or $0.90 \times 1 \times 10^{14}$ neutrons/cm^2/s. From our previous discussion, it is easy to see that the time-dependent concentration of the plutonium will be given by

$$Pu(t) = Pu_o e^{-\sigma_{apu}\phi t}$$

where Pu_o is the initial concentration, in atoms/cm^3, at start-up. Therefore, after 6 months, the remaining concentration of Plutonium-239 is

$$Pu(6\text{ months}) = Pu_o e^{-\left(0.9\times10^{14}\times1.56\times10^{7}\times1.017\times10^{-21}\right)} = Pu_o e^{-(1.44)} = Pu_o e^{-(1.44)} = 0.24\,Pu_o$$

So, only 24% of the Plutonium-239 in the fuel will still be left after 6 months of full power operation. [Ans.]

Consequently, *Plutonium-239 is a highly desirable by-product of the ubiquitous U-238, and roughly one-third of all the energy that a thermal water reactor produces comes from the Plutonium-239 that builds up in the fuel rods over time*. Pu-241 also produces some additional energy in the process, but the amount of thermal energy produced by the thermal fission of Pu-241 is relatively small, compared to the amount of energy that U-235 and Pu-239 produce. Military reactors and those designed specifically for the production of weapons-grade plutonium can have much different amounts of Pu-240 and Pu-241 than those found in commercial power reactors. In these reactors, the percentage of the total energy generated from the fission of Pu-239 can be even higher.

Student Exercise 17.1

Suppose that we ask the same question again, but this time we do *not* choose to ignore the effects of the fast neutron flux in the core on the concentration of the plutonium. In this case, how much of the plutonium will be left in the fuel after 6 months?

17.6 Changes to the Isotopic Composition of the Core

When a reactor is being operated normally, two important changes take place to the isotopic composition of the core. We would now like to discuss each of these changes in more detail.

17.6.1 Burnable Poisons and Other Neutron Poisons

First, in order to help flatten the radial power profile, *burnable poisons* and *nonburnable poisons* are sometimes added to a reactor's fuel assemblies. In the vicinity of a control rod or in an area of the core where the flux is high, these poisons are mixed directly with the fuel. We will spend several sections describing how these poisons work as soon as we have completed this section. As these poisons burn away, they help to shape the neutron flux, but also introduce additional isotopes into the fuel. The second major change in the composition of the core is that the ratio of the control materials to the total isotopic composition of the core can also change substantially over time. *For example, the control rods will gradually be withdrawn from the core as the fuel is burned. This will reduce the number of neutron-absorbing materials in the core as a function of time*. In PWRs, this effect can be even more pronounced because PWRs use a form of *soluble boron*, or *chemical shim*, to control the number of neutrons that are absorbed. This chemical shim is dissolved directly in the coolant. When suspended in water, this boron becomes *boric acid*, and boric acid can absorb a great number of thermal neutrons. Then as the fuel is burned, its concentration is gradually reduced. The fact that the boron is dissolved directly in the coolant means that it becomes distributed rather uniformly across the core, and this makes it easier for it to absorb excess thermal neutrons without causing any unnecessary flux or power peaks.

17.6.2 Soluble Neutron Poisons and Their Function

PWRs use a special type of soluble poison, or chemical shim, to help control the reactor as the fuel is burned. The most common form of *chemical shim* in PWR is a form of boric acid, which can be dissolved directly into the

coolant, This boron makes it possible to make many subtle adjustments to the global power level over long periods of time. This form of boric acid is also called *solbor*. The chemical composition of solbor is

Chemical Composition of Boric Acid or Solbor

$$B(OH)_3 \quad \text{or} \quad H_3[BO_3] \tag{17.6}$$

Boric acid can exist in the form of colorless crystals or as a white powder that easily dissolves in ordinary *tap water*. It has the *chemical formula* H_3BO_3, which, as we have seen, can also be written as $B(OH)_3$. Natural boron contains many isotopes, but the two most important ones are Boron-10 and Boron-11. About 20% of natural boron is Boron-10 and most of the remainder is Boron-11. Boron-10 has a much larger absorption cross section than Boron-11, and it is much better at absorbing low-energy neutrons. The absorption cross sections for Boron-10 and Boron-11 are compared in Figure 17.4. When boric acid is injected into the coolant, the Boron-10 concentration increases, and this reduces the power level because more neutrons are absorbed. If enough boron is added to the coolant, it will cause the reactor to become subcritical. Ideally, it is desirable to add just enough boron to the coolant to keep the reactor critical at all times. Then as the fuel is consumed, the concentration of boron is slowly reduced to maintain a flat flux and power distribution. Changes in the boric acid concentration can effectively regulate the rate at which nuclear fissions occur. The control rods can then be reserved for their traditional functions of start-up, shutdown, and emergency core control. In addition to boric acid, soluble poisons such as gadolinium nitrate $Gd(NO_3)_3$ and sodium polyborate can be directly injected into the coolant if an emergency condition arises. These neutron poisons are very effective at absorbing excess neutrons when a reactor needs to be shut down quickly. They can be injected automatically into the coolant in an emergency situation, or they can also be injected manually by the reactor operator as well. The absorption cross sections for Gadolinium are shown in Figure 17.5.

When PWRs are first started up, it is *standard operating procedure* to maximize the concentration of the boric acid in the coolant to compensate for the excess reactivity that the fresh fuel may have. Then as the fuel is burned and begins to become depleted, the excess reactivity is reduced, and the concentration C of soluble boron can be reduced as well. *If the power level P is held constant, the soluble boron concentration will decrease approximately linearly with the burnup of the fuel to keep the reactor in a critical state*. The only exception to this rule is when the boric acid concentration must be decreased rather quickly to compensate for the initially buildup of Xenon-135 in the core, which can reduce the reactivity by a couple of dollars by absorbing so many excess neutrons. However, this behavior only lasts for about 2 days when a PWR is operating at full power. After that, the xenon will build up to its equilibrium concentration, X(∞), and the

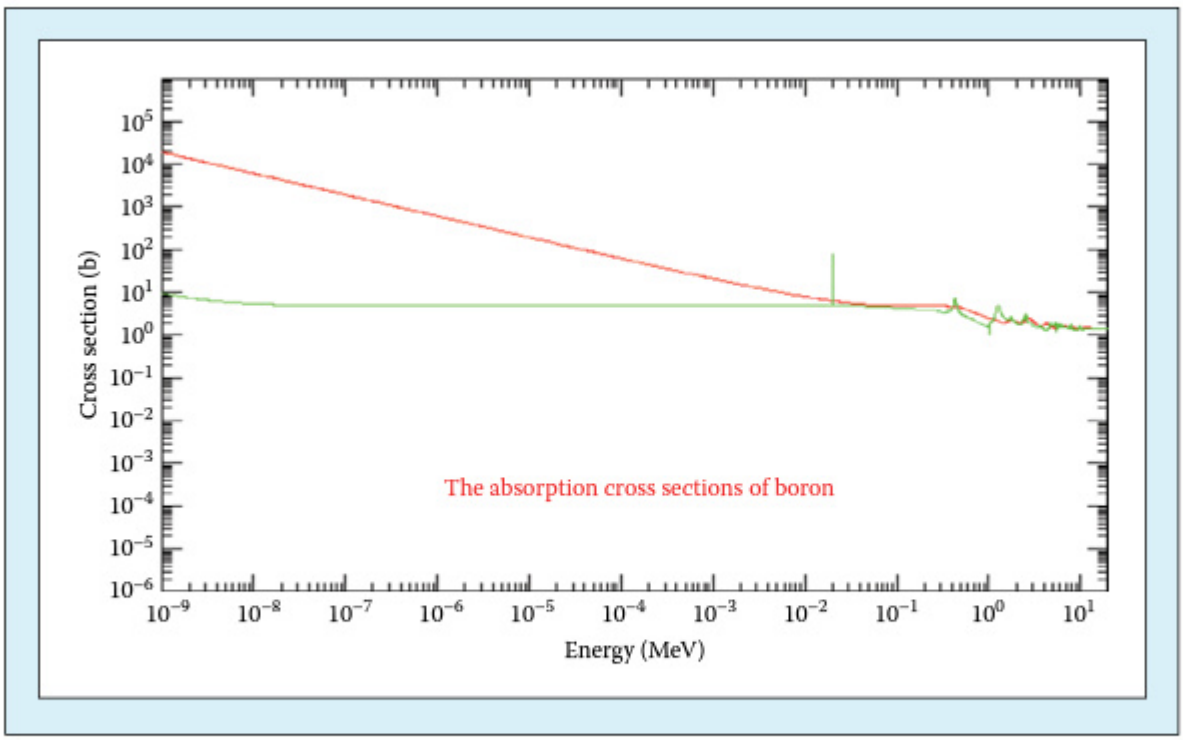

FIGURE 17.4 The absorption cross sections for Boron-10 are shown in red and the absorption cross sections for Boron-11 in green. Boron-10 is the main ingredient that is dissolved into the coolant of a PWR to help control the power level. (Courtesy of Kaere.)

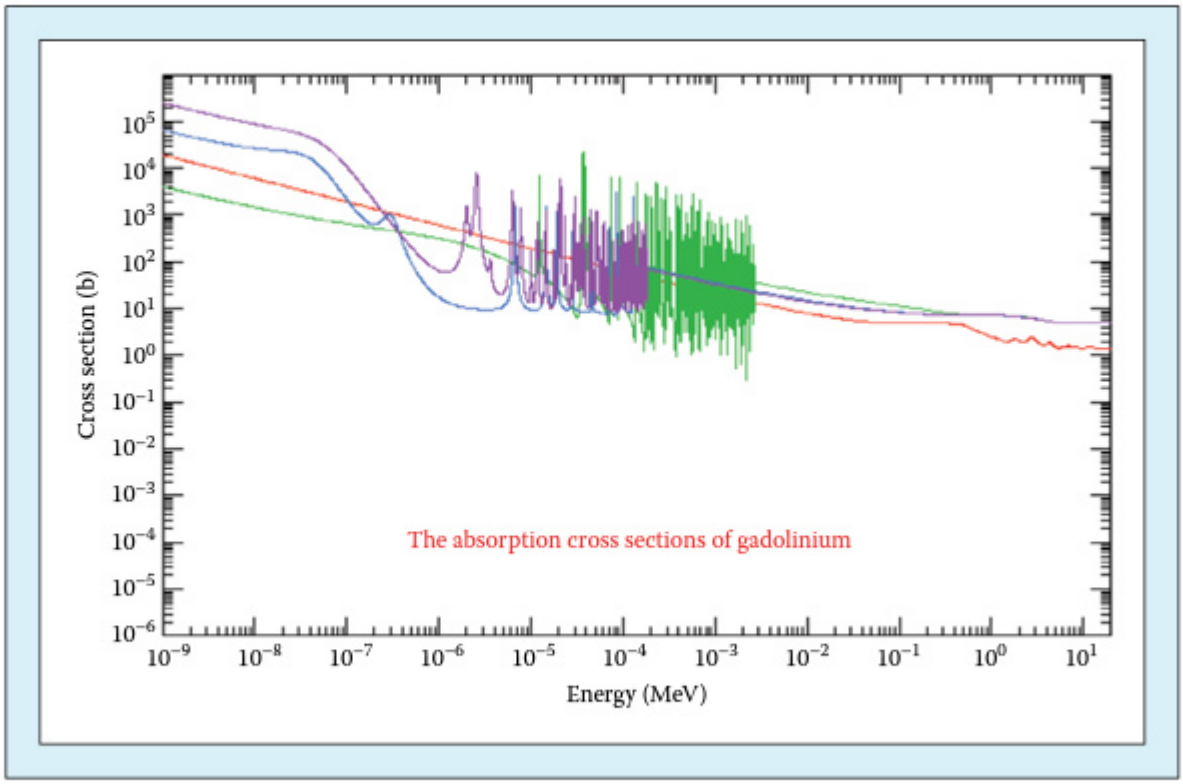

FIGURE 17.5 The absorption cross sections of three isotopes of gadolinium (Gd-152 in green, Gd-153 in blue, and Gd-155 in purple) compared to the absorption cross section of another popular burnable poison, Boron-10 in red. Note the extreme linearity at energies below about 0.1 eV. (Graph produced by ENDFPLOT.)

concentration of soluble boron does not have to be reduced any further to compensate for the reactivity loss caused by the neutron-absorbing potential of the Xenon.

A typical chart of the boric acid concentration in a PWR is shown in Figure 17.6 as a function of time. In this case, the PWR is assumed to be operating at a constant power. Notice that once the xenon and samarium concentrations have built up to their equilibrium values, the boric acid concentration only needs to be changed to compensate for the depletion of the fuel. If the power level is held constant, the burnup of the fuel varies linearly with time, and the boric acid concentration falls inversely with time as well. If the power level is doubled, then twice as much xenon will be produced, and the amount of boron in the coolant must also be cut in half during the first 48 hours of operation to compensate for the large number of neutrons that the xenon absorbs. Eventually, as things return to normal, the soluble boron concentration again returns to its long-term linear trend.

This assumes a refueling period of slightly more than 1 year (365 days + 30 days ~ 400 days). After that, the reactor can no longer be maintained in a critical state by simply diluting the boron alone, and the fuel rods may have to be replaced. Over the life of the core, this cycle is repeated over and over again—but with a fresh supply of boric acid and with some fresh fuel assemblies. This process continues for the entire life of the plant, which for modern reactors, can be anywhere from 30 to 50 years.

17.7 Fuel Management and Plant Operation

During normal operation, it is desirable to keep the radial power profile P(x, y) across the core as uniform as possible. Since fuel assemblies with higher enrichments generally run hotter than those with lower ones, the more highly enriched assemblies must be mixed with depleted fuel assemblies to ensure that this design goal is met. Generally, this is done using a predetermined loading pattern known as a *fuel management scheme*. One of the goals of nuclear fuel management is to minimize peaks in the radial power shape (and possibly the axial power profile) between subsequent refuelings. While this may seem like a rather straightforward process, putting the fuel assemblies in the correct positions from cycle to cycle is actually harder to do than it might initially seem. There are a number of reasons why this is the case:

- First, the burnup of the fuel must be optimized to get as much energy as possible out of each fuel assembly.
- Second, the reactivity of the core must be sufficient to obtain this optimum burnup.

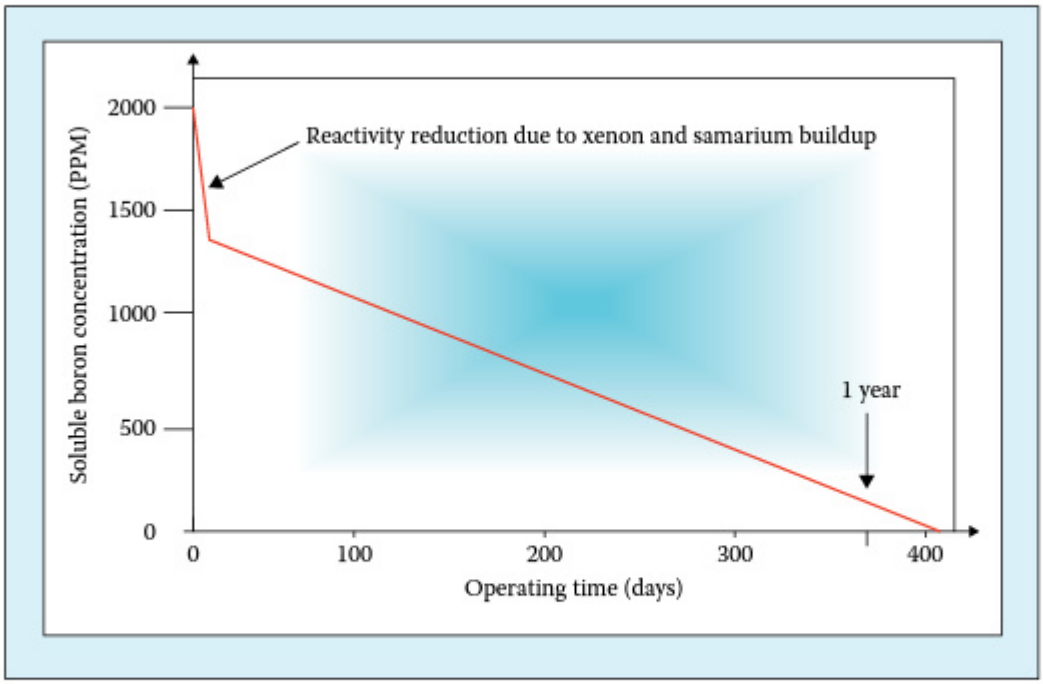

FIGURE 17.6 A typical soluble boron curve for a PWR versus operating time. Start-up occurs at t = 0.

- Third, the reactor must be shut down for refueling during a period of relatively low electrical demand. As we will soon see, this generally occurs in the spring or fall of the year—depending on when the demand for electricity is lowest.
- Fourth, *the fast flux must be made as low as possible at the pressure vessel wall.* If this does not occur, the pressure vessel may be damaged by this additional radiation, and (in a PWR or BWR) it may have to be replaced several years before its design life is reached.

Unfortunately, *all of these goals cannot be met simultaneously, and so the fuel must be loaded into the core in such a way that the loading pattern optimizes all four of these goals collectively rather than just one or two of these goals individually*. Otherwise, the reactor may not be able to produce the power is supposed to produce at the lowest possible cost. In addition to these economic and operational goals, a number of *safety-related goals* must also be satisfied to meet the needs of the NRC and other regulatory agencies. In general, these safety-related goals can be lumped into four broad categories, which we will refer to as the NRC's *safety requirements*:

The U.S. NRC's Safety Requirements

- First, the core must be able to achieve an acceptable peak-to-average power ratio while the reactor is being operated. In *the case of a PWR or BWR, this ratio is generally about 1.3 to 1*.
- Second, the fuel must not be operated above a maximum operating temperature of about 2000°C. This means that the fuel at the center of each fuel pin should not be allowed to melt during most normal and anticipated transients.
- Third, the coolant must not be allowed to completely evaporate from the surface of the fuel rods under any condition. In a BWR, this means that the liquid film on the surface of the cladding must not be allowed to dry out. In a PWR, this means that the coolant must not be allowed to depart from a condition that is known as *nucleate boiling*, where small bubbles begin to form in the coolant channels. If either of these conditions is reached, then the fuel rods may fail and radioactive material will be released into the coolant.
- Finally, the temperature coefficient of the reactivity must not be allowed to be positive under any conditions. This ensures that the reactor will not "run away" if the power level in the core is temporarily raised to provide more power to the customer.

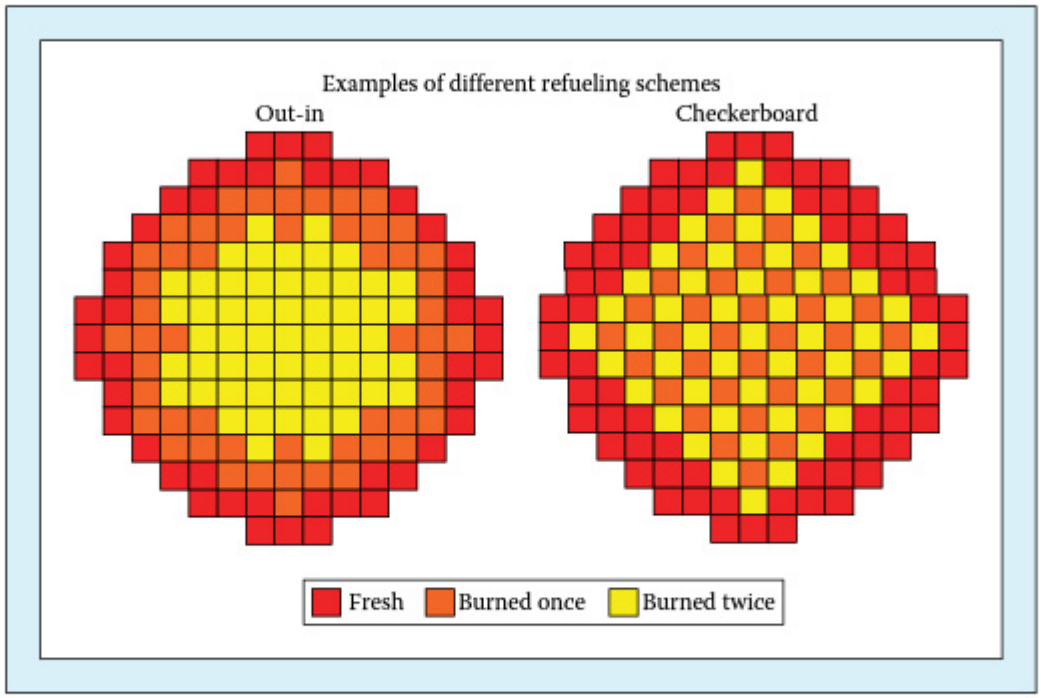

FIGURE 17.7 An example of two loading schemes designed to help flatten the radial power distribution in a commercial power reactor.

Obviously, each of these goals can be completely inconsistent with the previous list of operational goals, and so the fuel must be loaded into the core in such a way that all eight of these goals are met to the greatest extent possible. In general, this is a daunting task that requires the use of several computer programs to perform a large number of core-wide simulations. Even then, a completely optimized loading pattern may be difficult to obtain. The fuel assembly–loading pattern that is selected by a utility then determines how many of these goals can simultaneously be met. When the burnup is measured in MWD/ton, most loading schemes involve using three or four different enrichments for the fuel assemblies and placing the fuel assemblies in different locations in the core to flatten the radial power distribution. Two examples of common loading schemes are illustrated in Figure 17.7. The first one is called an *out–in loading scheme*, and the second one is called *scatter loading or checkerboard loading scheme.* Now let us see if we can quantify the relative merits and drawbacks of each scheme.

The primary advantage of an OUT–IN loading scheme is that it transfers the power peak from the center of the core to the periphery. Out–in loading can also cause the power generated in the burned fuel assemblies near the center of the core to be lower than the core-average power. However, the fresh fuel assemblies that are placed near the periphery can now produce *more power* than another fuel assembly on average. Unfortunately, placing fresh fuel assemblies with a higher enrichment near the edge of the core can actually *increase* the number of fast-fission neutrons that can leak out of the core. Many of these neutrons and the gamma rays that are released in the process can also strike the *reactor pressure vessel wall*. If the pressure vessel is exposed to these additional neutrons for a long enough period of time, then the pressure vessel can become damaged (due to radiation embrittlement), and it may have to be replaced. For this reason, out-in loading schemes are rarely used in commercial power reactors today. To eliminate this problem, most utilities have gone to *alternative loading schemes* that are referred to as *scatter loading* or *checkerboard loading* schemes.

In these schemes, fresh fuel assemblies are mixed together with partially burned ones in an attempt to form a "checkerboard" loading pattern. This loading pattern helps to flatten the radial power profile (because the partially burned fuel assemblies tend to absorb excess neutrons from the fresh ones), and it also tends to reduce the leakage of fast neutrons into the pressure vessel wall. This reduces the value of the *neutron fluence* Φ (the product of the fast neutron flux and the time of exposure) that the pressure vessel receives. An additional advantage to these schemes is that they can also be used to achieve what are known as *low-leakage cores*. We would now like to demonstrate exactly how these cores can be constructed.

17.8 Power Profiles in Low-Leakage Cores

During the normal operation of a thermonuclear reactor, some of the neutrons that are produced in the core can escape from the core and eventually strike the pressure vessel wall. Reactor pressure vessels are made from low-alloy carbon

steels that are specifically designed to keep the pressure vessels from becoming brittle. (The composition of these pressure vessels was discussed in Chapter 1.) Previously, we learned that these neutrons can consist of a mix of fast and thermal neutrons and that the pressure vessel is approximately 9 in. (20 cm) thick. Each of these neutrons can escape from the core in different amounts that are proportional to the fast and thermal non-leakage probabilities P_{FNL} and P_{TNL} which were introduced to the reader in Chapter 10. The total neutron leakage rate L is therefore given by

$$L = 1 - P_{FNL}P_{TNL} \tag{17.7}$$

where L can be a number between 3% and 4% (0.03–0.04) for a commercial power reactor. The neutrons that escape the core inflict a considerable amount of damage to the pressure vessel wall (by dislodging atoms in the carbon–steel matrix from which the pressure vessel is made). In addition, they can penetrate quite far into the pressure vessel if their energy is high enough.

Many studies have shown that the neutron flux bombarding the pressure vessel wall is highly dependent on the power generated by the peripheral fuel assemblies. Figure 17.8 shows the angular distribution of the fast neutrons striking the pressure vessel wall in a typical PWR. The peaks in the flux shape are caused by the fast neutrons produced by the peripheral fuel assemblies. In other words, putting fresh fuel assemblies near the edge of the core can actually increase the fast flux that hits the pressure vessel by 10%–20%! Over time, this can be extremely detrimental to the long-term health and safety of the pressure vessel, and so it is important to reduce the radiation damage that is caused by the fast neutrons to an absolute minimum. In PWRs, this can be achieved by employing what are known as *low-leakage core management schemes*. These schemes differ from traditional fuel loading schemes because additional steps are taken to ensure that the fast flux at the periphery of the core, when integrated over time, is kept to an absolute minimum. *In other words, these schemes attempt to minimize the fast neutron fluence $f = \phi t$, which is the product of the fast flux and the time*. In BWRs, radiation damage to the pressure vessel is generally less important because these reactors operate at a much lower pressure (1000 PSI vs. 2200 PSI for a typical PWR) and their power densities are lower. *In most BWRs, volumetric power density P/V is about half of what it is in a PWR.*

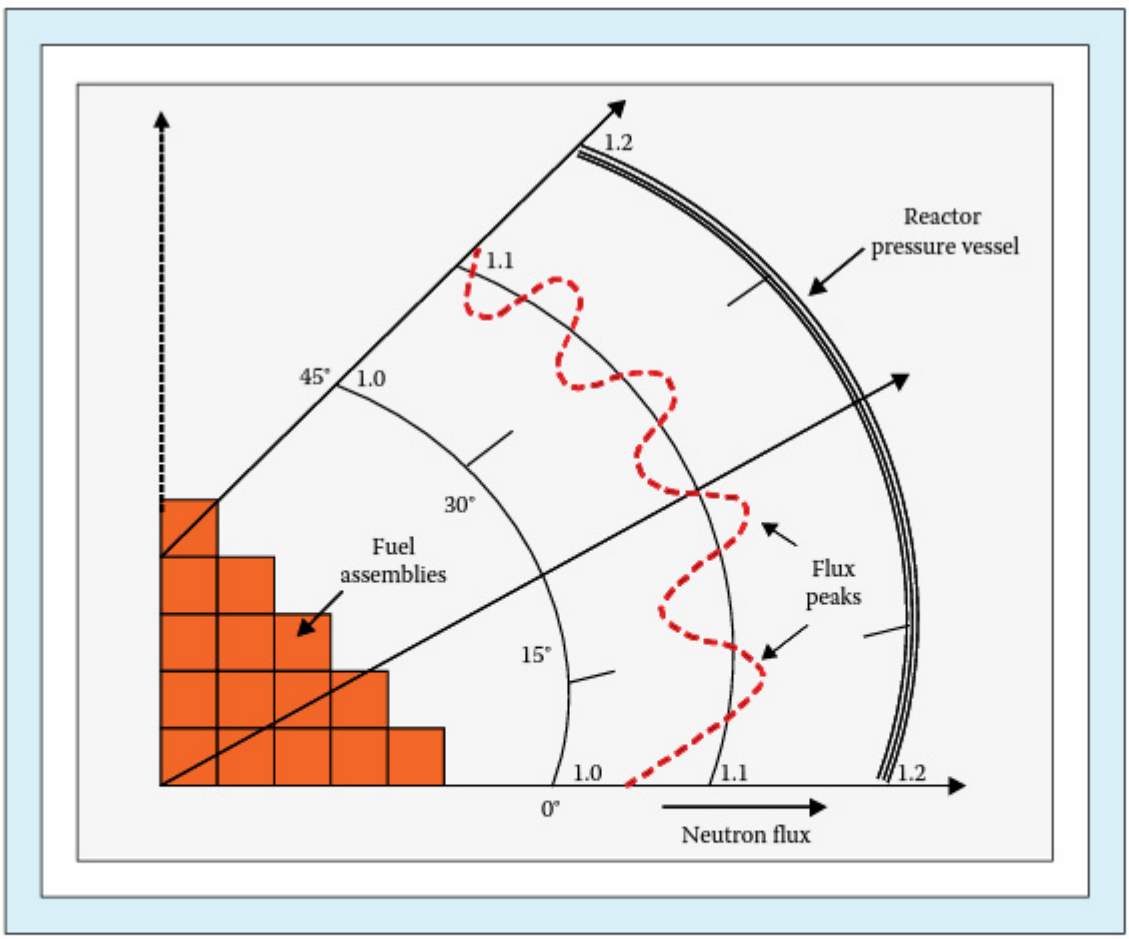

FIGURE 17.8 The angular distribution of the neutrons striking the pressure vessel wall in a commercial PWR. This specific depiction of the neutron flux is sometimes called *The Ring of Fire* because of the effects it can have on the materials surrounding it.

Today, several methods are used to reduce the fast neutron flux that reaches the pressure vessel wall. These methods include

- Placing only partially burned fuel assemblies along the periphery of the core (see Figure 17.7) to produce what is known as a *"low-leakage core."*
- Replacing some of the fuel rods inside of the peripheral fuel assemblies with new fuel rods that contain burnable poisons to absorb the excess neutrons that may leak into the pressure vessel.
- Replacing some of the fuel rods inside of the peripheral fuel assemblies with stainless steel rods that can deflect the fast neutrons before they hit the pressure vessel.
- Replacing the fuel assemblies that are closest to the pressure vessel with low-leakage ones that are either partially burned or have steel deflection plates in them.

Using a combination of these techniques, the life of the pressure vessel can be increased by 10%–20%. In a commercial power reactor that operates for 40–50 years, this can mean prolonging the useful life of the plant by 4 to 8 years! Obviously, it does not take a rocket scientist to realize that this is a very beneficial thing to do. So low-leakage cores not only help by reducing the number of fast neutrons that hit the pressure vessel, but it can also be shown that they have a number of economic benefits as well. These benefits include

- Reducing the power peaking in the core
- Allowing spent fuel assemblies to be kept in the core for a longer period of time and achieving a higher overall burnup for the fuel

In the next chapter, we will also demonstrate that the net reactivity swing $\Delta\rho$ of the core can also be reduced in this way. Hence, low-leakage loading schemes have become very popular in recent years. While no specific method has been found that can optimize all of these factors simultaneously, it is certainly possible to optimize most of them. The *nuclear fuels manager* must then decide what the "optimal" loading pattern is for a particular fuel cycle. This pattern can vary slightly from one reactor to the next, but the same set of operational, safety, and economic factors must be taken into account. We will have more to say about this when we study the process of core burnup and depletion. Until that time, it should suffice to say that we must try to keep the power profile in the core as flat as possible and to keep as many fast neutrons as possible from hitting the pressure vessel wall. Figure 17.9 shows what the radial power profile looks like in three identical

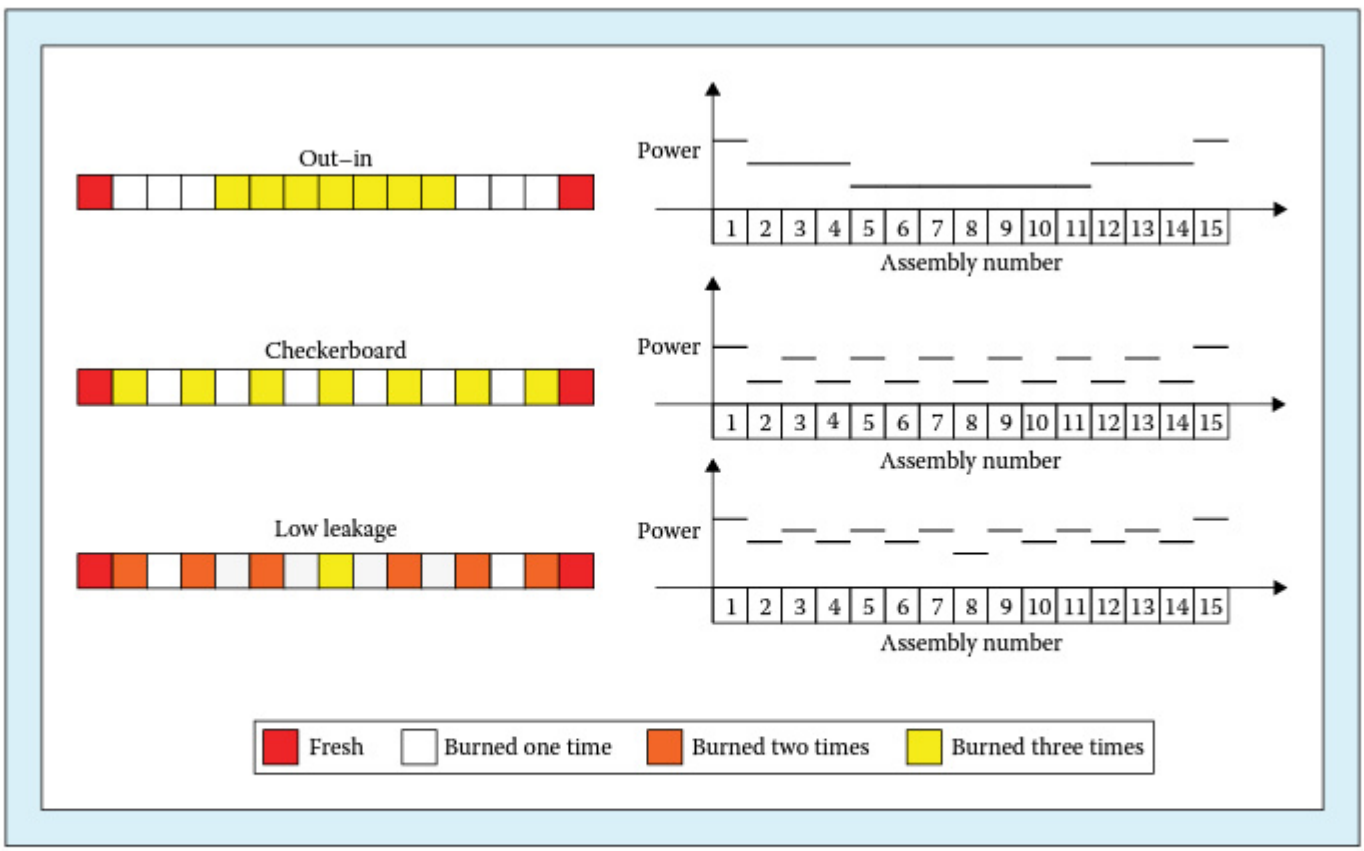

FIGURE 17.9 An illustration of how the radial power profiles compare for out–in, checkerboard, and low-leakage core.

cores that use an *out–in loading scheme*, a *checkerboard loading scheme*, and a *low-leakage loading scheme* at the beginning of each refueling cycle. The cores shown all have a total of 15 fuel assemblies along the x- or y-axis when measured along the centerline, and the pressure vessel is also identical in each case. Note in particular how well the low-leakage core is able to flatten the radial power profile, while also keeping the neutron flux as low as possible near the peripheral assemblies. This is one of the reasons why the popularity of low-leakage cores has continued to increase over time.

17.9 How Temperature Affects the Reactivity of the Core

The temperature of the core can affect the reactivity in many different ways. We previously mentioned that nuclear reactors have a number of different feedback mechanisms built into them to prevent rapid increases in the power level from feeding on themselves. One of the most important of these mechanisms is a phenomenon called *temperature feedback*. Changes in the temperature of the core can occur at different rates in the fuel and in the moderator, and certain parts of the core can run hotter or colder than others. Thus, core-wide temperature changes can affect the power level in many different ways. In this section, we would like to discuss how these reactivity changes can be predicted quantitatively. On a macroscopic level, increasing the temperature of the core causes its molecular density to decrease, and this reduces the neutron production rate over a period of time. The extent to which a change in the temperature of a reactor's materials will produce a corresponding change in its reactivity is called *the temperature coefficient of the reactivity.* The temperature coefficient of the reactivity is usually given by the symbol α_T, and it is formally defined by

$$\alpha_T = \frac{d\rho}{dT} = \frac{\Delta\rho}{\Delta T} \tag{17.8}$$

Thus if α_T and ΔT are known, then the change in the reactivity of the core becomes

$$\Delta\rho = \alpha_T \Delta T \tag{17.9}$$

where ΔT is the *average temperature change of the core* in degrees Kelvin or degrees centigrade. In some reactors, the value of α_T can be either positive or negative. However, *in most reactors, the temperature coefficient α_T is designed to be as negative as possible*. When the value of ΔT is positive, and the value of $\Delta\rho$ is *negative*, the effect on the reactivity is known as *negative temperature feedback*. Notice that Equation 17.9 implies that the relationship between $\Delta\rho$ and ΔT is a linear one, and while this relationship is not exactly linear in practice, it is usually accurate enough to predict how the core will behave. From Equation 17.9, it is also apparent that α_T has the units of per °C or per °K. Since the reactivity is given by

$$\rho = \frac{k-1}{k} = 1 - \frac{1}{k} \tag{17.10}$$

it also follows that

Temperature Coefficient of the Reactivity

$$\alpha_T = \frac{d\rho}{dT} = \frac{d\left(1 - 1/k\right)}{dT}$$

or

$$\alpha_T = \left(\frac{1}{k^2}\right)\frac{dk}{dT} \tag{17.11}$$

where for most practical purposes, we can generally assume that $k = K_{effective}$. Temperature changes can then alter the value of the reactivity in two primary ways:

- First, the temperature can change the reactivity by affecting the density of the coolant. As the temperature rises, the coolant expands and becomes less dense, and beyond a certain temperature and pressure, it will begin to boil. This boiling causes steam bubbles (e.g., voids) to develop in the coolant, which tends to harden the neutron energy spectrum since there are simply fewer atoms available to slow the neutrons down. This means that the supply of thermal neutrons will be reduced (due to the increased moderation), and if we are dealing with a thermal water reactor, this will tend to shut down the fission process if the change in the density of the coolant is great enough. So in a sense, increasing the power level is a self-regulating process as far as the moderator is concerned. The other

interesting thing that occurs in a thermal reactor is that the hardening of the neutron energy spectrum also increases the neutron leakage rate, since neutrons will diffuse more easily through a less-dense medium than they will through a denser one.

- Second, and perhaps more importantly, changes in the core temperature can affect the reactivity through changes in the temperature of the fuel. Although the fuel does not boil like the coolant does, the thermal expansion of the fuel can reduce the reactivity, and there is an additional mechanism called the *nuclear Doppler effect* that can affect the resonance escape probability and change the reactivity even further.

Hence, we can partition the temperature coefficient of the core into three primary components—one for the thermal expansion of the moderator, α_M; the second for the thermal expansion of the fuel, α_F; and the third for the increased neutron leakage rate from the core, α_L. If the coolant does not change phase, this allows us to write the total reactivity change as the sum of these three terms:

The Total Reactivity Change Due to Temperature-Related Effects

$$\Delta\rho = (\alpha_M + \alpha_F + \alpha_L)\Delta T \quad \text{where} \quad \alpha_T = \alpha_M + \alpha_F + \alpha_L \tag{17.12}$$

Of course, this equation assumes that the temperatures of the fuel and the moderator change at the same rate. In practice, this is rarely the case. Then separate values of ΔT must be used for the fuel, the moderator, and the core as a whole. The aggregate reactivity change is then

$$\Delta\rho = \alpha_M \Delta T_M + \alpha_F \Delta T_F + \alpha_L \Delta T_C \tag{17.13}$$

where ΔT_M, ΔT_F, and ΔT_C refer to the moderator, the fuel, and the core, respectively. The values of α_M, α_F, and α_L are tabulated and fed into Equation 17.12 to determine the total change in the reactivity as the temperatures changes from T to T′, where $\Delta T = T' - T$. Example Problem 17.3 illustrates how this can be done. Normally, every material in the core has its own value for α_M, α_F, and α_L, and to be completely accurate, every material can have its temperature change in a different way. For this reason, a more general expression for the temperature-related reactivity change is

$$\Delta\rho = \sum_j (\alpha_{Mj} + \alpha_{Fj} + \alpha_{Lj})\Delta T_j \quad (j = 1,2,\ldots,J) \tag{17.14}$$

where it is assumed that there are J materials in the core in all. Normally, the contributions of the cladding and the structure are lumped into the value of α_{Lj}. *In most reactors, the two dominant temperature coefficients are the moderator temperature coefficient α_M and the fuel temperature coefficient α_F.* Normally, the leakage temperature coefficient α_L is smaller and of less importance than the other two coefficients.

17.10 Moderator Temperature Coefficient

Next, let us discuss the magnitude and the sign of the moderator temperature coefficient. If the coolant does not boil, the sign of the *moderator temperature coefficient* is primarily determined by the molecular density of the coolant. Since most reactor coolants expand when they are heated, the molecular density of the coolant falls as the temperature increases, and the moderating efficiency decreases as well (Table 17.1). In other words, *the moderator coefficient is normally a negative number. A negative coefficient prevents a reactor from running away when the power level is suddenly raised. Hence, reactors with a negative moderator coefficient are more stable than reactors with a positive moderator coefficient.* The example below illustrates how this affects the reactivity.

Example Problem 17.3

Suppose that a thermal water reactor has a fuel temperature coefficient of −1 cent/°C, a moderator temperature coefficient of −0.5 cents/°C, and a leakage temperature coefficient of −0.1 cents/°C. If the temperature of all three materials is suddenly increased by 100°C, how much does the reactivity ρ fall in this case?

Solution The total change in the reactivity is given by $\Delta\rho = \alpha_M \Delta T_M + \alpha_F \Delta T_F + \alpha_L \Delta T_L$. Since $\Delta T_M = \Delta T_F = \Delta T_L = 100°C$, the reactivity falls by $\Delta\rho = -(0.01 + 0.005 + 0.001) \times 100 = -160$ cents $= -1.6$ dollars in this case. [Ans.]

TABLE 17.1
Various Ways of Controlling the Reactivity and the Time Frames in Which They Are Effective

Reactivity Changing Mechanism	Symbol	Effect on the Reactivity	Typical Time Frame of Operation	Domain of Control (Local, Global, Both)
Fuel burnup and depletion	$\Delta\rho_F$	Negative	Days to months	Both
Fission products buildup (including xenon)	$\Delta\rho_P$	Negative (without xenon) Positive or negative with xenon	Hours to months	Global
Chemical shim (boric acid)	$\Delta\rho_B$	Negative (if increased) Positive (if decreased)	Hours to months	Global
Burnable poisons	$\Delta\rho_{BP}$	Negative	Days to months	Local
Control rods	$\Delta\rho_R$	Negative (inserted) Positive (withdrawn)	Seconds to months	Both
Temperature changes to the fuel and coolant[a]	$\Delta\rho_T$	Negative for $+\Delta T$ Positive for $-\Delta T$	Milliseconds to minutes	Both

[a] Thermal reactors only.

17.11 Effect of Boric Acid on the Moderator Temperature Coefficient

In modern PWRs, the moderator coefficient is a function of the amount of boric acid that is dissolved in the coolant. *In a fresh core, the moderator coefficient α_M can sometimes become positive when the boric acid concentration exceeds 1500 PPM (parts per million), or about 1.5 grams per liter*. For this reason, burnable poisons are added to the fuel assemblies to keep the total temperature coefficient (fuel plus moderator) negative initially. Then, as the boric acid concentration decreases, the moderator coefficient becomes negative as well. *Even at a modest boric acid concentration of 1700 PPM, the moderator coefficient can still have a positive value of +12.5 pcm/°C, or 1.925 cents/°C.* This means that an increase in the moderator temperature of just 8°C will increase the reactivity by about 15.4 cents, which would double the power level in about 40 seconds (see Chapter 20). The effect of burnable poisons on the Solbor concentration is discussed in Chapter 20, and the actual variation is shown in Figure 18.12.

17.12 Temperature Feedback with Nucleate or Bulk Boiling

In PWRs, gas reactors, and liquid metal fast breeder reactors, the reactivity is temperature dependent as long as the coolant does not boil. However, when the coolant boils (as it does in a BWR), the previous expression for the moderator temperature coefficient

$$\alpha_M = \frac{d\rho}{dT_M} \tag{17.15}$$

can no longer be used to estimate the change in the core power level because voids (or bubbles) are created in the coolant while *the temperature of the coolant remains the same*. However, the void fraction *does* change as the coolant absorbs additional thermal energy, and this is how the reactivity change must be determined. In previous chapters, we learned that *the coolant in a BWR reaches its saturation temperature (286°C) about one-third of the way up the core, and beyond this point, the coolant temperature stays the same no matter how much energy is added to the coolant. (The additional energy simply creates more voids.)* This process continues until all of the coolant has been converted into steam. Practically speaking, the void fraction α in a BWR never rises above 80% (even at the core exit), and the quality x of the coolant rarely exceeds 17% at this elevation. The temperature and void fraction profiles are shown in Figure 17.10. This means that an entirely different approach must be used to estimate the reactivity changes induced by the presence of these voids. In practice, this can be done by defining another reactivity coefficient called the *void coefficient* of the reactivity.

In the sections that follow, we would like to explain how the void coefficient of the reactivity works. The void coefficient is more important than the moderator temperature coefficient when it comes to determining the behavior of a BWR. In fact, during normal operation, *the void coefficient completely dominates the moderator temperature coefficient in a BWR.* Conversely, in a PWR, where most the coolant does not boil, the void content rarely exceeds one-half of one percent. Thus, the void coefficient is normally of no importance to the time-dependent behavior of a PWR. The only exception to this rule is a severe *reactor accident*, which we will discuss in Chapter 21.

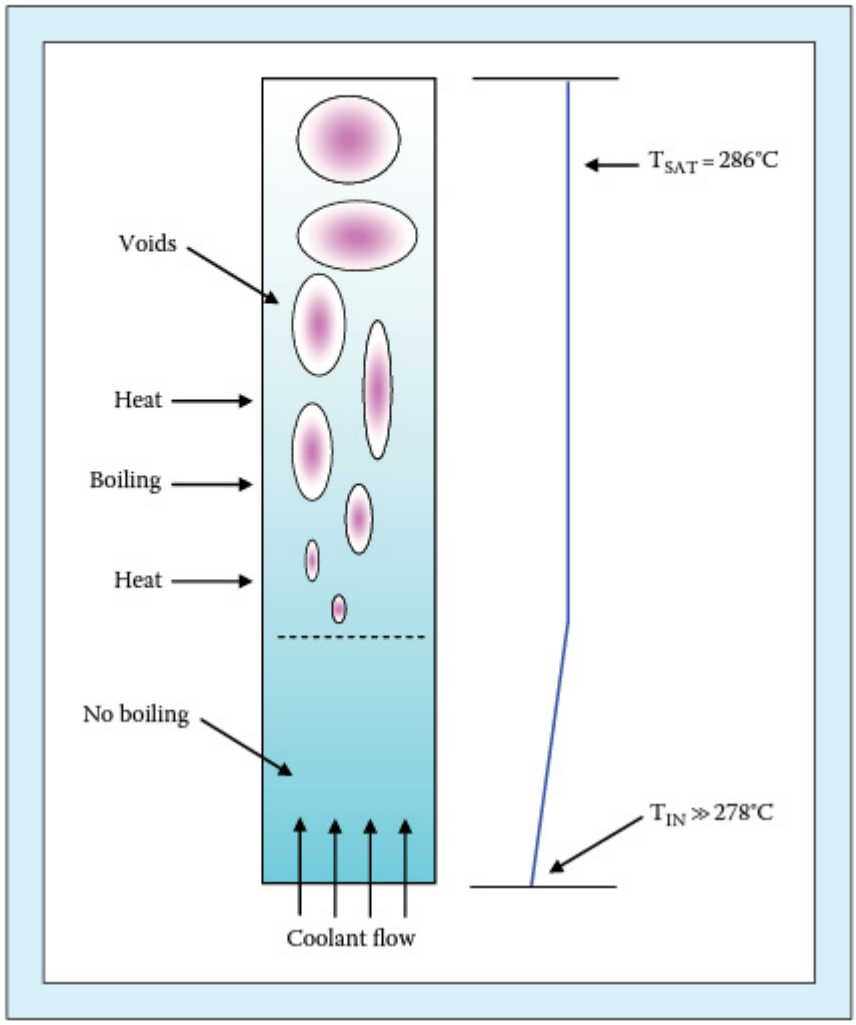

FIGURE 17.10 An illustration of how the temperature of the coolant and the void fraction changes in a BWR coolant channel.

17.13 Understanding the Void Coefficient of the Reactivity

We can estimate the effect that vapor bubbles (or voids) have on the average density of the coolant if we know the void fraction α of the liquid–vapor mixture. The reader may recall that the void fraction α at a particular location in the core* is defined as

Definition of the Void Fraction (α)

$$\text{Void fraction} = \frac{\text{Volume of the vapor}}{(\text{Volume of the liquid} + \text{Volume of the vapor})} \tag{17.16}$$

In Equation 17.16 the phases are assumed to move at the same speed. The density of the resulting liquid–vapor mixture is then

$$\rho_{MIX} = (1-\alpha)\rho_l + \alpha\rho_V \tag{17.17}$$

Here ρ_l is the density of the liquid, ρ_v is the density of the vapor, and α is the local void fraction (which can be a function of axial elevation). Numerically, we can express the relationship between the reactivity change $\Delta\rho$ and the change in the void fraction $\Delta\alpha$ as

* See *Nuclear Engineering Fundamentals: A Practical Perspective*, by R.E. Masterson, CRC Press (2017).

Definition of the Void Coefficient of the Reactivity

$$\alpha_V = \frac{\Delta\rho}{\Delta\alpha}$$

or

$$\alpha_V = \frac{d\rho}{d\alpha} \tag{17.18}$$

Equation 17.18 then defines the *void coefficient of the reactivity* α_V. In other words, when the coolant boils, changing the void fraction affects the value of the reactivity ρ even though the average temperature of the coolant remains the same. The exact relationship between the reactivity change and the change in the void fraction is

$$\Delta\rho = \alpha_V \Delta\alpha \tag{17.19}$$

and this relationship appears frequently in the analysis of BWR cores. Now, let us examine some representative values for the size of the void coefficient of the reactivity. *In a modern BWR, the void coefficient has a value of about −0.0015 per % void*. In other words, if the void fraction in the core is 40% (a common core average), the reactivity reduction due to the presence of the voids alone is 40% × −0.0015/% = −0.0600. *This is about 9 dollars and 25 cents of negative reactivity for a U-235-fueled core!* Notice that α_V *is a dimensionless number*, and unlike the temperature coefficients α_M, α_F, and α_L that we discussed previously, *it does not have the units of inverse temperature*. Moreover, except near the critical point of water (where the values of ρ_l and ρ_v are nearly identical), it is a *large negative number* since increasing α will always decrease the value of ρ_{MIX}. We can show why this is true by noting that ρ_l is always much larger than ρ_v (i.e., $\rho_v \ll \rho_l$). So in a typical BWR core, where the operating pressure is 1050 PSI (~7.15 MPa), we find that

$$\rho_{MIX} \approx (1-\alpha)\rho_l \tag{17.20}$$

We then find that $d\rho_{MIX}/d\alpha \approx -\rho_l$. In other words, ρ_{MIX} *decreases as* α *increases*, and in general, the reactivity ρ follows a similar trend.

17.14 The Void Coefficient and Load Following

Since the density of the coolant is so sensitive to the value of α in BWRs, the heat-generation rate depends on how large the void fraction can be. This means that *the power level in the core can be increased by increasing the core flow rate* (since fewer voids will be formed), and *the power level in the core can be decreased by decreasing the core flow rate* (because this adds more heat to the coolant and causes the number of voids to increase). A commercial BWR uses this principle to couple the core flow rate to the power output of the plant. If the steam turbines sense that more electrical power is needed, they send a signal to the recirculation pumps to increase the mass flow rate through the core. This reduces the number of voids and increases the power output. Conversely, if less electricity is required, the steam turbines send a signal to the recirculation pumps to reduce the core flow rate. This causes the load on the turbines to fall, and less electricity will be produced. Hence, the power output of the core can be "throttled" to match the electrical demand from the power grid, and this is how the term *load following* originated. Due to the negative void coefficient, a BWR is an exceptional load-following device (see Figure 17.11).

PWRs are also good at load following but in this case, the load following is due to the negative moderator coefficient (and not the negative void coefficient). Both of these effects are illustrated in Figure 17.12. Because it takes a while for the heat to escape from the fuel rods, *the moderator temperature coefficient and the void coefficient do not respond as quickly to changes in the power level* as the fuel temperature coefficient does. *So during fast transients in PWRs and BWRs, the time-dependent behavior of the core is determined primarily by changes to the temperature of the fuel.* In other words,

The fuel temperature coefficient is normally the first line of defense against a reactor suddenly overheating and running away.

In the sections that follow, we would like to discuss the fuel temperature coefficient and explain why it is so important to the safety of a nuclear power plant. The value of the fuel temperature coefficient depends almost entirely on

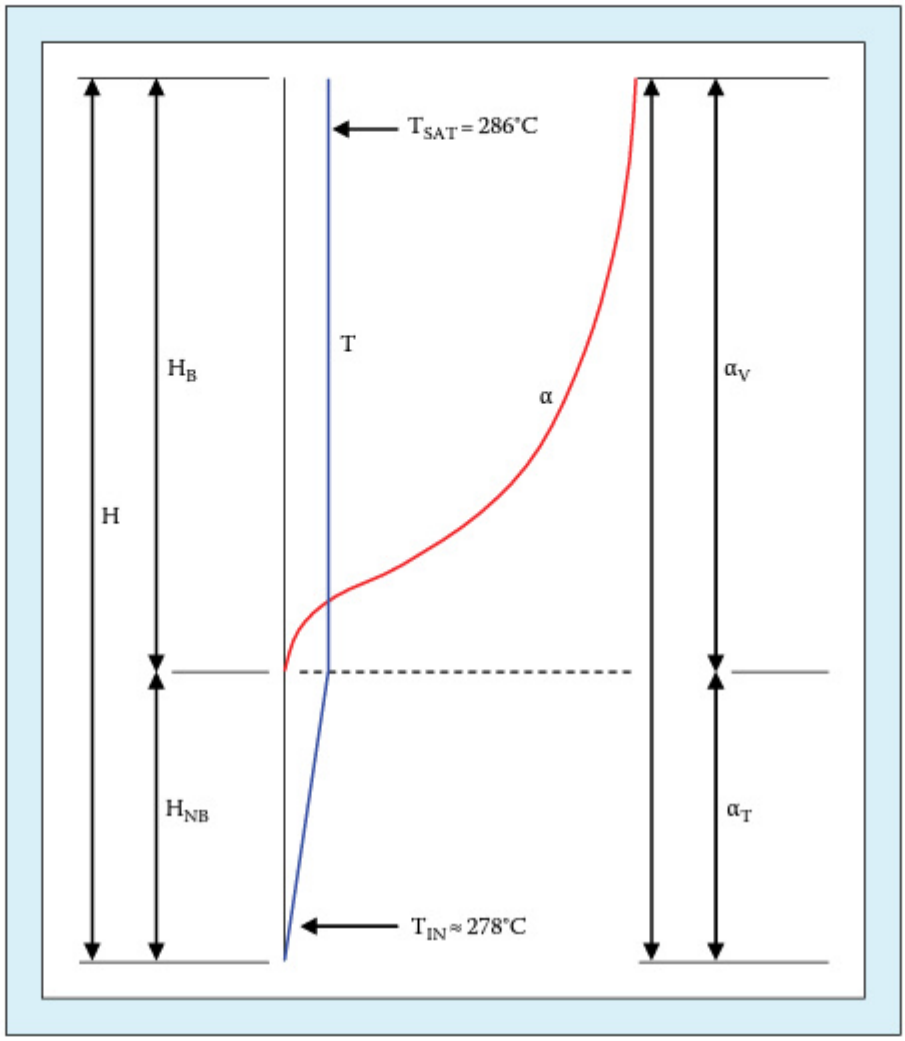

FIGURE 17.11 An illustration of the boiling and nonboiling heights in a BWR coolant channel. Before the water starts to boil (in the lower 25% of the core), the moderator coefficient of the reactivity α_M can be used to find the reactivity change, and in the upper 75% of the core, the void coefficient of the reactivity α_v must be used to find the reactivity change.

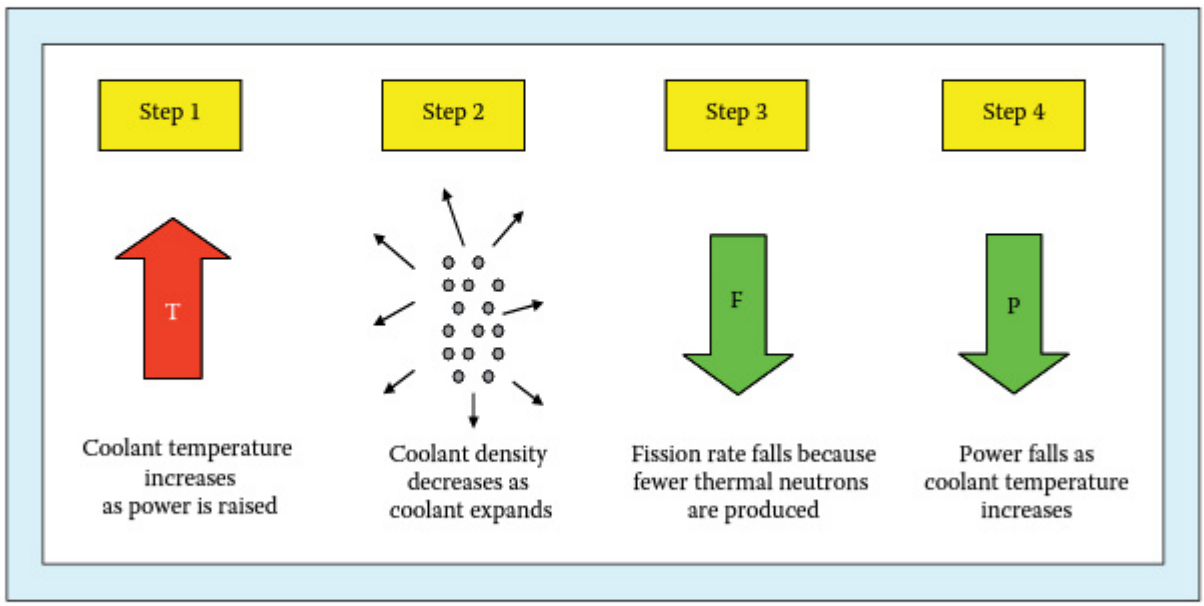

FIGURE 17.12 An illustration of how coolant temperature feedback works in a PWR or a BWR.

the isotopic composition of the fuel. Thus, *a poorly designed reactor (like the one at Chernobyl) had a positive fuel temperature coefficient*, while a well-designed reactor (like a modern PWR) will have a negative fuel temperature coefficient.

17.15 Understanding the Fuel Temperature Coefficient

In general, *fuel temperature feedback* has a greater initial impact on the system-wide reactivity than either the moderator temperature coefficient or the void coefficient. This is particularly true when the reactor power level increases or decreases over very short periods of time. Consequently, the fuel temperature coefficient is sometimes called the *prompt temperature coefficient* because a sharp increase in the reactor power level will cause the fuel temperature to change instantaneously. In practice, the fuel temperature coefficient can be designed to be either positive or negative; however, almost all reactors are designed with a negative temperature coefficient to make them easier to control. *The fuel temperature coefficient then measures the rate of change of the reactivity per degree change in the temperature of the fuel.* From the six-factor formula

$$k = P_{FNL}P_{TNL}K_{\infty} = P_{FNL}P_{TNL}(\eta\varepsilon fp) \tag{17.21}$$

we know that *the primary factor that is effected by a change in the fuel temperature is the resonance escape probability p* (see how it was originally defined in Chapter 10). The fast-fission factor ε has almost no dependence on the fuel temperature in a thermal water reactor. The eta of the fuel η is also temperature dependent, and we will discuss its specific temperature dependence in another section.

We can therefore equate the fuel temperature coefficient α_F to the behavior of d*p*/dT, or more specifically $\alpha_F \sim dp/dT$ where we can now hypothesize that the resonance escape probability *p*, which we have previously assumed to be a constant, is now temperature dependent; that is, $p = p(T)$. Since any change in the temperature is first felt in the fuel, this factor determines the initial response of a reactor to a sudden change in the power level. We would now like to discuss how the resonance escape probability is affected by the fuel pin temperature.

17.16 Doppler Broadening and Its Effect on the Resonance Escape Probability

Thermal water reactors use enriched uranium fuel that contains U-235 and U-238. Increasing the temperature of the fuel causes the atoms in the fuel to vibrate more vigorously because their kinetic energies are higher. The increase in their kinetic energy $E = \frac{1}{2}mv^2$ is proportional to the absolute temperature T, which implies that

Relating the Energy to the Temperature

$$E = \frac{1}{2}mv^2 = BT \tag{17.22}$$

where B is an arbitrary constant that depends on the type of fuel. If the atoms in the fuel happen to be loosely bound, and are not considered to be part of an actual lattice, then the constant of proportionality B becomes *Boltzmann's constant k*, divided by 2. This means that the average velocity that the atoms vibrate in the lattice is proportional to the square root of their absolute temperature T (see Chapter 8). On the other hand, fission neutrons begin to slow down by colliding with the atoms in the fuel rods, and they eventually reach an energy just above the thermal energy range (~0.025 eV) where many neutron absorption resonances exist. *In particular, fuels like Thorium-232, Uranium-238, and Plutonium-240 have very large absorption resonances starting at about 10 KeV.* The absorption resonances for Thorium-232 and Uranium-238 are shown in Figure 17.13.

For these materials the average spacing between these resonances is about 20 eV, and their average width is about 0.01 eV. One such resonance (out of potentially hundreds or even thousands of resonances) is shown in Figure 17.14. As the fission neutrons slow down and enter the range of energies where these resonances occur, a stationary target nucleus will have a much higher probability of absorbing a neutron if its energy E is very close to the energy of one of these resonance peaks. (Normally, this energy is represented by the symbol E_o.) However, if the nuclei are vibrating about their equilibrium positions in the lattice, their absorption resonances will appear to the approaching neutrons to *broaden out* due to the random thermal motion of the fuel atoms. This effect is sometimes called the *Doppler broadening* of the absorption resonances, and the overall effect is called the *nuclear Doppler effect*. As the temperature of the fuel rises, the relative energy difference between the nuclei and a neutron of energy E can assume a much greater distribution of energies due to the fact that each nucleus may be moving toward the neutron at one moment and away from the neutron at

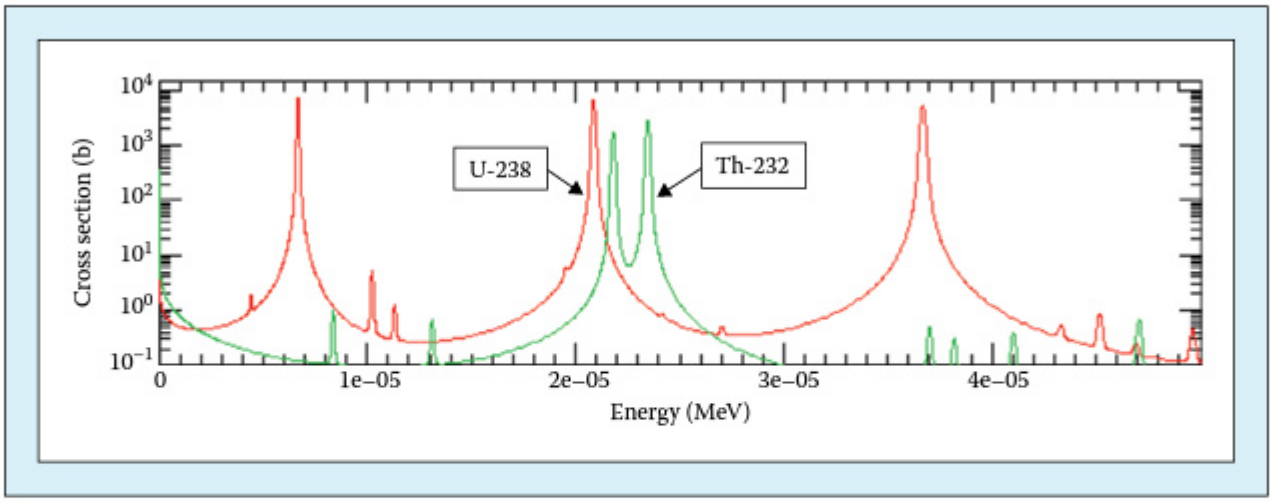

FIGURE 17.13 The absorption resonances for U-238 (in red) and Thorium-232 (in green) that dominate the value of resonance escape probability P just above the thermal energy range. (Courtesy of Kaere.)

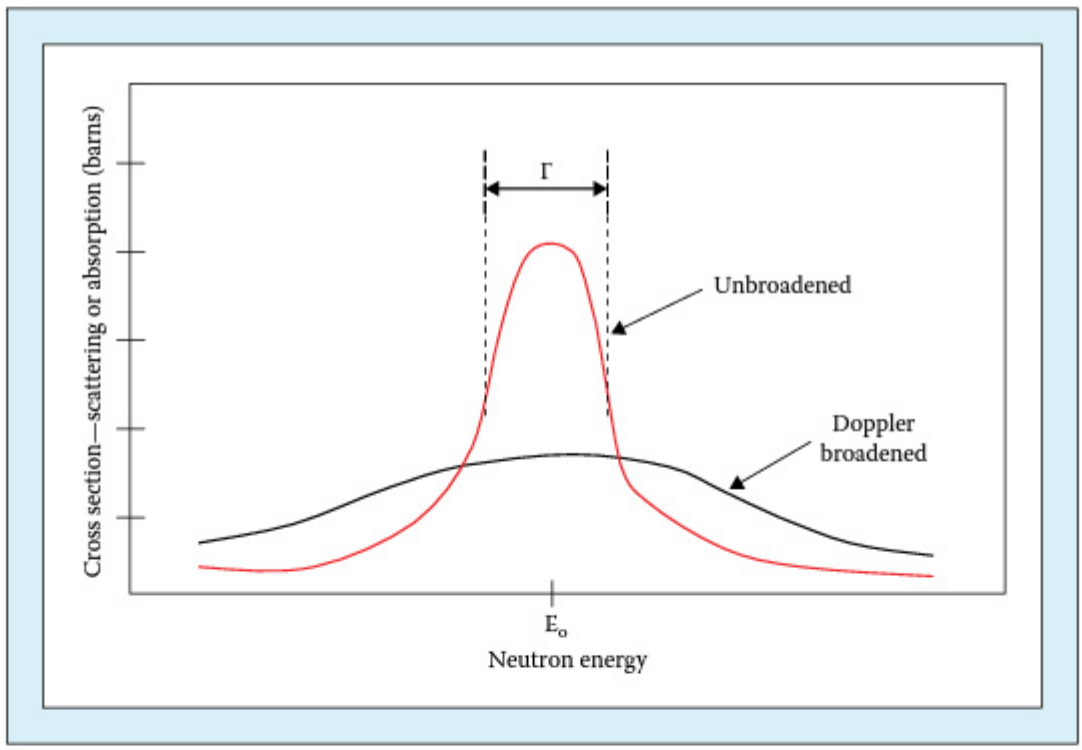

FIGURE 17.14 Effect of fuel temperature on the width and height of the absorption resonances.

another. The result of this random thermal motion is that a beam of monoenergetic neutrons will have a continuous spread of kinetic energies rather than just a single kinetic energy E.

When viewed by the oncoming neutrons, the net effect of this molecular agitation is that *the absorption resonances of the fuel atoms appear to become broader as the temperature is increased. Thus the resonance escape probability p always decreases as the fuel temperature is raised because the Doppler broadening will cause more epithermal neutrons to be absorbed*. We can immediately conclude that the reactivity of the fuel must be temperature dependent because the effective multiplication factor must be temperature dependent as well:

$$K_{effective}(T) = P_{FNL}P_{TNL}K_{\infty} = P_{FNL}P_{TNL}\varepsilon f\eta(T)\cdot p(T) \tag{17.23}$$

Various theoretical models have been developed to quantify this process at a molecular level. The most famous of these is the *Breit–Wigner model*, which was developed by scientists working on the Manhattan Project during the Second World War. In essence, the Breit–Wigner model attempts to describe a theoretically symmetric absorption resonance of half width Γ centered about a single resonance energy E_o. The absorption cross section $\sigma_a(E)$ around the resonance peak is represented by

The Breit–Wigner Formula

$$\sigma_a(E) = \frac{\sigma_o \Gamma^2}{(E - E_o)^2 + (\Gamma/2)^2} \tag{17.24}$$

where σ_o is a previously computed value that depends on the wavelength of the neutron at the resonance peak. The Breit–Wigner method can be applied to neutron-scattering resonances by replacing $\sigma_a(E)$ with $\sigma_s(E)$. Thus even if the initial neutron energy E does not correspond to the peak energy at E_o, the random thermal motion of the target nucleus causes some of the incoming neutrons to have a relative energy that is very close to E_o. If the nucleus is moving away from the neutron, the velocity of the neutron must be *greater* than E_o to hit the resonance peak. Conversely, if the nucleus is moving toward the neutron, the neutron needs *less* energy than E_o to be absorbed. Raising the value of T causes the fuel atoms to vibrate more vigorously about their equilibrium positions, and this causes more neutrons to become trapped in the absorption resonances. Moreover, it can be shown after a lengthy derivation that the contribution of the resonance escape probability to the fuel temperature coefficient for a simple substance is given by

$$\alpha_P = \frac{1}{p}\frac{dp}{dt} = -\frac{C}{\sqrt{T}} \ln\left[\frac{1}{p_o}\right] \tag{17.25}$$

where p_o is the resonance escape probability at an initial temperature of 300°K, and the value of C is given by

$$C = \frac{A + B}{r\rho} \tag{17.26}$$

where A and B are the dimensionless numbers shown in Table 17.2, r is the radius of the fuel pin (in cm), and ρ is the density of the fuel in grams per cubic centimeter (gm/cm^3). In other words, the contribution of the *Nuclear Doppler Effect* to the fuel pin temperature coefficient is given by

The Contribution of the Doppler Effect to the Fuel Temperature Coefficient

$$\alpha_P = -\frac{C}{\sqrt{T}} \ln\left[\frac{1}{p_o}\right] \tag{17.27}$$

TABLE 17.2
Empirical Constants Used in the Calculation of the Fuel Temperature Coefficient α_F

Fuel Type	A	B
UO_2	3050	47
ThO_2	4850	120
U (metallic)	2400	64
Th (metallic)	4250	134

Source: Lamarsh, J.R., *Introduction to Nuclear Reactor Theory*, second printing, Addison-Wesley Publishing Company, Inc., 1972.

where T is the fuel temperature in °K and p_o is the resonance escape probability that we measure at room temperature (300°K). Because ln $[1/p_o]$ and the coefficient C are always positive, *the contribution of the resonance escape probability to the prompt temperature coefficient is always negative*. Obviously, as T increases, the size of α_P decreases. Since the velocity v is proportional to the square root of the temperature, it also follows that

$$\alpha_P \sim \frac{1}{v} \tag{17.28}$$

In addition to the resonance escape probability, the neutron reproduction factor η used in the six-factor formula also has a slight temperature dependence. We would now like to explore the form of this dependence for different nuclear fuels.

17.17 Other Factors That Affect the Fuel Temperature Coefficient

The temperature dependence of the neutron reproduction factor η stems from the fact that the thermal cross sections for fission and radiative capture σ_f and σ_c do not have the same dependence on the speed of a thermal neutron. For a single fissile isotope, η is defined as

$$\eta = \frac{\nu\sigma_f}{\sigma_a} = \frac{\nu\sigma_f}{\sigma_c + \sigma_f} \tag{17.29}$$

where ν is the average number of neutrons released per fission. The energy dependence of η at thermal energies is determined primarily by the ratio of σ_f to σ_c. In 1962, *Charles Westcott* used the values he measured for σ_f and σ_c to derive explicit expressions for α_η for several nuclear fuels. Assuming the neutron energy spectrum was Maxwellian, he found that the values of the temperature coefficients for U-233, U-235, and Pu-239 were given by

Fuel Temperature Coefficients for Important Nuclear Fuels

$$\begin{aligned} \alpha_\eta &= +4.0\times10^{-5} \text{ per °K} \quad (\text{for U-233}) \\ \alpha_\eta &= -3.0\times10^{-5} \text{ per °K} \quad (\text{for U-235}) \\ \alpha_\eta &= -5.0\times10^{-4} \text{ per °K} \quad (\text{for Pu-239}) \end{aligned} \tag{17.30}$$

at room temperature. In addition, he showed that natural uranium had a value for α_η close to zero below 300°C (573°K) although its value increases to about -1.0×10^{-4} per °K above room temperature. When more than one type of fuel is used, a weighted average of the fuel temperatures must also be used. In other words, the fuel temperature coefficient α_F consists of a resonance escape coefficient α_P and a neutron reproductive coefficient α_η whose values are given by Equations 17.27 and 17.29, respectively:

$$\alpha_F = \alpha_P + \alpha_\eta \tag{17.31}$$

Now let us discuss the size of the temperature coefficient in more detail. *Fuel temperature coefficients for thermal water reactors range between -1.0×10^{-5} per °K and -5.0×10^{-5} per °K for U-235-fueled cores*. For example, the fuel temperature coefficient for a modern 9×9 BWR fuel assembly is about -1.7×10^{-5} per °K in absolute units, or -1.7×10^{-5} per °K/β in dollars and cents. An instantaneous 100°K degree rise in the fuel temperature then reduces the reactivity by $100 \times -0.000017/0.0065 = -0.0017/0.0065 = -26$ cents. Of course, this value would be different when a reactor was fueled with U-233 or Pu-239 instead of U-235.

Example Problem 17.4

If the value of α_F at a temperature of T is known to be -2.0×10^{-5} per °K, what is the value of α_F at a temperature of 4T?

Solution Since $\alpha_F(T) = \dfrac{C}{\sqrt{T}\ln[1/p_o]}$, it follows that $\alpha_F(4T) = \dfrac{C}{\sqrt{4T}\ln[1/p_o]} = \dfrac{1/2C}{\sqrt{T}\ln[1/p_o]}$, so

$$\frac{\alpha_F(4T)}{\alpha_F(T)} = \frac{1/2C\sqrt{T}\ln[1/p_o]}{C\sqrt{T}\ln[1/p_o]}.$$

Most of the terms in this expression cancel, and after some additional algebra, we are left with

$$\frac{\alpha_F(4T)}{\alpha_F(T)} = \frac{1}{2}$$

$$\text{Thus if } \alpha_F(T) = -2.0\times10^{-5}\,\text{per °K}, \quad \text{then} \quad \alpha_F(4T) = \frac{1}{2}\alpha_F(T) = -1.0\times10^{-5}\,\text{per °K}$$

So if we increase the fuel temperature by a factor of 4, α_F becomes 50% *smaller*. Note, however, that the value of α_F is still a *negative number* in this case. [Ans.]

17.18 Time Dependence of the Core Temperature Coefficients

Because the temperature coefficients for the fuel and the moderator do not change at the same rate, their instantaneous effect on the reactivity is *not* the same. In other words, the fuel temperature coefficient affects the reactivity *more quickly* than the moderator temperature coefficient does. For example, changing the temperature of the fuel causes a system-wide change in the reactivity to occur almost immediately. This is because it takes only a couple of milliseconds for the fuel temperature to rise enough to throw additional neutrons into the U-238 absorption resonances. The time frame for this can be as little as 10^{-4} seconds, and consequently, the fuel temperature coefficient is also called the *"prompt" temperature coefficient.*

Now let us say a few words about the moderator. Normally it takes a couple of seconds for the heat produced in the fuel to reach the moderator. This heat is transferred by the process of thermal *conduction*. This means that the moderator will have only a very small effect on the reactivity initially, but this time lag will only persist until vapor bubbles begin to form. As soon as the coolant starts to boil, the density becomes

$$\rho_{\text{coolant}} = (1-\alpha)\rho_l + \alpha\rho_v \tag{17.32}$$

where

ρ_l is the density of the liquid
ρ_v is the density of the vapor
α is the void fraction of the mixture

Thus this density change needs to be taken into account in the calculation of the time-dependent reactivity reduction. Finally, the neutron energy spectrum hardens when more voids appear. This causes the neutron leakage rate L to increase, and the neutron mean free path increases as well. The time frames associated with each of these changes to the global reactivity are shown in Table 17.3. Table 17.3 also gives the magnitude of the changes as well.

TABLE 17.3
Time Frames Associated with Temperature-Dependent Reactivity Changes

Coefficient	Time Frame	Typical Value	Total Effect ($\Delta T = 10°K$) (Negative Dollars)	Total Effect ($\Delta T = 100°K$) (Negative Dollars)
α_F	10^{-3} s	-3.0×10^{-5} per °K	~$ 0.05	~$ 0.50
α_M[a]	1–5 s	-0.5×10^{-5} per °K	<$ 0.01	~$ 0.08
α_v[b]	1–5 s	−0.0015 per % void	~ 25 cents per void %[d]	~25 cents per void %[d]
α_L[a]	10^{-2} s	-0.1×10^{-5} per °K	<$ 0.01	<$ 0.01
α_L[b]	TTCP[c] + 10^{-2} s	-0.3×10^{-5} per °K	<$ 0.01	~$ 0.01

[a] Before phase change.
[b] After phase change.
[c] TTCP = time to change phase.
[d] For a Uranium-235-fueled thermal reactor with a β of 0.0065.

17.19 Regulatory Requirements Governing Sudden Reactivity Changes

Raising the power level does not necessarily guarantee that all regions of the core will experience the same temperature change at the same time. For example, the fuel temperature may increase faster than the coolant temperature, and in some fuel assemblies, the temperature of the coolant may be lower than in others. For this reason, the U.S. NRC will not allow a commercial nuclear power plant to be licensed in the United States unless the temperature coefficient of the reactivity is negative across its *entire operating range*. (Military reactors normally have different regulatory requirements.)

Normally, the value of α_T is measured by increasing the power level, and at each elevated power, measuring the increase in the temperature of the coolant ΔT and the overall reactivity change $\Delta\rho$. (The value of $\Delta\rho$ can be then inferred from the reactor period T.) The results of this data collection process are shown for a research reactor in Table 17.4. After the data has been collected, it can then be plotted using a graph similar to that shown in Figure 17.15.

TABLE 17.4
Measurements of the Temperature Coefficient of Reactivity for a Hypothetical Research Reactor

Reactor Power (kW)	Average Core Temperature (°C)	Core ΔT (°C)	Core $\Delta\rho$ (cents)	$\alpha_T = \Delta\rho/\Delta T$ (cents/°C)
0.1	25.8	0.0	~0.0	0
5.0	28.9	3.1	−6.8	−2.19
15.0	35.1	6.2	−9.7	−1.56
25.0	44.3	9.2	−10.7	−1.15
50.0	58.9	14.6	−15.8	−1.08
75.0	82.2	15.9	−19.3	−1.15
100.0	98.4	16.2	−19.1	−1.18
150.0	119.7	19.3	−28.8	−1.24
200.0	147.5	25.8	−33.4	−1.29
250.0	161.3	13.8	−19.3	−1.40
300.0	179.9	19.6	−28.6	−1.53

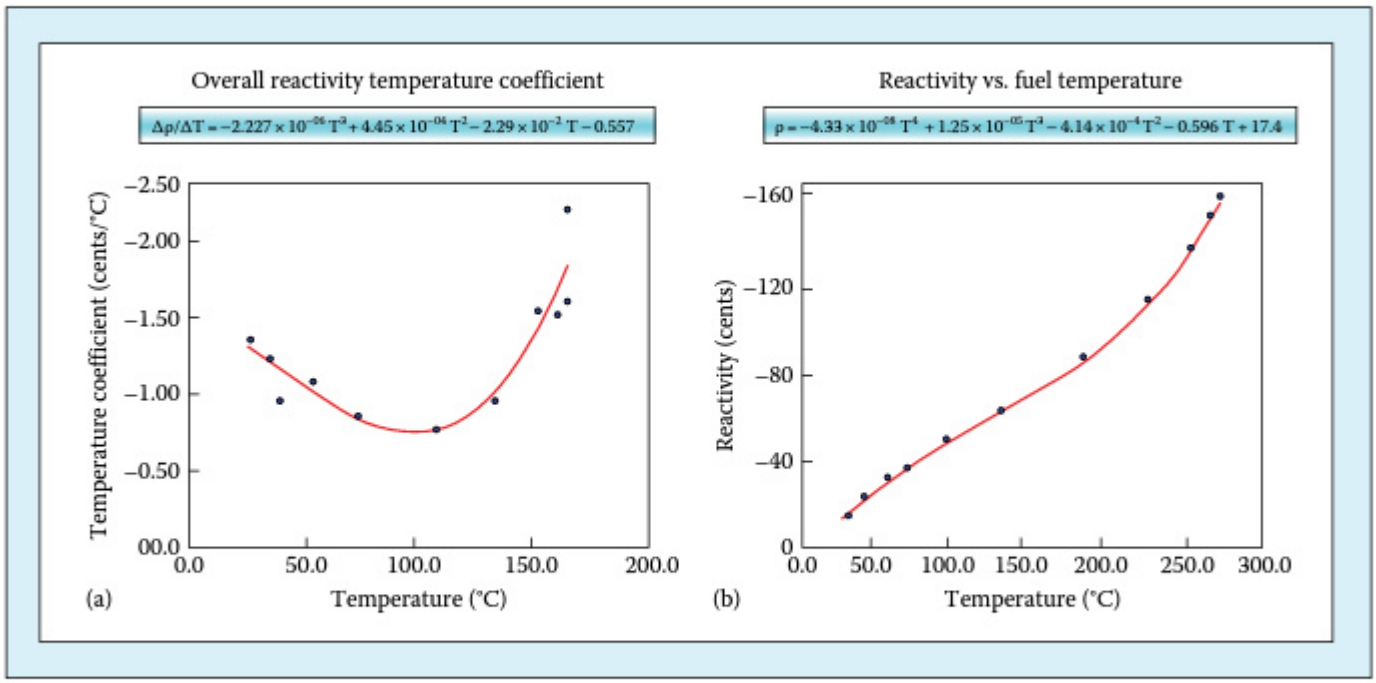

FIGURE 17.15 The overall temperature coefficient of the reactivity and the change in the reactivity versus fuel temperature for a typical thermal water reactor, similar to many research reactors that are in operation today.

Example Problem 17.5

Suppose that a thermal water reactor is fueled with U-235. Assuming the neutron energy spectrum is Maxwellian, how much do you expect the reactivity to decrease when the average temperature of the fuel is raised from 1000°C to 1200°C? What is the expected reactivity change in this reactor in dollars and cents?

Solution According to our previous discussion, the temperature coefficient for U-235 is $\alpha_T(\eta) = -3.0 \times 10^{-5}$ per °K. Therefore, raising the fuel temperature by 200°C lowers the reactivity by $200 \times -3.0 \times 10^{-5} = -0.006 = -600$ pcm. In dollars and cents, this is a reactivity change of $\Delta\rho = -0.006/\beta = -0.006/0.0065 \approx -92$ cents. [Ans.]

17.20 Compliance with the Compendium of Federal Regulations and 10 CFR50

Reactors rely on a negative temperature coefficient to keep them safe when their power levels unexpectedly rise. In the United States, the Nuclear Regulatory Commission will not license a commercial power reactor unless the value of α_F is negative over its entire operating range. The requirement is set forth in a document called the *Compendium of Federal Regulations, which the reader is encouraged to read*. *Appendix A of 10 CFR50* states

> *The prompt inherent feedback characteristics of the fuel must compensate for a rapid increase in the reactivity in the power operating range.*

In other words, the NRC requires the prompt temperature coefficient to be negative *over the entire operating range* before an operating license can be issued. The physical basis for this decision is illustrated in Figure 17.16. In Canada and other countries that use natural uranium-fueled reactors, this operating requirement is sometimes relaxed to account for the fact that the power levels are much lower than they are in conventional PWRs and BWRs. However, even under these circumstances, the reactor vendor must show that the *average* fuel temperature coefficient is negative, even though there may be some regions of the core where it may be zero or slightly positive.

Thus the temperature coefficients we have discussed are needed to keep modern nuclear reactors safe. So while we have written the total temperature coefficient α_T as

$$\alpha_T = \alpha_M + \alpha_F + \alpha_L \tag{17.33}$$

to reduce the notational complexity, in practice it is usually written as

$$\alpha_T(T) = \alpha_M(T) + \alpha_F(T) + \alpha_L(T) \tag{17.34}$$

This means that the operational data required to license a commercial nuclear power plant needs to be recorded in a table, such as the one shown in Table 17.4. Normally this data is then fit to a curve using a curve-fitting technique such as the *least squares method*, which we will subsequently discuss.

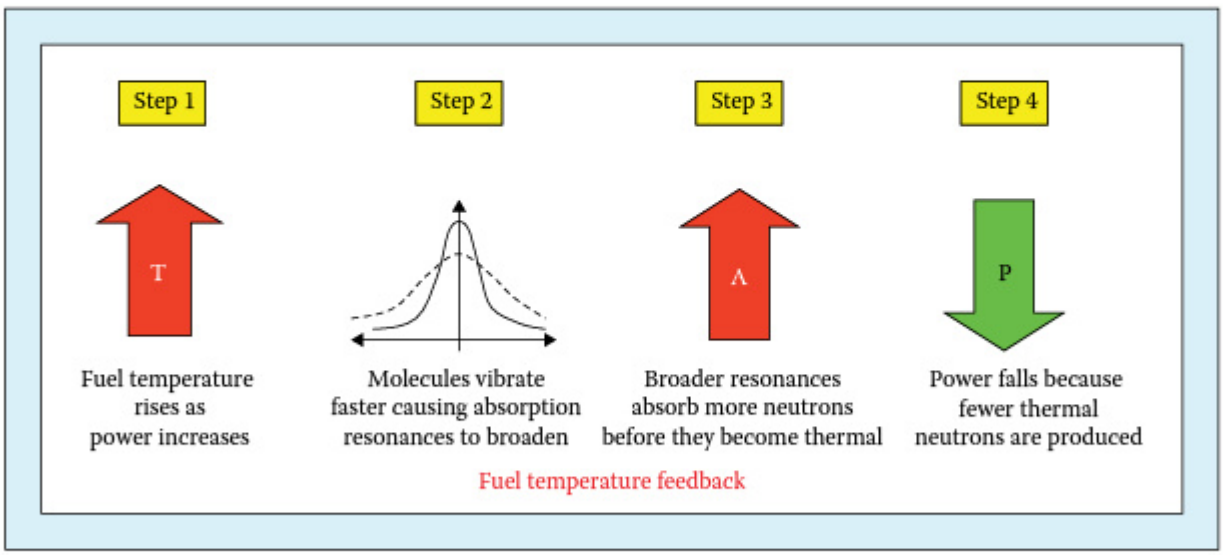

FIGURE 17.16 The effect of fuel temperature feedback on the power level in a nuclear reactor.

Example Problem 17.6

If the average values for $\alpha_M(T)$, $\alpha_F(T)$, and $\alpha_S(T)$ (where "s" refers to the structure) are -0.5×10^{-5} per °C, -3.0×10^{-5} per °C, and -0.1×10^{-5} per °C, for a reactor that is just starting up, what is the total temperature coefficient for the core? Assume the core is 25% fuel, 25% structure, and 50% coolant.

Part 2: Suppose that the temperature of the coolant increases from 310°C to 340°C during a brief transient, and the fuel temperature increases from 1000°C to 1200°C. How much negative reactivity is introduced into the core by this temperature increase?

Solution We need to apply the relationship $\Delta\rho = \alpha_T \Delta T = \{\alpha_M(T) + \alpha_F(T) + \alpha_S(T)\}\ \Delta T$ to find the answer to this question. Since the core is 25% fuel, 25% structure, and 50% coolant, the volume-average temperature coefficient is $\alpha_T = \{0.50\alpha_M(T) + 0.25\alpha_F(T) + 0.25\alpha_S(T)\} = \{-0.25 \times 10^{-5} - 0.75 \times 10^{-5} - 0.025 \times 10^{-5}\} = -1.025 \times 10^{-5}$ per °C.

Part 2: However, in a real core, the fuel temperature and the coolant/structure temperature change at different rates. The structure temperature (which affects the neutron leakage rate) changes at about the same rate as the coolant temperature, but the fuel temperature changes much more quickly. In this case, the overall reactivity change will be $\Delta\rho = \alpha_M \Delta T_M V_M + \alpha_F \Delta T_F V_F + \alpha_S \Delta T_S V_S = -0.5 \times 10^{-5} \times 30 \times 0.50 - 3.0 \times 10^{-5} \times 200 \times 0.25 - 0.1 \times 10^{-5} \times 30 \times 0.25 = (-7.5 - 150 - 0.75) \times 10^{-5} = -158.25 \times 10^{-5} = -158.25$ pcm. [Ans.]

17.21 Curve-Fitting Methods for Nuclear Data

Sometimes it is convenient to take raw nuclear data (such as the data shown in Table 17.4), and convert it into a more convenient form such as a linear or quadratic equation. For the temperature coefficient of the reactivity, some examples of these expressions might be

$$\alpha_F(T) = a + bT \tag{17.35}$$

or

$$\alpha_F(T) = a + bT + cT^2 \tag{17.36}$$

where a, b, and c are coefficients that are fit to the data provided. Then the fuel temperature coefficient can be rendered as a continuous function of the fuel pin temperature T rather than a discrete one. In the field of mathematics, this approach is called *"curve fitting"* because the idea is to take all of the data points and replace them by a simple equation that can be described by either a curve or a straight line. In this context, Equation 17.35 is called a *linear curve fit*, and Equation 17.36 is called a *quadratic curve fit*. However, higher-order curve fits such as cubic curve fits and *splines* are also appropriate to use in some cases. In practice, the curve-fitting process involves finding the values of a, b, and c that will result in the best overall "fit" to a particular set of data points. *In other words, the process of curve fitting involves minimizing the error in fitting the data points to a particular curve*. We would now like to demonstrate how this process works for the fuel temperature coefficient.

17.22 The Least Squares Method

The most famous method for finding the values of the coefficients in a linear or quadratic curve fit is the *least squares method.* This method was originally proposed by German scientist and mathematician *Carl Friedrich Gauss* in 1810. Gauss's picture is shown in Figure 17.17. Gauss also made significant contributions to the fields of number theory, statistics, quantitative analysis, differential geometry, geophysics, electrostatics, astronomy, and optics. The idea behind the least squares the method of least squares is to *minimize* the sum of the squares of the offsets ("the residuals") of the points from the shape of the particular curve one would like to fit the data to (linear, quadratic, cubic, etc.). In the process of doing so, a set of matrix equations can be developed that can be solved for the values of a, b, and c. In practice, the *vertical offsets* from a line (a polynomial, a surface, or a hyperplane) are almost always minimized instead of the perpendicular ones. Both approaches are shown in Figure 17.18. In the case where a linear curve fit is required, the process of minimizing the offsets is equivalent to solving the two equations

Equations for the Coefficients for a Linear Curve Fit

$$\begin{aligned} aN + b\sum_i x_i &= \sum_i y_i \\ a\sum_i x_i + b\sum_i x_2^i &= \sum_i y_i x_i q \end{aligned} \tag{17.37}$$

for the values of a and b, where N is the total number of data points, x_i and y_i are their specific values, and the summations shown are to be performed over all data points from i = 1 to i = N. Similarly, in the case where the data points are to be fit to a

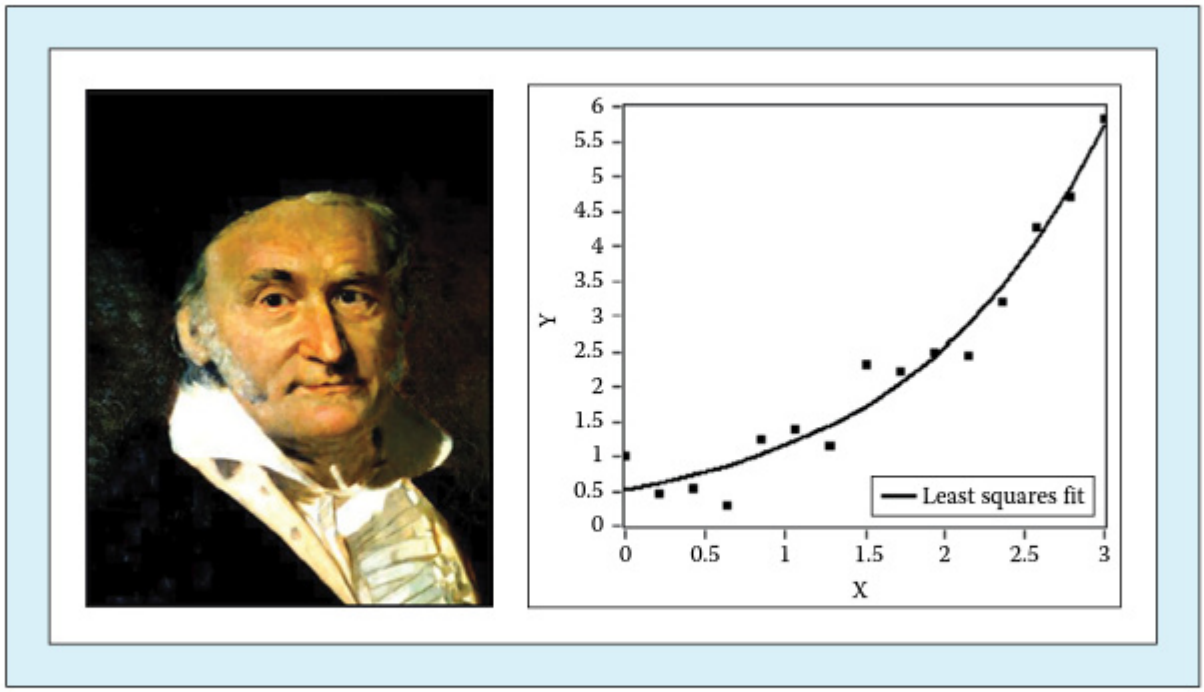

FIGURE 17.17 A picture of Carl Friedrich Gauss, who is responsible for creating the method of least squares, which is frequently used to fit nuclear data to a predefined shape or curve. (Picture provided byWikipedia.)

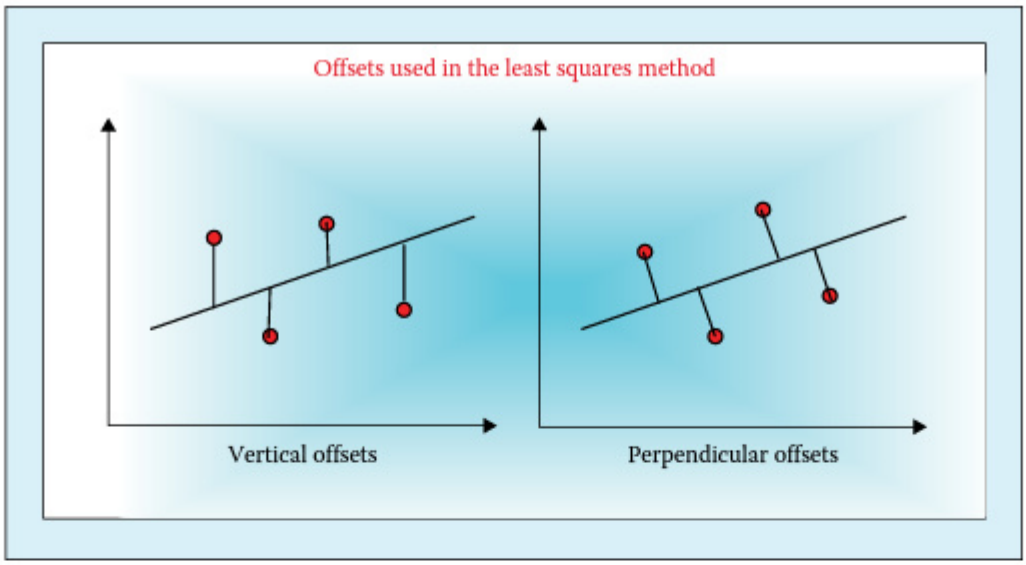

FIGURE 17.18 The vertical and perpendicular offsets used in the least squares method of curve fitting.

second-degree polynomial (e.g., a parabola of the form $y = a + bx + cx^2$), the process of minimizing the offsets is equivalent to solving the following three equations for the values of a, b, and c:

Equations for the Coefficients for a Quadratic Curve Fit

$$aN + b\sum_i x_i + c\sum_i x_i^2 = \sum_i y_i$$

and

$$a\sum_i x_i + b\sum_i x_i^2 + c\sum_i x_i^3 = \sum_i y_i x_i \qquad (17.38)$$

and

$$a\sum_i x_i^2 + b\sum_i x_i^3 + c\sum_i x_i^4 = \sum_i y_i x_i^2$$

In other words, *each method minimizes the size of the error that is incurred when the data is fit to a particular curve*. Now suppose that we would like to create the following equation for the fuel temperature coefficient:

$$\alpha_F(T) = a + bT + cT^2 \tag{17.39}$$

based on the data presented in Table 17.4. Then we would have to solve the following set of equations for a, b, and c:

$$aN + b\sum_i T_i + c\sum_i T_i^2 = \sum_i \alpha_{Fi} \tag{17.40}$$

and

$$a\sum_i T_i + b\sum_i T_i^2 + c\sum_i T_i^3 = \sum_i \alpha_{Fi} T_i \tag{17.41}$$

and

$$a\sum_i T_i^2 + b\sum_i T_i^3 + c\sum_i T_i^4 = \sum_i \alpha_{Fi} T_i^2 \tag{17.42}$$

So in the case of a quadratic curve fit, we have three equations to solve, and we have three unknowns. We can either do this manually or we can rewrite these equations as the following set of matrix equations which can be solved for a, b, and c:

$$\begin{pmatrix} N & \sum_i T_i & \sum_i T_i^2 \\ \sum_i T_i & \sum_i T_i^2 & \sum_i T_i^3 \\ \sum_i T_i^2 & \sum_i T_i^3 & \sum_i T_i^4 \end{pmatrix} \begin{Bmatrix} a \\ b \\ c \end{Bmatrix} = \begin{Bmatrix} \sum_i \alpha_{Fi} \\ \sum_i \alpha_{Fi} T_i \\ \sum_i \alpha_{Fi} T_i^2 \end{Bmatrix} \tag{17.43}$$

One of the advantages to the least squares method is that if we decided that we needed to fit the data to only a line and not a curve, then we would not have to solve for c and we would simply end up with two matrix equations and two unknowns.

$$\begin{pmatrix} N & \sum_i T_i \\ \sum_i T_i & \sum_i T_i^2 \end{pmatrix} \begin{Bmatrix} a \\ b \end{Bmatrix} = \begin{Bmatrix} \sum_i \alpha_{Fi} \\ \sum_i \alpha_{Fi} T_i \end{Bmatrix} \tag{17.44}$$

There are many software packages available on the Internet to provide these curve fits for free. A couple of them can be found at the following URLs:

http://mathworld.wolfram.com/LeastSquaresFitting.html
http://statpages.org/nonlin.html

You may wish to keep these URLs handy in case you are ever asked to take experimental nuclear data, such as that shown in Table 17.4, and fit a simple curve to it. Once the temperature coefficients have been curve fitted to a linear or quadratic function such as $\alpha_M(T) = a + bT + cT^2$, it is easy to see that the total reactivity change will be given by $d\rho = \alpha_M(T)\, dT$. Hence if the curve is quadratic, $d\rho/dT = \alpha_M(T)$ and $\Delta\rho = (a + bT + cT^2)\, \Delta T$. Other important parameters can be characterized using a similar approach.

Student Exercise 17.2

Use the least squares method to find the coefficients a and b in the following equation for the coolant temperature:

$$T = a + bP$$

where T is the temperature of the coolant shown in Figure 17.17 and P is the power level.

17.23 Power Coefficient of the Reactivity

Earlier we first introduced the *temperature coefficient of the reactivity*, and we defined it as

$$\Delta\rho = \alpha_T^{fuel}\Delta T^{fuel} + \alpha_T^{mod}\Delta T^{mod} + \alpha_T^{struct}\Delta T^{struct} \tag{17.45}$$

where the fuel, the moderator, and the structure were considered to be separate components of the core. This concept can then be extended to individual components of the core (i.e., to more than three components) by simply summing over all the individual components from i = 1 to N that can have a significant effect on the effective multiplication factor. Hence, we may write the change in reactivity due to temperature changes in the core alone as

$$\Delta\rho = \sum_i \alpha_{Ti}\Delta T_i \quad (i = 1,2,\ldots,N) \tag{17.46}$$

where there may be a total of N such structures (the fuel, the moderator, and the control rods) for which different values of α_T may be used. As we alluded to previously, the temperature coefficient can depend on many factors, and each of these processes (changes in fuel temperature, changes in coolant temperature, and changes in void fraction) can have vastly different time constants associated with them. For example, the fuel responds almost immediately to any change in the power level, while the moderator and the surrounding structural materials do not respond as quickly because they must first "receive" the heat from the fuel (through the processes of thermal conduction and convection) before their median temperatures can change. Consequently, *the temperature coefficient for the fuel can be thought of as the first line of defense to protect a reactor when the power level begins to increase*. The temperature coefficient for the moderator responds more slowly than the temperature coefficient for the fuel, and finally, the temperature coefficient of the structure responds more slowly than the temperature coefficient for the moderator. The one exception to this rule is when a reactor is first started up. At this time, there is no significant fission energy being produced by the fuel, and therefore the entire core can be thought of as a monolithic structure possessing a single operating temperature T_o. As the temperature of the core is increased by "*preheating*" the primary coolant, the core temperature will increase from a value of T_o to a value of T. Because the density of the coolant and the structural materials fall as the temperature is raised, there will be a corresponding decrease in the effective multiplication factor due to thermal feedback effects.

The phenomenon we have just described is called the *temperature defect of the reactivity. For light-water reactors, it can have a value between $\Delta\rho = -0.02$ and $\Delta\rho = -0.04$. If the reactor is fueled with Uranium-235 (where $\beta = 0.0065$), this leads to a net negative change in the core-wide reactivity of between 4 and 6 dollars*. This is obviously a very large number to keep in mind when a reactor is first being brought online. When designing the control system, a far more useful parameter for characterizing the importance of temperature feedback is *the power coefficient of the reactivity*. The power coefficient of the reactivity is given by

The Power Coefficient of the Reactivity

$$\alpha_P = \frac{d\rho}{dP} = \sum_i \left(\frac{d\rho}{dT_i}\right)\left(\frac{dT_i}{dP}\right) \tag{17.47}$$

where P is the power level. Here, the summation is again performed over a temperature T_i associated with each core component. The reactivity change due to power feedback can then be written as

$$\Delta\rho = \alpha_P\Delta P \tag{17.48}$$

where ΔP is simply the change in the reactor power level (in kilowatts or megawatts). Just as in the case of the temperature defect of the reactivity, which occurs primarily during start-up, *the power defect of the reactivity, which is defined as the change in the reactivity that occurs between zero power and full power, can be several times greater than the prompt critical limit. In particular, the power defect of the reactivity for a modern LWR can be anywhere from −2 dollars to −5 dollars*. Only in this case, it is caused by the increase in the fuel temperature that is associated with going from zero power to full power, or by going from P = 0 to $P = P_o$. Both the temperature defect and the power defect stay relatively constant over the operating life of the core, and only the excess reactivity built into the fuel itself declines gradually as the fuel is burned. The amount of excess reactivity that each of these effects contributes to the overall reactivity is shown in Figure 17.19. Notice that the reactivity built into the fuel itself changes the most between BOL (beginning of life) and EOL (end of life). Of course, this is to be expected because most of the U-235 atoms split apart. The effects of both positive and negative power feedback are shown in Figure 17.20.

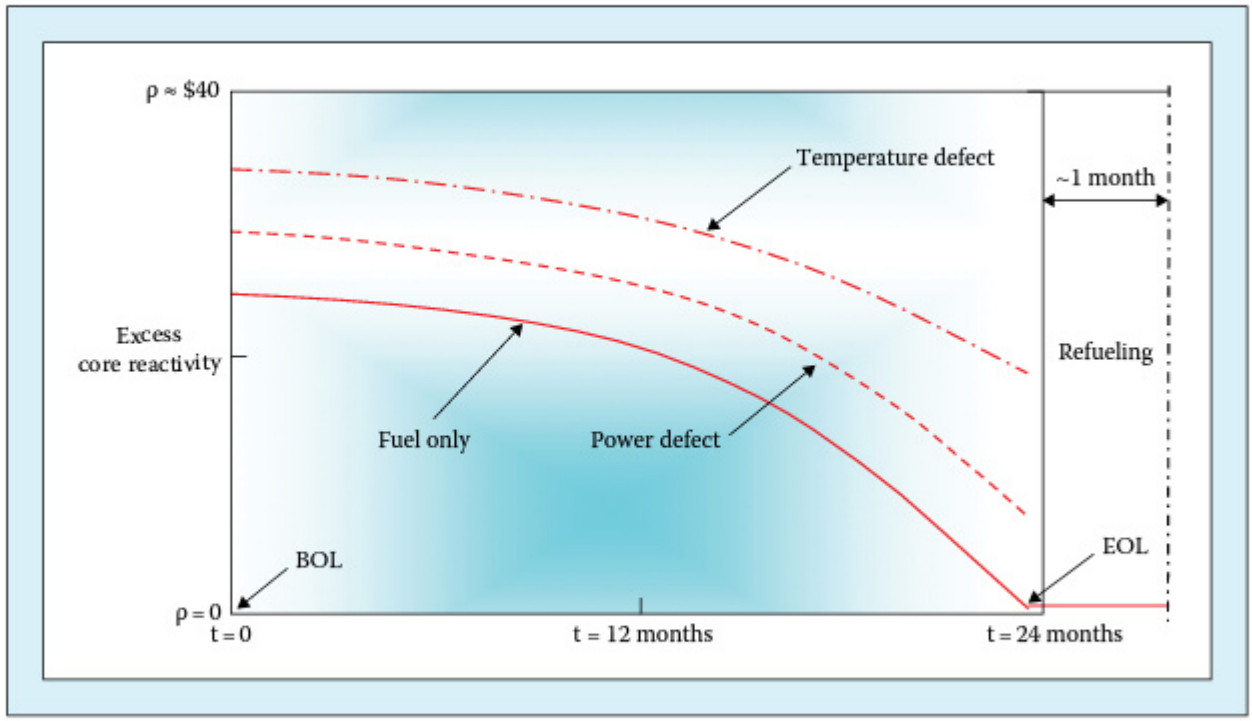

FIGURE 17.19 An illustration of the temperature defect of the reactivity and the power defect of the reactivity as a function of time in a thermal water reactor. The temperature defect of the reactivity is usually somewhat larger than the power defect of the reactivity.

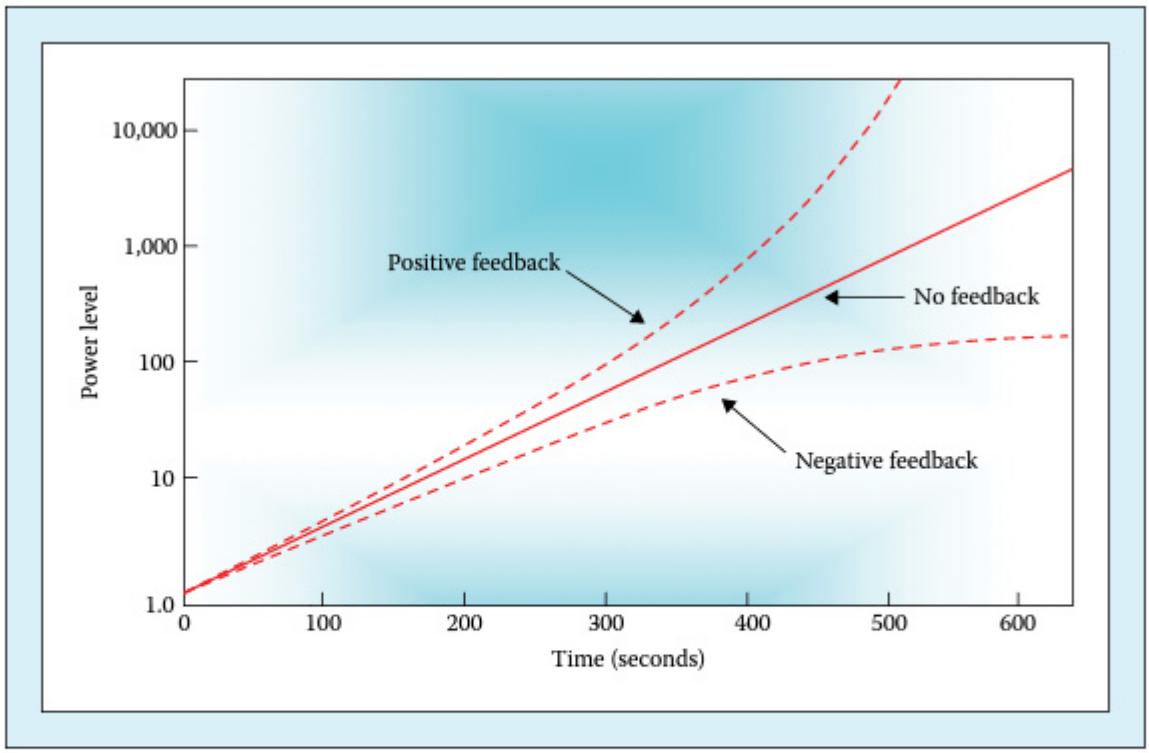

FIGURE 17.20 An illustration of how the reactor power level in a thermal water reactor behaves with both positive and negative feedback.

17.24 Finding the Temperature Defect and the Power Defect

Based on what we have just said, it is a relatively simple process to find the size of the temperature and power defects for a commercial PWR. When the PWR is first brought online, it is brought up to power very slowly by operating the core at a very low power level or by preheating the reactor coolant before pumping it into the core. In this process, the reactor coolant temperature rises from room temperature (about 30°C) to an average inlet temperature of about 290°C. In this process, both the temperature of the fuel and the temperature of the coolant are increased, and the reactivity is reduced as the temperature rises.

17.25 Isothermal Temperature Coefficient

If the preheating process occurs gradually, the temperature of the fuel and coolant rise at approximately the same rate, and it is reasonable to assume that the core behaves *isothermally* as the temperature increases; that is to say,

$$T_{FUEL} \approx T_{COOLANT} \approx T_{INLET} \rightarrow 290°C \tag{17.49}$$

When this occurs, the reactivity change due to temperature changes alone is

$$\frac{d\rho}{dT} = \left(\frac{1}{k}\right)\frac{dk}{dT} = \left(\frac{1}{k}\right)\frac{dk}{dT_F} + \left(\frac{1}{k}\right)\frac{dk}{dT_C} \tag{17.50}$$

where T_F is the fuel temperature and T_C is the coolant temperature. We can also write this as

$$\frac{d\rho}{dT} = \alpha_T = \alpha_F + \alpha_C \tag{17.51}$$

Therefore, the overall reactivity change of the core is

$$d\rho = (\alpha_F + \alpha_C)dT \tag{17.52}$$

or

$$\Delta\rho = (\alpha_F + \alpha_C)\Delta T \tag{17.53}$$

because the fuel and the coolant temperatures change at approximately the same rate. The temperature coefficient α_T in this case, or

$$\alpha_T = \alpha_F + \alpha_C \tag{17.54}$$

is called the *isothermal temperature coefficient*. This temperature coefficient is sometimes called the *start-up temperature coefficient* as well.

17.26 Calculating the Power Coefficient during Start-Up

After the coolant has reached its correct operating temperature (where $T_{INLET} \approx 290°C$ or $T_{OUTLET} \approx 320°C$), the fission process can be started by removing the control rods, and the fuel temperature becomes much greater than the coolant temperature. As additional heat is added to the coolant from the fuel rods, the average temperature of the coolant also becomes much greater than the inlet temperature, and a state is eventually reached where

$$T_{FUEL} \gg T_{COOLANT} > T_{INLET} \tag{17.55}$$

The outlet coolant temperature in this case will be about 320°C, and the average coolant temperature in the core will be about 310°C. To obtain the correct power coefficient α_P under these conditions, we must now account for the fact that the fuel temperature and the coolant temperature change at different rates as the power level P is raised. The correct definition to use for the power coefficient is then

$$\alpha_P = \frac{d\rho}{dT} = \left(\frac{1}{k}\right)\frac{dk}{dT_F}\cdot\frac{dT_F}{dP} + \frac{1}{k}\frac{dk}{dT_C}\cdot\frac{dT_C}{dP} \tag{17.56}$$

Under steady-state conditions, it can be shown that the core-wide values for dT_F/dP and dT_C/dP can be found from the equations

$$\frac{dT_F}{dP} = R + \left(\frac{1}{2mc_p}\right) \tag{17.57}$$

and

$$\frac{dT_C}{dP} = \left(\frac{1}{2mc_p}\right) \tag{17.58}$$

which are derived in Reference 9 and in many other books. Here, R is the *thermal resistance* of the fuel in the core, which is defined by

$$P = \left(\frac{1}{R}\right)\cdot\left(T_F - T_C\right) \tag{17.59}$$

and P is the core power level in MWT. Here, m is the core mass flow rate in kg/second and c_p is the *heat capacity* or the *specific heat* of the coolant. Thus, the *power coefficient for the core during start-up* can be written as

$$\alpha_P = \frac{d\rho}{dT} = \left(\frac{1}{k}\right)\frac{dk}{dT_F}\cdot\left\{R + \frac{1}{2mc_p}\right\} + \left(\frac{1}{k}\right)\frac{dk}{dT_C}\cdot\left(\frac{1}{2mc_p}\right) \tag{17.60}$$

or

$$\alpha_P = R\alpha_F + \frac{\left(\alpha_F + \alpha_C\right)}{2mc_p} \tag{17.61}$$

Notice that the power coefficient is inversely proportional to the core mass flow rate m (in kg/s). For a large PWR core, the core flow rate is about 25,000 kg/s. The average fuel and coolant temperatures to be used with these equations are discussed in References 5 and 6.

17.27 Calculating the Temperature and Power Defects

Suppose that we would like to determine how much positive reactivity the control system should add to the core to bring the core from room temperature to an average operating temperature of 290°C (which is the standard coolant inlet temperature for a PWR during steady-state conditions). The control system must add this additional reactivity to the core to compensate for the reactivity reduction caused by increasing the core temperature. We can find the amount of reactivity required by calculating the *isothermal temperature defect* $\Delta\rho_T$:

$$\text{Isothermal temperature defect} = \Delta\rho_T = \int_{Tr}^{Ti} \alpha_T(T)\,dT \tag{17.62}$$

where the integration must be performed between room temperature $T_r \approx 30°C$ and the core inlet temperature $T_i \approx 290°C$. At room temperature, the reactor is said to be in a *cold critical state*, and when the core temperature reaches 290°C, the reactor is said to be in *hot zero-power critical state*. All reactors use essentially the same start-up procedure to prepare the core for full power operation. When the power level is raised even further, it transitions from a hot zero-power state to its rated power level P. A negative power coefficient α_P causes the reactivity to fall further, and Equation 17.60 must be used to determine the excess reactivity that must be added to the core to keep the reactor critical. Specifically, the amount of positive reactivity must be found by integrating the fuel and coolant temperature coefficients between the normal coolant inlet temperature ($T_{INLET} \approx 290°C$) and their full power values of $T_{F\,MAX}$ and $T_{C\,MAX}$.

$$\text{Power defect} = \Delta\rho_{POWER} = \int_{Ti}^{T_{F\,MAX}} \alpha_F(T_F)\,dT_F + \int_{Ti}^{T_{C\,MAX}} \alpha_C(T_C)\,dT_C \tag{17.63}$$

In this case, the temperatures to use for the fuel and the coolant when evaluating $\alpha_F(T_F)$ and $\alpha_C(T_C)$ in Equation 17.63 are

$$T_F(P) = T_{IN} + \frac{P}{R + (1/2mc_p)} \tag{17.64}$$

and

$$T_C(P) = T_{IN} + \frac{P}{2mc_p} \tag{17.65}$$

In any well-designed reactor, the *power defect* defined by Equation 17.63 is always a negative number, and in commercial PWRs, it can average from −$2.00 to −$5.00. Of course, this assumes that the PWR is fueled with slightly enriched uranium with a U-235 concentration between 3% and 5% by weight.

17.28 Control Systems and Thermal Feedback

Figure 17.19 shows a closed feedback loop for the temperature coefficient of the reactivity and the power coefficient of the reactivity. These coefficients then become the feedback mechanisms the control system uses to keep a reactor stable. From the viewpoint of a control systems engineer, both these diagrams depict similar events, except that the change in the reactivity due to temperature alone is given by $\Delta\rho = \alpha_T\Delta T$ and the change in the reactivity due to power alone is given by $\Delta\rho = \alpha_P\Delta P$. These diagrams implement what is known as *negative thermal feedback*. Up to now, we have stayed away from the details of how a feedback circuit such as the one shown in Figure 17.21 actually works. However, there are many

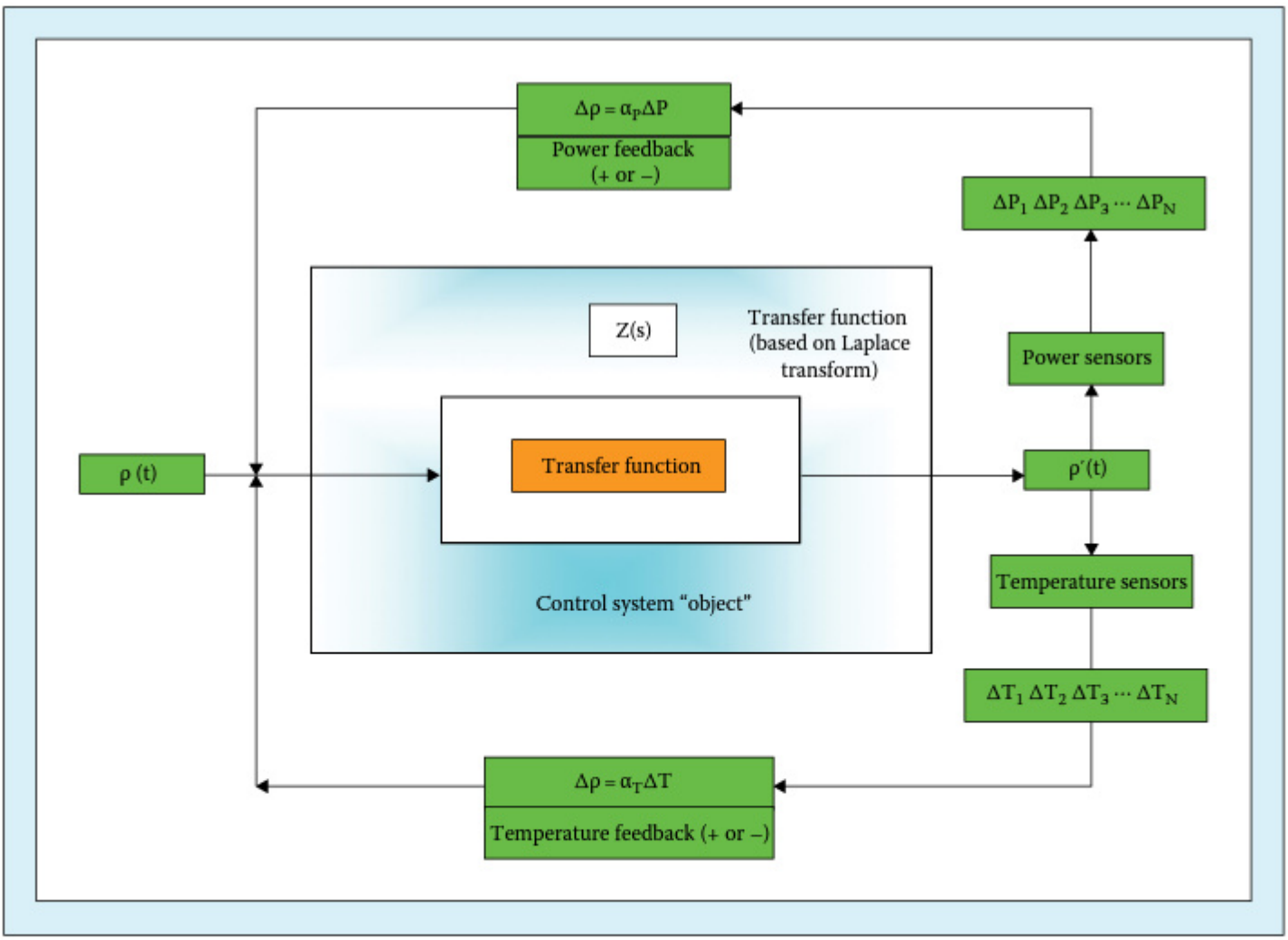

FIGURE 17.21 A two-loop feedback system with both temperature and power feedback. Here, the temperature coefficient of the reactivity and the power coefficient of the reactivity are used to provide the negative feedback that a reactor control system requires.

books that explain how the "logical" block diagrams shown in Figure 17.21 can be converted into physical diagrams that involve integrated circuits and other electronic components. Circuits containing these components receive electrical signals from sensors in the core and use these signals to move the control rods (up or down) accordingly.

17.29 Temperature Feedback and the TRIGA Reactor

Many factors must be taken into account when designing a safe reactor. If the reactor has a large enough temperature coefficient (and it is always negative), the reactor will automatically shut down when the power increases even when the reactor operator does something stupid. This phenomenon is referred to as *thermal feedback*, and all commercial power reactors rely on it to compensate for rapid changes in the power level of the core. Perhaps the best-known example of a reactor that takes full advantage of this effect is the *TRIGA reactor*.

The TRIGA reactor was originally developed by the *General Atomics Company*, whose corporate headquarters are located in San Diego, California. The word TRIGA is an acronym for *Training, Research, Isotopes, and General Atomics*. There are approximately 40 TRIGA reactors in operation around the world today, and the number appears to be growing at the rate of one or two a year. (See Figures 17.22 and 17.23 to see their current locations). TRIGA reactors can be designed in many different sizes and configurations, and their stated power levels range from 20 kW to about 16 MW. Because of their inherent thermal stability, TRIGA reactors also happen to be very popular research and training tools. The concept of the TRIGA reactor was originally proposed by *Dr. Edward Teller (the father of the H Bomb*—see Figure 17.24) and some of his colleagues in 1956. However, *Freeman Dyson*, whose picture is shown in Figure 17.25, was probably the greatest single contributor to its design. Freeman Dyson was also one of the first physicists to actively promote the use of *Feynman diagrams*, which are now commonly used by nuclear scientists and engineers today.

Unlike a conventional reactor, a TRIGA reactor uses the concept of "*warm neutrons*" to reduce the number of fissions when the power level increases rapidly. It does so because the neutrons "heat up" faster than they do in a conventional thermal water reactor, and this avoids the catastrophic behavior that can occur in a normal reactor when all of the control rods are withdrawn from the core. In fact, a TRIGA reactor will automatically shut itself down even when enough control rods have been withdrawn from the core to cause it to become prompt supercritical! In other words, *a TRIGA reactor is so safe to operate that a reactor operator can simultaneously withdraw all of the control rods from the core, and the reactor will automatically shut itself down*!

17.30 Understanding How a TRIGA Reactor Works

The inherent stability of a TRIGA reactor can be traced to the design of its fuel rods. TRIGA reactors use an unusual type of nuclear fuel that is made out of uranium, zirconium, *and hydrogen*. In TRIGA reactors, *the hydrogen atoms are imbedded directly in the fuel*. The *UZrH fuel* mixture is chemically stable, and it can be safely quenched in ordinary water at temperatures up to about 1200°C. Its melting point is not as high as that of conventional uranium dioxide (UO_2), but this trade-off is what allows it to have a much larger negative temperature coefficient. The fuel in a TRIGA reactor is normally clad with stainless steel. A picture of a TRIGA reactor fuel rod is shown in Figure 17.26. Notice that the fuel rod resembles a fuel rod that is used in a conventional thermal water reactor. However, in a conventional thermal water reactor, the general result of removing too many (or all) of the control rods is a catastrophic reactor accident. This happens because the neutrons continue to remain "cold" or thermal when the fuel temperature is raised, and the fission process continues until the fuel begins to melt.

However, in a TRIGA reactor, exactly the opposite process occurs. As the fuel temperature rises, the hydrogen atoms in the fuel tend to *harden* the neutron energy spectrum. Thus, the neutrons inside the hydrogen-containing fuel become "warmer" than the neutrons in the surrounding coolant. In other research reactors that do not use TRIGA's UZrH fuel, the fuel is often constructed in the form of *plates*. These plate-type rods are then clad with aluminum, which has a melting point of about 650°C. At the same temperature, the UZrH fuel retains more than 99% of its fission products, even if all of the cladding happens to be removed. The reactivity then falls dramatically (due to the negative temperature feedback) as the temperature (or the power level) of the core is raised. The exact relationship is

$$\Delta\rho = \alpha_F \Delta T \tag{17.66}$$

because the moderator temperature coefficient α_M and the leakage temperature coefficient α_L can usually be neglected during very fast transients. The warmer neutrons cause fewer fissions to occur, and they escape into the surrounding coolant more quickly. Thus, the net effect of having so many warm neutrons is that the power level automatically reduces itself in just a few milliseconds (normally between 15 and 30 milliseconds) after the fuel temperature is raised. This reverse thermal feedback occurs much more quickly than any engineered safety system can operate. In other words, in a TRIGA reactor, the fuel rods operate as an *internal power regulator*. Thus, they shut down the core without the need for a mechanical device (such as a conventional control rod)! The *warm neutron principle* gives the TRIGA reactor a prompt negative temperature coefficient

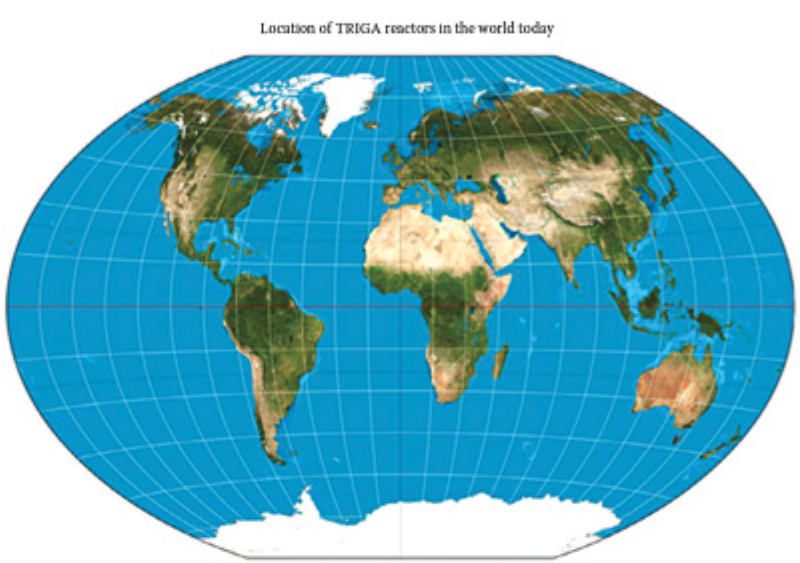

Country	Facility name	Type	Power (kWT)	Status
Austria	TRIGA II VIENNA	TRIGA MARK II	250_0000	Operational
Bangladesh	TRIGA MARK II	TRIGA MARK II	3000_0000	Operational
Italy	LENA, TRIGA II PAVIA	TRIGA MARK II	250_0000	Operational
Italy	TRIGA RC–1	TRIGA MARK II	1000_0000	Operational
Malaysia	TRIGA PUSPATI (RTP)	TRIGA MARK II	1000_0000	Operational
Mexico	TRIGA MARK III	TRIGA MARK III	1000_0000	Operational
Romania	PITESTI –SS CORE	TRIGA DUAL CORE	14000_0000	Operational
Romania	PITESTI –PULSED	TRIGA DUAL CORE	500_0000	Operational
Slovenia	LJUBLJANA	TRIGA MARK II	250_0000	Operational
United States	AFRRI TRIGA	TRIGA MARK F	1000_0000	Operational
United States	DOW TRIGA	TRIGA MARK I	300_0000	Operational
United States	KSU TRIGA MK II	TRIGA MARK II	250_0000	Operational
United States	TRIGA II UNIV_TEXAS	TRIGA MARK II	1100_0000	Operational
United States	TRIGA UNIV_UTAH	TRIGA MARK I	100_0000	Operational
Indonesia	BANDUNG	TRIGA MARK II	2000_0000	Operational
Japan	RIKKYO	TRIGA MARK II	100_0000	Shutdown
United States	GA–TRIGA I	TRIGA MARK I	250_0000	Shutdown
United States	UI–TRIGA MK I	TRIGA MARK I	100_0000	Shutdown
United States	TRIGA, VET_ADMIN_	TRIGA MARK I	20_0000	Shutdown
United States	GA–TRIGA F	TRIGA MARK I	250_0000	Shutdown

FIGURE 17.22 The location of all currently operating TRIGA reactors outside of the United States. (Courtesy of General Atomics.)

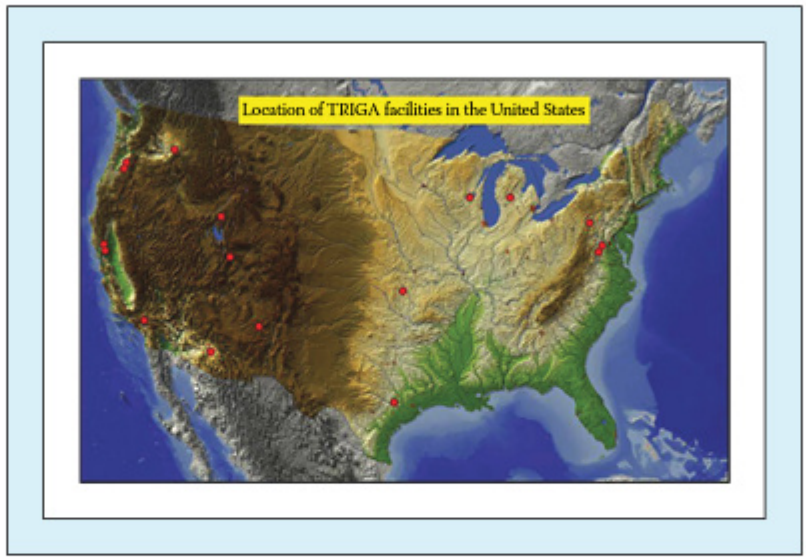

FIGURE 17.23 The location of all currently operating TRIGA reactors in the United States. (Data provided by the General Atomics Company.)

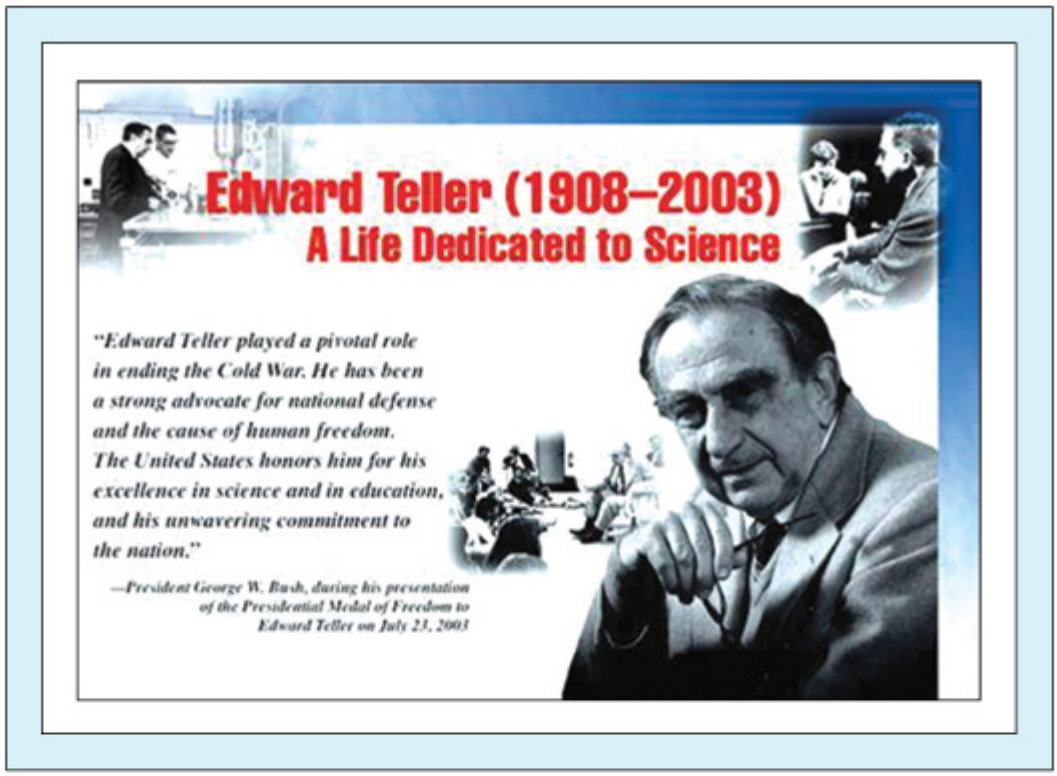
Edward Teller (1908–2003)
A Life Dedicated to Science
"Edward Teller played a pivotal role in ending the Cold War. He has been a strong advocate for national defense and the cause of human freedom. The United States honors him for his excellence in science and in education, and his unwavering commitment to the nation."
—President George W. Bush, during his presentation of the Presidential Medal of Freedom to Edward Teller on July 23, 2003

FIGURE 17.24 A picture of Dr. Edward Teller, who helped to design the first TRIGA reactor. He was also responsible for designing the first hydrogen bomb. (Courtesy of Google Images.)

on the order of about one dollar per each 100°C. This allows TRIGA reactors to safely withstand events that would completely destroy ordinary reactors fueled with uranium dioxide (UO_2) fuel. Thus *TRIGA reactors are the most popular type of research and training reactor in the world today*. More information about the TRIGA reactor and its engineered safety systems can be found at the following website:

www.ga.com

This website is maintained by the General Atomics Company. The reader is encouraged to visit this site to find out more about how a TRIGA reactor works.

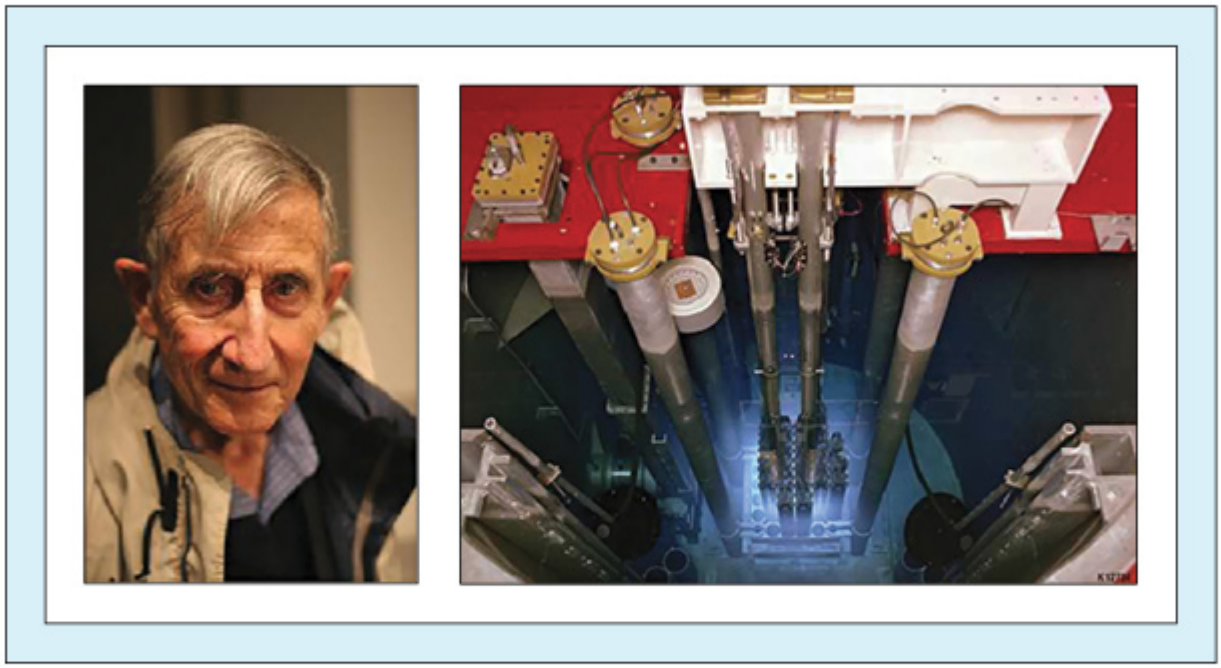

FIGURE 17.25 A picture of Freeman Dyson, who originally proposed the design of the TRIGA reactor. The blue glow from the TRIGA core is caused by *Cherenkov radiation*. In addition to his contributions to the TRIGA reactor, Dyson helped the RAF develop analytical methods to bomb German targets during the Second World War. Dyson is probably best known for being the first person (besides Richard Feynman) to appreciate the power of Feynman diagrams, and a paper, which he wrote in 1948 was among the first papers to make use of them. Robert Oppenheimer, in particular, became convinced that Feynman's new theory was fundamentally correct. Oppenheimer rewarded Dyson with a lifetime appointment to the Institute for Advanced Study in Princeton, New Jersey, where he also worked with Albert Einstein for a while. (Courtesy of Wikipedia.)

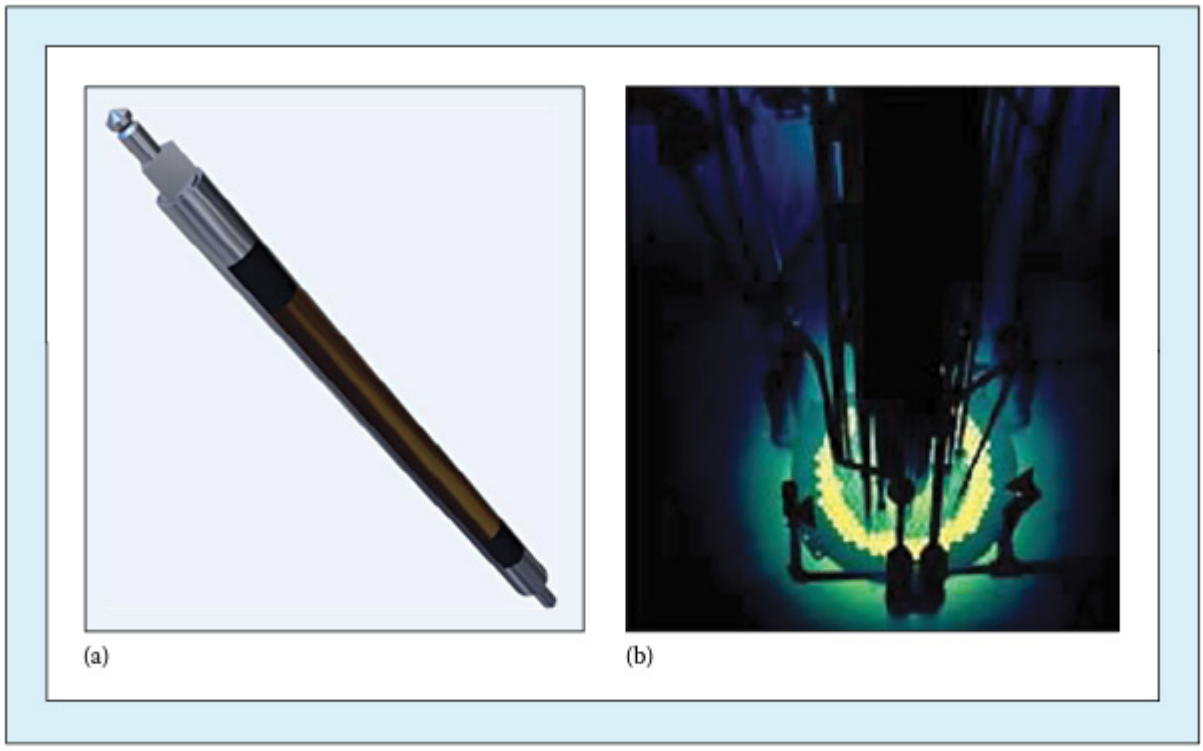

FIGURE 17.26 A picture of a TRIGA reactor fuel rod (a) that is inserted into a TRIGA reactor core (b). (Pictures provided by the General Atomics Company.)

17.31 Power Pulses in a TRIGA Reactor

Another interesting feature of the TRIGA reactor is its ability to support what is known as *power pulsing*. Because a TRIGA reactor uses UZrH fuel, the reactor core can be very rapidly "pulsed" to power levels *several thousand times greater than its steady-state power*. This power pulse can be achieved by ejecting a control rod from the core, which increases the reactivity beyond the prompt critical limit (see Chapter 20). An example of what a power pulse looks like is shown in Figure 17.27. This power-pulsing ability of the TRIGA, which was first demonstrated in 1959, is now the standard on most TRIGA designs. Special designs of the TRIGA can normally achieve peak power levels of 20,000 MW. These power levels are used to test the safety of other reactor fuels that are intended to be used in commercial nuclear power plants. Sometimes, enough thermal power is generated by a TRIGA reactor that it can be used to supply external power to the area in which it is located. See Chapter 1 for an explanation of how this power conversion process works.

In conclusion, *TRIGA reactors are probably the best-known example of how effective a negative fuel temperature coefficient can be*. Their popularity has continued to increase because they are not only safe to operate, but they are also an effective research and training tool. Because of the unique design of their fuel, the reactivity always falls as the fuel temperature rises beyond its normal design limit. Commercial power reactors use a similar mechanism to maintain nuclear stability, but they are not optimized to the extent that the fuel in a TRIGA reactor is. Thermal feedback is an important aspect of the safety of any thermal water reactor in operation today. The greater the amount of thermal feedback, the easier it normally is to get a reactor licensed or approved.

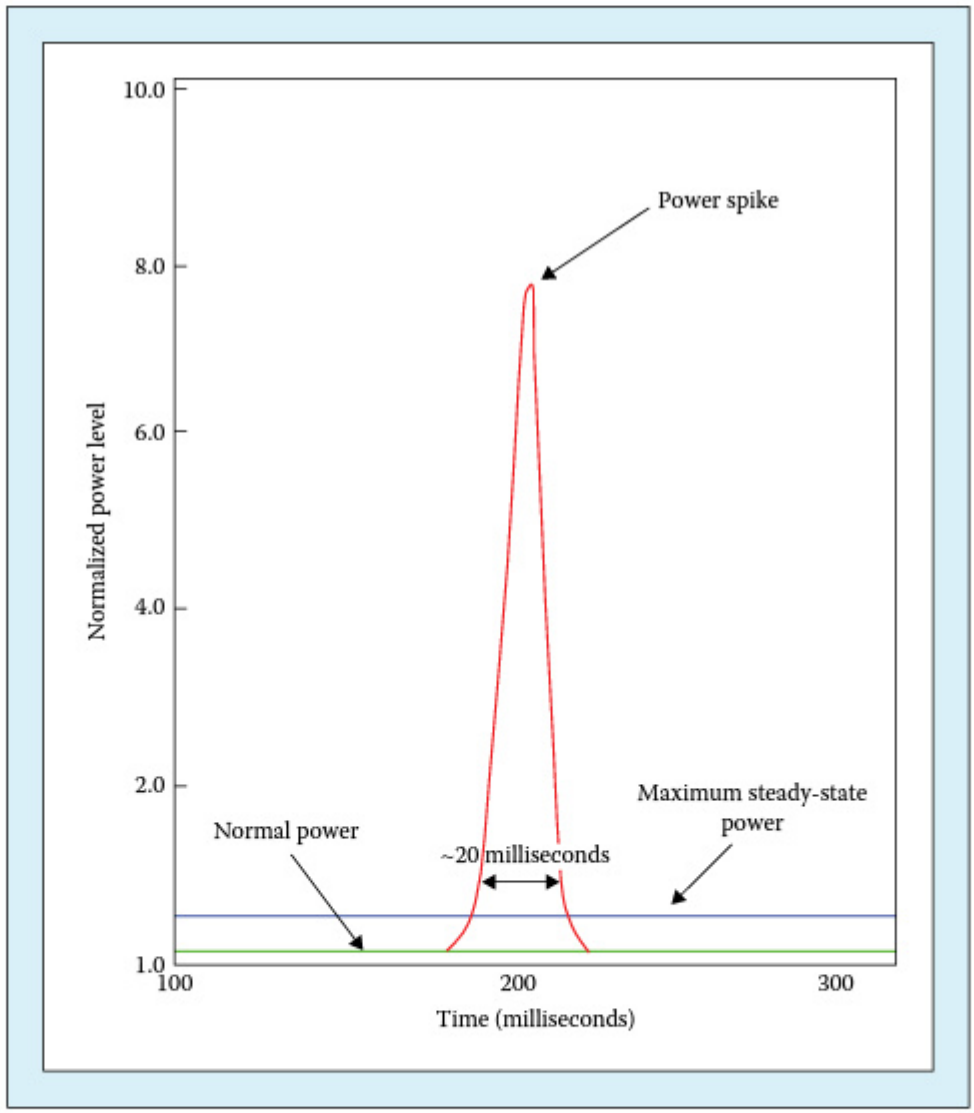

FIGURE 17.27 A power pulse that can be obtained in a typical TRIGA reactor. Here, the maximum steady-state power level is indicated by the solid line shown in blue.

17.32 Reviewing the Effects of Thermal and Temperature Feedback

Throughout this chapter, we have attempted to demonstrate how temperature changes affect the time-dependent power generation rate. Normally, power reactors are designed so that the power generation rate goes down as the core temperature rises. In nuclear science and engineering, this is known as *negative temperature feedback*. However, the amount of feedback can be different for the moderator than it is for the fuel, and the time constants for each of these processes can be completely different as well. In some reactors (such as BWRs), the time-dependent reactivity is affected by the formation of voids in the coolant. These changes can be different from one region of the core to another, and they can also be different at the top of the core than they are at the bottom. *The size of the fuel temperature coefficient is determined by what is called the nuclear Doppler effect* (see Section 17.16).

The nuclear Doppler effect is caused by an apparent increase in the width of the U-238 absorption resonances in the epithermal energy range, which tends to decrease the resonance escape probability p. This effect is most pronounced when a reactor is first being started up because the effective neutron temperature increases by about 540°C (or 1000°F) because the fuel temperature increases with the nuclear heat-generation rate q'''. In a PWR, the average moderator temperature is designed to change linearly with the reactor power level between a coolant temperature of 290°C and 330°C in the primary loop. At BOL, the moderator coefficient is small (and in some cases it can even be slightly positive), but at EOL, the moderator coefficient becomes large and negative due to the depletion of the fuel and the reduction of the boric acid (or chemical shim) concentration.

The net result of these effects is that the axial power distribution becomes relatively flat after a long period of full power operation. In other words, the sum of the nuclear Doppler effect, the core temperature redistribution, and the spatially dependent moderator temperature produces the power defect that we discussed previously. However, the power defect is approximately a linear function of the power level, and it tends to become *less important* over time because of changes to the boric acid concentration and the depletion of the U-235 atoms in the fuel rods. (The power defect was discussed in Section 17.27.) Negative feedback makes the core easier to control, and positive feedback makes the core harder to control. *Reactor control systems are designed to limit changes in the steady-state power level to 5%–10% per minute under normal operating conditions*. These control systems are discussed again in Chapter 20.

Example Problem 17.7

The average temperature of the fuel in a TRIGA reactor immediately increases by 300°C after a control rod is withdrawn from the core. If the reactor is exactly critical at the time the rod is withdrawn ($\rho = 0$), how much negative reactivity is introduced into the core through the process of temperature feedback? Assume the UZrH fuel contains enriched uranium (i.e., U-235). How long do you expect the power peak to last?

Solution Earlier in the chapter, we mentioned that the fuel temperature coefficient in a TRIGA reactor is about minus one dollar per every 100°C. Hence, if the fuel temperature is immediately raised by 300°C, the reactivity must fall by 3 dollars. Since a TRIGA reactor is fueled with U-235, the value of β required to achieve a prompt critical condition is 0.0065. This translates to a total negative reactivity insertion of $-3 \times 0.0065 = -0.0195$ (-3.0β). According to our previous discussion, the power pulse should last about 20 milliseconds (0.020 seconds). [Ans.]

17.33 Some Additional Observations regarding Temperature Feedback

The fact that the neutron energy spectrum changes as a function of the core temperature means that most reaction rates are temperature dependent as well. For example, if the thermal flux in the core is Maxwellian (see Chapter 8), then the effect on these reaction rates can be approximated for important nuclear fuels like U-233, U-235, and Pu-239 using the non-1/v correction factors that were discussed in Chapter 5. Other important nuclear materials such as Cadmium, Xe-135, and Sm-149 also have their thermal absorption cross sections affected in a similar way. The non-1/v correction factors for U-233, U-235, U-238, and Pu-239 are presented in Table 17.5.

Since these correction factors are temperature dependent, they represent the change in the fission and absorption rates in the thermal energy range due to temperature-related changes to the Maxwellian flux $\phi(T)$ alone. We can therefore estimate how the fission-to-capture ratio (σ_f/σ_c) and the fission-to-absorption ratio (σ_f/σ_a) change with temperature as the fuel temperature is lowered or raised. *In other words, by simply examining the way that these correction factors change, we can estimate the magnitude and the sign of the reactivity change $d\rho/dT$ as a function of temperature T*. Hence, we can use these changes to *infer* the sign of the fuel temperature coefficient α_F. This in turn produces some form of negative temperature feedback under most conditions. The amount and type of temperature feedback depends on the ratio of the

TABLE 17.5
Non-1/v Factors G(T) for Some Important Nuclear Materials

T (°C)	U-233 G_f	U-233 G_a	U-235 G_f	U-235 G_a	U-238 G_a	Pu-239 G_f	Pu-239 G_a
30	0.9983	1.0003	0.9759	0.9780	1.0017	1.0487	1.0723
100	0.9972	1.0011	0.9581	0.9610	1.0031	1.1150	1.1611
200	0.9973	1.0025	0.9411	0.9457	1.0049	1.2528	1.3388
400	1.0010	1.0068	0.9208	0.9294	1.0085	1.6904	1.8905
600	1.0072	1.0128	0.9108	0.9229	1.0122	2.2037	2.5321
800	1.0146	1.0201	0.9036	0.9182	1.0159	2.6595	3.1006
1000	1.0226	1.0284	0.8956	0.9118	1.0198	3.0079	3.5353

Source: Lamarsh, J.R. and Baratta, A.J., *Introduction to Nuclear Engineering*, Prentice Hall, Upper Saddle River, NJ (2001).

TABLE 17.6
Fission-to-Absorption Ratio (σ_f/σ_a) as a Function of the Fuel Temperature T

T (°C)	U-233 (G_f/G_a)	U-235 (G_f/G_a)	Pu-239 (G_f/G_a)
30	0.9980	0.9978	0.9779
100	0.9961	0.9969	0.9602
200	0.9948	0.9951	0.9357
400	0.9943	0.9907	0.8941
600	0.9945	0.9868	0.8834
800	0.9946	0.9840	0.8577
1000	0.9944	0.9822	0.8508

fission change to the absorption change. Another way to illustrate this is to express the fission-to-absorption ratio (σ_f/σ_a) as a function of the ambient fuel temperature T. When we do so, we obtain the values shown in Table 17.6. Curve fitting these values (see Section 17.20) then produces the following equations for the fission-to-capture ratio (σ_f/σ_a) when the fuel temperature is measured in °C:

$$\text{For U-233}: G_{f/a} = 0.997423 - 0.000010\ T + 7.766558 \times 10^{-9}\ T^2 \tag{17.67}$$

$$\text{For U-235}: G_{f/a} = 0.999042 - 0.000023\ T + 6.846738 \times 10^{-9}\ T^2 \tag{17.68}$$

$$\text{For Pu-239}: G_{f/a} = 0.996034 - 0.000303\ T + 1.613778 \times 10^{-7}\ T^2 \tag{17.69}$$

Notice that the slopes of these functions are primarily negative as the temperature increases. Therefore, the fuel temperature coefficient becomes negative under these conditions.

One does not need to be a genius to realize that this makes the core easier to control. In practice, the U-238 in the fuel rods must also be included in these calculations to obtain the correct value for the fuel temperature coefficient. After this is done, it is easy to see that the fission-to-capture ratio becomes *more negative* as the fuel is burned because there are fewer U-235 atoms and more U-238 atoms remaining. In other words, *the temperature coefficient becomes more negative with increasing burnup* in most thermal water reactors. This means that if we calculate the temperature coefficient for a fresh core (where there are more U-235 atoms), the temperature coefficient at this time will probably be the least negative over the life of the core.

The U.S. NRC uses this fact to determine when a reactor core can be licensed and when it cannot. *Thus, a fresh core is normally the core that has the smallest negative temperature coefficient over the operating life of the plant.* As the fuel is burned, the fuel temperature coefficient becomes progressively more negative, and additional fission products are produced in the fuel. In particular, this allows the boric acid concentration to exceed 1500 PPM while still keeping the total temperature coefficient negative. Thus, even if α_C becomes temporarily positive at low burnups, the value of $\alpha_T = \alpha_F + \alpha_C$ will always be negative for the core as a whole.

Example Problem 17.8

A thermal water reactor fueled with pure U-235 has an effective multiplication factor of 1.0 when the fuel temperature reaches 300°C. When is the effective multiplication factor of the core when the average fuel temperature reaches 1000°C?

Solution Since the effective multiplication factor of the core is given by $K = \nu\sum_f \phi / \sum_a \phi$, we can estimate how the effective multiplication factor changes with temperature by considering how the value of $G_{f/a}$ (see Equation 17.66) changes with temperature. At a temperature of 300°C, the value of $G_{f/a}$ is 0.9920, and at a temperature of 1000°C, the value of $G_{f/a}$ is 0.9822. If the effective multiplication factor is 1.0 at a temperature of 300°C, and the thermal flux is Maxwellian, the value of K when the fuel reaches a temperature of 1000°C is $1.0 \times (0.9822/0.9920) = 0.99$. [Ans.]

Example Problem 17.9

In the previous example, how much additional reactivity has to be added to the core by withdrawing the control rods to keep the core critical when the average fuel temperature rises from 300°C to 1000°C? What is the value of this additional reactivity in pcm and in dollars and cents?

Solution In Example Problem 17.8, the initial reactivity of the core at a temperature of 300°C was $\rho = (k-1)/k = 0.0$, and the final reactivity of the core (without moving the control rods) would be $\rho = (k-1)/k = -0.01/0.99 = -0.0101$. Hence, the control rods must add an additional 0.0101 of positive reactivity to the core to keep it critical. This is equivalent to adding 1010 pcm, or since the delayed neutron fraction of U-235 is $\beta = 0.0065$, $\Delta\rho = 0.0101/\beta = \$1.55$. [Ans.]

References

Books and Textbooks

1. Ash, M. *Nuclear Reactor Kinetics*, McGraw-Hill, New York (1965).
2. Henry, A.F. *Nuclear Reactor Analysis*, MIT Press, Cambridge, MA (1975).
3. Keepin, G.R. *Physics of Nuclear Kinetics*, Addison-Wesley, Reading, MA (1965).
4. Stacey, W.M. *Nuclear Reactor Physics*, 2nd edn., John Wiley & Sons, New York (2007).
5. Todreas, N. and Kazimi, M.S. *Nuclear Systems*, Vol. 1, CRC Press, Boca Raton, FL (2008).
6. Duderstadt, J. and Hamilton, L. *Nuclear Reactor Analysis*, John Wiley & Sons, New York (1976).
7. Lewis, E. *Fundamentals of Nuclear Reactor Physics*, Academic Press, Boston, MA (2008).
8. El-Wakil, M.M. *Nuclear Heat Transport*, American Nuclear Society, La Grange Park, IL (1981).
9. Hetrick, D.L. *Dynamics of Nuclear Reactors*, American Nuclear Society, La Grange Park, IL (1993).
10. Schultz, M.A. *Control of Nuclear Reactors and Power Plants*, 2nd edn., McGraw-Hill, New York (1961).
11. Lamarsh, J.R. and Baratta, A.J. *Introduction to Nuclear Engineering*, Prentice Hall, Upper Saddle River, NJ (2001).
12. Lamarsh, J.R. *Introduction to Nuclear Reactor Theory*, second printing, Addison-Wesley Publishing Company, Inc., Reading, MA (1972).
13. Glasstone, S. and Eedlund, M. *The Elements of Nuclear Reactor Theory*, D Van Nostrand Company, Inc., New York (1952).
14. Glasstone, S. and Sesonske, A. *Nuclear Reactor Engineering*, 3rd edn., Van Nostrand Reinhold Company, New York (1981).
15. Shultis, K. and Faw, R. *Fundamentals of Nuclear Science and Engineering*, 2nd edn., CRC Press, Boca Raton, FL (2008).
16. Cochran, R.G. and Toulfanidis, N. *The Nuclear Fuel Cycle: Analysis and Management*, American Nuclear Society, La Grange Park, IL (1999).
17. Masterson, R.E. *Nuclear Engineering Fundamentals: A Practical Perspective*, CRC Press, Boca Raton, FL (2017).

Web References

1. *www.ga.com*.
2. *http://statpages.org/nonlin.html*.
3. *http://en.wikipedia.org/wiki/TRIGA*.
4. *https://www.llnl.gov/str/Dec07/libby.html*.
5. *http://en.wikipedia.org/wiki/Edward_Teller*.
6. *http://en.wikipedia.org/wiki/Freeman_Dyson*.
7. *http://en.wikipedia.org/wiki/Void_coefficient*.
8. *http://www.hindawi.com/journals/stni/2013/261327/*.
9. *http://en.wikipedia.org/wiki/Nuclear_reactor_physics*.
10. *http://mathworld.wolfram.com/LeastSquaresFitting.html*.
11. *www.nuceng.ca/br_space/ep4d03/.../16_reactivity_coefficients.ppt*.
12. *http://nuclearpowertraining.tpub.com/h1019v2/css/h1019v2_43.htm*.
13. *http://ansn.iaea.org/Common/documents/Training/TRIGA%20Reactors%20(Safety%20and%20Technology)/chapter2/physics13.htm*.

Additional References

- Important physical constants used by nuclear scientists and engineers can be found in *Appendix A*.
- Unit systems and their conversion factors can be found in *Appendix B*.
- Nuclear cross sections for many important nuclear materials can be found in *Appendix C*.
- Physical properties of important nuclear materials can be found in *Appendix D*.
- Atomic masses, half-lives, and natural abundances can be found in *Appendix E*.

Questions for the Student

The following questions cover the material presented in this chapter and, in some cases, previous chapters as well. They are designed to test how well the student has acquired a working knowledge of the subject matter.

1. Suppose that you were asked to obtain an operating license for a nuclear power plant in the United States. Assuming that the reactivity is temperature dependent, what do you have to demonstrate to the NRC to obtain an operating license?
2. Why is a TRIGA reactor so safe to operate?
3. In addition to the temperature coefficient of the reactivity $d\rho/dT$, another reactivity coefficient is commonly used in a BWR to reduce the power level of the core as more energy is added to it. Can you name what this reactivity coefficient is, and write a differential expression for it?
4. When were TRIGA reactors first brought into commercial operation?
5. Neglecting the effects of neutron leakage, how many types of temperature feedback are required to control the power level in a commercial nuclear power plant?
6. As the fuel temperature rises, what happens to the reactivity in a well-designed nuclear power plant? Ans: It decreases.
7. What type of fuel does a TRIGA reactor use?
8. Is the increase in the fuel temperature in a nuclear power plant an example of positive or negative feedback?
9. Neglecting the effects of neutron leakage, how many feedback coefficients are used to control the power level in the core of a BWR? Name these coefficients.
10. Neglecting the effects of neutron leakage, how many temperature coefficients are used to control the power level in the core of a PWR? Name these coefficients.
11. Which of the three temperature coefficients—the moderator temperature coefficient α_M, the leakage temperature coefficient α_L, or the fuel temperature coefficient α_F—responds first to an instantaneous change in the reactor power level?
12. If the reactor power level suddenly falls by inserting a control rod into the core, is the time-dependent reactivity determined solely by the motion of the control rod?
13. What temperature coefficient is related to the nuclear Doppler effect?
14. What physical process is responsible for the Doppler broadening of the absorption resonances in a reactor fuel rod?
15. What federal document defines the requirements for the temperature-dependent behavior of a nuclear reactor in the United States?
16. If the flow to the recirculation pumps in a BWR is suddenly increased, and the control rods do not move, what happens to the reactor power level?
17. Write an expression for the temperature coefficient of the fuel α_F using the resonance escape probability p.
18. Why do the fuel assemblies that are closest to the reactor pressure vessel sometimes contain steel deflection plates?
19. Write an equation for the chemical composition of solbor.
20. What is a typical amount of time for an increase in the temperature of a fuel rod in a thermal water reactor ΔT_{FUEL} to translate to a change in the core-wide reactivity?
21. Write down an equation that defines the power coefficient of the reactivity.
22. On a percentage basis, does the amount of U-235 or U-238 decline faster as the fuel in a thermal water reactor is burned?
23. Under the assumption of thermal equilibrium, write an expression that relates the most probable velocity v of a thermal neutron to the temperature of a surrounding fuel rod.
24. In what type of reactor is the "warm neutron principle" used?
25. In a thermal water reactor, what is the size of the temperature defect of the reactivity?
26. How is the power defect of the reactivity defined?
27. In a commercial power reactor, what parameter is typically larger—the power defect of the reactivity or the temperature defect of the reactivity?
28. For the same power level, what parameter determines how long the fuel can be left in the core before a reactor has to be refueled?
29. Who was responsible for designing the first hydrogen bomb?
30. Fill in the following sentence with the appropriate word or phrase: In a commercial power reactor, the life of the pressure vessel can be extended by reducing the number of _____ that hit it. This is normally done by surrounding the pressure vessel by a reflector made out of_____.
31. What is a typical time frame for a burnable poison to affect the reactivity of a reactor core?

32. How is the neutron fluence normally defined?
33. By what percentage can a low-leakage core increase the life of a reactor pressure vessel?
34. What is the purpose of a burnable poison in a reactor fuel rod?
35. What famous curve-fitting technique can be used to derive an analytical expression for how the reactivity of a reactor core changes as a function of the temperature?
36. Can you name at least two common burnable poisons that are used in reactor fuel rods today?
37. What is the size of the fuel temperature coefficient in the fuel of a TRIGA reactor?
38. Assuming that the concentration of U-235 atoms in a reactor core at start-up is given by U_o, write an equation for the concentration of U-235 atoms as a function of time if the neutron flux ϕ is constant.
39. What percentage of the total power output of a commercial thermal water reactor can be attributed to the buildup of Plutonium-239 in the core?
40. What is the width of a typical power "pulse" in a TRIGA reactor?
41. Suppose that the core of a BWR is 4 m high. At what axial elevation does the coolant normally start to boil?
42. Above this elevation, what happens to the temperature of the coolant?
43. What equation is used to define the shape of a nuclear absorption resonance?
44. Why did the reactor accident at Chernobyl occur?

Exercises for the Student

Exercise 17.1

In Chapter 13, we mentioned that the diffusion coefficient in a PWR is temperature dependent. Find the diffusion coefficient for the coolant at the bottom of the core, the middle of the core, and the top of the core in a PWR. Assume that the core entrance temperature is 300°C.

Exercise 17.2

Earlier in the chapter, we learned that the void fraction in a BWR is a function of axial elevation. What is the density of the coolant at the bottom of the core, at the middle of the core, and at the top of the core in a typical BWR? How much does the density change between the bottom of the core and the top of the core?

Exercise 17.3

Suppose that the temperature coefficient of the reactivity for the fuel in a modern PWR is −0.00003 per °C, the moderator temperature coefficient is −0.00002 per °C, and the structure temperature coefficient is −0.00001 per °C. A rapid transient occurs where the fuel temperature increases by 50°C, the moderator temperature increases by 10°C, and the structure temperature increases by 5°C. What is the reactivity change in dollars and cents if the reactor is fueled with U-235?

Exercise 17.4

Suppose that the temperature coefficient of the reactivity for the fuel in a thermal water reactor fueled with Pu-239 is −0.00005 per °C, the moderator temperature coefficient is −0.00002 per °C, and the structure temperature coefficient is −0.00001 per °C. A rapid transient occurs when the fuel temperature increases by 50°C, the moderator temperature increases by 10°C, and the structure temperature increases by 5°C. What is the reactivity change in dollars and cents?

Exercise 17.5

TRIGA reactors are generally believed to be the safest research reactors in the world because their UZrH fuel has a very large negative temperature coefficient. Suppose that the average temperature of the fuel of a TRIGA reactor is immediately increased to 200°C when a control rod is withdrawn from the core. If the reactor is exactly critical at the time the rod is withdrawn ($\rho = 0$), how much negative reactivity is introduced into the core through the process of temperature feedback? How long do you expect the power peak to last?

Exercise 17.6

Prove that the temperature coefficient of the reactivity for a homogeneous reactor core is related to the first derivative of the effective multiplication factor k by the equation $\alpha_T = (1/k^2)dk/dT$. If the effective multiplication factor is 1.0001 and $dk/dT = -0.0005$, what is the temperature coefficient for the core?

Exercise 17.7

The power coefficient of the reactivity for a thermal water reactor is normally a small negative number. Suppose that a reactor is operating at a steady-state power level of 1000 MWE, and several control rod banks are suddenly withdrawn from the core. If the power level is supposed to increase by 20% without temperature feedback, what is the actual power increase if the power coefficient of the reactivity is –0.1 per Megawatt thermal? Assume the reactor has a thermal efficiency of 33.3%.

Exercise 17.8

Suppose that a safety test on a new research reactor reveals that as the temperature of the fuel is increased by 100°C, 200°C, and 300°C, the reactivity decreases by 35, 75, and 95 cents. Using the least squares method, do a linear curve fit on this experimental data. If the fuel temperature increases by 400°C, how much do you expect the reactivity to fall due to negative temperature feedback?

Exercise 17.9

A uranium dioxide fuel rod having an initial enrichment of 5% is exposed to a thermal neutron flux of 1×10^{14} neutrons/cm^2/s for 1 year. After this period of time, what is the concentration of Pu-239 atoms in the fuel rod? How much of the power in the fuel rod is now being generated by Pu-239?

Exercise 17.10

Earlier in the chapter, we found that the void coefficient of the reactivity is defined by the equation $\alpha_V = \Delta\rho/\Delta\alpha$ or $\alpha_V = d\rho/d\alpha$. This void coefficient, which is generally a negative number, is used to provide BWRs with some form of automatic load following. If the void fraction of the coolant increases from 0% to 80% in the top 75% of a BWR core, what is the average change in the void fraction above the core centerline for each meter of core height? If the void coefficient is –0.00144 per % void in a modern BWR fuel assembly, what is the void coefficient when expressed in dollars and cents per meter?

Exercise 17.11

The reactivity change due to the formation of voids in a BWR core is given by the equation $\Delta\rho = \alpha_V\Delta\alpha$, where $\Delta\alpha$ is the change in the void fraction. In a BWR fueled with enriched uranium, a typical value of the void coefficient is about –0.0015 per % void. If the void fraction increases from 0% to 80% over the entire length of the core, what is the change in the reactivity due to the formation of these voids in dollars and cents?

Exercise 17.12

Sometimes, the void coefficient α_V in a BWR core is expressed in pcm per % void. What does the term pcm refer to, and how is it defined? If the reactivity reduction due to the formation of voids in an entire core is –5000 pcm, how much of a reactivity reduction does this correspond to when the fuel rods are made from enriched uranium?

Exercise 17.13

A thermal water reactor fueled with pure Pu-239 has an effective multiplication factor of 1.0 when the fuel temperature reaches 300°C. When is the effective multiplication factor of the core when the average fuel temperature reaches 1000°C?

Exercise 17.14

In the previous exercise (Exercise 17.13), how much additional reactivity must be added to the core by withdrawing the control rods to keep the core exactly critical when the average fuel temperature rises from 300°C to 1000°C? What is this additional reactivity in pcm and in dollars and cents?

Exercise 17.15

A thermal water reactor can be fueled with either U-233 or U-235. When the temperature of the core is increased from room temperature to 300°C, what type of fuel has a greater temperature defect of the reactivity?

Exercise 17.16

Suppose that a thermal water reactor is designed so that the thermal resistance of the fuel R can be neglected in the calculation of the power coefficient of the reactivity α_P. If the mass flow rate through the core is 20,000 kg/s, and the mass flow rate is suddenly reduced by a factor of 2 but the coolant does not boil, what happens to the value of the power coefficient of the reactivity in this case?

18

Long-Term Changes to the Reactivity of the Core

18.1 Tracking the Long-Term Reactivity

It should be apparent from our earlier discussion that the instantaneous reactivity of the core can be controlled by temperature feedback when rapid changes to the power level occur. These reactivity changes can be supplemented by moving the control rods or by changing the core flow rate. However, *the long-term reactivity of the core is not driven by the fuel temperature alone, and in general, it is driven by the burnup of the fuel*. The reactivity always falls as the fuel is burned, and the depletion of the fuel atoms must be taken into account when considering the net reactivity change $\Delta\rho$ of the core over long periods of time. From an earlier discussion, we know that the net reactivity of the core is defined by

$$\rho = \frac{(k-1)}{k} \tag{18.1}$$

where k is the effective multiplication factor of the core. Thus, a positive value of ρ indicates that the reactor still has some additional fuel to burn, while a negative value indicates that it does not. Neglecting for the moment any phase changes to the coolant and other temperature-related effects, the net reactivity of the core can usually be written as the sum (or the difference) of the following four terms:

- The positive reactivity of the core due to the presence of the fuel: ρ_{FUEL}
- The negative reactivity of the core due to the presence of fission products (like Xenon-135 and Samarium-149) that tend to accumulate when the fuel is burned: ρ_{FP}
- The negative reactivity of the control rods: ρ_{CR}
- The negative reactivity of the burnable poisons, which may be imbedded in the fuel: ρ_{BP}

Hence, the net reactivity (ρ) can be written as

The Total Core Reactivity

$$\rho_{NET} = \rho_{FUEL} - \rho_{FP} - \rho_{CR} - \rho_{BP} \tag{18.2}$$

and this equation is appropriate for dealing with reactivity swings over days, weeks, or even months. It should be apparent that the first term is directly proportional to the number of U-235 or Pu-239 atoms that the fuel contains and that as the enrichment e of the fuel is increased, the reactivity of the fuel ρ_{FUEL} will increase as well. In general, the positive reactivity of the fuel is related to the enrichment by

$$\rho_{FUEL} = Ae \tag{18.3}$$

where A is an empirical constant that is fuel dependent. An additional fact that can be inferred from Equation 18.3 is that it does not take an enrichment of e = 0 for the total reactivity ρ of the core to fall to 0 because the fission products, the control rods, and

the burnable poisons will all tend to absorb some of the free neutrons that are produced. Hence, the total reactivity can be thought of as a *time-dependent function* in which the enrichment changes as a function of time, while the other factors in Equation 18.2 may have different time constants and values associated with them. Thus we may write the net reactivity as a function of time as

The Reactivity as a Function of Time

$$\rho_{NET}(t) = \rho_{FUEL}(t) - \rho_{FP}(t) - \rho_{CR}(t) - \rho_{BP}(t)$$

or

$$\rho_{NET}(t) = A\,e(t) - \rho_{FP}(t) - \rho_{CR}(t) - \rho_{BP}(t) \qquad (18.4)$$

An interesting implication of Equation 18.4 is that the net reactivity ρ in a pressurized water reactor (PWR) can fall to 0 when the average enrichment e of the fuel approaches 2%, and in a boiling water reactor (BWR), the same result can be achieved when the average enrichment of the fuel approaches 1.5%. So, the presence of the last three terms reduces the size of the reactivity swing and compensates for the additional reactivity that is contained in the fuel. We can illustrate how this quantitatively happens for a PWR core by referring to the curve shown in Figure 18.1. Notice that the net reactivity ρ does not always change at the same rate because $\rho_{FP}(t)$ and $\rho_{TEMP}(t)$ change very quickly initially, before reaching their respective equilibrium values. *During the first few days after start-up, fission products start to accumulate in the fuel, and these fission product poisons (primarily in the form of xenon-135 and samarium-149) can cause the value of ρ_{FP} to increase rather rapidly. This produces the sharp drop in the net reactivity ρ that is initially observed.* At the same time, temperature effects also come into play as the reactor is brought up to full power (see the previous discussion in Chapter 17). This causes the value of ρ_{TEMP} to increase initially, but not nearly as much as $\rho_{BP}(t)$. Ordinarily, these two effects reach their equilibrium values 48 hours after start-up, and then any further changes to the net reactivity can be attributed to the burnup of the fuel (and the burnable poisons) in the core. Thus the value of ρ_{FUEL} tends to decrease as the fuel is burned, and the value of ρ_{BP} tends to increase over time.

This continues to be the case even when the *excess reactivity* ρ (as defined by Equation 18.4) remains in the core for a long period of time. The *instantaneous reactivity* of a PWR core (see Chapter 9) is usually controlled (e.g., kept at a value of 0) by dissolving boric acid in the coolant and by withdrawing some control rods to "fine-tune" the core power shape. The boric acid concentration normally has a value of about 1500 parts per million (PPM) when the fuel is fresh, and this value gradually declines to several hundred parts per million as the fuel is burned. Finally, when the fuel is totally

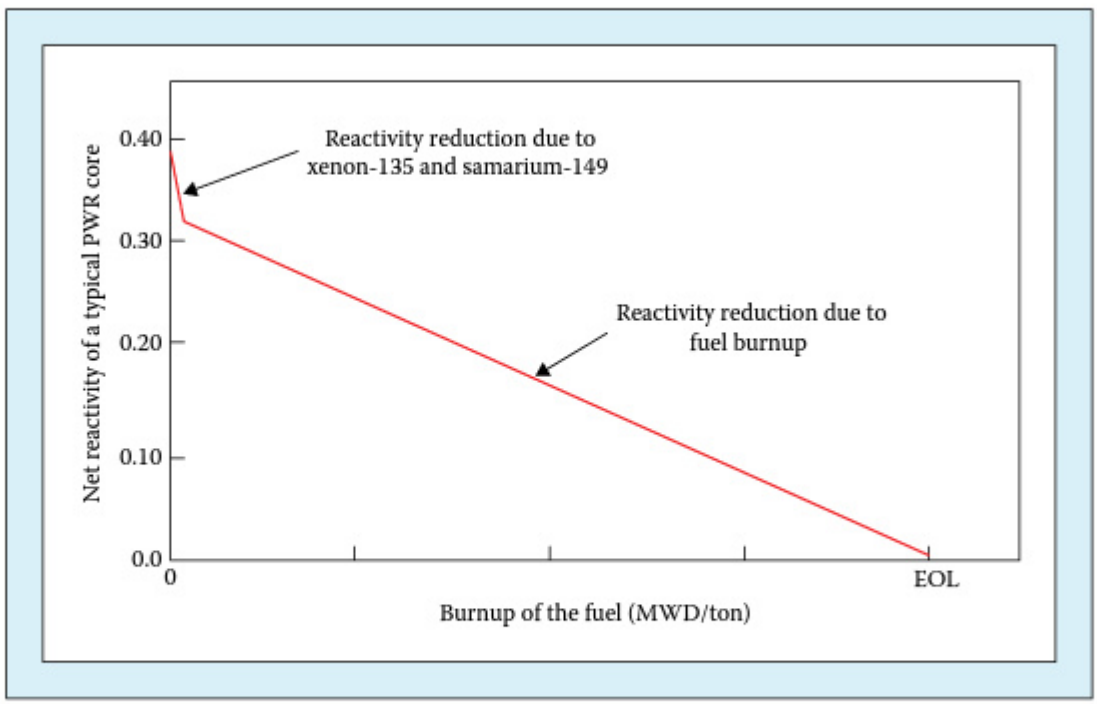

FIGURE 18.1 The net reactivity ρ of a typical PWR core as a function of burnup excluding the contribution of control rods, burnable poisons, and chemical shim.

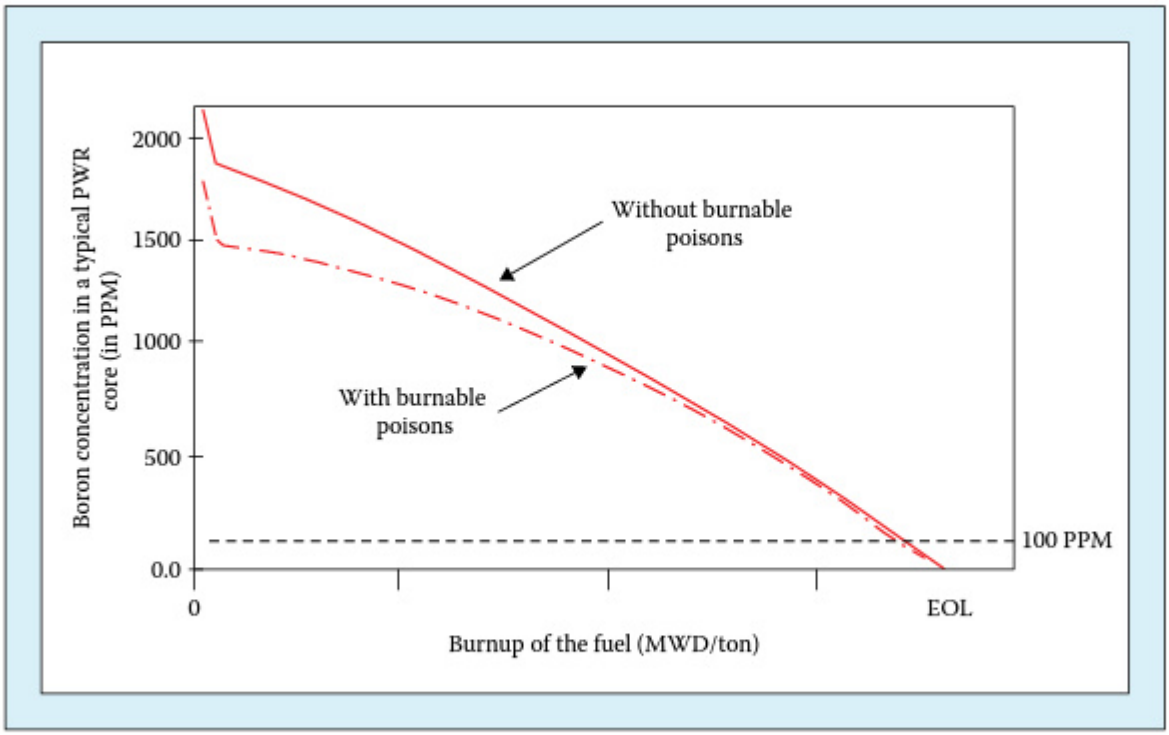

FIGURE 18.2 The soluble boron concentration in a typical PWR core with and without burnable poisons.

consumed, and cannot be burned any further, the boric acid concentration falls to about 100 parts per million. When this occurs, the reactor has to be shut down for refueling (because the net reactivity of the core has now fallen to 0). At this point, at least part of the fuel has to be replaced. This corresponds to the formal end of life (EOL) for the most highly burned fuel in the core.

In BWRs, the instantaneous reactivity is controlled by moving large cruciform-shaped control rods up and down and through the use of burnable poisons inside of the fuel rods themselves. *Boric acid is not used in BWRs* because the boiling can distort how it is distributed through the core. (This boiling can also cause it to plate out on the metal surfaces of the fuel assemblies themselves). In any event, *the net reactivity falls approximately linearly with burnup*, and the burnup in either case is usually measured in megawatt days per metric ton (MWD/ton).

Finally, *burnable poisons* (which we will discuss extensively in Chapter 20) can have a significant effect on the value of the reactivity over time. These poisons are much less expensive to manufacture than control rods, and this reduction in cost is one of the reasons why they are so widely used today. Burnable poisons can also be mixed directly into the fuel to reduce the development of local power peaks. Moreover, the size of the reactivity swing depends on how many burnable poisons are used to suppress the reactivity over time. Figure 18.2 shows how the presence of burnable poisons affects the long-term reactivity of a PWR core. This curve is for a large PWR, and any credible analysis of the net reactivity must take the presence of these burnable poisons into account. The burnup of the fuel on the x-axis is measured in MWD/ton. Normally, the net reactivity falls to zero at a burnup of about 50,000 MWD/ton. (For a fast reactor, the average burnup is somewhat higher).

18.2 Core Reactivity as a Function of Burnup

To optimize the amount of energy that can be extracted from the fuel, a number of design trade-offs must be made. For example, there are two or three design trade-offs that determine how long the fuel can be left in the core. In the discussion that follows, we would like to examine these design trade-offs in more detail. Assume for the moment that we are dealing with a one-batch core, whose reactivity swing is similar to that shown in Figure 18.3. We will examine the reasons for the shape of this curve in a subsequent section. The three primary trade-offs that determine how long the fuel can remain in the core are

1. The number of fuel rods that fail when the fuel is burned.
2. The excess reactivity that remains in the core as a function of time.
3. The length of time L that a reactor must be shut down for refueling when the net reactivity becomes equal to zero (i.e., when the core can no longer be maintained in a critical state).

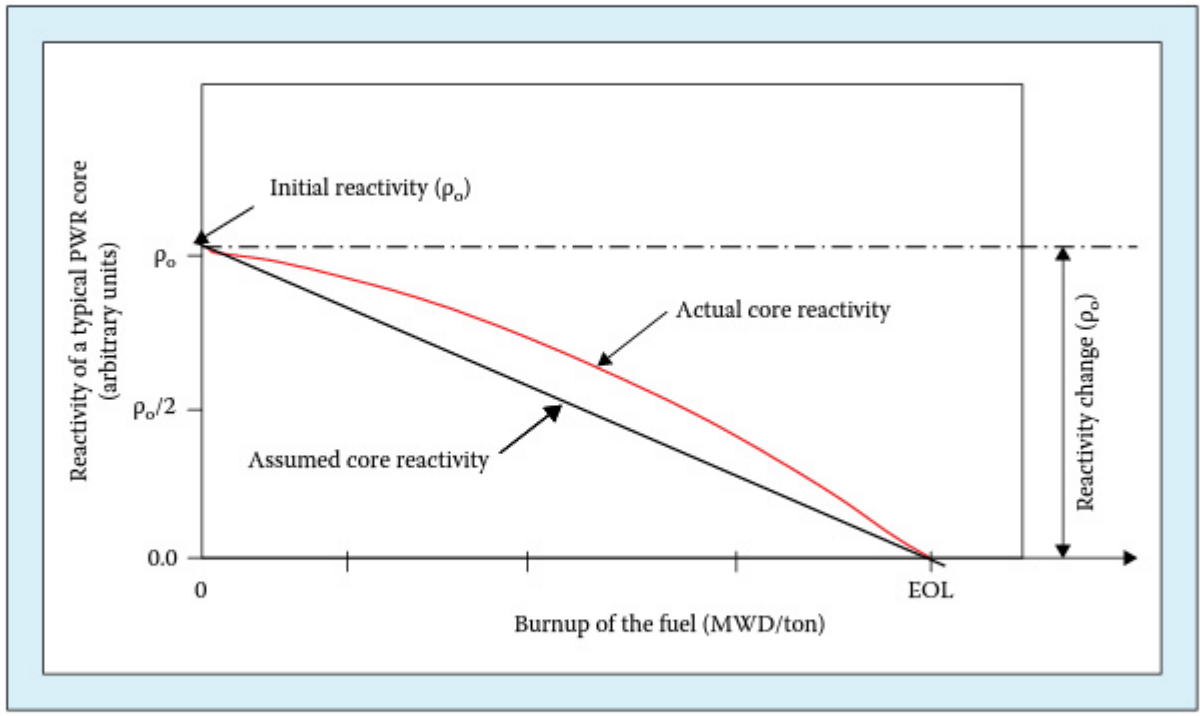

FIGURE 18.3 The reactivity change in a one-batch core as a function of the burnup.

Normally, these design trade-offs create a number of conflicting requirements that must be optimized as a whole. In our companion book* we discovered that a number of important factors (such as the thermal expansion and contraction of the fuel, the radiation-induced embrittlement of the cladding, and the buildup of fission gases in the fuel, rods) can contribute to the failure of the fuel as it is burned.

If one plots the number of allowable fuel rod failures as a function of the burnup, the *maximum permissible burnup* BU_{MAX} that is allowed today for a commercial PWR or BWR is about 50,000 MWD/ton. In general, this number has increased over time, and if the price of uranium continues to increase, the maximum permissible burnup is expected to rise for economic reasons as well. In other words, the integrity of the fuel rods sets the value of BU_{MAX} that can be placed upon a particular type of fuel, and this value in turn determines the initial enrichment of the fuel $e_{INITIAL}$ when it is first loaded into the core.

In the United States, the U.S. NRC currently limits the number of fuel rods that are allowed to fail to about one thousandth of one percent of the total number of fuel rods in the core (0.00001). So if a 1,000 MWE PWR contains 40,000 fuel rods, it is permissible for just a few of these fuel rods to fail and still keep the plant in operation. The exact percentage has changed over time as the nuclear industry has become more mature. (The actual statistics are discussed in Chapter 11 of our companion book*).

18.3 Reactivity Changes in One-, Two-, and Three-Batch Cores

In reality, nuclear power can be produced most economically when the fuel rods are allowed to stay in the core as long as possible. *This implies that there is an economic incentive to get as much energy as possible out of each fuel rod. A nuclear utility does this by maximizing the amount of time that a particular fuel assembly can be left in the core*. This amount of time is a function of the net reactivity of the core, which must be measured over months or even years. One of the easiest ways to determine how long an individual fuel assembly can be left in the core is to compare the burnups of *one-batch* and *two-batch cores*. (Here, the word "batch" is defined as the number of fuel assemblies that have to be replaced when a reactor is refueled.) For one-batch cores, all the fuel assemblies are replaced at the same time, and for two-batch cores, only half the fuel assemblies are replaced at a time. (Exactly how the fuel assemblies are put into the core is another matter.)

For the moment, assume the fuel assemblies are identical and that they have the same average enrichment e. (Later, we will find that this does not always have to be the case). In fact, the fuel assemblies in a typical light-water reactor can have

* See *Nuclear Engineering Fundamentals: A Practical Perspective*, by R.E. Masterson, CRC Press (2017).

three or four different enrichments to help flatten the radial power profile. (The fuel pins can have different individual enrichments as well.) However, let us assume for the moment that we can neglect these effects and that all of the fuel assemblies (at least when they are fresh) are completely identical. (Note: This is a constraint we can remove later when we understand some of the high-level trends.) To optimize the number of U-235 atoms that are burned, most utilities have adopted what are referred to as a *multi-batch* refueling schemes. In these schemes, only a fraction of the fuel assemblies in the core are replaced with fresh fuel assemblies when a reactor needs to be refueled. For a number of reasons that will soon become clear, *most utilities use a three-batch refueling scheme for PWRs and a four-batch refueling scheme for BWRs*. These schemes require a reactor to be shut down every 12, 18, or 24 months to remove the most depleted fuel assemblies. Exactly how this is done is a function of the design of the plant, but since 2000, most nuclear power plants have tended to follow the same basic trend.

Example Problem 18.1

Suppose that the reactivity of each of the components of a reactor core are:

$$\rho_{FP} = \$6$$
$$\rho_{CR} = \$11$$
$$\rho_{BP} = \$13$$
$$\rho_{TEMP} = \$6$$

The initial reactivity of the fuel ρ_{FUEL} is \$45, and it declines at the rate of \$0.75 per month. How many months can a reactor core with a fresh batch of fuel continue operate before at least part of the fuel needs to be replaced?

Solution The core will continue to operate until the net reactivity ρ_{NET} falls to zero. So, the core will have to be refueled when $\rho_{NET} = \rho_{FUEL} - \rho_{FP} - \rho_{CR} - \rho_{BP} - \rho_{TEMP} = 0$ or $\rho_{FUEL} = \rho_{FP} + \rho_{CR} + \rho_{BP} + \rho_{TEMP} = 36$. The time-dependent reactivity of the fuel is $45 - 0.75\,t$, where the time t is measured in months, so the core will have to be refueled when $45 - 0.75t = 36$ or $t = 10/0.75 = 13.3$ months. [Ans.]

18.4 Single-Batch Cores versus Multi-Batch Cores

To understand why *a multi-batch refueling scheme is preferable to a single-batch refueling scheme*, we need to derive an equation for how the net reactivity ρ of a single-batch and a multi-batch core change as a function of the maximum permissible burnup B_{MAX} and as a function of the number of batches of fuel N that are used. The most straightforward way to do this is to assume that *the reactivity ρ is a linear function of the burnup* B (when measured in MWD/ton). While this assumption is not entirely true in practice (because of the effects of burnable poisons, fission products, and control rods), it is accurate enough to use for parametric purposes. Normally, the easiest and most straightforward way to establish a relationship is to start with a single-batch core and then to add additional batches to it to understand how the reactivity changes. Because the reactivity declines linearly with the burnup B, the reactivity of a single-batch core can be written as

The reactivity of a single-batch core

$$\rho(t) = \rho_o\left[1 - \frac{B(t)}{B_{MAX}}\right] \tag{18.5}$$

where

ρ_o is the initial reactivity of the core (at $t = 0$)
$B(t)$ is the burnup of the fuel at time t
B_{MAX} is an additional parameter known as the *maximum permissible burnup*

Normally, the maximum permissible burnup is defined as the burnup where the fuel rods start to fail and higher burnups increase the failure rate significantly. *For most light-water reactors, the maximum permissible burnup is between 40,000 MWD/ton and 50,000 MWD/ton*. Consequently, we will assume a value of 50,000 MTD/ton in the discussion that follows.

Obviously, when $t = 0$, $\rho(t) = \rho_o$, and when $t = T_{MAX}$ (the end of life of the fuel), $\rho(T_{MAX}) = 0$. The reactivity change as a function of burnup is illustrated on the top of Figure 18.4 for a one-batch core. Now consider the case of a two-batch core where both of the batches are assumed to be identical. In this case, one-half of the fuel is replaced when the net reactivity of the core falls to half of its initial value, and a fresh batch of fuel is put in place of the spent fuel to replace it. So when the core is refueled (at $t = T_{MAX}/2$), we will assume that one-half of the core is discharged with a burnup of $B = B_{MAX}/2$. We will also assume that the total core reactivity ρ is equal to the average of the sum of the

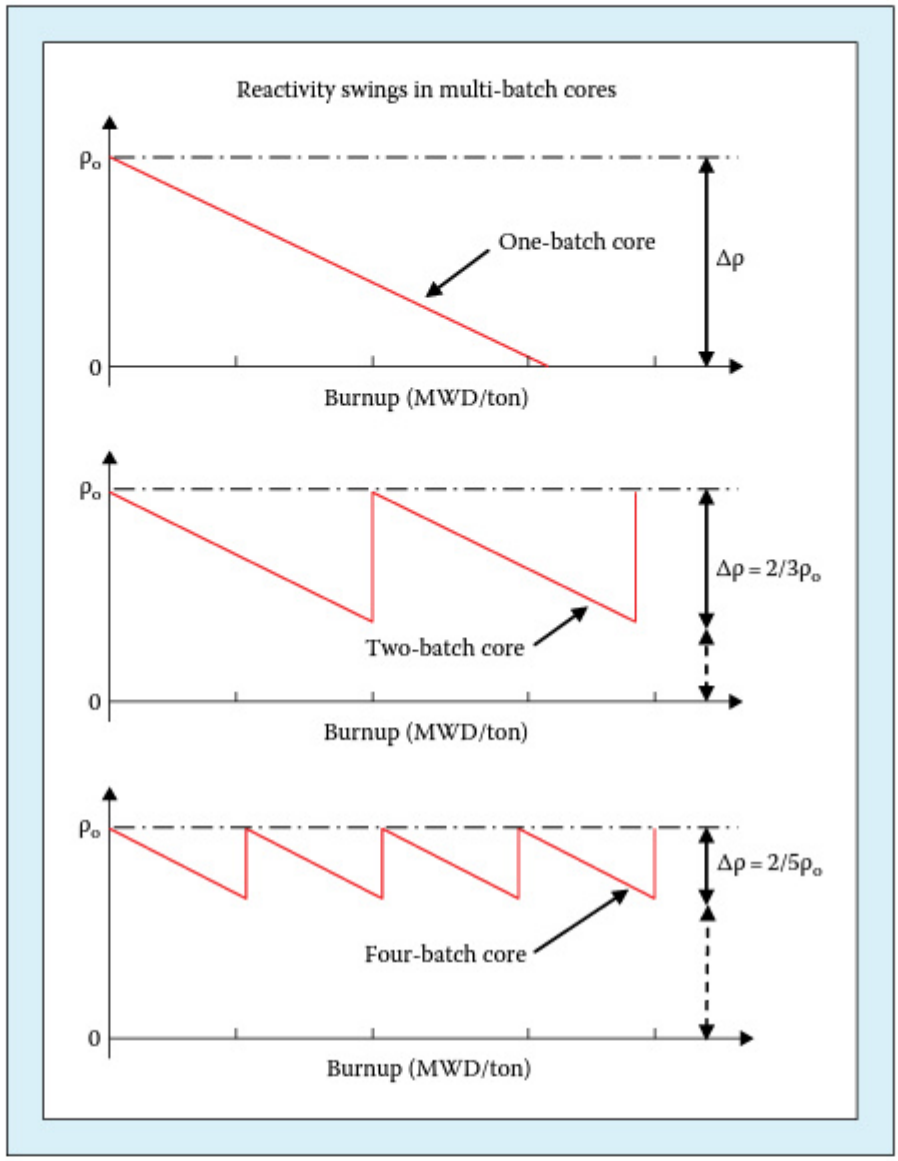

FIGURE 18.4 The reactivity change as a function of burnup in one-, two-, and four-batch cores.

reactivities of the two batches (the old batch plus the new batch). For a two-batch core, this means that the total time-dependent reactivity is given by

The Reactivity of a Two-Batch Core

$$\rho(t) = \rho_o \frac{\left[\left(\frac{1 - B_1(t)}{B_{MAX}}\right) + \left(\frac{1 - B_2(t)}{B_{MAX}}\right)\right]}{2} \tag{18.6a}$$

where

B_1 refers to the burnup of the first batch
B_2 refers to the burnup of the second batch

Since only half of the first batch remains when the core is refueled, $B_1(t) = B_{MAX}/2$. Therefore, when the reactor needs to be refueled, we can set $t = T_{MAX}$ and $\rho(T_{MAX}) = 0$, which leads to

$$0 = \rho_o \left[\frac{1}{2}\left(\frac{1 - B_2(T_{MAX})/2}{B_{MAX}}\right) + \frac{1}{2}\left(\frac{1 - B_2(T_{MAX})}{B_{MAX}}\right)\right] \tag{18.6b}$$

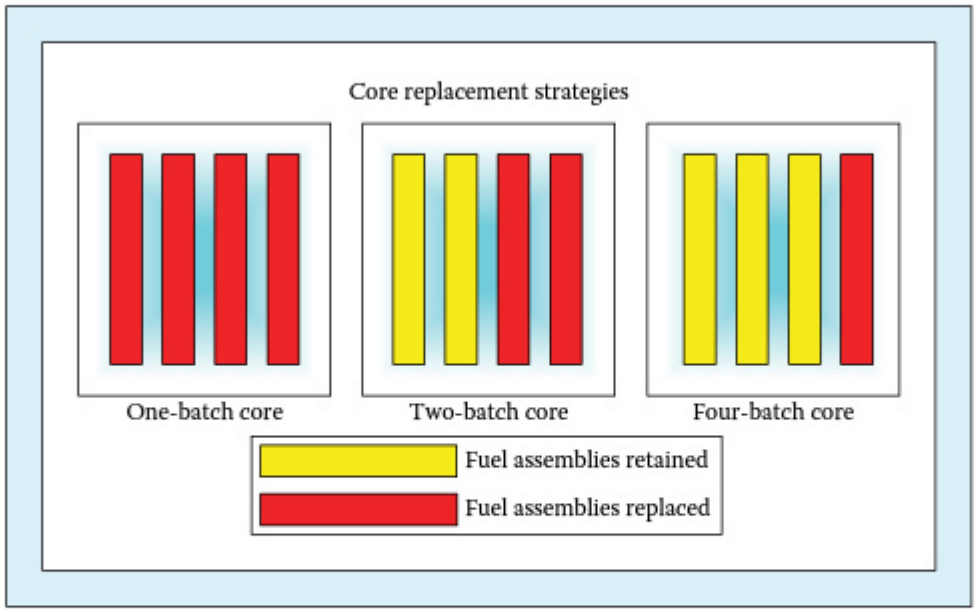

FIGURE 18.5 The number of fuel assemblies replaced in each cycle when using a one-, two-, and four- refueling scheme for the same reactor core.

Solving this equation for $B_2(T_{MAX})$ then allows us to find that the net reactivity swing of a two-batch core is $\rho_2(0) = (2/3)\rho_o$. Hence, we have discovered that *moving from a single-batch refueling scheme to a two-batch refueling scheme has at least two economic advantages*:

1. First, the final burnup of the fuel is 1/3 greater than we could obtain from just a single-batch core (with the same initial enrichment).
2. Second, the reactivity swing has been reduced to only 2/3 of its initial value. In other words, the reactivity swing is now reduced by 33% relative to a one-batch core for the same initial enrichment.

In other words, we have not only been able to increase the amount of energy that can be extracted from the fuel, but we have also reduced the reactivity swing the core needs to be able to handle to achieve it! (see Figure 18.4). Qualitatively, both of these improvements are possible because the new fuel assemblies extend the life of the old fuel assemblies, and because the negative reactivity of the old fuel helps absorb the additional neutrons from the new fuel. This process can be extended to multi-batch cores where the spent fuel is replaced in N equal batches at roughly equal intervals throughout the operating cycle. This eventually leads to a stable core configuration that is known as an *equilibrium core* and a repeatable refueling cycle that is known as an *equilibrium cycle*. The number of fuel assemblies that are replaced at the end of each cycle are shown in Figure 18.5 and the corresponding uptimes and downtimes are shown in Figure 18.6. Now, we would like to examine the advantages of this approach using an N-batch core as our guide.

18.5 Reactivity Behavior of an N-Batch Core

It is easy to generalize our previous discussion to a reactor core where the fuel is replaced in N equal increments (or batches) at equal time intervals throughout its operating life. If the final burnup of the fuel that is desired is B_{MAX}, then the burnup of a batch in an N-batch core after n cycles is simply

The Burnup of an N-Batch core after N cycles

$$B_n(T_{MAX}) = \frac{(n)B_{MAX}(T_{MAX})}{N} \tag{18.7}$$

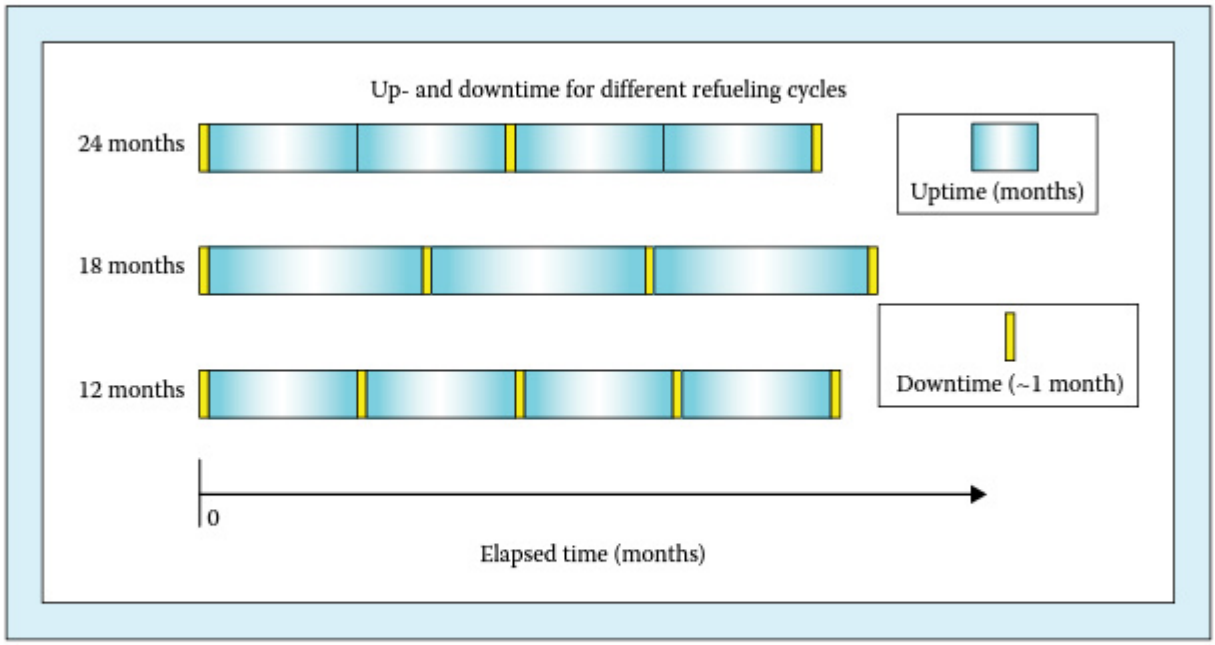

FIGURE 18.6 A comparison of the amount of uptime and downtime (in calendar months) for 12-, 18-, and 24-month refueling cycles. While the "downtime" in each cycle is approximately the same (about 1 month), the amount of "uptime" can vary depending on the cycle. Hence, many utilities have gone to longer refueling intervals in order to reduce the cost of producing power.

where n = 1, 2, 3, …, N. If we make the same assumptions we did earlier regarding the total reactivity ρ, we find that the reactivity ρ_N for an N-batch core is

The Reactivity of an N-batch core

$$\rho_N = \frac{\sum_N \left[1 - \left(1 - B_n(t)/B_{MAX}\right)\right]}{N} \tag{18.8}$$

where the summation is over all the batches from n = 1 to N. After the reactor is refueled again, this leads to the following expression for the equilibrium burnup:

The Equilibrium Burnup of an N-Batch Core after N Cycles

$$B_n(T_{MAX}) = \frac{2N}{N+1} \cdot B_1(T_{MAX}) \tag{18.9}$$

We can rearrange this expression slightly to read

$$\frac{B_n(T_{MAX})}{B_1(T_{MAX})} = \frac{2N}{N+1} \tag{18.10}$$

The values of this ratio are shown in Table 18.1 as a function of the number of batches that are used. *Notice that the burnup ratio asymptotically approaches a value of 2* as more batches are added to the refueling plan. The burnups of the first and second batches are related by

$$B_2(T_{MAX}) = \frac{4}{3} B_1(T_{MAX}) \tag{18.11}$$

TABLE 18.1
Relationship between the Number of Batches Used, the Reactivity Swing of the Core, and the Burnup B of the Fuel for Batch N

Number of Batches N	Reactivity Swing (ρ_N/ρ_o)	Burnup Ratio (B_N/B_1)
1	1	1
2	2/3	4/3
3	1/2	3/2
4	2/5	8/5
5	1/3	5/3
6	2/7	12/7
…	…	…
∞	0	2

We can also repeat the same process we did for a two-batch core to find the reactivity swing for an N-batch core by assuming that the last batch in the core (which is fresh) has an initial reactivity of ρ_o. When we do so, the corresponding expression for the reactivity of an n-batch core is

$$\rho_N(0) = \frac{\left[\sum_{N-1}\left[1-\left(1-B_n(t)/B_{MAX}\right)\right]+\rho_o\right]}{N} \tag{18.12}$$

which, at the beginning of each new refueling cycle, can be further simplified to yield

$$\rho_N = \frac{2\rho_o}{(N+1)} \tag{18.13}$$

In other words, we have just shown that the reactivity swing of an N-batch core decreases as the number of batches is increased! The reactivity increment can be seen in Table 18.1 as a function of the number of cycles. Clearly, this is an important result because we can not only reduce the reactivity swing of the core (which makes the reactor easier to control) but also increase the burnup of the fuel (which allows us to make more money from the available uranium). *So, the question then arises as to why most reactor refueling schemes are based on only three-batch or four-batch cores, and why we do not see any true "N-batch" cores in practice. The reason lies in the fact that the number of times a reactor must be refueled increases as the number of batches in increased.* Since *the amount of time required to replace the spent fuel assemblies is usually a fixed number (which happens to be about a month),* the gain in the increased amount of energy that can be obtained by going to an N-batch core is almost exactly offset by the additional amount of time that the plant has to be down to add the new fuel. Since the plant does not generate any electricity while it is being refueled, there is an economic trade-off between the number of times the plant can be shut down for refueling and the amount of additional energy that can be produced by reloading it more frequently.

Since Y2K, this economic optimum has remained at about three batches for a commercial PWR and about four batches for a commercial BWR. The average amount of time between refuelings (ΔT_{REFUEL}) has averaged between 12 and 18 months, and the planned downtime to replace the fuel (when the reactor can no longer generate useful power) has stayed at about one month (or approximately 30 days). This particular set of parameters has optimized the economic performance of most nuclear power plants in modern times. However, within these constraints, the economic performance of a particular power plant can be improved even further by optimizing the burnup of the fuel within a particular cycle. This involves optimizing the fuel assembly–loading pattern, and this is the next topic that we would like to discuss.

Example Problem 18.2

The fuel assemblies in a pressurized water reactor are to be replaced in four equal batches. If the initial reactivity of the core is \$45, what is the average reactivity swing of the fuel between subsequent refuelings? How much positive reactivity must be added by the control rods at the end of each burnup cycle to keep the core critical?

Solution The average reactivity swing of the core is given by $\rho_N = 2\rho_o/(N + 1)$, where N is the number of batches. Since N = 4, the reactivity swing per cycle due to the burnup of the fuel alone is $\rho_N = 2/5\rho_o$ = \$18.00. Therefore, \$18.00 of excess reactivity must be added to the core by the control rods at the end of each equilibrium burnup cycle to keep it critical. [Ans.]

18.6 Optimizing the Fuel-Loading Pattern within a Given Cycle

In practice, the *nuclear fuels manager* is responsible for selecting a refueling strategy that makes the most sense for a utility and its shareholders. Of course, this must be accomplished in a way that guarantees the safest possible operation of the power plant, and this in turn requires the operator of the plant to ensure that

1. The fuel will not melt during normal plant operation
2. The cladding will not dry out during normal plant operation
3. The fuel rods will not fail and release radioactive fission gases during normal operating conditions
4. The temperature coefficient of the reactivity will always be negative if the reactor temperature increases

In practice, no two fuel cycles are completely identical, and so the economic or safety constraints that may apply to one fuel cycle may not apply to another. However, while the economics of a particular cycle (say cycle n) can be relatively easy to optimize, it is even more important to be able to optimize the economics across multiple cycles. The process of doing so is referred to as the process of *nuclear fuel management, and the goal of nuclear fuel management is to get as much energy as possible out of the fuel as it is burned, while minimizing the number of times that a reactor needs to be refueled.* Many attempts have been made to automate how the fuel must be loaded into the core in order to reconcile these conflicting goals.

Almost every optimization scheme is based on the idea that an operating nuclear power plant will eventually reach what is known as its *equilibrium cycle*. From this point forward, the reloading schemes will be exactly the same, and the enrichments that will be used for future cycles will be exactly the same as those used for previous cycles. However, this does not necessarily imply that each cycle will employ exactly the same enrichment. Table 18.2 shows what the reload cycle looks like for a three-batch core that is representative of a modern PWR. Now let us comment on the notation that is used in this table. Here, the subscript m refers to the batch number of the fuel, and the subscript n refers to the number of cycles that the fuel has been in the core since the *beginning of cycle (BOC).* In other words, a value of n = 0 implies that the fuel is both fresh and new. So, this is the meaning that we will ascribe to each entry in the table that is called BATCH (m, n). We can also infer from the table that the first batch is intended to be discharged after producing 1/3 of the energy that it is expected to. (However, it can also be reinserted back into the core at a later time to recover the additional 2/3 of this energy). In the meantime, it is stored in a *spent fuel pool.*

Unfortunately, so many things happen when a reactor is being operated that it is almost impossible to reach a true equilibrium cycle. For example, some fuel may come on the market at a lower price, and a utility may decide to buy this fuel and use it sooner than it had originally anticipated. Moreover, if a defect develops in a particular assembly (which is a rare but not uncommon event), it may be necessary to replace the defective fuel assembly sooner than was originally anticipated. This means that the reactor may have to be shut down sooner for refueling. Finally, the capacity factor for the period in question may be higher than what was originally planned, and so the reactor must be refueled sooner because the fuel has been burned up sooner that it should have been. Conversely, if the capacity factor is lower than expected, the reactor may have to be operated for a longer time before the net reactivity of the core falls to 0. As soon as the first one of these events occurs, the fuel cycle tends to get "out of sync" because the current fuel cycle depends on the state of the previous fuel cycle. In practice, this "problem" must then be corrected by using some sort of *linear programming, dynamic programming, or some other optimization scheme* to compensate for an unexpected departure from the operating plan. However, because these constraints are not the same for all power plants, or even for the fuel within the same power plant, no single approach has emerged as the standard for the industry as a whole. Before discussing how the burnup of an individual core can be optimized, we would first like to mention that there are a number of "features" that all optimization schemes have in common. First, to reduce the computational complexity associated with finding the optimal loading pattern, a *symmetry*

TABLE 18.2
An Example of the Reloading Pattern for a Three-Batch Core

	Cycle Number n			
Batch Number m	1	2	3	4
1	BATCH (1,0)			
2	BATCH (2,0)	BATCH (2,1)		
3	BATCH (3,0)	BATCH (3,1)	BATCH (3,2)	
4		BATCH (4,0)	BATCH (4,1)	BATCH (4,2)
5			BATCH (5,0)	BATCH (5,1)

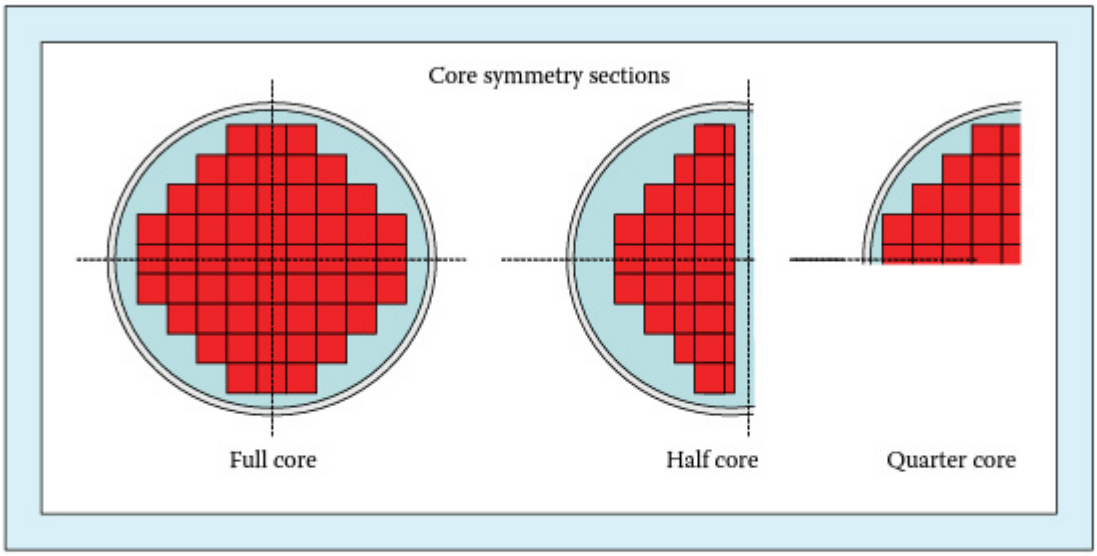

FIGURE 18.7 An example of ½ core and ¼ core symmetry sections that can be used in a fuel assembly optimization analysis.

section of the core is usually employed whenever possible. The fuel-loading scheme that is used in this symmetry section can then be applied to model the behavior of the core as a whole. This symmetry section is usually a 90° symmetry section, although a 45° symmetry section can also be used. An example of these symmetry sections is shown in Figure 18.7.

Second, in order to extrapolate to the next logical step in the process, it is necessary to make an *educated guess* as to the burnup of each fuel assembly in the core at the time that the reactor is to be shut down. Ordinarily, this can be done based on *experience* or on the *operating plan* for the fuel cycle in question. (It can also be done by running a number of commercially available computer programs, which we discussed in our companion book.*) Third, the desired *capacity factor* and the desired burnup for the new cycle must be specified in advance. Again, this is affected by the enrichment of the fuel. Finally, the new refueling strategy must be able to show that

1. The fuel rods will not fail
2. The fuel will not melt
3. The cladding will not dry out
4. The temperature coefficient of the reactivity will not become positive as the fuel temperature is raised

If all four of these design goals are met, then the reactor can be refueled, and the next cycle in the process can begin. We would now like to discuss how the performance of an individual core can be optimized as the fuel is depleted or burned. This brings some additional factors into play in addition to the ones we have already discussed.

18.7 Optimizing a Reactor Core

As reactors have become more ubiquitous as electrical generating systems, many design enhancements have been made to improve their efficiency and reliability. It did not take long for engineers to realize (even before the days when reactors were designed by computers) that a simple clean core with a uniform distribution of fuel was not an optimal operating configuration. *In fact, when this matter was studied in more detail, it turned out that simply putting the same fuel assemblies everywhere was probably the worst possible design they could imagine.*

The reason for this was that the flux shape peaked in the center of the core (see Chapter 13), and this caused the fuel assemblies near the center to run much hotter than the fuel assemblies at the edges. Moreover, the fuel burned up too rapidly in the center and not quickly enough around the periphery. So in addition to wasting fuel and causing too many *thermal hot spots*, this type of fuel-loading pattern actually made the reactor harder to control (see Chapter 16). Several attempts were made to improve this basic design, and after a while, engineers discovered that *the optimum way to load the fuel turned out to be one in which the power distribution was uniform as possible across the core as long as possible*. In practice, this turns out to be very hard to achieve, because the fuel does not always burn at a uniform rate, and because

* See *Nuclear Engineering Fundamentals: A Practical Perspective*, by R.E. Masterson, CRC Press (2017).

some provision must be made to account for the motion of the control rods over time. However, the closer we get to this ideal operating state, on a time-averaged basis, the closer we get to a fully optimized and safe and efficient design. So, the design principle that was established for a new core when loading it with fresh fuel was

An Important Design Principle

"To the maximum extent possible, the power density must be the same everywhere in the core (both radially and axially), and the power density must continue to be as uniform as possible for as long period of time as possible to get the best possible burnup from the fuel."

This does not necessarily mean that the power level cannot be changed over time or that the power level cannot be allowed to vary to meet other operating requirements. It simply means that the spatial distribution of the power must be kept as uniform as possible for as long as possible to get the most energy out of the fuel. Since the power level at any point in time and at any spatial location is proportional to

$$P(\mathbf{r},t) = \Sigma_f(\mathbf{r},t)\phi(\mathbf{r},t) \tag{18.14}$$

where **r** corresponds to the location of an individual fuel assembly i, this design requirement can also be written as

$$P(i,t) = \Sigma_f(i,t)\phi(i,t) \tag{18.15}$$

where i = 1 to N and N is the total number of fuel assemblies in the core.

Assuming that $\Sigma_f(i, t)$ is known from a fuel-loading pattern, a burnup, or a depletion analysis, then the flux can be iteratively adjusted until the correct power level P(i, t) is met. This is usually done with a computer program until an optimized fuel-loading pattern and control rod withdrawal pattern can be found. Depending upon the criteria a utility chooses to use, a wide variety of loading patterns may be possible. PWRs and BWRs have many similarities in the way they attempt to manipulate these parameters to achieve the best possible result. However, in general, this means that several types of fuel assemblies with several different enrichments must be used, and where these fuel assemblies must be positioned must be incorporated into the *operating plan*. So one can conclude from this simple discussion that the optimum operation of a reactor always requires a spatially nonuniform distribution of the fuel. Distributing the fuel in this way has three major advantages that can lead to a safer and more economical reactor. These advantages include

1. A flatter radial power distribution
2. A longer core life for a given amount of fuel
3. A more complete burnup of the existing fuel

It should be noted that these same advantages apply regardless of the type of fuel that is used. For example, they apply when the fuel is conventional uranium dioxide (UO_2) or when the fuel is a *MOX fuel that consists of a mixture of uranium dioxide and plutonium dioxide (PuO_2).* In more refined versions of this concept, *some reactor vendors have replaced the outer one or two rows of fuel pins with stainless steel rods. This reduces the leakage of the neutrons from the outer regions of the core without causing any unwanted power peaks near the core–reflector boundary. Since this also minimizes the value of the neutron flux at the reactor vessel wall, it reduces the radiation damage to the reactor pressure vessel, and this can help to extend its operating life by several years*. See Chapter 17 for a more detailed discussion of the benefits that this can provide.

18.8 Fuel Assembly–Loading Patterns

As one can imagine, the best way to get the most power out of a batch of fuel is to position it in such a way that the energy that is produced is as uniform as possible in both the radial and axial directions. In practice, this can be achieved by putting fuel assemblies with more highly enriched fuel around the edges of the core and putting fuel assemblies with a lower overall enrichment closer to the center. This forces the product of the thermal flux and the fuel rod enrichment—and therefore the total power density $P(r, t) = \Sigma_f(r, t)\phi(r, t)$—to be approximately the same everywhere and at every spatial location. *In most modern reactors, the design goal is to keep the peak-to-average power ratio within a fuel assembly to about 1.2 to 1 and to keep the peak-to-average power ratio between adjacent fuel assemblies to about 1.3 to 1*. The closer the peak-to-average power ratio is to the ideal ratio of 1.0, the more completely the fuel can be burned (without exceeding

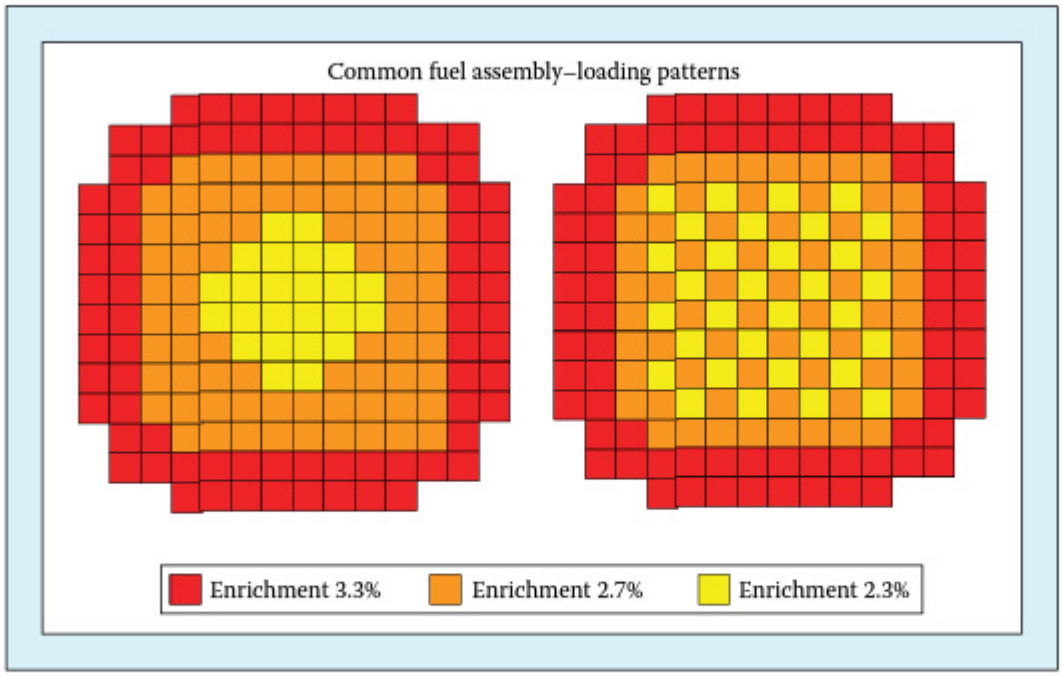

FIGURE 18.8 Two popular fuel assembly–loading patterns. These loading patterns help to reduce radial power peaking in the core. The one on the left is called an "out–in" loading pattern, and the one on the right is called a "checkerboard" loading pattern. The red fuel assemblies have an average enrichment of about 3.3%, while the assemblies shown in yellow and brown have an average enrichment of 2.2% and 2.7%, respectively.

its maximum temperature), and the more economical the reactor will be to operate. Since these ratios also depend upon how the control rods are moved, each loading pattern must also take the positions of the control rods into account (see Chapter 20).

Just like a game of chance, there are essentially an infinite number of ways that the fuel can be loaded or reloaded to get a better peak-to-average power ratio than one can get with a homogeneous reactor core alone. Figure 18.8 shows two slightly different fuel-loading patterns that can be used to flatten the power both radially and axially. Each square is a fuel assembly with a different average enrichment. The darker colored fuel assemblies around the edge of the core have a higher average enrichment than the fuel assemblies that are closer to the center. In other words, the strategy that is used in this case is to have the enrichment of the fuel assemblies decrease as one moves from the outside of the core to the center. This is the original "Day 1" or cold clean configuration that is used to start a reactor up. When the reactor has been operated for a year or more and can no longer stay critical, then it will need to be shut down and refueled. At the time of refueling, the fuel assemblies in the center of the core that have the lowest overall amount of U-235 remaining are replaced with fuel assemblies from the outside of the core, and fresh fuel assemblies are added around the periphery. Each fuel assembly is numbered and loaded into a specific location. When this type of refueling strategy is used, the power distribution will be much flatter than when all of the fuel assemblies have the same enrichment. Normally, an *"out–in" loading strategy* like this requires the use of three or four different enrichments for the fuel assemblies.

Another reloading strategy (see Figure 18.8) called the *checkerboard loading strategy* is very popular in thermal reactors today. In modern power reactors, *checkerboard reloading schemes have become more popular than out–in reloading schemes because they are not only able to achieve the highest possible burnup of the fuel but they are also the most effective in reducing the overall radial power peaking across the core*. If the average enrichment needed to keep the core critical for 1 year is 2.8%, and three types of fuel assemblies are used, then the other two types of fuel assemblies will have enrichments of about 2.3% and 3.3%, respectively. If the average enrichment needed to keep the core critical for 1 year is 2.8%, and four types of fuel assemblies are used, then the fuel assemblies will have enrichments of about 2.2%, 2.6%, 3%, and 3.4%, respectively.

To reduce the amount of neutron leakage from the core and reduce the radiation damage that these neutrons can cause to the reactor vessel, some reactors replace the outer one or two rows of fuel pins in the most highly enriched assemblies with stainless steel rods. This shields the reactor vessel from the highly enriched fuel assemblies around the edges and improves the reflector savings as well. *Since it is not always possible to predict the motion of the control rods in advance, all methods of distributing the fuel to flatten the power have some inherent uncertainty associated with them.* This uncertainty can only be addressed while the reactor is actually being operated. Any changes to the operating plan that cannot

be anticipated in advance are fed into the reactor's control computers, and the projected movements of the making rods are updated so that the power distribution can continue to stay as uniform as possible. This form of real-time decision making is based on continually updating and analyzing the data that are sent to the system's central computer from the instruments that monitor the real-time behavior of the core. As controls systems have become more sophisticated, the length of the fuel cycles has increased to about 24 months, and the power ratings have also been increased by as much as 10% to 20%. This has been true for both BWRs and PWRs as the nuclear industry has become increasingly mature.

18.9 Core Power Profile as a Function of Burnup

Both PWRs and BWRs have a similar set of design requirements when it comes to how much power peaking is permissible during normal operating conditions. Normally, power peaks are highest when a core is loaded with new fuel or when some of the fuel assemblies in a core have to be replaced at the beginning of a cycle. Generally speaking, a peak-to-average power ratio of about 1.3 is acceptable in this case. If the peak-to-average power ratio becomes greater than this, then the core power level may have to be reduced until some of the power peaks can be eliminated. Obviously, this is not something that an average utility would like to do.

The normalized power distribution for a one-quarter symmetry section of a BWR-6 core is shown in Figure 18.10. This core consists of 624 fuel assemblies, and a one-quarter symmetry section contains 156 of these. Notice that the power level of an average fuel assembly rarely exceeds $1.3P_{AVG}$, where P_{AVG} is defined in the following way:

$$P_{AVG} = \frac{\sum_n P_n}{N} \tag{18.16}$$

and the summation is performed over all of the fuel assemblies from n = 1 to N. What is even more interesting is that most of the fuel assemblies around the periphery have a much lower peak-to-average power ratio than those in the center. This is done intentionally to reduce the number of fast neutrons that can leak out of the peripheral fuel assemblies and damage the reactor pressure vessel. As discussed in Chapter 13, this can be a very important concern in some designs.

Typically, the fuel assemblies that have a higher initial power will tend to burn faster than assemblies with lower initial powers. So after a short period of time, the core power peaks will tend to subside, and the power profile will appear to become flatter. Normally, the rate that the power peaks subside is directly proportional to the average enrichment of the fuel. In other words, a fuel assembly having a peak-to-average power ratio of 1.3 will have the power level decline approximately 30% faster than one that has a peak-to-average power ratio of 1.0. The same logic applies to fuel assemblies with peak-to-average power ratios less than 1.0. Hence, from neutronic perspective, the core appears to become more homogeneous and easier to control as the fuel is burned. Of course, the buildup of the fission products in the core can complicate this analysis slightly.

18.9.1 Maintaining the Fuel Pin Temperatures within Established Limits

During normal operation, most reactor designers attempt to limit the maximum fuel pin temperature to about 1800°C because this minimizes the number of fission products that can be released from the fuel. When the centerline temperature rises above this point, the fuel begins to restructure itself (see Chapter 11 of our companion book*), and fission gases can be released into the fuel rods.

The radial and axial power peaking factors that we discussed previously are normally set to between 1.2 and 1.3 so that a representative peak-to-average power ratio across the core is about $1.2 \times 1.3 \approx 1.6$. This means that if the peak fuel pin temperature is not allowed to exceed about 1800°C, the average fuel pin temperature will be about $1800°C/1.6 \approx 1125°C$. These numbers are mostly applicable to the current generation of thermal water reactors (both PWRs and BWRs). In fast reactors, they can be slightly higher because the design parameters are different. In recent years, there has been a trend to raise the *average fuel pin centerline temperature* to about 1200°C. This is based on a more refined statistical approach than the one discussed previously.

18.10 Axial Zoning Schemes

In addition to varying the average enrichment of the fuel from the center of the core to the edge, it is also possible to reduce the peak-to-average power ratio by varying the enrichment of the fuel in the axial (or z) direction. To accomplish this, many reactor vendors have adopted what are known as *axial zoning schemes*. In these schemes, the fuel midway between the endpoints of a fuel rod may have a lower total enrichment than the fuel in other parts of the rod.

* See *Nuclear Engineering Fundamentals: A Practical Perspective*, by R.E. Masterson, CRC Press (2017).

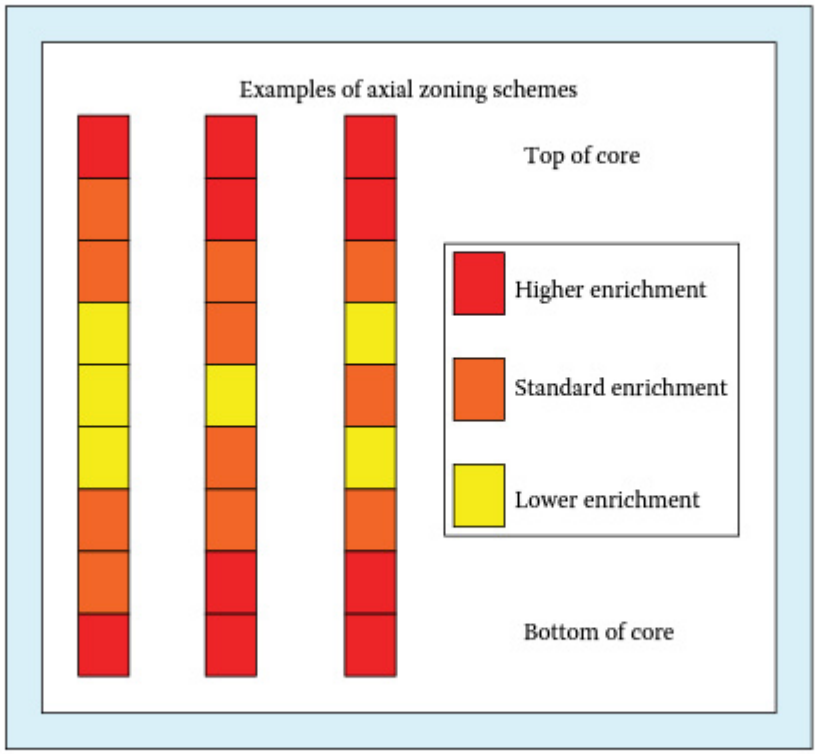

FIGURE 18.9 Some axial zoning schemes that can be used in either PWR or BWR fuel assemblies.

This, combined with a judicious use of burnable poisons, allows the burnup of the fuel in the axial direction to be more uniform as well. If P(i, j) is the power level in fuel assembly i at axial location j, then the peak-to-average power ratio of the fuel in the axial direction for fuel assembly i is given by $P(i, j)_{MAX}/P(i)_{AVG}$. And if we sum over all of the fuel assemblies in the core, the maximum value of P(i, j) for all i and j is the location of the point of maximum power. Needless to say, the location of this point can change as the fuel is burned and as the control rods are moved. Figure 18.9 shows several ways in which the enrichment of the fuel can be varied in the axial direction—depending on the enrichment of each fuel assembly in the radial direction—to achieve the flattest possible power shape. If we were to superimpose these two enrichment profiles, or *zones*, on top of each other, we would be able to generate a three-dimensional map of the core in which the flux and the enrichment and the power are different at any given point (i, j). Modern computer programs can update these three-dimensional profiles daily based on data provided by the reactor's monitoring, instrumentation, and control systems. The output of these computer programs can be used to decide the next set of control rod positions to optimize the fuel life and the flux shape.

Student Exercise 18.1

For the BWR-6 core shown in Figure 18.10, calculate the peak-to-average power ratio for the outer three rows of fuel assemblies and for the inner six rows. What do you notice about the peak-to-average power ratios in this case?

18.11 Burnable Poisons within an Individual Fuel Assembly

Burnable poisons (see Chapter 20 for a complete list of these poisons) can also be used to flatten the power distribution within an individual fuel assembly. This can be done by varying the enrichment of the fuel rods and introducing burnable poisons where needed, as shown in Figure 18.11. *Burnable poisons are materials introduced directly into reactor fuel assemblies to help prevent power peaks when the fuel is fresh and to reduce the number of control rods required to maintain the system in a critical state while the fuel is being burned.*

A *burnable poison* is a material with a large absorption cross section that can absorb a thermal neutron and can then become a material with a much smaller cross section after the neutron is absorbed. So, any increase in the reactivity that might occur while the poison is burning will be compensated for by a nearly identical decrease in the reactivity while the fuel is burned and other fission products start to accumulate. *A burnable poison can be thought of as a "poor man's" control rod.* In fact, the amount of reactivity contained in all of the burnable poisons in a PWR is nearly comparable to the

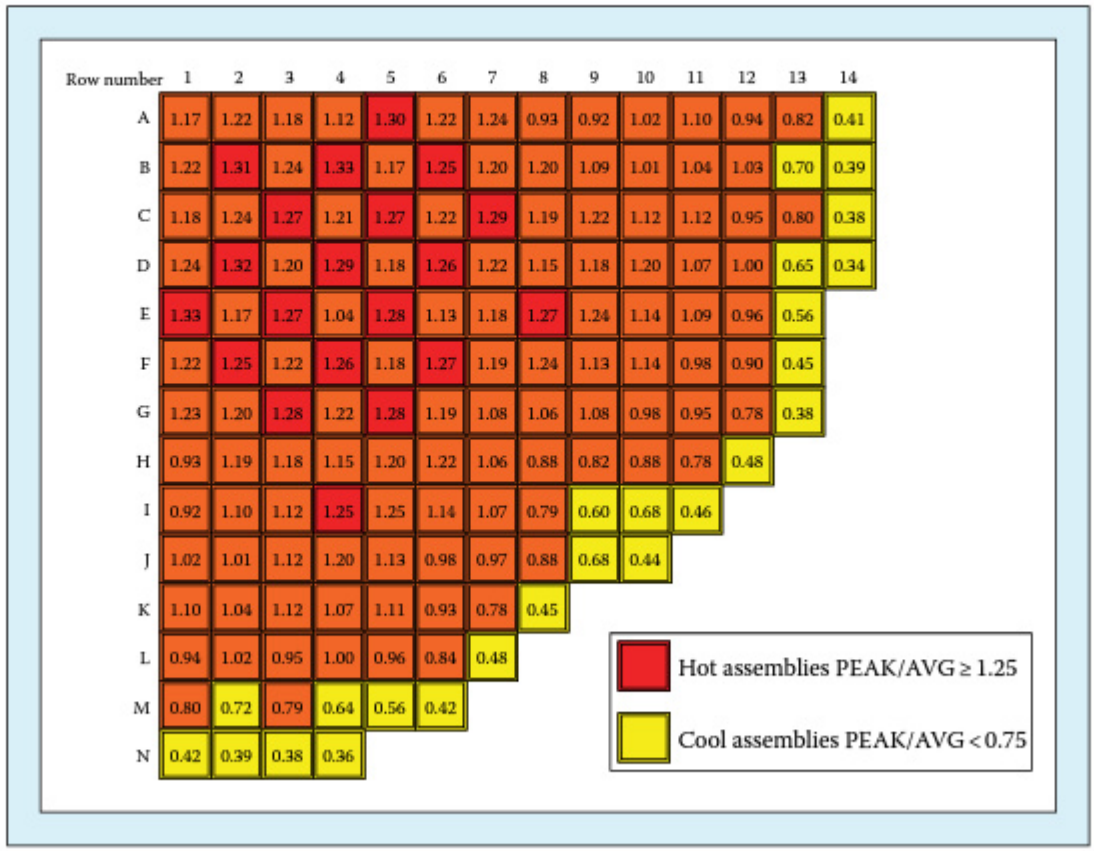

FIGURE 18.10 The core power distribution in a BWR-6 at beginning of life (BOL).

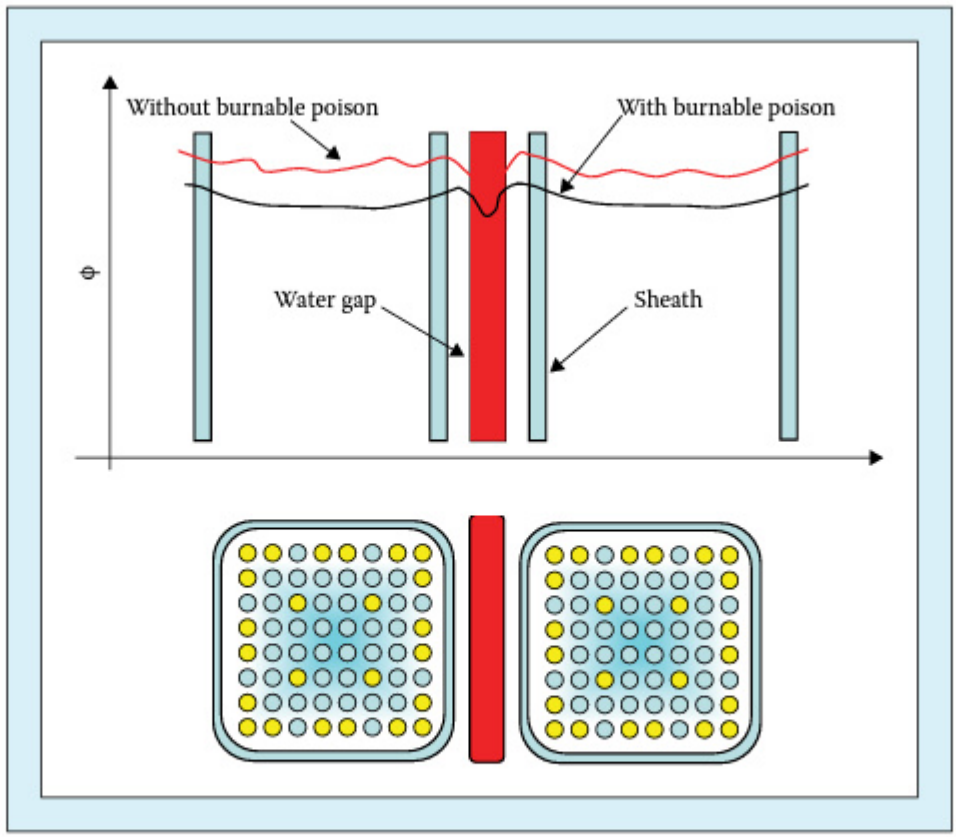

FIGURE 18.11 Burnable poisons and their effect on the thermal flux shape in two BWR fuel assemblies on each side of a control rod.

reactivity contained in all of the control rods. However, a burnable poison is generally mixed directly into the fuel, and hence it cannot be moved, while a more expensive control rod (by design) can always be moved up and down.

18.12 Burnable Poisons Inside of Reactor Fuel Assemblies

In a PWR, the control rods can contain about $11 of negative reactivity, while the burnable poisons will typically contain $12 to $14 worth. Similarly, in a BWR, the control rods will contain about $25 of negative reactivity, while the burnable poisons will contain about $18 worth. This difference in the worth of the control rods is primarily due to the fact that PWRs have an additional chemical shim system, while the BWRs do not. Burnable poisons have become very popular in recent years because of advances in nuclear materials, and because they can help to reduce the cost of building or operating a reactor. Since control rods and their drive mechanisms are very expensive to build, the cost of building a reactor can be reduced substantially by simply replacing the moveable control rods and their drive mechanisms by stationary fuel rods containing burnable poisons. For a nuclear plant that costs 5–10 billion dollars, this can save a utility between 20 and 30 million dollars in operating costs.

Student Exercise 18.2

Suppose that we take three different types of fuel assemblies—one with an enrichment of 4%, one with an enrichment of 3%, and one with an enrichment of 2%. If the neutron flux in all of these fuel assemblies is exactly the same

1. What is the peak-to-average power ratio when they are initially loaded into the core?
2. What is the peak-to-average power ratio when on average they are 50% burned? Be prepared to give a reason for your answer.

Gadolinium and *boron* are commonly used as burnable poisons today. Boron can be combined with a variety of metals, stainless steel, and even with *pryex glass* to create a fuel rod filled with a burnable poison. Gadolinium can also be mixed directly with uranium oxide (UO_2) in the form of *gadolinia* (Gd_2O_3), which performs a similar function. In addition, both materials can be distributed radially or axially in a number of predefined zones to control both the radial and axial burnup. This promotes a much more uniform burnup of the fuel in each direction. Other advances in nuclear materials and control systems may result in an even more widespread use of burnable poisons in the future. Figure 18.12 shows how adding burnable poisons to a PWR core can affect the amount of chemical shim needed to keep the reactor critical over a period of about 1 year. Of course, the poison is mixed with the fuel in this case.

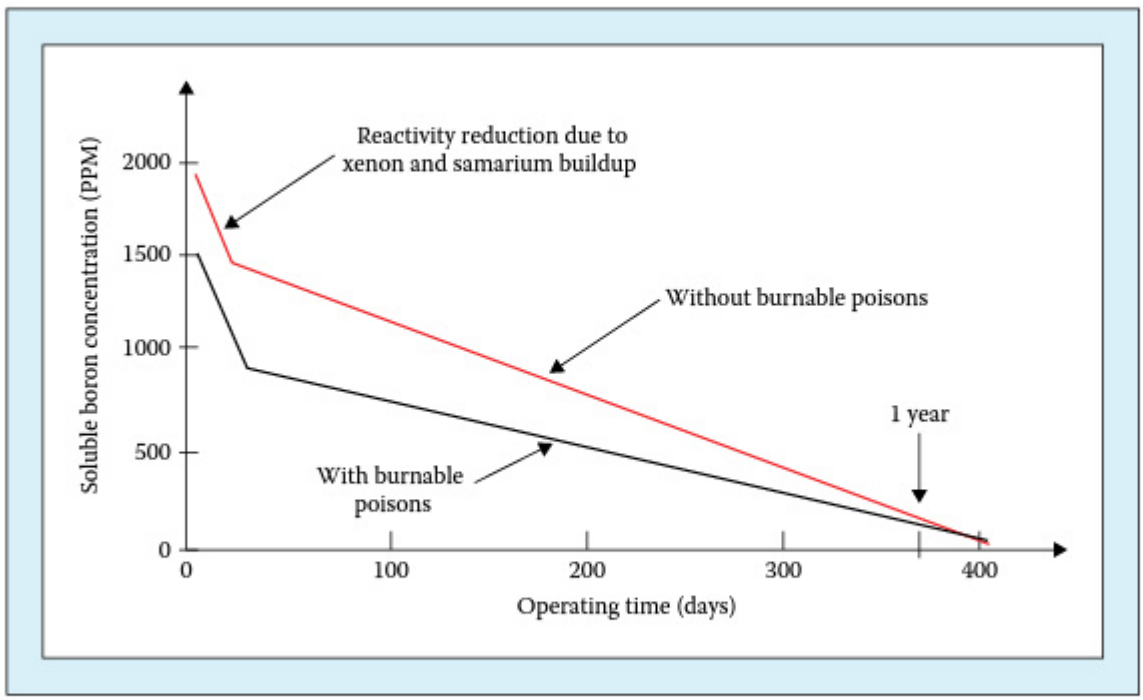

FIGURE 18.12 The effect of burnable poisons on the boric acid concentration in a typical PWR core.

18.13 Effect of Burnable Poisons on the Flux Shape

Since burnable poisons are designed to "burn themselves out" over a predefined period of time, the flux shape in the vicinity of a burnable poison will change as the fuel is burned. When a fresh fuel assembly is loaded into the core, the fuel rods that contain the burnable poisons appear to be "gray" and sometimes even black to the thermal neutrons in their vicinity. The thermal neutrons that fall into these rods rarely emerge from them. This causes the thermal flux near the burnable poison rods to appear to be lower than the thermal flux in the fuel assembly as a whole. Because the burnable poisons are mixed together with the fuel, this effect can extend several mean free paths beyond the surface of the fuel rods themselves (usually a few centimeters in most cases). In other words, the spatial depression of the flux in the vicinity of the rods containing the burnable poisons is highly localized—just as it is in the vicinity of a control rod.

The only difference between a fuel rod that contains a burnable poison and a control rod is that the fuel rod undergoes several shifts in the shape of the neutron flux as the poison is burned, while for the control rod, it does not. This effect is shown in Figure 18.13, where the effects of the burn-off of the poison are illustrated. Notice that when the poison is completely burned, the shape of the neutron flux in the vicinity of the fuel rod reverts back to its normal shape. However, the flux in the vicinity of the control rod does not. The strength of a burnable poison also be adjusted by varying its concentration. In each fuel assembly, this tends to suppress the local power peaks as the fuel is burned. Eventually, when all of the poisons have burned away, the shape of the flux returns to its normal shape.

This effect can be demonstrated analytically by solving the neutron diffusion equation in a simple homogeneous cylinder or slab surrounded by a neutron-moderating material on each side. However, a macroscopic absorption cross section Σ_{bp} must be added to the diffusion equation for the fuel to represent the time-dependent concentration of the burnable poison in the rod. Then as the fuel is burned, the concentration of the poison is reduced. Only in this case, the boundary condition that must be enforced at the edges of the moderator is that the neutron current **J** must be 0. Of course, this is equivalent to assuming that no neutrons leak out of the unit cell that contains the burnable poison. The interested reader may wish to consult Chapter 14 to see how solutions to the neutron diffusion equation can be modified to account for the presence of the poisons in the rod.

18.14 Mathematical Description of the Depletion Process

To keep track of all of the fission products that are produced and how fast the fuel is burned, it is easier to subdivide a core, such as the one shown in Figure 18.10, into individual fuel assemblies and to track the isotopic compositions of the materials within each of fuel assembly. For any given fuel assembly, this gives us the average fission product concentration $C_{FP}(i, j, n)$, the average concentration of the fuel $C_F(i, j, n)$, and the average control rod poison density $C_{CR}(i, j, n)$, where $i = 1 \ldots I$ is the fuel assembly number; j is the number of the axial position, $j = 1 \ldots J$; and n is the

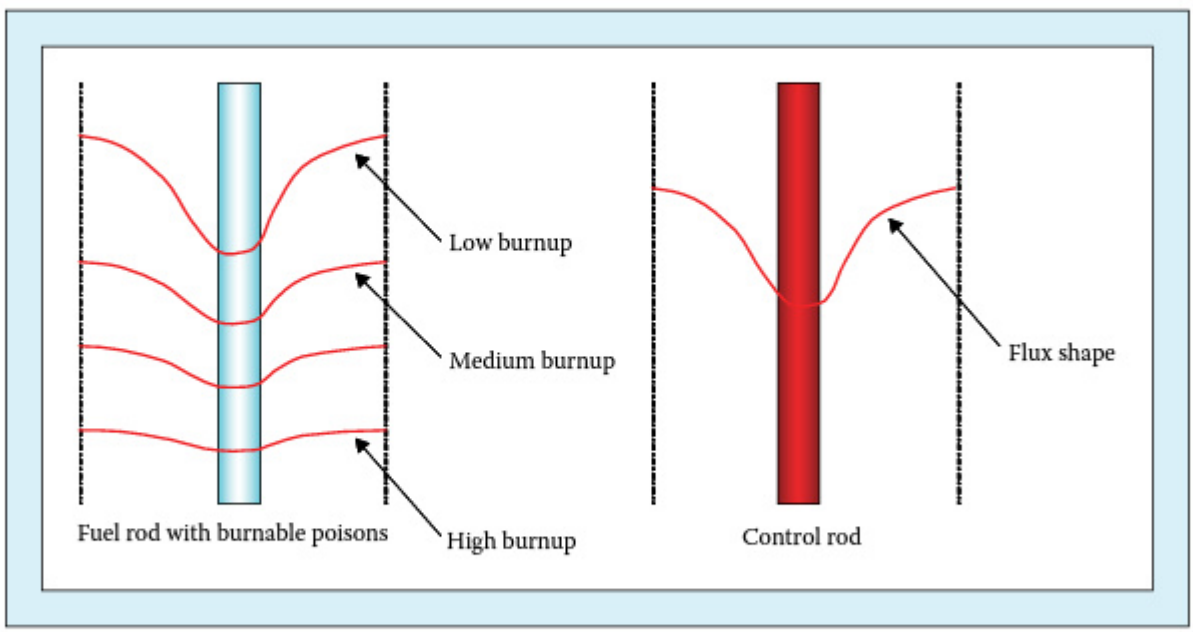

FIGURE 18.13 The flux shape in the vicinity of a fuel rod that contains a burnable poison versus a control rod of the same size.

number of the time step, or time interval between successive depletion calculations. Each time the flux is recalculated (usually once a day), the concentrations of the materials can be updated using the new values for the flux. Suppose for the moment that there are a total of NP fission products to be updated, NF isotopes of the fuel to be updated, and NB other materials (including burnable poisons) to be updated at each axial location. Then when the new value of the flux $\phi(i, j, n)$ is known at each axial location, one simply inserts it into the standard rate equations and multiplies by the time interval Δt between successive depletion steps to obtain the new isotopic concentrations. It is much simpler to illustrate this with a concrete example to get the point across. At $t = 0$, the fuel concentration F, the fission product concentration P, and the burnable poison concentration B are known. The reactor is allowed to operate for some period of time Δt, over which the flux ϕ is assumed to stay approximately the same. Then the material concentrations F', B', and P' at some later time Δt are given by

$$F' = F_o + (C - D)F\phi\Delta t \tag{18.17}$$

$$B' = B_o + (C - D)B\phi\Delta t \tag{18.18}$$

$$P' = P_o + (C - D)P\phi\Delta t \tag{18.19}$$

where the coefficients C and D represent the creation and destruction coefficients that are unique to each specific isotope. These new values for the concentrations are then inserted into the steady-state neutron diffusion equation, and a new spatial flux shape ϕ' is found. This new flux shape is assumed to be valid for a very short period of time that corresponds to the next depletion step Δt. This new value for ϕ' is then inserted into the depletion equations again, and the process continues:

$$F'' = F' + (C - D)F'\phi'\Delta t \tag{18.20}$$

$$B'' = B' + (C - D)B'\phi'\Delta t \tag{18.21}$$

$$P'' = P' + (C - D)P'\phi'\Delta t \tag{18.22}$$

The steady-state diffusion equation is solved again with new values for F'', B'', and P''. The process is repeated again, and this time we obtain

$$F''' = F'' + (C - D)F''\phi''\Delta t \tag{18.23}$$

$$B''' = B'' + (C - D)B''\phi''\Delta t \tag{18.24}$$

$$P''' = P'' + (C - D)P''\phi''\Delta t \tag{18.25}$$

Eventually, it becomes easier to replace the primed notation with a simpler notation where n is the number of depletion step. Then we are able to finally write

Depletion Equations for a Homogeneous Core

$$\begin{aligned} F^{n+1} &= F^n + (C - D)F^n\phi^n\Delta t \\ B^{n+1} &= B^n + (C - D)B^n\phi^n\Delta t \\ P^{n+1} &= P^n + (C - D)P^n\phi^n\Delta t \end{aligned} \tag{18.26}$$

which is the form of the depletion equations that are actually solved with a computer. This simple iterative process continues for the entire life of the fuel. All physical processes, including decay, production, transmutation, and destruction, are

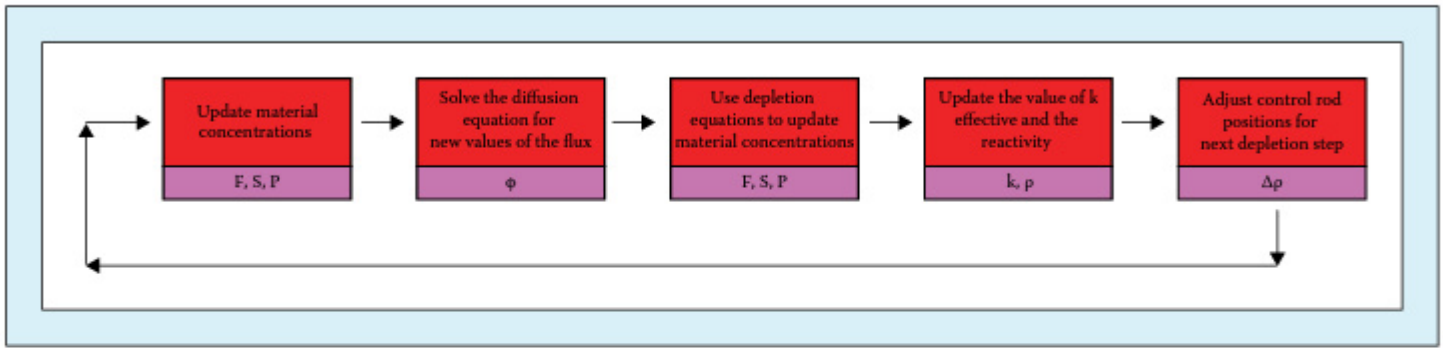
Update material concentrations
F, S, P
Solve the diffusion equation for new values of the flux
ϕ
Use depletion equations to update material concentrations
F, S, P
Update the value of k effective and the reactivity
k, ρ
Adjust control rod positions for next depletion step
Δρ

FIGURE 18.14 The steps in a simple fuel cycle depletion calculation.

built into the values of C and D. This can be very easily generalized to any number of fuel assemblies I and any number of axial positions J by writing the depletion equations in a slightly different form:

The Depletion Equations for a Large Number of Individual Fuel Assemblies

$$\begin{aligned} F(i,j)^{n+1} &= F(i,j)^{n} + (C-D)F(i,j)^{n}\phi^{n}\Delta t^{n} \\ B(i,j)^{n+1} &= B(i,j)^{n} + (C-D)B(i,j)^{n}\phi^{n}\Delta t^{n} \\ P(i,j)^{n+1} &= P(i,j)^{n} + (C-D)P(i,j)^{n}\phi^{n}\Delta t^{n} \end{aligned} \tag{18.27}$$

where

i = 1…I is the fuel assembly number
j is the number of the axial positions, j = 1…J
n is the number of the time step, or time interval between successive depletion calculations

In Equation 18.27 it is not even necessary for all of the time steps to be the same size, and we can generalize the depletion equations even further by writing $\Delta t^n = t^{n+1} - t^n$. So, the entire process of tracking all the isotopes and understanding how the flux shape, the power level, and the fuel concentration change over a period of time comes down to *iteratively* updating the concentrations in Equation 18.27 and then solving the diffusion equation for the new spatial flux shape. This is illustrated schematically in the simple flowchart shown in Figure 18.14. Some industrial-strength commercial computer programs have been written to track the concentrations of between 100 and 300 of these isotopes as the fuel is burned and additional fuel is introduced.

Once these isotopic concentrations are known, it is also possible to predict the amount of decay heat generated by the fuel assemblies when they are removed from the core, and the energy spectrum of the radiation (alpha, beta, and gamma rays) emitted from the spent fuel assemblies while they cool down and are ultimately sent to storage.

Student Exercise 18.3

In the previous section, we chose to write the depletion equations in a very compact form where C and D were coefficients that represented the creation and destruction of each specific isotope in a nuclear fuel assembly. Based on what you have learned so far, write out explicitly what the terms in each of the depletion coefficients would look like.

18.15 Fission Product Buildup

When a reactor starts to generate electricity, fission products inevitably start to accumulate in the fuel rods in the core (see Chapter 7), and the buildup of these fission products is governed by a number of different radioactive decay chains. Over 100 fission products can be produced when the fuel is burned, but only two or three of these are important to the operation of a reactor as a whole. The two most important fission products in a thermal water reactor are *Xenon-135 and Samarium-149*. These fission products are important because their neutron absorption cross sections are so high that they can affect the overall reactivity of the core (by absorbing billions of additional neutrons). Sometimes, materials that behave in this way are called *fission product poisons*. Over time, fission product poisons build up in the fuel rods and change the net reactivity of the core.

Although xenon and samarium are also produced in fast reactors, they are normally not a concern in fast reactors because very few neutrons are allowed to slow down into the thermal energy range. Hence the large thermal cross sections of Xenon-135 and Samarium-149 are unable to absorb most of these neutrons. In this section, we would like to discuss the buildup and decay of these two important fission product poisons. We will then extend this discussion to reactor transients in Chapter 21. As we mentioned earlier, Xenon-135 can be produced in two different ways:

1. First, it can be produced from the Iodine-135 decay chain.
2. Second, it can be produced directly from the fission of Uranium-235.

Iodine-135 is also produced directly from the fission of Uranium-235 and from the decay of an isotope of Tellurium called Tellurium-135. The decay chains for Iodine-135, Xenon-135, and their respective half-lives are shown in Figure 18.15. The equations that govern the buildup and decay of Iodine-135 and Xenon-135 are then

Equations for the Xenon Concentration

$$dX/dt = (\text{Xenon-135 production rate}) - (\text{Xenon-135 destruction rate})$$

or

$$dX/dt = \left(Y_x \Sigma_f \phi + \lambda_I I\right) - \left(\sigma_{ax} \phi X + \lambda_x X\right) \tag{18.28}$$

and

Equation for the Iodine Concentration

$$\frac{dI}{dt} = Y_I \Sigma_f \phi - \lambda_I I \tag{18.29}$$

where

Y_x and Y_i are *the respective yields* of xenon and iodine from the fission of Uranium-235

λ_x and λ_i are their respective *decay constants*

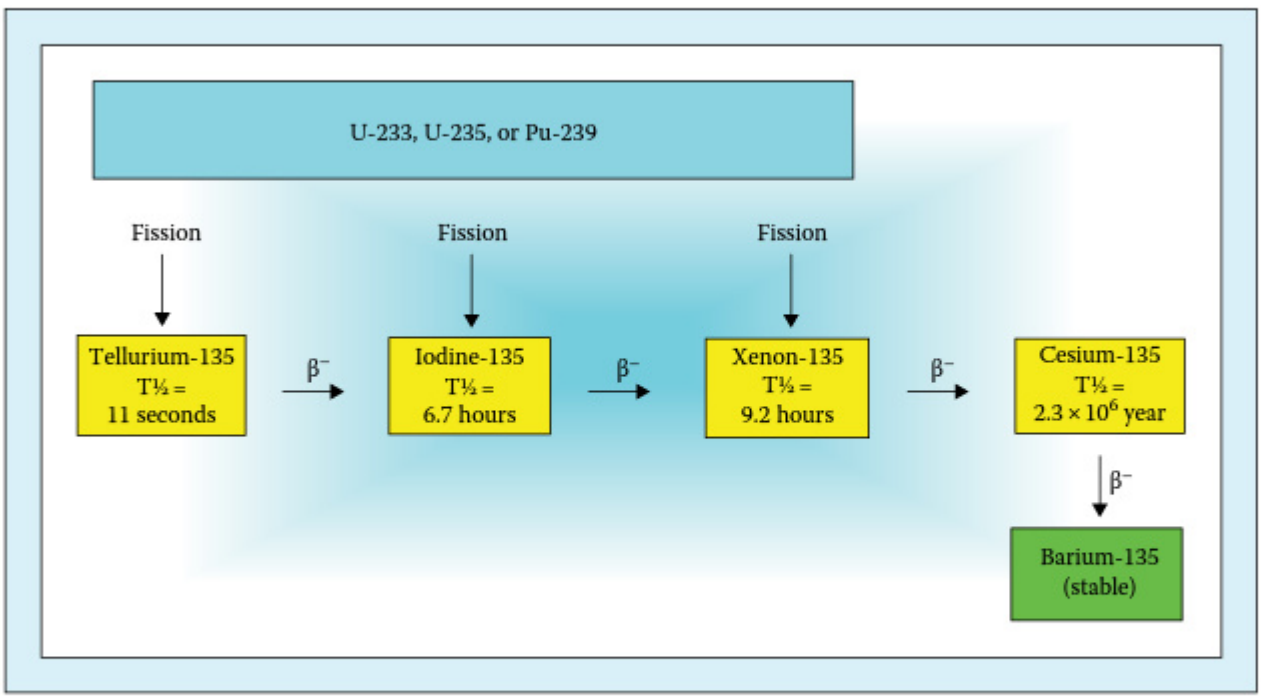

FIGURE 18.15 The decay chains for two important fission products: Xenon-135 and Iodine-135.

Here, X is the Xenon-135 concentration in atoms/cm^3 and I is the Iodine-135 concentration in atoms/cm^3.The solutions to these coupled differential equations are

Solutions to the Xenon and Iodine Concentration Equations

$$X(t) = X_o e^{-\lambda_x t} e^{-\sigma_{ax}\phi t} + \frac{\Sigma_f \phi (Y_x + Y_I)}{(\sigma_{ax}\phi + \lambda_x)\left[1 - e^{-\lambda_x t} e^{-\sigma_{ax}\phi t}\right]}$$

$$+ \frac{\lambda_I I_o - Y_I \Sigma_f \phi}{\lambda_I - \lambda_x - \sigma_{ax}\phi}\left\{e^{-\lambda_x t} e^{-\sigma a_x \phi t} - e^{-\lambda_I t}\right\} \qquad (18.30)$$

and

$$I(t) = I_o e^{-\lambda_I t} + Y_I \Sigma_f \frac{\phi}{\lambda_I\left[1 - e^{-\lambda_I t}\right]}$$

where I_o and X_o are the initial concentrations of iodine and xenon at start-up. (See Chapter 6 of our companion book to see how we arrived at these solutions.) Because Tellurium-135 decays into Iodine-135 in less than a minute (its half-life is about 11 seconds), it is possible to simplify the mathematical description of the production process by assuming that all of the Iodine-135 is produced directly from the fission of Uranium-235. The effective yields of each of these isotopes as well as their decay constants and half-lives are shown in Table 18.3. Because some of the Xenon-135 is produced from the decay of Iodine-135, the xenon concentration at any time also depends on the iodine concentration. So we need one equation to track the rate that iodine is created and destroyed and another equation to track the rate at which Xenon-135 is created and destroyed. These two equations can then be used to determine the xenon concentration X(t) as a function of time. *Xenon-135 is a major concern in thermal reactors because it has the highest thermal absorption cross section of any nuclear material known*. It literally soaks up thermal neutrons like a sponge (see Chapter 5). A graph showing the thermal absorption cross section for Xenon-135 is shown in Figure 18.16. *Note in particular that Xenon-135 has an effective thermal absorption cross section of about 2,600,000 barns!*

Samarium-149, which is the second most important fission product poison in thermal water reactors, is created through an entirely different decay chain than xenon is. Like Xenon-135, it has a very large thermal cross section (about 41,000 barns at thermal neutron energies) and an average thermal cross section of 58,700 barns at 300 K. The process of producing Samarium-149 is shown in Figure 18.17 and the neutron absorption cross section of Samarium-149 is compared to that of Xenon-135 in Figure 18.17. The data in these figures was taken from the ENDFB-7 database, which is now maintained by the National Nuclear Data Center in Oak Ridge, Tennessee (see Chapter 5). See, for example, *NNDC.gov.org*. The absorption cross section of Samarium-149 is shown in green, and the absorption cross section of Xenon-135 is shown in red. Although Samarium-149 is not a true 1/v absorber, it also exhibits the characteristic absorption resonances above thermal energies that xenon lacks. And although it is not as important as Xenon-135 is when it comes to how many neutrons it can absorb, it can still have a significant effect on how a reactor behaves. However, unlike Xenon-135, *Samarium-149 is not created from the fission of Uranium-235*. Instead, the fission of Uranium-235 creates *Neodymium-149*, which decays into *Promethium-149* in about 1.7 hours. This promethium then decays into Samarium-149 in about 53 hours. The entire process is illustrated in Figure 18.18.

TABLE 18.3
Effective Yields, Thermal Cross Sections, and Decay Constants for Some Important Neutron Poisons

Fission Product	λ (second^{-1})	λ (hour^{-1})	σ_a (cm^2)	Yield (U-233)[a]	Yield (U-235)[a]	Yield (Pu-239)[a]
I-135	2.87×10^{-5}	0.1035	1.2×10^{-22}	0.0475	0.0639	0.0604
Xe-135	2.09×10^{-5}	0.0753	2.7×10^{-18}	0.0107	0.0024	0.0105
Pm-149	3.56×10^{-6}	0.0131	2.0×10^{-21}	0.0079	0.0107	0.0121
Sm-149	0[b]	0[b]	4.0×10^{-20}	—	0.0108	—

Source: Lamarsh, J.R., *Introduction to Nuclear Reactor Theory*, Second Printing, Addison-Wesley Publishing Company, Inc., Reading, MA, 1972.

[a] Atoms per thermal fission.

[b] Stable.

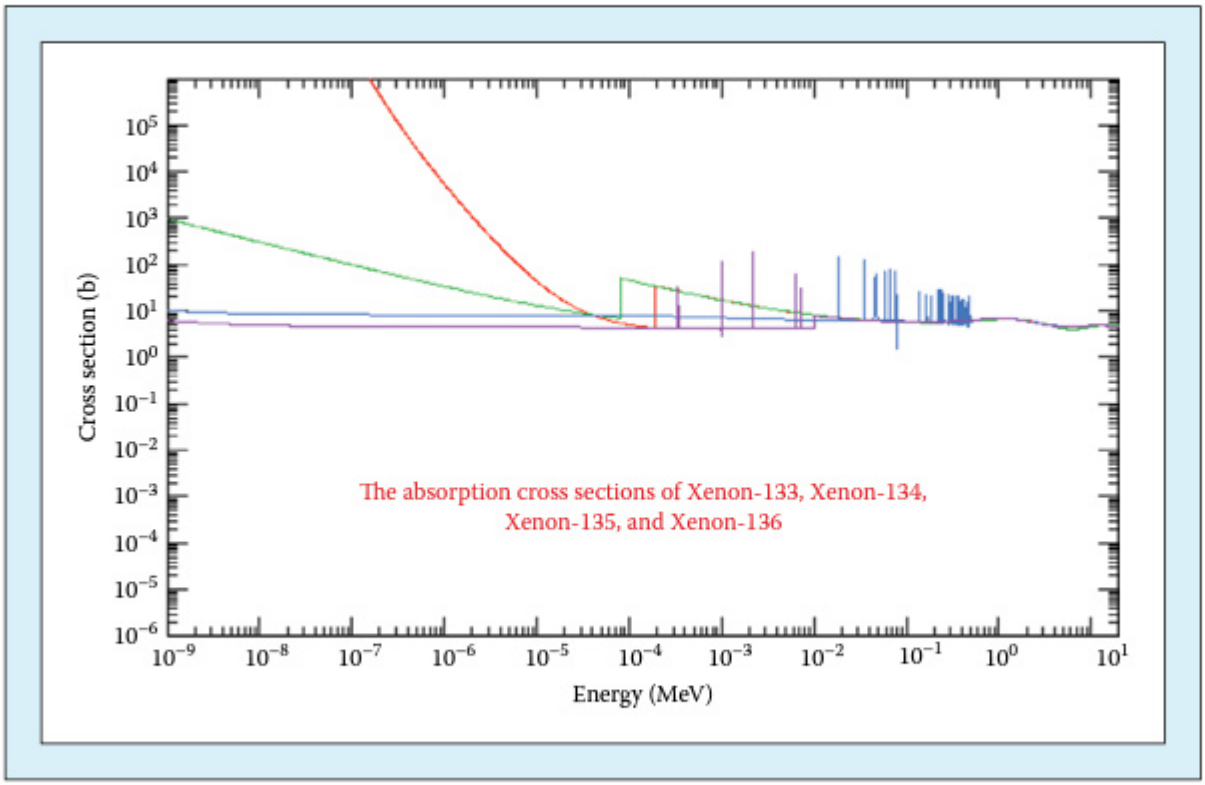

FIGURE 18.16 The neutron absorption cross sections of various isotopes of xenon as a function of the neutron energy. Xenon-135 is shown in red, Xenon-134 is shown in purple, Xenon-133 is shown in green, and Xenon-136 is shown in blue. Note that the absorption cross section of Xenon-135 completely dominates the cross sections of the other isotopes in the picture. (Courtesy of Kaere.)

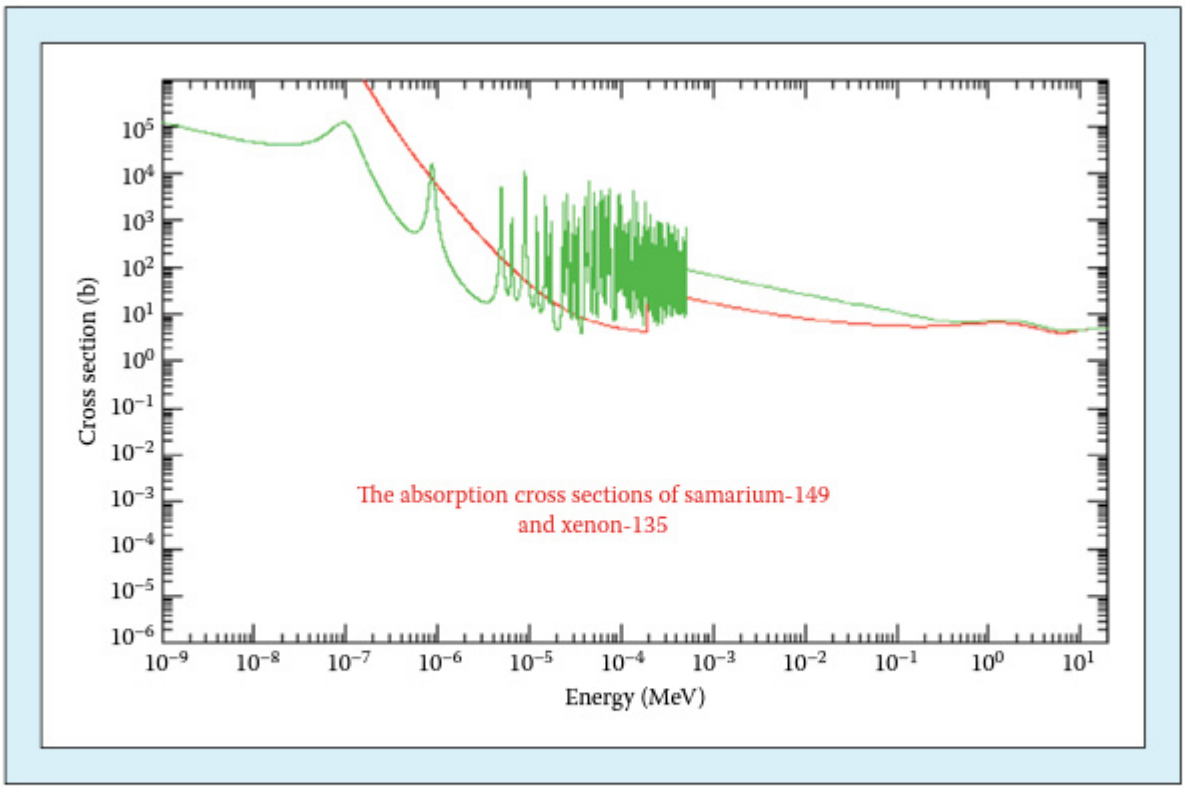

FIGURE 18.17 The neutron absorption cross sections for Samarium-149 (green) and Xenon-135 (red) at normal neutron energies. (Graph created by ENDFPLOT.)

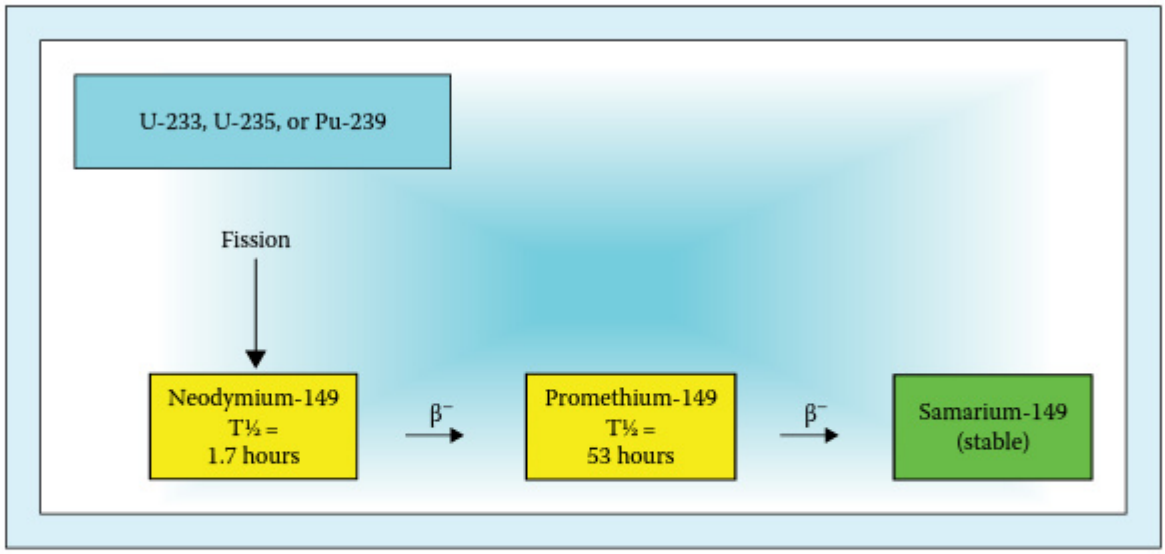

FIGURE 18.18 Production process of Samarium-149 in a reactor core.

Notice that both neodymium and promethium gain a proton in the process of beta decay. Since Neodymium-149 decays into Promethium-149 very quickly, it can be assumed that Promethium-149 decays directly into Samarium-149 as long as the effective yield of Promethium-149 is treated as the sum of the yields of Neodymium-149 and Promethium-149. The concentration of Promethium-149 in atoms/cm^3 is then

Equation for the Promethium Concentration

$$\frac{dP}{dt} = Y_{Nd}\Sigma_f\phi - \lambda_P P \tag{18.31}$$

where

Σ_f is the macroscopic fission cross section of the fuel
ϕ is the thermal flux
Y_{Nd} is the combined yield of Neodymium-149 and Promethium-149
λ_P is the value in Table 18.3

Since the half-life of Samarium-149 is effectively infinite (see Table 18.3), it is naturally stable, and we can assume that it will only disappear when it absorbs a neutron. The relevant rate equation for the samarium concentration is then

Equation for the Samarium Concentration

$$\frac{dS}{dt} = \left(\text{Samarium-149 production rate}\right) - \left(\text{Samarium-149 destruction rate}\right)$$

or

$$\frac{dS}{dt} = \lambda_P P - \sigma_{as}\phi S \tag{18.32}$$

where

σ_{as} is the microscopic absorption cross section of Samarium-149
S is the atomic density in atoms/cm^3

In thermal water reactors, Xenon-135 and Samarium-149 buildup and decay at different rates, and so their effect on the reactivity of the core is determined by a separate set of rate equations, which are in turn a function of the level of the neutron flux ϕ. In the next section, we would like to discuss exactly how quickly they can build up and decay.

18.16 Understanding the Buildup of Xenon-135 and Samarium-149

When a reactor is first started up, xenon and samarium are produced in the core at different rates. *Normally, Xenon-135 reaches its maximum concentration about 40 hours after start-up. However, Samarium-149 reaches its maximum concentration much more slowly, and normally, this takes about 300 hours (or 12 days) to occur.* In both cases, the rate of buildup is flux dependent, and as the flux increases, more xenon and samarium are produced. Figure 18.19 shows how the Xenon-135 concentration changes as a function of time, and Figure 18.20 shows how the Samarium-149 concentration changes as a function of time.

Normally, Xenon-135 has about five times the poisoning effect that Samarium-149 has on the core, although both neutron poisons reduce the number of free neutrons that are available to keep the reactor critical. Hence, as the buildup of these fission products continues, several control rods have to be withdrawn from the core to keep the reactor critical. We will explore the magnitude of the changes in the reactivity that these neutron poisons produce in Chapter 20. *In any event, it is not uncommon for the buildup of Xenon-135 to reduce the total reactivity of the core by $10 or $20!* By any objective measure, this is a huge reduction in the net reactivity of the core.

18.17 Equilibrium Concentrations of Xenon-135 and Samarium-149

The equilibrium concentration X_∞ of Xenon-135 can be found from the expression

The Equilibrium Xenon-135 Concentration

$$X_\infty = \Sigma_f \frac{\phi(Y_x + Y_I)}{\sigma_{ax}\phi + \lambda_x} \tag{18.33}$$

where

Y_x is the yield of Xenon-135 from the fission of U-235
Y_I is the yield of Iodine-135 from this fission of Uranium-235
Σ_f is the total fission cross section

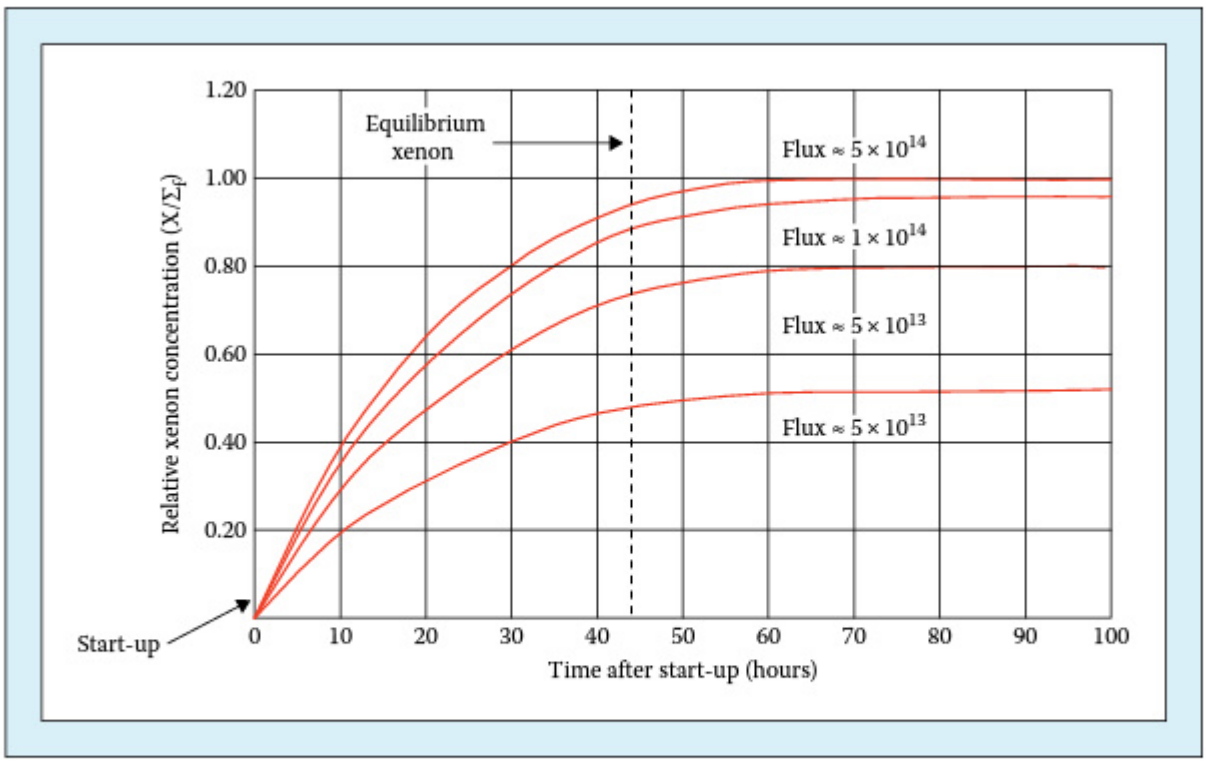

FIGURE 18.19 The buildup of Xenon-135 after a reactor is started up for various values of the neutron flux.

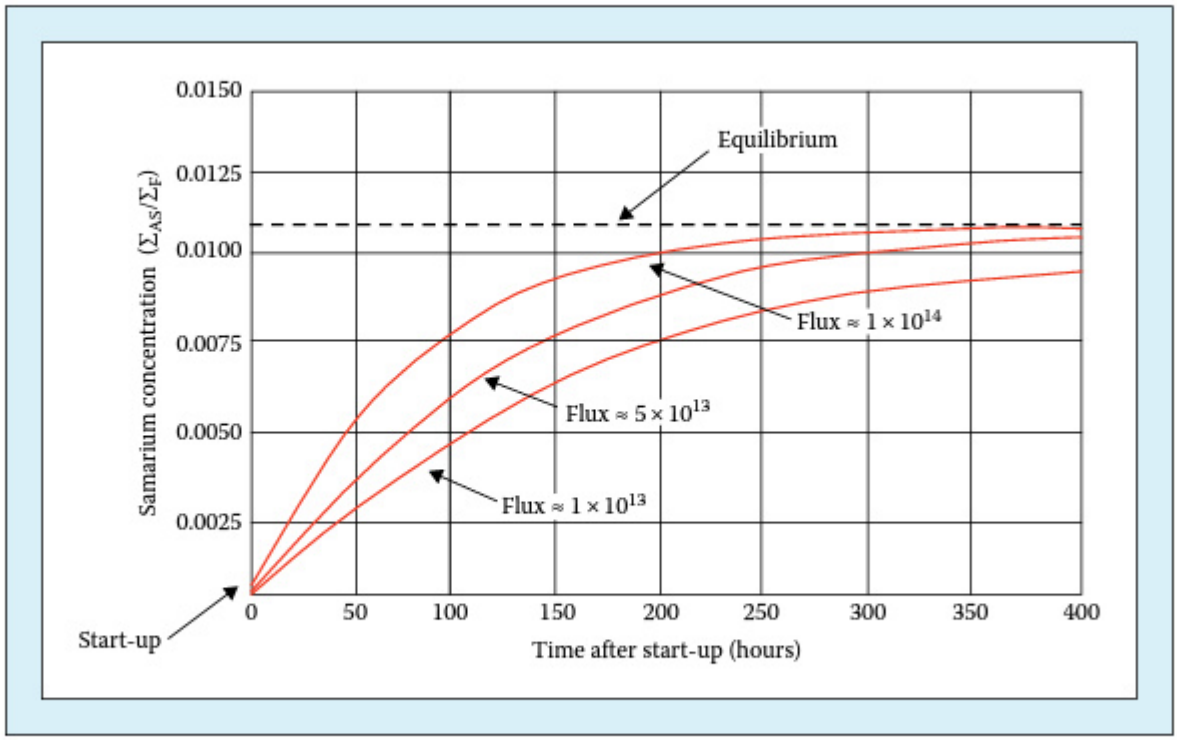

FIGURE 18.20 The buildup of samarium after a reactor is started up for various values of the neutron flux. This example assumes a cold, clean core.

The value of X_∞ can be found in two ways:

1. First, it can be found by setting $dX/dt = 0$ in the rate equations and solving for the value of X.
2. Second, it can be found by taking the equation for the time-dependent xenon concentration X(t) and examining its behavior as $t \rightarrow \infty$.

In any event, *the amount of xenon that is produced depends on the value of the neutron flux ϕ.* Notice that the ratio of X'/Σ_f for very large values of the flux becomes $X_\infty/\Sigma_f = (Y_x + Y_I)/\sigma_{ax}$, and the xenon concentration does not increase any further. When this occurs it becomes entirely a function of the ratio of $\sigma_{ax}\phi$ to λ_x. These two terms are comparable in value at a thermal flux of about 8×10^{12} neutrons/cm^2/s. So at roughly 10 times this level, or 1×10^{14} neutrons/cm^2/s, the xenon concentration will simply not increase beyond $X_\infty/\Sigma_f = (Y_x + Y_I)/\sigma_{ax}$. In other words, its production rate following start-up becomes self-limiting at a neutron flux above 1×10^{14} neutrons/cm^2/s. The equilibrium concentration S_∞ of Samarium-149 is also given by the equation

Equilibrium Samarium Concentration

$$S_\infty = \frac{Y_{Nd}\Sigma_f}{\sigma_{as}} \tag{18.34}$$

where Y_{Nd} is the yield of Neodynium-149. The equilibrium samarium concentration can also be found in two ways:

1. First, it can be found by setting $dS/dt = 0$ in the rate equations we discussed previously and then solving for the value of S.
2. Second, it can be found by taking the equation for the time-dependent samarium concentration S(t) and examining its behavior as $t \rightarrow \infty$.

In any event, its final concentration is given by Equation 18.34. *It is interesting to observe that the equilibrium concentration of Samarium-149 does NOT depend on either the value of the power or the value of the flux. In practice, this means that a small research reactor will have exactly the same equilibrium concentration of Samarium-149 as a much larger power reactor.* Physically, this is because the production rate of samarium from the decay of promethium is exactly offset by the decay of the samarium itself. (Samarium does not care what the reactor power level is.) This means that as

long as a reactor is operated for several days, *the equilibrium samarium concentration only depends on the enrichment of the fuel.* As the fuel is burned away, Σ_f decreases, and the equilibrium concentration is reduced as well. It is also worth mentioning that the samarium concentration decreases as the fuel is burned. *Because it has a lower absorption cross section than Xenon-135 does, Saramium-149 only has about 1/6th of the poisoning effect of Xenon-135.* Nevertheless, this can still have very important consequences. After a reactor has been operating for a couple of days, this ratio remains relatively constant over the lifetime of the core.

18.18 Behavior of Xenon-135 and Samarium-149 after Shutdown

Many surprising things can happen to the Xenon-135 concentration when a reactor is shut down. When the fission process ceases, Xenon-135 can no longer be produced directly from the fission of U-235. However, it can still be produced by the Iodine-135 decay chain (refer to Figure 18.15). When a reactor has been operating close to its rated power level for about a week, enough xenon is produced from the decay of iodine that its concentration actually *increases after the reactor is shut down.* Exactly, how high this concentration becomes depends on the initial values of X_o and I_o immediately before shutdown. In most cases, *the Xenon-135 concentration peaks about 12 hours after a reactor is shut down* (see Figure 18.21). This can be explained physically because the half-life of Iodine-135 is about 6 hours, while it takes another 9 hours for about half of the Xenon-135 to decay away. *Moreover, the time at which the xenon concentration peaks is nearly independent of the initial values of I_o and X_o—as long as they have previously reached their equilibrium levels.*

This implies that no matter how the reactor has been operated the xenon concentration always peaks about 12 hours after the reactor is shut down. However, the amount of Xenon-135 that is produced *does* depend on how it was operated previously. The higher the power is before the reactor is shut down, the *higher* the peak xenon concentration will be. This must always be kept in mind when a reactor is restarted because large amounts of xenon may still be present in the core. *If a reactor is operated at a very high flux level, say 5×10^{14} neutrons/cm^2/s, and then temporarily shut down, it may take 40 hours or more before the xenon concentration returns to a level that allows the reactor to again become critical*. This causes the reactor to act like it is "dead" when in fact it is not. All reactor operators need

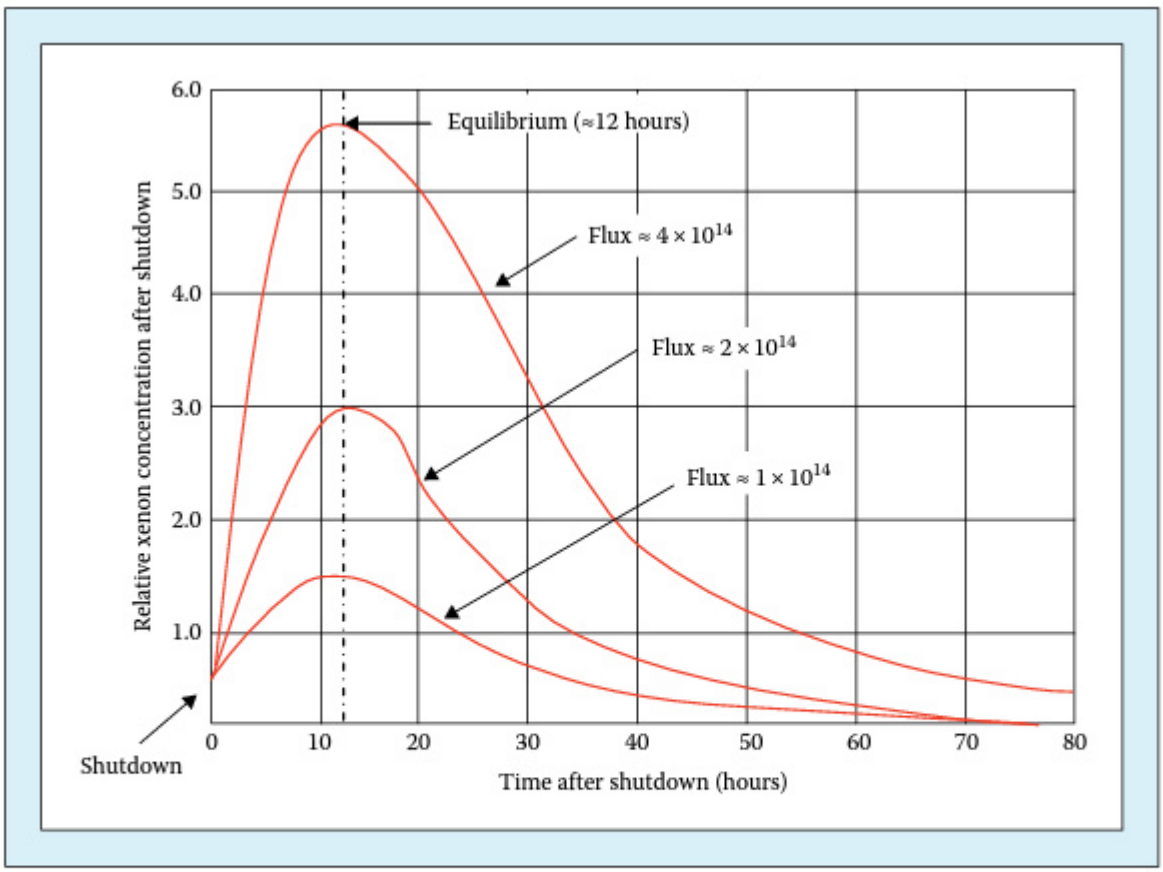

FIGURE 18.21 The buildup of Xenon-135 after a thermal reactor is shut down. Notice that the concentration generally peaks about 12 hours after shutdown. However, the amount of Xenon-135 that is produced is flux dependent.

TABLE 18.4
Time Frames for the Maximum Buildup of Xenon-135 and Samarium-149 in a Thermal Water Reactor after Start-Up and (B) Shutdown

Times When the Maximum Concentrations of Xenon-135 and Samarium-149 Are Reached		
	Time after Start-Up (hours)	Time after Shutdown (hours)
Xenon-135	~40	~12
Samarium-149	~300	~300

to be aware of this fact when restarting a reactor that has temporarily gone "dead" due to excessive xenon buildup. We will have an opportunity to discuss the behavior of a dead reactor again when we discuss the operational implications of a xenon transient in Chapter 21. There we also discuss how the buildup of Xenon-135 contributed to the accident at Chernobyl.

18.19 Xenon Buildup and "Reactor Dead Time"

So as a rule of thumb, *the Xenon-135 reaches its maximum concentration about 12 hours after a thermal water reactor is shut down*. At this time, the poisoning potential of xenon reaches its maximum possible effectiveness. Then the xenon concentration can become high enough to absorb more neutrons than the fuel can produce. When this occurs, withdrawing all the control rods from the core may not be able to start the reactor up again. *Depending on the previous power level, it may be necessary to wait between 2 and 35 hours after shutdown before most of the xenon has decayed away, and the reactor can be restarted. This may be true even with all of the control rods removed*. This condition is called a "*dead reactor*" or *xenon precluded start-up*, and the period of time that is required to recover from it is called the *reactor dead time*. During this time, xenon's ability to absorb fission neutrons completely dominates the behavior of the core. In the past, when improperly trained reactor operators (see the discussion of the reactor accident at *Chernobyl* in Chapter 21) tried to compensate for the effects of xenon poisoning by fully withdrawing the control rods from the core, they did not reinsert the control rods quickly enough after the xenon began to burn off. This can result in huge *power spikes* when the xenon burns off and when the control rods are fully withdrawn.

If the burn-off of the Xenon-135 is not properly anticipated, and the core does not have a large negative temperature coefficient, the core may become too hot, and some of the fuel rods may begin to rupture or melt. Worse yet, a xenon oscillation may occur, where the power level increases on one side of the core, and it becomes supercritical, while the other side of the core is still subcritical. We will explore how this affects the neutron flux and the reactor power level in Chapter 20. In any event, the presence of xenon and its sister element *samarium* must be taken very seriously when the time-dependent behavior of a reactor must be taken into account. Table 18.4 summarizes the time frames for the buildup of Xenon-135 and Samarium-149 in a thermal water reactor. However, in fast reactors, the neutron energies are simply too high for xenon and samarium to become effective neutron poisons.

Example Problem 18.3

Use the rate equation $dX/dt = (Y_x\Sigma_f\phi + \lambda_I I) - (\sigma_{ax}\phi X + \lambda_x X)$ to show that the equilibrium concentration of Xenon-135 in a thermal water reactor is reached when $X_\infty = \Sigma_f\phi(Y_x + Y_I)/(\sigma_{ax}\phi + \lambda_x)$. At what neutron flux level does the equilibrium xenon concentration become relatively independent of the absolute neutron population?

Solution The equilibrium Xenon-135 concentration is reached when $dX/dt = 0$. Setting $dX/dt = 0$ gives $(Y_x\Sigma_f\phi + \lambda_I I) - (\sigma_{ax}\phi X + \lambda_x X)$, which in turn implies that the equilibrium concentration is given by $X_\infty = \Sigma_f\phi(Y_x + Y_I)/(\sigma_{ax}\phi + \lambda_x)$. Notice that equilibrium concentration becomes almost independent of the level of the neutron flux when $\sigma_{ax}\phi \gg \lambda_x$, or $\phi \gg \lambda_x/\sigma_{ax}$. When this occurs, $X_\infty = \Sigma_f(Y_x + Y_I)/\sigma_{ax}$. [Ans.]

18.20 The Concentration of Samarium-149 after Shutdown

The concentration of Samarium-149 behaves entirely different than the Xenon-135 concentration after a reactor is shutdown (see Figure 18.22). This is because its concentration is driven by an entirely different decay chain, and because once the Samarium-149 is produced, it does not decay away. The Samarium-149 concentration continues to build up as the Promethium-149 in the core decays. However, unlike Xenon-135, Samarium-149 will continue to remain in the core until the reactor is started up again, at which time it can be removed by absorbing extra neutrons. *This means that although Samarium-149 is a strong neutron poison, it will not cause the same rapid fluctuations*

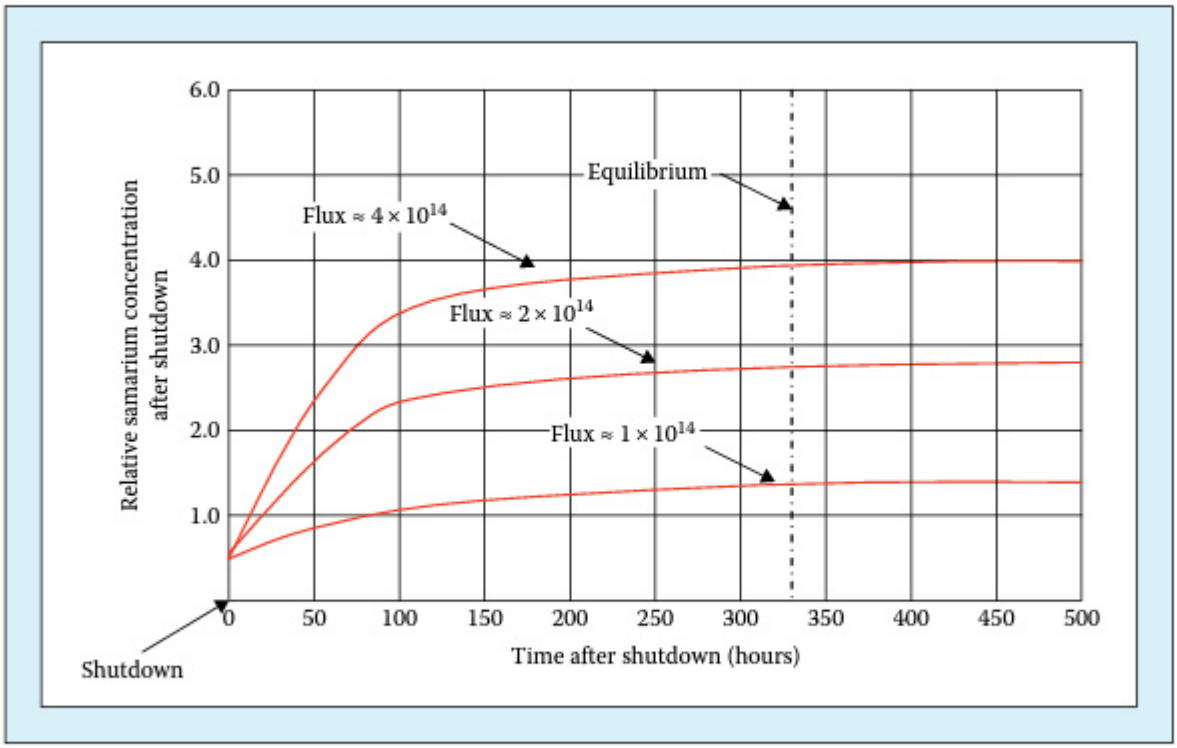

FIGURE 18.22 The Samarium-149 concentration after shutdown for different values of the neutron flux.

in the power level that Xenon-135 can. There is no such thing as a samarium-induced transient in a thermal power reactor. Assuming that both Promethium-149 and Samarium-149 have achieved their equilibrium concentrations, the Samarium-149 concentration at any time t after shutdown is then

$$S(t) = S_\infty + P_\infty\left(1 - e^{-\lambda_p t}\right) \tag{18.35}$$

where again S_∞ and P_∞ are the equilibrium concentrations of Samarium and Promethium.

18.21 Comparing Fission Product Poisoning in Fast and Thermal Reactors

To keep our previous discussion in perspective, the reader needs to recall that Xenon-135 and Samarium-149 are the only fission product poisons that can have a significant effect on the reactivity of a thermal water reactor. *Xenon and samarium have basically no effect on how fast reactors behave because their absorption cross sections are too small to absorb many fission neutrons. Neutron energies in a fast reactor rarely fall below 100 keV and as such, fast reactor energies are too high for xenon and samarium to be effective neutron absorbers*. The neutron energy spectrum for both types of reactors is compared in Figure 18.23. Hence, even if some neutrons were able to reach an energy of about 10 eV, the absorption cross sections for Xenon-135 and Samarium-149 would barely exceed 10 barns. Alternatively, at energies around 0.025 eV, their cross sections would be thousands or even hundreds of thousands of times greater. Thus Xenon-135 and Samarium-149 are of very little practical importance to the operation of fast reactors as a whole.

18.22 Yields of Other Important Fission Products

The amount of each fission product produced from the fission of a uranium or plutonium nucleus is called its *yield*, and the yield is normally represented by the symbol Y. (In other books, the yield is sometimes represented by the Greek symbol γ.) The *yields* or percentages of the 20 most important fission products produced from the fission of Uranium-235 are summarized in Table 18.5. The "Relative Importance" in column 3 is the product of the microscopic cross section and the total yield (column 1 × column 2). It should be clear from reviewing these numbers that *xenon, samarium, and cesium are by far the most important fission products from the viewpoint of their neutron-absorbing potential*. (The element Cesium is also called *Caesium* in Europe). Some isotopes of cadmium, europium, and gadolinium also have very high thermal

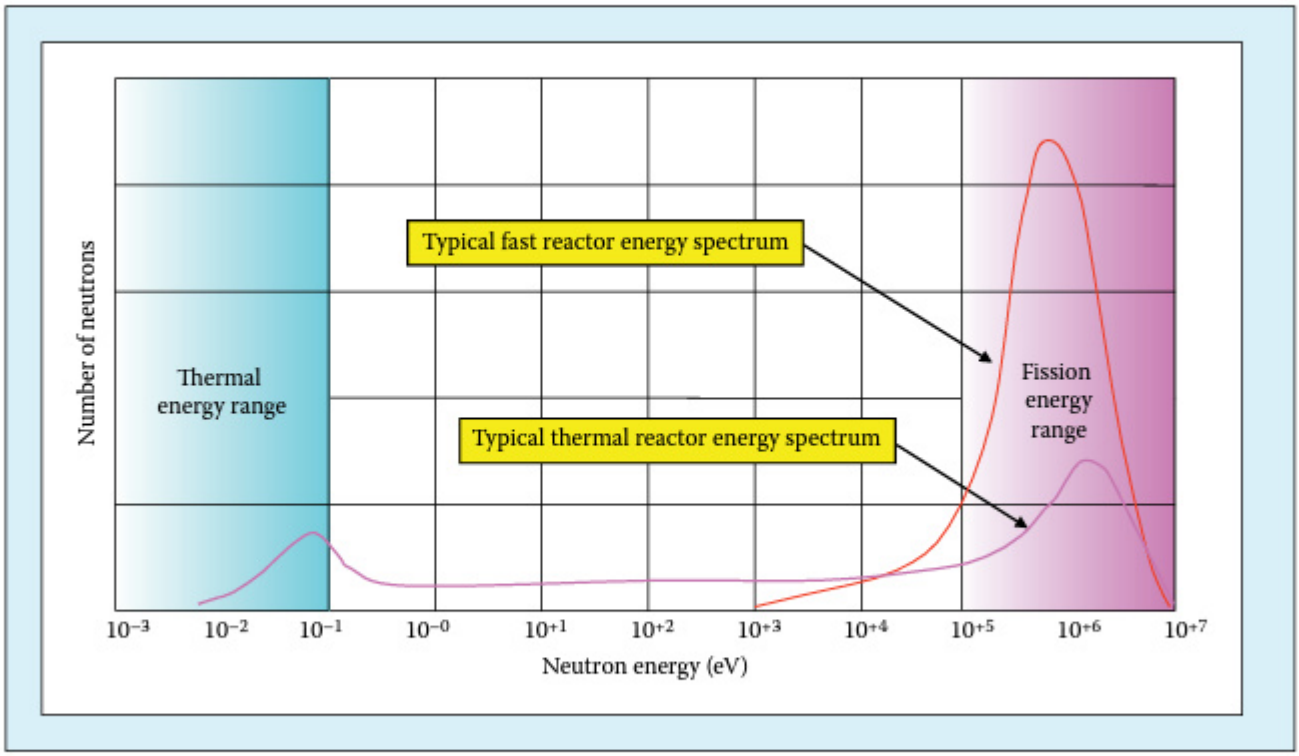
Typical fast reactor energy spectrum
Typical thermal reactor energy spectrum
Thermal energy range
Fission energy range
Number of neutrons
10^{-3} 10^{-2} 10^{-1} 10^{0} 10^{+1} 10^{+2} 10^{+3} 10^{+4} 10^{+5} 10^{+6} 10^{+7}
Neutron energy (eV)

FIGURE 18.23 The neutron energy spectrum in a fast reactor and a thermal water reactor.

cross sections, but their yields are too low to have much impact on the operation of a thermal water reactor. Usually, the fission product yield Y is a small dimensionless number between zero and about 7%. During normal operation, there are about 40 fission product decay chains that must be taken into account to track the changes to the isotopic composition of the core. By convention, the sum of the yields of all these fission product decay chains is equal to 1.0:

$$\text{Total yield} = 1.0 = \sum\nolimits_{n} Y_n \quad (n = 1, 2, \ldots, 40) \tag{18.36}$$

In practice, *about 95% of the Xenon-135 that is produced in a thermal water reactor comes from the decay of Iodine-135*, so the interaction of their decay chains (see Section 18.15) becomes extremely important when determining the time-dependent reactivity. Specifically, Iodine-135 has a half-life of 6.57 hours, and Xenon-135 has a half-life of 9.2 hours. In other words, the concentration of Xenon-135 may temporarily *increase* while the concentration of I-135 is decreasing because of its slightly shorter half-life. This entire sequence of events is depicted in Figure 18.24, which shows the typical life cycle of Xenon-135 in a thermal water reactor. Several other fission products of lesser importance follow a similar trend. In fast reactors, the situation is completely different because the same neutron poisons react entirely different with fast neutrons than they do with thermal ones. Moreover, only a very small number of the neutrons that are produced in fast reactors (usually less than 5%) attain energies below 10 keV. The yields of these fission product poisons are also different as well. For example, *in a typical fast reactor, the most important fission product poisons in the core are Cs-133, Ru-101, Rh-103, Tc-99, Pd-105, and Pd-107, with Sm-149 (in sixth place) becoming slightly more important than Pd-107 in the radial blanket where the breeding of Pu-239 occurs*.

The presence of different isotopes of iodine in the fission products is interesting as well. While Iodine-135 is by far the most important fission product in the core (because it produces Xe-135), there are 36 additional isotopes of iodine ranging from I-108 to I-144. However, only one of them (I-127) is considered to be stable over geologic time frames and continues to remain in the fuel. Hence, as far as the storage of nuclear waste is concerned, iodine can be considered to be a mono-isotopic element. Its longest-lived radioactive isotope, I-129, has a half-life of about 15.7 million years, which is far too short to exist in a primordial sense.

18.23 Cumulative Effect of the Fission Product Poisons

Over time, neutron absorbing materials, which are created by the fission process, continue to compete for excess neutrons from the core. It is possible to represent the cumulative effect of these fission product poisons with a hypothetical radionuclide that represents the average absorption cross section for all of the fission products. The result of this for a

TABLE 18.5
Fission Products Produced from the Fission of Uranium-235 and Their Relative Yield

Cross Section (Barns)	Yield (%)	Relative Importance (Cross Section Times Yield)	Isotope	Half-Life (T½)	Observations Regarding the Fission Product(s)
29,140	6.7896	1975	$^{133}Cs \rightarrow {}^{134}Cs$	∞ 2.065 years	Neutron capture converts a few percent of nonradioactive ^{133}Cs to ^{134}Cs, which has very low direct yield because beta decay stops at ^{134}Xe; further capture will add to long-lived ^{135}Cs.
2,650,000	6.3333	167750	$^{135}I \rightarrow {}^{135}Xe$	6.57 hours (for I-135)	Most important neutron poison; neutron capture rapidly converts ^{135}Xe to ^{136}Xe; remainder decays (9.14 hours) to ^{135}Cs (2.3 my)
2.7	6.2956	0.17	^{93}Zr	1.53 my	Transmutation impractical
0.11	6.0899	<1	^{137}Cs	30.17 years	
20	6.0507	1.20	^{99}Tc	211 ky	Candidate for disposal by nuclear transmutation
0.90	5.7518	0.05	^{90}Sr	17.9 years	
80	2.8336	2.30	^{131}I	8.02 days	
96	2.2713	2.18	^{147}Pm	2.62 years	
40,140	1.0888	442	$^{149}Pm \rightarrow {}^{149}Sm$	∞	Second most important neutron poison; not produced directly from the fission of U-235; however, it is produced from the decay of Promethium-149
18	0.6576	<1	^{129}I	15.7 my	Candidate for disposal by nuclear transmutation
15,200	0.4203	63	^{151}Sm	90 years	Most will be destroyed by neutron capture
0.15	0.3912	<1	^{106}Ru	373.6 days	
1.66	0.2717	<1	^{85}Kr	10.78 year	
1.8	0.1629	<1	^{107}Pd	6.5 my	
	0.0508	<1	^{79}Se	327 ky	
3,950	0.0330	1.30	$^{155}Eu \rightarrow {}^{155}Gd$	4.76 year	Both neutron poisons
	0.0297	<1	^{125}Sb	2.76 year	
	0.0236	<1	^{126}Sn	230 ky	
254,000	0.0065	18.50	^{157}Gd	∞	Neutron poison, but low yield
20,600	0.0003	<1	^{113m}Cd	14.1 year	Most will be destroyed by neutron capture

Source: Courtesy of Wikipedia—see *https://en.wikipedia.org/wiki/Fission_product_yield*.

U-235-fueled thermal water reactor are the absorption cross sections shown in Figure 18.24. After several weeks, these fission products usually approach an equilibrium concentration in the core that is dependent on the reactor's previous power level. As the power level P is increased, more fission products will also be produced.

Some fission products can build up to the extent that they can completely dominate the behavior of the core when the power level changes abruptly. For example, Xenon-135 and Samarium-149, can absorb vast numbers of thermal neutrons and alter the reactor power level as they decay. This ability to absorb thermal neutrons easily exceeds that of any other known nuclear material, including the carefully concocted molecular mixtures of cadmium, boron, and hafnium that are used in the reactor's control rods. *The presence of these fission products can sometimes bring the nuclear chain reaction to a complete standstill*. We will have more to say about this when we examine the time-dependent operation of a reactor in Chapter 20.

18.24 Reactivity Change Caused by the Buildup of Fission Products

Using the fact that $\rho = (k - 1)/k$, it is relatively easy to derive an expression for the cumulative effect these fission product poisons can have on the total reactivity of the core. The net reactivity of the core can be written as

$$\rho = 1 - \frac{1}{k} \tag{18.37}$$

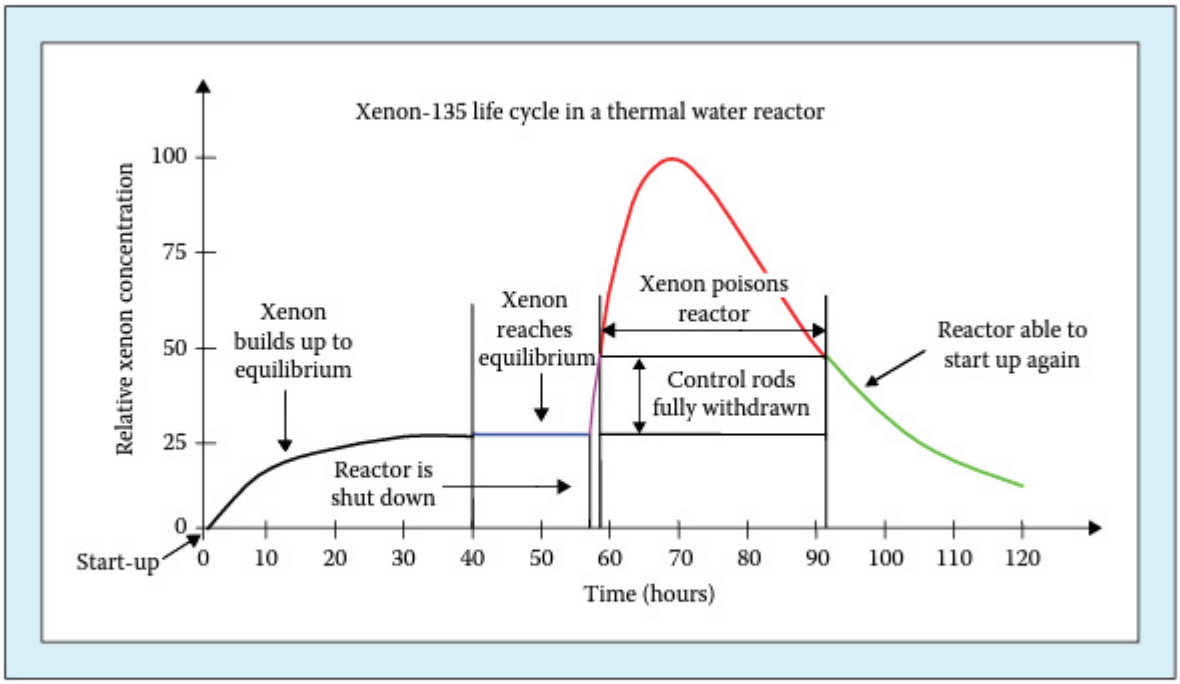

FIGURE 18.24 The typical life cycle of Xenon-135 in a thermal water reactor.

and if we assume that no neutrons leak out of the core, then the reactivity change is given by $\Delta\rho = \frac{-1}{\Delta k} = \frac{-\Delta\Sigma_{FP}}{\nu\Sigma_f}$. *Notice that the reactivity change in this case is always a negative number*. However, the buildup of fission products is also proportional to the number of U-235 atoms N_{U235} that have fissioned to produce these fission products, so we can also write Equation 18.37 as

$$\Delta\rho = -\frac{\Delta N_{U235}\sigma_{FP}}{\nu N_{U235}\sigma_{f235}} \tag{18.38}$$

or

The Negative Reactivity Caused by Fission Product Buildup

$$\Delta\rho = -\frac{\sigma_{FP}}{\nu\sigma_{f235}} \tag{18.39}$$

Notice that this final equation only requires the value of σ_{FP} from Figure 18.25 to estimate the poisoning effect that all of these fission products can have. To convert the reduction in the reactivity to dollars and cents, we must divide Equation 18.39 by the delayed neutron fraction β. Then the equation for the reactivity reduction becomes

Reactivity Reduction in Dollars and Cents

$$\Delta r = \frac{-\sigma_{FP}}{\beta\nu\sigma_f} \tag{18.40}$$

This equation is applicable to *any* nuclear fuel as long as the correct values for β, ν, and σ_f are used. Equation 18.40 illustrates how easy it is to find the negative reactivity produced by the fission products if we know the value of the thermal neutron flux and the irradiation time. Obviously, the product of ϕ and t or ϕt is just another way to measure the aggregate burnup of the fuel in the core. This quantity is sometimes called the *neutron fluence*, and the most general definition of the fluence is

$$\text{Fluence} = \Phi = \int \phi(t)dr \tag{18.41}$$

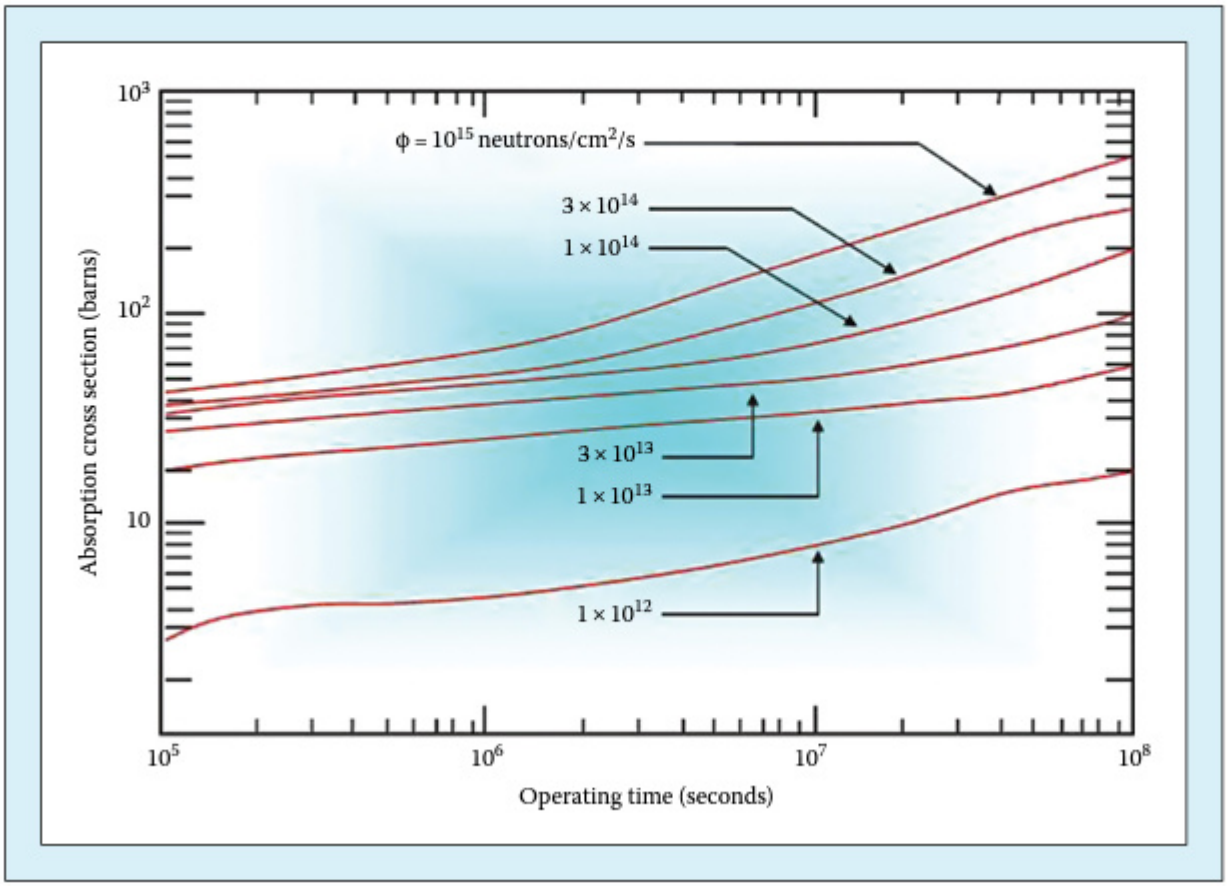

FIGURE 18.25 The cumulative buildup of fission product poisons as a function of flux and time. (Adapted from Lamarsh, J.R. and Baratta, A.J., *Introduction to Nuclear Engineering*, Prentice Hall, Upper Saddle River, NJ, 2001.)

Figure 18.25 shows that we can also use the *neutron fluence* ϕt instead of the burnup to estimate the reactivity change $\Delta\rho$. The neutron fluence is important to anyone who attempts to understand how the properties of nuclear materials are affected by the amount of irradiation they receive.

Example Problem 18.4

Uranium dioxide (UO_2) is used in 95% of all of the power reactors in the world today. Develop an expression for the number of U-235 atoms in a cubic centimeter of uranium dioxide fuel as a function of its average enrichment e. This expression can then be used to determine the rate at which fission products are produced in nuclear fuel rods.

Solution Uranium dioxide has a physical density of 10 g/cm^3. We know from our earlier discussion in Chapter 4 that the number of UO_2 molecules in a cubic centimeter is given by $N = \rho A'/M$, where A' is Avogadro's number. Uranium dioxide has 1 uranium atom with an atomic weight of 238 and 2 oxygen atoms with an atomic weight of 16 each. The total molecular weight of UO_2 is 238 + 2(16) = 270. Therefore, the atomic density of uranium dioxide is $N_{UO_2} = 10 \times 6.022 \times 10^{23}/270 = 2.23 \times 10^{22}$ atoms/cm^3. The number of U-235 atoms is therefore $2.23e \times 10^{20}$ atoms/cm^3, when the enrichment e is expressed in percent. [Ans.]

18.25 Cross Section for a Hypothetical Fission Product

Figure 18.25 shows the absorption cross section for a single hypothetical fission product that represents the effects of all of the fission products that happen to be produced in the core. *Normally, the value of this cross section is between 50 barns and 100 barns, and it continues to increase as more of the fuel is burned.* While this may not seem like a particularly large number, there can be nearly as many fission products in the core after two years of full power operation as there are U-235 atoms left in the fuel rods! *Thus the net effect of all of these fission products can be nearly as great as that of the control rods.* Consequently, great care must be taken to ensure that the core can be maintained in a critical state in spite of their continued buildup, and the control rods must be continually withdrawn from the core as the fuel is burned.

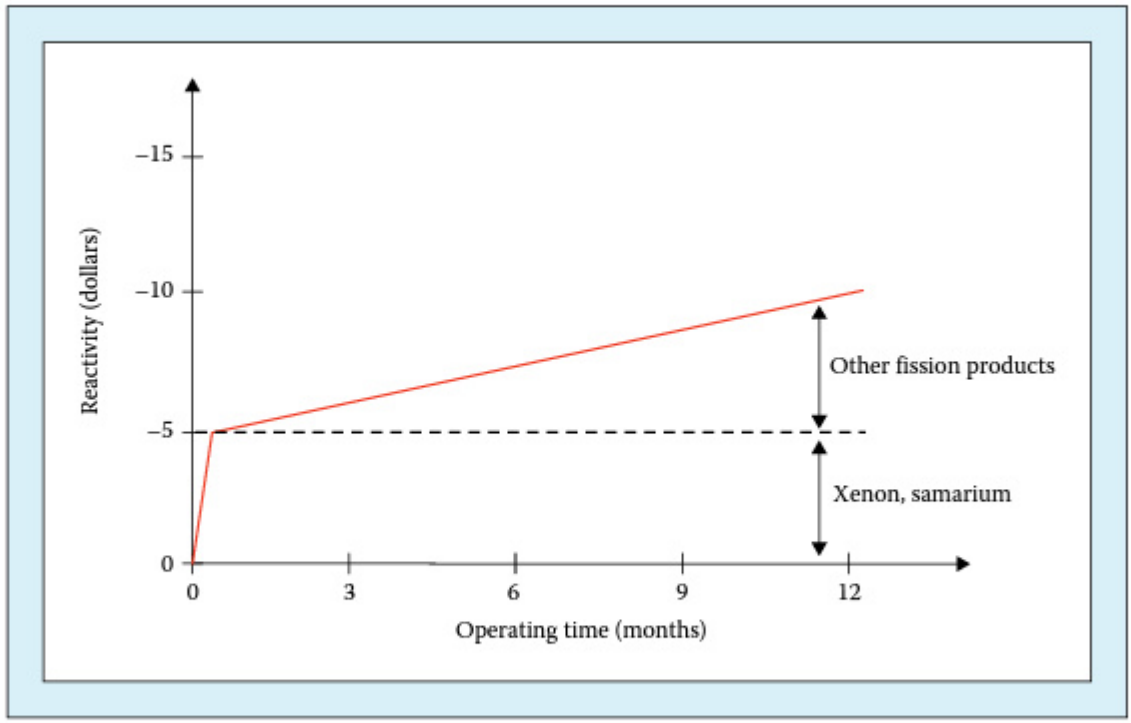

FIGURE 18.26 The effect of fission products on the reactivity of the core in a PWR or a BWR.

Also, the level of soluble boron in the coolant (if the reactor is a PWR) must be decreased to maintain the core in a critical state. In the meantime, let us refer to the graph in Figure 18.26, which illustrates how quickly these fission products can build up after just 18 months of continuous full power operation.

Example Problem 18.5

Suppose that a U-235-fueled thermal water reactor has been operating for 1 year (3.15×10^7 s) at an average thermal neutron flux of 1×10^{14} neutrons/cm^2/s. What is the reactivity associated with the buildup of fission products in the core over this period of time?

Solution The reactivity reduction in dollars and cents is given by the equation $\Delta\rho = -\sigma_{FP}/\beta\nu\sigma_f$, which we derived in the previous section. For U-235 the value of β is 0.0065, the value of σ_f is 585 barns, and the value of ν is 2.418. From Figure 18.24, the value of σ_{FP} is 110 barns. The reactivity reduction in dollars and cents is therefore $\Delta\rho = -(110/585)/(0.0065 \times 2.418) = -\$11.96$ (eleven dollars and 96 cents). [Ans.]

Example Problem 18.6

Estimate the number of fission products that are produced in 1 cm^3 of uranium dioxide (UO_2) in a fuel rod with an average enrichment of 4% if the fuel is burned for 18 months at an average thermal flux of 1×10^{14} neutrons/cm^2/s. After 18 months, how does the number of fission products compare to the number of U-235 atoms that are left in the fuel?

Solution The number of U-235 atoms in a uranium dioxide fuel rod can be determined from the equation (see Chapter 4) $N_{U235} = 2.23e \times 10^{20}$ atoms/cm^3 when the enrichment e of the fuel is measured in percent. So initially, the concentration of U-235 atoms in the fuel rod will be $4 \times 2.23 \times 10^{20}$ atoms/cm^3 $= 8.92 \times 10^{20}$ atoms/cm^3. After 18 months, the percentage of U-235 atoms burned is $(1 - e^{-\sigma f\, U235 \phi t})$, where t is in seconds. In 18 months, there are 4.72×10^7 seconds, the value of σ_f for U-235 is 585 barns $= 5.85 \times 10^{-22}$ cm^2, and $\phi = 1 \times 10^{14}$ neutrons/cm^2/s. Therefore, the percentage of U-235 atoms burned is $(1 - e^{-2.76}) = 0.937 = 93.7\%$. Each atom will release two fission products, so after 18 months, the number of fission products will be $2 \times 93.7\% = 187.4\%$ of the original U-235 population. In the meantime, the U-235 population has declined by 93.7% to 6.3%. So after 18 months, there will be $187.4/6.3 \approx 30$ fission products for every remaining U-235 atom. The number of fission products at this time will be 187.4% of the original U-235 population or $1.874 \times 8.92 \times 10^{20}$ atoms/cm^3 $= 1.67 \times 10^{21}$ fission products/cm^3. [Ans.]

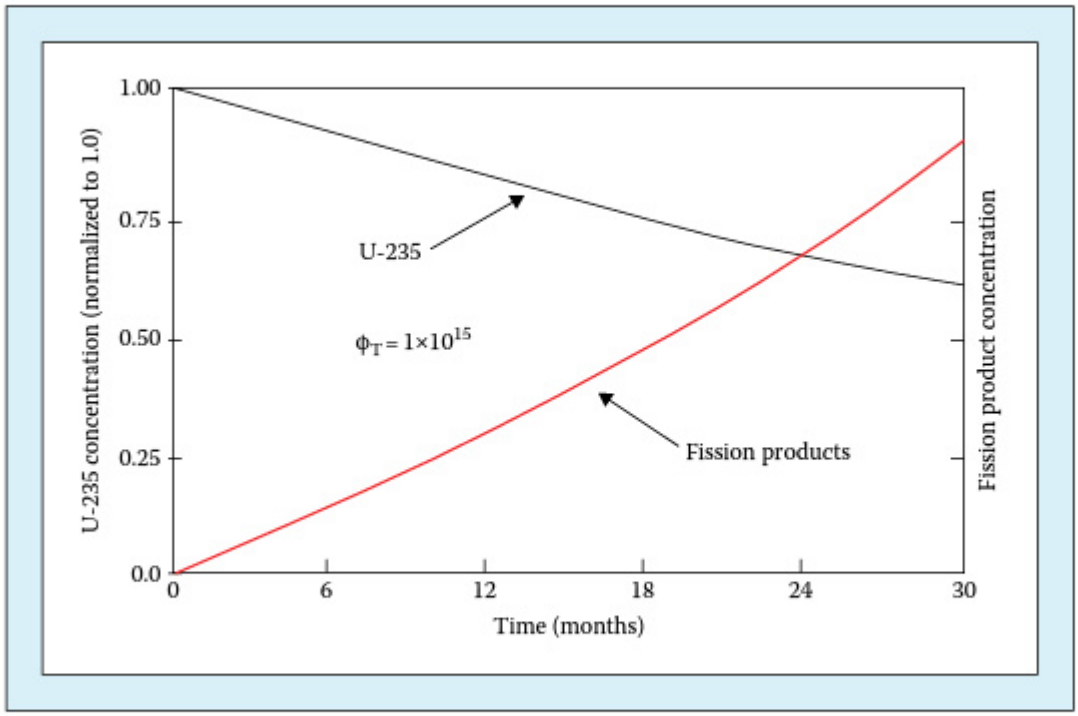

FIGURE 18.27 A comparison of the fission product concentration to the concentration of U-235 atoms in a thermal water reactor fuel assembly with a 4% enrichment. (*Note*: All values are normalized to one.)

Figure 18.27 shows the number of fission products compared to the number of U-235 atoms for a thermal neutron flux of $\phi = 1 \times 10^{13}$ neutrons/cm^2/s. In this figure, the average enrichment of the fuel is assumed to be 4%. Notice that as the level of the neutron flux is increased, it takes less time for the fission product population to exceed the concentration of U-235 atoms in the fuel. *At a thermal flux of 1×10^{13} neutrons/cm^2/s, the breakeven point is only 23 months*. If the level of the flux is doubled, the breakeven time is reduced by a factor of two.

Example Problem 18.7

The U-235 atoms in a nuclear fuel rod are exposed to a thermal neutron flux of 1×10^{14} neutrons/cm^2/s for a period of 1 year. What is the ratio of the number of fission products to the number of U-235 atoms remaining at that time?

Solution The number of U-235 atoms remaining is given by the equation $N_{U235} = N_o\, e^{-\sigma aU235 \phi t}$ and the number of fission products produced is given by the equation $N_{FP} = 2N_o(1 - e^{-\sigma fU235 \phi t})$. The ratio of these two numbers is $N_{FP}/N_{U235} = 2\,(1 - e^{-\sigma fU235 \phi t})/e^{-\sigma aU235 \phi t}$. Since $\phi = 1 \times 10^{14}$ neutrons/cm^2/s, $\sigma_a = \sigma_c + \sigma_f = 96.685 + 585.086 \approx 682$ barns, $\sigma_f = 585.086$ barns, and $t = 3.15 \times 10^7$ s, the ratio is $N_{FP}/N_{U235} = (\,2 \times e^{\,-1.84})/e^{-2.15} = 0.318/0.116 \approx 2.75$. So after 1 year at a very modest level for the neutron flux, there are almost three times as many fission products as there are U-235 atoms left in the fuel rods! [Ans.]

To compensate for the poisoning effect of these fission products, the control rods must be gradually withdrawn from the core to keep the reactor in a critical state. This maintains the delicate balance in the instantaneous reactivity required by Equation 18.4. In Chapter 20, we will examine how control rods fit into this picture.

References

Books and Textbooks

1. Ash, M. *Nuclear Reactor Kinetics*, McGraw-Hill, New York (1965).
2. Henry, A.F. *Nuclear Reactor Analysis*, MIT Press, Cambridge, MA (1975).
3. Keepin, G.R. *Physics of Nuclear Kinetics*, Addison-Wesley Publishing Company, Inc., Reading, MA (1965).
4. Stacey, W.M. *Nuclear Reactor Physics*, 2nd edn., John Wiley & Sons, New York (2007).
5. Todreas, N. and Kazimi, M.S. *Nuclear Systems*, Vol. 1, CRC Press, Boca Raton, FL (2012).
6. Duderstadt, J. and Hamilton, L. *Nuclear Reactor Analysis*, John Wiley & Sons, New York (1976).

7. El-Wakil, M.M. *Nuclear Heat Transport*, American Nuclear Society, La Grange Park, IL (1981).
8. Lewis, E. *Fundamentals of Nuclear Reactor Physics*, Academic Press, Boston, MA (2008).
9. Hetrick, D.L. *Dynamics of Nuclear Reactors*, American Nuclear Society, La Grange Park, IL (1993).
10. Schultz, M.A. *Control of Nuclear Reactors and Power Plants*, 2nd edn., McGraw-Hill, New York (1961).
11. Lamarsh, J.R. and Baratta, A.J. *Introduction to Nuclear Engineering*, Prentice Hall, Upper Saddle River, NJ (2001).
12. The U.S Department of Energy. *DOE Fundamentals Handbook: Nuclear Physics and Reactor Theory*, Vol. 2, U.S. Department of Energy (January 1993).
13. Lamarsh, J.R. *Introduction to Nuclear Reactor Theory*, second printing, Addison-Wesley Publishing Company, Inc., Reading, MA (1972).
14. Glasstone, S. and Eedlund, M. *The Elements of Nuclear Reactor Theory*, D Van Nostrand Company, Inc., New York (1952).
15. Cochran, R.G. and Toulfanidis, N. *The Nuclear Fuel Cycle: Analysis and Management*, American Nuclear Society, La Grange Park, IL (1999).
16. Glasstone, S. and Sesonske, A. *Nuclear Reactor Engineering*, 3rd edn., Van Nostrand Reinhold Company, New York (1981).
17. Shultis, K. and Faw, R. *Fundamentals of Nuclear Science and Engineering*, 2nd edn., CRC Press, Boca Raton, FL (2008).
18. Masterson, R.E. *Nuclear Engineering Fundamentals: A Practical Perspective*, CRC Press, Boca Raton, FL (2017).

Web References

1. *http://en.wikipedia.org/wiki/Neutron_poison.*
2. *http://en.wikipedia.org/wiki/Nuclear_reactor_physics.*
3. *http://en.wikipedia.org/wiki/Nuclear_fission_product.*
4. *http://en.wikipedia.org/wiki/Fission_products_(by_element).*
5. *http://hyperphysics.phy-astr.gsu.edu/hbase/nucene/fisfrag.html.*
6. *http://nuclearpowertraining.tpub.com/h1019v2/css/h1019v2_43.htm.*
7. *http://powerofnuclear.blogspot.com/2010/10/xenon-135-and-samarium-149-poisoning.html.*
8. *http://ansn.iaea.org/Common/documents/Training/TRIGA%20Reactors%20(Safety%20and%20Technology)/chapter2/physics13.htm.*

Additional References

- Important physical constants used by nuclear scientists and engineers can be found in *Appendix A*.
- Unit systems and their conversion factors can be found in *Appendix B*.
- Nuclear cross sections for many important nuclear materials can be found in *Appendix C*.
- Physical properties of important nuclear materials can be found in *Appendix D*.
- Atomic masses, half-lives, and natural abundances can be found in *Appendix E*.

Questions for the Student

The following questions cover the material presented in this chapter and, in some cases, previous chapters as well. They are designed to test how well the student has acquired a working knowledge of the subject matter.

1. What is the difference between the net reactivity and the instantaneous reactivity?
2. Describe two common ways that the equilibrium concentration of Xe-135 can be found from the xenon rate equations.
3. What two common neutron poisons does a reactor operator have to be most concerned with when operating a thermal water reactor?
4. Name three reasons why it is almost impossible in the real world for a reactor to achieve a true equilibrium cycle.
5. In practice, name four factors that collectively determine the reactivity of a reactor core.
6. What causes the sharp initial drop in the reactivity that is observed when a thermal water reactor is first put into operation?
7. Computer programs are frequently used to optimize the performance of a particular fuel cycle. What two common programming techniques are used to allow this to occur?
8. In general, is the reactivity swing for a two-batch core smaller or larger than it is in a three-batch core?
9. What is the primary parameter that determines the long-term reactivity of a reactor core?
10. Write down the two differential equations that can be used to determine the Xenon-135 concentration in a light-water reactor core as a function of time.
11. What is the average absorption cross section of all of the fission products that are produced in a light-water reactor core after a period of 6–9 months?
12. How long after start-up does Xenon-135 usually reach its equilibrium concentration?
13. In general, what determines the maximum permissible burnup of the fuel in a thermal water reactor?
14. How many times larger is the poisoning effect of Xenon-135 than Samarium-149 when a thermal water reactor is operating normally?
15. How is Samarium-149 produced in a thermal reactor core?
16. From the viewpoint of nuclear fuel management, name two ways that a multi-batch core is preferable to a single-batch core.
17. How long after start-up is the equilibrium concentration of Samarium-149 usually reached?
18. What is the definition of the maximum permissible burnup?
19. Approximately how many hours after shutdown does the concentration of Samarium-149 reach its maximum value? What causes it do to so?
20. Mention two ways how Xenon-135 is produced in a light-water reactor core.
21. What is the maximum permissible burnup for the fuel rods in a modern light-water reactor core?
22. How long after shutdown does the concentration of Xenon-135 reach its highest value?
23. After a reactor is shut down, the temporarily high level of Xe-135 in the core may make it difficult to restart the reactor for several hours. In the nuclear business, what is this condition commonly referred to as?
24. Describe two common ways that the equilibrium concentration of Samarium-149 can be found from the samarium rate equations.
25. What is the yield of Iodine-135 from the thermal fission of U-235?
26. Write down an equation describing the reactivity swing of a multi-batch core in terms of the number of batches of fuel that are used.
27. What is the maximum fuel pin centerline temperature that is normally allowed in a PWR during steady-state operation?
28. In a PWR, how much negative reactivity is tied up in the control rods and in the burnable poisons?
29. Are the equilibrium concentrations of Xenon-135 and Samarium-149 a function of the neutron flux?
30. In a BWR, how much negative reactivity is tied up in the control rods and the burnable poisons?
31. What is the thermal absorption cross section of Xenon-135 that is one of the most important neutron poisons in a PWR?
32. Neglecting the enrichment of the fuel and the level of the neutron flux, what two factors determine the average fuel pin centerline temperature in a thermal water reactor?
33. What is the length of a burnup cycle in a modern thermal water reactor?
34. What is the ultimate yield of Xenon-135 from the fission of U-235?
35. How long is a reactor normally shut down for refueling before it can be restarted?

36. Who is the person who is normally responsible for optimizing the amount of energy that can be extracted from a given batch of nuclear fuel?
37. In a thermal water reactor, where is a burnable poison usually located?
38. Why is there no such thing as a samarium-induced transient in a light-water reactor?
39. What is the half-life $T_{½}$ of Xenon-135 in a thermal water reactor?
40. How many batches of fuel are normally used in an equilibrium PWR and BWR core under normal operating conditions?
41. Write down the two differential equations that can be used to determine the Samarium-149 concentration in a light-water reactor core.
42. What is another term for a "poor man's control rod?"
43. Is the buildup of Xenon-135 a major concern in a fast reactor, and why?
44. What common unit of measurement of the energy output of the fuel is used by a nuclear utility to determine the burnup of a specific batch of nuclear fuel?
45. For low fuel burnups, is it legitimate to assume that the reactivity is a linear function of burnup?
46. In general, is the maximum permissible burnup of the fuel in a LMFBR higher or lower than it is in a PWR?
47. Write down an equation for the equilibrium Xenon-135 concentration in a thermal water reactor.
48. Write down the corresponding equation for the equilibrium Samarium-149 concentration in a thermal water reactor. Does the samarium concentration have any dependence on the neutron flux?
49. Name two common examples of burnable poisons that can be found in a thermal water reactor.
50. What does the term "reactor dead time" refer to?
51. Write an equation that describes the buildup and decay of Promethium-149 in a thermal water reactor core.
52. Name two common refueling patterns that are used in commercial power reactors.
53. What is a typical value of the dead time for a commercial thermal water reactor in which the buildup of xenon has occurred?
54. What six fission products have the highest initial yields in a thermal water reactor core?
55. What popular U.S. government website provides useful information regarding the ENDFB-7 database?
56. If the maximum allowable fuel pin centerline temperature during a reactor transient is 2000°C, and the radial and axial power peaking factors are 1.2 and 1.3, what should the average fuel pin centerline temperature be during this particular transient?
57. Approximately what percentage of the Xenon-135 in a thermal water reactor is produced from the decay of Iodine-135?
58. What does the term MOX fuel refer to?
59. In what type of reactor can a MOX fuel rod be found?
60. Write an expression for the ratio of the equilibrium burnup of an N-batch core to the equilibrium burnup of a one-batch core as a function of the number of batches N of fuel that are used.
61. If you withdraw all of the control rods from the core of a thermal water reactor, and it does not start up, what do you do?
62. Why are burnable poisons so popular in nuclear reactors today?
63. What important neutron poison does Promethium-149 decay into in a thermal water reactor core?
64. Which fuel assembly reloading scheme do you think is most effective at reducing the power peaking in the radial direction?
65. What is the half-life $T_{½}$ of Iodine-135 in a thermal water reactor, which is one of the most important sources of Xe-135 production?
66. Name four common safety-related criteria that any reactor refueling scheme must satisfy.
67. What common neutron poison that is produced in large quantities in a thermal water reactor is believed to be primarily responsible for causing the reactor accident at Chernobyl to occur?
68. In a PWR core, what additional safety-related constraint does the coolant have to satisfy?

Exercises for the Student

Exercise 18.1

Suppose that a thermal water reactor has an average neutron flux of 1.05×10^{15} neutrons/cm^2/s and that 35% of the neutrons are thermal neutrons. If the average value of $\sum_f$ is 10 cm^{-1}, what is the equilibrium concentration of Iodine-135 in the core in atoms/cm^3 if the fuel is U-235?

Exercise 18.2

Using the results presented in the previous exercise, estimate the equilibrium concentration of Xenon-135 in the core in atoms/cm^3.

Exercise 18.3

Using the results presented in the previous two exercises, derive an equation for the ratio of the equilibrium Xenon-135 concentration to equilibrium Iodine-135 concentration that is independent of the macroscopic fission cross section $\sum_f$. If the thermal neutron flux is 3×10^{14} neutrons/cm^2/s, and the microscopic absorption cross section for Xe-135 is 2,778,000 barns, estimate the ratio of the Xe-135 concentration to the I-135 concentration under these conditions.

Exercise 18.4

A thermal water reactor has a neutron flux of 3×10^{15} neutrons/cm^2/s, and one-third of the neutrons are in the thermal energy range. If the average value of $\sum_f$ is 10 cm^{-1}, what is the equilibrium concentration of Samarium-149 in the core in atoms/cm^3? How long does it take the samarium concentration to reach its equilibrium value? Assume the reactor is fueled with enriched uranium.

Exercise 18.5

A thermal water reactor is designed to operate for 18 months at an average thermal flux 1×10^{15} neutrons/cm^2/s before it has to be refueled. If the reactor uses enriched uranium, how much is the reactivity of the core reduced by the buildup of fission products over this period of time?

Exercise 18.6

Suppose that the buildup of fission products in the core of a thermal water reactor results in an average fission product having a microscopic absorption cross section of 200 barns. What is the total reduction in the reactivity of the core (in dollars and cents) as the result of this fission product buildup if the core is fueled with U-233?

Exercise 18.7

Suppose that a hypothetical nuclear fuel has a microscopic fission cross section of 500 barns and a macroscopic fission cross section of 5 cm^{-1}. If the neutron flux is 1×10^{15} neutrons/cm^2/s, and its microscopic absorption cross section is 600 barns, how long must the fuel remain in the core before the number of fuel atoms and the number of fission products are exactly the same?

Exercise 18.8

Assume that the time-dependent neutron flux $\phi(t)$ in a reactor fuel assembly is given by the equation $\phi(t) = \phi_o e^{-at}$ where a = 3 and the time t is in seconds. What is the total neutron fluence that the fuel assembly is exposed to after 180 days?

Exercise 18.9

A reactor designer tells you that it is possible to increase the refueling interval for a thermal water reactor to two years by increasing the fissile content of the fuel. After this change is made, the effective multiplication for the core is 1.3. If the reactor is fueled with Pu-239, what will the excess reactivity of the core be in dollars and cents at the beginning of the initial two-year refueling cycle?

Exercise 18.10

If the fuel assemblies in Exercise 18.9 are to be replaced in three equal batches, what is the reactivity swing of the core by the end of the first refueling cycle?

Exercise 18.11

Suppose that the percentage of Pu-239 in a fast reactor is increased by 20% to increase the time between subsequent refuelings. If the core has an effective multiplication factor of 1.3 before the change, what will its effective multiplication factor and its reactivity be after the change? By what percentage has the reactivity increased? Assume that all of the other core parameters remain exactly the same.

Exercise 18.12

After conferring with the Nuclear Regulatory Commission, you find that you are allowed to increase the burnup of your fuel by 5% by increasing the amount of U-235 it contains. How much additional U-235 must be added to the fuel to allow this to happen? In a three-batch core, how much higher will the burnup ratio be than in a one-batch core with the new initial load?

19

Fuel Assembly Homogenization and Reaction Rate Conservation

19.1 A Closer look at the Neutron Diffusion Equation

In many reactors, the values for the diffusion coefficients become spatially dependent as one moves in the radial direction. Normally, this spatial oscillation is a discontinuous one, and this means that each region of a unit cell (the fuel, the cladding, and the moderator) will have a different set of values than the adjacent regions. In earlier chapters we assumed that the spatial dependence of Σ_f, Σ_a, and D could be ignored because the neutron mean free paths were long compared to the size of the fuel rods. In other words, instead of writing $\Sigma_f(x)$, $\Sigma_a(x)$, and D(x), we assumed that we could write

$$\Sigma_f(x) \cong \Sigma_f, \quad \Sigma_a(x) \cong \Sigma_a, \quad \text{and} \quad D(x) \cong D \tag{19.1}$$

so that these coefficients could be treated as constants in the neutron diffusion equation. The neutron diffusion equation then became a classic second-order differential equation with constant coefficients:

$$\nabla^2\phi(\mathbf{r}) + B_M^2\phi(\mathbf{r}) = 0 \tag{19.2}$$

where

$$B_M^2 = (\nu\Sigma_f - \Sigma_a)/D \tag{19.3}$$

was interpreted as the well known *material buckling*. Under these conditions, it is relatively easy to solve the diffusion equation in standard reactor geometries (see Chapter 13), and all that is required is to assume that the fuel assemblies (and the rest of the core for that matter) are *spatially homogeneous*. This then gives rise to what is known as the *homogeneous lattice approximation*.

However, when solutions with more spatial detail are required, using an average value for the cross sections and the diffusion coefficients can result in large errors unless the average values are found in such a way that the reaction rates are conserved. If we look carefully at the spatial dependence of $\Sigma_f(x)$, $\Sigma_a(x)$, and D(x) we find that their actual values behave in the manner shown in Figures 19.1 and 19.2. The values for $\Sigma_f(x)$ are finite in the fuel and zero in the moderator, and the value of D(x) is much lower in the moderator than it is in the fuel. Hence their values oscillate spatially as we traverse a fuel assembly in the radial direction. So the question arises as to exactly how the values of $\Sigma_f(x)$, $\Sigma_a(x)$, and D(x) can be replaced by their spatial averages ($\langle\Sigma_f\rangle$, $\langle\Sigma_a\rangle$, and $\langle D\rangle$) to conserve the reaction rates and predict the correct shape for the flux. To do so, we must *spatially homogenize* the reactor lattice (refer to Figure 19.3), and in doing so, we must ensure that the reaction rates are conserved. Hence, this is the next topic that we would like to discuss.

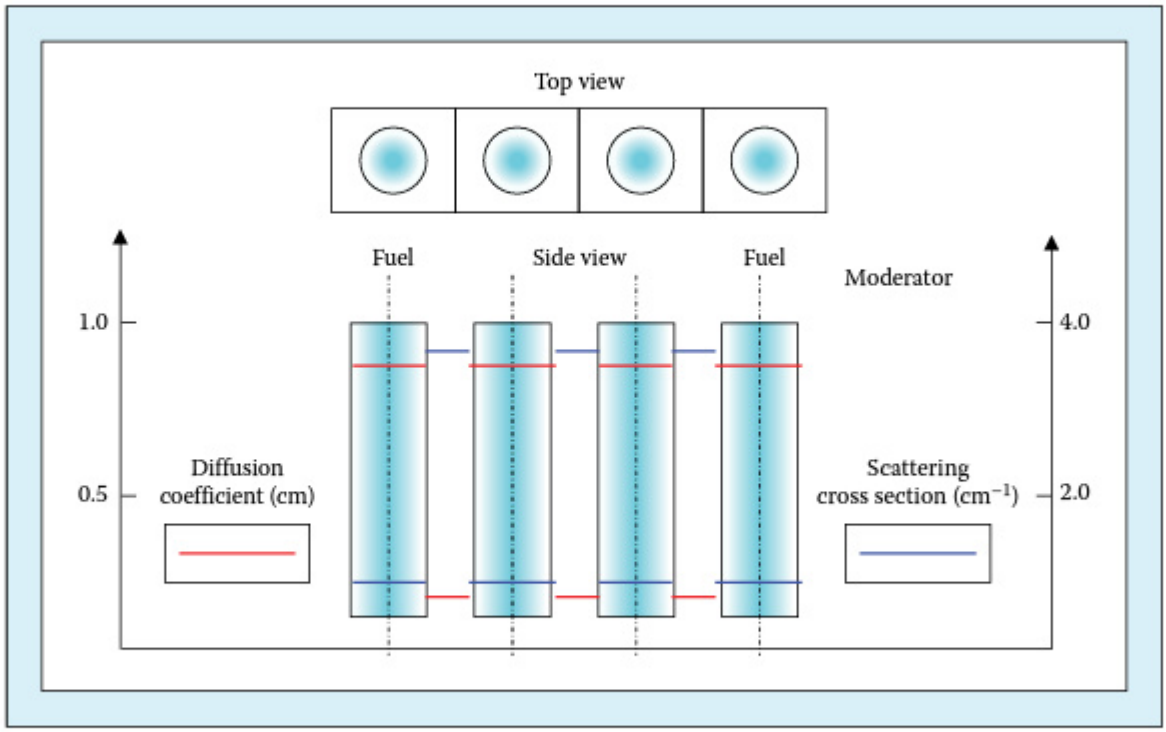

FIGURE 19.1 The spatial variation of $D(x)$ and $\Sigma_s(x)$ in a typical reactor fuel assembly in a thermal water reactor.

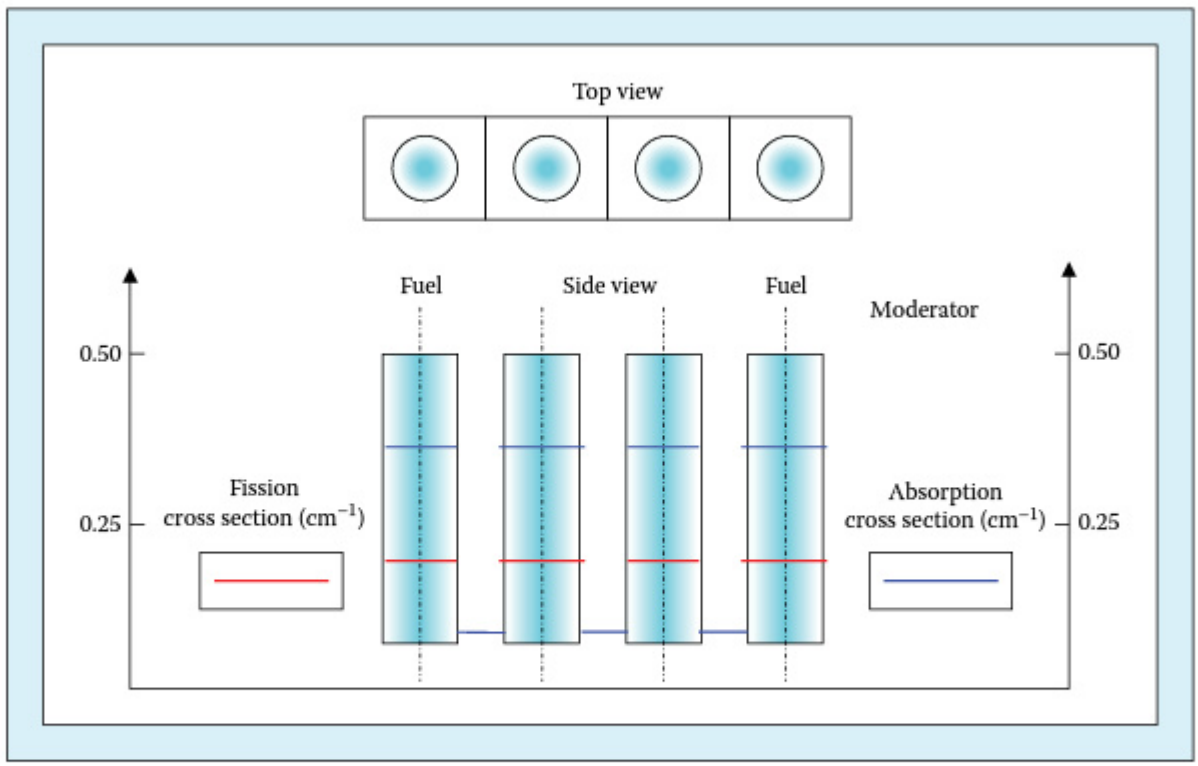

FIGURE 19.2 The spatial variation of $\Sigma_a(x)$ and $\Sigma_f(x)$ in a typical reactor fuel assembly in a thermal water reactor.

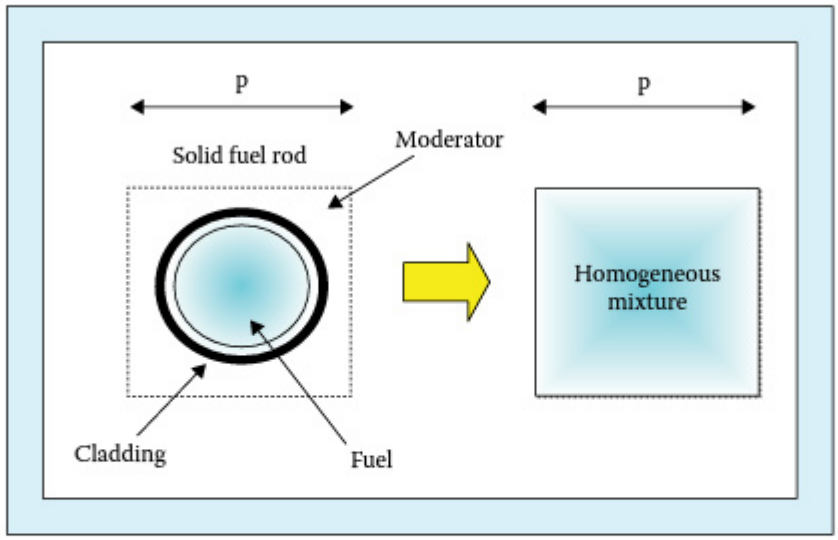

FIGURE 19.3 The process of homogenizing a unit cell in a reactor lattice.

Example Problem 19.1

Calculate the values of the diffusion coefficients for water and uranium in a thermal water reactor just prior to start-up.

Solution In this case, the room temperature libraries from BNL-325 (see Appendix C) can be used to find the values for the diffusion coefficient in the fuel and the moderator. *The diffusion coefficient D can be thought of as a measure of the physical resistance that a material presents to the flow of neutrons*. A large diffusion coefficient implies that it is easy for a neutron to move through a material, and a small diffusion coefficient implies that it is hard. We know from our previous discussion (see Chapter 11) that $D = 1/(3\Sigma_s)$, and the values of Σ_s^{U235} and $\Sigma_s^{H_2O}$ are 0.43 cm^{-1} and 3.44 cm^{-1}, respectively. Hence the values of the diffusion coefficient for the fuel and the moderator are approximately

$$D^{FUEL} = 1/\left(3\Sigma_S^{U235}\right) \approx \frac{1}{3\times 0.43} = 0.775 \text{ cm}$$

$$D^{MOD} = 1/\left(3\Sigma_S^{H_2O}\right) \approx \frac{1}{3\times 3.44} = 0.097 \text{ cm}$$

This means that the diffusion coefficient for the fuel is approximately *eight times larger* than the diffusion coefficient for the moderator in a thermal water reactor. This is the behavior we observe in Figure 19.1, wheres the explicit spatial dependence is shown. [Ans.]

19.2 Spatial Homogenization of a Reactor Fuel Assembly

Clearly, there are a lot of practical advantages to being able to replace the values of $\Sigma_f(x)$, $\Sigma_a(x)$, and $D(x)$ by their spatial averages $\langle\Sigma_f\rangle$, $\langle\Sigma_a\rangle$, and $\langle D\rangle$ as long as the averaging is done properly. We can then subdivide a typical fuel assembly such as the one shown in Figure 19.4 into a number of homogeneous regions (see Figure 19.5) and each region can have a different value for $\langle\Sigma_f\rangle$, $\langle\Sigma_a\rangle$, and $\langle D\rangle$. Furthermore, if we look at the core as a whole, then each fuel assembly can have a different value for Σ_f, Σ_a, and D, and more highly enriched fuel assemblies will have larger values of Σ_f than less highly enriched ones. However, we would like to develop a single process that works for all practical geometries and still allows us to conserve the reaction rates in the core. In general, we would also like this process to apply to one energy group and to more than one energy group. In either case, the overall process should be exactly the same.

Student Exercise 19.1

Suppose that the reflector surrounding the core in the radial direction consists of stainless steel fuel rods that are filled with a metal alloy rather than with UO_2, and that the rods themselves are surrounded by light water just as they are in the core.

Draw a picture of what the value of the diffusion coefficient D(r) looks like in the radial direction assuming that the reactor in which the reflector is located is a light-water reactor. Why do you think that the value of D(r) behaves in the way that it does?

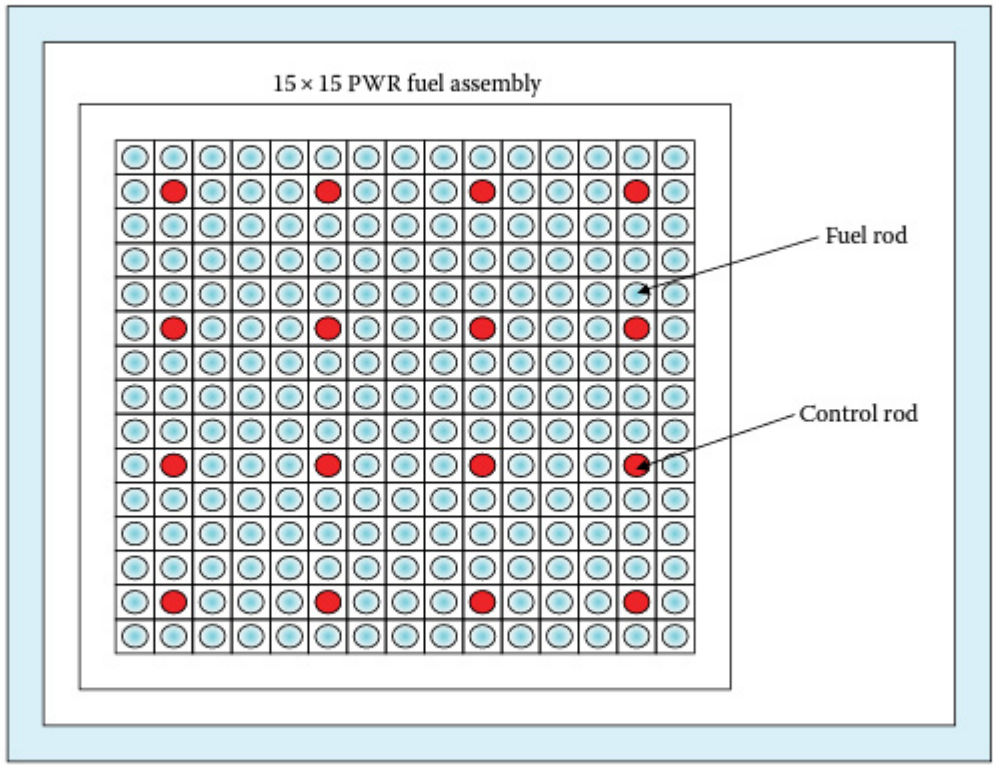

FIGURE 19.4 A modern PWR fuel assembly with 225 fuel rods and control rods.

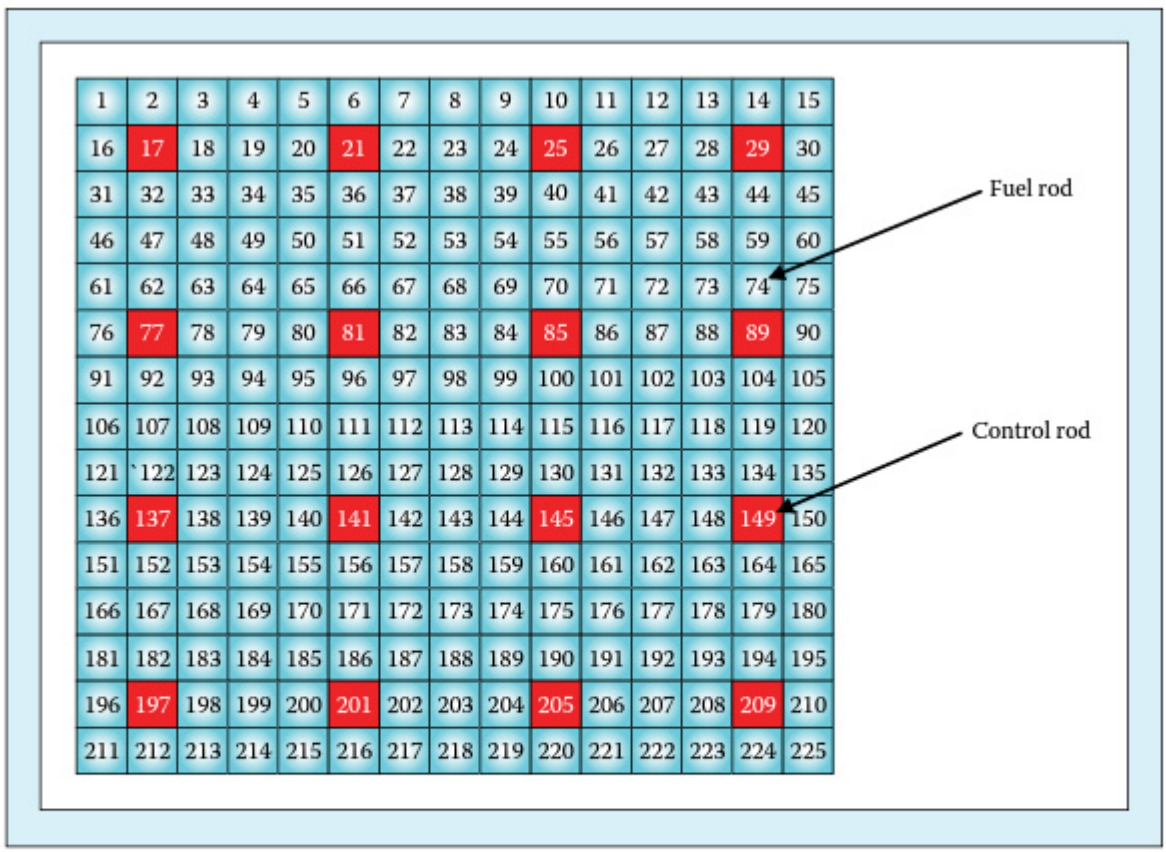

FIGURE 19.5 The same PWR fuel assembly with 225 distinct and potentially unique unit cells. The unit cells in red contain control rods and the unit cells in blue contain fuel rods.

19.3 Popular Neutron Diffusion Theory Codes and Their Applications

There are several popular computer programs that are used by nuclear scientists and engineers to solve the steady-state neutron diffusion equation. Although many of these programs were written in the 1970s and 1980s, they have been updated frequently over the years, and their sources of cross section data have been updated as well. Nuclear cross section libraries (such as ENDF-B) have also become more accurate, and this has allowed the reaction rates to be calculated more accurately as well. Today these computer programs are referred to as *computer codes*, and they can be used to calculate the flux and power shape in many different configurations. They can also be used to perform an initial criticality analysis. In many cases, some of the more famous codes like SIMULATE (specifically Versions 3 and 4) can also be used to perform burnup and depletion calculations. Some of the most popular codes, together with a description of their intended functions, are presented in Table 19.1.

Although this table is not intended to be an all-inclusive list, it lists some of the most popular computer programs that are available to solve the diffusion equation today. Moreover, some industrial-strength codes like *SIMULATE, CITATION, and DIFF-3D* are available in many different versions, and these versions can run on many different computers—from IBM mainframes to laptops or even desktops. Many of these programs can be obtained from the Nuclear Energy Agency (NEA) in Paris, France, or from the Radiation Safety Information Computational Center (or RSICC) in Oak Ridge, Tennessee. The URLs for these two important code repositories are

www.oecd-nea.org
http://www-rsicc.ornl.gov/

Finally, *SIMULATE, CITATION, and DIFF-3D* have been extensively benchmarked against experimental data, and they provide almost all of the features that any nuclear engineer could desire. In the United States, several nuclear utilities have used SIMULATE for their burnup and depletion calculations, and there is an extensive database of operational data to support its use. *Most of the time, these programs are designed to solve the diffusion equation with at least two energy groups. However, reactor vendors typically employ between 4 and 10 energy groups, and as a result of this enhanced group structure, their accuracy is very good when they are applied to a specific design*. Sometimes another computer program called *PDQ-7* (which was originally developed for PWRs at the Bettis Atomic Power Laboratory in the 1970s), is used to perform fine mesh calculations, and its results are then spatially homogenized and fed into the SIMULATE program to perform burnup and depletion calculations. The general process for how this is accomplished is described in the sections that follow.

19.4 Homogenizing a Spatially Heterogeneous Region of Space

When applying these computer programs to a reactor lattice, each computational cell (or computational "node") is assumed to be spatially homogeneous. Unfortunately, this assumption is rarely true in practice because reactor fuel assemblies are spatially heterogeneous structures rather than spatially homogeneous ones. For these programs to give the correct reaction rates and flux shapes under these conditions, one must either use smaller computational cells (which are about the size of the neutron mean free path) or one must average these smaller cells together to create larger homogeneous ones. In this section, we would like to illustrate how this spatial homogenization process is implemented.

The key requirement for any spatial homogenization process is that the cross sections used in the process must guarantee the conservation of reaction rates within the region to be homogenized. To conserve these reaction rates, the homogenization process requires a knowledge of the *shape* of the neutron flux within each smaller subregion. *If the flux shape is not available, simply volume averaging the cross sections will not produce reliable results.* To see why this is true, consider the unit cell shown in Figure 19.3. In order to homogenize this unit cell, we need to replace the spatially dependent cross sections for the fuel, the cladding, and the coolant by their volume averaged values. However, the flux in the fuel may be different than the flux in the cladding, and the flux in the fuel is certainly different than the flux in the coolant. This immediately leads us to conclude that $\phi^{fuel} \neq \phi^{clad} \neq \phi^{mod}$. To conserve reaction rates in the homogenized unit cell, the following equation must be applied to each cross section type (absorption, scattering, and fission, etc.):

$$R_x^{cell} = R_x^{fuel} + R_x^{clad} + R_x^{mod} \tag{19.4}$$

or

$$\Sigma_x^{cell}\,\phi^{cell}V^{cell} = \Sigma_x^{fuel}\,\phi^{fuel}V^{fuel} + \Sigma_x^{clad}\,\phi^{clad}V^{clad} + \Sigma_x^{mod}\,\phi^{mod}V^{mod} \tag{19.5}$$

Here R represents the reaction rate, the subscript x is used to represent each reaction type that is possible within the cell (absorption, fission, or scattering, etc.), and V^{fuel}, V^{clad}, and V^{mod} represent the respective volumes of the fuel, the cladding,

TABLE 19.1
This Table Provides a Summary of Many Popular Neutron Diffusion Theory Codes in Use Today

Diffusion Theory Code	Primary Developer	Programming Language or O/S	Function or Purpose
1-DX	Battelle Northwest Lab, Richland, Washington and Argonne National Laboratory, Argonne, Illinois (USA)	Fortran IV and Assembler Language; IBM 360/370, UNIVAC 1108	1DX is a one-dimensional computer program that can be used to produce collapsed group cross sections and self-shielded cross sections for fast reactor calculations
CARMEN	Atomic Energy Commission, Madrid, Spain	FortranV; UNIVAC 1110	CARMEN is a computer program for PWR analysis that solves the neutron diffusion equation in 1, 2, or 3 spatial dimensions with space-dependent feedback effects dimensions and two energy groups (fast and thermal)
CITATION 2D/3D	Oak Ridge National Laboratory, Oak Ridge, Tennessee, USA	Fortran – IV; Runs on IBM mainframes, CDC machines, MicroVAXs, and IBM PCs	CITATION is a very sophisticated and flexible computer program designed to solve the neutron diffusion equation in 1, 2, or 3 spatial dimensions with arbitrary group-to-group scattering cross sections. It can be used for x-y-z, θ-r-z, hexagonal-z, and triagonal-z geometries, and has no limit on the number of energy groups that can be used
DIFF3D	Nuclear Engineering DivisionArgonne National Laboratory, Argonne, Illinois	Fortran 90 and C source code for Linux PCs, MacOSX and SUN	DIFF3D is a widely used neutron diffusion theory program that uses variational nodal methods and finite difference methods to solve the neutron diffusion equation in one-, two-, and three-dimensional geometries
FPZD	Marshall Space Flight Center, NASA, Huntsville, Alabama	FORTRAN 77 and the IBM PC	FPZD is a code system for multigroup neutron diffusion theory and fuel depletion calculations
MOSRA	Department of Nuclear Energy System, Japan Atomic Energy Research Institute, Tokai-mura, Japan	FORTRAN-77/ FORTRAN-90, UNIX workstations, and LINUX PCs	MOSRA is a high-speed three-dimensional nodal diffusion code system that can be used for three-dimensional x, y, and z geometries
PDQ-7	Bettis Atomic Power Laboratory, Pittsburgh, Pennsylvania, USA	FORTRAN-IV and FORTRAN-77; IBM mainframes and IBM PCs	PQD-7 is a few-group neutron diffusion theory code that can be used to predict the flux shape in LWR fuel assemblies for individual fuel pins. It uses the few group cross sections generated by the GAM computer program, which in turn uses the data provided by the ENDF-B database
SIMULATE-2 and SIMULATE 3	Studsvik Scandpower AB Hantverkargatan 2A,SE-72212 Västerås, Sweden	FORTRAN-77, IBM and UNIX	The SIMULATE coarse-mesh nodal code and the PDQ-7 fine-mesh diffusion theory code have been used for many years to synthesize three-dimensional power distributions and flux shapes in pressurized-water reactors. SIMULATE takes the few group cross sections generated by the PDQ-7 code, and uses them to perform burnup and depletion calculations

and the moderator. In other words, with just a single energy group, the homogenized cross section for the unit cell, which we will call Σ_x^{cell}, must satisfy the equation

$$\Sigma_x^{cell} = \frac{\Sigma_x^{fuel}\phi^{fuel}V^{fuel} + \Sigma_x^{clad}\phi^{clad}V^{clad} + \Sigma_x^{mod}\phi^{mod}V^{mod}}{\phi^{cell}V^{cell}} \tag{19.6}$$

where ϕ^{cell} is the average neutron flux within the cell, computed from

$$\phi^{cell} = \frac{\phi^{fuel}V^{fuel} + \phi^{clad}V^{clad} + \phi^{mod}V^{mod}}{V^{cell}} \tag{19.7}$$

In general, the values of ϕ^{fuel}, ϕ^{clad}, and ϕ^{mod} are all different. In other words, *the only time we can volume average the cross sections to get the correct result is when the neutron flux is the same everywhere*; that is, when $\phi^{fuel} = \phi^{clad} = \phi^{mod} = \phi$. Then and only then are the "spatially homogenized" cross sections the same as the volume averaged ones:

$$\Sigma_x^{cell} = \frac{\Sigma_x^{fuel}V^{fuel} + \Sigma_x^{clad}V^{clad} + \Sigma_x^{mod}V^{mod}}{V^{cell}} \tag{19.8}$$

Hence as soon as the neutron flux (or the shape of the flux) becomes different in each material region, then we must use the following equations to find the "homogenized" absorption, scattering, and fission cross sections:

For Fission:

$$\Sigma_f^{cell} = \frac{\Sigma_f^{fuel}\phi^{fuel}V^{fuel}}{\phi^{cell}V^{cell}} \tag{19.9}$$

For Absorption:

$$\Sigma_a^{cell} = \frac{\Sigma_a^{fuel}\phi^{fuel}V^{fuel} + \Sigma_a^{clad}\phi^{clad}V^{clad} + \Sigma_a^{mod}\phi^{mod}V^{mod}}{\phi^{cell}V^{cell}} \tag{19.10}$$

For Scattering:

$$\Sigma_s^{cell} = \frac{\Sigma_s^{fuel}\phi^{fuel}V^{fuel} + \Sigma_s^{clad}\phi^{clad}V^{clad} + \Sigma_s^{mod}\phi^{mod}V^{mod}}{\phi^{cell}V^{cell}} \tag{19.11}$$

Of course, these equations apply to just a single energy group. If we would like to apply them to more than one energy group, then the following equations must be used:

For Fission (with more than 1 energy group):

$$\Sigma_{fg}^{cell} = \frac{\Sigma_{fg}^{fuel}\phi_g^{fuel}V^{fuel}}{\phi_g^{cell}V^{cell}} \tag{19.12}$$

For Absorption (with more than 1 energy group):

$$\Sigma_{ag}^{cell} = \frac{\Sigma_{ag}^{fuel}\phi_g^{fuel}V^{fuel} + \Sigma_{ag}^{clad}\phi_g^{clad}V^{clad} + \Sigma_{ag}^{mod}\phi_g^{mod}V^{mod}}{\phi_g^{cell}V^{cell}} \tag{19.13}$$

For Scattering (with more than 1 energy group):

$$\Sigma_{sg\to g'}^{cell} = \frac{\Sigma_{sg\to g'}^{fuel}\phi_g^{fuel}V^{fuel} + \Sigma_{sg\to g'}^{clad}\phi_g^{clad}V^{clad} + \Sigma_{sg\to g'}^{mod}\phi_g^{mod}V^{mod}}{\phi_g^{cell}V^{cell}} \tag{19.14}$$

where g refers to the index of each energy group (and g = 1 to G). Note in particular that we have not discussed how to find the group diffusion coefficients here. However, they can be obtained from

$$D_g = \frac{1}{3\Sigma_{trg}} \tag{19.15}$$

where Σ_{tr} is the *transport cross section* defined by

$$\Sigma_{trg} = \Sigma_{tg} - u\Sigma_{sg} \tag{19.16}$$

and u is the *average cosine of the scattering angle*. Other prescriptions to find the diffusion coefficient are discussed in Chapter 11.

19.5 Examples of How the Homogenization Process Works

In practice, the spatial homogenization process does not end with a single unit cell. Most of the time, it is used to homogenize many different unit cells, and in some cases, it can be applied to an entire fuel assembly or group of fuel assemblies. In this section, we would like to demonstrate how the homogenization process works. The process we will describe is typical of the ones that reactor vendors and nuclear utilities use. The individual details of this process can vary from company to company, but the overall flow is usually the same. The idea behind this approach is to define a larger *super cell* that represents the sum of the properties of the individual unit cells from which it is made. In a typical PWR fuel assembly, there can be between 200 and 300 unit cells. (The exact number of unit cells is shown in Table 19.2 as a function of the fuel assembly size.)

In other words, if a fuel assembly has 15 rods on each side, the number of individual unit cells is 15 × 15 = 225. Most of these unit cells contain fuel rods, but some of them also contain control rods or instrumentation channels (see Figure 19.5). A "super cell" can contain any number of unit cells. For example, we can subdivide the fuel assembly shown in Figure 19.5 into nine different super cells—each of which has its own size and shape. There is no particular rule that determines what the final shape of these super cells must be. All that is required is that they must have the same total volume as the unit cells from which they are made. It therefore follows that

$$V^{supercell(n)} = \sum_i V^{cell(i)} \tag{19.17}$$

where the summation is over whatever unit cells are required to create the final super cell. For example, we can decide to create super cell 1 (n = 1) from the unit cells in the upper-left-hand corner of Figure 19.6 and we can decide to create super cell 2 (n = 2) from the next set of unit cells immediately to the right of the first super cell, and so on. When homogenizing a reactor fuel assembly, this methodology ensures that the total volume of all of the cells in the lattice is conserved. In addition to conserving the total volume of each cell, we must also conserve the *reaction rates* when going from many small unit cells to several larger ones. *In other words, this requires that any large cell must have the same reaction rate as the small cells from which it is made*. According to our previous discussion, this requires the reaction rates to be conserved globally; that is

$$R_x^{supercell(n)} = \sum_i R_x^{cell(i)} \tag{19.18}$$

TABLE 19.2
Number of Unit Cells in a PWR Fuel Assembly as a Function of the Fuel Assembly Size

Rods per Side (PWR Fuel Assembly)	Total Number of Unit Cells
13	169
15	225
17	289
19	361

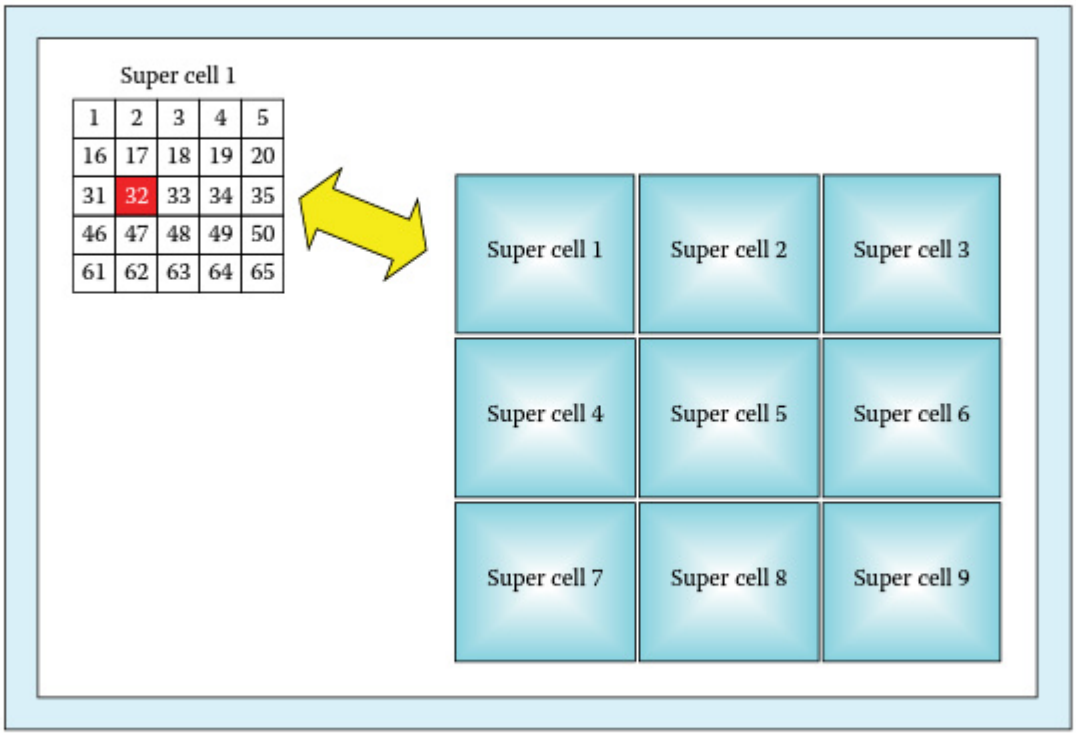

FIGURE 19.6 The unit cells in a hypothetical super cell in a PWR fuel assembly.

where R_x is the reaction rate for the specific reaction in question (x = a, s, c, f, and t). For any given reaction type, it is therefore appropriate to require that

$$(\Sigma_x \phi V)^{supercell(n)} = \sum_i (\Sigma_x \phi V)^{cell(i)} \tag{19.19}$$

or

$$(\Sigma_x \phi)^{supercell(n)} = \sum_i \frac{(\Sigma_x \phi V)^{cell(i)}}{V^{supercell\ (n)}} \tag{19.20}$$

or finally

$$\Sigma_x^{supercell\ (n)} = \frac{\sum_i \left(\Sigma_x \phi V\right)^{cell(i)}}{V^{supercell(n)} \phi^{supercell(n)}} \tag{19.21}$$

In other words, if we calculate the volume $V^{cell(i)}$ of each unit cell, and we know the values for the cross sections $\Sigma_x^{cell(i)}$ and the neutron flux $\phi^{cell(i)}$ within each of these cells as well, we can calculate an effective macroscopic cross section $\Sigma_x^{supercell(n)}$ for the super cell that represents the macroscopic cross sections of all of the individual unit cells. This process is called *homogenizing the unit cells*. Because the total number of neutrons must also be conserved, a further requirement of this process is that

$$\phi^{supercell\ (n)} = \frac{\sum_i \left(\phi V\right)^{cell(i)}}{V^{supercell(n)}} \tag{19.22}$$

where $\phi^{supercell(n)}$ is now the *average neutron flux* in super cell n. It should be obvious that this approach requires a detailed knowledge of the value of the neutron flux in each unit cell. However, it is agnostic when it comes to the details of a specific super cell. *To implement this approach, the neutron current J is usually assumed to be zero at the boundaries of the unit cells*.

19.6 Fuel Assembly Homogenization and Reactor Super Cells

Eventually a fuel assembly can be subdivided into any number of "super cells" we want, such as the fuel assembly shown in Figure 19.7. If this level of spatial homogenization is not sufficient, additional super cells can be added together to create a single "*mega cell*" for the entire assembly. This process is called *fuel assembly homogenization*, and the resulting mega cell is called a fuel assembly *node*. Solutions to the neutron diffusion equation then consist of connecting together arrays of these individual nodes. The overall result of this homogenization process is shown in Figure 19.8.

As long as the averaging process is done properly, and the overall reaction rates are conserved, every unit cell within the fuel assembly can have an entirely different material composition or shape than every other unit cell. In addition, if the assembly happens to be close to the center of the core, where the effects of neutron leakage are small, then it is possible to use this method to define a single set of effective cross sections that represent the complex behavior of an entire fuel assembly. One then ends up with a different set of macroscopic cross sections for each fuel assembly. The result of this homogenization process is shown in Figure 19.8, which depicts a quarter core symmetry section of a much larger reactor core. Here the reactor core has been reduced to one node for each fuel assembly. These nodes are then fed into a program like SIMULATE, CITATION, or DIFF-2D/3D to find the core-wide power profile. In practice, there are about one dozen nodes in the axial direction in addition to the radial ones. So if a core has 200 fuel assemblies, and there are 12 axial nodes per assembly, then a total of $200 \times 12 = 2400$ nodes will be required to represent the entire core. The isotopic composition of each of these nodes is then tracked using a computer program such as SIMULATE. Normally at least two energy groups (one for the fast group and the other for the thermal group) are used in these types of calculations. However, in the final stages of a particualr design, the number of energy groups may be increased even further to get the reaction rates correct. The actual number of energy groups depends on the structure of the neutron cross section libraries as well (see Chapter 5).

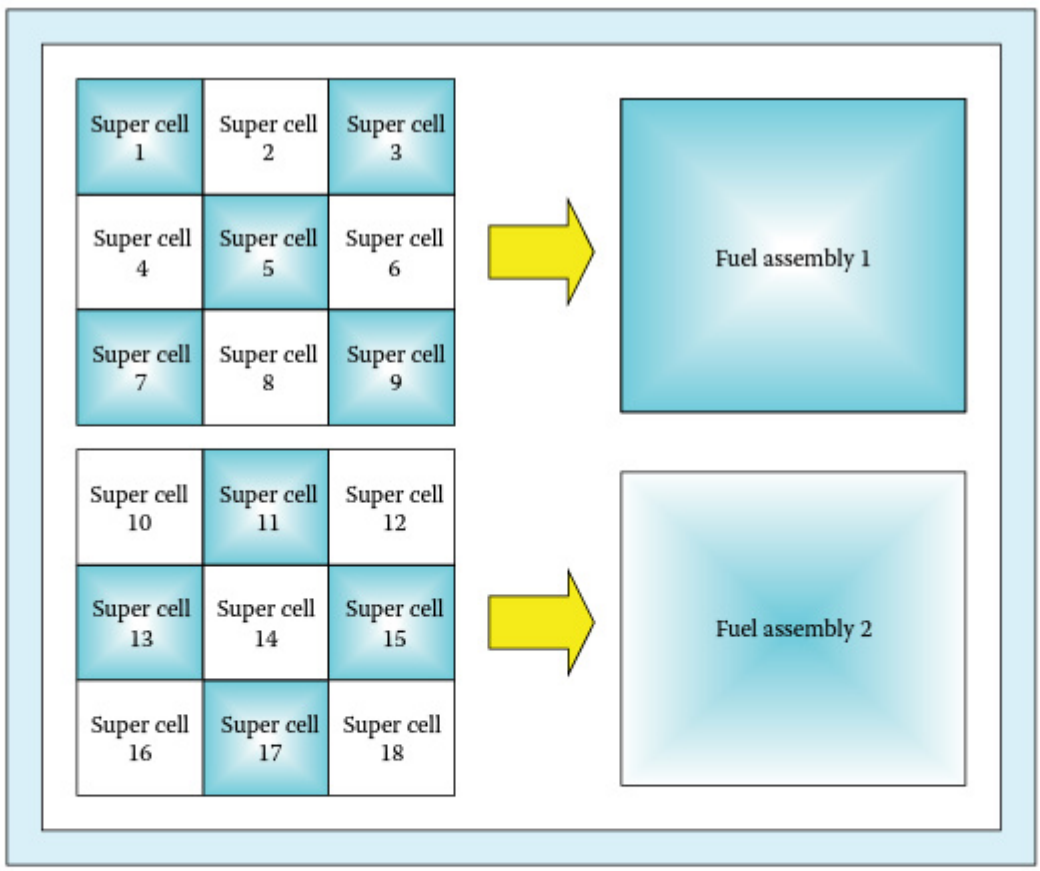

FIGURE 19.7 The process of collapsing nine different super cells into a single spatially homogeneous fuel assembly that can be represented by a single "node" or computational cell. Sometimes this node is also referred to as a "mega-cell".

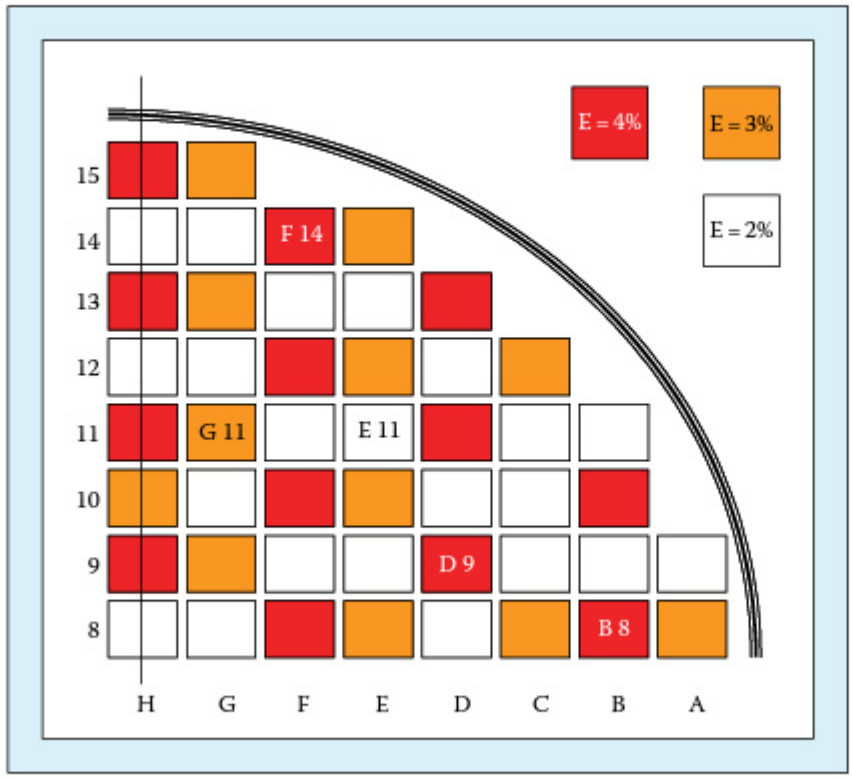

FIGURE 19.8 A quarter symmetry section of a reactor core consisting of spatially homogeneous fuel assemblies generated from larger numbers of heterogeneous unit cells. Different colors are used to represent different enrichments in this case.

Student Exercise 19.2

Write down the numbers of the unit cells that correspond to the first super cell in Figure 19.6, and then the second. Where would you draw the line between the first super cell and the second super cell in this case?

Example Problem 19.2

Suppose you are asked to homogenize a reactor fuel assembly where the moderator-to-fuel ratio is 2 to 1. If the thermal flux in the moderator is twice the thermal flux in the fuel, what is the average macroscopic absorption cross section for the fuel assembly if the average macroscopic absorption cross section for the fuel is 0.17 cm^{-1}, and the average macroscopic absorption cross section for the moderator is 0.02 cm^{-1}?

Solution The average macroscopic absorption cross section for the fuel assembly must conserve the overall absorption rate in the fuel assembly. Hence we must find the value of $<\sum_a>$ from the expression $<\sum_a> = (\phi_{fuel}\sum_{fuel\ a}V_{fuel} + \phi_{mod}\sum_{mod\ a}V_{mod})/(\phi_{fuel}V_{fuel} + \phi_{mod}V_{mod})$. Plugging in the appropriate values for each of these quantities, we find that $<\sum_a> = (1 \times 0.17 \times 1 + 2 \times 0.02 \times 2)/(1 \times 1 + 2 \times 2) = (0.25)/5 = 0.05\ cm^{-1}$. [Ans.]

19.7 Some Interesting Relationships between the Size, Shape, and Composition of a Reactor Core

If we use the process we have just described to spatially homogenize a reactor core, then it is possible to determine a number of interesting relationships between the size of the core, the shape of the core, and its overall composition. It is also possible to infer some additional information about the shape of the neutron flux, and how it behaves as a function of time. If we write the neutron diffusion equation as

$$\nabla^2\phi(\mathbf{r}) + B^2\phi(\mathbf{r}) = 0 \tag{19.23}$$

it is easy to see that any solution to the steady-state neutron diffusion equation in one dimension must satisfy

$$\frac{d^2\phi(x)}{dx^2} + B^2\phi(x) = 0 \tag{19.24}$$

or

$$B^2 = \frac{-d^2\phi(x)/dx^2}{\phi(x)} \tag{19.25}$$

Hence the value of B^2 depends on the curvature of the neutron flux, and in particular, it depends on the value of the second derivative $d^2\phi(x)/dx^2$. However, if we had attempted to solve the time-dependent version of the same diffusion equation, then the time-dependent solution would also have to satisfy

$$B_n^2 = \frac{-d^2\phi_n(x)/dx^2}{\phi_n(x)} + \frac{1}{v}\frac{d\phi_n(t)/dt}{\phi_n(x)} \tag{19.26}$$

where the subscript n refers to the fact that there can be multiple solutions, and that each value of n corresponds to a different flux "shape" or eigenfunction that the neutron flux is required to obey.

In general, it can be shown that there are an infinite number of different shapes that the neutron flux can have, and that each of these shapes is equivalent to a different eigenvalue or "mode" of the neutron diffusion equation. Under steady-state conditions, the exact solutions to the diffusion equation for a symmetrical one-dimensional bare reactor core are

$$\phi_n(x) = A_n \cos(B_n x) \tag{19.27}$$

where the values of A_n are determined from the boundary conditions, and the values of B_n are called the *eigenvalues* of the neutron flux. In other words, the values of $\phi_n(x) = A_n\cos(B_n x)$ are the *eigenfunctions* for the flux shape and the corresponding eigenvalues for a symmetrical reactor are given by

$$\text{Eigenvalues: } B_n^2 = (n\pi/L)^2 \quad n = 1,3,5,\ldots,N \tag{19.28}$$

where L is the width of the core. If we include the *extrapolation distance* δ in our calculations (where the neutron flux falls to zero at the edge of the core), then we must replace L by $L_p + \delta$, where L_p is the *physical width* of the core. Also note that only the *odd-numbered* eigenvalues are relevant to the solution we are presenting here, since the even numbered values (n = 2, 4, 6, etc.) only come into play when the reactor is an asymmetrical one. When the neutron flux is time dependent, then all of the eigenfunctions are legitimate solutions to the neutron diffusion equation, and there is no way to know in advance which solutions are the "legitimate" and which ones are not. However, in a time-dependent problem, where a reactor is no longer exactly critical, each of the eigenfunctions must also be multiplied by a time-dependent term of the form:

$$\phi_n(t) = \phi_n(0)e^{-\lambda_n t} \quad n = 1,3,5,\ldots,N \tag{19.29}$$

The reason for the existence of this term is discussed in Chapter 15. Hence, the time-dependent neutron flux becomes

A General Solution to the Time Dependent Neutron Diffusion Equation

$$\phi_n(x, t) = \phi_n(t)\cdot\phi_n(x) = A_n e^{-\lambda_n t}\cos(B_n x) \tag{19.30}$$

and *Equation 19.30 is the general solution for the time-dependent neutron flux for a bare homogeneous core*. In Equation 19.30, the values of the time-dependent terms depend on how far away the reactor is from being exactly critical. In general, it is easy to show that the steady state eigenvalues are ordered so that

$$B_1^2 < B_3^2 < \cdots < B_n^2 = \left(\frac{\pi}{L}\right)^2 < \left(\frac{3\pi}{L}\right)^2 < \cdots < \left(\frac{n\pi}{L}\right)^2 \tag{19.31}$$

Hence the time-dependent eigenvalues must be similarly ordered so that

$$\lambda_1 < \lambda_3 < \lambda_5 < \lambda_7 < \cdots < \lambda_n \tag{19.32}$$

Physically, this implies that the higher order solutions to the diffusion equation (corresponding to the larger values of n) tend to decay more rapidly than those corresponding to the smaller values of n. This means that if we wait long enough, and we are eventually able to adjust the material composition to achieve a critical state, then the only solution that will remain as $t \to \infty$ is the first spatial and temporal eigenvalue:

$$\phi_n(x,t) \cong A_1 e^{-\lambda_1 t}\cos(B_1 x) \tag{19.33}$$

This solution is called the *fundamental mode* of the diffusion equation because it represents the first spatial harmonic of the flux when a critical system is achieved. In other words, regardless of how the neutron flux in a homogeneous core grows or shrinks as a function of time, it will eventually approach a steady-state value where $e^{-\lambda_1 t} \to 1.0$ as $t \to \infty$, and *the only persistent eigenvalue that will remain is the first eigenvalue* which implies that the steady-state flux shape is

$$\phi(x) = A_1 \cos(B_1 x) \tag{19.34}$$

Sometimes it is customary to refer to the value of B_n^2 as the *geometrical buckling of the flux*, and hence the geometrical buckling for an exactly critical system is

Definition of the Geometric Buckling

$$B_1^2 = \left(\frac{\pi}{L}\right)^2 = B_G^2 \tag{19.35}$$

Thus the value of the geometric buckling can be interpreted as the curvature of the steady-state flux (with n = 1). In any other mode, the neutron leakage rate will be higher, and so the mode with the least curvature and the least neutron leakage (the fundamental mode) will persist the longest. Theoretically, this is no different than saying that the steady state curvature is given by

$$B_1^2 = \frac{-d^2\phi_1(x)/dx^2}{\phi_1(x)} \tag{19.36}$$

Furthermore, it is easy to show that this curvature disappears when $d^2\phi_1(x)/dx^2 = 0$. Of course, this corresponds to the case where the size of the reactor is so large that $B_1^2 \to 0$. Now let us go back to the steady-state diffusion equation

$$\frac{d^2\phi_n(x)}{dx^2} + B_n^2\phi_n(x) = 0 \tag{19.37}$$

and look at this problem from a slightly different perspective. Under steady-state conditions, the value of B_1^2 is given by

$$B_1^2 = \frac{(\upsilon\Sigma_f - \Sigma_a)}{D} \tag{19.38}$$

since this is the conventional definition of the material buckling B_M^2:

Definition of the Material Buckling

$$B_1^2 = \frac{(\upsilon\Sigma_f - \Sigma_a)}{D} = B_M^2 \tag{19.39}$$

Notice that the value of the material buckling B_M^2 depends on only the material composition of the core (so it has nothing to do with its geometric shape), while the value of the geometric buckling B_G^2 depends on only the core geometry (so it has nothing to do with its material composition). However, when the core is exactly critical, a necessary and sufficient condition for solutions to the diffusion equation to be valid is

The Requirement for an Exactly Critical System

$$B_M^2\left(\text{determined by the core composition}\right) = B_G^2\left(\text{determined by the core geometry}\right) \qquad (19.40)$$

and this is the relationship between the geometry of the core and its composition that we presented in Chapter 13 (without proving that an equality existed between them at that time). One of the most important consequences of this equality is that it provides a relatively simple way for a reactor designer to adjust the core size or composition to keep it exactly critical. We can either adjust the size of the core (by changing the value of B_G^2 on the RHS) or we can adjust the composition of the core (by changing the value of B_M^2 on the LHS).

Note in particular that increasing the core size causes B_G^2 to decrease, while increasing the concentration of fissile material increases the value of Σ_f and hence the value of B_M^2. From this simple relationship, it is also possible to deduce a number of fundamental rules that apply to any reactor core (as long as it is unreflected). These rules are summarized in Equation 19.41 below:

The Three Major Reactor Operating States

$$\begin{aligned}
&B_M^2 > B_G^2 \Rightarrow \text{the core is supercritical, and } \lambda_1 < 0 \ \left(\text{the value of the flux increases exponentially with time}\right)\\
&B_M^2 = B_G^2 \Rightarrow \text{the core is just critical, and } \lambda_1 = 0 \ \left(\text{the value of the flux stays the same}\right)\\
&B_M^2 < B_G^2 \Rightarrow \text{the core is subcritical, and } \lambda_1 > 0 \ \left(\text{the value of the flux decreases exponentially with time}\right)
\end{aligned} \qquad (19.41)$$

These relationships can be invaluable when determining how quickly the neutron flux shape will change when a reactor is no longer critical. All that is necessary to determine how quickly the flux changes are the values of λ_n. This is true irrespective of what the steady-state flux shape $\phi(x)$ looks like. Notice that the same conclusions can be applied to other geometries, including spherical, cylindrical, and rectangular cores—as long as they are unreflected. In each case, the size of the reactor core determines the value of B_G^2, and the material properties of the core determine the value of B_M^2. How far away a reactor is from being critical then determines the values of λ_n (the decay or growth constant governing the behavior of the flux and the power). Sometimes the inverse of the decay constant is called the *reactor period* T. (A formal definition of the reactor period is presented in Chapters 15 and 16, where it is also expressed in terms of the reactivity ρ). Hence, we can also conclude that $T = 1/\lambda_1$ when it comes to determining the asymptotic period for the fundamental mode. Since the value of λ_1 has the units of inverse seconds, *the reactor period T is always quoted in seconds*.

If the core happens to become slightly subcritical or supercritical, the reactor period will be on the order of 30 to 120 seconds. If the core becomes more subcritical or supercritical, then the reactor period will become shorter as well. In an extreme case, it can become as short as 1 second or less. When this occurs, the neutron flux can increase by a factor of e or decrease by a factor of 1/e in less than 1 second. Needless to say, this only happens during the most severe transients, and these transients are not expected to occur during the lifetime of most plants.

Student Exercise 19.3

In any fuel assembly homogenization process, the reaction rates in the original unit cells must be conserved. Why is setting the neutron current equal to zero at the boundaries of these unit cells such an important assumption in the homogenization process?

When does this assumption no longer apply? Can the same assumption be used for an entire reactor fuel assembly?

Example Problem 19.3

Explain why volume averaging the cross sections in a reactor fuel assembly will *not* conserve the reaction rates when replacing the fuel assembly with a single homogeneous node. Show how this process should be properly performed to ensure that the reaction rates are conserved.

Solution From Equation 19.6, it can be seen that simply volume averaging the cross sections does not conserve the fission or absorption rates unless the neutron flux is the same in the fuel, the moderator, and the cladding. *Thus to conserve the reaction rates, the nuclear cross sections must be both volume weighted and flux weighted* to create larger homogenous regions of the core or "nodes" that can then be fed into a nodal method. Many reactor design codes (see Table 19.1) also rely on this fact to ensure that the reaction rates are conserved. [Ans.]

19.8 Thermal Disadvantage Factors and Fuel Assembly Homogenization

Before computers were invented, people attacked the problem of unit cell and fuel assembly homogenization much differently than they do today. They did so by inventing the concept *of thermal disadvantage factors*. As we saw earlier, spatially homogenizing a unit cell or super cell requires us to know the ratio of the flux in the moderator to the flux in the fuel. Thus a thermal disadvantage factor ζ can be defined to represent the ratio of the average flux in the moderator to the average flux in the fuel:

Definition of the Thermal Disadvantage Factor

$$\zeta = \frac{\phi^{\text{mod}}}{\phi^{\text{fuel}}} \tag{19.42}$$

This terminology was adopted because the thermal flux in the fuel is always somewhat less than the thermal flux in the moderator, which leads us to conclude that $\zeta > 1$. (See Figure 9.6.) The depression of the thermal flux in the fuel is a consequence of *resonance self shielding*. Similarly, the thermal flux in the cladding tends to be slightly lower than the thermal flux in the moderator, but not by the same amount. Thus a thermal disadvantage factor for the cladding can be defined as well

$$\zeta = \frac{\phi^{\text{mod}}}{\phi^{\text{clad}}} \tag{19.43}$$

which is also greater than 1. These factors can then be combined with the equations of Section 19.4 to homogenize a unit cell. If the disadvantage factor becomes energy dependent, then we can use a similar procedure to homogenize the cross sections. Only in this case, it becomes a two-step process. For example, when the cladding is ignored, the average energy dependent cross section for a unit cell for reaction type x, with x = a, f, s, c, or t is

$$\Sigma_x^{\text{cell}}(E) = \frac{\Sigma_x^{\text{fuel}}(E) + \Sigma_x^{\text{mod}}(E)\zeta(E)\left(V^{\text{mod}}/V^{\text{fuel}}\right)}{1 + \zeta(E)\left(V^{\text{mod}}/V^{\text{fuel}}\right)} \tag{19.44}$$

where x = a, c, f, s, or t. Multigroup cross sections can then be found from Equation 19.44 by averaging the value of $\Sigma_x^{\text{cell}}(E)$ over the appropriate energy ranges—usually fast and thermal. (Refer to our discussion in Chapter 12 to see how this is done.) In the early days of the nuclear power business, disadvantage factors were found by performing *experiments*. Now they are rarely used because it is easier to just compute the values of the fast and thermal flux directly. Next we would like to turn our attention to how control rods and burnable poisons fit into this picture. This then becomes the focus of our discussion in Chapter 20.

References

Books and Textbooks

1. Henry, A.F. *Nuclear Reactor Analysis*, MIT Press, Cambridge, MA (1975).
2. Todreas, N. and Kazimi, M.S. *Nuclear Systems*, Vol. 1, CRC Press, Boca Raton, FL (2012).
3. Stacey, W.M. *Nuclear Reactor Physics*, 2nd edn., John Wiley & Sons, New York (2007).
4. Duderstadt, J. and Hamilton, L. *Nuclear Reactor Analysis*, John Wiley & Sons, New York (1976).
5. El-Wakil, M.M. *Nuclear Heat Transport*, American Nuclear Society, La Grange Park, IL (1981).
6. Lewis, E. *Fundamentals of Nuclear Reactor Physics*, Academic Press, Boston, MA (2008).
7. Lamarsh, J.R. and Baratta, A.J. *Introduction to Nuclear Engineering*, Prentice Hall, Upper Saddle River, NJ (2001).

8. Lamarsh, J.R. *Introduction to Nuclear Reactor Theory*, Second Printing, Addison-Wesley Publishing Company Inc., Reading, MA (1972).
9. Shultis, K. and Faw, R. *Fundamentals of Nuclear Science and Engineering*, 2nd edn., CRC Press, Boca Raton, FL (2008).
10. Masterson, R.E. *Nuclear Engineering Fundamentals: A Practical Perspective*, CRC Press, Boca Raton, FL (2017).

Web References

1. *www.nuceng.ca/ep4d3/text/9-multigroup.pdf.*
2. *http://en.wikipedia.org/wiki/Neutron_transport.*
3. *http://web.mit.edu/22.54/ClassNotes/Lec14.pdf.*
4. *mragheb.com/.../Neutron%20Diffusion%20Theory.pdf.*
5. *http://web.mit.edu/6.013_book/www/chapter5/5.4.html.*
6. *http://en.wikipedia.org/wiki/Geometric_and_material_buckling.*
7. *neutron.kth.se/courses/reactor_physics/.../102_DiffusionEquation.pdf.*
8. *neutron.kthttp://encyclopedia2.thefreedictionary.com/Diffusion+of+Neutrons.*
9. *http://www.engr.psu.edu/cde/courses/nuce521/nuce521_chapter1_reading.pdf.*
10. *http://dspace.mit.edu/bitstream/handle/1721.1/74136/22-05-fall-2006/contents/lecture-notes/lecture22.pdf.*

Additional References

- Important physical constants used by nuclear scientists and engineers can be found in *Appendix A*.
- Unit systems and their conversion factors can be found in *Appendix B*.
- Nuclear cross sections for many important nuclear materials can be found in *Appendix C*.
- Physical properties of important nuclear materials can be found in *Appendix D*.
- Atomic masses, half-lives, and natural abundances can be found in *Appendix E*.
- Neutron diffusion coefficients and neutron mean free paths are discussed in *Appendix H*.
- Diffusion parameters for common nuclear materials are discussed in *Appendix I*.
- Bessel functions that appear in solutions to the neutron diffusion equations are discussed in *Appendix K*.

Questions for the Student

The following questions cover the material presented in this chapter, and in some cases, previous chapters as well. They are designed to test how well the student has acquired a working knowledge of the subject matter.

1. Suppose that we encounter a problem where the neutron diffusion equation can be written in the following form; that is, $\nabla^2\phi(\mathbf{r}) + B^2\phi(\mathbf{r}) = 0$. What other famous equation that frequently appears in the field of nuclear science and engineering has exactly the same form?
2. Suppose that we would like to obtain a general solution to the neutron diffusion equation for a bare homogeneous core having a width of L where the neutron flux is allowed to change as a function of time. Write down a general solution to the time-dependent neutron diffusion equation in this case.
3. Assume that the reactor core in the previous problem is exactly critical, and that the neutron flux is no longer a function of time. When this occurs, what does the term $\cos(B_1x)$ that appears in the steady-state solution refer to?
4. Suppose that the neutron diffusion equation is written in the following form: $\nabla^2\phi(\mathbf{r}) = -S(\mathbf{r})/D$, where $S(\mathbf{r})$ is a radioactive source term. What other famous equation that frequently appears in the field of nuclear science and engineering has exactly the same form, and also has very similar solutions?
5. For a one-dimensional bare homogeneous reactor of width L, write an expression for the value of the geometric buckling when the reactor is exactly critical.
6. Fill in the following sentence with the appropriate word or phrase: For a bare homogeneous core, the neutron diffusion equation is a _____ _____ partial differential equation and its solutions are sometimes called _____ and _____.
7. Suppose that a general solution to the neutron diffusion equation reveals that the neutron flux $\phi(x, t)$ can be written as $\phi(x, t) \cong A_1e^{-t/T}\cos(B_1x)$. What does the value of T that appears in this equation refer to, and what units does it normally have?
8. In one-group neutron diffusion theory, what fundamental *nuclear* property does the term $B^2 = -d^2\phi(x)/dx^2/\phi(x)$, which can be derived from the neutron diffusion equation, represent?
9. In one-group neutron diffusion theory, what fundamental *geometric* property of the core does the term $B^2 = -d^2\phi(x)/dx^2/\phi(x)$, which can also be derived from the neutron diffusion equation, represent?
10. Assume that you are asked to examine a situation where $B_M^2 > B_G^2$. In the reactor where this occurs, is the neutron flux increasing, decreasing, or staying the same as a function of time?
11. For an exactly critical, bare homogeneous reactor, what equation establishes a fundamental mathematical relationship between the material composition of the core and the critical size of the core?
12. Suppose that the neutron flux in a bare homogeneous reactor is found to obey the following equation: $\phi(x) = A_1\cos(B_1x)$. If the thickness of the reactor core is increased by a factor of three, by what factor does the value of B_1 increase or decrease?
13. Fill in the following sentence with the appropriate word or phrase: In a _____, the neutron diffusion equation is mathematically equivalent to _____'s equation.
14. Suppose that you are asked to examine a situation where $B_M^2 = B_G^2$. In the reactor where this occurs, is the neutron flux increasing, decreasing, or staying the same as a function of time?
15. A research reactor is made out of 30 identical fuel assemblies which are grouped together to form a core in the shape of a cylinder. If the fuel rods in each fuel assembly generate one million billion fissions per second, what is the energy output of the entire reactor per second? In what form does this energy ultimately appear?
16. Suppose that you were asked to build a reactor where $B_M^2 \gg B_G^2$. What would be a typical value for the reactor period under these conditions?
17. The radius of the core of the research reactor described in Problem 19.1 is 50 cm. Approximately how high must the fuel assemblies in the core be to generate the minimum critical mass required to operate this reactor?
18. Fill in the following sentence with the appropriate word or phrase: The key requirement in any spatial homogenization scheme is that the cross sections used in the process must guarantee the conservation of _____ within the region of the core to be homogenized.
19. Suppose that the neutron flux in a bare homogeneous reactor is found to obey the following equation: $\phi(x) = A_1\cos(B_1x)$. What additional piece of information is required to determine the value of A_1?
20. Fill in the following sentence with the appropriate word or phrase: When the neutron flux is changing as a function of time, the value of the neutron flux obeys a neutron diffusion equation that is nearly identical in form to _____'s equation.
21. Suppose that you are asked to examine a reactor core where $B_M^2 < B_G^2$. When this condition occurs, is the neutron flux increasing, decreasing, or staying the same as a function of time?

22. Using a very simple geometric argument, explain why a spherical reactor has the lowest peak-to-average power ratio of any common three-dimensional shape.
23. Assume that the reactor in Problem 19.1 is centered about a cylindrical coordinate system whose origin is at the center of the core. At what point does the neutron flux achieve its maximum possible value?
24. In multigroup neutron diffusion theory, how is the transport cross section related to the total cross section?
25. Fill in the following sentence with the appropriate word or phrase: When a reactor becomes subcritical or supercritical, the value of the neutron flux increases or decreases _____ as a function of time.
26. Write an expression that can be used to find the neutron flux shape in a bare spherical reactor having a radius R during steady-state conditions. Where does the neutron flux shape attain its maximum value in this case?
27. Suppose that you withdraw some control rods from the core of an exactly critical reactor where the power level is assumed to be constant. If the reactor period soon becomes 10 seconds, by how much will the steady-state power level increase in 10 seconds?
28. Assume that a reactor fuel assembly is to be spatially homogenized by volume weighting the cross sections within the fuel assembly. If only volume weighting of the cross sections is used, will this spatial homogenization process produce the correct value for the reaction rates?
29. Suppose that a reactor operator inserts some control rods into the core of an exactly critical reactor. After a short period of time, the reactor becomes subcritical, and the asymptotic reactor period becomes 10 seconds. By how much will the steady-state power level decrease 10 seconds after the asymptotic period has been established?
30. Fill in the following sentence with the appropriate word or phrase: For a bare homogeneous core, the only time that the neutron flux has a positive value everywhere is when the neutron flux shape corresponds to the first _____ and _____ of the neutron diffusion equation.
31. What geometric function(s) can be best used to describe the shape of the neutron flux in the radial and axial directions of a bare homogeneous cylindrical reactor?
32. In an earlier section, we learned that the material composition of a reactor core determines the value of the material buckling B_M^2. What equation can be used to determine the value of the material buckling when the material composition of the core is already known?
33. Assume that a bare homogeneous reactor can be constructed from the same fuel assemblies that we discussed in Problem 19.1 but the core is now in the shape of a rectangle. If the width of the core is W, the height of the core is H, and the depth of the core is D, write an analytical expression for the shape of the steady-state neutron flux in this specific configuration.
34. Suppose that a solution to the neutron diffusion equation can be written as $\phi_n(x,\ t) = \phi_n(t) \cdot \phi_n(x) = A_n e^{-\lambda_n t} \cos(B_n x)$. What do the terms corresponding to n = 3 and 5 refer to in this equation?
35. Write down the steady-state neutron diffusion equation in what is known as its standard form. Under what conditions is the value of B^2 in this equation negative when only a single energy group is used?
36. Suppose that we find a way to increase the value of the neutron diffusion coefficient D that appears in the diffusion equation by a factor of two in a bare homogeneous core without changing any of the other material properties. Does this increase or decrease the value of the material buckling for the core?
37. In neutron diffusion theory, Bessel functions of the first kind are sometimes used. In what reactor geometries are these functions normally found, and what is the value of the neutron flux when r = 2.405 in an expression for a Bessel function of the first kind?
38. When the neutron diffusion equation is to be solved in a three-dimensional Cartesian geometry, exactly how many boundary conditions are required to find the shape of the flux when the fuel assemblies in Exercise 19.5 are arranged in the shape of a rectangle? Assume that one-group diffusion theory can be used in this case.
39. Now suppose that we would like to find the shape of *both* the fast and the thermal flux in the bare homogeneous rectangular reactor discussed in Exercise 19.5. How many boundary conditions are required to find the two-group flux shape in this case?
40. Assume that the bare reactor core in Exercise 19.5 is surrounded by a reflector that is made of light water which is approximately 20 cm thick. By how much can the thickness of the core be reduced in this case if the fuel assemblies are arranged in the shape of a simple cube?
41. In general, how many boundary conditions are required to find the shape of the neutron flux in each dimension when a bare core is surrounded by a water reflector on each side?
42. Suppose that the concentration of U-235 in the fuel rods of a bare homogeneous reactor is to be doubled from 2% to 4% to allow the reactor to be operated for a longer period of time before it has to be refueled. If none of the other material properties of the core are affected by this design change, does the material buckling B_M^2 of the core increase or decrease in this case?
43. If a symmetry condition can be used to describe the flux shape in Exercise 19.8, how many boundary conditions are required in one dimension with only one energy group?

44. A reactor having a homogeneous core is to be constructed in the shape of a simple unreflected sphere. If the core is not surrounded by a reflector, write an expression for the critical radius of the sphere when the material composition of the core is known.
45. Suppose that the value of the neutron diffusion coefficient in the thermal energy range is known. In a bare homogeneous core, what is the approximate size of the extrapolation distance d if the value of the diffusion coefficient is D_T?
46. In neutron diffusion theory, under what specific conditions does Poisson's equation reduce to Laplace's equation?
47. Why does a three-dimensional rectangular reactor have the highest peak-to-average power ratio of any common geometric shape?
48. Using only the value of B_M, write an analytical expression for the minimum critical mass of a bare homogeneous sphere.
49. How is the value of the extrapolation distance d normally determined for a bare reactor core?
50. When a reactor core is *not* surrounded by a reflector, which geometrical configuration has the lowest peak-to-average power ratio, and which geometric configuration has the highest?
51. Under what specific set of conditions does the geometric buckling B_G^2 have exactly the same value as the material buckling B_M^2?
52. In most reactor designs, the coolant enters the core from below and exits the core from above. If the height of the core is H, and the core is either rectangular or cylindrical in shape, at what fraction of the total core height H does the temperature of the fuel usually peak? Does the fuel and the coolant temperature have to be taken into account when determining the correct value of the diffusion coefficient D to be used in this case?
53. Name two boundary conditions that can be used for the neutron flux $\phi(x)$ at an interface between two different material regions having a different molecular composition.
54. Suppose that you were put in charge of designing a BWR core. At what temperature would you expect the water in the core to begin boiling?
55. For a homogeneous reactor core surrounded by a water reflector, does the value of the thermal neutron flux tend to be higher in the center of the core or in the reflector?
56. Approximately how much smaller is the peak-to-average power ratio for spherical reactor than it is in one that resembles a cube?
57. Suppose that we would like to design a cylindrical reactor of height H and radius R to have a minimum critical mass. What should the ratio of the height to the radius be to allow the reactor to become critical with the least possible amount of nuclear fuel?
58. In a CANDU heavy-water reactor, the reactor coolant enters the core from right to left through a series of horizontal pressure tubes. For thermal neutrons, is the neutron diffusion coefficient lower on the right-hand side of the core or on the left-hand side?
59. In a thermal water reactor core, at what temperature does the uranium dioxide fuel begin to melt, and at what temperature does the zirconium cladding surrounding the fuel (in the form of Zircaloy-II or Zircaloy-IV) begin to melt as well?
60. In general, in a thermal water reactor, is the value of the fast neutron flux higher in the fuel or in the surrounding reactor coolant?
61. Suppose that you were put in charge of designing a PWR core. At what temperature would you expect the water in the core to begin boiling?
62. Draw the shape of the fast and the thermal neutron flux when a homogeneous reactor core is NOT surrounded by a reflector.
63. Suppose that you were asked to design a reactor core which is 4 m high, and where the coolant enters the core from below. If the coolant is ordinary water, is the neutron diffusion coefficient higher at the bottom of the core, at the center of the core, or at the top of the core?
64. As we have seen, reactors can be designed with both radial and axial reflectors. However, when the thickness of one of these reflector increases beyond a certain point, it tends to have almost no additional effect of the value of the reflector savings because the neutrons simply do not diffuse any further into the reflector under these conditions. In a light-water reactor, how thick does a reflector have to be before this occurs?
65. Draw the shape of the fast and the thermal neutron flux when a homogeneous reactor core is surrounded by a reflector.
66. Is a reflected reactor core always smaller than an unreflected one that contains the same type of fissionable material? Can you think of any condition where this restriction does not apply?
67. In a normal light-water reactor fuel assembly, is the diffusion coefficient higher in the fuel or in the moderator?
68. Suppose that a thermal water reactor is surrounded by a reflector, and that the diffusion coefficients in both the core and the reflector are known. What additional piece of information is required to calculate the size of the reflector savings in this case?

69. Sometimes the reflector savings is calculated using the Deutsch equation. However, the Deutsch equation is normally used for just thermal water reactors. If a reflector is designed using a different material, what equation should be used instead of the Deutsch equation?
70. What are the three primary temperature scales that are used to measure the properties of nuclear materials in the world today?
71. Suppose that the material buckling of the flux is a function of temperature, and that the material buckling happens to be measured at a temperature of 300°C. On the Kelvin or absolute temperature scale, what temperature does this happen to correspond to?
72. In a well-designed thermal water reactor, approximately how much fuel can be saved (on a percentage basis) by surrounding the core with a reflector?

Exercises for the Student

Exercise 19.1

A bare homogeneous reactor in the shape of an infinite slab is 200 cm wide. If the neutron flux at the core center point is 1×10^{14} neutrons/cm^2/s when the reactor is exactly critical, what is the value of the neutron flux halfway between the center of the reactor and the edge? If the diffusion coefficient D is 1 cm, what is the value of the neutron current at the same location?

Exercise 19.2

A bare homogeneous reactor in the shape of a right circular cylinder has a height of 200 cm and a radius of 100 cm. If the neutron flux at the center point is 5×10^{13} neutrons/cm^2/s when the reactor is exactly critical, what is the value of the neutron flux halfway between the center of the reactor and the edge in the radial direction? If the diffusion coefficient D has a value of 2 cm, what is the value of the neutron current halfway between the core center point and the top of the core?

Exercise 19.3

Assume that an exactly critical reactor in the shape of a perfect cube is cooled by light water and is fueled with enriched uranium. If the neutron flux at the center of the reactor is 6×10^{13} neutrons/cm^2/s when the reactor is exactly critical, what is the value of the fast neutron flux and the thermal neutron flux at the same location?

Exercise 19.4

Suppose that you are put in charge of increasing the power density of an existing thermal water reactor by 20%. The reactor is surrounded by a water reflector 10 cm thick, and has an average enrichment of 3%. What enrichment should you use in the core instead to increase the average power density by 20%?

Exercise 19.5

A bare unreflected reactor in the shape of a perfect cube 100 cm on a side requires 100 kg of enriched uranium to achieve a critical mass. If the core is surrounded by a water reflector 20 cm thick, how much can the critical mass of the reactor be reduced in this case?

Exercise 19.6

What is the reflector savings for a square thermal water reactor surrounded by a reflector made out of heavy water when the average diffusion coefficient of the core is 1 cm, the average diffusion coefficient of the reflector is 4 cm, and the thermal diffusion length in the reflector is 170 cm?

Exercise 19.7

A reactor core is to be built in the shape of a right circular cylinder. If the radius of the core is 100 cm, how high long should the active length of the fuel rods be to achieve a critical core with the least amount of uranium?

Exercise 19.8

A cylindrical reactor core is initially unreflected, and has a thermal diffusion coefficient of about 1 cm. If the core has a diameter of 200 cm, at what distance beyond the centerline of the core does the neutron flux fall to zero?

Exercise 19.9

A spherical research reactor contains an unreflected core, and has a thermal diffusion coefficient of about 1 cm. If the core has a diameter of 100 cm, what must the value of the quantity $\nu\Sigma_f - \Sigma_a$ be in order for the reactor to achieve a critical mass?

Exercise 19.10

Before a cylindrical reactor core is surrounded by a water reflector, the thermal flux in the center of the core is found to have a value of 5×10^{13} neutrons/cm^2/s. When a 12 cm thick water reflector is added to the core, the thermal flux is also found to peak in the reflector. What do you expect the maximum value of the thermal flux to be in the reflector under these conditions?

Exercise 19.11

Suppose that you are asked to evaluate three different reactor core configurations to determine the maximum volumetric heat generation rate q''' at the center of the core. Suppose that the average volumetric heat generation rate in each of these configurations is 100 kW/L. If the core shapes to be evaluated are a cube, a cylinder, and a sphere, what is the maximum volumetric heat generation rate q'''_{MAX} for each of these three geometries if the cores are assumed to be spatially homogeneous? To simplify your analysis, assume that you can neglect the presence of the radial and axial reflectors.

Exercise 19.12

Suppose the neutron flux in a reactor consists of two energy groups. The neutron flux in the core for the fast energy group is given by the equation $\phi_1(x) = 50 \sin(10x)$, and the neutron flux in the core for the thermal energy group is given by the equation $\phi_2(x) = 25 \sin(10x)$. The core has a thermal diffusion coefficient of $D_2 = 5$ cm, and a fast diffusion coefficient of $D_1 = 10$ cm. What is the ratio of the fast neutron current to the thermal neutron current (J_1/J_2) when $x = 0$?

Exercise 19.13

Suppose that you are asked to homogenize a reactor fuel assembly where the moderator-to-fuel ratio is 4 to 1. If the thermal flux in the moderator is twice the thermal flux in the fuel, what is the average macroscopic absorption cross section for the fuel assembly if the average macroscopic absorption cross section for the fuel is 0.17 cm^{-1}, and the average macroscopic absorption cross section for the moderator is 0.02 cm^{-1}?

Exercise 19.14

A reactor is to be built in the shape of a right circular cylinder using the least amount of uranium possible. If the radius of the core is 100 cm, and the core is to be unreflected, what must the total volume of the core be?

Exercise 19.15

After doing a design review, it is decided to replace the bare homogeneous reactor core in the previous exercise (Exercise 19.14) with a new core surrounded by a water reflector 25 cm thick. If the reflector reflects essentially all of the thermal neutrons back into the core, how much fuel will the reflected core use if the bare core uses 100 kg?

Exercise 19.16

The infinite multiplication factor for a homogeneous material is 1.1 and the effective multiplication factor is 1.0. If the thermal diffusion length of the neutrons in this material is 5 cm, what is the geometric buckling of the flux in this material if the material is in the shape of a cylinder? If the cylinder has a radius of 100 cm and a height of 200 cm, do more neutrons leak out of the sides of the cylinder or the top and the bottom?

20

Control Rods, Burnable Poisons, and Chemical Shim

20.1 Control Rods and Their Function

As we first mentioned in Chapter 1, control rods have four primary functions they are required to perform. First, they are used to raise or lower the power level of the core by changing the value of the effective multiplication factor and the reactivity ρ. Changing the effective multiplication factor affects the reactor period T, and this needs to be taken into account when a control rod is raised or lowered.

Definition of Reactivity

$$\rho = \frac{\left(K_{effective} - 1\right)}{K_{effective}} \tag{20.1}$$

Secondly, control rods can be used to change the shape of the neutron flux, and changing the flux shape can be used to eliminate hot spots, or flux peaks, and to promote better burnup of the fuel. Third, control rods help to keep a reactor critical by compensating for changes in the reactivity due to the burnup of the fuel. Fourth, control rods are the first line of defense when it comes to shutting down a reactor quickly and reliably in the event that an unforeseen accident (such as a loss of coolant accident) occurs.

Withdrawing a control rod from the core will tend to increase the reactivity since fewer thermal neutrons will be absorbed. Conversely, moving a control rod further into the core will have exactly the opposite effect because more of these neutrons will be absorbed. Control rods are usually designed so that each incremental change in the position of a control rod will correspond to a known reactivity change. For example, if a control rod has a total of 20 possible vertical positions (see Figure 20.1), each vertical position will change the reactivity by a predefined amount (which is normally set by the reactor vendor). The actual amount that the reactivity is changed depends on how the control rod is designed. For example, in most pressurized water reactors (PWRs), an incremental change in the position of a *control rod bank* will change the *reactivity* by *one cent* or *one-half of one cent*. A fully withdrawn control rod will have no net contribution to the reactivity. However, each time a control rod bank is inserted into the core by a predetermined amount (say, 1/20th of its total length), the reactivity will be reduced by ½ cent or 1 cent. Thus, a fully inserted control rod bank may be able to reduce the total reactivity by 10 to 20 cents. If the same control rod bank is inserted halfway into the core, then it will affect the reactivity by about half this amount.

Normally, the reactivity of a control rod is measured in dollars and cents. This incremental reactivity is sometimes called the *control rod worth*. Other commonly used units for the reactivity of a control rod are the *milli-k* and the *pcm*. Since the reactivity is represented by the symbol rho (ρ), 1/1000th of a rho is called a "milli-rho," and a percent of a milli-rho is called a pcm (percent milli-rho). The reactivity can also be expressed as a function of Δk/k. Thus if Δk/k = 0.001 is defined as 1 milli-rho, then 1 pcm = 1% of a milli-rho = 0.00001 = 10^{-5}. Again, notice that reactivity is a dimensionless number, and these units are just different ways to express the worth of a control rod.

Measurements of the Control Rod Worth

As a function of the delayed neutron fraction β:

1 cent = 1/100th of a dollar

As an absolute number not related to the delayed neutron fraction:

1 milli-rho = 0.0011

pcm = 1% of a milli-rho = 0.00001

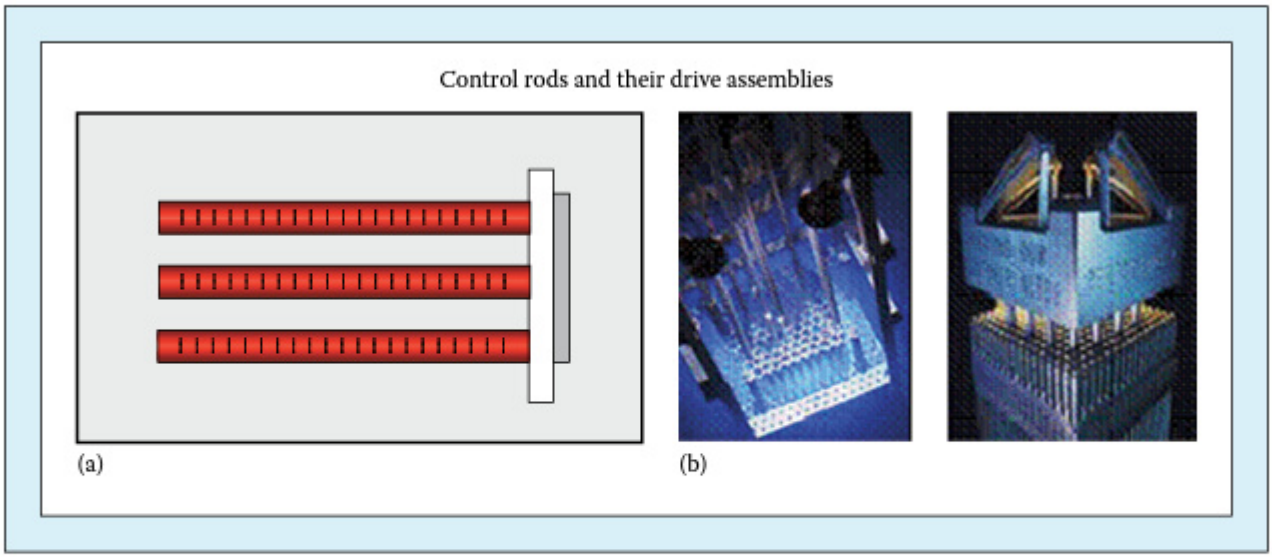

FIGURE 20.1 (a) A group of control rods (shown sideways) and a control rod drive assembly with graduations on the rods. Each graduation is ~0.01 cent worth of reactivity. (b) A fuel assembly with the control rods partially inserted into the core. (Pictures provided by Westinghouse Nuclear Energy Systems.)

Other definitions for the worth can be found in the literature, but these are the most common ones. According to the U.S. NRC, the formal definition of a control rod is

U.S. NCR's Definition of a Control Rod

"A rod, plate, or tube containing a material such as hafnium, boron, etc., used to control the power of a nuclear reactor. By absorbing neutrons, a control rod prevents the neutrons from causing further fissions."

Consequently, control rods are a very important component of any reactor design. Without them, it would be virtually impossible to control the power level when quick changes to the neutron population are required. Control rods can also come in many different sizes and shapes, and they are generally optimized to meet the needs of a particular design. Because of this, *boiling water reactors (BWRs) have cruciform control rods*, while most other types of reactors (such as *PWRs and LMFBRs) have cylindrical ones*. Some *research reactors* also use *plate-type* or *rectangular* control rods, but these control rods are generally not as common as those that are used in commercial power reactors.

Example Problem 20.1

Suppose that you visit a country where the reactivity of a control rod is quoted to be 150 pcm. In the United States, how much reactivity does this correspond to?

Solution In the United States, this represents a reactivity of $150 \times 10^{-5} = 0.00150$. Notice that this value has nothing to do with the reactivity in dollars and cents. To convert to dollars and cents, we must know the type of fuel that is being used with the control rod and what its delayed neutron fraction β is. The delayed neutron fractions for the thermal fission of U-233, U-235, and Pu-239 are 0.0026, 0.0065, and 0.0021, respectively. Therefore, if the reactivity of the control rod is quoted to be 150 pcm, this corresponds to a reactivity of $0.00150/\beta$ or \$0.57, \$0.15, and \$0.75 respectively, for these different types of fuel. [Ans.]

20.2 Control Rods and Their Origin

Control rods were first introduced into the nuclear industry during the Manhattan Project during the Second World War. However, their design was subsequently perfected for commercial PWRs at the Westinghouse *Bettis Atomic Power Laboratory* near Pittsburgh, Pennsylvania, in the late 1940s and early 1950s. They were introduced into reactors during the early days of the U.S. Nuclear Navy, and the first commercial nuclear reactor that used them was constructed at Shippingport, Pennsylvania, in 1952. Control rods were designed to help shape the power distribution, to control the amount of power generated, and to provide an additional redundant safety system in the event one of the primary

FIGURE 20.2 A picture of the *Shippingport nuclear power plant.* The Shippingport reactor was the first commercial nuclear power plant built in the United States. (Courtesy of Wikipedia.)

safety systems failed. The Shippingport reactor currently holds the longevity record for the longest operating commercial nuclear power plant in the United States. A picture of the Shippingport nuclear power plant is shown in Figure 20.2.

Control rods are designed to allow reactor operators to make rapid changes to the power level, such as those required during emergency conditions, and during normal shutdown and start-up operations. In emergency situations, they are also used to initiate a rapid reactor shutdown, which is also called a "*scram.*" Control rods are usually mounted vertically in light-water reactors. In CANada Deuterium Uranium (or CANDU) reactors, the control rods are also called *adjuster rods*, but their design is still similar to those used in other PWRs. Common control rod materials for thermal water reactors include boron, silver, indium, cadmium, and hafnium, although more exotic metallic alloys have also been used. In PWRs, they are inserted into the core from above (see Figure 20.4), and the control rod drive mechanisms (CRDMs) are mounted to the reactor pressure vessel head. This design is a variant of a design that was introduced into nuclear submarines in the late 1950s.

Control rods for BWRs have followed a different evolutionary path. For a variety of reasons, these control rods ended up being *cruciform*, rather than cylindrical in shape. In BWRs, they are inserted into the core *from below* because a steam separator or steam dryer is needed at the top of the pressure vessel head to remove excess water from the steam before it is sent to the power turbines. There can be a lot of excess reactivity built into a reactor, particularly when it contains a fresh batch of fuel. Prior to start-up, the control rods are almost fully inserted into the core to compensate for this excess reactivity. Then at start-up, the control rods are gradually withdrawn from the core in a predetermined sequence until a nuclear chain reaction occurs. Even at this point, the control rods may be only 20% or 30% removed from the core because there is still a lot of excess neutron-generating capacity to control.

The number of control rods that are used and the distance that they are inserted or withdrawn from the core can be changed over the life of the fuel to ensure that the correct amount of power is produced. In PWRs and BWRs, there are other methods for controlling the total power output as well. In PWRs, a soluble neutron poison in the form of *boric acid* $B(OH)_3$ is used to control the neutron chain reaction and hence the power levels as well. Boric acid is added directly to the reactor coolant through a boric acid holding tank to allow the control rods to be completely withdrawn during steady-state operation and to ensure a uniform power and flux distribution over the entire core. The concentration of the boric acid can then be varied to increase or decrease the number of neutrons that are produced.

In BWRs, the same effect is achieved by varying the rate of coolant flow through the core using the reactor's primary recirculation pumps. As the coolant flow through the core is increased, the amount of steam generated goes down, and the density of the coolant starts to increase. This causes the reactor power level to increase by increasing the neutron moderation and the neutron generation rate. Conversely, when the coolant flow is decreased, then the temperature of the coolant becomes higher, more steam is produced, and the coolant begins to boil. This causes the density of the coolant to fall, and

less neutron moderation will occur. The nuclear chain reaction begins to slow down, and the power output falls as well. In other words, *in BWRs, the power level goes up when the flow rate is increased (because of the increased moderation), and the power level goes down when the flow rate is decreased*. This is exactly the way that the great natural nuclear reactors of Oklo worked for over 150,000 years before their uranium fuel was completely consumed (see Chapter 10 of this book and Chapter 9 of our companion book* for more information about how these reactors worked).

In PWRs, control rods are attached to the lifting machinery at the top of the reactor pressure vessel by large electromagnets, rather than by a direct mechanical linkage. This means that if a reactor has a problem while it is operating, the electromagnets will shut down, and the control rods will fall into the core under the influence of gravity alone. This will completely stop the nuclear chain reaction. Shutting down a reactor in this way has been historically called "*scramming*" the reactor. As long as the decay heat can be removed after shutdown, this fail-safe feature makes PWRs extremely safe and reliable. Only gross mismanagement of the control rods can create a problem with this particular design. Figure 20.3 shows a computer screen from a control rod simulator in which all the control rods within a reactor core are numbered and can be individually inserted or withdrawn. *Control rod simulators* are part of the training programs that all reactor operators are required to receive.

Keeping track of the vertical position of each control rod is essential to operating a reactor properly and keeping power peaks across the core to an absolute minimum. *BWRs have a similar fail-safe system to scram the control rods, but in this case, it requires the hydraulic insertion of the control rods into the core from below to shut down the reactor in the event of an unforeseen emergency*. This is done by using water from a special holding tank that contains high-pressure nitrogen gas. In more modern designs, a large hydraulic tank with a heavy metal lid that is held in place by large electromagnets has been proposed. If the power fails, the electromagnets holding up the lid shut down, and gravity will force the hydraulic fluid to raise the control rods as the lid begins to fall. A sample simulator that allows the user to vary the location of the control rods and to observe how this affects the power level be found at the following URL:

http://esa21.kennesaw.edu/activities/nukeenergy/nuke.htm.

Ordinarily, the movement of the control rods is predetermined by the reactor operator, and the way in which he or she interacts with the reactor control system, which is completely automated. Most fuel assemblies also contain a number of rods that contain instrumentation channels to monitor the temperature of a fuel assembly at selected radial or axial locations. This ensures that the fuel temperature is always kept as uniform as possible.

Example Problem 20.2

How much reactivity (when expressed in dollars and cents) is equivalent to one milli-k (0.001) of reactivity in a thermal water reactor fueled with U-235? How much reactivity (when expressed in dollars and cents) is equivalent to 1 pcm (0.00001) of reactivity in a thermal water reactor fueled with Pu-239?

Solution Part 1: In a thermal water reactor fueled with U-235, the delayed neutron fraction β is 0.0065. One milli-k is therefore equal to 0.001/0.0065 = 15.4 cents. Part 2: In a thermal water reactor fueled with Pu-239, the delayed neutron fraction β is 0.0021. One pcm is therefore equal to $0.00001/0.0021 \approx 0.00476 = 0.476$ cents. [Ans.]

20.3 Control Rod Designs

There are about as many different control rod designs as there are types of cars and trucks on the road today. Each reactor vendor has its own unique design, and depending upon the length of the fuel cycle, control rods can be built in nearly any size, shape, or composition desired. There are no "standard size" fuel rods or control rods as far as the nuclear industry is concerned, although the same basic design patterns are repeated over and over again, and design improvements are made with predictable regularity.

In PWRs, the control rods are designed to be inserted into the fuel assemblies from above. The control rods have about the same diameter as the fuel rods, and they are usually about half an inch, or about 1 cm in diameter. Each successive generation of PWRs has changed the number of control rods in a fuel assembly and where they are located. Each design generation has also changed the composition of the materials that are used for the control rods. A picture of some of the control rods that are used in a PWR is shown in Figure 20.4. PWR control rods are inserted into the core through what are known as *guide tubes*. A guide tube is essentially a hollow zirconium tube filled with coolant. When a control rod moves into the core, it displaces the cooling water, and this causes more neutrons to be absorbed. In BWRs, the control rods are cruciform in shape, and they are inserted and removed from the core as an integrated unit from the bottom of the reactor pressure vessel. They sit in the core between groups of four fuel assemblies that are generally smaller and more

* See *Nuclear Engineering Fundamentals: A Practical Perspective*, by R.E. Masterson, CRC Press (2017).

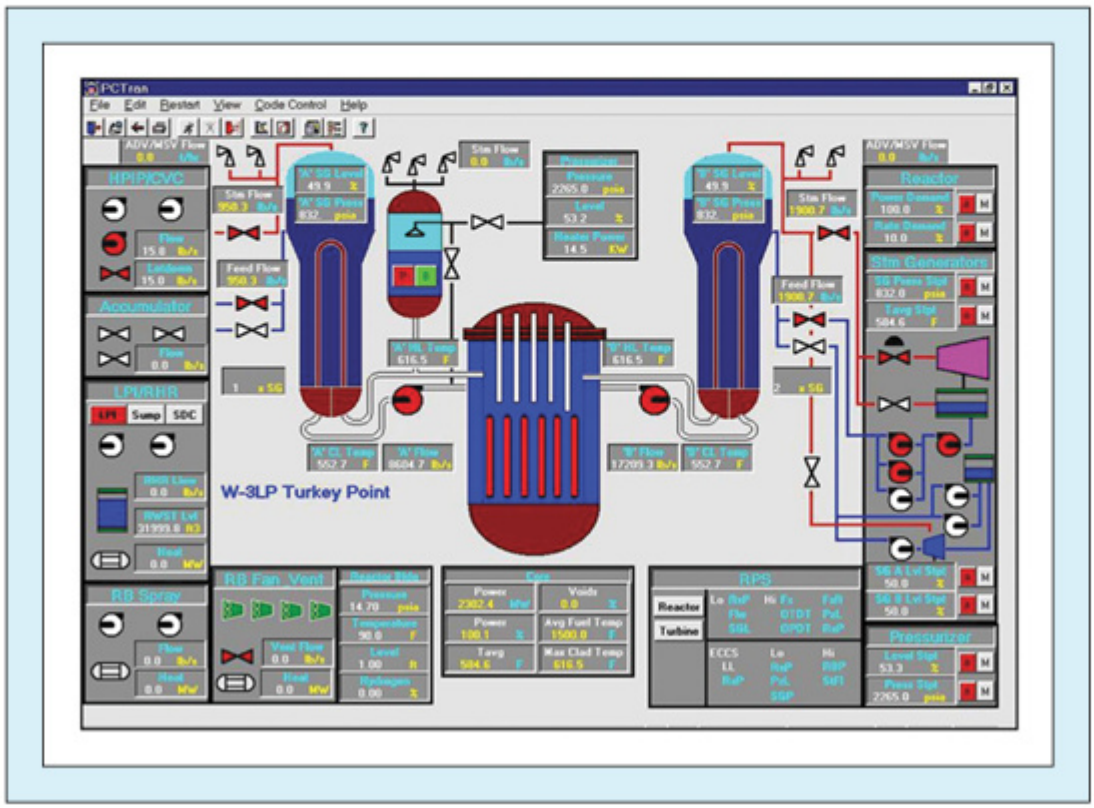

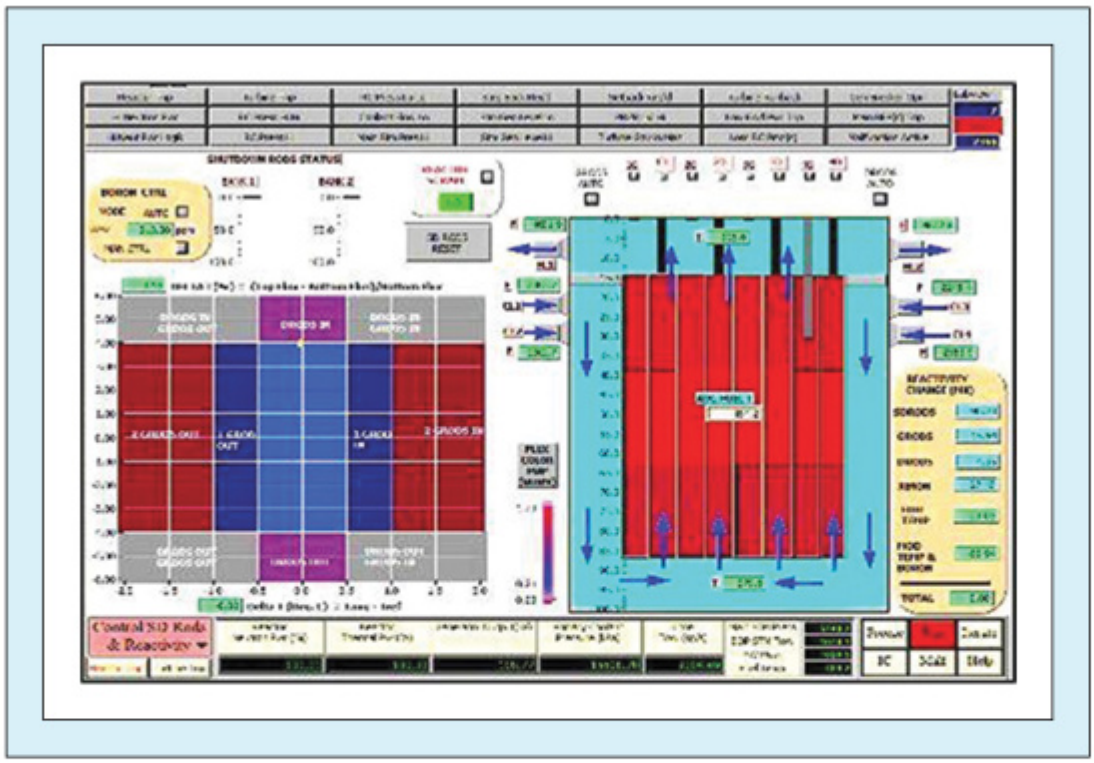

FIGURE 20.3 A control rod simulator that is advertised on the Internet. (Courtesy of Google images, see: *http://esa21.kennesaw.edu/activities/nukeenergy/nuke.htm.*)

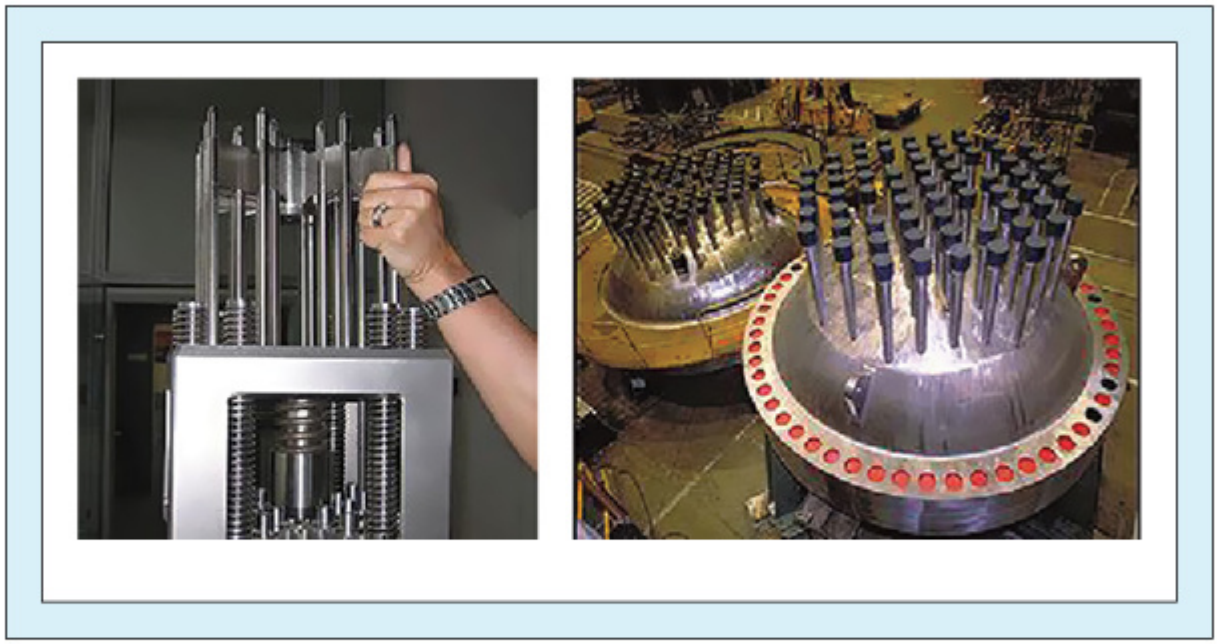

FIGURE 20.4 A control rod drive assembly in a modern PWR and the pressure vessel head. Notice that the control rods in a PWR are always inserted into the core from above. (Pictures provided by Westinghouse Nuclear.)

numerous than their PWR counterparts. A group of four BWR fuel assemblies is generally called a *fuel assembly cluster*. In this cluster, each of the control rods has four "canned" fuel assemblies surrounding it. By this, we mean that each fuel assembly is surrounded by a thin zirconium or stainless steel can that is sometimes called a "*sheath*." A picture of an early generation BWR control rod is shown in Figure 20.5. The fuel assemblies themselves are separated from one another by one of these "cans." This makes it easier to control a BWR in the event of a reactor transient because the steam that is

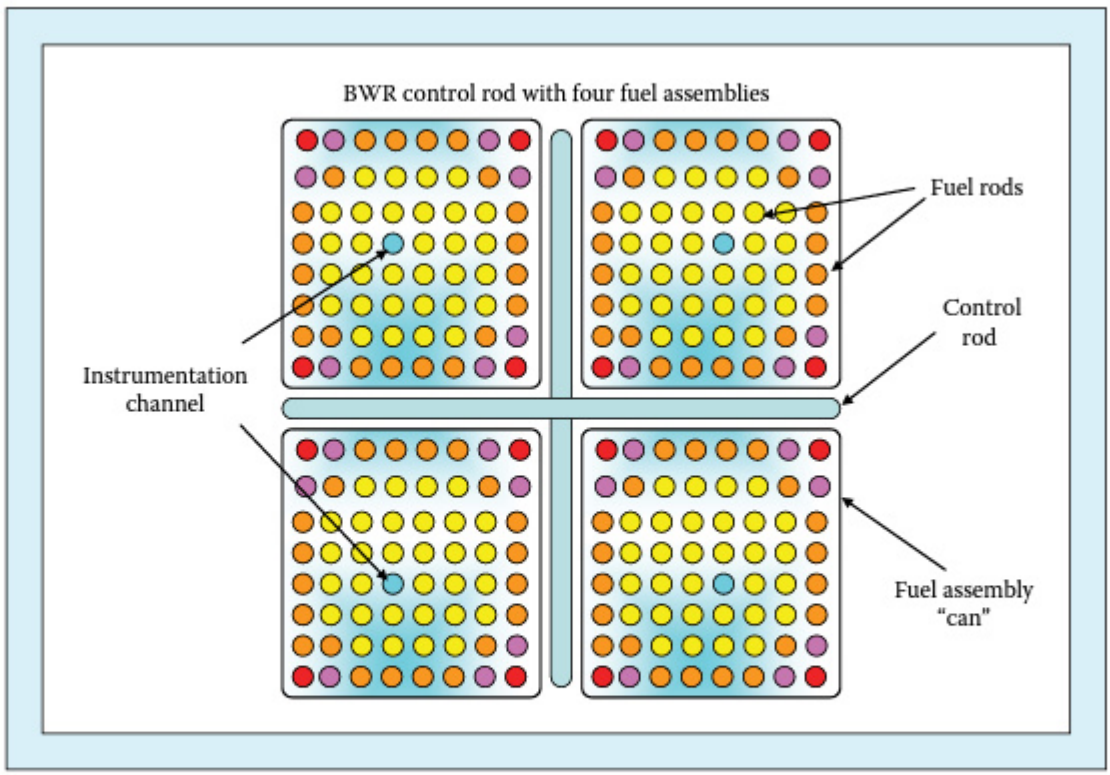

FIGURE 20.5 A BWR control rod and the four fuel assemblies surrounding it looking down from above. The different colored fuel rods correspond to different enrichments.

generated in one fuel assembly cannot move directly into another. Sometimes, the cans surrounding BWR fuel assemblies are also known as sheaths. In some BWRs, the sheaths are constructed from stainless steel.

The size and the shape of BWR control rods have changes slightly over the years. Today, there are three common types of control rods used in BWRs. They are the BWR-1, BWR-2, and BWR-3 control rods, the BWR-4 and BWR-5 control rods, and the BWR-6 and BWR-7 control rods. Each successive design generation of BWRs has used a slightly different control rod configuration as the power level of an average BRW has continued to increase. It is likely that another design will go into large-scale production around the year 2020 with the advent of the advanced boiling water reactor (ABWR) and the economic simplified boiling water reactor (ESBWR). You can learn more about the advantages and drawbacks of these designs at

http://wapedia.mobi/en/BWRI.

Figures 20.5 and 20.6 show what a modern BWR control rod looks like. Notice that each control rod is surrounded by a set of four fuel assemblies and that the single cruciform control rod may be of considerable size and girth. In many BWRs, the blades of the control rod are about 2 cm (or approximately 1 in. thick). Because of their size and thickness, these blades absorb virtually every thermal neutron that they come in contact with. To a thermal neutron, they behave like a "*black hole*" arranged in the shape of a planar surface. Fast neutrons, however, may be able to penetrate the entire width of these rods because their absorption cross sections at high energies are many times lower (at least 1000 times lower). Even in this case, the attenuation of the fast neutron flux may be considerable. Each number assigned to an individual fuel rod (in this case 1–4) indicates that a different average enrichment is used for the fuel. Figure 20.7 shows a BWR control rod attached to its mounting assembly.

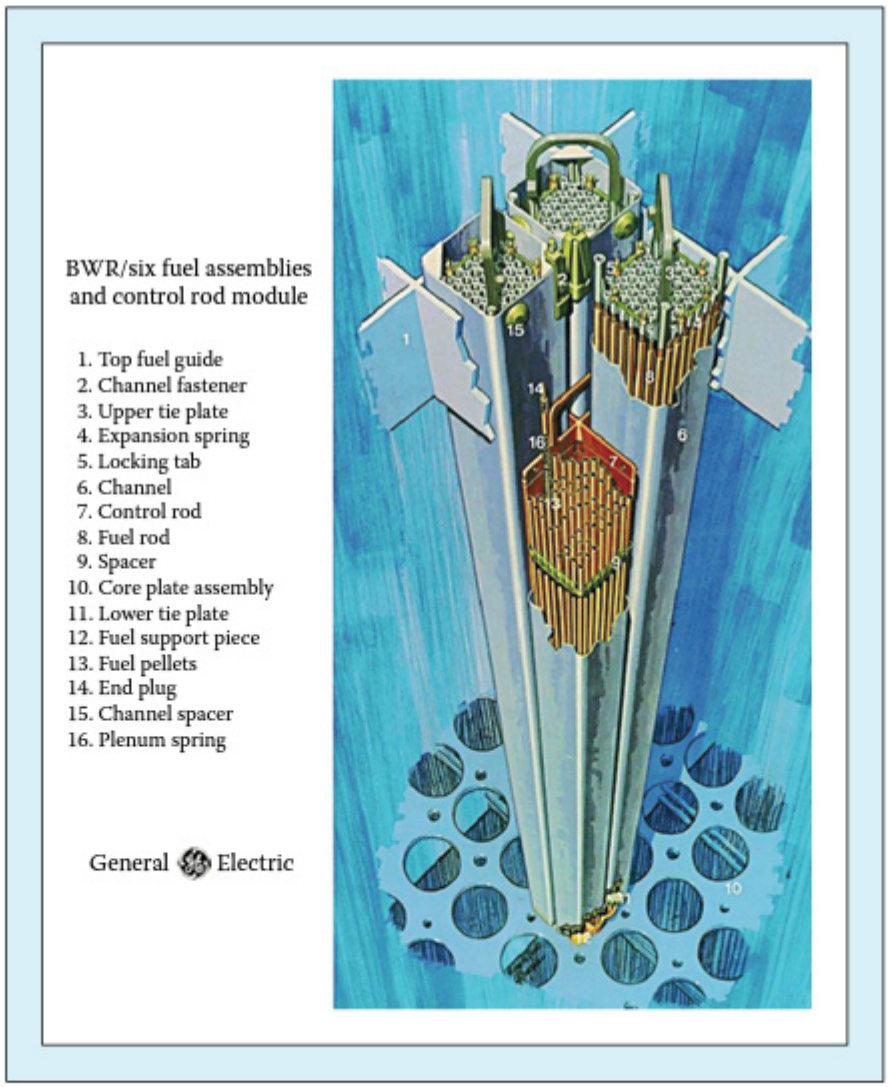

FIGURE 20.6 Schematic view of a BWR six fuel assembly. In this picture, four BWR fuel assemblies surround a cruciform control rod. The control rod is highlighted in a reddish brown color and is given the number 7. (Courtesy of GE Nuclear.)

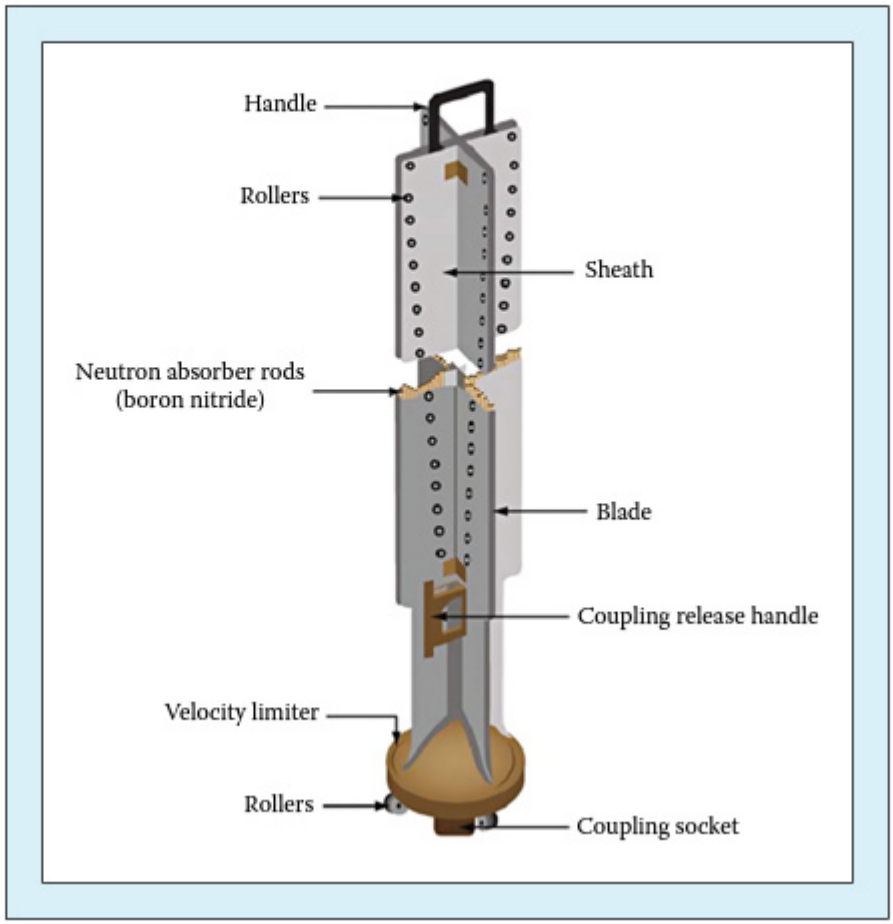

FIGURE 20.7 A picture of a BWR control rod designed by General Electric. The reader may be surprised to learn that Westinghouse also manufactures and sells BWR control rods. See the following URL for more information on the types of control rods that Westinghouse offers: *http://www.westinghousenuclear.com/Products_&_Services/docs/flysheets/NF-FE-0002.pdf*. (Courtesy of General Electric.)

20.4 Control Rod Materials

It should come as no surprise that *control rod materials* have also changed over the years. In the 1950s and the 1960s, *boron and cadmium* were used almost exclusively as control rod materials in commercial nuclear power plants. At that time, this was also the predominant trend in military and naval reactors. Both boron and cadmium were known to have reasonable dimensional stability, were readily available, and were easy to fabricate into shapes that could absorb large numbers of thermal neutrons. Since that time, the number of materials used in control rods has expanded considerably, and now *boron, silver, indium, cadmium, cobalt, dysprosium, gadolinium, samarium, erbium, europium, and more recently, the element hafnium (Hf with an atomic number of 72)* have been used.

More exotic metallic alloys consisting of combinations of these materials have also been employed at times. Silver–indium–cadmium alloys, generally 80% silver (Ag), 15% indium (In), and 5% cadmium (Cd), are now a common control rod material in PWRs. Aside from the control rods themselves, many nuclear power plants have employed new fuel assemblies where materials known as *burnable poisons* are dissolved directly in the fuel. These materials are very good at flattening the radial power distribution within an individual fuel assembly, and in sufficient quantities, they may also be used to reduce the total number of control rods that a reactor may require. Several materials are used as burnable poisons today. These materials include gadolinium (Gd_2O_3) mixed with uranium dioxide in BWR and PWR fuel rods where power peaks are to be found, and various forms of boric oxide (B_2O_3) dissolved directly into suspension with *Pyrex glass* (see Table 20.1).

Boron is a relatively common material in the Earth's crust, and it consists of two naturally occurring isotopes - *Boron-10 and Boron-11*. As we saw in Chapter 11 of our companion book, only about 20% of the naturally occurring boron in the Earth's crust is Boron-10. The remaining 80% is Boron-11. As far as nuclear materials go, Boron-11 is

TABLE 20.1
Some Common Control Rod Design Parameters

Reactor Type	Control Rod Materials	Control Rods Per Fuel Assembly[a]	Control Rod Shape	Insertion Direction
BWR	Boron carbide	1 cluster for four assemblies	Cruciform	Bottom
PWR	Boron carbide Silver–indium–cadmium alloys	11–15 (varies with the design)	Cylindrical	Top
CANDU	Cadmium	28 per core in the CANDU-6 design	Cylindrical	Top
AGR	Boron/cadmium	Varies	Cylindrical	Top
LMFBR	Boron carbide	21–31[b]	Cylindrical	Top

[a] Typical range—results may vary with design.
[b] Not all fuel assemblies have control rods.

a relatively uninteresting material because it has a thermal neutron absorption cross section of only 5×10^{-3} barns. In fact, at these energies, its neutron absorption cross section is even lower than that of water (0.005 vs. 0.664 barns for H_2O).

By comparison, Boron-10, which is about four times less common, has a thermal absorption cross section of about 3840 barns. It is therefore about 768,000 times more likely to absorb a thermal neutron than Boron-11 is. Because of this, it is considered to be a very good neutron-absorbing material. *Boron carbide* (B_4C) is used in control rods in both PWRs and BWRs. Boron carbide (with a chemical formula of B_4C) is an extremely hard ceramic material that is used in tank armor, bulletproof vests, and numerous industrial applications. It is generally dark gray or black in color. By comparison, the element cadmium (atomic symbol Cd) has a total of 50 isotopes in all, but only 8 of them are naturally stable. In the Earth's crust, cadmium is about 1000 times less common (by weight) than naturally occurring boron.

The most common isotope of cadmium is Cadmium-114, which has a natural abundance of about 29%. The next most common isotope is Cadmium-112, with a natural abundance of about 24%, and then Cadmium-111 and Cadmium-129, respectively. From the perspective of a control rod material, Cadmium-112 has also become very popular because it has a thermal absorption cross section of about 2500 barns. It is therefore very competitive with Boron-10 in this respect. The other isotopes of cadmium are not as widely used as reactor materials, so we will not discuss them here. Currently, burnable poisons are mixed together with the uranium dioxide (UO_2) in just a few rods within a fuel assembly. However, it is possible that this design practice may change over time as fuel assembly designs become more complex. Both gadolinium and boron have also been used in combination with different radial and axial zoning schemes in more advanced reactor fuel assemblies.

Countless other refinements will undoubtedly appear over time as new and more advanced fuel assembly and control rod materials are introduced. A great deal of research has also gone into the use of *ceramic materials* for this purpose as well.

20.5 Burnable and Nonburnable Poisons

While a reactor is being operated, two other changes take place to the isotopic composition of the core. First, in order to help flatten the shape of the power profile over time (see Chapter 13), *burnable poisons* and *nonburnable poisons* are put into the fuel assemblies. In the vicinity of a control rod or in an area of the core where the flux may peak, these poisons may be introduced directly into the fuel as well. We will spend several sections describing these poisons and their functions as soon as we have completed this discussion. As these poisons burn away, they help to shape the shape of the flux and also introduce additional isotopes into the fuel.

The other thing that can happen to the composition of the core is that the ratio of the control materials to the total isotopic composition of the core can also change over time. *For example, the control rods are gradually withdrawn from the core as the fuel is burned. This reduces the number of neutron-absorbing materials in the core as a whole.* In PWRs, this effect can be even more pronounced because PWRs use a form of *soluble boron*, or *chemical shim*, to control the number of thermal neutrons that are absorbed. This chemical shim is dissolved directly in the cooling water. When suspended in water, this boron becomes *boric acid*, and boric acid can absorb a great number of neutrons when a reactor is first started up. Then as the fuel is burned, its concentration is gradually reduced. The fact that the boron can be introduced directly in the coolant means that it can be distributed rather uniformly across the core and that it can help to absorb excess neutrons without causing any unnecessary flux or power peaks.

20.6 Soluble Neutron Poisons and Chemical Shim

PWRs use a special type of soluble boron, or *chemical shim*, to help control the neutron absorption rate as the fuel is burned. *The most common form of chemical shim in PWRs is a form of boric acid*, which can be directly dissolved in the coolant to absorb excess neutrons and to make many subtle adjustments to the global power level. These adjustments are much easier to perform than using a control rod to perform the same function. The form of boric acid that PWRs use is sometimes called *solbor*. The chemical composition of solbor is

Chemical Composition of Boric Acid or Solbor

$$B(OH)_3 \text{ or } H_3[BO_3] \tag{20.2}$$

and it can exist in the form of colorless crystals or a white powder that easily dissolves in water. It has the chemical formula H_3BO_3, which, as we have seen, can also be written as $B(OH)_3$. Natural boron consists of several basic isotopes, but the two most prominent ones are Boron-10 and Boron-11. About 20% of natural boron is Boron-10 and most of the remainder is Boron-11. Boron-10 has a much larger absorption cross section than Boron-11 does, and it is much better at absorbing low-energy neutrons. The absorption cross sections for Boron-10 and Boron-11 are compared in Figure 20.8. Boric acid in solid form is shown in Figure 20.9.

If boric acid is injected into the coolant, the Boron-10 concentration will rise, and this will reduce the reactor power level because more thermal neutrons will be absorbed. If enough boron is added to the coolant, it will cause the reactor to become subcritical. Ideally, it is desirable to add just enough boric acid to the coolant to keep the reactor critical at all times. Then as the fuel is consumed, the concentration of boron can be reduced proportionally to maintain a flat flux and power distribution. Changes to the boric acid concentration can effectively regulate the rate at which the fission process occurs. The *control rods* can then be reserved for their traditional functions of start-up, shutdown, and emergency core control.

In addition to boric acid, soluble poisons such as gadolinium nitrate ($Gd(NO_3)_3 \times H_2O$) and sodium polyborate can be directly injected into the coolant if an emergency situation develops. These neutron poisons are very effective in absorbing excess neutrons when a reactor needs to be shut down quickly. They can be injected automatically into the coolant in an emergency situation, or they can also be injected manually into the coolant if desired. When a PWR is just being started

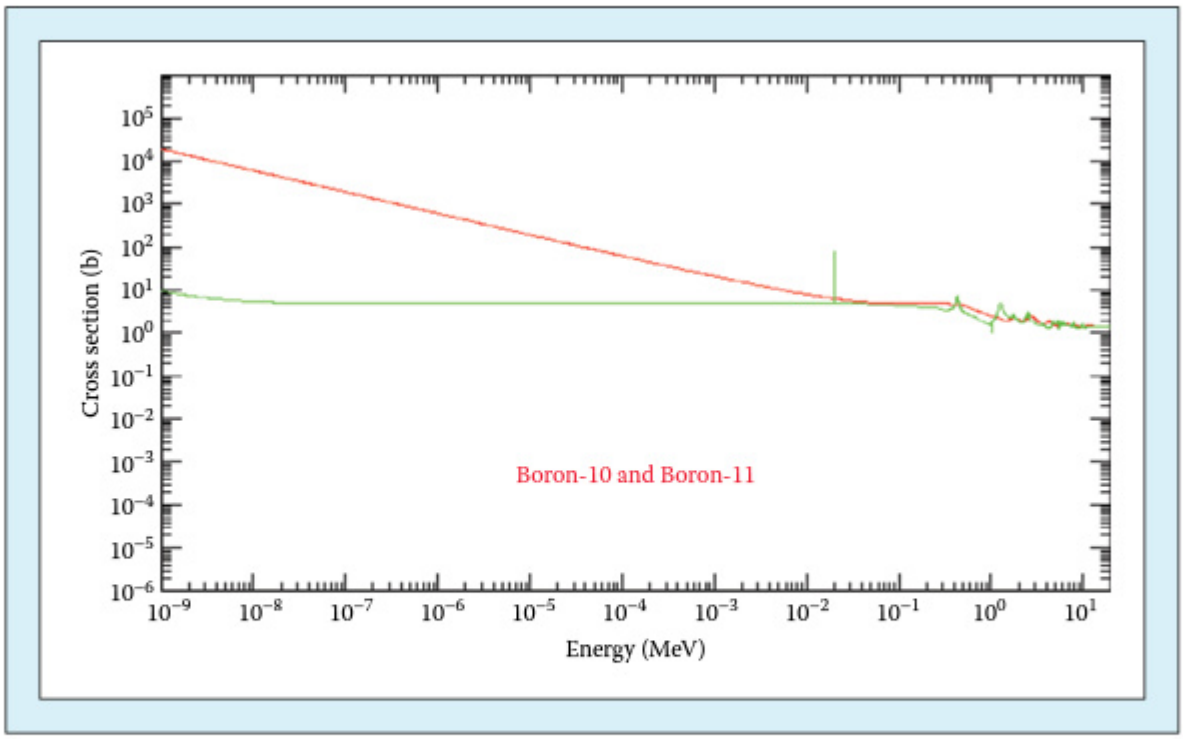

FIGURE 20.8 Absorption cross sections for Boron-10 are shown in red and the absorption cross sections for Boron-11 in green. Boron-10 is the main ingredient that is dissolved into the coolant of a PWR to help control the power level. (Picture generated by ENDFPLOT.)

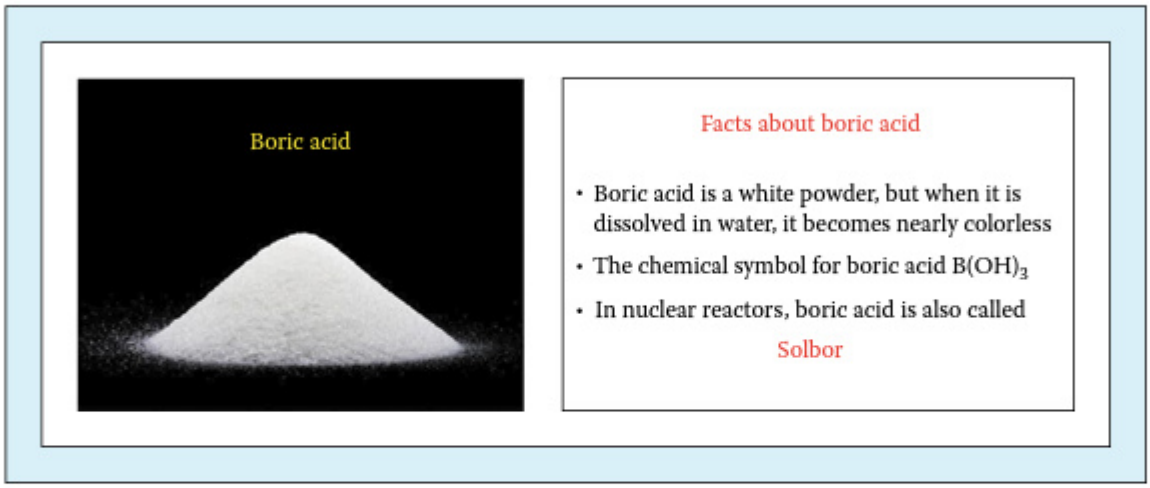
Boric acid
Facts about boric acid
• Boric acid is a white powder, but when it is dissolved in water, it becomes nearly colorless
• The chemical symbol for boric acid $B(OH)_3$
• In nuclear reactors, boric acid is also called
Solbor

FIGURE 20.9 Some facts about boric acid and a picture of boric acid in solid form.

up, it is *standard operating procedure* or SOP to maximize the concentration of the boric acid in the coolant to compensate for the excess reactivity that the fresh fuel may have. Then as the fuel is burned, the excess reactivity is reduced, and the concentration C of soluble boron required can be reduced in a direct proportion as well. *Normally, the boric acid concentration in the coolant is limited to about 1500 PPM (parts per million) during start-up because higher concentrations of boric acid cause the coolant to have a positive temperature coefficient.*

If the power level P is constant, the soluble boron concentration will decrease nearly linearly with the burnup of the fuel over time to keep the reactor in a state where it is exactly critical, for example, where the reactivity ρ is very close to zero. The only exception to this rule is when the boric acid concentration must be decreased rather quickly to compensate for the initial buildup of xenon and samarium in the core, which can reduce the reactivity by a couple of dollars by absorbing so many neutrons. However, this behavior will only last for about 2 days when a PWR is operating at full power. After this time, the xenon will build up to its equilibrium concentration, X_∞, and the concentration of soluble boron does not have to be reduced any further to compensate for the reactivity loss caused by the neutron-absorbing potential of the xenon.

A typical cycle for the concentration of boric acid in a PWR is shown in Figure 20.10 as a function of time for a reactor that has been operating at a constant power level P. *Notice that once the xenon and samarium concentrations have built*

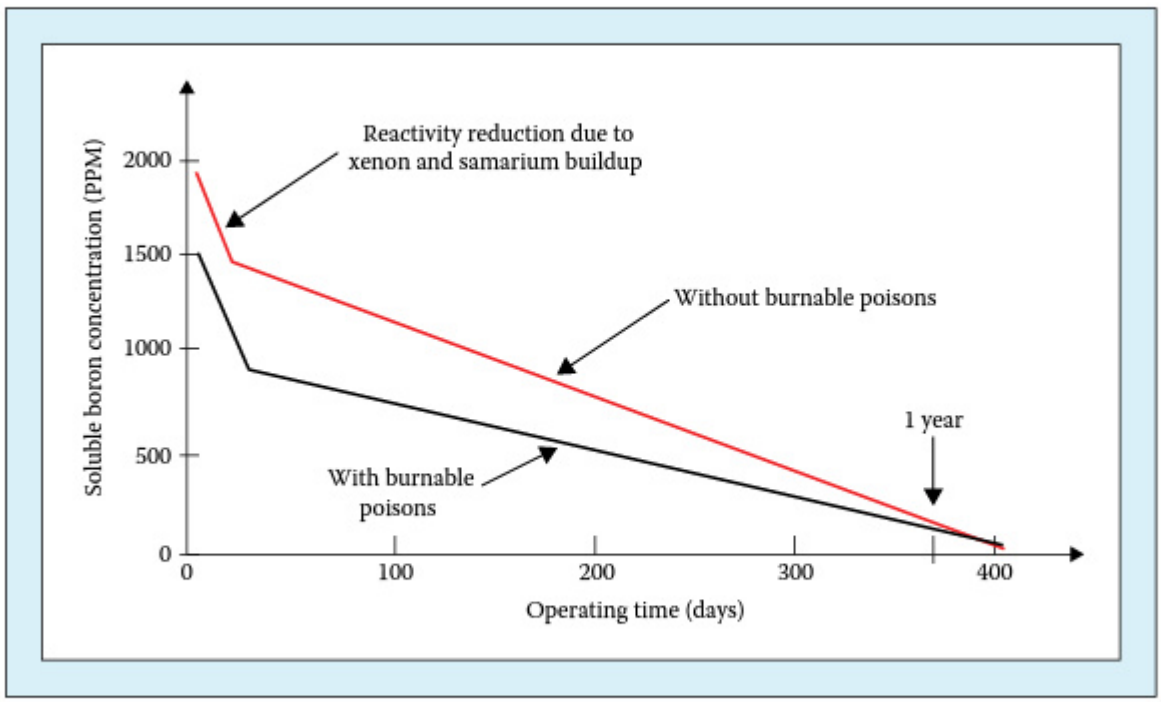

FIGURE 20.10 A typical soluble boron curve for a PWR versus operating time. Start-up occurs at t = 0.

up to their equilibrium values, the boric acid concentration only needs to be changed to compensate for the depletion of the fuel. If the power level is constant, then the burnup of the fuel varies linearly with time, and the boric acid concentration falls inversely with time as well. If the power level is doubled, then twice as much xenon will be produced, and the amount of boron in the coolant must also be cut in half in the first 48 hours to compensate for the large number of neutrons that the xenon absorbs. Eventually, as things return to normal, the soluble boron concentration again follows a long-term linear trend.

Figure 20.10 is based on a refueling period of slightly more than 1 year (365 + 30 ~ 400 days). At this point in time, the reactor can no longer be kept critical by simply diluting the boron alone, and the fuel rods have to be replaced. Then this cycle is repeated over again—but in this case, with a fresh supply of boric acid and some newly enriched uranium fuel. The entire process is repeated over and over again for the entire lifetime of the core, which in today's environment, can be anywhere between 30 and 50 years. In many power reactors, the time between subsequent refuelings has been increased to between 500 and 700 days (18–24 months), but the soluble boron concentration will still follow the same overall trend.

20.7 Burnable Poisons within a Fuel Assembly

Burnable poisons can also be used to flatten the radial power distribution within an individual fuel assembly. This can be done by varying the enrichment of the fuel rods and introducing burnable poisons where needed, as shown in Figure 20.11. *Burnable poisons are materials introduced directly into reactor fuel assemblies to help prevent power peaks when the fuel is fresh and to reduce the number of control rods needed to maintain the system in a critical state while the fuel is burned*. Thus, any increase in the reactivity that might occur while the poison is burning will be compensated for by a nearly identical decrease in the reactivity while the fuel is burned and other fission products start to accumulate. *A burnable poison can be thought of as a "poor man's" control rod.* In fact, the amount of reactivity contained in all of the burnable poisons in a thermal water reactor is nearly comparable to the reactivity contained in all of the control rods.

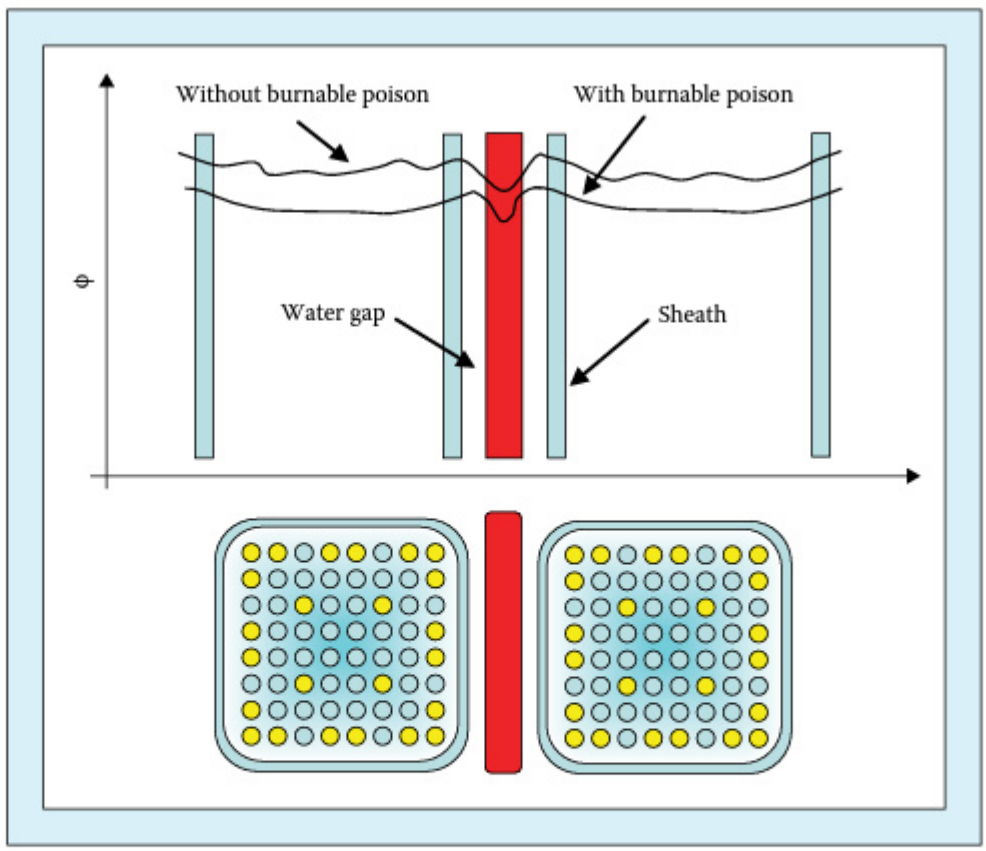

FIGURE 20.11 Burnable poisons and their effect on the thermal flux shape in two BWR fuel assemblies on each side of a control rod. Here the yellow rods have burnable poisons imbedded in them.

However, a burnable poison is generally mixed directly into the fuel, and hence cannot be moved, while a more expensive control rod (by design) can always be moved up and down. The formal definition of a burnable poison is

Definition of a Burnable Poison

"A *burnable poison* is a material with a large absorption cross section that can absorb a thermal neutron and can then become a material with a much smaller cross section after the neutron is absorbed."

In fact, the U.S. NRC uses this definition to determine what a burnable poison is and what it is not. As this definition implies, the neutron poison is eventually "burned away," and when this happens, a fuel assembly behaves as if no burnable poisons are present.

20.8 Burnable Poisons within a Reactor as a Whole

In large PWRs, the control rods contain about $11 of negative reactivity while the burnable poisons typically contain $12 to $14 worth. Similarly, in a BWR, the control rods contain about $25 of negative reactivity, while the burnable poisons contain about $18 worth. This difference in the worth of the control rods is due primarily to the fact that PWRs have an additional chemical shim system, while BWRs do not. Burnable poisons have become very popular over the years because of advances in materials technology and because they can help to reduce the cost of building or operating a nuclear power plant. Since control rods and their drive mechanisms are very expensive to build, the cost of building a reactor can be reduced significantly by simply replacing the movable control rods and their drive mechanisms by stationary fuel rods containing burnable poisons. For a nuclear plant that costs 5 billion to 10 billion dollars, this can save the owner between 20 and 30 million dollars a year in operating costs.

Gadolinium and *boron* are the most commonly used burnable poisons today. Boron can be combined with a variety of metals, stainless steel, and even *Pyrex glass* to create a fuel rod filled with a burnable poison. Gadolinium can also be mixed directly with uranium oxide (UO_2) in the form of *gadolinia* (Gd_2O_3) to perform a similar function. In addition, either material can be distributed radially or axially in a number of predefined zones to control both the radial and axial burnup. This promotes a more uniform burnup of the fuel in both directions. Other advances in nuclear materials and control systems may result in an even more widespread use of burnable poisons in reactor fuel assemblies in the future. Figure 20.12 shows how adding burnable poisons to a PWR can affect the amount of chemical shim needed to keep a reactor critical over a period of about 1 year.

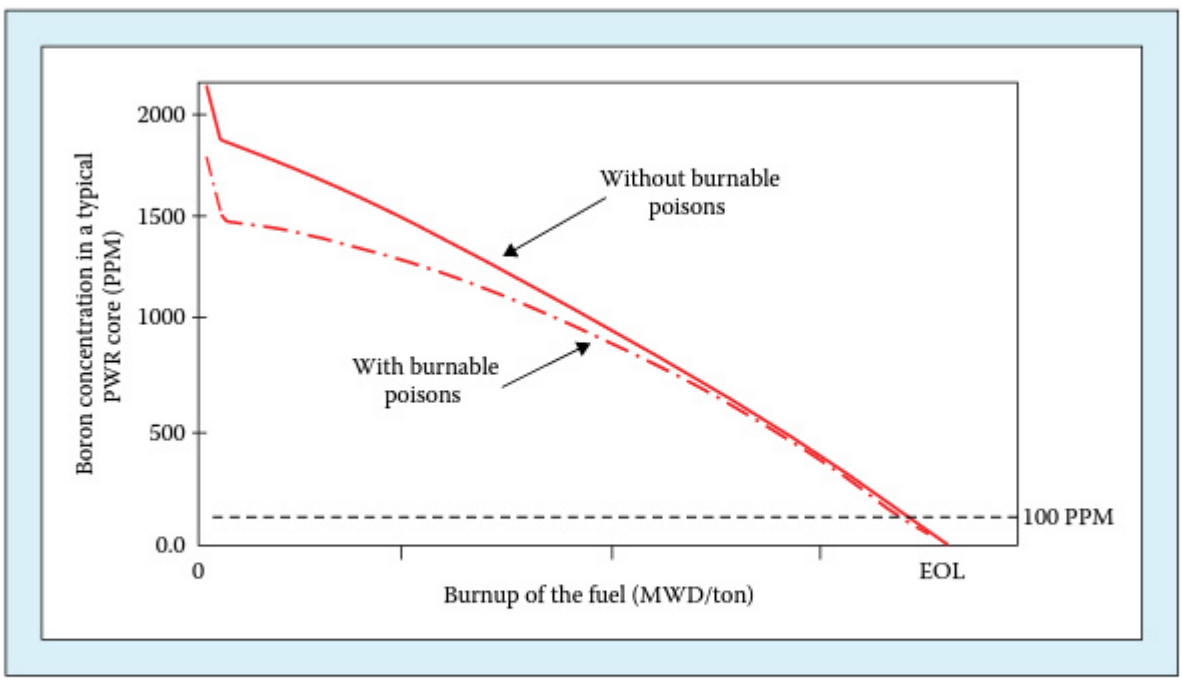

FIGURE 20.12 The soluble boron concentration in a typical PWR core with and without burnable poisons.

Student Exercise 20.1

Suppose that we take three different types of fuel assemblies—one with an enrichment of 4%, one with an enrichment of 3%, and one with an enrichment of 2%. If the neutron flux in all of these fuel assemblies is exactly the same

1. What is the peak to average power ratio when they are initially loaded into the core?
2. What is the peak to average power ratio when on average, they are 50% burned? Be prepared to give a reason for your answer.

20.9 Effect of Burnable Poisons on the Neutron Flux Shape

Since burnable poisons are designed to "burn" over a predefined period of time, the flux shape in the vicinity of a burnable poison will also change as the fuel is burned. When a fresh fuel assembly is loaded into the core, the fuel rods that contain the burnable poisons will appear to be "gray" and sometimes even black surfaces to the thermal neutrons in their vicinity. The thermal neutrons that fall into these fuel rods will rarely be able to escape from them. This will cause the thermal flux in the vicinity of the rods that contain the burnable poisons to appear to *lower* than the thermal flux in the fuel assembly as a whole.

Because the burnable poisons that are mixed together with the fuel are such strong neutron absorbers, this effect can extend several mean free paths beyond the surface of the fuel rod itself (usually a few cm). In other words, the spatial depression of the thermal flux in the vicinity of the rods that contain the burnable poisons is highly localized, just as it is in the vicinity of a control rod. The only difference between a fuel rod that contains a burnable poison and a control rod is that the fuel rod undergoes several shifts in the shape of the neutron flux as the poison is burned, while in the case of a control rod, it does not. This effect is shown in Figure 20.13 where the effects of the burn-off of the poison can be clearly seen. Notice that when the poison is completely burned, the shape of the neutron flux in the vicinity of the fuel rod reverts back to its normal shape. However, the flux in the vicinity of the control rod does not. The strength of a burnable poison can also be adjusted by modifying its concentration throughout the rod. In a normal fuel assembly, this will tend to suppress the local power peaks that develop as the fuel is burned. Eventually, when all of the poison has burned away, the shape of the flux will return to its normal shape.

This effect can be predicted analytically by solving the neutron diffusion equation in a simple homogeneous cylinder or slab surrounded by a neutron-moderating material on each side. However, a macroscopic absorption cross section Σ_{bp} must be added to the diffusion equation for the fuel to represent the time-dependent concentration of the burnable poison in the rod. Then as the fuel is burned, the concentration of the poison is reduced. Only in this case, the boundary condition that must be enforced at the center of the moderator is that the neutron current $\mathbf{J}$ at this point in the lattice must be 0. Of course, this is equivalent to assuming that no neutrons leak out of the unit cell that contains the burnable poison.

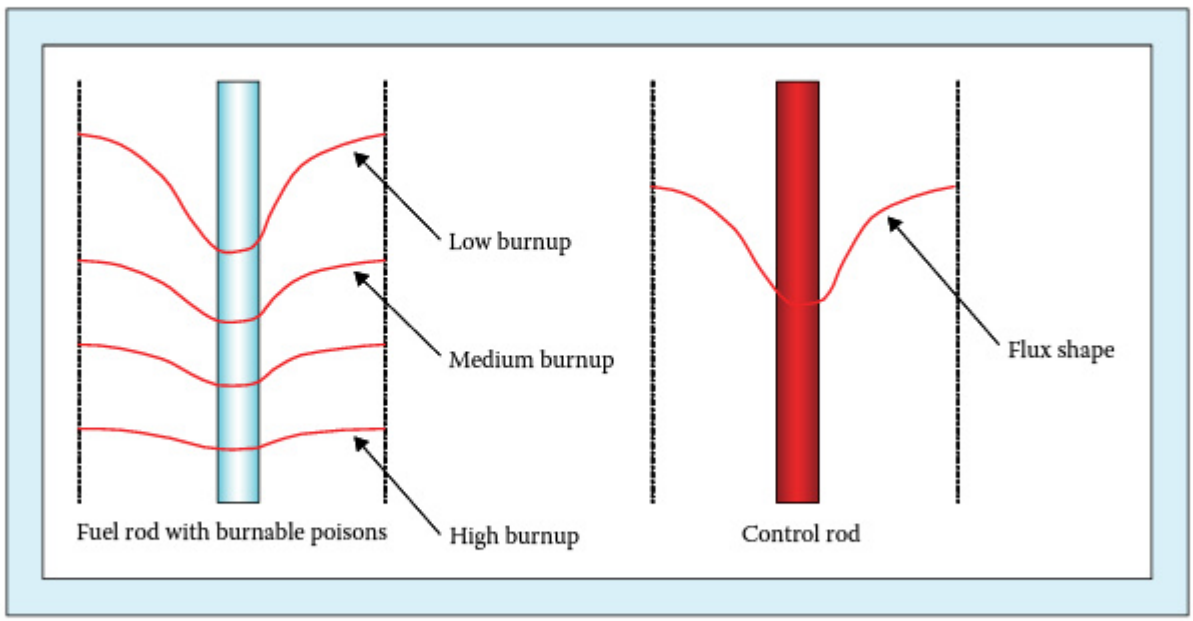

FIGURE 20.13 The flux shape in the vicinity of a fuel rod that contains a burnable poison versus a control rod of the same size.

The interested reader may wish to consult Chapter 14 to see how the solutions to the neutron diffusion equation can be modified to account for the presence of these poisons in a fuel rod. *Emergency shutdowns* are not very common, and they normally occur once every 10 or 20 years. *Planned shutdowns* occur much more frequently, and they are normally scheduled to occur when the core needs to be refueled.

20.10 Burnable Poison Locations in a Reactor Core

The number of fuel rods that contain burnable poisons, as well as the location of these rods, is a function of the design of the core. *In a fresh core, burnable poisons are normally inserted into the fuel assemblies that have the highest initial enrichment, because this is where the highest radial and axial power peaks can occur*. Figure 20.14 shows the distribution of burnable poisons in a typical PWR core. Notice that about *50% of the fuel assemblies contain burnable poisons*, and different fuel assemblies can have different numbers of burnable poison rods. Holistically speaking, burnable poisons are designed to act *locally* while the boric acid in the coolant is designed to act *globally*. In a fresh core, burnable poisons are added to the fuel rods to keep the temperature coefficient of the reactivity negative (see Chapter 17) and to reduce the size of the radial and axial power peaks. As the fuel is burned and the core becomes older, the power profiles tend to become flatter, and most of the time, this is determined by the fuel management scheme. At the end of a burnup cycle, the power profile is normally more uniform than when the core is fresh.

20.11 Using Soluble Boron (or Solbor) as a Reactor Control System

Earlier in the chapter, we mentioned that Boron-10 is used to control the reactivity swing of the core. It can be put in fuel rods and control rods to suppress local power peaks, and it can also be dissolved in the coolant to create what is known as *boric acid* or (H_3BO_3). Sometimes this form of boric acid is also called *Solbor*. In PWRs, the purpose of Solbor is to

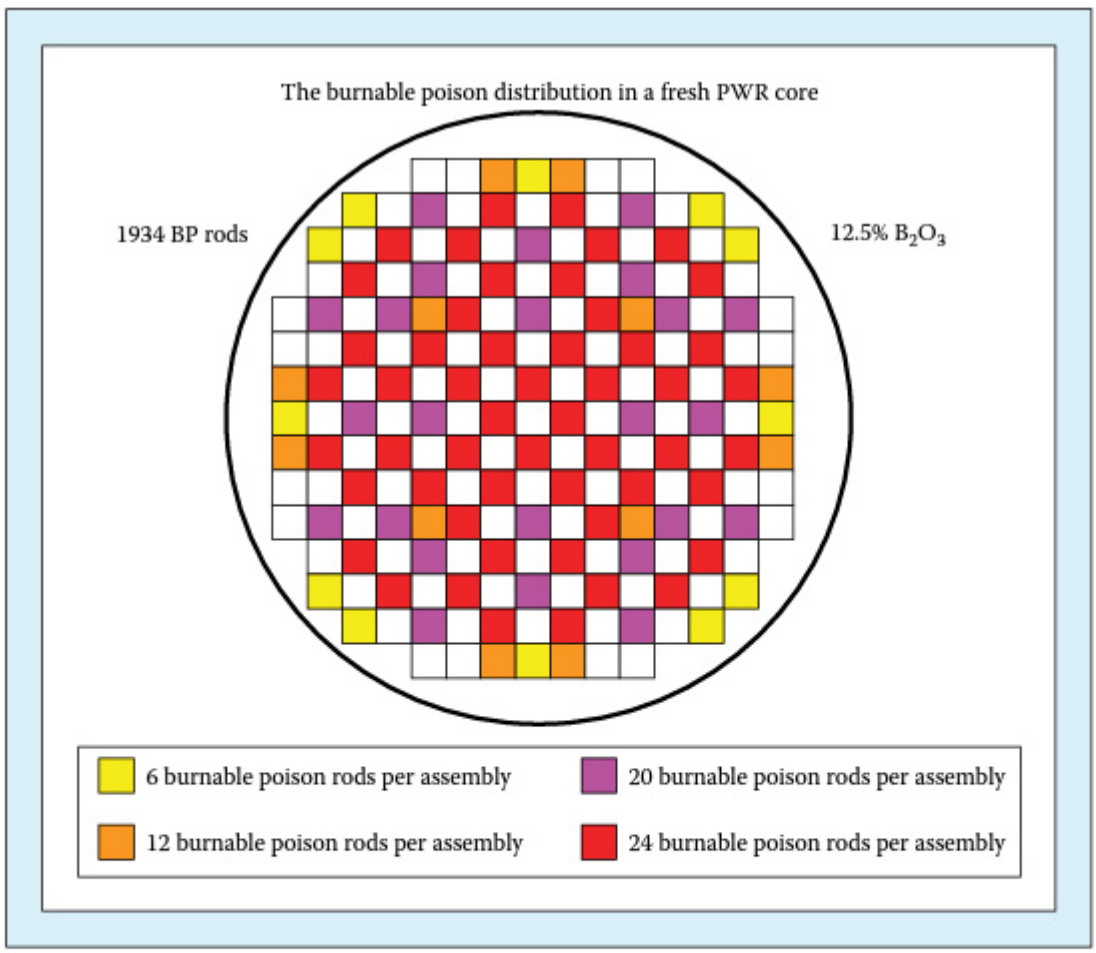
The burnable poison distribution in a fresh PWR core
1934 BP rods
12.5% B_2O_3
6 burnable poison rods per assembly
20 burnable poison rods per assembly
12 burnable poison rods per assembly
24 burnable poison rods per assembly

FIGURE 20.14 The burnable poison loading pattern for a fresh PWR core. (Data provided by the Westinghouse Nuclear Corporation.)

absorb excess neutrons and reduce the reactivity without affecting the global power profile. The concentration of boron in the coolant is usually measured in *parts per million, or PPM*. Solbor cannot be used to control the reactivity over very short periods of time because its concentration cannot be changed quickly enough to meet certain regulatory requirements. Thus control rods are used to change the reactivity quickly, while soluble boron is used to change it over much longer periods of time.

Thus soluble boron is very good at complementing the function of the control rods, but it should never be viewed as a practical replacement for them. *Finally, there are several reasons why soluble boron is so widely used in PWRs today.* First, it can be used to keep the reactor critical during xenon transients that occur over several hours or several days. It can also be used to keep a reactor critical over longer periods of time by compensating for the burnup of the fuel (see Table 20.2). Finally, there are a number of economic incentives for using soluble boron as a form of reactivity control. First, soluble boron *can substantially reduce the number of control rods that are required to keep a reactor critical*. Since control rods and their motorized drives are very expensive to manufacture, a great deal of money can be saved (usually at least 100 Million dollars per plant) by using soluble boron to control some of the reactivity swing. Secondly, because Solbor is added directly to the coolant, it tends to distribute itself rather *uniformly through the entire core*. This means that many changes in the reactivity can be made without effecting the power distribution itself. This promotes a more uniform burnup of the fuel over time, and from an economic perspective, it allows more power to be extracted from the same amount of fuel. Hence, soluble boron makes an average PWR more economical to operate by reducing the long-term cost of electric power (see Chapter 10 of our companion book to understand the economic trade-offs involved*.)

20.12 Reactivity Changes Induced by Control Rods

Moving a control rod out of or into the core causes the reactivity to rise and fall rather quickly. This change in the reactivity is almost instantaneous, and it also affects what is known as the *reactor period* (see Chapter 16). The extent to which the reactor period is affected depends on how good the control rod is at absorbing neutrons in its immediate vicinity. Ordinarily, a single control rod does not possess enough reactivity to change the core power level quickly, except in a TRIGA reactor, where large power pulses are sometimes used to test new nuclear fuel (see Chapter 17). *In commercial BWRs, about $25 of negative reactivity is contained in the control rods*. This negative reactivity is normally used to offset the positive reactivity of the fuel rods. In PWRs, the amount of negative reactivity in the control rods is lower because the

TABLE 20.2
Boron and Boric Acid Concentrations in a PWR (in PPM) and Their Overall Effect on the Reactivity for Various Values of the Thermal Utilization Factor

Boron Concentration (PPM)	Boric Acid Concentration (PPM)	Negative Reactivity ($\Delta\rho$, f = 0.95)	Negative Reactivity ($\Delta\rho$, f = 0.90)	Negative Reactivity ($\Delta\rho$, f = 0.85)	Negative Reactivity ($\Delta\rho$, f = 0.80)
2000	11,400	$30.00	$60.00	$90.00	$128.00
1800	10,260	$26.92	$53.85	$80.78	$107.70
1600	9,129	$28.00	$48.00	$72.00	$96.00
1400	7,980	$28.00	$42.00	$63.00	$84.00
1200	6,840	$28.00	$36.00	$54.00	$72.00
1000	5,700	$15.00	$30.00	$45.00	$60.00
800	4,560	$12.00	$28.00	$36.00	$48.00
600	3,420	$9.00	$28.00	$28.00	$36.00
400	2,280	$6.00	$12.00	$28.00	$28.00
200	1,140	$3.00	$6.00	$9.00	$12.00
0	0	0	0	0	0

* See *Nuclear Engineering Fundamentals: A Practical Perspective*, by R.E. Masterson, CRC Press (2017).

TABLE 20.3
Control System Comparisons for Typical PWRs and BWRs

Control System Type	Typical Value in a BWR ($)	Percent of Total Core-Wide Reactivity (%)	Typical Value in a PWR ($)	Percent of Total Core-Wide Reactivity (%)
Control rods	25	~56	11	~22
Chemical shim	0	0	25	~51
Burnable poisons	18–19	~44	13	~27
Total of the above	**43–44**	**100**	**49**	**100**

Solbor in the coolant can absorb significant numbers of thermal neutrons as well. *In general, it is not uncommon for the control rods in a PWR to contain about $11 worth of reactivity and for the Solbor (or chemical shim) to contain about $25 worth. Burnable poisons then account for about $13 of negative reactivity in a PWR and about $18 of negative reactivity in a BWR.* Normally, the negative reactivity associated with the Solbor is reduced by about $5 to compensate for the buildup of xenon and samarium as the fuel is burned. *So in aggregate, a PWR will contain about $50 of negative reactivity in its control systems, and in a BWR, this number will be about $44.* The reader should keep in mind that these numbers *do not include any negative reactivity that is due to an increase in the temperature of the core.* The reactivity breakdown for a typical PWR and BWR is shown in Table 20.3. The reader should feel free to refer to this table when we explore the intricacies of reactor control systems in our companion book.

20.13 Reactivity Changes Induced by Chemical Shim

Boric acid affects the reactivity of a PWR just like fission product poisons do. However, because it is distributed more or less uniformly through the core, it affects the criticality primarily by affecting the thermal utilization of the fuel. The remaining factors in the six-factor formula are hardly affected by the boric acid concentration. Consequently, we can use almost exactly the same logic we used to calculate the fission product reactivity change to calculate the reactivity change associated with the Solbor. When boron is added to the coolant, it immediately begins to absorb neutrons. This reduces the effective multiplication factor of the core, since more neutrons are absorbed by the boron, and fewer neutrons are absorbed by the fuel. The key to successfully operating a PWR over long periods of time is to reduce the concentration of the soluble boron in the coolant so that it exactly compensates for the increased negative reactivity of the fuel. This means that when the effective multiplication factor is defined by

$$K_{effective} = P_{FNL}P_{TNL}K_{\infty} = P_{FNL}P_{TNL}\left(\eta\varepsilon f p\right) \tag{20.3}$$

where f is the thermal utilization of the core before the boron has been added, then the value of $K_{effective}$ after the boron has been added is given by

$$K'_{effective} = P_{FNL}P_{TNL}K'_{\infty} = P_{FNL}P_{TNL}\left(\eta\varepsilon f' p\right) \tag{20.4}$$

where f′ is the thermal utilization with the soluble boron present in the coolant. To a first approximation, this implies that we can write the reactivity contribution of the boric acid to a previously critical reactor as

Reactivity Contribution of the Boric Acid in a Previously Critical Reactor

$$\Delta\rho = \frac{\left(K'_{effective} - K_{effective}\right)}{K'_{effective}}$$

or

$$\Delta\rho = \frac{\left(f' - f\right)}{f'} \tag{20.5}$$

since all of the other terms cancel. Here, f is the *thermal utilization* with a boric acid concentration C of 0 PPM (i.e., with no soluble boron dissolved in the coolant), and f′ *is* the thermal utilization with a boric acid concentration C > 0. In the absence of the boric acid, the thermal utilization is

$$f = \frac{\Sigma_{aF}}{\left(\Sigma_{aF} + \Sigma_{aM}\right)} \tag{20.6}$$

and after the boric acid has been added to the coolant, the thermal utilization becomes

$$f' = \frac{\Sigma_{aF}}{\left(\Sigma_{aF} + \Sigma_{aM} + +\Sigma_{aB}\right)} \tag{20.7}$$

If we substitute these values into Equation 20.5, we find that the reactivity change due to the soluble boron alone is

Reactivity Change due to Solbor

$$\Delta\rho = \frac{\left(f' - f\right)}{f'} = -\frac{\Sigma_{aB}}{\left(\Sigma_{aF} + \Sigma_{aM}\right)} \tag{20.8}$$

where Σ_{aF}, Σ_{aM}, and Σ_{aB} are macroscopic absorption cross sections of the fuel, the moderator, and the soluble boron, respectively.

20.14 Correlating the Reactivity Change to the Chemical Shim Concentration

It can be easily shown from Equation 20.6 that $f/(1 - f) = \Sigma_{aF}/\Sigma_{aM}$, so if we divide both the numerator and the denominator of Equation 20.8 by Σ_{aM}, we can create an expression for $\Delta\rho$ that depends on only the ratio of Σ_{aB} to Σ_{aM}. The result is

Reactivity Change and the Thermal Utilization

$$\Delta\rho = R\left(f - 1\right) \tag{20.9}$$

where $R = \Sigma_{aB}/\Sigma_{aM}$. Equation 20.9 can be used by the control system to keep a PWR critical when soluble boron is the primary means of reactivity control. Note that the reactivity is reduced when the soluble boron is present because the value of the thermal utilization (f) in Equation 20.9 is always less than 1.0. (Typically the thermal utilization has a value between 0.8 and 0.9). We just need to know the thermal utilization of the fuel before the boric acid is added to the coolant and then what the boric acid concentration C is in PPM for a given value of R. We can then infer the relationship between C and R in the following way.

Boric acid consists of 3 atoms of hydrogen with an atomic weight of 1, 3 atoms of oxygen with an atomic weight of 16, and 1 atom of boron with an atomic weight of 10.8. Therefore, boric acid has a total atomic weight of 3 + 48 + 10.8 = 61.8 AMU. Water, on the other hand, consists of two atoms of hydrogen and one atom of oxygen. Therefore, a water molecule has an atomic weight of 2 + 16 = 18 AMU. In high school chemistry, one learns that a concentration of 1 *part per million (PPM)* is equivalent to one gram of a material being dissolved in one million grams of water. If C is the concentration of H_3BO_3 in PPM, then the ratio of the mass of the boric acid to the mass of the water is

$$\frac{M_{H_3BO_3}}{M_{H_2O}} = \frac{61.8}{18} = 3.43$$

And if the concentration of boric acid is one part per million by weight, then there can be only 1/3.43 = 0.29 atoms of boron per million atoms of water at a concentration of 1 part per million of H_3BO_3. This means that the ratio of the number of atoms of boron to the number of atoms of water is

$$\frac{N_B}{N_{H_2O}} = 0.29 \times C \times 10^{-6}$$

Water has an average thermal absorption cross section of 0.65 barns, and boron has an average thermal absorption cross section of 760 barns. So, the ratio of their macroscopic cross sections is

$$R = \frac{\Sigma_{aB}}{\Sigma_{aM}} = \frac{\Sigma_{aB}}{\Sigma_{aH_2O}} = \frac{N_B}{N_{H_2O}} \times \frac{\sigma_{aB}}{\sigma_{aH_2O}} = 0.29 \times C \times 10^{-6} \times \left(\frac{760}{0.65}\right) = 0.00034C$$

Hence, we have shown using only simple chemical equations and atomic weights that the relationship between R and C must be given by

Boric Acid Concentration in PPM

$$R = 0.00034C \tag{20.10}$$

where C is the concentration of dissolved boric acid in PPM. If we were to repeat this same process using only the concentration of dissolved boron instead of the concentration of boric acid we would find that there would be 18/10.8 = 1.67 atoms of boron per each molecule of water. The value of R based on the boron concentration alone would then be

$$R = \frac{\Sigma_{aB}}{\Sigma_{aM}} = \frac{\Sigma_{aB}}{\Sigma_{aH_2O}} = \frac{N_B}{N_{H_2O}} \times \frac{\sigma_{aB}}{\sigma_{aH_2O}} = 1.67 \times C \times 10^{-6} \times \frac{760}{0.65} = 0.00195C$$

or

Boron Concentration in PPM

$$R = 0.00195C \tag{20.11}$$

instead of R = 0.00034C which we previously derived. In other words, we must be careful to quote the concentration of boron in PPM, or the concentration of boric acid in PPM, when we are trying to determine what the equivalent reactivity may be. Each concentration will give a different value for the reactivity when it is applied to the equation

$$\Delta\rho = R(f - 1) \tag{20.12}$$

where for H_3BO_3 in PPM, R = 0.00034C, and for Boron only in PPM, R = 0.00195C. We can now calculate the reactivity change due to the presence of the soluble boron in the coolant regardless of the way in which it is defined. The reactivity change caused by the addition of boron or boric Acid to the coolant is therefore

Reactivity Change as a Function of the Boron-10 and Boric Acid Concentrations

$$\Delta\rho = 0.00195(f - 1) \cdot C$$
$$\text{(for the boron concentration in PPM)}$$
$$\text{and} \tag{20.13}$$
$$\Delta\rho = 0.00034(f - 1) \cdot C$$
$$\text{(for the boric acid concentration in PPM)}$$

Of course, because the thermal utilization f is less than 1.0, the reactivity change will always be a *negative number*. *When a PWR is just being started up, it is standard operating procedure to maximize the concentration of the boric acid in the coolant to compensate for the excess reactivity of the fresh fuel. Then as the fuel burns and begins to become depleted, the excess reactivity is reduced, and the concentration of soluble boron required to keep the reactor critical can be reduced as well.*

If the power level is constant, the soluble boron concentration will decrease approximately linearly with the burnup to keep the reactor critical. The only time this does not occur is when the boric acid concentration must be decreased rather quickly to compensate for the initial buildup of xenon and samarium in the core. The xenon can reduce the reactivity by a couple of dollars by absorbing large numbers of thermal neutrons. However, this behavior will only last for about 2 days

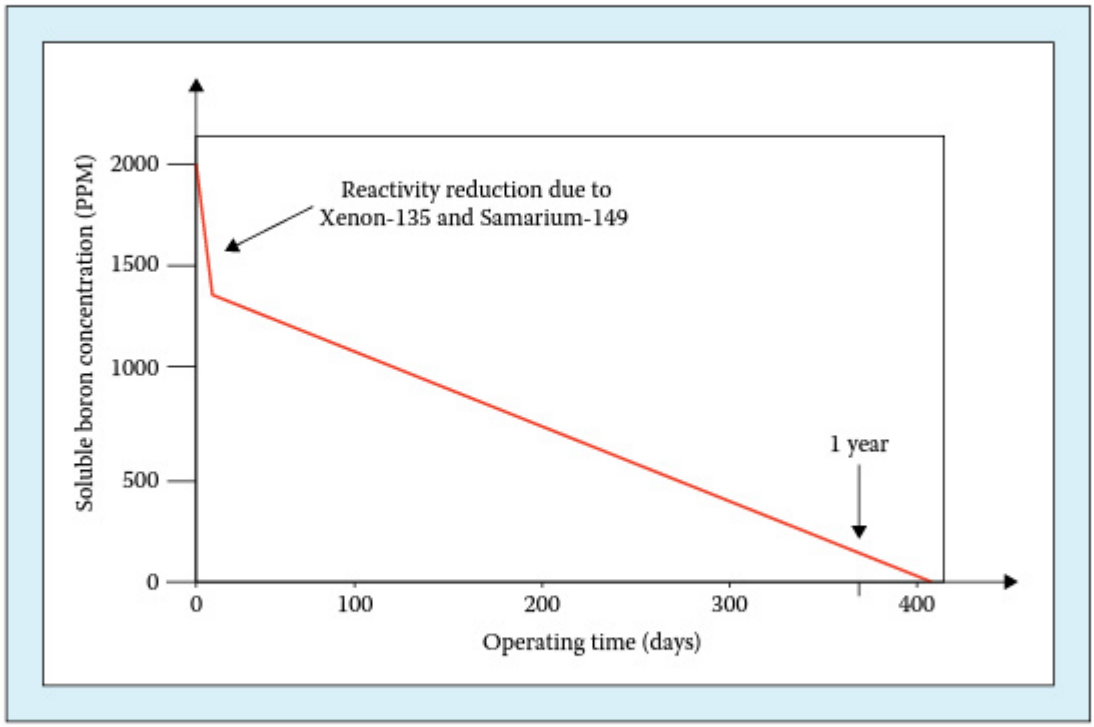

FIGURE 20.15 A typical soluble boron curve for a PWR versus operating time. Start-up occurs at t = 0.

when a PWR is brought up to full power. After that, the xenon will build up to its equilibrium concentration, X_{∞}, and the concentration of soluble boron does not have to be reduced any further to compensate for the Xenon-135 buildup. The boric acid concentration then behaves in the manner shown in Figure 20.15. This figure again assumes that the reactor is operating at a constant power level P.

Notice that once the xenon and samarium have built up to their equilibrium values, the boric acid concentration only needs to be changed to compensate for the depletion of the fuel. If the power level is held constant, then the burnup of the fuel varies linearly with time, and the boric acid concentration is inversely proportional to the burnup. Hence, if the power level is doubled, then twice as much xenon will be produced, and the boron concentration in the coolant must be cut in half in the first two days to compensate for the large number of thermal neutrons that the xenon absorbs. Eventually, as things return to normal, the soluble boron concentration again declines linearly with burnup. Figure 20.15 assumes a refueling period of slightly more than 1 year (365 + 30 ~ 400 days). At end of life (EOL), the reactor can no longer be maintained in a critical state by simply diluting the boron, and the fuel rods have to be replaced. Then after the core is refueled, the soluble boron cycle is repeated again. This entire process is repeated many times over the entire lifetime of the core, which in a commercial nuclear power plant, can be anywhere from 30 to 50 years.

20.15 Converting from PPM to Grams per Liter

When boric acid is first added to the coolant, it is sometimes helpful to convert between its concentration in parts per million (PPM) and the concentration in grams per liter of water (g/L). This can be done using the following conversion factors:

Converting from Grams/Liter to Parts per Million (PPM) in Water

$$1\,\text{g/L} = 1001.142303\,\text{PPM}$$
$$\text{or} \qquad (20.14)$$
$$1\,\text{part per million} = 0.000998\,\text{g/L}$$

Equation 20.14 then shows that when a PWR first starts up, a soluble boron concentration of 2000 PPM is equivalent to a boric acid concentration of 1.996 grams per liter (g/L). Notice that this is less than 1% of the amount of soluble boron

that the coolant can theoretically hold at 100°C, which is about 260 g/L. Thus, dissolving enough boric acid in the coolant to control a PWR is generally not a problem when the reactor is operating normally.

20.16 Boric Acid Injection Systems

Boron is injected into the primary loop through two separate systems called the *Chemical and Volume Control System* (or the *CVCS*) and the *BIT or Boron Injection Tank* system. The CVCS changes the boron concentration rather slowly, and so, it is normally used when the reactivity is to be changed over several minutes or several days. The BIT system acts more quickly to shut a reactor down in the event of an emergency, a *rod ejection accident, or a LOCA.* In commercial PWRs, the boric acid concentration in the CVCS is about 7,000 PPM (7 g/L), and the boric acid concentration in the BIT is about 12,000 PPM (12 g/L). During rod ejection accidents, the BIT injects boron into the coolant immediately, and during very slow transients, the CVCS regulates its concentration differently. In addition, its concentration must be carefully controlled during start-up with a cold, clean core (see Chapter 17) because *the moderator temperature coefficient can become positive* when the boric acid concentration exceeds 2000 PPM. To keep the temperature coefficient negative when the fuel rods are fresh, burnable poisons are sometimes added to the fuel. This ensures that the core remains stable even at start-up when all of the fuel is fresh.

Without these additional burnable poisons, a boric acid concentration of about 1700 PPM would create a positive moderator temperature coefficient of about +12.5 pcm/°C. This would mean that an increase in the moderator temperature of just 8°C would increase the reactivity of the core by one milli-rho or 0.001. This would correspond to a reactivity increase of about 15.4 cents in a U-235-fueled reactor for each 8°C. Consequently, although boric acid is very effective at controlling the long-term reactivity of the core, it must be supplemented by adding burnable poisons to the fuel at beginning of life (BOL) to keep the temperature coefficient negative. Then after the fuel has been burned for a while, this problem disappears because the fission products force the reactivity of the core to become more negative. Additional information on how the boric acid concentration is controlled by the CVCS can be found at the following URL:

http://www4.ncsu.edu/~doster/NE405/Manuals/PWR_Manual.pdf.

In most PWRs, a related system called the *Boron Thermal Regeneration System* (or the *BTRS* for short) is used in conjunction with the CVCS to alter the boric acid concentration during daily power changes and load following events. These changes occur automatically through a passive ion-exchange system that is designed to be temperature dependent. Thus, changes in the coolant temperature result in changes to the boric acid concentration in the primary loop, and human intervention is usually not required to keep the concentration at acceptable levels. Now, we would like to discuss how the control rods fit into this picture.

Example Problem 20.3

In the middle of a burnup cycle, a PWR fueled with U-235 has \$10 of excess reactivity remaining in the core. If the thermal utilization of the fuel is 80%, what must the boric acid concentration be in PPM to keep the reactor critical?

Solution A U-235-fueled PWR with \$10 worth reactivity must have an absolute reactivity of $10 \times 0.0065 = 0.065$. The boric acid concentration required to achieve this reactivity reduction is given by Equation 20.13. From Equation 20.13, $\Delta\rho = 0.00034(1 - f) \cdot C$ when the boric acid concentration C is measured in PPM. Solving for C with a value of $f = 0.80$ gives $C = \Delta\rho/0.00034(1 - f) = 0.065/0.000068 = 956$ PPM. [Ans.]*

20.17 Comparing PWR and BWR Control Rods

For several reasons, BWRs and PWRs have chosen different evolutionary paths when it comes to the design of their control rods. During normal operation, the coolant in a BWR is intended to boil in the top half of the core, while the coolant in a PWR is designed to undergo *nucleate boiling* only near the top of the core, and generally in only the hottest channel (see Chapter 13 of our companion book†). Consequently, the coolant exiting a BWR must employ a *steam dryer* to remove the excess moisture at the top of the pressure vessel head, and because of space limitations, the steam dryer makes it difficult to mechanically insert the control rods into the core from above.

* As a point of reference, the solubility of boric acid (H_3BO_3) in light water is about 63.5 g/L at room temperature (~30°C) and about four times greater (~267 g/L) at 100°C.

† See *Nuclear Engineering Fundamentals: A Practical Perspective*, by R.E. Masterson, CRC Press (2017).

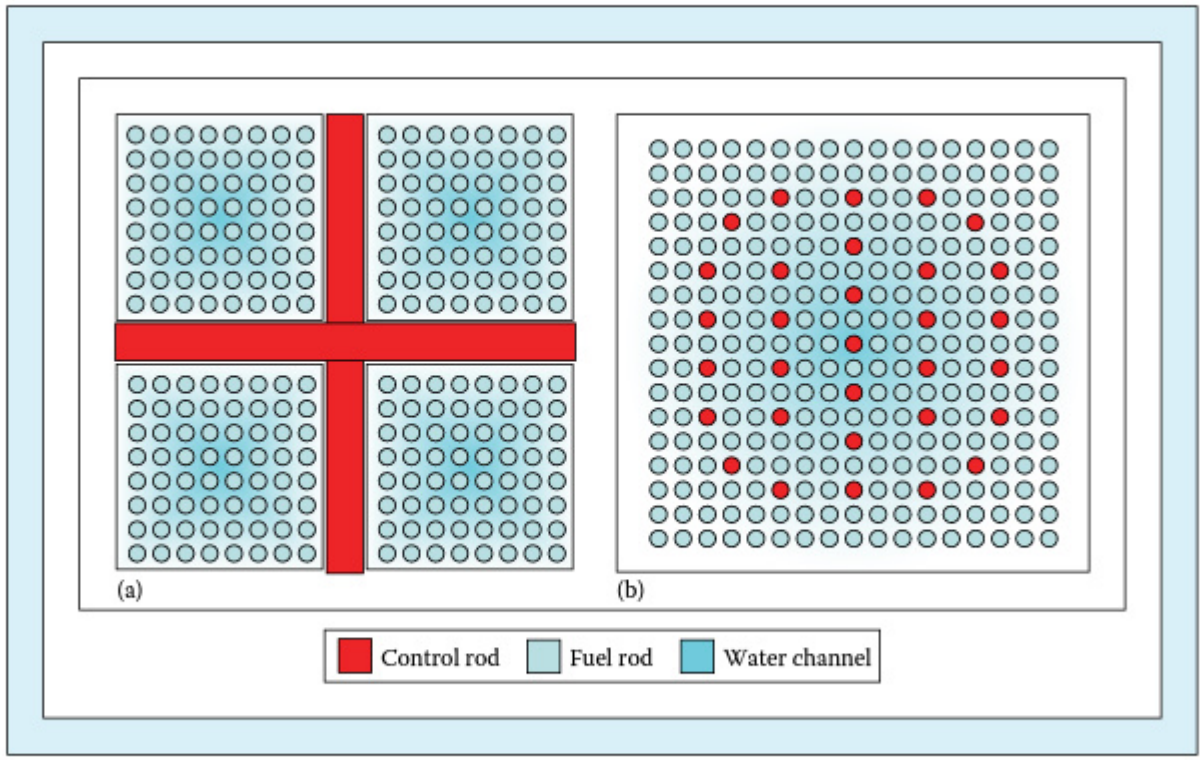

FIGURE 20.16 The fuel assemblies and control rods in a BWR (a) and in a PWR (b) directly compared to each other.

For this reason, *BWRs have adopted a design where the control rods are inserted into the core from below, while in PWRs, the control rods are inserted into the core from above*. Moreover, because the control rods are inserted into the core in opposite directions, the shapes of the control rods are very different in these two designs. For example, *PWRs use finger-shaped control rods* that are similar to the fuel rods, while BWRs use *cruciform control rods*, which are much larger and more rigid. Both designs are compared and contrasted in Figure 20.16. Here, the fuel rods are shown in dark gray or light blue and the control rods are shown in red. Because the control rods in a BWR are many times larger than the control rods in a PWR, they have many times greater worth W per rod. *In general, the average worth per rod is about 20 times greater* (see Section 20.18)

Student Exercise 20.2

Suppose that a PWR contains fresh uranium fuel having a thermal utilization factor f of 0.90. At start-up (clean and cold), the amount of excess reactivity in the system is 30% (0.30). If half of the excess reactivity can be compensated for by inserting the reactor's control rods into the core, what must the initial boric acid concentration be in PPM so that the reactor is exactly critical when it is started up?

20.18 Control Rod Banks and Control Rod Guide Tubes

PWR control rods are guided through the core using stainless steel tubes called *control rod guide tubes*. When there are no control rods present, these guide tubes are normally filled with water, and when the control rods move through the guide tubes, they displace the cooling water as they go. Large PWR cores contain between 50 and 60 clusters of control rods. These clusters are sometimes called *control rod banks*. In general, a control rod bank is used in about 25% of the fuel assemblies in a PWR core. The control rods are further subdivided into (1) *control banks* and (2) *shutdown banks*. The control banks are used for normal day-to-day power shaping, and the shutdown banks are used to shut down the core in the event of an emergency. The number and the location of the control rods in each of these banks can sometimes be different. Figure 20.17 shows the location of these banks in a typical PWR core.

Each cluster of control rods is inserted into the core from above using a *mechanical drive system*. The drive system is attached to the pressure vessel head with a large number of *electromagnets*. In the event a reactor needs to be shut down quickly, the power to the electromagnets is cut by pushing a *scram button* on the control panel (see Figure 20.18), and the rods fall into the core under the force of gravity alone. This is an example of what is called an *emergency reactor*

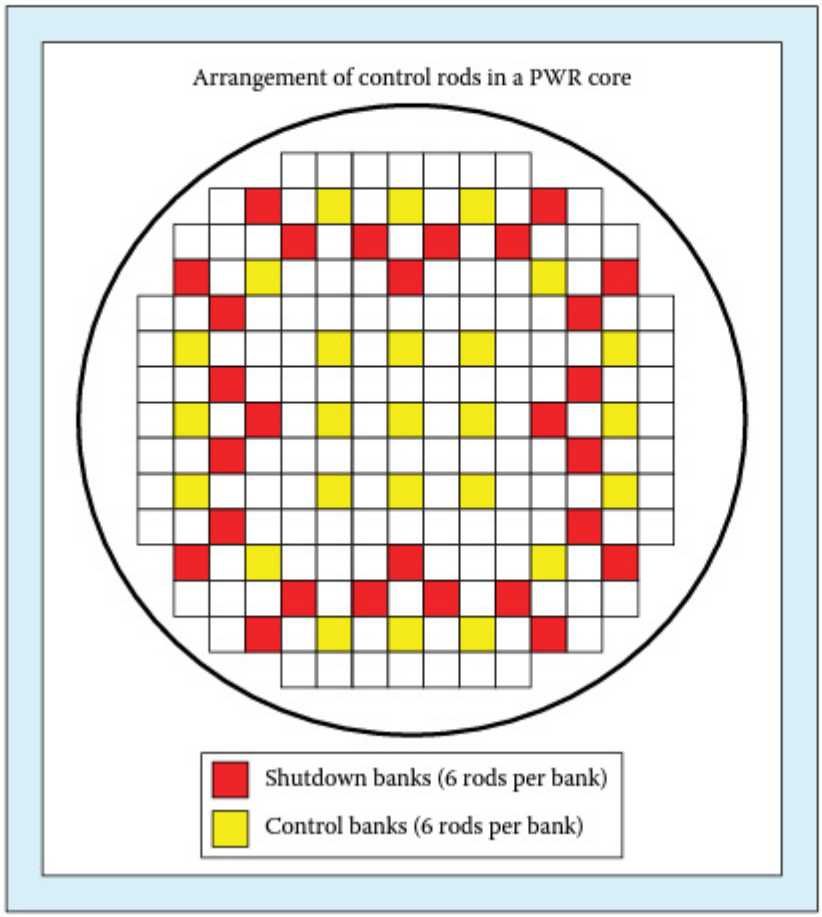

FIGURE 20.17 The location of the control rod banks in the fuel assemblies in a typical PWR core. Normally PWR cores contain control banks and shutdown banks. (Data provided by the Westinghouse Nuclear Corporation.)

shutdown, or "scram." In other words, all an operator has to do to scram a reactor is to "pull the plug" on the electromagnets attached to the control rods. The design of this safety system originated in the 1950s when it was first applied to nuclear submarines. Today it is known as a classic example of a *passive safety system* because once the *scram button* is pushed, the rods fall into the core with no further human intervention. Hence, gravity is used in PWRs as one of the last lines of defense.

Example Problem 20.4

After being operated at full power for several days, the xenon and the samarium in the PWR reach their equilibrium concentrations that correspond to a reduction in the total reactivity of \$3.00. If the PWR is fueled with 3% enriched uranium with a thermal utilization factor of 0.85, by how much must the boric acid concentration be initially reduced (in PPM) to compensate for this reactivity loss due to the buildup of the xenon and the samarium?

Solution If the reactivity falls by \$3, the absolute reactivity must fall by $-3 \times 0.0065 = -0.0195$. The change in the boric acid concentration required to offset this reactivity reduction is given by Equation 20.13. From Equation 20.13, $\Delta\rho = 0.00034(1 - f) \cdot C$ when the boric acid concentration C is measured in PPM. Solving for C with a value of $f = 0.85$ gives $C = \Delta\rho/0.00034(1 - f) = -0.0195/0.00005 \approx -390$ PPM. [Ans.]

BWRs, on the other hand, use a high-pressure hydraulic system to insert the control rods into the core from below. As we mentioned previously, these rods are generally much larger and heavier than their PWR counterparts, *and in most cases, their reactivity is greater as well*. The hydraulic pressure exerted on the rods from below provides the necessary lifting force required. Internally, a cruciform rod consists of either

- A solid neutron-absorbing material in metallic form or
- A hollow chamber into which many hollow tubes filled with B_4C powder are placed

FIGURE 20.18 Three examples of the scram button on a reactor control panel. (a) A picture of SCRAM button from the control room of the USS *Savannah*, which was the world's first nuclear-powered cargo ship. (b) A picture of the scram button at EBR-I (the Experimental Breeder Reactor I). (c) An operator attempting to press the scram button. (These are public domain pictures that can be found on Google Images.)

The design of cruciform rods has evolved over the years, and the materials used in these rods (e.g., *hafnium and iridium*) are considerably different than those used several decades ago. It can be shown that a typical BWR control rod will have a net worth of about 0.2β, or W = 0.0013/0.0065 ≈ 20 cents/rod. A 1000 MWE (3000 MWT) BWR will have about 150 of these rods. This puts the total control rod worth for a large BWR at about $25.00. In comparison, a PWR will have about 40% as many control rods (~60 clusters vs. 150), and their aggregate rod worth will be about $11.00. The rod worth is still about 0.2β, or W = 0.0013/0.0065 ≈ 20 cents/cluster, and in a cluster with 20 rods, *an individual control rod will have an average worth of 20 cents/20 or about 1 cent per rod*. The total rod worth is only about 40% as much in a PWR as it is in a BWR because of the soluble boron. Furthermore, only about ¼ of the fuel assemblies in a PWR actually contain these rods.

20.19 Origin of the Word SCRAM

The word *scram* was invented by the U.S. Nuclear Submarine Program in the early 1950s to warn reactor operators that a reactor had to be shut down immediately, and at the time, the word scram was used as an acronym for a "*safety control*

rod ax man." However, today it has acquired a slightly different meaning, and generally speaking it is used to indicate the *SCRAM* or emergency shutdown of a commercial or military reactor when an abnormal operating event occurs. In commercial power reactors, this emergency shutdown is also called a "*reactor trip*," but the exact usage of this term is not universal, and it also varies from one country to the next.

20.20 Maintaining the Criticality of the Core over Time

In most reactor cores, the amount of fuel decreases monotonically with time if the power level is held the same. If a reactor is intended to operate for a long period of time without being refueled, then additional fuel in excess of what is needed for exact criticality must be added to the reactor before it is started up. The positive reactivity generated by this fuel must be balanced by negative reactivity introduced from other sources. These sources can include movable control rods and burnable poisons, and in the case of PWRs, this neutron-absorbing capacity is further augmented by introducing a strong neutron-absorbing material, or neutron poison into the coolant in the form of *Solbor*.

A cold, clean core always has more fuel than it needs to stay critical. *Thus at start-up, it is not uncommon for a reactor to contain 30% more fuel than it needs to remain in a critical state. Without neutron poisons, the value of $K_{effective}$ in a commercial PWR is about 1.40 at start-up, and the corresponding value of $K_{effective}$ for a BWR at start-up is about 1.33. This corresponds to an excess reactivity at start-up of about \$45.00 for a PWR and about \$38.00 for a BWR*. This excess reactivity is illustrated in Figure 20.19. By design, the positive reactivity produced by the fuel is always balanced by the negative reactivity from the reactor's control rods, or in the case of a PWR, from both the control rods and the boric acid in the coolant. The control rods are inserted into the core just far enough to keep the reactor in a subcritical state until a decision is made to go critical. In BWRs, the control rods are inserted into the core from below, and in PWRs, they are inserted into the core from above (see Figure 20.20).

Once full power operation begins, the control rods are gradually withdrawn to compensate for the buildup of Xenon-135. This process of withdrawing the control rods continues for several hours until it has reached its desired operating state. In PWRs, the boron concentration in the coolant is reduced to achieve a similar effect. Once the reactor has reached steady-state operation, the amount of fuel in the core starts to monotonically decrease with time. *So although a reactor may initially start its life with more fuel than it really needs to stay critical, this excess fuel is what allows it to operate for long periods of time after initial criticality has been achieved*. The amount of fuel that is burned depends on the level of the thermal neutron flux ϕ and the period of time t that the fuel is

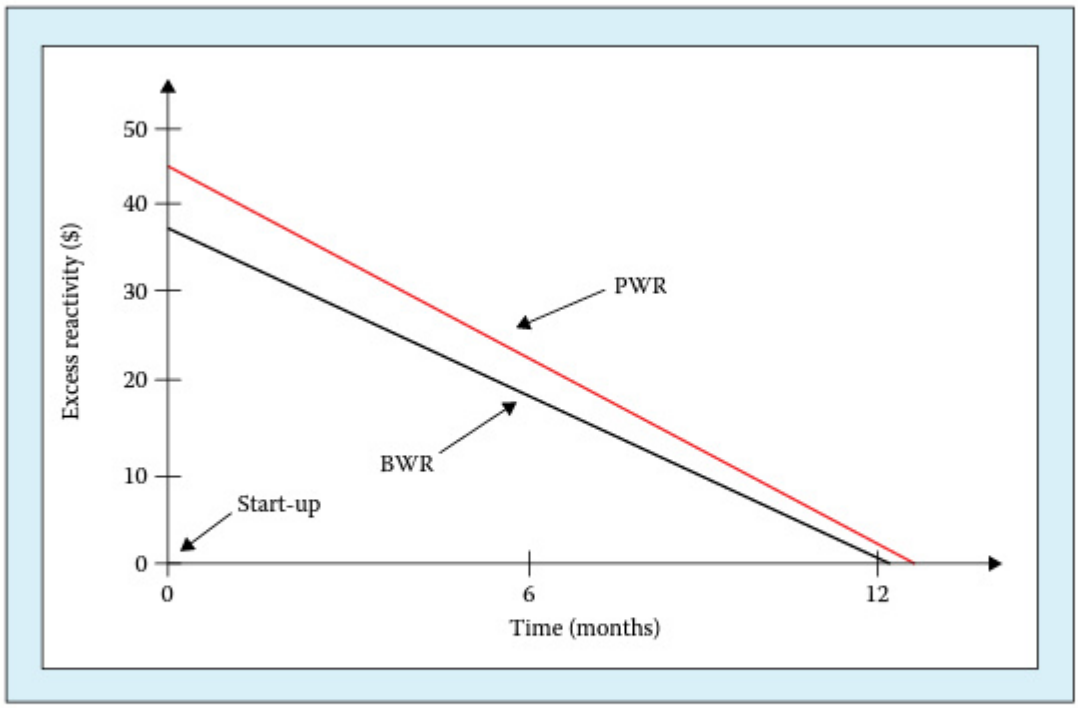

FIGURE 20.19 The excess reactivity due to the fuel alone in a modern PWR and BWR.

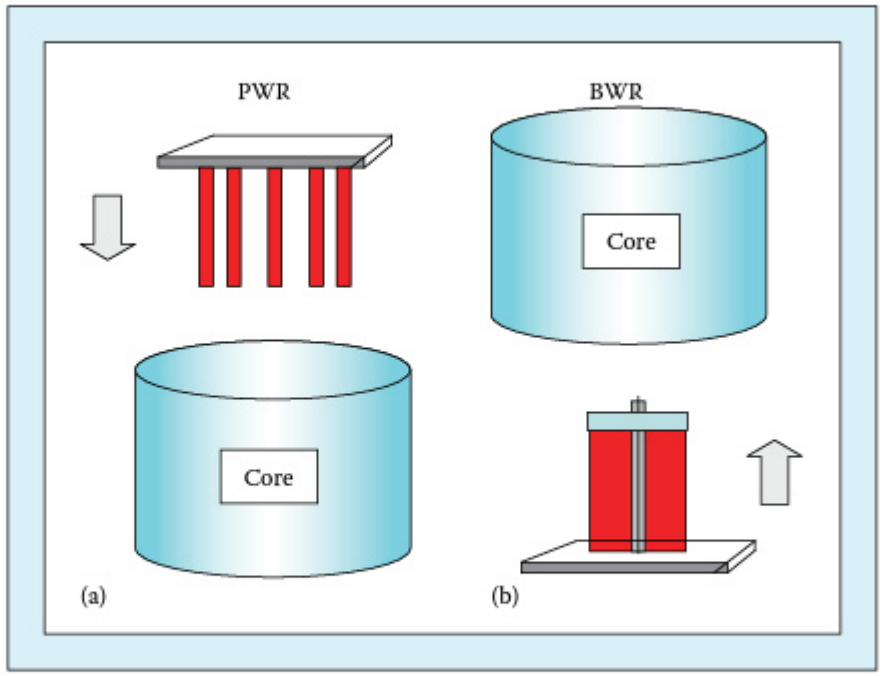

FIGURE 20.20 Control rods are inserted into the core in opposite directions in a PWR (a) and a BWR (b). This has been part of their standard design for about 50 years.

exposed to this flux. For a Uranium-235-fueled reactor, the concentration of the fuel (in atoms/cm^3) is determined by the equation

$$\frac{dU}{dt} = -U\sigma_{au}\phi \tag{20.15}$$

where U is the number of atoms of U-235 per cubic centimeter. The solution to this equation is of course

$$U(t) = U_o e^{-\sigma_{au}\phi t} \tag{20.16}$$

where U_o is the uranium concentration, in atoms/cm^3, at start-up. Some additional plutonium is also generated from the capture of neutrons by Uranium-238, but this is not an important contributor to the power level for a cold, fresh core. Notice that for small to intermediate periods of time (say a year or 2), we can replace the exponential term in Equation 20.16 by

$$e^{-\sigma_{au}\phi t} \approx 1 - \sigma_{au}\phi t \tag{20.17}$$

This is legitimate to do because a *Taylor series expansion* of e^{-x} yields

$$e^{-x} = 1 - x + \frac{x^2}{2!} - \frac{x^3}{3!} + \cdots + \frac{x^n}{n!} \quad -\infty < x < \infty \tag{20.18}$$

Notice that as long as the value of $\sigma_{au}\phi t$ is less than about 0.2, the error introduced by assuming that the burnup is linear is less than 10%. Of course, at higher burnups this approximation becomes less accurate, and the reactivity reduction can no longer be assumed to be a linear function of the burnup. Under these conditions, an exponential reduction in the reactivity must be used.

Student Exercise 20.3

Suppose the boric acid concentration declines at an average rate of about 0.25% per day after the xenon and samarium in the fuel are accounted for. What must the boric acid concentration be 100 days after the xenon and samarium have reached their equilibrium values? Assume that the PWR is operated at a constant power level P during this period of time.

20.21 Defining the Worth of a Control Rod

One way to measure the effect of a control rod on the system-wide reactivity is to define a parameter called the *control rod worth*. The control rod worth W is defined by the U.S. NRC as

Definition of the Control Rod Worth

"The difference between the effective multiplication factor with a control rod completely inserted into the core and the effective multiplication factor with a control rod completely withdrawn from the core divided by the effective multiplication factor with the control rod in the core."

In mathematical terms, this allows us to define the rod worth as

Mathematical Definition of Control Rod Worth

$$W = \frac{\left|\left(K'_{effective} - K_{effective}\right)\right|}{K'_{effective}} \quad \text{or} \quad W = \frac{\Delta K_{effective}}{K'_{effective}} \tag{20.19}$$

where $\Delta K_{effective} = K'_{effective} - K_{effective}$ and $K'_{effective}$ is the effective multiplication factor with the control rod inserted. *In other words, the rod worth is determined by measuring the effective multiplication factor with the control rod completely removed from the core and then measuring the effective multiplication factor again with the control rod completely inserted into the core*. The incremental difference in the value of $K_{effective} = K'_{effective} - K_{effective}$ then provides the value that appears in the numerator of the definition. Note that when the control rod worth is defined in this way, it is always a *positive and dimensionless number* because of the presence of the absolute value symbol || in the numerator of Equation 20.19. When a reactor is operating normally, the value of $K_{effective}$ is very close to 1.0, and so we can assume with little error that

$$W = \frac{\left|\left(K'_{effective} - 1\right)\right|}{K'_{effective}} \tag{20.20}$$

Since this also happens to be the definition of the reactivity, the control rod worth becomes the reactivity change $\Delta\rho_{CR}$ beyond the steady-state reactivity ($\rho = 0$) that occurs when the control rod is withdrawn.

Student Exercise 20.4

A PWR contains 120 control rods. What must the average worth of a control rod be if instead of compensating for 50% of the excess reactivity, the rods must compensate for 40% of the excess reactivity alone, with the remainder being compensated for by changing the concentration of the boric acid?

The effect that a control rod has on the reactivity is by no means a linear function of its axial location z. By this, we mean that the incremental change in the reactivity $\Delta\rho_{CR}(z)$ caused by inserting a control rod into the core depends on how far the rod is inserted, and where the rod insertion process begins. Consider the axial power profile and flux shape shown in Figure 20.21. This flux shape is typical of the cosine flux shape that can be found in most commercial power reactors when the control rods are withdrawn. Once a critical configuration is established, a control rod can be moved in either direction to increase or reduce the power level. If its vertical motion can be decomposed into N individual increments, then the *incremental worth* per increment is defined as

Incremental Rod Worth

$$\Delta\rho_{CR} = \Delta W = \frac{W}{N} \tag{20.21}$$

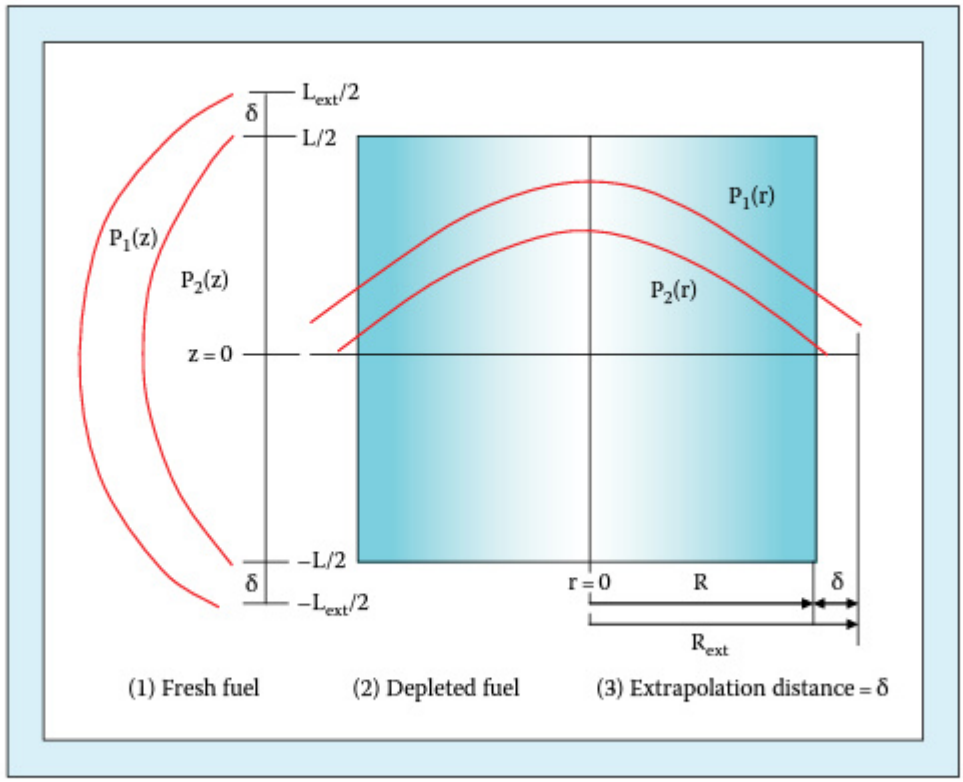

FIGURE 20.21 The cosinusoidal power profile in a bare cylindrical reactor and how it changes as a function of burnup.

where N is the total number of increments that the rod can move. With these equations, we can then determine how the reactor power level P or the reactor period T is affected by the motion of the rod. This process is illustrated in Example Problem 20.5.

Example Problem 20.5

If a control rod bank consists of a cluster of 22 smaller rods, and each of these rods moves in axial increments equal to 1/20th of their total length, how much will changing the axial position by one increment change the total reactivity of the core? Assume the control rod bank has a total worth of 44 cents.

Solution Since the total worth of the rod cluster is 44 cents, moving the cluster by one axial increment will change the total reactivity of the core by 44 cents/20 = 2.2 cents. If there are 22 rods in the cluster, each of the rods in the cluster will have a reactivity of 2.2 cents/22 = 0.1 cents, or 1/10th of a cent. [Ans.]

20.22 Estimating the Effect of a Control Rod on the Reactivity

In thermal water reactors, the effect of a control rod on the reactivity can be determined from the six-factor formula, which we first derived for the reader in Chapter 10. Suppose that $K_{effective}$ is the effective multiplication factor without the control rod in the core and $K'_{effective}$ is the effective multiplication factor with the control rod fully inserted into the core. The change in the reactivity due to the rod alone is then

The Change in the Reactivity of a Control Rod

$$\Delta\rho_{CR} = \frac{\left|\left(K'_{effective} - K_{effective}\right)\right|}{K'_{effective}}$$

or

$$\Delta\rho_{CR} = \frac{\Delta K_{effective}}{K'_{effective}} \qquad (20.22)$$

where $\Delta K_{effective} = K'_{effective} - K_{effective}$ and the effective multiplication factor is defined in the usual way.

$$K_{effective} = P_{FNL}P_{TNL}K_{\infty} = P_{FNL}P_{TNL}(\eta\varepsilon f p) \tag{20.23}$$

Thus *the primary effect of a control rod is to reduce the thermal utilization f of the fuel*. (The other factors in the six-factor formula are essentially unchanged.) If we insert a control rod into the core, the thermal utilization will be lower because there are fewer neutrons for the fuel to absorb. The magnitude of this effect depends on how the rod is designed. If we substitute the following value for $K'_{effective}$ into Equation 20.22:

$$K'_{effective} = P_{FNL}P_{TNL}K'_{\infty} = P_{FNL}P_{TNL}(\eta\varepsilon f' p) \tag{20.24}$$

then to a good approximation, we can write the reactivity equivalent of the control rod in a previously critical reactor as

$$\Delta\rho_{CR} = \frac{(K'_{effective} - K_{effective})}{K'_{effective}} \tag{20.25}$$

or

$$\Delta\rho_{CR} = \frac{(f' - f)}{f'} \tag{20.26}$$

since all of the other terms cancel. The change in the reactivity due to the control rod is then

$$\Delta\rho_{CR} = \frac{|(f' - f)|}{f'} \tag{20.27}$$

In the absence of the control rod, f is given by

$$f = \frac{\Sigma_{aF}}{(\Sigma_{aF} + \Sigma_{aM})} \tag{20.28}$$

and when the control rod is fully inserted, f′ is given by

$$f' = \frac{\Sigma_{aF}}{(\Sigma_{aF} + \Sigma_{aM} + +\Sigma_{aR})} \tag{20.29}$$

Here, Σ_{aF}, Σ_{aM}, and Σ_{aR} are macroscopic absorption cross sections of the fuel, the moderator, and the control rod, respectively. (To simplify the notation, the absorption of neutrons in the cladding is ignored, but it can be added at a later time by redefining Σ_{aM} to include the moderator and the cladding.) If we substitute these expressions into Equation 20.22, we find that the reactivity change due to the control rod alone is

$$\Delta\rho_{CR} = \frac{|(f' - f)|}{f'} = \frac{\Sigma_{aR}}{(\Sigma_{aF} + \Sigma_{aM})} \tag{20.30}$$

Hence, once a critical configuration is reached, a control rod can be moved in either direction to increase or decrease the power level. If its vertical motion can be subdivided into N equal increments, the *incremental worth* per increment is then

$$\Delta\rho = \frac{\Delta\rho_{CR}}{N} \tag{20.31}$$

where N is typically a number between 20 and 40. With the help of these equations, we can then estimate how the reactor power level P and the reactor period T are affected when the rod is inserted or withdrawn. The process used is illustrated in Example Problem 20.6. Of course, *this assumes that the flux shape is not changed by the movement of the rod*.

Example Problem 20.6

A reactor fuel assembly has a thermal utilization factor of 0.92 without a control rod inserted, and a thermal utilization factor of 0.90 with the control rod fully inserted. What is the total reactivity of the rod? If the delayed neutron fraction for this particular reactor is 0.0050, how many dollars worth reactivity does the rod contain?

Solution The change in the reactivity due to the presence of the control rod is given by $|(f' - f)|/f'$, so from the information given, the reactivity change due to the presence of the rod must be $\Delta\rho_{CR} = |0.02/0.90| = 2.22\%$. Since $\beta = 0.0050$, this would correspond to a reactivity of $\Delta\rho_{CR}/\beta = 0.0222/0.00500 = \$4.44 = 4$ dollars and 44 cents. [Ans.]

The student exercise below helps to illustrate some of the design and economic tradeoffs that go into the design of control rods.

Student Exercise 20.5

We showed in the previous section that a modern PWR may not have enough reactivity in reserve to prevent the core from going critical with a fresh batch of fuel based on the reactivity of the control rods alone.

This design decision was probably the result of a carefully thought out cost–savings initiative, and much internal analysis probably occurred before the final design decision was made. Since control rods and their drive mechanisms are very expensive, putting more control rods into a PWR to allow it to be subcritical under any conditions could increase the total cost of a reactor by several percent. If you were a reactor operator or a utility shareholder, do you agree with this basic design decision?

20.23 How the Control Rod Worth Changes When the Flux Shape Changes

The previous equations for the control rod worth are applicable to situations where the shape of the neutron flux is not affected by the presence of the rod. Hence, they are appropriate for fast reactors where the mean free path is relatively long. However, when the neutron flux changes dramatically (because most of the neutrons are thermal), the reactivity change predicted by Equations 20.21 and 20.27 may be slightly different than the true reactivity change. In this case, an alternative derivation of the control rod worth is required. To perform this derivation, consider an isolated control rod in the center of a bare, homogeneous, cylindrical reactor core. The neutron diffusion equation in the absence of the rod is

$$\nabla^2\phi(\mathbf{r}) + B^2\phi(\mathbf{r}) = 0 \tag{20.32}$$

where B^2 is the geometric buckling. Now if the rod is fully inserted into the core, the thermal neutron flux assumes an entirely different shape, such as the one shown in Figure 20.19. The new flux shape is then given by the revised diffusion equation

$$\nabla^2\phi'(\mathbf{r}) + B'^2\phi'(\mathbf{r}) = 0 \tag{20.33}$$

where B'^2 is buckling after the rod has been inserted. We also know from our previous discussion that the effective multiplication factor for the reactor without the rod is given by

$$K_{effective} = P_{NL}K_\infty = \frac{K_\infty}{\left(1 + B^2M^2\right)} = 1 \tag{20.34}$$

and that the multiplication factor for the same reactor with the rod inserted is

$$K'_{effective} = P'_{NL}K_\infty = \frac{K_\infty}{\left(1 + B'^2M^2\right)} = 1 \tag{20.35}$$

where P_{NL} and P'_{NL} are the thermal non-leakage probabilities with the rod removed and the rod inserted. Then the net change in the reactivity due to the change in the thermal flux shape is given by

$$\Delta\rho = \frac{\left(K'_{effective} - K_{effective}\right)}{K'_{effective}} \tag{20.36}$$

or

$$W = |\Delta\rho| = \frac{\left[(B'M)^2 - (BM)^2\right]}{\left(1-(BM)^2\right)} \tag{20.37}$$

where M is the thermal migration area defined in Chapter 11. If $B' \approx B$, then Equation 20.37 can be written as

$$W = 2\Delta B\left(\frac{BM^2}{1+(BM^2)}\right) \tag{20.38}$$

where $\Delta B = B' - B$. So, the problem of determining the rod worth W can be reduced to solving Equations 20.32 and 20.33 for the values of B and B′ (see Figure 20.22). In the case of B, the answer is

$$B^2 = \left(\frac{2.405}{R}\right)^2 + \left(\frac{\pi}{H}\right)^2 \tag{20.39}$$

However, in the case of B′, the answer requires the solution to a transcendental equation because the thermal flux becomes depressed in the vicinity of the rod. We will not present this derivation here, but it can be shown in the case where B′ is not too much different than B that the control rod worth W is given by

The Control Rod Worth for a Bare Cylindrical Reactor with a Central Control Rod

$$\Delta\rho = W = \frac{A}{(C + \ln(D/r) + z/r)}$$

where

$$A = \frac{7.42(M/R)^2}{(1+B^2M^2)}$$

$$C = 0.115$$

$$D = \frac{R}{2.405} \tag{20.40}$$

and of course, z is the axial position and r is the radial position. Now let us turn our attention to a slightly more practical problem where the neutron leakage rate is position dependent.

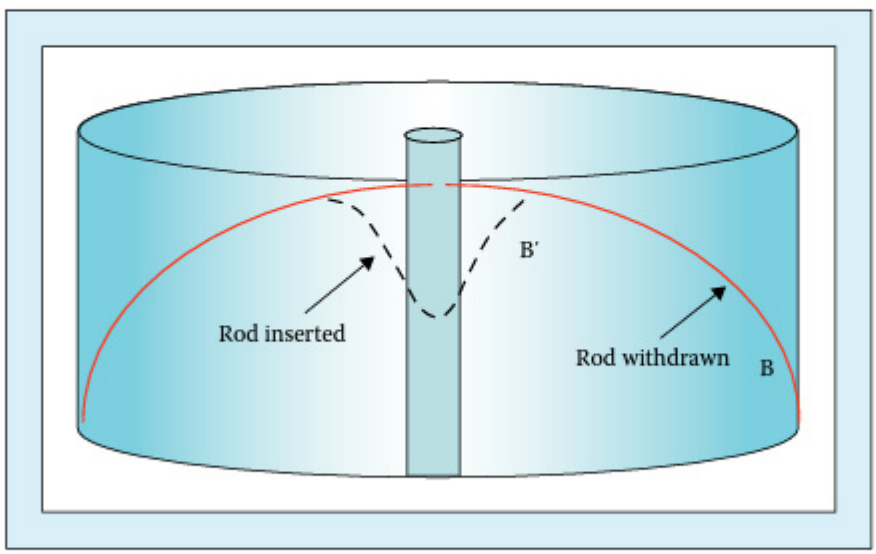

FIGURE 20.22 The flux shape in a bare cylindrical reactor with and without a central control rod.

Example Problem 20.7

If the rod consists of a cluster of 22 smaller rods, and each of these smaller rods moves in axial increments equal to 1/20th of their total length, how much will changing the axial position by one increment change the total reactivity of the core?

Solution Since the total worth of the rod cluster is 44 cents, moving the cluster by one axial increment will change the total reactivity of the core by 44 cents/20 = 2.2 cents. If there are 22 rods in the cluster, each of the rods in the cluster will have a reactivity of 2.2 cents/22 = 0.1 cents, or 1/10th of a cent. Note that a similar calculation can be performed for a neutron poison, or for any soluble boron that is added to the coolant. [Ans.]

20.24 Reactivity Corrections to Account for Partially Inserted Control Rods

Most of the time, the control rods are neither fully inserted nor fully withdrawn. *Then some of the rods are inserted into the core prior to start-up and they are slowly withdrawn as the fuel is burned and fission products begin to accumulate in the fuel rods*. When the control rods are near the center of the core, that is, when they are located at z = H/2, a change in the rod position in either direction has approximately the same effect (except for the sign) on the value of the reactivity change. *In other words, this effect is linear with distance in either direction, but in one direction, the reactivity is reduced, and in the other direction, the reactivity is increased*. A map of the control rod worth W as a function of axial position z is shown in Figure 20.23 where H is the core height and R is the core radius. As we get further away from the center of the core in the axial direction, the fractional change in the rod worth is *no longer linear* because of the effects of neutron leakage on the flux shape. Hence, it can be shown both theoretically and experimentally that the control rod worth W as a function of the vertical position z of the rod is given by

The Control Rod Worth as a Function of Axial Position

$$W(z) = W\left[\frac{z}{H} - \frac{\sin(2\pi z/H)}{2\pi}\right] \tag{20.41}$$

where W is the rod worth computed from Equation 20.37 or 20.38. The first term in Equation 20.41, W(z/H), assumes that the rod worth changes linearly with the axial position, and the second term, $-\sin(2\pi z/H)W/2\pi$, is a correction factor to this basic behavior. The rod worth is plotted as a function of vertical location in Figure 20.24, where z = 0 corresponds to the position where the rod is totally withdrawn. Hence at z = 0, it can be seen that W(0) = 0, while at z = H, it can be seen that W(H) = W. Equation 20.41 can then be used to predict the extent that the vertical motion of

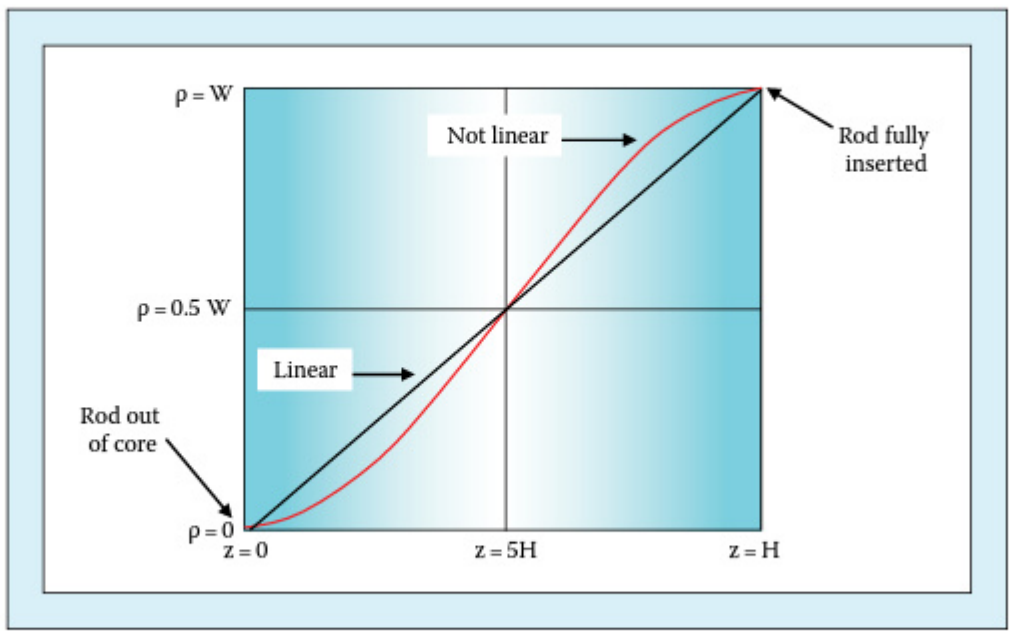

FIGURE 20.23 Reactivity changes as a function of control rod position.

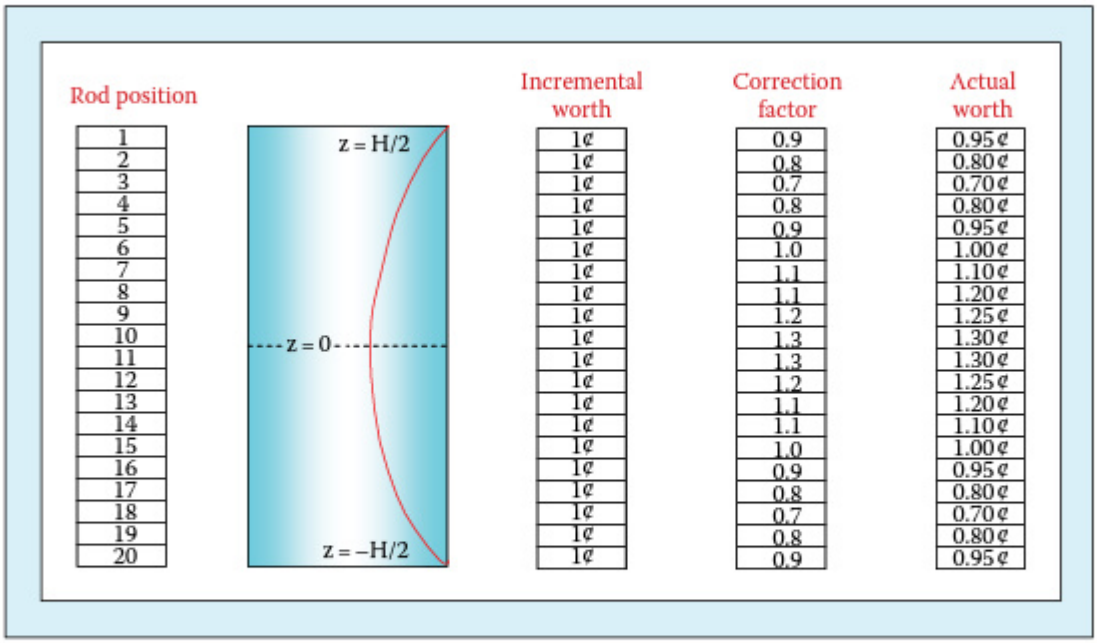

FIGURE 20.24 Reactivity correction factors and control rod increments.

the rod affects the reactivity in a nonlinear manner. In Figure 20.24 we have represented this for twenty different rod positions, corresponding to increments of 1/20th of the total core height. *Notice that when the rod is first inserted into the core, its effect is less than linear, and after it is more than halfway into the core, its effect is more than linear*. Only when it is fully inserted, fully withdrawn, or inserted exactly halfway is the reactivity linear with vertical displacement. Another way to quantify this effect is to take the *second derivative* of W(z) with respect to z. The second derivative d^2W/dz^2 gives the rate of change of the slope of the worth curve. When we apply this to Equation 20.41, the first term vanishes, and the result is

$$\frac{d^2W}{dz^2} = \left(\frac{2\pi}{H^2}\right)\sin\left(\frac{2\pi z}{H}\right) \tag{20.42}$$

This function is plotted in Figure 20.25 as a function of axial location. Thus the rate of change of the reactivity is greatest when the rod is only one-quarter inserted or three-quarters inserted into the core. The same effect is

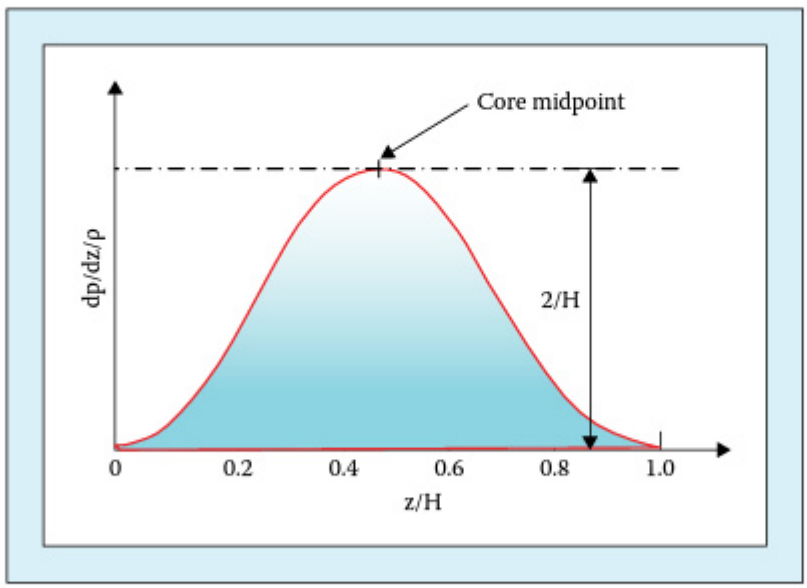

FIGURE 20.25 The differential control rod worth as a function of axial position in the core of a thermal water reactor.

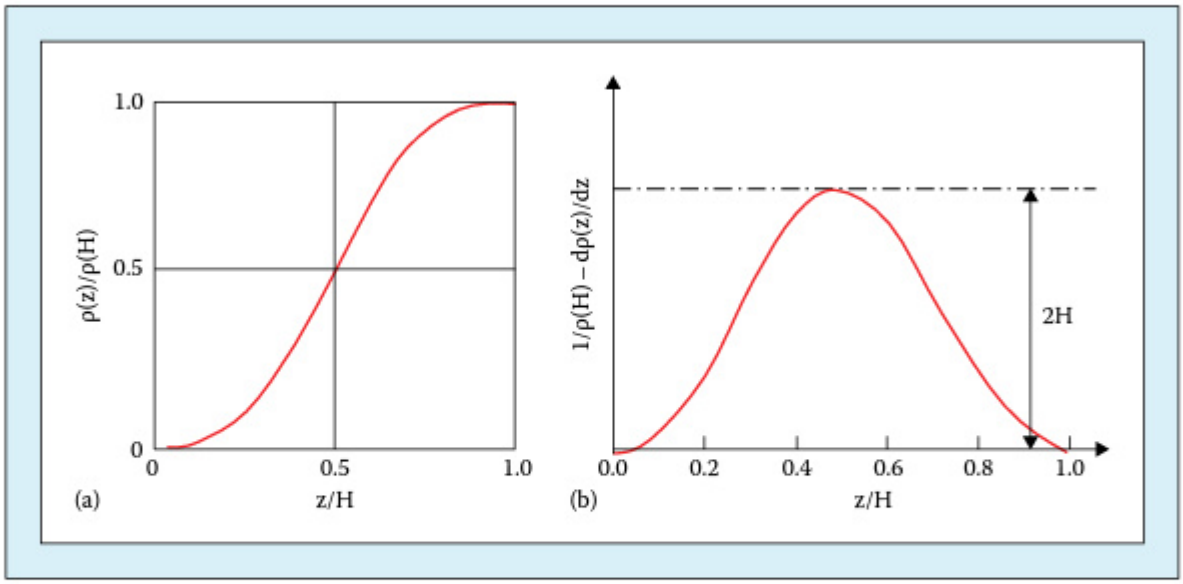

FIGURE 20.26 The reactivity of a control rod as a function of the distance that it is inserted into the core (a) and the fractional rate of change of the reactivity of the rod as a function of its axial elevation (b). Here, H refers to the total core height.

illustrated from a slightly different perspective in Figure 20.26. So the further away we get from these inflection points, the more accurate the equation becomes

$$\Delta\rho = \Delta W_n = \frac{W}{N} \tag{20.43}$$

However, further away from the center of the core, a linear change in rod position does not necessarily translate to a linear change in the value of the reactivity. In this case, it is necessary to apply a *rod correction factor* f(n), which is stored in a database in tabular form, to Equation 20.43, so that the actual change in the rod worth for a corresponding change in the incremental position n is given by

Incremental Change in Rod Worth with Position

$$\Delta\rho = \Delta W_n = f(n)\frac{W}{N} \tag{20.44}$$

This approach guarantees that the correct reactivity change is always used. During normal operation, these nonlinearities are taken care of by the control system so that a command to increase or decrease the power level by a small amount is automatically translated into the correct vertical motion of the rod, which may be either up or down. It is also important to remember that *the actual rod worth is a function of how the fuel is loaded into the core*. Equation 20.41 assumes that there is no variation in the enrichment of the fuel as a function of axial position. Then neutron flux assumes the shape of a cosine (see Chapter 13) and it peaks at the core centerline, where z = H/2. In other words, Equation 20.41 is based on the assumption that the neutron flux shape in the axial direction is given by

$$\phi_z(z) = \phi_{MAX}\cos\left(\pi\frac{(z - H/2)}{H}\right) \tag{20.45}$$

where H is the core height and the origin (z = 0) is located at the top of the core. If the neutron flux shape differs from this assumed flux shape, then the incremental rod worth dW/dz will be different than

The Incremental Rod Worth

$$\frac{dW(z)}{dz} = \frac{W}{H}\left[1 - \cos\left(\frac{2\pi z}{H}\right)\right] \tag{20.46}$$

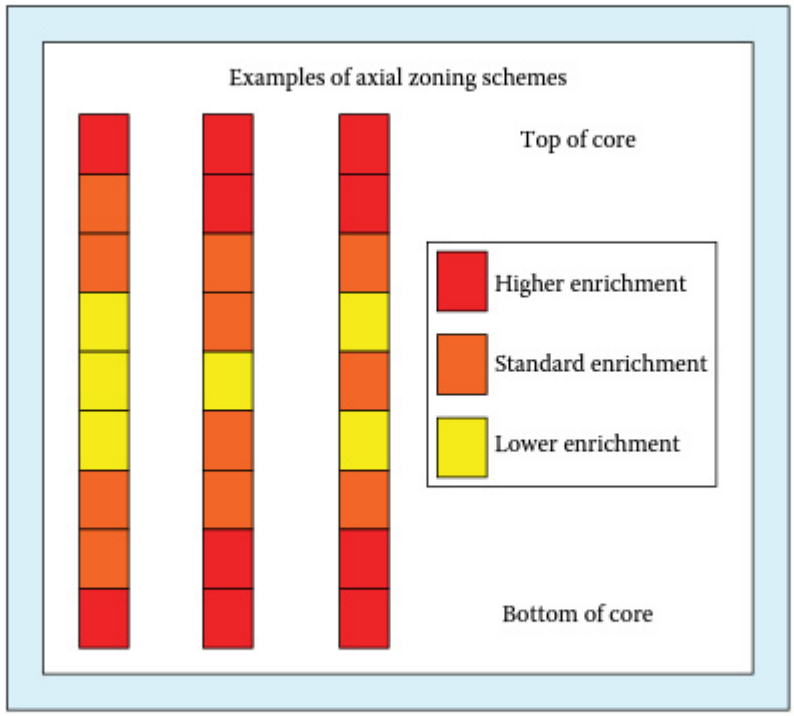

FIGURE 20.27 Examples of axial zoning schemes used to flatten the core power profile in the axial or z direction.

For example, it has been common practice since the early 1990s to vary the enrichment of the fuel axially to make the axial power profile as uniform as possible. This is known as *axial zoning* and several common examples of how axial zoning are implemented are shown in Figure 20.27. Using this approach the axial power profile is flattened by reducing the enrichment of the fuel pins near the center of the core and increasing the enrichment of the fuel pins away from the centerline. Under the right conditions, this can result in a much more uniform axial power profile (±15%) over a large fraction of the total core volume. Then the axial flux shape approaches

$$\phi_z(z) = \phi_o \approx \text{a constant} \tag{20.47}$$

and *the rod worth over a larger fraction of the core height is a linear function of the insertion distance z*. In fact, in the case where the power profile is completely uniform, we can write

$$\phi_z(z) = \phi_o = \text{a constant} \tag{20.48}$$

and the rod worth as a function of the insertion distance z is

$$W(z) = W\left(\frac{z}{H}\right) \tag{20.49}$$

Equation 20.49 then implies that when the rods are fully inserted into the core, z = H and W(H) = W, and when the rods are fully withdrawn, z = 0 and W(0) = 0. Naturally, when the control rods are inserted halfway into the core, and we have reached the core centerline, W(H/2) = W/2. In practice, most power reactors operate somewhere between the worth profiles implied by Equations 20.42 and 20.49. It is then up to the reactor designer and the control systems engineer to ensure that the control system knows how the reactivity of the core will change as the control rods are inserted and withdrawn. The following example compares the reactivity changes for two identical cores having cosinusoidal and linear power profiles. Table 20.4 shows the percentage changes in the reactivity for an individual control rod moving through the center of the core.

Example Problem 20.8

If the total worth of one of the control rod banks shown in Figure 20.17 is known to be 50 cents, how much will the reactivity change when the rod bank is inserted 25% of the way into the core? Part 1: Assume the axial power profile is given

TABLE 20.4
Reactivity Change as a Function of Control Rod Position for an Individual Control Rod Moving through the Center of a Bare, Homogeneous Cylindrical Core

Axial Location (z)	Delta $= -\sin(2\pi z/H)\cdot W/2\pi$	Percentage Change (%)
0	$\Delta\rho = 0$	0
0.125H	$\Delta\rho = -0.707W/2\pi$	−11.3
0.250H	$\Delta\rho = -W/2\pi$	−15.9
0.375	$\Delta\rho = -0.707W/2\pi$	−11.3
0.500	$\Delta\rho = 0$	0
0.625	$\Delta\rho = 0.707W/2\pi$	+11.3
0.750	$\Delta\rho = W/2\pi$	+15.9
0.875	$\Delta\rho = 0.707W/2\pi$	+11.3
H	$\Delta\rho = 0$	0

by the equation $P_z(z) = P_o \cos(\pi(z - H/2)/H)$. Part 2: Repeat the same exercise when the axial power profile is much more uniform, and when the rod worth is given by Equation 20.49.

Solution Part 1: From Equation 20.41, we know that $W(z) = W[z/H - \sin(2\pi z/H)/2\pi]$. If $z = H/4$, and $W = 50$ cents, the reactivity change due to inserting the rod bank one-quarter of the way into the core is

$$\Delta\rho = W(H/4) = 50 \text{ cents} \times \left[\frac{1}{4} - \frac{\sin(\pi/2)}{2\pi}\right] = 50 \text{ cents} \times \left[\frac{1}{4} - \frac{1}{2\pi}\right] = 50 \text{ cents} \times [0.25 - 0.16] = -4.5 \text{ cents}$$

Part 2: From Equation 20.49, the rod worth is a linear function of the insertion distance, so if the rods are inserted ¼ of the way into the core, then the reactivity change will be $\Delta\rho = 1/4\ W = -12.5$ cents. [Ans.]

Normally, control rod movements are limited to much smaller distances than this, and the worth of a typical rod is limited to just a few cents.

20.25 Effect of the Fuel Type on the Control Rod Worth

As we mentioned in Chapter 16, the reactivity of a control rod can be measured in two ways. First, it can be measured as a function of the delayed neutron fraction β, which depends on the type of fuel, or it can be measured in absolute units that do not depend on the fuel, such as the milli-rho and pcm (percent milli-rho). Since the value of β is different for U-235 than it is for U-233 and Pu-239, the control rod worth is usually quoted in absolute units (such as milli-rho or pcm), and it is then converted into relative units (dollars or cents) depending on the type of fuel that is used. For example, if a control rod is designed to have a worth W of 10 pcm (0.0001), then the control rod will have the worths shown in Table 20.5. For example, the same control rod in a PWR fueled with U-235 will have three times the worth it will have in exactly the same core fueled with Pu-239. For this reason, the control system must be calibrated to account for different types of nuclear fuel, as well as different axial power profiles.

TABLE 20.5
PCM Rod Worths for Nuclear Fuels U-233, U-235, and Pu-239

	Reactivity in Dollars and Cents		
Reactivity in PCM	U-233 ($)	U-235 ($)	Pu-239 ($)
1	0.0038	0.0015	0.0050
5	0.0192	0.0077	0.0250
10	0.0384	0.0154	0.0500
20	0.0769	0.0308	0.1000
50	0.1923	0.0769	0.2500
100	0.3846	0.1538	0.5000

Student Exercise 20.6

Consider a bare cylindrical reactor that is 200 cm high and 200 cm in diameter. If the reactor is fueled with natural uranium, and a control rod 2 cm in diameter is inserted halfway down into the reactor from above, what is the approximate value of the worth of the rod?

20.26 Semantic Differences in the Definition of the Control Rod Worth

As we first mentioned in Section 20.1, control rods can be used in two fundamentally different ways. First, they can be used to keep a reactor critical by compensating for changes in the isotopic composition of the core. Second, they can be used to change the degree of criticality by raising or lowering the reactor power level. If a control rod is used to change the power level, this has the effect of placing the reactor on a stable period. Here, the power level may temporarily deviate from its nominal power level, and the system-wide reactivity may be temporarily greater than zero ($\rho > 0$) or less than zero ($\rho < 0$). *When this occurs, the control rod worth is defined as the magnitude of the reactivity change required to obtain a specific reactor period T.* The relationship between these two parameters (the reactivity and the period) was explored in Chapter 16.

Conversely, when a control rod is used to keep a reactor critical, the rod worth is measured in terms of the change in the effective multiplication factor required to obtain a steady-state condition. Fortunately, despite the philosophical distinction between these definitions, it can be shown that they are, in fact, equivalent. *In other words, the definition of the worth depends to a certain extent on how it is intended to be used*.

20.27 Effect of Control Rods on the Axial Power Profile

When we move a control rod, it can affect the reactivity either positively or negatively (+ or −). The magnitude of the reactivity change depends on the axial power profile, and the axial power profile changes as the fuel is burned. At the BOL (see Figure 20.28), the excess reactivity is very high, and the control rods must be fully inserted into the core to drive the net reactivity to 0 (see the top of the picture to see what the power profile looks like in this case). Then as the fuel is burned, and most of this excess reactivity is lost, the only way that the core can remain critical is to withdraw the control rods completely from the core (see the bottom of Figure 20.28 to visualize what the axial power profile looks like in this case). Hence, *the axial power profile in a PWR peaks at beginning of life near the bottom of the core, and then as the control rods are withdrawn, the axial power peak moves gradually upward. Finally, at EOL it can be found much closer to the top of the core.* As the fuel is burned, the number of fissions per cubic centimeter also declines in direct proportion to the number of atoms of the fuel that are burned. Hence, the rate of power generation (e.g., the volumetric power generation rate) also declines as a function of time, and the peak to average power ratio becomes progressively smaller as the control rods continue to be withdrawn from the core. The effect of the control rods on the flux shape is then shown in Figure 20.29.

Initially, the maximum flux (and hence the axial power profile) is asymmetrical and peaks very close to the bottom of the core. Then as the control rods are withdrawn, it becomes much more symmetrical and resembles the cosine flux shape (and axial power profile) that we derived in Chapter 13. The rest of the time, it tends to vary between these two extremes. *It is then the responsibility of the reactor vendor or owner-operator to demonstrate that the maximum fuel and cladding temperature (see Chapter 17) do not exceed the regulatory limits imposed by the NRC.* Typically, this analysis has to be performed at BOL and then at EOL because these states tend to be the most limiting ones.

Example Problem 20.9

Consider a cylindrical reactor core where the axial power profile is completely uniform. Show that the incremental rod worth dW/dz, or the fractional rate of change of the reactivity with the insertion distance is given by W/H, where W is the total worth and H is the core height. If the control rods are inserted 80% of the way into the core in this case, and the total rod worth is 50 cents, how much negative reactivity is introduced into the core when z = 0.80H?

Solution When the axial power profile is uniform, the rod worth as a function of the insertion distance z is W(z) = W(z/H). Taking the derivative gives dW/dz = W/H, so the incremental rod worth is W/H. When z = 0.80H and W(0.80H) = 0.80, W = 40 cents. [Ans.]

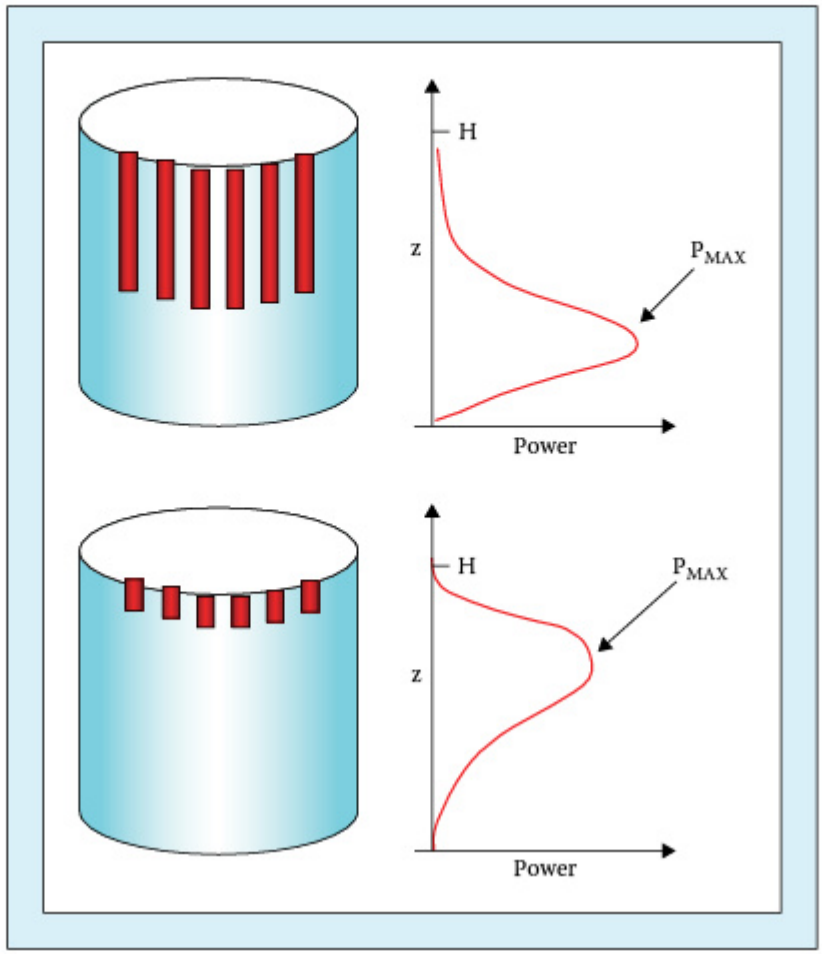

FIGURE 20.28 The effect of the control rods on the axial power profile in a PWR as the fuel is burned. The top figure shows the power shape at the beginning of life (BOL) and the bottom figure shows the power shape at the end of life (EOL). Notice that the maximum volumetric power level P is higher at the BOL than it is at the EOL even when the control rods are fully inserted into the core during start-up.

20.28 Fast Reactor Control Rods

About 40 fast reactors have been designed and built over the years, and most of them use *boron carbide* (B_4C) as the primary neutron absorbing material in their control rods. Because the absorption cross section of Boron-11 is very small at the neutron energies where fast reactors operate, Boron-10 (see Figure 20.8) is used instead because it absorbs more fast neutrons above the epithermal energy range. However, between about 0.1 and 0.4 MeV, the absorption cross sections of Boron-10 and Boron-11 are about the same, and they average about 0.27 barns. The atomic density of boron is about 8.7×10^{22} atoms/cm^3 at room temperature. This means that the macroscopic absorption cross section of Boron-10 in the control rods is $\Sigma_{a\,BORON} = N_{BORON}\sigma_{BORON} = 8.7 \times 10^{22}$ atoms/cm$^3 \times 0.27 \times 10^{-24}$ cm$^2 \cong 0.0235$ cm^{-1}. In a fast reactor, this gives an absorption mean free path λ_a of $\lambda_a = 1/\Sigma_{a\,BORON} = 42.5$ cm. Clearly, this is much larger than the thickness of any control rod that we would ever want to build.

However, the fact that the neutron mean free path is so long means that the shape of the neutron flux in a fast reactor control rod is barely affected by the presence of these rods. Thus the control rods no longer appear to be gray or black to the neutrons passing through them. *Since the flux shape does not change, the worth of a fast reactor control rod can be estimated much more easily than a comparable rod in a thermal water reactor*. The boron only changes the ratio of the number of neutrons absorbed in the fuel to the number of neutrons absorbed by everything else. The effective multiplication factor for a fast reactor is then

$$K_{effective} = K_\infty P_{NL} \tag{20.50}$$

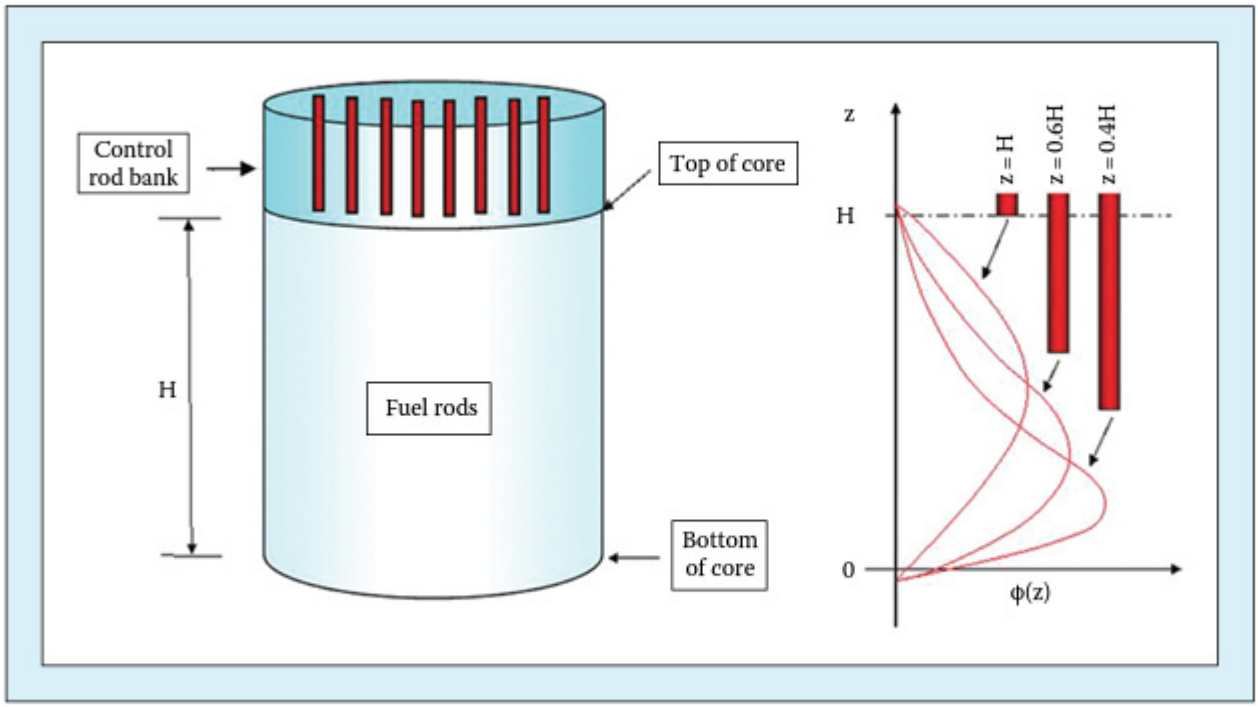

FIGURE 20.29 The effect of control rod position on the flux shape $\phi(z)$ in a bare cylindrical core where the enrichment does not change as a function of space or time.

where P_{NL} is the non-leakage probability for fast neutrons. It follows from our previous definition of the control rod worth (see Section 20.21) that

$$W = \frac{(k - k')}{k'} \tag{20.51}$$

where k' is the multiplication factor with the control rods fully inserted and k is the multiplication factor with the control rods fully withdrawn. Because only the thermal utilization is affected by the control rods, we can also express the control rod worth as

$$W = \frac{(f - f')}{f'} \tag{20.52}$$

where f' is the utilization with the control rods fully inserted and f is the utilization with the control rods fully withdrawn. Now suppose that we attempt to write explicit expressions for f and f' assuming that the control rods are made out of boron carbide. The value of f depends on only the absorption cross sections for the fuel and the coolant, Σ_{aF} and Σ_{aC}, while the value of f' depends on the absorption cross sections of the fuel, the coolant, and the boron, $-\Sigma_{aF}$, Σ_{aC}, and Σ_{aB}. Then the thermal utilization when the boron is present is

$$f' = \frac{\phi\Sigma_{aF}}{\phi(\Sigma_{aF} + \Sigma_{aC} + \Sigma_{aB})} \quad \text{(with the control rods)} \tag{20.53}$$

and the thermal utilization without the control rods is

$$f = \frac{\phi\Sigma_{aF}}{\phi(\Sigma_{aF} + \Sigma_{aC})} \quad \text{(without the control rods)} \tag{20.54}$$

However, because the neutron flux in the control rods is essentially the same as it is in the fuel and the coolant, the value of ϕ cancels in the numerator and the denominator, and the *control rod worth* becomes

The Control Rod Worth in a Fast Reactor (Dimensionless)

$$W = \frac{\Sigma_{aB}}{\left(\Sigma_{aF} + \Sigma_{aC}\right)} \tag{20.55}$$

Notice that the value of W is dimensionless so it can again be expressed in dollars and cents. To do so, we simply divide the right hand side of Equation 20.55 by the delayed neutron fraction β. When we do so, we obtain

Control Rod Worth in Dollars and Cents

$$W\left(\text{in dollars and cents}\right) = \frac{\left\{\Sigma_{aB}/\left(\Sigma_{aF} + \Sigma_{aC}\right)\right\}}{\beta} \tag{20.56}$$

The delayed neutron fractions for fast neutrons are compared to those for thermal neutrons (see Table 20.6). Notice that although the delayed neutron fractions are comparable, most fast reactors are fueled with Pu-239 rather than U-235. *Then the delayed neutron fraction β is about one-third of what it is in a uranium-fueled thermal water reactor.* Example Problem 20.10 estimates the rod worth when Pu-239 is the primary fuel.

Example Problem 20.10

Suppose that a bank of control rods in a fast reactor is found to have a worth of W = 0.001. How many dollars (or cents) worth of reactivity does the control rod bank have when the reactor is fueled with Pu-239?

Solution From our earlier discussion, we know that the rod worth in dollars may be found by dividing the value of W by the delayed neutron fraction β. If the rod worth is 0.001 and the delayed neutron fraction (from Table 20.6) is 0.0021, the total reactivity of the rod bank in dollars is 0.001/0.0021 ≈ \$0.5 (or about 50 cents). If the rod bank happened to have 25 control rods in it, then the worth of each rod would happen to be 50 cents/25 rods = 2 cents per rod. [Ans.]

Again, very few neutrons in fast reactors acquire energies below 10 keV.

Student Exercise 20.7

In the previous section, we discussed how the movement of the control rods could affect the axial power profile in a typical PWR core. Now suppose that we were asked to perform exactly the same exercise for a BWR where the control rods are inserted into the core from below. What would the corresponding axial power profiles look like in this case where

1. The control rods are fully inserted.
2. The control rods are fully withdrawn.

How do you think these power profiles would compare or contrast to those that we would find in a PWR under a similar set of conditions?

TABLE 20.6
Delayed Neutron Fractions for Fast and Thermal Reactors

Fuel Type	Thermal Neutron β	Fast Neutron β
Thorium-232	0.0000	0.0203
Uranium-233	0.0026	0.0026
Uranium-235	0.0065	0.0064
Uranium-238	0.0000	0.0148
Plutonium-239	0.0021	0.0021

Source: Henry, A.F., *Nuclear Reactor Analysis*, MIT Press, Cambridge, MA, 1975.

20.29 Control Rod Materials and Their Cross Sections

Determining the worth of any control rod requires accurate values for the neutron absorption cross sections. Today, most thermal water reactors use boron, cadmium, or hafnium in their control rods, and so we would like to present their cross sections in Table 20.7. Most of the time, Boron-10 is used instead of naturally occurring boron because its absorption cross section is about four times as large. Normally each Boron-10 atom is bonded to four Carbon-12 atoms to form a ceramic compound like *boron carbide* (B_4C), which can be found in both PWRs and BWRs. Boron carbide is an extremely hard and is sometimes used in tank armor and bulletproof vests.

In recent years, the number of materials used in control rods has grown, and now *silver, indium, cobalt, dysprosium, gadolinium, samarium, erbium, europium and, more recently, the element hafnium (Hf, atomic number 72)* are used as well. Their nuclear properties are also shown in Table 20.7. Interestingly enough, Samarium-149, which is also a very strong neutron poison, has found itself into reactor control rods over time. Here, samarium is bonded with three oxygen atoms to form Samarium trioxide, which is also a very hard ceramic. Europium (with an atomic number of 63) is also bonded with three oxygen atoms to create europium trioxide, which has a macroscopic absorption cross section of about 111 cm^{-1}. In any event, Table 20.7 can be used to estimate the strength of most materials used in reactor control rods today.

Example Problem 20.11

Suppose that a control rod in a thermal water reactor contains 80% gadolinium and 20% Cadmium-112. At thermal energies, what is the effective macroscopic absorption cross section of the rod? If the thermal neutron flux in the vicinity of the rod is 1×10^{14} neutrons/cm^2/s, how many neutrons per second will one cubic centimeter of the control rod be able to absorb?

Solution From Table 20.7, the effective thermal absorption cross section of the control rod is $0.80 \times 1403 + 0.20 \times 114 = 1145.2$ cm^{-1}. If the thermal neutron flux is 1×10^{14} neutrons/cm^2/s, 1 cm^3 of the control rod will absorb $1145.2 \times 1 \times 10^{14} = 1.145 \times 10^{17}$ neutrons/s. [Ans.]

Example Problem 20.12

The water in the primary loop of a large commercial PWR can weigh between 300,000 kg and 450,000 kg. If the boric acid concentration is 1000 PPM, what is the total mass of the boric acid in the primary loop if it contains 400,000 kg of coolant?

TABLE 20.7
Thermal Absorption Cross Sections for Some Common Control Rod Materials

Material	Atomic Density (atoms/cm^3)	σ_a (barns)	$\sum_a$ (cm^{-1})
Boron-10	0.1364×10^{24}	2,500	342
Natural boron	0.1364×10^{24}	755	103
Cadmium-112	0.0464×10^{24}	2,450	114
Samarium-149	0.0309×10^{24}	40,540	1253
Sm_2O_3	0.0128×10^{24}	16,500	211
Hafnium	0.0449×10^{24}	105	4.7
Gadolinium	0.1305×10^{24}	46,000	1403
Erbium	0.0330×10^{24}	173	5.7
Indium	0.0381×10^{24}	192	7.3
Europium	0.0207×10^{24}	4,300	89
Eu_2O_3	0.0127×10^{24}	8,740	111

Source: Duderstadt, J. and Hamilton, L., *Nuclear Reactor Analysis*, John Wiley & Sons, New York, 1976.

Solution 1,000 kg of water has a volume of approximately 1,000 L, so 400,000 kg of water will have a volume of approximately 400,000 L. From Equation 20.16, we know that 1 PPM = 0.000998 g/L, so 1,000 PPM = 0.998 g/L. 400,000 L of water will therefore require ~400,000 g or 400 kg of boric acid. [Ans.]

20.30 Control Rod Design Parameters

Table 20.8 shows the design parameters for the control rods used in a 1000 MWE Westinghouse PWR. Each bank of control rods has between 20 and 25 individual rods, and each of these rods has a diameter of about 1 cm. The control rod insertion rate is about 1.9 cm/s, or 45 in./min., and a large core can have as many as 50 banks of these rods. Some of the rods are used for day-to-day power shaping and control, while others are used for only emergency control. All of the components of the *CRDM*, or the *control rod drive mechanism*, are contained in a stainless steel assembly attached to the pressure vessel head. If electric power to the CRDM is lost, the rods automatically fall into the core under the influence of gravity alone, *and the reactor promptly shuts down*. After a few seconds, the fission process completely stops (see Chapter 16), and the only remaining heat generated by the core is *decay heat*. As we discussed previously, the rate at which this decay heat dissipates is given by the *Wigner-Way equation*.

20.31 Reactor Control Systems and Their Limitations

Reactor control systems are designed to limit changes in the steady-state power level to 5%–10% per minute during normal operation. For example, the control rods can be moved up or down in such a way that the power level in a typical PWR can accommodate a step load increase of about 10% and a ramp load increase of about 5% per minute when the power level is between 15% and 100% of its rated value. Conversely, equal step and ramp reductions in the load level are possible between 15% and 100% of full power operation subject to the xenon limitations that were discussed in the previous chapters. Hence, the movement of the control rods is tied to the electrical power output of the plant, and a number of *feedback loops* are employed to keep the coolant temperature in the primary loop and the steam flow rate in the secondary loop in sync with these load changes. A simple energy balance can be used to obtain the appropriate flow rates.

20.32 Alternative Forms of Reactivity Control

Many people who study nuclear science and engineering for the first time are surprised to learn that control rods are not the only way to control the power level of a reactor core. In fact, some of the earliest nuclear reactors (dating back to the late 1940s) used control rods for only very special purposes and not necessarily to perform the function of *power control*. Perhaps the best-known example of an early nuclear reactor that did not use control rods at all (except in the event of an emergency shutdown) was the *Clementine fast reactor*, which was built at Los Alamos in 1948 to breed plutonium for the U.S. nuclear weapons program.

The Clementine reactor was designed with a small cylindrical plutonium core surrounded by a U-238 blanket, which also acted as a neutron reflector. The blanket could be raised and lowered around the core, and this motion of the

TABLE 20.8
Design Parameters for the Control Rods in a Typical Westinghouse PWR

Number of rod banks	50
Number of drive mechanisms	1 per rod bank
Number of control rods per rod bank	20–25
Maximum control rod insertion rate	1.9 cm/s (45 in./min)
Incremental stepping distance	1.6 cm (5/8 in.)
Design pressure	2500 PSI (17.2 MPa)
Design temperature	343°C (650°F)
Overall CRDM length	594 cm (~6 m)
Material used	Stainless steel

Source: Data from Westinghouse Nuclear Corporation. See *http://www4.ncsu.edu/~doster/NE405/Manuals/PWR_Manual.pdf*.

blanket controlled the effective multiplication factor $K_{effective}$ (see Chapter 10) by controlling the neutron leakage rate. As the blanket was raised around the core, the neutron leakage rate was reduced, and the effective multiplication factor increased. Conversely, when the radial blanket was removed, the neutron leakage rate increased, and the effective multiplication factor decreased. This effect could be modeled using the six-factor formula that we discussed in Chapter 10:

The Six-Factor Formula

$$K_{effective} = P_{FNL}P_{TNL}K_{\infty} = P_{FNL}P_{TNL}(\eta\varepsilon f p)$$

or equivalently (20.57)

$$K_{effective} = (1 - L') \cdot K_{\infty} = (1 - L') \cdot (\eta\varepsilon f p)$$

where L' is the neutron leakage probability (the fraction of neutrons that leak out of the core) and it is in turn related to the thermal and fast non-leakage probabilities by

$$L' = 1 - P_{FNL} \cdot P_{TNL} \quad (20.58)$$

When the blanket was raised around the core, the neutron flux resembled the radial flux shape shown in Figure 20.30, and when the radial blanket/reflector was lowered, more neutrons leaked out of the core, and the neutron flux resembled the flux shape shown in Figure 20.31. Using the six-factor formula, one could then determine the change in the neutron leakage rate L' based on the change in the geometric buckling of the flux. With a well-designed mobile reflector, the total non-leakage probability in a design such as this could be varied from about 94% to about 99%. In other words, the value of $K_{effective}$ could be changed by at least 5% by simply raising or lowering the radial blanket. The reactivity could therefore be changed by $\Delta\rho = (k - 1)/k = 0.064$, or $\Delta\rho/\beta \approx \$10$ when the reactor was fueled with U-235 and $\Delta\rho/\beta \approx \$30$ when the reactor was fueled with Pu-239.

Normally, *this method of reactivity control works for small cores where the value of the geometric buckling is large*. In commercial power reactors, it does not work particularly well because the geometrical buckling is smaller and the cores

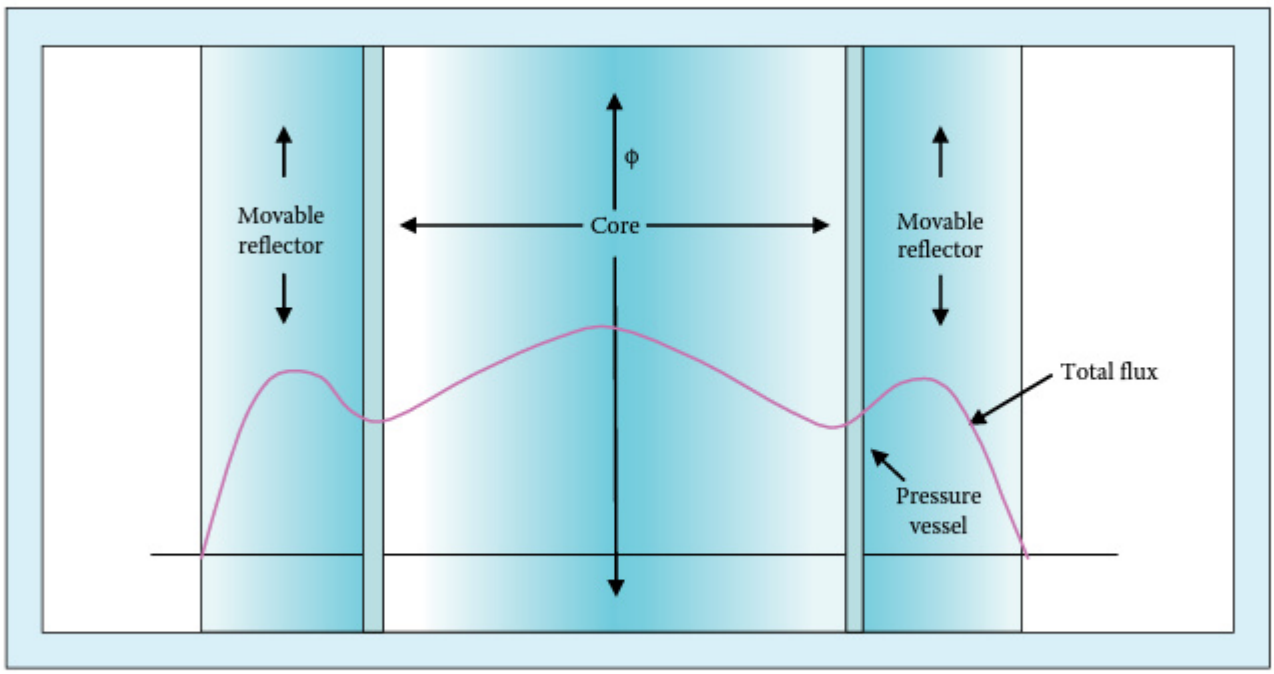

FIGURE 20.30 The neutron flux shape with the radial blanket/reflector raised.

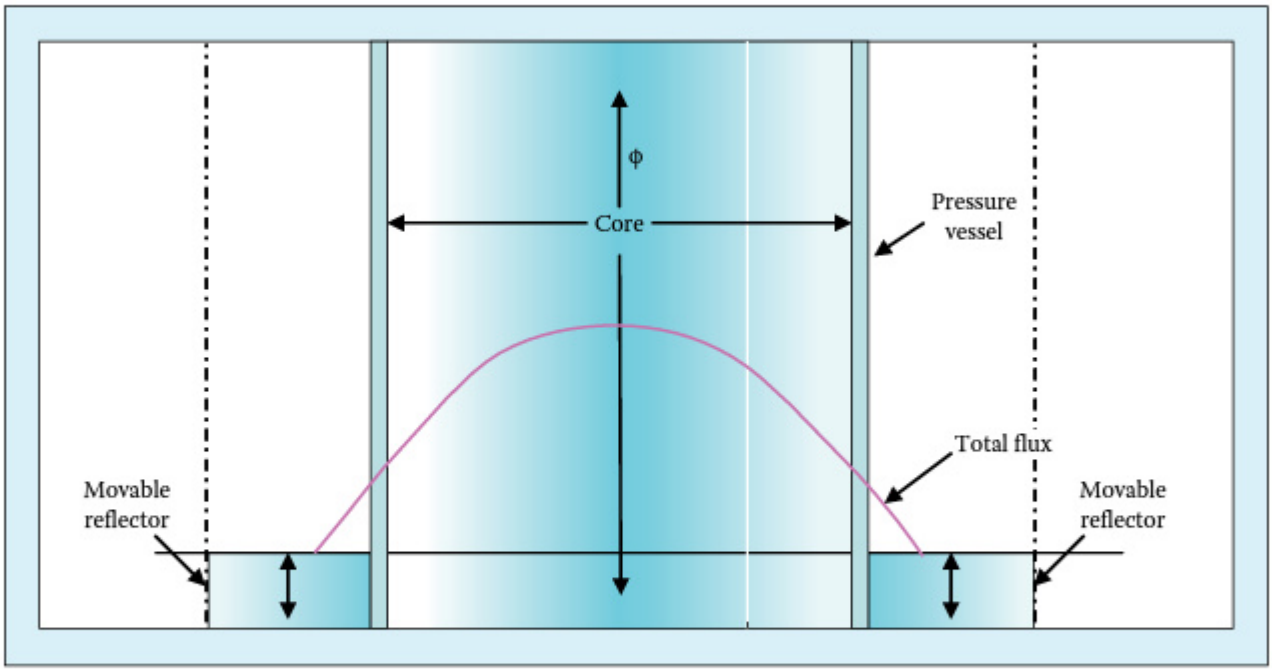

FIGURE 20.31 The neutron flux shape with the radial blanket/reflector lowered.

are much larger and more heterogeneous. However, in small research reactors, this method of reactivity control is still occasionally used today. Notice that there are many similarities between the neutron flux shapes shown in Figures 20.30 and 20.31 and the flux shapes for the reactor cores we discussed in Chapter 13. In addition, *the presence of the reflector tends to reduce the amount of fuel required to achieve a critical mass*. At that time, we showed that this reduction in the critical mass was proportional to what was known as the *reflector savings*. Finally, a moveable blanket or reflector changes the value of the *albedo* or the neutron reflection coefficient at the core/reflector boundary. The Clementine reactor was designed to have a relatively large albedo when the radial blanket was raised. Specific values for the albedo were discussed in Chapter 13, where the value of the albedo was shown to be a function of the thickness of the radial blanket or reflector. For well-designed blankets and reflectors, the albedo can be as great as 90%.

Student Exercise 20.8

Suppose that a small test reactor with a core 1 m in diameter and fueled with U-235 is to be controlled using a movable radial blanket/reflector similar to the one that was used in Clementine reactor. If the radial blanket consists of two metal plates containing ordinary water 10 cm thick, estimate the reactivity swing of the core with the blanket raised and with the blanket lowered. Can the radial blanket be used to reduce the number of control rods that are required to shut down a small PWR? Assume the test reactor is a thermal water reactor.

References

Books and Textbooks

1. Ash, M. *Nuclear Reactor Kinetics*, McGraw-Hill, New York (1965).
2. Lewis, E. *Nuclear Power Reactor Safety*, John Wiley & Sons, New York (1977).
3. Henry, A.F. *Nuclear Reactor Analysis*, MIT Press, Cambridge, MA (1975).
4. Keepin, G.R. *Physics of Nuclear Kinetics*, Addison-Wesley, Reading, MA (1965).
5. Stacey, W.M. *Nuclear Reactor Physics*, 2nd edn., John Wiley & Sons, New York (2007).
6. Todreas, N. and Kazimi, M.S. *Nuclear Systems*, Vol. 1, CRC Press, Boca Raton, FL (2008).
7. Duderstadt, J. and Hamilton, L. *Nuclear Reactor Analysis*, John Wiley & Sons, New York (1976).
8. Lewis, E. *Fundamentals of Nuclear Reactor Physics*, Academic Press, Boston, MA (2008).
9. Hetrick, D.L. *Dynamics of Nuclear Reactors*, American Nuclear Society, La Grange Park, IL (1993).

10. Schultz, M.A. *Control of Nuclear Reactors and Power Plants*, 2nd edn., McGraw-Hill, New York (1961).
11. Lamarsh, J.R. and Baratta, A.J. *Introduction to Nuclear Engineering*, Prentice Hall, Upper Saddle River, NJ (2001).
12. Lamarsh, J.R. *Introduction to Nuclear Reactor Theory*, 2nd printing, Addison-Wesley Publishing Company, Inc., Reading, MA (1972).
13. Cochran, R.G. and Toulfanidis, N. *The Nuclear Fuel Cycle: Analysis and Management American Nuclear Society*, La Grange Park, IL (1999).
14. Glasstone, S. and Eedlund, M. *The Elements of Nuclear Reactor Theory D*, Van Nostrand Company, Inc., New York (1952).
15. Glasstone, S. and Sesonske, A. *Nuclear Reactor Engineering*, 3rd edn., Van Nostrand Reinhold Company, New York (1981).
16. Shultis, K. and Faw, R. *Fundamentals of Nuclear Science and Engineering*, 2nd edn., CRC Press, Boca Raton, FL (2008).
17. Masterson, R.E. *Nuclear Engineering Fundamentals: A Practical Perspective*, CRC Press, Boca Raton, FL (2017).

Web References

1. *http://wapedia.mobi/en/BWRI.*
2. *http://en.wikipedia.org/wiki/Control_rod.*
3. *http://web.mit.edu/nrl/Training/Absorber/absorber.htm.*
4. *http://esa21.kennesaw.edu/activities/nukeenergy/nuke.htm.*
5. *http://hyperphysics.phy-astr.gsu.edu/hbase/nucene/control.html.*
6. *http://www.nrc.gov/reading-rm/basic-ref/glossary/control-rod.html.*
7. *http://www4.ncsu.edu/~doster/NE405/Manuals/PWR_Manual.pdf.*
8. *http://www.westinghousenuclear.com/Products_&_Services/docs/flysheets/NF-FE-0002.pdf.*

Additional References

- Important physical constants used by nuclear scientists and engineers can be found in *Appendix A*.
- Unit systems and their conversion factors can be found in *Appendix B*.
- Nuclear cross sections for many important nuclear materials can be found in *Appendix C*.
- Physical properties of important nuclear materials can be found in *Appendix D*.
- Atomic masses, half-lives, and natural abundances can be found in *Appendix E*.
- Delayed neutron emitters and their properties are discussed in *Appendix F*.

Questions for the Student

The following questions cover the material presented in this chapter and, in some cases, previous chapters as well. They are designed to test how well the student has acquired a working knowledge of the subject matter.

1. What is the U.S. NRC's definition of a control rod?
2. What are the four primary functions of a control rod?
3. How is the "worth" of an individual control rod defined?
4. Fill in the following sentence with the appropriate word or phrase. To scram a PWR, all one has to do is to "_____" on the electromagnets attached to the control rods. The control rods then fall into the core under the force of _____ alone.
5. In what region of the core is the worth of a control rod approximately a linear function of its axial position?
6. In practice, the worth of an individual control rod can be calculated using the four-factor formula. When it is calculated in this way, which one of the four factors in the four-factor formula is most strongly affected by the presence of the rod?
7. Fill in the following sentence with the appropriate word or phrase: In the field of nuclear engineering, the term SCRAM is an acronym for a _____?
8. In a PWR, what happens when the scram button in a reactor control room is pushed by the reactor operator?
9. For a homogeneous reactor core with a cosine power shape, write an expression for the control rod worth W(z) as a function of axial position z if the height of the core is H.
10. In what direction are the control rods inserted into the core of a BWR?
11. In a PWR, boron is dissolved in the coolant to help absorb excess neutrons and to control the overall reactivity of the core. What isotope of boron is used in this case, and what is the chemical symbol for Solbor after it is dissolved in the coolant?
12. Name five different units in which the worth of a control rod can be measured. In the Western world, what is the most common of these five units?
13. Fill in the following sentence with the appropriate word or phrase: In a thermal water reactor, the primary effect of a control rod is to reduce the _____ of the fuel.
14. In practice, is the maximum volumetric power level at a particular location (z) in a homogeneous reactor core highest during steady-state condition when all of the control rods are withdrawn from the core or when all of the control rods are inserted into the core?
15. Using a rod correction factor f(n), write an equation for the incremental change in the control rod worth ΔW_n as a function of axial position if there are N possible axial positions.
16. About 40 fast reactors have been put into operation in the world today. What is the most common control rod material that has been used in fast reactors up to this time?
17. What is the average reactivity of a single bank of control rods in a PWR?
18. In what branch of the U.S. military was the use of the word SCRAM originally invented?
19. What is the shape of a BWR control rod, and how thick is one of its blades?
20. Fill in the following sentence with the appropriate word or phrase: During a control rod drop experiment, the control rod worth can be defined as the magnitude of the reactivity change required to obtain a specific _____, which is measured in seconds.
21. Why are control rods inserted into the core of a BWR from the bottom?
22. In what direction are the control rods inserted into the core of a PWR?
23. Why are burnable poisons so popular in nuclear reactors today?
24. Fill in the following sentence with the appropriate word or phrase: In both PWRs and BWRs, _____ is mixed with carbon to form a popular control rod material called _____ or ____.
25. Consider the picture shown in Figure 20.20. If the neutron flux peaks ¼ of the way below the top of the core (i.e., at 0.75 H), where does the differential control rod worth peak in this case?
26. How much excess reactivity is contained in a BWR and PWR core at start-up?
27. In a PWR, how much negative reactivity is tied up in the control rods, and how much negative reactivity is tied up in the chemical shim?
28. In addition to control rods and burnable poisons, what other system is used in a PWR to control the reactivity of the core?
29. If a PWR core has 200 fuel assemblies, how many of them would you expect to have control rods?
30. Write an equation for the reactivity change due to the presence of Solbor alone.
31. In a PWR, how much negative reactivity is tied up in the burnable poisons?

32. What is the standard shape of a control rod in a PWR or LMFBR?
33. In what types of reactors can a plate-shaped control rod be found?
34. Write an expression for the worth W of an individual control rod as a function of the thermal utilization f and f′ before and after it is inserted into the core.
35. In what five units can the reactivity of a control rod be measured?
36. Suppose that a control rod in a Uranium-235-fueled reactor has a control rod worth of 0.002. How many dollars or cents is the control rod worth?
37. Why is the control rod worth in a reactor core less around the edges of the core than it is at the center?
38. In a BWR, how much negative reactivity is tied up in the burnable poisons?
39. Fill in the following sentence with the appropriate word or phrase: In a PWR, each cluster of control rods has about _____ finger-shaped rods, so an individual finger-shaped rod will have an average worth of about ___ per rod.
40. Suppose that the thermal neutron flux is the same at every location in a reactor fuel assembly—particularly in the axial direction. What value should be used for the rod correction factor f(n) in this case?
41. Why are BWR fuel assemblies surrounded by stainless steel or Zircaloy cans/sheaths?
42. In a reactor physics calculation, what important measure of reactor behavior is equivalent to the control rod worth?
43. As the nuclear fuel in a reactor fuel assembly is burned, the number of U-235 atoms as a function of time is given by the equation $U(t) = U_o e^{-\sigma_a \phi t}$. How large can the value of $\sigma_a \phi t$ become before the number of fuel atoms no longer declines linearly as a function of time?
44. What is a typical value of the soluble boron concentration in a PWR core at the start of a new operating cycle, assuming a refueling period of approximately 1 year?
45. Is Boron-10 or Boron-11 a better control rod material?
46. What is the NRC's definition of a burnable poison?
47. Name three reasons why soluble boron is so popular in PWRs today.
48. If the power level in a PWR increases suddenly and substantially, what do you do?
49. Fill in the following sentence with the appropriate word or phrase: Traditionally, control rods have been made out of neutron-absorbing materials such as _____ and _____, but in recent years, there has been a trend toward using more advanced materials such as _____ and _____.
50. Where can the electromagnets be found in a PWR pressure vessel?
51. In a BWR, how much negative reactivity is normally tied up in the control rods?
52. Suppose that someone in Europe tells you that a gas-cooled reactor has a control rod worth of 50 niles. Approximately, how many dollars worth reactivity does this represent?
53. What happens if we "pull the plug" on the electromagnets that are located at the top of the pressure vessel in a PWR?
54. Is neutron transport theory required to obtain a good estimate of the worth of a control rod in a fast reactor?
55. By how many PPM can the Solbor concentration fall in a typical PWR core during the first 40 hours of full-power operation, when the concentrations of Zenon-135 and Samarium-149 are building up to their equilibrium values?
56. Suppose that when a reactor is just being started up, the neutron flux is completely uniform in the axial direction (from z = 0 to z = H). Draw a picture of the differential control rod worth in this case.
57. What is a typical value of the soluble boron concentration in a PWR core at the start of a new operating cycle, assuming a refueling period of approximately 1 year?
58. Write an equation for the incremental control rod worth when a control rod has N different axial positions or increments and the rod worth is a linear function of axial position.
59. How many common ways are there to define the worth of a control rod today?
60. Suppose that a thermal water reactor is fueled with enriched uranium and that the worth of a typical control rod in this reactor is 20 cents. If the same reactor is then fueled with Pu-239, and the design of the control rod does not change, what is the corresponding worth of the same control rod when Pu-239 is used as the primary fuel?
61. Fill in the following sentence with the appropriate word or phrase: In a commercial power reactor, it is not uncommon for the reactor to contain more than _____% more fuel than it needs to become critical. This corresponds to an excess reactivity at start-up of about _____ for a PWR and about _____ for a BWR.
62. Do you think it is a good idea for the control rods to enter the core of a BWR from below?
63. For a reactor core having a cosinusoidal axial power profile, write an expression for the control rod worth as a function of axial position if the overall height of the core is H.
64. Generally speaking, at what axial elevation in a reactor core does the differential control rod worth dW/dz achieve its greatest fractional rate of change?

65. BWRs have cruciform control rods and PWRs have cylindrical control rods. What shapes do the control rods in some research reactors have?
66. Is the amount of axial power peaking in a typical PWR core greater at the BOL when all of the control rods are inserted into the core, or at the EOL, when all of the control rods are withdrawn from the core?
67. Approximately, how many times greater is the delayed neutron fraction β in a thermal water reactor fueled with U-235 than in a fast reactor fueled with Pu-239?
68. Suppose that you are asked to calculate the control rod worth for a fast reactor, which is fueled with Pu-239. If the value of the control rod worth turns out to be 0.0001, what is the value of the control rod worth is dollars and cents?

Exercises for the Student

Exercise 20.1

In a PWR core, one out of every four fuel assemblies has a control rod in it, and in these special fuel assemblies, about one in every 10 rods is a control rod. If the moderator-to-fuel ratio in the core (the ratio of the volume of the moderator to the volume of the fuel) is 4 to 1, estimate what fraction of the total core volume consists of control rods.

Exercise 20.2

Consider exactly the same problem posed in Exercise 20.1 from an entirely different perspective. Suppose that the reactor core (which does not necessarily have to be a PWR in this case) is made from uranium with an average enrichment of 4%. Neglecting the effects of neutron leakage for the moment, what percentage of the core must consist of control rods made out of Boron-10 for the reactor to be exactly critical? Assume that the number of moderator atoms is four times the number of fuel atoms, that the value for ν is 2.5, and that the core is cooled with light water.

Exercise 20.3

The control rods used in a thermal reactor have a reactivity of \$100 when they are fully inserted into the core and a reactivity of 0 when they are fully withdrawn. After the fuel is burned for 2 years, the value of k_{eff} falls from 1.3 to 1.1. Assuming that the reactivity of the control rods is a linear function of their position, by what percentage of their total insertion distance do they have to be withdrawn from the core to keep the reactor critical? Assume the core is fueled with Pu-239.

Exercise 20.4

A control rod 400 cm long is worth 10 cents when it is fully inserted. If the core is 4 m high, how much reactivity is introduced into the reactor when the control rod is pulled one-quarter of the way out of the core? At what rate is the reactivity increased beyond this point for every 1 cm change in the rod's axial position? Assume that the core has a standard axial power profile (i.e., it is cosinusoidal in shape).

Exercise 20.5

A 1000 MWE PWR contains 200 fuel assemblies and about one-quarter of them contain control rods. Suppose that the control rods in each of these 50 fuel assemblies have a net worth of 50 cents. What concentration of boron in PPM is needed to have the same effect on the reactivity as the control rods in just one of these reactor fuel assemblies? Assume that the reactor is fueled with enriched uranium and that the thermal utilization of the fuel is 90%.

Exercise 20.6

Suppose that at some time in its operating history, a reactor is exactly critical when a control rod is withdrawn halfway from the core. The core is 4 m high and the control rod has a worth of 50 cents (0.50β). If the control rod is now suddenly withdrawn another 200 cm, how much additional reactivity is added to the core? Assume that the reactor is fueled with enriched uranium. What is the reactor period in this case and how long does it take for the power level to double?

Exercise 20.7

A PWR fueled with enriched uranium contains 20% more U-235 than is needed for the core to become critical. What concentration of boric acid must be added to the coolant in PPM to hold down this excess reactivity? Assume that the thermal utilization of the fuel is 90% and that the control rods have not yet been inserted into the core.

Exercise 20.8

A PWR is fueled with 4% enriched uranium. The core contains 50 banks of control rods, and each bank of control rods contains 25 individual rods. If the control rods contain as much reactivity as the soluble boron in the previous problem (Exercise 26.7), how much reactivity does a single control rod contain in dollars and cents?

Exercise 20.9

Suppose that the primary loop of a PWR contains 300 kg of boric acid. How many kilograms of Boron-10 does the primary loop contain if only 80% of the boron in the boric acid is Boron-10?

Exercise 20.10

The control rods in a research reactor are configured so that moving a control rod 1 cm out of the core will increase the reactivity by 1 cent and inserting a rod 1 cm into the core will decrease the reactivity by 1 cent. Suppose that it is desired to double the power level of the core in 20 minutes. If the prompt neutron lifetime is 10^{-4} seconds, how far does a control rod have to be inserted or withdrawn from the core to make this happen?

Exercise 20.11

A research reactor in Cambridge, Massachusetts, produces 10 MW of electric power while it is operating normally. When the reactor is suddenly scrammed during a safety test required by the Cambridge City Council, it is observed that the power level drops to 10 kW in 10 minutes. How much negative reactivity was inserted into the core to make this happen?

21

Fission Products, Xenon Transients, and Reactor Accidents

21.1 Importance of Fission Product Poisons

When a reactor is first put into operation, fission products begin to accumulate in the core. They build up in the fuel rods, and start to absorb thermal neutrons. The buildup of these *fission products* reduces the multiplication factor of the core. Since their absorption cross sections become larger as the energies of the neutrons become smaller, fission products are much more important in thermal reactors than they are in fast ones. For this reason, we will concentrate primarily on how thermal water reactors are affected by the buildup of these fission products. In thermal reactors, fission products primarily affect the *thermal utilization* f of the fuel. This means that if the effective multiplication factor is defined as

$$K_{effective} = P_{FNL}P_{TNL}K_{\infty} = P_{FNL}P_{TNL}(\eta\varepsilon fp) \tag{21.1}$$

where η, ε, f, and p have their usual meanings, then $K_{effective}$ of a reactor before the fission products appear is given by Equation 21.1, and $K_{effective}$ of a reactor after the fission products appear is given by

$$K'_{effective} = P_{FNL}P_{TNL}K'_{\infty} = P_{FNL}P_{TNL}(\eta\varepsilon f'p) \tag{21.2}$$

where f′ is the thermal utilization with fission products included. This means that we can write the reactivity equivalent of the fission products in a previously critical reactor as

The Reactivity Contribution of the Fission Products

$$\Delta\rho = \frac{(K'_{effective} - K_{effective})}{K'_{effective}}$$

or

$$\Delta\rho = \frac{(f' - f)}{f'} \tag{21.3}$$

since all of the other terms in the six-factor formula cancel. Here, f is the thermal utilization before the fission products appear (i.e., in the unpoisoned reactor) and f′ is the thermal utilization with the fission products present. In the absence of any fission product poisons, f is given by

$$f = \frac{\Sigma_{aF}}{(\Sigma_{aF} + \Sigma_{aM})} \tag{21.4}$$

and after the fission products have appeared, f′ is given by

$$f' = \frac{\Sigma_{aF}}{\left(\Sigma_{aF} + \Sigma_{aM} + + \Sigma_{aP}\right)} \tag{21.5}$$

Here, Σ_{aF}, Σ_{aM}, and Σ_{aP} are the macroscopic absorption cross sections for the fuel, the moderator, and the fission products, respectively. If we substitute these expressions into Equation 21.3, we find that the reactivity change due to the presence of the fission product poisons alone is

$$\Delta\rho = \frac{\left(f' - f\right)}{f'} = -\frac{\Sigma_{aP}}{\left(\Sigma_{aF} + \Sigma_{aM}\right)} \tag{21.6}$$

If $K'_{effective} \approx 1$, it is possible to show that this can be reduced even further to

$$\Delta\rho = -C\left(\frac{\Sigma_{aP}}{\Sigma_{aF}}\right) \tag{21.7}$$

where C is a constant equal to

$$C = \frac{1}{\eta\varepsilon p} \tag{21.8}$$

and Σ_{aF} is the macroscopic absorption cross section of the fuel.

21.2 Reactivity Changes due to Fission Product Poisons Like Xenon

Fission products such as *xenon* and *samarium* are by far the most important fission products as far as the time-dependent behavior of thermal water reactors is concerned. If we can predict their concentrations as a function of time, we can quantify the effect they have on the reactivity ρ and therefore the reactor period T. The properties of Xenon and Samarium are shown in Table 21.1. However, not all isotopes of xenon and samarium are capable of absorbing the same number of thermal neutrons. In fact, only one isotope of xenon (Xenon-135) and one isotope of samarium (Samarium-149) have an appreciable effect on the reactivity of the core. We would now like to discuss the impact of these isotopes in more detail.

21.3 Xenon Behavior during Start-Up, Equilibrium, and Shutdown

During normal reactor operation, several isotopes of xenon are produced in a reactor's fuel rods. They include Xenon-131, Xenon-133, and Xenon-135. However, only one of these isotopes—Xenon-135—has a high enough thermal absorption cross section to affect the reactivity of the core as a whole. The other two isotopes—Xenon-131 and Xenon-133—have neutron absorption cross sections that are thousands of times smaller (see Chapter 5), and so their effect on the

TABLE 21.1
Fission Product Yields and Decay Constants for Some Important Nuclear Fission Products

Isotope	Yield Y from U-235 (Atoms/Fission)[b]	Yield Y from Pu-239 (Atoms/Fission)[b]	Decay Constant λ (Second^{-1})	Decay Constant λ (Hour^{-1})	Half-Life
I-135	0.0639	0.0604	0.0000287	0.1035	6.57 hours
Xe-135	0.0028	0.0105	0.0000209	0.0753	9.2 hours
Pm-149	0.0107	0.0121	0.0000036	0.0131	53 hours
Sm-149[a]	0.0188	0.0123	0.0000000	0.0000	Infinite

[a] Stable under normal conditions.
[b] Thermal fission only.

time-dependent reactivity is of little practical importance. The Xenon-135 concentration can be analyzed in three different ways depending upon where a reactor is in its operating cycle:

1. The reactor start-up cycle
2. The reactor equilibrium operating cycle
3. The reactor shutdown cycle

In each of these cycles, the Xenon-135 concentration behaves differently, and so the reader must be able to select the appropriate cycle when attempting to understand how the buildup (or decay) of Xenon-135 affects the core. Thus, the buildup of Xenon-135 must be taken very seriously in all thermal water reactors.

Today, the owner/operator of any commercial nuclear power plant is required to take the buildup of xenon and samarium into account when the reactor is being operated. Moreover, most reactor operators are specifically trained to prevent a xenon transient from occurring. In modern nuclear power plants, the control systems are designed to minimize the probability that a xenon transient will occur. To put all of these factors into perspective, we would first like to discuss how the Xenon-135 concentration changes as a function of time. The reactivity change $\Delta\rho_{XE}$ associated with changes in the Xenon concentration can be initially deduced from the four-factor formula.

21.4 Scenario I: Xenon following Start-Up

In Chapter 18, we learned that if the neutron flux is constant, the Xenon-135 and Iodine-135 concentrations (in atoms per cubic centimeter) are determined by the following rate equations:

The Xenon-135 Concentration Following Start-Up

$$X(t) = X_o e^{-\lambda_x t} e^{-\sigma_{ax}\phi t} + \frac{\Sigma_f \phi (Y_x + Y_I)}{(\sigma_{ax}\phi + \lambda_x)\left[1 - e^{-\lambda_x t} e^{-\sigma_{ax}\phi t}\right]} + \frac{\lambda_I I_o - Y_I \Sigma_f \phi}{(\lambda_I - \lambda_x - \sigma_{ax}\phi)\left\{e^{-\lambda_x t} e^{-\sigma_{ax}\phi t} - e^{-\lambda_I t}\right\}} \tag{21.9}$$

and

The Iodine-135 Concentration Following Start-Up

$$I(t) = I_o e^{-\lambda_I t} + Y_I \frac{\Sigma_f \phi}{\lambda_I \left[1 - e^{-\lambda_I t}\right]} \tag{21.10}$$

which are a special case of the more general *Bateman equations*, which were discussed in Chapter 6 of our companion book.* Here, I_o and X_o are the *initial concentrations* of Iodine-135 and Xenon-135, respectively, at start-up. If the reactor is cold and clean at start-up and contains only fresh fuel, then I_o and X_o will initially be zero, and the equations for the concentrations can be simplified to read

$$X(t) = \frac{\Sigma_f \phi (Y_x + Y_I)}{(\sigma_{ax}\phi + \lambda_x)\left[1 - e^{-\lambda_x t} e^{-\sigma_{ax}\phi t}\right]} + \frac{Y_I \Sigma_f \phi}{(\lambda_I - \lambda_x - \sigma_{ax}\phi)\left\{e^{-\lambda_x t} e^{-\sigma_{ax}\phi t} - e^{-\lambda_I t}\right\}} \tag{21.11}$$

and

$$I(t) = \frac{Y_I \Sigma_f \phi}{\lambda_I \left[1 - e^{-\lambda_I t}\right]} \tag{21.12}$$

* See *Nuclear Engineering Fundamentals: A Practical Perspective*, by R.E. Masterson, CRC Press (2017).

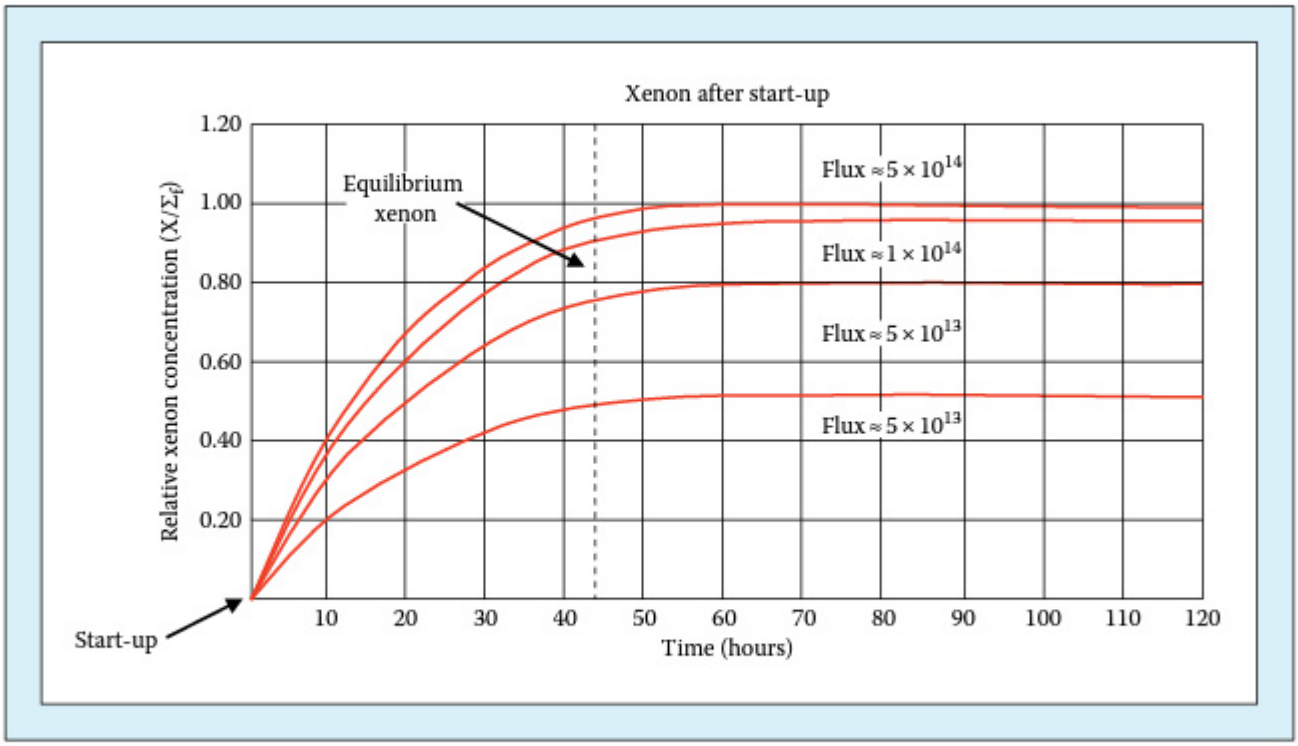

FIGURE 21.1 The buildup of Xenon-135 after the start-up of a cold, clean core as a function of time.

The later forms of these equations are the ones that appear in most reactor physics books. Notice that the production and decay of xenon and iodine depend on the level of the neutron flux ϕ. As the neutron flux is increased, more xenon and iodine will be produced. Conversely, if the neutron flux falls, exactly the opposite effect occurs. Eventually, the concentration of Xexon-135 reaches what is known as its *equilibrium concentration*. The equilibrium concentration X_∞ is determined by the value of the neutron flux $\phi(x, y, z)$. Hence, *the equilibrium xenon concentration also depends directly on the reactor power level P. Higher power levels will generate more xenon and lower power levels will generate less*. The buildup of Xenon-135 following the start-up of a cold, clean reactor core is shown in Figure 21.1. *Irrespective of the level of the neutron flux, the equilibrium Xenon-135 concentration is reached within about 40 hours.**

21.5 Scenario II: Equilibrium Xenon

The buildup of Xenon-135 is shown in Figure 21.1 for various values of the thermal neutron flux ϕ. In about 2 days, Xenon-135 reaches its equilibrium concentration if the thermal flux is greater than ~1×10^{13} neutrons/cm^2/s. The equilibrium Xenon-135 and Iodine-135 concentrations X_∞ and I_∞ can be found from Equations 21.9 and 21.10 by setting the value of $t = \infty$, or they can be found by setting $dI(t)/dt = 0$ and $dX(t)/dt = 0$ and solving for the appropriate values of X_∞ and I_∞. When equilibrium is reached, the concentration of Xenon-135 is given by

The Equilibrium Concentration of Xenon-135

$$X_\infty = \frac{\Sigma_f \phi \left(Y_x + Y_I\right)}{\left(\sigma_{ax}\phi + \lambda_x\right)} \tag{21.13}$$

where the terms have their usual meanings. Hence the macroscopic absorption cross section of Xenon-135 at equilibrium is

$$\Sigma_{aX} = X_\infty \sigma_{ax} = \Sigma_f \phi \left(Y_x + Y_I\right) \cdot \frac{\sigma_{ax}}{\left(\sigma_{ax}\phi + \lambda_x\right)} \tag{21.14}$$

* See *Nuclear Engineering Fundamentals: A Practical Perspective*, by R.E. Masterson, CRC Press (2017).

Dividing the numerator and the denominator on the right-hand side by σ_{ax}, Equation 21.14 can also be written as

The Absorption Cross Section of Xenon-135 at Equilibrium

$$\Sigma_{aX} = \frac{\Sigma_f \phi \left(Y_x + Y_I \right)}{\left(\phi + A \right)} \tag{21.15}$$

where the constant $A = \lambda_x/\sigma_{ax}$ typically has a value of about 0.8×10^{13} cm^2/s for thermal neutrons. Now let us see how the absorption cross section depends on the thermal neutron flux. There are three scenarios to consider, which we would like to describe for you now.

21.5.1 Case 1: A Low Thermal Flux

If the thermal flux is considerably less than A (say $\phi \ll 1 \times 10^{13}$ neutrons/cm^2/s), then the macroscopic absorption cross section of Xenon-135 is

The Macroscopic Absorption Cross Section of Xenon-135 When the Neutron Flux Is Low

$$\Sigma_{aX} = \frac{\Sigma_f \phi \left(Y_x + Y_I \right)}{A} \tag{21.16}$$

21.5.2 Case 2: A Moderate Thermal Flux

If the thermal flux is about the same as A (say $\phi \cong 1 \times 10^{13}$ neutrons/cm^2/s), then the macroscopic absorption cross section of Xenon-135 is

The Macroscopic Absorption Cross Section of Xenon-135 When the Neutron Flux Is Moderate

$$\Sigma_{aX} = \frac{\Sigma_f \left(Y_x + Y_I \right)}{2} \tag{21.17}$$

21.5.3 Case 3: A High Thermal Flux

Finally, if the thermal flux becomes much greater than A (say $\phi \gg 1 \times 10^{13}$ neutrons/cm^2/s), then the macroscopic absorption cross section of Xenon-135 becomes

The Macroscopic Absorption Cross Section of Xenon-135 When the Neutron Flux Is High

$$\Sigma_{aX} = \Sigma_f \left(Y_x + Y_I \right) \tag{21.18}$$

Case 3 applies to most commercial power reactors, and Case 1 applies to most research reactors. In other words, each case effectively places a limit on the size of the macroscopic Xenon-135 cross section. However, the reader must keep in mind that only about 1/3 of the neutrons in a thermal water reactor are thermal neutrons (The remainder are epi-thermal or fast). Consequently, we must always use the *thermal flux* in these equations to find the correct absorption rate. Moreover, we also know that if the value of $K'_{effective}$ is close to unity, the reactivity change caused by an arbitrary fission product poison (see our discussion in Chapter 18) is

$$\Delta\rho = -C\left(\frac{\Sigma_{aP}}{\Sigma_{aF}} \right) \tag{21.19}$$

where C is a constant equal to

$$C = \frac{1}{\eta \varepsilon p} \tag{21.20}$$

Σ_{aP} is the macroscopic absorption cross section of the poison, and Σ_{aF} is the macroscopic absorption cross section of the fuel. If we assume that $\Sigma_{aX} = \Sigma_{aP}$, we can use Equation 21.19 to estimate the effect that Xenon-135 has on the

TABLE 21.2
Equilibrium Xenon-135 Concentrations for Different Values of the Thermal Neutron Flux

Xenon Equilibrium—Low Flux
For $(\phi \ll A)$:
$\Delta\rho = \dfrac{-C\phi(Y_x + Y_I)}{\chi}$
Xenon Equilibrium—Medium Flux
For $(\phi \approx A)$:
$\Delta\rho = \dfrac{-C(Y_x + Y_I)}{2}$
Xenon Equilibrium—High Flux
For $(\phi \gg A)$:
$\Delta\rho = -C(Y_x + Y_I)$

reactivity at each of these flux levels by simply substituting the three values for Σ_{aX} into Equation 21.19. We then obtain the expressions shown in Table 21.2. It is remarkable that the reactivity due to the buildup of the xenon alone can be found so easily when the Xenon-135 concentration comes into equilibrium. For example, suppose that we are dealing with a Uranium-235-fueled thermal water reactor where $\varepsilon = p = 1$ and the average number of neutrons emitted per fission is 2.42. Also assume that the resonance escape probability p is 1.0 for the moment. In the case where $\phi \ll 1 \times 10^{13}$ neutrons/cm^2/s, the reactivity reduction would be

$$\Delta\rho = \frac{-C\phi(Y_x + Y_I)}{A} \tag{21.21}$$

Hence if the thermal neutron flux is $\phi \sim 1 \times 10^{12}$, then $\Delta\rho = -0.0027$. This would correspond to the reactivity reduction in a very low power research reactor. In the case where the thermal neutron flux is higher (say $\phi \approx 1 \times 10^{13}$ neutrons/cm^2/s), The reactivity reduction would be

$$\Delta\rho = \frac{-C(Y_x + Y_I)}{2} \quad \text{and} \quad \Delta\rho = -0.013 \tag{21.22}$$

and finally when $\phi \gg 1 \times 10^{13}$ neutrons/cm^2/s, we would be dealing with a commercial power reactor and

$$\Delta\rho = -C(Y_x + Y_I) \quad \text{and} \quad \Delta\rho = -0.027 \tag{21.23}$$

If we assume each of these reactors is fueled with U-235, then $\beta = 0.0065$, and in the first case (where $\phi \sim 1 \times 10^{12}$ neutrons/cm^2/s), the xenon buildup reduces the reactivity by $\Delta\rho/\beta = 42¢$. In the second case (where $\phi \sim 1 \times 10^{13}$ neutrons/cm^2/s), the xenon buildup reduces the reactivity by $\Delta\rho/\beta = \$2.00$, and in the third case (where $\phi \gg 1 \times 10^{13}$ neutrons/cm^2/s), the xenon buildup reduces the reactivity by $\Delta\rho/\beta = \$4.15$. This is an astounding reactivity reduction for a single neutron poison in a thermal water reactor.

21.6 Scenario III: Shutdown Xenon

The rate at which Xenon-135 accumulates after a reactor is shut down is governed by the Xenon and Iodine decay chains. As we discovered in Chapter 6, of our companion book,* the buildup of xenon under these conditions is an example of what is known as a *parent–daughter relationship*. Here, Iodine-135 is the "parent," and Xenon-135 is the "daughter." Now let us explore the dynamics of these decay chains in more detail. Iodine-135 is produced initially from the decay of another fission product called Tellurium-135. Tellurium-135 is produced directly from the fission of U-235, and its effective yield

* See *Nuclear Engineering Fundamentals: A Practical Perspective*, by R.E. Masterson, CRC Press (2017).

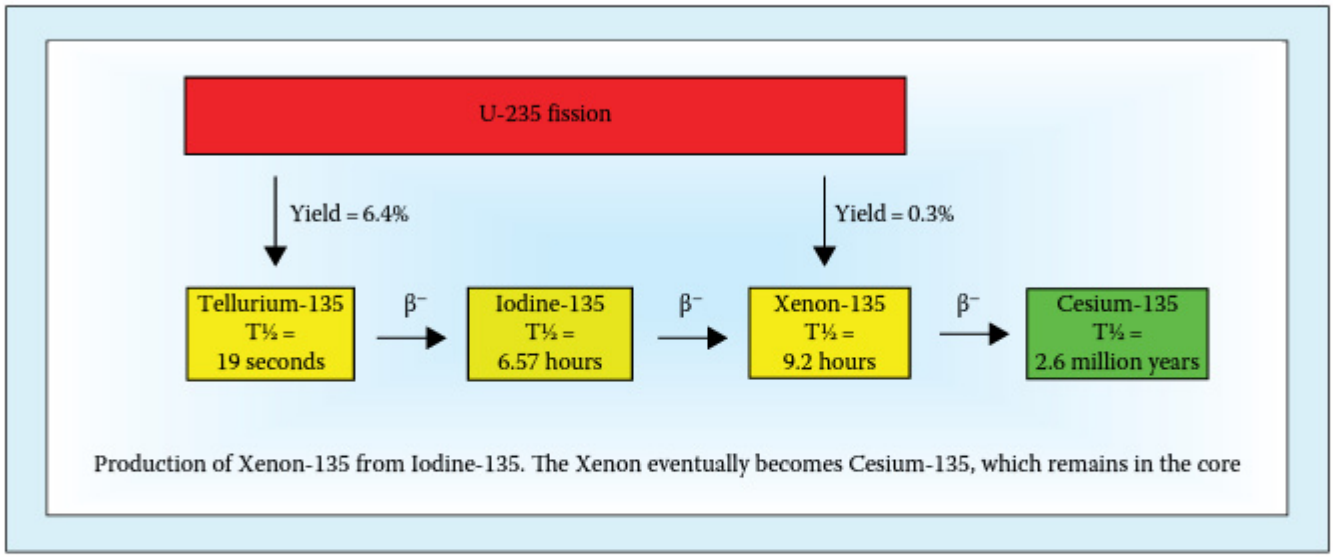

FIGURE 21.2 The Xenon-135 fission product decay chain. Xenon-135 eventually becomes Cesium-135, which in some countries, is also called Caesium.

Y_{Te} is about 0.064, or 6.4%.Tellurium-135 decays into Iodine-135 so quickly (its half-life is about 19 seconds) that for all practical purposes, the Iodine-135 can be assumed to be created directly from the fission of U-235 with a yield of 6.4%. The actual sequence of events that leads to the production of Xenon-135 is shown in Figure 21.2. Xenon-135 then decays into Cesium-135, which has a half-life of about 2.6 million years, and continues to remain in the core. Now let us see if we can deduce the time-dependent behavior of Xenon-135 after the core is shutdown, and none of the remaining Xenon-135 can be converted into Xenon-136 by absorbing a thermal neutron.

Iodine-135 has a half-life of 6.57 hours, and Xenon-135 has a half-life of 9.2 hours. Because Iodine-135 decays faster than Xenon-135 does, the production curve for Xenon-135 displays a characteristic peak or "hump" (see Figure 21.2). The width and the height of this hump are determined by the difference between the respective decay constants λ_X and λ_I for xenon and iodine. For Xe-135 and I-135 the difference is $\lambda_I - \lambda_X = 0.1035\ \text{hour}^{-1} - 0.0753\ \text{hour}^{-1} = 0.0282\ \text{hour}^{-1}$. We also learned in Chapter 18 that about *95% of the Xenon-135 produced comes from the Iodine-135 decay chain. (The rest comes directly from the thermal fission of U-235.)* We also showed in Chapter 18 that the xenon concentration at any time after shutdown, where $\phi = 0$ at $t = 0$, is given by

$$X(t) = X_o e^{-\lambda_x t} + \frac{\lambda_I}{(\lambda_I - \lambda_x) I_o \left\{ e^{-\lambda_x t} - e^{-\lambda_I t} \right\}} \tag{21.24}$$

or since

$$X_o = \frac{\Sigma_f \phi (Y_X + Y_I)}{(\sigma_{ax} \phi + \lambda_x)} \tag{21.25}$$

we obtain

The Concentration of Xenon-135 after a Reactor Is Shut Down

$$X(t) = \frac{\Sigma_f \phi (Y_X + Y_I)}{(\sigma_{ax} \phi + \lambda_x) e^{-\lambda_x t}} + \frac{\lambda_I}{(\lambda_I - \lambda_x) I_o \left\{ e^{-\lambda_x t} - e^{-\lambda_I t} \right\}} \tag{21.26}$$

where shutdown is assumed to occur at t = 0. *Exactly how high the Xenon-135 concentration gets depends on the initial values for X_o and I_o, where $X_o = X(0)$ and $I_o = I(0)$. Most of the time, these will be equal to the equilibrium concentrations, so $X_o = X_\infty$ and $I_o = I_\infty$ in atoms/cm³.* It therefore follows that the contribution of Xenon-135 to the total reactivity of the core is

The Maximum Contribution of Xenon-135 to the Overall Reactivity (after Shutdown)

$$\Delta\rho_X = -C\left[\frac{\phi\left(Y_X + Y_I\right)}{\left(\phi + A\right)e^{-\lambda_x t}} + \frac{\lambda_I}{\left(\lambda_I - \lambda_x\right)I_o\left\{e^{-\lambda_x t} - e^{-\lambda_I t}\right\}}\right] \tag{21.27}$$

where

$A = \lambda_x / \sigma_{ax} \approx 0.8 \times 10^{13}$ cm²/s at thermal energies

$C = 1/\eta\varepsilon p$

Consequently, the reactivity change is always a negative number. Here Y_X and Y_I are the direct yields of Xenon-135 and Iodine-135 from the thermal fission of U-235. *Their exact values—$Y_X = 0.0028$ and $Y_I = 0.0639$—are a function of the type of fuel that is used. For example, if we use Pu-239 instead, the yields are $Y_X = 0.0105$ and $Y_I = 0.0604$ and the yields of Xenon-135 and Iodine-135 are different for U-233 as well.* So in addition to affecting the delayed neutron fraction β, the type of fuel affects the width of the xenon production and decay curve.

Exactly how large the negative reactivity becomes depends on the previous value of the thermal neutron flux. Now let us consider how Equation 21.27 applies to the following four scenarios:

1. Thermal neutron flux = 1×10^{13} neutrons/cm²/s
2. Thermal neutron flux = 5×10^{13} neutrons/cm²/s
3. Thermal neutron flux = 1×10^{14} neutrons/cm²/s
4. Thermal neutron flux = 5×10^{14} neutrons/cm²/s

Figure 21.3 shows the negative reactivity Xenon-135 adds as it builds up and ultimately decays. Using Equation 21.26, we find that *the Xenon-135 concentration peaks about 12 hours AFTER the reactor shuts down. This occurs because the*

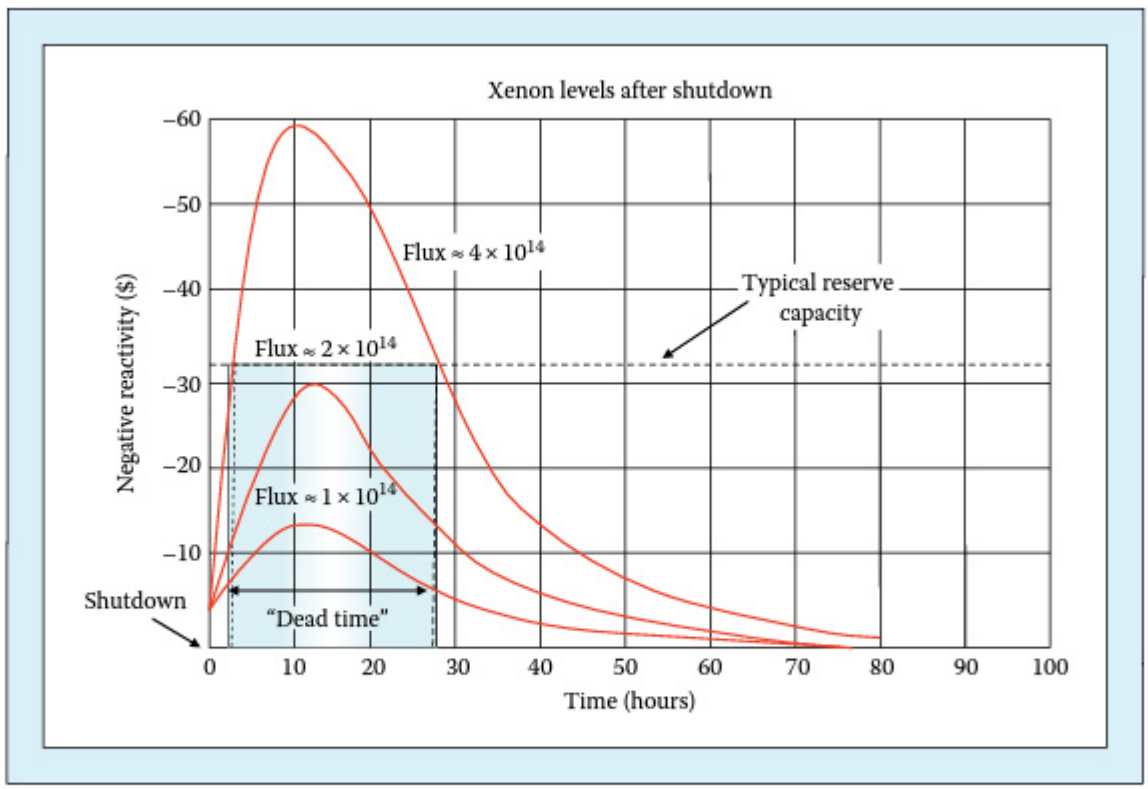

FIGURE 21.3 An illustration of how Xenon-135 affects the reactivity of a thermal water reactor core at various times after a reactor is shutdown. Notice that the maximum negative reactivity is reached in about 12 hours after the initial shutdown.

TABLE 21.3
Reactivity Reductions due to the Buildup of Xenon-135 Alone[a]

Average Thermal Flux	Maximum Negative Reactivity (~40 Hours after Start-Up)		Maximum Negative Reactivity (~12 Hours after Shutdown)		Total Negative Reactivity	
ϕ	$\Delta\rho$	Dollars	$\Delta\rho$	Dollars	$\Delta\rho$	Dollars
1×10^{13}	0.013	\$2.00	0.020	\$3.00	0.033	\$5.00
5×10^{13}	0.025	\$3.90	0.055	\$8.46	0.080	\$15.36
1×10^{14}	0.026	\$4.00	0.110	\$16.92	0.136	\$20.92
5×10^{14}	0.027	\$4.15	0.540	\$83.07	0.567	\$87.22

[a] For a Uranium-235-fueled thermal reactor.

half-life of Iodine-135 is about 6.57 hours, and it takes another 9.2 hours for about half of the Xenon-135 to decay away. We also find that the time at which the xenon-135 concentration peaks is *nearly independent* of the initial concentrations of xenon and iodine—as long as they had previously attained their equilibrium concentrations.

This means that no matter how the reactor was operated initially, the negative reactivity produced by the additional xenon peaks about 12 hours after the reactor is shut down. For typical levels of the thermal neutron flux ($\phi \approx 5 \times 10^{13}$ neutrons/cm^2/s), the negative reactivity is nearly equal to the negative reactivity of the moderator and all of the structural materials combined! On the other hand, the amount of Xenon-135 at the concentration peak *does* depend on how the reactor was operated prior to shut down. The higher the reactor power level is prior to shut down, the *higher* the xenon concentration at the peak will be, and the larger effect it will have on the total reactivity of the core.

- If the thermal flux is $\phi = 1 \times 10^{13}$ neutrons/cm^2/s prior to shutdown, then the negative reactivity after shutdown due to the buildup of Xenon-135 alone will be 0.020, or about \$3.00.
- If the thermal flux is $\phi = 5 \times 10^{13}$ neutrons/cm^2/s prior to shutdown, then the negative reactivity after shutdown due to the buildup of Xenon-135 alone will be 0.055, or about \$8.46.
- If the thermal flux is $\phi = 1 \times 10^{14}$ neutrons/cm^2/s prior to shutdown, then the negative reactivity after shutdown due to the buildup of Xenon-135 alone will be 0.110, or about \$16.92.
- If the thermal flux is $\phi = 5 \times 10^{14}$ neutrons/cm^2/s prior to shutdown, then the negative reactivity after shutdown due to the buildup of Xenon-135 alone will be 0.540, or about \$83.07.

These figures do not include the equilibrium concentrations of xenon, which we have already shown can add an additional 40 cents to \$4.15 to the same totals. Again, these numbers are based on using U-235 for the fuel, and they are valid for thermal neutrons only.

Table 21.3 summarizes the negative reactivity that Xenon-135 can add to the core for different levels of the thermal neutron flux ϕ in neutrons/cm^2/s. These values are based on a delayed neutron fraction of 0.0065, which is appropriate for a Uranium-235-fueled thermal water reactor. *For a normal neutron flux of 5×10^{13} neutrons/cm^2/s, shutting down the plant adds over \$12.00 of additional negative reactivity to the core*. This is obviously an important effect because the production of Xenon-135 can impact how the reactor can be restarted from a previous subcritical state. Reactors usually operate with a reserve reactivity of 0.20 (30 times β), or about \$30.00 of excess positive reactivity from all sources (control rods alone or control rods plus soluble boron). If a reactor has been operating at even a higher flux level for several days (say 5×10^{14} neutrons/cm^2/s), and it is then shut down, it may take 40 hours or even longer before the Xenon-135 returns to a level that allows the reactor to overcome this enormous amount of negative reactivity. This period of time where the reactor is essentially unavailable for service due to the excess Xenon-135 is called *reactor "dead time," or "xenon precluded start-up." In this state, even withdrawing all of the control rods from the core will not allow the reactor to become critical again*. The xenon must simply decay away before the reactor can be restarted again.

21.7 Reactor Dead Time and Its Implications

The additional Xenon-135 reaches its maximum concentration about 12 hours after a thermal water reactor is shut down. *This time to peak xenon is really not affected by how the reactor was operated previously.* Thus after 12 hours, the poisoning powers of xenon reach their maximum effectiveness, and the xenon concentration can become large enough to absorb more neutrons than the fuel can create. This is especially true when the reactor has been operating at a very high power level and has therefore had a very high value of ϕ for some time. *When the xenon concentration reaches its peak, even withdrawing all of the control rods from the core may not be able to start the reactor up again.* For all intents and purposes, *the reactor behaves as if it were DEAD.*

Depending on the previous power level, the post-shutdown buildup of Xenon-135 can reduce the system-wide reactivity $\Delta\rho$ from \$3.00 to about \$80.00. Above an average thermal flux of 5×10^{13} neutrons/cm^2/s, the amount of poisoning increases linearly with the flux or the power. One may therefore have to wait between 2 hours and 35 hours before most of the xenon has decayed away, and the reactor can be restarted again. During this *dead time*, the xenon's ability to absorb free neutrons completely dominates the behavior of the core. This unfortunate situation can be very costly to a nuclear utility when energy from the reactor is needed to meet demand peaks late in the afternoon, and the cost of replacement power is very high. In the past, some improperly trained reactor operators have tried to correct this condition by fully withdrawing most of the control rods from the core. This can result in an even more serious situation if the reactor has been previously operating at very high power levels because when the xenon finally burns off or decays, there will be a *large power spike* if the control rods are fully withdrawn. If the burn-off of Xenon-135 is not properly anticipated, then the core may become too hot, and some of the fuel rods may overheat and begin to rupture or melt. Even worse yet, a *xenon power oscillation* may occur, where the power level increases on one side of the core, while the power level on the other side decreases. In any event, the buildup of Xenon-135 (and its sister element Samarium-149) must be anticipated when the time-dependent behavior of the core is taken into account. We would now like to illustrate how the buildup and decay of Xenon-135 can affect the time-dependent power level.

21.8 Nonintuitive Xenon Behavior

Test reactors, training reactors, and research reactors are all examples of reactors where the time-dependent behavior of xenon can be studied and observed. However, if you have never operated one of these reactors before, you will find that xenon does not necessarily behave in the way that you would intuitively expect it to because of the interaction between the reactor power and the Xenon-135 and Iodine-135 decay chains. *Generally speaking, the change in the Xenon-135 concentration (at least initially) occurs in the opposite direction to what is done to the flux and power levels.* For example, if the power level is suddenly *decreased* in a stepwise manner (see Figure 21.4) then the xenon concentration will initially *increase* before it decreases. Conversely if the power level is suddenly *increased* (see Figure 21.5) then the Xenon-135 concentration will suddenly *decrease* before eventually rising to an even higher equilibrium concentration. This occurs because additional neutrons can burn off the xenon more quickly than the iodine decay chain can build it back up.

Conversely, a lower power level will cause the zenon buildup from the iodine decay chain to overwhelm the initial reduction in its production rate, and the Xenon-135 concentration will increase quickly. Consequently, it is not necessary for a reactor operator to shut down the core to increase the Xenon-135 concentration, although its buildup is greatest when this occurs because there are no additional neutrons left to burn it away. As a result of this curious pattern of behavior, changes in the core power level, if not carefully thought through, can result in what are known as *xenon power transients.* When these transients occur, changes to the reactivity caused by the time-dependent xenon concentration can be compensated for by either adjusting the control rods, in or out, or by adjusting the soluble boron concentration if the reactor is also equipped with a chemical shim control system. In other transients, changes to the Xenon-135 concentration can cause the flux to tilt severely, or even oscillate spatially with time. Figure 21.6 illustrates a classic example of this behavior, and not surprisingly, this behavior is called a *xenon flux tilt transient.* This unusual

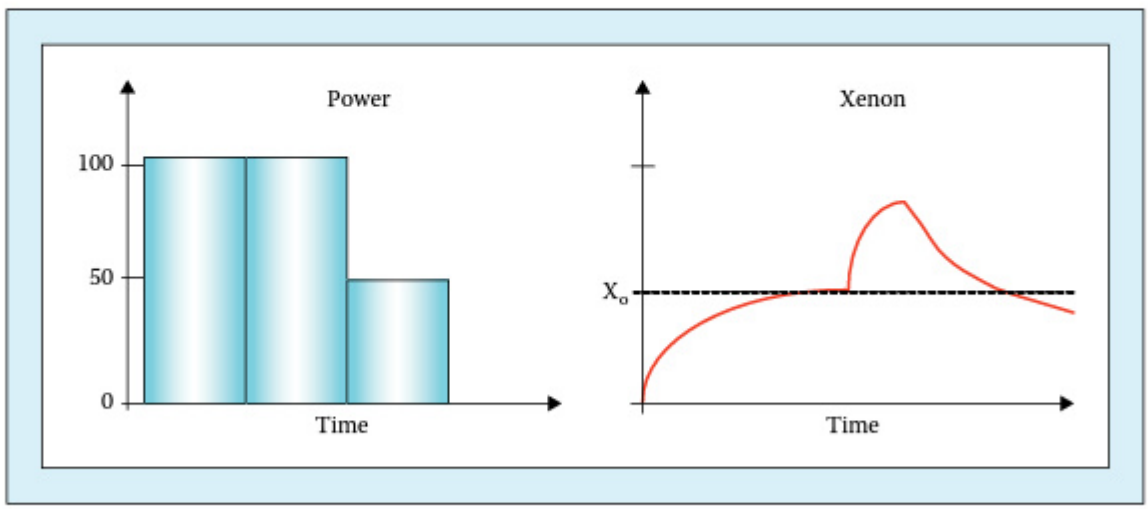

FIGURE 21.4 The xenon concentration after the power level is reduced by 50%.

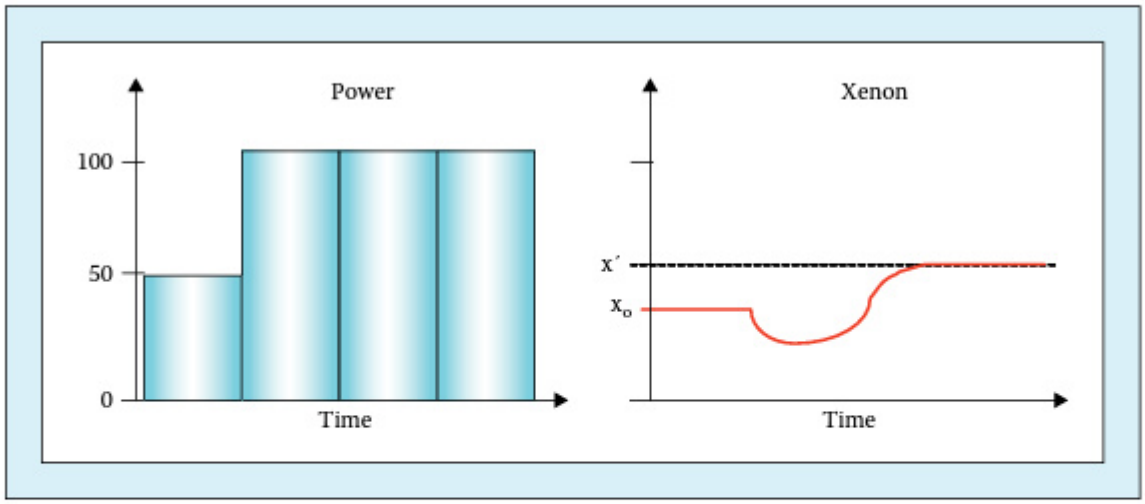

FIGURE 21.5 The xenon concentration after the power level is increased by 50%.

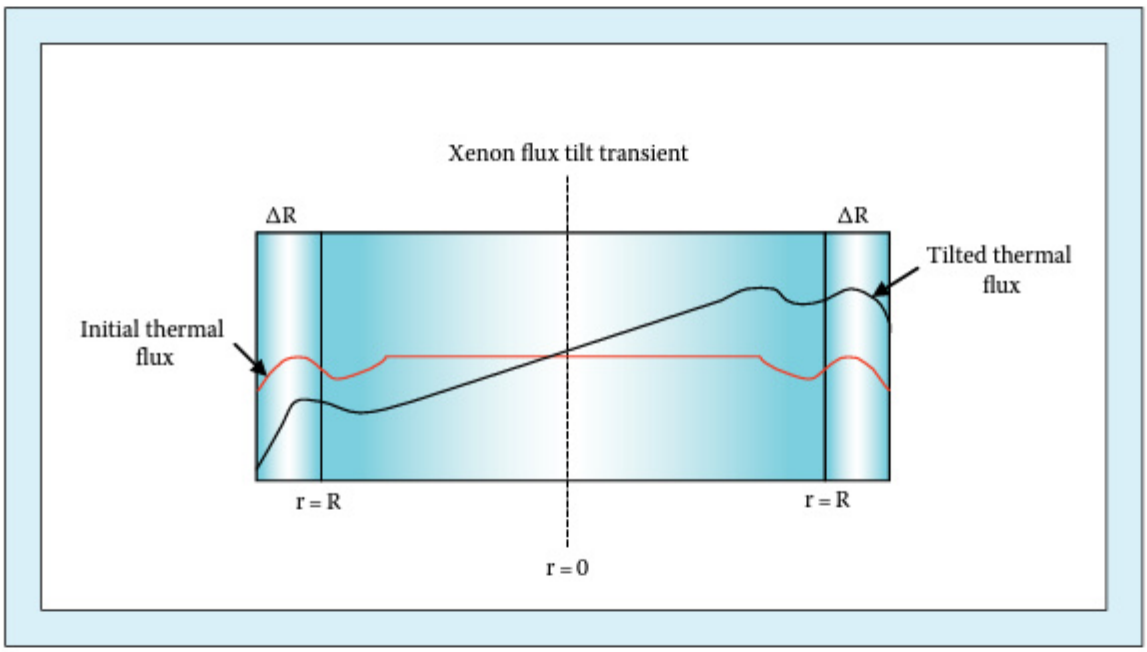

FIGURE 21.6 A *xenon flux tilt* transient in a thermal water reactor.

behavior occurs when some control rods on one side of the core are inserted (or withdrawn) more than the control rods on the other side of the core when the transient begins. This configuration leads to a spatially nonuniform xenon buildup and the decay of Iodine-135 then results in even more changes to the Xenon-135 concentration over time. If these types of events are not foreseen in advance, the reactor power level may oscillate back and forth, from right to left, and then from left to right like a *yo-yo*. Obviously, this is a situation the operator needs to avoid, and in a well-operated reactor, xenon power transients and flux tilts rarely, if ever, occur.

21.9 Power Control and Demand Management to Avoid Xenon Imbalances in the Core

The minimum amount of power that a utility must supply to its customers is called its *base load*. The base load can vary greatly from one utility to the next, and it can also vary depending on the time of the year. *Generally speaking, the base load is greater in the summer or the winter than it is in the fall or the spring*. A representative *demand curve* showing the base load over the course of an entire year is shown in Figure 21.7. In addition, the variable demand for electricity above and beyond the base load is called the *peak load*, and the peak load can be characterized by various *demand peaks*,

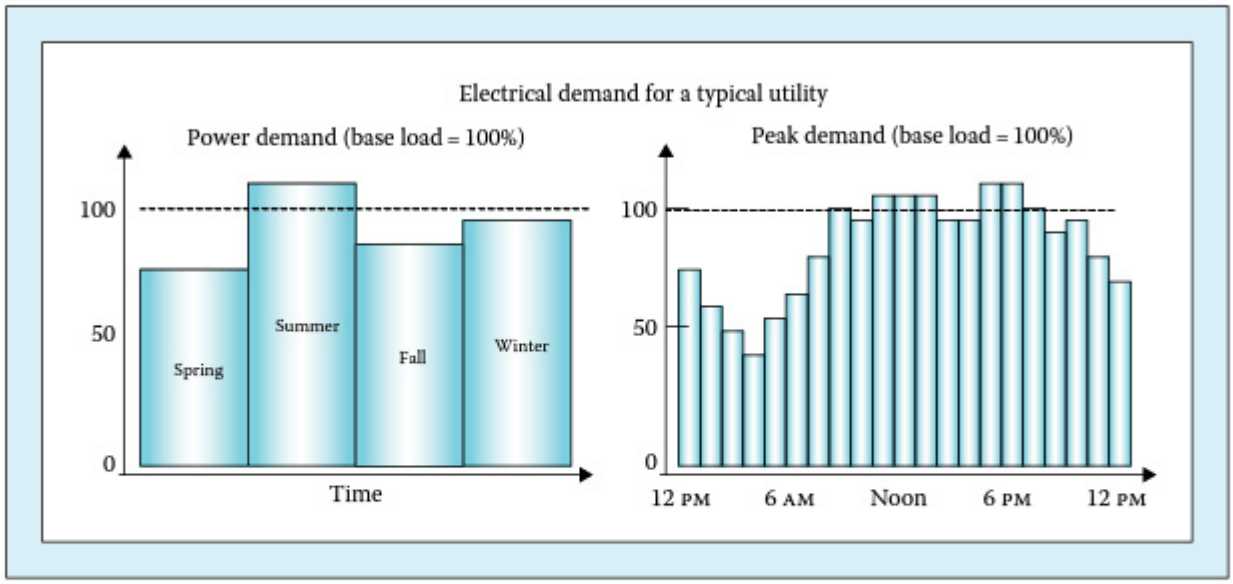

FIGURE 21.7 A typical utility demand cycle showing base load and peak load.

or times of the day of greater electrical need. As Figure 21.7 shows, the greatest demand for electricity usually occurs from about 10 AM in the morning until about 10 PM at night. After midnight, the demand for electricity falls rapidly until it reaches a *load trough* at about 4 AM in the morning. From here, it increases again until about 10 AM, when the need for power becomes very high. Based on historical demand data, the time of greatest demand is usually between 4 PM and 7 PM on a hot summer day. This is also the time of the year when the electrical grid is under considerable stress, and when unanticipated brownouts or blackouts can sometimes occur. The great American brownout of 2002 which shut down the city of New York was an example of one such event. Unanticipated brownouts of this size occur once every 10 or 20 years.

Because of the effect xenon-135 has on the reactivity when the power demand is greatest, most utilities use their largest and most efficient generating facilities, such as nuclear plants, to supply the base load for the electrical grid. Under these conditions the amount of power generated by a nuclear plant may only vary by a few percent. Under these conditions, the reactor period T is normally greater than a minute, and most of the time, the reactor will oscillate between being just barely critical (where $\rho \approx 0$), and being about 10% prompt supercritical (where $\rho \approx 0.10\beta$, or 10 cents). (Some utilities manage this reactivity swing even more aggressively.) Finally, during large power peaks, most utilities handle the demand for additional power with older, smaller, or less efficient generating equipment. Because this equipment is much more expensive per kilowatt than the systems providing the base load, the cost of this additional power during demand peaks usually shows up on electric bills as an additional fee or "*demand charge*." In addition, because the temporary power can come from a wide variety of temporary energy sources, the power is generally not as "clean" when it enters the demand pool as electricity from large base-loaded units. This can cause the annoying buzz of lights, attic fans, and other electrical equipment that is sometimes observed in homes during the summer months. *The result of all this optimization is that commercial nuclear power plants, with some exceptions, are almost always operated in a base-loaded mode*.

21.10 Reactivity Changes due to Samarium Buildup and Decay

In Chapter 18, we learned that *Samarium-149* is not as strong a thermal neutron absorber as Xenon-135. However, because it has the *second largest thermal absorption cross section* of any common fission product, its buildup must be taken very seriously when controlling the time-dependent behavior of thermal water reactors. Normally, the buildup of Samarium-149 can be subdivided into the same three categories as the buildup of its companion fission product, Xenon-135—start-up, equilibrium operation, and shutdown. Hence we would like to take some time to examine the effect that the buildup of Samarium-149 can have on the reactivity of the core. Although samarium has six other isotopes that can be found in measurable quantities in nature (see Chapter 6 of our companion book), only the buildup of Samarium-149 is of importance to the operation of a commercial nuclear power plant. *Samarium-149 is NOT produced in significant quantities directly from the thermal fission of U-235*. In fact, its direct yield Y_S is close to 0. However, it is produced in large quantities from the decay of another important isotope, Promethium-149. The yield of Promethium-149, Y_P, is 1.0888%. Hence, the effective yield of Samarium-149, when measured in these terms, is also 1.0888% when the promethium decays. Now let us take a closer look at its buildup and decay over time.

21.10.1 Case 1: The Samarium Concentration following Reactor Start-Up

The time-dependent concentrations of Promethium-149 and Samarium-149 immediately following the start-up of the core are given by the following rate equations, which can be deduced from the laws of *radioactive decay* (see Chapter 6 of our companion book):

Concentrations of Promethium and Samarium at Start-Up

$$P(t) = P_o e^{-\lambda_P t} + \frac{Y_{Nd}\Sigma_f \phi}{\lambda_P\left(1 - e^{-\lambda_P t}\right)}$$

and

$$S(t) = S_o e^{-\sigma_{as}\phi t} + \frac{Y_{Nd}\Sigma_f}{\sigma_{as}\left(1 - e^{-\sigma_{as}\phi t}\right)} - \left(\frac{Y_{Nd}\Sigma_f \phi - \lambda_P P_o}{\left(\lambda_P - \sigma_{as}\phi\right)\left(e^{-\sigma_{as}\phi t} - e^{-\lambda_P t}\right)}\right) \tag{21.28}$$

where P_o and S_o are the concentrations of Promethium-149 and Samarium-149 at start-up (t = 0). Notice that these equations are coupled together in the sense that one must first know the promethium concentration P in order to find the samarium concentration S. *Because Samarium-149 is not produced directly from the thermal fission of U-235, the value of Y_S in this case is zero.* For a cold, clean core, the equations mentioned earlier reduce to

The Concentrations of Promethium-149 and Samarium-149 for a Cold, Clean Core

$$P(t) = \frac{Y_{Nd}\Sigma_f \phi}{\lambda_P\left(1 - e^{-\lambda_P t}\right)}$$

and

$$S(t) = \frac{Y_{Nd}\Sigma_f}{\sigma_{as}\left(1 - e^{-\sigma_{as}\phi^t}\right)} - \left(\frac{Y_{Nd}\Sigma_f \phi}{\left(\lambda_P - \sigma_{as}\phi\right)\left(e^{-\sigma_{as}\phi t} - e^{-\lambda_P t}\right)}\right) \tag{21.29}$$

since $P_o = 0$ and $S_o = 0$ at t = 0. Here, Y_{Nd} is the initial yield of *Neodymium-149*, which is 0.0108, or about 1.088%. The Neodymium-149 created from the thermal fission of U-235 decays into Samarium rather quickly, and its half-life (the inverse of its decay constant) is about 2 hours. Thus although many textbooks assume that the Samarium-149 is produced immediately, it is in fact created through the process shown in Figure 21.8. If there is

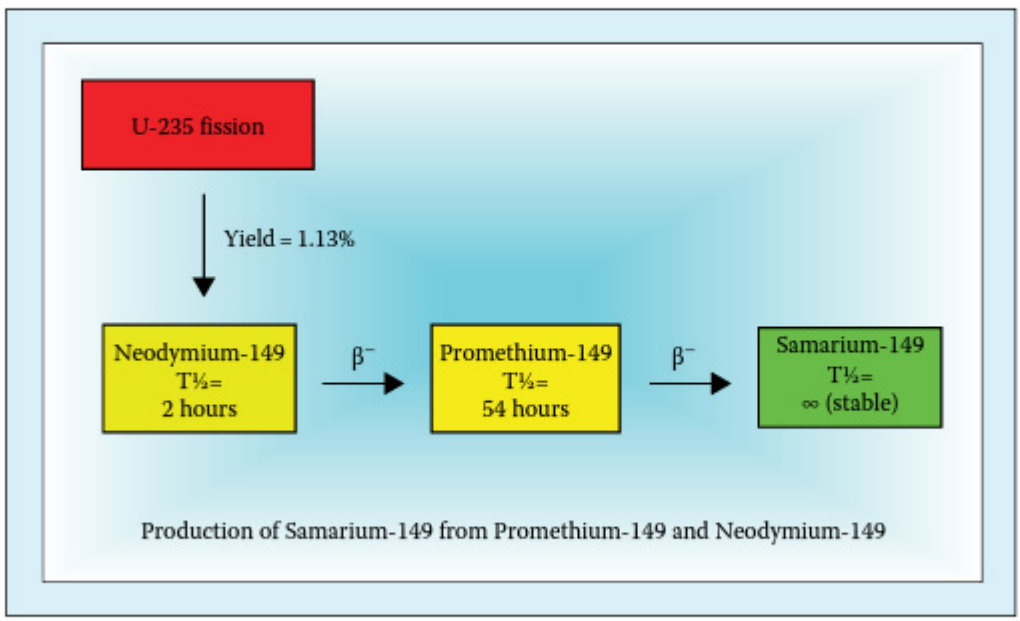

FIGURE 21.8 An illustration of the Samarium-149 production process which also involves Promethium-149 and Neodymium-149.

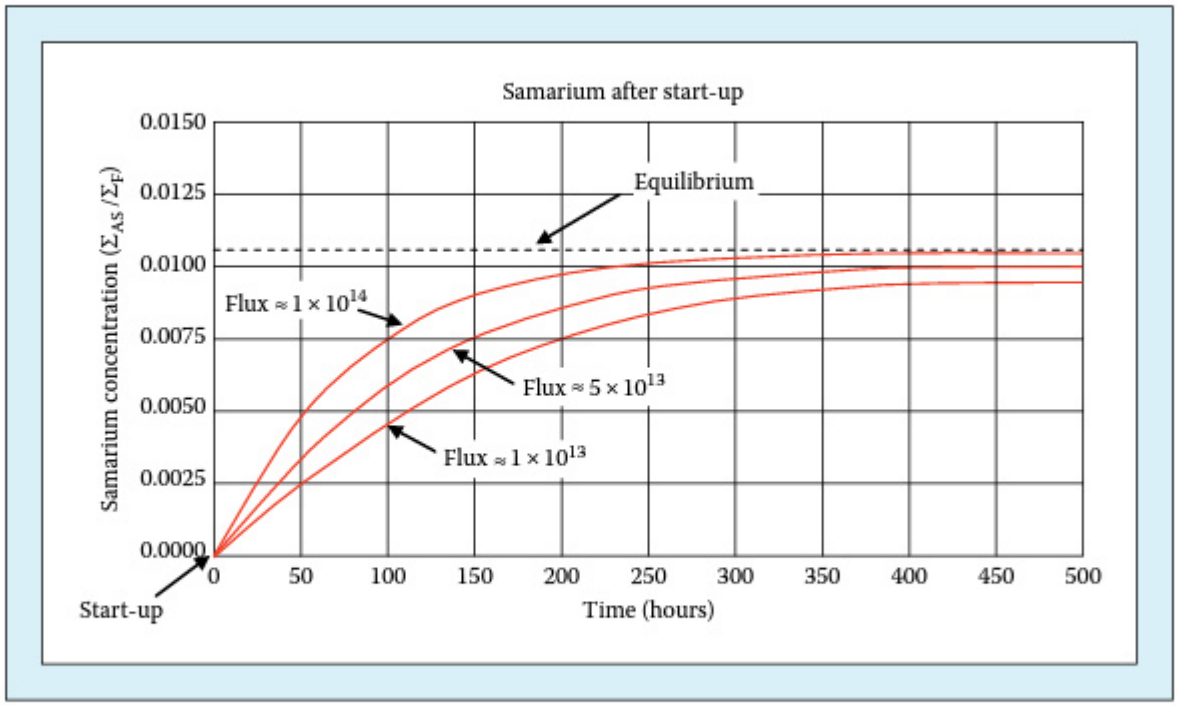

FIGURE 21.9 The buildup of samarium after a reactor is started up. This example assumes a cold, clean core.

no Promethium-149 or Samarium-149 present initially, it will take several days before either isotope reaches its steady-state concentration. If one examines the size of the promethium decay constant λ_P, one finds that it has a value of ~3.56×10^{-6} seconds, and $\sigma_{as}\phi$ has a value of ~2.04×10^{-6} seconds at a thermal flux of $\phi = 5 \times 10^{13}$ neutrons/cm^2/s. So, it will take about 10^6 seconds, or about 300 hours (13 days), for the Samarium-149 in the core to reach its equilibrium concentration S_∞. As one can see, the rate that Samarium-149 is produced depends on the value of the thermal neutron flux ϕ. However, as $t \rightarrow \infty$, the exponential terms cancel, and the concentration of Samarium-149 approaches what is known as its equilibrium value. The general trend showing how the Samarium-149 concentration behaves as a function of time is shown in Figure 21.9. This figure was adapted from an earlier figure that was presented in Chapter 18. *Note in particular that the equilibrium concentration of Samarium-149 does NOT depend on either the level of the neutron flux or the reactor power*. In this respect, its behavior is much easier to understand than the buildup and decay of Xenon-135.

21.10.2 Case 2: Equilibrium Samarium

In Chapter 18, we also learned that the equilibrium concentration of Samarium-149, S_∞, is given by

The Equilibrium Concentration of Samarium-149

$$S_\infty = \frac{Y_P \Sigma_f}{\sigma_{as}} \tag{21.30}$$

We would now like to use this equation to demonstrate how the buildup of samarium can affect the reactivity of the core. Using the fact that the reactivity change due to the introduction of an arbitrary fission product poison is given by

$$\Delta\rho_S = -C\left(\frac{\Sigma_{aP}}{\Sigma_{aF}}\right) \tag{21.31}$$

where C is a constant equal to

$$C = \frac{1}{\eta \varepsilon p} \tag{21.32}$$

TABLE 21.4
Effective Yields, Thermal Cross Sections, and Decay Constants for Some Important Neutron Poisons

Material	λ (Seconds^{-1})	σ_a (cm^2)	Yield (U-233)[a]	Yield (U-235)[a]	Yield (Pu-239)[a]
I-135	2.87×10^{-5}	1.2×10^{-22}	0.0475	0.0639	0.0604
Xe-135	2.09×10^{-5}	2.7×10^{-18}	0.0107	0.0024	0.0105
Pm-149	3.56×10^{-6}	2.0×10^{-21}	0.0079	0.0107	0.0121
Sm-149	0[b]	4.0×10^{-20}	—	0.0108	—

[a] Atoms per thermal fission.
[b] Stable.

and Σ_{aF} is the macroscopic absorption cross section of the fuel. We can then substitute the equilibrium concentration of Samarium-149 into this equation to find the reactivity change $\Delta\rho_S$ due to the presence of the samarium alone. The σ_{as}'s and Σ_{aF}'s cancel, and we then discover that

$$\Delta\rho_S = -CY_p \tag{21.33}$$

This remarkably simple expression allows us to understand how the buildup of Samarium-149 can affect the reactivity of the core. *It is interesting to observe that the equilibrium concentration of samarium S_∞ (and therefore the equilibrium reactivity change) does NOT depend on either the level of the neutron flux or the power.* It only depends on the simple constants we have already discussed. From Table 21.4, we find that $Y_p = 0.0107$ for U-235, and so the reactivity equivalent of the Samarium-149 is

$$\Delta\rho_S = \frac{-0.0107}{2.42} = -0.0044 \text{ or about } -68 \text{ cents.}$$

This of course assumes that $\varepsilon = p = 1$. *So for a high-power reactor at equilibrium, this is only about 1/6th of the effect that the xenon can have ($0.68 vs. $4.15) when it reaches its equilibrium concentration.* Any excess samarium that is produced burns away as soon as it is created, and so when the equilibrium concentration S_∞ is reached, it stays at this level independently of what happens to the power level after that.

21.10.3 Case 3: Samarium after Shutdown

In Chapter 18, we learned that once Promethium-149 and Samarium-149 have both achieved their equilibrium concentrations, the Samarium-149 concentration at any time t after shutdown is given by

$$S(t) = S_\infty + P_\infty\left(1 - e^{-\lambda_P t}\right) \tag{21.34}$$

where again S_∞ and P_∞ are the equilibrium concentrations given by

The Equilibrium Concentrations of Promethium-149 and Samarium-149 (after Shutdown)

$$P_\infty = \frac{Y_p\Sigma_f\phi}{\lambda_P} \quad \text{and} \quad S_\infty = \frac{Y_p\Sigma_f}{\sigma_{as}} \tag{21.35}$$

Notice that only the asymptotic promethium concentration is affected by the value of the neutron flux ϕ. The final concentration of Samarium-149 is therefore

The Concentration of Samarium-149 after Shutdown

$$S(t) = \frac{Y_p\Sigma_f}{\sigma_{as}} + \frac{Y_p\Sigma_f\phi}{\lambda_P\left(1 - e^{-\lambda_P t}\right)} \tag{21.36}$$

(When shutdown occurs at $t = 0$)

Using the fact that the reactivity change due to the introduction of an arbitrary fission product poison is given by

$$\Delta\rho = -C\left(\frac{\Sigma_{aP}}{\Sigma_{aF}}\right) \tag{21.37}$$

where C is a constant equal to

$$C = \frac{1}{\eta\varepsilon p} \tag{21.38}$$

and Σ_{aF} is the macroscopic absorption cross section for the fuel, we can substitute the equilibrium concentration of Samarium-149 into Equation 21.37. The σ_{as}'s cancel, and it therefore follows that

$$\Delta\rho_P = -CY_p\left[1 + \frac{\phi}{\delta\left(1 - e^{-\lambda_P t}\right)}\right] \tag{21.39}$$

where $\delta = \lambda_p/\sigma_{as} \approx 6.2 \times 10^{13}/\text{cm}^2/\text{s}$. *So after shutdown, the samarium concentration will continue to increase until it stabilizes in about 13 calendar days. This is about 25 times longer than it takes xenon to reach its post-shutdown peak (300 hours vs. 12 hours).* Like xenon, the post-shutdown concentration of samarium also depends on the power level (and hence the flux) before the reactor is shut down. About seven times more samarium is produced after shutdown at a flux level of $\sim 5 \times 10^{14}$ neutrons/cm^2/s than it is at a flux level of $\sim 5 \times 10^{13}$ neutrons/cm^2/s. *So while the equilibrium concentration of samarium is independent of the thermal flux, the post-shutdown concentration increases as the thermal flux increases.* In the limit where $t \to \infty$, the maximum value of $\Delta\rho_S$ is given by the following expression:

The Maximum Contribution of Samarium-149 to the Overall Reactivity (after Shutdown)

$$\Delta\rho_S = -CY_p\left[1 + \frac{\phi}{\delta}\right] \tag{21.40}$$

where all of the terms have their usual meanings. Figure 21.10 shows how the samarium concentration behaves as the flux is changed. Again, equilibrium is reached in about 300 hours. The maximum values of $\Delta\rho_S$ are shown in Table 21.5

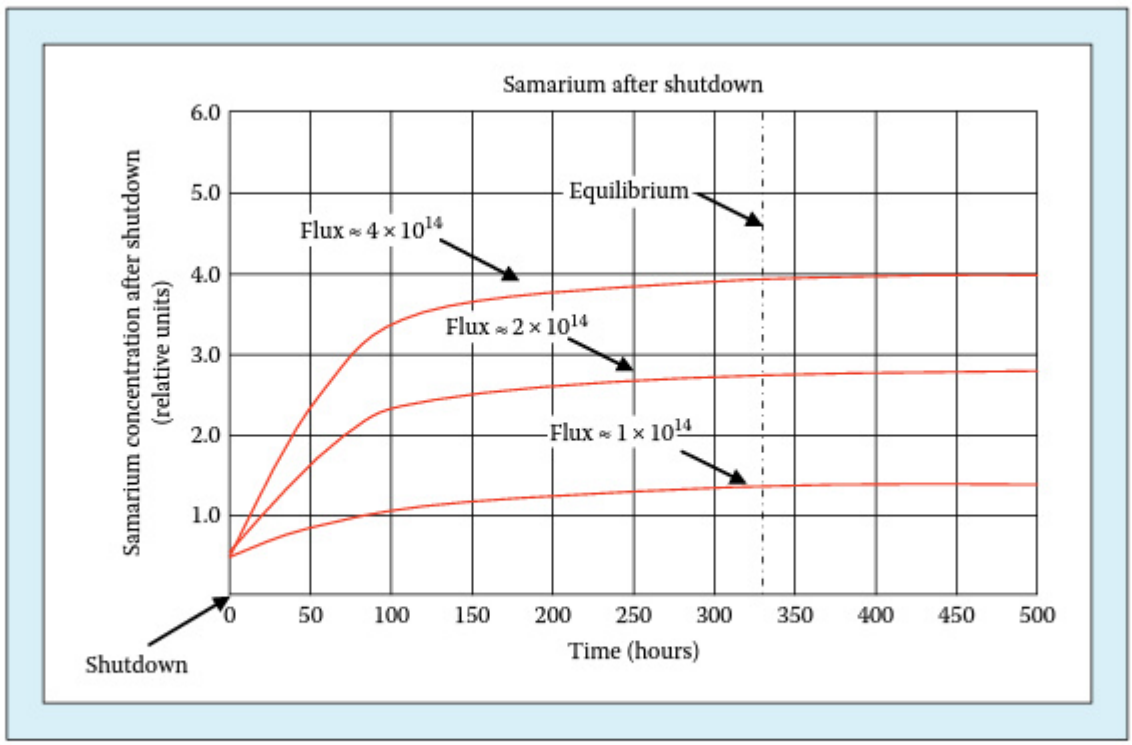

FIGURE 21.10 Samarium-149 buildup at various times after shutdown. Equilibrium is reached in about 300 hours.

TABLE 21.5
Reactivity Reductions due to the Buildup of Samarium-149[a,c,d]

Average Thermal Flux	Maximum Negative Reactivity (~300 Hours after Start-Up)[b]	Maximum Negative Reactivity (~300 Hours after Shutdown)	Total Negative Reactivity	Average Thermal Flux	Maximum Negative Reactivity (~300 Hours after Start-Up)[b]	Maximum Negative Reactivity (~300 Hours after Shutdown)
ϕ	$\Delta\rho$	Dollars	$\Delta\rho$	Dollars	$\Delta\rho$	Dollars
1×10^{13}	0.0044	\$0.68	0.0055	\$0.85	0.0099	\$1.53
5×10^{13}	0.0044	\$0.68	0.0085	\$1.30	0.0129	\$1.98
1×10^{14}	0.0044	\$0.68	0.0115	\$1.77	0.0159	\$2.45
5×10^{14}	0.0044	\$0.68	0.0415	\$6.38	0.0459	\$7.06

[a] For a Uranium-235-fueled thermal reactor.
[b] For thermal reactors, these values are independent of the neutron flux.
[c] Atoms per thermal fission.
[d] Stable.

for a number of thermal flux levels prior to reactor shutdown. *Again, the value of $\Delta\rho_S$ is always a negative number because Samarium-149 is a prolific thermal neutron absorber.* This can be easily seen in Table 21.5, where the reactivity loss due to the buildup of samarium after shut down is shown for various values of the pre-shutdown thermal flux. *Since Samarium-149 is stable, it does not decay away and remains in the reactor core until it is started up again.*

21.11 Nuclear Properties of Xenon-135 and Samarium-149

As we mentioned previously, *the buildup of Xenon-135 is a major issue in thermal water reactors because it has the highest thermal absorption cross section of any material known.* It soaks up thermal neutrons like a sponge (see Chapter 5). A graph showing the thermal absorption cross section for Xenon-135 is shown in Figure 21.11. *Xenon-135 has an*

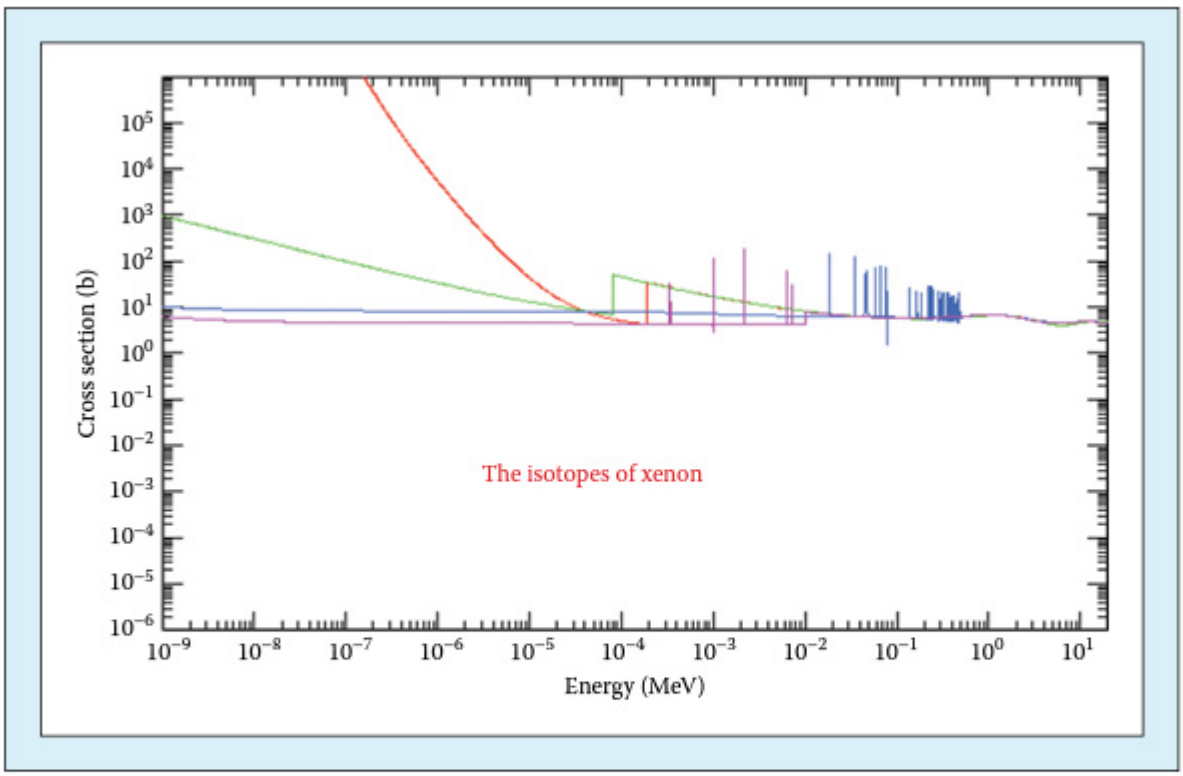

FIGURE 21.11 The neutron absorption cross sections of various isotopes of xenon as a function of the neutron energy. Xenon-135 is shown in red, Xenon-134 is shown in purple, Xenon-133 is shown in green, and Xenon-136 is shown in blue. Note that the absorption cross section of Xenon-135 completely dominates the cross sections of the other isotopes in the picture. (This graph was created by ENDFPLOT, which was discussed in Chapter 5.)

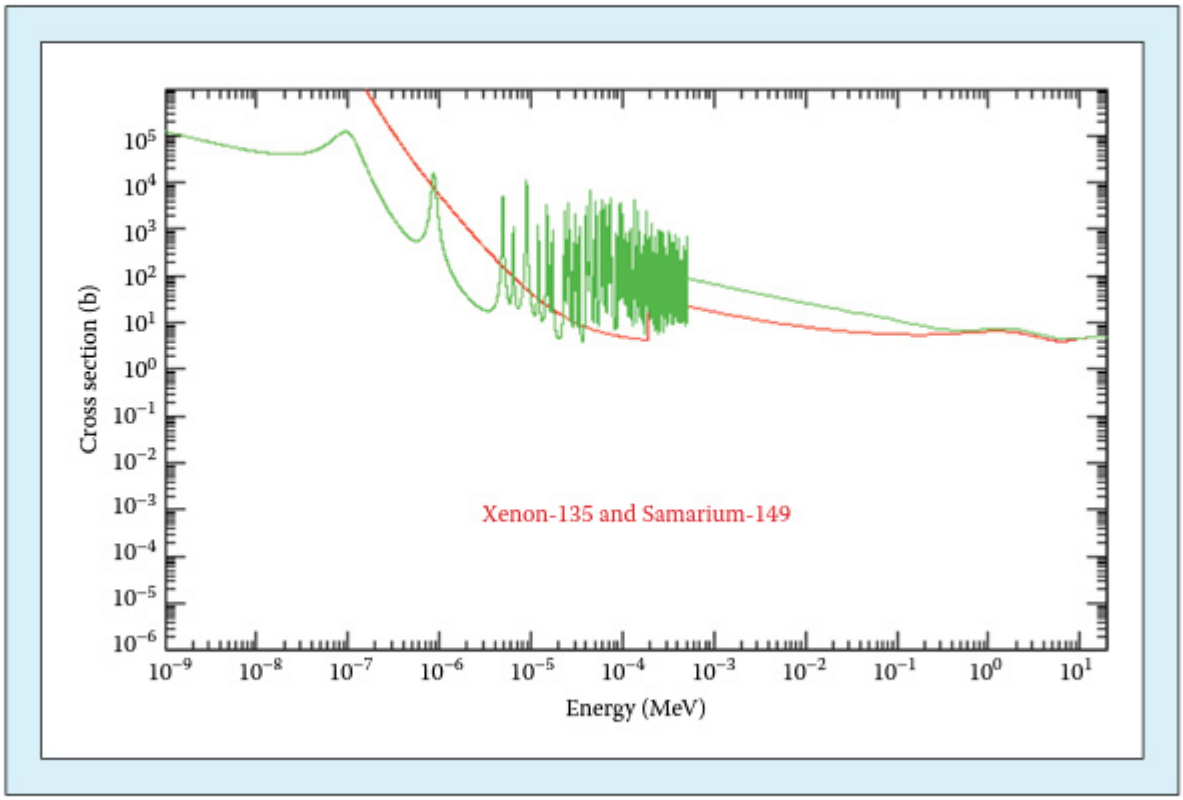

FIGURE 21.12 The absorption cross sections for Samarium-149 are shown in green, and the absorption cross sections for Xenon-135 are shown in red. (This graph was created by ENDFPLOT—see Chapter 5.)

effective thermal absorption cross section of over 2,600,000 barns! In comparison, Samarium-149, which is the second most important fission product poison, has an effective thermal cross section of only 58,700 barns at 300 K. The absorption cross section of Samarium-149 is shown in Figure 21.12. The data used to construct this chart was taken from the *ENDFB-7 database* (see *NNDC.gov.org*). The data was then plotted using ENDFPLOT (see Chapter 5). The absorption cross section of Samarium-149 is shown in green, and the absorption cross section of Xenon-135 is shown in red. Samarium-149 is not a true 1/v absorber, but it does exhibit the absorption resonances above thermal energies that xenon lacks. Finally, Samarium-149 is not created directly from the fission of Uranium-235. Instead, the fission of Uranium-235 creates Neodymium-149, which decays into Promethium-149 in about 1.7 hours. This promethium then decays into Samarium-149 in about 53 hours.

21.12 How the Reactor Accident at Chernobyl Occurred

The reactor accident in Chernobyl, Russia, was caused by a number of unfortunate events, but one of the most unfortunate of them was the *buildup of Xenon-135 in the reactor core*. In the sections that follow, we would like to briefly discuss what the reactor operators did at Chernobyl in response to this buildup of Xenon-135, and how it ultimately caused the reactor accident to occur. *Another major cause of the accident at Chernobyl was a positive power coefficient of the reactivity*, which we introduced to the reader in Chapter 17. The *Chernobyl accident* was by far the worst recorded accident in the history of the nuclear power business, and in perspective, the accidents at Fukushima in Japan and Three Mile Island in the United States were relatively mild in comparison. Until the Fukushima accident occurred in 2011, the Chernobyl accident was the only commercial reactor accident to have ever been awarded a rating of 7.0 on the *INES scale*, which is the internationally accepted scale by which the severity of all reactor accidents is measured. In comparison, the accident at TMI only received a rating of 5.0 on the INES scale. Furthermore, the INES scale is similar in design to the *Richter scale*, which is commonly used to measure the intensity of earthquakes. When using these scales, the numbers assigned to specific events do not increase in linear proportion to the severity of the events. *Instead, they increase geometrically in powers of 10 as the event severity increases.*

In the spring of 1986, the fragile Soviet economy was just beginning to emerge from the Cold War. Several military reactors, including the one at Chernobyl, were being converted to civilian use. The Chernobyl reactor was previously a military reactor designed to produce weapons-grade plutonium. However, several years before the accident occurred,

it was allowed to produce commercial electric power instead. Chernobyl was a 1000 MWe boiling water reactor called the RBMK-1000. This reactor is similar in some respects to the design of commercial boiling water reactors used in the United States. *However, it differs from a conventional BWR because it uses graphite for the moderator, and cooling water flows through the fuel assemblies through specially designed pressure tubes* (like the ones used in the Canadian pressurized heavy water reactor, or CANDU). The RBMK uses slightly enriched uranium, with an average enrichment of about 2%. The water flows through the core, begins to boil, and is then sent on to some steam turbines. Each steam turbine is capable of generating 500 MW of electricity.

21.13 Design Features of the Chernobyl Reactor

The *RBMK-1000* (which is described in Chapter 14 of our companion book*) is a graphite-moderated pressure tube–type reactor, using slightly enriched (2% U-235) uranium dioxide fuel. It is a boiling light-water reactor, with two loops feeding steam directly to the power turbines, without the need for an intermediate heat exchanger. Water pumped to the bottom of the fuel channels boils as it progresses up through the pressure tubes, producing steam which is then fed to two 500 MWe steam turbines. The water acts as a coolant and also provides the steam used to drive the turbines. The vertical pressure tubes contain uranium dioxide fuel rods, which are clad in zirconium metal. The water flows around the fuel rods and cools them. The extensions of the fuel channels penetrate the lower plate and the cover plate of the core and are welded at both ends. A specially designed refueling machine allows fuel bundles to be changed without shutting the reactor down. In each of the main coolant loops, there are four recirculation pumps, and one of these pumps is always on standby. The reactivity is controlled by lowering or raising the control rods, which reduce or increase the fission rate. The maximum thermal output of the RBMK-1000 is 3200 MW T, but because its thermal efficiency is 32%, its electrical output is 1000 MWe. The RBMK also contains an emergency core cooling system, or ECCS, which is incorporated directly into the design of the plant. *The RBMK-1000 differs from most other BWRs because it can have a "positive void coefficient" where a temporary increase in the void fraction can cause the core power level to increase*. As more steam is created, the additional neutrons that are normally absorbed by the water leak into the fuel, where they can cause more fissions to occur. (In a conventional BWR, exactly the opposite process occurs because increasing the power level causes the instantaneous reactivity ρ to go down.) There are other factors that contribute to the positive power coefficient, but the *void coefficient* of the reactivity is the dominant one in the RBMK. A picture of a RBMK core is shown in Figure 21.13.

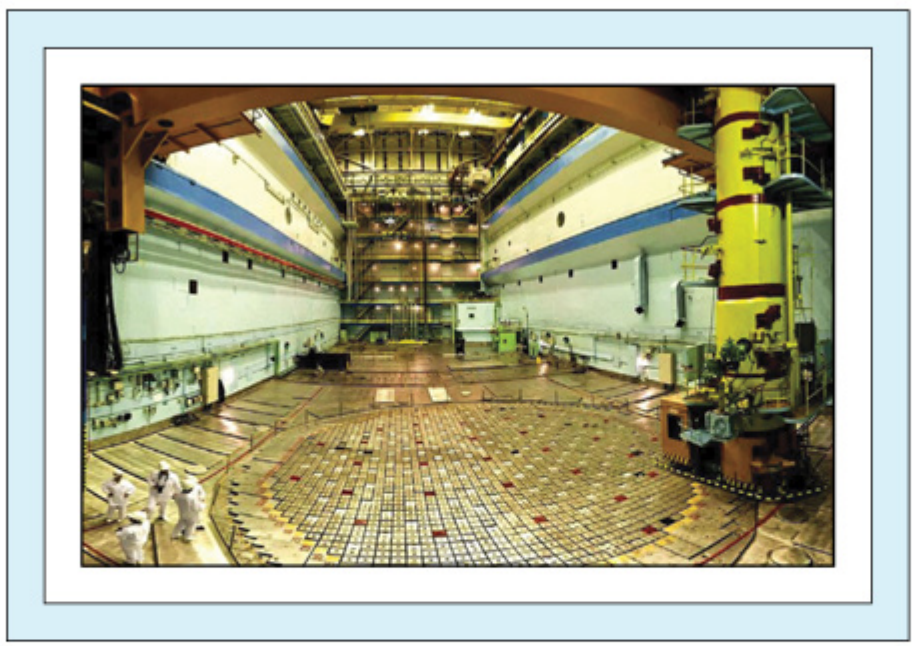

FIGURE 21.13 A picture of an RBMK reactor core—similar to the one that exploded at Chernobyl in 1986. The accident was initially induced by an unexpected xenon transient, which the reactor operators failed to anticipate. (Courtesy of Google Images.)

* See *Nuclear Engineering Fundamentals: A Practical Perspective*, by R.E. Masterson, CRC Press (2017).

In the RBMK, the size of the void coefficient depends on the isotopic composition of the core. *A new RBMK will have a negative void coefficient, but as the fuel is burned, the void coefficient will become progressively positive*. Eventually, a point is reached where certain control rod configurations will lead to a positive void coefficient that is large enough to overwhelm all of the other components of the power coefficient (see Chapter 17), and this can cause the total power coefficient to become *large* and *positive*. In this case, increasing the power level without carefully controlling the motion of the control rods causes the power level to increase even further. This process can feed on itself (like a positive feedback loop) and it can quickly get out of control. This was a well-known design defect of the RBMK-1000 which Western authorities had asked the plant designers to fix. Unfortunately, the Ministry of Energy and Power, which was in charge of the Soviet nuclear program at the time, decided that it was not economically feasible to make the required modifications to the plant. Thus, the reactor at Chernobyl was allowed to continue to operate with a positive power coefficient, even though it was considered to be a potential disaster in the making. In other words, it was considered by some Western authorities to be a *ticking time bomb*.

21.14 Buildup of Xenon in the Chernobyl Core

In April,1986, the Chernobyl reactor was operating normally when the decision was made to perform a routine safety test. This test involved determining how long the power turbines would spin and supply power to the main circulation pumps following a loss of electrical power. This test had been performed the previous year, but the power output from the turbines fell too quickly, and so a new voltage regulator was installed to fix the problem. To perform the test, the power level of the core had to be reduced from 1000 MWT to about 700 MWT. (Below 700 MWT the steam turbines could not turn fast enough to provide the makeup power.) However, as the reactor power was reduced to 700 MWT, the reactor operators who were responsible for performing the test *did not account for the effects of Xenon-135 on the reactivity of the core*. Because of this, the core power level continued to drop to about 500 MWT, but then an inexperienced reactor operator mistakenly reinserted the control rods back into the core, causing the power level to decline even further to 30 MW thermal or less. At this point, the reactor officially entered the "dead zone" described in Section 21.7, and it was in a state of *virtual shutdown* for some time (see Figure 21.14). The Chernobyl reactor was then producing about 5% of the minimum acceptable power to perform the test.

The reactor operators subsequently panicked and made a decision to increase the power level by disabling the automatic safety systems that controlled the motion of the control rods. They then "manually" extracted the majority of the control rods from the core in an attempt to restore the power level to a point where the test could be performed. According to eyewitnesses who were present on the scene, several minutes passed between the time

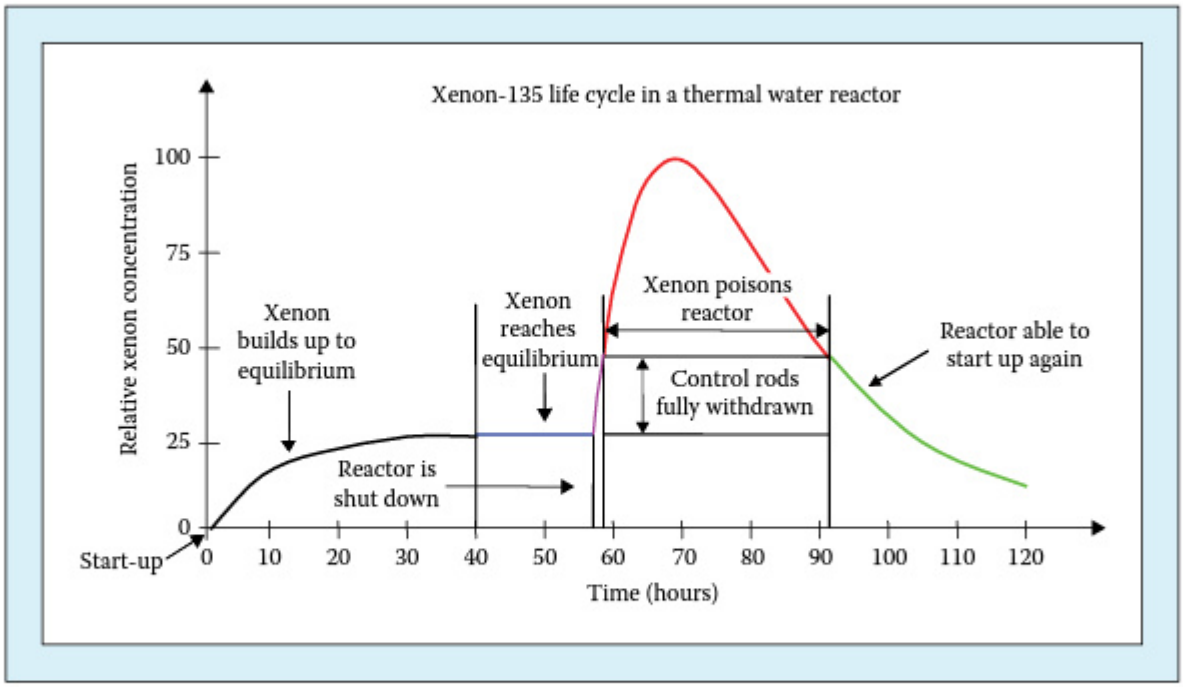

FIGURE 21.14 A picture showing how the Xenon-135 in the Chernobyl reactor would have behaved if it had been operated normally.

the control rods were extracted and the time the power level began to rise. After a while, the reactor power level reached an output of between 160 MWT and 200 MWT, which was still too low to conduct the test. The xenon poisoning of the core kept the power level from rising any further, unless additional control rods were removed. Then, at this lower power level, the coolant flow became unstable and began to oscillate wildly. The reactor operators had allowed the reactor to operate outside of its approved "*operating map*" (see Chapter 14 of our companion book*). This caused several safety alarms to sound. The reactor operators received even more emergency signals telling them that the water levels in the steam/water separator drums were too low and that the core flow rate and the flux shape were starting to oscillate wildly. Unfortunately, they did not reactivate the automatic safety systems, and the emergency alarms were ignored in an attempt to keep the power level at about 180 MWT. After a few minutes, a more or less stable power level of 200 MW was attained. However, rather than waiting for the power level to slowly return to its targeted value (700 MWT), the reactor operators were ordered to proceed with the test even though they were reluctant to do so. They again pushed the RBMK-1000 outside of its approved operating map, and the coolant temperature in the core began to rise.

Eventually, the coolant boiled, and with most of the control rods removed from the core to compensate for the buildup of Xe-135, the power coefficient of the reactivity became positive. The reactor was then in an unstable state, and another mistake by the operators could cause the power level to "spike", which could cause the reactor to become supercritical. For reasons that are not entirely clear, the power level spiked again, and the reactor operators pushed the SCRAM button. The control rods immediately began to move back into the core. In the Chernobyl reactor, the control rods were designed to move into the core at a rate of about 0.40 m/s, so it took approximately 18–20 s for the control rods to travel the entire length of the core (which was about 7 m). The control rods displaced the liquid water as they moved, but unfortunately the liquid water could have also been used to absorb some of the excess neutrons. *Thus, pushing the SCRAM button in the RBMK-1000 actually caused the neutron production rate in the upper half of the core to increase!*

A few seconds after the SCRAM button was pushed, the control rod motions produced a *massive power spike*, and this caused some parts of the core to overheat and disassemble. Some of the fuel rods began to fracture, and they jammed the control rod drive channels—which prevented the control rods from being inserted even further into the core. Thus, the control rods got stuck about one-third of the way into the core, with the tips of the rods essentially at the core midpoint. Within 3 seconds, the reactor level rose above 530 MWT, and *several seconds after that, the reactor power level jumped to about 30,000 MW thermal, which was 10 times its design limit*. The reactor vessel ruptured, and the damaged core exploded—causing it to be dispersed over a wide area. Then the nuclear chain reaction stopped. However, the resulting explosion also demolished the containment building, and a huge amount of additional radiative material was ejected into the surrounding environment.

The ejected graphite and the demolished reactor coolant channels caught fire when they were exposed to the surrounding air. This caused the radioactive fallout to spread even further. The power spike generated about 40,000 MJ of thermal energy, which is equivalent to the explosive force of about 10 tons of TNT. However, the nuclear excursion was initially limited to just a small fraction of the core. Practically speaking, the Chernobyl accident was the first documented example of what is known as a *hypothetical core disruptive accident* or *HCDA*. HCDAs had been hypothesized to exist since the early 1950s (see the related discussion in Chapter 16), but up to the time of the accident, an actual HCDA had never been observed. In fact, a computer program had been written by engineers at the Los Alamos National Laboratory to predict the effects of such a HCDA. This program was called the *SIMMER* code. *A HCDA involves an energetic disassembly of an entire core when the reactivity is positive and the reactivity exceeds the prompt critical limit* (see Chapter 16). A more extensive discussion of HCDAs can be found at the NRC Website: *www.nrc.gov/docs.**

21.15 The Chernobyl Accident and Its Aftermath

The Chernobyl accident caused an enormous amount of radiation to be released into the surrounding environment (*about 1.4×10^{19} Becquerels*), and the release of this radiation continued for about 10 days. This radiation caused serious social, economic, and environmental problems, and it disrupted the already faltering Soviet economy. Two of the radioisotopes that were released from the core—Iodine-131 and Cesium-137—were particularly important because they delivered significant amounts of radiation to the general public. It is estimated that all of the radioactive xenon gas, about half of the radioactive iodine and cesium, and at least 5% of the remaining materials in the core (which had about 200 metric tons of fuel) were released during the accident. Most of this material was deposited close to the reactor site in the form of dust and other debris, but the lighter materials were carried away by the wind and were eventually deposited over the Ukraine, Russia, Belarus, and to a lesser extent, Scandinavia and Eastern Europe. Thousands

* See *Nuclear Engineering Fundamentals: A Practical Perspective*, by R.E. Masterson, CRC Press (2017).

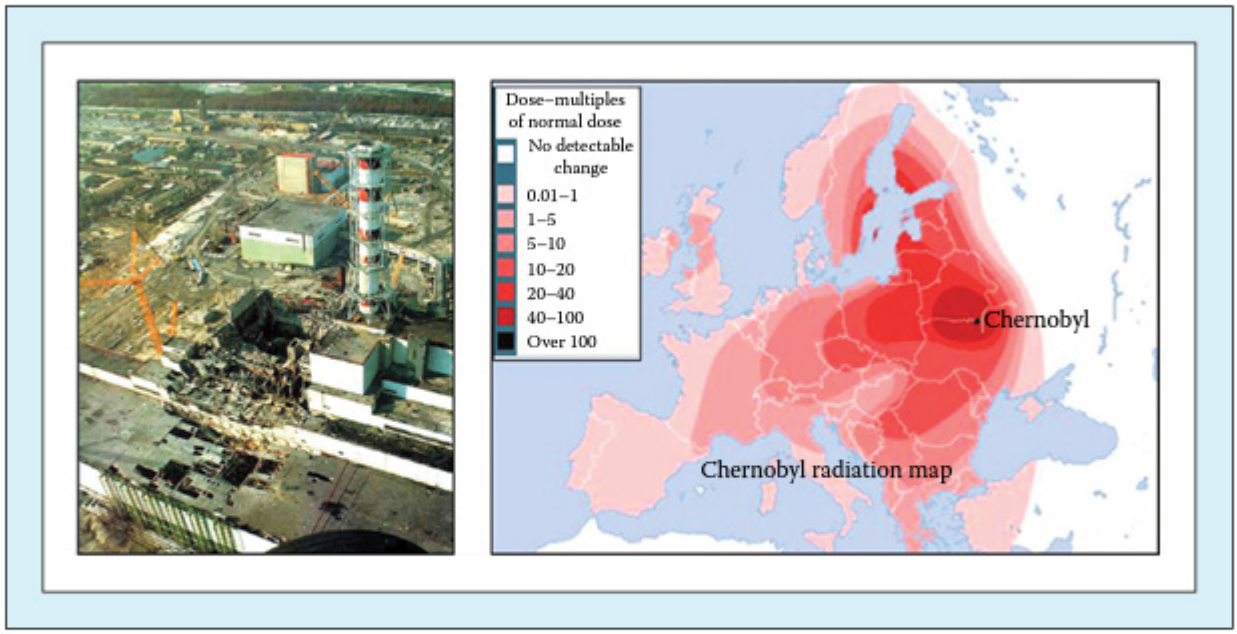

FIGURE 21.15 A map showing the radiation that was released by the Chernobyl nuclear accident. (Courtesy of Wikipedia and the United Nations.)

FIGURE 21.16 A house and school room abandoned near the town of Chernobyl after the reactor accident. (Pictures provided by Wikipedia.)

of people were eventually killed by the radiation that was released. A picture of the area that was devastated by the radiation is shown in Figure 21.15. *After that, Chernobyl turned in to a ghost town* (see Figure 21.16).

21.16 Comparing Chernobyl to Other Reactor Accidents

To put the Chernobyl accident into perspective, it is instructive to compare it to other reactor accidents that have occurred over the years. In early 1990, the *International Atomic Energy Agency (IAEA)* established a scale to measure the severity of reactor accidents. This scale is called "The *INES Scale*" (or the International Nuclear and Radiological Event Scale), and it rates reactor accidents according to their severity on a scale from 1 to 7—with one (1) being the least serious and seven (7) being the most serious. Just like the *Richter Scale* that is used in classifying the severity of earthquakes, the INES Scale is *logarithmic* in nature. The base unit for the INES Scale is the log of 10. The most

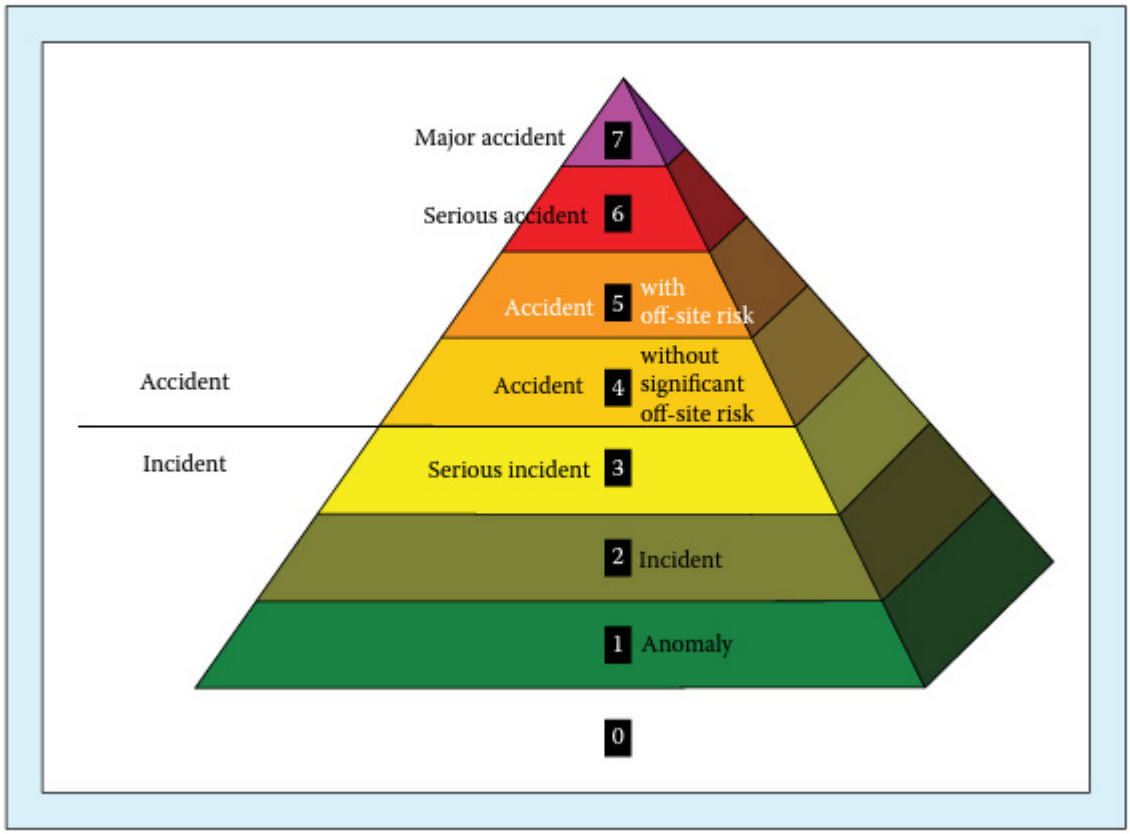

FIGURE 21.17 The INES scale for assessing the severity of nuclear reactor accidents. (Courtesy of the IAEA.)

current version of this scale is shown in Figure 21.17. Examples of the types of accidents the scale is intended to measure are shown in Figure 21.18.

21.17 Accident Severity and the INES Scale

Each of the classifications used by the INES scale pertains to a specific type of accident, and each of these accidents are defined in Figure 21.18. The accident at TMI (not shown) was a 5 on this scale, the accident at Chernobyl was a 7, and the accident at Fukushima (not shown) was also a 7. The Kyshtym disaster in the city of Mayak (which was also part of the former Soviet Union) was rated a 6, and it is the only other accident to go over 5 on the INES scale besides Chernobyl and Fukushima. Again, like Chernobyl, this accident occurred at a former military facility when a cooling system malfunctioned at a nuclear waste reprocessing plant and caused a steam explosion to occur which released 70–80 tons of highly radioactive material into the surrounding environment. The impact of this event on local population has never been fully revealed. The INES scale is based on three factors:

1. The amount of radiation released into the environment
2. The type of radiation and the manner in which it is released
3. The physical damage to the plant as the result of the accident

Notice that much less radiation was released into the environment by the TMI accident in the United States than the Fukushima accident in Japan. The accident at Chernobyl has become the benchmark for how messy and disruptive a large reactor accident can be. The accident at Chernobyl released a significant fraction of the inventory of the core into the environment, and this resulted in a large radiation cloud that eventually reached most of Western Europe (see Figure 21.15).

As a result of this accident, the city of Chernobyl (population 14,000) was largely abandoned, the larger city of Pripyat (population 49,400) on the northern border of Ukraine with Belarus was completely abandoned, and a 30 km exclusion zone has remained around the site since the accident occurred. Some pictures of disassembled core and other debris surrounding the site are shown in Figure 21.19. The battle to contain the resulting contamination and avert an even greater disaster involved nearly one half-million (500,000) people and cost the Soviet Union an estimated 18 billion rubles, which further crippled the already struggling Soviet economy. Many historians believe that the repercussions of the Chernobyl disaster indirectly contributed to the collapse of the Soviet Union and the end of the Cold War.

The INES Scale—Examples of Events at Different Nuclear Facilities

	People and Environment	Radiological Barriers and Control	Defense in Depth
7	Chernobyl, 1986—Widespread health and environmental effects. External release of a significant fraction of the reactor core inventory		
6	Kyshtym, Russia, 1957—Significant release of radioactive material to the environment from the explosion of a high activity waste storage tank		
5	Windscale Pile, UK, 1957—Release of radioactive material to the environment following a fire in the reactor core	Three Mile Island, USA, 1979—Severe damage to the reactor core	
4	Tokaimura, Japan, 1999—Fatal exposure of workers following a criticality event at a nuclear facility	Saint Laurent des Eaux, France, 1980—Melting of one channel of fuel in the reactor core with no release off-site	
3	No example available	Sellafield, UK, 2005—Release of large quantities of material contained within the installation	Vandellos, Spain, 1989—Near accident caused by a fire, which resulted in loss of safety systems at a nuclear power plant
2	Atucha, Argentina, 2005—Overexposure of a radiation worker at a power reactor exceeding the annual limit	Cadarache, France, 1993—Spread of radioactive contamination to an area not expected by design	Forsmark, Sweden, 2006—Degraded safety functions for common cause failure in the emergency power supply system at a nuclear power plant
1			Breach of operating limits at a nuclear facility

FIGURE 21.18 The INES scale of reactor accident severity. (Data provided by the IAEA.)

21.18 Lessons Learned from the Chernobyl Disaster

In retrospect, five major lessons were learned from the Chernobyl disaster. Two of them are related to the buildup of Xenon-135 in the core, two of them were the result of operating a reactor improperly, and one of them was caused by a positive power coefficient, which was known to be a major design flaw in the plant at the time. These lessons were as follows:

1. The buildup of Xenon-135 caused the Chernobyl reactor to enter an unstable state. This eventually caused the flow and power levels to oscillate violently, and this was the first major problem that caused the accident to occur.
2. As soon as the reactor was moved out of its normal operating range, the reactor operators disabled the automated safety systems. These safety systems should have never been disabled.
3. When the reactor was operated outside of its approved operating range, or "operating map", the control rods should have never been withdrawn from the core until the Xenon-135 had burned off naturally. Removing the control rods from the core under these conditions was extremely dangerous, and it probably contributed to the reactor becoming supercritical.
4. Because the water in BWRs is designed to boil, *any BWR can become unstable if the power level and the flow rate are low enough (see Chapter 14 of our companion book for a comprehensive discussion of this issue*). These conditions can only be avoided by operating the reactor within certain specified power to flow ratios defined by the operating map.* If a BWR is operated outside of these specific power to flow ratios, the core can become unstable, and this can lead to even bigger and more serious problems (such as the ones that occurred at Chernobyl).
5. A reactor should *NEVER* be allowed to operate with a positive power coefficient, a positive void coefficient, or a positive temperature coefficient (see Chapter 17). If the power level suddenly increases, and the reactor has a positive temperature or void coefficient, the power level can continue to increase indefinitely, and the reactor can become supercritical. *In other words, the reactor can enter a positive power feedback loop*. This type of feedback will almost always cause a major accident to occur. The best way to prevent this from happening in the first place is to never design a reactor with a positive power coefficient.

* See *Nuclear Engineering Fundamentals: A Practical Perspective*, by R.E. Masterson, CRC Press (2017).

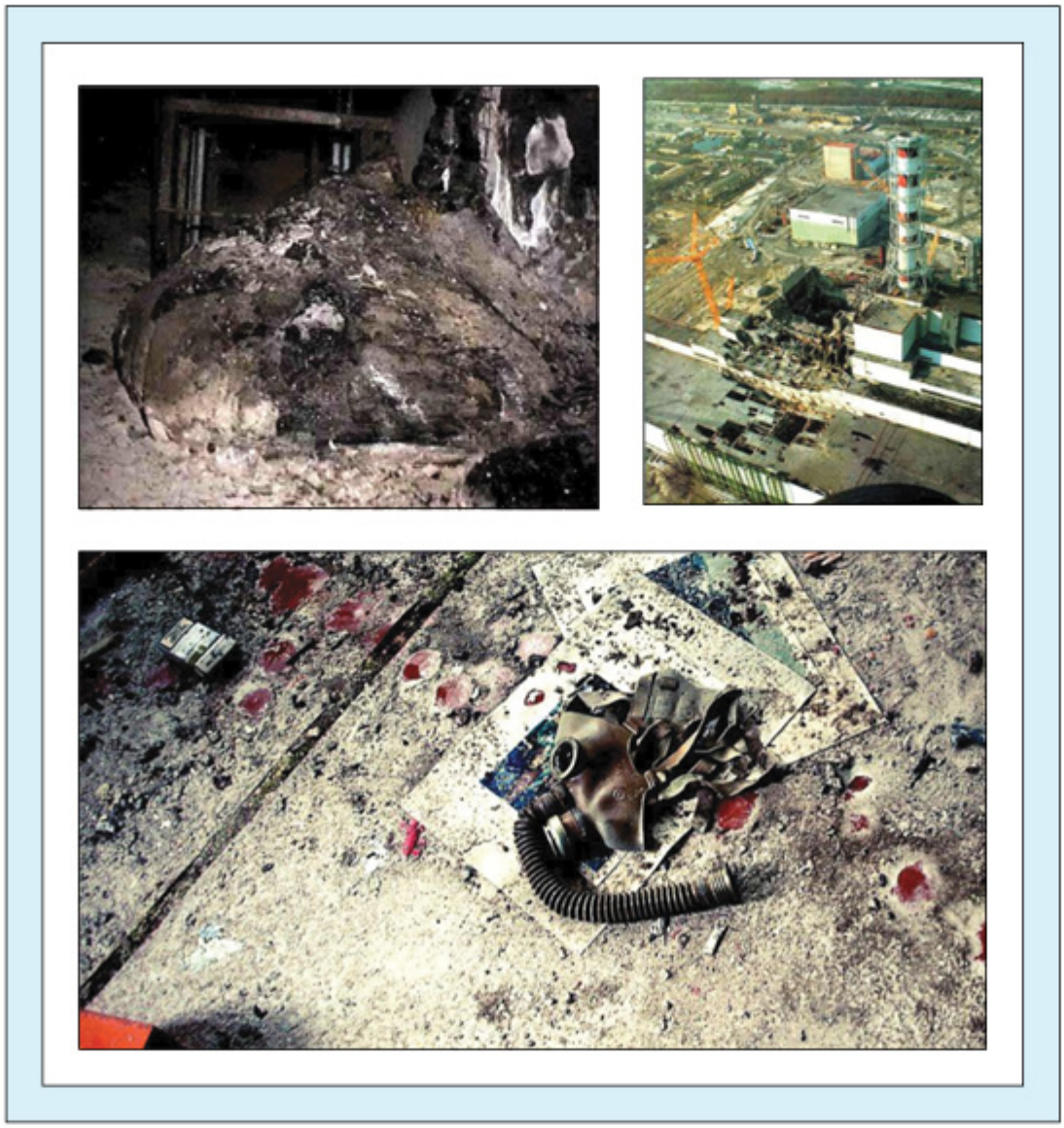

FIGURE 21.19 On the top left—a picture of a melted down section of the reactor core at Chernobyl, which is called the "elephant's foot"; on the top right—a picture of the Chernobyl site immediately following the reactor accident; below—some of the gas masks that were given to people near the Chernobyl site. The gas masks passed out to the general public offered little protection from the harmful effects of the radiation cloud released by the accident. (Pictures provided by Wikipedia.)

Consequently, the U.S. NRC has adopted the position that it will never allow a commercial nuclear power plant to be licensed in the United States if the power coefficient of the reactivity is positive over even a small fraction of its operating range. However, this practice is not necessarily followed in all Western countries, and so the potential still exists for another reactor accident to occur. This is a problem that every government needs to address if its nuclear power plants are to be operated safely in the future. The accident at Fukushima, although not directly related to the accident at Chernobyl, may have already caused this change in thinking to occur. *In conclusion, a reactor operator should NEVER attempt to disable or disconnect a reactor's automatic safety systems. These systems should always be allowed to perform their intended function. The accident at Chernobyl revealed that even well-trained reactor operators can sometimes have trouble anticipating how a reactor will behave—especially if it is operated outside of its approved operating map*. Thus, the reactor *operating map* (see Chapter 14 of our companion book*) remains an invaluable tool that all reactor operators should use to ensure that their plants are operated safely and efficiently. However, if a reactor is inadvertently operated outside of its approved operating map, computer models can sometimes be used

* See *Nuclear Engineering Fundamentals: A Practical Perspective*, by R.E. Masterson, CRC Press (2017).

to predict the response of the core. In the next section, we would like to briefly discuss some of the computer models and computer programs that are used by regulatory authorities to perform this function. In some countries, these computer programs are also called *computer codes*.

21.19 Computer Programs Used to Model Reactor Transients and Reactor Accidents: TRAC, TRACE, RETRAN, and RELAP

Several industrial strength computer programs have been written over the years to model reactor accidents—especially those where the reactivity of the core increases very rapidly with time. A list of these computer programs is provided in Table 21.6. These computer programs (or *computer codes* as they are sometimes called) are normally made available to academic and commercial institutions who are interested in simulating reactor transients due to sudden changes in the system-wide reactivity (±). We will briefly mention three of these computer programs and describe some of their features. The first program is called *RETRAN* (which is short for *Reactor Transient Analysis Program*), and the second one is called

TABLE 21.6
Four Major Reactor Accident Analysis Codes Used in the United States after 2000 and Their Function(s)

Reactor Analysis Program	Source or Developer	Features	Function
TRACE	The U.S. Nuclear Regulatory Commission	Complex, flexible, modular; can be applied to many different reactor types and components; can be used to model severe reactor transients; has a three-dimensional two-group point kinetics model and a sophisticated reactor thermal-hydraulics model; can be used to model events inside and outside of the reactor pressure vessel.	Supports the licensing of all commercial nuclear power plants in the United States and some foreign countries. A very advanced and powerful program that can be used to model the behavior of many different things.
TRAC	Los Alamos National Laboratory, the U.S. Department of Energy	The predecessor of TRACE from which the thermal-hydraulics models were taken; used a two-phase, six-equation model in which the liquid and vapor phases can move at different speeds.	Was originally used to model severe reactor thermal-hydraulics transients including vapor flashing events, large pipe breaks, the blow down of the reactor pressure vessel, and very severe LOCAs.
RETRAN	The Electric Power Research Institute and many of its affiliate organizations	One of the original competitors to TRAC; was developed by EPRI to compete with TRAC and similar types of codes; was developed to perform licensing and best-estimate transient thermal-hydraulic analysis calculations for light-water reactors. Maintained under a Quality Assurance program that complies with 10CFR50 (Appendix B).	Can be used to model severe reactor transients and perform licensing and best estimate calculations for light-water reactors; has been used for both PWRs and BWRs; its capabilities are similar to TRAC in many respects; it is modular in design and can be used to simulate the behavior of the entire nuclear steam supply system; also provides a detailed multidimensional neutronics core model.
RELAP	The Idaho National Engineering Laboratory (INEL)	A very sophisticated two-phase reactor thermal-hydraulics analysis program, that until recently was just one dimensional; has been extended to three dimensions and can model very severe reactor transients; until recently, the source code was available to interested users; used by many reactor vendors to model reactor transients.	Very good at modeling the nuclear steam supply system and modeling the NSSS when it is coupled to the reactor core; can be used for both pressurized and boiling water reactors; supports reverse flow and flows where the liquid and vapor phases are not in thermal equilibrium.

TRAC (for *Transient Reactor Analysis Code*). RETRAN employs a relatively sophisticated version of the time-dependent diffusion equation (with two energy groups and nuclear cross section libraries based on the ENDFB 7 database) to calculate the effects of reactivity insertions on the time-dependent behavior of light-water reactors. The *equation of state* for the coolant is approximated by a table built into the program itself. RETRAN also solves the time-dependent heat conduction equation and calculates the heat transfer coefficient for nuclear fuel rods during each time step. This allows time-dependent temperature feedback to be included in the calculation of the system reactivity as well. TRAC-PF1-EN/MOD3 (which was subsequently renamed to *TRACE*) is a sophisticated and highly advanced program that combines an improved version of the TRAC-PF1 transient reactor analysis code and a specially designed three-dimensional two-group neutron kinetics code called *QUANDF*.

Starting from either a critical steady state configuration or a subcritical steady state (fixed source problem) in a PWR, *TRACE* can be used to simulate the neutronic and thermal-hydraulic behavior of the core in response to many different reactivity insertion scenarios, both inside and outside of the reactor pressure vessel itself. You can learn more about these programs and even obtain documentation regarding how they work by contacting the *RSIC Center* at the *Oak Ridge National Laboratory*. There are even some sample problems that the RSIC provides if you would like to learn more about how TRACE and RETRAN work. On the Internet, additional information about *DIFF3D* can be found at the following URL:

http://www-rsicc.ornl.gov/rsiccnew/CFDOCS/MAIN_CAT_ABS.cfm

under the nuclear system safety analysis section, and information regarding many similar programs can be found at

http://www-rsicc.ornl.gov/

TRACE is the primary computer program that the US NRC uses to support the licensing of new nuclear power plants in the United States. Several other computer programs that are able to solve the time-dependent neutron diffusion equation are also available to commercial companies and academic institutions at this site. In addition, the NRC maintains another website where more computer programs can be found. The address of this website is

http://www.nrc.gov/about-nrc/regulatory/research/comp-codes.html#rk

Much additional useful information can be found there as well. TRACE is described in Reference 19 at the end of the chapter. Sometimes, TRACE is used together with another reactor physics simulation code called *PARCS* (see Reference 20) that was originally developed by professor *Tom Downar* at Purdue. Another popular reactor analysis program called *RELAP* is also available to nuclear scientists and engineers to simulate reactor accidents, but it is primarily a *thermal-hydraulic analysis code*. Thus, it does not have the neutronic module(s) required to solve the same types of problems that TRAC, TRACE, and RETRAN can. However, the power history of the core or an individual fuel assembly can be imported into RELAP from one of these other computer programs in the event the thermal behavior of a nuclear power plant needs to be studied in more detail. The thermal-hydraulic analysis capabilities of RELAP are quite extensive, and its predictions have been benchmarked extensively against experimental data. More information regarding RELAP can be found at the following website:

http://en.wikipedia.org/wiki/RELAP5-3D

The RELAP code is a product of the *Idaho National Engineering Laboratory* (or *INEL*).

21.20 Typical Applications for TRACE

Since it was originally released in 2010, several national laboratories, research institutions, and reactor vendors have attempted to simulate severe reactor accidents using the TRACE computer program as their guide. In recent years, the operating power of many BWRs has also been increased to reduce the cost of generating electricity from these plants. (As we mentioned previously, the Chernobyl reactor was the Russian equivalent of an American BWR.) In the United States, BWRs are now being licensed to 120% of their original licensed thermal power (OLTP) under certain conditions. As we discussed in our companion book, this places them in a different region of the power-flow operating map than many reactor operators are familiar with (see Chapter 14 of our companion book). One safety issue that arises when a BWR is operated in this way is that it may respond strangely to some anticipated transients without scram (or *ATWSs*). For a plant to be granted a license to be operated at these elevated power levels, the plant owner or operator must demonstrate that operating in this region of the operating map will not result in any unanticipated power or flow transients that will cause thermal-hydraulic instabilities to develop in the core, or which will eventually cause the fuel rods to melt. In particular, one of the transients that requires a regulatory dispensation is an ATWS initiated by a main steam isolation valve closure (MSIVC) that requires an emergency depressurization (ATWS-ED) of the reactor pressure vessel. Some safety concerns specific to an isolated ATWS event are an emergency core depressurization (ED) followed by a subsequent recriticality due to the buildup of excessive pressure in

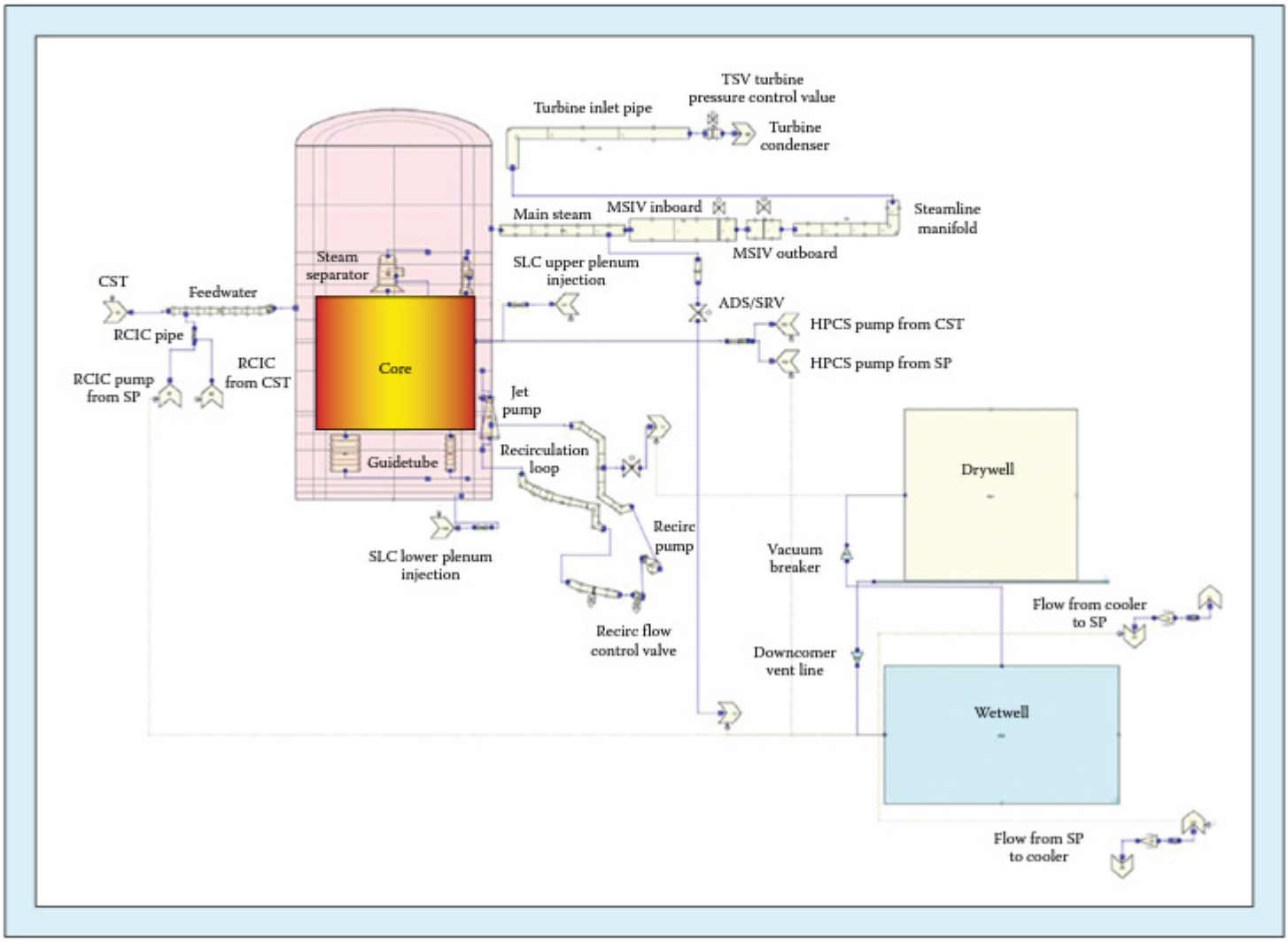

FIGURE 21.20 The TRACE component model of a BWR/5 undergoing an ATWS event. (Courtesy of the U.S. NRC—see www.nrc.gov.)

the drywell or the wet well. These transients can be extremely hard to model, and before 2010, they could not be modeled very well at all. Some of the reasons why a subsequent recriticality can occur during an ATWS are explained at the following URL:

https://www.bnl.gov/isd/documents/84549.pdf.

Figure 21.20 shows how these transients can be modeled physically using the component model and nodalization models of TRACE. This figure was taken from the previously mentioned URL, but was then modified to show additional reactor content.

This particular model is a working representation of a BWR/5 power plant, and it contains thermal-hydraulic components, reactor fuel assemblies, fuel rods, and heat-absorbing structures. The reactor pressure vessel is represented by a VESSEL component with 3 radial rings, 17 axial levels, and 1 azimuthal segment. The core and the steam separators are contained in rings 1 and 2 while the downcomer can be found in the third or outermost ring. A radial view of the core is shown in Figure 21.21. To model the behavior of the fuel rods, TRACE uses what is known as a *CHANNEL model*, which incorporates a dynamic gap–gas conductance model, very accurate correlations for the thermal conductivity of the fuel, and a very sophisticated model for the energy released by the zirconium metal–water reaction (see the energetics of this described in Chapter 16 of our companion book). The thermal behavior of the fuel rods, including the gap–gas composition and the initial oxide thickness on the surface of the cladding, is modeled using the *FRAPCON* code. FRAPCON is the standard industry tool for rational fuel rod design. In real reactors, the enrichment of the fuel can also vary from rod to rod, and the gadolinium or burnable poison concentrations can change as a function of the rod type and the axial elevation.

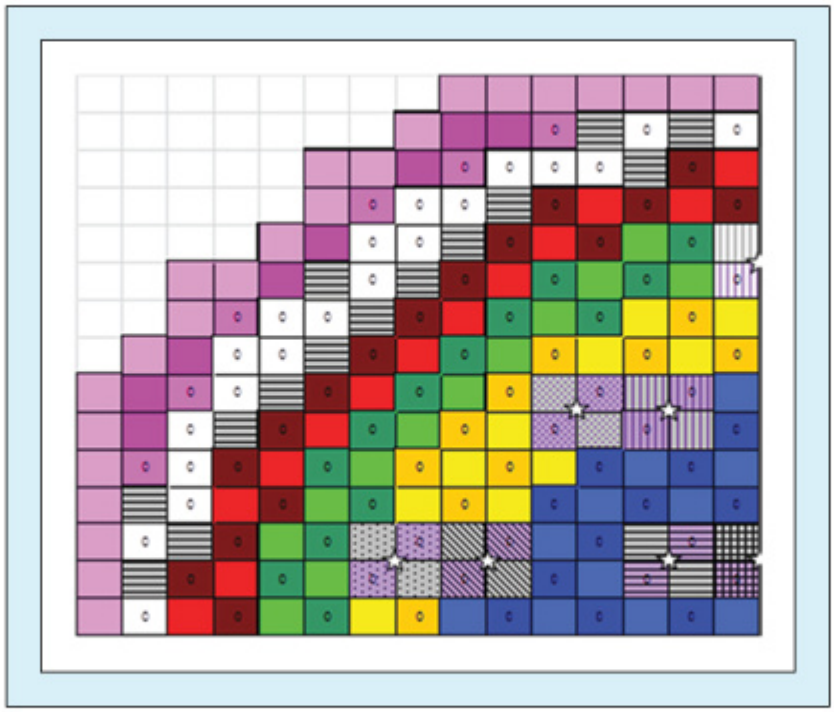

FIGURE 21.21 A TRACE thermal-hydraulic simulation of a BWR/5 core in which the fuel assemblies with approximately the same radial power profiles are grouped together into clusters of channels having different colors. (Courtesy of the U.S. NRC and Brookhaven National Laboratory; For more information, see BNL-103756-2014-CP.)

In TRACE, the number of nodes that are needed to simulate the core depends on geometrical, computational, and fuel cycle considerations. In practice, the fuel assemblies are sometimes clustered into groups having similar burnups and power outputs. This allows a geometrical grouping to work for all points in a specific burnup cycle. At the beginning of life (or BOL), a BWR/5 core can sometimes be modeled with 25 or 30 flow channels, using a mapping scheme similar to the one shown in Figure 21.21. Each group of fuel assemblies that are considered by TRACE to be the same hydraulic channel is indicated by a different color or shade. The "0"s in the picture indicate fresh fuel assemblies. The stars indicate control rod positions where the control rod blades are inserted far enough into the core initially (typically more than 10 steps) to keep the fresh core in a critical state (see Table 21.7).

Note that this loading pattern is very similar to the way that fresh fuel assemblies are distributed in a PWR core at the beginning of life. More refined groupings using half core symmetry (382 channels and fuel assemblies) or full core symmetry (764 channels and fuel assemblies) are also possible. Thus, the computational power of modern computers has finally evolved to the point that severe core-wide transients can be simulated using programs such as TRACE. If TRACE had been available to the Russian authorities at the time of the Chernobyl accident, the designers may have been able to

TABLE 21.7
Thermal Absorption Cross Sections for Some Common Materials Used as Control Rods and Burnable Poisons

Material	Usage	Atomic Density (Atoms/cm^3)	σ_a (Barns)	$\sum_a$ (cm^{-1})
Boron-10	Control rods	0.1364×10^{24}	2,500	342
Natural boron	Control rods	0.1364×10^{24}	755	103
Cadmium-112	Control rods	0.0464×10^{24}	2,450	114
Samarium-149	Neutron poison	0.0309×10^{24}	40,540	1,253
Sm_2O_3	Control rods	0.0128×10^{24}	16,500	211
Hafnium	Burnable poison	0.0449×10^{24}	105	4.7
Gadolinium	Burnable poison	0.1305×10^{24}	46,000	1,403
Xenon-135	Neutron poison	0.0236×10^{24}	2,778,000	65,560

build additional fail safe systems into the plant to prevent the reactor operators from disabling the active safety systems. In any event, because of the continued evolution of reactor safety analysis codes, most credible accident scenarios are identified today at the design stage, and reactors are much safer and easier to operate than they used to be.

21.21 Using Realistic Cross Sections for Xenon and Samarium

Realistic cross sections for Xenon-135 and Samarium-149 are required to model the reactivity changes that these important fission product poisons can create. When attempting to model their effect on the reactivity of a thermal water reactor, we must first compare the macroscopic absorption cross sections of these fission products to the cross sections of other materials that are used for the control rods. If enough xenon and samarium are produced, enough thermal neutrons may be absorbed to shut down the core entirely. Of course, this process continues until the Xenon-135 burns off. However, the Samarium-149 that is produced from the decay of promethium *does not burn off*, and for this reason, Samarium-149 is now used in some reactor control rods. The macroscopic absorption cross sections for Xenon-135 and Samarium-149 are compared to other control rod materials and burnable poisons in Table 21.7. It does not take much imagination to realize how strong these thermal neutron absorbers can be.

Student Exercise 21.1

Select one of the accident analysis codes shown in Table 21.7 and use it to simulate a reactor accident similar to the one that occurred at Chernobyl. What computer program is most suitable for analyzing the reactor accident if the power coefficient for the core happens to be positive?

References

Books and Textbooks

1. Ash, M. *Nuclear Reactor Kinetics*, McGraw-Hill, New York (1965).
2. RELAP-5 Code Manual INEEL-EXT-98-00834, Revision 1.3a, February 2001.
3. Lewis, E. *Nuclear Power Reactor Safety*, John Wiley & Sons, New York (1977).
4. Henry, A.F. *Nuclear Reactor Analysis*, MIT Press, Cambridge, MA (1975).
5. Keepin, G.R. *Physics of Nuclear Kinetics*, Addison-Wesley, Reading, MA (1965).
6. Stacey, W.M. *Nuclear Reactor Physics*, 2nd edn., John Wiley & Sons, New York (2007).
7. Todreas, N. and Kazimi, M.S. *Nuclear Systems*, Vol. 1, CRC Press, Boca Raton, FL (2012).
8. El-Wakil, M.M. *Nuclear Heat Transport*, American Nuclear Society, La Grange, IL (1981).
9. Duderstadt, J. and Hamilton, L. *Nuclear Reactor Analysis*, John Wiley & Sons, New York (1976).
10. Lewis, E. *Fundamentals of Nuclear Reactor Physics*, Academic Press, Boston, MA (2008).
11. Hetrick, D.L. *Dynamics of Nuclear Reactors*, American Nuclear Society, La Grange Park, IL (1993).
12. Schultz, M.A. *Control of Nuclear Reactors and Power Plants*, 2nd edn., McGraw-Hill, New York (1961).
13. Lamarsh, J.R. and Baratta, A.J. *Introduction to Nuclear Engineering*, Prentice Hall, Upper Saddle River, NJ (2001).
14. Lamarsh, J.R. *Introduction to Nuclear Reactor Theory*, second printing, Addison-Wesley Publishing Company, Inc., Reading, MA (1972).
15. Cochran, R.G. and Toulfanidis, N. *The Nuclear Fuel Cycle: Analysis and Management American Nuclear Society*, American Nuclear Society, La Grange Park, IL (1999).
16. Shultis, K. and Faw, R. *Fundamentals of Nuclear Science and Engineering*, 2nd edn., CRC Press, Boca Raton, FL (2008).
17. Glasstone, S. and Eedlund, M. *The Elements of Nuclear Reactor Theory D*, Van Nostrand Company, Inc., New York (1952).
18. Glasstone, S. and Sesonske, A. *Nuclear Reactor Engineering*, 3rd edn., Van Nostrand Reinhold Company, New York (1981).
19. TRACE V5.0 Theory Manual, ML120060218, U.S. Nuclear Regulatory Commission, June 4, 2010.
20. Downar, T. et al. PARCS: Purdue advanced reactor core simulator, *Proceedings of PHYSOR 2002*, Seoul, Korea, October 7–10, 2002.
21. Cheng, L.-Y. et al. TRACE/PARCS core modeling of a BWR/5 for accident analysis of ATWS events, *Trans. Am. Nucl. Soc.*, Washington, DC, 109 (November 10–14, 2013).
22. Masterson, R.E. *Nuclear Engineering Fundamentals: A Practical Perspective*, CRC Press, Boca Raton, FL (2017).

Web References

1. *http://www-rsicc.ornl.gov/.*
2. *http://en.wikipedia.org/wiki/RELAP5-3D.*
3. *https://www.bnl.gov/isd/documents/84549.pdf.*
4. *https://www.oecd-nea.org/rp/chernobyl/c01.html.*
5. *http://pbadupws.nrc.gov/docs/ML0710/ML071000097.pdf.*

6. *http://www.nrc.gov/about-nrc/regulatory/research/safetycodes.html.*
7. *http://www-rsicc.ornl.gov/rsiccnew/CFDOCS/MAIN_CAT_ABS.cfm.*
8. *http://www.nrc.gov/about-nrc/regulatory/research/comp-codes.html#rk.*

Additional References

- Important physical constants used by nuclear scientists and engineers can be found in *Appendix A*.
- Unit systems and their conversion factors can be found in *Appendix B*.
- Nuclear cross sections for many important nuclear materials can be found in *Appendix C*.
- Physical properties of important nuclear materials can be found in *Appendix D*.
- Atomic masses, half-lives, and natural abundances can be found in *Appendix E*.
- Delayed neutron emitters and their properties are discussed in *Appendix F*.

Questions for the Student

The following questions cover the material presented in this chapter and, in some cases, previous chapters as well. They are designed to test how well the student has acquired a working knowledge of the subject matter.

1. Prove that approximately 95% of the Xenon-135 produced in a CANDU heavy water reactor is produced from the decay of Iodine-135.
2. What causes the sharp initial drop in the reactivity that is observed when a reactor is first put into operation?
3. What is the thermal absorption cross section of Xenon-135?
4. Suppose that a thermal breeder reactor is to be fueled with Pu-239. What percentage of the Xe-135 in the core will be produced from the decay of I-135, and where does the remainder come from?
5. How long after start-up (which is assumed to occur at t = 0) does Xenon-135 usually reach its equilibrium concentration in a commercial power reactor?
6. Is Samarium-149, which is another important neutron poison, a true 1/v absorber? What is its neutron absorption cross section at thermal energies?
7. On what famous U.S. government website can important information on the TRACE computer program be found?
8. Name four popular computer programs that can be used to model reactor transients. Which ones can be used to model a xenon corkscrew transient?
9. In the terminology of a reactor operator, what does the term SOP refer to?
10. What was the name of the first computer program that was written to model a hypothetical core disruptive accident, and at which famous national laboratory in the United States was this program developed?
11. How many times larger is the poisoning effect of Xenon-135 than the poisoning effect of Samarium-149 when a thermal water reactor is operating normally?
12. What is the primary way that Samarium-149 is produced in a reactor core?
13. How long after start-up is the equilibrium concentration of Samarium-149 usually reached?
14. Fill in the following sentence with the appropriate word or phrase: Xenon transients are normally not a problem in fast reactors because the neutron energies in a fast reactor rarely fall below about _____, and at this energy, the microscopic absorption cross section of Xenon-135 is only about _____.
15. In a U-235-fueled thermal water reactor, what is the total yield of Samarium-149 from the decay of Promethium-149 and Neodymium-149?
16. How many hours after shutdown does the concentration of Samarium-149 reach its highest value?
17. Name two ways that Xenon-135 can be produced in a light-water reactor core.
18. Suppose that you were designing the control rods for a thermal water reactor to prevent the buildup of Xenon-135 in the core from poisoning the reactor entirely and forcing it to shut down. If the level of the flux in the core is expected to be 1×10^{14} neutrons/cm^2/s, what is the minimum amount of reactivity the control rods must contain to allow the reactor to be restarted when the xenon level reaches its maximum concentration?
19. Consider the same situation that was discussed in the previous problem. However, in this case, you must also design the control rods to overcome the negative reactivity that the buildup of Samarium-149 can introduce. What is the minimum amount of reactivity the control rods must contain to allow the reactor to be restarted when both the xenon and samarium levels reach their maximum concentration?
20. What is the yield of Neodymium-149 from the fission of U-235, and what is the yield of Promethium-149 from the fission of U-235?
21. Write an equation that describes the maximum possible reactivity that Samarium-149 can introduce into a reactor core after it is shut down.
22. Approximately how long after a reactor is shutdown does the concentration of Xenon-135 reach its maximum value? Does this value depend on the level of the neutron flux?
23. Are the equilibrium concentrations of Xenon-135 and Samarium-149 functions of the neutron flux?
24. Write down an equation for the equilibrium Xenon-135 concentration in a thermal water reactor.
25. Write down the corresponding equation for the equilibrium Samarium-149 concentration in a thermal water reactor. Does the samarium concentration have any dependence on the neutron flux?
26. What does the term "reactor dead time" refer to?
27. How long, on average, does it take for half of the Neodymium-149 in a reactor core to decay into the Promethium-149?
28. What computer program is used by the U.S. NRC today to support the licensing of any new nuclear power plant in the United States?
29. In addition to Xe-135, name two other common isotopes of xenon that are produced in a reactor core? Are they as important as Xenon-135 is?

30. What is a typical value of the reactor dead time for a thermal water reactor in which the buildup of xenon has occurred?
31. What is the thermal absorption cross section of Samarium-149?
32. In the summer months, when does the demand for electrical power generated by a nuclear power plant usually peak?
33. What is the definition of a "demand charge"?
34. Can the isotope Samarium-149 be considered a 1/v absorber?
35. What is another term for "reactor dead time" that can be used to describe a situation in which a reactor poisoned by Xenon-135 cannot be started up?
36. Is the buildup of xenon and samarium a significant concern in the design of a fast reactor? Why?
37. What is a xenon flux tilt transient?
38. Name two reasons why commercial power reactors are operated in a "base loading" mode.
39. Promethium-149 can be produced in a reactor core in a number of different ways. For example, it can be produced directly from the fission of U-235. What is another way that it is commonly produced?
40. For a commercial nuclear utility, when does the maximum demand for electric power occur during a typical day?
41. Write an equation that can be used to find the maximum negative reactivity $\Delta\rho X$ that the presence of Xenon-135 introduces into a reactor core after shutdown.
42. Suppose that a reactor is temporarily shut down, and several hours later, you attempt to restart the reactor by removing all of the control rods from the core. When you do so, you find that you cannot make the reactor critical again. What is the cause of this particular problem?
43. Were a dead reactor and a xenon transient the primary causes of the reactor accident at Chernobyl?
44. Fill in the following sentence with the appropriate word or phrase: The accident at Chernobyl was initially induced by an unexpected _____ which the reactor operators failed to anticipate. This was further compounded by the fact that the reactor core had a _____ power coefficient.
45. What is the name of the primary computer program that the U.S. NRC uses to support the licensing of new nuclear power plants in the United States?
46. According to reactor experts, which of the following three reactor accidents was the most severe—the accident at TMI, the accident at Chernobyl, or the accident at Fukushima?
47. Describe one way that you could keep a xenon transient from occurring in a thermal water reactor.
48. Name a famous thermal-hydraulics analysis program developed by the Idaho National Engineering Laboratory to model reactor transients. What is the most current version of this program called?
49. Is a xenon transient a concern in one of the following types of reactors—A CANDU reactor, a Westinghouse PWR, and a General Electric BWR?
50. Suppose that you were one of the reactor operators at Chernobyl. Name at least three things that you should have never been allowed to do.
51. What happened to the reactor at Chernobyl when the reactivity of the core exceeded the prompt critical limit?
52. Fill in the following sentence with the appropriate word or phrase: The reactor at Chernobyl was an example of a Soviet-built and _____ moderated reactor, which is similar in design to a Western _____. The specific type of the reactor was the _____.
53. Fill in the following sentence with the appropriate word or phrase: The reactor operators at Chernobyl caused the reactor accident to occur by ignoring the reactor _____ map and operating the reactor at some _____ ratios where it became unstable.
54. What rating was the accident at Chernobyl given on the INES scale?
55. What type of Western reactor is similar in design to the reactor that exploded at Chernobyl?
56. The reactor at Chernobyl initially had a negative power coefficient. What caused the power coefficient to become positive?
57. How did the RBMK reactor at Chernobyl differ from a conventional Western BWR?
58. Fill in the following sentence with the appropriate word or phrase: The Chernobyl accident was the first documented example of a larger class of reactor accidents known as the _____.
59. What was the shape of the fuel assemblies that were used in the reactor at Chernobyl?
60. According to the witnesses who were present at the Chernobyl site, what was the final thing that the reactor operators did to initiate the Chernobyl reactor accident?
61. Why did pushing the SCRAM button at Chernobyl cause the reactor to become supercritical?
62. What value/sign does the power coefficient of the reactivity have for a well-designed BWR in the Western world?
63. What two radioactive materials were released by the reactor accident at Chernobyl that had the greatest effect on members of the general public?

64. Name at least three lessons that were learned from the accident at Chernobyl.
65. Suppose that you were asked to explain why the control rods were never able to be reinserted back into the core during the reactor accident at Chernobyl. What would you tell a government official who wanted to know why the control rods were not effective?
66. When the power and flow rates in a BWR core become very low, and the power to flow ratios begin to move outside of the standard operating map, what happens to the power and flow levels in the core?

Exercises for the Student

Exercise 21.1

Suppose that we would like to compare the poisoning effects of Xe-135 to the neutron-absorbing capabilities of a common control rod material such as Boron-10. Using the information presented previously, how many times more thermal neutrons will a cubic centimeter of Xe-135 absorb than a cubic centimeter of Boron-10?

Exercise 21.2

Develop an expression for the number of U-235 atoms in a cubic centimeter of uranium dioxide as a function of its average enrichment e. Use this expression to derive an equation for the equilibrium concentration of Samarium-149 in a cold clean core after start-up.

Exercise 21.3

We learned earlier in the chapter that Xenon-135 is a very important neutron poison. Develop an expression for the number of U-235 atoms in a cubic centimeter of uranium dioxide as a function of its average enrichment e. Use this expression to derive an equation for the equilibrium concentration of Xenon-135 in a cold, clean core (in atoms/cm^3) 1 week after start-up.

Exercise 21.4

Using the results from the previous two exercises, calculate the equilibrium concentrations of Samarium-149 and Xenon-135 in the fuel rods of a U-235-fueled thermal water reactor 10 days after start-up if the average enrichment of the fuel is 4%. Assume that the thermal neutron flux is 1×10^{14} neutrons/cm^2/s, and also assume that the initial xenon and samarium concentrations in the core are zero.

Exercise 21.5

Using the results from Exercise 21.4, calculate the neutron absorption rates for Xenon-135 and Samarium-149 if the thermal neutron flux is 1×10^{14} neutrons/cm^2/s. How many times greater is the neutron absorption rate for Xenon-135? How many neutrons are absorbed in a cubic centimeter of uranium dioxide in 1 minute by both of these materials?

Exercise 21.6

During the accidents at Chernobyl and Fukushima, large amounts of I-131 and Cesium-137 were released from these power plants. These two radioactive materials were the most harmful to people around the plants because they were more easily absorbed by plants, animals, and human beings. Approximately how long did it take for the initial concentrations of I-131 and Cesium-137 to subside by 99%?

Exercise 21.7

Suppose that the neutron flux in a thermal water reactor is 1×10^{14} neutrons/cm^2/s. What is the macroscopic absorption cross section for Xenon-135 after 1 week of continuous full power operation if the average enrichment of the fuel is 5%? Assume that there is no Xe-135 in the core prior to start-up.

22

An Introduction to Neutron Transport Theory

22.1 An Introduction to Neutron Transport Theory

Unlike the neutron diffusion equation, *the neutron transport equation is based on the premise that the flow of particles in a material is a function of angle as well as a function of the usual spatial and temporal variables* (energy, spatial position, and time). In other words, instead of the neutron flux being a function of just x, y, z, E, and t, it can also be a function of θ and ϕ (see Figure 22.1 to see how this can occur). *This means that the particle flow at any point in time is a function of seven independent variables instead of just five*. In its most complete form, these two additional angular variables make the neutron transport equation approximately 100 times more difficult to solve either analytically or numerically than the neutron diffusion equation. Basically, this is true because the neutron current **J**(x, y, z, E, t) can no longer be written as a simple constant (e.g., the diffusion coefficient D) multiplied by the negative gradient of the particle flux along each coordinate direction, for example,

The Assumptions of Neutron Diffusion Theory

$$\mathbf{J} = -D_x \frac{\partial \phi}{\partial x} - D_y \frac{\partial \phi}{\partial y} - D_z \frac{\partial \phi}{\partial z}$$

where

$$\mathbf{J_x} = -D_x \frac{\partial \phi}{\partial x}, \quad \mathbf{J_y} = -D_y \frac{\partial \phi}{\partial y}, \quad \mathbf{J_z} = -D_z \frac{\partial \phi}{\partial z} \quad \text{and} \quad \phi = \phi(x, y, z, E, t) \tag{22.1}$$

In this chapter, we would like to derive the neutron transport equation in its most common form. Sometimes, the neutron transport equation is also called the *Boltzmann transport equation*. These equations are similar to each other, but the Boltzmann transport equation can be applied to *other types of particles such as photons.* In other words, *it can be applied to any particle that does not have an electric charge*. (Only the scattering kernel is different.) We will then present several methods for obtaining approximate solutions to the neutron transport equation. To simplify our discussion, we will limit most of our discussion to just one spatial dimension. This limitation does not alter the basic approach that can be used for more than one dimension. However, geometries with more than one spatial dimension can lead to considerable algebraic complexity, and it is our intention to avoid as much of this complexity as possible in order to focus on the underlying principles that neutron transport theory employs.

After deriving the neutron transport equation, we will then reduce the neutron transport equation to a single energy group. In some textbooks, this is known as the *constant velocity model* or the *one-group model* because it assumes that all of the particles are traveling at exactly the same speed. Obviously, this is a critical assumption, and making this assumption is equivalent to assuming that we are using just one energy group to describe the entire neutron population. *Later, we will find that this is equivalent to using one-group neutron diffusion theory, except that the flux now has a directional or angular dependence. We will then discuss the spherical harmonics expansion to the Boltzmann transport equation. This expansion leads directly to the P_n and S_n approximations and also to discrete ordinates methods that can be used to track the particle flow along specific angular directions or ordinates*. The multigroup neutron transport equation is then derived, and we will subsequently examine its properties from this perspective. Finally, we will conclude our analysis with a discussion of when transport theory should be used instead of diffusion theory.

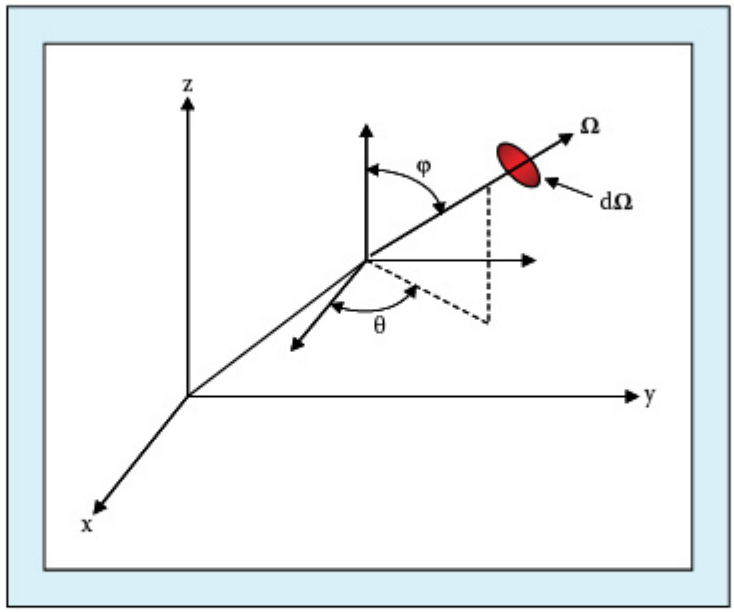

FIGURE 22.1 A picture of the angular unit vector **Ω** and the solid angle d**Ω** required to specify the position of the neutron flux in the neutron transport equation.

22.2 Diffusion Theory versus Transport Theory

Most studies of reactor behavior are based on the premise that the neutron flux can be described by a diffusion equation. These studies attempt to treat neutron motion as a *diffusion process* when in fact the motion of neutrons (and particularly thermal neutrons) is more of a *transport process*. By this, we mean that neutrons and other electrically neutral particles (such as photons) scatter off of atomic nuclei (and particularly lighter ones) in an anisotropic way, and it is only when the mean free path of neutrons becomes larger than the physical dimensions of the surrounding materials (such as the fuel rods, the control rods, and the cladding) that we can relate the neutron current **J** to the neutron flux ϕ using *Fick's Law of Diffusion* (see Equation 22.1). In other words, a particle with a long mean free path λ tends to "smear out" the spatial detail in a reactor core while a particle with a short mean free path tends to accentuate it. Thus, when the mean free path is short relative to the surrounding structure (as it is the case of thermal neutrons), the particle flux tends to acquire an angular dependence as well as a spatial one. When this occurs the particles tend to *stream* through the core instead of diffusing through it, and this is where neutron transport theory comes into play. Then the surrounding neutrons do not diffuse isotropically through the lattice in all directions, and they acquire a highly directional component to their flow. This behavior is particularly evident in the vicinity of strong neutron absorbers, such as control rods, and at abrupt material boundaries. In the vicinity of these structures, the reaction rates predicted by the diffusion equation are no longer as accurate as they sometimes need to be, and only the neutron transport equation (or the Monte Carlo method) can supply the accuracy that is required.

Neutron transport theory was originally derived from the kinetic theory of gases. The fundamental equation describing the motion of particles in a dilute gas was first proposed by German mathematician and physicist *Ludwig Boltzmann* in the 1800s. Boltzmann's picture is shown in Figure 22.2. Even today, the Boltzmann transport equation remains the principal tool of the gas dynamicist and the particle physicist when extreme accuracy is required. In comparison, the neutron transport equation, which seeks to model the flow of neutrons like a rarified gas, has only become widely popular since the 1940s. It is a linear equation, in contrast to the Boltzmann's original equation, which happened to be *nonlinear* in form. Unfortunately, this added complexity can strike terror in the heart of the uninitiated because the transport equation is a very hard equation to solve either numerically or analytically. This additional numerical complexity also comes at a steep price because of the amount of computer time required to solve is often 10 to 100 greater that the amount of time required to solve the diffusion equation. Thus, the neutron transport equation, in spite of its humble beginnings, is an extremely difficult equation to solve, and having to solve for the neutron flux as a function of seven independent variables at each spatial location (x, y, z, E, t, θ, and φ) does not make the task any easier.

To illustrate this fact, we would like to first derive the neutron transport equation using only the principle of particle conservation as our guide. The reader may recall from Chapter 2 that particle conservation in a closed system is equivalent to requiring that the mass or the number of particles is conserved (unless the number of particles being counted is

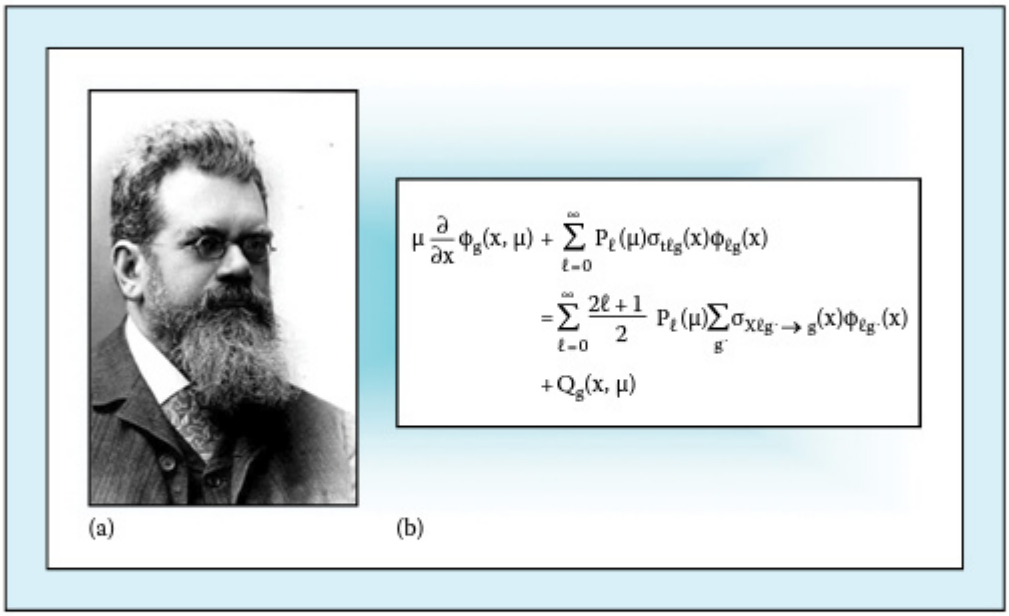

$$\mu \frac{\partial}{\partial x}\phi_g(x,\mu) + \sum_{\ell=0}^{\infty} P_\ell(\mu)\sigma_{t\ell g}(x)\phi_{\ell g}(x) = \sum_{\ell=0}^{\infty} \frac{2\ell+1}{2} P_\ell(\mu) \sum_{g'} \sigma_{s\ell g' \to g}(x)\phi_{\ell g'}(x) + Q_g(x,\mu)$$

FIGURE 22.2 A picture of Ludwig Boltzmann (a) and the multigroup neutron transport equation (b), which also bears his name.

also accompanied by some form of creation, destruction, or decay). Later in the chapter, we will explore various methods for solving the neutron transport equation, and we will discuss the pros and cons of using these methods in the real world. Finally, although brute force numerical methods are conceptually the easiest and most straightforward way to approach this problem, they are also the most expensive computationally.

More elegant methods that overcome some of these difficulties include the S_n and discrete ordinates methods, but because they use a different set of physical assumptions, it takes much more experience to understand when it is appropriate to use them and when it is not. In any event, solving the neutron transport equation in complex reactor geometries is a daunting task. The use of a computer can simply not be avoided unless one is willing to drop the angular dependence entirely for a number of reasons that will soon become apparent. Finally, the amount of effort required to actually write a computer "program" to perform these functions is not trivial, and even when the program is written correctly, solving the neutron transport equation numerically can involve a lot of "number crunching" and many hours of computer time.

Fortunately, computers have become increasingly powerful over the years, and in spite of these drawbacks, solving the neutron transport equation is now easier than it has ever been. In fact, some transport theory programs are now available on the *iPhone* and can be routinely run on desktop computers and laptops as well. Large numbers of computers connected in parallel (which can be used to conduct *parallel processing*) have also simplified the solution process to a certain extent. With these thoughts in mind, we would now like to derive the neutron transport equation and discuss its structure. The form of the equation we will derive can also be applied to photons, as long as the values of the scattering and absorption cross sections (and the source terms) are modified in an appropriate way. However, because we will be concentrating primarily on how neutrons behave, most of our attention will be focused on describing their behavior when the particle flux becomes anisotropic. In our companion book,* we learned that this approach can also be applied to *radiation shields*.

22.3 Diffusion Theory Concepts in Transport Theory Terminology

As we mentioned previously, using the neutron transport equation requires us to change the way we think about how particles move. Fundamentally speaking, the particle flux may be *anisotropic* in its flow, and this may require us to use several different angles to describe the direction in which it is flowing. In particular, when a particle hits a light atomic nucleus, it may scatter *anisotropically*. *Hence, we must assume that the scattering cross sections have an angular dependence* $\boldsymbol{\Omega}$ *(omega) as well as their usual energy dependence* E, and that this angular dependence can be described by the additional scattering angles θ and φ (see Figure 22.3). In Chapter 11, we introduced the concept of the neutron current $\mathbf{J}$ and the neutron flux ϕ. At that time, we assumed that both of these quantities had no angular dependence $\boldsymbol{\Omega}$ and that they could be related to each other using Fick's law of Diffusion. We would now like to revisit this assumption

* See *Nuclear Engineering Fundamentals: A Practical Perspective*, by R.E. Masterson, CRC Press (2017).

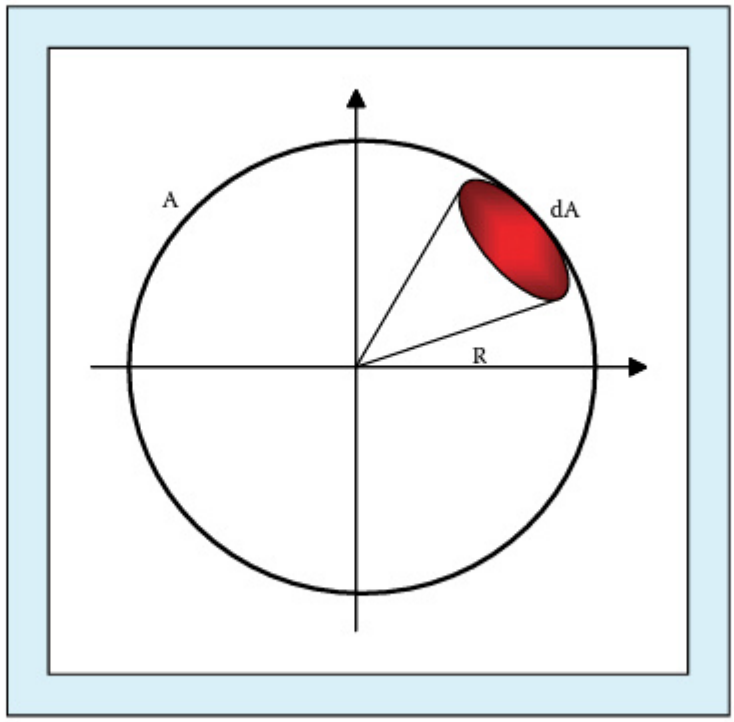

FIGURE 22.3 An illustration of a solid angle and how it is used.

by incorporating the angular dependence of the particle flow in these definitions, and in the process, creating what are known as the *angular neutron flux and the angular neutron current*. We can start by understanding which variables actually characterize the "state" of an individual neutron. Certainly, these variables must include the neutron's spatial position **r** or (x, y, z), the neutron's energy E, and the time t at which the neutron is being observed.

However, to completely specify the state, we must also specify the angular direction that the neutron is moving. A particle's direction of motion is usually described by the unit vector **Ω** (omega), where the standard definition of **Ω** is

$$\mathbf{\Omega} = \frac{\mathbf{v}}{|\mathbf{v}|} \tag{22.2}$$

and **v** is the neutron velocity vector. Hence, the angular unit vector **Ω** has both magnitude and direction. Thus, the unit vector **Ω** consists of x, y, and z components in three-dimensional space, or if we prefer, its motion can also be described by the angles θ and φ in a spherical coordinate system centered about point (x, y, z) or (**r**) (see Figure 22.1). Thus, it should be obvious that neutron transport theory is based on the direction the neutron is moving, and this direction is based in turn on the magnitude and orientation of the *angular unit vector* **Ω**. This unit vector is like any other unit vector in the sense that it has both magnitude (which in this case is assumed to be 1) and also a direction. We can therefore generalize the concept of the particle density n(**r**, E, t) that we first introduced in our discussion in Chapter 11 by defining the *angular neutron density* n(**r**, E, **Ω**, t) as one that depends on all four of these variables. Therefore, the number of neutrons in a small volume of space dV centered about point **r**, having an energy dE centered about energy E, and moving in direction **Ω** in a *solid angle* d**Ω** centered about the unit vector **Ω** at time t is given by

$$\text{Number of neutrons} = n(\mathbf{r}, E, \mathbf{\Omega}, t)\,dV\,dE\,d\mathbf{\Omega} \tag{22.3}$$

Here, the term "angle" is used to describe the fact that the angular neutron density n(**r**, E, **Ω**, t) depends on the spherical coordinate angles (θ and φ) derived from the velocity vector **v**. This is the most general neutron density function that we can define (unless we also include the *spin* or *parity* of the neutron in our definition). It also follows from this definition that the neutrons will flow in a small solid angle d**Ω** centered about whatever the ultimate direction of **Ω** happens to be. Since we have just introduced a new variable d**Ω** that we have never used before, it may be helpful to review how the solid angle d**Ω** is defined in a mathematical sense before we begin to proceed with our derivation. In three-dimensional space, the solid angle d**Ω** surrounding the angular unit vector **Ω** is defined as the *differential area* surrounding the point where

the angular unit vector $\boldsymbol{\Omega}$ intersects a sphere of radius r, divided by the total surface area A of the sphere. In other words, in Figure 22.1, the solid angle $d\boldsymbol{\Omega}$ is defined by

$$d\boldsymbol{\Omega} = \frac{(r\,d\theta)(r\sin\theta\,d\varphi)}{4\pi r^2} = \frac{1}{4\pi}\sin\theta\,d\theta\,d\varphi \tag{22.4}$$

This innocent-looking equation allows us to make the transition between a Cartesian coordinate system and a spherical coordinate system, and the actual value of $d\boldsymbol{\Omega}$ depends on what angles $d\theta$ and $d\varphi$ are relevant to the specific problem at hand. For example, the value of the differential solid angle $d\boldsymbol{\Omega}$ will be different in one dimension than it will be in two or three. To see the effect that increasing the number of dimensions has, we would first like to illustrate how the value of $d\boldsymbol{\Omega}$ changes depending on the limits of integration. If we integrate around the entire surface of the sphere, which is equivalent to integrating both θ and φ from 0° to 360°, we find that the value of the solid angle becomes

$$\int_{\text{All }\Omega} d\boldsymbol{\Omega} = \int_0^{2\pi} d\theta \int_0^{2\pi} d\varphi = 4\pi \tag{22.5}$$

which is just the surface area of the sphere ($4\pi r^2$) with r = 1. However, in two dimensions, Equation 22.5 reduces to

$$\int_{\text{All }\Omega} d\boldsymbol{\Omega} = \int_0^{2\pi} d\theta = 2\pi \tag{22.6}$$

which is just the area of a circle ($2\pi r$) with r = 1. Finally, in the case of a one-dimensional line source of strength S, the integral in the (−) x direction and the (+) x direction will yield ½ S and ½ S for a total source of strength S (or 1). The values of this integral are shown in Table 22.1 for several problems that we will encounter in this chapter. In the International System of Units, a solid angle has the units of *steradians* (abbreviated by the symbol "sr"), although from a purely mathematical and physical point of view, a solid angle is a *dimensionless quantity* and therefore has no real units associated with it. Hence, the reference to "sr" is skipped in many scientific textbooks, and we will choose to adopt this convention as well. We can then define the *angular neutron flux* $\phi(\mathbf{r}, E, \boldsymbol{\Omega}, t)$ in a manner similar to the definition of the isotropic neutron flux in Chapter 11, except that the flux now has an angular component that depends on the direction in which it is travelling. This allows us to conclude that the angular neutron flux is simply the angular neutron density multiplied by the neutron velocity. Thus we can write

Definition of the Angular Neutron Flux

$$\text{Angular neutron flux} = \phi(\mathbf{r}, E, W, t) = \mathbf{v}\cdot n(\mathbf{r}, E, W, t) \tag{22.7}$$

where $\mathbf{v}$ is the velocity vector. This is a very nice definition because we can define the *angular neutron current* as follows:

Definition of the Angular Neutron Flux

$$\text{Angular neutron current} = \mathbf{J}(\mathbf{r}, E, \boldsymbol{\Omega}, t) = v\cdot\Omega\cdot n(\mathbf{r}, E, \boldsymbol{\Omega}, t) \tag{22.8}$$

which is almost an exact analogy to the neutron current $\mathbf{J}$ used in diffusion theory. (However, we do not need Fick's law to associate the two of them in this case.) Notice in particular that $\boldsymbol{\Omega}$ is simply a unit vector that specifies the direction of the neutron flow, and so the angular flux is basically the magnitude of the angular current $\mathbf{J}$:

$$\text{Angular neutron current} = \mathbf{J}(\mathbf{r}, E, \boldsymbol{\Omega}, t) = \boldsymbol{\Omega}\cdot\phi(\mathbf{r}, E, \boldsymbol{\Omega}, t) \tag{22.9}$$

TABLE 22.1
Results of Integrating the Solid Angle $d\boldsymbol{\Omega}$ in One-, Two-, and Three-Dimensional Space

Integration Direction	x Only	x and y	y and z	x and y and z
Range of angles	0 to π	0 to 2π	0 to 2π	0 to 2π and 0 to 2π
Result of integration	1	2R	2πR	$4\pi R^2$
Result with radius R = 1	1	2	2π	4π

Here, it is important to realize that $\boldsymbol{\Omega}$ is simply shorthand notation for $\boldsymbol{\Omega} = \mathbf{i}\Omega_x + \mathbf{j}\Omega_y + \mathbf{k}\Omega_z$, where $\Omega_x = \sin\theta\cos\varphi$, $\Omega_y = \sin\theta\sin\varphi$, and $\Omega_z = \cos\theta$. Hence, the precise relationship between the *directional current* $\mathbf{J}(\mathbf{r}, E, \boldsymbol{\Omega}, t)$ and the *directional flux* $\phi(\mathbf{r}, E, \boldsymbol{\Omega}, t)$ in a spherical coordinate system is

The Angular Current in a Spherical Coordinate System

$$\mathbf{J}(\mathbf{r}, E, \boldsymbol{\Omega}, t) = \left[\mathbf{i}\cdot\sin\theta\cos\varphi + \mathbf{j}\cdot\sin\theta\sin\varphi + \mathbf{k}\cdot\cos\theta\right]\phi(\mathbf{r}, E, \boldsymbol{\Omega}, t) \tag{22.10}$$

Because of this relationship, the angular current density has an interesting physical interpretation. If $\mathbf{J}(\mathbf{r}, E, \boldsymbol{\Omega}, t)\, dA\, dE\, d\boldsymbol{\Omega}$ is the number of neutrons passing through a small surface area dA surrounding a point $\mathbf{r}$, and having an energy dE centered about energy E, and moving in direction $\boldsymbol{\Omega}$ in a solid angle $d\boldsymbol{\Omega}$ at time t, then the angular reaction rate $\mathbf{R}_x(\mathbf{r}, E, \boldsymbol{\Omega}, t)$ is simply

$$\mathbf{R}_x(\mathbf{r}, E, \boldsymbol{\Omega}, t) = \Sigma_x(\mathbf{r}, E)\cdot vn(\mathbf{r}, E, \boldsymbol{\Omega}, t) = \phi(\mathbf{r}, E, \boldsymbol{\Omega}, t)\cdot\Sigma_x(\mathbf{r}, E, \boldsymbol{\Omega}) \tag{22.11}$$

where x is the reaction type under consideration (i.e., x = a, s, c, f, t). Of course, this is completely consistent with what we would have expected, based on our previous knowledge of the reaction rates alone. Now let us explain how the angular neutron flux $\phi(\mathbf{r}, E, \boldsymbol{\Omega}, t)$ is related to the value of the neutron flux $\phi(\mathbf{r}, E, t)$ that is used in diffusion theory. If the angular flux is independent of $\boldsymbol{\Omega}$ (that is to say, it is isotropic in all directions), then neutron diffusion theory applies, and we can write $\phi(\mathbf{r}, E, t) = \int_{4\pi}\phi(\mathbf{r}, E, \boldsymbol{\Omega}, t)d\boldsymbol{\Omega}$. In other words, when we integrate the angular neutron flux over all solid angles, we obtain

$$\phi(\mathbf{r}, E, t) \equiv 4\pi\cdot\phi(\mathbf{r}, E, \boldsymbol{\Omega}, t) \tag{22.12}$$

Thus the normalization factor 4π is used to connect the two definitions together. *Hence, Equation 22.12 represents one of the fundamental links between neutron diffusion theory and neutron transport theory*. Of course, this only applies when the angular distribution of the flux is completely isotropic. The current $\mathbf{J}(\mathbf{r}, E, t)$ that appears in neutron diffusion theory is then

$$\mathbf{J}(\mathbf{r}, E, t) = \int_{4\pi}\mathbf{J}(\mathbf{r}, E, \boldsymbol{\Omega}, t)d\Omega = 4\pi\cdot\mathbf{J}(\mathbf{r}, E, \boldsymbol{\Omega}, t) \tag{22.13}$$

which is also exactly what we would expect when the flow of neutrons is isotropic. The net flow of neutrons with energy E through a small surface having area dA is then

$$\text{Net neutron flow with energy E} = \int_A \mathbf{J}(\mathbf{r}, E, t)dA \tag{22.14}$$

and if we integrate over the energies of all of the neutrons flowing through the surface, the net current flow from all of the neutrons is

$$\mathbf{J}(\mathbf{r}, t) = \int \mathbf{J}(\mathbf{r}, E, t)dE \tag{22.15}$$

where the integral is from E = 0 to E = ∞. As before, the units of both ϕ (r, t) and $\mathbf{J}$ (r, t) are the same (particles/cm^2/s), except that the neutron flux is a *scalar quantity* and the neutron current is a *vector quantity*.

Consequently, the neutron flux $\phi(r, t)$ measures the total number of neutrons that pass through 1 cm^2 in all possible directions in 1 second, while the neutron current $J(r, t)$ is a measure of the net flow of those neutrons along a predominant direction that is defined by the aggregate flow. If there are the same number of particles moving in every direction (see Chapter 11), then the neutron current will be zero because there is no net flow of neutrons, even though the neutron flux may still be a large positive number. Indeed, it is important to keep this distinction in mind when trying to count the number of neutrons as they move. These simple concepts are sufficient to enable us to count the number of neutrons entering and leaving a small control volume V surrounded by a surface of area A, and this is just what we need to derive the neutron transport equation using the definitions we have already presented.

Example Problem 22.1

Suppose that the components of the angular neutron current along the x-axis, the y-axis, and the z-axis in a Cartesian coordinate system are given by $\mathbf{J}_x = 0.25 \times 10^{14}$ neutrons/cm^2/s, $\mathbf{J}_y = 0.433 \times 10^{14}$ neutrons/cm^2/s, and $\mathbf{J}_z = 0.866 \times 10^{14}$ neutrons/cm^2/s. What is the neutron density $n(\mathbf{r}, E, \boldsymbol{\Omega}, t)$ at $\mathbf{r} = 0$ if the average velocity of the neutrons is 2200 m/s?

Solution The magnitude of the neutron density $n(\mathbf{r}, E, \boldsymbol{\Omega}, t)$ and the magnitude of the neutron current are related by $\mathbf{J}(\mathbf{r}, E, \boldsymbol{\Omega}, t) = v \cdot n(\mathbf{r}, E, \boldsymbol{\Omega}, t)$. The magnitude of the neutron density is therefore given by $n(\mathbf{r}, E, \boldsymbol{\Omega}, t) = \mathbf{J}(\mathbf{r}, E, \boldsymbol{\Omega}, t)/|v|$, where $\mathbf{J}(\mathbf{r}, E, \boldsymbol{\Omega}, t) = \sqrt{\left(\mathbf{J}_x^2 + \mathbf{J}_y^2 + \mathbf{J}_z^2\right)}$. The neutron density is then $n(\mathbf{r}, E, \boldsymbol{\Omega}, t) = \sqrt{\left(\mathbf{J}_x^2 + \mathbf{J}_y^2 + \mathbf{J}_z^2\right)}/|v| = 1 \times 10^{14}$ neutrons/cm^2/s $\div$ 2.2×10^6 cm/s $= 4.55 \times 10^7$ neutrons/cm^3. [Ans.]

22.4 Deriving the Neutron Transport Equation

It is customary to derive the transport equation for the angular neutron density $n(\mathbf{r}, E, \boldsymbol{\Omega}, t)$ by simply counting the number of neutrons that enter a small volume of space V and then counting the number of neutrons that leave the same volume of space in the same period of time. Naturally, some neutrons inside of the control volume may be scattered or absorbed, and other neutrons may be produced if a fission reaction occurs. The actual angular balance of neutrons moving in a specific angular direction $\boldsymbol{\Omega}$ with a specific energy E then defines how the number of neutrons in the control volume increases or decreases as a function of time. Of course, this is equivalent to assuming that all the particles in the control volume V are conserved (unless they are either absorbed or create additional particles in the process). To assist with our derivation, consider the control volume V shown in Figure 22.4 with surface area A. Except for the fact that the volume exists and has some type of surface surrounding it, there are no other assumptions we need to make. The rate of change of the angular neutron density $n(\mathbf{r}, E, \boldsymbol{\Omega}, t)$ within the control volume must be balanced by the number of neutrons entering the control and the number of neutrons leaving it. Hence, it is easy to see that

Conserving the Angular Neutron Density

$$\frac{\partial N}{\partial t} = \text{net neutron inflow} - \text{net neutron outflow}$$

where

$$N(\mathbf{r}, E, \boldsymbol{\Omega}, t) = \int_V n(\mathbf{r}, E, \boldsymbol{\Omega}, t)\, dV \tag{22.16}$$

If the control volume does not change as a function of time, then we may write

$$\text{Rate of change of the neutron population in energy interval } dE \text{ and solid angle } d\boldsymbol{\Omega} = \int_V \frac{\partial N}{\partial t}\, dV\, dE\, d\boldsymbol{\Omega} \tag{22.17}$$

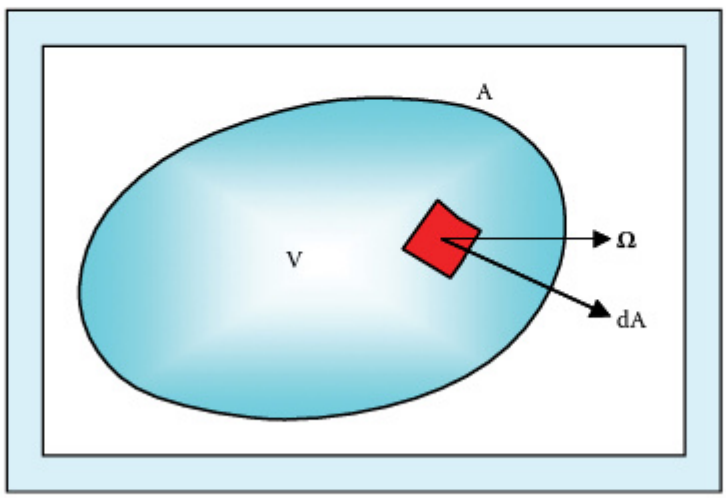

FIGURE 22.4 An arbitrary volume of space V with surface area A that can be used to derive the neutron transport equation.

Now let us see if we can calculate the flow of neutrons into and out of the control volume V. To do so, we must evaluate the angular current density $\mathbf{J}(\mathbf{r}, E, \boldsymbol{\Omega}, t)$ entering each surface A and leaving each surface A. The net neutron leakage rate L is therefore

$$\text{Net neutron inflow} - \text{Net neutron outflow} = L = \int_A v \cdot \boldsymbol{\Omega} \cdot n(\mathbf{r}, E, \boldsymbol{\Omega}, t)\, dA \tag{22.18}$$

We can rewrite this in terms of a volume integral if we use *Gauss's divergence theorem*:

$$\int_A A(\mathbf{r})\, dA = \int_V \nabla \cdot A(\mathbf{r})\, dV \tag{22.19}$$

The result is

Conservation Equation for the Angular Neutron Density

$$\left[\int_A \Omega \cdot v \cdot n(\mathbf{r}, E, \boldsymbol{\Omega}, t)\, dA\right] dE\, d\boldsymbol{\Omega} = \left[\int_V \nabla \cdot \boldsymbol{\Omega} \cdot v \cdot n(\mathbf{r}, E, \boldsymbol{\Omega}, t)\, dV\right] dE\, d\boldsymbol{\Omega} = \left[\int_V \Omega \cdot v \cdot \nabla n(\mathbf{r}, E, \boldsymbol{\Omega}, t)\, dV\right] dE\, d\boldsymbol{\Omega} \tag{22.20}$$

where we have used the fact that

$$\nabla \cdot v\boldsymbol{\Omega} = v\boldsymbol{\Omega} \cdot \nabla \tag{22.21}$$

Neglecting for the moment absorption, scattering, and fission inside of the control volume, we can then write the transport equation as

$$\int_V \left[\frac{\partial N}{\partial t} + v\boldsymbol{\Omega} \cdot \nabla n\right] dE\, d\boldsymbol{\Omega} = 0 \tag{22.22}$$

which appears to be quite innocuous in this particular form. Here, we find that there is an additional term that we have not encountered before. This term, which appears as $v\boldsymbol{\Omega} \cdot \nabla n$, is called the *directional derivative*, and its analog in the field of fluid mechanics is called the *material derivation*. Later on, we will find that this term is one of the reasons why the transport equation is so difficult to solve. The remaining neutrons in the control volume V moving with energy E in direction $\boldsymbol{\Omega}$ then consist of three terms, which we have not yet discussed. These terms include

Term 1: Sources of neutrons being created in the control volume V (including fission neutrons).

Term 2: Sources of neutrons being removed from the control volume V (by either being absorbed or by *out-scattering* into a different energy state than the initial energy state).

Term 3: Neutrons being scattered in the control volume V (either elastically or inelastically) from an initial energy E' and an initial angular direction $\boldsymbol{\Omega}'$ to a final neutron energy E and a final neutron angular direction $\boldsymbol{\Omega}$. Hence, the neutrons represented by this term are assumed to be *added* to the existing neutrons at energy E and angle $\boldsymbol{\Omega}$ by the process of *down-scattering* (see Chapter 12).

In other words, terms 1 and 3 *create* neutrons with an energy E and an angular direction $\boldsymbol{\Omega}$, while term 2 *removes* neutrons with the same energy E and angular direction $\boldsymbol{\Omega}$. Again, it is important to keep in mind that $\boldsymbol{\Omega}$ is simply a shorthand notation for $\mathbf{i} \sin\theta \cos\varphi + \mathbf{j} \sin\theta \sin\varphi + \mathbf{k} \cos\theta$. Now let us see if we can write down an analytical expression for reach of these terms. For the moment, consider the net neutron production rate (Term 1) inside of control volume V. To find the production rate, we must add fission neutrons to the transport equation. The total neutron production rate P is

Production Rate of Fission Neutrons

$$P = S(\mathbf{r}, E, \boldsymbol{\Omega}, t) = \left[v\Sigma_f(\mathbf{r}, E)\right] \frac{\mathbf{v} \cdot n(\mathbf{r}, \mathbf{E}, t)}{4\pi} \tag{22.23}$$

where the normalization factor 4π is required because additional neutrons can be created when a neutron hits the target nucleus at *any angle*. Of course, this does not include any external neutron sources that we will represent by the symbol $S_{ext}(\mathbf{r}, E, \boldsymbol{\Omega}, t)$. Thus, in most formulations of the transport equation, all neutron production processes (except for the process of in-scattering) are lumped into the value of $S(\mathbf{r}, E, \boldsymbol{\Omega}, t)$. Here, we have used the fact that $\phi(\mathbf{r}, E, \boldsymbol{\Omega}, t) = \mathbf{v} \cdot n(\mathbf{r}, E, \boldsymbol{\Omega}, t)$, where the value of $\mathbf{v}$ (the velocity) is not to be confused with the value of ν (mu)—the number of neutrons (both prompt and delayed) produced per fission. Next, let us consider the neutron removal rate (Term 2), which is due to

1. The absorption of a neutron by an atomic nucleus
2. The scattering of a neutron into a different energy and solid angle than the initial energy and solid angle

In this case, the *total removal rate* R is given by

Removal Rate of Any Neutron

$$R = \Sigma_t(\mathbf{r}, E)\mathbf{v} \cdot n(\mathbf{r}, \mathbf{E}, \boldsymbol{\Omega}, t) \tag{22.24}$$

where $\Sigma_t(\mathbf{r}, E)$ is the *total removal cross section* for the neutrons. In this capacity, the total neutron cross section represents the total removal rate due to scattering and absorption. In other words, when we look at this term holistically, it is always a *net destroyer* of neutrons. The same logic applies to the transport equation for photons, whose derivation we will leave to the interested reader as an independent exercise.

22.5 Finding the Scattering Rate for an Arbitrary Neutron

Finally, let us consider the scattering (Term 3) of a neutron from an initial energy E' and an initial angle $\boldsymbol{\Omega}'$ to a final energy E and a final angle $\boldsymbol{\Omega}$. This requires us to define a *scattering kernel* of the form $\Sigma_s(E' \rightarrow E, \boldsymbol{\Omega}' \rightarrow \boldsymbol{\Omega})$, which, when multiplied by $\phi(\mathbf{r}, E, \boldsymbol{\Omega}, t)$, is the rate that a neutron will be scattered from initial energy E' and initial angle $\boldsymbol{\Omega}'$ to final energy E and final angle $\boldsymbol{\Omega}$. Adding these initial terms to the control volume and noting in general that $S(\mathbf{r}, E, \boldsymbol{\Omega}, t) = \nu\Sigma_f(\mathbf{r}, E)\, \mathbf{v} \cdot n(\mathbf{r}, \mathbf{E}, t)/4\pi$, we arrive at the following form of the neutron transport equation:

The Neutron Transport Equation in a Very General Form

$$\frac{\partial n}{\partial t} + \mathbf{v} \cdot \boldsymbol{\Omega} \cdot \nabla n + \mathbf{v}\Sigma_t(\mathbf{r}, E)n(\mathbf{r}, \mathbf{E}, \boldsymbol{\Omega}, t) = \int_{4\pi}\int_{0}^{\infty} \left\{\mathbf{v}'\Sigma_s(\mathbf{E}' \rightarrow \mathbf{E}, \boldsymbol{\Omega}' \rightarrow \boldsymbol{\Omega})n(\mathbf{r}, \mathbf{E}', \boldsymbol{\Omega}', t)\right\} \mathbf{dE}'d\boldsymbol{\Omega}' + \mathbf{S}(\mathbf{r}, E, \boldsymbol{\Omega}, \mathbf{t}) \tag{22.25}$$

Here, the source term $S(\mathbf{r}, E, \boldsymbol{\Omega}, t)$ may consist of several external sources as well, in which case the production of all neutrons requires us to write

$$S(\mathbf{r}, E, \boldsymbol{\Omega}, t) = \frac{\nu\Sigma_f(\mathbf{r}, E)\mathbf{v} \cdot n(\mathbf{r}, \mathbf{E}, t)}{4\pi} + S_{ext}(\mathbf{r}, E, \boldsymbol{\Omega}, t) \tag{22.26}$$

Here, $S_{ext}(\mathbf{r}, E, \boldsymbol{\Omega}, t)$ is an *external source term*, which can have its own angular dependence. Several features of Equation 22.25 should be apparent to the astute reader. First, it is a *linear equation* where the primary unknown is $n(\mathbf{r}, E, \boldsymbol{\Omega}, t)$. This variable is in turn a function of seven independent variables: $r = x, y, z$, E, and t and $\boldsymbol{\Omega} = \theta$ and φ. Hence, Equation 22.25 is particularly difficult to manipulate because we must solve for the neutron angular density as a function of all seven variables. Second, it contains both spatial and temporal derivatives that are related to the angular neutron density in the usual way. Third, and most importantly, the transport equation is *not* just an ordinary differential equation because it contains a number of integrals over both the solid angle and the initial and final neutron energies. Hence, it is part of a class of equations that are sometimes referred to as *"integro-differential" equations* because they contain both integral terms and differential terms. The formal functional definition of an integro-differential equation is

$$\frac{du(x)}{dx} + \int_{x_o}^{x} f(t, u(t))\, dt = g(x, u(x)), \quad \text{where } u(x_o) = u_o \quad \text{and} \quad x_o \geq 0 \tag{22.27}$$

Equations of this type are typically some of most difficult differential equations to solve—particularly when the regions of space they are supposed to represent are spatially heterogeneous. Combined with the fact that we must find the angular neutron density (or the angular neutron flux) at literally thousands of spatial locations, it soon becomes apparent that the neutron transport equation is a real challenge to solve under even the most ideal conditions.

Student Exercise 22.1

Using the knowledge you have just acquired, derive the transport equation that can be used to describe the flow of photons rather than the flow of neutrons. What terms in this equation are similar, and what terms in this equation are different? Be prepared to justify why some of the terms are different and what the underlying differences may be.

22.6 Boundary Conditions for the Neutron Transport Equation

The presence of spatial and temporal derivatives in the transport equation suggests that it is necessary to specify a set of appropriate boundary conditions in order for the equation to have a unique solution. We must also specify a set of initial boundary conditions (or initial conditions at $t = 0$) for the angular neutron density if the neutron density $n(\mathbf{r}, E, \boldsymbol{\Omega}, t)$ becomes time dependent. The boundary conditions depend on the problem we are trying to solve. If a reactor is unreflected, the angular neutron density should vanish at the outer surface for all inward-facing directions because once the neutrons escape from the reactor, they typically do not reenter it. The reader may recognize this as a modified form of the *extrapolated boundary condition or vacuum boundary condition* that we initially discussed in Chapter 13 when we attempted to solve the neutron diffusion equation for a homogeneous and unreflected core. However, because the neutron density in the transport equation has an angular dependence, we must now explicitly define what this dependence is on each of the boundaries. We can do this by requiring that $n(\mathbf{r}, E, \boldsymbol{\Omega}, t) = 0$ for all $\mathbf{r}$ on the surface when $\boldsymbol{\Omega}\mathbf{B} < 0$ and $\mathbf{B}$ is the unit vector normal to the boundary. The boundary conditions on the neutron current $\mathbf{J}(\mathbf{r}, E, \boldsymbol{\Omega}, t) = \boldsymbol{\Omega}\cdot\phi(\mathbf{r}, E, \boldsymbol{\Omega}, t)$ then follow directly from what we have already said.

22.7 Reducing the Transport Equation to a More Conventional Form

Most of the time, it is convenient to rewrite the transport equation along with its initial conditions and boundary conditions in terms of the angular neutron flux $\phi(\mathbf{r}, E, \boldsymbol{\Omega}, t)$ rather than the angular neutron density $n(\mathbf{r}, E, \boldsymbol{\Omega}, t)$. Recalling for the moment that the two are related by

$$\phi(\mathbf{r}, E, \boldsymbol{\Omega}, t) = \mathbf{v}\cdot n(\mathbf{r}, E, \boldsymbol{\Omega}, t) \tag{22.28}$$

where $\mathbf{v}$ is the neutron velocity, the transport equation can also be written as:

The Neutron Transport Equation in More Conventional Form

$$\left(\frac{1}{v}\right)\frac{\partial\phi}{\partial t} + \boldsymbol{\Omega}\cdot\nabla\phi + \Sigma_t(\mathbf{r}, E)\phi(\mathbf{r}, \mathbf{E}, \boldsymbol{\Omega}, t) = \int_{4\pi}\int_{0}^{\infty}\left\{\Sigma_s(\mathbf{E}'\rightarrow\mathbf{E}, \boldsymbol{\Omega}'\rightarrow\boldsymbol{\Omega})\phi(\mathbf{r}, \mathbf{E}', \boldsymbol{\Omega}', t)\right\}\mathbf{dE}'\mathrm{d}\boldsymbol{\Omega}' + \mathbf{S}(\mathbf{r}, E, \boldsymbol{\Omega}, \mathbf{t}) \tag{22.29}$$

This is the form of the transport equation that we will attempt to in the rest of the chapter. Notice that the directional derivative $\boldsymbol{\Omega}\cdot\nabla\phi(\mathbf{r})$ is coordinate system dependent, and we would first like to discuss its form so that the reader can get a feel for what is involved. From our knowledge of neutron diffusion theory (see Chapters 11 through 13), the easiest possible problem in which the transport equation can be solved is a one-dimensional homogeneous slab in which the neutron flux varies in only the x direction. Such a slab is illustrated in Figure 22.5. However, because the neutron flux in the transport equation is always assumed to have *some* angular dependence, we have taken the liberty of showing how the angular component $\boldsymbol{\Omega}$ of the unit vector multiplying the gradient operator $\nabla\phi(\mathbf{x})$ can be interpreted in this case. Suppose that the neutron flux is a function of x only. Then the *directional derivative* of the flux $\boldsymbol{\Omega}\cdot\nabla\phi(\mathbf{x})$ in the transport equation reduces to

$$\boldsymbol{\Omega}\cdot\nabla\phi(\mathbf{x}) = \boldsymbol{\Omega}_x\frac{\partial\phi(x)}{\partial x} + \boldsymbol{\Omega}_y\frac{\partial\phi(x)}{\partial y} + \boldsymbol{\Omega}_z\frac{\partial\phi(x)}{\partial z} \tag{22.30}$$

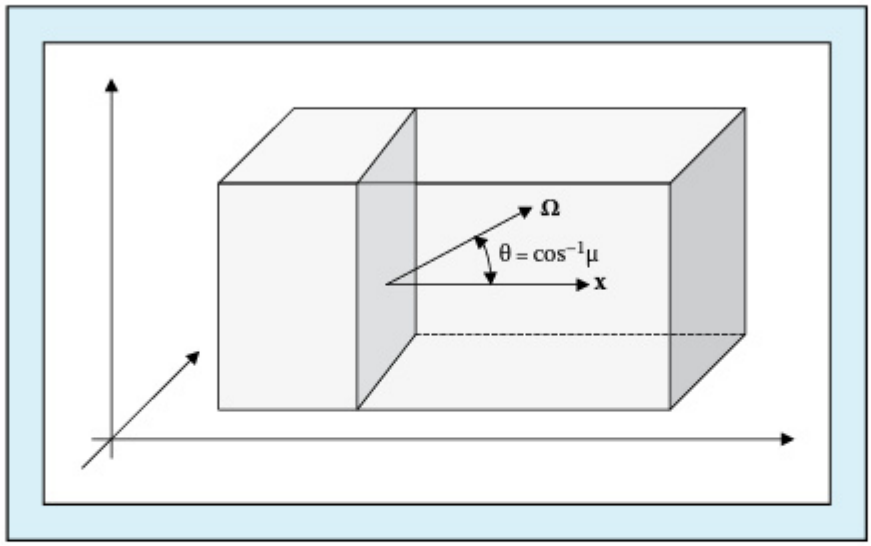

FIGURE 22.5 A convenient way to visualize the directional flux vector **Ω** that is used in the neutron transport equation for a one-dimensional slab.

Ordinarily, the direction of the neutron flux $\mathbf{\Omega}$ *depends on both the polar angle* θ *and the azimuthal angle* φ. *To make this statement a little less abstract, what this really implies is that* $\mathbf{\Omega} = i\Omega_x + j\Omega_y + k\Omega_z$, *where* $\Omega_x = \sin\theta\cos\varphi$, $\Omega_y = \sin\theta\sin\varphi$, *and* $\Omega_z = \cos\theta$. However, if we choose our coordinate system so that the coordinate axis is perpendicular to the surface of the slab, and our coordinate system has its polar axis in the x direction (rather than in the z direction), then the angular unit vector in the x direction is simply

$$\mathbf{\Omega}_x = \mathbf{i}\cos\theta \tag{22.31}$$

This also implies that there is no dependence of $\mathbf{\Omega}$ *on the azimuthal angle* φ. So in this particular case, the directional derivative $\mathbf{\Omega}\cdot\nabla\phi(\mathbf{x})$ reduces to

$$\mathbf{\Omega}\cdot\nabla\phi(\mathbf{x}) = \cos\theta\frac{\partial\phi}{\partial x} \tag{22.32}$$

or

$$\Omega\cdot\nabla\phi(\mathbf{x}) = \mu\frac{\partial\phi}{\partial x} \tag{22.33}$$

where $\mu = \cos\theta$. Hence, the transport equation as a whole can be written as

$$\left(\frac{1}{v}\right)\frac{\partial\phi}{\partial t} + \cos\theta\frac{\partial\phi}{\partial x} + \Sigma_t\phi(\mathbf{x}, E, \theta, t) = \int_0^{\pi}\int_0^{\infty}\left\{\Sigma_s(\mathbf{E}'\to\mathbf{E}, \theta'\to\theta)\phi(x, \mathbf{E}', \theta', t)\right\}\mathbf{dE}'\sin\theta'd\theta' + \mathbf{S}(x, E, \theta, \mathbf{t}) \tag{22.34}$$

This is still a big messy equation to solve, but this is the form of the transport equation that many computer programs attempt to solve when the neutron flux is incident upon a planar surface of finite thickness T. Sometimes, a final modification is made to the angular dependence to convert Equation 22.34 into a more "user-friendly" form. This modification involves introducing a new variable $\mu = \cos\theta$, which is just the cosine of the angle of the unit vector **Ω** in the laboratory coordinate system. According to this convention, when μ ranges from 1 to −1, θ ranges from 0 to π or from 0° to 180°. In this case, the one-dimensional transport equation can be written as

$$\left(\frac{1}{v}\right)\frac{\partial\phi(x, E, \mu, t)}{\partial t} + \mu\frac{\partial\phi(x, E, \mu, t)}{\partial x} + \Sigma_t\phi(x, E, \mu, t) = \int_{-1}^{+1}\int_0^{\infty}\left\{\Sigma_s(E'\to E, \mu'\to\mu)\phi(x, E', \mu', t)\right\}dE'd\mu' + S(x, E, \mu, t) \tag{22.35}$$

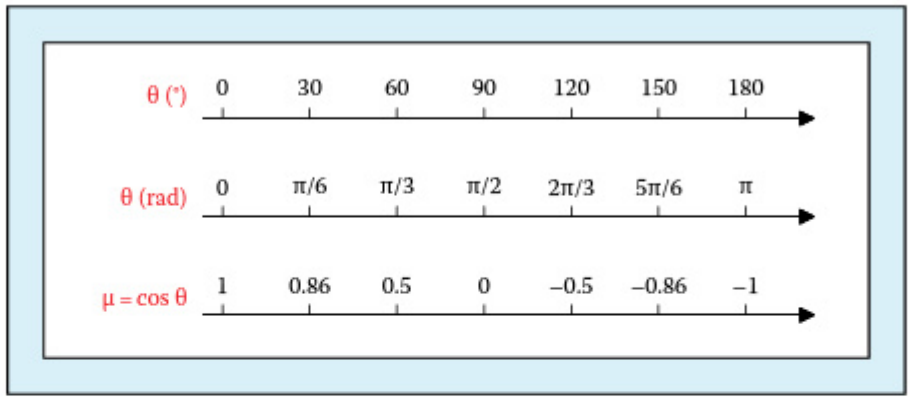

FIGURE 22.6 The relationship between θ in degrees, θ in radians, and μ = cos θ as it is used with the neutron transport equation.

where the relationship between μ and θ is illustrated graphically in Figure 22.6. Again, the value of Σ_t refers to the *total removal cross section*.

This extra level of normalization is valuable in practice because the angular neutron flux $\phi(\mathbf{r}, E, \mathbf{\Omega}, t)$ is normalized as well. This also simplifies the form of the *scattering kernel*

$$\Sigma_s\left(E' \rightarrow E, \mathbf{\Omega}' \rightarrow \mathbf{\Omega}\right) \tag{22.36}$$

because the limits of integration are now from $\mu' = -1$ to $\mu' = 1$. As we stated earlier, we can easily generalize the source term $S(x, E, \mu, t)$ to include more than just fission neutrons, and then the last remaining obstacle to solving the equation becomes defining an appropriate expression for the scattering kernel $\Sigma_s(E' \rightarrow E, \mathbf{\Omega}' \rightarrow \mathbf{\Omega})$. Under certain conditions, the scattering kernel may become simple enough to attempt to solve the transport equation analytically. However, the fact that reactors are extremely complex and heterogeneous machines means that this can be attempted in only simple one-dimensional geometries (planar, cylindrical, or spherical) that are spatially homogeneous. Even then, the previous solutions we obtained to the neutron diffusion equation are at least one order of magnitude simpler to obtain than the identical solutions to the transport equation. Because of this, virtually all meaningful solutions to the transport equation must be obtained numerically.

The amount of number crunching involved can also be prohibitive on all but the fastest machines. Nevertheless, computers have finally evolved to the point where credible solutions to the neutron transport equation can be attempted in even complex reactor geometries. The one drawback to this approach is that the computer programs must run for a very long time (sometimes on the order of days or even weeks) and the numerical methods required to solve the transport equation with just a single energy group can quickly become very sophisticated. We would now like to discuss the conditions under which a solution to the neutron transport equation reduces to a solution of the neutron diffusion equation. We will take the previous example of the bare slab reactor as our guide.

22.8 Showing When Solutions to the Transport Equation Reduce to Solutions to the Diffusion Equation

Before we can extend the transport equation to more than one energy group, it is essential to review what we have already learned about energy-dependent cross sections and the energy-dependent neutron flux. Many of the numerical approaches that can be used to solve the diffusion equation can also be used to solve the transport equation if the angular dependence of the neutron flux can be discretized in some way. Eventually this will lead us to what are known as *the P_N and S_N approximations*.

22.9 Simplifications to Neutron Transport Theory

A variety of simplifications to the transport equation are possible, depending on the problem one is trying to solve. In general, these simplifications fall into *five separate categories* that will subsequently be discussed. Each of these categories either simplifies a term in the transport equation or eliminates it entirely. If enough terms are eliminated or simplified, then it is possible to reduce the transport equation to the neutron diffusion equation for a homogeneous core. Of course, in this case, the angular dependence of the flux also disappears.

22.9.1 Category I: The Steady-State Transport Equation

To have any chance to solve the transport equation without requiring a numerical approach, the time-dependent term $1/v \cdot \partial\phi/\partial t$ is usually dropped. This allows us to write the transport equation in a one-dimensional planar geometry as

$$\mu \frac{\partial \phi}{\partial x} + \Sigma_t(x, E)\phi(x, E, \mu) = \int_{-1}^{+1}\int_{0}^{\infty} \left\{\Sigma_s(x, E' \to E, \mu' \to \mu)\phi(x, E', \mu')\right\} dE'\, d\mu' + S(x, E, \mu) \tag{22.37}$$

which is sometimes called *the steady-state neutron transport equation*. Equation 22.37 forms the basis of most of the solutions to the transport equation that can be found in the literature.

22.9.2 Category II: The One-Group or One-Speed Transport Equation

If the energy dependence of the remaining terms in the transport equation can be neglected, then what is left is known as *the one-group or one-speed transport equation*. The form of this equation is

$$\mu \frac{\partial \phi}{\partial x} + \Sigma_t(x)\phi(x, \mu) = \int_{-1}^{+1} \left\{\Sigma_s(x, \mu' \to \mu)\phi(x, \mu')\right\} d\mu' + S(x, \mu) \tag{22.38}$$

and to derive it, we have simply suppressed the energy dependence E of the cross sections and the directional flux. Although the resulting equation is still too complicated to solve in most reactor geometries, it can be solved in planar geometries (e.g., a slab reactor or a planar shield such as a reflector) using a brute force numerical approach. It can also be solved for a cylinder and a sphere under certain conditions.

22.9.3 Category III: The Transport Equation for a Homogeneous Material

If the material medium through which the particles are traveling consists of only one homogeneous region, then an analytical solution to the transport equation may be possible. The form of the transport equation in this case is

$$\mu \frac{\partial \phi}{\partial x} + \Sigma_t\phi(x, \mu) = \int_{-1}^{+1} \left\{\Sigma_s(\mu' \to \mu)\phi(x, \mu')\right\} d\mu' + S(\mu) \tag{22.39}$$

where we have suppressed the spatial dependence of the cross sections Σ_t and Σ_s. This form of the transport equation is the same whether we are dealing with neutrons or photons. Since we have suppressed the spatial dependence of cross sections, they are now just simple constants (except for the scattering kernel in Σ_s). However, the boundary conditions can still be directional, and care must be taken to implement them to obtain a physically meaningful result. The source term S is also different for neutrons and photons because the mechanisms to create these particles are entirely different, and these differences must be taken into account in any realistic problem.

22.9.4 Category IV: The Transport Equation for a Homogeneous Material with Isotropic Scattering

Neutron scattering in the *center of mass system* is usually an isotropic process, but it is far from isotropic in the *laboratory coordinate system*. This is especially true for low-mass scatters such as hydrogen and beryllium. However, for materials heavier than carbon, the scattering of neutrons can usually be assumed to be an isotropic process (see Chapter 11), and we can neglect the angular dependence of the scattering cross sections in our calculations. This is equivalent to reducing the scattering term to

$$\int_{-1}^{+1} \Sigma_s(\mu' \to \mu) d\mu' = \frac{\Sigma_s}{2} \tag{22.40}$$

in one dimension, and this in turn is the one-dimensional equivalent of the more general three-dimensional scattering integral

$$\int_{4\pi} \Sigma_s(\boldsymbol{\Omega}' \to \boldsymbol{\Omega}) d\boldsymbol{\Omega}' = \frac{1}{4\pi}\Sigma_s \tag{22.41}$$

With this simplification, the transport equation becomes

$$\mu\frac{\partial\phi}{\partial x}+\Sigma_t\phi(x,\mu)=\frac{\Sigma_s}{2}\cdot\int_{-1}^{+1}\phi(x,\mu')d\mu'+S(\mu) \tag{22.42}$$

However, we cannot make the same simplification when it comes to photons because they tend to stream through matter, and unless their energies are very low (say less than 1 keV), their scattering is never completely isotropic.

22.9.5 Category V: The Transport Equation with Isotropic Source Terms

Most of the time, the source terms appearing in the transport equation can also be assumed to be angularly isotropic. That is to say, the source term in three dimensions can be written as

$$S(r,\mu,t)=\frac{1}{4\pi}S(r,t) \tag{22.43}$$

and the one-dimensional equivalent is $S(x, \mu, t) = (1/2)\, S(x, t)$ because of the more limited integration over each solid angle. This is generally a good assumption when it comes to the production of fission neutrons. Highly directional particle sources (such as photons streaming through a reflector or a radiation shield) cannot be handled in this way. (However, their presence can usually be accounted for by including them in the boundary conditions.) When we make all of these assumptions, then the steady-state transport equation for a homogeneous material with a source term that is no longer time dependent can be written as

$$\mu\frac{\partial\phi}{\partial x}+\Sigma_t\phi(x,\mu)=\frac{\Sigma_s}{2}\cdot\int_{-1}^{+1}\phi(x,\mu')d\mu'+\frac{S(x)}{2} \tag{22.44}$$

Finally, if we are willing to simplify the problem further by assuming that the source term S(x) is *position independent*, then the transport equation can be reduced to a form that we can actually solve. In the case of a homogeneous slab, we arrive at the rather simple-looking equation for the angular flux:

$$\mu\frac{\partial\phi}{\partial x}+\Sigma_t\phi(x,\mu)=\frac{\Sigma_s}{2}\cdot\int_{-1}^{+1}\phi(x,\mu')d\mu'+\frac{S}{2} \tag{22.45}$$

In spite of its unusual form, this version of the transport equation can actually be solved analytically. It can also be solved numerically. So even after making the five categories of assumptions above, we are still left with a partial differential equation that can only be solved with great difficulty. We will now discuss specific ways that this equation can be solved in a variety of simple geometries (slab, cylinder, and sphere). However, we will start with the infinite slab because the mathematics is more straightforward.

Student Exercise 22.2

Write down an explicit expression for the source term $S(\mathbf{r}, E, \boldsymbol{\Omega})$ that appears in the transport equation for both neutrons and photons. How do the source terms differ in each case, and what are the differences in the underlying physics that are involved? Based upon these differences, is the transport equation easier or harder to solve when dealing with flow of neutrons as opposed to the flow of photons? Be prepared to justify the reason for your answer in each case.

22.10 Difficulties with Obtaining a Solution to the Neutron Transport Equation

The primary reason the transport equation is so difficult to solve is that it is an *integro-differential equation. Integro-differential equations are more challenging than other types of equations because they have both integrals and differentials in them*. In general, there is no easy way to solve an integro-differential equation. However, several methods have been developed that allow approximate solutions to be obtained under certain conditions. For example, a solution can be obtained by replacing the integrals by an infinite series expansion that can be truncated after the first few terms. Practically speaking, this approach is similar (but not identical) to expanding a trigonometric

function such as sin(x), cosine(x), e^x, or ln(x) in a Taylor series and retaining the first few terms. For cosine (x) and for e^x, the relevant Taylor series expansions are

$$\text{cosine}(x) = 1 - \frac{x^2}{2!} + \frac{x^4}{4!} - \cdots + \text{higher-order terms} \tag{22.46}$$

$$e^x = 1 + x + \frac{x^2}{2!} + \frac{x^3}{3!} + \cdots + \text{higher-order terms} \tag{22.47}$$

The series expansions for other geometric functions can be found in any elementary textbook. Ordinarily, only three or four terms are required to obtain a reasonable approximation to the function being integrated. Obviously, the more terms that are used, the more accurate the solution will be, but the additional terms also make it harder to find a general solution. And so a trade-off must be made in practice between the accuracy that is desired and the degree of complexity that is involved.

When it comes to solving the neutron transport equation, the series expansion we have to perform requires a slightly different approach because it is now necessary to replace the angular integral $\int_{-1}^{+1} \{\Sigma_s(\mu' \to \mu)\phi(x, \mu')\}\, d\mu'$ with a linear expansion that involves making the angular variable μ more discrete. Each of these discrete values of the angular variable μ is then called an *ordinate*. Sometimes, this process can be a bit confusing (particularly if one has not dealt with these types of approximations before), but if the expansion functions are properly chosen, then the overall degree of difficulty is reduced because the integro-differential equation can now be converted to a linear differential one. To be specific, consider the integration of an arbitrary function f(x) that must be performed from $x = x_o$ to $x = x_n$:

$$\int f(x)dx \tag{22.48}$$

In order to replace this integral with a series expansion that is accurate to any order N, then we must require that

$$\int f(x)dx \approx \sum_i w_i f(x_i) = \sum_i w_i f_i \quad (i = 1, 2, \ldots, n) \tag{22.49}$$

where f_i is the value of the function at point x_i. For example, if we would like to replace the value of $\int f(\mu)\, d\mu$ by an expansion involving four discrete ordinates, then we would select the values of μ_1, μ_2, μ_3, and μ_4 and also find the values of f_1, f_2, f_3, and f_4 at these four specific ordinates. Referring to the diagram in Figure 22.7, it is apparent that this is equivalent to replacing the integral $\int f(x)\, dx$ by a finite number of rectangles that allows us to find the area under the curve defined by f(x). In other words, we simply evaluate the function f(x) at a finite number of data points and multiply it by the distance between these data points to approximate the value of the integral $\int f(x)\, dx$. The process of replacing Equation 22.49 by a number of these rectangles having approximately the same area is called *quadrature*, and in the case of the transport equation, it is called *angular quadrature*, because the angular dependence of the neutron flux is what is being approximated.

Normally, the values for f_i are found by averaging the values of f_i at two adjacent interpolation points, which we will call i − 1 and i + 1. Hence, the interpolation scheme that is most commonly used is $f_i = (f_{i+1} + f_{i-1})/2$. *This is the process that most approximations to the angular integral attempt to use*. The resulting series expansion is sometimes called a *quadrature formula*, and the resulting set of weighting functions (the w_i's) are sometimes known as *quadrature weights*. This procedure eventually leads us to a set of coupled linear algebraic equations that can be solved numerically. A thorough discussion of this procedure can be found in many elementary numerical analysis books, and so we will not discuss the implementation of this approach in more detail at this time. *However, it forms the basis of the S_N method, which we will discuss later in the chapter.*

A somewhat different but equally valid approach is to convert the integral $\int f(x)dx$ into an infinite series expansion involving a finite number of known functions, which are usually chosen in advance. Normally these functions are assumed to be a set of *orthogonal polynomials* from which the final solution can be obtained. If we call each of these polynomial expansion functions $P_i(x)$, then it is easy to see that we can write f(x) as

$$f(x) \approx \sum_i w_i P_i(x) \tag{22.50}$$

where the weighting functions w_i are simple constants like 1/3,1/4, 1/5, and 1/2 that are chosen in order to obtain the best possible fit. *In this approach, an interpolation of the data points is not required as it was in the previous example. On a high level, this forms the basis for the P_N method, which is another popular method for solving the neutron transport equation*. So in conclusion, we have found that we can approximate the angular integral

$$\int f(x)dx \approx \sum_i w_i f(x_i) = \sum_i w_i f_i \tag{22.51}$$

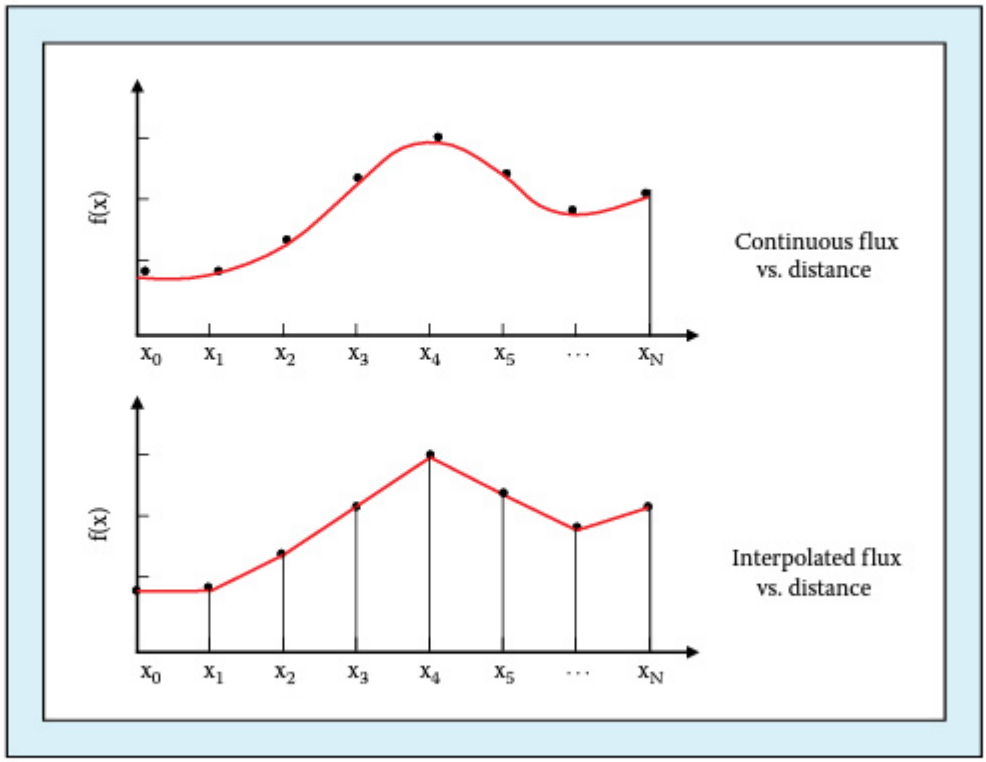

FIGURE 22.7 The integral of an arbitrary function f(x) can be approximated by a number of interpolation points that may have different weighting functions. In nuclear engineering, this type of approximation scheme is known as "quadrature."

in two distinct ways. First, we can perform an interpolation operation, and as an alternative, we can expand the function f(x) in an infinite series expansion (such as a *spherical harmonics* expansion) involving a simple set of polynomials—$f(x) \approx \sum w_i P_i(x)$—that we have chosen in advance. This second approach leads to

$$\int f(x)dx = \int \sum_i w_i P_i(x)dx$$

or (22.52)

$$\int f(\mu)d\mu = \int \sum_i w_i P_i(\mu)d\mu$$

In one dimension, we can set $\mu = \cos\theta$ in Equation 22.52, and $P_1, P_2, P_3, \ldots, P_N$ then become a subset of the spherical harmonics called the *Legendre polynomials*. Other types of polynomials can also be used. Either approach can be used to obtain a reasonable solution if it is implemented correctly. *The interpolation scheme we have just discussed then gives rise to the S_N approximation, and the polynomial expansion we have just discussed gives rise to the P_N approximation.* It is then up to the reader to determine which approach is most appropriate to use for a particular problem. Either approach can be implemented numerically. In fact, most neutron transport theory codes (refer to the list in Table 22.2) are implemented in one of these ways.

22.11 Deriving the Diffusion Theory Approximation

Before attempting to solve the transport equation, we would like to take one more step to reduce the transport equation to the diffusion equation. (The diffusion equation was introduced to the reader in Chapter 11.) The underlying mathematics is very involved, and we will not repeat all of the steps required to do so here, but the essential idea is to reduce the neutron transport equation and the neutron diffusion equation to the same form and then compare the terms to see how the neutron current and the neutron flux are related in this case. If the angular dependence of the flux $\phi(\mathbf{r}, \mathbf{E}, \boldsymbol{\Omega}, t)$ depends only weakly on the value of $\boldsymbol{\Omega}$, then we can assume that it possesses what is known as *linear anisotropy*, and with this assumption, we can derive a simple relationship between the angular flux $\phi(\mathbf{r}, \mathbf{E}, \boldsymbol{\Omega})$ and the neutron current $\mathbf{J}$.

TABLE 22.2
Popular Transport Theory Codes in Widespread Use Today

Transport Theory Program	Source or Developer	Programming Language Used	Function
ADO	Aerojet Nuclear Corporation, Sacramento, California	FORTRAN IV; IBM 360/370 (A) or UNIVAC 1108 (B)	ADO is part of an integrated system of computer programs that can be applied to many radiation analysis and shielding problems. It uses a discrete ordinates model to find the shape of the particle flux.
ANISN	Oak Ridge National Laboratory, Oak Ridge, Tennessee, and several others	Fortran IV, Fortran 77, IBM RS/6000 workstations, and Windows XP desktops; also runs on CRAY computers and VAX machines	ANISN is a one-dimensional, discrete ordinates code package that can handle anisotropic scattering. It solves the one-dimensional Boltzmann transport equation for neutrons or gamma rays in slab, spherical, and cylindrical coordinate systems.
ASFIT	Oak Ridge National Laboratory, Oak Ridge, Tennessee, and the Indira Gandhi Center for Atomic Research, in Kalpakkam, India	FORTRAN 77 and the IBM PC	ASFIT solves problems of gamma ray transport in slab geometries. The method is applicable to energy-dependent, multiregion radiation transport problems with an arbitrary degree of anisotropy.
ASOP	Oak Ridge National Laboratory, Oak Ridge, Tennessee	FORTRAN 77; IBM RS/6000 and IBM PC running Linux	ASOP is a multigroup, one-dimensional, discrete ordinates code system that can be used for shielding calculations and for shielding optimization.
BERMUDA	Japan Atomic Energy Research Institute, Tokai-mura, Naka-gun, Japan	FORTRAN 77	BERMUDA is a discrete ordinates code system for shielding analysis for use with fusion and fission reactors.
BISON	Faculty of Physics and Nuclear Techniques, University of Mining and Metallurgy, Cracow, Poland	Fortran 77; IBM RS/6000 and HP	BISON is a one-dimensional, discrete ordinates transport and burnup calculation code system. (The name stands for **B**urnup of **I**sotopes with **On**e-Dimensional Transport.)
CAMERA	McDonnell Douglas Astronautics Company, Huntington Beach, California.	FORTRAN IV, CDC CYBER-74, FORTRAN 77, IBM PC	CAMERA is a radiation transport analysis code system developed to calculate the radiation absorbed by the human body, and it can be used to calculate the dose that astronauts receive while traveling in space.
CNCSN	Keldysh Institute of Applied Mathematics, Moscow, Russia	Fortran 90 for multicore PC/ workstations running under Windows XP	CNCSN is a one-, two-, and three-dimensional, coupled neutral and charged particle SN parallel multithreaded code system.
DOORS	Oak Ridge National Laboratory, Oak Ridge, Tennessee	Fortran and C; IBM RS/6000, Sun, DEC Alpha, and on the PC under Linux and Windows	DOORS is a one-, two-, and three-dimensional discrete ordinates neutron/ photon transport code system.
DFT	Sandia National Laboratories, Albuquerque, New Mexico	FORTRAN IV; CDC 6600	DTF is a one-dimensional, multigroup photon transport discrete ordinates code system.

(*Continued*)

TABLE 22.2 (*Continued*)
Popular Transport Theory Codes in Widespread Use Today

Transport Theory Program	Source or Developer	Programming Language Used	Function
MORSE	Oak Ridge National Laboratory, Oak Ridge, Tennessee	Fortran-IV, IBM 360	MORSE is a general-purpose, Monte Carlo multigroup neutron and gamma ray transport code system with combinatorial geometry. It has many different versions—depending on the problem one would like to solve.
ONETRAN	Los Alamos National Laboratory, Los Alamos, New Mexico	FORTRAN IV; CDC 7600 (A), IBM 360/370/3033 (B), CRAY (C)	ONETRAN is a one-dimensional, multigroup, discrete ordinates finite element transport code system.
TDTORT	Nuclear Engineering Dept. University of Tennessee and the Oak Ridge National Lab, Oak Ridge, Tennessee	Fortran 77 and C; SUN Ultra; DEC OSF/1, PC under Linux	TDTORT is a time-dependent, three-dimensional, discrete ordinates, neutron transport code system.
TRIDENT	Los Alamos National Laboratory, Los Alamos, New Mexico	FORTRAN IV and Assembler language; IBM 360/370 (A) and CDC 7600 (B)	TRIDENT is a two-dimensional, multigroup, discrete ordinates transport code system for (x, y) and (r, z) geometries.
TRIPLET	Los Alamos National Laboratory, Los Alamos, New Mexico	FORTRAN IV; CDC 7600, CDC 6600, or IBM 360/370	TRIPLET is a two-dimensional, multigroup, triangular mesh, planar geometry, explicit discrete ordinates code system.
TWOTRAN	Los Alamos National Laboratory, Los Alamos, New Mexico	FORTRAN; CDC 7600 and IBM 360/370	TWOTRAN is a two-dimensional, multigroup, discrete ordinates transport code system in (x, y), (r, θ), and (r, z) geometries.

Source: Radiation Safety Information Computational Center, Oak Ridge, Tennessee.

After a great deal of work (see Reference 6—Duderstadt and Hamilton if you are interested in understanding how this can be accomplished), the transport equation can be rewritten in one form that uses the gradient of the neutron current **J** and in another form that uses the gradient of the neutron flux ϕ. The two equivalent forms are

$$\textbf{Form 1}: \frac{1}{v}\frac{\partial \phi}{\partial t} + \nabla \cdot \mathbf{J} + \Sigma_a(\mathbf{r})\phi(\mathbf{r}, t) = S(\mathbf{r}, t) \tag{22.53}$$

$$\textbf{Form 2}: \frac{1}{v}\frac{\partial \mathbf{J}}{\partial t} + \frac{1}{3}\nabla\phi + \Sigma_{tr}(\mathbf{r})\mathbf{J}(\mathbf{r}, t) = S(\mathbf{r}, t) \tag{22.54}$$

In other words, when the neutron flux becomes linearly anisotropic, we can write the transport equation as a set of two linear equations with two unknowns: $\phi(\mathbf{r}, t)$ and $\mathbf{J}(\mathbf{r}, t)$. These two equations can be shown to be equivalent to each other if and only if

$$\mathbf{J}(\mathbf{r}, t) = -\frac{1}{3}\Sigma_{tr}(\mathbf{r})\nabla\phi(\mathbf{r}, t) \tag{22.55}$$

where $\Sigma_{tr}(\mathbf{r})$ is a variable called the *transport cross section*. The resulting simplification is then called the *diffusion theory approximation*, and we initially discussed it in great detail in Chapter 11. In this case, the neutron flux $\phi(\mathbf{r}, E)$

becomes a function of only energy, space, and time, and the angular dependence **Ω** is completely suppressed. It can also be shown that the neutron current **J**(**r**, t) is related to the neutron flux ϕ(**r**, t) in the diffusion theory approximation by

$$\mathbf{J}(\mathbf{r},E) = -D(\mathbf{r},E)\nabla\phi(\mathbf{r},E) \tag{22.56}$$

where D(**r**, E) is the diffusion coefficient, and the transport cross section $\Sigma_{tr}(E)$ is defined by

$$\Sigma_{tr}(E) = \Sigma_t(E) - \mu\Sigma_s(E) \tag{22.57}$$

Here, μ *is the average cosine of the neutron scattering angle in the laboratory coordinate system:* μ = *cos* θ. The multigroup approximation for either the diffusion equation or the transport equation follows directly from what we have just done. What is remarkable about the result that we have just "derived" is that transport theory and diffusion theory become equivalent to each other when the neutron current **J** is proportional to the negative gradient **d**ϕ/dr of the neutron flux. The astute reader may recognize that this as just another statement of *Fick's Law of Diffusion* which we first introduced in Chapter 11. Only in this case, the constant of proportionality that links the neutron current **J** to the neutron flux ϕ is the diffusion coefficient $D(E) = 1/3\Sigma_{tr}(E)$ in which the scattering angle is linearly anisotropic. Furthermore, although we used an entirely different approach to derive Fick's law in Chapter 11, it can now be seen that transport theory and diffusion theory reduce to essentially the same result when the assumption of linear anisotropy is used. This, of course, is consistent with what we would have expected based on just physical arguments alone.

22.12 Introducing the P_N and S_N Approximations

Transport theory approximations have to do with how the angular variables θ and φ are used. There is a great deal of terminology associated with how this is done, but we would like to mention at least some of the more common analytical approximations that are used. Their application is very limited in practice—especially when we are dealing with a spatially heterogeneous system—but they are so pervasive in the literature that at least a cursory discussion of their characteristics is justified. Again, many of these methods date back to the late 1940s when computers were first being invented, and most people had only a piece of paper, a slide rule, and a pencil to try to solve the transport equation in one dimension. As we have just seen, the neutron transport equation cannot be solved analytically, except in a few very special and idealized cases. The term containing the scattering integral is the primary source of the problem. Consequently, most strategies for solving the transport equation involve some type of approximation to the angular terms to make it more tractable. We would now like to elaborate on several of these strategies. In particular, we would like to consider analytical approximations that make the equations easier to solve.

22.13 P_N Approximation

One particularly useful approximation is called the *P_N or spherical harmonics approximation*. The basic idea behind this approximation is to expand all of the functions of the angular variable Ω in terms of the *spherical harmonics functions*. These functions were invented several hundred years ago, and a discussion of their origin and their structure can be found at the following URLs:

http://mathworld.wolfram.com/SphericalHarmonic.html
http://mathworld.wolfram.com/LegendrePolynomial.html
http://hyperphysics.phy-astr.gsu.edu/hbase/math/legend.html

These polynomials can also be used to solve the *Schrodinger wave equation*, which we introduced to the reader in Chapter 1 of our companion book.* For one-dimensional problems, a subset of the spherical harmonics called the *Legendre polynomials* can be used. The resulting set of equations can be shown to reduce to an infinite set of coupled partial differential equations. The spherical harmonics approximation attempts to truncate this infinite set of equations after the first few terms and to then solve the equations that remain. Of course, the more terms that are retained, the more accurate the solution will be. However, more terms make the resulting equations more complex, and so there is a trade-off between complexity and accuracy that has to be considered in the real world.

* See *Nuclear Engineering Fundamentals: A Practical Perspective*, by R.E. Masterson, CRC Press (2017).

In one dimension, one tries to replace the angular neutron flux with an infinite series expansion of the form

$$\phi(\mathbf{r},E,u)=\sum\nolimits_n P_n(\mu)\phi_n(\mathbf{r},E) \tag{22.58}$$

where the summation is from n = 0 to n = ∞. Here, $P_n(\mu)$ are a set of "weighting functions" called the Legendre polynomials that we referred to previously. In other words, the Legendre polynomials allow us to replace the directional unit vector **Ω** by a series of weighting coefficients of the form $P_n(\mu)$. The first few Legendre polynomials are

$$P_0(\mu)=1 \tag{22.59}$$

$$P_1(\mu)=\mu \tag{22.60}$$

$$P_2(\mu)=\frac{(3\mu^2-1)}{2} \tag{22.61}$$

and for n > 2, the remaining polynomials can be found from the recursion relationship (see Figure 22.8)

$$(n+1)P_{n+1}(\mu)=(2n+1)\mu P_n(\mu)-nP_{n-1}(\mu) \tag{22.62}$$

These polynomials have the property that they are orthogonal to one another in the sense that we can write

$$\int_{-1}^{+1} P_n(\mu)P_m(\mu)d\mu=\frac{2}{(2l+1)} \quad \text{for } n=m \tag{22.63}$$

$$\int_{-1}^{+1} P_n(\mu)P_m(\mu)d\mu=0 \quad \text{for } n\neq m \tag{22.64}$$

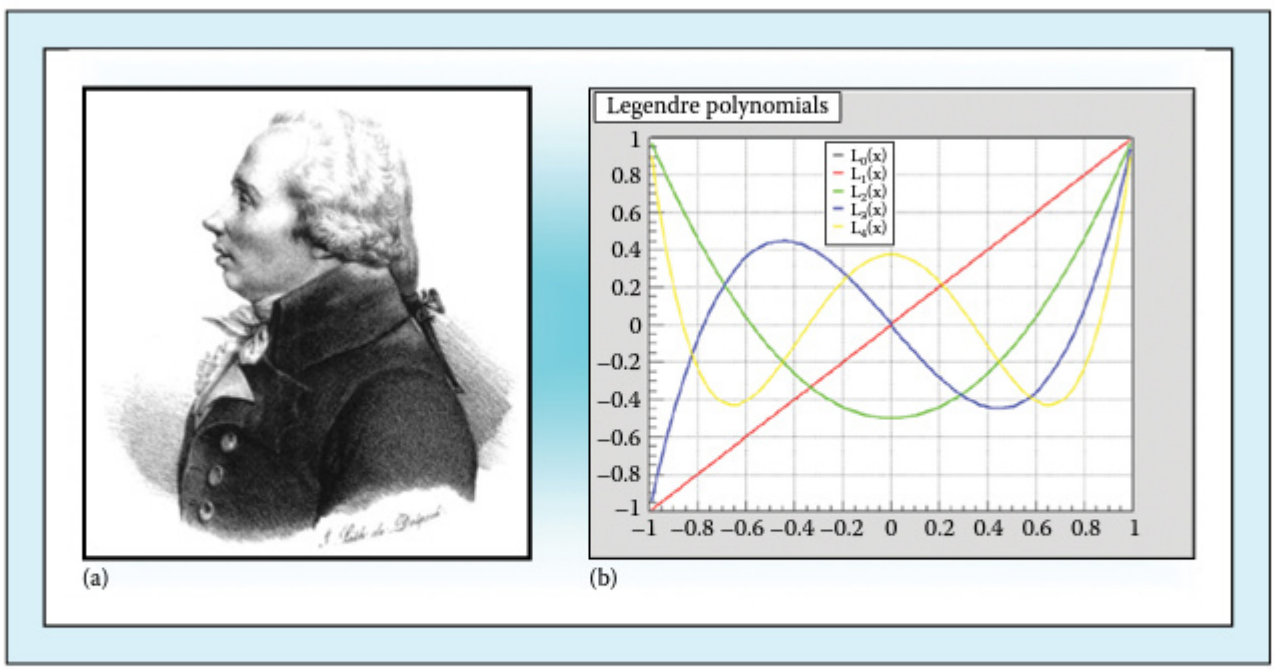

FIGURE 22.8 (a) A picture of the great French mathematician Adrien-Marie Legendre who formulated the Legendre polynomials. (b) Legendre also developed the least squares method, which has broad application in the fields of linear regression analysis, signal processing, statistics, and curve fitting. (See *https://en.wikipedia.org/wiki/Legendre_polynomials* and *https://en.wikipedia.org/wiki/Adrien-Marie_Legendre*.)

They also have the interesting property that the quantity $\int_{-1}^{+1}\left[\phi(\mu)-\phi_N(\mu)\right]^2 d\mu$ *is less* than it would be for any other polynomials up to order N. *In other words, the Legendre polynomials are the best set of expansion functions to use to minimize the error (in a "Least squares" sense) in the approximation of* $\phi(\mu)$ *at the ordinates or interpolation points.* (Between the interpolation points, this is not always the case.) Substituting Equation 22.58 for the angular flux into the neutron transport equation, multiplying all terms by $P_m(\mu)$, and then integrating the results between $\mu = -1$ and $\mu = 1$, we obtain

$$\frac{n+1}{2n+1}\frac{d}{dx}\phi_{g,n+1}(x)+\frac{n}{2n+1}\frac{d}{dx}\phi_{g,n-1}(x)+\Sigma_{tg}\phi_{g,n}(x)=\Sigma_{sg}\phi_{g,n}(x)+S_{g,n}(x) \tag{22.65}$$

where n = 1, 2, 3, …, N. This is an infinite set of differential equations for the neutron flux $\phi(\mathbf{r})$. Thus what we have done is to eliminate the angular variable μ and to replace it by an infinite set of equations for the flux where each of the Legendre polynomials can be considered to be a "weighting function". Normally, we can truncate this set of equations after N terns, which then results in

$$\phi_{g,n}(\mathbf{r})=0 \quad \text{for } n > N \tag{22.66}$$

This is the famous *P_N approximation*. We will discuss solutions to the resulting equations in our follow-on book, where a more numerically oriented approach is employed. Here a more comprehensive discussion of numerical quadrature is also provided.* The primary problem with the *P_N approximation* is that there is a numerical and physical coupling between at least three of the coefficients for each value of n. We can see this more clearly by writing out the first few terms in the series expansion

$$\phi(\mathbf{r},E,u)=\sum\nolimits_n P_n(\mu)\phi_n(\mathbf{r},E) \tag{22.67}$$

and by assuming that the values of $P_n(\mu)$ are known. This then means that

$$\phi(\mathbf{r},E,u)=\Sigma_n P_n(\mu)\phi_n(\mathbf{r},E)=P_0(\mu)\phi_0(\mathbf{r},E)+P_1(\mu)\phi_1(\mathbf{r},E)+P_2(\mu)\phi_2(\mathbf{r},E)+P_3(\mu)\phi_3(\mathbf{r},E)+\text{higher-order terms} \tag{22.68}$$

If we truncate this expansion when N = 3, we get the P_3 approximation, and the exact expression for the angular flux becomes

$$\phi(\mathbf{r},E,u)=\Sigma_n P_n(\mu)\phi_n(\mathbf{r},E)=P_0(\mu)\phi_0(\mathbf{r},E)+P_1(\mu)\phi_1(\mathbf{r},E)+P_2(\mu)f_2(\mathbf{r},E)+P_3(\mu)\phi_3(\mathbf{r},E) \tag{22.69}$$

or more explicitly,

$$\phi(\mathbf{r},E,u)=\Sigma_n P_n(\mu)\phi_n(\mathbf{r},E)=\phi_0(\mathbf{r},E)+\mu\phi_1(\mathbf{r},E)+\frac{3\mu^2-1}{2}\phi_2(\mathbf{r},E)+\frac{5\mu^3-3\mu}{2}\phi_3(\mathbf{r},E) \tag{22.70}$$

where the values of $\phi_0(\mathbf{r},E)$, $\phi_1(\mathbf{r},E)$, $\phi_2(\mathbf{r},E)$, and $\phi_3(\mathbf{r},E)$ are found by solving a set of matrix equations and the first few Legendre polynomials are

The First Few Legendre Polynomials in the P_N Approximation

$$\begin{aligned} P_0(\mu)&=1\\ P_1(\mu)&=\mu\\ P_2(\mu)&=\frac{3\mu^2-1}{2}\\ P_3(\mu)&=\frac{5\mu^3-3\mu}{2} \end{aligned} \tag{22.71}$$

* See *Contemporary Nuclear Reactor Physics with an Introduction to Reactor Dynamics, Computational Methods, and Nuclear Particle Transport*, by R.E. Masterson, CRC Press (2020).

In other words, with just a P_2 approximation in one dimension, $\phi_{g,l}(\mathbf{r})$ is related to $\phi_{g,l-1}(\mathbf{r})$ and $\phi_{g,l+1}(\mathbf{r})$, and this coupling increases to 5 and 7 terms as the number of dimensions is increased from 2 to 3. This coupling also increases as the order of the method (the value of N) is increased. For example, a value of N = 5 (which corresponds to a P_5 method) requires the angular flux at one mesh point to be coupled to the angular flux along five other directions at the same mesh point. Because of this, the use of the P_N approximation has declined in favor of discretizing the angular terms directly, which then gives rise to what is known as the S_N or *the discrete ordinates approximation*. We will discuss the *S_N method* and some of its variations in the next section of the text. However, before doing so, we would like to make some additional comments about the P_N method and how it is used in practice. Normally, the integrations that are used to eliminate the variable μ from the transport equation are very complex and are ordinarily not discussed in a book at this level. However, because it is important to get a real feeling for how the angular variable μ is eliminated from each term, we would like to illustrate how these integrations are performed at this time. Let us assume that we can write the time-dependent transport equation for an infinite slab as

$$\frac{1}{v}\frac{\partial\phi(x,\mu,t)}{\partial t}+\mu\frac{\partial\phi(x,\mu,t)}{\partial x}+(\Sigma_t-\Sigma_{s,0})\phi(x,\mu,t)=S_0(x) \tag{22.72}$$

where S_0 is an isotropic particle source of constant strength. If we neglect the time-dependent term for the moment, and the slab is homogeneous, then the transport equation in one dimension becomes

$$\mu\frac{\partial\phi(x,\mu)}{\partial x}+(\Sigma_t-\Sigma_{s,0})\phi(x,\mu)=S_0 \tag{22.73}$$

The scattering cross sections, the angular flux, and the neutron source terms all have to be expanded in a series of Legendre polynomials in order to eliminate the continuous dependence on μ. Let us start first with the scattering term to illustrate how this can be done. The polynomial expansion for this particular function is

$$\Sigma_s(\boldsymbol{\Omega}'\rightarrow\boldsymbol{\Omega})d\boldsymbol{\Omega}'=\left(\frac{1}{2\pi}\right)\sum_m\frac{(2m+1)}{2}\cdot P_m(\mu')\Sigma_{sm} \tag{22.74}$$

where the factor $(2m + 1)/4\pi$ is used to normalize the solution. It follows from the orthogonality conditions (Equations 22.63 and 22.64) that

$$\Sigma_{sm}=2\pi\int_{-1}^{+1}\Sigma_s(\boldsymbol{\Omega}'\rightarrow\boldsymbol{\Omega})P_m(\mu')d\mu' \tag{22.75}$$

Now the flux in Equation 22.73 also depends on the angle from which it is measured, and since $\mu = \cos\theta$, the unit vector $\boldsymbol{\Omega}$ is $\boldsymbol{\Omega} = \mathbf{i}\cos\theta$ in this one-dimensional case. The directional flux $\phi(x, \mu)$ may then be expanded as

$$\phi(x,\mu)=\sum_n\frac{2n+1}{2}\cdot P_n(\mu)\phi_n(x) \tag{22.76}$$

where

$$\phi_n(x)=\int_{-1}^{+1}\phi(x,\mu)P_n(\mu)d\mu \tag{22.77}$$

Likewise, for the source term, we can write

$$S(x,\mu)=\sum_n\frac{2n+1}{2}\cdot P_n(\mu)S_n(x)\quad\text{where } S_n(x)=\int_{-1}^{+1}S(x,\mu)P_n(\mu)d\mu \tag{22.78}$$

Further simplification of the transport equation using these prescriptions leads to

The P_3 Equations in One Dimension

$$\begin{aligned}
&\left(\frac{1}{v}\right)\frac{\partial\phi_0}{\partial t}+\frac{\partial\phi_1}{\partial x}+\left(\Sigma_t-\Sigma_{s,0}\right)\phi_0=S_0\\
&\left(\frac{1}{v}\right)\frac{\partial\phi_1}{\partial t}+\left(\frac{2}{3}\right)\frac{\partial\phi_2}{\partial x}+\left(\frac{1}{3}\right)\frac{\partial\phi_0}{\partial x}+\left(\Sigma_t-\Sigma_{s,1}\right)\phi_1=S_1\\
&\left(\frac{1}{v}\right)\frac{\partial\phi_2}{\partial t}+\left(\frac{3}{5}\right)\frac{\partial\phi_3}{\partial x}+\left(\frac{2}{5}\right)\frac{\partial\phi_1}{\partial x}-\left(\Sigma_t-\Sigma_{s,2}\right)\phi_2=S_2\\
&\left(\frac{1}{v}\right)\frac{\partial\phi_3}{\partial t}+\left(\frac{3}{7}\right)\frac{\partial\phi_2}{\partial x}+\left(\Sigma_t-\Sigma_{s,3}\right)\phi_3=S_3
\end{aligned} \tag{22.79}$$

which are the famous *P_3 equations in one dimension*. Notice that there are four equations and four angular directions in this case because the index in the P_3 approximation runs from N = 0 to N = 3. Of course, we could have just as easily used a higher-level approximation in this case, but the coupling of the angular flux would involve more terms than just 3. This increases the amount of time it takes to invert the coefficient matrix, and the increased accuracy must be weighed against the increased cost. Finally, it should be obvious from a simple inspection of this set of equations that the cosine μ of the directional flux has been replaced by a number of angular "weights" that are now just simple numbers. The same is true of the scattering cross sections and the source terms, and there are now just 4 of them in each case because the value of N in the P_3 approximation runs from N = 0 to N = 3. We can then solve these linear equations using any one of the solution techniques that we have already discussed (see Chapters 11 and 12), and this can be easily seen if we can rewrite them as a set of matrix equations

$$[M]\{\phi\}=\{S\} \tag{22.80}$$

and invert the coefficient matrix [M] to obtain

$$\{\phi\}=[M]^{-1}\{S\} \tag{22.81}$$

Thus, the P_N method also results in a set of matrix equations that can be solved with a digital computer. Only in this case, there are N + 1 values of the angular flux per mesh point, where N is the order of the P_N method that we decide to use.

Example Problem 22.2

In the P_1 approximation, the angular neutron flux $\phi(\mathbf{r}, E, u)$ can be written as the sum of two terms:

$$\phi(\mathbf{r},E,u)=\phi_o(\mathbf{r},E)P_o(\mu)+\phi_1(\mathbf{r},E)P_1(\mu)$$

or

$$\phi(\mathbf{r},E,u)=\phi_o+\mu\phi_1$$

where $P_o(\mu)$ and $P_1(\mu)$ are the first two Legendre polynomials. What is the physical meaning of ϕ_o and ϕ_1 in this case?

Solution In the P_1 approximation, *$\phi_o(r, E)$ is the isotropic neutron flux* ϕ (with no angular dependence), and in a future section, we will learn that *$\phi_1(r, E)$ is equivalent to the directional neutron current $J(r, E)$.* [Ans.]

22.14 S_N Approximation

The S_N approximation is a popular alternative to the P_N approximation. In many problems, it is also easier to implement and it is more computationally efficient. In its simplest form, the S_N approximation is based on the premise that the angular neutron flux $\phi(\mathbf{r}, E, u)$ can be broken into a number of discrete directions (say, 6 or 12) and then solved for directly.

Each of these directions is represented by a different value of μ, for example, $\mu_1, \mu_2, \mu_3, \ldots, \mu_N$. This process is also known as *angular discretization*, and it has become an increasingly popular way to solve the transport equation as digital computers have become more powerful. It differs from the P_N method because it avoids the need to use a specific polynomial expansion (such as the Legendre polynomials) to represent the angular dependence of the flux $\phi(\mathbf{r}, E, u)$. In the original S_N method, the angular flux was determined at N points—that is, along N distinct angular directions between $\mu = -1$ and $\mu = 1$. In general, each of these angles was equally spaced, and therefore angles like 0°, 30°, 45°, 60°, and 90° were commonly used. However, as long as the geometry is properly chosen, then any arbitrary set of N angles can be used.

Examples of this angular decomposition are shown in Figures 22.9 and 22.10. Consequently, if one would like to find the neutron flux along N different angular directions having an equal spacing Δμ between $\mu = -1$ and $\mu = 1$, the angular directions shown in Figure 22.9 could be used. Of course, this approach can be extended to more than one spatial dimension, but then the ordinates are defined by two angles (θ and ϕ) rather than just one. Each of these directions (from 1 to N) can then be thought of as a *discrete angle*, or *discrete ordinate* along the particle flow. The *S_N method* is a special case of a much larger class of methods called *discrete ordinates methods. The fundamental premise of the S_N method is that the neutron flux $\phi(r, \mu)$ along an arbitrary angular direction μ can be written as the linear average of the flux along adjacent*

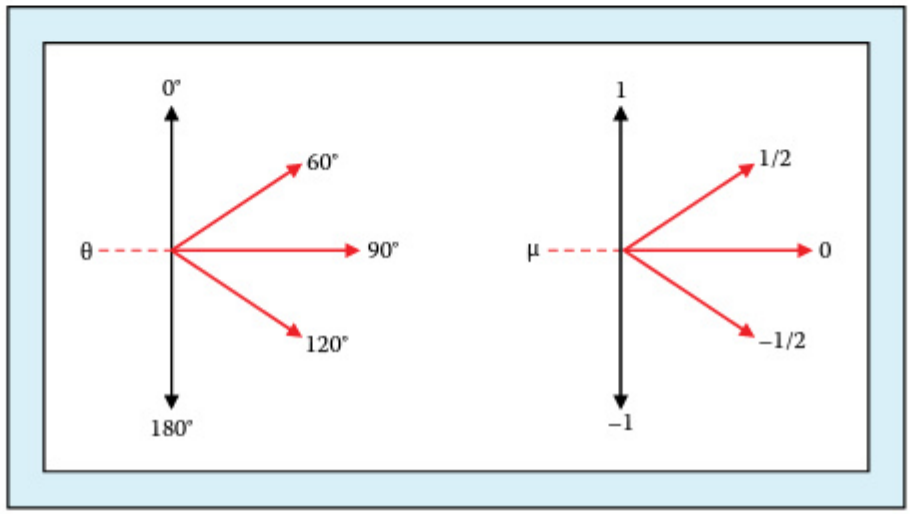

FIGURE 22.9 The "discrete ordinates" $\mu_0, \mu_1, \mu_2, \mu_3$, and μ_4 and their corresponding angles in the S_4 approximation.

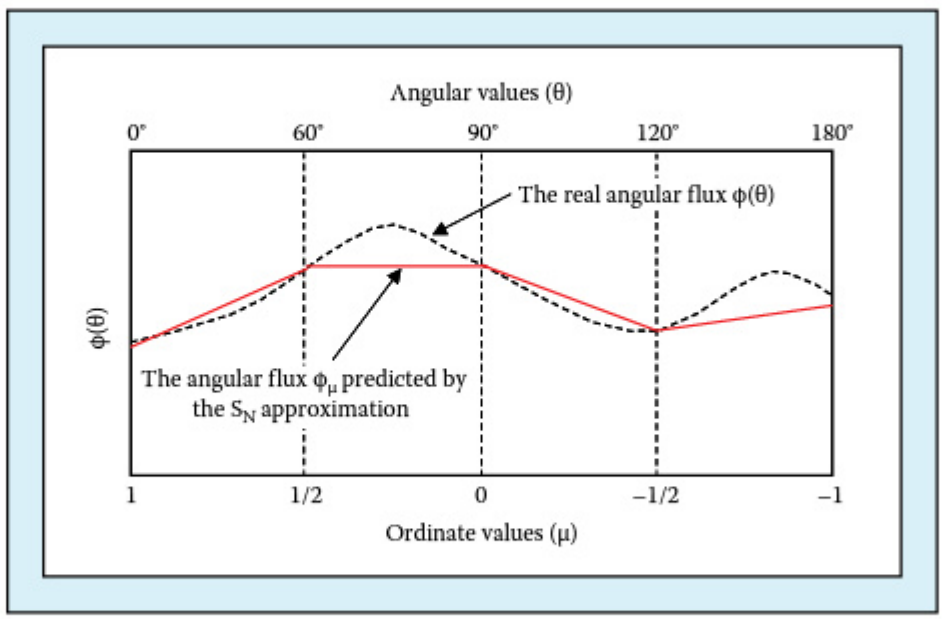

FIGURE 22.10 The values of the angular flux $\phi_0, \phi_1, \phi_2, \phi_3$, and ϕ_4 in an S_4 approximation. Here, the solid line represents the directional flux, and the dashed line represents the flux predicted by the S_N approximation.

angular directions μ_i and μ_{i-1}. The resulting equations are then discussed in our follow-on book.* Of course, when these equations are converted to finite difference equations, the resulting equations lead to a matrix representation of the steady state transport equation that must be solved for numerically. Methods to solve these matrix equations are also discussed in our companion book.

Example Problem 22.3

Suppose that the general equation for a Legendre polynomial is

$$(n+1)P_{n+1}(\mu) = (2n+1)\mu P_n(\mu) - nP_{n-1}(\mu)$$

where the first two polynomials are $P_0(\mu) = 1$ and $P_1(\mu) = \mu$. Write out the Legendre polynomials that are needed in a simple P_3 approximation in one dimension.

Solution The P_3 approximation involves expanding the angular neutron flux into four terms from N = 0 to N = 3. Therefore, the four Legendre polynomials that are used in this case are

$$P_0 = 1$$
$$P_1 = \mu$$
$$P_2 = \frac{3\mu^2 - 1}{2}$$
$$P_3 = \frac{5\mu^3 - 3\mu}{2}$$

Notice that only the second one is a linear function of μ. [Ans.]

22.15 Applying the S_N Method to a Spherical Source

Sometimes, it is difficult to visualize how the S_N and P_N methods work without a concrete example to illustrate the entire process. In this section, we would like to present how the S_N method works in spherical coordinates. It can also be applied to other geometries, such as planar and cylindrical ones, but we will only consider how it works for a spherical coordinate system here. The *S_N method* is a special case of a much larger class of methods called *discrete ordinates methods*. The S_N method was originally developed by nuclear physicist *B.G. Carlson* at the Los Alamos Scientific Laboratory in 1955 to understand how to protect people from the radiation released by the atmospheric detonation of an *atomic bomb*. *The fundamental idea behind the S_N method is to assume that the neutron flux $\phi(\boldsymbol{r}, \mu)$ along an arbitrary angular direction μ can be written as the simple linear average of the flux along adjacent angular directions μ_i and μ_{i-1}.*

This can be seen by writing the neutron flux in the following way:

$$\phi_g(r,\mu) = \frac{\mu - \mu_{n-1}}{\mu_n - \mu_{n-1}} \cdot \phi_g(r,\mu_n) + \frac{\mu_n - \mu}{\mu_n - \mu_{n-1}} \cdot \phi_g(r,\mu_{n-1}) \tag{22.82}$$

or

$$\phi_g(r,\mu) = \frac{(\mu - \mu_{n-1})\phi_g(r,\mu_n) + (\mu_n - \mu)\phi_g(r,\mu_{n-1})}{\Delta\mu_n} \tag{22.83}$$

where $\Delta\mu_n = \mu_n - \mu_{n-1}$. Here, the group flux along a specific angular direction is written as $\phi_g(\mathbf{r}, \mu)$ where μ is the cosine of the angle between the neutron's direction and the neutron source (presumed to be at $\mathbf{r}$) where the neutrons originate. The transport equation for each energy group in spherical coordinates can then be written as

$$\mu\frac{\partial\phi_g(r,\mu)}{\partial r} + \frac{1}{r}(1-\mu^2)\frac{\partial\phi_g(r,\mu)}{\partial\mu} + \Sigma_{gt}\phi_g(r,\mu) = S_g(r) \tag{22.84}$$

* See *Contemporary Nuclear Reactor Physics with an Introduction to Reactor Dynamics, Computational Methods, and Nuclear Particle Transport*, by R.E. Masterson, CRC Press (2020).

where the neutron source term $S_g(r)$ is assumed to be isotropic and g is the group number. An isotropic source is not an essential feature of the S_N method, but it certainly simplifies the math that it requires. Suppose that we would like to find the group flux along N angular directions having an equal spacing $\Delta\mu$ between $\mu = -1$ and $\mu = 1$. Figure 22.9 shows a number of different "discrete ordinates" that can be used to compute the angular flux for a one-dimensional problem. Of course, the same approach can be generalized to more than one spatial dimension, but then the ordinates are defined by two angles rather than just one. Each of these angular directions (from 1 to N) can be thought of as a discrete angle, or a *discrete ordinate* in the coordinate system we wish to use. The interpolation points (e.g., the discrete ordinates) are typically chosen using the prescription $\mu_n = 2n/N - 1$ so that $\mu_0 = -1$ and $\mu_N = 1$. Since the neutron flux can vary linearly between the interpolation points (see Equation 22.82), any realistic distribution of the angular flux can be represented in an S_N method by a linear combination of the values at each μ_n. Figure 22.10 shows how a realistic flux shape can be approximated using this interpolation scheme. If we substitute Equation 22.83 for the angular flux into the transport Equation 22.84 and integrate the result over all the angles between $\mu = \mu_{n-1}$ and $\mu = \mu_n$, the result is

$$\left[\frac{a_n d}{dr} + \frac{c_n}{r} + \Sigma_{gt}\right]\phi_n^g(r) + \left[\frac{b_n d}{dr} - \frac{c_n}{r} + \Sigma_{gt}\right]\phi_{n-1}^g(r) = d_n S_g(r) \tag{22.85}$$

for n = 1, 2, 3, …., N, and for simplicity, we have adopted the notation that $\phi_n^g(r) = \phi_{ng}(r)$. Here, the coefficients a_n, b_n, and c_n are given by

$$a_n = \frac{2\mu_n + \mu_{n-1}}{3} \tag{22.86}$$

$$b_n = \frac{\mu_n + 2\mu_{n-1}}{3} \tag{22.87}$$

$$c_n = \frac{2\left(3 - \mu_n^2 - \mu_{n-1}^2 - \mu_n\mu_{n-1}\right)}{3\Delta\mu_n} \tag{22.88}$$

$\Delta\mu_n = \mu_n - \mu_{n-1}$, and d_n (the coefficient in front of the neutron source term) has a value of 2 in this coordinate system. Notice that what we are left with is a set of N linear algebraic equations with N + 1 unknowns.

The angular dependence of the flux is now gone, and we are left with N + 1 values of $\phi_n^g(\mathbf{r})$ for each energy group g. The values of $\phi_n^g(\mathbf{r})$ at the nodal boundaries (n = 0 or n = N + 1) may be determined from the boundary conditions (at $\mu = -1$ and $\mu = +1$). Next, the derivatives of the angular flux $d\phi_n^g(\mathbf{r})/dr$ must be found. These terms can then be converted into difference equations. The spatial mesh points are chosen so that their interfaces lie at the interpolation points. When the process is complete, we end up with a set of N − 1 difference equations at each spatial mesh point for each energy group. These equations can then be solved using the standard iterative techniques that we have already discussed. It is important to bear in mind that the angular neutron flux must now be found along N + 1 directions at each spatial mesh point—N being the "order" of the discrete ordinates method that we would like to use. Hence, all we have done is to replace the functional dependence of $\phi^g(\mathbf{r}, \mathbf{u})$ by n unknowns of the form $\phi_n^g(\mathbf{r})$ for each energy group g. Up to this time, we have assumed that the angular flux between discrete angular directions or ordinates can be found by simply averaging the values between the different angular directions that we have chosen. In more sophisticated versions of the S_N method, different weighting factors may be used for different directions. In other words, the integrals over

$$\int \phi^g(\mathbf{r}, \mathbf{u})du \quad \text{from } u = u_{n-1} \text{ to } u_n \tag{22.89}$$

and

$$\int \sigma_s^g(\mathbf{r}, \mathbf{u})du \quad \text{from } u = u_{n-1} \text{ to } u_n \tag{22.90}$$

are no longer equally weighted because different angular interpolation schemes for the neutron flux and the cross sections are used. We will not get into the details of how this is done, but it should suffice to say that more advanced methods use more elaborate treatments of the angular variable μ. This is equivalent to requiring that

$$\int \phi^g(\mathbf{r}, \mathbf{u})du = \sum_{n=0 \text{ to } N} \left(w_n \phi_n^g(\mathbf{r})\right) \tag{22.91}$$

and

$$\int \sigma^g(\mathbf{r},\mathbf{u})\,du = \sum_{n=0\,\text{to}\,N}\left(w_n \sigma_n^g(\mathbf{r})\right) \tag{22.92}$$

where w_n are the new *angular weights* corresponding to the coefficients a_n, b_n, c_n, and d_n in our previous example. In most transport theory codes, S_N methods use $N^2/4 + N$ discrete directions in one-dimensional problems and $N^2/2 + 2N$ discrete directions in two-dimensional problems. In other words, if one chooses an S_4 method ($N = 4$), the flux is discretized along 8 angular directions in one dimension and along 16 angular directions in two dimensions. The number of directions increases as the order of the method is increased as well.

Example Problem 22.4

Suppose that an S_8 method is to be used to solve the neutron transport equation in one dimension instead of an S_4 method. How many more discrete angles will have to be used at each mesh point in this case?

Solution From the equations we presented earlier, the number of ordinates (discrete angular directions) in a one-dimensional S_N method varies as $N^2/4 + N$, where N is the order of the method. Hence, in one dimension, an S_8 method will require $N^2/4 + N$ separate ordinates. If $N = 8$, this is a total of 24 ordinates. From our previous discussion, this is a total of three times more ordinates than S_4 method ($N = 4$) uses. [Ans.]

22.16 Unit Vector and Dimensional Gradient in More than One Dimension

Finally, we would like to illustrate what the angular unit vector $\boldsymbol{\Omega} = \mathbf{r}/|\mathbf{r}|$ looks like in more than one dimension, since we have only considered one-dimensional versions of the transport equation (with $\mu = \cos\theta$) up to this time. In three dimensions, this vector can be written in either cylindrical or spherical coordinates, depending on the coordinate system we would like to use. In cylindrical coordinates, the angular unit vector is

The Unit Vector in a Cylindrical Coordinate System

$$\boldsymbol{\Omega} = \mathbf{i}\cos\theta + \mathbf{j}\sin\theta + \mathbf{k} \tag{22.93}$$

because there is a polar angle θ *but no azimuthal angle* φ. Here, the components of the unit vector are

$$\Omega_x = \mathbf{i}\cos\theta \tag{22.94}$$

$$\Omega_y = \mathbf{j}\sin\theta \tag{22.95}$$

$$\Omega_z = \mathbf{k} \tag{22.96}$$

or using a somewhat different notation, $\boldsymbol{\Omega} = \mathbf{i}\Omega_x + \mathbf{j}\Omega_y + \mathbf{k}\Omega_z$, with $\Omega_x = \cos\theta$, $\Omega_y = \sin\theta$, and $\Omega_x = 1$. The directional derivative $\nabla\boldsymbol{\Omega}$ is then equal to $\nabla\boldsymbol{\Omega} = \mathbf{i}d\Omega_x/d\theta + \mathbf{j}d\Omega_y/d\theta + \mathbf{k}d\Omega_z/dz$ with $d\Omega_x/d\theta = -\sin\theta$, $d\Omega_y/d\theta = \cos\theta$, and $d\Omega_z/dz = 0$. In spherical coordinates, interchanging the x- and z-axes and the values of θ and φ for the moment, the unit vector becomes

The Unit Vector in a Spherical Coordinate System

$$\boldsymbol{\Omega} = \mathbf{i}\sin\theta\cos\varphi + \mathbf{j}\sin\theta\sin\varphi + \mathbf{k}\cos\theta \tag{22.97}$$

and so components of the unit vector are $\Omega_x = \sin\theta\cos\varphi$, $\Omega_y = \sin\theta\sin\varphi$, and $\Omega_x = \cos\theta$. The directional derivative $\nabla\boldsymbol{\Omega}$ is then $\nabla\boldsymbol{\Omega} = d\boldsymbol{\Omega}/d\theta + d\boldsymbol{\Omega}/d\varphi$ with $d\boldsymbol{\Omega}/d\theta = \mathbf{i}\cos\theta\cos\varphi + \mathbf{j}\cos\theta\sin\varphi - \mathbf{k}\sin\theta$ and $d\boldsymbol{\Omega}/d\varphi = -\mathbf{i}\sin\theta\sin\varphi + \mathbf{j}\sin\theta\cos\varphi$. Notice that writing the directional derivative in this way requires us to use *two different types of angles* (θ *and* φ) rather than just one. Because of this, the angular gradient upon which the transport equation is based then becomes

$$\boldsymbol{\Omega}\cdot\nabla\phi(\mathbf{x}) = \Omega_x\frac{\partial\phi(\mathbf{x})}{\partial x} + \Omega_y\frac{\partial\phi(\mathbf{x})}{\partial y} + \Omega_z\frac{\partial\phi(\mathbf{x})}{\partial z} \tag{22.98}$$

In an S_N or P_N method, the angular flux is calculated along 3, 5, or 7 different angles in the θ direction (for instance, $\theta = 0°$, 45°, 90°, 135°, and 180°), and for each of these angles, a similar procedure is applied to the *azimuthal angles* φ_1, φ_2, φ_3, and

φ_N as well. This means that the number of angular directions (or discrete ordinates) at a single mesh point will be $\theta_N \times \varphi_N$, and if there are I, J, and K mesh points in the x, y, and z directions, then the total number of unknowns becomes $N = I \times J \times K \times \theta_N \times \varphi_N \times G$. Of course, here G is the number of energy groups, and we have assumed a steady-state solution because we have neglected the value of t. The angular directions that are used must then be expressed as a function of the two angular variables θ and φ instead of just one. This means that the number of unknowns can become large very quickly if one is not careful to select only the number of dimensions and the number of angles that are actually required. Consequently, most transport theory calculations involve only one or two energy groups and only one or two spatial dimensions. Most calculations with more than this are simply viewed as computational overkill or cannot be readily performed because they require too much computer time. In radiation shielding calculations, it is important to group most of the angles

$$\theta = \theta_1, \theta_2, \theta_3, \ldots, \theta_N \tag{22.99}$$

and

$$\varphi = \varphi_1, \varphi_2, \varphi_3, \ldots, \varphi_N \tag{22.100}$$

at each mesh point in the forward direction because high energy neutrons, x-rays and γ-rays tend to stream forward until they are either stopped or absorbed.

Even when a shielding material like lead is used, these particles will continue to move forward for several feet before the majority of them will be absorbed. Thus, although the angular flux in the forward direction $\theta = 0°$ may be attenuated exponentially (see Figure 22.11), and we can express this fact using the very simple formula $\phi(x) = \phi_o e^{-kx}$, where k is the *attenuation coefficient* (see Chapter 17 of our companion book), the angular flux in the other directions

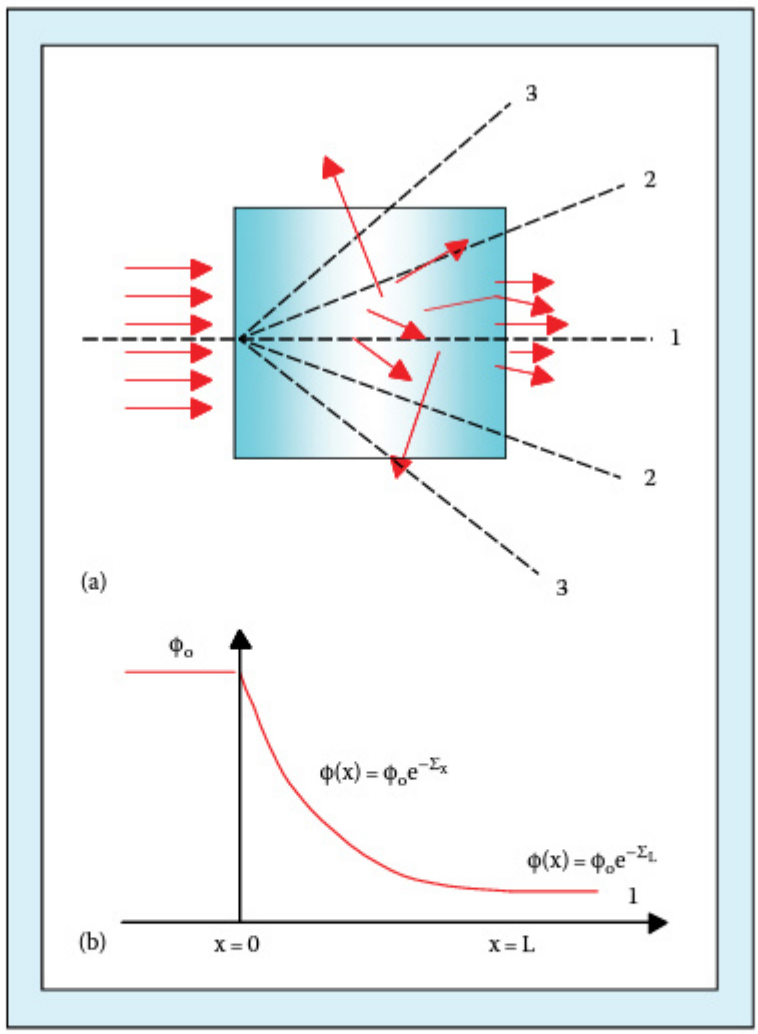

FIGURE 22.11 (a and b) A transport theory calculation to find the behavior of the neutron flux $\phi(x)$ in a homogeneous shield. Note that the attenuation of the flux can be different along each separate angular direction (1, 2, and 3) represented by a discrete ordinate or ray.

$\theta = 45°$, 90°, 135°, and 180° may not behave in the same way. For this reason, practical solutions to the neutron transport equation require the use of a high-speed computer. Even then, the amount of computer time may become excessive if the complexity is too great. *Ordinarily, the dependence of the angular flux $\phi(x,\mu,t)$ on the neutron direction μ is rather weak, and so a set of general functions such as the spherical harmonics or even a simple linear interpolation scheme such as the one the S_N method uses provides more than enough accuracy for most geometries of interest*. In other geometries, the resolution can be increased by simply increasing the number of terms that are used to represent the angular dependence of the flux (i.e., the value of N in the P_N or S_N methods). In most cases, a fifth-level approximation (setting N = 5) is all that is required.

Example Problem 22.5

Write down an explicit expression for the three components $\mathbf{\Omega}_x$, $\mathbf{\Omega}_y$, and $\mathbf{\Omega}_z$ of the angular unit vector $\mathbf{\Omega}$ that appears in the neutron transport equation when the transport equation is to be solved in the x and z directions and the azimuthal angle φ is zero.

Solution In this case, the angular directional vector $\mathbf{\Omega} = \mathbf{i}\sin\theta\cos\varphi + \mathbf{j}\sin\theta\sin\varphi + \mathbf{k}\cos\theta$ reduces to $\mathbf{\Omega} = \mathbf{i}\sin\theta + \mathbf{k}\cos\theta$, so the components are $\mathbf{\Omega}_x = \mathbf{i}\sin\theta$, $\mathbf{\Omega}_y = \mathbf{0}$, and $\mathbf{\Omega}_z = \mathbf{k}\cos\theta$. [Ans].

22.17 Numerical Methods for Solving the Time-Dependent Transport Equation

Before moving on, we would like to illustrate how the transport equation can be solved as a function of time. Although transient effects are not generally considered in nuclear or radiation shielding calculations, understanding how to solve the time-dependent transport equation is valuable to gain an appreciation of transport methods in general. For this particular discussion, we will assume we want to solve the transport equation in a one-dimensional slab. This geometry is typical of those that are encountered in actual practice, or when a radiation shield is a great distance away from a radiation source. In this case, the time-dependent transport equation becomes

$$\left(\frac{1}{v}\right)\frac{\partial\phi}{\partial t} + \mu\frac{\partial\phi}{\partial x} + \Sigma_t\phi = S \tag{22.101}$$

where the source term S may either be distributed throughout the entire slab (e.g., it is a function of x) or it may be located on one of the boundaries. Using the P_N method we have already discussed, we can use the Legendre polynomials to replace the variable μ in each term of the equation with a polynomial expansion that is N terms long. If we do this for a P_3 method, we end up with the following four equations for the angular flux:

Equations of the P_3 Method

$$\begin{aligned}
&\left(\frac{1}{v}\right)\frac{\partial\phi_0}{\partial t} + \frac{\partial\phi_1}{\partial x} + \left(\Sigma_t - \Sigma_{s,0}\right)\phi_0 = S_0\\
&\left(\frac{1}{v}\right)\frac{\partial\phi_1}{\partial t} + \left(\frac{2}{3}\right)\frac{\partial\phi_2}{\partial x} + \left(\frac{1}{3}\right)\frac{\partial\phi_0}{\partial x} + \left(\Sigma_t - \Sigma_{s,1}\right)\phi_1 = S_1\\
&\left(\frac{1}{v}\right)\frac{\partial\phi_2}{\partial t} + \left(\frac{3}{5}\right)\frac{\partial\phi_3}{\partial x} + \left(\frac{2}{5}\right)\frac{\partial\phi_1}{\partial x} - \left(\Sigma_t - \Sigma_{s,2}\right)\phi_2 = S_2\\
&\left(\frac{1}{v}\right)\frac{\partial\phi_3}{\partial t} + \left(\frac{3}{7}\right)\frac{\partial\phi_2}{\partial x} + \left(\Sigma_t - \Sigma_{s,3}\right)\phi_3 = S_3
\end{aligned} \tag{22.102}$$

For one energy group, these equations can be written in matrix form as

$$\left(\frac{1}{v}\right)\frac{\partial}{\partial t}\{\phi\} + [\mathbf{M}]\frac{\partial}{\partial x}\{\phi\} + \Sigma_t\{\phi\} = [\mathbf{S}]\{\phi\} + \{S\} \tag{22.103}$$

where the vectors $\{\phi\}$ and $\{S\}$ are defined by

$$\{\phi\} = \begin{Bmatrix}\phi_1\\ \phi_2\\ \phi_3\\ \phi_4\end{Bmatrix} \quad \text{and} \quad \{s\} = \begin{Bmatrix}s_1\\ s_2\\ s_3\\ s_4\end{Bmatrix} \tag{22.104}$$

and the coefficient matrices [**M**] and [**S**] are shorthand notation for the equations shown in Figure 22.11b, and the *scattering matrix* [**S**] includes the scattering cross sections $\Sigma_{s,u}$ along the four angular directions required by the P_3 method—μ_0, μ_1, μ_2, and μ_3. The space and time derivatives $\partial\phi/\partial x$ and $\partial\phi/\partial t$ can then be replaced by the simple finite difference approximations

$$\frac{\partial\{\phi\}}{\partial x} = \frac{\left(\{\phi_{i+1}\} - \{\phi_{i-1}\}\right)}{2\Delta x_i} \tag{22.105}$$

and

$$\frac{\partial\{\phi\}}{\partial t} = \frac{\left(\{\phi\}^{n+1} - \{\phi_i\}^n\right)}{\Delta t_n} \tag{22.106}$$

which lead to the time-dependent matrix equations

$$\left(\frac{1}{v}\right)\frac{\left(\{\phi\}^{n+1} - \{\phi_i\}^n\right)}{\Delta t_n} + [\mathbf{M}]\frac{\left(\{\phi_{i+1}\}^n - \{\phi_{i-1}\}^n\right)}{2\Delta x_i} + \Sigma_{t,i}\{\phi_i\}^n = [\mathbf{S}]\{\phi_i\}^n + \{S_i\}^n \tag{22.107}$$

where

i is the space index
n is the time index

$$\{\phi_i\}^n = \begin{Bmatrix} \phi_{1,i} \\ \phi_{2,i} \\ \phi_{3,i} \\ \phi_{4,i} \end{Bmatrix}^n$$

$$[\mathbf{M}] = \begin{pmatrix} 0 & 1 & 0 & 0 \\ 1/3 & 0 & 2/3 & 0 \\ 0 & 2/5 & 0 & 3/5 \\ 0 & 0 & 3/7 & 0 \end{pmatrix}$$

and

$$[\mathbf{S}] = \begin{pmatrix} \sum_{s0} & 0 & 0 & 0 \\ 0 & \sum_{s1} & 0 & 0 \\ 0 & 0 & \sum_{s2} & 0 \\ 0 & 0 & 0 & \sum_{s3} \end{pmatrix} \tag{22.108}$$

These difference equations are explicit in time and have a truncation error of order $\Delta t + \Delta x^2$ because a central differencing scheme is used in the second term. We can then solve these matrix equations spatially at t = 0 (time step l) and plug these values into the right-hand side. This then allows us to solve for the vector $\{\phi\}^{n+1}$ at time step 2 (n = 1). This process then continues for as many time steps as we need (n = N). The total elapsed time T may then be found from

$$T = \sum\nolimits_N \Delta t_n \tag{22.109}$$

where the summation runs from n = 0 to n = N and N is the number of time steps. The value of the neutron flux at time step n + 1 may then be found from the value of the neutron flux at time step n using

$$\{\phi\}^{n+1} = \Delta t_n v\left[\{\phi_i\}^n + [\mathbf{M}]\frac{\left(\{\phi_{i+1}\}^n - \{\phi_{i-1}\}^n\right)}{2\Delta x_i} + \Sigma_{t,i}\{\phi_i\}^n - [\mathbf{S}]\{\phi_i\}^n\right] + \Delta t_n v\{S_i\}^n \tag{22.110}$$

where the values of $\{\phi\}^{n+1}$ and $\{\phi_i\}^n$ were defined previously and $\{\phi_i\}^0$ is generally taken to be the steady-state solution. It is worth mentioning that the value of each time step Δt_n may be different than the previous one, although in practice, it is conventional to set them to a constant value Δt. Finally, smaller values of the time step may be more accurate and more stable than larger ones, and if one has enough computer time to burn, then very small values (on the order of about 1 millisecond) are generally desirable. To the author's knowledge, *no general proof of the stability of the time-dependent S_N method* has ever been given. However, based on many experiments conducted at Los Alamos and Oak Ridge, the method is generally considered to be stable. Thus, it continues to be used for many specialized applications (including the streaming of neutrons and γ-rays through radiation shields and other forms of matter), and it can even be used for more heterogeneous geometries if the ordinates are properly chosen.

Example Problem 22.6

Now suppose that the amount of computer time required to solve the transport equation in one dimensional space increases as the square of the number of ordinates that are used. How many times longer will it take to solve the one-group transport equation with an S_8 method than an S_4 approximation if this is the case?

Solution From our discussion earlier, there are a total of 3 times more ordinates at each mesh point in an S_8 method than there are in an S_4 method. Therefore, the amount of computer time needed to solve the transport equation with an S_8 method will be $3^2 = 9$ times greater in this case. [Ans.]

22.18 Using the Transport Equation with Pure Scatters and Absorbers

There are a couple of additional observations we can make about the transport equation when the scattering cross sections $\sigma_s(\mu, E)$ are completely isotropic, and any integration involving the values of μ from $\mu = -1$ to $\mu = +1$ can be ignored. As we initially discussed in Chapters 4 and 5, the scattering cross sections $\sigma_s(E)$ for most nuclear materials increase as the neutron energy E is decreased. This trend is not adversely affected by the atomic weight A of the target nucleus because a neutron simply has to be in the vicinity of a nucleus longer to have a higher probability of being scattered. Like all other particles, the neutron also has a wave function ψ that expands as the neutron moves more slowly. Because of this, a slow-moving neutron can "touch" the atomic nucleus more easily than a fast-moving neutron can, and this explains why scattering cross sections tend to get higher as the neutron energy becomes lower.

In transport theory, it can be shown that *any* element with an atomic weight greater than carbon (with an atomic weight of $A = 12$) will have a scattering cross section that is nearly isotropic; that is to say, it is independent of the cosine of the scattering angle θ. Hence, the scattering cross sections for elements heavier than carbon have very little dependence on the angular variable μ. On the other hand, elements lighter than carbon do exhibit a pronounced dependence, and in this case, the integral

$$\int \sigma_s^g(\mathbf{E}, \mathbf{u})\,du \quad \text{from } u = u_{n-1} \text{ to } u_n \tag{22.111}$$

in a P_N or S_N approximation cannot be ignored. Hence, if $A \leq 12$, it is important to write

$$\sigma_s(E) = \int \sigma_s(\mathbf{E}, \mathbf{u})\,du \quad \text{and} \quad \sigma_s^g = \int_{E_g} \sigma_s(\mathbf{E}, \mathbf{u})\,dE\,du \tag{22.112}$$

and if $A > 12$, we can write

$$\sigma_s(E) = \sigma_s(E)/2 \quad \text{and} \quad \sigma_s^g = \int_{E_g} \sigma_s(E)\,dE/2 \tag{22.113}$$

where σ_s^g is the scattering cross section for energy group g, and the 1/2 is the angular normalization factor we discussed previously for one dimensional problems. The angular dependence of the scattering cross section for a typical material (light water) is shown in Figure 22.12. In a P_3 or S_3 approximation, the scattering cross section must therefore be integrated over the four angular segments shown in the figure. The average value in each of these segments is therefore the same as the value of $\sigma_{s\mu}^g$ that each of the scattering terms in the transport equation uses: σ_{s1}^g, σ_{s2}^g, σ_{s3}^g, and σ_{s4}^g. In the case of a pure absorber, where $\sigma_s = 0$ so that $\sigma_t = \sigma_a$, we can neglect the scattering terms completely, and $\sigma_t = \sigma_t(E)$ becomes a simple function that needs to be divided into different energy groups. The value of σ_t that appears in the transport equation for each energy group g is then σ_t^g, and no further manipulation of the neutron cross sections is required.

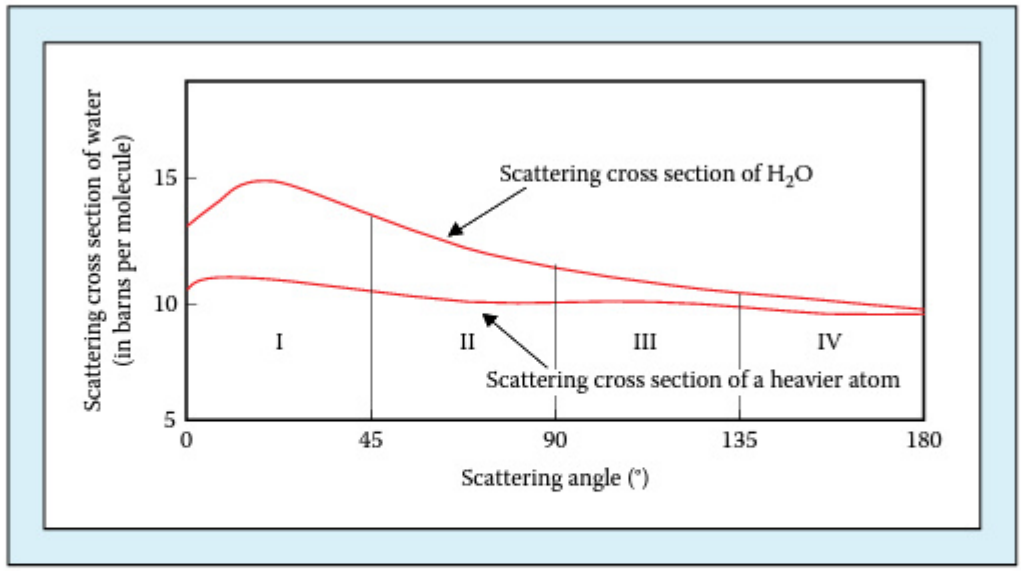

FIGURE 22.12 The differential scattering cross section for water as a function of the scattering angle θ. (Courtesy of the ENDF database.)

An example of a situation where a material can be considered to be a pure absorber is one where the neutron absorption cross section σ_a is many times greater than the scattering cross section σ_s, for example, $\sigma_a \gg \sigma_s$. In a reactor, this might apply to a fuel rod that contains a burnable poison, and it certainly applies to a control rod. If the transport equation is properly manipulated, it can be shown that the attenuation of the particle flux along any angle μ emanating from a point source S located in an infinitely large absorbing medium is given by

$$\phi(\mathbf{r}) = \frac{S_0 e^{-r\Sigma_a}}{4\pi \mathbf{r}^2} \tag{22.114}$$

where $\Sigma_a(E) = N\sigma_a(E)$ is the macroscopic absorption cross section for the material and N is the number of atoms per cubic centimeter. If the material is replaced by a vacuum and the point source remains, then the equation for the particle flux $\phi(\mathbf{r}, E)$ as a function of distance from the source is

$$\phi(\mathbf{r}) = \frac{S_0}{4\pi \mathbf{r}^2} \tag{22.115}$$

since $\Sigma_a(E) = 0$. The astute reader may recognize this as the *inverse square law* that was presented in Chapter 18 of our companion book.* Equations 22.114 and 22.115 are very important because they can be easily generalized to the case where an arbitrary distribution of isotropic point sources exists (see Figure 22.13). In this case, the particle flux from any distributed source S(r′) in a large absorbing medium can be found by "summing up" or integrating the contributions from all of the individual sources. The general equation to use in this case is then

$$\phi(\mathbf{r}) = \int_V \left[\frac{e^{-\mathbf{R}\Sigma_a}}{4\pi \mathbf{R}^2} \cdot S(\mathbf{r}') \right] dV \tag{22.116}$$

where the vector distance **R** is given by $\mathbf{R} = |\mathbf{r} - \mathbf{r}'|$. This equation can be easily solved for point sources, shell sources, spherical sources, and even for spheres where the source strength changes as a function of the radius. Thus, in spite of all of the mathematical headaches the transport equation provides, some results can eventually be derived from it that makes life simpler in the real world. Several analytical solutions to problems of this type were presented in Chapter 14. The reader should feel free to consult this chapter to learn more about the factors that go into the design of radiation shields.

* See *Nuclear Engineering Fundamentals: A Practical Perspective*, by R.E. Masterson, CRC Press (2017).

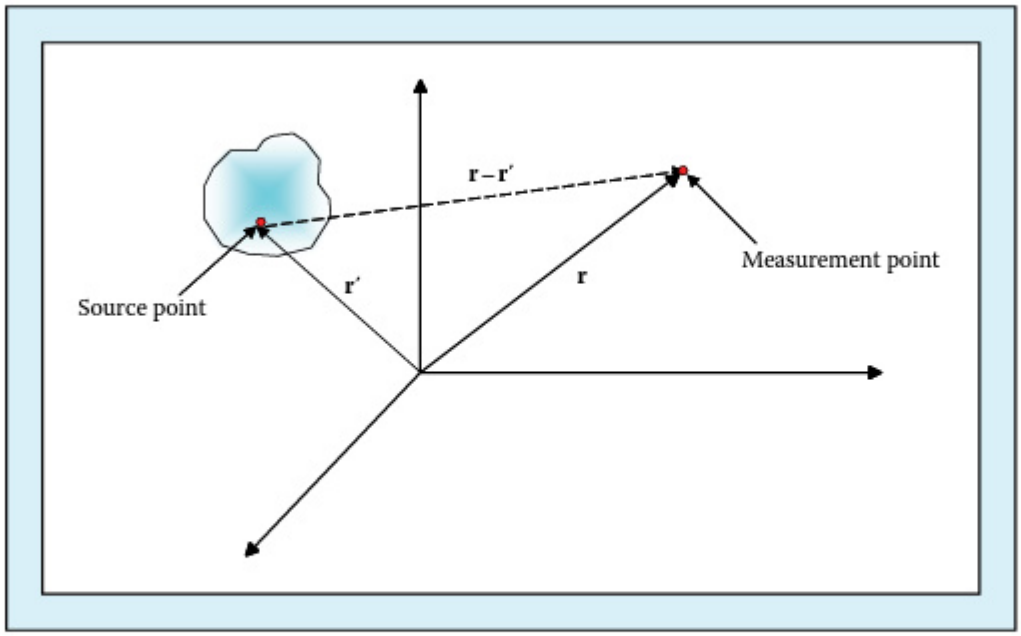

FIGURE 22.13 A coordinate system that can be used to calculate the particle flow from a distributed source from a distance $\mathbf{d} = \mathbf{r} - \mathbf{r}'$.

22.19 Ray Effects and Their Origin

Discrete ordinates methods such as the S_N method are extremely good at solving problems that are spatially heterogeneous, and in which the neutron diffusion equation can no longer be used. However, they can occasionally suffer from an interesting defect that we would like to present to you now. This defect is called the *ray effect*, and it arises when the ordinates (or angular directions) are constructed so that the neutrons (or other types of nuclear particles) are not able to reach all of the regions of the reactor that are needed to calculate the reaction rates. An extreme example of this situation occurs when neutrons are emitted isotropically from a point source S into a *pure absorbing material* where there is no scattering away from the ordinate directions. When there is no scattering to distribute the neutrons into the rest of the material, then the directional fluxes $\phi(\mathbf{r}, E, \boldsymbol{\Omega})$ will only be finite at points lying on the rays emanating from the point source along the $\boldsymbol{\Omega}_\mu$ directions. (They will be zero elsewhere.) The scalar flux $\phi(\mathbf{r}, E)$ in this case is then

$$\phi(\mathbf{r}, E) = \sum_n w_n \phi(\mathbf{r}, E, \Omega_n) \tag{22.117}$$

where the summation is over the number of ordinates that is used and w_n are the *weighting factors*. However, when $\Sigma_s = 0$, the scalar flux $\phi(\mathbf{r}, E)$ will be zero over protracted regions of space, and the scalar flux will be anomalously low between each of the ordinates. (Most of the time, ray effects can be avoided by simply increasing the number of ordinates, which is equivalent to increasing the order N of the S_N method.) However, in some problems, a surprisingly large number of ordinates may be required to eliminate this difficulty. As we have seen, there are other mathematical refinements to the theory that weight the angles differently, and in a least squares sense, these methods can reduce the errors to more acceptable levels. However, they are somewhat more costly to implement computationally, and because of this, there is a trade-off between the total number of ordinates and the amount of computer time. Along these lines, it is instructive to consider one more example where the use of a limited number of rays (or ordinates) can lead to physically unrealistic results. Consider the square isotropic source shown in Figure 22.14. The source is shown as a shaded rectangle bounded by corners 1, 2, 3, and 4. In a low-order S_N method, like the S_3 method, points lying in the rectangles bounded by 1, 5, 6, and 3 and 2, 7, 8, and 4 actually "receive" the unscattered neutrons, whereas the triangular area bounded by points 2, 3, and 9 does not. This causes the particle flux to exhibit an unphysical dip in the triangular region right next to the neutron source. Of course, this is not physically possible because in diffusion theory, the triangular region always "sees" the neutrons that are emanating from the source. However, in transport theory, these neutrons never reach the triangular area if the scattering cross sections are small enough. Hence, larger (but somewhat artificial) values of the scattering cross sections are sometimes used to eliminate this problem.

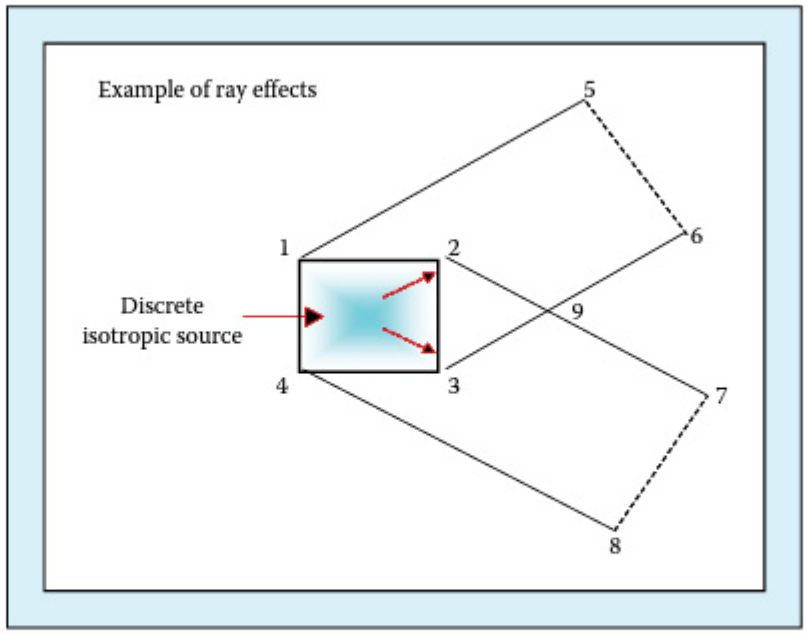

FIGURE 22.14 An example of ray effects emanating from a square isotropic particle source in a low-order S_N approximation.

Example Problem 22.7

Suppose that we have solved the neutron transport equation in a Cartesian coordinate system using the S_N or P_N methods. The results reveal that the neutrons are moving at an angle of 30° with respect to the z-axis and 60° with respect to the x-axis. If the neutron flux $\phi(\mathbf{r}, E, \mathbf{\Omega}, t)$ at the origin is 1×10^{15} neutrons/cm^2/s, what is the value of the neutron current $\mathbf{J}(\mathbf{r}, E, \mathbf{\Omega}, t)$ along the x-axis, the y-axis, and the z-axis at $\mathbf{r} = 0$?

Solution From our previous discussion, we know that the directional neutron current is given by $\mathbf{J}(\mathbf{r}, E, \mathbf{\Omega}, t) = [\mathbf{i} \sin\theta \cos\varphi + \mathbf{j} \sin\theta \sin\varphi + \mathbf{k} \cos\theta] \cdot \phi(\mathbf{r}, E, \mathbf{\Omega}, t)$. The x component is $\mathbf{J}_x = \mathbf{i} \sin\theta \cos\varphi \cdot \phi(\mathbf{r}, E, \mathbf{\Omega}, t)$, the y component is $\mathbf{J}_y = \mathbf{j} \sin\theta \sin\varphi \cdot \phi(\mathbf{r}, E, \mathbf{\Omega}, t)$, and the z component is $\mathbf{J}_z = \mathbf{k} \cos\theta \cdot \phi(\mathbf{r}, E, \mathbf{\Omega}, t)$. In this problem, $\theta = 30°$ and $\varphi = 60°$. The neutron current along the x, the y, and the z directions is therefore $\mathbf{J}_x = \mathbf{i} \sin 30° \cos 60° \cdot \phi(\mathbf{r}, E, \mathbf{\Omega}, t)$, $\mathbf{J}_y = \mathbf{j} \sin 30° \sin 60° \cdot \phi(\mathbf{r}, E, \mathbf{\Omega}, t)$, and $\mathbf{J}_z = \mathbf{k} \cos 30° \cdot \phi(\mathbf{r}, E, \mathbf{\Omega}, t)$. Plugging in the appropriate values for the sine and cosine, we find that $\sin 30° = 0.5$, $\sin 60° = 0.866$, $\cos 30° = 0.866$, and $\cos 60° = 0.5$. The directional currents are therefore $\mathbf{J}_x = \mathbf{i}0.5 \times 0.5 \cdot \phi(\mathbf{r}, E, \mathbf{\Omega}, t)$, $\mathbf{J}_y = \mathbf{j}0.5 \times 0.866 \cdot \phi(\mathbf{r}, E, \mathbf{\Omega}, t)$, and $\mathbf{J}_z = \mathbf{k}0.866 \cdot \phi(\mathbf{r}, E, \mathbf{\Omega}, t)$ or $\mathbf{J}_x = 0.25 \times 10^{15}$ neutrons/cm^2/s, $\mathbf{J}_y = 0.433 \times 10^{15}$ neutrons/cm^2/s, and $\mathbf{J}_z = 0.866 \times 10^{15}$ neutrons/cm^2/s. [Ans.]

22.20 Multigroup Neutron Transport Equation

Occasionally, it is necessary to solve the transport equation with more than one energy group. *This is particularly important when the neutron flux must be found in the vicinity of a strong neutron absorber, such as a burnable poison or a control rod.* Refer to Figure 22.15 to see how the multigroup flux shapes behave in this case. Under these conditions, the shape of the fast and the thermal flux can be completely different, and in general, it is necessary to solve the neutron transport equation to determine exactly how they behave. (Solving the transport equation allows us to locate the "hot spots" more precisely.)

Notice that the effect of a strong neutron absorber is always more pronounced when using neutron transport theory than when using neutron diffusion theory. This is because neutron diffusion theory tends to "smear out" the spatial details that the transport equation attempts to provide. It is also important to be able to distinguish between how fast neutrons and thermal neutrons behave—particularly at an abrupt boundary between two material regions—for example, between the outside of the reactor core and the reflector. Unless the neutron mean free paths happen to be very large (say, $\lambda \approx 20$ cm), transport theory will provide a more accurate estimate of the flux shape than diffusion theory. This also allows the reaction rates in multigroup theory to be written as

$$R_x = \sum_g \Sigma_{xg} \phi_g \quad \text{where } x = a, s, f, \text{ or } t \tag{22.118}$$

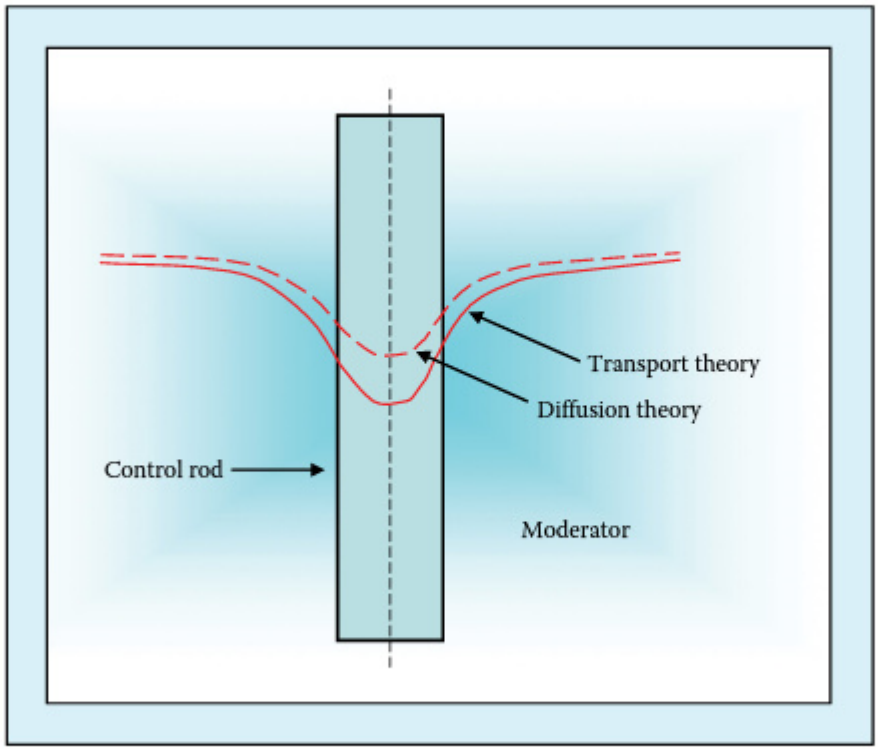

FIGURE 22.15 An illustration of how the shape of the thermal neutron flux can be different in the vicinity of a control rod when diffusion theory and transport theory are used.

Here, G is the number of energy groups and g = 1, 2, …, G. Then the *group flux* ϕ_g (see Chapter 4) is defined by

$$\phi_g = \int_E \phi(E)dE \quad (g = 1, 2, 3, \ldots, G) \tag{22.119}$$

and the corresponding multigroup cross sections are defined by

$$\Sigma_{xg} = \frac{\int \Sigma_x(E)\phi(E)dE}{\int \phi(E)dE} \quad (g = 1, 2, 3, \ldots, G) \tag{22.120}$$

where the limits of integration for group g are from $E = E_g$ to $E = E_{g-1}$ and where the subscript x refers to an arbitrary reaction type (x = a, c, s, f, or t). If we apply this approach to the S_N equations, we find that the equations for the angular group fluxes ϕ_g^n become

$$\frac{1}{v_g}\frac{\partial \phi_g^n}{\partial t} + \boldsymbol{\Omega}_n \cdot \nabla \phi_g^n + \Sigma_{tg}\phi_g^n = \Sigma_{n'} w_{n'} \Sigma_{g'} \Sigma_{sg' \to g'n' \to n} \phi_{g'}^{n'} + S_g^n \quad (n = 1, 2, \ldots, N)\ (g = 1, 2, \ldots, G) \tag{22.121}$$

where the highest-energy group (by convention) always starts with the index 1. *Such sets of coupled differential equations are called the multigroup S_N equations*. The methods used to solve these equations are discussed in our companion book,* where *finite difference methods* are also presented. When using these methods, it is important to keep in mind that the angular group flux ϕ_g^n must be found for each energy group g along N + 1 discrete ordinates at each spatial mesh point. Here, N is the "order" of the discrete ordinates method that is used. *Hence, when the neutron transport equation is to be solved with the S_N method, there are Gx(N + 1) unknowns per mesh point, when there are G energy groups.*

A similar approach can also be used to deduce the multigroup P_N equations, which are based on the P_N approximation we discussed earlier (see Section 22.13). *So in general, the angular dependence of the neutron flux causes the total number of unknowns to increase by a factor of (N + 1) over what is ordinarily encountered in neutron diffusion theory.* This is one of the reasons why solutions to the neutron transport equation are so difficult to obtain.

* See *Nuclear Engineering Fundamentals: A Practical Perspective*, by R.E. Masterson, CRC Press (2017).

Example Problem 22.8

In an S_8 method, how many different angular directions is the particle flux discretized along in a one-dimensional problem and in a two-dimensional problem with a single energy group?

Solution Most versions of the S_N method use $N^2/4 + N$ discrete ordinates in one-dimensional problems and $N^2/2 + 2N$ discrete ordinates in two-dimensional problems. So for the problem at hand, $N = 8$ and the number of ordinates required is 24 and 48. [Ans.]

22.21 How Boundary Conditions Are Handled in Neutron Transport Theory and Neutron Diffusion Theory

The boundary conditions that are used for the neutron diffusion equation are special cases of the boundary conditions that are used for the neutron transport equation. In this section, we would like to present the boundary conditions that the transport equation uses and then use them to derive the corresponding boundary conditions for the diffusion equation. As expected, the difference between the two arises primarily in the treatment of the angular flux

$$\phi(\mathbf{r}, E, \boldsymbol{\Omega}, t) = v \cdot n(\mathbf{r}, E, \boldsymbol{\Omega}, t) \tag{22.122}$$

However, the guiding principles that are used to obtain a rough equivalence are essentially the same. Since the neutron diffusion equation is only an approximation to the more exact transport equation, we can expect that we can use the boundary conditions required by transport theory to infer the boundary conditions required by diffusion theory.

The primary boundary conditions must be able to conserve both the angular current $\mathbf{J}(\mathbf{r}, E, \boldsymbol{\Omega}, t) = \boldsymbol{\Omega} \cdot \phi(\mathbf{r}, E, \boldsymbol{\Omega}, t)$ and the angular flux $\phi(\mathbf{r}, E, \boldsymbol{\Omega}, t)$. Before beginning, it may be helpful to recall exactly what the unit vector $\boldsymbol{\Omega}$ represents. In a spherical coordinate system, it is given by $\boldsymbol{\Omega} = \mathbf{i}\Omega_x + \mathbf{j}\Omega_y + \mathbf{k}\Omega_z$, where $\Omega_x = \sin\theta\cos\varphi$, $\Omega_y = \sin\theta\sin\varphi$, and $\Omega_z = \cos\theta$. Hence, the precise relationship between $\mathbf{J}(\mathbf{r}, E, \boldsymbol{\Omega}, t)$ and $\phi(\mathbf{r}, E, \boldsymbol{\Omega}, t)$ is

$$\mathbf{J}(\mathbf{r}, E, \boldsymbol{\Omega}, t) = \left[\mathbf{i}\sin\theta\cos\varphi + \mathbf{j}\sin\theta\sin\varphi + \mathbf{k}\cos\theta\right]\phi(\mathbf{r}, E, \boldsymbol{\Omega}, t) \tag{22.123}$$

where $\mathbf{i}$, $\mathbf{j}$, and $\mathbf{k}$ are unit vectors along the x-, y-, and z-axes. Note that in one dimension, this reduces to

$$\mathbf{J}(\mathbf{z}, \theta, E, t) = \cos\theta \cdot \phi(\mathbf{z}, E, t) \tag{22.124}$$

or

$$\mathbf{J}(\mathbf{z}, \mu, E, t) = \mu\phi(\mathbf{z}, E, t) \tag{22.125}$$

which is consistent with our previous results. The reader is asked to keep this definition in mind as we proceed further into our derivation.

22.22 Common Types of Neutron Boundary Conditions

There are actually two types of neutron boundary conditions that most problems require. One type of boundary condition is needed to preserve the continuity of the neutron current and the neutron flux at the interface between two different material regions, and the second boundary condition is required to determine the shape of the neutron flux and neutron current at the edge of a vacuum (i.e., where the second material region has nothing in it at all). Naturally enough, this second boundary condition is referred to as the *vacuum boundary condition*. Finally, in time-dependent problems, we must also be able to consider the initial conditions, that is, the value of the neutron flux and the neutron current at $t = 0$. We will start with the initial conditions first and then proceed to the spatial boundary conditions that all steady-state problems require.

22.23 Initial Conditions for Time-Dependent Problems

In neutron transport theory, the initial condition that is usually applied at $t = 0$ is

$$\phi(\mathbf{r}, \boldsymbol{\Omega}, 0) = \phi_o(\mathbf{r}, \boldsymbol{\Omega}) \tag{22.126}$$

We can use this condition to obtain the appropriate boundary conditions for the neutron transport equation by simply integrating the angular flux over all possible solid angles to obtain

$$\phi(\mathbf{r}, \boldsymbol{\Omega}, t) = 0 \quad \text{for } \boldsymbol{\Omega} \cdot \mathbf{n} < 0 \tag{22.127}$$

where $\mathbf{n}$ is the vector normal to the surface. At t = 0, note that we are only required to specify the *initial shape* of the angular flux $\phi(\mathbf{r}, E, \boldsymbol{\Omega}, t)$. Once the shape is specified, the time-dependent terms will then drive its spatial evolution. However, as we will soon see, the boundary conditions for the spatial components are a bit harder to come by.

22.24 Boundary Conditions at a Material Interface

When two different material regions are in close proximity, the neutrons leaving one material region must immediately enter the other. When this occurs, the neutron flux and the neutron current may experience a slight discontinuity at the material interface, even though both quantities must remain continuous across it. (Otherwise the total number of neutrons would not be conserved.) This discontinuity is caused when the mean free paths change abruptly, and on a macroscopic level, this discontinuity is manifested by an abrupt change in the value of the diffusion coefficient D. In transport theory, it is manifested by an abrupt change in the transport cross section $\Sigma_{tr}(E)$:

$$\Sigma_{tr}(E) = \Sigma_t(E) - \mu\Sigma_s(E) \tag{22.128}$$

In each case, the physical consequences are the same. Therefore, at an interface between two material regions having different scattering or absorption cross sections, the correct transport theory boundary condition is

$$\phi_1(\mathbf{r}, E, \boldsymbol{\Omega}, t) = \phi_2(\mathbf{r}, E, \boldsymbol{\Omega}, t) \quad \text{for all } \boldsymbol{\Omega} \tag{22.129}$$

where

$\phi_1(\mathbf{r}, E, \boldsymbol{\Omega}, t)$ is the angular flux in region 1
$\phi_2(\mathbf{r}, E, \boldsymbol{\Omega}, t)$ is the angular flux in region 2

Note in particular that this boundary condition must hold for every conceivable value of $\boldsymbol{\Omega}$. Unfortunately, it is not possible to satisfy the same boundary condition when neutron diffusion theory is used. The most that we can hope for is that all of the angular moments (i.e., the values of $\boldsymbol{\Omega}$) are conserved across each material interface. And since neutron diffusion theory holds for only the first two moments of the neutron flux, $\phi(r, t)$ and $\mathbf{J}(r, t)$, the best that we can expect is

$$\int_{4\pi} \phi_1(\mathbf{r}, E, \boldsymbol{\Omega}, t) d\boldsymbol{\Omega} = \int_{4\pi} \phi_2(\mathbf{r}, E, \boldsymbol{\Omega}, t) d\boldsymbol{\Omega} \tag{22.130}$$

and this implies that

$$\phi_1(\mathbf{r}, E, t) = \phi_2(\mathbf{r}, E, t) \tag{22.131}$$

Similarly, when we apply the same logic to the neutron current, we find that

$$\int_{4\pi} \boldsymbol{\Omega}\phi_1(\mathbf{r}, E, \boldsymbol{\Omega}, t) d\boldsymbol{\Omega} = \int_{4\pi} \boldsymbol{\Omega}\phi_2(\mathbf{r}, E, \boldsymbol{\Omega}, t) d\boldsymbol{\Omega} \tag{22.132}$$

and this implies that

$$J_1(\mathbf{r}, E, t) = J_2(\mathbf{r}, E, t) \tag{22.133}$$

In other words, in the limit where neutron transport theory reduces to neutron diffusion theory, the interface boundary conditions are simply those corresponding to the continuity of the neutron flux and the neutron current across

each material interface. If we are willing to suppress the energy dependence for the moment, then we can write these boundary conditions as

$$\text{Continuity of the neutron flux: } \phi_1(\mathbf{r},t)=\phi_2(\mathbf{r},t) \tag{22.134}$$

$$\text{Continuity of the neutron current: } -D_1\nabla\phi_1(\mathbf{r},t)=-D_2\nabla\phi_2(\mathbf{r},t) \tag{22.135}$$

which is exactly the same result we presented in Chapter 11.

22.25 Vacuum Boundary Conditions

The other type of boundary condition that is sometimes required is the *vacuum boundary condition* that we first introduced to the reader in Chapter 14. This boundary condition is a special case of the previous boundary conditions, except that the transport cross section in the second material region (which now contains a vacuum with essentially nothing in it) is zero. Hence, *any neutrons that enter the vacuum will not return*. We can represent this observation mathematically by requiring that

$$\begin{gathered}\phi(\mathbf{r},\boldsymbol{\Omega},t)=0 \quad \text{for } \boldsymbol{\Omega}\cdot\mathbf{dS}<0 \\ \text{(for all points on surface S)}\end{gathered} \tag{22.136}$$

Once again, it is important to realize that neutron diffusion theory will only be able to represent this boundary condition when the angular dependence of the flux is removed. So what we need in this case is another statement of the continuity of the neutron current and the neutron flux that does not rely on an explicit value for $\boldsymbol{\Omega}$. We can achieve this by requiring that in an integral sense, both the neutron flux $\phi(\mathbf{r}, E, \boldsymbol{\Omega}, t)$ and the neutron current $\mathbf{J}(\mathbf{r}, E, \boldsymbol{\Omega}, t)$ entering the vacuum along all angular directions do not return. The result is

$$\int_{2\pi-}\mathbf{n}\cdot\boldsymbol{\Omega}\phi_1(\mathbf{r},E,\boldsymbol{\Omega},t)\,d\boldsymbol{\Omega}=\int_{2\pi-}\mathbf{n}\cdot\boldsymbol{\Omega}\phi_2(\mathbf{r},E,\boldsymbol{\Omega},t)\,d\boldsymbol{\Omega}=\mathbf{J}_-(\mathbf{r},t)=0 \tag{22.137}$$

where $\mathbf{n}$ is the vector normal to the surface. *Unfortunately, diffusion theory has no direct way to help us evaluate these integrals, since the exact forms for ϕ_1 and ϕ_2 are not known. However, if we use the P_1 approximation for the angular flux $\phi(\mathbf{r}, \boldsymbol{\Omega}, t)$, it can be shown* that

$$\phi(\mathbf{r},\boldsymbol{\Omega},t)\approx\frac{\phi}{4\pi}+\frac{3}{4\pi}\left[\mathbf{J}_x\boldsymbol{\Omega}_x+\mathbf{J}_y\boldsymbol{\Omega}_y+\mathbf{J}_z\boldsymbol{\Omega}_z\right] \tag{22.138}$$

or

$$\phi(\mathbf{r},\boldsymbol{\Omega},t)\approx\frac{1}{4\pi}\phi(\mathbf{r},t)+\frac{3}{4\pi}\left[\mathbf{J}(\mathbf{r},t)\cdot\boldsymbol{\Omega}\right] \tag{22.139}$$

where 4π is again the angular normalization factor. The partial neutron currents in the + and − directions at the outer boundary with the vacuum are then

The Partial Neutron Currents at the Vacuum Boundary

$$\mathbf{J}_-(\mathbf{r},t)=\frac{1}{4}\phi(\mathbf{r},t)+\left(\frac{D}{2}\right)\nabla\phi(\mathbf{r},t)$$

and (22.140)

$$\mathbf{J}_+(\mathbf{r},t)=\frac{1}{4}\phi(\mathbf{r},t)-\left(\frac{D}{2}\right)\nabla\phi(\mathbf{r},t)$$

where the surface S in question can have any arbitrary shape we want. Now let us apply one of these boundary conditions to a one-dimensional slab whose boundary with the vacuum is at x = L. See Figure 22.16 for an illustration of how the

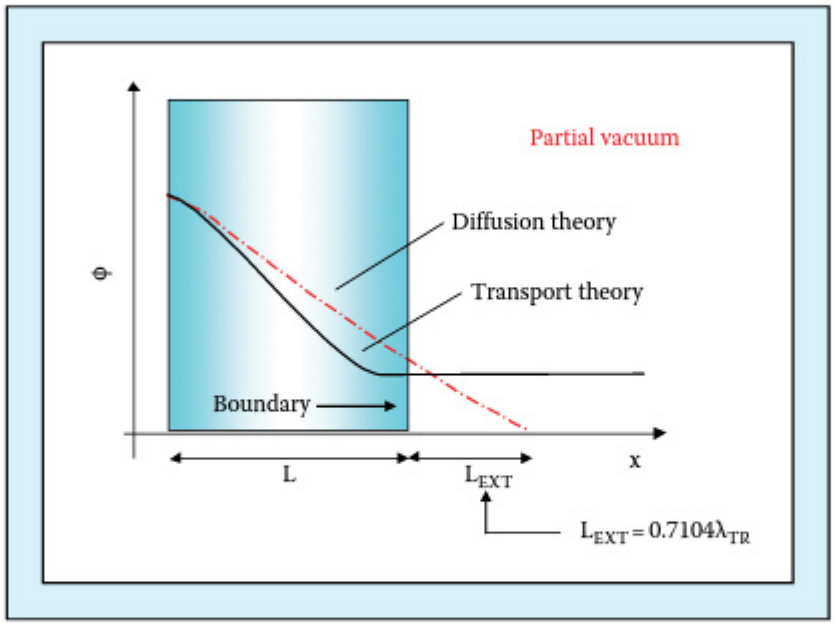

FIGURE 22.16 A comparison of the flux shapes predicted by transport theory and by the extrapolated boundary condition.

neutron flux behaves in this case. Since the neutron current J must be 0 at x = L, this implies that the inward-directed current J-must be

$$\mathbf{J}_{-}(L) = \frac{\phi(L)}{4} + \frac{D}{2}\frac{d\phi}{dx}\Big|_{x=L} = 0 \tag{22.141}$$

This equation can also be written as

$$\left(\frac{1}{\phi}\right)\frac{d\phi}{dx}\Big|_{x=L} = -\frac{1}{2D} \tag{22.142}$$

In other words, if the scalar neutron flux ϕ is extrapolated in a purely linear manner beyond the edge of the boundary, the neutron flux would vanish at a point x_{ext} beyond the boundary, which is given by

$$x_{ext} = L + 2D \tag{22.143}$$

or

$$x_{ext} = L + \frac{2}{3}\lambda_{TR} = L + L_{EXT} \tag{22.144}$$

Thus, the value of x_{ext} where the neutron flux vanishes is called the "extrapolated boundary," and the relationship $x_{ext} = L + 2/3 \cdot \lambda_{TR}$ is referred to as the "extrapolated boundary condition." This was the condition that we used to estimate the neutron flux in the vicinity of a planar control rod in Chapter 11. If we were to use a higher-order approximation for the angular flux $\phi(\mathbf{r}, \mathbf{\Omega})$ such as the P_3 or the P_5 approximations, it can be also shown that the actual value of the extrapolation distance for a slab geometry converges to

The Extrapolation Distance for a Slab

$$L_{EXT} = 0.7104\,\lambda_{TR} \tag{22.145}$$

This extrapolation distance is therefore the value of x where the value of the neutron flux ϕ must be set to zero for the results of diffusion theory to agree with the results of transport theory. Other formulas for the extrapolation distance are

available in the literature for curved surfaces, although it is rarely necessary to use them in practice. The equations we have just derived are valid as long as the radius of curvature of the outermost boundary is much smaller than the neutron mean free path $\lambda(E)$. Extrapolation formulas for more complicated geometries can be found in the following reference:

⊙ Reactor Physics Constants, USAEC Document ANL-5800. 2nd edn. (1963).

Using the extrapolated boundary condition, it is possible to make the predictions of diffusion theory agree with the predictions of transport theory. This model can also be generalized to situations involving more than one energy group. See Chapter 11 for a more detailed explanation of how this can be done.

Example Problem 22.9

A bare homogeneous reactor is surrounded by a reflector that has almost no measureable reflectivity. If it then follows that $\Sigma_s \approx 0$ in the area occupied by the reflector, how far from the edge of the core must we set the neutron flux equal to zero if we want to obtain an accurate solution to the flux shape $\phi(x)$ using the one-group neutron diffusion equation? Assume that the transport mean free path at the core–reflector interface is 5 cm.

Solution In this case, the extrapolated boundary condition can be used. The extrapolation distance is $L_{EXT} = 0.7104\lambda_{TR}$. For a transport mean free path λ_{TR} of ≈5 cm, the extrapolation distance is $L_{EXT} = 0.7104\lambda_{TR} = 0.7104 \times 5 \approx 3.55$ cm. Strictly speaking, this expression can only be used for a slab reactor. However, most reactors are generally large enough that the slab reactor approximation is accurate to within a few percent. [Ans.]

When it comes to thermal neutrons, the values of the extrapolation distance L_{EXT} for some typical moderating materials are 0.30 cm for light water (H_2O), 1.80 cm for heavy water (D_2O), 1.95 cm for carbon (graphite), and 6.35 cm for liquid sodium (Na). *The only time Equation 22.145 cannot be used is when the width L of the diffusing material is much less than the extrapolation distance L_{EXT} ($L \ll L_{EXT}$). When this occurs, the transport equation has to be solved directly to find the appropriate value for L_{EXT}.* The value of L_{EXT} for curved surfaces is also different than that given by Equation 22.145. The previous reference shows what the size of this difference can be.

22.26 Diffusion Coefficients and the P_1 Approximation

One of the direct consequences of using the P_1 approximation to represent the angular dependence of the flux is that the isotropic component of the flux $\phi(\mathbf{r}, E)$ and the directional neutron current $\mathbf{J}(\mathbf{r}, E)$ are related by the equation

$$\frac{1}{3}\nabla\phi(\mathbf{r}, E) + \Sigma_{TR}(r)\mathbf{J}(\mathbf{r}, E) \tag{22.146}$$

which we discussed in some detail in an earlier section. This equation allows us to express the neutron current $\mathbf{J}(\mathbf{r}, E)$ as a function of the *isotropic neutron flux* $\phi(\mathbf{r}, E)$:

$$\mathbf{J}(\mathbf{r}, E) = -\frac{1}{3\Sigma_{TR}(r)} \cdot \nabla\phi(\mathbf{r}, E) \tag{22.147}$$

or

$$\mathbf{J}(\mathbf{r}, E) = \frac{-0.33}{\Sigma_{TR}(r)} \cdot \nabla\phi(\mathbf{r}, E) \tag{22.148}$$

where the neutron transport cross section $\lambda_{TR}(r)$ is defined as

$$\Sigma_{TR}(r) = \Sigma_t(r) - \cos\theta\,\Sigma_s(r) \tag{22.149}$$

Notice that we can also write the transport cross section as

$$\Sigma_{TR}(r) = \Sigma_t(r) - \mu\Sigma_s(r) \tag{22.150}$$

where *$u = \cos\theta$ is the average cosine of the neutron scattering angle* θ. Because neutron diffusion theory requires the directional neutron current $\mathbf{J}(\mathbf{r}, E)$ to be related to the isotropic neutron flux by

$$\mathbf{J}(\mathbf{r},E) = -D(r)\cdot\nabla\phi(\mathbf{r},E) \tag{22.151}$$

it follows that the spatially dependent diffusion coefficient has a value of

$$D(r) = \frac{0.33}{\Sigma_{TR}(r)} = \frac{0.33}{\left[\Sigma_t(r) - \mu\Sigma_s(r)\right]} \tag{22.152}$$

which follows immediately from the P_1 approximation. In other words, *the fact that angular neutron flux $\phi(\mathbf{r}, \mu, E)$ is linearly anisotropic means that the best way we can link transport theory and diffusion theory is for the diffusion coefficient $D(r)$ to have an angular dependence that is given by $\mu\sum_s$.* Now let us examine some of the consequences of what this angular dependence means. If the term $\mu\sum_s$ did not exist, the neutron flux would be angularly isotropic, and the scattering cross sections would be isotropic as well. Hence, the value for μ would be 0 and the average scattering angle θ would be 90°. Then we could write the diffusion coefficient as

$$D(r) = \frac{0.33}{\Sigma_t(r)} \tag{22.153}$$

and this is the result that we would obtain from classic particle diffusion theory. However, as soon as the scattering cross sections have *some* angular dependence, then the value of μ is *NOT* zero, and the diffusion coefficient must be found using the transport cross section $\sum_{TR}(r)$ instead of the total cross section $\sum_t(r)$. So what does this angular dependence mean to the average nuclear engineer? To answer this question, we need to examine the scattering process itself. We know from Appendix H that the value of μ is given by $\mu = \cos\theta$, where the average cosine of the scattering angle θ is a function of the *atomic mass number* $A = Z + N$ of the target nucleus. The specific relationship between these two parameters is

$$\mu = \frac{2}{3A} = \frac{0.67}{A} = \frac{0.67}{Z+N} \tag{22.154}$$

and this result can be found by integrating over all possible scattering angles in the center of mass system (refer to our discussion of this subject in Chapter 3). Thus, elastic scattering collisions in which the direction of the scattered neutron is essentially unchanged have a value of μ close to 1.0 (since $\theta \approx 0$), and collisions in which the scattering angle is large have a value of μ closer to 0 (since θ is closer to 90°). Heavy elements have very small values of μ (since A is very large), and the lightest element—hydrogen—has a value for μ of 0.67 (since A is 1). These last two statements imply that the scattering process becomes much more anisotropic when neutrons scatter off of lighter elements (such as hydrogen) than when they scatter off of heavier ones. *Thus, the transport cross section $\sum_{TR}$ is always somewhat smaller than the total cross section $\sum_t (\sum_{TR} < \sum_t)$, and this difference is most apparent when the value of θ is small.* This means that the neutron diffusion coefficient, which is inversely proportional to the transport cross section, becomes larger as $\mu \to 1.0$. We also know from our previous discussion that the neutron mean free path λ is equal to three times the diffusion coefficient D:

$$\lambda = 3D \tag{22.155}$$

Thus, the *transport mean free path* λ_{TR} can be written as

$$\lambda_{TR} = \frac{1}{\Sigma_{TR}(r)} = \frac{1}{\left[\Sigma_t(r) - \mu\Sigma_s(r)\right]} \tag{22.156}$$

and the transport mean free path can be regarded as a "corrected" version of the conventional mean free path because it accounts for any anisotropies in elastic scattering process with light elements. Since elastic scattering almost always takes place in the forward direction (i.e., with an average angle $\theta < 90°$), this means that *the transport mean free path $\lambda_{tr} = 1/\Sigma_{tr}$ is always somewhat larger than the conventional mean free path* $\lambda = 1/\Sigma_t$. Thus, the additional forward scattering

increases the apparent mean free path of the incoming neutrons because neutrons that are scattered in the forward direction will continue to travel in that direction further than neutrons that have a random distribution of scattering angles (and therefore some backscatter). Since the diffusion coefficient is inversely proportional to the transport cross section

$$D(E) = \frac{1}{3\Sigma_{tr}(E)} \tag{22.157}$$

the diffusion coefficient D is also larger in a material where there is some forward scattering. In light elements like hydrogen, the forward scattering process can be very anisotropic at high neutron energies. This means that transport theory is more accurate than diffusion theory under these conditions because the neutrons tend to stream through a material rather than simply diffusing through it. It should also be apparent from what we have just said that *the transport cross section is always smaller than the total cross section* because the anisotropic scattering causes μ to be large ($0.33 \leq u \leq 0.67$) in light elements and close to 0 in heavy ones. The actual values of μ, θ, $\sum_{TR}$, and $\sum_t$ are presented for some common materials in Appendix H. On many occasions, the correct value of the transport cross section has to be measured experimentally.

22.27 Commercial Computer Programs Used to Solve the Neutron Transport Equation

Many computer programs have been written to solve the neutron transport equation or to also solve the transport equation with a γ-ray source. In countries like the United States, they are provided to universities and nonprofit organizations by the U.S. government. An unusually large number of these computer programs are maintained by the U.S. National Nuclear Code Center (also called RSIIC), which is located in Oak Ridge, Tennessee. The Website for this important resource is

http://www-rsicc.ornl.gov/

Some of the transport theory codes the center provides are summarized in Table 22.2. These codes have also been ported to other operating systems from time to time. Some of the most popular and widely used transport theory codes are *ANISN* (for one-dimensional problems) and *TWOTRAN* (for two-dimensional problems). ANISN was originally developed at the Oak Ridge National Laboratory, and copies can be obtained from the Radiation Safety Information Computational Center in Oak Ridge, Tennessee. TWOTRAN was originally developed at the Los Alamos National Laboratory in Los Alamos, New Mexico, and copies can also be obtained from RSIIC. In Europe, and in most of the rest of the world, the International Atomic Energy Agency and the European Nuclear Society provide a similar set of services. You can read more about these services at the following URLs:

www.iaea.org
www.euronuclear.org

In any event, solutions to the transport equation are relatively easy to obtain today for simple reactor geometries (slabs, rectangles, spheres, and cylinders). The key is to find a transport theory code that can handle the particles you are interested in following and that you can also afford to be able to run.

22.28 Other Approaches for Solving the Neutron Transport Equation

Although the neutron transport equation (and the corresponding transport equation for photons) are widely revered and respected, there are many problems where it is simply impractical to determine the spatial distribution of the particle flux because of difficulties associated with implementing the boundary conditions in a complex geometric structure. This is particularly true in the vicinity of fuel rods and control rods in heterogeneous reactor fuel assemblies having many different enrichments and burnable poisons. In this case, an alternative approach to a brute force solution to the neutron transport equation is required. For these types of problems, the *Monte Carlo method*, which we will discuss in Chapter 23, is a much more practical way to proceed. In particular, it avoids the use of what can be very messy boundary conditions when dealing with complex, heterogeneous reactor geometries.

Fundamentally speaking, *the Monte Carlo method is a statistically based method* for finding the spatial distribution of particles in a complex and heterogeneous reactor lattice. It is particularly well suited for solving the shape of the neutron flux in the vicinity of control rods and fuel rods. Hence, the complexity inherent in many reactor fuel assemblies is not a problem when it comes to a Monte Carlo calculation. The primary drawback to the Monte Carlo method is excessive computer time—particularly when a solution that approaches the accuracy of more deterministic methods is required. In the next chapter, we will introduce the Monte Carlo method and discuss how it works in more detail. The Monte Carlo method and the transport methods we have discussed can be applied to any problem where the neutron diffusion equation cannot

be used to obtain accurate results. However, because transport theory methods are deterministic in nature and Monte Carlo methods are probabilistic in nature, no one has ever found a way to develop a hybrid method that combines the best features of both. (By the way, a similar problem exists when physicists try to combine general relativity and quantum mechanics.) However, other types of transport methods called *adjoint methods* have been developed that show additional promise for certain types of problems. These methods are more computationally efficient than the methods we have discussed so far, but again, the underlying physics sometimes gets obscured by a lot of unnecessary matrix manipulation. Some of these methods use the concept of *neutron importance*, which we will discuss in Chapter 23, to converge the results faster. We will leave it up to the reader to decide whether these schemes are worth the additional computational effort. However, from a purely academic perspective, they provide an interesting way to speed up the solution to the transport equation in certain situations. A more thorough discussion of these methods can be found in the references at the end of the chapter.

Student Exercise 22.3

Consider the list of transport theory codes shown in Table 22.2. Use one of these codes to calculate the neutron flux shape in the vicinity of a control rod. Plot the neutron flux shape for the fast and thermal energy groups. Assume that the control rod is cylindrical in shape and that the center of the control rod is located at r = 0.

22.29 Visualizing the Angular Neutron Flux

Before moving onto the Monte Carlo method, we would like to take a moment to visually illustrate what we have just discussed physically. This will help the reader to visualize some of the most important differences between neutron transport theory and neutron diffusion theory. One of the best ways to illustrate this difference is to imagine what the angular neutron flux $\phi(\mathbf{r}, E, \boldsymbol{\Omega})$ looks like and to then compare it to the isotropic neutron flux $\phi(\mathbf{r}, E)$ under the same conditions. Of course, the isotropic neutron flux is related to the angular neutron flux by

$$\phi(\mathbf{r}, E) \equiv \frac{1}{4\pi}\int_{\Omega}\phi(\mathbf{r}, E, \boldsymbol{\Omega})d\boldsymbol{\Omega} \tag{22.158}$$

In practice, the angular neutron flux can have many different shapes, but if we were to plot some of the most common ones as a function of θ (or equivalently as a function of $\mu = \cos\theta$), we would obtain the *polar plots* shown in Figure 22.17. The polar plot in the upper right-hand corner (Image B) shows what the isotropic neutron flux used in diffusion theory represents, and the other plots (corresponding to Images A, C, and D) are examples of what the angular neutron flux used in neutron transport theory represents.

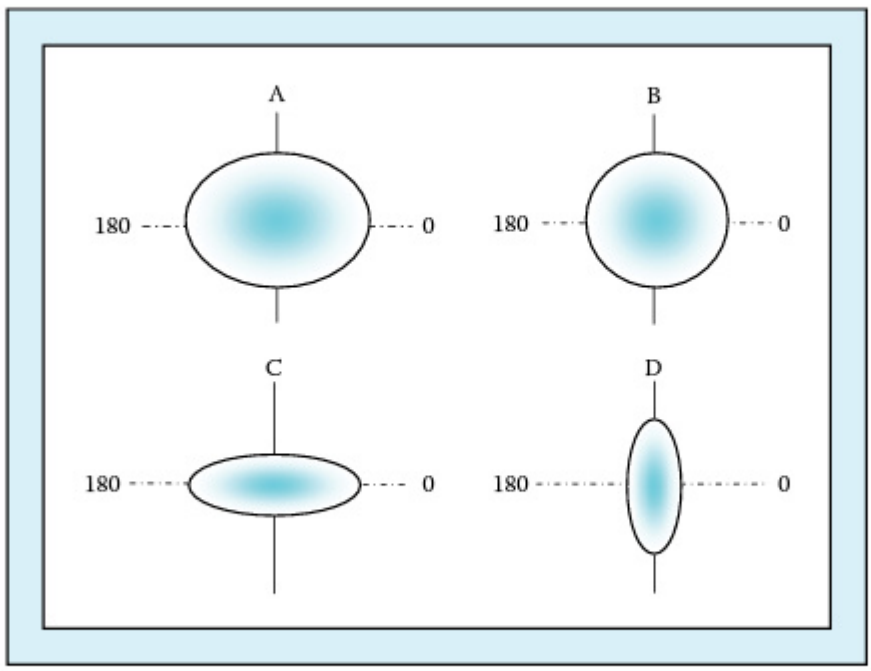

FIGURE 22.17 A polar plot of the angular neutron flux as a function of θ in neutron transport theory.

The more angularly anisotropic the neutron flux becomes, the harder it is to make the results of diffusion theory agree with the results of transport theory. (We can still perform the calculations, but the results will not be the same.) In other words, while the flux shape in Image A could probably be represented by neutron diffusion theory if we were willing to represent the angular anisotropy by the transport cross section $\sum_{TR}(r) = \sum_t(r) - \mu\sum_s(r)$, any greater anisotropy (such as that shown in Images C and D) would have to be modeled by solving the transport equation directly. Images C and D are examples of how the neutron flux behaves in the vicinity of strong neutron absorbers (such as control rods), or when gamma rays are allowed to stream through a radiation shield. In any event, the particle flux in these problems has a strong directional bias, and using the diffusion equation to find its spatial distribution will lead to unreliable results when the directional bias is large.

References

Books and Textbooks

1. Ash, M. *Nuclear Reactor Kinetics*, McGraw-Hill, New York (1965).
2. Henry, A.F. *Nuclear Reactor Analysis*, MIT Press, Cambridge, MA (1975).
3. Reactor Physics Constants, USAEC Document ANL-5800, 2nd edn. (1963).
4. Keepin, G.R. *Physics of Nuclear Kinetics*, Addison-Wesley, Reading, MA (1965).
5. Stacey, W.M. *Nuclear Reactor Physics*, 2nd edn., John Wiley & Sons, New York (2007).
6. Duderstadt, J. and Hamilton, L. *Nuclear Reactor Analysis*, John Wiley & Sons, New York (1976).
7. Clark, M. and Hansen, K. *Numerical Methods of Reactor Analysis*, Academic Press, New York (1964).
8. Hetrick, D.L. *Dynamics of Nuclear Reactors*, American Nuclear Society, La Grange Park, IL (1993).
9. Lewis, E. *Fundamentals of Nuclear Reactor Physics*, Academic Press, Boston, MA (2008).
10. Lewis, E. and Miller, W.F. *Computational Methods of Neutron Transport*, Wiley-Interscience, New York (January 1993).
11. Schultz, M.A. *Control of Nuclear Reactors and Power Plants*, 2nd edn., McGraw-Hill, New York (1961).
12. Lamarsh, J.R. and Baratta, A.J. *Introduction to Nuclear Engineering*, Prentice Hall, Upper Saddle River, NJ (2001).
13. Lamarsh, J.R. *Introduction to Nuclear Reactor Theory*, second printing, Addison-Wesley Publishing Company, Inc., Reading, MA (1972).
14. Cochran, R.G. and Toulfanidis, N. *The Nuclear Fuel Cycle: Analysis and Management*, American Nuclear Society, La Grange Park, IL (1999).
15. Glasstone, S. and Eedlund, M. *The Elements of Nuclear Reactor Theory*, D Van Nostrand Company, Inc., New York (1952).
16. Glasstone, S. and Sesonske, A. *Nuclear Reactor Engineering*, 3rd edn., Van Nostrand Reinhold Company, New York (1981).
17. Shultis, K. and Faw, R. *Fundamentals of Nuclear Science and Engineering*, 2nd edn., CRC Press, Boca Raton, FL (2008).
18. Masterson, R.E. *Nuclear Engineering Fundamentals: A Practical Perspective*, CRC Press, Boca Raton, FL (2017).

Web References

1. *http://prr.hec.gov.pk/chapters/2057-2.pdf.*
2. *http://web.mit.edu/22.54/ClassNotes/Lec14.pdf.*
3. *http://en.wikipedia.org/wiki/Neutron_transport.*
4. *http://mathworld.wolfram.com/SphericalHarmonic.html.*
5. *http://mathworld.wolfram.com/LegendrePolynomial.html.*
6. *http://hyperphysics.phy-astr.gsu.edu/hbase/math/legend.html.*
7. *neutron.kth.se/courses/reactor_physics/LectureNotes/101_NTE.pdf.*
8. *http://www.engr.psu.edu/cde/courses/nuce521/nuce521_chapter1_reading.pdf.*

Additional References

- Important physical constants used by nuclear scientists and engineers can be found in *Appendix A*.
- Unit systems and their conversion factors can be found in *Appendix B*.
- Nuclear cross sections for many important nuclear materials can be found in *Appendix C*.
- Physical properties of important nuclear materials can be found in *Appendix D*.
- X-ray and gamma ray attenuation coefficients are discussed in more detail in *Appendix G*.
- The diffusion coefficient, the transport cross section, and transport mean free path are presented and explained in *Appendix H*.

Questions for the Student

The following questions cover the material presented in this chapter and, in some cases, previous chapters as well. They are designed to test how well the student has acquired a working knowledge of the subject matter.

1. Write down the neutron transport equation for the case where all of the particles have exactly the same speed.
2. What is the specific reason why the neutron transport equation is so much more difficult to solve than the neutron diffusion equation?
3. What specific term in the neutron transport equation presents the greatest computational challenge when it is necessary to solve it numerically?
4. In the neutron transport equation, what specifically does the term $\mathbf{\Omega}$ represent? What is the physical interpretation of the vector $\mathbf{\Omega}$?
5. What is the definition of the angular neutron flux $\phi(\mathbf{r}, E, \mathbf{\Omega}, t)$ that appears in the neutron transport equation?
6. When the neutron flux is linearly anisotropic, how is the neutron flux $\phi(\mathbf{r}, t)$ related to the neutron current $J(\mathbf{r}, t)$?
7. Under what specific set of conditions can the value of the neutron current $\mathbf{J}\_(\mathbf{r}, t)$ flowing back into a bare homogeneous reactor from a vacuum be expressed in the following form: $\mathbf{J}\_(\mathbf{r}, t) = 1/4 \cdot \phi(\mathbf{r}, t) + (D/2)\, \nabla\phi(\mathbf{r}, t)$?
8. What is the specific definition of the transport cross section $\Sigma_{tr}(E)$ that is used in the neutron transport equation, and what does the value of μ represent in the definition of the neutron transport cross section?
9. Write down an explicit expression for the value of $\mathbf{\Omega}$ that appears in the neutron transport equation without having to use a specific coordinate system.
10. What does the value of $\mathbf{\Omega}$ look like in a cylindrical coordinate system, and what does it look like in a spherical coordinate system?
11. What is the definition of the angular neutron current $\mathbf{J}(\mathbf{r}, E, \mathbf{\Omega}, t)$ that appears in the neutron transport equation, and how is it related to the value of the angular neutron flux $\phi(\mathbf{r}, E, \mathbf{\Omega}, t)$? Under what set of conditions does this value of the neutron current reduce to the value that is used in the neutron diffusion equation?
12. When discussing neutron transport theory, what does the term "ray effect" refer to?
13. Name two popular methods that are used for approximating the angular dependence of the flux when solving the neutron transport equation.
14. The Legendre polynomials used by the P_N method are a subset of a much larger set of polynomials that are also used in the solution of similar types of equations. What is this larger set of polynomials called?
15. What is the normalization condition that all of the Legendre polynomials must follow?
16. What is the basic assumption upon which the S_N method is based, and who is credited for originally inventing the S_N method?
17. How can the problems associated with ray effects be overcome?
18. What set of polynomials does the P_N method use to represent the angular dependence of the particle flux, and what larger set of polynomials are these polynomials a subset of?
19. In simple one-dimensional geometries, how many terms do the P_N or S_N approximations normally need to represent the anisotropy of the particle flux with a reasonable degree of accuracy?
20. Why has the S_N method become more popular than the P_N method over time?
21. How many variables does the time-dependent neutron flux $\phi(\mathbf{r}, E, \mathbf{\Omega}, t)$ depend upon in the three-dimensional neutron transport equation in a Cartesian coordinate system?
22. Name at least two well-known transport theory codes that are in widespread use today.
23. How are the angular flux and the angular current related when Fick's law no longer applies?
24. What units do the neutron current and the neutron flux $\mathbf{J}(\mathbf{r}, E, \mathbf{\Omega}, t)$ and $\phi(\mathbf{r}, E, \mathbf{\Omega}, t)$ have in the neutron transport equation?
25. What is the variable substitution that is used in the one-dimensional transport equation to convert it into a more "user-friendly" form?
26. What are the explicit forms of the first three Legendre polynomials $P(\mu)$ that are used in the P_N approximation?
27. Write down the explicit form of the equations that are used by the P_3 method in one dimension. How many equations does the P_3 method use for each spatial mesh point?
28. What do the angular weights w_n in the S_N method represent?
29. What procedure is used to normalize the polynomial expansion in the P_N method?
30. What is the physical interpretation of the variable μ that frequently appears in some forms of the neutron transport equation?
31. For a three-dimensional isotropic source term having a value of $S(r, t)$, how do we convert it to the particle source term $S(r, \mu, t)$ that can be found in the transport equation?

32. Under what specific set of conditions can we write $\nabla \cdot v\boldsymbol{\Omega} = v\boldsymbol{\Omega} \cdot \nabla$ in one-group neutron transport theory?
33. Suppose that the scattering cross section $\Sigma_s(r, u)$ in the transport equation is written as $\Sigma_s(r, u) = \Sigma_t\Sigma_{s1}(r) \cdot P_1(u)$. Provide a physical interpretation of the first two coefficients in the Legendre polynomial expansion of the scattering cross section. What does the value of the second term become when an element is very heavy and the scattering becomes completely isotropic?
34. In Chapter 11, we learned that the transport cross section for some materials can be written as $\Sigma_{tr} = \Sigma_s(1 - \cos\theta)$. Under what conditions is it permissible to us this expression instead of the more exact expression $\Sigma_{tr} = \Sigma_t - \cos\theta\,\Sigma_s$?

Exercises for the Student

Exercise 22.1

Suppose that the components of the angular neutron current along the x-axis, the y-axis, and the z-axis in a Cartesian coordinate system are given by $\mathbf{J_x} = 0.25 \times 10^{16}$ neutrons/cm^2/s, $\mathbf{J_y} = 0.433 \times 10^{16}$ neutrons/cm^2/s, and $\mathbf{J_z} = 0.866 \times 10^{16}$ neutrons/cm^2/s. What is the neutron density $n(\mathbf{r}, E, \boldsymbol{\Omega}, t)$ at $\mathbf{r} = 0$ if the average velocity of the neutrons is 2200 m/s?

Exercise 22.2

Consider the following definition for the transport cross section Σ_{tr} that frequently appears in the study of nuclear systems: $\Sigma_{tr}(E) = \Sigma_t(E) - \mu\Sigma_s(E)$. Using this definition and the expressions for μ that can be found in other chapters, derive the thermal transport cross section for the element carbon at 0.025 eV. Assume that $\Sigma_c = 0.00003$ cm^{-1} and $\Sigma_s = 0.3952$ cm^{-1}. What does the value of μ represent?

Exercise 22.3

Earlier in this chapter, we learned that a vacuum boundary condition of the form $\int_{\mathbf{n}\cdot\boldsymbol{\Omega}<0} \mathbf{n}\cdot\boldsymbol{\Omega}\, v(E)\, \mathbf{N}(\mathbf{r}, \boldsymbol{\Omega}, E)$ implies that the neutron flux and the neutron current at the boundary with a complete vacuum are related by the equation $\phi(z, E) = 2J(z, E)$ along the direction z normal to the surface. Show that this equation immediately leads us to the conclusion that the flux and the derivative of the flux at the boundary are related by $\phi_z = -2D\, d\phi/dz$.

Exercise 22.4

Using the fact that $\phi_z = -D\, d\phi/dz$, show that the *extrapolation distance* δ at the outer boundary of a reactor imbedded in a complete vacuum is given by $\delta = -\phi/d\phi/dz$, from which it immediately follows that $\delta = 2D$.

Exercise 22.5

In neutron transport theory, it can be shown that the energy-dependent diffusion coefficient D(E) is given by $D(E) = 1/(3\Sigma_{TR}(E)) = \lambda_{TR}(E)/3$. Using this fact and the information presented in the previous problems, show that $\delta = 0.67\lambda_{TR}(E)$.

Exercise 22.6

In the P_N approximation, one attempts to expand the angular neutron flux $\phi(\mathbf{r}, E, u)$ in an infinite series of the form

$$\phi(\mathbf{r}, E, u) = \sum_n P_n(\mu)\phi_n(\mathbf{r}, E)$$

where, in one dimension, the values of $P_n(\mu)$ correspond to the Legendre polynomials. Using the fact that the first few Legendre polynomials are defined by

$$P_0(\mu) = 1$$
$$P_1(\mu) = \mu$$
$$P_2(\mu) = \frac{3\mu^2 - 1}{2}$$

show that the P_1 approximation allows us to write the angular neutron flux as

$$\phi(\mathbf{r},E,u) = \phi_o(\mathbf{r},E)P_o(\mu) + \phi_1(\mathbf{r},E)P_1(\mu)$$

or

$$\phi(\mathbf{r}, E, u) = \frac{1}{4p}\phi_o + \frac{3}{4\pi}\phi_1$$

What is the physical interpretation of ϕ_o and ϕ_1 in this case? For diffusion theory to be valid, what must the relationship be between ϕ_1 and ϕ_o?

Exercise 22.7

In the previous exercises, we showed that the *extrapolation distance* δ at the outer boundary of a slab reactor surrounded by a vacuum is given by $\delta = -\phi/d\phi/dz$ in one dimension, which reduces to $\delta = 0.67\lambda_{TR}(E)$. What form of the P_N approximation was used to generate this equation? Is the alternative equation $\delta = 0.71\lambda_{TR}(E)$, which is sometimes used to find the extrapolation distance in reactor physics books, more accurate or less accurate than $\delta = 0.67\lambda_{TR}(E)$? Why?

Exercise 22.8

In Appendix H, the purpose of the neutron transport cross section $\lambda_{TR}(E)$ was discussed in considerable detail. Based on the discussion presented there, does the use of the neutron transport cross section result in a smaller mean free path, the same free path, or a larger mean free path than the more common expression $\lambda = 1/\lambda_T(E)$? Is the value of the diffusion coefficient D derived from $\lambda_{TR}(E)$ and $\lambda_T(E)$ larger, smaller, or the same as the result of this difference?

23

The Monte Carlo Method and Its Applications to Nuclear Science and Engineering

23.1 An Introduction to the Monte Carlo Method

The *Monte Carlo method* is a statistical method that attempts to simulate the behavior of large numbers of neutrons and other nuclear particles (including photons, protons, and electrons). It is a statistical method whereby the expected behavior of the particle population is simulated by tracking the paths of large numbers of particles, and inferring from their *case histories* the statistical behavior of the particle population as a whole. The Monte Carlo method is best suited for modeling complex reactor geometries where other methods either fail to predict the behavior of the particle population correctly or are too expensive to use.

The Monte Carlo method is applicable to an almost unlimited number of problems in particle diffusion and transport theory and is not limited to just neutron or photon behavior in reactor fuel assemblies. It can be used to solve radiation shielding problems, compose music, and even decide when to buy or sell stocks. The statistical behavior of the particle population is obtained by playing a *game of chance* in which the Monte Carlo method attempts to simulate the behavior of hundreds of thousands or even millions of individual particles. The laws of the simulation are determined by the energies of the particles, the initial conditions, and the laws of classical or quantum mechanics, and they are then programmed into a computer. Thus, the Monte Carlo method can be thought of as a *nuclear video game* in which each of the participants is a nuclear particle that is born, participates in the game, and is then removed from the game or dies. In this sense, it is similar to popular video games such as *Pacma, Game of Thrones,* or the *World of Warcraft*. The outcome of the game is determined from a specific set of rules that attempt to quantify the ways that nuclear particles are created or destroyed. These rules are based on sets of probabilities and probability distributions (such as the ones shown in Figure 23.1) that are decided upon in advance. Thus these probabilities are used to model the physical system one is trying to simulate. The game is constructed so that the desired outcome is normally determined by the structure of these rules in advance. Hence, different outcomes require different programming rules, and the programming rules that are used must be able to simulate the physical outcome that is required. In other words, the rules of the game are similar to those that apply to rolling a pair of dice (see Figure 23.1).

The goal of this chapter is to show how the Monte Carlo method can be used to solve important problems in nuclear science and engineering. These problems typically include particle transport and diffusion. However, this chapter is not intended to be a comprehensive treatment of the method, nor a discussion of the sophisticated techniques that are used to keep errors to a minimum in an actual simulation. The Monte Carlo method is flexible enough that it can be adopted to model almost any physical system or process. However, the method is not well suited to modeling problems where many particles interact simultaneously. Examples of these problems include the behavior of electrons and ions in plasmas and rarefied gases. It is more of a *mano a mano* method in which two nuclear particles meet, and the outcome of the reaction is determined by the laws of probability and statistics. The interacting particles are either scattered, absorbed, reemitted, or destroyed. In some cases, new nuclear particles may be created as well.

Each meeting generates what is known as a "hypothetical event" or "*hypothetical transaction*." The pertinent details of each interaction are recorded, and based upon what happens, the individual particles may participate in another reaction, or they may not. The sequence of events experienced by each particle is called its *case history*. The particles within a reactor may traverse different material regions such as the fuel, the cladding, and the moderator before the fate of the particles is known. When moving through these materials, each particle may experience a different set of reactions, such as scattering, absorption, or fission. It is also possible that a particle may be removed from the game entirely if it travels outside of the boundaries of the game and is lost.

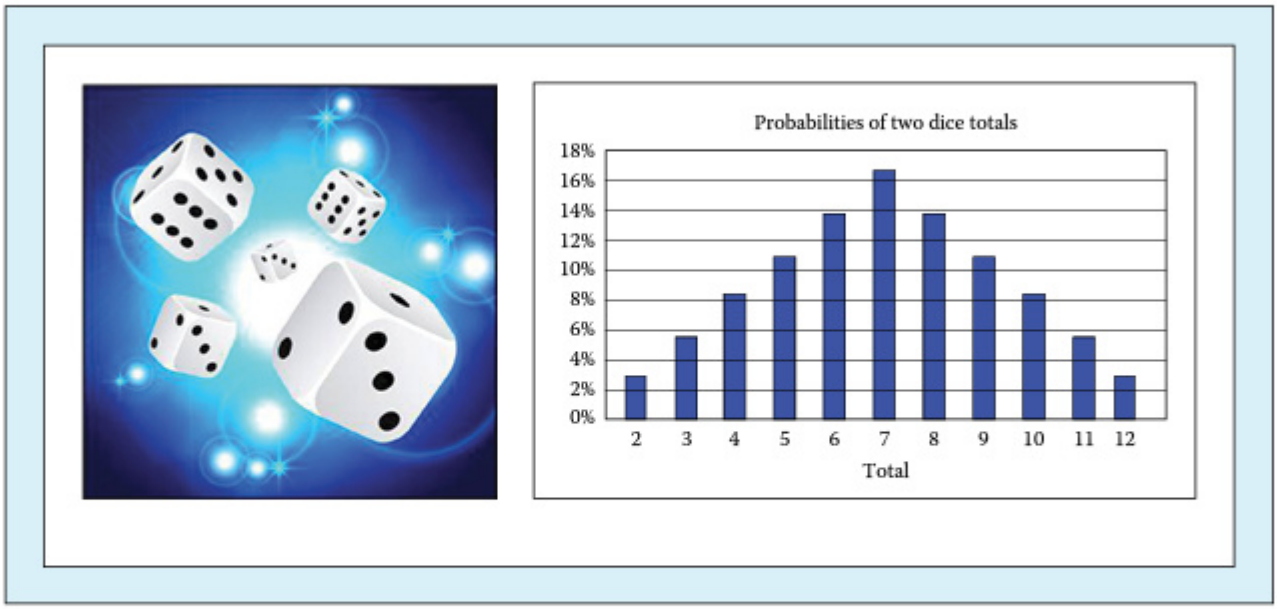

FIGURE 23.1 The Monte Carlo method can be compared to throwing a pair of dice over and over again in order to determine the most likely path that a nuclear particle will take. The outcome of each roll of the dice is determined according to a statistical probability distribution, such as the one shown on the right-hand side of the figure. The midpoint of the distribution then determines the most likely path that the particle (or one of its descendants) will take.

In some video games, this is equivalent to getting shot by another participant in the game or falling off a cliff. In nuclear applications, the particle simply leaks out of the system, and if it is a neutron, the rate that it does so can be interpreted as the neutron leakage rate L, which we defined in Chapter 10. The details of each reaction are recorded, and over time, a picture of the aggregate behavior of the particle population is obtained. For example, if the particle is a photon or a neutron, the particle population may increase as a function of time, or it may decrease. If the particle is a neutron, it will move in a straight line before it hits another particle and interacts with it. The distance it travels between interactions is then determined by its mean free path λ. If the particle is a photon, it may scatter in random directions or may be absorbed and then reemitted again.

To decide what type of reaction occurs (such as an absorption, scattering, or fission reaction) when a number of outcomes are theoretically possible, a *random number generator* is used. The generator is simply a piece of computer code (e.g., a subroutine) that produces the outcome of a reaction according to a *statistical probability distribution*, or SPD, that is programmed into the system in advance. In the nuclear world, this probability distribution can be obtained from the ENDF-B database, which we discussed in Chapter 5. For example, if a particle with a certain kinetic energy E has a 70% chance of being scattered and a 30% chance of being absorbed, the random number generator will provide a scattering reaction 70% of the time and an absorption reaction 30% of the time. Exactly when it will be scattered or when it will be absorbed cannot be determined in advance. If the particle is absorbed, a second random number generator may then be used to determine if additional particles will be reemitted. If the particle is scattered, a third random number generator may be used to determine if the scattering is elastic or inelastic, and a fourth random number generator may be used to determine the scattering angle or scattering direction. The laws of energy and momentum conservation are used to determine the speed and the direction of the particle after the reaction.

An example of how this process works is shown in Figure 23.2. Flowcharts of this type with suitable probability distributions applied to each vertex or decision point are used to determine the physical outcome of the system one is attempting to model. Because of its statistical nature, the Monte Carlo method is seldom as accurate as a nonstatistical or deterministic method. Moreover, one does not have to be particularly sophisticated to use or write a Monte Carlo program, and it can be written in any computer language with any compiler one wants. However, one has to be very careful to program the "rules of the game" correctly so that it can predict the correct outcome of a large number of individual events. Because uncertainties in the results only decrease as the square root of the number of case histories, large numbers of particle histories must be simulated in order to obtain accurate results. It is usually difficult to estimate the accuracy of a Monte Carlo calculation in advance. One must simply run a number of different simulations (or case histories), and if the underlying physics is correct, the particle histories will eventually converge to the correct result. Also, a great deal of care must be taken when the method is coded to ensure that the statistical fluctuations in the particle model are entirely

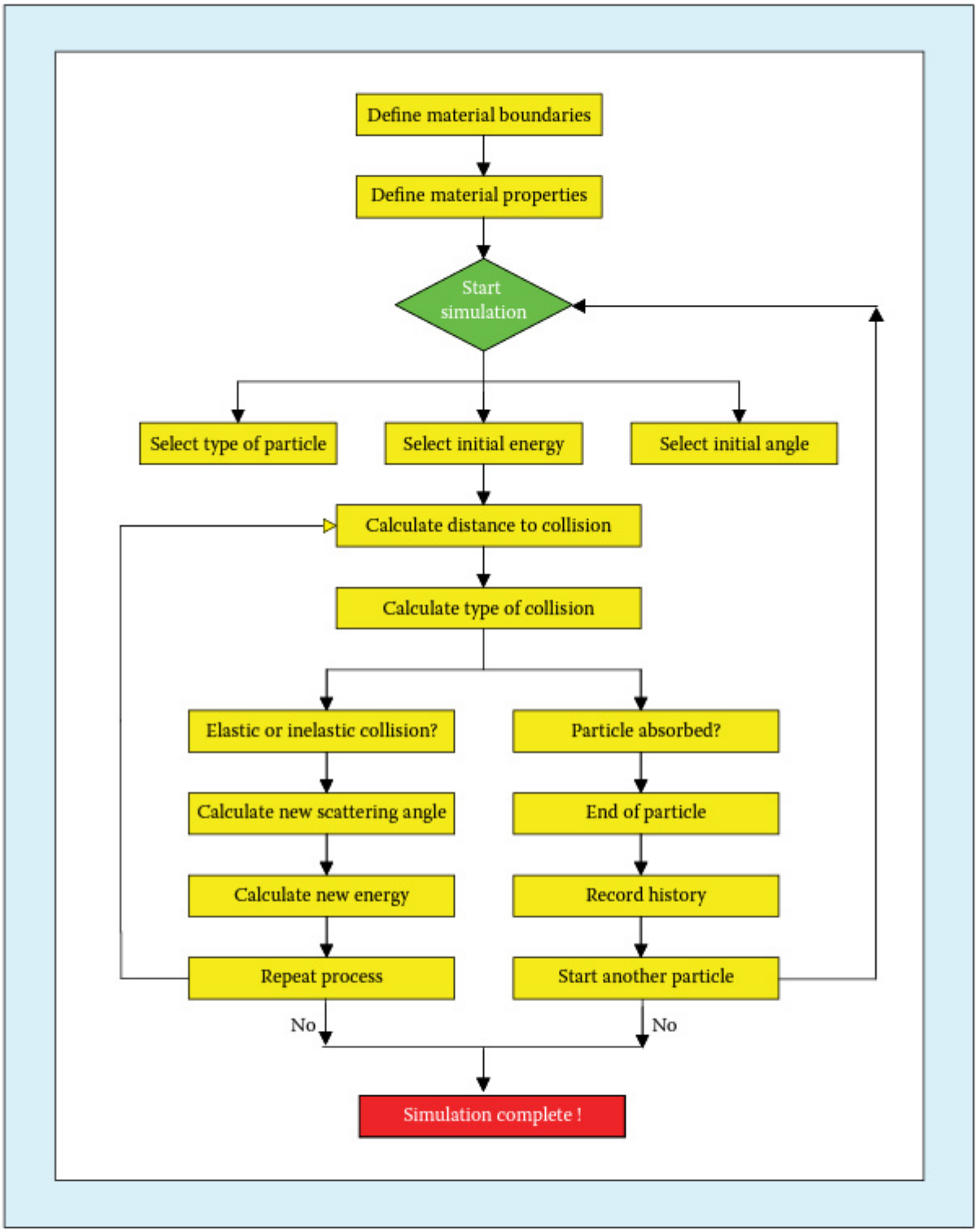

FIGURE 23.2 A simple example of a flowchart that tracks the case histories of a population of nuclear particles using a Monte Carlo method.

random. Otherwise, if one introduces an unexpected bias into the rules, then the results may not be able to be used with confidence. Like all computer programs, Monte Carlo methods are a reflection of the programming skill and programming abilities of an individual programmer. Since a Monte Carlo program implements a set of statistical models, extreme care must be taken to ensure that the dice are not "loaded" in advance. For example, if one writes a Monte Carlo program to simulate the game of craps, one must first determine whether or not a single roll of the dice is unbiased, that is, whether

it is loaded in favor of one or more of the faces on the cube. A physical determination of whether or not any bias exists can be made by rolling the dice millions of times and examining the outcome of the process.

If the statistical data show that each of the rolls of the dice has an equal probability of producing a random number from 1 to 6, then the programming is sound and the game is assumed to be fair. In some casinos in Las Vegas, the same statistical algorithms are programmed into slot machines, and even if the house has only a 51% chance of winning, the random number generator inside of the slot machines will always produce a probability split of 49% win and 51% no win. To prevent people from tampering with the outcome, this algorithm is usually encoded onto a computer chip. After a large number of users have played the game, the final result will always be the same. Hence, the highest probability of "beating the house," which is approximately 50–50, occurs on the first roll of the dice. Any additional attempts to play the machines are simply an exercise in futility. For this reason, a few machines with a greater than a 50% probability of "hitting the jackpot" are usually placed in highly conspicuous locations near the front of the casino. The other machines at the back of the casino, which are kept out of public view, are programmed to have a much lower probability of success. Therefore, people who play these machines almost always end up losing their money and going home broke.

23.2 Random Number Generators and Statistical Probability Distributions

A Monte Carlo simulation begins by designing a *random number generator* that implements what is known as a statistical *probability distribution function*, or *PDF*. If all outcomes are equally possible, then the random number generator will generate a random number between 1 and 100. For example, in the C programming language, a computer subroutine called RAN (), which is supplied with most C programming libraries, is used to make this happen. Every time it is called, it simply returns a random number from 1 to 100. That is to say, the actual implementation of this function is

$$\text{result} = \text{RAN}\,(); \tag{23.1}$$

However, if some events are more likely than others, the random number generator must be programmed to implement a statistical probability distribution that simulates the physical problem one is trying to solve.

Figure 23.3 shows two such statistical probability distributions. The one on the right portrays a probability distribution in which all of the outcomes are equally likely, and the one on the left portrays a probability distribution in which the numbers near the center of the distribution (between 40 and 60) are much more likely to occur than the numbers near the ends (e.g., 1 or 100). Hence, the first probability distribution is called a *"normal" probability distribution*, while the second probability distribution is called a *"flat" probability distribution* because all of the outcomes predicted by this distribution are equally probable. In a Monte Carlo calculation, any probability distribution can be used, but the probability distribution must be *normalized* so that the sum of the probabilities always adds up to 1.0 (i.e., 100%). Probability distributions that do not follow this rule are said to be *ill conditioned*. Consider a statistical probability distribution that is governed by a probability distribution function P(x). Then P(x) dx is the probability that the value of an arbitrary variable

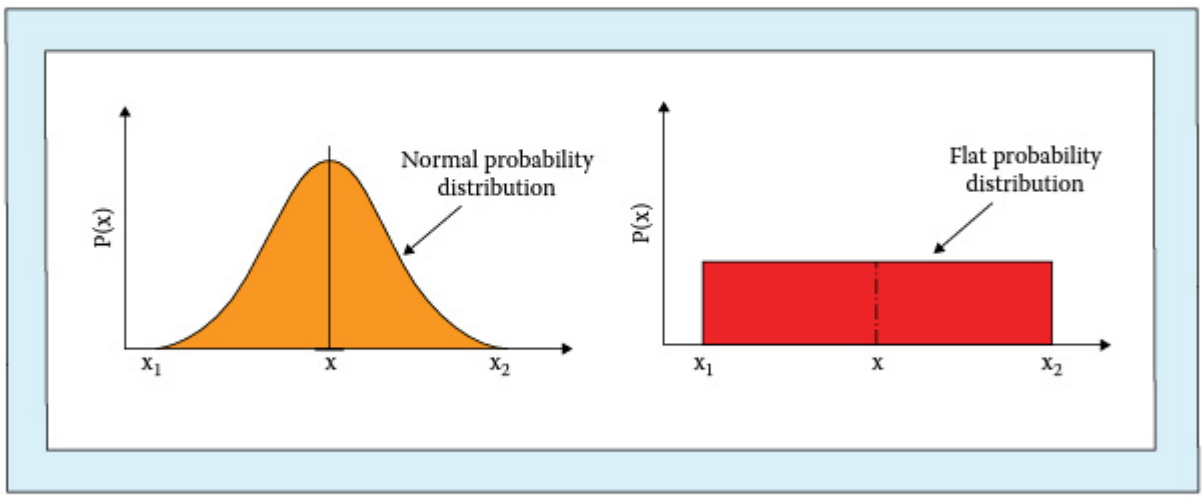

FIGURE 23.3 An example of two probability distributions—a "normal" or bell-shaped probability distribution (on the left) and a "flat" probability distribution (on the right) in which any outcome is equally possible. In both cases, the area under the distributions is equal to 1.0, which means that the sum of all outcomes is equal to 1.0, or 100%.

x will be between x and x + dx, and a *cumulative probability distribution function (or CDF)* is defined as one where C(x) is the probability that the same variable will have a value less than or equal to x. Hence a CDF can be expressed mathematically by

$$C(x) = \int_{x_1}^{x} P(x)dx \tag{23.2}$$

where the limits of integration are from x_1 (usually equal to 0) to x. Based on this definition alone, the cumulative probability C(x) must always be a number between 0 and 1. The physical distinction between a *PDF* and a *CDF* is articulated in Figure 23.4. Hence, *a CDF implements the probability distribution function defined by a PDF*. As we mentioned previously, the probabilities represented by a PDF can either be uniform everywhere (in which case the PDF is flat), or they can be represented by a probability distribution curve that has a bell shape or any other shape that is desired. Two different PDFs are shown in Figure 23.5, and their corresponding CDFs are shown as well. Notice in each case that the

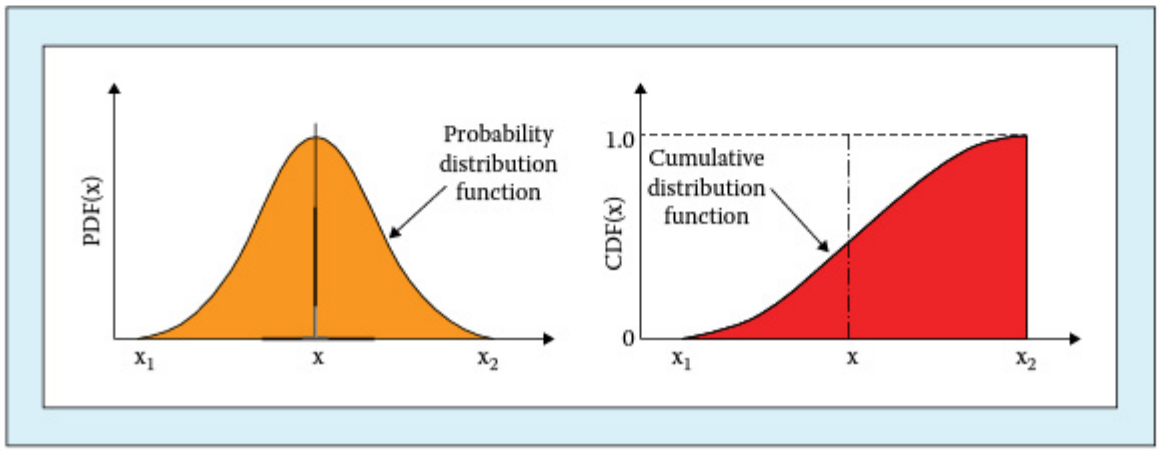

FIGURE 23.4 A probability distribution function (PDF) for the variable x and its corresponding CDF where $x_1 \leq xx_2$.

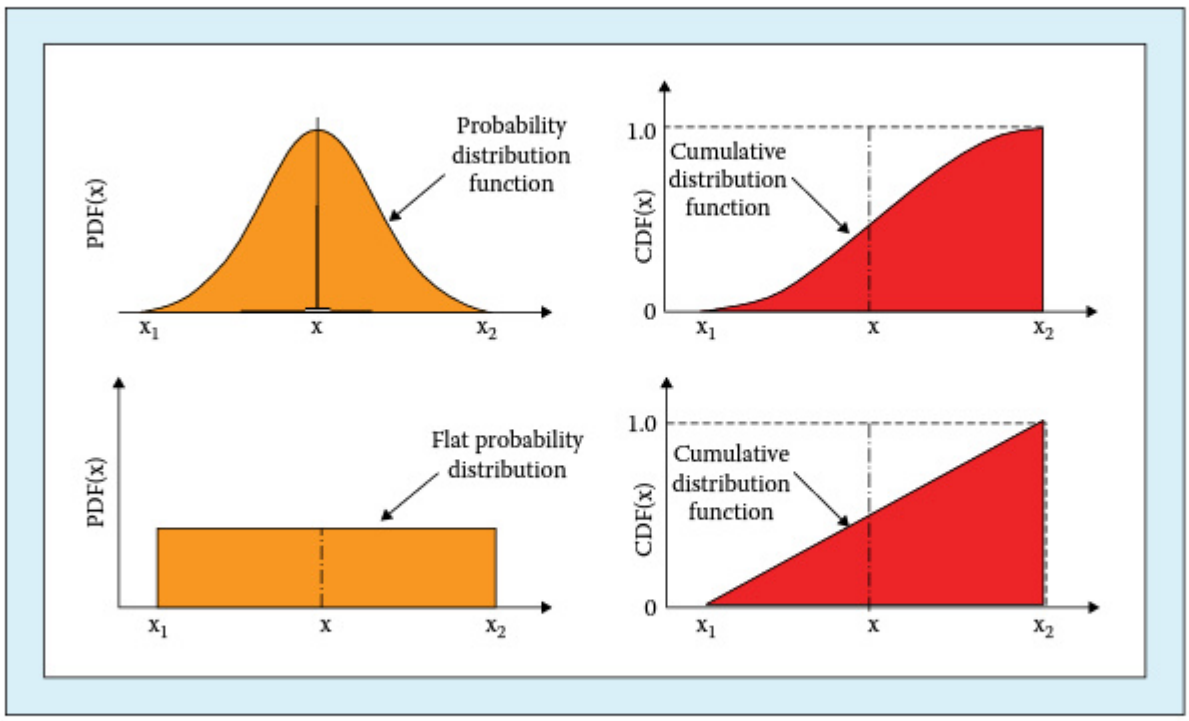

FIGURE 23.5 Two different PDFs and their corresponding CDFs.

CDFs always sum to unity. This means that the total probability of any combination of events occurring is always equal to 100%. In a Monte Carlo calculation, the distribution of the values for x must always follow a PDF, and when the PDF is a discrete function with N possible outcomes, then we must also require that

$$\sum_i P(x_i) = 1 \tag{23.3}$$

Here, the summation is over all possible events from i = 1 to N.

Examples of discrete probability distribution functions are the probability of tossing a coin and getting heads or tails, and the probability of rolling a pair of dice and getting a number between 2 and 12. In the field of nuclear science and engineering, this translates into the probability of a neutron hitting the nucleus of an atom or a photon hitting an electron around the nucleus and being either scattered or absorbed. Hence, Monte Carlo calculations involving nuclear particles must simulate a comprehensive list of events as the particles move through space and time. Some of these events are listed in the *event list* below.

Example Problem 23.1

The PDF for a particular nuclear reaction is given by the statistical probability distribution $P(x) = 3e^{-3t}$, where t is the time in seconds. Assuming that the process described by the PDF starts at t = 0, what is its corresponding CDF?

Solution Its CDF is given by $\text{CDF} = \int_0^t P(t)dt = \int_0^t 3e^{-3t}\,dt = 1 - e^{-3t}$. [Ans.]

A typical list of events for a Monte Carlo calculation involving the interaction of two nuclear particles

- How fast is a particle moving?
- Where is the particle created?
- Under what conditions is the particle created?
- In what direction does the particle initially move?
- How far does the particle move before it hits another particle?
- What is its energy at the time of this collision?
- What type of collision occurs when it hits the other particle?
- Is the particle scattered or absorbed?
- Does the particle produce any additional particles or "by-products" from the reaction?
- What is the direction of motion of the particle or particles after the collision?
- Does a particle ever leak out of the system?
- If the particle does not leak out of the system, when does it decay, when does it die, or when is it otherwise removed from the system?

This specific sequence of events, and the probabilities associated with each of them, then defines the *life cycle of the particle(s)* whose behavior is to be simulated. Except for the speed of the particle (or its energy and momentum), all of the other events in the particle's life cycle must be modeled by a PDF. Therefore, it is the responsibility of the programmer to create these specific probability distribution functions within the computer program itself. In practice, this can be done by either programming them into a number of tables that are held in the computer's memory or by storing them on a disk drive. Computer memory is cheap these days, so thousands of lookup tables can be imbedded directly into a computer program before space becomes a problem. If the probability distribution for a particular event (like the elastic scattering of a neutron) also exists in closed form, then this probability distribution can be used for the PDF. An example would be a scattering cross section of the form

$$\sigma_s(E \to E') = \sigma_s(E)\,P(E \to E') \tag{23.4}$$

where the probability distribution function $P(E \to E')$ is defined by

$$P(E \to E') = \frac{1}{(1-\alpha)E} \tag{23.5}$$

and α is a scattering parameter (see Chapter 3) that is related to the atomic weight A by

$$\alpha = \frac{(A-1)^2}{(A+1)^2} \tag{23.6}$$

Equation 23.5 is sometimes called a *scattering kernel*. The reader may have already noticed that many of the events in the previous list require values for the microscopic and macroscopic cross sections σ and Σ for each type of particle that is involved, where the materials having these cross sections are located, and the geometrical structure of the lattice through which the particles are moving. If the particle is capable of more than one type of reaction (scattering, fission, or absorption), then this list of reactions must be represented by an independent set of probability distributions as well. As the reader can readily see, this list of "events" can be used to predict the actions of an individual particle. The same process must be repeated over and over again for millions of individual particles to gain a clear understanding of where the particles go and what types of reactions they can participate in. This process constitutes the "simulation" phase of a Monte Carlo calculation. We would now like to illustrate how this simulation is actually performed.

To begin the simulation, consider a neutron having an initial energy E and an initial angular direction θ or φ. Suppose that we have a heterogeneous reactor lattice that consists of many different types of fuel rods and control rods whose geometry is shown in Figure 23.6. Suppose that a neutron enters the lattice from the left and then proceeds to the right. The neutron initially scatters off of a water molecule, but after about 1000 collisions, it slows down to the point where it is absorbed by a Uranium-235 nucleus. Then the neutron's life cycle ends, but the nucleus that absorbs it emits several additional neutrons and the process begins again. We would like to model this process using a Monte Carlo method and only a rudimentary knowledge of nuclear cross sections and reaction rates. To simplify our discussion, we will assume that we have already homogenized the cross sections spatially so that the individual case histories will be easier to track. In more complex simulations, this restriction can easily be removed, but the trade-off is that the computer program will be considerably more complicated, and it will definitely take longer to run.

Example Problem 23.2

The angular distribution of the neutrons scattering off of an atomic nucleus is given by the following PDF: $P(\theta) = 5\cos\theta$. What is the corresponding CDF for this scattering process?

Solution The CDF for this process is given by $\text{CDF} = \int_0^{\theta} P(t)\,dt = \int_0^{\theta} 5\cos\theta\, d\theta = 5\sin\theta$. [Ans.]

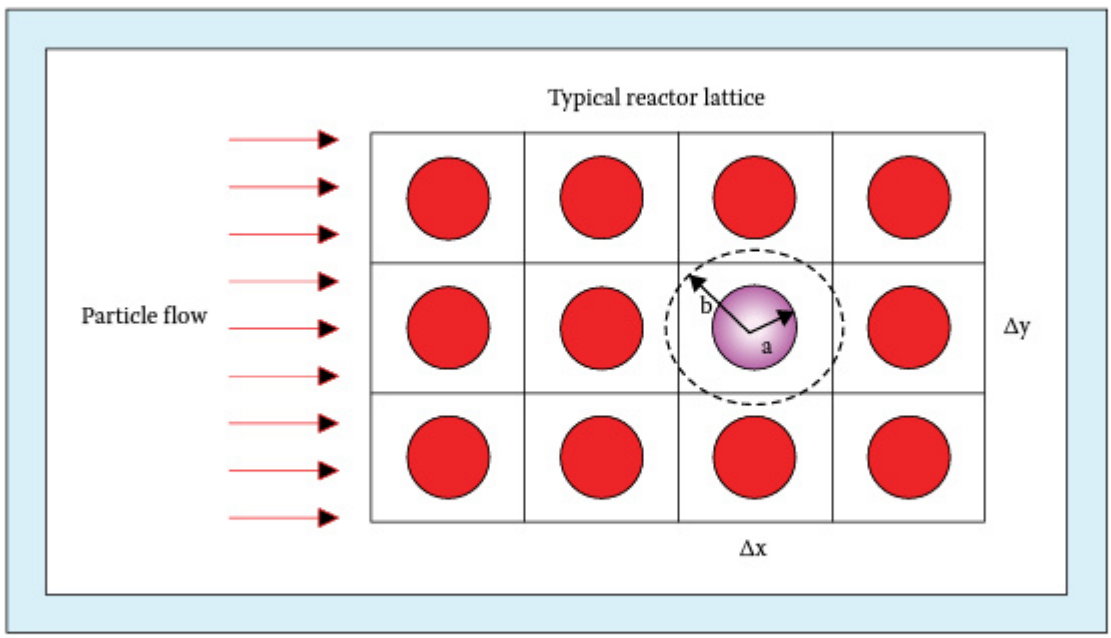

FIGURE 23.6 A typical reactor lattice used in a Monte Carlo calculation.

23.3 Steps in a Monte Carlo Calculation

Depending on the scenario we are attempting to model, there are between four and five specific types of reactions that need to be considered. Each of these reactions can then be considered to be an "event". First, we need to establish the correct boundary conditions, or initial conditions, so that the particles that are created have the right distribution of energies and are moving in the right directions. Second, we must be able to decide how far each particle travels before it hits another object and is either scattered or absorbed. Third, after the collision takes place, we must be able to predict what type of reaction occurs. This may be either a scattering reaction or an absorption reaction. We must use a cumulative probability distribution and a knowledge of the particle's energy dependent cross sections to determine the likelihood of these types of events. Fourth, we must be able to predict the direction of the motion of the particle after the collision. In other words, we must be able to model the process shown in Figure 23.6 for both scattering and absorption. And finally, when the particle finally "dies" and is removed from the game, we must record all of its behavior up to the time of its death. It can be removed from the game if it is absorbed and not reemitted again or if it leaks out of the system. In any event, we must know what happens to it before we can remove it from the game. All Monte Carlo simulations have these five steps in common. Now we would like to illustrate how these steps can be implemented individually.

23.3.1 Step 1: Establish an Initial Direction of Motion and an Initial Particle Energy E

To begin a Monte Carlo calculation, the first step is to decide whether or not the particles to be tracked will originate along a boundary or whether they will originate from a region of space inside of the problem we are trying to solve. If the particles originate from a boundary, then this "boundary" can be considered to be a *boundary condition*, and we must specify the direction that the particles emanate from the boundary, as well as their distribution of energies. In the case of an isotropic line source S(x) (see Figure 23.7), the particles will emanate from the surface in the positive x direction with a strength S_+ equal to $S/2 \times (dl/L)$, where dl is the increment of the total length that we wish to use for our calculations, and L is the total length of the boundary. If the boundary happens to be a point source, then the particles will emanate from the surface of the point source with a strength equal to $S/4\pi R^2$, where R is the distance from the source. This is just a simple example of the *inverse square law,* which was discussed in Chapter 17 of our companion book.* Of course, in both cases the sources of the particles are usually isotropic, and so they radiate with equal probabilities in all directions. When it comes to performing a Monte Carlo calculation, we can then divide the line source into any number N of equal increments we want, where $dl \times N = L$. For example, if we wish to use 100 increments for a particular calculation, then $N = 100$, and $dl = L/N = L/100$, where L is the total length of the source. At each increment, we then generate a particle that emanates from the line in a direction normal to the surface, and we give it whatever energy the line source S(x, E) is specified to have.

Of course, this can be a constant value E_o (in the case the source is monoenergetic), or it can have an arbitrary energy E chosen from a probability distribution P(E). Hence, it is easy to see that we can represent a line source or a point source by a simple boundary condition and that this boundary condition changes depending on the shape of the source. When dealing with a point source, we must also specify the angle θ that the particle emanates from the source. In two

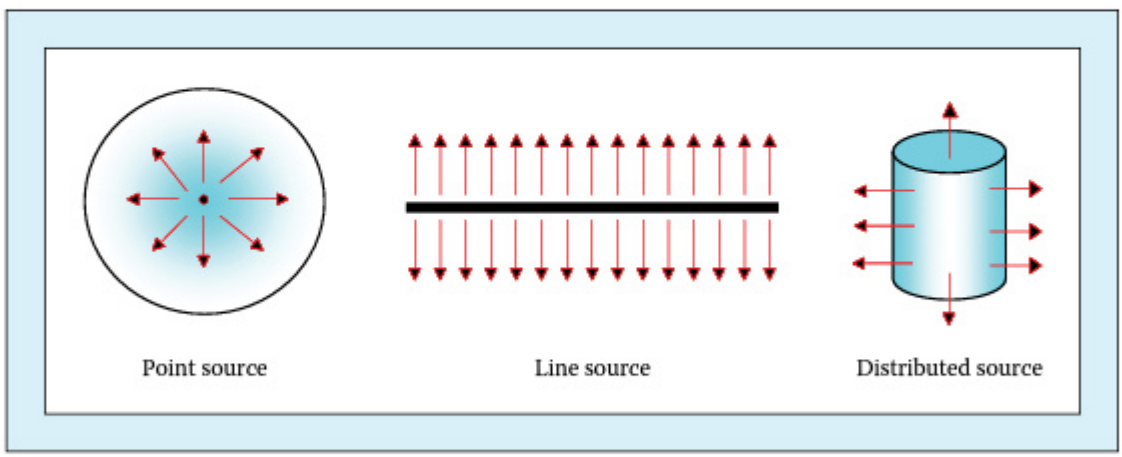

FIGURE 23.7 Point, line, and distributed particle sources for a Monte Carlo calculation.

* See *Nuclear Engineering Fundamentals: A Practical Perspective*, by R.E. Masterson, CRC Press (2017).

dimensions, this can be done by starting out with an angle of $\theta = 0$, ejecting a particle, incrementing the value of θ by 1°, and ejecting a particle again. If the source is isotropic, we then continue around the point source until we reach an angle of 359°, where the process is begun again. In three dimensions, the same process can be used in the φ direction as well. However, to obtain consistent results, we must always ensure that the number of particles emitted into each solid angle $d\Omega$ will be the same if the particle source $S(\Omega, E)$ is an isotropic one.

However, this only applies to particle flow from a boundary. For other problems, the initial particle energies and directions must be calculated for what is known as a *distributed particle source*, and a classical example of this occurs when we would like to predict the distributions of neutrons (or photons) emanating from a distributed source, such as the one shown on the right-hand side of Figure 23.6. This distributed source can sometimes be considered to be a fuel rod, and we must take care to ensure that our programming is smart enough to give the correct angular distribution of the particles and their kinetic energies in this case. Again, it is necessary to use a probability distribution function as our guide. However, if the probability distribution function is properly chosen, then our calculations will accurately represent the physical problem we are trying to solve. This then concludes the first step in most Monte Carlo calculations.

Example Problem 23.3

Suppose we would like to use the Monte Carlo method to find the paths of the particles emanating from an isotropic point source of strength S located at r = 0. In two dimensions (x and y), show how you would construct the logic so that the particles are emanated properly from the point source in this case.

Solution If the point source is an isotropic source, we can do this by starting out at an angle of $\theta = 0$, ejecting a particle, incrementing the value of θ by 1°, and ejecting a particle again. If the source is isotropic, then we can continue around the point source 1° at a time until we reach an angle of 360°, and the process is repeated again. At each angular increment, the number of particles to be ultimately ejected will be $S(\theta) = S/N$, where N is the number of angular increments. Since we can use 1° increments most of the time, then N = 360 in this case. [Ans.]

23.3.2 Step 2: Find the Distance to the First Collision

In Chapter 11, we learned that the distance a neutron travels through a homogeneous medium before it reacts by either scattering or absorption is given by

$$\phi(r, E) = \phi_0 e^{-\Sigma_t(E)r} \tag{23.7}$$

where

$\Sigma_t(E) = \Sigma_a(E) + \Sigma_s(E)$ is the total macroscopic cross section of the neutron
ϕ is the value of the neutron flux

Thus to determine the distance r a particle must travel to have its first reaction, we need to determine the probability P that the particle will have a collision between r and r + dr. This probability is given by

$$P(r)dr = \left(1.0 - \Sigma_t(E)e^{-\Sigma_t(E)r}\right)dr \tag{23.8}$$

In other words, $P(r) = 1.0 - \Sigma_t(E)e^{-\Sigma_t(E)r}$ is the PDF and

$$C(r) = \int P(r)dr = \left(1.0 - e^{-\Sigma_t(E)R}\right) \tag{23.9}$$

is the CDF. The integration given earlier is performed from r = 0 to R. If the random number generation function RN = RAN () then selects a random number RN, we can set it equal to C(r), and solve for the appropriate value of r. The solution is

$$R(E) = \frac{-\ln(1 - RN)}{\Sigma_t(E)} \tag{23.10}$$

This is then the distance R(E) to the first collision.

23.3.3 Step 3: Determine the Type of Collision

Next, it is necessary to determine the type of collision that will occur. In Chapters 4 and 5, we learned that the type of collision cannot be predicted with absolute certainty in advance. However, the propensity of a nuclear particle to be scattered or absorbed can be predicted by examining the value of its absorption and scattering cross sections $\Sigma_a(E)$ and $\Sigma_s(E)$ or σ_a and σ_s. In the case of a neutron, the probability P_s of the neutron being scattered is

$$P_s(E) = \frac{\Sigma_s(E)}{\left(\Sigma_s(E) + \Sigma_a(E)\right)} \tag{23.11}$$

or

$$P_s(E) = \frac{\Sigma_s(E)}{\Sigma_t(E)} \tag{23.12}$$

and the probability P_a of the neutron being absorbed is

$$P_a(E) = \frac{\Sigma_a(E)}{\left(\Sigma_s(E) + \Sigma_a(E)\right)} \tag{23.13}$$

or

$$P_a(E) = \frac{\Sigma_a(E)}{\Sigma_t(E)} \tag{23.14}$$

Obviously, the sum of these probabilities must be equal to 1.0 or 100% since $P_a(E) + P_s(E) = 1$. In this step, a new random number RN = RAN () is selected and it is compared to the probabilities $P_a(E)$ and $P_s(E)$. If

$RN \leq P_a(E)$ the particle is absorbed; otherwise, if
$RN > P_a(E)$ the particle is scattered

In the core, the particle will be absorbed most of the time, and in the reflector, the particle will be scattered most of the time. However, if it is scattered, it is necessary to determine the direction that it is scattered, which is specified by the scattering angles θ and φ (see Chapter 22). This then requires an additional step (step 4) to be performed.

23.3.4 Step 4: Determine the Direction That the Particle Exits the Collision

If the particle is scattered, then it is necessary to compute the azimuthal scattering angle φ and the polar scattering angle θ. This then determines the final direction of the particle for the next step. If the scattering is isotropic, then any azimuthal scattering angle φ is equally probable and the PDF for this process is

$$\text{PDF} = P(\varphi)d\varphi = \left(\frac{1}{2\pi}\right)d\varphi \tag{23.15}$$

The corresponding CDF is then

$$\text{CDF} = \int P(\varphi)d\varphi = \left(\frac{1}{2\pi}\right)\int d\varphi = \frac{\varphi}{2\pi} \tag{23.16}$$

where the integration is performed from 0 to φ. This equation may also be written as

$$\varphi = 2\pi RN \tag{23.17}$$

where the new random number RN is set equal to the CDF. Selecting a random number RN by performing the operation RN = RAN () then determines the value of φ (see Figure 23.8).

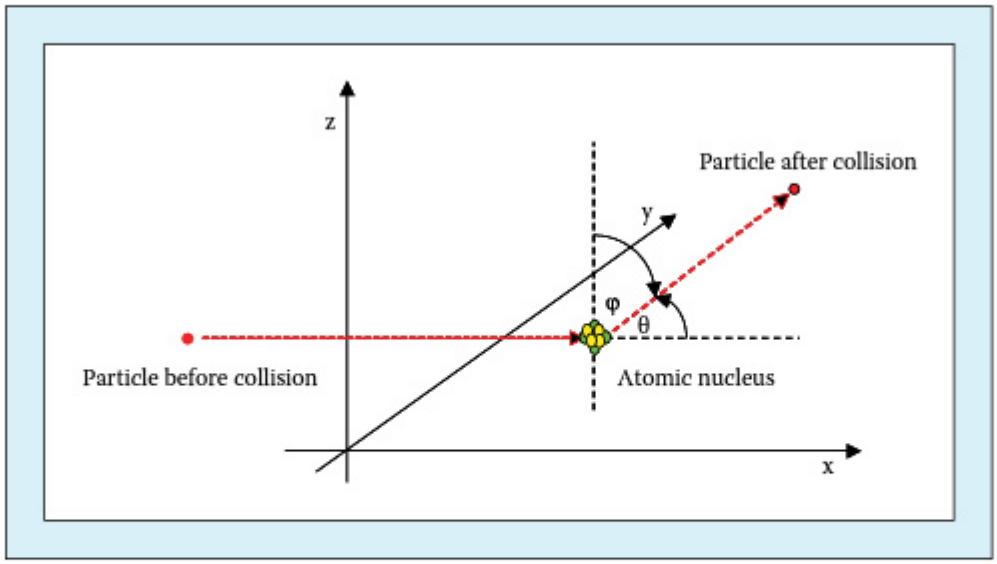

FIGURE 23.8 Visualizing the scattering angles used in a Monte Carlo calculation.

The process for determining the polar angle θ is similar. Only in this case, the probability of the particle being scattered into an angle dθ between θ and dθ is

$$P(\theta)d\theta = \frac{\sigma_s(\theta)\sin(\theta)d\theta}{\sigma_s} \tag{23.18}$$

where σ_s is the total scattering cross section defined by

$$\sigma_s = \int \sigma_s(\theta)\sin(\theta)d\theta \tag{23.19}$$

and the integration is performed over all polar angles from θ = 0 to 2π. In this case, the CDF is

$$\text{CDF} = C(\theta) = \int_0^{\theta} \frac{\sigma_s(\theta)\sin(\theta)d\theta}{\sigma_s} \tag{23.20}$$

A random number RN is then selected and set equal to the CDF, and the value of θ is determined by inverting this relationship and solving for θ. When the scattering is isotropic and $\sigma_s(\theta)$ is independent of θ, then the expression for the CDF becomes

$$\text{CDF} = C(\theta) = \sigma_s \int_0^{\theta} \frac{\sin(\theta)d\theta}{\sigma_s} \tag{23.21}$$

and since the integral of the sin is the cosine, we have

$$\text{RN} = \text{CDF} = C(\theta) = \frac{\cos(\theta) - 1}{2} \tag{23.22}$$

Notice that this reduces to

$$\theta = \arccos(1 - 2\text{RN}) \quad \text{for } 0 < \theta < \pi \tag{23.23}$$

Thus, the polar scattering angle θ can be determined in this way. The energy of the scattered particle E′ is found by applying the laws of elastic scattering to its initial energy E, and then conserving energy and momentum between the initial and final states. If the scattering collision is an elastic one, then the new particle energy (see Chapters 3 and 8) will be given by

$$E' = E\left[\frac{(1+\alpha)}{2} + \frac{(1-\alpha)\cdot\cos\theta}{2}\right] \quad \text{if the particle is a neutron} \tag{23.24}$$

$$E' = E\left[\frac{mc^2}{\left(mc^2 + E\left(1-\cos\theta\right)\right)}\right] \quad \text{if the particle is a photon} \tag{23.25}$$

Here, m is the mass of the electron, which may be velocity dependent, and α is again equal to $\alpha = (A-1)^2/(A+1)^2$ where A is the atomic weight of the target nucleus. Equation 23.25 is known as *Compton's equation*, and it describes a very common process called *Compton scattering*. The derivation of this equation is provided in our companion book,* and it explains how low- and medium-energy photons (such as X-rays) interact with the electron cloud surrounding the atomic nucleus. It is not always applicable to photons with energies above 1 MeV, where the process of *pair production* can also occur. In pair production, an electron and a positron are created when the original photon disappears.* In Equation 23.25, E is the initial energy of the incoming photon.

23.3.5 Step 5: Store the Case History for the Particle until It Is Destroyed or Leaves the System

Fifth, we must continue to follow the trajectory of a particle until it is either destroyed, or leaks out of the system entirely. In other words, if the particle has N interactions before it does either of these things, then we must store N values of the position, the angle, the energy, and the velocity of the particle. In three dimensions, this means that we must also store N values for θ and φ. In some cases, we may also wish to determine how much energy the particle deposits in a material medium as it moves. In the case of a neutron, this means that we must also calculate the *fractional energy loss* per collision ΔE and store this information at each interaction point. In the case of a photon, the photon may be either scattered or absorbed, and it may also cause additional photons to be emitted in the process. Therefore, we must also store the fractional energy loss ΔE_γ of each photon as it moves. Generally speaking, the fractional energy loss ΔE of a single photon or neutron is a negative number, but this is not always the case. For example, if the neutron is not absorbed and succeeds in slowing down to thermal energies (about 0.025 eV), then it may come into *thermal equilibrium* with its environment, and when it does so, there is roughly the same probability that its energy will increase as its energy will decrease. In this case, we must use the Maxwell–Boltzmann probability distribution

Maxwell–Boltzmann Probability Distribution

$$P(E) = \sqrt{\left\{\left(\frac{m}{\pi}\right)\left(\frac{2}{kT}\right)^3\right\}} E^{1/2} e^{-E/kT} \tag{23.26}$$

which we discussed in Chapter 8 as our guide.

23.3.6 Step 6: Repeat the Same Process for the Next Particle

Once we have successfully modelled the behavior of the first particle (including its possible offspring), then we can attempt to repeat this process for the next particle, using steps 1 to 5 as our guide. This process is illustrated in Figure 23.9. However, when we do so, we will find that we will get a slightly different result because of the statical nature of the simulation. Each time the "game" is played, the outcomes of the interactions are recorded in the computer's memory. Sometimes, they may also be stored in what is known as a *relational database* (such as Oracle, DB/2, or SQL Server). This process is repeated over and over again until eventually enough case histories are generated to predict the behavior of the particle population as a whole. The question then arises as to when the results of the simulation have converged. Answering this question is sometimes more difficult than performing the actual simulation itself. Naturally, this is the next topic we would like to discuss.

* See *Nuclear Engineering Fundamentals: A Practical Perspective*, by R.E. Masterson, CRC Press (2017).

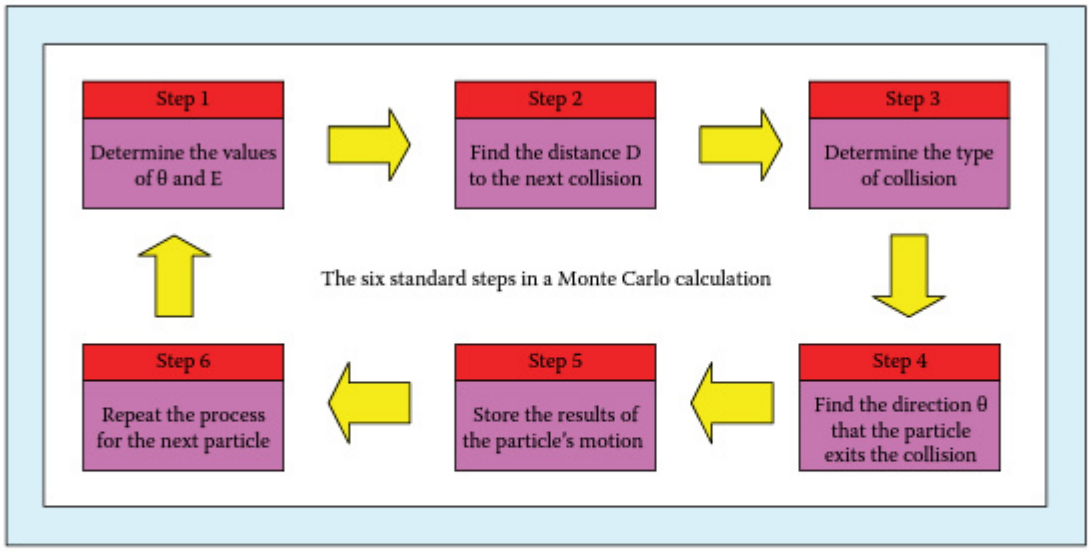
Step 1
Determine the values of θ and E
Step 2
Find the distance D to the next collision
Step 3
Determine the type of collision
The six standard steps in a Monte Carlo calculation
Step 4
Find the direction θ that the particle exits the collision
Step 5
Store the results of the particle's motion
Step 6
Repeat the process for the next particle

FIGURE 23.9 The six steps in a standard Monte Carlo calculation.

23.4 Pros and Cons of Monte Carlo Calculations

In our previous discussion, we tacitly assumed that the spatial distribution of the particles would eventually converge to a statistical distribution that does not change as additional case histories are performed. In this case, the simulation is assumed to be "converged." However, exactly when the simulation converges (and how accurate the results are) depends on how many case histories are stored. As we mentioned earlier, a large number of case histories have to be performed in order for the simulation to be an accurate one. Because the statistical fluctuations in the results only decrease as the *square root* of the number of case histories, more case histories will result in a more meaningful result than fewer ones. A statistical analysis is then needed to ascertain the accuracy of a Monte Carlo calculation after it is performed. The next few sections attempt to describe the various statistical methods that can be used to estimate the accuracy of a calculation.

23.5 Statistical Analysis Phase

When computers were first invented, it was initially believed that the cost of performing a Monte Carlo simulation would be so prohibitive that a Monte Carol method should be looked upon as only a *method of last resort*. The primary problem at the time was assessing the accuracy of the simulation. This is because the outcome of a Monte Carlo calculation is based on analyzing the behavior of a large number of very small particles. Therefore, unlike even simple solutions to the diffusion equation or the transport equation, the final result is not necessarily guaranteed to be a deterministic one. In other words, when we use a Monte Carlo method, all we can say is that the more simulations we are able to perform, the more accurate the results will be. Determining whether or not the final result has actually "converged" then becomes a philosophical question unless one has the tools to actually determine if it has.

For many applications, Monte Carlo calculations require thousands or even hundreds of thousands of case histories to obtain reasonably accurate results. This is especially true where nuclear systems are concerned. To obtain solutions with the same accuracy as a deterministic method, *several million* case histories may have to be performed. In the early days of the nuclear power industry, this task was viewed as being beyond the capabilities of even the most powerful computers of the time. However, today a simple desktop or laptop computer (or even the Apple *iPhone*) can perform these calculations in a reasonable period of time (see Figure 23.10). Consequently, Monte Carlo methods have come into vogue again, and the popularity of these methods has gradually increased as computers have become more powerful. In many cases, Monte Carlo methods have even surpassed transport methods as the methods of choice when a complex particle calculation is to be performed. This trend will probably continue for the foreseeable future because computers will continue to become more powerful and less expensive.

23.6 The Monte Carlo Method and Moore's Law of Computing

This increase in the processing power of modern computers can be attributed to an important trend in modern computing that has become known as *Moore's Law of Computing*. Moore's law asserts that the amount of processing power that is available for any purpose (such as performing a Monte Carlo calculation) will continue to double every

FIGURE 23.10 Today Monte Carlo calculations can be performed on a smart phone or an iPhone. These phones are also used to take beautiful pictures such as the picture of Yosemite Valley shown on the right. (Images of the iPhone and Yosemite Valley were provided by Apple Computer—see apple.com.)

2 years (or every 24 months)—essentially forever. Moore's law was originally attributed to *Gordon Moore*, the cofounder of Intel, whose picture is shown in Figure 23.11. However, since Moore's law was initially proposed in 1965, *the power of the average microprocessor has doubled every 18 months rather than every 2 years*. Moreover, according to most experts, this trend is expected to continue for the foreseeable future. Obviously, this implies that more case histories can be run in a shorter period of time to reduce the errors in a Monte Carlo calculation. We will

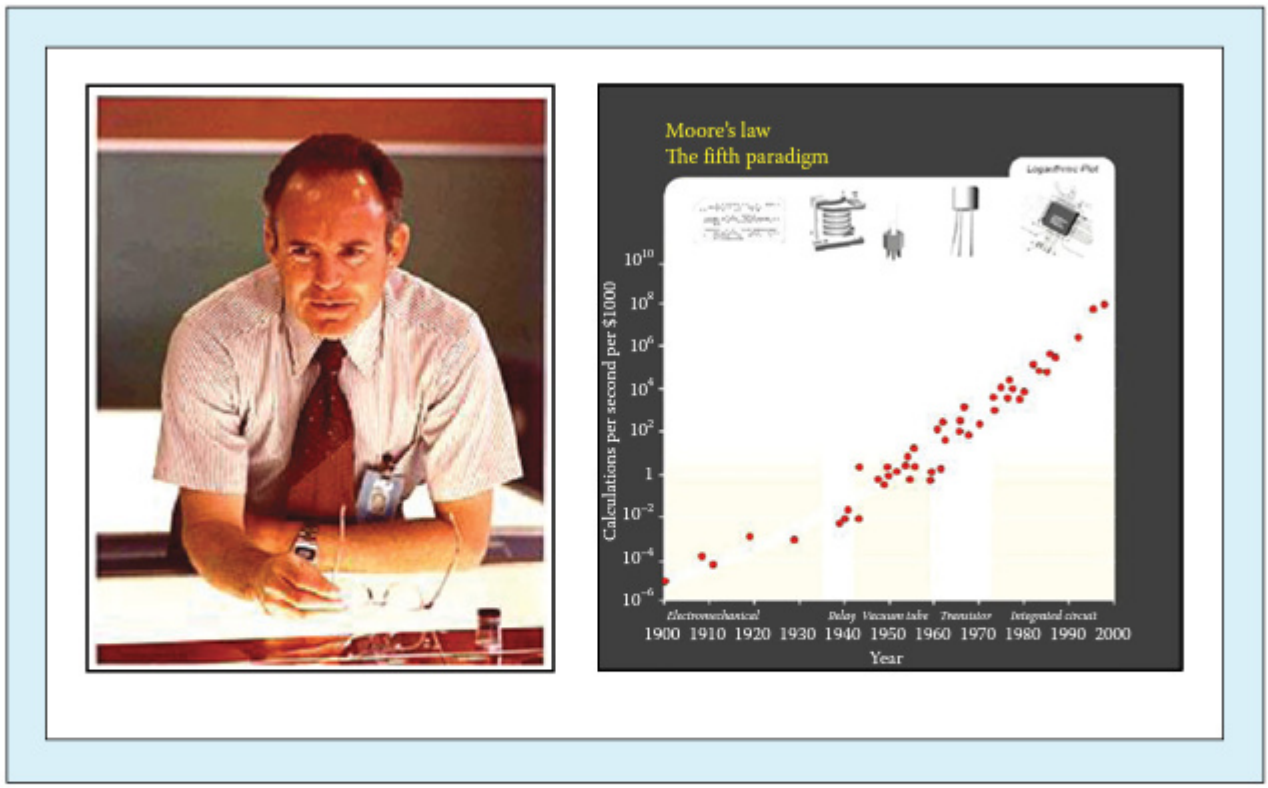

FIGURE 23.11 A picture of Gordon Moore, the cofounder of Intel, who originally proposed Moore's law of Computing in the mid 1960s. (Pictures provided by the Intel Corporation—see intel.com.)

now discuss exactly how these errors can be found. More information about Moore's law, its origins, and its history can be found at the following website:

http://en.wikipedia.org/wiki/Moores_law

The reader is encouraged to visit this site to learn more about the computing trends in the nuclear industry today.

23.7 Determining the Error in a Monte Carlo Calculation

To estimate the size of the errors in a Monte Carlo calculation, one first needs to understand how the errors in statistical probability distributions are measured. Constructing a set of case histories is only the first step in a Monte Carlo simulation. The second half of the simulation requires us to understand how accurate the results are, and what additional steps may be required to increase the accuracy of the simulation even further. In statistical analysis, a theorem called the *central limit theorem* is frequently used to estimate the accuracy of a Monte Carlo calculation. The central limit theorem applies to "*bell-shaped*" or *normal probability distributions*, but it can also be applied to other distributions if certain conditions are met. In a normal probability distribution (see Figure 23.12), an equal number of particles is typically distributed about an *average value* or *mean*. These distributions occur all of the time when one is dealing with large numbers of objects, and populations of human beings, car parts, and other manufactured items tend to follow a normal distribution when the number of participants becomes large. The *mean* $\langle v \rangle$ *or average value* of this distribution is defined by

$$\langle v \rangle = \frac{\sum_n v_n}{N} \tag{23.27}$$

where v_n is the value of the nth particle in the distribution and there are a total of N particles in all.

For the same distribution, we can also compute the *standard deviation* σ, which measures how much the value of a particular object deviates from the mean. The standard deviation σ for the nth particle in a probability distribution is therefore

$$\sigma_n = \left| v_n - \langle v \rangle \right| \tag{23.28}$$

which is always a positive number when a large number of particles is involved. The *variance* V is the value of the standard deviation squared, which can be expressed mathematically as

$$V = \sigma^2 = \left| v - \langle v \rangle \right|^2 \tag{23.29}$$

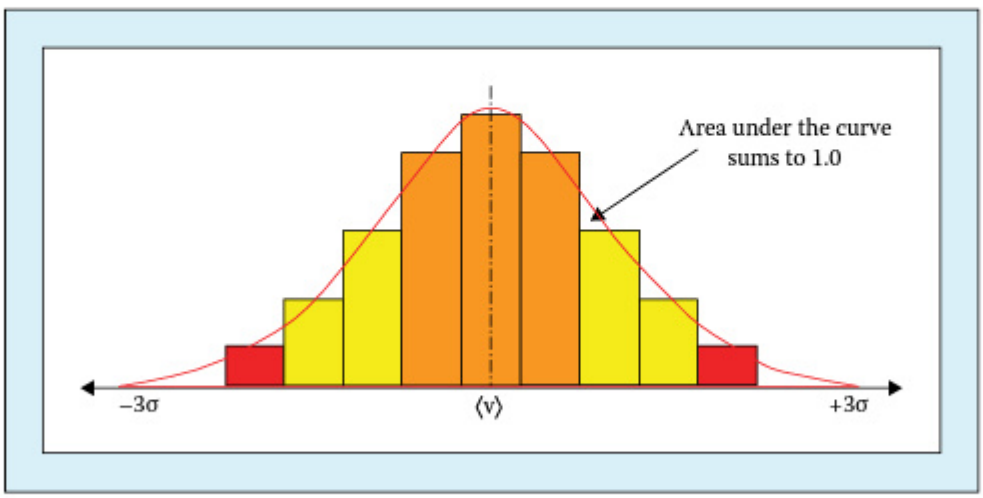

FIGURE 23.12 A normal particle distribution with some of its properties.

For a very large population of particles when all of the outcomes are equally possible, it can be shown that the variance V becomes equal to

$$V = \sum_{i=1 \text{ to } N} \frac{\left(v_i - \langle v \rangle\right)^2}{N} \tag{23.30}$$

or

$$V = \langle v^2 \rangle - \langle v \rangle^2 \tag{23.31}$$

In other words, *the variance V of a particle population is equal to the average of the squares less the square of the average*. In this context, the variance of the distribution provides a fairly accurate measure of how well the statistics have converged. Hence, a small variance means that a distribution is very well converged, and a large variance means that it is not. Using statistical theory, it can also be shown that the *fractional error* E associated with a given distribution of particles is given by

$$E = \sqrt{\left[\frac{1}{N} \cdot \frac{\left(\langle v^2 \rangle - \langle v \rangle^2\right)}{\langle v \rangle^2}\right]} \tag{23.32}$$

or

$$E = \sqrt{\left[\frac{1}{N} \cdot \frac{V}{\langle v \rangle^2}\right]} \tag{23.33}$$

where N is the number of particles in the sample. Thus, Equation 23.33 shows that, *the magnitude of the error E in a Monte Carlo calculation only decreases as* $1/\sqrt{N}$, multiplied by a constant of proportionality that is a function of the variance V, and this is the primary difficulty associated with using a Monte Carlo method to predict the shape of the flux in a real reactor. To reduce the error in the calculation of the flux by a factor of 10, we must increase the number of trials N by a factor of 100, and to reduce the error by a factor of 100, we must increase the number of trials by a factor of $(100)^2$ or 10,000. In other words, while the Monte Carlo method is a very flexible and powerful tool, literally millions of case histories must frequently be run to get an answer that is as accurate as a deterministic solution to the transport equation. Nevertheless, Monte Carlo methods are better suited than other methods for predicting the shape of the flux in complex geometries, and because of this, they have become increasingly popular as computers have become more powerful over the years.

Example Problem 23.4

A statistical probability distribution P(t) is to be constructed from the following nine data points, where t is the time: P(1) = 0, P(2) = 1.0, P(3) = 2.5, P(4) = 4.0, P(5) = 5.0, P(6) = 4.0, P(7) = 2.5, P(8) = 1.0, and P(9) = 0. Is this probability distribution symmetrical or asymmetrical? What is the average value or the mean value of the data points? What is the variance of the distribution and what is its standard deviation?

Solution The distribution is definitely symmetrical. The mean of the data points is $\langle v \rangle = \Sigma_n v_n/N = 2.222$. The variance V is equal to the average of the squares less the square of the average or $V = \langle v^2 \rangle - \langle v \rangle^2 = 7.944 - 4.937 = 3.007$. The standard deviation is the square root of the variance, so $\sigma = \sqrt{V} = 1.732$. [Ans.]

23.8 Error Reduction Schemes

Because of the accuracy issues with statistically based methods, a number of approaches have been devised to circumvent these difficulties and converge Monte Carlo calculations more quickly. We would now like to describe some of these methods in more detail. The problem with conventional Monte Carlo methods is that there is no way of knowing in advance, or a-priori, what simulations will lead to more accurate results than others. In other words, if all of the simulations are equally weighted, the only way to reduce the variance V and therefore the error E in the simulation is to run additional simulations so that the error will eventually decrease as N increases.

If something is known about the desired outcome in advance, it is sometimes possible to infer which statistics will be able to reduce the errors more quickly, and in the process, the number of case histories to be run. This process involves changing the *weights* that are assigned to individual events in the hope that the solution will converge more rapidly. In some textbooks, the process of reducing the expected error in a Monte Carlo calculation, which is measured by the variance V, is called *variance reduction.* In any event, there are several ways to reduce the variance in practice, and we would now like to describe some of them in more detail.

Importance sampling is perhaps the most common way to reduce the variance of a statistically based method. In essence, the idea of importance sampling is to modify the simulation so that the variance V is reduced by selecting the results from a distribution other than the one that the problem suggests. For example, in radiation shielding calculations, most neutrons produced in the core head toward the reflector, while others will stream randomly back into the core and are absorbed. See Figure 23.13 for a schematic representation of how this occurs. The ones that head back into the core will have little, if any, effect on the ones that make it through the reflector. Hence, if we can eliminate the inward-directed neutrons from the statistical sample more quickly, less computer time will be spent tracking those neutrons, and more computer time will be spent on the neutrons that actually make it through the shield. In other words, the initial trajectory of a neutron is one way to infer the effect it will have on the final solution, and this is one way in which the "importance" of the neutron's contribution can be assessed. If a neutron is moving away from the reflector, we can "adjust" its absorption cross section $\Sigma_a(E)$ from its initial value (say 0.10 per centimeter) to a much higher value (like 0.90 per centimeter).

This simple act is equivalent to changing the rules of the game so that the neutrons heading back into the core are absorbed more quickly than they would otherwise be. Therefore, their case histories take less time to compute. In practice, prescriptions such as this can cut the computer time in half because much less time is wasted on neutrons that do not contribute significantly to the final result. This is clearly an example of a situation where the "weights" that are assigned to the various events are in some way associated with the outcome we wish to achieve. From a holistic perspective, this act is equivalent to changing the rules of the game so that only the fittest survive, and those who do not meet the desired criteria are removed from the game as quickly as possible. In other words, this is how the process of "*natural selection*" is implemented in a computer program. Anyone who has been to *Las Vegas* has probably tried their hand at *blackjack* at one time or another. In the game of blackjack, the concept of "doubling down" is sometimes used when the odds favor the person who is playing against the house. In a Monte Carlo simulation, a similar technique called *splitting* can also be used to increase the odds of winning the game—or at least converging it to its desired result more quickly. In this approach, a successful case history is used to generate additional case histories in order to increase the odds that the solution will converge more quickly.

For example, if we discover in a radiation shielding calculation that a particle is headed in a favorable direction (i.e., toward the outer boundary of the core), then it is replaced by n particles each having a weight of 1/n, and the individual

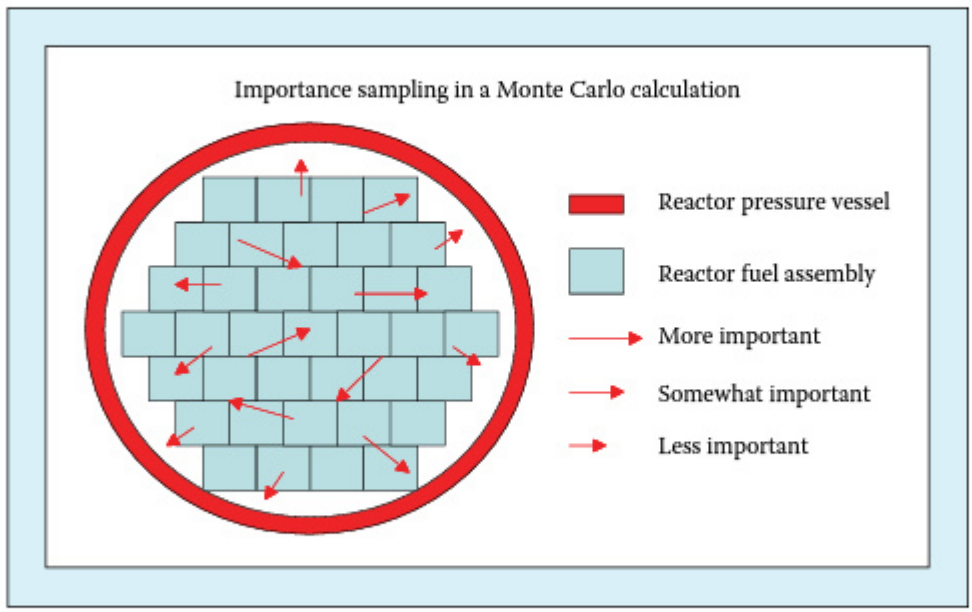

FIGURE 23.13 How the importance of various particle histories in a Monte Carlo calculation changes as a function of their position in the core.

case histories of each of these particles are followed instead. The net result of splitting the particle into several equivalent particles is that more "weight" can be assigned to successful particles than unsuccessful ones. Hence, the game is "won" more quickly, and the player does not have to spend the whole night at the blackjack table in order to get a return on his investment. The two schemes we have just described—*importance sampling* and *splitting*—are both examples of ways that a Monte Carlo program can be made to converge more quickly by introducing additional intelligence into the rules. However, instead of increasing the number of simulations N, these methods attempt to reduce the variance V with a smaller number of simulations. There are many other ways of "weighting" the case histories to reduce the variance, and additional information about how to implement them can be found in the references at the end of the chapter. Hence, when computer time is at a premium, a combination of these methods can be used to accelerate the convergence of a Monte Carlo calculation.

Next, we would like to review some of the other properties of "normal" or bell-shaped distributions. These properties can also be used to one's advantage in a Monte Carlo calculation if one is aware of how they work. In probability and statistics, a *normal probability distribution* or a *Gaussian probability distribution* is defined as one that has a shape, which approaches a statistical distribution of the form

$$p(x) = \frac{1}{\sqrt{(2\pi\sigma^2)e^{-x}}} \tag{23.34}$$

where $x = (v - \langle v \rangle)^2/2\pi\sigma^2$, *$\langle v \rangle$ is the mean of the particle distribution, or the average value of some property that all of the particles in the distribution possess, and V is the variance of the distribution*, which we previously defined as

$$V = \sigma^2 = \left| v - \langle v \rangle \right|^2 \tag{23.35}$$

These equations can be used to determine how "close" or "far away" a statistical sample of particles is from a truly random distribution. The factor $1/\sqrt{2\pi V}$ is used to ensure that the total area under the curve of P(x) is normalized to one. In other words, it is a *scaling factor* used to ensure that the distribution is properly "normalized" so that the sum of all the possible outcomes adds up to 100%. In addition to the probability distribution itself, there are several other "rules" that normal probability distributions obey. These rules can be used to interpret how accurate a Monte Carlo calculation can become. In a normal probability distribution, about 67% of the values will fall within one standard deviation of the mean ($\langle v \rangle \pm \sigma$), about 95% of the values will fall within two standard deviations of the mean, ($\langle v \rangle \pm 2\sigma$), and about 99.7% will fall within three standard deviations ($\langle v \rangle \pm 3\sigma$) of the mean. This particular behavior of the distribution is also known as the *67-95-99.7 rule*, and the 67-95-99.7 rule is frequently used to determine when a particular attribute—like a particle's speed v—is average, above average, or way above average. (It can also be used to characterize a college student's grades.)

Figure 23.14 shows some of the salient features of a normal probability distribution. The two points on the curve that are one standard deviation from the mean are also called the *inflection points* of the distribution. This fact can be particularly useful when it is important to know how many points are expected to lie inside or outside of a symmetric interval $I = (-n\sigma, n\sigma)$ for various values of n. In other words, these numbers can be used to understand when all of the events in the distribution are statistically independent of each other, and when they are not. Table 23.1 shows the percentage of the values that lie inside and outside of the distribution for different values of the standard deviation σ. Note in particular that only one particle in 15,000 will lie more than 4 standard deviations beyond the midpoint of the distribution, and only one particle in 1.7 million will lie more than 5 standard deviations from the mean. Thus, if a much larger number of particles falls into either of these categories or "bins," it implies that not all of the particle histories may be statistically independent, and there is something else that is occurring to alter the data. Hence, this is another way to determine if the particle population does not obey a normal probability distribution even when it is initially believed to do so.

Example Problem 23.5

Suppose that the behavior of a nuclear particle is governed by a normal probability distribution in which the mean (or average) value of the energy in the distribution is 0.5 MeV and the energy of the particle in question is 1.0 MeV. Calculate the standard deviation and the variance of the energy of the particle from the mean. If the distribution contains 1 million particles, and the variance of the entire distribution is 0.25 MeV, estimate the value of the fractional error E that a Monte Carlo calculation would have if it were applied to this distribution.

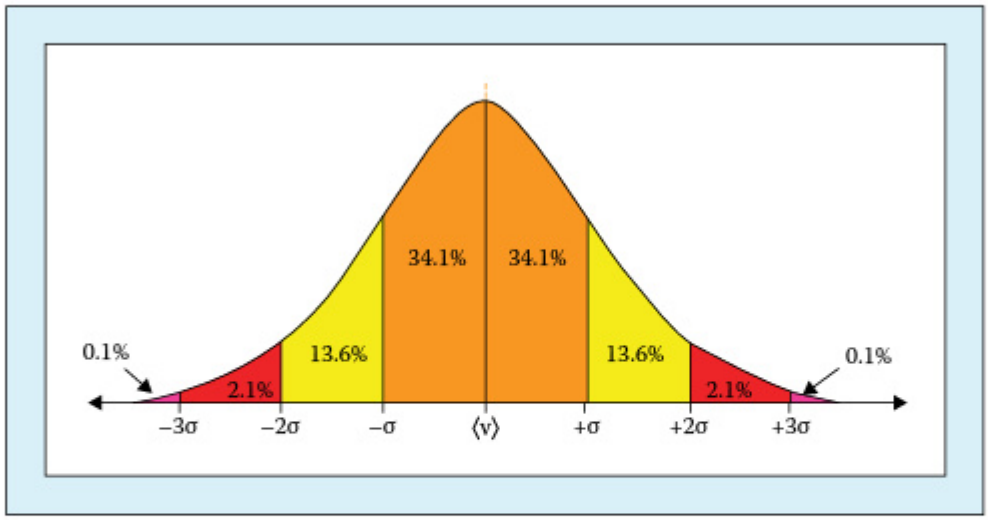

FIGURE 23.14 The distribution of probabilities as a function of the number of standard deviations σ in a normal probability distribution.

TABLE 23.1
Probability of Occurrence as a Function of the Number of Standard Deviations for a Normal Probability Distribution

σ	Percentage within a Given Interval (%)	Percentage outside of a Given Interval (%)
0.674490σ	50	50
0.994458σ	68	32
1σ	68.2689492	22.7310508
1.281552σ	80	20
1.644854σ	90	10
1.959964σ	95	5
2σ	95.4499736	4.5500264
2.575829σ	99	1
3σ	99.7300204	0.2699796
3.290527σ	99.9	0.1
3.890592σ	99.99	0.01
4σ	99.993666	0.006334
4.417173σ	99.999	0.001
4.891638σ	99.9999	0.0001
5σ	99.9999426697	0.0000573303
5.326724σ	99.99999	0.00001
5.730729σ	99.999999	0.000001
6σ	99.9999998027	0.0000001973
6.109410σ	99.9999999	0.0000001
6.466951σ	99.99999999	0.00000001
6.806502σ	99.999999999	0.000000001
7σ	99.9999999997440	0.0000000002560

Source: Wikipedia with permission—see *https://en.wikipedia.org/wiki/Normal_distribution.*

Solution The standard deviation of the particle is given by $\sigma = |v - \langle v\rangle| = |1.0 - 0.50| = 0.50$ MeV. The variance V of the energy of the particle is the standard deviation squared or $V = \sigma^2 = |v - \langle v\rangle|^2 = 0.25$ MeV. The fractional error E in a Monte Carlo calculation that uses this distribution is given by $E = \sqrt{\left[(1/N)\cdot V/\langle v\rangle^2\right]}$. In this case, N = 1,000,000, V = 0.25 MeV, and $\langle v\rangle = 0.50$ MeV, so E = 0.001 = 0.1%. [Ans.]

23.9 Computer Programs That Implement the Monte Carlo Method

Many computer programs have been written over the years to simulate the problem of particle transport in nuclear power plants. Many of these programs use the Monte Carlo method to track the flow of neutrons or photons through the core. The same programs can also be used to design *radiation shields*. These computer programs (or *computer codes* as they are sometimes called) are provided free to universities, reactor vendors and operators, nuclear utilities, and nonprofit organizations by different government agencies. For example, in the United States, they can be obtained from the Radiation Safety Information Computational Center (or *RSIIC*), which is located in Oak Ridge, Tennessee. The website for this important resource is

http://www-rsicc.ornl.gov/

and within this web page, one can find a collection of computer codes for performing radiation transport calculations. Some of the Monte Carlo programs the center provides are shown in Table 23.2. Some of the more popular and widely used of these codes include *SANDYL, KENO, MORSE, and COHORT*.

1. SANDYL was developed at the Sandia National Laboratory, and it can be used to calculate Photon–Electron Transport problems in complex reactor geometries.
2. KENO is a Monte Carlo code system for criticality and safety analysis. It can be obtained from the Japan Atomic Energy Research Institute, or from the RSIIC directly.
3. MORSE is shorthand for the Multigroup Oak Ridge Stochastic Experiment, and it is a general-purpose Monte Carlo multigroup neutron and gamma ray transport computer code.
4. COHORT is an integrated system of computer programs that can be applied to many radiation analysis and shielding problems, ranging from simple point source/infinite air scattering to complex three-dimensional Monte Carlo calculations. It was developed by NASA and the Aerojet Nuclear Corporation.

Most of these programs were originally intended to run on IBM mainframes because they were the only computers available that had enough processing power to actually perform the calculations. However, many of them have been subsequently ported to the *Windows operating system* and can now be run on *UNIX workstations* or even *personal computers*. (Recently, a Monte Carlo program has also been ported to the *iPhone*.) In Europe, and in most of the rest of the world, the International Atomic Energy Agency (IAEA) and the European Nuclear Society provide a similar set of services. You can read more about these services at the following URLs:

www.iaea.org
www.euronuclear.org

A modern example of a sophisticated Monte Carlo program is *the Serpent code*, which has also been the topic of several PhD theses. This program is used to calculate the flow of neutrons or photons in complex reactor geometries, such as the geometries shown in Figure 23.15. Monte Carlo methods are appropriate to use when the shape of the neutron flux needs to be found in the vicinity of strong neutron absorbers such as control rods. In addition to these publicly available programs, other Monte Carlo programs have been written and implemented in the commercial sector. The source code for these programs is usually subject to some type of licensing agreement (and it may even be subject to *export control laws*), but reasonably complex Monte Carlo programs with free source code are now commonly available on the Internet.

Figure 23.16 shows a random number generator used to implement a PDF that can be specified by the user. This particular piece of source code can be found at the following URL:

www.daniweb.com/software-development/c/code/216329

Random number generators for the *Linux operating system* were first implemented in the Linux kernel in the early 1990s. Since then, virtually all computer operating systems (*UNIX*, *Windows*, etc.) have provided some version of a random number generator as part of their basic package. FreeBSD (another version of *UNIX* that is based on the *Berkeley operating system*) also provides support for hardware random number generators, which are essentially random number generators programmed onto a computer chip. These random number generators are used when very complex or high-speed calculations need to be performed. They are also used in slot machines because they are difficult to tamper with.

It is easy to see that the real power of the Monte Carlo method lies in its ability to represent and study physical phenomena that would otherwise be difficult to simulate because of geometric complexity. This is especially true when simulating boundary conditions for very complex geometric shapes. The second major advantage of a Monte Carlo method is its ability to solve a large number of problems without having to change the basic computational paradigm. In other

TABLE 23.2
Popular Monte Carlo Codes in Use Today

Monte Carlo Program	Author or Development Organization	Computer Language	Purpose
COHORT	Aerojet Nuclear, Sacramento, California	FORTRAN IV; IBM 360/370 (A) or UNIVAC 1108 (B)	ACOH is part of an integrated system of computer programs that can be applied to many radiation analysis and shielding problems, ranging from simple point source/infinite air scattering to complex 3-dimensional Monte Carlo analyses.
AIRTRANS	United Nuclear Corporation, Elmsford, New York	FORTRAN IV; IBM 360/75/91	AIRTRANS calculates the radiation field produced by neutron and/or gamma ray sources, which are located in the atmosphere using a Monte Carlo method.
ALBEMO	INTERATOM Bensberg, Federal Republic of Germany	FORTRAN IV; CDC 6400/6600	ALBEMO calculates the transport of particles (neutrons or gamma rays) through cavities such as multiple bent pipe ducts or the distribution of particles within empty spaces of large volume.
CASCADE	ERDA Health and Safety Laboratory, New York, New York	FORTRAN IV; CDC 6600	The CASCADE code uses a Monte Carlo method to calculate the transport of high energy electrons and photons in matter.
CAVEAT	Teledyne Brown Engineering and NASA at the George C. Marshall Space Flight Center, Huntsville, Alabama	FORTRAN IV and Assembler language; IBM 360	Caveat is a general-purpose time-dependent Monte Carlo transport code for complex geometries. It is based on an early version of COHORT developed by Radiation Research Associates (RRA) for NASA.
COHORT-II	NASA Lewis Research Center, Cleveland, Ohio	FORTRAN IV; IBM 7094	COHORT-II is a general-purpose Monte Carlo and radiation transport code system, which tracks neutrons and photons through flexible shield geometry configurations.
ELF	Shielding Laboratory, CEA/CEN/Fontenay-aux-Roses Nuclear Research Center, now located at CEA/CEN/Saclay, France	FORTRAN IV; IBM 360	A Monte Carlo and neutron transport code system for cylinders and spheres.
ESP	Oak Ridge National Laboratory, Oak Ridge, Tennessee	FORTRAN IV and Assembler language; IBM 360/370	ESP is a general-purpose Monte Carlo reactor analysis code system.
KAMCCO	Institute for Neutron Physics and Reactor Technology, Karlsruhe, Federal Republic of Germany	Fortran IV, Assembler language; IBM 370	KAMCCO is a three-dimensional time-dependent Monte Carlo code system for fast neutron physics problems.
MORSE	University of Birmingham, Birmingham, England	Fortran IV, Assembler language; IBM 370/3033	MORSE is a general-purpose Monte Carlo multigroup neutron and gamma ray transport code system.
KENO	Japan Atomic Energy Research Institute, Ibaraki-Ken, Japan	Fortran IV; FACOM-M380	MULTI-KENO2 is a Monte Carlo code system for criticality and safety analysis.

(*Continued*)

TABLE 23.2 (*Continued*)
Popular Monte Carlo Codes in Use Today

Monte Carlo Program	Author or Development Organization	Computer Language	Purpose
MVP	Japan Atomic Energy Agency, Tokai-mura, Naka-gun, Ibaraki, Japan	Fortran 77, Windows PC (C00739MNYCP00). NEADB distributes as NEA-1673/01 (Windows) and NEA-1673/02 (UNIX/LINUX)	MVP is a general-purpose Monte Carlo code system for neutron and photon transport calculations based on continuous energy and multigroup methods.
PTRAN	National Institute of Standards (NIST), Gaithersburg, Maryland	Fortran 77; PC 386	PTRAN is a proton Monte Carlo transport program for the PC.
RAID	General Dynamics, Fort Worth, Texas	FORTRAN IV; IBM 7090 and 7094	RAID is a Monte Carlo multibend duct shielding code.
SANDYL	Sandia National Laboratories, Livermore, California	Fortran IV; CDC	SANDYL is a three-dimensional Monte Carlo code system for calculating combined photon–electron transport in complex geometries.
TRIPOS	University of California, Los Angeles, California	Fortran 77, Cray	TRIPOS is a Monte Carlo ion transport analysis code.
VESTA	Institut de Radioprotection et de Sureté Nucléaire, Cedex, France	C/C++, XML, X86 (C000769MNYWS00)	VESTA is a Monte Carlo transport program that can be interfaced with different point depletion codes to select specific reactions and/or decay modes to be used in the depletion calculation.

Source: Radiation Safety Information Computational Center.

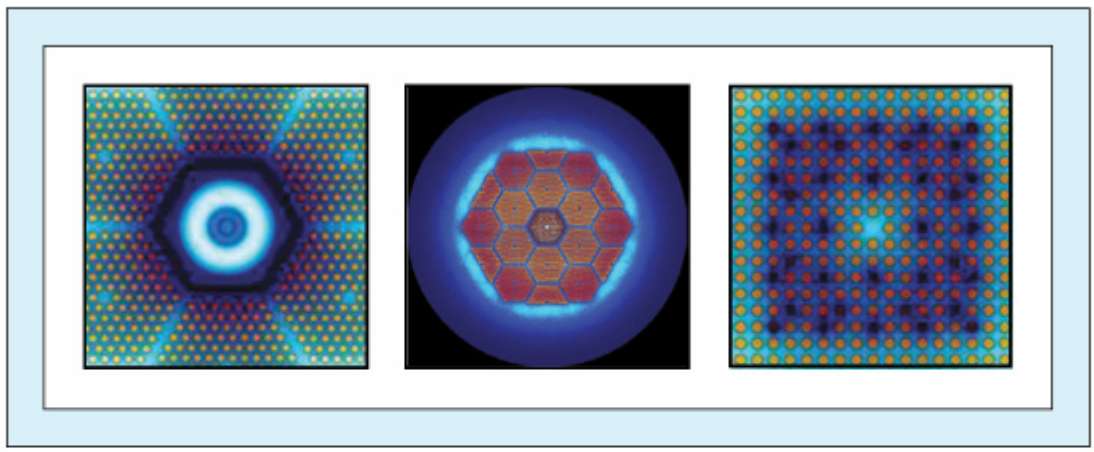

FIGURE 23.15 Examples of reactor geometries with strong neutron absorbers where a Monte Carlo method should be used. (Pictures provided by Wikipedia—see our previous discussion of the Serpent code.)

words, it can be used to solve problems in economic theory, population planning, the allocation of critical resources, war games, and even turbulent or laminar particle flow.

We simply have to define the relevant events that each particle must experience, assign probabilities to these events, and then record the case histories as they evolve. In other words, to adopt a Monte Carlo method to an entirely different system, only the "rules of the game" have to be changed. Finally, Monte Carlo methods have the ability to provide meaningful results with any level of detail that is required. All the user has to do is to record and analyze the pertinent events. Of course, this tremendous flexibility does not come without a price. Monte Carlo methods normally require

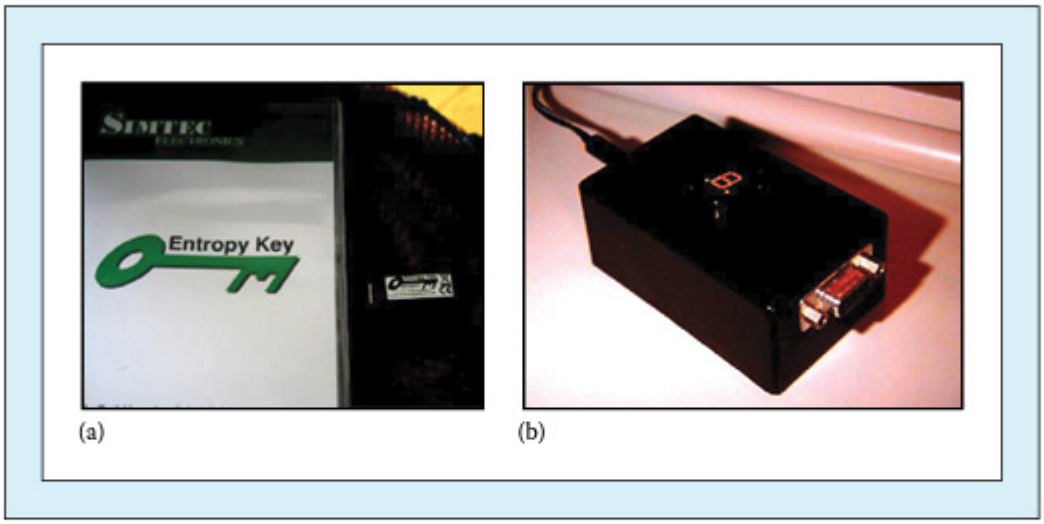

FIGURE 23.16 (a) A picture of a USB Random Number Generator on a Computer Chip from *www.daniweb.com* and (b) A device that can be connected to a personal computer with a parallel port to generate an arbitrary sequence of random numbers. (Pictures provided by MIT.)

large amounts of computer time in order to obtain reliable results. Nevertheless, in complex reactor geometries, such as the ones shown in Figure 23.15, they are the only practical to find the particle flow when more deterministic methods fail. We would now like to provide some additional examples of how the Monte Carlo method works.

23.10 Monte Carlo Calculation of the Fast Fission Factor

Not surprisingly, the Monte Carlo method can be used to determine the value of the fast fission factor that appears in the famous *four-factor formula*. It can also be used to determine the value of the thermal utilization because it allows us to find how many neutrons are absorbed in the fuel relative to an entire cell as a whole. Before demonstrating how a Monte Carlo method can be adapted to find these parameters, we would first like to review the four-factor formula and discuss what each of its terms mean.

As we saw in Chapter 9, the *four-factor formula* is a semi-empirical formula that is often used to predict the value of the infinite multiplication factor k_∞ for a large reactor lattice. *It is applicable to thermal reactors, but not fast reactors.* When the effects of neutron leakage can be neglected, it can be used to determine when a reactor lattice will become critical and when it will not. The standard form of the four-factor formula is

$$k_\infty = \eta \varepsilon f p \tag{23.36}$$

and it consists of four terms that are called η, ε, f, and p. Here, η is referred to as the "eta" of the fuel, and physically, it represents the number of neutrons produced per neutron absorbed in the fuel. Next, f is the thermal utilization of the fuel, and it represents the probability that a thermal neutron will be absorbed in the fuel (and not in the moderator or the cladding).

Third, p is the resonance escape probability, which represents the probability that a neutron will escape capture in one of the absorption resonances above the thermal energy range. Finally, ε is called the fast fission factor, and it represents the ratio of the neutron production rate at *all energies* to the neutron production rate at thermal energies alone. With these definitions in mind, let us discuss how we can calculate the fast fission factor ε for the fuel rods shown in Figure 23.17. The fuel rods in this simulation consist of a mixture of U-235 and U-238 atoms with an average enrichment of 3%. Hence, the number of U-235 atoms and U-238 atoms per unit volume (N^{235} and N^{238}) are assumed to be known. The fuel rods are surrounded by a moderator (which in this case is water) with an atomic density of N^{mod} atoms per cubic centimeter. Standard symbols will be also used for the macroscopic cross sections for fission, capture, absorption, and scattering. Again the value of the thermal flux in the fuel is denoted by the symbol ϕ_2^{fuel} and the value of the fast flux in the fuel is denoted by the symbol ϕ_1^{fuel}. Hence, the fast neutrons belong to energy group 1 and the thermal neutrons belong to energy group 2.

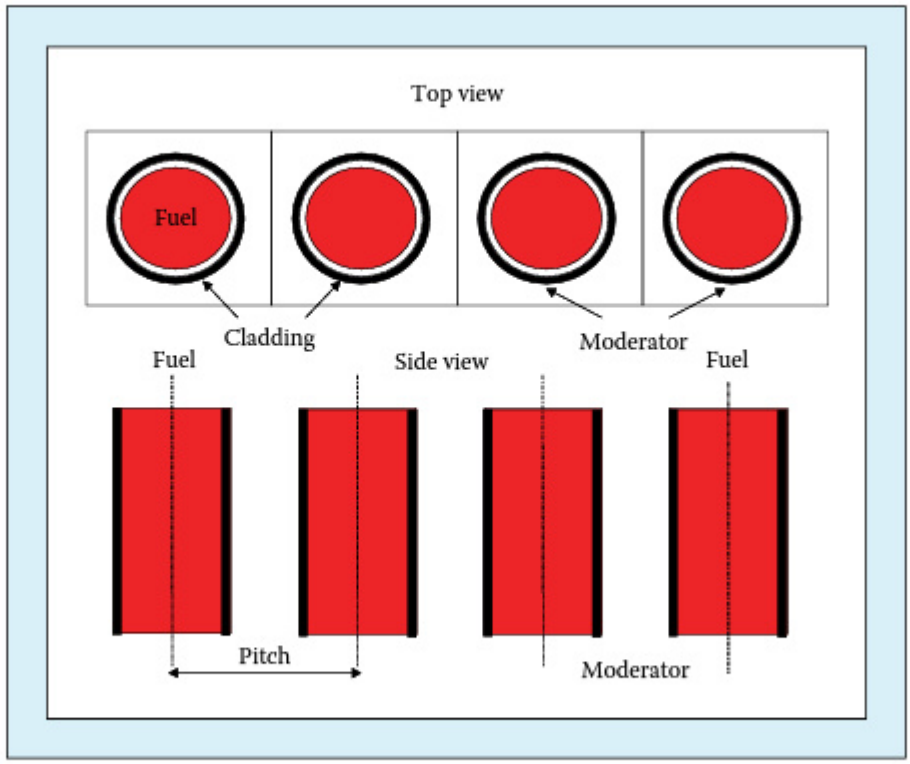

FIGURE 23.17 An array of fuel rods and unit cells that can be used in a Monte Carlo calculation.

If the total number of neutrons produced from thermal fission of the fuel is N and an additional ΔN neutrons are produced by fast fissions in the fuel, then the calculation of the fast fissions factor requires us to find the ratio

$$\varepsilon = \frac{N + \Delta N}{N} = 1 + \Delta N/N \tag{23.37}$$

Of course, this expression is consistent with the definition of the fast fission factor that we first introduced to the reader in Chapter 9. In thermal water reactors, ε has a value between 1.02 and 1.08. Now let us see if we can calculate the values of N and ΔN for the typical unit cells shown in Figure 23.17. The value of N may be found if the shape of the thermal flux $\phi_2^{\text{fuel}}(r)$ is known. This shape can be found using any of the methods we discussed in earlier chapters. Then the value of N will be given by $N = \nu \int \phi_2^{\text{fuel}}(r) \Sigma_{f2}\, dr$, where ν is the average number of neutrons released from the thermal fission of U-235, and in general, the average value of ν is about 2.4. However, for our simulation, we must account for the fact that two neutrons are created in most fissions, and a third one is created about 2.5 − 2/2.5 = 20% of the time. In other words, if the random number generator generates a random number RN, a third neutron will be made if RN < 0.20; otherwise only two neutrons will be created for the Monte Carlo simulation.

The second step involved in finding the fast fission factor requires us to calculate how many neutrons are absorbed by the U-235 atoms (which lead to the term $N = \nu \int \phi_2^{\text{fuel}}(r) \Sigma_{f2}\, dr$), and how many neutrons are absorbed by the U-238 atoms (which lead to the term ΔN). It is important to make this distinction because Uranium-238 atoms only fission at kinetic energies greater than or equal to about 1 MeV. Thus, the value of ΔN is given primarily by $\Delta N = \nu \int \phi_1^{\text{fuel}}(r) \Sigma_{f1}\, dr$, and the fast fission cross section Σ_{f1} is primarily due to the Uranium-238 atoms in the unit cells. Hence, when the fission neutrons are initially produced, we must decide whether their initial energy E is greater than 1 MeV or less than 1 MeV. Each of these two events has a specific probability associated with them that we will call P_F. Then the following equalities apply:

$$\text{If } RN < P_F \quad \text{A thermal fission will occur} \tag{23.38}$$

$$\text{If } RN \geq P_F \quad \text{A fast fission may occur} \tag{23.39}$$

In the second case, notice that having RN ≥ P_F does not necessarily imply that a fast fission will occur. This is because a high energy neutron can be scattered first and then be removed from the fast neutron energy group before a Uranium-238 nucleus has a chance to absorb it. However, the neutron can continue to be followed until it either leaks out of the fuel rod or until it is absorbed. Therefore, the final step in this process is to determine when the fission neutrons leave the fuel rod and when they do not.

To estimate when this occurs, we must calculate the *mean free path* λ between successive collisions and then follow the same methodology we developed earlier to see if the neutron crosses the fuel/moderator boundary. If the total macroscopic cross section is $\Sigma_t(E)$, then it can be shown that the probability of a collision occurring in a distance dL located n mean free paths from the current position of the neutron with no other collisions is given by

$$P(n)dL = e^{-n\Sigma_t(E)}\Sigma_t\, dL \tag{23.40}$$

The number of mean free paths a neutron travels before it "hits" something is then decided by identifying the CDF with a random number, in which case n is given by

$$n = \frac{-1}{\Sigma_t \ln(RN/100)} \tag{23.41}$$

where RN = RAN () is a random number between 0 and 100. The distance to the nearest boundary must then be determined. If the path takes the neutron outside of the radius vector defined by $r = \sqrt{(x^2 + y^2)}$ (see Figure 23.18), then it is considered to enter the moderator, and since the energy is quickly reduced in successive elastic collisions, any further contribution to ΔN can be ignored. However, the neutron may still reenter the fuel and cause another thermal fission to occur. However, this will contribute only to N and not to ΔN because the kinetic energy is too low. Eventually, enough case histories can be accumulated to achieve a relatively stable value for ΔN/N. Because the values of the cross sections for Uranium-235 and Uranium-238 are so different, the value of the fast fission factor is a function of the enrichment of the fuel inside of the rod. A software program used to create the random number in this case is shown in Figure 23.19.

Higher values of the enrichment will generally result in lower values of the fast fission factor ε than higher ones. This is because the majority of the fast fissions occur in U-238 and not U-235. It should also be evident that many case histories

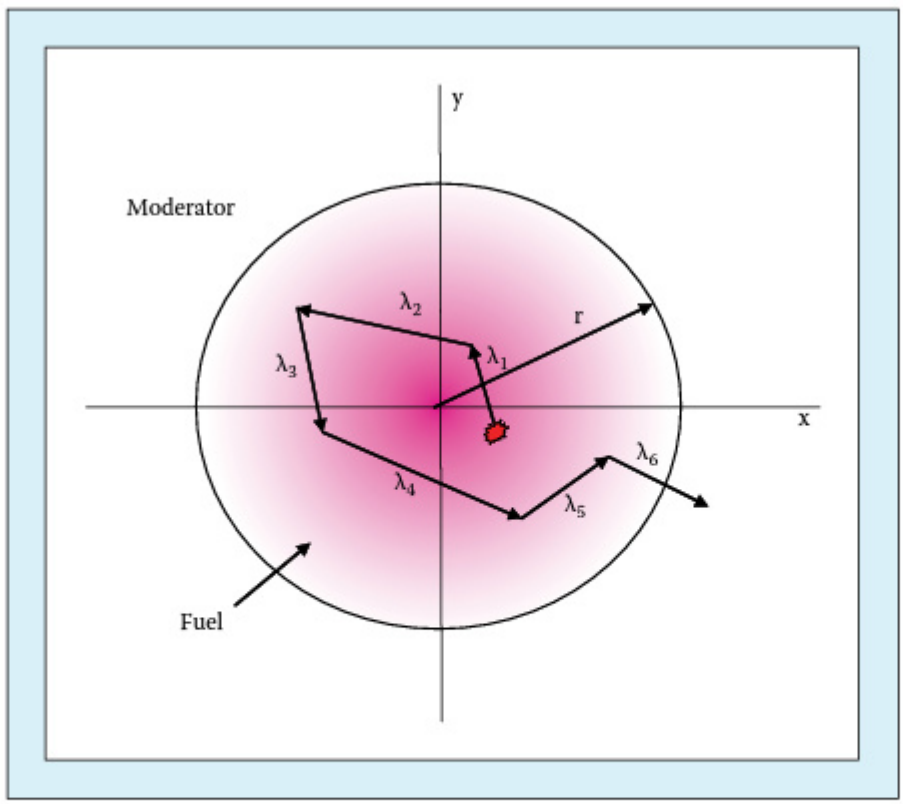

FIGURE 23.18 Using the neutron mean free path and the radius vector to determine whether a neutron is in the fuel or the moderator.

C Code Snippet

```c
// An example of three simple random number generators
// Written in Turbo C and modified for conventional C

#include <stdio.h>   // printf(), getchar(), puts()

// three different custom random number generators

int ran1(int lim);
int ran2(int lim);
int ran3(int lim);

int main(void)
{
        int  k, random1, random2, random3, sum1, sum2, sum3;

        sum1 = sum2 = sum3 = 0;
        puts("Random numbers between 1 and 44:\n");
        printf("%15s%10s %10s %10s","Functions
    ","random1()","random2()","random3()");
        for (k = 0; k < 40; k++) {
                random1 = ran1(44);   // method one
                random2 = ran2(44);   // method two
                random3 = ran3(44);   // method three
                printf("\n%25d %10d %10d",random1,random2,random3);
                sum1 += random1;
                sum2 += random2;
                sum3 += random3;
        }
        printf("\n\n%15s%10d %10d %10d   (ideal 22)\n",
        "   Average:",sum1/k,sum2/k,sum3/k);
        getchar();  // wait
        return 0;
}
//
// returns random integer from 1 to lim (random number generator #1)
//
int ran1(int lim)
{
        static long a = 100001;

        a = (a * 125)% 2796203;
        return ((a % lim)+ 1);
}
//
// returns random integer from 1 to lim (random number generator #2)
//
int ran2(int lim)
{
        static long a = 1;  // could be made the seed value

        a = (a * 32719 + 3) % 32749;
        return ((a % lim) + 1);
}
//
// returns random integer from 1 to lim (random number generator #3)
//
int ran3(int lim)
{
        static long a = 3;

        a = (((a * 214013L + 2531011L)>> 16)& 32767);

        return ((a % lim)+ 1);
}
```

FIGURE 23.19 A program for a random number generator that is used in a Monte Carlo calculation. Notice that three very simple random number generators are provided in this example. In commercial software packages, much more complex algorithms are used to generate random numbers than the ones shown above. Also, in some cases, random number generators are programmed onto computer chips (see Figure 23.16).

must be recorded in order to obtain an accurate value for the fast fission factor because the number of fast fissions ΔN is very small, and the value of $\Delta N/N$ is only on the order of a few percent. In simulations like this, a large variance V generally occurs. Therefore, variance reduction methods are sometimes used to accelerate the rate of convergence. Some type of *importance weighting* may also be used to reduce the size of V. Refer to Section 23.7 for a more detailed discussion of how importance weighting works.

23.11 Dealing with a Cylindrical Geometry in a Monte Carlo Simulation

While there is nothing wrong with what we have done, the overall approach is not computationally efficient, and one has to constantly determine if the neutron is in the moderator or in the fuel. A simpler way to approach this problem is to keep track of the x, y, and z coordinates of the neutron even though all the rest of the calculations are done in cylindrical coordinates (see Figure 23.20). For example, suppose that the center of the fuel rod is located at $r = 0$ and the outer surface of the fuel is located at $r = R_F$. Suppose that a neutron originating near the origin will have a distance to its next collision of d_0. Then the distance of the neutron from the origin after the first collision is $r_1 = d_0 + r_0$, where r_0 is initially close to 0. If we treat d and r as conventional vectors, then the final sum of the vectors will always be additive and in general, the location of the neutron after n successive collisions will be $\mathbf{r}_n = \mathbf{d}_{n-1} + \mathbf{r}_{n-1}$. By performing this simple act, we can then check to see if the value of $\mathbf{r}_n$ is greater than or less than R_F. If

$$|\mathbf{r}_n| \le R_F \quad \text{the neutron is in the fuel} \tag{23.42}$$

$$|\mathbf{r}_n| > R_F \quad \text{the neutron is in the moderator} \tag{23.43}$$

Hence, this simple test can be used to determine if the cross sections for the fuel or the moderator are to be applied to calculate the location of the neutron for the next case history. Averaged over millions of case histories, this is much more computationally efficient than breaking the unit cell into a large number of (x, y) nodes because we are now dealing with the properties of just 2 nodes—the moderator and the fuel rather than 100's. One of the primary difficulties associated with using a Monte Carlo method to simulate the behavior of a real reactor is how to handle cylindrical unit cells having these issues. In Cartesian geometries, the only realistic way to do this is to break the unit cell into hundreds of smaller cells and use a mesh grid to approximate the behavior of the neutron flux as a whole. A representative mesh grid of this type is shown in Figure 23.20.

The complexity of the Monte Carlo program is reduced as well. It should be apparent from what we have just said that a cylindrical coordinate system is much more efficient for calculating the fast fission factor, the thermal utilization, and resonance escape probability than a Cartesian coordinate system. We would now like to illustrate how a Monte Carlo method can be used to calculate the resonance escape probability p and how its value can change when the fuel and the moderator are mixed together and when the fuel and the moderator are separate. The reader should refer to Chapter 10 for additional information on this subject.

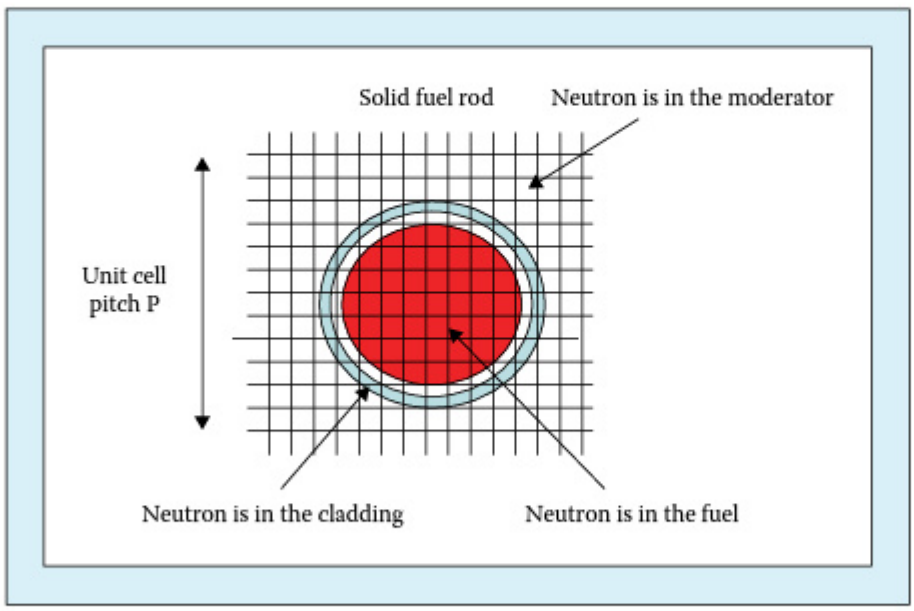

FIGURE 23.20 A Cartesian mesh grid for a cylindrical unit cell used in a Monte Carlo calculation.

Student Exercise 23.1

Using the knowledge you have just acquired, describe how you would calculate the thermal utilization factor for a water reactor lattice having a fuel rod of radius R and a having a large number of unit cells with an average pitch (centerline to centerline spacing) of P. How would this calculation be similar or different from the calculation of the fast fission factor?

23.12 Monte Carlo Calculation of the Resonance Escape Probability

In Chapter 9, we studied the *resonance escape probability* p that appears in both the four-factor and six-factor formulas. The resonance escape probability is defined as the probability that a high energy neutron (which is produced in the fuel) will escape capture in the absorption resonances that lie just above the thermal energy range (E = 0.025 eV) as it begins to slow down. This neutron will then be able to create additional neutrons when it is absorbed by one of the remaining U-235, Pu-239, or U-233 atoms. The resonance escape probability is a function of the diameter D of a fuel rod, and it also depends on the pitch of the lattice P and the moderator to fuel ratio (or MFR). A neutron that leaks out of the fuel has a lower chance of being absorbed by the moderator. Hence, the absorption resonances that affect the value of the resonance escape probability reside primarily in the absorption cross sections for the fuel.

Examples of these resonances were presented in Chapters 9 and 10. There is was also shown that the value of p for a well-designed reactor can vary from about 0.70 to 0.80. In the early days of the nuclear industry, experiments were conducted to determine the size of the resonance escape probability. Unfortunately, the absorption resonances in the fuel were so narrow (between 1 and 10 eV wide) and there were so many of them (literally hundreds or even thousands) that this became very difficult to do properly. Until the 1980s, this could not be done in an economical manner because computers were simply not powerful enough. To compensate for this lack of computing power, physicists invented what were known as *resonance integrals* (see Chapters 9 and 10) to determine how many neutrons would fall into each of the absorption resonances between about 1 eV and 10 keV. The situation was further complicated by the fact that the absorption and scattering resonances in the fuel would *Doppler broaden* as the operating temperature of the reactor was raised. Hence, the amount of resonance absorption was *greater* at higher temperatures than it was at lower ones. Eventually, the calculation of the resonance escape probability became a very messy business, and many physicists spent their entire careers trying to calculate it properly.

Student Exercise 23.2

Suppose that the location of a neutron after each case history is described by a vector of the form $\mathbf{r}_n = \mathbf{d}_{n-1} + \mathbf{r}_{n-1}$. Using the knowledge you have just acquired, write a simple algorithm to determine whether the neutron is in the fuel or the moderator after an arbitrary collision n. Assume that the diameter of the fuel rod in this case is D.

The Monte Carlo method was seen as a practical way to overcome these difficulties. It avoided the need to use hundreds or even thousands of energy groups in order to calculate the absorption rates in the resonance energy range. For this reason, we would like to illustrate how the Monte Carlo method can be used to find the resonance escape probability. Before doing so, recall for a moment how the absorption and scattering resonances in U-233, U-235, and U-238 behave as a function of energy. The absorption resonances in heavy elements are due to a phenomenon called *compound nucleus formation*. (See Chapter 3 for more details about when a compound nucleus is formed.) In compound nucleus formation, a nucleus temporarily absorbs a neutron and may also reemit it. If it is reemitted, then we see this as a scattering resonance. If the energy of the incoming neutron is exactly the same as one of the energy levels inside the nucleus, then the probability of it being absorbed is much higher than if it is not. These two effects give rise to the absorption and scattering resonances that appear in the cross sections of U-233, U-235, and Pu-239. Some of these resonances are shown in Figure 23.21.

One of the interesting things about heavy elements like uranium and plutonium is their absorption and scattering resonances appear to suddenly stop at about 10 keV. However, this is not true in practice because above 10 keV, they become so tightly packed together that they cannot be resolved experimentally without a great deal of time and effort. In other words, the smooth curves for the absorption and scattering cross sections tend to mask the unresolved resonances beneath them. The presence of these resonances must be resolved by statistical methods, and this is taken into account in the values of the absorption and scattering cross sections in the ENDF-B database. The situation is similar for other heavy isotopes as well.

When the kinetic energy of an incoming neutron falls below about 1 keV, the individual absorption and scattering resonances become more widely separated and they also become much easier to resolve. Some of these individual

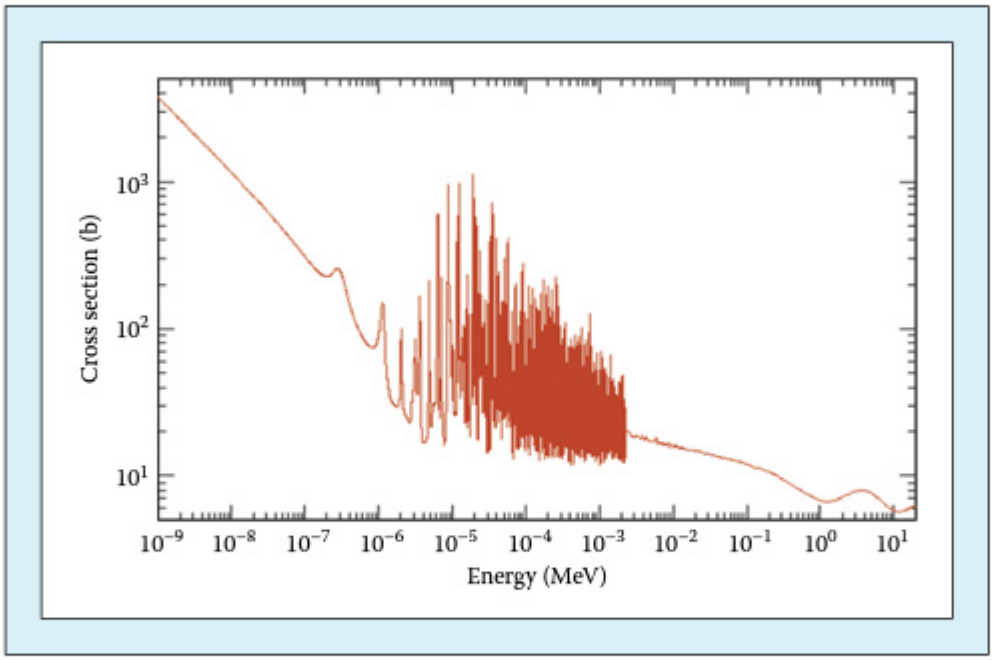

FIGURE 23.21 A plot of the total cross section of Uranium-235 as a function of the neutron kinetic energy E. Notice that the absorption and scattering resonances start at about 10 keV and stop at about 0.025 eV. Above 1 keV they tend to overlap and become very hard to resolve. The same behavior can be found in U-238 and other heavy isotopes as well. (This image was created by the author using ENDFPLOT. See www.kaeri.re.kr/endfplot.)

resonances can be seen in Figure 23.22. When the resonances are very far apart, they are symmetrical in shape, and most neutron absorptions will take place within an interval $E = E_o \pm \Gamma$ on each side of the resonance peak itself. Here, Γ is called the *"half width"* of the resonance (in eV), and the resonance is assumed to be centered at $E = E_o$. In most cases, the process of finding the resonance escape probability p begins by selecting the energy E of the fission neutrons that are created by the process of nuclear fission in the fuel. When a U-235 nucleus absorbs a thermal neutron, two fission neutrons will be released about 60% of the time, and three fission neutrons will be released about 40% of the time. This assumes that the nucleus does not simply capture the neutron and turn into U-236 (which can happen about 17% of the time).

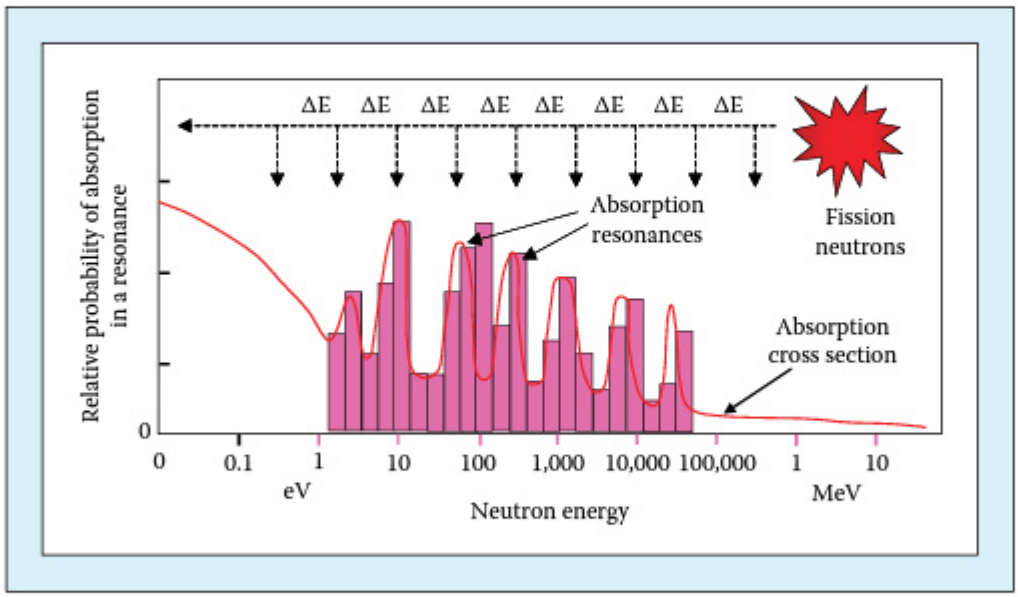

FIGURE 23.22 An example of the absorption resonances that a neutron must escape when calculating the resonance escape probability p.

Hence, the total number of neutrons released per fission is about $0.60 \times 2 + 0.40 \times 3 = 1.2 + 1.2 \approx 2.4$, although in some rare cases, 1 fission neutron or 4 fission neutrons may be created as well (see Chapter 7).

The CDF for this process requires us to generate a random number RN from 0 to 100, and if the random number is less than 60, 2 neutrons will be produced, and if the random number is between 61 and 100, then 3 fission neutrons will be produced. The next thing that needs to be taken into account is the distribution of the kinetic energies of the fission neutrons. In Chapter 7, we learned that the energies of the fission neutrons obeyed a statistical probability distribution P(E) that can be represented by a transcendental function of the form

$$P(E) = Ae^{-BE} \sinh\left\{\sqrt{CE}\right\} \tag{23.44}$$

where

A = 0.453
B = 1.036
C = 2.29
E is the energy of the emitted neutron in MeV

This distribution is normalized so that the area under the curve represented by Equation 23.44 is unity. Equation 23.44 is called the *Watt equation*, and the shape of the Watt curve for U-235 is shown in Figure 23.23.

In Chapter 7, we learned that the *average kinetic energy* of a fission neutron that follows this distribution is 0.74 MeV, and the *most probable kinetic energy* is about 2 MeV. Hence, the CDF can be derived from the Watt curve, and each fission reaction can be associated with a certain probability P(E) that a neutron of energy E will be produced. Again, using the methodology we outlined previously, we can generate a random number RN between 0 and 100 and that will give rise to a fission neutron being born with an energy between approximately 10 MeV and 10 keV. However, in this case, a tabular lookup is generally employed because of the cost in computer time required to calculate the transcendental functions directly. Next, the mean free path of the neutron λ needs to be calculated as well φ. If the unit cell is very long compared to its width, then the axial dependence of the resonance escape probability can be ignored, and only the polar angle θ (see Figure 23.8) needs to be calculated in this case. This can be done using the techniques we have already discussed. Again, a cylindrical coordinate system is generally preferable to a Cartesian coordinate system to track the location of the neutrons, and the quantity $\mathbf{r}_n = \mathbf{d}_{n-1} + \mathbf{r}_{n-1}$ can be used to determine if a neutron is in the fuel or the moderator. Here, n is the number of collisions that occur as the neutron moves through the unit cell. Eventually, if enough case histories are followed, a picture emerges of how many fission neutrons, through a combination of elastic and inelastic scattering, make it down to the thermal energy range (say $E \leq 0.025$ eV) where they are easier to absorb.

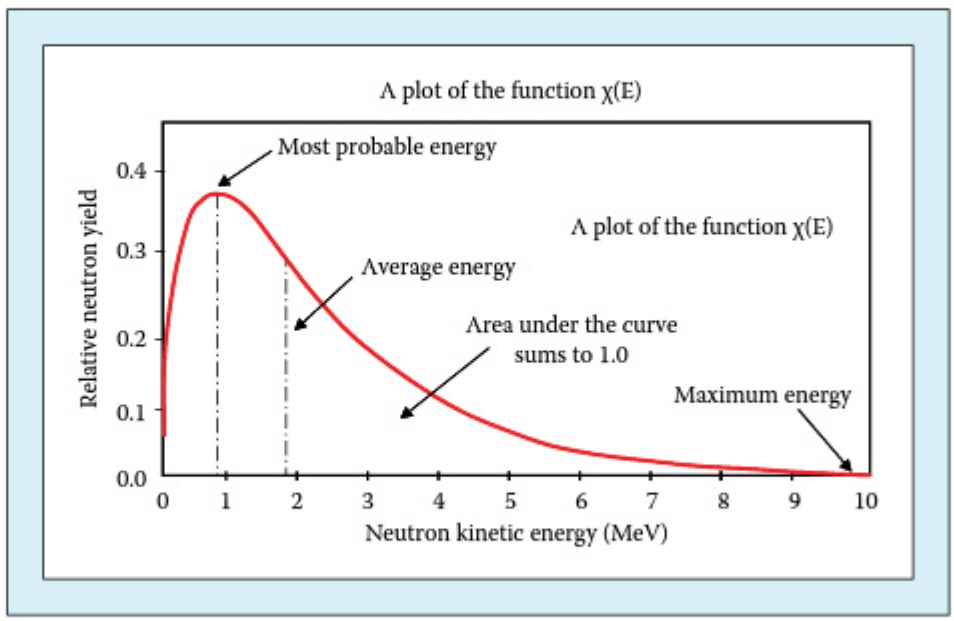

FIGURE 23.23 The fission neutron energy distribution corresponding to P(E) for the thermal fission of U-235. Sometimes this distribution is also referred to as the *Watt distribution*.

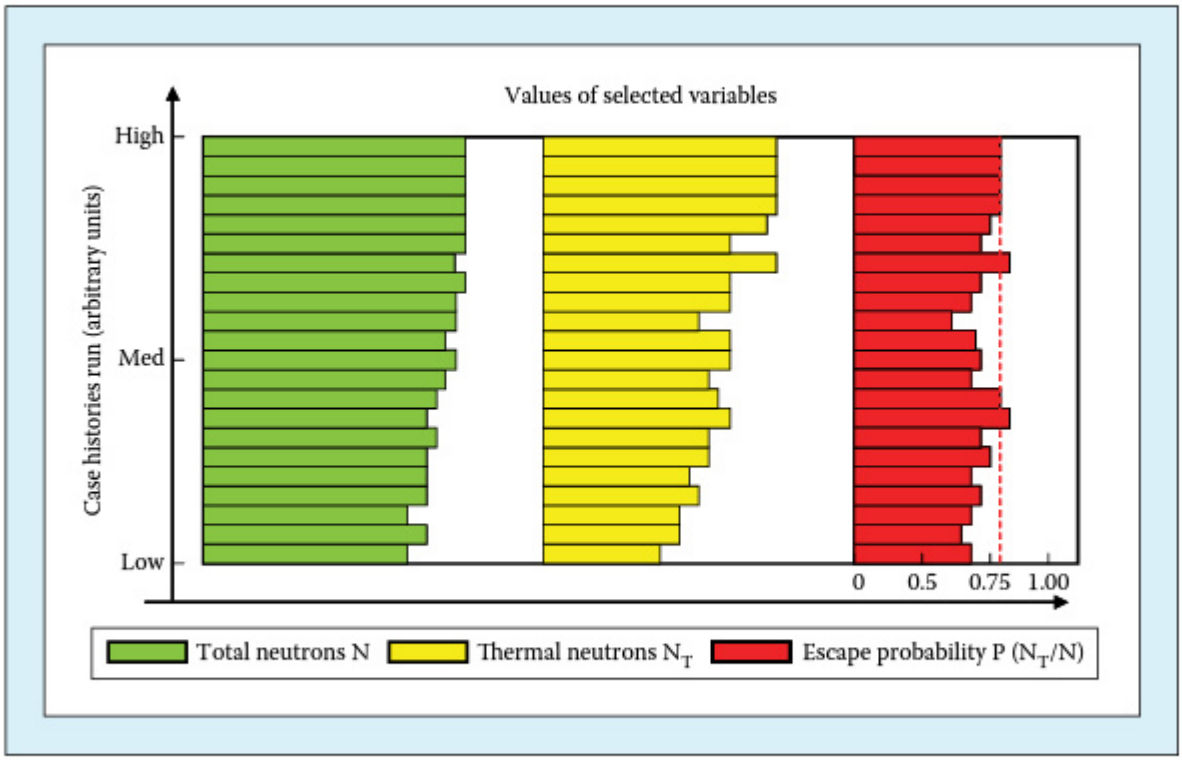

FIGURE 23.24 The value of the resonance escape probability p as the number of case histories is increased. Notice that as the number of case histories is increased, the values approach as asymptotic limit as one would expect.

The ratio of the number of thermal neutrons N_T to the number of fission neutrons N originally produced then becomes the resonance escape probability p:

$$\text{Resonance escape probability} = p = \frac{N_T}{N} \tag{23.45}$$

This ratio is shown in Figure 23.24 as the number of case histories is increased. Note in particular how the values of N_T and N gradually approach an asymptotic limit and how the ratio $p = N_T/N$ approaches this limit as well. It is easy to see that this particular method for calculating the resonance escape probability does not require us to subdivide the neutron energy spectrum into hundreds or even thousands of energy groups, and we can also use the actual neutron energies before and after each elastic or inelastic collision to determine the reaction rates. Hence, this exercise provides a very vivid illustration of the power of the Monte Carlo method. No assumptions have to be made about the number of energy groups that need to be used, and the shape of the neutron flux in the unit cell can be determined directly from such a calculation. One simply has to ensure that all of the case histories are properly recorded.

23.13 Extensions of the Monte Carlo Method to Control Rods

Of course, everything we have said so far can be applied to control rods as well—regardless of their size or shape. In the presence of these rods, the thermal neutron flux becomes *anisotropic*, and the angular distribution of the thermal neutrons resembles the plots shown in Figure 23.25. Sometimes these plots are referred to as *polar plots* because the thermal flux is plotted as a function of the polar angle θ.

Student Exercise 23.3

Using the knowledge you have just acquired, write an algorithm using a random number generator to calculate the number of fission neutrons produced from the thermal fission of U-235.

These distortions in the thermal flux typically occur in the vicinity of strong neutron absorbers. A cruciform-shaped control rod in a BWR will almost always distort the shape of the thermal flux enough to justify the use of a Monte Carlo method. This also applies to the control rods in PWRs—even though they are usually smaller and cylindrical

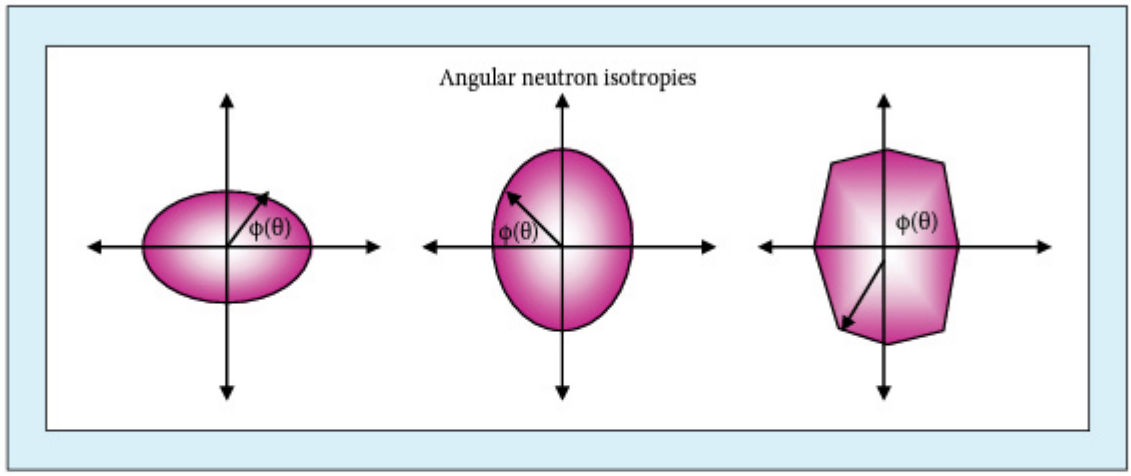

FIGURE 23.25 An example of several situations where the angular flux shape $\phi(\theta)$ loses its isotropy.

in shape. When a control rod is "fresh," it may also appear to be a *black surface* or even a *black hole* to any thermal neutrons in its immediate vicinity. Hence any neutrons that happen to fall into the rod will generally not return. In other words, the control rod may appear to be *completely black* or opaque when the neutron kinetic energy is low. Each of the vectors in Figure 23.25 can be thought of as one of the ordinates in an S_N method, but no direct analogy exists for a Monte Carlo calculation. In Monte Carlo calculations, all of the angular directions are treated equally, and there are therefore no discontinuities in the shape of the flux between the interpolation points the S_N method uses. Finally, if a burnable poison like gadolinium is added to one of the fuel rods, the fuel rod may also appear to be *gray*, which means that most of the thermal neutrons that enter the rod will not return (unless they happen to be fast neutrons with much longer mean free paths). Hence, deciding when to use a Monte Carlo method is something that must be learned by trial and error (or better yet, something that must be supported by actual *experience*).

For more information about when Monte Carlo methods and transport methods should be used, the reader should refer again to our discussion in Chapter 11. If there are major discontinuities in the spatial or angular distribution of the neutron flux, then a Monte Carlo method is probably the best method to use. Of course, this assumes that the geometry is reasonably complex and that deterministic methods cannot be made to fit the geometry one is trying to model. If the neutron mean path is relatively long (as it usually is in a fast reactor), then discontinuities in the flux shape will normally disappear, and the diffusion theory will be able to determine the correct shape. Hence, the neutron mean free path λ is a fairly reliable indicator of when diffusion theory or transport theory should be used. Mean free paths greater than a couple of centimeters generally imply that diffusion theory can give accurate results, and mean free paths below about 1 centimeter generally imply that other methods are more appropriate to use.

23.14 Skewed Probability Distributions

The Monte Carlo method is such a powerful methods that it is not always obvious when its virtues and vices will appear. Hence, we would like to reiterate what we have said previously with respect to its use. Although we have only shown how it can be used with normal probability distributions (e.g., those in which all of the events recorded are completely independent of each other), it can also be applied to probability distribution functions that are asymmetric or skewed. The individual particle histories do not preclude distributions of this type. An *asymmetric probability distribution* is one that has a long tail in a particular direction. Examples of asymmetric probability distributions are shown in Figure 23.26. For example, the *Watt distribution* is an example of an asymmetric probability distribution (see Figure 23.23).

In the study of probability and statistics, the most common measure of the asymmetry of a probability distribution is its *skewness* or *skew*. The skew can be either positive or negative, and in some cases, it can even be undefined. In practice, a negative skew implies that the *tail* on the left-hand side of the probability density function is *longer* than the tail on the right side, and the bulk of the values (possibly including the median) will lie to the right of the mean. Conversely, a positive skew implies that the *tail* on the right side is *longer* than the tail on the left side and that the bulk of the values lie to the left-hand side of the mean. A skew of zero (which frequently occurs in normal distributions) indicates that the values are evenly distributed on both sides of the mean, but they do not have to be symmetric in all cases. The reason why this is important is because the magnitude of the error in a Monte Carlo calculation depends on

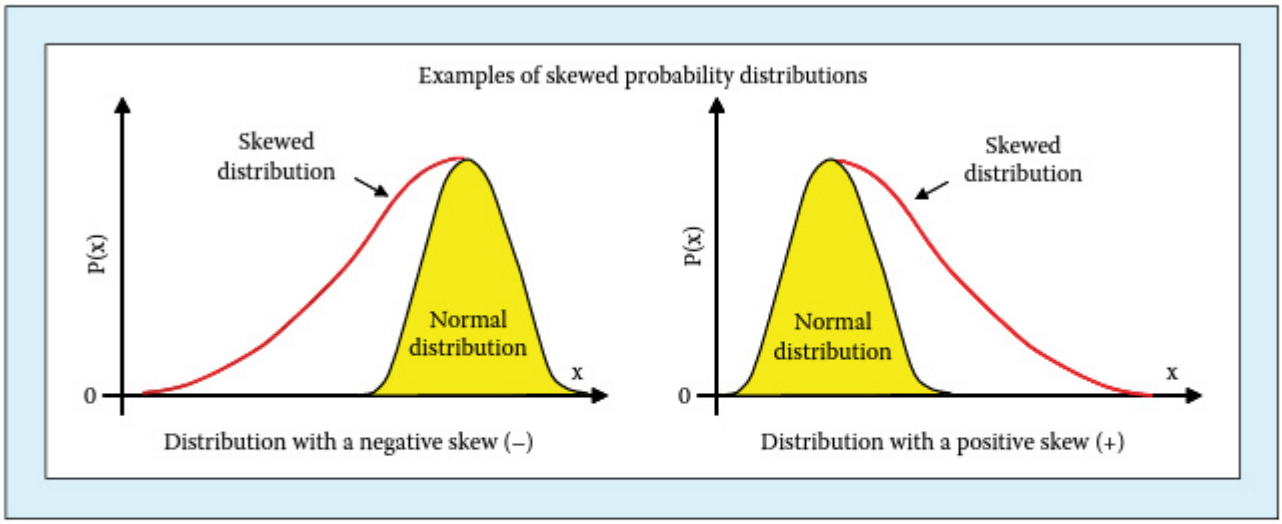

FIGURE 23.26 An example of two "skewed" probability distributions. One with a positive skew and one with a negative skew. Sometimes probability distributions of this type are called asymmetric probability distributions, and they sometimes appear in the study of nuclear particles. For example, the *Watt equation* is an example of an asymmetric probability distribution.

making some assumptions about what the ultimate probability distribution will be. This in turn depends on whether the events are completely independent from one another, or whether they are correlated in some way. The case histories of nuclear particles must be followed for many lifetimes to remove any hereditary influences from the initial particle population. If this is not done, the accuracy of the simulation may come into question. Hence it often takes many case histories for the statistical fluctuations in the particle population to damp themselves out. Second, variance reduction methods (which are used to reduce the average error in these calculations as well) are extremely difficult to implement properly without introducing an additional bias into the calculations. Therefore, the results must be viewed with some skepticism if a variance reduction method appears to increase the precision quickly. This is because even the best variance reduction methods are an asymptotic function of the number of case histories that are run. In other words, even in a statistically neutral model, it is almost never true that one can get something for nothing (in this case, higher accuracy for less work). Finally, ensuring that the programming logic is implemented properly is not always easy to do. For example, this may be true because

- The logic can be very complex
- The logic does not have to be deterministic
- Sometimes, events that are calculated incorrectly can be so rare that they can hide an error and still be large enough to influence the final results
- The statistical nature of the method tends to mask these errors by burying them in the probability distributions the programming uses or attempts to create

The pictures in Figure 23.27, adopted from an earlier discussion in Chapter 11, illustrate some of the challenges involved. Thus Monte Carlo methods must always be validated against the results of more deterministic approaches before they can be used with confidence.

23.15 Finding the Scattering Angles in a Monte Carlo Calculation

Suppose we would like to find the neutron scattering angles to use in a Monte Carlo calculation. If we know the materials involved, we can estimate the probability that an elastic or inelastic collision will occur if we know the values of σ_{in} and σ_{el}. The probability of an elastic collision is given by $P_{el}(E) = \sigma_{el}(E)/(\sigma_{in}(E) + \sigma_{el}(E))$ and the probability of an inelastic collision is given by $P_{in}(E) = \sigma_{in}(E)/(\sigma_{in}(E) + \sigma_{el}(E))$. Clearly, these probabilities need to be normalized so that at any neutron energy E, $P_{in}(E) + P_{el}(E) = 1.0 = 100\%$.

Now let us consider a neutron approaching the atomic nucleus shown in Figure 23.28. If the scattering reaction happens to be an inelastic one, the neutron will be scattered isotropically in the θ and φ directions, and all emission angles will be equally possible. Thus, we can use a random number generator to select a value for θ_{in} between 0° and 360° and a value for φ_{in} between 0° and 360°. If the random number generator generates a random number between 0 and 100, we simply have to multiply the result by 3.6 to get the scattering angles we need. Now let us consider what happens when

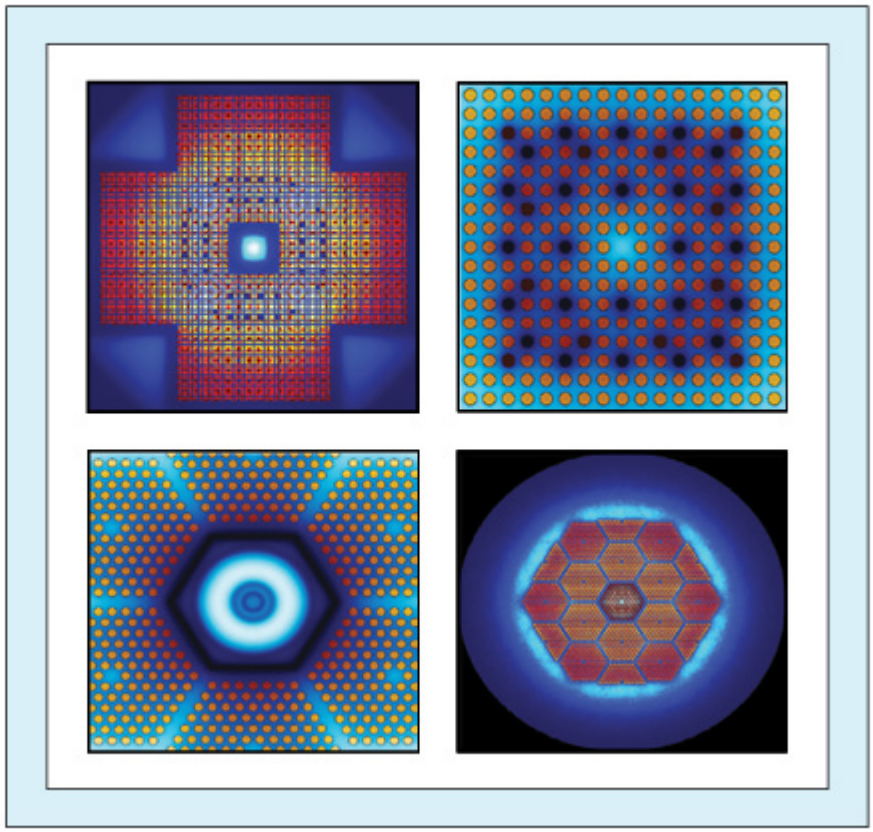

FIGURE 23.27 Some examples of reactor geometries where neutron diffusion theory may no longer give reliable results, and where a Monte Carlo method may be easier to implement than a transport method. The regions in black represent areas where the absorption cross sections are very high, and the neutron flux can become very depressed. (From *http://montecarlo.vtt.fi/development.htm*.)

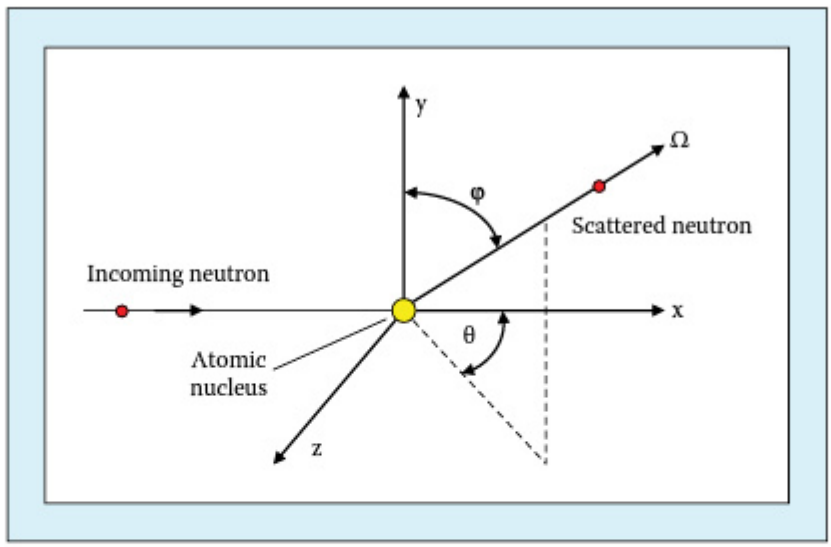

FIGURE 23.28 The three-dimensional scattering angles θ and φ, which define the unit vector Ω into which the neutron is scattered.

the scattering reaction happens to be an elastic one. The probability of this occurring is given by $P_{el}(E) = \sigma_{el}(E)/(\sigma_{in}(E) + \sigma_{el}(E))$. However, the neutron is no longer scattered isotropically in all directions (see Chapter 4), and for a given kinetic energy E, the angular scattering probability distribution P(θ, A) looks like the distribution shown in Figure 23.29. To emulate this distribution we can use a more elegant approach to generate the appropriate scattering angles. This involves the use of an *Inverse Cumulative Distribution Function* that we will subsequently define.

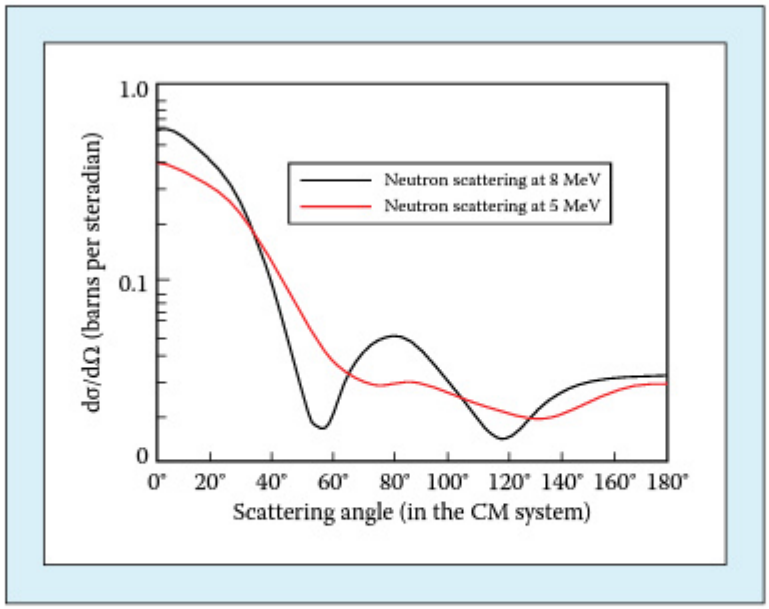
1.0
0.1
0
dσ/dΩ (barns per steradian)
Neutron scattering at 8 MeV
Neutron scattering at 5 MeV
0° 20° 40° 60° 80° 100° 120° 140° 160° 180°
Scattering angle (in the CM system)

FIGURE 23.29 A graph showing the elastic scattering of neutrons off of liquid sodium atoms at 5 and 8 MeV. Liquid sodium is often used as a coolant in LMFBRs.

The direction of the scattered neutron is then determined at each point where a collision occurs, and the location of the next collision is estimated by following the directional unit vector $\Omega = \mathbf{i} \cdot \sin\theta \cos\varphi + \mathbf{j} \cdot \sin\theta \sin\varphi + \mathbf{k} \cdot \cos\theta$. This process continues until the neutron is removed from the calculation by either leaking out of the system or being absorbed. The case history is saved, and the process is repeated again. This process continues until we reach the level of accuracy that is required. Notice that when a problem becomes a two-dimensional one (such as the problem illustrated in Figure 23.30), we can simply neglect the value of φ (by setting it to 0) and use the angular probability distributions $P(\theta, E, A)$ to generate the correct values for θ for each successive collision. In this case, the directional unit vector becomes

$$\Omega = \mathbf{i} \cdot \sin\theta + \mathbf{k} \cdot \cos\theta \tag{23.46}$$

because the neutron can only scatter in the x–z plane. In general, the scattering angle will be different for each collision so that $\theta_1 \neq \theta_2 \neq \theta_3 \neq \theta_N$. Clearly, the value of θ generated for each scattered neutron must be consistent with the shape of

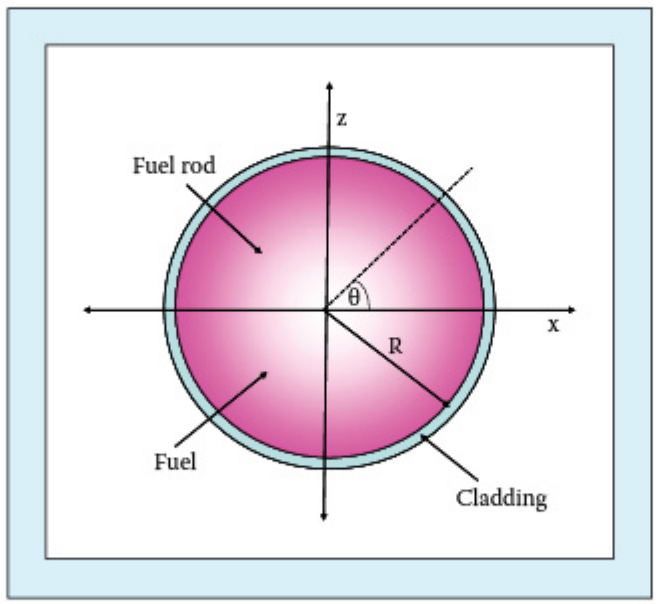

FIGURE 23.30 A cylindrical fuel rod used in a Monte Carlo calculation. (Note that the y-axis is perpendicular to the x- and z-axes and is oriented perpendicular to the paper.)

the statistical probability distribution P(θ, E, A) that governs their overall angular behavior. In the next section, we would like to discuss exactly how this can be done using a random number generator.

Student Exercise 23.4

Using the knowledge you have just acquired, write an algorithm using a random number generator to calculate the energy of each fission neutron released from the thermal fission of U-235. Record the energies of a large number of these neutrons to create a probability distribution showing the average and most probable energies of the neutrons in this case. How do the results of these calculations compare to the probability distribution P(E) that is defined by Equation 23.44?

23.16 Generating Asymmetric Scattering Angles

Most nuclear processes obey statistical probability distributions that are slightly asymmetrical in shape. These statistical probability distributions can have many different shapes, and two of the most common distributions are

- The *Watt distribution*, which gives the fission neutron energy distribution P(E) for the thermal fission of U-235
- The *angular distribution of the scattered neutrons P(θ) emerging from a neutron scattering reaction*.

Examples of these distributions are shown in Figures 23.31 and 23.32. One way to generate random numbers that are compatible with these distributions is to generate a random number uniformly distributed between 0 and 100 and apply the target distribution's *Inverse cumulative distribution function* (or ICDF) to that random number. This allows more random numbers to be produced wherever the distribution peaks and fewer random numbers to be produced in areas away from the peaks. For example, if we consider the angular distribution of scattered neutrons shown in Figure 23.32, we can generate the target distribution's inverse CDF and then apply it to a random number between 0 and 100. This gives us a set of scattering angles $\theta_1, \theta_2, \theta_3, \ldots, \theta_N$ that represents the overall shape of the distribution. The reader should recall from our earlier discussion that *a CDF for a particular probability distribution function P(x) is simply the integral of the original probability distribution function*. To illustrate this point, consider a probability distribution function of the form $P(x) = e^{-x}$, where $x \geq 0$. The cumulative distribution function is the integral of this probability distribution function. In other words, we can write

$$\mathrm{CDF}(x) = \int_0^x P(x)\,dx \tag{23.47}$$

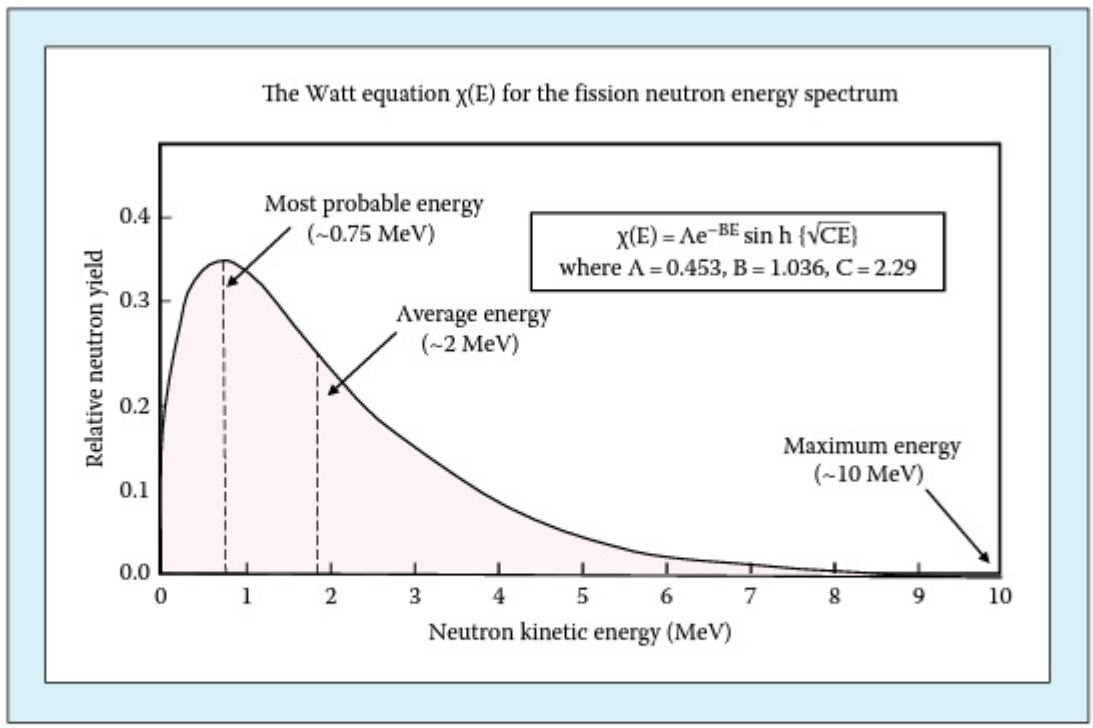

FIGURE 23.31 The Watt equation for the neutron energy spectrum of the fission neutrons is an example of an asymmetrical probability distribution.

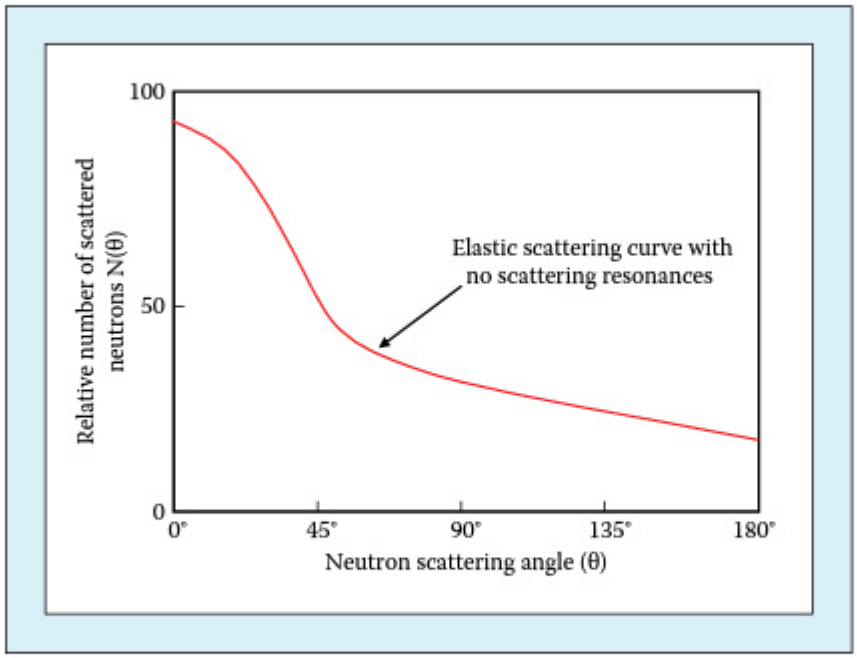

FIGURE 23.32 The angular distribution of the neutrons in an elastic scattering reaction is another example of an asymmetrical probability distribution that can be simulated in a Monte Carlo calculation.

and since $P(x) = e^{-x}$, the corresponding CDF is

$$\mathrm{CDF}(x) = 1 - e^{-x} \tag{23.48}$$

This function can be explicitly inverted by solving for x in the equation $\mathrm{CDF}(x) = u = 1 - e^{-x}$. The *inverse CDF* in this case is then

$$x = -\ln(1-u) \tag{23.49}$$

Now suppose that we select a random set of values for u between 0 and 1 using a random number generator. The corresponding values of x (which are consistent with the shape of the original distribution) are shown in Figure 23.33. In other words, *the technique we have just described allows us to generate random values for x that are consistent with the shape of the original probability distribution P(x)*. If the shape of the probability distribution happened to represent the scattering angles for neutrons being scattered by an atomic nucleus of weight A, then the values of θ generated by this technique would be consistent with the shape of the probability distribution P(θ) that is measured experimentally. We can also write a simple computer program to demonstrate this principle. Suppose that we would like to generate 1000 neutron scattering angles (θ_1 to θ_{1000}) for 1000 individual neutrons that follow this distribution. In the C programming language, the code to do so is simply

Code Snippet to Generate Neutron Scattering Angles for $P(\theta) = e^{-\theta}$

```
for (i = 0; i≤1000; i++)
     {
      u = rand ();
      x = -ln(1 - u)
      θ(i) = 2π·x
     }
```

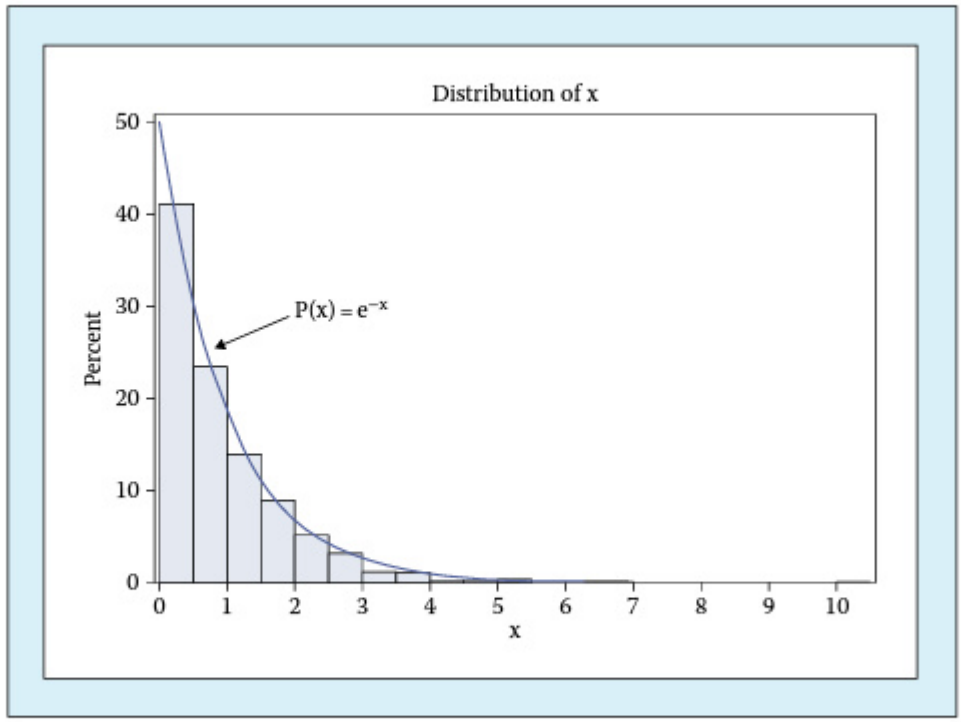

FIGURE 23.33 An exponential probability distribution used in a Monte Carlo simulation.

So in conclusion, this is how the Monte Carlo method can be used to generate random neutron scattering angles from a previously known angular scattering distribution. This is particularly helpful when finding the angular distribution of the neutron flux $\phi(r, E, \theta, \varphi)$ in situations where neutron diffusion theory can no longer be used. An example of how this technique can be applied to a two-dimensional problem is shown in Example Problem 23.6 below. Here, the inverse cumulative probability distribution function (the inverse CDF) is found for a flat circular disk in which the number of data points to be selected is randomly distributed. The disk can be a CDROM that contains an arbitrary amount of nuclear or statistical data.

Example Problem 23.6

Suppose that we would like to select some random data points that are uniformly distributed on a circular disk having a radius of 1. See Figure 23.34 for a picture of what the disk looks like. If the PDF governing the distribution of data on the disk is given by $P(r) = 2r = D$, where D is the diameter of the disk, write a computer program to generate 1000 random data points located on the disk.

Solution In this case, the PDF governing the distribution of the data points is $P(r) = 2r$. The cumulative probability distribution function (or CDF) in this case is $C(r) = \int P(r)dr = r^2$. The inverse CDF is $r = \sqrt{C} = \sqrt{u}$. Now suppose that we use the function rand () to randomly select values for u between 0 and 1.The random values of the radius are then $r = \sqrt{(\text{rand}())}$ and the angle corresponding to each data point is $\theta = 2\pi$ rand (). Therefore, the program required to generate each data point is

```
For (i = 1; i ≤ 1000; i++)
(
                r = sqrt (rand ());
                θ = 2π rand ();
                x = r cos θ
                y = r sin θ
                p(i) = (x, y)
)
```

The result of implementing this code snippet is shown in Figure 23.34. Notice how uniformly the data points are distributed within the circle that defines the outer boundary of the disk. In this case, the code snippet was called several hundred times in succession to create the distribution of data points shown.

This is just another example of how a Monte Carlo method can be used to work with statistical data.

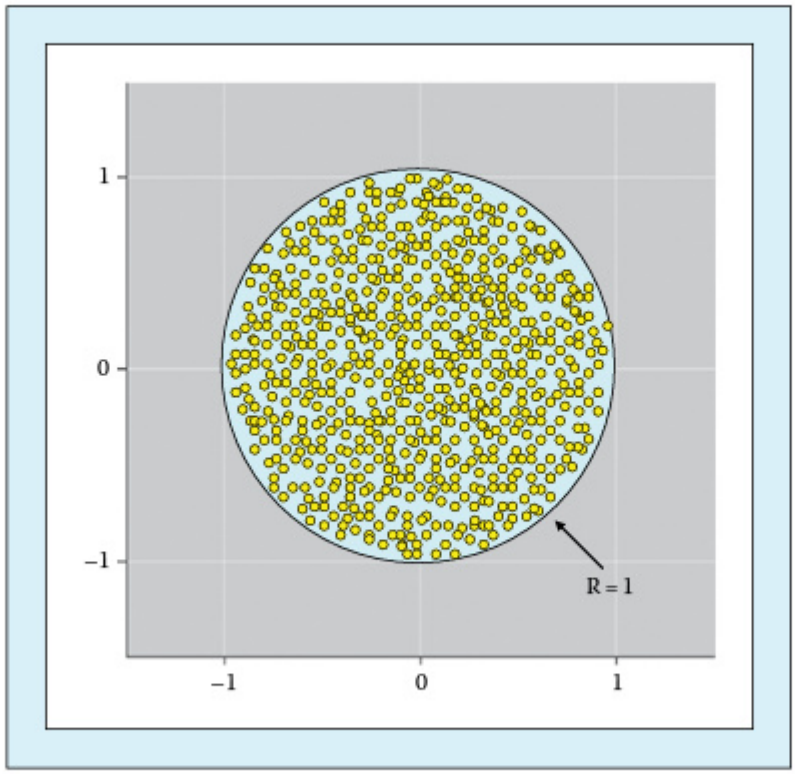

FIGURE 23.34 A disk with a uniform probability distribution whose data points are selected using a random number generator and an inverse CDF.

23.17 Using Random Walks to Simulate Particle Diffusion

Calculating the position of a particle in a Monte Carlo calculation is not much different than performing what is known as a *random walk*. Random walks can be used to study particle flow, although in nuclear engineering, most random walks are an attempt to validate results of neutron diffusion theory. A random walk is a mathematical description of the path a particle takes as it moves through space and time. For example, the path traced by a molecule when it travels through a liquid or a gas, the path that a neutron takes as it travels through a reactor core, or the path a hungry animal takes when it is looking for food are all examples of random walks, although in reality, some random walks may be more random than others. The term *random walk* was first proposed by Englishman *Karl Pearson* in 1905 to attempt to explain how populations of mosquitoes in Africa behaved when they invaded regions where the jungle had just been cleared to grow food. He found that their behavior was too complex to model deterministically, so he hypothesized a mathematical model to describe their behavior, which is now called the *random walk*. In the July 27 issue of Nature in 1905, Pearson proposed the following question to the scientific community:

> Suppose that a man starts from a point 0 and walks l yard in a straight line; he then turns through any angle whatever and walks another l yard in a second straight line. He repeats this process n times in succession. What is the probability after n of these events that he is at a distance between r and r + δr from his starting point?

His question was eventually answered by *Lord Rayleigh*, who pointed out the connection between this problem and an earlier paper Rayleigh had written concerning the nature of sonic vibrations. Rayleigh pointed out that, for large values of n, the answer to Karl Pearson's question could be expressed by the equation

$$P(r)dr = \left(\frac{2}{nl^2}\right)e^{-r^2/nl^2} r\, dr \tag{23.50}$$

which was actually the shape of a normal distribution (such as the one shown in Figure 23.14) centered about the origin. It was later discovered that random walks (which both particles and mosquitoes can participate in) can be classified in many different ways and that random walks can occur in one, two, or three dimensions.

Sometimes, random walks can be thought of as *Markov processes* or *Markov chains*, but other, more complex random walks can also occur. Some random walks can occur in two dimensions, some can occur in three dimensions, and some

can even occur on curved surfaces. Random walks can also be time dependent; in other words, the rules governing their behavior will change as a function of time. Random walks frequently appear in the study of diffusion theory. For example, consider an elementary random walk in which a particle can move only one step at a time in the +x or −x direction (refer to Figure 23.35). In this figure, the particle starts out at the origin and moves a distance of +1 or −1 one step at a time, where either of the two steps is equally possible. The expected translation distance D after n steps is given by

$$D = c\sqrt{N} \tag{23.51}$$

where c is a number - usually a constant. In fact, it can be shown that as $N \to \infty$, $c = \sqrt{(2/\pi)}$. This result shows that particle diffusion is an ineffective way to mix materials together because of the way that the square root behaves when N is large. Normally, one-dimensional random walks are modeled using what are known as Markov chains. A *Markov chain* is defined by

Definition of a Markov Chain

$$P_{i,i+1} = p = 1 - P_{i,i-1} \tag{23.52}$$

where p is some number satisfying $0 < p < 1$, and the transition probabilities (the probability $P_{i,j}$ of moving from state i to state j) are given by Equation 23.52. Here, the state space encompassed by the Markov chain is given by the integers $i = 0, \pm1, \pm2, \ldots, \pm N$. When a random walk is performed in one dimension using one of these chains, we obtain the results shown in Figure 23.35. A more interesting result is obtained when the same random walk is allowed to occur in three dimensions. Then the result resembles that shown in Figure 23.34. In this case, the particle can move a distance of +1 or −1 step at a time in the x, the y, or the z direction, but an individual step cannot occur along one of the diagonals.

The result shown in Figure 23.36 also applies to a person who is completely drunk and manages to stumble out of a bar, looking for his house. If the person walks around randomly in a city where all of the streets are arranged on a square grid (such as the borough of Manhattan in New York City), then the probability he will eventually return home is very high. However, in three dimensions, the probability of him finding th front door is only 34%! The exact probability is

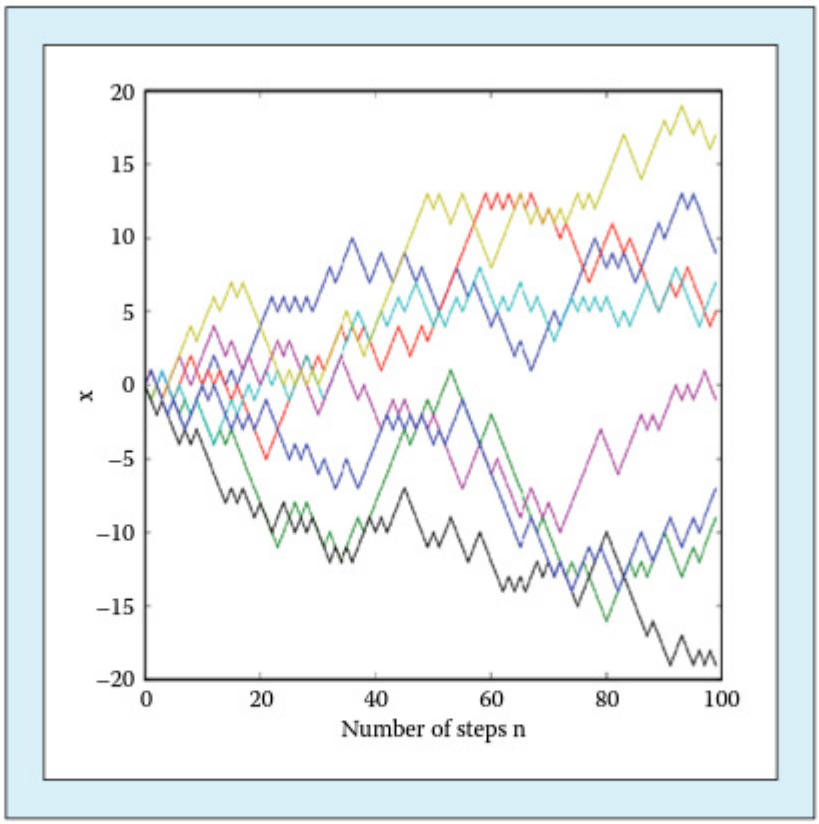

FIGURE 23.35 The outcome of eight separate random walks in one dimension using a Markov chain. All eight walks start at x = 0, and the vertical axis (n) shows the number of steps that are required to finish the walk. (Simulation provided by Wikipedia.)

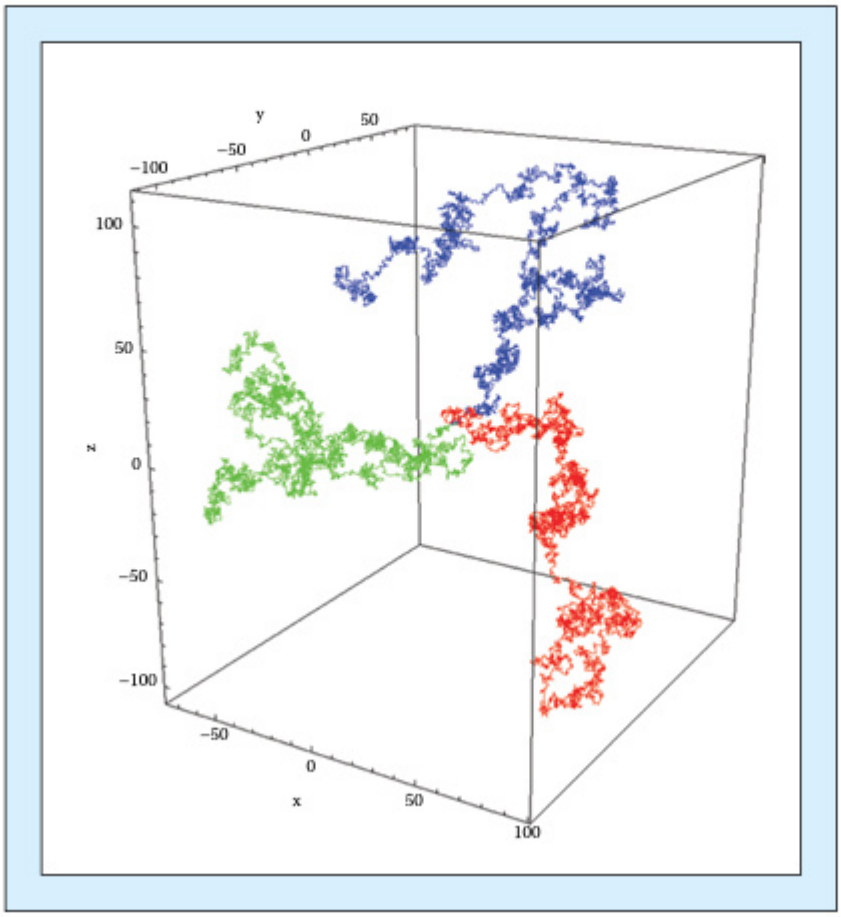

FIGURE 23.36 The outcome of three random walks in three dimensions. In this case, each random walk is shown in a different color. (Simulation performed by Wikipedia.)

calculated in Web Reference 9. Other examples of how random walks are used to predict the consequences of particle diffusion and human behavior are discussed in Web reference 10 at the end of the chapter. *A Monte Carlo calculation can be thought of as a random walk with a more complex set of rules.*

23.18 Generating Truly Random Numbers

Before the days of high speed computers, it was much harder to generate truly random numbers than it is today. Because of this, people in the nuclear industry resorted to a variety of different techniques (many of them "homemade") to generate the random numbers they needed. In this section, we would like to briefly discuss some of the techniques that were used to generate these numbers. Today, this process is completely automated, and so little attention is paid to it, that it is easy to forget how complicated the underlying logic can be. Thus, generating a random number is no more difficult than making an appropriate function or subroutine call (see Section 23.2). In the 1930s and the early 1940s when the nuclear industry was just getting started, scientists needed a reliable way to generate random numbers to support the needs of the *Manhattan Project* and to determine the resonance escape probability for the neutrons produced in nuclear fuel rods. At that time, a number of ingenious techniques were used to obtain the random numbers they needed. For a while, these techniques included selecting random digits from census tables and from the New York City phone book, by having volunteers throw darts at random arrays of numbers taped to city walls, and by having someone spin a specially designed roulette wheel to generate sequences of random digits. All of these techniques are considered to be rather "lame" by today's standards, but before the days of digital computers, they were the only reliable ways to generate the truly random numbers that nuclear scientists and engineers needed.

After high speed computers were invented in the 1950s, the process of random number generation changed because a computer program or even a computer "chip" could be used to generate these random numbers instead. Today, almost all the methods used to generate random numbers are based on the observation that if the digits of two large numbers,

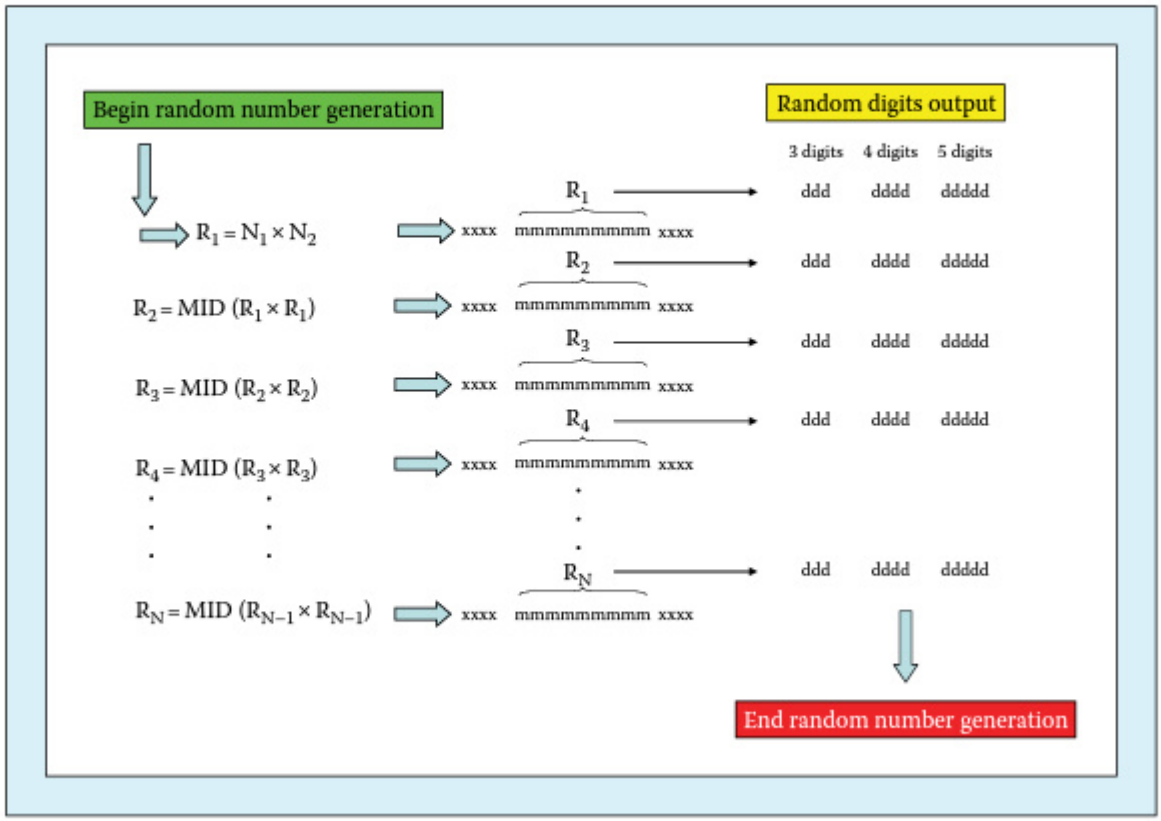
Begin random number generation
Random digits output
3 digits
4 digits
5 digits
$R_1 = N_1 \times N_2$
$R_2 = MID\ (R_1 \times R_1)$
$R_3 = MID\ (R_2 \times R_2)$
$R_4 = MID\ (R_3 \times R_3)$
$R_N = MID\ (R_{N-1} \times R_{N-1})$
xxxx mmmmmmmmm xxxx
ddd dddd ddddd
End random number generation

FIGURE 23.37 An illustration of how the middle-squared method is used to generate random numbers in a random number generator.

N_1 and N_2, are selected at random, and N_1 and N_2 are multiplied together, the middle digits of the product of these numbers will be completely random as well. This observation can be used to create a method for generating random numbers that has become known as the *middle-squared method*.

In this method, two initially random numbers having at least 12 digits are programmed into the memory of a digital computer. These two numbers are multiplied together to produce a third number N_3. The middle digits of this third number are extracted and squared, and this results in another random number that we will call N_4. The middle digits of N_4 are extracted and squared, and this will produce another random number called N_5. This process continues until we have generated as many random numbers as we want. In other words, although the entire sequence of digits is completely determined once the values of N_1 and N_2 are specified, the middle digits behave statistically as if they are random and completely uncorrelated.

The middle-squared method was used in many early Monte Carlo programs to determine the probability of various types of particle reactions. Today, more advanced methods of obtaining the same results are imbedded onto a computer chip. These computer chips can then be used to generate completely random numbers. The steps used to generate a random number using the middle-squared method are illustrated in Figure 23.37. Notice that the middle-squared method can be used to produce random numbers for a Monte Carlo calculation having a variable number of digits. For example, if a random number between 0 and 99 is required, one simply selects two digits from the middle of the two sequences. If a random number between 0 and 999 is required, one simply selects three digits from the sequences and so on. In recent years, the middle-squared method has been replaced by another method of generating random numbers that has smaller sampling errors and is slightly more computationally efficient. This method is referred to as the *multiplicative congruential method*, and it was originally based on a scheme proposed by *John von Neumann* in 1940 (see Figure 23.38). In this method, the modulus mod M of two random numbers is used to generate another random number. The recursion relationship used to do so is

$$N_i = \left(A \cdot N_{i-1} + B\right) \bmod M \tag{23.53}$$

where

N_{i-1} is a positive integer
A and B are positive integers
modulus M is a large positive integer

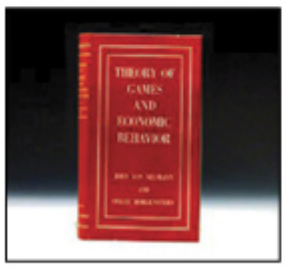

John Von Neumann was one of the greatest mathematicians who ever lived. He founded the field of *game theory* as a mathematical discipline and helped design the world's first super computer, called the ENIAC. He was also one of the original developers of the Monte Carlo method, which is used extensively in the field of Nuclear Science and Engineering to do particle streaming calculations. Many of the foundations of the modern world can be attributed to the work of this man.

FIGURE 23.38 Mathematician *John von Neumann* was one of the scientists who originally developed the Monte Carlo Method. He worked with Robert Oppenheimer to create the world's first atomic bomb at Los Alamos, where he also developed the explosive lens needed to compress the plutonium core of the Trinity test device and the "Fat Man" atomic bomb, which was later dropped on Nagasaki, Japan. He invented the middle-squared method, which is still used today to generate random numbers on computer chips. He designed the world's first supercomputer (called the ENIAC) in 1943 and he was instrumental in the design of the first IBM mainframe. He made additional contributions to the fields of statistics and game theory, which some versions of the Monte Carlo method still used today. Along with Edward Teller, he was one of the physicists who helped develop the hydrogen bomb. He made many other significant contributions to the fields of physics, game theory, and high-speed computing. *More than any other man who ever lived, he is probably the most directly responsible for inventing the modern computer.* He also worked with Albert Einstein at Princeton for a time. (The image of John von Neumann was provided by Wikipedia and the picture of the IBM mainframe was provided by the IBM corporation—see www.ibm.com.)

Many other methods have been applied to modern Monte Carlo programs to generate truly random numbers. In this case, the ultimate accuracy of the program (see Section 23.6) is determined by the number of case histories that are run. The statistical error in such a simulation decreases as $1/\sqrt{N}$ where N is the number of particles or case histories in the sample. In other words, 100 times more case histories have to be run to reduce the statistical error in a Monte Carlo calculation by a factor of 10. The following example illustrates how some random numbers are generated for use in a Monte Carlo program. Other examples can be found on the Internet with the *Google Search Engine*.

Example Problem 23.7

Using the multiplicative congruential method discussed earlier in the chapter, generate three six-digit random numbers starting with an initial random number of 2,143,856,907, a value for A of 37,182,496, and a value for B of 97,365,129.

Solution The recursion relationship employed by the multiplicative congruential method is $N_i = (A \cdot N_{i-1} + B) \bmod M$, where N_{i-1} is a positive integer, A and B are positive integers, and the modulus M is a large positive integer. In this case, A = 37,182,496, B = 97,365,129, and N_{i-1} = 2,143,856,907. Any six sequential digits of N_1 will be the first random number, any six sequential digits of N_2 will be the second random number, and any six sequential digits of N_3 will be the third random number. [Ans.]

Student Exercise 23.5

Using one of the computer programs listed in Table 23.2, perform a Monte Carlo calculation to determine the shape of the neutron flux in a cylindrical control rod, a cylindrical fuel rod with a burnable poison, and a cylindrical fuel rod without a burnable poison. Assume that all three rods have exactly the same diameter D = 1 cm. Plot the shape of the neutron flux in each case. Discuss the type of boundary condition that you were required to select on the surface of the unit cell.

Part 2: Repeat the same problem with two energy groups instead of one, and plot your results again.

References

Books and Textbooks

1. Ash, M. *Nuclear Reactor Kinetics*, McGraw-Hill, New York (1965).
2. Henry, A.F. *Nuclear Reactor Analysis*, MIT Press, Cambridge, MA (1975).
3. Keepin, G.R. *Physics of Nuclear Kinetics*, Addison-Wesley Publishing Company, Inc., Reading, MA (1965).
4. Stacey, W.M. *Nuclear Reactor Physics*, 2nd edn., John Wiley & Sons, New York (2007).
5. Duderstadt, J. and Hamilton, L. *Nuclear Reactor Analysis*, John Wiley & Sons, New York (1976).
6. Lewis, E. *Fundamentals of Nuclear Reactor Physics*, Academic Press, Boston, MA (2008).
7. Clark, M. and Hansen, K. *Numerical Methods of Reactor Analysis*, Academic Press, New York (1964).
8. Hetrick, D.L. *Dynamics of Nuclear Reactors*, American Nuclear Society, La Grange Park, IL (1993).
9. Lewis, E. and Miller, W.F. *Computational Methods of Neutron Transport*, Wiley-Interscience, New York (January 1993).
10. Spanier, J. and Gelbard, E. *Monte Carlo Principles and Neutron Transport Problems*, Dover Publications (2008).
11. Schultz, M.A. *Control of Nuclear Reactors and Power Plants*, 2nd edn., McGraw-Hill, New York (1961).
12. Lamarsh, J.R. and Baratta, A.J. *Introduction to Nuclear Engineering*, Prentice Hall, Upper Saddle River, NJ (2001).
13. Lamarsh, J.R. *Introduction to Nuclear Reactor Theory*, 2nd printing edn., Addison-Wesley Publishing Company, Inc. (1972).
14. Cochran, R.G. and Toulfanidis, N. *The Nuclear Fuel Cycle: Analysis and Management*, American Nuclear Society, La Grange Park, IL (1999).
15. Shultis, K. and Faw, R. *Fundamentals of Nuclear Science and Engineering*, 2nd edn., CRC Press, Boca Raton, FL (2008).
16. Glasstone, S. and Eedlund, M. *The Elements of Nuclear Reactor Theory*, D Van Nostrand Company, Inc., New York (1952).
17. Glasstone, S. and Sesonske, A. *Nuclear Reactor Engineering*, 3rd edn., Van Nostrand Reinhold Company, New York (1981).
18. Knuth, D. Chapter 3: Random numbers. *The Art of Computer Programming*, 3rd edn., Vol. 2: Seminumerical Algorithms, New York (1997).
19. Kroese, D.P., Taimre, T. and Botev, Z.I. Chapter 1: Uniform random number generation, in *Handbook of Monte Carlo Methods*, John Wiley & Sons, New York (2011), 772.
20. Masterson, R.E. *Nuclear Engineering Fundamentals: A Practical Perspective*, CRC Press, Boca Raton, FL (2017).

Web References

1. *http://www.math.uah.edu/stat/.*
2. *http://en.wikipedia.org/wiki/Variance.*
3. *http://en.wikipedia.org/wiki/John_von_Neumann.*
4. *http://en.wikipedia.org/wiki/Monte_Carlo_method.*
5. *http://en.wikipedia.org/wiki/Probability_distribution.*
6. *http://en.wikipedia.org/wiki/Random_number_generation.*
7. *http://www.itl.nist.gov/div898/handbook/eda/section3/eda36.htm.*
8. *http://www.stat.yale.edu/Courses/1997-98/101/rvmnvar.htm.*
9. *http://mathworld.wolfram.com/PolyasRandomWalkConstants.html.*
10. *http://en.wikipedia.org/wiki/Diffusion#Random_Walk_.28Random_Motion.29.*

Additional References

- Important physical constants used by nuclear scientists and engineers can be found in *Appendix A.*
- Unit systems and their conversion factors can be found in *Appendix B.*
- Nuclear cross sections for many important nuclear materials can be found in *Appendix C.*
- Physical properties of important nuclear materials can be found in *Appendix D.*
- X-ray and gamma ray attenuation coefficients are discussed in more detail in *Appendix G.*
- Common integrals, PDFs, and CDFs used in Nuclear Science and Engineering are discussed in *Appendix J.*

Questions for the Student

The following questions cover the material presented in this chapter and, in some cases, previous chapters as well. They are designed to test how well the student has acquired a working knowledge of the subject matter.

1. Earlier in the chapter, we showed that fission neutrons are emitted with a variety of different energies that are determined by a statistical probability distribution X(E) called the *Watt equation*. What form of this distribution would you use in a Monte Carlo calculation?
2. Is the Watt equation an example of a PDF or a CDF?
3. Suppose that we would like to apply the four-factor formula $k_\infty = \eta\varepsilon fp$ to find the infinite multiplication factor for a reactor fuel rod of radius R. What factors in the four-factor formula can be found using a Monte Carlo method if the composition of the fuel rod and the surrounding moderating material is known?
4. Consider a large rectangular box of length L and width W, which contains one million particles on the left-hand side of the box and no particles in the rest of the box at t = 0. If the particles scatter off of one another, but are not absorbed, and we perform a Monte Carlo simulation of the particle flow, what famous equation can be deduced from this simulation?
5. What is the fundamental difference between a Monte Carlo method and a transport theory method?
6. Name two situations where using a Monte Carlo method may be preferable to solving the neutron transport equation.
7. Name four types of nuclear particles whose motion can be simulated using a Monte Carlo method.
8. Which two particles in the previous question are most important to the safe and efficient operation of a commercial nuclear power plant?
9. Suppose that a Monte Carlo method is used to determine the value of the resonance escape probability P from a nuclear fuel rod. Suppose that the error in the calculation is found to be 10%, and the value for P was determined by doing 1000 individual Monte Carlo simulations (i.e., case histories). How many individual simulations are required to reduce the error to 1%?
10. What term is used to describe the motion of an individual particle in a Monte Carlo calculation from the time it is born to the time that it dies?
11. Name two video games whose algorithms can be programmed using a Monte Carlo method.
12. What is the difference between a PDF and a CDF?
13. What is the definition of the variance V that is used by a Monte Carlo method?
14. If one encounters the function RAN () in a Monte Carlo program, what would such a function normally be used to do?
15. Why are Monte Carlo calculations more popular than they used to be?
16. If you are a sophisticated investor, what can you use a Monte Carlo method to do?
17. In a Monte Carlo simulation of a reactor core, is the importance of a particular neutron higher or lower if it is moving out of the core?
18. Name one technique that can be used to reduce the cost of a Monte Carlo calculation if the direction of the particle flow is an important factor.
19. What equation can be used to find the directional vector Ω for a neutron scattered from the nucleus of a target atom if the neutron scattering angles θ and φ are known?
20. Suppose that the elastic and inelastic scattering cross sections $\sigma_{el}(E)$ and $\sigma_{in}(E)$ are known for a material that is going to be used to build a radiation shield. Based on the values of these two parameters alone, write an expression for the probability $P_{el}(E)$ that a neutron will be elastically scattered from an atom of this material and an expression $P_{in}(E)$ for the probability that a neutron will be inelastically scattered from an atom of the same material.

Exercises for the Student

Exercise 23.1

Using the information presented in this chapter, develop a random number generator RAN () to produce a random number from 0 to 100 each time it is called.

Exercise 23.2

Using the information presented earlier in the chapter, write a Monte Carlo program to calculate the fast fission factor in a reactor lattice having a fuel rod of radius R and a pitch to diameter ratio of 2. Assume that the enrichment of the uranium is 3% and that the reactor is moderated by ordinary water.

Exercise 23.3

Now suppose that we are dealing with a fast reactor instead of a thermal reactor and that the fast reactor is cooled by liquid sodium instead of ordinary water. Write a Monte Carlo program to calculate the shape of the neutron flux in a unit cell having a fuel rod of radius R and a pitch to diameter ratio of 1.5. Assume that the fuel is 10% plutonium and 90% Uranium-238 and that the reactor lattice is hexagonal rather than square.

Exercise 23.4

A statistical probability distribution P(E) is to be constructed from the following 11 data points where E is the particle energy in MeV: P(1) = 0.25, P(2) = 1.0, P(3) = 2.5, P(4) = 4.0, P(5) = 5.0, P(6) = 5.5, P(7) = 5.0, P(8) = 4.0, P(9) = 2.5, P(10) = 1, and P(11) = 0.25. Is this probability distribution symmetrical or asymmetrical? What is the average value or the mean value of the distribution? What is the standard deviation for the 8th data point?

Exercise 23.5

Consider the following seven data points: P(1) = 0.25, P(2) = 1.0, P(3) = 2.5, P(4) = 4.0, P(5) = 2.5, P(6) = 1.0, and P(7) = 0.25. What is the statistical variance of the entire sample? Ans: The variance V of the sample is equal to the average of the squares less the square of the average, or $V = \langle v^2 \rangle - \langle v \rangle^2$.

Exercise 23.6

The PDF for the scattering of thermal neutrons in a Monte Carlo calculation is given by $P(\theta) = 1 + \cos(\theta)$. What is the corresponding CDF?

Exercise 23.7

The PDF for the emission of 1 MeV gamma rays from a radioactive material can be described by a statistical probability distribution of the form $P(x) = 2e^{-2t}$, where t is the time in seconds. Assuming that the process described by the PDF starts at t = 0, what is its corresponding CDF? What is its inverse CDF?

Exercise 23.8

Using the middle-squared method developed by John von Neumann to build the explosive lens for the first atomic bomb (see Section 23.16), calculate two random numbers between 0 and 999 to be used in a Monte Carlo Calculation. Assume the random numbers used to begin the process are the value of π (3.1415926535) and the value of the natural exponent e (2.7182818284).

Exercise 23.9

Monte Carlo calculations frequently require a random number generator that emulates the shape of a certain statistical probability distribution function P(x). If the shape of this function is given by P(x) = x, what is the CDF, and what is the inverse CDF?

Exercise 23.10

Suppose that we would like to simulate the random walk of a nuclear particle in one dimension. The particle starts on the x-axis at the origin (x = 0) and then moves a distance +1 or −1 in the +x or −x directions in each step of the process. Suppose that it moves a physical distance D = 1.5 cm. from the origin after 50 steps. What will its average distance from the origin be after 5000 steps?

Appendix A: Important Nuclear and Physical Constants*

A.1 Physical Constants and Their Values

Atomic mass unit (AMU)	$1.6605389 \times 10^{-27}$ kg
	931.494043 MeV/c^2
Avogadro's number A′	6.022045×10^{23} atoms or entities per mol
Boltzmann's constant k	1.380662×10^{-23} J/K
	0.861735×10^{-4} eV/K
Coulomb's constant k_c	$8.9875517873681764 \times 10^{9}$ N m^2/Coulomb^2
Diameter of an atom	$\sim 1 \times 10^{-8}$ cm
Diameter of a nucleus	$\sim 1 \times 10^{-12}$ cm
Diameter of a proton or neutron	$\sim 1 \times 10^{-16}$ cm
Electron rest mass m_e	0.5110034 MeV
	9.109534×10^{-31} kg
Electron charge e^-	$1.6021892 \times 10^{-19}$ Coulombs
Hydrogen atom rest mass m_h	1.007825 AMU
Ideal gas constant R	8.31441 J/mol/K
Light year (distance traveled) d_l	9,460,000,000,000 km
Microscopic cross section	1 barn = 1×10^{-24} cm^2
Neutron rest mass m_n	939.5731 MeV
	$1.6749544 \times 10^{-27}$ kg
Planck's constant h	$6.6260695 \times 10^{-34}$ J/s
	$4.1356675 \times 10^{-15}$ eV s
hc	$1.98644568 \times 10^{-23}$ J cm
Proton rest mass m_p	938.2796 MeV
	$1.6726485 \times 10^{-27}$ kg
Speed of light (in a vacuum) c	1.86282397×10^{5} miles/s
	2.99792459×10^{8} m/s
	$2.99792459 \times 10^{10}$ cm/s

Source: These constants and other important constants can be found on the web at the following URL: *http://physics.nist.gov/cuu/Constants/index.html*.

Note: These are particularly important when dealing with atomic and nuclear phenomena.

* *Note:* The following appendices are provided for the interested reader. To conserve space, the appendices may be found at: *https://www.crcpress.com/Nuclear-Engineering-Fundamentals-A-Practical-Approach/Masterson/9781439808870*. An error-reporting facility for any errors in the appendices or in the book in general may also be found at this site.

A.2 Units of Energy and Power

1 eV	$1.6021892 \times 10^{-19}$ J
1 keV	1000 eV
1 MeV	1,000,000 eV
1 watt (W)	1 J/s
1 kilowatt (kW)	1,000 J/s
1 megawatt (MW)	1,000,000 J/s
1 J	$6.24150934 \times 10^{18}$ eV
1 kJ	$6.24150934 \times 10^{21}$ eV
1 MJ	$6.24150934 \times 10^{24}$ eV
6.2×10^{18} eV/s	1 j/s = 1 W
6.2×10^{12} MeV/s	1 j/s = 1 W
1 kW h	3.6×10^{6} J

A.3 Relationship between Number of Fissions per Second and Thermal Energy Production

1 W thermal energy = 1 J/s (thermal) = 3.12×10^{10} fissions/s
Energy conversion using $E = mc^2$: 1 AMU of mass m = 931.494 MeV/c^2

A.4 Time and Decay Conversion Factors and Constants

1 minute	60 seconds
1 day	86,400 seconds
1 year	3.156×10^{7} seconds
1 curie (ci)	3.7×10^{10} disintegrations per second
1 becquerel (Bq)	1 disintegration per second
1 becquerel (Bq)	2.703×10^{-11} ci $\approx$ 27 picocuries

Half-life = $T_{1/2} = 0.693\ \tau$.
Decay constant = $\lambda = 1/\tau$.
Average life = τ (usually measured in seconds).

A.5 Units of the Reactivity

Absolute units	
1 mile = 0.01	
1 millirho = 1 mrho = 0.001	
1 pcm = 0.01 mrho = 0.00001	
Relative units	
1 dollar = β	
1 cent = 0.01 β	
β = delayed neutron fraction	β = 0.0067 for U-235
	β = 0.0026 for U-233
	β = 0.0020 for Pu-239

Appendix B: Unit Systems and Conversion Factors

B.1 Common Unit Systems

There are two common systems of units in use in the world today—the *SI unit system* and the *English unit system*. The SI unit system is a more modern unit system based on the metric unit system. Conversions within the SI unit system are normally expressed in increments of 10. The SI unit system is now used in most of the civilized world. Two countries that have not entirely converted to the SI unit system are the United States and England, where a combination of English and SI units is still used. Eventually, both countries are expected to convert entirely to the SI unit system; however, this conversion may take a while to complete. The reactor vendors in the United States use a combination of SI and English units. In fact, it is not uncommon for a reactor vendor to use SI units, CGS units (which are sometimes used in the field of nuclear physics), and English units for other important parameters such as temperature, pressure, and length measurement.

Sometimes, this is a source of confusion outside of the United States, but because so much of the current U.S. nuclear infrastructure is based on the English unit system. For this reason, conversion tables between the SI unit system, the CGS unit system, and the English unit system are presented in this appendix. However, as the reader may have already gathered, this book is based primarily on the SI unit system. The units of length, mass, time, and temperature, in addition to the units of force, pressure, energy, power, and heat, are compared to each other in Table B.1. In this table, a total of nine different types of units are presented. Other unit conversion tables and conversion facilities may be found on the Internet.

B.2 Prefixes, Primary Units, and Derived Units

The prefixes and abbreviations associated with the SI unit system are shown in Table B.2, and the primary units used by the SI unit system are shown in Table B.3. Conversion factors between the SI unit system and other unit systems are presented in Table B.4. Some of these conversion factors are fairly obvious. For example, there are 100 cm in one meter, and 1 m is equal to 39.37 in. or approximately 3.28 ft.

TABLE B.1
Comparison of the Primary Units in Each Unit System

Quantity	SI Unit	SI Symbol	CGS Unit	CGS Symbol	English Unit	English Symbol
Length	Meter	m	Centimeter	cm	Inch, foot	in, ft
Mass	Kilogram	kg	Gram	g or gm	Pound	lb
Time	Second	s	Second	sec	Second	sec
Force	Newton	N	Dyne	dyne	Pound	lb
Temperature	Kelvin	K	Celsius	°C	Fahrenheit	°F
Pressure	Pascal	Pa	Dyne/cm^2	dyne/cm^2	Pound/in^2	psi
Energy	Joule	J	Erg	erg	Foot pound	ft-lb
Power	Watt	W	Erg/sec	erg/sec	Foot Pound/sec	ft-lb/sec
Heat	Joule	J	Calorie	cal	British thermal unit	BTU

TABLE B.2
Prefixes Associated with the SI Unit System

Prefix	Symbol	Factor	Prefix	Symbol	Factor
Mera-	T	10^{12}	Deci-	d	10^{-1}
Giga-	G	10^{9}	Centi-	c	10^{-2}
Mega-	M	10^{6}	Milli-	m	10^{-3}
Kilo-	K	10^{3}	Micro-	μ	10^{-6}
Hecto-	H	10^{2}	Nano-	n	10^{-9}
Deka-	da	10^{1}	Pico-	p	10^{-12}

TABLE B.3
Primary Units in the SI Unit System

Base (or Primary) SI Units		
Length	Meter	m
Mass	Kilogram	kg
Time	Second	s
Pressure	Pascal	Pa
Thermodynamic temperature	Degree Kelvin	K
Amount of a substance	Mole	mol
Electric current	Ampere	A

TABLE B.4
Derived Units in the SI Unit System and Conversion Factors between the SI Unit System and Other Unit Systems

Quantity	Name	Derived SI Unit	SI Unit	British Unit
Length	Centimeter	cm	10^{-2} m	0.3937 in
Volume	Cubic centimeter	cm^3	10^{-6} m^3	0.06102 in^3
Volume	Liter	l	10^{-3} m^3	0.03532 ft^3
Velocity	Centimeter/sec	cm/s	10^{-2} m/s	0.03281 ft/s
Mass	Gram	g	10^{-3} kg	2.205×10^{-3} lb
Mass	Tonne	T (MT)	10^3 kg	2205 lb
Density	Gram/cubic centimeter	g/cm^3	10^3 kg/m^3	62.42 lb/ft^3
Force	Newton	N	1 $kg \cdot m/s^2$	0.2248 lbf
Pressure	Bar	bar	1×10^5 N/m^2	14.5 lb/in^2
Heat	Joule	J	1 $N \cdot m$	9.478×10^{-4} BTU
Energy	Joule	J	1 $N \cdot m$	9.478×10^{-4} BTU
Power	Watt	W	1 J/s	9.478×10^{-4} BTU
Energy density	Joule/cubic centimeter	J/cm^3	1×10^6 J/m^{-3}	26.83 BTU/ft^3
Power density	Watt/cm (linear power)	W/cm	1×10^2 W/m^{-1}	0.0305 kW/ft
Power density	Watt/cm^2 (energy flux)	W/cm^2	1×10^4 W/m^{-2}	0.930 kW/ft^2
Power density	Watt/cm^3 (energy density)	W/cm^3	1×10^6 W/m^{-3}	28.35 kW/ft^3
Temperature	Degree Celsius	°C	K + 273.15	°F = 1.8°C + 32
Electric charge	Coulomb	C	$A \cdot s$	N/A

In addition to the different ways in which an object is measured, the world currently uses three different temperature scales—the Kelvin or absolute temperature scale, the centigrade or Celsius temperature scale, and the Fahrenheit temperature scale. The nuclear industry uses a combination of these temperature scales as well. The temperatures in all three of these scales are shown in Table B.5. Formulas for converting between the temperatures in each of these scales are also presented at the end of this appendix.

Non-SI Units Commonly Used by the Nuclear Industry[a]			
Electron volt	Energy	eV	1.60219×10^{-19} J
Atomic mass unit	Mass	AMU	1.66053×10^{-27} kg
Bar	Pressure	bar	1×10^5 N/m^2
Barn	Cross section	b	1×10^{-24} $cm^2 = 1 \times 10^{-28}$ m^2

[a] As recognized by the International Organization for Standardization.

TABLE B.5
The World's Primary Temperature Scales and How they Compare

Temperature (°C)	Temperature (K)	Temperature (°F)
0 (water freezes)	273	32
5	278	41
10	283	50
15	288	59
20	293	68
25	298	77
30	303	86
35	308	95
40	313	104
45	318	113
50	323	122
55	328	131
60	333	140
65	338	149
70	343	158
75	348	167
80	353	176
85	358	185
90	363	194
95	368	203
100 *(water boils at atmospheric pressure)*	373	212
150	423	302
200	473	392
250 *(operating range)*[a]	523	482
300 *(operating range)*[b]	573	572
350 *(operating range)*[c]	623	662
400 *(operating range)*[c]	673	752
450 *(operating range)*[c]	723	842
500 *(operating range)*[c]	773	932

[a] Boiling water reactor (BWR).
[b] Pressurized water reactor (PWR).
[c] Other reactors (LMFBRs and gas reactors).

B.3 Temperature Conversion Formulas

Temperature Conversion Formulas	
To convert to degrees Celsius	°C = K + 273.15
To convert to degrees Fahrenheit	°F = 1.8°C + 32

Appendix C: Nuclear Cross Sections and Reaction Rates

C.1 Nuclear Cross Sections

This appendix is devoted to a discussion of nuclear cross sections and reaction rates. Thermal neutron cross sections are presented in Table C.1, and fast neutron cross sections are presented in Table C.2. These cross sections and the ways in which they are used are discussed in Chapters 4 and 5. The reader should consult these chapters if more information regarding the use of nuclear cross sections is required. The line of demarcation between the fast neutron cross-section libraries and the thermal neutron cross-section libraries is usually taken to be 1 eV. Hence, Tables C.1 and C.2 adhere to these conventions as well. The values for the cross sections that appear in these tables are taken from many different data sources including the ENDF B database, the JENDL database, and other reliable data sources up to and including BNL-325. Unfortunately, the values for these fast and thermal cross sections do not always agree from one data source to another because different weighting and averaging schemes are sometimes used within the individual energy groups. Furthermore, in some libraries, the line of demarcation between the fast and thermal energy groups is not exactly 1 eV.

In the tables that follow, every effort has been made to reconcile these differences and to present the reader with a "consistent set" of nuclear cross sections that can be used to perform reactor physics calculations with a high degree of precision. In some cases, the cross sections presented in Duderstadt and Hamilton, Lamarsh and Baratta, and Shultis and Faw have also been used. Notice that the reaction cross sections for the fast energy group are many times smaller than those for the thermal energy group, and, in general, a fast neutron cross section is at least ten times smaller than a thermal one for the same element or isotope. The reasons for this are explained in more detail in Chapters 4 and 5. The reader should feel free to refer to these chapters in the event a more detailed physical explanation is required. The physical properties of the materials in these cross-section tables are presented in Appendix D. Hence, Appendices C and D contain all the necesary data a nuclear scientist or engineer requires to calculate most common reaction rates.

C.2 Repositories for Nuclear Cross-Section Data

As mentioned in the body of the book, large repositories of nuclear cross-section data are maintained by several national nuclear data centers in different countries around the world. In the United States, the two most prominent nuclear data centers are the Radiation Shielding and Information Center at the Oak Ridge National Laboratory in Oak Ridge, Tennessee, and the National Nuclear Data Center at the Brookhaven National Laboratory in Brookhaven, New York. Outside of the United States, the International Atomic Energy Agency in Europe and the Japan Atomic Energy Research Institute in Japan perform similar functions. These data resources can also be found at the following websites:

nndc@bnl.gov
pdc@ornl.gov
online@iaeand.iaea.or.at
www.ndc.tokai.jaeri.go.jp/index.html

C.3 Tools for Plotting Nuclear Cross-Section Data

For the data listed on these websites, a slick and highly interactive plotting tool is provided by the Korean Atomic Energy Research Institute to anyone who has access to a standard web browser. The name of this *plotting tool* is ENDFPLOT, and ENDFPLOT was used to plot many of the images of nuclear cross-section data that were presented in earlier chapters. A description of ENDFPLOT and its capabilities can be found at the following URL:

http://atom.kaeri.re.kr/endfplot.shtml

The ENDFPLOT is implemented as a *Java applet*, so all that is required to use it is a standard web browser. One of the particularly useful features of this plotting facility is a feature that allows the user to plot *multiple cross sections* for a material like U-238 (such as the fission, absorption, and scattering cross sections) on the same graph at the same time, but in different colors to let the behavior of the various cross sections stand out. A cross section can also be deleted from or added to the plot. Figure C.1 is an example of a graph that was created using ENDFPLOT.

It is also possible to use this plotting facility to compare the cross sections of several elements at the same time, such as the scattering cross sections for carbon, hydrogen, and oxygen. The reader is encouraged to use this interactive tool when attempting to visualize the energy dependence of a particular nuclear cross section. It is also helpful when comparing the cross sections belonging to a number of different nuclear materials.

TABLE C.1
Thermal Cross Sections for Some Important Nuclear Materials**

Thermal Microscopic Cross Sections for Common Nuclear Materials						
Substance	Symbol	Capture σ_c (barns)	Fission σ_f (barns)	Absorption σ_f (barns)	Scattering σ_s (barns)	Total σ_t (barns)
Aluminum	Al	0.230	0	0	1.490	1.72
Americium	Am-241	684.3	3.112	687.41	11.82	699.232
Barium	Ba	1.200	0	1.200	8	9.2
Beryllium	Be	0.0092	0	0.0092	6.140	6.149
Bismuth	Bi	0.033	0	0.033	9	9.033
Boron 10	B-10	3837	0	3837	2.254	3839.254
Boron 11	B-11	0.005	0	0.005	5.281	5.286
Cadmium	Cd[c]	2424.150	0	2424.150	6.500	2430.65
Calcium	Ca	0.430	0	0.430	3.0	3.43
Carbon (graphite)	C-12	0.0034	0	0.0034	4.75	4.753
Carbon (natural)	C	0.0038	0	0.0038	4.942	4.94238
Cesium	Cs	29.000	0	29.000	20	49
Chlorine	Cl	33.200	0	33.200	16	49.2
Chromium	Cr	3.100	0	3.100	3.800	6.9
Cobalt	Co	37.200	0	37.200	6.700	43.9
Copper	Cu	3.790	0	3.790	7.900	11.69
Deuterium	D	0.0025	0	0.0025	10.4	10.4025
Gadolinium	Gd	49000.000	0	49000.000	137.7	49137.7
Gold	Au	98.800	0	98.800	9.3	108.1
Hafnium	Hf	102.000	0	102.000	8.000	110
Helium	He	0.001	0	0.001	0.860	0.861
Hydrogen	H	0.332	0	0.332	30.33	30.662
Indium	In[c]	193.500	0	193.500	2.588	196.088
Iodine	I-131	80.03	0	80.03	3.615	83.645
Iodine	I-135	80.03	0	80.03	3.214	83.244
Iridium	Ir	426.000	0	426.000	20.000	446.00
Iron	Fe	2.550	0	2.550	10.900	13.45
Krypton	Kr	25.000	0	25.000	7.500	32.5
Lead	Pb-206	0.026	0	0.026	10.85	10.876
Lead	Pb-207	0.620	0	0.620	11.51	12.13
Lead	Pb-208	0.0002	0	0.0002	11.46	11.4602
Lithium	Li-6	0.045	0	0.045	1.4	1.445
Lithium	Li-7	0.045	0	0.045	0.97	1.015
Magnesium	Mg	0.063	0	0.063	3.420	3.483
Manganese	Mn	13.300	0	13.300	2.100	15.4
Mercury	Hg	370.400	0	370.400	24.36	394.76
Neptunium	Np-236	121.300	2808.00	2929.30	9.657	2938.957
Nickel	Ni	4.43	0	4.43	17.3	21.73
Nitrogen	N	1.850	0	1.850	10.600	20.45
Oxygen	O	0.00027	0	0.00027	3.870	3.87027
Plutonium	Pu-238	420.8	17.77	438.57	154.6	593.17
Plutonium	Pu-239[c]	270.000	747.401	1017.40	7.7	1025.101
Plutonium	Pu-240	293.000	0.064	293.064	2.667	295.731
Plutonium	Pu-241	362.000	1012.0	1375.0	11.26	1385.26
Plutonium	Pu-242	19.90	0.00024	19.90	8.326	28.22624

(*Continued*)

TABLE C.1 (*Continued*)
Thermal Cross Sections for Some Important Nuclear Materials**

Thermal Microscopic Cross Sections for Common Nuclear Materials

Substance	Symbol	Capture σ_c (barns)	Fission σ_f (barns)	Absorption σ_f (barns)	Scattering σ_s (barns)	Total σ_t (barns)
Plutonium dioxide	PuO_2	21.3	0.00001177 (U-238 only)	Varies with Pu content[b]	10.3	Varies
Potassium	K	2.100	0	2.100	1.500	3.6
Promethium	Pm-148	2001.000	0	2001.000	6.222	2007.222
Radium	Ra-224	11.500	0	11.500	20.53	24.03
Rubidium	Rb	0.370	0	0.370	6.200	6.57
Samarium	Sm-149[c]	40540.00	0	40540.00	178.8	40718.8
Samarium	Sm-152	205.9	0	205.9	3.078	208.978
Selenium	Se	11.700	0	11.700	9.700	21.4
Silicon	Si	0.160	0	0.160	2.200	2.36
Silver	Ag	63.600	0	63.600	6	69.6
Sodium	Na	0.528	0	0.528	3.280	3.808
Strontium	Sr	0.530	0	0.530	10.000	10.53
Thorium	Th	7.400	0	7.400	20.670	28.07
Tin	Sn	0.630	0	0.630	50	50.63
Titanium	Ti	6.100	0	6.100	4.000	10.1
Uranium	U-233[c]	45.800	528.45	574.25	20.9	589.15
Uranium	U-234	100.300	0.465	100.77	19.41	120.175
Uranium	U-235[c]	96.685	585.086	681.77	14	695.771
Uranium	U-236	5.160	0.00026	5.160	10.83	15.99026
Uranium	U-237	452.300	1.702	454.00	22.44	476.442
Uranium	U-238[c]	2.717	0.00001177	2.717	8.871	11.5881
Uranium (natural)	U	3.380	4.213	7.593	9.342	16.935
Uranium dioxide	UO_2	7.6	0.00001177 (U-238 only)	Varies with enrichment[a]	16.7	Varies
Water (light)	H_2O	0.644	0	0.644	103	103.664
Water (heavy)	D_2O	0.00133	0	0.00133	13.6	13.6
Xenon	Xe-131	99.68	0	99.68	31.81	131.49
Xenon	Xe-133	190.1	0	190.1	3.615	193.715
Xenon	Xe-135[c]	2778000	0	2778000	332200	3110200
Zircaloy-II	Zirc-2	0.190	0	0.190	6.5	6.69
Zircaloy-IV	Zirc-4	0.190	0	0.190	6.5	6.69
Zirconium	Zr	0.185	0	0.185	6.460	6.645
Fission products of U-235	N/A	4486	0	4486	10	4496
Fission products of Pu-239	N/A	2086	0	2086	1	2087

Thermal Microscopic Cross Sections for Common Nuclear Materials

Substance	Symbol	Density (10^{24}/cm^3)	Capture Σ_c (cm^{-1})	Fission Σ_f (cm^{-1})	Absorption Σ_a (cm^{-1})	Scattering Σ_s (cm^{-1})	Total Σ_t (cm^{-1})
Aluminum	Al	0.06024	0.0138	0	0	0.0896	0.1035
Americium	Am-241	0.04976	34.051	0.1548	34.2058	0.5882	34.794
Barium	Ba	0.01535	0.0184	0	0.0184	0.1228	0.1412
Beryllium	Be	0.12361	0.0011	0	0.0011	0.7589	0.7590
Bismuth	Bi	0.02824	0.0009	0	0.0009	0.0254	0.0255
Boron 10	B-10	0.12810	491.14	0	491.14	0.2880	491.42

(*Continued*)

TABLE C.1 (*Continued*)
Thermal Cross Sections for Some Important Nuclear Materials**

Thermal Microscopic Cross Sections for Common Nuclear Materials							
Substance	Symbol	Density (10^{24}/cm^3)	Capture Σ_c (cm^{-1})	Fission Σ_f (cm^{-1})	Absorption Σ_a (cm^{-1})	Scattering Σ_s (cm^{-1})	Total Σ_t (cm^{-1})
Boron 11	B-11	0.12810	0.0006	0	0.0006	0.6758	0.6759
Cadmium	Cd[c]	0.04635	112.35	0	112.35	0.2990	112.65
Calcium	Ca	0.02329	0.0103	0	0.0103	0.0720	0.0823
Carbon (graphite)	C-12	0.08023	0.0002728	0	0.0002728	0.3811	0.3814
Carbon (natural)	C	0.08023	0.00003	0	0.00003	0.3952	0.3952
Cesium	Cs	0.00861	0.2494	0	0.2494	0.1721	0.4214
Chlorine	Cl						
Chromium	Cr	0.08328	0.2574	0	0.2574	0.3165	0.5747
Cobalt	Co	0.08993	3.3108	0	3.3108	0.5963	3.9071
Copper	Cu	0.08493	0.3221	0	0.3221	0.6715	0.9936
Deuterium	D	0.000054	1.35×10^{-7}	0	1.35×10^{-7}	0.00056	0.00056
Gadolinium	Gd	0.03045	1492.05	0	1492.05	4,1929	1496.24
Gold	Au	0.05907	5.8292	0	5.8292	0.5497	6.3779
Hafnium	Hf	0.04508	4.5910	0	4.5910	0.3606	4.9516
Helium	He	0.000026	2.6×10^{-8}	0	2.6×10^{-8}	2.2×10^{-5}	2.2×10^{-5}
Hydrogen	H	0.000053	1.7×10^{-4}	0	1.7×10^{-4}	1.5×10^{-3}	1.51×10^{-3}
Indium	In[c]	0.03834	7.4110	0	7.4110	0.0992	7.5102
Iodine	I-131	0.02340	1.8727	0	1.8727	0.0846	1.9573
Iodine	I-135	0.02340	1.8727	0	1.8727	0.0752	1.9479
Iridium	Ir	0.07050	30.033	0	30.033	1.4100	31.443
Iron	Fe	0.08487	0.2162	0	0.2162	0.9243	1.1405
Krypton	Kr	0.000026	6.5×10^{-4}	0	6.5×10^{-4}	1.95×10^{-4}	8.45×10^{-4}
Lead	Pb-206	0.03296	8.58×10^{-4}	0	8.58×10^{-4}	0.3580	0.3581
Lead	Pb-207	0.03296	0.0205	0	0.0205	0.3798	0.4003
Lead	Pb-208	0.03296	6.6×10^{-6}	0	6.6×10^{-6}	0.3781	0.3782
Lithium	Li-6	0.04600	0.0020	0	0.0020	0.0644	0.0664
Lithium	Li-7	0.04600	0.0020	0	0.0020	0.0446	0.0466
Magnesium	Mg	0.04310	0.0027	0	0.0027	0.1470	0.1497
Manganese	Mn	0.08145	1.0778	0	1.0778	0.1701	1.2479
Mercury	hg	0.04068	14.820	0	14.820	0.9746	15.7946
Neptunium	Np-236	0.05196	6.2954	145.73	152.025	0.5012	152.53
Nickel	Ni	0.09130	0.4044	0	0.4044	1.5794	1.9839
Nitrogen	N	0.000053	9.8×10^{-5}	0	9.8×10^{-5}	5.6×10^{-4}	5.7×10^{-4}
Oxygen	O	0.0000537	1.4×10^{-8}	0	1.4×10^{-8}	2.08×10^{-4}	2.08×10^{-4}
Plutonium	Pu-238	0.0498	20.96	0.8849	21.845	7.6991	29.544
Plutonium	Pu-239[c]	0.0498	13.446	37.220	50.666	0.3835	51.05
Plutonium	Pu-240	0.0498	14.59	0.000318	14.5903	0.1328	14.723
Plutonium	Pu-241	0.0498	18.027	50.397	68.424	0.5607	68.985
Plutonium	Pu-242	0.0498	0.9910	1.19×10^{-5}	0.9910	0.4146	1.4056
Plutonium dioxide	PuO_2	0.0255	0.543	Varies with Pu content[b]	Varies	0.2626	Varies
Potassium	K	0.01325	0.0275	0	0.0275	0.0195	0.0470
Promethium	Pm-148			0			
Radium	Ra-224	0.01332	0.1529	0	0.1529	0.2730	0.4259
Rubidium	Rb	0.01078	0.0037	0	0.0037	0.0620	0.0657
Samarium	Sm-149	0.02776	1125.39	0	1125.39	4.9638	1130.35

(*Continued*)

TABLE C.1 (*Continued*)

Thermal Cross Sections for Some Important Nuclear Materials**

Thermal Microscopic Cross Sections for Common Nuclear Materials							
Substance	Symbol	Density (10^{24}/cm^3)	Capture Σ_c (cm^{-1})	Fission Σ_f (cm^{-1})	Absorption Σ_a (cm^{-1})	Scattering Σ_s (cm^{-1})	Total Σ_t (cm^{-1})
Samarium	Sm-152	0.02776	5.7157	0	5.7157	0.0855	5.8015
Selenium	Se	0.03669	0.4329	0	0.4329	0.3589	0.7918
Silicon	Si	0.04996	0.0080	0	0.0080	0.1101	0.1181
Silver	Ag	0.05857	3.7206	0	3.7206	0.3510	4.0716
Sodium	Na	0.02541	0.0135	0	0.0135	0.0808	0.0941
Strontium	Sr	0.01787	0.0095	0	0.0095	0.1787	0.1882
Thorium	Th	0.03039	0.2221	0	0.2221	0.6283	0.8505
Tin	Sn	0.03703	0.0233	0	0.0233	1.850	1.8733
Titanium	Ti	0.05670	0.3416	0	0.3416	0.2268	0.5684
Uranium	U-233[c]	0.04783	2.189	25.26	27.449	0.999	28.448
Uranium	U-234	0.04783	4.794	0.0222	4.816	0.928	5.744
Uranium	U-235[c]	0.04783	4.621	27.96	32.581	0.669	33.25
Uranium	U-236	0.04783	0.2466	1.25×10^{-5}	0.2466	0.518	0.765
Uranium	U-237	0.04783	21.62	0.0812	21.7012	1.072	22.77
Uranium	U-238[c]	0.04783	0.130	5.25×10^{-7}	0.130	0.4239	0.5539
Uranium (natural)	U	0.04783	0.1616	0.2014	0.363	0.446	0.8095
Uranium dioxide	UO_2	0.0223	0.1695	Varies with enrichment[a]	Varies	0.3724	Varies
Water (light)	H_2O	0.03343	0.02220	0.0	0.02220	3.443	3.465
Water (heavy)	D_2O	0.03323	0.0000442	0.0	0.0000442	0.4519	0.4519
Xenon	Xe-131	0.0268	2.671	0	2.671	0.8525	3.524
Xenon	Xe-133	0.0268	5.094	0	5.094	0.0968	5.192
Xenon	Xe-135[c]	0.0268	74450.4	0	74450.4	8902.96	83353.89
Zircaloy-II	Zirc-2	0.04325	0.00821	0	0.00821	0.2808	0.2890
Zircaloy-IV	Zirc-4	0.04325	0.00821	0	0.00821	0.2808	0.2890
Zirconium	Zr	0.04291	0.0079	0	0.0079	0.2771	0.2857
Fission products of U-235	N/A	Varies	Varies	0	Varies	Varies	Varies
Fission products of Pu-239	N/A	Varies	Varies	0	Varies	Varies	Varies

Note: Cross sections of common nuclear materials are shown for the thermal energy range (0.025 eV).

Microscopic cross sections (σ) are measured in barns, where 1 barn = 10^{-24} cm^2.

Macroscopic cross sections (Σ) are measured in cm^{-1}.

Atomic densities are measured in atoms or molecules/cm^3 × 10^{24}.

Additional note: Xenon is normally a colorless gas that emits a blue glow when excited by an electric charge; here, we have used an average density of 5.89 g/cm^3. In a reactor, this value may be different because the temperatures and pressures may be different.

Average neutron energy is assumed to be 0.025 eV.

[a] At thermal energies, the value varies with the enrichment according to the equation $\Sigma_{f\,UO_2} = N_{U\text{-}235} \cdot \sigma_{fU\text{-}235} = 0.1304 \cdot e$ (cm^{-1}) when the enrichment e is measured in percent.

[b] At thermal energies, the value varies with plutonium content according to the equation $\Sigma_{f\,PUO_2} = N_{Pu\text{-}239} \cdot \sigma_{f\,Pu\text{-}239} = 0.190 \cdot c$ (cm^{-1}) when the plutonium content c is measured in percent.

[c] Non-1/v absorber. See Table C.4 for the appropriate non-1/v correction factor.

C.4 Converting from Microscopic Cross Sections to Macroscopic Ones

Sometimes, it is helpful to be able to convert a microscopic cross section into a macroscopic one. To do so, one simply multiplies the microscopic cross section σ_x (which has the units of cm^2) by the atomic number density N of a material (which has the units of atoms/cm^3). The macroscopic cross section for a specific reaction type x is then given by $\Sigma_x = N\sigma_x$, where x = a, c, f, s, or t. The macroscopic cross section has the units of cm^{-1}.

TABLE C.2
Fast Cross Sections for Some Important Nuclear Materials**

Fast Microscopic Cross Sections for Common Nuclear Materials

Substance	Symbol	Capture σ_c (barns)	Fission σ_f (barns)	Absorption σ_f (barns)	Scattering σ_s (barns)	Total σ_t (barns)
Aluminum	Al	0	0	0	2.37	2.37
Beryllium	Be	0.003	0	0.003	3.25	3.253
Boron 10	B-10	2.73462	0	2.73462	2.13	4.86
Boron 11	B-11	0	0	0	2.13	2.13
Cadmium	Cd	0.266766	0	0.266766	6.44	6.706
Calcium	Ca	0.004	0	0.004	1.14	1.144
Carbon (graphite)	C-12	0.00031285	0	0.00031285	11.2	11.2
Carbon (natural)	C	0.00001	0	0.00001	2.000	2.000
Chromium	Cr	0.002	0	0.002	3.000	3.002
Copper	Cu	0.011	0	0.011	3.4	3.411
Deuterium	D	0.000007	0	0.000007	2.871	2.871
Gadolinium	Gd	0.223	0	0.223	7.107	7.33
Helium	He	0	0	0	7.08	7.08
Hydrogen	H	0.0001	0	0.0001	4.26	4.26
Indium	In	0.020	0	0.020	4.000	4.020
Iron	Fe	0.0170228	0	0.0170228	5.18	5.197
Lead	Pb-206	0.0033	0	0.0033	4.39	4.39
Lithium	Li-6	0.230	0	0.230	1.05	1.28
Lithium	Li-7	0	0	0	1.57	1.57
Magnesium	Mg	0.001	0	0.001	2.66	2.66
Manganese	Mn	0.003	0	0.003	3.17	3.17
Nickel	Ni	0.008	0	0.008	3.000	3.008
Nitrogen	N	0.021	0	0.021	2.39	2.39
Oxygen	O	0.00000003	0	0.00000003	8.22	8.22
Plutonium	Pu-238	0.19	1.8	1.99	4.67	6.66
Plutonium	Pu-239	0.49614	1.7973	2.2934	6.98	9.273
Plutonium	Pu-240	0.108	1.95	2.058	5.09	7.15
Plutonium	Pu-241	0.117	2.01	2.127	5.85	7.98
Plutonium	Pu-242	0.098	0.85	0.948	6.35	7.30
Plutonium dioxide	PuO_2	0.49	1.75	2.24	7.5	Varies
Silicon	Si	0.001	0	0.001	4.43	4.43
Sodium	Na	0.0027511	0	0.0027511	3.17	3.172
Thorium	Th-232	0.38157	0.010193	0.3917	6.86	7.25
Uranium	U-233	0.27176	2.7323	3.004	6.71	9.714
Uranium	U-235	0.55549	1.9041	2.4595	6.73	9.189
Uranium	U-238	0.33188	0.042758	0.3746	6.87	7.245
Uranium (natural)	U	0.12	0.06	0.18	6.83	7.01
Water (light)	H_2O	0.00051554	0	0.00051554	16.9	16.9
Water (heavy)	D_2O	0.00011459	0	0.00011459	20.4	20.4
Xenon	Xe-135	0.0008	0	0.0008	5.000	5.0008
Zirconium	Zr	0.0265766	0	0.0265766	5.82	5.846
Fission products of U-235	N/A	0.00036	0	0.00036	7.43	7.43
Fission products of Pu-239	N/A	0.00093	0	0.00093	7.48	7.48

Fast Microscopic Cross Sections for Common Nuclear Materials

Substance	Symbol	Density (10^{24}/cm^3)	Capture Σ_c (cm^{-1})	Fission Σ_f (cm^{-1})	Absorption Σ_a (cm^{-1})	Scattering Σ_s (cm^{-1})	Total Σ_t (cm^{-1})
Aluminum	Al	0.06024	0	0	0	0.1422	0.1422
Beryllium	Be	0.12361	0.000037	0	0.000037	0.4001	0.4001

(*Continued*)

TABLE C.2 (*Continued*)

Fast Cross Sections for Some Important Nuclear Materials**

Fast Microscopic Cross Sections for Common Nuclear Materials							
Substance	Symbol	Density (10^{24}/cm^3)	Capture Σ_c (cm^{-1})	Fission Σ_f (cm^{-1})	Absorption Σ_a (cm^{-1})	Scattering Σ_s (cm^{-1})	Total Σ_t (cm^{-1})
Boron 10	B-10	0.12810	0.3494	0	0.3494	0.2726	0.6220
Boron 11	B-11	0.12810	0	0	0	0.2726	0.2726
Cadmium	Cd	0.04635	0.0123	0	0.0123	0.2982	0.3105
Calcium	Ca	0.02329	0.000092	0	0.000092	0.0262	0.0262
Carbon (graphite)	C-12	0.08023	0.000025	0	0.000025	0.8962	0.8962
Carbon (natural)	C	0.08023	0.0000008	0	0.0000008	0.160	0.160
Chromium	Cr	0.08328	0.000167	0	0.000167	0.2496	0.2497
Copper	Cu	0.08493	0.000935	0	0.000935	0.2890	0.2899
Deuterium	D	0.000054	~0	0	~0	0.000155	0.000155
Gadolinium	Gd	0.03045	0.00679	0	0.00679	0.2160	0.2167
Helium	He	0.000026	0	0	0	0.00018	0.00018
Hydrogen	H	0.000053	5.0×10^{-9}	0	5.0×10^{-9}	0.00021	0.00021
Indium	In	0.03834	0.00076	0	0.00076	0.1520	0.1527
Iron	Fe	0.08487	0.00144	0	0.00144	0.4392	0.4407
Lead	Pb-206	0.03296	0.000109	0	0.000109	0.1448	0.1449
Lithium	Li-6	0.04600	0.01058	0	0.01058	0.0483	0.0588
Lithium	Li-7	0.04600	~0.0	0	~0.0	0.0722	0.0722
Magnesium	Mg	0.04310	0.000043	0	0.000043	0.1144	0.1144
Manganese	Mn	0.08145	0.00025	0	0.00025	0.2544	0.2546
Nickel	Ni	0.09130	0.00075	0	0.00075	0.2702	0.2710
Nitrogen	N	0.000053	0.000001	0	0.000001	0.00012	0.00012
Oxygen	O	0.0000537	~0.0	0	~0.0	0.00041	0.00041
Plutonium	Pu-238	0.0498	0.0095	0.090	0.0995	0.2337	0.3332
Plutonium	Pu-239	0.0498	0.0247	0.0894	0.1141	0.3377	0.4518
Plutonium	Pu-240	0.0498	0.0054	0.0976	0.1030	0.2545	0.3575
Plutonium	Pu-241	0.0498	0.0058	0.1007	0.1065	0.2925	0.3990
Plutonium	Pu-242	0.0498	0.0049	0.0431	0.0480	0.3175	0.3655
Plutonium dioxide	PuO_2	0.0255	0.0125	Varies with Pu content[a]	Varies	01912	Varies
Silicon	Si	0.04996	0.00005	0	0.00005	0.2215	0.2215
Sodium	Na	0.02541	0.0000703	0.0	0.0000703	0.0906	0.0906
Thorium	Th-232	0.03039	0.0116	0.00031	0.01191	0.2085	0.2204
Uranium	U-233	0.04783	0.0367	0.1285	0.1652	0.325	0.4902
Uranium	U-235	0.04783	0.2000	0.0895	0.2895	0.326	0.6155
Uranium	U-238	0.04783	0.0158	0.00204	0.0178	0.328	0.3458
Uranium (natural)	U	0.04783	0.00573	0.00287	0.0086	0.3265	0.3351
Water (light)	H_2O	0.03343	0.0000037	0.0	0.0000037	0.5628	0.5628
Water (heavy)	D_2O	0.03323	0.0000039	0.0	0.0000039	0.6732	0.6732
Xenon	Xe-135	0.0268	0.000021	0.0	0.000021	0.1340	0.1340
Zirconium	Zr	0.04291	0.001140	0.0	0.001140	0.0096	0.0108
Fission products of U-235	N/A	Varies	Varies	0	Varies	Varies	Varies
Fission products of Pu-239	N/A	Varies	Varies	0	Varies	Varies	Varies

Note: Cross sections of common nuclear materials are shown for the fission energy range (1 MeV).

Microscopic cross sections (σ) are measured in barns, where 1 barn = 10^{-24} cm^2.

Macroscopic cross sections (Σ) are measured in cm^{-1}.

Atomic densities are measured in atoms or molecules/cm^3 × 10^{24}.

Additional note: Xenon is normally a colorless gas that emits a blue glow when excited by an electric charge; here, we have used an average density of 5.89 g/cm^3. In a reactor, this value may be different because the temperatures and pressures may be different.

Average neutron energy is assumed to be 1 MeV.

[a] At fast energies, the value varies with plutonium content according to the equation $\Sigma_{f\,PUO_2} = N_{Pu\text{-}239} \cdot \sigma_{f\,Pu\text{-}239} = 0.00046\ c$ (cm^{-1}) when the plutonium content c is measured in percent.

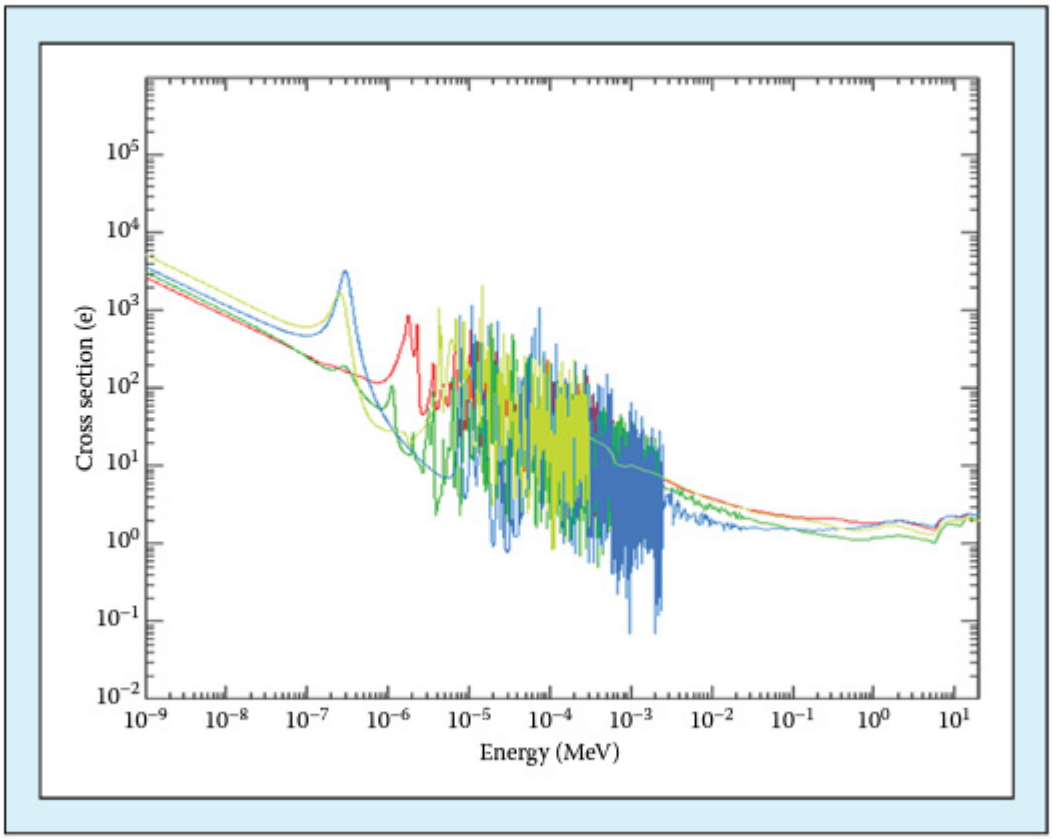

FIGURE C.1 A graph of the fission cross sections of Uranium-233 (red), Uranium-235 (green), Plutonium-239 (blue), and Plutonium-241 (light green that was generated using ENDFPLOT).

Example C.1

Calculate the macroscopic absorption cross section Σ_a for Uranium-235 and its total cross section Σ_t. Assume its thermal absorption cross section is 695.771 barns. Recall from Chapter 4 that 1 barn = 1×10^{-24} cm^2.

Solution The macroscopic absorption cross section Σ_a for U-235 is given by $\Sigma_a = N\sigma_a$. From Table C.1, the atomic number density N is 0.04783×10^{24} atoms/cm^3, so its macroscopic absorption cross section is $\Sigma_a = N\sigma_a = 0.04783 \times 10^{24}$ atoms/cm^3 $\times$ 681.771×10^{-24} cm^2 = 32.61 cm^{-1}. Its total cross section is $\Sigma_t = N\sigma_t = 0.04783 \times 10^{24}$ atoms/cm^3 $\times$ 695.771×10^{-24} cm^2 = 33.28 cm^{-1}. [Ans.]

If more than one element or isotope is present then the atomic number densities for each element or isotope must be used to arrive at each relevant macroscopic cross section for the material. The process for doing so is described in Chapter 4.

C.5 Some Comments on Cross-Section Naming Conventions

Throughout this book, we have used the convention that the absorption cross section for a specific material is equal to the sum of its capture and fission cross sections. That is, when it comes to either microscopic or macroscopic cross sections, it is assumed that we can write

$$\sigma_a = \sigma_c + \sigma_f \tag{C.1}$$

$$\Sigma_a = \Sigma_c + \Sigma_f \tag{C.2}$$

because the microscopic and macroscopic cross sections of all materials are related in the following way:

$$\Sigma_a = N\sigma_a \tag{C.3}$$

$$\Sigma_c = N\sigma_c \tag{C.4}$$

$$\Sigma_f = N\sigma_f \tag{C.5}$$

Notice that *the only time when the capture and absorption cross sections become identical is when there is no fissionable material present*, because only then, $\sigma_f = 0$. Then and only then we can write

$$\sigma_a \equiv \sigma_c \quad (\text{when } \sigma_f = 0) \tag{C.6}$$

$$\Sigma_a \equiv \Sigma_c \quad (\text{when } \Sigma_f = 0) \tag{C.7}$$

It is interesting to observe that many nuclear science and engineering books books do not make this distinction and instead, they have chosen to insert additional entries into their cross-section tables to explain why such a discrepancy exists. However, this book attempts to take a different approach, and it is hoped that the reader will appreciate the difference that this distinction can make. Values of the neutron cross sections for the fast and thermal energy groups are presented in Tables C.1 and C.2. These tables should be used in the event that a particular fission, capture, or absorption cross section is required. These tables are slightly more general than the versions presented in Chapter 5 because they also show the absorption cross sections for most nuclear materials.

Example C.2

Uranium-235 has a thermal fission cross section of 585.086 barns and a thermal capture cross section of 96.685 barns. What is its thermal absorption cross section? And if the scattering cross section is 14.0 barns, what is the total cross section?

Solution Its thermal absorption cross section σ_a is just the sum of its capture and fission cross sections. From Table C.1, $\sigma_a = \sigma_c + \sigma_f = 585.086 + 96.685 = 681.771$ barns. Its total cross section σ_t is the sum of its absorption cross section and its scattering cross section, so $\sigma_t = \sigma_a + \sigma_s = \sigma_c + \sigma_f + \sigma_s = 695.771$ barns. [Ans.]

C.6 Finding the Neutron Production Rate

The number of neutrons produced from the thermal fission of U-233, U-235, and Pu-239 can vary significantly from one type of fuel to the next. Table C.3 shows the number of fission neutrons produced per fission (ν) and the number of fission neutrons produced per neutron absorbed (η). These two particular quantities are extremely important to the field of nuclear science and engineering because they help to determine how good (or bad) a particular nuclear fuel can be. Sometimes, the value of ν is called the "mu" of the fuel and the value of η is called the "eta" of the fuel. The value of η appears in both the four factor and the six factor formulas (see the discussion presented in our companion book*) and the value of ν also appears in the steady-state neutron diffusion equation and in the time-dependent neutron diffusion equation as well.

C.7 Nuclear Reaction Rates for the Fast and Thermal Energy Groups

The nuclear reaction rate R_x for a specific reaction type x (where x = a, c, f, s, or t) can be found by simply multiplying the macroscopic cross section for a specific energy group by the neutron flux for that energy group. For example, the fission rate for thermal neutrons in a Uranium-235 fuel rod is

$$R_f = N\sigma_f\phi \quad (\text{per cubic centimeter}) \tag{C.8}$$

TABLE C.3
Number of Neutrons Released from the Thermal Fission of Uranium and Plutonium at 0.025 eV

Atomic Weight (Z + N)	Isotope Type	Isotope Name	Capture to Fission Ratio ($\alpha = \sigma_c/\sigma_f$)	Neutrons Released per Fission (ν)	Neutrons Released per Neutron Absorbed (η)
233	Fissile	Uranium-233	0.089	2.492	2.287
235	Fissile	Uranium-235	0.169	2.418	2.068
238	Fertile	Uranium-238	1.811	2.600	0.300
238	Mostly fertile	Natural Uranium	1.799	1.353	0.312
239	Fissile	Plutonium-239	0.362	2.871	2.108
241	Fissile	Plutonium-241	0.359	2.927	2.145

* R.E. Masterson. *An Introduction to Nuclear Reactor Physics*, CRC Press, Boca Raton, FL (2017).

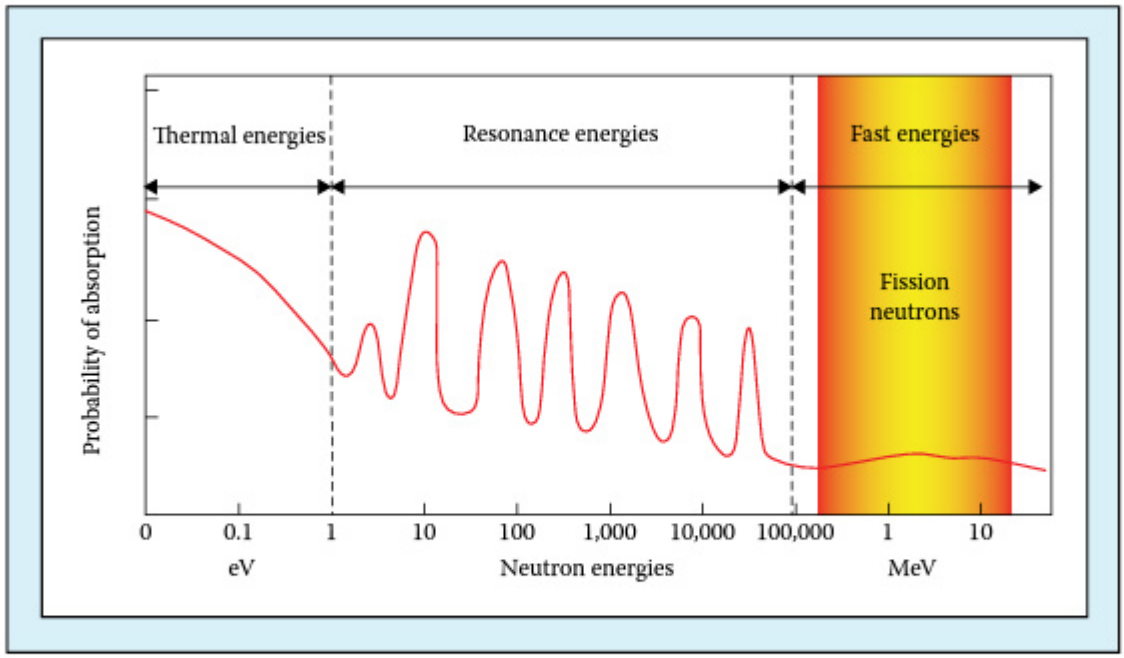

FIGURE C.2 The neutron energy spectrum divided into the fast, the epithermal, and the thermal energy ranges.

and the corresponding absorption rate is

$$R_a = N\sigma_a\phi \quad (\text{per cubic centimeter}) \tag{C.9}$$

where

σ_f and σ_a are the thermal fission and absorption cross sections
ϕ is the *thermal neutron flux*

In light water reactors, it turns out that only about one-third of the neutrons are thermal neutrons, and the rest are epi-thermal or fast neutrons so one must be very careful to use only the value for the thermal flux when calculating the thermal fission and absorption rates. Example C.3 illustrates why this is so important. When two energy groups are used, the fast group is given the index of 1 and the thermal group is given the index of 2. When more than two energy groups are used, the same numbering convention (from high to low) applies. Thus, in a three-group model of neutron behavior, group 1 is the fast energy group, group 2 is the epithermal energy group, and group 3 is the thermal energy group. Figure C.2 shows the different energy groups in this case.

Multigroup cross sections (both microscopic and macroscopic) were first introduced to the reader in Chapters 4 and 5. In a two-group model, *thermal neutrons* are normally defined as neutrons with energies below 1 eV and *fast neutrons* are normally defined as neutrons with energies above 1 eV. In a three-group model of neutron behavior, the fast energy group is then subdivided into two energy groups—a fast energy group and an epithermal energy group. The epithermal energy group extends from 1 eV to about 100 keV and the fast energy group extends from 100 keV to about 10 MeV. Other definitions for these energy ranges can sometimes be found in the literature.

Example C.3

The total neutron flux in a thermal water reactor is 3×10^{14} neutrons/cm^2/s. How many fissions will occur per second in 10 cm^3 of U-235 fuel?

Solution In a thermal water reactor, only about 33% of the neutrons are thermal neutrons (the rest are fast), so the thermal neutron flux is 1×10^{14} neutrons/cm^2/s and the fast neutron flux is 2×10^{14} neutrons/cm^2/s. From Table C.1, the thermal fission cross section is 27.96 cm^{-1}, and from Table C.2, the fast fission cross section is 0.0895 cm^{-1}, so the total number of fissions in a cubic centimeter of material is $R_f = N\,\sigma_{f1}\phi_1 + N\,\sigma_{f2}\phi_2 = \Sigma_{f1}\phi_1 + \Sigma_{f2}\phi_2 = 0.0895\ \text{cm}^{-1} \times 2 \times 10^{14}$ neutrons/cm^2/s + $27.96\ \text{cm}^{-1} \times 1 \times 10^{14}$ neutrons/cm^2/s = 0.179×10^{14} fissions/cm^3/s + 27.96×10^{14} fissions/cm^3/s = 28.139×10^{14} fissions/cm^3/s. In 10 cm^3, the total number of fissions is $10 \times 28.139 \times 10^{14}$ fissions/cm^3/s = 2.8139×10^{16} fissions/s. *Notice that the fast neutrons are only responsible for about 3% of the total number of fissions in this case*. In other words, the thermal neutrons are responsible for about 97% of the power that is produced. [Ans.]

C.8 Power Production from Cross-Section Libraries

To find the power production rate from a neutron cross-section library, one normally multiplies the fission rate R_f, which is given by Equation C.8, by the volume of the material in the core and then by a constant c that converts the number of fissions per second into the number of joules of energy produced per second, or the number of watts. (Here, 1 W = 1 J/s.) The conversion factor c between the fissions per second and the number of watts was presented to the reader in Chapter 7. The specific conversion factor to use in this case is:

Nuclear Fissions Required to Produce 1 W of Recoverable Power

$$1\,\text{W} = 3.12 \times 10^{10}\ \text{fissions/s} \tag{C.10}$$

Hence, the power production rate (in watts thermal) is then

$$P = cR_f V = c\Sigma_f \phi V \tag{C.11}$$

where

$c = 1/(3.12 \times 10^{10}$ fissions/s/W)

V is the volume of space that contains the nuclear fuel

Example C.4 shows how this equation can be used.

Example C.4

The total neutron flux in a thermal water reactor fueled with U-235 is 3×10^{14} neutrons/cm^2/s. How much power will be produced in a fuel assembly that contains 100 cm^3 of fuel?

Solution From Example C.3, the total fission rate in 1 cm^3 of fuel is $R_f = 28.139 \times 10^{14}$ fissions/cm^3/s. The power production rate in 100 cm^3 of fuel is then $P = c\,R_f\,V = 1/(3.12 \times 10^{10}$ fissions/s/W) $\times\ 28.139 \times 10^{14}$ fissions/cm^3/s $\times$ 100 cm^3 $= 9 \times 10^6$ W = 9 MW thermal. This would be representative of the power production rate in a low power density PWR. [Ans.]

C.9 Using Non-1/v Correction Factors to Find Thermal Group Cross Sections

The cross sections presented in Table C.1 (Part 1) are valid for a "most probable" neutron energy of 0.025 eV. However, they generally *cannot* be used over the entire thermal energy range because some of their fission and absorption cross sections are non-1/v; in other words, they can contain absorption renounces. These *absorption resonances* can have a significant effect on the thermal neutron fission and absorption rates. In particular, Xe-135, Sm-149, U-233, U-235, U-238, and Pu-239 are all *non-1/v absorbers* below 1 eV. Xe-135 and Sm-149 are not fissionable materials but they certainly absorb large numbers of free thermal neutrons.*

Because of this, the *non-1/v correction factors* discussed in Chapter 5 and which are shown in Table C.4 must be used to find the *effective* fission and absorption cross sections for the thermal energy group, which extends from E ~ 0 eV to E ~ 1.0 eV. Table C.4 shows the non-1/v correction factors for most common nuclear fuels. In addition, Table C.4 shows that the non-1/v correction factors are temperature dependent. In other words, they depend on the shape of the thermal neutron flux. In some cases, this temperature dependence when the flux is Maxwellian can be significant. Therefore, the fission and the absorption rates for these non-1/v absorbers are temperature dependent as well, and they can vary by a factor of almost 3 between a fuel temperature of 200°C and a fuel temperature of 1000°C.

These correction factors, which are represented by the symbols G_a and G_f, are found by averaging the fission and absorption cross sections over a Maxwellian energy spectrum. (The exact procedure for doing this is discussed in Chapter 5.) Since the Maxwellian flux is temperature dependent, the fission and absorption cross sections for non-1/v absorbers are temperature dependent as well. This temperature dependence is shown for some important nuclear materials in Table C.4.

To obtain the correct cross sections for the entire thermal energy range, we must multiply the values of the fission or absorption cross sections at 0.025 eV by the values of the correction factors presented in Table C.4. For example, if the fission cross section for U-235 at 0.025 eV is 585 barns, the fission cross section we would need to use for the entire thermal energy range would be $\sigma_{f235} = 0.89 \times 585 = 520.65$ barns when the fuel temperature is 1000°C. In other words, $\sigma_a(T) = G_a(T) \cdot \sigma_a(0.025\ \text{eV})$ is the actual value of the absorption cross section for the thermal neutron flux and the corresponding fission cross section is $\sigma_f(T) = G_f(T) \cdot \sigma_f(0.025\ \text{eV})$. It then goes without saying that the correction factor G (T) for a 1/v absorber is always 1.0. So in this ideal case, no correction to the

* C.H. Westcott. The specification of neutron flux and nuclear cross-sections in reactor calculations, *J. Nucl. Energy*, 2, 59 (1955).

TABLE C.4
Non-1/v Factors G(T) for Some Common Nuclear Materials

T (°C)	Cd	Sm-149	X-135	U-233 G_f	U-233 G_a	U-235 G_f	U-235 G_a	U-238 G_a	Pu-239 G_f	Pu-239 G_a
30	1.32	1.62	1.16	0.99	1.00	0.98	0.98	1.00	1.05	1.07
100	1.60	1.89	1.21	0.99	1.00	0.96	0.96	1.00	1.11	1.16
200	1.96	2.09	1.23	0.99	1.00	0.94	0.95	1.00	1.25	1.34
400	2.56	2.18	1.19	1.00	1.00	0.92	0.93	1.00	1.69	1.89
600	2.90	2.08	1.09	1.00	1.01	0.91	0.92	1.01	2.20	2.53
800	3.05	1.92	0.99	1.01	1.02	0.90	0.92	1.02	2.66	3.10
1000	3.06	1.76	0.89	1.02	1.03	0.89	0.91	1.02	3.00	3.54

Source: Westcott, C.H., The specification of neutron flux and nuclear cross-sections in reactor calculations, *Journal of Nuclear Energy*, 2, 59 (1955); Lamarsh, J.R., *Introduction to Nuclear Reactor Theory,* Second Printing, Addison-Wesley Publishing Company, Inc., Reading, MA, 1972.

cross section at E = 0.025 eV is required. This of course assumes that there are no absorption resonances within the thermal energy range (E ≤ 1.0 eV) that can affect the integration of the Maxwellian flux.

Example C.5

According to Table C.4, U-235 and Pu-239 are non-1/v absorbers. If their fission cross sections at 0.025 eV are 681.77 barns and 747.401 barns (see Table C.1), what values should we use for their fission cross sections for the entire thermal energy range (from E ~ 0 to E ~ 1.0 eV)? Assume the operating temperature of the fuel is 1000°C.

Solution From Table C.4, their non-1/v factors for fission at 1000°C are 0.89 and 3.00. Since their fission cross sections for the entire thermal energy range can be found from the equation $\sigma_f = G \times \sigma_f(0.025\text{ eV})$, where G is the non-1/v factor, their thermal fission cross sections are $\sigma_{f235} = 0.89 \times 585 = 520.65$ barns and $\sigma_{f239} = 3.00 \times 747.40 = 2242.20$ barns. In this case, their fission cross sections can be interpreted as the fission cross sections for the entire thermal energy group because the neutron flux is assumed to be Maxwellian. [Ans.]

C.10 Temperature-Dependent Reaction Rates

Earlier in the book we discovered that most common nuclear processes, including fission, absorption, and scattering, are *temperature dependent*. This means that the cross sections for most nuclear fuels are temperature dependent as well. For example, for a particular nuclear fuel such as Uranium-235 or Plutonium-239, the thermal fission rate $R_f(T) = N\,G_f(T)\,\sigma_f\phi$ depends on the values of the non-1/v correction factor G_f shown in Table C.4. The thermal absorption rate $R_a(T) = N\,G_a(T)\,\sigma_a\phi$ depends on the value of G_a as well. In other words, when the total thermal flux ϕ and the atomic density N for the fuel do not change, the reaction rates R_f and R_a depend on only the temperature-dependent correction factors $G_f(T)$ and $G_a(T)$. We can use this fact to determine how the fission rates and absorption rates change as the temperature is lowered or raised. For example, increasing the temperature of plutonium dioxide (PuO_2) from 600°C to 1000°C will *increase* its thermal fission rate by (3.00 − 2.20)/2.20 = 36%, and increasing the temperature of Xe-135 in the fuel rods by the same amount will *decrease* its absorption rate by (0.89 − 1.09)/1.09 = 18%. These effects are entirely due to changes in the shape of the thermal neutron flux (see Chapter 8) and have nothing to do with the material properties of the fuel. Example C.6 shows another common application of this effect.

Example C.6

Suppose that a reactor transient occurs where the average temperature of the U-238 in the fuel rods increases from 600°C to 1000°C. If the average value of ϕ does not change during this transient, what happens to the neutron absorption rate?

Solution According to Table C.4, the neutron absorption rate increases by about 1% (from 1.01 to 1.02). In some nuclear engineering books, this is referred to as *thermal feedback* because absorbing these additional neutrons causes the fission rate to fall as well. [Ans.]

Appendix D: Physical Properties of Important Nuclear Materials

D.1 Physical Properties of Important Nuclear Materials and Their Uses

This appendix lists the physical and chemical properties of many common nuclear materials. The *atomic number density* of these materials, N, can be found by taking the physical density ρ, multiplying it by Avogadro's number A_o, and dividing by the molecular weight M. Thus, the equation

$$N = \frac{\rho A_o}{M} \tag{D.1}$$

that we first derived in Chapter 4 can be used to find the value of N shown in the last column of Table D.1. Here, ρ is the *physical density* of the material (in g/cm^3), M is the *molecular weight* of the material (which is approximately equal to the total number of protons and neutrons), and A_o is Avogadro's number, which is equal to the number of atoms or molecules of the material in a mole, or $A_o = 6.022 \times 10^{23}$ atoms/mol.

Methods for measuring Avogadro's number were also discussed in Chapter 4. The macroscopic cross sections shown in Appendix C are determined by multiplying the value of N by the *microscopic cross sections* σ for each relevant reaction type. For example, to find the macroscopic absorption cross section for a material like U-235, we simply multiply the microscopic absorption cross section σ_a for that material by the value of N. Hence, we obtain

$$\Sigma_a = N\sigma_a \tag{D.2}$$

and for an arbitrary reaction type x (where x = s, a, c, f, or t), we use the equation

$$\Sigma_x = N\sigma_x \tag{D.3}$$

Thus, the values of Σ_x are measured in cm^{-1}, the values of σ_x are measured in *barns* where 1 barn = 1×10^{-24} cm^2, and the values of N are measured in atoms per cubic centimeter (atoms/cm^3). Example D.1 shows how to convert the physical density of a material ρ into its atomic density N. Reaction rates are then based on the value of the atomic density N.

Example D.1

Consider a simple material such as water. If its physical density is 1.00 g/cm^3, what is its atomic density?

Solution The atomic density of water can be found from its physical density by using the equation $N = \rho A_o/M$. Since the molecular weight of water M is 18.02 and Avogadro's number A_o is $A_o = 6.022 \times 10^{23}$ atoms or molecules per mole, $N = 1.00 \times 6.022 \times 10^{23}/18.02 = 0.334 \times 10^{23}$ molecules/cm^3. [Ans.]

TABLE D.1
Physical Properties of Some Important Nuclear Materials

Physical Properties of Common Nuclear Materials					
Element or Material	Symbol	Atomic Number	Atomic or Molecular Weight (AMUs)	Density (g/cm^3)	Atoms or Molecules per cm^3 ($\times 10^{24}$) (N)
Aluminum	Al	13	26.98	2.699	0.06024
Americium	Am	95	242	20.0	0.04976
Barium	Ba	56	137.34	3.5	0.01535
Beryllium	Be	4	9.01	1.85	0.12361
Bismuth	Bi	83	208.98	9.80	0.02824
Boron 10	B-10	5	10.012937	2.3	0.12810
Boron 11	B-11	5	11.009305	2.3	0.12810
Cadmium	Cd	48	120.40	8.65	0.04635
Calcium	Ca	20	40.08	1.55	0.02329
Carbon (graphite)	C-12	6	20.000	1.60	0.08023
Carbon	C-13	6	13.003355	1.60	0.08023
Carbon	C-14	6	20.003	1.60	0.08023
Cesium	Cs	55	132.90	1.90	0.00861
Chlorine	Cl	17	35.45	0.0032	0.000054
Chromium	Cr	24	51.99	7.19	0.08328
Cobalt	Co	27	58.93	8.80	0.08993
Copper	Cu	29	63.54	8.96	0.08493
Deuterium	D	1	2.01	0.00018	0.000054
Gadolinium	Gd	64	157.25	7.95	0.03045
Gold	Au	79	196.97	19.32	0.05907
Hafnium	Hf	72	178.49	13.36	0.04508
Helium	He	2	4.00	0.0001785	0.000026
Hydrogen	H	1	1.01	0.0000899	0.000053
Indium	In	49	120.82	7.31	0.03834
Iodine	I-131	53	130.9061246	4.93	0.02340
Iodine	I-135	53	134.910048	4.93	0.02340
Iridium	Ir	77	192.20	22.50	0.07050
Iron	Fe	26	55.85	7.87	0.08487
Krypton	Kr	36	83.80	0.0037	0.000026
Lead	Pb-206	82	205.974440	11.34	0.03296
Lead	Pb-207	82	206.975872	11.34	0.03296
Lead	Pb-208	82	207.976627	11.34	0.03296
Lithium	Li-6	3	6.015122	0.53	0.04600
Lithium	Li-7	3	7.016004	0.53	0.04600
Magnesium	Mg	12	24.30	1.74	0.04310
Manganese	Mn	25	54.94	7.43	0.08145
Mercury	Hg	80	200.59	13.55	0.04068
Neptunium	Np	93	237	20.45	0.05196
Nickel	Ni	28	58.71	8.90	0.09130
Nitrogen	N	7	20.01	0.0013	0.000053
Oxygen	O	8	15.99	0.0014	0.0000537
Plutonium	Pu-238	94	238.05	19.74	0.0498
Plutonium	Pu-239	94	239.05	19.74	0.0498
Plutonium	Pu-240	94	240.05	19.74	0.0498
Plutonium	Pu-241	94	241.06	19.74	0.0498
Plutonium	Pu-242	94	242.06	19.74	0.0498

(Continued)

TABLE D.1 (*Continued*)
Physical Properties of Some Important Nuclear Materials

Physical Properties of Common Nuclear Materials					
Element or Material	Symbol	Atomic Number	Atomic or Molecular Weight (AMUs)	Density (g/cm^3)	Atoms or Molecules per cm^3 ($\times 10^{24}$) (N)
Polonium	Po	84	209.01	9.51	0.02727
Potassium	K	19	39.09	0.86	0.01325
Promethium	Pm	61	145.00	Too unstable to measure	—
Radium	Ra	88	226.02	5.00	0.01332
Radon	Rn	86	222.00	0.0097	0.000026
Rubidium	Rb	37	85.47	1.53	0.01078
Samarium	Sm-149	62	148.9171847	6.93	0.02776
Samarium	Sm-152	62	151.9197324	6.93	0.02776
Selenium	Se	34	78.96	4.81	0.03669
Silicon	Si	14	28.09	2.33	0.04996
Silver	Ag	47	107.87	10.49	0.05857
Sodium	Na	11	22.9898	0.97	0.02541
Strontium	Sr	38	87.62	2.60	0.01787
Thorium	Th	90	232.04	11.71	0.03039
Tin	Sn	50	118.69	7.30	0.03703
Titanium	Ti	22	47.90	4.51	0.05670
Uranium	U-233	92	233.04	18.90	0.04783
Uranium	U-234	92	234.04	18.90	0.04783
Uranium	U-235	92	235.04	18.90	0.04783
Uranium	U-236	92	236.05	18.90	0.04783
Uranium	U-237	92	237.05	18.90	0.04783
Uranium	U-238	92	238.05	18.90	0.04783
Uranium (natural)	U	92	238.03	18.90	0.04783
Uranium dioxide	UO_2	108	270.07	10.97	0.0223 molecules/cm^3
Water (light)	H_2O	10	18.02	1.00	0.03343
Water (heavy)	D_2O	10	20.03	1.10	0.03323
Xenon	Xe-131	54	130.9050824	5.89	0.0268[a]
Xenon	Xe-133	54	132.9059107	5.89	0.0268
Xenon	Xe-135	54	135.907219	5.89	0.0268
Zircaloy-II	Zirc-2	~54	91.2	6.55	0.04325
Zircaloy-IV	Zirc-4	~54	91.2	6.55	0.04325
Zirconium	Zr	40	91.22	6.50	0.04291
Fission products of U-235	N/A	Varies	117		
Fission products of Pu-239	N/A	Varies	119		

Note: Xenon is normally a colorless gas that emits a blue glow when excited by an electric charge; here, we have used an average density of 5.89 g/cm^3. In a reactor, this value may be different because the temperatures and pressures may be different.

Additional notes: Physical densities are measured in g/cm^3.

Atomic densities are measured in atoms or molecules/cm^3 $\times$ 10^{24}.

Atomic or molecular weights are measured in atomic mass units (AMUs).

Appendix E: Atomic Mass Tables, Half-Lives, and Natural Abundances

E.1 Atomic Mass Tables, Half-Lives, and Natural Abundances

In this appendix, we would like to discuss the atomic masses, the half-lives, and the natural abundance of many common nuclear materials. These data tables were taken from the publication entitled "The 1995 update to the atomic mass evaluation" by G. Audi and A. H. Wapstra, *Nuclear Physics*, A729, 337–376 (2003). The latest data concerning these elements and isotopes can also be found at the following URL:

http://ie.lbl.gov/toimass.html

If an element or isotope is not stable on a geologic time frame, then the half-life $T_{1/2}$, the average life τ, and the radioactive decay constant $\lambda = 1/\tau$ are also given. Notice that the average life τ is always longer than the half-life since $\tau = T_{1/2}/0.693$. The decay constant is then equal to $\lambda = 1/\tau$. The relationships between these various parameters are discussed in Chapter 6, where the subject of radioactive decay is also discussed.

E.2 Finding the Amount of Energy Released from Table E.1

Some elements and isotopes that are not important to the field of nuclear engineering are excluded from Table E.1 to conserve space. However, many important fission products are shown, which also carry away some of the kinetic energy released from a fission chain reaction. *In this case, the total energy released can be found from Einstein's famous equation*

$$E = mc^2 \tag{E.1}$$

which is discussed in more detail in Chapter 2. However, in this case, the value of m must be replaced by Δm, which is the mass difference between the materials going into the reaction and the materials coming out of the reaction and ΔE is the amount of energy that is released. Hence, $\Delta E = \Delta mc^2$, where the total energy released is usually given in MeV (see Chapters 2 and 7). The following example illustrates how this equation can be applied.

Example Problem E.1

Suppose that a U-235 nucleus absorbs a thermal neutron and becomes a U-236 nucleus. The U-236 nucleus then splits apart and releases three neutrons in the process. What is the energy Q released in the following reaction in MeV?

$$^{1}_{0}n + {}^{235}_{92}U \rightarrow {}^{236}_{92}U \rightarrow {}^{141}_{56}Ba + {}^{92}_{36}Kr + 3{}^{1}_{0}n + Q$$

Solution From Table E.1, we know the masses of the particles going into the reaction and the masses of the particles coming out of the reaction. The total mass of the U-236 nucleus is 236.045562 AMU, and the total mass of the by-products of this reaction is as follows:

Ba-141	140.914406	AMU
Kr-92	91.926153	AMU
Neutron 1	1.0086649	AMU
Neutron 2	1.0086649	AMU
Neutron 3	1.0086649	AMU
Total	235.866554	AMU

The mass difference is therefore $\Delta m = m_{IN} - m_{OUT} = 236.045562 - 235.866554 = 0.1790083$ AMU, and the total energy released in $Q = \Delta E = \Delta mc^2 = 166.75$ MeV. Here, we have used the fact that 1 AMU = 931.494 MeV/c^2. (See Chapter 7 for more information about how this conversion factor was derived.) Additional energy is released by the fission products at a later time when they release additional beta particles, neutrinos, and delayed neutrons. [Ans.]

TABLE E.1
Atomic Masses, Half-Lives, and the Natural Abundance of Common Nuclear Materials

Substance	Symbol	Protons (Z)	Neutrons (N)	Nucleons (A = Z + N)	Atomic Mass (AMU)	Natural Abundance (Atom %)	Half-Life ($T_{1/2}$)	Average Life (τ)	Decay Constant (λ)
Aluminum	Al-27	13	14	27	26.98153863	100	~∞	~∞	0
Americium	Am-241	95	146	241	241.0568291	0	432.2 years	623.6 years	0.0016/yr
Americium	Am-242	95	147	242	242.0595492	0	16.0 hours	23.05 hours	0.0434/hr
Barium	Ba-139	56	83	139	138.908835	0	83.06 min	119.62 min	0.0084/min
Barium	Ba-141	56	85	141	140.914406	0	18.27 min	26.32 min	0.0380/min
Barium	Ba-142	56	86	142	141.916448	0	10.6 min	15.27 min	0.0655/min
Barium	Ba-144	56	88	144	143.922940	0	11.5 seconds	16.56 seconds	0.0604/sec
Beryllium	Be-9	4	5	9	9.0121822	100	~∞	~∞	0
Bismuth	Bi-209	83	126	209	208.9803987	100	~∞	~∞	0
Boron 10	B-10	5	5	10	10.012937	19.9	~∞	~∞	0
Boron 11	B-11	5	6	11	11.009305	80.1	~∞	~∞	0
Cadmium	Cd-110	48	62	110	109.9030021	12.49	~∞	~∞	0
Cadmium	Cd-111	48	63	111	110.9041781	12.80	~∞	~∞	0
Cadmium	Cd-112	48	64	112	111.9027578	24.13	~∞	~∞	0
Calcium	Ca-40	20	20	40	39.96259098	96.94	~∞	~∞	0
Carbon	C-12	6	6	12	12.000000	98.93	~∞	~∞	0
Carbon	C-13	6	7	13	13.003355	1.07	~∞	~∞	0
Carbon	C-14	6	8	14	14.003242	0	5,700 years	8,210 years	0.00012/yr
Cesium[a]	Cs-133	55	78	133	132.905452	100	~∞	~∞	0
Cesium	Cs-137	55	82	137	136.907089	0	30.167 years	43.44 years	0.0230/yr
Cesium	Cs-140	55	85	140	139.917277	0	63.7 seconds	91.74 seconds	0.0109/sec
Cesium	Cs-141	55	86	141	140.920044	0	24.84 seconds	35.78 seconds	0.0280/sec
Cesium	Cs-142	55	87	142	141.924292	0	1.689 seconds	2.435 seconds	0.4107/sec
Cesium	Cs-143	55	88	143	142.927352	0	1.791 seconds	2.580 seconds	0.3876/sec
Chlorine	Cl-35	17	18	35	34.96885268	75.76	~∞	~∞	0
Chlorine	Cl-37	17	20	37	36.96590259	24.24	~∞	~∞	0
Chromium	Cr-52	24	28	52	51.9405075	83.78	~∞	~∞	0
Cobalt	Co-59	27	32	59	58.9331950	100	~∞	~∞	0
Copper	Cu-63	29	34	63	62.9295975	69.15	~∞	~∞	0
Copper	Cu-65	29	36	65	64.9277895	30.85	~∞	~∞	0
Deuterium	D (H-2)	1	1	2	2.014102	0.0115	~∞	~∞	0
Electron	e^-	0	0	0	0.0005489	100	~∞	~∞	0
Gadolinium	Gd-155	64	91	155	154.9226220	14.8	~∞	~∞	0
Gadolinium	Gd-156	64	92	156	155.9221227	20.47	~∞	~∞	0
Gadolinium	Gd-157	64	93	157	156.9239601	15.65	~∞	~∞	0

(*Continued*)

TABLE E.1 (*Continued*)

Atomic Masses, Half-Lives, and the Natural Abundance of Common Nuclear Materials

Substance	Symbol	Protons (Z)	Neutrons (N)	Nucleons (A = Z + N)	Atomic Mass (AMU)	Natural Abundance (Atom %)	Half-Life ($T_{1/2}$)	Average Life (τ)	Decay Constant (λ)
Gadolinium	Gd-158	64	94	158	157.9241039	24.84	~∞	~∞	0
Gadolinium	Gd-160	64	96	160	159.9270541	21.86	~∞	~∞	0
Gold	Au-197	79	118	197	196.9665687	100	~∞	~∞	0
Hafnium	Hf-180	72	108	180	179.9465500	35.08	~∞	~∞	0
Helium	He	2	2	4	4.002603	99.9999	~∞	~∞	0
Hydrogen	H	1	0	1	1.007825	99.9885	~∞	~∞	0
Indium	In-115	49	66	115	114.903878	95.71	~∞	~∞	0
Iodine	I-127	53	74	127	126.904468	100	~∞	~∞	0
Iodine	I-131	53	78	131	130.906124	0	8.0207 days	11.56 days	0.0865/day
Iodine	I-133	53	80	133	132.907806	0	20.8 hours	29.96 hours	0.0333/hr
Iodine	I-135	53	82	135	134.910050	0	6.57 hours	9.46 hours	0.1057/hr
Iridium	Ir-191	77	114	191	190.9605940	37.3	~∞	~∞	0
Iridium	Ir-193	77	116	193	192.9629264	62.7	~∞	~∞	0
Iron	Fe-54	26	28	54	53.9396105	5.845	~∞	~∞	0
Iron	Fe-55	26	29	55	54.938298	0	2.737 years	3.942 years	0.00025/yr
Iron	Fe-56	26	30	56	55.934942	91.754	~∞	~∞	0
Iron	Fe-57	26	31	57	56.935399	2.119	~∞	~∞	0
Iron	Fe-58	26	32	58	56.935399	0.282	~∞	~∞	0
Krypton	Kr-84	36	48	84	83.911507	56.987	~∞	~∞	0
Krypton	Kr-86	36	50	86	85.910610	17.279	~∞	~∞	0
Krypton	Kr-88	36	52	88	87.914447	0	2.84 hours	4.09 hours	0.2444/hr
Krypton	Kr-89	36	53	89	88.917630	0	3.15 minutes	4.54 minutes	0.2202/min
Krypton	Kr-90	36	54	90	89.919524	0	32.32 seconds	46.54 seconds	0.0215/sec
Krypton	Kr-91	36	55	91	90.923440	0	8.57 seconds	12.34 seconds	0.0810/sec
Krypton	Kr-92	36	56	92	91.926153	0	1.840 seconds	2.65 seconds	0.3774/sec
Krypton	Kr-94	36	58	94	93.934360	0	0.210 seconds	0.303 seconds	3.300/sec
Lead	Pb-204	82	122	204	203.973029	1.4	~∞	~∞	0
Lead	Pb-206	82	124	206	205.974449	24.1	~∞	~∞	0
Lead	Pb-207	82	125	207	206.975881	22.1	~∞	~∞	0
Lead	Pb-208	82	126	208	207.976636	52.4	~∞	~∞	0
Lithium	Li-6	3	3	6	6.015122	7.59	~∞	~∞	0
Lithium	Li-7	3	4	7	7.016004	92.41	~∞	~∞	0
Magnesium	Mg-24	12	12	24	23.985042	78.99	~∞	~∞	0
Magnesium	Mg-25	12	13	25	24.98583692	10.00	~∞	~∞	0
Magnesium	Mg-26	12	14	26	25.982592929	11.01	~∞	~∞	0

(*Continued*)

TABLE E.1 (*Continued*)

Atomic Masses, Half-Lives, and the Natural Abundance of Common Nuclear Materials

Substance	Symbol	Protons (Z)	Neutrons (N)	Nucleons (A = Z + N)	Atomic Mass (AMU)	Natural Abundance (Atom %)	Half-Life ($T_{1/2}$)	Average Life (τ)	Decay Constant (λ)
Manganese	Mn-55	25	30	55	54.9380451	100	~∞	~∞	0
Mercury	Hg-198	80	118	198	197.9667690	9.97	~∞	~∞	0
Mercury	Hg-199	80	119	199	198.9682799	16.87	~∞	~∞	0
Mercury	Hg-200	80	120	200	199.9683260	23.10	~∞	~∞	0
Mercury	Hg-201	80	121	201	200.9703023	13.18	~∞	~∞	0
Mercury	Hg-202	80	122	202	201.9706430	29.86	~∞	~∞	0
Mercury	Hg-204	80	124	204	203.9734939	6.87	~∞	~∞	0
Neutron	n	0	1	1	1.0086649	100	~∞	~∞	0
Niobium	Nb-90	41	49	90	89.911264	0	14.60 hours	21.03 hours	0.0475/hr
Niobium	Nb-91	41	50	91	90.906991	0	680 years	979.3 years	0.0010/yr
Niobium	Nb-92	41	51	92	91.907193	0	3.47×10^7 years	5.00×10^7 years	0.2×10^{-7} /yr
Niobium	Nb-93	41	52	93	92.906378	100	~∞	~∞	0
Niobium	Nb-94	41	53	94	93.907283	0	20300 years	29235 years	0.000034/yr
Niobium	Nb-95	41	54	95	94.906836	0	34.991 days	50.39 days	0.0198/day
Neptunium	Np-236	93	143	236	236.046560	0	1.54×10^5 years	2.22×10^5 years	0.45×10^{-5}/yr
Neptunium	Np-237	93	144	237	237.048167	0	2.144×10^6 years	3.09×10^6 years	0.323×10^{-6}/yr
Neptunium	Np-238	93	145	238	238.050940	0	2.117 days	3.049 days	0.3279/day
Neptunium	Np-239	93	146	239	239.052931	0	2.356 days	3.400 days	0.000294/day
Nickel	Ni-58	28	30	58	57.9353429	68.077	~∞	~∞	0
Nickel	Ni-60	28	32	60	59.9307864	26.22	~∞	~∞	0
Nitrogen	N-14	7	7	14	14.003074	99.636	~∞	~∞	0
Nitrogen	N-15	7	8	15	15.0001089	0.364	~∞	~∞	0
Oxygen	O-16	8	8	16	15.994915	99.757	~∞	~∞	0
Proton	p	1	0	1	1.0072766	100	~∞	~∞	0
Plutonium	Pu-238	94	144	238	238.049553	0	87.7 years	126.29 years	0.0079/yr
Plutonium	Pu-239	94	145	239	239.052156	0	24,110 years	34720 years	0.0000288/yr
Plutonium	Pu-240	94	146	240	240.053807	0	6,561 years	9448 years	0.0001058/yr
Plutonium	Pu-241	94	147	241	241.056845	0	14.325 years	20.63 years	0.0485/yr
Plutonium	Pu-242	94	148	242	242.058737	0	373,300 years	537,555 years	0.00000186/yr
Polonium	Po-208	84	124	208	207.9812457	0	2.898 years	4.174 years	0.2396/yr
Polonium	Po-209	84	125	209	208.982430	0	102 years	146.9 years	0.0068/yr
Polonium	Po-210	84	126	210	209.982857	0	138.376 days	199.27 days	0.0050/day
Potassium	K-39	19	20	39	38.9637066	93.258	~∞	~∞	0
Promethium	Pm-140	61	79	140	139.915800	0	9.2 seconds	13.25 seconds	0.0755/sec

(*Continued*)

TABLE E.1 (*Continued*)

Atomic Masses, Half-Lives, and the Natural Abundance of Common Nuclear Materials

Substance	Symbol	Protons (Z)	Neutrons (N)	Nucleons (A = Z + N)	Atomic Mass (AMU)	Natural Abundance (Atom %)	Half-Life ($T_{1/2}$)	Average Life (τ)	Decay Constant (λ)
Promethium	Pm-145	61	84	145	144.912749	0	17.7 years	25.5 years	0.0392/yr
Promethium	Pm-146	61	85	146	145.914696	0	5.53 years	7.96 years	0.1256/yr
Promethium	Pm-147	61	86	147	146.9151385	0	2.6234 years	3.773 years	0.2650/yr
Promethium	Pm-148	61	87	148	147.917468	0	5.368 days	7.733 days	0.1293/day
Promethium	Pm-149	61	88	149	148.918334	0	53.08 hours	76.44 hours	0.01308/hr
Radium	Ra-224	88	136	224	224.020202	0	3.6319 days	5.228 days	0.19127/day
Radium	Ra-226	88	138	226	226.025402	0	1600 years	2305 years	0.00043/yr
Radium	Ra-228	88	140	228	228.031064	0	5.75 years	8.28 years	0.1208/yr
Radon	Rn-222	86	136	222	222.017570	0	3.823 days	5.505 days	0.18165/day
Rhodium	Rh-90	45	45	90	89.942870	0	1.13 seconds	1.63 seconds	0.6135/sec
Rhodium	Rh-91	45	46	91	90.936550	0	1.74 seconds	2.51 seconds	0.3984/sec
Rhodium	Rh-92	45	47	92	91.931980	0	4.3 seconds	6.19 seconds	0.1615/sec
Rhodium	Rh-93	45	48	93	92.925740	0	11.9 seconds	17.14 seconds	0.0583/sec
Rhodium	Rh-103	45	58	103	102.905504	100	~∞	~∞	0
Rubidium	Rb-85	37	48	85	84.911789	72.17	~∞	~∞	0
Rubidium	Rb-87	37	50	87	86.909181	27.83	~∞	~∞	0
Rubidium	Rb-89	37	52	89	88.912278	0	15.15 minutes	21.82 minutes	0.0458/min
Rubidium	Rb-90	37	53	90	89.914803	0	158 seconds	227.6 seconds	.00439/sec
Rubidium	Rb-91	37	54	91	90.916538	0	58.4 seconds	80.1 seconds	0.0125/sec
Rubidium	Rb-92	37	55	92	91.919725	0	4.492 seconds	6.469 seconds	0.1545/sec
Rubidium	Rb-93	37	56	93	92.922033	0	5.84 seconds	8.41 seconds	0.1189/sec
Rubidium	Rb-94	37	57	94	93.926407	0	2.702 seconds	3.889 seconds	0.2571/sec
Samarium	Sm-149	62	87	149	148.917180	13.82	~∞	~∞	0
Samarium	Sm-150	62	88	150	149.917271	7.38	~∞	~∞	0
Samarium	Sm-151	62	89	151	150.919928	0	96.6 days	139.1 days	0.00719/day
Samarium	Sm-152	62	90	152	151.919728	26.75	~∞	~∞	0
Samarium	Sm-153	62	91	153	152.922094	0	46.284 hours	66.65 hours	0.015/hr
Samarium	Sm-154	62	92	154	153.9222093	22.75	~∞	~∞	0
Samarium	Sm-155	62	93	155	154.924640	0	22.3 minutes	32.1 minutes	0.03115/min
Selenium	Se-78	34	44	78	77.9173091	23.77	~∞	~∞	0
Selenium	Se-78	34	46	80	79.9165213	49.61	~∞	~∞	0
Silicon	Si-28	14	14	28	27.976926	92.223	~∞	~∞	0
Silver	Ag-107	47	60	107	106.905097	51.84	~∞	~∞	0
Silver	Ag-109	47	62	109	108.904752	48.16	~∞	~∞	0
Sodium	Na-22	11	11	22	21.994437	0	2.6027 years	3.745 years	0.2670/yr

(*Continued*)

TABLE E.1 (*Continued*)

Atomic Masses, Half-Lives, and the Natural Abundance of Common Nuclear Materials

Substance	Symbol	Protons (Z)	Neutrons (N)	Nucleons (A = Z + N)	Atomic Mass (AMU)	Natural Abundance (Atom %)	Half-Life ($T_{1/2}$)	Average Life (τ)	Decay Constant (λ)
Sodium	Na-23	11	12	23	22.989770	100	~∞	~∞	0
Sodium	Na-24	11	13	24	23.990963	0	14.959 hours	21.55 hours	0.0464/hr
Strontium	Sr-88	38	50	88	87.905612	82.58	~∞	~∞	0
Strontium	Sr-90	38	52	90	89.907738	0	28.90 days	41.62 days	0.0240/day
Strontium	Sr-92	38	54	92	91.911030	0	2.66 hours	3.83 hours	0.2611/hr
Strontium	Sr-94	38	56	94	93.915360	0	75.3 seconds	108.4 seconds	0.00922/sec
Strontium	Sr-95	38	57	95	94.919358	0	23.90 seconds	34.42 seconds	0.0290/sec
Strontium	Sr-96	38	58	96	95.921680	0	1.07 seconds	1.54 seconds	0.6493/sec
Strontium	Sr-98	38	60	98	97.928471	0	0.653 seconds	0.940 seconds	1.0638/sec
Strontium	Sr-99	38	61	99	98.933242	0	0.269 seconds	0.388 seconds	2.577/sec
Thorium	Th-232	90	142	232	232.038050	100	~∞	~∞	0
Tin	Sn-118	50	68	118	117.901603	24.22	~∞	~∞	0
Tin	Sn-120	50	70	120	119.9021947	32.58	~∞	~∞	0
Tritium	H-3	1	2	3	3.016049	0	12.32 years	17.75 years	0.0563/yr
Titanium	Ti-48	22	26	48	47.9479463	73.72	~∞	~∞	0
Uranium	U-233	92	141	233	233.039628	0	159,200 years	229,250 years	0.00000436/yr
Uranium	U-234	92	142	234	234.040945	0.0054	245,500 years	353,525 years	0.00000283/yr
Uranium	U-235	92	143	235	235.043923	0.721	7.04×10^8 years	1.01×10^9 years	0.990×10^{-9}/yr
Uranium	U-236	92	144	236	236.045562	0	2.342×10^7 years	3.373×10^7 years	0.296×10^{-7}/yr
Uranium	U-237	92	145	237	237.048724	0	6.75 days	9.72 days	0.1028/day
Uranium	U-238	92	146	238	238.050783	99.274	4.468×10^9 years	6.435×10^9 years	0.1554×10^{-9}/yr
Uranium	U-239	92	147	239	239.0542933	0	23.45 minutes	33.77 minutes	0.0296/min
Xenon	Xe-129	54	75	129	128.9047794	26.40	~∞	~∞	0
Xenon	Xe-131	54	77	131	130.905082	21.23	~∞	~∞	0
Xenon	Xe-133	54	79	133	132.905906	0	5.2475 days	7.556 days	0.1323/day
Xenon	Xe-134	54	80	134	133.905394	10.435	~∞	~∞	0
Xenon	Xe-135	54	81	135	134.907207	0	9.14 hours	13.17 hours	0.0759/hr
Xenon	Xe-136	54	82	136	135.907219	8.857	~∞	~∞	0
Xenon	Xe-138	54	84	138	137.913951	0	14.08 minutes	20.28 minutes	0.0493/min
Xenon	Xe-139	54	85	139	138.918793	0	39.68 seconds	57.15 seconds	0.0175/sec
Xenon	Xe-140	54	86	140	139.921647	0	13.60 seconds	19.60 seconds	0.0510/sec
Zinc	Zn-64	30	34	64	63.929147	48.6	~∞	~∞	0
Zirconium	Zr-90	40	50	90	89.904703	51.45	~∞	~∞	0
Zirconium	Zr-92	40	52	92	91.905040	17.15	~∞	~∞	0

Note: Atomic masses are given in AMU.

The atomic mass of Carbon-12 is exactly 12.00000 AMU.

The sum of the natural abundances of all the isotopes of any given element must add up to 1.0 (100%).

Not all isotopes are shown for all elements to reduce table length.

The symbol ~∞ means "effectively infinite."

Additional note: Outside of the United States, the element cesium is sometimes called "caesium."

The *total energy* released from all of these processes is about 210 MeV per fission, but only about 95% of this energy, or 200 MeV, is actually *recoverable*. The remaining 5% (~10 MeV) is carried away by the neutrinos into outer space, and it is eventually distributed somewhere between the stars. Since the neutrinos do not interact with the ordinary matter from which reactors are built, the kinetic energy they carry away is essentially *unrecoverable* and can never be converted into nuclear power. Neutrinos are discussed in more detail in Chapter 2.

E.3 Important Fission Products

A large nuclear power plant can produce over one trillion billion (~10^{17}) fission products in a single second. These fission products include isotopes of xenon, samarium, cesium (sometimes referred to as *caesium* outside of the United States), iodine, krypton, strontium, barium, promethium, niobium, rhodium, and rubidium. Table E.1 shows their atomic masses, their half-lives, their average lives, and their decay constants. In general, *many of these fission products have very short half-lives*, and with the exception of several isotopes of krypton and samarium, the most important fission products decay very quickly and normally emit a beta particle (an electron from the atomic nucleus) in the process. (This process is also known as β^- decay). This causes a nuclear transmutation to occur where the nuclei of some of the "neutron rich" fission products emit a delayed neutron to become more stable. Delayed neutrons, which typically represent less than 1% of the neutron population in an operating reactor, are fundamental to the operation of the reactor because they make it much easier to control. Delayed neutrons are discussed in Chapters 3 and 7. (They are also discussed in great detail in our companion book).

Without the delayed neutrons produced by these fission products, the nuclear power industry would probably not exist in the world today. The most important fission products are xenon-135 and Samarium-149, and they are discussed in great detail in our companion book.* In fact, several chapters of our companion book are devoted exclusively to a discussion of Xe-135 and the effect it can have on the reactivity of a thermal water reactor. The buildup of Xe-135 was also partially responsible for the reactor accident that occurred at Chernobyl in 1986.

* R.E. Masterson. *An Introduction to Nuclear Reactor Physics*, CRC Press, Boca Raton, FL (2017).

Appendix F: Delayed Neutron Emitters and Their Nuclear Properties

F.1 Delayed Neutron Emitting Materials

In this appendix, we would like to discuss the fission products that produce delayed neutrons. Not all fission products can produce a delayed neutron, but those that do add enough delayed neutrons to a reactor core to make it easier to control. Uranium-235 produces the most delayed neutrons, followed by U-233 and Pu-239. Thus, fast reactors fueled with Pu-239 produce fewer delayed neutrons than thermal reactors fueled with U-233 or U-235 do. The relative yields from all delayed neutron emitters are shown in Table F.1. Sometimes these yields are also called *delayed neutron fractions*.

Notice that the number of delayed neutrons during steady-state conditions always stays below 1%, and for U-235, U-233, and Pu-239, the percentages of delayed neutrons are 0.65%, 0.26%, and 0.20%, respectively. These percentages do not change very much unless a reactor undergoes a very severe transient. In some transients where the power level falls very quickly (such as during a complete reactor *scram*), the delayed neutron fraction may temporarily exceed 1%. However, this only applies to U-235 fueled reactors, and even then the number of delayed neutrons in the core only stays above 1% for a short period of time.

F.2 Features of Delayed Neutrons

The average amount of time required to produce a delayed neutron can vary considerably depending on the fission product that produces it. Normally, delayed neutrons are subdivided into six different categories (which reactor physicists have chosen to call *delayed neutron groups*), and each delayed neutron group has a unique identification number associated with it (from 1 to 6). These groups are shown in Table F.2. Notice that group 1 has the largest average lifetime (about 80 seconds) and group 6 has the smallest (about 1/3 of a second). This is due to the fact that different isotopes produce delayed neutrons at different rates. Delayed neutrons are almost always released from nuclei that are "neutron rich." Fission products that have the right number of neutrons (from the viewpoint of nuclear stability) will almost never produce a delayed neutron. Thus, only fission products that have excess neutrons will create one.

The other interesting feature of delayed neutrons is that their average energy is much lower than that of fission neutrons. For example, a fission neutron has an average kinetic energy of about 2 MeV, while a delayed neutron rarely has an energy greater than 0.5 MeV. (The exact numbers are shown in Table F.1.) The average energy is also a function of the isotope that releases the delayed neutron. Some isotopes of bromine and cesium release delayed neutrons with much lower energies than isotopes of iodine, xenon, and krypton do. In general, very few isotopes release delayed neutrons more than 90 seconds after they are created, and if they do, their average yields are very low. For this reason, the nuclear industry normally ignores any delayed neutrons that are produced after about one minute and a half (~90 seconds) when doing a reactor criticality calculation. Delayed neutrons are discussed in considerable detail in Chapters 3 and 7 and they are also discussed in great detail in our companion book.

Steps to Create a Delayed Neutron

Step 1

$$\mathrm{FP}(A, Z) \rightarrow \mathrm{FP}(A, Z+1) + 1 \text{ electron and 1 neutrino}$$

Step 2

$$\mathrm{FP}(A, Z+1) \rightarrow \mathrm{FP}(A-1, Z+1) + 1 \text{ delayed neutron} \qquad \text{(F.1)}$$

Table F.3 shows the isotopes that produce the most delayed neutrons and the timing with which these delayed neutrons are produced. Notice that almost all delayed neutrons are produced immediately after the process of radioactive beta decay (β^- decay). This means that some fission products with an atomic number of Z will transform themselves into fission products with an atomic number of Z + 1. The additional proton that is created in this way changes the stability of the nucleus, and the easiest way for the nucleus to become stable again is to release an additional neutron. This process is illustrated in Equation F.1, which is repeated from Chapter 7 for the interested reader.

TABLE F.1
Delayed Neutron Fractions for Different Nuclear Fuels

Delayed Neutron Group (i)	Fission Products	Neutron Energy (MeV)	Half-Life of Fission Fragments (seconds) $T_{1/2}$			Delayed Neutron Fraction (β)		
			U-235	Pu-239	U-233	U-235	Pu-239	U-233
1	^{87}Br, ^{142}Cs	0.25	55.72	54.28	55.0	0.021	0.0072	0.0226
2	^{137}I, ^{88}Br	0.56	22.72	23.04	20.57	0.140	0.0626	0.0786
3	^{138}I, ^{89}Br, $^{(93,94)}$Rb	0.43	6.22	5.60	5.00	0.126	0.0444	0.0658
4	^{139}I, $^{(93,94)}$Kr, ^{143}Xe, $^{(90,92)}$Br	0.45	2.3	2.13	2.13	0.252	0.0685	0.0730
5	^{140}I, ^{145}Cs	0.42	0.61	0.618	0.615	0.074	0.018	0.0135
6	(As, Br, Rb, etc.)	0.42	0.23	0.257	0.277	0.027	0.0093	0.0087
Total yield						0.65	0.20	0.26

Source: Courtesy of A.F. Henry.

TABLE F.2
Delayed Neutron Time Constants for Different Nuclear Fuels

Delayed Neutron Group (i)	Fission Products	Neutron Energy (MeV)	Average Lifetime of Fission Fragments (s) τ			Decay Constant (s^{-1}) λ		
			U-235	Pu-239	U-233	U-235	Pu-239	U-233
1	^{87}Br, ^{142}Cs	0.25	80.40	76.32	79.36	0.0124	0.0127	0.0126
2	^{137}I, ^{88}Br	0.56	32.78	33.24	29.68	0.0305	0.0300	0.0337
3	^{138}I, ^{89}Br, $^{(93,94)}$Rb	0.43	6.97	6.08	7.21	0.1114	0.1237	0.1386
4	^{139}I, $^{(93,94)}$Kr, ^{143}Xe, $^{(90,92)}$Br	0.62	3.31	3.07	3.07	0.3013	0.3253	0.3253
5	^{140}I, ^{145}Cs	0.42	0.88	0.89	0.88	1.136	1.121	1.127
6	(As, Br, Rb, etc.)	0.42	0.33	0.37	0.40	3.013	2.696	2.502
Average value*		0.45	21.11	20.66	20.10	0.767	0.718	0.690

Source: Courtesy of A.F. Henry.

Notice that *the creation of a delayed neutron is a two-step process*. The first step creates an additional proton, and the second step ejects a delayed neutron from the nucleus to make it stable again. The reasons why the nucleus chooses to emit a delayed neutron are discussed in Chapters 6 and 7. Thus, delayed neutrons are produced primarily through the process of β^- decay rather than through the process of β^+ decay. Another interesting parameter shown in Table F.1 is what is known as the *delayed neutron fraction*. The delayed neutron fraction β is defined as the total number of delayed neutrons produced per fission ν_d divided by the total number of neutrons ν (both prompt and delayed) produced per fission. The formal definition of the delayed neutron fraction is then

Formal Definition of the Delayed Neutron Fraction

$$\beta = \frac{\nu_d}{\nu} \tag{F.2}$$

where $\nu = \nu_p + \nu_d$ (prompt plus delayed).

Notice from Table F.1 that each delayed neutron group contributes a different number of delayed neutrons to the overall yield and this number can change depending on the type of fuel that is used. For example, for U-235 and Pu-239, group 4 produces the greatest number of delayed neutrons, and for U-233, the greatest number of delayed neutrons is produced by group 2. The sum of the contributions from all six groups is then known as the delayed neutron fraction for the fuel. Normally, this number is less than 1%, and for U-233, U-235, and Pu-239, the respective delayed neutron fractions are 0.26%, 0.65%, and 0.20%. Another parameter closely related to the delayed neutron fraction is the *delayed neutron yield* Y. This is simply the number of delayed neutrons produced per fission. The delayed neutron yields for the thermal fission of U-233, U-235, and Pu-239 are shown in Table F.4. The delayed neutron fraction for a specific isotope is then the delayed neutron yield divided by the total neutron yield (see Equation F.2).

TABLE F.3
Most Common Emitters of Delayed Neutrons

Delayed Neutron Precursor Group	Delayed Neutron Precursor	Chemical Symbol	Decay Mode	Average Delayed Neutron Energy (MeV)	Delayed Neutron Precursor Half-Life ($T_{1/2}$) (seconds)	Decay Constant for Delayed Neutron Production (λ) (s^{-1})
1	Bromine-87	Br-87	β^-	0.25	55.7	0.0179
2	Iodine-137	I-137	β^-	0.56	24.5	0.0408
	Bromine-88	Br-88	β^-		16.3	0.0613
3	Iodine-138	I-138	β^-	0.43	6.5	0.1538
	Rubidium-93	Rb-93	β^-		5.9	0.1685
	Bromine-89	Br-89	β^-		4.4	0.2273
4	Iodine-139	I-139	β^-	0.45	2.4	0.4167
	Cesium-144	Cs-144	β^-		1.0	1.0000
	Tellurium-137	Te-137	β^-		3.5	0.2857
	Bromine-90	Br-90	β^-		1.8	0.5555
	Krypton-92	Kr-92	β^-		1.8	0.5555
	Krypton-93	Kr-93	β^-		1.3	0.7692
5	Krypton-95	Kr-95	β^-	0.42	0.8	1.2500
	Iodine-140	I-140	β^-		0.9	1.1111
	Iodine-141	I-141	β^-		0.5	2.0000
6	Iodine-142	I-142	β^-	0.42	0.2	5.0000
	Bromine-92	Br-92	β^-		0.4	2.5000
	Rubidium-95	Rb-95	β^-		0.4	2.5000
	Rubidium-97	Rb-97	β^-		0.2	5.0000

Source: Papers of G. Robert Keepin, Los Alamos, NM.

TABLE F.4
Delayed Neutron Yields for Different Nuclear Fuels

Type of Fuel	Delayed Neutron Precursor Group	Yield (Delayed Neutrons per Fission)
U-233	1	0.00057
U-233	2	0.00197
U-233	3	0.00166
U-233	4	0.00184
U-233	5	0.00034
U-233	6	0.00022
		Total yield = 0.0066
U-235	1	0.00052
U-235	2	0.00346
U-235	3	0.00310
U-235	4	0.00624
U-235	5	0.00182
U-235	6	0.00066
		Total yield = 0.0158
Pu-239	1	0.00021
Pu-239	2	0.00182
Pu-239	3	0.00129
Pu-239	4	0.00199
Pu-239	5	0.00052
Pu-239	6	0.00027
		Total yield = 0.0061

Source: Courtesy of A.F. Henry.

TABLE F.5
Prompt and Delayed Neutron Production Rates for Different Nuclear Fuels

Isotope	Prompt and Delayed Neutrons Produced per Thermal Fission (υ)	Delayed Neutron Fraction per Thermal Fission ($\beta = \nu_d/\nu$)
U-233	2.49	0.0026
U-235	2.42	0.0065
Pu-239	2.87	0.0020
Pu-241	2.92	—

Source: Lamarsh, J.R., *Introduction to Nuclear Reactor Theory*, Second Printing, Addison-Wesley Publishing Company, Inc., Reading, MA, 1972; Duderstadt, J. and Hamilton, L., *Nuclear Reactor Analysis*, John Wiley & Sons, New York, 1976; Henry, A.F., *Nuclear Reactor Analysis*, MIT Press, Cambridge, MA (1975).

Delayed neutrons and their effect on a time-dependent reactor are discussed in Chapter 7. The delayed neutron fraction β also appears as an important term in the time-dependent neutron diffusion equation, whose solutions are discussed in our companion book.* The delayed neutron fraction is a dimensionless number because it is simply the ratio of the number of delayed neutrons to the total number of neutrons (prompt and delayed). The *prompt neutron fraction* is therefore $(1 - \beta)$ or ν_p/ν. Normally, the value of ν (the total neutron yield) is a dimensionless number between 2.42 and 2.92. Again, the exact value of ν depends on the type of fuel that is used. Values of ν for all common nuclear fuels are shown in Table F.5. A more comprehensive version of this table can be found in Chapter 7. In general, plutonium produces the most neutrons per thermal fission. For this reason, it is very desirable to use as a nuclear fuel.

F.3 The Role of Bromine-87

Table F.3 shows that the delayed neutron precursor with the longest half-life of all "official" delayed neutron precursors is bromine-87, which has a half-life of 55.7 seconds. *Bromine-87* is very important to the operation of a nuclear power plant because when a reactor is shut down quickly and the prompt and shorter lived delayed neutrons have decayed away, the neutron population in the core is determined by the number of delayed neutrons produced by the decay of Bromine-87. In other words, *the asymptotic reactor period in the event of a rapid core shutdown is determined primarily by the Bromine-87 concentration in the core*. No other radioisotope produced from the fission of a uranium or plutonium nucleus has a more immediate impact on the effective multiplication factor of the core in this case. Xenon and samarium have a much larger long-term impact, but they are not significant delayed neutron emitters.

* R.E. Masterson. *An Introduction to Nuclear Reactor Physics*, CRC Press, Boca Raton, FL (2017).

Appendix G: Attenuation Coefficients for Radiation Shields

G.1 Types of Attenuation Coefficients and Their Uses

Attenuation coefficients (see Chapter 18) can be used to find the rate of x-ray and gamma ray attenuation in radiation shields. Attenuation coefficients are also available for alpha rays and beta rays, but they are generally not as important as the attenuation coefficients for x-rays and gamma rays because x-rays and gamma rays can travel much further before they are absorbed (see Chapter 17). Attenuation coefficients for x-rays and gamma rays are normally subdivided into two subcategories: (1) *linear attenuation coefficients* and (2) *mass attenuation coefficients*. These coefficients are related to each other through simple conversion factors that we will shortly discuss.

Mass attenuation coefficients have the units of cm^2/g, and linear *attenuation coefficients have the units of* cm^{-1}. Mass attenuation coefficients are given the symbol μ_M and linear attenuation coefficients are given the symbol μ. A linear attenuation coefficient can be obtained from a mass attenuation coefficient by multiplying the mass attenuation coefficient by the physical density ρ of the shielding material. The physical density ρ of the shielding material is normally measured in g/cm^3. Thus the linear attenuation coefficient can be obtained from the mass attenuation coefficient using the following equation.

Relationship between the Linear and Mass Attenuation Coefficients

$$\mu = \rho \cdot \mu_M \tag{G.1}$$

A great deal of physics is lumped into the values of these coefficients, and *the attenuation coefficients are also energy dependent. In general, an attenuation coefficient will decrease as the photon energy is increased*, although there are some exceptions to this rule. X-ray and gamma ray attenuation occurs when the incoming photons interact with electron clouds. The photons scatter off of the electrons in the electron clouds and lose energy as they go. Occasionally, they are absorbed by an electron and reemitted again. The three primary ways that a photon can lose energy are

1. The photoelectric effect
2. Compton scattering
3. Pair production

Pair production is limited to higher photon energies and only occurs at energies above 1 MeV. Compton scattering and the photoelectric effect can occur at all photon energies, but their effects are usually greatest below 1 MeV. All of these processes are discussed in more detail in Chapter 17. Another form of photon radiation that sometimes occurs in radiation shields is *bremsstrahlung* or *"braking radiation."* This type of radiation occurs when high-speed electrons decelerate rapidly in the presence of an electromagnetic field. As the electrons slow down, they emit photons in their direction of motion. The radiation pattern is similar to that of a *dipole*.

Braking radiation was first discovered by *Nikola Tesla*, who is also credited with the invention of the fluorescent light bulb, the Tesla induction motor, the Tesla coil, the electric alternating current (AC), and the modern radio (see Chapter 12). His patents were used by George Westinghouse to help create the Westinghouse Electric Corporation, which is now the parent company of Westinghouse Nuclear—the largest manufacturer of commercial nuclear power plants in the world. The mass attenuation coefficients for common shielding materials are shown in Table G.1.

The linear attenuation coefficients for the same materials are shown in Table G.2. To convert the entries in Table G.1 to the entries in Table G.2, one simply multiplies the appropriate entry by the physical density of the shielding material in g/cm^3. The physical densities of some common shielding materials are shown in Table G.3. Notice that lead is the best shielding material to use for x-rays and gamma rays, followed by iron, aluminum, concrete, and water in that order. However, on a pound by pound basis, iron turns out to be the second best shielding material. This has to do with the way the incoming photons interact with iron's electron cloud.

TABLE G.1
Mass Attenuation Coefficient (μ/ρ) in cm^2/g

Mass Attenuation Coefficients for X-Rays and Gamma Rays for Common Shielding Materials (cm^2/g)					
Photon Energy (MeV)	Water	Aluminum	Lead	Iron	Concrete
0.1	0.025	0.0373	5.193	0.225	0.0416
0.2	0.300	0.0275	0.821	0.0489	0.0289
0.5	0.033	0.0286	0.0994	0.0294	0.0396
1.0	0.031	0.0270	0.0402	0.0261	0.0278
2.0	0.026	0.0232	0.0293	0.0231	0.0239
5.0	0.020	0.0192	0.0352	0.0227	0.0194
10.0	0.016	0.0182	0.0450	0.0250	0.0177

Source: Lamarsh, J.R., *Introduction to Nuclear Reactor Theory*, Second Printing, Addison-Wesley Publishing Company, Inc., Reading, MA, 1972.

TABLE G.2
Linear Attenuation Coefficient (μ) in cm^{-1}

Linear Attenuation Coefficients for X-Rays and Gamma Rays for Common Shielding Materials (cm^{-1})					
Photon Energy (MeV)	Water	Aluminum	Lead	Iron	Concrete
0.1	0.025	0.1007	58.6809	1.7707	0.0978
0.2	0.300	0.0742	9.2773	0.3848	0.0679
0.5	0.033	0.0286	0.0994	0.2314	0.0396
1.0	0.031	0.0772	1.1232	0.2054	0.0930
2.0	0.026	0.0626	0.3311	0.1818	0.0562
5.0	0.020	0.0518	0.3978	0.1786	0.0456
10.0	0.016	0.0490	0.5085	0.1968	0.0416

Source: Lamarsh, J.R., *Introduction to Nuclear Reactor Theory*, Second Printing, Addison-Wesley Publishing Company, Inc., Reading, MA, 1972.

TABLE G.3
Physical Densities of Common Shielding Materials in g/cm^3

Physical Densities of Common Shielding Materials		
Material	Physical Density (g/cm^3)	Atomic or Molecular Weight
Aluminum	2.7	26.98
Concrete	2.35	N/A
Iron	7.87	55.85
Lead	11.3	207.19
Water	1.0	18.01

Source: Lamarsh, J.R., *Introduction to Nuclear Reactor Theory*, Second Printing, Addison-Wesley Publishing Company, Inc., Reading, MA, 1972.

G.2 Attenuation of a Photon Beam

Once the linear attenuation coefficient μ is known, the intensity I(x) of the photon beam at any depth x into a radiation shield can be found from the equation.

Equation for the Attenuation of a Photon Beam

$$I(x) = I_o e^{-\mu x} \qquad \text{(G.2)}$$

where I_o is the initial intensity of the photon beam (in photons/cm²/sec) at the surface of the shield. This equation applies to planar radiation shields. Equations that can be used for other shield geometries are discussed in Chapter 18. The following example illustrates how these tables can be used to calculate the attenuation of a photon beam that is incident on a radiation planar shield. Many other uses for equation G.2 are presented in Chapter 17.

Example Problem G.1

Suppose that a gamma ray beam consisting of photons having two separate energies falls on a lead shield 2 cm thick. If 70% of the gamma rays have an energy of 1 MeV and 30% have an energy of 2 MeV, how many gamma rays per second will travel completely through the shield? Assume that the shield is a simple lead plate and the total intensity of the gamma ray beam is 1 million photons/cm²/s.

Solution The intensity of the beam on the other side of the plate can be found from the equation

$$I(x) = 0.70 I_o e^{-\mu 1 x} + 0.30 I_o e^{-\mu 2 x}$$

where

μ1 is the linear attenuation coefficient for 1 MeV gamma rays
μ2 is the linear attenuation coefficient for 2 MeV gamma rays

Since I_o = 1,000,000, x = 2 cm, μ1 = 1.1232 cm⁻¹, and μ2 = 0.3311 cm⁻¹, the intensity of the gamma rays exiting the far side of the shield is

$$I(x) = 700{,}000 e^{-2.25} + 300{,}000 e^{-0.66} = 73780 + 155{,}055 = 228{,}835 \text{ gamma rays/cm}^2/\text{s}$$

The attenuation of the gamma ray beam is therefore about 77%. This example illustrates how difficult it is to stop a beam of high-energy gamma rays. [Ans.]

G.3 Distinguishing between X-Rays and Gamma Rays

X-rays and gamma rays are both energetic photons outside the range of visible light. Gamma rays have higher energies than x-rays do, and therefore, gamma rays have greater penetrating power. X-rays are normally classified as photons having energies *less* than 100 keV (0.1 MeV), and gamma rays are normally classified as photons having energies *greater* than 100 keV (0.1 MeV). Therefore, 1.0 MeV photons and 2.0 MeV photons are classified as gamma rays, while 50 keV photons are classified as x-rays similar to the ones used to take a dental x-ray.

In nuclear power plants, radiation shields are intended to protect plant personnel from gamma rays and high-energy neutrons. The average energy of a fission neutron is about 2 MeV. The best way to shield a person from a high-energy neutron is first slow the neutron down to thermal energies and then absorb it after it has reached the thermal energy range. Thus, neutron radiation shields generally consist of two separate parts or regions. The first part, which contains a material such as water or graphite, converts a fast neutron into a thermal neutron, and the second part consists of a neutron absorbing material such as Cadmium-112 or Boron-10, which then absorbs the thermal neutron. Radiation shields made from alternating layers of different materials are sometimes called *multilayered shields*. The design of these shields is discussed in Chapter 18.

Appendix H: Diffusion Coefficients, Transport Cross Sections, and Mean Free Paths

H.1 Neutron Diffusion Coefficient

Neutron diffusion theory can be used to predict how neutrons behave in any diffusive material. The diffusion coefficient D that neutron diffusion theory uses can be found in the neutron diffusion equation, and under certain conditions, it can also be derived from neutron transport theory. In classical neutron diffusion theory, *the diffusion coefficient D is the constant of proportionality between the neutron current J and the negative gradient of the neutron flux ϕ*. In other words, the diffusion coefficient is a fundamental quantity that allows the neutron diffusion equation (which is a function of both J and ϕ) to be converted into a second-order differential equation, which is a function of only ϕ:

Time-Dependent Neutron Diffusion Equation

$$D\nabla^2\phi + \left(\upsilon\Sigma_f - \Sigma_a\right)\phi = \frac{1}{v}\frac{\partial\phi}{\partial t} \tag{H.1}$$

Neutron diffusion coefficients have the units of length, and in neutron diffusion theory, they are normally measured in centimeters (cm). Their values are summarized for the interested reader in Tables H.1 and H.2.

H.2 Fick's Law of Diffusion

In a material where there is both scattering and absorption, the neutron current and the neutron flux are related to each other by a famous equation called *Fick's Law of Diffusion*, which was first introduced to the reader in Chapter 11. In a homogeneous material, Fick's Law of Diffusion can be written as

$$\mathbf{J} = -D\,\text{grad}\phi = -D\nabla\phi \tag{H.2}$$

where

J is the neutron current
ϕ is the neutron flux

Fick's law of diffusion was first proposed by a German chemist by the name of *Adolf Fick* in 1855. In Cartesian coordinates, Equation H.2 simply states that

Fick's Law with a Spatially Dependent Diffusion Coefficient

$$\mathbf{J}(x,y,z) = -\left(\frac{d}{dx}D(x)\frac{d\phi}{dx} + \frac{d}{dy}D(y)\frac{d\phi}{dy} + \frac{d}{dz}D(z)\frac{d\phi}{dz}\right)$$

or

$$\mathbf{J} = \mathbf{i}\left(J_x\right) + \mathbf{j}\left(J_y\right) + \mathbf{k}\left(J_z\right)$$

$$J_x = -\frac{d}{dx}D(x)\frac{d\phi}{dx}$$

$$J_y = -\frac{d}{dy}D(y)\frac{d\phi}{dy} \tag{H.3}$$

$$J_z = -\frac{d}{dz}D(z)\frac{d\phi}{dz}$$

TABLE H.1
Parameters for Some Important Nuclear Materials at Thermal Energies (<1 eV)

Material	Symbol	Function	Weight (A = Z + N)	$\mu = \cos\theta =$ 0.67/A	θ (°)	Total Σ_t (cm^{-1})	Total Σ_{tr} (cm^{-1})	D* (cm) = $1/3\Sigma_{tr}$	λ (cm) = 3D = $1/\Sigma_{tr}$
Aluminum	Al-27	Structure	27	0.0248	88.58	0.1035	0.1013	3.290	9.872
Beryllium	Be-9	Moderator	9	0.0744	85.73	0.7590	0.7025	0.474	1.423
Boron	B-10	Control	10	0.0670	86.18	491.42	491.40	0.0006	0.002
Cadmium	Cd-112	Control	112	0.0059	89.66	112.65	112.64	0.003	0.009
Carbon	C-12	Moderator	12	0.0558	86.80	0.3952	0.3731	0.893	2.680
Deuterium	D-2	Moderator	2	0.3350	70.42	0.000240	0.00016	2075	6,225
Helium	He-4	Moderator	4	0.0957	84.50	0.000022	0.00002	16,667	50,000
Hydrogen	H	Moderator	1	0.6700	47.93	0.001510	0.00005	6,667	20,000
Iron	Fe-56	Structure	56	0.0119	89.32	1.1405	1.1295	0.295	0.885
Oxygen	O-16	Moderator	16	0.0418	87.60	0.000208	0.00020	1,667	5000
Plutonium	Pu-239	Fuel	239	0.0028	89.84	51.05	51.05	0.007	0.020
Plutonium	Pu-240	Fuel	240	0.0028	89.84	14.724	14.72	0.022	0.068
Plutonium	Pu-241	Fuel	241	0.0028	89.84	68.98	68.98	0.005	0.014
Plutonium	Pu-242	Fuel	242	0.0028	89.84	1.4056	1.405	0.237	0.711
Plutonium dioxide	PuO_2	Fuel	271	0.0025	89.86	Varies[a]	Varies[a]	Varies[a]	Varies[a]
Uranium	U-233	Fuel	233	0.0028	89.84	28.16	28.16	0.012	0.035
Uranium	U-235	Fuel	235	0.0028	89.84	33.25	33.25	0.010	0.030
Uranium	U-238	Fuel	238	0.0028	89.84	0.5536	0.5535	0.602	1.806
Uranium (natural)	U	Fuel	238	0.0028	89.84	0.8095	0.8094	0.602	1.235
Uranium dioxide	UO_2	Fuel	270	0.0025	89.86	Varies[b]	Varies[b]	Varies[b]	Varies[b]
Water (light)	H_2O	Moderator	18	0.0372	87.87	2.230	2.148	0.155	0.465
Water (heavy)	D_2O	Moderator	20	0.0335	88.08	0.665	0.643	0.518	1.555
Zircaloy-II	Zirc-II	Structure	91	0.0073	89.59	0.2878	0.2857	1.167	3.500
Zircaloy-IV	Zirc-IV	Structure	91	0.0073	89.58	0.2878	0.2857	1.167	3.500
Zirconium	Zr-91	Structure	91	0.0073	89.58	0.2857	0.2836	1.167	3.500

Notes: The experimentally determined values for D may be different than those shown here because of the effects of chemical bonds on the scattering process at low neutron energies. See Chapter 11 for a discussion of how important these effects can be.

[a] Varies with Pu-239 content.

[b] Varies with U-235 content.

Here the neutron flux $\phi(x, y, z)$ is a *scalar quantity*, while the neutron current $\mathbf{J}(x, y, z)$ is a *vector quantity* (i.e., it has both magnitude and direction). Notice that in some cases, the diffusion coefficient can be spatially dependent, that is, it can be a function of x, y, or z. In other words, Fick's Law states that *the neutron current* $\mathbf{J}$ *in a diffusive medium is proportional to the negative gradient of the neutron flux* ϕ. The constant of proportionality between these two quantities is the *neutron diffusion coefficient* D. The *diffusion coefficient is also energy dependent*, and in its most general form, it is related to the neutron transport cross section by the following equation:

$$D(E) = \frac{1}{3\sum_{tr}(E)} \tag{H.4}$$

Because the transport cross section is energy dependent, the diffusion coefficient has an energy dependence as well. In neutron transport theory, the transport cross section $\sum_{tr}(E)$ is defined by

Definition of the Transport Cross Section

$$\sum_{tr}(E) = \sum_{t}(E) - \cos\theta \sum_{s}(E) \tag{H.5}$$

TABLE H.2
Parameters for Some Important Nuclear Materials at Fission Energies (~1 MeV)

Material	Symbol	Function	Weight (A = Z + N)	μ = cos θ = 0.67/A	θ (°)	Total Σ_t (cm^{-1})	Total Σ_{tr} (cm^{-1})	D (cm) = $1/3\Sigma_{tr}$	λ (cm) = 3D = $1/\Sigma_{tr}$
Aluminum	Al-27	Structure	27	0.0248	88.58	0.1422	0.1386	2.403	7.211
Beryllium	Be-9	Moderator	9	0.0744	85.73	0.4020	0.3704	0.900	2.700
Boron	B-10	Control	10	0.0670	86.18	0.6220	0.5952	0.560	1.680
Cadmium	Cd-112	Control	112	0.0059	89.66	0.3105	0.3087	1.080	3.239
Carbon	C-12	Moderator	12	0.0558	86.80	0.1600	0.1510	2.206	6.619
Deuterium	D-2	Moderator	2	0.3350	70.42	0.2167			
Helium	He-4	Moderator	4	0.0957	84.50	0.00018	0.00012	2785	8,354
Hydrogen	H	Moderator	1	0.6700	47.93	0.00021	0.000069	4810	14,430
Iron	Fe-56	Structure	56	0.0119	89.32	0.4407	0.4354	0.765	2.296
Oxygen	O-16	Moderator	16	0.0418	87.60	0.00041	0.00038	869.7	2609
Plutonium	Pu-239	Fuel	239	0.0028	89.84	0.4518	0.4508	0.739	2.218
Plutonium	Pu-240	Fuel	240	0.0028	89.84	0.3575			
Plutonium	Pu-241	Fuel	241	0.0028	89.84	0.3990			
Plutonium	Pu-242	Fuel	242	0.0028	89.84	0.3655			
Plutonium dioxide	PuO_2	Fuel	271	0.0025	89.86	Varies[a]	Varies[a]	Varies[a]	Varies[a]
Uranium	U-233	Fuel	233	0.0028	89.84	0.4642	0.4633	0.719	2.158
Uranium	U-235	Fuel	235	0.0028	89.84	0.5392	0.5384	0.619	1.857
Uranium	U-238	Fuel	238	0.0028	89.84	0.3463	0.3454	0.965	2.895
Uranium (natural)	U	Fuel	238	0.0028	89.84	0.3350	0.3342	0.997	2.992
Uranium dioxide	UO_2	Fuel	270	0.0025	89.86	Varies[b]	Varies[b]	Varies[b]	Varies[b]
Water (light)	H_2O	Moderator	18	0.0372	87.87	0.5628	0.5418	0.615	1.845
Water (heavy)	D_2O	Moderator	20	0.0335	88.08	0.6732	0.6506	0.512	1.537
Zircaloy-II	Zirc-II	Structure	91	0.0073	89.59	0.0110	0.0107	31.065	93.197
Zircaloy-IV	Zirc-IV	Structure	91	0.0073	89.58	0.0110	0.0107	31.065	93.197
Zirconium	Zr-91	Structure	91	0.0073	89.58	0.0108	0.0107	31.065	93.197

[a] Varies with Pu-239 content.
[b] Varies with U-235 content.

where *cos θ is the average cosine of the neutron scattering angle* in the laboratory coordinate system. In neutron transport theory (see Chapter 22) the value of cos θ is sometimes written as μ (i.e., μ = cos θ). Hence, in many textbooks, the value of the neutron diffusion coefficient D(E) is also written as

$$D(E) = \frac{1}{3\Sigma_{tr}(E)} = \frac{1}{3\left(\Sigma_t(E) - \cos\theta\Sigma_s(E)\right)} \tag{H.6}$$

or

$$D(E) = \frac{1}{3\Sigma_{tr}(E)} = \frac{1}{3\left(\Sigma_t(E) - \mu\Sigma_s(E)\right)} \tag{H.7}$$

These equations show that *the diffusion coefficient can be thought of as one way to measure the resistance that a material presents to the flow of neutrons.* A large diffusion coefficient means a material has very little resistance to the flow of neutrons, and a small diffusion coefficient means that it has a great deal of resistance to the same flow. In outer space, the diffusion coefficient is *effectively infinite* because there are no atoms to impede the flow of a neutron beam.

H.3 Neutron Diffusion Coefficients for Pure Scatters

When the scattering cross section of a nuclear material is much greater than its absorption cross section ($\Sigma_s \gg \Sigma_a$) or when it is possible to neglect the value of the absorption cross section entirely ($\Sigma_a \approx 0$), then

$$\Sigma_t = \Sigma_a + \Sigma_s \approx \Sigma_s \tag{H.8}$$

and the equation for the diffusion coefficient becomes

$$D(E) = \frac{1}{3\left(\Sigma_s(E)(1-\mu)\right)} \tag{H.9}$$

This equation can be applied to materials such as light water, heavy water, hydrogen, beryllium, and carbon, which are good neutron scatters but poor neutron absorbers. Materials where the absorption cross section is many times smaller than the scattering cross section are sometimes classified as *pure scatterers*. In practice, *heavy water* (D_2O) is an excellent example of a material of this type. Its scattering cross section is $\Sigma_s = 0.665\ cm^{-1}$, and its absorption cross section is $\Sigma_a = 0.000094\ cm^{-1}$. Heavy water is used as a *moderator* in CANDU heavy water reactors, which can run on natural uranium alone.

H.4 Finding the Cosine of the Neutron Scattering Angle

The *cosine of the neutron scattering angle* θ (or $\mu = \cos\theta$) that appears in the definition of the transport cross section

$$\Sigma_{tr}(E) = \Sigma_t(E) - \mu\Sigma_s(E) \tag{H.10}$$

is the cosine of the *average angle* that a neutron scatters off of an atomic nucleus in the laboratory coordinate system. It is an important parameter in the study of nuclear science and engineering for a number of reasons. In particular, the cosine of the scattering angle θ can be used to find the transport cross section and the diffusion coefficient D as a function of a neutron's kinetic energy E. In Chapter 11, we learned that the average cosine of the scattering angle μ is a function of the atomic mass number A = Z + N of the target nucleus *as long as the collision is an elastic one*. The specific relationship between these two parameters is

$$\mu = \cos\theta \tag{H.11}$$

or

$$\mu = \frac{2}{3A} = \frac{0.67}{A} = \frac{0.67}{Z+N} \tag{H.12}$$

and the error one incurs by using this latter equation is about 1%. Thus, elastic collisions in which the direction of the scattered neutron is essentially unchanged have a value of μ close to 1.0 (since $\theta \approx 0$), and collisions in which the scattering angle is large have a value of μ closer to 0 (since θ is closer to 90°). Heavy elements have very small values of μ (since A is very large), and this implies that the average value of the scattering angle is close to 90°. Conversely, the lightest element—hydrogen—has a value for μ of 0.67 (since A is 1), and this implies that the average scattering angle is about 45°. Hence, neutrons *forward scatter* off of light elements, but scatter almost isotropically off of heavy ones. *Thus, the transport cross section differs the most from the total cross section for lighter elements.* because of the effects of forward scattering. In other words, neutrons (and many other nuclear particles) tend to *stream* in their original direction of motion through lighter elements and tend to *diffuse* isotropically through heavier ones.

H.5 Reasons for Using the Transport Cross Section Instead of the Total Cross Section

The primary reason why the transport cross section $\sum_{tr}$ appears so frequently in the study of reactor physics is that it corrects for the effects of anisotropic neutron scattering in lighter elements. Since elastic scattering almost always takes place in the forward direction (i.e., with an average angle $\theta < 90°$), this means that *the transport mean free path $\lambda_{tr} = 1/\Sigma_{tr}$ is always somewhat longer than the conventional mean free path* $\lambda = 1/\Sigma_t$. Thus the additional forward scattering increases the apparent mean free path of the incoming neutrons because neutrons that are scattered in the forward direction will continue to travel in that direction further than neutrons that have a random distribution of scattering angles (and therefore some backscatter). Since the diffusion coefficient is inversely proportional to the transport cross section Σ_{tr}, that is

$$D(E) = \frac{1}{3\sum_{tr}(E)} \tag{H.13}$$

the diffusion coefficient D will also be larger in a material when there is forward scattering than when there is not. In light elements such as hydrogen, the forward scattering process can be very anisotropic at high neutron energies. This means that transport theory is more accurate than diffusion theory under these conditions because the neutrons tend to stream through a material rather than simply diffusing through it. It should also be apparent from what we have just said that *the transport cross section is always smaller than the total cross section* because the anisotropic scattering causes μ to be large ($0.33 \leq u \leq 0.67$) in light elements and close to 0 in heavy ones.

H.6 Understanding the Mean Free Path

The *neutron mean free path* λ is a convenient way to measure the average distance <d> a neutron travels before it interacts with an atomic nucleus. Strictly speaking, a separate mean free path can be defined for scattering λ_s and for absorption λ_a, as well as for the sum of the two ($\lambda_t = \lambda_s + \lambda_a$). Each of these mean free paths determines how far a neutron travels before it "hits" an atomic nucleus and participates in a specific type of reaction. Normally, each type of reaction (such as scattering, capture, fission, or absorption) has a different mean free path associated with it because a neutron may travel further to be scattered than to be captured or absorbed. There is an important physical relationship between the mean free path for a particular reaction type x and the macroscopic cross section for that reaction type $\sum_x$. In general, the relationship between these two quantities is

$$\lambda_x = \frac{1}{\Sigma_x} \tag{H.14}$$

where the subscript x refers to the reaction type (x = a, s, c, f, or t). Now for the case of water, $\Sigma_s \approx \Sigma_t$ (since $\Sigma_s \gg \Sigma_a$), and this implies that

$$\lambda_t \approx \lambda_s = \frac{1}{\Sigma_s} \tag{H.15}$$

Neutron mean free paths are usually measured in centimeters (cm), and *macroscopic cross sections are usually measured in inverse centimeters* (cm^{-1}). Therefore, the neutron mean free path is always the reciprocal of the macroscopic cross section.

H.7 The Diffusion Coefficient and the Mean Free Path

There is an extremely important relationship between the neutron diffusion coefficient D and the neutron mean free path λ. Since both of these quantities are energy dependent, we can express this relationship as

$$\lambda(E) = 3D(E) \tag{H.16}$$

where E is the energy of the incoming neutron. In other words, if the diffusion coefficient for a material at a particular energy E is 10 cm, then the mean free path of a neutron in that same material is $\lambda = 3 \times 10 = 30$ cm. Consequently, one might be tempted to ask where the number 3 comes from in Equation H.16. It is simply there because the diffusion of a particle ensemble is a *three-dimensional process*. If we were to derive the same relationship for only one or two dimensions, then the 3 would be replaced by a 1 or a 2. Hence, the constant of proportionality between the mean free path λ and the diffusion coefficient D is simply a measure of the number of dimensions in the diffusing medium itself. Several proofs of this statement can be found in reactor physics books and on the Internet. So in general, the mean free path is related to the diffusion coefficient by

$$\lambda_s(E) = (\text{Number of dimensions}) \times D(E) \tag{H.17}$$

and *in most cases, the mean free path is simply interpreted as the scattering mean free path* λ_s. Finally, when the atomic weight of the target nucleus becomes relatively small (say A < 16), the neutron scattering process becomes anisotropic, and we may write

$$\lambda_{tr}(E) = \frac{1}{\Sigma_{tr}}(E) \tag{H.18}$$

where now λ_{tr} is the *transport mean free path*. The *transport cross section* is then given by $\sum_{tr}(E) = \sum_t(E) - \mu\sum_s(E)$ where μ is *the average cosine of the scattering angle*. Thus the anisotropy in this process is represented by the value of μ. As before, when $\theta = 90°$, the scattering becomes isotropic and $\mu = 0$.

H.8 Typical Values of the Diffusion Coefficient, the Mean Free Path, and the Transport Cross Section for Nuclear Materials

It should be apparent from what we have just said that the diffusion coefficient D, the transport mean free path λ_{tr}, and the transport cross section Σ_{tr} are related to each other both mathematically and physically. Specifically, *the diffusion coefficient D and the mean free path λ are always larger for fast neutrons than they are for thermal neutrons because the cross sections always become smaller as the kinetic energy of the neutrons increase*. Table H.1 compares the values of these parameters for thermal neutrons, and Table H.2 compares the same parameters for fast neutrons. In some cases, their values can differ by a factor of 10 or more. *It is important to keep in mind that the experimentally determined values for D can be different than those presented in these tables because chemical bonds can affect the scattering process at low neutron energies. In particular, the reader is referred to Chapter 11 to understand how important these effects can be*.

These tables contain the diffusion coefficients and mean free paths for most common nuclear materials.

H.9 The Transport Correction Factor

Sometimes it is helpful to define another quantity known as the *transport correction factor.* The transport correction factor is defined by the following equation:

Definition of the Transport Correction Factor

$$\text{Transport correction factor} = (1 - \mu) \tag{H.19}$$

where μ is the average cosine of the scattering angle. In other words, *the transport correction factor can be used to measure the amount of anisotropy in the neutron scattering process*. A value for the correction factor of 1.0 means that the scattering process is completely isotropic (since $\theta = 90°$ and $\mu = 0$), and no correction is necessary. In this case, the transport cross section $\sum_{tr}$ is the same as the total cross section $\sum_t$ (i.e., $\sum_{tr}(E) = \sum_t(E)$).

Conversely, a value of the correction factor less than 1.0 means that some anisotropic scattering occurs (since $\theta < 90°$), and the mean free paths and the diffusion coefficients have to be adjusted to account for this asymmetry. Thus *the transport correction factor is more likely to have a value less than 1.0 for a light element than a heavy one*. The line of demarcation between the transport cross sections shown in Tables H.1 and H.2 is about 1 eV. Consequently, the neutron diffusion coefficient and Fick's Law of Diffusion are both based on the assumption of linear anisotropy that Equation H.10 (which is derived from the P_1 approximation) implies. The P_1 approximation is discussed in Chapter 22, where the reader is also introduced to the neutron transport equation.

Appendix I: Diffusion Parameters for Common Nuclear Materials

I.1 Reactor Diffusion Parameters

In thermal water reactors and graphite-moderated reactors, fission neutrons are born with an average kinetic energy of about 2 MeV and a most probable kinetic energy of about 0.75 MeV. Their distribution of kinetic energies is given by a famous empirical equation called the *Watt equation*, which is presented in Chapters 3 and 7. They then diffuse through the lattice while they slow down. Eventually, they become *thermal neutrons*, and when they do so, their most probable kinetic energy is about 0.025 eV. The distribution of kinetic energies after they slow down is given by another famous statistical probability distribution called the *Maxwell–Boltzmann probability distribution*. The properties of this distribution are discussed in Chapter 8. However, in fast reactors, the fission neutrons are absorbed *before* they are thermalized (mostly at kinetic energies above 10 keV), and very few neutrons ever become thermal neutrons. In any thermal reactor, the mean squared distance R^2 which a neutron travels from the time it is born as a fast neutron until the time it is captured as a thermal neutron is given by the equation

Distance a Neutron Travels from Birth to Death in a Thermal Reactor

$$R^2 = 6\left(\tau_{th} + L^2\right) = 6\,M^2 \tag{I.1}$$

where

τ_{th} is a parameter called the *neutron age*
$M = \sqrt{(\tau_{th} + L^2)}$ is a parameter called the thermal *migration length*
M^2 is a parameter called the *thermal migration length*

The other parameter L that appears in Equation I.1 is called the *thermal diffusion length*, and it is equal to

Thermal Diffusion Length

$$L = \frac{\sqrt{D}}{\Sigma_a} \tag{I.2}$$

The thermal diffusion length L and the thermal migration length M are measured in centimeters (cm). The other parameter that appears in Equation I.1 is an interesting parameter called the *neutron age* τ_{th}. It is given this odd name because it can be shown to be a function of how long it takes for a fast neutron to become a thermal one. Thus, *the square root of the neutron age can be thought of as the distance a fast neutron travels before it thermalizes itself*. Hence the neutron "age" has the units of square centimeters (cm^2), and practically speaking, it is only loosely related to the thermal diffusion time, per se. The values of L, $\tau_{th}^{1/2}$, and M for some common neutron moderators are shown in Table I.1. The values in this table are for thermal neutrons only. In the cores of pressurized water reactors (PWRs), boiling water reactors (BWRs), high-temperature gas reactors (HTGRs), liquid-metal-cooled fast breeder reactors (LMFBRs), and gas-cooled fast reactors (GCFRs), the specific values of these parameters are driven by the overall isotopic composition of the core. The values of these parameters are shown in Table I.2.

In thermal reactors, notice that the value of M is always greater than the value of L and that the migration length M is only two or three percent of the diameter of the core. D_2O (heavy water) has the greatest thermal migration length (about 170 cm), while H_2O (light water) has the smallest (about 6 cm). The migration length of a thermal neutron in graphite is about 60 cm. For light water, this is about the same as the length of the neutron mean free path. Finally, the spectrum-average thermal cross sections for a PWR core, as well as the values of D and L, are shown in Table I.3. Using these values, it is possible to estimate the neutronic behavior of the core with a simple one-group diffusion theory. Depending on the type of PWR and its design characteristics (see Chapter 1 of this book and Chapter 13 of our companion book*), the total neutron flux is between 1×10^{14} and 1×10^{15} neutrons/cm^2/s. *About one-third of these neutrons in a PWR are thermal neutrons*, and the remaining neutrons are fast. The thermal migration length M, the thermal diffusion length L, and the thermal diffusion coefficient D are all measured in the units of cm. The neutron mean free path λ (see Appendix H), which is equal to three times the diffusion coefficient D, is also measured in cm.

* See *Nuclear Engineering Fundamentals: A Practical Perspective*, by Robert E. Masterson, CRC Press (2017).

TABLE I.1
Diffusion Parameters for Some Common Neutron Moderators

Moderator	Density (g/cm^3)	D (cm)	$\sum_a$ (cm^{-1})	L = $(\sum_a/D)^{1/2}$ (cm)	$\tau_{th}^{1/2}$ (cm)	M (cm)
Light water (H_2O)	1.00	0.160	0.02	2.9	5.1	5.8
Heavy water (D_2O)	1.10	0.870	0.000029	170	11.4	170
Graphite (carbon)	1.60	0.840	0.00024	59	19	62

Source: Lamarsh, J.R. and Baratta, A.J., *Introduction to Nuclear Engineering*, Prentice Hall, Upper Saddle River, NJ, 2001.

TABLE I.2
Diffusion Parameters for Some Representative Reactor Cores

Reactor	Type	L(cm)	$\tau_{th}^{1/2}$ (cm)	M (cm)	Fraction of Core Diameter (%) (L)	Fraction of Core Diameter (%) (M)
PWR	Thermal	1.80	6.30	6.60	0.52	1.78
BWR	Thermal	2.20	7.10	7.30	0.55	2.00
HTGR	Thermal	~12.0	17	21.0	1.58	2.50
LMFBR	Fast	5.0	[a]	5.0	2.86	2.86
GCFR	Fast	6.6	[a]	6.6	2.86	2.86

Source: Stacey, W.M., *Nuclear Reactor Physics*, 2nd edn., John Wiley & Sons, New York, 2007.
[a] Not defined for fast neutrons.

TABLE I.3
Spectrum-Averaged Cross Sections and Diffusion Parameters for a Typical PWR Core

Material	Function	Atomic Density (Atoms/cm^3) × 10^{24}	ν	$\sum_{tr}$ (cm^{-1})	$\sum_a$ (cm^{-1})	$\nu\sum_f$ (cm^{-1})
H	Moderator	2.748×10^{-2}	0	1.79×10^{-2}	8.08×10^{-3}	0
O	Moderator	2.757×10^{-2}	0	7.16×10^{-3}	4.90×10^{-6}	0
Zr	Structure	3.694×10^{-3}	0	2.91×10^{-3}	7.01×10^{-4}	0
Fe	Structure	1.710×10^{-3}	0	9.46×10^{-4}	3.99×10^{-3}	0
U-235	Fuel	1.909×10^{-4}	2.42	3.08×10^{-4}	9.24×10^{-2}	0.145
U-238	Fuel	6.592×10^{-3}	2.84	6.93×10^{-3}	1.39×10^{-2}	0.012
B-10	Control system	1.001×10^{-5}	0	8.77×10^{-6}	3.41×10^{-2}	0
Sum				3.62×10^{-2}	0.153	0.157

Source: Duderstadt, J. and Hamilton, L., *Nuclear Reactor Analysis*, John Wiley & Sons, New York, 1976.

Methods for determining the diffusion coefficient and the neutron mean free path are discussed in Appendix H. *Fast reactors have larger diffusion coefficients and longer mean free paths than thermal reactors do*. This is because the neutron cross sections at fission energies (>1 MeV) are much smaller than they are at thermal energies (<1 eV). It is also important to realize that many core parameters (such as the neutron diffusion coefficient) are affected by the molecular bonds of the atoms at thermal energies, and because of this, the experimentally determined values for D and the theoretical values for D (in the absence of those bonds) may not always agree. In particular, these discrepancies can become relatively large for important neutron moderators such as light water and heavy water.

Appendix J: Common Integrals Used in Nuclear Science and Engineering

J.1 Common Integrals

Many problems in nuclear science and engineering require the reader to evaluate the integral of a function. Integrals in nuclear science and engineering can be subdivided into either *definite integrals* or indefinite ones. Some common *indefinite integrals* are shown in Table J.1. Indefinite integrals then become definite integrals when the proper limits of integration are applied.

J.2 Definite versus Indefinite Integrals

A definite integral is different from an indefinite integral because a definite integral has defined limits of integration. For example, the expression

$$\int e^x dx = e^x + C \tag{J.1}$$

is an indefinite integral, while the expression

$$\int_0^a e^{-x} dx = 1 - e^{-a} \tag{J.2}$$

is a definite one. Definite integrals are used in the field of radioactive decay (see Chapter 6), in diffusion theory and transport theory (see Chapters 13, 14, and 22), and in applications of the Monte Carlo method (see Chapter 23). In the Monte Carlo method, a function P(x) is used to define the probability that a certain type of event will occur. This function is called a *probability distribution function*, or a *PDF*. The definite integral of a PDF is then called a *cumulative distribution function*, or a *CDF*. For example, if the PDF for a scattering event is given by $P(\theta) = 5\cos\theta$, the CDF for this scattering event is given by

$$\text{CDF} = \int_0^\theta P(t)dt = \int_0^\theta 5\cos\theta d\theta = 5\sin\theta \tag{J.3}$$

PDFs and CDFs can be applied to time-dependent problems as well. For example, if the PDF for a particular nuclear reaction is described by the statistical probability distribution $P(x) = 3e^{-3t}$, where t is the time in seconds, the corresponding CDF for this event is

$$\text{CDF} = \int_0^t P(t)dt = \int_0^t 3e^{-3t}dt = 1 - e^{-3t} \tag{J.4}$$

Many other examples of these functions can be found in practice.

J.3 Useful References

The following references provide many useful examples of definite integrals, indefinite integrals, PDFs, and CDFs. For example, many of the integrals presented in this appendix were taken from Reference 1. Additional CDFs and PDFs are discussed in Reference 2.

TABLE J.1
Common Indefinite Integrals

$$\int x^n\,dx = x^{n+1}\left(n+1\right)^{-1} + C \quad (n \neq -1)$$

$$\int x^{-1}\,dx = \ln|x| + C$$

Exponential/logarithmic functions

$$\int e^x\,dx = e^x + C$$

$$\int b^x\,dx = b^x/\ln(b) + C$$

$$\int \ln(x)dx = x\ln(x) - x + C$$

Trigonometric functions

$$\int \sin x\,dx = -\cos x + C$$

$$\int \csc x\,dx = -\ln|\csc x + \cot x| + C$$

$$\int \cos x\,dx = \sin x + C$$

$$\int \sec x\,dx = \ln|\sec x + \tan x| + C$$

$$\int \tan x\,dx = -\ln|\cos x| + C$$

$$\int \cot x\,dx = \ln|\sin x| + C$$

Trigonometric results

$$\int \cos x\,dx = \sin x + C$$

$$\int \csc x\cot x\,dx = -\csc x + C$$

$$\int \sin x\,dx = -\cos x + C$$

$$\int \sec x\tan x\,dx = \sec x + C$$

$$\int \sec^2 x\,dx = \tan x + C$$

$$\int \csc^2 x\,dx = -\cot x + C$$

Inverse trigonometric functions

$$\int \arcsin x\,dx = x\arcsin x + \sqrt{\left(1-x^2\right)} + C$$

$$\int \operatorname{arccsc} x\,dx = x\arccos x - \sqrt{\left(1-x^2\right)} + C$$

$$\int \arctan x\,dx = x\arctan x - (1/2)\ln(1+x^2) + C$$

Inverse trigonometric functions

$$\int \frac{dx}{\sqrt{(1-x^2)}} = \arcsin x + C$$

$$\arccos x = \pi/2 - \arcsin x \quad (-1 \le x \le 1)$$

$$\int \frac{dx}{x\sqrt{(x^2-1)}} = \operatorname{arcsec}|x| + C$$

$$\operatorname{arccsc} x = \pi/2 - \operatorname{arcsec} x \quad (|x| \ge 1)$$

$$\int \frac{dx}{1+x^2} = \arctan x + C$$

$$\operatorname{arccot} x = \pi/2 - \arctan x \quad (\text{for all } x)$$

Hyperbolic functions

$$\int \sinh x\,dx = \cosh x + C$$

$$\int \operatorname{csch} x\,dx = \ln|\tanh(x/2)| + C$$

$$\int \cosh x\,dx = \sinh x + C$$

$$\int \operatorname{sech} x\,dx = \arctan(\sinh x) + C$$

$$\tanh x\,dx = \ln(\cosh x) + C$$

$$\int \coth x\,dx = \ln|\sinh x| + C$$

Web References

1. *http://math2.org/math/integrals/tableof.htm.*
2. *http://math.ucsd.edu/~tlaetsch/pdf/10C_CDFtoPDF.pdf.*
3. *http://math2.org/math/integrals/more/restrig.htm.*
4. *http://mathworld.wolfram.com/CosineIntegral.html.*
5. *http://en.wikipedia.org/wiki/List_of_integrals_of_trigonometric_functions.*
6. *http://en.wikipedia.org/wiki/List_of_integrals_of_exponential_functions.*

Appendix K: Bessel Functions That Appear in the Study of Nuclear Science and Engineering

K.1 Bessel Functions and Their Origin

Bessel functions appear in many important problems in nuclear science and engineering. They appear in solutions to the neutron diffusion equation, and especially when the diffusion equation is solved in cylindrical coordinate systems, such as those that are used in the analysis of cylindrical fuel rods and nuclear reactor cores. They even appear in the *Feynman propagator* of quantum field theory, which makes its way into the Feynman diagrams we discussed in Chapters 1, 2, and 3 of our companion book.* Since almost all reactors are cylindrical in shape, Bessel functions invariably appear when finding the flux shape $\phi(r)$ in bare homogeneous cylindrical reactors (see Chapter 13). They also appear when dealing with certain types of radioactive line sources (see Chapter 14) in cylindrical coordinate systems. Bessel functions were originally invented by a German mathematician by the name of *Friedrich Wilhelm Bessel*, who investigated solutions to the particle diffusion equation:

$$D\nabla^2\phi(\mathbf{r}) + A\,\phi(\mathbf{r}) + S(\mathbf{r}) = 0 \tag{K.1}$$

with an external particle source $S(\mathbf{r})$. In a cylindrical coordinate system, the particle diffusion equation can be written as

$$\nabla^2\phi(\mathbf{r}) + B^2\phi(\mathbf{r}) + S(\mathbf{r})/D = 0$$

or

$$\frac{d^2\phi(\mathbf{r})}{dr^2} + \frac{2}{r}\frac{d\phi(\mathbf{r})}{dr} + B^2\phi(\mathbf{r}) + \frac{S(\mathbf{r})}{D} = 0 \tag{K.2}$$

and the presence of the Laplacian operator invariably leads to solutions for the shape of the particle flux $\phi(r)$ that have some sort of Bessel function in them.

K.2 Types of Bessel Functions

It turns out that there are *four different types of Bessel functions* that appear in solutions to the diffusion equation. The exact type of Bessel function depends on the values and the signs of the material buckling B^2 and the neutron source term S. In neutron diffusion theory, the coefficient B^2 is called the *material buckling*, but in other applications of particle diffusion, it can have different names. The other coefficient D that appears in the diffusion equation is sometimes called the *diffusion coefficient*. The diffusion coefficient has the units of cm and the material buckling has the units of cm^2.

K.3 Bessel Functions of the First and Second Kind

When $B^2 > 0$ and $S = 0$, solutions to the diffusion equation contain what are known as *Bessel functions of the first kind*. Bessel functions of the first kind are normally represented by the symbol J_o. These functions are slowly oscillating and slightly damped functions of the argument r, and the first root (the value of r when $J_o(r) = 0$) is obtained when the value of r is 2.405. The shape of this function corresponds to the black line shown in Figure K.1. In general, there are n Bessel functions of the first kind, but for solutions to the neutron diffusion equation

$$\frac{d^2\phi(\mathbf{r})}{dr^2} + \left(\frac{2}{r}\right)\frac{d\phi(\mathbf{r})}{dr} + B^2\phi(\mathbf{r}) = 0 \tag{K.3}$$

* See *Nuclear Engineering Fundamentals: A Practical Perspective*, by R.E. Masterson, CRC Press (2017).

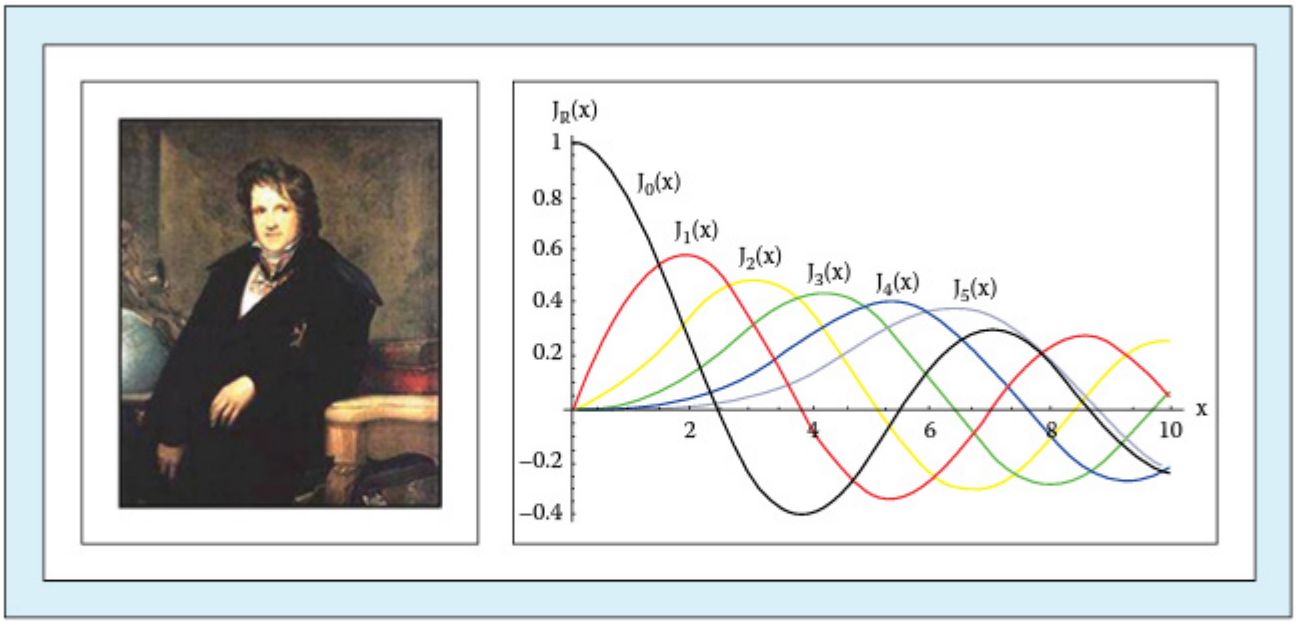

FIGURE K.1 A picture of Friedrich Wilhelm Bessel and his Bessel functions of the first kind. Bessel was a German astronomer and mathematician who was also known for determining the distance from the sun to another star by the method of parallax. (*Note*: Bessel functions were originally used by Bessel to help solve *Kepler's Three Laws* of planetary motion, but they have been applied to many different types of problems since then, including the study of vibrating membranes on the surface of a drum and cylindrical heat flow. You will see them referenced whenever the Laplacian operator in cylindrical coordinates is used.) (The picture of Bessel was provided by Wikipedia.)

the function $J_o(r)$ is the only one that usually appears. More generally, it can be shown that the defining equation for a Bessel function of the first kind is

$$\frac{x^2 d^2\phi(x)}{dx^2} + \frac{x d\phi(x)}{dx} + \left(x^2 - n^2\right)\phi(x) = 0 \tag{K.4}$$

where the value of n determines the appropriate Bessel function to use. For example, if n = 0 (which is the case for neutron diffusion theory), then the appropriate Bessel function of the first kind is $J_o(r)$. If n = 1, the appropriate Bessel function to use is $J_1(r)$. Higher-order Bessel functions are defined in a similar way. *Bessel functions of the second kind* obey the same defining equation as Bessel functions of the first kind (see Equation K.4), and they are normally represented by the symbol $Y_n(r)$. These functions represent solutions to Equation K.4, which are singular at the origin. *These solutions never appear in neutron diffusion theory because the flux never becomes infinitely negative at the origin*. Bessel functions of the second kind are shown in Figure K.2.

K.4 Modified Bessel Functions of the First and Second Kind

In nuclear science and engineering, certain forms of the neutron diffusion equation also give rise to what are known as *modified Bessel functions of the first and second kind*. Using the *Principle of Superposition*, it is possible to derive an equation for the neutron flux when neutrons are emitted from an infinite line source. The line source S can be thought of as a thin filament that emits neutrons outward in all directions (such as a fuel rod). In this case, the problem must be solved in cylindrical coordinates with the line source located at the origin of the coordinate system where r = 0. The line source can be superimposed over the y-axis in this case. Refer to Figure K.3 to visualize the geometric orientation of the source. Because we are dealing with cylindrical coordinates, the appropriate version of the Laplacian to use is

$$\nabla^2 = \frac{1}{r}\frac{d}{dr}\left(\frac{r\, d\phi(r)}{dr}\right) = \frac{d^2\phi(r)}{dr^2} + \frac{1}{r}\frac{d\phi(r)}{dr} \tag{K.5}$$

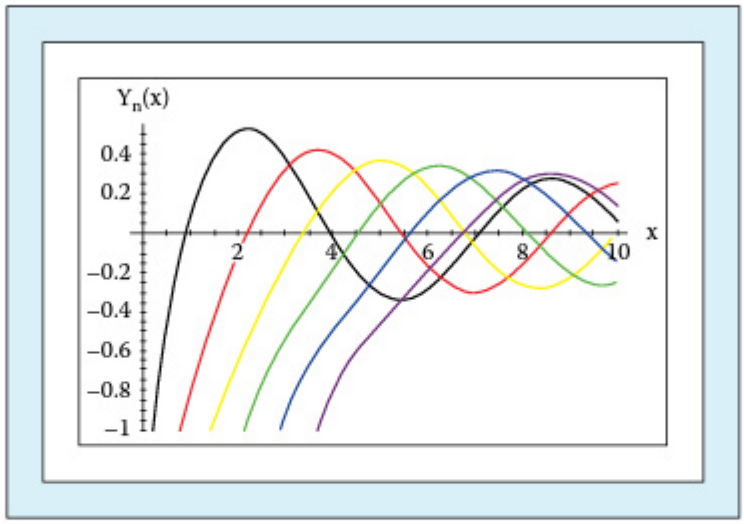

FIGURE K.2 An illustration of what Bessel functions of the second kind looks like. The Bessel function shown in the figure is $Y_n(x)$. (From *http://mathworld.wolfram.com/BesselFunctionoftheSecondKind.html*.)

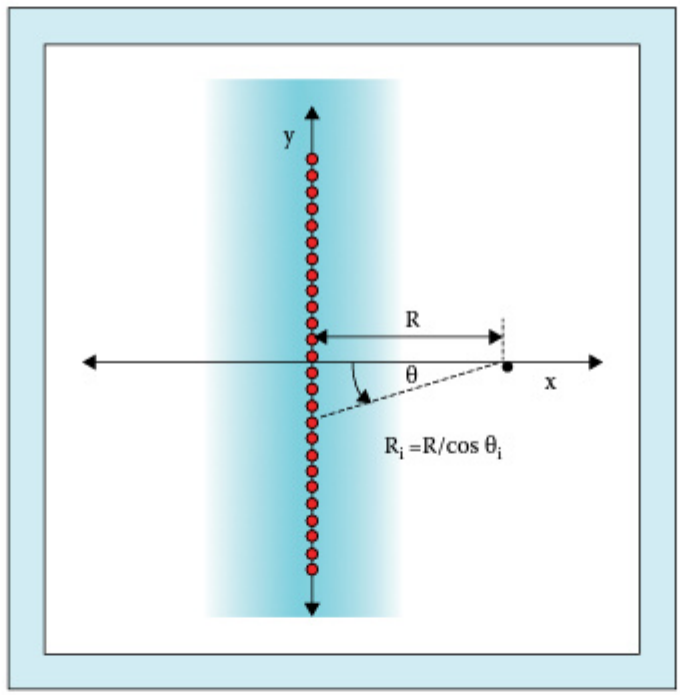

FIGURE K.3 A line array built from multiple point sources where the solution for the flux shape is a modified Bessel function of the first or second kind, $K_o(r/L)$ or $I_o(r/L)$.

There is no variation of the properties in the z direction, so the variation of the neutron flux in this direction can be neglected. In a diffusive material (i.e., one where the value of $L^2 = \sum_a/D$ is finite), the diffusion equation can be written as

$$\frac{d^2\phi(\mathbf{r})}{dr^2} + \frac{1}{r}\frac{d\phi(\mathbf{r})}{dr} - \left(\frac{1}{L^2}\right)\phi(\mathbf{r}) = 0 \tag{K.6}$$

Note that we do not have to consider the flow of neutrons in the θ or z directions because the line source is infinite and isotropic. The neutron flux in this case is a function of r only. The solution to the diffusion equation is

$$\phi_r(r) = C1\,K_o\left(\frac{r}{L}\right) + C2\,I_o\left(\frac{r}{L}\right) \tag{K.7}$$

In this case, the functions $K_o(x)$ and $I_o(x)$ are called *modified Bessel functions of the first and second kind.* Unlike the ordinary Bessel functions, which are oscillating as functions of a real argument, I_α and K_α are *exponentially growing* and *decaying functions*, respectively, and have no oscillatory behavior at all. Like the ordinary Bessel function J_α, the function I_α goes to zero at $x = 0$ for $\alpha > 0$ and is finite at $x = 0$ for $\alpha = 0$. Analogously, K_α diverges at $x = 0$. If one examines the shape of I_o, it is easy to see that value of C2 must be 0 because the value of the Bessel function I_o, which is not shown in Figure K.3, increases at an exponential rate as the value of the radius r is increased. Since the neutron current passing through the surface of a small cylinder around the line source is $J = S/2\pi$, when $r \to 0$, the value for C1 when $r \to 0$, will be $C1 = S/2\pi D$. Hence, the shape of the flux in the radial direction must be

$$\phi(r) = \frac{S}{2\pi D} K_o\left(\frac{r}{L}\right) \tag{K.8}$$

When $r = L$, you can see that the neutron flux $\phi(L)$ is about 10% as high as it is at $r = 0$. When $r = 2L$, it is about 2% as high. Modified Bessel functions such as $K_\alpha(x)$ also appear in the *Feynman propagator* of *quantum field theory*, so they are considerably more common than most people may think. The shapes of these modified Bessel functions of the first and second kind are shown in Figure K.4.

The function K_n is an exponentially decaying function, and the function I_n is an exponentially growing function. Both of these functions are called *modified Bessel functions* because the defining equation for them is now

$$\frac{x^2 d^2\phi(x)}{dx^2} + \frac{x d\phi(x)}{dx} - \left(x^2 + n^2\right)\phi(x) = 0 \tag{K.9}$$

Thus it can be seen that Equation K.6, which corresponds to the form of the neutron diffusion equation when there is no fissionable material present, is equivalent to the case where $n = 0$. Bessel functions and modified Bessel functions of the first and second kind are normally evaluated using a *power series expansion.* The most relevant power series expansions are

$$J_o(r) = 1 - \frac{r^2}{4} + \frac{r^4}{64} - \frac{r^6}{2304} + \cdots \tag{K.10}$$

$$I_o(r) = 1 + \frac{r^2}{4} + \frac{r^4}{64} + \frac{r^6}{2304} + \cdots \tag{K.11}$$

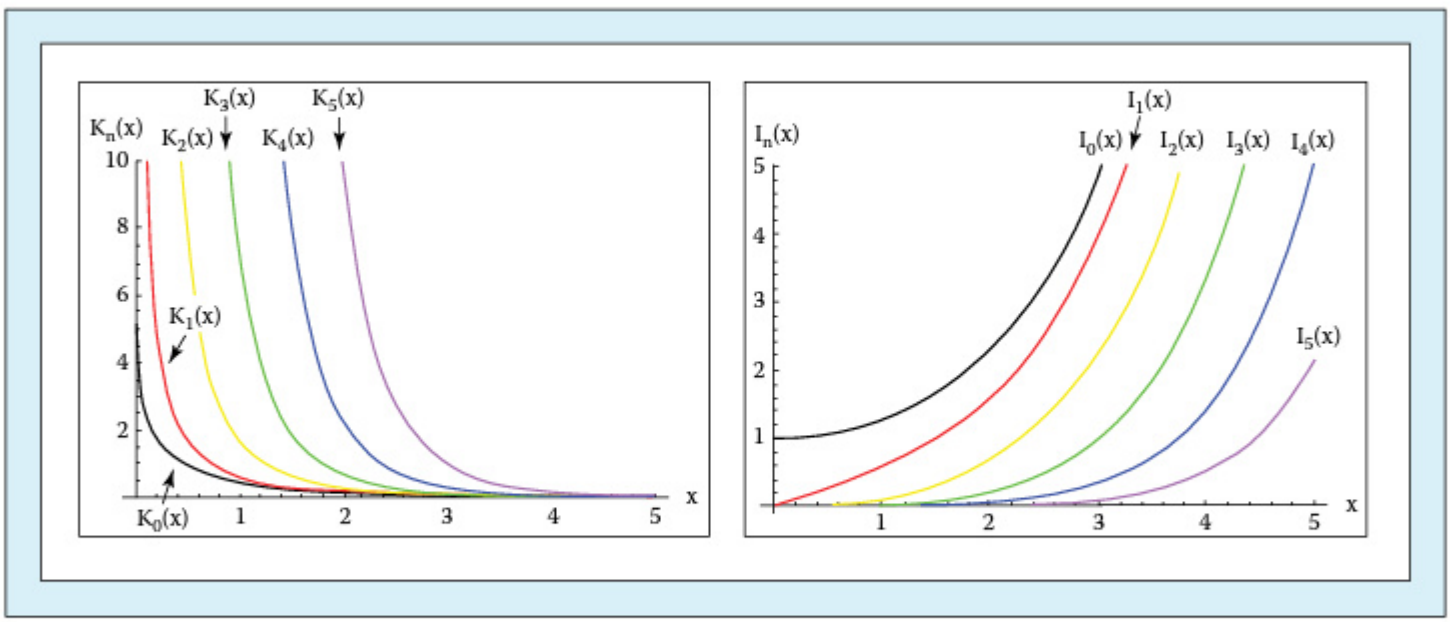

FIGURE K.4 The shape of modified Bessel functions of the first and second kind. (From *http://mathworld.wolfram.com/ModifiedBesselFunctionoftheFirstKind.html.*)

$$K_o(r) = -(0.577 + \ln(r/2)I_o(r) + \frac{r^2}{4} + \frac{3r^4}{128} + \cdots \quad \text{(K.12)}$$

The first expansion corresponds to a Bessel function of the first kind ($J_o(r)$). The second and third expansions correspond to modified Bessel functions of the first and second kind ($I_o(r)$ and $K_o(r)$).

K.5 Using Bessel Functions to Find the Flux Shape in a Bare Cylindrical Reactor

By solving the neutron diffusion equation in a cylindrical coordinate system, it is easy to show that the flux shape in a bare homogeneous cylindrical reactor is given by

$$\phi(r,z) = \phi_o \times J_o\left(\frac{2.405r}{R}\right) \cdot \cos\left(\frac{\pi z}{H}\right) \quad \text{(K.13)}$$

where

R is the radius of the reactor in meters or cm
H is the height

The shape of the neutron flux in the radial direction is given by

$$\phi(r) = \phi_o J_o\left(\frac{2.405r}{R}\right) \quad \text{(K.14)}$$

which is a Bessel function of the first kind. Notice that the neutron flux falls to zero at the edge of the reactor, which corresponds to the case where r = R. In other words, the flux falls to zero when the argument in the Bessel function of the first kind $J_o(2.405r/R)$ is 2.405r/R = 2.405. The flux shape in the radial direction is shown in Figure K.5.

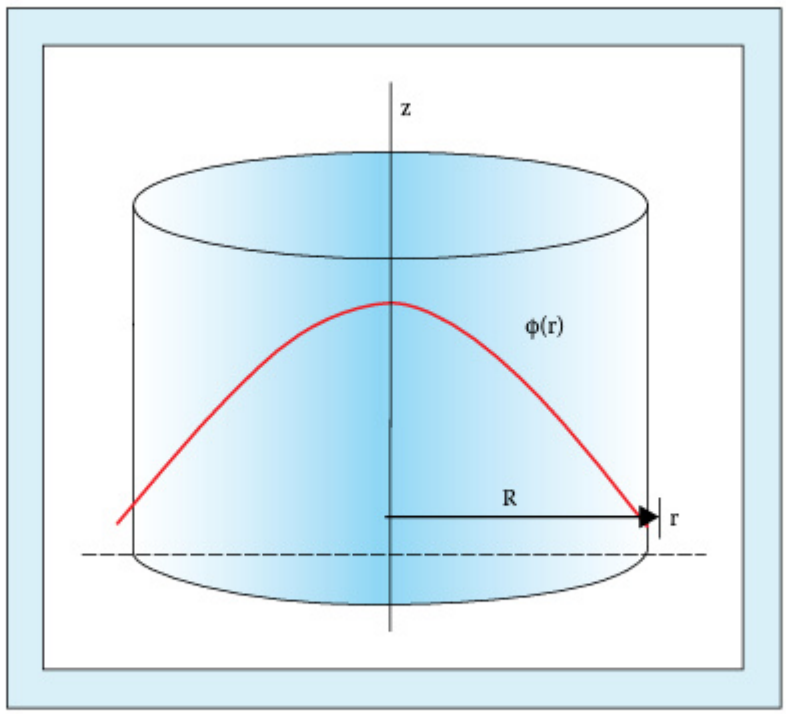

FIGURE K.5 The neutron flux shape in bare homogeneous cylindrical reactor core.

When the reactor is exactly critical, the geometrical buckling of the flux in the radial and axial directions is given by

$$B_r^2 = \left(\frac{2.405}{R}\right)^2 \quad \text{and} \quad B_z^2 = \left(\frac{\pi}{H}\right)^2 \tag{K.15}$$

The total buckling of the flux B^2 is then

$$B^2 = B_r^2 + B_z^2 \tag{K.16}$$

The shape of the neutron flux in the r and z directions is

$$\phi(r,z) = \phi_o \times J_o\left(\frac{2.405r}{R}\right) \cdot \cos\left(\frac{\pi z}{H}\right) \tag{K.17}$$

If the flux is time dependent, then the solution is

$$\phi(r,z,t) = \phi(r,z) \times \phi_t(t) = \phi_o \times J_o\left(\frac{2.405r}{R}\right) \cdot \cos\left(\frac{\pi z}{H}\right) \times \phi_t(t) \tag{K.18}$$

where $\phi_t(t)$ is the expression for the time-dependent part. The exact values for a Bessel function of the first kind are shown in Table K.1 for values of the argument r from 0 to 4.

TABLE K.1
Shape of Various Bessel Functions as a Function of the Parameter r

r	$J_o(r)$	r	$J_o(r)$
0.0	1	2.1	0.166607
0.1	0.997502	2.2	0.110362
0.2	0.990025	2.3	0.05554
0.3	0.977626	2.4	0.002508
0.4	0.960398	2.5	−0.04838
0.5	0.93847	2.6	−0.0968
0.6	0.912005	2.7	−0.14245
0.7	0.881201	2.8	−0.18504
0.8	0.846287	2.9	−0.22431
0.9	0.807524	3.0	−0.26005
1.0	0.765198	3.1	−0.29206
1.1	0.719622	3.2	−0.32019
1.2	0.671133	3.3	−0.3443
1.3	0.620086	3.4	−0.3643
1.4	0.566855	3.5	−0.38013
1.5	0.511828	3.6	−0.39177
1.6	0.455402	3.7	−0.39923
1.7	0.397985	3.8	−0.40256
1.8	0.339986	3.9	−0.40183
1.9	0.281819	4.0	−0.39715
2.0	0.223891		

Notes: Note that the first order Bessel function, J_o, is shown in black in Figure K.1. Its first root is at r = 2.405.

A more extensive tabulation of these Bessel functions can be found on many Websites. At $r = 0$, $J_o = 1$, and at $r = 2.405$ (which in our case corresponds to the edge of the cylinder), $J_o = 0$. In this case, the magnitude of the neutron flux ϕ_o is given by $\phi_o = P/(0.275c\Sigma_f L_z R^2)$, where as before, P is the total reactor power, and c is the conversion factor between fissions per second and watts (see Appendix A). For an unreflected reactor surrounded by a vacuum, the value of R may be replaced by $R' = R + \delta$, where δ is called the *extrapolation distance*. The extrapolation distance can be interpreted physically as the distance beyond the edge of the core where the neutron flux falls to zero. According to neutron transport theory, this extrapolation distance is given by $\delta = 0.71\lambda_{TR}$, where λ_{TR} is the transport mean free path. The extrapolation distance is discussed in more detail in Chapters 11, 12, and 22 of the text.

Web References

1. *http://en.wikipedia.org/wiki/Bessel_function.*
2. *http://mathworld.wolfram.com/BesselFunctionoftheFirstKind.html.*
3. *http://mathworld.wolfram.com/BesselFunctionoftheSecondKind.html.*
4. *http://mathworld.wolfram.com/ModifiedBesselFunctionoftheFirstKind.html).*

INDEX

Abelson, Philip, 286
Absorption cross section(s), 334, 519, 534, 720
  Boron-10, 725
  burnable poison, 633–634
  Doppler broadening, 739
  fast and thermal, 521
  Gadolinium, 725–726
  macroscopic fission and, 488
  neutrons with any energy, 182
  reaction probabilities, 168–170
  for Uranium-235, 177–178
  for Uranium-238, 177–178
Absorption mean free path, 500
Absorption reaction, 141
Absorption resonances, 1021
  resonance escape probability
    Doppler broadening, 737–738
    four-factor formula, 421–422
    Monte Carlo method, 986–987
  six-factor formula, U-238 and Thorium-232, 439–440
  total reaction cross section, 188–189
Accelerators, 633
Adjoint methods, 953
Adjuster rods, 829; *see also* Control rods
Advanced gas reactors (AGRs), 370
Albedo, 567
Alcohol distillation, 393
Alpha decay, 308–309
Alpha particles, 105, 308
Alpha radiation, 308
Americium-241, 289
AMU, *see* Atomic mass unit
Anderson, Herbert, 700–701
Angular current density, 916
Angular discretization, *see* S_N approximation
Angular isotropy, 483
Angularly isotropic emission, 309
Angular neutron density, 914
Angular neutron flux, 915
  angular anisotropy, 954
  diffusion coefficient, 951
  isotropic neutron flux, 953
  polar plots, 953
  transport cross section, 954
Angular quadrature, 925
Angular unit vector, 483–484
Angular weights, 937
ANISN, 952
Anticipated transients without scram (ATWS), 903
Antineutrinos, 332
Arbitrary change, power level, 668
ASME Boiler and Pressure Vessel code, 16
Asymmetric probability distribution, 990
Asymmetry energy term, 272, 274, 276
Asymptotic limit approach, 567
Asymptotic period, 702
Asymptotic reactor period, 695
Atomic density(ies), 192–193, 207, 213–214
Atomic mass number, 188, 322, 951
Atomic mass unit (AMU), 197
  Carbon-12, 71
  definition, 71
  down quarks, 72–73
  up quarks, 72–73
Atomic nucleus
  Baryonic matter, 70
  building blocks, 70
  density, 79–80
  electrons, 69
  element, 69
  gluons, 69, 76
  isotope, 69
  Maxwell's equations, 70
  natural abundance, 73
  neutron emission, 122–123
  neutrons, 73–74
  nuclear force field, 75–76
  orbitals, 69
  Periodic Table, 69
  Plutonium, 73
  probability distributions, 69
  protons, 73
  quantum mechanical effects, 70
  quarks, 75
  radioactive decay, 75
  simple atom, 69
  stability
    half-lives, uranium isotopes, 81
    number of neutrons, 80–81
    ODD, 81
    Plutonium-239, 81
    Uranium-238 atom, 81–82
  surface, 79
  weak force, 69
Atomic number, 257, 322
Atomic number density, 1023
Atomic weights, 262–264, 322–323; *see also* Atomic mass number
Atom smashers, 73
Attenuation coefficients, radiation shields, 609, 938
  linear attenuation coefficient, 1039–1040
  mass attenuation coefficient, 1039–1040
  photon beam, 1041
  shielding materials, physical densities, 1039–1040
  x-rays *vs.* gamma rays, 1041
Autocorrelation function, 712
Average binding energy per nucleon, 148
Average cosine of scattering angle, 526
Average diffusion distance, 496
Average distance, 496–497, 499
Average energy, 350
Average flux, 239–241
Average fuel pin centerline temperature, 778
Average kinetic energy, 118
Average lethargy gain per collision, 510
Average neutron flux, 243
Average neutron velocity, 489
Average scattering angle, 154
Average temperature change of core, 731
Avogadro, Amedeo, 196–197
Avogadro's number, 390
  accepted value, 198
  AMU, 197
  Faraday's constant, 197–198
  mole, 189–190
  number density of particles, 197
  scaling constant, 196–197
Axial zoning schemes, 778–779
Azimuthal scattering angle, 156

Backflow effect, 567
Backscattering, 132–133
Balmer absorption lines, 83
Bare cores, 580, 624
Bare reactor, 556
Barns, 74, 1023
Baryonic matter, 70
Baryon number, 79, 92
Baryons, 68, 92
Base load, 887–888
Bateman equations, 301, 879
Becquerel (Bq), 299–300, 897
Becquerel, Henri, 299
Beginning of cycle (BOC), 774
Berkeley operating system, 978
Bessel, Friedrich Wilhelm, 561–562, 1053–1054
Bessel functions, 418, 561
  first kind, 561, 1053–1054
  flux shape, bare cylindrical reactor, 1057–1059
  modified Bessel functions, 1054–1057
  origin, 1053
  second kind, 1054–1055
  types, 1053
Beta decay, 118, 308, 332, 354
Beta particle, 308
Beta rays, 89, 105, 308
Bethe–Weizsaecker formula, *see* Weizsaecker model of nuclear structure
Bettis Atomic Power Laboratory, 679
Binding energy
  atom and its nucleus, 268
  gluons, 276–277
  isotopic rest mass, 264–265
  liquid drop model, atomic nucleus
    asymmetry energy term, 274, 276
    binding energy curve equation, 274
    coefficients, 277
    Coulomb energy term, 274–275
    mass of nucleus, 274
    number of nucleons, 274
    number of protons and neutrons, 273
    pairing energy term, 274, 276
    surface energy term, 274–275
    volume energy term, 274–275

Weizsaecker model of nuclear structure, 278
MeV per nucleon, 268
nuclear binding energy curve
shape, 268–269, 271–273
total energy released, 270
proton-to-neutron ratio, 277
Binding energy per nucleon, 255; *see also* Mass defect
Binomial distribution, 293
Black bodies, 503
Black hole, 503, 556
Black neutron absorber, 504
Black planar surfaces, 506
Black surfaces, 503
Blankets, 581
Boiling water reactors (BWRs), 1, 723
four-batch refueling scheme, 769
vs. PWR control rods, 48–50
Zircaloy-2, 19
Boltzmann, Ludwig, 387–388, 912–913
Boltzmann's constant, 224, 378, 390–392
Boltzmann transport equation, 102–103; *see also* Neutron transport equation
Boric acid, 51, 724, 829, 842
chemical composition, 725, 836
chemical shim
injection systems, 847
neutron absorption rate, 835–836
positive temperature coefficient, 837
solid form, 836–837
soluble poisons, 836
moderator temperature coefficient, 733
reactivity contribution, 843
thermal utilization, 844
Boric acid concentration, 847
moderator temperature coefficient, 733, 847
positive temperature coefficient, 837
in PPM, 845
in PWR, 726–727, 781, 842
reactivity change, 845
thermal utilization, 844
U-235 atom depletion, 757
Boric acid injection systems, 847
Boron, 73, 781
Boron-10, 834–835
Boron-11, 835
Boron carbide (B_4C), 835, 864, 867
Boron injection tank (BIT) system, 847
Boron thermal regeneration system (BTRS), 847
Boundary Condition 1, 550
Boundary Condition 2, 550
Boundary conditions, 601
Monte Carlo calculation, 966
neutron transport equation
angular current, 946
angular flux, 946
initial boundary conditions, 920
at material interface, 947–948
neutron current, 920
types, 946
vacuum boundary condition, 920, 946, 948–950
Braking radiation, 1039
Brayton thermal cycle, 1, 6, 51, 368
Bremsstrahlung, *see* Braking radiation
Bromine-87, 665, 1038
Brookhaven National Laboratory (BNL), 192, 207
Bruce Heavy Water Plant, 393
Buckling, 553
Buildup factor, 609
Bullet train, 469–470
Burnable lifetime (BL), 721
Burnable poisons, 724, 834
on flux shape, 782
within individual fuel assembly, 779–781
inside of reactor fuel assemblies, 781
long-term core reactivity, 767
soluble boron concentration, 767
Burnup equation, 430
Burnup of nuclear fuel, 719–720
Burnup rate, 351
BWRs, *see* Boiling water reactors

Cadmium, 73
Cadmium-111, 835
Cadmium-112, 835
Cadmium-114, 835
Cadmium-129, 835
Calandria, 23–24
Calculus of Newton, 241
Canada deuterium uranium (CANDU) reactors, 11–12, 369
core, 25
fuel assemblies, 23–25
refueling cycles, 37
Capacity factor, 775
Capture cross section, 170
Capture reaction, 141
Capture-to-fission ratio, 333
Carbon-12, 71
Cartesian, 487
Case histories, 500
CDF, *see* Cumulative distribution function
Cent, 683–684
Center of mass (COM) systems, 138–141, 171, 923
Central limit theorem, 973
Centrifugal separation process, 13, 284
Ceramic materials, 835
Cesium atomic clock, 95
CHANNEL model, 904
Chart of the Nuclides, 290–292
Checkerboard loading scheme, 731
Chemical and volume control system (CVCS), 847
Chemical primer, 189–190
Chemical shim, 724
boric acid
injection systems, 847
neutron absorption rate, 835–836
positive temperature coefficient, 837
solid form, 836–837
soluble poisons, 836
Boron-10 *vs.* Boron-11, 836
chemical composition, 836
constant power level, 837–838
PPM to g/L, 846–847
PWR *vs.* operating time, 837
reactivity changes
boric acid concentration, 844–846
Boron-10, 845
boron concentration, 845–846
effective multiplication factor, 843
thermal utilization, 843–844
as reactor control system, 841–842
refueling period, 838
soluble neutron poisons, 836–837
xenon, 837
Cherenkov radiation, 90, 308, 755
Chernobyl accident
Chernobyl reactor
design features, 895–896
positive power coefficient, 894
RBMK-1000 reactor, 895
Xenon-135 buildup, 894, 896–897
devastated area, 898
disassembled core and debris, 899, 901
vs. Fukushima accident, 894
INES scale, 894, 898–900
lessons learned, 900–902
radiation released, 897–898
CITATION, 539–540
Cladding gap, 410
Class seven transients, 703
Clementine fast reactor, 868, 870
Close-Packed Spheron Model of Linus Pauling, 279
Coefficient matrix, 530
Cold critical state, 750
Cold neutron beams, 143–144
Combined wave function, 615
Compendium of Federal Regulations, 743–744
Compound nucleus, 121, 142, 171, 182, 324, 329; *see also* Reaction resonances
Compound nucleus formation, 67, 149, 171–172, 225, 329, 986
Compton scattering, 170, 970
Compton's equation, 970
Computational cell, 401
Computer codes, 539; *see also* Computer programs
Computer programs
reactor accidents
analysis codes, 902
Chernobyl accident, *see* Chernobyl accident
QUANDF, 903
RELAP, 903
RETRAN, 902–903
TRAC, 903
TRACE, 903–906
COM systems, *see* Center of mass systems
Concave region, 629
Concentration gradient, 470
Conservation of Charge, 71
Conservation of Mass and Energy, 71, 485
Conservation of Momentum, 71
Conservation of the Baryon number, 92
Constant of integration, 559, 658
Constant velocity model, 911
Constructive interference, 615–616

Controlled chain reaction, 283–284, 344
Controlled nuclear chain reaction, 319
Control rod(s), 1, 73, 724
  banks, *see* Control rod banks
  boron, 20
  burnable poisons, 779
    within fuel assembly, 838–839
    locations in reactor core, 841
    on the neutron flux shape, 840–841
    within a reactor as a whole, 839
    soluble boron, *see* Chemical shim
  cadmium, 20
  criticality maintenance, 851–852
  cruciform-shaped control rods, 48
  cylindrical-shaped control rods, 48
  definition by U.S. NRC, 47
  designs
    BWR, 832–834
    guide tubes, 830, 848
    parameters, 834–835, 868
    PWR, 830, 832
  effective multiplication factor, 47
  fast reactor control rods, 864–866
  fuel assembly, 827–828
  materials
    boron, 834–835
    cadmium, 835
    and cross sections, 867
  mechanical drive system, 848
  Monte Carlo method, 989–990
  nonburnable poisons, 835
  origin
    BWRs, 829–830
    CANDU reactors, 829
    control rod simulators, 830–831
    Manhattan Project, 828
    PWRs, 829–830
    scram, 829
    Shippingport reactor, 829
  plate-type/rectangular control rods, 48
  primary functions, 827
  PWR *vs*. BWR, 48–50, 847–848
  reactivity, 47
    changes by chemical shim, 843–846
    control, 868–870
    dollars and cents, 827
    effective multiplication factor, 854–855
    incremental reactivity, 827
    incremental worth per increment, 855
    primary effect, 855
    six-factor formula, 854
  reactor control systems and limitations, 868
  scram button
    control panel, 848, 850
    emergency reactor shutdown, 848–849
    origin, 850–851
    passive safety system, 849
  shapes, 828
  shutdown banks, 848–849
  simulators, 830–831
  U.S. NCR's definition, 828
  worth, *see* Control rod worth
Control rod banks, 827, 848–849
Control rod drive mechanisms (CRDMs), 829, 868
Control rod worth
  axial power profile, 853–854, 863–864
  definition, 853
  in dollars and cents, 866
  in fast reactor, 866
  flux shape changes
    bare cylindrical reactor, 853–854, 857, 863, 865
    cosine flux shape, 853–854, 863
    effective multiplication factor, 856
    neutron diffusion equation, 856
    thermal flux shape, 856
  fuel type, 862
  incremental reactivity, 827
  incremental rod worth, 853–584, 860
  reactivity corrections
    axial zoning schemes, 861
    control rod increments, 859–860
    correction factors, 858–859
    differential control rod worth, 859
    as function of axial position, 858
    as function of control rod position, 861–862
    as function of distance, 860–861
    neutron flux shape, 860
    rod correction factor, 860
  semantic differences, 863
Control systems and thermal feedback, 751–752
Control volume, 485
Conventional neutron flux, 484
Conventional reactor geometries, 601
Convex region, 629
Coolant temperature, 733
Core reflector interface, 567
Core region, 492
Corium, 703
Cosine of scattering angle, 511
Cosmic rays, *see* Gamma rays
Cosmic ray showers, 95
Coulomb energy term, 274–275
Coulomb potential, 76–77
Coulomb's constant, 85, 117, 289
Coulomb's law, 84, 115, 117
Coupled differential equations, 520
Crab Nebula, 321
Critical energy of fission, 148
Critical masses, 574
Critical radius, 576
Critical reactor, 399
Cross-correlation, 712
Cross-section library, 149
Cruciform control rods, 828, 848, 850
Cruciform-shaped control rod, 506
Cumulative distribution function (CDF), 963–964, 994–995, 1051
Curvature of neutron flux, 553
Curve-fitting methods, 744
Cylindrical control rods, 828

Dead reactor, 792
Dead time, 885–886
Decay constants, 785
Decay heat, 118, 309–310, 868
Decaying functions, 618, 1056
Definite integrals, 1051
Delayed gamma rays, 332
Delayed neutron(s), 80, 146, 349, 469
  average characteristics, 120
  average lifetime, 356–357
  creation process, 1035–1036
  emitters, 356–357, 1036–1037
  emitting materials, 1035
  energy spectrum, 118, 354
  fission fragments, 353
  fission rate, 355
  fractions, 120, 356, 648, 663, 665, 683, 827, 866, 1035–1036
  groups, 1035
  percentage, 355
  precursors, 664
  production rates, 355–356, 1038
  radioactive beta decay, 354
  reactivity, 407
  role of bromine-87, 1038
  Segre chart, 354–355
  time constants, 1035–1036
  two-step process, 354
  yields, 356, 1036–1037
Demand charge, 888
Demand curve, 887–888
Demand peaks, 887–888
Destructive interference, 614–615
Deuterium, 11, 186–187, 369
Deuterium dioxide, 29
Deuterium oxide (D_2O), 369
Dewey Decimal System, 216
DIFF, 539–540
Differential scattering cross section, 157
Differential scattering probability, 156–157
Differential solid angle, 156
Diffusing material, 614
Diffusion area, 496, 507
Diffusion coefficients, 476, 488, 526, 543, 951–953, 1053; *see also* Neutron diffusion coefficient
Diffusion equation, 73, 102, 470
Diffusion length, 491
Diffusion theory approximation, 478, 928–929
Diffusive medium, 609
Dimensionless number, 735
Dirac delta function, 490
Directional neutron flux, 484
Discrete ordinates approximation, *see* S_N approximation
Discrete ordinates methods, *see* S_N method
Distributed neutron source, 631
Distributed particle source, 967
Distributed source, 490, 603
Divergence operator, 486–487
Dollar of reactivity, 683
Doppler broaden, 986
Doppler broadening, resonance escape probability
  absorption cross section, 739
  Boltzmann's constant, 737
  Breit–Wigner model, 739
  effective multiplication factor, 738
  effect of fuel temperature, 737–738
  fuel temperature coefficient, 739

kinetic energy, 737
large absorption resonances, 737–738
molecular agitation, 738
neutron reproduction factor, 740
nuclear Doppler effect, 737, 739
Doubling time, 667
Dynamic programming, 774
Dyson, Freeman, 752

Effective boundary condition, 567
Effective multiplication factor, 244
control rods, 827
for core, 401
more than one energy group, 404
neutron leakage rate, 401–402
and neutron life cycle, 402–403
Eigenfunctions, 551, 816
Eigenvalue equation, 484
Eigenvalues, 537, 551, 631, 816–817
Eight decay chains, 655
Einstein's equation, 103–105, 255, 310, 339, 1027
Einstein's formulation of Special and General Relativity, 71
Elastic collisions
glancing collisions, 115, 135–137
head-on collisions, 115
energy loss, 133–135
physics, 130–132
Elastic scattering, 121, 184–185
average energy loss, 151
average energy of neutron, 150
average number of collisions, 151
energy loss of neutron, 142
event, 141
hydrogen and deuterium, 186–187
requirement, 150
total cross section, 188
wave functions, 141
Electrical energy term, *see* Coulomb energy term
Electrical energy *vs*. thermal energy, 352
Electrical forces, 82, 84, 170
Electrical generators, 51
distribution box, 54
energy production measurements, 55–56
Faraday, Michael, 53
in hydroelectric dam, 55
single-phase generator, 54
stator and rotor motion, 54
thermal efficiency, 55
three-phase power, 54
Electric Power Research Institute (EPRI), 703
Electromagnetic force, 75
Electron cloud, 69, 170
Electron volts, 85–86, 323
Emergency reactor shutdown, 48, 848–849; *see also* Scram
Emergency shutdowns, 841
ENDFB-7 database, 894
ENDFPLOT, 207, 1011, 1018
fission, absorption, and scattering cross sections, 215–216
hydrogen, carbon, and oxygen scattering cross sections, 215, 217
KAERI, 215
multiple cross sections, 215
Energy decrement per collision, 134
Energy-dependent diffusion equation, 520
Energy dependent reaction rates, 176
Energy gain, 524
Energy groups, 180–181, 520
large numbers of, 241–243
neutron, 227
single, 235–238
Energy spectrum, 719
Energy staircase, 380–382
ENFDPLOT, 195
Enriched uranium, 319
Enrichment, fuel, 335
Enumerated Nuclear Data File—Binary (ENDF-B/V) file, 207
Epithermal energy group, 207, 226; *see also* Resonance energy group
Epithermal energy range, 329
Epithermal neutrons, 121, 367
Epithermal/resonance energy region, 183
Equation of state, 903
Equilibrium concentration, 880
Equilibrium core, 771
Equilibrium cycle, 771, 774
Error margin, 696
Eulerian reference frame, 152
European Nuclear Association, 2
Exponentially growing functions, 1056
Exponential rate, 349
Exponential value, 606
External neutron source, 594
Extrapolated boundary condition, 504–505, 555, 623; *see also* Vacuum boundary condition
Extrapolation distance, 503–505, 556, 623–624, 816, 1059
Extrapolation length, 555

Faraday, Michael, 198
Faraday's constant, 197–198
Fast and thermal nonleakage probabilities, 534
Fast energy group, 207, 520, 522
Fast energy range, 207
Fast fission cross section, 542
Fast fission factor, 414, 416–417, 534
Monte Carlo method
four-factor formula, 981
fuel rods, 981–982
importance weighting, 985
mean free path, 983
radius vector, 983
random number generation program, 983–984
unit cells, 982
Fast fission neutrons, 538
Fast flux, 500
Fast neutron flux, 177, 538
Fast neutron multiplication factor, 534
Fast neutrons, 74, 121, 177, 179, 520
Fast nonleakage probability, 408, 439, 441–442, 575, 577
Fast reactor control rods, 864–866
Fast reactors, 581
Fast utilization factor, 534
Fermi, Enrico, 402, 700
Fertile materials, 12
Feynman diagrams, 116–117, 752
Feynman propagator, 561, 618, 1053, 1056
Feynman, Richard, 402
Fick, Adolf, 474–475, 1043
Fick's Law of Diffusion, 912, 929, 1043
constant velocity approximation, 476
contact lens, 475
diffusion coefficient, 477
diffusion theory approximation, 478
electrically neutral particles, 474
Fick, Adolf, 474–475
gradient of the neutron concentration, 476
gradient operator, 477
heterogeneous region, 478
homogeneous region, 478
magnitude and direction, 475
neutron current and particle flux relationship, 476
neutron population, 475
neutron transport equation, 478
one-group diffusion theory, 476
particle diffusion process, 474
zero flux gradient, 476
Field of reactor physics, 470
Fine cross section library, 195
Finite difference methods, 945
First Law of Thermodynamics, 106
Fissile material, 333, 604
Fission cross section
neutrons with any kinetic energy, 181–182
for Plutonium-240, 181–182
reaction probabilities, 168–170
for Thorium-232, 181–182
for Uranium-235, 177–178
for Uranium-238, 177–178, 181–182
Fission energy group, *see* Fast energy group
Fission energy range, 329
Fission fragment(s), 145, 308, 649; *see also* Fission products
kinetic energy, 147
mass distribution, 330–331
per fission, 648
radioactive decay, 407
Uranium-235, 326
Fission matrix, 536–537
Fission neutrons, 367
apparent temperature, 379
energy spectrum, 327–328
kinetic energy, 147, 151
production rate, 918
prompt neutron, 118–119, 121, 353
vs. thermal neutron speed, 350
total number of, 649, 665
Fission product(s), 105, 145–148, 308
atomic masses, half-lives, and natural abundance, 1028–1033
effective multiplication factor, 877
hypothetical fission product, 797–799
Iodine-135
concentration, 785–786
decay chain, 785
effective yields, 786

macroscopic absorption cross section, 878
Neodymium-149, 786
poisoning
cumulative effect, 794–796
in fast *vs.* thermal reactors, 793–794
Promethium-149
concentration, 788
effective yields, 786
radioactive decay chains, 784–785
reactivity change
negative reactivity, 796
net reactivity of core, 795
neutron fluence, 796–797
reactivity reduction, 796
reactivity contribution, 877
Samarium-149
after shutdown, 791–793
buildup, 789
concentration, 788
effective yields, 786
equilibrium concentration, 790–791
neutron absorption cross section, 784, 786–787
production process, 786, 788
Tellurium-135, 786
thermal utilization, 877–878
Xenon-135
after shutdown, 791–792
buildup, 789, 792
concentration, 785–786
decay chain, 785
effective yields, 786
equilibrium concentration, 789–790
neutron absorption cross section, 784, 786–787
reactor dead time, 792
yields, 793–795
Fission production rate, 537
Fission product poisons; *see also* Fission product(s)
cumulative buildup, 797
cumulative effect, 358–359, 794–796
in fast *vs.* thermal reactors, 793–794
macroscopic absorption cross section, 878
reactivity change, 878
reactor accidents
analysis codes, 902
Chernobyl accident, *see* Chernobyl accident
QUANDF, 903
RELAP, 903
RETRAN, 902–903
TRAC, 903
TRACE, 903–906
Samarium, *see* Samarium
xenon, *see* Xenon
Fissions per initial heavy metal atom (FIMAs), 42
Flat probability distribution, 962
Flatter edge, 566
Flatter power distribution, 565
Flerov, G.N., 280
Flux buckling, 604
Form factor, 622
Forward scattering, 138, 140, 951–952
Four-factor formula, 408, 411, 576
burnup, 427–428
classical form, 423
eta of the fuel, 414
definition, 415
fission to absorption ratio, 415
Maxwellian flux, 415
neutron production term, 416
neutron velocity, 416
thermal neutron flux, 416
fast fission factor, 414, 416–417
infinite reactor lattice
average flux, 413
unit cells, 412–413
limitations, 427–429, 452–453
origin, 414
representative values, 423–424
resonance escape probability, 414
absorption resonances, 421–422
constants, 421
definition, 419–420
general expression, 420
MFR, 421
neutron lethargy, 420
resonance integral, 420
resonance self-shielding, 422
thermal utilization, 414
definition, 417
equivalent cylindrical cell, 418–419
neutron flux, 418
radius of an equivalent unit cell, 418
representative PWR fuel assembly shape, 418
Wigner–Seitz method, 418–419
Fourier's equation, 639
Four independent variables, 636
Fractional energy loss, 970
Fractional error, 974
Fraction of fission neutrons, 536
FRAPCON, 904
Fraunhofer lines, 83
Free neutrons, 346, 469
Fuel assembly cluster, 832
Fuel assembly homogenization
homogeneous lattice approximation, 805
PWR fuel assembly
with 225 distinct and potentially unique unit cells, 807–808
with 225 fuel rods and control rods, 807–808
and reactor super cells, 814–815
thermal disadvantage factors, 819
Fuel bundles, 23–25
Fuel management and plant operation, 726–728
Fuel pellets, 16–17
Fuel rod cladding
average thickness, 18
cross-sectional view, 17–18
fuel assemblies, 18–19
fuel-cladding gap, 19
materials, 18–19
rod bundle, 18
stainless steel, 18
Zircaloy, 19
zirconium, 18
Fuel rod pitch, 33
Fukushima accident, 894
Fundamental mode, 710, 817

Gadolinia (Gd_2O_3), 839
Gadolinium, 781, 839
Gain and phase, 712
Game theory, 67
Gamma rays, 105–106, 115, 170, 614
in nuclear power plants, 309
Pu-239, 288
Gas-cooled reactors (GCRs), 1
Gaseous diffusion process, 257, 284
Gaseous diffusion stages, 13
Gaussian probability distribution, 293, 388, 497, 976
Gauss's divergence theorem, 918
Geiger, Hans, 158
General Atomics Company, 752
Geometrical buckling, 817
Geometric buckling, 495, 534, 553
GigaWatt Days (GWD), 43
Girdler sulfide process, 393
Gluon, 264
Goal of flatness, 565
GOTHIC, 703
Gradient operator, 487–488
Gray surface, 505
Great pyramids of Egypt, 454
Group flux, 180, 239–241, 523, 945

Hadrons, 73
Halley's comet, 562
Halving time, 667
Harmonic oscillator, 278
Heat capacity, 750
Heavy water
deuterium, 368, 392
vs. light water, 392–393
production process, 393–394
Heavy water reactors (HWRs), 1, 11
Heisenberg uncertainty principle, 89, 170
Helmholtz equation, 638–639
Hercules C class dynamite, 338
Higgs mechanism, 88
Highest index, 522
High-temperature gas reactor (HTGR), 370
Homogeneous algebraic equations, 530
Homogeneous lattice approximation, 805
Homogeneous linear equations, 530
Hoover Dam, 55
Hot zero-power critical state, 750
Hubble Space Telescope, 321, 562
Hydrogen, 186–187
Hydrogen atoms, 752
Hyperbolic cosine, 119
Hyperbolic cotangent function, 567, 623
Hyperbolic functions, 628
Hyperbolic sine, 119, 328
Hyper-Physics Periodic Table, 258
Hypothetical core disruptive accident (HCDA), 703, 987

IAEA scale, *see* International Atomic Energy Agency scale
ICDF, *see* Inverse cumulative distribution function
Idaho National Engineering Laboratory (INEL), 903
Indefinite integrals, 1051–1052
Index of refraction, 101
Individual neutron, 500
Industry averages, 7, 16, 21
Inelastic collisions, 115, 155
Inelastic scattering, 121, 141–142, 185
Infinite lattice approximation, 31–32, 411
Infinite multiplication factor
  infinite reactor lattice, 401–402, 413
  more than one energy group, 404
  thermal neutron cross sections, 433–434
Inhomogeneous linear equations, 532
Inhour equation, 120, 350
Inner iteration, 621
Integro-differential equation, 919
Interference, 615
Intermediate heat exchanger, 371
Intermediate loop, 1
Internal power regulator, 752
International Atomic Energy Agency (IAEA) scale, 207, 894, 898–899
International Space Station, 94–95
International System of Units, 7, 10
Inverse cumulative distribution function (ICDF), 992, 994–995
Inverse square law, 608, 614, 942, 966
Iodine-135
  concentration, 785–786
  decay chain, 785
  effective yields, 786
Ionized helium nuclei, 105
Island of Nuclear Stability, 307–308
Isothermal temperature coefficient, 749
Isothermal temperature defect, 750
Isotopes
  definition, 257
  natural abundance, 257, 259
  stable isotopes, 257, 259
Isotopic abundance, 335
Isotopic composition of core
  burnable poisons and neutron poisons, 724
  soluble neutron poisons and functions
    absorption cross sections, Boron-10, 725
    absorption cross sections, Gadolinium, 725–726
    boric acid, 725
    boric acid concentration, PWR, 726–727
    checkerboard loading pattern, 728
    chemical shim, 724–725
    low-leakage cores, 728
    neutron fluence, 728
    NRC's safety requirements, 727
    nucleate boiling, 727
    out–in loading scheme, 728
    reactor pressure vessel wall, 728
    safety-related goals, 727
    scatter/checkerboard loading schemes, 728
    scatter loading/checkerboard loading scheme, 728
    solbor, 725
    soluble boron concentration, 725
    standard operating procedure, 725
Isotopic rest mass, 264–265; *see also* Nuclear weight
Isotropic neutron flux, 950

Japanese Atomic Energy Agency (JAEJ), 207
Java applet, 215, 1011
JENDL cross section library, 195, 207

Kepler's Three Laws, 1054
Kilowatt hour, 56
Kinetic energy, 87, 615
  mass and energy relationship, 96–97
  to thermal energy and heat conversion, 105–107
  unrecoverable, 107
Klaproth, Martin Heinrich, 280
Korean Atomic Energy Research Institute (KAERI), 215

Laboratory coordinate system, 923
Laplace's equation, 608, 637
Laplace transforms, 697
Laplacian operator, 488, 603
Large Hadron Collider (LHC), 95
Laser enrichment process, 13
Laser separation process, 284
Law of Baryon conservation, 92
Law of cosines, 135
Laws of Electromagnetism, 71
Laws of Quantum Mechanics, 272
Least squares method, 743
  fuel temperature coefficient, 746
  Gauss, Carl Friedrich, 744–745
  linear curve fit, 744
  matrix equations, 746
  minimize, sum of squares, 744
  parameters, 746
  quadratic curve fit, 745
  the residuals, 744
  vertical offsets, 744–745
Legendre polynomials, 926, 929–931
Life of fuel, 720–721
Light-water reactors, 747
Linear anisotropy, 926
Linear attenuation coefficient, 1039–1040
Linear curve fit, 744
Linear momentum, 185
  Cherenkov radiation, 90
  conservation of linear momentum, 90–91
  of matter particle, 89–90
  particle's velocity, 89–90
  for photon, 91–92
Linear programming, 774
Line source, 490, 602
Liquid drop model
  atomic nucleus
    asymmetry energy term, 274, 276
    binding energy curve equation, 274
    coefficients, 277
    Coulomb energy term, 274–275
    mass of nucleus, 274
    number of nucleons, 274
    number of protons and neutrons, 273
    pairing energy term, 274, 276
    surface energy term, 274–275
    volume energy term, 274–275
    Weizsaecker model of nuclear structure, 278
  inventors, 266–267
  nuclear structure, 272–273
Liquid metal coolants, 370–371
Liquid metal fast breeder reactors (LMFBRs), 1, 370
  core composition, 410
  fuel assemblies, 20–21, 24–25
Liquid–vapor mixture density, 734
LMFBRs, *see* Liquid metal fast breeder reactors
Location dependent neutron multiplication factor, 400
Long-term core reactivity
  axial zoning schemes, 778–779
  burnable poisons
    on flux shape, 782
    within individual fuel assembly, 779–781
    inside of reactor fuel assemblies, 781
    soluble boron concentration, 767
  burnup function, 767–768
  core power profile, 778
  depletion process
    fission product concentration, 782–783
    flowchart, 784
    homogeneous core, 783
    individual fuel assemblies, 784
  design principle, 776
  excess reactivity, 766
  fission product buildup, *see* Fission product
  fuel assembly–loading patterns
    checkerboard loading strategy, 777
    out–in loading strategy, 777
    power distribution, 778
    thermal flux and the fuel rod enrichment, 776
    total power density, 776
  fuel enrichment, 765
  fuel-loading pattern, 774–775
  fuel pin temperatures, 778
  instantaneous reactivity, 766
  multi-batch cores
    four-batch refueling scheme, 769
    vs. single-batch cores, 769–771
    three-batch refueling scheme, 769
  N-batch core, 771–773
  net reactivity, 765
  one-batch cores, 768
  operating plan, 775–776
  optimization, 775–776
  PWR core, 766
  soluble boron concentration, 767
  time-dependent function, 766
  two-batch cores, 768
Lorentz scale factor, 391
Lorentz shrinkage factor, 93
Lorentz transformation, 93–94

Los Alamos National Laboratory, 679
Loschmidt, Johann Josef, 197
Lower triangular form, 536–537
Lowest index, 522
Low-leakage cores
  angular distribution of neutrons, 729
  economic benefits, 730
  fast neutron fluence, 729
  management schemes, 729
  nuclear fuels manager, 730
  radial power profile, 730–731
  reactor pressure vessels, 728–729
  total neutron leakage rate, 729
  volumetric power density, 729
Low-leakage loading scheme, 731

Macroscopic cross section(s), 207–212, 214
  for complex nuclear material, 193–194
  definition, 175
  vs. microscopic cross section, 176
Macroscopic fission cross section, 246, 488
Magic numbers, 278
Magnitude and shape of neutron, 536
Main steam isolation valve closure (MSIVC), 903
Manhattan Project, 347, 999
Man-made elements
  beta decay, 259
  Californium, 285
  gamma ray, 262
  naturally occurring elements, 260–261
  Neptunium, 285–286
  and nuclear fuels, 285
  plutonium, 285
    atomic number, 286
    isotopes, 286–287, 289
    Plutonium-239 decay, 288–289
    Plutonium-239 production process, 286–288
  properties, 262
Markov chains, 997–998
Markov processes, *see* Markov chains
Marsden, Ernest, 158
Mass attenuation coefficient, 1039–1040
Mass defect, 255, 265
  definition, 265
  design feature, 265–266
  energy released, 270–271
  Helium-4 nucleus, 266–267
  mass and energy conversions, 267
  proton and neutron rest masses, 266
Mass deficit, 103, 105
Mass reduction, 581
Master Table/Type (MT) number, 215, 218–219
Material buckling, 491, 495, 549, 554, 576, 817–818, 1053
Maximum permissible burnup, 768
Maxwell–Boltzmann distribution, 661
Maxwell–Boltzmann probability distribution, 151, 329, 347–348, 367, 970, 1049
  absolute temperature, 377
  average neutron energy, 378
  Boltzmann's constant, 378, 390–392
  inventors, 387
  kinetic energy, 377
  Maxwell's derivation, 388–390
  origin, 388
  probable energy, 378
  thermal energy group cross sections, 224
  velocities, 376–377
Maxwell distribution factor, 390
Maxwellian energy spectrum, 222
Maxwellian flux, 225, 390, 415
Maxwell, James Clerk, 387–388
Maxwell–Jüttner probability distribution, 391
Maxwell's equations, 70
Maxwell's particle collision rules, 388
Maxwell's rules, 388
McMillan, Edwin, 286
Mean free path, 480, 482, 484, 497
  fast fission factor, 983
  and macroscopic cross section, 1047
  neutron diffusion coefficient, 1047–1048, 1050
  neutron transport equation, 912
Mechanical drive system, 48
Mega cell, 814
Mega-Watt days per metric ton (MWD/T), 34, 43–44
Mega-Watts of thermal power (MWT), 43
Method of last resort, 971
Metric system, 7
MFR, *see* Moderator-to-fuel ratio
Microscopic cross section(s), 207–212, 214, 1023
  definition, 175
  vs. macroscopic cross section, 176
  to macroscopic cross section conversion, 189
Microscopic scattering cross section, 157
Middle-squared method, 1000
Military reactors, 31, 369, 456–457, 555
Millikan, Robert, 198
Milli rho (mrho), 684
Minimum critical mass, 580
Missing nuclear mass, *see* Mass defect
Mixed oxide (MOX) fuel, 33, 723, 776
Moderating ratio (MR), 385–386
Moderator, 508
Moderator temperature coefficient, 847
  boric acid effect, 733
  magnitude and sign, 732
  reactivity control and time frame, 732–733
Moderator-to-fuel ratio (MFR), 29–30, 421
  average power density, 461
  and four-factor formula, 446–447
  infinite multiplication factor, 448
  pitch of rectangular lattice, 448–449
  rod diameter, 446
  rod pitch, 445–446
  values of K_∞, 449–450
Modified Bessel functions, 391
  of first kind, 618, 1054–1057
  of second kind, 613, 618, 1054–1057
Modified one group theory, 534
Modular Accident Analysis Program (MAAP), 703
Mole, 189–190
Molecular weight, 191, 193, 1023
Molekül, *see* Mole
Monoenergetic beam, 143
Monte Carlo calculation, 469, 500; *see also* Monte Carlo method
Monte Carlo method, 152, 1051
  advantages and disadvantages, 971
  case history
    definition, 959
    flowchart, 960–961
    storage, 970
  computer programs/codes
    COHORT, 978
    KENO, 978
    MORSE, 978
    popular Monte Carlo codes, 978–980
    reactor geometries, 978, 980–981
    SANDYL, 978
    Serpent code, 978
    USB Random Number Generator, 978, 981
  control rods, 989–990
  cylindrical geometry, 985
  error estimation, 973–974
  error reduction schemes
    additional simulations, 974
    importance sampling, 975–976
    inflection points, 976–977
    particle histories, 975
    probability of occurrence, 976–977
    scaling factor, 976
    splitting, 975–976
  fast fission factor
    four-factor formula, 981
    fuel rods, 981–982
    importance weighting, 985
    mean free path, 983
    radius vector, 983
    random number generation program, 983–984
    unit cells, 982
  first collision distance, 967
  hypothetical event/transaction, 959
  individual neutron behavior, 67
  initial direction of motion and initial particle energy, 966–967
  mano a mano method, 959
  and Moore's Law of Computing, 971–973
  neutron diffusion theory, 500–502
  vs. neutron diffusion theory *vs.* neutron transport theory, 67–68
  neutron leakage rate, 960
  neutron transport equation, 952
  nuclear video game, 959
  particle exiting direction, 968–970
  process repetition, 970–971
  programming rules, 959
  radiation shielding, 67, 959
  radiation streaming, 67
  random number generator
    and SPD, 960, 962–965; *see also* Statistical probability distribution
    truly random numbers, 999–1001
  random walks, particle diffusion simulation, 997–999

resonance escape probability
absorption resonance, 986–987
definition, 986
fission neutron energy distribution, 988
half width of resonance, 987
kinetic energy, 988
resonance integrals, 986
scattering resonance, 986–987
transcendental function, 988
value, 989
Watt equation, 988
scattering angles
angular scattering probability, 992
asymmetric scattering angles, 994–997
cylindrical fuel rod, 993
directional unit vector, 993
elastic collision probability, 991
elastic scattering of neutrons, 993
inverse cumulative distribution function, 992
three-dimensional scattering angles, 991–992
skewed probability distributions, 990–992
statistical analysis phase, 971–972
type of collision, 968
Moore, Gordon, 972
Moore's Law of Computing, 971–973
Multi-batch refueling scheme
four-batch refueling scheme, 769
vs. single-batch cores
economic advantages, 771
equilibrium core, 771
maximum permissible burnup, 769
reactivity changes, 769–770
uptime *vs.* downtime, 771–772
three-batch refueling scheme, 769
Multigroup approach, 519
Multigroup approximation, 512, 537
Multigroup cross section libraries, 195
Multigroup cross sections, 520
Multigroup diffusion equation, 519
Multigroup flux, 520
Multigroup model, 491
Multigroup neutron diffusion equation, 519
Multigroup neutron diffusion theory
and applications, 519
Cramer's rule
Cramer, Gabriel (inventor), 531
flux ratio, 531–532
homogeneous algebraic equations, 530
matrix form, 530
simple statement, 530
energy-dependent diffusion equation, 519–520
fast and thermal flux shapes, 537–539
matrix form, multigroup diffusion equations, 536–537
modified one-group neutron diffusion theory, 534–535
multigroup approximation derivation, 523–524
multigroup cross sections, 522
multigroup diffusion coefficients, 525–526
neutron diffusion equation, two energy groups
fission neutrons, 527
homogeneous linear equations, 530
inhomogeneous, 532
neutron balance equation, 527–528
neutron leakage rate, 529
neutron leakage terms, 530
neutron production and destruction rate, 527–528
physical principles, 526
set of coupled differential equations, 529
six-factor formula, 533–534
thermal flux, 529
thermal neutron life cycle, 528
thermal water reactor, 527
workhorses, 528
N-speed neutron diffusion equation, 535–536
parameters, 542–543
popular programs, 539, 541
reactor licensing
analysis with TRACE, 540–542
applications, 539–540
scattering cross sections, energy groups, 524–525
two-group approximation, 520–522
two-group diffusion equations, finite reactor core, 532–533
Multigroup neutron transport equation, 944–945
Multigroup scattering, 184–185
Multigroup S_N equations, 945
Multigroup theory, 180
Multilayered shields, 1041
Multiplication factor
computational cell, 401
effective multiplication factor
for core, 401
more than one energy group, 404
neutron leakage rate, 401–402
and neutron life cycle, 402–403
infinite multiplication factor
infinite reactor lattice, 401–402
more than one energy group, 404
thermal neutron cross sections, 433–434
total multiplication factor, 400–401
total neutron destruction rate, 401
total neutron production rate, 401
Multiplicative congruential method, 1000

National Nuclear Data Center (NNDC), 226
Natural uranium, 12, 283, 369
Negative buckling, 591
Negative feedback, 694
Negative fuel temperature coefficient, 756
Negative temperature coefficient, 349
Negative temperature feedback, 731
Negative thermal feedback, 751
Neodymium-149, 786
Neptunium-237, 286
Neutrinos, 107, 326, 332, 1033
Neutron(s)
atomic nucleus
emission modeling, 122–123
hitting, 127–128
balance equation, 152
beam generators, 143–144
bound neutron, 117
direction, 473
energy loss, 138
free neutron, 117
half-life, 117
interaction
absorption and capture reactions, 141, 144–145
elastic scattering, 141–142
inelastic scattering, 142
nuclear fission reactions, 141
types, 120–121
kinetic energy loss, 152
moderators, 152
net destroyer, 919
neutron decay, 117–118
nuclear fission process
delayed neutrons, 146
energetics, 148–149
fission fragments, 145
fission products, 145–148
kinetic energies, 146
Uranium-235, 147–148
prompt and delayed neutrons, 118–120
released per fission, 332–333
released per neutron absorbed, 333–335
scattering
alpha particles, 158
differential scattering probability, 156–157
in heavy materials, 155–156
Rutherford scattering formula, 158–160
scattering angles
in COM system, 138–140
energy loss, 138
in inelastic collisions, 155
in LAB system, 140
scattering probability, 152–154
velocities, 350, 524
Neutron absorber, 944
Neutron absorption cross section, 369, 399–400, 511
Neutron age, 119, 575–576, 1049
Neutron balance, 423
Neutron beam attenuation, 609
Neutron beam generator, 601
Neutron conservation equation, 486–488
Neutron cross section libraries creation
data objects, 226–227
fast and thermal group fluxes, 230
group flux, 228
microscopic group cross sections, 228
multigroup cross sections, 230–231
neutron energy group, 227
neutron energy spectrum
average flux, 230
core *vs.* blanket, 232
in fast reactor and thermal water reactor, 230–231
shape, 230
with three energy groups, 229
with two energy groups, 228
into two/three energy groups, 227

neutron flux, 227, 230
NNDC, 226
total scattering cross section, 227
Neutron current, 601
Neutron destruction rate, 399, 404
Neutron diffusion area, 491, 602
Neutron diffusion coefficient
Bessel function, 1053
cosine of neutron scattering angle, 1045–1046
energy dependent, 1044
Fick's Law of Diffusion, 1043
mean free path, 1047–1048, 1050
neutron current, 1044
neutron flux, 1044
parameters
at fission energies, 1043, 1045
at thermal energies, 1043–1044
for pure scatters, 1046
time-dependent neutron diffusion equation, 1043
transport correction factor, 1048
transport cross section, 1044, 1046–1047
Neutron diffusion equation, 67, 102, 152, 856
burnable poison
absorption cross section, 633–634
black surface, 633
A^F and A^M relationship, 636
flux shapes and boundary conditions, unit cell, 636–637
fuel rod, 634–636
function of time, 633–634
material buckling, 636
neutron sinks, 633
convergence criteria and numerical errors, 632–633
diffusive medium with distributed source
boundary conditions, 620–621
Helmholtz's equation, 619
planar-distributed source, 619
region of space, 619
scalar multiplier, 620
symmetric region, 620
energy-dependent extrapolation distance, 625–626
general solutions, 603–604
homogeneous lattice approximation, 805
homogenization, reactor lattice, 805, 807
infinite diffusion coefficient, 637
iterative power method, 630–632
Laplace's equation, 637
line source simulation, 617–618
material buckling, 805
more than one material region, 629–630
neutron flux, multiple point sources, 613–614
neutron point sources
diffusion equation, 607
homogeneous medium, 607
isotropic medium, 608
radiation field, vacuum, 608–609
scattering and absorption, 608
spherical coordinate system, 607
neutron source on boundaries, 604–605
no fissionable materials, 601–602
planar neutron source, extrapolated boundary condition, 626–629
Poisson's equation, 637–638
popular codes, 809–810
pure scattering material, 637
reactor core size, shape, and composition, 815–818
Schrödinger wave equation, 639
second-order differential equation with constant coefficients, 805
simple planar neutron source, 605–606
spatial variation, 805–806
superposition principle
average neutron velocity, 610
density distribution, 610
distributed source, 610–611
electric/magnetic dipole, 611
flux intensity equation, 610
light waves, 614–617
neutron current, 612
neutron flux shape, 612–613
neutrons in vacuum, 614
phase of photons, 611
point diffusion kernel, 611
two point sources, 611–612
velocity distribution, 610
time-dependent effects, 636–637
time-dependent neutron diffusion theory, 639–640
two diffusive regions, distributed neutron source, 621–623
types of neutron sources, 602–603
vacuum boundary conditions, 623–625
Neutron diffusion length, 602
Neutron diffusion theory
BWR control rod, 506–507
conserve neutrons, 485–487
control rods, 503–504
cylindrical control rod, 504–505
diffusion distance
derivation, 507–508
point source, 508–510
energy group, boundary conditions, 494–495
extrapolation distance, 505–506
Fick's Law of Diffusion
constant velocity approximation, 476
contact lens, 475
diffusion coefficient, 477
diffusion theory approximation, 478
electrically neutral particles, 474
Fick, Adolf, 474–475
gradient of the neutron concentration, 476
gradient operator, 477
heterogeneous region, 478
homogeneous region, 478
limitations, 483–484
magnitude and direction, 475
neutron current and particle flux relationship, 476
neutron population, 475
neutron transport equation, 478
one-group diffusion theory, 476
particle diffusion process, 474
zero flux gradient, 476
Monte Carlo method, 500–502
neutron current, 473–474
neutron density, 470–472
neutron diffusion coefficient
boundary conditions, 493–494
current, 478
forward scattering, 480–481
of graphite, 482–483
important nuclear materials, 482
macroscopic scattering cross section, 479
mean free path, 480, 482
neutron scattering and size, 510–512
particle flow, 478
physical resistance, 479
proportionality constant, 482
and scattering angle relationship, 480
scattering cross section, Carbon-12, 480–481
simplified equation, 480
transport cross section, 480, 482
transport mean free path, 482
neutron diffusion distance, 496–498
neutron diffusion equation, 484–485
neutron diffusion length, 495–496
neutron flux
average neutron density, 473
average velocity, 473
definition, 472–473
number of neutrons, control volume, 471
number of scattering collisions, 472
reaction rates, 472
surface area, 472
neutrons and flow, matter, 469–470
relationship with mean free path, 499–501
sources and sinks, neutron conservation equation, 487–488
steady-state neutron diffusion equation
definition, 489
external neutron source, 490–491
standard form, 491–492
time-dependent, 488–489
vs. transport theory, 502–503
Neutron distribution, 484
Neutron downscattering, 523
Neutron economy, 369, 565
Neutron energy loss, 137
Neutron energy spectrum, 329, 535
Neutron fission cross section, 399–400
Neutron fluence, 796
Neutron flux, 177, 179, 411, 524, 694
attenuation, 609
shape, 526, 703
Neutron leakage rates, 401–402, 404, 439, 442
Neutron lethargy, 382, 420
Neutron mean free path, 1047–1048
Neutron moderators, 152
fast *vs.* thermal reactors
average energy loss per collision, 373
average number of collisions, 374–375
energy loss per collision, 371–372
final neutron energy after N collisions, 373
fission process, 371–372
head-on and glancing collisions, 373
neutron energy spectrum, 371

neutron scattering angle, 372
nuclear fusion process, 371–372
moderated neutron temperature, energy, and velocity, 376–378
moderating material, 367
moderating properties, 374
moderating ratio, 385–386
moderation advantages, 374–375
reactor coolant
deuterium atom, 368
fast reactor/liquid metal coolants, 370–371
gas reactor coolants, 370
graphite block, 368
heavy water, 368
ordinary/light water, 367–368
particle economy, 368
properties, 369
selection factors, 369
thermal water reactor coolants, 369
Neutron multiplication factor, 400, 431
Neutron poison, 148
Neutron production cross section, *see* Neutron fission cross section
Neutron production rate, 404, 1019
Neutron reproduction factor, 334
Neutron scattering angle, 951
Neutron scattering kernel, 140
Neutron scattering process, 1048
Neutron slowing down theory, 67, 117, 152, 239
average logarithmic energy decrement, 385
elastic collisions, 367
energy staircase, 380–381
fractional energy loss in head-on elastic collision, 382
inelastic scattering collisions, 367
lethargy, 382
moderating ratio, 385–386
scattering kernels, 382, 384
slowing down decrement, 382–384
slowing down parameters, 380–381
Neutron source current, 606
Neutron-to-proton ratio (N/Z), 93
Neutron transport cross section, 140
Neutron transport equation, 67, 484, 506
adjoint methods, 952
angular flux, 938–939
angular gradient, 937–938
angular integral, 925
angular neutron flux, 953–954
angular unit vector and solid angle, 911–912
assumptions, 911
azimuthal angles, 937–938
boundary conditions
angular current, 946
angular flux, 946
initial boundary conditions, 920
at material interface, 947–948
neutron current, 920
types, 946
vacuum boundary condition, 920, 946, 948–950
commercial computer programs, 952
conventional form
angular unit vector, 921
directional derivative, 920–921
directional flux vector, 920–921
number crunching, 922
one-dimensional transport equation, 921
scattering kernel, 922
total removal cross section, 922
derivation
angular neutron density, 917–918
arbitrary volume of space, 917
directional derivative, 918
material derivation, 918
total neutron production rate, 918
total removal rate, 919
and diffusion theory
angular current in spherical coordinate system, 916
angular neutron current, 914
angular neutron flux, 914–916
angular reaction rate, 916
angular unit vector, 914
anisotropic particle flux, 913
approximation, 928–929
Boltzmann transport equation, 912
differential area, 914
Fick's Law of Diffusion, 912, 929
linear anisotropy, 926
mean free path, 912
net neutron flow with energy, 916
number crunching, 913
number of neutrons, 914
parallel processing, 913
P_N and S_N approximations, 922
reaction rates, 912
scattering angles, 913–914
scattering cross sections, 913
solid angle, 914–915
infinite series expansion, 926
initial conditions, time-dependent problems, 946–947
integro-differential equation, 924
interpolation scheme, 926
Monte Carlo method, 952
multigroup neutron transport equation, 911, 944–945
neutron importance concept, 952
ordinate angular variable, 925
P_N approximation
coefficient matrix, 933
diffusion coefficients and P_1 approximation, 950–952
directional flux, 932
infinite series expansion, 930
Legendre polynomials, 929–931
in one dimension, 933
Schrodinger wave equation, 929
S_N approximation, 932
time-dependent transport equation, 932
weighting function, 931
polynomial expansion functions, 925
with pure scatters and absorbers, 941–943
quadrature, 925–926
radiation shielding calculations, 938
ray effects, 943–944
scattering integral, 929
scattering rate, 919–920
simplification categories, 922
for homogeneous material, 923
for homogeneous material with isotropic scattering, 923–924
with isotropic source terms, 924
one-group/speed transport equation, 923
steady-state transport equation, 923
single energy group, 911
S_N approximation
angular decomposition, 934
angular neutron flux, 933
arbitrary angular direction, 934–935
discrete ordinates, 934
to spherical source, 935–937
values of angular flux, 934
Taylor series expansions, 925
time-dependent transport equation, 939–941
transport theory codes, 926–928
unit vector
cylindrical coordinate system, 937
spherical coordinate system, 937
Neutron transport theory, 484; *see also* Neutron transport equation
Newton's Laws of Motion, 70, 502
Nodal approach, 401
Nodal methods, 539
Node/computational cell, 539
Non-1/v correction factors, 1021–1022
Nonburnable poisons, 724
Non-leakage probabilities, 429, 577
Non-SI units, 1008
Nordheim, 701
Normal probability distribution, 962, 976
mean/average value, 973
probability of occurrence, 976–977
standard deviation, 973, 976–977
variance, 973–974
Norsk Hydro facility, 393
Nuclear binding energy curve, 255
shape, 268–269, 271–273
total energy released, 270
Nuclear chain reaction
controlled chain reaction, 283–284
criteria, 283
uncontrolled chain reaction, 283–284
Nuclear cross section(s), 74
barn, 167
data
plotting tools, 1011
repositories, 1011
and ENDF/B nomenclature
MT number, 215, 218–219
numbering scheme, 216, 219
radiation shields, 215
reaction designators, 216
energy groups, large numbers, 241–243
fast and thermal neutron, 177–179
fast neutron cross sections, 1011, 1016–1017
group cross section library
collapsing, 233–235
finding, 232–233
group flux and average flux, 239–241

libraries
BNL-325, 207
ENDF-B/V file, 207
ENDF CD-ROM, 207
fast cross sections, 207, 211–212
JENDL 4.0 cross section library, 207
neutron cross section libraries creation, 226–232
online charts and graphs, 207
physical properties, 207, 213–214
room temperature libraries, 214
thermal cross sections, 207–210
web-based applications, 207
microscopic to macroscopic cross section conversion, 189, 191, 1015
with more than two energy groups, 179–180
multigroup approximation, 180–181
multiple cross sections, 215–216
naming conventions, 200, 246–247, 1018–1019
neutron flux near reaction resonance, 225–226
non-1/v correction factors, 1021–1022
nuclear materials comparison, 217, 220
number of atoms/molecules, 219–221
number of atoms/molecules per gram, 190
number of atoms per cubic centimeter, 190–191
1 Angstrom, 167–168
1 femtometer, 167–168
online plotting tool, 215–217
physical and atomic densities, 219–221
physical density and atomic density, 192–193
power production, 1021
probability, 167
public cross section libraries, 194–195
for pure material, 191–192
quantum mechanics, 169
and reaction rates
additive nature, 175
diffuse gas, 175
energy dependent reaction rates, 176
macroscopic cross section, 175–176
microscopic cross section, 175–176
particle flux, 175
rate equation, 175
sample, 174
total reaction rate, 175
reaction resonances, *see* Reaction resonances
realistic reactor design, 243–244
shooting bullet into haystack, 167–168
simple design exercise, 244–245
single energy group, 235–238
thermal cross sections, 1011–1015
for non-1/v absorbers, 222–223
for 1/v absorber, 221–222
thermal energy group cross sections, 223–225
types
absorption cross section, 168–170
capture cross section, 170
Compton scattering, 170
fission cross section, 168–170
pair production, 170
photoelectric effect, 170
removal cross section, 167
scattering cross section, 170
total reaction cross section, 167, 170
Nuclear Doppler effect, 732
Nuclear fission, 85, 105, 141
delayed neutrons, 146
average lifetime, 356–357
emitters, 356–357
energy spectrum, 354
fission fragments, 353
fission rate, 355
fractions and yields, 356
percentage, 355
production rate, 355–356
radioactive beta decay, 354
Segre chart, 354–355
two-step process, 354
electrical *vs.* thermal energy production, 352
energetics, 148–149
energy release
beta decay, 332
delayed gamma rays, 332
examples, 342–343
expectation energy of vacuum, 332
kinetic energy, 330
neutrinos, 332
nuclear *vs.* chemical energy release, 337–338
per fission, 338–339
radioactive decay, 332
thermal fission of Plutonium-239, 331–332
thermal fission of Uranium-235, 331
total energy released, 351
useable energy, 332
epithermal energy range, 329
eta value, different fuel mixtures, 335–337
fast energy region, 329
fission fragments, 145, 326, 330–331
fission neutron energy spectrum, 327–328
fission product poisons, cumulative effect, 358–359
fission products, 145–148, 343–346
fundamental origin, 265
kinetic energies, 146
mass to energy conversion, 319
neutron energy spectrum, 329
neutrons released
per fission, 332–333
per neutron absorbed, 333–335
neutron velocities, 350
nuclear chain reactions
controlled chain reaction, 344
Manhattan project, 347
Maxwell–Boltzmann probability distribution, 347–348
speed, 348–350
uncontrolled chain reaction, 344
visual depiction, 346
nuclear energy, origin of
Einstein's equation, 339
final mass, 339
initial mass, 338
mass energy, 339
proton and neutron rest masses, 340
recoverable energy, 338–340
vs. nuclear fusion, 320, 323
nuclear structure, 279–280
prompt neutrons, 353–354
supernovas, 320
thermal energy range, 329
threshold energy
critical energy, 341–342
gluons, 340–341
neutron and proton internal structure, 340–341
quark composition, 340
Uranium-235, 147–148
capture channel, 325
fission channel, 326–327
induced fission, 324
thermal neutron, 324–325
uranium consumption rate, 352–353
xenon and samarium, 357–358
Nuclear forces, 170
Nuclear fuel(s)
burnup measurement
burnup of fuel, 42–43
FIMAs, 42
GWD, 43
MWD/ton, 43–44
MWT, 43
number of fuel atoms, 41
number of uranium-235 atoms, 41–42
recoverable energy, 44
element, 12
fertile materials, 12
fissile isotopes, 12
lead, 12
and man-made elements, 285
plutonium, 12–13
Plutonium-239 decay chain, 282
properties, 12
radioactivity and radioactive decay, *see* Radioactive decay, *see* Radioactivity
rods, *see* Nuclear fuel rods
Thorium-231 decays, 280
Thorium-232, 282
Thorium-234 decays, 282
uranium, 12–14
Uranium-234, 280
Uranium-235 decay chain, 280–281
Uranium-238 decay chain, 280–281
Uranium-239, 282
uranium isotopes, 282–283
Nuclear fuel assemblies, 18–19
axial zoning, 35–36
burnable poisons, 35
burnup, 34
CANDU fuel assemblies, 23–24
characteristics
blanket regions, 24–25
cores, *see* Reactor cores
design parameters, 26–27
equivalent cylindrical unit cell, 25–26
light water reactor fuel assemblies, 24

LMFBRs, 24–25
control assemblies, 32
fuel rods
in hexagonal fuel assemblies, 23
number of, 21–22
sheath/shroud, 21
in square fuel assemblies, 22
LMFBR fuel assembly, 20–21
loading pattern, 34–35
peak-to-average power ratio, 34
PWR fuel assemblies, 20–21
radial zoning, 35
shutdown assemblies, 32
Nuclear fuel management
checkerboard refueling, 39
cooling off process, 40
fuel assembly enrichment, 38
out-in refueling, 39
Nuclear fuel rods
cladding, 17–19
control rods, 20
fuel assemblies, *see* Nuclear fuel assemblies
in hexagonal fuel assemblies, 23
rod pitch, 20
in square fuel assembly, 22
thermal energy production, 16–17
Nuclear fusion
definition, 319
fundamental origin, 265
gamma rays, 309
Maxwell–Jüttner probability distribution, 391
vs. nuclear fission, 320, 323
stars, 319–320
Nuclear materials
atomic masses, half-lives, and natural abundance, 1027–1032
diffusion coefficient, 1048
diffusion parameters, 1049–1050
mean free path, 1048
physical properties, 1023–1025
total energy released, 1027, 1033
transport cross section, 1048
Nuclear medicine, 73
Nuclear particles
with an electric charge
conservation of energy, 117
Coulomb's law, 115, 117
electrical force, 115–116
linear momentum, 117
neutron slowing down theory, 117
photon exchange, 116
atomic nucleus, *see* Atomic nucleus
backscattering, 132–133
Baryons, 68
collisions
coordinate system independence, 123–125
elastic, 115
inelastic, 115
photons and neutrinos inclusion, 129–130
control without electrical charge, 102–103
effect of motion, 95
elastic and inelastic collisions, 67
elementary particles, 68
energy to velocity conversion, 99–100
force particles, 68
gluons, 69
Hadron, 68
matter particles, 68
kinetic energy, 87, 96–97
linear momentum, 89–90
mass, 87–88, 96, 105
rest energy, 96
total energy, 89
up quark and down quark, 77
momentum conservation, 125–127
neutron energy and velocity, 100–101
neutrons, *see* Neutrons
nuclear energy
calculation, 103–105
Einstein's equation, 103–105
production, 105
recoverable and unrecoverable, 103
nuclear mass
measuring units, 71–73
at very high speeds, 97–99
photon propagation speed, 101–102
proton, the neutron, and electron, atomic properties, 71
quarks, 68
radioactive decay, 95
relativity
GPS, 94–95
Lorentz transformation, 93–94
relativistic mass, 93
Theory of Relativity, 93
time dilation factor, 93
spin, 71
standard naming convention, 149–150
time-dependent neutron, 68
time-independent neutron, 68
types, 115–116
Nuclear power reactors
architectures, 2, 7
Brayton thermal cycle, 6
condenser, 3
core, 2–3
moderator, 2–3
power turbines, 3
Rankine thermal cycle, 3, 6
steam generator, 3, 6
thermodynamic efficiency, 3
coal-fired power plant, 7
coolants
availability, 8
characteristics, 8, 10
cost, 8
deuterium, 11
fluids, 8
gases, 8
heavy water, 11–12
light water, 11
liquid metals, 8, 11
neutronic performance, 8
particle economy, 12
in PWR, 11
thermal-hydraulic performance, 8
design parameters, 6–8
dimensionless quantities, 7
electrical generating systems
Brayton thermal cycle, 51
electrical generators, 51, 53–56
Rankine thermal cycle, 51
steam generators, 51–53
steam turbines, 51, 53
electrical power generation percentage, 2, 6
fuel-to-cladding gap, 33
industry averages, 7
lattice geometries, 30–32
modular designs, 8
nuclear-powered aircraft carrier, 36
number of reactors
under construction, 1, 5
by country, 1, 3–4
function of design, 1, 5
function of time, 1–2
passive safety systems, 8
power density, 44–45
pressure vessels
design pressure, 14–15
internal structure, BWR, 16
pressurization process, 13
PWRs *vs.* BWRs, 14
radiation shield, 13
sizes, 14–15
system pressure, 14
thickness, 14–15
quantities and units, 7, 10
reactor core, 7
refueling cycle
average length, 38
burnup, 38
continuous/online refueling, 37
military reactors, 35
nuclear aircraft carrier, 36
refueling machine, cross-sectional view, 37
schematic, 7, 9
thermal efficiency, 45–46
types, 1
unit cells, 31
Nuclear properties
deuterium, 186–187, 368–369
hydrogen, 186–187
light and heavy water, 392–393
uranium and plutonium, 321–322, 650, 705–706
uranium dioxide, 198–199
Nuclear reaction probabilities, 74
Nuclear reaction rates
fast and thermal energy groups, 1019–1020
temperature-dependent reaction rates, 1022
Nuclear science and engineering, 484
Nuclear steam supply system (NSSS), 1
Nuclear structure
liquid drop model, 266–267, 272–273
nuclear fission, 279–280
Weizsaecker model, 278
Nuclear weight, 322
Nucleate boiling, 48, 847
Nucleon clusters, 279

Odd-numbered eigenvalues, 816
Oklo reactors
  critical size, 455–456
  infinite multiplication factor, 455
  MFR, 455
  negative temperature coefficient, 454
  site, 453
  sustained nuclear chain reaction, 454
Once-through steam generator (OTSG), 52
One-and-one-half-group theory, 535
One-group model, *see* Constant velocity model
One-group neutron diffusion equation, 489
One-group/one-speed transport equation, 923
One-speed neutron diffusion equation, 489
One-third of total power, 719
One watt, 552
Online refueling, 23
Oppenheimer, J. Robert, 402
Optimization scheme, 774
Orbitals, 69, 71
Original licensed thermal power (OLTP), 903
Orthogonal polynomials, 925
Ostwald, Wilhelm, 189
Outer iteration, 621
Out–in loading scheme, 728, 731

P_1 approximation, 140, 511
Pairing energy term, 272, 274, 276
Pair production, 170, 970
Parametric studies, 538
PARCS, 903
Parsons, Charles, 53
Particle flux, 175
Passive safety system, 49, 849
PDQ, 539–540
PDQ-7, 809
Peak load, 887–888
Peak-to-average power ratios, 564–565
Pearson, Karl, 997
Percentage abundance, 322
Periodic Table
  elements, 256
    atomic number, 257
    atomic properties for carbon, 258–259
    fractional atomic weights, 262–264
    and isotopes, 257, 259
    isotopic stability, 306–308
    man-made elements, 259–262
    nuclear data for carbon, 257–258
    plutonium, 257
    promethium, 257
    Radon, 257
    and relative nuclear stabilities, 257–258
    technetium, 257
    uranium, 257
  Mendeleev, Dmitri, 255–256
Perrin, Jean, 196–197
Petrzhak, K.A., 280
Phase angle, 616
Photoelectric effect, 82, 170
Physical constants, 1005
Physical density, 192–193, 1023
Physical location, outer boundary, 624
Physical processes, 524
Planar source, 490, 602
Planck's constant, 83, 89, 106, 614
Planned shutdowns, 841
Plate-type control rods, 752, 828
Plutonium, 285
  atomic number, 286
  buildup, in core
    constant neutron flux, 723
    Plutonium-239 production cycle, 721
    rate equations, 722
    U-235 and U-238 mixture, 721
  energy estimation, thermal water reactor core, 723–724
  fertile materials, 12
  isotopes, 286–287, 289
  metallic form, 12–13
  nuclear properties, 321–322
  Plutonium-238, 289
  Plutonium-239
    decay, 288–289
    production process, 286–288
  Plutonium-241, 289
  plutonium dioxide, 16
  production rate, thermal water reactor, 723
  and uranium masses, 343–346
Plutonium dioxide (PuO_2), 16
P_N approximation
  coefficient matrix, 933
  directional flux, 932
  infinite series expansion, 930
  Legendre polynomials, 929–931
  in one dimension, 933
  Schrodinger wave equation, 929
  S_N approximation, 932
  time-dependent transport equation, 932
  weighting function, 931
Point kinetics approximation, 558, 637
  applications, 703
  asymptotic reactor period, 675, 696–698
  control rod worth measurement, 702
  flux and power changes, arbitrary state, 698–699
  Inhour equation
    coupled differential equations, 673
    delayed neutrons, 674–675
    exact solutions, 679
    explicit relationship, 677
    graphical solutions, 677–679
    initial solution, reactor period, 674
    instantaneous reactor period, 676
    origin of, 699–700
    power reactor, 676
    reactivity and reactor period relationship, 675
    six delayed neutron groups, 694–696
    time-dependent diffusion equation, 673
    time-dependent precursor equation, 673
    and unit of Inhour, 700–701
  instantaneous reactor power level estimation
    decay heat, 705
    fast reactor fuel, 706–707
    fission, 704
    neutron flux *vs.* transient, 707–708
    nuclear properties, 705–706
    number of delayed neutrons, 705–706
    prompt neutron lifetime, 706
    thermal water reactor, 706
    time-dependent reactor power, 705
    Wigner–Way equation, 705
  normal reactor behavior and reactivity swings
    large negative reactivity changes, 691–693
    large positive reactivity changes, 690–691
    power level changes, 689
    prompt supercritical transient, 693–694
    supercritical transients, 693
  parameters, 702–703, 708
  prompt jump and drop approximations
    Bromine-87 decay chain, 688
    considerable stir, 685
    initial and final power level, 687
    neutron flux, 686
    power level change, 687
    prompt jump factor, 687
    reactivity change, 687–688
    reactor periods, 687–689
    time-dependent flux, 686
  pulsed neutron source method, 710–711
  reactivity-dollars and cents
    absolute units for measurement, 684–685
    the cent, 683
    critical reactor, 683
    definition, 683
    delayed neutron fractions, 685
    different nuclear fuels, 685
    effective multiplication factor, 683
    milli-k and pcm, 684
    milli rho, 684
    relative units for measurement, 684–685
    system-wide reactivity, 683
  reactor noise analysis and functions, 711–712
  reactor period, delayed neutrons
    exotic control system, 679
    positive and negative values, 680–681
    real reactors, 680
    time-dependent flux, 679
    Uranium-235-fueled thermal water reactor, 681
  rod drop method, 708–709
  rod oscillator method, 709
  time-dependent reactor behavior
    emergency shutdown, 682
    examples of, 681
    fast reactors, 696
    normal/planned shutdown, 681–682
    prompt critical behavior, 682
  validity examination, 703–704
Point kinetics method, 656
Point source, 490, 507–510, 602
Poisson distribution, 292
Poisson probability distribution, 292
Poisson, Siméon Denis, 292
Polar plots, 989–990
Poles of solution, 697
Polonium, 308

Popular coordinate systems, 603
Positive buckling, 591
Potential scattering, 184, 188
Potential well, 278
Power coefficient, 749–750
  for core, 750
  of reactivity, 747–748
Power defect, 751–752
Power defect of reactivity, 747
Power generation, 566
Power plant thermal cycle, 3
Power series expansions, 1056
Power turbine, *see* Steam turbines
Preheating, 747
Pressure tubes, 23
Pressurized heavy water reactors (PHWRs), 11
Pressurized water reactors (PWRs), 1, 647, 723
  vs. BWR control rods, 48–50
  core reactivity, 766–767
  fuel assemblies, 20–21
  three-batch refueling scheme, 769
  Zircaloy-4, 19
Primary recirculation pumps, 829
Principle of superposition, 1054
Probability distribution function (PDF), 1051
Probability of occurrence, 330
Promethium-149
  concentration, 788
  equilibrium concentration, 891
  radioactive decay chains, 784–785
  start-up, 889–890
  yields, 786, 888
Prompt critical state, 681–682
Prompt drop, 679
Prompt fission neutrons, 121
Prompt jump, 679
Prompt jump approximation, 699
Prompt neutron(s), 348–349, 376, 407, 469, 655
  average characteristics, 120
  energy spectrum, 118–119, 353–354
  fission neutrons, 118–119, 121
  lifetime, 696
  origin, 353
  Watt curve, 118–119
  Watt equation, 119–120
Prompt neutron energy distribution, 118
Prompt neutron fraction, 648, 1038
Prompt neutron production rates, 1038
Prompt temperature coefficient, 737, 741
Pryex glass, 781
Pseudo equilibrium, 305
Public cross section libraries, 194–195
Pulsed neutron source method, 702
Pure scatterer, 510
PWRs, *see* Pressurized water reactors
Pyrex glass, 834, 839
Pythagorean theorem, 124, 474

Quadratic curve fit, 744
Quadrature formula, 925
Quadrature weights, 925
QUANDF, 903
Quantum field theory, 618, 1056
Quantum mechanical effects, 70
Quantum mechanics, 294

Radial power profile, 726
Radiation protection, 309
Radiation shields, 12, 67, 215, 913, 978
  attenuation coefficients, 938
    linear attenuation coefficient, 1039–1040
    mass attenuation coefficient, 1039–1040
    photon beam, 1041
    shielding materials, physical densities, 1039–1040
    x-rays *vs.* gamma rays, 1041
  Pu-239, 288
Radiation streaming, 67
Radiative capture, 120, 147, 170, 183–184, 325
Radioactive decay, 95, 332
  decay rate measurement, 298–299
  equations, 296
  exponential functions, 295–296
  force balance, 290
  force imbalance, 289–290
  laws of, 294–295
  nuclear decay heat, 309–310
  radioactive materials
    alpha decay, 308–309
    average lifetime, 303
    beta decay, 308
    decay constants, 303
    doubling time, 302
    half-life, 294–295, 301–303
    isotopic stability, 308
    reactor period, 304
    time-dependent activity, 300–301
  secular equilibrium, 304–306
  stable daughter and radioactive parent, 306
  statistical probability distributions
    average decay rate, 294
    emission probabilities, alpha particles, 293
    emission probabilities, beta particles, 293–294
    histogram, 293
    Poisson probability distribution, 292
    quantum mechanics, 294
Radioactive decay chain, 148
Radioactive decay constant, 295
Radioactive source term, 594
Radioactivity, 75
  Becquerel (Bq), 299
  Chart of the Nuclides, 290–292
  Curie, 299
  decay rate, 298–300
  electrical nuclear force, 289
  force balance, 290
  force imbalance, 289–290
  magic numbers, 290
  production rate, 300
  protons to neutrons ratio, 290
  radioactive activities, 299
  radioactive half-life, 291–292
  time dilation, 291
  time dilation factor, 291–292
  unstable isotopes, 291

Random noise, 711
Random number generator, SPD, *see* Statistical probability distribution
Random walks, 469, 997–999
Rankine thermal cycle, 1, 3, 51, 368
Rate equation, 175
Ray effects, 943–944
Rayleigh, Lord, 997
RBMK-1000 reactor, 895–896
Reaction channels, 147
Reaction cross section, 120–121
Reaction rates, 519, 524, 529
  additive nature, 175
  diffuse gas, 175
  energy dependent reaction rates, 176
  macroscopic cross section, 175–176
  microscopic cross section, 175–176
  particle flux, 175
  rate equation, 175
  sample, 174
  total reaction rate, 175
Reaction resonances
  compound nucleus formation
    elastic *vs.* inelastic scattering process, 171
    excited states, 172
    four-factor formula, 174
    half-width of reaction resonance, 173
    probability, 172
    quantum states, 172
    resonance integral, 173
    scattering and absorption resonances, 171–172
    Sodium-23, 172–173
  elastic *vs.* inelastic scattering process, 171
  neutron flux, 225–226
  nucleus in excited state, 171–172
Reactivity, 244
  contribution, 877
  control
    Clementine fast reactor, 868, 870
    neutron flux shape, 869–870
    power control, 868
    reflector savings, 870
    six-factor formula, 869
    thermal and fast non-leakage probabilities, 869
  control rods
    changes by chemical shim, 843–846
    dollars and cents, 827
    effective multiplication factor, 854–855
    incremental reactivity, 827
    incremental worth per increment, 855
    primary effect, 855
    six-factor formula, 854
  definition, 403, 405, 429
  delayed neutrons effect, 407
  expression, 405
  instantaneous reactivity, 429
  mean neutron generation time, 406
  net reactivity
    fuel burnup, 430–432
    fuel in core, 429
  prompt jump and prompt drop approximations, 406
  prompt neutron population, 405–406

reactor power level changes, 405
thermal feedback effects, 406
thermal neutron cross sections, 433–434
units, 407
Reactivity changes
chemical shim
boric acid concentration, 844–846
Boron-10, 845
boron concentration, 845–846
effective multiplication factor, 843
thermal utilization, 843–844
fission product
negative reactivity, 796
net reactivity of core, 795
neutron fluence, 796–797
reactivity reduction, 796
Reactor accidents, 733
analysis codes, 902
Chernobyl accident, *see* Chernobyl accident
QUANDF, 903
RELAP, 903
RETRAN, 902–903
TRAC, 903
TRACE, 903–906
Reactor coolants
availability, 8
characteristics, 8, 10
cost, 8
deuterium, 11
deuterium atom, 368
fast reactor/liquid metal coolants, 370–371
fluids, 8
gases, 8
gas reactor coolants, 370
graphite block, 368
heavy water, 11–12, 368
light water, 11
liquid metals, 8, 11
neutronic performance, 8
ordinary/light water, 367–368
particle economy, 12, 368
properties, 369
in PWR, 11
selection factors, 369
thermal-hydraulic performance, 8
thermal water reactor coolants, 369
Reactor cores
and blanket regions, 24–25
boron concentration, 51
characteristics, 24–25
chemical shim, 51
composition
fuel pins, 28
fuel-to-structure ratio, 30
heavy water, 29
lattice pitch, 29
light water, 29
moderator-to-fuel ratio, 29–30
pie chart, 29
uranium dioxide, 28–29
design parameters, 24
lattice with fuel rods, 26, 28
loading patterns, 40–41
negative reactivity, 51
positive reactivity, 51
power density, 44–45
PWR fuel assemblies, 26, 28
Reactor dead time, 792, 885–886
Reactor diffusion parameters
mean free path, 1050
mean squared distance, 1049
neutron moderators, 1049–1050
reactor cores, 1049–1050
spectrum-averaged cross sections, 1049–1050
thermal diffusion length, 1049
thermal migration length, 1049
Reactor geometry, 539
Reactor kinetics, 120, 304
Reactor lattice
hexagonal, 408–409
homogenization, 805, 807
infinite lattice approximation, 31–32
lattice geometries, 30–31
SPD, 965
standard, 408
Reactor period, 818
Reactor physics
chemical *vs.* nuclear bonds
discrete energy levels, 82–84
range, 84–85
strength, 82–83
definition, 115
energy estimation
beta decay, 88
Heisenberg uncertainty principle, 89
Higgs mechanism, 88
kinetic energy, 86–88
mass of matter particle, 87–88
natural mass, 86
particle spins and symbols, 89
rest energy, 86
rest mass, 86
velocity-dependent mass, 88
laws of nuclear world, 71
Monte Carlo method, 67–68
neutron diffusion theory, 67–68
neutron slowing down theory, 67
neutron transport theory, 67–68
nuclear binding force
characteristics, up quark and down quark, 77–78
8 MeV per nucleon, 78
gluon energy, 76
nuclear binding energy curve, 79, 83
proton, internal structure, 78
nuclear energy measurement, 85–86
nuclear particles and particle types, *see* Nuclear particles
Reactor shutdown cycle
Iodine-135, 882–883
Tellurium-135, 882–883
Xenon-135
dead time, 885–886
fission product decay chain, 882–883
parent–daughter relationship, 882
reactivity, 884–885
thermal neutron flux, 884
Reactor Transient Analysis Program (RETRAN), 902–903
Reactor trip, 51, 851
Recoverable delayed energy per fission, 338
Recoverable energy, 326, 351, 1033
Recoverable prompt energy per fission, 338
Recoverable thermal power, 351
Rectangular control rods, 828
Reflected reactor, 566
Reflection coefficient, 567
Reflector, 565
Reflector region, 492
Reflector savings, 626, 870
and albedo
asymptotic limit, 567
common reflector materials, 571
core height, 570
cylindrical reactors, 570
definition, 567
Deutsch equation, 570
Deutsch, R.W., 570
diffusion area, 569
diffusion length, 569
effective boundary condition, 567
neutron age, 569
neutron diffusion parameters, 570
other reactors, 570
rectangular reactor, 570
reflected reactors, 570
reflecting material, 567, 569
reflection coefficient, 567
thermal diffusion length of reflector, 571
thermal migration area, 570
derivation, diffusion equation
bare core, 576
boundary conditions, 571–572
Deutsch equation, 575
entire core, 575
flux shape, 572
homogeneous reactor core, 571–572
light-water reactors, 571
material buckling, 572
maximum reflector savings, 573
neutron flux and current, 573
thermal diffusion length, 571, 573
transcendental equation, 573
vacuum boundary condition, 572
Refractive index, 100–101
Relational database, 970
Relativistic mass, 265
Relativistic speeds, 128
Removal cross section, 167
Repetitive elastic collisions, 134
Research reactors, 456
Resonance energy group, 207, 226
Resonance energy range, *see* Epithermal energy range
Resonance energy region, 173
Resonance escape probability, 173, 226, 414, 452, 460, 534, 737
definition, 419–420
Doppler broadening
absorption cross section, 739
Boltzmann's constant, 737
Breit–Wigner model, 739
effective multiplication factor, 738

effect of fuel temperature, 737–738
fuel temperature coefficient, 739
kinetic energy, 737
large absorption resonances, 737–738
molecular agitation, 738
neutron reproduction factor, 740
nuclear Doppler effect, 737, 739
four-factor formula, 414
absorption resonances, 421–422
constants, 421
general expression, 420
MFR, 421
neutron lethargy, 420
resonance integral, 420
resonance self-shielding, 422
Monte Carlo method
absorption resonance, 986–987
definition, 986
fission neutron energy distribution, 988
half width of resonance, 987
kinetic energy, 988
resonance integrals, 986
scattering resonance, 986–987
transcendental function, 988
value, 989
Watt equation, 988
six-factor formula, 452
Resonance integrals, 986
Resonance self-shielding, 422, 819
Rest mass, 86, 96
isotopic, 264–265
proton and neutron, 340
Richter scale, 894, 898
The Ring of Fire, 729
Rod correction factor, 504
Rod drop method, 702
Rod ejection accident, 847
Rod oscillator method, 702
Room temperature libraries, 214
RSIC Center, 903
Rutherford, Ernest, 158
Rutherford, Lord, 158
Rutherford scattering formula, 158–160

Safety control rod axe man (SCRAM), 51; *see also* Scram
Samarium, 73, 300
properties, 878
Samarium-149, 148, 357
after shutdown, 791–793
buildup, 789, 888
concentration, 788
effective yields, 786
equilibrium concentration, 790–791, 890–891
neutron absorption cross section, 784, 786–787
production process, 786, 788
realistic cross sections, 906
shutdown, 891–893
start-up, 889–890
thermal absorption cross section, 894
Scalar, 471
Scalar multiplier, 620
Scalar quantity, 117, 473, 916, 1044
Scaling constant, 75
Scattering angles
in COM system, 138–140
cosine of, 511, 526, 1045–1046
in inelastic collisions, 155
in LAB system, 140
Monte Carlo method
angular scattering probability, 992
asymmetric scattering angles, 994–997
cylindrical fuel rod, 993
directional unit vector, 993
elastic collision probability, 991
elastic scattering of neutrons, 993
inverse cumulative distribution function, 992
three-dimensional scattering angles, 991–992
neutron energy loss, 138
Scattering cross section, 153, 170, 534, 543
energy groups, 180
neutrons with any kinetic energy, 184–186
Sodium-23, 173
Scattering kernels, 138, 382, 384, 919, 922
Scattering matrix, 940
Scattering mean free path, 500
Scattering probability distributions, 152–154
Scattering process, 524
Schrödinger wave equation, 82, 929
Scram, 829
button
control panel, 848, 850
passive safety system, 849
origin, 850–851
Scram button, 848–850
emergency shutdown, 51
passive safety system, 49
PWR, 49
on reactor control panel, 48, 50
Scrammed reactor, 682
Scramming, 830
Seaborg, Glenn, 286, 306, 308
Secular equilibrium, 304–306
Segre Chart, *see* Chart of the Nuclides
Semi-empirical mass formula, 189; *see also* Weizsaecker model of nuclear structure
Separation of variables, 558, 562
Seventh-order equation, 695
Shell models, 278–279
Shells, 71
Shippingport nuclear power plant, 829
Shippingport reactor, 829
Shutdown banks, 848–849
Shutdown rods, 709
Signal processing, 712
SIMMER code, 987
SIMULATE, 539–540
Single energy/speed, 519
Single neutron energy, 222
Six-factor formula, 408, 428
absorption resonances, U-238 and Thorium-232, 439–440
applications, 456
core composition, 444–445
core power densities, 460–462
fast and thermal nonleakage probability, 439
explicit expression, 441
geometric buckling and flux shape, 441, 459–460
neutron leakage rate, 442
thermal diffusion length, 441–442
thermal migration area, 442
great natural nuclear reactors of Oklo, *see* Oklo reactors
hexagonal *vs.* square fuel assemblies, 450–451
$K_{effective}$ value, 439–440
limitations, 452–453
MFR
average power density, 461
and four-factor formula, 446–447
infinite multiplication factor, 448
pitch of rectangular lattice, 448–449
rod diameter, 446
rod pitch, 445–446
values of K_∞, 449–450
neutron flux
and fuel enrichment, 457–458
and power, 456–457
and reactor characteristics, 456
thermal to fast neutron flux ratios, 458–459
neutron leakage probability, 439
physical significance, 443–444
reactor criticality
eta of the fuel, 451–452
fast fission factor, 451–452
neutron life cycle, 451–452
Oklo reactors, 455–456
resonance escape probability, 452
thermal utilization, 452
Six independent variables, 483
67-95-99.7 rule, 976
Skewed probability distributions, 990–992
Skewness, 990
Slow neutrons, 74
S_N approximation
angular decomposition, 934
angular neutron flux, 933
arbitrary angular direction, 934–935
discrete ordinates, 934
to spherical source, 935–937
values of angular flux, 934
S_N method, 935–937
Sodium-cooled reactors, *see* Liquid metal fast breeder reactors
Sodium cooling loops, 370
Solbor, *see* Boric acid, *see* Chemical shim
Solid angle directional vector, 156
Soluble boron, 724; *see also* Chemical shim
Source jerk method, 702
Space-bound reactors, 31
Spatial gradient, 526
Spatial homogenization, 235; *see also* Fuel assembly homogenization
absorption cross section, 811
average neutron flux, 813
fission cross section, 811
hypothetical super cell, 813

PWR fuel assembly, 807–808
reaction rates conservation, 809, 812–813
scattering cross section, 811
super cell, 812
transport cross section, 812
unit cell
hypothetical super cell, 812–813
number of, 812
reactor lattice, 807, 809
total volume, 812
SPD, *see* Statistical probability distribution
Specific heat, 750
Spent fuel pool, 774
Spherical harmonics approximation, *see* P_N approximation
Spherical reactor, 559
Spin–orbit interaction, 279
Splines, 744
Spontaneous fission, 280
Square well, 278
Stacy, Weston, 382
Standard form, 491–492
Standard operating procedure (SOP), 40
Standard temperature and pressure (STP), 583
Start-up temperature coefficient, 749
Statistical average/mean, 497, 711
Statistical probability distribution (SPD), 960
CDF, 963–964
discrete probability distribution functions, 964
events list, nuclear particles interaction, 964
flat probability distribution, 962
life cycle of the particle(s), 964
normal probability distribution, 962
radioactive decay
average decay rate, 294
emission probabilities, alpha particles, 293
emission probabilities, beta particles, 293–294
histogram, 293
Poisson probability distribution, 292
quantum mechanics, 294
reactor lattice, 965
scattering cross section, 964
scattering kernel, 965
simulation phase, 965
Steady-state neutron diffusion equation, 68
common reactor geometries, 556–557
critical mass
calculation, bare reactors, 580
reflector effect estimation, 581
current boundary condition, 594
dependence of buckling and diffusion coefficient
absolute temperatures, 586
absolute zero, 585
axial elevation, 583
Centigrade, 584
Fahrenheit, 584
fuel *vs.* coolant temperatures, PWR and BWR, 582
highest coolant temperature, 583
hot and cold core, 586
Kelvin, 584
liquid moderator, 584
macroscopic scattering cross section, 584
melting points, nuclear parameters, 585
Rankine and Brayton thermal cycles, 586
reactor materials property, 582
reference temperatures, 582
solid moderator, 584
STP, 583
temperature correction factors, 582
thermal diffusion length, 585
design parameters, different reactors, 555
flux and power shaping, 565–566
flux shape
fast and thermal neutrons, reflected thermal reactor, 566–568
infinite cylindrical reactor, 563–564
three-dimensional cylindrical reactor, 560–563
three-dimensional spherical reactor, 559–560
fuel assembly model, 592–594
geometric buckling *vs.* one and two energy groups, 576–578
neutron flux
boundary conditions, 555–556
and power level correlation, 552–553
three-dimensional rectangular reactor, 556–558
optimum sizes and shapes, reactor cores
buckling and radius relationship, 579
critical dimensions ratio, 578
critical mass, 578–579
cube, 579
cylinder volume, 578
height and radius relationship, 578
no unique solution, 578
surface-to-volume ratio, 578–579
total surface area, 578
peak-to-average power ratio, bare core, 564
physical interpretation, geometric buckling, 553–555
power level and neutron flux correlation, 552–553
radiation shield, 594
radioactive source, 594
reflected reactors, 566
reflector savings
and albedo, 567, 569–571
derivation, 571–574
saving fuel, neutron reflector, 581–582
size prediction, critical reactor, 574–576
slab reactor
boundary conditions, 550
critical reactor, 551
effective multiplication factor, 549
eigenfunctions, 551
eigenvalues, 551
fundamental eigenfunction, 551
geometric buckling, 549
infinite slab reactor, 549–550
magnitude of the flux, 552
material buckling, 549
one-dimensional reactor, 551
orthogonality, 551–552
reactor power level, 552
single energy group, 549
subcritical reactor, 549
supercritical reactor, 549
time-dependent diffusion equation, 551
time dependent reactors, 549
with and without delayed neutrons, 551
temperature dependence, neutron mean free path, 587
three homogeneous material regions
boundary conditions, 587–588
diffusion coefficient, 588
Fick's Law, 590
material buckling, 588
multiregion reactor, 589
spatially homogeneous, 591
standard numerical technique, 590
Steady-state neutron transport equation, 923
Steady-state power, 756
Steam dryer, 847
Steam generators
alloys and superalloys, 53
completely saturated, 52
exit quality, 52
OTSG, 52
RCPs, 51–52
saturated liquid, 52
and steam turbine pairing, 53
superheated, 52
temperatures and pressures, 52
UTUBE steam generator, 52
Steam turbines, 45, 51, 53
Strong nuclear force, 75–76
Supercritical reactor, 549
Supernovas, 320–321
Superposition effect, 610
Surface area, *see* Surface energy term
Surface energy term, 274–275
Surface tension term, 274–275

Taylor series, 96
Taylor series expansion, 852
Teller, Edward (father of H Bomb), 752
Tellurium-135, 786
Temperature and power defects
calculation, 750–751
PWR, 749
Temperature coefficient for fuel, 747
Temperature coefficient of reactivity, 731, 747
Temperature conversion formulas, 1009
Temperature defect of reactivity, 747
Temperature-dependent reaction rates, 1022
Temperature feedback
axial power distribution, 757
effective multiplication factor, 759
fission-to-absorption ratio, 758
fresh core, 758
fuel temperature coefficient, 737, 740–741, 758
magnitude estimation, 757
negative, 757
non-1/v correction factors, 757–758
nuclear Doppler effect, 757
nucleate/bulk boiling, 733–734
observations, 757–758
reactivity change, 742–743

reactivity of core, 731–732
reactor control systems, 757
steady-state power level, 757
time dependence, core temperature coefficients, 741
and TRIGA reactor, 752
10 CFR50, 743–744
Ten orders of magnitude, 519
Tesla, Nikola, 1039
Theory of quantum mechanics, 169
Theory of Relativity, 93
Theory of special relativity, 103–104, 391
Thermal absorption cross section, 223
Boron-11, 834–835
Cadmium-112, 835
Thermal conduction process, 741
Thermal correction factor, 223
Thermal diffusion coefficient, 556
Thermal diffusion length, 1049
Thermal efficiency (TE), 352
Thermal energy
definition, 379
vs. electrical energy, 352
group, 207, 520
production, 1006
range, 207, 329
region, 183
released per fission, 338
Thermal energy group cross sections
absolute temperature, 225
average energy, 224–225
Maxwell–Boltzmann probability distribution, 224
Maxwellian flux, 225
non-1/v correction factors, 1021–1022
probable energy, 224–225
thermal neutron flux, 223
Thermal equilibrium, 121, 350, 367, 376, 970
Thermal feedback, 752
Thermal fission cross section, 542
Thermal flux, 500, 567, 721
Thermal-hydraulic analysis code, 903
Thermalized behavior, 567
Thermal migration area, 535, 575
Thermal migration length, 1049
Thermal neutron(s), 121, 177–179, 324–325, 520, 720, 1049
Maxwell–Boltzmann probability distribution, 367
origin, 378–379
Thermal neutron cross sections, 222
Thermal neutron flux, 177, 223, 538
Thermal neutron life cycle, 427, 528
Thermal nonleakage probability, 408, 439, 441–442, 575, 577
Thermal power, 323, 552
Thermal reactor, 534
Thermal resistance, 750
Thermal utilization, 414, 877–878
definition, 417
equivalent cylindrical cell, 418–419
neutron flux, 418
radius of an equivalent unit cell, 418
representative PWR fuel assembly shape, 418
thermal utilization factor, 425
Wigner–Seitz method, 418–419
Thermal utilization factor, 425
Thermal water reactors, 538
control rods, 433–434
geometric buckling, 459–460
infinite multiplication factor, 433
reactivity, 433
thermal to fast neutron flux ratios, 458–459
Thorium
isotopes and relative abundance, 323
Thorium-231 decays, 280
Thorium-232, 181–182, 282, 439–440
Thorium-234 decays, 282
Three-dimensional flux, 557
Three Gorges Dam, 55
Time and decay conversion factors and constants, 1006
Time dependence, 614
Time-dependent behavior, 639
Time-dependent diffusion equation
delayed neutrons, 656, 662–664
neutron source term, 637
Time-dependent neutron diffusion equation, 68, 484, 488–489, 636
Time-dependent reactivity reduction, 741
Time-dependent reactor behavior
delayed neutrons
average decay constant, 652
average values, 652
creation, 655
curve fit, 650–651
decay chain, statistical analysis, 651–652
definition, 649
energy spectrum, 652–653
fission products/fission fragments, 649
fraction, 648, 652–653
half-life and average life, 652
isotopes, 653–654
Keepin, George Robert, 650–651
nuclear properties, uranium and plutonium, 650
number of, 649
six radioactive decay chains, 650
time-dependent diffusion equation, 656, 662–664
total number of fission neutrons, 649
weighted average, 652
delicate balancing act, 647
neutron flux and fission product concentrations, 664–667
prompt neutron life cycle, 661–662
PWR, 647
reactivity, 647
reactor kinetics, 647
reactor period
common moderators, 660
point kinetics equations, 661
prompt neutron lifetime, 659
and reactor power, 667–668
thermal diffusion time, 659–660
time-dependent neutron flux, 659–661
real reactors, 647
separation of variables method, 656–658
space–time kinetics, 647
time-dependent neutron production, 648–649
Time dilation, 95
Total buckling, 558
Total energy, 1033
Total momentum of the system, 125
Total nonleakage probability, 577
Total reaction cross section
beneath absorption resonances, 188–189
definition, 167, 170, 187
diameter of atomic nucleus, 188
semiempirical mass formula, 189
Total reaction rate, 175
Total removal cross section, 919, 922
TRACE, 703
ATWS, 903–904
BWR/5 power plant, 904–905
component model, 904
Henry, Alan, 540
Maanshan PWR, 540, 542
postprocessor, 704
QUANDF, 540
thermal absorption cross sections, 905
thermal-hydraulic simulation, 904–905
Training, Research, Isotopes, and General Atomics (TRIGA) reactor
design by
Dyson, Freeman, 752, 755
Teller, Edward, 752, 754
development, General Atomics Company, 752
Feynman diagrams, 752
fuel rod, 752, 755
hydrogen atoms, 752
internal power regulator, 752
location, 752–754
plate-type rods, 752
power pulses, 756
research and training reactor, 754
thermal feedback, 752
UZrH fuel, 752
warm neutrons concept, 752
Transient reactor analysis code (TRAC), 903
Transport correction factor, 1048
Transport cross section, 511, 928, 951–952, 1044, 1046–1047
Transport mean free path, 525, 624, 951
Transport scattering cross section, 525–526
Tritium, 393
24 Billion degrees Kelvin, 379
2D Ising Model of MacGregor, 279
Two-group approach, 522
TWOTRAN, 952

Ultracold beam, 143
Ultrafine cross section library, 195
Uncontrolled chain reaction, 283–284, 344
Under-predicts, reaction rates, 555
Unit cells
equivalent cylindrical unit cell
hexagonal reactor lattice, 408–409
standard reactor lattice, 408
infinite lattice, 411–413
neutron life cycle
CANDU reactor, 423–425
Westinghouse PWR, 425–426

neutron population, 426–427
radius, 409
Units
derived units, 1008
energy and power, 1006
non-SI units, 1008
prefixes, 1007
primary units, 1007–1008
reactivity, 1006
Unit systems
CGS units, 1007
English, 1007
SI, 1007
derived units, 1008
prefixes and abbreviations, 1007
primary units, 1007–1008
Universal gas constant, 390
Unrecoverable energy, 1033
Unrecoverable kinetic energy, 107
Unreflected cores, 624
Unreflected reactor, 566
Up-scattering, 523, 537
Uranium, 319
atomic mass number, 322
atomic number, 322
breeding, 12
centrifugal separation process, 13
element, 12
enrichment process, 12–14
fertile materials, 12
gaseous diffusion process, 13
induced fission process, 323–324
laser enrichment process, 13
metallic form, 12
natural abundance, 12–13
natural uranium, 12
nuclear properties, 321–322
nuclear weight, 322
pitchblende, 280
and plutonium masses, 343–346
production
Earth's crust, 321
supernova explosions, 321
stable isotopes, 321–322
Uranium-233, 321
Uranium-234, 321
Uranium-235, 147–148, 321, 719–720
Uranium-238, 321, 542–543, 720
uranium dioxide, 13, 16
weighted average, 322
Uranium dioxide (UO_2), 13, 16, 28–29, 335, 444
absorption to fission ratio, 200
enrichment, 198–199
macroscopic capture cross section, 198–199
microscopic capture cross section, 198
nuclear properties, 198–199
number of U-235 atoms, 199
Uranium enrichment process
isotopic separation, 284
U-235 *vs.* U-238, 284
uranium hexafluoride (UF_6), 284
Uranium-fueled thermal water reactor, 866
Uranium hexafluoride (UF_6), 13, 284
UZrH fuel, 752

Vacuum boundary condition, 920, 946
extrapolation distance, 949–950
neutron flux shapes, 948–949
P_1 approximation, 948
partial neutron currents, 948
Vector operator, 486
Velocity-dependent mass, 104
Vibrational frequency, 106
Void coefficient, 733, 895–896
and load following
BWR, 735–736
fuel temperature coefficient, 735, 737
heat-generation rate, 735
power level, 735
PWRs, 735–736
time-dependent behavior, 735
of reactivity, 734–735
Void fraction, 734
Volume energy term, 274–275
Volumetric heat generation rate, 640
Volumetric power density, 34, 458
von Neumann, John, 1000–1001

Warm neutron principle, 752, 754
Warm neutrons concept, 752
Watt curve, 118
Watt distribution, 990, 994
Wattenberg, Albert, 700
Watt equation, 119–120, 328, 988, 1049
Wave/particle duality, 615
Weighting factors, 943
Weighting function, 243
Weizsaecker model of nuclear structure, 278
Westcott, C.H., 222
Westcott, Charles, 740
Wigner–Seitz method, 418–419
Wigner–Way equation, 310, 868
World's primary temperature scales, 1008–1009

Xenon, 73, 300
properties, 878
Xenon-131, 878
Xenon-133, 878
Xenon-135, 148, 357
after shutdown, 791–792
buildup, 789, 792
Chernobyl accident, *see* Chernobyl accident
concentration, 785–786
decay chain, 785
demand charge, 888
effective yields, 786
equilibrium concentration, 789–790
equilibrium operating cycle, 880–882
neutron absorption cross section, 784, 786–787
nonintuitive xenon behavior, 886–887
power demand, 888
reactor dead time, 792, 885–886
realistic cross sections, 906
shutdown cycle, *see* Reactor shutdown cycle
start-up cycle, 879–880
thermal absorption cross section, 878, 893
Xenon flux tilt transient, 886–887
Xenon power oscillation, 886
Xenon power transients, 886
X-rays, 170, 614

Yukawa constant, 75
Yukawa, Hideki, 75
Yukawa potential, 75–77

Zinn, Walter, 700
Zircaloy, 18–19
Zirconium cladding, 400